U.S. Department
of Commerce

Volume 102
Number 1
January 2004

Fishery Bulletin

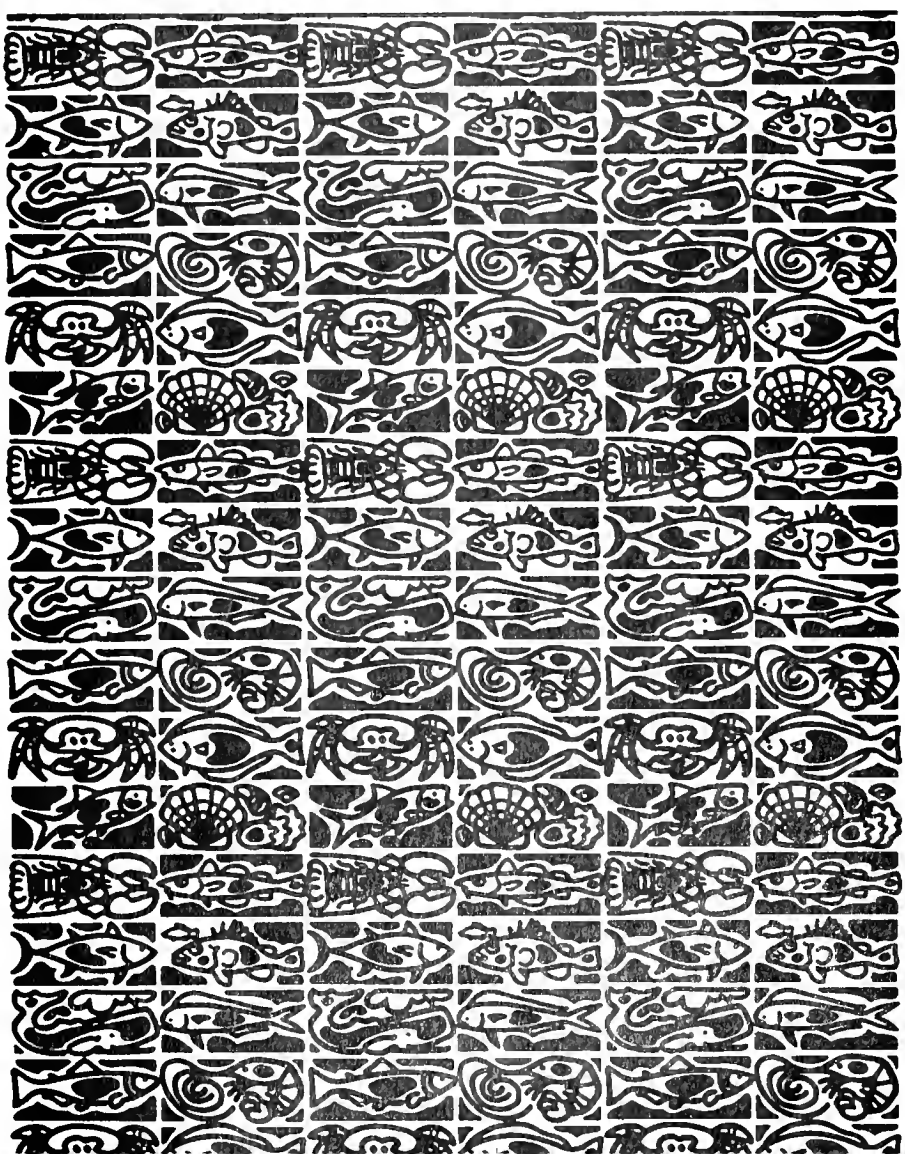

The *Fishery Bulletin* (ISSN 0090-0656) is published quarterly by the Scientific Publications Office, National Marine Fisheries Service, NOAA, 7600 Sand Point Way NE, BIN C15700, Seattle, WA 98115-0070. Periodicals postage is paid at Seattle, WA, and at additional mailing offices. POSTMASTER: Send address changes for subscriptions to Fishery Bulletin, Superintendent of Documents, Attn.: Chief, Mail List Branch, Mail Stop SSOM, Washington, DC 20402-9373.

The Secretary of Commerce has determined that the publication of this periodical is necessary according to law for the transaction of public business of this Department. Use of funds for printing of this periodical has been approved by the Director of the Office of Management and Budget.

For sale by the Superintendent of Documents, U.S. Government Printing Office, Washington, DC 20402. Subscription price per year: $55.00 domestic and $68.75 foreign. Cost per single issue: $28.00 domestic and $35.00 foreign. **See back for order form.**

Fishery Bulletin

***Fishery Bulletin* web site: www.fishbull.noaa.gov**

The *Fishery Bulletin* carries original research reports and technical notes on investigations in fishery science, engineering, and economics. It began as the Bulletin of the United States Fish Commission in 1881; it became the Bulletin of the Bureau of Fisheries in 1904 and the *Fishery Bulletin* of the Fish and Wildlife Service in 1941. Separates were issued as documents through volume 46, the last document was No. 1103. Beginning with volume 47 in 1931 and continuing through volume 62 in 1963, each separate appeared as a numbered bulletin. A new system began in 1963 with volume 63 in which papers are bound together in a single issue of the bulletin. Beginning with volume 70, number 1, January 1972, the *Fishery Bulletin* became a periodical, issued quarterly. In this form, it is available by subscription from the Superintendent of Documents, U.S. Government Printing Office, Washington, DC 20402. It is also available free in limited numbers to libraries, research institutions, State and Federal agencies, and in exchange for other scientific publications.

U.S. Department of Commerce
Seattle, Washington

Volume 102
Number 1
January 2004

Fishery Bulletin

Contents

Articles

Notes

The effects of size-selective fisheries on the stock dynamics of and sperm limitation in sex-changing fish

Suzanne H. Alonzo

Institute of Marine Sciences and the Center for Stock Assessment Research (CSTAR)
University of California Santa Cruz
1156 High Street
Santa Cruz, California 95064
E-mail address: shalonzo@ucsc.edu

Marc Mangel

Department of Applied Mathematics and Statistics
Jack Baskin School of Engineering and the Center for Stock Assessment Research (CSTAR)
University of California Santa Cruz
1156 High Street
Santa Cruz, California 95064

Abstract—Fisheries models have traditionally focused on patterns of growth, fecundity, and survival of fish. However, reproductive rates are the outcome of a variety of interconnected factors such as life-history strategies, mating patterns, population sex ratio, social interactions, and individual fecundity and fertility. Behaviorally appropriate models are necessary to understand stock dynamics and predict the success of management strategies. Protogynous sex-changing fish present a challenge for management because size-selective fisheries can drastically reduce reproductive rates. We present a general framework using an individual-based simulation model to determine the effect of life-history pattern, sperm production, mating system, and management strategy on stock dynamics. We apply this general approach to the specific question of how size-selective fisheries that remove mainly males will impact the stock dynamics of a protogynous population with fixed sex change compared to an otherwise identical dioecious population. In this dioecious population, we kept all aspects of the stock constant except for the pattern of sex determination (i.e. whether the species changes sex or is dioecious). Protogynous stocks with fixed sex change are predicted to be very sensitive to the size-selective fishing pattern. If all male size classes are fished, protogynous populations are predicted to crash even at relatively low fishing mortality. When some male size classes escape fishing, we predict that the mean population size of sex-changing stocks will decrease proportionally less than the mean population size of dioecious species experiencing the same fishing mortality. For protogynous species, spawning-per-recruit measures that ignore fertilization rates are not good indicators of the impact of fishing on the population. Decreased mating aggregation size is predicted to lead to an increased effect of sperm limitation at constant fishing mortality and effort. Marine protected areas have the potential to mitigate some effects of fishing on sperm limitation in sex-changing populations.

Manuscript approved for publication 23 July 2003 by Scientific Editor.

Manuscript received 20 October 2003 at NMFS Scientific Publications Office.

Fish. Bull. 102:1–13 (2004).

Fisheries models are generally used to predict the impact of fishing on stock dynamics and yield (Quinn and Deriso, 1999; Haddon, 2001). Classic models have focused mainly on growth, fecundity, and survival of species, without considering the impact of mating patterns on reproduction, survival, and recruitment. It is now recognized that life-history strategies and mating behavior will affect stock dynamics. Even so, general quantitative predictions regarding the effect of specific life-history patterns on fished populations are limited and further theory is needed (Levin and Grimes, 2002). It is likely that management strategies taking into account a species' reproductive behavior will greatly improve our ability to manage stocks (e.g. Beets and Friedlander, 1999). We would also like to know when the mating behavior and reproductive strategies of a stock will be worth investigating and when traditional management techniques will be sufficient. For example, in a management context, how do sex-changing stocks differ from separate-sex species? Here, we take an initial step toward generating a theory of the combined effect of life history and mating patterns on stock dynamics by focusing on the potential for and effect of sperm limitation in a protogynous (female to male) sex-changing stock. We focus on protogyny for this article because numerous protogynous species are commercially important, namely red porgy (*Pagrus pagrus*), gag grouper (*Mycteroperca microlepis*), and California sheephead (*Semicossyphus pulcher*).

Sex-changing fish present a unique challenge for management because size-selective fisheries have the potential to drastically reduce reproductive rates and population size at levels of fishing that would not pose a problem for dioecious (separate-sex) species (Huntsman and Schaaf, 1994; Armsworth, 2001; Fu et al., 2001). On the other hand, protogynous stocks may be less sensitive to the removal of large individuals if females are not fished and fertilization rates remain high. Many commercially important species are known to change sex (Bannerot et al., 1987; Shapiro, 1987; Coleman et al., 1996; Brule et al., 1999; Adams et al., 2000; Armsworth, 2001; Fu et al., 2001). Previous models have shown that sex-changing fish may be vulnerable to fishing (Bannerot et al., 1987; Huntsman and Schaaf, 1994; Armsworth, 2001; Fu et al., 2001).

Complications arise because the effect of fishing on a sex-changing species is mediated by many aspects of their reproductive biology, such as sex ratio, size-dependent fecundity, spawning aggregation size, and reproductive skew. Furthermore, patterns of sex change have cascading effects on the sex ratio, social interactions, population

fecundity, and male sperm production—all of which can affect stock dynamics. Thus, we cannot treat sex change as an isolated aspect of a species. Instead, we must consider sex change within the context of the mating system and the life history of the species to make general predictions. Behaviorally appropriate models are required to generate constructive qualitative and quantitative theory. Past theory has indicated that sex-changing populations exhibit stock dynamics that often differ from those of dioecious populations (Bannerot et al., 1987; Huntsman and Schaaf, 1994; Armsworth, 2001; Fu et al., 2001). Furthermore, protogynous stocks are predicted to be sensitive to fishing pattern and may exhibit nonlinear dynamics that could lead to population crashes (Armsworth, 2001). However, it is not known which aspects of the mating behavior and life history pattern of sex-changing stocks drive these differences. Here we focus on comparing a protogynous stock with an otherwise identical dioecious population to determine the effect of mating aggregation size, fertilization rates, and life history pattern on stock dynamics.

Size-selective (or age-selective) fisheries can impact a species through a decrease in spawning stock biomass, in general and through the removal of highly fecund larger and older individuals, in particular (Sadovy, 2001). However, in protogynous species, fisheries that preferentially remove large males can also change the population sex ratio; however, the exact effect of fishing pressure on stock dynamics in a protogynous species is complex. At one extreme, the complete removal of males from the population would cause a stock to crash, potentially making sex-changing species more vulnerable than dioecious species in the face of high fishing pressures. At the other extreme, sex-changing species may be less affected by size-selective fisheries if female fecundity limits recruitment and males are not removed in such numbers as to reduce mating or fertilization rates. Currently, there is no theory that predicts the potential for sperm limitation in protogynous stocks as a function of gamete production, fertilization rates, and mating pattern.

It has been suggested that marine reserves may be a viable management option for species where highly fecund older individuals are critical to reproduction (Levin and Grimes, 2002). However, no theory exists that can predict the impact of marine reserves on stock dynamics in sex-changing species. We consider the impact of a no-take marine reserve on the stock dynamics. We compare the effect of setting aside 0–30% of the spawning population in a reserve. We assume that larval production is exported from within the reserve to the rest of the population and determine whether the reserve can mediate some of the effects of fishing outside the reserve because this represents the optimal scenario for marine reserves. We also compare mean catch rates in the presence and absence of a reserve as a function of fishing mortality.

Spawning-per-recruit (SPR) measures are often used to estimate the impact of fishing on a stock (Parkes, 2000; Jennings et al., 2001). Ideally, a spawning-per-recruit measure would keep track of per-recruit production of larvae or eggs (Jennings et al., 2001). However, spawning stock biomass per recruit (SSBR) is commonly used to estimate the reproductive output per recruit at different intensities of fishing. One assumes that the biomass of mature fish is linearly related to reproductive output, which may be the case when egg production limits biomass and fecundity increases linearly with biomass. In protogynous stocks, overfishing of males alone may decrease fertilization rates and hence reproductive output without affecting either female biomass or egg production. Thus, in protogynous stocks or sex-selective fisheries, classic measures of spawning per recruit may misrepresent the impact of fishing on the stock's reproduction and hence population stability (Punt et al., 1993). We examine a variety of per-recruit measures and determine their ability to predict changes due to exploitation in mean population size.

In this study, we describe a general approach using sex- and size-dependent individual-based simulation models that predict reproduction, size distribution, and sex ratio in fished populations as a function of mating system and sex-change pattern. We examine the case where sex change occurs at a specific size threshold. We recognize that plastic and socially mediated sex-change patterns have been observed, and our results will apply only to species with fixed sex change. We explore the impact of mating aggregation size, sperm production, and asymptotic fertilization rates on the predicted stock dynamics in the presence of exploitation. We make predictions regarding the effects of fishing on population size, reproduction, sex ratio, size distribution, and fertilization rates. We also compare our results to previous work and discuss future directions.

Methods

We used an individual-based simulation to predict the size distribution, individual and population fecundity, population sex ratio, fertilization rate, and population size as a function of fishing mortality (Fig. 1). Individuals vary in age, size, sex, and mating site. Population size varies as a function of baseline survival, fishing mortality, reproduction, and larval recruitment. Reproduction depends on the pattern of sex change, mating system, sex ratio, mating site, and fecundity (or fertility) of individual males and females. For each annual time period, we determined individual survival, the size and age of these individuals in the next time period, and the total production of surviving offspring by those individuals. Initial analyses showed that a stationary size, sex, and age distribution is found within approximately 50 time periods and is independent of the initial population conditions. Thus, we simulated 100 time periods prior to examining the impact of fishing on stock dynamics to ensure that the population had already reached the stationary size and sex distribution for that scenario and set of parameters. We then examined the model for 100 reproductive seasons in the presence of fishing with a constant mean fishing mortality. Because a number of elements of the model were stochastic, we examined 20 simulations for each scenario and set of parameter values. Initial analyses indicated that 20 simulations were more than sufficient to lead to low variability in the key measures of interest. We assumed that reproduction occurs at the level of the mating

group at different reproductive sites. Individual survival, maturation, sex change, and mating site were determined stochastically as described below.

Fishing and adult survival

We assumed that adult survival is density independent but depends on fishing selectivity, fishing mortality, and baseline adult mortality in the absence of fishing. For simplicity, we assumed that age and size do not affect nonfishing adult mortality μ_A. We assumed that the fishery is size selective; we let L represent fish size, F represent annual fishing mortality, L_f represent the size at which there is 50% chance an individual of that size will be taken, and r represent the steepness of the selectivity pattern. Then fishing selectivity per size class $s(L)$ is given by

$$s(L) = \frac{1}{1+\exp\left(-r(L-L_f)\right)} \tag{1}$$

and adult annual survival becomes

$$\sigma(L) = \exp\left(-\mu_A - Fs(L)\right). \tag{2}$$

We assumed that fishing does not differentially affect the sexes independent of size. We recognize, however, that for some species this may not be the case. We also assumed that fishing occurs each year prior to reproduction and can represent either pulse or continuous fishing with an annual mortality F. We let $N_a(t)$ represent the number of individuals in age class a at time t so that population size $N(t) = \Sigma_a N_a(t)$.

Population dynamics

We assumed that the number of larvae that enter the population is determined by the production of fertilized eggs $P(t)$ and the probability that those larvae will survive to recruit. $P(t)$ is determined by the adult fecundity and fertilization rates described below. For computational tractability, we also assumed that a population ceiling $N_{\max}$ exists (Mangel and Tier, 1993, 1994). However, we chose $N_{\max}$ large enough that the stable population size was below the ceiling. Larval survival has both density-independent and density-dependent components (e.g. Cowen et al., 2000; Sale, 2002). We used a Beverton-Holt recruitment function to determine larval survival to the next age class (Quinn and Deriso, 1999; Jennings et al., 2001). Larvae represented the zero-age class $N_0(t)$ and thus the number of larvae surviving to recruit in any year t is given by

$$N_0(t) = \begin{cases} (\alpha P(t))/(1+\beta P(t)) & \text{if } (\alpha P(t))/(1+\beta P(t)) + \sum_{a=1} N_a(t) \le N_{\max} \\ \max\left(0, N_{\max} - \sum_{a=1} N_a(t)\right) & \text{if } (\alpha P(t))/(1+\beta P(t)) + \sum_{a=1} N_a(t) > N_{\max}, \end{cases} \tag{3}$$

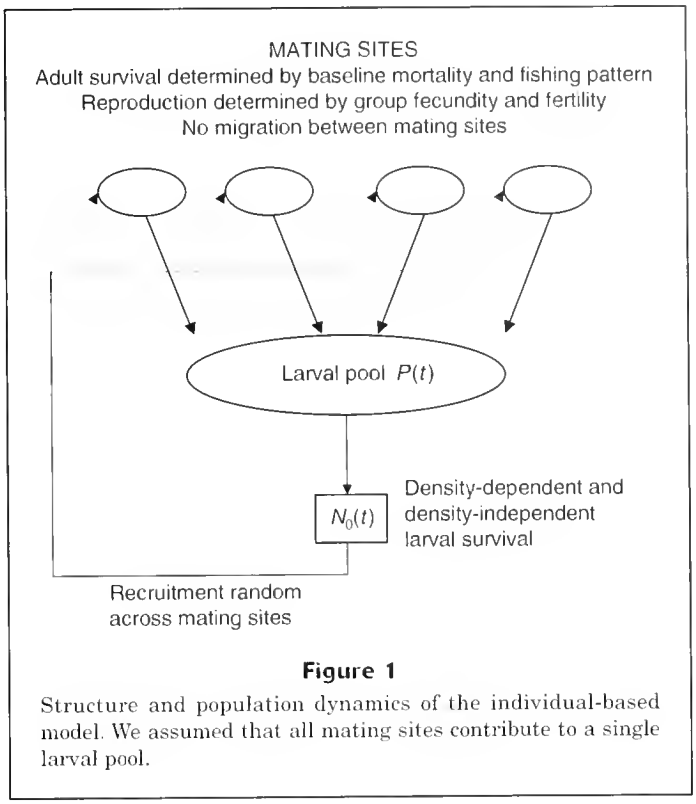

Figure 1

Structure and population dynamics of the individual-based model. We assumed that all mating sites contribute to a single larval pool.

where α gives density-independent survival; and β determines the strength of the density-dependence in the larval phase. In this function, we used the number of fertilized eggs produced, $P(t)$, rather than spawning stock size. We selected parameter values for larval survival that allowed the mean population size to be stationary near the ceiling in the absence of fishing. We assumed a single larval pool and that larvae recruit to mating sites at random (Fig. 1). The population was open between mating sites and we were simulating the entire stock. Thus, there was no emigration to or immigration from outside populations.

Growth dynamics

We assumed that all larvae enter the population at the same size, L_0. We assumed that growth is deterministic and independent of sex or reproductive status. We used a discrete time version of the von Bertalanffy growth equation (Beverton, 1987, 1992) to determine growth between age classes of surviving adults in which $L_{\inf}$ represents the asymptotic size and k is the growth rate. Then an individual of length $L(t)$ at time t will grow in the next time period to size $L(t+1)$ as follows:

$$L(t+1) = L_{\inf}(1+\exp(-k)) + L(t)\exp(-k). \tag{4}$$

Mating system

We assumed that reproduction occurs at the level of the mating group, and we examined the effect of varying mating group size and the number of mating sites. We assumed

that juveniles and adults exhibit site fidelity but that larvae settle randomly among mating sites. We also assumed that the population carrying capacity is split equally among the mating sites and that the total capacity of all mating sites exceeds the maximum population size in the absence of fishing as determined by adult mortality and the recruitment function. Therefore, mating sites do not limit recruitment but may affect reproductive rates. We examined three cases: 1) the entire population mates at one site (one mating site with up to 1000 individuals); 2) a few large mating groups exist (10 sites with a maximum of 100 individuals per site); and 3) many small mating aggregations exist (20 mating sites with a maximum of 50 individuals per site). For simplicity, we assumed that within a mating site, individuals mate in proportion to their fertility and fecundity. Therefore, large males and females have higher expected reproductive success. However, we assumed that all males that are large enough to change sex have a chance of reproducing proportional to their fertility. This is equivalent to assuming that females exhibit a mate choice threshold (Janetos, 1980) that has evolved with the size-at-sex change and that females have an equal probability of mating with males above this size threshold. However, a large male mating advantage clearly still exists. We also assumed that fishing mortality remains constant as mating aggregation size varies. Thus, we assumed that fishing effort per site does not increase as the number of mating sites decreases. An alternative would be to assume that total fishing mortality increases as the number of mating aggregations decreases.

Maturity

The probability that an individual matures $p_m(L)$ is determined by size. Once an individual matures, she remains female until sex change (see below). We let L_m represent the length at which 50% of the individuals will have matured.

$$p_m(L) = \frac{1}{1+\exp(-q(L-L_m))}, \quad (5)$$

where q determines the steepness of the probability function.

Sex change

The probability of sex change, $p_c(L)$, is a logistic function of absolute size L

$$p_c(L) = \frac{1}{1+\exp(-\rho(L-L_c))}, \quad (6)$$

where L_c represents the size at which 50% of the individuals will change sex from female to male and ρ is a constant.

Reproduction

We assumed that female fecundity $E(L)$ depends on individual size according to the allometric relationship

$$E(L)=aL^b, \quad (7)$$

where a and b are constants.

Once an individual has changed sex (as determined by the sex change rule described above) sperm production (in millions) $S(L)$ is given by

$$S(L)=cL^d, \quad (8)$$

where c and d are constants.

Size-dependent fecundity has been measured in many fish species (e.g. Gunderson, 1997). A general allometric relationship between sperm production and size has not been established. Therefore, we assumed that male gamete production increases with size at the same rate as that for females (b=d). We also assumed that males produce many more sperm at any body length than females produce eggs. Clearly, other possible patterns exist. We examined the case where males produce from 10^2 to 10^6 sperm for every egg produced by a female. In the pelagic spawning wrasse (*Thalassoma bifasciatum*), large males release approximately 1000 times more sperm than females release eggs (Schultz and Warner, 1991; Warner et al., 1995).

We used recently published data on sperm production and fertilization rates in the bluehead wrasse (*Thalassoma bifasciatum*) to generate a biologically appropriate fertilization function for our model (Warner et al., 1995; Petersen et al., 2001). It is critical to consider a biologically appropriate form for the function to express fertilization rates when considering the potential for sperm limitation. The probability an egg will be fertilized is an increasing function of the number of sperm available for that mating (Fig. 2). The number of eggs released per mating also affects the fertilization rate (Fig. 2). For simplicity, we calculated the average expected fertilization rate per mating site based on the total production of sperm and eggs at the site. We let S represent the number of sperm released (in millions) and E the number of eggs released at each mating site. We assumed that the proportion of eggs fertilized per mating site p_F is given by

$$p_F = \frac{S}{1+(\kappa E+\chi)S}, \quad (9)$$

where κ and χ are constants fitted to the data.

The number of eggs fertilized per group is $p_F E$ and the total production of fertilized eggs, $P(t)$, is the sum of the number of eggs fertilized in all mating groups.

Measures of spawning stock biomass per recruit

To measure the impact of fishing on stock dynamics, we computed the total spawning stock biomass per recruit starting from the beginning of fishing for the next 50 years. We used the generally recognized pattern that fish wet weight tends to be approximately proportional to the cube of fish length (Gunderson, 1997) to convert fish length, L, into relative biomass, $B(L)$~L^3. Then we calculated total female and male spawning stock biomass

per recruit (SSBR). We also kept track of the total fecundity (egg production per recruit), fertility (sperm production per recruit), and eggs fertilized per recruit.

Marine reserves

We examined the effect of no-take marine reserves on the predicted stock dynamics by comparing the stock dynamics in the presence and absence of reserves. Without a reserve, individuals at all mating sites are subject to fishing. In the presence of a no-take marine reserve, we "protect" a percentage of the mating sites (and thus the population) from fishing. We examined cases in which 0%, 10%, 20%, and 30% of mating sites were protected from fishing. We assumed that the population is completely open among mating sites. Thus, eggs produced from all mating sites enter one larval pool and recruitment occurs randomly between mating sites. Clearly other possibilities exist and could be considered in future analyses, but this case represents a reasonable baseline situation to consider because many marine fish have pelagic larval phases. We also recognize that these analyses ignore the effect of interactions between species within the reserve on stock dynamics. We examined two situations. In the first case, reduced fishing effort occurs when mean fishing mortality is decreased in the presence of reserves because fishing mortality (F) at the unprotected sites remains the same as before the reserve. In the second case, the redistribution of fishing effort occurs when mean fishing mortality across all sites remains the same because fishing mortality increases at the unprotected sites.

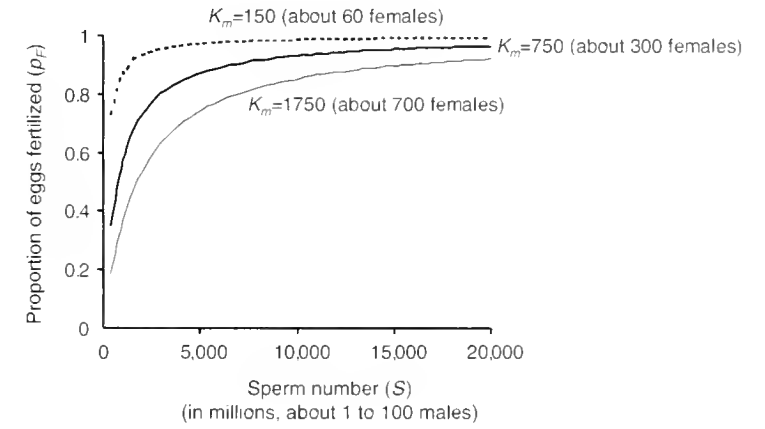

Figure 2

Fertilization rate as a function of the number of eggs and sperm per mating site. The saturation parameter $K_m=\kappa E+\chi$ is taken from Equation 9.

Comparison of sex-changing stocks and dioecious stocks

Ideally, we would like to distinguish the effects of sex change in isolation from the confounding effects of mating pattern, sex ratio, survival, growth, and population fecundity on stock dynamics. To differentiate whether sex change in isolation or other aspects of the mating system determine the predicted stock dynamics, we also examined a version of the model described above for a population where sex is fixed at birth. In this dioecious population, we keep all aspects of the stock constant except for the pattern of sex determination (whether the species changes sex or is dioecious). One would generally expect a dioecious population with no differences between the sexes in mortality to exhibit a 50:50 sex ratio (Fisher, 1930; Trivers, 1972; Charnov, 1982). However, we wanted to control for all differences between the dioecious and protogynous stocks other than the sex-determination pattern. Therefore, we considered the same sex ratio at maturity (0.67=the proportion of adults that are female) as found in the sex-changing population in the absence of fishing. Assuming no sex-specific differences in survival to maturity, this is the same as assuming a 0.67 sex ratio at birth. In this model, individuals remain one sex (determined randomly at birth) throughout their lifetime. Fishing is size but not sex selective. We assumed that males mature at the same size as females.

Parameter values

We used previous research on California sheephead (Labridae, *Semicossyphus pulcher*), a commercially important sex-changing fish, to provide evolutionarily and ecologically reasonable parameters for the model. Although the growth, survival, and reproduction of this species have been studied, less is known about the factors that induce sex change and mating behavior. In this species, sex change occurs at approximately 30 cm although the exact pattern varies among populations (Warner, 1975; Cowen, 1990). It is not known whether sex change is fixed or socially mediated. Because nothing is known about fertilization rates in the California sheephead, we generated κ and χ (Eq. 9) by fitting a line through the estimated values of K_m for small and large bluehead wrasse females as a function of their mean egg production (see Table 1 and Fig. 2; Warner et al., 1995; Petersen et al., 2001). For parameter values and sensitivity analyses see Table 1.

Results

We present the average across 20 simulations of the mean population measures of the last 50 years for each simulation. The variation around the mean in all measures considered was very low (hundredths of a percent of the mean or less). For the spawning per recruit (SPR) measures we give the mean value across the first 50 years of fishing to ensure that the entire cohort had died before the end of the simulation. When the ratio of sperm to eggs is 10^4 to 10^6, a single male can fertilize all of the eggs in the population. When the ratio of sperm to eggs is 10^2, sperm limitation occurs even in the absence of fishing. Therefore, we present results for the case where the ratio of sperm to eggs is 10^3

Table 1

The following parameters were used in the model.

Parameter	Baseline values	Definition and source
Growth		
k	0.05	growth rate (based on Cowen, 1990)
L_{inf}	90 cm	asymptotic size (based on Cowen, 1990)
L_0	8 cm	larval size at recruitment
Population		
N_{max}	1000	maximum population size
μ_A	0.35	adult mortality (based on Cowen, 1990)
α	0.0001	density-independent larval mortality
β	$\alpha/(1-\exp(-\mu_A))N_{max}$ (3.33×10^{-7})	larval recruitment function parameter (see text)
Fishing		
r	1 (0.1)	steepness of selectivity curve
L_f	30 (25, 35)	length at which 50% chance a fish will be removed
F	0–3	fishing mortality
Reproduction		
a	7.04	constant in the fecundity relationship (Warner, 1975)
b	2.95	exponent in the fecundity relationship (Warner, 1975)
c	$10^{-3}a$ ($10^{-2}a$, $10^{-4}a$)	constant in the sperm production function (measured in millions of sperm)
d	b	exponent in the fertility relationship (Warner, 1975)
κ	0.000003	slope of fertilization function parameter
χ	0.09	intercept of fertilization function parameter (based on Peterson et al., 2001) see text for details
Maturity		
L_m	20 cm	length at which 50% of fish mature (Warner, 1975; Cowen, 1990)
q	1	shape parameter in the maturity function
Sex change		
L_c	30 cm	length at which 50% of fish change sex (Warner, 1975; Cowen, 1990)
ρ	1	shape parameter in the sex change function

and fertilization rates are 100% in the absence of fishing, but the population must have multiple males for high fertilization rates. For all the results presented in our study we assumed a fixed sex-change pattern, mating among males and females at each site proportional to gamete production, and larval export among mating sites. We also assumed, unless otherwise noted, a sharp size-selective fishing pattern (r=1) and that the probability of sex change and removal of sex-changing fish by the fishery are centered at the same mean size or L_f=L_c. Clearly, the results presented in our study may not apply to cases where these assumptions are not met.

General patterns predicted by the model

First, we examined the general effect of fishing mortality on the sex-changing stock for the case when one mating site exists. When L_f= L_c, eggs produced per recruit decrease only slightly with fishing mortality (e.g. a 3% drop as fishing mortality increased from 0 to 3, Fig. 3A). However, the mean number of eggs fertilized (both total and per recruit) decreases sharply as fishing mortality increases (e.g. a 30% drop as fishing mortality increased from 0 to 3, Fig. 3A). The number of recruits per year decreases as well. As fishing mortality increases, male spawning stock biomass per recruit decreases dramatically, whereas changes in female spawning stock biomass would be practically undetectable (90% drop for male SSBR, compared with a 3% drop for female SSBR as F increases from 0 to 3, Fig. 3B). Because of the drop in male SSBR, total spawning stock biomass (males and females) per recruit also decreases as fishing mortality increases. Sperm production per recruit is predicted to decrease with increasing fishing mortality (Fig. 3C).

Sensitivity of stock dynamics to fishing pattern

In general, mean population size decreases as fishing pressure increases (Fig. 4A). The adult sex ratio (measured as

the percentage of mature individuals that are female) also increases as fishing mortality increases (Fig. 4B) and the mean size of adults in the population decreases. These patterns depend on fishing being size selective, which causes a disproportional take of males. If the size-selectivity of the fishery targeted smaller size classes (L_f<L_c), a decline in annual biomass removed by the fishery is predicted with increasing F and the stock is predicted to crash at a relatively low fishing mortality (Fig. 4C). If the fishery is less selective (r=0.1, L_f=L_c), the population is also predicted to crash for most fishing mortalities. Thus, allowing some proportion of mature males to consistently escape fishing is critical even at low fishing mortality. As fishing mortality increases, the predicted biomass removed by the fishery increases with diminishing returns (Fig. 4C). When L_f=L_c, the biomass removed by the fishery does not continue to increase with F because all males above the size at sex change are being removed by the fishery. In this case, the males in the population are essentially breeding only once before they are taken by the fishery. For the range of fishing mortality considered, we did not observe a decline in biomass taken with increasing F unless L_f<L_c or r=0.1. If more size classes are allowed to escape fishing (L_f>L_c), the general patterns remain the same, but for the same fishing mortality (F), the effect of fishing on the population is less (Fig. 4). Female biomass does not decrease much with fishing mortality when L_f=L_c even though some females are removed by the fishery because the probability of a female changing sex is the probability of it being fished. Therefore, female loss due to the fishery affects male biomass rather than female biomass in the population.

Sperm limitation and production

The removal of large males from the population is predicted to cause sperm limitation and decreased fertilization rates (Fig. 3, A and C), leading to a decrease in mean population size (Fig. 4A). The degree to which the fertilization rate and thus the population size decreases depends to a great extent on the pattern of sperm production and fertilization. We assumed that only a few males are needed to fertilize the eggs of many females (Fig. 2). We also assumed that per-capita reproduction and recruitment are high even at a low population size (Barrowman and Myers, 2000). Thus, protogynous populations with lower sperm production or fertilization rates would experience greater effects from fishing than predicted in the present study. Similarly, populations with lower production or survival would experience larger decreases in population size even with the same level of sperm limitation and fishing. In general, however, the removal of males alone from a protogynous population with a fixed sex change is predicted to cause decreased fertilization rates and lower mean population size even when the fertilization rate function is asymptotic and individual male sperm production is high.

Mating aggregation size

As mating aggregation size decreased and fishing mortality and effort remained constant, the effect of fishing on the population increased. As described above, we assumed that fishing effort would not be concentrated on the few large mating aggregations and thus increase total fishing mortality. The sex ratio, mean size, mean fecundity, and mean fertility all remained the same across different mating aggregation sizes with constant fishing mortality. However, the mean fertilization rate and number of fertilized eggs per recruit decreased with mating group size (Fig. 5) even though male biomass and SSBR remained the same. Both predicted mean population size and biomass taken decreased as fishing mortality increased (Fig. 5). This pattern was generated by sperm limitation in small mating groups. Smaller groups have higher probabilities that sperm production within the group will not be sufficient to fertilize the eggs produced within the mating group. Small mating aggregations may not only be sperm limited but also be male limited and fail to reproduce completely; populations with small group sizes (50 individuals or less) were predicted to become extinct in

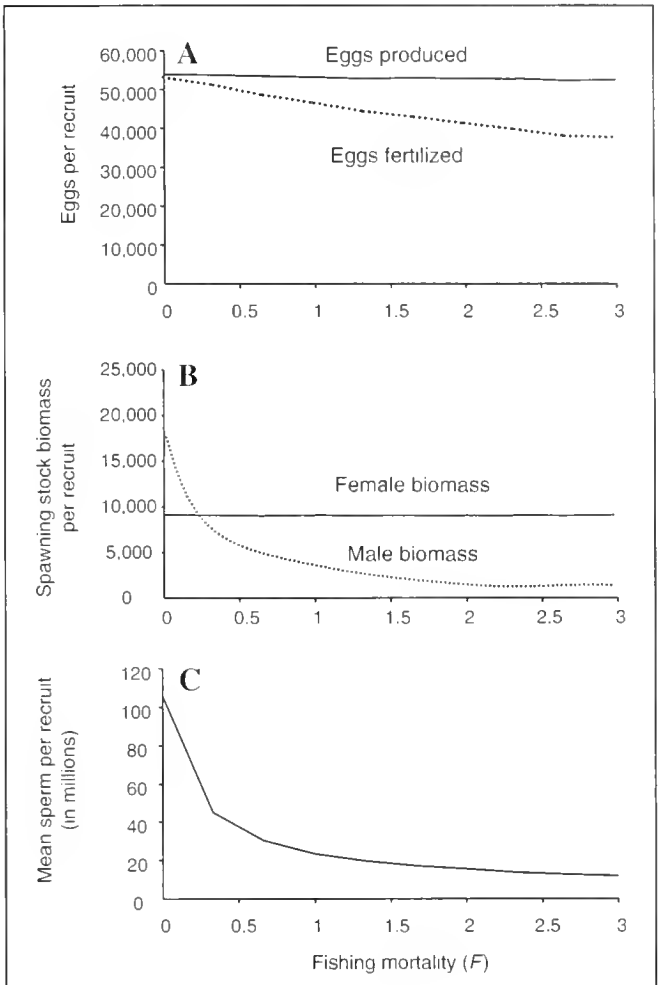

Figure 3

Spawning-per-recruit measures. Results are presented for the sex-changing stock with one mating site when L_f = L_c and r=1. Means across 20 simulations are given. For details see the general text.

5–25% of the simulations as fishing mortality (F) increased from 0 to 1. The impact of mating group size on stock dynamics is thus predicted to be nonlinear. A threshold mating aggregation size appeared to exist below which sperm limitation and reproductive failure become common.

Spawning-per-recruit measures

For size-selective fishing, the spawning stock biomass per recruit of females is not predicted to decrease significantly with increased fishing mortality as long as some male size classes escape fishing ($L_f \geq L_c$). However, male biomass per recruit and sperm production per recruit are both predicted to decrease. Although egg production is not predicted to decrease with increasing size-selective fishing pressure, the number of fertilized eggs is predicted to decrease. When all male size classes are fished ($L_f \geq L_c$), the stock is predicted to crash and therefore clearly female biomass and egg production are predicted to decrease with fishing mortality. In general, the predicted decrease in mean population size and reproduction is driven for the most part by decreased sperm production and consequently a reduction in the number of eggs fertilized per recruit. The relationships between fishing pressure and the classic spawning-per-recruit measures do not indicate the true effect that fishing is predicted to have on the protogynous population (Fig. 6). When $L_f \geq L_c$, female spawning stock biomass per recruit and eggs produced per recruit showed almost no effect of fishing on the population, even as mean population size decreased. Because of the size-selective fishing pattern, total and male biomass per recruit decreased with fishing mortality and decreasing mean population size. However, male and total biomass per recruit did not reflect the increased effect of fishing on populations with smaller mating aggregations. The production of fertilized eggs per recruit decreased with increased fishing pressure and decreased more sharply for smaller mating aggregations. Only the number of fertilized eggs per recruit could assess the predicted effect of fishing on the protogynous population. Thus, classic SPR measures were predicted to fail in the presence of sperm limitation to assess the impact of fishing on a protogynous stock.

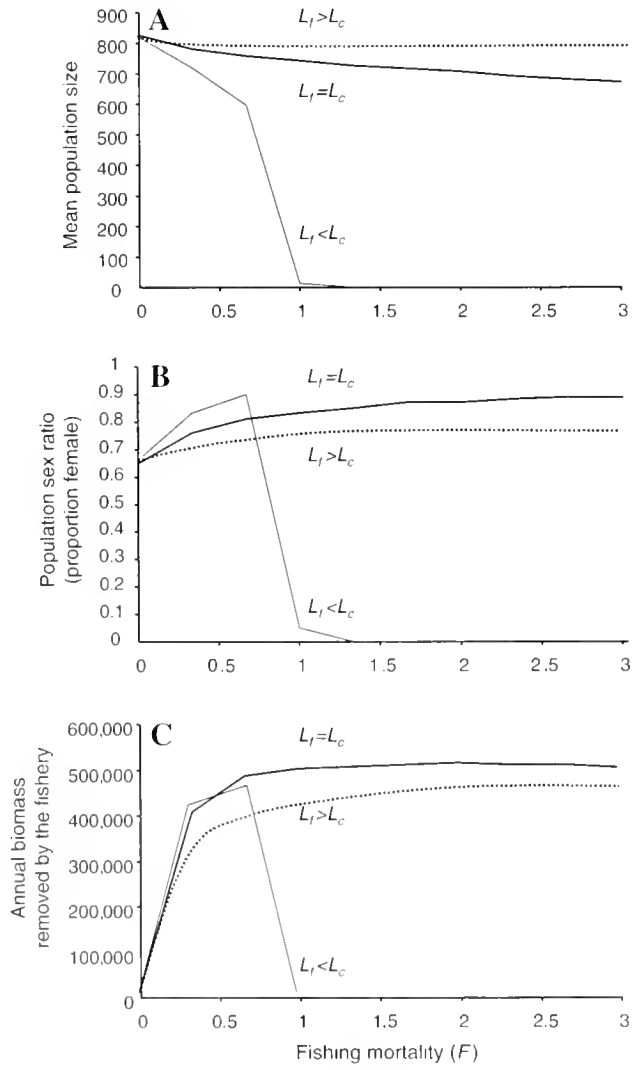

Figure 4

The effect of size-selective fishing on stock dynamics. We present results for the sex-changing stock with one mating site when r=1. Means across 20 simulations are given. For details see the general text.

Marine reserves and fishery management

In the situation considered in this study, the pattern of fishing is more important to stock dynamics than the presence of marine reserves. We assumed a size-selectivity that allowed on average 50% of individuals of sex-changing size to escape the fishing gear. Thus, although the sex ratio does increase (become more female) by 20–40%, all males are not lost from the population (when $L_f \geq L_c$ and r=1). If fishing selectivity occurs at a smaller size, then the effects on the population are predicted to be much greater and the protogynous stock would suddenly become more affected than the dioecious population. For example, at L_f=25 cm the protogynous stock is predicted to crash whenever $F \geq 1$. This occurs not because of a reduction in the production of eggs but rather because of a failure to fertilize the eggs produced by surviving females. When males of all size classes are fished, populations can become male limited and fertilization rates drop drastically. A decrease in the production of fertilized eggs can lead to a decrease in female biomass, but it is the removal of males rather than females that causes this decline.

When fishing effort is not redistributed after the formation of a reserve, the impact of fishing on the mean population size and SPR measures is predicted to decrease (e.g. Fig. 7A). However, if fishing effort is redistributed among unprotected areas, the benefit of the reserves to the protogynous stock decreases (Fig. 8A). Protecting some sites allows large males to

escape fishing and thus increases the production of fertilized eggs at the population level. However, yield decreased proportionally to the percentage of sites protected by the reserve unless fishing effort is redistributed among the remaining sites. We assumed that fish do not move between sites after the larval stage, and thus larger and older individuals do not leave the reserve and become exposed to fishing. Although this assumption is clearly appropriate for some species, it is important to realize that the dynamics and predictions would differ for more closed populations or migratory species. For the fishing pattern and biological scenario examined in this study, marine reserves are not predicted to increase biomass available to the fishery (Figs. 7B and 8B).

Dynamics of dioecious versus protogynous stocks

In the dioecious stock with a single randomly mating aggregation, both male and female biomass per recruit and fecundity or fertility per recruit are predicted to decrease as fishing mortality increases (Fig. 6). Because both egg production and sperm production decrease with increased fishing pressure in the dioecious stock, the number of eggs fertilized per recruit did not differ much from the other SPR measures. Thus, SSBR and eggs per recruit also indicated the impact of fishing on the stock in dioecious stocks with large mating aggregations. The percent drop in population size and fertilized egg production is predicted to be much greater in dioecious species and occurred more quickly than in the sex-changing stock because of a reduction in overall population fecundity even in the absence of decreased fertilization rates. However, dioecious stocks are predicted to exhibit larger mean population size for the same fishing mortality and to support a larger fishery because of the additional egg production of large fecund females. At very small mating aggregations, sperm limitation is predicted even in the dioecious stock and fertilized eggs per recruit become a better indicator of stock dynamics in the presence of fishing. Dioecious stocks are also predicted to benefit from marine no-take reserves through the protection of large fecund females (Fig. 7).

Discussion

In this study we developed a general framework that examines the consequences to

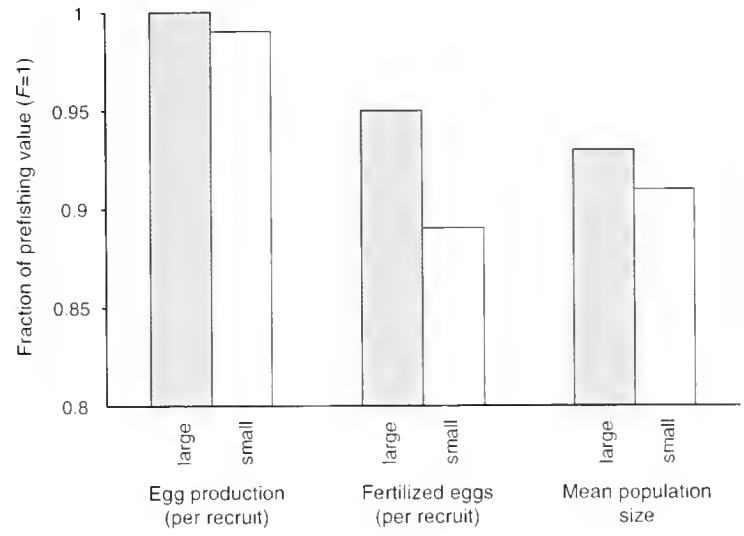

Figure 5

Mating aggregation size affects the response to fishing. Large (one large mating aggregation) and small (10 smaller mating aggregations) situations are compared. Percent change in the presence of fishing (from F=0 to F=1) in egg production per recruit, mean fertilized egg production per recruit, and mean population size are given. Total population fecundity and mean body size are lower for the smaller mating aggregations.

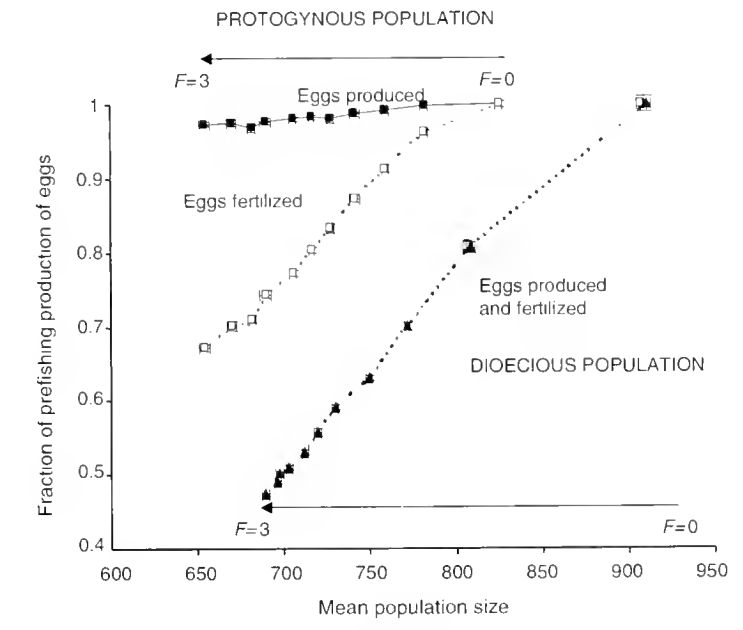

Figure 6

Spawning-per-recruit (SPR) measures in a protogynous (squares) and dioecious (triangles) stock: Mean egg production per recruit (filled) and mean fertilized eggs per recruit (open) are shown for a randomly mating population with one large mating group. Error bars indicate the standard error of the mean. For the dioecious population, the two SPR measures overlap.

fisheries management of a behaviorally and evolutionary reasonable life-history and sex-change pattern. We based our assumptions and parameter values on patterns observed in natural populations that have presumably evolved given the life history tradeoffs and expected reproductive success associated with these behaviors. However, we made various assumptions that affect the predicted patterns such as a fixed sex-change pattern, male mating success proportional to sperm production, and a very resilient recruitment function. Despite these assumptions, a number of general patterns emerge.

Life-history pattern is important but not sufficient to predict stock dynamics

In general, we predicted that a protogynous stock with fixed sex change will respond to the same fishing pressure differently than an otherwise identical dioecious stock. Understanding the life history of the population is clearly important to our understanding of stock dynamics. However, it is not possible to classify protogynous stocks simply as more or less sensitive to fishing. The differences between dioecious and sex-changing fish are relatively complex, and it is not the case that one life history is expected to be more or less vulnerable to fishing. Although the sex change and fishing pattern are important, they must be seen in the context of the mating system, reproductive behavior, and population dynamics of the species. If no male size classes escape fishing, then the sex-changing population will be much more sensitive to fishing and may crash even at low fishing mortality. When some male size classes escape fishing, an identical dioecious stock is predicted to experience a greater decrease in mean population size than the protogynous population. However, the protogynous species is predicted to be much more sensitive to mating aggregation size and sperm limitation. Protogynous stocks are predicted to benefit from marine protected areas at high levels of fishing mortality where sperm limitation is common at fished mating sites. In contrast, the dioecious stock is predicted to derive a greater benefit of marine reserves even at low fishing mortality because of the protection of large fecund females (Fig. 7). Although the sex-changing population is predicted to be less sensitive to fishing mortality overall, it is clearly very important to understand the exact details of the sex-change pattern and the size-selectivity of fishing in relation to sex change. It will also be important to understand the mating system and patterns of fertilization success and sperm production in males when managing a protogynous stock. Given the sensitivity of the sex-changing stock to the size-selective pattern of fishing, we recommend the precautionary approach of keeping fishing mortality sufficiently low so that some males of all size classes always escape fishing (Fig. 4C). Clearly, protogynous stocks cannot be managed as if they were dioecious.

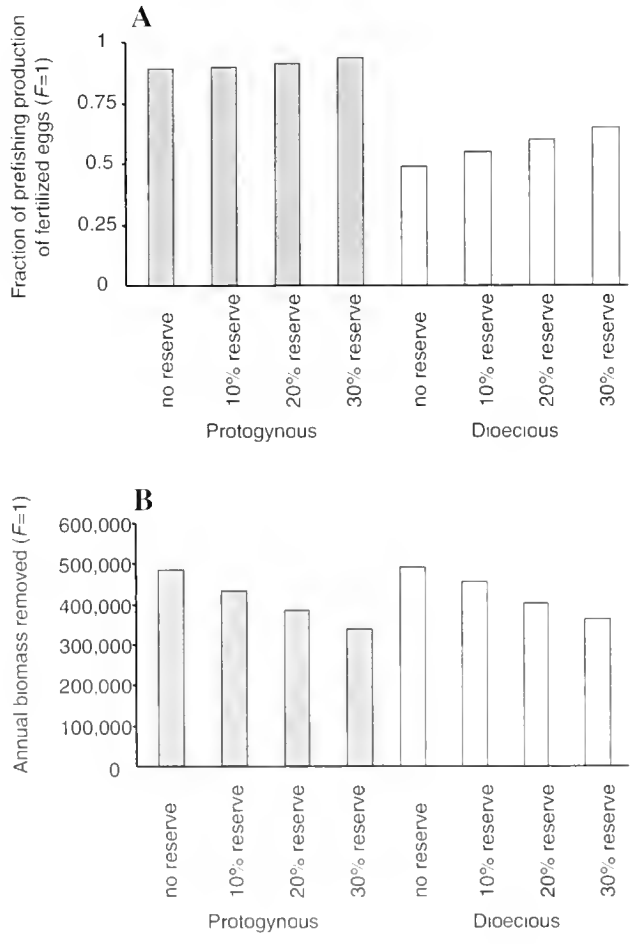

Figure 7

The effect of marine reserves on protogynous and dioecious populations when fishing effort is decreased (case 1). (**A**) Percent change in the presence of fishing (F=1) in the production of fertilized eggs compared to in the absence of fishing. (**B**) Annual biomass removed by the fisheries varies with marine reserve and sex-change pattern. Numbers shown are for 10 mating sites when F=1.

Sperm limitation and mating aggregation size affect stock dynamics

The removal of large males from the population can cause sperm limitation, decreased fertilization rates, and decreased population size even in a resilient species with high sperm production. Sperm limitation will increase as mating group size decreases. In the present model, even small males produced relatively large amounts of sperm. If males are removed, populations with lower sperm production are predicted to be more sensitive to the removal of large fertile males. Our assumption of fertilization rates determined by total egg and sperm production per mating site will, if anything, have underestimated the potential for sperm limitation. Other mating systems and reproductive behaviors could lead to greater sperm limitation than predicted in our study. For example, species that have not evolved under sperm competition should be more affected by the removal of large males than

species with sperm competition because of decreased allocation to sperm production. Pair spawning among individuals could also lead to decreased fertilization rates. Reproductive behaviors often found in sex-changing species, such as territoriality, female choice, resource-defense polygyny, and mate monopolization, all lead to skewed reproductive success for males and could further decrease fertilization rates. Sperm limitation is predicted to occur, and an understanding of such factors as fertilization rate, sperm production, mating skew, and mating group size will increase our ability to understand and predict stock dynamics.

Traditional spawning-per-recruit measures can fail in the presence of sperm limitation

Although problems exist with traditional spawning-per-recruit measures in general (Parkes, 2000), they are especially problematic for sex-changing stocks. In the dioecious stock, the relationship between female and total spawning stock biomass per recruit exhibits a roughly linear relationship with population size. In the sex-changing stock, female fecundity does not reflect the changes in mean population size. Although total or male spawning stock biomass per recruit did decrease with decreased population size, the fit between these measures will depend greatly on the size-dependent sperm production of males, mating aggregation size, and other factors determining the potential for sperm limitation. Male or total spawning stock biomass per recruit alone cannot predict sperm limitation and thus will fail to predict the potential population crashes that may result. We conclude that any measure of spawning per recruit in a sex-changing species that does not consider sperm limitation and reduced fertilization rates has the potential to underestimate the impact of fishing on the population. The number of eggs produced or female spawning stock biomass can remain relatively unchanged in the face of high fishing mortality even as the population is predicted to decline. However, the failure of classic spawning-per-recruit measures in the presence of declines due to sperm limitation or decreased fertilization rate will not be limited to protogynous stocks. Although sperm production patterns and fertilization rates are not known for many commercially important species, this information can be collected to develop a general sense of how sperm production depends on individual size. We also have a general sense of the factors that are expected to affect fertilization rates (Birkhead and Møller, 1998) and these can be easily studied in any species where spawning grounds are accessible to researchers. It is clear that new management measures must be developed for sex-changing species that consider the potential for sperm limitation because biomass alone may miss the potential for rapid population crashes. One purpose of theory is to tell us what we need to know more about and to stimulate further research. Our results clearly indicate that we need to know more about sperm production and fertilization rates when managing protogynous stocks.

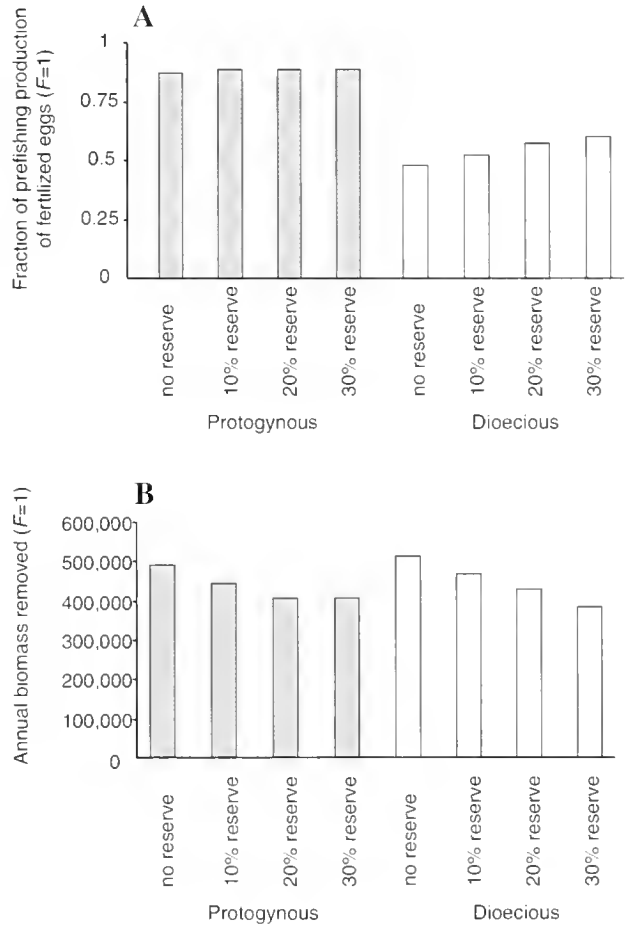

Figure 8

The effect of marine reserves on protogynous and dioecious populations when fishing effort is redistributed (case 2). (**A**) Percent change in the presence of fishing (F=1) in the production of fertilized eggs compared to percent change in the absence of fishing. (**B**) Annual biomass removed by the fisheries varies with marine reserve and sex-change pattern. Numbers shown are for 10 mating sites when F=1.

Marine reserves and size-selective fishing can be used to manage protogynous stocks

Marine reserves clearly have the potential to decrease the impact of fishing on populations. Large highly fecund or fertile individuals may be protected from size-selective fisheries. However, the benefits of a marine reserve will be significantly decreased if fishing effort is simply redistributed to unprotected sites (Figs. 7 and 8; Guenette and Pitcher, 1999; Apostolaki et al., 2002). It is usually recognized that the larval export and import dynamics will be crucial to whether reserves increase mean population size. We predict that the degree to which stocks respond to no-take reserves will also depend on their life-history pattern, mating system, and size-dependent fecundity and fertility. The protection of large and fecund (or fertile)

fish will certainly increase reproduction and decrease the impact of fishing on the population. However, the benefit of marine reserves will be much greater in populations where larger or older individuals play a key role in reproduction. Given the predicted extreme sensitivity of the protogynous population to the pattern of size-selective fishing, marine protected areas could represent a precautionary management strategy to ensure that some males are not subject to fishing mortality.

A comprehensive approach to stock dynamics

Managing fishing on stocks of sex-changing fish will require considering the sex-change pattern. However, one must also consider the sex change pattern within the context of the mating system. Although the pattern of sex determination does affect the stock dynamics, simple statements regarding whether dioecious or sex-changing populations are more sensitive to fishing are not possible. The differences among dioecious and sex-changing stocks are complex, and the management of these stocks will depend as much on their mating system, the type of fishing strategies used to capture them, and mating aggregation size as on the sex determination pattern. Classic SPR measures cannot measure sperm limitation and reduced fertilization rates, and thus will not always measure or predict the impact of fishing mortality on the population. Rather than relying on measures of spawning stock biomass per recruit alone, management groups should also monitor protogynous sex-changing stocks for a reduction in fertilization rates

Acknowledgments

We thank Phil Levin, Alec McCall, Steve Ralston, and Bob Warner for their comments on an earlier version of this manuscript. This research was supported by National Science Foundation grant IBN-0110506 to Suzanne Alonzo and the Center for Stock Assessment Research (CSTAR).

Literature cited

Adams, S., B. D. Mapstone, G. R. Russ, and C. R. Davies.
2000. Geographic variation in the sex ratio, sex specific size, and age structure of *Plectropomus leopardus* (Serranidae) between reefs open and closed to fishing on the Great Barrier Reef. Can. J. Fish. Aquat. Sci. 57:1448–1458.

Apostolaki, P., E. J. Milner-Gulland, M. K. McAllister, and G. P. Kirkwood.
2002. Modelling the effects of establishing a marine reserve for mobile fish species. Can. J. Fish. Aquat. Sci. 59: 405–415.

Armsworth, P. R.
2001. Effects of fishing on a protogynous hermaphrodite. Can. J. Fish. Aquat. Sci. 58:568–578.

Bannerot, S., W. F. Fox, and J. E. Powers.
1987. Reproductive strategies and the management of snappers and groupers in the gulf of Mexico and Caribbean. *In* Tropical snappers and groupers: biology and fisheries management (J. J. Polovina and S. Ralston, eds.), p. 561–603. Westview Press, Boulder, CO.

Barrowman, N. J., and R. A. Myers.
2000. Still more spawner-recruitment curves: The hockey stick and its generalizations. Can. J. Fish. Aquat. Sci. 57: 665–676.

Beets, J., and A. Friedlander.
1999. Evaluation of a conservation strategy: a spawning aggregation closure for red hind, *Epinephelus guttatus*, in the U.S. Virgin Islands. Environ. Biol. Fishes 55:91–98.

Beverton, R. J. H.
1987. Longevity in fish: some ecological and evolutionary considerations. *In* Evolution of longevity in animals. (A. D. Woodhead and K. H. Thompson, eds.) p. 161–185. Plenum, New York, NY.
1992. Patterns of reproductive strategy parameters in some marine teleost fishes. J. Fish Biol. 41 (suppl. B):137–160.

Birkhead, T. R., and A. P. Moller.
1998. Sperm competition and sexual selection, 826 p. Academic Press, San Diego, CA.

Brule, T., C. Deniel, T. Colas-Marrufo, and M. Sanchez-Crespo.
1999. Red grouper reproduction in the southern Gulf of Mexico. Trans. Am. Fish. Soc. 128:385–402.

Charnov, E. L.
1982. The theory of sex allocation, 355 p. Princeton Univ. Press, Princeton, NJ.

Coleman, F. C., C. C. Koenig, and L. A. Collins.
1996. Reproductive styles of shallow-water groupers (Pisces: Serranidae) in the eastern Gulf of Mexico and the consequences of fishing spawning aggregations. Environ. Biol. Fishes 47:129–141.

Cowen, R. K.
1990. Sex change and life history patterns of the labrid, *Semicossyphus pulcher*, across an environmental gradient. Copeia 1990:787–795.

Cowen, R. K., K. M. M. Lwiza, S. Sponaugle, C. B. Paris, and D. B. Olson.
2000. Connectivity of marine populations: Open or closed? Science 287:857–859.

Fisher, R. A.
1930. The genetical theory of natural selection, 272 p. Clarendon Press, Oxford.

Fu, C., T. J. Quinn, II, and T. C. Shirley.
2001. The role of sex change, growth and mortality in *Pandalus* population dynamics and management. ICES J. Mar. Sci. 58:607–621.

Guenette, S., and T. J. Pitcher.
1999. An age-structured model showing the benefits of marine reserves in controlling overexploitation. Fish. Res. 39:295–303.

Gunderson, D. R.
1997. Trade-off between reproductive effort and adult survival in oviparous and viviparous fishes. Can. J. Fish. Aquat. Sci. 54:990–998.

Haddon, M.
2001. Modelling and quantitative methods in fisheries, 406 p. Chapman and Hall, Boca Raton, FL.

Huntsman, G. R., and W. E. Schaaf.
1994. Simulation of the impact of fishing on reproduction of a protogynous grouper, the graysby. No. Am. J. Fish. Manag. 14:41–52.

Janetos, A. C.
1980. Strategies of female mate choice: a theoretical analysis. Behav. Ecol. Sociobiol. 7:107–112.

Jennings, S., M. J. Kaiser, and J. D. Reynolds.
2001. Marine fisheries ecology, 417 p. Blackwell Science, Oxford.

Levin, P. F., and C. B. Grimes.
2002. Reef fish ecology and grouper conservation and management. *In* Coral reef fishes: dynamics and diversity in a complex ecosystem (P. F. Sale, ed.) p. 377–390. Academic Press, Amsterdam.

Mangel, M., and C. Tier.
1993. A simple direct method for finding persistence times of populations and application to conservation problems. Proc. Nat. Acad. Sci. USA 90:1083–1086.
1994. Four facts every conservation biologist should know about persistence. Ecology 75:607–614.

Parkes, G.
2000. Understanding SPR and its use in U.S. fishery management, 62 p. Center for marine conservation, Washington D.C.

Petersen, C. W., R. R. Warner, D. Y. Shapiro, and A. Marconato.
2001. Components of fertilization success in the bluehead wrasse, *Thalassoma bifasciatum*. Behav. Ecol. 12: 237–245.

Punt, A. E., P. A. Garratt, and A. Govender.
1993. On an approach for applying per-recruit measures to a protogynous hermaphrodite, with an illustration for the slinger *Chrysoblephus puniceus* (Pisces: Sparidae). S. Afr. J. Sci. 13:109–119.

Quinn, T. J., and R. B. Deriso.
1999. Quantitative fish dynamics, 542 p. Oxford Univ. Press, New York, NY.

Sadovy, Y.
2001. The threat of fishing to highly fecund fishes. J. Fish Biol. 59:90–108.

Sale, P. F.
2002. The science we need to develop more effective management. *In* Coral reef fishes: dynamics and diversity in a complex ecosystem (P. F. Sale, ed.) p. 361–376. Academic Press, Amsterdam.

Schultz, E. T., and R. R. Warner.
1991. Phenotypic plasticity in life-history traits of female *Thalassoma bifasciatum* (Pisces: Labridae): 2. Correlation of fecundity and growth rate in comparative studies. Environ. Biol. Fishes 30:333–344.

Shapiro, D. Y.
1987. Reproduction in groupers. *In* Tropical snappers and groupers: biology and fisheries management (J. J. Polvina and S. Ralston, eds.) p. 295–328. Westview Press, Boulder, CO.

Trivers, R. L.
1972. Parental investment and sexual selection. *In* Sexual selection and the descent of man (B. Campbell, ed.), p. 136–179. Aldine-Atherton, Chicago.

Warner, R. R.
1975. The reproductive biology of the protogynous hermaphrodite *Pimelometopon pulchrum* (Pisces: Labridae). Fish. Bull. 73:262–283.

Warner, R. R., D. Y. Shapiro, A. Marcanato, and C. W. Petersen.
1995. Sexual conflict: Males with highest mating success convey the lowest fertilization benefits to females. Proc. R. Soc. Lond. B. Biol. Sci. 262:135–139.

Abstract—We present a growth analysis model that combines large amounts of environmental data with limited amounts of biological data and apply it to *Corbicula japonica*. The model uses the maximum-likelihood method with the Akaike information criterion, which provides an objective criterion for model selection. An adequate distribution for describing a single cohort is selected from available probability density functions, which are expressed by location and scale parameters. Daily relative increase rates of the location parameter are expressed by a multivariate logistic function with environmental factors for each day and categorical variables indicating animal ages as independent variables. Daily relative increase rates of the scale parameter are expressed by an equation describing the relationship with the daily relative increase rate of the location parameter. *Corbicula japonica* grows to a modal shell length of 0.7 mm during the first year in Lake Abashiri. Compared with the attainable maximum size of about 30 mm, the growth of juveniles is extremely slow because their growth is less susceptible to environmental factors until the second winter. The extremely slow growth in Lake Abashiri could be a geographical genetic variation within *C. japonica*.

An environmentally based growth model that uses finite difference calculus with maximum likelihood method: its application to the brackish water bivalve *Corbicula japonica* in Lake Abashiri, Japan

Katsuhisa Baba

Hokkaido Hakodate Fisheries Experiment Station
1-2-66, Yunokawa, Hakodate
Hokkaido 042-0932, Japan
E-mail address: babak@fishexp.pref.hokkaido.jp

Toshifumi Kawajiri

Nishiabashiri Fisheries Cooperative Association
1-7-1, Oomagari, Abashiri
Hokkaido 093-0045, Japan

Yasuhiro Kuwahara

Hokkaido Abashiri Fisheries Experiment Station
31, Masuura, Abashiri
Hokkaido 099-3119, Japan.

Shigeru Nakao

Graduate School of Fisheries Sciences
Hokaido University
3-1-1, Minato, Hakodate
Hokkaido 041-8611, Japan

Manuscript approved for publication
14 August 2003 by Scientific Editor.

Manuscript received 20 October 2003
at NMFS Scientific Publications Office.

Fish. Bull. 102:14–24 (2004).

Extreme fluctuations, both short-term and seasonal, in food availability (e.g. phytoplankton density) make it difficult to determine relationships between the growth of filter-feeding bivalves and environmental factors (Bayne, 1993). However, it is becoming easier to acquire large amounts of environmental data through the use of data loggers, submersible fluorometers, or remote-sensing satellites, which enable environmental monitoring at daily or subdaily intervals. The development of these devices could solve difficulties in data collection. However, analytical methods that combine large amounts of environmental data with limited amounts of biological data (e.g. shell length) are not yet well developed. We present an environmentally based growth model that combines such unbalanced data sets. This model is useful in elucidating relationships between environmental factors and growth of filter feeders from field data.

Complex box models, such as ecophysiological models, can derive the relationships between environmental factors and the growth of filter-feeding bivalves (Campbell and Newell, 1998; Grant and Bacher, 1998; Scholten and Smaal, 1998). These models are useful for estimating impacts of cultivated species on an ecosystem or the carrying capacity of a species (or both) (Dame, 1993; Héral, 1993; Grant et al., 1993). They are suitable for animals that have been widely studied, such as *Mytilus edulis*, because they are derived by integrating a huge amount of ecophysiological knowledge acquired mainly from laboratory experiments. However, extrapolation of such knowledge to natural conditions is still controversial (Jørgensen, 1996; Bayne, 1998). Our model treats complicated eco-

physiological processes as a black box; we constructed the model directly from fluctuations in environmental factors and growth rates. Our approach is reasonable for animals for which ecophysiological knowledge is limited, especially when the main purpose of investigation is to derive the relationships between environment and growth.

We applied the model to a single cohort of *Corbicula japonica* juveniles spawned in August 1997. We did not consider any bias caused by adjacent cohorts because *C. japonica* failed to spawn in 1995, 1996, and 1998 in Lake Abashiri owing to low water temperatures during the spawning season (Baba et al., 1999). Such investigations provide important basic information, such as the shape of the distribution of a single cohort, and the relationship between growth rate and expansion rate of size variation in a single cohort.

Corbicula spp. are harvested commercially in Japan. The annual catch ranged from 19,000 to 27,000 metric tons in 1996 to 2000 (Ministry of Agriculture, Forestry and Fisheries[1]), of which *C. japonica* was the main species. *Corbicula japonica* is distributed in brackish lakes and tidal flats of rivers from the south of Japan to the south of Sakhalin (Kafanov, 1991), is a dominant macrozoobenthos in these lakes, and has important roles in bioturbation and energy flow (Nakamura et al., 1988; Yamamuro and Koike, 1993). Juvenile *C. japonica* growth is fast in southern habitats. Their spats collected in Lake Shinji, which lies in the southern part of its range, grow to a mean shell length of around 6.7 mm in natural conditions by the first winter (Yamane et al.[2]). In northern habitats, growth is also believed to be fast; Utoh (1981) reported that mean shell length at the first annual mark was around 5.7 mm in Lake Abashiri. In Utoh's study differences between the shell lengths at the first annual marks and the shell lengths of individuals aged to be one year were also reported. The purposes of the present study are to elucidate juvenile growth and its relationship to environmental factors in Lake Abashiri.

Materials and methods

Overview of the model

Our model expresses relative growth rate for *C. japonica* by a sigmoid function with environmental factors and animal ages as independent variables. Modeling processes in general follow five steps: 1) Shell lengths of a single cohort are summarized by an adequate probability density function, which is expressed by a location parameter and a scale parameter; 2) Daily relative increase rate of the location parameter (dRIRL) is approximated by a sigmoid function with environmental factors and animal ages as independent variables; 3) Daily relative increase rate of the scale parameter is approximated by a simple function with the dRIRL as an independent variable; 4) The model is optimized by a maximum likelihood method; and 5) The best model is selected by Akaike information criterion (AIC). The AIC is an information-theoretic criterion extended from Fisher's likelihood theory and is useful for simultaneous comparison of models (Akaike, 1973; Burnham and Anderson, 1998).

Study site and sampling method

To collect juveniles of *C. japonica* spawned in August 1997, sediments were sampled with a 0.05-m^2 Smith–McIntyre grab once or twice a month from September 1997 to July 1999 at a depth of 3.5–4.0 m in Lake Abashiri (Fig. 1). The habitat of *C. japonica* is restricted to areas shallower than 6-m depth because the deeper area, the lower stratum of the lake, is covered by anoxic polyhaline water. We assumed that the selectivity of the sampling gear on *C. japonica* juveniles was negligible because the gear grabs the juveniles with the sediment. Because the magnitude of spawning in 1997 was relatively small (Baba et al., 1999), we selected a sampling site where we found abundant settled juveniles in our preliminary investigations. Samples could not be obtained during winter because of ice cover. Sediments were washed with tap water on 2- mm and 0.125-mm mesh sieves from September 1997 to October 1998, and on 4.75-mm and 0.125-mm mesh sieves from April to July 1999. To separate the juveniles from the retained sediments, we treated the sediments with zinc chloride solution as described by Sellmer (1956). Then we sorted the juveniles under a binocular microscope. Identification of the cohort spawned in 1997 was quite easy because *C. japonica* failed to spawn in 1995, 1996, and 1998 owing to low water temperatures during the spawning season (Baba et al., 1999). We considered all the individuals that passed through the larger-mesh sieves and that were retained on the smaller-mesh sieve as the 1997 cohort. Shell lengths were measured under a profile projector (V-12, Nikon Ltd., Chiyoda, Tokyo) at 50× magnification with a digital caliper (Digimatic caliper, Mitsutoyo Ltd., Kawasaki, Kanagawa), which has a 0.02-mm precision.

Environmental factors

Values for water temperature (°C), water fluorescence (fluorescence equivalent to uranin density, μg/L), salinity (psu, practical salinity unit), and turbidity (equivalent to kaolin density, ppm) were obtained for 0.1-m intervals from unpublished data at the Abashiri Local Office of the Hokkaido Development Bureau.[3] The variables were measured by a submersible fluorometer (Memory Chlorotec, ACL-1180-OK, Alec Electronics Ltd., Kobe, Hyogo) at four sites in Lake Abashiri at intervals of about one week (Fig. 1). The average values of each variable between the depths of 1 m and 6 m were used for later analyses. Values between the measured dates were interpolated linearly

[1] Ministry of Agriculture, Forestry and Fisheries. 1996–2002. Statistics on fisheries and water culture production. Association of Agriculture and Forestry, 1-2-1 Kasumigaseki, Chiyoda, Tokyo 100-0013, Japan.

[2] Yamane, K., M. Nakamura, T. Kiyokawa, H. Fukui, and E. Shigemoto. 1999. Experiment on the artificial spat collection. Bull. Shimane Pref. Fish. Exp. Stn., p. 232–234. Unpubl. rep. Shimane Prefectural Fisheries Experimental Station, 25-1 Setogashima, Hamada, Shimane 697-0051, Japan. [In Japanese.]

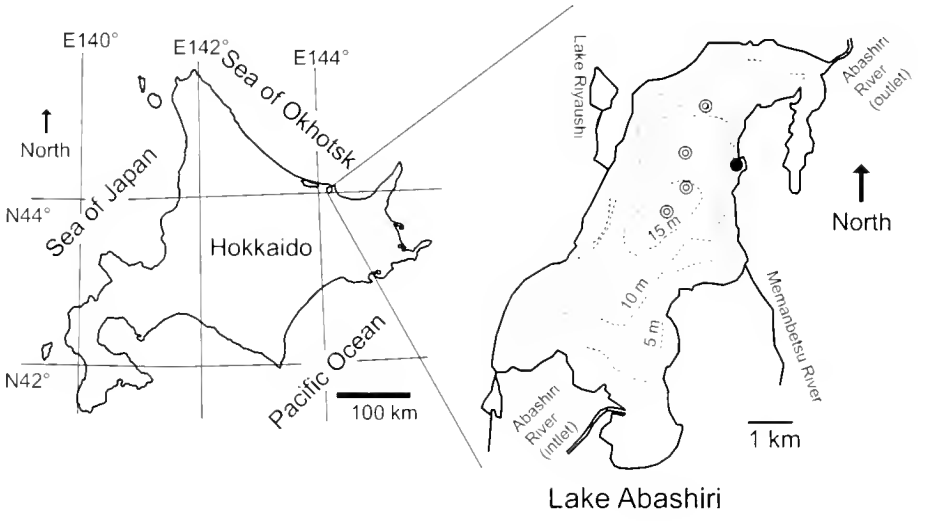

Figure 1

Location of sampling site for *Corbicula japonica* juveniles in Lake Abashiri, Japan (●). Environmental factors—water temperature, water fluorescence, salinity, and turbidity—were measured at four sites, designated by ◎.

for subsequent analysis with the environmentally based growth model. The water fluorescence reflects the density of phytoplankton.

Model structure

Modeling the distribution of a single sample Normal distribution is usually used to describe a single cohort in fishes and aquatic invertebrates (e.g. Pauly, 1987; Founier and Sibert, 1990; Yamakawa and Matsumiya, 1997). However, an adequate function to describe a single cohort of each animal should be selected to avoid biases caused by any inadequacies of the function. Probability density functions of many distributions are applicable for that purpose, and the appropriate can be selected among easily calculable functions to ensure convergence of the model. Characteristics of many distributions are well described by Evans et al. (1993). We used two distributions: normal distribution and largest extreme value distribution. The normal distribution is symmetric. The largest extreme value distribution is asymmetric with a longer tail toward the larger side. These are expressed by a location parameter and a scale parameter.

To use all the information inherent in data, parameters of the distribution functions are estimated from raw data (e.g. lengths), not from summarized data such as length frequency. This estimation method is described by Sakamoto et al. (1983). The most adequate distribution is selected by AIC. Log-likelihood functions of the distributions take the following forms:

Normal distribution

$$\log_e L_{normal}(a,b) = \sum_{i=1}^{n} \log_e \left\{ \frac{1}{\sqrt{2\pi b^2}} \exp\left[-(l_i - a)^2 / 2b^2\right] \right\}, \quad (1)$$

Largest extreme value distribution

$$\log_e L_{largest}(a,b) = \sum_{i=1}^{n} \log_e \left\{ (1/b)\exp\left[-(l_i - a)/b\right] \times \exp\left\{-\exp\left[-(l_i - a)/b\right]\right\} \right\}, \quad (2)$$

where n = number of data;
l_i = length of ith individual;
a = location parameter; and
b = scale parameter.

The location parameter is a mean in the normal distribution. The location parameter is a mode in the largest extreme distributions. The scale parameter is a standard deviation in the normal distribution.

The AIC is calculated by

$$\text{AIC} = -2 \log_e (\textit{maximum likelihood}) + 2m, \quad (3)$$

where m = number of parameters to be estimated.

The model with the minimum AIC is the best model. A difference of more than 1 or 2 is regarded as significant in terms of AIC (Sakamoto et al., 1983).

Modeling the change in the location Values of the location and scale parameters usually increase with the growth of an animal. The relative increase rate in a certain time step is defined as

[3] Abashiri Local Office of the Hokkaido Development Bureau, 2-6-1 Shinmachi, Abashiri, Hokkaido 093-0046, Japan.

$$r_i = (P_i - P_{i-1}) / P_{i-1}, \tag{4}$$

where r_i = relative increase rate of a parameter in the ith time step; and
P_i = parameter value after the ith time step.

Relationships between the parameter value and the relative increase rate of the parameter can be expressed by

$$\begin{aligned} P_1 &= P_0(1+r_1) \\ P_2 &= P_1(1+r_2) = P_0(1+r_1)(1+r_2) \\ P_3 &= P_2(1+r_3) = P_0(1+r_1)(1+r_2)(1+r_3) \\ &\vdots \\ P_n &= P_0\prod_{i=1}^{n}(1+r_i), \end{aligned} \tag{5}$$

where P_0 = parameter value at the first sampling;
P_i = parameter value after the ith time step; and
r_i = relative increase rate of the parameter in the ith time step.

We used one day as the time step in this study. In our environmentally based growth model, we assumed that the daily relative increase rate of location parameter (dRIRL) depends on the age of the animal and on environmental factors for each day. Sigmoid functions that take values between 0 and a certain maximum are empirically appropriate for expressing the relationships between the dRIRL and independent variables, especially for measures such as shell length that do not show negative growth. Therefore, using categorical variables indicating animal ages and environmental factors for each day as independent variables, we express the dRIRL by the multivariate logistic function

$$s_i = s_{\max} / \left\{1+\exp\left[-\left(\sum_{j=1}^{n_A}\alpha_j A_j + \sum_{k=1}^{n_E}\beta_k E_{ki}\right)\right]\right\}, \tag{6}$$

where s_i = dRIRL on the ith day from the first sampling;
$s_{\max}$ = potential maximum dRIRL of the animal;
α_j, β_k = coefficients of each independent variable;
A_j = categorical variable (a dummy variable indicating animal ages) that takes the value 1 or 0;
E_{ki} = the kth environmental factor on the ith day from the first sampling;
n_A = number of age categories; and
n_E = number of environmental factors.

The categorical variable takes the value of 1 when the animal is the category, otherwise it takes 0. The multivariate logistic function with $s_{\max} = 1$ is used for logistic regressions (Sokal and Rohlf, 1995). A method of giving a value to the categorical variable is described by Zar (1999).

Modeling the change in scale The daily relative increase rate of scale parameter (dRIRS) and dRIRL must be correlated because the dRIRS is larger when the dRIRL is larger. Therefore, we estimated the dRIRS from an equation expressing the relationship to the dRIRL. We tested two functions,

$$t_i = \begin{cases} \gamma_1 + \gamma_2 s_i & (\gamma_1 + \gamma_2 s_i > 0) \\ 0 & (\gamma_1 + \gamma_2 s_i \le 0) \end{cases} \tag{7}$$

and

$$t_i = \begin{cases} (s_i - \gamma_1)^{\gamma_2} & (s_i - \gamma_1 > 0) \\ 0 & (s_i - \gamma_1 \le 0) \end{cases}, \tag{8}$$

where t_i = dRIRS on the ith day from the first sampling;
γ_1, γ_2 = coefficients of the equations; and
s_i = dRIRL on the ith day from the first sampling.

Model estimation

Likelihood function The location and scale parameters at the first sampling (a_0 and b_0), the coefficients of Equation 6 ($s_{\max}$, α_j and β_k), and the coefficients of Equations 7 and 8 (γ_1 and γ_2) are estimated as values that maximize total log-likelihood. The total log-likelihood is evaluated by the adequate probability density function selected in the first step. The log-likelihood functions take the following forms:

Normal distribution

$$\begin{aligned} &\log_e L_{normal}(a_0, b_0, s_{\max}, \alpha_j, \beta_k, \gamma_1, \gamma_2) \\ &= \sum_{q=1}^{N}\sum_{i=1}^{n_q}\log_e\left\{\frac{1}{\sqrt{2\pi\hat{b}_q^2}}\exp\left[-(l_{qi}-\hat{a}_q)/2\hat{b}_q^2\right]\right\}; \end{aligned} \tag{9}$$

Largest extreme value distribution

$$\begin{aligned} &\log_e L_{largest}(a_0, b_0, s_{\max}, \alpha_j, \beta_k, \gamma_1, \gamma_2) \\ &= \sum_{q=1}^{N}\sum_{i=1}^{n_q}\log_e\left\{(1/\hat{b}_q)\exp\left[-(l_{qi}-\hat{a}_q)/\hat{b}_q\right]\right. \\ &\left.\times\exp\left\{-\exp\left[-(l_{qi}-\hat{a}_q)/\hat{b}_q\right]\right\}\right\}, \end{aligned} \tag{10}$$

where a_0, b_0 = values of the location and scale parameters, respectively, at the first sampling;
$s_{\max}$, α_j, β_k = coefficients of Equation 6;
γ_1, γ_2 = coefficients of Equations 7 and 8;
N = number of samplings;
n_q = number of data at the qth sampling;
$\hat{a}_q$ = location parameter at the qth sampling estimated by Equation 5 (r_i=s_i);
$\hat{b}_q$ = scale parameter at the qth sampling estimated by Equation 5 (r_i=t_i); and
l_{qi} = length of the ith individual at the qth sampling.

AIC is used to select significant environmental factors, the age categorization, and the equation to express the

relationship between dRIRL and dRIRS, i.e. Equation 7 or 8.

Confidence intervals To evaluate uncertainties of coefficient values and model selection, we estimated the 95% confidence intervals of all coefficients—i.e. a_0, b_0, s_{max}, α_j, β_k, γ_1, and γ_2—based on profile likelihood. For example, the 95% confidence interval of a_0—$a_{0,95}$—was estimated as an interval that suffices in the following equation:

$$2\Big\{\max \log_e L(\hat{a}_0,\hat{b}_0,\hat{s}_{\max},\hat{\alpha}_j,\hat{\beta}_k,\hat{\gamma}_1,\hat{\gamma}_2) - \max \log_e L(\hat{a}_0,\hat{b}_0,\hat{s}_{\max},\hat{\alpha}_j,\hat{\beta}_k,\hat{\gamma}_1,\hat{\gamma}_2 \mid a_0 = \alpha_{0,96})\Big\} \le \chi_1^2(0.05), \quad (11)$$

where $x_1^2(0.05)$ = value of a chi-squared distribution at an upper probability of 0.05 with one degree of freedom, i.e. 3.84.

The characteristics of the interval are explained by Burnham and Anderson (1998).

We used Microsoft Excel (Microsoft Corp., Redmond, WA) as the analysis platform, and Solver (Microsoft Corp., Redmond, WA) as the nonlinear optimization tool.

Model selection

We used three procedures for model selection to achieve the best model. First, we constructed an *a priori* set of base models based on biological variables; then we selected the best base model. Fixation of the base model drastically decreases possible candidate models to be tested. To test all possible combinations of independent variables and model forms is quite impractical. Second, we excluded insignificant factors from the best base model. Third, we checked the significance of environmental factors that were not included in the base models. If one was significant, we included it in the best base model. All of these procedures were performed by AIC. The construction of the *a priori* set of candidate models is partially subjective, but it is an important part of the model construction (Burnham and Anderson, 1998).

Seasonal growth in bivalves is influenced by water temperature and food supply (Bayne and Newell, 1983). The growth rate of *Corbicula fluminea* changes with age (McMahon, 1983). Therefore, we constructed base models combining water temperature, water fluorescence, and categorical variables indicating age for the independent variables of Equation 6. We tested two types of categorization of age. The first segregates ages based on real age, i.e. two categories: 0+ or 1+. The second segregates ages in relation to winter, i.e. three categories: before the first winter, from the first to the second winter, and after the second winter. For the real-age categorization, age was segregated based on 1 September, because the spawning season was in August 1997. For the winter-base age categorization, we segregated ages based on 1 January. No biases should have occurred because of the segregation date of the winter base categorization and because the growth of *C. japonica* is negligible during winter. Four base models were constructed combining the two types of age categorization and two types of equations expressing the relationship between the dRIRL and the dRIRS, i.e. Equations 7 or 8. We selected the best base model by AIC.

To check the significance of each environmental factor and age categorization, we removed the independent variables one by one from the best base model and re-optimized the model. When the model was significantly improved by the removal in terms of AIC, the effect of the variable was insignificant on the model; therefore we excluded it.

To check the significance of salinity and turbidity, which were not included in the base models, we included them one at a time into the best base model and re-optimized the model. When the model was improved by the inclusion, the effect of the variable was significant on the model; therefore we included it.

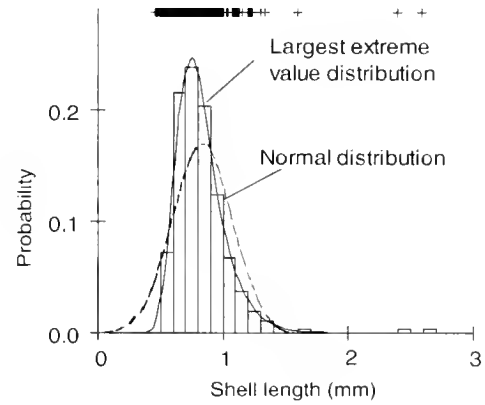

Figure 2

Two distributions fitted by the maximum-likelihood method to the shell lengths of *Corbicula japonica* juveniles spawned in 1997 and sampled on 22 April 1999. Raw data are shown by +. The shell length composition is shown by the histogram.

Results

Modeling the distribution of a single sample

The largest extreme value distribution was the best in terms of AIC except for data sampled on 13 May 1998 (results are not shown). The exception is due probably to the small sample size (n=38) on that date. The largest extreme value distribution was therefore used to evaluate likelihood in later analyses: we selected Equation 10 from Equations 9 and 10. The result of fitting the two distributions to the shell lengths sampled on 22 April 1999 is shown in Figure 2 as a representative example. The largest extreme value distribution is apparently better than the normal distribution for describing the single cohort of *C. japonica* spawned in 1997.

Table 1

Values of location and scale parameters at the first sampling, coefficients, log-likelihood, and AIC of models constructed based on the largest extreme value distribution. The best AIC among four base models (models 1–4) is enclosed by a single line. The best AIC of all models is enclosed by a double line. dRIRL = daily relative increase rate of location parameter, dRIRS = daily relative increase rate of scale parameter. Temp. = water temperature, WF = water fluorescence, Sal. = salinity, Turb. = turbidity, C1 = before the first winter, C2 = from the first to the second winter, C3 = after the second winter.

Model no.	Parameters at 1st sampling		Max. dRIRL	Age categorization			Environmental factors				Expressing relationship between dRIRS and dRIRL				
	a_0	b_0	s_{max}	A_1 α_1	A_2 α_2	A_3 α_3	Temp. β_1	WF β_2	Sal. β_3	Turb. β_4	γ_1	γ_2	Eq. no	Log-L	AIC
				0+	1+										
1	0.299	0.040	0.012	−62.6	−23.7		0.16	2.61			0.0000	1.686	7	850.4	−1682.9
2	0.297	0.040	0.011	−56.1	−22.1		0.20	2.44			0.0001	0.887	8	852.3	−1686.5
				C1	C2	C3									
3	0.299	0.042	0.011	−16.8	−16.7	−9.1	0.61	0.41			−0.0076	2.902	7	950.4	−1880.9
4	0.299	0.042	0.011	−17.5	−17.6	−9.6	0.65	0.42			0.0034	0.760	8	952.2	−1884.4
4.1	0.299	0.042	0.011	−18.3[1]		−10.0	0.68	0.44			0.0034	0.760	8	952.2	−1886.3
4.2	0.297	0.038	0.005	127.9	−26.8[1]		0.34	4.15			0.0000	0.895	8	735.0	−1451.9
4.3	0.295	0.037	0.008	−47.3	−16.3	−8.8		1.47			0.0033	0.766	8	848.9	−1679.9
4.4	0.299	0.041	0.013	-4.9	-8.9	-4.9	0.40				0.0020	0.806	8	909.6	-1801.1
4.5	0.299	0.042	0.011	−16.7[1]		−9.1	0.62	0.42	−0.25		0.0033	0.762	8	952.4	−1884.8
4.6	0.299	0.042	0.011	−18.5[1]		−10.2	0.68	0.44		0.007	0.0034	0.760	8	952.2	−1884.4

[1] One common coefficient was used for the two categorical variables.

Model selection and application

Model 4 was the best in terms of AIC among four base models (Table 1, models 1–4); ages were categorized in relation to winter; and the relationship between dRIRL and dRIRS was expressed by Equation 8.

Four models were made by removing each independent variable from model 4 (Table 1, models 4.1 to 4.4). The effect of one age categorization—segregation of ages between the first and second winters—was insignificant on the model, because the model was significantly improved by its removal in terms of AIC. The effects of the other independent variables were significant on the model, because the model was significantly worse by their removal in terms of AIC. The effects of salinity and turbidity were insignificant on the model, because adding each variable made the model significantly worse in terms of AIC (Table 1, models 4.5 and 4.6). Consequently, model 4.1 was the best model to describe the relationships among environmental factors, ages, and growth of *C. japonica* juveniles spawned in 1997.

The coefficient value for age categorization of before the second winter (−18.3) is much smaller than that of after the second winter (−10.0) (Table 1). This difference suggests that the growth response of *C. japonica* juveniles is much less susceptible to environmental factors before the second winter than after.

Peaks of the dRIRL corresponded with peaks of water fluorescence, when the water temperature was warmer than about 10°C, especially before the second winter (Fig. 3, B and C). Therefore, food supply is the most influential factor when the water temperature is above about 10°C. The slow growth or no growth during winter is due to the low water temperatures. The dRIRL reached a plateau after 30 May 1999. This was due to two factors: water fluorescence was relatively intense after 30 May 1999 (Fig. 3B); and the growth response of *C. japonica* to the environmental factors was more susceptible after the second winter than before.

The confidence limits of all the coefficients seem to be reasonably estimated by the profile likelihood method (Table 2). These results also guarantee the convergence of the model because the model was frequently optimized to seek each confidence limit with different starting values. We repeated the optimization at least 20 times to seek each confidence limit. On other models, we also confirmed the convergences as well.

The largest extreme value distributions estimated by model 4.1 fitted the shell lengths of *C. japonica* juveniles very well (Fig. 4).

Discussion

Model formulation and application

Largest extreme value distribution is apparently better than normal distribution to describe the single cohort of *C. japonica* that spawned in 1997. This distribution has a mode and a longer tail toward the larger side. If the shell

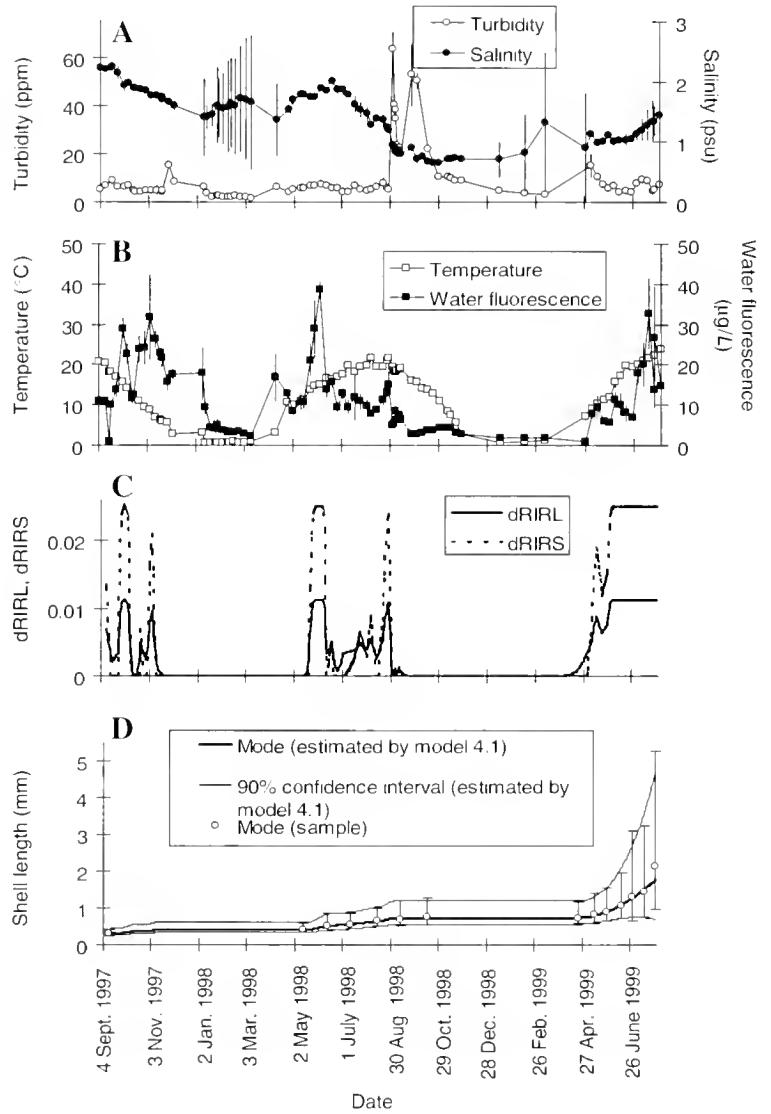

Figure 3

Environmental fluctuations and prediction of the growth of *Corbicula japonica* juveniles spawned in 1997 in Lake Abashiri by the best model (Model 4.1 in Table1). (**A**) Insignificant environmental factors (factors excluded in the model selection), turbidity (equivalent to kaolin density, ppm) and salinity (psu, practical salinity unit). (**B**) Significant environmental factors (factors included in the model selection), temperature (°C) and water fluorescence (equivalent to uranin density, µg/L). (**C**) Daily relative increase rate of location parameter (dRIRL) and daily relative increase rate of scale parameter (dRIRS) estimated by the model. (**D**) Growth of *Corbicula japonica*; vertical bars represent 90% confidence intervals for the shell lengths of the samples.

length distribution becomes asymmetric during growth, skewness of the distribution would increase according to growth. However, there is no correlation between the skewness and the means of the shell lengths. Therefore, we thought that the shell length distribution of the cohort was already asymmetric just after settlement. Such a distribution might be influenced by fluctuations in larval settlement during the spawning season; and larval settlement would be influenced by fluctuations in larval supply from the water column. During the spawning season of 1997, the average planktonic larval density gradually increased from 26 ind/m^3 on 25 July to a maximum of 603 ind/m^3 on

Table 2

95% confidence limits of location and scale parameters at the first sampling and coefficients of the best model constructed based on the largest extreme value distribution (models 4.1 in Table 1) estimated by profile likelihood method. dRIRL = daily relative increase rate of location parameter, dRIRS = daily relative increase rate of scale parameter, Temp. = water temperature, WF = water fluorescence, Sal. = salinity, Turb. = turbidity.

	Parameters at 1st sampling		Max. dRIRL	Age categorization			Environmental factors				Expressing relationship between dRIRS and dRIRL	
				A_1	A_2	A_3	Temp.	WF	Sal.	Turb.		
	a_0	b_0	s_{max}	α_1	α_2	α_3	β_1	β_2	β_3	β_4	γ_1	γ_2
Lower 95 %	0.294	0.039	0.010	−26.6[1]		−14.6	0.41	0.27			0.0027	0.734
Upper 95 %	0.304	0.045	0.013	−11.5[1]		−6.4	1.00	0.64			0.0039	0.793

[1] One common coefficient for the two categorical variables.

13 August. Then it sharply decreased to 3 ind/m^3 on 19 August (Baba et al., 1999). Such a pattern of larval-density fluctuation might have caused the asymmetric distribution of shell lengths of the settled juveniles. Another possible factor that influenced the shapes of the shell length distributions and the relationship between dRIRL and dRIRS is size-dependent mortality, e.g. predations and fisheries. Size-dependent mortality has been reported in several marine bivalves (e.g. Nakaoka, 1996). Potential predators of *C. japonica* are fishes, such as Japanese dace (*Tribolodon hakonensis*) (also known as big-scaled Pacific redfin, FAO), Pacific redfin (*Tribolodon brandtii*), common carp (*Cyprinus carpio*), and the So-iny mullet (*Liza haematocheila*) (Kawasaki[4]). In our study, the size-dependent mortality was negligible because the range of the shell lengths observed in this study was very narrow.

The shape of the distribution to describe a single cohort should be determined from the data. In contrast, single cohorts are usually separated from multicohort data by assuming a normal distribution of lengths in a single cohort (e.g. Fournier and Sibert, 1990). Therefore, it is possible that multicohort analysis done without selection of an adequate distribution to describe a single cohort causes substantial bias in estimations of various stock features of animal populations, such as age composition, growth, mortality, and recruitment. In our preliminary analyses, we also tested smallest extreme value distribution, inverse Gaussian distribution, and lognormal distribution. The inverse Gaussian distribution was the best for two samples; the lognormal distribution, was the best for two samples; the largest extreme value distribution was the best for ten samples. Therefore, it is reasonable to select the largest extreme value distribution. We selected a single distribution for our analyses, otherwise a discontinuous point would have appeared in the growth curve.

Relatively large confidence intervals were obtained in the coefficients of the linear component of Equation 6, i.e. α_j, and β_k (Table 2). The relatively large confidence intervals may indicate that the number of estimated coefficients is somewhat larger than the number of samplings. Therefore, to estimate these coefficients more precisely, we may need to investigate more cohorts spawned in other years in future investigations.

Growth of *C. japonica*

We identified extremely slow growth in *C. japonica* juveniles, which grew to a modal shell length of 0.7 mm during the first year in Lake Abashiri, which lies at 43.7°N. Spats of *C. japonica* collected from 1992 to 1997 in Lake Shinji, which lies at 35.5°N, grew to a mean shell length of 6.7 mm in natural conditions by the first winter (Yamane et al.[2]). Using environmental factors measured in Lake Shinji from 1990 to 1998 at monthly intervals (Seike[5]), we simulated the growth of *C. japonica* with model 4.1. *Corbicula japonica* grew to a mean shell length of 1.4 mm (standard error, 0.37) by the first winter in the simulations. Therefore, the large difference in juvenile growth between the two habitats cannot be explained by environmental differences because the results of the simulation were apparently an underestimate. We think that the extremely slow growth of the juveniles (prolonged phase of meiobenthic development) in Lake Abashiri is probably a geographical variation, which is genetically determined, within *C. japonica*. However, there remains a possibility that the juvenile growth differences depend on other environmental factors not measured in this study. Therefore, the geographical

[4] Kawasaki, K. 1997. Lagoon structure and fish production in Ogawara-ko Lagoon. *In* Final reports on fisheries in Ogawara-ko Lagoon (Tohoku Construction Corporation ed.), p. 4–33. Unpubl. rep. Construction Office for Takasegawa General Development of Tohoku Regional Construction Bureau, 3 Ishido, Hachinohe, Aomori 039-1165, Japan.

[5] Seike, Y. 1990–98. Gobiusu: monthly report of water quality in Lake Shinji and Lake Nakaumi. Unpubl. rep. Faculty of Science and Engineering, Shimane University, 1060 Nishikawatsu, Matsue, Shimane 690-0823, Japan.

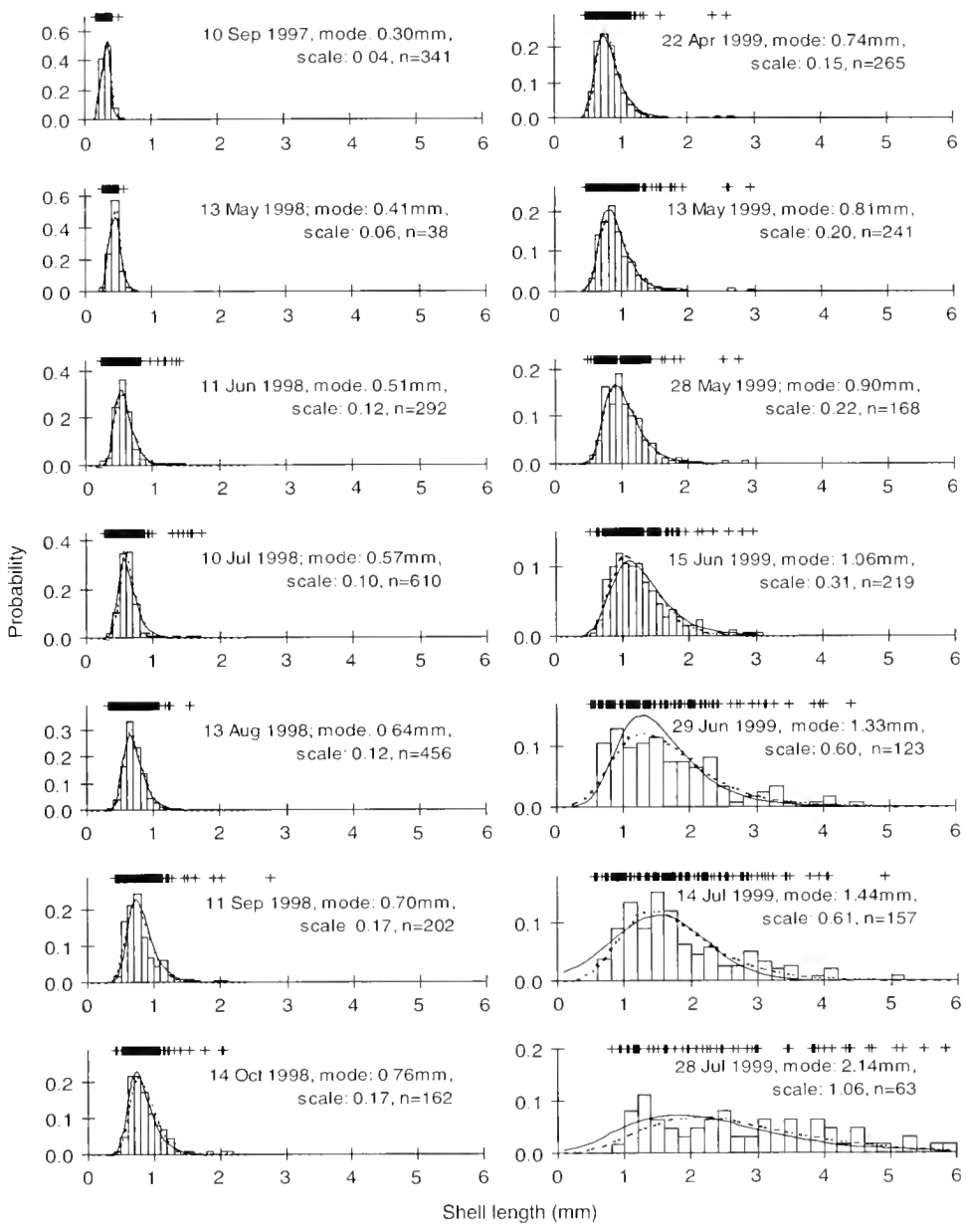

Figure 4

Shell-length compositions of a single cohort of *Corbicula japonica* spawned in 1997. The raw data (shell lengths) are shown by +. The largest extreme value distribution estimated by the best model (model 4.1 in Table 1) is shown by a solid line. The largest extreme value distribution independently fitted by the maximum likelihood method is shown by a dashed line. The sampling date and values of location parameter (mode) and scale parameter independently fitted by the maximum likelihood method are shown in each panel.

variation should be validated by reciprocal transplantations or laboratory experiments (or both) in future investigations. Prolonged phases of meiobenthic development have been reported in some marine bivalves (Nakaoka, 1992; Harvey and Gage, 1995). However, a prolonged phase of meiobenthic development as a geographical variation is rarely reported.

In many species of bivalve, populations from higher latitudes have a slower initial growth rate; but longevity and ultimate size in these populations are frequently greater than at lower latitudes (Newell, 1964; Seed, 1980). The extremely slow growth of *C. japonica* juveniles in Lake Abashiri may be an extreme example of this phenomenon. In Lake Abashiri, *C. japonica* failed to spawn in ten out of 21 years for which

data were available because of low water temperatures during the summer spawning season (Baba et al., 1999). This means that a long life span is essential to sustain populations of *C. japonica* in northern habitats. We think that a long life span is the ultimate factor for the extremely slow growth rate of *C. japonica* juveniles in Lake Abashiri.

The growth response of *C. japonica* juveniles is much less susceptible to environmental factors before the second winter than after and is the proximate factor for an extremely slow growth rate. *Nuculoma tenuis*, a detritus feeder, develops its palp proboscides, its feeding apparatus, during the prolonged phase of meiobenthic development (Harvey and Gage, 1995). The change of growth susceptibility to environmental factors in young ages may suggest that some functional morphological changes occur in *C. japonica*, also a filter feeder. In our preliminary analyses, we could not find a better model when we used different values of s_{max} in Equation 6 between ages instead of categorical variables indicating ages. Therefore, we conclude that the difference in growth rates between ages is not due to a difference in potential maximum growth rate, at least in the range of the shell length observed in our study. When our model is applied to a wider range of the shell lengths or other species, it is best to examine the age dependence of s_{max}.

Acknowledgments

We express our thanks to T. Kato, Vice-Head of the River Improvement Section in the Abashiri Local Office of the Hokkaido Development Bureau, for providing environmental data on Lake Abashiri. We also thank the reviewers of Fishery Bulletin for providing helpful suggestions on our manuscript.

Literature cited

Akaike, H.
1973. Information theory and an extension of the maximum likelihood principle. *In* Second international symposium on information theory (B. N. Petrov and F. Csaki, eds.), p. 267–281. Akademiai Kiado, Budapest.

Baba, K., T. Kawajiri, and Y. Kuwahara.
1999. Effects of water temperature and salinity on spawning of the brackish water bivalve *Corbicula japonica* in Lake Abashiri, Hokkaido, Japan. Mar. Ecol. Prog. Ser. 180: 213–221.

Bayne, B. L.
1993. Feeding physiology of bivalves: time dependence and compensation for changes in food availability. *In* Bivalve filter feeders and marine ecosystem processes (R. F. Dame ed.), p. 1–24. Springer Verlag, New York, NY.
1998. The physiology of suspension feeding by bivalve molluscs: an introduction to the Plymouth "TROPHEE" workshop. J. Exp. Mar. Biol. Ecol. 219:1–19.

Bayne, B. L., and R. C. Newell.
1983. Physiological energetics of marine molluscs. *In* The Mollusca, 4(1) (A. S. M. Saleuddin and K. M. Wilbur eds.), p. 407–515. Academic Press, New York, NY.

Burnham, K. P., and D. R. Anderson.
1998. Model selection and inference, 349 p. Springer, New York, NY.

Campbell, D. E., and C. R. Newell.
1998. MUSMOD, a production model for bottom culture of the blue mussel, *Mytilus edulis* L. J. Exp. Mar. Biol. Ecol. 219:171–203.

Dame, R. F.
1993. The role of bivalve filter feeder material fluxes in estuarine ecosystems. *In* Bivalve filter feeders in estuarine and coastal ecosystem processes: NATO ASI Series (R. F. Dame ed.), p. 245–269. Springer-Verlag, Berlin, Heidelberg.

Evans, M., N. Hastings, and B. Peacock.
1993. Statistical distribution, 170 p. John Wiley & Sons, New York, NY.

Fournier, D. A., and J. R. Sibert.
1990. MULTIFAN a likelihood-based method for estimating growth parameters and age composition from multiple length frequency data sets illustrated using data for southern bluefin tuna (*Thunnus maccoyii*). Can. J. Fish. Aquat. Sci. 47:301–317.

Grant, J., and C. Bacher.
1998. Comparative models of mussel bioenergetics and their validation at field culture sites. J. Exp. Mar. Biol. Ecol. 219:21–44.

Grant, J., M. Dowd, K. Thompson, C. Emerson, and A. Hatcher.
1993. Perspectives on field studies and related biological models of bivalve growth and carrying capacity. *In* Bivalve filter feeders in estuarine and coastal ecosystem processes: NATO ASI Series (R. F. Dame ed.), p. 371–420. Springer-Verlag, Berlin, Heidelberg.

Harvey, R., and J. D. Gage.
1995. Reproduction and recruitment of *Nuculoma Tenuis* (Bivalvia: Nuculoida) from Loch Etive, Scotland. J. Moll. Stud. 61:409–419.

Héral, M.
1993. Why carrying capacity models are useful tools for management of bivalve molluscs culture. *In* Bivalve filter feeders in estuarine and coastal ecosystem processes: NATO ASI Series (R. F. Dame ed.), p. 455–477. Springer-Verlag, Berlin, Heidelberg.

Jørgensen, C. B.
1996. Bivalve filter feeding revisited. Mar. Ecol. Prog. Ser. 142:287–302.

Kafanov, A. I.
1991. Bivalves on continental shelf and continental slope of Northern Pacific, p. 81–82. Science Acad. USSR, Vladivostok.

MacMahon, R. F.
1983. Ecology of an invasive pest bivalve, *Corbicula*. *In* The Mollusca, 6(12) (W. D. Russell-Hunter, ed.), p. 505–561. Academic Press, Orlando, FL.

Nakamura, M., M. Yamamuro, M. Ishikawa, and H. Nishimura.
1988. Role of the bivalve *Corbicula japonica* in the nitrogen cycle in a mesohaline lagoon. Mar. Biol. 99: 369–374.

Nakaoka, M.
1992. Age determination and growth analysis based on external shell rings of the protobranch bivalve *Yoldia notabilis* Yokoyama in Otsuchi Bay, Northeastern Japan. Benthos Res. 43:53–66.
1996. Size-dependent survivorship of the bivalve *Yoldia notabilis* (Yokoyama, 1920): the effect of crab predation. J. Shellfish Res. 15:355–362.

Newell, G. E.
1964. Physiological aspects of the ecology of intertidal molluscs. *In* Physiology of Mollusca (K. M. Wilbur and C. M. Yonge eds.), p. 59–81. Academic Press, London.

Pauly, D.
1987. A review of the ELEFAN system for analysis of length

frequency data in fish and aquatic invertebrates. *In* Length-based methods in fisheries research (D. Pauly and G. R. Morgan eds.), p. 7–34. ICLARM conference proceedings 13, 688 International Center for Living Aquatic Resource Management, Manila, Philippines and Kuwait Institute for Scientific Research, Safet, Kuwait.

Sakamoto, Y., M. Ishiguro, and G. Kitagawa.
1983. Statistics based on information amount (Jouhouryou Toukei Gaku), 236 p. Kyoritu Shuppan, Tokyo. [In Japanese.]

Scholten, H., and A. C. Smaal.
1998. Responses of *Mytilus edulis* L. to varying food concentrations: testing EMMY, an ecophysiological model. J. Exp. Mar. Biol. Ecol. 219:217–39.

Seed, R.
1980. Shell growth and form in the Bivalvia. *In* Skeletal growth of aquatic organisms (D. G. Rhoads ed.), p. 23–67. Plenum Press, New York, NY.

Sellmer, G. P.
1956. A method for the separation of small bivalve molluscs from sediments. Ecology 37:206.

Sokal, R. R. and F. J. Rohlf.
1995. Biometry, 3rd ed., 887 p. W. H. Freeman and Company, New York, NY.

Utoh, H.
1981. Growth of the brackish water bivalve, *Corbicula japonica* Prime, in Lake Abashiri. Sci. Rep. Hokkaido Fish. Exp. Stn. 23:65–81. [In Japanese.]

Yamakawa, T., and Y. Matsumiya.
1997. Simultaneous analysis of multiple length frequency data sets when the growth rates fluctuate between years. Fish. Sci. 63:708–714.

Yamamuro, M., and I. Koike.
1993. Nitrogen metabolism of the filter-feeding bivalve *Corbicula japonica* and its significance in primary production of a brackish lake in Japan. Limnol. Oceanogr. 38: 997–1007.

Zar, J. H.
1999. Biostatistical analysis, 663 p. Prentice Hall, Upper Saddle River, NJ.

Abstract—Information is summarized on juvenile salmonid distribution, size, condition, growth, stock origin, and species and environmental associations from June and August 2000 GLOBEC cruises with particular emphasis on differences related to the regions north and south of Cape Blanco off Southern Oregon. Juvenile salmon were more abundant during the August cruise as compared to the June cruise and were mainly distributed northward from Cape Blanco. There were distinct differences in distribution patterns between salmon species: chinook salmon were found close inshore in cooler water all along the coast and coho salmon were rarely found south of Cape Blanco. Distance offshore and temperature were the dominant explanatory variables related to coho and chinook salmon distribution. The nekton assemblages differed significantly between cruises. The June cruise was dominated by juvenile rockfishes, rex sole, and sablefish, which were almost completely absent in August. The forage fish community during June comprised Pacific herring and whitebait smelt north of Cape Blanco and surf smelt south of Cape Blanco. The fish community in August was dominated by Pacific sardines and highly migratory pelagic species. Estimated growth rates of juvenile coho salmon were higher in the GLOBEC study area than in areas farther north. An unusually high percentage of coho salmon in the study area were precocious males. Significant differences in growth and condition of juvenile coho salmon indicated different oceanographic environments north and south of Cape Blanco. The condition index was higher in juvenile coho salmon to the north but no significant differences were found for yearling chinook salmon. Genetic mixed stock analysis indicated that during June, most of the chinook salmon in our sample originated from rivers along the central coast of Oregon. In August, chinook salmon sampled south of Cape Blanco were largely from southern Oregon and northern California; whereas most chinook salmon north of Cape Blanco were from the Central Valley in California.

Manuscript approved for publication 30 June 2003 by Scientific Editor.

Manuscript received 20 October 2003 at NMFS Scientific Publications Office.

Fish. Bull 102:25–46 (2004).

Juvenile salmonid distribution, growth, condition, origin, and environmental and species associations in the Northern California Current*

Rick D. Brodeur
Northwest Fisheries Science Center
National Marine Fisheries Service, NOAA
2030 S. Marine Science Drive
Newport, Oregon 97365
E-mail address: Rick.Brodeur@noaa.gov

Joseph P. Fisher
College of Ocean and Atmospheric Sciences
Oregon State University
Corvallis, Oregon 97331

David J. Teel
Northwest Fisheries Science Center
National Marine Fisheries Service, NOAA
Seattle, Washington 98112

Robert L. Emmett
Northwest Fisheries Science Center
National Marine Fisheries Service, NOAA
2030 S Marine Science Drive
Newport, Oregon 97365

Edmundo Casillas
Northwest Fisheries Science Center
National Marine Fisheries Service, NOAA
Seattle, Washington 98112

Todd W. Miller
Cooperative Institute for Marine Resources Studies
Oregon State University
Newport, Oregon 97365

The need to understand the direct and indirect linkages between oceanographic conditions and salmon survival in the marine environment has increased with the listing of many West Coast salmon stocks as threatened or endangered. Recent studies have shown that long-term changes in climate affect oceanic structure and produce abrupt differences in salmon marine survival and returns (Francis and Hare, 1994; Mantua et al., 1997). A major regime shift in the subarctic and California Current ecosystems during the late 1970s may have been a factor in reducing ocean survival of salmon in the Pacific Northwest and in increasing marine survival in Alaska (Hare et al., 1999). Fluctuations in mortality of salmon in the freshwater and marine environments have been shown to be almost equally significant sources of annual salmonid recruitment variability (Bradford, 1995). Unlike in the freshwater environment, the physical and biological mechanisms and factors in the marine environment that cause mortality of salmon are largely unknown. Predation, inter- and intraspecific competition, food availability, smolt quality and health, and physical ocean conditions likely influence survival of salmon in the marine environment. Thus, increasing our understanding of nearshore ocean environments, their linkages to oceanographic conditions, and the role they play in salmonid survival, could provide management options for increasing adult returns. Characterization of the space-time variability of the environmental conditions that smolts encounter when they enter the nearshore ocean, and the eventual survival of these smolts will allow us to identify which biotic and abiotic ocean conditions are correlated with various ocean survival levels.

Many anadromous salmonid populations along the west coast of the United States have declined over the last few decades (Nehlsen et al., 1991), and most stocks show a regional north-south pattern in degree of extinction risk (Kope and Wainwright, 1998). This pattern suggests that both marine habitat conditions and mesoscale climate patterns affect salmonid population status (e.g. Lawson, 1993). A dramatic example is the population trend of coho salmon (*Oncorhynchus kisutch*) along the Oregon coast. Populations along the coast north of Cape Blanco (43°N) have exhib-

* Contribution number 364 of the U.S. GLOBEC program, NEP Office, Oregon State University, Corvallis, OR.

ited a strong decline in size and survival in the mid-1990s; whereas populations south of Cape Blanco have not shown this trend (Lewis[1]). This finding suggests that these two populations have experienced different ocean conditions.

The quality of the marine habitat (in terms of habitat complexity, prey density, and temperature) undoubtedly influences fish growth and condition. Growth and indices of condition can be used as measures of habitat quality for juvenile salmon and to identify essential links between oceanographic conditions and survival of salmon populations during the critical juvenile life history phase. Measures such as growth (growth rate, size variation, and allometric relationships) (Lorenzen, 1996; McGurk, 1996) and accumulation of energetic reserves used in growth and sustenance during the low-productivity winter periods have been used previously to characterize habitat quality and to describe how it ultimately affects the individual and the population (Perry et al., 1996; Paul and Willette, 1997). Environmental factors are known to affect growth, reproduction, survival, and ultimately population recruitment (Hinch et al., 1995; Marschall and Crowder, 1995; Friedland and Haas, 1996). As such, fish condition, growth rate, and size in the pre-adult stages are parameters that can be used to identify the influence of natural and anthropogenic ocean conditions on marine survival.

Much of our current knowledge of the dominant nekton of the pelagic ecosystem off the coasts of Oregon and Washington is derived from a series of 17 cruises conducted by Oregon State University (OSU) from 1979 to 1985. These collections, consisting of >900 quantitative purse seine sets in the northern California Current, were made to examine geographic distributions and temporal trends of the dominant nekton and how these relate to physical and biotic conditions at the time of capture. The primary purpose of these cruises was to collect data for assessment of the abundance, distribution, growth, migration, and ecology of juvenile salmon in coastal waters. Data on the distribution, migration and growth of juvenile salmon from these cruises have been summarized in Fisher and Pearcy (1988; 1995), Pearcy and Fisher (1988, 1990), and Pearcy (1992). Analysis of the nonsalmonid data includes studies on their abundance and distribution (Brodeur and Pearcy, 1986; Emmett and Brodeur, 2000), feeding habits (Brodeur et al., 1987) and interannual variability in relation to oceanographic conditions (Brodeur and Pearcy, 1992). In addition, the distribution of juvenile salmon (mainly coho and chinook salmon [*O. tshawytscha*]) has been studied more recently as a component of a multiyear Columbia River Plume study (Emmett and Brodeur, 2000; Teel et al., 2003; Brodeur et al., 2003). However, all these cruises extended only as far south as Cape Blanco, with the exception of one cruise (July 1984), which extended as far south as Eureka, California, but included only a few collections south of Cape Blanco (Pearcy and Fisher, 1990). Thus, the region south of Cape Blanco is almost completely unknown in terms of juvenile salmon distribution, pelagic nekton, and biological oceanography in general, despite being an area of very strong upwelling and high productivity. Also, the fine-scale distribution of juvenile salmon in relation to environmental variables has not been studied in any detail.

The California Current is not homogeneous but rather can be divided into distinct subunits or regions, each with its own physical and biological characteristics (U.S. GLOBEC, 1994). A break between the northernmost two regions occurs at Cape Blanco, where the equatorward upwelling jet veers sharply off the shelf and into the California Current (Barth et al., 2000). The upwelling zone north of the cape is narrow, extending out about 30 km, whereas south of Cape Blanco, it can extend up to 100 km offshore. This area also appears to represent a faunal break for some zooplankton communities (McGowan et al., 1999; Peterson and Keister, 2002) and is a break point for alternative salmon migration strategies (Weitkamp et al., 1995; Weitkamp and Neely, 2002).

During the summer of 2000, we conducted broad-scale sampling and fine-scale process studies from central Oregon to northern California to examine the distribution of juvenile salmon and associated species in relation to environmental conditions. This was one component of a multidisciplinary U.S. Global Ocean Ecosystem Dynamics (GLOBEC) Northeast Pacific study examining the northern California Current ranging in scope from the physics up to the top trophic levels (Batchelder et al., 2002). We were interested in examining the distribution of juvenile salmon north and south of Cape Blanco, the origin of these fish, and any regional differences in growth and condition of salmon across the range of sampling. Evidence exists that the physical conditions and the associated biota are different within this geographical scale. Thus, analyses of the relationship between oceanographic conditions and the response of resident biota can provide insights into the linkages associated with physical and biological processes that shape the biological community, and in particular, those associated with salmon recruitment.

Methods

Field surveys

Surveys were conducted over two time periods—early summer (29 May–18 June, 2000) and late summer (28 July–15 August, 2000). Each survey consisted of a mesoscale grid along designated GLOBEC transects that had been monitored for several years and by fine-scale process sampling at stations of interest based on features observed in the physical environment (fronts or eddies) or by acoustic sampling conducted by two accompanying oceanographic vessels (RV *Wecoma* and RV *New Horizon*). Further details on the physical and biological conditions occurring at the time of our sampling have been reported by Batchelder et al. (2002).

For the mesoscale survey, stations were established at 1, 5, 10, 15, 20, 25 and 30 nautical miles from shore on each of five transects. Inclement weather, particularly

[1] Lewis, M. A. 2002. Stock assessment of anadromous salmonids 2001. Monitoring program report OPSW-ODFW-2002-04, 57 p. Oregon Dept. Fish Wildlife, Portland, OR 97207.

during the first cruise, prevented us from sampling all the stations along each transect. At each station, a Nordic 264 rope trawl built by Nor'Eastern Trawl Systems, Inc. (Bainbridge Island, WA) was towed in surface waters by a chartered fishing vessel (FV *Sea Eagle*) at a speed of 6 km/h. This rope trawl has a maximum mouth opening of approximately 30 m × 18 m. Mesh sizes ranged from 162.6 cm in the throat of the trawl near the jib lines to 8.9 cm in the codend. To maintain catches of small fish and squid, a 6.1-m long, 0.8-cm mesh knotless liner was sewn into the codend. All tows were 30 minutes in duration. All fish and squid caught were counted and measured at sea. After fork length (FL) was measured to the nearest mm, all juvenile salmon were immediately frozen for later determinations of growth, condition, food habits, genetic analysis, and assessment of pathological condition.

The physical and biological environment was monitored and sampled at each station immediately prior to setting the trawl. A CTD (conductivity, temperature, and depth) cast was made with a Sea-Bird SBE 19 Seacat profiler to 100 m at deep stations or within 10 m of the bottom at shallow stations. Chlorophyll and nutrient samples were collected from 3 m depth with a Niskin water sampler. A neuston tow with a 1-m^2 mouth containing 333-μm mesh net was towed for 5 minutes out of the wake of the vessel at each station. General Oceanics flow meters were placed inside the net to measure the amount of water sampled. Additional details on the analysis of these neuston trawls are available in Reese et al.[2]

Condition and growth analysis

Each salmonid was remeasured (FL to the nearest mm) and weighed (to the nearest 0.1 g) in the laboratory. A portion of hepatic and muscle tissue was excised, placed in individual capsules, frozen in liquid nitrogen, and stored at –80°C until analyzed. The bioenergetic health of juvenile salmon was evaluated by assessing changes in water content (as a surrogate measure of fat accumulation) of liver and muscle to estimate dry tissue weight. The water content was determined by drying tissue samples to a constant weight at 105°C. The accumulation of energy reserves during the growth season (energy reserves of salmon in August in relation to salmon collected in June) that would enhance survival of juveniles during the winter when food availability is lower was also measured. The condition of juvenile salmon was assessed by examining weight residuals (by using either the wet weight or dry weight) derived from the allometric relationship between length and weight of individual juvenile salmon after logarithmic transformation (Jakob et al., 1996) of salmon captured in June and August. Wet-weight residuals are representative of the traditional condition index of animals and are a reflection of somatic tissue growth. Dry-weight residuals are responsive to accumulation of fat stores and are a reflection of the bioenergetic health of the individual animal (Sutton et al., 2000; Post and Parkinson, 2001).

To contrast growth characteristics during 2000 in different latitudinal ranges of the California Current, we compared ocean growth rates of juvenile coho salmon south and north of Cape Blanco in the GLOBEC study area, and in the area from Newport, Oregon, north to northern Washington. The physical and biological characteristics of these three regions of the coastal ocean differ greatly (U.S. GLOBEC, 1994), and these differences may impact the distribution and abundance of prey of juvenile salmonids and therefore may also affect salmonid growth. Data north of Newport, Oregon, were collected during a separate study of the Columbia River plume and the adjacent coastal ocean (hereafter called the "plume study") using the same trawl and a similar sampling strategy as in the GLOBEC study (see Emmett and Brodeur [2000] and Teel et al. [2003] for details).

Scales were examined from 45 juvenile coho salmon caught during the June and August 2000 GLOBEC cruises and 252 juvenile coho salmon caught during the 2000 plume cruises. The scales were mounted on gummed cards from which acetate impressions were made. Using a video camera attached to a compound microscope and Optimas® imaging software (vers. 5.1, Optimas Inc., Seattle, WA) we measured the distance (scale radius) along the anterior-posterior axis of each scale from the focus (F) to the ocean entry mark (OE) and to the scale margin (Fig. 1). The fork-length of each fish at the time of ocean entry (FL_{OE}) was estimated from the scale radius (SR_{OE}) at ocean entry using the Fraser and Lee back-calculation method (Ricker, 1992):

$$FL_{OE} = \frac{(FL - 36.07)}{SR} \times SR_{OE} + 36.07,$$

where FL = length at capture;
SR = scale radius at capture; and
36.07 = the intercept from a regression of SR on FL for juvenile coho salmon caught in the ocean (Fig. 2A).

In an analogous fashion, fish weight at time of ocean entry (Wt_{OE}) was back-calculated from the estimated fish fork length at ocean entry (FL_{OE}):

$$\ln(Wt_{OE}) = \frac{(\ln(Wt) + 12.633)}{\ln(FL)} \times \ln(FL_{OE}) - 12.633,$$

where Wt = weight at capture; and
–12.633 = the intercept from a linear regression of $\ln(Wt)$ on $\ln(FL)$ for juvenile coho salmon caught in the ocean (Fig. 2B).

The growth rate in FL,

$$(FL - FL_{OE})/\Delta d,$$

[2] Reese, D. C., T. W. Miller, and R. D. Brodeur. 2003. Community structure of neustonic zooplankton in the northern California Current in relation to oceanographic conditions, 22 p. Unpubl. manuscript. Northwest Fisheries Science Center, NMFS, 2030 S. Marine Science Drive, Newport, OR 97365.

Figure 1

Scale from a 352-mm FL male juvenile coho salmon (*Oncorhynchus kisutch*) caught during the August 2000 GLOBEC cruise showing the axis of measurement (black line), the focus (F), the mark of ocean entry (OE), and the scale margin (SM).

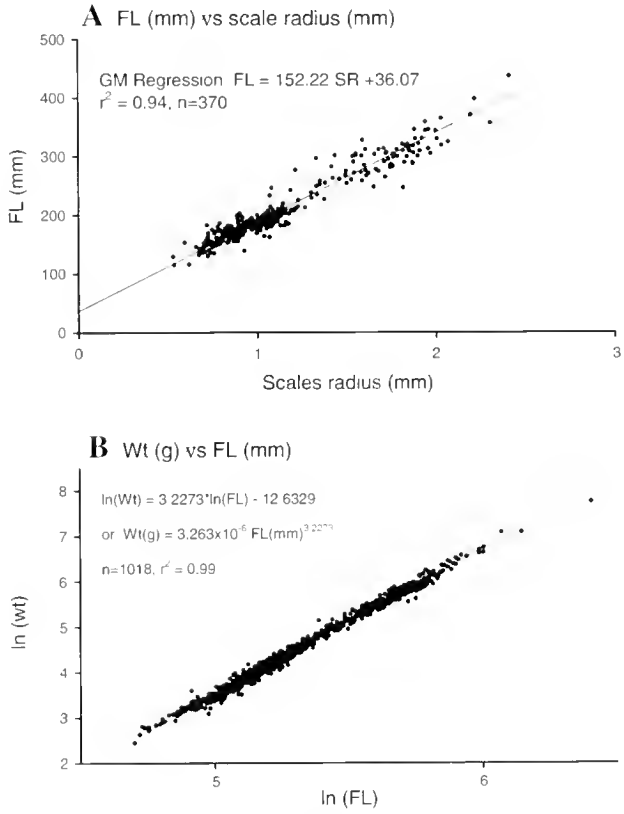

Figure 2

(**A**) Regression of fork length (FL) on scale radius and, (**B**) regression of $\ln(Wt)$ on $\ln(FL)$ for juvenile coho salmon (*Oncorhynchus kisutch*) caught during the May 1998–September 2000 Columbia River plume study.

and the instantaneous growth rate in weight:

$$G = \left(\ln(Wt) - \ln(Wt_{OE})\right) / \Delta d,$$

where Δd = estimated days between ocean entry and capture, were estimated for each salmon.

The meaning of the instantaneous growth rate G can be stated as follows: if salmon growth is exponential between ocean entry and capture, then

$$\frac{Wt}{Wt_{OE}} = e^{G \cdot \Delta d},$$

and at any *instant* the fish's weight increases at the *rate* of G of its body weight per day. G can be multiplied by 100 to give the instantaneous growth rate in terms of percentage of body weight per day.

Although the dates of ocean entry of individual fish were unknown, seaward migration of coho salmon smolts in California, Oregon, and Washington rivers occurs mainly between mid-April and mid-June, and there is no consistent latitudinal trend in timing of the migration (Weitkamp et al., 1995). Peak downstream migration of coho salmon smolts was between mid-May and very early June in the Columbia River estuary, 1978–83 (Dawley et al., 1985), and in the lower Trinity River, California, 1997–2000 (USFWS[3]). In 2000, peak downstream migration of mainly nonhatchery coho salmon smolts at 13 monitoring sites in coastal Oregon rivers north of Cape Blanco occurred from April 2 to May 20; median peak migration occurred 26 April (Solazzi et al.[4]) From the information available on timing of seaward migration of coho salmon smolts, we used an ocean entry date of 15 May when calculating Δd and estimating ocean growth rates of unmarked coho salmon from scales.

In addition to estimating growth rates of juvenile coho salmon from scales, we also estimated instantaneous growth rates in weight between hatchery release and capture in the ocean of 28 coded-wire–tagged (CWT) juvenile coho salmon:

[3] USFWS (U.S. Fish and Wildlife Service). 2001. Juvenile salmonid monitoring on the mainstem Klamath River at Big Bar and mainstem Trinity River at Willow Creek, 1997–2000, 106 p. Annual report of the Klamath River Fisheries Assessment Program. Arcata Fish and Wildlife Office, Arcata, CA 95521.

[4] Solazzi, M. F., S. L. Johnson, B. Miller, and T. Dalton. 2002. Salmonid life-cycle monitoring project 2001. Monitoring program report OPSW-ODFW-2002-2, 25 p. Oregon Dept. Fish and Wildlife, Portland, OR 97207.

$$G = (\ln(Wt) - \ln(Wt_R)) / \Delta d,$$

where Wt = weight of the CWT fish at capture;
Wt_R = the average weight of fish in the CWT group at time of release; and
Δd = days between hatchery release and capture in the ocean.

Estimated growth rates of these CWT fish, of known release date and known average release weight were used to validate the growth rates estimated from scale analysis

Our analysis of the growth of chinook salmon based on scale characteristics is not far enough advanced to report in this article. We plan to present these data in a later article.

Contribution of hatchery coho salmon to catches

The total numbers, percentages of marked fish (any external fin clips or internal tags) and grand average weights of hatchery coho salmon smolts released in 2000 are summarized for different release regions in Appendix Table 1. These data were used to compare the estimated average weights of fish at time of ocean entry (from scale analysis) with the average weights of hatchery fish at time of release, and also to estimate the proportions of hatchery coho salmon in our catches. We calculated the expected percentage ($E\%$) of marked fish in each catch if 100% of the fish were hatchery fish:

$$E\% = \sum R_i \times A_i,$$

where R_i = the proportional contribution of region i to the catch (this paper for the GLOBEC catches, and from Teel et al., 2003 for the plume study catches); and
A_i = the percentage of hatchery fish that were marked in region i (from Appendix Table 1).

The percentage of hatchery fish in each catch sample ($H\%$) was then estimated as

$$H\% = \frac{O\%}{E\%} \times 100,$$

where $O\%$ = observed percentage of marked fish.

Genetic analysis

The freshwater origins of juvenile chinook and coho salmon and steelhead (*O. mykiss*) were studied by using standard methods of genetic mixed stock analysis (Milner et al., 1985; Pella and Milner, 1987). According to the methods described by Aebersold et al. (1987), samples of eye, liver, heart, and skeletal muscle were extracted from frozen whole juvenile salmon and analyzed with horizontal starch-gel protein electrophoresis. Data from previous studies characterizing genetic (allozyme) differences among spawning populations in California and the Pacific Northwest were then used as baseline data to estimate the stock compositions of our ocean caught mixed-stock samples. Baselines consisted of 32 gene loci and 116 populations for chinook salmon (Teel et al.[5]), 58 loci and 49 populations for coho salmon (Teel et al., 2003), and 55 loci and 57 populations for steelhead (Busby et al., 1996). Estimates of stock compositions were made by using the maximum likelihood procedures described by Pella and Milner (1987) and the Statistical Package for Analyzing Mixtures (Debevec et al., 2000). Estimates of individual baseline populations were then summed to estimate contributions of regional stock groups. Precision of the stock composition estimates was estimated by bootstrapping the estimates 100 times with resampling of the baseline and mixture genetic data as described in Pella and Milner (1987).

Habitat and assemblage analysis

The raw numbers of fish and squid caught from each trawl were converted to densities based on the volume filtered per trawl to standardize for differences in effort between tows. Density contours of juvenile salmon and other nekton were produced using specialized graphics programs. We then tested whether the habitat associations of the dominant salmonids were significantly different from the total habitat sampled by following the methods outlined in Perry and Smith (1994). This procedure involved comparing the cumulative distributions of salmon catch with observed environmental conditions (temperature, salinity, chlorophyll-*a* at one meter, water depth, and neuston displacement volume). We performed 5000 randomizations of the data and used the Cramér-von Mises test statistic recommended by Syrjala (1996) as being robust to the effects of inordinately large catches.

To explore the relationship between juvenile salmon and other fish species and environmental variables, we used several types of multivariate analyses (McCune and Grace, 2002). Original data from each of the two cruises formed complimentary species and environmental matrices. The June and August cruises were analyzed individually to look at spatial patterns of species composition in relation to environmental gradients (Gauch, 1982). To avoid spurious effects of rare species, we excluded species from the data matrix that had a frequency of occurrence of less than 10% of the possible occurrences for each cruise (McCune and Grace, 2002). To minimize the effect of very large catches, the data were log transformed. Stations with no species present were eliminated from the data set to allow for analysis of sample units in species space. Data transformations and their effects on the summary statistics were examined prior to analysis. Analyses of data were performed by using PC-ORD version 4.28 (McCune and Mefford, 1999).

Agglomerative hierarchical cluster analysis (AHCA) using the Bray-Curtis dissimilarity measure and Wards

[5] Teel, D. J., P. A. Crane, C. M. Guthrie, III, A. R. Marshall, D. M. Van Doornik, W. D. Templin, N. V. Varnavskaya, and L. W. Seeb. 1999. Comprehensive allozyme database discriminates chinook salmon from around the Pacific Rim. (NPAFC document 440), 25 p. Alaska Department of Fish and Game, Division of Commercial Fisheries, 333 Raspberry Road, Ancorage, AK 99518.

linkage function was applied to arrange the nekton species assemblages and stations into cluster groups. The cutoff level to form optimal groups within the species and station dendrograms was based on several criteria: 1) biological meaning; 2) significance tests of groups using a multi-response permutation procedure (MRPP); and 3) comparison of cutoff level MRPP results with those groups obtained from one cutoff level below and above the level of interest. A nonparametric procedure, MRPP compares the *a priori* groupings from AHCA and tests the hypothesis of no difference between the groups. For cluster analysis of stations, indicator species analysis (ISA) was used to determine nekton species strongly associated with individual groups. ISA assigns indicator values to each species according to relative abundance and frequency, then tests the significance (Monte-Carlo permutation test) of the highest species-specific indicator value assigned to a particular group.

Nonmetric multidimensional scaling (NMS; Kruskal, 1964) was used to ordinate sample units in species space and to compare station cluster groups to environmental gradients. NMS was chosen for this analysis because it is robust to data that are non-normal and that have high numbers of zeros. Initial runs of NMS from both cruise datasets resulted in three-dimensional solutions. Subsequent reapplication of NMS using a three-dimensional solution (Sorensen distance, 400 maximum iterations, and 40 runs with real data) was applied for the final ordinations. To examine the environmental or station factors associated with each NMS axis that may have affected the distribution of the dominant taxa, we correlated the NMS station and species scores to a suite of environmental variables including water depth, distance offshore, latitude, surface temperature, surface salinity, chlorophyll-*a* concentration, and neuston zooplankton settled volumes. Pearson and Kendall correlations with each ordination axis were used to measure strength and direction of individual species and environmental parameters.

Results

Distribution of juvenile salmon and other species

We collected a total of 18,852 nekton individuals: two cephalopod, one agnathan, two elasmobranch, and 57 fish taxa from 163 surface trawls (see Table 1 for scientific names of all species). With the exception of market squid in June and blue shark in August, most of the nonteleost nekton occurred in only a few collections. Substantially fewer fish were caught in the June cruise than in the August cruise, but the diversity was much higher in the June cruise. The catch in June was dominated by forage fishes such as Pacific herring, surf and whitebait smelt, and juvenile rockfishes, sablefish, and flatfishes. Salmonids, mainly juvenile chinook and coho salmon and steelhead, comprised a relatively minor proportion of the catches (only 114 juvenile salmonids; 1.9 % of the total).

The August cruise was dominated by several large catches of Pacific sardine (Table 1). Jack mackerel was the most common nonsalmonid caught. Many of the juvenile fish taxa caught during the June cruise were absent during the August cruise; those that did occur (sablefish, rex sole) were much lower in abundance. Mesopelagic fishes of the family Bathylagidae and Myctophidae were collected only during the August cruise, mainly because of the inclusion of more offshore stations and occasional collections during nondaylight hours. As in the earlier cruise, salmonids comprised a relatively minor percentage of the catch (3.1%) but were more common and abundant during this survey.

Juvenile chinook salmon were broadly distributed latitudinally during both cruises, but their distribution was mainly restricted to nearshore stations within the 100-m isobath (Fig. 3). Coho salmon juveniles were more common north of Cape Blanco during both cruises and were found generally farther offshore than chinook salmon juveniles (Fig. 3). In contrast, steelhead juveniles were found mainly south of Cape Blanco, especially in June, but their zonal distribution overlapped that of coho salmon juveniles.

Size and condition of juvenile salmon

Fork length of yearling chinook salmon averaged 227 ±42 mm FL in June and 230 ±30 mm FL in August and averaged 135 ±12 mm FL for subyearling chinook salmon in August, whereas juvenile coho salmon averaged 162 ±32 mm FL in June and 286 ±46 mm FL in August (Table 2). No significant differences in fork length of juvenile chinook or coho salmon north or south of Cape Blanco were evident.

Juvenile coho salmon weighed significantly more on a wet-weight basis for a given fork length in the region north of Cape Blanco compared to juveniles captured south of Cape Blanco (Fig. 4). This pattern was also similar and significant when evaluated on a dry-weight basis (bioenergetic growth). Although the stock composition in the two regions could account for some of these differences, the growth responses likely reflect habitat-specific features in the region north of Cape Blanco that benefit coho salmon. No difference in condition of yearling chinook salmon captured north or south of Cape Blanco, on either a wet- or dry-weight basis, was evident (Fig. 4). Information regarding size and condition of subyearling chinook salmon are not presented because few subyearling chinook salmon were caught in June and all but one subyearling chinook salmon in August were caught in the region south of Cape Blanco, OR. Insufficient subyearling chinook salmon were available for an analysis comparable to that done for yearling chinook and coho salmon.

Proportions of wild and hatchery coho salmon

Most of the juvenile coho salmon caught during the plume study north of Newport, Oregon, originated in hatcheries (Table 3). In June and September 2000 we estimated that wild fish comprised only 10% and 25%, respectively, of the catch. Wild fish, however, comprised a proportionally much higher percentage of the catch of coho salmon in the GLOBEC study area in June north of Cape Blanco (67%), and in August south of Cape Blanco (61%), than in the plume study area farther to the north. Most jacks and

Table 1

Phylogenetic listing of nekton catch in numerical composition, frequency of occurrence (F.O.) and size range caught for each cruise. (j) indicates juvenile stage; (a) adult. ML = mantle length, TL = total length, FL = fork length, SL = standard length (in mm).

			June (84 stations)			August (79 stations)		
Class and Family	Common name	Scientific name	Number	F.O.	Size range	Number	F.O.	Size range
Cephalopoda								
Onychoteuthidae	Pacific clubhook squid	*Onychoteuthis borealijaponicus*	19	6	21–80 ML	302	6	21–227 ML
Loliginidae	Market squid	*Loligo opalescens*	301	14	33–122 ML	1	1	35 ML
Agnatha								
Petromyzontidae	Pacific lamprey	*Lampetra tridentata*				1	1	625 TL
Chondrichthyes								
Alopiidae	Thresher shark	*Alopias vulpinus*	1	1	36–576 TL			
Carcharhinidae	Blue shark	*Prionace glauca*				18	10	1300–1660 TL
Osteichthyes								
Xenocongridae	Eel leptocephalus	*Thalassenchelys coheni*	3	1	214–243 TL	2	2	260–305 TL
Clupeidae	Pacific herring	*Clupea pallasi*	1022	9	127–195 FL			
	Pacific sardine	*Sardinops sagax*	7	2	237–260 FL	10,327	15	178–290 FL
Engraulididae	Northern anchovy	*Engraulis mordax*				49	12	148–165 FL
Salmonidae	Chinook salmon (j,a)	*Oncorhynchus tshawytscha*	56	18	121–780 FL	252	26	109–910 FL
	Coho salmon (j,a)	*Oncorhynchus kisutch*	35	15	122–580 FL	111	25	210–736 FL
	Cutthroat trout (j,a)	*Oncorhynchus clarki*	1	1	186 FL	3	3	258–341 FL
	Steelhead trout (j,a)	*Oncorhynchus mykiss*	22	8	176–284 FL	36	13	261–430 FL
Osmeridae	Smelt (j)	Osmeridae	14	4	37–52 SL	74	5	31–50 SL
	Surf smelt	*Hypomesus pretiosus*	846	8	128–184 FL	351	7	140–187 FL
	Whitebait smelt	*Allosmerus elongatus*	946	6	60–114 FL	79	3	76–132 FL
Bathylagidae	Popeye blacksmelt	*Bathylagus ochotensis*				1	1	76 SL
Paralepidae	Slender barracudina	*Lestidium ringens*				3	1	72–76 SL
Myctophidae	Northern lampfish	*Stenobrachius leucopsarus*				96	4	14–70 SL
	Bigfin lanterfish	*Symbolophorus californiensis*				61	4	89–102 SL
	Blue laternfish	*Tarletonbeania crenularis*				10	3	33–87 SL
Gadidae	Gadid (j)	Gadidae	10	3	42–58 SL	13	3	53–57 SL
	Pacific cod (j)	*Gadus macrocephalus*	23	1	38–60 SL			
	Pacific tomcod (j)	*Microgadus proximus*	6	4	35–55 SL	8	2	49–80 SL
Scomberesocidae	Pacific saury	*Cololabis saira*	26	1	182–229 FL	66	6	131–194 FL
Atherinidae	Jacksmelt	*Atherinopsis californiensis*				1	1	302 FL
Trachipteridae	King-of-the-salmon (j)	*Trachipterus altivelis*	2	2	71–270 SL	12	2	40–83 SL
Gasterosteidae	Threespine stickleback	*Gasterosteus aculcatus*	1	1	60 SL			
Scorpaenidae	Pacific ocean perch (j)	*Sebastes alutus*	1	1	33 SL			
	Darkblotched rockfish (j)	*Sebastes crameri*	154	14	29–54 SL	1	1	53 SL
	Yellowtail rockfish (j)	*Sebastes flavidus*	1350	24	20–63 SL	1	1	18 SL
	Shortbelly rockfish (j)	*Sebastes jordani*	1	1	37 SL			
	Black rockfish (j,a)	*Sebastes melanops*	1	1	30 SL	1	1	335 FL
	Bocaccio (j)	*Sebastes paucispinis*	20	5	21–36 SL			
	Canary rockfish (j)	*Sebastes pinniger*	27	5	22–39 SL			
	Bank rockfish (j)	*Sebastes rufus*	8	1	16–28 SL			
	Stripetail rockfish (j)	*Sebastes saxicola*	13	3	32–37 SL			
Hexagrammidae	Lingcod (j)	*Ophiodon clongatus*	20	9	76–81 FL			
Anoplopomatidae	Sablefish (j)	*Anoplopoma fimbria*	182	14	55–136 FL	4	2	173–241 FL

continued

Table 1 (continued)

Class and Family	Common name	Scientific name	June (84 stations)			August (79 stations)		
			Number	F.O.	Size range	Number	F.O.	Size range
Cottidae	Irish lord (j)	*Hemilepidotus* spp.	2	1	38–40 FL			
	Cabezon (j)	*Scorpeanichthys marmoratus*	12	7	33–38 SL			
	Pacific staghorn sculpin	*Leptocottus armatus*	1	1	180 TL			
Agonidae	Sturgeon poacher (j)	*Podothecus acipenserinus*				1	1	80 TL
Cyclopteridae	Pacific spiny lumpsucker	*Eumicrotremus orbis*				1	1	253 TL
Carangidae	Jack mackerel	*Trachurus symmetricus*	111	3	364–583 FL	839	20	227–589 FL
Bramidae	Pacific pomfret	*Brama japonica*				5	2	387–434 FL
Anarhichadidae	Wolf-eel (j)	*Anarrhichthys ocellatus*	15	13	215–555 TL	8	7	442–582 TL
Ammodytidae	Pacific sandlance	*Ammodytes hexapterus*	4	4	45–82 SL			
Zaprodidae	Prowfish (j)	*Zoprora silenus*	1	1	68 SL			
Scombridae	Chub mackerel	*Scomber japonicus*				74	6	266–421 FL
Centrolophidae	Medusafish	*Icichthys lockingtoni*	3	3	37–50 SL	8	6	87–129 FL
Bothidae	Sanddabs (j)	*Cithorichthys* spp.	23	13	35–43 SL	3	2	269–288 TL
	Pacific sanddab (j)	*Cithorichthys sordidus*	32	4	32–44 SL			
	Speckled sanddab (j)	*Citharichthys stigmaeus*	60	10	30–43 SL			
Pleuronectidae	Dover sole (j)	*Microstomus pacificus*	2	2	40–50 SL	3	1	27–34 SL
	Sand sole (j)	*Psettichthys melanostictus*	3	3	22–39 SL			
	Slender sole (j)	*Eopsetta exilis*				1	1	66 SL
	Starry flounder	*Platichthys stellatus*				2	1	349–399 TL
	Curlfin sole (j)	*Pleuronichthys decurrens*	5	3	25–31 SL			
	English sole	*Parophrys vetulus*	1	1	303 TL			
	Rex sole (j)	*Errex zachirus*	581	12	34–79 SL	48	11	44–70 SL
Molidae	Ocean sunfish	*Mola mola*				1	1	620 TL
Total			5974			12,878		

about one half of the nonjacks caught north of Cape Blanco in August were hatchery fish.

Two factors, however, may have lead to inaccuracies in estimation of hatchery-wild ratios of coho salmon in the GLOBEC study area. First, because of low sample sizes, the data were pooled from both June and August catches for the genetic stock analysis; therefore we do not know the proportional contributions of the different release areas to the catches in either month alone. Second, all the fish released from Klamath River and Trinity River hatcheries had been clipped on the maxillary. We were unaware that the maxillary clip was being used, did not look for it, and consequently may have classified fish with this mark as unmarked. Therefore, the proportion of hatchery fish in the catch of coho salmon during GLOBEC may have been higher than is shown in Table 3.

Age and growth of juvenile coho salmon

Forty-three percent (24 of 56) of the juvenile coho salmon caught during the August GLOBEC cruise were precocious males ("jacks") according to the testes-weight to body-weight criteria of Pearcy and Fisher (1988). This is a much higher percentage of jacks than found among juvenile fish caught in September 2000 in the plume study off Oregon and Washington, where only 4.5% of fish (6 of 132) were precocious males or females according to the same criteria. Because the jacks were considerably larger than the nonjacks, average growth rates of the two groups were reported separately.

Estimated average growth rates in FL between ocean entry and capture were higher for fish caught in the August 2000 GLOBEC cruises (1.56–2.22 mm/d) than for fish caught in any other cruises (Table 3). The fish caught in August 2000 were also larger when they entered the ocean (average170–178 mm FL) than fish caught in other cruises (average154–160 mm FL). Average growth rate of jacks from north of Cape Blanco (2.22 mm/d), was significantly higher (*t*-test, $P<0.05$) than growth rates of nonjacks (1.56–1.67 mm/d). Growth rates of nonjacks north and south of Cape Blanco were not significantly different (*t*-test, $P<0.05$). The combination of large size at ocean entry

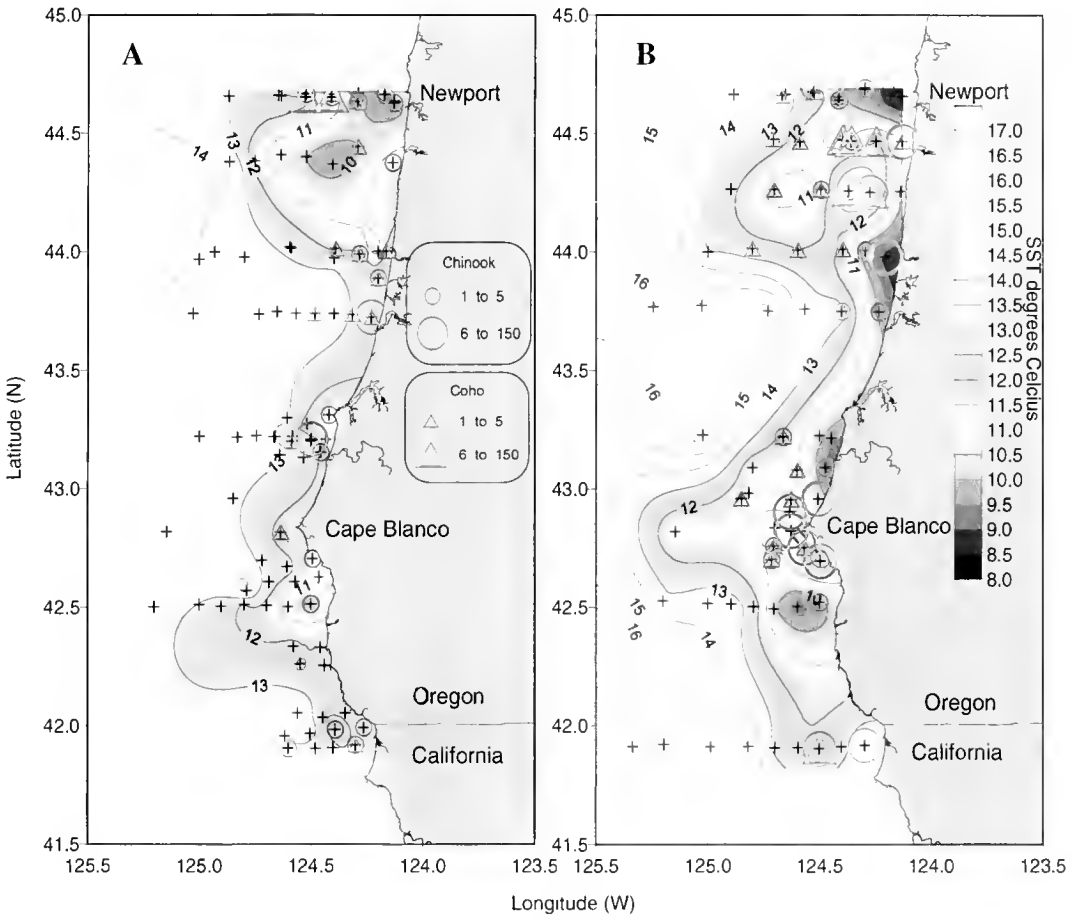

Figure 3

Catch distribution for juvenile coho (*Oncorhynchus kisutch*) and chinook salmon (*O. tshawytscha*) for the (**A**) June and (**B**) August cruise overlaid on surface temperature contours. Plus signs are stations sampled where no salmon were caught.

and favorable conditions for growth in the ocean probably contributed to the very high percentage of jack coho salmon in August 2000 in the GLOBEC study area.

Estimated average growth rates between ocean entry and capture of juvenile coho salmon were higher in the GLOBEC area than in the plume study area (t-tests, $P<0.05$). For fish caught in June, average growth rate was 1.06 mm/d and 0.63 mm/d in the GLOBEC and plume study areas, respectively. For fish caught in August or September, average growth rate was 1.57–2.22 mm/d in the GLOBEC study area and 1.17 mm/d plume in the study area (Table 3). The higher growth rates of coho salmon caught in the GLOBEC study area suggests that in 2000 conditions for growth were better there than those in the plume study area farther north off Oregon and Washington. Average instantaneous growth rates in weight were also higher (t-tests, $P<0.05$) for the fish caught in the June and August 2000 GLOBEC cruises (2.0 and 2.1–2.8% body wt/d, respectively) than for the fish caught in the June and September 2000 plume study cruises (1.2 and 1.7 % body wt/d, respectively; Table 4A).

In addition, the average condition index (CI) of juvenile coho salmon in June was significantly higher (t-test, $P=0.03$) in the GLOBEC study area (1.12, $n=32$, SD=0.087) than in the plume study area (1.07, $n=245$, SD=0.117). Similarly, the average CI of nonjack juvenile coho salmon was higher (t-test, $P=0.002$) in August in the GLOBEC study area (1.24, $n=32$, SD=0.096) than in September in the plume study area (1.18, $n=132$, SD=0.100). Both the high instantaneous growth rates in weight and the high CI of juvenile coho salmon caught in the GLOBEC study area suggest that conditions for growth of coho salmon in this area were very good in 2000. Growth rates estimated from the few CWT fish caught during these cruises (Table 4B) were similar to, and help validate, the growth rates estimated from scales (Table 4A).

Average weights at time of ocean entry back-calculated from scales for coho salmon caught in June in the GLOBEC area and in all months in the plume study area (Table 4A) were slightly higher than the average weights of hatchery coho salmon at time of release (Appendix Table 1). For example, in the plume study area, average back calculated weights at ocean entry ranged from 37.5 g to 42.4 g (Table 4A)—slightly higher than the expected average weights at release of about 32–33 g based on the stock composi-

Table 2

Summary of mean, standard deviation, and range of FL measured in the field, weight measured in the laboratory, and condition index (CI) of subyearling (age 0.0) and yearling (age 1.0) chinook salmon and yearling (age 1.0) coho salmon caught during the June and August cruises north (N) and south (S) of Cape Blanco (latitude 42.837°). Precocious coho salmon are indicated with a "J".

	Field FL (mm)				Laboratory weight (g)			C.I. (wt× 10^5/ FL^3)	
	n	Mean	SD	Range	Mean	SD	Range	Mean	SD
Chinook (age 0.0)									
June (N)	1	121	—	—	18	—	—	1.04	—
August (N)	1	172	—	—	70	—	—	1.37	—
August (S)	125	134	12	109–175	28	9	12–70	1.10	0.08
Chinook (age 1.0)									
June (N)	27	229	42	144–280	178	91	33–306	1.32	0.10
June (S)	1	174	—	—	67	—	—	1.28	—
August (N)	54	229	26	187–318	164	72	80–468	1.32	0.09
August (S)	35	231	35	190–349	176	94	80–535	1.32	0.07
Coho (age 1.0)									
June (N)	30	161	33	122–276	56	51	19–292	1.13	0.08
June (S)	2	172	0	172–172	49	1	48–49	0.95	0.01
August (N-J)	24	365	31	310–415	690	209	375–1198	1.38	0.12
August (N)	24	285	51	210–385	326	188	97–766	1.26	0.10
August (S)	8	293	33	239–334	308	103	157–433	1.19	0.05

Table 3

Catch, percentage of the catch that was marked, estimated percentage of hatchery origin, size of scale sample, FL at ocean entry (OE) back calculated from scales, FL at capture, and estimated growth rate in FL while in the ocean for juvenile coho salmon caught during the 2000 GLOBEC and Columbia River plume studies. All length data are from the scale sample only. An ocean entry date of 15 May was used when calculating growth rate in FL.

Cruise	Catch (*n*)	Marked	Estimated % hatchery origin	Scale sample (*n*)	Back-calculated FL at OE (mm) mean (SD)	FL at capture (mm) mean (SD)	Growth rate (mm/d) mean (SD)
GLOBEC							
June 2000	32	32%	33%	11	155 (29.0)	177 (42.3)	1.06 (1.01)
Aug 2000							
North of C. Blanco							
Jacks	24	71%	74%	19	170 (22.8)	370 (28.1)	2.22 (0.35)
Nonjacks	24	46%	48%	9	178 (21.6)	309 (46.1)	1.67 (0.51)
South of C. Blanco							
Nonjacks	8	38%	39%	6	178 (13.0)	303 (29.3)	1.56 (0.22)
Plume study							
May 2000	165	68%	76–80%[1]	79	157 (16.5)	166 (17.7)	0.97 (1.15)
Jun 2000	245	76%	90%	97	160 (14.5)	185 (23.4)	0.63 (0.53)
Sep 2000	132	65%	75%	76	154 (19.0)	305 (24.9)	1.17 (0.23)

[1] No genetic stock analysis was available. The higher estimate assumes the same stock composition as in June, the lower estimate assumes that all hatchery fish were from the Columbia River.

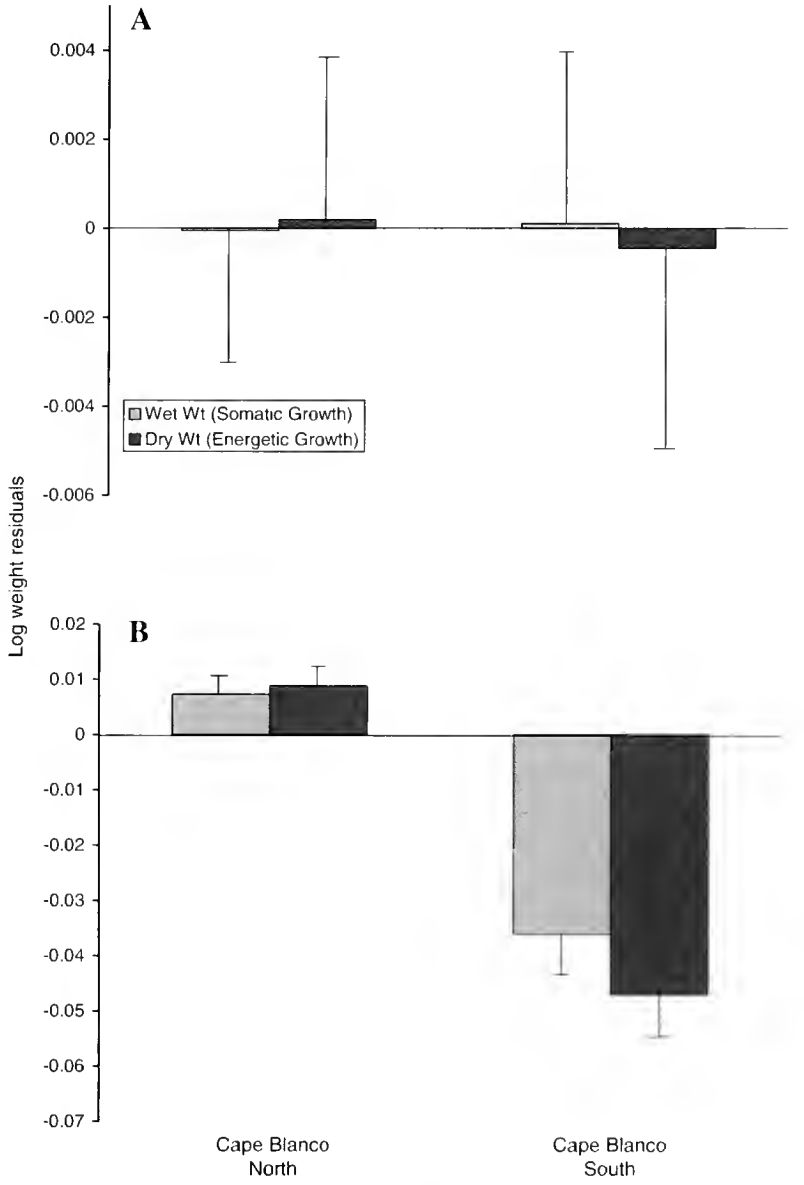

Figure 4

Wet and dry weight residuals (+1 standard error) for (**A**) yearling chinook (*Oncorhynchus tshawytscha*) and (**B**) juvenile coho salmon (*O. kisutch*) collected North and South of Cape Blanco. Weight residuals are derived from the linear relationship between fork length and wet or dry weight (log-transformed data) of juvenile salmon captured in June and August.

tion of these catches (Teel et al., 2003) and the release weights (Appendix Table 1). Similarly, the back-calculated weight at ocean entry in June in the GLOBEC area (45.5 g) was slightly higher than the expected average weight at hatchery release (about 41 g) based on the stock composition (Table 5) and the average release weights. These fairly small differences between back-calculated size at ocean entry and average size at release could be due to growth during downstream migration, selectively higher mortality of small smolts, or a bias in the back-calculation procedure.

However, the average back-calculated weights at time of ocean entry of fish caught in August in the GLOBEC study area (60–69 g) were over two standard deviations above the average weights of hatchery fish released from the Oregon coast or northern California—the main contributors to this catch (Appendix Table 1). These were obviously atypical coho salmon, and the very high proportion of jacks (preco-

Table 4

(**A**) Weights at ocean entry (OE) back-calculated from scales, weights at capture, and estimated instantaneous rates of growth while in the ocean (*G*) for juvenile coho salmon caught during the 2000 GLOBEC and Columbia River plume studies. An ocean entry date of 15 May was used when calculating growth rate. (**B**) Similar data for CWT fish. Growth rates of the CWT coho salmon were estimated for the periods between hatchery release and capture in the ocean.

		Back-calc. Wt. at OE (g)	Weight at capture (g)	*G*
A Cruise	*n*	mean (SD)	mean (SD)	mean (SD)
GLOBEC				
June 2000	11	45.5 (26.8)	78.0 (76.4)	0.020 (0.015)
Aug 2000				
North of C. Blanco				
Jacks	19	68.9 (27.2)	719.7 (200.0)	0.028 (0.005)
Nonjacks	9	59.5 (26.3)	419.2 (177.2)	0.023 (0.006)
South of C. Blanco				
Nonjacks	6	60.3 (12.8)	336.2 (96.2)	0.021 (0.002)
Plume study				
May 2000	79	39.4 (10.8)	47.9 (14.6)	0.020 (0.024)
Jun 2000	97	42.4 (12.5)	71.9 (33.3)	0.012 (0.009)
Sep 2000	75	37.5 (13.7)	347.2 (158.3)	0.017 (0.003)
		Wt. at release (g)	Wt. at capture (g)	*G*
B Cruise	*n*	mean (SD)	mean (SD)	mean (SD)
GLOBEC				
Jun 2000	4	44.4 (1.3)	86.6 (30.9)	0.018 (0.005)
Aug 2000	3	35.6 (9.8)	395.7 (215.0)	0.024 (0.003)
Plume study				
Jun 2000	11	28.3 (4.5)	66.1 (32.3)	0.012 (0.005)
Sep 2000	10	33.4 (10.9)	392.4 (283.3)	0.018 (0.002)

cious, sexually developed males) among the fish was probably a consequence of their very large size at ocean entry and their high rates of growth in the ocean.

Freshwater origins of juvenile salmonids

Allozyme data were collected from samples of 247 chinook salmon, 88 coho salmon, and 58 steelhead. Genetic mixed stock analyses indicated that chinook salmon in June were predominately (54%, SD=0.18) from rivers and hatcheries along the mid Oregon coast, an area immediately north of Cape Blanco (Table 5, Fig. 5). In August, chinook salmon were largely from rivers that enter the sea south of Cape Blanco. Fish from the Sacramento and San Joaquin rivers in northern California were estimated to comprise 90% (SD=0.07) of the chinook salmon sampled in August north of Cape Blanco. The largest concentration of chinook salmon we sampled was south of Cape Blanco in August, and these fish were mostly from rivers in southern Oregon (53%, SD=0.10) and the Sacramento and San Joaquin rivers (20%, SD=0.05). Chinook salmon from the Columbia River Basin were also present, but were estimated to comprise only 18% (SD=0.15) of the June sample and 8% (SD=0.05) of the August sample north of Cape Blanco. Recoveries of hatchery chinook salmon bearing coded-wire tags (CWT) provided direct evidence of stock origins for ten fish, all taken in trawls north of Cape Blanco (Table 5). These data reveal that hatchery fish released from the Umpqua River on the central Oregon coast (n=6), Columbia River Basin (n=3) and Sacramento River (n=1) contributed to our sample of chinook salmon. The proportion of CWT fish from the Umpqua River in our August catch north of Cape Blanco (8%) indicated that the contribution of mid Oregon coastal fish was underestimated in the genetic analysis likely because of the small size of the mixture sample.

Genetic estimates of coho salmon indicated that most fish originated from coastal Oregon rivers north of Cape Blanco (47%, SD=0.10) and from the Columbia River (13%, SD=0.08) (Table 5). However, a substantial proportion (40%, SD=0.09) of coho salmon were from coastal rivers south of Cape Blanco, a region that includes spawning populations in the Rogue and Klamath rivers. Eight coho salmon in our sample contained CWTs and showed that fish from

Table 5

Estimated percentage stock compositions, samples sizes, and recoveries of coded wire tags (CWTs) for chinook and coho salmon and steelhead sampled in trawl surveys along the Oregon and California coasts in 2000. Some of the major baseline stocks are given for coastal stock groups. None of the steelhead sampled contained coded wire tags.

	June (n=35) Entire Study Area			August (n=157) South of Cape Blanco			August (n=55) North of Cape Blanco		
Chinook salmon stock group	Est.	SD	CWT	Est.	SD	CWT	Est.	SD	CWT
Columbia and Snake Rivers	18	0.15	2	3	0.03		8	0.05	1
North Oregon coast (Nehalem, Trask, Alsea, and Siuslaw Rivers)	0	0.00		0	0.00		0	0.00	
Mid Oregon coast (Umpqua, Coquille, Sixes, and Elk Rivers)	54	0.18	3	3	0.03		1	0.02	3
South Oregon coast (Rogue, Chetco, and Winchuck Rivers)	26	0.16		53	0.10		0	0.00	
Klamath and Trinity Rivers	0	0.00		14	0.07		0	0.00	
North California Coast (Mad, Eel, and Mattole Rivers)	2	0.05		7	0.07		1	0.04	
Sacramento and San Joaquin Rivers	0	0.00		20	0.05		90	0.07	1

	June and August (n=88) Entire study area		
Coho salmon stock group	Est.	SD	CWT
Columbia River	13	0.08	2
North and Mid Oregon coast (Nehalem, Siletz, Alsea, Umpqua, and Coos Rivers)	47	0.10	5
Rogue and Klamath Rivers	40	0.09	1
North California Coast (Mad, Russian, Little, and Scott Rivers)	0	0.00	

	June and August (n=58) Entire study area	
Steelhead trout stock group	Est.	SD
Columbia and Snake Rivers	0	0.00
North and Mid Oregon coast (Nehalem, Siletz, Alsea, Umpqua, Coos, and Coquille Rivers)	1	0.03
South Oregon coast (Elk, Rogue, Chetco, and Winchuck Rivers)	53	0.08
Smith, Klamath, and Trinity Rivers	0	0.00
North California Coast (Mad, Eel, and Ten Mile Rivers)	10	0.05
Sacramento and San Joaquin Rivers	14	0.05
Central and South California Coast (San Lorenzo River and Scott, Pauma, and Gaviota Creeks	3	0.02
Unknown	19	—

hatcheries in the Umpqua River (n=5), Rogue River (n=1), and Columbia River (n=2) were in our study area.

Genetic analysis of steelhead samples showed that a large proportion were from the Rogue River and nearby coastal streams (53%, SD=0.08). Steelhead from the Sacramento and San Joaquin rivers (14%, SD=0.05) and northern California coastal rivers (10%, SD=0.05) were also present. Estimates for steelhead originating from rivers north of Cape Blanco and from south of the San Francisco Bay were near zero. Approximately 19% of the steelhead mixture was not allocated to any source population, suggesting that our baseline data for the species is incomplete. No steelhead in our collections contained CWTs.

Species associations of juvenile salmonids and other species

From cluster analysis of species based on station assemblages (Fig. 6), MRPP of both sample periods showed strong within-group agreement (P<0.0001) at the first level (two groups); all subsequent groups had sequentially higher levels of within-group agreement. As a result, the cutoff level was determined by balancing a lower percent information remaining (<30%) in the model while retaining biologically meaningful groups. For June this cutoff resided at the second level (three groups) and for August, at the third level (four groups). For the June cruise, all salmonids includ-

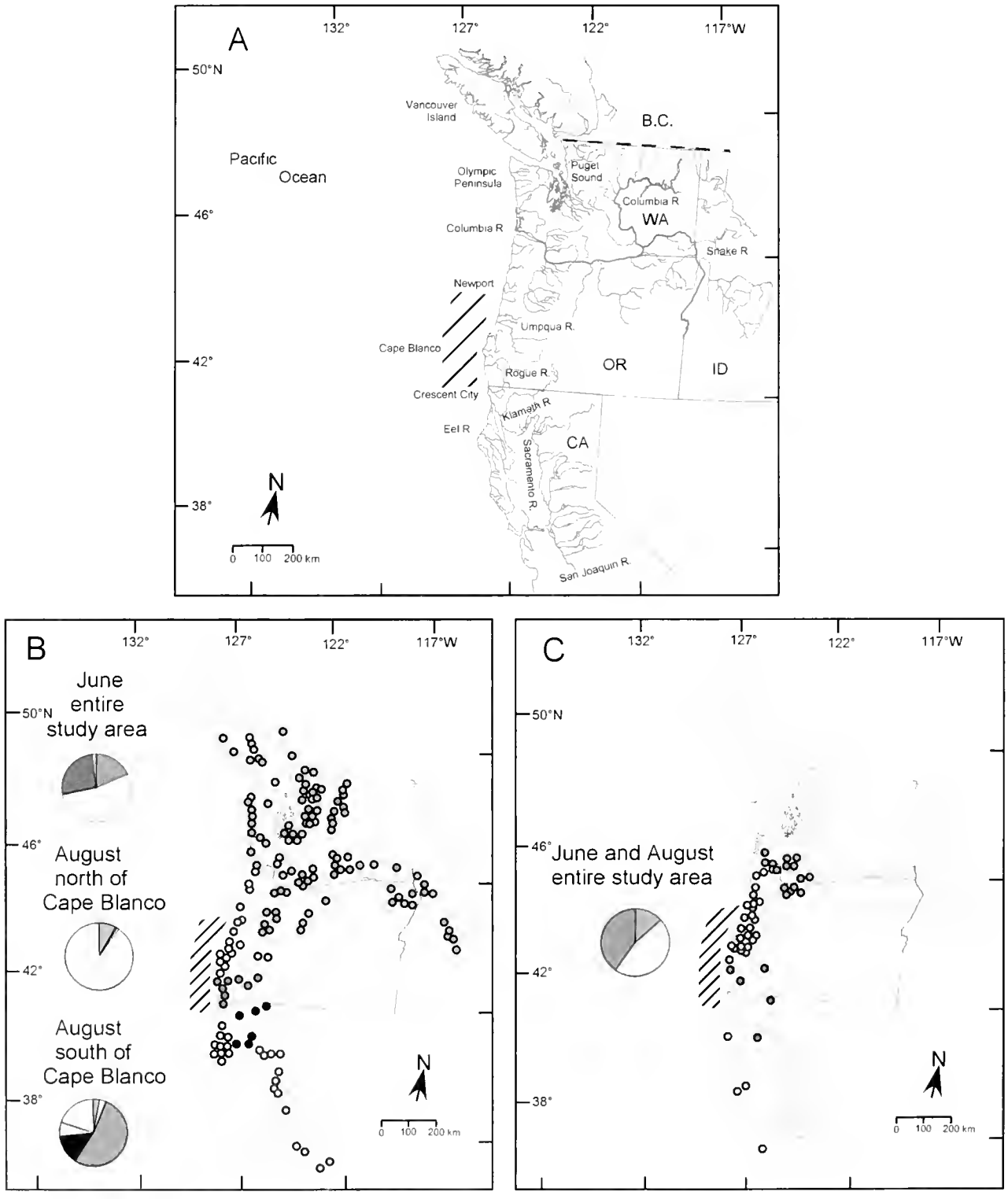

Figure 5

(**A**) Map of study area and location of GLOBEC sampling (hatching). (**B**) Stock compositions of chinook salmon (*Oncorhynchus tshawytscha*). Stock groups are North of Columbia River (grey), Columbia River Basin (green), north Oregon coast (pink), mid Oregon coast (yellow), south Oregon coast (dark blue), Klamath River Basin (black), north California coast (light blue), and Central Valley (red). (**C**) Stock compositions of coho salmon (*O. kisutch*). Stock groups are Columbia River (green), mid and north Oregon coast (dark pink), Rogue and Klamath rivers (blue), and north California coast (orange).

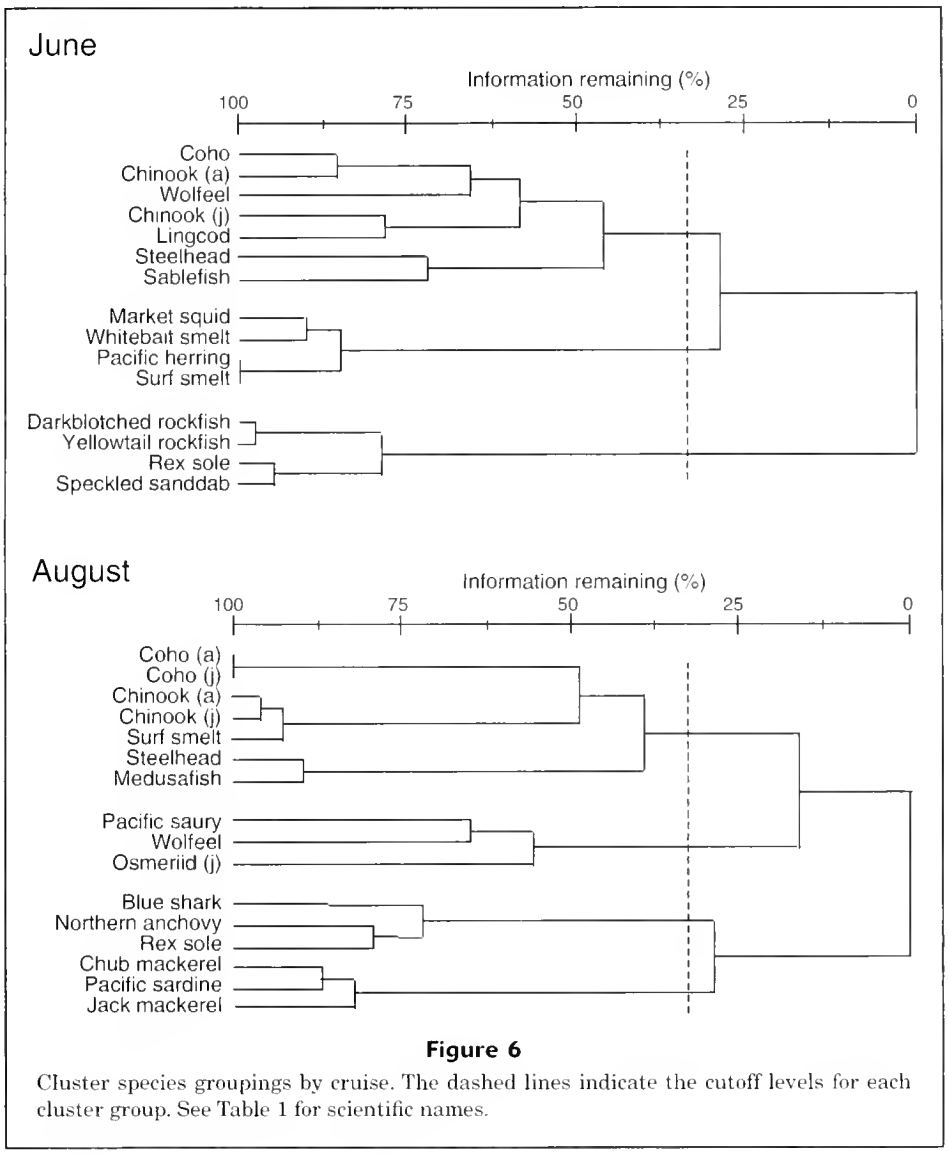

Figure 6

Cluster species groupings by cruise. The dashed lines indicate the cutoff levels for each cluster group. See Table 1 for scientific names.

ing steelhead were classified within the same grouping that included several pelagic juvenile taxa, including wolf-eel, lingcod, and sablefish (Fig. 6). Two other clusters that were not associated with juvenile salmon included a southern inshore group consisting of market squid, Pacific herring, and two species of smelt and an offshore northern group consisting primarily of juvenile rockfish and rex sole. For the August cruise, all salmonid juveniles and adults again clustered together in one large group with surf smelt and medusafish (Fig. 6). The remaining three groups were much smaller and consisted primarily of offshore pelagic species.

Cluster analysis of stations based on species assemblages, and subsequent examination of the cutoff level using MRPP, resulted in three groupings from both sample periods (Fig. 7). MRPP revealed strong within-group agreement for all levels ($P<0.0001$); however, delineation at three groups was based on maintaining lower percent information remaining (<30%) and still having a meaningful level of resolution. There was some measure of geographic separation among the three groups (Fig. 7). In June, group A was predominantly inshore and mostly in the southern half of the sampling area, group B was found mainly in the middle shelf region and was more northern, and group C was found predominantly offshore. In August, group A consisted of only three stations, all south of Cape Blanco, whereas groups B and C both spanned the entire shelf and offshore region and had no particular north-south affinity (Fig. 7). ISA of the groups from both sampling periods showed that only groups A and C had indicator species (Tables 6 and 7), whereas the intermediate groups had none.

Ordination analyses and environmental correlates

NMS ordination of the June sampling period (Fig. 8A) revealed most of the variance in the data: axes 1 and

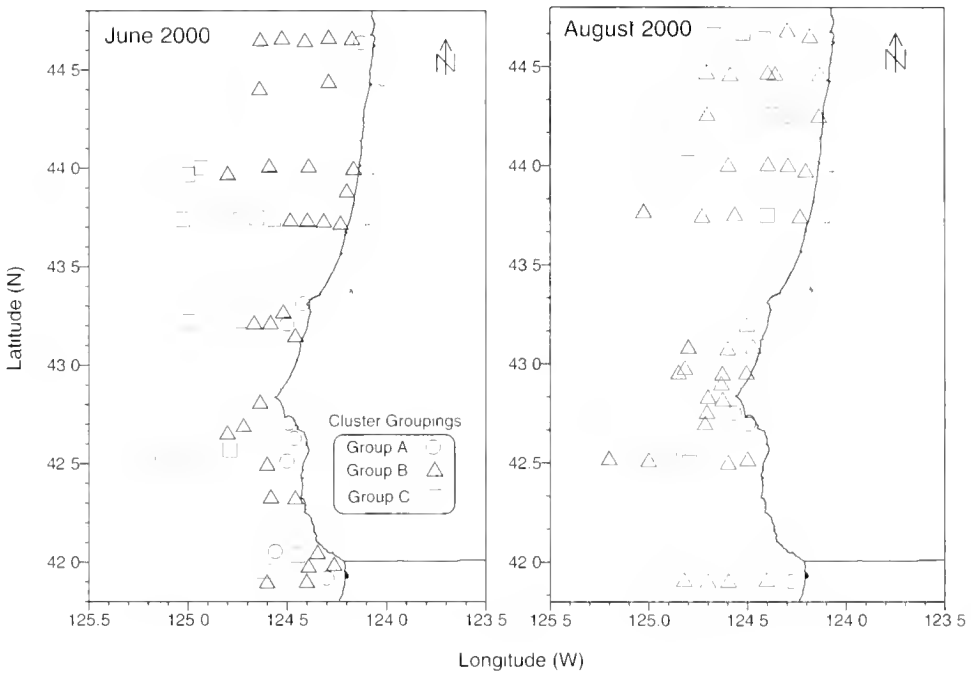

Figure 7

Map showing locations of cluster station groupings by cruise.

Table 6

Indicator species analysis showing indicator values for dominant pelagic nekton captured in pelagic trawls during June 2000 and mean, standard deviations (SD), and *P*-values for each cluster grouping. Cluster Group B did not have any species that were determined to be indicators of that group.

Group	Species	Observed indicator value (IV)	Indicator value IV from randomized groups		
			Mean	SD	*P*-value
A	chinook (age 0.0)	61.0	15.7	6.54	<0.001
A	lingcod	26.1	12.6	5.67	0.024
A	Pacific herring	71.7	12.8	5.88	<0.001
A	surf smelt	86.5	11.8	5.59	<0.001
A	whitebait smelt	31.5	10.4	5.55	0.007
A	market squid	50.8	15.0	6.20	<0.001
C	darkblotched rockfish	66.8	15.8	6.31	<0.001
C	rex sole	46.0	15.0	6.24	0.002
C	sablefish	31.1	16.2	6.32	0.035
C	speckled sanddab	52.5	13.4	5.94	0.001
C	yellowtail rockfish	98.8	19.0	6.30	<0.001

3 represented 31% and 23%, respectively (stress=16.3). Temperature, depth and salinity best explained the ordination of stations, representing a cross shelf gradient from nearshore high levels of salinity to increasing temperature and depth offshore. Ordination of August stations (Fig. 8B) represented 42% of the variance in the data, and 23% of the variance was loaded on axis 2 and 19% on axis 3 (stress=19.4). As with June, salinity increased toward the coast and temperature and depth increased off the shelf. The groups derived from the cluster analysis tended to group together in multivariate space, with the exception of group B in the June cruise (triangles in Fig. 8A).

Table 7

Indicator Species Analysis showing indicator values for dominant pelagic nekton captured in pelagic trawls during August 2000 and mean, standard deviations (SD), and *P*-values for each cluster grouping. Cluster Group B did not have any species that were determined to be indicators of that group.

Group	Species	Observed indicator value (IV)	Indicator value IV from randomized groups		
			Mean	SD	*P*-value
A	chinook (age 1.0)	76.5	21.3	11.18	0.004
A	chinook (age 0.0)	80.4	22.1	11.62	0.003
A	surf smelt	97.9	12.4	8.21	<0.001
C	chub mackerel	33.3	12.8	8.88	0.021
C	jack mackerel	73.7	23.0	11.86	0.006

Table 8

Results of statistical tests for habitat associations between juvenile salmon and environmental or station variables from each cruise in 2000. Fish marked by zeros indicate subyearlings and those marked with one indicate yearlings. Shown are the *P*-levels for 5000 randomizations of the cumulative frequency of the habitat variable and the proportion of the standardized salmon catch associated with each habitat observation. Results are based on the Cramer von-Mises test statistic determined from binned data for depth and neuston biomass. Significance values <0.05 are shown in boldface.

Cruise	Taxon and age	Surface temp.	Surface salinity	1-m chlorophyll	Bottom depth	Neuston biomass
Jun	chinook (age 1.0)	0.30	0.60	0.13	0.18	0.13
	coho (age 1.0)	0.33	0.48	0.21	0.17	0.31
Aug	chinook (age 0.0)	0.36	0.25	0.13	0.35	0.42
	chinook (age 1.0)	**0.04**	**<0.01**	**<0.01**	**0.02**	0.29
	coho (age 1.0)	0.68	**0.04**	0.07	**0.02**	0.45

There were few instances where the habitat associations of juvenile salmon were significantly different from the distribution of environmental variables sampled (Table 8). None of the variables were significant for yearling chinook and coho salmon in the June sampling (no subyearling salmon were caught during that cruise). In August, all the variables except neuston biomass were significant for yearling chinook salmon. These fish were collected at cooler temperatures, higher salinities, higher chlorophyll-*a* concentrations, and at shallower depths than have been typically recorded (Fig. 9). Coho salmon juveniles were found in higher salinities and shallower depths than at the sampled habitat (Fig. 9). These results correlated with the capture of juvenile chinook salmon and to a lesser with extent coho salmon at nearshore stations in the upwelling zone.

Discussion

Understanding the mechanisms underlying the dynamics of multispecies communities is one of the biggest challenges in ecology. Most communities contain many interacting species, each of which is likely to be affected by multiple biotic and abiotic factors. In order to effectively characterize a system, we need to differentiate variability resulting from both temporal and spatial factors. Our observations took place during two time periods of about 20 days each and thus were not synoptic "snapshots" of the system. Indeed, during our June sampling, conditions changed markedly from the beginning to the end of the cruise because of the arrival of an anomalous major southwest storm (Batchelder et al., 2002), which likely completely altered the hydrography and biology of the system. Thus, short-term temporal variability may obscure patterns observed over the spatial scale of our sampling.

The pelagic nekton community sampled during these cruises was not that different from what had previously been shown for purse seine and trawling collections off the coast of Oregon and Washington (Brodeur and Pearcy, 1986; Emmett and Brodeur, 2000; Brodeur et al., 2003). The early summer nekton community was dominated by coastal forage fishes such as smelts and Pacific herring, but also comprised juveniles of many rockfish, sculpin, and flatfish species. These winter-spring spawning species eventually settle out to demersal habitats sometime in summer (Shenker, 1988; Doyle, 1992), which may in part explain the paucity of these taxa in the August cruise. In contrast, the August nekton community consisted of large,

highly migratory species such as Pacific sardines, jack mackerel, and chub mackerel. Pacific sardine, which was almost completely absent from the system in the 1980s, has undergone a substantial resurgence and is now one of the most abundant species off the coast in summer (Brodeur et al., 2000; Emmett and Brodeur, 2000; McFarlane and Beamish, 2001). It should be noted, however, that some of the differences between cruises could be accounted for by the inclusion of substantially more offshore stations during the second cruise. Our results from the community analyses suggest that juvenile salmon tend to co-occur with each other and with a variety of other pelagic nekton, including adult salmon, and that this spatial overlap varies temporally. Brodeur et al. (2003), in analyzing community structure based on previous pelagic sampling data off Oregon and Washington, arrived at similar results. In both studies, the geographic boundaries of the pelagic assemblages often overlap and are not as distinct as demersal assemblages. However, the pelagic environment is much more spatially and temporally heterogeneous than the demersal environment, and many of the species examined in our study are highly mobile and are likely to respond quickly to changing conditions. Research is presently underway to examine the trophic interactions among salmonids and with other sympatric nekton species in order to determine what ecological relationships (e.g. predation, competition), if any, are occurring in this system.

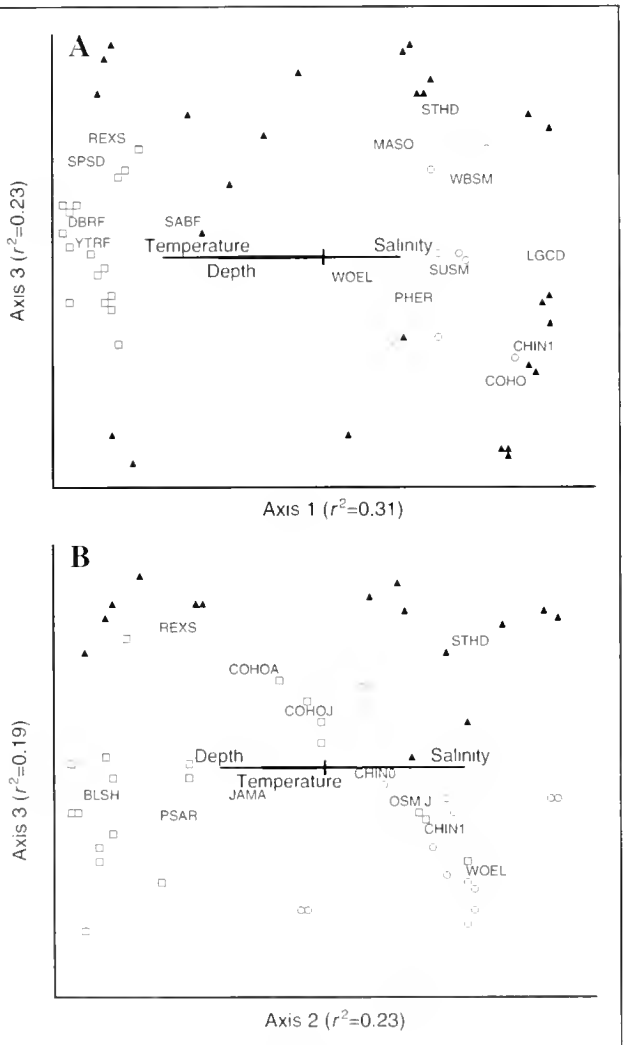

Figure 8

Nonmetric multidimensional scaling (NMS) ordination plot of stations and nekton species with environmental parameters from June (**A**) and August (**B**) 2000 GLOBEC cruises. Station symbols denote: onshore (○), mid-shelf (▲), and slope (□) groupings; Species abbreviations denote the following taxa: CHIN 0 (chinook, age 0), CHIN 1 (chinook, age ≥1.1), STHD (steelhead trout), SUSM (surf smelt), PSAU (Pacific saury), WOEL (wolf-eel juvenile), OSM J (osmerid juvenile), REXS (rex sole, larval), MEDF (medusafish), PSAR (Pacific sardine), JAMA (jack mackerel), CHMA (chub mackerel), NANC (northern anchovy), BLSH (blue shark).

From the results of our sampling, we concluded that juvenile salmonids, with the possible exception of steelhead, occupy the cool, high salinity, inshore upwelling regions off the southern Oregon coast. However, particularly for the June cruise, many of the coho and chinook salmon juveniles collected may have recently entered the ocean with little time to disperse offshore, so that the capture location may not reflect true habitat preferences. Moreover, the vertical dimensions of our trawl also precluded us from sampling the nearshore, subtidal regions where some subyearling chinook may reside shortly after entering the ocean.

Salmon and steelhead differed considerably in stock composition. The pattern for coho salmon was similar to that of chinook salmon in that fish from sources both north and south of Cape Blanco contributed to our catches. However, steelhead from rivers north of Cape Blanco were absent, presumably having migrated offshore and north shortly after entering the sea, as shown by Pearcy et al. (1990). Although our stock composition estimates for steelhead should be viewed with caution because of an incomplete genetic baseline and a relatively small number of samples, our findings support Pearcy et al.'s suggestion that steelhead from rivers south of Cape Blanco have a unique marine distribution and reside throughout the summer in the upwelling zone off northern California and southern Oregon.

Our study revealed seasonal shifts in the abundance and stock composition of juvenile salmonids. Although salmonids comprised small portions of the vertebrate catches of both the June and August cruises, juvenile chinook salmon, coho salmon, and steelhead were much more abundant later in the summer, likely indicating that fish moving into our study area are from shoreline or riverine habitats. The greater abundance of chinook salmon in late summer can be explained in part by the northern migration of fish that originated in rivers south of our study area. Chinook salmon from the Sacramento and San Joaquin rivers in California's Central Valley comprised substantial proportions in the August catches both south (20%) and north (90%) of Cape Blanco. In contrast, the few chinook salmon caught in June were mostly (54%) from streams that enter the sea immediately north of Cape Blanco such as the Umpqua, Coquille, Sixes, and Elk rivers. Chinook salmon

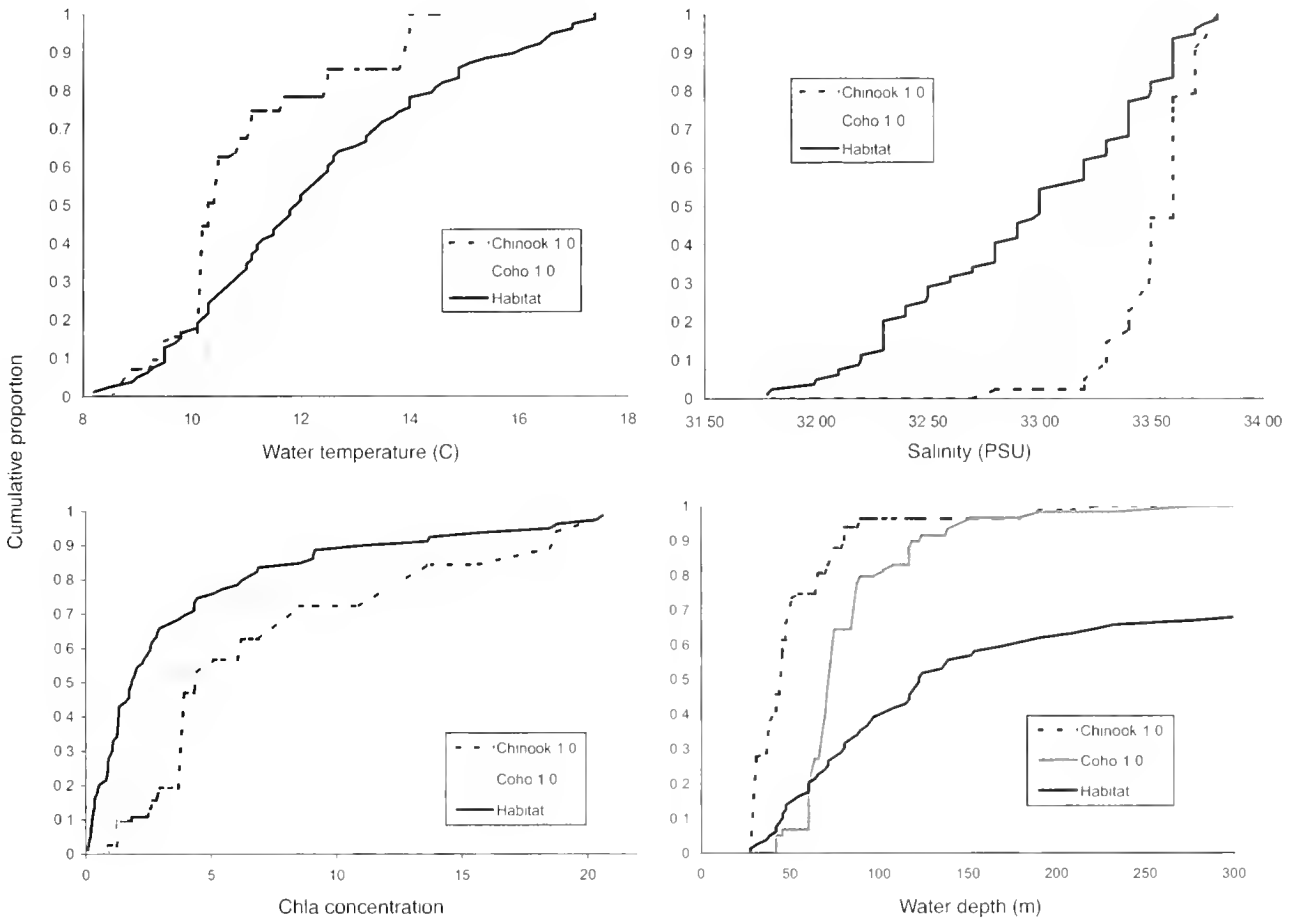

Figure 9

Cumulative distribution curves for salmon and environmental or station variables. Only the August variables that showed at least one significant difference are included. See Table 8 for results of the statistical tests.

from these rivers are known to primarily migrate north of our study area along the coast (Nicholas and Hankin, 1988). By August, fish from these stocks were nearly absent from our samples. Oregon rivers south of Cape Blanco, an area that includes the Rogue, Chetco, and Winchuck rivers, produce chinook salmon with a more southerly pattern of ocean migration (Nicholas and Hankin, 1988; Myers et al., 1998). Chinook salmon from these rivers were found throughout the summer and contributed 53% to our largest catches of chinook salmon along transects south of Cape Blanco in August.

Results from our 2000 GLOBEC cruises identified Cape Blanco as an important breakpoint in salmonid life-history variation. Stock distributions of both juvenile salmon and steelhead indicated that different migration patterns of fish originating from southern and northern rivers are evident during their early marine phase. Our August survey also revealed sharp contrasts in life-history type and freshwater origin between the juvenile chinook salmon population in the marine area north of Cape Blanco and that to the south. Chinook salmon captured north of Cape Blanco were nearly all yearlings and largely from the Sacramento River drainage. Subyearlings predominated in our catches south of Cape Blanco and included a much larger proportion of fish from coastal streams in southern Oregon and northern California.

Comparisons of our results with similar studies conducted further north show differences in salmonid migrations on a somewhat broader geographic scale. In several years of sampling during the summers of 1981 through 1985 off the central Oregon to northern Washington coast, most juvenile chinook salmon bearing CWTs were from Columbia River hatcheries (Pearcy and Fisher, 1990; Fisher and Pearcy, 1995). Only one tagged chinook salmon from a river south of Cape Blanco (Klamath River) was captured. Pearcy and Fisher also found that juvenile coho salmon were largely from the Columbia River and that smaller contributions were from coastal rivers north of Cape Blanco. Their findings have been corroborated by more recent surveys in the same region (Emmett and Brodeur, 2000) using genetic

data (Teel et al., 2003). Samples from subsequent cruises will be used to examine the persistence of such fine- and broad-scale geographic structure in the juvenile migrations of salmonid stocks.

A major source of error in our estimates of growth rates of juvenile coho salmon back-calculated from scales was uncertainty of when individual fish entered the ocean. We used a single date of ocean entry for all fish (15 May), but individual fish, of course, entered the ocean at different times over the course of a month or more. Consequently, coefficients of variation were relatively large (84–119% and 75–120% of mean growth rate in FL and weight, respectively) for fish caught in May and June, when errors in estimated growth periods likely were large in relation to the actual growth periods. Conversely, coefficients of variation were relatively small (14–30% and 10–26% of growth rate in FL and weight, respectively) for fish caught in August or September, when errors in estimated growth periods likely were small in relation to the actual growth periods. (Note the decrease in standard deviation of mean growth rates with month of capture in Tables 3 and 4A). Growth rates of CWT coho salmon between hatchery release and capture in the ocean (Table 4B) were very similar to the growth rates of unmarked salmon estimated from scales for the same months and areas. In addition, the growth rates of the former group (CWT coho salmon) helped to validate the growth rates of the latter group (Table 4A).

Significant differences in growth and condition of juvenile coho salmon indicate that different oceanographic environments exist north and south of Cape Blanco. The length of the fish indicated that substantial growth occurred in juvenile coho salmon during the study period. Assessment of other growth features (condition) revealed that juvenile coho salmon grew better north of Cape Blanco. Because we included measurement of condition in both the June and August period in the evaluation, changes in stock composition, described earlier, may be partly responsible for this observation. Although genetic stock composition was different between months, month of sampling was not a significant factor, suggesting that stock composition is not likely a significant factor affecting the difference in condition (a performance metric) of juvenile salmon north and south of Cape Blanco.

Several lines of evidence further support the hypothesis that areas north of Cape Blanco benefit juvenile yearling chinook and coho salmon. There were greater numbers of juvenile yearling chinook and coho salmon to the north of Cape Blanco. Although our overall sampling effort was greater north of Cape Blanco, in the mesoscale portion of our survey designed to assess general distribution patterns, more yearling chinook and coho salmon were captured north of Cape Blanco. Secondly, when we evaluated the growth rate of juvenile coho salmon in the GLOBEC region compared to juveniles captured off northern Oregon and Washington, juveniles from the GLOBEC region grew much better. The similar tracking of resource (distribution and abundance) and performance (measured in terms of either somatic and energetic growth or growth rate) metrics for juvenile yearling chinook salmon and coho salmon north of Cape Blanco suggests that habitat quality in this region was better. The results of this study help define the biogeographical zones for salmon growth and establish regional-based management strategies for depleted salmon stocks.

Acknowledgments

We thank the captain and crew of the FV *Sea Eagle* for their expert help in conducting the trawling operations under sometimes adverse weather conditions. We are grateful to Jackie Popp-Noskov, Paul Bentley, Marcia House, and Becky Baldwin for assistance in field sampling. Donald Van Doornik and David Kuligowski collected the genetic data. We thank Anne Marshall for the use of unpublished chinook salmon allele frequency data. Stephen Smith and Alex De Robertis helped with the statistical analysis. Earlier versions of this manuscript were improved by the helpful comments of two anonymous journal reviewers. Research was conducted as part of the U.S. GLOBEC program and was jointly funded by the National Science Foundation (Grant no. OCE-0002855) and the National Oceanic and Atmospheric Administration (NOAA). We also acknowledge the Bonneville Power Administration for funding the plume study.

Literature cited

Aebersold, P. B., G. A. Winans, D. J. Teel, G. B. Milner, and F. M. Utter.
1987. Manual for starch gel electrophoresis: a method for the detection of genetic variation. NOAA Tech. Rep. NMFS 61, 19 p.

Batchelder, H. P., J. A.Barth, M. P. Kosro, P. T. Strub, R. D. Brodeur, W. T. Peterson, C. T. Tynan, M. D. Ohman, L. W. Botsford, T. M. Powell, F. B. Schwing, D. G. Ainley, D. L. Mackas, B. M. Hickey, and S. R. Ramp.
2002. The GLOBEC Northeast Pacific California Current System program. Oceanogr. 15:36–47.

Barth, J. A., S. D. Pierce, and R. L. Smith.
2000. A separating coastal upwelling jet at Cape Blanco, Oregon and its connection to the California Current System. Deep-Sea Res. 47(part II):783–810.

Bradford, M. J.
1995. Comparative review of Pacific salmon survival rates. Can. J. Fish. Aquat. Sci. 52:1327–1338.

Brodeur, R. D., P. J. Bentley, R. L. Emmett, T. Miller, and W. T. Peterson.
2000. Sardines in the ecosystem of the Pacific Northwest. Proc. sardine 2000 symposium. Pacific States Marine Fish. Comm., p. 90–102. [Available from Pacific States Marine Fisheries Commission, Portland, OR.]

Brodeur, R. D., J .P. Fisher, Y. Ueno, K. Nagasawa, and W. G. Pearcy.
2003. An east-west comparison of the Transition Zone coastal pelagic nekton of the North Pacific Ocean. J. Oceanog. 59(4):415–434.

Brodeur, R. D., H. V. Lorz, and W. G. Pearcy.
1987. Food habits and dietary variability of pelagic nekton off Oregon and Washington, 1979–1984. NOAA Tech. Rep. NMFS 57, 32 p.

Brodeur, R. D., and W. G. Pearcy.
1986. Distribution and relative abundance of pelagic non-

salmonid nekton off Oregon and Washington, 1979–1984. NOAA Tech. Rep. NMFS 46, 85 p.

1992. Effects of environmental variability on trophic interactions and food web structure in a pelagic upwelling ecosystem. Mar. Ecol. Prog. Ser. 84:101–119.

Busby, P. J., T. C. Wainwright, G. J. Bryant, L. Lierheimer, R. S. Waples, F. W. Waknitz, and I. V. Lagomarsino.

1996. Status review of west coast steelhead from Washington, Idaho, Oregon, and California. NOAA Tech. Memo. NMFS-NWFSC-27, 261 p.

Dawley, E. M., R. D. Ledgerwood, and A. Jensen.

1985. Beach and purse seine sampling of juvenile salmonids in the Columbia River estuary and ocean plume, 1977–1983. Vol. 1, Procedures, sampling effort, and catch data. NOAA Tech. Memo. NMFS F/NWC-74, 260 p.

Dehevec, E. M., R. B. Gates, M. Masuda, J. Pella, J. Reynolds, and L. W. Seeb.

2000. SPAM (Version 3.2): Statistics program for analyzing mixtures. J. Hered. 91:509–511.

Doyle, M. J.

1992. Neustonic ichthyoplankton in the northern region of the California Current ecosystem. Calif. Coop. Oceanic Fish. Invest. Rep. 33:141–161.

Emmett, R. L., and R. D. Brodeur.

2000. The relationship between recent changes in the pelagic nekton community off Oregon and Washington and physical oceanographic conditions. Bull. North Pac. Anadr. Fish. Comm. 2:11–20.

Fisher, J. P., and W. G. Pearcy.

1988. Growth of juvenile coho salmon (*Oncorhynchus kisutch*) off Oregon and Washington, USA in years of differing coastal upwelling. Can. J. Fish. Aquat. Sci. 45: 1036–1044.

1995. Distribution, migration, and growth of juvenile chinook salmon, *Oncohychus tshawytscha*, off Oregon and Washington. Fish. Bull. 93:274–289.

Francis, R. C., and S. R. Hare.

1994. Decadal-scale regime shifts in large marine ecosystems of the Northeast Pacific: a case for historical science. Fish. Oceanogr. 3:279–291.

Friedland, K. D., and R. E. Haas.

1996. Marine post-smolt growth and age at maturity of Atlantic salmon. J. Fish Biol. 48:1–15.

Gauch, H. G., Jr.

1982. Multivariate analysis in community ecology. Cambridge Univ. Press, N.Y. 298 p.

Hare, S. R., N. J. Mantua, and R. C. Francis.

1999. Inverse production regimes: Alaska and West Coast salmon. Fisheries 24:6–14.

Hinch, S. G., M. C. Healey, R. E. Diewert, K. A.Thomson, R. Hourston, M. A. Henderson, and F. Juanes.

1995. Potential effects of climate change on marine growth and survival of Fraser River sockeye salmon. Can. J. Fish. Aquat. Sci. 52:2651–2659.

Jakob, E. M., S. D. Marshall, and G. W. Uetz.

1996. Estimating fitness: a comparison of body condition indices. Oikos 77: 61–67.

Kope, R., and T. Wainwright.

1998. Trends in the status of Pacific salmon populations in Washington, Oregon, California, and Idaho. North Pac. Anadr. Fish. Comm. Bull. 1:1–12.

Kruskal, J. B.

1964. Nonmetric multidimensional scaling: a numerical method. Psychometricka 29:115–129.

Lawson, P. W.

1993. Cycles in ocean productivity, trends in habitat quality, and the restoration of salmon runs in Oregon. Fisheries 18:6–10.

Lorenzen, K.

1996. The relationship between body weight and natural mortality in juvenile and adult fish: A comparison of natural ecosystems and aquaculture. J. Fish Biol. 49: 627–647.

Mantua, N. J., S. R. Hare, Y. Zhang, J. M. Wallace, and R. C. Francis.

1997. A Pacific interdecadal oscillation with impacts on salmon production. Bull. Am. Meteorol. Soc. 78: 1069–1079.

Marschall, E. A., and L. B. Crowder.

1995. Density-dependent survival as a function of size in juvenile salmonids in streams. Can. J. Fish. Aquat. Sci. 52:136–140.

McCune, B., and J. B. Grace.

2002. Analysis of ecological communities, 300 p. MjM Software Design, Gleneden Beach, OR.

McCune, B., and M. J. Mefford.

1999. PC-ORD, multivariate analysis of ecological data, users guide, 237 p. MjM Software Design, Gleneden Beach, OR.

McFarlane, G. A., and R. J. Beamish.

2001. The re-occurrence of sardines off British Columbia characterises the dynamic nature of regimes. Prog. Oceanogr. 49:151–165.

McGowan, J. A., D. B. Chelton, and A. Conversi.

1999. Plankton patterns, climate, and change in the California Current. *In* Large marine ecosystems of the Pacific Rim: assessment, sustainability, and management (K. Sherman and Q. Tang, eds.), p. 63–105. Blackwell Science, Malden, MA.

McGurk, M. D.

1996. Allometry of marine mortality of Pacifc salmon. Fish. Bull. 94:77–88.

Milner, G. B., D. J. Teel, F. M. Utter, and G. A. Winans.

1985. A genetic method of stock identification in mixed populations of Pacific salmon, *Oncorhynchus* spp. Mar. Fish. Rev. 47:1–8.

Myers, J. M., R. G. Kope, G. J. Bryant, D. J. Teel, L. J. Lierheimer, T. C. Wainwright, W. S. Grant, F. W. Waknitz, K. Neely, S. T. Lindley, and R. S. Waples.

1998. Status review of chinook salmon in Washington, Idaho, Oregon, and California. NOAA Tech. Memo. NMFS-NWFCS-35, 443 p.

Nehlsen, W., J. E. Williams, and J. A. Lichatowich.

1991. Pacific salmon at the crossroads: stocks at risk from California, Oregon, Idaho, and Washington. Fisheries 16: 4–21.

Nicholas, J. W., and D. G. Hankin.

1988. Chinook salmon populations in Oregon coastal river basins: Description of life histories and assessment of recent trends in run strengths. Oregon Department of Fish and Wildlife, Fish Division Information Report 88-1, 359 p.

Paul, A. J., and T. M. Willette.

1997. Geographical variation in somatic energy content of migrating pink salmon fry from PWS: a tool to measure nutritional status. *In* Proceedings of the international symposium on the role of forage fishes in marine ecosystems. Alaska Sea Grant College Program, Report 97-01, p. 707–720. Univ. Alaska, Fairbanks, AK.

Pearcy, W. G.

1992. Ocean ecology of North Pacific salmonids, 179 p. Univ. Washington Press, Seattle, WA.

Pearcy, W. G., R. D. Brodeur, and J. P. Fisher.

1990. Distribution and biology of juvenile cutthroat trout

(*Oncorhynchus clarki clarki*) and steelhead (*O. mykiss*) in coastal waters off Oregon and Washington. Fish. Bull. 88: 697–711.

Pearcy, W. G., and J. P. Fisher.
1988. Migrations of coho salmon, *Oncorhynchus kisutch*, during their first summer in the ocean. Fish. Bull. 86: 173–195.
1990. Distribution and abundance of juvenile salmonids off Oregon and Washington, 1981–1985. NOAA Tech. Rep. NMFS 93:1–83.

Pella, J., and G. B. Milner.
1987. Use of genetic marks in stock composition analyses. *In* Population genetics and fishery management, (N. Ryman and F. Utter, eds.), p. 247–276. Washington Sea Grant, Univ. Washington Press, Seattle, WA.

Perry, R. I., B. Hargreaves, B. J. Waddell, and D. L. Mackas.
1996. Spatial variations in feeding and condition of juvenile pink and chum salmon off Vancouver Island, British Columbia. Fish. Oceanogr. 5:73–88.

Perry, R. I., and S. J. Smith.
1994. Identifying habitat associations of marine fishes using survey data: an application to the Northwest Atlantic. Can. J. Fish. Aquat. Sci. 51:589–602.

Peterson, W. T., and J. E. Keister.
2002. The effect of a large cape on distribution patterns of coastal and oceanic copepods off Oregon and northern California during the 1998-1999 El Niño-La Niña. Prog. Oceanogr. 53:389–411.

Post, J. R., and E. A. Parkinson.
2001. Energy allocation strategy in young fish: allometry and survival. Ecology 82:1040–1051.

Ricker, W. E.
1992. Back-calculation of fish lengths based on proportionality between scale and length increments. Can. J. Fish. Aquat. Sci. 49:1018–1026.

Shenker, J. M.
1988. Oceanographic associations of neustonic larval and juvenile fishes and Dungeness crab megalopae off Oregon. Fish. Bull. 86:299–317.

Sutton, S. G., T. P. Bult, and R. L. Haedrich.
2000. Relationship among fat weight, body weight, water weight, and condition factors in wild Atlantic salmon parr. Trans. Am. Fish. Soc. 129:527–538.

Syrjala, S. E.
1996. A statistical test for a difference between the spatial distributions of two populations. Ecology 77:75-80.

Teel, D. J., D. M. Van Doornik, D. R. Kuligowski, and W. S. Grant.
2003. Genetic analysis of juvenile coho salmon (*Oncorhynchus kisutch*) off Oregon and Washington reveals few Columbia River wild fish. Fish. Bull. 101:640–652.

U.S. GLOBEC.
1994. A science plan for the California Current. U.S. GLOBEC Rep. 11, 134 p. Univ. California, Berkeley, CA.

Weitkamp, L., and K. Neely.
2002. Coho salmon (*Oncorhynchus kisutch*) ocean migration patterns: insight from marine coded-wire tag recoveries. Can. J. Fish. Aquat. Sci. 59:1100–1115.

Weitkamp, L. A., T. C. Wainright, G. J. Bryant, G. B. Milner, D. J. Teel, T. G. Kope, and R. S. Waples.
1995. Status review of coho salmon from Washington, Oregon, and California. NOAA Tech. Memo. NMFS-NWFSC-24, 258 p.

Appendix Table 1

Summary of releases of coho salmon smolts in 2000 by region. This summary of releases of all hatchery coho salmon smolts by region was calculated from data in the Pacific States Marine Fisheries Commission Regional Mark Information System (http://www.rmis.org/ [accessed 5 April 2003]) and in USFWS 2001 (see Footnote 2 in the general text).

	No. of release groups	Total fish released	Release weight (g)	
			Marked	mean (SD)
All British Columbia	250	13,612,715	71.4%	19.6 (5.7)
Washington: St. Juan de Fuca, Puget Sound, Skagit River, Nooksack River, etc.	83	15,316,299	86.4%	29.1 (19.7)
Washington:				
North of Columbia River to Cape Flattery	63	7,630,257	76.7%	31.6 (5.3)
Columbia River	140	29,879,137	89.0%	32.0 (6.4)
Oregon Coast north of Cape Blanco	14	809,962	95.6%	41.6 (7.4)
Southern Oregon and Northern California: Rogue, Klamath, and Trinity Rivers	5	745,060	99.8%[1]	42.1 (4.4)

[1] 100% of the fish released from Klamath and Trinity Rivers were clipped on the maxillary.

Spatial and temporal variation in the diet of the California sea lion (*Zalophus californianus*) in the Gulf of California, Mexico

Francisco J. García-Rodríguez
David Aurioles-Gamboa

Centro Interdisciplinario de Ciencias Marinas-Instituto Politécnico Nacional
Departamento de Biología Marina y Pesquerías
Apdo. Postal 592
La Paz, Baja California Sur, México
E-mail address (for F. J. García-Rodríguez): fjgrodri@cibnor.mx

Abstract—Between June 1995 and May 1996 seven rookeries in the Gulf of California were visited four times in order to collect scat samples for studying spatial and seasonal variability California sea lion prey. The rookeries studied were San Pedro Mártir, San Esteban, El Rasito, Los Machos, Los Cantiles, Isla Granito, and Isla Lobos. The 1273 scat samples collected yielded 4995 otoliths (95.3%) and 247 (4.7%) cephalopod beaks. Fish were found in 97.4% of scat samples collected, cephalopods in 11.2%, and crustaceans in 12.7%. We identified 92 prey taxa to the species level, 11 to genus level, and 10 to family level, of which the most important were Pacific cutlassfish (*Trichiurus lepturus*), Pacific sardine (*Sardinops caeruleus*), plainfin midshipman (*Porichthys* spp.), myctophid no. 1, northern anchovy (*Engraulis mordax*), Pacific mackerel (*Scomber japonicus*), anchoveta (*Cetengraulis mysticetus*), and jack mackerel (*Trachurus symmetricus*). Significant differences were found among rookeries in the occurrence of all main prey ($P \leq 0.04$), except for myctophid no. 1 ($P > 0.05$). Temporally, significant differences were found in the occurrence of Pacific cutlassfish, Pacific sardine, plainfin midshipman, northern anchovy, and Pacific mackerel ($P < 0.05$), but not in jack mackerel ($\chi^2 = 2.94$, df=3, $P = 0.40$), myctophid no. 1 ($\chi^2 = 1.67$, df= 3, $P = 0.64$), or lanternfishes ($\chi^2 = 2.08$, df=3, $P = 0.56$). Differences were observed in the diet and in trophic diversity among seasons and rookeries. More evident was the variation in diet in relation to availability of Pacific sardine.

Manuscript approved for publication 9 October 2003 by Scientific Editor.
Manuscript received 20 October 2003 at NMFS Scientific Publications Office.
Fish. Bull. 102:47–62 (2004).

The population of the California sea lion (*Zalophus californianus*), in the Gulf of California numbers approximately 23,000 individuals, 82% of which inhabit the northern region of the gulf above latitude 28° (Aurioles-Gamboa and Zavala-González, 1994). In this region are found the most important reproductive areas and the highest pup production of the Gulf. Aurioles-Gamboa and Zavala-González (1994) suggested that the high concentration of animals in this region is related to high abundance of pelagic fish such as Pacific sardine (*Sardinops caeruleus*) (also known as South American pilchard, FAO), Pacific mackerel (*Scomber japonicus*), Pacific thread herring (*Opisthonema libertate*), and anchoveta (*Cetengraulis mysticetus*) (Cisneros-Mata et al., 1987[1]; Cisneros-Mata et al., 1991[2]; Cisneros-Mata et al., 1997[3]).

Despite the importance of the northern gulf region, feeding studies of the California sea lion at Gulf of California rookeries have been few and have been conducted at different time periods. Researchers have studied sea lion diet in Los Islotes (Aurioles-Gamboa et al., 1984; García-Rodríguez, 1995), Los Cantiles (Isla Angel de la Guarda), Isla Granito (Sánchez-Arias, 1992; Bautista-Vega, 2000), and Isla Racito (Orta-Dávila, 1988). These studies have shown that sea lions consume a variety of prey and that differences exist between the diet of sea lions found at different rookeries within the Gulf of California. At Los Islotes, the most important prey were cusk eel (*Aulopus bajacali*), bigeye bass (*Pronotogrammus eos*), threadfin bass (*Pronotogrammus multifasciatus*), and splitail bass (*Hemanthias* sp.) (Aurioles-Gamboa et al., 1984; García-Rodríguez, 1995). At Los Cantiles and Isla Granito important prey were lanternfish (*Diaphus* sp.), northern anchovy (*Engraulis mordax*), Pacific cutlassfish (*Trichiurus nitens*), shoulderspot (*Caelorinchus scaphopsis*), and Pacific whiting (*Merluccius productus*) (Sanchez-Arias, 1992; Bautista-Vega, 2000), whereas at Isla Racito, important prey were Pacific sardine (*Sardinops caeruleus*), Pacific mackerel (*Scomber japonicus*), grunt (*Haemulopsis* spp.), rockfish (*Sebastes*

[1] Cisneros-Mata, M. A., J. P. Santos-Molina, J. A. De Anda M., A. Sánchez-Palafox, and J. J. Estrada. 1987. Pesquería de sardina en el noroeste de México (1985/86). Informe Técnico, 79 p. Centro Regional de Investigaciones Pesqueras de Guaymas. INP. SEPESCA. Calle 20 No. 605 Sur Col. La Cantera. Guaymas, Son. CP. 85400.

[2] Cisneros-Mata, M. A., M. O. Nevarez-Martínez, G. Montemayor-López, J. P. Santos-Molina, and R. Morales-Azpeitia. 1991. Pesquería de sardina en el Golfo de California de 1988/89–1989/90. Informe Técnico, 80 p. Centro Regional de Investigaciones Pesqueras de Guaymas. INP. SEPESCA. Calle 20 No. 605 Sur Col. La Cantera. Guaymas, Son. CP. 85400.

[3] Cisneros-Mata, M. A., M. O. Nevárez-Martínez, M. A. Martínez-Zavala, M. L. Anguiano-Carranza, J. P. Santos-Molina, A. R. Godínez-Cota, and G. Montemayor-López. 1997. Diagnosis de la pesquería de pelágicos menores del Golfo de California de 1991/92 a 1995/96. Informe Técnico, 59 p. Centro Regional de Investigaciones Pesqueras de Guaymas. INP. SEMARNAP. Calle 20 No. 605 Sur Col. La Cantera. Guaymas, Son. CP. 85400.

spp.), and Pacific whiting (*Merluccius* spp.) (Orta-Dávila, 1988).

Some California sea lion prey are important fisheries resources in Mexico. The Pacific sardine, for example, is the target of a fishery begun in 1967 and which, along with the northern anchovy, contributed to most of the volume of the catch (200,870 t during the 1995–96 season) obtained in the Gulf (Cisneros-Mata et al.[3]). The central and northern regions of the Gulf of California harbor the greatest abundance of sea lions and schooling fishes, such as the sardine and anchovy. Because of this, knowledge of sea lion feeding habits and their temporal and spatial variability is relevant to understanding the potential interaction between sea lions and fisheries in the area (Orta-Dávila, 1988; Sánchez-Arias, 1992; Bautista-Vega, 2000).

In this article, we present the results of concurrent diet studies conducted at various rookeries and haulout areas of sea lions in the northern rookeries of the Gulf of California to examine the prey consumed, and spatial and temporal variability in their diet.

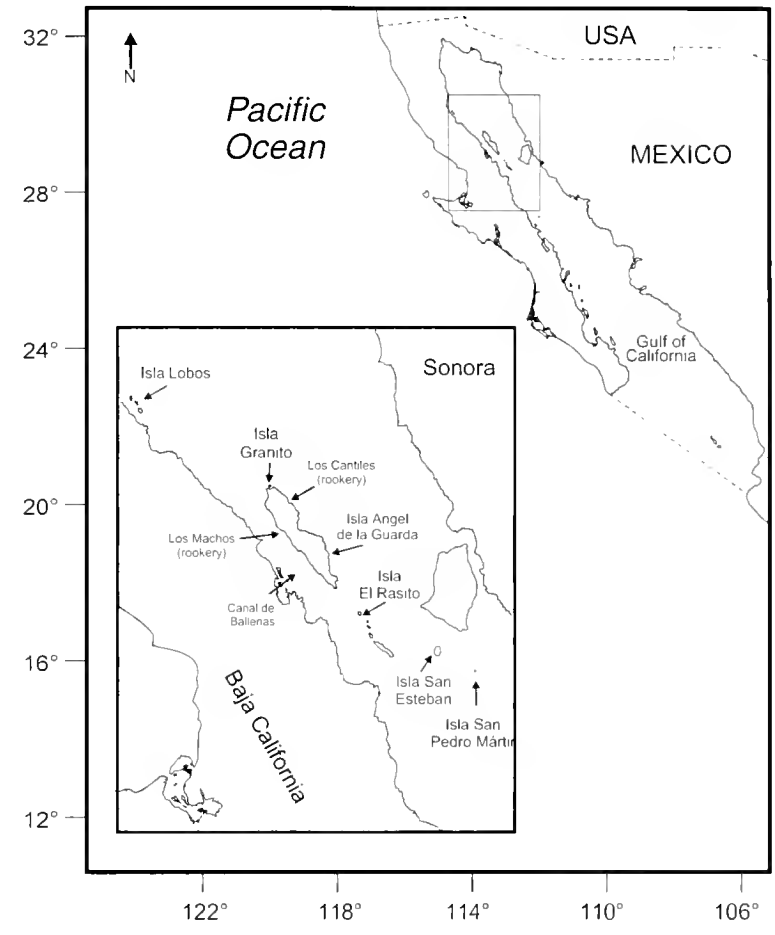

Figure 1

Map of Baja California showing location of California sea lion rookeries that were studied in the Gulf of California.

Materials and methods

Scat samples of California sea lions were collected at Isla San Pedro Mártir (SPM, 28°24′00″N, 112°25′3″W), Isla San Esteban (EST, 28°42′00″N, 112°36′00″W), Isla Rasito (RAS, 28°49′30″N, 112°59′30″W), Isla Granito (GRA, 29°34′30″N, 113°32′15″W), Isla Lobos (LOB, 30°02′30″N, 114°, 28′30″W), and at two colonies of Isla Angel de la Guarda known as Los Machos (MAC, 29°20′00″N, 113°30′00″W), and Los Cantiles (CAN, 29°32′00″N, 113°29′00″W, Fig. 1). The total number of California sea lions in these seven rookeries was approximately 15,000 animals (that were hauled out) of which about 12.2% inhabit San Pedro Mártir, 34.7% San Esteban, 2.8% El Rasito, 10.0% Los Machos, 8.7% Los Cantiles, 11.0% Isla Granito, and 20.6% Isla Lobos (Aurioles-Gamboa and Zavala-González, 1994). All the animals were spread out along the shoreline of each island, except at Isla Angel de la Guarda, where they were clustered within two areas: Los Cantiles, on the eastern shoreline and Los Machos on the western shoreline.

Scat samples were obtained at reproductive and nonreproductive haulout areas between June 1995 and May 1996. At El Rasito, sampling was done only at one reproductive area; fresh and dried samples were collected (Fig. 2). If for any reason a scat was not collected (because it was found in pieces or in poor condition), it was destroyed and the site was cleared to avoid collection during subsequent trips. All fresh and dried samples collected were pooled to represent each sampling period. We assumed that the diet information corresponded to a time period close to the collection trip, but some dried scats could have been deposited shortly after the last collection.

Scats were stored in plastic bottles and then dried shortly thereafter to prevent decomposition of fish otoliths and other hard parts (which were used in subsequent prey identification) until the scats could be processed at a later date. The samples were processed by soaking in a weak biodegradable detergent solution for 1 to 7 days before being sifted through nested sieves of 2.00-, 1.18-, and 0.5-mm mesh size. Fish bones and scales, eye lenses of fish and squid, otoliths, cephalopod beaks, and crustacean fragments were extracted from the samples. Cephalopod beaks were stored in 70% ethanol, and the other items were dried and stored in vials. Sagittal otoliths and cephalopod beaks were used to identify teleost fish and cephalopods, respectively. Identifications were made by using photographs and diagrams from Clarke (1962), Fitch (1966), Fitch and Brownell (1968), and Wolff (1984), as well as voucher specimen material from the 1) Center Interdisciplinario de Marinas Ciencias (CICIMAR), 2) Instituto Tecnólogico y de Estudios Superiores de Monterrey, Guaymas, 3) Los Angeles County Museum of Natural History, California, and 4) Centro de Investigación Científica y de Educación Superior de Ensenada (CICESE), Baja California, Mexico. Prey species identifed to family level were coded by using

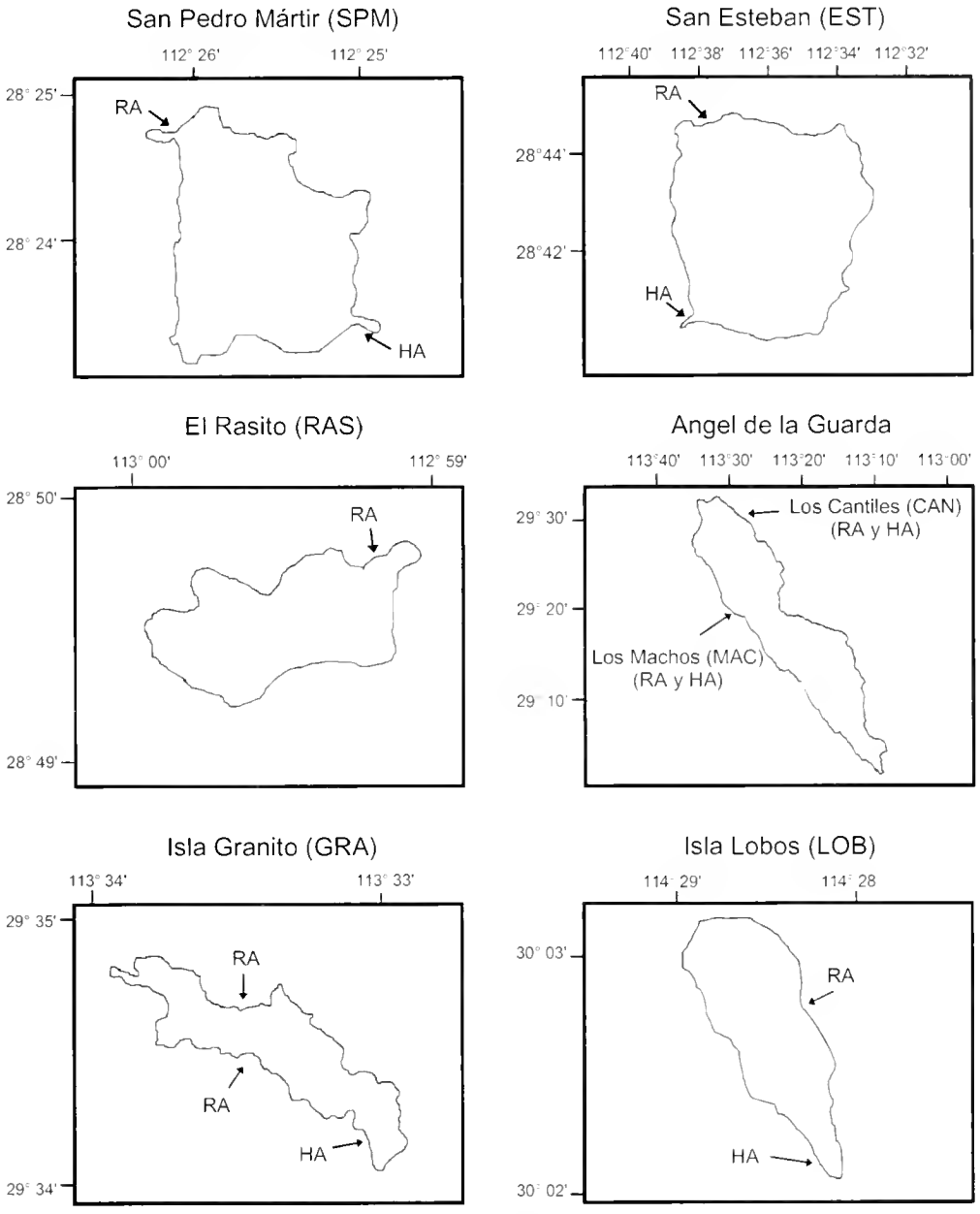

Figure 2

Location of sites where samples of California sea lion scats were collected at each island. RA = reproductive area; HA = haulout area.

the family name plus a sequential number. Otoliths from prey species that were not identified to species, genus, or family level were coded with "fish species" plus a number.

Three indices were used to describe the diet of sea lions. Percent number (PN) represents the percentage of the number of individuals for each prey taxon over the total number of individuals found in all scat samples. Percent of occurrence (PO) represents the percentage of scats having a given prey taxon and indicates the percentage of the population that is consuming a particular prey species. The third index, index of importance (IIMP) incorporates PN and PO and is defined as

$$\mathrm{IIMP}_i = \frac{1}{U}\sum_{j=1}^{U}\frac{X_{ij}}{X_j}, \qquad (1)$$

where x_i = number of individuals of taxon i in scat j;
X_j = total number of individuals from all taxa found in scat j; and
U = total number of samples with prey.

The IIMP, developed for scat analysis (García-Rodríguez, 1999), was used to determine the importance of prey species, their spatial and temporal variation in the diet,

diversity of prey estimates, and measures of similarity among rookeries. Crustaceans were not incorporated into the IIMP index because it was not possible to quantify the number of individuals in the samples.

We used the IIMP Index because it is less sensitive to changes in the number of prey in an individual scat compared to PN. For example, if a scat contains a single prey taxon, the IIMP does not change regardless of the number of individuals of that taxon, in that scat. However, as one increases the number of individuals of a given prey taxon in the scat, the PN will also increase for that prey. The IIMP allows each scat to contribute an equal amount of information, whereas PN can be dominated by a few scats with a large number of a single prey-taxon otoliths. In this manner the IIMP is similar to the split-sample frequency of ocurrence (SSFO) index, developed by Olesiuk (1993), where each scat is treated as a sampling unit and does not assume, as does PN, that the distribution of prey hard parts between scats is uniform. However, with the SSFO index, each prey taxon in a given scat is given an equal weight for that scat. If only one species occurs in a sample, its occurrence is scored as 1, if two species occur, each occurrence is scored as 0.5, and so forth (Olesiuk, 1993). The IIMP index incorporates more information than the SSFO index, regardless of the number of individuals of each taxon in the scat.[4]

Percent number (PN) was used only to show differences between broad prey groups (fishes and cephalopods) and PO was used to review the temporal and spatial changes from each main prey (those with average IIMP of at least 10% at any rookery). For all estimations, a single otolith (right or left) or single cephalopod beak (upper or lower) represented one individual prey. We tested the hypothesis that the occurrence of the main prey was independent of the rookery and of the date collection using contingency tables and an estimator of chi-square (χ^2) (Cortés, 1997).

Total length of the otoliths (mm) and the linear equation obtained by Alvarado-Castillo[5] were used to estimate the length of the Pacific sardine (total length mm=7.41+(47.24×otolith length mm); r=0.85, n=2740). Insufficient data did not allow estimating the size of specimens from May. All estimated lengths were transformed using log10, followed by an ANOVA among sampling periods. The size of Pacific sardine consumed by California sea lion was compared to those caught in the commercial fishery. We chose to estimate the size of Pacific sardines because of the broad information available concerning age and growth and other aspects about the fishery and because we found many sardine otoliths in good condition.

Spatial and temporal correlation in composition of diet was compared by using the Spearman rank correlation coefficient (R_S) (Fritz, 1974). Pairs of IIMP values were used for each prey taxon in a pair of sampling events (rookeries or sampling dates) to examine the correlation among them. This analysis was limited to prey that had an IIMP value of 10% or more. Cluster analysis of average IIMP data for the seven rookeries was used to assess the similarity of the diet among rookeries. The dendrogram for the cluster analysis was based on relative Euclidean distances and unweighted pair-grouping methods (UPGMA) strategy (Ludwig and Reynolds, 1988). We included only prey that, for at least one occasion, had IIMP values ≥10%.

Trophic diversity was evaluated by using diversity curves (Hurtubia, 1973) developed from IIMP index data. For each date and colony, the cumulative diversity was calculated for increasing numbers of sequentially numbered (but we assumed randomly deposited and collected) scat samples. The diversity curves also allowed us to evaluate sample size (Hurtubia, 1973; Hoffman, 1978; Magurran, 1988, Cortés, 1997) by identifying the point at which the curve flattens. The diversity was estimated by using the Shannon index:

$$H' = -\sum_{i=1}^{S} p_i \ln p_i, \quad (2)$$

where H' = trophic diversity;
S = total number of prey taxa; and
P_i = $IIMP_i$, and represents the relative abundance of taxon i obtained from each scat and pooled from scat 1 up to the total number of scats collected.

The values of trophic diversity were then plotted against the number of pooled scats.

Results

Identification of prey

The 1273 scat samples collected during June 1995 through May 1996 (Table 1) yielded fish remains in 97.4% of the samples, cephalopod remains in 11.2%, and crustacean remains in 12.7%. Fish and cephalopods represented 95.3% and 4.7%, respectively, of the 5242 individual prey (excluding crustaceans). The occurrence and number of these prey groups changed temporally and spatially (Fig. 3). We identified 92 prey taxa to the species level, 11 to the genus level, and 10 to family level from 851 scats (Table 2). Remaining scats had damaged prey structures in a condition that prevented us from identifying species to the genus or family level.

We found nine main prey with IIMP average values ≥10% (Table 3): the Pacific cutlassfish (*Trichiurus lepturus*), the Pacific sardine (*Sardinops caeruleus*), the plainfin midshipman (*Porichthys* spp.), myctophid no. 1, the northern anchovy (*Engraulis mordax*), Pacific mackerel (*Scomber japonicus*), the anchoveta (*Cetengraulis mysticetus*), jack mackerel (*Trachurus symmetricus*), and the lanternfish (unid. myctophid).

[4] García-Rodríguez, F. J., and J. De la Cruz-Agüero. In prep. An index to measure the specie prey importance of California sea lion (*Zalophus californianus*) based on scat samples.

[5] Alvarado-Castillo, R. Unpubl. data. Departamento de Biología y Pesquerías, Centro Interdisciplinario de Ciencias Marinas. Avenida IPN S/N Col. Palo Playa de Santa Rita, La Paz, Baja California Sur, Mexico 23070.

Table 1
Number of scats collected at each rookery for each sampling period.

	June 1995	September 1995	January 1996	May 1996	Total
San Pedro Mártir (SPM)	22	33	88	29	172
San Esteban (EST)	50	66	91	67	274
El Rasito (RAS)	11	56	58	25	150
Los Cantiles (CAN)	20	58	47	35	160
Isla Granito (GRA)	24	20	41	19	104
Los Machos (MAC)	39	32	36	0	107
Isla Lobos (LOB)	72	139	72	23	306
Total	238	404	433	198	1273

Spatial and temporal variability of the main prey

The importance (IIMP) of the Pacific cutlassfish was greater in Los Cantiles (28.4%), Isla Lobos (20.8%), and Isla Granito (48.5%) than at other sites (Fig. 4). The Pacific sardine was the dominant prey at Los Machos and to the south. There was a significant correlation across the seasons between Los Machos and El Rasito (r=0.998, P=0.04), but not between Los Machos and Isla Granito (r=0.602, P=0.59). The IIMP of sardine was also correlated between El Rasito and San Esteban (r=0.95, P=0.04). The plainfin midshipman did not show a clear pattern, but its presence in the diet increased northeastward from Isla Angel de la Guarda. Lanternfishes, especially myctophid no. 1, were the dominant prey at San Pedro Mártir, San Esteban, and El Rasito. The presence of Pacific mackerel was positively correlated with the presence of the Pacific sardine. The anchoveta was only found at Isla Lobos, and jack mackerel at El Rasito, San Pedro Mártir, and Isla Granito.

The changes in the PO of the main prey coincided with the variations of the IIMP. The occurrence of Pacific cutlassfish, Pacific sardine, plainfin midshipman, northern anchovy, Pacific mackerel, and jack mackerel was significantly different (P<0.04) among rookeries. Myctophid no. 1 showed no significant difference in ocurrence (χ^2=11.04, df=6, P=0.09); but when all lanternfishes were pooled, their occurrence among rookeries was significantly different (χ^2=11.13, df=6, P=0.04). We found significant temporal differences in the occurrence of Pacific cutlassfish, Pacific sardine, plainfin midshipman, northern anchovy, and Pacific mackerel (P<0.05), but no significant differences were found among seasons in the occurrence of jack mackerel (χ^2=2.94, df=3, P=0.40), myctophid no. 1 (χ^2=1.67, df=3, P=0.6428), or lanternfish (χ^2=2.08, df=3, P=0.5562).

Size of Pacific sardine consumed by sea lions

The estimated size of the Pacific sardine found in scat was between 101.8 mm and 179.7 mm (mean length of 150.4 mm ±13.7 mm). Significant differences were found among sampling periods (F=4.79, df=2, P=0.01), specifically between June and January (Newman-Keuls test; P=0.04) and between September and January (Newman-Keuls test; P=0.01). The average size was 147.4 mm (±16.1 mm) in June, 151.7 mm (±13.0 mm) in September, and 136.5 mm (±13.7 mm) in January (Fig. 5). A similar pattern was found in Los Cantiles, Los Machos, and Isla Granito.

Spatial and temporal correlation in diet

We identified 25 prey taxa that had an IIMP index value of ≥10% (Table 3) for a given collection. The Spearman rank correlation coefficient of IIMP between any pair of rookeries during June, September, January, and May was not significant (P>0.08). There was no positive correlation among any pair of sampling periods for any rookery (P>0.14), except between January and May at San Pedro Mártir (R_S=0.64, P<0.05) and El Rasito (R_S=0.66, P<0.05) and between January and June as well as between January and May at Isla Lobos (R_S=0.56, P=0.05; and R_S=0.59, P=0.05, respectively).

The similarity in diet was related to the distance between rookeries. A clustering for the seven rookeries was obtained from these 25 prey taxa (Fig 6). We arbitrarily used a "cut-off" distance of 0.3 and 0.4 on the dendrogram as reference points for identifying clusters. The group obtained by using the first distance (0.3) showed four feeding areas: one located in the south (area I: San Pedro Mártir, San Esteban, and El Rasito), another in Canal de Ballenas (area II: Los Machos) and two in the north (area III: Los Cantiles and Isla Lobos; and area IV: Isla Granito). When the second distance (0.4) was used, the seven rookeries grouped into two clusters: 1) the southern region and Canal de Ballenas, and 2) the region north of Angel de la Guarda.

Spatial and temporal variability in trophic diversity

Temporal variability in trophic diversity was evident between the rookeries (Fig. 7). In general, two patterns could be differentiated: one in which the diversity varied little throughout the year and the other in which diversity was high in January and low in September. The rookeries San Pedro Mártir and Isla Lobos showed the first pattern and Los Machos and Isla Granito (and to a lesser extent, San Esteban and El Rasito) showed the second pattern. In September, when diversity was low, the dominant prey at

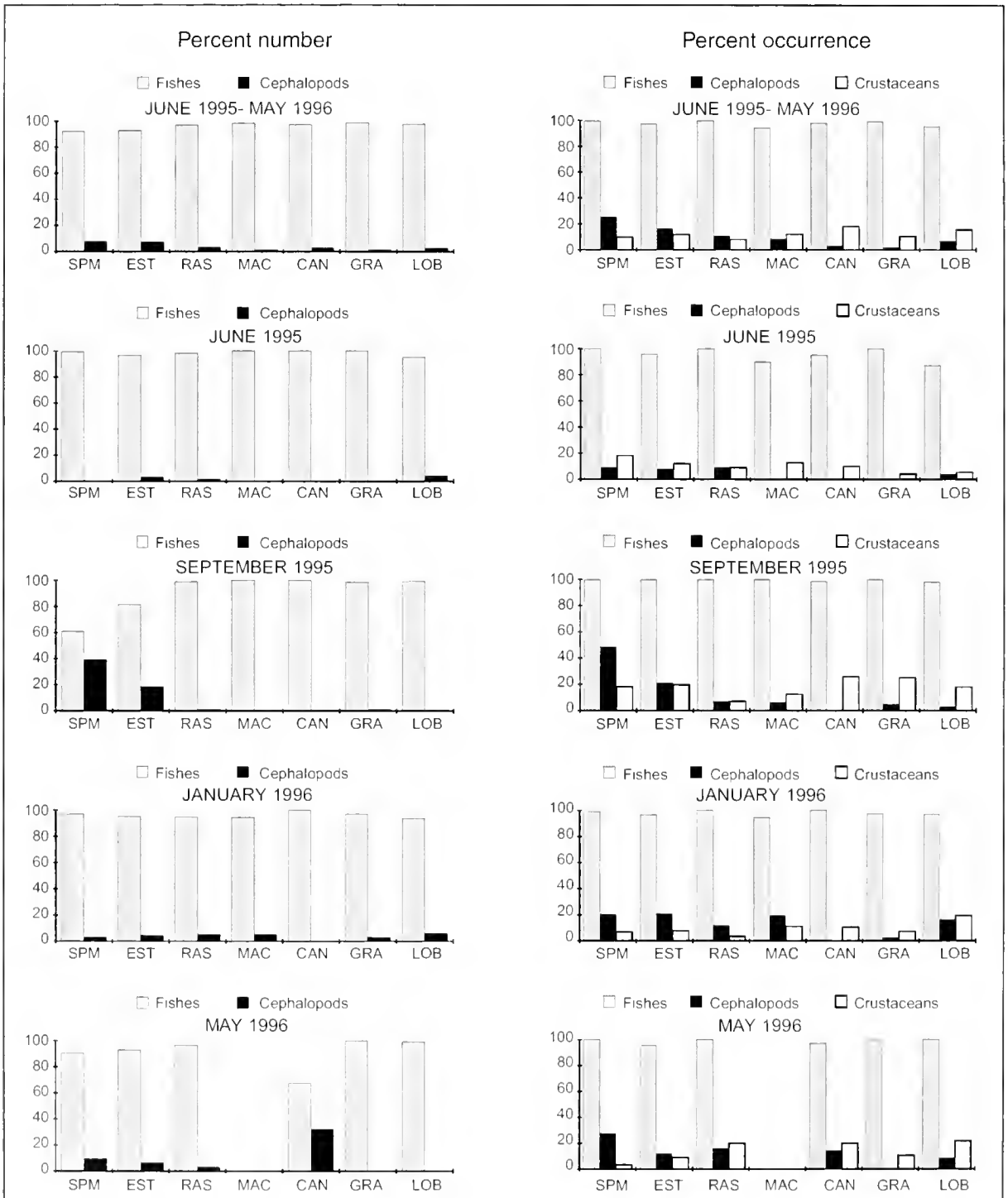

Figure 3

Percent number (PN) and percent occurrence (PO) index values for fishes, cephalopods, and crustaceans found in samples of California sea lion scats collected at seven rookeries in the Gulf of California, Mexico, for all sampling periods combined and for each sampling period.

San Esteban, El Rasito, and Los Machos was Pacific sardine, whereas at Isla Granito, it was Pacific cutlassfish (Fig. 4). The curves obtained for Los Cantiles showed a clear pattern of diversity only in September, although the trend in the January curve would suggest a higher diversity in January than in September.

Table 2

Prey of California sea lion identified from scat samples collected at Isla San Pedro Martir, Isla San Esteban, Isla El Rasito, Los Cantiles, Isla Granito, Los Machos and Isla Lobos from June 1995 through May 1996. *n* ind. = number of individuals in the sample; PN = percent number; n occurr = number of occurrences; PO = percentage of occurrence; IIMP = index of importance.

Scientific name	Common name	*n* Ind.	PN	*n* Occurr.	PO	IIMP
Trichiurus lepturus	Pacific cutlassfish	306	5.837	128	15.041	16.392
Sardinops caeruleus	Pacific sardine	358	6.829	88	10.341	10.020
Porichthys spp.	midshipman	456	8.699	95	11.163	9.297
Myctophid no. 1	lanternfish	714	13.621	119	13.984	7.901
Engraulis mordax	northern anchovy	430	8.203	43	5.053	5.199
Scomber japonicus	Pacific mackerel	103	1.965	42	4.935	3.403
Cetengraulis mysticetus	anchoveta	410	7.821	15	1.763	2.404
Loliolopsis diomedeae	squid	77	1.469	35	4.113	2.399
Trachurus symmetricus	jack mackerel	111	2.118	41	4.818	2.273
Merluccius spp.	Pacific whiting	55	1.049	25	2.938	2.206
Pontinus spp.	scorpionfish	61	1.164	26	3.055	1.842
Enoploteuthid no. 1	squid	95	1.812	23	2.703	1.754
Caelorinchus scaphopsis	shoulderspot	65	1.240	25	2.938	1.728
Octopus sp. no. 1	octopus	24	0.458	17	1.998	1.614
Sebastes macdonaldi	Mexican rockfish	42	0.801	18	2.115	1.496
Citharichthys sp no. 1	sanddab	120	2.289	23	2.703	1.220
Fish species no. 1	—	49	0.935	25	2.938	1.153
Haemulopsis leuciscus	white grunt	176	3.357	21	2.468	1.093
Peprilus snyderi	salema butterfish	163	3.110	33	3.878	1.025
Prionotus spp.	searobin	12	0.229	9	1.058	0.855
Prionotus stephanophrys	lumptail searobin	53	1.011	14	1.645	0.814
Argentina sialis	Pacific argentine	19	0.362	13	1.528	0.754
Fish species no. 2	—	55	1.049	27	3.173	0.737
Hemanthias peruanus	splittail bass	60	1.145	22	2.585	0.602
Fish species no. 3	—	9	0.172	6	0.705	0.592
Micropogonias ectenes	slender croaker	13	0.248	9	1.058	0.547
Lepophidium spp.	cusk-eel	9	0.172	3	0.353	0.532
Fish species no. 4	—	10	0.191	3	0.353	0.511
Sebastes exsul	buccanner rockfish	15	0.286	10	1.175	0.505
Cranchiid no. 2	Squid	20	0.382	12	1.410	0.501
Haemulon flaviguttatum	yellowspotted grunt	11	0.210	3	0.353	0.468
Selar crumenophthalmus	bigeye scad	24	0.458	12	1.410	0.431
Fish species no. 5	—	33	0.630	19	2.233	0.384
Paralabrax sp. no. 1	sea bass	9	0.172	5	0.588	0.373
Synodus sp. no. 3	lizardfish	10	0.191	3	0.353	0.341
Lepophidium prorates	prowspine cusk-eel	5	0.095	4	0.470	0.335
Fish species no. 6	—	9	0.172	5	0.588	0.324
Synodus sp. no. 1	lizardfish	25	0.477	10	1.175	0.324
Octopus sp, no. 2	octopus	8	0.153	7	0.823	0.308
Gonatus berryi	squid	5	0.095	5	0.588	0.274
Mugil cephalus	striped mullet	1	0.019	1	0.118	0.265
Paranthias colonus	Pacific creole-fish	1	0.019	1	0.118	0.265
Balistes polylepis	finescale triggerfish	13	0.248	4	0.470	0.245
Physiculus nematopus	charcoal mora	30	0.572	12	1.410	0.244
Hemanthias spp.	sea bass	9	0.172	6	0.705	0.234
Fish species no. 7	—	10	0.191	8	0.940	0.233
Uroconger varidens	conger eel	8	0.153	5	0.588	0.189
Larimus spp.	drum	8	0.153	6	0.705	0.174
Apogon retrosella	barspot cardinalfish	5	0.095	4	0.470	0.173
Dosidicus gigas	squid	8	0.153	5	0.588	0.171

continued

Table 2 (continued)

Scientific name	Common name	*n* Ind.	PN	*n* Occurr.	PO	IIMP
Merluccius productus	Pacific whiting	1	0.019	1	0.118	0.167
Fish species no. 8	—	2	0.038	2	0.235	0.159
Synodus sp. no. 2	lizardfish	12	0.229	5	0.588	0.132
Scorpaena sonorae	Sonora scorpionfish	2	0.038	1	0.118	0.130
Eucinostomus spp.	mojarra	13	0.248	5	0.588	0.129
Fish species no. 9	—	3	0.057	3	0.353	0.127
Cynoscion reticulatus	striped weakfish	23	0.439	7	0.823	0.124
Fish species no. 10	—	10	0.191	1	0.118	0.122
Caulolatilus affinis	bighead tilefish	4	0.076	3	0.353	0.114
Paralabrax auroguttatus	goldspotted sand bass	18	0.343	4	0.470	0.110
Fish species no. 11	—	3	0.057	2	0.235	0.102
Cranchiid no. 5	squid	1	0.019	1	0.118	0.097
Bodianus diplotaenia	mexican hogfish	1	0.019	1	0.118	0.087
Prionotus sp. no. 1	searonbin	2	0.038	2	0.235	0.087
Strongylura exilis	california needlefish	1	0.019	1	0.118	0.083
Synodus spp.	lizardfish	6	0114	5	0.588	0.146
Fish species no. 12	—	3	0.057	3	0.353	0.074
Fish species no. 13	—	2	0.038	1	0.118	0.065
Fish species no. 14	—	3	0.057	1	0.118	0.060
Fish species no. 15	—	2	0.038	1	0.118	0.058
Fish species no. 16		2	0.038	2	0.235	0.056
Porichthys sp. 1	midshipman	1	0.019	1	0.118	0.052
Fish species no. 17	—	5	0.095	3	0.353	0.049
Calamus brachysomus	Pacific porgy	5	0.095	2	0.235	0.043
Fish species no. 18	—	1	0.019	1	0.118	0.042
Fish species no. 19	—	5	0.095	2	0.235	0.041
Ophididae no. 1	—	1	0.019	1	0.118	0.040
Fish species no. 20	—	5	0.095	3	0.353	0.039
Sebastes sinesis	blackmouth rockfish	2	0.038	1	0.118	0.039
Symphurus spp.	tonguefish	3	0.057	1	0.118	0.038
Fish species no. 21	—	2	0.038	1	0.118	0.036
Pronotogrammus multifasciatus	threadfin bass	8	0.153	2	0.235	0.029
Fish species no. 22	—	2	0.038	2	0.235	0.027
Fish species no. 23	—	2	0.038	1	0.118	0.021
Orthopristis reddingi	Bronze-striped grunt	16	0.305	1	0.118	0.020
Fish species no. 24	—	2	0.038	1	0.118	0.020
Fish species no. 25	—	1	0.019	1	0.118	0.016
Cranchiidae no. 4	squid	2	0.038	2	0.235	0.014
Fish species no. 26	—	2	0.038	2	0.235	0.014
Histioteuthis heteropsis	squid	1	0.019	1	0.118	0.014
Scorpaenidae no. 1	—	1	0.019	1	0.118	0.011
Fish species no. 27	—	3	0.057	2	0.235	0.011
Fish species no. 28	—	1	0.019	1	0.118	0.010
Fish species no. 29	—	1	0.019	1	0.118	0.008
Cranchiidae no. 3	squid	1	0.019	1	0.118	0.006
Bollmannia spp.	goby	1	0.019	1	0.118	0.006
Fish species no. 30	—	1	0.019	1	0.118	0.005
Cranchiidae no. 1	squid	1	0.019	1	0.118	0.004
Paralabrax maculatofasciatus	spotted sand bass	1	0.019	1	0.118	0.003
Ophidion scrippsae	basketweave cusk-eel	1	0.019	1	0.118	0.003
Physiculus spp.	cod, codling, mora	2	0.038	1	0.118	0.003
Ophididae no. 2	—	4	0.076	1	0.118	0.002
Unid. Carangidae	jacks	8	0.153	3	0.353	0.141

continued

Table 2 (continued)

Scientific name	Common name	*n* Ind.	PN	*n* Occurr.	PO	IIMP
Unid. Engraulidae	anchovies	1	0.019	1	0.118	0.248
Unid. Haemulidae	grunts	13	0.248	11	1.293	0.509
Unid. Labridae	wrasses	1	0.019	1	0.118	0.005
Unid. Mycthophidae	lanternifishes	216	4.121	71	8.343	4.895
Unid. Ophididae	cusk-eel	2	0.038	1	0.118	0.098
Unid. Scianidae	drums	13	0.248	9	1.058	0.643
Unid. Scorpaenidae	scorpionfishes	30	0.572	18	2.115	1.078
Unid. Serranidae	sea bass	13	0.248	6	0.705	0.176
Unid. Triglidae	searobins	1	0.019	1	0.118	0.002
	Unid. fishes	39	0.744	16	1.880	1.819
	Unid. cephalopods	4	0.076	4	0.470	0.373
	Unid. fishes (very eroded)	381	7.268	231	27.145	
	Remains of cephalopods			14	1.645	
	Remains of crustaceans			162	19.036	

Discussion

Stomach acids attack otoliths, affecting their size and number and consequently the estimate of prey occurrence and importance. Erosion of otoliths during digestion has been analyzed in studies of pinnipeds in captivity. Bowen (2000) reviewed nine studies that estimated the proportion of otoliths recovered in scat samples to obtain a prey-number correction factor (NCF). He found that NCF is greater than 1.0 because many prey species are not recovered in the scat samples. Additionally, the erosion level can be significantly different among prey species (Bowen, 2000) because of differences in the shape and microstructure of otoliths. Therefore, estimates of biomass based on scat analysis should be carefully interpreted because the consumption of some prey species can be under- or overestimated. Correction factors are needed to compensate for differential erosion for the prey species of each pinniped.

In this study the most important prey of California sea lions were pelagic fish with small, thin, and fragile otoliths (Nolf, 1993). The lanternfish also have small otoliths—perhaps smaller than those of any other prey taxa found in the scats. Their true importance in California sea lion feeding may be underestimated because of erosion caused by stomach acids (Da Silva and Neilson, 1985; Murie and Lavigne, 1985; Jobling and Breiby, 1986; Jobling, 1987; Tollit et al., 1997). Similarly, the presence of cephalopods may have been underestimated because their jaws are composed of chitin, which is harder to digest, and frequently are regurgitated (Pitcher, 1980; Hawes, 1983). However, the high resistence to digestion of cephalopod beaks allows recovery of them in good shape. Thus they are a good choice to use in such diet analyses (Lowry and Carretta, 1999).

A numerical index of prey species importance may over- or underestimate the dominance of prey species in the diet because it does not consider the weight of the prey. For IIMP, a numerical index that assumes a similar weight for all prey species, the true importance of the individual large prey in the diet can be underestimated and the importance of individual small prey can be overestimated. This problem is also present when the PO, PN, and the SSFO index are used because these are all based only upon the number and occurrence of otoliths and cephalopods beaks. As when using PN, and the SSFO, the IIMP does not work for species that cannot be enumerated, such as crustaceans.

Given the tendencies of the trophic diversity curves, the sample size was suitable in almost all cases. However, at San Pedro Mártir a few more samples would have been useful to fully depict the diet. At Los Cantiles, except during September 1995, the samplings should have been more intense because the flattened portion of the diversity curves are not clear. The information, therefore, that comes from those samples could be biased. However, the number of scats that we analyzed contained a high percentage of the consumed species, especially the main prey.

The results of this study indicate that the California sea lion consumed mainly fish and some crustaceans and cephalopods. According to the PN index, fish were more important than cephalopods in the diet of sea lions. In addition, fish were more frequent (PO) than crustacean and cephalopods.

Crustaceans were represented in a similar manner in scats from all rookeries. Cephalopods, however, were more important at San Pedro Mártir and San Esteban, probably because they are more common towards the southern gulf. Species of the suborder Oegopsida, which includes oceanic species (Roper and Young, 1975), were most commonly found in scats from these rookeries. Orta-Dávila (1988) and Sánchez-Arias (1992) have also noted the low consumption of cephalopods at the northern rookeries. Fish were the most diverse and commonly eaten prey. In contrast to cephalopods, fish were slightly less important in the southern region.

The availability and abundance of the various prey resources influenced the diet of the sea lions in the Gulf

Table 3

Prey of California sea lions having IIMP index values ≥10% in at least one sampling period for seven rookeries in the Gulf of California, Mexico. Blank indicate that species were not recorded in diet; "—" means unavailable data.

	Prey species	June 1995	September 1995	January 1996	May 1996	Average
San Pedro	*Engraulis mordax*	29.7		2.1	0.5	8.1
Martir	myctophid no. 1	29.0	10.5	9.0	20.5	17.3
	Porichthys spp.	11.2	2.0	6.8	15.5	8.9
	Prionotus stephanophrys	0.6	3.3	3.3	10.9	4.5
	enopleoteuthid no.1		27.3	0.8		7.0
	Sebastes macdonaldi		10.4			2.6
	Haeumulopsis leuciscus			16.7	6.0	5.7
San Esteban	*Trichiurus lepturus*	24.9	3.4		3.0	7.8
	Sardinops caeruleus	10.0	34.1		4.2	12.1
	unid. Myctophidae	13.79	3.4	4.3	10.9	8.1
	myctophid no. 1	2.8	11.8	8.9	18.8	10.6
	enopleoteuthid no. 1		16.9			4.2
	Sebastes macdonaldi		2.1	9.7	1.4	3.3
	fish species no. 1			1.7	11.0	3.2
El Rasito	*Porichthys* spp.	26.2	4.0	2.3		8.1
	unid. Myctophidae	16.4	1.5	8.1	16.4	10.6
	Scomber japonicus	13.8	3.2	3.7	2.5	5.8
	Pontinus spp.	11.5	5.1	4.1	10.9	7.9
	Octopus sp. no.1	11.5		2.9	7.7	5.5
	myctophid no. 1	6.6	5.1	21.4	6.8	10.0
	Sardinops caeruleus	1.6	40.1	0.9	7.3	12.5
	Trachurus symmetricus		22.0	5.0	23.4	12.6
	Caelorinchus scaphopsis		3.6	13.5	10.5	6.9
Los Machos	*Sardinops caeruleus*	21.0	64.1	16.8	—	34.0
	Scomber japonicus	19.0		10.9	—	10.0
	Merluccius spp.	15.4		8.2	—	7.9
	Trichiurus lepturus	11.7	5.4		—	5.7
	Sebastes macdonaldi	1.8		11.3	—	4.4
Los Cantiles	*Porichthys* spp.	66.7	15.5			20.6
	Trichiurus lepturus	22.2	38.2		53.1	28.4
	Engraulis mordax	3.7	0.4	14.3		4.6
	myctophid no. 1		17.6	4.8		5.6
	Sardinops caeruleus		6.8	19.0		6.5
	fish species no. 3		0.9	14.3		3.8
	unid. fishes		0.9	19.0		5.0
	unid. Scianidae			14.3		3.6
	Lepophidium spp.			14.		3.5
	Loliolopsis diomedeae				21.1	5.3
Isla Granito	*Engraulis mordax*	49.3	7.8			14.3
	Trichiurus lepturus	22.0	70.1	2.0	100.0	48.5
	unid. myctophidae	1.7	1.1	12.6		3.9
	Sardinops caeruleus	0.9		18.7		4.9
	Porichthys spp.	0.5	18.2	4.6		5.8
	Cutharichthys sp. no. 1			21.7		5.4
Isla Lobos	*Cetengraulis mysticetus*	32.7	0.1	6.8	27.8	16.9
	Trichiurus lepturus	25.2	27.7	15.8	14.3	20.8
	Porichthys spp.	9.0	10.3	23.2	35.5	19.5
	Loliolopsis diomedeae	4.9	2.2	11.6	3.5	5.6
	Peprilus snyderi		23.5	5.2		7.2

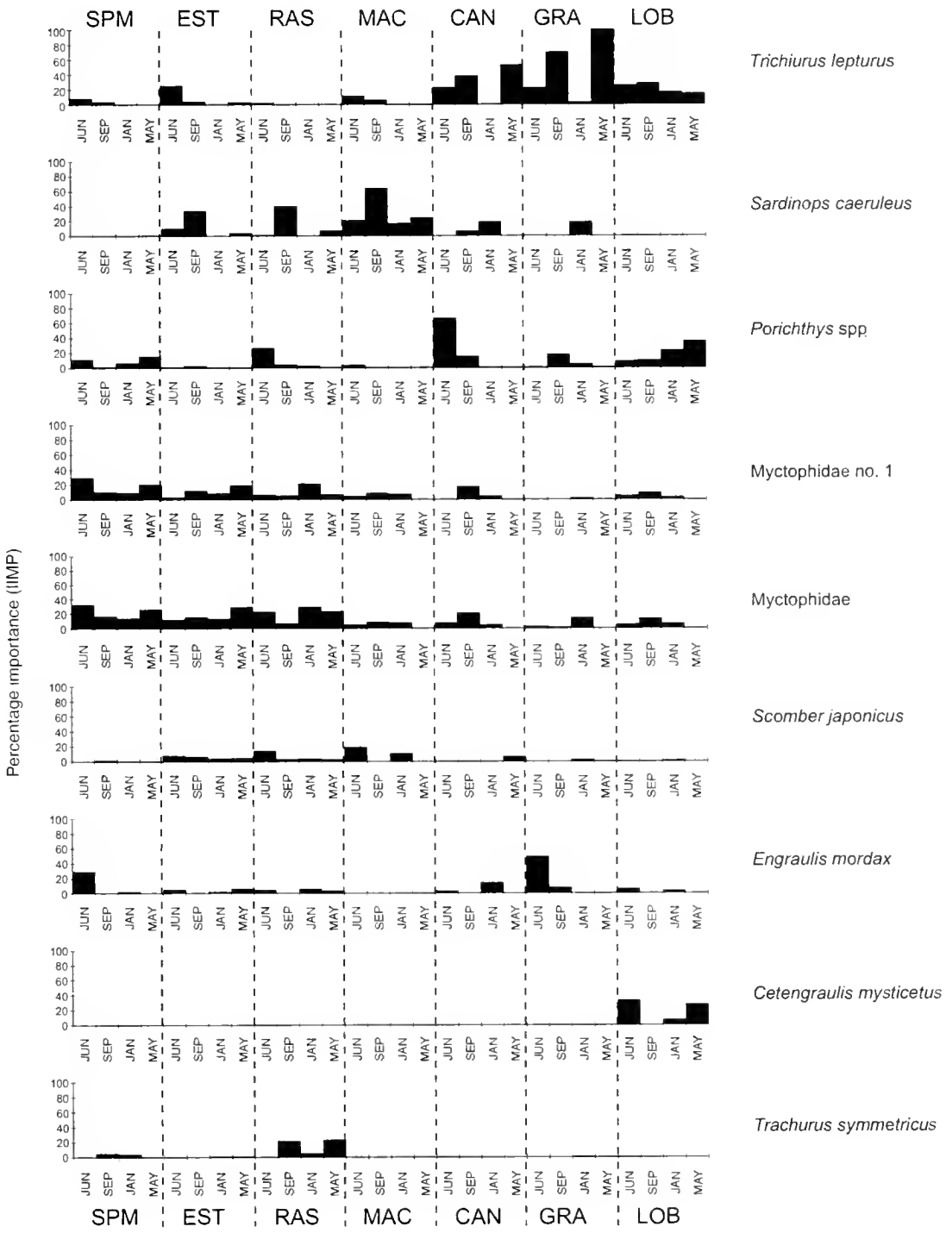

Figure 4

Index of importance (IIMP) for nine prey species identified from samples of California sea lions scats collected at seven rookeries in the Gulf of California, Mexico, during June and September 1995, and January and May 1996.

of California. The distribution pattern of Pacific sardine closely agrees with its importance in the sea lions diet. The Pacific sardine occurred in high concentrations around Angel de la Guarda and Isla Tiburon during the summer and along the coast of southern Sonora during the winter, where spawning occurs (Cisneros-Mata et al.[3]). Sardines

were consumed in the Canal de Ballenas region during the summer (September), when they are very abundant. Larger size Pacific sardines were consumed by sea lions most frequently during the summer when adult sardines occur more frequently in the Canal de Ballenas. As adult sardine left Canal de Ballenas (Cisneros-Mata et al., 1997), the proportion of young individuals in the diet of sea lions increased. The fish eaten by sea lions were apparently smaller than those captured by the commercial fisheries. The average estimated size of the sardines consumed was 150.4 mm, whereas the average size of commercially caught fish during the 1995–96 season was 162.4 mm (Cisneros-Mata et al.[3]). This 7% difference in size may have been caused by an underestimation of otolith size because of digestive erosion (Jobling and Breiby, 1986). If this is so, then the size of Pacific sardines consumed by sea lions is similar to the size of those captured by the fishery.

Isla Lobos was the only rookery where Pacific sardine was not consumed. This finding differs from those of Cisneros-Mata et al.[3] which show the Pacific sardines present as far north as Isla Lobos. However, their study period was during the 1991–92 El Niño episode, whereas our study occurred during normal oceanographic conditios in 1995–96.

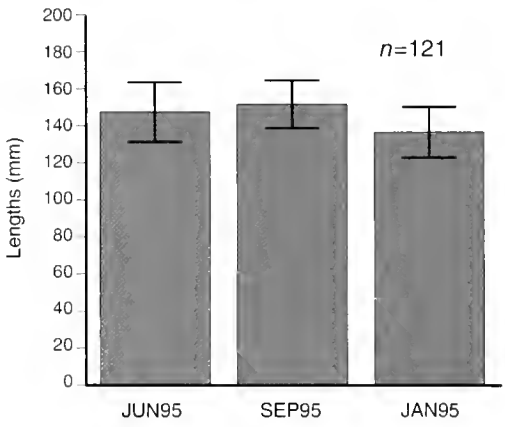

Figure 5

Size of Pacific sardine (*Sardinops caeruleus*) estimated from otoliths found in California sea lions scats collected in Isla San Esteban, El Rasito, Granito, Los Cantiles, and Los Machos. One standard deviation is indicated from each mean.

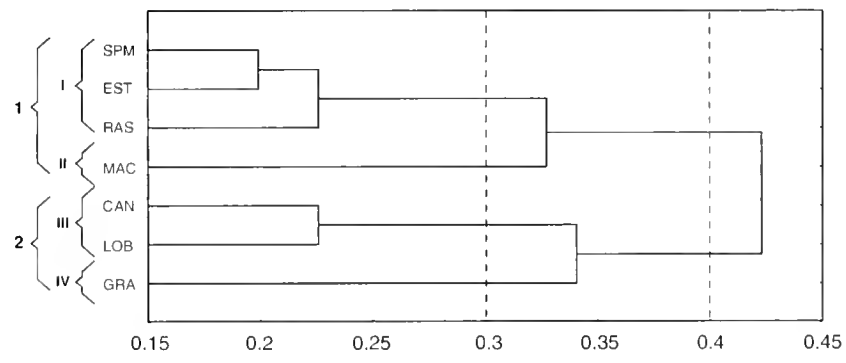

Figure 6

Dendrogram of cluster analysis of seven rookeries determined with Euclidean distance (computed from the IIMP of the 25 prey that had on at least one occasion a value ≥10%) and the UPGMA (unweighted pair-grouping methods) strategy. The vertical lines represent the points of references to delimit the groups.

Less is known about the spatial and temporal availability of other important prey. As with commercial captures (Arvizu-Martinez, 1987), Pacific mackerel occurred together with Pacific sardine. Similar variations in occurrence for both species have been noticed from stomach content analyses of the giant squid (*Dosidicus gigas*) (Ehrhardt, 1991). Lanternfishes were abundant north of Isla Angel de la Guarda (Robison, 1972); however they were not important in the diet of the California sea lion in this region. Their greater importance in the diet at southern rookeries was probably due to the absence of more preferred prey such as Pacific sardine, Pacific cutlassfish, or anchoveta. The consumption of northern anchovy tended to be less important towards Canal de Ballenas, where Pacific sardine reached its maximum importance. The low spatial overlap of these two species has also been noted in other studies. The anchoveta was present only at Isla Lobos. This is an estuarine-lagoon species, typical of coastal lagoons of northern Sinaloa and Sonora (Castro-Aguirre et al., 1995). The presence of this prey in Isla Lobos is possibly due to the sandy coast (Walker, 1960), which is similar to that of the Sinaloa-Sonora coast.

The diet of California sea lions differed among rookeries, probably due to differences in feeding sites and prey availability. Antonelis et al. (1990) studied the foraging characteristics of the northern fur seal (*Callorhinus ursinus*) and the California sea lion at San Miguel Island and found differences between foraging areas among species. The northern fur seal was found most frequently foraging in oceanic water within 72.4 km from the island, whereas Californinia sea lions forgaged more often in the shallower neritic zone, within 54.2 km from the island. Different foraging distances in California sea lions from San Miguel Island were found by Melin and DeLong (1999). During the nonbreeding season a higher percentage of foraging locations occurred at distances less than 100 km, whereas during the breeding season most of the foraging locations occurred at distances greater than 100 km. These differences are probably due to the increased California sea lion population in San Miguel; this increase in population forces sea lions to exploit new areas as a density-dependent response to population

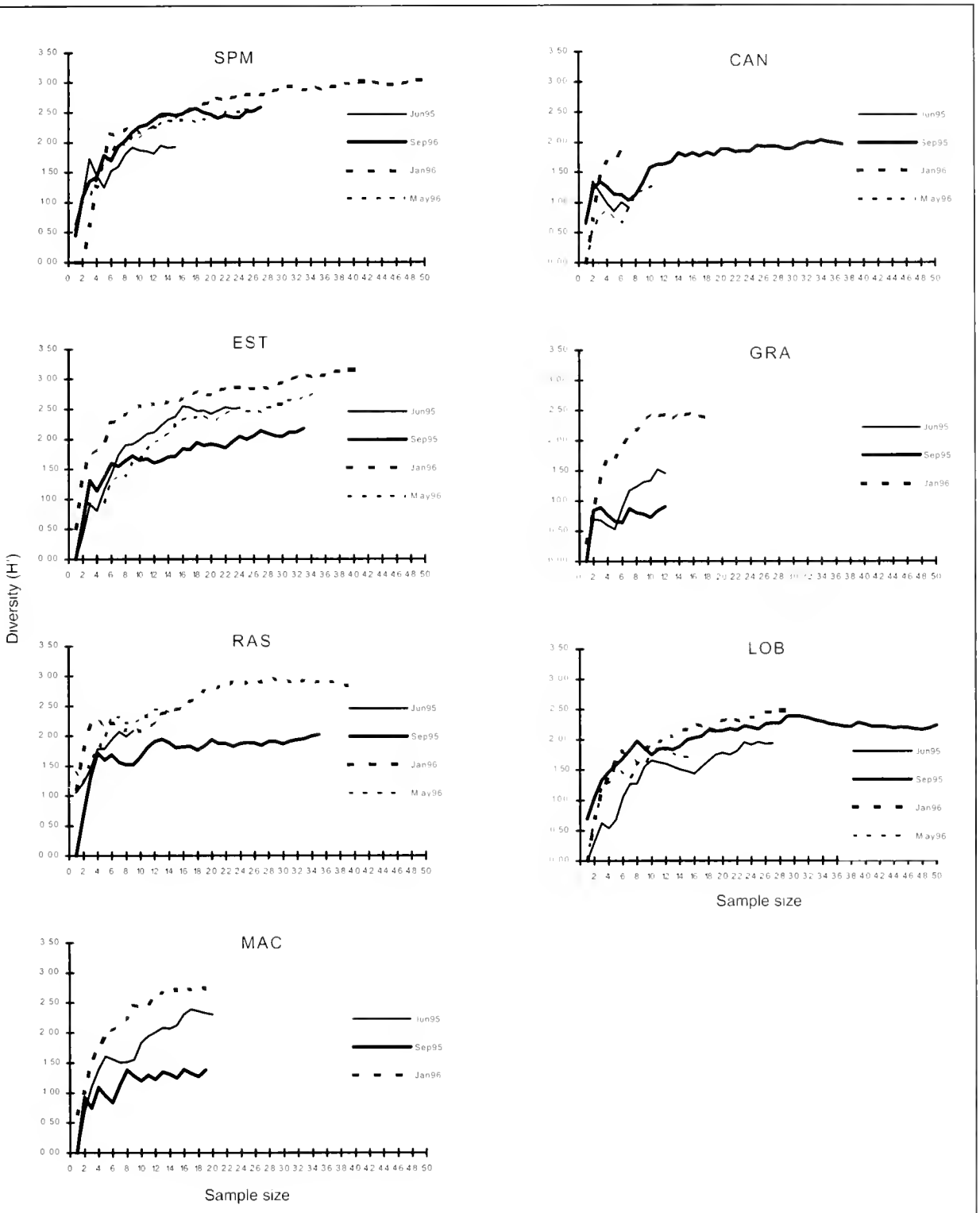

Figure 7

Trophic diversity curves for California sea lions determined from scat samples collected at seven rookeries in the Gulf of California, Mexico. SPM = San Pedro Mártir; EST = San Esteban; RAS = Isla Rasito; MAC = Los Machos; CAN = Los Cantiles; GRA = Isla Granito; LOB = Isla Lobos.

growth. Although, these differences could also be due to variability in the distribution of prey (Melin and DeLong, 1999), as suggested by Antonelis and Fiscus (1980), foraging areas might change with season and annual variations in prey availability and abundance.

Foraging areas in the Gulf of California could lie closer to rookeries than those recorded for San Miguel Island sea lions because the diet was different among rookeries in spite of the shorter distance between them (54.2 km). At Los Islotes, Baja California Sur, adult females fed within 20 km of the colony (Durán-Lizárraga, 1998). Kooyman and Trillmich (1986a, 1986b) reported similar data in sea lion colonies of the Galapagos Islands. In the northern region of the Gulf of California, feeding range could be shorter than that at Los Islotes because of the higher concentration of food at high nutrient concentrations (phosphate, nitrate, nitrite, and silicate) in Canal de Ballenas that is associated with strong tidal mixing (Alvarez-Borrego, 1983).

Four foraging zones were discerned from dietary differences in sea lions from the seven rookeries studied. Zone I, which included San Pedro Mártir, San Esteban, and El Rasito, was characterized by the consumption of lanternfish; zone II, which included Los Machos was characterized by the consumption of Pacific sardine and Pacific mackerel; zone III, which included Isla Granito, by the consumption of Pacific cutlassfish and the northern anchovy; and zone IV, Los Cantiles and Isla Lobos, was characterized by the consumption of the plainfin midshipman and the Pacific cutlassfish. These four zones may indicate differences in habits used by sea lions or may indicate different oceanographic conditions exploited by sea lions. The eastern coast of the Gulf of California displays high photosynthetic pigment concentrations, associated with upwelling induced by winds from the northwest in the winter. These conditions may make Canal de Ballenas one of the most important for the distribution of Pacific sardine during the summer.

Trophic diversity varied spatially and temporally. San Pedro Mártir and Isla lobos sea lions seem to depend on a more stable feeding areas compared to sea lions at rookeries on Isla Granito and Los Machos, where changes in diversity of consumed species indicated that sea lions feed on fewer species during certain times of the year. Similar results in relation to the changes in diversity were also noticed in the rookeries of the Channel Islands and Farallon Islands, California (Bailey and Ainley, 1982; Antonelis et al., 1984; Lowry et al., 1990; Lowry et al., 1991). Perhaps the tendency to have the highest values of diversity and little seasonal variation at San Pedro Mártir is the result of this rookery being located in a zone of transition between two biogeographical areas. This geographical position confers greater environmental heterogeneity and greater ecological diversity (Walker, 1960).

California sea lions in the upper region of the Gulf of California obtain the main portion of their diet from a relatively small number of species. The decrease in abundance of any of these food resources can seriously affect the population, particularly at Isla Granito and Los Machos because sea lions from these rookeries depend on a few species.

Acknowledgments

We wish to thank Secretaria de Marina, Armada de Mexico, for its great support during the field activities, and the Consejo Nacional de Ciencia y Tecnologia (CONACYT) for funding this study under grant number 26430-N. The Secretaria de Medio Ambiente, Recursos Naturales y Pesca (SEMARNAP) provided permits for field work (DOO.-700-(2)01104 and DOO.-700(2).-1917). We would like to thank Robert Lavenberg and Jeff Siegel for allowing us the use of otoliths from the collection at the Natural Museum History of Los Angeles County and also Lawrence Barnes for his logistical support during the stay of first author at Los Angeles; we also thank Manuel Nava for allowing us the use of otoliths from the collection in Tecnologico de Monterrey, Campus Guaymas. We are also grateful to Unai Markaida for his assistance in prey identification based on the examination of cephalopods beaks. We thank Mark Lowry for commenting on an earlier draft of the paper, Norman Silverberg for reviewing the manuscript in English, and two anonymous reviewers for their valuable suggestions and criticism. The first author would like to thank Centro Interdisciplinario de Ciencias Marinas-IPN for a scholarship (PIFI, Programa Institucional para la Formación de Investigadores) assigned for postgraduate studies.

Literature cited

Alvarez-Borrego, S.
1983. Gulf of California. *In* Estuaries and enclosed seas (B. H. Ketchum, ed.), p 427–449. Elsevier Scientific Publishing Co., Amsterdam.

Antonelis, G. A, and C. H. Fiscus.
1980. The pinnipeds of the California Current. Calif. Coop. Oceanic Fish. Invest. Rep. 21:68–78.

Antonelis, G. A., C. H. Fiscus, and R. L. DeLong.
1984. Spring and summer prey of California sea lions, *Zalophus californianus*, at San Miguel Island, California 1978–79. Fish. Bull. 82:67–75.

Antonelis, G. A., B. S. Stewart, and W. F. Perryman.
1990. Foraging characteristics of females northern fur seals (*Callorhinus ursinus*) and California sea lion (*Zalophus californianus*). Can J. Zool. 68:150–158.

Arvizu-Martınez, J.
1987. Fisheries activities in the Gulf of California, México. Calif. Coop. Oceanic Fish. Invest. Rep. 28:32–36.

Aurioles-Gamboa, D., C. Fox, F. Sinsel, and G. Tanos.
1984. Prey of sea lions (*Zalophus californianus*) in the bay of La Paz, Baja California Sur, México. J. Mammal. 65(3): 519–21.

Aurioles-Gamboa, D., and A. Zavala-González.
1994. Algunos factores ecológicos que determinan la distribución y abundancia del lobo marino de California, *Zalophus californianus*, en el Golfo de California. Ciencias Marinas 20(4):535–553.

Bailey, K. M., and D. G. Ainley.
1982. The dynamics of California sea lion predation on Pacific hake. Fish. Res. 1:163–176.

Bautista-Vega, A. A.
2000. Vartiación estacional en la dieta del lobo marino común, *Zalophus californianus*, en las Islas Ángel de la Guarda y Granito, Golfo de California, México. Tesis de Licenciatura,

113 p. Universidad Nacional Autónoma de México. México, D.F.

Bowen, W. D.
2000. Reconstruction of pinniped diets: accounting for complete digestion of otoliths and cephalopod beaks. Can. J. Fish. Aquat. Sci. 57:898–905.

Castro-Aguirre, J. L., E. F. Balart, and J. Arvizu-Martinez.
1995. Contribución al conocimiento del origen y distribución de la ictiofauna del Golfo de California, México. Hidrobiológica 5(1-2):57–78.

Clarke, M. R.
1962. The identification of cephalopod "beaks" and the relationship between beak size and total body weight. Bull. British Museum (Natural History) Zoology 8(10):419–480.

Cortés, E.
1997. A critical review of methods of studying fish feeding based on analysis of stomach contents: application to elasmobranch fishes. Can. J. Fish. Aquat. Sci. 54:726–738.

Da Silva, J., and J. D. Neilson.
1985. Limitations of using otoliths recovered in scats to estimate prey consumptions in seals. Can. J. Fish. Aquat. Sci. 42:1439–1442.

Durán-Lizárraga, M. E.
1998. Caracterización de los patrones de buceos de alimentación de lobo marino *Zalophus californianus* y su relación con variables ambientales en la Bahía de La Paz, B.C.S. Tesis de Maestria, 82 p. CICIMAR, La Paz, B.C.S., México.

Ehrhardt, N. M.
1991. Potential impact of a seasonal migratory jumbo squid (*Dosidicus gigas*) stock on a Gulf of California sardine (*Sardinops sagax caerulea*) population. Bull. Mar. Sci. 49(1–2):325–332.

Fitch, J. E.
1966. Additional fish remains, mostly otoliths, from a Pleistocene deposit at Playa del Rey, California. Los Angeles County Mus., Cont. in Sci. (119):1–16.

Fitch, J. E., and R. L. Brownell.
1968. Fish otoliths in Cetacean stomachs and their importance in interpreting feeding habits. J. Fish. Res. Board Canada. 25(12):2561–2574.

Fritz, E. S.
1974. Total diet comparison in fishes by Spearman rank correlation coefficients. Copeia (1974):210–214.

García-Rodríguez, F. J.
1995. Ecología alimentaria del lobo marino de California, *Zalophus californianus californianus* en Los Islotes, B.C.S., México. Tesis de Licenciatura, 106 p. Universidad Autónoma de Baja California Sur. La Paz, B.C.S., México.
1999. Cambios espaciales y estacionales en la estructura trófica del lobo marino de California, *Zalophus caliornianus*, en la región de la grande islas, Golfo de California. Tesis de Maestria, 73 p. CICIMAR. La Paz, B.C.S, México.

Hawes, D.
1983. An evaluation of California sea lion scat samples as indicators of prey importance. Master's thesis, 50 p. San Francisco State Univ., San Francisco, CA.

Hoffman, M.
1978. The use of Pielou's method to determine sample size in food studies. *In* Fish food habits studies: proceedings of the second Pacific Northwest technical workshop (S. J. Lipovsky and C. A. Simenstad, eds.), p 56–61. Washington Sea Grant Publication, Seattle, WA.

Hurtubia, J.
1973. Trophic diversity measurement in sympatric predatory species. Ecology 54(4):885–890.

Jobling, M.
1987. Marine mammal faeces samples as indicators of prey importance—a source of error in bioenergetics studies. Sarsia 72:255–260.

Jobling, M., and A. Breiby.
1986. The use and abuse of fish otoliths in studies of feeding habits of marine piscivores. Sarsia 71:265–274.

Kooyman, G. L., and F. Trillmich.
1986a. Diving behavior of Galapagos fur seals. *In* Fur seals: maternal strategies on land and at sea (R. L. Gentry and G. L. Kooyman, eds), p. 186–195. Princeton Univ. Press, New Jersey, NJ.
1986b. Diving behavior of Galapagos sea lions. *In* Fur seals—maternal strategies on land and at sea (R. L. Gentry and G. L. Kooyman, eds.), p. 209–220. Princeton Univ. Press, Princeton, NJ.

Lowry, M. S., and J. V. Carretta.
1999. Market squid (*Loligo opalescens*) in the diet of California sea lions (*Zalophus californianus*) in southern California (1981–1995). Calif. Coop. Oceanic Fish. Invest. Rep. 40:196–207.

Lowry, M. S., C. W. Oliver, C. Macky, and J. B. Wexler.
1990. Food habits of California sea lions *Zalophus californianus* at San Clemente Island, California, 1981–86. Fish. Bull. 88:509–521.

Lowry, M. S., B. S. Stewart, C. B. Heath, P. K. Yochem, and J. M. Francis.
1991. Seasonal and annual variability in the diet of California sea lions *Zalophus californianus* at San Nicolas Island, California, 1981–86. Fish. Bull. 89:331–336.

Ludwig, J. A., and J. F. Reynolds.
1988. Statistical ecology: a primer on methods and computing, 338 p. John Wiley and Sons, New York, NY.

Magurran, A. E.
1988. Ecological diversity and its measurement, 178 p. Princeton Univ. Press, Princeton, NJ.

Melin, S. R., and R. L. DeLong.
1999. At-sea distribution and diving behavior of California sea lion females from San Miguel Island, California. *In* Proceeding of the fifth California islands symposium (D. R. Browne, K. L. Mitchell, and H. W. Chaney, eds.), p. 407–402. Santa Barbara Museum of Natural History, Santa Barbara, CA.

Murie, D. J., and D. M. Lavigne.
1985. A technique to recovery of otoliths from stomach contents of piscivorous pinnipeds. J. Wildl. Manag. 49: 910–912.

Nolf, D.
1993. A survey of perciform otoliths and their interest for phylogenetic analysis, with an iconographic synopsis of the Percoidei. Bull. Mar. Sci. 52(1):220–239.

Olesiuk, P. F.
1993. Annual prey consumption by harbor seals (*Phoca vitulina*) in the Strait of Georgia, British Columbia. Fish. Bull. 91:491–515.

Orta-Dávila, F.
1988. Hábitos alimentarios y censos globales del lobo marino (*Zalophus californianus*) en el Islote El Racito, Bahía de las Ánimas, Baja California. México durante octubre 1986–1987. Tesis de Licenciatura, 59 p. Universidad Autónoma de Baja California. Ensenada, B.C.

Pitcher, K. W.
1980. Stomach contents and feces as indicators of harbour seal, *Phoca vitulina*, foods in the Gulf of Alaska. Fish. Bull. 78:797–798.

Robison, B. H.
1972. Distribution of the midwater fishes of the Gulf of California. Copeia (1972):449–61
Roper, C. F. E., and R. E. Young.
1975. Vertical distribution of pelagic cephalopods. Smithsonian Contribution to Zoology 209(51):31.
Sanchez-Arias, M.
1992. Contribución al conocimiento de los hábitos alimentarios del lobo marino de California *Zalophus californianus* en las Islas Angel de la Guarda y Granito, Golfo de California, México. Tesis de Licenciatura, 63 p. Universidad Nacional Autonoma de Mexico. México, D.F.
Tollit, D. J., M. J. Steward, P. M. Thompson, G. J. Pierce, M. B. Santos, and S. Hughes.
1997. Species and size differences in the digestion of otoliths and beaks: implications for estimates of pinniped diet composition. Can. J. Fish. Aquat. Sci. 54:105–119.
Walker, B. W.
1960. The distribution and affinities of the marine fish fauna of the Gulf of California. System. Zool. 9(3):123–133.
Wolff, G. A.
1984. Identification and estimation of size from the beaks of 18 species of cephalopods from the Pacific Ocean. NOAA Tech. Rep. NMFS 17, 49 p.

Recruitment and spawning-stock biomass distribution of bay anchovy (*Anchoa mitchilli*) in Chesapeake Bay*

Sukgeun Jung
Edward D. Houde
University of Maryland Center for Environmental Science
Chesapeake Biological Laboratory
1 Williams St., P.O. Box 38
Solomons, Maryland 20688
E-mail address (for S. Jung): jung@cbl.umces.edu

Abstract—Recruitment of bay anchovy (*Anchoa mitchilli*) in Chesapeake is related to variability in hydrological conditions and to abundance and spatial distribution of spawning stock biomass (SSB). Midwater-trawl surveys conducted for six years, over the entire 320-km length of the bay, provided information on anchovy SSB, annual spatial patterns of recruitment, and their relationships to variability in the estuarine environment. SSB of anchovy varied sixfold in 1995–2000; it alone explained little variability in young-of-the-year (YOY) recruitment level in October, which varied ninefold. Recruitments were low in 1995 and 1996 (47 and 31×10^9) but higher in 1997–2000 (100 to 265×10^9). During the recruitment process the YOY population migrated upbay before a subsequent fall-winter downbay migration. The extent of the downbay migration by maturing recruits was greatest in years of high freshwater input to the bay. Mean dissolved oxygen (DO) was more important than freshwater input in controlling distribution of SSB and shifts in SSB location between April–May (prespawning) and June–August (spawning) periods. Recruitments of bay anchovy were higher when mean DO was lowest in the downbay region during the spawning season. It is hypothesized that anchovy recruitment level is inversely related to mean DO concentration because low DO is associated with high plankton productivity in Chesapeake Bay. Additionally, low DO conditions may confine most bay anchovy spawners to the downbay region, where production of larvae and juveniles is enhanced. A modified Ricker stock-recruitment model indicated density-compensatory recruitment with respect to SSB and demonstrated the importance of spring-summer DO levels and spatial distribution of SSB as controllers of bay anchovy recruitment.

Manuscript approved for publication 30 September 2003 by Scientific Editor.
Manuscript received 20 October 2003 at NMFS Scientific Publications Office.
Fish. Bull. 102:63–77 (2004).

Recruitment for marine fishes is variable and is regulated or controlled by a combination of density-dependent and density-independent processes. It has been hypothesized that density-independent processes dominate from the egg to larval stages whereas density-dependent control by predation may be more important in the juvenile stage (Sissenwine, 1984; Houde, 1987). Density-dependent processes may be stock dependent, regulated by adult abundances, or dependent on abundances of the early-life stages (Ricker, 1975). In estuarine systems, where hydrological conditions (e.g. dissolved oxygen, temperature, and circulation) vary widely, the roles of density-independent physical factors on fish recruitments may be dominant, making it difficult, but still important, to partition density-dependent and density-independent processes, particularly for short-lived small pelagic fishes such as anchovies and sardines.

Bay anchovy (*Anchoa mitchilli*) (Engraulidae) is a coastal species distributed broadly in the western Atlantic from Maine to Mexico. This small fish is the most abundant and ubiquitous fish in Chesapeake Bay, the largest estuary on the east coast of North America (Houde and Zastrow, 1991; Able and Fahay, 1998). It is not fished, yet there is evidence that recruitment is variable (Newberger and Houde, 1995). It feeds on zooplankton—primarily copepods and other small crustacea—and is a major prey of piscivores, including several economically important fishes (Baird and Ulanowicz, 1989; Luo and Brandt, 1993; Hartman and Brandt, 1995). Male and female bay anchovy in Chesapeake Bay mature at 40–45 mm fork length (44–50 mm total length) at about 10 months of age, and peak spawning occurs in July (Zastrow et al., 1991). Most eggs are produced by age-1 individuals (Luo and Musick, 1991; Zastrow et al., 1991). Bay anchovy may survive to age 3+ and reach approximately 100 mm length and 5 g wet weight (Newberger and Houde, 1995; Wang and Houde, 1995).

Newberger and Houde (1995) noted large differences in annual survey abundances of bay anchovy that apparently resulted from variability in annual recruitments. In Chesapeake Bay, abundance, growth, and mortality rates of bay anchovy eggs and larvae vary temporally and spatially (Dorsey et al., 1996; MacGregor and Houde, 1996; Rilling and Houde, 1999a, 1999b). Individual-based models were developed to test the hypothesis that recruitment of bay anchovy is determined by variable growth and mortality during early-life stages that are regulated by density-dependent processes (Wang et al., 1997; Cowan et al., 1999; Rose et al., 1999). In previous research, there was little knowledge of levels of spawning stock biomass or density-independent environmental factors that may control recruitment through their effects on spatial and temporal variability in growth and mortality of prerecruit anchovy.

* Contribution 3696 of the University of Maryland Center for Environmental Science, Chesapeake Biological Laboratory, Solomons, MD 20688.

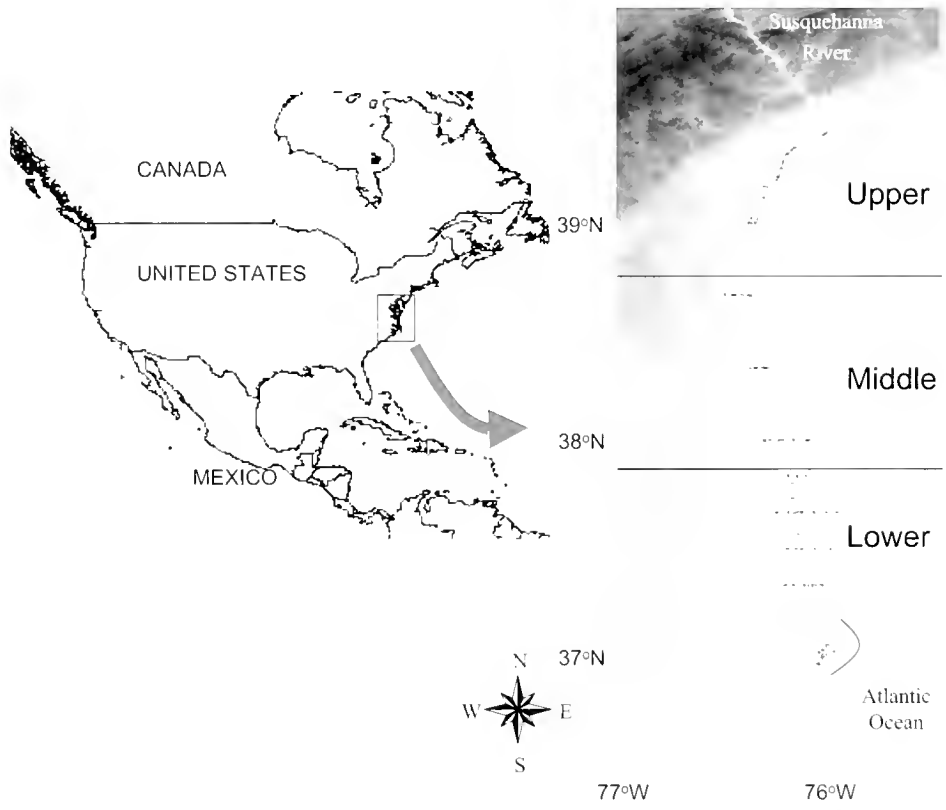

Figure 1

Chesapeake Bay and stations sampled by the midwater trawl in the 1995–2000 surveys. Horizontal lines indicate boundaries of three designated regions.

We evaluated environmental factors, spatial distribution of spawning stock biomass (SSB), and possible ontogenetic migrations of prerecruits (Dovel, 1971; Loos and Perry, 1991; Wang and Houde, 1995; Kimura et al., 2000) with respect to bay anchovy recruitment variability. Our objectives were 1) to estimate annual and regional variability in bay anchovy recruitment, 2) to evaluate effects of hydrological conditions (mainly, freshwater input, and dissolved oxygen concentration) on stage-specific distribution, ontogenetic migration, and recruitment, and 3) to identify mechanisms and describe patterns or trends in the bay anchovy recruitment process. Data were obtained in a six-year, multidisciplinary research program conducted throughout Chesapeake Bay.

Materials and methods

Study area

Chesapeake Bay is a coastal plain estuary of partially mixed fresh water and sea water. Its 320-km mainstem varies in width from about 6 to 50 km (Fig. 1). The Bay is shallow; less than 10% of its area is >18 m deep and approximately 50% is <6 m deep. More than 80% of the freshwater entering the bay is from tributaries on its northern and western sides (Chesapeake Bay Program[1]). Salinity grades from near-full seawater at the mouth of the bay to freshwater near its head. Water temperatures reach 28–30°C in mid summer, and fall to 1–4°C in late winter (Murdy et al., 1997). Despite shallow depth, the bay usually has a strongly developed pycnocline, and has seasonally strong vertical gradients in temperature, salinity, and dissolved oxygen.

Surveys

Trawl surveys were conducted three times annually over the entire bay (April–May, June–August, and October), 1995–2000 (Table 1, Fig. 1). Midwater-trawl (MWT) fish collections[2] were made on transects in three regions: the lower bay (37°05′N–37°55′N), middle bay (37°55′N–38°45′N), and upper bay (38°45′N–39°25′N). As defined, the lower bay contains 51% of water volume, the middle bay 32%, and the upper bay 17% (Fig. 1). The number of midwater trawl sta-

[1] Chesapeake Bay Program. 2000. Chesapeake Bay: Introduction to an ecosystem. U.S. Environmental Protection Agency, publ. EPA 903-R-00-001, 30 p. EPA, 410 Severn Ave, Suite 109, Annapolis, MD 21403.

[2] Trophic interactions in estuarine systems, midwater trawl survey. University of Maryland Center for Environmental Science, Chesapeake Biological Laboratory. http://www.chesapeake.org/ ties/mwt [accessed 15 October 2003].

Table 1

Cruise dates, mean temperatures (°C), salinities (psu), and dissolved oxygen (mg/L), integrated from surface to bottom, and pooled standard errors for individual cruises, years, seasons, and regions of Chesapeake Bay, 1995–2000. CV = coefficient of variation for annual means.

	Temperature	SE	Salinity	SE	Oxygen	SE
Cruise date (departure)						
28 Apr 95	13.88	0.11	15.01	0.42	8.53	0.13
23 Jul 95	28.13	0.12	15.48	0.44	6.50	0.14
28 Oct 95	17.26	0.12	17.39	0.45	7.59	0.14
28 Apr 96	13.87	0.10	10.84	0.36	10.21	0.11
17 Jul 96	24.66	0.11	11.80	0.41	7.43	0.13
22 Oct 96	16.10	0.10	11.26	0.36	8.55	0.11
20 Apr 97	10.93	0.13	11.41	0.50	10.01	0.16
11 Jul 97	25.28	0.13	13.59	0.51	7.10	0.16
29 Oct 97	14.64	0.13	18.19	0.51	8.01	0.16
11 Apr 98	12.26	0.12	8.90	0.44	9.95	0.14
04 Aug 98	26.15	0.12	12.89	0.46	7.01	0.15
19 Oct 98	18.60	0.13	16.64	0.49	8.64	0.15
19 Apr 99	11.97	0.13	13.51	0.49	10.04	0.16
26 Jun 99	23.52	0.15	16.02	0.56	5.75	0.18
23 Oct 99	16.30	0.14	17.38	0.53	8.87	0.17
29 Apr 00	12.95	0.17	12.51	0.64	8.98	0.20
25 Jul 00	24.26	0.14	14.06	0.53	5.17	0.17
17 Oct 00	17.89	0.15	16.73	0.56	7.63	0.18
Year						
1995	19.76	0.07	15.96	0.25	7.54	0.08
1996	18.21	0.06	11.30	0.22	8.73	0.07
1997	16.95	0.08	14.40	0.29	8.37	0.09
1998	19.00	0.07	12.81	0.27	8.53	0.08
1999	17.26	0.08	15.64	0.30	8.22	0.10
2000	18.36	0.09	14.43	0.33	7.26	0.11
CV	5.8%		12.5%		7.2%	
Season						
April–May	12.64	0.05	12.03	0.20	9.62	0.06
June–August	25.33	0.05	13.97	0.20	6.49	0.06
October	16.80	0.05	16.27	0.20	8.22	0.06
Region of bay						
Lower	18.40	0.04	21.19	0.16	8.15	0.05
Middle	18.33	0.05	14.06	0.19	8.33	0.06
Upper	18.04	0.06	7.02	0.23	7.85	0.07

tions per survey ranged from 24 to 52 (six-year total=597). Additional baywide surveys (August 1997 and September 1998) and partial surveys (June 1997, July 1998, and July 1999) also provided data (total stations =146).

An 18-m^2 mouth-opening midwater trawl (MWT), with 3-mm codend mesh was deployed from the stern of the 37-m research vessel *Cape Henlopen*. All trawling was conducted at night. Standardized tows of 20-min duration were conducted and the trawl was deployed at graded depth intervals from surface to bottom (2 minutes at each depth interval) in order to provide a sample of fish from the entire water column. Fish catches (or subsamples) were counted, measured (to the nearest 1.0 mm), and weighed on deck immediately after a tow.

Abundance and biomass of bay anchovy recruits and spawners

We separated bay anchovy catches into YOY and spawners based on total length (TL). The minimum length of bay anchovy retained by the MWT was 21 mm TL, which we also defined as the minimum TL for recruited YOY bay

anchovy. Modal lengths of young-of-the-year (YOY) bay anchovy cohorts were determined from length-frequency distributions in MWT catches and a modal analysis (Bhattacharya, 1967; King, 1995). Based on the modal analysis of summer and fall survey data, the maximum TL of YOY bay anchovy and, therefore, the minimum TL of spawners, were estimated (Table 2).

Length-dependent gear selectivity for bay anchovy was adjusted by comparing catches of the MWT and a 2-m^2 Tucker trawl with catches from 707-μm meshes at the same stations during a September 1998 baywide survey. The length-specific MWT:Tucker-trawl catch ratios (N_{MWT}/N_{TT}=catch per unit of effort MWT ÷ catch per volume of water Tucker trawl) for anchovies 21–70 mm TL indicated that both gears fished with a consistent selectivity for bay anchovy of 30–48 mm TL, and with a slight decrease in N_{TT} for 48–70 mm TL. However, the values of N_{MWT}/N_{TT} were lower by factors of 1~7 for 21–30 mm TL fish, indicating that small anchovies were collected less efficiently by the MWT. We concluded that length classes of anchovies >30 mm TL were equally vulnerable to the MWT and those >48 mm TL were less vulnerable to the Tucker trawl. Accordingly, we adjusted MWT catches of ≤30 mm TL anchovy by multiplying them by a weighting factor estimated from the regression of values of N_{MWT}/N_{TT} for 21–30 mm TL bay anchovy.

$$(\textit{Weighting factor}) = -0.59\ TL + 19.08, \qquad (r^2=0.96)$$

where TL = total length.

The weighting factor equals 1.0 for anchovy >30 mm TL because MWT selectivity is constant for anchovy >30 mm TL. To estimate water sampled in a 20-min MWT tow,

$$D_N = N_{MWT}/V_{MWT} = (1/s) \times N_{TT}/V_{TT}$$

and

$$V_{MWT} = s \times (N_{MWT}/N_{TT}) \times V_{TT},$$

where D_N = the concentration of 31–48 mm TL bay anchovy at a station (i.e. number/m^3);
N_{MWT} = the number of 31–48 mm TL bay anchovy collected per 20-min MWT tow at a station;
V_{MWT} = the effective water volume sampled by a 20-min MWT tow (m^3);
N_{TT} = the number of 31–48 mm TL bay anchovy collected by the 2-m^2 Tucker trawl at the same station;
s = vulnerability to the Tucker trawl (s=1 if all bay anchovies in water volume, V_{TT}, are collected); and V_{TT} is the volume filtered by the Tucker trawl (m^3) estimated from a flowmeter in its mouth.

The mean of N_{MWT}/N_{TT} for 30–48 mm TL bay anchovy during the September 1998 survey indicated that V_{MWT} = 4961 m^3, if 30–48 mm TL bay anchovy did not significantly avoid the mouth of the 2-m^2 Tucker trawl (i.e. s=1). Assuming s=1 (i.e. V_{MWT}=4961 m^3), we estimated "relative" baywide abundance and biomass of YOY and spawners for the 18 surveys from 1995 to 2000.

Table 2

Estimated maximum total lengths of young-of-the-year bay anchovy (mm) from Chesapeake Bay, based on analysis of length-frequency distributions.

Year	Date	Length (mm)
1995	23 Jul	52
	28 Oct	69
1996	17 Jul	57
	22 Oct	68
1997	11 Jul	30
	2 Aug	56
	29 Oct	66
1998	4 Aug	50
	7 Sep	62
	19 Oct	69
1999	26 Jun	30
	23 Oct	65
2000	25 Jul	52
	17 Oct	67

To coarsely estimate a typical value of s, "absolute" baywide spawner biomasses in June–August were estimated for 1995–2000 according to an egg production method (Parker, 1985; Rilling and Houde, 1999a). Bay anchovy eggs had been collected in a 1-m^2 Tucker trawl during the same surveys and provided estimates of egg abundance. The coverage of stations and sampling design for the Tucker trawl was comparable to that of the MWT, but the Tucker trawl was deployed during both day and night. We presumed that all eggs collected between 00:00 and 20:00 h had been spawned near a midnight peak (00:00 h) (Zastrow et al., 1991) and decreased in abundance at a mean instantaneous mortality (reported for bay anchovy eggs in Chesapeake Bay as M = 0.066/h; Dorsey et al., 1996). Based on the estimated number of eggs spawned at 00:00 h for each station, the regional mean weight of individual spawners (defined by the minimum TL in Table 2) in MWT catches, and the reported fecundity-weight relationship for females (Zastrow et al., 1991), we were able to coarsely estimate "absolute" baywide spawner biomass. We assumed that the spawning fraction of adult females per day was essentially 1.0 (i.e. all adult females participated in spawning, Zastrow et al., 1991) and the fecundity-weight relationship was constant over years.

Comparison of the baywide estimates of spawner biomass in June–August based on the egg production method ("absolute" biomass) with estimates based on the MWT catch-per-unit-of-effort ("relative" biomass) indicated that, on average, for 1995 to 2000, s is equal to 0.20. Therefore, the mean effective water volume fished by a 20-min MWT tow was 4961 × 0.20 = 989 m^3.

Because N_{MWT} of bay anchovy was highly variable, even at stations on the same sampling transect, and a mixed model (SAS version 6.12, SAS Inst. Inc., Cary, NC) including spatial covariance (variogram) did not significantly improve precision in annual, seasonal, and regional means or differences of N_{MWT}, a stratified sampling design (Steel and Torrie, 1980), i.e. stratum = region, was adopted. Based on the mean effective water volume ($= s \times V_{MWT}$), we estimated regional "absolute" abundance and biomass (number and wet weight) and related standard errors of the linear combination by regional subvolumes (Samuels, 1989) of bay anchovy ≥21 mm TL for all MWT surveys from 1995 to 2000 by multiplying regional mean MWT catch by $V_r/989$, where V_r represents the water volume (m^3) in each bay region (Cronin, 1971):

$$N_{total} = (N_l \times V_l + N_m \times V_m + N_u \times V_u)/(s \times V_{MWT}) \times V_{total}$$

$$SE_N = Sc_N \sqrt{V_l^2/n_l + V_m^2/n_m + V_u^2/n_u},$$

where N_{total} = baywide absolute abundance;
N_l, N_m, N_u = mean values of N_{MWT} for the lower (l), middle (m), and upper (u) bay;
V_l, V_m, V_u = bay subvolumes for the lower (l), middle (m), and upper (u) bay (from Cronin, 1971), $V_l = 26.7 \times 10^9$ m^3, $V_m = 16.8 \times 10^9$ m^3, $V_u = 8.7 \times 10^9$ m^3, $V_{total} = V_l + V_m + V_u = 52.1 \times 10^9$ m^3;
SE_N = standard error of N_{total};
n_l, n_m, n_u = number of midwater trawl stations for the lower (l), middle (m), and upper (u) bay;
Sc_N = pooled standard deviation of N_{MWT} = square root of mean squares within groups in analysis of variance table = $\sqrt{(SS_l + SS_m + SS_u)/(n_{total} - 3)}$, where SS_l, SS_m, SS_u = sum of squares of N_{MWT} for the lower (l), middle (m), and upper (u) bay, and $n_{total} = n_l + n_m + n_u$.

Environmental factors

Depth profiles of temperature, salinity, and dissolved oxygen (DO) concentration were determined from conductivity-temperature-depth (CTD) casts at sampling stations. DO data were adjusted by calibrating against Winkler titration data from water samples collected in Niskin bottles deployed with the CTD cast. However, DO data from the CTD could not be adjusted for the 1999 summer and all calendar year 2000 cruises because Winkler titrations were not conducted. To estimate regional means for the water column, we averaged temperature, salinity, and DO values by integrating the observed values with respect to depth, after dividing the water column into "above pycnocline" and "subpycnocline" layers.

Ontogenetic migration

We analyzed length-frequency distributions along the south-north axis of the bay (i.e. by latitude) to delineate possible ontogenetic migrations of YOY and adult bay anchovy. To parameterize the distribution of YOY and adult abundance and biomass, we estimated the biomass-weighted mean latitudes of occurrence for each length class (3-mm interval).

$$\bar{L}_{B,l} = \sum_k B_{k,l} L_k / \sum_k B_{k,l},$$

where $\bar{L}_{B,l}$ = biomass-weighted mean latitude of a length class, l;
L_k = latitude of the station, k; and
B = biomass (g, wet weight) per 20-min tow.

We devised a metric to parameterize the location of bay anchovy SSB. We assumed that the baseline boundary for SSB distribution during the spring was at the mouth of the bay (37°00′N). Then, the upbay difference between biomass-weighted mean latitude of SSB (in decimal units) in Jun–August and the baseline for SSB during the spring (ΔL) was calculated:

$$\Delta L = \left(\begin{array}{c} \text{biomass-weighted mean latitude of} \\ \text{SSB in June – August} \end{array} \right) - 37.00.$$

Recruitment model

As an exploratory step, a correlation analysis was undertaken to examine the relationships between bay anchovy SSB, migration patterns, and recruitment levels with respect to regional and depth-layer-specific mean temperature, mean salinity, mean DO, their gradients, and monthly mean freshwater flow from the Susquehanna River. Cross-correlations revealed that SSB migration pattern (ΔL), regional mean DO concentrations, and October YOY recruitment level were closely correlated. Regional mean DO concentration provided the best fit to YOY recruitment level in October when baywide SSB also was included as an explanatory variable in multiple regressions. However, because there is uncertainty in the uncalibrated DO measurements in 1999 and 2000, we did not use regional mean DO in our recruitment model. Instead, we developed a modified Ricker-type stock-recruitment model (Ricker, 1975) that included ΔL as an explanatory variable:

$$R_y = a\, S \exp(-\beta_1 S - \beta_2 \Delta L) + \varepsilon_y \quad \text{(modified Ricker model)}$$

where R_y = recruitment level = October YOY abundance in each year (1995–2000);
y; a, β_1 and β_2 = regression coefficients;
S = estimated baywide SSB (male+female) in metric tons for April–May; and
ε_y = the error term.

In this model, if ΔL is held constant, R_y is maximum at $S = 1/\beta_1$. Although no abiotic factor was included explicitly in the model, ΔL is strongly correlated with regional mean DO and serves as a proxy for it. For the modified Ricker model, collinearity, and jackknife influence diagnostic tools were

Table 3

Seasonal mean freshwater flow entering Chesapeake Bay from the Susquehanna River (m^3/s). Data source: http://va.water.usgs.gov/chesbay/RIMP/adaps.html.

Period	1995	1996	1997	1998	1999	2000
Jan–Mar	1289	2495	1474	2563	1325	1379
Apr–Jun	728	1702	920	1625	791	1627
Jul–Sep	238	768	239	334	294	393
Oct–Dec	923	2230	746	194	642	504
Annual mean	795	1799	845	1179	763	976

applied to evaluate reliability of the regression model (Belsley et al., 1980; SAS, 1989).

Results

Environmental factors

Stream flows from the Susquehanna River (Table 3) varied annually and seasonally. Freshwater stream flows were higher in 1996 and 1998 than in other years. Baywide mean values of water temperature, salinity, and DO concentration, averaged from surface to bottom, varied annually, seasonally, and regionally (Table 1). Annually, mean temperature was highest in 1995 and lowest in 1997. Mean salinity was highest in 1995 and lowest in 1996. Mean DO concentration was highest in 1996 and lowest in 2000. Regionally, salinity was more variable than temperature and DO concentration. Seasonally, temperature and DO concentration were more variable than salinity. Temperature was highest in the June–August period, the spawning season of bay anchovy. Seasonally, salinity increased progressively from April–May to October. Mean DO concentration was consistently lowest in June–August.

Trends in abundance and recruitment

Estimates of bay anchovy abundance reported in our study are for the entire mainstem of Chesapeake Bay. The estimated recruitment levels (baywide abundance of YOY bay anchovy >30 mm TL in October) varied ninefold and were low in 1995 and 1996 (47.5 $\pm$16.6 and 30.6 $\pm 8.6 \times 10^9$ individuals) but much higher in 1997–2000 (99.6 $\pm$12.4 to 264.8 $\pm 32.6 \times 10^9$). Baywide estimates of bay anchovy biomass for individuals >30 mm TL increased from April to October in each year (Table 4). October baywide biomass varied sevenfold from 27.1 $\pm 5.5 \times 10^3$ to 192.9 $\pm 20.4 \times 10^3$ tons and was highest in 1998 and lowest in 1996.

Estimated spawning stock biomass (SSB) in April–May was lowest in 1995 (3.3 $\pm 1.1 \times 10^3$ tons), and highest in 1997 (20.1 $\pm 5.3 \times 10^3$ tons), indicating sixfold variability. SSB in June–August was lowest in 1996 (2.4 $\pm 0.2 \times 10^3$ tons), and highest in 1997 (21.1 $\pm 2.3 \times 10^3$ tons). The SSBs in April–May and June–August did not show any obvious relationship to YOY abundance (recruitment) in October.

Ontogenetic migration

The length-specific mean locations (latitudes of occurrence) of bay anchovy revealed an apparent ontogenetic migration. Small juveniles of bay anchovy tended to move upbay and were located primarily upbay until they were approximately 45 mm TL, after which they began to move downbay (Fig. 2). In April–May, age-1 bay anchovy <60 mm TL, consisting of individuals recruited from the previous year, varied annually in their mean latitude of occurrence, whereas large (≥age 1, ≥60 mm TL) bay anchovy had relatively stable locations near the boundary between the lower and middle bay regions, centered at latitude 37°40′N (Fig. 2A). Compared to April–May, age-1+ bay anchovy in June–August were more variable in their annual mean locations, but both YOY and adult bay anchovy tended to occur upbay of latitude 38°00′N, except in year 2000 (Fig. 2B). In 1997 and 1999, when annual mean temperatures were lowest (Table 1), YOY bay anchovy were too small to be sampled by the MWT in June–August and are not represented in Figure 2B. In October, mean latitudes of occurrence (Fig. 2C) indicated a consistent distribution pattern and an apparent ontogenetic migration by YOY anchovy. The most probable explanation for the observed latitudinal distributions was that small YOY bay anchovy tended to move upbay initially, but then downbay at about 45 mm TL. Distribution of age-1+ individuals in October was variable.

The SSB of bay anchovy (excludes YOY) from 1995 to 2000 was centered near 38°00′N in April–August except in June–August of 1995 and 1996, when the SSB was centered farther upbay (Fig. 3A). In 2000, the migration pattern differed from other years. Spawning bay anchovy in 2000 were located farther downbay in July than in April (Fig. 3A). The April–May location of prespawning SSB was mostly explained by the mean flow of the Susquehanna River from June of the previous year to February of the current year (r^2=0.94, P=0.0012; Fig. 3B). But, in June–August, the mean location of spawning fish was more strongly and significantly related to the subpycnocline-layer mean

Table 4

Baywide abundance and biomass estimates for bay anchovy >30 mm TL (young-of-the-year + adult). SE = standard error.

		Abundance ($\times 10^9$)		Biomass ($\times 10^3$ metric tons)	
Year	Period	Estimate	SE	Estimate	SE
1995	April–May	2.1	0.7	3.3	1.1
	June–August	57.8	28.1	32.6	17.5
	October	47.5	16.6	51.9	21.0
1996	April–May	4.9	1.1	8.9	2.0
	June–August	5.3	1.6	3.7	1.3
	October	30.6	8.6	27.1	5.5
1997	April–May	11.8	3.3	20.1	5.3
	June–August	9.4	2.3	21.1	5.0
	October	99.6	12.4	85.6	10.8
1998	April–May	3.5	0.7	6.1	1.3
	June–August	14.4	4.5	17.0	7.9
	October	264.8	32.6	192.9	20.4
1999	April–May	6.9	1.4	10.6	2.2
	June–August	5.5	1.2	10.6	2.4
	October	124.5	28.3	115.3	25.0
2000	April–May	6.2	4.1	13.0	6.6
	June–August	144.6	51.2	56.0	17.0
	October	169.1	43.7	152.9	40.0

DO during that same period in the middle bay (r^2=0.75, P=0.02; Fig. 3C).

Correlations

Correlation analyses suggested that regional mean DO concentrations are the most important environmental correlate associated with spatial distribution of SSB and recruitment processes of bay anchovy. The mean locations (latitudes of occurrence), abundances, and biomasses for YOY and adult bay anchovy were analyzed with respect to environmental variables (Table 5). Recruitment levels (YOY abundance) in October were consistently inversely correlated with DO concentrations in the lower and middle bay in June–August (r=–0.13 to –0.89). Biomass-weighted mean latitude of SSB (age 1+) in April–May was consistently and positively correlated with regional salinities in April–May (r=0.30 to 0.88). On the other hand, in June–August, surface-layer mean salinity in the lower Bay and subpycnocline-layer mean DO in the lower and middle bay were significantly and positively correlated with mean latitude of SSB or ΔL (r=0.82 to 0.91). Baywide SSB in April–May and June–August tended to be negatively correlated with water temperature in April–May (r=–0.45 to –0.90).

Recruitment model

Although SSB alone did not correlate significantly with recruitment level, mean DO in June–August was significantly related to the mean latitude of SSB in June–August (or ΔL) and bay anchovy recruitment level in October (Figs. 3C and 4). ΔL was selected as the explanatory variable, rather than DO, because DO data were uncalibrated in 1999 and 2000. The correlation observed between ΔL and DO (Fig 3C) suggested that ΔL can serve as a proxy for DO in the stock-recruitment model. Including ΔL and SSB for April–May in a modified Ricker model provided a good fit to bay anchovy recruitment levels observed from 1995 to 2000 (Fig. 5). The model is

$$R_y = 365\, S \exp(-0.19\, S\, 1.35\, \Delta L) \quad \text{(modified Ricker model)}.$$

In the model, if ΔL is held constant, predicted recruitment level of bay anchovy is maximum when baywide SSB in April–May is approximately 5.3×10^3 tons. Collinearity and influence diagnostic statistics did not indicate collinearity between the two independent variables (S and ΔL), or that an observation in any year had a dominating influence on parameter estimates.

Discussion

Complex environmental processes and biological interactions control bay anchovy recruitment in Chesapeake Bay. Dissolved oxygen (DO), freshwater flow, salinity, and temperature acting on prerecruits and adults are important factors affecting bay anchovy distribution and levels of recruitment. Spawning stock size also is related to recruit-

ment level. Our results have demonstrated that there is a strong spatial component in the recruitment dynamics of bay anchovy. Although fish recruitment processes historically have been difficult to understand, our six-year, spatially extensive research has provided new insights into processes that control bay anchovy recruitment.

Ontogenetic migration pattern

It is apparent that ontogenetic migration plays a role in the spatial and temporal patterns in abundance, biomass, and production of bay anchovy. There are several lines of evidence. Rilling and Houde (1999a), in a baywide analysis, reported that mean density of eggs and larvae in June and July 1993 was very high in the lower Chesapeake Bay compared to more upbay sites. Dovel (1971) and Loos and Perry (1991) reported possible upbay or upriver migration of bay anchovy larvae and juveniles in the mainstem and tributaries of the Bay. Recent otolith microchemical analyses have strongly supported the hypothesis that an upbay ontogenetic migration by small YOY anchovy (≥25 mm, late larvae and small juveniles) occurs (Kimura et al., 2000). In the middle Hudson River estuary (Schultz et al., 2000) and Chesapeake Bay (North and Houde, in press), selective tidal-stream transport was suggested as a mechanism for up-estuary movements of bay anchovy larvae. Our conceptual model of the bay anchovy life cycle includes migration patterns in the bay based on available knowledge and evidence (Fig. 6).

It is uncertain what benefits YOY bay anchovy derives from upbay migration in summer and whether the migration is passive or active before a subsequent reverse migration in the fall. To explain upbay movements of estuarine fishes, Dovel (1971) proposed that there is a "critical zone" of low salinity and high prey production in the upper bay, which is important as a nursery for bay anchovy and other fish species. In late spring and early summer, age-1 and age-1+ bay anchovy mature and move upbay while spawning, although the year 2000, when mean freshwater streamflow during the previous fall-winter was lowest, was an exception. Recruited YOY bay anchovy apparently overwinter primarily, but not entirely, downbay until spring.

There remains a possibility of significant immigration to the bay by adult bay anchovy in some years from the coastal ocean or tidal tributaries of the bay. Without such immigration, baywide adult abundance would decrease continuously during the April–October period through natural mortality. However, in two years of our six-year study, 1995 and 1998, estimated adult abundance increased substantially from April to July, and in 1999 adult abundance increased from June to October, implying significant immigration to the bay in those years (Jung, 2002).

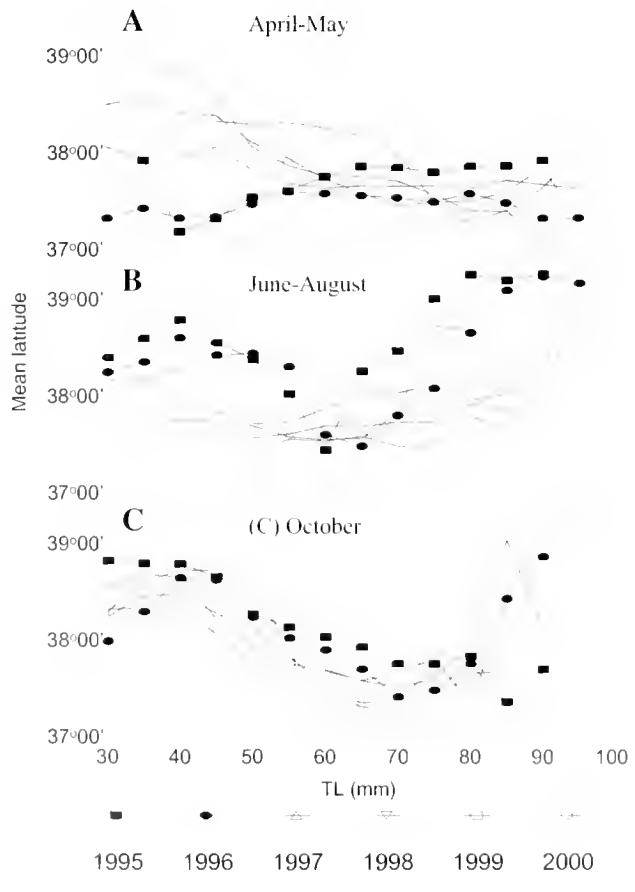

Figure 2

Abundance-weighted mean latitude of occurrence of bay anchovy (*Anchoa mitchilli*) in Chesapeake Bay, 1995–2000.

Recruitment control and regulation

The modified Ricker recruitment model that included SSB and ΔL as explanatory variables provided a good fit to bay anchovy recruitments. Although the model fitted well, there were only six years of data, and the underlying mechanisms explaining relationships between the distribution and level of SSB, hydrological conditions, and density-dependent regulatory processes in recruitment of bay anchovy are not yet clear. Nevertheless, correlations and the recruitment model clearly indicated a density-dependent effect of SSB level and also implicated environmental factors (at the mesoscale) that are related to mean DO concentration, latitudinal distribution of SSB (ΔL), and the recruitment level of bay anchovy (Fig. 4).

The modified Ricker model for bay anchovy (Fig. 5) indicates a density-compensatory stock-recruitment relationship (Ricker, 1975), although we do not know at what life stages density-dependent processes are most important. Without accounting for the controlling effect of ΔL and mean DO on a regional scale, the density-dependence might have gone undetected (Fig. 4). Recent individual-based models suggest that density-dependent processes during early-life stages could stabilize bay anchovy recruitments (Wang et al., 1997; Cowan et al., 1999; Rose et al., 1999). At the small scales of several meters modeled by Wang et al. (1997) and Cowan et al. (1999), larval-stage feeding

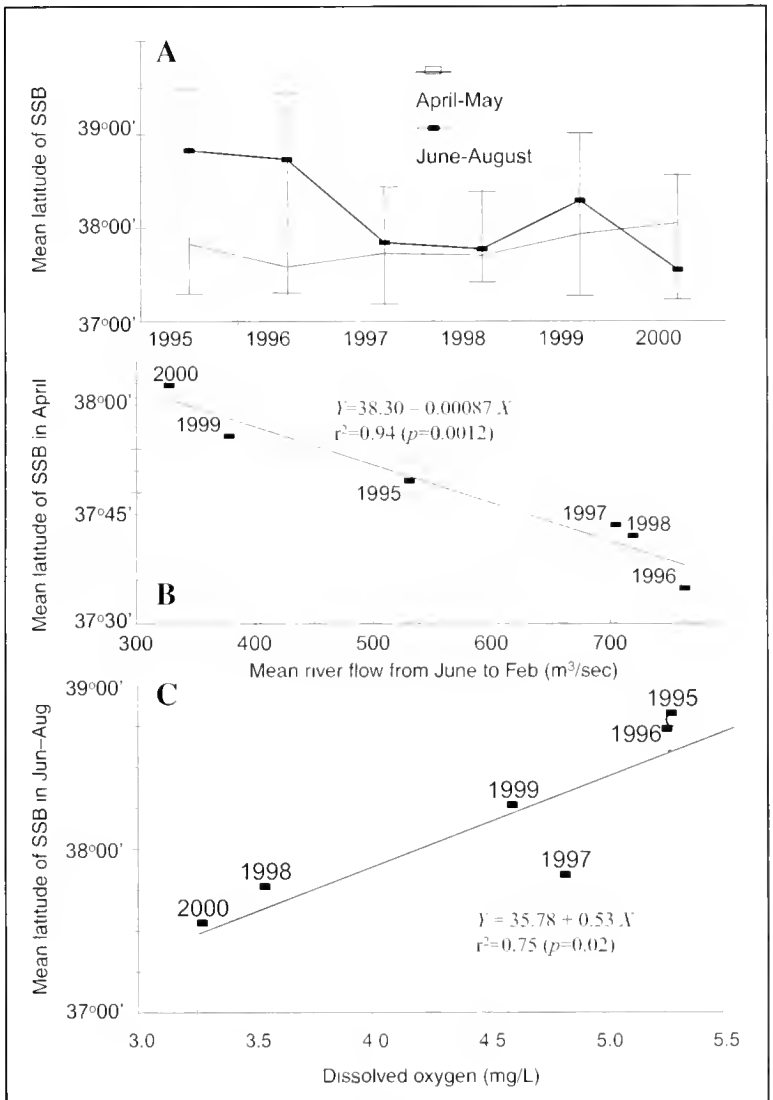

Figure 3

Mean location (latitude) of adult bay anchovy (*Anchoa mitchilli*) spawning stock biomass (SSB) in Chesapeake Bay. (**A**) Mean latitude and standard deviation in April–May and in June–August. The upper vertical bar represents mean + standard deviation for June–August, and the lower vertical bar represents mean–standard deviation for April–May. (**B**) Mean latitude in April–May and mean Susquehanna River flow from June of the previous year to February of the current year. (**C**) Mean latitude in June–August and mean dissolved oxygen in the subpycnocline layer of the middle bay in June–August.

processes were important and high adult SSB could produce abundant first-feeding larvae with subsequent density-dependent food competition. In Tampa Bay, Florida, Peebles et al. (1996) hypothesized that bay anchovy's size-specific fecundity is directly related to prey availability for adults. Modeled results of Rose et al. (1999) suggested that density-dependent growth of bay anchovy larvae and juveniles in Chesapeake Bay would lead to density-dependent survival of these stages. Hunter and Kimbrell (1980) and Alheit (1987) proposed that cannibalism by adults on eggs and larvae provides a degree of density-dependent regulation in anchovies of the genus *Engraulis*. Analyses of feeding by adult bay anchovy did not indicate that pelagic fish eggs were a significant part of bay anchovy diet (Vazquez-Rojas, 1989; Klebasko, 1991), although no specific study of cannibalism has been undertaken.

We propose three hypotheses that may explain the relationships among regional DO concentration, the latitudinal shift in SSB distribution during the spawning season (ΔL), and recruitment levels of bay anchovy in October. The

hypotheses are the following: 1) averaged DO concentration is inversely related to levels of plankton productivity in a region and high plankton productivity favors high recruitments of planktivorous bay anchovy; 2) low dissolved oxygen concentrations can restrict spatial distribution of bay anchovy SSB to the lower bay insuring high egg and

Table 5

Cross-correlation coefficients for bay anchovy distribution and abundance with respect to region- and layer-specific means of temperature, salinity, and dissolved oxygen from 1995 to 2000. Mean latitude is biomass-weighted mean latitude of occurrence of bay anchovy. Abundance and biomass are baywide total estimates. ΔL = (mean latitude in June–August) –37.00. Abbreviations are as follows: SAL = salinity, TEM = water temperature, OXY = dissolved oxygen; the fourth and fifth digits: 04 = April–May, 07 = June–August; the sixth character: L = lower bay, M = middle bay, U = upper bay; The last character: S = layer above the pycnocline, B = layer below the pycnocline. * = significant at $\alpha = 0.05$.

	Young-of-the-year		Adult			
	Mean latitude	Abundance	Mean latitude		Biomass	
	October	October	April–May	June–August (or ΔL)	April–May	June–August
SAL04LS	0.29	–0.43	0.74	0.26	–0.17	–0.52
SAL04MS	0.45	–0.63	0.30	0.71	–0.41	–0.22
SAL04US	0.27	–0.60	0.42	0.53	–0.18	–0.02
SAL04LB	–0.24	0.01	0.88*	–0.16	–0.14	–0.31
SAL04MB	0.08	–0.17	0.59	0.33	–0.39	–0.05
SAL04UB	0.29	–0.61	0.45	0.46	–0.03	0.05
SAL07LS	0.83*	–0.75		0.91*		–0.46
SAL07MS	–0.12	0.06		0.14		0.31
SAL07US	0.06	–0.03		–0.04		–0.33
SAL07LB	0.70	–0.75		0.64		–0.11
SAL07MB	–0.41	0.60		–0.31		0.19
SAL07UB	0.15	–0.20		0.01		–0.42
TEM04LS	0.16	–0.25	–0.03	0.65	–0.90*	–0.48
TEM04MS	0.50	–0.46	0.14	0.65	–0.71	–0.85*
TEM04US	0.53	–0.32	–0.36	0.52	–0.56	–0.85*
TEM04LB	0.29	–0.49	0.19	0.71	–0.72	–0.45
TEM04MB	0.22	–0.42	0.39	0.47	–0.55	–0.62
TEM04UB	0.40	–0.26	–0.39	0.48	–0.60	–0.77
TEM07LS	–0.49	–0.04		0.11		0.45
TEM07MS	–0.16	–0.21		0.47		0.14
TEM07US	–0.29	–0.08		0.39		0.38
TEM07LB	–0.68	0.24		–0.11		0.38
TEM07MB	–0.24	–0.10		0.37		–0.04
TEM07UB	–0.45	0.16		0.21		0.46
OXY04LS	0.63	–0.22	–0.80	0.39	–0.10	–0.30
OXY04MS	–0.27	0.56	0.23	–0.81	0.55	–0.04
OXY04US	–0.43	0.41	–0.30	–0.30	0.30	0.88*
OXY04LB	0.93*	–0.68	–0.59	0.63	0.04	–0.38
OXY04MB	0.47	–0.35	–0.31	–0.09	0.70	–0.12
OXY04UB	–0.57	0.65	–0.32	–0.46	0.21	0.78
OXY07LS	0.18	–0.30		0.29		0.32
OXY07MS	0.01	–0.13		0.29		0.56
OXY07US	0.23	–0.32		0.50		0.10
OXY07LB	0.67	–0.48		0.82*		–0.28
OXY07MB	0.72	–0.89		0.87*		–0.04
OXY07UB	0.01	0.16		0.21		0.37

larval production there; and 3) density-depensatory predator satiation occurs when concentrations of bay anchovy larvae and juveniles at the mesoscale (10–100 km) are high in relation to satiation potential of predators, which favors larval production and high anchovy recruitments.

First, averaged DO level in the bay or its regions may be an indicator of ecosystem metabolism and secondary production. DO level in the subeuphotic layer is an indicator of respiration and secondary production by planktonic and benthic communities (Kemp and Boynton, 1980; Kemp et al., 1992). Recruitment levels of bay anchovy increased substantially in 1997 and in subsequent years. We speculate that enhanced detrital production potentially increased zooplankton prey abundances in the subsequent year and that associated elevated levels of respiration by detrital microorganisms and zooplankton contributed to low mean DO. Increased zooplankton prey abundances, in turn, may have promoted production of larval and juvenile bay anchovy in 1997 and 1998. Thus, increased prey availability, associated with low mean DO concentration, could have enhanced recruitment (Fig. 4).

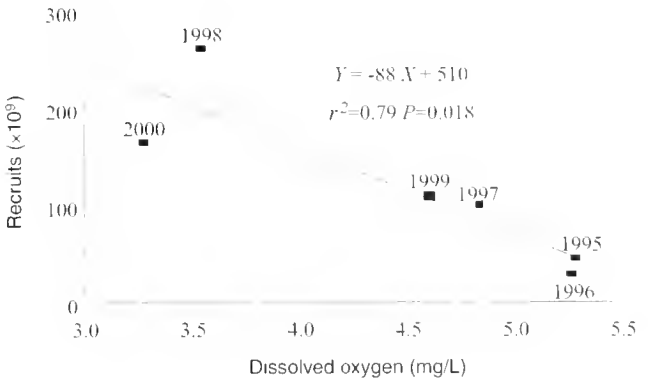

Figure 4

Relationship between mean dissolved oxygen below the pycnocline in the middle Chesapeake Bay during the June–August period and recruitment level of bay anchovy in October. r^2 = coefficient of determination.

The second hypothesis proposes that spatial restriction of SSB by low DO is a factor controlling bay anchovy recruitment. Based on our results, hypoxic conditions in the bay appear to define the distribution and potential for upbay migration of bay anchovy SSB (Fig. 3C). In years when the baywide subpycnocline mean DO level was low, spawning bay anchovy tended to be most concentrated in the lower bay (Table 5, Fig. 3, A and C), possibly because hypoxia in deeper waters of the mid-bay region discouraged upbay migration. The region selected by adult anchovy as the predominant spawning area and its variability played

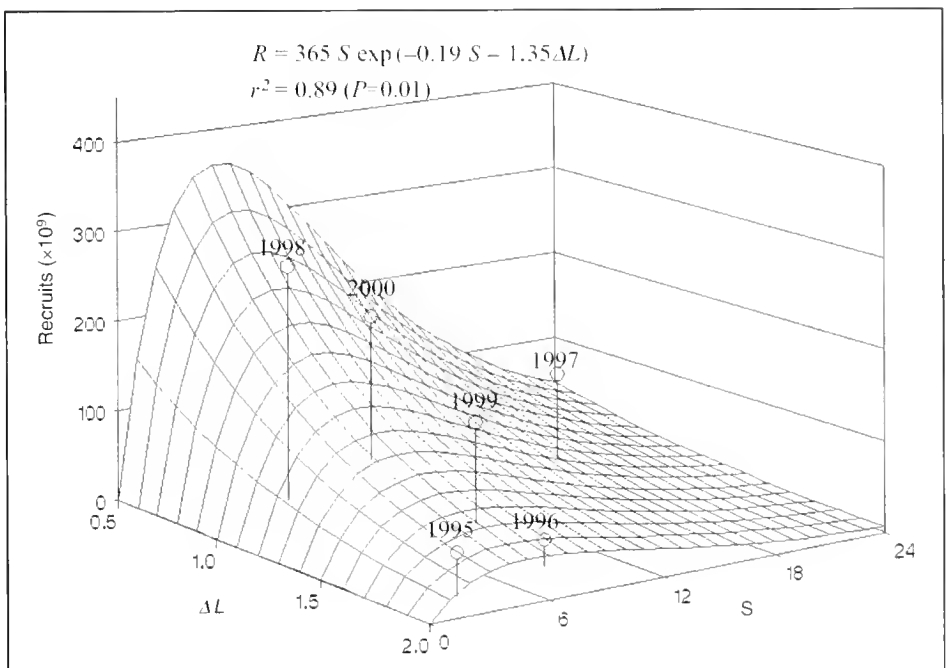

Figure 5

Stock-recruitment model (modified Ricker model). R = baywide number of recruits in October ($\times 10^9$). ΔL = location of bay anchovy (*Anchoa mitchilli*) spawning stock biomass in June–August in relation to the baseline latitude at the mouth of the bay, 37°00′N. S = baywide spawning stock biomass (SSB $\times 10^3$ metric tons for April–May). Balloon symbols are observed data from 1995 to 2000.

a strong role in controlling YOY recruitment levels. The four highest recruitment years in our series had the lowest mean subpycnocline DO levels and had distribution patterns of SSB that differed little between the prespawning April–May and spawning June–August periods (Fig. 4). Although we do not fully understand how DO, and possibly hypoxic conditions, affect migratory behavior and distribution patterns of bay anchovy, hypoxia in Chesapeake Bay has been demonstrated in other research to affect spatial and temporal patterns of fish abundance, including bay anchovy (Breitburg, 1992; Keister et al., 2000).

Our third hypothesis proposes that predation is an important regulator of fish recruitment in early-life stages (Sissenwine, 1984; Bailey and Houde, 1989). We hypothesize that abundant and spatially concentrated larval or juvenile anchovy, as observed in the lower bay, could promote early-life survival by satiating predators, even if some predators migrate to areas where larval and juvenile anchovy are abundant. At mesoscale distances of 10–100 km, distribution of predators (e.g. YOY and age-1 weakfish [*Cynoscion regalis*]) may be important. If the maximum number of prey that can be eaten by predators is reasonably constant, the effect of predation can be density-dependent (Hilborn and Walters, 1992), i.e. predation mortality rate decreases as prey density increases.

In support of the third hypothesis, a correspondence analysis on fish species assemblages by year, season, region, and life stage (Jung and Houde, 2003) indicated that distributions and abundances of YOY weakfish, a major predator of bay anchovy in Chesapeake Bay (Hartman and Brandt, 1995), and YOY bay anchovy were closely associated spatially, seasonally, and annually in our six-year study. The major spawning area of bay anchovy is spatially restricted. If predator migration to the area is limited, then as the supply of larvae and juveniles increases, it may saturate predator demand, the condition necessary for depensation to be important.

It may seem contradictory to propose that density-compensation with respect to SSB (the negative sign of β_1) and density-depensation with respect to ΔL (the second or third hypothesis) can act simultaneously during larval and juvenile stages. Under this circumstance, the number of surviving postlarval anchovies is hypothesized to decrease because of food limitation when larval abundance is high, reducing subsequent predation-related mortality rate on postlarvae and small juveniles. Low abundance of anchovy early-life stages will lead to the opposite effect (Fig. 7). The proposed opposing responses of the early-larval and late-larval–juvenile stages are explained by differences in the spatial scales of distribution and densities of life stages of bay anchovy (Fig. 7). The spatial scale of processes that affect distributions of late-stage larvae and juveniles is large compared to that for early-stage larvae because of the increased dispersal and swimming ability of juveniles. Comparing early-larval and late-larval–juvenile stages of bay anchovy, we propose that effects of prey concentration (the first hypothesis) and SSB level (density-compensation) act primarily on the dynamics of early-larval stages, whereas predation mortality and the inhibitory effects of low DO (density-depensation; the second and third hypotheses) are more important regulators and controllers, respectively, during late-larval and juvenile stages.

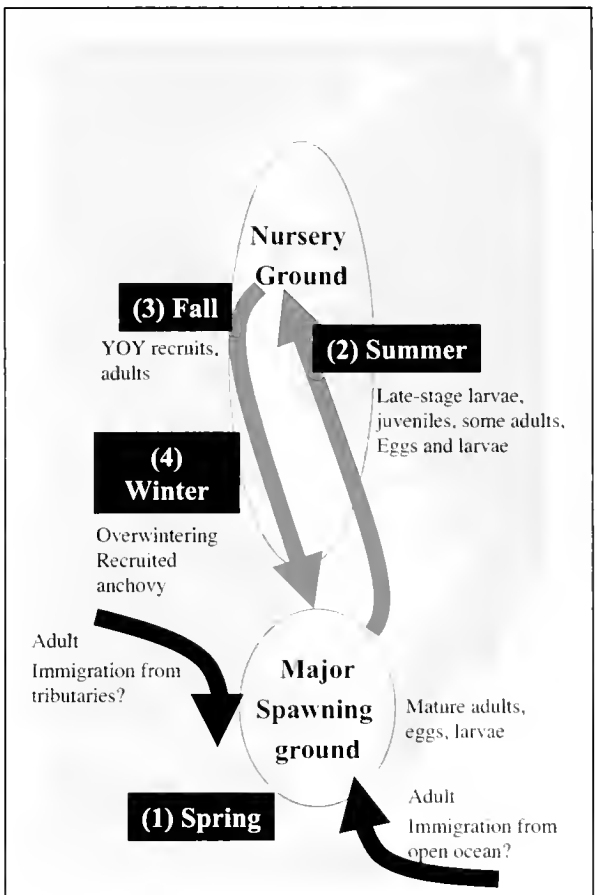

Figure 6

Conceptual model representing bay anchovy (*Anchoa mitchilli*) life cycle and ontogenetic migration within Chesapeake Bay, and possible immigration of adults from tributaries and coastal ocean.

The three hypotheses that relate DO, SSB distribution, and recruitment of bay anchovy are not mutually exclusive. If low mean DO level is an indicator of enhanced prey production and availability to larvae and juveniles, increased prey productivity in the lower bay could enhance bay anchovy recruitment potential by supplying enough zooplankton prey to spawning adults, larvae, and juveniles. At the same time, low mean DO in the mid-Bay could confine most spawning bay anchovy to the lower bay, thus increasing spawning and larval production there, and possibly enhancing survival of juveniles by predator satiation. Ultimately, other hypotheses may provide better explanations of the relationships between regional mean DO, latitudinal shifts in distribution of spawners, abundances of spawners, and recruitment of bay anchovy. For example, abundant gelatinous organisms, such as the scyphomedusa (*Chrysaora quinquecirra*) and the lobate ctenophore (*Mnemiopsis leidyi*), can be important predators on early-stage anchovy and competitors with juveniles and adults (Purcell et al.,

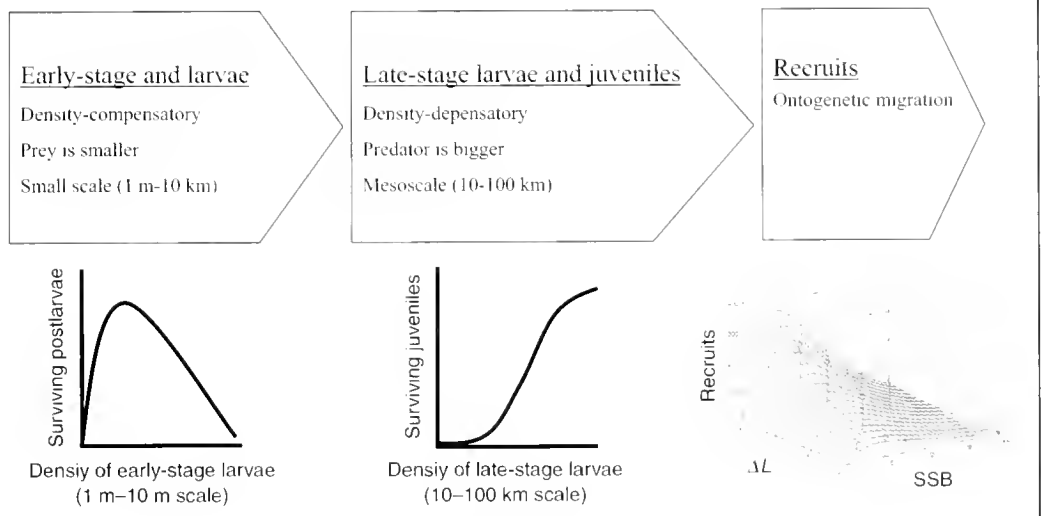

Figure 7

Hypotheses and conceptual model of the bay anchovy (*Anchoa mitchilli*) recruitment process in Chesapeake Bay. The density-compensatory process acts at a small spatial scale during the early-larval stages, whereas the density-depensatory process acts at a broader spatial scale during late-stage larval and juvenile stages. The ontogenetic migration is controlled by dissolved oxygen levels and other hydrological factors.

1994), but their potential role with respect to bay anchovy recruitment could not be defined in our study. For the present, it is clear that most spawning occurs in the lower and mid Chesapeake Bay, from which larval and juvenile anchovies disperse upbay. We hypothesize that food availability is the major factor controlling production of bay anchovy early-larval stages whereas predation becomes more important during late-larval and juvenile stages. Our results and hypotheses implicate density-related processes, operating at different spatial scales, as regulators of recruitment of bay anchovy in Chesapeake Bay.

Acknowledgments

We thank S. Leach, E. North, J. Hagy, C. Rilling, J. Cleveland, A. Madden, D. O'Brien, B. Pearson, D. Craige, T. Auth, and the able crew of RV *Cape Henlopen* for assistance in field surveys. T. Miller and E. Russek-Cohen provided comments and assistance on statistical analyses. This research was supported by a U.S. National Science Foundation, Land Margin Ecosystem Research (LMER) program grant, "Trophic interactions in estuarine systems (TIES)" (grant DEB94-12113). Additional support was provided by NSF Grant OCE-9521512 and by National Oceanic and Atmospheric Administration grant NOAA, NA17OP2656.

Literature cited

Able, K. W., and M. P. Fahay.
1998. The first year in the life of estuarine fishes in the Middle Atlantic Bight, 342 p. Rutgers Univ. Press, New Brunswick, NJ.

Alheit, J.
1987. Egg cannibalism versus egg predation: their significance in anchovies. S. Afr. J. Mar. Sci. 5:467–470.

Bailey, K. M., and E. D. Houde.
1989. Predation on eggs and larvae of marine fishes and the recruitment problem. Adv. Mar. Bio. 25:1–83.

Baird, D., and R. E. Ulanowicz.
1989. The seasonal dynamics of the Chesapeake Bay ecosystem. Ecol. Monogr. 59:329–364.

Belsley, D. A., E. Kuh, and R. E. Welsch.
1980. Regression diagnostics: identifying influential data and sources of collinearity, 292 p. John Wiley and Sons, Inc., New York, NY.

Bhattacharya, C. G.
1967. A simple method of resolution of a distribution into Gaussian components. Biometrics 23:115–135.

Breitburg, D. L.
1992. Episodic hypoxia in Chesapeake Bay: Interacting effects of recruitment, behavior, and physical disturbance. Ecol. Monogr. 62:525–546.

Cowan, J. H., K. A. Rose, E. D. Houde, S. B. Wang, and J. Young.
1999. Modeling effects of increased larval mortality on bay anchovy population dynamics in the mesohaline Chesapeake Bay: evidence for compensatory reserve. Mar. Ecol. Prog. Ser. 185:133–146.

Cronin, W. B.
1971. Volumetric, areal, and tidal statistics of the Chesapeake bay estuary and its tributaries, 15 p. Chesapeake Bay Institute, Johns Hopkins Univ., Baltimore, MD.

Dorsey, S. E., E. D. Houde, and J. C. Gamble.
1996. Cohort abundances and daily variability in mortality of eggs and yolk-sac larvae of bay anchovy, *Anchoa mitchilli*, in Chesapeake Bay. Fish. Bull. 94:257–267.

Dovel, W. L.
1971. Fish eggs and larvae of the upper Chesapeake Bay. Chesapeake Biological Laboratory, special report 4, 71 p. Natural Resource Institute, Univ. Maryland, College Park, MD.

Harding, L. W., M. E. Mallonee, and E. S. Perry.
2002. Toward a predictive understanding of primary productivity in a temperate, partially stratified estuary. Estuar. Coast. Shelf Sci. 55:437–463.

Hartman, K. J., and S. B. Brandt.
1995. Predatory demand and impact of striped bass, bluefish, and weakfish in the Chesapeake Bay: applications of bioenergetics models. Can. J. Fish. Aquat. Sci. 52: 1667–1687.

Hilborn, R., and C. J. Walters.
1992. Stock and recruitment. *In* Quantitative fisheries stock assessments: choice, dynamics, and uncertainty (R. Hilborn and C. J. Walters, eds.), p. 241–296. Chapman & Hall, New York, NY.

Houde, E. D.
1987. Fish early life dynamics and recruitment variability. Am. Fish. Soc. Symp. 2:17–29.

Houde, E. D., and C. E. Zastrow.
1991. Bay anchovy. *In* Habitat requirements for Chesapeake Bay living resources, 2nd ed. (S. L. Funderburk, J. A. Mihursky, S. J. Jordan, and D. Riley, eds.), p. 8.1 to 8.14. Living Resources Subcommittee, Chesapeake Bay Program, Annapolis, MD.

Hunter, J. R., and C. A. Kimbrell.
1980. Egg cannibalism in the northern anchovy, *Engraulis mordax*. Fish. Bull. 78:811–816.

Jung, S.
2002. Fish community structure and the spatial and temporal variability in recruitment and biomass production in Chesapeake Bay. Ph.D. diss., 349 p. Univ. Maryland, College Park, MD.

Jung, S., and E. D. Houde.
2003. Spatial and temporal variability of pelagic fish community structure and distribution in Chesapeake Bay, U.S.A. Estuar. Coast. Shelf Sci. 58:335–351.

Keister, J. E., E. D. Houde, and D. L. Breitburg.
2000. Effects of bottom-layer hypoxia on abundances and depth distribution of organisms in Patuxent River, Chesapeake Bay. Mar. Ecol. Prog. Ser. 205:43–59.

Kemp, W. M., and W. R. Boynton.
1980. Influence of biological and physical processes on dissolved oxygen dynamics in an estuarine system: implications for measurement of community metabolism. Estuar. Coast. Mar. Sci. 11:407–431.

Kemp, W. M., P. A. Sampou, J. Garber, J. Tuttle, and W. R. Boynton.
1992. Seasonal depletion of oxygen from bottom waters of Chesapeake Bay: roles of benthic and planktonic respiration and physical exchange processes. Mar. Ecol. Prog. Ser. 85:137–152.

Kimura, R., D. H. Secor, E. D. Houde, and P. M. Piccoli.
2000. Up-estuary dispersal of young-of-the-year bay anchovy *Anchoa mitchilli* in the Chesapeake Bay: inferences from microprobe analysis of strontium in otoliths. Mar. Ecol. Prog. Ser. 208:217–227.

King, M.
1995. Fisheries biology, assessment and management, 341 p. Fishing News Books, Oxford.

Klebasko, M. J.
1991. Feeding ecology and daily ration of bay anchovy, *Anchoa mitchilli* in the mid-Chesapeake Bay. M.S. thesis, 103 p. Univ. Maryland, College Park, MD.

Loos, J. J., and E. S. Perry.
1991. Larval migration and mortality rates of bay anchovy in the Patuxent River. *In* Larval fish recruitment and research in the Americas: proceedings of the 13th annual fish conference, 21–26 May 1989, Merida, Mexico (R. D. Hoyt, ed.), p. 65–76. NOAA Technical Report NMFS 95.

Luo, J., and S. B. Brandt.
1993. Bay anchovy *Anchoa mitchilli* production and consumption in mid-Chesapeake Bay based on a bioenergetics model and acoustic measurement of fish abundance. Mar. Ecol. Prog. Ser. 98:223–236.

Luo, J., and J. Musick.
1991. Reproductive biology of the bay anchovy in Chesapeake Bay. Trans. Am. Fish. Soc. 120:701–710.

MacGregor, J. M., and E. D. Houde.
1996. Onshore-offshore pattern and variability in distribution and abundance of bay anchovy *Anchoa mitchilli* eggs and larvae in Chesapeake Bay. Mar. Ecol. Prog. Ser. 138: 15–25.

Murdy, E. O., R. S. Birdsong, and J. A. Musick.
1997. Fishes of Chesapeake Bay, 324 p. Smithsonian Institution Press, Washington, D.C. and London.

Newberger, T. A., and E. D. Houde.
1995. Population biology of bay anchovy *Anchoa mitchilli* in the mid Chesapeake bay. Mar. Ecol. Prog. Ser. 116:25–37.

North, E. W., and E. D. Houde.
In press. Transport and dispersal of bay anchovy (*Anchoa mitchilli*) eggs and larvae in Chesapeake Bay. Estuar. Coast. Shelf Sci..

Parker, K.
1985. Biomass model for the egg production method. *In* An egg production method for estimating spawning biomass of pelagic fish: application to the northern anchovy, *Engraulis mordax* (R. Lasker, ed.), p. 5–7. NOAA Tech. Rep. NMFS 36.

Peebles, E. B., J. R. Hall, and S. G. Tolley.
1996. Egg production by the bay anchovy *Anchoa mitchilli* in relation to adult and larval prey fields. Mar. Ecol. Prog. Ser. 131:61–73.

Purcell, J. E., D. A. Nemazie, S. E. Dorsey, E. D. Houde, and J. C. Gamble.
1994. Predation mortality of bay anchovy *Anchoa mitchilli* eggs and larvae due to scyphomedusae and ctenophores in Chesapeake Bay. Mar. Ecol. Prog. Ser. 114 :47–58.

Ricker, W. E.
1975. Computation and interpretation of biological statistics of fish population. Bull. Fish. Res. Board Can. 191: 1–382.

Rilling, G. C., and E. D. Houde.
1999a. Regional and temporal variability in distribution and abundance of bay anchovy (*Anchoa mitchilli*) eggs, larvae, and adult biomass in the Chesapeake Bay. Estuaries 22: 1096–1109.
1999b. Regional and temporal variability in growth and mortality of bay anchovy, *Anchoa mitchilli*, larvae in Chesapeake Bay. Fish. Bull. 97:555–569.

Rose, K. A., J. H. Cowan, M. E. Clark, E. D. Houde, and S. B. Wang.
1999. An individual-based model of bay anchovy population dynamics in the mesohaline region of Chesapeake Bay. Mar. Ecol. Prog. Ser. 185:113–132.

SAS Institute Inc.
1989. SAS/STAT user's guide, version 6, 4th ed., 1686 p. SAS Institute Inc., Cary, NC.

Samuels, M. L.
1989. Statistics for the life sciences, p. 409–42. Prentice-Hall, Inc., Upper Saddle River, NJ.
Schultz, E. T., R. K. Cowen, K. M. M. Lwiza, and A. M. Gospodarek.
2000. Explaining advection: Do larval bay anchovy (*Anchoa mitchilli*) show selective tidal-stream transport? ICES J. Mar. Sci. 57:360–371.
Sissenwine, M. P.
1984. Why do fish populations vary? *In* Exploitation of marine communities (R. M. May, ed.), p. 59–94. Springer-Verlad, Berlin.
Smith, E. M., and W. M. Kemp.
2001. Size structure and the production/respiration balance in a coastal plankton community. Limnol. Oceanogr. 46: 473–485.
Steel, R. G. D., and J. H. Torrie.
1980. Principles and procedures of statistics. A biometrical approach. 2nd ed., 633 p. McGraw-Hill Inc. New York, NY.
Vazquez-Rojas, A. V.
1989. Energetics, trophic relationships and chemical composition of bay anchovy, *Anchoa mitchilli* in the Chesapeake Bay. M.S. thesis, 166 p. Univ. Maryland, College Park, MD.
Wang, S. B., J. H. Cowan, K. A. Rose, and E. D. Houde.
1997. Individual-based modelling of recruitment variability and biomass production of bay anchovy in mid-Chesapeake Bay. J. Fish Biol. 51 (suppl. A):121–134.
Wang, S. B., and E. D. Houde.
1995. Distribution, relative abundance, biomass and production of bay anchovy *Anchoa mitchilli* in the Chesapeake Bay. Mar. Ecol. Prog. Ser. 121:27–38.
Zastrow, C. E., E. D. Houde, and L. G. Morin.
1991. Spawning, fecundity, hatch-date frequency and young-of-the-year growth of bay anchovy *Anchoa mitchilli* in mid-Chesapeake Bay. Mar. Ecol. Prog. Ser. 73:161–171.

Coupling ecology and economy: modeling optimal release scenarios for summer flounder (*Paralichthys dentatus*) stock enhancement

G. Todd Kellison

David B. Eggleston

Department of Marine, Earth, and Atmospheric Sciences,
North Carolina State University
Raleigh, North Carolina 27695-8208
Present address (for G. T. Kellison, contact author): National Park Service/Biscayne National Park
9700 SW 328th St, Homestead, Florida 33033

E-mail address (for G. T. Kellison): todd_kellison@nps.gov

Abstract—Increasing interest in the use of stock enhancement as a management tool necessitates a better understanding of the relative costs and benefits of alternative release strategies. We present a relatively simple model coupling ecology and economic costs to make inferences about optimal release scenarios for summer flounder (*Paralichthys dentatus*), a subject of stock enhancement interest in North Carolina. The model, parameterized from mark-recapture experiments, predicts optimal release scenarios from both survival and economic standpoints for varyious dates-of-release, sizes-at-release, and numbers of fish released. Although most stock enhancement efforts involve the release of relatively small fish, the model suggests that optimal results (maximum survival and minimum costs) will be obtained when relatively large fish (75–80 mm total length) are released early in the nursery season (April). We investigated the sensitivity of model predictions to violations of the assumption of density-independent mortality by including density-mortality relationships based on weak and strong type-2 and type-3 predator functional responses (resulting in depensatory mortality at elevated densities). Depending on postrelease density, density-mortality relationships included in the model considerably affect predicted postrelease survival and economic costs associated with enhancement efforts, but do not alter the release scenario (i.e. combination of release variables) that produces optimal results. Predicted (from model output) declines in flounder over time most closely match declines observed in replicate field sites when mortality in the model is density-independent or governed by a weak type-3 functional response. The model provides an example of a relatively easy-to-develop predictive tool with which to make inferences about the ecological and economic potential of stock enhancement of summer flounder and provides a template for model creation for additional species that are subjects of stock enhancement interest, but for which limited empirical data exist.

Manuscript approved for publication 17 July 2003 by Scientific Editor.

Manuscript received 20 October 2003 at NMFS Scientific Publications Office.

Fish. Bull. 102:78–93 (2004).

Commercially important marine fish and invertebrate populations are declining worldwide in response to overexploitation and habitat degradation (Rosenberg et al., 1993; FAO 1998). This reduction in harvestable fishery resources has stimulated increasing interest in the use of hatchery-reared (HR) animals to enhance wild stocks (Munro and Bell, 1997; Travis et al., 1998; Cowx, 1999; Kent and Drawbridge, 1999). Unfortunately, many stock enhancement programs proceed before ecological concerns are adequately addressed (Blankenship and Leber, 1996), and without the identification of goals or the evaluation of the success of enhancement efforts (Cowx, 1999). If fishery managers can satisfactorily determine that enhancement efforts will have no ecologically significant negative ramifications, then managers should establish specific, quantifiable goals and objectives of enhancement efforts as part of a responsible approach to stock enhancement (Blankenship and Leber, 1996; Heppell and Crowder, 1998). Once such goals have been established, managers should identify stocking approaches that will lead to the most cost-efficient realization of enhancement goals—a process that can be accomplished with the aid of coupled ecological and economic models. Although numerous (advanced) models (conceptual and species-specific) exist to predict the biological and ecological impact of alternative enhancement scenarios (e.g. Botsford and Hobbs, 1984; Salvanes et al., 1992; Barbeau and Caswell, 1999; Sutton et al., 2000), there are few models (of which we are aware) that have attempted to link the biological and ecological results of stocking efforts (e.g. addition of biomass to a stocked population) with the economic costs associated with various release scenarios (e.g. Botsford and Hobbs, 1984; Hobbs et al., 1990; Hernandez-Llamas, 1997; Kent and Drawbridge, 1999). Such a link is critical to the responsible use of funding to rebuild or manage fisheries, and for the comparison of predicted costs of enhancement versus alternative management techniques.

In North Carolina, there has been recent interest in stock enhancement with summer flounder (*Paralichthys dentatus*) (Waters, 1996; Rickards, 1998; Waters and Mosher, 1999; Burke et al., 2000; Copeland et al.[1]) because of a combination of heavy commercial and recreational exploitation, established techniques for mass hatchery-rearing (Burke et al., 1999), and considerable knowledge of summer flounder life history (Powell and Schwartz, 1977; Burke et al., 1991; Burke, 1995). Nevertheless, there have been no large-scale release experiments (and subsequent collection of data) by which to make empirical inferences about stock enhancement potential for this species. We present a compartmental model, parameterized from mark-recapture field experiments,

[1] Copeland, B. J., J. M. Miller, and E. B. Waters. 1998. The potential for flounder and red drum stock enhancement in North Carolina. Summary of workshop, 30–31 March, 1998, 22 p. [Available from North Carolina State Univ, Raleigh, NC 27695.]

Table 1

Range of numbers of summer flounder (*Paralichthys dentatus*) released (and resulting postrelease densities), sizes-at-release, and dates of release simulated in the model.

Number released	Postrelease density	Size-at-release	Dates of release
100–400,000	0.001–4.0	30–80 mm	1 April–15 July

that incorporates size of fish released, date-of-release, and number of fish released to calculate 1) predicted numbers of survivors and 2) economic costs associated with varying release scenarios under density-independent mortality. We investigated the sensitivity of model predictions to violations of the assumption of density-independent mortality because there is abundant evidence that mortality rates, or processes underlying mortality rates (e.g. growth), are affected by density-dependent relationships in the wild (see, for recent examples, Buckel et al., 1999; Bystroem and Garcia-Berthou, 1999; Jenkins et al., 1999; Kimmerer et al., 2000). We did so by repeating model simulations under varying density-mortality relationships (depensatory in nature at elevated densities), using experimental evidence from our own field studies and published observations for similar species to parameterize density-mortality relationships. Additionally, we used a scenario in which the density-mortality relationship changed over time to make inferences about the effect of more complex density-mortality relationships on postrelease mortality of juvenile summer flounder. Finally, we generated predicted temporal patterns of field densities under varying density-mortality relationships and compared them with observed (in the field) patterns to determine whether model output under the considered density-mortality relationships matched actual patterns in the field. The model provides an example of a relatively easy-to-develop predictive tool with which to make inferences about the ecological and economic potential of stock enhancement with summer flounder and provides a template for model creation for additional species that are subjects of stock enhancement interest, but for which limited empirical data exist.

Materials and methods

Background

In North Carolina, wild summer flounder recruit to shallow-water estuarine nursery habitats from February to May, after which small juvenile (20–35 mm total length [TL]) densities range from ~0.1 to 1.0 fish/m^2 (Burke et al., 1991; Kellison and Taylor[2]). Juveniles subsequently make an ontogenetic habitat shift to deeper waters (Powell and Schwartz, 1977), apparently after reaching a total length of ~80 mm (Kellison and Taylor[2]). By mid-July, densities of juvenile summer flounder in the shallow water nursery habitats are near zero (Kellison and Taylor[2]).

Model pathway

Our compartmental model simulated the daily mortality and growth of different-size hatchery-reared (HR) fish released in the field over a 105-day period (1 April to 15 July, based on observed field abundances) in a hypothetical release habitat of 10 hectares. The model predicted the percentage of released fish surviving and economic cost-per-survivor under 2730 release scenarios for a specified number of fish released (see below). To begin the model, a value of number of fish released (NFR) ranging from 100 to 400,000 (Table 1) was chosen (Fig. 1), resulting in postrelease densities (assuming even postrelease distribution) of 0.001–4.0 fish/m^2. These values included a range of densities of juvenile summer flounder observed in wild nursery habitats (~0–1 fish/m^2; mean ~0.05 fish/m^2; Kellison and Taylor[2]), but also included unusually high densities (>1 fish/m^2) in order to examine how such release strategies would affect model output (we did not examine densities >4 fish/m^2 because of a lack of data on fish response to resource limitation likely to occur as densities increased past values for which we had empirical growth data). Each group of NFR was initially assigned a "size-(TL) at-release" of 30 mm (the smallest size-at-release simulated in the model), after which a size-dependent economic cost associated with the release of the 30-mm-TL fish was calculated (see below). The release group was then assigned a minimum Julian "day of release" of 92 (corresponding to 1 April, the earliest release date simulated in the model). A range of Julian days of release was included in the model because field-estimated growth rates were dependent on Julian day (Kellison, 2000), and growth rates are potentially important to the determination of mortality rates (Rice et al. 1993). With this model, we then calculated daily mortality and growth (described below) in the hypothetical release habitat over the number of days at large (DAL), where

$$DAL = 197 \text{ (the Julian day corresponding to 15 July)} - 92 \text{ (Julian release day)},$$

and output a number of survivors and a calculated cost-per-survivor (CPS), where

$$CPS = \textit{cost associated with release} \div \textit{predicted number of survivors},$$

[2] Kellison, G. T., and J. C. Taylor. 2000. Unpubl. data. Department of Marine, Earth, and Atmospheric Sciences, North Carolina State University, Raleigh, NC 27695-8208.

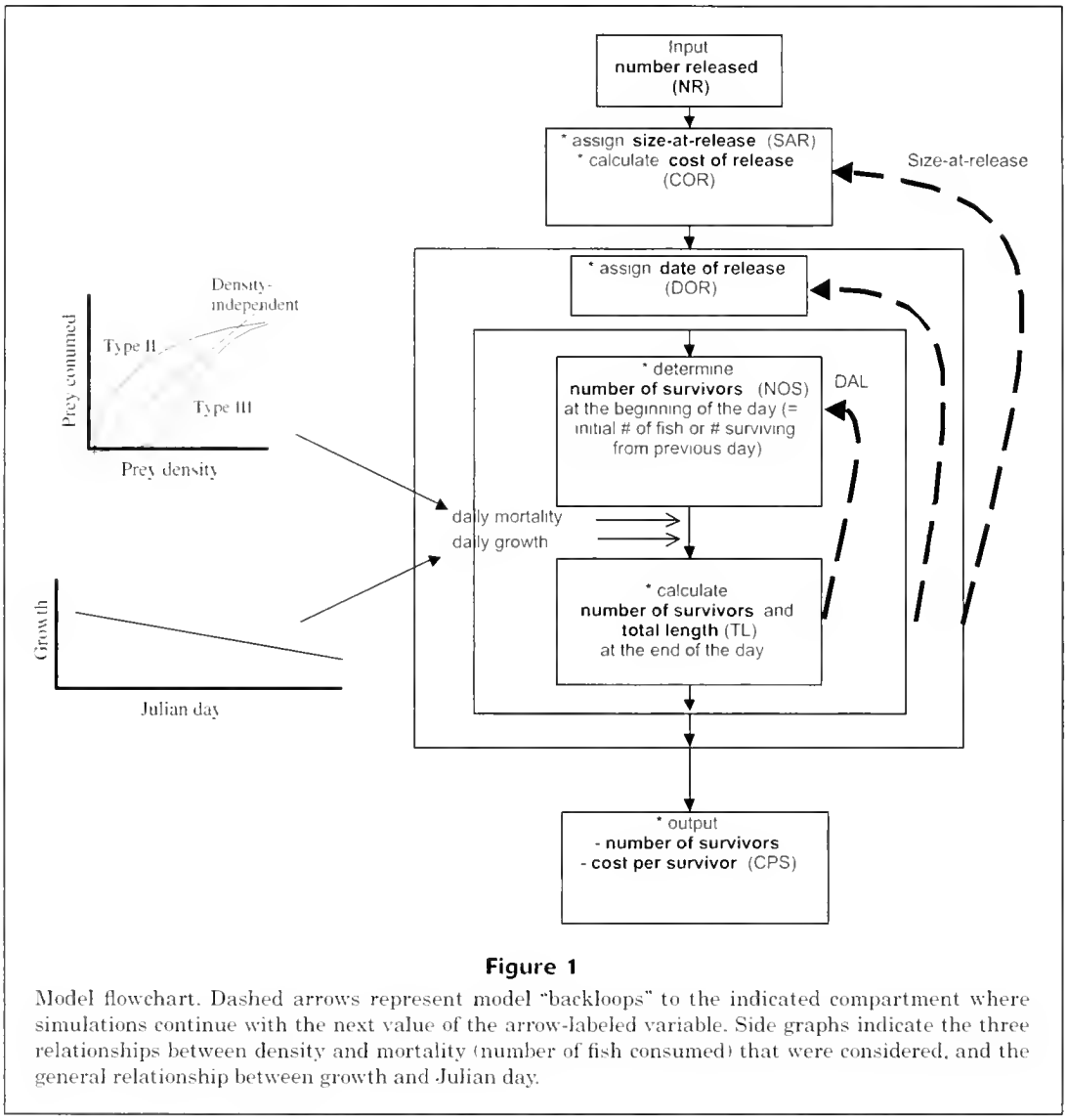

Figure 1

Model flowchart. Dashed arrows represent model "backloops" to the indicated compartment where simulations continue with the next value of the arrow-labeled variable. Side graphs indicate the three relationships between density and mortality (number of fish consumed) that were considered, and the general relationship between growth and Julian day.

for the initial release scenario of fish size = 30 mm TL, Julian day = 92, and an NFR input determined by the modeler). The model then looped back to the "date-of-release" step and simulated the release of the 30-mm-TL fish for Julian release days 93–197, outputting a predicted number of survivors and cost-per-survivor for each release date. The model then repeated all previous steps under sequentially larger size-at-release scenarios, looping back to the "size-at-release" step and simulating the release of fish ranging in size from 32–80 mm TL fish in steps of 2 mm TL. The model output was a predicted number of survivors and economic cost-per-survivor for each release day (92–197) for each size-at-release (Fig. 1). Thus, for each input NFR, there were 26 size-at-release possibilities × 105 Julian days of release possibilities, which resulted in 2730 simulations, each of which resulted in a predicted number of survivors and cost-per-survivor for that particular release scenario. For each input NFR, the results from the 2730 simulations were plotted on two response surfaces, with an x-axis of size-at-release, a y-axis of date-of-release, and a z-axis of either 1) predicted number of survivors (NOS), or 2) cost-per-survivor (CPS), to identify release scenarios resulting in the maximum predicted number of survivors and minimum cost-per-survivor, respectively. The scenarios resulting in the maximum predicted number of survivors and minimum cost-per-survivor were not necessarily identical.

Calculation of mortality, growth, survival, and economic costs associated with release

During each day at large (DAL), released fish were subjected to a density-independent daily mortality rate of 0.02153, derived from postrelease mark-recapture data of HR summer flounder (Kellison et al., 2003b). In deriving this value, mean postrelease densities were used to estimate a total number of survivors from experimental releases. Daily survival was then calculated with the equation

$$NFR \times S_D^{DAL} = NOS,$$

where NFR = number released;
S_D = daily survival;
DAL = days at large (from release date until Julian day 197); and
NOS = estimated number of survivors.

Daily mortality (M_D) was then calculated from the equation

$$M_D = 1 - S_D.$$

At the end of each simulated day, all fish that were alive increased in growth according to the equation

$$G_D = -0.0061 \times \text{Julian day} + 1.2487,$$

which was derived from mark-recapture data (Kellison, 2000), and in which G_D is daily growth in millimeters. Fish reaching 80 mm TL during the model (i.e. by 15 July) were considered to make an ontogenetic habitat shift to deeper waters. These fish were then subjected to one half year of natural mortality to simulate mortality-related losses from deeper-water habitats (M=0.28; Froese and Pauley, 2001). Remaining fish, now having survived ~one year of natural mortality, were considered to be survivors (available to the commercial fishery), which is a conservative assumption because 1-yr-old summer flounder are only partially recruited to the commercial fishery. All fish not reaching a total length of 80 mm were assumed to perish.

To determine size-dependent economic costs of fish production, we used the following regression equation derived for Japanese flounder (*Paralichthys olivaceus*) by Sproul and Tominaga (1992) because equivalent economic data for summer flounder were unavailable:

$$C_{PF} = 14.24 + 1.234 \times TL,$$

where C_{PF} = the cost per fish in Japanese yen (¥); and
TL = the total length of the HR fish.

Costs were then converted into US$ by using an exchange rate of 106.7¥ per 1 US$ (universal currency converter). We feel use of this cost-of-fish-production equation is appropriate because the Japanese flounder is closely related and similar in life history traits to the summer flounder (Tanaka et al., 1989; Burke et al., 1991), resulting in similar optimal rearing practices for hatchery-reared Japanese and summer flounder (Burke et al., 1999), and thus likely similar rearing costs. Additionally, the scale of Japanese flounder hatchery production is similar to, or greater than, other government subsidized hatchery production programs (e.g. red drum in Texas, cod in Norway [Svåsand, 1998]).

Density-mortality relationships

We tested the sensitivity of the model results (optimal predicted number of survivors and cost-per-survivor estimates under varying NFRs) to violations of the assumption of density-independent mortality by incorporating varying types and strengths of density-dependent mortality (depensatory in nature at elevated densities; see below) into the model. As a basis for these sensitivity analyses, we assumed that predation was the driving mechanism underlying the postrelease mortality of HR summer flounder under the densities examined (Kellison et al., 2000; Kellison et al., 2003b). Thus, we made daily mortality rates correspond to either a type-2 or type-3 predator functional response (Holling, 1959; see Lindholm et al., 2001 for example), in which proportional mortality due to predation decreases with increasing density (type-2 response) or increases initially with increasing density, reaches a zenith, and then decreases with increasing density (type-3 response) (Fig. 2). Both type-2 and type-3 responses result in decreasing (depensatory) mortality at elevated prey densities due to predator satiation. We did not include scenarios in which mortality increased at elevated densities (as would be expected when densities reached those likely to result in resource limitation) because we did not include in the model elevated release densities likely to result in resource limitation. We parameterized the daily mortality curves so that each response (type 2 or 3) incorporated the daily mortality rate of 0.02153. These mortality curves contain mortality values that are within ranges reported in the literature for other species of juvenile marine fishes (Bax, 1983; Houde, 1987; Nash, 1998; Rose et al., 1999). To make further inferences about the importance of density-dependent mortality to model results, we included a 1) weak and 2) strong form of each functional response (types 2 and 3) (Fig. 2), as well as scenarios in which the response shifted temporally from 3) type 2 to 3, and 4) type 3 to 2 at the midpoint of the nursery season (Julian day 145). We included both the weak and strong forms of the type-2 and type-3 functional responses to determine the extent to which variation in the strength of the functional response would affect model predictions. The strength of the functional response could vary because of annual variation in the presence or abundance of prey or because predators could affect the density-mortality relationship (see, for example, Hansen et al., 1998).

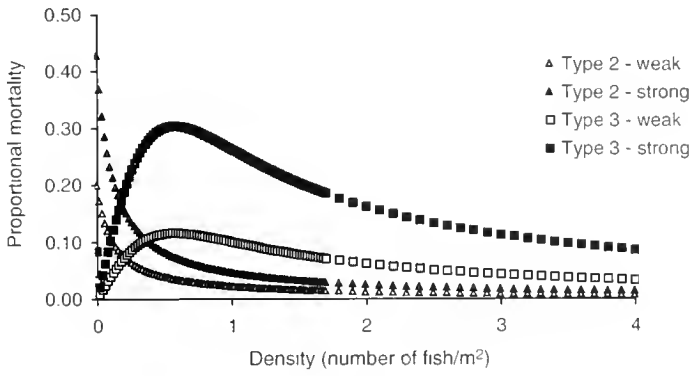

Figure 2

Proportional mortality curves for juvenile summer flounder corresponding to weak and strong type-2 and type-3 mortality responses.

For example, a strong positive (compensatory) density-mortality relationship driven by predators might become weaker in years when predator abundance was lower than average. We included the temporally shifting functional response scenarios to determine the extent to which temporal variation in the form of the functional response would affect model predictions. Temporal variation in the form of the functional response might occur because of temporal changes in the predator community, or because of changing predator-prey size dynamics (e.g. Stoner, 1980; Black and Hairston, 1988). For example, as the nursery season for summer flounder progresses, proportionately greater numbers of juveniles grow to sizes at which they are capable of preying on smaller juveniles (Kellison, personal obs.). If cannibalistic summer flounder exhibit a different predatory functional response from that of the predator guild community predominating earlier in the season, then the density-mortality relationship may change seasonally.

We replicated all model simulations over each of the six density-mortality relationships (weak and strong types 2 and 3, and shifting patterns [type 2 to 3 and type 3 to 2]) to determine optimal release scenarios (maximum number of survivors, minimum cost-per-survivor) under each relationship. We then compared results to those obtained under density-independent mortality to make inferences about the importance of density-mortality relationships to model results.

Correspondence between predicted and observed temporal abundance patterns

Different density-mortality relationships may result in distinct temporal patterns of abundance (e.g. rapid versus more gradual declines in abundance) depending on initial densities. We generated predicted patterns of temporal field abundance of juvenile summer flounder under density-independent mortality and four additional density-mortality relationships (governed by weak and strong type 2 and 3 functional responses) and under varying initial densities (0.1, 0.3, and 0.5 fish/m^2) to examine whether the different density-mortality relationships would result in distinct temporal patterns of abundance. We used 1998–99 field data and logarithmic or polynomial regression models to generate curves that best fitted (based on r^2 values) observed (from natural nursery sites) temporal declines in abundance under varying initial densities. We compared the best-fit curves to those predicted by the model under density-independent and four additional density-mortality relationships. These comparisons allowed us to make qualitative inferences about which density-mortality relationship(s) resulted in the best match between predicted and observed temporal patterns of abundance.

Model assumptions

The assumptions of the model are the following:

1 Daily mortality is independent of size. Although there is strong evidence that mortality of fishes in the wild is size-dependent (Lorenzen, 2000), particularly in regard to the importance of size to susceptibility to predation (see, for example, Elis and Gibson, 1995; Furuta, 1999; Manderson et al., 1999), we found no evidence (from recaptures of released hatchery-reared fish) of size-selective daily mortality for juvenile summer flounder ranging in size from ~30–80 mm TL in shallow-water nursery areas (Kellison et al., 2003a). Implications for violations of this assumption are addressed in the "Discussion" section.

2 Daily growth is independent of fish density. We based this assumption on field experiments that indicated no growth limitation at densities roughly equal to the maximum densities explored in the model (Kellison et al., 2003b). Similar findings (i.e. no food-limitation or density-dependent growth) have been reported for similar-size plaice in shallow-water nursery habitats (van der Veer and Witte, 1993).

3 Economic cost per fish (C_{PF}) is independent of the number of fish acquired for release (i.e. within the range of numbers of fish released in model simulations, there is no decrease in cost per fish as the number of fish acquired from the production hatchery for release increases). This assumption is likely to be valid over changes in numbers of fish released common to stock enhancement programs (Sproul and Tominaga, 1992) but may not be valid as numbers released change over orders of magnitude because of economy of scale (Adams and Pomeroy 1991; Garcia et al., 1999).

4 There is no emigration from the release habitat until fish exhibit an ontogenetic shift in habitat at 80 mm TL. Although pre-ontogenetic habitat shift emigration may not truly be zero, we feel that it is also unlikely that pre-ontogenetic habitat-shift emigration accounts for more than a minimal amount of loss of released fish from the habitat of release, as supported by several points. First, rates of pre-ontogenetic shift emigration in wild juveniles are apparently low (Kellison and Taylor[2]), suggesting that large-scale spatial migrations may not be part of the behavioral repertoire of early juvenile summer flounder. Second, irregular temporally replicated sampling outside of experimental release sites resulted in zero captures of emigrating hatchery-reared fish (Kellison et al., 2003b). Third, emigration rates of closely related HR Japanese flounder (*Paralichthys olivaceus*) are reported to be very low (Tominaga and Watanabe, 1998). In combination, these points suggest that our zero emigration assumption is appropriate.

5 Fish that do not grow to 80 mm TL during the model period (i.e. by 15 July) do not survive. Although this assumption cannot be examined with our field data, data do show that juvenile summer flounder are absent from shallow-water nursery habitats by mid to late July (Kellison et al.[3]). Thus, all fish have either perished or made ontogenetic habitat shifts to deeper habitats by this time. Our field observations suggest that the deeper habitats to which larger flounder

[3] Kellison, G. T., J. C. Taylor, and J. S. Burke. 2000. Unpubl. data. Department of Marine, Earth, and Atmospheric Sciences, North Carolina State Univ., Raleigh, NC 27695-8208.

make ontogenetic habitat shifts are inhabited by relatively high densities of potential predators (e.g. blue crabs, age 1+ flounders, red drum [*Sciaenops ocellatus*], searobin [*Prionotus* sp.], and lizardfish [*Synodus* sp.]), which may be considerably less abundant in shallow-water habitats. These relatively large and abundant predators would presumably expose small migrating fish to high rates of predation (see, for example, Elis and Gibson, 1995; Furuta, 1999; Manderson et al., 1999). This assumption is supported by research with the congener Japanese flounder (*Paralichthys olivaceus*). Although a range of sizes of hatchery-reared Japanese flounder may survive within relatively shallow nursery habitats, fishes less than 90 mm TL moving into relatively deep waters are poorly represented in subsequent age classes, most likely due to predation-induced mortality (Yamashita et al., 1994; Furuta, 1999).

6 There is no relationship between length of rearing period (time spent in the hatchery environment) and probability of postrelease mortality related to behavioral deficits (Olla et al., 1998). Hatchery-specific selection pressures may result in HR fish that are behaviorally selected to survive in the hatchery and not in the wild (see Olla et al., 1998; Kellison et al., 2000; for discussion). We assume that behavioral deficits are not exacerbated with time spent in the hatchery (i.e. behavioral deficits are equal for all sizes-at-release).

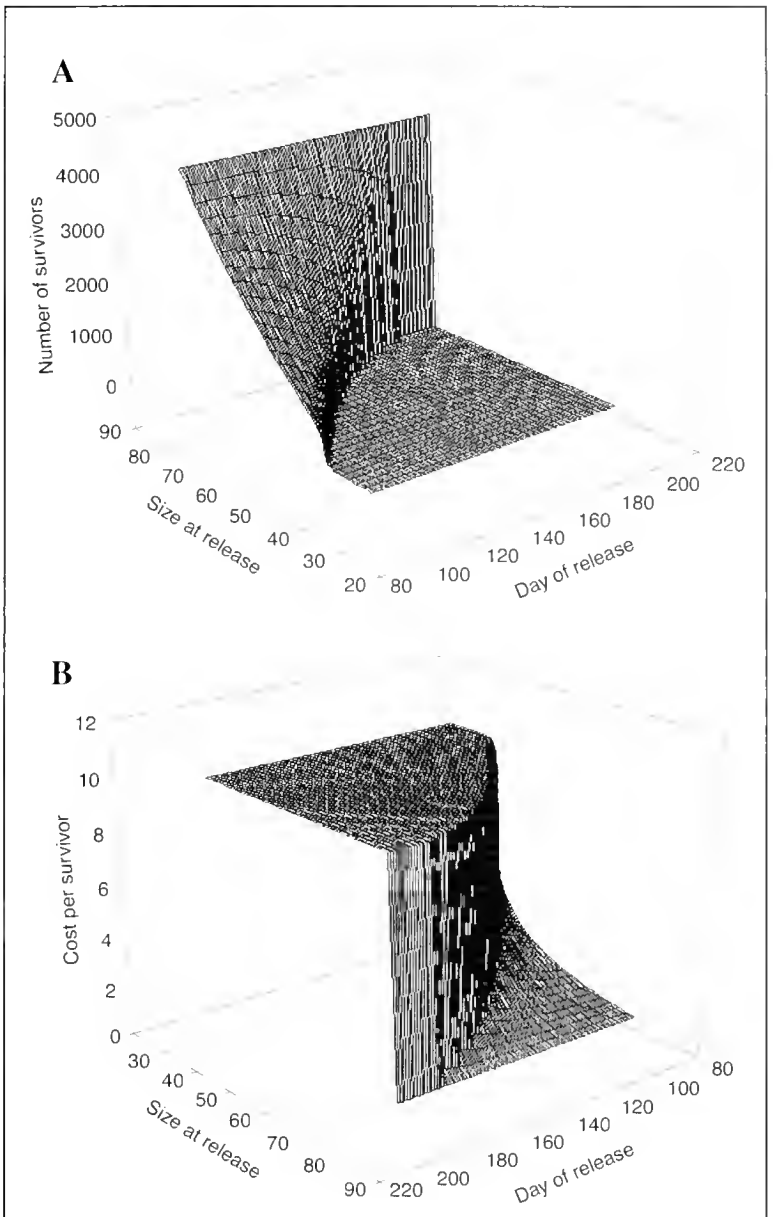

Figure 3

Response surfaces of (**A**) number of fish survivors (summer flounder) and (**B**) cost-per-survivor (CPS) as a function of date of release and size at release at number released (NR) = 5000 (postrelease density=0.05) under density-independent mortality. CPS values greater than $10 were set equal to $10 for ease of presentation.

Results

The most important factor affecting the number of survivors (and therefore percent survival) was size-at-release because the greatest numbers and percentages of survivors were always produced by releasing the largest fish possible (80 mm TL in the model). Number of survivors decreased with decreasing size-at-release and with increasing Julian day of release (Fig. 3A). The cost-per-survivor (CPS) was also most affected by size-at-release, such that CPS decreased with increasing size-at-release (Fig. 3B). CPS generally increased with increasing Julian day of release (Fig. 3B), although this effect was less important than the effect of size-at-release. Because mortality was originally assumed to be density-independent, the optimal cost-per-survivor did not vary with the number of fish released (Fig. 4), and the relationship between number of fish released and number of survivors was linear (Fig. 4), such that the maximum number of survivors were generated from the greatest number of fish released (NFR=400,000).

Sensitivity of model predictions to violations of density-independent mortality assumption

Model results varied considerably under the various density-mortality relationships (Fig. 5, A and B), indicating the importance of knowledge of the relationship between numbers of fish released (density) and mortality in the wild to predicting optimal release scenarios. Variation in model output was dependent on the type and strength of

the density-mortality relationship. For example, at postrelease densities of 0.5 fish/m^2 (NFR=50,000), survival of released flounder under density-independent mortality was ~28% higher than that predicted under strong type-3 mortality, but only ~2% higher than that predicted under weak type-2 mortality (Fig. 5A). At postrelease densities of 0.001 fish/m^2 (NFR=100), survival of released flounder under density-independent mortality was ~41% higher than that predicted under strong type-2 mortality, but ~2% less than that predicted under strong type-3 mortality (Fig. 5A). In contrast, when postrelease densities were relatively high, there was less of an impact of density-mortality relationship on postrelease survival and costs associated with stock enhancement. For example, at postrelease densities of three fish/m^2 (NFR=300,000), survival of released flounder differed by less than 4% between density-independent, weak or strong type-2, and weak type-3 mortality, although survival under strong type-3 mortality was ~9% less than that predicted under density-independent mortality and ~11% less than that predicted under strong type-2 mortality (Fig. 5A). Thus, the model results were most sensitive to violations of the assumption of density-independent mortality at low densities of fish released in the field.

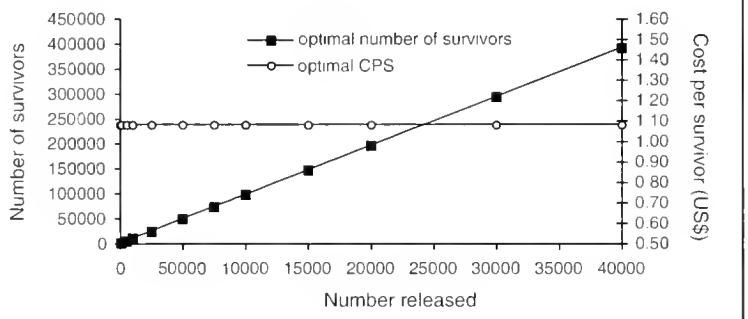

Figure 4

Optimal number of fish survivors and cost-per-survivor as a function of varying numbers of summer flounder released under density-independent mortality.

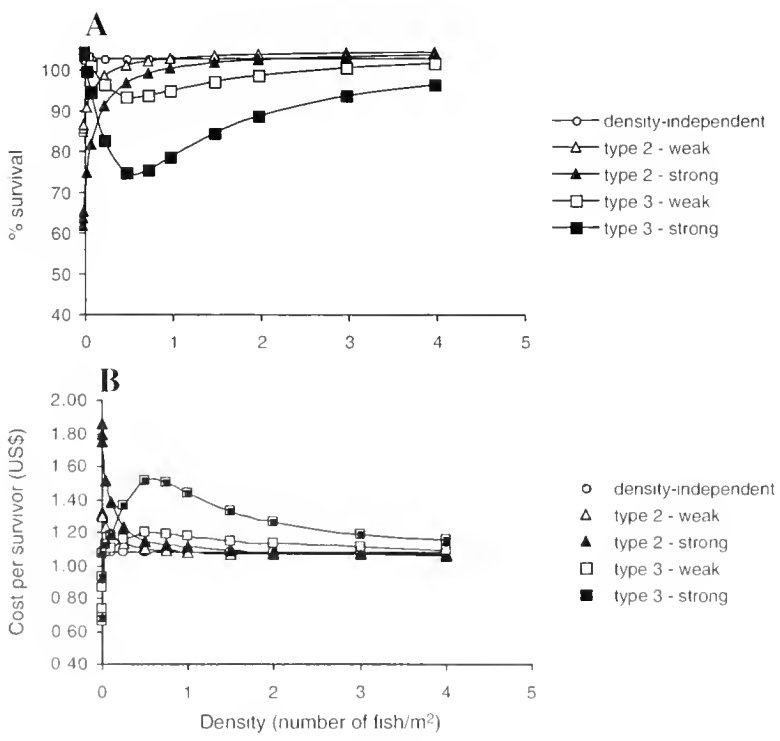

Figure 5

(A) Optimal percent survival and (B) optimal cost-per-survival (US$) as a function of postrelease density under density-independent and varying density-dependent mortality relationships for summer flounder.

Type-2 mortality As with density-independent mortality, the most important factor affecting number of survivors and cost per survivor under type-2 mortality was size-at-release (Fig. 6, A and B). In all simulations, the greatest number of survivors was produced by releasing the largest fish possible. Number of survivors decreased with increasing Julian day of release (Fig. 6A). There was a considerable interaction between size-at-release and number of fish released, such that low postrelease densities were subjected to relatively high proportional mortality. Thus, when fish were released in low numbers and at small sizes, the fish were subjected to relatively high proportional mortality rates for long periods of time (while they grew towards the 80-mm-TL ontogenetic shift size) and consequently produced few or no survivors (Fig. 6A). Optimal release scenarios under strong type-2 mortality produced substantially lower (>40% in some cases) percent survival (and therefore substantially higher cost-per-survivor) estimates at low to moderate numbers released (NFR=100–50,000; postrelease density=0.001–0.5 fish/m^2) than under density-independent mortality (Fig. 5, A and B). Differences in percent survival estimates (and thus cost-per-survivor estimates) between density-independent survival and weak or strong type-2 mortality declined to less than 5% when the numbers released increased to 25,000 (postrelease density=0.25 fish/m^2) under weak type-2 mortality and 75,000 (postrelease density=0.75 fish/m^2) under strong type-2 mortality (Fig. 5A). Thus, model predictions under density-independent mortality differed most from predictions under mortality governed by

a type-2 predator functional response when postrelease densities were relatively low.

Type-3 mortality As in all other simulations, the most important factor affecting number of survivors under type-3 mortality was size-at-release, such that the greatest numbers of survivors were always produced by releasing the largest fish possible (Fig. 7A). Number of survivors decreased with increasing Julian day of release (Fig. 7A). Percent survival was considerably lower (>25% in some cases) under type-3 mortality than under density-independent mortality at moderate to high numbers released (NFR=10,000–400,000) (Fig. 5A).

In nearly all simulations, the lowest CPS values were produced by releasing the largest fish possible (Fig. 7B). The exceptions to the "large size = optimal CPS" rule occurred when postrelease densities were small (corresponding to numbers released of 100, 500, and 1000) and the mortality curve was type 3 (weak or strong). In these instances, mortality was sufficiently low at low release densities (Fig. 7B) so that the difference in overall survival between small- and large-released fish was small enough to be overridden by the increased cost of the larger fish, and the minimum CPS was obtained when small (42–44 mm TL) fish were released (e.g. Fig. 7B).

At low numbers released (NFR=100–1000), optimal cost-per-survivor was considerably lower (>45% in some cases) under type-3 mortality than under density-independent mortality (Fig. 5A). As NFR increased, CPS under type-3 mortality became greater (~40% in some cases) than that achieved under density-independent mortality (Fig. 5B).

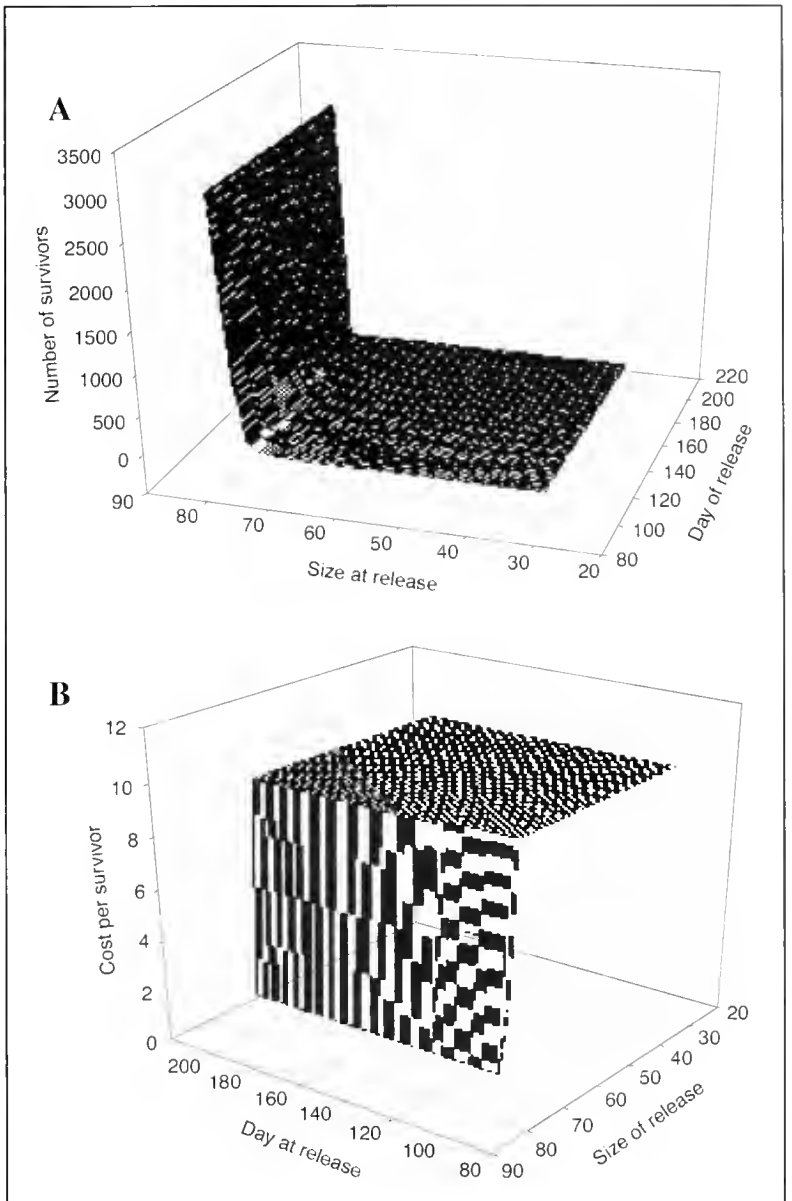

Figure 6

Response surfaces of (**A**) number of fish (summer flounder) survivors and (**B**) cost-per-survivor (CPS) as a function of date of release and size at release at number released (NR) = 5000 (postrelease density=0.05) under a strong type-2 functional response. CPS values greater than $10 were set equal to $10 for ease of presentation.

Temporal shift in functional response from type 2 to type 3, and from type 3 to type 2 The optimal numbers of survivors under varying numbers released were identical, and optimal CPS values nearly identical, when the form of the functional response changed from a type 2 to a type 3, and from a type 3 to a type 2, midway through the juvenile nursery season (Fig. 8, A and B). The differences at low postrelease densities between optimal CPS values under shifting type 2 to type 3 and type 3 to type 2 scenarios (Fig. 8A) occurred because initial mortality under the type-3 functional response was sufficiently low that the difference in overall survival between small- and large-released fish was small enough to be overridden by the increased cost of the larger fish (Fig. 8A). The minimum CPS was obtained when small (42–44 mm TL) fish were released (in all other cases, optimal results were obtained when size-at-release was maximized) (Fig. 8A). The major difference between the two shifting scenarios is that the release dates producing optimal results for a given number of fish released varied depending on the direction of the shifting functional response. For example, when the functional response shifted from a type 2 to a type 3, a release of 100,000 HR organisms achieved optimal results when release occurred early in the season (Julian day ≤145) (Fig. 9A). When the functional response shifted from a type 3 to a type 2, a release of 100,000 HR summer flounder achieved optimal results only when releases occurred later in the season (Julian day >145) (Fig. 9B). When the

functional response shifted from a type 3 to a type 2, releasing 100,000 HR organisms prior to Julian day 146 resulted in markedly decreased survival (and therefore increased CPS) compared to results obtained from releases after day 146 (e.g. releasing on Julian day 92 resulted in a decrease in number of survivors and an increase in CPS of 22.8% and 29.7%, respectively) (Fig. 9B). Thus, date-of-release had a significant effect on the results (and therefore in determining optimal release strategies) when the relationship between density and mortality changed temporally, suggesting that the presence of a temporal shift in the functional response of the predator guild would have considerable effects on the number of survivors and CPS for stock enhancement efforts with juvenile summer flounder.

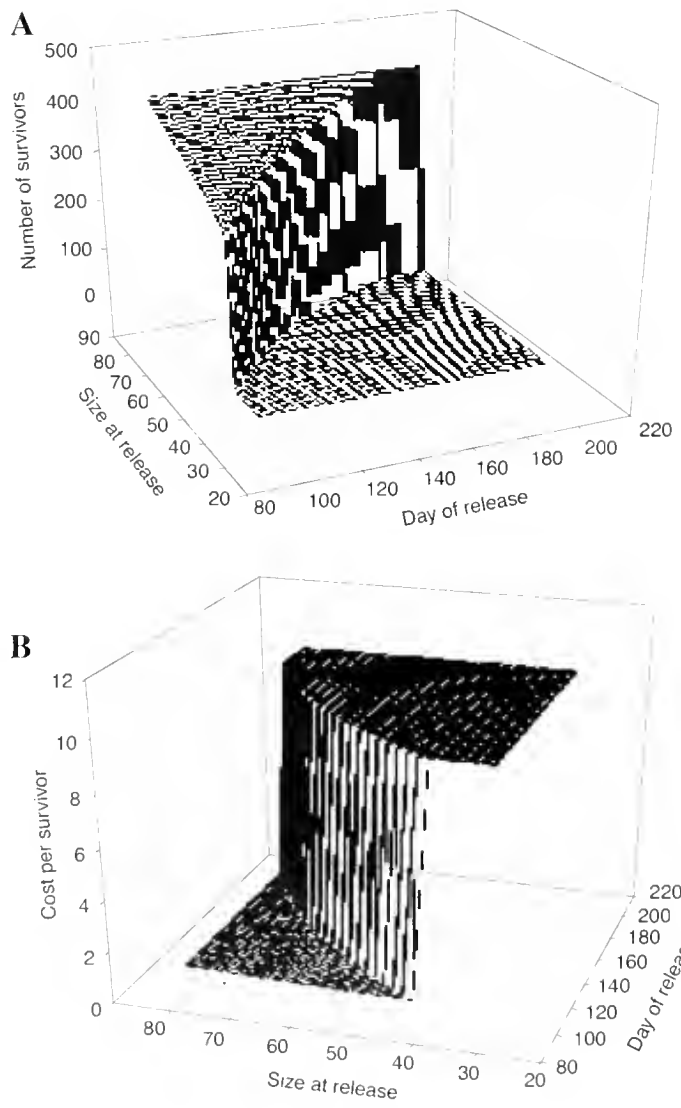

Figure 7

Response surfaces of (**A**) number of fish (summer flounder) survivors and (**B**) cost-per-survivor (CPS) as a function of date of release and size at release at number released (NR) = 500 (postrelease density=0.005) under a strong type-3 functional response. CPS values greater than $10 were set equal to $10 for ease of presentation.

Correspondence between predicted and observed temporal abundance patterns

Under the assumption of a type-2 functional response, predicted declines in juvenile summer flounder density over time were rapid when initial density was relatively low (i.e. 0.1 fish/m^2) (Fig. 10, A and B). These predictions contrast with those observed in the field, in which declines at relatively low initial densities were gradual (compare Fig. 10A and 10B to Fig. 10F). Under the assumption of a type-3 functional response, predicted declines were rapid when initial density was relatively high (i.e. 0.5 fish/m^2) (Fig. 10, C and D). These results generally contrast with those observed in the field, in which declines at relatively high densities were much less rapid than those predicted under a strong type-3 functional response, and somewhat less rapid than those predicted under a weak type-3 functional response (Figs. 10F and 11). Under density-independent mortality, there was little difference in predicted declines in juvenile summer flounder density over time between the three initial density levels (0.1, 0.3, and 0.5 fish/m^2); in each case there was a gradual decrease in density over time (Fig. 10E). These results were similar to those observed in the field, although declines at relatively high densities in the field were somewhat more rapid than those predicted under density-independent mortality (compare Figs. 10E and 10F). Thus, a density-mortality relationship lying between that generated under density-independence and that generated under the weak type-3 functional response in the model would most closely predict the temporal declines observed in the field.

Discussion

Implications for stock enhancement of summer flounder

Regardless of the relationship between density and mortality, size-at-release was the most important variable in the model affecting survival and costs associated with stock enhancement of summer flounder. The model predicts that under all release scenarios, 1) survival will be maximized and 2) costs associated with stock enhancement (i.e. cost per survivor) will be minimized when HR fish are released at the largest size possible. From a survival standpoint, these results are not

surprising. Larger fish spend fewer days than smaller fish in the wild nursery habitats before making an ontogenetic habitat shift to deeper waters and thus are susceptible to daily natural mortality for fewer numbers of days than are smaller fish. Thus, total mortality of smaller fish is greater than that of larger fish. Additionally, although we chose to make mortality independent of size in the model, abundant literature suggests that natural mortality (especially due to predation) may decrease with increasing size by mechanisms such as enhanced resistance to starvation, decreased vulnerability to predators, and better tolerance of environmental extremes (Sogard, 1997; Hurst and Conover, 1998; Lorenzen, 2000). Thus, the difference in predicted survival between 1) relatively large and relatively small fish and 2) fish released early versus late in the season in our model would be even greater if larger summer flounder suffered lower natural mortality than smaller fish. Furthermore, the daily mortality estimate used in the density-independent simulations and to parameterize the different types of density-mortality relationships may have been an underestimate of daily mortality (Kellison, 2000). If a greater estimate of daily mortality had been used, the difference in predicted survival between relatively large and relatively small fish in our model would have been further exacerbated because smaller fish spend longer amounts of time in the model growing to the 80-mm-TL ontogenetic shift size. These conclusions are supported by empirical research demonstrating that relatively large released HR fish suffer lower mortality than relatively small HR fish released in the field (e.g. Yamashita et al., 1994; Leber, 1995; Willis et al., 1995; Tominaga and Watanabe, 1998; Svåsand et al., 2000).

Although the survival predictions of the model (total mortality decreases with increasing size-at-release) are not surprising, the economic (cost-per-survivor) predictions were unexpected. The paradigm for stock enhancement strategy is that the rearing of relatively large fish for release is cost prohibitive, so that mass releases of relatively small, inexpensive-to-rear fish are a better strategy than the release of larger, expensive-to-rear fish (Kellison, personal obs.). Thus, relatively small juveniles are released in virtually all current stock enhancement programs (e.g. Russell and Rimmer, 1997; Masuda and Tsukamoto, 1998; McEachron et al., 1998; Svåsand, 1998; Serafy et al., 1999). Nevertheless, large-scale hatcheries and grow-out facilities are using ever-increasing technology to minimize the costs associated with the production of relatively large fishes (Sproul and Tominaga, 1992). Thus, for species for which 1) hatcheries are capable of producing relatively large fish at relatively low costs (as is likely for summer flounder), and 2) postrelease survival rates increase with release size, release scenarios utilizing the largest fish possible may maximize the potential (i.e. produce maximum survival at minimum costs) of stock enhancement efforts. In these cases, the "small fish maximize stock enhancement potential" paradigm might be replaced with a "large fish maximize potential" paradigm. As a caveat, this "large fish" strategy may be limited by spatial limitations of hatcheries in producing large numbers of relatively large fish. Because reared fish generally must

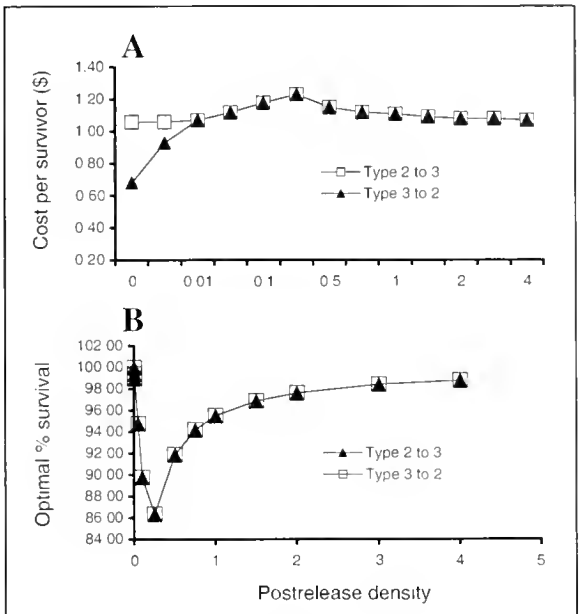

Figure 8

Optimal (**A**) economic cost-per-survivor and (**B**) percent survival of released hatchery-reared summer flounder under temporally shifting functional responses of type 2 to type 3 and type 3 to type 2.

be kept below critical densities in hatchery environments because of water quality and fish interaction issues (e.g. cannibalism), larger fish necessarily require more space than smaller fish for rearing. If the demand for space to rear large quantities of large fish can be realized, then the model simulations indicate that stock enhancement strategies in which size-at-release is maximized will produce the maximum number of survivors.

Although not as important as size-at-release, Julian day of release had a significant effect on survival and cost-per-survivor in the model, such that enhancement efforts were always more successful (more survivors, lower costs) when fish were released at the earliest Julian day possible. These results occurred because growth in the model decreased with increasing Julian Day. Although the mechanisms underlying this decrease in growth with increasing Julian day are unknown, they may be related to decreased prey availability or metabolic efficiency as temperatures increase with increasing Julian day (Malloy and Targett, 1994a, 1994b; Fujii and Noguchi, 1996; Howson, 2000). Thus, for a given size-at-release, fish released earlier in the season experienced greater growth rates than fish of the same size-at-release released later in the season and therefore reached the 80-mm-TL ontogenetic shift size faster (over a period of fewer days) than fish released later in the season. Thus, fish released earlier in the season were susceptible to natural mortality for fewer days than fish released later in the season and therefore suffered lower total mortality. These results emphasize the importance of knowledge of possible time-dependent growth in the field prior to stock enhancement efforts.

Is density important? Effects of varying density-mortality relationships

Our results suggest that the relationship between density and mortality has the potential to significantly affect optimal release scenarios associated with stock enhancement efforts. Because the original simulations were performed under density-independent mortality, the number of survivors originally increased linearly with the number released, resulting in a density-independent cost-per-survivor. Thus, when mortality is independent of density (over a given range of densities) for a target species for stock enhancement, managers will maximize the number of survivors produced by releasing the greatest number of fish possible within that range for a given size class. When mortality varied with density of released fish, the number of survivors and cost-per-survivor depended on the density-mortality relationship. In some cases, optimal results (maximum survival and minimum cost) differed depending on whether the response variable was number of survivors or cost-per-survivor. Under the assumption of a strong type-3 functional response and under relatively low postrelease densities, survival was optimized (maximized) by releasing the largest fish (80 mm TL) possible; however, cost-per-survivor was optimized (minimized) by releasing smaller fish (42–44 mm TL). This result occurred because mortality at low postrelease densities was sufficiently low that the difference in total mortality attributed to the longer "susceptibility" period of the smaller fish was insufficient to override the economic advantage of releasing smaller fish. Simulations under shifting functional responses (type 2 to type 3 and type 3 to type 2) produced optimal results similar to those obtained when nonshifting type-2 or type-3 functional responses were employed because densities were generally reduced to such low numbers by the time the shift occurred that the changing density-mortality relationship was inconsequential. Importantly, when functional responses shifted temporally, the predicted number of survivors and economic cost per survivor was at times very dependent on date of release, suggesting that identifying or ruling out shifting functional responses in the wild may be critical to accurate prediction of response variables (survivors and economic costs) associated with stock enhancement. Although we are not aware of reports in the literature of shifting functional responses in the wild, we are also not aware of studies that have tested for such a phenomenon, possibly because of the logistical difficulties inherent in identifying a shifting functional response.

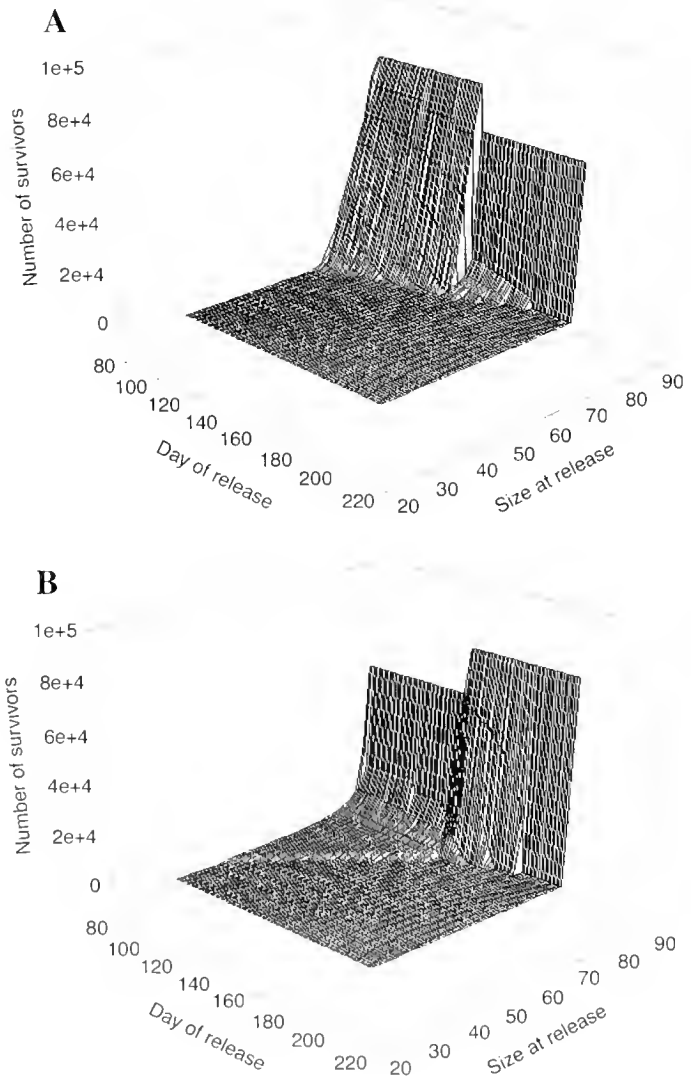

Figure 9

(**A**) Response surface of optimal number of summer flounder survivors as a function of date of release and size at release at number released (NR) = 100,000 (postrelease density=1.0 fish/m^2) under the assumption of a temporally shifting functional responses from type 2 to type 3. (**B**) Response surfaces of optimal number of survivors as a function of date of release and size at release at number released (NR) = 100,000 (postrelease density=1.0 fish/m^2) under the assumption of a temporally shifting functional responses from type 3 to type 2.

Correspondence between predicted and observed temporal abundance patterns

Predictions of field abundance patterns of juvenile flounder density over time were noticeably different under density-independent mortality and density-dependent mortality governed by type-2 and type-3 functional responses. For example, our simulations predict that fish density should decrease rapidly under relatively low initial densities if the functional response is type 2, decrease rapidly at relatively high initial densities if the functional response is type 3, and

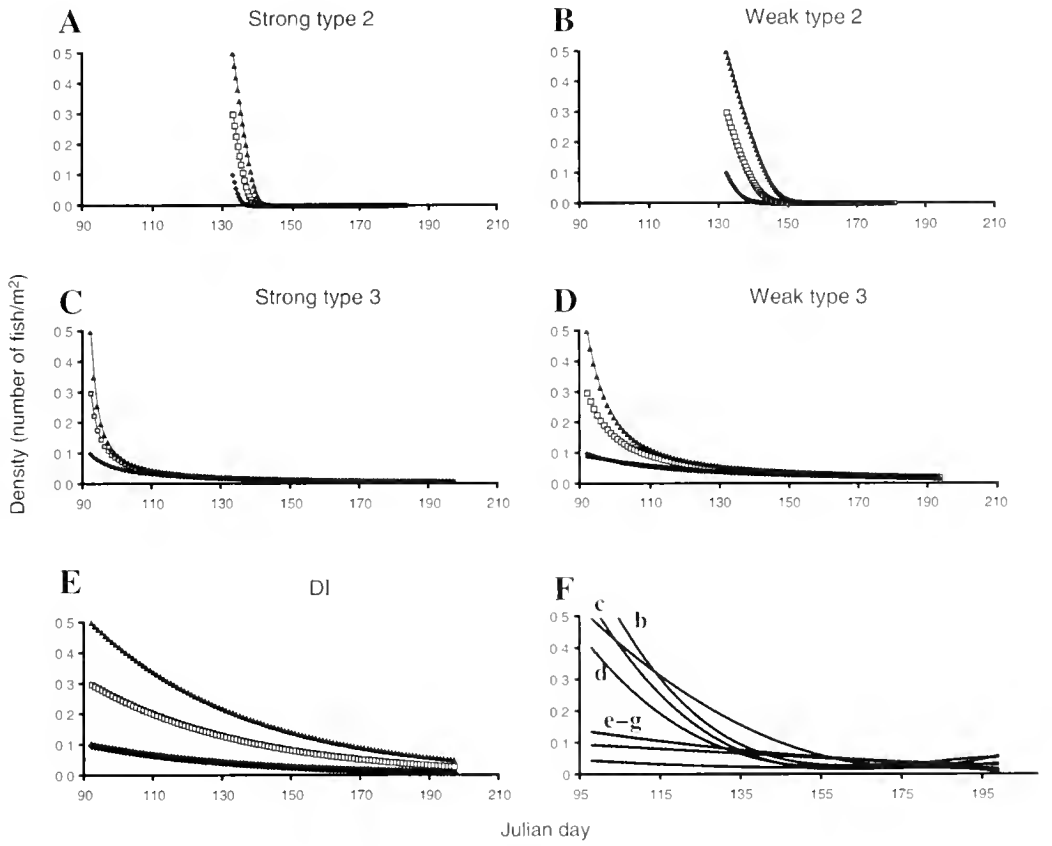

Figure 10

Predicted temporal trends in summer flounder abundance under initial densities of 0.5, 0.3, and 0.1 fish/m^2 under the assumption of a functional response that is a (**A**) strong type 2, (**B**) weak type 2, (**C**) strong type 3, (**D**) weak type 3, and under the assumption of (**E**) density-independent (DI) mortality. The curves in (**F**) are best fitted (highest r^2 value) to data collected in Duke Beach 1999 (curve a, r^2=0.82), Haystacks Marsh 1999 (curve b, r^2=0.73), Prytherch Marsh 1999 (curve c, r^2=0.82), Towne Beach 1999 (curve d, r^2=0.91), Radio Beach 1999 (curve e, r^2 = 0.27), Duke Beach 1998 (curve f, r^2=0.31), and Prytherch 1998 (curve g, r^2=0.16) (see Fig. 11 for data).

gradually decrease regardless of initial density if mortality is density independent. From examinations of temporal abundance patterns from several nursery sites (see Kellison et al., 2003b, for site descriptions), it is evident that observed declines at relatively low initial densities are similar to predicted declines under both density-independent mortality and a weak type-3 functional response; whereas observed declines at relatively high initial densities are somewhat less gradual than predicted under density-independent mortality, but somewhat more gradual than predicted under the weak type-3 functional response. These results suggest that model predictions made under the assumption of a weak type-3 response may give reasonably accurate but conservative predictions of juvenile summer flounder mortality and economic costs associated with stock enhancement for comparison with alternative management methods. As a caveat, although we found no evidence of size-dependent daily mortality over the range of fish sizes examined in this study, it is very likely that such a relationship exists to some extent (Sogard, 1997; Lorenzen, 2000). Incorporating size-dependent mortality into the model would decrease the slopes of the predicted temporal abundance curves but should not change the conclusion that the observed data lie somewhere between values predicted under density-independent mortality and those governed by a weak type-3 functional response, respectively. Additionally, because the portions of the curves used to delineate between temporal abundances expected under density-independent versus varying density-mortality relationships are from early in the growth season (later parts of the curve converge on very low densities) and because nearly all fish in these portions of the curves are at sizes well below that at which ontogenetic emigration occurs, the exclusion of emigration from these simulations should not affect the general conclusions reached. These issues could be clarified with further field trials to investigate the dependence of daily mortality rates on fish size.

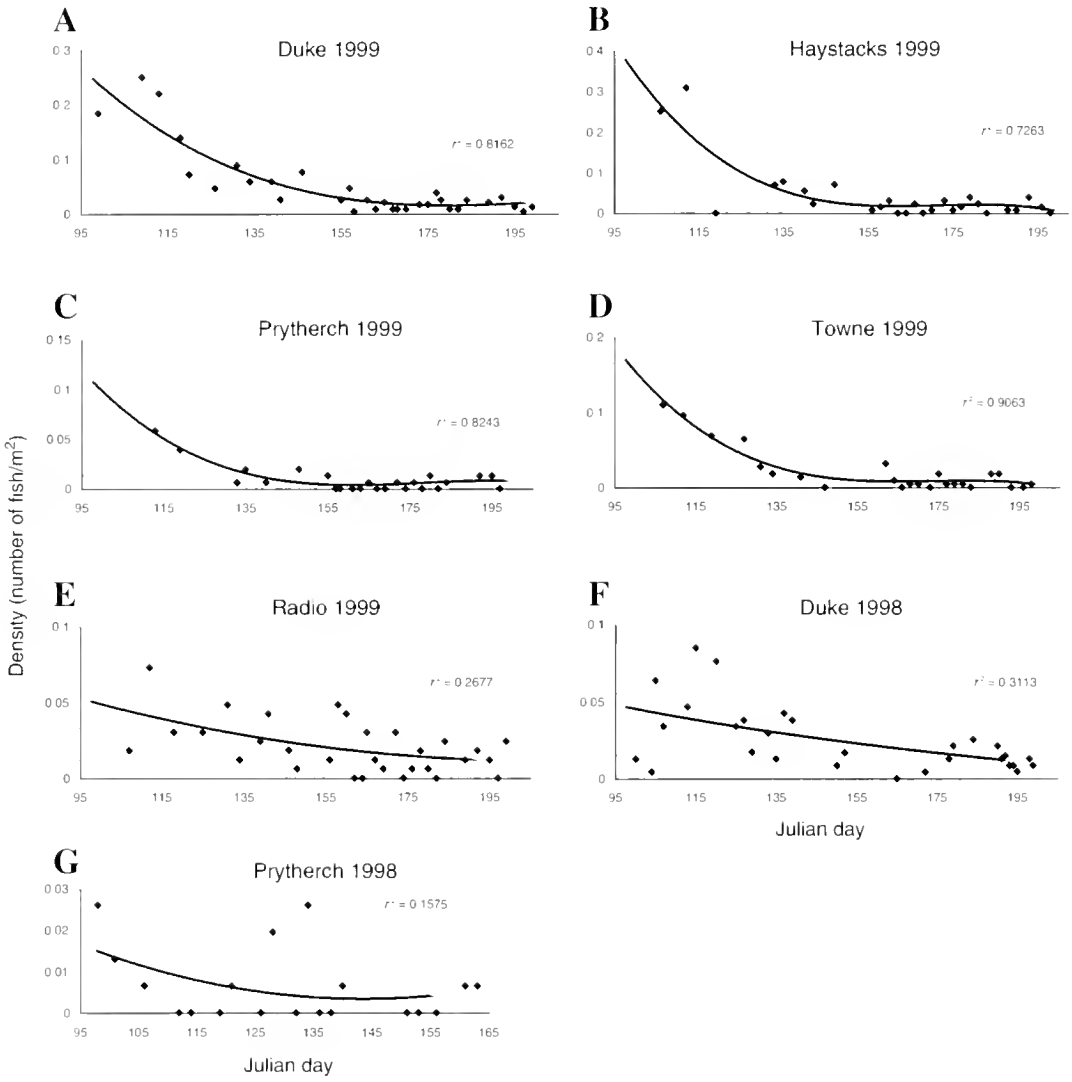

Figure 11

Temporal density patterns from (**A**) Duke Beach, 1999; (**B**) Haystacks Marsh, 1999; (**C**) Prytherch Marsh, 1999; (**D**) Towne Beach, 1999; (**E**) Radio Beach, 1999; (**F**) Duke Beach, 1998; and (**G**) Prytherch Marsh 1998. Densities are corrected for gear bias (see Kellison, 2000).

Model utility and implications

Although model results varied considerably under the various density-mortality relationships, the overall predictions that survival would be maximized and economic costs minimized when relatively large fish were released early in the season were unaffected by the density-mortality relationship. These results suggest that managers may use this model to make inferences about optimal release scenarios even if density-mortality relationships are unknown. Additionally, these results have important implications for the cost efficiency of stock enhancement programs. Managers can use the model to determine the release scenarios under which they can 1) maximize the number of survivors, given a financial limit (e.g. given a budget of x dollars, what release scenario or scenarios will produce the greatest number of survivors?), and 2) minimize costs, given a goal of number-of-survivors-produced (e.g. given a goal of producing x survivors, what release scenario or scenarios will be most cost efficient?).

In conclusion, the compartmental model used in this study provides an example of a relatively easy-to-develop predictive tool with which to make inferences about the ecological and economic potential of stock enhancement, in relation to alternative management approaches, to rebuild depleted fisheries.

Acknowledgments

We thank Brian Burke (NCSU) for tutelage in the use of Visual Basic, Mike Denson (South Carolina Department of Natural Resources) and Pete Schuhmann (UNC-Wilmington) greatly contributed to the editing of an earlier version of this manuscript. Mark Wuenschel, Michael Martin, Brian Degan, Lisa Etherington, and Mikael Currimjoe provided valuable laboratory and field assistance necessary for parameter estimation. This project was partially funded by the University of North Carolina at Wilmington/North Carolina State University Cooperative Ph.D. Program, and a grant from the National Science Foundation (OCE 97-34472) to D. Eggleston.

Literature cited

Adams, C. M., and R. S. Pomeroy.
1991. Scale economies in hard clam aquaculture. J. Shellfish Res. 10:307–308.

Barbeau, M. A., and H. Caswell.
1999. A matrix model for short-term dynamics of seeded populations of sea scallops. Ecol. Appl. 9:266–287.

Bax, N. J.
1983. Early marine mortality of marked juvenile chum salmon (*Oncorhynchus keta*) released into Hood Canal, Puget Sound, Washington, in 1980. Can. J. Fish. Aquat. Sci. 40:426–435.

Black, R. W. II, and N. G. Hairston Jr.
1988. Predator driven changes in community structure. Oecologia 77:468–479.

Blankenship, H. L., and K. M. Leber.
1996. A responsible approach to marine stock enhancement. *In* Developing and sustaining world fisheries resources: the state of science and management (D. A. Hancock, D. C. Smith, A. Grant, and J. P. Beumer, eds.), p. 485–491. CSIRO, Collingwood, Australia.

Botsford, L. W., and R. C. Hobbs.
1984. Optimal fishery policy with artificial enhancement through stocking: California's white sturgeon as an example. Ecol. Model. 23:293–312.

Buckel, J. A., D. O. Conover, N. D. Steinberg, and K. A. McKown.
1999. Impact of age-0 bluefish (*Pomatomus saltatrix*) predation on age-0 fishes in the Hudson River estuary: evidence for density-dependent loss of juvenile striped bass (*Morone saxatilis*). Can. J. Fish. Aquat. Sci. 56:275–287.

Burke, J. S.
1995. Role of feeding and prey distribution on summer and southern flounder in selection of estuarine nursery habitats. J. Fish Biol. 47:355–366

Burke, J. S., J. M. Miller, and D. E. Hoss.
1991. Immigration and settlement pattern of *Paralichthys dentatus* and *P. lethostigma* in an estuarine nursery ground, North Carolina, U.S.A. Neth. J. Sea Res. 27:393–405.

Burke, J. S., J. P. Monaghan, and S. Yokoyama.
2000. Efforts to understand stock structure of summer flounder (*Paralichthys dentatus*) in North Carolina, USA. J. Sea Res. 44:111–122.

Burke, J. S., T. Seikai, Y. Tanaka, and M. Tanaka.
1999. Experimental intensive culture of summer flounder, *Paralichthys dentatus*. Aquaculture 176: 135–144.

Bystroem, P., and E. Garcia-Berthou.
1999. Density dependent growth and size specific competitive interactions in young fish. Oikos 86: 217–232.

Cowx, I. G.
1999. An appraisal of stocking strategies in the light of developing country constraints. Fish. Manag. Ecol. 6: 21–34.

Elis, T., and R. N. Gibson.
1995. Size-selective predation of 0-group flatfishes in a Scottish coastal nursery ground. Mar. Ecol. Prog. Ser. 127:27–37.

FAO (Food and Agriculture Organization of the United Nations).
1998. Summary: The state of world fisheries and aquaculture. http://www.fao.org/WAICENT/FAOINFO/FISHERY/FISHERY.HTM. [Accessed: June 1998.]

Froese, R., and D. Pauly, eds.
2001. FishBase. World wide web electronic publication. http://www.fishbase.org. [Accessed: January 2001.]

Fujii, T., and M. Noguchi.
1996. Feeding and growth of Japanese flounder (*Paralichthys olivaceus*) in the nursery ground. *In* Proceedings of an international workshop: survival strategies in early life stages of marine resources, p. 141–154. A. A. Balkema Publishers, Brookfield, VT.

Furuta, S.
1999. Seasonal changes in abundance, length distribution, feeding condition and predation vulnerability of juvenile Japanese flounder, *Paralichthys olivaceus*, and prey mysid density in the Tottori coastal area. Nippon Suisan Gakkaishi 65:167–174.

Garcia, L. MaB., R. F. Agbayani, M. N. Duray, G. V. Hilomen-Garcia, A. C. Emata, and C. L. Marte.
1999. Economic assessment of commercial hatchery production of milkfish (*Chanos chanos* Forsskål) fry. J. Applied Ichthyol. 15:70–74.

Hansen, M. J., M. A. Bozek, J. R. Newby, S. P. Newman, and M. D. Staggs.
1998. Factors affecting recruitment of walleyes in Escanaba Lake, Wisconsin, 1958–1996. North Am. J. Fish. Manag. 18:764–774.

Heppell, S. S., and L. B. Crowder.
1998. Prognostic evaluation of enhancement programs using population models and life history analysis. Bull. Mar. Sci. 62:495–507.

Hernandez-Llamas, A.
1997. Management strategies of stocking density and length of culture period for the Catarina scallop *Argopecten circularis* (Sowerby): A bioeconomic approach. Aquacult. Res. 28:223–229.

Hobbs, R. C., L. W. Botsford, and R. G. Kope.
1990. Bioeconomic evaluation of the culture/stocking concept for California halibut. The California halibut, *Paralichthys californicus*, resource and fisheries, 1990, p. 417–450. Cal. Dep. Fish Game Fish. Bull., vol. 174.

Holling, C. S.
1959. Some characteristics of simple types of predation and parasitism. Canadian Entomologist 91: 385–398.

Houde, E. D.
1987. Fish early life history dynamics and recruitment variability. Am. Fish. Soc. Symp. 2:17–29.

Howson, U. A.
2000. Nursery habitat quality for juvenile paralichthyid flounders: Experimental analysis of the effects of physicochemical parameters. Ph.D. diss., 129 p. Univ. Delaware, Newark, DE. 129 p.

Hurst, T. P., and D. O. Conover.
1998. Winter mortality of young-of-the-year Hudson River bass (*Morone saxatilis*): Size-dependent patterns and effects on recruitment. Can. J. Fish Aquat. Sci. 55: 1122–1130.

Jenkins, T. M. Jr., S. Diehl, K. W. Kratz, and S. D. Cooper.
1999. Effects of population density on individual growth of brown trout in streams. Ecol. 80:941–956.

Kellison, G. T.
2000. Evaluation of stock enhancement potential for summer flounder (*Paralichthys dentatus*): an integrated laboratory, field and modeling study. Ph.D. diss., 196 p. NC State Univ., Raleigh, NC.

Kellison, G. T., D. B. Eggleston, and J. S. Burke.
2000. Comparative behaviour and survival of hatchery-reared versus wild summer flounder (*Paralichthys dentatus*). Can. J. Fish. Aquat. Sci. 57:1870–1877.

Kellison, G. T., D. B. Eggleston, J. C. Taylor, and J. S. Burke.
2003a. An assessment of biases associated with caging, tethering, and habitat-specific trawl sampling of summer flounder (*Paralichthys dentatus*). Estuaries 26:64–71.

Kellison G. T., D. B. Eggleston, J. C. Taylor, J. S. Burke, and J. A. Osborne.
2003b. Pilot evaluation of summer flounder stock enhancement potential using experimental ecology. Mar. Ecol. Prog. Ser. 250:263–278.

Kent, D. B., and M. A. Drawbridge.
1999. Developing a marine ranching programme: A multidisciplinary approach. Marine ranching: Global perspectives with emphasis on the Japanese experience. FAO fisheries circular 943:66–78. FAO, Rome.

Kimmerer, W. J., J. H. Cowman Jr., L. W. Miller, and K. A. Rose.
2000. Analysis of an estuarine striped bass (*Morone saxatilis*) population: influence of density-dependent mortality between metamorphosis and recruitment. Can. J. Fish. Aquat. Sci. 57:478–486.

Leber, K. M.
1995. Significance of fish size-at-release on enhancement of striped mullet fisheries in Hawaii. J. World. Aquacult. Soc. 26:143–153.

Lindholm, J. B., P. J. Auster, M. Ruth, and L Kaufman.
2001. Modeling the effects of fishing and implications for the design of marine protected areas: juvenile fish responses to variation in seafloor habitat. Conserv. Biol. 15:424–437.

Lorenzen, K.
2000. Allometry of natural mortality as a basis for assessing optimal release size in fish stocking programmes. Can. J. Fish. Aquat. Sci. 57:2374–2381.

Malloy, K. D., and T. E. Targett.
1994a. The use of RNA:DNA ratios to predict growth limitation of juvenile summer flounder (*Paralichthys dentatus*) from Delaware and North Carolina estuaries. Mar. Biol. 118:367–375.
1994b. Effects of ration limitation and low temperature on growth, biochemical condition, and survival of juvenile summer flounder from two Atlantic Coast nurseries. Trans. Am. Fish. Soc. 123:182–193.

Manderson, J. P., B. A. Phelan, A. J. Bejda, L. L. Stehlik, and A. W. Stoner.
1999. Predation by striped searobin (*Prionotus evolans*, Triglidae) on young-of-the-year winter flounder (*Pseudopleuronectes americanus*, Walbaum): examining prey size selection and prey choice using field observations and laboratory experiments. J. Exp. Mar. Biol. Ecol. 242:211–231.

Masuda, R., and K. Tsukamoto.
1998. Stock enhancement in Japan: review and perspective. Bull. Mar. Sci. 62:337–358.

McEachron, L. W., R. L. Colura, B.W. Bumguardner, and R. Ward.
1998. Survival of stocked red drum in Texas. Bull. Mar. Sci. 62:359–368.

Munro, J. L., and J. D. Bell.
1997. Enhancement of marine fisheries resources. Rev. Fish. Sci. 5:185–222.

Nash, R. D. M.
1998. Exploring the population dynamics of Irish Sea plaice, *Pleuronectes platessa* L., through the use of Paulik diagrams. J. Sea Res. 40:1–18.

Olla, B. L., M. W. Davis, and C. H. Ryer.
1998. Understanding how the hatchery environment represses or promotes the development of behavioural survival skills. Bull. Mar. Sci. 62:531–550.

Powell, A. B., and F. J. Schwartz.
1977. Distribution of paralichthid flounders (Bothidae: Paralichthys) in North Carolina estuaries. Chesapeake Sci. 18: 334–339.

Rice, J. A., T. J. Miller, K. A. Rose, L. B. Crowder, E. A. Marschall, A. S. Trebitz, and D. L. DeAngelis.
1993. Growth rate variation and larval survival: Inferences from an individual-based size-dependent predation model. Can. J. Fish. Aquat. Sci. 50:133–142.

Rickards, W. L.
1998. Sustainable flounder culture and fisheries: a regional approach involving Rhode Island, New Hampshire, Virginia, North Carolina, and South Carolina. *In* Nutrition and technical development of Aquaculture, Nov. 1998, p. 17–20. Sea Grant, Durham, NH.

Rose, K. A., J. H. Cowan Jr, M. E. Clark, E. D. Houde, and S-B Wang.
1999. An individual-based model of bay anchovy population dynamics in the mesohaline region of Chesapeake Bay. Mar. Ecol. Prog. Ser. 185:113–132.

Rosenberg, A. A., M. J. Fogarty, M. P. Sissenwine, J. R. Beddington, and J. G. Shepard.
1993. Achieving sustainable use of renewable resources. Science 262:828–829.

Russell, D. J., and M. A. Rimmer.
1997. Assessment of stock enhancement of barramundi *Lates calcarifer* (Bloch) in a coastal river system in far northern Queensland, Australia. Developing and sustaining world fisheries resources. *In* Developing and sustaining world fisheries resources: the state of science and management, p. 498–503. CSIRO, Collingwood (Australia).

Salvanes, A. G. V., D. L. Aksnes, and J. Giske.
1992. Ecosystem model for evaluating potential cod production in a west Norwegian fjord. Mar. Ecol. Prog. Ser. 90: 9–22.

Serafy, J. E., J. S. Ault, T. R. Capo, and D. R. Schultz.
1999. Red drum, *Sciaenops ocellatus* L., stock enhancement in Biscayne Bay, FL, USA: assessment of releasing unmarked early juveniles. Aquacult. Res. 30:737–750.

Sogard, S. M.
1997. Size-selective mortality in the juvenile stage of teleost fishes: a review. Bull. Mar. Sci. 60: 1129–1157.

Sproul, J. T., and O. Tominaga.
1992. An economic review of the Japanese flounder stock enhancement project in Ishikari Bay, Hokkaido. Bull. Mar. Sci. 50:75–88.

Stoner, A.W.
1980. Feeding ecology of *Lagodon rhomboides* (Pisces: Sparidae): variation and functional responses. Fish. Bull. 78: 337–352.

Sutton, T. M., K. A. Rose, and J. J. Ney.
2000. A model analysis of strategies for enhancing stocking success of landlocked striped bass populations. N. Am. J. Fish. Manag. 20:841–859.

Svasand, T.
1998. Cod enhancement studies in Norway—background and results with emphasis on releases in the period 1983–1990. Bull. Mar. Sci. 62:313–324.
Svasand, T. S., T. Kristiansen, T. Pedersen, A. G. V Salvanes, R. Engelsen, G. Naevdal, and M. Nodtvedt.
2000. The enhancement of cod stocks. Fish Fisheries 1: 173–205.
Tanaka, M., T. Goto, M. Tomiyama, and H. Sudo.
1989. Immigration, settlement and mortality of flounder *Paralichthys olivaceus* larvae and juveniles in a nursery ground, Shijiki Bay, Japan. Neth. J. Sea Res. 24:57–67.
Tominaga, O., and Y. Watanabe.
1998. Geographical dispersal and optimum release size of hatchery-reared Japanese flounder *Paralichthys olivaceus* released in Ishikari Bay, Hokkaido, Japan. J. Sea Res. 40: 73–81.
Travis, J., F. C. Coleman, C. B. Grimes, D. Conover, T. M. Bert, and M. Tringali.
1998. Critically assessing stock enhancement: an introduction to the Mote Symposium. Bull. Mar. Sci. 62: 305–311.
van der Veer, H. W., and J. I. Witte.
1993. The "maximum growth/optimal food condition" hypothesis: A test for 0-group plaice *Pleuronectes platessa* in the Dutch Wadden Sea. Mar. Ecol. Prog. Ser. 101: 81–90.
Waters, E. B.
1996. Sustainable flounder culture and fisheries. NC Sea Grant Publication UNC-SG-96-14, 12 p. Sea Grant, Raleigh, NC.
Waters, E. B., and K. Mosher, eds.
1999. Flounder aquaculture and stock enhancement in North Carolina: issues, opportunities and recommendations. NC Sea Grant Publication, UNC-SG-99-02, 24 p. Sea Grant, Raleigh, NC.
Willis, S. A., W. W. Falls, C. W. Dennis, D. E. Roberts, and P. G. Whitechurch.
1995. Assessment of season of release and size-at-release on recapture rates of hatchery-reared red drum. Uses and effects of cultured fishes in aquatic ecosystems. Am. Fish. Soc. Symp. 15:354–365.
Yamashita, Y., S. Nagahora, H. Yamada, and D. Kitigawa.
1994. Effects of release size on survival and growth of Japanese flounder *Paralichthys olivaceus* in coastal waters off Iwate Prefecture, northeastern Japan. Mar. Ecol. Prog. Ser. 105:269–276.

Sex-specific growth and mortality, spawning season, and female maturation of the stripey bass (*Lutjanus carponotatus*) on the Great Barrier Reef

Jacob P. Kritzer

School of Marine Biology & Aquaculture
and CRC Reef Research Centre–Effects of Line Fishing Project
James Cook University
Townsville, Queensland 4811, Australia
Present address: Department of Biological Sciences
University of Windsor
401 Sunset Avenue
Windsor, Ontario N9B 3P4, Canada

E-mail address: kritzer@uwindsor.ca

Abstract—Sex-specific demography and reproductive biology of stripey bass (*Lutjanus carponotatus*) (also known as Spanish flag snapper, FAO) were examined at the Palm and Lizard island groups, Great Barrier Reef (GBR). Total mortality rates were similar between the sexes. Males had larger L_∞ at both island groups and Lizard Island group fish had larger overall L_∞. Female:male sex ratios were 1.3 and 1.1 at the Palm and Lizard island groups, respectively. The former is statistically different from 1, but is unlikely significantly different in a biological sense. Females matured on average at 2 years of age and 190 mm fork length at both locations. Female gonadal lipid body indices peaked from August through October, preceding peak gonadosomatic indices in October, November, and December that were twice as great as in any other month. However, ovarian staging revealed 50% or more ovaries were ripe from September through February, suggesting a more protracted spawning season and highlighting the different interpretations that can arise between gonad weight and gonad staging methods. Gonadosomatic index increases slightly with body size and larger fish have a longer average spawning season, which suggests that larger fish produce greater relative reproductive output. Lizard Island group females had ovaries nearly twice as large as Palm Island group females at a given body size. However, it is unclear whether this reflects spatial differences akin to those observed in growth or effects of sampling Lizard Island group fish closer to their date of spawning. These results support an existing 250 mm minimum size limit for *L. carponotatus* on the GBR, as well as the timing of a proposed October through December spawning closure for the fishery. The results also caution against assessing reef-fish stocks without reference to sex-, size-, and location-specific biological traits.

Manuscript approved for publication 22 July 2003 by Scientific Editor.

Manuscript received 22 July 2003 at NMFS Scientific Publications Office.

Fish Bull. 102:94–107 (2004).

Lutjanid snappers are among the most prominent species comprising the catch of hook-and-line fisheries on tropical reefs worldwide (Dalzell, 1996). A notable exception is the line fishery on Australia's Great Barrier Reef (GBR). There, the finfish catch, and therefore the majority of fisheries research, is dominated by coral trouts of the genus *Plectropomus* (Mapstone et al.[1]). However, the GBR finfish harvest is diverse and the catch of many secondary species has risen steadily since the early 1990s (Mapstone et al.[1]). Furthermore, over the past decade, the GBR fishery has changed with the advent of the lucrative Asian live reef-fish market. At present, only a handful of the many species harvested on the GBR are exported to the live reef-fish market. However, continued expansion of the trade coupled with the depletion of fish stocks in other source nations (Bentley[2]) has the potential to introduce demand for a wider range of species. Even in the absence of changes in the species composition of live reef-fish exports, increased demand for secondary species due to changes in either domestic preferences or availability of primary species has the potential to elevate harvest of currently nontarget species (Kritzer, 2003).

Effective multispecies management of the GBR fishery will ultimately require understanding the biology of more than simply the primary target species. For example, spawning closures of the fishery have been proposed for nine-day periods around the new moon in October, November, and December on the rationale that this will protect spawning activity of a wide range of harvested species (Queensland Fisheries Management Authority[3]). Yet, spawning season information for species beyond the common coral trout (*P. leopardus*) (Ferreira, 1995; Samoilys, 1997) is nearly nonexistent. The GBR fishery is in a fortunate position with respect to management of many species for which exploitation is still at relatively low levels because baseline biological characteristics can be estimated before stock structure is drastically altered by fishing. These data can then be used in both formulating management strategies and monitoring effects of fishing.

[1] Mapstone, B. D., J. P. MacKinlay, and C. R. Davies. 1996. A description of the commercial reef line fishery log book data held by the Queensland Fisheries Management Authority. Report to the Queensland Fisheries Management Authority, 480 p. Primary Industries Building, GPO Box 46, Brisbane, Queensland 4001, Australia.

[2] Bentley, N. 1999. Fishing for solutions: can the live trade in wild groupers and wrasses from Southeast Asia be managed? TRAFFIC Southeast Asia report, 143 p. Unit 9-3A, 3rd Floor, Jalan SS23/11, Taman SEA, 47400 Petaling Jaya, Selangor, Malaysia.

[3] Queensland Fisheries Management Authority. 1999. Queensland coral reef fin fish fishery. Draft management plan and regulatory impact statement, 80 p. Primary Industries Building, GPO Box 46, Brisbane, Queensland 4001, Australia.

One of the most prominent secondary species in the GBR fishery is the stripey bass (*Lutjanus carponotatus*) (Spanish flag snapper, FAO). In relation to other large predators on the GBR, *L. carponotatus* is highly abundant on inshore reefs, common on mid-continental shelf reefs, and absent from outer-shelf reefs (Newman and Williams, 1996; Newman et al., 1997; Mapstone et al.[4]). Although this affinity for inshore reefs has the potential to make the species more susceptible to recreational fishing, the limited available data do not suggest that it is heavily exploited by the recreational fleet (Higgs, 1993) in relation to the commercial fleet (Mapstone et al.[1]). *Lutjanus carponotatus* has a broad-based diet, consuming a wide variety of smaller reef fishes and invertebrates (Connell, 1998). Its role as a predator coupled with its abundance, particularly on inshore reefs, suggests that the species might have an important ecological function on the GBR in addition to its role as a fishery resource.

Davies (1995) and Newman et al. (2000) have collected basic demographic data for *L. carponotatus* on the northern and central GBR, respectively. They both reported a pronounced asymptote in the growth trajectory and that most growth occurred over the first three to five years and little subsequent growth over a lifespan that can reach 15 to 20 years. Newman et al. (2000) also reported a heavily male-biased sample and larger body sizes among males. Unlike age and growth data, no information on reproduction of *L. carponotatus* has been available despite that fact that existing (minimum size limits) and proposed (spawning closures) fisheries regulations are based largely on reproductive traits (Queensland Fisheries Management Authority[3]).

Specific aims of this study were 1) to estimate sex ratios and sex-specific schedules of growth and mortality; 2) to estimate age- and size-specific schedules of female maturation; 3) to identify the spawning season; and 4) to determine whether reproductive output is proportional to body size by examining the ovary weight-body weight relationship and the average spawning duration of large and small fish. All traits were estimated at the Palm Island group on the central GBR. Additionally, sex-specific growth and female maturity schedules were also examined at the Lizard Island group on the northern GBR to develop spatial comparisons.

Materials and methods

Field methods

Size, age, and reproductive data were obtained for 465 *L. carponotatus* collected by spear fishing on fringing reef slopes during monthly fishery independent sampling at Pelorus, Orpheus, and Fantome Islands in the Palm Island group on the central GBR (Fig. 1) from April 1997 through March 1998. No sampling took place in January 1998 because of severe flooding in the area. To develop spatial comparisons, samples of 118 and 18 fish were obtained in October 1997 and April 1999, respectively, by spear fishing at the Lizard Island group approximately 400 km north of the Palm Island group (Fig. 1). Fish were collected from depths of 2 to 15 m by teams of two to four scuba divers. *Lutjanus carponotatus* most commonly inhabits depths less than 15 m (Newman and Williams, 1996); therefore sampling efforts encountered the majority of the population. Fish were targeted as encountered, without preference based on size, in order to collect as representative a sample as possible. Fish <150 mm fork length (FL) were rare in the samples because they were infrequently observed on reef slopes (Kritzer, 2002). Therefore, supplemental spear fishing on reef flats targeting smaller fish was conducted at the Palm Island group (n=24) in April and December 1999 and at the Lizard Island group (n=25) in May 1999 to obtain growth data for size classes against which the primary sampling was biased.

Total weight (TW, g) and FL (mm) of each specimen were recorded. Ovaries and testes of small lutjanids on the GBR are characterized by a lipid body running along the length of each lobe, akin to that found in tropical acanthurids (Fishelson et al., 1985). Gonads and these associated lipid bodies were removed and preserved in FAAC (formaldehyde 4%, acetic acid 5%, calcium chloride 1.3%). Sagittal otoliths were removed, cleaned, and stored for later analyses.

Gonad processing and ovarian staging

The lipid body was removed from each ovary or testis after fixation and the weight of the gonad (GW) and lipid body (LW) were measured to the nearest 0.01 g. A gonadosomatic index (GSI) and lipidsomatic index (LSI; after Lobel, 1989) were calculated for each sample as the percentage of TW represented by GW and LW, respectively. Features of whole fixed ovaries including color, speckling, and surface texture were noted as potential criteria for macroscopic staging after comparison with samples processed histologically. Sex of the April 1999 Lizard Island group samples was determined macroscopically only, and was therefore used in sex-specific growth analyses but not in analysis of maturity. Fish <150 mm FL had undeveloped gonads and sex of these specimens was not determined or assigned a reproductive stage.

A subsample of 131 ovaries spanning the range of gonad sizes and external appearances were prepared for histological examination. Samoilys and Roelofs (2000) found that medial gonad sections were adequate for determination of reproductive status. Therefore, a medial section was removed from one gonad lobe, dehydrated, and embedded in paraffin. Embedded ovarian tissues were sectioned at 5 μm and stained with hematoxylin and eosin. Ovaries were staged on the basis of the most advanced oocyte stage present (West, 1990). Additional features used in histological staging included the presence of brown bodies and atretic

[4] Mapstone, B. D., A. M. Ayling, and J. H. Choat. 1998. Habitat, cross shelf and regional patterns in the distributions and abundances of some coral reef organisms on the northern Great Barrier Reef. Great Barrier Reef Marine Park Authority research publication 48, 71 p. GPO Box 1379, Townsville, Queensland 4810, Australia.

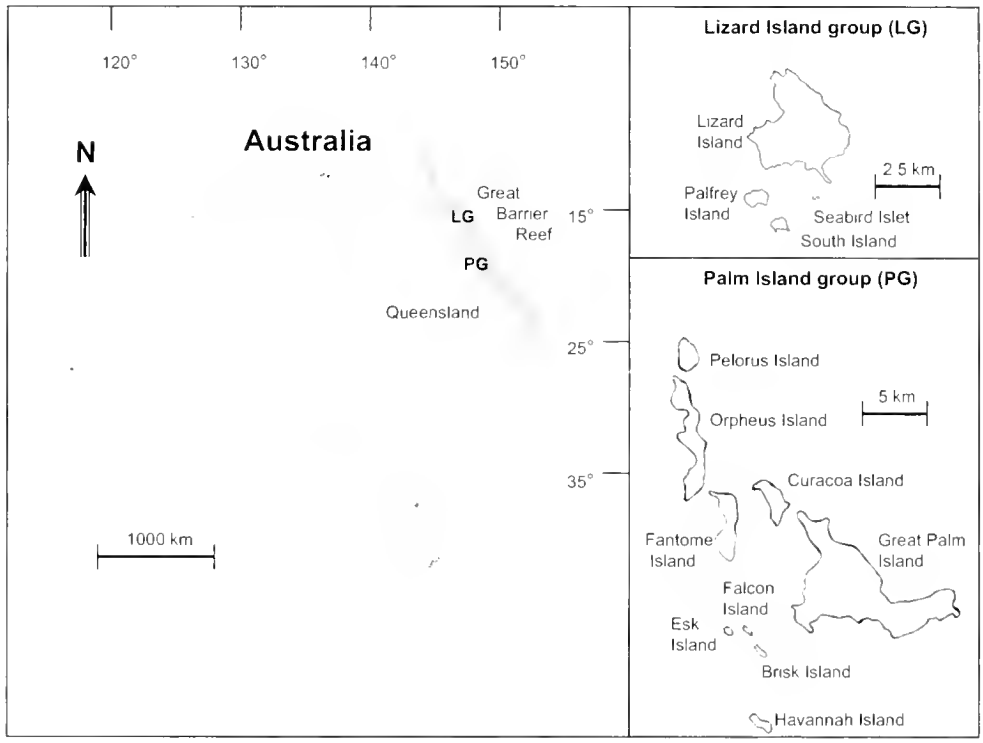

Figure 1

Location of the Palm Island group (PG) and Lizard Island (LG) group within the Great Barrier Reef off the coast of Queensland, Australia.

oocytes and, in the case of inactive ovaries, the relative thickness of the gonad wall and the compactness of the ovarian lamellae (Samoilys and Roelofs, 2000). For those samples processed histologically, macroscopic features were compared within and between reproductive stages to determine whether any macroscopic characteristics could be used to accurately stage ovaries

Age determination

Ages of fish were determined in order to estimate age-based schedules of growth, mortality, and maturation. Otoliths lacking broad, opaque macro-increments were processed to enumerate finer presumed daily micro-increments. These otoliths were ground by hand first from the anterior end and then the posterior end through a progressively finer series of P1200 sandpaper, 12-μm lapping film, and 9-μm lapping film until a thin section through the nucleus remained. Micro-increments were enumerated on two independent occasions. If the two counts for one specimen did not deviate by more than 5% of their mean, the mean was used as the age estimate. Otherwise, a third reading was performed and the mean of this and the more similar of the first two readings was used as the age estimate, again provided that the counts differed by no more than 5% of their mean.

Macro-increments in the otoliths of *L. carponotatus* have been validated as annuli by tetracycline labeling (Cappo et al., 2000). A pilot analysis indicated that age estimates did not differ between readings of whole left and right otoliths (paired t-test: df=59; t=0.60; P=0.55); therefore one otolith was randomly selected from each sample for age determination. All otoliths were initially read whole. A second pilot analysis compared whole and sectioned age estimates for a subsample of *L. carponotatus* otoliths. This comparison suggested that whole readings began to drastically underestimate age beyond approximately sectioned age 12 (see Kritzer, 2002). To capitalize on both the greater efficiency of whole readings and the greater accuracy of sectioned readings, whole readings were used for all fish except for those for which any whole reading exceeded 10 or for which there was not agreement in at least two out of three independent whole readings. If at least two out of three independent readings of either whole or sectioned otoliths (as appropriate) agreed, then that value was used as the age estimate. Ferreira and Russ (1994) have described the whole- and sectioned-otolith preparation and reading methods used in the present study.

Sex-specific demography

Early growth of *L. carponotatus* was estimated by linear regression of FL on age for those samples processed to read subannual micro-increments. Separate regressions were performed for the Palm and Lizard island groups and these were compared by analysis of covariance (ANCOVA). Because of the undeveloped nature of the gonads of the smallest fish, early growth was estimated without refer-

ence to sex. Sex ratios at each island group were compared with an expected ratio of 1:1 by χ^2 goodness-of-fit tests by using all specimens (i.e. immature and mature) whose sex could be determined.

Lifetime growth parameters were estimated for males and females from each island group by fitting the von Bertalanffy growth function (VBGF),

$$L_t = L_\infty\left(1-\exp\left(-K(t-t_0)\right)\right),$$

where L_t = FL at age t;
L_∞ = the mean asymptotic FL;
K = the Brody growth coefficient; and
t_0 = the age at which fish have theoretical FL of 0.

Growth functions were fitted by nonlinear least-squares regression of FL on age by using samples for which sex was determined. Because VBGF parameter estimates can be sensitive to the range of ages and sizes used (see Ferreira and Russ, 1994, for an empirical example), a common t_0 equivalent to the x-intercept of the early growth estimates was used in all models (see "Results" section). Although the sex-specific sample sizes at the Lizard Island group were smaller (n=65 for females; n=62 for males), VBGF parameter estimates achieved high precision at sample sizes between 50 and 100 (Kritzer et al., 2001); therefore the Lizard Island group data were included in the analysis. Growth parameters were compared by plotting 95% confidence regions of the parameters K and L_∞ (Kimura, 1980) for each sex from each location and assessing the degree of overlap.

Sex-specific total mortality rates, Z, were estimated by using the age-based catch curve of Ricker (1975) as the slope of a linear regression of natural log-transformed frequency on age class. Everhart and Youngs (1981) proposed that catch curve analysis should exclude age classes with n<5 and Murphy (1997) proposed that age structures used in catch curves should be truncated at the first age class with n<5. Alternatively, Kritzer et al. (2001) proposed that a sample should contain an average of at least ten fish per age class irrespective of age class-specific sample sizes. Therefore catch curves were fitted by two different methods for each sex at the Palm Island group. The first catch curve began at the modal age class and stopped before the first age class with n < 5. The second catch curve likewise began at the modal age class but included all age classes that were thereafter represented in the data set. Sex-specific sample sizes for the Lizard Island group were too small by any of these criteria and this location was excluded. Mortality estimates for Palm Island group fish were compared between the fitting methods within each sex as well as between sexes by ANCOVA.

Reproductive biology

Maturation schedules of female fish were estimated for each island group by fitting a logistic model,

$$P_i = 1/\left(1+\exp(a-ri)\right),$$

where P_i = the proportion of mature fish in age or 20-mm size class i;
a adjusts the position of the curve along the abscissa; and
r determines its steepness.

Age- and size-specific maturity functions were used to estimate the mean age, t_{50}, and size, L_{50}, at which 50% of females are mature at each island group.

Monthly mean LSI and GSI values of mature Palm Island group fish were plotted separately for males and females to determine seasonal patterns of energy storage and the peak spawning period of *L. carponotatus*. The proportion of specimens at each mature female reproductive stage in each month was also plotted to examine ovarian development patterns throughout the year and the degree of spawning activity occurring outside of peak months.

To examine whether relative reproductive output increases with body size, GW and GSI for stage-IV ovaries collected during peak spawning months were regressed against TW. Residual plots were used to assess deviation from a linear relationship and to identify three outliers, which were removed from the regression analysis. Regression slopes were compared between the two island groups by ANCOVA. Also, mean GSI values and the proportion of Palm Island group females with stage-IV ovaries during spawning months were compared between females ≤230 mm FL and those >230 mm FL to examine whether the duration of spawning varies between size classes (*nota bene*: 230 mm FL is approximately the mean size of mature Palm Island group females and splits each month's sample approximately in half).

Results

Ovarian staging

Five female reproductive stages were identified through histological analysis (Table 1) and were based largely on the scheme of Samoilys and Roelofs (2000). Ovarian stages I (immature) and II (resting mature) have similar oocyte stages. These can be distinguished by the presence of brown bodies or atretic oocytes, which are typically products of prior spawning (e.g. Ha and Kinzie, 1996; Adams et al., 2000) and are usually absent from stage-I ovaries. However, these structures will not necessarily persist in ovaries that have spawned, and in fact were rare among the samples; therefore identification of immature females was based primarily on structural organization of the ovary. Stage-I ovaries typically have a thin ovarian wall and more compacted oocytes, whereas ovaries that have previously spawned tend to have a thicker ovarian wall and a more disorganized arrangement of oocytes (Table 1). Also, there were distinct size differences between stage-I ovaries and other stages. The mean GW of stage-I ovaries was approximately one-third that of stage-II ovaries, and mean GSI was approximately one-half of that at stage II (Table 1), and the distribution of body sizes of fish at stage I had much lower minimum, maximum, and modal size

Table 1

Description of histological and macroscopic features (after fixation in a formaldehyde, acetic acid, calcium chloride solution) of ovarian developmental stages of *Lutjanus carponotatus*. Stage definitions and descriptions are largely a modification of the scheme proposed by Samoilys and Roelofs (2000). Mean ovary weight (GW) and gonosomatic index (GSI) for the larger Palm Island group sample are provided.

	Stage	Histological features	Macroscopic features
Inactive	I Immature	Relatively thin ovarian wall; lamellae well packed; only darkly purple staining previtellogenic oocyte stages (oogonia and perinucleolar stages) present.	Always even white color over entire surface; smooth surface texture; lobes quite small (typically <2 cm long) and thin (mean GW=0.33 g; mean GSI=0.24%).
	II Resting	Relatively thick ovarian wall; spaces between lamellae common; only previtellogenic oocyte stages and possibly brown bodies and few atretic vitellogenic oocytes present.	Even white to cream or tan color over gonad surface; surface may be smooth or somewhat convoluted; small white stage II ovaries are difficult to distinguish from stage I without histology (mean GW=1.01 g; mean GSI=0.43%).
Active	III Ripening	Most advanced oocytes are at yolk globule or migratory nucleus stage; atretic oocytes or brown bodies possibly present.	Color sometimes white but more often cream to tan; surface is commonly convoluted; difficult to distinguish from stage II without histology (mean GW=1.18 g; mean GSI=0.53%).
	IVa Ripe	Most advanced oocytes at yolk vesicle stage; atretic oocytes or brown bodies possibly present.	Color tan to brown or mustard with opaque speckles that become larger and more dense as late stage oocytes become more numerous; convoluted surface sometimes with prominent vascularization (mean GW=4.04 g; mean GSI=1.39%).
	IVb Running ripe	Similar to stage IVa but large, irregularly shaped, clear to lightly coloured hydrated oocytes are present.	External appearance identical to stage IVa and can only be differentiated histologically (no samples found at Palm Island group).

classes compared with the distribution of body sizes of fish at stage II (Fig. 2).

Stage-III (ripening) ovaries contain oocytes at the yolk vesicle vesicle stage, which some authors classify as vitellogenic (e.g. Samoilys and Roelofs, 2000) and others classify as previtellogenic (e.g. West 1990). Like stage-II ovaries, stage-III ovaries can, but do not necessarily, contain brown bodies or atretic oocytes as evidence of probable prior spawning. Although the fish might not have spawned previously, stage III is considered to be a mature stage in the present study because the appearance of yolk vesicles is associated with the initial development of the yolk globule and represents advanced development of the oocyte beyond perinucleolar stages (West, 1990). Therefore, the fish is preparing for spawning and will soon be part of the mature population if it is not already. Mean age and size of stage-II (4.4. years and 219 mm FL), stage-III (5.0 years and 222 mm FL), and stage-IV (6.5 years and 261 mm FL) females were much more similar to one another than they were to stage-I females (1.9 years and 119 mm FL). Moreover, size-frequency distributions of fish at stages II, III, and IV showed considerable overlap and similarity with one another and were all quite distinct from the size-frequency distribution for stage-I females (Fig. 2). This suggests a division between immature fish and those that are spawning or are nearly ready to do so. The pronounced difference in GW and GSI between stage-I and stage-III ovaries and similarity in these metrics between stage-II and stage-III fish (Table 1) further support this division.

Most immature ovaries and all ripe ovaries could be identified macroscopically. Because certain macroscopic features were common to multiple ovarian stages, additional histological features was required to separate the largest immature from the smallest resting ovaries and all ripening from resting ovaries among the samples remaining after the initial comparison between histological and macroscopic features. Only one ovary with fully hydrated oocytes, collected at the Lizard Island group, was found among the samples prepared for histological analysis; therefore stages IVa and IVb were treated as a single stage. Stage IV sufficiently represents final development toward spawning on the broad seasonal time scale adopted in this study but encompasses a wide range of ovarian characteristics and would need to be divided into more detailed stages for finer temporal scale studies of lunar or diel spawning patterns. No samples exhibited features of truly "spent" ovaries.

Sex-specific demography

Differences were not apparent in early growth of *L. carponotatus* between the island groups (ANCOVA: df=1, 46; F=1.07; P=0.301); therefore the data were pooled to

estimate an early growth rate of 0.76 mm/d, assuming daily periodicity of micro-increments (Fig. 3). This rate of growth represents quite rapid growth, given that fish are adding 100 mm of length in around 4 months, increasing from approximately 20 to 120 mm FL (Fig. 3). The x-intercept of the early growth curve (=–17.98 d) was divided by 365 d/yr to estimate a common t_0 (=–0.049 yr) for all VBGF models.

Although size at age for both sexes at both island groups was characterized by substantial individual variability, different growth trajectories were evident for males and females (Fig. 4, A and B). Estimates (Table 2) and 95% joint confidence regions (Fig. 4C) for the VBGF parameters indicated that the primary differences in these trajectories at each island group lay in L_∞ (which indicated that males grow larger than females). In contrast, the common range of K values spanned by the sexes within each island group indicated similar curvature (Table 2, Fig. 4C). However, use of a common t_0 restricts the range of possible fitted K values (Kritzer et al., 2001). In addition to the differences between the sexes, the data revealed a general pattern of larger body sizes at the Lizard Island group (Table 2, Fig. 4).

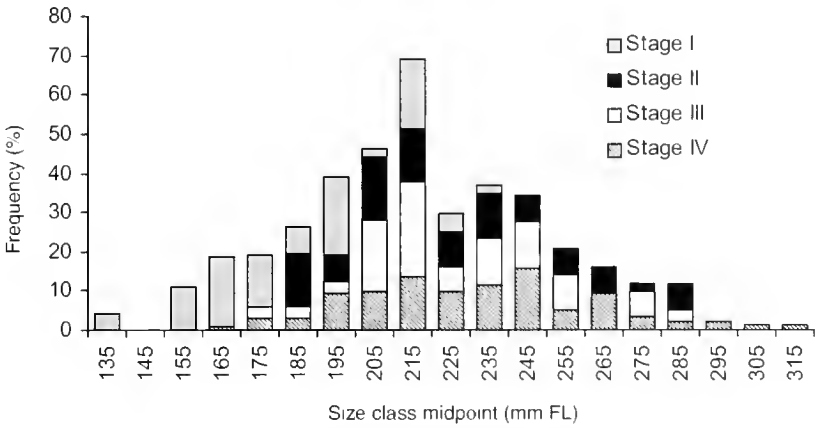

Figure 2

Size-frequency distributions of female Palm Island group *Lutjanus carponotatus* at each of the four stages of ovarian development. Stage descriptions are provided in Table 1.

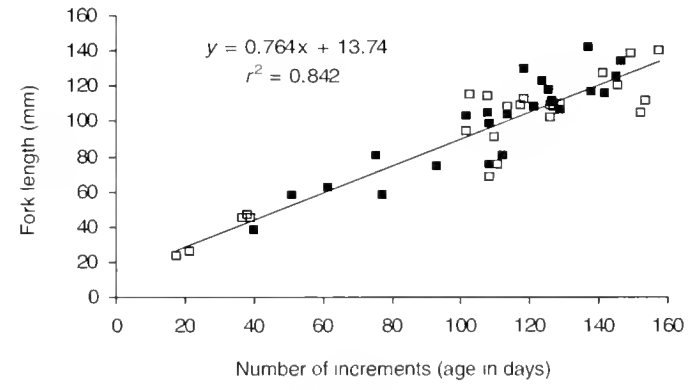

Figure 3

Fork length at microincrement count for *Lutjanus carponotatus* lacking the first annulus at the Palm (□; n=24) and Lizard (■; n=25) island groups. Periodicity of increments is presumed to be daily. Data from each island group are distinguished, but a pooled linear growth curve is presented as separate growth curves did not differ (ANCOVA: df=1, 46; F=1.07; P=0.301).

Mortality estimates at the Palm Island group were slightly higher when all age classes beyond 1 year were included compared with exclusion of age classes with $n < 5$ (Fig. 5). These higher mortality estimates contrast with Murphy's (1997) finding that truncation of the age structure results in higher least-squares estimates of Z. The differences between mortality rates estimated with and without age classes with $n < 5$ were minor for both males (ANCOVA: df=1, 20; F=0.009; P=0.92) and females (ANCOVA: df=1, 23; F=1.35; P=0.26). Therefore, for comparisons between the sexes, the estimates that included all age classes greater than 1 yr were used. In contrast to the sex-specific growth differences, Z estimates of 0.26/yr and 0.29/yr (Fig. 5) corresponding to annual survivorship of 77% and 75% for females and males, respectively, at the Palm Island group were similar between the sexes (ANCOVA: df=1, 27; F=0.505; P=0.483). Murphy's (1997) results also suggested that least-squares mortality estimates are likely to be around 30% less than the true mortality rate when n = 200 and the true Z = 0.2/yr. Correcting these mortality estimates based upon this potential bias results in Z estimates up to 0.37/yr and 0.41/yr for females and males, respectively, with corresponding annual survivorship of 69% and 66%. However, the catch curve estimates (Fig. 5) corresponded well with estimates based upon Hoenig's (1983) empirically derived relationship between Z and maximum age, t_{max} (females: t_{max}=18 yr, Z=0.23/yr; males: t_{max}=16 yr; Z=0.26/yr).

The observed female-to-male sex ratios of 1.3 and 1.1 were close to unity at the Palm and Lizard Island groups, respectively (Table 2). However, χ^2 tests suggest this ratio is statistically different from 1 at the Palm Island group (df= 1; χ^2=7.74; P=0.005) but not at the Lizard Island group (df=1; χ^2=0.031; P=0.86).

Age and size at maturity

Although there was some indication that Palm Island group females mature at slightly younger ages and smaller sizes

than Lizard Island group females, maturation schedules were generally similar (Fig. 6). At both island groups, age 2 was the age at both earliest maturity and 50% maturity, and 93–100% of females had matured by age 4 (Fig. 6A, Table 3). Thus, maturation was rapid, beginning early in life and ending within a 2-year period with nearly all members of a cohort mature. Length-specific maturation schedules also exhibited similarity between the island groups with mature fish first appearing in the 160–179 mm FL size class, estimated 50% maturation in the 180–199 mm FL size class, and 93–100% maturity at the 220–239 mm FL size class (Fig. 6B, Table 3).

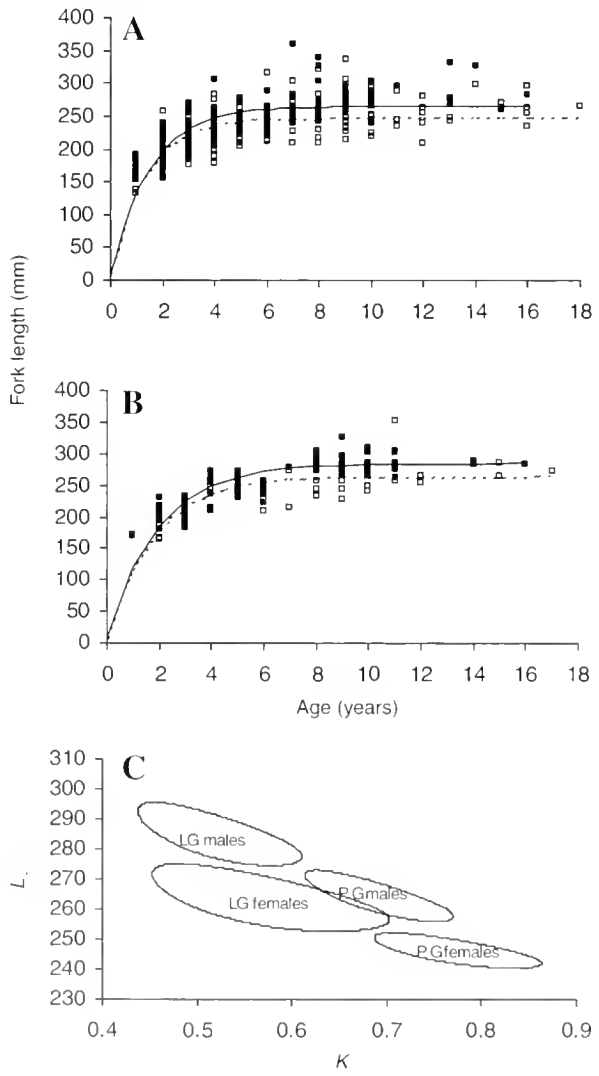

Figure 4

Fork length at age and estimated von Bertalanffy growth curves for male (■, solid lines) and female (□, broken lines) *Lutjanus carponotatus* at the Palm (**A**) and Lizard (**B**) island groups and estimated 95% joint confidence regions of the parameters K and L_∞ (**C**). Parameter estimates are presented in Table 2.

Spawning season

Mature female LSI values were highest in August through October with a maximum in September (Fig. 7A). The peak in GSI lagged that of LSI by two months with the highest values occurring from October through December and with a maximum in November (Fig. 7A). The absence of a January sample unfortunately leaves some ambiguity as to whether GSI, and therefore presumably spawning activity, would still be high at this time or if it would have begun to decline. Male GSI values also exhibited a November maximum (Fig. 7B). Male LSI values, however, did not show any clear trend of increase and decline throughout the year and peaks in April, May, and August that did not correlate with future GSI values as clearly as seen in the female data (Fig. 7). Unlike LSI values for females, monthly mean male LSI values were always greater than the corresponding GSI values.

The seasonal pattern of *L. carponotatus* spawning activity suggested by monthly trends in the proportions of mature ovarian stages can be interpreted as different from that suggested by GSI values. The lowest GSI values in the October–December peak period were close to twice as great as the next highest values in September and February (Fig. 7A). However, the percentage of stage-IV ovaries in the September sample was greater than 50%, which is well over half the percentage of the October sample; whereas the February sample comprised approximately the same percentage of stage-IV ovaries as October (Fig. 8). Also, more than 50% of the March sample was stage-IV ovaries (Fig. 8), whereas its GSI value was close to that of the months with relatively few ripe ovaries (Fig. 7A). Furthermore, September and March had the highest proportions of ripening (stage-III) females and thus far fewer resting mature (stage-II) females than the April to August period of limited spawning activity (Fig. 8). Therefore, regardless of whether September, February, and March are defined as nonspawning months or months of limited spawning activity based upon GSI, analysis of ovarian stage frequencies suggests these to be periods of greater spawning activity than might be predicted with GSI. Clearly, the presence of advanced oocytes is a much better indication of imminent spawning than any measure of gonad size; therefore the reproductive stage-frequency data undoubtedly provide the more accurate picture of *L. carponotatus* spawning patterns.

Of 59 ovaries staged from the October 1997 Lizard Island group sample, eight were at stage I, two were at stage II, and 49 (96% of mature females in the sample) were at stage IV. This finding suggests that the island groups share at least October as a common period of active spawning.

Reproductive differences between locations and among size classes

The variation in GW among females of like body sizes during peak spawning months increased to some degree with increasing TW, but there was a generally homogeneous spread of data around the predicted regression

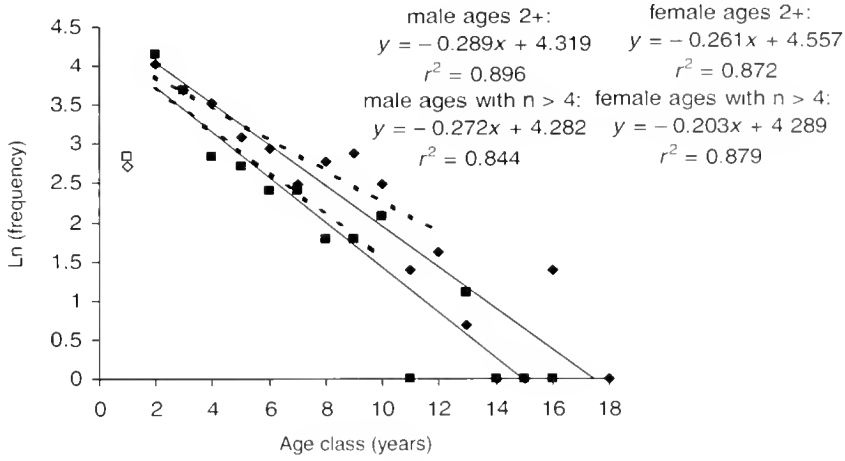

Figure 5

Age-based catch curves for female (■, higher elevation lines) and male (♦, lower elevation lines) *Lutjanus carponotatus* at the Palm Island group fitted to all age classes >1 (solid lines) and age classes >1 with n >4 (dashed lines). Open symbols represent age class 1, which was not used in the analysis.

Table 2

Sex-specific von Bertalanffy growth parameters for *Lutjanus carponotatus* at the Palm and Lizard Island groups, Great Barrier Reef. n is sample size; $\bar{L}_F$ is the mean fork length (mm); K is the Brody growth coefficient (per yr); L_∞ is the mean asymptotic fork length (mm); a common t_0 of –0.049 yr was used in all growth models. Standard errors are provided below parameter estimates.

	n	$\bar{L}_F$	K	L_∞	r^2
Palm Island group					
females	263	224.2	0.77	246.3	0.515
		(2.11)	(0.032)	(2.25)	
males	202	224.7	0.69	264.3	0.629
		(2.78)	(0.028)	(3.26)	
sex ratio	1.3:1				
Lizard Island group					
females	65	239.9	0.56	263.5	0.618
		(4.76)	(0.043)	(4.24)	
males	62	256.4	0.51	284.8	0.714
		(4.77)	(0.032)	(4.03)	
sex ratio	1.1:1				

lines across body sizes (Fig. 9A). This suggests that on average GW at stage IV during peak spawning months is a linear function of TW. Lizard Island group fish generally had larger ovaries at a given size than did Palm Island group fish (Fig. 9A), a difference supported by ANCOVA (df=1, 125; F=34.7; P<0.001). In fact, regression slopes of 0.25 and 0.52 suggest relative ovary weights at the Lizard Island group were approximately twice as large as those at the Palm Island group. There were no differences in the GW-TW relationship among October, November, and December at the Palm Island group, and therefore the differences in this relationship between the island groups was consistent whether only the Palm Island group October data were used or whether the October through December data were used.

Although GW is a linear function of TW, the nonzero regression constants (Fig. 9A) mean that GW is not a constant proportion of TW. Consequently, GSI increases with increasing TW (Fig. 9B). The relationship between TW and GSI is not strong, with regression slopes close to zero and low r^2 values at both island groups (Fig. 9B). Despite this, the relationship is statistically strong at both the Palm (ANOVA: df=1,82; F=12.70; P=0.006) and Lizard (ANOVA: df= 1,42; F=22.95; P<0.0001) Island groups. Also, there is

some suggestion that, like the GW-TW relationship, the GSI-TW relationship varies between the island groups, although to a much lesser extent (ANCOVA: df=1,125; F=7.44; P=0.007).

There is some indication that larger fish spawn over a longer period at the Palm Island group. During the September–February spawning season, mean GSI values were always higher for mature Palm Island group females >230 mm FL compared with mature females ≤230 mm FL at the same location (Fig. 10). This pattern is likely due in part to the higher relative gonad weights of larger fish (Fig. 9B) but also seems to be driven by greater proportions of stage-IV ovaries among larger mature females in September, October, and February compared with fish ≤230 mm FL (Fig. 10). During these months, 13%, 13% and 25% more large fish were at stage IV, respectively, than were small fish.

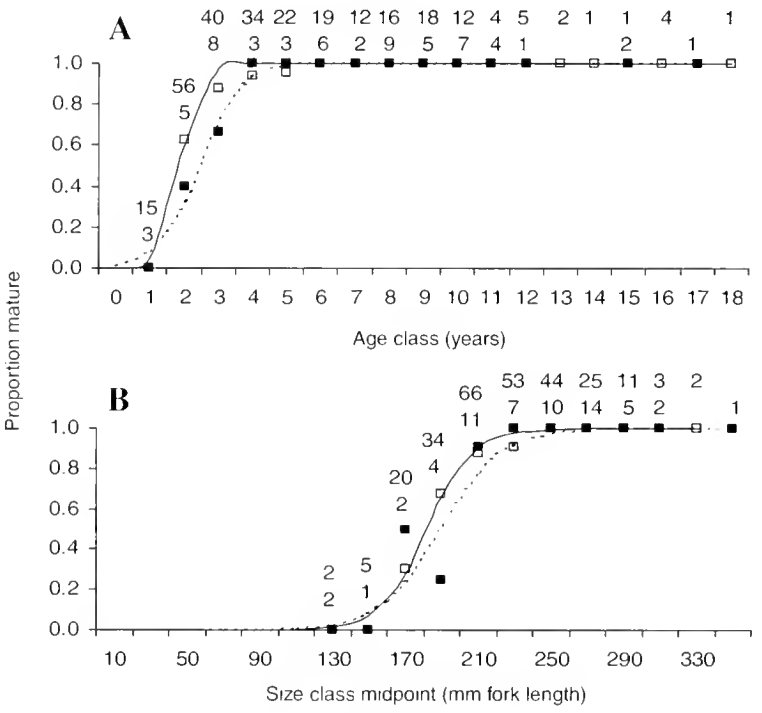

Figure 6

Proportion of mature female *Lutjanus carponotatus* and estimated age-specific (**A**) and size-specific (**B**) logistic maturation schedules at the Palm (■, solid lines) and Lizard (□, broken lines) island groups. Sample sizes for the Palm (top value) and Lizard (lower value) Island groups are presented above the data for each age or size class. Parameters of the maturity functions are provided in Table 3.

Discussion

Demography and reproduction of *L. carponotatus*

Growth of *L. carponotatus* is rapid for the first two years of life, slows over the next two years, and nearly ceases by age 4. The slowing and cessation of growth coincide with the ages at 50% and 100% maturity, respectively, and support the argument of Day and Taylor (1997) that maturation represents a pivotal physiological transformation and consequently a fundamental shift in the growth trajectory. Further supporting the idea that reproductive development occurs at the expense of somatic growth is the apparently longer average spawning season among larger fish that have ceased most somatic growth. The limited growth over much of the lifes-

Table 3

Parameters of age- and size-specific logistic maturation schedules and estimated ages and fork lengths at 50% maturity of female *Lutjanus carponotatus* at the Palm and Lizard Island groups, Great Barrier Reef. a adjusts the position of the logistic function along the abscissa; r determines the steepness of the logistic function; t_{50} is the age at 50% maturity; L_{50} is the fork length at 50% maturity. Standard errors are provided below parameter estimates.

	a	r	r^2	t_{50} or L_{50}
Age-specific				
Palm Island group	6.40	3.42	0.985	1.9 years
	(1.42)	(0.12)		
Lizard Island group	4.16	1.73	0.990	2.4 years
	(0.48)	(0.19)		
Size-specific				
Palm Island group	14.72	0.081	0.994	182 mm
	(1.49)	(0.008)		
Lizard Island group	11.61	0.061	0.908	189 mm
	(3.84)	(0.020)		

pan of *L. carponotatus* can explain the apparently constant mortality rate over many age classes (evidenced by high catch curve r^2 values) given that mortality is often largely a function of body size (Roff, 1992).

The development and regression of visceral fat stores preceding increases in ovary weight is a pattern that has been observed in other reef fishes, including tropical surgeonfishes (Acanthuridae: Fishelson et al., 1985) and groupers (Serranidae: Ferreira, 1995) and temperate rockfishes (Scorpaenidae: Guillemot et al., 1985). These patterns suggest that the stored lipid is fuelling the energetic costs of spawning. The lack of a similar pattern for males supports the idea that energetic costs associated with production of sperm are low in relation to eggs (Wootton, 1985) thus enabling male *L. carponotatus* to attain larger sizes, as also reported by Newman et al. (2000). Alternatively, males might spawn more frequently throughout the year than females and the lack of seasonal patterns in lipid storage among males might reflect a more regular energetic demand that precludes energy storage. In any case, these sex-specific growth patterns, coupled with similar mortality rates between the sexes and sex ratios that are at unity or that are at most only slightly female-biased (see below), suggest that females are limiting reproduction of this species. Therefore stock dynamics should be modeled in terms of female biology (Hilborn and Walters, 1992).

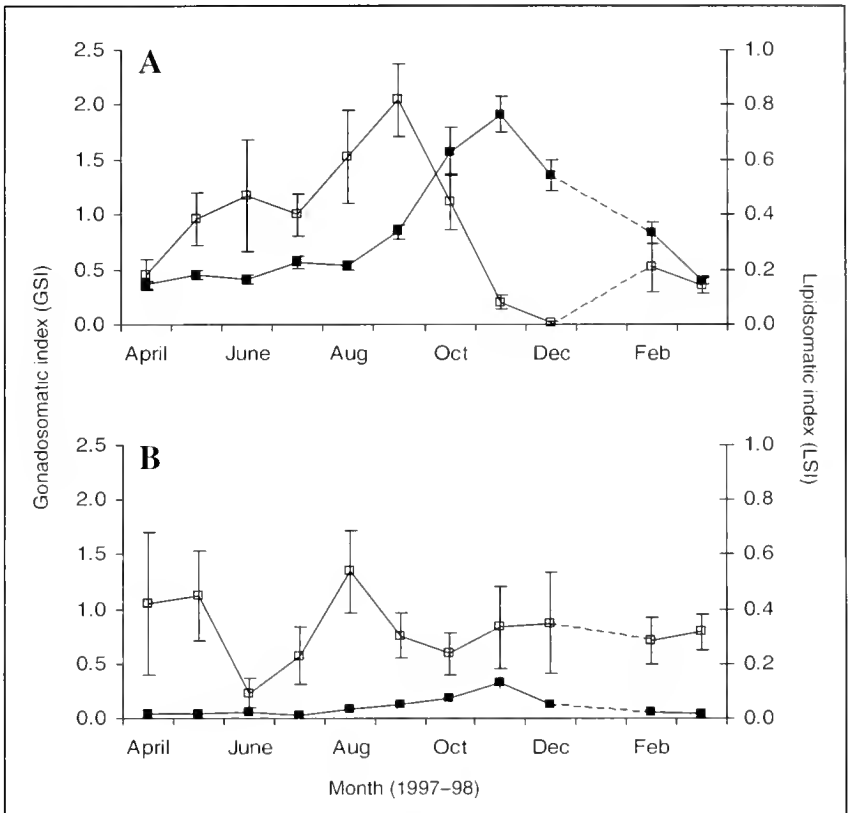

Figure 7

Monthly mean gonadosomatic index (GSI ±SE; ■) and lipidsomatic index (LSI ±SE; □) values for mature female (**A**) and all male (**B**) *Lutjanus carponotatus* at the Palm Island group.

The apparently female-biased sex ratio at the Palm Island group starkly contrasts with the heavily male-biased sex ratio reported for mid-shelf reefs of the central GBR by Newman et al. (2000). However, neither a male- nor female-biased sex ratio would be expected from a nonhermaphrodite that is not known to possess a complex mating system such as defense of females or territories. It is possible that the spawning sex ratio (i.e. excluding juveniles) is closer to unity if males mature earlier than females, but this ratio is not possible to assess because male maturation has not yet been examined for this species. The difference between the sex ratio reported in this study and that by Newman et al. (2000) might be due to variation in mating systems across a cross-shelf density gradient (Newman and Williams, 1996). Alternatively, the sampling by traps and line fishing conducted by Newman et al. (2000) could be more heavily biased toward males than the sampling by spear fishing used in the present study because of larger size, wider gape, or more aggressive behavior toward bait among males (Cappo and Brown, 1996). Furthermore, it is likely that a female-biased sex ratio as observed at the

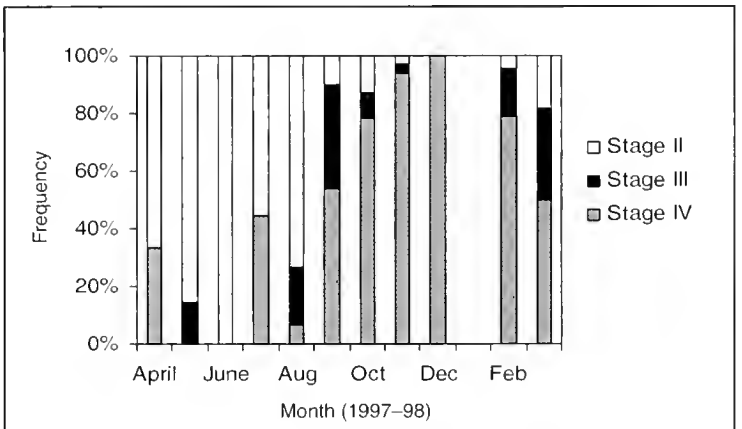

Figure 8

Monthly frequencies of ovarian stages of mature *Lutjanus carponotatus* at the Palm Island group. Stage descriptions are provided in Table 1.

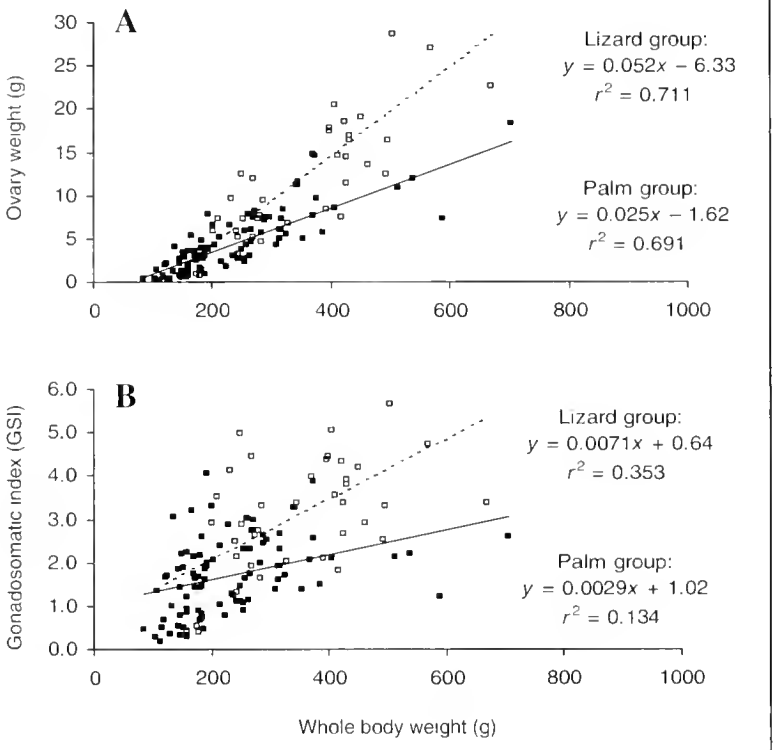

Figure 9

Fixed ovary weight (**A**) and gonadosomatic index (**B**) at fresh whole body weight for mature female *Lutjanus carponotatus* at ovarian stage IV (see Table 1) collected during peak spawning months (Oct–Dec) at the Palm (■, solid lines) and Lizard (□, dashed lines) island groups.

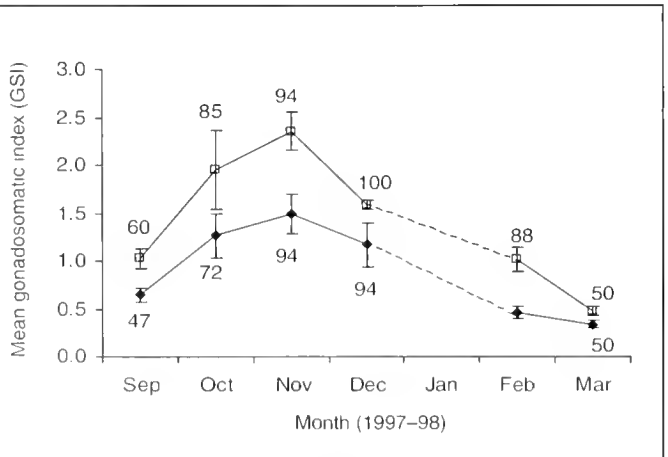

Figure 10

Mean gonadosomatic index (GSI ±SE) for mature female *Lutjanus carponotatus* at the Palm Island group during the September through March spawning season for small (≤230 mm fork length; ■) and large (≤230 mm fork length; □) size classes. The percentage of fish at stage IV (see Table 1) is indicated above each data point.

Palm Island group is not a prevalent feature of *L. carponotatus* populations. Rather, the strong statistical suggestion of a sex ratio quite different from unity might be due to the fact that sex ratios often show temporal variability (e.g. Stergiou et al., 1996) coupled with the propensity to achieve statistically significant differences when using large sample sizes (Johnson, 1999).

Maturation schedules and sex-specific growth differences were consistent between the island groups, but overall growth patterns differed, with Lizard Island group fish reaching larger asymptotic body sizes. Given the vast distance between the island groups, these differences might be due to inherent genetic differences between the populations. Or, effects of temperature (the Palm Island group sits at a higher latitude), turbidity, freshwater run-off (the Palm Island group sits closer to a river mouth and has more developed mangrove systems), or other environmental factors could be driving the differences. Of course, these possibilities are not mutually exclusive.

The larger ovaries observed among Lizard Island females might be due to further spatial differences or might be an effect of timing of sampling. The temporal resolution of sampling aimed to identify the extent of the spawning season but was too coarse to account for intramonth differences in ovarian development. Large changes in ovary size might occur within stage IV, and the final progression to immediate prespawning stages can be rapid (e.g. Davis and West, 1993). The Lizard Island group sample was collected from 17 to 23 October 1998, whereas the corresponding Palm Island group sample was collected from 11 to 12 October 1998. The October 1998 new moon was on the 20th, and *P. leopardus*, the only GBR species for which lunar spawning patterns have been reported, spawns primarily around the new moon (Samoilys, 1997). If *L. carponotatus* spawning is also centered around the new moon, the spatial differences in ovary weight at body weight might be due to more advanced development toward full hydration within the Lizard Island group sample. In fact, the higher proportion of stage-IV ovaries within the October Lizard Island group sample (96%) compared with the October Palm Island group sample (78%), coupled with the higher relative ovary weights at the Lizard Island group in October, can be taken as preliminary evidence that *L. carponotatus* spawns at the new moon.

Comparison with other reef fishes

The growth differences between male and female *L. carponotatus* contrast with a general trend of larger body sizes among female lutjanids observed in Atlan-

tic, Caribbean, and Hawaiian species (Grimes, 1987). However, the pattern observed in the present study seems common in the Indo-Pacific where males frequently (Davis and West, 1992; McPherson and Squire, 1992; Newman et al., 1996, 2000), but not universally (Hilomen, 1997), are the larger sex. As noted above, these differences are consistent with predictions based on energetic costs of producing sperm and eggs.

Lutjanus carponotatus spawning patterns identified by using both GSI and ovarian stage frequencies show pronounced seasonal differences: there are at least five months of very limited or no spawning activity from April through August. This finding supports Grimes's (1987) observation that continental lutjanid populations tend to have more restricted spawning seasons than populations associated with oceanic islands, which spawn more or less continuously throughout the year. Although seasonal patterns exist, the prominence of ripe gonads over seven months from September through March suggests an extended spawning season and supports the general observation that tropical reef fishes spawn over longer periods within the year than do cooler water species (Lowe-McConnell, 1979). However, a study with finer temporal resolution is needed to verify that spawning actually occurs in months with a high proportion of stage-IV ovaries.

Female *L. carponotatus* mature on average at approximately 75% of their mean asymptotic size, 54% of their maximum observed size, and 11% of their maximum longevity. The relative size at maturity contrasts with Grimes's (1987) observations that shallow-water continental lutjanid populations like those of *L. carponotatus* on the GBR typically mature at smaller relative sizes (≈42% maximum size) compared to deep-water populations associated with oceanic islands (≈50% maximum size). Two sympatric shallow-water species, *L. russelli* (Sheaves, 1995) and *L. fulviflamma* (Hilomen, 1997), likewise contrast with the general familial trend and mature at approximately 50% and 75% of their maximum size, respectively. Hence, a general pattern of relative size at maturity might exist among shallow-water lutjanids in the GBR region that is different from those regions covered by Grimes's (1987) review. Lutjanids on the GBR are generally lightly fished (Mapstone et al.[1]); therefore the geographic difference in sizes at maturity might be due to fishing pressure selecting for smaller sizes at maturity in other regions.

The relative age at maturity of *L. carponotatus* cannot be as readily placed in a broader familial context given that ages at maturity were not widely estimated for lutjanids at the time of Grimes's (1987) review. However, an array of published studies suggests that many tropical and subtropical demersal fishes share the absolute, but not relative, ages of *L. carponotatus* at 50% and 100% maturity at 2 and 4 years, respectively. These include other small gonochores on the GBR (Sheaves, 1995; Hart and Russ, 1996; Hilomen, 1997), as well as a range of gonochores in other regions (Grimes and Huntsman, 1980; Davis and West, 1993; Ross et al., 1995) and hermaphrodites on the GBR and elsewhere (Ferreira, 1993, 1995; Bullock and Murphy, 1994). The ubiquity of this maturity schedule, despite a wide array of maximum body sizes (160–1200 mm) and longevities (6–56 years) among these species, perhaps suggests a common physiological threshold toward which many species gravitate in order to maximize lifetime reproductive success. More comprehensive analysis of life history trade-offs (e.g. Roff, 1992) is needed to test this hypothesis.

Fisheries management

Harvest of *L. carponotatus* is currently restricted to fish greater than 250 mm total length (approximately 233 mm FL) with the aim of allowing 50% of fish to spawn at least once, and this regulation is proposed to remain after revision by the GBR fishery management plan (Queensland Fisheries Management Authority[3]). The estimated size at 50% maturity of 190 mm FL suggests that the regulation is meeting its objective. However, the objective itself might not adequately protect the reproductive potential of *L. carponotatus* and similar species if individuals require multiple spawning years to ensure sufficient replenishment of the stock. The extensive longevities of many reef fishes have been hypothesized to be a mechanism for coping with low and irregular recruitment rates through a process dubbed the "storage effect" (Warner and Chesson, 1985). The rationale behind the storage effect hypothesis is that fish must reproduce during many breeding seasons in order to endure poor recruitment years and realize high reproductive success during the unpredictable and intermittent good recruitment years. If this process is important for population dynamics of *L. carponotatus* and other species, management will need to protect an intact natural population structure in some areas within the fishery. Protecting older age classes cannot be achieved by using maximum size limits for species like *L. carponotatus* that have a pronounced asymptote in the growth trajectory because body sizes are similar over a broad range of age classes and size is therefore poorly correlated with age. Protecting natural age structure could be accomplished through a system of strategically designed marine protected areas that allow some populations to experience natural survival free of fishing mortality.

Proposed closures of the GBR line fishery during nine-day periods around the new moon in October, November, and December are aimed at protecting spawning activity and particularly spawning aggregations of *P. leopardus* and other harvested species (Queensland Fisheries Management Authority[3]). *Lutjanus carponotatus* shares a peak spawning period during these months with *P. leopardus* (Ferreira, 1995; Samoilys 1997) and several other sympatric exploited species (McPherson et al., 1992; Sheaves, 1995; Hilomen, 1997; Brown et al.[5]). In addition, the larger ovaries of the Lizard Island group fish, which were collected closer to the new moon, may indicate that, like *P. leopardus* (Samoilys, 1997), *L. carponotatus* spawns at

[5] Brown, I. W., P. J. Doherty, B. Ferreira, C. Keenan, G. McPherson, G. Russ, M. Samoilys, and W. Sumpton. 1994. Growth, reproduction and recruitment of Great Barrier Reef food fish stocks. Final report to the Fisheries Research and Development Corporation, FRDC Project 90/18, Queensland Department of Primary Industries, 154 p. Southern Fisheries Centre, GPO Box 76, Deception Bay, Queensland 4508, Australia.

the new moon. Therefore, the timing of the proposed spawning closures seems appropriate. However, it is not known whether *L. carponotatus* aggregate to spawn; therefore the goal of protecting spawning aggregations might not be relevant for this species. In fact, the prevalence and ecological importance of spawning aggregations for any species on the GBR is largely unknown; therefore the efficacy of the proposed closures is difficult to predict.

Beyond the implications for management regulations, these data have implications for modeling *L. carponotatus* stock dynamics. In particular, the results suggest that reproductive output by a unit of *L. carponotatus* biomass cannot be predicted on the basis of that biomass alone. Relative ovary weight increases slightly with increasing body size and there is evidence that larger fish spawn more frequently. The greatest difference in the proportion of ripe ovaries between size classes occurred in February 1998 after severe flooding in January. It is possible that the lower proportion of ripe ovaries among small fish in February was due to stresses caused by changes in salinity or increased run-off and is not a regular trait. However, increased resilience to environmental stresses that allows more frequent spawning would also increase the relative reproductive success of large fish. Therefore, a population comprising fewer larger fish is likely to show greater annual egg production than a population with equivalent biomass that comprises more numerous but smaller fish. Additionally, the sex-specific patterns reported in this study further suggest gross biomass might be an inadequate index of replenishment potential and that female biomass needs to be considered. Therefore, stock structure, in terms of sex ratio and the frequency of size classes, and not simply overall biomass needs to be considered when predicting reproductive potential.

Acknowledgments

I thank the numerous assistants who participated in fieldwork, as well as Sam Adams and Sue Reilly for assistance with histological examinations. The manuscript was greatly improved by comments from Howard Choat, Carl Walters, Tony Fowler, Campbell Davies, Sam Adams, Bruce Mapstone, an anonymous thesis examiner, and two anonymous reviewers. This work was conducted while the author was supported by an international postgraduate research scholarship from the Commonwealth of Australia and a postgraduate stipend from the CRC Reef Research Centre. Final preparation of the manuscript took place while the author was supported by a postdoctoral fellowship funded jointly by the University of Windsor and the Canadian National Science and Engineering Research Council (collaborative research opportunity grant no. 227965-00) to Peter Sale and others).

Literature cited

Adams, S., B. D. Mapstone, G. R. Russ, and C. R. Davies.
2000. Geographic variation in the sex ratio, sex specific size, and age structure of *Plectropomus leopardus* (Serranidae) between reefs open and closed to fishing on the Great Barrier Reef. Can. J. Fish. Aquatic Sci. 57: 1448–1458.

Bullock, L. H., and M. D. Murphy.
1994. Aspects of the life history of the yellowmouth grouper, *Mycteroperca interstitialis*, in the eastern Gulf of Mexico. Bull. Mar. Sci. 55:30–45.

Cappo, M., and I. W. Brown.
1996. Evaluation of sampling methods for reef fish of commercial and recreational interest. CRC Reef Research Centre Technical Report 6, 72 p.

Cappo, M., P. Eden, S. J. Newman, and S. Robertson.
2000. A new approach to validation of periodicity and timing of opaque zone formation in the otoliths of eleven species of *Lutjanus* from the central Great Barrier Reef. Fish. Bull. 98:474–488.

Connell, S. D.
1998. Patterns of piscivory by resident predatory reef fish at One Tree Reef, Great Barrier Reef. Mar. Freshw. Res. 49:25–30.

Dalzell, P.
1996. Catch rates, selectivity and yields of reef fishing. *In* Reef fisheries (N. V. C. Polunin and C. M. Roberts, eds.), p. 161–192. Chapman and Hall, London.

Davies, C. R.
1995. Patterns of movement of three species of coral reef fish on the Great Barrier Reef. Ph.D. diss, 212 p. James Cook University, Queensland, Australia.

Davis, T. L. O., and G. J. West.
1992. Growth and mortality of *Lutjanus vittus* (Quoy and Gaimard) from the North West Shelf of Australia. Fish. Bull. 90:395–404.
1993. Maturation, reproductive seasonality, fecundity, and spawning frequency in *Lutjanus vittus* (Quoy and Gaimard) from the North West Shelf of Australia. Fish. Bull. 91: 224–236.

Day, T., and P. D. Taylor.
1997. Von Bertalanffy's growth equation should not be used to model age and size at maturity. Am. Nat. 149: 381–393.

Everhart, W. H., and W. D. Youngs.
1981. Principles of fishery science, 349 p. Cornell Univ. Press, Ithaca, NY.

Ferreira, B. P.
1993. Reproduction of the inshore coral trout *Plectropomus maculatus* (Perciformes: Serranidae) from the central Great Barrier Reef, Australia. J. Fish Biol. 42:831–844.
1995. Reproduction of the common coral trout *Plectropomus leopardus* (Serranidae: Epinephelinae) from the central and northern Great Barrier Reef, Australia. Bull. Mar. Sci. 56: 653–669.

Ferreira, B. P., and G. R. Russ
1994. Age validation and estimation of growth rate of the coral trout, *Plectropomus leopardus*, (Lacepede 1802) from Lizard Island, northern Great Barrier Reef. Fish. Bull. 92:46–57.

Fishelson, L., W. L. Montgomery, and A. A. Myrberg.
1985. A new fat body associated with the gonad of surgeonfishes (Acanthuridae: Teleostei). Mar. Biol. 86:109–112.

Grimes, C. B.
1987. Reproductive biology of the Lutjanidae: a review. *In* Tropical snappers and groupers: biology and fisheries management (J. Polovina and S. Ralston., eds.), p. 239–294. Westview Press, London.

Grimes, C. B., and G. R. Huntsman.
1980. Reproductive biology of the vermilion snapper,

Rhomboplites aurorubens, from North Carolina and South Carolina. Fish. Bull. 78:137–146.

Guillemot, P. J., R. J. Larson, and W. H. Lenarz.
1985. Seasonal cycles of fat and gonad volume in five species of northern California rockfish (Scorpaenidae: *Sebastes*). Fish. Bull. 83:299–311.

Ha, P. Y., and R. A. Kinzie.
1996. Reproductive biology of *Awaous guamensis*, an amphidromous Hawaiian goby. Environ. Biol. Fish. 45:383–396.

Hart, A. M. and G. R. Russ.
1996. Response of herbivorous fishes to crown-of-thorns *Acanthaster planci* outbreaks. III. Age, growth, mortality and maturity indices of *Acanthurus nigrofuscus*. Mar. Ecol. Prog. Ser. 136:25–35.

Higgs, J. B.
1993. A descriptive analysis of records of the recreational reef-line fishery on the Great Barrier Reef. M.Sc. thesis, 128 p. James Cook Univ., Queensland, Australia.

Hilborn, R., and C. J. Walters.
1992. Quantitative fisheries stock assessment: choice, dynamics and uncertainty, 570 p. Kluwer Academic, Boston, MA.

Hilomen, V. V.
1997. Inter- and intra-habitat movement patterns and population dynamics of small reef fishes of commercial and recreational significance. Ph.D. diss., 277 p. James Cook Univ., Queensland, Australia.

Hoenig, J. M.
1983. Empirical use of longevity data to estimate mortality rates. Fish. Bull. 82:898–902.

Johnson, D. H.
1999. The insignificance of statistical significance testing. J. Wildlife Manag. 63:763–772.

Kimura, D. K.
1980. Likelihood methods for the von Bertalanffy growth curve. Fish. Bull. 77:765–776.

Kritzer, J. P.
2002. Variation in the population biology of stripey bass *Lutjanus carponotatus* within and between two island groups on the Great Barrier Reef. Mar. Ecol. Prog. Ser. 243:191–207.
2003. Biology and management of small snappers on the Great Barrier Reef. *In* Bridging the gap: a workshop linking student research with fisheries stakeholders (A. J. Williams, D. J. Welch, G. Muldoon, R. Marriott, J. P. Kritzer, and S. Adams eds.), p. 62–80. CRC Reef Research Centre, Townsville, Queensland, Australia.

Kritzer, J. P., C. R. Davies, and B. D. Mapstone
2001. Characterizing fish populations: effects of sample size and population structure on the precision of demographic parameter estimates. Can. J. Fish. Aquat. Sci. 58: 1557–1568.

Lobel, P. S.
1989. Ocean current variability and the spawning season of Hawaiian reef fishes. Env. Biol. Fish. 24:161–171.

Lowe-McConnell, R. H.
1979. Ecological aspects of seasonality in fishes of tropical waters. Symp. Zool. Soc. Lond. 44:219–241.

McPherson, G. R., and L. Squire
1992. Age and growth of three dominant *Lutjanus* species of the Great Barrier Reef inter-reef fishery. Asian Fish. Sci. 5:25–36.

McPherson, G.R., L. Squire, and J. O'Brien
1992. Reproduction of three dominant *Lutjanus* species of the Great Barrier Reef inter-reef fishery. Asian Fish. Sci. 5:15–24.

Murphy, M. D.
1997. Bias in Chapman-Robson and least-squares estimators of mortality rates for steady state populations. Fish. Bull. 95:863–868.

Newman, S. J., and D. M. Williams
1996. Variation in reef associated assemblages of the Lutjanidae and Lethrinidae at different distances offshore in the central Great Barrier Reef. Environ. Biol. Fish. 46: 123–138.

Newman, S. J., D. M. Williams, and G. R. Russ
1996. Age validation, growth and mortality rates of the tropical snappers (Pisces: Lutjanidae) *Lutjanus adetii* (Castelnau, 1873) and *L. quinquelineatus* (Bloch, 1790) from the central Great Barrier Reef, Australia. Mar. Freshw. Res. 47:575–584.
1997. Patterns of zonation of assemblages of the Lutjanidae, Lethrinidae and Serranidae (Epinephilinae) within and among mid-shelf and outer-shelf reefs in the central Great Barrier Reef. Mar. Freshw. Res. 48:119–128.

Newman, S. J., M. Cappo, and D. M. Williams
2000. Age, growth and mortality of the stripey, *Lutjanus carponotatus* (Richardson) and the brown-stripe snapper, *L. vitta* (Quoy and Gaimard) from the central Great Barrier Reef, Australia. Fish. Res. 48:263–275.

Ricker, W. E.
1975. Computation and interpretation of biological statistics of fish populations, 382 p. Bull. Fish. Res. Board Can. 191.

Roff, D.A.
1992. The evolution of life histories, 535 p. Chapman and Hall, New York, NY.

Ross, J. L., T. M. Stevens, and D. S. Vaughan
1995. Age, growth, mortality, and reproductive biology of red drums in North Carolina waters. Trans. Am. Fish. Soc. 124:37–54.

Samoilys, M. A.
1997. Periodicity of spawning aggregations of coral trout *Plectropomus leopardus* (Pisces: Serranidae) on the northern Great Barrier Reef. Mar. Ecol. Prog. Ser. 160: 149–159.

Samoilys, M. A., and A. Roelofs.
2000. Defining the reproductive biology of a large serranid, *Plectropomus leopardus*. CRC Reef Research Centre Technical Report 31, 36 p.

Sheaves, M.
1995. Large lutjanid and serranid fishes in tropical estuaries: are they adults or juveniles? Mar. Ecol. Prog. Ser. 129: 31–40.

Stergiou, K. I., P. Economidis, and A. Sinis.
1996. Sex ratio, spawning season and size at maturity of red bandfish in the western Aegean Sea. J. Fish. Biol. 49: 561–572.

Warner, R. R., and P. L. Chesson.
1985. Coexistence mediated by recruitment fluctuations: a field guide to the storage effect. Am. Nat. 125:769–787.

West, G.
1990. Methods of assessing ovarian development in fishes: a review. Aust. J. Mar. Freshw. Res. 41:199–222.

Wootton, R. J.
1985. Energetics of reproduction. *In* Fish energetics: new perspectives (P. Tytler and P. Calow, eds.), p. 231–254. Croom Helm, London.

Examination of the foraging habits of Pacific harbor seal (*Phoca vitulina richardsi*) to describe their use of the Umpqua River, Oregon, and their predation on salmonids

Anthony J. Orr
Adria S. Banks
Steve Mellman
Harriet R. Huber
Robert L. DeLong
National Marine Mammal Laboratory
Alaska Fisheries Science Center, NMFS, NOAA
7600 Sand Point Way NE
Seattle, Washington 98115
E-mail address (for A. J. Orr, contact author): tony.orr@noaa.gov

Robin F. Brown
Oregon Department of Fish and Wildlife
2040 S. E. Marine Science Drive
Newport, Oregon 97365

Abstract—The increase in harbor seal (*Phoca vitulina richardsi*) abundance, concurrent with the decrease in salmonid (*Oncorhynchus* spp.) and other fish stocks, raises concerns about the potential negative impact of seals on fish populations. Although harbor seals are found in rivers and estuaries, their presence is not necessarily indicative of exclusive or predominant feeding in these systems. We examined the diet of harbor seals in the Umpqua River, Oregon, during 1997 and 1998 to indirectly assess whether or not they were feeding in the river. Fish otoliths and other skeletal structures were recovered from 651 scats and used to identify seal prey. The use of all diagnostic prey structures, rather than just otoliths, increased our estimates of the number of taxa, the minimum number of individuals and percent frequency of occurrence (%FO) of prey consumed. The %FO indicated that the most common prey were pleuronectids, Pacific hake (*Merluccius productus*), Pacific staghorn sculpin (*Leptocottus armatus*), osmerids, and shiner surfperch (*Cymatogaster aggregata*). The majority (76%) of prey were fish that inhabit marine waters exclusively and fish found in marine and estuarine areas (e.g. anadromous spp.) which would indicate that seals forage predominantly at sea and use the estuary for resting and opportunistic feeding. Salmonid remains were encountered in 39 samples (6%); two samples contained identifiable otoliths, which were determined to be from chinook salmon (*O. tshawytscha*). Because of the complex salmonid composition in the Umpqua River, we used molecular genetic techniques on salmonid bones retrieved from scat to discern species that were rare from those that were abundant. Of the 37 scats with salmonid bones but no otoliths, bones were identified genetically as chinook or coho (*O. kisutch*) salmon, or steelhead trout (*O. mykiss*) in 90% of the samples.

Manuscript approved for publication 9 October 2003 by Scientific Editor.
Manuscript received 20 October 2003 at NMFS Scientific Publications Office.
Fish. Bull. 102:108–117 (2004).

The Pacific harbor seal (*Phoca vitulina richardsi*) is found along the west coast of North America from the Aleutian Islands, Alaska, to the San Roque Islands, Baja California (King, 1983; Reeves et al., 1992). Before the passage of the Marine Mammal Protection Act (MMPA) of 1972, harbor seals in Oregon were kept at relatively low numbers (fewer than 500 animals in 1968) because of bounties offered by the state and harassment from commercial and sport fishermen (Pearson and Verts, 1970). Since passage of protective legislation, harbor seals in Oregon have increased an average of 6% to 7% annually between 1978 and 1998, although, in recent years, numbers appear to be leveling at about 8000 individuals (Brown and Kohlmann, 1998).

The rapid increase in harbor seal numbers has revived fishery-managers' interest in seal diet because of the potential for increased consumption of commercial fish species. In addition, there has been a heightened concern about greater harbor seal abundance in rivers and estuaries during migrations of depressed salmonid populations because of the potential negative impact on the recovery of these fishes (NMFS, 1997). Because of the tenuous status of many salmonid (*Oncorhynchus* spp.) species along the west coast, the National Marine Fisheries Service (NMFS) recommended that the United States Congress modify the MMPA to allow lethal removal of seals from river mouths where they may prey on depressed salmonid populations (NMFS, 1997). Predation of salmonids by harbor seals in Oregon has been documented (Brown, 1980; Harvey, 1987; Brown et al., 1995; Riemer and Brown, 1997; Beach et al.[1]). The proportion of salmonids in the diet of harbor seals varied from 1% to 30% depending on area, season, and sampling method (NMFS, 1997).

Pinniped prey consumption can be determined from direct observations in some systems, if prey is consumed at

[1] Beach, R., A. Geiger, S. Jefferies, S. Treacy, and B. Troutman. 1985. Marine mammals and their interactions with fisheries of the Columbia River and adjacent waters, 1980–1982. NWAFC (Northwest Alaska Fisheries Science Center) processed rep. NWAFC 85-04, 316 p. NWAFC, National Marine Fisheries Service, Seattle, WA, 98115.

the surface (Bigg et al., 1990); however, consumption is typically determined by examining scat (fecal) samples. In the past, species-specific sagittal otoliths found in scats were used exclusively to determine the identification of prey taxa. However, because otoliths can be partially or completely digested, or are not present in scats (because the head of the prey was not consumed), they are not always an adequate representation of diet. Recently, investigators have begun to use additional structures (e.g. cranial elements, vertebrae) recovered from scats to identify prey (e.g. Olesiuk et al., 1990; Cottrell et al., 1996; Riemer and Brown, 1997; Browne et al., 2002; Lance et al.[2]). These structures usually are more common than otoliths and frequently can be identified to species; however, bones of some species can be identified to family only (e.g. salmonids). Consequently, the National Marine Mammal Laboratory (NMML) collaborated with the Conservation Biology Molecular Genetics Laboratory (CBMGL; Northwest Fisheries Science Center, Seattle, WA) to develop molecular genetic identification of salmonid species (Purcell et al., 2004). Because of the complex salmonid species composition in the Umpqua River, genetic identification was vital to distinguish species that were rare from those that were abundant.

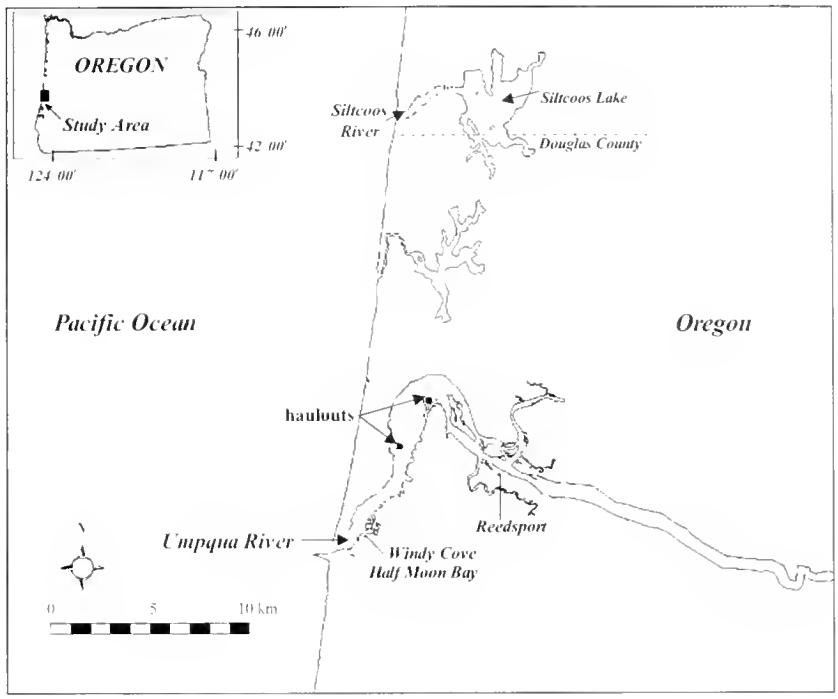

Figure 1

Map of the lower section of the Umpqua River, Oregon, where scat samples were collected at two haulout sites during 1997 and 1998.

The original impetus of this study was to assess the impact of harbor seal predation on the recovery of the Umpqua River sea-run cutthroat trout (*O. clarkii*) that were listed as endangered under the Endangered Species Act (ESA) during 1996 (Johnson et al., 1999). Umpqua River cutthroat trout were removed from the ESA in 2000 because they were identified to be part of the larger Oregon Coast evolutionary significant unit (U.S. Fish and Wildlife Service, 2000). The present study was continued despite the "delisting" of cutthroat trout because the Umpqua is inhabited year-round by harbor seals that haul out several kilometers upriver and is, thus, ideal for determining whether the presence of a pinniped species within a system is indicative of substantial feeding on fish species of concern within that environment. In addition, the Umpqua River contains several other salmonid species whose status is precarious (NMFS, 1997). Therefore, the development of genetic identification techniques was considered valuable for this system, as well as for future foraging studies in which species-specific identification may be desirable but impossible by way of conventional identification methods.

The objectives of this study were 1) to determine by an examination of diet if harbor seals that haul out in the Umpqua River feed primarily in the river or elsewhere, and 2) to apply genetic techniques to identify salmonid prey species.

Materials and methods

Study area

The Umpqua River, located in southern Oregon (Fig. 1), is a natal river for sea-run cutthroat trout, as well as chinook (*O. tshawytscha*), coho (*O. kisutch*) salmon, and steelhead trout (*O. mykiss*). The Umpqua estuary is also inhabited year-round by approximately 600–1000 harbor seals and has been designated as an area where pinnipeds and salmonids significantly co-occur (NMFS, 1997). Scat samples for this study were collected from two haulouts located within 4.8 km of the river's mouth and within 1.6 km of each other (Fig. 1).

Scat collection and analysis

Samples were collected during two seasons: "spring" (March through June) and "fall" (August to December). "Spring" corresponded to the migration of anadromous cutthroat trout adults and some juveniles to the ocean and "fall" coincided approximately with the freshwater return of spawning anadromous adults. The migratory and spawn-

[2] Lance, M., A. Orr, S. Riemer, M. Weise, and J. Laake. 2001. Pinniped food habits and prey identification techniques protocol. AFSC Proc. Rep. 2001-04, 36 p. AFSC, NMFS, NOAA. 7600 Sand Point Way NE, Seattle, WA 98115.

Table 1

Collection dates of harbor seal scats and numbers of scats with identifiable prey remains, without identifiable remains, and without remains from the Umpqua River, Oregon, during 1997 and 1998. Fall and spring periods correspond to timing of cutthroat trout runs on the Umpqua River.

Collection dates	With identifiable remains	Without identifiable remains	Without remains	Total
Fall, 1997				
16–23 Sep	26	1	2	29
27 Sep–6 Oct	5	0	3	8
12–24 Oct	31	0	7	38
31 Oct–10 Nov	21	0	6	27
12–25 Nov	36	0	10	46
Total	119	1	28	148
Spring 1998				
24–25 Mar	27	5	2	34
13–15 Apr	59	5	7	71
26–27 Apr	45	4	4	53
13–14 May	41	0	4	45
27–28 May	12	0	1	13
11–12 Jun	35	2	1	38
Total	219	16	19	254
Fall 1998				
5–6 Aug	142	1	1	144
19–20 Aug	111	1	3	115
6–9 Sep	28	3	3	34
19–21 Sep	13	0	0	13
7–8 Oct	19	0	1	20
Total	313	5	8	326

ing periods of chinook and coho salmon, and steelhead trout also occur during these times.

During fall 1997, all harbor seal scats present at the haulouts were collected every other day during the daytime low tide, weather permitting (Table 1). In 1998, biweekly attempts were made to pick a minimum of 50 scats during low tides at the haulout sites (Table 1). Scats were collected, placed in individual plastic bags, and frozen for later processing. At the laboratory samples were thawed and rinsed in nested sieves (1.0 mm, 0.71 mm, and 0.5 mm in 1997; 1.4 mm, 1.0 mm, and 0.5 mm in 1998). Fish structures were dried and stored in glass vials and cephalopod remains were stored in vials with 70% isopropyl or ethyl alcohol.

Prey were identified to the lowest possible taxon by using sagittal otoliths, skeletal, and cartilaginous remains from fish and beaks and statoliths from cephalopods. Other invertebrate remains were discarded from analysis because of the uncertainty of identifying them as primary or secondary prey. Unknown prey were categorized as "unidentified" and "unidentifiable" (Browne et al., 2002). Items that were categorized as "unidentifiable" were excluded from analyses because they could not be distinguished from prey already identified in the sample. Otoliths, beaks, and diagnostic bones were identified by using an extensive reference collection at the NMML and voucher samples verified by Pacific Identifications (Victoria, British Columbia).

After identification, otoliths were separated by side (left, right, or unknown) and enumerated to determine minimum number of specific prey. Unique diagnostic structures (e.g. quadrates, angulars, basioccipitals, vomers) were used for identification and enumeration of fish. Non-unique skeletal structures such as gillrakers and teeth were used to identify but not enumerate taxa (i.e. their presence indicated only a single individual) unless the structures were from different size classes. Vertebrae were treated like other non-unique structures; however, for salmon, if the number of vertebrae reflected more than one individual, then they were used for enumeration. Cephalopod beaks were separated by side (upper, lower, or unknown) and enumerated to determine number of prey.

To discern where harbor seals were feeding, identified prey were categorized as those exclusively found in rivers or estuaries (e.g. gobiids, cyprinids), those found exclusively in marine waters (e.g. gadids, myxinids), and those that could potentially be found in either environment (e.g. anadromous species, osmerids, petromyzontids) by using Eschmeyer et al. (1983). A seal was considered to feed in the river-estuary system if all the prey taxa identified in the scat were definitely or could potentially be found in the system. For example, a sample containing remains of peamouth chub (*Mylocheilus caurinus*), threespine stickleback (*Gasterosteus aculeatus*), river lamprey (*Lampetra ayresii*), and chinook salmon would be classified as a riverine-

estuarine species because these prey items could feasibly be consumed in the river. It was assumed that the seal was feeding in the marine environment if a sample contained exclusively marine prey, such as Pacific hagfish (*Eptatretus stoutti*), Pacific hake (*Merluccius productus*), and rockfish (*Sebastes* spp.). If a scat comprised prey taxa that potentially could be found in a riverine-estuarine system or marine waters (e.g. salmonids, osmerids), as well as those found exclusively in marine waters, then it was assumed that the feeding environment was marine or mixed.

Salmonid skeletal remains were sent to the CBMGL for species identification. Remains to be analyzed genetically were selected by number or size (or both) to represent different species or individuals present in each scat. For example, if a scat had 95 approximately equal-size vertebrae (a salmonid has approximately 65 vertebrae; Butler, 1990), then at least two vertebrae (potentially representing at least two individuals) were sent for genetic identification. Also, if a sample had a very large gillraker and three small vertebrae, then the gillraker and one vertebra were sent for genetic identification. The size of diagnostic structures was also used to categorize salmon remains as juvenile or adult, when possible. The CBMGL identified salmonid species by direct sequencing of mitochondrial DNA or analysis of restriction fragment length polymorphism (Purcell et al., 2004).

The abundance of prey taxa in harbor seal diet for each period was described by using the minimum number of individuals (MNI) and percent frequency of occurrence (%FO). We compared the effect of including bone on the number of prey consumed by estimating MNI using the greater number of right or left otoliths and then again using all diagnostic skeletal remains. Cephalopod MNI was estimated from the greater number of upper or lower beaks. The %FO of prey taxon i was defined as

$$\%FO_i = \frac{\sum_{k=1}^{s} O_{ik}}{s} \times 100,$$

where O_{ik} = absence (0) or presence (1) of taxon i in scat k; and

s = the total number of scats that contained identifiable prey remains.

The presence of taxon i in scat k was determined by using otoliths and then again using all structures. To account for variability in diet, point estimates of %FO for a prey taxon were determined during each sampling period and then averaged for each season.

Results

Scats

Over 725 scats were collected during all periods. The number of scats collected with identifiable remains was 119 (99%; n=148) in fall 1997, 219 (93%; n=254) in spring 1998, and 313 (98%; n=326) in fall 1998 (Table 1). Of the 651 samples with identifiable prey remains, 605 (93%) contained fish bones, 347 (53%) had fish otoliths, 231 (36%) contained remains from cartilaginous fish, and 41 (6%) had cephalopod beaks. A majority (65% fall 1997, 65% spring 1998, 63% fall 1998) of scats with identifiable remains had one to three prey taxa present and less than 4% contained more than ten taxa. Approximately 40 prey taxa, representing at least 25 families, were identified throughout the study (Tables 2 and 3).

For nearly all prey taxa, MNI was greater when all skeletal remains were identified than when otoliths were used exclusively (Table 2). For several species, such as Pacific hake, Pacific herring (*Clupea pallasii*), and Pacific sardine (*Sardinops sagax*), MNI at least tripled when all structures were used for enumeration (Table 2). For most salmonids, cartilaginous fishes, three-spine stickleback, Irish lords (*Hemilepidotus* spp.), and Pacific mackerel (*Scomber japonicus*), no otoliths were recovered; therefore other skeletal elements had to be used for identification (Table 2). For a few prey, such as cyprinids, gobiids, and butter sole (*Isopsetta isolepis*), only otoliths were recovered (Table 2).

Foraging habits

The %FO for most prey taxa was greater when all structures were used than when just otoliths were used (Table 3). The %FO indicated that the prey most frequently consumed were pleuronectids, Pacific hake, Pacific staghorn sculpin (*Leptocottus armatus*), osmerids, and shiner surfperch (*Cymatogaster aggregata*). Prey frequently found in scats included those that were exclusively marine (e.g. Pacific hake, rex sole (*Glyptocephalus zachirus*), English sole (*Parophrys vetulus*), and myxinids), and those that occur in both marine and estuarine waters (e.g. Pacific staghorn sculpin, and shiner surfperch [Table 3]). Only 24% of scats were composed entirely of prey taxa that could be found in riverine-estuarine systems (Fig. 2). Consequently, a majority of the scats contained prey species that were exclusively marine ($\bar{x}$=25.3%) or were a mixture of marine and potentially marine species ($\bar{x}$=50.8%; Fig. 2).

Salmonids

Salmonid remains were found in only 6% (39/651) of the samples. Five chinook smolts were identified from otoliths in two samples collected during fall 1997; in the remaining 37 samples, salmonid bones were unidentifiable to species with conventional techniques. With the cooperation of CBMGL, we examined 116 salmonid bones using molecular genetic techniques. Species identification was successful for 67% (78/116) of the bones and teeth from 90% (35/39) of the scat samples that contained salmonid structures. In the four samples that remained unidentified, three contained only a single salmonid bone that failed to produce any DNA. Most of the other bones where DNA could not be extracted were small or fragmented and highly digested. Seventeen of the samples contained chinook salmon bones (including the two samples with chinook salmon otoliths); 11 contained coho salmon bones, four contained steelhead trout bones, and three contained bones from two salmonid

Table 2

Minimum number of individuals (MNI) of fish prey derived from sagittal otoliths and all structures retrieved from harbor seal scats collected at the Umpqua River during 1997 and 1998. *s* represents the number of scats with identifiable remains. na indicates taxon did not have sagittal otoliths to be used for identification.

		Fall 1997 (*s*=119)		Spring 1998 (*s*=219)		Fall 1998 (*s*=313)	
Family	Species	MNI otoliths	MNI all structures	MNI otoliths	MNI all structures	MNI otoliths	MNI all structures
Ammodytidae	Pacific sand lance	205	208	317	321	3	7
Bothidae	Pacific sanddab	12	13	9	9	1	2
Clupeidae	American shad	1	2	4	11	1	15
	Pacific herring	6	22	3	10	121	345
	Pacific sardine	0	0	50	235	39	185
Cottidae	Pacific staghorn sculpin	44	65	25	48	30	85
	unidentified cottid	0	0	0	0	0	8
Cyprinidae	peamouth chub	1	1	4	4	4	4
Embiotocidae	shiner surfperch	104	109	209	274	23	104
Engraulididae	northern anchovy	1	3	0	0	1	2
Gadidae	Pacific hake	1	35	10	44	58	199
	Pacific tomcod	9	21	19	52	8	26
Gasterosteidae	threespine stickleback	0	1	0	0	0	0
Gobiidae	unidentified gobiid	2	2	1	1	0	0
Hexagrammidae	lingcod	0	1	0	0	1	1
Myxinidae	Pacific hagfish	0	20	0	13	0	61
Ophidiidae	spotted cusk-eel	0	0	4	4	2	2
Osmeridae	unidentified osmerid	42	54	14	41	105	132
Petromyzontidae	Pacific lamprey	na	5	na	89	na	41
	river lamprey	na	2	na	1	na	0
Pholididae	saddleback gunnel	3	7	1	3	0	1
Pleuronectidae	English sole	38	41	37	39	75	84
	Dover sole	1	4	5	6	27	51
	slender sole	1	1	18	24	28	42
	butter sole	1	1	15	15	2	2
	rex sole	19	44	44	53	96	125
	petrale sole	0	0	0	0	1	1
	starry flounder	10	17	8	12	6	31
Rajidae	unidentified rajid	na	1	na	7	na	4
Scombridae	Pacific mackerel	0	2	0	3	0	2
Scorpaenidae	*Sebastes* spp.	0	15	6	19	2	3
Trichodontidae	Pacific sandfish	0	0	0	1	2	3
Zoarcidae	unidentified zoarcid	0	0	0	0	2	2
Salmonidae	coho salmon						
	unknown	0	4	0	0	0	0
	juvenile	0	1	0	4	0	2
	adult	0	0	0	1	0	3
	Steelhead or rainbow trout						
	unknown	0	0	0	2	0	2
	juvenile	0	0	0	0	0	1
	chinook salmon						
	unknown	5	6	0	0	0	3
	juvenile	0	5	0	2	0	5
	adult	0	1	0	0	0	0
	unidentified salmonid						
	unknown	0	2	0	1	0	2
	juvenile	0	1	0	0	0	1

Table 3

Mean percent frequency of occurrence (%FO) of common prey recovered from harbor seal scat samples collected at haulout sites in the Umpqua River, Oregon, during 1997 and 1998. SD indicates standard deviation.

		Fall 1997	Spring 1997	Fall 1998
Family	Species	Mean (±SD)	Mean (±SD)	Mean (±SD)
Ammodytidae	Pacific sand lance	12.5 ±8.3	12.6 ±8.3	9.1 ±8.9
Bothidae	Pacific sanddab	11.4 ±7.5	4.1 ±2.5	3.0 ±3.2
Clupeidae	American shad	4.3 ±0.6	13.0 ±2.3	5.3 ±3.1
	Pacific herring	16.9 ±13.7	7.3 ±6.9	35.9 ±21.8
	Pacific sardine	0	16.1 ±12.2	17.9 ±9.1
Cottidae	Pacific staghorn sculpin	23.9 ±8.5	21.0 ±19.0	11.8 ±4.5
	unidentified cottid	16.5 ±20.4	3.2 ±0.7	0.8 ±0.1
Cyprinidae	peamouth chub	3.8	2.3 ±0.6	2.8
Embiotocidae	shiner surfperch	18.2 ±8.2	23.6 ±19.4	7.0 ±2.9
Engraulididae	northern anchovy	5.5 ±3.2	0	2.1 ±2.0
Gadidae	Pacific hake	27.9 ±9.7	17.0 ±5.7	41.6 ±25.5
	Pacific tomcod	15.4 ±7.8	16.1 ±7.0	12.3 ±8.3
Gasterosteidae	threespine stickleback	2.8	0	0
Gobiidae	unidentified gobiid	7.7	1.7	0
Hexagrammidae	lingcod	3.8	0	0.7
Loliginidae	market squid	12.8 ±10.2	3.5 ±1.3	0
Myxinidae	Pacific hagfish	17.5 ±7.9	6.7 ±3.5	16.5 ±9.4
Octopodidae	*Octopus rubescens*	3.8 ±1.4	8.3 ±2.6	8.4 ±7.0
Ophidiidae	spotted cusk-eel	0	0	0.9
Osmeridae	unidentified osmerid	20.8 ±11.3	14.6 ±8.2	19.5 ±10.0
Petromyzontidae	Pacific lamprey	7.7 ±8.2	20.5 ±10.1	8.2 ±2.9
	river lamprey	5.6	3.7	0
Pholididae	saddleback gunnel	14.7 ±16.9	2.6 ±0.3	5.3
Pleuronectidae	English sole	21.9 ±1.7	8.7 ±5.2	17.5 ±12.0
	Dover sole	7.4 ±5.9	4.6 ±0.7	13.5 ±13.6
	slender sole	0	11.0 ±7.2	14.9 ±14.9
	butter sole	3.8	7.2 ±3.7	1.4
	rex sole	27.4 ±12.1	14.2 ±9.6	19.9 ±20.5
	petrale sole	0	0	0.7
	starry flounder	15.8 ±7.4	3.7 ±1.0	5.8 ±1.2
Rajidae	unidentified rajid	2.8	5.0 ±1.6	2.8
Scombridae	Pacific mackerel	3.8 ±1.4	4.6 ±4.0	0.8 ±0.1
Scorpaenidae	*Sebastes* spp.	15.7 ±8.3	9.1 ±2.6	2.1
Trichodontidae	Pacific sandfish	0	1.7	2.1
unidentifed bothid/ pleuronectid	unidentified flatfish	38.5 ±15.9	20.2 ±10.3	14.8 ±2.5
Zoarcidae	unidentified zoarcid	0	0	1.4
Salmonidae	coho salmon			
	unknown	5.8 ±3.6	0	0
	juvenile	4.8	3.3 ±2.3	0.7
	adult	0	2.4	6.2 ±6.2
	steelhead/rainbow trout			
	unknown	0	2.7 ±1.4	0.7
	juvenile	0	0	0.9
	adult	0	0	0.9
	chinook salmon			
	unknown	7.6 ±3.5	0	0.8 ±0.1
	juvenile	4.0 ±1.1	3.4	3.6 ±3.0
	adult	4.8	0	0
	unidentified salmonid(s)			
	unknown	4.3 ±0.6	2.4	0.8 ±0.1
	juvenile	4.8	0	7.7

species (two with coho and chinook salmon and one with coho salmon and steelhead trout, Table 2). No cutthroat trout were identified with conventional or molecular genetic techniques.

Using otoliths and other diagnostic skeletal structures, we enumerated at least 54 individual salmonids in 39 scats (Table 2). All individuals identified as adults (n=5) were coho salmon, except one chinook salmon from spring 1997. Individual juveniles identified as steelhead trout (n=1), coho salmon (n=7), chinook salmon (n=12), or unidentified salmonids (n=2) were present during all periods. Because of the difficulty of determining age from size-variable structures such as gillrakers and teeth, most individuals (n=27) were designated as "unknown age."

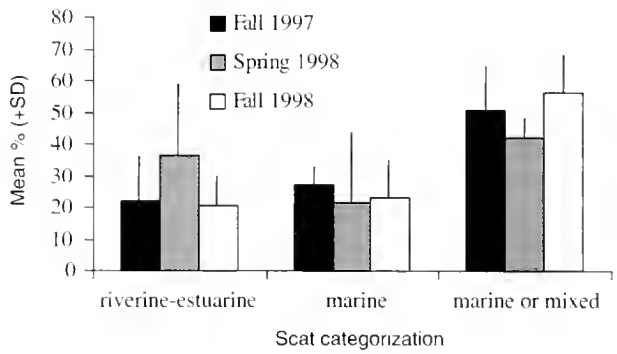

Figure 2

Mean percentage plus standard deviation (SD) of scats that were classified as "riverine-estuarine" (i.e. samples composed of prey taxa that are exclusively or potentially (e.g. anadromous species, osmerids) found in rivers or estuaries), "marine" (i.e. samples composed exclusively of prey that inhabit marine waters), and "marine or mixed" (i.e. samples composed of prey taxa exclusively found in marine waters or those that might inhabit marine waters at some stage in their life).

Discussion

Investigating diet is essential to assessing the role of harbor seals in marine and freshwater ecosystems in order to quantify their interactions with fisheries and determine their impact on the recovery of endangered species. All methods used to investigate diet of seals and other pinnipeds have some limitations (Murie and Lavigne, 1985, 1986; Harvey, 1989). With scats, it is assumed that the relative frequency of prey identified from undigested remains reflects the frequency of prey eaten (Tollit et al., 1997). However, several investigators have determined that this assumption may be seriously biased in several ways (Hawes, 1983; da Silva and Neilson, 1985; Jobling, 1987; Dellinger and Trillmich, 1988; Harvey, 1989; Pierce and Boyle, 1991; Cottrell et al., 1996; Tollit et al., 1997; Bowen, 2000; Orr and Harvey, 2001). No diet study can estimate detrimental or lethal impacts to prey resulting from harassment by pinnipeds. In addition, once a prey is captured, a seal might consume only the soft tissue (especially of larger prey), which would not leave identifiable evidence in scats. Additionally, because skeletal remains from different prey species pass through the alimentary canal and erode at different rates they may not reflect the true number or proportions of prey consumed (Hawes, 1983; Harvey, 1989; Pierce and Boyle, 1991; Cottrell et al., 1996; Tollit et al., 1997). Therefore, predation estimates determined from scat samples should be regarded as a measure of minimum impact. Although there are complications inherent in the use of scats to describe the diet of seals, scat analysis remains useful because many scats can be collected quickly, with minimum effort and without harm to the animals (Harvey, 1989).

Scats

Recently, skeletal remains other than otoliths and beaks have begun to be used to identify and enumerate prey of pinnipeds (e.g. Olesiuk et al., 1990; Cottrell et al., 1996; Riemer and Brown, 1997; Browne et al., 2002). There are constraints, however, for using all skeletal elements to identify prey species, including the need for a reference collection and the extensive training of personnel to identify digested prey structures (Cottrell et al., 1996). Moreover, there is usually a bias in the recovery and recognition of prey structures from different taxa (Cottrell et al., 1996; Laake et al., 2002). This bias may be a significant problem in estimating relative abundance of prey or biomass consumption by harbor seals and is the reason these indices were not considered in this study.

Despite these complications, the use of all available structures increased our estimates of prey diversity, MNI, and %FO for most prey taxa. Examination of all diagnostic structures also allowed us to consider a greater sample size because 93% of scats with identifiable remains contained bones, whereas only 53% of scats contained otoliths. Species not represented by otoliths, such as salmonids (during 1998) and cartilaginous fishes, were detected because all structures were used. In addition, the MNI of important prey such as Pacific hake, Pacific herring, and Pacific sardine would have been greatly underestimated had otoliths been used exclusively because the MNI derived by using all structures was at least threefold greater. Although there are complexities associated with estimating MNI from all structures, this method avoids the use of numerical correction factors determined from recovery rates of otoliths fed to captive seals during laboratory experiments (Browne et al., 2002). Results from captive experiments are highly variable between repeated trials for the same individual and among different individuals (Harvey, 1989; Bowen et al., 2000; Orr and Harvey, 2001).

Foraging habits

Harbor seals in the lower Umpqua River consumed prey from over 35 taxa; however, only a few prey taxa were dominant in their diet, as reflected by %FO. Overall, the five most abundant families of prey were Clupeidae, Cot-

tidae, Embiotocidae, Gadidae, and Pleuronectidae. These are similar to those reported in other studies of harbor seal diet in Oregon (Riemer and Brown, 1997; Browne et al., 2002; Riemer et al.[3,4]).

It was evident by the presence of prey like Pacific hake, Pacific sardine, hagfish, and various flatfishes that seals fed offshore in pelagic and demersal areas. Harbor seals also consumed prey (e.g. Pacific staghorn sculpin) commonly found inshore or in estuarine waters. The NMFS recommendations to remove pinnipeds from systems where endangered prey also occur, rely on the assumption that pinnipeds are primarily feeding (on ESA-listed species) in that system. Our study indicated that this was not the case. Although the seals at the Umpqua hauled out several kilometers up river, they foraged primarily at sea.

Because of the life histories of many of the prey taxa, our foraging habitat categories must be considered estimations of where the prey might have been consumed. For example, we estimated that 24% of scats contained prey attributable to the riverine-estuarine environment. However, this may actually be an overestimation because some of these species potentially inhabit the marine environment at some time in their life and may have been consumed there. Additionally, scats categorized as marine or mixed may reflect that the seal fed solely in the marine environment (because all the taxa can potentially be found in marine waters) or fed at sea and within the river. Nevertheless, these categories are useful for a broad apportioning of foraging habitat. Even though we were able to determine that approximately 76% of the scats contained marine and potentially marine prey taxa, we were unable to assess whether this reflected a seal population with homogeneous or heterogeneous foraging patterns. In other words, because the scats could not be attributed to a particular individual, we had no way of discerning: 1) whether the entire seal population foraged roughly three-fourths of the time at sea and one-fourth of the time in the river, or 2) whether 76% of the seals fed at sea whereas 24% foraged closer to shore and in the river. This distinction may be important if only a subgroup of seals is feeding in the river and preying on fish that are seasonally abundant in the estuary, such as salmonids. Studies that incorporate radio- or satellite-telemetry or genetic identification of individual prey items in scats may reveal these distinctions in the future.

Because the seals haul out almost 5 km upriver and have been observed as far as 32 km upriver, it is clear that seals use the river environment. However, the prevalence of marine fish remains in the scat samples indicates that the seals that haul out at the Umpqua River do not feed exclusively in the river. The predominance of marine prey may reflect a foraging strategy in which the effort required to find marine sources of food is offset by the energy gained by exploiting large aggregations of marine schooling fish (e.g. Pacific hake and Pacific sardine). In this scenario, the seals in the Umpqua estuarine-riverine system may depend on marine resources while taking advantage of protected estuarine waters that provide a sheltered place to rest and occasionally feed.

Salmonids

We used two methods to estimate the number of salmonids eaten by harbor seals: prey remains and genetic analyses of scat samples. Analysis of skeletal remains was of limited value because the majority of salmonid structures recovered from scat samples were bones, which could be identified only to family. This study represents a novel application of genetic techniques to identify salmonid species from bones found in scats. These techniques allowed us to determine species for a majority of the salmonid samples that would have otherwise remained unidentified because they did not contain otoliths.

Salmonid bones or otoliths were found in 6% of the harbor seal scats collected during our study—a finding that is comparable to the 5% found by Laake et al. (2002) at the Columbia River. However, it is about one-half of what was found by Riemer and Brown (13%; 1997) at selected sites in Oregon. Brown et al. (1995) found salmonids in 12% of gastrointestinal tracts of harbors seals taken incidentally by commercial salmon gillnet fishing operations, and Roffe and Mate (1984) observed that salmonids made up 30% of the prey for harbor seals surface feeding in the Rogue River. Regardless of sampling method, in these studies, most of the salmonids could be identified only to family because few otoliths were recovered and genetic techniques to identify bones to species had not yet been developed.

Salmonids are present in the Umpqua River year-round although species and age composition change throughout the year. In this study, most salmonid prey of known age were juveniles; however, we could determine age of only one-half of the individuals. Juveniles are found in the Umpqua River system year-round and may be easier for seals to catch than adults. Alternatively, perhaps seals did not consume many adult skeletal elements because adult salmonids are large fish, which may be ripped apart rather than swallowed whole.

Our sampling seasons encompassed at least some portion of the migrations of all salmonids, all of which (except cutthroat trout) were prey of harbor seals. The fact that portions of all migrations were included in the sampling design was noteworthy because there were a large number of seals in the river throughout the year and yet we found no evidence through genetic or otolith identification that seals consumed cutthroat trout in the Umpqua River. The genetic identification tools developed and applied in our collaboration with CBMGL were useful in discerning

[3] Riemer, S. D., R. F. Brown, and M. I. Dhruv. 1999. Monitoring pinniped predation on salmonids in the Alsea and Rogue River estuaries: fall, 1997. *In* Pinniped predation on salmonids: preliminary reports on field investigations in Washington, Oregon, and California, p. 104–152. Compiled by National Marine Fisheries Service, Northwest Region. [Available from ODFW, 7118 NE Vandenberg Avenue, Corvallis, OR 97330.]

[4] Riemer, S. D., R. F. Brown, and M. I. Dhruv. 1999. Monitoring pinniped predation on salmonids in the Alsea and Rogue River estuaries: fall, 1998. *In* Pinniped predation on salmonids: preliminary reports on field investigations in Washington, Oregon, and California, p. 153–188. Compiled by National Marine Fisheries Service, Northwest Region. [Available from ODFW, 7118 NE Vandenberg Avenue, Corvallis, OR 97330.]

scarce from abundant salmonids. These techniques may be useful in identifying other pinniped prey that lack species-specific structures and would allow managers to better assess the impact of pinniped predation on threatened or endangered species.

Acknowledgments

This study was proposed and initiated in collaboration with Joe Scordino. Scat collection and harbor seal counts were conducted by Lawrence Lehman, Kirt Hughes, Merrill Gosho, Sharon Melin, and Robert DeLong. The U.S. Coast Guard Umpqua River Station provided boat storage and a location for keeping a chest freezer during the 1997 field season. We would like to thank the Oregon Institute of Marine Biology, Charleston, OR, where the samples collected during 1997 were processed. We greatly appreciate the collaboration with Conservation Biology Molecular Genetics Laboratory, which resulted in the identification of our salmon remains based on genetic methods. We would also like to thank Susan Reimer who kindly helped us with difficult identifications, as well as Lawrence Lehman and Jason Griffith for their verification of bone and otolith identifications. We thank Patience Browne, Patrick Gearin, John Jansen, Mark Dhruv, and three anonymous reviewers for providing helpful comments on earlier drafts of this manuscript.

Literature cited

Bigg, M. A., G. Ellis, P. Cottrell, and L. Milette.
1990. Predation by harbour seals and sea lions on adult salmon in Comox Harbour and Cowichan Bay, British Columbia. Can. Tech. Rep. Fish. Aquat. Sci. 1769, 31 p.

Bowen, W. D.
2000. Reconstruction of pinnipeds diets: accounting for complete digestion of otoliths and cephalopod beaks. Can. J. Fish. Aquat. Sci. 57:898–905.

Brown, R. F.
1980. Abundance, movements and feeding habits of the harbor seal, *Phoca vitulina*, at Netarts Bay, Oregon. M.S. thesis, 69 p. Oregon State Univ., Corvallis, OR.

Brown, R. F., S. D. Riemer, and S. Jefferies.
1995. Food of pinnipeds collected during the Columbia River Area Commercial Salmon Gillnet Observation Program, 1991–1994. ODFW (Oregon Dep. Fish Wildlife), Wildlife Diverstiy Program Tech. Rep. 95-6-01, 16 p.

Brown, R. F., and S. Kohlmann.
1998. Trends in abundance and current status of the Pacific harbor seal (*Phoca vitulina richardsi*) in Oregon: 1977–1998. ODFW, Wildlife Diverstiy Program Tech. Rep. 98-6-01, 16 p.

Browne, P., J. L. Laake, and R. L. DeLong.
2002. Improving pinniped diet analyses through identification of multiple skeletal structures in fecal samples. Fish. Bull. 100:423–433.

Butler, U. L.
1990. Distinguishing natural from cultural salmonid deposits in Pacific Northwest North America. Ph.D. diss., 218 p. Univ. of Washington, Seattle, WA.

Cottrell, P. E., A. W. Trites, and E. H. Miller.
1996. Assessing the use of hard parts in faeces to identify harbour seal prey: results of captive-feeding trials. Can. J. Zool. 74:875–880.

da Silva, J., and J. Neilson.
1985. Limitations of using otoliths recovered in scats to estimate prey consumption in seals. Can. J. Fish. Aquat. Sci. 42:1439–1442.

Dellinger, T., and F. Trillmich.
1988. Estimating diet composition from scat analysis in otariid seals (Otariidae): is it reliable? Can. J. Zool. 66: 1865–1870.

Eschmeyer, W. N., E. S. Herald, and H. Hammann.
1983. A field guide to Pacific Coast fishes of North America, 336 p. Houghton Mifflin Co., Boston, MA.

Harvey, J. T.
1987. Population dynamics, annual food consumption, movements and dive behaviors of harbor seals, *Phoca vitulina richardsi*, in Oregon. Ph.D. diss., 177 p. Oregon State Univ., Corvallis, OR.
1989. Assessment of errors associated with harbor seal (*Phoca vitulina*) faecal sampling. J. Zool., Lond. 219: 101–111.

Hawes, S.
1983. An evaluation of California sea lion scat samples as indicators of prey importance. M.S. thesis. 50 p. San Francisco State Univ. San Francisco, CA.

Jobling, M.
1987. Marine mammal faeces samples as indicators of prey importance—a source of error in bioenergetics studies. Sarsia 72:255–260.

Johnson, O., M. Ruckelshaus, W. Grant, F. Waknitz, A. Garrett, G Bryant, K. Neely, and J. Hard.
1999. Status review of coastal cutthroat trout from Washington, Oregon, and California. NOAA Tech. Memo. NMFS-NWFSC-37, 292 p.

King, J.
1983. Seals of the world, 240 p. Comstock Publishing Assoc., Cornell Univ. Press, New York, NY.

Laake, J. L., P. Browne, R. L. DeLong, and H. R. Huber.
2002. Pinniped diet composition: a comparison of estimation models. Fish. Bull. 100:434–447.

Murie, D., and D. Lavigne.
1985. A technique for the recovery of otoliths from stomach contents of piscivorous pinnipeds. J. Wildl. Manag. 49: 910-912.
1986. Interpretation of otoliths in stomach content analyses of phocid seals: Quantifying fish consumption. Can. J. Zool. 64:1152–1157.

NMFS (National Marine Fisheries Service).
1997. Investigation of scientific information on the impacts of California sea lions and Pacific harbor seals on salmonids and on the coastal ecosystem of Washington, Oregon, and California. NOAA Tech. Memo. NMFS-NWFSC-28, 172 p.

Olesiuk, P. F., M. A. Bigg, G. M. Ellis, S. J. Crockford, and R. J. Wigen.
1990. An assessment of the feeding habits of harbour seals (*Phoca vitulina*) in the Strait of Georgia, British Columbia, based on scat analysis. Can. Tech. Rep. Fish. Aquat. Sci. 1730, 135 p.

Orr, A. J., and J. T. Harvey.
2001. Quantifying errors associated with using fecal samples to determine the diet of the California sea lion (*Zalophus californianus*). Can. J. Zool. 79:1080–1087.

Pearson, J., and B. Verts.
1970. Abundance and distribution of harbor seals and northern sea lions in Oregon. Murrelet 51:1–5.
Pierce, G. J., and P. R. Boyle.
1991. A review of methods for diet analysis in piscivorous marine mammals. Ocean. Mar. Biol. Ann. Rev. 29:409–486.
Purcell, M, G. Mackey, E. LaHood, H. Huber, and L. Park.
2004. Molecular methods for the genetic identification of salmonid prey from Pacific harbor seal (*Phoca vitulina richardsi*) scat. Fish. Bull. 102:213–220.
Reeves, R., B. Stewart, and S. Leatherwood.
1992. The Sierra Club handbook of seals and sirenians, 359 p. Sierra Club Books, San Francisco, CA.
Riemer, S. D., and R. F. Brown.
1997. Prey of pinnipeds at selected sites in Oregon identified by scat (fecal) analysis, 1983–1996. ODFW Wildlife Diversity Program Tech. Rep. 97-6-02, 34 p.
Roffe, T., and B. Mate.
1984. Abundances and feeding habits of pinnipeds in the Rogue River, Oregon. J. Wildl. Manag. 48:1262–1274.
Tollit, D. J., M.J. Steward, P. M. Thompson, G. J. Pierce, M. B. Santos, and S. Hughes.
1997. Species and size differences in the digestion of otoliths and beaks: implications for estimates of pinniped diet composition. Can. J. Fish. Aquat. Sci. 54:105–119.
U. S. Fish and Wildlife Service.
2000. Endangered and threatened wildlife and plants; final rule to remove the Umpqua River cutthroat trout from the list of endangered wildlife. Federal Register: 26 April 2000, 65(81:24420–24422.

Abstract—Larval development of the sidestriped shrimp (*Pandalopsis dispar*) is described from larvae reared in the laboratory. The species has five zoeal stages and one postlarval stage. Complete larval morphological characteristics of the species are described and compared with those of related species of the genus. The number of setae on the margin of the telson in the first and second stages is variable: 11+12, 12+12, or 11+11. Of these, 11+12 pairs are most common. The present study confirms that what was termed the fifth stage in the original study done by Berkeley in 1930 was the sixth stage and that the fifth stage in the Berkeley's study is comparable to the sixth stage that is described in the present study. The sixth stage has a segmented inner flagellum of the antennule and fully developed pleopods with setae. The ability to distinguish larval stages of *P. dispar* from larval stages of other plankton can be important for studies of the effect of climate change on marine communities in the Northeast Pacific and for marine resource management strategies.

Larval development of the sidestriped shrimp (*Pandalopsis dispar* Rathbun) (Crustacea, Decapoda, Pandalidae) reared in the laboratory

Wongyu Park

School of Fisheries and Ocean Sciences
University of Alaska Fairbanks
Juneau, Alaska, 99801-8677
E-mail address: wpark@uaf.edu

R. Ian Perry

Pacific Biological Station,
Fisheries and Oceans
Nanaimo, British Columbia, V9R 5K6, Canada

Sung Yun Hong

Department of Marine Biology
Pukyong National University
Pusan, 608-737, Korea

Sixteen species of the genus *Pandalopsis* have been recognized in the Southwestern Atlantic and North Pacific Oceans (Komai, 1994; Jensen, 1998; Hanamura et al., 2000). Most members of the genus attain a large body size and are valuable as commercial fishery resources (Holthuis, 1980; Baba et al., 1986). In the North Pacific, *P. dispar*, *P. ampla*, *P. aleutica*, *P. longirostris*, *P. lucidirimicola*, and *P. spinosior* have been reported. Of these, *Pandalopsis dispar* is an important component of the commercial shrimp fisheries along with several species of the genus *Pandalus*. Commercial landings of shrimp during 1999 totaled approximately 19 million tons (PSMFC, 1999).

Knowledge of the life histories of these species, including the duration and growth of their larvae, is important for stock assessment and management. However, remarkably little is known about their early life histories because most species of the genus live at considerable depths. Of the 16 *Pandalopsis* species, the larvae of only three species have been described partly or completely from plankton samples or from larvae reared in the laboratory. The larvae of *Pandalopsis japonica* were described completely from specimens reared in the laboratory by Komai and Mizushima (1993). Kurata (1964) described the first stage of *P. coccinata* from plankton samples and from larvae hatched in the laboratory. Thatje and Bacardit (2000) assumed that larvae of *P. ampla* occurring in Argentine waters were similar to those of *P. dispar* and *Pandalopsis coccinata*. Berkeley (1930) described four larval stages of *P. dispar* based on samples collected in British Columbia coastal waters. The first stage was obtained from ovigerous females, whereas the larvae of the other stages were separated from plankton samples. In addition, the stage described as the fifth stage was not clearly defined.

In this study, we describe the complete series of larval stages of *P. dispar* using specimens reared in the laboratory.

Materials and methods

Ovigerous females of *Pandalopsis dispar* were collected on 25 March

Manuscript approved for publication 23 June 2003 by Scientific Editor.

Manuscript received 20 October 2003 at NMFS Scientific Publications Office.

Fish. Bull. 102:118–126 (2004).

1999 by using a small shrimp trawl fished at depths of about 40 m near Gabriola Island in the vicinity of the Pacific Biological Station, Nanaimo, British Columbia (latitude 49°13', longitude 123°55'). Water temperature at the collection site was around 9°C, and salinity was 29.0‰. The females were each kept in a 20-L jar with seawater. The larvae hatched on 1 April 1999. Hundreds of larvae hatched from one female. Of these, one hundred newly hatched larvae were transferred into individual 250-mL jars. To obtain samples for drawing and descriptions, a total of 150 larvae from the female were reared in a 20-L jar. Newly hatched *Artemia* nauplii were used to feed the larvae. We used filtered natural seawater from 40 m depth without adjusting the water temperature or salinity. Water temperature during the rearing experiments ranged from 8.7°C to 12.2°C (mean 10.5°C). Salinity during the rearing experiments ranged from 26.0‰ to 31.0‰ (mean 28.9‰). The water in each jar was changed daily.

All drawings were made with a drawing tube attached to a microscope. Carapace length (CL) was measured with an ocular micrometer from the posterior edge of the orbital arch to the middorsal posterior edge of the carapace. The anatomical terms used in this paper are from Pike and Williamson (1969) and Haynes (1985).

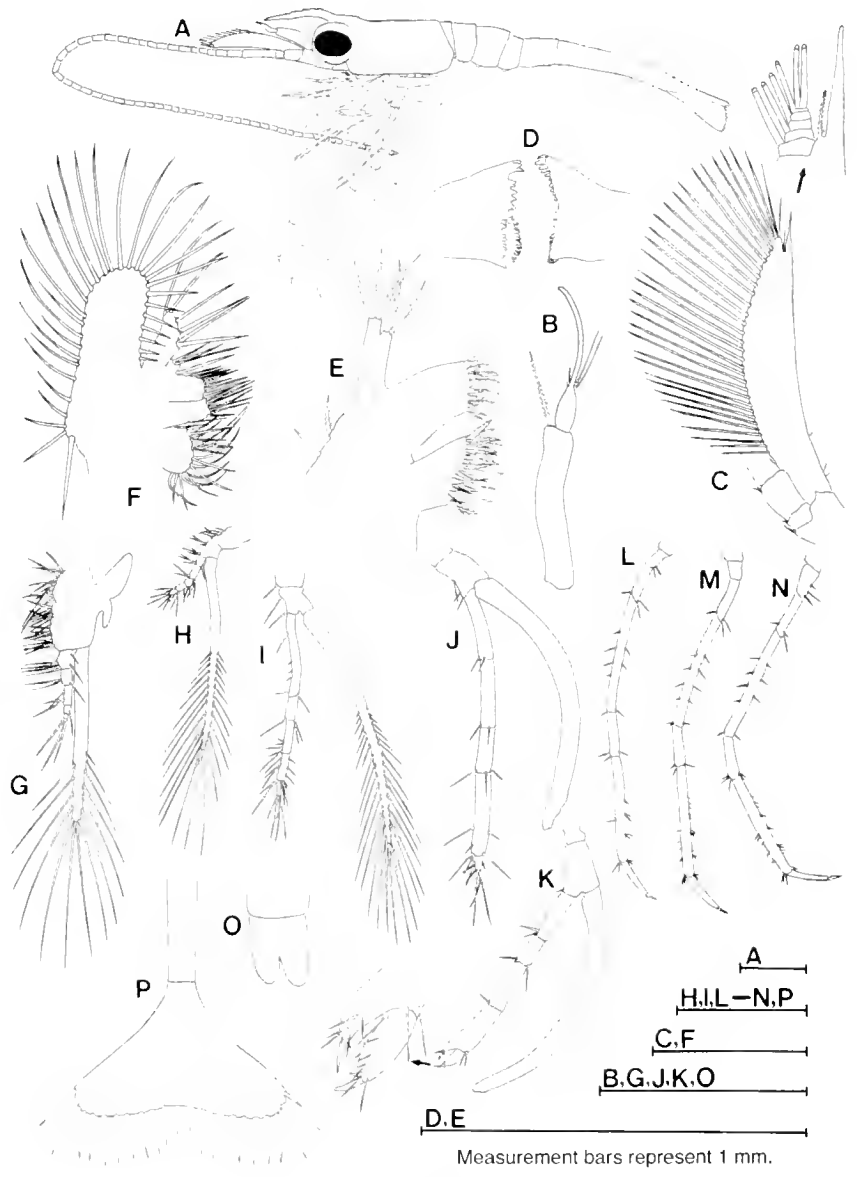

Figure 1

Results

In the complete larval development of *Pandalopsis dispar* there are five zoeal stages. In addition, there is one postlarval stage. The duration of each larval stage and the survival rate of *P. dispar* are shown in Table 1.

Larval description

First stage

Carapace (Fig. 1A) Carapace length (CL), 1.6 mm (SD: 0.06 mm, n=89); with concave lateral margin; rostrum long, well developed and directed forward and upward; weak

Table 1

Duration of each larval stage of *Pandalopsis dispar* at 8.7–12.2°C (mean 10.5°C) and 26.0–31.0‰ (mean 28.9‰). Stage 6 is a postlarval stage.

Stage	Mean duration (day)	Range (day)	Number of larvae observed
1	10.7	9–15	89
2	8.9	8–11	81
3	9.5	8–14	67
4	10	9–12	59
5	10.8	10–13	51
6	10.5	9–12	48

dorsal denticles and bare ventral tubercles on rostrum; rostrum about 0.7 times as long as carapace.

Eyes (Fig. 1A) Sessile.

Abdomen (Fig. 1A) 5 somites plus telson.

Antennule (Fig. 1, A and B) Peduncle unsegmented with a strong seta at distromesial margin; outer flagellum with 2+2 short aesthetascs.

Antenna (Fig. 1, A and C) Longer than the whole body length; flagellum segmented throughout its length; outer-distal corner terminated with an acute spine and a minute seta; inner-distal margin 5-segmented with 1, 1, 1, 1, 2 setae; inner margin fringed with 28–29 setae.

Mandible (Fig. 1D) Asymmetrical; without the same arrangement of denticles, however, almost the same size; incisor process not separated from molar process; armed with several teeth on molar part.

Maxillule (Fig. 1E) Coxal and basal endite with serially developed strong spines and multiple setae; endopod with 2+3 terminal setae

Maxilla (Fig. 1F) Palp with 2, 1, 1, 2 setae; coxal endite with 6 distal setae; basal endite with 8 distal setae; broad scaphognathite with narrow posterior lobes having long naked setae.

First maxilliped (Fig. 1G) Endites separated by shallow notch and with multiple setae; bilobed epipod; endopod 4-segmented with 6, 3, 3, 4 setae; exopod with 14 plumose natatory setae; terminal segment with 3 terminal spines and 1 subterminal spine.

Second maxilliped (Fig. 1H) Coxa with 7 setae; basis with 3 setae; no epipod; endopod 5 segmented with 5, 5, 2, 4, 4 setae; exopod with 27 plumose natatory setae.

Third maxilliped (Fig. 1I) Coxa with 1 seta; basis with 2 setae; endopod 5-segmented with various number of setae; exopod with 34–36 plumose natatory setae.

Pereiopods (Fig. 1, J–N) 1st pereiopod (Fig. 1J) not chelate; 3 long terminal spines on dactylus; dactylus short; propodus longer than carpus; exopod without natatory setae; endopod of 2nd pereiopod chelated (Fig. 1K); chela with numerous small spines; ischium and carpus of pereiopods 3–5 (Fig. 1, L–N) longer than 1st and 2nd ones; propodus armed with several minute spines.

Pleopods (Fig. 1O) Bilobed buds, not functional.

Telson (Fig. 1P) Triangular form; broadened at the end, posterolateral margin with 11+12 (12+12, 11+11) marginal spines; each spine with fine hairs.

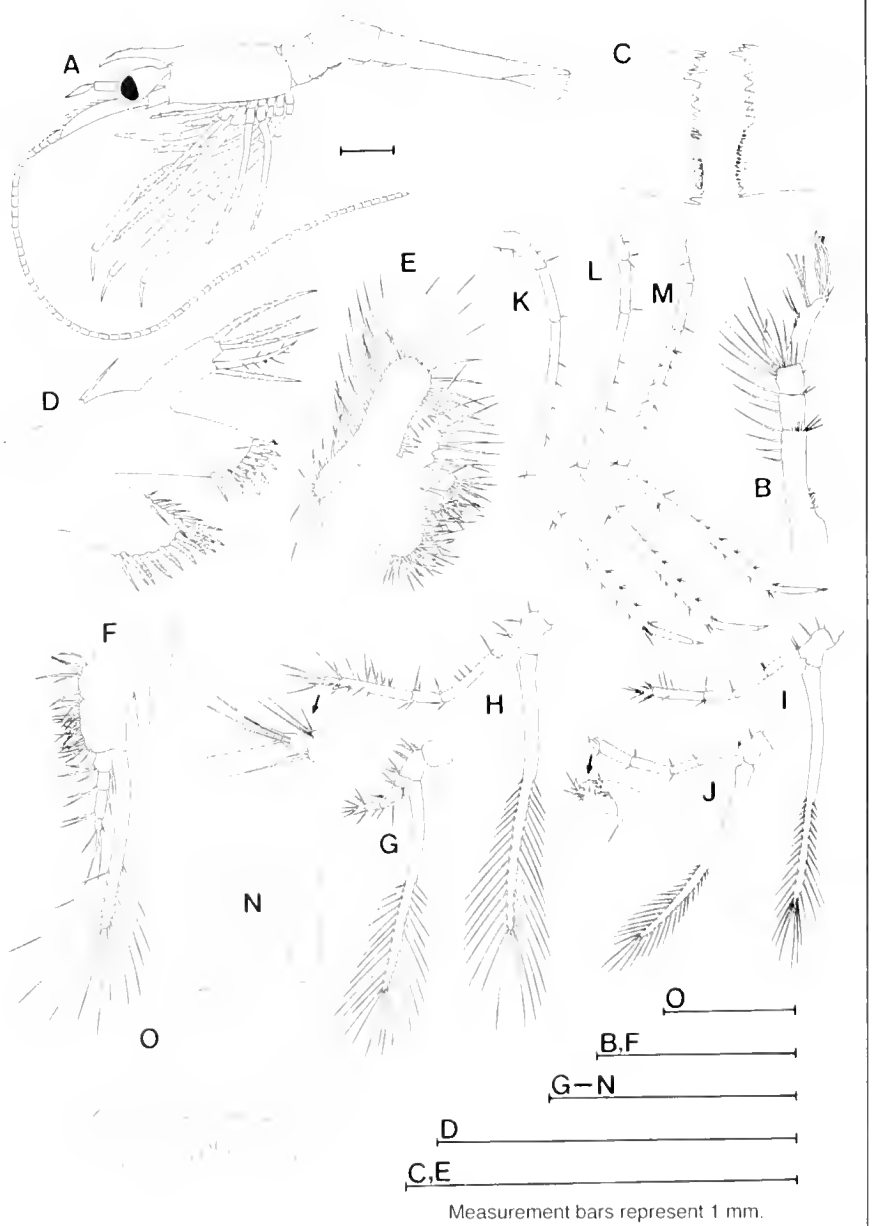

Figure 2

Second stage

Carapace (Fig. 2A) CL, 2.2 mm (SD: 0.11, n=81); rostrum not strongly curved upwards; 5–6 prominent dorsal denticles and 3–4 weak ventral spines; rostrum shorter than carapace; supraorbital spine present.

Eyes (Fig. 2A) Stalked; separated from carapace.

Antenna (Fig. 2A) General shape unchanged; longer than that of 1st stage.

Antennule (Fig. 2B) Peduncle 3-

segmented; inner flagellum with 2 distal setae; outer flagellum with 2, 3, 4, 2 aesthetascs on inner margin.

Mandible (Fig. 2C) General shape unchanged; bigger than that of 1st stage.

Maxillule (Fig. 2D) Coxal and basal endite with serially developed strong spines and multiple setae; endopodite with 2+3 spines; a strong subterminal seta.

Maxilla (Fig. 2E) Palp with 2, 2, 2, 3 setae; broad scaphognathite with narrow posterior lobe having a long naked seta; coxal endite with 6 distal setae; basal endite with 7 distal setae.

First maxilliped (Fig. 2F) Epipod bilobed; endopod with 3+1, 2+1, 2+1, 3 setae; exopod unsegmented with 14 plumose natatory setae.

Second maxilliped (Fig. 2G) One long and several intermediate sized spines in basal endite; endopod 5-segmented; exopod with 24 plumose natatory setae.

Third maxilliped (Fig. 2H) Endopod 5-segmented, armed with many spines; exopod of 36 plumose natatory setae.

Pereiopods (Fig. 2, I–M) Not chelate; 1st pereiopod of 4 spines in basal endite; 3 strong and two weak spines in dactylus of 1st pereiopod; general shape unchanged from 2nd pereiopod through 5th pereiopod.

Pleopods (Fig. 2N) Bilobed buds, not functional; no seta and hair on buds; no further development from the 1st stage.

Telson (Fig. 2O) Unchanged.

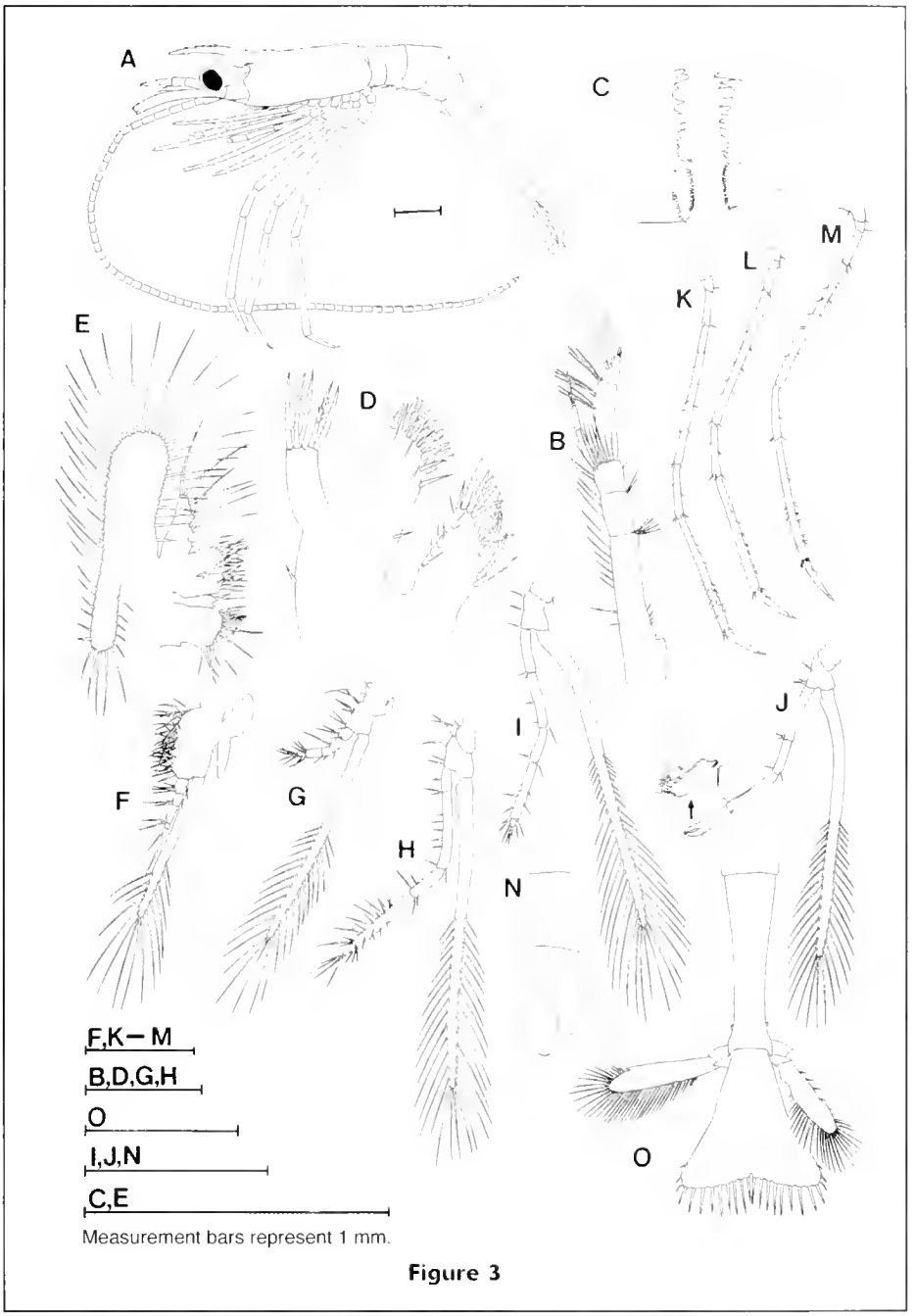

Figure 3

Third stage

Carapace (Fig. 3A) CL, 2.7 mm (SD: 0.12, n=67); longer rostrum than that of 2nd stage; almost 0.9 times as long as carapace; rostrum with 5-6 dorsal spines and 1-2 ventral spines.

Antennule (Fig. 3B) Inner flagellum 2-segmented with 0, 2 setae; outer flagellum 2-segmented with 3+3+3, 3+3 aesthetascs.

Antenna (Fig. 3A) General shape unchanged; longer than 2nd stage.

Mandible (Fig. 3C) Molar and incisor processes present; incisor process with 6-9 teeth; molar process with heavy teeth on biting edge.

Maxillule (Fig. 3D) Palp with 2+3 setae; a small subterminal spine; basal and coxal endite with numerous spines.

Maxilla (Fig. 3E) Protopodite unsegmented; palp with 1, 2, 2, 1+2 setae and with 4 lobes; broad scaphognathite with narrow posterior lobe bearing numerous setae.

First maxilliped (Fig. 3F) Epipod bilobed; endopod 4-segmented with 4, 2, 2, 2 setae; exopod with 15–16 plumose natatory setae;

Second maxilliped (Fig. 3G) Coxal endite with an epipod and a strong spine; endopod 5-segmented with 3, 2, 2, 4, 6 setae exopod with setae.

Third maxilliped (Fig. 3H) Coxal endite with one long and

one short spine; basal endite with 2 long and 2 intermediate sized spines; endopod 5-segmented with numerous setae; exopod with 25–26 plumose natatory setae.

Pereiopods (Fig. 3, I–M) General shape unchanged except addition of setae.

Pleopods (Fig. 3N) Buds biramous; much longer than that of 2nd stage.

Uropods (Fig. 3O) Biramous; endopod with a fused spine at distal quarter of outer margin and numerous setae on inner distal margin; exopod with 4 spines on outer margin and numerous setae on inner distal margin.

Telson (Fig. 3O). With 12 pairs of posterolateral spines plus a median spine.

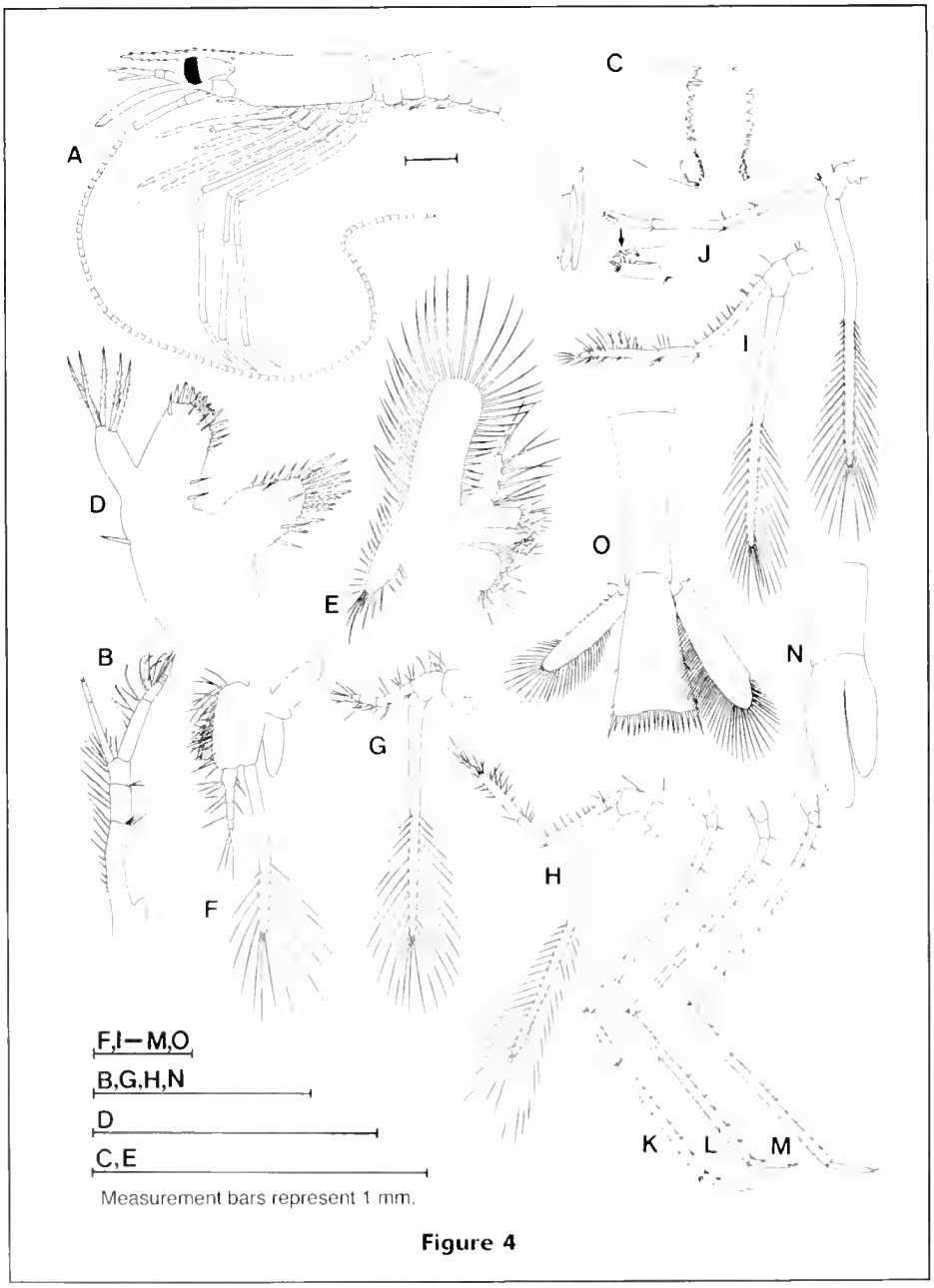

Figure 4

Fourth stage

Carapace (Fig. 4A) CL, 3.1 mm (SD: 0.13, n=59); Rostrum slightly longer than carapace and directed forward; rostrum with 15 dorsal spines and 6 ventral spines.

Antenna (Fig. 4A) General shape unchanged; longer than that of 3rd stage.

Antennule (Fig. 4B) Much longer inner flagellum than that of 3rd stage; inner flagellum about 0.9 times as long as outer flagellum, 2-segmented with 0, 2 setae; outer flagellum 6-segmented with 1, 2, 2, 3, 4 aesthetascs.

Mandible (Fig. 4C) Similar to third stage.

Maxillule (Fig 4D) General shape unchanged except addition of setae on endites.

Maxilla (Fig. 4E) Palp with 3, 2, 2, 3 setae; endites and scaphognathite added numerous setae.

First maxilliped (Fig. 4F) Expod with 15 plumose natatory setae.

Second maxilliped (Fig. 4G) Basal endite with an epipod and a long spine; exopod with 28–29 plumose natatory setae.

Third maxilliped (Fig. 4H) Expopod with 36–37 plumose natatory setae.

Pereiopods (Fig. 4, I–M) Number of spines increased.

Pleopods (Fig. 4N) Lobes much longer than those of third stage.

Uropods (Fig. 4O) Endopod and exopod with numerous setae on inner distal margin.

Telson (Fig. 4O) With 12 pairs of spines on posterolateral margin; a pair of lateral spines at distal third.

Fifth stage

Carapace (Fig. 5A) CL, 3.6 mm (SD: 0.15, n=51); Rostrum directed forward and upward, slightly longer than carapace; rostrum with 17–18 dorsal spines and 7–8 ventral spines.

Antennule (Fig. 5B) Inner flagellum 3-segmented and about 0.9 times as long as outer flagellum; outer flagellum with 2+2+3+3+3+2+3+5 aesthetascs and distal third 6-segmented.

Mandible (Fig. 5C) More advanced development than that of 6th; not much change in biting surface.

Maxillule (Fig. 5D) General shape unchanged except addition of setae on endites.

Maxilla (Fig. 5E) General shape unchanged.
First maxilliped (Fig. 5F) Exopod with 16 plumose natatory setae.
Second maxilliped (Fig. 5G) Exopod with 31–33 plumose natatory setae.
Third maxilliped (Fig. 5H) Exopod with 46–48 plumose natatory setae.
Pereiopods (Fig. 5, I–M) Ischium slightly expanded in first pereipod.
Pleopods (Fig. 5N) Much more developed than pleopods of 4th stage; exopod with 13, 1 setae; endopod with 6 setae and vestiges of appendix interna.
Uropod (Fig. 5O) Exopod with numerous minute spines on outer margin
Telson (Fig. 5O) Both lateral margins parallel; 19 terminal spines; 2 pairs of lateral spines.

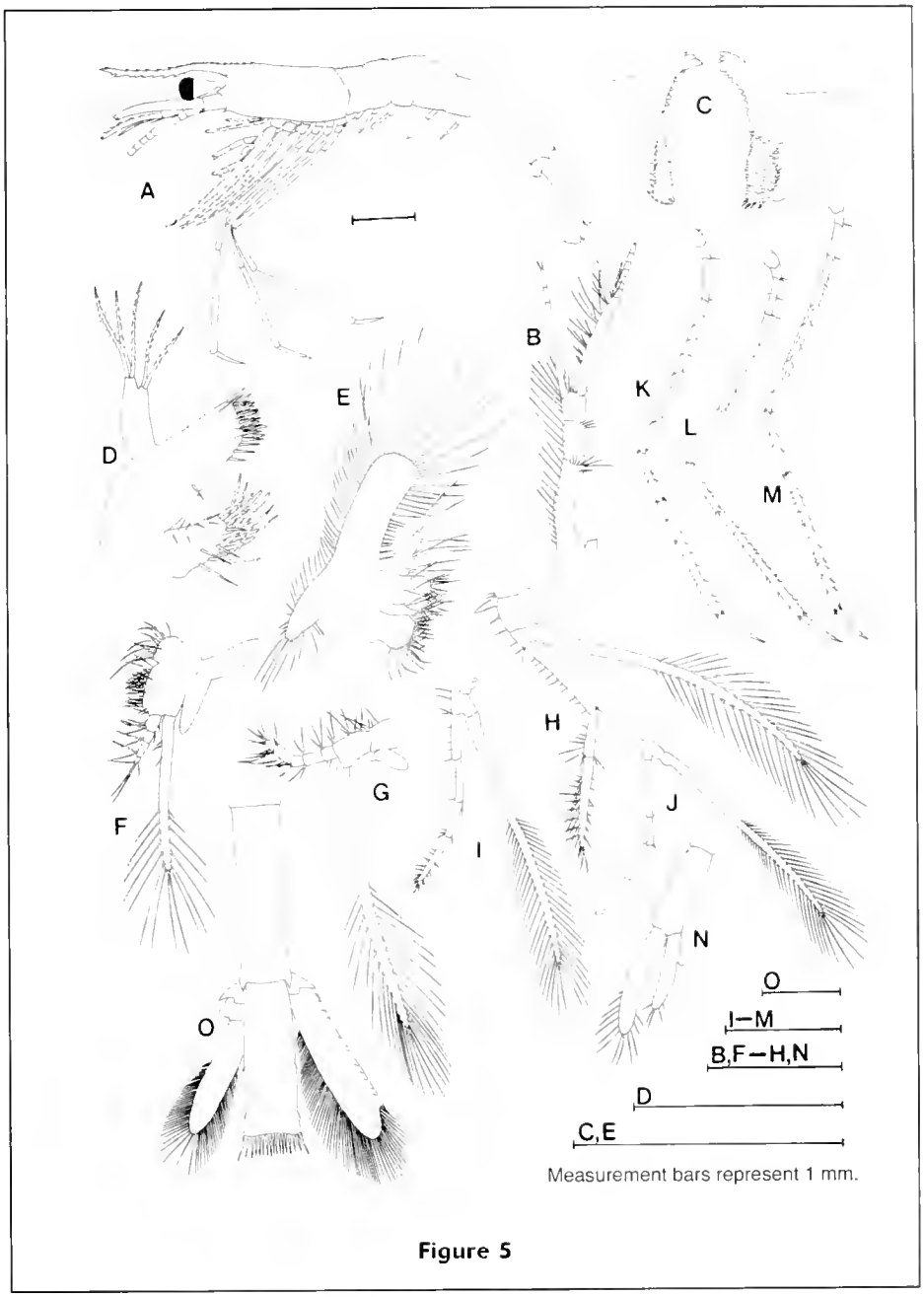

Figure 5

Sixth stage

Carapace (Fig. 6A) CL, 4.0 mm (SD: 0.21, n=48); adult-like.
Antennule (Fig. 6B) Inner flagellum as long as outer flagellum; inner flagellum with multisegments; outer flagellum with numerous segments.
Mandible (Fig. 6C) Incisor part separated from molar process and extended anteriorly.
Maxillule (Fig. 6D) 9 terminal spines on basal endite.
Maxilla (Fig. 6E) Palp with 2, 2, 2, 1+2 spines; broad scaphognathite with narrow posterior lobe bearing 3 long setae.
First maxilliped (Fig. 6F) Exopodite with 4+2, 2, 2 3 long and 1 short spines.
Second maxilliped (Fig. 6G) Basal endite with 2 long spines; vestigial dactylus.
Third maxilliped (Fig. 6H) Propodus armed with many spines; dactylus with 2 spines.
Pereiopods (Fig. 6, I–M) 1st pereipods with subchelated terminal segment; 1st pereiopod with slightly expanded ischium.
Pleopods (Fig. 6N) Endopod and exopod with numerous plumose natatory setae; endopod with epipod almost adult-like.
Uropods (Fig. 6O) Biramous; larger than those of fifth stage; adult-like.
Telson (Fig. 6O) Telson with 20 terminal spines and 4 pairs of lateral spines.

Discussion

The first stage larva of *Pandalopsis dispar* described by Berkeley (1930) is identical to the larva described in the present study. However, we found that she overlooked some important characteristics. She described the first stage larva as having 24 setae on the margin of the telson. We found, however, that the number of setae is variable, and that the larvae have 11+12, 12+12, or 11+11 marginal

setae. Of these, 11+12 pairs are more common than the others.

Berkeley (1930) described the fifth stage based on plankton materials. In the present study, what was described by Berkeley (1930) as the fifth stage larva turned out to be the sixth stage because the larvae of this stage have fully developed pleopods. Although the larvae of the fifth stage have somewhat natatory setose on their pleopods, they appear not to be completely functional. Compared to the larvae of *P. japonica*, *P. dispar* has one more stage than that of *P. japonica*. The pleopod development of *P. japonica* from the fourth stage to the fifth stage is very obvious, whereas that of *P. dispar* has another stage and the changes in its features between the fourth and sixth stages are easily seen.

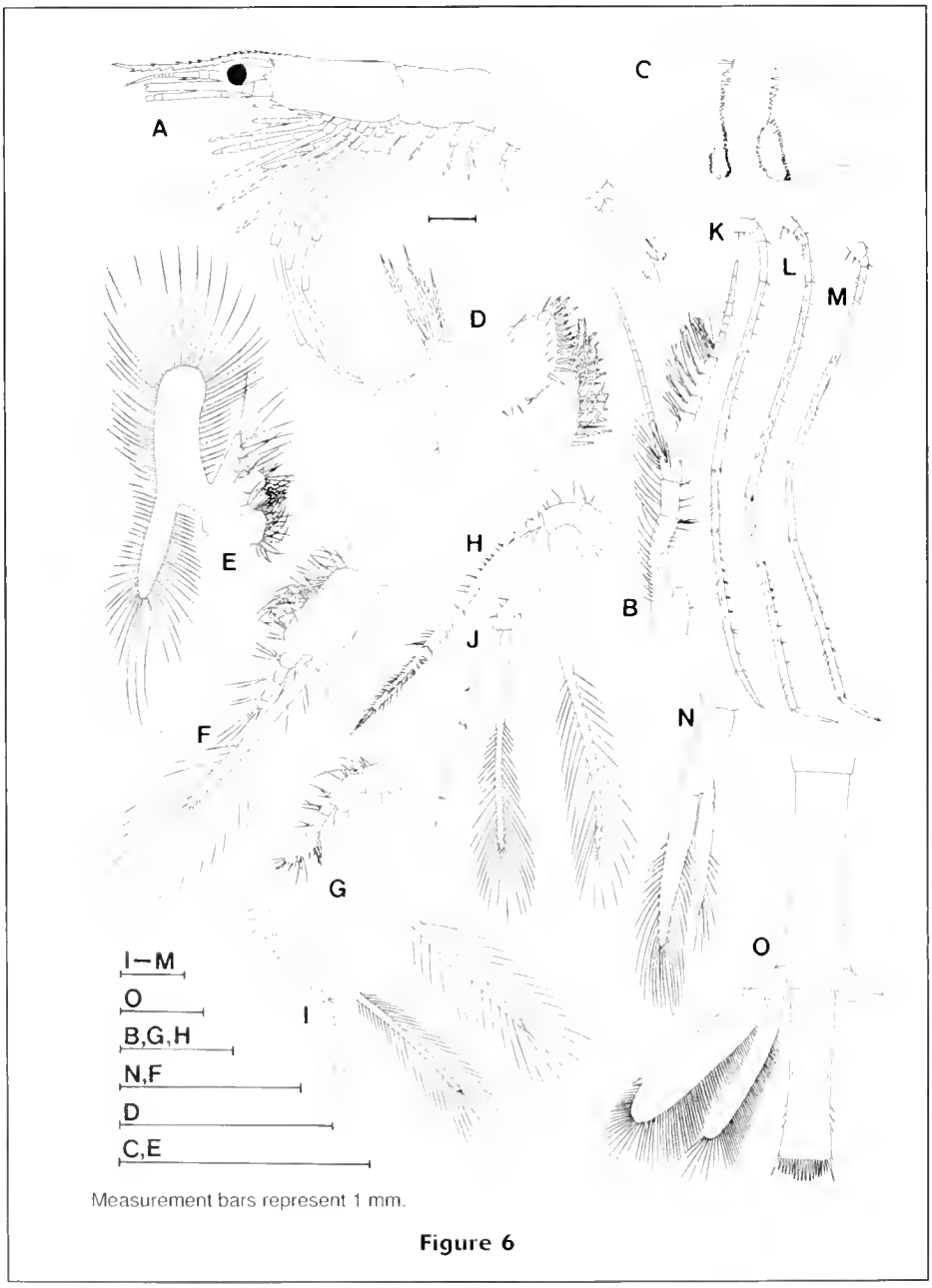

Figure 6

The major characteristics of the six larval stages of *P. dispar* are summarized in Table 2. This table can be used for the identification of the larval stages of this species. Komai (1994) reviewed the morphological characters of the first larval stage of three *Pandalopsis* spp.: *P. dispar*, *P. coccinata*, and *P. japonica*. The larvae of *P. dispar* at this stage are quite different from those of the other two species. The larvae of *P. dispar* have a triangular telson, whereas those of *P. coccinata* and *P. japonica* have a semicircular telson.

The adults of the genus *Pandalopsis* differ from those of other pandalid shrimps by having a laminated expansion on the first pereiopod (Schmit, 1921; Butler, 1980). This character is also present in larvae of *P. coccinata* and *P. japonica*, whereas it is not present in larvae of *P. dispar*. From the third stage the ischium does indicate expansion, however, it is not distinctive. It is assumed that in *P. dispar*, the expansion should be distinctive after the larval stages.

In *P. coccinata* and *P. japonica* the ischium of the first pereiopod has a laminated expansion; however, in *P. dispar* it has no lamination. The structure of the ischium of the first pereiopod can be a diagnostic feature of *P. dispar* in addition to the shape of the telson.

Interspecific variation in the larval stages of pandalid shrimp is large, ranging from three to thirteen stages (Rothlisberg, 1980; Komai and Mizushima, 1993). Haynes (1980, 1985) assumed that *P. dispar* might have seven pelagic stages, or at least more than four. The present study has determined that *P. dispar* has five zoeal stages prior to the juvenile stage.

Pandalopsis dispar is one of the four principal target species of shrimp trawl fisheries in both offshore and inshore areas of the NE Pacific Ocean (PICES, 2001) but has undergone very large fluctuations in abundance, particularly in Alaska where it was reduced to extremely low levels during the late 1980s and through the 1990s. These fluctuations appear to have been associated first with climate fluctuations (Anderson, 2000), and second with intense harvesting (Oresanz et al., 1998). Anderson (2000) has suggested that pandalid shrimp population changes are one of the early in-

Table 2

Major characters of *Pandalopsis dispar* larvae.

Characters		Larval stage[1] 1	2	3	4	5	6 (postlarva)
Antenna flagellum	Inner	One strong spine	One peduncle with a few small spines	2 segments	2 segments	3 segments	Multisegmented over 14
	Outer	Not segmented	Slightly developed	2 segments	6 segments	7 segments	12 segments
Telson		12+11, 12+12, or 11+11		10 pairs of terminal spines, 2 pairs of uropods	One spine on each midlateral margin	2 spines on each lateral margin	4 spines on each lateral margin
Pleopod development		Wide as much as long	Longer than wide	Almost separated lobes	Longer lobes than those of stage 3	Lobes separated completely with natatory setae	Adult-like, with many natatory setae on both lobes

[1] Eyes of the first stage are sessile on carapace, whereas those of the second and later stages are stalked.

dicators of shifts in marine communities in this region. Orensanz et al. (1998) have suggested it is important to recognize that crustacean stocks can have multiscale spatial structures; species have possibly both widely distributed populations (such as in the oceanic offshore) and populations with discrete and localized distributions (as may occur in the nearshore inlets).

The ability to distinguish the larval stages of *Pandalopsis dispar* from routine plankton samples is therefore of use in studying both these problems of population fluctuations and population distributions. Early identification of trends in strong versus weak year classes can provide rapid indications of possible changes in large-scale climate conditions. Unambiguous identification of planktonic stages of *P. dispar* is also essential for studies of the spatial structure of its populations, for studies of transport pathways and potential mixing rates among populations, and ultimately for understanding the metapopulation structure of these populations. This latter point is critical for the development of improved management approaches, which may include identification of reproductive refugia (Orensanz et al., 1998).

Acknowledgments

We wish to thank Jim Boutillier and Steve Head for their support with this study. This study was supported by the Korea Research Foundation Grant (KRF-2002-013-H00005).

Literature cited

Anderson, P. J.
2000. Pandalid shrimp as indicators of ecosystem regime shift. J. Northw. Atl. Fish. Sci. 27:1–10.

Baba, K., K. Hayashi, and M. Toriyama.
1986. Decapod crustaceans from continental shelf and slope around Japan, 336 p. Japan Fisheries Resource Conservation Association, Tosho Printing Co. Ltd., Tokyo.

Berkeley, A.
1930. The post-embryonic development of the common pandalids of British Columbia. Cont. Can. Bio. Fish., New Series 6:79–163.

Butler, T. H.
1980. Shrimps of the Pacific coast of Canada. Can. Bull. Fish. Aquat. Sci. 202, 280 p.

Hanamura, Y., H. Khono, and H. Sakai.
2000. A new species of the deepwater pandalid shrimp of the genus *Pandalopsis* (Crustacea: Decapoda: Pandalidae) from the Kuril Islands, North Pacific. Crust. Res. 29:27–34.

Haynes, E.
1980. Larval morphology of *Pandalus tridens* and summary of the principal morphological characteristics of North Pacific pandalid shrimp larvae. Fish. Bull. 77:625–640.

Haynes, E.
1985. Morphological development, identification, and biology of larvae of Pandalidae, Hippolytidae and Crangonidae (Crustacea: Decapoda) of the northern North Pacific Ocean. Fish. Bull. 83:253–288.

Holthuis, L. B.
1980. Shrimps and prawns of the world, an annotated catalogue of species of interest to fisheries. FAO species Catalogue. FAO Fish. Syn. 125, FIR/S 125 Vol.1, 271 p.

Jensen, G. C.
1998. A new species of the genus *Pandalopsis* (Decapoda: Caridea: Pandalidae) from the Eastern Pacific, with notes on its natural history. Species Diversity 3:81–88.

Komai, T.
1994. Deep-sea shrimps of the genus *Pandalopsis* (Decapoda: Caridea: Pandalidae) from the Pacific Coast of eastern Hokkaido, Japan with the description of two new species. J. Crust. Biol. 14:538–559.

Komai, T., and T. Mizushima.
1993. Advanced larval development of *Pandalopsis japonica*

Balss, 1914 (Decapoda: Caridea: Pandalidae) reared in the Laboratory. Crustaceana 64:24–39.

Kurata, H.
1964. Larvae of deacapod Crustacea of Hokkaido. 3. Pandalidae. Bull. Hokkaido Reg. Fish. Res. Lab. 28:23–34.

Orensanz, J. M., J. Armstrong, D. Armstrong, and R. Hilborn.
1998. Crustacean resources are vulnerable to serial depletion—the multifaceted decline of crab and shrimp fisheries in the greater Gulf of Alaska. Rev. Fish Biol. Fisheries 8: 117–176.

Pike, R. B., and D. I. Williamson.
1964. The larvae of some species of Pandalidae (Decapoda). Crustaceana 6:265–284.

PICES.
2001. Commercially important crabs, shrimps and lobsters of the North Pacific Ocean. PICES Scientific Report 19, 79 p. North Pacific Marine Science Organization, Sidney, B.C., Canada

PSMFC (Pacific States Marine Fisheries Commission).
1999. 52nd annual report of the Pacific States Marine Fisheries Commission (A. J. Didier, ed.), 37 p. Pacific States Marine Fisheries Commission, Gladston, OR.

Rothlisberg, P. C.
1980. A complete larval description of *Pandalus jordani* Rathbun (Decapoda, Pandalidae) and its relation to other members of the genus *Pandalus*. Crustaceana 38:19–48.

Schmitt, W. L.
1921. The marine decapod Crustacea of California with special reference to the decapod Crustacea collected by the United States Bureau of Fisheries Steamer "Albatross" in connection with the biological survey of San Francisco bay during the years 1912–1913. Univ. California, Publ. Zool., vol. 23, 470 p.

Thatje, S., and R. Bacardit.
2000. Larval development of *Austropandalus grayi* (Cunningham, 1871) (Decapoda, Caridea, Pandalidae) from the southwestern Atlantic Ocean. Crustaceana 73:609–628.

Sources of age determination errors for sablefish (*Anoplopoma fimbria*)*

Donald E. Pearson
Santa Cruz Laboratory
National Marine Fisheries Service
110 Shaffer Road
Santa Cruz, California 95060
E-mail address: Don.Pearson@Noaa Gov

Franklin R. Shaw
Alaska Fisheries Science Center
National Marine Fisheries Service
7600 Sand Point Way NE
Seattle, Washington 98118

Abstract—This study was undertaken to resolve problems in age determination of sablefish (*Anoplopoma fimbria*). Aging of this species has been hampered by poor agreement (averaging less than 45%) among age readers and by differences in assigned ages of as much as 15 years.

Otoliths from fish that had been injected with oxytetracycline (OTC) and that had been at liberty for known durations were used to determine why age determinations were so difficult and to help determine the correct aging procedure. All fish were sampled from Oregon southwards, which represents the southern part of their range. The otoliths were examined with the aid of image processing.

Some fish showed little or no growth on the otolith after eight months at liberty, whereas otoliths from other fish grew substantially. Some fish lay down two prominent hyaline zones within a single year, one in the summer and one in the winter. We classified the otoliths by morphological type and found that certain types are more likely to lay down multiple hyaline zones and other types are likely to lay down little or no zones. This finding suggests that some improvement could be achieved by detailed knowledge of the growth characteristics of the different types.

This study suggests that it may not be possible to obtain reliable ages from sablefish otoliths. At the very least, more studies will be required to understand the growth of sablefish otoliths.

Manuscript approved for publication 14 July 2003 by Scientific Editor.

Manuscript received 20 October 2003 at NMFS Scientific Publications Office.

Fish Bull. 102:127–141 (2004).

Sablefish (*Anoplopoma fimbria*) are a valuable groundfish resource off the west coast of North America. The fishery in California, Oregon, and Washington is tightly regulated according to periodic stock assessments. Between 1990 and 1998 landings averaged more than 8000 metric tons per year and an average exvessel (retail) value of 12.5 million dollars per year (PFMC, 1999).

Sablefish are distributed in the northeastern Pacific Ocean from Baja California to the Bering Sea and southeast to northern Japan (Miller and Lea, 1972). Males and females are sexually mature between 55 and 67 cm, although there is considerable variation (Fujiwara and Hankin 1988a; Hunter et al., 1989). Off Washington, Oregon, and California, sablefish spawn from October through April and spawning peaks in January and February. Sablefish are oviparous, releasing eggs that float near the surface (Hunter et al., 1989). After hatching, larvae and juveniles inhabit surface waters offshore for several years after which they migrate inshore and settle to the bottom.

Sablefish are found on the continental slope and are commercially fished at depths from 200 to 1400 meters (Leet et al., 1992). Adult sablefish feed on fish, cephalopods, and crustaceans (Laidig et al., 1998). They reach a maximum length of 102 cm (Miller and Lea, 1972) and are believed to be a very long-lived species (possibly 100 years or more).

Many physical features have been used to age this species, including scales, finrays, thin-sectioned otoliths, and broken and burned otoliths, but all methods have resulted in less than 45% agreement among readers (Lai, 1985; Fujiwara and Hankin 1988b; Kimura and Lyons, 1991; Heifetz et al., 1999). The broken and burned otolith method (Chilton and Beamish, 1982) is the principal method used in aging of the species in both the United States and Canada. Typically, age readers agree on ages less than 50% of the time, and for fish older than 7 years, agreement drops to less than 15% (Kimura and Lyons, 1991).

There have been repeated efforts at validating sablefish ages and developing aging criteria. Beamish et al. (1983) successfully used oxytetracycline (OTC) marking to validate ages and repeated his experiment in 1995 when additional marked fish were recovered (MacFarlane and Beamish, 1995). Lai (1985) validated the use of otoliths for aging sablefish. Fujiwara and Hankin (1988b) examined otolith growth characteristics to help refine aging criteria. Heifetz et al. (1999) validated the currently accepted aging practices and examined sources of error in the aging of sablefish. Kastelle et al. (1994) used radiometric methods to generally validate the aging criteria currently used. Even with all of these studies that have validated age

* Contribution 119 from the Santa Cruz Laboratory, National Marine Fisheries Service, Santa Cruz, CA 95060.

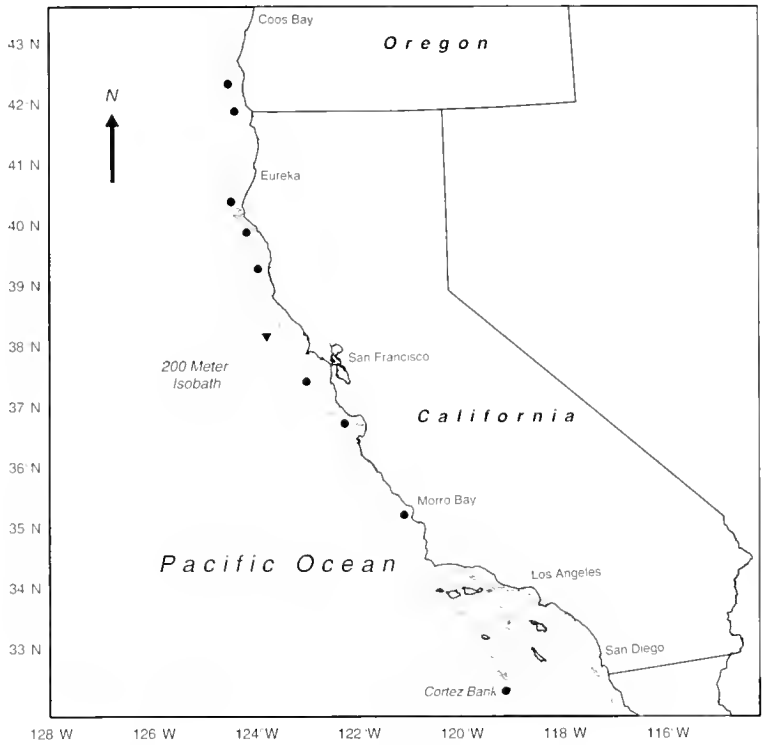

Figure 1

Map of California and southern Oregon showing the locations (black dots) of sablefish sampling and tagging in September and October of 1991.

determinations, independent age readings seldom are in agreement. This suggests that the methods used to validate the ages were insufficient to allow development of precise aging criteria. The lack of reliable age data has made stock assessments difficult and controversial (Crone et al., 1997), and in addition, accurate aging is needed to support ecological and habitat studies.

In September and October of 1991, a tagging and oxytetracycline (OTC) injection study was included as part of a fish trap survey of the abundance of sablefish in southern Oregon and California. The purpose of this study was to attempt, once more, to improve our ability to reliably age sablefish, thereby improving our ability to manage the species.

Methods

Capture, tagging, injection, and recovery

In September 1991, the fisheries research vessel *Alaska* was chartered by the National Marine Fisheries Service to conduct a trap survey from Coos Bay, Oregon, to Cortez Bank, California (Fig. 1). A total of nine sites were visited. At each site seven strings of ten traps were deployed in various depths between 250 and 1900 meters. The traps were retrieved after 24 hours, the catch was removed, and the traps reset for an additional 24 hours. All the sablefish were counted, otoliths were removed from the first 20 arbitrarily selected fish at each station, and the rest of the fish were tagged with blue spaghetti tags. Three of every four tagged fish were injected intraperitoneally with 30 mg of OTC per kilogram of fish (Beamish et al., 1983) and the fourth fish was used as a control. A complete description of the survey can be found in Parks and Shaw (1994).

A scientist visited the major commercial fishing ports in California and southern Oregon to make port samplers, commercial dealers, and fishermen aware of the importance of the study and to explain handling procedures in the study. A $50.00 reward was offered for the return of whole tagged fish.

When a tagged fish was returned, the port sampler measured it (fork length in mm), determined the sex, and removed the otoliths. The otoliths were cleaned and stored in painted glass vials (because the OTC mark was light labile) with a 50% ethanol solution.

Processing of the otoliths

Two pairs of otoliths were initially selected to develop the procedures to be used in the study. It was found that the OTC mark was very faint and upon heating (as required by conventional age determination methods), the mark disappeared. Accordingly, we developed a method to obtain images of the otoliths before and after heating, and to superimpose the two images of the same otolith; the first viewed under UV light and, the second, after heating, under white light.

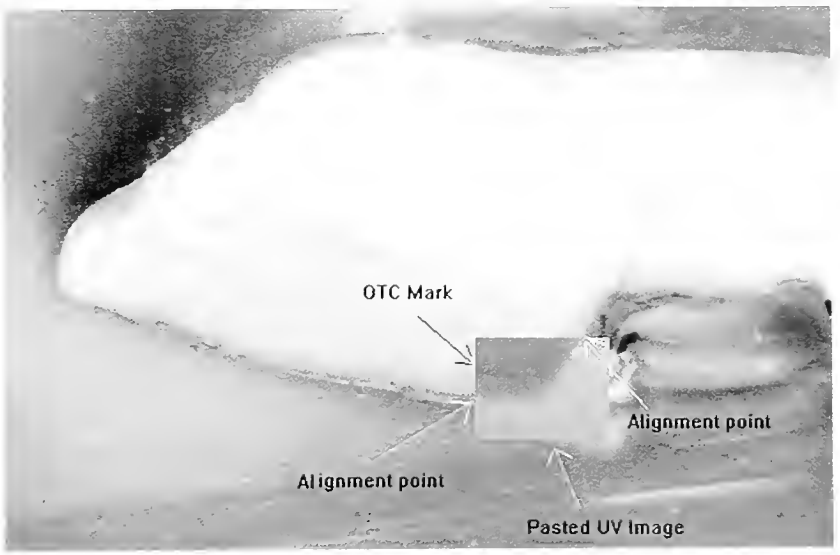

Figure 2

Composite image of a sablefish otolith. The otolith was first viewed under UV light and an image was captured. It was then baked and a second image was captured by using white light. Then a small rectangle from the UV image was electronically cut and pasted on the image of the baked otolith. The flourescent mark produced by the OTC appears as a dark line on the UV section. Points on the otolith used for correct positioning of the pasted section are shown.

The otoliths were embedded in epoxy casting resin. After the resin hardened, the blocks containing the otoliths were sliced in half across the dorsoventral axis with a diamond saw.

Images were captured in a two-stage process. The first stage used ultraviolet light to reveal the OTC mark, and the second stage used white light to reveal the growth marks used for age determination. In the first stage, the room was completely darkened and an image of the otolith, including the OTC mark, was captured by using a video camera capable of capturing images under low light conditions. We used an ultraviolet lamp which produced a strong beam of light at 365 angstroms. The otolith was viewed on a compound microscope using reflected light. The camera and image processing system were connected to a PC computer equipped with a frame grabber card. A version of NIH Image, a public domain image processing software (Scion Corporation, Frederick, MD), was used to process the images.

The embedded otolith was placed on the microscope and a drop of mineral oil was placed on the surface of the otolith. The limited amount of UV light available to the camera required the use of frame averaging. Usually 30 frames were sufficient to produce a sharp view of the otolith and the fluorescing mark. In some cases, the mark was too faint to allow an image to be captured. When there was sufficient fluorescence, two composite images were captured, one at 4× and one at 40×.

In the second stage, the same embedded otolith was placed in a small toaster oven at 270°C and heated for 20 to 25 minutes until it had turned dark brown. This baking process enhanced the growth rings for visual analysis and approximated what age readers see using the break and burn method; however, the latter process results in darker hyaline zones than those obtained with this method. After cooling, the otolith was viewed under white light. A second set of images was then captured. A section of each UV image was then electronically cut and pasted onto the image captured under visible light. With some experimentation it was found that the pasted sections could be aligned exactly over the visible light images, creating a final composite image as shown in Figure 2.

Initial examination of the otoliths

Initially, all OTC-marked otoliths were examined with knowledge of the year and season of release, but without any other information about the fish. Composite UV and white light images were obtained as previously described. The age reader determined the following: whether or not the OTC mark was visible; whether the OTC mark was in a hyaline or opaque zone; the number of annual hyaline zones visible beyond the OTC mark (and whether or not the edge was included in the count); edge type (hyaline, narrow opaque, wide opaque, or unidentifiable), and the shape of the otolith. In some cases the OTC mark could not be identified or the mark was too faint to be captured as a composite image; these specimens were excluded from subsequent analyses.

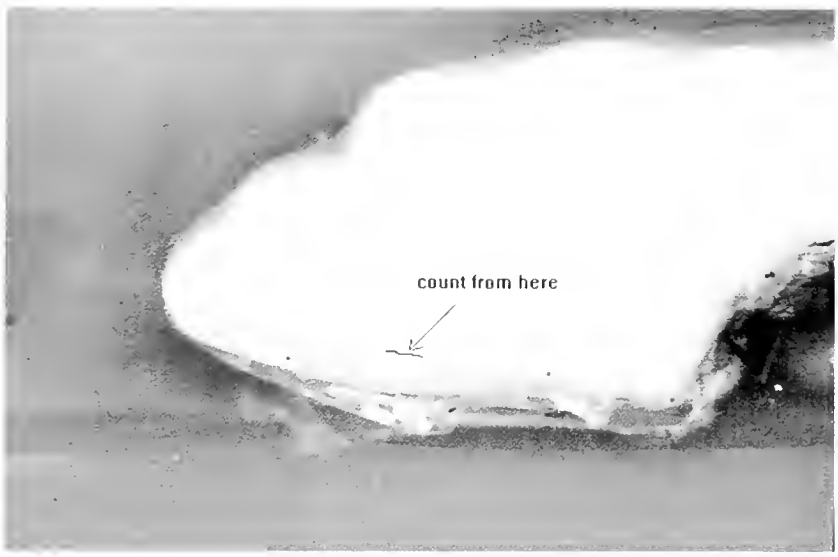

Figure 3

Example of an image of a baked sablefish otolith which has been annotated with a mark. The image is an example of one of the images provided to three researchers in order to obtain cross-reading comparisons.

Following standard age determination procedures (Chilton and Beamish, 1982), if a hyaline zone was not visible on the edge between January and March, then the edge was counted. If a mark was not visible on the edge between April and May and there was a wide opaque zone, then the edge was counted as a mark. If a mark was visible on the edge and the month was after May, the edge was not counted. This procedure is used to properly assign the fish to an annual cohort. Because the reader was not given the month of recapture, the ages were adjusted based on the count of hyaline zones, the month of recapture, and whether the edge had been counted. This adjustment provided a corrected reader count of annual marks. The corrected count was compared to the number of annual marks that would have been present if marks were laid down annually.

Previous experience suggested that there are different patterns of sablefish otolith growth. We attempted to classify and characterize these different types of growth patterns based on morphology of the otoliths as seen in cross section. After the otoliths had been examined, we developed a standard classification scheme of morphological classes and types which could be used to classify the most commonly observed morphological types. The otoliths were re-examined and reclassified to see if difficulties and discrepancies in aging were associated with morphological type. It was hoped that this process could be used to refine the aging criteria and improve precision.

Because sample size was small, we used a Fisher exact test (Agresti, 1990) to test for independence of morphological type versus tendency to over-estimate, correctly estimate, or under-estimate the number of annual marks. The columns in the test indicated whether the fish had been over-aged, correctly aged, or under-aged. The rows in the test were the four morphological types identified in this study.

Examination of the otoliths by the age readers

To determine how age readers would count the marks on the otoliths, we selected a subsample of 25 otoliths to be aged at four West Coast fisheries laboratories. The otolith selection was based on having good quality images and otoliths. The images of the baked otoliths (not the composite images) were annotated with a mark (Fig. 3). The mark was placed in a location which could be readily located on the actual otolith by the readers—on the zone just inside of the OTC mark. Readers were given the following: a set of printed images, an electronic file of the images for viewing on a computer screen, the embedded otolith, the month of capture, the size and sex of the fish from which the otolith came, and a set of instructions for examining the otoliths. Readers were not told where the mark on the image was placed in relation to where the OTC mark was in order to reduce bias from readers who may have known when the fish were injected and recaptured. Readers were asked to provide the following: the number of annual marks visible outside the mark on the image, whether the edge was counted, how confident they were of their readings, and any comments they might have.

Three readers participated in this analysis, two of whom had extensive, long-term experience in aging sablefish. The readings and age determination criteria (including edge count criteria) were compared to each other and to the time known to have passed between OTC marking and recapture.

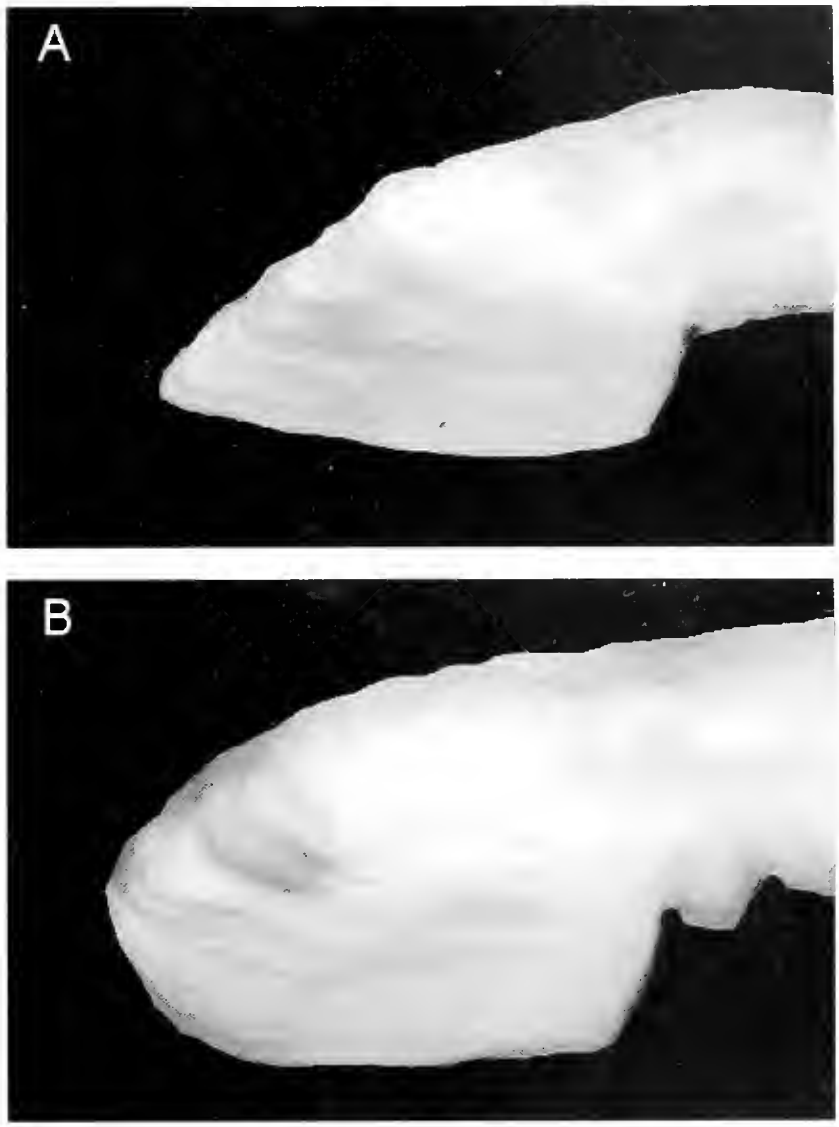

Figure 4

Images of four otolith morphological types. (**A**) Otolith is a wide type, (**B**) otolith is a wide, wedge subtype. (**C**) otolith is a thick type, and (**D**) otolith is a thick, wedge subtype.

To determine if age determination difficulties were related to sex, size, area of capture, depth of capture, or otolith morphological type; Fisher exact tests were performed. In each test, the variables were compared to whether the fish had been correctly aged, over aged, or under aged.

Results

Recoveries

A total of 2575 fish were tagged at the nine sites, and 368 tagged fish were recaptured. Of the recaptured fish, 284 had been injected with OTC. Of the 284 injected fish, usable otoliths were recovered from 191 fish; for the remaining fish, otoliths either were not recovered or were too badly damaged during removal to be used.

Otolith morphological types

After examination of all the otoliths, "wide" and "thick" morphological types were identified, and each type had a "wedge" subtype (Fig. 4). Each otolith in the study was then classified according to this scheme.

The wide type (Fig. 4A) is characterized by new growth that steadily increases cross sectional width along the dorsal and ventral surfaces. In the wedge subtype (Fig. 4B), initial growth increases the width, but the most

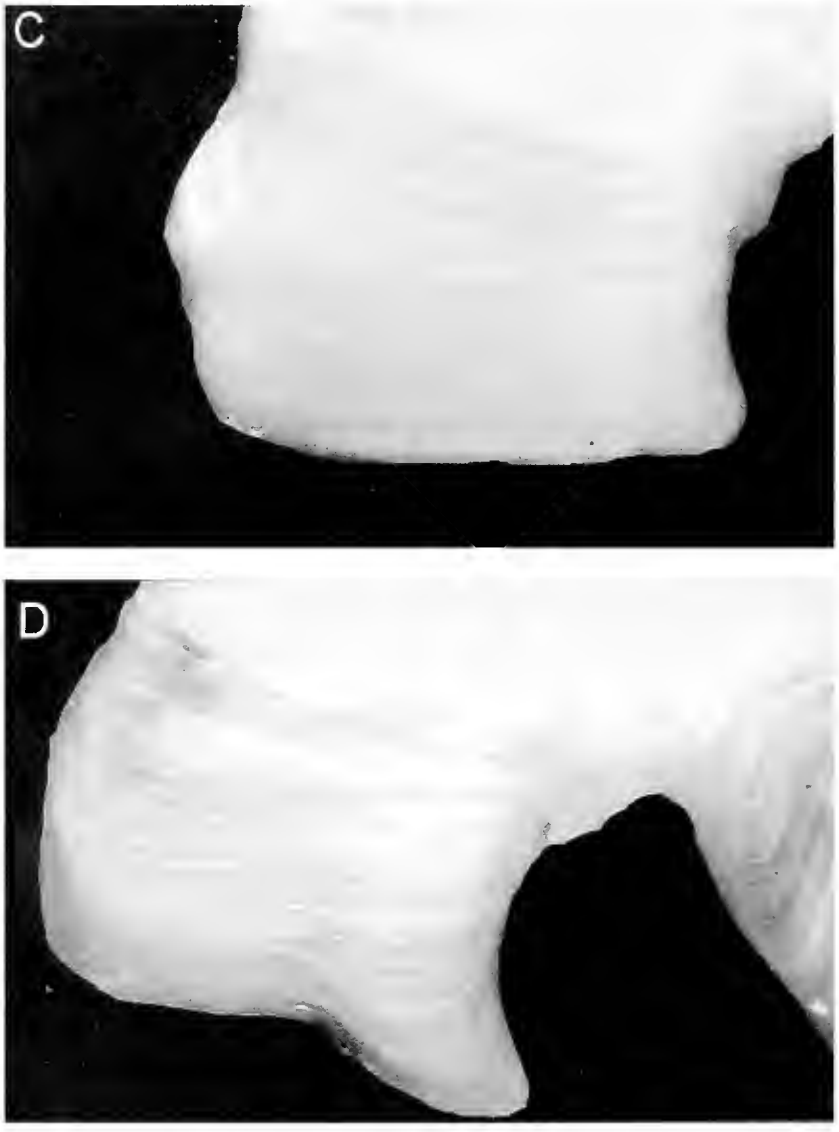

Figure 4 (continued)

recent growth is concentrated on the medial or lateral surface at the sulcus, decreasing towards the dorsal and ventral surfaces, resulting in a wedgelike appearance.

The thick type (Fig. 4C) is characterized by new growth that increases the thickness of the otolith without increasing the cross sectional width, causing the annulii to appear closely spaced on the lateral surfaces. In the wedge subtype (Fig. 4D), the most recent growth is concentrated at the sulcus and narrows towards the dorsal and ventral surfaces, forming a wedge shape.

It should be noted that these types and subtypes are not always clearly defined. It should also be noted that classification to the subtype is based on the most recent one or more hyaline zones. A wedge subtype is formed when a single hyaline zone widens near the sulcus and comes to a point at the outer edge.

Of the 191 otoliths examined, 63 (33.0%) were classified as "wide" types, 76 (39.7%) were classified as "wide, wedge subtypes," 32 (16.8%) were classified as "thick" types, 5 (2.6%) were classified as "thick, wedge subtypes,' and 15 (7.9%), could not be classified by this scheme.

Position of the OTC mark

There was no detectable OTC mark in 22 of 191 otoliths. The absence of marks appeared to be a random event, occurring in otoliths from several different recovery years and equally likely to be found among different sexes, otolith types, different depths, and locations.

Of the 169 otoliths with detectable marks, the OTC mark was found in a hyaline zone in 129 otoliths (76.3%), in an opaque zone in 36 otoliths (21.3%), and could not be reli-

Table 1

Frequency of otoliths with an OTC mark appearing on the edge versus those with the marks inside the edge. All fish were injected between September and October of 1991.

Year	Month	Mark on edge	Mark not on edge
1991	Oct	2	1
	Nov	1	3
	Dec	4	2
1992	Jan	2	4
	Feb	1	6
	Mar	7	4
	Apr	3	1
	May	7	26
	Jun	2	
	Jul	1	7
	Aug	1	4
	Sep	1	2
	Oct	5	
	Nov	3	
	Dec		

ably determined in four otoliths (2.4%) because the marks were between a hyaline and opaque zone. Of the 36 otoliths with the mark in an opaque zone, the mark occurred just after a hyaline zone in four otoliths. In 24 of the 36 otoliths with the mark in an opaque zone, the mark was on the edge where it can be difficult to determine whether it is opaque or hyaline. In no case did the reader indicate that the mark was in a hyaline zone at the edge and thus the edge appeared to be opaque in most cases.

The OTC mark occurred on the otolith edge in 30 of the otoliths recaptured prior to 1993 (up to 16 months after injection). Examination of the monthly distribution of otoliths with marks on the edge (Table 1) indicated that some fish exhibited little or no otolith growth for substantial lengths of time.

Otoliths from fish recaptured in 1992 with marks on the edge (i.e. showing little growth) were examined and classified by morphological type (Table 2). This examination indicated that the thick type is more likely to have little growth

Table 3

Number of visible hyaline zones occurring after an OTC mark on otoliths from fish recaptured in 1992. This is shown by three-month interval to show the progression of development of the hyaline zones. All fish were injected in September and October of 1991.

	No. of hyaline zones		
Interval	0	1	2
Jan–Mar	12	8	1
Apr–Jun	5	14	4
Jul–Sep	6	2	
Oct–Dec	3	1	

because 32% of the otoliths with marks on the edge were the thick type, yet they made up only 17% of the otoliths in the study. Conversely, only 18% of the otoliths with the mark on the edge were of the wide type; however, they made up 33% of the otoliths in the study. This trend was not statistically significant, however, because the *P*-value was 0.106.

Number of visible hyaline zones

The number of prominent hyaline zones after the OTC mark for fish recaptured in 1992 at three-month intervals is shown in Table 3. This distribution shows the otoliths that had no detectable growth but also shows that a hyaline zone forms in many fish during the winter. It also shows that in some fish, a summer hyaline zone is formed; however, the sample size for October–December was small and this is a period when a summer hyaline zone would be expected to be fully visible.

The number of visible and prominent hyaline zones after the OTC mark for fish recaptured after 1992 (Table 4), compared with the number of zones which should have been counted, showed that if a reader had counted each of the prominent hyaline zones as an annulus, the count would have overestimated the age of the fish. An example of an otolith with a larger number of prominent hyaline zones than expected is shown in Figure 5. It should be noted that a reader would not necessarily have counted each of the

Table 2

Number of otoliths in 1992 with OTC marks on the edge by otolith morphological type. Also shown is the overall percentage of the morphological types in the present study. All fish were injected in September and October 1991.

	Otolith type							
	Wide		Wide, wedge		Thick		Thick, wedge	
	No.	Percent	No.	Percent	No.	Percent	No.	Percent
1992 otoliths	4	18	10	45	7	32	1	5
Otoliths in this study	63	33	76	40	32	17	5	3

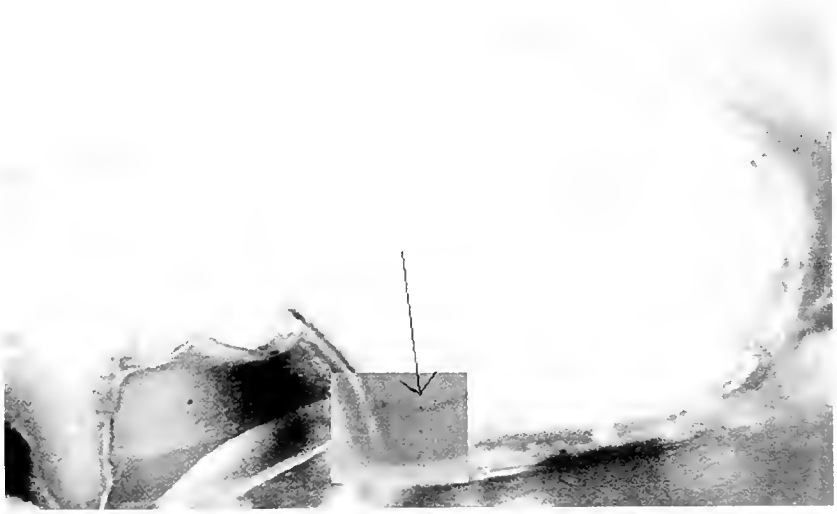

Figure 5

Image of a sablefish otolith having more prominent hyaline zones than should have been present. The fish was caught after eight months at liberty. A single hyaline zone should have formed; however, there is a zone on the edge and one midway between the dark OTC mark.

Table 4

Counts of the number of prominent hyaline zones versus the number of annual hyaline zones that should have been present after an OTC mark. These counts are for fish recaptured more than 15 months after initial capture. Agreement between counts and number of expected annual hyaline zones is shown in bold.

		No. of prominent hyaline zones										
Year	Expected number	0	1	2	3	4	5	6	7	8	9	10
1993	2	3	1	**7**	6	4	3					
1994	3	2		1	**5**	2	1	3	1			
1995	4	1				**2**		5	1	2	1	
1996	5					1	**1**		1	2		
1997	6				1			**1**	1		2	1

Table 5

Percent and number (in parentheses) of sablefish otoliths with more hyaline zones than were expected, with the expected number of hyaline zones (correct count), and with fewer hyaline zones than were expected for each otolith type.

Otolith type	More zones	Expected number of zones	Fewer zones
Thick	10.3% (3)	41.4% (12)	48.3% (14)
Thick, wedge	0 (0)	40.0% (2)	60.0% (3)
Wide	39.3% (22)	48.2% (27)	12.5% (7)
Wide, wedge	35.2% (25)	45.1% (32)	19.7% (14)

prominent hyaline zones as an annulus (they might have considered them to be checks). In many of these otoliths, there were less prominent zones that were not counted and which were interpreted as checks.

Thick type otoliths and thick, wedge subtype otoliths tend to have fewer visible hyaline zones than expected (Table 5). In contrast, wide type and the wide, wedge subtype otoliths are more likely to have more hyaline zones than expected. The Fisher exact test yielded a significant P-value of 0.001.

Blind comparisons of reader counts

A comparison of the counts of annual hyaline zones for each reader to the expected number of annual hyaline zones

Table 6

Comparison of number of annual hyaline zones counted by reader 1 versus the expected number of annual hyaline zones that should have been counted. Agreement with the expected counts are shown in bold.

	Reader 1 count						
Expected count	1	2	3	4	5	6	7
1	**2**	7	2	1			
2		**2**	4	1	1		
3		1			1		
4				**2**			
5			1				

Table 7

Comparison of number of annual hyaline zones counted by reader 2 versus the expected number of annual hyaline zones that should have been counted. Agreement with the expected counts are shown in bold.

	Reader 2 count						
Expected count	1	2	3	4	5	6	7
1		5	2	3	1	1	
2			3	2	2		1
3			**1**	1			
4						1	1
5					**1**		

Table 8

Comparison of number of annual hyaline zones counted by reader 3 versus the expected number of annual hyaline zones which should have been counted. Agreement with the expected counts are shown in bold.

	Reader 3 count						
Expected count	1	2	3	4	5	6	7
1	**10**	2					
2	2	**1**	3	1	1		
3	1	1					
4	2						
5	1						

after the OTC mark are shown in Tables 6, 7, and 8. In these tables, it is assumed that the readers should not have counted the zone in which the OTC mark occurred because that mark is presumed to have formed in the summer of 1991. Readers 1 and 2 tended to overestimate, whereas reader 3 (the least experienced age reader) had generally good agreement. Reader 1 agreed with the expected count 24% of the time, reader 2 agreed with the expected count 4% of the time, and reader 3 agreed with the expected count 44% of the time. The result for reader 3 is deceptive, however, because that reader did not follow accepted methods of when to count the edge.

Reader 1 and reader 2 agreed on whether to count the edge of the otolith in 24 of 25 otoliths (Table 9). Reader 3 agreed with reader 1 on whether to count the edge in 16 of 25 otoliths and 17 of 25 otoliths with reader 2. Had reader 3 followed accepted practice, agreement with the expected count would have been much less.

Efforts to determine what factors (depth of capture, location of capture, sex, size of the fish, and otolith morphological type) resulted in a miscount of the true number of annual marks were inconclusive. We first corrected the count for the fact that all readers counted the mark in which the OTC mark had occurred by subtracting one from their counts, and we then eliminated the readings from reader 3 because of his lack of experience and anomalous age determination criteria. Then we examined the relationship of how many otoliths had been over-aged, correctly aged, and under-aged to the above factors. Depth of capture was divided into two groups: less than 600 m and 600 or more m. Location was divided into two groups: north and south of latitude 39 north. Sizes were divided into two groups: <55 cm FL and ≥55 cm FL. And finally, we tested each of the four otolith morphological types.

We used Fisher exact tests to determine the probability that differences were due to chance alone. There were no detectable differences from the null hypothesis for depth, sex, or location of capture (Table 10); however, there was some evidence that fish length and otolith morphological type might be related to miscounting. Small fish showed a slightly greater tendency to be over counted (more rings than should have been present) than larger fish (P=0.150). Otolith morphological type showed some departure from randomness; thick types appeared to be more likely to be undercounted (fewer rings than should have been present) and wide types were more likely to be over counted (P=0.066).

Discussion

Position of mark

There was no visible mark on 22 of the 191 otoliths (11.5%). Beamish et al. (1983) reported that 14 of 129 OTC-injected fish (10.9%) had no detectable mark. They attributed this to improper handling of the fish after recapture. The similarity in the number of otoliths failing to show the OTC mark between their study and our study suggests that some portion of the population may not absorb sufficient OTC to produce a visible mark.

The finding that most of the OTC marks were in a hyaline zone is important. This indicates that many of the sablefish in our study laid down a prominent hyaline zone in the summer. Age readers who conventionally assume that an annual mark is laid down only in the winter

Table 9

Blind reading results of 25 sablefish otoliths by 3 readers. All fish had been captured and injected with OTC in September and October of 1991. The counts they provided are the number of annual marks outside of the OTC mark. "Expected count" indicates how many winter hyaline zones should have been present. The columns labeled "Edge" refer to whether or not the edge was included in the age reader's counts.

			Reader 1		Reader 2		Reader 3	
Fish ID no.	Recapture date	Expected count	Count	Edge	Count	Edge	Count	Edge
10375	4 May 92	1	2	Y	2	Y	1	N
10030	14 May 92	1	1	Y	2	Y	1	N
10267	17 May 92	1	2	Y	3	Y	1	N
10408	17 May 92	1	2	Y	2	Y	2	Y
10417	18 May 92	1	2	Y	3	Y	1	N
10630	25 May 92	1	4	Y	4	Y	1	N
12148	26 May 92	1	3	Y	4	Y	1	N
12176	26 May 92	1	2	Y	5	Y	1	N
12431	26 May 92	1	2	Y	2	Y	2	Y
10568	29 Jul 92	1	1	N	2	N	1	N
11121	1 Oct 92	1	2	N	6	N	1	N
11117	16 Oct 92	1	3	N	4	N	1	N
10400	12 Jan 93	2	3	Y	5	Y	3	Y
10370	14 Jan 93	2	4	Y	4	Y	3	Y
10870	15 Feb 93	2	2	Y	7	Y	5	Y
10246	15 Apr 93	2	3	N	3	Y	3	Y
11735	16 May 93	2	3	Y	3	Y	2	Y
11586	18 May 93	2	2	Y	4	Y	4	Y
11106	3 Aug 93	2	3	N	3	N	1	N
10617	2 Dec 93	2	5	N	5	N	1	N
10580	23 May 94	3	2	Y	4	Y	2	Y
10714	9 Dec 94	3	5	N	3	N	1	N
11516	3 Aug 95	4	4	N	7	N	1	N
11524	16 Dec 95	4	4	N	6	N	1	N
11761	25 Apr 96	5	3	Y	5	Y	3	N

Table 10

Comparison of the number of fish under counted, correctly counted, and over counted by two experienced age readers versus depth of capture, location (north or south of 39 degrees latitude), sex, fork length, and otolith morphological type. The *P*-value from the Fisher exact test is shown, indicating the level of significance.

	Under counted	Correctly counted	Over counted	*P*
Depth				
<600 meters	7	14	15	0.987
>600 meters	3	6	5	
Location				
South	4	8	10	0.606
North	3	12	7	
Sex				
Male	3	2	5	0.381
Female	7	18	15	
Length				
<55 cm	4	11	15	0.150
≥55 cm	6	6	5	
Otolith type				
Thick	4	2	2	0.066
Thick, wedge	1	1	0	
Wide	2	5	11	
Wide, wedge	3	12	7	

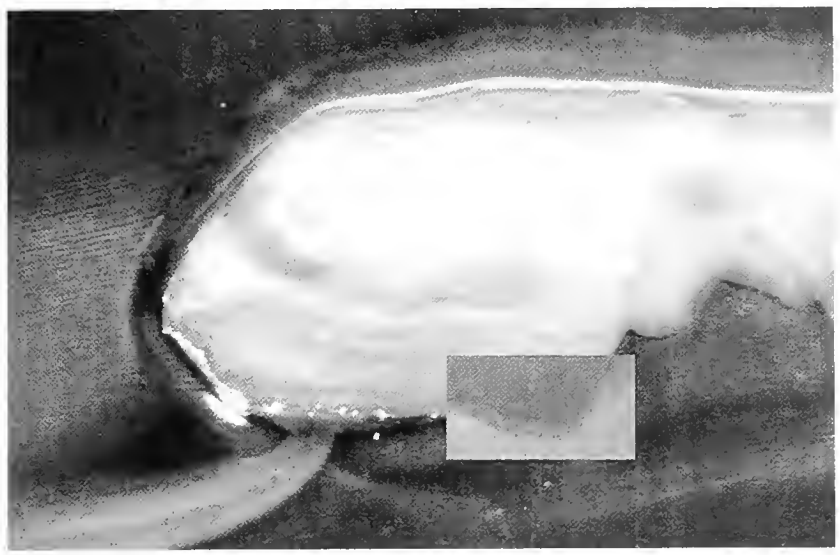

Figure 6

Image of a baked sablefish otolith with an electronically pasted section taken from an image captured under UV light. The dark OTC mark is clearly located within a hyaline zone, and the hyaline zone persists through the entire otolith. The fish was injected with OTC on 5 October 1991.

would probably mis-age these fish. Because the age readers who examined the otoliths without knowledge of the recapture information were not informed that the point they were counting from was just inside the summer mark, it was interesting to note that all three of them counted the hyaline zone in which the OTC mark had occurred as an annual hyaline zone in all cases. In other words, the summer hyaline zone did not appear to be a check to the readers. The readers indicated that the manner of preparation of the otoliths (embedded and baked) was not the manner in which they were accustomed to view otoliths and may have influenced their results. The fact that the hyaline zones were not as dark with the baking method as opposed to the burning method may have influenced the readers age estimates; however, some otolith burns can be quite light and experienced readers recognize the various levels of burning, particularly when cross reading otoliths from other age readers. Readers sometimes use multiple sections and are free to manipulate the otolith to improve viewing, which was not possible in the present study. Beamish et al. (1983) indicated that when readers knew how many marks to look for, they were able to identify false annual marks (checks). According to their study, a check is not persistent throughout the otolith. In Figure 6, the hyaline zone in which the OTC mark appeared clearly persists throughout the otolith. If the hyaline zone which contained the OTC mark began to be laid down in the winter, then there would be very little time for the formation of a wide opaque zone to form after injection in the fall. Because the age readers counted the hyaline zone in which the OTC mark occurred, they clearly assumed that it was not a check. If the age readers had known that the hyaline zone (in which the OTC mark occurred) had formed in the summer, then they presumably would not have counted it. It is therefore of interest to see the effect on agreement between reader counts minus the hyaline zone where the OTC mark occurred and the actual number of hyaline zones that should have been present. When we adjusted the reader counts by subtracting one year from their original counts and compared their adjusted counts to the expected number of annual marks (Table 11), agreement for readers 1 and 2 improved, whereas it decreased for reader 3 (the least experienced reader).

Also of importance is the fact that on some otoliths, even after eight months at liberty, no growth had occurred, as evidenced by the fact that the OTC mark was on the edge. For example, otoliths from two fish, recaptured after eight months at liberty showed marked differences in otolith growth (Fig. 7). On otolith A there was no detectable growth with the OTC mark on the edge, whereas on otolith B there was substantial growth. The OTC marks on both otoliths were very prominent. These otoliths came from similar fish; that is, otolith A came from a 597-mm female fish caught in 680 meters of water at 40°52′ latitude, and otolith B came from a 610-mm female fish caught in 480 meters of water at 41°54′ latitude. This provides strong evidence that otolith growth, and presumably fish growth, varies greatly among individual sablefish. Beamish et al. (1983) reported that the OTC mark was on or near the edge in 28 otoliths (18.1%) of 154 fish which had been at liberty for two to three years. In a similar time interval, we found that 34 of 126 (27.0%) had the OTC marks on or near the edge. Both the finding of a summer hyaline zone and the differences in growth of the otolith among individual fish

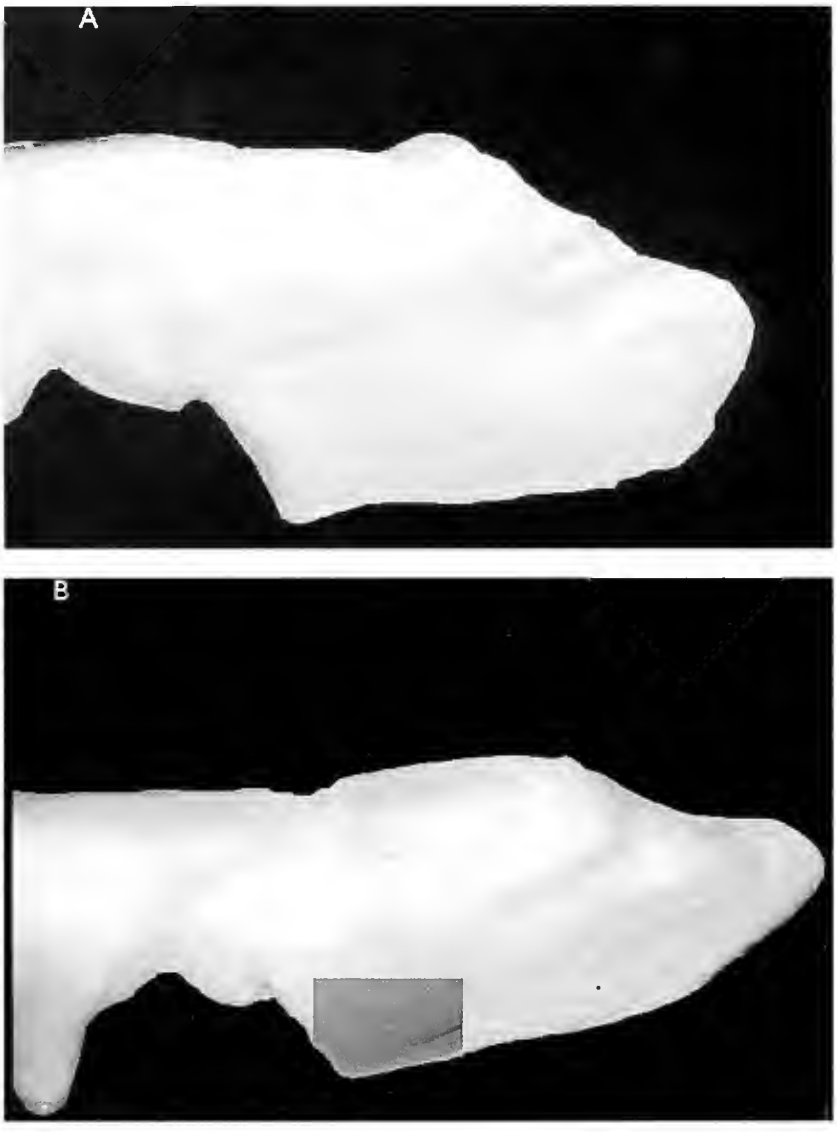

Figure 7

Images of otoliths from two sablefish showing differences in otolith growth rate. Both fish were injected with OTC in early October of 1991 and were recaptured in May of 1992. (**A**) Otolith was from a 597-mm female caught in 680 meters of water at 40°52′ latitude. (**B**) Otolith was from a 610-mm female fish caught in 480 meters of water at 41°52′ latitude. The OTC mark in A was on the edge, whereas the position of the OTC mark in B is shown on the insert.

are important factors in developing reliable and consistent age determination criteria.

The importance of using the same age determination criteria among readers cannot be overestimated. In the blind comparison, the readers were asked whether they had included the edge in their count of annual zones. With standard age determination methods, if no hyaline material is visible on the edge up to about May, then the edge is counted. This procedure is based on the assumption that a zone is in the process of forming but is not yet clearly visible. On the other hand, if hyaline material is observed on the edge after May, it is not counted because it is assumed to be either a check or the beginning of the next winter's hyaline zone. Reader 1 and reader 2 (the two most experienced age readers) agreed on whether to count the edge 96% of the time, indicating that they were using the same criteria. Reader 3, however, agreed with reader 1 only 64% of the time and with reader 2 only 68% of the time which suggests that reader 3 was using different edge-interpretation criteria.

Table 11

Percent agreement between number of hyaline zones counted by three age readers and the number which should have been present. Also shown is the effect of removing the count of a hyaline zone which formed in the summer and which should not have been counted as an annual mark.

Reader 1		Reader 2		Reader 3	
Original	Corrected	Original	Corrected	Original	Corrected
24%	44%	4%	36%	44%	20%

Effect of ages on stock assessments

Crone et al. (1997) noted that one of the problems with stock assessments of sablefish is that the size at 50% sexual maturity is between 55 and 67 cm (age 5–7) and that there is considerable variability in the these estimates. Further, they noted that there has been difficulty in determining age-specific selectivity because of problems with the ages used in previous assessments. Crone et al. (1997) further noted that there is a considerable discrepancy in ages among the age determination laboratories on the west coast. Finally, the model used to perform stock assessments has estimated that in order to obtain a good fit with the data, the actual level of aging error should be higher than has been reported. The lack of reliable age data has been used to criticize stock assessments.

Age and length at sexual maturity has been found to vary substantially by depth (Fujiwara and Hankin, 1988a). Fujiwara and Hankin found that both males and females had a length of 550 mm for the length at 50% sexual maturity in shallow water (<600 meters). In depths greater than 600 m, the size at 50% sexual maturity was 450 mm for males and 500 mm for females. To determine age, they used sectioned otoliths and methods that may not have been directly comparable to the methods used in other studies or the methods used in the present study; nonetheless, they found that both males and females matured at a younger age in deeper water. Saunders et al. (1997) also reported differences in length at maturity related to depth and location of capture. Methot[1] found that ontogenetic movement into deeper water for spawning was more closely related to age than size. If sexual maturity is more closely related to age than length as suggested by Methot, then unreliable ages may explain the variable maturity schedule for sablefish. In our study, fish were captured over a 900 nmi range at depths from 200 to more than 1000 m. If depth is related to growth of sablefish, then it is possible that the different morphometric types of otoliths observed in our study may also be a function of depth. If depth is responsible for the morphological types, it also suggests that reliability of ages may be a function of the depth at which the sablefish are found. Further, if depth influences growth, a fish which changes its depth over time, may exhibit different patterns of growth throughout its life which would further complicate the problem of determining reliable ages.

Potential sources of error in this study

This study used sablefish caught in the southern part of the sablefish range. Many species show latitudinal variation in growth (June and Reintjes, 1959; White and Chittenden, 1977; Leggett and Carscadden, 1978; Shepherd and Grimes, 1983; Pearson and Hightower, 1991). It is possible that the results of this study do not apply to the northern portion of their range.

Another potential source of error in our study is the effect of tagging on the growth of the sablefish. MacFarlane and Beamish (1990) found that tagged sablefish grew slower than untagged fish. If this is true, then the results of this study are much more difficult to interpret. MacFarlane and Beamish did not use OTC and as a result they based their ages on conventional aging methods. If they had injected the fish, it would have been interesting to note whether the ages for the fish in their study would have been interpreted differently. If fish do grow differently after tagging, many age, growth, and validation studies will need to be re-evaluated.

Conclusion

Obtaining accurate ages, with reasonable precision, for sablefish is very difficult. Previous aging studies of sablefish have obtained results similar to ours, even when the readers knew how many annual marks should have been present (Beamish et al. 1983; MacFarlane and Beamish, 1995). We found that some fish lay down two marks a year and others may not lay down any. We also found that certain morphological types of otoliths may be indicative of slow growing fish and others may be indicative of rapidly growing fish (assuming otolith growth relates to fish growth).

The fact that agreement among readers or with the correct age consistently ranges between 30% and 45% suggests that this imprecision may be inherent in sablefish aging. A substantial fraction of the population may not be able to be reliably aged: some otoliths do not appear to grow and others grow very rapidly, laying down prominent summer hyaline zones that even experienced age readers cannot differentiate from winter hyaline zones.

[1] Methot, R. D. 1995. Geographic patterns in growth and maturity of female sablefish off the U.S. west coast. Unpubl. manuscript, 39 p. NOAA, NMFS, Northwest Fisheries Science Center, Seattle, WA.

We believe the wide type and wide, wedge subtypes are often over-aged, and the thick type and thick, wedge subtypes are occasionally under-aged and further propose that readers be made aware that a hyaline zone typically forms in the winter, but that it is not uncommon for a second mark to form in the summer.

Another, less desirable approach, would be for age readers to record the morphological type of otolith as a routine part of aging. Users of the data could then incorporate this information into their studies by using a correction factor for fish likely to be under-aged and for fish likely to be over-aged. This factor could be in the form of an aging error matrix as suggested by Heifetz et al. (1999). This approach may not be practical until more data are available on the true effect on ages for the morphological types described in this study, including how many years would need to be added or subtracted for each type. Finally, a more complete description of the morphological types would be needed to assist the age readers.

Acknowledgments

We would like to express our gratitude to Delsa Anderl (Alaska Fisheries Science Center), Kristin Munk (Alaska Department of Fish and Game), Shayne MacLellan (Pacific Biological Station, Canadian Department of Fisheries and Oceans), and Bruce Pederson (Oregon Department of Fish and Wildlife) for participating in the otolith blind reading component of this paper. We would also like to thank Dan Kimura and Craig Kastelle of the Alaska Fisheries Science Center for their assistance in developing the design of this study. We would like to thank Michael Mohr (Southwest Fisheries Science Center, Santa Cruz, CA) for his valuable contribution to the statistical analyses used in this study. This study could not have been completed without the support of Gary Stauffer (Alaska Fisheries Science Center) who provided funding for the recovery of the sablefish. Additionally, this study would never have been completed without the assistance of numerous commercial market samplers, port biologists, commercial fishermen, and dealers who were responsible for collecting and processing the sablefish when they were caught. And finally, we would like to thank William Lenarz (Southwest Fisheries Science Center, retired) for his support of this study.

Literature cited

Agresti, A.
1990. Categorical data analysis, 558 p. Wiley, New York, NY.

Beamish, R. J., G. A. MacFarlane, and D. E. Chilton.
1983. Use of oxytetracycline and other methods to validate a method of age determination for sablefish. *In* Proceedings of the second international sablefish symposium, p. 95–116. Alaska Sea Grant Rep. 83-8, Univ. Alaska, Fairbanks, AK.

Chilton, D. E., and R. J. Beamish.
1982. Age determination methods for fishes studied by groundfish program at the Pacific Biological Station. Can Spec Publ. Fish. Aquat. Sci. 60:19–22.

Crone, P. R., R. D. Methot, R. J. Conser, R. R. Lauth, and M. E. Wilkins.
1997. Status of the sablefish resource off the U.S. Pacific Coast in 1997. Appendix G *in* Status of the Pacific Coast groundfish fishery through 1997 and recommended acceptable biological catches for 1998, 135 p. Pacific Fisheries Management Council 1998.

Fujiwara, S., and D. G. Hankin.
1988a. Sex ratio, spawning period, and size and age at maturity of sablefish Anoplopoma fimbria off northern California. Nippon Suisan Gakkaisha 54(8):1333–1338.
1988b. Aging discrepancy related to asymmetrical otolith growth for sablefish *Anoplopoma fimbria* in northern California. Nippon Suisan Gakkaishi 54(1):27–31.

Heifetz, J., D. Anderl, N. E. Maloney, and T. L. Rutecki.
1999. Age validation and analysis of aging error from marked and recaptured sablefish, *Anoplopoma fimbria*. Fish. Bull. 97:256–263.

Hunter, J. R., B. J. Macewicz, and C. A. Kimbrell.
1989. Fecundity and other aspects of the reproduction of sablefish, *Anoplopoma fimbria*, in central California waters. CalCOFI Rep. 30, 1989, p. 61–72.

June, F. C., and J. W. Reintjes.
1959. Age and size composition of the menhaden catch along the Atlantic coast of the United States, 1952–55; with a brief review of the commercial fishery. U.S. Fish and Wildl. Serv., Spec. Sci. Rep. Fish. 317, 65 p.

Kastelle, C. R. D. K. Kimura, A. E. Nevissi, and D. R. Gunderson.
1994. Using Pb-210/Ra-226 disequilibria for sablefish, *Anoplopoma fimbria*, age validation. Fish. Bull. 92:292–301.

Kimura, D. K., and J. J. Lyons.
1991. Between-reader bias and variability in the age determination process. Fish. Bull. 89:53–60.

Lai, H. L.
1985. Evaluation and validation of age determination for sablefish, pollock and yellowfin sole; optimum sampling design using age-length key; and implications of aging variability in pollock. Ph.D. diss., 426 p. Univ. Washington, Seattle, WA

Laidig, T. E., P. B. Adams, and W. M. Samiere.
1998. Feeding habits of sablefish, *Anoplopoma fimbria*, off the coast of Oregon and California. NOAA Tech. Rep NMFS 130:65–79.

Leet, W. S., C. M. Dewees, and C. W. Haugen.
1992. California's living marine resources and their utilization. Calif. Seagrant Publication UCSGEP-92-12, 257 p. Univ. California Davis, Davis, CA.

Leggett, W. C., and J. E. Carscadden.
1978. Latitudinal variation in reproductive characteristics of American shad (*Alosa sapidissima*): evidence for population specific life history strategies in fish. J. Fish. Res. Board Can. 35:1469–1478.

Macfarlane, G. A., and R. J. Beamish.
1990. Effect of an external tag on growth of sablefish (*Anoplopoma fimbria*), and consequences to mortality and age at maturity. Can. J. Fish. Aquat. Sci. 47:1551–1557.
1995. Validation of the otolith cross-section method of age determination for sablefish (*Anoplopoma fimbria*) using oxytetracycline. *In* Recent developments in fish otolith research (D. H. Secor, J. M. Dean, and S. E. Campana, eds.), p. 319–329. Univ. South Carolina Press, Columbia, SC.

Miller, D. J., and R. N. Lea.
1972. Guide to the coastal marine fishes of California. CDFG (Calif. Dep. Fish and Game) Fish Bull. 157, 249 p.

Parks, N. B., and F. R. Shaw.
1994. Relative abundance and size composition of sablefish

(*Anoplopoma fimbria*) in the coastal waters of California and southern Oregon, 1984–1991. NOAA Tech. Memo NMFS-AFSC-35, 38 p.

Pearson, D. E., and J. E. Hightower.
1991. Spatial and temporal variability in growth of widow rockfish (*Sebastes entomelas*). NOAA Tech. Mem. NOAA-TM-NMFS-SWFSC-167, 43 p.

PFMC (Pacific Fishery Management Council).
1999. Status of the Pacific Coast groundfish fishery through 1999 and recommended acceptable biological catches for 2000, 232 p. Pacific Fishery Management Council, Portland, Oregon.

Saunders, M. W., B. M. Leaman, G. A. McFarlane.
1997. Influence of ontogeny and fishing mortality on the interpretation of sablefish, *Anoplopoma fimbria*, life history. NOAA Tech Rep. NMFS 130:81–92.

Shepherd, G., and C. B. Grimes.
1983. Geographic and historic variations in growth of weakfish, *Cynoscion regalis*, in the middle Atlantic bight. Fish. Bull. 81:4:803–813.

White, M. L., and M. E. Chittenden.
1977. Age determination, reproduction, and population dynamics of the Atlantic croaker, *Micropogonius undulatus*. Fish. Bull. 75:109–123.

Growth, mortality, and hatchdate distributions of larval and juvenile spotted seatrout (*Cynoscion nebulosus*) in Florida Bay, Everglades National Park

Allyn B. Powell
Robin T. Cheshire
Elisabeth H. Laban
National Ocean Service
National Oceanic and Atmospheric Administration
Center for Coastal Fisheries and Habitat Research
101 Pivers Island Road
Beaufort, North Carolina 28516
E-mail address (for A. B. Powell): allyn.powell@noaa.gov

James Colvocoresses
Patrick O'Donnell
Florida Fish and Wildlife Commission
Florida Marine Research Institute
2796 Overseas Highway, Suite 119
Marathon, Florida 33050

Marie Davidian
Room 209, Patterson Hall
2501 Founder's Drive
North Carolina State University
Raleigh, North Carolina 27695

Abstract—Life history aspects of larval and, mainly, juvenile spotted seatrout (*Cynoscion nebulosus*) were studied in Florida Bay, Everglades National Park, Florida. Collections were made in 1994–97, although the majority of juveniles were collected in 1995. The main objective was to obtain life history data to eventually develop a spatially explicit model and provide baseline data to understand how Everglades restoration plans (i.e. increased freshwater flows) could influence spotted seatrout vital rates. Growth of larvae and juveniles (<80 mm SL) was best described by the equation $\log_e$ *standard length* = −1.31 + 1.2162 ($\log_e$ *age*). Growth in length of juveniles (12–80 mm SL) was best described by the equation *standard length* = −7.50 + 0.8417 (*age*). Growth in wet weight of juveniles (15–69 mm SL) was best described by the equation $\log_e$ *wet-weight* = −4.44 + 0.0748 (*age*). There were no significant differences in juvenile growth in length of spotted seatrout in 1995 between three geographical subdivisions of Florida Bay: central, western, and waters adjacent to the Gulf of Mexico. We found a significant difference in wet-weight for one of six cohorts categorized by month of hatchdate in 1995, and a significant difference in length for another cohort. Juveniles (i.e. survivors) used to calculate weekly hatchdate distributions during 1995 had estimated spawning times that were cyclical and protracted, and there was no correlation between spawning and moon phase. Temperature influenced otolith increment widths during certain growth periods in 1995. There was no evidence of a relationship between otolith growth rate and temperature for the first 21 increments. For increments 22–60, otolith growth rates decreased with increasing age and the extent of the decrease depended strongly in a quadratic fashion on the temperature to which the fish was exposed. For temperatures at the lower and higher range, increment growth rates were highest. We suggest that this quadratic relationship might be influenced by an environmental factor other than temperature. There was insufficient information to obtain reliable inferences on the relationship of increment growth rate to salinity.

Manuscript approved for publication 23 June 2003 by Scientific Editor.
Manuscript received 20 October 2003 at NMFS Scientific Publications Office.
Fish. Bull. 102:142–155 (2004).

The spotted seatrout (*Cynoscion nebulosus*) is an important recreational fish in Florida Bay and spends its entire life history within Florida Bay (Rutherford et al.,1989). The biology of adult spotted seatrout in Florida Bay is well known (Rutherford et al., 1982, 1989), as are the distribution and abundance of juveniles in the bay, including a description of the juvenile habitats and their diets (Hettler, 1989; Chester and Thayer, 1990; Thayer et al., 1999; Florida Department of Environmental Protection[1]). The temporal and spatial distribution and abundance of larval spotted seatrout in Florida Bay and adjacent waters, and the spatial and temporal spawning habits of these larvae also have been determined (Powell et al., 1989; Rutherford et al., 1989; Powell, 2003).

The early life history of spotted seatrout in other south Florida estuaries also has been well documented. Peebles and Tolley (1988) described the distribution, growth, and mortality of larval spotted seatrout in Naples and Fakahatchee Bays, and McMichael and Peters (1989) described the size distribution, growth, spawning, and diet of spotted seatrout in Tampa Bay.

Information on growth and mortality of larval and juvenile spotted seatrout in Florida Bay is lacking. Research on these topics would enhance our understanding of the entire life history of this valuable species, and in particular aid in eventually developing a spatially explicit model for spotted seatrout that is highly desired by the Program Management Committee for the South Florida Ecosystem Restoration Prediction and Modeling Program. In addition, these life history studies could help clarify juvenile growth and survival and provide needed information for the restoration

[1] Florida Department of Environmental Protection. 1996. Fisheries-independent-monitoring program, 1995 annual report, 58 p. Florida Department of Environmental Protection, Florida Marine Research Institute, 100 8th Avenue SE, St. Petersburg, FL 33701.

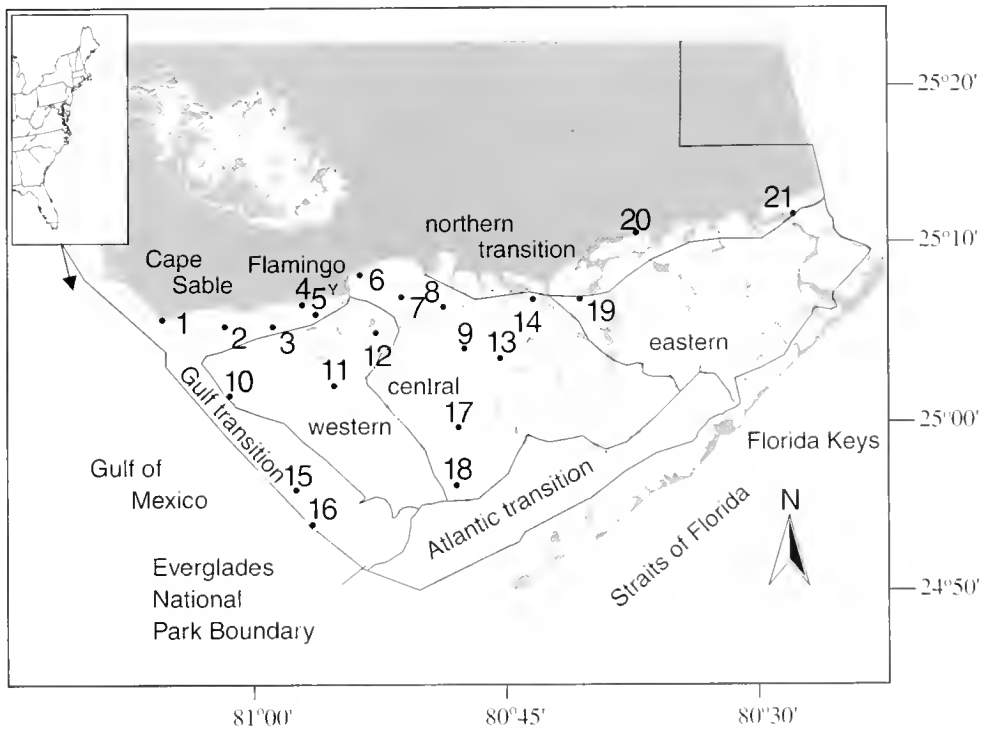

Figure 1

Location of sampling sites for spotted seatrout (*Cynoscion nebulosus*) in Florida Bay, Everglades National Park, Florida, including Florida Bay Subdivisions.

of the Everglades, including a return of historic freshwater flows into Florida Bay.

Two conceptual frameworks have been advanced to couple the role of growth and mortality in influencing cohort dynamics. Anderson (1988), in a review of hypotheses relating survival of prerecruits to recruitment, advocated a growth-mortality hypothesis as a rational framework for early life history studies that address recruitment variability. This concept predicts that survival of a cohort is directly related to growth rates during the early life stages. The growth-mortality framework, which includes several important integrated components and is based on bioenergetic principles of growth and ecological theory that predict growth rate, is directly related to survival. If it can be demonstrated that survival is a function of growth during the early life stage, then a valuable tool becomes available for examining mechanisms influencing recruitment of marine fishes.

Another framework suggests that the mortality rate does not operate alone in determining stage-specific survival, but it is the mortality:growth (M:G) ratio (mortality per unit of growth) that determines stage-specific survival (see citations in Houde, 1997). Houde (1997) advanced the idea of using the M:G ratio as an estimator of production and potential survivorship especially in early life stages when both mortality and growth are high and variable. This concept was partly based on the strong coupling of growth and mortality demonstrated by Ware (1975) who argued that when growth rate is poorer than average, larvae would be exposed to sources of mortality over a longer period and hence their mortality rate would increase. Growth and mortality values for successive cohorts would tend to form a cluster of points around a regression of mortality on growth based on average values for a particular species.

Our intent is not to test the growth-mortality hypothesis (*sensu* Hare and Cowen, 1997) as outlined by Anderson (1988), nor fully to develop the M:G ratio concept (Houde, 1997), but rather to use these concepts as a framework for our study. The major goal is to provide information on growth and survival of larval and, mainly, juvenile spotted seatrout that can ultimately be used to develop a spatially explicit model that can be linked to Everglades restoration activities. Therefore, the major objectives of this paper are 1) to determine overall growth rates of larval and juvenile spotted seatrout in Florida Bay; 2) to determine and compare juvenile growth rates geographically; 3) to estimate natural mortality rates of juveniles; 4) to estimate hatchdate distributions; 5) to compare cohort growth and mortality rates and G:M ratios for juveniles; and 6) to evaluate the effects of salinity and temperature on otolith growth—a surrogate for somatic growth.

Methods and materials

Field collections

Larval fish used for otolith microstructure analysis were collected from September 1994 through July 1997, mainly in the Gulf transition, western, and central subdivisions (Table 1, Fig. 1). These subdivisions designated by the

Table 1

Florida Bay sampling stations where otoliths from spotted seatrout were collected. Included are numbers (n) of larvae and juveniles used in the otolith microstructure analysis, and subdivisions as defined by the South Florida Ecosystem Restoration Prediction and Modeling Program, Program Management Committee.

Station number	Latitude (degrees and minutes)	Longitude (degrees and minutes)	Florida Bay subdivisions	Location	Juveniles (n)	Larvae (n)
1	25 06.81	81 05.27	Gulf transition	Cape Sable	—	4
2	25 06.37	81 01.42	Gulf transition	Middle Ground	1	10
3	25 06.40	80 58.58	Gulf transition	Conchie Channel	—	4
4	25 07.70	80 56.90	Gulf transition	Bradley Key	119	—
5	25 07.12	80 56.07	western	Murray Key	4	8
6	25 08.11	80 50.95	central	Snake Bight	3	—
7	25 09.45	80 53.42	central	Snake Bight	4	—
8	25 07.50	80 48.51	central	Rankin Lake	12	—
9	25 05.06	80 47.30	central	Roscoe Key	20	—
10	25 02.30	81 .1.12	Gulf transition	Sandy Key	49	—
11	25 02.90	80 55.00	western	Johnson Key Basin	125	—
12	25 06.00	80 52.50	western	Palm Key Basin	110	—
13	25 04.50	80 45.15	central	Whipray Basin	2	62
14	25 08.00	80 43.20	central	Crocodile Point	9	—
15	24 56.70	80 57.20	Gulf transition	Schooner Bank	2	—
16	24 54.70	80 56.31	Gulf Transition	Sprigger Bank	—	8
17	25 00.40	80 47.68	central	Sid Key Bank	6	—
18	24 57.03	80 47.52	central	Twin Key Basin	6	—
19	25 07.98	80 40.48	eastern	Madeira Point	1	—
20	25 11.85	80 37.15	northern	Little Madeira Bay	8	—
21	25 13.00	80 27.80	eastern	Shell Key	5	—

South Florida Ecosystem Restoration Prediction and Modeling Program, Program Management Committee, were based on modifications of the benthic mollusc community (Turney and Perkins, 1972). In 1994 and 1995, we used 60-cm bongo nets fitted with 0.333-mm mesh fished from the port side of a 5.4-m boat. Beginning in 1996, we used a paired 60-cm bow-mounted push net with 0.333-mm mesh nets similar to that described by Hettler and Chester (1990).

Juvenile spotted seatrout were obtained from monitoring programs established by the NOAA Center for Coastal Fisheries and Habitat Research (NOAA) and Florida Marine Research Institute (FMRI). NOAA collections were made from May 1995 through September 1997. Juveniles were collected with an otter trawl towed between two 5-m boats. The otter trawl measured 3.4 m (headrope) and was fitted with a 3.2-mm mesh tailbag with 6-mm mesh. FMRI collections were made in 1995 with a seine and a trawl. The 21.4-m center-bag drag seine was fitted with a 1.8 m × 1.8 m × 1.8 m bag of 3.2-mm mesh. The 6.1-m (headrope) otter trawl was fitted with a body of 38.1-mm stretch mesh and a 3.2-mm mesh tailbag. The majority of juveniles (86%) from NOAA and FMRI collections were collected in 1995.

Otolith microstructure analysis

Otolith processing Otolith removal and preparation generally followed the methods of Secor et al. (1991). All otoliths, except for the right sagitta, were mounted on a slide with mounting media and archived. The right sagittal otolith was embedded for transverse sectioning or polishing (or both). The left sagitta was embedded for transverse sectioning if the right was damaged. Sagittae were read with a light microscope at 1000× magnification under oil immersion. The first increment was determined as that following the core increment; which was defined as a well-defined dark increment surrounding the core (Powell et al., 2000). Two blind counts of increments were made by one reader and if the counts differed by more than 5, then the otolith was read again. If the counts were within the acceptable range, the two counts were averaged. Based on a previous validation study (Powell et al., 2000), 2.5 days were added to the increment counts to obtain the daily age. A total of 582 sagittal otoliths were aged. This total included 96 from larval collections from September 1994 through July 1997, 139 juveniles from NOAA collections from June 1995 through September 1997, and 347 from FMRI collections from June 1995 through December 1995.

Increment widths were measured on 347 otoliths from FMRI collections (1995) by using image analysis. The measuring path consisted of two segments: a ventral path from the core to the 21st increment and a ventral-medial path along the sulcus, from the 21st increment to the edge (Fig. 2). The 21st increment was selected as the transition point in these measuring paths by test reading 30 otolith sections representing the entire range of sample fish

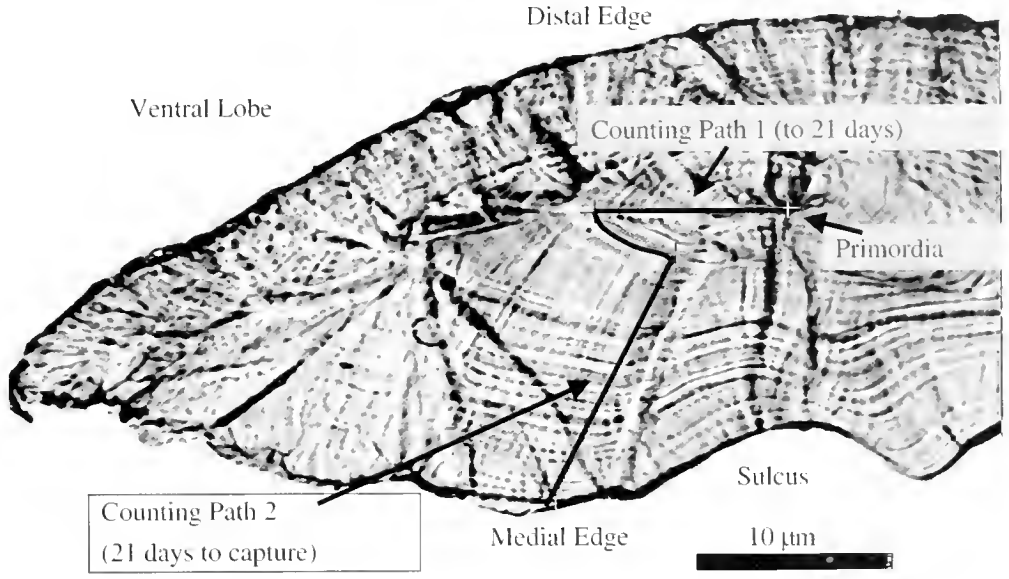

Figure 2

Transverse polished section of a spotted seatrout (*Cynoscion nebulosus*) (18 mm SL; age 48 days) otolith showing the counting paths.

lengths. In all samples, the 21st increment could easily be traced in both measuring paths and in all samples the first 21 increments could be measured within the same image. Increment widths were averaged over a 7-day period. Age estimates were also obtained and we eliminated any otolith used to measure increment widths if the difference in total increment count between the two methods (counts obtained directly from the microscope versus those attained by image analysis) was greater than 7 days or 10%. On this basis, 117 otoliths were removed from the increment width analysis.

We believed counts obtained directly from the microscope were more accurate than those obtained by summing the number of increments measured on the computer monitor with the image analysis system. Counting increments directly through the microscope lens allows the reader to optically section the otolith (by varying the focus), which helps in detecting daily increments. "Frozen" multiple images are a result of using the image analysis; hence optical sectioning is not possible.

Data analysis Data from all years and sources were used for 1) overall growth (i.e. larval and juvenile); 2) juvenile growth; and 3) estimates of juvenile mortality. Data from NOAA larval and juvenile collections were used to estimate a body-length–otolith-radius relationship. Data from 1995 FMRI and NOAA collections, which was the most complete data set, were used for growth comparisons between cohorts, and hatchdate distributions. Data from 1995 FMRI collections were used for 1) growth comparisons between geographical subdivisions; 2) estimating a wet-weight–age relationship to compute the ratio of wet-weight specific-growth to mortality (G:M ratios), which assesses the relative recruitment potential of individual cohorts (Houde, 1996; Rilling and Houde, 1999; Rooker et al., 1999); and 3) determining the influence of temperature on otolith increment width. We used the FMRI data set exclusively for the above analyzes because collections were spatially more localized and wet weights were available.

Natural mortality (M) estimates were derived by regressing $\log_e$ unadjusted numbers on age classes (5-day bins); the resulting slope provided an estimate of total mortality (Ricker, 1975). However, on the basis of the age-frequency distributions (Fig. 3), we considered juveniles ≥40 days old fully recruited to our gear and juveniles ≥90 days old appeared to avoid our gear. Hence, only juveniles between 40 and 90 days old were used to calculate mortality.

Hatchdate distributions were computed on a weekly basis and adjustments for mortality were made on individual juveniles by the equation

$$N_o = N_t / e^{-Zt},$$

where N_0 = estimated number at hatching;
N_t = number at time t (N_t=1 because N_0 was calculated for each individual fish);
Z = instantaneous daily mortality coefficient; and
t = age in days.

Spotted seatrout cohorts were divided into weekly units, but comparisons between cohort growth was done on a monthly basis because of inadequate numbers for weekly comparisons. A test of heterogeneity of slopes was imple-

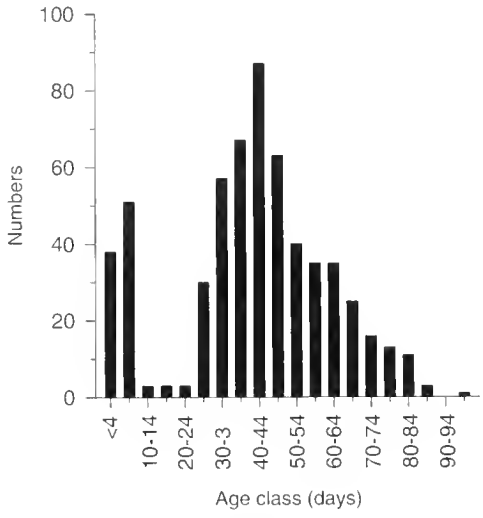

Figure 3

Frequency distribution of spotted seatrout (*Cynoscion nebulosus*) age classes used in determining minimum age at full recruitment to the sampling gear, and mortality.

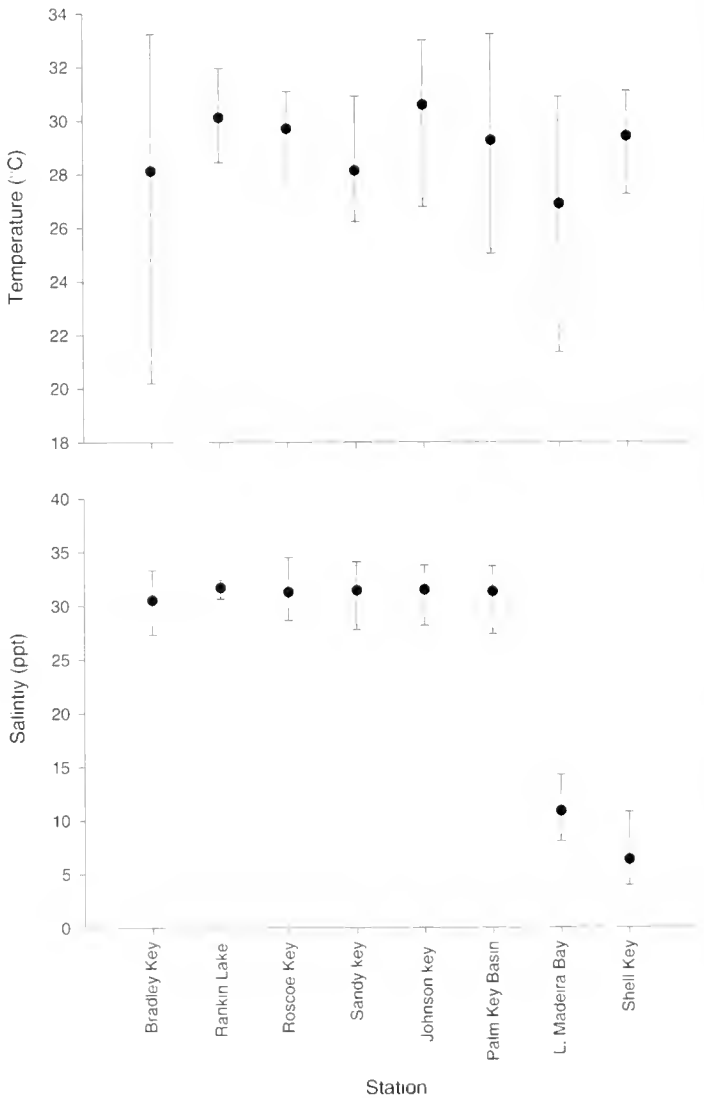

Figure 4

Mean and ranges of temperature and salinity data by station used in the otolith microstructure longitudinal analysis (relationship between increment width and temperature and salinity). For station locations relative to subdivisions, see Table 1 and Figure 1.

mented by using a generalized linear model (SAS/STAT software, version 6.12, SAS Institute, Cary, NC) to test if growth differed among cohorts. A general linear test (Neter et al., 1983) was used to compare growth between three geographical subdivisions (Gulf transition, western, and central). This test is a function of the error sum of squares of the reduced model minus the error sum of squares of the full model. Adequate numbers of juveniles were not available to compare growth in eastern and northern subdivisions (Table 1). Circular statistics (Batschelet, 1981) were used to determine if spawning, as determined from hatchdate distributions, was uniform over the lunar month. The phase of the moon for 1995 was identified by the fraction illuminated (U. S. Naval Observatory Applications Department, 1997). A 3-point moving average was used to test if spawning was cyclical.

Cohorts (1995) were categorized according to the following hatchdates: cohort A, 29 March–2 May ("April"); cohort B, 3 May–6 June ("May"); cohort C, 7 June–4 July ("June"); cohort D, 5 July–1 August ("July"); cohort E, 2 August–5 September ("August"); cohort F, 6 September–3 October ("September").

Comparisons of the relative recruitment potential of individual cohorts (G:M ratios) between all cohorts were unresolved. Although cohort mortality estimates could be generated, they were appropriate (by analyzing r^2 and P-values from regression analysis) for only three cohorts (cohorts B, D, and F).

A random coefficient model was used to investigate the relationship between growth rate of otoliths with age and temperature from juveniles collected in 1995. Most fish were exposed to salinities in a narrow range between 28 and 34 ppt; only 9 fish were exposed to salinities in the 5–13 ppt range (Fig. 4). Consequently, there was insufficient information to obtain reliable inferences on the relationship of growth rate to salinity or the relationship to salinity and temperature for growth information obtained by using either otolith measuring path. This was a disappointment because growth responses to salinity were considered an important objective in relation to proposed Everglades water management activities. Thus, investigation was restricted to the relationship of growth with temperature. A separate model was fitted for the first (1–21 increments)

and second (22–60 increments) measuring paths because otolith increment width changed at a constant (age-independent) rate for each path. We did not include fish with >60 increments because the relationship past this number was determined for only 10% of the fish and included obvious outliers. Letting Y_{ij} be the otolith width measurement for fish i at age a_{ij}, where j indexes time, the model for each path was

$$Y_{ij} = \alpha_{0i} + \alpha_{1i} a_{ij} + e_{ij},$$

where α_{0i} and α_{1i} are the fish-specific intercept and slope describing the relationship between increment width and age for fish i, and e_{ij} is a normally distributed error term; thus, α_{1i} is the growth rate for fish i over the measuring path. Temperature exhibited only negligible change for any given fish over the measuring path; thus, temperature for fish i was summarized as t_i, the average temperature over the path for that fish. To determine an appropriate model for the relationship between intercept and growth rate and temperature, a preliminary analysis was performed in which ordinary least squares estimates of α_{0i} and α_{1i} were obtained separately for each fish i and plotted against temperature. For the first measuring path (1–21 increments), the appropriate model was

$$\alpha_{0i} = \beta_{00} + \beta_{01} t_i + b_{0i}, \alpha_{1i} = \beta_{10} + \beta_{11} t_i + \beta_{12} t_i^2 + b_{1i},$$

where b_{0i} and b_{1i} are normally distributed random effects, allowing growth rates for fish at the same temperature to vary across fish. For the second measuring path (22–60 increments), the appropriate model was,

$$\alpha_{0i} = \beta_{00} + \beta_{01} t_i + \beta_{02} t_i^2 + b_{0i}, \alpha_{1i} = \beta_{10} + \beta_{11} t_i + \beta_{12} t_i^2 + b_{1i}.$$

By substitution, these considerations yielded models 1 and 2 for the first and second paths, respectively:

$$Y_{ij} = (\beta_{00} + \beta_{01} t_i) + (\beta_{10} + \beta_{11} t_i + \beta_{12} t_i^2)\, a_{ij} + b_{0i} + b_{1i} a_{ij} + e_{ij} \quad (1)$$

$$Y_{ij} = (\beta_{00} + \beta_{01} t_i + \beta_{02} t_i^2) + (\beta_{10} + \beta_{11} t_i + \beta_{12} t_i^2)\, a_{ij} + b_{0i} + b_{1i} a_{ij} + e_{ij} \quad (2)$$

thus representing otolith increment width in each case as having a straight line relationship with age, where the slope (age-independent growth rate) depends on average temperature according to a quadratic relationship. The random effects allow observations on the same fish to be correlated, whereas observations across fish are independent. Models 1 and 2 were implemented in SAS Proc Mixed (SAS/STAT software, version 6.12, SAS Institute, Cary, NC).

Daily temperature records were obtained from the United States Department of Interior's National Park Service, Florida Bay monitoring stations and averaged over a 7-day period. In 1995, temperature records were available only for Johnson Key Basin (JKB), Whipray Basin (WB), Little Blackwater Sound (LBS), and Little Madeira Bay (LMB), but spotted seatrout were also collected at other sites (Table 1). Daily temperatures were estimated for Sandy Key (SK) and Roscoe Keys (RK) from values recorded during sampling trips because both these stations are not in close proximity to National Park Service monitoring sites. Sandy Key values were regressed on JKB values (same dates). Sandy Key temperatures were collected from January 1994 through August 1996. The regression model for temperature was $SK = 0.76 + 0.9536\, JKB$ [r^2=0.89; n=25]. Roscoe Key values were regressed on WB values (same dates). Roscoe Key temperatures were collected from January 1994 through August 1996. The regression model for temperature was $RK = 5.60 + 0.7976\, WB$ [r^2=0.87; n=31]. Temperature values were available at Murray Key (MK) in 1997. To attain values for our 1995 analysis we regressed MK on JKB (same dates). The temperature regression model was $MK = 0.77 + 0.9680$ JKB [r^2=0.99; n=342].

We reported measurements in standard length (SL). For preflexion and flexion larvae, standard length was measured from the tip of the snout to the tip of the notochord. For postflexion larvae and juveniles, standard length was measured from the tip of the snout to the base of the hypural plate.

Results

Overall growth of larvae and juveniles (<80 mm SL) was best described by the equation $\log_e$ *standard length* = −1.31 + 1.2162 ($\log_e$ *age*) [n=582; r^2=0.97]. Growth in body length of juveniles (12–80 mm SL) was best described by the linear equation *standard length* = −7.50 + 0.8417 (*age*) [n=486; r^2=0.84]; hence, juveniles between approximately age 20–100 days grew on average 0.84 mm/d. There were no significant differences in juvenile growth in body length among three geographical subdivisions [F^4_{327}=0.756; n=333] (Table 2), but there was a significant growth difference in length for one of six 1995 cohorts (Table 3, Fig. 5). Growth in wet weight of juveniles (15–69 mm SL) was best described by the equation $\log_e$ *wet weight* = −4.44 + 0.0748 (*age*) [n=347, r^2=0.84]. There was a significant growth difference in wet weight for one cohort (Table 4, Fig. 6).

Weekly 1995 hatchdate distributions, determined by using daily instantaneous mortality (0.0585, Fig. 7), indicated juveniles in collections (i.e. survivors) were from spawning that was cyclical and protracted (Fig. 8). The most intense successful spawning occurred during 21–27 June (9.2% of total). Using a 3-point moving average, we observed three similar cycles (Fig. 8). From data on survivors, ~25% of juveniles were spawned by late May, 50% by early July, and 75% by late August and from data on cohorts, three cohorts (cohorts C, D, and E; early June–late August) comprised 55% of the total estimated spawn of spotted seatrout. There was no correlation between spawning and moon phase (periodic regression r^2=0.019, P=0.754) (Fig. 8).

The relative recruitment potential (G:M ratio) of the 1995 year class estimated from the wet-weight specific growth coefficient (0.0748) and the instantaneous daily mortality rate (0.0585, Fig. 7) was 1.28. The G:M ratio for three cohorts (B, May; D, July; and F, September) was greater than the ratio for the total 1995 year class because mortal-

Table 2

Summary of growth data used to compare growth in length of spotted seatrout among three Florida Bay subdivisions. Growth was best described by the linear equation: *standard length* = a + b (age in days).

Subdivision	Intercept	Slope	n	r^2	Size range (mm SL)
Gulf transition	−11.07	0.8914	139	0.86	16–69
Central	−12.23	0.9298	49	0.80	15–63
Western	−10.56	0.8834	145	0.85	17–69

Table 3

Summary of statistics for a test for heterogeneity of slopes for cohort somatic growth rates of spotted seatrout. Cohorts were categorized according to month of hatchdate (see text). The base parameter is cohort F and all parameter estimates are deviations from the base cohort. For growth equations, see Figure 5.

Parameter	Estimate	Standard error	t-value	P-value
Intercept	−7.97270	3.02829	−2.63	0.0088
Cohort A	−0.86811	4.31970	−0.20	0.8408
Cohort B	−11.85849	3.91387	−3.03	0.0026
Cohort C	1.65094	3.86470	0.43	0.6695
Cohort D	−6.70820	4.74936	−1.41	0.1586
Cohort E	1.02077	3.50931	0.29	0.7713
Slope	0.82088	0.05613	14.62	<0.001
Cohort A	0.04054	0.08604	0.47	0.6378
Cohort B	0.24578	0.07106	3.46	0.0006
Cohort C	−0.00113	0.07091	−0.02	0.9873
Cohort D	0.15741	0.08730	1.80	0.0721
Cohort E	0.04544	0.06821	0.67	0.5058

Table 4

Summary of statistics for a test for heterogeneity of slopes for cohort wet-weight growth rate of spotted seatrout. Cohorts were categorized according to month of hatch date (see text). The base parameter is cohort F and all parameter estimates are deviations from the base cohort. For growth equations, see Figure 6.

Parameter	Estimate	Standard error	t-value	P-value
Intercept	−4.27384	0.23763	−17.99	<0.0001
Cohort A	0.10201	0.37014	0.28	0.7830
Cohort B	−0.46348	0.34092	−1.36	0.1749
Cohort C	−0.27866	0.32116	−0.87	0.3862
Cohort D	−0.19540	0.38352	−0.51	0.6108
Cohort E	−0.38260	0.29853	−1.28	0.2009
Slope	0.06974	0.00439	15.88	<0.0001
Cohort A	0.00195	0.00729	0.27	0.7889
Cohort B	0.00679	0.00622	1.09	0.2754
Cohort C	0.00502	0.00575	0.87	0.3835
Cohort D	0.00759	0.00702	1.08	0.2808
Cohort E	0.01188	0.00564	2.11	0.0359

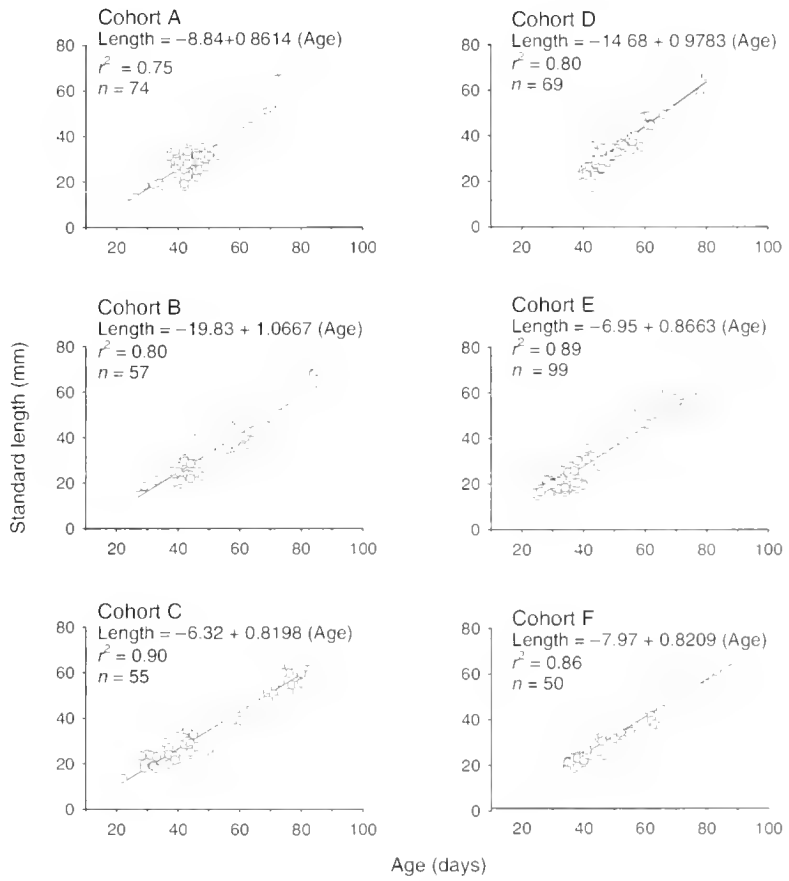

Figure 5

Comparison of growth in standard length among six spotted seatrout (*Cynoscion nebulosus*) cohorts collected in 1995. See text for cohort hatchdates.

Table 5

Daily growth (wet weight in grams) rates and daily mortality rates for three cohorts in Florida Bay in 1995. Cohorts were categorized according to month of hatchdate (see text). The G:M ratio derived from the growth and mortality rates is also presented. For growth equations and associated r^2 values, see Figure 6.

Cohort	Hatchdate month	Growth rate	Mortality rate	r^2	G:M ratio	Size range (mm SL)
B	May	0.0765	0.0445	0.54	1.72	28–62
D	July	0.0773	0.0565	0.82	1.37	37–68
F	September	0.0697	0.0354	0.67	1.97	37–66

ity rates appeared relatively low compared to the overall mortality rate (0.0585) for juveniles (Table 5). However, differences in mortality rates among these three cohorts were not significant (F^1_{21}=1.414). There were no significant differences in weight-specific coefficients among the three cohorts (B, D, and F) (Table 4), but a significant difference in length-specific coefficients among the three cohorts was found (Table 3). Cohort B (May) had a significantly higher growth rate than the other two cohorts.

There was a close relationship between otolith radius and body length (Fig. 9). A linear equation with the sagittal ventral radius, had a similar r^2 as a curvilinear equation with the sagittal dorsal radius. However, we were unable to measure increment widths along this plane and instead used a combination of a ventral path and a ventral medial path.

As an initial demonstration that otolith increment width increased with age along the 1–21 increment measuring path and decreased along the 22–60 increment path, simpli-

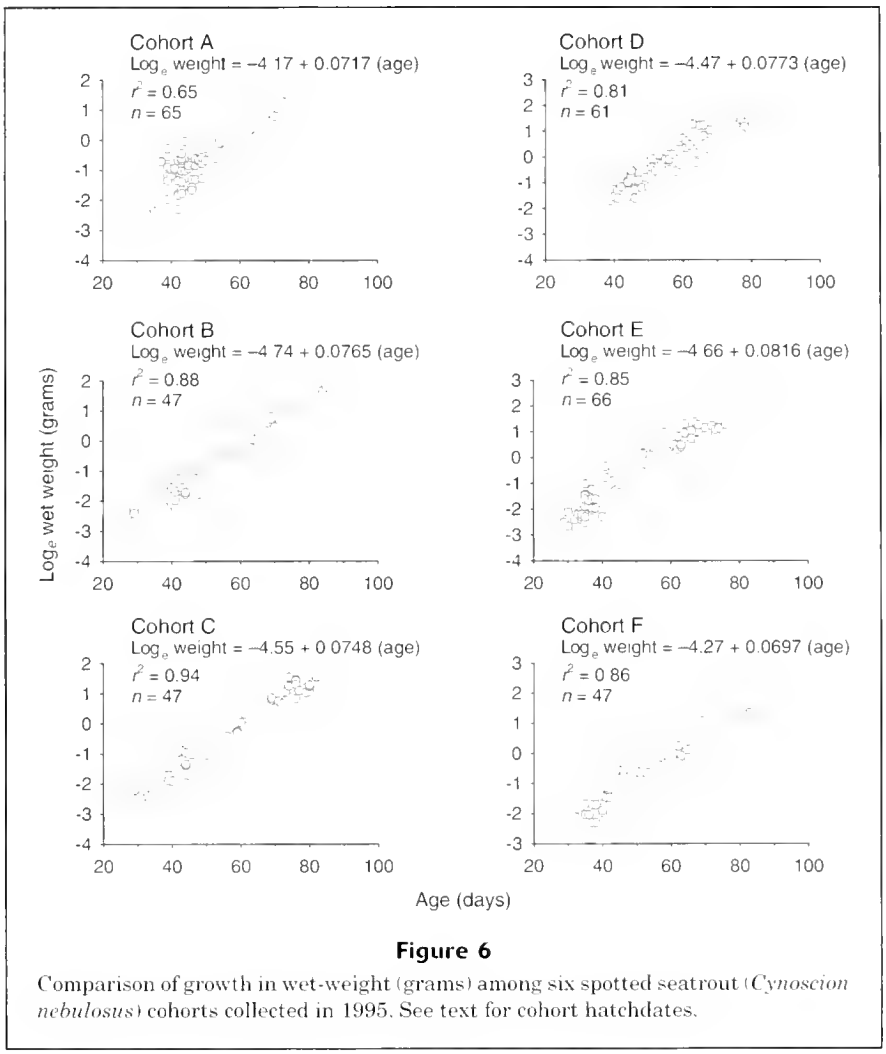

Figure 6

Comparison of growth in wet-weight (grams) among six spotted seatrout (*Cynoscion nebulosus*) cohorts collected in 1995. See text for cohort hatchdates.

fied versions of Equations 1 and 2 (see above) were fitted, in which all coefficients of temperature were set equal to zero, so that Equations 1 and 2 represent simple linear relationships with age. For the first path, the estimate of slope was 0.153 μm/d (P<0.0001); that for the second path was –0.065 μm/d (P<0.0001). Addition of quadratic terms to each model was not supported (P=0.81 and 0.12, respectively). For the first path, whether intercept or growth rate were associated with temperature was determined by testing whether the parameters β_{01}, β_{11}, and β_{12} were equal to zero. There was no evidence that any of these parameters were different from zero (P=0.45, 0.35, and 0.42, respectively); the latter two may indicate that the data do not support the contention that growth rate depends on temperature in this range (1–21 d). For the second path, tests of β_{02}=0 and β_{12}=0 offered strong evidence that these parameters are different from zero (P<0.001 in each case). In particular, these results suggested for the age range 22–60 d, otolith growth rates decrease. The extent of the decrease is strongly associated with average temperature according to a quadratic relationship such that growth rates were more steeply decreasing with age for lower temperatures and then became shallower at higher temperatures. In summary, for temperatures at the lower and higher end of the observed temperature range, otolith growth rates for the age range 22–60 d were higher than they were in the middle of the observed temperature range.

Discussion

Growth in body length of juvenile spotted seatrout in Florida Bay was faster than growth of juveniles from Tampa Bay (Table 6, McMichael and Peters, 1989). Florida Bay is generally considered an oligotrophic system (Fourqurean and Robblee, 1999). Nevertheless, seagrass beds in western Florida Bay, where juvenile spotted seatrout are most common (Chester and Thayer, 1990), are significantly more dense than beds in northwestern Florida waters, slightly north of Tampa Bay (Iverson and Bittaker, 1986). Increased growth of juveniles in Florida Bay could be attributed to the dense seagrass beds that provide habitat for epifaunal crustaceans (Holmquist et al., 1989; Matheson et al., 1999), which are important in the diet of juve-

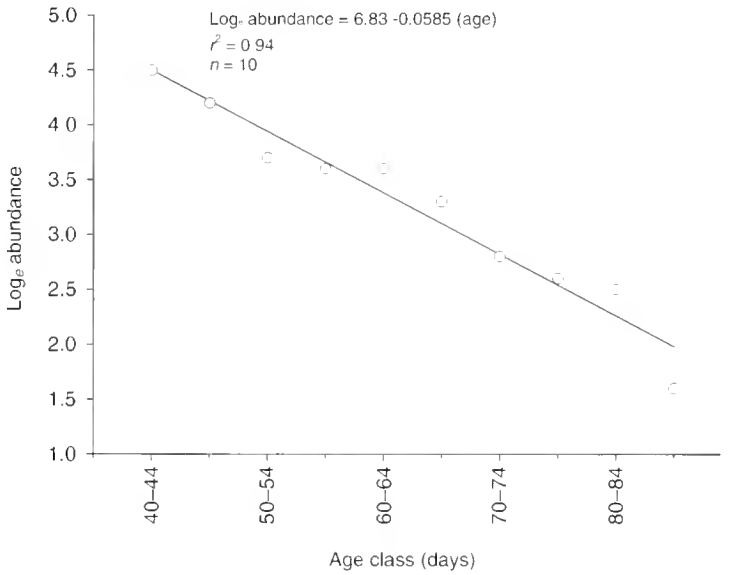

Figure 7

Catch curve of juvenile spotted seatrout (*Cynoscion nebulosus*) used to estimate daily instantaneous mortality (Z). Z = slope = –0.0585. Spotted seatrout were fully recruited to the gear at age 40–44 days.

Table 6

Comparison of spotted seatrout growth (size in mm SL at age) between Tampa Bay, Florida (McMichaels and Peters, 1989) and Florida Bay, Florida (this study).

	Age (days)								
Area	10	20	30	40	50	60	70	80	90
Tampa Bay	5.1	10.2	15.3	20.3	25.4	30.5	35.6	40.7	45.8
Florida Bay	4.4	10.3	16.9	23.3	31.4	39.2	47.2	55.6	64.1

nile spotted seatrout (Hettler, 1989; McMichael and Peters, 1989). Additionally, warmer water temperatures have been observed in Florida Bay (Boyer et al., 1999) compared to Tampa Bay (McMichael and Peters, 1989); these warmer temperatures could enhance growth if adequate food is available (Warren, 1971). However, our study and that of McMichael and Peters (1989) were quite a few years apart; hence differences that we observed could also be accounted for by interannual variability. In addition, differences in growth could also be attributed to differences in sampling gear between the two studies.

Florida Bay is a heterogenous ecosystem and consists of ecologically distinct regions (Phlips and Badylak, 1996; Fourqurean and Robblee, 1999); however, we did not detect any differences in growth of juvenile spotted seatrout among our three subdivisions. In general, juvenile collections from the central subdivision were from stations that were spatially dispersed; whereas, juvenile collections in the western and Gulf transition subdivisions were from relatively few stations (Table 1). Normally, the central subdivision is characterized by the highest salinities in the bay and the western and the Gulf transition are characterized by high salinities (Orlando et al., 1997). However, in our study, salinities in the three subdivisions were moderate and similar (Fig 4), and growth rates estimated for the three subdivisions could be useful as baseline rates, particularly in the central subdivision where salinities are commonly hyperhaline (Orlando et al., 1997).

The spawning habits of spotted seatrout throughout their entire range are generally similar. They have a protracted spawning season, are multiple spawners, and reach sexual maturity at an early age. Initiation of spawning might be temperature dependent, with water temperatures between 20° and 23°C necessary to initiate reproductive development (Brown-Peterson and Warren, 2001). Hatchdate distributions calculated for spotted seatrout in

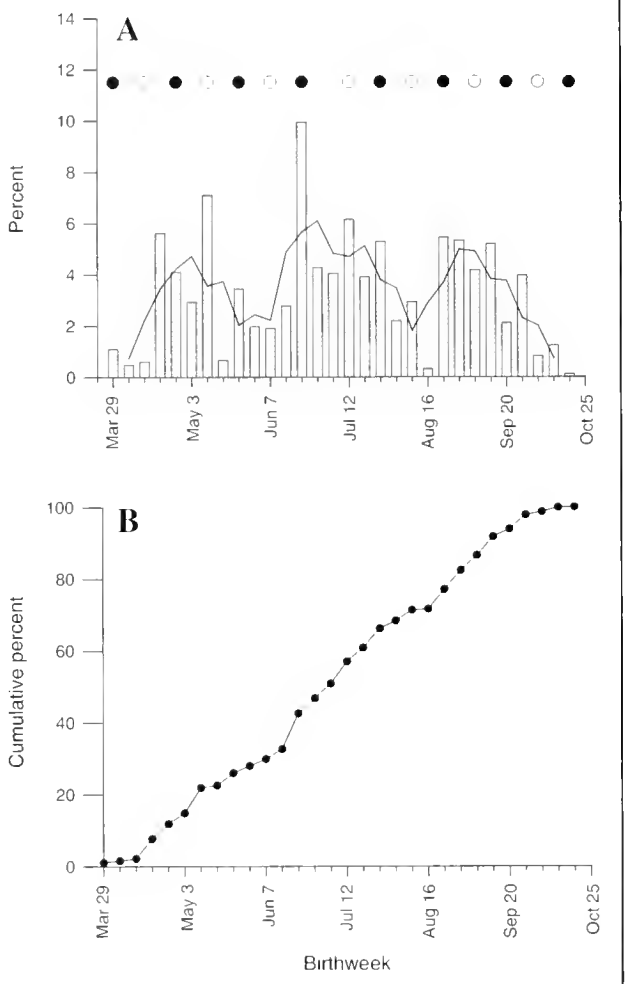

Figure 8

(**A**) Spotted seatrout (*Cynoscion nebulosus*) (n=417) weekly hatchdate distributions adjusted for mortality, including moon phases (●=new moon; ○=full moon), and 3-point moving average (solid line) of hatchdate distributions. (**B**) Cumulative frequency of spotted seatrout (n=417) hatchdate distributions.

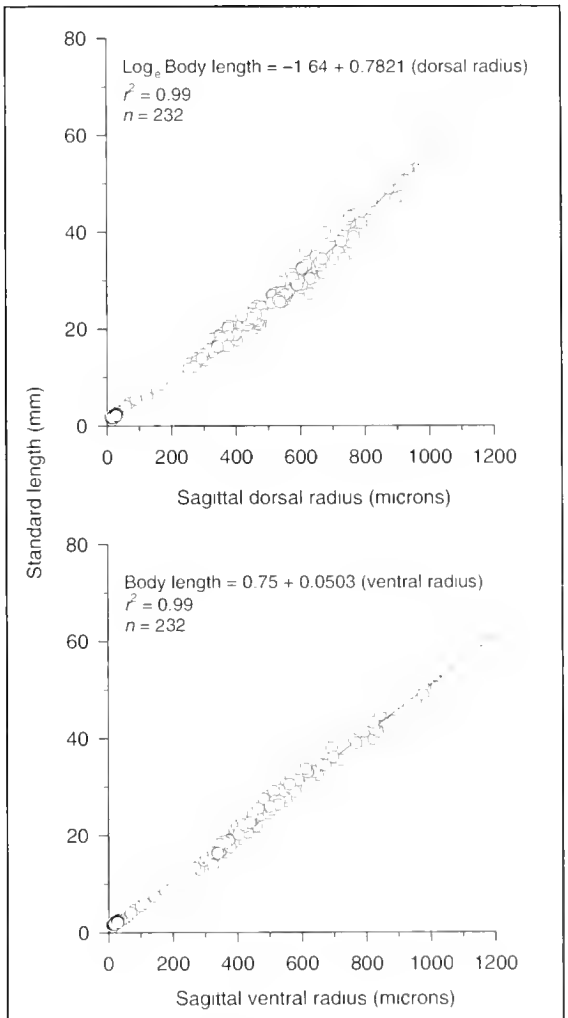

Figure 9

The relationship between sagittal otolith radius and standard length (top), and sagittal ventral radius and standard length (bottom) for spotted seatrout (*Cynoscion nebulosus*).

Florida Bay in this study along with early stage larval collections (Powell, 2003) indicate that spotted seatrout spawn between March and October (based on hatchdate distributions) and that the majority of spawning occurs between 27° and 35°C , with very little spawning between 20° and 26°C (based on early stage larval collections). Spawning peaks, based on larval collections in 1994–96, occurred in June, August, and September (Powell, 2003), and early May, late June, and late August through early September based on 1995 hatchdate distributions (this study). However, Stewart (1961) reported that spotted seatrout in Florida Bay spawned throughout the year and that spawning peaked in spring and fall. Another larval fish study in Florida Bay indicated that some spawning occurs as early as February and continues into December (Rutherford et al., 1989).

Peak spawning activity of spotted seatrout is highly variable (McMichael and Peters, 1989; Brown-Peterson and Warren, 2001). McMichael and Peters (1989) observed two spawning peaks: spring and summer. Older fish participate in two peak spawning periods (Tucker and Faulkner, 1987), and a portion of the larger spring-spawned fish (age-1+) enter the spawning population during their second summer, augmenting the number of summer spawning fish.

We found that spawning activity and moon phase were uncorrelated, which is not in concordance with observations of McMichael and Peters (1989). They found that distinct peaks in spawning (based on hatchdate distributions of larval spotted seatrout) occurred at monthly intervals, and this periodicity might coincide with moon phase. However, this monthly periodicity was not observed when their data for juvenile spotted seatrout were examined. Moreover, statistical tests were not performed on the data in their study.

Our inferences, from this study, in relation to spotted seatrout peak spawning are based on hatchdate distributions and should be viewed with caution because hatchdates are based on survivors. Differential survival for early life history stages can bias results. Hatchdate distributions are valuable when compared to egg or recently hatched larval densities and might suggest processes responsible for differential cohort survivorship. Because spotted seatrout undergo a protracted spawning period and because there is high variation associated with icthyoplankton samples (Cyr et al., 1992), intensive and extensive sampling of recently hatched larvae would be required over a long duration to answer these process-oriented mortality questions.

The daily instantaneous mortality rate of juvenile spotted seatrout was higher in Florida Bay than those reported from northwestern Florida systems (Nelson and Leffler, 2001). Mortality rates of juvenile spotted seatrout from Florida Bay were 5.7%/d; whereas, for the other systems, rates approximated 3%/d. In general, mortality rates might increase with increasing estuarine temperatures (Houde and Zastrow, 1993). Although we were unable to estimate instantaneous daily mortality rates for larval spotted seatrout, these data have been estimated for larvae (3.5–6.5 mm) in two southwestern Florida estuaries (Peebles and Tolly, 1988). Highly variable rates were reported between the two Florida estuaries (Naples Bay: 0.70 or 50%/d; and Fakahatchee area: 0.37 or 31%/d). Houde (1996) reported a generalized instantaneous daily mortality rate for marine fish larvae of 0.239 (21%/d). Estimating mortality rates for larval spotted seatrout in Florida Bay will be critical for calculating G:M ratios in order to evaluate stage-specific survival and to develop credible spatially explicit models.

Mortality rates of spotted seatrout cohorts could be calculated for only three of six cohorts (B, May; D, July; and F, September) because slopes were significantly different from zero for only these cohorts. Furthermore, mortality rates of two of the three cohorts (B and F) were associated with low r^2 values (Table 5); hence the G:M ratios along with the mortality rates for these three cohorts should be considered "rough" estimates. Attaining more accurate mortality estimates for spotted seatrout would be valuable in linking cohort variability with potential recruitment and stage-specific survival. For example, larval cohorts of bay anchovy (*Anchoa mitchilli*) from Chesapeake Bay, a temperate estuary, exhibit growth rates that are temporally variable and mortality rates that are spatially and temporally variable (Rilling and Houde, 1999). Temperature, zooplankton prey and gelatinous predators are believed to influence growth and mortality rates of the bay anchovy. For striped bass (*Morone saxatilis*) in a subestuary of Chesapeake Bay, cohorts exhibited highly variable seasonal G:M ratios that were strongly influenced by temperature (Houde, 1997). In a subtropical estuary, cohort-specific mortality rates for juvenile red drum varied temporally; early and late season cohorts exhibited the highest mortality rates, which coincided with highest growth rates and G:M ratios for midseason cohorts (Rooker et al., 1999). We agree with Houde (1997) that future research should focus on the variability and causes of variability in growth and mortality, both of which interact to determine stage-specific survival. The developmental stage or age where G:M variability is greatest, along with the relationship of this variability to recruitment, need to be determined for spotted seatrout in Florida Bay. No doubt a relationship exists between G:M ratios and recruitment. Future research should also determine if cohort G:M ratios and somatic growth rates are seasonally or spatially variable. If they are, then a limited spatial and temporal sampling program could be designed to annually evaluate G:M ratios at highly variable stages or ages as an index of year-class strength of spotted seatrout in Florida Bay. Such an index could be verified by examining year-class catch rates on an annual basis or by virtual population analysis.

In our study there was little temporal difference in growth of juvenile spotted seatrout cohorts. Larval growth and mortality, which was not treated adequately in our study, could be influenced by copepod prey—an important dietary component of larval spotted seatrout (McMichael and Peters, 1989). The copepod *Acartia tonsa* is dominant in Florida Bay, but egg production rates for this species are low in the bay compared to those in other systems (Kleppel et al., 1998). We suspect the "bottleneck" to recruitment of spotted seatrout could occur during the larval stage. Hence, future research should examine mortality and growth of larval and recently settled spotted seatrout; in particular the patterns of larval production potential (G:M ratios). Research in these areas should increase our understanding of the degree of variability in stage-specific survival and recruitment of spotted seatrout in Florida Bay (Houde, 1996).

For most species, especially those with protracted spawning habits, it is most informative to analyze cohort growth and mortality. For example, striped bass and bay anchovy cohorts in Chesapeake Bay exhibit highly variable growth rates, mortality rates, and stage durations (Rutherford and Houde, 1995; Rilling and Houde, 1999). This variability could cause differential survival for cohorts and result in frequency distributions of survivor hatchdates that do not resemble recently hatched larvae or egg-production frequency distributions (e.g. Crecco and Savoy, 1985; Rice et al., 1987).

We are unable to interpret the significance of the absolute value of the G:M ratio for juvenile spotted seatrout, because interannual comparisons were not made, but we presented the ratio for future comparisons. Generally, the G:M ratio is <1.0 during the early larval stage, indicating a decline in biomass. However, the G:M ratio of a cohort will eventually exceed 1.0 as a result of a relative decline in mortality as larvae grow (Houde and Zastrow, 1993). Clearly, stage specific analysis of the spotted seatrout from egg through juvenile stage would have been more informative in determining when the maximum G:M ratio occurs (when cohort biomass increases at a maximum rate) and in providing insight into stage-specific dynamics of spotted seatrout (Houde, 1997). A constraint of our study was our inability to estimate larval mortality rates; hence early life history stage dynamics could not be examined.

Size-selective mortality in the juvenile life history stages can have important consequences for recruitment. Sogard (1997) argued that "within-cohort size-selective mortality"

is more evident in the juvenile stage than during the egg and larval stages when random mortality independent of fish size is more likely to occur (e.g. dispersal of eggs and larvae away from suitable nursery areas). In addition, variation in size, which provides a "template" for size-selective processes, increases during the juvenile stage as larval size is constrained by egg size. Sogard (1997) cited a number of recent studies that suggest the early juvenile period plays a greater role in determining year-class strength than previously thought.

We were unable to determine if salinity influenced increment width (a surrogate for somatic growth) at early life stages. Understanding the relationship between salinity and growth is critical because Everglades restoration will most likely result in increased freshwater flows to Florida Bay, and during low rainfall periods, salinities in the north central portion of the bay can exceed 45 ppt (Orlando et al., 1997; Boyer et al., 1999). But, salinities were moderate and similar at most stations where juvenile trout were collected in the bay during 1995 (Fig. 4). Very few fish were collected at low salinities: in fact, juvenile spotted seatrout are not commonly collected at low-salinity stations (Table 1; Florida Department of Environmental Protection[1]), and hyperhaline conditions were not observed in 1995. Therefore, we were only able to determine if temperature could influence increment widths. The curvilinear relationship between otolith growth rate and temperature, although a statistically strong relationship, is difficult to explain biologically. Temperature could mask other factors, e.g. temporal variability in prey and predator availability, and optimal temperatures for growth (Rooker et al., 1999). We were able to demonstrate that one cohort grew faster than five other cohorts, possibly indicating differential prey availability in 1995. An individual-based bioenergetics model for spotted seatrout now in preparation (Wuenschel et al.[2]) should add to our understanding of the effects of salinity and temperature on larval and juvenile spotted seatrout

Acknowledgments

We are especially grateful to Al Crosby, Mike Greene, Mike LaCroix, and other Beaufort staff that participated in the field work. We thank James Waters of the NMFS Southeast Fisheries Science Center for computer programing assistance and Jon Hare of our laboratory for performing the circular statistics. We are grateful to Dean Ahrenholz, Jon Hare, Patti Marraro, Joseph Smith, and three anonymous reviewers for their valuable reviews of the manuscript. We also thank Steve Bobko at Old Dominion University for the image analysis macro used to obtain otolith increment widths.

[2] Wuenschel, M. J., R. G. Werner, D. E. Hoss, and A. B. Powell. 2001. Bioenergetics of larval spotted seatrout (*Cynoscion nebulosus*) in Florida Bay. Florida Bay Science Conference, April 23–26, 2001, p. 215–216. Westen Beach Resort, Key Largo, Florida. Abstract. Center for Coastal Fisheries and Habitat Research, Beaufort Laboratory, 101 Pivers Island Road, Beaufort, NC 28516.

Literature cited

Anderson, J. T.
1988. A review of size dependent survival during pre-recruit stages of fishes in relation to recruitment. J. Northw. Atl. Fish. Sci. 8:55–66.

Batschelet, E.
1981. Circular statistics in biology, 371 p. Academic Press, New York, NY.

Boyer, J. N., J. W. Fourqurean, and R. D. Jones.
1999. Seasonal and long-term trends in the water quality of Florida Bay (1989–1997). Estuaries 22:417–430.

Brown-Peterson, N. J., and J. W. Warren.
2001. The reproductive biology of spotted seatrout, *Cynoscion nebulosus*, along the Mississippi Gulf Coast. Gulf Mexico Sci. 2001:61–73.

Chester, A. J., and G. W. Thayer.
1990. Distribution of spotted seatrout (*Cynoscion nebulosus*) and gray snapper (*Lutjanus griseus*) juveniles in seagrass habitats of western Florida Bay. Bull. Mar. Sci. 46:345–357.

Crecco, V., and T. Savoy.
1985. Effects of biotic and abiotic factors on growth and relative survival of young American shad, *Alosa sapidissima*, in the Connecticut River. Can. J. Fish. Aquat. Sci. 42: 1640–1648.

Cyr, H., J. A. Downing, S. Lalonde, S. B. Baines, and M. L. Price.
1992. Sampling larval fish: choice of sample number and size. Trans. Am. Fish. Soc. 121:356–368.

Fourqurean, J. W., and M. B. Robblee.
1999. Florida Bay: a history of recent ecological changes. Estuaries 22:345–357.

Hare, J. A., and R. K. Cowen.
1997. Size, growth, development, and survival of the planktonic larvae of *Pomatomus saltatrix* (Pisces: Pomatomidae). Ecology 78:2415–2431.

Hettler, W. F., Jr.
1989. Food habits of juveniles of spotted seatrout and gray snapper in western Florida Bay. Bull. Mar. Sci. 44: 152–165.

Hettler, W. F., and A. J. Chester.
1990. Temporal distribution of ichthyoplankton near Beaufort Inlet, North Carolina. Mar. Ecol. Prog. Ser. 68: 157–168.

Holmquist, J. G., G. V. N. Powell, and S. M. Sogard.
1989. Decapod and stomatopod communities of seagrass-covered mud banks in Florida Bay: inter- and intra-bank heterogeneity with special reference to isolated subenvironments. Bull. Mar. Sci. 44:251–262.

Houde, E. D.
1996. Evaluating stage-specific survival during the early life of fish. *In* Survival strategies in early life stages of marine resources (Y. Watanabe, Y. Yamashita, and Y. Oozeki, eds.), p. 51–66. Balkema, Brookfield, VT.
1997. Patterns and consequences of selective processes in teleost early life histories. *In* Early life history and recruitment of fish populations (R. C. Chambers and E. A. Trippel, eds.), p. 173–196. Chapman and Hall, London.

Houde, E. D., and C. E. Zastrow.
1993. Ecosystem-and taxon-specific dynamic and energetic properties of larval fish assemblages. Bull. Mar. Sci. 53: 290–335.

Iverson, R. L., and H. F. Bittaker.
1986. Seagrass distributions and abundances in eastern Gulf of Mexico coastal waters. Estuar. Coast. Shelf Sci. 1986:577–602.

Kleppel, G. S., C. A. Burkart, L. Houchin, and C. Tomas.
1998. Egg production of the copepod *Acartia tonsa* in Florida Bay during summer. 1. The roles of food environment and diet. Estuaries 21:328–339.

Matheson, R. E., Jr., S. M. Sogard, and K. A. Bjorgo.
1999. Changes in seagrass-associated fish and crustacean communities on Florida Bay mud banks: the effects of recent ecosystem changes? Estuaries 22:534–551.

McMichael, R. H., Jr., and K. M. Peters.
1989. Early life history of spotted seatrout, *Cynoscion nebulosus* (Pisces: Sciaenidae), in Tampa Bay, Florida. Estuaries 12:98–110.

Nelson, G. A., and D. Leffler.
2001. Abundance, spatial distribution, and mortality of young-of-the-year spotted seatrout (*Cynoscion nebulosus*) along the Gulf Coast of Florida. Gulf Mex. Sci. 19:30–42.

Neter, J., W. Wasserman, and M. H. Kutner.
1983. Applied linear regression models, 547 p. Richard D. Irwin, Inc., Homewood, IL.

Orlando, S. P., Jr., M. B. Robblee, and C. J. Klein.
1997. Salinity characteristics of Florida Bay: a review of the archived data set (1955–1995), 33 p. Office of Ocean Resources Conservation and Assessments, NOAA, Silver Spring, MD.

Peebles, E. B., and S. G. Tolley.
1988. Distribution, growth and mortality of larval spotted seatrout, *Cynoscion nebulosus*: a comparison between two adjacent estuarine areas of southwest Florida. Bull. Mar. Sci. 42:397–410.

Phlips, E. J., and S. Badylak.
1996. Spatial variability in phytoplankton standing crop and composition in a shallow inner-shelf lagoon, Florida Bay, Florida. Bull. Mar. Sci. 58:203–216.

Powell, A. B.
2003. Larval abundance and distribution, and spawning habits of spotted seatrout, *Cynoscion nebulosus*, in Florida Bay, Everglades national Park, Florida. Fish. Bull. 101: 704–711.

Powell, A. B., D. E. Hoss, W. F. Hettler, D. S. Peters, and S. Wagner.
1989. Abundance and distribution if ichthyoplankton in Florida Bay and adjacent waters. Bull. Mar. Sci. 44:35–48.

Powell, A. B., E. H. Laban, S. A. Holt, and G. J. Holt.
2000. Validation of age estimates from otoliths of larval and juvenile spotted seatrout, *Cynoscion nebulosus*. Fish. Bull. 98:650–654.

Rice, J. A., L. B. Crowder, and M. E. Holey.
1987. Exploration of mechanisms regulating larval survival in Lake Michigan bloater: a recruitment analysis based on characteristics of individual larvae. Trans. Am. Fish. Soc. 116:481–491.

Ricker, W. E.
1975. Computation and interpretation of biological statistics of fish populations. Bull. Fish. Res. Board. Can. 191, 382 p.

Rilling, G. C., and E. D. Houde.
1999. Regional and temporal variability in growth and mortality of bay anchovy, *Anchoa mitchilli*, larvae in Chesapeake Bay. Fish. Bull. 97:555–569.

Rooker, J. R., S. A. Holt, G. J. Holt, and L. A. Fuiman.
1999. Spatial and temporal variability in growth, mortality, and recruitment potential of postsettlement red drum, *Sciaenops ocellatus*, in a subtropical estuary. Fish. Bull. 97:581–590.

Rutherford, E. S., and E. D. Houde.
1995. The influence of temperature on cohort-specific growth, survival, and recruitment of striped bass, *Morone saxatilis*, larvae in Chesapeake Bay. Fish. Bull. 93:315–332.

Rutherford, E. S., E. B. Thue, and D. G. Buker.
1982. Population characteristics, food habits and spawning activity of spotted seatrout, *Cynoscion nebulosus*, in Everglades National Park, 48 p. United States Park Service, South Florida Research Center Report T-668, Homestead, Florida.

Rutherford, E. S., T. W. Schmidt, and J. T. Tilmant.
1989. Early life history of spotted seatrout (*Cynoscion nebulosus*) and gray snapper (*Lutjanus griseus*) in Florida Bay, Everglades National Park, Florida. Bull. Mar. Sci. 44:49–64.

Secor, D. H., J. M. Dean, and E. H. Laban.
1991. Manual for otolith removal and preparation for microstructural analysis, 85 p. Belle W. Baruch Institute for Marine Biology and Coastal Research Technical Publication 1990-01.

Sogard, S. M.
1997. Size-selective mortality in the juvenile stage of teleost fishes: a review. Bull. Mar. Sci. 60:1129–1157.

Stewart, K. W.
1961. Contributions to the biology of the spotted seatrout (*Cynoscion nebulosus*) in the Everglades National Park, Florida. M.S thesis, 103 p. Univ. Miami, Coral Gables, FL.

Thayer, G. W., A. B. Powell, and D. E. Hoss.
1999. Composition of larval, juvenile and small adult fishes relative to change in environmental conditions in Florida Bay. Estuaries 22:518–533.

Tucker, J. W., Jr., and B. E Faulkner.
1987. Voluntary spawning patterns of captive spotted seatrout. Northeast Gulf Sci. 9:59–63.

Turney, W. J., and B. F. Perkins.
1972. Molluscan distribution in Florida Bay. Sedimenta III, 37 p. Rosenstiel School of Atmospheric Science, Univ. of Miami, FL.

U. S. Naval Observatory Applications Department.
1997. Fraction of the moon illuminated. [Available at http//aa.usno.navy.mil/data/docs/Moon Fraction.html.] Last accessed 17 December 2001.

Ware, D. M.
1975. Relation between egg size, growth, and natural mortality of larval fish. J. Fish. Res. Board Can. 32:2503–2512.

Warren, C. E.
1971. Biology and water pollution control, 434 p. W. B Saunders Company, Philadelphia, PA.

Abstract—Age and growth of the night shark (*Carcharhinus signatus*) from areas off northeastern Brazil were determined from 317 unstained vertebral sections of 182 males (113–215 cm total length [TL]), 132 females (111.5–234.9 cm) and three individuals of unknown sex (169–242 cm). Although marginal increment (MI) analysis suggests that band formation occurs in the third and fourth trimesters in juveniles, it was inconclusive for adults. Thus, it was assumed that one band is formed annually. Births that occur over a protracted period may be the most important source of bias in MI analysis. An estimated average percent error of 2.4% was found in readings for individuals between two and seventeen years. The von Bertalanffy growth function (VBGF) showed no significant differences between sexes, and the model derived from back-calculated mean length at age best represented growth for the species (L_∞=270 cm, K= 0.11/yr, t_0=−2.71 yr) when compared to the observed mean lengths at age and the Fabens' method. Length-frequency analysis on 1055 specimens (93–260 cm) was used to verify age determination. Back-calculated size at birth was 66.8 cm and maturity was reached at 180–190 cm (age 8) for males and 200–205 cm (age ten) for females. Age composition, estimated from an age-length key, indicated that juveniles predominate in commercial catches, representing 74.3% of the catch. A growth rate of 25.4 cm/yr was estimated from birth to the first band (i.e. juveniles grow 38% of their birth length during the first year), and a growth rate of 8.55 cm/yr was estimated for eight- to ten-year-old adults.

Manuscript approved for publication 26 June 2003 by Scientific Editor.

Manuscript received 20 October 2003 at NMFS Scientific Publications Office.

Fish. Bull. 102:156–167 (2004).

Age determination and growth of the night shark (*Carcharhinus signatus*) off the northeastern Brazilian coast

Francisco M. Santana

Rosangela Lessa

Universidade Federal Rural de Pernambuco (UFRPE)
Departamento de Pesca, Laboratório de Dinâmica de Populações Marinhas - DIMAR
Dois Irmãos, Recife-PE, Brazil, CEP 52171-900

E-mail address (for R. Lessa, contact author): rplessa@ig.com.br

The night shark (*Carcharhinus signatus*) is a deepwater coastal or semi-oceanic carcharhinid that is found in the western Atlantic Ocean along the outer continental or insular tropical and warm temperate shelves, at depths exceeding 100 meters (Bigelow and Schroeder, 1948). The species has been recorded from Delaware to Florida, the Caribbean sea (Cuba), and northern South America (Guayana) (Compagno, 1984). It has also been recorded in southern Brazil, Uruguay, and Argentina (Krefft, 1968; Compagno, 1984; Marín et al., 1998), and on the seamounts off northeastern Brazil (02°16′ to 04°05′S and 033°43′ to 037°30′W, Menni et al., 1995) where it is called "toninha."

Since 1991, tuna longline vessels have targeted the night shark in northeastern Brazil (Hazin et al., 1998) because of its highly prized fins, the increasing value of shark meat in the local market, and their relatively large abundance and accessability on seamounts (Menni et al., 1995). This species is most important in the area, making up 90% of catches over shallow banks (CPUE, in number, is 2.94/100 hook), and only 15% of catches on the surrounding deep area, yielding 0.04/100 hook (Amorim et al., 1998).

Information on this species is restricted to taxonomic descriptions (Bigelow and Schroeder 1948; Cadenat and Blache, 1981; Compagno, 1984, 1988), and some biological aspects (Guitart Manday, 1975; Hazin et al., 2000). Night sharks reach >270–280 cm maximum total length (TL) (Compagno, 1984; Branstetter, 1990). Off northeastern Brazil, females mature at 200–205 cm TL, males at 185–190 cm. Litter sizes range from 10 to 15 pups and the gestation period may last one year (Hazin et al., 2000). The assumed size-at-birth off the United States is 60–65 cm TL (Compagno, 1984; Branstetter, 1990). Age and growth have not been estimated.

The aim of this study is to present the first growth curve for *Carcharhinus signatus* from vertebral and length-frequency analyses. This information will permit the use of age-based stock assessment methods for the management of the species in the Exclusive Economic Zone (EEZ) off Brazil.

Materials and methods

Sampling data and vertebrae were collected from November 1995 to November 1999 from commercial landings (Natal, Brazil) caught in deep (Aracati, Dois Irmãos, Fundo, Sirius) and shallow (Pequeno, Leste, and Sueste) seamounts with depths between 38 to 370 m at the summits (Fig. 1).

Commercial vessels were equipped with ~30 km Japanese-style multifilament longline gear (Suzuki et al., 1977). On average, each vessel used 970–980 hook per day; mainline sets began at ~02:00 h and ended at ~06:00 h. The retrieval of gear began at noon and finished by dusk. The Brazilian sardinella (*Sardinella brasiliensis*), margined flyingfish (*Cypselurus cyanopterus*), and squid (*Loligo* sp.) were used as bait (Hazin et al., 1998).

A total of 1055 individuals, landed whole, eviscerated, or as carcasses (headless and finless), were sampled. The interdorsal space (posterior dorsal

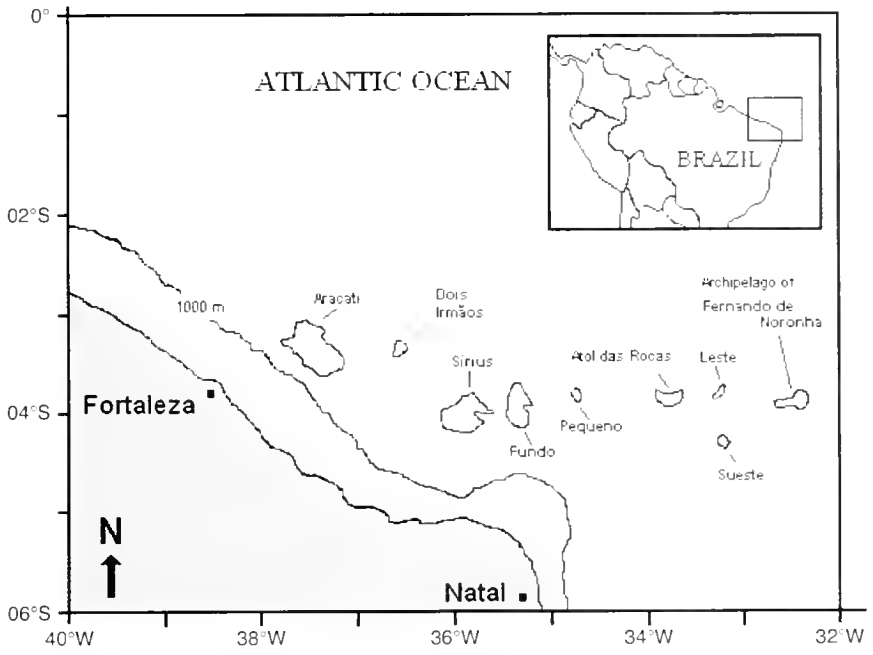

Figure 1

Location of the sampling area for the night shark (*C. signatus*) collected off northeastern Brazil.

fin base to origin of the second dorsal fin [IDS, cm]), total length (snout to a perpendicular line from the tip of the upper caudal fin [TL, cm]) and fork length (snout to fork of tail [FL, cm]) were measured. In carcasses, only IDS was measured, and IDS, FL, and TL were recorded for eviscerated or whole individuals. A set of five or six vertebrae were removed from below the first dorsal fin in 317 specimens. Total length was measured as the "natural length" (without depressing the tail) according to Garrick (1982).

To estimate TL for carcasses, relationships from subsamples of IDS versus TL and FL versus TL were established for males and females separately. Linear regressions derived for each sex were tested for homogeneity and analyzed for covariances (ANCOVA), resulting in TL=1.2049 FL + 1.7972 (r^2=0.944, n=668, P=0.41) and TL = 3.3467 IDS + 30.879 (r^2=0.824; n=764, P=0.161). Whenever length is mentioned hereafter, we always refer to TL.

Vertebrae were processed by removing excess tissue, fixed in 4% formaldehyde for 24 hours, and preserved in 70% alcohol. Each vertebra was embedded in polyester resin and the resulting block was cut to about a 1-mm thick section containing the nucleus by using a Buehler® low speed saw. Initially, alizarin-red-s stained sections (Gruber and Stout, 1983) were compared to unstained sections from the same individuals to define the best contrast for narrow and broad zones. In the first procedure, sections were immersed overnight in an aqueous solution of alizarin red s and 0.1% NaOH at a ratio of 1:9 and then rinsed in running tap water. In stained sections, narrow zones were visible as dark red and broad zones as light red, whereas in unstained sections translucent (narrow) and opaque (broad) zones were visible under transmitted light. Unstained sections produced comparable results to alizarin stained sections and were used for band observation in the study.

Bands counted in each section and distances from the focus to the margin of each narrow zone were recorded. Vertebral radius (VR) was measured by using a binocular dissecting microscope equipped with an ocular micrometer. Measurements were made at 10× magnification (1 micrometer unit=1 mm) with both reflected and transmitted light. The same reader read sections from the same specimen twice at different times without knowledge of the individual size or previous count. Whenever the counts differed between the two readings, a third reading was used for back-calculation of size-at-age.

The index of average percentage error (IAPE) (Beamish and Fournier, 1981) to compare reproducibility of age determination between readings was calculated.

$$IAPE = 1/N \sum \left(1/R \sum \left(|X_{ij} - X_j| / X_j \right) \right) \times 100,$$

where N = the number of fish aged;
R = the number of readings;
X_{ij} = the mean age of j^{th} fish at the i^{th} reading; and
X_j = the mean age calculated for the j^{th} fish.

Marginal increment (MI) analysis to determine the time of band formation was used. The analysis was restricted to 1995–97, when samples were collected every month. The distance from the final band to the vertebral's edge (MI) was expressed as a percentage of the distance between the last two bands formed on vertebrae (Crabtree and Bullock, 1998). The distance between the last and the penultimate band was divided by the distance between the nucleus and the

last band for each vertebra that was measured, and we then calculated the mean of this number for the entire sample:

$$\sum\left((R_{n-1})-R_n\right)/n = 0.13 (\mathrm{SE}=0.0009).$$

The expected distance between the last (R_n) and the penultimate (R_{n-1}) bands was estimated as a function of the distance between the vertebral nucleus and the last band (MI). The percent marginal increment (PMI) was calculated as

$$PMI = \left[MI/(0.13\times R_n)\right]\times 100.$$

Analysis of variance to test for differences in PMI by month was used. *Post-hoc* tests (Tukey honest significant differences ([HSD]) were performed to indicate which months were different.

Characterization of the vertebral edge was used to determine the time period of band formation (Carlson et al., 1999). Under reflected light, a narrow dark zone (MI 0), a narrow light zone (MI 0.1 to 0.5), and a broad light zone (MI 0.6 to 1) were observed. Absolute marginal increments (MI) were also analyzed by trimester for juveniles aged four and five years, and for adults (more than eight years) to confirm the time of translucent zone formation.

The relationship between VR and TL was calculated by sex, tested for normality, and compared by ANCOVA (Zar, 1996). The final regression in both sexes did not pass through the origin, thus suggesting that the Fraser-Lee method was the most appropriate for back-calculation (Ricker, 1969).

$$[TL]_n = (R_n/VR)([TL]-a)+a,$$

where $[TL]_n$ = the back-calculated length at age n;
R_n = vertebral radius at the time of the ring n;
VR = the vertebral radius at capture;
TL = the length at capture; and
a = the intercept on the length axis.

A von Bertalanffy growth function (VBGF) (von Bertalanffy, 1938) was fitted to back-calculated and observed length-at-age data with the following equation.

$$L_t = L_\infty\left[1-e^{-k(t-t_0)}\right],$$

where L_t = predicted length at age t;
L_∞ = mean asymptotic total length;
K = growth rate constant; and
t_0 = the age when length is theoretically zero.

To obtain parameters of VBGF, data were analyzed by using FISHPARM (Prager et al., 1987) for nonlinear least-squares parameter estimation. The Kappenman's method (1981), based on the sum of squares of the differences between observed and predicted lengths from a growth model, was used for comparing male and female growth curves. In addition, likelihood-ratio tests were used to compare parameter estimates of the von Bertalanffy equation between sexes (Cerrato, 1990).

Von Bertalanffy parameters (L_∞, K) were also estimated by the method of Fabens (1965) usually employed for recapture data and which takes into account the size at birth (L_0) instead of t_0. This method reconfigures VBGF and forces the regression through a known size at birth:

$$L_t = L_\infty(1-be^{-Kt}),$$

where $b = (L_\infty - L_0)/L_\infty$.

We used Fabens routine for growth increment data analysis of the FAO-ICLARM stock assessment tools (FISAT) program (Gayanilo et al., 1996), assuming that the time intervals ($=\Delta t$) for each size-at-age class were equal and had a periodicity identical to that obtained from the vertebral analysis.

The lengths of 1055 individuals were divided into 5-cm intervals and analyzed by the Shepherd method (1987) with the length-frequency data analysis program (LFDA). Initial values of L_∞ were based on results from maximal lengths in the sample and from literature (Compagno, 1984). K values ranging from 0.05 to 1.8 were used as input into the program, which was run repeatedly until the highest score function was obtained. The L_∞ and K values were then used to calculate t_0 (Sparre et al., 1989):

$$t_0 = t+(1/K)\left(\ln\left[L_\infty - lt\right]\right)/L_\infty).$$

Using an age-length key, based on 317 individuals for which vertebrae were read, we evaluated the age composition of the sample (Bartoo and Parker, 1983). Maximal ages in the sample were calculated by employing the inverted VBGF (Sparre et al., 1989). Further, the formula by Fabens (1965) [5(ln2)/K] for longevity estimation was used. All statistical inferences were made at a significance level of 0.05.

Results

The total sample size consisted of 1055 individuals: (551 males [93–248 cm], 499 females [110–252 cm], and 5 individuals of undetermined sex [169–260 cm]) (Fig. 2). Of these, vertebrae were removed from 317 specimens (182 males [113–215 cm], 132 females [111.5–234.9 cm], and 3 individuals of undetermined sex [169–242 cm]).

Differences in the relationship between VR and TL between sexes were not found to be significant (P=0.811). The regression for the overall sample showed a linear relationship: TL = 13.523VR + 41.824 (r^2=0.89; n=317), indicating that vertebrae are suitable structures for age determination, and methods based on direct proportion are appropriate for back-calculation.

The average percentage error, calculated between two readings, ranged from 0% to 4.5% in vertebrae with 2 to 17 bands and the average IAPE for the overall sample was 2.4%. Coefficient of variation (CV) between readings for total sample was 6.88%.

Monthly PMI analysis, for the entire sample, indicated that bands were formed from June to October, when high-

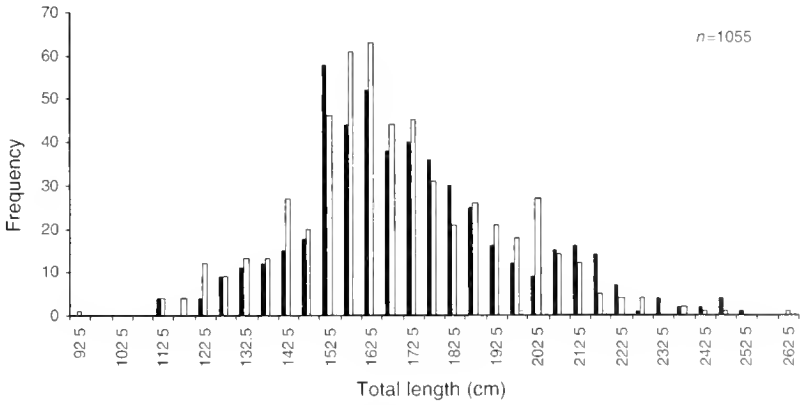

Figure 2

Length-frequency distribution for the night shark (*C. signatus*) caught off northeastern Brazil between 1995–99 (black bars=females; white bars = males; grey bars = undetermined sex).

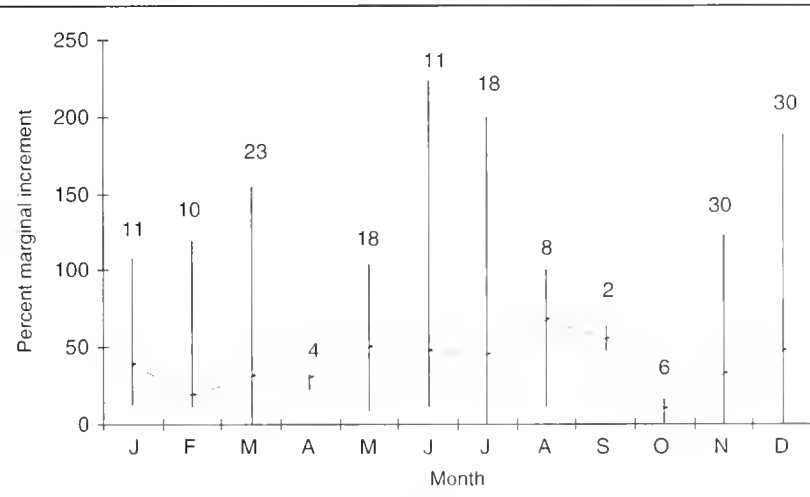

Figure 3

Percent marginal increments means (-) with the minimum and maximum values for the night shark (*C. signatus*) caught from 1995 to 1997 off northeastern Brazil (n=171). The number of individuals sampled per month is shown above the vertical bars.

est mean values are reached (Fig. 3). These values are followed by the lowest mean PMI in October, indicating that the new translucent zone forms from that point on. Monthly PMIs showed significant differences throughout the year (P=0.0463) and *post-hoc* comparisons detected differences in February, April, September, and October. Furthermore, monthly categorization of vertebral edges indicated that the highest frequency of broad light edges (MI 0.6–1) appears from July through December and narrow dark edges (MI 0) from March through December, with the exception for months of May and August (Fig. 4). Trimonthly frequency distribution of absolute marginal increments (MIs) was carried out for juveniles, revealing four and five bands, and for adults, revealing more than eight bands. For the former group, a higher number of broader increments and fully formed bands in the third and fourth trimesters were observed (Fig. 5). For adults, an unclear pattern was observerd perhaps because a smaller sample size was obtained.

Because there was no complete agreement on the time of band formation among different MI analysis for juveniles and adults, age was assigned by assuming an annual pattern of band deposition. The birth mark present in all analyzed vertebrae was not taken into account for age assignation. Under this assumption, band counts indicate relative age (years).

Mean observed lengths-at-age were higher than mean back-calculated lengths for males and females and were likely due to the strong variation in size for each age class (Table 1). The tendency of back-calculated lengths of older

Table 1

Mean back-calculated (BC) and observed length-at-age (OL) data for male and female night sharks (*C. signatus*) collected off northeastern Brazil (SD=standard deviation).

	Females		Males	
Age (yr)	BC (cm) ±SD	OL (cm) ±SD	BC (cm) ±SD	OL (cm) ±SD
0	66.8 ±1.78	—	67.3 ±1.41	—
1	91.9 ±1.31	—	92.3 ±1.37	—
2	113.4 ±2.13	122.5 ±16.93	113.3 ±1.48	120.1 ±4.21
3	128.8 ±2.21	132.9 ±9.77	128.6 ±1.54	135 ±8.91
4	142.7 ±2.41	149.8 ±7.75	142.4 ±1.94	151.5 ±9.72
5	154.7 ±2.92	160.7 ±7.21	154.5 ±2.7	157.5 ±7.86
6	165.9 ±3.46	166.8 ±10.32	166.3 ±3.25	167.5 ±8.1
7	176.8 ±3.4	179.8 ±9.56	177.4 ±2.64	177.6 ±9.34
8	185.9 ±3.71	184.9 ±9.12	187.4 ±2.22	189.8 ±6.53
9	194.8 ±3.82	197.1 ±6.49	195.8 ±2.25	199.9 ±5.26
10	202 ±4.75	208.2 ±3.89	202.4 ±2.78	204.3 ±3.13
11	206.9 ±5.56	202	209.8	212.5 ±3.54
12	215.7 ±2.4	218	—	—
13	222.2	—	—	—
14	226.9	—	—	—
15	231.7	234.4 ±0.63	—	—

fish in the early years to be systematically lower than younger ones at the same age (Lee's phenomenon) was not evident (Tables 1 and 2).

Using back-calculated lengths-at-age (Table 3), we plotted male and female growth curves separately and then tested the data; no indication of significant differences in growth was observed between sexes with both the Kapenman's (P>0.05) and likelihood ratio tests (Table 4). Data were then treated together, incorporating individuals of undetermined sex. VBGFs derived from observed length at age were not tested because of missing values in different age classes. The method of Fabens for combined sexes, fitted to back-calculated data, provided L_∞ and K, by using b = 0.781, L_0= 62.5 cm (Compagno, 1984) and, Δt = 1 year (Table 2).

Parameters from back-calculation were close to those derived from length-frequency analysis for 1055 specimens, whereas observed lengths and the Fabens method, provided the most varying parameters with lowest correlation and highest coefficients of variation (Table 2).

The smallest specimen in the vertebral sample showing two complete bands in sections was 111.5 cm, close to the estimated mean back-calculated length at age two of 113.7 cm (Table 3). Size at maturity, 185–190 cm for males and 200–205 cm for females, corresponded to 8- and 10-year-old individuals, respectively (Fig. 6). The largest and oldest specimen whose vertebrae were used, was 242 cm, which corresponded to 17-year-old individual.

A growth rate of 25.4 cm/yr was estimated from birth to the first band—a rate that corresponded to 38% of the birth length (the length at birth being 66.8 cm). Also, a mean rate of 8.55 cm/yr was calculated for 8- to 10-year-old individuals, when maturity is achieved (Table 3).

Considering mature individuals >185 cm, the age composition for the vertebral samples (n=317) indicated that 17.3% of specimens were adults (Table 5). Instead, for the total sample (n=1055), where the age ranged between 2 to ≥17 years, adults corresponded to 25.3% of the total sample

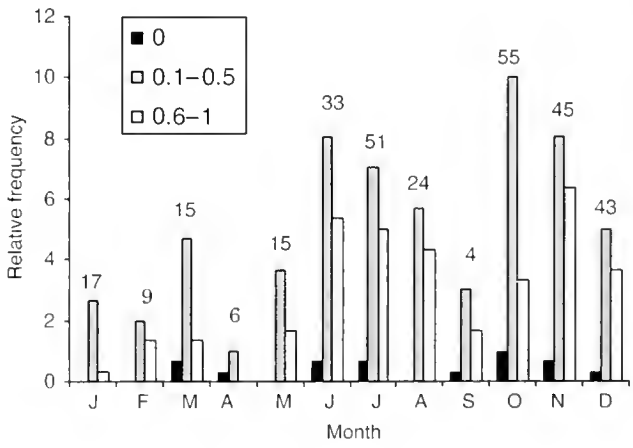

Figure 4

Categorization of edges by month for the night shark (*C. signatus*) off northeastern Brazil.

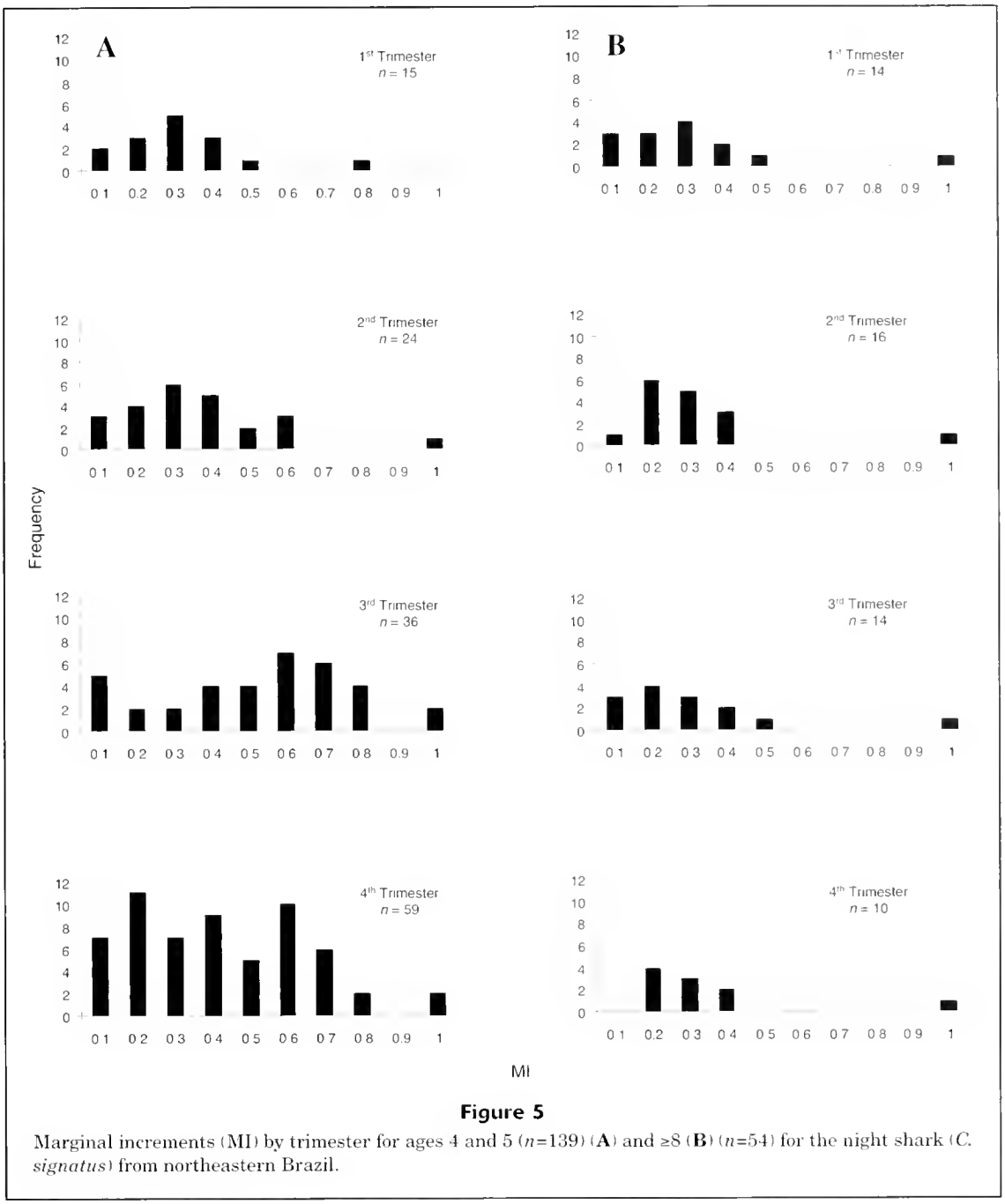

Figure 5

Marginal increments (MI) by trimester for ages 4 and 5 (n=139) (**A**) and ≥8 (**B**) (n=54) for the night shark (*C. signatus*) from northeastern Brazil.

(Fig. 7). According to the inverted back-calculated VBGF the oldest specimen in the sample was 31.7 years old (260 cm), whereas longevity was 31.5 years.

Discussion

Validating the time of band formation is considered critical when using hard parts for age estimates (Brothers, 1983), and validation is successful when growth zones are shown to form annually in all age groups of the population (Beamish and McFarlane 1983). Marginal increment analysis, carried out on younger and faster growing individuals, cannot always be used for validating older age groups, and therefore all ages must be ascertained (Brothers, 1983). In the present study, we obtained significant differences in marginal increments for the total sample. However, the significance level of the test (P=0.046) was close enough to 0.05 to cause us to suspect that the distributions could have been similar. The time of band formation varied when different age groups were analyzed separately, despite suggestions that bands are completed in the third and

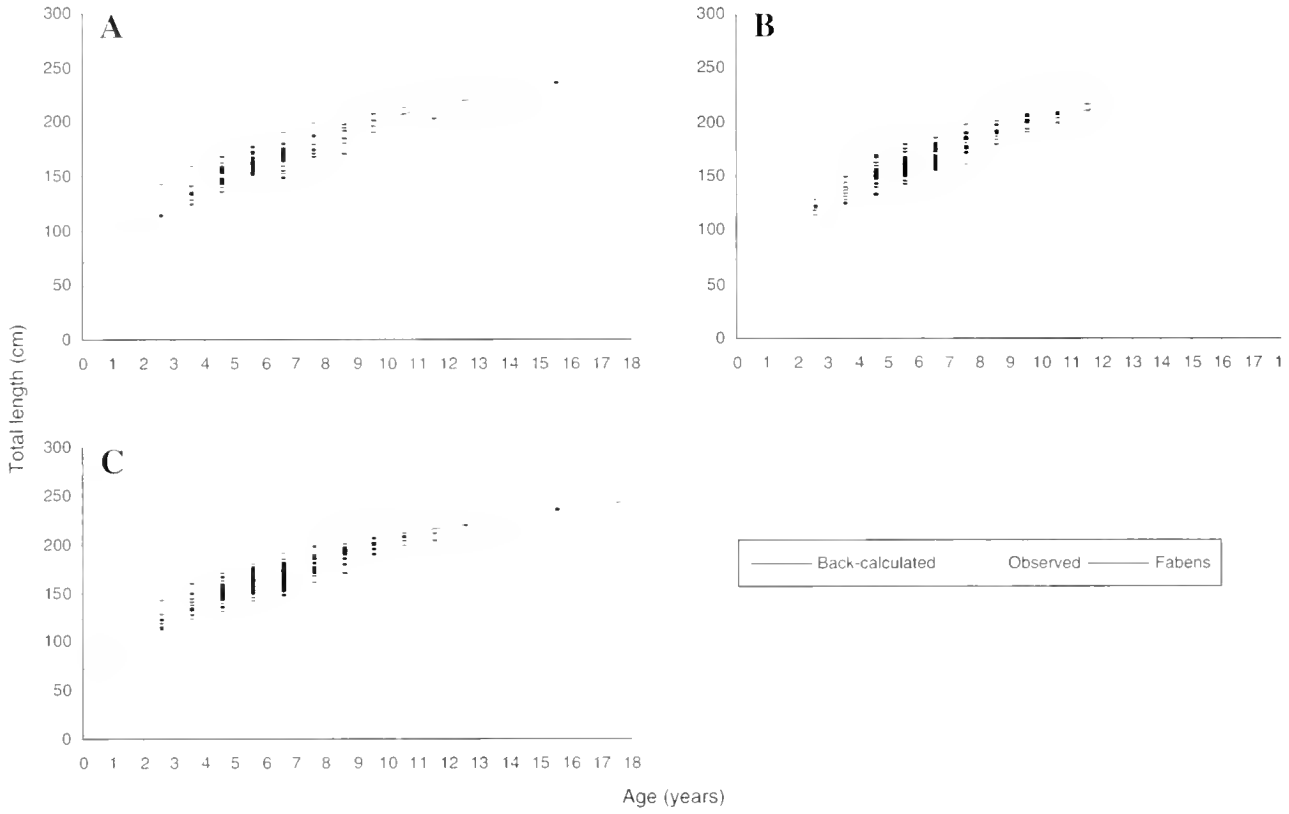

Figure 6

Growth curves generated from (**A**) females, (**B**) males, and (**C**) sexes combined for the night shark (*C. signatus*) off the northeastern Brazil.

Table 2

Von Bertalanffy parameters derived from back-calculated lengths (BC), observed lengths (OL), lengths from the Fabens method, and the length-frequency data analysis (LFDA) package for the pooled database (SE is standard error; CV is coefficient of variation).

Methods	Sex	L_∞ (cm)	SE	CV	K(/year)	SE	CV	t_0(year)	SE	CV	r^2
BC	Males	256.5	5.56	0.022	0.124	0.007	0.055	−2.538	0.119	0.047	0.999
	Females	265.4	4.15	0.016	0.114	0.005	0.045	−2.695	0.127	0.047	0.999
	Both	270	2.78	0.01	0.112	0.003	0.031	−2.705	0.099	0.037	0.999
OL	Males	306.1	37.71	0.117	0.076	0.02	0.267	−4.663	0.882	0.189	0.995
	Females	297.1	26.71	0.09	0.077	0.018	0.235	−4.853	0.977	0.201	0.99
	Both	289.9	7.6	0.026	0.085	0.006	0.077	−4.395	0.348	0.079	0.998
Fabens	Both	285.3	15.69	0.055	0.08	0.016	0.2	—	—	—	—
LFDA	Both	270.9	—	—	0.106	—	—	—	—	—	—

fourth trimesters (new bands begin to form in this period) in juveniles. Results were inconclusive for adults. For *C. obscurus* (Natanson et al., 1995), *C. plumbeus* (Sminkey and Musick 1995), *C. porosus* (Batista and Silva, 1995; Lessa and Santana, 1998), *C. acronotus* (Carlson et al., 1999), and *I. oxyrhynchus* (Lessa et al., 2000), inconclusive results for MI analysis were obtained. The inability to demonstrate the periodicity of band deposition in adult sharks

in the present study is similar to the outcome for *C. limbatus* older than four years (Wintner and Cliff, 1996). For the last mentioned species, the problem was circumvented by restricting MI analysis to juveniles (Killam and Parsons, 1989).

Age was assigned by assuming an annual pattern of deposition, as commonly occurs for most carcharhinids like *C. brevipinna* and *C. limbatus*, *Rhizoprionodon terraenovoe* (Branstetter et al., 1987; Branstetter and Stiles, 1987), *Negaprion brevirostris* (Gruber and Stout, 1983), and *C. longimanus* (Seki et al., 1998; Lessa et al., 1999c). Three sources of bias generally occur with MI analysis: 1) sample sizes are small for any particular month or for any age class (Cailliet, 1990); 2) data are collected over a too long a period causing variability on account of annual marks that are not formed at the same time (Brothers, 1983) and 3) births occur over a long period (Brothers, 1983). All these may have biased MI analysis in the present study.

Research carried out in the study area by Hazin et al. (2000) indicated that copulation takes places throughout the austral summer. Embryos measuring 10 to 40 cm were collected in February, whereas 31.8 to 37.2 cm embryos were found in June. This remarkable variability in embryo size during the gestation period suggests that birth period lasts several months. Furthermore, with an estimated back-calculated birth length of 66.8 cm, individuals measuring ~40 cm in February will be born long before individuals that measured 37.2 cm in June. Such a protracted parturition period could lead to differences in MI of the same cohort. Thus, after an assumed ~12 months gestation period, individuals are born with birth dates varying by several months. Moreover, no significant differences in MI analysis was found for *C. porosus* and *I. oxyrhynchus*, which also have a protracted birth seasons (Lessa et al., 1999a, 1999b).

A comparison of growth model parameters by using known size information, such as size-at-birth and maximum observed size, can be

Table 3

Back-calculated and observed length-at-age data (cm) for combined sexes of the night shark (*C. signatus*) caught off northeastern Brazil. Numbers in parentheses are the number of individuals examined for each category of band count.

		Vertebral band count																
Age (yr)	*n*	0 (317)	1 (317)	2 (317)	3 (307)	4 (285)	5 (236)	6 (146)	7 (80)	8 (54)	9 (31)	10 (16)	11 (7)	12 (4)	13 (3)	14 (3)	15 (3)	16 (1)	17 (1)
Back calculated																			
2	10	65.1	90	112.1															
3	22	65.7	90.9	112.8	127.1														
4	49	57.8	93.5	115.4	130.9	144.2													
5	90	67.6	92.5	113.8	128.9	142.1	154												
6	66	67.6	91.6	112.1	126.7	139.7	151.6	162.3											
7	26	68.2	92.2	113.2	128.2	141.3	153.4	164.6	174.7										
8	23	68.5	92.6	113.4	128.2	141.9	153.9	165.3	175.9	185.1									
9	15	67.8	93.3	114.4	130.1	143.9	156	167.5	178.1	187.7	196.3								
10	9	67.1	93.2	112.9	127.9	141.5	153.6	165	175.7	185.6	194.3	201.6							
11	3	66.9	93	112.4	128.5	143.4	157.3	169	178.4	187	194.2	201.4	206.7						
12	1	64.3	90.8	110.7	129.2	143.8	155.7	167.7	178.3	187.5	195.5	202.1	208.7	214					
15	2	66.3	91.5	115.3	131	145.9	159.6	171.8	182.1	190.2	197.7	205.2	211.3	217.4	222.2	226.9	231.7		
17	1	65.5	93.3	119.7	133.6	146.1	157.2	168.3	179.4	189.2	198.9	207.2	214.2	219.8	225.3	229.5	233.7	237.8	240.6
Mean		66.8	92.2	113.7	129.2	143.1	155.2	166.8	177.8	187.5	196.1	203.5	210.2	217.1	223.8	228.2	232.7	237.8	240.6
SD		1.316	1.127	2.224	1.924	1.978	2.358	2.833	2.362	1.83	1.896	2.603	3.229	2.882	2.213	1.796	1.376	—	—
Observed																			
Mean		—	—	120.9	133.9	150.7	159	167.4	177.8	188.3	199	205.2	209	218	—	—	234.4	—	242
SD		—	—	8.765	9.185	8.803	7.688	9.003	9.354	7.556	5.641	3.509	6.557	0	—	—	0.629	—	0

Table 4

Likelihood ratio tests comparing estimates of von Bertalanffy parameters for males (noted as 1) and females (noted as 2) for *C. signatus* in the linear constraints.

Hypothesis	Linear constraints	Residual SS	χ^2_r	df	P
HΩ	none	60536.4			
Hω1	$L_{\infty 1} = L_{\infty 2}$	10511	0.049	1	0.996
Hω2	$K_1 = K_2$	10524.3	0.047	1	0.996
Hω3	$t_{01} = t_{02}$	10205.6	0.122	1	0.999
Hω4	Same L_∞, K, and t_0	24301.2	0.164	3	0.973

useful as a method of verification (Cailliet et al., 1983). Although no specimens younger than 2-years-old were caught (perhaps due to the gear selection bias), the presumed size at birth was about 60–65 cm (Compagno, 1984), which is similar to the estimated size in the present study (66.8 cm). Also, the estimated L_∞ value (270 cm), derived from the back-calculated or observed VBGF is close to the maximum size of 276 cm mentioned by Bigelow and Schroeder (1948), 280 cm off Cuba (Compagno, 1984), and 275 cm by Garrick (1985).

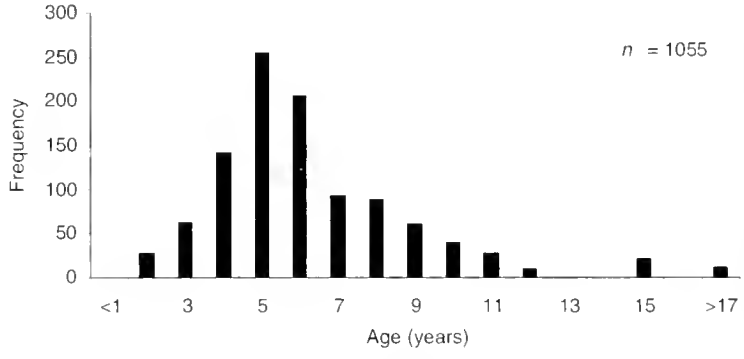

Figure 7

Age composition for the night shark (*C. signatus*) collected off northeastern Brazil.

Mean observed length-at-age is generally higher than back-calculated mean length-at-age (Bonfil et al., 1993; Lessa and Santana, 1998), leading to lower values of L_∞ and higher values of K. However, in the present study, although mean observed length-at-age is higher than mean back-calculated lengths, parameters derived from back-calculation provided a lower L_∞ and a higher K value. Inconsistency of the observed length-at-age set is attributed to the missing values in for ages 0, 1, 13, 14, and 16. This led to a VBGF which provided an unrealistic birth size of 90 cm and which present a flatter shape than the back-calculated curve.

Von Bertalanffy growth parameters generated from both back-calculation and by the Fabens method were all considered suitable and were of the same magnitude. However, taking into account 1) parameters close to those derived for length-frequency analysis, and 2) the best statistical fit, the back-calculated VBGF was chosen as best representing growth in the species.

Comparisions of biological features such as maturity size and maximum sizes have been used for inferences in growth and to explain differences between sexes (Natanson et al., 1995; Natanson and Kohler, 1996; Lessa et al., 2000). The studied species shows a disparity of ~15 cm in maturity sizes between sexes (Hazin, et al., 2000), corresponding to ~2 years. In addition, the largest specimen, for which sex was determined, was a 252-cm female and the largest male was 248 cm. These disparities, however, did not bring about differences in growth between sexes, as indicated by results of both tests used. Such a result can be explained by the number of juveniles used for age determination (~83%). Thus, the number of adults was not high enough to bring about any differences in the growth equation although differences frequently occur after maturity, caused by different growth rates between sexes (Natanson et al., 1995; Sminkey and Musick, 1995).

Assuming that the time elapsed between birth and the band corresponding to age 1 is one year, the species grows 38% of its birth length during the first year. This growth rate is close to that (50%) generally assumed (Branstetter 1990; Cortés, 2000). Furthermore, the estimated K value falls within the range suggested by the first author, and according to him, the night shark is a relatively fast growing species, presenting a life strategy similar to that of *C. falciformis*, and apparently depending on rapid growth for adequate neonate survival due to vulnerability to predation from large sharks.

In summary, considering the increasing fishing effort on the night shark as a targeted species and that catches are mainly composed by juveniles (representing 74.7% of specimens in landings), we believe that the K-selected characteristics of the species (including late maturity, long gestation period, and low fertility) should be taken into account in determining the management of this resource. Demographic analyses will be required for the examination of consequences of current levels of exploi-

Table 5

Age-length key (in percentages) for the night shark (*C. signatus*) caught off northeastern Brazil. Numbers in parentheses are the number of individuals examined in each age class.

		Age (years)															
TL (cm)	*n*	2 (10)	3 (22)	4 (49)	5 (90)	6 (66)	7 (26)	8 (23)	9 (15)	10 (9)	11 (3)	12 (1)	13 —	14 —	15 (2)	16 —	17 (1)
112.5	3	100	—	—	—	—	—	—	—	—	—	—	—	—	—	—	—
117.5	1	100	—	—	—	—	—	—	—	—	—	—	—	—	—	—	—
122.5	6	66.7	33.3	—	—	—	—	—	—	—	—	—	—	—	—	—	—
127.5	8	12.5	87.5	—	—	—	—	—	—	—	—	—	—	—	—	—	—
132.5	9	—	66.7	33.3	—	—	—	—	—	—	—	—	—	—	—	—	—
137.5	5	—	60	40	—	—	—	—	—	—	—	—	—	—	—	—	—
142.5	11	9.1	9.1	63.6	18.2	—	—	—	—	—	—	—	—	—	—	—	—
147.5	16	—	12.5	62.5	12.5	12.5	—	—	—	—	—	—	—	—	—	—	—
152.5	42	—	—	28.6	61.9	9.5	—	—	—	—	—	—	—	—	—	—	—
157.5	39	—	2.6	20.5	56.4	20.5	—	—	—	—	—	—	—	—	—	—	—
162.5	37	—	—	8.1	51.4	37.8	2.7	—	—	—	—	—	—	—	—	—	—
167.5	26	—	—	15.4	34.6	34.6	11.5	3.8	—	—	—	—	—	—	—	—	—
172.5	29	—	—	—	20.7	48.3	31	—	—	—	—	—	—	—	—	—	—
177.5	21	—	—	—	19	52.4	14.3	14.3	—	—	—	—	—	—	—	—	—
182.5	9	—	—	—	—	33.3	33.3	33.3	—	—	—	—	—	—	—	—	—
187.5	12	—	—	—	—	8.3	41.7	41.7	8.3	—	—	—	—	—	—	—	—
192.5	8	—	—	—	—	—	—	62.5	37.5	—	—	—	—	—	—	—	—
197.5	12	—	—	—	—	—	16.7	50	25	8.3	—	—	—	—	—	—	—
202.5	7	—	—	—	—	—	—	—	71.4	14.3	14.3	—	—	—	—	—	—
207.5	9	—	—	—	—	—	—	—	33.3	66.7	—	—	—	—	—	—	—
212.5	2	—	—	—	—	—	—	—	—	50	50	—	—	—	—	—	—
217.5	2	—	—	—	—	—	—	—	—	—	50	50	—	—	—	—	—
222.5	—	—	—	—	—	—	—	—	—	—	—	—	—	—	—	—	—
227.5	—	—	—	—	—	—	—	—	—	—	—	—	—	—	—	—	—
232.5	2	—	—	—	—	—	—	—	—	—	—	—	—	—	100	—	—
237.5	—	—	—	—	—	—	—	—	—	—	—	—	—	—	—	—	—
>242.5	1	—	—	—	—	—	—	—	—	—	—	—	—	—	—	—	100

lation to ensure the sustainability of the night shark in northeastern Brazil.

Acknowledgments

The present research was funded by Ministério do Meio Ambiente-MMA, Secretaria da Comissão Interministerial para os Recursos do Mar-SECIRM in the scope of Programa Nacional de Avaliação do Potencial Sustentável de Recursos Vivos–REVIZEE. We are grateful to Norte Pesca S. A. and to Conselho Nacional de Desenvolvimento Científico e Tecnológico-CNPq for scholarships and research grants (Procs: 301048/83, 38.0726/96-3 and 820652/87-3).

Literature cited

Amorim, A. F., C. A. Arfelli, and L. Fagundes.
1998. Pelagic elasmobranchs caught by longliners off Southern Brazil during 1974–97: an overview. Mar. Freshw. Res., 49:621–632.

Batista, V. S., and T. C. Silva.
1995. Age and growth of juveniles of junteiro shark *Carcharhinus porosus* in the coast of Maranhão, Brazil. Rev. Bras. de Biol. 55 (suppl. 1):25–32.

Bartoo, N. V., and K. E. Parker.
1983. Reduction of bias generated by age-frequency estimation using the von Bertalanffy growth equation. *In* Proceedings of the international workshop on age determination of oceanic pelagic fishes: tunas, billfishes, and sharks (E. D. Prince and L. M. Pulos, eds.), p. 25–26. NOAA Technical Report NMFS 8.

Beamish, R. J., and D. A. Fournier.
1981. A method for comparing the precision of a set of age determinations. Can. J. Fish. Aquat. Sci., 38: 982–983.

Beamish, R. J., and G. A. McFarlane.
1983. Validation of age determination estimates: The forgotten requirement. *In* Proceedings of the international workshop on age determination of oceanic pelagic fishes: tunas, billfishes, and sharks (E. D. Prince and L. M. Pulos, eds.), p. 29–33. NOAA Technical Report NMFS circular 8.

Bigelow, H. B., and W. C. Schroeder.
1948. Fishes of the western North Atlantic, lancelets, cyclostomes, sharks, 576 p. Memoirs of Sears Foundation for Marine Research 1.

Bonfil, R., R. Mena, and D. Anda.
1993. Biological Parameters of Commercially Exploited Silky Shark, *Carcharhinus falciformis*, from the Campeche Bank, Mexico. NOAA Technical Report NMFS 115:73–76.

Branstetter, S.
1990. Early life-history implications of selected carcharhinoid and lamnoid sharks of the northwest Atlantic. *In* Elasmobranchs as living resources: advances in the biology, ecology, systematics, and the status of the fisheries (H. Pratt, S. Gruber, and T. Taniuchi, eds.), 17–28. NOAA Technical Report NMFS 90.

Branstetter, S., J. A. Musick, and J. A. Colvocoresses.
1987. A comparison of the age and growth of the tiger shark, *Galeocerdo cuvieri*, from off Virginia and from the northwestern gulf of Mexico. Fish. Bull. 85:269–279.

Branstetter, S., and R. Stiles.
1987. Age and growth estimates of the bull shark, *Carcharhinus leucas*, from Northern Gulf of Mexico. Environ. Biol. Fish. 20(3):169–181.

Brothers, E. B.
1983. Summary of round table discussions on age validation. *In* Proceedings of the international workshop on age determination of oceanic pelagic fishes: tunas, billfishes, and sharks (E. D. Prince, L. M. Pulos, eds.), p. 35–44. NOAA Technical Report NMFS 8.

Cadenat J., and J. Blache.
1981. Requins de Méditerranée et d Atlantique. Faune tropicale, 330 p. ORSTOM (Office de Recherche Scientifique et Technique d'Outre-Mer) 21.

Cailliet, G.
1990. Elasmobranch age determination and verification: an updated review. *In* Elasmobranchs as living resources: advances in biology, ecology, systematics and the status of the fisheries (H. L. Pratt Jr., S. H. Gruber, and T. Taniuchi, eds.), p. 157–165. NOAA Technical Report NMFS 90.

Caillet, G., K. L. Martin, D. Kusher, P. Wolf, and B. A. Welden.
1983. Techniques for enhancing vertebral bands in age estimation of California elasmobranchs. *In* Proceedings of the international workshop on age determination of oceanic pelagic fishes: tunas, billfishes, and sharks (E. D. Prince, L. M. Pulos, eds.), p. 157–165. NOAA Technical Report NMFS 8.

Carlson, J. K., E. Cortés, and A. G. Johnson.
1999. Age and growth of the blacknose shark *Carcharhinus acronotus* in the eastern Gulf of Mexico. Copeia 1999(3): 684–691.

Cerrato, R. M.
1990. Interpretable statistical tests for growth comparisons using parameters in the von Bertalanffy equation. Can. J. Fish. Aquat. Sci. 47(7):1416–1426.

Compagno, L. J. V.
1984. FAO species catalogue. Vol. 4: Sharks of the world, Part 2: Carcharhiniformes. FAO Fisheries Synopsis 125: 251–655. FAO, Rome.
1988. Sharks of the order Carcharhiniformes, 486 p. Princeton Univ. Press, Princeton, NJ.

Cortes, E.
2000. Life history and correlations in sharks. Rev. Fish. Sci. 8(4):299–344.

Crabtree, R. E., and L. H. Bullock.
1998. Age, growth, and reproduction of black grouper, *Mycteroperca bonaci*, in Florida waters. Fish. Bull. 96: 735–753.

Fabens, A. J.
1965. Properties and fitting of the von Bertalanffy growth curve. Growth 29:265–289.

Gayanilo, F. C. Jr., P. Sparre, and D. Pauly.
1996. FAO ICLARM stock assessment tools. User's manual. FAO computerized information series (Fisheries) 8, 126 p and 3 diskettes. FAO, Rome.

Garrick, J. A. F.
1982. Sharks of the genus *Carcharhinus*. NOAA Tech. Rep. NMFS circular, 194 p.
1985. Additions to a revision of the shark genus *Carcharhinus*: Synonymy of the *Aprionodon* and *Hypoprion* and descriptions of as new species of Carcharhinus (Carcharhinidae). NOAA Tech. Rep. NMFS 34, 26 p.

Gruber, S., and R. Stout.
1983. Biological materials for the study of age and growth in tropical marine elasmobranch, the lemon shark, *Negaprion brevirostris* (Poey). *In* Proceedings of the international workshop on age determination of oceanic pelagic fishes: tunas, billfishes, and sharks (E. D. Prince, and L. M. Pulos, eds.), 193–205. NOAA Technical Report NMFS 8.

Guitart Manday, D.
1975. Las pesquerias pelago-oceanicas de corto radio de acción en la région noroccidental de Cuba. ser. Oceanol. Acad. Cienc. Cuba 31, 26 p.
Hazin, F. H. V., J. R. Zagaglia, M. Broadhurst, P. Travassos, and T. R. Q. Bezerra.
1998. Review of a small-scale pelagic longline fishery off northeastern Brazil. Mar. Fish. Rev. 60(3):1–8.
Hazin, F. H., F. Lucena, T. S. L. Souza, C. Boeckman, M. Broadhurst, and R. Menni.
2000. Maturation of the night shark, *Carcharhinus signatus*, in the south-western equatorial Atlantic Ocean. Bull. Mar. Sci. 66(1):173–185.
Kappenman, R. F.
1981. A method for growth curve comparisons. Fish. Bull. 79:95–101.
Killam, K. A., and G. R. Parsons.
1989. Age and growth of the blacktip shark, *Carcharhinus limbatus*, near Tampa Bay, Florida. Fish. Bull. 87:845–857.
Krefft, G.
1968. Neue und erstmalig nachgewiesene Knorpelfische aus dem Archibenthal des Südwestatlantiks, einsliesslich einer Diskussion einiger *Etmopterus*-Arten Südlicher Meere. Arch. Fischereiwiss. 19(1):1–72.
Lessa, R., and F. M. Santana.
1998. Age determination and growth of the smalltail shark *Carcharhinus porosus* from northern Brazil. Mar. Freshw. Res. 49:705–711.
Lessa, R., V. Batista, and Z. Almeida.
1999a. Occurrence and biology of the daggernose shark *Isogomphodon oxyrhynchus* (Chondrichthyes: Carcharhinidae) off the Maranhão Coast (Brazil). Bull. Mar. Sci. 64(1):115–128.
Lessa, R., F. Santana, R. Menni, and Z. Almeida.
1999b. Population structure and reproductive biology of the smalltail shark (*Carcharhinus porosus*) off Maranhão. Mar. Freshw. Res. 50:383–388.
Lessa, R., F. M. Santana, and R. Paglerani.
1999c. Age, growth and stock structure of the oceanic whitetip shark, *Carcharhinus longimanus*, from the southwestern Equatorial Atlantic. Fish. Res. 42:21–30.
Lessa, R., F. M. Santana, V. Batista, and Z. Almeida.
2000. Age and growth of the daggernose shark, *Isogomphodon oxyrhynchus*, from northern Brazil. Mar. Freshw. Res. 51:339–347.
Marín, Y., F. Brum, L. F. Barea, and J. F. Chocca.
1998. Incidental catch associated with swordfish longline fisheries on the South-West Atlantic Ocean. Mar. Freshw. Res. 49:633–639.
Menni, R. C., F. H. V. Hazin, and R. P. Lessa.
1995. Occurrence of the night shark *Carcharhinus signatus*, and the pelagic stingray *Dasyatis violacea* off northeastern Brazil. Neotropica 41(105–106):105–110.
Natanson, L. J., J. G. Casey, and N. E. Kohler.
1995. Age and growth estimates for the dusky shark, *Carcharhinus obscurus*, in the western North Atlantic Ocean. Fish. Bull. 93:116–126.
Natanson, L. J., and N. E. Kohler.
1996. A preliminary estimate of age and growth of the dusky shark *Carcharhinus obscurus* from the South-West Indian Ocean, with comparisons to the Western North Atlantic population. S. Afr. J. Mar. Sci. 17: 217–224.
Prager, M. M., S. B. Saila, and C. M. Recksiek.
1987. FISHPARM: a microcomputer program for parameter estimationof nonlinear models in fishery science. Technical Report. 870:1–37. Dep. Oceanography, Old Dominion Univ., Norfolk, VA.
Ricker, W. E.
1969. Effects of size-selective mortality and sampling bias on estimates of groowth, mortality, production and yield. J. Fish. Res. Board Can. 26(3):479–541.
Seki, T., T. Taniuchi, H. Nakano, and M. Shimizu.
1998. Age, growth and reproduction of the oceanic whitetip shark, *Carcharhinus longimanus* from the Pacific Ocean. Fish. Sci. 64(1):14–20.
Shepherd, J. G.
1987. A weakly parametric method for estimating growth parameters from length composition data. *In* Length-based methods in fisheries research. ICLARM (International Center for Living Resources Management) conference proceedings 13 (D. Pauly and G. Morgan, eds.), p. 113–119. ICLARM, Manila, and the Kuwait Institute for Scientific Research, Safat, Kuwait.
Sminkey, T. R., and J. A. Musick.
1995. Age and growth of the sandbar shark, *Carcharhinus plumbeus*, before and after population depletion. Copeia 1995(4):871–883.
Sparre, P., E. Ursin, and S. C. Venema.
1989. Introduction to tropical fish stock. Part 1. Manual. FAO Fisheries Tech. Paper 306.1, 337 p. FAO, Rome.
Suzuki, Z., Y. Warashima, and M. Kishida.
1977. The comparison of catches by regular and deep tuna longline gear in the western and central equatorial Pacific. Bull. Far Seas Fish. Res. Lab. 15:51–89.
von Bertalanffy, L.
1938. A quantitative theory of organic growth. Hum. Biol. 10:181–213.
Wintner, S., and G. Cliff.
1996. Age and growth determination of the blacktip shark, *Carcharhinus limbatus*, from the east coast of South Africa. Fish. Bull. 94:135–144.
Zar, J. H.
1996. Biostatistical analysis, 3rd ed., 662 p. Prentice Hall, Upper Saddle River, NJ.

Distribution and biology of prowfish (*Zaprora silenus*) in the northeast Pacific

Keith R. Smith
David A. Somerton
Mei-Sun Yang
Daniel G. Nichol
Alaska Fisheries Science Center
National Marine Fisheries Service
7600 Sand Point Way NE
Seattle, Washington 98115
E-mail address (for K. R. Smith, contact author) Keith.Smith@noaa.gov

Abstract—The prowfish (*Zaprora silenus*) is an infrequent component of bottom trawl catches collected on stock assessment surveys. Based on presence or absence in over 40,000 trawl catches taken throughout Alaskan waters southward to southern California, prowfish are most frequently encountered in the Gulf of Alaska and the Aleutian Islands at the edge of the continental shelf. Based on data from two trawl surveys, relative abundance indicated by catch per swept area reaches a maximum between 100 m and 200 m depth and is much higher in the Aleutian Islands than in the Gulf of Alaska. Females weigh 3.7% more than males of the same length. Weight-length functions are W (g) = 0.0164 $L^{2.92}$ (males) and W = 0.0170 $L^{2.92}$ (females). Length at age does not differ between sexes and is described by $L = 89.3(1 - e^{-0.181(t+0.554)})$, where L is total length in cm and t is age in years. Females reached 50% maturity at a length of 57.0 cm and an age of 5.1 years. Prowfish diet is almost entirely composed of gelatinous zooplankton, primarily scyphozoa and salps.

Manuscript approved for publication 20 September 2003 by Scientific Editor.
Manuscript received 20 October 2003 at NMFS Scientific Publications Office.
Fish. Bull. 102:168–178 (2004).

Current taxonomy distinguishes the prowfish (*Zaprora silenus*, Fig. 1) as the only species and the only genus of the family Zaproridae. Other families in the encompassing suborder Zoarcoidei include Bathymasteridae (ronquils), Cryptacanthodidae (wrymouths), Pholidae (gunnels), and Stichaeidae (pricklebacks). Systematics of most families within Zoarcoidei, and of the suborder itself within the order perciforms, is uncertain (Nelson, 1994). Prowfish (adult) physical features include an elongate, laterally compressed body; a high convex brow and interorbital area ending with a short blunt snout; and a distinctive protruding area below a slightly upturned terminal mouth. Fins consist of: a long, moderately high dorsal fin; a moderately long anal fin; a discrete truncate caudal fin with a short, broad peduncle; and moderately large, rounded pectoral fins (pelvic fins are absent). Teeth are small, sharp, and close-set in a single row attached only to the jaws. Scales are ctenoid. Numerous distinctive large round pores occur on the sides and top of the head. Color is olive-gray to brown dorsally, shading lighter below, suffused on the sides and back with many small dark spots (Clemens and Wilby, 1961; Eschmeyer et al, 1983; Hart, 1973; Kessler, 1985). The maximum length reported is more than 1 m (Tokranov, 1999).

Since its original description (Jordan, 1897), the prowfish has been observed infrequently despite numerous and extensive bottom trawl surveys comprising thousands of net deployments off Alaska and the west coast of North America. It is not clear whether this lack of documentation indicates a species of low abundance or a preference by prowfish for a habitat, such as rough rock substrate or steep bottom gradients, that is poorly sampled by bottom trawl surveys. Nevertheless, the species is common enough to be considered representative of the ichthyofauna of certain benthic biotopes within its range (Allen and Smith, 1988; Tokranov, 1999). It has been encountered at locations along the outer continental shelf and upper slope ranging in a long arc from San Miguel Island, California, north through the Gulf of Alaska, west through the Bering Sea and Aleutian Islands to the Asiatic shelf, thence south to Hokkaido, at depths of 10–675 m (Allen and Smith, 1988; Hart, 1973). In addition to occurring in the catches on biological surveys, prowfish have been taken incidentally, and occasionally processed, in commercial fishing operations on the outer continental shelf (Smith, pers. obs.; Berger[1]).

Prowfish are known to be pelagic as pre-adults (Hart, 1973; Doyle et al, 2002). After larval transformation at 30 mm (Matarese et al., 1989), juveniles maintain close proximity to the medusae of pelagic cnidarians (Scheffer, 1940). Brodeur (1998) observed juveniles swimming near the bells of scyphomedusae *Cyanea capillata* and *Chrysaora melanaster* and retreating

[1] Berger, J. 2002. Personal commun. Alaska Fisheries Science Center, National Marine Fisheries Service, 7600 Sand Point Way NE, Bldg 4, Seattle, WA 98115-0070.

Figure 1

Aquarium prowfish specimen, National Marine Fisheries Service, Kodiak Laboratory, Kodiak, AK. Photograph by Jan Haaga.

behind the tentacles or within the bells of these jellyfish when approached by a remotely operated vehicle, apparently as a means of protection from predators. Prowfish are also believed to later become demersal and have a preference for rocky areas (Tokranov, 1999).

The association with scyphomedusae and other large gelatinous zooplankton exhibited by juveniles may continue throughout their lives, because such prey are reported to constitute a considerable portion of the prowfish diet (Carollo and Rankin, 1998). In the stomachs of 16 juveniles of 5–13.3 cm total length captured at midwater depths in Prince William Sound in 1995, Sturdevant[2] found prey biomass was composed principally of hyperiid amphipods but also found unquantifiable gelatinous matter which was thought to be the remains of jellyfish tentacles.

Little is known regarding possible predators of prowfish, the relative frequency of prowfish among prey items, or the sizes of prowfish consumed. Prowfish have been found in the diets of diving seabirds and have comprised 25% of food biomass delivered to tufted puffin (*Lunda cirrhata*) chicks (Sturdevant[2]). Yang (1993) found prowfish in only 0.3% of 467 stomachs of Pacific halibut (*Hippoglossus stenolepis*) taken by bottom trawl in the Gulf of Alaska in 1990, accounting for 0.03% (by weight) of total food present. Orlov (1998) found prowfish in 0.13% of stomachs of white-blotched skate (*Bathyraja maculata*) caught by bottom trawl off the Northern Kuril Islands and Southeastern Kamchatka in 1996. In comparisons of proximate composition among 17 taxa of forage-size fish from the northeastern Pacific (Van Pelt et al, 1997; Payne et al, 1999), juvenile prowfish averaged highest in moisture content (86–88% by weight) and relatively low in lipids (10.8±1.3%, dry weight analysis).

In this study we examined information on this little-known species, investigating spatial and depth distributions, size frequency, growth, reproduction, and diet in the waters off Alaska.

Materials and methods

Data and sample collection

Data used in this investigation were collected during bottom trawl surveys for groundfish and invertebrate stocks conducted by the Resource Assessment and Conservation Engineering (RACE) Division of the Alaska Fisheries Science Center (AFSC), National Marine Fisheries Service. Areas surveyed were the continental shelf and upper slope of the eastern Bering Sea, Aleutian Islands region (AI), Gulf of Alaska (GOA), and west coast of North America from Washington to California. Trawl catches were sorted to species, weighed, and individuals were counted, following procedures described in Wakabayashi et al. (1985).

[2] Sturdevant, M. V. 1999. Forage fish diet overlap, 1994–1996. *Exxon Valdez* oil spill restoration project final report (restoration project 97163C), 184 p. Alaska Fish. Sci. Cent., Auke Bay Laboratory, Natl. Mar. Fish. Serv., NOAA, Juneau, AK. [Available by order no. PB2000-100700 from Natl. Tech. Info. Serv, 5285 Port Royal Rd., Springfield, Virginia 22161.]

To characterize prowfish distribution we obtained catch data from 42,601 bottom trawl deployments (hauls) executed from 1953 through 2000 using a variety of net designs. We used these data to determine presence or absence of prowfish at each haul location. Previous observations have indicated that prowfish tend to be pelagic as larvae and become demersal as adults (Matarese et al., 1989; Hart, 1973). A full accounting of prowfish distribution by life stage is beyond the scope of this investigation, which focuses on adults. Therefore we confined our observations to haul catches taken on bottom, as opposed to in mid-water or at the surface.

On two of the bottom trawl surveys, one in the Gulf of Alaska from 22 May to 30 July 1996, and the other in the Aleutian Islands from 10 June to 11 August 1997, additional prowfish data were collected. Consistency between these surveys in sampling procedures and equipment (Martin, 1997, and Stark[3]) facilitated subsequent data comparisons.

Density of prowfish at each sampling location was estimated as the number caught divided by the km^2 of area swept by the trawl (catch per unit of effort, or CPUE). Research vessels on both surveys employed the standard RACE Division model poly-Nor'eastern high-opening bottom trawl net with roller gear, and hauls were made during daylight. Net configuration and bottom contact during trawling were monitored by Scanmar instrumentation. Data were obtained from 807 hauls in the Gulf of Alaska and 408 hauls in the Aleutian Islands. The average area swept per haul was 0.025 km^2 in the GOA and 0.024 km^2 in the AI.

All prowfish were sorted to sex by examination of the gonads and then length (total length; cm) was measured. Sample sizes were 84 males and 90 females for the Gulf of Alaska; 396 males and 431 females for the Aleutian Islands. Whole-body weights (g) of 83 male and 88 female prowfish from the Gulf of Alaska were measured and the sagittal otoliths were removed and stored in 50% ethanol. Whole ovaries from a representative subsample of 39 of the females were removed, frozen, and later stored in 10% buffered formalin solution.

Diet composition was examined from stomach contents of 76 individuals (18 from the Gulf of Alaska and 58 from the Aleutian Islands). Stomachs containing food and with no signs of regurgitation or net-feeding (e.g. the stomach was in an inverted or flaccid state or there was the presence of prey in the mouth or around the gills) were removed and preserved in 10% buffered formalin.

Laboratory procedures

Standard otolith-preparation techniques for age determination were modified to accommodate the relatively small size of prowfish otoliths (usually <5 mm long). An anterior portion of each otolith was removed by a transverse cut with scalpel perpendicular to the sagittal axis and anterior to the nucleus. The remainder, which contained the nucleus, was baked at 300–475°C for up to 17 min or heated over an alcohol flame to enhance visibility of annuli. The otoliths were then individually mounted on slides by completely embedding them in clear thermoplastic posterior end down. On hardening, each mount was wet-sanded on increasingly fine grades of sandpaper (400–2000 grit), parallel to the slide, until the surface intersected the otolith nucleus (transverse section). Preparing readable mounts was a delicate procedure; besides cutting and polishing the small otoliths precisely without fracturing them, precise heating temperature and time were especially critical to expose annuli without again causing fractures or burning the otolith. Our method had advantages over the standard "break and burn" method of simply coating the surface of a temporarily mounted specimen with oil to enhance visibility of annuli, in lieu of polishing. It allowed a more precise intersection of the nucleus by the viewed surface and eliminated the need to remove oil from specimens intended for further viewing in order to prevent blurring of annuli. After preparation, slides were placed in sufficient water to cover the surface scratches and were examined under a dissecting microscope with reflected light. Age in years was determined by counting the annuli or hyaline bands according to the criteria described in Chilton and Beamish (1982).

Prowfish ovaries were prepared for histological examination by removing a small portion from the middle of each ovary, which was then embedded in paraffin, sectioned at 6 μm, and stained with hematoxylin and eosin. The histological slides were examined under a compound microscope and donor females were classified as either sexually immature or mature based on the presence of yolk in the oocytes (i.e. vitellogenesis).

Prowfish stomachs were processed by first neutralizing the 10% formalin used for initial fixation and then by immediately transferring the stomachs into 70% ethanol. The food was removed, blotted with a paper towel, and examined with a dissecting microscope. Prey items were sorted to the lowest practical taxonomic level and then weighed to the nearest 0.1 gm. The percentage of total prey weight which each taxon comprised, as well as the percentage of stomachs containing each taxon, was calculated for each haul sample and then estimated for each of the two regions as the average of the per-haul percentages.

Analysis of data

The distribution of prowfish density over depth in the Gulf of Alaska and the Aleutian Islands was determined by calculating the mean CPUE for each 20-m depth interval from 20 m to 480 m. Both surveys utilized a stratified sampling design in which sampling density (hauls per unit area) varied by geographical subarea (Martin, 1997; Stark[3]). To compensate for this variation, the CPUE of each haul was weighted by the inverse of the sampling density in that geographic stratum. The mean bottom depth as weighted by prowfish density was calculated for each of the two regions as the weighted average of the midpoints of the depth intervals, where the weighting factors were the interval-mean CPUE values.

[3] Stark, J. 1998. Report to industry: fishing log for the 1997 bottom trawl survey of the Aleutian Islands. AFSC Proc. Rep. 98-06, 96 p. Alaska Fish. Sci. Cent., Natl. Mar. Fish. Serv., NOAA, 7600 Sand Point Way NE, Bldg. 4, Seattle, WA 98115-0070.

Frequency distributions of prowfish total length, separated by sex and region, were calculated as the weighted percent of measurements within 10-cm length intervals. The weighting factors were calculated for each fish measurement as the inverse of geographic-stratum sampling (i.e. haul) density, multiplied by the inverse of the individual haul area that was swept. Also, differences in mean length between sexes or regions were examined by using analysis of variance (ANOVA)[4] to test the significance of statistical differences based on the weighted lengths. Because potential grouping of prowfish by size could affect within-haul variance, source haul (i.e. that in which each measured fish was caught) was included in analyses as a possible random variable affecting length. Variances in length between regions and sexes were each tested for significance against variance among hauls. The significance of the haul variable was also checked by testing variance among hauls against that among measurements.

The relationship of body weight (g; W) to total length (cm; L) was assumed to be an exponential function:

$$W = e^{\alpha} L^{\beta},$$

for which the parameters α and β were estimated from the data by first log-transforming both variables and then calculating the intercept and slope of the least squares linear regression:

$$\ln(W) = \alpha + \beta \ln(L).$$

To determine whether the relationship differed by sex, analysis of covariance (ANCOVA; Statgraphics Plus, Manugistics, Inc., Rockville, MD) was used to compare the fit of a model with two regression lines, each with a sex-specific intercept and slope, to the fit of a two-line model with sex-specific intercepts and a common slope (null hypothesis). If no significant difference was observed, then a second test was performed by testing the latter model against the null hypothesis of a common regression line with single intercept and slope for both sexes combined. The relationships in the best-fit model were then transformed back to exponential form.

Prowfish growth was described by fitting the von Bertalanffy function to length (L) and age (year; t) data by using nonlinear least squares. The function is

$$L = L_{\infty}(1 - e^{-k(t - t_0)}),$$

where L_{∞} = asymptotic maximum length;
k = a constant (per year) affecting model early growth rate; and
t_0 = hypothetical age at 0 length.

To determine whether parameters differed between prowfish sexes, we fitted the function separately to the data from each sex as well as to the data for both sexes combined. A likelihood ratio test was then used to determine whether the separate-sex model fitted the data significantly better than the combined-sex model (Kimura, 1980). Significance of the likelihood ratio was based on the chi-squared statistic with degrees of freedom equal to the difference in number of parameters between the two models.

The proportion of prowfish females that were mature (P_{mat}) at a given length or age was described with logistic functions of the form $P_{mat} = 1/(1 + e^{\alpha + \beta X})$, where X is either length (L) or age in years (t), and α and β are function parameters. The models were fitted to the data by using maximum likelihood. After the relationships were estimated, the length and age at which 50% of females were mature were estimated by setting $P_{mat} = 0.5$ in each function and solving for X. The 95% confidence interval for each estimate was calculated by using the delta method (Seber, 1973).

Results

Geographic distribution

Prowfish distribution in the waters off Alaska, as indicated by their presence at 1528 out of a total of 35,159 historical bottom trawl locations, is shown in Figure 2. The total count of individuals in catches was 11,401. Distribution south of approximately 50°N latitude off Vancouver Island is not shown because here 6 of 7442 bottom trawl hauls caught a total of 8 prowfish. The southernmost occurrence was at 34°13.4'N latitude near San Miguel Island, southern California. Prowfish were taken at depths ranging from 24 m to 801 m but most frequently appeared in catches close to the break between the continental shelf and upper continental slope near 200 m depth.

Prowfish CPUE was greater than zero at 64 of 807 haul locations in the Gulf of Alaska in 1996 and at 48 of 408 locations in the Aleutian Islands in 1997. Over all areas at the depths fished the range of per-haul CPUE was 0–547.5 prowfish/km^2 (average=6.7 prowfish/km^2) in the GOA and 0–5220.1 prowfish/km^2 (average=65.1 prowfish/km^2) in the AI. The average CPUE within 20-m bottom depth intervals in each region indicated that fish tend to be most concentrated at intermediate depths (Fig. 3). Depth at trawl locations ranged from 20 to 479 m for the GOA and from 22 to 474 m for the AI, and prowfish were collected at 34–252 m (GOA) and 89–258 m (AI), respectively. The CPUE-weighted average bottom depth was 163.8 m for the GOA and 150.3 m for the AI.

The CPUE values within 20-m depth intervals (Fig. 3) indicated that the regional difference in mean density was largely due to differences at the same depth rather than differences between regions in the amount of area available at a given bottom depth.

Length distribution

Length-frequency histograms by region and sex for prowfish from the Gulf of Alaska (84 males, 90 females) and Aleutian Islands (396 males, 431 females) are shown in Figure 4. Analysis of variance tests for a difference in mean length

[4] Unless otherwise specified, ANOVA, log-likelihood, and nonlinear regression analyses were accomplished by using Systat 10 software (Systat 10 Statistics I, SPSS Inc.,Chicago, IL).

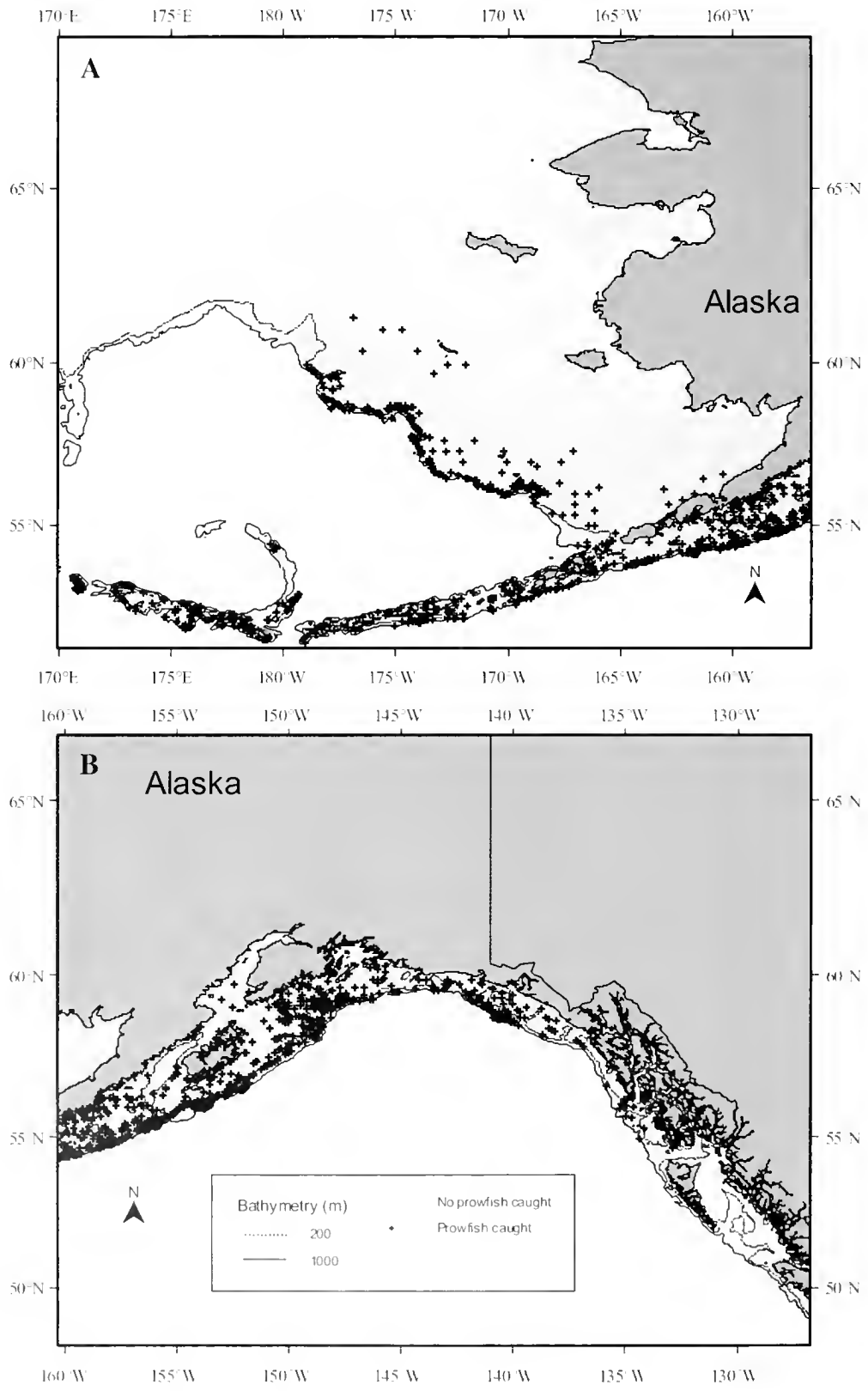

Figure 2

Locations of Alaska Fisheries Science Center groundfish survey bottom trawls (prior to year 2001) in (**A**) the eastern Bering Sea and the Aleutian Islands region and (**B**) the Gulf of Alaska, indicating trawls in which prowfish occurred.

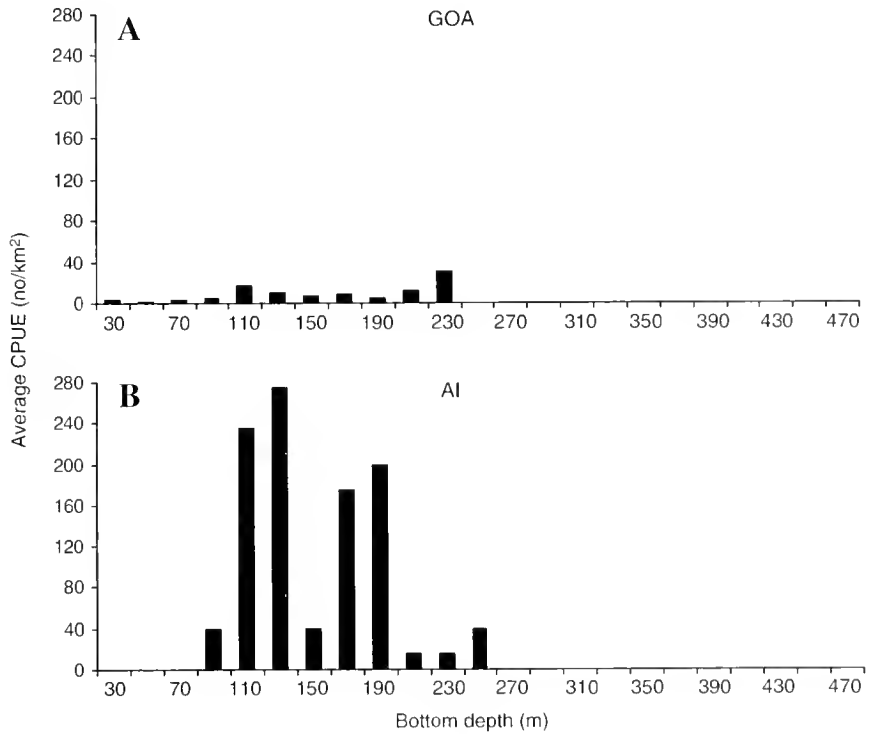

Figure 3

Average prowfish catch per unit of effort (CPUE; no/km^2) within 20-m intervals over the range of trawl depths of 20–479 m in the Gulf of Alaska (GOA) in 1996 (**A**) and 22–474 m in the Aleutian Islands (AI) in 1997 (**B**). The mean of interval midpoints, each weighted by interval average CPUE, was 163.8 m for the GOA and 150.3 m for the AI.

between sexes were not significant for either the GOA (P=0.83) or the AI (P=0.76). Although the weighted mean for both sexes combined was 61.0 cm (range: 11–90 cm) in the GOA and 51.9 cm (range: 25–87 cm) in the AI, the difference in length between regions was not significant (P=0.11). Grouping of prowfish of similar size within hauls was highly significant in both the GOA and the AI (P<<0.01).

Weight-length relationship

In the between-sex ANCOVA comparison of the linearized (i.e. log-transformed) weight-to-length relationships based on prowfish caught in the Gulf of Alaska, the slopes were not significantly different between sexes (P=0.38). However, the difference in intercepts was significant (P=0.044). Thus the best fitting model varied by sex with two regression lines of equal slope but with sex-specific intercepts. The equivalent functions in terms of the untransformed variables (Fig. 5) were

$$W_{males} = 0.0164 \times L^{2.922},$$

and

$$W_{females} = 0.017 \times L^{2.922}.$$

The model indicated that adult females are, on average, 3.7% heavier than males of the same length.

Age and growth

Readable otolith specimens were produced for 138 prowfish (71 males, 67 females) of the 172 from which samples were collected. Production of readable specimens did not appear related to fish size or age. The likelihood ratio test for a difference between males and females in the relationship of length to age was not significant (P=0.53), indicating that there was no difference in growth between sexes. The best-fit von Bertalanffy function (Fig. 6) had the following parameters (with 95% confidence intervals): L_∞ = 89.33 ±6.5 cm; k = 0.18 ±0.05/year; and t_0 = –0.55 ±0.12 year.

Female maturity

The proportions of females that were mature were highly significant logistic functions of length and age (P<0.005; Fig. 7). The fitted functions of length and age were

$$P_{mat} = 1/(1 + e^{371.14 - 6.51L});$$

and

$$P_{mat} = 1/(1 + e^{9.66 - 1.90t}).$$

The theoretical length and age at which 50% of females were mature, with respective 95% confidence limits, were 57.0 ±0.4 cm and 5.1 ±0.7 years.

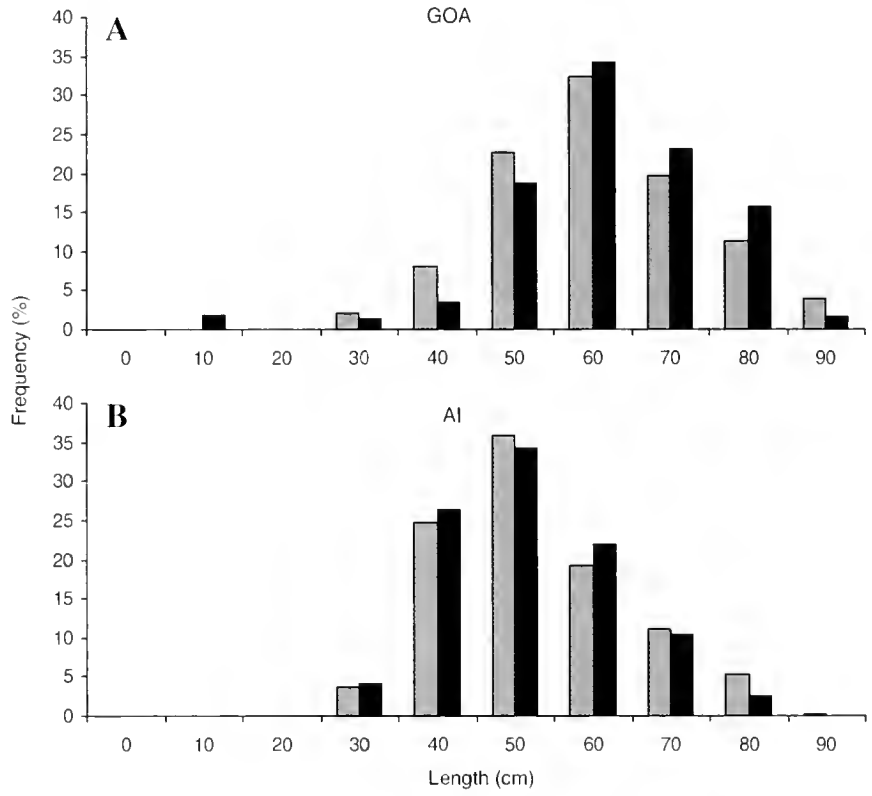

Figure 4

Frequency distribution of total lengths of (**A**) 84 male and 90 female prowfish from the Gulf of Alaska (GOA; 1996) and (**B**) 396 males and 431 females from the Aleutian Islands (AI; 1997). Gray bars show the percentage of male lengths and black bars the percentage of female lengths within continuous 10-cm intervals (e.g. 25–35 cm).

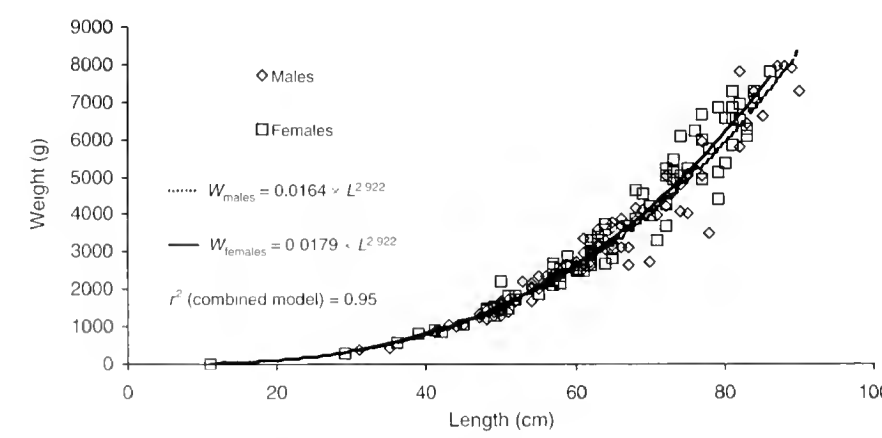

Figure 5

Prowfish body weight (W) fitted by an exponential function of fish total length (L) and sex. Data for males (n=83) are shown by diamonds and the fitted model by a dashed line. Data for females (n=88) are shown by squares and the fitted model by a solid line.

Food habits

Fish used for diet study averaged 63.8 cm in total length (range: 49–87 cm) in the Gulf of Alaska and 56.9 cm (range: 30–79 cm) in the Aleutian Islands. The contents of 18 prowfish stomachs from the Gulf of Alaska and 58 from the Aleutian Islands showed that jellyfish (99% and 31%

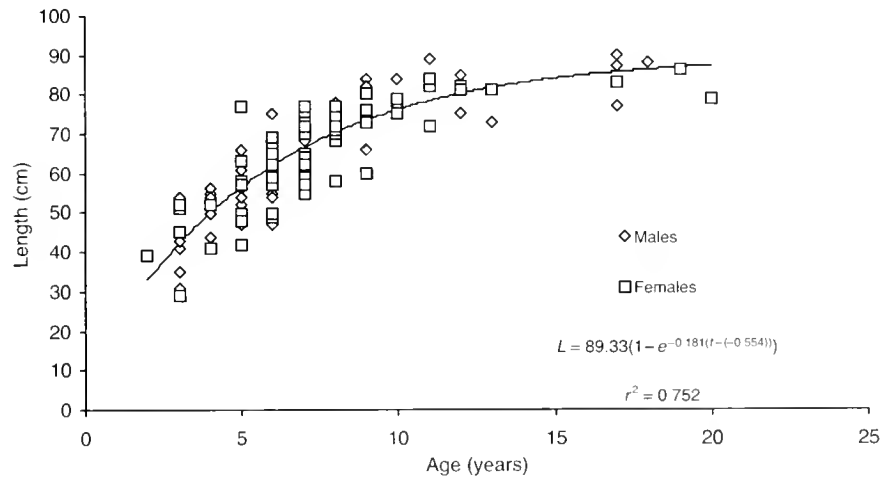

Figure 6

Prowfish total length (L) fitted by a von Bertalanffy function of age (t). Data for males (n=71) are shown by diamonds; data for females (n=67) are shown by squares. The fitted model is shown by a solid line.

Table 1

Mean percent weight (%W) and mean percent frequency of occurrence (%FO) of the prey items from 18 prowfish stomachs collected in the Gulf of Alaska (GOA; 1996; total prey weight=299 g) and 58 stomachs from the Aleutian Islands area (AI; 1997; total prey weight=1446.6 g). Sample prowfish had an average total length of 63.8 cm (range: 49–87 cm) from the GOA and and 56.9 cm (range: 30–79 cm) from the AI.

	GOA (n=18)		AI (n=58)	
Prey name	% W	% FO	% W	% FO
Scyphozoa (jellyfish)	98.84	100	30.45	29.88
Ctenophora (comb jelly)			0.09	1.23
Polychaeta (worm)			0.03	5.8
Calanoida (copepod)	0.26	28.13	0.04	29.14
Thysanoessa raschii (euphausiid)			0.05	6.67
Mysidacea Mysida (mysid)	0.01	3.13		
Hyperiidea (amphipod)			0.19	33.46
Gammaridea (amphipod)			0.12	30.49
Themisto sp. (amphipod)	0.32	28.57	0.14	36.91
Salpa sp. (pelagic salp)			34.06	46.79
Larvacea (pelagic tunicate)	0.13	12.5		
Sebastes sp. (rockfish) larvae, 5–8 mm long	0.43	42.86		
Microsomus pacificus (Dover sole) eggs	0.01	3.13		
Unidentified organic material			34.84	32.59

by weight of total food in the two regions, respectively) and gelatinous pelagic tunicates (*Salpa* spp.; 34% in the Aleutian Islands area only) were the most important food (Table 1). Although calanoid copepods and *Themisto* sp. (amphipod) were both often present in GOA specimens (28.13% and 28.57% of stomachs, respectively), they were not important food in terms of weight. The same was true in the AI for calanoid copepods, *Themisto* sp., gammaridean amphipods, and hyperiidean amphipods (29.14%, 36.91%, 30.49%, and 33.46% respectively). Mysids and larvaceans from GOA specimens as well as ctenophors, polychaetes, and euphasiids from AI specimens occurred in trace amounts. *Sebastes* larvae (5–8 mm standard length), the only fish species found, were found in 43% of Gulf of Alaska stomachs but made up only 0.43% of prey weight. Some Dover sole (*Microstomus pacificus*) eggs had also been consumed.

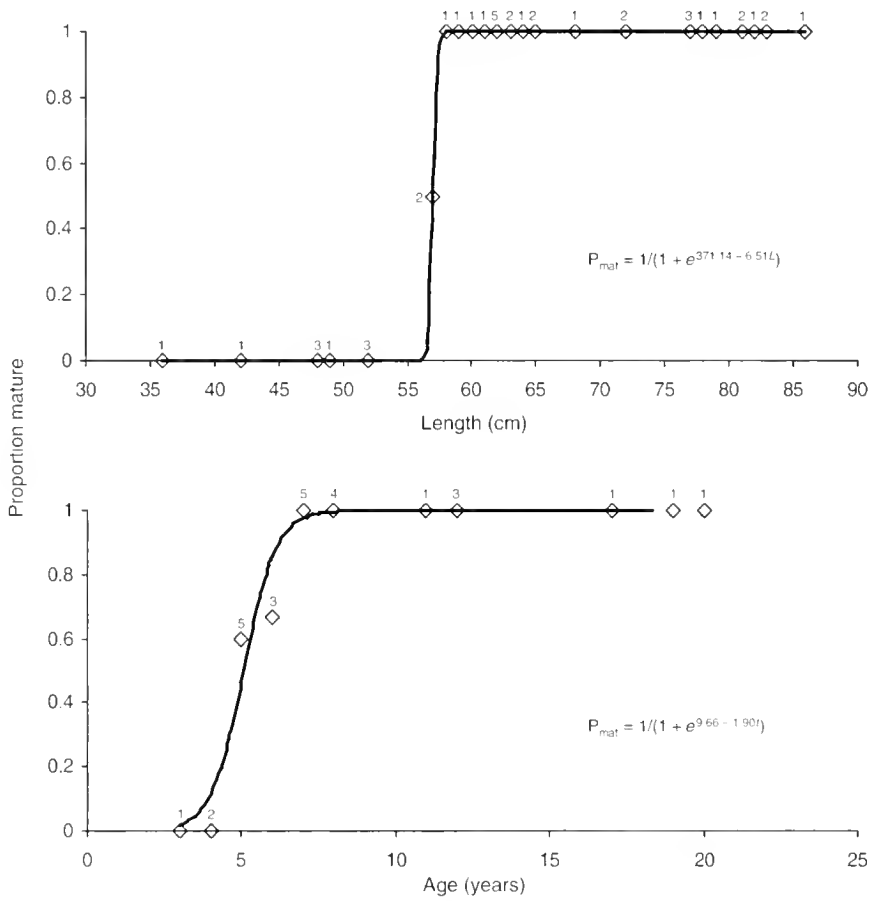

Figure 7

Proportion of female prowfish mature (P_{mat}) as logistic functions of length (L) and age (t). Data points based on 39 maturity-at-length and 27 maturity-at-age observations are shown by diamonds, and numbers of females of each cm-length and year-age class are shown next to the corresponding symbol. The fitted logistic models are shown by solid lines. The length and age at which $P_{mat} = 0.5$ with 95% confidence limits are 57.0 ±0.4 cm and 5.1 ±0.7 years.

Discussion

Geographic distribution

Historically occurring in the catch in AFSC bottom trawl surveys in areas of the eastern Bering Sea, Aleutian Islands, and Gulf of Alaska regions, prowfish were also observed more rarely farther south along the West Coast as far as the vicinity of San Miguel Island, California. This is the apparent southern limit of their range in the northeastern Pacific (Allen and Smith, 1988). They were most often encountered in the vicinity of the edge of the continental slope near 200 m depth (Fig. 2), although our data increase the maximum known depth of occurrence from 675 m (Allen and Smith, 1988) to 801 m. As indicated by survey CPUE, prowfish density was greatest between the depths of 100 m and 240 m (Fig. 3). Our distribution data show similarities with those of Tokranov (1999), who studied >300 bottom trawls executed in 1995–97 on the shelf and slope off the southern Kamchatka Peninsula and northern Kuril Islands, in which adult prowfish were taken at 100–480 m. Tokranov often found fish concentrated in areas of high-relief, rocky bottom—a common feature of the shelf edge in the Gulf of Alaska and Aleutian Islands regions. Such areas near the shelf break may be important prowfish habitat. Underwater videos taken in the northeast Gulf of Alaska by the Alaska Department of Fish and Game (Brylinsky[5]) show numerous adult fish resting on or just above this type of substrate.

Density was greater in the AI than in the GOA, over all bottom depths combined and in most cases by individual depth interval (Fig. 3). One reason may be that preferred habitat comprises a larger proportion of the Aleutian Is-

[5] Brylinsky, C. 2000. Pers. commun. Alaska Department of Fish and Game, 304 Lake Street, Sitka, AK 99835.

lands area. Because of the lack of a relatively broad shelf in the region, a larger proportion of trawls are in or near areas of steep seafloor gradient and therefore likely over rough bottom (Fig. 2).

Length distribution

In both the Gulf of Alaska and the Aleutian Islands, few prowfish <40 cm in length were captured (Fig. 4). This paucity of small prowfish is not due to size selection by the trawl net mesh because the codend is lined with small mesh (1.3 cm stretched measure) webbing that retains small individuals of other species. A different explanation, based on the observations of Brodeur (1998) and Scheffer (1940), is that pre-adult prowfish are pelagic, remaining in proximity with large coelenterates and thus avoiding bottom trawls. Thus, the minimum capture length may indicate the length at which prowfish recruit to a demersal habitat. Our data showed no statistically significant length difference between sexes, in contrast with the data of Tokranov (1999) who suggested a length dimorphism where females are generally longer than males.

Weight-length relationship

The best-fitting model of weight versus length predicts that for any length, female prowfish are, on average, 3.7% heavier than males (Fig. 5). It seems unlikely that this relationship exists over all developmental stages because our samples were almost all adults and such a (relative) difference might not remain constant during all ontogenetic sexual divergence. What is more certain is simply the existence of some small degree of length-weight dimorphism (females slightly heavier at a given length). Also, this dimorphism is not likely to stem primarily from a sexual difference in gonad weight because the maximum proportion of total female body weight composed of ovarian tissue was only 2.7%. Thus the difference is due to other morphological or behavioral differences.

Growth

There was no significant difference between sexes in length versus age. The predicted length of a prowfish of given age based on our samples was higher than that indicated by Tokranov (1999). In our study 5-year-old and 9-year-old fish averaged 56.6 cm and 73.5 cm in length, respectively. Tokranov (1999) considered that prowfish growth determined from otoliths of 102 specimens from the Northwest Pacific indicated a comparatively fast-growing species reaching an average length of 44.6 cm by 5 years of age and 67 cm after 9 years. These data suggest prowfish are indeed relatively fast growing and that growth rates for the Gulf of Alaska are faster than those for off southeastern Kamchatka and the northern Kuril Islands. Alternatively, size-dependent mortality from such elements as incidental capture by commercial fishing may affect the two populations differently.

Historically, two other prowfish have been aged from otoliths: a male 84 cm long taken near Eureka, CA (Fitch and Lavenberg, 1971), and a female 50.1 cm long (standard length) from off Monterey (Cailliet and Anderson, 1975). The ages estimated were 12 and 3 years, respectively. After converting the standard length record to an estimate of total length for the second specimen of 58 cm by using a ratio described by Baxter,[6] both lengths are slightly greater than our predictions for the same ages, albeit near the limits of our data range. This finding contrasts with the predictions of lesser length at a given age presented by Tokranov (1999).

Maturity

Little previous data exist with which to compare our observations of female prowfish rate of maturation. Cailliet and Anderson (1975) examined the ovaries of their 50.1-cm 3-year-old female specimen for vitellogenesis and predicted an age at first spawning of 4 years, slightly less than the lower 95% confidence limit of 4.4 years for our expected average age at 50% maturity.

Food habits

Our observation that gelatinous zooplankton was the largest constituent in the contents of prowfish stomachs (Table 1) is supported by Tokranov (1999), who found that the two most common prey taxa among the contents of 102 stomachs of adult specimens from the northwestern Pacific were Scyphozoa (59.6–62.0% of stomachs) and Ctenophora (6.0–15.4% of stomachs). Anecdotal observations have also been made of the feeding behavior of an aquarium specimen over an approximate 2-year period (Carollo and Rankin, 1998). When first obtained, the fish ate only various jellyfish species, rejecting other food, including a variety of live invertebrates. In our food samples, we observed other taxa, such as invertebrates and small fish, but these were a minor part, possibly first captured by jellyfish and then secondarily ingested by prowfish. Carollo and Rankin (1998) found that the aquarium specimen would ingest such items when eating the bells of *Chrysaora melanaster* in which such food had previously been placed, indicating the possibility of this occurring naturally. Possibly more reflective of the unnatural circumstances, the specimen later began accepting such items outside the bells of jellyfish.

Apparent adaptations of the prowfish to a diet of gelatinous zooplankton include the small, sharp, close-set teeth in a single row attached only to the jaws, which are capable of a 180-degree gape, and the large rough-scaled lips (Clemens and Wilby, 1961; Hart, 1973; Carollo and Rankin, 1998).

Acknowledgments

We are grateful for the expert advice given by Alaska Fisheries Science Center colleagues Delsa Anderl and Nancy

[6] Baxter, R. 1990. Unpubl. manuscript. Annotated key to the fishes of Alaska, 803 p. [Available from Sera Baxter, Box 182, Seldovia, AK 99663.]

Roberson regarding age-reading of prowfish otoliths, and by AFSC colleagues Kathy Mier and Susan Piquelle regarding statistical analyses of data.

Literature cited

Allen, James M., and Gary B. Smith.
1988. Atlas and zoogeography of common fishes in the Bering Sea and Northeastern Pacific. NOAA Tech. Rep. NMFS 66, 151 p.

Brodeur, R. D.
1998. In situ observations of the association between juvenile fishes and scyphomedusae in the Bering Sea. Mar. Ecol. Prog. Ser. 163:11–20.

Cailliet, G. M., and M. E. Anderson.
1975. Occurrence of prowfish *Zaprora silenus* Jordan, 1896 in Monterey Bay, California. Calif. Fish Game 61(1):60–62.

Carollo, M., and P. Rankin.
1998. The care and display of the prowfish, *Zaprora silenus*. Drum and Croaker 29:3–6.

Clemens, W. A., and G. V. Wilby.
1961. Fishes of the Pacific coast of Canada. Fish. Res. Board Can. Bull. 68, 2nd ed., 443 p.

Chilton, D. E., and R. J. Beamish.
1982. Age determination methods for fishes studied by the groundfish program at the Pacific Biological Station. Can. Spec. Pub. Fish. Aquat. Sci. 60, 102 p.

Doyle, M. J., K. L. Meir, M. S. Bushy, and R. D. Brodeur.
2002. Regional variation in springtime ichthyoplankton assemblages in the northeast Pacific Ocean. Progress in Oceanography 53 (2–4):247–281

Eschmeyer, W. N., E. S. Herald, and H. Hammann.
1983. A field guide to Pacific Coast fishes of North America, 336 p. Peterson field guide ser. Houghton Mifflin, Boston, MA.

Fitch, J. E., and R. J. Lavenberg.
1971. Marine food and game fishes of California, 179 p. U.C. Press, Berkeley, CA.

Hart, J. L.
1973. Pacific fishes of Canada. Fish. Res. Board Can. Bull. 180, 740 p.

Jordan, D. S.
1897. Notes on fishes little known or new to science. Proc. Calif. Acad. Sci., 2nd ser., 6:203–205.

Kessler, D. W.
1985. Alaska's saltwater fishes and other sea life: a field guide, 358 p. Alaska Northwest, Anchorage, AK

Kimura, D. K.
1980. Likelihood methods for the von Bertalanffy growth curve. Fish. Bull. 77:765–776.

Martin, M. H.
1997. Data report: 1996 Gulf of Alaska bottom trawl survey. NOAA Tech. Memo. NMFS-AFSC-82, 235 p.

Matarese, A. C., A. W. Kendall, D. M. Blood, and B. M. Vinter.
1989. Laboratory guide to early life history stages of northeast pacific fishes. NOAA Tech. Rep. NMFS 80, 652 p.

Nelson, J. S.
1994. Fishes of the world, 3rd ed., 600 p. John Wiley, New York, NY..

Orlov, A. M.
1998. On feeding of mass species of deep-sea skates (*Bathyraja* spp., Rajidae) from the Pacific waters of the Northern Kurils and Southeastern Kamchatka. J. Icthyol. 38(8): 635–644.

Payne, S. A., B. A. Johnson, and R. S. Otto.
1999. Proximate composition of some north-eastern Pacific forage fish species. Fish. Oceanogr. 8(3): 159–177.

Scheffer, V. B.
1940. Two recent records of *Zaprora silenus* Jordan from the Aleutian Islands. Copeia 1940(3):203.

Seber, G. A. F.
1973. The estimation of animal abundance, 506 p. Hafner Press, New York, NY.

Tokranov, A. M.
1999. Some features of biology of the prowfish *Zaprora silenus* (Zaproridae) in the Pacific waters of the Northern Kuril Islands and Southeastern Kamchatka. J. Ichthyol. 39(6):475–478.

Van Pelt, T. I., J. F. Piatt, B. K. Lance, and D. D. Roby.
1997. Proximate composition and energy density of some North Pacific forage fishes. Comp. Biochem. Physiol. 118A(4):1393–1398.

Wakabayashi, K., R. G. Bakkala and M. S. Alton.
1985. Methods of the U.S.–Japan demersal trawl surveys. *In* Results of cooperative U.S.–Japan groundfish investigations in the Bering Sea during May–August 1979 (R. G. Bakkala and K. Wakabayashi, eds.), p. 7–26. Int. North Pac. Fish. Comm. Bull. 44.

Yang, Mei-Sun.
1993. Food habits of the commercially important groundfishes in the Gulf of Alaska in 1990. NOAA Tech. Memo. NMFS-AFSC-22, 150 p.

Fish lost at sea: the effect of soak time on pelagic longline catches

Peter Ward

Ransom A. Myers

Department of Biology
Dalhousie University
Halifax, B3H 4JI Canada
E-mail address (for P. Ward): ward@mathstat.dal.ca

Wade Blanchard

Department of Mathematics and Statistics
Dalhousie University
Halifax, B3H 44 Canada

Abstract—Our analyses of observer records reveal that abundance estimates are strongly influenced by the timing of longline operations in relation to dawn and dusk and soak time—the amount of time that baited hooks are available in the water. Catch data will underestimate the total mortality of several species because hooked animals are "lost at sea." They fall off, are removed, or escape from the hook before the longline is retrieved. For example, longline segments with soak times of 20 hours were retrieved with fewer skipjack tuna and seabirds than segments with soak times of 5 hours. The mortality of some seabird species is up to 45% higher than previously estimated.

The effects of soak time and timing vary considerably between species. Soak time and exposure to dusk periods have strong positive effects on the catch rates of many species. In particular, the catch rates of most shark and billfish species increase with soak time. At the end of longline retrieval, for example, expected catch rates for broadbill swordfish are four times those at the beginning of retrieval.

Survival of the animal while it is hooked on the longline appears to be an important factor determining whether it is eventually brought on board the vessel. Catch rates of species that survive being hooked (e.g. blue shark) increase with soak time. In contrast, skipjack tuna and seabirds are usually dead at the time of retrieval. Their catch rates decline with time, perhaps because scavengers can easily remove hooked animals that are dead.

The results of our study have important implications for fishery management and assessments that rely on longline catch data. A reduction in soak time since longlining commenced in the 1950s has introduced a systematic bias in estimates of mortality levels and abundance. The abundance of species like seabirds has been over-estimated in recent years. Simple modifications to procedures for data collection, such as recording the number of hooks retrieved without baits, would greatly improve mortality estimates.

Manuscript approved for publication 22 September 2003 by Scientific Editor.

Manuscript received 20 October 2003 at NMFS Scientific Publications Office.

Fish. Bull. 102:179–195 (2004).

Our knowledge of large pelagic fish in the open ocean comes primarily from tagging and tracking experiments and from data collected from longline fishing vessels since the 1950s. Abundance indices for pelagic stocks are often derived from analyses that model catch as a function of factors such as year, area, and season. However, the amount of time that baited hooks are available to fish is likely to be another important factor influencing catch rates (Deriso and Parma, 1987).

The activity of many pelagic animals and their prey vary with the time of day. Broadbill swordfish, for example, feed near the sea surface at night. They move to depths of 500 m or more during the day (Carey, 1990). Other species may be more active in surface waters during the day (e.g. striped marlin) or at dawn and dusk (e.g. oilfish). Longline fishing crews take a keen interest in the timing of their fishing operations and soak time (the total time that a baited hook is available in the water). However, assessments have not accounted for those factors in estimating the abundance or mortality levels of target species or nontarget species.

In many assessments that use pelagic longline catch rates, fishing effort is assumed to be proportional to the number of hooks deployed. The effects of soak time and timing may have been omitted because a clear demonstration of their effects on pelagic longline catch rates is not available. The few published accounts on soak time in pelagic longline fisheries have been based on limited data and a few target species. For example, in analyzing 95 longline operations or "sets" by research vessels Sivasubramaniam (1961) reported that the catch rates of bigeye tuna increased with soak time, whereas yellowfin tuna catch rates were highest in longline segments with intermediate soak times.

In contrast to the limited progress in empirical studies, theoretical approaches are well developed for modeling factors that may influence longline catch rates. Soon after large-scale longlining commenced, Murphy (1960) published "catch equations" for adjusting catch rates for soak time, bait loss, escape, hooking rates, and gear saturation. He suggested that escape rates could be estimated from counts of missing hooks and hooks retrieved without baits. Unfortunately, such data are rarely collected from pelagic longline operations.

More recently, hook-timers attached to longline branchlines have begun to provide information on the time when each animal is hooked and also whether animals are subsequently lost, e.g. Boggs (1992), Campbell et al.[1,2] Such data are particularly useful to under-

[1] Campbell, R., W. Whitelaw, and G. McPherson. 1997. Domestic longline fishing methods and the catch of tunas and non-target species off north-eastern Queensland (1st survey: October–December 1995). Report to the Eastern Tuna and Billfish Fishery MAC. 71 p. Australian Fisheries Management Authority, PO Box 7051, Canberra Business Centre, ACT 2610, Australia.

[2] *See next page.*

standing the processes affecting the probability of capture and escape.

The purpose of our study is to determine whether variations in the duration and timing of operations bias abundance and mortality estimates derived from longline catch rates. We present a theoretical model that is then related to empirical observations of the effects of soak time on catch rates. The strength in our approach is in applying a random effects model to large data sets for over 60 target and nontarget species in six distinct fisheries. We also investigate the survival of each species while hooked because preliminary analyses suggested that the effects of soak time on catch rates might be linked to mortality caused by hooking (referred to as "hooking mortality").

Factors affecting catch rates

To aid interpretation of our statistical analysis of soak time effects, we first developed a simple model to illustrate how the probability of catching an animal may vary with soak time.

The probability of an animal being on a hook when the branchline is retrieved is a product of two probability density functions: first the probability of being hooked and then the probability of being lost from the hook.[3] Influencing the probability of being hooked are the species' local abundance, vulnerability to the fishing gear, and the availability of the gear. Catches will deplete the abundance of animals within the gear's area of action, particularly for species that have low rates of movement. Movement will also result in variations in exposure of animals to the gear over time—for instance, as they move vertically through the water column in search of prey (Deriso and Parma, 1987).

Other processes that will reduce the probability of being hooked include bait loss and reduced sensitivity to the bait (Fernö and Huse, 1983). Longline baits may fall off hooks during deployment, deteriorate over time and fall off or they may lose their attractant qualities. They may be removed by target species, nontarget species, or other marine life, such as squids. Hooked animals may also escape by severing the branchline or breaking the hook. Sections of the longline may become saturated when animals are hooked, reducing the number of available baits (Murphy, 1960; Somerton and Kikkawa, 1995). After an animal has been hooked, it may escape, fall off the hook, be removed by scavengers, or it may remain hooked until the branchline is retrieved.

Some of the processes affecting the probability of an animal being on a hook when the the branchline is retrieved are species-specific, whereas other processes may affect all species. For example, bait loss during longline deployment will reduce the catch rates of all species. In contrast, the probability of a hooked animal escaping may be species-dependent; some species are able to free themselves from the hook whereas other species are rarely able to do this.

Our simple model of the probability of an animal being on a hook is based on a convolution of the two time-related processes described above: 1) the decay in the probability of capture with the decline in the number of baits that are available; and 2) gains due to the increased exposure of baits to animals and losses due to animals escaping, falling off, or being removed by scavengers.

The probability of an animal being on a hook when the branchline is retrieved is the integral of the probability density functions of capture and retention:

$$\pi(T) = \int_{t=0}^{T} P_c(t) P_r(T-t)\,dt, \tag{1}$$

where $\pi(T)$ = the "catch rate" or probability of an animal being on a hook when the branchline is retrieved at time T (T is the total soak time of the hook);
$P_c(t)$ = the probability density function of an animal being captured at time t; and
$P_r(t)$ = the probability density function of a captured animal being retained on the hook for a length of time t.

The probability density function of capture can be approximated with an exponential function:

$$P_c(t) = P_0 e^{-\alpha t}, \tag{2}$$

where P_0 = the probability of capture when the hook is deployed (t=0); and
α = a parameter determining the rate of change in capture probability over time.

After the animal is hooked, the probability density function of an animal being retained after capture can be approximated as

$$P_r(t) = e^{-\beta(t)}, \tag{3}$$

where β = the "loss rate," a parameter determining the rate of change in the probability of an animal being retained after it has been captured.

Substituting approximations 2 and 3 into Equation 1 gives

$$\begin{aligned}\pi(T) &= \int_{t=0}^{T} P_0 e^{-\alpha t} e^{-\beta(T-t)} dt \\ &= \frac{P_0}{\beta-\alpha}\left[e^{-\alpha T} - e^{-\beta T}\right].\end{aligned} \tag{4}$$

[2] Campbell, R., W. Whitelaw, and G. McPherson. 1997. Domestic longline fishing methods and the catch of tunas and nontarget species off north-eastern Queensland (2nd survey: May–August 1996). Report to the Eastern Tuna and Billfish Fishery MAC, 48 p. Australian Fisheries Management Authority, PO Box 7051, Canberra Business Centre, ACT 2610, Australia.

[3] In discussing continuous variables we use the terms "probability" and "probability density function" interchangeably.

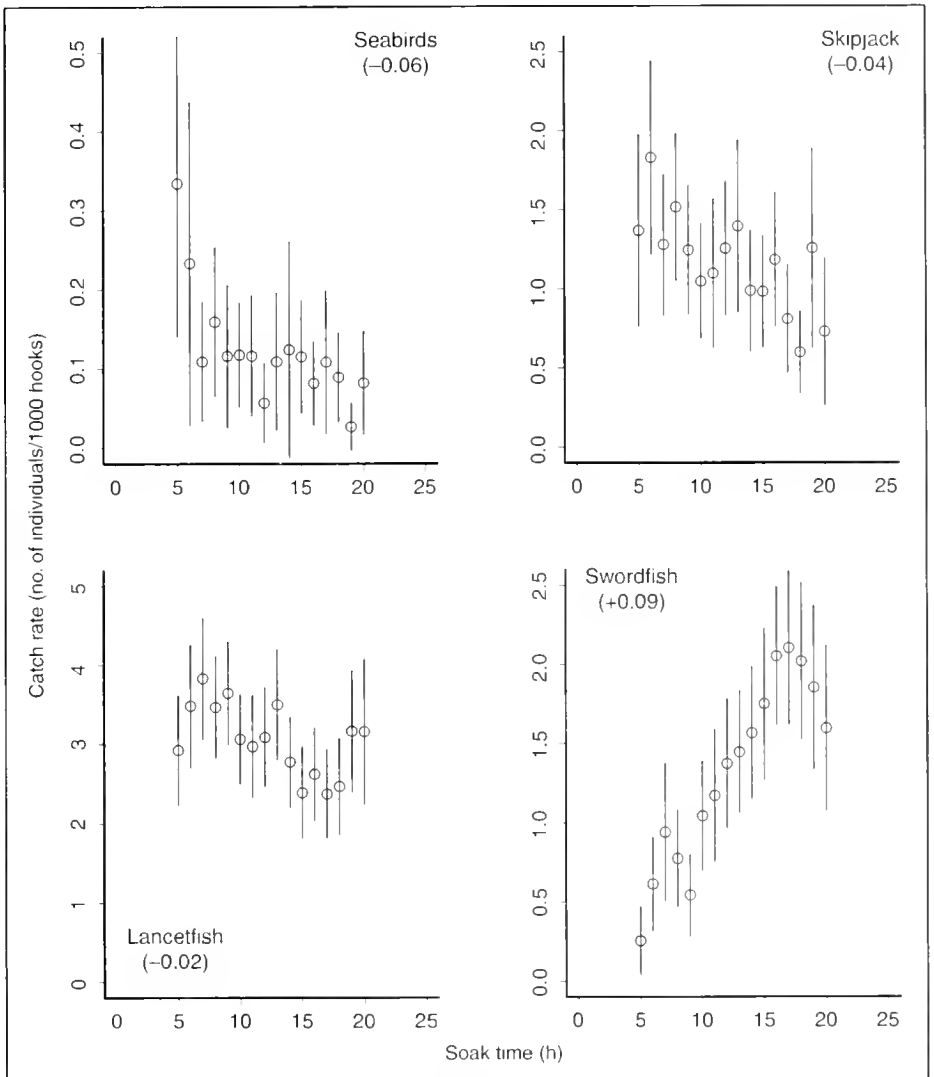

Figure 1

Mean catch rates plotted against soak time for skipjack tuna, long-nosed lancetfish, and swordfish in the South Pacific yellowfin tuna fishery and for "other seabirds" in the South Pacific bluefin tuna fishery. To reduce variability, the estimates were limited to longline segments with more than 25 hooks and soak times of 5–20 hours. Vertical bars are 95% confidence intervals for the mean hourly catch rate. In parentheses are the soak-time coefficients from random effects models (note that the soak-time coefficient is not the same as the slope coefficient of a regression of the data presented in this graph).

Our model is similar to the parabolic catch model examined by Zhou and Shirley (1997). It is simpler than catch equations developed by other authors because it does not include specific terms for the loss of baits, for fish competition, and gear saturation.

Preliminary plots of observer data indicated a variety of patterns in the relationship between catch rates and soak time (e.g. Fig. 1). By varying the values of P_0 (probability of capture), α (capture rate), and β (loss rate), our simple catch equation (Eq. 4) can mimic the observed patterns (Fig. 2). However, estimates of P_0, α , and β are not available. Instead, we used the empirical approach described in the following section to model the effect of soak time on catch rates. The relationship of soak time to catch rate represents the product of the probability of capture and the probability of being retained.

One approach to investigating the effects of soak time on catch rates is to fit linear regressions to aggregated data like those presented in Figure 1. Such an approach, however, would violate assumptions of independence (within each longline operation, catch rates in consecutive segments will be related), normality (these are binomial data), and homogeneity of variance (for binomial data, the variance is dependent on the mean).

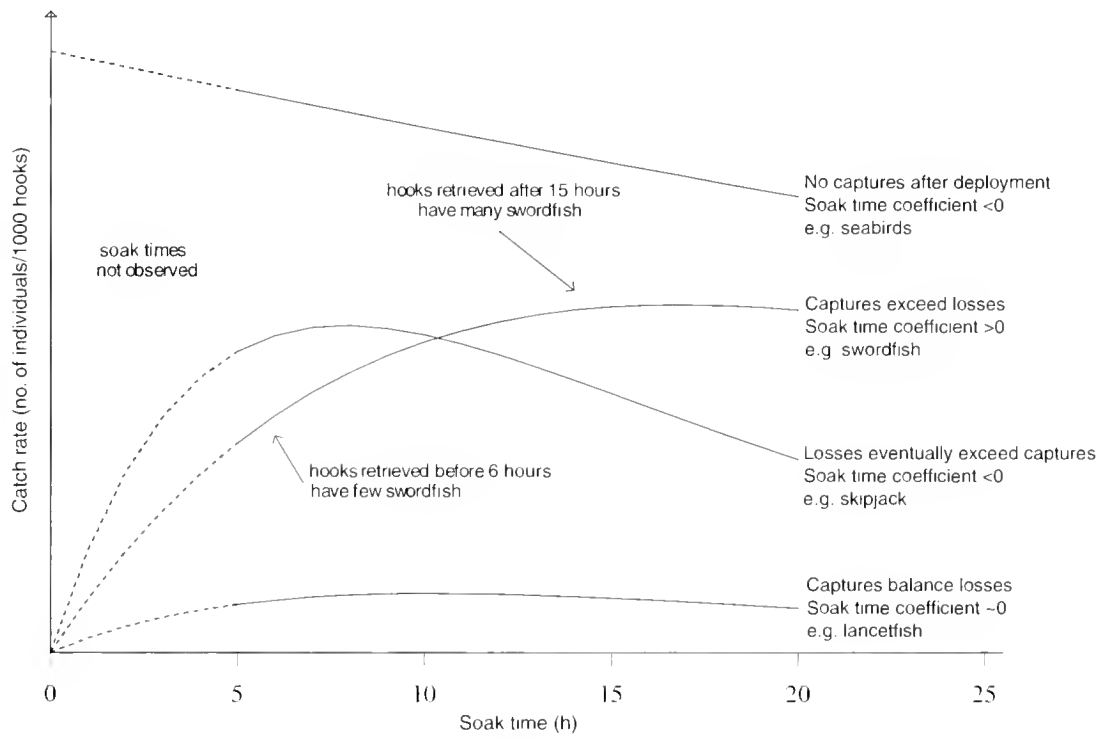

Figure 2

Illustration of different patterns in the theoretical relationship between longline catch rates and soak time. The probability of an animal being on a hook when a branchline is retrieved (the "catch rate") is estimated from Equation 4 by using soak times (T) ranging from 0 to 20 hours and three different combinations of values for P_0 (probability of capture), α (capture rate), and β (loss rate). For seabirds, the probabilities were estimated from Equation 6. The probabilities are not on the same scale for all species.

Another approach might be to fit separate logistic regressions to each operation and then to combine the parameter estimates. This would overcome the problems of normality and homogeneity of variance. However, the separate regressions would not incorporate information that is common to all operations.

Instead, we used a logistic regression with random effects. The key advantage in using random-effects models in this situation is that they carry information on the correlation between longline segments that is derived from the entire data set of operations.

Data and methods

Fisheries

We analyzed observer data from six different fisheries in the Pacific Ocean to determine the effects of soak time and timing on longline catch rates (Table 1, Fig. 3). These fisheries involve two different types of longline fishing operation: 1) distant-water longlining involves trips of three months or longer and the catch is frozen on board the vessel; and 2) fresh-chilled longlining, which involves small vessels (15–25 m) undertaking trips of less than four weeks duration, and the catch is kept in ice, ice slurries, or in spray brine systems. The fresh-chilled longliners deploy shorter longlines with fewer hooks (~1000 hooks) than the distant-water longliners (~3000 hooks per operation) (Ward, 1996; Ward and Elscot, 2000).

The six fisheries share many operational similarities, such as the types of bait used and soak time. However, they are quite different in terms of targeting, which is determined by fishing practices, e.g. the depth profile of the longline, timing of operations and the area and season of activity. South Pacific bluefin tuna longliners operate in cold waters (10–16°C) in winter to catch southern bluefin tuna. In the South Pacific yellowfin tuna longliners target tropical species, such as yellowfin and bigeye tuna, in warmer waters (19–22°C) (Ward, 1996). To target bigeye tuna, longlines in the Central Pacific bigeye fishery are deployed in the early morning with hook depths ranging down to about 450 m. The depths of the deepest hook are much shallower (~150 m) in the North Pacific swordfish fishery where the longlines are deployed late in the afternoon and retrieved early in the morning (Boggs, 1992).

Observer data

National authorities and regional organizations placed independent observers on many longliners operating in the six fisheries during the 1990s. The observer data consisted of records of the species and the time when each animal was brought on board. We restricted analyses to operations where the last hook that had been deployed was retrieved first ("counter-retrieved"), where there was no evidence of stoppages due to line breaks or mechanical failure, and where there was continuous monitoring by an observer. Combined with records of the number of hooks deployed and start and finish times of deployment and retrieval, the observer data allowed calculation of soak time and catch rates of longline segments. We aggregated catches and the number of hooks into hourly segments. The soak time was estimated for the midpoint of each hourly segment.

The Central Pacific bigeye tuna and North Pacific swordfish fisheries differed from the other four fisheries in the species that were recorded and the method of recording the time when each animal was brought on board. Observers reported catches according to a float identifier in the Central and North Pacific fisheries. Therefore we estimated soak times for each longline segment from the time when each float was retrieved. For those fisheries, observers reported the float identifier only for tuna, billfish, and shark (Table 2). Data are available for protected species, such as seals, turtles, and seabirds but were not sought for the present study.

We assumed a constant rate of longline retrieval throughout each operation. The number of hooks retrieved during each hourly segment was the total number of hooks divided by the duration of monitoring (decimal hours). For each species we analyzed only the operations where at least one individual of that species was caught.

Longline segments that involved a full hour of monitoring had several hundred hooks. Segments at either end of the longline involved less than an hour of monitoring and had fewer hooks. Catch rates may become inflated in segments with very small numbers of hooks. Therefore we arbitrarily excluded segments where the observer monitored less than 25 hooks.

For four of the fisheries, data were available on survival rates, allowing the investigation of the relationship between soak time and hooking mortality. For the Western Pacific and South Pacific fisheries, observers reported whether the animal was alive or dead when it was brought on board. We calculated survival rate (the number alive divided by the total number reported dead or alive) for species where data were available on the life status of more than ten individuals.

Generalized linear mixed model

Logit model We applied a generalized linear mixed model to the observer data. The model is based on a logistic regression, with the catch (y) on each hook assumed to have a binomial distribution with $y \sim b(n, \pi)$. π is the expected value of the distribution for a specified soak time. We refer to it as the probability of catching an animal or

Table 1

Summary of the six fisheries analyzed, showing the mean number of hooks per operation, mean duration of operations, mean catch rate of all species, the period of observer data, and the total number of longline operations. For the two Western Pacific fisheries, the catch rates are for the most common species only. NP = North Pacific; CP = Central Pacific; WP = Western Pacific; and SP = South Pacific.

Fishery name	Fleet	Area	Target species	Period	No. of operations	Hooks per operation	Duration (h)	Catch rate (no. of fish per 1000 hooks)
NP swordfish[1]	U.S. fresh-chilled	North Pacific	swordfish	1994–2002	1539	812	21	51
CP bigeye tuna[1]	U.S. fresh-chilled	Central Pacific	bigeye tuna, albacore	1994–2002	3243	1865	19	23
WP bigeye tuna	fresh-chilled (various flags)	Western Pacific	bigeye tuna, yellowfin tuna	1990–2001	1915	1620	21	28
WP distant	distant-water (various flags)	Western Pacific	bigeye tuna, yellowfin tuna	1990–2001	234	2347	22	30
SP yellowfin tuna	Japan distant-water	northeastern Australia	yellowfin tuna, bigeye tuna	1992–97	1419	3130	22	40
SP bluefin tuna	Japan distant-water	southeastern Australia	southern bluefin tuna	1992–97	666	3086	22	23

[1] We used the number of hooks between floats to distinguish the North Pacific swordfish fishery (<15 hooks between floats) from the Central Pacific bigeye tuna fishery (16 or more hooks between floats).

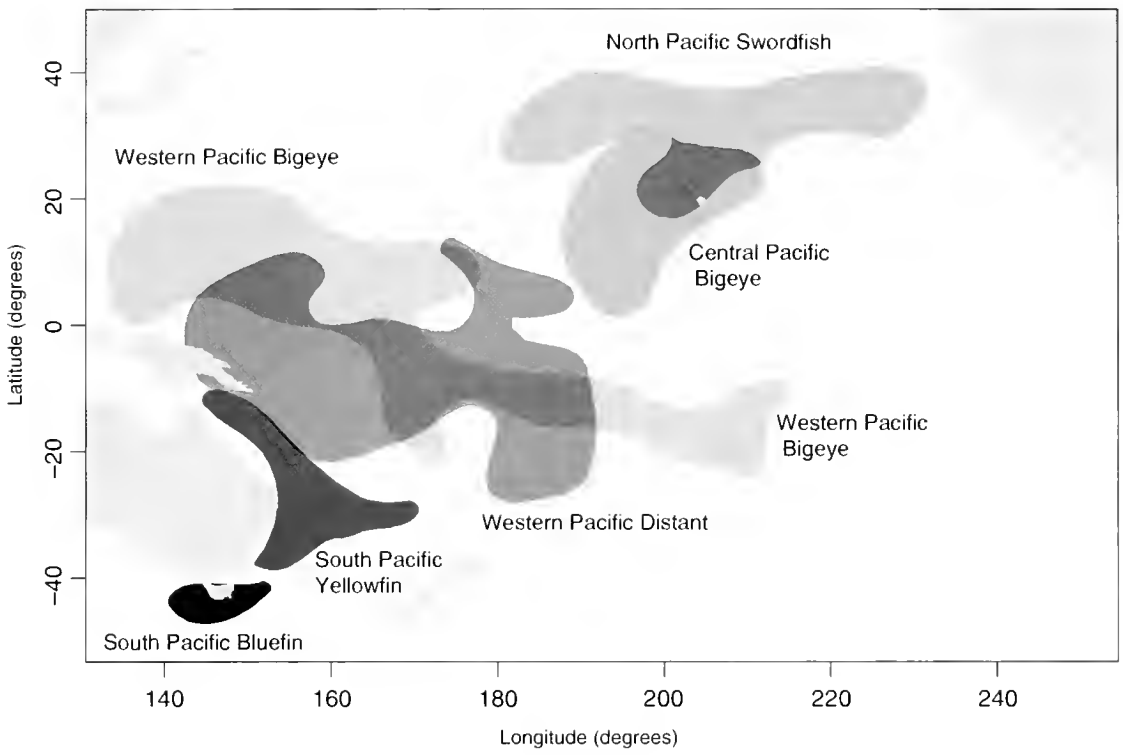

Figure 3
Geographical distribution of the observer data analyzed for each fishery.

the expected number of animals per hook. For each longline segment (j) within each operation (i), we link $\pi_{i,j}$ to a linear predictor ($\eta_{i,j}$) through the equation

$$\pi_{i,j} = \frac{e^{\eta_{i,j}}}{(1+e^{\eta_{i,j}})},$$

$\eta_{i,}$ is then modeled as a function of soak time:

$$\eta_{i,j} = \beta_0 + \beta_1 T_{i,j}, \quad (5)$$

where $T_{i,j}$ = the hook's soak time (decimal hours) in longline segment j;
β_0 = the intercept; and
β_1 = the slope coefficient, which we term the "soak time coefficient."

Modeling the probability of a catch on each individual hook would result in large numbers of zero observations and thus test the limits of current computer performance. Therefore we aggregated hooks and catches into hourly segments for each longline operation.

We assumed that each longline segment had the same configuration and that the probability of capture was the same for each segment within a longline operation. The assumption may be violated where segments pass through different water masses or where they differ in depth profile or baits. Saturation of segments with animals will also alter the capture probability between segments. The effects of water masses, depth profiles, baits, and gear saturation were not analyzed in the present study.

Capture probability may also vary through the differential exposure of segments to the diurnal cycle of night and day. The addition of dawn and dusk as fixed effects allowed us to model diurnal influences on catch rates.

Fixed effects To explore factors that might affect the relationship between soak time and catch rate, we added four fixed effects to the logit model: year, season, and, as mentioned above, whether the segment was available at dawn or dusk. A full model without interaction terms would be

$$\eta_{i,j} = \beta_0 + \beta_1 T_{i,j} + \beta_2 A_{i,j} + \beta_2 P_{i,j} + \beta_3 S_{i,j} + \beta_4 Y_{i,j} + O_i,$$

where $T_{i,j}$ = the hook's soak time (decimal hours) in longline segment j;
$A_{i,j}$ = an indicator of whether the hook was exposed to a dawn period;
$P_{i,j}$ = an indicator of whether the hook was exposed to a dusk period;
$S_{i,j}$ = the season (winter or summer);
$Y_{i,j}$ = the year;
O_i = the random effect for operation that we modeled as an independent and normally distributed variable (see "Random effects" section); and
β_0–β_4 are parameters (fixed effects) to be estimated. We refer to β_1 as the "soak time coefficient."

Table 2

List of common and scientific names of the species analyzed. Also shown is the number of individuals of each species analyzed in each fishery. A dash indicates that the species was not analyzed in the present study; it does not necessarily mean that the species was not taken in the fishery. In particular, observer data on the time of capture were not available for "other bony fish" in the North Pacific swordfish and Central Pacific bigeye tuna fisheries. NP = North Pacific; CP = Central Pacific; WP = Western Pacific; SP = South Pacific; LN = long-nosed; and SN = short-nosed.

		Fishery					
Common name	Species	NP swordfish	CP bigeye tuna	WP bigeye tuna	WP distant	SP yellowfin tuna	SP Bluefin tuna
Tuna and tuna-like species							
Albacore	*Thunnus alalunga*	9707	23,128	14,194	11,976	21,550	1399
Bigeye tuna	*Thunnus obesus*	5409	45,476	9814	2581	1846	–
Butterfly mackerel	*Gasterochisma melampus*	—	—	—	—	—	533
Skipjack tuna	*Katsuwonus pelamis*	546	13,882	1456	445	691	—
Slender tuna	*Allothunnus fallai*	—	—	—	—	—	28
Southern bluefin	*Thunnus maccoyii*	—	—	—	—	1030	10,537
Yellowfin tuna	*Thunnus albacares*	2811	21,654	16,029	4689	12,454	—
Wahoo	*Acanthocybium solandri*	383	5508	1345	—	308	—
Billfish							
Black marlin	*Makaira indica*	25	41	353	226	160	—
Blue marlin	*Makaira nigricans*	981	2379	1467	529	179	—
Sailfish	*Istiophorus platypterus*	49	193	706	399	151	—
Shortbill spearfish	*Tetrapturus angustirostris*	543	5467	529	398	654	—
Striped marlin	*Tetrapturus audax*	1963	8332	681	182	724	—
Swordfish	*Xiphias gladius*	22,457	1680	1472	287	1173	92
Other bony fish							
Barracouta	*Thyrsites atun*	—	—	—	—	53	—
Barracudas	*Sphyraena* spp.	—	—	707	153	—	—
Escolar	*Lepidocybium flavobrunneum*	1208	3983	1343	878	1726	84
Great barracuda	*Sphyraena barracuda*	32	743	303	442	92	—
Lancetfish (LN)	*Alepisaurus ferox*	2788	30,136	325	419	2868	610
Lancetfish (SN)	*Alepisaurus brevirostris*	—	—	155	84	257	59
Lancetfishes	*Alepisaurus* spp.	—	—	1431	98	—	—
Long-finned bream	*Taractichthys longipinnis*	—	—	—	—	—	292
Mahi mahi	*Coryphaena hippurus*	17,463	19,090	1436	211	447	—
Oilfish	*Ruvettus pretiosus*	555	1091	420	456	653	900
Opah	*Lampris guttatus*	68	4724	527	129	80	213
Pomfrets	Family Bramidae	—	—	623	60	—	40
Ray's bream	*Brama brama*	—	—	—	—	1074	10,547
Ribbonfishes	Family Trachipteridae	—	—	—	—	—	22
Rudderfish	*Centrolophus niger*	—	—	—	—	—	90
Sickle pomfret	*Taractichthys steindachneri*	—	—	122	21	—	—
Slender barracuda	*Sphyraena jello*	—	—	—	—	121	—
Snake mackerel	*Gempylus serpens*	1971	9881	256	44	—	—
Snake mackerels	Family Gempylidae	—	—	456	10	—	—
Southern Ray's bream	*Brama* spp.	—	—	—	—	—	28
Sunfish	*Mola ramsayi*	—	—	—	—	249	99
Sharks and rays							
Bigeye thresher shark	*Alopias superciliosus*	149	1930	145	61	—	—
Blacktip shark	*Carcharhinus limbatus*	—	—	445	125	—	—
Blue shark	*Prionace glauca*	31,503	31,413	5601	1628	1689	12,797
Bronze whaler	*Carcharhinus brachyurus*	—	—	—	—	116	—
Crocodile shark	*Pseudocarcharias kamoharai*	—	—	153	73	—	—

continued

Table 2 (continued)

Common name	Species	Fishery					
		NP swordfish	CP bigeye tuna	WP bigeye tuna	WP distant	SP yellowfin tuna	SP Bluefin tuna
Sharks and rays (continued)							
Dog fishes	Family Squalidae	—	—	—	—	—	60
Dusky shark	*Carcharhinus obscurus*	—	112	—	—	20	—
Grey reef shark	*Carcharhinus amblyrhynchos*	—	—	282	64	—	—
Hammerhead shark	*Sphyrna* spp.	—	—	142	191	22	—
Long finned mako	*Isurus paucus*	—	83	108	15	—	—
Oceanic whitetip shark	*Carcharhinus longimanus*	568	2373	2376	384	142	—
Porbeagle	*Lamna nasus*	—	—	—	—	27	1011
Pelagic stingray	*Dasyatis violacea*	2374	2849	1212	248	534	109
Pelagic thresher shark	*Alopias pelagicus*	—	—	77	34	—	—
School shark	*Galeorhinus galeus*	—	—	—	—	—	143
Short finned mako	*Isurus oxyrinchus*	476	685	408	169	432	128
Silky shark	*Carcharhinus falciformis*	25	1433	5396	2406	8	—
Silvertip shark	*Carcharhinus albimarginatus*	—	—	168	74	—	—
Thintail thresher shark	*Alopias vulpinus*	—	74	—	—	—	31
Thresher shark	*Alopias superciliosus*	—	—	415	—	93	18
Tiger shark	*Galeocerdo cuvier*	—	—	56	18	38	—
Velvet dogfish	*Zameus squamulosus*	—	—	—	—	—	156
Whip stingray	*Dasyatis akajei*	—	—	78	15	—	—
Seabirds							
Albatrosses	Family Diomedeidae	—	—	—	—	—	88
Petrels	Family Procellariidae	—	—	—	—	—	29
Other seabirds	Family Procellariidae	—	—	—	—	38	200
All operations	104,054		238,340	73,212	30,222	51,699	40,343

To maintain a focus on the effects of soak time, the models were limited to simple combinations of fixed effects and interaction terms. Dawn and dusk were added to various models of each species in each fishery. To reduce complexity, year and season were limited to models of seven species (bigeye tuna, oilfish, swordfish, blue shark, albacore, southern bluefin tuna, long-nosed lancetfish) in the two South Pacific fisheries. The seven species represented four taxonomic groups and the full range of responses observed in preliminary analyses of the soak-time–catch-rate relationship.

Random effects We added random effects to all models to allow catch rates of segments within each longline operation to be related. The random effects model assumes that there is an underlying distribution from which the true values of the probability of catching the species, π, are drawn. The distribution is the among-operation variation or "random effects distribution." The operations are assumed to be drawn from a random sample of all operations, so that the random effects (O_i) in the relationship between catch rate and soak time for each operation (i) are independent and normally distributed with $O_i \sim N(0, \sigma^2)$. The random effects and various combinations of the fixed effects were added to the linear predictor presented in Equation 5.

For each species in the South Pacific yellowfin tuna data set we compared the performance of models under an equal correlation structure with that of models under an autoregressive correlation structure. Under an autoregressive structure, catch rates in the different hourly segments within the operations are not equally correlated. For example, the correlation between segments might be expected to decline with increased time between segments. However, we used an equal correlation structure for all models because the Akaike's information criterion (AIC) and Sawa's Bayesian information criterion (BIC) indicated that there was no clear advantage in using the autoregressive structure rather than an equal correlation structure.

Implementation We implemented the models in SAS (version 8.0) using GLIMMIX, a SAS macro that uses iteratively reweighted likelihoods to fit generalized linear

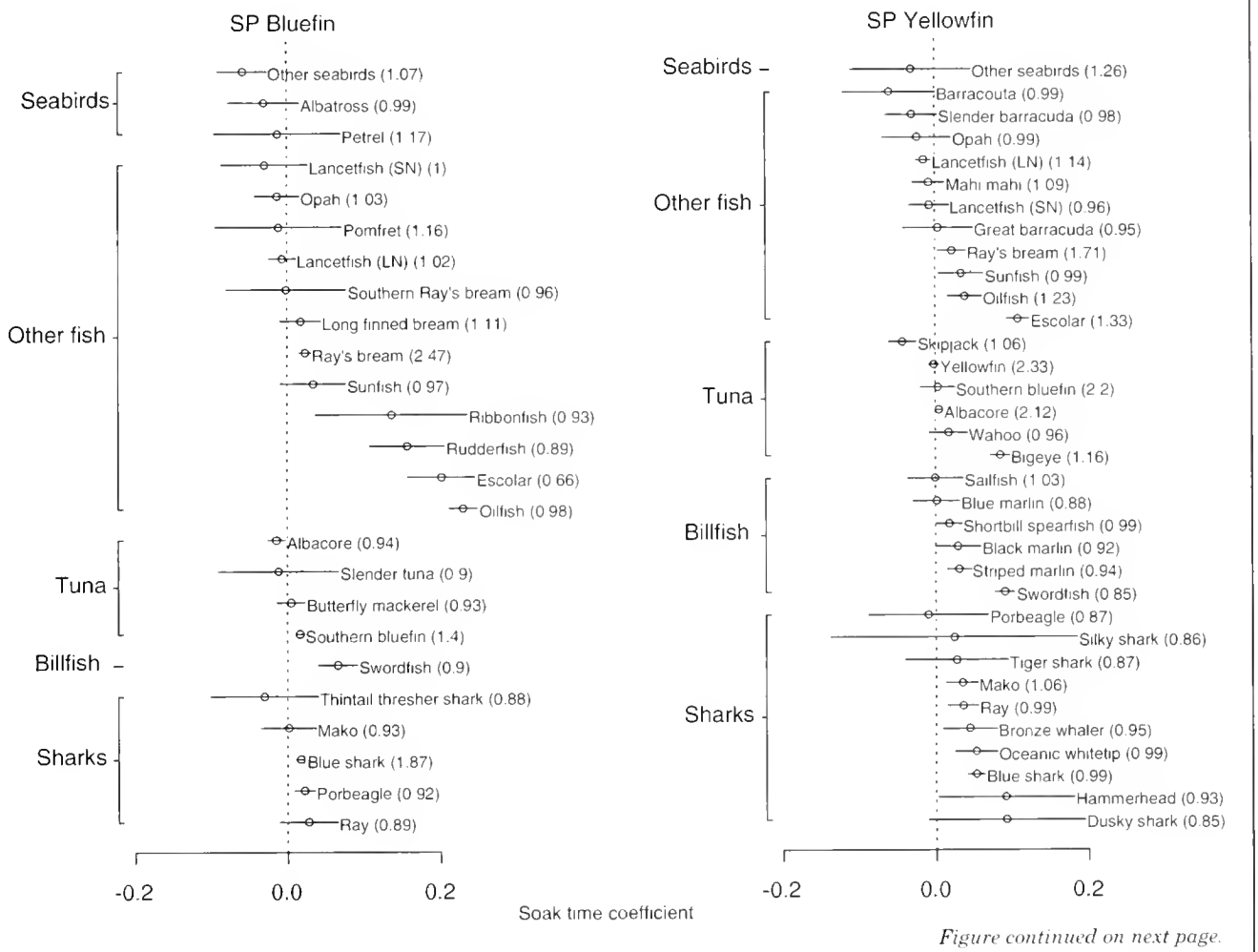

Figure continued on next page.

Figure 4

Coefficients for the effect of soak time on the catch rates of the most abundant species in each fishery. The coefficients are from random effects models where soak time is the only factor. Horizontal bars are 95% confidence intervals for the estimated coefficient. The dispersion parameter is shown in parentheses (it is 1.00 for species that are distributed as predicted by the model, but may be higher for species that have a more clumped distribution along the longline).

mixed models (Wolfinger and O'Connell, 1993). To judge the performance of the various model formulations, we checked statistics, such as deviance and dispersion, and examined scatter plots of chi-square residuals against the linear predictor (η) and QQ plots of chi-square residuals. We used the AIC and BIC to compare the performance of the various model formulations.

Variance in the binomial model depends on only one parameter, P. A dispersion parameter is therefore necessary to allow the variance in the data to be modeled. In effect, the dispersion parameter scales the estimate of binomial variance for the amount of variance in the data. The dispersion parameter will be near one when the variance in the data matches that of the binomial model. Values greater than one ("over-dispersion") imply that the species may have a clumped distribution along the longline.

Results

Soak time

For most species, soak time had a positive effect on catch rates (Fig. 4). In addition to being statistically significant, the effect of soak time made a large difference to catch rates at opposite ends of the longline. In the South Pacific yellowfin tuna fishery, for example, the expected catch rates of swordfish can vary from 0.6 (CI ±0.1) per 1000 hooks (5 hours) to 1.9 (CI ±0.3) per 1000 hooks (20 hours) (Table 3). A soak time of 5 hours and 3500 hooks (if that were possible) would result in a total catch of about two swordfish. In contrast, almost seven swordfish are expected from a longline operation of the same number of hooks with 20 hours of soak time.

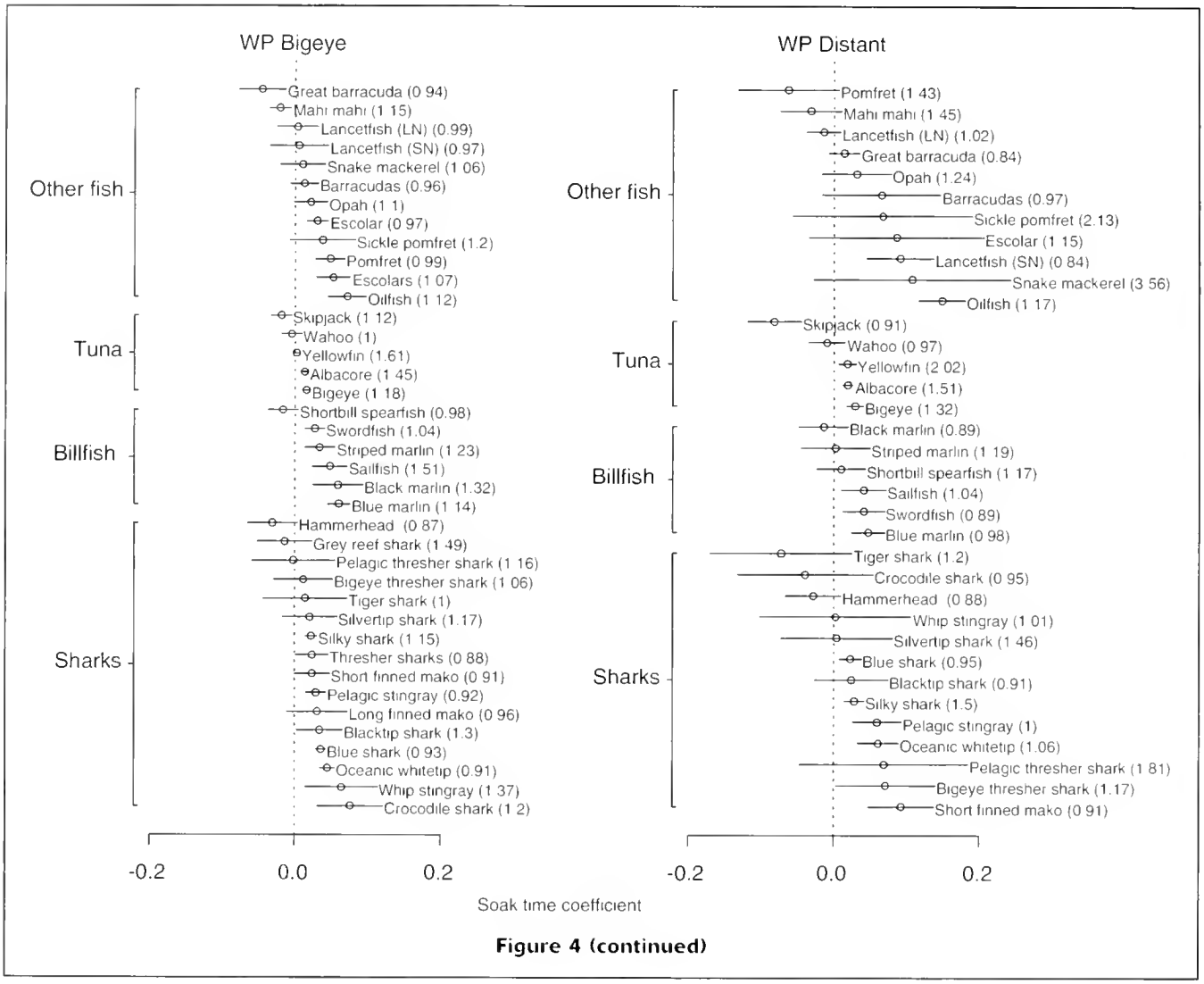

Figure 4 (continued)

For some species (e.g. seabirds, skipjack tuna, and mahi mahi), soak time had a negative effect on catch rates that was often statistically significant (Fig. 4). For skipjack tuna in the Western Pacific distant fishery, for example, catch rates decreased from 1.3 (CI ±0.2) per 1000 hooks for a soak time of 5 hours to 1.0 (CI ±0.1) per 1000 hooks (20 hours). Soak time had a small or statistically insignificant effect on catch rates for several species, such as yellowfin tuna and shortbill spearfish.

Fixed effects

Exposure to dusk had a positive effect on the catch rates for most species (Fig. 5). Dusk often had a negative effect on the catch rates of billfish, such as striped marlin and sailfish. For most species, however, the effect of dawn was weaker, and it influenced the catch rates of fewer species.

Like soak time, timing made a substantial difference to catch rates (Table 4). For a soak time of 12 hours in the South Pacific yellowfin fishery, for example, longline segments exposed to both dawn and dusk have a catch rate of 2.0 (CI ±0.5) escolar per 1000 hooks. The catch rate is 0.8 (CI ±0.1) per 1000 hooks for segments that were not exposed to dawn or dusk.

The effects of timing on catch rates were most pronounced in the South Pacific bluefin tuna fishery. The fishery also showed the greatest range in soak time coefficients, and the coefficients tended to be larger than those of other fisheries (Fig. 4).

Separately, the fixed effects often had statistically significant relationships with catch rates of the seven species that we investigated in detail. However, the interaction between soak time and each fixed effect was less frequently significant. Season was significant, for example, in none of the six models that included a soak-time–season interaction term. By comparison, season was significant in six of the 18 models that included season as a factor but not with a soak-time–season interaction term. The effect of soak time was not significant for southern bluefin tuna in any model for the South Pacific bluefin tuna fishery. It was significant

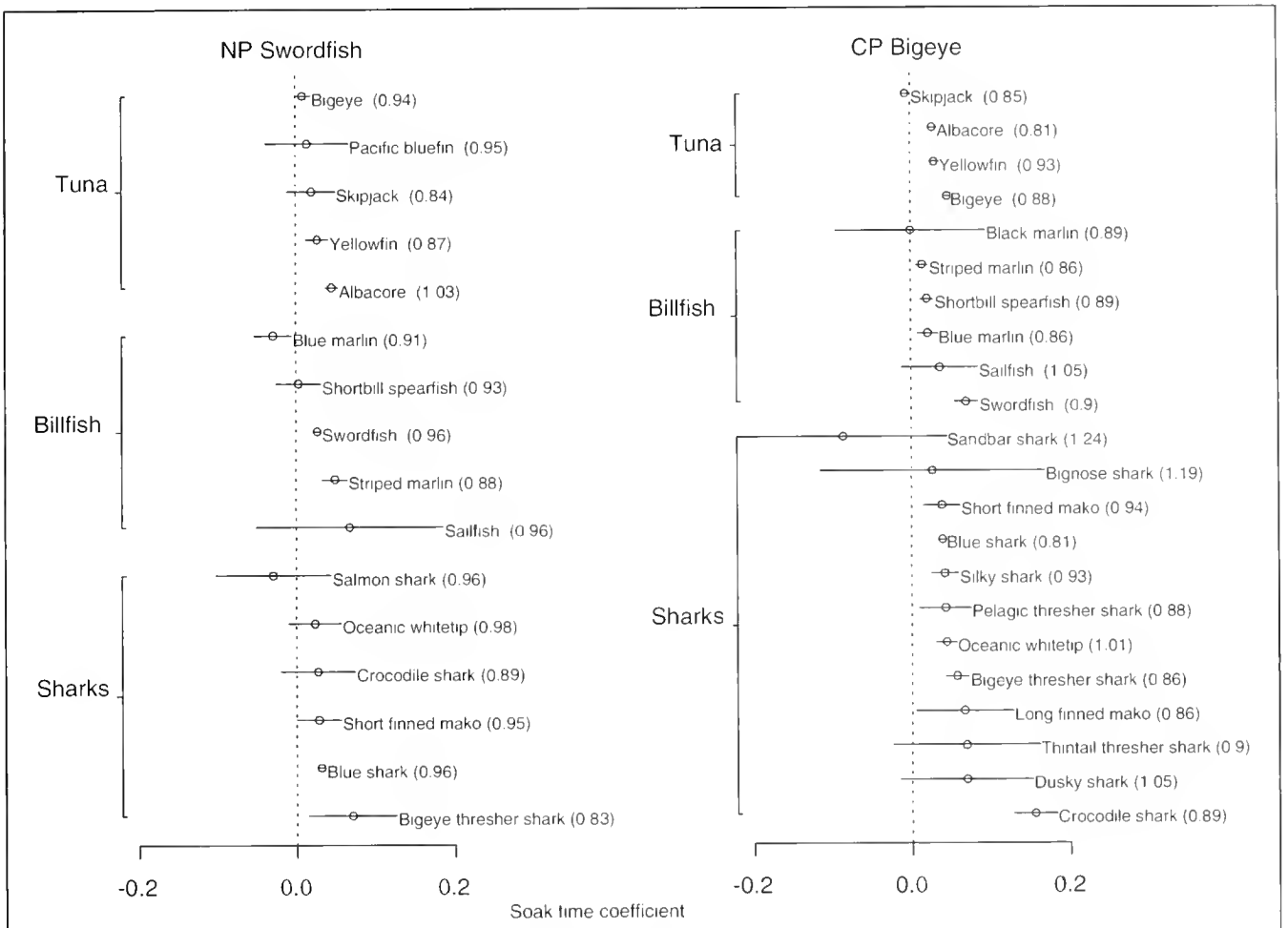

Figure 4 (continued)

in 36 of the 48 models for the other six species. We concluded that the fixed effects modified the intercept of the soak-time–catch-rate relationship, but they rarely altered the slope of the relationship.

Akaike's information criterion (AIC) and Sawa's Bayesian information criterion (BIC) both indicated that models with soak time as the only variable were the most or second most parsimonious model. This was the case for all models, except for several models of albacore and long-nosed lancetfish. Therefore the following discussion concentrates on the effects of soak time and timing on catch rates.

Discussion

In considering results of the random effects models, we examined patterns in the effects of soak time and timing among taxonomic groups, the mechanisms that may cause the patterns, and their implications. First, however, we investigated whether the effects were consistent for the same species between fisheries.

Comparison of fisheries

The effect of soak time was consistent for several species between the fisheries, despite significant differences in fishing practices and area and season of activity. For example, the soak time coefficients for species in the South Pacific yellowfin tuna fishery were very similar to those of the same species in the Central Pacific bigeye tuna fishery (r=0.79) (Fig. 6).

Several species had a narrow range of soak time coefficients over all the fisheries analyzed. Estimates of the coefficient of yellowfin tuna, for example, ranged from 0.00 (CI ±0.01) in the South Pacific yellowfin fishery to 0.04 (CI ±0.01) in the North Pacific swordfish fishery. A coefficient of 0.04 is equivalent to a difference of 1.3 yellowfin tuna per 1000 hooks between longline segments with soak times of 5 and 20 hours. The range in coefficients is also small for other abundant and widely distributed species, such as albacore (r=0.00–0.05) and blue shark (r=0.01–0.05).

For many species, however, the correlation between soak-time coefficients from different fisheries was poor (Fig. 6).

Table 3

Examples of the effect of soak time on expected catch rates of species in the South Pacific yellowfin tuna fishery. The expected catch rates (number per 1000 hooks) are predicted from the soak-time coefficient for each species for longline segments exposed to a dusk period with a soak time of 5 or 20 hours. Figure 4 shows the 95% confidence intervals for soak-time coefficients used to calculate the expected catch rates. LN = long-nosed; SN = short-nosed.

	Soak time (h)	
Species	5	20
Tuna and tuna-like species		
Albacore	15.5	13.4
Bigeye tuna	1.1	2.3
Skipjack tuna	1.3	1.0
Southern bluefin tuna	5.2	5.5
Yellowfin tuna	8.4	7.7
Billfish		
Black marlin	0.4	1.6
Blue marlin	1.2	0.4
Sailfish	0.8	1.0
Shortbill spearfish	1.0	1.6
Striped marlin	0.8	1.0
Swordfish	0.6	1.9
Other bony fish		
Barracouta	0.8	0.7
Escolar	0.8	3.1
Great barracuda	0.9	1.1
Lancetfish (LN)	2.7	2.4
Lancetfish (SN)	1.6	1.4
Mahi mahi	1.0	0.9
Oilfish	0.8	2.2
Opah	0.7	0.5
Ray's bream	1.8	2.0
Slender barracuda	1.7	1.6
Sunfish	0.6	1.3
Wahoo	1.0	1.1
Sharks and rays		
Blue shark	1.1	2.0
Bronze whaler	0.7	0.8
Dusky shark	0.4	0.8
Hammerhead	0.2	1.8
Mako	0.6	0.8
Oceanic whitetip	0.5	0.9
Porbeagle	1.2	1.1
Pelagic stingray	0.9	1.2
Thresher shark	0.6	1.0
Tiger shark	0.5	0.5

Table 4

Examples of the effect of timing on expected catch rates of species in the South Pacific yellowfin tuna fishery. The expected catch rates (number per 1000 hooks) are predicted from the soak-time coefficient for each species for a longline operation with a soak time of 12 hours. The different catch rates are for longline segments exposed to neither the dawn or dusk period, for dawn only, and for dawn and dusk periods. LN = long-nosed; SN = short-nosed.

	Period		
Species	Neither period	Dawn only	Dawn + dusk
Tuna and tuna-like species			
Albacore	12.3	14.0	16.5
Bigeye tuna	0.9	1.2	2.1
Skipjack tuna	1.4	1.2	1.0
Southern bluefin tuna	3.8	2.9	4.1
Yellowfin tuna	7.7	7.6	8.0
Billfish			
Black marlin	1.2	0.6	0.4
Blue marlin	0.4	1.0	1.4
Sailfish	0.8	0.7	0.7
Shortbill spearfish	1.3	0.9	0.9
Striped marlin	0.8	0.9	0.9
Swordfish	0.5	0.7	1.3
Other bony fish			
Barracouta	1.1	1.2	0.7
Escolar	0.8	1.0	2.0
Great barracuda	1.0	0.8	0.8
Lancetfish (LN)	2.8	2.7	2.5
Lancetfish (SN)	1.2	1.1	1.3
Mahi mahi	1.2	1.3	1.1
Oilfish	0.8	1.1	1.8
Opah	0.5	0.5	0.6
Ray's bream	0.8	0.7	1.6
Slender barracuda	2.0	1.5	1.2
Sunfish	0.8	0.6	0.7
Wahoo	1.2	1.3	1.1
Sharks and rays			
Blue shark	1.3	1.4	1.4
Bronze whaler	0.6	0.9	1.0
Dusky shark	0.1	0.1	0.6
Hammerhead	0.4	0.2	0.3
Mako	0.7	0.8	0.8
Oceanic whitetip	0.7	0.8	0.7
Porbeagle	1.0	0.6	0.6
Pelagic stingray	0.9	0.9	1.1
Thresher shark	0.6	0.6	0.7
Tiger shark	0.4	0.5	0.7

For a few species (e.g. tiger shark) the poor correlation may have been a function of small sample sizes and the wide confidence intervals of the estimates. For other species the estimates were well determined, yet poorly correlated, e.g. the coefficient for short-nosed lancetfish was 0.09 (CI ±0.05) in the Western Pacific distant fishery compared to 0.01 (CI ±0.04) in the Western Pacific bigeye tuna fishery. Therefore, we urge caution in applying our estimates to the same species in longline fisheries in other areas.

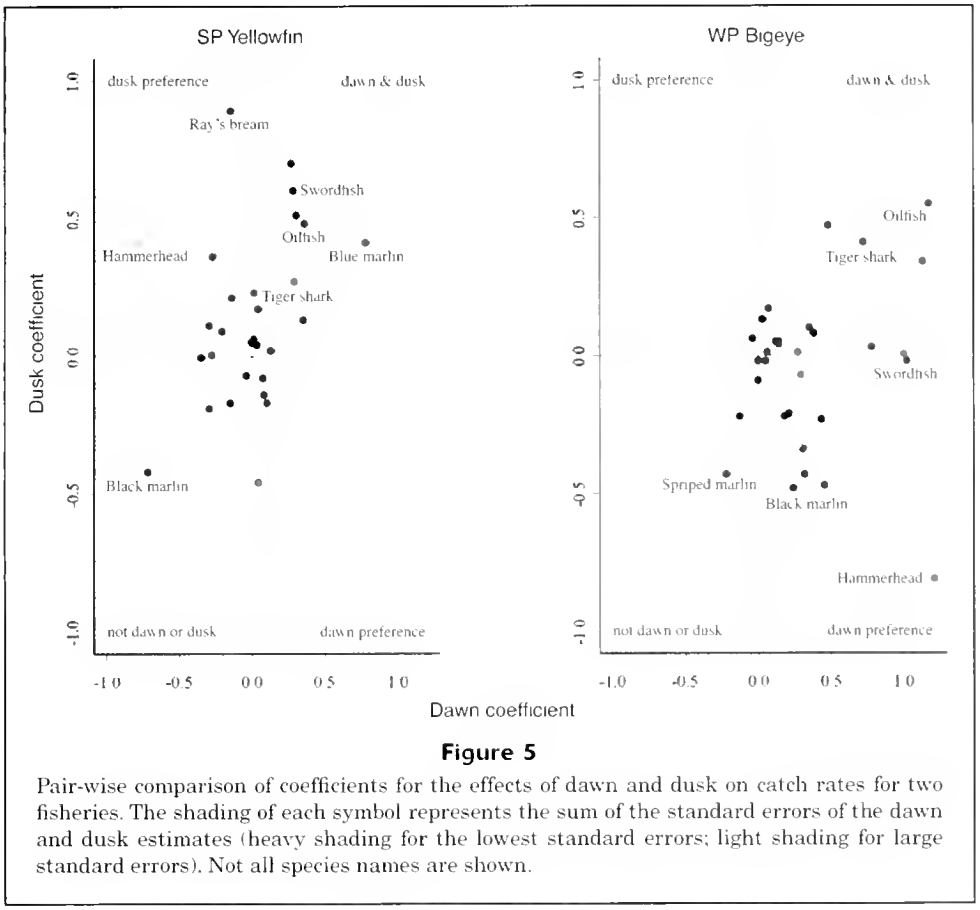

Figure 5

Pair-wise comparison of coefficients for the effects of dawn and dusk on catch rates for two fisheries. The shading of each symbol represents the sum of the standard errors of the dawn and dusk estimates (heavy shading for the lowest standard errors; light shading for large standard errors). Not all species names are shown.

Underlying mechanisms

The broad taxonomic groups taken by longline each represent a wide range of life history strategies and feeding behaviors. Nevertheless, the results show a tendency for soak time to have a positive effect on catch rates of most shark species (Fig. 4). It also had a positive effect on catch rates of many billfish species, including striped marlin, black marlin, and swordfish. There is no clear pattern in the effect of soak time on catch rates of tuna or other bony fish. It had a negative effect on the four seabird groups.

The results imply that the ability of a species to stay alive and to escape or avoid scavengers while hooked is important in determining the catch that is actually brought on board. The effect of soak time is significantly correlated with the ability of a species to survive while hooked on the longline in the four fisheries with data on survival (Fig. 7). Soak time has a strong, positive effect on catch rates of species like blue shark, which are almost always alive when branchlines are retrieved. Species like skipjack tuna and seabirds are usually dead. Soak time had a negative effect on their catch rates. The opposite trend would be expected if escape is a significant process that affects catch rates; if escape is important, soak time should have a *negative* affect on the catch rates of the most active species. Therefore removal by scavengers is likely to be more important than escape in determining catch rates for many species.

Longline branchlines are usually 20–30 m in length, allowing considerable room for a live, hooked animal to evade predators or scavengers. Or, scavengers may be attracted by immobile and dead animals. The scavenger avoidance hypothesis is attractive, but it is difficult to test with observer data. Data from hook-timer experiments may help to estimate the total number of animals that are lost or removed from the longline. Data presented by Boggs (1992) showed a large number of hook-timers that were triggered but which did not hold an animal when the branchline was retrieved, e.g. his data show that 2–4% of hook-timers on 10,236 branchlines that had "settled" were activated but did not have an animal. It is unclear whether the triggering of hook-timers was due to equipment malfunction or whether it represents high loss rates. Of particular significance to the question of loss rates is the fact that current hook-timer technology does not identify the species that were lost and whether they were alive or dead.

We noticed that soak-time coefficients tended to be poorly correlated between fisheries and that the effects of soak time on catch rates were most pronounced in the South Pacific bluefin tuna fishery. Our scavenging hypothesis might explain those observations as evidence that the activities of scavengers vary between fisheries. For example, blue shark might be an important scavenger. They are most abundant in temperate areas (Last and Stevens, 1994). Our analyses showed a predominance of negative soak-time coefficients

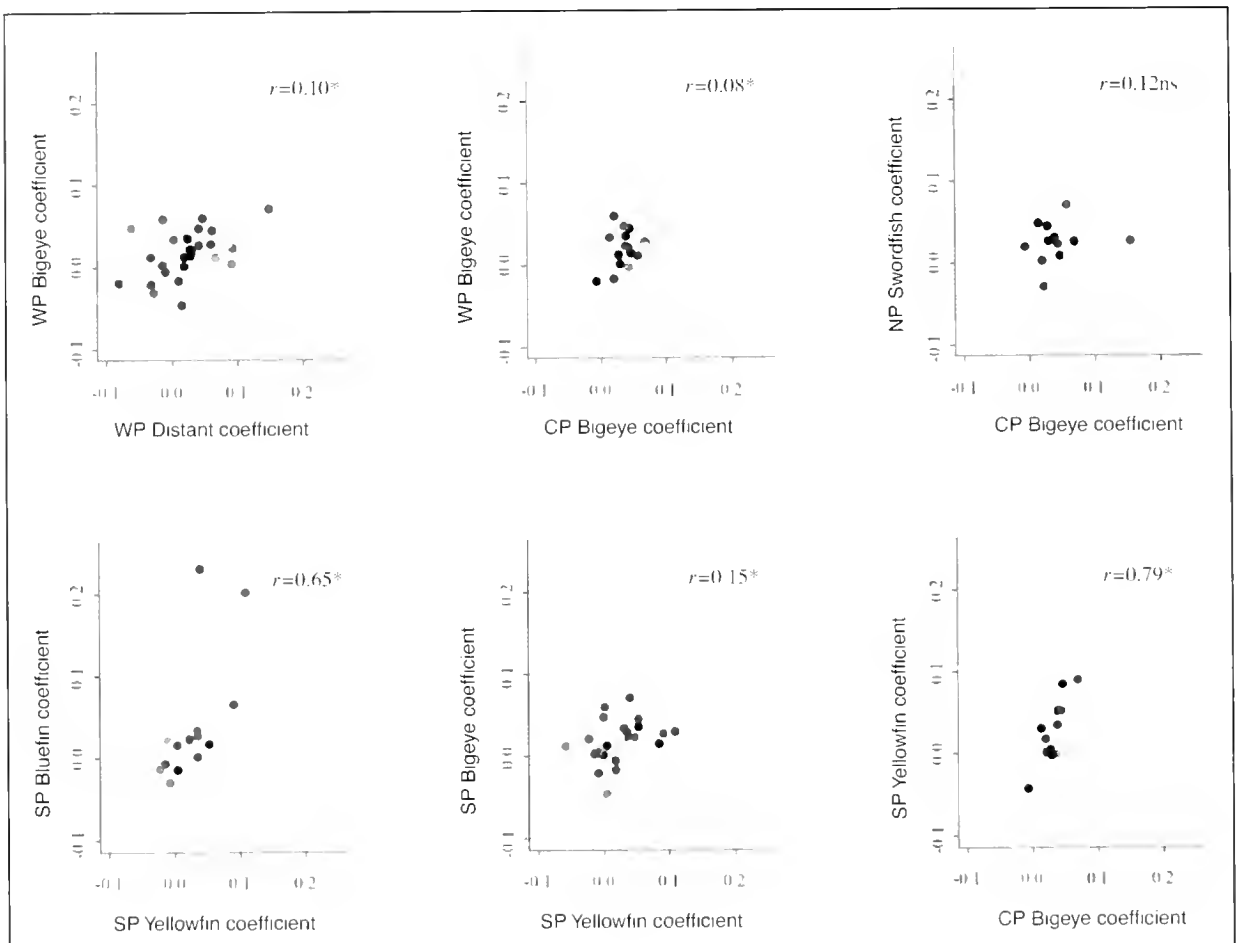

Figure 6

Pair-wise comparison of soak time coefficients for species that were common to fisheries. The coefficients are from random effects models where soak time is the only factor. The shading of each symbol represents the size of the standard error of the estimate. "*r*" is the correlation coefficient of a linear regression of coefficients (* indicates that the regression slope is significantly different from one at the 95% level, whereas "ns" indicates that the null hypothesis, that the regression slope equals one, cannot be rejected).

in the South Pacific bluefin tuna fishery—perhaps indicating that loss rates may be particularly high where blue shark are abundant.

Nevertheless, there are other plausible explanations for the differences in soak-time effects between fisheries. The movement of branchlines caused by wave action will cause animals to fall off hooks, especially when branchlines are near the sea surface. Rough seas are frequently experienced in the North Pacific swordfish and South Pacific bluefin tuna fisheries where the soak-time effects were most pronounced.

Another source of loss might be the breakage of longline branchlines. The animal's teeth or rostrum might abrade the branchline causing the branchline to fail and allowing the animal to escape. In this regard it is noteworthy that Central Pacific bigeye tuna longliners often use wire for the end of branchlines or "leader" whereas North Pacific wwordfish longliners use monofilament nylon leaders (Ito[4]).

Mortality estimates

The results of our study show that longline catch rates that are not adjusted for the effects of soak time will underestimate the level of mortality of several species because they are lost after being hooked. The soak time effect was negative for albatrosses and other seabirds. This finding agrees with field observations (e.g. Brothers, 1991) that most seabirds are taken during longline deployment in the brief period after the bait is cast from the vessel until the bait sinks beyond the depth that seabirds can dive to. Those observations indicate that counts of seabirds when they are brought on board do not cover the total number hooked because many fall off or are removed by scavengers or are lost during the operation.

[4] Ito, R. 2002. Personal commun. National Marine Fisheries Service (NOAA), 2570 Dole Street, Honolulu Hawaii 96822-2396.

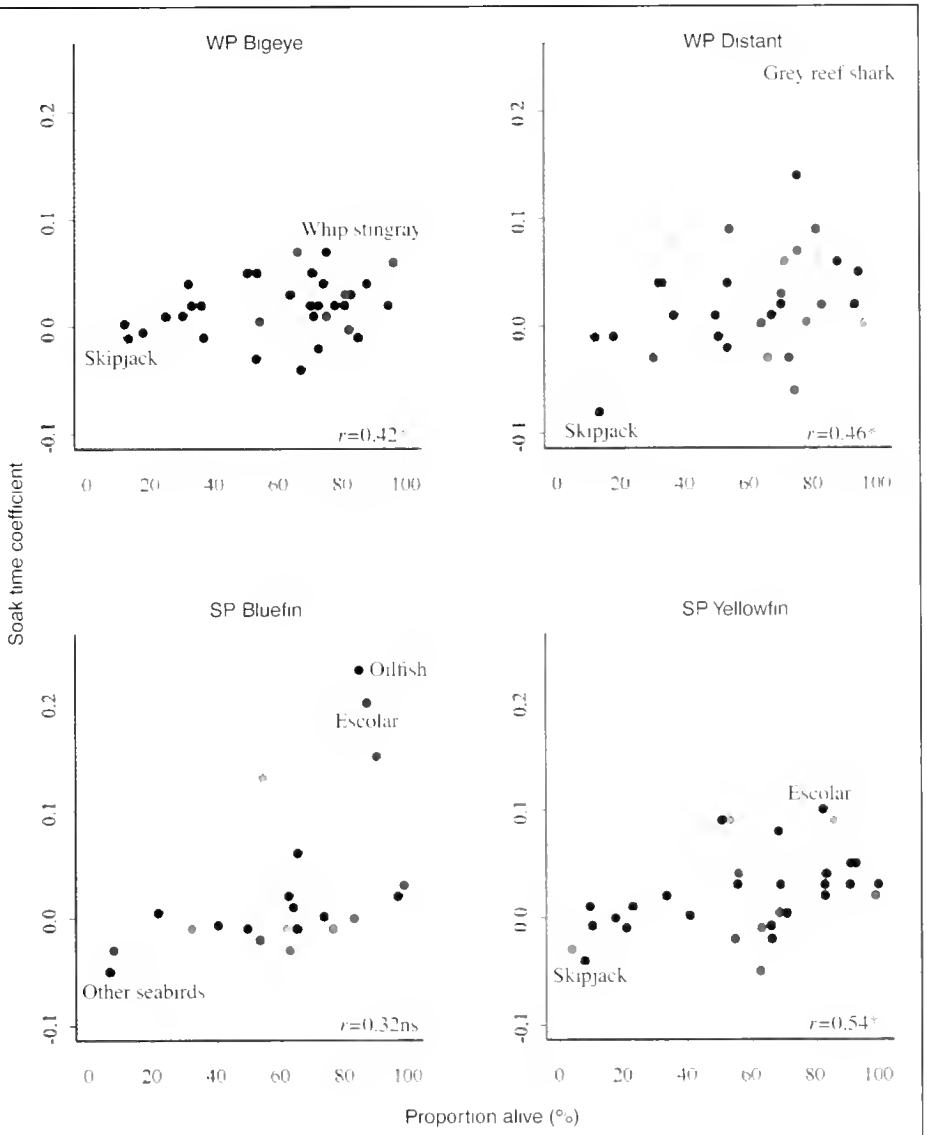

Figure 7

Soak-time coefficients plotted against the proportion of each species reported to be alive when brought on board. Not included are species where less than ten individuals for the fishery had a record of life status. The coefficients are from random effects models where soak time is the only factor. The shading of each symbol represents the size of the standard error of the estimate. The proportion alive is assumed to be measured without error. "r" is the correlation coefficient of a linear regression of coefficients (* indicates that the regression slope is significantly different from zero at the 95% level).

Seabirds provide a unique case for estimating loss rates because they are only caught when the longline is deployed (Brothers, 1991). Within minutes of the branchline being deployed, the capture rate (α in Eq. 4) falls to zero whereas the loss rate β might be constant or it might vary. Therefore, the probability of a seabird being on a hook when the branchline is retrieved is

$$\pi(T) = e^{-\beta T}. \quad (6)$$

We estimated a soak-time coefficient of –0.0302 (CI ±0.0462) for albatrosses in the South Pacific bluefin tuna fishery. Substituting 0.0302 for β in Equation 6 and 10.4 hours for T (the average soak time of hooks deployed by the longliners), we estimated that 27% of albatrosses are lost after being hooked but before the branchlines are retrieved. The loss rate is about 12% for petrels (β=0.0123) and 45% for other seabirds (β=0.0582). It is about 26% for other seabirds in the South Pacific yellowfin tuna fishery (β=0.0307, T=10.0 hours).

For fishes and sharks, we do not know how the probability of capture, or capture rate, or loss rate varies during a longline operation. However, hook–timer experiments

and observer programs may provide estimates of those parameters. Broad limits for the probability of capture may also be obtained if observers were to report the number of branchlines that are retrieved with missing baits or missing hooks.

For most species, capture rates must balance or outweigh loss rates. In this case, captures result from the increased exposure of animals to the longline as a result of movement and, perhaps, the dispersal of chemical attractants during the operation. However, we must stress that losses are also likely to be occurring for the species that have positive coefficients. The analyses indicate the relative levels of loss between longline segments of varying soak time. Other than those for seabirds, we cannot estimate the levels of catch that are lost.

Adding to the uncertainty over loss rates is the unknown fate of lost animals. For seabirds it is known that most drown soon after being hooked. The few seabirds that survive while hooked eventually drown during longline retrieval (Brothers, 1991). However, it is not known whether other lost animals are dead or alive.

Results of our analyses may also be useful for monitoring programs. Observers are increasingly being placed on longliners to collect data on bycatch and to independently verify data reported in logbooks. A sampling approach is necessary in some fisheries because observers are often unable to monitor the entire longline retrieval. Indications that catch rates of some species at the end of the retrieval are double those at the beginning necessitate care in designing observer monitoring protocols and in the interpretation of the data. Observers could also collect information on the number of hooks retrieved without baits. Such data would greatly improve the estimates of α and β required for the theoretical model. For the empirical model, catch rate data from research surveys where longline segments have very short (<4 hour) soak times would improve estimates of soak-time coefficients.

Historical changes

The interaction of year and soak time was rarely significant for the random effects models of the seven species examined in detail. This might suggest that soak-time–catch-rate relationships are stable over time. However, the range of years that we analyzed was limited to 1992–97. Over larger time scales there have been large variations in the abundance of individual species and the mix of species comprising the pelagic ecosystem. We cannot predict how soak-time–catch-rate relationships would change with those long-term variations.

Our original motivation for examining the effects of soak time was the hypothesis that the number of hooks per operation and soak time have increased since longlining commenced and that this may have resulted in an overestimation of billfish catch rates in early years. Ward[5] presented information on temporal trends in soak time and timing for several longline fleets. Although there is uncertainty over the early operations, the available information indicates significant historical changes in Japan's distant-water longline operations. Average soak time shows a decline from over 11.5 hours before 1980 to 10.0 hours in the 1990s. For species with a negative soak-time coefficient, this apparently modest reduction in soak time would inflate catch rate estimates for recent years. It would result in reduced catch-rate estimates for species with positive coefficients. For example, the expected catch rate for swordfish is 0.94 (CI ±0.06) per 1000 hooks for a soak time of 11.5 hours compared to 0.82 (CI ±0.06) per 1000 hooks for 10.0 hours.

More significant may be changes in the timing of operations. During 1960–80 most baits used with Japan's distant-water longliners were available to fish at dawn whereas about 50% were also available at dusk. Longlines were deployed and retrieved at later times in the 1990s so that about 30% of baits were available at dawn and about 70% available at dusk. In the case of swordfish, the changes in timing would moderate the effects of reduced soak time. The expected catch rate for swordfish is 0.89 per 1000 hooks in the early operations compared to 0.83 per 1000 hooks in the later operations.

Conclusions

The results have important implications for fishery management and assessments that rely on longline catch data. Modifications to data collection, such as recording the number of hooks with missing baits during longline retrieval, would greatly improve mortality estimates. The mortality of species like seabirds is significantly higher than previously estimated. Such underestimation may be particularly critical for the assessment and protection of threatened species of seabirds. Furthermore, the changes in timing and reduction in soak time have resulted in a systematic bias in estimates of mortality levels and abundance indices for many species. For species like swordfish, where soak time has a positive effect on catch rates, the stocks might be in better shape than predicted by current assessments (if assessments were solely based on catch and effort data). The opposite situation would occur for species with negative soak-time coefficients: assessments that use long time-series of longline catch data will over-estimate the species' abundance so that population declines are more severe than previously believed.

Acknowledgments

Grants from the Pew Charitable Trust, Pelagic Fisheries Research Program, and the Killam Foundation provided financial support for this work. Peter Williams (Secretariat of the Pacific Community), U.S. National Marine Fisheries Service staff (Kurt Kawamoto, Brent Miyamoto, Tom Swenarton, and Russell Ito) and Thim Skousen (Australian Fisheries Management Authority) provided observer data and operational information on the fisheries. We are espe-

[5] Ward, P. 2002. Historical changes and variations in pelagic longline fishing operations. http://fish.dal.ca/~myers/pdf papers.html. [Accessed 22 February 2003.]

cially grateful to the observers who collected the data used in this study and thank the masters, crew members, and owners of longliners for their cooperation with the observer programs. Pierre Kleiber, Ian Jonsen, Julia Baum, Boris Worm and an anonymous referee provided many useful comments on the manuscript.

Literature cited

Boggs, C. H.
1992. Depth, capture time, and hooked longevity of longline-caught pelagic fish: timing bites of fish with chips. Fish. Bull. 90:642–658.

Brothers, N.
1991. Albatross mortality and associated bait loss in the Japanese longline fishery in the Southern Ocean. Biol. Conserv. 55:255–268.

Carey, F. G.
1990. Further acoustic telemetry observations of swordfish. Mar. Recr. Fish. 13:103–22. Sportfishing Institute, Washington D.C.

Deriso, R. B., and A. M. Parma.
1987. On the odds of catching fish with angling gear. Trans. Am. Fish. Soc. 116:244–256.

Fernö, A., and I. Huse.
1983. The effect of experience on the behaviour of cod (*Gadus morhua* L.) towards a baited hook. Fish. Res. (Amst.) 2: 19–28.

Last, P. R., and J. D. Stevens.
1994. Sharks and rays of Australia. CSIRO Australia. 513 pages + color plates.

Murphy, G. I.
1960. Estimating abundance from longline catches. J. Fish. Res. Board Can. 17:33–40.

Sivasubramaniam, K.
1961. Relation between soaking time and catch of tunas in longline fisheries. Bull. Jpn. Soc. Sci. Fish. 27:835–845.

Somerton, D. A., and B. S. Kikkawa.
1995. A stock survey technique using the time to capture individual fish on longlines. Can. J. Fish. Aquat. Sci. 52: 260–267.

Ward, P. J.
1996. Japanese longlining in eastern Australian waters, 1962–90, 249 p. Bureau of Resource Sciences, Canberra.

Ward, P., and S. Elscot.
2000. Broadbill swordfish: status of world fisheries, 242 p. Bureau of Rural Sciences, Canberra.

Wolfinger, R. and M. O'Connell.
1993. Generalized linear mixed models: a pseudo-likelihood approach. J. Stat. Comput. Simul. 48:233–243.

Zhou, S., and T. C. Shirley.
1997. A model expressing the relationship between catch and soak time for trap fisheries. N. Am. J. Fish. Manag. 17: 482–487.

Abstract—Annual mean fork length (FL) of the Pacific stock of chub mackerel (*Scomber japonicus*) was examined for the period of 1970–97. Fork length at age 0 (6 months old) was negatively correlated with year-class strength which fluctuated between 0.2 and 14 billion in number for age-0 fish. Total stock biomass was correlated with FL at age but was not a significant factor. Sea surface temperature (SST) between 38–40°N and 141–143°E during April–June was also negatively correlated with FL at age 0. A modified von Bertalanffy growth model that incorporated the effects of population density and SST on growth was well fitted to the observed FL at ages. The relative FL at age 0 for any given year class was maintained throughout the life span. The variability in size at age in the Pacific stock of chub mackerel is largely attributable to growth during the first six months after hatching.

Effects of density-dependence and sea surface temperature on interannual variation in length-at-age of chub mackerel (*Scomber japonicus*) in the Kuroshio-Oyashio area during 1970–1997

Chikako Watanabe

Akihiko Yatsu

National Research Institute of Fisheries Science
Fisheries Research Agency
2-12-4 Fukuura, Kanazawa
Yokohama 236-8648, Japan
E-mail address (for C. Watanabe) falconer@affrc.go.jp

Variability in growth of marine fishes has been attributed to the effects of density-dependence or environmental factors such as water temperature, or to the effects of both factors (e.g. Moyle and Cech, 2002). Size-at-age data are crucial because they are necessary for stock assessment methods such as virtual population analysis, yield per recruit, and spawning-per-recruit analyses (Pauly, 1987; Mace and Sissenwine, 1993; Haddon, 2001) and are possibly useful for detecting regime shifts as well (Yatsu and Kidoroko, 2002). Around Japan, the effects of population density and sea water temperature on fish growth have been shown for the Pacific stock of chub mackerel (*Scomber japonicus*) (Iizuka, 1974), Japanese Spanish mackerel (*Scomberomorus niphonius*) (Kishida, 1990), the Pacific and Tsushima Current stocks of Japanese sardine (*Sardinops melanostictus*) (Hiyama et al., 1995; Wada et al., 1995), and Japanese common squid (*Todarodes pacificus*) (Kidokoro, 2001).

The Pacific stock of chub mackerel is one of the most important commercially exploited fish populations in Japan and has been managed by the total allowable catch (TAC) system in Japan since 1997. Chub mackerel seasonally migrate along the Pacific coast of Japan from Kyushu to Hokkaido. They spawn in the coastal waters around Izu Islands and off southwestern Japan between February and June (Fig. 1, Watanabe, 1970; Usami, 1973; Murayama et al., 1995; Watanabe et al., 1999). Adult fish (after spawning) and their offspring migrate eastward along the Pacific coast with the Kuroshio Current. Juvenile mackerel of about 6 months old usually recruit to the purse-seine and set-net fisheries off the coast of northeastern Japan at the end of summer (Fig. 1, Odate, 1961; Kawasaki, 1966; Watanabe, 1970; Iizuka, 1974). The total catch of the Pacific stock of chub mackerel increased during the 1960s and 1970s, peaked at 1.5 million metric tons in 1978, and then declined to 2.3 thousand tons in 1990 (Fig. 2). The estimated total biomass increased in the 1970s from 2.8 million tons in 1970 to 5.9 million tons in 1977, and the consecutive occurrences of large year classes exceeded 7 billion age-0 (6-month-old) fish in the early and mid 1970s. In 1990, the biomass was reduced to a minimum of 0.2 million tons in 1990 (Table 1, Fig. 2; Yatsu et al.[1]). Relatively large year classes occurred in 1992 (2.8 billion fish) and 1996 (4.5 billion fish), and the total biomass increased in the mid 1990s, but it remained at about 10% of the level attained in the mid 1970s (Yatsu et al.[1]).

On the basis of year-class strength and variations in fork length (FL) at ages 0–2 for the 11 year classes present from 1963 to 1973, Iizuka (1974) suggested an effect of density-dependent growth on young chub mackerels. In

[1] Yatsu, A., C. Watanabe, and H. Nishida. 2001. Stock assessment of the Pacific stock of chub mackerel in fiscal 2000 year. *In* Stock assessment report, p. 64–87. [In Japanese. Available from Fisheries Research Agency, 2-12-4 Fukuura, Kanazawa, Yokohama 236-8648, Japan.]

Manuscript approved for publication 22 September 2003 by Scientific Editor.
Manuscript received 20 October 2003 at NMFS Scientific Publications Office.
Fish. Bull. 102:196–206 (2004).

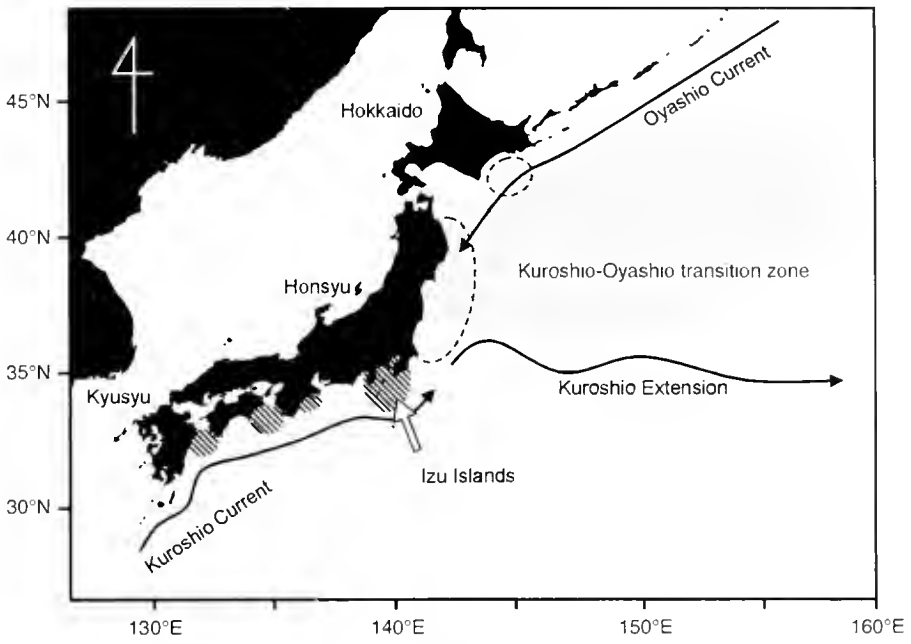

Figure 1

Distribution of the Pacific stock of chub mackerel (*Scomber japonicus*) and major oceanographic features around Japan. The hatched areas show spawning grounds. The dotted areas show feeding grounds. Major purse-seine fishing grounds are surrounded by dashed lines. The fishing grounds around the eastern coast of Hokkaido failed in 1977 with the decline in biomass (Hirai, 1991).

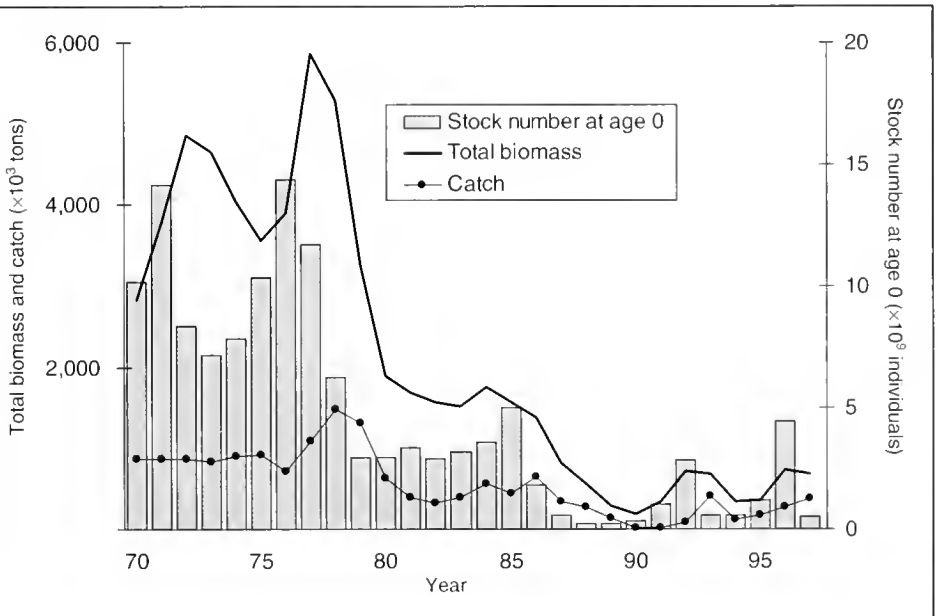

Figure 2

Total biomass, total catch, and year-class strength for the Pacific stock of chub mackerel (*Scomber japonicus*) (Yatsu, et al.[1]). Year-class strength was represented by the stock in number at age 0, estimated by virtual population analysis (Yatsu, et al.[1]).

this study we describe the variation in FL at age of the Pacific stock of chub mackerel in the Kuroshio–Oyashio area, using data from 1970 to 1997 when the stock biomass fluctuated between 0.2 and 5.9 million metric tons. We use these data to evaluate the effects of population density and sea surface temperature on FL at age.

Materials and methods

Biological data

Biological data have been compiled since 1964 for purse-seine, set-net, dip-net catches, and other catches by national fisheries research institutes and local government fisheries experimental stations in Japan. Fork length (FL) was measured for one thousand to 100 thousand fish per year and body weight (BW) and gonad weight were measured for 10–100% of these fish. The monthly FL compositions and the relationships of FL to BW were established for each year with this data set. Year-specific age-length keys from 1970 to 1994 were adopted from the reports of cooperative research on Pacific mackerel by local government agencies in Chiba, Kanagawa, Shizuoka, and Tokyo.[2] Between 1995 and 1997, age-length keys were developed by national fisheries research institutes and local government fisheries experimental stations.

For calculating the mean FL for ages 0, 1, 2, 3, 4, 5, and 6 years and older, we used data from the purse-seine fishery of northeastern Japan during September–December for 28 years, from 1970 to 1997. The catch of this fishery in these four months constituted 26–80% (the 28-year mean is about 63%) of the total annual catch of the Pacific stock of chub mackerel. Catch in number at FL class i (cm) of each month were calculated by

$$n_{a,i} = C_a \frac{d_{a,i}}{\sum_{k=1}^{50} d_{a,k} w_{a,k}}, \quad (1)$$

where $n_{a,i}$ = catch in number at FL class i (cm) {= 1, . . . , k, . . 50} of month a {= *Sep.*, *Oct.*, *Nov.*, *Dec.*};
$d_{a,i}$ = frequency at FL class i of month a;
$w_{a,i}$ = a mean weight of each FL class derived from the FL-BW relationship; and
C_a = a total catch of month a.

We then summed $n_{a,i}$ of 4 months to derive the annual catch in number at FL class i:

$$n_i = \sum_{a\ Sep}^{Dec} n_{a,i}, \quad (2)$$

where n_i = the annual catch in number at FL class i.

Using the age-length key, we converted n_i to catch at FL class i at age j:

$$n_{i,j} = n_i \times r_{i,j}, \quad (3)$$

where $n_{i,j}$ = the annual catch in number at FL class i at age j; and
$r_{i,j}$ = the proportion of age j at FL class i ($r_{i,0} + r_{i,1} + \cdots + r_{i,k} = 1$).

From $n_{i,j}$, we calculated the mean and variance of FL at age j:

$$l_j = \frac{\sum_{i=1}^{k} n_{i,j} l_{i,j}}{\sum_{i=1}^{k} n_{i,j}} \quad (4)$$

and

$$Var(l_j) = \frac{\sum_{i=1}^{k} n_{i,j} (l_{i,j} - l_j)^2}{\left(\sum_{i=1}^{k} n_{i,j}\right) - 1}, \quad (5)$$

where l_j = mean FL at age j; and
$l_{i,j}$ = mean FL at FL class i at age j.

Sea surface temperature

Time-series data for sea surface temperature (SST, temperatures averaged over 10 days for 1° latitude × 1° longitude blocks over the northwestern North Pacific between 0–53°N and 110–180°E since 1950) were provided by the Oceanographical Division of the Japan Meteorological Agency. The SST data for each block was averaged for periods of three months (i.e. January–March, April–June, July–September, and October–December). The relationship between the SST of each block and FL at age 0 were examined from 1970 to 1997.

Autocorrelation

For correlation analysis, effective sample sizes (n^*) were calculated for all time series data to take autocorrelation into account. n^* was computed by the formula (Pyper and Peterman, 1998):

$$\frac{1}{n^*} = \frac{1}{n} + \frac{2}{n} \sum_{j=1}^{n-5} r_{XX}(j) r_{YY}(j), \quad (6)$$

where $r_{XX}(j)$ and $r_{YY}(j)$ are the autocorrelations of X and Y at lag j, defined here with the additional weighting factor proposed by Pyper and Peterman (1998):

$$r_{XX}(j) = \frac{n}{n-j} \frac{\sum_{t=1}^{n-j} (X_t - \bar{X})(X_{t+j} - \bar{X})}{\sum_{t=1}^{n} (X_t - \bar{X})^2}. \quad (7)$$

Growth model

We used the modified von Bertalanffy growth model to incorporate the effects of population density and sea sur-

[2] Age-length keys. *In* Kanto Kinkai no Masaba ni tuite, Appendix 1, vol. 30, 30 p. [In Japanese. Available from Kanagawa Prefectual Fisheries Research Institute, Jyogashima, Misaki, Miura, Kanagawa 238-0237, Japan.]

face temperature according to Millar and Myers,[3] who nvestigated three formulations of the modified von Bertalanffy equations: 1) a reversible effect on the growth constant k; 2) a reversible effect on the asymptotic length L_∞; and 3) an irreversible effect on L_∞ or k. We tested two of the models, 1 and 2, to investigate the effect of population density and SST. We did not test model 3 because we did not consider that the environmental effects on growth were permanent. Mean length at age i of year-class y was estimated with the following formulas:

Model 1: reversible environmental effect on k

$$\hat{L}_{i,y} = L_\infty(1-e^{-k_{0,y}t_0}) \quad (8)$$

$$\hat{L}_{i,y} = \hat{L}_{i-1,y} + (L_\infty - \hat{L}_{i-1,y})(1-e^{-k_{i-1,y}}) \quad (9)$$

$$k_{i,y} = k + \beta_1 T_{i+y} + \beta_2 D_{i,y}. \quad (10)$$

Model 2: reversible environmental effect on L_∞

$$\hat{L}_{0,y} = L_{\infty 0,y}(1-e^{-kt_0}) \quad (11)$$

$$\hat{L}_{i,y} = \hat{L}_{i-1,y} + (L_{\infty i,y} - \hat{L}_{i-1,y})(1-e^{-k}) \quad (12)$$

$$L_{\infty i,y} = L_\infty + \beta_1 T_{i+y} + \beta_2 D_{i,y}, \quad (13)$$

where t_0 = the age at length 0 (year);
L_∞ = the asymptotic length; and
k = the growth coefficient;
$L_{\infty i,y}$ = L_∞ at age i of year-class y;
$k_{i,y}$ = k at age i of year-class y;
T_{i+y} = the sea surface temperature in year i+y; and
$D_{i,y}$ = a population density presented by the number of stock at age i of year-class y.

These variables were z-score standardized. The model parameters α_1 and β_2 were estimated to represent the effects of T_{i+y} and $D_{i,y}$ on k or L_∞.

The parameters were estimated by maximizing the likelihood function which is represented by

$$L(i,y) = \hat{L}_{i,y} + \varepsilon_i, \quad (14)$$

$$\varepsilon_i \sim N(0,\sigma_i^2), \quad (15)$$

and

$$L(L_\infty,k,t_0,\beta_1,\beta_2,\sigma_i^2) = \prod_y \prod_i \left[2\pi\sigma_i^2\right]^{-\frac{1}{2}} \exp\left[-\frac{\left\{L(i,y)-\hat{L}_{i,y}\right\}^2}{2\sigma_i^2}\right]. \quad (16)$$

[3] Millar, R. B., and R. A. Myers. 1990. Modeling environmentally induced change in growth for Atlantic Canada cod stock. ICES CM 1990/G:24.

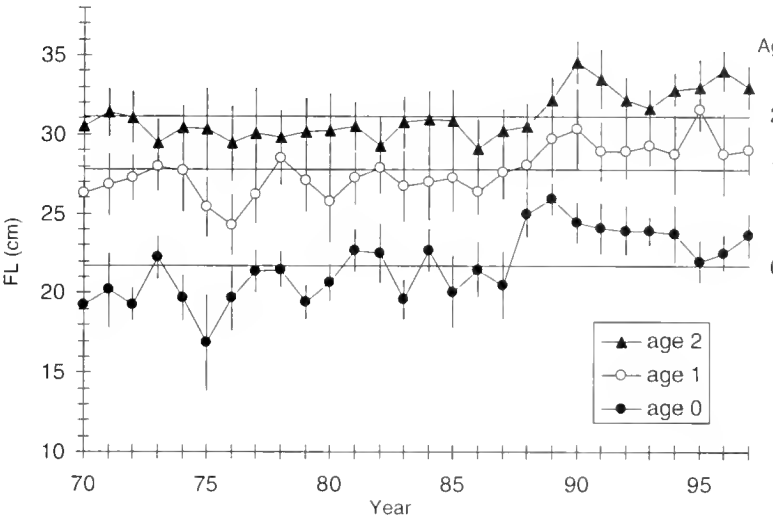

Figure 3

Interannual fluctuations in mean fork length (FL) at age 0, age 1, and age 2 for chub mackerel (*Scomber japonicus*) in 1970–97. Horizontal lines show the 28 year mean FL at age 0, 1, and 2, respectively. Vertical bars show standard deviations.

We ran the models with all possible combinations of explanatory variables (T, D, T, and D), and compared AIC with that obtained with the base parameters (L_∞, t_0, k).

Results

Fork length at age

Mean FL at age 0 varied substantially over the time series examined. For example, it ranged from 16.9 (Sd ±3.0) cm in 1975 to 25.9 (Sd ±1.0) cm in 1989. The mean FL for the 28 years period was 21.7 (±2.1) cm (coefficient of variation: CV=9.8%, Table 1, Fig. 3). The FL-at-age-0 values were smaller than the 28-year mean FL for the 1970s, varied around the mean in the early and mid 1980s, reached a maximum in 1989, and were at about 22–24 cm in the 1990s (Fig. 3).

Mean FL at age 1 was similarly variable; it ranged from 24.3 (±1.9) cm in 1976 to 31.6 (±1.4) cm in 1995. The 28-year mean FL was 27.7 (±1.6) cm (CV=5.6%, Table 1). The trend in interannual variability was similar to that in age 0, i.e. it was smaller in the 1970s and larger in the 1990s (Fig. 3). In age-2 fish the 28-year minimum FL of 29.1 (±1.8) cm was observed in 1986 and the maximum of 34.5 (±1.3) cm was observed in 1990 (the 28-year mean FL=31.1 (±1.5) cm, CV=4.7%, Table 1, Fig. 3).

In fish age 3 and older, mean FL varied year-to-year in a manner similar to that found in the younger ages (Table 1). Annual mean FLs for 3-, 4-, and 5-year-olds were 33.7 (±1.3) cm (3.8%), 36.2 (CI ±1.4) cm (CV=4.0%), and 38.5 (CI ±1.5) cm (CV=3.8%), respectively (Table 1). The mean FLs for ages 0–5 of each year were significantly different among different years (one-way ANOVA, $P<0.01$).

Table 1

Total biomass, year class strength (stock number at age 0; Yatsu, et al.[1]), SST, and mean fork length (FL) of *Scomber japonicus* from 1970 to 1997. Blanks show the lack of data.

Year	Total Biomass (10^3 t)	Stock number at age 0 (10^6 individuals)	SST (°C)[1]	Mean FL (SD) cm					
				0	1	2	3	4	5
1970	2833	10,199	11.5	19.2 (2.6)	26.3 (1.8)	30.5 (2.4)	34.2 (1.7)	37.7 (1.6)	40.5 (1.4)
1971	3781	14,138	10.9	20.2 (2.3)	26.8 (1.9)	31.4 (1.5)	34.3 (1.6)	37.7 (1.6)	40.4 (1.3)
1972	4860	8342	13.2	19.3 (1.0)	27.2 (1.4)	31.1 (1.6)	34.3 (1.5)	37.3 (1.7)	40.0 (1.5)
1973	4650	7154	11.1	22.2 (1.4)	27.9 (1.5)	29.4 (1.6)	31.2 (1.8)	33.1 (2.0)	36.1 (1.9)
1974	4048	7854	10.5	19.7 (1.4)	27.7 (2.5)	30.4 (1.4)	31.9 (1.7)	33.9 (1.8)	37.6 (1.7)
1975	3558	10,353	12.3	16.9 (3.0)	25.4 (1.8)	30.3 (2.6)	32.7 (1.6)	33.8 (1.6)	35.5 (1.7)
1976	3896	14,402	11.5	19.7 (2.0)	24.3 (1.9)	29.4 (2.4)	33.7 (1.9)	35.3 (1.8)	38.1 (1.8)
1977	5868	11,701	10.9	21.4 (1.3)	26.2 (1.8)	30.1 (2.8)	33.5 (2.2)	35.7 (1.7)	37.4 (1.4)
1978	5285	6249	10.0	21.5 (1.1)	28.5 (1.7)	29.8 (1.6)	32.1 (2.3)	34.5 (2.1)	36.1 (1.9)
1979	3250	2931	12.3	19.5 (1.1)	27.1 (2.0)	30.2 (2.0)	33.0 (1.7)	35.2 (1.6)	37.2 (1.3)
1980	1898	2952	11.3	20.7 (1.1)	25.8 (2.6)	30.3 (2.2)	32.4 (1.8)	33.9 (1.8)	35.6 (1.6)
1981	1683	3374	9.4	22.7 (1.3)	27.2 (1.7)	30.5 (1.5)	33.1 (2.1)	36.5 (1.8)	38.0 (1.5)
1982	1567	2883	10.8	22.5 (1.8)	27.9 (1.6)	29.3 (1.8)	33.6 (2.2)	36.6 (1.6)	38.3 (1.4)
1983	1516	3175	11.5	19.6 (1.2)	26.7 (2.2)	30.8 (1.6)	33.6 (1.5)	35.5 (2.0)	37.8 (1.2)
1984	1759	3605	9.3	22.7 (1.3)	27.0 (2.4)	31.0 (1.8)	34.8 (1.9)	36.6 (1.8)	38.2 (2.0)
1985	1565	4998	11.4	20.1 (2.2)	27.3 (2.1)	30.9 (1.9)	33.3 (1.9)	37.4 (1.7)	39.0 (1.8)
1986	1373	1833	9.7	21.5 (1.7)	26.4 (1.4)	29.1 (1.8)	32.5 (2.4)	35.9 (2.1)	38.9 (1.9)
1987	812	583	10.9	20.5 (2.1)	27.6 (1.7)	30.2 (1.3)	32.8 (1.6)	36.4 (2.3)	39.2 (0.8)
1988	555	236	11.4	24.9 (1.4)	28.1 (1.5)	30.5 (1.4)	32.8 (1.7)	36.8 (1.6)	40.1 (1.2)
1989	289	219	9.8	25.9 (1.0)	29.7 (2.3)	32.2 (1.4)	34.6 (1.5)	35.7 (1.5)	39.2 (1.5)
1990	185	356	11.7	24.4 (1.3)	30.3 (2.6)	34.5 (1.3)	35.8 (1.5)	38.2 (1.1)	39.7 (0.8)
1991	338	1017	12.2	24.1 (1.6)	28.9 (1.8)	33.5 (1.9)	35.5 (1.2)	36.7 (1.9)	39.0 (1.8)
1992	724	2839	9.7	24.0 (1.6)	29.0 (1.7)	32.1 (1.4)	34.1 (1.5)	37.5 (1.6)	40.5 (1.6)
1993	685	589	10.7	23.9 (0.9)	29.3 (1.3)	31.7 (1.1)	33.2 (0.5)		
1994	343	547	11.3	23.7 (1.7)	28.8 (2.5)	32.8 (1.0)	34.6 (0.8)	35.9 (0.7)	39.1 (1.0)
1995	351	1183	11.3	22.0 (1.3)	31.6 (1.4)	32.9 (1.8)	35.5 (1.8)	38.0 (1.3)	39.2 (0.8)
1996	726	4452	9.9	22.5 (1.1)	28.7 (2.5)	34.1 (1.2)	36.1 (1.1)	37.8 (0.9)	39.7 (0.7)
1997	682	529	9.9	23.6 (1.4)	29.0 (1.5)	33.0 (1.3)	35.4 (1.7)	37.6 (0.7)	38.6 (0.5)
28-year mean of FLs at ages				21.7 (2.1)	27.7 (1.6)	31.1 (1.5)	33.7 (1.3)	36.2 (1.4)	38.5 (1.5)

[1] SST during April–June in the waters bounded by 38–40°N and 141–143°E.

Mean growth increments I of each year class from age 0 (6 months old) to ages 1–5 (I_{0-t}) showed significantly negative correlations (Table 2). Correlations between the two variables tended to increase with age: –0.69 for I_{0-1}, –0.71 for I_{0-2}, –0.80 for I_{0-3}, and –0.77 for I_{0-4}.

The relative FL at age 0 for any given year class was maintained throughout the life span. A correlation between the mean FL at age 0 and age 1 within each year class (1970 to 1996 year class) was positive and statistically significant ($P<0.05$, Fig. 4). Similarly, the positive correlations between the mean FL at age 0 and age 3 (1970 to 1994 year class, $P<0.01$, Fig. 4), and age 0 and age 4 (1970 to 1993 year class, $P<0.05$, Fig. 4) were significant ($P<0.05$, Fig. 4).

Correlation between FL and population density

Population densities represented by stock in number at age 0 and total biomass were negatively correlated to FL at age. Negative correlations between the logarithm of abundance of age 0 ($\ln N_0$) and FL at ages were relatively high in age 0 to 3 (–0.69 to –0.83, Table 3) and low in age 4 and 5 (–0.63 and –0.64, Table 3). Correlations were statistically significant for ages 0, 2, and 3 (Table 3). Negative correlations between the logarithm of total biomass and FL at ages were relatively high at ages 0 to 2 (–0.73 to –0.75) and moderate for age 3 to 5 (–0.50 to –0.52, Table 4). However, the relationships were not statistically significant for all ages (Table 4).

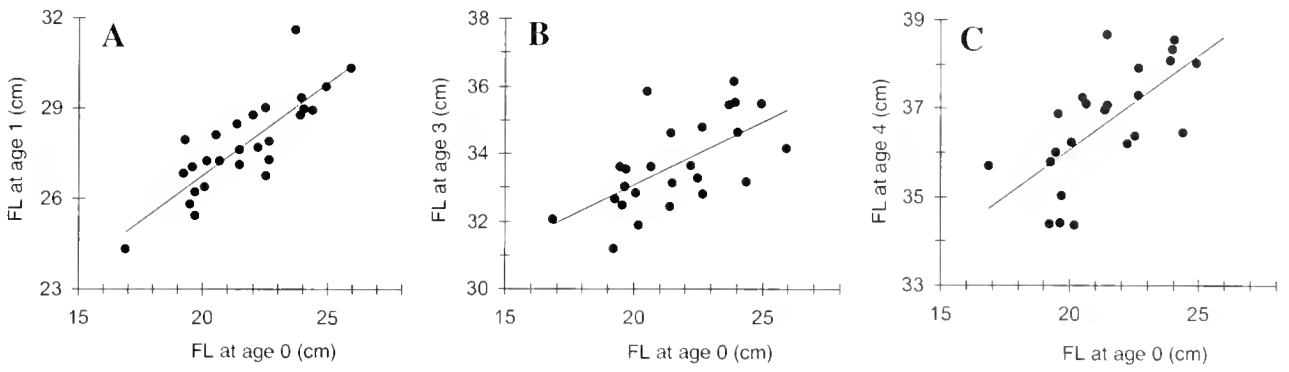

Figure 4

Scatter plots of FL at age 1 (**A**), age 3 (**B**) and age 4 (**C**) on FL at age 0 for chub mackerel (*Scomber japonicus*). Correlations between FL at age 1 with age 0 (r=0.83, n=28, actual sample size n^*=8, df=6), age 3 with age 0 (r=0.62, n=26, n^*=11, df =9) and age 4 with age 0 (r=0.67, n=24, n^*=10) were all significant at $P < 0.05$.

Table 2

Correlation of FL at age 0 and growth increment after age 0. n = actual sample size. n^* and degree of freedom (df) show the effective n and df when the data were corrected for autocorrelation (Pyper and Peterman, 1998). Significance level: **, P<0.01.

Growth increment	r	r^2	n	n^*	df
Ages 0–1	−0.69**	0.48	27	21	19
Ages 0–2	−0.71**	0.51	26	25	23
Ages 0–3	−0.80**	0.64	25	23	21
Ages 0–4	−0.77**	0.59	23	24	22
Ages 0–5	−0.78**	0.61	22	22	20

Table 3

Correlation between the natural logarithm of the abundance of age 0 and mean FL for each age. n = actual sample number. n^* and degree of freedom (df) show the significant n and df when autocorrelation was considered (Pyper and Peterman, 1998). Significance levels: *, $P < 0.05$.

Age	r	r^2	n	n^*	df
0	−0.75*	0.57	28	8	6
1	−0.69	0.48	27	7	5
2	−0.83*	0.69	26	6	4
3	−0.71*	0.51	25	9	7
4	−0.63	0.40	23	8	6
5	−0.64	0.40	22	6	4

Correlation between FL and SST

Growth in the first six months of life was correlated with SST. We detected significant negative correlation between FL-at-age 0 and SST between April and June in the waters bounded by 38–40°N and 141–143°E (r=−0.45, r^2=0.20, n=28, n^*=27, df=25, P<0.05, Fig. 5). The SST between July and September of this area was also negatively correlated with FL at age 0 although the correlation coefficient was not significant at 5% level.

Table 4

Correlation between natural logarithm of total biomass and mean FL for each age. n = actual sample size. n^* and dgree of freedom (df) show the effective n and df when the data were corrected for autocorrelation (Pyper and Peterman, 1998). No correlations were significant (P>0.05).

Age	r	r^2	n	n^*	df
0	−0.74	0.38	27	6	4
1	−0.73	0.32	27	6	4
2	−0.75	0.36	27	5	3
3	−0.52	0.26	27	11	9
4	−0.51	0.26	26	9	7
5	−0.50	0.22	26	7	5

Growth analysis

Model 1 that incorporated SST (T) and population density (D) gave a minimum Akaike's information criterion (AIC) of 457.68 (Table 5) and the model was expressed by

$$\hat{L}_{t,y} = 43.98\left\{1-\exp(-2.585)\exp\left(-\sum_{t=0}^{5} k_{t,y}\right)\right\} \quad (17)$$

$$k_{t,y} = 0.271 - 0.008T_{t+y} - 0.21D_{t,y}. \quad (18)$$

This model estimated the FL at ages 0–5 well (Fig. 6). The AIC of model 1 incorporating T and D was smaller than the AIC of model 2; therefore the environmental factors had an affect on k rather than L_∞.

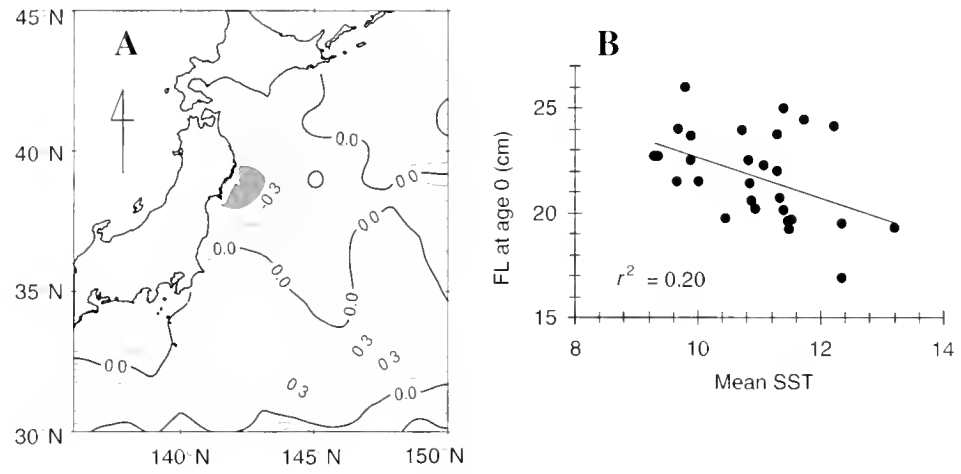

Figure 5

(**A**) Map to show correlation between sea surface temperatures (SST) and mean fork length (FL) at age 0 for chub mackerel (*Scomber japonicus*). The dotted area indicates the negative correlation coefficient r above 0.4. The contour interval is 0.1 of the correlation coefficient and positive contours are shown as dashes. (**B**) Relationship between mean SST for the area 38°–40°N and 141–143°E from April to June and mean FL at age 0. Correlation was significant at the 5% level (r=–0.45, n=28, n'=27, df=25).

To investigate the effect of T and D, we calculated the total effect on k for year-class y according to Sinclair et al. (2002):

$$\frac{\sum_{t=0}^{5}\beta_1 T_{t+y}}{6} \text{ for } T, \text{ and } \frac{\sum_{t=0}^{5}\beta_2 D_{t,y}}{6} \text{ for } D.$$

Discussion

Estimated population abundance of age-0 fish and total biomass may explain density-dependent growth. FL at age 0, 2, and 3 of the Pacific stock of chub mackerel were negatively correlated with the number of age-0 recruits. Correlations between biomass and FL at ages 0–5 were low and not significant. Therefore, year-class strength is indicated to have a greater negative influence on the growth of the Pacific stock of chub mackerel than total biomass, as reported for the Atlantic mackerel (*Scomber scombrus*) (Agnalt, 1989; Overholtz, 1989; Neja, 1995) and Atlantic herring (*Clupea harengus*) (Toresen, 1990).

Density-dependent growth in fish populations seems to be a common phenomenon for pelagic fishes found in the temperate waters of Japan. The FL at age 0 of the 1963–69 year classes ranged from 16 to 20 cm, and were smaller than those of the 1970s, possibly indicating density-dependent growth (Iizuka, 1974). According to Honma et al. (1987), the stock abundance of the Pacific stock of chub mackerel from 1963 to 1969 was larger than it was in the 1970s. Wada et al. (1995) and Hiyama et al. (1995) found negative relationships between total biomass and body length in the Pacific and Tsushima Current stock of the Japanese sardine (*Sardinops melanostictus*). Kishida (1990) demonstrated a density-dependent relationship between the growth and total stock density (CPUE) of Japanese Spanish mackerel (*Scomberomorus niphonius*).

Our results do not agree with the positive effect of sea water temperature on somatic growth that has been shown for several species, including Japanese common squid (Kidokoro, 2001), Atlantic herring (Moores and Winters, 1981; Toresen, 1990), and Atlantic cod (*Gadus morhua*) (Brander, 1995; Dutil et al., 1999; Rätz et al. 1999; Otterson et al., 2002).

Table 5

Summary of statistics from the estimation of growth for chub mackerel (*Scomber japonicus*). AIC = Akaike's information criterion.

Model	Variables	No. of unknown parameters	Log likelihood	AIC
1	$L_\infty, k, t_0, \sigma_1 \ldots \sigma_5$	9	–280.20	578.40
	$L_\infty, k, t_0, \sigma_1 \ldots \sigma_5, \beta_1$	10	–270.10	560.20
	$L_\infty, k, t_0, \sigma_1 \ldots \sigma_5, \beta_2$	10	–222.38	464.77
	$L_\infty, k, t_0, \sigma_1 \ldots \sigma_5, \beta_1, \beta_2$	11	–217.84	457.68
2	$L_\infty, k, t_0, \sigma_1 \ldots \sigma_5$	9	–280.20	578.40
	$L_\infty, k, t_0, \sigma_1 \ldots \sigma_5, \beta_1$	10	–268.63	557.25
	$L_\infty, k, t_0, \sigma_1 \ldots \sigma_5, \beta_2$	10	–224.01	468.02
	$L_\infty, k, t_0, \sigma_1 \ldots \sigma_5, \beta_1, \beta_2$	11	–220.81	463.62

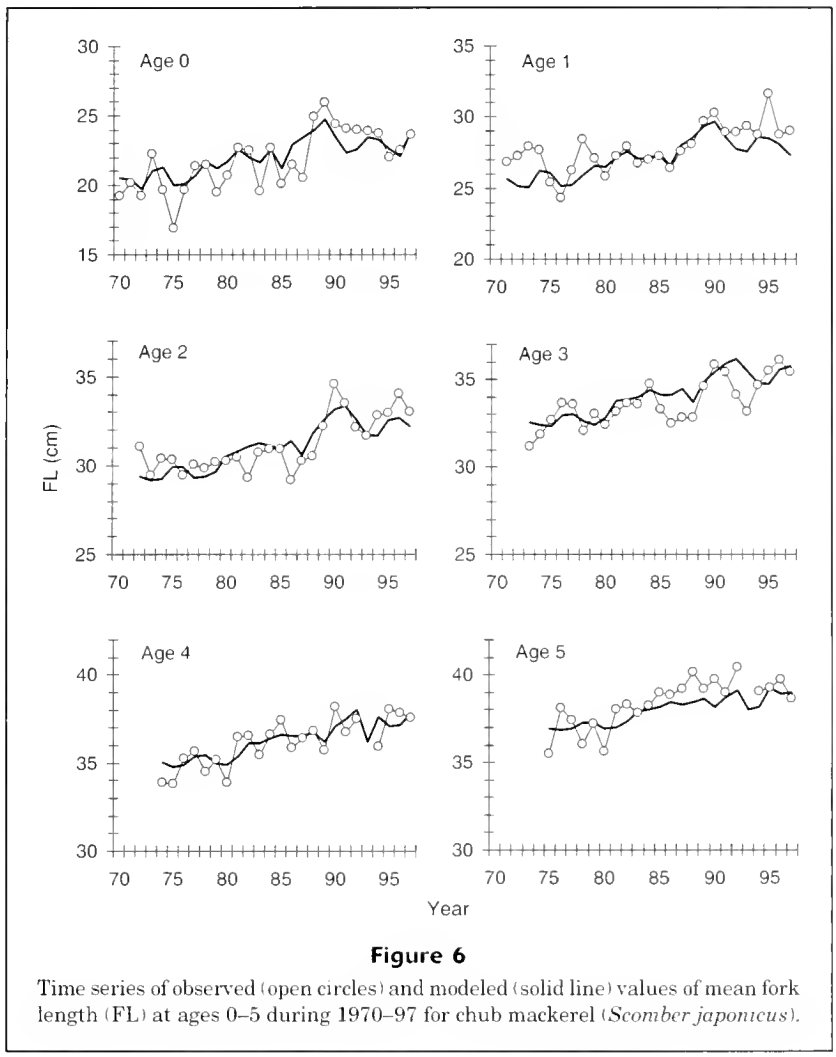

Figure 6

Time series of observed (open circles) and modeled (solid line) values of mean fork length (FL) at ages 0–5 during 1970–97 for chub mackerel (*Scomber japonicus*).

There was a positive correlation between FL at age 0 and 1°×1° block SST in the waters of 32–34°N and 144–149°E, located south of the Kuroshio Extension flowing eastward at the latitude of 35–37°N from April to June (Figs. 1 and 5A). But the correlation coefficient was not significant, and this area was not considered to be inhabited by juvenile mackerel (Watanabe, 1970). Thus, we considered that the SST in the waters of 32–34°N and 144–149°E was not a significant factor on the variation of FL at age 0.

The low SST in the waters bounded by 38–40°N and 141–143°E is indicative of a large inflow of Oyashio Current waters (Hirai and Yasuda, 1988), which is a cold water current and has high productivity (Odate, 1994), into the Kuroshio–Oyashio transition zone, where is one of the main feeding grounds of mackerels (Odate, 1961; Watanabe, 1970; Watanabe and Nishida, 2002; Fig. 1). Thus, we hypothesized that the large inflow of Oyashio current waters into the Kuroshio–Oyashio transition zone improved the feeding condition and accelerated the growth of juvenile mackerel. Jobling (1988) suggested a parabolic relationship between water temperature and fish growth. The range of SST in this area, which was negatively correlated with FL at age 0 of mackerel, was 9–13°C (Table 1). This temperature range is near the lowest nonstressful temperatures for mackerel (10–12°C, Schaefer, 1986). Thus, we do not consider that the negative relationship between growth and SST was the result of suppressed growth by the high ambient temperature.

In mackerel, maximum egg production appears to have shifted to later in spring during the 1990s, as compared to the late 1970s and 1980s, resulting in a shorter period of growth and thus smaller fish (Fig. 8, Mori et al.[4]; Kikuchi and Konishi[5]; Ishida and Kikuchi[6]; Zenitani et al.[7]; Kubota et al.[8]). In the early 1970s, the main spawning period was

[4] Mori, K., K. Kuroda, and Y. Konishi. 1988. Monthly egg production of the Japanese sardine, anchovy, and mackerels off the southern coast of Japan by egg censuses. Datum Collect. Tokai Reg. Fish. Res. Lab. 12:1–321. [In Japanese. Available from National Research Institute of Fisheries Science, 2-12-4 Fukuura, Kanazawa, Yokohama 236-8648, Japan.]

[5] *See next page.*

[6] *See next page.*

[7] *See next page.*

[8] *See next page.*

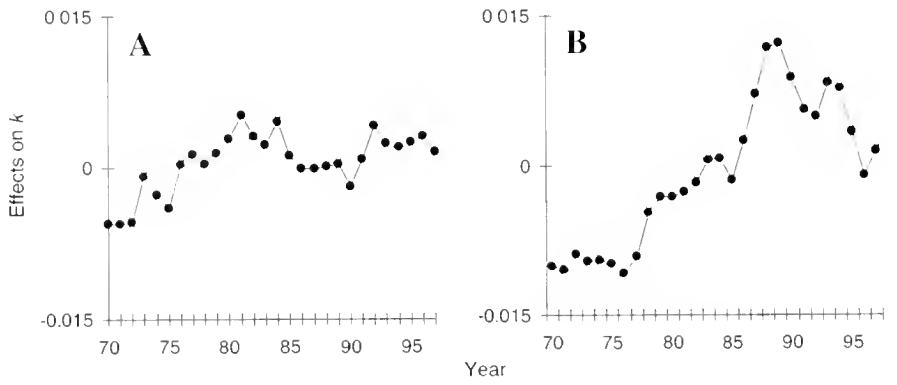

Figure 7

The total effect of (**A**) mean SST for the area of 38–40°N and 141–143°E from April to June, and (**B**) population density on k for each year class of chub mackerel (*Scomber japonicus*).

also in April (Kuroda[9]). Delayed spawning in the 1990s should have resulted in a reduction in the mean FL at ages during September–December in the 1990s compared to the 1970s and 1980s; however the present study showed the opposite result (Table 1). We hypothesize that the effect of the shift of spawning period on the FL at ages may have been overwhelmed by the effect of population density (Fig.7).

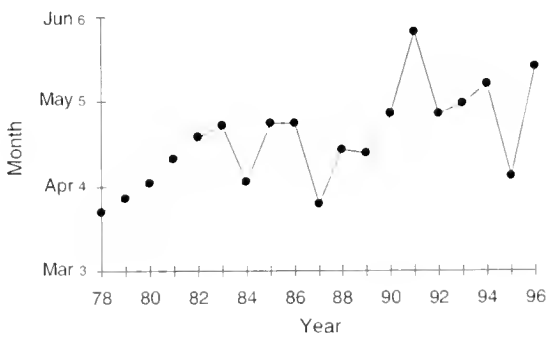

Figure 8

Interannual variation in the peak period (weighted monthly means) of egg production for the Pacific stock of chub mackerel (*Scomber japonicus*), which includes a small portion from the eggs of spotted mackerel (*Scomber australasicus*) (Mori et al.[4]; Kikuchi and Konishi[5]; Ishida and Kikuchi[6]; Zenitani et al.[7]; Kubota et al.[8]).

The estimated FL at age from our growth model, with the use of AIC, fitted well to the observed FL at age (Fig. 6). Mean growth increments I of each year class from age 0 (6 months old) to ages 1–5 (I_{0-t}) were significant and negatively correlated with FL at age 0 (Table 2), indicating that the growth rate of mackerel had changed from year to year for a given year class. This negative correlation indicated that the effects of population density and SST was temporal, and influenced k rather than L_∞. The negative correlation between FL at age 0 and growth increments also suggested that the FL at age of mackerel approximated the asymptotic length. Thus, mackerel growth was best fitted to the modified von Bertalanffy growth model with the temporal environmental effect on k (Table 5).

[5] Kikuchi, H., and Y. Konishi. 1990. Monthly egg production of the Japanese sardine, anchovy, and mackerels off the southern coast of Japan by egg censuses: January, 1987 through December, 1988, 72 p. National Research Institute of Fisheries Science, Tokyo. [In Japanese. Available from National Research Institute of Fisheries Science, 2-12-4 Fukuura, Kanazawa, Yokohama 236-8648, Japan.]

[6] Ishida, M. and H Kikuchi. 1992. Monthly egg production of the Japanese sardine, anchovy, and mackerels off the southern coast of Japan by egg censuses: January, 1989 through December, 1990, 86 p. National Research Institute of Fisheries Science, Tokyo. [In Japanese. Available from National Research Institute of Fisheries Science, 2-12-4 Fukuura, Kanazawa, Yokohama 236-8648, Japan.].

[7] Zenitani, H., M. Ishida, Y. Konishi, T. Goto, Y. Watanabe, and R. Kimura. 1995. Distributions of eggs and larvae of Japanese sardine, Japanese anchovy, mackerels, round herring, jack mackerel and Japanese common squid in the waters around Japan, 1991 through 1993. Resources Management Research Report Series A-2, 368 p. National Research Institute, Japan Fisheries Agency, Tokyo. [In Japanese. Available from National Research Institute of Fisheries Science, 2-12-4 Fukuura, Kanazawa, Yokohama, 236-8648 Japan.]

[8] Kubota, H., Y. Oozeki, M. Ishida, Y. Konishi, T. Goto, H. Zenitani, and R. Kimura. 1999. Distributions of eggs and larvae of Japanese sardine, Japanese anchovy, mackerels, round herring, jack mackerel and Japanese common squid in the waters around Japan, 1994 through 1996, 352 p. Resources Management Research Report Series A-2., National Research Institute, Japan Fisheries Agency, Tokyo. [In Japanese. Available from National Research Institute of Fisheries Science, 2-12-4 Fukuura, Kanazawa, Yokohama 236-8648, Japan.]

[9] Kuroda, K. 2002. Personal commun. 1-1-3-406, Kasumi, Narashino, Chiba 275-0022, Japan

The effect of population density on growth of mackerel was higher than the effect of SST (Fig. 7, Table 6). Our result agreed with the results for Japanese sardine (Wada et al., 1995) and Atlantic cod (Sinclair et al., 2002). Particularly, the effect of population density was significant in the late 1980s, which resulted in a remarkable increase in FL at age 0 (Figs. 3 and 7).

The relative size at age 0 was carried over to older ages (Fig. 4), indicating that the cohorts that were small at age 0 could not compensate for this early small size. Iizuka (1974) reported that the trend of growth established at age 0 for chub mackerel was maintained until age 2 for the 1963–73 year classes. Toresen (1990) demonstrated from length data that a trend in rate of growth for a given year class of Norwegian herring was determined at the immature stage and was consistent after maturation. Total length of Hokkaido-Sakhalin herrings (*Clupea pallasii*) at age 5 and older was positively correlated with the length at age 4 (Watanabe et al., 2002). Because fish first mature at age 4, this implied that the trend in total length of each year class was determined by the age at maturity. From these results we hypothesize that the variability in size at age in the Pacific stock of chub mackerel is largely attributable to growth before maturity, especially during the first 6 months after hatching.

Acknowledgments

We would like to thank K. Meguro of Chiba Prefecture Governmental Office and K. Kobayashi of Shizuoka Prefecture Governmental Office for providing insights into chub mackerel's growth and into age determination. We also thank T. Akamine, M. Suda, and N. Yamashita of the National Research Institute of Fisheries Science for advice on the statistical analysis. We also thank Y. Watanabe and C. B. Clarke of the Ocean Research Institute, University of Tokyo, for their constructive comments on this manuscript.

Literature cited

Agnalt, A. -L.
1989. Long-term changes in growth and age at maturity of mackerel, *Scomber scombrus* L., from the North Sea. J. Fish Biol. 35 (suppl. A):305–311.

Brander, K. M.
1995. The effect of temperature on growth of Atlantic cod (*Gadus morhua* L.). ICES J. Mar. Sci. 52:1–10.

Dutil, J. -D., M. Castonguay, D. Gilbert, and D. Gascon.
1999. Growth, condition, and environmental relationships in Atlantic cod (*Gadus morhua*) the northern Gulf of St. Lawrence and implications for management strategies in the Northwest Atlantic. Can. J. Fish. Aquat. Sci. 56: 1818–1831.

Haddon, M.
2001. Modelling and quantitative methods in fisheries, 406 p. Chapman&Hall/CRC, New York, NY.

Hirai, M.
1991. Fisheries oceanographic study on purse-seine fishing-grounds for chub mackerel in the Sanriku coastal waters. Bull. Tohoku Natl. Fish. Res. Inst. 53:59–147. [In Japanese.]

Hirai, M., and I. Yasuda.
1988. Interannual variability of the temperature field at 100 m depth near the east coast of Japan. Bull. Otsuchi Ocean Res. Center, Univ. Tokyo. 14:184–186.

Hiyama, Y., H. Nishida, and T. Goto.
1995. Interannual fluctuations in recruitment and growth of the sardine, *Sardinops melanostictus*, in the Sea of Japan and adjacent waters. Res. Popul. Ecol. 37(2):177–183.

Honma, M., Y. Sato, and S. Usami.
1987. Estimation of the population size of the Pacific mackerel by the cohort analysis. Bull. Tokai Reg. Fish. Res. Lab. 121:1–11. [In Japanese.]

Iizuka, K.
1974. The ecology of young mackerel in the north-eastern sea of Japan IV. Estimation of the population size of the 0-age group and the tendencies of growth patterns on 0, I, and II age groups. Bull. Tohoku Reg. Fish. Res. Lab. 34: 1–16. [In Japanese.]

Jobling, M.
1988. A review of the physiological and nutritional energetics of Cod, *Gadus morpha* L., with particular reference to growth under farmed conditions. Aquaculture, 70:1–19.

Kawasaki, T.
1966. Structure of the Pacific population of the mackerel. Bull. Tokai Reg. Fish. Res. Lab. 47:1–34. [In Japanese.]

Kidokoro, H.
2001. Fluctuations in body size and abundance of Japanese common squid (*Todarodes pacificus*) in the Sea of Japan. GLOBEC report 15:42.

Kishida, T.
1990. Relationship between growth and population density of Japanese Spanish mackerel in the central and western waters of the Seto Inland Sea. Bull. Nansei Natl. Fish. Res. Inst. 23:35–41. [In Japanese.]

Mace, P. M., and M. O. Sissenwine.
1993. How much spawning per recruit is enough? Can. Spec. Publ. Fish. Aquat. Sci. 120:101–118

Moores, J. A., and G. H. Winters.
1981. Growth patterns in a Newfoundland Atlantic herring (*Clupea harengus harengus*) stock. Can. J. Fish. Aquat. Sci. 39:454–461.

Moyle, P. B., and J. J. Cech Jr.
2002. Fishes: An introduction to ichthyology. 4th ed., 612 p. Prentice Hall, Englewood Cliffs, NJ.

Murayama, T., I. Mitani, and I. Aoki.
1995. Estimation of the spawning period of the Pacific mackerel *Scomber japonicus* based on the changes in gonad index and the ovarian histology. Bull. Jpn. Soc. Fish. Oceanogr. 59:11–17. [In Japanese.]

Neja, Z.
1995. The stock size and changes in the growth rate of the northwest Atlantic mackerel (*Scomber scombrus* L.) in 1971–1983. Acta Ichthyologica et Piscatoria 25:113–121.

Odate, K.
1994. Zooplankton biomass and its long-term variation in the western north Pacific ocean, Tohoku sea area, Japan. Bull. Tohoku Natl. Fish. Res. Inst. 56, 115–173. [In Japanese.]

Odate, S.
1961. Study on the larvae of the fishes in the north-eastern sea area along the Pacific coast of Japan. Part 1. Mackerel. *Pneumatophorus japonicus* (Houttuyn). Bull. Tohoku Reg. Fish. Res. Lab. 19:98–108. [In Japanese.]

Otterson, G., K. Helle, and B. Bogstad.
2002. Do abiotic mechanisms determine interannual vari-

ability in length-at-age of juvenile Arcto-Norwegian cod? Can. J. Fish. Aquat. Sci. 59:57–65.

Overholtz, W. J.
1989. Density-dependent growth in the northwest Atlantic stock of Atlantic mackerel (*Scomber scombrus*). J. Northw. Atl. Fish. Sci. 9:115–121.

Pauly, D.
1987. Application of information on age and growth of fish to fishery management. *In* Age and growth of fish (R. C. Summerfelt and G. E. Hall, eds.) p.495–506. Iowa State Univ Press, Ames, IA.

Pyper, B. J., and R. M. Peterman.
1998. Comparison of methods to account for autocorrelation in correlation analyses of fish data. Can. J. Fish. Aquat. Sci. 55:2127–2140.

Ratz, H. -J., M. Stein, and J. Lloret.
1999. Variation in growth and recruitment of Atlantic cod (*Gadus morhua*) off Greenland during the second half of the twentieth century. J. Northw. Atl. Fish. Sci. 25:161–170.

Schaefer, K. M.
1986. Lethal temperature and the effect of temperature change on volitional swimming speeds of chub mackerel, *Scomber japonicus*. Copeia 1986:37–44.

Sinclair, A. F., D. P. Swain, and J. M. Hanson.
2002. Disentangling the effects of size-selective mortality, density, and temperature on length-at-age. Can. J. Fish. Aquat. Sci. 59:372:382.

Toresen, R.
1990. Long-term changes in growth of Norwegian spring-spawning herring. J. Cons. Int. Explor. Mer 47:48–56.

Usami, S.
1973. Ecological studies of life pattern of the Japanese mackerel, *Scomber japonicus* Houttuyn: on the adult of the Pacific subpopulation. Bull. Tokai Reg. Fish. Res. Lab. 76: 71–178. [In Japanese.]

Wada, T., Y. Matsubara, Y. Matsumiya, and N. Koizumi.
1995. Influence of environment on stock fluctuations of Japanese sardine, *Sardinops melanostictus*. Can. Spec. Publ. Fish. Aquat. Sci. 121:387–394.

Watanabe, C., and H. Nishida.
2002. Development of assessment techniques for pelagic fish stocks: applications of daily egg production method and pelagic trawl in the northwestern Pacific ocean. Fisheries Science. 68:97–100.

Watanabe, C., T. Hanai, K. Meguro, R. Ogino, Y. Kubota, and R. Kimura.
1999. Spawning biomass estimates of chub mackerel *Scomber japonicus* of Pacific subpopulation off central Japan by a daily egg production method. Nippon Suisan Gakkaishi 65(4):695–702. [In Japanese.]

Watanabe, T.
1970. Morphology and ecology of early stages of life in Japanese common mackerel, *Scomber japonicus* Houttuyn, with special reference to fluctuation of population. Bull. Tokai Reg. Fisb. Res. Lab. 62:1–283. [In Japanese.]

Watanabe, Y., Y. Hiyama, C. Watanabe, and S. Takayanagi.
2002. Inter-decadal fluctuations in length-at-age of Hokkaido-Sakhalin herring and Japanese sardine in the Sea of Japan. PICES Scientific Report 20:63–67.

Yatsu, A., and H. Kidokoro.
2002. Coherent low frequency variability in biomass and in body size of Japanese common squid, *Tadorodes padificus*, during 1964–2002, 89 p. Abstracts of PICES 11th annual meeting.

Latitudinal and seasonal egg-size variation of the anchoveta (*Engraulis ringens*) off the Chilean coast

Alejandra Llanos-Rivera

Leonardo R. Castro

Laboratorio de Oceanografía Pesquera y Ecología Larval
Departamento de Oceanografía
Universidad de Concepción
Casilla 160-C, Concepción, Chile

E-mail address (for L. R. Castro, contact author): lecastro@udec.cl

The anchoveta *Engraulis ringens* is widely distributed along the eastern South Pacific (from 4° to 42°S; Serra et al., 1979) and it has also supported one of the largest fisheries of the world over the last four decades. However, there are few interpopulation comparisons for either the adult or the younger stages. Reproductive traits, such as fecundity or spawning season length, are known to vary with latitude for some fish species (Blaxter and Hunter, 1982; Conover, 1990; Fleming and Gross, 1990; Castro and Cowen, 1991), and latitudinal trends for some early life history traits, such as egg size and larval growth rates, have been reported for others clupeiforms and other fishes (Blaxter and Hempel, 1963; Ciechomski, 1973; Imai and Tanaka, 1987, Conover 1990, Houde 1989). However, there is no published information on potential latitudinal trends during the adult or the early life history of the anchoveta, even though this type of information may help in understanding recruitment variability, especially during recurring large scale events (such as El Niño or La Niña) that affect the entire species range.

Egg volume has been found to vary widely among species and among populations of the same species. For fish that broadcast planktonic or benthic eggs, egg size often varies as the spawning season progresses (Bagenal, 1971), and the magnitude of this variation depends on the species. For instance, the egg volume of the pelagic spawners *Engraulis anchoita* and *Solea solea* decreases 23% and 38%, respectively, throughout the spawning season (Ciechomski, 1973; Rijnsdorp and Vingerhoed, 1994). Maternal and environmental factors may also affect egg volume (Bagenal, 1971; Thresher, 1984; Rijnsdorp and Vingerhoed, 1994; Chambers and Waiwood, 1996; Chambers, 1997). Variations in size of the spawning females and shifts in energy allocation from reproduction to growth as the spawning season progresses may influence the egg volume (Wootton, 1990). Alternatively, seasonal variations in photoperiod, seawater temperature, and food supply during the spawning season may affect the reproductive output (Wootton, 1990).

Scarce information exists on the variability of egg sizes for fishes in the Humboldt Current. In this extensive area, the heavily exploited anchoveta *Engraulis ringens* is the dominant small pelagic species. Throughout this range, three major stocks are recognized: the northern stock off northern Peru (the largest); the central stock off southern Peru and northern Chile (mid-size), and the southern stock off central Chile (the smallest of the three). For the entire distribution of anchoveta, the main spawning season is from July through September, but may extend to December or January (Cubillos et al., 1999). The wide latitudinal range and prolonged spawning period suggest the possibility of egg-size variation, as observed in other clupeifoms (Blaxter and Hempel, 1963; Ciechomski, 1973; Imai and Tanaka, 1987). Egg size correlates with larval characteristics such as larval length at hatching, the time to first feeding, and time before irreversible starvation (Shirota, 1970; Ware, 1975; Hunter, 1981; Marteinsdottir and Able, 1992). To explore whether differences in potential early-life-stage survival would exist among populations and (or seasons), the objective of our research was to determine whether variations in some early-life-stage characteristics occur among populations of *E. ringens* along its distribution. In this study, we 1) report changes in egg size throughout the anchoveta spawning season as well as for the peak months of the spawning season, 2) evaluate whether egg size varies with respect to latitude, and 3) evaluate whether differences in larval length and yolksac volume occur in hatching larvae from the two major spawning stocks along Chile (central and southern stocks).

Materials and methods

We collected anchovy eggs from four locations along the coastal zone (<20 nmi offshore) off northern and central Chile during the austral winter and spring spawning seasons 1995–97 (Fig. 1). Eggs were collected with a Calvet net (150 μm mesh) in Iquique and Antofagasta (northern Chile), with a standard conical net (330 μm) in Valparaíso and with either a Tucker trawl (250 μm mesh) or a standard bongo net (500 μm) in Talcahuano. The shorter axis of the anchovy eggs varied from 0.563 mm (SD=0.032) in Iquique to 0.657 mm (SD=0.027) in Talcahuano. Consequently, egg extrusion from the nets was ruled out as a potential source of variation in our collections. Egg size (length and width) was measured with an ocular micrometer on a dissecting microscope at 25× magnification. Upon collection, all eggs were preserved in 5% buffered formalin. Previous studies on anchoveta eggs have reported no egg size shrinkage or shape changes with formalin preservation (Fisher, 1958). Similarly, reports on this species and other anchovies show that egg-size variations throughout their development do not occur (*Engraulis ringens*, Fisher, 1958; *Engraulis japonica*, Imai and Tanaka, 1987). We tested this hypothesis using eggs that we collected in northern Chile and found no size differences among different egg stages (ANOVA, n=535, P=0.1176).

Manuscript approved for publication
12 August 2003 by Scientific Editor.

Manuscript received 20 October 2003
at NMFS Scientific Publications Office.

Fish. Bull. 102:207–212 (2004).

Egg volume was calculated considering the anchovy egg as an ellipsoid ($V=4\pi \times a \times b \times c/3$, where a, b and c are the ellipse radii).

Statistical analyses included one-way ANOVA tests for volume differences among eggs spawned in three subperiods during the spawning season (initial, middle, and final) in Valparaíso and Talcahuano (1996–97). We did not have samples from the start of the spawning season in 1996 for Valparaíso; thus, we used samples collected in late June 1995 for this subperiod (Table 1). Variations in the egg-size frequency distributions between contiguous subperiods were also tested with nonparametric tests (Kolmogorov-Smirnov test). Changes in egg volume with latitude were tested by using egg sizes measured at four localities (20°, 23°, 33°, and 36°S) during the peak spawning months (initial subperiod). The same statistical tests were used as in the previous objective (ANOVA, Kolmogorov-Smirnov test).

To evaluate the relationship between egg size and larval length at hatching, live eggs from ichthyoplankton samples from the field in August 2000 were transported to the laboratory and reared at the normal mixed-layer temperature off Antofagasta and Talcahuano (15°C and 12°C, respectively) (Escribano et al., 1995; Castro et al., 2000). A subsample of the incubated egg batch was preserved in 5% formalin and measured at the beginning of the experiments. The rest of the eggs were placed in 1-L flasks and incubated until hatching under 12h/12h photoperiod. This procedure was repeated twice (4 days apart) in each zone. From each rearing experiment, 30 just-hatched larvae (max. 30 min from hatch) were anesthetized and measured (notochord length) under a dissecting microscope with the aid of an ocular micrometer. Additionally, yolksac sizes of recently hatched larvae were measured and volume estimated as one half of an ellipsoid by using the algorithms given above.

Results

A total of 7196 anchovy eggs were measured. The egg size tended to decrease as the spawning season progressed (Fig. 2). From late June through January the mean volume decreased by about 20% in Valparaíso and by about 10% in Talcahuano (ANOVA, $P<0.05$)(Table 1). The size-frequency distribution between consecutive subperiods (initial, middle, and final) also differed in both areas (Kolmogorov-Smirnov test, $P<0.05$). The mean size of the eggs in Valparaíso was smaller than in Talcahuano during all subperiods (Table 1), and the largest difference between areas was at the end of the spawning season (15%).

During the spawning peak (spawning commencement), when the eggs were larger, the mean anchoveta egg size increased with latitude (ANOVA, $P<0.01$; Fig. 3). At Iquique (20°S), the mean egg volume was 21% smaller than at Antofagasta (23°S), 49% smaller than at Valparaíso (33°S), and 56% smaller than the eggs from Talcahuano (36°S), the southernmost location (Table 2). The egg-size frequency distribution differed between adjacent areas (Kolmogorov-Smirnov test, $P<0.05$). Interestingly, the smallest

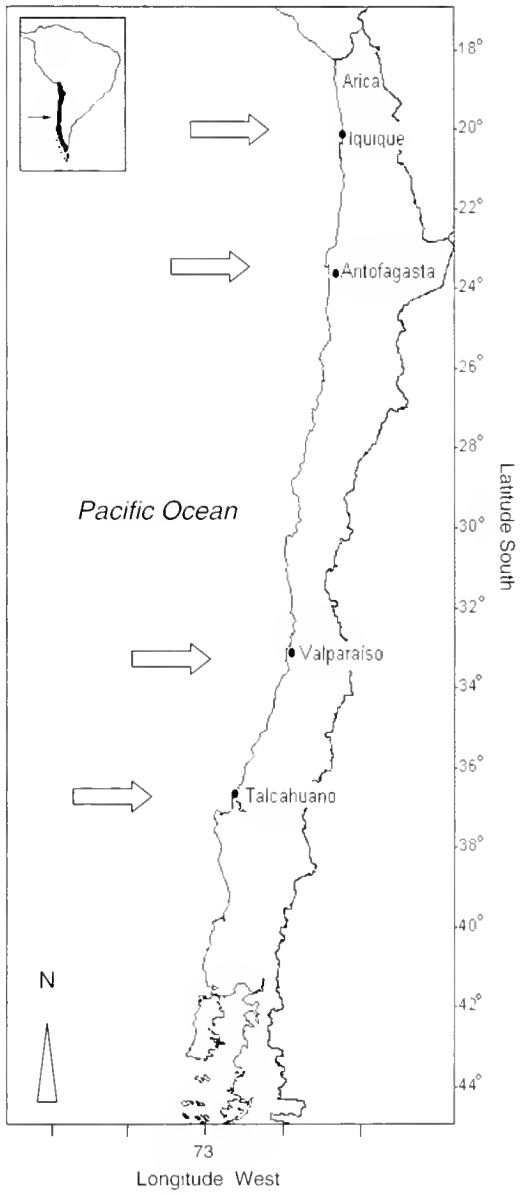

Figure 1

Areas where anchoveta eggs were collected to determine egg-size variations along the Chilean coast. Arrows show the locations depicted in Table 2.

egg sizes measured in Iquique (<0.19 mm^3) did not occur in Talcahuano. Similarly, the largest sizes determined in Talcahuano (>0.30 mm^3) did not occur in Iquique, at the lowest latitude.

Larval length at hatching determined in the rearing experiments at normal field temperatures was greater for the southernmost population (Talcahuano) (Table 3). The mean larval size for the southern location (2.70 mm notochord length) was 8.2% greater than the larvae hatched from eggs collected at the northern experimental location (Antofagasta, 2.50 mm). Furthermore, the yolksac volume in the recently hatched larvae in Talcahuano (0.130 mm^3)

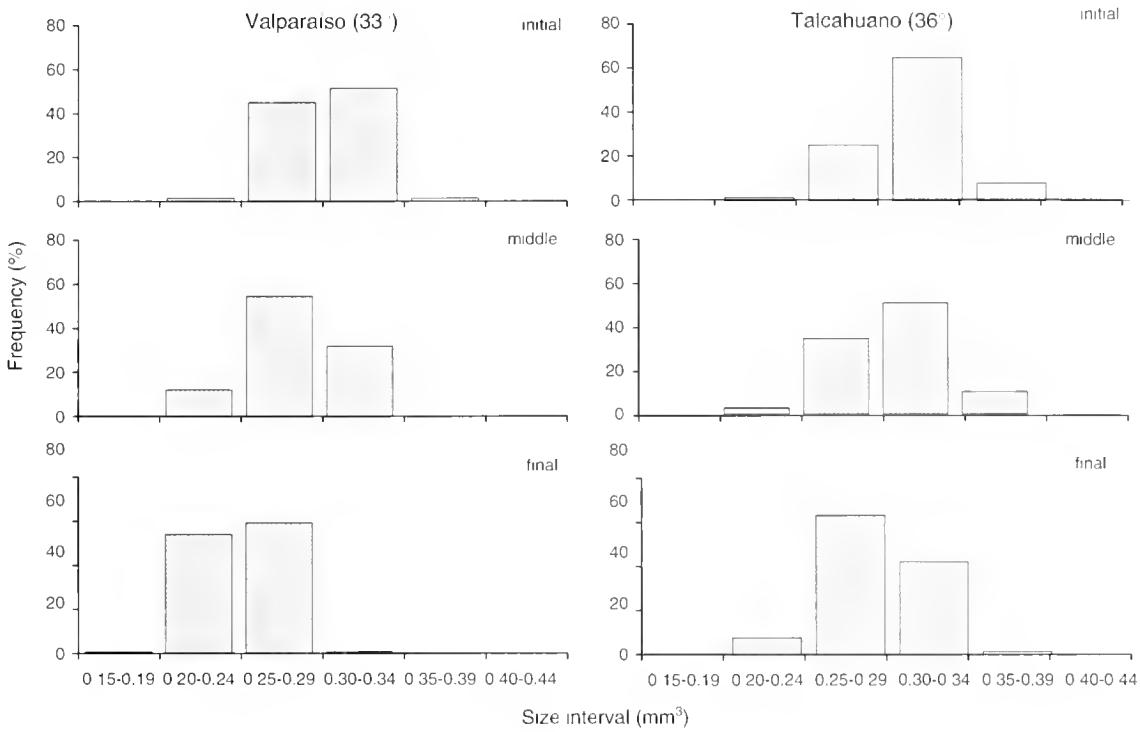

Figure 2

Seasonal variation in egg size of the anchoveta (*E. ringens*) off Valparaiso and Talcahuano. *Y*-axis is frequency over the total number of eggs measured at each locality. Initial, middle, and final are subperiods within the spawning season (see Table 2).

Table 1

Mean volume of *Engraulis ringens* eggs at the beginning, middle, and end of the spawning season off Valparaiso and Talcahuano, central Chile. SD = standard deviations. *n* = number of eggs measured.

	Valparaiso			Talcahuano		
	June 1995	October 1996	December 1996	August 1996	October 1996	January 1997
Volume (mm^3)	0.298	0.281	0.247	0.312	0.308	0.286
SD	0.026	0.029	0.022	0.030	0.034	0.029
n	62	759	630	1833	718	1099

was much larger (33% larger) than the yolk volume of the larvae hatched in Antofagasta (0.098 mm^3).

Discussion

The results of this study identified several trends that are related to egg-size variation. First, egg size tends to decrease with the progression of the spawning season. Second, egg size increases with latitude during the peak spawning period. Third, larval size at hatching is smaller in the northern latitude populations. Fourth, the yolk sac of recently hatched larvae is much larger than expected (based on the larval size at hatching) in the southern population.

A number of hypotheses have been proposed to explain egg-size variations in fish that spawn at multiple times as the reproductive season progresses. It has been proposed that in clupeiforms, the decrease in egg size may result from maternal reduction of energy reserves over the spawning season, a switch in the stored energy from reproduction to growth, seasonal changes in the age structure of the spawning population, or changes during ovogenesis that are correlated with temperature (Blaxter and Hunter, 1982; Chambers, 1997, for a recent review). In the anchoveta *E. ringens*, published data suggest that some

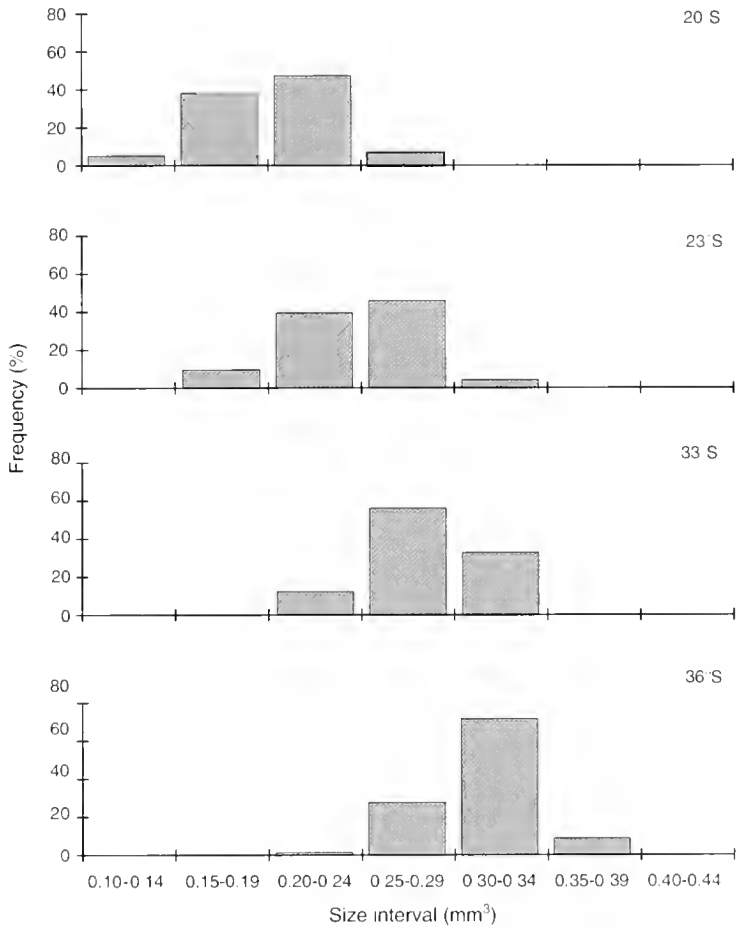

Figure 3

Latitudinal variation in egg size of the anchoveta (*E. ringens*) along northern and central Chile during the peak months of the spawning season. Y-axis is frequency over the total number of eggs measured at each locality.

of these factors co-occur. For instance, changes in growth rates for yearly cohorts during the spawning season (low at the beginning, fast at the end) have been documented for the southernmost population (Cubillos et al., 2001). Alternatively, variations in the population age structure during the spawning season have also been reported as the 1.5 year-old new recruits begin to spawn in early summer (late December–January, Cubillos et al., 1999, 2001). Changes in environmental factors affecting the spawning adults also correlate with the egg-size variations. The photoperiod and nearsurface temperatures increase as the spawning season progresses from mid-winter to late spring.

Larger egg size at the beginning of the spawning season in winter may be advantageous for these offspring because the chances of survival increase with the larger sizes of the hatching larvae. According to Cushing (1967), larger size larvae should be favored over smaller larvae in seasons with variable environmental conditions. In the Talcahuano area, strong fluctuations in the hydrographic regime occur during winter as strong north wind storms alternate with short periods of south winds, and also because of the increased river flow to the coastal zone (Castro et al., 2000). Larval food, although variable, seems to be sufficient to support most of the larval growth demands for larger exogenous feeding larvae during winter (Hernandez and Castro, 2000). For recently hatched larvae, however, the picture might be slightly different because, in addition to food supply variability, the strong turbulent environmental conditions may jeopardize first feeding success. In these highly variable areas, therefore, larger larval size at hatching and larger yolk reserves may be even more important than in other less hydrographically variable areas and seasons.

A remarkable increase in egg size at the peak spawning season occurred with respect to latitude. Egg from the northernmost (20°S) latitude were at a maximum 55% larger than eggs from the southernmost (36°S) latitude. Latitudinal variations in egg size have been previously reported for other anchovies (i.e. *Engraulis anchoita*; Ciechomski, 1973). However, egg-size variations for fishes

Table 2

Width, length, and volume of anchoveta eggs collected at different latitudes along the Chilean coast during the peak months of the spawning season. SD = standard deviations. *n* = number of eggs measured.

	Width (mm)		Length (mm)		Volume (mm^3)		
Latitude and area	mean	SD	mean	SD	mean	SD	*n*
20° Iquique	0.563	0.032	1.201	0.076	0.201	0.031	1670
23° Antofagasta	0.597	0.030	1.293	0.083	0.243	0.034	425
33° Valparaíso	0.643	0.023	1.373	0.064	0.298	0.026	62
36° Talcahuano	0.657	0.027	1.377	0.063	0.312	0.030	1833

Table 3

Morphological characteristics of recently hatched *Engraulis ringens* larvae from rearing experiments at normal field temperatures in Antofagasta (15°C) and Talcahuano (12°C). SD = standard deviations. *N* = number of eggs measured. Exp. = experiment.

		Egg volume (mm^3)		Larval length at hatching (mm)		Yolksac size at hatching (mm^3)	
		Exp. 1	Exp. 2	Exp. 1	Exp. 2	Exp. 1	Exp. 2
Antofagasta							
15°C	Mean	0.264	0.260	2.49	2.50	0.099	0.096
	SD	(0.023)	(0.023)	(0.170)	(0.104)	(0.012)	(0.012)
	n	358	325	30	30	30	30
Talcahuano							
12°C	Mean	0.302	0.292	2.71	2.69	0.126	0.134
	SD	(0.023)	(0.026)	(0.111)	(0.103)	(0.016)	(0.017)
	n	254	66	30	30	30	30

are not necessarily always associated with latitude (i.e. north Atlantic herring stocks) because local environmental conditions that trigger spawning (i.e. specific temperature or others) may have a stronger effect in some species (Chambers, 1997). Because of the extremely wide distribution range of the anchoveta (4–42°S) and its residence along an almost linear coast oriented exactly north–south, we proposed that any potential differences in egg size due to specific local conditions is probably over-driven by the larger scale changes in environmental conditions associated with latitude.

The strong latitudinal gradient in egg size of the anchoveta may be an adaptive measure if different egg sizes are favored at different latitudes or if there is a correlation between egg size and adult life history traits that maximize net reproductive output. Unfortunately, an analysis of the anchoveta in which fecundity, age of first reproduction, longevity, or other adult traits are compared in relation to latitude has not yet been carried out. The timing and length of the spawning season seem to be similar for the northern (Iquique, 20°S) and southern (Talcahuano, 36°S) stocks along Chile, despite the different temperatures at which anchoveta spawn (Castro et al., 2001). The decrease in egg size coincides with known temperature effects on physiological rates (Houde, 1989) and on ecological factors related to the need of anchoveta at early life stages to remain in nearshore environments (Bakun, 1996). At lower latitudes, the sea temperature is higher and the seaward surface Ekman transport is stronger and therefore eggs and larvae in such conditions would likely develop rapidly. Alternatively, anchovy egg and larvae at higher latitudes are retained nearshore in winter (because the Ekman transport is negative, Castro et al., 2000) but are exposed to lower temperatures and to strong turbulence that may not facilitate the first feeding of recently hatched larvae and subsequent rapid larval development. Larger eggs, larger larvae at hatching, and more energy reserves may be the favored early life history strategy in southern populations. How the latitudinal variations in environmental characteristics affect the rest of the life history traits of the different populations of *Engraulis ringens*, one of the most important fish species in the world in terms of catches, remains to be assessed.

Acknowledgments

We acknowledge help from R. Escribano (U. Antofagasta), G. Claramunt (U. Arturo Prat), and F. Balbontín (U. of Valparaíso) who facilitated ichthyoplankton collections.

H. Moyano (U. of Concepcion) allowed the use of his laboratory and optical material. This study was financed by the project FONDECYT 1990470 to L. R. Castro. E. Tarifeño, and R. Escribano. Alejandra Llanos-Rivera was also partially supported by the Graduate School of the Universidad de Concepcion.

Literature cited

Bagenal, T.B.
1971. The interrelation of the size of fish eggs, the date of spawning and the production cycle. J. Fish Biol. 3: 207–219

Bakun, A.
1996. Patterns in the ocean. Ocean processes and marine population dynamics, 233 p. California Sea Grant College Publ., NOAA in Cooperation with the Centro de Investigaciones Biologicas del Noreste, La Paz, BCS, Mexico.

Blaxter, J., and G. Hempel.
1963. The influence of egg size on herring larvae (*Clupea harengus* L.). J. Con. Perm. Int. Explor. Mer 28: 211–240.

Blaxter, J. H. S., and J. R. Hunter
1982. The biology of clupeoid fishes. Adv. Mar. Biol. 20: 3–194.

Castro, L. R., and R. K. Cowen
1991. Environmental factors affecting the early life history of bay anchovy (*Anchoa mitchilli*) in Great South Bay, New York. Mar. Ecol. Prog. Ser. 76:235–247.

Castro, L. R., G. R Salinas, and E. H. Hernández.
2000. Environmental influences on winter spawning of the anchoveta, *Engraulis ringens*, off Central Chile. Mar. Ecol. Prog. Ser. 197:247–258.

Castro, L. R., A. Llanos, J. L. Blanco, E. Tarifeño, R. Escribano, and M. Landaeta.
2001. Latitudinal variations in spawning habitat characteristics: influence on the early life history traits of the anchoveta, *Engraulis ringens*, off northern and central Chile. GLOBEC Report 16:42–45.

Chambers, R. C.
1997. Environmental influences on egg and propagule sizes in marine fishes. *In* Early life history and recruitment in fish populations (R. C. Chambers and E. A. Trippel, eds.), p. 63–102. Chapman & Hall, London.

Chambers, R. C., and K. Waiwood.
1996. Maternal and seasonal differences in egg sizes and spawning characteristics of captive Atlantic cod, *Gadus marhua*. Can. J. Fish. Aquat. Sci. 53:1986–2003.

Ciechomski, J. de
1973. The size of the eggs of the Argentine anchovy, *Engraulis anchoita* (Hubbs & Marini) in relation to the season of the year and the area of spawning. J. Fish Biol. 5:393–398.

Conover, D.
1990. The relation between capacity for growth and length of the growing season: evidence for and implications of countergradient variation. Trans. Am. Soc. 119:416–430.

Cubillos, L. A., D. Arcos, D. Bucarey, and M. Canales.
2001. Seasonal growth of small pelagic fish off Talcahuano, Chile (37°S, 73°W): a consequence of their reproductive strategy to seasonal upwelling? Aquat. Living Resour. 14:1–10.

Cubillos, L. A., M. Canales, D. Bucarey, A. Rojas, and R. Alarcón.
1999. Reproductive period and mean size at first maturity for *Strangomera bentincki* and *Engraulis ringens* from 1993 to 1997, off central-southern Chile. Invest. Mar. 27:73–85. [In Spanish.]

Cushing, D. H.
1967. The grouping of herring populations. J. Mar. Biol. Assoc. U.K. 47:193–208

Escribano, R., L. Rodriguez, and C. Irribarren
1995. Temporal variability of sea temperature in bay of Antofagasta, Northern Chile (1991–1995). Estud. Oceanol. 14:39–47. [In Spanish.]

Fisher, W.
1958. Huevos, crias y primeras prelarvas de la anchoveta *Engraulis ringens* Jenyns. Rev. Biol. Mar. 8 (1-2-3):111–124.

Fleming, I. A., and M. Gross.
1990. Latitudinal clines: a trade-off between egg number and size in pacific salmon. Ecology 71(1):1–11.

Hernández, E. H., and L. R. Castro.
2000. Larval growth of the anchoveta, *Engraulis ringens*, during the winter spawning season off central Chile. Fish. Bull. 98:704–710.

Houde, E. D.
1989. Comparative growth, mortality and energetics of marine fish larvae: temperature and implied latitudinal effects. Fish. Bull. 87:471–495.

Hunter, J. R.
1981. Feeding ecology and predation of marine fish larvae. *In* Marine fish larvae (R. Lasker, ed.), p. 34–77. Univ. Washington Press, Seattle, WA.

Imai, Ch., and S. Tanaka.
1987. Effect of sea water temperature on egg size of Japanese anchovy. Nippon Suisan Gakkaishi 53(12): 2169–2178.

Marteinsdottir, G., and K. Able.
1992. Influence of egg size on embryos and larvae of *Fundulus heteroclitus* (L.). J. Fish Biol. 41:883–896.

Rijnsdorp, A., and B. Vingerhoed.
1994. The ecological significance of geographical and seasonal differences in egg size in sole *Solea solea* (L.). Neth. J. Sea Res. 32(3/4):255–270.

Serra J., O. Rojas, M. Aguayo, F. Inostroza, and J. Cañon.
1979. Anchoveta (*Engraulis ringens*). *In* Estado actual de las principales pesquerias nacionales. Bases para un desarrollo pesquero, 36 p. Corporacion de fomento de la produccion. Instituto de Fomento Pesquero. Santiago, Chile.

Shirota, A.
1970. Studies on the mouth size of fish in the larval and fry stages. Bull. Jap. Soc. Sci. Fish. 36:353–368.

Thresher, R. E.
1984. Reproduction in reef fishes, 399 p. T.F.H. Publications, Inc. Ltd., The British Crown Colony of Hong Kong.

Ware, D. M.
1975. Relation between egg size, growth, and natural mortality of larval fish. J. Fish. Res. Board Can. 32: 2503–2512.

Wootton, R.
1990. Ecology of teleost fishes, 404 p. Chapman & Hall. London.

Molecular methods for the genetic identification of salmonid prey from Pacific harbor seal (*Phoca vitulina richardsi*) scat

Maureen Purcell

Greg Mackey

Eric LaHood

Conservation Biology Molecular Genetics Laboratory
Northwest Fisheries Science Center
National Marine Fisheries Service, NOAA
2725 Montlake Blvd. E.
Seattle, Washington 98112-2097

Harriet Huber

National Marine Mammal Laboratory
Alaska Fisheries Science Center
National Marine Fisheries Service, NOAA
7600 Sand Point Way NE
Seattle, Washington 98115

Linda Park

Conservation Biology Molecular Genetics Laboratory
Northwest Fisheries Science Center
National Marine Fisheries Service, NOAA
2725 Montlake Blvd. E.
Seattle, Washington 98112-2097

E-mail address (for L. Park, contact author): linda.park@noaa.gov

Twenty-six stocks of Pacific salmon and trout (*Oncorhynchus* spp.), representing evolutionary significant units (ESU), are listed as threatened or endangered under the Endangered Species Act (ESA) and six more stocks are currently being evaluated for listing.[1] The ecological and economic consequences of these listings are large; therefore considerable effort has been made to understand and respond to these declining populations. Until recently, Pacific harbor seals (*Phoca vitulina richardsi*) on the west coast increased an average of 5% to 7% per year as a result of the Marine Mammal Protection Act of 1972 (Brown and Kohlman[2]). Pacific salmon are seasonally important prey for harbor seals (Roffe and Mate, 1984; Olesiuk, 1993); therefore quantifying and understanding the interaction between these two protected species is important for biologically sound management strategies. Because some Pacific salmonid species in a given area may be threatened or endangered, while others are relatively abundant, it is important to distinguish the species of salmonid upon which the harbor seals are preying. This study takes the first step in understanding these interactions by using molecular genetic tools for species-level identification of salmonid skeletal remains recovered from Pacific harbor seal scats.

Most studies of harbor seal food habits rely on morphological identification of indigestible parts (e.g. otoliths and bones) from scat. Otoliths can be used to identify fish species (Ochoa-Acuna and Francis, 1995) but are not always present in scats, which can result in an underestimate of the number of species and the number of fish consumed (Harvey, 1989). Skeletal remains in scat are much more common and generally bones can be identified to the species level (Cottrell et al., 1996). Morphological identification is possible to the family level only with Pacific salmonid bones; however, genetic markers have the ability to discriminate between species, and the feasibility of extracting DNA from bones has been clearly demonstrated (Hochmeister et al., 1991).

Mitochondrial DNA (mtDNA) has been widely employed in systematic studies (reviewed by Avise, 1994) making it ideal for animal species identification. In this study, we explored three regions of the mitochondrial genome that have been previously characterized in Pacific salmonids (Shedlock et al., 1992; Domanico and Phillips, 1995; Parker and Kornfield, 1996). DNA sequencing of these regions provided an unambiguous way to determine species identity. Because high throughput sequencing can be prohibitively expensive for laboratories with limited facilities, restriction fragment length polymorphism (RFLP) analysis was also explored as an alternative for species identification. A previous study had established a species-specific polymerase chain reaction (PCR) test for Pacific Northwest salmon and coastal trout species (McKay et al., 1997). The PCR test is based on the initial amplification of an approximately 1000-bp fragment of the nuclear growth hormone 2 gene. The degraded state of the DNA isolated from bones recovered from scat has generally limited successful PCR to amplicons of 300 bp or less (data not shown). Furthermore, the amount of DNA isolated from bone fragments can be quite small; mtDNA is present in higher copy number per cell than is nuclear DNA. Thus, we considered mtDNA it to be a more

[1] http://www.nwr.noaa.gov/1salmon/salmesa/specprof.htm. [Accessed June 17, 2003.]

[2] Brown, R. F., and S. G. Kohlman. 1998. Trends in abundance and current status of the Pacific harbor seal (*Phoca vitulina richardsi*) in Oregon: 1977–1998. ODFW (Oregon Department of Fish and Wildlife) Wildlife Diversity Program Technical Report, 98-6-01, 16 p. [Available from ODFW, 7118 NE Vandenberg Ave. Corvallis, OR 97333.]

Manuscript approved for publication 9 October 2003 by Scientific Editor.

Manuscript received 20 October 2003 at NMFS Scientific Publications Office.

Fish. Bull. 102:213–220 (2004).

appropriate target for our assay. We chose to explore smaller regions of the mitochondrial genome, including the d-loop (Shedlock et al., 1992), a portion of the 16s ribosomal gene (Parker and Kornfield, 1996), and a region spanning the cytochrome oxidase III, t-RNA glycine, and ND3 genes (hereafter, referred to as COIII/ND3) (Domanico and Phillips, 1995). Significant interspecific variation but not intraspecific variation was observed in the COIII/ND3 region among salmonid species in previous studies, making it a particularly good candidate region for the development of diagnostic markers (Domanico and Phillips, 1995).

In the first phase of the study, we developed and validated the genetic tools for species identification by using frozen or ethanol-preserved tissues collected from known species and populations. In the second phase, we applied these tools to the identification of bone remains from harbor seal scats collected at the Umpqua River (Oregon). A number of Pacific salmonid species are present in the Umpqua River but of particular concern were the sea-run cutthroat (*Oncorhynchus clarki*) that were listed as endangered under the ESA during 1996 (Johnson et al., 1999). Here we report the method associated with these two phases of the project. The salmonid bones that were identified genetically were incorporated into a larger study of the harbor seal diet and are reported in a companion paper (Orr et al., 2004).

Materials and methods

Salmonid tissue samples of known species have been collected over the past decade by geneticists from the Conservation Biology Molecular Genetics Laboratory (NOAA/NMFS/NWFSC) or generously donated by others (see "Acknowledgments" section) and maintained either frozen at –80°C or preserved in 95% ethanol. Reference populations were chosen to represent the geographic range of chinook salmon (*O. tshawytscha*), coho salmon (*O. kisutch*), sockeye salmon (*O. nerka*), pink salmon (*O. gorbuscha*), chum salmon (*O. keta*), steelhead (*O. mykiss*), coastal cutthroat trout (*O. clarki clarki*), and Yellowstone cutthroat trout (*O. clarki bouvieri*) (collection information is listed in Table 1). Tissues were extracted with either a standard phenol and chloroform extraction (Sambrook et al., 1989) or by using the DNAeasy 96-well tissue kit (Qiagen, Valencia, CA), following the manufacturer's instruction for tissue preparations. PCR primers were either taken directly from the published studies or designed from the reported sequences (Table 2). All primers were cycled with 2.5 mM $MgCl_2$, 0.8 mM dNTPs, 0.04 μM primers, 0.25 units of *Taq* DNA polymerase (Promega, Madison, WI), 20–40 ng of DNA, and cresol red loading buffer (final concentration 2% sucrose and 0.005% cresol red) for 35–45 cycles of 94°C for 45 seconds, 55°C for 45 seconds, and 72°C for 1 minute.

A single individual of each salmonid species listed in Table 1 was sequenced for both the 16s rRNA and COIII/ND3 regions. For DNA sequencing, the PCR products were purified with an Ultrafree MC column (Millipore, Beverly, MA) and resuspended in 20 μL of sterile water. The purified product (1–10 μL depending on band intensity) was manually sequenced by using the USB ThermoSequenase cycle sequencing kit (Cleveland, OH), following the manufacturer's instructions. MACDNASIS (Miraibio Inc., Alameda, CA) and SEQUENCHER (Gene Codes Corp., Ann Arbor, MI) were used for sequence alignment and identification of diagnostic restriction enzyme cut sites.

RFLP analysis of the unpurified COIII/ND3 PCR product was performed in the presence of a cresol red loading buffer. Restriction digests were incubated for 6 to 12 hours at 37°C for *Dpn* II, *Sau* 96I, *Fok* I, *Ase* I, at 50° for *Apo* I, and at 60°C for *Bst* NI with the supplied buffers (NEB, Beverly, MA) and 1–5 units of enzyme. Restricted products were electrophoresed in a 4% 3:1 high-resolution and medium-resolution agarose gel (Continental Laboratory Products, San Diego, CA). DNA bands on the agarose gels were visualized with SYBR Gold, following the manufacturer's instructions (Molecular Probes, Eugene, OR).

Personnel from the National Marine Mammal Laboratory (NMML) collected and processed harbor seal scat samples from the Umpqua River (Orr et al., 2004). NMML researchers identified bone remains to either family or species level by using morphological characteristics of skeletal remains (Orr et al., 2004). From 39 harbor seal scats, 116 bones were identified morphologically to the genus *Oncorhynchus* and subjected to DNA analysis for species identification. For a positive DNA extraction control, we simulated digestion by treating coastal cutthroat bones (collected from Cowlitz Trout Hatchery, Winlock, WA) in a mixture of laboratory-grade trypsin (a digestive enzyme), baking soda, and water for 1 to 2 days. These trypsin-treated bones from a coastal cutthroat trout were used as positive DNA extraction and amplification control.

To prepare samples for DNA extraction, bones were soaked in 10% sodium hypochlorite for 10 minutes to destroy any contaminating DNA that may have adhered to the outside of the bone and were rinsed twice in sterile water. Bones ranged in weight from 0.1 to 105.6 mg and included teeth, vertebrae, gillrakers, radials, and bone fragments (hereafter, all bony parts and teeth will be referred to as "bone"). The bones were decalcified overnight in 0.5M EDTA solution (Hochmeister et al., 1991); fragile or small fragments were not decalcified. The EDTA was removed and the decalcified samples were extracted with the QIAamp tissue extraction kit (Qiagen, Valencia, CA) according to the manufacturer's instructions with the following modifications: 1) samples were proteinase K digested overnight or until completely digested; 2) 10 mg/μL yeast t-RNA carrier was added to the extractant before placement on the QIAQuick column; and 3) DNA was eluted in a reduced volume (50–100 μL) of buffer AE. Negative controls containing no tissue were simultaneously processed to verify that the extraction was free of contaminating DNA. The trypsin-treated coastal cutthroat bones were used as positive extraction and PCR controls.

Five to ten microliters of the extracted DNA were used in each amplification reaction. Amplification success was determined by electrophoresis through a 2% agarose gel followed by staining with ethidium bromide or the more sensitive SYBR Gold (Molecular Probes). Species identifi-

Table 1

Species, locations, and sample sizes (n) examined for RFLP analysis.

Species	Population	Location	n
Chinook	Walker Creek	Upper Frasier River, British Columbia	10
	Grovers Creek Hatchery	Puget Sound, Washington	12
	Lookingglass Hatchery	Snake River, Oregon	12
	Carson Hatchery	Columbia River, Washington	12
	Abernathy Hatchery.	Columbia River, Washington	11
	Upper Sacramento Mainstem	Sacramento River, California	10
Coho	Edison Creek	Oregon Coast	13
	Sandy River	Columbia River, Oregon	15
	North Fork Moclips River	Washington Coast	15
	Minter Creek Hatchery	Puget Sound, Washington	15
	Yakoun River	Queen Charlotte Island, British Columbia	7
Sockeye	Nehalem Ponds	Oregon Coast	4
	Redfish Lake	Snake River, Idaho	4
	Alturas Lake	Snake River, Idaho	2
	Ozette Lake	Washington Coast	14
	Lake Wenatchee	North Cascades,Washington	10
	Babine Lake	Central British Columbia	2
	Kamchatka River	Kamchatka Peninsula, Russia	9
Chum	Hamma Hamma River	Hood Canal, Washington	11
	Frosty Creek	Alaskan Peninsula	12
	Utka River	Chucotka Peninsula, Russia	9
	Miomote River	West Honshu, Japan	11
Pink	Nisqually River	South Puget Sound, Washington	6
	Snohomish River Even Year	North Puget Sound, Washington	12
	Skagit River	North Puget Sound, Washington	7
	Hood Canal Hatchery	Hood Canal, Washington	9
Steelhead	Gaviota Creek	South California Coast	4
	Coquille River	Oregon Coast	8
	Upper Tucannon River	Snake River, Washington	12
	Finney Creek	Puget Sound, Washington	12
	Quinault Hatchery	Washington Coast	12
	Tigil River	Kamchatka Peninsula, Russia	12
Cutthroat[1]	Alsea River	Oregon Coast	2
	Alsea Hatchery	Oregon Coast	3
	Duwamish River	Puget Sound Washington	12
	Yellowstone River	Yellowstone River, Montana	5

[1] Cutthroat trout from the Yellowstone River are a different subspecies (*O. clarki bouvieri*) from the Washington and Oregon coastal cutthroat trout (*O. clarki clarki*).

cation was accomplished by sequencing of either the d-loop or the COIII/ND3 region. RFLP analysis was performed as described above with the following modifications: *Bst* NI was excluded because it is redundant with *Dpn* II, the enzyme amount was reduced to 0.4–1.0 units per reaction, and incubation time did not exceed 2 hours. The COIII/ND3 primers are specific to the family Salmonidae. To test the possibility that the failure to obtain amplification with the COIII/ND3 primers was due to morphological misidentification of an *Oncorhynchus* species we used the 16s primers that are conserved across a broad set of taxa from Platyhelminthes through Chordata (Parker and Kornfield, 1996).

Results

The COIII/ND3 and 16s sequences were confirmed for all seven salmonid naturally present in the Pacific Northwest (Figs. 1 and 2) and deposited in Genbank (COIII/ND3: AF294827-AF294833; 16S: AF296341-AF296347). Two chinook salmon were sequenced representing two *Dpn* II

Table 2

Primer sequences, size of amplified product in base pairs, and references for mitochondrial loci used in this study.

Locus	Primer sequences (5′ to 3′)	Product size	Reference
d-loop	P2: tgt taa acc cct aaa cca g P4: gcc gaa tgt aaa gca tct ggt	230	Shedlock et al., 1992
COIII/ ND3	F: tta caa teg ctg acg gcg R: gaa aga gat agt ggc tag tac tg	368	Domanico and Phillips, 1995
16sV	F: tac ata aca cga gaa gac c R: gtg att gcg ctg tta tcc	260	Parker and Kornfield, 1997

Table 3

Restriction fragment length polymorphisms of the cytochrome oxidase III and ND3 region digested with six restriction enzymes. The "A" haplotype does not cut with the enzyme, "B" cuts with the enzyme, and "C" cuts with the enzyme but at a different site than "B."

Species	*Dpn* II	*Sau* 96I	*Fok* I	*Ase* I	*Apo* I	*Bst* NI
Chinook	A/B[1]	B	B	A	A	A
Coho	A	A	B	A	A	A
Sockeye	A	A	A	A	C	B
Chum	A	A	A	B	C	A
Pink	C	A	A	B	C	C
Steelhead	A	A	A	B	B	A
Cutthroat	A	A	A	A	A	A

[1] Spring-running chinook from the Columbia and Snake Rivers were polymorphic for the *Dpn* II cut site. Spring chinook from Carson Hatchery (derived from the upper Columbia River spring-running ESU [evolutionary significant unit]) had the "A" haplotype at a frequency of 0.91 (n=12) and spring chinook from Lookingglass Hatchery (Snake River spring-summer-running ESU) had the "A" haplotype at a frequency of 0.83 (n=12). All other chinook samples from Table 1 were invariant for the "B" haplotype.

haplotypes (A and B) and their sequences are presented in Figure 1; the chinook salmon individuals were from the Upper Columbia River summer and fall ESU (Methow River, WA). A second intraspecific polymorphism in chinook salmon was observed at position 341 between our ND3 sequence and the published sequence (Domanico and Phillips, 1995) (Fig.1). Sufficient nucleotide variation exists in the d-loop (Shedlock et al., 1992) and in the COIII/ND3 region (Fig. 1) to distinguish among the salmon species by sequencing; both regions were used for bone identification.

Six restriction enzymes were selected from the COIII/ ND3 sequence that appeared to distinguish among all the species (*Dpn* II, *Sau* 96I, *Fok* I, *Ase* I, *Apo* I, and *Bst* NI) (Fig. 1). The *Dpn* II and *Bst* NI cut patterns are redundant in that only one of these enzymes is required for species identification when used in conjunction with the other four enzymes (however, only *Dpn* II exhibits the intraspecific chinook polymorphism, see below). Haplotype patterns for all species are listed in Table 3. The haplotypes were scored with a simple alphabetic system: "A" was uncut (368 base-pair (bp) band) and "B" was cut (the size differed depending on enzyme). A few of the enzymes had an alternative cut site, and the resulting haplotype we labeled "C." The "B" haplotype produced by *Apo* I occurs in steelhead and the bands migrate at 300 and 68 bp, whereas the bands of the "C" haplotype in sockeye, chum, and pink salmon migrate at 250 and 118 bp. The enzyme *Bst* NI also has two cut patterns: the sockeye salmon "B" haplotype bands migrate at 282 and 87 bp and the "C" haplotype bands in pink salmon migrate at 271 and 98 bp. The *Dpn* II "B" haplotype in chinook salmon creates two fragments, 290 and 80 bp; the "C" haplotype in pink salmon creates three fragments, 292, 53, and 24 bp.

To confirm that the restriction enzyme polymorphisms were diagnostic within each species, we surveyed all seven Pacific salmon species representing multiple populations spanning a large geographic range (Table 1). No intraspecific polymorphisms were detected among populations with the exception of chinook salmon (Tables 1 and 3). A single intraspecific polymorphism was found with the *Dpn* II enzyme in chinook salmon lineages in the Columbia and Snake River basins (Tables 1 and 3). Chinook salmon from the Snake River spring-summer run (Lookingglass

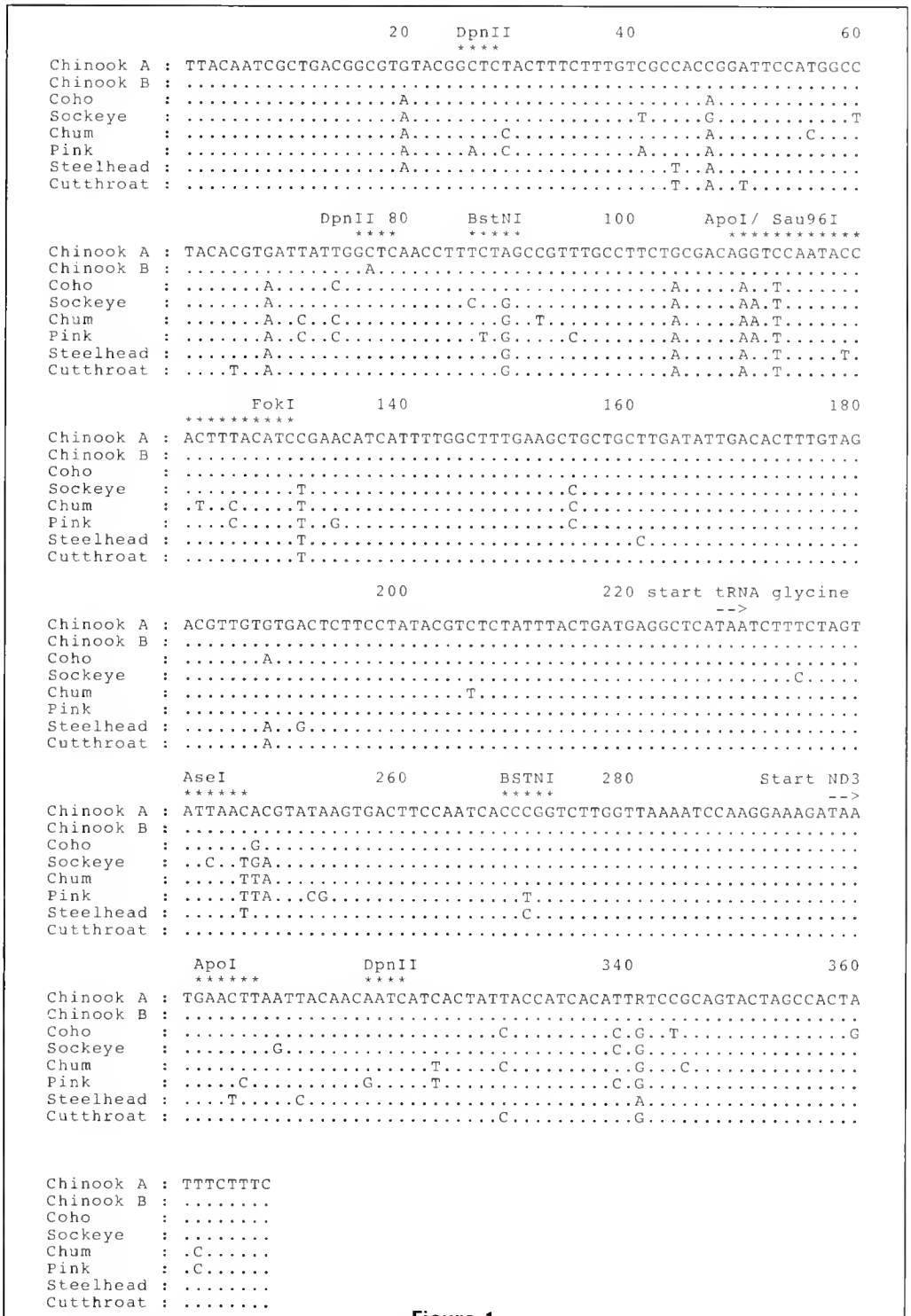

Figure 1

Aligned sequences of the 3' region of the cytochrome oxidase III gene (COIII), the tRNA glycine gene, and the 5' region of the ND3 gene for seven species of the genus *Oncorhynchus*. The cutthroat trout sequence is represented by the coastal cutthroat subspecies (*O. clarki clarki*). Chinook "A" refers to the "A" *Dpn* II haplotype; chinook "B" refers to the "B" *Dpn* II haplotype. Sequence identity relative to the chinook salmon "A" sequence is denoted by dots; nucleotide substitutions are indicated. The arrow at basepair (bp) 230 is the start of the tRNA glycine gene and the arrow at bp 300 is the start of the ND3 gene. Stars above the sequence correspond to restriction enzyme cut sites used in this study. At position 341 in chinook, the R represents an A or G.

```
                              20                  40                  60
Chinook    : GGAGCTTTAGACACCAGGCAGATCACGTCAAACAACCTTGAATTAACAAGTAAAAACGCAGT
Coho       : .........................................G.....................
Sockeye    : ............................................................
Chum       : ..........................................C.................
Pink       : ..............C............A...A..........................
Steelhead  : ............................G...........................
Cutthroat  : ............................G...........................


                          80                  100                 120
Chinook    : GACCCCTAGCCCATATGTCTTTGGTTGGGGCGACCGCGGGGGAAAATTAAGCCCCCATGTGG
Coho       : ............................................................
Sockeye    : ...........G................................................
Chum       : ..........................................A.................
Pink       : ..........................................A.................
Steelhead  : ............................................................
Cutthroat  : ...................................T............C............


                        140                 160                 180
Chinook    : ATGGGGGCATGCCCCCACAGCCAAGAGCCACAGCTCTAAGCACCAGAATATCTGACCAAAAA
Coho       : ..............T............T...A.............................
Sockeye    : ............................................................
Chum       : ....................G.....T...................T.............
Pink       : ...........T.........G.....T..............C..................
Steelhead  : ....................G.....T................................T.
Cutthroat  : ....................G.....T..G.............................


                      200                 220
Chinook    : TGATCCGGCAAACGCCGATCAACGGACCGAGTTACCCTAG....
Coho       : ..........................................
Sockeye    : ..........................................
Chum       : ..........................................
Pink       : .........G................................
Steelhead  : .........G................................
Cutthroat  : ..........................................
```

Figure 2

Aligned sequences of a variable portion of the 16s gene for seven species of the genus *Oncorhynchus*. Sequence identity in relation to the chinook salmon "A" sequence is denoted by dots; nucleotide substitutions are indicated.

Hatchery) and hatchery stocks descended from the Upper Columbia River spring run (Carson Hatchery) had the "A" (uncut) haplotype at a frequency of 83% and 91%, respectively, whereas those from the Lower Columbia River ESU were invariant for the "B" (cut) haplotype. The "B" haplotype was also invariant in the other lineages examined (Sacramento River, CA; Puget Sound, WA; and the Fraser River, BC). Despite this *Dpn* II polymorphism, the haplotype patterns were still chinook-specific.

Extractions from the trypsin-treated cutthroat trout bones, used as positive controls, were amplified consistently, but of the 116 salmonid bones from harbor seal scats, only 78 (67%) were amplified. Failed samples were repeated several times with all possible primer sets. Because each scat contained multiple bones, we were able to amplify bones representing 35 of the 39 scats (90%). The smallest bone we successfully amplified was a 0.2-mg tooth and the largest was a 21.8-mg vertebra. There did not appear to be a relationship between bone size and DNA extraction success; no significant difference in mean bone size was detected between 32 bones that either amplified or failed (P=0.280; unpaired t-test; SYSTAT 8.0 [Chicago, IL]). The bone samples that failed to amplify repeatedly were also tested by using the evolutionarily conserved 16s primers. Some samples were still refractory to PCR, indicating that the overall DNA quality or quantity was insufficient for this assay; however, those samples that did amplify were identified by sequencing as salmon. In an unrelated study using river otter bones (data not presented), one bone sample morphologically identified as salmonid yielded a sequence with 100% identity to the published 16s sequence available for Northern squawfish (*Ptychocheilus oregonensis*) (Simons and Mayden, 1998).

After verifying the specificity of the RFLP analysis for differentiating the Pacific salmon species, the assay was applied to the bone samples. Restriction enzyme digestion required some modification when applied to bone. On occasion, the restriction enzyme protocol developed for the fresh tissue resulted in degradation of the amplified bone PCR product. Enzyme amount and digestion times were scaled back for the analysis of the bone samples. The *Fok* I enzyme proved the most difficult for the bone samples, which was likely due to nonspecific restriction that occurs when the enzyme is present at a high concentration in relation to its target or if the reaction is allowed to digest for more than two hours. In some cases, only very weak amplification was achieved with the bone samples and it was difficult to get digestion without degradation. Although sequencing was the main technique used for bone identification, 23 bones in this study were identified by using the RFLP technique. Fourteen of these 23 bones were additionally confirmed by sequencing and the two techniques gave matching results.

Discussion

This study focused on the development of tools for the genetic identification of Pacific salmon skeletal remains recovered from harbor seal scats. These tools help to determine the diet of marine mammals and can also be used to address direct management questions regarding interspecific interactions in rivers such as the Umpqua River where salmonid species of concern (cutthroat trout) occur with protected marine mammal species. The harbor seal diet in the Umpqua River consisted of nonsalmonid fish and chinook, coho, and steelhead; no cutthroat trout were observed in the scat samples (Orr et al., 2004). The majority of salmonid species identifications were possible only by using genetic methods because very few otoliths were recovered in the Umpqua River scats. A number of other sites exist were this technology may also be applicable. In Hood Canal (WA) the summer chum salmon run is listed as threatened under the ESA. A report of seal diets in Hood Canal determined that 27% of the fish consumed by harbor seals were salmonids (Jeffries et al.[3]). The study used both bones and otoliths, but only 25% of the samples contained otoliths that allowed species-level identification. In the Alsea River (OR), coho salmon are listed as threatened. A report by Riemer et al.[4] indicated that 6% of fish consumed by pinnipeds in the Alsea River are salmonids; none of the salmonid remains were morphologically identifiable to species.

Extraction of DNA from bones can be done with a commercially available kit with minor modifications. In our study, only 67% of the bone DNA extracts could be amplified by PCR. PCR failure could be due to DNA degradation during the digestive process or to environmental exposure after defecation. However, multiple bones are often present in scats and we were able to amplify DNA from at least one bone representative from 35 out of the 39 scats examined. Sequencing or RFLP analyses of the COIII/ND3 locus are both viable methods of identifying the seven common *Oncorhynchus* species. This study used manual sequencing with radioactivity and we did have better results using this method compared to the RFLP method. A recently published study also identified restriction enzymes in the cytochrome B gene that distinguish among the salmonid species (Russell et al., 2000). The study reported diagnostic RFLP differences among these species but did not confirm the lack of intraspecific variation in a wide geographic survey of each species. The goal of the cytochrome B RFLP assay designed by Russell et al. (2000) was to identify salmon species found in processed food products but the primers may also prove useful in species identification of bone remains. The 16s primer set is also valuable for bones that are morphologically unidentifiable. However for salmonid species identification, the 16s region contains fewer diagnostic nucleotide substitutions in relation to the d-loop and the COIII/ND3 region. Overall, the techniques established here would be useful for further study of marine mammal diets and may have the potential for forensic application.

[3] Jeffries, S. J., J. M. London, and M. M. Lance. 2000. Observations of harbor seal predation on Hood Canal summer chum salmon run 1998–1999. Annual progress report to Pacific States Marine Fisheries Commission, 39 p. [Available from WDFW, Marine Mammals Investigations, 7801 Phillips Rd. SW, Tacoma, WA 98498.]

[4] Riemer, S. D., R. F. Brown, B. E. Wright and M. I. Dhruv. 1999. Monitoring pinniped predation on salmonids at Alsea River and Rogue River, Oregon: 1997–1999. Oregon Department of Fish and Wildlife, Marine Mammal Research Program, Corvallis, OR, 36 p. [Available from ODFW, 7118 NE Vandenberg Ave., Corvallis, OR 97333.]

Acknowledgments

The authors acknowledge Robert Delong for suggesting this study. Jon Baker at the Northwest Fisheries Science Center and Paul Spruell at the University of Montana kindly provided cutthroat DNA. James Shaklee at the Washington Department of Fish and Wildlife kindly provided pink salmon samples. Sam Wasser and Virginia Butler provided advice on the recovery of DNA from scat and bone samples. Gail Bastrup assisted in technical aspects of this study.

Literature cited

Avise, J. C.
1994. Molecular markers, natural history, and evolution, p. 44–91. Chapman and Hall, New York, NY.

Cottrell, P. E., A. W. Trites, and E. H. Miller.
1996. Assessing the use of hard parts in faeces to identify harbour seal prey: results of captive-feeding trials. Can. J. Zool. 74:875–880.

Domanico, M. J., and R. B. Phillips.
1995. Phylogenetic analysis of Pacific salmon (genus *Oncorhynchus*) based on mitochondrial DNA sequence data. Mol. Phylogenet. Evol. 4:366–371.

Harvey, J. T.
1989. Assessment of errors associated with harbour seal (*Phoca vitulina*) faecal sampling. J. Zool. 219:101–111.

Hochmeister, M. N., B. Budowle, U. V. Borer, U. Eggmann, C. T. Comey, and R. Dirnhofer.
1991. Typing of deoxyribonucleic acid (DNA) extracted from compact bone from human remains. J. Forensic Sci. 36: 1649–1661.

Johnson, O., M. Ruckelshaus, W. Grant, F. Waknitz, A. Garrett, G. Bryant, K. Neely, and J. Hard.
1999. Status review of coastal cutthroat trout from Washington, Oregon, and California. NOAA Tech. Memo. NMFS-NWFSC-37, p 138–139.

McKay, S. J., M. J. Smith, and R. H. Devlin.
1997. Polymerase chain reaction-based species identification of salmon and coastal trout in British Columbia. Mol. Mar. Biol. Biotechnol. 6:131–140.

Ochoa-Acuna, H., and J. M. Francis.
1995. Spring and summer prey of the Juan Fernandez fur seal, *Arctocephalus philippii*. Can. J. Zool. 73:1444–1452.

Olesiuk, P. F.
1993. Annual prey consumption by harbor seals (*Phoca vitulina*) in the Strait of Georgia, British Columbia. Fish. Bull. 91:491–515.

Orr, A., A. Banks, S. Mellman, and H. Huber.
2004. Examination of Pacific harbor seal (*Phoca vitulina richardsi*) foraging habits to describe their use of the

Umpqua River, Oregon, and their predation on salmonids. Fish. Bull. 102:108–117.

Parker, A., and I. Kornfield.
1996. An improved amplification and sequencing strategy for phylogenetic studies using the mitochondrial large subunit rRNA gene. Genome 39:793–797.

Roffe, T., and B. Mate.
1984. Abundance and feeding habits of pinnipeds in the Rogue River, OR. J. Wildl. Manag. 48:1262–1274.

Russell, V. J., G. L. Hold, S. E. Pryde, H. Rebbein, J. Quinteiro, M. Rey-Mendez, C. G. Sotelo, R. Perez-Martin, A. T. Santos, and C. Rosa.
2000. Use of restriction fragment length polymorphism to distinguish between salmon species. J. Agricult. Food Chem. 48:2184–2188.

Sambrook, J., E. F. Fritsch, and T. Maniatis.
1989. Molecular cloning: a laboratory manual, p. 9.17–9.19. Cold Spring Harbor Laboratory, Cold Spring Harbor, NY.

Shedlock, A. M., J. D. Parker, D.A. Crispin, T. W. Pietsch, and G. C. Burmer.
1992. Evolution of the salmonid mitochondrial control region Mol. Phylogenet. Evol. 1:179–192.

Simons, A. M., and R. L. Mayden.
1998. Phylogenetic relationships of the western North American phoxinins (Actinopterygii: Cyprinidae) as inferred from mitochondrial 12S and 16S ribosomal RNA sequences. Mol. Phylogenet. Evol. 9:308–329.

Diel vertical migration of the bigeye thresher shark (*Alopias superciliosus*), a species possessing orbital retia mirabilia

Kevin C. Weng

Barbara A. Block

Tuna Research and Conservation Center
Hopkins Marine Station of Stanford University
120 Oceanview Boulevard
Pacific Grove, California 93950

E-mail address (for K. C. Weng): kevin.cm.weng@stanford.edu

The bigeye thresher shark (*Alopias superciliosus*, Lowe 1841) is one of three sharks in the family Alopiidae, which occupy pelagic, neritic, and shallow coastal waters throughout the tropics and subtropics (Gruber and Compagno, 1981; Castro, 1983). All thresher sharks possess an elongated upper caudal lobe, and the bigeye thresher shark is distinguished from the other alopiid sharks by its large upward-looking eyes and grooves on the top of the head (Bigelow and Schroeder, 1948). Our present understanding of the bigeye thresher shark is primarily based upon data derived from specimens captured in fisheries, including knowledge of its morphological features (Fitch and Craig, 1964; Stillwell and Casey, 1976; Thorpe, 1997), geographic range as far as it overlaps with fisheries (Springer, 1943; Fitch and Craig, 1964; Stillwell and Casey, 1976; Gruber and Compagno, 1981; Thorpe, 1997), age, growth and maturity (Chen et al., 1997; Liu et al., 1998), and aspects of its reproductive biology (Gilmore, 1983; Moreno and Moron, 1992; Chen et al., 1997).

Limited information on the movement patterns of bigeye thresher sharks has been obtained from mark-recapture studies by using conventional tags. The longest straight-line movement of a conventionally tagged bigeye thresher shark to date is 2767 km from waters off New York to the eastern Gulf of Mexico (Kohler and Turner, 2001). The bigeye thresher shark has been captured on longlines set near the surface at night (0 m to 65 m, Fitch and Craig, 1964; Stillwell and Casey, 1976; Thorpe, 1997; Buencuerpo et al., 1998) and at 400 m to 600 m during the day (Nakamura[1]). There is no published information available regarding its habitat and behavior, although Francis Carey tracked a bigeye thresher with an acoustic tag for six hours (Carey[2]).

Endothermy is a rare trait in fishes and has been demonstrated only in tunas (Thunnini), billfishes (Xiphiidae, Istiophoridae), and lamnid sharks (Lamnidae) (Carey and Teal, 1969; Carey, 1971, 1982a; Block, 1991). In all endothermic fishes, the blood supply to aerobic tissues such as slow-twitch swimming muscle, visceral organs, extraocular muscles, retina, and brain occurs by counter-current heat exchangers known as retia mirabilia. The vascular supply reduces heat loss to the environment and enables heat conservation in metabolically active tissues (Carey, 1971). Lamnid sharks have retia mirabilia in the circulatory anatomy supplying the slow-oxidative swimming muscles, viscera, brain, and eyes (Burne, 1924; Block and Carey, 1985; Tubbesing and Block, 2000). In many lamnid species, tissue temperatures significantly above ambient have been recorded from freshly captured specimens and through telemetry studies of swimming animals (Carey, 1971; Carey et al., 1981, 1982, 1985; McCosker, 1987; Goldman, 1997; Tubbesing and Block, 2000).

The anatomy of alopiid sharks suggests that endothermy may occur in this family. The bigeye thresher and the common thresher (*Alopias vulpinus*) have centrally located slow-oxidative muscle and primitive retia mirabilia supplying blood to them (Carey, 1982b; Bone and Chubb, 1983). Burne (1924) noted a coiling of the pseudobranchial artery supplying the orbit and cranial regions in the common thresher. No internal tissue temperature measurements have been taken for free-swimming thresher sharks to ascertain whether heat is conserved in oxidative tissues. A freshly caught bigeye thresher shark was found to have a body-core thermal excess of 4°C (Carey, 1971); thus the species may have the ability to conserve metabolic heat.

In this study we present electronic tagging data on the movements, diving behavior, and habitat preferences of the bigeye thresher shark based on two individuals studied with pop-up satellite archival tags. In addition, we provide a brief description of the orbital rete mirabile of the species. The presence of this highly developed rete mirabile within the orbital sinus suggests a physiological mechanism to buffer the eyes and brain from the large temperature changes associated with diel vertical migration, potentially conferring enhanced physiological performance.

Materials and methods

The movements of two bigeye thresher sharks were monitored with pop-up satellite archival tags (PAT tag version 2.00, Wildlife Computers, Redmond, WA; Gunn and Block, 2001; Marcinek et al., 2001). The first shark was captured on a longline set in the Gulf of Mexico at 26.5°N, 91.3°W on 12 April

[1] Nakamura, I. 2002. Personal commun. Institut National des Sciences et Technologies de la Mer, 28 rue 2 Mars 1934, 2025 Salammbo, Tunisia.

[2] Carey, F. G. (deceased). 1990. Personal commun. Woods Hole Oceanographic Institution, Woods Hole, MA 02543.

Manuscript approved for publication 15 August 2003 by Scientific Editor.

Manuscript received 20 October 2003 at NMFS Scientific Publications Office.

Fish. Bull. 102:221–229 (2004).

2000 in waters with a surface temperature of 21.9°C. The longline set contained 184 hooks set at depths between 70 m and 90 m and was made at 06:00 h and retrieved at 09:00 h. Circle hooks (L2045 20/0 circle hook, Eagle Claw, Denver, CO) were used to avoid hooking of the gut, and the shark in this study was hooked in the corner of the jaw. Hooks were baited with squid, and chemical light sticks were attached to every other line. The mass of the shark was visually estimated at 170 kg by an experienced commercial longline fisherman, which corresponds to a fork length of 229 cm, and a total length of 377 cm, based on the weight-length relationship of Kohler et al. (1995). According to this size estimation and the published size-at-maturity data (Chen et al., 1997; Liu et al., 1998), the shark was mature. The sex of the shark was not determined. The second shark was captured by hook-and-line gear near Hawaii at 19.5°N, 156.0°W on 13 May 2003 in waters with a surface temperature of 25.5°C. A baited circle hook set at a depth of 40 m was taken by the shark at 02:00 h. The mass of the shark was estimated at 200 kg by an experienced sportfishing captain, which corresponds to a fork length of 242 cm, and a total length of 400 cm (after Kohler et al., 1995). Given this size, the shark was mature (Chen et al., 1997; Liu et al., 1998), but its sex was not determined.

Each pop-up satellite archival tag was attached to a titanium dart (59 mm × 13 mm) with a 17 cm segment of 136-kg monofilament line (300-lb test extra-hard Hi-Catch, Momoi Fishing Net Mfg. Co. Ltd., Ako City, Hyogo prefecture, Japan). The dart was inserted into the dorsal musculature of the shark at the base of the first dorsal fin, such that the tag trailed behind the fin. Following attachment of each tag, the fishing line was cut near the hook and both sharks swam away vigorously. Tagging locations were recorded by using the vessel's global positioning system. After the Gulf of Mexico shark was tagged, a depth-temperature recorder (ABT-1, Alec Electronics, Kobe, Japan) was used to determine the temperature-depth profile of the upper 200 m of the ocean at the release site, at a resolution of 1 m.

The pop-up satellite archival tag deployed in the Gulf of Mexico was programmed to collect pressure and temperature data at two-minute intervals, which the on-board software (PAT software version 1.06, Wildlife Computers, Redmond, WA) summarized into six-hour bins. This version of PAT software did not permit light-based geolocation. The summary data for each time interval comprised percentage distributions of time-at-depth and time-at-temperature, and profiles of temperature-at-depth. Temperature-depth profiles for this generation of software were recorded at intervals by measuring a single temperature at depths of 0, 25, 50, 75, 100, 125, 150, 200, 250, 300, 350, and 400 meters for the deepest dive. A mean temperature-depth profile was obtained by calculating the mean temperature at each specified depth for all profiles taken during the track. The endpoint position of the shark's track was obtained from the tag's radio transmissions to the Argos satellites. The six-hour bins were later combined into 12-hour bins representing day (06:00 to 17:59 h local time) and night (18:00 to 05:59 h local time). At the time and place of tag deployment, sunrise occurred at 05:45 h and sunset at 18:28 h; whereas at the popup time and position, sunrise occurred at 05:02 h and sunset at 18:55 h (U.S. Naval Observatory), such that the day and night bin cutoffs were always within one hour of true sunrise and sunset.

The pop-up satellite archival tag deployed off Hawaii collected data at 30-second intervals and summarized them into four-hour bins (PAT software version 2.08e, Wildlife Computers, Redmond, WA). The data were later combined into day and night bins as for the first tag, and the actual sunrise and sunset times were within one hour of 06:00 h and 18:00 h, respectively (U.S. Naval Observatory). The tag measured the minimum and maximum temperature at the surface, maximum depth, and six intermediate depths, for the deepest dive in each time interval. Temperature-depth profiles for each time interval were later constructed by using the maximum temperature at each depth for all profiles taken during the track, and a curve was fitted by using a LOWESS (locally weighted regression smoothing) function (Cleveland, 1992). Version 2.08e PAT software collected light data for geolocation; however the diel dive pattern of the shark prevented the calculation of accurate positions.

The vascular circulation to the brain and eyes was examined in two bigeye thresher sharks: one common thresher shark and one pelagic thresher shark (*Alopias pelagicus*). A female bigeye thresher (1.5 m fork length) was captured off Cape Hatteras, North Carolina, and a male (1.4 m fork length) was captured in the Gulf of Mexico. The circulatory systems of the bigeye threshers were injected with latex to aid in identifying the blood vessels. A male common thresher (1.3 m fork length) was captured off Cape Hatteras, North Carolina, and was examined without being frozen or preserved. An immature female pelagic thresher shark (1.37 m fork length) was captured in the Indian Ocean. The orbital retia mirabilia were prepared from casts of the vascular circulation that were removed from the orbit.

Results

One bigeye thresher shark was tracked in the Gulf of Mexico for 60 days, and another in the Hawaiian Archipelago for 27 days, by using pop-up satellite archival tags. Both tags released from the sharks as programmed and transmitted summary information to Argos satellites. The tag deployed in the Gulf of Mexico popped up on 10 June 2000 at 27.95°N, 89.54°W (Fig. 1A). The shark moved a straight-line distance of 320 km during the track, starting from the central Gulf in depths exceeding 3000 m and moving to waters 150 km south of the Mississippi Delta where depths were approximately 1000 m. The second shark was tagged off the Kona coast of Hawaii and the tag released on 9 June 2003 at 24.2°N, 165.6°W, northeast of French Frigate Shoals, a straight-line distance of 1125 km from the deployment position (Fig. 1B).

The depth and temperature distributions of the bigeye thresher sharks showed a strong diel movement pattern (Fig. 2). The Gulf of Mexico shark spent the majority of the daytime (84% [±2.3%], mean [±1 SE]) below the thermocline between 300 m and 500 m and the majority of nighttime (80% [±4.7%], mean [±1 SE]) in the mixed layer

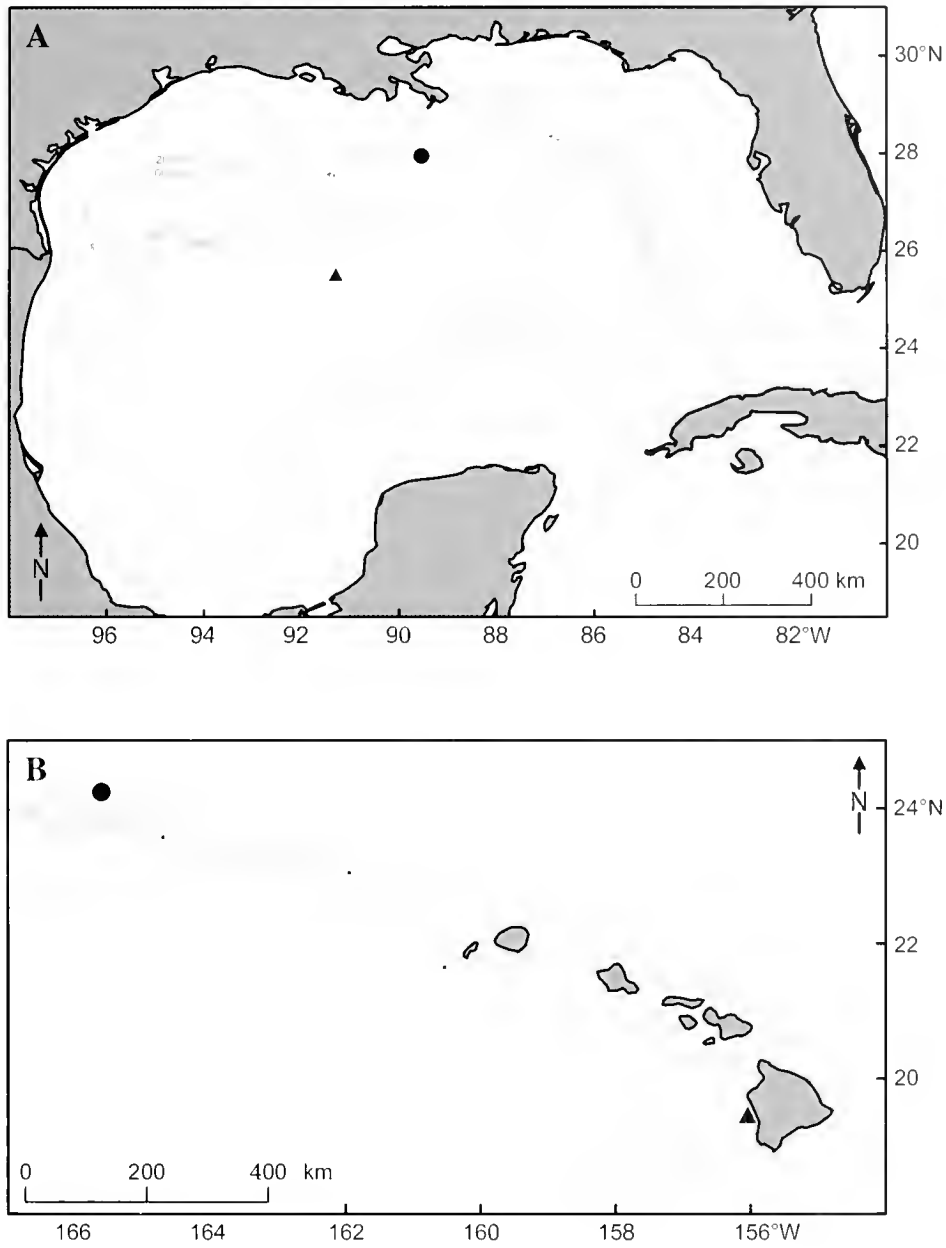

Figure 1

Deployment (▲) and end-point (●) positions for the two pop-up satellite archival tags attached to bigeye thresher sharks. Both tags surfaced on the programmed dates and transmitted data to Argos satellites. Pressure sensors in the tags confirmed that the tags remained attached to the sharks for the duration of the tracks. (**A**) In the Gulf of Mexico a shark was tagged and released on 12 April 2000 and the tag surfaced on 10 June 2000. The shark moved a straight-line distance of 320 km during the 60-day track. (**B**) In the Hawaiian Archipelago a shark was tagged on 13 May 2003 off Kona, Hawaii, and the tag surfaced on 9 June 2003 northeast of French Frigate Shoals. The shark moved a straight-line distance of 1125 km during the 27-day track.

and upper thermocline between 10 m and 100 m (Fig. 2A). The shark spent most of the daytime in deeper waters of 6°C to 12°C (70% [±4.4%], mean [±1 SE]), and most of the nighttime in shallower waters from 20°C to 26°C (70% [±2.7%], mean [±1 SE]) (Fig. 2B). A temperature-depth profile taken by the tag during the first day of the shark's track closely matched a profile taken from the vessel with a bathythermograph (Fig. 3A). The mean temperature-depth profile for the 60-day track (Fig. 3B), when compared with the shark's depth preferences (Fig. 2A), indicated that

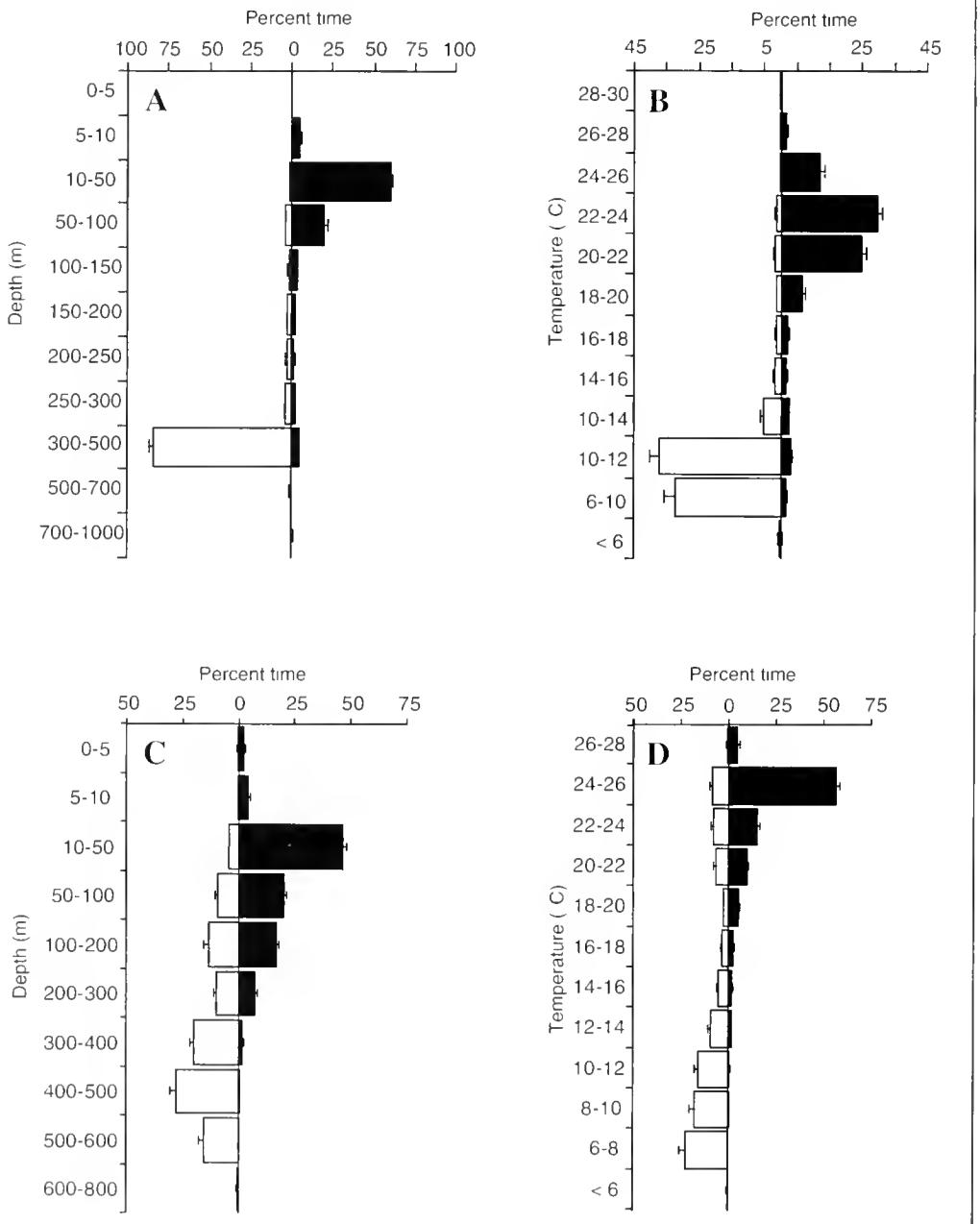

Figure 2

Depth and temperature distributions of two bigeye thresher sharks showing diel vertical migration. The tags recorded depth and temperature at two-minute (**A, B**) or 30-second (**C, D**) intervals; data are summarized into a series of bins for the full duration of each track. (A) Depth distribution for the Gulf of Mexico shark is shown as the percentage of day (□) and night (■) spent within depth bins ranging from the surface to 1000 m. Error bars are 1 SE. (B) Temperature distribution for the Gulf of Mexico shark is shown as the percentage of day (□) and night (■) spent within temperature bins ranging from 6°C to 30°C. The shark occupied cool waters during the day and warm waters during the night, a consequence of its deep daytime and shallow nighttime habitats. Error bars are 1 SE. (**C**) Depth distribution for the Hawaii shark showing diel vertical migration. The shark spent most of the daytime at the base of the thermocline and most of the nighttime in the mixed layer and upper thermocline. (**D**) Temperature distribution for the Hawaii shark showing cool daytime and warm nighttime water temperatures.

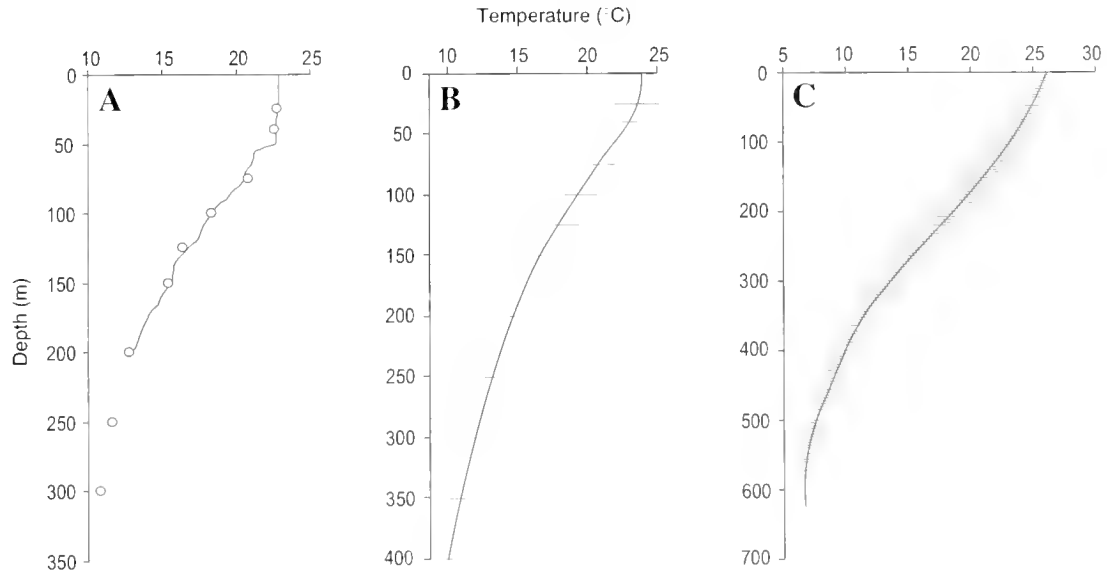

Figure 3

Temperature-depth profiles characterizing the thermal habitat of two bigeye thresher sharks. (**A**) Profiles of the Gulf of Mexico taken with a bathythermograph (——) sampling at 1-m intervals deployed from the fishing vessel after the tagging event, and by the pop-up satellite archival tag (○) during the first day it was attached to the bigeye thresher shark. The two profiles are similar, indicating that the pop-up satellite archival tag is capable of characterizing thermal habitat. (**B**) Average temperature-depth profile for the 60-day track of the bigeye thresher shark in the Gulf of Mexico, showing a mixed layer shallower than 50 m and a thermocline extending beyond 400 m where waters were 10°C. The curve was fitted by using a LOWESS function and error bars are 1 SD, because 1 SE bars are invisible at this scale. (**C**) Average temperature-depth profile for the 27-day track of the bigeye thresher shark in the Hawaiian Archipelago, showing a shallow mixed layer a thermocline extending to approximately 600 m where waters were 6°C. Curve was fitted by using a LOWESS function and error bars are 1 SD, because 1 SE bars are invisible at this scale.

the shark spent most of the daytime below the maximum gradient of the thermocline where temperatures were approximately 10°C. On 25 April and 25 May 2000 the shark spent two hours of the day in waters between 4°C and 6°C. The Hawaii shark showed a similar diel vertical migration, with a lesser contrast between day and night (Fig. 2, C and D). The shark's modal nighttime depth was between 10 m and 50 m, whereas its modal daytime depth was between 400 m and 500 m (Fig. 2C). The temperature-depth profile for the Hawaii shark (Fig. 3C) indicated that it spent nighttime above the thermocline and daytime below it.

The bigeye thresher shark possesses a large arterial plexus between the posterior part of the eye and the wall of the orbital sinus, which appears to be a rete mirabile (Fig. 4). The orbital rete is bathed in venous blood from the orbital sinus and its anterior surface is contoured to the posterior surface of the eye. The sources of venous input to the orbital sinus remain unknown but are most likely within the surrounding extraocular muscles, which are large and comprise numerous aerobic muscle fiber types, and the retina. The rete shown in Figure 4 measures 72 mm by 49 mm by 19 mm. A reduced structure of similar form is also found in the pelagic thresher shark, but is not present in the common thresher. The orbital rete of the bigeye and pelagic threshers is larger in absolute size and occupies a greater cross sectional proportion of the orbital sinus than the lamnid orbital rete noted by Burne (1924). The arterial vessels form a finer and more orderly meshwork than those in the lamnid sharks (Block and Carey, 1985; Tubbesing and Block, 2000) and appear similar in physical structure to the mammalian carotid rete used for brain cooling (Baker, 1982).

Discussion

Observations of the biological features of the bigeye thresher shark are rare and our knowledge of the species is based primarily on incidental catches in fisheries. Using pop-up satellite archival tags we were able to record behavior for a total of 87 days, and for individual periods up to 60 days without recapturing or following the study animals. We observed a pronounced diel alternation between warm shallow waters and cool deep waters and a rete mirabile that may confer physiological benefits during deep dives by stabilizing brain and eye temperatures.

The depth data obtained for the bigeye thresher shark shows a striking pattern of diel vertical migration. The bigeye thresher shark's vertical movement pattern is distinct from those of most other sharks for which observations

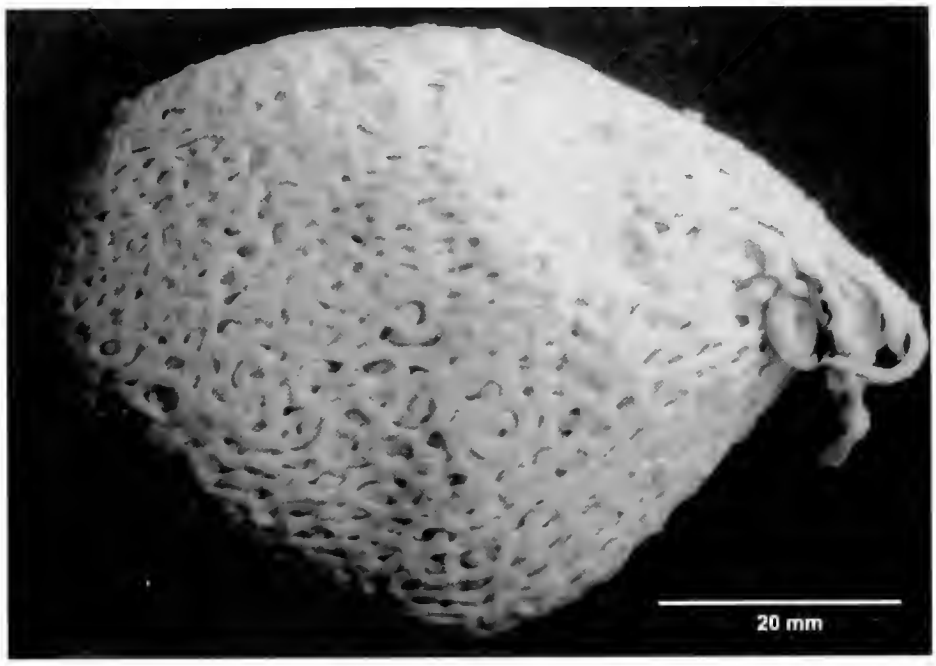

Figure 4

Orbital rete of a bigeye thresher shark, showing the highly developed arterial network. The rete was injected with latex so that the arterial structure (72 mm by 49 mm by 19 mm) could be photographed. The structure of the rete and its position in the orbital sinus suggest that it may be a heat exchanging vascular plexus. Retention of metabolic heat in the eyes and brain would buffer these sensitive organs from the large ambient temperature swings that occur as a result of the bigeye thresher shark's diel vertical migrations. A smaller but similar structure is found in *A. pelagicus* but not in *A. vulpinus*.

exist. In satellite or acoustic tracks, diel vertical migration was not observed for white sharks (*Carcharodon carcharias*; Carey et al., 1982; Goldman and Anderson, 1999; Boustany et al., 2002), salmon sharks (*Lamna ditropis*; Block et al.[3]), shortfin mako (*Isurus oxyrhynchus*; Carey, 1982b; Holts and Bedford, 1993), blue (*Prionace glauca*, Carey, 1982b; Carey and Scharold, 1990), sixgill (*Hexanchus griseus*; Carey and Clark, 1995), tiger (*Galeocerdo cuvier*; Tricas et al., 1981; Holland et al., 1999), Pacific angel (*Squatina californica*; Standora and Nelson, 1977), whale (*Rhincodon typus*; Gunn et al., 1999), or scalloped hammerhead sharks (*Sphyrna lewini*; Klimley, 1993).

Diel vertical migration has been observed in the swordfish (*Xiphias gladius*; Carey and Robison, 1981; Carey[4]), the megamouth shark (*Megachasma pelagios*; Nelson et al., 1997), and the school shark (*Galeorhinus galeus*; West and Stevens, 2001). Carey and Robison (1981) and Carey[4] studied swordfish in both the Pacific and Atlantic Oceans, acoustically tracking fish that moved from the surface at night to over 600 m during day. A megamouth shark showed a strong diel vertical migration when tracked acoustically off southern California (Nelson et al., 1997) with shallow nighttime and deep daytime distribution in a vertical range of 20 m to 160 m. West and Stevens (2001) studied school sharks in southern Australia using archival tags and noted that they ascended in the water column at night.

The ambient temperature at the modal day- and nighttime depths of the two bigeye thresher sharks differed by 15° to 16°C, requiring them to be eurythermal. The sharks spent most of the nighttime in shallow waters warmer than 20°C and commonly spent 8 or more hours during the daytime in deep waters cooler than 10°C. The coolest waters occupied had temperatures between 4°C and 6°C. The bigeye thresher sharks tracked in our study spent a higher proportion of their time in waters below 10°C than did white sharks (Carey et al., 1982; Boustany et al., 2002) and mako sharks (Carey and Scharold, 1990; Klimley et al., 2002).

The presence of a rete mirabile in the cranial region may indicate a mechanism for heat conservation. Heat conservation in the brain and eyes would enable the big-

[3] Block, B. A., K. G. Goldman, and J. A. Musick. 1999. Unpubl. data. Hopkins Marine Station of Stanford University, 120 Oceanview Boulevard, Pacific Grove, CA 93950.

[4] Carey, F. G. 1990. Further acoustic telemetry observations of swordfish. *In* Planning the future of billfishes; proceedings of the second international billfish symposium, 1–5 August 1988, Kailua-Kona, Hawaii (R. H. Stroud, ed.), p. 103–122. National Coalition for Marine Conservation, 3 North King St., Leesburg, VA 20176.

eye thresher shark to prolong its foraging time beneath the thermocline, as we observed for both of the sharks tagged in our study. The retina and brain are extremely temperature sensitive in most vertebrates and the large changes in depth and temperature recorded would impose significant effects on the biochemical processes occurring in these tissues (Block and Carey, 1985; Block, 1994). Delayed responses to retinal stimulation can be caused by cooling, whereas increased noise and random firing of neurons can be caused by warming—both responses having adverse affects on sensory function (Konishi and Hickman, 1964; Friedlander et al., 1976; Prosser and Nelson, 1981).

Anatomical and physiological adaptations to warm the brain and eyes have evolved independently in divergent pelagic fish lineages, including the lamnid sharks (Block and Carey, 1985), billfishes of the Xiphiidae and Istiophoridae (Carey, 1982a; Block, 1983) and some scombrid fishes (Linthicum and Carey, 1972). A cranial rete mirabile also has been identified in mobulids (Schweitzer and Notarbartolo di Sciara, 1986) and is thought to be a heat exchanger (Alexander, 1995, 1996). Although it is premature to suggest that the orbital rete of the bigeye thresher shark is a heat exchanger without direct evidence of elevated tissue temperatures in the brain and eyes, the structure is larger than the rete mirabile of lamnid sharks, for which elevated brain and eye temperatures have been demonstrated (Block and Carey, 1985). The anatomical arrangement of an arterial plexus in an orbital sinus is correlated with heat conservation strategies in other vertebrates (Baker, 1982). The phylogenetic relationships of the alopiid and lamnid sharks (Compagno, 1990; Naylor et al., 1997) suggest that endothermic traits evolved independently in the two families.

This note presents new information on the depth and ambient temperature preferences of the bigeye thresher shark based on observations of two individuals, as well as the anatomy of the orbital rete mirabile, which appears to function as a vascular heat exchanger. Behavior of many organisms varies with ontogeny, season and location; therefore the present study should be considered as only the beginning of an understanding of the bigeye thresher shark's physical habitat preferences and adaptations to temperature change. Further studies on individuals of different sizes and in different regions will enhance our understanding of the behavior, and morphological and physiological adaptations, of the bigeye thresher shark to variations in temperature.

Acknowledgments

This research was supported by grants from the National Marine Fisheries Service, the National Fish and Wildlife Federation and the Packard Foundation. The authors wish to thank Captain David Price and crew of the FV *Allison*, and Captain John Bagwell and crew of the FV *Silky*. Shana Beemer provided scientific assistance on the cruise and Captain McGrew Rice assisted in tagging and releasing the Gulf of Mexico shark. This research was conducted under Scientific Research Permit TUNA-SRP-2000-002, issued by the Office of Sustainable Fisheries, National Marine Fisheries Service, Silver Spring, MD 20910.

Literature cited

Alexander, R. L.
1995. Evidence of counter-current heat exchanger in the ray, *Mobula tarapacana* (Chondrichthyes: Elasmobranchii: Batoidea: Myliobatiformes). J. Zool. (Lond) 237:377–384.
1996. Evidence of brain-warming in the mobulid rays, *Mobula tarapacana* and *Manta birostris* (Chondrichthyes: Elasmobranchii: Batoidea: Myliobatiformes). Zool. J. Linn. Soc. 118:151–164.

Baker, M. A.
1982. Brain cooling in endotherms in heat and exercise. Annu. Rev. Physiol. 44:85–96.

Bigelow, H. B., and W. C. Schroeder.
1948. Sharks. *In* Fishes of the western North Atlantic, part one (A. Parr and Y. Olsen, eds), p. 59–546. Sears Found. Mar. Res., Yale Univ., Mem. 1.

Block, B. A.
1983. Brain heaters in the billfish. Am. Zool. 23:936.
1991. Endothermy in fish: thermogenesis ecology and evolution. *In* Biochemistry and molecular biology of fishes. Volume 1: Phylogenetic and biochemical perspectives (P. Hochachka and T. Mommsen, eds.), p. 269–311. Elsevier, Amsterdam.
1994. Thermogenesis in muscle. Annu. Rev. Physiol. 56: 535–577

Block, B. A., and F. G. Carey.
1985. Warm brain and eye temperatures in sharks. J. Comp. Physiol. B. Biochem. Syst. Environ. Physiol. 156: 229–236.

Bone, Q., and A. D. Chubb.
1983. The retial system of the locomotor muscles in the thresher shark (*Alopias vulpinus*). J. Mar. Biol. Assoc. U.K. 63:239–242.

Boustany, A. M., S. F. Davis, P. Pyle, S. D. Anderson, B. J. Le Boeuf, and B. A. Block.
2002. Satellite tagging: expanded niche for white sharks. Nature 415:35–36.

Buencuerpo, V., S. Rios, and J. Moron.
1998. Pelagic sharks associated with the swordfish, *Xiphias gladius*, fishery in the eastern North Atlantic Ocean and the strait of Gibraltar. Fish. Bull. 96:667–685.

Burne, R. H.
1924. Some peculiarities of the blood vascular system of the porbeagle shark (*Lamna cornubica*). Philos. Trans. R. Soc. Lond. B. Biol. Sci. 212B:209–257.

Carey, F. G.
1971. Warm bodied fish. Am. Zool. 11:135–143.
1982a. A brain heater in the swordfish (*Xiphias gladius*). Science 216:1327–1329.
1982b. Warm fish. *In* A companion to animal physiology; 5th international conference on comparative physiology; Sandbjerg, Denmark, July 22–26, 1980 (C. R. Taylor, K. Johansen and L. Bolis, eds.), p. 216–234. Cambridge Univ. Press, Cambridge, England; New York, NY.

Carey, F. G., J. G. Casey, H. L. Pratt, D. Urquhart, J. E. McCosker, J. A. Seigel, and C. C. Swift.
1985. Temperature, heat production and heat exchange in lamnid sharks. *In* Biology of the white shark (J. A. Seigel and C. C. Swift, eds.), p. 92–108. Mem. South. Calif. Acad. Sci., vol. 9, Fullerton, CA.

Carey, F. G., and E. Clark.
1995. Depth telemetry from the sixgill shark, *Hexanchus griseus*, at Bermuda. Environ. Biol. Fishes 42:7–14.

Carey, F. G., J. W. Kanwisher, O. Brazier, G. Gabrielson, J. G. Casey, and H. L. J. Pratt.
1982. Temperature and activities of a white shark, *Carcharodon carcharias*. Copeia 1982:254–260.

Carey, F. G., and B. H. Robison.
1981. Daily patterns in the activities of swordfish, *Xiphias gladius*, observed by acoustic telemetry. Fish. Bull. 79: 277–292.

Carey, F. G., and J. V. Scharold.
1990. Movements of blue sharks (*Prionace glauca*) in depth and course. Mar. Biol. 106:329–342.

Carey, F. G., and J. M. Teal.
1969. Mako and porbeagle: warm-bodied sharks. Comp. Biochem. Physiol. 28:199–204.

Carey, F. G., J. M. Teal, and J. W. Kanwisher.
1981. The visceral temperatures of mackerel sharks (Lamnidae). Physiol. Zool. 54:334–344.

Castro, J. I.
1983. The sharks of North American waters, 180 p. Texas A&M Univ. Press, College Station, TX.

Chen, C.-T., K.-M. Liu, and Y.-C. Chang.
1997. Reproductive biology of the bigeye thresher shark, *Alopias superciliosus* (Lowe, 1839)(Chondrichthyes: Alopiidae), in the northwestern Pacific. Ichthyol. Res. 44: 227–235.

Cleveland, W. S., E. Grosse, and W. M. Shyu.
1992. Local regression models. Chapter 8 *in* Statistical models in S (J. M. Chambers and T. J. Hastie eds.), 608 p. Wadsworth & Brooks/Cole, Pacific Grove, CA.

Compagno, L. J. V.
1990. Relationships of the megamouth shark, *Megachasma pelagios* (Lamniformes: Megachasmidae), with comments on its feeding behavior. *In* Elasmobranchs as living resources: advances in the biology, ecology, systematics, and the status of the fisheries (H. L. J. Pratt, S. H. Gruber, and T. Taniuchi, eds.), p. 357–379. NOAA Technical Report 90.

Fitch, J. E., and W. L. Craig.
1964. First records for the bigeye thresher (*Alopias superciliosus*) and slender tuna (*Allothunnus fallai*) from California, with notes on eastern Pacific scombrid otoliths. Calif. Fish Game 50:195–206.

Friedlander, M. J., N. Kotchabhakdi, and C. L. Prosser.
1976. Effects of cold and heat on behavior and cerebellar function in goldfish. J. Comp. Physiol. A Sens. Neural. Behav. Physiol. 112:19–45.

Gilmore, R. G.
1983. Observations on the embryos of the longfin mako, *Isurus paucus* and the bigeye thresher, *Alopias superciliosus*. Copeia 1983:375–382.

Goldman, K. J.
1997. Regulation of body temperature in the white shark, *Carcharodon carcharias*. J. Comp. Physiol. B. Biochem. Syst. Environ. Physiol. 167:423–429.

Goldman, K. G., and S. D. Anderson.
1999. Space utilization and swimming depth of white sharks, *Carcharodon carcharias*, at the South Farallon Islands, central California. Environ. Biol. Fishes 56:351–364.

Gruber, S. H., and L. J. V. Compagno.
1981. Taxonomic status and biology of the bigeye thresher, *Alopias superciliosus*. Fish. Bull. 79:617–640.

Gunn, J. S., J. D. Stevens, T. L. O. Davis, and B. M. Norman.
1999. Observations on the short-term movements and behaviour of whale sharks (*Rhincodon typus*) at Ningaloo Reef, Western Australia. Mar. Biol. 135:553–559.

Gunn, J. S., and B. A. Block.
2001. Advances in acoustic, archival and satellite tagging of tunas. *In* Tunas: physiology, ecology and evolution (B. A. Block and E. D. Stevens, eds.), p. 167–224. Academic Press, San Diego, CA.

Holland, K. N., B. M. Wetherbee, C. G. Lowe, and C. G. Meyer.
1999. Movements of tiger sharks (*Galeocerdo cuvier*) in coastal Hawaiian waters. Mar. Biol. 134:665–673.

Holts, D. B., and D. W. Bedford.
1993. Horizontal and vertical movements of the shortfin mako shark, *Isurus oxyrinchus*, in the southern California bight. Aust. J. Mar. Freshw. Res. 44:901–909.

Klimley, A. P.
1993. Highly directional swimming by scalloped hammerhead sharks, *Sphyrna lewini*, and subsurface irradiance, temperature, bathymetry, and geomagnetic field. Mar. Biol. 117:1–22.

Klimley, A. P., S. C. Beavers, T. H. Curtis, and S. J. Jorgensen.
2002. Movements and swimming behavior of three species of sharks in La Jolla Canyon, California. Environ. Biol. Fishes 63:117–135.

Kohler, N. E., J. G. Casey, and P. A. Turner.
1995. Length-weight relationships for 13 species of sharks from the western North Atlantic. Fish. Bull. 93:412–418.

Kohler, N. E., and P. A. Turner.
2001. Shark tagging: A review of conventional methods and studies. Environ. Biol. Fishes 60:191–223.

Konishi, J., and C. P. Hickman.
1964. Temperature acclimation in the central nervous system of rainbow trout (*Salmo gairdnerii*). Comp. Biochem. Physiol. 13:433–442.

Linthicum, D. S., and F. G. Carey.
1972. Regulation of brain and eye temperatures by the bluefin tuna. Comp. Biochem. Physiol. A Comp. Physiol. 43:425–433.

Liu, K.-M., P.-J. Chiang, and C.-T. Chen.
1998. Age and growth estimates of the bigeye thresher shark, *Alopias superciliosus*, in northeastern Taiwan waters. Fish. Bull. 96:482–491.

Marcinek, D. J., S. B. Blackwell, H. Dewar, E. V. Freund, C. Farwell, D. Dau, A. C. Seitz, and B. A. Block.
2001. Depth and muscle temperature of Pacific bluefin tuna examined with acoustic and pop-up satellite archival tags. Mar. Biol. 138:869–885.

McCosker, J. E.
1987. The white shark, *Carcharodon carcharias*, has a warm stomach. Copeia 1987:195–197.

Moreno, J. A., and J. Moron.
1992. Reproductive biology of the bigeye thresher shark *Alopias superciliosus* Lowe 1839. Aust. J. Mar. Freshat. Res. 43:77–86.

Naylor, G. J. P., A. P. Martin, E. G. Mattison, and W. M. Brown.
1997. Interrelationships of lamniform sharks: Testing phylogenetic hypotheses with sequence data. *In* Molecular systematics of fishes (T. D. Kocher and C. A. Stepien, eds.), p. 199–218. Academic Press, San Diego, CA.

Nelson, D. R., J. N. McKibben, W. R. Strong Jr., C. G. Lowe, J. A. Sisneros, D. M. Schroeder, and R. J. Lavenberg.
1997. An acoustic tracking of a megamouth shark, *Megachasma pelagios*: A crepuscular vertical migrator. Environ. Biol. Fishes 49:389–399.

Prosser, C. L., and D. O. Nelson.
1981. Role of nervous systems in temperature adaptation of poikilotherms. Annu. Rev. Physiol. 43:281–300.
Schweitzer, J., and G. Notarbartolo di Sciara.
1986. The *rete mirabile cranica* in the genus *Mobula*: a comparative study. J. Morphol. 188:167–178.
Springer, S.
1943. A second species of thresher shark from Florida. Copeia 1943:54–55.
Standora, E. A., and D. R. Nelson.
1977. A telemetric study of the behavior of free swimming Pacific angel sharks *Squatina californica*. Bull. South. Calif. Acad. Sci. 76:193–201.
Stillwell, C. E., and J. G. Casey.
1976. Observations on the bigeye thresher shark, *Alopias superciliosus*, in the western North Atlantic. Fish. Bull. 74:221–225.
Thorpe, T.
1997. First occurrence and new length record for the bigeye thresher shark in the northeast Atlantic. J. Fish Biol. 50: 222–224.
Tricas, T. C., L. R. Taylor, and G. Naftel.
1981. Diel behavior of the tiger shark *Galeocerdo cuvier* at French Frigate Shoals Hawaiian Islands USA. Copeia 1981:904–908.
Tubbesing, V. A., and B. A. Block.
2000. Orbital rete and red muscle vein anatomy indicate a high degree of endothermy in the brain and eye of the salmon shark. Acta Zool. (Stockh.) 81:49–56.
West, G. J., and J. D. Stevens.
2001. Archival tagging of school shark, *Galeorhinus galeus*, in Australia: Initial results. Environ. Biol. Fishes 60: 283–298.

Fishery Bulletin

Guidelines for contributors

Content of papers

Articles

Articles are reports of 10 to 30 pages (double spaced) that describe original research in one or a combination of the following fields of marine science: taxonomy, biology, genetics, mathematics (including modeling), statistics, engineering, economics, and ecology.

Notes

Notes are reports of 5 to 10 pages without an abstract that describe methods and results not supported by a large body of data. Although all contributions are subject to peer review, responsibility for the contents of articles and notes rests upon the authors and not upon the editor or the publisher. It is therefore important that authors consider the contents of their manuscripts carefully. Submission of an article is understood to imply that the article is original and is not being considered for publication elsewhere. Manuscripts must be written in English. Authors whose native language is not English are strongly advised to have their manuscripts checked for fluency by English-speaking colleagues prior to submission.

Preparation of papers

Text

Title page should include authors' full names and mailing addresses (street address required) and the senior author's telephone, fax number, e-mail address, as well as a list of key words to describe the contents of the manuscript. **Abstract** must be less than one typed page (double spaced) and must not contain any citations. It should state the main scope of the research but emphasize the author's conclusions and relevant findings. Because abstracts are circulated by abstracting agencies, it is important that they represent the research clearly and concisely. **General text** must be typed in double-spaced format. A brief introduction should state the broad significance of the paper; the remainder of the paper should be divided into the following sections: Materials and methods, Results, Discussion (or Conclusions), and Acknowledgments. Headings within each section must be short, reflect a logical sequence, and follow the rules of multiple subdivision (i.e. there can be no subdivision without at least two subheadings). The entire text should be intelligible to interdisciplinary readers; therefore, all acronyms and abbreviations should be written out and all lesser-known technical terms should be defined the first time they are mentioned. The scientific names of species must be written out the first time they are mentioned; subsequent mention of scientific names may be abbreviated. Follow *Scientific style and format: CBE manual for authors, editors, and publishers* (6th ed.) for editorial style and the most current issue of the *American Fisheries Society's common and scientific names of fishes from the United States and Canada* for fish nomenclature. Dates should be written as follows: 11 November 1991. Measurements should be expressed in metric units, e.g. metric tons (t). The numeral one (1) should be typed as a one, not as a lower-case el (l).

Footnotes

Use footnotes to add editorial comments regarding claims made in the text and to document unpublished works or works with local circulation. Footnotes should be numbered with Arabic numerals and inserted in 10-point font at the bottom of the first page on which they are cited. Footnotes should be formatted in the same manner as citations. If a manuscript is unpublished, in the process of review, or if the information provided in the footnote has been conveyed verbally, please state this information as "unpubl. data," "manuscript in review," and "personal commun.," respectively. Authors are advised wherever possible to avoid references to nonstandard literature (unpublished literature that is difficult to obtain, such as internal reports, processed reports, administrative reports, ICES council minutes, IWC minutes or working papers, any "research" or "working" documents, laboratory reports, contract reports, and manuscripts in review). If these references are used, please indicate whether they are available from NTIS (National Technical Information Service) or from some other public depository. Footnote format: author (last name, followed by first-name initials); year; title of report or manuscript; type of report and its administrative or serial number; name and address of agency or institution where the report is filed.

Literature cited

The literature cited section comprises works that have been published and those accepted for publication (works in press) in peer-reviewed journals and books. Follow the name and year system for citation format. In the text, write "Smith and Jones (1977) reported" but if the citation takes the form of parenthetical matter, write "(Smith and Jones, 1977)." In the literature cited section, list citations alphabetically by last name of senior author: For example, Alston, 1952; Mannly, 1988, Smith, 1932; Smith, 1947, Stalinsky and Jones, 1985. Abbreviations of journals should conform to the abbreviations given in the *Serial sources for the BIOSIS previews database*. Authors are responsible for the accuracy and completeness of all citations. Literature citation format: author (last name, followed by first-name initials); year; title of report or article; abbreviated title of the journal in which the article was published, volume number, page numbers. For books, please provide publisher, city, and state.

Tables

Tables should not be excessive in size and must be cited in numerical order in the text. Headings in tables should be short but ample enough to allow the table to be intelligible on its own. All unusual symbols must be explained in the table legend. Other incidental comments may be footnoted (use italic arabic numerals for footnote markers). Use asterisks only to indicate probability in statistical data. Place table legends on the same page as the table data. We accept tables saved in most spreadsheet software programs (e.g. Microsoft Excel). Please note the following:

- Use a comma in numbers of five digits or more (e.g. 13,000 but 3000).
- Use zeros before all decimal points for values less than one (e.g. 0.31).

Figures

Figures include line illustrations, computer-generated line graphs, and photographs (or slides). They must be cited in numerical order in the text. Line illustrations are best submitted as original drawings. Computer-generated line graphs should be printed on laser-quality paper. Photographs should be submitted on glossy paper with good contrast. All figures are to be labeled with senior author's name and the number of the figure (e.g. Smith, Fig. 4). Use Helvetica or Arial font to label anatomical parts (line drawings) or variables (graphs) within figures; use Times Roman bold font to label the different sections of a figure (e.g. **A**, **B**, **C**). Figure legends should explain all symbols and abbreviations seen within the figure and should be typed in double-spaced format on a separate page at the end of the manuscript. We advise authors to peruse a recent issue of *Fishery Bulletin* for standard formats. Please note the following.

- Capitalize the first letter of the first word of axis labels.
- Do not use overly large font sizes to label axes or parts within figures.
- Do not use boldface fonts within figures.
- Do not create outline rules around graphs.
- Do not use horizontal lines through graphs.
- Do not use large font sizes to label degrees of longitude and latitude on maps.
- Indicate direction of degrees longitude and latitude on maps (e.g. 170°E).
- Avoid placing labels on a vertical plane (except on y axis).
- Avoid odd (nonstandard) patterns to mark sections of bar graphs and pie charts.

Copyright law

Fishery Bulletin, a U.S. government publication, is not subject to copyright law. If an author wishes to reproduce any part of *Fishery Bulletin* in his or her work, he or she is obliged, however, to acknowledge the source of the extracted literature.

Submission of papers

Send four printed copies (one original plus three copies)—clipped, *not stapled*—to the Scientific Editor, at the address shown below. Send photocopies of figures with initial submission of manuscript. Original figures will be requested later when the manuscript has been accepted for publication. Do not send your manuscript on diskette until requested to do so.

Dr. Norman Bartoo
National Marine Fisheries Service, NOAA
8604 La Jolla Shores Drive
La Jolla, CA 92037

Once the manuscript has been accepted for publication, you will be asked to submit a software copy of your manuscript. The software copy should be submitted in WordPerfect or Word format (in Word, save as Rich Text Format). Please note that we do not accept ASCII text files.

Reprints

Copies of published articles and notes are available free of charge to the senior author (50 copies) and to his or her laboratory (50 copies). Additional copies may be purchased in lots of 100 when the author receives page proofs.

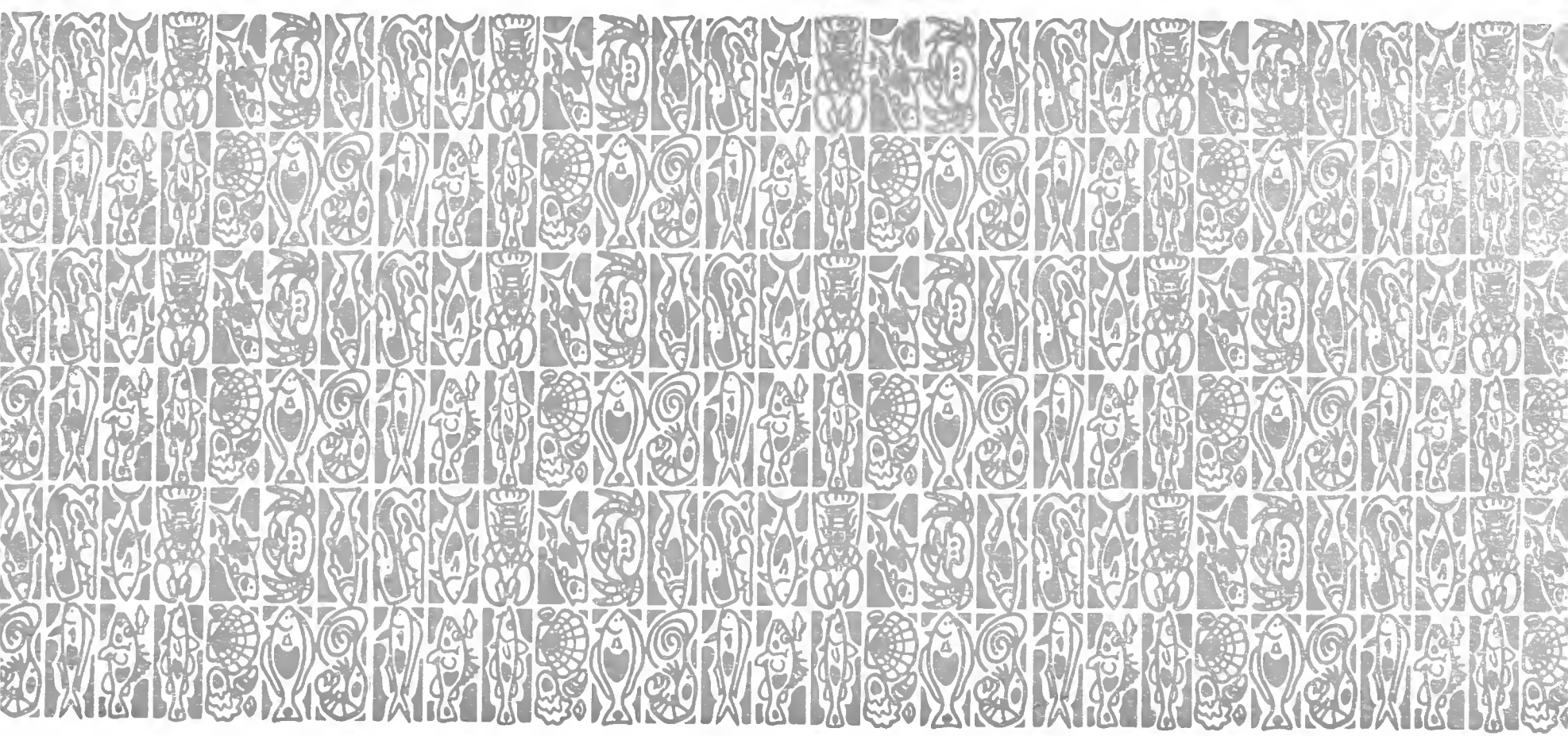

U.S. Department
of Commerce

Volume 102
Number 2
April 2004

Fishery Bulletin

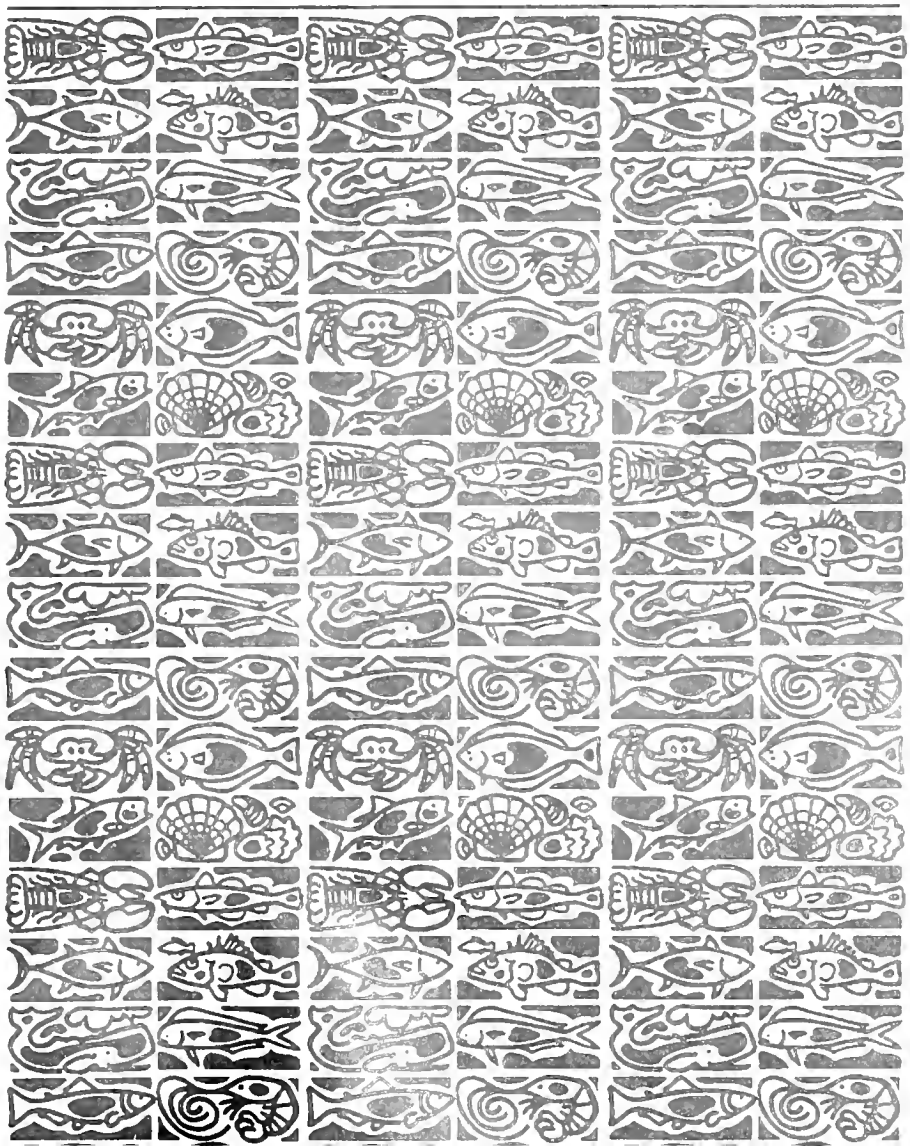

The *Fishery Bulletin* (ISSN 0090-0656) is published quarterly by the Scientific Publications Office, National Marine Fisheries Service, NOAA, 7600 Sand Point Way NE, BIN C15700, Seattle, WA 98115-0070. Periodicals postage is paid at Seattle, WA, and at additional mailing offices. POSTMASTER: Send address changes for subscriptions to Fishery Bulletin, Superintendent of Documents, Attn.: Chief, Mail List Branch, Mail Stop SSOM, Washington, DC 20402-9373.

The Secretary of Commerce has determined that the publication of this periodical is necessary according to law for the transaction of public business of this Department. Use of funds for printing of this periodical has been approved by the Director of the Office of Management and Budget.

For sale by the Superintendent of Documents, U.S. Government Printing Office, Washington, DC 20402. Subscription price per year: $55.00 domestic and $68.75 foreign. Cost per single issue: $28.00 domestic and $35.00 foreign. **See back for order form.**

Fishery Bulletin

***Fishery Bulletin* web site: www.fishbull.noaa.gov**

The *Fishery Bulletin* carries original research reports and technical notes on investigations in fishery science, engineering, and economics. It began as the Bulletin of the United States Fish Commission in 1881; it became the Bulletin of the Bureau of Fisheries in 1904 and the *Fishery Bulletin* of the Fish and Wildlife Service in 1941. Separates were issued as documents through volume 46; the last document was No. 1103. Beginning with volume 47 in 1931 and continuing through volume 62 in 1963, each separate appeared as a numbered bulletin. A new system began in 1963 with volume 63 in which papers are bound together in a single issue of the bulletin. Beginning with volume 70, number 1, January 1972, the *Fishery Bulletin* became a periodical, issued quarterly. In this form, it is available by subscription from the Superintendent of Documents, U.S. Government Printing Office, Washington, DC 20402. It is also available free in limited numbers to libraries, research institutions, State and Federal agencies, and in exchange for other scientific publications.

U.S. Department of Commerce
Seattle, Washington

Volume 102
Number 2
April 2004

Fishery Bulletin

Contents

Articles

Notes

Abstract—We estimated the total number of pantropical spotted dolphin (*Stenella attenuata*) mothers killed without their calves ("calf deficit") in all tuna purse-seine sets from 1973–90 and 1996–2000 in the eastern tropical Pacific. Estimates were based on a tally of the mothers killed as reported by color pattern and gender, several color-pattern-based frequency tables, and a weaning model. Over the time series, there was a decrease in the calf deficit from approximately 2800 for the western-southern stock and 5000 in the northeastern stock to about 60 missing calves per year. The mean deficit per set decreased from approximately 1.5 missing calves per set in the mid-1970s to 0.01 per set in the late-1990s. Over the time series examined, from 75% to 95% of the lactating females killed were killed without a calf. Under the assumption that these orphaned calves did not survive without their mothers, this calf deficit represents an approximately 14% increase in the reported kill of calves, which is relatively constant across the years examined. Because the calf deficit as we have defined it is based on the kill of mothers, the total number of missing calves that we estimate is potentially an underestimate of the actual number killed. Further research on the mechanism by which separation of mother and calf occurs is required to obtain better estimates of the unobserved kill of dolphin calves in this fishery.

Manuscript approved for publication 7 January 2004 by Scientific Editor.

Manuscript received 20 January 2004 at NMFS Sceintific Publications Office.

Fish. Bull. 102:233–244 (2004).

Annual estimates of the unobserved incidental kill of pantropical spotted dolphin (*Stenella attenuata attenuata*) calves in the tuna purse-seine fishery of the eastern tropical Pacific

Frederick Archer

Tim Gerrodette

Susan Chivers

Alan Jackson

Southwest Fisheries Science Center
National Marine Fisheries Service
8604 La Jolla Shores Dr.
La Jolla, California 92037

E-mail address (for F. Archer): eric.archer@noaa.gov

In the eastern tropical Pacific (ETP), yellowfin tuna (*Thunnus albacares*) are frequently found swimming under schools of pantropical spotted (*Stenella attenuata*) and spinner (*S. longirostris*) dolphins. For the past four decades, the ETP yellowfin tuna fishery has made use of this association by chasing the more visible dolphins at the surface and using purse-seines to encircle the schools "carrying" the tuna (NRC, 1992). The large bycatch of dolphins in this fishery has become widely known as the "tuna-dolphin issue" (Gerrodette, 2002). During the 1960s, the number of dolphins killed by the fishery was estimated to be 200,000–500,000 per year (Wade, 1995), and two stocks of spotted and spinner dolphins were reduced to fractions of their previous sizes (Smith, 1983; Wade et al.[1]). A long history of technological innovations by fishermen, laws and fishing regulations, dolphin quotas, eco-labeling of "dolphin-safe" tuna, and a comprehensive international observer program (Gosliner, 1999; Hall et al., 2000; Gerrodette, 2002) has reduced the dolphin bycatch to less than 1% of its former level. The reported bycatch in recent years is less than 2000 dolphins per year for all species combined (IATTC, 2002).

Although the reported kill has dramatically decreased, recent studies suggest that there is little evidence that the stocks are growing close to expected rates (Wade et al.[1]). One hypothesis for this lack of recovery has been that there are unobserved kills of dolphins during tuna purse-seine sets. Archer et al. (2001) presented evidence of an under-representation of suckling spotted and spinner dolphin calves in a sample of tuna purse-seine sets in the eastern tropical Pacific. Given that some of these missing calves are still dependent on their mothers for nutrition, it is likely that once separated they would die and this under-representation represents some degree of unobserved kill.

In Archer et al. (2001), the sample of sets examined was limited to those sets in which all of the animals killed had biological data collected by technicians aboard the tuna vessel. Calves still dependent on their mothers in the kill were identified by five intervals of body length, chosen to cover a range of

[1] Wade, P. R., S. B. Reilly, and T. Gerrodette. 2002. Assessment of the population dynamics of the northeastern offshore spotted and the eastern spinner dolphin populations through 2002. National Oceanographic and Atmospheric Administration Administrative Report LJ-02-13, 58 p. Southwest Fisheries Science Center, 8604 La Jolla Shores Dr., La Jolla, CA 92037.

calf sizes. Because of this approach, it was not possible to derive a single estimate of the number of missing calves or to extrapolate their estimate to sets not used in this analysis.

In the current study, we present a different method of estimating the number of missing calves in each set where offshore spotted dolphins (*S. attenuata attenuata*) were killed. For brevity, we call the shortage of calves in the kill in relation to the number of lactating females in the kill the "calf deficit." We examined the western-southern and northeastern offshore stocks separately according to the geographic boundaries described by Dizon et al. (1994). As they age, spotted dolphins change color through five color phases (Perrin, 1970). We used the color-phase frequency distribution of the kill in conjunction with age- and color-based frequency distributions from a sample of the kill to estimate the total number of missing calves in each stock, along with confidence intervals derived from bootstrap replications. This method also allowed us to examine the calf deficit from sets in recent years from which we did not have biological samples and to examine the time series of available years for evidence of a trend in the calf deficit.

Methods

Since 1973, observers have been randomly placed on tuna purse-seine vessels. For each spotted dolphin killed during an observed set, observers attempted to record the sex and the color phase of the dolphin (neonate, two-tone, speckled, mottled, and fused, see Perrin, 1970). From the National Marine Fisheries Service (NMFS) set log database, we obtained the number of northeastern and western-southern offshore spotted dolphins (by gender and color phase) killed in every observed set from 1973 to 1990. The Inter-American Tropical Tuna Commission (IATTC) provided the same data from 1996 to 2000.

Proration

In each set, color phase or gender (or both) may not have been recorded for some dolphins. Assuming that the distribution of the demographic composition of this missing data is equivalent to the overall demographic composition of the kill, we allocated the number of dolphins of unknown color phase (nu) to unknown gender in each color phase (ngu_c) according to the following formula.

$$ngu'_c = ngu_c + \left(nu \frac{N_c}{\sum_c N_c} \right), \quad (1)$$

where c = one of the five color phases (neonate to fused);
N_c = the total number of dolphins in each color phase in the entire data set; and
ngu'_c = the new number of dolphins in each color phase where gender is unknown, including the individuals of prorated unknown color phase

The number of male (nm'_c) or female (nf'_c) dolphins in a color phase was calculated as

$$nm'_c = nm_c + \left(ngu'_c \cdot \frac{Nm_c}{Nm_c + Nf_c} \right), \quad (2)$$

$$nf'_c = nf_c + \left(ngu'_c \cdot \frac{Nf_c}{Nm_c + Nf_c} \right), \quad (3)$$

where Nm_c and Nf_c are the total number of males and females, respectively, observed in that color phase in the entire data. Table 1 gives the sample size of sets for both stocks by year, as well as the fraction of the kill of unknown gender and color phase that were prorated as described above.

Number of suckling calves

As time permitted, NMFS observers would also collect biological data from a subset of the kill. For this study, we used ages estimated from teeth collected for a study of spotted dolphin growth and reproduction (Myrick et al., 1986). The specimens used were a random sample of all male and female spotted dolphins collected between 1973 and 1978 for which total body length was recorded and teeth were collected. However, additional specimens with lengths less than 150 cm were selected in order to match as closely as possible the length distribution of the aged sample to the underlying length distribution of the spotted dolphins in the kill. This was necessary because observers did not generally collect teeth from smaller, younger animals. Later, another sample of female spotted dolphins was selected from specimens collected in 1981. Specimens were aged as described in Myrick et al. (1986).

The final data set used in our analyses included age estimates for 1094 female spotted dolphin specimens and 798 male specimens. Of these, 649 females and 457 males belonged to the northeastern stock and had color phase recorded. These 1106 dolphins were used to generate the age frequency distribution for each color phase (F_{ac}, Table 2),

$$F_{ac} = \frac{S_{ac}}{\sum_a S_{ac}}, \quad (4)$$

where S_{ac} = the number of samples of age a in color phase c.

The oldest age recorded was 36 years.

To derive an age distribution for the dolphins killed in each tuna set, we estimated the number of dolphins in each age class (n_a) as

$$n_a = \sum_c (F_{ac} \cdot n'_c), \quad (5)$$

where n'_c = the sum of nm'_c and nf'_c (the number of males and females in each color phase after proration from Equations 2 and 3).

Table 1

Sample sizes of NMFS (1973–1990) and IATTC (1996–2000) observed sets with spotted dolphin kill made on two stocks of pantropical spotted dolphins (*Stenella attenuata*) by year.

	Northeastern stock				Western-southern stock			
Year	Number of sets with kill	Observed kill	Fraction of kill of unknown color phase	Fraction of kill of unknown gender	Number of sets with kill	Observed kill	Fraction of kill of unknown color phase	Fraction of kill of unknown gender
1973	332	5242	0.09	0.31	75	1199	0.17	0.34
1974	515	5864	0.16	0.23	92	1715	0.10	0.31
1975	554	8073	0.31	0.19	75	1702	0.30	0.20
1976	239	2376	0.24	0.25	356	6293	0.27	0.23
1977	467	2146	0.23	0.26	528	3358	0.18	0.32
1978	224	1016	0.18	0.41	329	3998	0.37	0.34
1979	218	1045	0.38	0.27	168	1262	0.40	0.14
1980	165	1132	0.45	0.28	106	1206	0.73	0.13
1981	121	815	0.46	0.13	112	1346	0.48	0.12
1982	171	1696	0.51	0.22	159	1966	0.37	0.38
1983	12	177	0.80	0.08	35	148	0.32	0.35
1984	43	294	0.37	0.25	71	961	0.48	0.15
1985	186	2625	0.39	0.40	54	381	0.49	0.13
1986	150	1816	0.48	0.28	132	1818	0.60	0.22
1987	630	3327	0.25	0.31	175	1768	0.62	0.14
1988	207	1142	0.18	0.27	107	479	0.36	0.34
1989	293	1096	0.29	0.25	323	2793	0.48	0.14
1990	157	515	0.16	0.31	121	829	0.35	0.13
1996	273	724	0.27	0.44	161	374	0.18	0.54
1997	163	393	0.15	0.42	274	738	0.24	0.48
1998	161	260	0.21	0.51	125	236	0.19	0.46
1999	189	317	0.18	0.58	88	159	0.11	0.56
2000	146	291	0.23	0.47	115	250	0.20	0.61

In Equation 4, an age distribution was generated for each color phase, and then the number of dolphins in each age class was summed across all color phases.

To estimate the number of calves in each set, we used this age distribution in conjunction with a weaning model developed from a study of the stomach contents and ages of calves (Archer and Robertson, in press). The model predicts the probability that an animal of a given age (a) will be suckling:

$$P(milk)_a = \frac{1}{1+e^{1.90-2.6a}}. \quad (6)$$

The estimated number of calves (N_{calf}) in a set is then

$$N_{calf} = \sum_{a=0}^{3} \left(n_a \cdot P(milk)_a\right). \quad (7)$$

In our estimate of N_{calf} we chose to use only the first four age classes (0 to 3) because $P(milk)_4$ was extremely small (2×10^{-4}). These age classes allowed us to decrease computational time without significantly affecting the estimates.

Number of lactating females

Observers visually examined the mammaries of the 649 females used in the age distribution above (Eq. 4) for the presence of milk as part of the suite of biological data collected. Using these data in conjunction with the color phase of these females, we calculated the fraction of lactating females in each color phase ($Flac_c$),

$$Flac_c = \frac{Slac_c}{Sfem_c}, \quad (8)$$

where $Slac_c$ and $Sfem_c$ = the number of females that were lactating and the total number of females in color phase c of the samples examined.

$Flac_c$ was 0.00, 0.01, 0.04, 0.22, and 0.50 for neonate, two-tone, speckled, mottled, and fused specimens, respectively. The estimated number of lactating females (N_{lac}) in a set was then

$$N_{lac} = \sum_c (nf_c' \; Flac_c) \quad (9)$$

Calf deficit

As described in Archer et al. (2001), the calf deficit (D) in each set was calculated by subtracting the number of calves (N_{calf}) from the number of lactating females (N_{lac}). If this value was zero or less, then D was set to zero to indicate that there were enough calves to account for all lactating females killed (Fig. 1),

$$D = \begin{cases} N_{lac} - N_{calf} & \text{if } N_{lac} > N_{calf} \\ 0 & \text{if } N_{lac} \leq N_{calf} \end{cases}. \quad (10)$$

We calculated three deficit-based fractions: 1) the mean deficit per set (D_s); 2) the mean deficit per dolphin killed (D_k); and 3), the mean deficit per lactating female killed (D_l):

$$D_s = \frac{\sum D}{ObsSets}, \quad (11)$$

$$D_k = \frac{\sum D}{ObsKill}, \quad (12)$$

$$D_l = \frac{\sum D}{EstLacKill}, \quad (13)$$

where $\sum D$ = the total observed calf deficit in each year;
ObsSets = the number of observed sets used in the analysis, including those sets without a dolphin kill;
ObsKill = the number of dolphins killed in the observed sets; and
EstLacKill = the total estimated number of lactating females killed.

The above analysis was conducted each year. Estimation error was evaluated with 20,000 bootstrap replicates for each year. For each replicate, the sets within that year were randomly resampled. The frequency tables F_{ac} and $Flac_c$ were also recalculated by resampling the list of biological specimens. The parameters for the weaning model, $P(milk)_a$, were estimated again by resampling the 29 calves and by fitting the logistic model to the new data set as described in Archer and Robertson (in press). All resampling was done with replacement. N_{calf}, N_{lac}, and D were estimated as described above for each set, and D_s, D_k, and D_l were calculated for the replicate. The 95% confidence intervals for N_{calf}, N_{lac}, D, D_s, D_k, and D_l were estimated from the 2.5% and 97.5% quantiles of the distributions of the bootstrap replicate values.

The total calf deficit (D_{total}) was estimated as the deficit per dolphin killed (D_k) multiplied by the total number of dolphins killed (N_{killed}) by stock each year,

$$D_{total} = D_k \times N_{killed}. \quad (14)$$

Table 2

Age-class frequency distribution for each color phase (F_{ac}).

Age (yr)	Neonate	Two-tone	Speckled	Mottled	Fused
0	0.80	0.12	0	0	0
1	0.20	0.32	0	0	0
2	0	0.31	0.04	0	0
3	0	0.16	0.18	0.01	0
4	0	0.05	0.14	0.02	0
5	0	0.02	0.13	0.03	0
6	0	0	0.13	0.04	0.01
7	0	0	0.06	0.05	0
8	0	0	0.10	0.06	0
9	0	0	0.06	0.07	0.01
10	0	0	0.01	0.10	0.01
11	0	0	0.01	0.14	0.03
12	0	0	0.01	0.08	0.02
13	0	0	0.04	0.07	0.03
14	0	0	0.03	0.07	0.03
15	0	0	0	0.06	0.06
16	0	0.01	0.01	0.06	0.07
17	0	0	0.01	0.03	0.07
18	0	0	0	0.01	0.07
19	0	0	0	0.03	0.09
20	0	0	0	0.03	0.07
21	0	0	0	0.01	0.08
22	0	0	0	0	0.06
23	0	0	0.01	0	0.07
24	0	0	0	0.01	0.04
25	0	0	0	0.01	0.04
26	0	0	0	0	0.04
27	0	0	0	0.01	0.03
28	0	0	0	0.01	0.02
29	0	0	0	0	0.01
30	0	0	0	0.01	0.02
31	0	0	0	0	0.01
32	0	0	0	0	0
33	0	0	0	0	0.01
34	0	0	0	0	0
35	0	0	0	0	0
36	0	0	0	0	0.01

For the period 1973–84, annual values of N_{killed} for each stock were provided by the IATTC (Joseph[2]). For 1984–90 and 1996–2000, values were published by IATTC (2002). In the bootstrap estimation of the 95% CI around D_{total}, for the 1973–90 period, each replicate was randomly sampled from a normal distribution by using the estimated total kill standard error. For 1996–2000, the total kill was reported to be exact; therefore the total kill was used without variance in all replicates.

[2] Joseph, J. 1994. Letter of September 6 to Michael Tillman, 2 p. Southwest Fisheries Science Center, 8604 La Jolla Shores Dr., La Jolla, CA 92037.

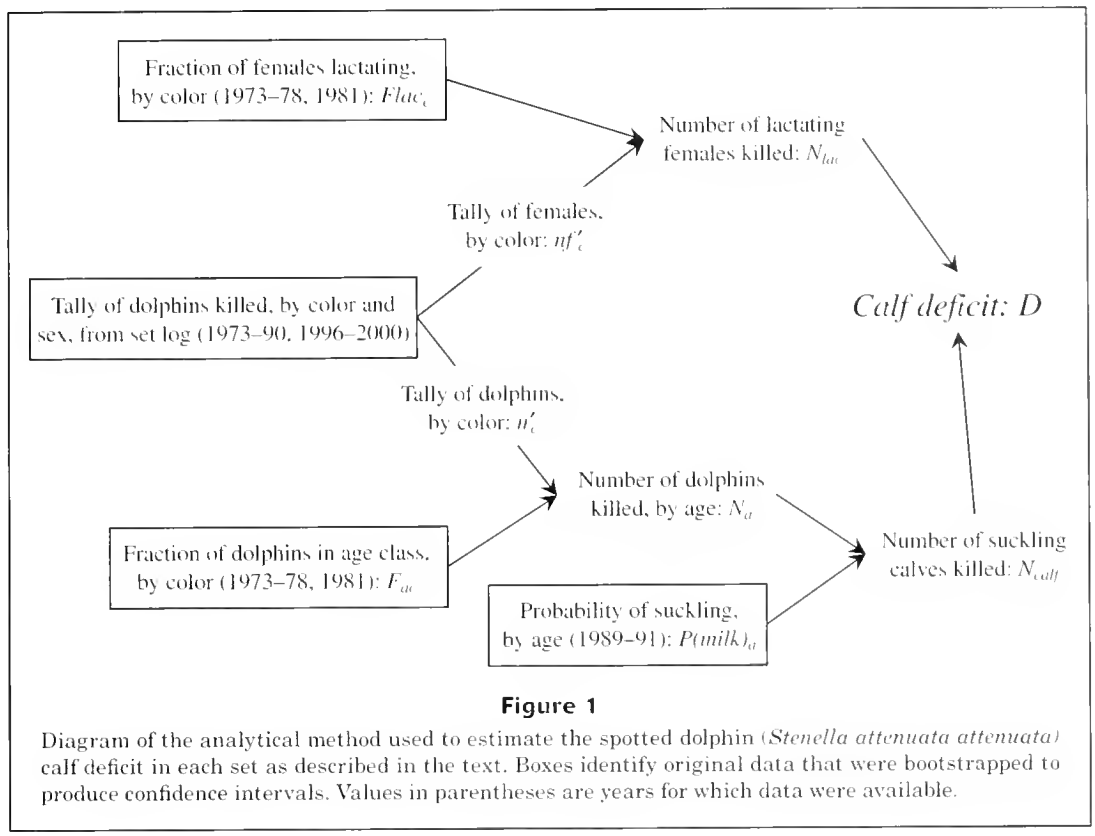

Figure 1

Diagram of the analytical method used to estimate the spotted dolphin (*Stenella attenuata attenuata*) calf deficit in each set as described in the text. Boxes identify original data that were bootstrapped to produce confidence intervals. Values in parentheses are years for which data were available.

In a subset of the sets that we examined, every individual killed had been examined and biological samples had been collected from it; therefore, we knew the actual number of lactating females killed. There were 1108 of these "100% sampled" sets on the northeastern stock, and 697 on the western-southern stock from 1973 to 1990. We evaluated the accuracy of our frequency-based method by conducting a paired *t*-test between our estimate of the number of lactating females and the number observed in each of these sets.

Stomach-content data were not available for every animal in these 100%-sampled sets; therefore, we did not know the actual number of suckling calves. However, we also used paired *t*-tests to compare our estimate of the number of suckling calves in each set with the number of animals smaller than 122 cm, which was the estimated length at which the probability of milk in the stomach was 0.5, given the weaning model of Archer and Robertson (in press). Likewise, our estimate of the calf deficit was compared with the deficit as estimated by using a cutoff length of 122 cm. These tests were done to determine if the method in the present study would produce significantly different results from the method used in the previous study. Paired *t*-tests were conducted for each year separately, as well as for all years combined. A power analysis was also performed for these paired *t*-tests to determine the minimum detectable difference at which we could reject the null hypothesis of no difference between methods given observed sample sizes and variability.

Results

The calf deficit as a fraction of the number of dolphins killed (D_k) increased slightly during the mid-1970s but remained relatively constant throughout the rest of the time series at approximately 0.14 missing calves per dolphin killed for both stocks (Fig. 2). The total calf deficit (D_{total}) as estimated from the annual kill decreased from highs of approximately 5000 in the mid-1970s down to 2000–3000 by the early 1980s (Fig. 3). In the late 1980s, this value increased to approximately 5000 in northeastern spotted dolphins (Table 3A) and approximately 2800 in the western-southern stock (Table 3B), reflecting an increase in the reported kills. In the last five years of the time series (1996–2000), the estimated total deficit was approximately 60 missing calves.

The mean deficit per set (D_s) for northeastern spotters over all years was 1.03 missing calves per set, and the median was 0.30 (Fig. 4). For western-southern spotted dolphins, the mean was 1.28 missing calves per set, and the median was 0.33. The estimated mean deficit per set was approximately 1.5 in the mid-1970s and decreased over time to 0.01–0.02 at the end of the time series (Fig. 4). For both stocks, 75–95% of lactating females killed were not killed with their calf (Fig. 5).

In the sets that were 100%-sampled, for all years combined, there was no significant difference between the observed and the estimated number of lactating females killed in either stock (Table 4). The results of paired *t*-tests

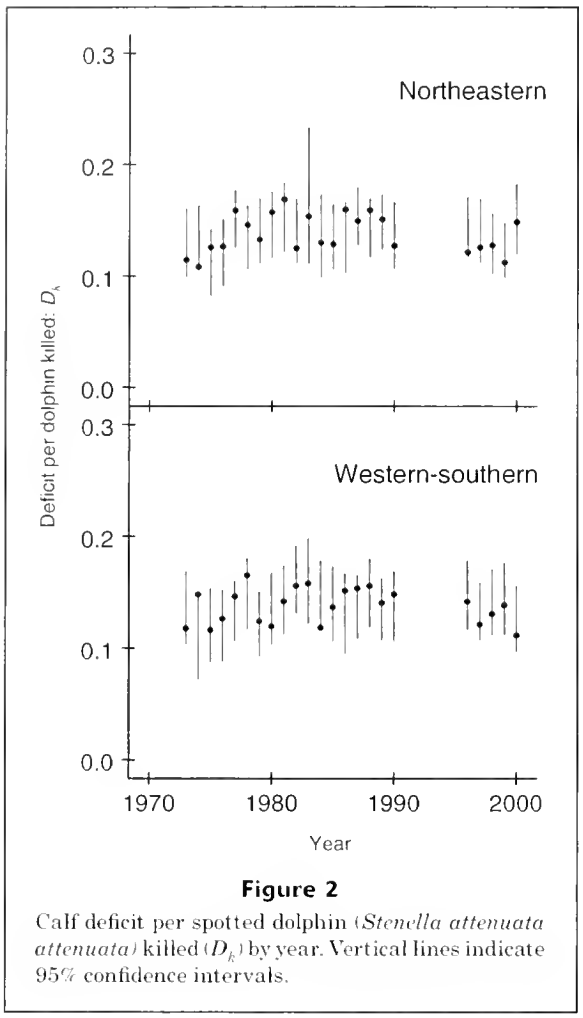

Figure 2

Calf deficit per spotted dolphin (*Stenella attenuata attenuata*) killed (D_k) by year. Vertical lines indicate 95% confidence intervals.

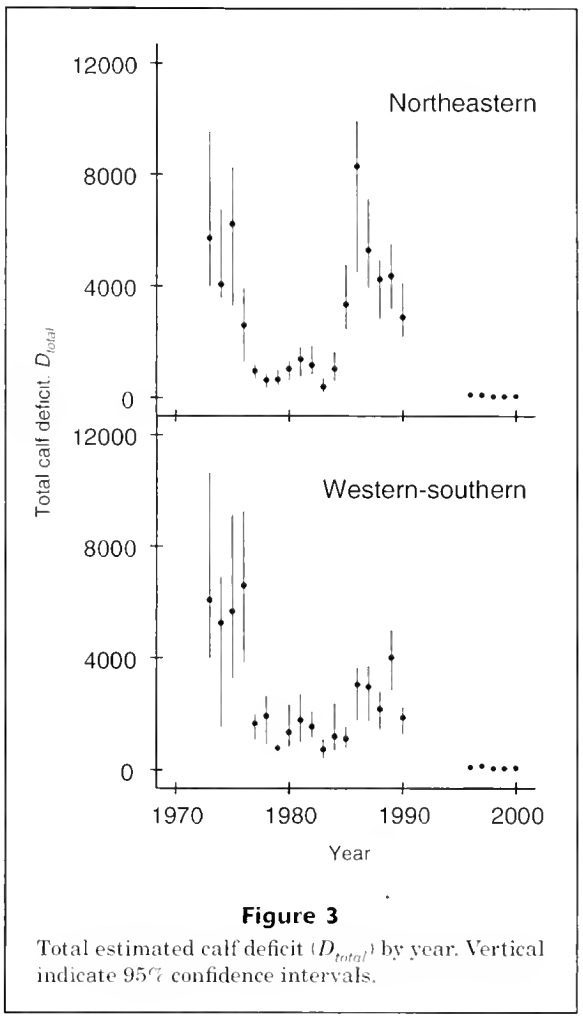

Figure 3

Total estimated calf deficit (D_{total}) by year. Vertical indicate 95% confidence intervals.

by year indicated that the observed number of lactating females in each set was significantly greater ($P \leq 0.05$) than the estimated number in 1977 for the northeastern and the western-southern stocks and in 1979 for the western-southern stock. The difference was significantly less in 1984 for the western-southern stock. Using 0.1 as our type-2 error level, we determined through power analysis that the minimum detectable difference ($\alpha=0.05$) between the mean observed and estimated number of lactating females per set across all years was approximately 0.08 and 0.09 in the northeastern and western-southern stocks respectively.

The observed number of calves per set, defined as the number of dolphins less than 122 cm, was significantly greater for both stocks, for all years combined, than the values estimated in this paper (Table 5). The overall mean difference was 0.17 calves per set for the northeastern stock and 0.12 for the western-southern stock. About half of the years showed a significant difference for each stock. In the comparison of the calf deficit by year, only a few years showed significant differences in either stock (Table 5). However, the estimated deficit tended to be larger than the observed deficit. The paired *t*-test for all years combined was significant for the northeastern stock, although the mean difference was only −0.06 missing calves per set. The minimum detectable difference from the power analysis for the mean number of calves per set and mean calf deficit per set across all years was 0.06 and 0.08 respectively for both stocks.

Discussion

In the present study, we present an estimate of the number of missing dependent northeastern and western-southern offshore spotted dolphin calves in the tuna purse-seine kill from 1973 to 1990 and from 1996 to 2000. The total number of missing calves decreased through the time series, which, because we estimated the calf deficit as a function of the size of the kill, was a direct result of the large reduction in the annual dolphin kill by the fishery. Between 1973 and 2000, the shortage of calves in the kill remained at a relatively constant fraction of the kill, about 14%, for both stocks of pantropical spotted dolphins (Fig. 2). On the assumption that suckling calves do not survive separation from their mother (Archer et al., 2001;

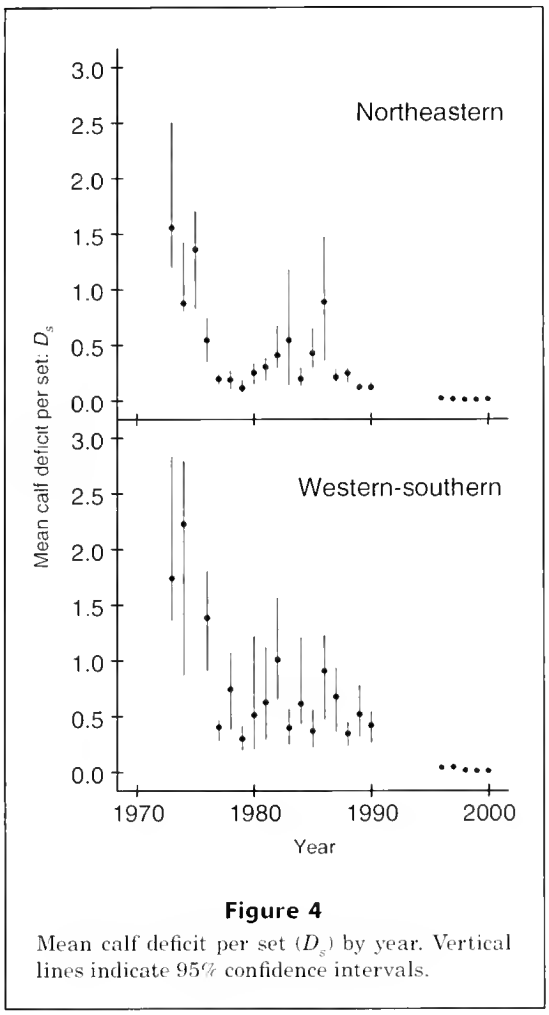

Figure 4

Mean calf deficit per set (D_s) by year. Vertical lines indicate 95% confidence intervals.

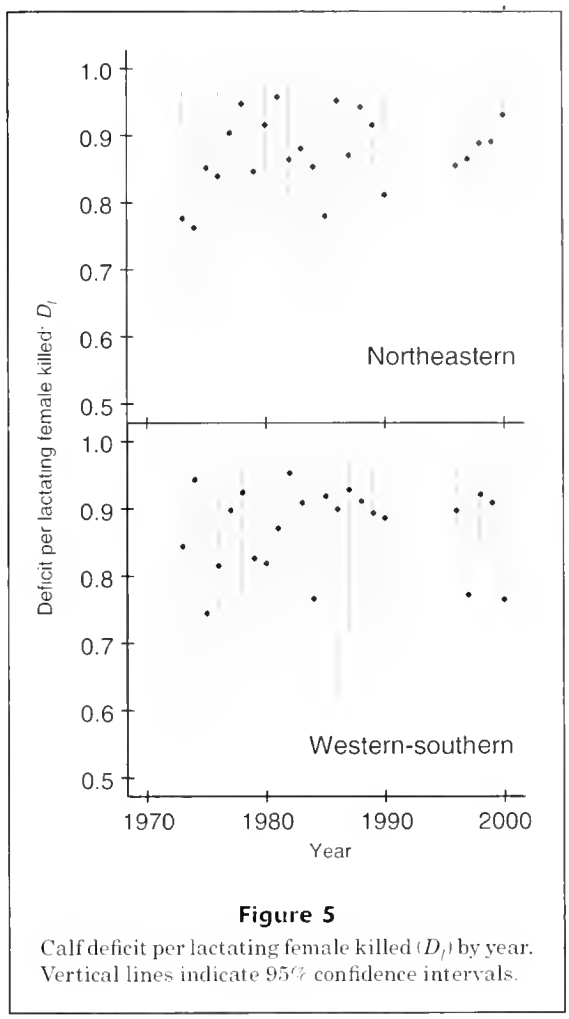

Figure 5

Calf deficit per lactating female killed (D_f) by year. Vertical lines indicate 95% confidence intervals.

Edwards[3]), the estimated calf deficit represents an approximately 14% underestimate of the reported kill.

The calf deficit in the present study was estimated from the number of dependent calves and lactating females killed by using age-color frequency tables and data on the stomach contents of weaning calves. Specimens used to derive the age and color table were collected from 1973 to 1978 and 1981, and specimens used for the weaning model were collected between 1989 and 1991. If the distributions of these samples were not representative of all years that we examined, then our results may be biased. However, the results of a study to construct the annual age distribution of the kill (Archer and Chivers[4]) indicated that there is no significant difference in the age-color frequency table across years. The sample size for the stomach data (29 calves) was too small to examine differences between years.

Our finding of no significant difference between our estimates of the number of lactating females and the observed tally of lactating females in sets where the entire kill was sampled validates this portion of our estimation procedure. However, because the number of suckling calves present in these 100%-sampled sets was not recorded, we were unable to validate the method used to generate these estimates in a similar manner.

The results of our paired *t*-tests indicated that the observed number of animals smaller than 122 cm tended to be greater than the number we estimated. This is most likely a result of the difference between how calves were counted in each method. Archer et al. (2001) considered all animals under a series of cutoff values to be calves that were dependent on suckling for survival. In the present study, the weaning model that we used (Archer and Rob-

[3] Edwards, E. F. 2002. Behavioral contributions to separation and subsequent mortality of dolphin calves chased by tuna purse-seiners in the eastern tropical Pacific Ocean. National Oceanographic and Atmospheric Administration Administrative Report LJ-02-28, 34 p. Southwest Fisheries Science Center, 8604 La Jolla Shores Dr., La Jolla, CA 92037.

[4] Archer, F., and S. J. Chivers. 2002. Age structure of the northeastern spotted dolphin incidental kill by year for 1971 to 1990 and 1996 to 2000. National Oceanographic and Atmospheric Administration Administrative Report LJ-02-12, 18 p. Southwest Fisheries Science Center, 8604 La Jolla Shores Dr., La Jolla, CA 92037.

Table 3

Estimated calf deficit per kill (D_k) and total calf deficit. Total number of spotted dolphins killed reported by the IATTC (2002) and Joseph (footnote 2 in the general text). Values in parentheses are 95% lower and upper confidence intervals.

Stock and year	Estimated calf deficit in observed sets	Observed dolphin kill	Mean calf deficit per kill (D_k)	Total number of NE spotted dolphins killed (±SE)	Estimated total calf deficit
A Northeastern (NE) stock					
1973	599 (464,964)	5242 (3947,6820)	0.11 (0.10,0.16)	49928 ±8899	5709 (3972,9532)
1974	634 (583,1027)	5864 (4943,6916)	0.11 (0.10,0.16)	37410 ±4222	4046 (3573,6708)
1975	1014 (618,1269)	8073 (6578,9965)	0.13 (0.08,0.14)	49399 ±8809	6206 (3297,8254)
1976	300 (196,408)	2376 (1786,3079)	0.13 (0.09,0.15)	20443 ±4721	2583 (1284,3903)
1977	341 (249,416)	2146 (1743,2622)	0.16 (0.13,0.18)	5937 ±690	943 (656,1167)
1978	148 (83,209)	1016 (684,1431)	0.15 (0.11,0.16)	4226 ±827	616 (336,836)
1979	138 (96,226)	1045 (680,1629)	0.13 (0.11,0.17)	4828 ±817	640 (428,963)
1980	178 (107,239)	1132 (724,1637)	0.16 (0.12,0.18)	6468 ±962	1016 (622,1300)
1981	137 (84,173)	815 (560,1122)	0.17 (0.12,0.18)	8096 ±1508	1366 (753,1774)
1982	212 (155,347)	1696 (1126,2395)	0.12 (0.11,0.17)	9254 ±1529	1155 (833,1840)
1983	27 (7,59)	177 (35,410)	0.15 (0.11,0.23)	2460 ±659	377 (169,678)
1984	38 (26,57)	294 (191,417)	0.13 (0.10,0.17)	7836 ±1493	1017 (608,1602)
1985	337 (235,508)	2625 (1839,3529)	0.13 (0.11,0.16)	25975 ±3210	3338 (2447,4748)
1986	290 (119,478)	1816 (859,3440)	0.16 (0.10,0.17)	52035 ±8134	8297 (4496,9935)
1987	497 (397,667)	3327 (2777,4002)	0.15 (0.13,0.18)	35366 ±4272	5280 (3949,7106)
1988	182 (122,215)	1142 (880,1462)	0.16 (0.12,0.17)	26625 ±2744	4234 (2825,4907)
1989	165 (120,217)	1096 (871,1371)	0.15 (0.12,0.17)	28898 ±3108	4357 (3186,5492)
1990	65 (53,90)	515 (421,632)	0.13 (0.11,0.17)	22616 ±2575	2875 (2176,4085)
1996	88 (76,142)	724 (568,926)	0.12 (0.12,0.17)	818	99 (96,139)
1997	49 (42,69)	393 (331,461)	0.13 (0.11,0.17)	721	91 (81,121)
1998	33 (26,41)	260 (230,296)	0.13 (0.10,0.16)	298	38 (30,46)
1999	36 (30,48)	317 (282,357)	0.11 (0.10,0.15)	358	40 (35,53)
2000	43 (32,58)	291 (247,342)	0.15 (0.12,0.18)	295	44 (35,54)

continued

Table 3 (continued)

Stock and year	Estimated calf deficit in observed sets	Observed dolphin kill	Mean calf deficit per kill (D_k)	Total number of NE spotted dolphins killed (±SE)	Estimated total calf deficit
B Western-southern (WS) stock					
1973	141 (110,229)	1199 (836,1638)	0.12 (0.10,0.17)	51,712 ±10,721	6076 (3993–10,633)
1974	254 (100,318)	1715 (939,2733)	0.15 (0.07,0.15)	35,499 ±10,309	5254 (1554,6890)
1975	197 (123,322)	1702 (1104,2434)	0.12 (0.09,0.15)	48,837 ±10,055	5664 (3285,9121)
1976	795 (524,1036)	6293 (4925,7860)	0.13 (0.09,0.15)	52,206 ±8883	6595 (3833,9223)
1977	491 (345,563)	3358 (2860,3906)	0.15 (0.11,0.16)	11,260 ±1186	1647 (1098,1959)
1978	660 (342,949)	3998 (2508,5922)	0.17 (0.12,0.18)	11,610 ±2553	1917 (932,2614)
1979	157 (104,216)	1262 (939,1643)	0.12 (0.09,0.15)	6,254 ±1229	776 (438,1138)
1980	144 (59,344)	1206 (411,2542)	0.12 (0.10,0.17)	11,200 ±2430	1339 (831,2320)
1981	191 (90,340)	1346 (577,2416)	0.14 (0.11,0.17)	12,512 ±2629	1775 (1010,2682)
1982	306 (198,474)	1966 (1337,2734)	0.16 (0.13,0.19)	9869 ±1146	1536 (1156,2088)
1983	23 (15,33)	148 (99,206)	0.16 (0.12,0.20)	4587 ±928	724 (418,1087)
1984	114 (80,224)	961 (526,1513)	0.12 (0.12,0.18)	10,018 ±2614	1183 (712,2352)
1985	52 (32,79)	381 (225,570)	0.14 (0.11,0.17)	8089 ±951	1105 (781,1524)
1986	275 (143,373)	1818 (1065,2784)	0.15 (0.10,0.17)	20,074 ±2187	3037 (1776,3617)
1987	271 (147,374)	1768 (1068,2661)	0.15 (0.11,0.16)	19,298 ±2899	2959 (1754,3695)
1988	75 (51,96)	479 (368,605)	0.16 (0.12,0.18)	13,916 ±1741	2166 (1453,2785)
1989	392 (242,589)	2793 (1819,4277)	0.14 (0.11,0.16)	28,560 ±2675	4011 (2861,4977)
1990	123 (78,160)	829 (582,1128)	0.15 (0.11,0.17)	12,578 ±1015	1864 (1283,2236)
1996	53 (42,71)	374 (308,448)	0.14 (0.12,0.18)	545	77 (64,97)
1997	89 (72,132)	738 (598,931)	0.12 (0.11,0.16)	1044	126 (112,165)
1998	31 (25,42)	236 (192,288)	341 (0.11,0.17)	44	0.13 (38,58)
1999	22 (16,32)	159 (123,209)	0.14 (0.11,0.18)	253	35 (28,44)
2000	28 (22,44)	250 (189,330)	0.11 (0.10,0.15)	435	48 (42,67)

Table 4

Annual mean observed and mean estimated number of lactating females per set in 100% sampled sets. Values in parentheses are 95% lower and upper confidence intervals assuming a normal distribution of differences. Bold type indicates significant difference from zero ($P \leq 0.05$) in the paired t-tests.

	Northeastern stock				Western-southern stock			
Year	No. of sets	Observed	Estimated	Difference (95% CI)	No. of sets	Observed	Estimated	Difference (95% CI)
1973	116	0.55	0.61	−0.06 (−0.17,0.05)	21	1.19	1.30	−0.11 (−0.63,0.42)
1974	98	0.51	0.54	−0.03 (−0.13,0.07)	16	0.75	0.81	−0.06 (−0.36,0.24)
1975	99	0.57	0.48	0.09 (−0.05,0.22)	14	1.07	0.92	0.15 (−0.46,0.77)
1976	51	0.28	0.35	−0.08 (−0.18,0.02)	90	0.500	0.502	−0.002 (−0.119,0.115)
1977	167	0.55	0.46	**0.09 (0.01,0.15)**	163	0.49	0.37	**0.12 (0.03,0.21)**
1978	82	0.37	0.40	−0.03 (−0.14,0.08)	93	0.50	0.52	−0.02 (−0.19,0.13)
1979	75	0.47	0.46	0.01 (−0.13,0.14)	61	0.64	0.47	**0.17 (0.01,0.33)**
1980	54	0.39	0.38	0.01 (−0.11,0.13)	34	0.50	0.44	0.06 (−0.09,0.20)
1981	41	0.53	0.74	−0.21 (−0.81,0.38)	38	0.66	0.64	0.02 (−0.16,0.19)
1982	36	0.62	1.18	−0.56 (−1.40,0.27)	33	0.30	0.44	−0.14 (−0.37,0.10)
1983	33	1.33	2.14	−0.81 (−7.89,6.28)	6	0.17	0.57	−0.40 (−1.57,0.77)
1984	4	0.25	0.49	−0.24 (−0.67,0.18)	29	0.48	1.08	**−0.60 (−0.96, −0.23)**
1985	70	0.34	0.50	−0.16 (−0.36,0.06)	17	0.35	0.50	−0.15 (−0.49,0.20)
1986	45	0.71	0.47	0.24 (−0.04,0.51)	28	0.61	0.42	0.19 (−0.01,0.38)
1987	121	0.43	0.46	−0.03 (−0.18,0.11)	30	0.27	0.46	−0.19 (−0.44,0.06)
1988	6	0.44	0.57	−0.13 (−0.59,0.35)	—	—	—	—
1989	24	0.96	1.03	−0.07 (−0.59,0.44)	15	0.93	0.96	−0.03 (−0.68,0.64)
1990	16	0.56	0.47	0.09 (−0.25,0.44)	9	0.67	0.93	−0.26 (−0.94,0.42)
All	1108	0.50	0.53	−0.03 (−0.08,0.02)	697	0.545	0.546	−0.001 (−0.053,0.051)

ertson, in press) estimated the probability that a calf of a given age class was still suckling. Given that body length has a near linear relationship with age in these young age classes (Perrin, 1976), this meant that for any chosen length of independence, each individual smaller than that cutoff value would only be counted fractionally, in effect correcting for the probability that an animal of a given age is not suckling. This procedure caused the method in this paper to tally fewer "calves" in each set than in the previous study. A secondary result of this effect was that the mean deficit per set estimated in the present study tended to be slightly higher than that presented by Archer et al. in 2001.

We estimated the total number of missing calves as a function of the number of dolphins killed in each stock (Table 3). Prior to 1995, only a fraction of the purse-seine trips carried scientific observers. To estimate the number killed in each stock, kill rates from the observed trips were applied to unobserved trips, stratified by area and stock (IATTC, 2002; Joseph, 1994[2]). Since 1995 it has been reported that all dolphin sets have been observed, and that the number of dolphins killed is therefore known without error (IATTC, 2002).

The total calf deficit could also be estimated as a function of the number of sets by multiplying the total number of sets made on each stock by D_s (Fig. 4). In the only study to estimate the number of sets made on each stock annually, Archer et al.[5] used a relatively simple proration scheme of unobserved sets derived from ratios of the number of sets made on each stock in observed sets. However, because Archer et al.[5] did not stratify unobserved sets by area, basing the total calf deficit on these estimates would produce a different result from that presented in Table 3. Because the estimates of the kill by stock included stratification by area, estimates of the total calf deficit calculated by multiplying the kill estimates by D_k are likely to be more accurate. It is important to realize that the deficit that we present is directly related to the kill observed in the sets that we used. In other words, if proration schemes for unobserved sets were the same for the number of sets made and the number of dolphins killed, estimates of the total calf deficit with either D_s or D_k would be equivalent.

Wade et al.[1] explored the effects of 50% and 100% additional fisheries-related mortality on the assessment of the northeastern spotted dolphin stock. The assumption of additional mortality led to higher estimates of maximum

[5] Archer, F., T. Gerrodette, and A. Jackson. 2002. Preliminary estimates of the annual number of sets, number of dolphins chased, and number of dolphins captured by stock in the tuna purse-seine fishery in the eastern tropical Pacific, 1971–2000. National Oceanographic and Atmospheric Administration Administrative Report LJ-02-10, 26 p. Southwest Fisheries Science Center, 8604 La Jolla Shores Dr., La Jolla, CA 92037.

Table 5

Annual mean number of dolphins killed ≤122 cm (calves killed based on length) and estimated number of suckling calves (calves based on weaning model) per set in 100% sampled sets (first line for each year). Mean deficit per set using 122 cm as cutoff length (calf deficit based on length) and calf deficit as estimated in this article (calf deficit based on weaning model) on second line for each year. Values in parentheses are 95% lower and upper confidence intervals assuming a normal distribution of differences. Differences in bold indicate significant difference from zero ($P \leq 0.05$) in the paired t-test.

	Northeastern stock				Western-southern stock			
		Calves killed based on length	Calves killed based on weaning model			Calves killed based on length	Calves killed based on weaning model	
Year	No. of sets	Calf deficit based on length	Calf deficit based on weaning model	Difference (95% CI)	No. of sets	Calf deficit based on length	Calf deficit based on weaning model	Difference (95% CI)
1973	116	0.54	0.21	**0.33 (0.18,0.50)**	21	0.33	0.06	**0.27 (0.01,0.55)**
		0.35	0.48	**−0.13 (−0.26,−0.03)**		1.00	1.25	−0.25 (−0.79,0.29)
1974	98	0.39	0.05	**0.34 (0.20,0.47)**	16	0.56	0.09	0.47 (−0.53,1.47)
		0.36	0.50	**−0.14 (−0.26,−0.03)**		0.56	0.74	−0.18 (−0.61,0.25)
1975	99	0.57	0.15	**0.42 (0.20,0.64)**	14	0.29	0.11	0.18 (−0.03,0.39)
		0.46	0.40	0.04 (−0.05,0.16)		0.93	0.83	0.10 (−0.45,0.66)
1976	51	0.18	0.11	0.07 (−0.01,0.15)	90	0.13	0.07	**0.06 (0.001,0.13)**
		0.28	0.31	−0.03 (−0.14,0.06)		0.49	0.47	0.02 (−0.10,0.15)
1977	167	0.10	0.03	**0.07 (0.02,0.12)**	163	0.17	0.06	**0.11 (0.06,0.16)**
		0.51	0.45	0.06 (−0.01,0.14)		0.46	0.35	0.11 (0.03,0.20)
1978	82	0.17	0.03	**0.14 (0.05,0.23)**	93	0.18	0.05	**0.13 (0.04,0.23)**
		0.35	0.39	−0.04 (−0.14,0.07)		0.43	0.50	−0.07 (−0.22,0.09)
1979	75	0.09	0.04	0.05 (−0.02,0.13)	61	0.31	0.13	**0.18 (0.04,0.32)**
		0.44	0.43	0.01 (−0.11,0.13)		0.51	0.37	0.14 (−0.03,0.31)
1980	54	0.16	0.03	**0.13 (0.02,0.25)**	34	0.00	0.01	**−0.01 (−0.02,−0.003)**
		0.373	0.371	0.002 −0.115,0.119)		0.50	0.44	0.06 (−0.08,0.21)
1981	41	0.105	0.110	−0.005 (−0.194,0.185)	38	0.05	0.04	0.01 (−0.04,0.07)
		0.53	0.65	−0.12 (−0.57,0.31)		0.63	0.62	0.01 (−0.17,0.20)
1982	36	0.44	0.21	0.23 (−0.10,0.55)	33	0.06	0.02	0.04 (−0.04,0.12)
		0.44	1.00	−0.56 (−1.27,0.14)		0.27	0.42	−0.15 (−0.37,0.08)
1983	33	0.00	0.14	0.14 (−0.64,0.36)	6	0.17	0.04	0.13 (−0.31,0.57)
		1.33	2.00	−0.67 (−7.25,5.91)		0.17	0.56	−0.39 (−1.56,0.76)
1984	4	0.00	0.02	−0.02 (−0.08,0.04)	29	0.14	0.04	0.10 (−0.01,0.21)
		0.25	0.49	−0.24 (−0.67,0.18)		0.35	1.04	−0.69 (−1.13,−0.26)
1985	70	0.13	0.04	**0.09 (0.02,0.15)**	17	0.06	0.04	0.02 (−0.06,0.10)
		0.29	0.47	−0.18 (−0.39,0.03)		0.35	0.49	−0.14 (−0.48,0.21)
1986	45	0.13	0.04	**0.09 (0.01,0.17)**	28	0.04	0.03	0.01 (−0.04,0.06)
		0.64	0.44	0.20 (−0.04,0.44)		0.57	0.39	0.18 (−0.02,0.38)
1987	121	0.14	0.02	**0.12 (0.05,0.20)**	30	0.23	0.08	**0.15 (0.02,0.30)**
		0.38	0.45	−0.07 (−0.22,0.07)		0.27	0.43	−0.16 (−0.41,0.09)
1988	6	0.11	0.12	−0.01 (−0.23,0.22)	—	—	—	—
		0.33	0.50	−0.17 (−0.62,0.28)				
1989	24	0.22	0.13	0.09 (−0.11,0.29)	15	0.47	0.20	**0.27 (0.05,0.49)**
		0.87	0.95	−0.08 (−0.60,0.43)		0.73	0.82	−0.09 (−0.66,0.48)
1990	16	0.31	0.21	0.10 (−0.18,0.38)	9	0.89	0.17	0.72 (−0.18,1.62)
		0.56	0.41	0.15 (−0.20,0.51)		0.33	0.77	−0.44 (−1.15,0.27)
All	1108	0.25	0.08	**0.17 (0.13,0.20)**	697	0.18	0.06	**0.12 (0.09,0.16)**
		0.42	0.48	**−0.06 (−0.10,−0.01)**		0.49	0.51	−0.02 (−0.08,0.03)

growth rates and lower estimates of the current size of the population in relation to carrying capacity. Wade et al.[1] did not model the calf deficit estimated in our present study, but the effect of 14% additional mortality would probably be less than the 50% additional mortality that was modeled. The 50% mortality was spread over all age classes, and additional mortality due to missing calves should be assigned to the first two year classes only. The important question is whether the calf deficit in the kill represents the main effect of mother-calf separation by the fishing process. As outlined in Archer et al. (2001), the mechanism by which suckling calves are separated from their mothers is unknown. If separation is simply a function of the number of lactating females killed, then the deficit presented here is an accurate representation of the number of "missing" calves.

However, there is some evidence that separation can occur without the mother being killed. In the early days of the backdown procedure, purse-seine skippers reported that "Babies swim around the outside of the net pushing to get back in probably because their mothers are still inside" (Gehres[6]). It is unclear whether these calves were separated prior to encirclement or were released early during backdown, prior to their mothers. Regardless, given that dolphins exhibit some of their fastest swimming during a set immediately upon release from the net (Chivers and Scott[7]), separated calves waiting immediately outside the net may risk separation if their mothers join the rest of the school rapidly swimming away from the net. If this, or any of the other scenarios regarding the manner in which permanent separation can occur without the mother being killed (Archer et al., 2001), then the calf deficit underestimates the actual number of orphaned calves. Future research should focus on the mechanism of calf separation because a better understanding of this process is the only way we will be able to estimate the magnitude of the unobserved calf mortality and its subsequent effects on the population.

Acknowledgments

The authors wish to thank Michael Scott and Nick Vogel of the IATTC for providing data as well as Jay Barlow and Bill Perrin for helpful reviews and analytical suggestions.

[6] Gehres, L. E. 1971. Letter of July 2 to Alan R. Longhurst, 2 p. Southwest Fisheries Science Center, 8604 La Jolla Shores Dr., La Jolla, CA 92037.

[7] Chivers, S. J., and M. D. Scott. 2002. Tagging and tracking of *Stenella* spp. during the 2001 Chase Encirclement Stress Studies cruise. National Oceanographic and Atmospheric Administration Administrative Report LJ-02-33, 21 p. Southwest Fisheries Science Center, 8604 La Jolla Shores Dr., La Jolla, CA 92037.

Literature cited

Archer, F., T. Gerrodette, A. Dizon, K. Abella and S. Southern.
2001. Unobserved kill of nursing dolphin calves in a tuna purse-seine fishery. Mar. Mamm. Sci. 17:540–554.

Archer, F., and K. M. Robertson.
In press. Age and length at weaning and development of prey preferences of pantropical spotted dolphins, *Stenella attenuata*, from the eastern tropical Pacific. Mar. Mamm. Sci.

Dizon, A. E., W. F. Perrin, and P. A. Akin.
1994. Stocks of dolphins (*Stenella* spp. and *Delphinus delphis*) in the eastern tropical Pacific: a phylogeographic classification. NOAA Tech. Rep. NMFS-119, 20 p.

Gerrodette, T.
2002. Tuna-dolphin issue. *In* Encyclopedia of marine mammals (W. F. Perrin, B. Wursig, and J. G. M. Thewissen, eds.), p. 1269–1273. Academic Press, San Diego, CA.

Hall, M. A., L. A. Dayton, and K. I. Metuzals.
2000. Bycatch: problems and solutions. Mar. Poll. Bull. 41:204–19.

IATTC (Inter-American Tropical Tuna Commission).
2002. Annual report of the Inter-American Tropical Tuna Commission 2000, 171 p. IATTC, La Jolla, CA.

Gosliner, M. L.
1999. The tuna-dolphin controversy. *In* Conservation and management of marine mammals (J. R. Twiss Jr., and R. R. Reeves, eds.), p. 120–155. Smithsonian Institution Press, Washington and London.

Myrick, Jr., A. C., A. A. Hohn, J. Barlow, and P. A. Sloan.
1986. Reproductive biology of female spotted dolphins, *Stenella attenuata*, from the eastern tropical Pacific. Fish. Bull. 84:247–259.

NRC (National Research Council).
1992. Dolphins and the tuna industry, 176 p. National Academy Press, Washington, D.C.

Perrin, W. F.
1970. Color patterns of the eastern Pacific spotted porpoise *Stenella graffmani* Lonnberg (Cetacea, Delphinidae). Zoologica (NY) 54:135–149.

Perrin, W. F., J. M. Coe, and J. R. Zweifel.
1976. Growth and reproduction of the spotted porpoise, *Stenella attenuata*, in the offshore eastern tropical Pacific. Fish. Bull. 74:229–269.

Smith, T.
1983. Changes in size of three dolphin (*Stenella* spp.) populations in the eastern tropical Pacific. Fish. Bull. 81:1–13.

Wade, P. R.
1995. Revised estimates of incidental kill of dolphins (Delphinidae) by the purse-seine tuna fishery in the eastern tropical Pacific, 1959–1972. Fish. Bull. 93:345–354

Abstract—*Psednos rossi* new species (Teleostei: Liparidae) is described from two specimens collected in the North Atlantic Ocean off Cape Hatteras, North Carolina, at depths of 500–674 m. *Psednos rossi* belongs to the *P. christinae* group, which includes six other species and is characterized by 46–47 vertebrae and the absence of a coronal pore. *Psednos rossi* differs from those six species by having characters unique within the genus: straight spine, body not humpbacked at the occiput, and a very large mouth with a vertical oral cleft. Other distinguishing characters include a notched pectoral fin with 15–16 rays, eye 17–19% SL, and color in life orange-rose. With *P. rossi*, the genus *Psednos* as currently known includes 26 described and five undescribed species of small meso- or bathypelagic liparids from the Atlantic, Pacific, and Indian Oceans.

A remarkable new species of *Psednos* (Teleostei: Liparidae) from the western North Atlantic Ocean

Natalia V. Chernova

Zoological Institute
Russian Academy of Sciences
Universitetskaya nab. 1
St. Petersburg 199034, Russia

David L. Stein

NOAA/NMFS Systematics Laboratory
Smithsonian Institution
P.O. Box 37012
National Museum of Natural History, MRC-0153
Washington, D.C. 20013-7012
E-mail address (for D. L. Stein, contact author): david.stein@noaa.gov

Manuscript approved for publication 7 January 2004 by Scientific Editor.

Manuscript received 20 January 2004 at NMFS Scientific Publications Office.

Fish. Bull. 102:245–250 (2004).

The liparid genus *Psednos* Barnard 1927 is a group of meso- and bathypelagic snailfishes distinguished from the genus *Paraliparis* by having the infraorbital canal of the cephalosensory system interrupted behind the eye and usually having a pronounced dorsal curvature of the spine, producing a "humpbacked" body. *Psednos* are small, easily damaged, and often misidentified as juvenile *Paraliparis*. Until 1978, the genus was known only from two specimens of a single species (*Psednos micrurus* Barnard 1927) collected off Cape Point, South Africa. Two additional specimens were collected in the southern Indian Ocean and reported by Stein (1978). No further specimens or species were described until Andriashev (1992) described another new species. Since then, active searches for material from collections around the world have yielded many specimens from the Atlantic, Pacific, and Indian Oceans. To date, 25 species have been described (Andriashev, 1992, 1993; Chernova, 2001; Stein et al., 2001; Chernova and Stein, 2002) and an additional five are undescribed (one in Stein et al., 2001, three in Chernova and Stein, 2002, all in poor condition; and another that is currently being described by Stein). In this article, we describe an especially noteworthy species of the genus from two specimens collected from the North Atlantic off Cape Hatteras, North Carolina.

Materials and methods

All characters available for both specimens were studied. Characters and terms used were described by Andriashev (1992), Chernova (2001), Stein et al. (2001), and Chernova and Stein (2002). Counts were made from a radiograph of the holotype and from each specimen where possible; vertebral counts include the urostyle. The first caudal vertebra is that with the haemal spine supporting the first anal-fin ray. The posterior tip of the lower jaw in *Psednos* forms a distinct and prominent ventrally directed angle, the retroarticular process (Chernova, 2001). Counts and proportions are given as a percentage of standard length (SL) and head length (HL). Nonstandard measurements are the following: distance from mandible to anus (from anterior tip of mandible to center of anus); distance from anus to anal-fin origin (from center of anus to anal-fin origin); interorbital width (measured between upper margins of eyes); postocular head length (distance from posterior margin of eye to tip of opercular flap).

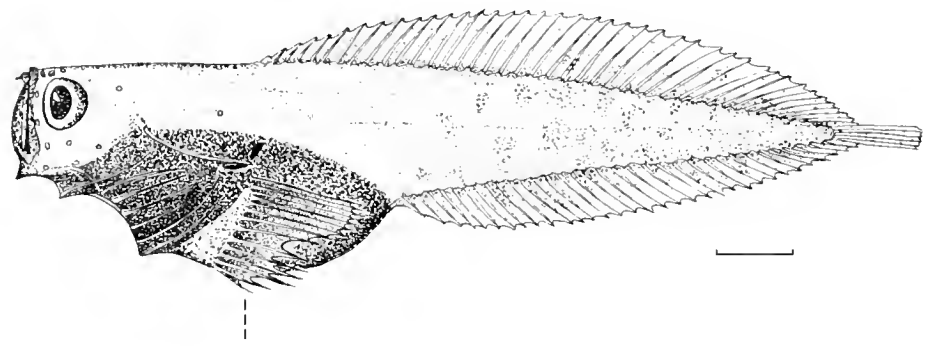

Figure 1

Psednos rossi n.sp., paratype, USNM 372727. Adult, 51.8 mm SL, 57.2 mm TL. Sta. CH-01-047, off Cape Hatteras. Scale 5 mm. Infraorbital pore 6 not shown owing to damage.

We selected the smaller specimen to serve as the holotype owing to its better condition (skin, pores, shape of head) and the availability of more characters. Unfortunately, it is distorted and does not look natural; therefore the undistorted larger (adult) specimen, the paratype, is illustrated. It is also more useful to have a drawing of an adult for comparison with other *Psednos* specimens.

In these small fishes, precise counts of number of tooth rows are possible only in disarticulated cleared and stained specimens; thus, we provide approximate counts. Similarly, the drawing of the gill arch of the paratype was made without dissection by viewing through an opening in the branchiostegal membrane.

Although Andriashev (1986) and Andriashev and Stein (1998) demonstrated the importance of the pectoral girdle in distinguishing among species and in explaining liparid relationships, we did not dissect, clear, and stain a pectoral girdle from these specimens owing to the high probability of damaging them and destroying other characters (Chernova, 2001; Chernova and Stein, 2002). The new species is so easily distinguished from congeners that it is not necessary for a diagnosis of the species to look at additional characters that the pectoral girdle can provide. Future specimens should be used to study these characters.

The holotype and paratype are permanently deposited in the Division of Fishes, Smithsonian Institution, National Museum of Natural History (USNM collection).

Results

Psednos rossi, n.sp.

Holotype

USNM 372726, juvenile, 37.2 mm SL, TL?, Sta. EL-00-033, off Cape Hatteras (The Point), 35°30.036′N, 74°46.497′W, 500–674 m over about 900 m depth, 23 July 2000, Tucker trawl. Good condition but distorted.

Paratype

USNM 372727, adult (sex not identified), 51.8 mm SL, 57.2 mm TL, Sta. CH-01-047, off Cape Hatteras (The Point), 35°28.93′N, 74°45.93′W, 628–658 m over 1090–704 m depth, 24 Aug. 2001, Tucker trawl. Throat slightly damaged, head slightly compressed, skin on head partly missing.

Diagnosis

Vertebrae 47, dorsal-fin rays 42–44, coronal pore absent. Mouth vertical, symphysis of upper jaw above level of eye. Body not humpbacked, vertebral column not curved behind cranium. Gill cavity enlarged. Anus on vertical behind head. Pectoral fin notched, rays 8+2+5–6. Eye 17–19% HL.

Description

Counts and proportions are given in Table 1. Head large, about one-third SL, its depth less than, and its width equal to or a little greater than, its length (Fig. 1). Head depth slightly greater than its width. Mouth very large, distinctly superior. Jaws almost vertical, at angle of about 90° to horizontal. Symphysis of upper jaw above level of eye. Ascending process of premaxilla horizontal, its distal end almost above center of eye. Posterior tip of lower jaw exactly below symphysis of upper jaw. Posterior (lower) end of mouth cleft well below level of lower margin of eye. When mouth closed, ventral surface of lower jaw forms entire frontal surface of head. Lower jaw included. Symphyseal process present at lower jaw symphysis, projecting forward prominently; retroarticular processes of lower jaw large, acute, directed anteroventrally (Fig. 2A). Teeth large, sharp, spear-shaped, strongly curved inward (Fig. 2B), in (smaller) holotype in approximately 22 and 24 (32 and 35) rows on upper and lower jaw; 5 (8–9) teeth in first full row near symphyses of both jaws. Snout short, 1.5 (1.0) times eye diameter. Olfactory rosette (7 lobes) and nostril above anterior third of eye. Eyes not large, close to upper

Table 1

Counts and proportions for the holotype and paratype of *Psednos rossi* new species. Proportions are in % of standard length (SL) followed by % head length (HL, in parentheses).

	USNM 372726 Holotype 37.2 mm SL	USNM 372727 Paratype 51.8 mm SL
Vertebrae	47	—
Dorsal-fin rays	44	42
Anal-fin rays	35	33
Pectoral-fin rays	16 [L] 15 [R]	15 [L, R]
Caudal-fin rays	6	6
Gill rakers	—	10
Head length	32.3	29.9
Head width	22.0 (68.1)	13.5 (45.2)
Head depth	23.7 (73.4)	17.4 (58.2)
Body depth	21.5 (66.6)	25.1 (83.9)
Body depth at anal-fin origin	13.4 (41.5)	17.0 (56.8)
Predorsal-fin length	29.6 (91.6)	26.6 (89.0)
Preanal-fin length	47.8 (148.0)	48.3 (161.5)
Mandible to anus	34.9 (108.0)	36.7 (122.7)
Anus to anal fin origin	23.7 (73.4)	21.2 (70.9)
Upper pectoral-fin lobe length	13.4 (41.5)	13.5 (45.2)
Pectoral-fin notch ray length	8.1 (25.1)	—
Lower pectoral-fin lobe length	9.4 (29.1)	—
Eye diameter	5.4 (16.7)	5.8 (19.4)
Snout length	8.1 (25.0)	7.7 (25.8)
Interorbital width	13.4 (42.0)	11.2 (37.4)
Postocular head length	18.8 (58.0)	19.3 (64.5)
Upper jaw length	16.1 (49.8)	12.5 (41.8)
Lower jaw length	16.1 (49.8)	13.5 (45.2)
Gill opening length	5.4 (16.7)	5.4 (18.1)
Opercle length	13.4 (41.5)	12.5 (41.8)

contour of head. Interorbital space flat, 2.5 (1.9) times eye diameter. Gill opening short, 1.0 (0.9) times eye diameter, at 45° angle, entirely above pectoral-fin base and slightly anterior to it (distance between ventral end of gill opening and base of upper pectoral ray about equal to length of gill opening). Opercular flap small, acute. Opercle very long, directed ventrally and posteriorly, its tip below level of posterior end of lower jaw. Interopercle of similar length, visible externally, its anterior tip projecting anteriorly from ventral contour of head (Fig. 1). Long opercle, interopercle and elongated branchiostegal rays support membranes of enlarged branchial cavity that appears externally as a black posterior part of head. Branchial cavity length slightly more than half head length. Branchiostegal rays (4+2) long and distinctly visible externally. Gill rakers modified, closely but irregularly set, mostly alternating (especially on gill arch one), often paired on the outer and inner sides of each gill arch (central part of arches two and three); plates flattened, triangular, similar in shape to those in *P. pallidus* or *Psednos* sp.1 of Chernova and Stein (2002, Figs. 9 and 13), spinule-bearing surface directed internally, flat and longitudinally oval. Spinules closely set, usually in two longitudinal rows, each of five to eight spinules, often with a few additional spinules in between (Fig. 2C).

Sensory pores difficult to see because of thin transparent skin (damaged in paratype). Nasal pores 2, the posterior on a vertical through center of eye. Paired nasal bones (through which the nasal canals run) long, tubular, and visible externally. Coronal pore absent. Lacrimal bones (bearing anterior portion of infraorbital canal) large, visible externally, slightly prominent anteriorly. Infraorbital canal (better preserved in holotype) interrupted behind eye, infraorbital pores 6 (5+1), posteriormost above posterior margin of eye (Fig. 2A). In paratype, skin behind eye missing. Preoperculomandibular pores 6 (3 on lower jaw + 3 on preopercular area). Two temporal pores present: t_1 a short distance behind posterior margin of eye, and t_{sb}, the suprabranchial pore, above and in front of gill opening (Fig. 2A).

Pectoral fin notched, of 16 (15) rays. Upper lobe of 8 (8) rays, the 2 (2) notch rays more widely spaced and placed exactly at middle of fin base. In holotype, left lower pectoral lobe with 6, on right 5, rays. In paratype, 5 rays on each side. Bases of lower-lobe rays stronger and thicker than those of upper-lobe rays. Level of uppermost pectoral ray below horizontal through lower end of upper jaw. Base of pectoral fin close to vertical, lowest ray almost directly below uppermost. Upper-lobe rays not reaching anal fin origin, lower-lobe rays not reaching vertical through ends of upper lobe rays. In holotype, length of notch rays 1.7 times in upper pectoral-fin lobe length, lower pectoral-fin lobe 1.4 times in it.

Body not humpbacked, dorsal contour of back almost straight; spine horizontal, its anterior end not dorsally curved (Fig. 3). Neural spines of vertebrae 1–4 neither longer nor broader than those posterior, unlike other species (see Fig. 5 in Chernova, 2001). Maximum body depth 4.2 (4.0) times in standard length and 1.6 (1.5) times depth at anal-fin origin. In holotype, occiput slightly swollen (Fig. 3); in paratype, dorsal outline of head and back in front of dorsal fin origin almost perfectly flat (Fig. 1), possibly an age-related difference. Abdominal part of body long, preanal length almost half of standard length. Interneural of first dorsal-fin ray between neural spines 3 and 4. Dorsal and anal fins moderately deep, maximum depth of erect dorsal fin in paratype 8.9 times in SL, 2.7 times in head length (damaged in holotype). Dorsal and anal fins overlapping about one-third of caudal-fin length. Anus on vertical behind head, slightly behind base of uppermost pectoral ray. Skin transparent. Gelatinous subcutaneous tissue weakly developed. In holotype (smaller specimen) body not as deep and jaws longer than in the paratype (larger specimen). Differences in head width and interorbital width are great because head of paratype was slightly compressed during fixation. Other proportions similar to those of holotype.

Body color in alcohol pale; under magnification, slightly dusky blotches of dots present caudally in paratype and absent in holotype. Head musculature pale. Black peritoneum visible through body wall. Mouth and gill cavities, gill arches, tongue, and both jaws black; gill rakers pale. Musculature of pectoral girdle appears pale on lateral surface of belly. Color in life orange-rose.

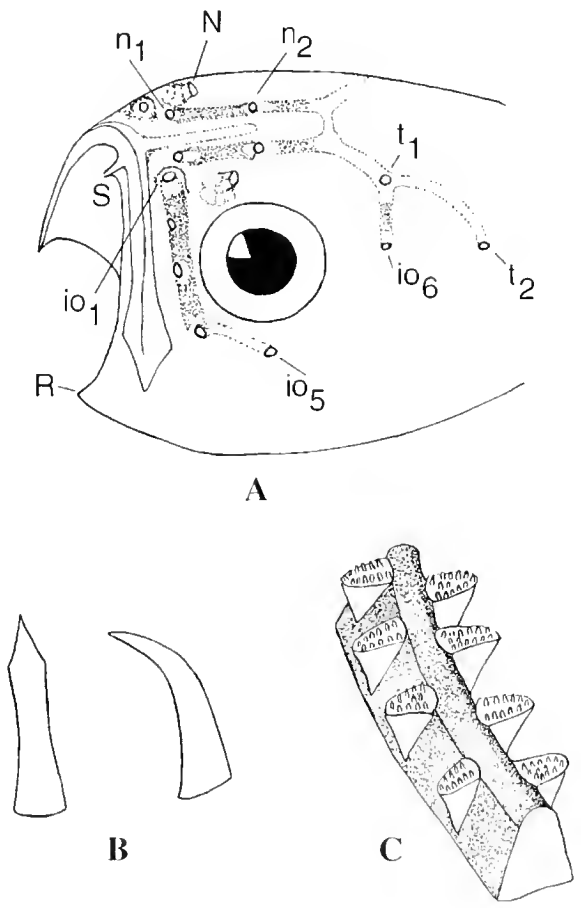

Figure 2

Details of anatomy of *Psednos rossi*. (**A**) Cephalic pores and prominent features of head. Portions of sensory canals passing through bones are stippled. N = nostril and olfactory rosette; io = infraorbital pores, n = nasal pores, t = temporal pores; S = symphyseal knob; R = retroarticular process. (**B**) Teeth of paratype: (left) frontal view; (right) lateral view. Tooth length about 0.25 mm. (**C**) First gill arch of paratype, USNM 372727, right side; view from inside of gill cavity. Raker height about 0.3 mm.

Distribution

Western North Atlantic off Cape Hatteras, mesopelagic at depths of 500–674 m.

Etymology

The patronym "rossi" after Steve W. Ross, who initially notified us of the captures and furnished the specimens to us for examination.

Comparative notes

Psednos rossi seems to belong to the *P. christinae* group (see Chernova, 2001; Chernova and Stein, 2002), including *P. andriashevi*, *P. barnardi*, *P. christinae*, *P. dentatus*, *P. groenlandicus*, and *P. harteli*. Species of this group are characterized by vertebrae 46–47, dorsal-fin rays 38–42, anal-fin rays 33–35, and coronal pore absent (versus the *P. micrurus* group having vertebrae 40–44, dorsal-fin rays 34–38, anal-fin rays 28–33, and coronal pore present) (Chernova, 2001). *Psednos rossi* distinctly differs from the other species of the *christinae* group in at least having occiput not swollen (vs. greatly swollen), not humpbacked because the vertebral column is straight (vs. humpbacked owing to the greatly curved anterior part of the spine), mouth vertical with jaws at 90° to horizontal, symphysis of upper jaw above level of eye (vs. a more or less oblique mouth at an angle of 30–45° and the upper jaw, symphysis on a horizontal with the lower half of the eye); and anus

Figure 3

Radiograph of *Psednos rossi* n.sp., holotype, USNM 372726. Juvenile, 37.2 mm SL. Sta. EL-00-033, off Cape Hatteras.

behind the head (vs. anus below the posterior third of the head). The very oblique, almost vertical mouth occurs often in species of the *P. micrurus* group, five of which have the mouth at 75–85° to the horizontal (*P. anoderkes, P. cathetostomus, P. microps, P. mirabilis, P. sargassicus*). However, they all differ as described above.

Discussion

The physical features of *Psednos rossi* are unique in the genus. The straight vertebral column and body are outside the previous diagnosis of the genus, because all previously known species are humpbacked owing to the curved spinal column. Nevertheless, *P. rossi* clearly belongs in *Psednos* rather than *Paraliparis* because it has the other generic characters of *Psednos* (Chernova, 2001); particularly, its sensory canal system and pores are of *Psednos* type, having an interrupted infraorbital canal behind the eye. We suggest that its remarkable body shape is an extreme transformation of the usual *Psednos* body shape and is associated with the change of the mouth from oblique and of normal size to vertical and very large. In this process the anterior movement of the bony elements of the jaws greatly enlarges the branchial cavity.

The morphology of *Psednos rossi* invites speculation about its ecology. The very large superior mouth with vertical jaws, eyes located close to the dorsal contour of the head and oriented to look forward and up, and straight body suggest adaptation to feeding on detritus and animals (such as copepods) above it in the water column. These adaptations, similar to those of hatchetfishes (family Sternoptychidae), are highly advantageous for a mesopelagic mode of life. Sudden opening of the very large vertical lower jaw could produce a strong orobranchial suction, simultaneously bringing food into the mouth and thus saving energy for this fish, which is probably a poor swimmer.

Work over the last several years has made it clear that *Psednos* species exist at mesopelagic depths in the North Atlantic, Indian, North Pacific, and South Pacific Oceans. We confidently expect discovery of additional species from meso- and bathypelagic waters.

Acknowledgments

We wish to thank S. W. Ross, K. J. Sulak, and J. V. Gartner Jr. for collecting the specimens, bringing them to our attention, and loaning them to us for description. Collections were supported by the U.S. Geological Survey, State of North Carolina, North Carolina Coastal Reserve Program, and the Duke/UNCW Oceanographic Consortium. The figures are drawn by the senior author, who was supported by the Russian Science Foundation Grants 02-04-48669 and 00-15-07794.

Literature cited

Andriashev, A. P.

1986. Review of the snailfish genus *Paraliparis* (Scorpaeniformes: Liparididae) of the Southern Ocean, 204 p. Theses Zoologicae 7, Koeltz Scientific Books, Koenigstein

1992. Morphological evidence for the validity of the antitropical genus *Psednos* Barnard (Scorpaeniformes, Liparidae) with a description of a new species from the eastern North Atlantic. UO, Tokyo 41:1–18.

1993. The validity of the genus *Psednos* Barnard (Scorpaeniformes, Liparidae) and its antitropical distribution area. Vopr. Ikhtiol. 33 (1):5–15 [in Russian.] J. Ichthyol. 33 (5):81–98. [English translation.]

Andriashev, A. P., and D. L. Stein.

1998. Review of the snailfish genus *Careproctus* (Liparidae, Scorpaeniformes) in Antarctic and adjacent waters. Contr. Sci. Nat. Hist Mus. Los Angeles Cty. 470:1–63.

Chernova, N. V.
2001. A review of the genus *Psednos* (Pisces, Liparidae) with description of ten new species from the North Atlantic and southwestern Indian Ocean. Bull. Mus. Comp. Zool. 155:477–507.

Chernova, N. V., and D. L. Stein.
2002. Ten new species of *Psednos* (Pisces, Scorpaeniformes: Liparidae) from the Pacific and North Atlantic Oceans. Copeia 2002 (3):755–778.

Stein, D. L.
1978. The genus *Psednos* a junior synonym of *Paraliparis*, with a redescription of *Paraliparis micrurus* (Barnard) (Scorpaeniformes: Liparidae). Matsya 4:5–10.

Stein, D. L., N. V. Chernova, and A. P. Andriashev.
2001. Snailfishes (Pisces: Liparidae) of Australia, including descriptions of 30 new species. Rec. Austr. Mus. 53:341–406.

Age and growth of sailfish (*Istiophorus platypterus*) in waters off eastern Taiwan

Wei-Chuan Chiang
Chi-Lu Sun
Su-Zan Yeh
Institute of Oceanography
National Taiwan University
No. 1, Sec. 4, Roosevelt Road
Taipei, Taiwan 106
E-mail address (for C. L. Sun, contact author) chilu@ntu.edu.tw

Wei-Cheng Su
Taiwan Fisheries Research Institute
No. 199, Ho-Ih Road
Keelung, Taiwan 202

Abstract—Age and growth of sailfish (*Istiophorus platypterus*) in waters off eastern Taiwan were examined from counts of growth rings on cross sections of the fourth spine of the first dorsal fin. Length and weight data and the dorsal fin spines were collected monthly at the fishing port of Shinkang (southeast of Taiwan) from July 1998 to August 1999. In total, 1166 dorsal fins were collected, of which 1135 (97%) (699 males and 436 females) were aged successfully. Trends in the monthly mean marginal increment ratio indicated that growth rings are formed once a year. Two methods were used to back-calculate the length of presumed ages, and growth was described by using the standard von Bertalanffy growth function and the Richards function. The most reasonable and conservative description of growth assumes that length-at-age follows the Richards function and that the relationship between spine radius and lower jaw fork length (LJFL) follows a power function. Growth differed significantly between the sexes; females grew faster and reached larger sizes than did males. The maximum sizes in our sample were 232 cm LJFL for female and 221 cm LJFL for male.

Manuscript approved for publication 22 December 2003 by Scientific Editor.
Manuscript received 20 January 2004 at NMFS Scientific Publications Office.
Fish. Bull. 102(2): 251–263 (2004).

The sailfish (*Istiophorus platypterus*) is distributed widely in the tropical and temperate waters of the world's oceans. According to data from longline catches, sailfish are usually distributed between 30°S and 50°N in the Pacific Ocean, and highest densities are found in the warm Kuroshio Current and its subsidiary currents. This species has a tendency to be found close to the coast and near islands (Nakamura, 1985). During the 1990s the annual landings of sailfish off Taiwan ranged between 600 and 2000 metric tons, of which approximately 54% came from waters off Taitung (eastern Taiwan). Sailfish are seasonally abundant from April to October (peak abundance from May to July) and contribute substantially to the economic importance of the eastern coast of Taiwan where this species is taken primarily by drift gill nets, although they are also caught by set nets, harpoons, and as incidental bycatch in inshore longline fisheries.

Age and growth of sailfish caught in recreational fisheries in the Atlantic Ocean have been studied by using various methods, including length-frequency analysis (de Sylva, 1957), analysis of release-recapture data (Farber[1]), and inferences from observed marks on hard parts, such as spines (Jolley, 1974, 1977; Hedgepeth and Jolley, 1983) and otoliths (Radtke and Dean, 1981; Radtke, 1983; Prince et al., 1986). In contrast, very few attempts have been made to age sailfish in the Pacific Ocean. Koto and Kodama (1962) estimated the growth of sailfish caught with longlines from 1952 to 1955 in the East China Sea using length-frequency analysis, and Alvarado-Castillo and Félix-Uraga (1996, 1998) used the fourth spine of the first dorsal fin to estimate age and growth of sailfish caught from 1989 to 1991 in the recreational fishery off Mexico. However, western Pacific sailfish have not been aged with calcified structures in any previous study.

The aging of fishes, and consequently the determination of their growth and mortality rates, is an integral component of modern fisheries science (Paul, 1992). Mortality and growth rates provide quantitative information on fish stocks and are needed for stock assessment methods such as yield-per-recruit and cohort analysis (Powers, 1983).

The objectives of this study were to estimate age and growth of sailfish by counting growth rings on cross sections of the fourth spine of the first dorsal fin and to determine which of the Richards function and the standard von Bertalanffy growth function best represents growth of sailfish in waters off eastern

[1] Farber, M. I. 1981. Analysis of Atlantic billfish tagging data: 1954–1980. Unpubl. manuscr. ICCAT workshop on billfish, June 1981. Southeast Fisheries Center Miami Laboratory, National Marine Fisheries Service, NOAA, 75 Virginia Beach Drive, Miami, FL 33149.

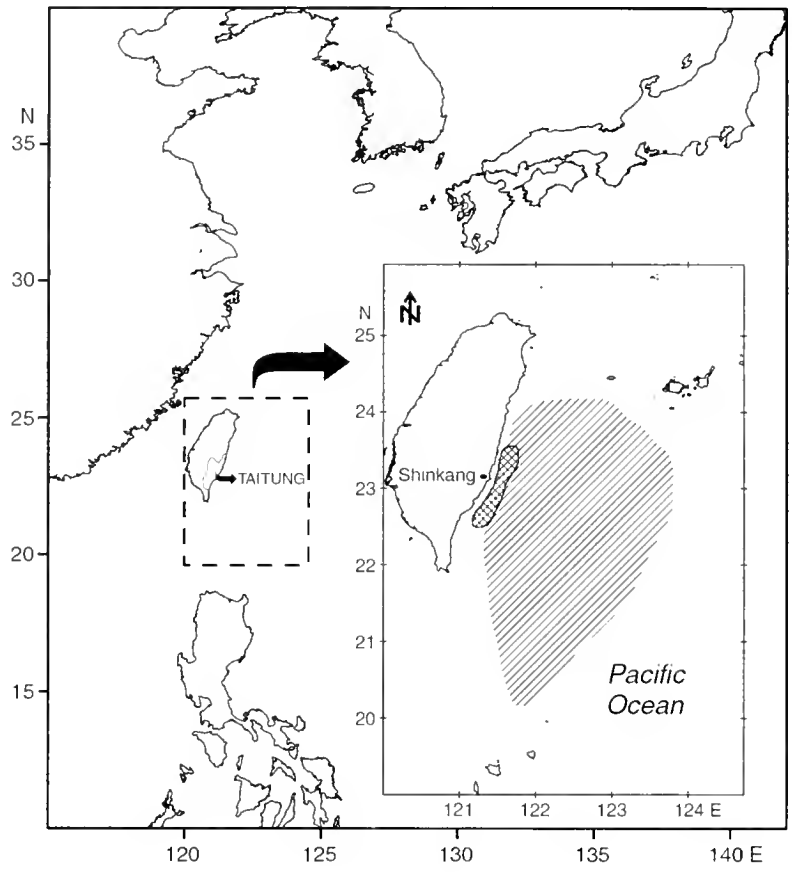

Figure 1

Fishing grounds of the gillnet (cross lines) and longline (oblique lines) fishing boats based at Shinkang fishing port.

Taiwan. This information could be used to determine the age composition of the catch and to assess the status of sailfish in these waters by using yield-per-recruit or sequential population analysis techniques.

Materials and methods

Materials

Data on total length (TL), eye fork length (EFL), lower jaw fork length (LJFL) (in cm), round weight (RW) (in kg) and the first dorsal fins of male and female sailfish were collected monthly at the fishing port of Shinkang (Fig. 1) from July 1998 to August 1999. In total, 304 TLs, 1166 LJFLs, 1166 RWs, and 1166 dorsal fins were collected. The dorsal fins were kept in cold storage before being boiled to remove surrounding tissue and to separate the fourth spines. Three cross sections (thickness 0.75 mm) were taken successively along the length of each spine with a low-speed "ISOMET" saw (model no. 11-1280) and diamond wafering blades, at a location equivalent to 1/2 of the maximum width of the condyle base measured above the line of maximum condyle width (Fig. 2A) (Ehrhardt et al., 1996; Sun et al., 2001, 2002). The sections were immersed in 95% ethanol for several minutes for cleaning, placed on disposable paper to air dry, and then stored in a labeled plastic case for later reading. Spine sections were examined with a binocular dissecting microscope (model: Leica-MZ6) under transmitted light at zoom magnifications of 10–20× depending on the sizes of the sections. The most visible one of these three sections was read twice, approximately one month apart. If the two ring counts differed, the section was read again, and if the third ring count differed from the previous two ring counts, the spine was considered unreadable and discarded. The precision of reading was evaluated by using average percent error (APE) (Beamish and Fournier, 1981; Campana, 2001) and coefficient of variation (CV) (Campana, 2001) statistics.

Images of the cross sections were captured by using the Image-Pro Image analysis software package (Media Cybernetics, Silver Spring MD, 1997) in combination with a dissecting microscope equipped with a charged coupled device (CCD) camera (model: Toshiba IK-630) and a Pentium II computer equipped with a 640×480 pixel frame grab card and a high-resolution (800×600 pixel) monitor.

The distance from the center of the spine section to the outer edge of each growth ring was measured in microns with the Image-Pro software package after calibration against an optical micrometer. The center of the spine

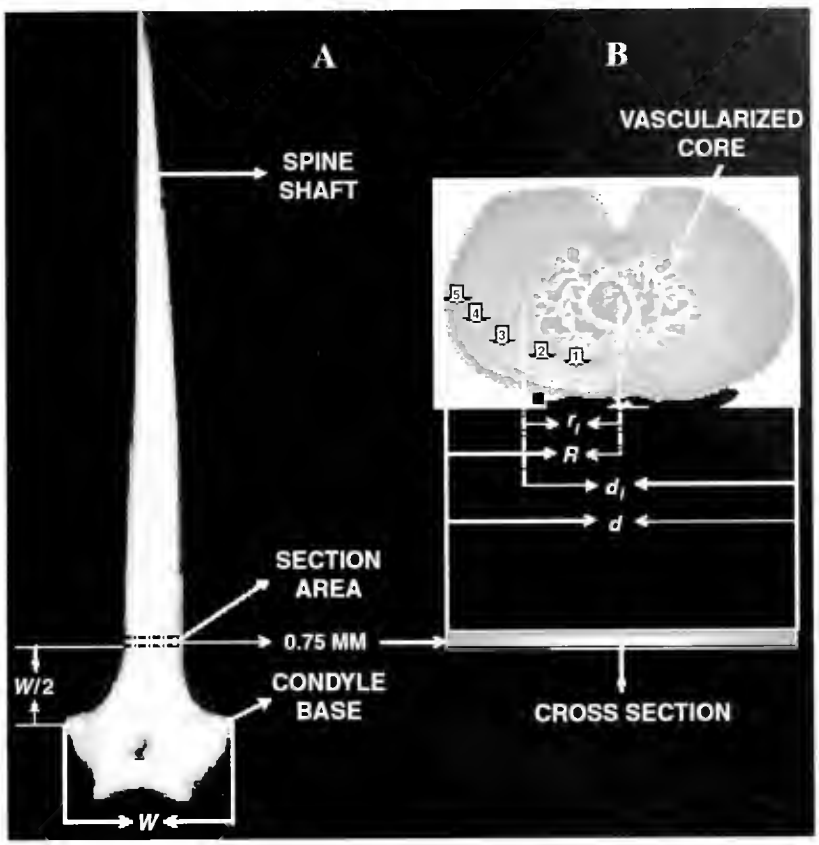

Figure 2

Schematic diagram of the fourth dorsal spine of sailfish (*I. platypterus*) and the location of the cross section (**A**), and a cross section showing the measurements taken for age determination of sailfish (**B**). W = maximum width of condyle base, R = radius of spine, r_i = radius of ring i, d = diameter of spine, d_i = diameter of ring i. The vascularized core and growth rings (1, 2, 3, 4, 5) are also shown.

section was estimated according to the methods of Cayré and Diouf (1983) (Fig. 2B). The distances (d_i) were then converted into radii (r_i) by using the equation (Megalofonou, 2000; Sun et al., 2001):

$$r_i = d_i - (d/2),$$

where r_i = radius of the ring i;
d_i = distance from the outside edge of ring i to the opposite edge of the cross section; and
d = diameter of the spine.

False growth rings were defined according to criteria of Berkeley and Houde (1983), Tserpes and Tsimenides (1995), and Ehrhardt et al. (1996).

Accounting for missing early rings

The first several growth rings of the larger specimens may be obscured because of the large size of the vascularized core of the spine. The number of early but missing growth rings was therefore estimated by the replacement method applied to Pacific blue marlin (*Makaira nigricans*) by Hill et al. (1989). This method involved first compiling ring radii statistics from younger specimens that had at least the first or second ring visible. Radii of the first four visible rings from samples that had missing early rings were then compared with the radii for these younger specimens. When the radii of at least two successive rings of the first four visible rings each fitted well within one standard deviation from the mean radii of each of two or more rings from the data compiled from the younger specimens, the number of missing rings was computed as the difference between the ring counts for the matched radii compiled from younger specimens and those for the specimen of interest.

Validation

The marginal increment ratio (MIR), which was used to validate the rings as annuli, was estimated for each

specimen by using the following equation (Hayashi, 1976, Prince et al., 1988; Sun et al., 2002):

$$MIR = (R - r_n)/(r_n - r_{n-1}),$$

where R = spine radius; and
r_n and r_{n-1} = radius of rings n and $n-1$.

The mean MIR and its standard error were computed for each month by sex for all ages combined, and also for the ages 1–5 and 6–11 for males and 1–5 and 6–12 for females.

Growth estimation

Growth for males and females was estimated by back-calculation of lengths at presumed ages. Two methods were used. Method 1 was based on the assumption that the relationship between spine radius (R) and LJFL (L) is linear, i.e., $L=a_1+b_1R$ (Berkeley and Houde, 1983; Sun et al., 2002), whereas method 2 was based on the assumption that this relationship is a power function, i.e., $L=a_2R^{b_2}$ (Ehrhardt, 1992; Sun et al., 2002). The parameters of the relationships were estimated by maximum likelihood, assuming log-normally distributed errors. Akaike's information criterion (AIC, Akaike, 1969) was used to select which of the linear and power functions best represented the data:

$$AIC = -2\ln L + 2p,$$

where $\ln L$ = logarithm of likelihood function evaluated at the maximum likelihood estimates for the model parameters, and
p = number of model parameters.

The equations used to back-calculate the lengths at presumed ages were

$$L_n = \begin{cases} a_1 + \left(\frac{r_n}{R}\right)(L - a_1) & \text{linear relationship} \\ \left(\frac{r_n}{R}\right)^{b_2} L & \text{power relationship} \end{cases},$$

where L_n = LJFL when ring n was formed;
L = LJFL at time of capture; and
r_n = radius of ring n.

The standard von Bertalanffy growth function (standard VB) (von Bertalanffy, 1938) and the Richards function (Richards, 1959) were then fitted to the mean back-calculated male and female lengths-at-age from methods 1 and 2, assuming additive error.

Standard VB:

$$L_t = L_\infty\left(1 - e^{-k(t-t_0)}\right),$$

Richards function:

$$L_t = L_\infty\left(1 - e^{-K(1+m)(t-t_0)}\right)^{\frac{1}{1+m}},$$

where L_t = the mean LJFL at age t;
L_∞ = the asymptotic length;
t_0 = the hypothetical age at length zero;
k and K = the growth coefficients; and
m = the fourth growth-equation parameter.

An analysis of residual sum of squares (ARSS) was used to test whether the growth curves for the two sexes were different (Chen et al., 1992; Tserpes and Tsimenides, 1995; Sun et al., 2001), and the log-likelihood ratio test was used to determine whether the Richards function provided a statistically superior fit to the data than the length-at-age standard VB growth function.

Results

Of the 1166 dorsal spines sampled, 1135 (97%) (699 males and 436 females) were read successfully. The average percent error (APE) was 6.31% (5.91% for males and 6.93% for females) and the coefficient of variation (CV) was 8.93% (8.36% for males and 9.81% for females). Of the 31 spines that could not be read, 22 were considered unreadable because the existence of multiple rings made the identification of annuli difficult or resulted in aging discrepancies between readings, and the remaining nine spines were unreadable because of abnormal growth.

The length-frequency and weight-frequency distributions for the 1166 individuals are shown in Figure 3. These individuals ranged from 78 to 221 cm LJFL (mean=177.62, SD=16.13, n=720) or 1 to 49 kg RW (mean=22.13, SD=5.68) for the males and from 80 to 232 cm LJFL (mean=179.96, SD=17.90, n=446) or 2 to 58 kg RW (mean=23.65, SD=7.34) for the females. The females were significantly larger than the males (t-test, $P<0.05$). Table 1 summarizes the relationships between EFL and LJFL and TL, and that between LJFL and weight. The latter relationship differed significantly between males and females (analysis of covariance; $P<0.05$).

At least the first or second ring in 417 (60%) of male spines and 300 (69%) of female spines was visible. The ring radii statistics by sex is summarized in Figure 4. All other specimens were assigned inner rings and final age estimates based upon these data. The mean ring radii by age group, for males and females, after correction for missing early rings, are listed in Table 2. The maximum age of the sampled sailfish, after correction for missing early rings, was 11 years for males and 12 years for females. The maximum ages before correction were 8 years for both sexes.

The monthly means of the marginal increment ratio (MIR) for males of all ages during May–August were high (~0.72) but declined markedly thereafter and reached a minimum of 0.46 in November (Fig. 5). Similarly, the MIR for females dropped from 0.71 in September to a minimum of 0.47 in November (Fig. 6). The monthly means of MIR did not differ significantly from each other over the period December–March (ANOVA, P_{σ}=0.86, P_{φ}=0.96). However, the monthly means of MIR from April through August for males and from April through September for females were

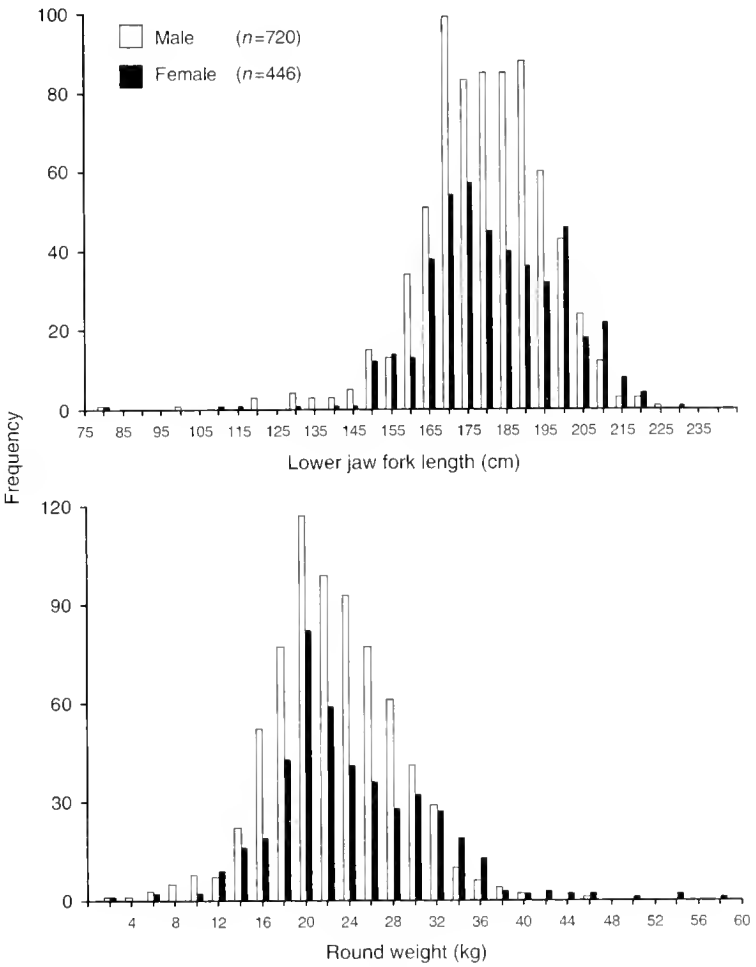

Figure 3

The size-frequency distributions by 5-cm intervals (upper figure) and by 2-kg intervals (lower figure) for male and female sailfish (*I. platypterus*) collected from the waters off eastern Taiwan.

significantly higher than those from September through November for males (*t*-test, $P<0.001$) and from October through November for females (*t*-test, $P<0.001$). Also, the mean MIR in November was significantly lower than that in December (*t*-tests, $P_{♂}<0.05$, $P_{♀}<0.05$). The trends in the monthly means of MIR when the data were split into ages 1–5 and 6+ were similar to those for all ages combined. The results in Figures 5 and 6 indicate that one growth ring is formed each year, most likely from September to November for males and from October to November for females.

Figure 7 shows the sex-specific relationships between LJFL and spine radius based on method 1 (linear regression) and method 2 (power function). The relationships for males and females are significantly different (method 1: $F_{698,435}=56.07$, $P<0.01$; method 2: $F_{698,435}=59.93$, $P<0.01$). According to AIC, the power function provides a better fit to the data (ΔAIC=38.57 and 30.96 for males and females, respectively). Therefore, the most parsimonious representation of the data is the power function with separate parameters for males and females.

The mean back-calculated lengths-at-age obtained from methods 1 and 2 are listed in Table 3. After the first year of life, the growth rates of both sexes slow appreciably. However, females still grow faster and consequently reach larger sizes than males. The standard VB and the Richards function for males and females are shown in Figure 8 and the corresponding parameter estimates are listed in Table 4. The growth curves for males differ significantly from those for females ($F=99.86$ $P<0.05$ and $F=107.38$ $P<0.05$ for the standard VB curve [methods 1 and 2], and $F=144.01$ $P<0.05$ and $F=48.43$ $P<0.05$ for the Richards function [methods 1 and 2]). The Richards function provides a statistically superior fit to the data (log-likelihood ratio test; $P<0.001$) when method 2 is used to back-calculate length-at-age but not when method 1 is used.

Table 1

Linear relationships ($Y=a+bX$) among total length (TL, cm), lower jaw fork length (LJFL, cm) and eye fork length (EFL, cm), and the log-linear length-weight (round weight, RW, kg) relationships for sailfish in the waters off eastern Taiwan. Values in parentheses are standard errors.

Y	X	a	b	n	LJFL range (cm)	RW range (kg)	r^2
Male							
TL	LJFL	19.660 (6.334)	1.205 (0.037)	184	78–211		0.854
TL	EFL	24.782 (6.176)	1.364 (0.042)	184	78–211		0.854
EFL	LJFL	−5.196 (0.772)	0.893 (0.004)	720	78–221		0.983
$\log_{10}$RW	$\log_{10}$LJFL	−5.381 (0.080)	2.985 (0.036)	720	78–221	1–46	0.906
Female							
TL	LJFL	6.728 (9.351)	1.286 (0.055)	120	109–210		0.824
TL	EFL	6.754 (9.505)	1.489 (0.064)	120	109–210		0.820
EFL	LJFL	−2.209 (0.802)	0.876 (0.004	446	80–232		0.989
$\log_{10}$RW	$\log_{10}$LJFL	−5.338 (0.103)	2.970 (0.046)	446	80–232	2–58	0.905

Discussion

Age estimate determined from dorsal-fin spines

Dorsal-fin spines appear to be useful for aging sailfish. They are easily sampled without reducing the economic value of the fish and can also be read easily (the growth rings stand out clearly). In contrast, scales cannot be used to age sailfish because scale deposition patterns change as sailfish age (Nakumura, 1985), and otoliths are extremely small and fragile and are often difficult to locate (Radtke, 1983). Reading otoliths is more time consuming and expensive than reading spines and spines can also be easily stored for future re-examination (Compeán-Jimenez and Bard, 1983; Sun et al., 2001, 2002).

The problems associated with the fin-spine aging method used in this study were the possible existence of false rings and the presence of the vascularized core which can obscure early growth rings in larger fish. These problems were also noted by Berkeley and Houde (1983), Hedgepeth and Jolley (1983), Tserpes and Tsimenides (1995), Megalofonou (2000), and Sun et al. (2001, 2002). However, Tserpes and Tsimenides (1995) and Megalofonou (2000) noted that experienced readers can overcome the problem of multiple rings by determining whether the rings are continuous around the circumference of the entire spine section and by judging their distance from the preceding and following rings. We observed false rings in spines for all age classes larger than age two, which we read without problem by using these guidelines. The missing early growth rings in larger specimens were accounted for by compiling ring radii statistics for younger specimens for which at least the first or second ring was visible and by comparing the radii of the first several visible rings of the specimens that had missing early rings to the mean radii and standard deviations of the compiled data. Similar approaches for solving the problem of missing rings have also been used for Pacific blue marlin (Hill et al., 1989).

Marginal increment ratio (MIR) analysis is the most commonly applied method for age validation (Campana, 2001). The MIR analysis conducted for sailfish suggested that one growth ring is formed each year from September to November for males and from October to November for females. Spawning for sailfish in the waters east of Taiwan lasts from April through September (Chiang and Sun[2]). This is exactly the period when growth is low, as indicated by the narrow and translucent rings. Similar findings have been reported for skipjack tuna (Antoine et al., 1983), swordfish (Ehrhardt, 1992; Tserpes and Tsimenides, 1995), and bigeye tuna (Sun et al., 2001). Although the timing of annulus formation coincides with spawning season for sailfish in the eastern Taiwan, annulus deposition

[2] Chiang, W. C., and C. L. Sun. 2000. Sexual maturity and sex ratio of sailfish (*Istiophorus platypterus*) in the eastern Taiwan waters. Abstracts of contributions presented at the 2000 annual meeting of the Fisheries Society of Taiwan, Keelung, Taiwan, 16–17 December 2000, 15 p. The Fisheries Society of Taiwan, 199 Hou-Ih Road, Keelung, 202 Taiwan.

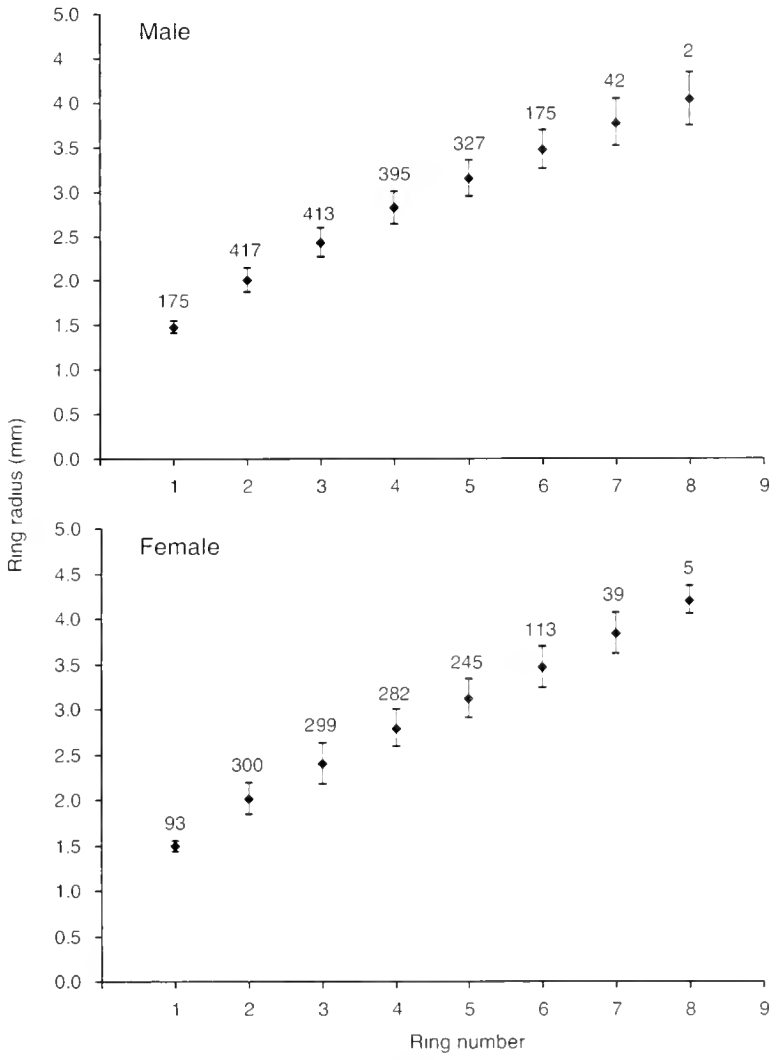

Figure 4

Mean (±1 SD) ring radius for male and female sailfish (*I. platypterus*) collected from the waters off eastern Taiwan that had at least the first or second ring present. The numbers above the vertical bars are the sample sizes.

may also be related to sailfish migration and environmental factors, as suggested by Sun et al. (2002) for swordfish. The MIR analysis provides only a partial age validation; complete validation requires either mark-recapture data or the study of known-age fish (Beamish and McFarlane, 1983; Prince et al., 1995; Tserpes and Tsimenides, 1995; Sun et al., 2001, 2002).

Selection of a growth curve

Female sailfish are typically larger for similar ages in males and grow faster than males, and the length-weight relationship differs significantly between the sexes. Similar results have been reported for east Pacific Ocean sailfish (Hernández-Herrera and Ramírez-Rodríguez, 1998), Indian Ocean sailfish (Williams, 1970) and Atlantic Ocean sailfish (Beardsley et al., 1975; Jolley, 1974, 1977; Hedgepeth and Jolley, 1983).

The Richards function appears to fit the data better than the standard VB curve (Fig. 8) and provides a more realistic description of growth for animals of age 0. The standard VB curve is commonly used to describe asymptotic growth in fish but did not fit the back-calculated lengths for fish younger than three (Table 4, Fig. 8).

Further discussion of growth curves will likely focus on method 2 (i.e., a power function relationship between spine radius and LJFL) because it provides a better fit to the data than method 1. Ehrhardt (1992), Ehrhardt et al.

Table 2

Mean radius of each ring for male and female sailfish in the waters off eastern Taiwan. Roman numerals indicate the number of rings. Numbers in parentheses are the number of specimens for which the specified ring was readable. "—"means no data owing to vascularization at core area.

Age class	Sample size	Mean radius (mm) of each ring											
		I	II	III	IV	V	VI	VII	VIII	IX	X	XI	XII
Male													
1	1	1.54 (1)											
2	4	1.53 (4)	2.08 (4)										
3	18	1.45 (12)	2.02 (18)	2.51 (18)									
4	68	1.49 (45)	2.02 (68)	2.48 (68)	2.91 (68)								
5	171	1.48 (62)	2.00 (152)	2.40 (171)	2.79 (171)	3.14 (171)							
6	198	1.46 (41)	2.02 (133)	2.44 (188)	2.83 (198)	3.17 (198)	3.49 (198)						
7	130	1.42 (10)	1.96 (38)	2.42 (94)	2.80 (123)	3.18 (128)	3.50 (130)	3.82 (130)					
8	74	1.44 (1)	1.96 (4)	2.44 (36)	2.79 (62)	3.14 (72)	3.48 (74)	3.81 (74)	4.09 (74)				
9	22	—	—	—	2.69(11)	3.02 (16)	3.37 (22)	3.70 (22)	4.02 (22)	4.29 (22)			
10	9	—	—	—	—	—	3.09 (5)	3.55 (8)	3.39 (8)	4.23 (9)	4.48 (9)		
11	3	—	—	—	—	—	2.90 (2)	3.28 (2)	3.74 (3)	4.04 (3)	4.33 (3)	4.50 (3)	
Mean		1.47	2.00	2.43	2.81	3.16	3.48	3.79	4.05	4.25	4.45	4.50	
SD		0.07	0.14	0.16	0.18	0.20	0.22	0.23	0.23	0.21	0.15	0.15	
Growth increase			0.53	0.43	0.38	0.34	0.32	0.31	0.26	0.20	0.20	0.05	
Female													
1	1	1.51 (1)											
2	1	1.58 (1)	2.23 (1)										
3	17	1.44 (15)	2.00 (17)	2.47 (17)									
4	38	1.48 (17)	2.00 (37)	2.39 (38)	2.80 (38)								
5	146	1.49 (46)	1.98 (132)	2.39 (146)	2.80 (146)	3.12 (146)							
6	107	1.52 (11)	2.05 (74)	2.45 (102)	2.84 (107)	3.17 (107)	3.48 (107)						
7	64	1.52 (2)	2.08 (34)	2.55 (59)	2.95 (64)	3.29 (64)	3.60 (64)	3.89 (64)					
8	35	1.53 (1)	2.02 (4)	2.40 (10)	2.76 (29)	3.17 (33)	3.53 (34)	3.86 (35)	4.16 (35)				
9	17	—	1.91 (1)	2.36 (4)	2.79 (10)	3.07 (16)	3.40 (17)	3.76 (17)	4.07 (17)	4.38 (17)			
10	7	—	—	—	—	2.81 (4)	3.10 (7)	3.46 (7)	3.84 (7)	4.23 (7)	4.55 (7)		
11	1	—	—	—	—	—	3.31 (1)	3.82 (1)	4.25 (1)	4.44 (1)	4.74 (1)	4.95 (1)	
12	1	—	—	—	—	—	—	3.88 (1)	4.12 (1)	4.49 (1)	4.81 (1)	5.14 (1)	5.32 (1)
Mean		1.49	2.01	2.44	2.83	3.16	3.50	3.84	4.10	4.35	4.60	5.04	5.32
SD		0.06	0.17	0.25	0.23	0.24	0.27	0.27	0.29	0.32	0.41	0.13	
Growth increase			0.52	0.43	0.39	0.33	0.34	0.34	0.26	0.25	0.25	0.44	0.28

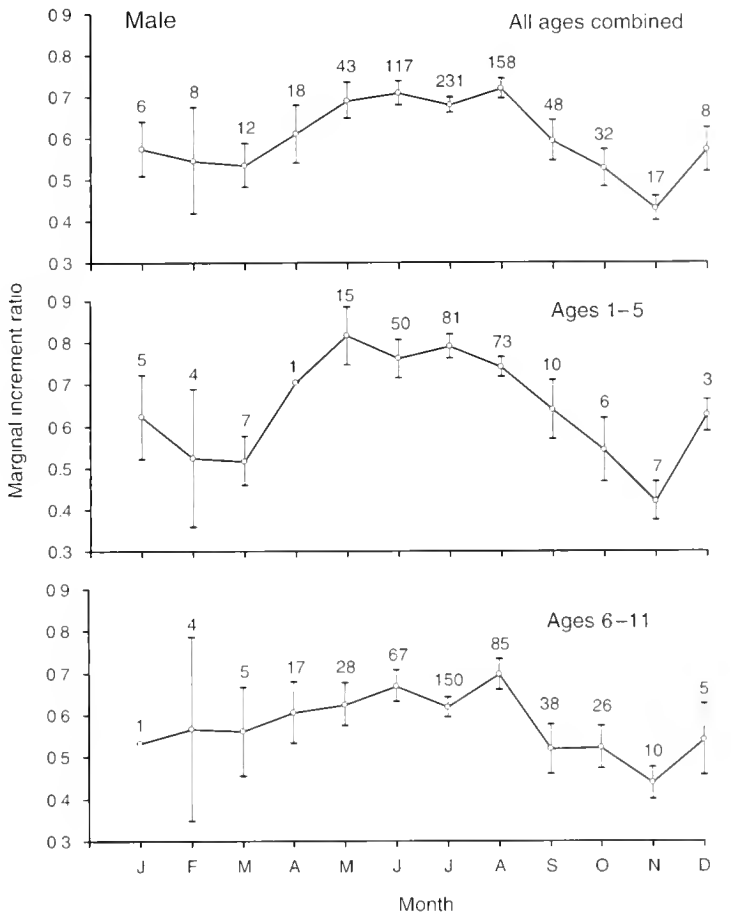

Figure 5

Monthly means of marginal increment ratio for male sailfish (*I. platypterus*) in the waters off eastern Taiwan for all ages combined and for age classes 1–5 and 6–11, respectively. Vertical bars are ±1 SE; numbers above the vertical bars are sample sizes.

Table 3

Mean back-calculated lower jaw fork lengths at age for sailfish in the waters off eastern Taiwan.

	Back-calculated length (cm)								
	Method 1		Method 2			Method 1		Method 2	
Age (yr)	Male	Female	Male	Female	Age (yr)	Male	Female	Male	Female
1	108.53	113.41	99.90	103.51	7	181.11	185.36	181.86	186.09
2	125.70	130.79	121.79	126.32	8	188.99	192.82	189.84	193.67
3	138.82	143.90	137.27	141.96	9	194.98	200.60	196.59	201.47
4	150.80	156.02	150.56	155.54	10	200.78	207.85	201.74	208.81
5	161.78	166.22	162.12	166.38	11	208.05	213.29	209.14	214.66
6	171.63	176.60	172.18	177.12	12		217.15		219.05

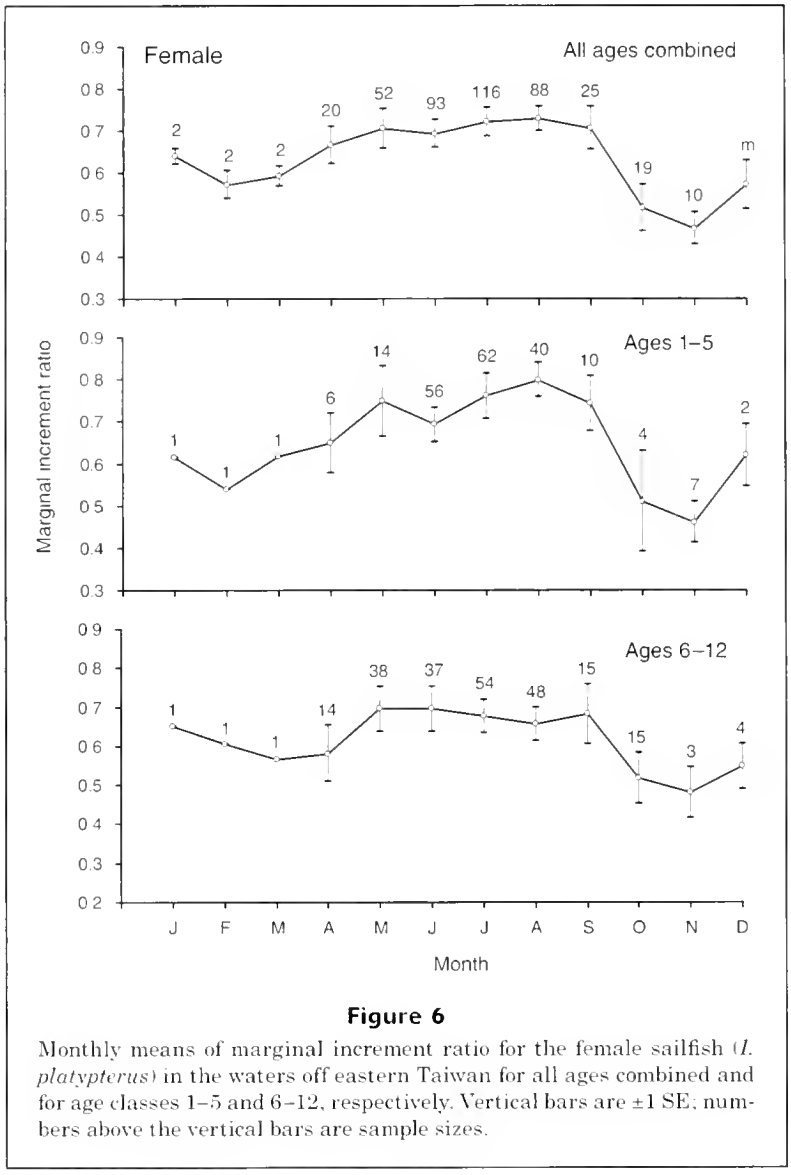

Figure 6

Monthly means of marginal increment ratio for the female sailfish (*I. platypterus*) in the waters off eastern Taiwan for all ages combined and for age classes 1–5 and 6–12, respectively. Vertical bars are ±1 SE; numbers above the vertical bars are sample sizes.

(1996), and Sun et al. (2002) favored method 2 because they believed it to be more biologically realistic. When the back-calculated lengths-at-age are generated with this method the Richards function provides a statistically superior fit to the length-at-age data. Therefore, the parameter estimates for the Richards function with method 2 listed in Table 4 are recommended as the most appropriate for calculating the age composition of sailfish in the waters to the east of Taiwan. It is perhaps worth noting that the t_0 values estimated for the Richards function with method 2 are much closer to zero than those estimated for the Richards function with method 1.

Comparison with previous studies

Figure 9 compares the age-length relationships of this paper with those for Atlantic (de Sylva, 1957; Hedgepeth and Jolley, 1983; Farber[1]) and Pacific sailfish (Koto and Kodama, 1962; Alvarado-Castillo and Félix-Uraga, 1998). De Sylva (1957) and Koto and Kodama (1962) used length-frequency analysis and concluded that sailfish are a very fast growing and short-lived species. However, they likely underestimated age and overestimated growth rate when their results are compared with those of other more recent studies.

The maximum ages found in this study (11 years for males and 12 years for females) are close to the maximum longevity of at least 13 years proposed by Prince et al. (1986) based on tagging data. Farber[1] analyzed Atlantic billfish tagging data and suggested that the asymptotic size was essentially reached by age 3 (Hedgepeth and Jolley, 1983), whereas the present study found a more gradual increase in length with age, in common with the results of Hedgepeth and Jolley (1983).

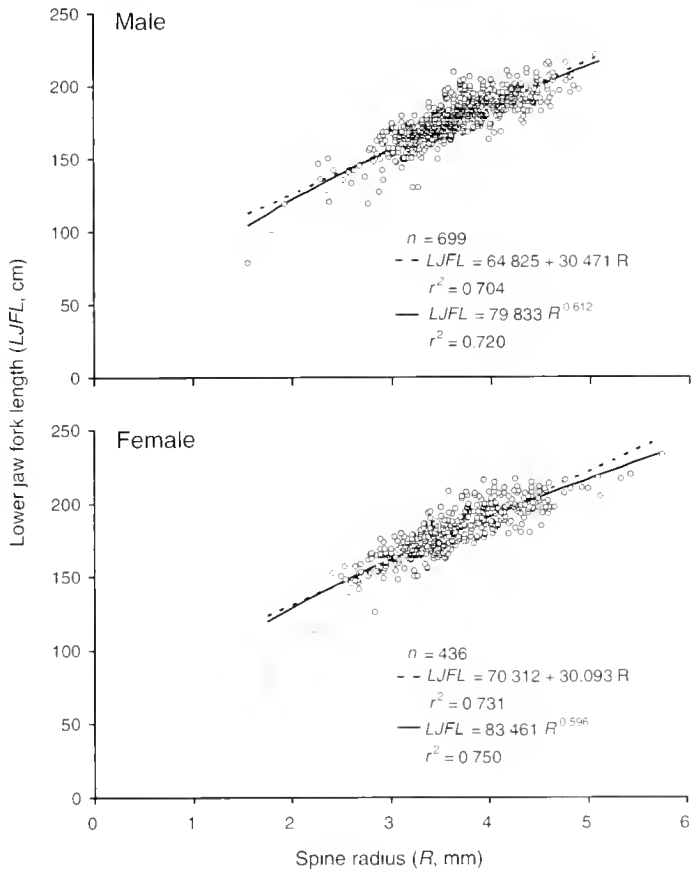

Figure 7

Relationship between lower jaw fork length and spine radius for male and female sailfish (*I. platypterus*) in the waters off eastern Taiwan.

Table 4

Parameter estimates and standard errors (in parenthesis) for the standard von Bertalanffy growth function and the Richards function for sailfish in the waters off eastern Taiwan.

	Standard von Bertalanffy growth function				Richards function			
	Method 1		Method 2		Method 1		Method 2	
Parameter	Male	Female	Male	Female	Male	Female	Male	Female
L_∞	252.6	261.4	240.4	250.3	271.8	280.4	294.0	343.8
	(3.652)	(3.397)	(3.794)	(4.278)	(22.713)	(19.882)	(29.607)	(47.921)
k	0.115	0.110	0.145	0.138				
	(0.005)	(0.004)	(0.008)	(0.008)				
t_0	−3.916	−4.207	−2.781	−2.990	−2.473	−2.608	−0.704	−0.468
	(0.143)	(0.147)	(0.154)	(0.186)	(0.931)	(0.896)	(0.279)	(0.186)
K					0.051	0.049	0.023	0.011
					(0.034)	(0.030)	(0.013)	(0.007)
m					−0.551	−0.578	−1.288	−1.639
					(0.472)	(0.436)	(0.308)	(0.243)

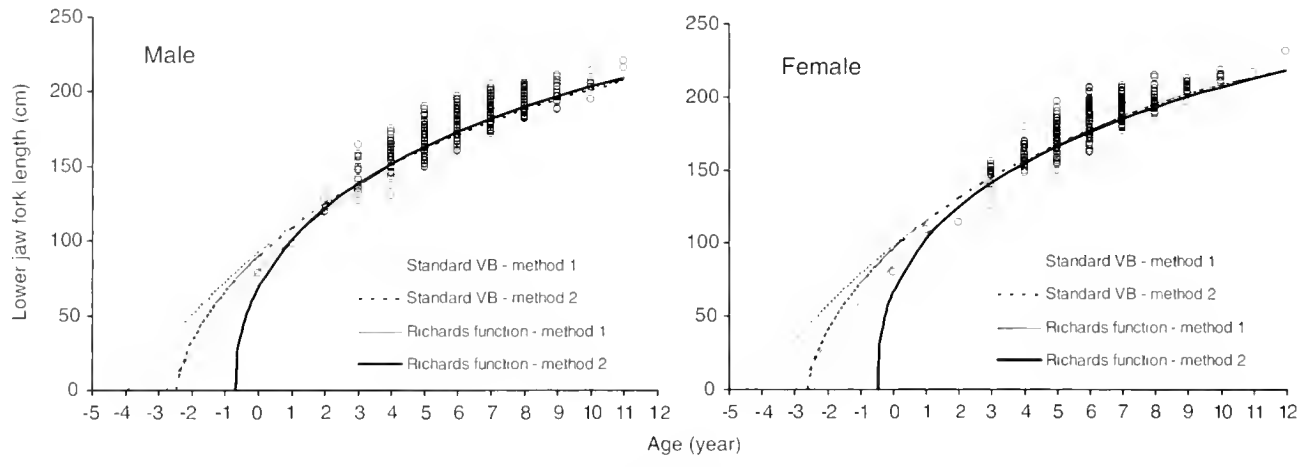

Figure 8

Observed and back-calculated length-at-age and standard von Bertalanffy and Richards function model-predicted growth curves for male and female sailfish (*I. platypterus*) in the waters off eastern Taiwan.

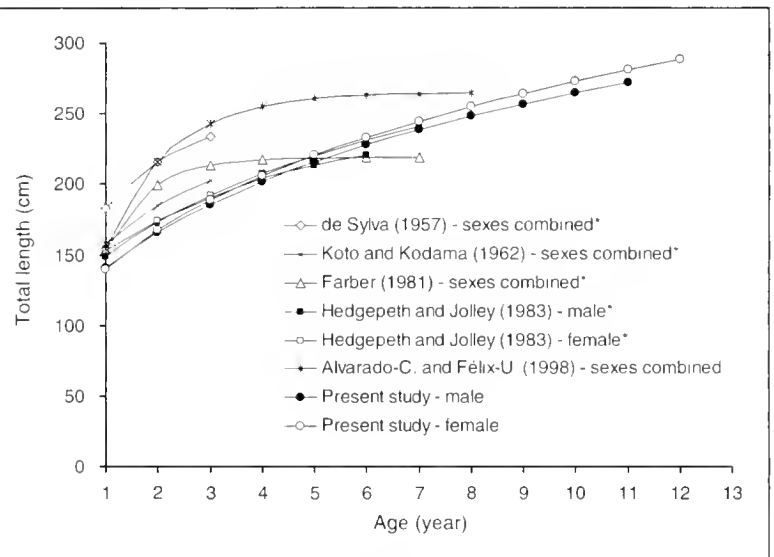

Figure 9

A comparison of the growth curves for sailfish (*I. platypterus*) estimated by different authors. (* Data from Table 1 of Hedgepeth and Jolley, 1983.)

Even though the aging method used in the present study is the same as that of Hedgepeth and Jolley (1983) and Alvarado-Castillo and Félix-Uraga (1998), there are nevertheless differences in the estimated length-at-age. This difference could be due to spatial differences in growth, the range of ages and sizes used in the analysis, or the form of the growth model applied. The size range in the present study is broader than those in previous studies and the growth curve is based on the Richards function rather than the standard VB function. Therefore, we believe that our growth parameter estimates are more appropriate for use in stock assessments of the sailfish population in the western Pacific Ocean.

Acknowledgments

The authors express sincere gratitude to André Punt, School of Aquatic and Fishery Sciences, University of Washington, for his valuable comments and comprehensive editing of the manuscript. This study was in part supported financially by the "Fisheries Agency, Council of Agriculture, Taiwan," through grant 91AS-2.5.1-F1(7) to Chi-Lu Sun.

Literature cited

Akaike, H.
1969. Fitting autoregressive models for prediction. Ann. Inst. Stat. Math. 21:243–247.

Alvarado-Castillo, R. M., and R. Félix-Uraga.
1996. Age determination in *Istiophorus platypterus* (Pisces: Istiophoridae) in the south of the Gulf of California, Mexico. Rev. Biol. Trop. 44:233–239.
1998. Growth of *Istiophorus platypterus* (Pisces: Istiophoridae) from the south of the Gulf of California. Rev. Biol. Trop. 46:115–118.

Antoine, L. M., J. J. Mendoza, and P. M. Cayré.
1983. Progress of age and growth assessment of Atlantic skipjack tuna, *Euthynnus pelamis*, from dorsal fin spines. NOAA Tech. Rep. NMFS 8:91–97.

Beamish, R. J., and D. A. Fournier.
1981. A method for comparing the precision of a set of age determinations. Can. J. Fish. Aquat. Sci. 38:982–983.

Beamish, R. J., and G. A. McFarlane.
1983. Validation of age determination estimates, the forgotten requirement. NOAA Tech. Rep. NMFS 8:29–33.
Beardsley, G. L., N. R. Merrett, and W. J. Richards.
1975. Synopsis of the biology of sailfish, *Istiophorus platypterus* (Shaw and Nodder, 1791). NOAA Tech. Rep. NMFS SSRF 675:95–120.
Berkeley, S. A., and E. D. Houde.
1983. Age determination of broadbill swordfish, *Xiphias gladius*, from the Straits of Florida, using anal fin spine sections. NOAA Tech. Rep. NMFS 8:137–146.
Campana, S. E.
2001. Accuracy, precision and quality control in age determination, including a review of the use and abuse of age validation methods. J. Fish. Biol. 59:197–242.
Cayré, P. M., and T. Diouf.
1983. Estimated age and growth of little tunny, *Euthynnus alletteratus*, off the coast of Senegal, using dorsal find spine sections. NOAA Tech. Rep. NMFS 8:105–110.
Chen, Y., D. A. Jackson, and H. H. Harvey.
1992. A comparison of von Bertalanffy and polynomial functions in modelling fish growth data. Can. J. Fish. Aquat. Sci. 49:1228–1235.
Compeán-Jimenez, G., and F. X. Bard.
1983. Growth of increments on dorsal spines of eastern Atlantic bluefin tuna, *Thunnus thynnus*, and their possible relation to migratory patterns. NOAA Tech. Rep. NMFS 8:77–86.
de Sylva, D. P.
1957. Studies on the age and growth of the Atlantic sailfish, *Istiophorus americanus* (Cuvier), using length-frequency curves. Bull. Mar. Sci. Gulf Caribb. 7:1–20.
Ehrhardt, N. M.
1992. Age and growth of swordfish, *Xiphias gladius*, in the northwestern Atlantic. Bull. Mar. Sci. 50:292–301.
Ehrhardt, N. M., R. J. Robbins, and F. Arocha.
1996. Age validation and estimation of growth of swordfish, *Xiphias gladius*, in the northwest Atlantic. ICCAT (International Commission for the Conservation of Tunas) Col. Vol. Sci. Pap. 45(2):358–367.
Hayashi, Y.
1976. Studies on the red tilefish in the east China sea—I. A fundamental consideration for age determination from otoliths. Bull. Jap. Soc. Sci. Fish. 42:1237–1242.
Hedgepeth, M. Y., and J. W. Jolley Jr.
1983. Age and growth of sailfish, *Istiophorus platypterus*, using cross section from the fourth dorsal spine. NOAA Tech. Rep. NMFS 8:131–135.
Hernández-Herrera, A., and M. Ramírez-Rodríguez.
1998. Spawning seasonality and length at maturity of sailfish (*Istiophorus platypterus*) off the Pacific coast of Mexico. Bull. Mar. Sci. 63:459–467.
Hill, K. T., G. M. Cailliet, and R. L. Radtke.
1989. A comparative analysis of growth zones in four calcified structures of Pacific blue marlin, *Makaira nigricans*. Fish. Bull. 87:829–843.
Jolley, J. W., Jr.
1974. On the biology of Florida east coast Atlantic sailfish, (*Istiophorus platypterus*). NOAA Tech. Rep. NMFS SSRF 675:81–88.
1977. The biology and fishery of Atlantic sailfish, *Istiophorus platypterus*, from southeast Florida. Fla. Mar. Res. Publ. 28, 31 p.
Koto, T., and K. Kodama.
1962. Some considerations on the growth of marlins, using size-frequencies in commercial catches. 1. Attempts to estimate the growth of sailfish. Rep. Nankai. Reg. Fish. Res. Lab. 15:97–108.
Megalofonou, P.
2000. Age and growth of Mediterranean albacore. J. Fish. Biol. 57:700–715.
Nakamura, I.
1985. FAO species catalogue. Billfish of the world. An annotated and illustrated catalogue of marlins, sailfishes, spearfishes, and swordfishes known to date. FAO Fish. Synop. 125(5), 65 p
Paul, L. J.
1992. Age and growth studies of New Zealand marine fisheries, 1921–90: a review and bibliography. Aust. J. Mar. Freshw. Res. 43:879–912.
Powers, J. E.
1983. Some statistical characteristics of ageing data and their ramification in population analysis of oceanic pelagic fishes. NOAA Tech. Rep. NMFS 8:19–24.
Prince, E. D., D. W. Lee, C. A. Wilson, and S. A. Berkeley.
1988. Use of marginal increment analysis to validate the anal spine method for ageing Atlantic swordfish and other alternatives for age determination. ICCAT Col. Vol. Sci. Pap. 27:194–201.
Prince, E. D., D. W. Lee, C. A. Wilson, and J. M. Dean.
1986. Longevity and age validation of a tag-recaptured Atlantic sailfish, *Istiophorus platypterus*, using dorsal spines and otoliths. Fish. Bull. 84:493–502.
Prince, E. D., D. W. Lee, C. J. Cort, G. A. McFarlane, and A. Wild.
1995. Age validation evidence for two tag-recaptured Atlantic albacore, *Thunnus alalunga*, based on dorsal, anal, and pectoral finrays, vertebrae, and otoliths. *In* Recent developments in fish otolith research (D. H. Sector, J. M. Dean, and S. E. Campana, eds.), p. 375–396. Univ. South Carolina Press, Columbia, SC.
Radtke, R. L.
1983. Istiophorid otoliths: extraction, morphology, and possible use as ageing structures. NOAA Tech. Rep. NMFS 8:123–129.
Radtke, R. L., and J. M. Dean.
1981. Morphological features of the otoliths of the sailfish, *Istiophorus platypterus*, useful in age determination. Fish. Bull. 79:360–367.
Richards, F. J.
1959. A flexible growth function for empirical use. J. Exp. Bot. 10:290–300.
Sun, C. L., C. L. Huang, and S. Z. Yeh.
2001. Age and growth of the bigeye tuna, *Thunnus obesus*, in the western Pacific Ocean. Fish. Bull. 99:502–509.
Sun, C. L., S. P. Wang, and S. Z. Yeh.
2002. Age and growth of swordfish (*Xiphias gladius* L.) in the waters around Taiwan determined from anal-fin rays. Fish. Bull. 100:822–835.
Tserpes, G., and N. Tsimenides.
1995. Determination of age and growth of swordfish, *Xiphias gladius* L., 1758, in the eastern Mediterranean using anal-fin spines. Fish. Bull. 93:549–602.
von Bertalanffy, L.
1938. A quantitative theory of organic growth (Inquiries on growth laws. II). Hum. Biol. 10:181–213.
Williams, F.
1970. The sport fishery for sailfish at Malindi, Kenya, 1958–1968, with some biological notes. Bull. Mar. Sci. 20(4):830–852.

Abstract—A density prediction model for juvenile brown shrimp (*Farfantepenaeus aztecus*) was developed by using three bottom types, five salinity zones, and four seasons to quantify patterns of habitat use in Galveston Bay, Texas. Sixteen years of quantitative density data were used. Bottom types were vegetated marsh edge, submerged aquatic vegetation, and shallow nonvegetated bottom. Multiple regression was used to develop density estimates, and the resultant formula was then coupled with a geographical information system (GIS) to provide a spatial mosaic (map) of predicted habitat use. Results indicated that juvenile brown shrimp (<100 mm) selected vegetated habitats in salinities of 15–25 ppt and that seagrasses were selected over marsh edge where they co-occurred. Our results provide a spatially resolved estimate of high-density areas that will help designate essential fish habitat (EFH) in Galveston Bay. In addition, using this modeling technique, we were able to provide an estimate of the overall population of juvenile brown shrimp (<100 mm) in shallow water habitats within the bay of approximately 1.3 billion. Furthermore, the geographic range of the model was assessed by plotting observed (actual) versus expected (model) brown shrimp densities in three other Texas bays. Similar habitat-use patterns were observed in all three bays—each having a coefficient of determination >0.50. These results indicate that this model may have a broader geographic application and is a plausible approach in refining current EFH designations for all Gulf of Mexico estuaries with similar geomorphological and hydrological characteristics.

Manuscript approved for publication 22 December 2003 by Scientific Editor.

Manuscript received 20 January 2004 at NMFS Scientific Publications Office.

Fish. Bull. 102:264–277 (2004).

A habitat-use model to determine essential fish habitat for juvenile brown shrimp (*Farfantepenaeus aztecus*) in Galveston Bay, Texas

Randall D. Clark

John D. Christensen

Mark E. Monaco

Biogeography Program
Center for Coastal Monitoring and Assessment
National Center for Coastal Ocean Science
National Ocean Service, NOAA
Silver Spring, Maryland 20910

E-mail address (For R. D. Clark): Randy.Clark@noaa.gov

Philip A. Caldwell

Geoffrey A. Matthews

Thomas J. Minello

Fishery Ecology Branch
Galveston Southeast Fisheries Science Center Laboratory
National Marine Fisheries Service, NOAA
Galveston, Texas 77550

Shallow estuarine habitats, whose complexity promotes survival and growth, are used by many young fish and macroinvertebrate species (Boesch and Turner, 1984). A complete understanding of how these habitats sustain species productivity is unknown and has become a focal point of federal fishery management programs. The National Marine Fisheries Service (NMFS) has developed guidelines to identify essential fish habitat (EFH) for all federally managed species based on four levels of available information that encompass the ecological linkages between habitats and fishery production. Examination of habitat-use patterns (habitat-related densities) are needed to determine which habitats are likely to be most essential. These patterns are measurable and can be reasonable indicators of habitat value. Relative habitat values have been estimated by comparing animal densities under the assumption that high densities reflect greater habitat quality and preferred habitat (Pearcy and Myers, 1974; USFWS, 1981; Zimmerman and Minello, 1984; Sogard and Able, 1991; Baltz et al., 1993).

Considerable bottom-type variation exists in northern Gulf of Mexico estuaries, including intertidal marsh, submerged aquatic vegetation, oyster reef, mangroves, tidal mudflats, and subtidal bay bottom. Within each of these habitats, environmental and structural gradients may affect the functional role or importance of these habitats for particular species. To understand these relationships, fisheries independent monitoring (FIM) data are needed to determine species-habitat affinities that provide evidence that not all habitats are of equal importance for the maintenance of a population (Monaco et al., 1998; Minello 1999; Beck et al., 2001). Habitat affinities may change with spatial and temporal fluctuations of environmental variables, such as salinity and temperature (Copeland and Bechtel, 1974; Baltz et al., 1998).

In this study we developed predictive models that estimate brown shrimp (*Farfantepenaeus aztecus*, formerly *Penaeus aztecus* [see Perez-Farfante and Kensley, 1997]) habitat-use patterns and interactions as a function of density-independent processes in Galveston Bay, Texas. Previous com-

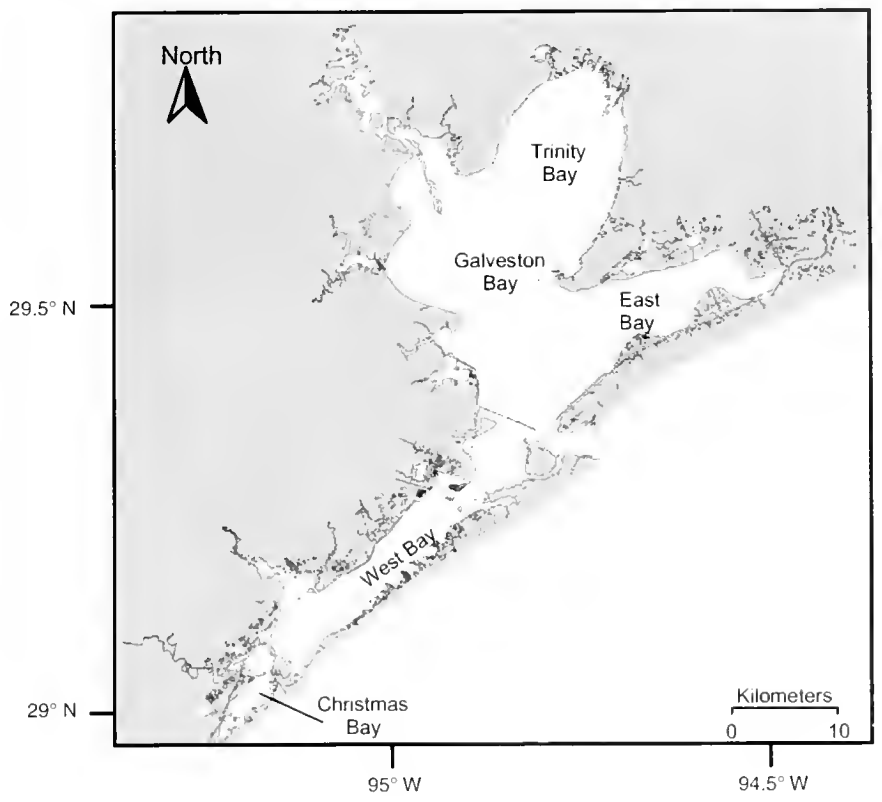

Figure 1
Map of Galveston Bay, Texas.

parisons of brown shrimp densities among different bottom types in Louisiana and Texas estuaries have been conducted within limited temporal and spatial scales (Peterson and Turner, 1994; Zimmerman et al., 1984; Zimmerman et al., 1990b; Rozas and Minello, 1998; Minello, 1999).

Our work expands upon these studies by developing a multivariate bottom-type use and environmental model incorporated into a geographic information system (GIS) that provides a spatial assessment of habitat use. In addition, the model is designed to be transferable to other northern Gulf of Mexico estuaries and thus would allow fishery managers to identify the relative importance of habitat types for population maintenance and recruitment into the fishery.

Materials and methods

Geographic setting

The Galveston Bay complex (Fig. 1) encompasses approximately 2020 km^2 and is one of the largest estuaries in the northern Gulf of Mexico (NOAA, 1989). Comprising several major embayments, including Trinity, Galveston, East, and West bays, the complex contains many smaller interconnecting subbays, rivers, streams, tidal creeks, wetlands, reefs, and tidal flats around its periphery. The bay bottom is mostly flat and shallow (mean depth is approximately 2 m) and has slightly elevated oyster reefs, elevated dredge material areas, river channels, and deeper dredged navigation channels.

Data collection

Sixteen years (1982–97) of brown shrimp density data were analyzed to quantify areas of potential EFH. A total of 46,080 brown shrimp were captured during this time period with a mean total length of 27.5 mm (Fig. 2). Data from published studies by Czapla (1991), Minello et al. (1991), Minello and Zimmerman (1992), Minello and Webb (1997), Rozas and Minello (1998), Zimmerman et al. (1984, 1989, 1990a, 1990b), Zimmerman and Minello (1984), and various unpublished sources from the Galveston Laboratory of the National Marine Fisheries Service were combined to comprise a comprehensive density database of associated bottom-type and environmental data that would support model development and GIS analyses. All samples were collected by using a drop trap sampler, described in Zimmerman et al. (1984), which employs large cylinders (1.0 or 2.6 m^2 area) released from a boom affixed to a boat to entrap organisms. This quantitative technique samples fishes and macro-invertebrates in highly structured shallow-water habitats such as salt marshes, seagrass beds, and oyster reefs where the efficiency of conventional trawl and bag-seine gear is diminished.

Habitat mapping

The underlying spatial framework for incorporating model predictions into the GIS consisted of six maps: four salinity periods, one bathymetric map, and one map defining bottom-type distribution. All GIS maps were developed in Universal Transverse Mercator projection, UTM, datum-1983, zone-15, using ArcView 3.1 (Redlands, CA) software. Each map consisted of 10 × 10 m grid cells where each cell contained pertinent salinity, depth, or bottom-type information.

Salinity maps were developed from depth-averaged salinity models by using historical Galveston Bay data collected during 1979–90 (Orlando et al., 1993). Four salinity periods were identified to represent typical salinity conditions under average seasonal freshwater inflow: low (March–June), increasing (July), high (August–October), and decreasing (November–February). Five isohalines were developed to display spatial salinity distribution (Christensen et al.[1]): 0–0.5, 0.51–5, 5.1–15, 15.1–25, and >25 parts per thousand (ppt) (Fig. 3).

Bottom types from the drop sample database were divided into three categories:

Marsh edge (ME)	intertidal marsh within 5 meters of open water habitat. This category consisted primarily of saltmarsh cord grass (*Spartina alterniflora*), and smaller proportions of salt meadow-grass (*Spartina patens*), black needlerush (*Juncus roemerianus*), salt grass (*Distichlis spicata*), bullrushes (*Scirpus* spp.), and cattails (*Typha* spp.);
Submerged aquatic vegetation (SAV)	consisted primarily of shoalgrass (*Halodule wrightii*), wigeongrass (*Ruppia maritima*), and a sporadic distribution of wild celery (*Vallisneria americana*);
Shallow non-vegetated bottom (SNB)	generally restricted to waters less than 1 meter deep, including creeks, ponds, shoreline, and open bay habitat.

Density data for other bottom types were limited and were not used in the analysis.

Wetland maps, used in the creation of the bottom type map in the GIS, were obtained from the U.S. Fish and Wildlife Service's national wetland inventory (NWI). The NWI maps were obtained as vector files, created by digitizing boundaries between wetland types from 1989 aerial photographs and classified by using the classification scheme of Cowardin et al. (1979). Regularly flooded emergent vegetation and submerged aquatic vegetation distributions from the NWI maps of Galveston Bay were chosen to represent ME and SAV, respectively, from the drop sample database. Nonvegetated open water areas with depths greater than 1 m were eliminated throughout the bay to reflect depth range from the drop sample database. This elimination was done by plotting approximately 400,000 depth soundings obtained from the National Geophysical Data Center (NGDC), and a bathymetric grid map was developed in 1-m contours with ArcView 3.1 (6 nearest neighbors, power=2). The nonvegetated open water map from NWI was overlaid with the bathymetric map and only those areas within the 1-m contour were extracted and added to the bottom-type map (Fig. 4).

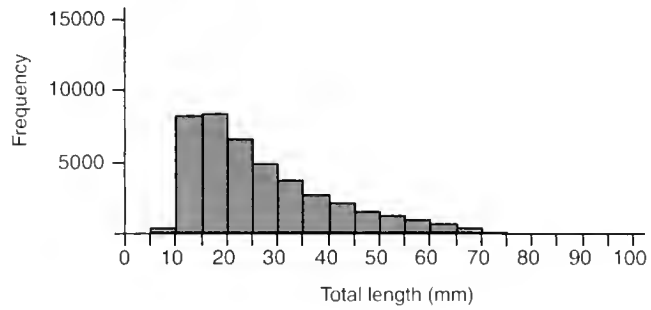

Figure 2

Total-length frequency distribution for juvenile brown shrimp captured in drop traps within Galveston Bay (1982–97).

Two maps were used to plot (map) seasonal model predictions, bottom type, and the respective salinity period. The salinity maps did not completely correspond temporally with seasons defined by cluster analysis of *in situ* temperature recordings from the density database. Salinity periods were chosen to correlate with temporal seasons based on maximum monthly overlap to develop the seasonal prediction maps: low salinity (spring); increasing salinity (summer); high salinity (fall); and decreasing salinity (winter).

The total area of Galveston Bay (2020 km^2) was determined by combining the total areas for regularly flooded emergent vegetation, irregularly flooded emergent vegetation, SAV, and open water classifications from NWI data. The bottom-type map reflects the study area and totaled 565.6 km^2 after excluding all areas >1 m in depth and with irregularly flooded emergent vegetation: SNB = 476.2 km^2, ME = 84.9 km^2, and SAV = 4.5 km^2. Initially, NWI's SAV classification totaled 5.7 km^2, but the final SAV coverage was reduced to 4.5 km^2 based on SAV mapping by White et al. (1993).

Regression modeling

ANOVA and Tukey-Kramer multiple means comparisons were used to determine if mean density varied significantly by bottom type, salinity zone, and season. Multiple regression with significant predictors was used to predict mean log density. The model was then applied to the GIS maps

[1] Christensen, J. D., T. A. Battista, M. E. Monaco, and C. J. Klein. 1997. Habitat suitability modeling and GIS technology to support habitat management: Pensacola Bay, Florida Case Study, 58 p. NOAA/NOS Strategic Environmental Assessments Division, Silver Spring, MD.

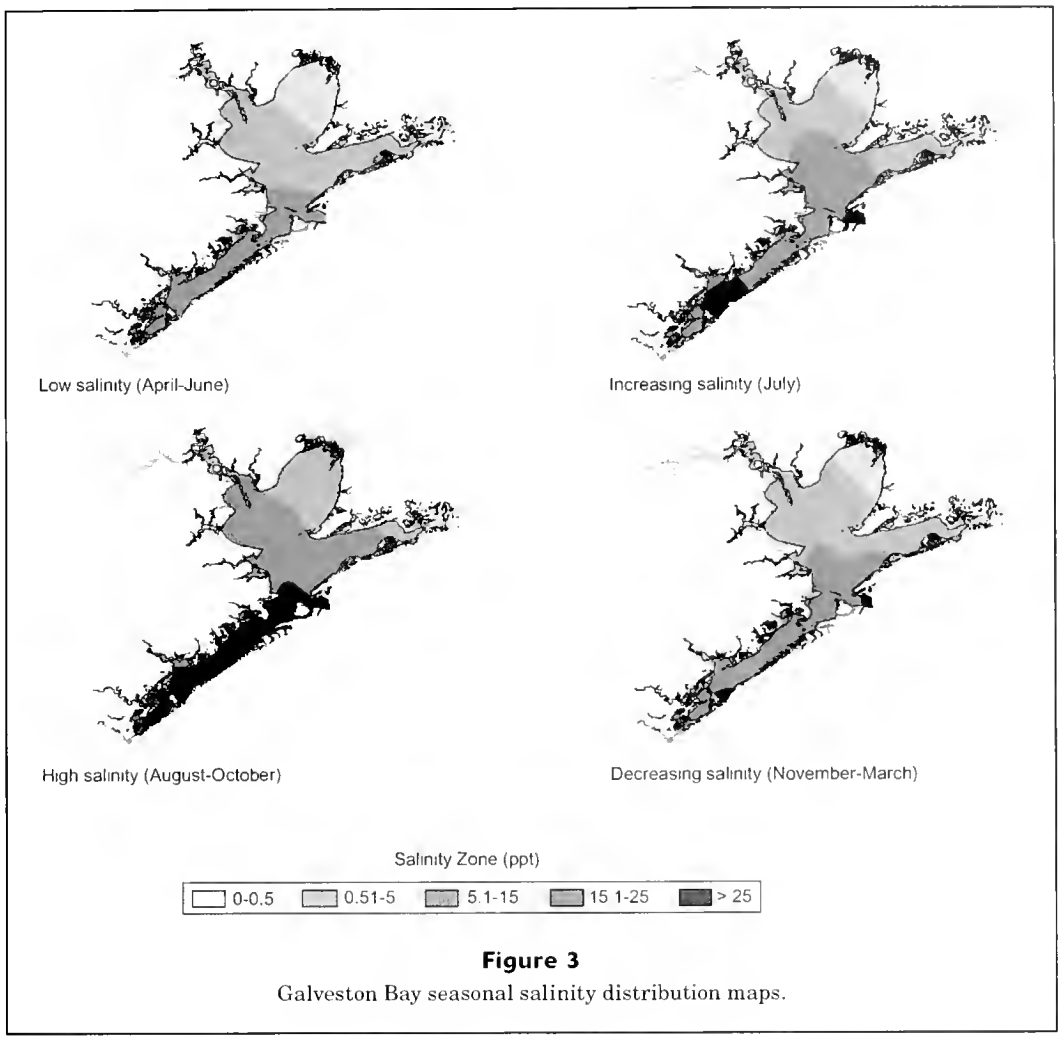

Figure 3
Galveston Bay seasonal salinity distribution maps.

to spatially display model predictions in each 10 × 10 m cell. The resulting values for each cell (predicted mean log density) were converted to numbers/m^2 and reclassified into 5 percentiles based on their resultant distribution: 0–20%, 21–40%, 41–60%, 61–80%, and 81–100%. All statistical analyses were conducted with JMP statistical software (SAS Institute, Cary, NC).

Due to difficulties in creating continuous salinity and temperature contour maps in GIS, these variables were classified as follows: salinity was classified by one of the five isohaline zones described previously and analyzed as such to determine its influence on brown shrimp distribution; and water temperature was classified by season determined by cluster analysis and analyzed to examine possible temporal effects of brown shrimp distribution.

Spatial patterns were evaluated by comparing the predicted mean log density values with the observed mean log density values from Galveston Bay drop samples. Additionally, the model's predictive performance was assessed by comparing the predicted mean log density values with observed mean log density values from samples collected in Matagorda, Aransas, and San Antonio bays using the same collection method. With this approach, the assumption was made that brown shrimp modeled in Galveston Bay respond similarly to the range of biotic and abiotic factors in the other bay systems.

Drop sample data collected during July–September 1984 (n=128), and April–June 1985 (n=144) from West Bay (ME, SNB) and Christmas Bay (ME, SAV, and SNB) were used to examine bottom-type preference or selectivity. Tukey-Kramer multiple comparisons test was used to compare log density patterns in areas where ME and SAV occurred together and in areas where SAV was not present.

Results

Brown shrimp model

ANOVA and Tukey-Kramer pair-wise comparisons showed significant differences in brown shrimp log density between the three bottom types, five salinity zones, and four seasons (Fig. 5). Multiple regression models were run with these discreet variables (Mahon and Smith, 1989;

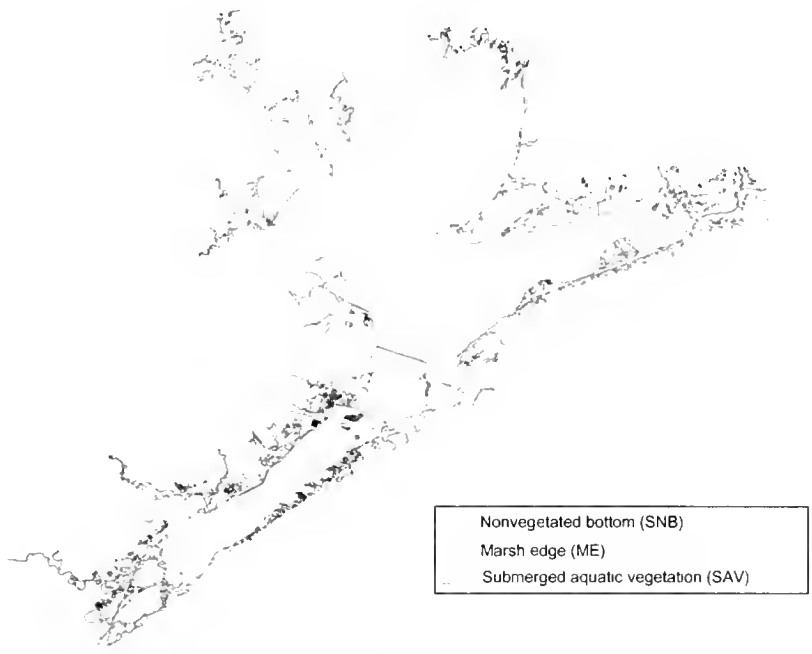

Figure 4

Spatial distribution of Galveston Bay bottom types used in the multivariate regression model.

Table 1

Results of the least squares multiple regression model for predicting seasonal brown shrimp density in Galveston Bay, Texas. * = significant at $P < 0.05$.

Model fit	r^2	Mean	Observations (n)	Mean square error	
	0.73	0.47	47	0.20	
			ANOVA		
Source	df	Sum of squares	Mean square	F ratio	Prob > F
Model	17	5.74	0.33	8.43	
Error	29	1.61	0.04		
Total	46	6.90			<0.0001*
			Effects		
Source	df	Sum of squares		F ratio	Prob > F
Season	3	1.85		15.43	<0.0001*
Bottom type	2	0.61		7.57	0.0023*
Salinity zone	4	3.15		19.68	<0.0001*
Bottom type × Salinity zone	8	0.86		2.69	0.0242*

Krumgalz et al., 1992; Garrison, 1999) and we tested for possible interactions between the variables. Only the interaction between bottom type and salinity zone yielded statistically significant results. ANOVA results for the model including the bottom-type and salinity-zone interaction term (Table 1) and variable coefficients (Table 2) fitted

Table 2

Variable coefficients (log +1) derived from brown shrimp multivariate regression model. ME = marsh edge; SAV = submerged aquatic vegetation; SNB = shallow nonvegetated bottom.

y-intercept	Bottom type	Season	Salinity zone	Bottom type × salinity zone
0.335	0.113 (ME)	0.239 (spring)	−0.525 (0–0.5)	−0.104 (ME/0–0.5)
	0.043 (SAV)	0.165 (summer)	−0.147 (0.5–5)	−0.055 (SAV/0–0.5)
	−0.156 (SNB)	−0.045 (fall)	0.079 (5–15)	0.159 (SNB/0–0.5
		−0.359 (winter)	0.286 (15–25)	0.273 (ME/0.5–5)
			0.307 (>25)	−0.396 (SAV/0.5–5)
				0.123 (SNB/0.5–5)
				−0.030 (ME/5–15)
				0.049 (SAV/5–15)
				−0.018 (SNB/5–15)
				−0.119 (ME/15–25)
				0.288 (SAV/15–25)
				−0.168 (SNB/15–25)
				−0.018 (ME/>25)
				0.114 (SAV/>25)
				−0.096 (SNB/>25)

the data well ($r^2=0.73$, $n=47$). Overall, density predictions were highest in the spring, declined through summer and fall, and reached the lowest values during winter (Fig. 6). SNB density predictions were highest in the >25 ppt salinity zone and declined as salinity declined in the estuary. ME density predictions exhibited similar density prediction trends; however, a smaller peak was observed in the 0.5–5 ppt salinity zone. This result may be an artifact of two fall samples that exhibited high density within this salinity zone. Density predictions within SAV were near zero in the lower two salinity zones, peaked in the 15–25 ppt salinity zone, and slightly decreased in the >25 ppt salinity zone.

Model prediction maps

For all seasons, highest density predictions corresponded with ME and SAV bottom types within the region of the bay with highest salinity—Christmas and West bays (Fig. 7). Density predictions decreased within all bottom types as salinity declined in the middle and upper regions of the bay. Spring density predictions were the highest; maximum values were predicted within ME (6.14/m^2) and SAV (14.49/m^2) located in Christmas and West bays (Fig. 7). Density predictions steadily declined through the middle bay and declined to 1/m^2 or less within SAV and SNB in the upper region of the bay (Trinity Bay) where salinities were less than 5 ppt. Density predictions during summer, fall, and winter were lower than those observed during the spring but exhibited similar spatial trends—higher predictions within the high salinity vegetated bottom types, and decreasing with decreasing salinity.

Model performance

Spatial patterns were assessed by plotting predicted mean density values from the model and observed mean density

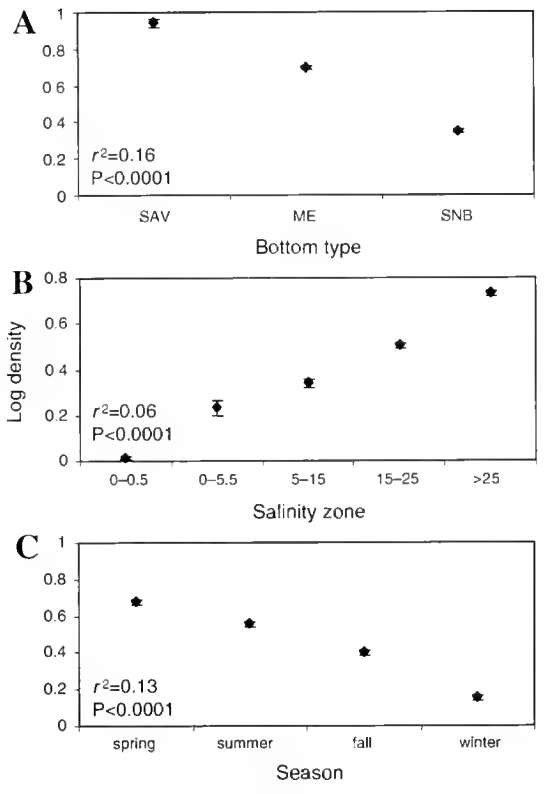

Figure 5

Analysis of variance and Tukey–Kramer pair-wise comparisons of brown shrimp density between (**A**) bottom type, (**B**) salinity zone and, (**C**) season. Mean densities are represented by solid diamonds and lines determine standard error. SAV = submerged aquatic vegetation; ME = marsh edge; SNB = shallow nonvegetated bottom.

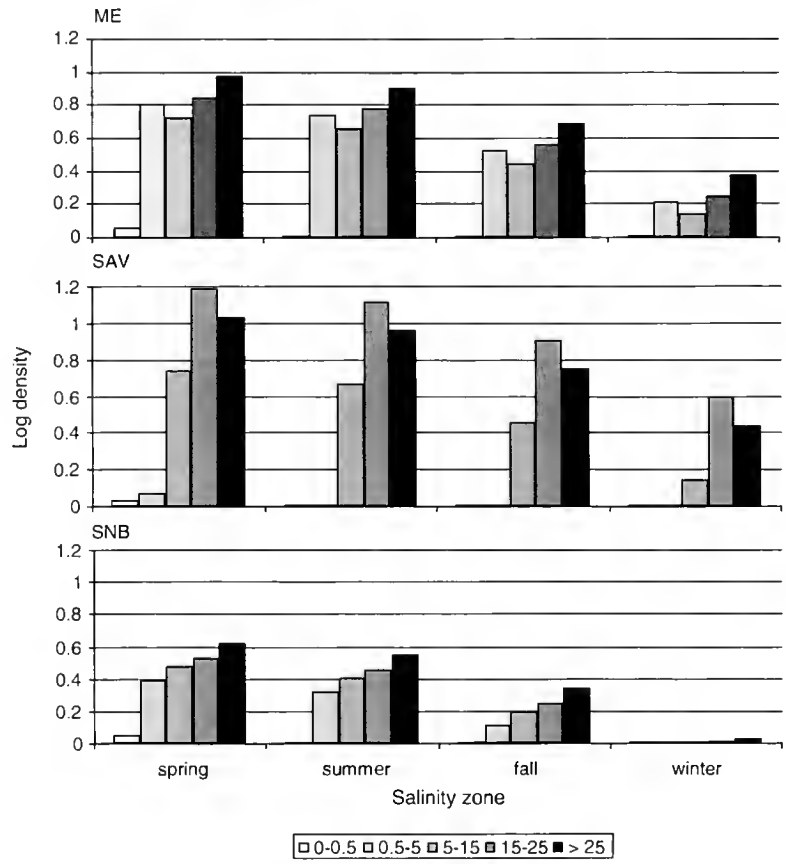

Figure 6

Seasonal density predictions for brown shrimp (*F. aztecus*) by bottom type and salinity zone. ME = marsh edge; SAV = submerged aquatic vegetation; SNB = shallow nonvegetated bottom.

values from drop sample data collected in Galveston Bay. Regression analysis from this plot exhibited a strong positive relationship (r^2=0.83, P<0.0001) between predicted and observed density data (Fig. 8). This analysis was performed to verify how the model represented the observed density data.

Model performance and transferability were assessed by regressing predicted mean density values from the Galveston Bay model on observed mean density values from drop sample data collected in Matagorda, San Antonio, and Aransas bays (Fig. 9). Regression analysis produced a positive relationship for the entire drop sample data from these bays combined (r^2=0.56) and individually: Matagorda—r^2=0.54; San Antonio—r^2=0.57; and Aransas—r^2=0.56. In Aransas and San Antonio bays, brown shrimp densities were greatest during the spring within the SAV bottom type and within salinities >15 ppt. In Matagorda Bay, brown shrimp densities were greatest in the spring within ME bottom types in waters >15 ppt. No SAV samples were taken in this estuarine system.

Use of bottom types

Results from spring (1985) and fall (1984) drop samples within Christmas and West Bay (in lower Galveston Bay) bottom types revealed significantly greater brown shrimp densities in Christmas Bay SAV than adjacent ME and SNB (P<0.0001). Brown shrimp densities in West Bay ME were not significantly different from Christmas Bay SAV but were significantly greater than densities within adjacent SNB and Christmas Bay ME and SNB bottom types (Fig. 10).

The model results were also used to roughly estimate an overall population of approximately 1.3 billion juvenile brown shrimp in Galveston Bay during the spring season, by multiplying predicted densities by bottom-type area (Table 3). Total area of bottom types in Galveston Bay were as follows: 4.5 km^2 (SAV); 84.9 km^2 of marsh edge (ME); and 1627.2 km^2 of nonvegetated bottom (29% [476.2 km^2] of the latter area was considered SNB). On the basis of predicted densities in different salinity regimes, we estimated that there would be 51.0 million shrimp

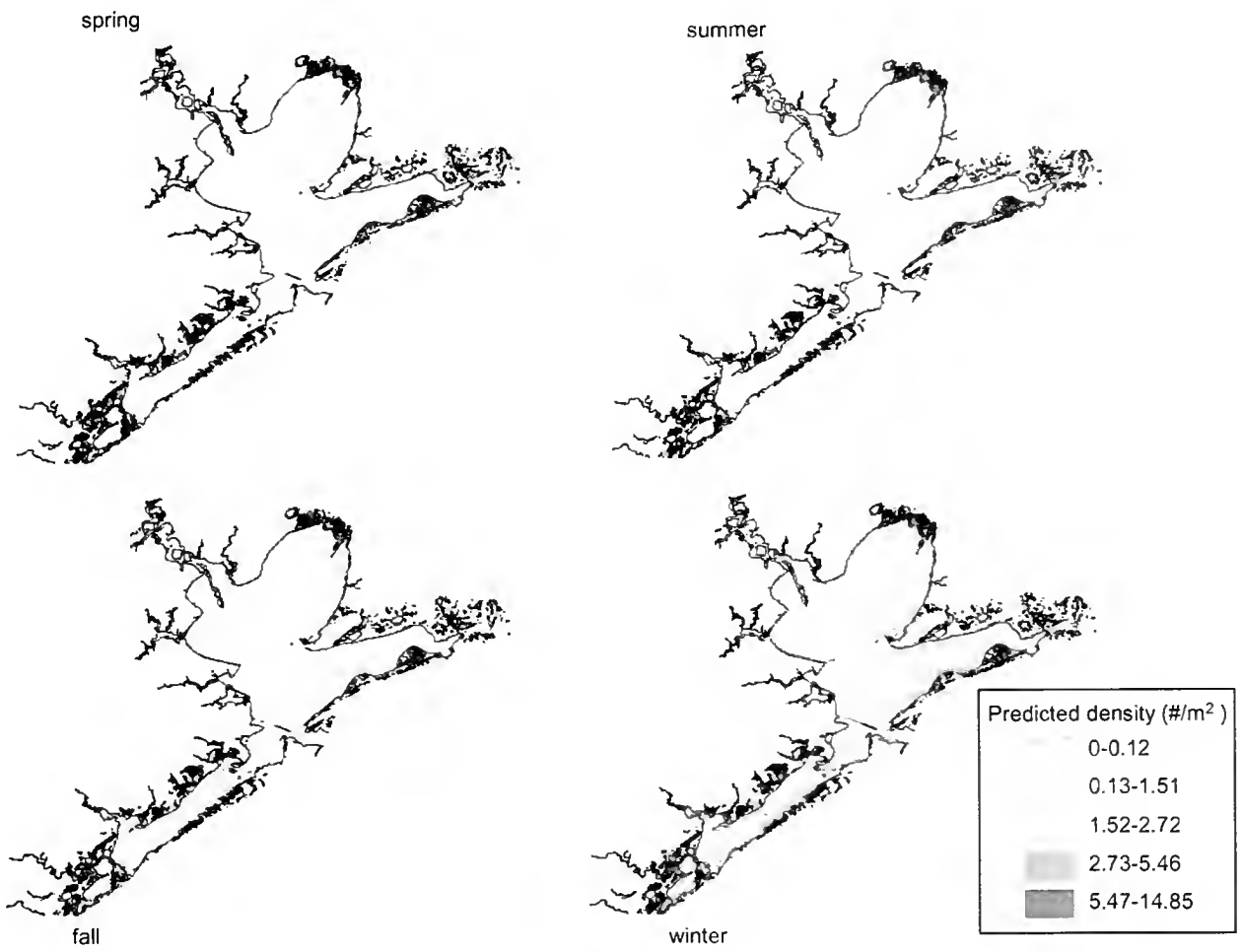

Figure 7

Seasonal spatial distribution maps of predicted densities for brown shrimp (*F. aztecus*).

in SAV and 858.7 million shrimp in SNB. We used marsh edge densities to estimate 473.5 million shrimp in regularly flooded vegetation or about 55,700 shrimp per hectare of this habitat type.

Discussion

Various factors are considered important in defining nursery areas for juvenile estuarine-dependent organisms; however, the specific contributions of these factors are poorly understood (Beck et al., 2001). Specific combinations of physiochemical conditions and cyclic primary production that are related to food availability, growth, and sanctuary from predation often define optimal environments (Miller and Dunn, 1980). Barry et al. (1999) considered prey availability to be a necessary component defining the nursery function of estuarine habitats. Shrimp and blue crab production has been correlated with the availability of wetland habitat in estuaries (Turner, 1977; Zimmerman et al., 2000). In the present study, brown shrimp were most abundant in the lower bay where vegetated habitats were most abundant. Zimmerman et al. (1990b) reported that benthic infauna are most abundant in vegetated habitats within lower Galveston Bay and are nutritionally important for penaeids (Zein-Eldin and Renaud, 1986; McTigue and Zimmerman, 1991, 1998). In addition, field and laboratory experiments have shown that brown shrimp growth is positively correlated with the abundance of marsh epiphytes and phytoplankton (Gleason and Zimmerman, 1984).

Most estuarine nekton are adaptable to the highly dynamic environmental conditions exhibited within estuaries (Gifford, 1962; Tagatz, 1971; Zimmerman et al., 1990b). These organisms are commonly found in a wide range of salinities and temperatures and are most affected by sudden changes in these environmental conditions

Table 3

Estimated area (km^2) of each bottom type and salinity zone combination sampled during spring (March–May), and estimated brown shrimp population based on spring density predictions from the model. ME = marsh edge; SAV = submerged aquatic vetetation; SNB = shallow nonvegetated bottom.

Bottom type	Salinity zone (ppt)	Bottom type area (km^2)	Density estimate (number/m^2)	Population estimate (millions)	Shrimp/ha. (thousands)
ME	0–0.5	1.4	0.14	0.2	1428
	0.5–5	1.6	5.50	8.8	55,000
	5–15	22.4	4.44	99.4	44,375
	15–25	59.5	6.14	365.3	61,394
	>25	0	8.46	0	0
	Total 84.9		473.5	55,771	
SAV	0–0.5	1.0	0.09	0.09	9000
	0.5–5	0.03	0.18	0.005	1667
	5–15	0.02	4.56	0.09	45,000
	15–25	3.5	14.52	50.8	145,142
	>25	0	9.91	0	0
	Total 4.5		51.0	114,680	
SNB	0–0.5	29.6	0	0	0
	0.5–5	54.2	1.01	54.7	10,092
	5–15	183.6	1.61	295.6	16,100
	15–25	203.3	2.41	489.9	24,097
	>25	5.5	3.37	18.5	33,636
	Total 476.2		858.7	18,032	
Total	565.6			1383.2	24,455

(Christensen et al., 1997). In laboratory experiments, Zein-Eldin and Aldrich (1965) concluded that higher salinities are more favorable for brown shrimp. Salinities of 20 ppt or greater were considered optimum in data from Louisiana (Barrett and Gillespie, 1973).

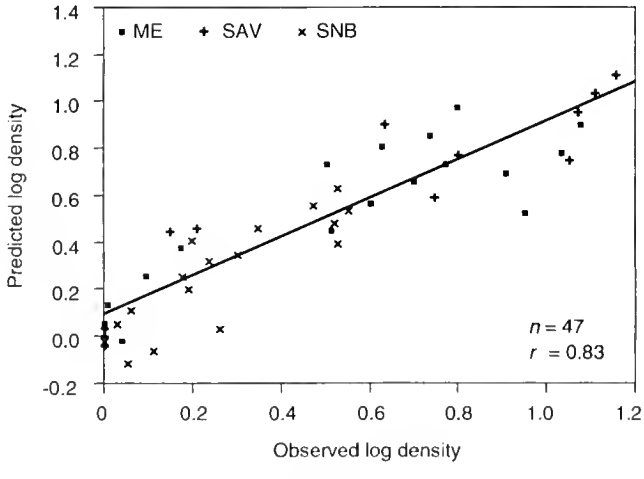

Figure 8

Relationship between predicted and observed densities of brown shrimp (*F. aztecus*) in Aransas, Matagorda and San Antonio bays and predicted densities from the Galveston Bay model. ME = marsh edge; SAV = submerged aquatic vegetation; SNB = shallow nonvegetated bottom.

In the present study, brown shrimp were captured throughout Galveston Bay, but highest densities were observed in the lower bay where salinities were greater than 15 ppt. This spatial trend was further strengthened by greater abundance of vegetated bottom types in the lower portions of the bay, where nearly half of the total marsh edge and 90% of seagrass beds are located (Fig. 4). These bottom types are regularly inundated and provide stable substrate for brown shrimp prey (epiphytic algae and infauna), whereas seasonal oligohaline marsh and SAV habitats in the upper bay may not promote favorable conditions for prey organisms (Zimmerman et al., 1990b). Therefore, salinity effects and the greater availability of vegetated habitats in the lower bay may work in a complementary manner to provide nursery areas for brown shrimp in Galveston Bay.

Previous attempts to examine spatial patterns of abundance and to determine linkages between organisms and habitat included the development of habitat suitability index (HSI) models. Early methods were derived by the U.S. Fish and Wildlife Service (USFWS) for freshwater species, where the HSI was defined as a numerical index that represented the capacity of a given habitat to support a selected species. The scale of HSI values (0–1.0) reflects a linear relationship between suitability and carrying capacity

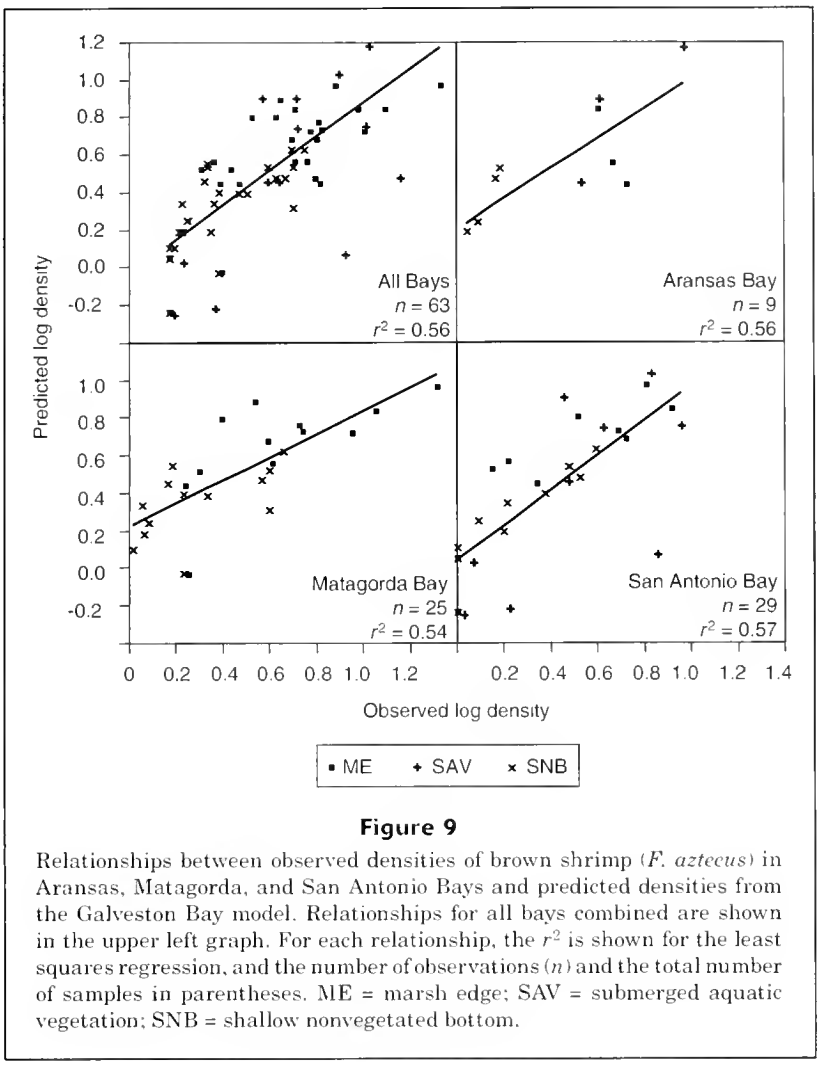

Figure 9

Relationships between observed densities of brown shrimp (*F. aztecus*) in Aransas, Matagorda, and San Antonio Bays and predicted densities from the Galveston Bay model. Relationships for all bays combined are shown in the upper left graph. For each relationship, the r^2 is shown for the least squares regression, and the number of observations (n) and the total number of samples in parentheses. ME = marsh edge; SAV = submerged aquatic vegetation; SNB = shallow nonvegetated bottom.

(USFWS, 1981). Recently, Christensen et al.[1] and Brown et al., 2000, developed suitability indices, based on literature reviews and expert opinion, and raster-based GIS models that produce a spatial view of relative suitability. The Florida Fish and Wildlife Conservation Commission-Marine Research Institute (FMRI) and the National Ocean Service's Center for Coastal Monitoring and Assessment (NOS/CCMA) collaborated to develop a suite of quantitative HSI modeling approaches, using fisheries-independent monitoring catch-per-unit-of-effort (CPUE) data (Rubec et al., 1998, 1999, 2001). These studies used an unweighted geometric mean formula as part of the HSI models to assess overall suitability. This approach assigns equal weight to all factors by using scaled suitability indices as inputs to the model. The regression approach used in this study more appropriately weights density according to the factors in the model and allows a more robust technique to elucidate spatial patterns of habitat use by using actual CPUE data. In addition, the method described in our study can support more complex analyses, such as interaction effects or trophic relationships (or both).

Our ANOVA (Table 1) revealed that season, bottom type, salinity, and the interaction between salinity and bottom type are significant factors that influence the distribution of juvenile brown shrimp in Galveston Bay. The addition of the interaction effect to the model increases the coefficient of determination from 0.63 to 0.73. Without this term in the model, predicted values for brown shrimp density are overestimated compared to the observed density data. Seagrass beds in salinities greater than 15 ppt supported significantly greater densities of brown shrimp than did marsh edge. However, in locations with salinities less than 15 ppt, brown shrimp densities were not significantly different between the two bottom types. These results indicate significantly lower use among all the bottom types analyzed in the fresher portion of the estuary. It is likely that salinity and a combination of other environmental factors directly or indirectly (or directly and indirectly) affect abundance on bottom types and habitat quality in this region. The results indicate that SAV supports greater brown shrimp density than do ME and SNB; however, SAV accounts for less than 1% of the total bottom type within

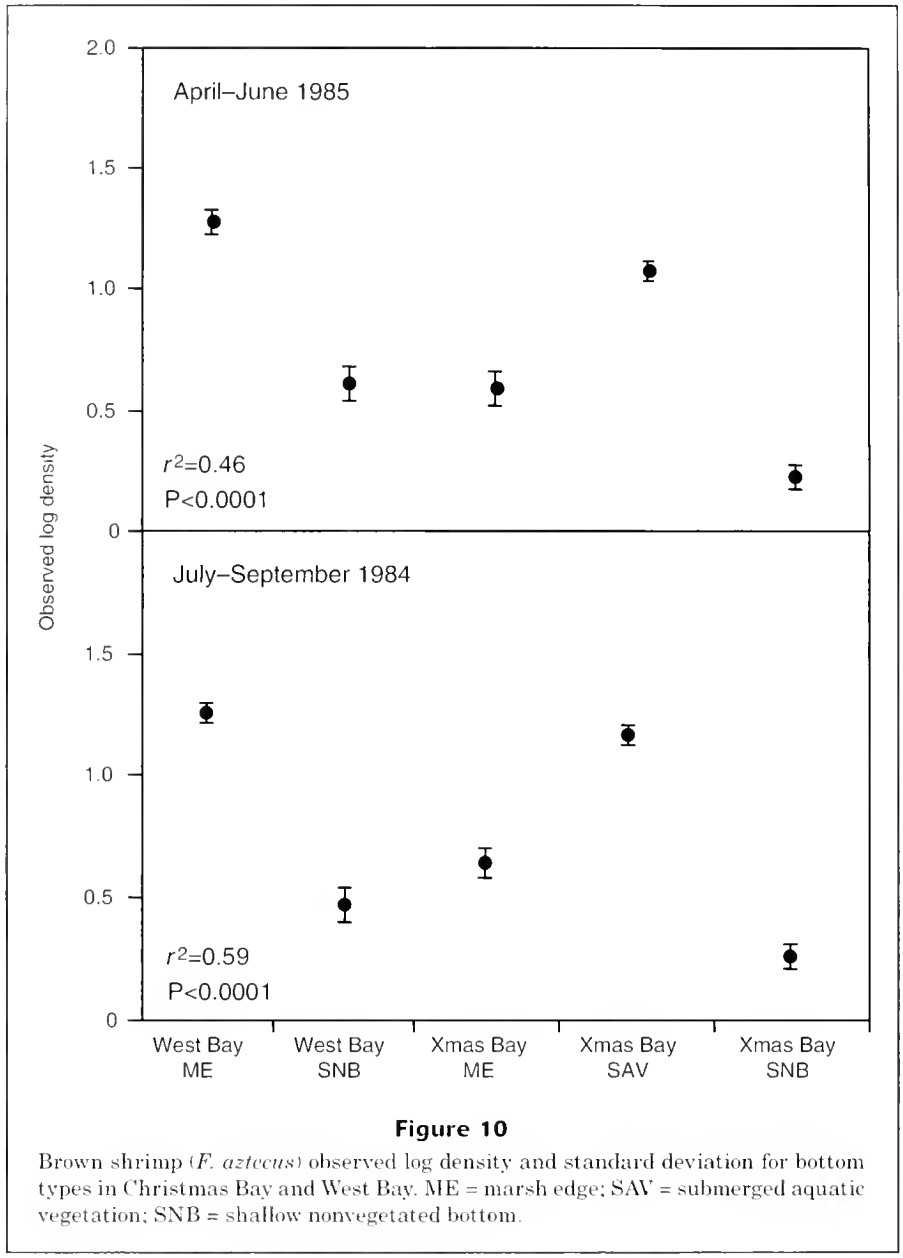

Figure 10

Brown shrimp (*F. aztecus*) observed log density and standard deviation for bottom types in Christmas Bay and West Bay. ME = marsh edge; SAV = submerged aquatic vegetation; SNB = shallow nonvegetated bottom.

Galveston Bay. Our data suggest that brown shrimp select SAV over ME when these habitats co-occur (Christmas Bay) and select ME when grassbeds are absent (West Bay) (Fig. 10). Habitat submergence time may explain high SAV use in Christmas Bay (Rozas and Minello, 1998). Subtidal grassbeds may provide more continuous refuge and food supply at both low and high tides than the marsh surface, which can be accessed only during high tides. Additionally, brown shrimp were significantly smaller in SAV ($\bar{x}$=17 mm) than in ME ($\bar{x}$=25 mm) (*t*-test, $P<0.001$), which may imply ontogenetic changes in habitat or trophic requirements (Conrow et al., 1990; Thomas et al., 1990; Rozas and Minello, 1999). Differences in the use of bottom types may correspond with the population's size distribution at the time of sampling. Additional research is needed to reveal ontogenetic habitat shifts and relationships among shallow estuarine bottom types (McIvor and Rozas, 1996).

Assessment of the model performance was based on FWS HSI theory where there is a positive relationship between HSI value and the carrying capacity of the available habitat. In the present study, the relationship equates high brown shrimp densities with optimal habitat conditions that promote high carrying capacity. Therefore, low densities would reflect a low suitability or a low capacity to support the population. Comparisons of predicted density with that of observed values from Galveston Bay, and other Texas bays (Figs. 7 and 8) agree with FWS theory by exhibiting a strong relationship between density and suitable habitat as determined from the model. Model performance and transferability were examined by applying

the Galveston Bay model (with interaction term) to brown shrimp density data from Aransas, Matagorda, and San Antonio bays. The results indicated similar habitat-use patterns in Aransas and San Antonio bays; there were higher densities in high-salinity seagrass beds and a declining density as salinity decreased in these bay systems. No SAV samples were taken in Matagorda Bay; however, the model performed well in predicting greater brown shrimp density in higher-salinity marsh-edge habitats. Our analysis suggests that although the empirical model is complex, it is general enough to be applicable across a broader range of habitat types. The model results may, however, have some geographic limitations. For instance, the model may not perform well within the Laguna Madre in south Texas, where freshwater inflow is diminished and hypersaline conditions exist. This conclusion is consistent with Rubec et al. (1999), who used similar methods to demonstrate that HSI models are applicable across estuaries in central Florida. Our results are promising in view of previous efforts where predictions of nekton abundance with empirical models have proven difficult.

Currently, estuarine EFH for most federally managed species in the Gulf of Mexico exists as mapped estimates of relative abundance from NOS's estuarine living marine resources (ELMR) database (GMFMC, 1998; Nelson and Monaco, 2000). The entire Galveston Bay complex was considered EFH for brown shrimp based on ELMR relative abundance data. Our model, generated by using brown shrimp density data, provides a more spatially resolved delineation of EFH (in waters <1 m depth) for brown shrimp <100 mm.

The analyses described in the present study focused on bottom types in waters less than 1 m which comprise about 25% of the available habitat in Galveston Bay. Trawl CPUE data from Texas Parks and Wildlife Department (TPWD) were analyzed to compare abundance and distribution patterns in waters >1 m. These trawls (3.8-cm stretched mesh) do not capture small size classes (<50 mm TL) of brown shrimp efficiently; thus the trawl analysis provides information only on larger size classes (mean=89 mm). However, few individuals in smaller size classes of shrimp (<50 mm TL) are likely to inhabit deeper bay waters; density estimates of small nekton, including shrimp, decline rapidly with depth (Mock, 1966; Baltz et al., 1993; Rozas, 1993; Rozas and Zimmerman, 2000). In addition, these CPUE values are likely underestimates of brown shrimp density; catch efficiency for shrimp in trawls can be roughly estimated at 20% (Zimmerman et al., 1984; Rozas and Minello, 1997). Despite these problems, shrimp abundance estimates in water >1 m appear low; abundance estimates from TPWD trawl data in deep open-bay waters were almost two orders of magnitude lower than densities in shallow water habitats.

Brown shrimp population estimates from the present study (Table 3) were highest in the lower bay (224,568 per ha.). Seagrass beds accounted for more than 60% of the estimate (145,142 per ha.) and marsh edge and nonvegetated bottom types combined were estimated at approximately 79,000 per ha. As noted earlier, the NWI regularly flooded emergent vegetation classification is not all marsh edge but is a complex of SNB, marsh edge, and inner marsh with different shrimp densities associated with each of these microhabitat types. Minello and Rozas (in press) modeled small-scale density patterns on the marsh surface in a 437-ha. salt marsh of lower Galveston Bay and applied these data to a GIS analysis of marsh landscape patterns. In this highly fragmented marsh complex that was 37% SNB and 63% marsh vegetation, they estimated brown shrimp populations at 37,000 per ha. We could not estimate brown shrimp populations in irregularly flooded emergent vegetation, although the areal coverage of this habitat type was large. Compared with the regularly flooded wetlands, overall densities of brown shrimp in these irregularly flooded systems should be relatively low because of higher marsh surface elevations (Rozas and Reed, 1993; Minello et al., 1994; Minello and Webb, 1997) and restricted tidal access (Rozas and Minello, 1999). We also were unable to assess the contribution of oyster reef as habitat for brown shrimp. Coen et al. (1999), however, reported brown shrimp on oyster reefs, and Powell (1993) estimated that there was 108 km^2 of this habitat in Galveston Bay.

Our modeling results provide evidence that estuarine habitat types are discriminately used by brown shrimp. The success of transferring our empirical model from Galveston Bay to adjacent bay systems in Texas suggests that the model has a broad application and can possibly be used to simulate patterns of habitat use in systems that lack sufficient density data. Continuing collections of density data in Gulf estuaries are necessary to make additional interestuary comparisons and to determine whether these habitat-use patterns differ throughout the distributional range of brown shrimp. The use of other habitat types also needs to be examined. For example, other available habitat types from Galveston Bay, such as oyster reef and inner marsh, and from other Gulf estuaries, such as mangrove, calcium carbonate rock formations, and sponge communities, may be important habitats for this federally managed species.

Acknowledgments

Funding and support for this work was provided by the Southeast Region of NOAA's National Marine Fisheries Service, The Southeast Fisheries Science Center, and the Biogeography Program of the National Ocean Service. We would like to thank Pete Sheridan, Lawrence Rozas, Ken Heck, and Roger Zimmerman for providing access to published and unpublished data sets. John Boyd helped with construction of the nekton density database.

Literature cited

Baltz, D. M., J. W. Fleeger, C.F. Rakocinski, and J. N. McCall. 1998. Food, density, and microhabitat: factors affecting growth and recruitment potential of juvenile saltmarsh fishes. Environ. Biol. Fish. 53:89–103.

Baltz, D. M., C. Rakocinski, and J. W. Fleeger. 1993. Microhabitat use by marsh-edge fishes in a Louisiana estuary. Environ. Biolog. Fish. 36:109–126.

Barret, B. B., and M. C. Gillespie.
1973. Primary factors which influence commercial shrimp production in coastal Louisiana. La. Wild Life Fish. Comm., Tech. Bull. 9, 28 p.

Barry, J. P., M. M. Yoklavich, G. M. Cailliet, D. A. Ambrose, and B. S. Antrim.
1999. Trophic ecology of the dominant fishes in Elkhorn Slough, California, 1974–1980. Estuaries 19:115–138.

Beck, M. W., K. L. Heck Jr., K. Able, D. Childers, D. Eggleston, B. M. Gillanders, B. Halpern, C. Hays, K. Hoshino, T. Minello, R. Orth, P. Sheridan, and M. Weinstein.
2001. The identification, conservation, and management of estuarine and marine nurseries for fish and invertebrates. Bioscience 51:633–641.

Boesch, D. F., and R. E. Turner.
1984. Dependence of fishery species on salt marshes: The role of food and refuge. Estuaries 7:460–468.

Brown, S. K., K. R. Buja, S. H. Jury, M. E. Monaco, and A. Banner.
2000. Habitat suitability index models for eight fish and invertebrate species in Casco and Sheepscot Bays, Maine. N. Am. J. Fish. Manag. 20:408–435.

Christensen, J. D., M. E. Monaco, and T. A. Lowery.
1997. An index to assess the sensitivity of Gulf of Mexico species to changes in estuarine salinity regimes. Gulf Res. Rep. 9(4):219–229.

Coen, L. D., M. W. Luckenbach, and D. L. Breitburg.
1999. The role of oyster reefs as essential fish habitat: a review of current knowledge and some new perspectives. *In* Fish habitat: essential fish habitat and rehabilitation (L. R. Benaka, ed.), p. 438–454. Am. Fish. Soc., Symposium 22, Bethesda, MD.

Conrow, R. A., V. Zale, and R. W. Gregory.
1990. Distributions and abundances of early life stages of fishes in a Florida lake dominated by aquatic macrophytes. Trans. Am. Fish. Soc. 119:521–528.

Copeland, B. J., and T. J. Bechtel.
1974. Some environmental limits of six gulf coast estuarine organisms. Contrib. Mar. Sci. 18:169–204.

Cowardin, L. J., V. Carter, F. C. Golet, and E. T. Laroe.
1979. Classification of wetlands and deepwater habitats of the United States. U.S. Fish Wildl. Serv. Biol. Serv. Program FWS/OBS-79/31, 131 p.

Czapla, T. E.
1991. Diets and prey selection of pinfish and southern flounder in a *Halodule wrightii* seagrass meadow. Ph.D. diss., 119 p. Texas A&M Univ., College Station, TX

Garrison, L. P.
1999. Vertical migration behavior and larval transport in brachyuran crabs. Mar. Ecol. Prog. Ser. 176:103–113.

Gifford, C. A.
1962. Some aspects of osmotic and ionic regulation in the blue crab, *Callinectes sapidus*, and the ghost crab, *Ocypode albicans*. Publ. Inst. Mar. Sci. 8:97–125.

Gleason, D. F., and R. J. Zimmerman.
1984. Herbivory potential of postlarval brown shrimp associated with salt marshes. J. Exp. Mar. Biol. Ecol. 84: 235–246.

GMFMC (Gulf of Mexico Fishery Management Council).
1998. Generic amendment for addressing essential fish habitat requirements. Prepared by the GMFMC, October 1998, 34 p.

Krumgalz, B. S., G. Fainshtein, and A. Cohen.
1992. Grain size effect on anthropogenic trace metal and organic matter distribution in marine sediments. Sci. Total Environ. 116(1–2):15–30.

Mahon, R. and R. W. Smith.
1989. Comparison of species composition in a bottom trawl calibration experiment. J. Northw. Atl. Fish. Sci. 9:73–79.

McIvor, C. C., and L. P. Rozas.
1996. Direct nekton use of intertidal saltmarsh habitat and linkage with adjacent habitats: a review from the southeastern United States. *In* Estuarine shores: evolution, environments and human alterations (K. F. Nordstrom and C. T. Roman, eds.), p. 311–334. John Wiley and Sons, Ltd., Chichester, England.

McTigue, T. A., and R. J. Zimmerman.
1991. Carnivory versus herbivory in juvenile *Penaeus setiferus* (Linnaeus) and *Penaeus aztecus* (Ives). J. Exp. Mar. Biol. Ecol. 15:1–16.
1998. The use of infauna by juvenile *Penaeus aztecus* (Ives) and *P. setiferus* (Linnaeus). Estuaries 21:160–175.

Miller, J. M., and M. L. Dunn.
1980. Feeding strategies and patterns of movement in juvenile estuarine fishes. *In* Estuarine perspectives (V. S. Kennedy, ed.), p. 437–448. Academic Press, New York, NY.

Minello, T. J.
1999. Nekton densities in shallow estuarine habitats of Texas and Louisiana and the identification of essential fish habitat. *In* Fish habitat: essential fish habitat and rehabilitation (L. Beneka, ed.), p. 43–75. Am. Fish. Soc., Bethesda, MD.

Minello, T. J., and L. P. Rozas.
In press. Nekton populations in Gulf Coast wetlands: fine-scale spatial distributions, landscape patterns, and restoration implications. Ecol. Appl.

Minello, T. J., and J. W. Webb Jr.
1997. Use of natural and created *Spartina alterniflora* salt marshes by fishery species and other aquatic fauna in Galveston Bay, Texas, USA. Mar. Ecol. Prog. Ser. 151:165–179.

Minello, T. J., J. W. Webb Jr., R. J. Zimmerman, R. B. Wooten, J. L. Martinez, T. J. Baumer, and M. C. Patillo.
1991. Habitat availability and utilization by benthos and nekton in Hall's Lake and West Galveston Bay. NOAA Tech. Memo. NMFS-SEFC-275, 37 p.

Minello, T. J., and R. J. Zimmerman.
1992. Utilization of natural and transplanted Texas salt marshes by fish and decapod crustaceans. Mar. Ecol. Prog. Ser. 90:273–285.

Minello, T. J., R. J. Zimmerman, and R. Medina.
1994. The importance of edge for natant macrofauna in a created salt marsh. Wetlands 14:184–198.

Mock, C. R.
1966. Natural and altered estuarine habitats of penaeid shrimp. Proceedings of the Gulf and Caribbean Fisheries Institute, 19th annual session, p. 86–98. Gulf and Caribbean Fish. Inst., Fort Pierce, FL.

Monaco, M. E., S. B. Weisberg, and T. A. Lowery.
1998. Summer habitat affinities of estuarine fish in US mid-Atlantic coastal systems. Fish. Manag. Ecol. 5:161–171.

NOAA (National Oceanic and Atmospheric Administration).
1989. Estuaries of the United States: vital statistics of a natural resource base, 79 p. Strategic Environmental Assessments Division, National Ocean Service (NOS), NOAA, Rockville, MD.

Nelson, D. M., and M. E. Monaco.
2000. National overview and evolution of NOAA's estuarine living marine resources (ELMR) Program. NOAA Tech. Memo. NOS NCCOS CCMA 144, 60 p. Center for

Coastal Monitoring and Assessment, NOS, NOAA, Silver Spring, MD.

Orlando, S. P. Jr., L. P. Rozas, G. H. Ward, and C. J. Klein.
1993. Salinity characteristics of Gulf of Mexico estuaries, 209 p. Office of Ocean Resources and Conservation and Assessment, NOAA, Silver Spring, MD.

Pearcy, W. G., and S. S. Myers.
1974. Larval fishes of Yaquina Bay, Oregon: a nursery ground for marine fishes? Fish. Bull. 72:201–213.

Perez-Farfante, I., and B. Kensley.
1997. Penaeoid and sergestoid shrimps and prawns of the world; keys and diagnoses for the families and genera. Memoires du Muséum National d'Histoire Naturelle, tome 175, 233 p.

Peterson, G. W., and R. E. Turner.
1994. The value of salt marsh edge vs. interior as a habitat for fish and decapod crustaceans in a Louisiana tidal marsh. Estuaries 17:235–262.

Powell, E. N.
1993. Status and trends analysis of oyster reef habitat in Galveston Bay. *In* Proceeding, second state of the bay symposium (R. W. Jensen et al., eds.), p. 207–209. Galveston Bay National Estuary Program, Houston, TX.

Rozas, L. P.
1993. Nekton use of salt marshes of the southeast region of the United States. *In* Proc. 8th symp. coastal and ocean management (O. T. Magoon, W. S. Wilson, H. Converse, and L. T. Tobin, eds.), p. 528–537. Coastal Zone '93 Conference, Am. Soc. Civil Eng., New Orleans, LA.

Rozas, L. P., and T. J. Minello.
1997. Estimating densities of small fishes and decapod crustaceans in shallow estuarine habitats: a review of sampling design with focus on gear selection. Estuaries 20: 199–213.
1998. Nekton use of salt marsh, seagrass, and nonvegetated habitats in a south Texas (USA) estuary. Bull. Mar. Sci. 63(3):481–501.
1999. Effects of structural marsh management on fishery species and other nekton before and during a spring drawdown. Wetl. Ecol. Manag. 7: 121–139.

Rozas, L. P., and D. J. Reed.
1993. Nekton use of marsh-surface habitats in Louisiana (USA) deltaic salt marshes undergoing submergence. Mar. Ecol. Prog. Ser. 96:147–157.

Rozas, L. P., and R. J. Zimmerman.
2000. Small-scale patterns of nekton use among marsh and adjacent shallow nonvegetated areas of the Galveston Bay estuary, Texas (USA). Mar. Ecol. Prog. Ser. 193:217–239.

Rubec, P. J., M. S. Coyne, R. H. McMichael Jr., and M. E. Monaco.
1998. Spatial methods being developed in Florida to determine essential fish habitat. Fisheries 23(7):21–25.

Rubec, P. J., J. C. W. Bexley, H. Norris, M. S. Coyne, M. E. Monaco, S. G. Smith, and J. S. Ault.
1999. Suitability modeling to delineate habitat essential to sustainable fisheries. Am. Fish. Soc. Symp. 22:108–133.

Rubec, P. J., S. G. Smith, M. S. Coyne, M. White, A. Sullivan, T. MacDonald, R. H. McMichael Jr., M. E. Monaco, and J. S. Ault.
2001. Spatial modeling of fish habitat suitability in Florida estuaries. *In* Spatial processes and management of marine populations (G. H. Kruse, N. Bez, A. Booth, M. W. Dorn, S. Hills, R. N. Lipcus, D. Pelltier, C. Roy, S. J. Smith, and D. Witherell, eds.), p. 1–18. Sea Grant report AK-SG-01-02. Univ. Alaska, Fairbanks, AK.

Sogard, S. M., and K. W. Able.
1991. A comparison of eelgrass, sea lettuce macroalgae, and marsh creeks as habitats for epibenthic fishes and decapods. Estuar. Coast. Shelf Sci. 33:501–519.

Tagatz, M. E.
1971. Osmoregulatory ability of blue crabs in different temperature-salinity combinations. Ches. Sci. 12:14–17.

Thomas, J. L., R. J. Zimmerman, and T. J. Minello.
1990. Abundance patterns of juvenile blue crabs (*Callinectes sapidus*) in nursery habitats of two Texas bays. Bull. Mar. Sci. 46:115–125.

Turner, R. E.
1977. Intertidal vegetation and commercial yields of penaeid shrimp. Trans. Am. Fish. Soc. 106:411–416.

USFWS (U.S. Fish and Wildlife Service).
1981. Standards for the development of habitat suitability index models for use with the habitat evaluation procedures. Report 103, ESM release 1-81, 66 p. Division of Ecological Services, USFWS, Washington, DC.

White, W. A., T. A. Tremblay, E. G. Wermund Jr., and L. R. Handley.
1993. Trends and status of wetland and aquatic habitats in the Galveston Bay System, Texas, 225 p. Galveston Bay National Estuary Program, Galveston, TX.

Zein-Eldin, Z. P., and D. V. Aldrich.
1965. Growth and survival of postlarval *Penaeus aztecus* under controlled conditions of temperature and salinity. Biol. Bull. (Woods Hole) 129:199–216.

Zein-Eldin, Z. P., and M. L. Renaud.
1986. Inshore environmental effects on brown shrimp, *Penaeus aztecus*, and white shrimp, *P. setiferus*, populations in coastal waters, particularly Texas. Mar. Fish. Rev. 48:9–19.

Zimmerman, R. J., and T. J. Minello.
1984. Densities of *Penaeus aztecus*, *P. setiferus* and other natant macrofauna in a Texas salt marsh. Estuaries 7: 421–433.

Zimmerman, R. J., T. J. Minello, T. J. Baumer, and M. C. Castiglione.
1989. Oyster reef as habitat for estuarine macrofauna. NOAA Tech. Memo., NMFS-SEFC-249, 16 p.

Zimmerman, R. J., T. J. Minello, M. C. Castiglione, and D. L. Smith.
1990a. The use of *Juncus* and *Spartina* marshes by fisheries species in Lavaca Bay, Texas, with reference to effects of floods. NOAA Tech. Memo., NMFS-SEFC-251, 40 p.
1990b. Utilization of marsh and associated habitats along a salinity gradient in Galveston Bay. NOAA Tech. Memo., NMFS-SEFC-250, 68 p.

Zimmerman, R. J., T. J. Minello, and L. P. Rozas.
2000. Salt marsh linkages to productivity of penaeid shrimps and blue crabs in the northern Gulf of Mexico. *In* Concepts and controversies in tidal marsh ecology (M. P. Weinstein and D.A. Kreeger, eds.), p. 293–314. Kluwer Academic Publ., Dordrecht, The Netherlands.

Zimmerman, R. J., T. J. Minello, and G. Zamora.
1984. Selection of vegetated habitat by *Penaeus aztecus* in a Galveston Bay salt marsh. Fish. Bull. 82:325–336.

Translocation as a strategy to rehabilitate the queen conch (*Strombus gigas*) population in the Florida Keys

Gabriel A. Delgado
Claudine T. Bartels
Robert A. Glazer
Florida Fish and Wildlife Conservation Commission
Florida Marine Research Institute
2796 Overseas Highway, Suite 119
Marathon, Florida 33050
E-mail address (for G. A. Delgado): gabriel.delgado@fwc.state.fl.us

Nancy J. Brown-Peterson
Department of Coastal Sciences
College of Science and Technology
The University of Southern Mississippi
P.O. Box 7000
Ocean Springs, Mississippi 39566

Kevin J. McCarthy
National Marine Fisheries Service, NOAA
75 Virginia Beach Drive
Miami, Florida 33149

Abstract—Queen conch (*Strombus gigas*) stocks in the Florida Keys once supported commercial and recreational fisheries, but overharvesting has decimated this once abundant snail. Despite a ban on harvesting this species since 1985, the local conch population has not recovered. In addition, previous work has reported that conch located in nearshore Keys waters are incapable of spawning because of poor gonadal condition, although reproduction does occur offshore. Queen conch in other areas undergo ontogenetic migrations from shallow, nearshore sites to offshore habitats, but conch in the Florida Keys are prevented from doing so by Hawk Channel. The present study was initiated to determine the potential of translocating nonspawning nearshore conch to offshore sites in order to augment the spawning stock. We translocated adult conch from two nearshore sites to two offshore sites. Histological examinations at the initiation of this study confirmed that nearshore conch were incapable of reproduction, whereas offshore conch had normal gonads and thus were able to reproduce. The gonads of nearshore females were in worse condition than those of nearshore males. However, the gonadal condition of the translocated nearshore conch improved, and these animals began spawning after three months offshore. This finding suggests that some component of the nearshore environment (e.g., pollutants, temperature extremes, poor food or habitat quality) disrupts reproduction in conch, but that removal of nearshore animals to suitable offshore habitat can restore reproductive viability. These results indicate that translocations are preferable to releasing hatchery-reared juveniles because they are more cost-effective, result in a more rapid increase in reproductive output, and maintain the genetic integrity of the wild stock. Therefore, translocating nearshore conch to offshore spawning aggregations may be the key to expediting the recovery of queen conch stocks in the Florida Keys.

Manuscript approved for publication 24 November 2003 by Scientific Editor.
Manuscript received 20 January 2004 at NMFS Scientitific Publications Office.
Fish. Bull. 102:278–288 (2004).

The queen conch (*Strombus gigas*) is a large marine gastropod harvested intensively throughout the Caribbean for its meat and shell. In the Florida Keys, conch once supported commercial and recreational fisheries, but overharvesting severely depleted the population. The harvesting of conch has been banned in Florida since 1985, but the population has not recovered to levels that can support exploitation (Glazer and Berg, 1994; Berg and Glazer, 1995; Glazer and Delgado, 2003). Intensive fishing may invoke depensatory mechanisms as densities are reduced, limiting the ability of conch to locate mates and increasing the chance of recruitment failure (Appeldoorn, 1995). This seems to be the case in Florida because the lack of recovery has been attributed to diminished recruitment due in part to small spawning aggregations (Stoner et al., 1997; Stoner and Ray-Culp, 2000).

Queen conch occur in the various oceanside habitats of the Florida Keys archipelago with the exception of Hawk Channel (Glazer and Berg, 1994). This naturally occurring deep-water channel runs parallel to the Florida Keys, between the island chain and the offshore reef tract. The substrate on the bottom of Hawk Channel is predominantly soft sediment, which is poor conch habitat; consequently, Hawk Channel serves as a barrier to migration and isolates nearshore from offshore conch aggregations (Glazer and Berg, 1994). We have been monitoring queen conch stocks throughout the Florida Keys since 1987, and despite extensive surveys, we have never observed reproductive activity among conch in nearshore aggregations (Glazer and Berg, 1994). Conversely, reproductive behavior has been commonly observed among conch in offshore aggregations (Glazer and Berg, 1994). Moreover, a preliminary histological examination of conch from these two regions indicated that the gonads of offshore conch were capable of undergoing gametogenesis, whereas the gonads of nearshore conch were nonfunctional (Glazer and Quintero,

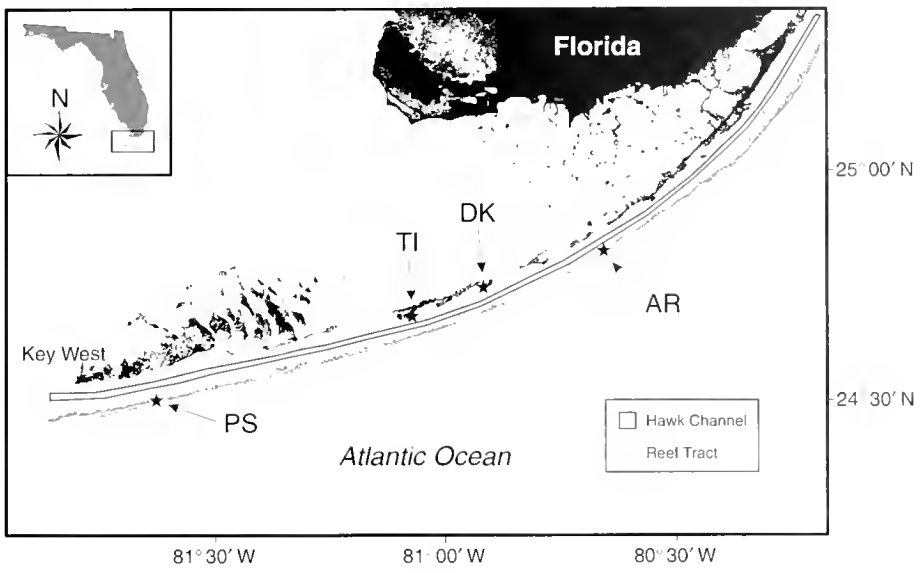

Figure 1

Queen conch (*Strombus gigas*) translocation sites in the Florida Keys (adapted from McCarthy et al. 2002). The nearshore region is the stretch of water on the landward side of Hawk Channel; the offshore region is the stretch of water on the other side of the channel, contiguous with the Atlantic Ocean. Nearshore conch were translocated from Tinglers Island (TI) to Alligator Reef (AR) and from Duck Key (DK) to Pelican Shoal (PS).

1998; McCarthy et al., 2002). In a metapopulation context, the nearshore region in the Florida Keys can be considered a "blackhole sink" for larval recruitment because conch that settle there do not spawn and thus do not contribute to the reproductive output of the stock (*sensu* Morgan and Botsford, 2001).

In 1990, the Florida Fish and Wildlife Conservation Commission's (FWC) Florida Marine Research Institute constructed an experimental hatchery to test the feasibility of rehabilitating queen conch stocks in the Florida Keys by releasing hatchery-reared juveniles. A series of experiments to determine the best size of juveniles, time of release, and area to release hatchery-reared juvenile conch were conducted, and a cost-benefit analysis was performed. Unfortunately, the high mortality of conch after release, coupled with high production costs, caused us to examine alternate strategies (Glazer and Delgado, 2003).

Translocation is defined as the intentional introduction or reintroduction of animals in an attempt to establish, reestablish, or augment a population in order to aid in the recovery of a native species whose numbers have been reduced by overharvesting or habitat loss (or both) (Griffith et al., 1989). This method of population recovery has been used to facilitate the recovery of numerous species of birds and mammals (Griffith et al., 1989) and several aquatic species, including cutthroat trout (Harig et al., 2000) and corals (Edwards and Clark, 1999; Rinkevich, 1995; van Treeck and Schuhmacher, 1997). Nest translocations have also proven effective in efforts to recover sea turtles (Garcia et al., 1996).

The present study was initiated to determine the potential of translocating nonspawning nearshore conch to offshore sites as a method to augment spawning aggregations and as an aid in the recovery of the queen conch population in the Florida Keys. However, this strategy will be beneficial only if the translocated conch regain their reproductive capacity. To test this approach, we translocated adult conch from the nearshore region into existing offshore breeding aggregations and examined changes in reproductive behavior (i.e., mating and spawning) and gonadal development.

Materials and methods

Translocations and reproductive behavior

During March 1999, we translocated adult conch from nearshore aggregations to aggregations offshore. Nearshore aggregations were located at Tinglers Island (24°41′N, 81°05′W; water depth <1–2 m) and Duck Key (24°45′N, 80°55′W; water depth <1–2 m) (Fig. 1). The habitat at the two nearshore sites was characterized as a matrix of hard-bottom and *Thalassia testudinum* patches. Offshore aggregations were located at Alligator Reef (24°51′N, 80°37′W; water depth 9–11 m) and Pelican Shoal (24°30′N, 81°37′W; water depth 5–7 m) (Fig. 1). The habitat at the offshore sites consisted of back-reef rubble, sandy plains, and patches of *Thalassia testudinum*.

We tagged 44 adult conch at Tinglers Island; 23 were translocated to Alligator Reef, and 21 were rereleased at

Table 1

The number of gonadal tissue samples taken from resident nearshore, resident offshore, and translocated nearshore queen conch, by sex and season.

	Spring		Summer		Fall	
	Females	Males	Females	Males	Females	Males
Resident nearshore	13	12	14	12	10	6
Resident offshore	22	20	19	20	25	15
Translocated nearshore	—	—	12	12	13	4

Table 2

Index and definitions used to quantify gonadal maturity in queen conch. This index is patterned after the maturity scale developed by Egan (1985). The dashed line separates the scores 1–5 from 6–8 that were combined for statistical analyses.

Gonadal condition	Score	Definition
Early development	1	primary and cortical alveolar oocytes in females; spermatogonia and spermatocytes in males
Mid development	2	vitellogenesis beginning in females; spermatozoa present in males
Late development	3	fully developed oocytes in females, none in oviduct; all stages of spermatogenesis, no spermatozoa in vas deferens
Ripe	4	oocytes in oviduct for females; spermatozoa in vas deferens for males
Spent	5	reabsorption of vitellogenic oocytes in females; empty lobules, residual spermatozoa in males
Atresia	6	reabsorption of oocytes and no vitellogenesis in females; reabsorption of spermatozoa in males
Regressed	7	only primary oocytes in females; only primary spermatogonia in males
No tissue	8	no gonadal tissue development and no germ cells present; this is an abnormal condition in adult females and males

Tinglers Island. We also tagged 132 adult conch at Duck Key; 73 were translocated to Pelican Shoal, and 59 were re-released at Duck Key. In addition, 100 resident offshore conch were tagged *in situ* at both Alligator Reef and Pelican Shoal. Conch were tagged with individually numbered tags that were secured to the shell spires by Monel wire; in addition, colored flagging tape was similarly attached to facilitate recapture.

Reproductive behavior of tagged queen conch was monitored at each of the four sites on a weekly basis, weather permitting, from March 1999 through November 1999. Offshore sites were surveyed by using SCUBA; nearshore sites were surveyed by snorkeling. Mating activity was quantified by counting the number of tagged individuals (both males and females) copulating; spawning activity was quantified by counting the number of tagged females laying egg masses. Data from the two nearshore sites were pooled and data from the two offshore sites were pooled. Data were also pooled by season: spring consisted of March, April, and May; summer consisted of June, July, and August; and fall consisted of September, October, and November.

Histological examinations

Gonadal tissue samples from adult conch were collected for histological examination at the initiation of the study (spring; the start of the breeding season), during July–August (summer; breeding season), and during October (fall; the end of the breeding season) in order to assess gonadal development in relation to time after translocation. We collected approximately 40 resident offshore conch during each season (Table 1). However, because of the small size of the nearshore aggregations and the small number of nearshore conch translocated offshore, we collected about 20 individuals from these two groups each season (Table 1). We did not determine the sex of the animals before sample collection; therefore the breakdown by sex is not exactly even (Table 1).

A one-cm^3 piece of tissue from the middle of the gonad of each animal was placed in a labeled plastic cassette and preserved in 10% neutral buffered formalin. After 7 to 14 days in fixative, the tissue samples were rinsed overnight in freshwater. The samples were then dehydrated in a se-

ries of graded ethanols (one change of 60% ethanol and two changes of 70% ethanol for two hours each) and loaded into an automatic tissue processor (Shandon Hypercenter XP, Shandon Scientific Ltd., Pittsburgh, PA) for dehydration, clearing, and paraffin infiltration. Tissues were embedded in Paraplast Plus (Fisher Scientific, Pittsburgh, PA) and sectioned at 4 μm with a rotary microtome. Two serial sections from each tissue sample were mounted on glass slides, allowed to dry overnight, and stained with hematoxylin 1 and eosin Y (Richard Allen Inc., Richland, MI). All laboratory procedures followed approved standard operating procedures developed under the Good Laboratory Practices guidelines (EPA and FDA guidelines).

A detailed histological inspection of each sample was made to assess the stage of gonadal maturity and the percentage of gametogenic tissue. Each animal was given a score from 1 to 8 to quantify gonadal maturity (Table 2). This index was derived from a maturity scale developed by Egan (1985). Because of the small number of animals collected, gonadal maturity scores from 1 to 5 were combined to group animals that would be capable of spawning or had recently spawned (Table 2). Scores from 6 to 8 were combined to group animals that would not spawn again in a season or were not capable of spawning (Table 2). In addition, the percentage of gametogenic tissue present (i.e., the percentage of ovarian or testicular tissue occupying the available space of the section) was visually estimated by using the following index: <25%, 25–50%, 51–75%, and >75%. For statistical analyses, this index was reduced to two categories: <50% and >50%.

Statistical analyses

We evaluated differences in reproductive behavior (mating and spawning) between resident nearshore and translocated nearshore conch for each season by using Fisher's exact test because it is not sensitive to small sample sizes (Zar, 1996). We also examined differences in gonadal condition (i.e., gonadal maturity and the percentage of gametogenic tissue) between resident nearshore and resident offshore conch for each season by using Fisher's exact test. Males and females were analyzed separately. In order to assess the effectiveness of the translocations to the offshore region, we used Fisher's exact test to compare the gonadal condition of translocated nearshore conch with the gonadal condition of resident nearshore conch in summer and in fall. Again, the sexes were analyzed separately. All tests were run on SPSS 9.0 (SPSS Inc., Chicago, IL) for Windows. Results were considered significant if $P<0.05$.

Results

Reproductive behavior: mating

Approximately 84% of the tagged resident nearshore conch, 69% of the tagged translocated nearshore conch, and 88% of the tagged resident offshore conch were observed at least once during monitoring. Resident nearshore conch and translocated nearshore conch were not observed mating during any of the field surveys; conversely, resident offshore conch were observed mating throughout the study (Table 3). The mating frequency of resident offshore conch was highest during the spring (5.3%) and decreased during subsequent seasons to 0.9% in the fall (Table 3). All observed mating occurred between resident offshore animals.

Table 3

Percentage of mating (the number of males and females mating divided by the total number of conch observed during that season) and spawning (the number of females spawning divided by the total number of females observed during that season) in nearshore conch and offshore conch by season (adapted from McCarthy et al., 2002). Numbers in parentheses represent the number of observations; *P* represents the probabilities from Fisher's exact test of differences in reproductive behavior between resident nearshore and translocated nearshore conch. The asterisk (*) indicates that the test was statistically significant. N/A indicates that statistical analyses were not conducted because no mating or spawning was observed among either resident nearshore or translocated nearshore animals.

	Offshore conch	Nearshore conch		
	Resident	Resident	Translocated	*P*
Mating				
Spring	5.3 (95)	0.0 (37)	0.0 (19)	N/A
Summer	2.4 (467)	0.0 (106)	0.0 (81)	N/A
Fall	0.9 (232)	0.0 (20)	0.0 (51)	N/A
Spawning				
Spring	46.2 (39)	0.0 (6)	0.0 (10)	N/A
Summer	16.8 (191)	0.0 (34)	12.2 (41)	0.041
Fall	5.2 (97)	0.0 (9)	18.5 (27)	0.214

Reproductive behavior: spawning

Neither resident nearshore females nor translocated nearshore females were observed spawning during the spring (Table 3). However, by summer, translocated nearshore females had attained the capacity to spawn and had a significantly higher spawning frequency than resident nearshore females (12.2% vs. 0.0%, respectively) (Table 3). During the fall, spawning frequency of translocated nearshore females peaked at 18.5%, whereas resident nearshore females had still not exhibited any spawning behavior (Table 3). However, this difference was not statistically significant because of the small number of resident nearshore conch observed (Table 3). Looking at individual performance instead of spawning frequency, seven (or about 14%) of the approximately 50 nearshore females translocated offshore were observed spawning at least once during the study period.

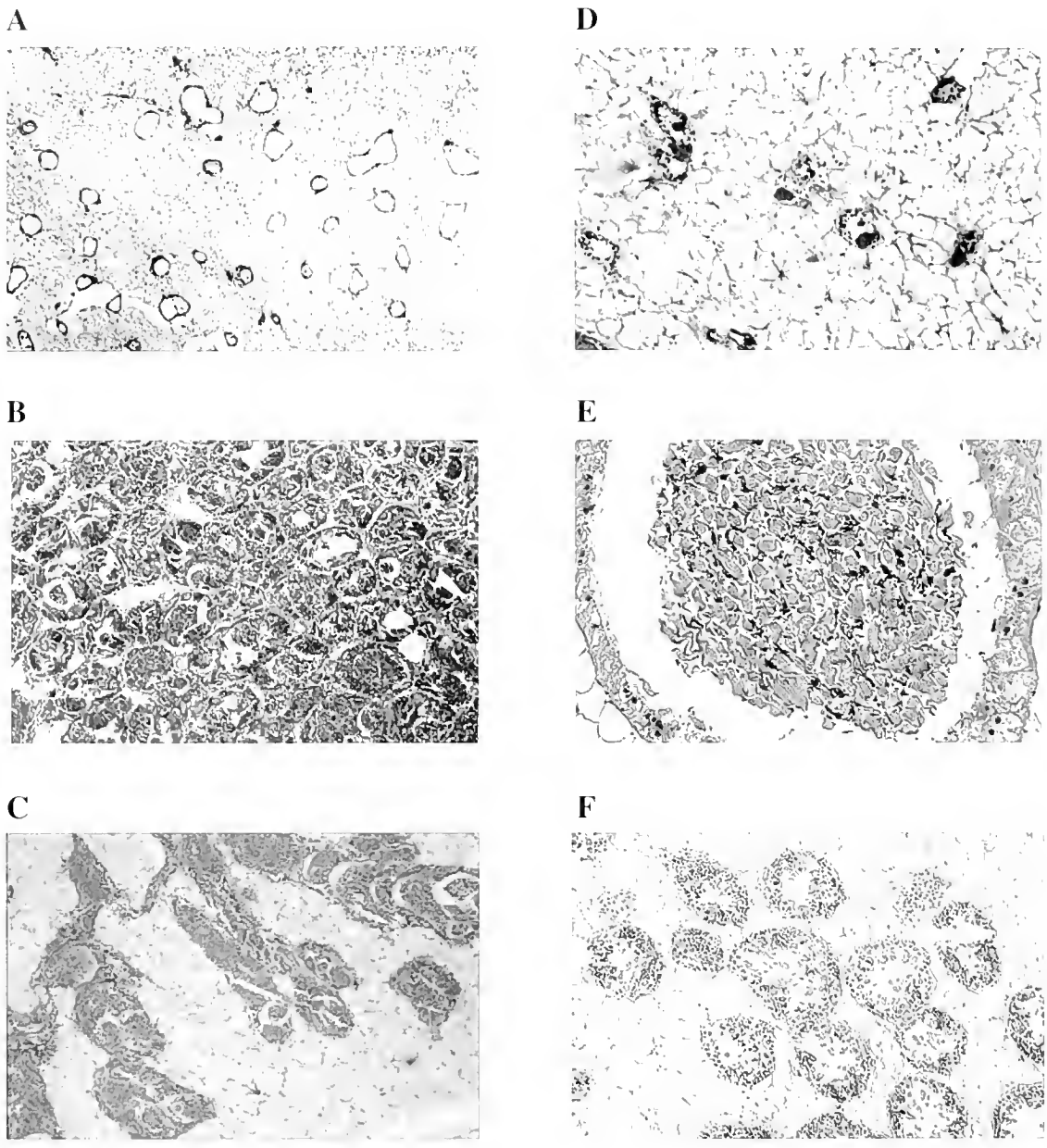

Figure 2

Photomicrographs of the gonadal condition of resident nearshore, resident offshore, and translocated nearshore queen conch (*Strombus gigas*). (**A**) Resident nearshore female during spring, no tissue and <25% gametogenic tissue. (**B**) Resident offshore female during spring, ripe and >75% gametogenic tissue. (**C**) Translocated nearshore female during summer, late development and 25–50% gametogenic tissue. (**D**) Resident nearshore male during spring, early development and <25% gametogenic tissue. (**E**) Resident offshore male during spring, ripe and >75% gametogenic tissue. (**F**) Translocated nearshore male during summer, ripe and 25–50% gametogenic tissue.

Resident offshore females were observed spawning throughout the study (Table 3). Their spawning frequency peaked during the spring at 46.2% and decreased during subsequent seasons to 5.2% in the fall (Table 3).

Histology: females

Histological examinations revealed that the gonadal condition of resident nearshore and resident offshore female

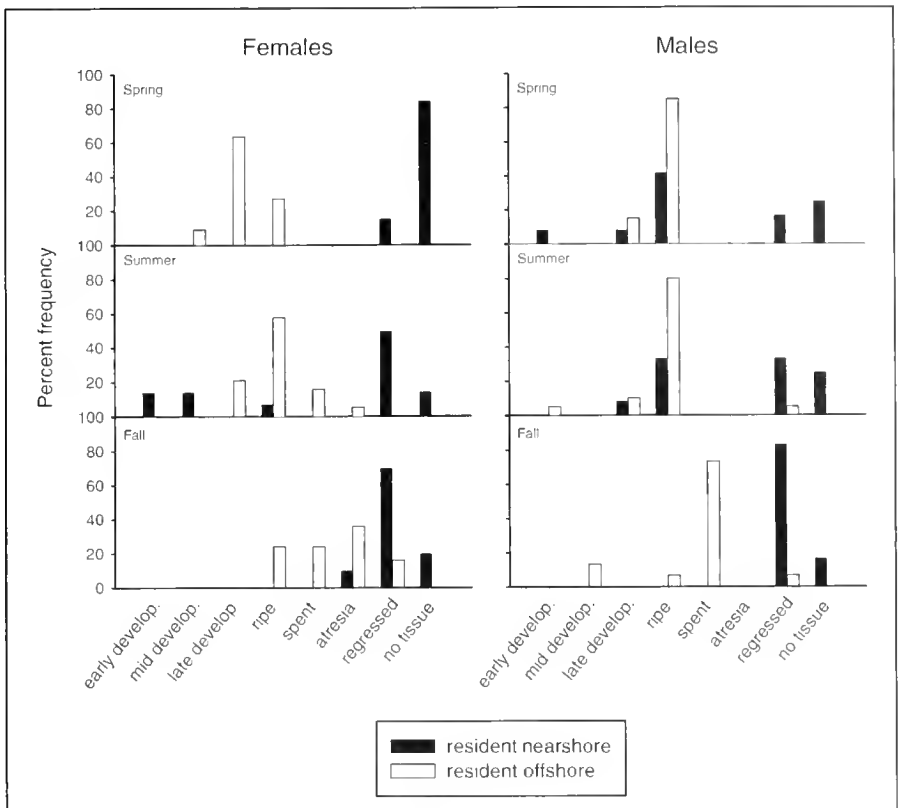

Figure 3

Gonadal maturity of resident nearshore and resident offshore queen conch (*Strombus gigas*) by sex and season. The dotted line separates the categories that were combined for statistical analyses.

conch were markedly different at the beginning of the study (Fig. 2, A and B). There were significant differences in gonadal maturity between resident offshore and resident nearshore female conch during the spring, summer, and fall (Table 4). During the spring, the gonads of most resident offshore females were categorized as being in late development; by summer most were ripe and by fall most were either spent, in atresia, or regressed (Fig. 3). In contrast, the gonads of most resident nearshore females contained no germ cells during the spring (Fig. 3). By summer, the gonads of some resident nearshore females were found to be in the early stages of development, but most females were still incapable of spawning, and by fall, all the resident nearshore females sampled were incapable of spawning (Fig. 3). There were also significant differences in the percentage of gametogenic tissue between resident offshore and resident nearshore females during the spring, summer, and fall (Table 4). The gonads of most resident offshore females contained >75% gametogenic tissue throughout the study period, whereas those of most resident nearshore females had <25% (Fig. 4).

The gonadal condition of translocated nearshore females (Fig. 2C) improved when compared with the gonadal condition of resident nearshore females (Fig. 2A). There were significant differences in gonadal maturity between translocated nearshore and resident nearshore females during both the summer and fall (Table 5). There was

Table 4

Probabilities from Fisher's exact test of differences in gonadal maturity and the percentage of gametogenic tissue between resident nearshore and resident offshore conch by sex and season. *n* represents the total number of observations. Asterisks (*) indicate that the test was statistically significant.

	Females		Males	
	n	*P*	*n*	*P*
Gonadal maturity				
Spring	35	<0.001*	32	0.004*
Summer	33	<0.001*	32	0.002*
Fall	35	0.006*	21	<0.001*
% gametogenic tissue				
Spring	35	<0.001*	32	<0.001*
Summer	33	<0.001*	32	<0.001*
Fall	35	0.002*	21	<0.001*

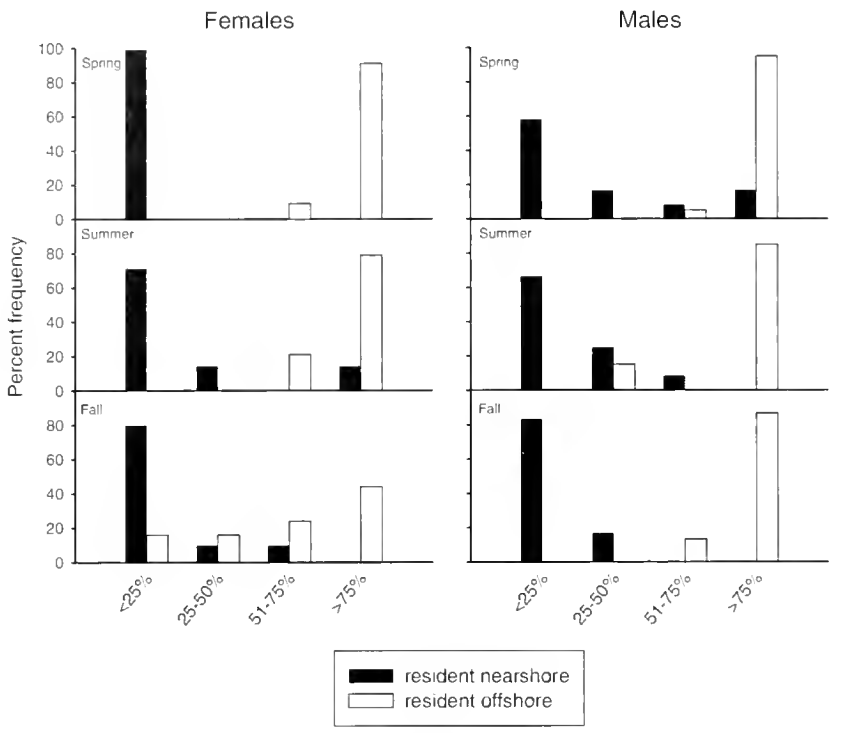

Figure 4

The percentage of gametogenic tissue of resident nearshore and resident offshore queen conch (*Strombus gigas*) by sex and season. The dotted line separates the categories that were combined for statistical analyses.

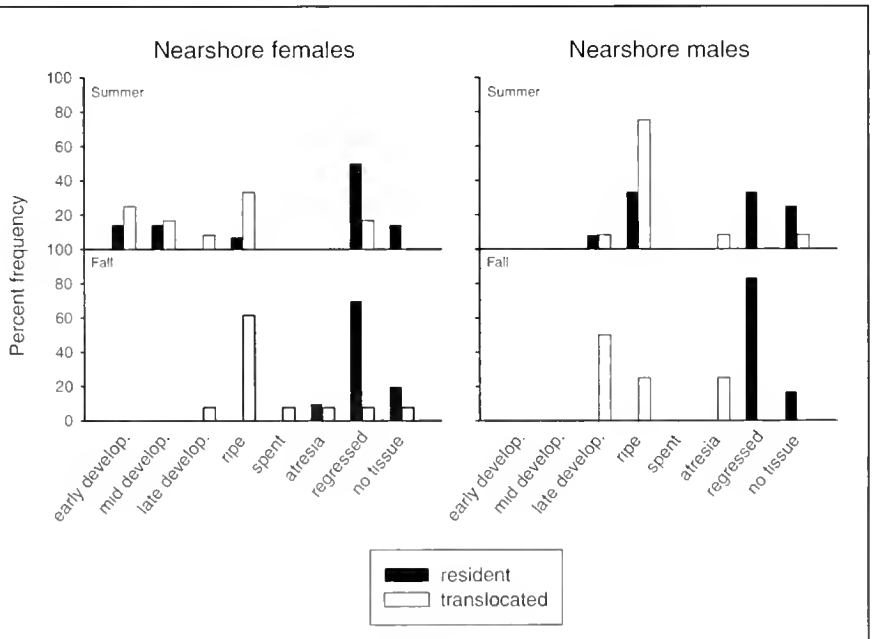

Figure 5

Gonadal maturity of resident nearshore and translocated nearshore queen conch (*Strombus gigas*) by sex and season. The dotted line separates the categories that were combined for statistical analyses.

a higher percentage of translocated nearshore females in some stage of gonadal development than resident nearshore females during the summer; in fact, about 30% of the translocated females were ripe (Fig. 5). By fall, the differences were even more extreme; over 60% of the translocated nearshore females were ripe, whereas all of the resident nearshore females were incapable of reproducing (Fig. 5). Although there was a significant difference in gonadal maturity between translocated nearshore and resident nearshore females during the summer, there was no significant difference in the percentage of gametogenic tissue (Table 5 and Fig. 6). However, by fall, there were significant differences in the percentage of gametogenic tissue between translocated nearshore and resident nearshore females (Table 5). Most translocated nearshore females had developed >75% of the gonad, whereas most resident nearshore females still had <25% gametogenic tissue (Fig. 6).

Histology: males

There were marked differences in gonadal condition of resident nearshore and resident offshore male conch (Fig. 2, D and E). There were significant differences in gonadal maturity between resident offshore and resident nearshore male conch during the spring, summer, and fall (Table 4). During the spring and summer, the gonads of most resident offshore males were categorized as ripe; by fall most were spent (Fig. 3). In contrast, at least half of the resident nearshore males were not capable of spawning during the spring and summer, although some were in the early stages of testicular development and some were even ripe (Fig. 3). However, all the sampled resident nearshore males were incapable of spawning by fall and none were identified as spent (Fig. 3). Histological examinations also revealed significant differences in the percentage of gametogenic tissue between resident offshore and resident nearshore males during the spring, summer,

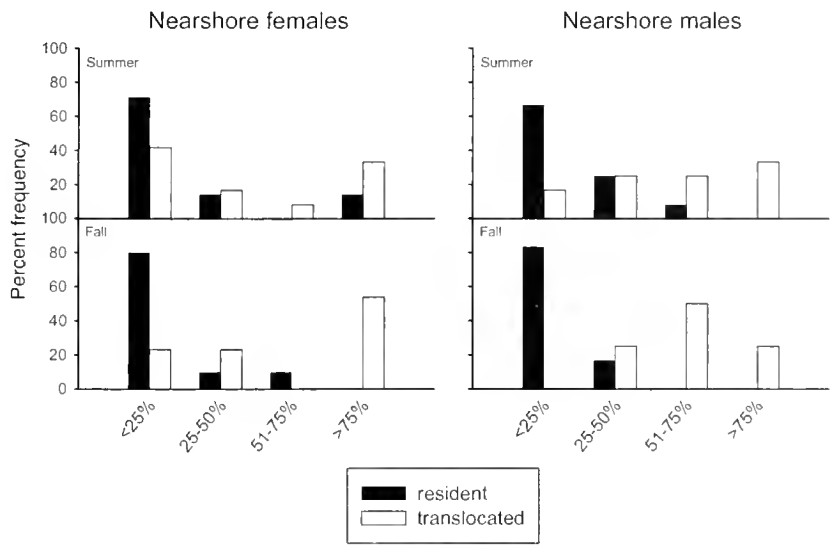

Figure 6

The percentage of gametogenic tissue of resident nearshore and translocated nearshore queen conch (*Strombus gigas*) by sex and season. The dotted line separates the categories that were combined for statistical analyses.

and fall (Table 4). Most resident offshore males had >75% gametogenic tissue throughout the study period, whereas most resident nearshore males had <25% (Fig. 4).

The gonadal condition of translocated nearshore males (Fig. 2F) improved in relation to the gonadal condition of resident nearshore males (Fig. 2D). There were significant differences in gonadal maturity between translocated nearshore and resident nearshore males during both the summer and fall (Table 5). Almost 80% of the translocated nearshore males were ripe during the summer, whereas about half of the resident nearshore males were incapable of reproducing (Fig. 5). By fall, most translocated nearshore males were still capable of reproduction, whereas none of the resident nearshore males were (Fig. 5). There were also significant differences in the percentage of gametogenic tissue between resident nearshore and translocated nearshore males during the summer and fall (Table 5). During the summer, the gonads of most of the resident nearshore males contained <25% gametogenic tissue, whereas translocated nearshore males were divided equally among the four gametogenic tissue categories (Fig. 6). During the fall, the gonads of most of the resident nearshore males still had <25% gametogenic tissue; however, most translocated nearshore males had developed >50% of the gonad (Fig. 6).

Table 5

Probabilities from Fisher's exact test of differences in gonadal maturity and the percentage of gametogenic tissue between resident nearshore and translocated nearshore conch by sex and season. *n* represents the total number of observations. Asterisks (*) indicate that the test was statistically significant.

	Females		Males	
	n	*P*	*n*	*P*
Gonadal maturity				
Summer	26	0.019*	24	0.045*
Fall	23	<0.001*	10	0.033*
% gametogenic tissue				
Summer	26	0.130	24	0.014*
Fall	23	0.038*	10	0.033*

Discussion

In the nearshore region of the Florida Keys, adult queen conch had severe deficiencies in reproductive behavior and gonadal development. Histological examinations of resident nearshore conch revealed that most were incapable of reproducing, whereas resident offshore conch exhibited a normal reproductive cycle (as described by Egan, 1985, and Stoner et al., 1992). Furthermore, our results suggest that female conch may be more sensitive to the negative effects of nearshore conditions than male conch. For example, during the spring and summer, some resident nearshore males were ripe (although their reproductive output would have been severely reduced because of a low percentage of gametogenic tissue), whereas the gonads of

most resident nearshore females contained no germ cells. The latter condition may have been due to the fact that egg production is more costly bioenergetically than sperm production (Ricklefs, 1990).

Mating and spawning do not occur among resident nearshore conch presumably because of their retarded gonadal development; however, the translocation of nearshore conch to the offshore region mitigated the deleterious effects that the nearshore environment had on their gonadal development. The reproductive tissues of translocated nearshore conch began to develop during the summer after the conch had spent about three months offshore. Most translocated female conch were in the early stages of gonadal development, whereas most translocated male conch were ripe. We believe this difference in gonadal development is due to the fact that the starting gonadal condition of nearshore females was worse than the starting condition of male conch. By fall, after six months offshore, most translocated females had become ripe. In addition, the percentage of gametogenic tissue in the gonads of both sexes increased through the summer and fall.

In conjunction with the improvement in gonadal condition, nearshore females translocated to the offshore region were observed spawning during the summer and fall; however, no mating was observed among nearshore conch translocated offshore. Resident offshore conch also had low mating frequencies (<6%). Similarly low mating frequencies have been reported in the Virgin Islands (Randall, 1964) and the Bahamas (Stoner et al., 1992). We suspect that the lack of observations of nearshore conch mating in the offshore region may have been an artifact of the low probability of encountering that activity due to the small number of nearshore conch translocated offshore. Nevertheless, we believe mating must have occurred because translocated nearshore conch were observed spawning. However, it is unknown if queen conch are capable of laying unfertilized egg masses.

The beginning of reproductive activity in queen conch is linked to the start of spring, when water temperatures begin rising (Randall, 1964; Stoner et al., 1992; Weil and Laughlin, 1984). This same seasonal pattern was observed in our study with resident offshore conch. They exhibited the highest mating and spawning frequencies during the spring and reproductive behavior decreased during the ensuing seasons. However, compared with the spawning pattern of resident offshore conch, peak spawning in translocated nearshore conch was delayed; peak spawning occurred during the fall. Nevertheless, there was evidence to suggest that the timing of reproductive behavior of both resident offshore and translocated nearshore conch might eventually become similar. Our results indicated that it takes at least three months after translocation for the negative effects of the nearshore environment to be mitigated and for gonadal maturation to occur. The out-of-phase spawning may have been prevented if the translocations had occurred earlier in the year (e.g., January, instead of March).

Identifying the causative factor or factors that inhibit the reproductive viability of nearshore queen conch requires further study. However, the juxtaposition of the nearshore conch aggregations with human population centers suggests that anthropogenic changes to the nearshore region may be partially responsible. Decreased reproductive output caused by anthropogenic contaminants has been observed in several marine invertebrates, including dogwinkles (*Nucella lapillus*) (Bryan et al., 1987; Gibbs and Bryan, 1986), scallops (Gould et al., 1988), sea urchins (Krause, 1994; Thompson et al., 1989), and shrimps and crabs (Wilson-Ormond et al., 1994). For example, chronic exposure to tributyltin has been shown to sterilize females of several species of mollusks (Matthiessen and Gibbs, 1998), and sublethal levels of copper greatly inhibited gamete production and maturation in scallops (Gould et al., 1988). There have also been numerous reports implicating eutrophication in nearshore habitat degradation in the Florida Keys (Lapointe et al., 1990; Lapointe and Clark, 1992; Szmant and Forrester, 1996); however, very little is known about the effects of increased nutrient levels at the organismal level.

The retarded gonadal condition in nearshore queen conch may also be due to environmental factors such as suboptimal habitat, poor food quality, or temperature extremes associated with shallow water. Research on bivalves has shown that habitat, diet, and food quality directly affect gamete production (Le Pennec et al., 1998; Madrones-Ladja et al., 2002). As they increase in age and size, queen conch undergo ontogenetic migrations from shallow, nearshore sites to deeper-water habitats (Randall, 1964; Sandt and Stoner, 1993; Stoner, 1989; Weil and Laughlin, 1984). It has been hypothesized that as conch grow larger and require more food, they migrate to take advantage of the augmented food supply in more productive offshore habitats (Sandt and Stoner, 1993; Stoner, 1989). However, nearshore queen conch in the Florida Keys are prevented from migrating offshore by Hawk Channel (Glazer and Berg, 1994). Therefore, translocating nearshore conch offshore would, in effect, link these isolated environments.

The implications of this study are of particular importance to the FWC-Florida Marine Research Institute's ongoing queen conch stock restoration program. Translocating naturally recruiting nearshore conch to offshore areas would be more cost effective than hatchery production of juvenile conch, especially because production costs are eliminated and survival of translocated conch is likely to be much greater than that of hatchery outplants (see Stoner, 1997, for a review of juvenile mortality in stock enhancement efforts). Translocations would also have a more immediate effect on reproductive output than would the release of hatchery-reared conch. A translocation program would focus on moving large juveniles and adults offshore, whereas a hatchery program must release small juveniles (to minimize production costs) that would then have to survive to maturity. Consequently, translocations would quickly alleviate the depensatory mechanisms described by Appeldoorn (1995) that can affect the recovery of queen conch stocks. Finally, translocations provide the added benefit of maintaining the genetic diversity of the population. Hatchery-reared conch are typically derived from a few egg masses and there is a concurrent loss in

rare alleles (Allendorf and Ryman, 1987). However, the use of wild conch to enhance the spawning aggregations eliminates this problem.

Queen conch appear to be a prime candidate for rehabilitation by translocation because they meet the criteria associated with successful translocations reported by Griffith et al. (1989). These factors include release within the historical range of the species or into areas of increased habitat quality (or both). Additionally, herbivorous animals stand a greater chance of translocation success than do carnivores or omnivores. Lastly, wild animals translocate more successfully than captive-bred animals. According to these parameters, queen conch are ideally suited for translocations.

However, before a full-scale translocation program can be implemented, there are some theoretical considerations that must be addressed. For example, Stoner and Ray-Culp (2000) reported that conch reproductive behavior reached an asymptotic level near 200 conch/ha.; therefore, it would seem advantageous to enhance reproductive aggregations to that density. However, without high habitat quality, translocations have low success rates regardless of how many animals are released (Griffith et al., 1989). First, we must ascertain if offshore habitats can support the added number of conch or if the translocated or native animals (or both) will simply disperse after release because of density-dependent factors (e.g., intraspecific competition for limited resources). Conch grazing has been shown to significantly reduce the biomass of seagrass macrodetritus and epiphytes (Stoner, 1989). In addition, the effects of removing nearshore conch from the nearshore environment need to be investigated.

Additionally, if increased recruitment is the ultimate goal of the translocation program, larvae must survive and be retained within the Florida Keys. At this point, it is unknown whether larvae produced from translocated nearshore conch are viable or as viable as the larvae produced by native offshore conch. Furthermore, the relative contribution of local and upstream sources to recruitment is unknown. Stoner et al. (1996, 1997) suggested that most of the queen conch larvae entering the Florida Keys come from upstream sources. If this is indeed the case, then local translocations will not be as effective as an international or regional management strategy. However, mechanisms for larval retention in the Florida Keys have been described by Lee and Williams (1999), who suggested that the periodic formation of gyres in the lower Keys may facilitate the retention and recruitment of locally produced larvae. If larvae are retained within the Florida Keys system, any increase in local larval production will increase larval supply and may increase recruitment. Therefore, translocation sites should be located in the lower Keys in order to ensure maximum larval retention and recruitment.

The present study has shown that translocation may be a viable method for rehabilitating queen conch populations in the Florida Keys. We have demonstrated that nearshore conch that were translocated offshore regained some of their reproductive capacity and abilities. Therefore, moving conch from nearshore larval sinks to offshore larval sources may be the key to expediting the recovery of queen conch stocks. Further research (e.g., larval retention studies, studies on the effect of water quality on larval survival, carrying capacity studies) and monitoring will determine the efficacy of this restoration strategy.

Acknowledgments

John Hunt, William Sharp, James Colvocoresses, Allan Stoner, and one anonymous reviewer provided insightful comments on the manuscript. Judy Leiby and Jim Quinn provided editorial comments. We thank Mary Enstrom and Sherry Dawson of The Nature Conservancy (TNC) as well as the numerous TNC volunteers who participated in the field surveys. Meaghan Darcy and other staff members at the Florida Marine Research Institute assisted in the field and in sample processing. This project was funded by Partnerships for Wildlife Grant no. P-3 from the U.S. Fish and Wildlife Service and by the Florida Fish and Wildlife Conservation Commission.

Literature cited

Allendorf, F. W., and N. Ryman.
1987. Genetic management of hatchery stocks. *In* Population genetics and fishery management (N. Ryman and F. Utter, eds.), p. 141–59. Washington Sea Grant, Washington D.C.

Appeldoorn, R. S.
1995. Potential depensatory mechanisms operating on reproductive output in gonochoristic molluscs, with particular reference to strombid gastropods. ICES Mar. Sci. Symp. 199:13–18.

Berg, Jr., C. J., and R. A. Glazer.
1995. Stock assessment of a large marine gastropod (*Strombus gigas*) using randomized and stratified towed-diver censusing. ICES Mar. Sci. Symp. 199:247–258.

Bryan, G. W., P. E. Gibbs, G. R. Burt, and L. G. Hummerstone.
1987. The effects of tributyltin (TBT) accumulation on adult dog-whelks, *Nucella lapillus*: Long-term field and laboratory experiments. J. Mar. Biol. Assoc. U.K. 67:525–544.

Edwards, A. J. and S. Clark.
1999. Coral transplantation: a useful management tool or misguided meddling? Mar. Pollut. Bull. 37:474–487.

Egan, B. D.
1985. Aspects of the reproductive biology of *Strombus gigas*. M.S. thesis, 147 p. Univ. British Colombia, Vancouver, Canada.

Garcia, A., R. Adaya, and G. Ceballos.
1996. Sea turtle conservation in Cuixmala, Jalisco: the role of nest translocation in small beaches. Bull. Ecol. Soc. Am. 77:155.

Gibbs, P. E., and G. W. Bryan.
1986. Reproductive failure in populations of the dog-whelk, *Nucella lapillus*, caused by imposex induced by tributyltin from antifouling paints. J. Mar. Biol. Assoc. U.K. 66:767–777.

Glazer, R. A., and C. J. Berg Jr.
1994. Queen conch research in Florida: an overview. *In* Queen conch biology, fisheries, and mariculture (R. S. Appeldoorn and B. Rodriguez, eds.), p. 79–95. Fundación Cientifica Los Roques, Caracas, Venezuela.

Glazer, R. A., and G. A. Delgado.
2003. Towards a holistic strategy to managing Florida's queen conch (*Strombus gigas*) population. *In* El Caracol *Strombus gigas*: conocimiento integral para su manejo sustentable en el Caribe (D. Aldana Aranda, ed.), p. 73–80. CYTED (Programa Iberoamericano de Ciencia y Technología para el Desarrollo), Yucatán, México.

Glazer, R. A., and J. Quintero.
1998. Observations on the sensitivity of queen conch to water quality: implications for coastal development. Proc. Gulf Carib. Fish. Inst. 50:78–93.

Gould, E., R. J. Thompson, L. J. Buckley, D. Rusanowsky, and G. R. Sennefelder.
1988. Uptake and effects of copper and cadmium in the gonad of the scallop *Placopecten magellanicus*: concurrent metal exposure. Mar. Biol. 97:217–223.

Griffith, B., J. M. Scott, J. W. Carpenter, and C. Reed.
1989. Translocation as a species conservation tool: status and strategy. Science 245:477–480.

Harig, A. L., K. D. Fausch, and M. K. Young.
2000. Factors influencing success of greenback cutthroat trout translocations. North Am. J. Fish. Manag. 20:994–1004.

Krause, P. R.
1994. Effects of an oil production effluent on gametogenesis and gamete performance in the purple sea urchin (*Strongylocentrotus purpuratus* Stimpson). Environ. Toxicol. Chem. 13:1153–1161.

Lapointe, B. E. and M. W. Clark.
1992. Nutrient inputs from the watershed and coastal eutrophication of the Florida Keys. Estuaries 15:465–476.

Lapointe, B. E., J. D. O'Connell, and G. Garrett.
1990. Nutrient couplings between on-site sewage disposal systems, groundwaters, and nearshore surface waters of the Florida Keys. Biogeochem. 10:289–307.

Le Pennec, M., R. Robert, and M. Avendano.
1998. The importance of gonadal development on larval production in pectinids. J. Shellfish Res. 17:97–101.

Lee, T. N., and E. Williams.
1999. Mean distribution and seasonal variability of coastal currents and temperature in the Florida Keys with implications for larval recruitment. Bull. Mar. Sci. 64:35–56.

Madrones-Ladja, J. A., M. R. dela Peña, and N. P. Parami.
2002. The effect of micro algal diet and rearing condition on gonad maturity, fecundity, and embryonic development of the window-pane shell, *Placuna placenta* Linnaeus. Aquaculture 206:313–321.

Matthiessen, P., and P. E. Gibbs.
1998. Critical appraisal of the evidence for tributyltin-mediated endocrine disruption in mollusks. Environ. Toxicol. Chem. 17:37–43.

McCarthy, K. J., C. T. Bartels, M. C. Darcy, G. A. Delgado, and R. A. Glazer.
2002. Preliminary observation of reproductive failure in nearshore queen conch (*Strombus gigas*) in the Florida Keys. Proc. Gulf Carib. Fish. Inst. 53:674–680.

Morgan, L. E. and L. W. Botsford.
2001. Managing with reserves: Modeling uncertainty in larval dispersal for a sea urchin fishery. *In* Spatial processes and management of marine populations (G. H. Kruse, N. Bez, A. Booth, M. W. Dorn, S. Hills, R. N. Lipcius, D. Pelletier, C. Roy, S. J. Smith, and D. Witherell, eds.), p. 667–684. Alaska Sea Grant, AK-SG-01-02. Univ. Alaska, Fairbanks, Alaska.

Randall, J. E.
1964. Contributions to the biology of the queen conch, *Strombus gigas*. Bull. Mar. Sci. 14:246–295.

Ricklefs, R. E.
1990. Ecology. 3rd ed., 896 p. W.H. Freeman and Co., New York, NY.

Rinkevich, B.
1995. Restoration strategies for coral reefs damaged by recreational activities: the use of sexual and asexual recruits. Restoration Ecology 3:241–251.

Sandt, V. J. and A. W. Stoner.
1993. Ontogenetic shift in habitat by early juvenile queen conch, *Strombus gigas*: patterns and potential mechanisms. Fish. Bull. 91:516–525.

Stoner, A. W.
1989. Winter mass migration of juvenile queen conch *Strombus gigas* and their influence on the benthic environment. Mar. Ecol. Prog. Ser. 56:99–104.
1997. The status of queen conch, *Strombus gigas*, research in the Caribbean. Mar. Fish. Rev. 59:14–22.

Stoner, A. W., R. A. Glazer, and P. J. Barile.
1996. Larval supply to queen conch nurseries: relationships with recruitment process and population size in Florida and the Bahamas. J. Shellfish Res. 15:407–420.

Stoner, A. W., N. Mehta, and T. N. Lee.
1997. Recruitment of *Strombus* veligers to the Florida Keys reef tract: relation to hydrographic events. J. Shellfish Res. 16:19–29.

Stoner, A. W. and M. Ray-Culp.
2000. Evidence for allee effects in an over-harvested marine gastropod: density-dependent mating and egg production. Mar. Ecol. Prog. Ser. 202:297–302.

Stoner, A. W., V. J. Sandt, and I. F. Boidron-Metairon.
1992. Seasonality in reproductive activity and larval abundance of queen conch, *Strombus gigas*. Fish. Bull. 90:161–170.

Szmant, A. M., and A. Forrester.
1996. Water column and sediment nitrogen and phosphorous distribution patterns in the Florida Keys, USA. Coral Reefs 15:21–41.

Thompson, B. E., S. M. Bay, J. W. Anderson, J. D. Laughlin, D. J. Greenstein, and D. T. Tsukada.
1989. Chronic effects of contaminated sediments on the urchin *Lytechinus pictus*. Environ. Toxicol. Chem. 8:629–637

van Treeck, P. and H. Schuhmacher.
1997. Initial survival of coral nubbins transplanted by a new coral transplantation technology-options for reef rehabilitation. Mar. Ecol. Prog. Ser. 150:287–292.

Weil, E., and R. Laughlin.
1984. Biology, population dynamics, and reproduction of the queen conch *Strombus gigas* Linne in the Archipielago de los Roques National Park. J. Shellfish Res. 4:45–62.

Wilson-Ormond, E. A., M. S. Ellis, and E. N. Powell.
1994. The effect of proximity to gas producing platforms on size, stage of reproductive development and health in shrimp and crabs. J. Shellfish Res. 13:306.

Zar, J. H.
1996. Biostatistical analysis, 3rd ed., 662 p. Prentice Hall, Upper Saddle River, NJ.

Genetic differentiation among Atlantic cod (*Gadus morhua*) from Browns Bank, Georges Bank, and Nantucket Shoals

Christopher Lage

Department of Biological Sciences
Murray Hall
University of Maine
Orono, Maine 04469

Kristen Kuhn

Irv Kornfield

School of Marine Sciences
Murray Hall
University of Maine
Orono, Maine 04469

E-mail address (for I. Kornfield, contact author): irvk@maine.edu

Abstract—This study examines genetic variation at five microsatellite loci and at the vesicle membrane protein locus, pantophysin, of Atlantic cod (*Gadus morhua*) from Browns Bank, Georges Bank, and Nantucket Shoals. The Nantucket Shoals sample represents the first time cod south of Georges Bank have been genetically evaluated. Heterogeneity of allelic distribution was not observed ($P>0.05$) between two temporally separated Georges Bank samples indicating potential genetic stability of Georges Bank cod. When Bonferroni corrections ($\alpha=0.05$, $P<0.017$) were applied to pairwise measures of population differentiation and estimates of F_{ST}, significance was observed between Nantucket Shoals and Georges Bank cod and also between Nantucket Shoals and Browns Bank cod. However, neither significant differentiation nor significant estimates of F_{ST} were observed between Georges Bank and the Browns Bank cod. Our research suggests that the cod spawning on Nantucket Shoals are genetically differentiated from cod spawning on Browns Bank and Georges Bank. Managers may wish to consider Nantucket Shoals cod a separate stock for assessment and management purposes in the future.

Manuscript approved for publication 5 November 2003 by Scientific Editor.

Manuscript received 20 January 2004 at NMFS Scientific Publications Office.

Fish. Bull. 102:289–297 (2004).

The Atlantic cod (*Gadus morhua*) is a migratory gadid found on both sides of the North Atlantic. In the Northwest Atlantic, cod are distributed nearly continuously along the continental shelf from Greenland to North Carolina, spawning in relatively discrete, temporally stable areas, and different regions are regarded as different management units defined primarily by latitude and bathymetry (Ruzzante et al., 1998). Atlantic cod historically supported economically important fisheries in the Northwest Atlantic (Halliday and Pinhorn, 1996). In U.S. waters, cod are assessed and managed as two stocks: 1) Gulf of Maine and 2) Georges Bank and southward (including Nantucket Shoals). Growth rates differ between the two stocks; growth is slower in the Gulf of Maine compared to growth in Georges Bank (Pentilla et al., 1989); each stock is exploited by the same gear type and may show similar biological responses towards such gear selection. Although both stocks support important commercial and recreational fisheries, each is overexploited and remains at a low biomass level (Mayo and O'Brien, 1998; O'Brien and Munroe, 2001; Mayo et al., 2002). Overexploitation may result in significant life-history changes such as a decline in time to reproductive maturity which has been observed in Georges Bank cod (O'Brien, 1998); such changes may be a compensatory response to overfishing but may also be influenced by shifts in underlying genetic control (Policansky, 1993).

Commercial fisheries are conducted year round, using primarily otter trawls and gill nets. The Canadian fishery on Georges Bank is managed under an individual quota system. United States cod fisheries are managed under the New England Fishery Management Council's Northeast Multispecies Fishery Management Plan (FMP)[1] as implemented by the U.S. Federal Register, 50 CFR Part 648 (U.S. Federal Register, 2003). Under this FMP, cod are included in a complex of 15 groundfish species managed by time and area closures, trip limits, gear restrictions, minimum size limits, days-at-sea restrictions, and a permit moratorium. The FMP's goal is to reduce fishing mortality to levels that will allow stocks within the complex to initially rebuild above minimum biomass thresholds, and, ultimately, to remain at or near target levels.

When ecological and evolutionary processes are responsible for stock structuring, it is necessary to incorpo-

[1] New England Fishery Management Council. 2003. Northeast Multispecies Fishery Management Plan. NEFMC, 50 Water St., Mill 2, Newburyport, MA, 01950

rate them into strategies designed to manage exploited species (Avise, 1998). High dispersive capabilities of many marine fish often correlate with low levels of population divergence over vast areas (Ward et al., 1994; Graves, 1998) and may be particularly true for species characterized by high fecundity, large population size, and potentially long-distance egg and larval dispersal. Although marine fish predominantly have high dispersal rates and low levels of population structuring, migratory species with continuous distributions may develop and maintain stock structure if they show fidelity to natal spawning sites or limited egg and larval dispersal. Fidelity to natal grounds has been shown in Greenland-Iceland cod (Frank, 1992) and Georges Bank haddock (Polacheck et al., 1992). Genetic divergence between areas originates when populations are formed or through the restriction of gene flow. Cod in some regions are known to migrate long distances, whereas in other regions they are nearly stationary (Lear and Green, 1984). Tagging studies in the Gulf of Maine show little exchange between the region east of Browns Bank and Georges Bank, and the inner Gulf of Maine (Hunt et al., 1999); however exchange has been reported among Bay of Fundy, southern Nova Scotia, Browns Bank, and Georges Bank populations (Klein-MacPhee, 2002). Such exchange among cod from different management areas may be important for stock assessments and management practices. Determining underlying genetic structure of spawning stocks is paramount to the conservation and management of overexploited species.

In the last 30 years the use of molecular-based studies in fisheries science has become common (Shaklee and Bentzen, 1998). In cod, a number of studies have used allozymes (Moller, 1968; Jamieson, 1975; Cross and Payne, 1978; Dahle and Jorstad, 1993), but their use and sensitivity are limited because of weak statistical power resulting from low levels of polymorphism and because of processes of balancing selection (Mork et al., 1985; Pogson et al., 1995). Mitochondrial DNA (mtDNA) characterization among Northwest Atlantic cod indicates that there is limited, albeit significant, population structuring throughout most the species' range (Smith et al., 1989; Carr and Marshall, 1991; Pepin and Carr, 1993; Carr et al., 1995; Arnason and Palsson, 1996). Genetic divergence at the vesicle membrane protein locus, pantophysin (*Pan*I), originally called *GM*798 and identified as synaptophysin (*Syp*I) (Fevolden and Pogson, 1997), has been reported among populations of cod from the Northwest Atlantic (Pogson, 2001; Pogson et al., 2001), Norway and the Arctic (Fevolden and Pogson, 1997), and Iceland (Jonsdottir et al., 1999, 2002). High levels of variation have been reported at nuclear RFLP loci (Pogson et al., 1995; Pogson et al., 2001), and especially at microsatellite loci (Bentzen et al., 1996; Ruzzante et al., 1996a, 1996b, 1997, 1998; Beacham et al., 1999; Miller et al., 2000; Ruzzante et al., 2000, 2001). By using microsatellites, significant genetic structuring has been detected among cod populations on major continental shelves and on neighboring banks that are separated by deep channels and have gyre-like circulation patterns hypothesized to act as retention mechanisms for eggs and larvae (Ruzzante et al., 1998). Although both Browns and Georges Bank maintain persistent gyre-like circulation patterns that may act to retain eggs and larvae, they are separated by the Fundian Channel (>260 m) which may pose a barrier to juvenile and adult migration (Klein-MacPhee, 2002). Evaluation of Northwest Atlantic haddock by using microsatellites showed similarly significant stock structuring from Newfoundland to Nantucket Shoals (Lage et al., 2001). Current assessment and management of cod in U.S. waters combine Georges Bank with the regions to its south including Nantucket Shoals. This study investigates genetic stock structure among cod from this region and provides additional insight for scientists and managers.

Materials and methods

Sampling

Samples of adult cod were collected through the U.S. National Marine Fisheries Service and the Canadian Department of Fisheries and Oceans groundfish surveys between 1994 and 2000. Adult cod were obtained from each of the following spawning grounds (Fig. 1): Browns Bank (July 1994, n=30), Georges Bank (March 1994, n=48; March 1999, n=96; Σn=144), and Nantucket Shoals (March 2000, n=97). Blood or tissue (or both) was obtained from individual fish and preserved in 95% ethanol for subsequent DNA extraction.

DNA extraction, amplification, and visualization

DNA was extracted by using either a Qiamp DNA Mini Kit (Qiagen Inc., Valencia, CA) or by following a published protocol designed for nucleated blood cells (Ruzzante et al., 1998). Five microsatellite loci—*Gmo*1, *Gmo*132 (Brooker et al., 1994), *Gmo*8, *Gmo*19, *Gmo*34 (Miller et al., 2000), and the pantophysin locus, *Pan*I (Fevolden and Pogson, 1997; Pogson, 2001)—were used to evaluate genetic diversity. Polymerase chain reactions (PCR) of all loci were performed in an Eppendorf Mastercycler Gradient thermal cycler. Final concentrations of reagents in a 25 μL PCR cocktail were as follows: ~10 ng of genomic DNA, 1×PCR buffer pH 9.5 [10 mM KCl, 20 mM Tris-HCl pH 8.3, 10 mM $(NH_4)_2SO_4$], 1.5 mM $MgCl_2$, 200 μM each dNTP, 0.15 μM forward primer, 0.15 μM reverse primer (unlabeled for the *Pan*I locus and 5'-labeled with a TET, FAM, or HEX ABI dye for all microsatellite loci), and 0.75 units of Taq DNA polymerase. PCR conditions were as follows: initial 5 min at 95°C, 30 cycles of denaturing at 95°C for 1 min, annealing at 50°C (*Gmo*8, *Gmo*19, and *Gmo*34), 55°C (*Pan*I), and 57°C (*Gmo*1 and *Gmo*132) for 1 min 30 s, and extending at 72°C for 1 min 30 s with a final extension of 72°C for 10 min. *Gmo*19 and *Gmo*34, as well as *Gmo*1 and *Gmo*132, were multiplexed in two 25 μL PCR reactions. Flourescent microsatellite PCR products were visualized on an ABI377 automated DNA sequencer (Perkin-Elmer Corporation, Foster City, CA) and were analyzed by using GeneScan (vers. 2.1) and Genotyper (vers. 2.1) software programs (Perkin-Elmer Corporation, Foster City, CA). *Pan*I PCR

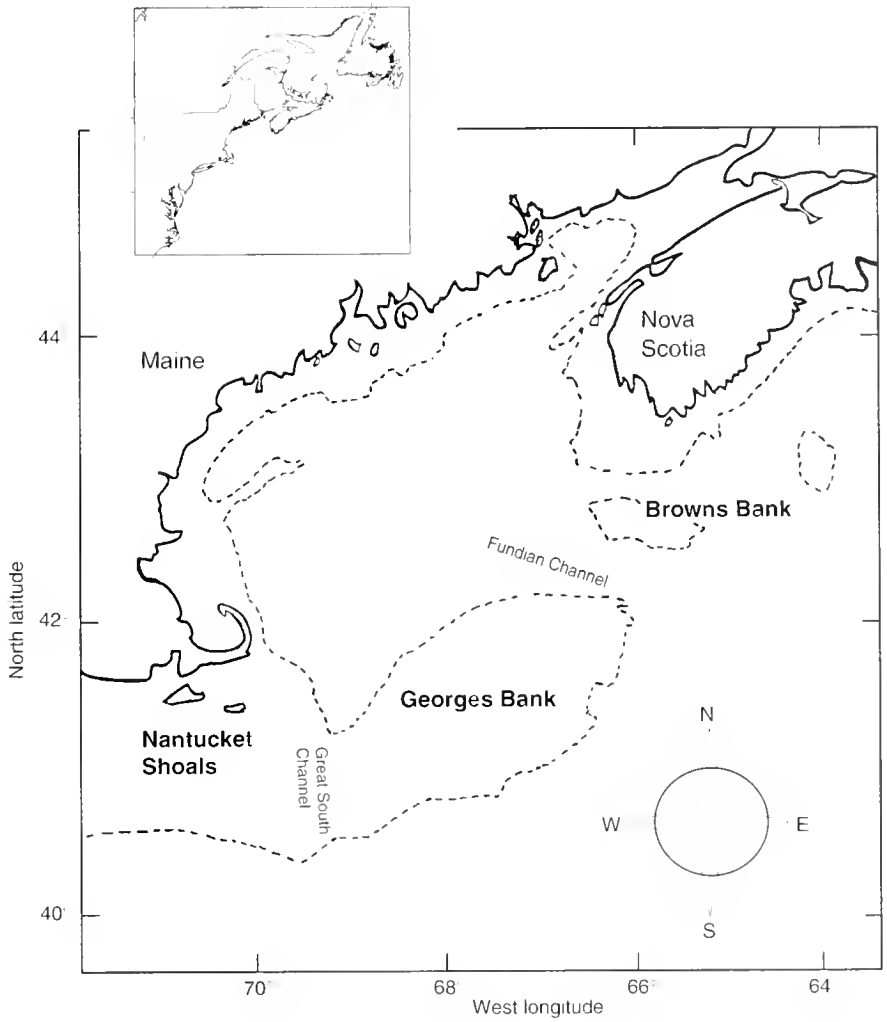

Figure 1

Map of Northwest Atlantic sampling regions for Atlantic cod (*Gadus morhua*). Dashed lines indicate the 100-m isobath.

products were digested with the restriction endonuclease *Dra*I for at least 2 hours at 37°C and visualized on 2% agarose gels to determine presence of $Pan\text{I}^{A}$ or $Pan\text{I}^{B}$ (or both) allelic variants.

Genetic analyses

Samples were tested for conformation to Hardy-Weinberg equilibrium (HWE) expectations by the Markov chain method (Guo and Thomson, 1992) by resampling 2000 iterations per batch for 200 batches with GENEPOP vers. 3.1d (CEFE/CNRS, Montpelier, France; available at http://www.cefe.cnrs-mop.fr/) (Raymond and Rousset, 1995); the null hypothesis tested was random union of gametes within a population. All loci were tested for genotypic disequilibrium across the entire data set, as well as for individual populations by using Markov chain resampling with 2000 iterations per batch for 200 batches in GENEPOP vers. 3.1d; the null hypothesis tested was that the genotypes at one locus are independent from genotypes at the other locus.

Tests of allelic and genotypic differentiation among and between population samples were conducted by using FSTAT 2.9.1 (UNIL, Lausanne, Switzerland; available at http://www.unil.ch/izea/softwares/fstat.html) (Goudet, 1995); the null hypothesis tested was homogeneous distributions across samples. Because alleles can be considered as independent when samples conform to HWE, it is valid to permute alleles among samples to test for population differentiation. On the other hand, when HWE is rejected within samples, alleles within an individual cannot be considered independent, and thus permuting genotypes among samples is the only valid permutation scheme. In both cases, contingency tables were generated and classified by using the log-likelihood statistic G (Goudet et al, 1996). Estimates of among- and between-sample F_{ST}'s were generated according to Weir and Cocherham (1984) with FSTAT vers. 2.9.1 and GENETIX vers. 4.04 (available

Table 1

Genetic variation in sampled populations of Atlantic cod (*Gadus morhua*) and *P*-value (in parentheses) for among sample population differentiation. n = observed number of alleles; H_0 = observed heterozygosity; F_{ST} = the among-sample *P*-value); bp = base pairs; * = significant deviation from HWE (α=0.05, P<0.0083); † = P <0.05; ‡ P= ≤0.001

			Browns Bank		Georges Bank		Nantucket Shoals			
Locus	Σn	Allelic range	H_0	n	H_0	n	H_0	n	F_{ST}	Differentiation
*Pan*I	2	*Pan*I^A/*Pan*I^B	0.0385	2	0.0397	2	0.0222	2	−0.0052 (0.767)	0.7820
*Gmo*1	5	96–110 bp	0.1000	4	0.1319	5	0.1505	5	0.0019 (0.307)	0.3210
*Gmo*8	23	118–201 bp	0.8929	17	0.8370	19	0.8444	20	0.0001 (0.437)	0.5200
*Gmo*19	26	120–237 bp	0.8846	17	0.8148*	25	0.7975*	23	−0.0021 (0.857)	0.8320
*Gmo*34	11	82–120 bp	0.7778	5	0.5683	11	0.6630	7	−0.0033 (0.797)	0.8400
*Gmo*132	21	105–155 bp	0.8333	13	0.8214	17	0.7727	16	0.0255 (0.000)‡	0.0010‡
All loci	88	—	—	—	—	—	—	—	0.0047 (0.001)‡	0.0240†

at http://www.univ-montp2.fr/~genetix/genetix/genetix.htm) (Belkhir et al.[2]). Significance of F_{ST} estimates was determined with 2000 randomizations. Tests of population differentiation and estimations of F_{ST} were calculated at each locus individually and at all loci combined. To correct for simultaneous comparisons, standard Bonferroni corrections were applied by using a global significance level of 0.05 (Rice, 1989).

Results

Genetic variation

Observed numbers of alleles, allelic ranges, heterozygosities, and deviations from HWE are presented in Table 1. All tests of genotypic linkage disequilibrium were nonsignificant at the global and population levels. When Bonferroni corrections for multiple tests were applied to tests of HWE (α=0.05, P<0.0083), the pooled Georges Bank sample deviated significantly at *Gmo*19, and the Nantucket Shoals sample deviated at *Gmo*8 and at *Gmo*19. Interestingly, these two loci have the greatest variation based on number of alleles and heterozygosity. In each case, the cause of deviation was due to an excess of homozygotes. Population samples that generally conform to expectations of random mating but show a lack of concordance to HWE at one or more loci may be due to a number of processes including null alleles, genetic drift, admixture, selection, and insufficient sampling (e.g., Ruzzante, 1998). Possible explanations of homozygote excess include sample admixture (Wahlund effect) or drift; however these explanations are unlikely because one would expect to see similar results at all loci. More likely explanations are the presence of null alleles or selection. Deviations of HWE at *Gmo*8 and *Gmo*19 were not observed in all population samples, indicating that null alleles were not present at a global-level but may be present at the population-level for these two loci. Subsequently, any significant population structuring observed at these loci should be viewed with caution (see below).

Population structure

Tests of population structure are shown in Table 2. Although *Gmo*8 and *Gmo*19 showed significant deviations from HWE, they did not support any significant population structuring even when tests of population differentiation were performed without assuming conformation to HWE (i.e., permuting among genotypes rather than alleles). Heterogeneity of allelic distribution was not observed (P>0.05) between the 1994 and 1999 Georges Bank samples at each locus individually and at all loci combined, thus indicating potential genetic stability of Georges Bank cod. These samples were subsequently pooled to form a single Georges Bank population sample to facilitate statistical analyses by allowing for better estimations of allele frequencies and by reducing the number of pairwise tests. Tests of population differentiation among samples showed significant divergence at *Gmo*132 (P<0.01) and at all loci combined (P<0.05). When Bonferroni corrections were applied to pairwise measures of divergence (α=0.05, P<0.017), significance was observed between Nantucket Shoals and Georges Bank at *Gmo*132 and at all loci combined, and also between Nantucket Shoals and Browns Bank at *Gmo*132. No significant differentiation was observed between individual or pooled Georges Bank samples and the Browns Bank sample.

Significant among-population F_{ST} values were estimated at *Gmo*132 (0.0255, P<0.001) and at all loci combined (0.0047, P<0.01). When Bonferroni corrections were applied, significant pairwise-population F_{ST} values were estimated between Nantucket Shoals and Browns Bank at *Gmo*132 (0.0624, P<0.001) and at all loci combined

[2] Belkhir K., P. Borsa, L. Chikhi, N. Raufaste, and F. Bonhomme. 2002. GENETIX 4.04, logiciel sous Windows TM pour la génétique des populations. Laboratoire Génome, Populations, Interactions, CNRS UMR 5000, Université de Montpellier II, Montpellier (France).

Table 2

Genetic structuring in sampled populations of Atlantic cod (*Gadus morhua*): Above diagonal are *P*-values for pairwise differentiation. Below diagonal are pairwise F_{ST} values; upper values are for all loci combined; lower values are for *Gmo*132. * = $P < 0.0167$ ($\alpha = 0.05$ for three comparisons); ** = $P \leq 0.001$.

	Browns Bank	Georges Bank	Nantucket Shoals
Browns Bank	—	0.5440	0.2970
	—	0.1120	0.0020*
Georges Bank	0.0012	—	0.0030*
	0.0124	—	0.0010**
Nantucket Shoals	0.0114*	0.0045*	—
	0.0624**	0.0226**	—

(0.0114, $P<0.017$), and between Nantucket Shoals and Georges Bank at *Gmo*132 (0.0226, $P<0.001$) and at all loci combined (0.0045, $P<0.017$). Estimates of F_{ST} values between Browns Bank and Georges Bank samples were all nonsignificant. No significant genetic structuring was observed in any comparison when *Gmo*132 was excluded from the analysis.

Discussion

Georges Bank, a large, shallow offshore bank located along the southern edge of the Gulf of Maine off the U.S. and Canadian coasts (Fig. 1), supports a large fish biomass. High primary productivity and tightly bound system energetics on the bank result in relatively stable levels of overall biomass and total fish production, although major shifts in species composition routinely occur (Fogarty and Murawski, 1998). The largest spawning aggregation of cod on Georges Bank is found on the Northeast Peak, a gravel region that is an important habitat for the early demersal phase of cod, and may represent a limiting resource for this stock (Lough and Bolz 1989; Langton et al., 1996). The bank maintains its own circulation pattern in a slow clockwise gyre which may act as a transportation and retention mechanism for planktonic eggs and larvae (Smith and Morse, 1984; Lough and Bolz, 1989). There may be exchange of biota among regions by episodic fluxes of shelf water carrying eggs and larvae away from the Scotian Shelf and Browns Bank onto Georges Bank (Cohen et al., 1991; Townsend and Pettigrew, 1996; Bisagni and Smith, 1998). Once on Georges Bank, planktonic eggs and larvae may, depending on depth, be entrained and transported to gravel settlement sites along the western edge of Georges Bank (Smith and Morse 1984; Lough and Bolz, 1989; Werner et al., 1993). However, wind-driven advection may cause egg and larval loss from the Northeast Peak and southern flank of Georges Bank (Lough et al., 1989). Cod spawned in the Gulf of Maine usually drift southeasterly towards Georges Bank because of the counterclockwise Gulf of Maine gyre, but the extent of egg and larval exchange between these regions is unknown (Serchuk et al., 1994).

Cod have been found from the surface to depths greater than 450 meters; however few cod proximate to the Gulf of Maine occur deeper than 180 meters (Klein-MacPhee, 2002). Browns Bank and Georges Bank are bathymetrically separated by the relatively deep (>260 meters) Fundian Channel which may act as a barrier to adult migration, whereas Georges Bank and Nantucket Shoals are separated by the relatively shallow (<100 meters) Great South Channel. Although the latter channel is probably not a significant barrier to adult migration, it is an area of strong recirculation towards Georges Bank and could limit egg and larval dispersal. Tagging studies show little exchange of adults between the inner Gulf of Maine and the region east of Browns Bank and Georges Bank (Hunt et al., 1999), but limited exchange has been reported among the Bay of Fundy, southern Nova Scotia, Browns Bank, and Georges Bank (Klein-MacPhee, 2002).

The likelihood of determining correct population structure increases when population differentiation is stable over time (Waples, 1998). Results from this study are concordant with observations of temporal stability of microsatellite variation observed in Atlantic cod (Ruzzante et al., 1996a, 1997, 2001). Tests of population differentiation and subdivision cannot reject the maintenance of genetic homogeneity among Georges Bank cod from 1994 to 1999 and thus may indicate some degree of temporal genetic stability among adult Georges Bank cod.

Our results indicate that cod from Nantucket Shoals are genetically distinct from those from Browns Bank and Georges Bank, and cod from the two Banks are more genetically similar. The observed lack of heterogeneity between Browns Bank and Georges Bank is consistent with gene flow—perhaps due to episodic larval transport and some level of limited adult exchange. Nantucket Shoals cod may be genetically distinct because of egg and larval isolation by entrainment in the Georges Bank gyre or because of limited movement of adults between regions (or a combination of both). Eggs and larvae spawned on Nantucket Shoals most likely do not enter the Georges Bank gyre system; these early life history forms may be retained on the shoals or transported to the southwest by prevailing circulation (Fogarty and Murawski, 1998). Some North Atlantic cod stocks have shown substantial differences in

growth rate, reproductive capacity, and maturity schedules related to temperature (Brander, 1994). Cod within our study zone generally avoid water temperatures greater than 10°C, but Nantucket Shoals cod are abundant in temperatures as warm as 15°C (Klein-MacPhee, 2002). This differential thermal tolerance may support genetic structuring of Nantucket Shoals cod by selecting against individuals from other areas.

Closely related gadid species such as cod and haddock may exhibit similar patterns of population genetic structuring associated with similar life histories, selective pressures, and ecological constraints. Our results are concordant with a previous study suggesting that haddock from Browns Bank and Georges Bank are genetically similar and that haddock from Nantucket Shoals are distinct (Lage et al., 2001). However, Ruzzante et al. (1998) observed significant genetic differentiation between cod from Browns Bank and Georges Bank. Our results do not agree with this previously observed heterogeneity between Browns Bank and Georges Bank and may be due to the examination of different loci, different sampling comparisons, or small sample sizes used in both studies (or to a combination of these variables) (Ruzzante, 1998; Smouse and Chevillon, 1998).

Among loci, the greatest genetic differentiation was observed at locus *Gmo*132. Indeed, observed statistical significance of population differentiation and F_{ST} depends entirely on *Gmo*132. Length variation at *Gmo*132 is a function of mutations in the repetitive array and of an indel in a flanking region (Ruzzante et al., 1998) causing bimodal allele distributions in some populations. When compared to other microsatellite loci, *Gmo*132 has shown the greatest differentiation among other Northwest Atlantic cod populations (Bentzen et al., 1996; Ruzzante et al., 1998, 2001) and among Northwest Atlantic haddock populations (Lage et al., 2001) by an order of magnitude. Other loci examined have not shown similarly strong measures of population structuring. Observed genetic structuring may be due to forces currently determining regional larval and adult distributions, including bathymetry and oceanographic patterns. However, because similar genetic structuring is not observed at all loci, another potential explanation is that structuring at *Gmo*132 is due to forces that acted during the formation of populations rather than to forces presently maintaining strong reproductive isolation. Once genetic structure was generated during the formation of these populations subsequent to the last ice age, biological and oceanographic forces may have maintained such structure; other loci may show an absence of structure simply because it may not have been present when populations were formed. Pogson et al. (2001) reported that the recent age of populations, rather than extensive gene flow, may be responsible for weak population structure in Atlantic cod, and that interpreting limited genetic differences among populations as reflecting high levels of ongoing gene flow should be made with caution. This suggests that the observed lack of heterogeneity between Browns Bank and Georges Bank may not be due to high levels of ongoing gene flow, but to similarities between recently generated populations maintained by small but adequate levels of gene flow.

Alternatively, significant structuring associated with *Gmo*132 in both cod and haddock may suggest that selection is acting at this or at a linked locus. Although microsatellites themselves may be generally considered neutral, there is, in theory, potential for physical linkage or drift-generated linkage disequilibrium between microsatellite and functional loci. There is however, recent evidence of selection acting directly on microsatellite loci in tilapia in high-salinity environments. Streelman and Kocher (2002) found a strong functional genotype-environment interaction and suggested that microsatellite repeats of varying length might induce promoter conformations that differ in their capacity to bind transcriptional regulators. A potential selective mechanism to support the observed genetic structuring of Nantucket Shoals cod (and haddock) may be differential thermal tolerance, although this hypothesis remains untested.

There is strong evidence for an unusual mix of balancing and directional selection at the pantophysin (*Pan*I) locus in cod but no evidence of stable geographically varying selection among North Atlantic populations (Pogson, 2001; Pogson et al., 2001). In the present study, the *Pan*I locus showed little variation and no significant genetic structuring (Table 1). The observed lack of geographic structuring at *Pan*I provides no evidence for local adaptation. However, our observations may be due to strong balancing selection among the geographically proximate populations examined or, if *Pan*I is not under selection, insufficient variation to resolve genetic structure. Alternatively, this observed lack of genetic divergence at *Pan*I could be due to similarities among recently generated populations of North Atlantic cod.

Our research suggests that the cod spawning on Nantucket Shoals are genetically differentiated from cod spawning on Browns Bank and Georges Bank. Managers may wish to consider Nantucket Shoals cod as a separate stock for assessment and management purposes in light of current practices that combine Georges Bank with regions to the south as one management unit. Cod from within the Gulf of Maine can potentially migrate along the coast to Nantucket Shoals where there is little geographic barrier to adult movement. If this is true, the Nantucket Shoals sample that we analyzed may actually be representative of a mixed Gulf of Maine and Nantucket Shoals population. Additional analyses are needed to evaluate the hypothesis that Nantucket Shoals cod are genetically distinct from cod spawning within the Gulf of Maine. Further studies should address the issues of temporal stability and robust sampling and should incorporate cod samples from within the Gulf of Maine.

Acknowledgments

We thank three anonymous reviewers for their insightful comments. We thank the captains, crews, and scientists from the Canadian Department of Fisheries and Oceans and the United States. National Marine Fisheries Service. In particular, we would like to thank Chris Taggart, Nina Shepard, and Holly McBride for assistance in obtaining

samples. IK thanks Maryhaven for support. This work was funded by OCE9806712 from the U.S. National Science Foundation.

Literature cited

Arnason, E., and S. Palsson.
1996. Mitochondrial cytochrome b DNA sequence variation of Atlantic cod (*Gadus morhua*) from Norway. Mol. Ecol. 5:715–724.

Avise, J. C.
1998. Conservation genetics in the marine realm. J. Hered. 89:377–382.

Beacham, T. D., J. Brattey, K. M. Miller, L. D. Khai, and R. E. Withler.
1999. Population structure of Atlantic cod (*Gadus morhua*) in the Newfoundland and Labrador area based on microsatellite variation. DFO Canadian Stock Assessment Secretariat Research Document 99/35:1–32.

Bentzen, P., C. T. Taggart, D. E. Ruzzante, and D. Cook.
1996. Microsatellite polymorphism and the population structure of Atlantic cod (*Gadus morhua*) in the northwest Atlantic. Can. J. Fish. Aquat. Sci. 53:2706–2721.

Bisagni, J. J., and P. C. Smith.
1998. Eddy-induced flow of Scotian Shelf water across Northeast Channel, Gulf of Maine. Continental Shelf Res. 18:515–539.

Brander, K. M.
1994. Patterns of distribution, spawning, and growth in North Atlantic cod: the utility of inter-regional comparisons. International Council for the Exploration of the Seas (ICES) Marine Science Symposia 198:406–413.

Brooker, A. L., D. Cook, P. Bentzen, J. M. Wright, and R. W. Doyle.
1994. The organization of microsatellites differs between mammals and cold water fishes. Can. J. Fish. Aquat. Sci. 51:1959–1966.

Carr, S. M., and H. D. Marshall.
1991. Detection of intraspecific DNA sequence variation in the mitochondrial cytochrome b gene of Atlantic cod (*Gadus morhua*) by the polymerase chain reaction. Can. J. Fish. Aquat. Sci. 48:48–52.

Carr, S. M., A. J. Snellen, K. A. Howse, and J. S. Wroblewski.
1995. Mitochondrial DNA sequence variation and genetic stock structure of Atlantic cod (*Gadus morhua*) from bay and offshore locations on the Newfoundland continental shelf. Mol. Ecol. 4:79–88.

Cohen, E. B., D. G. Mountain, and R. O'Boyle.
1991. Local-scale versus large-scale factors affecting recruitment. Can. J. Fish. Aquat. Sci. 48:1003–1006.

Cross, T. F., and R. H. Payne.
1978. Geographic variation in Atlantic cod, *Gadus morhua*, off Eastern North America: a biochemical systematics approach. J. Fish. Res. Board Can. 35:117–123.

Dahle, G., and K. E. Jorstad.
1993. Haemoglobin variation in cod- a reliable marker for Arctic cod (*Gadus morhua* L.). Fish. Res. 16:301–311.

Fevolden, S. E., and G. H. Pogson.
1997. Genetic divergence at the synaptophysin (*Syp1*) locus among Norwegian coastal and north-east Arctic populations of Atlantic cod. J. Fish. Biol. 51:895–908.

Fogarty, M. J., and S. A. Murawski.
1998. Large-scale disturbance and the structure of marine systems: fishery impacts on Georges Bank. Ecol. Appl. 8:S6–S22.

Frank, K. T.
1992. Demographic consequences of age-specific dispersal in marine fish populations. Can. J. Fish. Aquat. Sci. 49:2222–2231.

Goudet, J.
1995. FSTAT (vers. 1.2): a computer program to calculate F-statistics. J. Hered. 86:485–486.

Goudet, J., M. Raymond, T. De Meeus, and F. Rousset.
1996. Testing divergence in diploid populations. Genetics 144:933–940.

Graves, J. E.
1998. Molecular insights into population structure of cosmopolitan marine fishes. J. Hered. 89:427–437.

Guo, S. W., and E. A. Thomson.
1992. Performing the exact test of Hardy-Weinberg proportions for multiple alleles. Biometrics 48:361–372.

Halliday, R. G., and A. T. Pinhorn.
1996. North Atlantic fishery management systems: a comparison of management methods and resource trends. J. Northw. Atl. Fish. Sci. 20:1–143.

Hunt, J. J., W. T. Stobo, and F. Almeida.
1999. Movement of Atlantic cod, *Gadus morhua*, tagged in the Gulf of Maine area. Fish. Bull. 97:842–860.

Jamieson, A.
1975. Enzyme type of Atlantic cod stocks on the North American banks. *In* Isozymes IV: Genetics and evolution (C. L. Markert (ed.), p. 491–515. Academic Press, New York, NY.

Jonsdottir, O. D. B., A. K. Imsland, A.K., Danielsdottir and G. Marteinsdottir.
2002. Genetic heterogeneity and growth properties of different genotypes of Atlantic cod (*Gadus morhua* L.) at two spawning sites off south Iceland. Fish. Res. 55:37–47.

Jonsdottir, O. D. B., A. K. Imsland, A.K., Danielsdottir, V. Thorsteinsson, and G. Naevdal.
1999. Genetic differentiation among Atlantic cod in south and south-east Icelandic waters: synaptophysin (*Syp1*) and haemoglobin (*Hbl*) variation. J. Fish. Biol. 54:1259–1274.

Klein-MacPhee, G.
2002. Cods. Family Gadidae. *In* Bigelow and Shroeder's fishes of the Gulf of Maine III (B. B. Collette and G. Klein-MacPhee, eds.), p. 223–260. Smithsonian Institution Press, Washington D.C.

Lage, C. R., M. Purcell, M. Fogarty, and I. Kornfield.
2001. Microsatellite evaluation of haddock (*Melanogrammus aeglefinus*) stocks in the northwest Atlantic ocean. Can. J. Fish. Aquat. Sci. 58:982–990.

Langton, R. W., R. S. Steneck, V. Gotceitas, F. Juanes, and P. Lawton.
1996. The interface between fisheries research and habitat management. N. Am. J. Fish. Manag. 16:1–7.

Lear, W. H., and J. M. Green.
1984. Migration of the "northern" Atlantic cod and the mechanisms involved. *In* Mechanisms of migration in fishes (J. D. McCleave, ed.), p. 309–315. Plenum, New York, NY.

Lough, R. G., and G. R. Bolz.
1989. The movements of cod and haddock larvae onto the shoals of Georges Bank. J. Fish. Biol. (suppl. A) 35:71–79

Lough, R. G., P. C. Valentine, D. C. Potter, P. J. Auditore, G. R. Bolz, J. D. Jielson, and R. I. Perry.
1989. Ecology and distribution of juvenile cod, and haddock in relation to sediment type and bottom currents on eastern Georges Bank. Mar. Ecol. Prog. Ser. 56:1–12.

Mayo, R. K., and L. O'Brien.
1998. Atlantic cod. *In* Status of fishery resources off the northeastern United States for 1998 (S. H. Clark, ed.), p. 49–52. NOAA Tech. Memo. NMFS-NE-115.

Mayo, R. K., E. M. Thunberg, S. E. Wigley, and S. X. Cadrin.
2002. The 2001 assessment of the Gulf of Maine Atlantic cod stock. Northeast Fish. Sci. Cent. Ref. Doc. 02-02, 154 p.

Miller, K. M., K. D. Le, and T. D. Beacham.
2000. Development of tri- and tetranucleotide repeat microsatellite loci in Atlantic cod (*Gadus morhua*). Mol. Ecol. 9:238–239.

Moller, D.
1968. Genetic diversity in spawning cod along the Norwegian coast. Hereditas 60:1–32.

Mork, J., Ryman, N., Stahl, G., Utter, F. and G. Sundness.
1985. Genetic variation in Atlantic cod (*Gadus morhua*) throughout its range. Can. J. Fish. Aquat. Sci. 42:1580–1587.

O'Brien, L.
1998. Factors influencing rates of maturation in the Georges Bank and the Gulf of Maine Atlantic cod stocks. NAFO Sci. Counc. Res. Doc. 98/104, 34 p.

O'Brien, L., and N. J. Munroe.
2001. Assessment of the Georges Bank Atlantic cod stock for 2001. Northeast Fish. Sci. Cent. Ref. Doc. 01-10, 126 p.

Pentilla, J. A., G. A. Nelson, and J. M. Burnett III.
1989. Guidelines for estimating lengths at age for 18 northwest Atlantic finfish and shellfish species. NOAA Tech. Memo. NMFS-F/NEC-66, 39 p.

Pepin, P., and S. M. Carr.
1993. Morphological, meristic, and genetic analysis of stock structure in juvenile Atlantic cod (*Gadus morhua*) from the Newfoundland shelf. Can. J. Fish. Aquat. Sci. 50:1924–1933.

Pogson, G. H.
2001. Nucleotide polymorphism and natural selection at the pantophysin (*Pan*I) locus in the Atlantic cod, *Gadus morhua* (L.). Genetics 157:317–330.

Pogson, G. H., K. A.Mesa, and R. G. Boutilier.
1995. Genetic population structure and gene flow in the Atlantic cod, *Gadus morhua*: a comparison of allozyme and nuclear RFLP loci. Genetics 139:375–385.

Pogson, G. H., C. T. Taggart, K. A. Mesa, and R. G. Boutilier.
2001. Isolation by distance in the Atlantic cod, *Gadus morhua*, at large and small geographic scales. Evolution 55:131–146.

Polacheck, T., D. Mountain, D. McMillan, W. Smith, and P. Berrien.
1992. Recruitment of the 1987 year class of Georges Bank haddock (*Melanogrammus aeglefinus*): the influence of unusual larval transport. Can. J. Fish. Aquat. Sci. 49: 484–496.

Policansky, D.
1993. Fishing as a cause of evolution in fishes. *In* The exploitation of evolving populations (T. K. Stokes, J. M. McGlade, and R. Law, eds.), p. 2–18. Springer-Verlag, Berlin.

Raymond, M., and F. Rousset.
1995. GENEPOP (vers. 1.2): population genetics software for exact tests and eumenism. J. Hered. 86:248–249.

Rice, W. R.
1989. Analyzing tables of statistical tests. Evolution 43: 223–225.

Ruzzante, D. E.
1998. A comparison of several measures of genetic distance and population structure with microsatellite data: bias and sampling variance. Can. J. Fish. Aquat. Sci. 55:1–14.

Ruzzante, D. E., C. T. Taggart, and D. Cook.
1996a. Spatial and temporal variation in the genetic composition of a larval cod (*Gadus morhua*) aggregation: cohort contribution and genetic stability. Can. J. Fish. Aquat. Sci. 53:2695–2705.

Ruzzante, D. E., C. T. Taggart, and D. Cook.
1998. A nuclear basis for shelf- and bank-scale population structure in northwest Atlantic cod (*Gadus morhua*): Labrador to Georges Bank. Mol. Ecol. 7:1663–1668.

Ruzzante, D. E., C. T. Taggart, D. Cook, and S. Goddard.
1996b. Genetic divergence between inshore and offshore Atlantic cod (*Gadus morhua*) off Newfoundland: microsatellite DNA variation and antifreeze level. Can. J. Fish. Aquat. Sci. 53:634–645.

Ruzzante, D. E., C. T. Taggart, D. Cook, and S. Goddard.
1997. Genetic differentiation between inshore and offshore Atlantic cod (*Gadus morhua*) off Newfoundland: a test and evidence of temporal stability. Can. J. Fish. Aquat. Sci. 54:2700–2708.

Ruzzante, D. E. C. T. Taggart, R. W. Doyle, and D. Cook.
2001. Stability in the historical pattern of genetic structure of Newfoundland cod (*Gadus morhua*) despite the catastrophic decline in population size from 1964 to 1994. Cons. Genetics 2:257–269.

Ruzzante, D. E., J. S. Wroblewski, C. T. Taggart, R. K. Smedbol, D. Cook, and S. V. Goddard.
2000. Bay-scale population structure in coastal Atlantic cod in Labrador and Newfoundland, Canada. J. Fish. Biol. 56:431–447.

Serchuk, F. M., M. D. Grosslein, R. G. Lough, D. G. Mountain, and L. O'Brien.
1994. Fishery and environmental factors affecting trends and fluctuations in the Georges Bank and Gulf of Maine Atlantic cod stocks: an overview. ICES Mar. Sci. Symp. 198:77–109.

Shaklee, J. B., and P. Bentzen.
1998. Genetic identification of stocks of marine fish and shellfish. Bull. Mar. Sci. 62:589–621.

Smith, P. J., A. J. Birley, A. Janieson, and C. A. Bishop.
1989. Mitochondrial DNA in the Atlantic cod, *Gadus morhua*: lack of genetic divergence between eastern and western populations. J. Fish. Biol. 34:369–373.

Smith, W., and W. W. Morse.
1984. Retention of larval haddock *Melanogrammus aeglefinus* in the Georges Bank region, a gyre-influenced spawning area. Mar. Ecol. Prog. Ser. 24:1–13.

Smouse, P. E., and C. Chevillon.
1998. Analytical aspects of population-specific DNA fingerprinting for individuals. J. Hered. 89:143–150.

Streelman, J. T, and T. D. Kocher.
2002. Microsatellite variation associated with prolactin expression and growth of salt-challenged tilapia. Physiol. Genomics 9:1–4.

Townsend, D. W., and N. R. Pettigrew.
1996. The role of frontal currents in larval fish transport on Georges Bank. Deep-Sea Res.II. 43:1773–1792.

United States Federal Register.
2003. 50 CFR Part 648. [Available at http://www.gpoaccess.gov; accessed 1 May 2003.]

Waples, R. S.
1998. Separating the wheat from the chaff: patterns of

genetic differentiation in high gene flow species. J. Hered. 89:438–450.

Ward, R. D., M. Woddwark, and D. O. F. Skibinski.
1994. A comparison of genetic diversity levels in marine, freshwater, and anadromous fishes. J. Fish. Biol. 44: 213–232.

Weir, B. S., and C. C. Cockerham.
1984. Estimating F-statistics for the analysis of population structure. Evolution 38:1358–1370.

Werner, F. E., F. H. Page, D. R. Lynch, J. W. Loder, R. G. Lough, R. I. Perry, D. A. Greenberg, and M. Sinclair.
1993. Influences of mean advection and simple life behavior on the distribution of cod and haddock early life stages on Georges Bank. Fish. Oceanogr. 2:43–64.

Conserving oyster reef habitat by switching from dredging and tonging to diver-harvesting

Hunter S. Lenihan
Bren School of Environmental Science and Management
University of California, Santa Barbara
Santa Barbara, California 93106-5131
E-mail address: Lenihan@bren.ucsb.edu

Charles H. Peterson
Institute of Marine Sciences
University of North Carolina at Chapel Hill
Morehead City, North Carolina 28557

Abstract—A major cause of the steep declines of American oyster (*Crassostrea virginica*) fisheries is the loss of oyster habitat through the use of dredges that have mined the reef substrata during a century of intense harvest. Experiments comparing the efficiency and habitat impacts of three alternative gears for harvesting oysters revealed differences among gear types that might be used to help improve the sustainability of commercial oyster fisheries. Hand harvesting by divers produced 25–32% more oysters per unit of time of fishing than traditional dredging and tonging, although the dive operation required two fishermen, rather than one. *Per capita* returns for dive operations may nonetheless be competitive with returns for other gears even in the short term if one person culling on deck can serve two or three divers. Dredging reduced the height of reef habitat by 34%, significantly more than the 23% reduction caused by tonging, both of which were greater than the 6% reduction induced by diver hand-harvesting. Thus, conservation of the essential habitat and sustainability of the subtidal oyster fishery can be enhanced by switching to diver hand-harvesting. Management schemes must intervene to drive the change in harvest methods because fishermen will face relatively high costs in making the switch and will not necessarily realize the long-term ecological benefits.

Manuscript approved for publication 25 November 2003 by Scientific Editor.
Manuscript received 20 January 2004 at NMFS Scientific Publications office.
Fish. Bull. 102:298–305 (2004).

Commercial fishing for demersal fishes and benthic invertebrates, such as mollusks and crabs, is commonly undertaken with bottom-disturbing gear that can inflict damage to seafloor habitats (Dayton et al., 1995; Engel and Kvitek, 1995; Jennings and Kaiser, 1998; Watling and Norse, 1998). Habitat damage from dredges and analogous gear, designed to excavate invertebrates that are partially or completely buried beneath the surface of the seafloor, is generally much more severe than the damage caused by bottom trawls (Collie et al., 2000). Furthermore, impacts on and recovery from bottom-disturbing fishing gear vary with habitat type; generally smaller effects and more rapid rates of recovery are found for infauna in sedimentary habitats and the most severe and long-lasting damage in biogenic habitats that emerge from the seafloor (Peterson et al., 1987; Collie et al., 2000). Such biogenic habitats include seagrass beds, fields of sponges and bryozoans, and invertebrate reefs. Biogenic reefs that provide important ecosystem services such as habitat for other organisms include not only tropical coral reefs but also temperate reefs constructed by oysters (Bahr and Lanier, 1981; Lenihan et al., 2001), polychaetes like *Petaloproctus* (Wilson, 1979; Reise, 1982), and vermetid gastropods (Safriel, 1975). The recovery of such emergent invertebrate reefs is a slow process because of the relative longevity of the organisms that provide structure for the reef after they die and because of the nature of reefs as accumulations of multiple generations of reef builders.

One widespread temperate reef builder, the American oyster (*Crassostrea virginica*, also known as the "eastern oyster," Am. Fish. Soc.), has been especially affected by bottom-disturbing fishing gear as the target of fisheries. More than one hundred years of dredging and tonging oysters in the Chesapeake Bay and Pamlico Sound have caused severe degradation of the oyster reef matrix (deAlteris, 1988; Hargis and Haven, 1988), such that reef area and elevation have been dramatically reduced (Rothschild et al., 1994; Lenihan and Peterson, 1998). Reduction in reef height has a serious consequence for the oyster population because one function of naturally tall subtidal oyster reefs is to elevate the oysters up into the mixed surface layer of the estuary; this layer of mixed surface water allows them to avoid mass mortality from persistent exposure to seasonally anoxic and hypoxic bottom water (Lenihan and Peterson, 1998). Reef height and structure also control reef hydrodynamics (e.g., flow speed, turbulent mixing, and particle delivery and deposition), which influence oyster population dynamics and production (Lenihan, 1999). Consequently, harvest-related reef destruction and degradation are considered major factors that have led to declines of American oys-

ters in many estuaries located along the coasts of the Atlantic Ocean and Gulf of Mexico (Lukenbach et al., 1999).

Loss of oysters and the biogenic habitat that they provide appears from archaeological and paleontological evidence to be a worldwide phenomenon in temperate estuaries (Jackson et al., 2001). Oyster loss hurts not only the oyster fishery but, more importantly, imperils the ecosystem services provided by the oysters. These include, especially, the provision of emergent habitat and reef-dependent prey resources for many fish and crustacean populations of commercial and recreational importance (Peterson et al., 2000; Lenihan et al., 2001; Peterson et al., 2003), the filtration of estuarine waters (Newell, 1988), and the promotion of estuarine biodiversity by provision of hard-bottom habitat in fields of mobile sediments (Wells, 1961).

Because of the importance of restoring and sustaining oysters and their reefs to serve both the oyster fishery and the ecosystem, we designed a field test of the habitat impacts of three oyster harvesting methods: dredging, tonging, and hand extraction by divers (diver-harvesting). Our study is a gear comparison, in which we assess not only the traditional response variable of quantitative harvest per unit of effort with each gear but also the degree of reef habitat damage induced by the extraction of the oysters (analogous to Peterson et al., 1983). We additionally examine the quality of the oysters harvested as a function of gear type. The results indicate that diver-harvesting is a more environmentally sound way of harvesting oysters than traditional methods with dredges and tongs and may be more compatible with conserving oyster reef habitat.

Methods

Study site

Gear comparisons were conducted on subtidal oyster reefs in the Neuse River estuary, North Carolina (35°00′20″N, 76°33′50″W). Environmental conditions of this estuary are well described elsewhere (Paerl et al., 1998; Lenihan, 1999). Briefly, the estuary is mesohaline, an optimal habitat for the American oyster, and was once an important oyster fishery ground (Lenihan and Peterson, 1998). The estuary contains remnants of many large, natural subtidal oyster reefs that have been intensely mined by oyster harvesting gear for over a century. Dredging is the most common fishing practice. Mining of the reef matrix has combined with sediment loading and eutrophication-associated hypoxia (Paerl et al., 1998) to degrade the oyster reef habitats and greatly reduce oyster populations (Lenihan and Peterson, 1998). In harvested areas, reefs that were 2–3 m tall in quantitative surveys in the late 1800s (n=8 reefs) were all <1 m tall in our survey conducted in 1994—a modification of habitat caused entirely by the removal of oysters and shells during harvesting with dredges and tongs (Lenihan and Peterson, 1998). To help maintain oyster harvests, the North Carolina Division of Marine Fisheries (NCDMF) restores oyster reefs throughout many locations in the estuary by creating piles of oyster shell, or marl, on the seafloor. These restored oyster reefs are also targeted by oyster fishermen using dredges and, less often, using manual oyster tongs (Marshall[1]).

Experimental oyster reefs

Gear comparisons were conducted in March 1996 on 16 subtidal oyster reefs that had previously been created in July 1993 as part of a reef restoration experiment (Lenihan and Peterson, 1998; Lenihan, 1999) in collaboration with NCDMF. The experimentally restored reefs (referred to as "experimental reefs" in this gear-comparison study) were piles of oyster shells 1 m tall, 6–7 m in diameter (28.3–38.5 m^2 in area), and generally hemispherical in shape. Natural subtidal reefs located elsewhere in the estuary are typically larger, rectangular biogenic structures, ranging from 8–13 m wide and 20–30 m long. Experimental reefs were constructed in 3–4 m of water on a firm and sandy bottom, and were separated by at least 50 m. From the time of their construction until use in our experiments, the restored oyster reefs remained research sanctuaries, protected from commercial and recreational shellfishing.

As oysters settle and undergo metamorphosis on the shells of other (live and dead) oysters, to which they are attracted by chemical cues (Tamburri et al., 1992), they help cement together and add to the shell matrix of the reef over years. Prior to our harvest treatments, the experimentally restored reefs were colonized by at least three generations of oysters, many of which grew to adult size (range of oyster sizes on experimental reefs at the start of our experiment: 2–11 cm in shell height). Consequently, the shell matrices of the reefs had become somewhat cohesive, although probably less so than natural oyster reefs. In February 1996, before initiation of experimental harvests, there was no significant difference in the mean density of adult (>1 cm in shell height) oysters (mean ±SD 179.1 ±18.4/m^2) among the four sets of four experimental reefs randomly selected to receive the four harvesting treatments (one-way ANOVA; $F_{3,12}$=0.29; mean square error=285.06; P=0.83). Experimental reefs in the Neuse River usually had slightly higher oyster densities nearer their base and larger oysters near the crest (see Lenihan, 1999).

Experimental harvests

We compared three types of oyster-harvesting techniques: dredging, hand-tonging, and diver-harvesting. In March 1996, each of 16 reefs was either dredged, tonged, diver-harvested, or left unharvested as a control (four replicates of each treatment). Experimental dredging and hand-tonging were conducted in the manner applied by commercial oyster fishermen. The dredge, 25 kg in weight and 1 m in width, was pulled behind a powerboat operated by NCDMF personnel with commercial oyster-dredging experience. Hand-tonging was also conducted by a professional oyster

[1] Marshall, M. 1999. Personal commun. North Carolina Division of Marine Fisheries, 3431 Arendell St., Morehead City, NC 28557.

fisherman, R. A. Cummings. Oysters and shell material collected by dredges and tongs were separated aboard the boat on a culling board, using the common culling techniques (i.e., breaking apart oysters and shell with hammers, mallets, and chisels). As mandated by law, oyster shell and undersized oysters (<7 cm in height) were thrown overboard above the reef from which they had been collected.

Hand collections of oysters were conducted by scuba divers (J. H. Grabowski and H. S. Lenihan). Unlike professional oyster divers in Chesapeake Bay and other areas, who rake large quantities of shell and attached oysters into baskets that are pulled aboard ship to be culled, the divers in this trial adopted a different method designed to preserve reef habitat. Instead of collecting shell and oysters indiscriminately, the divers chose only those oysters that appeared alive and of market-size. Selected oysters were hand picked from the reef and placed in heavy plastic mesh baskets that, when full, were subsequently pulled aboard the boat with haul lines.

To standardize fishing effort, each of the 12 harvested reefs was harvested for 2 hours, regardless of the number of oysters collected. A 2-h harvest period for each 28.3–38.5 m^2 reef was considered to be a thorough but not excessive level of harvesting by the professional fishermen. The numbers of oysters collected in the final three or four dredge hauls and oyster tongs were typically lower (by ~10–20%) than the preceding dredge hauls and tongs. This reduction in the catch per unit of effort was great enough that a fisherman foraging optimally would normally cease harvesting at that time and move on to another reef. Similarly, after 2 hours of diver-harvesting, most of the clearly visible market-size oysters had been harvested.

Quantifying reef structure

Measurements of oyster reef height and diameter were conducted on all 16 experimental reefs both before and after application of the three fishing methods. In February 1996, the preharvest height and radius of each oyster reef were measured by scuba divers using a custom-made "square angle," consisting of two pieces (2 m and 5 m long) of 3-cm wide steel angle-iron, each with an attached 1-m long carpenter's level. Both pieces of angle iron were marked at 1-cm intervals. The 5-m long (cross) piece was attached to the 2-m long (upright) piece by a roller-joint. The roller-joint allowed the cross piece to move up and down the upright piece, thus providing a measure of reef height, and to move horizontally in relation to the upright piece, thus providing a measurement of reef radius. The 2-m long piece also had a 0.75-m long piece of angle iron attached perpendicularly near its bottom so that it would not sink into the seafloor when placed upright.

One diver held the 2-m long angle iron perpendicular to the seafloor at the edge of a reef, while the other diver placed the 5-m long angle iron parallel to the seafloor, so that one end rested on the highest point of a reef and the other end met the upright angle iron at the reef's edge. The height and radius of the reef were then measured by recording the height at which the cross piece met the upright piece, and the distance at which the upright piece met the cross-piece. For each reef, a mean diameter was calculated by measuring three separate radii (oriented at three compass bearings, all 120° apart), multiplying the radii by two to estimate diameters, and then averaging the three diameters. This averaging procedure was undertaken because the reefs were not perfectly circular. Measurements of reef height and radius were repeated in March, two–five days after experimental harvests were completed.

Sampling oyster populations

We sampled live and dead oysters on each treatment and control reef before (late February 1996) and immediately after (late March) experimental harvests to estimate the proportion of oysters incidentally killed but not harvested by each harvesting treatment. Specifically, oyster data was collected within 30 hours of the application of the harvest treatment on each replicate reef. Densities of live and dead oysters were quantified by divers who haphazardly placed eight 0.5-m^2 weighted PVC quadrats on the reef surface at haphazard locations and recorded the number of live and dead oysters greater >1 cm in height. The density of dead oysters was measured by counting the number of oyster shells that were articulated and appeared relatively fresh (i.e., not black in color or decayed), or oysters with somatic tissue exposed because of cracked, broken, or punctured shells. Oysters with exposed somatic tissue almost certainly die because of predation by fishes and crabs in the Neuse River estuary (Lenihan, 1999; and see Lenihan and Micheli, 2000). Mean proportions of dead oysters were computed (dead oysters/dead+alive oysters), as well as mean densities of live and dead oysters on each reef.

Catch per unit of effort

The relative efficiency of each harvesting method was determined by comparing the numbers of bushels (1 bushel=36.4 L) of market-size oysters taken per hour of fishing. We quantified numbers of bushels for each harvesting method aboard the boat by placing oysters of legal size in premeasured mesh baskets. After being counted, and upon termination of the harvest trial, many of the oysters were returned to other nearby reefs not involved in the experiment.

Statistics

One-way analysis of variance (ANOVA) was used to compare the following across harvest treatments and controls: 1) changes in mean reef height and diameter; 2) catch per unit of effort; 3) the proportion of oysters found dead on reefs before harvest; 4) the proportion of oysters found dead on reefs after harvest; and 5) the absolute difference in the proportion of oysters found dead before versus after harvesting (|*after* minus *before*|). Data from all treatment (dredging, tonging, and diver-harvesting; n=4 for each treatment) and the control (n=4) reefs were used in

Table 1

Results of one-way ANOVAs comparing differences in reef height (cm), reef diameter (cm), and catch per unit of effort (number of oysters collected per hour) among experimental reefs harvested by different methods (dredging, tonging, diver-harvesting, and controls). df = degrees of freedom; ms = mean square; F = F-value; P = P-value; ss = sum of squares. Partial r^2= treatment ss/total ss.

		Reef height				Reef diameter				Catch per unit of effort			
Source	df	ms	F	P	partial r^2	ms	F	P	partial r^2	ms	F	P	partial r^2
Harvesting treatment	3	0.09	36.90	0.0001	0.90	0.07	15.79	0.0002	0.80	3.21	17.84	0.0001	0.11
Residual	12	0.003				0.005				0.08			
Total	15			Total ss: 0.31					0.27				9.64

the ANOVA. Before ANOVA, homogeneity of variances was tested by using Cochran's method (α=0.05). All data passed this test. After ANOVA, *post hoc* differences among means were compared by using Student-Newman-Keuls (SNK) tests (α=0.05).

Results

Reef height and diameter

Dredge harvesting on experimental reefs removed the largest amount of shell material from the reefs, based on the reduction of reef height (Fig. 1A) and on the qualitative assessment of increases in numbers of oyster shells found on the seafloor around the reefs. Hand-tonging removed an intermediate amount of reef materials, and diver-harvesting removed far less shell matrix than either dredging or tonging. All harvesting methods reduced the height of restored oyster reefs (Fig. 1A), but dredging (34% of reef height) and tonging (23%) had greater impacts than did diver-harvesting (6%). ANOVA demonstrated significant differences among harvest treatments in mean change in reef height (Table 1); all harvest treatments induced a loss in reef height as compared with unharvested control reefs (SNK; P<0.05). Dredging reduced reef height more than any other treatment (SNK, P<0.05), and tonging reduced reef height more than diver-harvesting (SNK, P<0.05). The reduction in reef height caused by diver-harvesting was small (mean ±SD: 6 ±3 cm). However, diver-harvesting nearly eliminated the veneer of live market-size oysters on reefs, which provides substantial structure on reef surfaces.

Oyster harvesting either slightly increased or slightly decreased reef diameter, depending upon method (Fig. 1B). Reef material was apparently removed from edges of reefs by tonging, thereby reducing reef diameter. Shell was spread around the reefs by dredging, thereby increasing reef diameter after application of that harvesting method. The effects of oyster harvesting on reef diameter proved significant (Table 1). Tonging significantly reduced reef size compared with controls and the other two harvesting treatments (SNK; P<0.05), whereas dredging

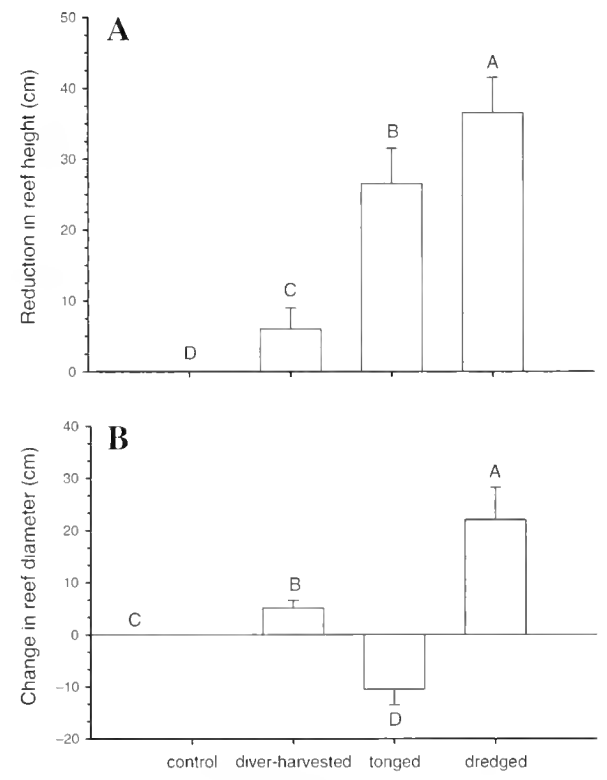

Figure 1

Modification of reef size and structure caused by various harvesting techniques. (**A**) Mean (+SE) reduction in the height of experimentally restored oyster reefs caused by three types of oyster harvesting: hand-harvesting by divers, hand tonging, and dredging. Dredges are pulled behind power boats. Reefs were located in the Neuse River estuary, North Carolina. Letters represent results of SNK *post hoc* tests: dredged>tonged>diver-harvested>control at P<0.05. (**B**) Mean (+SE) change in the diameter of experimental oyster reefs caused by different oyster-harvesting techniques. Letters represent results of SNK *post hoc* tests: dredged>diver-harvested>control>tonged at P<0.05.

Table 2

Results of one-way ANOVAs comparing differences in the proportion of oysters found dead ("mortality") on reefs before and after harvesting by different methods (dredging, tonging, diver-harvesting, and controls), and the absolute difference ([*after–before*]) in the proportion of dead oyster found before versus after harvesting. df = degrees of freedom; ms = mean square; F = F-value; P = P-value; ss = sum of squares. Partial r^2 = treatment ss/total ss.

	Before mortality					After mortality				Difference in mortality			
Source	df	ms	F	P	partial r^2	ms	F	P	partial r^2	ms	F	P	partial r^2
Harvesting treatment	3	0.001	0.49	0.69	0.11	0.02	7.90	0.004	0.58	0.01	7.56	0.004	0.57
Residual	12	0.001				0.002				0.08			
Total	15			Total ss: 0.01					0.08				0.04

increased reef diameter compared to the other treatments (SNK; $P<0.05$). The increase in diameter of diver-harvested reefs was also greater than that for controls (SNK; $P<0.05$). The substantial increase in shell material (with oysters of all sizes) spread out on the seafloor on dredged reefs indicates that the collection efficiency of dredges is less than 100%.

Catch per unit of effort

Catch per unit of effort of oysters included the time required to collect oysters from the reef and the time needed to separate (i.e., cull) them from undersized oysters and shell material. Two of the harvesting methods, hand-tonging and oyster dredging, are one-man operations in which one fisherman can operate the harvesting gear, cull oysters, and drive the boat. Therefore, measurements of catch per unit of effort for dredging and tonging represent the numbers of bushels of oysters one fisherman can collect per hour. In contrast, scuba diving is rarely attempted alone and it is usually necessary for someone else to tend the diver (e.g., helping him or her in and out of the water) and to haul oysters up to the boat when given a signal by the diver on the reef. Divers should preferably work as a team using the "buddy" system for safety reasons. Data for diver-collections are given in bushels per hour collected by one diver but hauled up to the boat and culled by a second person.

There was a significant difference in the numbers of bushels collected per hour by the different harvesting techniques (Table 1). Diver-harvesting had a higher catch efficiency than all other treatments (SNK; $P<0.05$; Fig. 2). Diver-harvesting was about 25% more time efficient than dredge harvesting and 32% more efficient than tonging. There was no statistically significant difference in efficiency between dredging and tonging (SNK; $P>0.05$).

Incidental oyster mortality

The proportion of oysters found dead on experimental reefs in February 1996 (~20%), prior to experimental harvesting, was similar to that found on other nearby experimental and natural reefs in the Neuse River estuary in preceding years (e.g., Lenihan and Peterson, 1998; Lenihan 1999). In February, the proportions of dead oysters did not differ among the four sets of reefs destined to be experimentally harvested (Table 2, Fig. 3A). In contrast, there was a large and statistically significant difference in the proportions of dead oysters on the reefs after harvesting (Table 2, Fig. 3A). The proportions of dead oysters on reefs that had been tonged and dredged were significantly greater than on diver-harvested and control reefs (SNK; $P<0.05$).

Before-after-control-impact (BACI) comparison of the change in proportions of dead oysters from before to after harvesting ([*after–before*]), a direct estimate of incidental mortality caused by harvesting gear, showed a similar pattern to mortality inferred from *in situ* proportions of dead oysters in March after harvesting (Table 2, Fig. 3B).

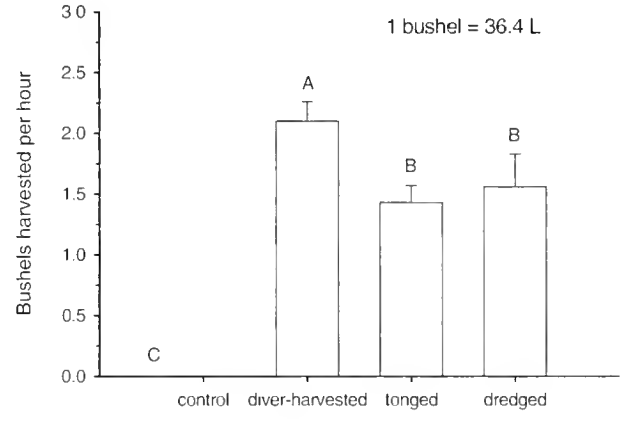

Figure 2

Mean (+SE) number of bushels collected per hour on experimental reefs by different oyster-harvesting techniques. Letters represent results of SNK *post hoc* tests: diver-harvested>dredged and tonged>control at $P<0.05$.

A significant treatment effect in the *after* period (Table 2) indicated that the change over time in proportion of dead oysters varied among harvest treatments. Tonging and dredging increased the fraction of dead among *in situ* oysters on reefs (SNK; $P<0.05$; Fig. 3B), but diver-harvesting did not. Immediately after harvesting, divers found that many oysters on tonged and dredged reefs had been broken open, severely cracked, or punctured.

Discussion

Our comparisons of gear revealed relatively unambiguous differences in their harvesting efficiency for oyster dredges, tongs, and hands of divers. Dredging and tonging had similar and statistically indistinguishable catch efficiencies, which seems reasonable given that both techniques are commonly employed in the same locations and times in the oyster fishery. Presumably, fishermen choose between these two gears on the basis of personal preference, history, and skill, as well as on the basis of water depth, bottom type, and other factors that did not vary in our study. Diver-harvesting of oysters resulted in higher rates of harvest per hour, but this enhancement in catch efficiency required the presence of two people, one diver beneath the surface and another person on deck involved in hauling baskets of oysters onto the deck and culling out marketable oysters. Because the increase in efficiency was only 25–32%, this enhancement falls short of the 100% required to compensate each fisherman to the same degree that dredging and tonging provide. Nevertheless, the immediate economics of diver-harvesting could prove competitive or even superior if the single deckhand could serve two or more divers, which seems likely from our experience with the workload on deck, and if the oysters taken are priced more favorably because of larger size or less damage, which seems possible. A complete short-term economic comparison would need to include higher costs for fuel in dredging and costs of filling air tanks for diving, as well as depreciation of gear.

This discussion of the basic efficiencies and economics of the methods of commercial oyster fishing is based upon short-term considerations only. That short-term time perspective is the cause of failures to achieve sustainability in fisheries quite generally (Ludwig et al., 1993; Botsford et al., 1997). We show that adoption of hand-harvesting by divers would result in substantially less fishery-induced reduction in reef height by a factor of four to six, implying greater preservation of the habitat and thus a more sustainable fishing practice. Our data on the changes in area covered by reefs as a function of harvest treatment revealed only small differences among treatments. The height of a reef is a critical variable in sustaining the reef as an engine of oyster production because short reefs can be easily covered by sediment (Lenihan, 1999), can be abraded by sediment transport (Lenihan, 1999), and can fail to extend above hypoxic bottom waters (Lenihan and Peterson, 1998). Tall reefs (i.e., reefs not degraded by harvesting) produce faster flow speeds and more turbulence for oyster populations, which in turn increase oyster growth rate, increase

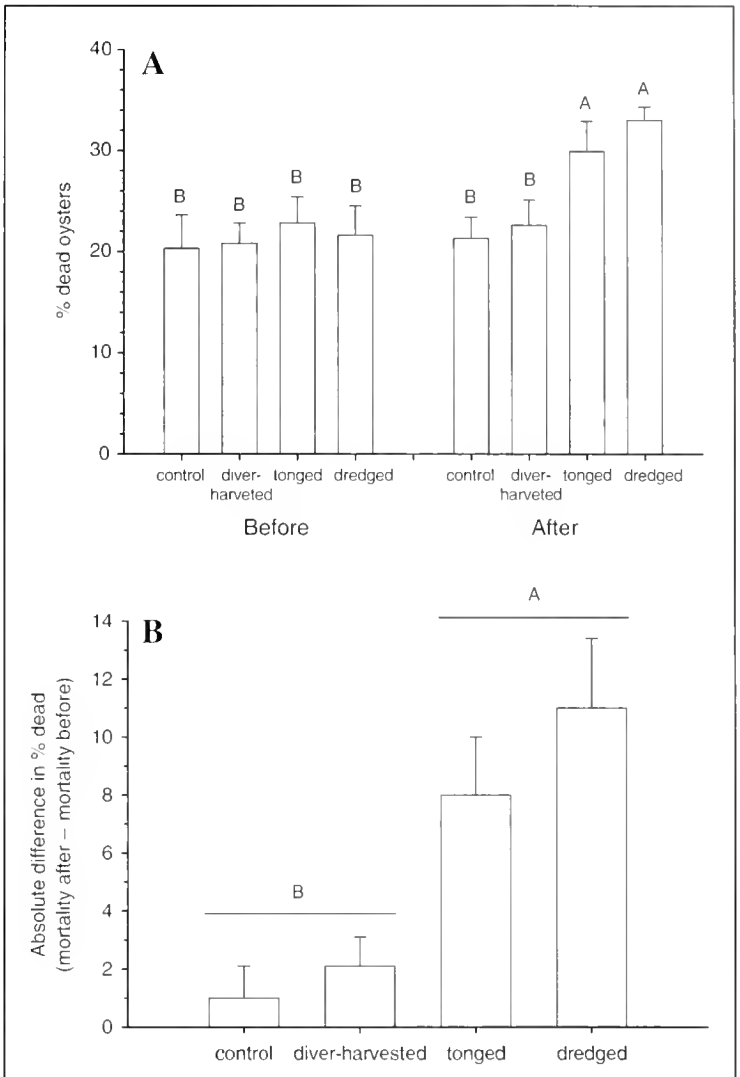

Figure 3

Mortality of oysters caused by various harvesting techniques. (**A**) Mean (+SE) % dead within oyster populations on experimental reefs before and after being harvested by three different harvesting techniques: dredging, tonging, and diver-harvesting. Control reefs were not harvested. Letters represent results of SNK *post hoc* tests: dredged, after>tonged, after>all other treatments at $P<0.05$. There was no difference among treatments before harvesting. (**B**) Mean (+SE) absolute difference in the % dead oysters on experimental reefs before and after harvesting. Difference calculated by: [% *after*–% *before*]. Letters represent results of SNK *post hoc* tests: dredged and tonged>diver-harvested and control at $P<0.05$.

physicalogical condition, reduce disease incidence and intensity, and decrease mortality (Lenihan, 1999). Consequently, assessment of economics of the oyster fishery over longer time frames would likely demonstrate higher returns from practicing diver-harvesting, assuming that this technique conserved reef structure. Diver-harvesting also killed fewer of the oysters that remained on the bottom, thereby sustaining future harvests better through reduced wastage and by retention of more live oysters that would produce more reef material.

Although the relative advantage of diver-harvesting for conserving reef structure is evident, the absolute conservation of reef habitat under the various oyster harvesting methods is not clear from our study. Our data on impacts of diver-harvesting revealed slight declines in reef height, but whether these same declines would apply to an older reef, as opposed to a recently restored reef, is open to question. The level of cementation that binds the shells of the reef is not as great on recently restored reefs, making them more susceptible to degradation with physical disturbance. Our study measured only the immediate drop in reef elevation after fishing at a level that removed a large fraction of legally marketable oysters. In a well-managed fishery, this drop in reef elevation would represent virtually an entire season's decline, after which substantial reef growth would occur through recruitment and growth of smaller oysters before a new harvesting season. Thus, a healthy oyster reef may well be able to compensate for the modest reduction in elevation caused by diver-harvesting. If so, oyster reef sanctuaries now being created throughout the Chesapeake Bay (Luckenbach et al., 1999) could conceivably be opened to diver-harvesting (without implements) and still preserve the reef services to the ecosystem. This possibility deserves to be evaluated in order to minimize conflicts between the goals of restoring oyster reef habitat for conservation purposes and restoring oyster reefs for the restoration of lost fisheries.

Application of the results of our gear comparisons to management of oyster fisheries will likely encounter some impediments. Although various artisanal fisheries worldwide have employed free diving as a fishing technique and some modern fisheries, including the American oyster fishery, involve the use of scuba, diving is not a skill possessed by most oyster fishermen and probably is not a method under consideration for oyster fishing in general. In addition, the peak of oyster harvesting season on the Atlantic and Gulf coasts is usually during winter months (e.g., November–March) when water temperatures in estuaries are quite low (0–10°C). Such conditions require cold-water diving equipment (e.g., dry-suits), which will further increase the cost of this new harvesting technique. Thus acceptance of diver-harvesting by the industry would require training in diving skills and safety, education and demonstration of the advantages of this gear, and perhaps even investment of public funds to defray costs of the transition from traditional dredges and tongs to scuba or hookah. Because the gains of switching to diver-harvesting accrue to the industry over the long term, while individual fishermen who switch may suffer economically in the short-term, gear choice represents a modified example of the tragedy of the commons (Ludwig et al., 1993). Only when armed with some form of ownership rights and an attendant long-term perspective would an individual oyster fisherman choose to switch to diver-harvesting. The precipitous declines of over 99% in oyster landings in mid-Atlantic estuaries (Rothschild et al., 1994; Lenihan and Peterson, 1998) mean that oyster fishermen can hardly be expected to bear the costs of switching fishing methods. Therefore, government intervention would be required to convert subtidal oyster dredge and tong fisheries into diver-harvesting operations for two reasons; the need for compensation of start-up costs and the need to overcome the tragedy of the commons. Given the dire state of oyster fisheries today (Rothschild et al., 1994), the habitat destruction in these declines (deAlteris, 1988; Hargis and Haven, 1998; Rothschild et al., 1994; Lenihan and Peterson, 1998), the broad ecosystem services provided by healthy oyster reefs (Jackson et al., 2001; Lenihan et al. 2001), and the very real potential for restoring oysters and their reefs (Luckenbach et al., 1999; Lenihan, 1999), a mandate to switch fishing methods for subtidal oyster fisheries could pay large dividends.

Acknowledgments

We thank Mike Marshall, Jeff French, and those many NCDMF people working on deck for initially creating experimental reefs to our specifications and for later applying the experimental dredge harvesting treatment. We thank Robert A. Cummings for applying the hand-tonging treatment, and Jonathan H. Grabowski for helping with diver-harvesting of reefs. This work was funded by the North Carolina General Assembly through the Cooperative Institute of Fisheries Oceanography (to C. H. Peterson), and NOAA-Chesapeake Bay Program Oyster Disease Program (to H. S. Lenihan, C. H. Peterson, and F. Micheli).

Literature cited

Bahr, L. M., and W. P. Lanier.
1981. The ecology of intertidal oyster reefs of the South Atlantic coast: a community profile. U.S. Fish Wildl. Serv. Office of Biological Services FWS/OBS-81/15.

Botsford, L. W., J. C. Castilla, and C. H. Peterson.
1997. The management of fisheries and marine ecosystems. Science 277:509–515.

Collie, J. S., S. J. Hall, M. J. Kaiser, and I. R. Poiner.
2000. A quantitative analysis of fishing impacts on shelf-sea benthos. J. Anim. Ecol. 69:785–798.

Dayton, P. K., S. F. Thrush, M. T. Agardy, and R. J. Hoffman.
1995. Environmental effects of marine fishing. Aquat. Conserv. Mar. Fresh. Ecosyst. 5:205–232.

deAlteris, J. T.
1988. The geomorphologic development of Wreck Shoal, a subtidal oyster reef of the James River, Virginia. Estuaries 11:240–249.

Engel, J., and R. G. Kvitek.
1995. Effects of otter trawling on a benthic community in

Monterey Bay National Marine Sanctuary. Conserv. Biol. 12:1204–1214.

Hargis, W. J., Jr., and D. S. Haven.
1988. The imperiled oyster industry of Virginia: a critical analysis with recommendations for restoration. Special report 290 in applied marine science and ocean engineering, 145 p. Virginia Sea Grant Marine Advisory Services, Virginia Institute of Marine Science, Gloucester Point, VA.

Jackson, J. B. C., M. X. Kirby, W. H. Berger, K. A. Bjorndal, L. W. Botsford, B. J. Bourque, R. H. Bradbury, R. Cooke, J. Erlandson, J. A. Estes, T. P. Hughes, S. Kidwell, C.B. Lange, H. S. Lenihan, J. M. Pandolphi, C. H. Peterson, R. S. Steneck, M. J. Tegner, and R. R. Warner.
2001. Historical overfishing and the recent collapse of coastal ecosystems. Science 293:629–638.

Jennings, S., and M. J. Kaiser.
1998. The effects of fishing on marine ecosystems. Adv. Mar. Biol. 34:201–352.

Lenihan, H. S.
1999. Physical-biological coupling on oyster reefs: how habitat structure influences individual performance. Ecol. Monogr. 69:251–276.

Lenihan, H. S., and F. Micheli.
2000. Biological effects of shellfish harvesting on oyster reefs: resolving a fishery conflict by ecological experimentation. Fish. Bull. 98:86–95.

Lenihan, H. S., and C. H. Peterson.
1998. How habitat degradation through fishery disturbance enhances impacts of hypoxia on oyster reefs. Ecol. Appl. 8:128–140.

Lenihan, H. S., C. H. Peterson, J. E. Byers, J. H. Grabowski, G. W. Thayer, and D. R. Colby.
2001. Cascading of habitat degradation: oyster reefs invaded by refugee fishes escaping stress. Ecol. Appl. 11:764–782.

Luckenbach, M. A., R. Mann, and J. A. Wesson (eds.).
1999. Oyster reef restoration: a synopsis and synthesis of approaches, 366 p. Virginia Institute of Marine Sciences Press, Gloucester Point, VA.

Ludwig, D., R. Hilborn, and C. Walters.
1993. Uncertainty, resource exploitation, and conservation: lessons from history. Science 260:17–18.

Newell, R. I. E.
1988. Ecological changes in the Chesapeake Bay: Are they the result of overharvesting the American oyster, *Crassostrea virginica*? *In* Understanding the estuary: advances in Chesapeake Bay research (M. P. Lynch, E. C. Krome, eds.), p. 536–546. Chesapeake Bay Research Consortium, Publ 129 CBP/TRS 24/88, Gloucester Point, VA.

Paerl, H. W., J. L. Pinckney, J. M. Fear, and B. L. Peierls.
1998. Ecosystem responses to internal and watershed organic matter loading: consequences for hypoxia in the eutrophying Neuse River Estuary, North Carolina, USA. Mar. Ecol. Prog. Ser. 166:17–25.

Peterson, C. H., H. C. Summerson, and S. R. Fegley.
1983. The relative efficiency of tow clam rakes and their contrasting impacts on seagrass biomass. Fish. Bull. 81:429–434.
1987. Ecological consequences of mechanical harvesting of clams. Fish. Bull. 85:281–298.

Peterson, C. H., H. C. Summerson, E. Thomson, H. S. Lenihan, J. H. Grabowski, L. Manning, F. Micheli, and G. Johnson.
2000. Synthesis of linkages between benthic and fish communities as a key to protecting essential fish habitat. Bull. Mar. Sci. 66:759–774.

Peterson, C. H., J. H. Grabowski, and S. P. Powers.
In press. Quantitative enhancement of fish production by oyster reef habitat: restoration valuation. Mar. Ecol. Prog. Ser.

Reise, K.
1982. Long-term changes in the macrobenthic invertebrate fauna of the Wadden Sea: are polychaetes about to take over? Neth. J. Sea Res. 16:29–36.

Rothschild, B. J., J. S. Ault, P. Goulletquer, and M. Héral.
1994. Decline of the Chesapeake Bay oyster population: a century of habitat destruction and overfishing. Mar. Ecol. Prog. Ser. 111:29–39.

Safriel, U. N.
1975. The role of vermetid gastropods in the formation of Mediterranean and Atlantic reefs. Oecologia 20:85–101.

Tamburri, M. N., R. K. Zimmer-Faust, and M. L. Tamplin.
1992. Natural sources and properties of chemical inducers mediating settlement of oyster larvae: a re-examination. Biol. Bull. 183:327–337.

Watling L., and E. A. Norse.
1998. Disturbance of the seabed by mobile fishing gear: a comparison to forest clearcutting. Cons. Biol. 12:1180–1197.

Wells, H. W.
1961. The fauna of oyster reefs with special reference to the salinity factor. Ecol. Monogr. 31:239–266.

Wilson, W. H., Jr.
1979. Community structure and species diversity of the sediment reefs constructed by *Petaloproctus socialis* (Polychaeta: Maldanidae). J. Mar. Res. 37:623–641.

Fecundity, egg deposition, and mortality of market squid (*Loligo opalescens*)

Beverly J. Macewicz
J. Roe Hunter
Nancy C. H. Lo
Erin L. LaCasella

Southwest Fisheries Science Center
National Marine Fisheries Service, NOAA
8604 La Jolla Shores Drive
La Jolla, California 92037-1508

E-mail address (for B. J. Macewicz): Bev.Macewicz@noaa.gov

Abstract—*Loligo opalescens* live less than a year and die after a short spawning period before all oocytes are expended. Potential fecundity (E_P), the standing stock of all oocytes just before the onset of spawning, increased with dorsal mantle length (L), where $E_P = 29.8L$. For the average female squid (L of 129 mm), E_P was 3844 oocytes. During the spawning period, no oogonia were produced; therefore the standing stock of oocytes declined as they were ovulated. This decline in oocytes was correlated with a decline in mantle condition and an increase in the size of the smallest oocyte in the ovary. Close agreement between the decline in estimated body weight and standing stock of oocytes during the spawning period indicated that maturation and spawning of eggs could largely, if not entirely, be supported by the conversion of energy reserves in tissue. *Loligo opalescens*, newly recruited to the spawning population, ovulated about 36% of their potential fecundity during their first spawning day and fewer ova were released in subsequent days. *Loligo opalescens* do not spawn all of their oocytes; a small percentage of the spawning population may live long enough to spawn 78% of their potential fecundity.

Loligo opalescens are taken in a spawning grounds fishery off California, where nearly all of the catch are mature spawning adults. Thirty-three percent of the potential fecundity of *L. opalescens* was deposited before they were taken by the fishery (December 1998–99). This observation led to the development of a management strategy based on monitoring the escapement of eggs from the fishery. The strategy requires estimation of the fecundity realized by the average squid in the population which is a function of egg deposition and mortality rates. A model indicated that the daily total mortality rate on the spawning ground may be about 0.45 and that the average adult may live only 1.67 days after spawning begins. The rate at which eggs escape the fishery was modeled and the sensitivity of changing daily rates of fishing mortality, natural mortality, and egg deposition was examined. A rapid method for monitoring the fecundity of the *L. opalescens* catch was developed.

Manuscript approved for publication 19 December 2003 by Scientific Editor.

Manuscript received 20 January 2004 at NMFS Scientific Publications Office.

Fish. Bull. 102:306–327 (2004).

Many loliginid squid populations depend entirely upon the reproductive output of the preceding generation because individuals live less than a year (Yang et al., 1986; Hatfield, 1991, 2000; Natsukari and Komine, 1992; Arkhipin, 1993; Arkhipin and Nekludova, 1993; Jackson, 1993, 1994; Jackson et al., 1993; Boyle et al., 1995; Jackson and Yeatman, 1996; Jackson et al., 1997; Moltschaniwskyj and Semmens, 2000; Semmens and Moltschaniwskyj, 2000). In California waters, *Loligo opalescens* (market squid, also known as the opalescent inshore squid [FAO]) live only 6–12 months (Butler et al., 1999) and die after spawning (McGowan, 1954; Fields, 1965). Thus, fecundity of *L. opalescens* is a critical life history trait and, in addition, must be known in order to estimate the biomass with either egg deposition or larval production methods (Hunter and Lo, 1997). *Loligo opalescens* is one of the most valuable fishery resources in California waters and is monitored under the Coastal Pelagics Species Fishery Management Plan of the Pacific Fishery Management Council as market squid.

Laptikhovsky (2000) pointed out that squid fecundity estimates would be biased if the females spawned ova prior to capture, if oocytes remained in the ovary after death, or if some of the standing stock of oocytes were lost because of atresia. Previous field work on squid fecundity has been limited to the traditional method of simply counting oocytes or ova (or both) of animals taken on the spawning grounds, and none of the biases identified by Laptikhovsky (2000) have been evaluated (Boyle and Ngoile, 1993; Coelho et al., 1994; Guerra and Rocha, 1994; Boyle et al., 1995; Collins et al., 1995; Moltschaniskyj, 1995; Lopes et al., 1997; Laptikhovsky, 2000). On the other hand, laboratory studies (Ikeda et al., 1993; Bower and Sakurai, 1996; Sauer et al., 1999; and Maxwell and Hanlon, 2000) have indicated that oocytes remain in the ovaries after spawning and death. Additionally, atresia was found to occur in all stages of oocytes of *Loligo vulgaris reynaudii* (Melo and Sauer, 1998). Modern approaches to estimating lifetime fecundity in fishes take the potential biases of past spawning history, residual fecundity, and atresia into account (Hay et al., 1987; Hunter et al., 1992; Macewicz and Hunter, 1994; Kjesbu et al., 1998). The initial objectives of the present study were to estimate the fecundity of *L. opalescens* by using a modern approach that considers such biases, and to provide a histological description of those aspects of ovarian structure upon which modern fecundity analyses are based. As our work progressed, we realized that it might be practical to manage the market squid fishery by monitoring egg escapement based on fecundity measurements. Thus, we added two new objectives: to conduct a preliminary evaluation of the use of egg escapement as a tool for management of the market squid fishery; and to develop a method

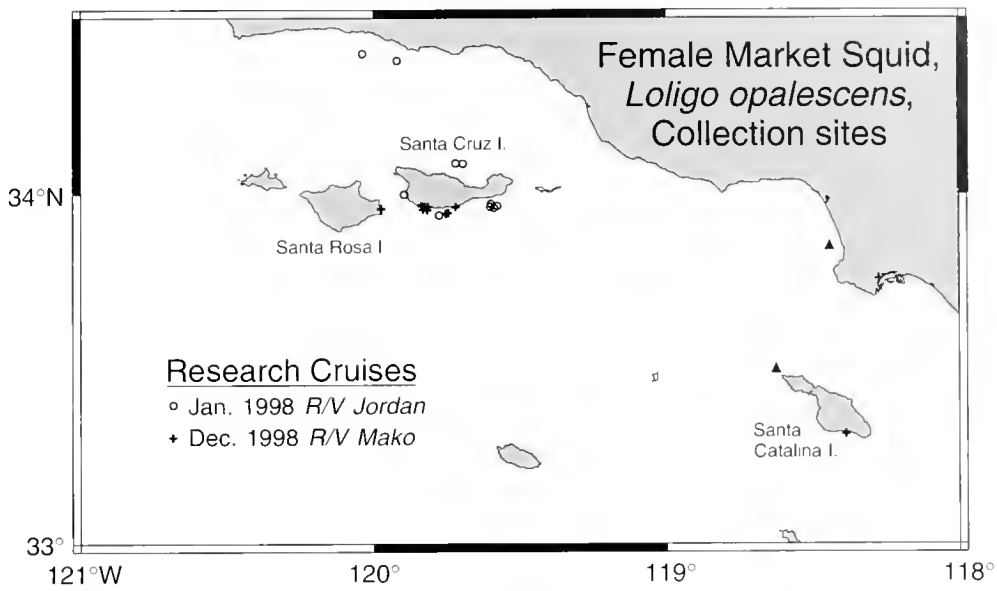

Figure 1

Collection locations for female *Loligo opalescens* during two joint research cruises during 1998 by California Department of Fish & Game (CDF&G) and National Marine Fisheries Service (NMFS) and for three immature females (triangles) collected during February 2000 (CDF&G).

to monitor the fecundity of the catch that avoids the costly process of counting all oocytes and ova.

In this study we consider four aspects of the fecundity of *L. opalescens*: potential fecundity, minimum residual fecundity, maximum fecundity, and the fecundity deposited by the average female in the population. *Potential fecundity*, or *potential lifetime fecundity*, is the standing stock of all oocytes in the ovary just before the onset of the first ovulation. Because *L. opalescens* are semelparous, the standing stock of all oocytes in the ovary just before first ovulation equals their potential lifetime fecundity. Clearly, once ovulation and spawning (deposition of ova in egg capsules on the sea floor) begin, the standing stock of oocytes can no longer be considered a measure of the potential fecundity of the female. *Minimum residual fecundity* is the minimum number of oocytes that might be expected to remain in the ovary at death. Because ovaries of dying *L. opalescens* contain oocytes (Knipe and Beeman, 1978), only a portion of the potential fecundity will be spawned in their lifetime. We use ancillary information on *L. opalescens* (an index of mantle condition and extent of ovarian development) to project what the minimum residual may be. *Maximum fecundity* (potential fecundity less the minimum residual fecundity) is the maximum number of eggs a female might be expected to deposit in a lifetime. We also estimate the fraction of the potential fecundity deposited by the average female, a key vital rate we approximate by modeling the daily rates of total mortality and egg deposition. Lastly, the term "standing stock of oocytes" is used throughout this article to indicate the total number of oocytes at all stages in an ovary. Whether the standing stock of a particular female is to be considered a potential fecundity, a residual fecundity, or something in between, depends upon ancillary information (i.e., presence of postovulatory follicles in the ovary, ova in the oviduct, mantle condition, or the level of ovarian maturity).

Materials and methods

We collected *Loligo opalescens* during two southern California research cruises in 1998 (7–15 January and 3–10 December) (Fig. 1). Most specimens were taken at night by using trawls, jigging, or by removing them from commercial purse-seine catches at sea; some specimens were collected during the day by using bottom trawls. We measured dorsal mantle length (mm), weighed the whole body (g), and classified the ovary and preserved it with viscera and oviduct attached in 10% neutral buffered formalin. To determine reproductive state we decided not to use the familiar ovary classification systems but rather tabulated gross anatomical characters and, later on, selected the most useful characteristics. See Table 1 for characters selected for scoring.

Preserved ovaries and oviducts were reclassified in the laboratory and weighed (to nearest 0.001 g). A piece of the preserved ovary from each of the 135 female *L. opalescens* from January and the 117 females from December was sectioned and stained (hematoxylin and eosin). Analyses of the histological sections included identification of the oocytes in the various development stages (I–VI) as described by Knipe and Beeman (1978), and identification of atresia and postovulatory follicles (Fig. 2). We use the term "ova" to indicate an ovulated mature oocyte (stage VI).

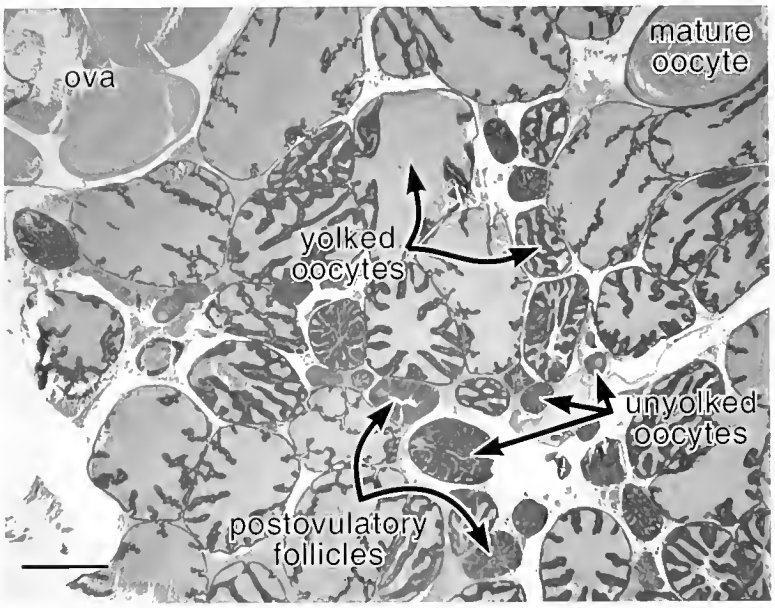

Figure 2

Slide of the ovary (stained with hematoxylin and eosin) of a mature spawning female *L. opalescens*. Bar = 1.0 mm.

Table 1

Classification system for the gross anatomical characteristics of the reproductive system of female market squid (*Loligo opalescens*).

Female organs	Character	Grade
Nidamental gland	length	millimeters
Accessory nidamental gland	color	0=clear, 1=whitish, 2= pink, 3=peach, 4=reddish-orange
Oviduct	number of large clear eggs	1=none, 2=1–20, 3=21–200, 4=>200
Ovary	number of large clear oocytes	1=none, 2=1–20, 3=21–200, 4=>200
Ovary	number of opaque or white oocytes	1=none, 2=1–20, 3=21–200, 4=>200

Postovulatory follicles were classified as either new, degenerating, or very degenerative. We assigned the females to one of the following reproductive categories on the basis of the histology of their ovaries (numerical stages in Knipe and Beeman, 1978):

Immature — Ovary contains only unyolked oocytes; oocyte development ranged from stages I (oogonia) to IV (follicular invagination oocyte) and requires microscopic examination.

Mature preovulatory — No postovulatory follicles are present. Ovaries contain oocytes with yolk (stage V, yolking begins about 1.1 mm in size); ovary usually contains unyolked oocytes.

Mature spawning — Ovary contains postovulatory follicles (POFs) of any degree of degeneration (none to extensive); more than one degenerative POF class may be present. Oocyte development stages III–VI are often present but stages Ic–II are rare. (2% of the ovaries have late stage Ic oocytes and none have any of the earliest stages, Ia or Ib.)

In some histological sections of ovaries we saw 1–10 yolking oocytes (development stage V) with a broken follicle layer, and the yolk seemed to be oozing out between the other oocytes. Because this may have been an artifact of handling, we did not use such females to estimate fecundity.

We used the gravimetric method (Hunter et al., 1985, 1992) to estimate the standing stock of oocytes in 98 *L. opalescens* ovaries. The gravimetric method overestimated the total number of oocytes of *Loligo pealeii*, but the difference between a count of all oocytes and a weight-based estimate was slight (Maxwell and Hanlon, 2000). We did not compare our estimates with a count of all oocytes in the ovary because we used a portion of the ovary for our histological examinations, and each value is the mean of the counts from two tissue samples (average coefficient of variation between samples was 0.12). All oocytes in each tissue sample were macroscopically classified (Fig. 3) as either unyolked, yolked, mature, or atretic; they were then counted by class and all stages were summed. "Atretic" was defined as oocytes in the alpha stage of atresia (Hunter and Macewicz, 1985b), recognizing, however, that poor preservation can create oocytes of similar macroscopic appearance. The number of ova in the oviduct was also counted directly (usually when n was less than 300) or the mean number was estimated from two tissue samples by using the gravimetric method. To illustrate the form of the oocyte-size distribution in the ovary, we measured (to 0.01 mm) the major axis of all the oocytes in one tissue sample from each ovary of six females by using a digitizer linked by a video camera to a dissection microscope. In all other ovaries used for fecundity estimation, we measured only the smallest and largest oocyte in the sample. The length of the major axis of the smallest oocyte (D) was used as an index of the extent of ovarian maturity. D is a crude index of time elapsed during the spawning period—as long as oocyte maturation continues throughout the spawning period and no new oocytes are produced—both of which appear to be true for *L. opalescens*.

To monitor body condition we cut a tissue sample disc from the mantle using a number 11 cork borer (area of 251.65 mm^2) and removed the outer dermis and the inner membrane. The mantle sample discs were frozen and subsequently dried at 56°C to a constant weight. An index of mantle condition (C) was calculated as the weight of the dry mantle in milligrams divided by disc surface area and is expressed as mg/mm^2.

We evaluated the extent that body reserves might be used to support egg production by comparing dry weight of the eggs and capsules to prespawning female body dry weight. For these calculations we made the following measurements: 1) the mean dry weight of one squid egg was 0.00177 g, including a fraction of the egg capsule because the value is based on the dry weight of 34 egg capsules (1–2 days old) containing 2 to 403 eggs each (total of 7341 eggs, capsules collected from La Jolla Canyon 6 July and 11 September 2000); 2) the relationship of dorsal mantle length (L) and whole-body wet weight (W_w) for immature and mature preovulatory females of $W_w = 0.000051L^{2.8086}$, where W_w is in grams and L is in mm (Fig. 4); and 3) the mean wet weight to dry weight conversion factor of 0.24 (2SE=0.001), based on the wet and dry weights of mantle tissue sampled from 214 mature females. The latter conversion factor was constant regardless of mantle condition index; apparently, in *L. opalescens*, starvation does not result in the replacement of muscle tissue with water as it does in fishes (Woodhead, 1960).

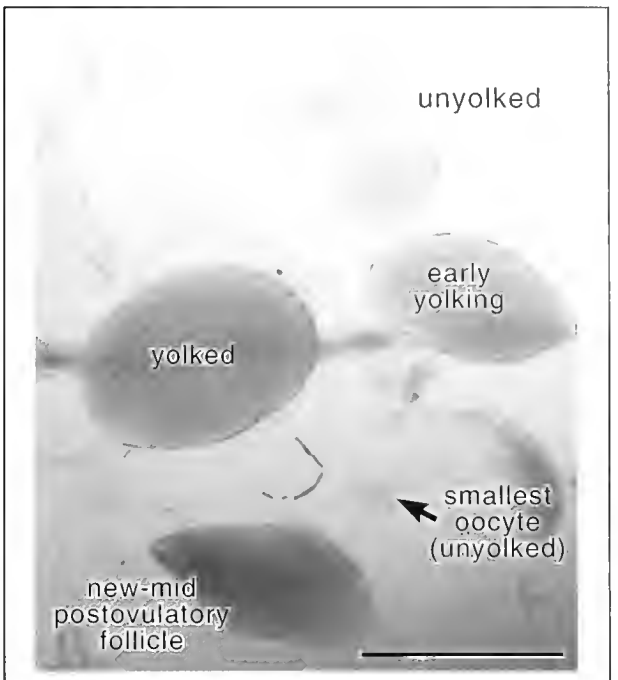

Figure 3

Whole *L. opalescens* oocytes as viewed under a dissection microscope used for counting and classifying oocytes. Bar = 1.0 mm.

In addition to the specimens taken during the research surveys, we also estimated the fecundity of 60 *L. opalescens* from the commercial catch sampled by California Department of Fish & Game (CDF&G) during 1998 and 1999. Landed specimens were not analyzed histologically because their ovarian tissues had begun to deteriorate before preservation. The 60 females were selected by dorsal mantle length and mantle condition index to provide a wide and uniform distribution of length and mantle condition. The number of oocytes in the ovaries was estimated (as described above) and the number of ova in the oviducts were predicted from oviduct weight (Fig. 5). CDF&G also provided data on the dry mantle disc weights of 1275 mature females taken from the catch from December 1998 through December 1999 as random samples taken during the Southern Californian Bight market squid fishery. About 100,000 tons of market squid were landed during this sampling period .

Modeling egg deposition

To identify egg deposition and mortality rates most consistent with our current understanding of spawning biology, we developed a model to estimate the proportion of the potential fecundity deposited by a cohort in its lifetime. The mean proportion of the potential fecundity deposited is the proportion of eggs deposited weighted by the propor-

tion of the cohort that died. Both the proportion of eggs deposited and squid that died were expressed as negative exponential functions. The cumulative eggs deposited up to elapsed time t (days) for a mature female *L. opalescens* is the difference of two terms: $E_{SP,t} = E_P - E_{YD,t}$ where $E_{SP,t}$ is the total eggs deposited by one female up to time t, E_P is the potential fecundity, and $E_{YD,t}$ is the standing stock of oocytes in the ovary plus the standing stock of ova in the oviduct remaining in the body at time t. If we assume that $E_{YD,t}$ declines at an exponential rate from E_P: $E_{YD,t} = E_P e^{-vt}$, where v is the daily rate of eggs deposited, then $E_{SP,t} = E_P(1-e^{-vt})$. We constructed the cumulative egg deposition curve as $Q_{SP,t} = E_{SP,t}/E_P = 1-e^{-vt}$. Assuming the mortality (survival) curve for the squid is e^{-zt}, where z is adult daily total mortality rate ($z=m+f$, where m is natural and f is fishing mortality), we computed the mean fraction of the potential fecundity deposited ($Q_{SP,t}$):

$$Q_{SP} = \frac{\int_0^{t_{\max}} ze^{-zt}(1-e^{-vt})dt}{\int_0^{t_{\max}} ze^{-zt}dt} \quad (1)$$

$$= 1 - \frac{z(1-e^{-(z+v)t_{\max}})}{(z+v)(1-e^{-zt_{\max}})} \cong \frac{v}{z+v} \text{ for large } t_{\max},$$

where $t_{\max}$ is the total elapsed time (days).

The mean fraction of the potential fecundity that remains in the average female (standing stock of oocytes and ova) over her lifetime is $1 - Q_{SP}$, and mean Q_{SP} is always less than one because of mortality. The mean duration of the spawning period in days is computed as the elapsed time corresponding to the mean fraction of eggs deposited (Q_{SP}: Eq. 1 and by setting $Q_{SP}=1-e^{-vt}$):

$$t_{Q_{SP}} = \ln(1 - Q_{SP})/(-u). \quad (2)$$

We evaluated various rates of adult daily total mortality (z) and egg deposition (v) using these models to determine the combination of rates that would provide estimates of fecundity nearest to our observed field data.

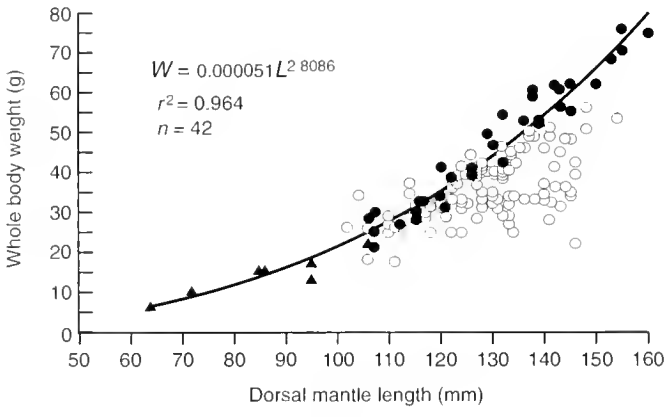

Figure 4

Female squid whole body weight (W) as a function of dorsal mantle length (L) for the 158 females with fecundity analyses. The line expresses the length-weight relation of females before weight losses associated with spawning and was fitted to the combined data for immature females (solid triangles), mature preovulatory females (solid circles), and mature females judged by their mantle condition to be new recruits to the spawning ground (solid circles). Open circles indicate females that have spawned.

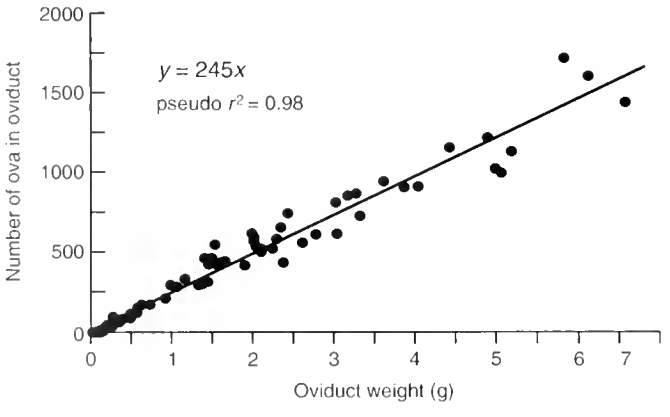

Figure 5

Number of ova in each oviduct shown as a function of the oviduct weight; n equals 91 mature females, pseudo r^2 = 1 – *residual ss/total ss*.

Modeling the effect of fishing effort on egg escapement

In theory we could manage the market squid fishery by monitoring egg escapement, that is, the fraction of the fecundity realized by the average female. Under such a management scheme, egg escapement would be maintained at a specified level by changing fishing effort whenever escapement of eggs fell below it. In this section we develop a model to explore the relative effects of fishing effort on egg escapement. We use this model to discuss some of the biological issues related to using egg escapement as a management tool.

In the modeling process, we follow one cohort of spawners. The elapsed time 0 is defined as the time when squid start spawning. The total escapement of eggs for a given elapsed time (t_k in days) is the sum of three sources of egg escapement: E_C, the total number of eggs deposited by mature females in the catch; E_M, the total number of eggs deposited by mature females dying of natural causes; and E_A, the total number of eggs deposited by females

alive and not taken by the fishery up to time t_k, and $t_k < t_{max}$. The egg escapement rate, R_{e,t_k}, up to time t_k is the sum of the three sources of egg escapement divided by the total number of eggs that would have been spawned if no fishery existed (E):

$$R_{e,t_k} = \frac{E_C + E_M + E_A}{E}. \quad (3)$$

Egg escapement rate at the maximum elapsed time (t_{max}) is

$$R_{e,t_{max}} = \frac{E_C + E_M}{E}, \quad (4)$$

where $t_k = t_{max}$.

Because there are no survivors at time t_{max}, no eggs can be deposited and E_A is zero.

Each term in Equation 3 can be expressed as functions of the mean cumulative number of eggs deposited up to time t_k, $\overline{E_{SP,t_k}} = \overline{E_P} - \overline{E_{YD,t_k}} = \overline{E_P}(1-e^{-vt_k})$, and total mortality ($z$) of the cohort; z includes both natural morality (m) and fishing mortality (f). For practicality, we considered cases when $t_k = t_{max}$, where E_A is zero. For formulas of any t_k, see appendix. The total number of eggs deposited by the females in the catch (E_C) is

$$E_C = \int_0^{t_{max}} \overline{E_{SP,t}} N_0 e^{-(m+f)t} f dt = \overline{E_P} N_0 \int_0^{t_{max}} (1-e^{-vt}) e^{-(m+f)t} f dt \quad (5)$$

$$= \overline{E_P} N_0 f \frac{v}{(m+f)(m+f+v)}, \quad (6)$$

where $\overline{E_P}$ = the mean number of oocytes in the ovary per mature female prior to spawning; and
N_0 = the number of mature females at time 0.

From the fishery data, we can estimate the total number of eggs deposited by the females in the catch (E_C) as

$$\hat{E}_C = N_C\left(\hat{\overline{E_P}} - \hat{\overline{E_{YD}}}\right), \quad (7)$$

where $\hat{\overline{E_P}}$ and $\hat{\overline{E_{YD}}}$ = sample estimates from the catch; and
N_C = the total number of spawners in the catch.

The total number of eggs deposited by *L. opalescens* prior to death due to natural mortality (E_M) is

$$E_M = \int_0^{t_{max}} \overline{E_{SP,t}} N_0 e^{-(m+f)t} m dt = \overline{E_P} N_0 \int_0^{t_{max}} (1-e^{-vt}) e^{-(m+f)t} m dt$$

$$= \overline{E_P} N_0 m \frac{v}{(m+f)(m+f+v)} \quad (9)$$

The total eggs that would be deposited for the cohort without fishing mortality is

$$E = \int_0^{t_{max}} \overline{E_{SP,t}} N_0 m e^{-mt} dt = \overline{E_P} N_0 \int_0^{t_{max}} (1-e^{-vt}) m e^{-mt} dt \quad (10)$$

$$E = \overline{E_P} N_0 \frac{v}{m+v}, \quad (11)$$

where t_{max} (days) = the maximum elapsed time; and
time 0 = the time at the onset of egg deposition.

Egg escapement based on Equation 4 is

$$R_{e,t_{max}} = \frac{\frac{f}{(m+f)(m+f+v)} + \frac{m}{(m+f)(m+f+v)}}{\frac{v}{v+m}} = \frac{m+v}{m+f+v}. \quad (12)$$

Thus, egg escapement reduces down to a simple ratio, $\frac{m+v}{m+f+v}$, involving three daily instantaneous rates: natural mortality (m), egg deposition (v), and fishing mortality (f). $R_{e,t_{max}} = 1$ when there is no fishing and thus $R_{e,t_k} < 1$ with fishing mortality. The lower bound of the egg escapement rate for the cohort is equal to the ratio of the eggs escaping the fishery (E_C) to the total eggs deposited if no fishery existed (E):

$$R_e = E_C / E. \quad (13)$$

Results

Oocyte maturation and production

Immature ovaries contain many small unyolked oocytes with a pronounced peak at about 0.15 mm in size distribution (Fig. 6A). As development continues and vitellogenesis begins, the peak diminishes and shifts to a larger size class of unyolked oocytes (Fig. 6B). Just before the onset of spawning, the size distribution of oocytes becomes relatively flat without pronounced modes (Fig. 6C) and remains so through the rest of the spawning period (Fig. 6, D–F). The standing stock of oocytes declines throughout the spawning period. The minimum size of oocytes in the ovary gradually increases after the onset of yolking, indicating that new oocytes are not produced. We saw no primary oogonia in our histological sections of mature ovaries, another indication that new oocytes are not produced in mature ovaries. Knipe and Beeman (1978) reached the

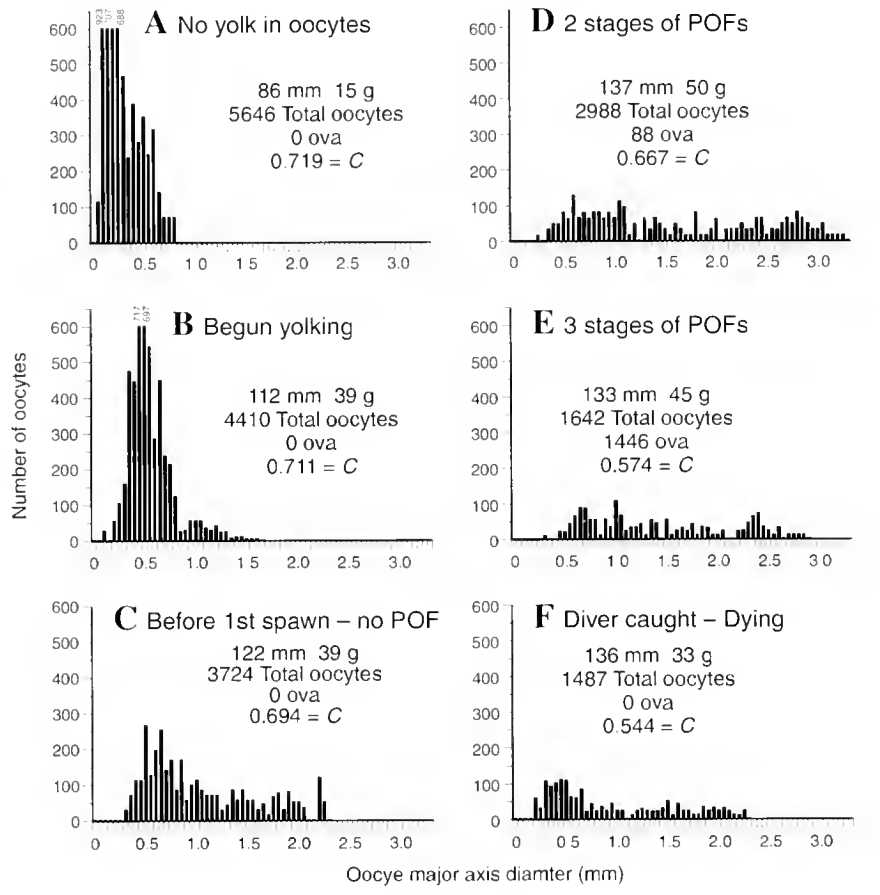

Figure 6

Oocyte-size distribution for six female *Loligo opalescens*. Dorsal mantle length (mm), body weight (g), the total number of oocytes in the ovary, and the number of ova are indicated for each specimen. (**A**) Female that is immature. (**B** and **C**) Females that are considered to be mature and preovulatory because neither has postovulatory follicles (POFs) in their ovaries nor ova in their oviducts. Although the oocytes have just begun yolking in the ovary of female B, female C has well-yolked oocytes and is close to its first ovulation. (**D–F**) Females are mature spawning females and their ovaries contained postovulatory follicles. Female F was caught by a scuba diver and appeared to be dying.

same conclusion from their histological analysis of *L. opalescens* ovaries. Thus, potential fecundity in *L. opalescens* probably becomes fixed near the onset of spawning. Not all oocytes are deposited, however, because all spawning females had some oocytes and many oocytes were counted in the ovary of a dying female (Fig. 6F).

In *L. opalescens* the migration of the oocyte nucleus begins early in the maturation process shortly before the onset of vitellogenesis, whereas in fishes, migration is near the end of vitellogenesis. The follicle of a migratory-nucleus-stage oocyte (late stage IV) of *L. opalescens* has a very large granulosa cell layer (in relation to the size of the oocyte) and is highly folded and perhaps fully developed. Subsequent maturation of the oocyte seems to consist primarily of the massive addition of yolk and fluid and the consequent stretching and unfolding of the follicle, ending with the formation of a chorion. Apparently, the formation of the chorion compacts the yolk because many mature oocytes (endpoint of stage V) have a smaller major axis than advanced yolked oocytes prior to chorion formation. Thus, maximum oocyte size is not a good proxy for oocyte maturation in *L. opalescens* and is not an indicator of the time remaining before spawning of the next batch. More importantly, the ovary of *L. opalescens* seems well adapted for rapid oocyte vitellogenesis, maturation, and spawning because nuclear migration and follicle cell proliferation is completed at an early stage.

Ovulation appears to occur in small batches. The distribution of oocyte sizes in spawning *L. opalescens* was flat (e.g., Fig. 6, D–F) and lacked the separate and distinct mode of hydrated oocytes that is typical in fishes. Batch sizes of mature oocytes ranged from 5 to 246 and averaged 50 (n=72

females). The maximum number of mature oocytes (246) was never close to the maximum number of ova (1726) in the oviduct. In addition, spawning females with 900 or more ova in their oviduct had in every case three or more distinctly different stages of postovulatory follicles in their ovaries (Table 2). Thus the oviduct is probably filled by a series of ovulation bouts separated by enough time to produce distinct age classes of degenerating follicles in the ovary.

Potential fecundity (E_P)

Potential fecundity (E_P) is the standing stock of oocytes of all stages in the ovary of a mature female just prior to the first ovulation. Finding females at this point in their reproductive cycle was difficult because nearly all specimens had already ovulated. The ovaries of 94% of the 247 mature females, from our research cruises, contained postovulatory follicles, indicating that they had recently ovulated and would not be suitable for estimating E_P. As can be seen in Figure 7A, spawning females had fewer oocytes in their ovaries than did mature preovulatory females. The relation between fecundity and squid size is best expressed in terms of dorsal mantle length (L) because *L. opalescens* lose weight during spawning (Figs. 4, 7C). The data from thirteen mature preovulatory females were used to establish the relationship between potential fecundity and L:

$$E_P = 85.62L - 6715, \qquad [r^2 = 34.3\%] \qquad (14)$$

where L = dorsal mantle length in mm.

Because the constant was not significant (P=0.146) and the coefficient was (P=0.036), we forced the regression through zero which resulted in the equation

$$E_P = 29.8L. \qquad (15)$$

Thus, the average female (129 mm) according to Equation 15 had a potential fecundity of 3844 oocytes (SE=317).

Clearly it would be preferable if the sample size for the estimate of potential fecundity were larger because thirteen females may not accurately represent the *L. opalescens* stock. Although the landed catch provides an unlimited supply of specimens, histological detection of postovulatory follicles is not possible because of deterioration of the ovaries. An alternative approach is to use mantle condition of mature females from the catch as a proxy for the preovulatory state. As can be seen in Figure 7C, the mantle condition index (C) of mature females declines as oocyte maturation continues and females deposit eggs. The mature preovulatory females (n=11, two discs were lost) had a mean C of 0.73 mg/mm^2 (SE=0.02). We believe that the twenty-two mature females from the landed catch with $C \geq 0.7$ mg/mm^2 had not begun to deposit eggs (Table 3). Because many of them had ovulated, we combined our estimates of the standing stock of oocytes (E_Y) with those of ova (E_D) to calculate total fecundity ($E_Y + E_D = E_{YD}$), and then regressed total fecundity on length. Although the regression was not significant, the average total fecundity of 3890 oocytes (Table 3) was within 5% of the potential fecundity of 4083 oocytes computed by substituting the mean length of the twenty-two females (137 mm) in Equation 15. The close agreement between these two values increases our confidence that the potential fecundity equation is accurate despite the low n. On the other hand, this rough comparison is not a substitute for increasing the sample size of specimens analyzed histologically, because females from the catch may have spawned some of their ova before they were captured.

Table 2

Percentage of spawning female market squid classed by the number of eggs in their oviducts and by the number of ages (stages of degeneration) of postovulatory follicles (POFs) in their ovaries.

Number of eggs in the oviduct	Number of females	Percentage of females	
		1 or 2 ages of POFs	≥3 ages of POFs
0	1	100	0
1–300	36	22	78
301–600	20	35	65
601–900	10	20	80
901–1200	7	0	100
1201–1500	2	0	100
1501–1800	2	0	100

Maximum fecundity ($E_P - E_R$)

Few if any *L. opalescens* live to realize their full potential fecundity (E_P). The literature on *L. opalescens* indicates that females that were described as "spawned out," dying, or dead had oocytes in all stages of development except the earliest previtellogenic stage (Knipe and Beeman 1978). In addition, all the spawning females that we collected had some oocytes in their ovaries. Thus, the maximum fecundity that *L. opalescens* might be expected to realize is the potential fecundity less an estimate of the number of oocytes that might be left in the ovary at death (residual fecundity [E_R]). To estimate residual fecundity we examined the relationship of the standing stock of oocytes in the spawning period with mantle condition index (C), size of the smallest oocyte (D), and dorsal mantle length (L).

The standing stock of oocytes in ovaries of mature females declines rapidly with decreasing mantle condition, between a C of 0.8 and 0.6 mg/mm^2, and more gradually over lower mantle conditions (Fig. 7C). A curvilinear relationship also exists between oocyte standing stock and the size of the smallest oocyte (Fig. 7B). Thus the number of past spawnings (decline in oocyte standing stock) appears to be inversely correlated with C and directly correlated with the extent of ovarian maturation as measured by D. To quantify how the standing stock of oocytes changes during the spawning period we fitted a nonlinear model to the fecundity data of 75 mature spawning females (Fig. 7) from our research cruises:

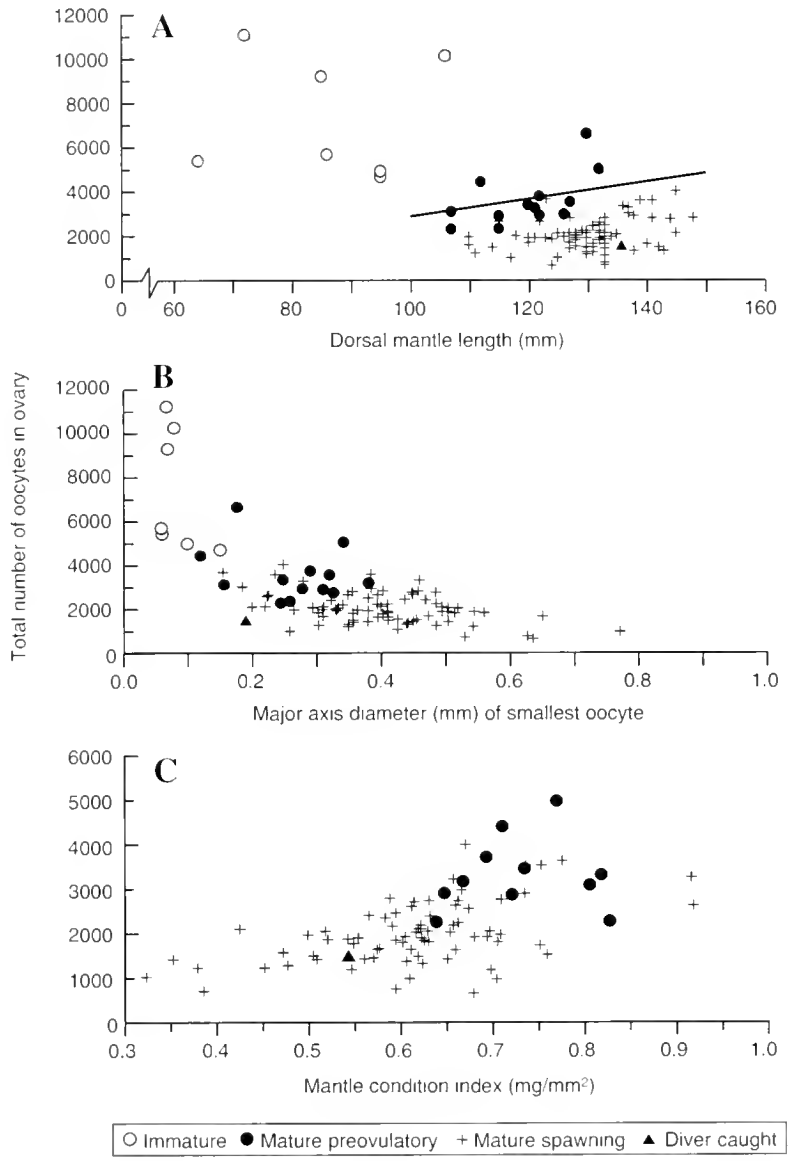

Figure 7

The number of oocytes in ovaries of 98 *Loligo opalescens* as a function of dorsal mantle length (**A**) and the diameter of the major axis of the smallest oocyte (**B**). In (**C**), the number of oocytes is plotted as a function of mantle condition index (the dry weight per surface area of a mantle tissue disc) for 87 mature females (4 discs were lost and the 7 immature were not included). Line in A expresses potential fecundity as a function of length (E_P=29.8L) for the 13 mature preovulatory females (solid circles); open circles represent immature females; plus signs represent spawning females; and the triangle represents a dying mature female.

$$E_R = 30283e^{(-1.24D - 6.19C - 0.024L + 0.059LC)}, \quad (16)$$

where C = mantle condition index;
D = size of the smallest oocyte; and
L = dorsal mantle length.

Substituting into the model (Fig. 8) the maximum observed D (0.771 mm) and the minimum observed C (0.323 mg/mm^2) from our research survey data set, we estimated that a female *L. opalescens* with L of 129 mm may have a minimum residual fecundity of 834 oocytes (CV=0.12).

Table 3

Mean fecundity, gonad weight, and dorsal mantle length for 60 mature female market squid (*Loligo opalescens*) sampled at the ports December 1998 to December 1999.

Mantle condition index (mg/mm^2)		Fecundity (mean number)			Mean gonad weight (g)	Dorsal mantle length (mm)		Number of females
Class	Mean	Oocytes in ovary (E_Y)	Ova in oviduct (E_D)	Total (E_{YD})		Mean	Range	
0.347–0.499	0.432	1134	231	1365	2.215	132	106–146	22
0.500–0.699	0.613	2072	522	2594	4.959	125	102–154	16
0.700–0.951	0.824	2589	1301	3890	8.988	137	106–160	22
0.347–0.951	0.624	1917	701	2618	5.397	132	102–160	60

A 129-mm *L. opalescens* with a potential fecundity of 3844 oocytes would have a maximum fecundity of 3010 eggs (3844–834 eggs) or about 78% of the potential fecundity. Very few females would be expected to deposit 78% of their potential because this maximum is based on extreme values for both mantle condition index and ovarian maturation. In a much larger set of mantle samples from the catch (Table 4), only 1.5% of the females had values of C less than 0.35 mg/mm^2. Clearly very few squid live to deposit 78% of their potential fecundity.

Another approach is to count the number of oocytes remaining in the ovaries of females presumed, from their behavior and appearance, to be dying. Although *L. opalescens* has been observed to be dying or dead on the bottom on video from a remotely operated vehicle (Cossio[1]), capturing such females was not attempted at the time. A female *L. opalescens* (136 mm) believed to be dying was opportunistically collected by a diver 6 July 2000 on the La Jolla Canyon spawning grounds (McGowan, 1954). There were no ova and the ovary contained 1487 oocytes—substantially more oocytes than our estimate of the minimum residual fecundity. In fact, the female had deposited only about 63% of her potential fecundity.

Table 4

Distribution of mantle condition index for 1275 mature female *L. opalescens* sampled from the landed catch from December 1998 to December 1999.

Mantle condition index (mg/mm^2)	Mature females	
	Number	Percentage
0.263–0.299	4	0.3
0.300–0.349	15	1.2
0.350–0.399	29	2.3
0.400–0.449	54	4.2
0.450–0.499	91	7.1
0.500–0.549	128	10.0
0.550–0.599	207	16.2
0.600–0.649	210	16.5
0.650–0.699	216	16.9
0.700–0.749	137	10.7
0.750–0.799	94	7.4
0.800–0.849	53	4.2
0.850–0.899	18	1.4
0.900–0.949	10	0.8
0.950–0.999	6	0.5
1.000–1.043	3	0.2

Role of body reserves

We used weight relationships to evaluate the extent to which body reserves might be used to support the reproduction of spawning female *L. opalescens*. In these crude energetic calculations we did not include metabolism, conversion efficiencies, or caloric values of tissues. We used the average dry weight of squid eggs, length to body weight conversion, potential fecundity equation, and the conversion factor from wet to dry mantle weight. We assumed preovulatory mantle condition index (C) for an average mature female of 130 mm was 0.798 mg/mm^2, the mean for valnes (n=41) of $C \geq 0.700$ mg/mm^2 in the our fecundity data set. We calculated that the potential fecundity of a 130-mm *L. opalescens* (i.e., 3874 encapsulated eggs) has a dry weight of 6.86 g which is equivalent to 64.8% of the whole-body dry weight (10.58 g) of that female just before spawning. If mantle condition is reduced in proportion to the dry weight of all the eggs, our hypothetical female would have a C of about 0.281mg/mm^2 ($0.798 \times [(10.58-6.86)/10.58]$). This end point ($C$=0.281, egg=0) and the beginning point for the mature preovulatory female (C=0.798, eggs=3874) create a hypothetical

[1] Cossio, A. 2000. Personal commun. Southwest Fisheries Science Center, National Marine Fisheries Service, 8604 La Jolla Shores Dr., La Jolla, CA 92037

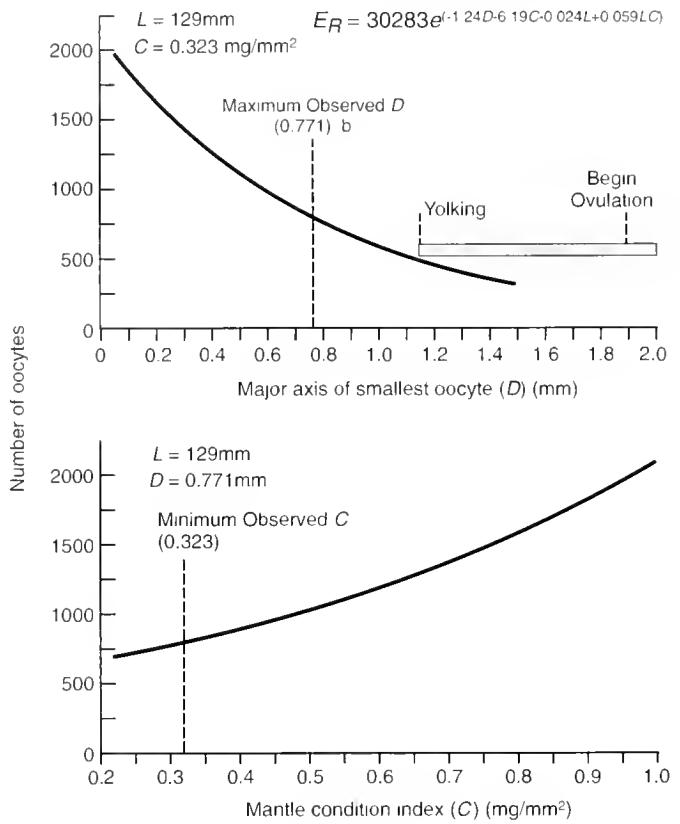

Figure 8

Changes in the standing stock of oocytes predicted by Equation 16 (equation also given at top of panel) when major axis of smallest oocyte (D) is varied and mantle condition index (C) held constant (upper panel), and when C is varied and D held constant (lower panel). The major axis size of oocyte when yoking begins and when ovulation begins is also indicated, as are the maximum observed D and minimum observed C. Substitution of the latter two values into the equation yields the standing stock of oocytes of females close to the end of their reproductive activity and is considered to be a minimum estimate of residual fecundity.

line that expresses oocyte standing stock for the average mature female of 130 mm as a function of mantle condition. In addition to the hypothetical line, we plotted the total standing stock of oocyte and ova (E_{YD}) and mantle condition index for all 147 mature females used for direct fecundity determinations (Fig. 9). Our hypothetical line, based on direct proportionality between egg dry weight and body dry weight, follows the general trend in the data, indicating that energy reserves in mantle tissue may largely support the production and spawning of eggs. Of course, actual energy costs would be higher because metabolism, other somatic tissue, and conversion efficiency of mantle tissue to eggs are not considered. The lowest observed C in the fecundity data set was 0.323 and the lowest C observed in the 1275 mature females from the landed catch was 0.263. Using the above preovulatory C (0.798 mg/mm^2), we determined that these values of C are equivalent to 60% and 67% losses in body dry weight for these individuals. Fields (1965) suggested body wet weight declined by as much as 50%, which is consistent with our results.

These rough calculations support the long held belief that oocyte maturation is supported primarily by body reserves. Some feeding occurs during spawning; *L. opalescens* has been observed feeding under lights at night on the spawning grounds (Butler[2]). Maxwell and Hanlon (2000) observed *L. pealeii* feeding between egg-laying bouts when they were held in the laboratory. Feeding between spawning bouts by the more robust spawners that may migrate on and off the grounds each day seems quite

[2] Butler, J. 2000. Personal commun. Southwest Fisheries Science Center, National Marine Fisheries Service, 8604 La Jolla Shores Dr., La Jolla, CA 92037.

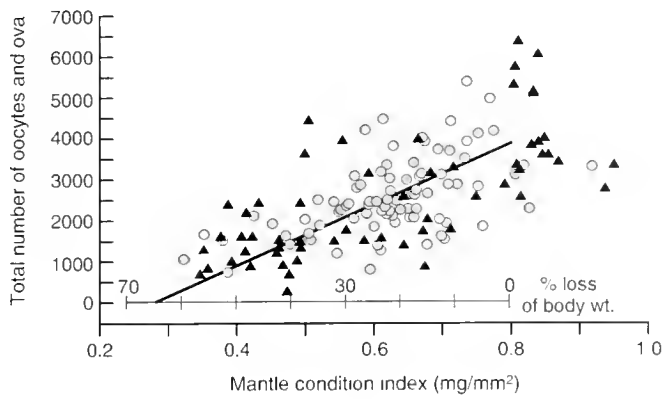

Figure 9

Standing stock of oocytes and ova as a function of mantle condition index for 60 mature females taken in the fishery (triangles) and 87 mature females taken in research surveys (circles). The line (not drawn to the data points plotted) represents a possible relation if losses in body weight were equivalent to the weight of the spawn released, computed for an average female (130 mm) where the starting point is her potential fecundity of 3874 oocytes and ends with 0 eggs and a mantle condition index of 0.281 mg/mm^2.

possible, but it seems unlikely for the nearly exhausted *L. opalescens* that are near the end of their life.

Longevity and egg deposition rates

Inferences regarding the longevity of adult spawning *L. opalescens* are the best proxy we have for the mortality rates of spawning adults. Previous observers (McGowen, 1954; Fields, 1965) suggested that females deposited all their eggs in one night and death soon followed. On the other hand, it is unreasonable to expect that a reduction of 60% in body weight and the maturation and deposition of up to 78% of the potential fecundity could take place in 24 hours. Our data on fecundity and mantle condition show an initial rapid decline in the number of oocytes followed by a more gradual decline (Fig. 7C), indicating an initial period of intense egg laying may be followed by a longer one where fewer eggs are deposited. It is also important to recognize that ovaries of spawning animals contain a wide range of oocyte sizes (Fig. 6), including many small unyolked oocytes (0.3–1 mm) that may mature and be deposited during the spawning period. It is unlikely that all these processes (body resorption, dynamic changes in rates of egg deposition, and maturation of small unyolked oocytes) could occur in one 24-hour period. Spawning periods longer than two weeks also seem unlikely because mature *L. opalescens* females may require extensive feeding periods and prolonged absences from the spawning grounds; these behaviors are inconsistent with our energetic analysis in the preceding section. Our analysis indicated that the observed reduction in eggs can be fairly well explained by the observed reduction in squid dry weight.

Egg deposition rates provide another way to infer the longevity of spawning squid. The best evidence for the rate of egg deposition is provided by females judged, on the basis of their high mantle condition ($C \geq 0.700$ mg/mm^2), to be new recruits to the spawning grounds. Considering only those new recruits that have ovulated (postovulatory follicles present or ova in the oviduct), the difference between their average oocyte standing stock (E_Y=2571) and their average potential fecundity (E_P=4020) was equivalent to a reduction of 1449 oocytes or 36% of their potential fecundity (Table 5). If the difference is spawned in 24 hours or less, then 36% can be considered as an average for the first day of egg deposition. Instead of using the reduction of oocyte standing stock, one could consider the standing stock of ova (E_D) to be equivalent to the first day (24-hour period) of spawning in these new recruits. Their average E_D was 1073 or 27% of their potential fecundity. Thus depending on the criteria, the first day of spawning might be 27% to 36% of the potential fecundity. We prefer 36% because it is unaffected by any losses due to egg deposition.

The standing stock of ova (E_D) of spawning females with lower mantle condition (C<0.7 mg/mm^2) averaged 9% of their potential fecundity. If the average E_D from these females is a crude measure of daily egg deposition rates after the first day, then we calculate it would take seven additional days [(100%–36%)/9%] to use up the remaining potential fecundity or a total spawning period of eight days. Eight days is an extreme value because an adult *L. opalescens* has never been taken with zero oocytes. The minimum residual fecundity was 22% of the potential which is roughly equivalent to about two days of egg deposition. Thus, six days may be a better guess of the maximum longevity of spawning *L. opalescens*.

Table 5

The mean fecundity for various classes of mantle condition for spawning *Loligo opalescens* and the grand mean weighted by the frequency of mantle condition classes in fisbery samples 1998–99.

Class of mantle condition (mg/mm^2)	Number of spawning females	Mean fecundity (SE)			Dorsal mantle length in mm	Mean potential fecundity[1] (SE)	Number of eggs deposited $E_{SP} = E_P - E_{YD}$	Weighting factors (Table 4)
		Oocytes in ovary (E_Y)	Ova in oviduct (E_D)	Total (E_{YD})	Mean (SE)			
≤0.499	31	1212 (93)	207 (40)	1419 (100)	133 (2.08)	3954 (384)	2535	0.151
0.500–0.699	70	2008 (84)	437 (49)	2496 (100)	128 (1.20)	3813 (340)	1317	0.597
≤0.700	34	2571 (202)	1073 (109)	3657 (210)	135 (2.37)	4020 (385)	363	0.252
0.323–0.951	135	1967 (83)	544 (47)	2541 (102)	131 (1.01)	3897 (336)	1356	
				2599[2]	129.5	3859 (320)	1260[3]	

[1] Potential fecundity (E_P) estimated by $E_P = 29.8L$, where L = dorsal mantle length in millimeters.

[2] Product of population E_P and weighted average of the fraction of potential fecundity remaining in spawners):
$3859 \times [(1419/3954 \times 0.151) + (2496/3813 \times 0.597) + (3657/4020 \times 0.252)] = 2599$; or the population E_P less $E_{SP(weighted)}$ which is 3859–1260.

[3] Weighted average of the number of eggs deposited $[(2535 \times 0.151) + (1317 \times 0.597) + (363 \times 0.252)]$.

Probably very few females would be expected to survive six days because only a small percentage of the spawning population (Table 4) met the mantle criteria for minimum residual fecundity.

In summary, our best guess of the maximum longevity of squid on the spawning grounds is about six days. Our best description of daily egg deposition is a rate that ends the first day with 36% of the potential fecundity deposited and averages about 9% of the potential per day over the remaining five days and where only a small percentage of the females live to deposit 78% or more of their potential fecundity.

Egg escapement

We examine the spawning dynamics of *Loligo opalescens* from the standpoint of possibly using fecundity of the catch to monitor and ultimately regulate escapement of eggs from the fishery. The key variable in this approach is the fraction of the potential fecundity that is actually deposited as eggs on the bottom because this value can be directly estimated from the fecundity of the catch. Two other important parameters are the daily rate of total mortality (z) on the spawning grounds and the daily rate of egg deposition (v). Neither of these parameters can be directly estimated but they are approximated by values that are most consistent with our observations by using a model (Eq. 1). Our observations consist of the fecundity of the catch and the inferences regarding longevity and egg deposition, presented in the previous section. We use our approximations for egg deposition and total mortality in a second model (Eq. 12) to gain an idea of how natural mortality and fishing mortality may affect egg escapement. Lastly, we present a rapid method for monitoring the fecundity of the catch which does not require direct counting of oocytes or ova.

Fraction of the potential fecundity spawned (Q_{SP}) In a spawning population of *L. opalescens*, the mean standing stock of oocytes and ova ($\overline{E_{YD}}$), when expressed as a fraction of potential fecundity, is equivalent to the fraction of the potential fecundity of the population that remains in the spawners ($\overline{E_{YD}}/\overline{E_P}$). When subtracted from one ($1-[\overline{E_{YD}}/\overline{E_P}]$), the difference becomes the fraction of the potential fecundity of the population that is actually spawned (Q_{SP}). For this interpretation to be correct, samples must be randomly drawn from the population and represent all spawners according to their abundance on the spawning grounds—from the newly recruited to those that have been spawning for extended periods.

Neither the females taken from our research cruises nor those used to estimate fecundity from the landed catch were random samples of the spawning population. First, not all of the specimens taken during the two research cruises were from the spawning grounds. Second, the 60 females from the commercial catch were not randomly chosen but were selected to represent a full range of L and C. However, by weighting our fecundity estimates by a random sample of mantle condition from the fishery, it was possible to approximate a random fecundity sample of spawners. The population we used for weighting was based on the mantle condition index (C) of 1275 randomly taken specimens from the commercial catch sampled December 1998 through December 1999 (Table 4). The weighted and unweighted mean standing stocks of oocytes and ova ($\overline{E_{YD}}$) were similar (Table 5), indicating that our previous selection of specimens by C did not introduce a large bias. For the unweighted data, $\overline{E_{YD}}$ was 2541 and was 2599

Table 6

Estimates of number of days of egg deposition, the mean number of eggs deposited, mean standing stocks of oocytes and ova remaining in female *L. opalescens*, mean number of eggs deposited at the end of the first night (all means are expressed as a fraction of the potential fecundity), for various combinations of possible egg deposition (v) and total adult mortality (z) rates. Model provided estimate nearest observed data when $z = 0.45$, $v = 0.25$, and $t_{max} = 8$ days.

Daily total mortality (z)	Daily egg deposition rate (v)	Fraction of potential fecundity deposited Q_{SP} (Equation 1)	Fraction of potential fecundity remaining in females $(1-Q_{SP})$	Mean number of nights of egg deposition $t_{Q_{SP}}$ (Equation 2)	Fraction of eggs deposited at the end of the first night $(1-e^{-v})$	Days to reach 78% eggs deposited
0.2	0.25	0.458	0.542	2.45	0.221	6.057
0.2	0.45	0.617	0.383	2.13	0.362	3.365
0.2	0.65	0.706	0.294	1.88	0.478	2.329
0.45	0.25	0.341	0.659	1.67	0.221	6.057
0.45	0.45	0.486	0.514	1.48	0.362	3.365
0.45	0.65	0.580	0.420	1.33	0.478	2.329
0.8	0.25	0.237	0.763	1.08	0.221	6.057
0.8	0.45	0.359	0.641	0.99	0.362	3.365
0.8	0.65	0.447	0.553	0.91	0.478	2.329
Observed		0.326 (SE 0.075)	0.674		0.36	6.0

when the data were weighted by the distribution of mantle conditions in the catch. The mean fraction of the potential fecundity deposited (Q_{SP}) by *L. opalescens* was 0.326 (1–2599/3859). That much of the fecundity had escaped (eggs were deposited) before the market squid were taken by the fishery does not seem unreasonable because 22–36% of E_P may be deposited during the first day of spawning. The mean Q_{SP} is an important index because it measures egg escapement as a fraction of potential fecundity over its lifetime (Eq. 1). It is used in subsequent sections to identify a daily total mortality rate and egg escapement rate for the average female in the population that best characterizes the sampled *L. opalescens* population.

Preferred mortality and egg deposition rates We used Equation 1 to evaluate which combination of a range of plausible values for the rates of daily total mortality (z of 0.2, 0.45, and 0.8) and daily egg deposition (v of 0.25, 0.45, and 0.65) provides an estimate closest to observed Q_{SP} ($\overline{E_{SP}/E_P}$) (Table 6). The combination of an adult daily total mortality (z) rate of 0.45, a daily egg deposition (v) rate of 0.25, and using a $t_{\max}$ of 8 days gave an estimate that was most consistent with the observed value for Q_{SP} of 0.326 (Table 6, Fig. 10). This combination of rates also gave an egg depletion of 78% of the potential fecundity in 6 days which was consistent with our best guess for maximum longevity and maximum fecundity. On the other hand, the model (using $1-e^{-vt}$ and t=1) predicts that about 22% of the potential is deposited by the end of the first 24 hours (day 1) which is less than our preferred estimate (36%) based on the reduction in standing stock of oocytes but is closer to the one based on the standing stock of ova (27%). A possible biological explanation for the difference might be that some of the ova produced during the first day of deposition might remain in the oviduct and then be deposited on the second day. Regardless of the uncertainties regarding the fit for the initial day of egg deposition, a daily total mortality rate of 0.45 and daily egg deposition rate of 0.25 are most consistent with the field data known at the present time. This means that the average spawning period is very short; the average female lives only 1.67 days after spawning begins (ln(0.659)/–0.25; Eq. 2). It is interesting that 1.67 days for the average animal is not a radical departure from Fields's (1965) original conclusion of a single night of spawning.

Egg escapement from the fishery In *L. opalescens*, where the fishery targets spawning adults that die after spawning, it is important to know the effect of fishing mortality on the egg escapement rate with respect to the lifetime fecundity deposited, $R_{e,t_{\max}}$ (Eq. 12). However, not all terms in Equation 12 are observable and it may be practical to manage the fishery by monitoring the fraction of the potential fecundity that is deposited on the bottom (Q_{SP}= $1-[\overline{E_{YP}/E_P}]$). Nevertheless, we examined the potential effects of fishing mortality (f) on the egg escapement rate, $R_{e,t_{\max}}$, when natural mortality (m) is 0.1, 0.25, or 0.4, and egg deposition (v) is 0.25, 0.45, or 0.65 (Fig. 11). Because our preferred rates from the previous section are v = 0.25 and z = 0.45, then m is <0.45 with fishing because $z = m + f$. If we use v = 0.25 and set daily natural mortality rate high (m=0.4), then f is 0.05 and $R_{e,t_{\max}}$ is 93%. Doubling the fishing mortality (to 0.1) produces an absolute difference of 6% in egg escapement (Fig. 11C). Thus at a high m of 0.4, escapement is relatively insensitive to changes in daily

fishing mortality. At lower natural mortalities, a change in fishing mortality has a greater effect on escapement. At m = 0.1 and f = 0.35 $R_{e,t_{max}}$ is 50%. Doubling the fishing morality to 0.7 $R_{e,t_{max}}$ would be 33%, producing a loss of 17% in escapement (Fig. 11A). Increasing the rate of daily egg deposition (v) from our preferred value of 0.25 to 0.65 also diminishes the effect of fishing mortality on escapement but the effect of fishing on egg escapement is most marked at the low natural mortality of m = 0.1 and is relatively minor when natural mortality reaches m = 0.4. Thus, uncertainties regarding the true initial values of egg deposition seem relatively unimportant at these high mortality rates. It is important to remember that in this discussion that we are discussing daily mortality rates that last only a few days or weeks of the life of a semelparous animal; hence the rates are very high and resemble the typical daily mortality rates of small pelagic fish eggs (Alheit, 1993) that also exist for short periods.

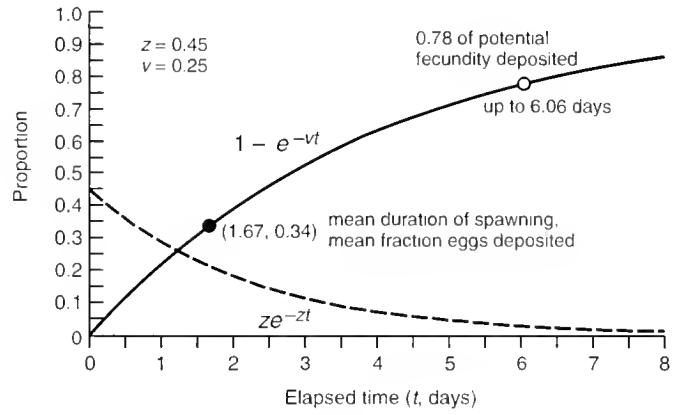

Figure 10

The cumulative egg release curve (solid line) and the density function of longevity on the spawning grounds of adult females (dashed line) of *Loligo opalescens* for a total mortality rate (z) of 0.45 and a egg release rate (v) of 0.25. The plotted solid circle represents mean egg deposition estimated by the model as a proportion of the potential fecundity and model estimate of the mean duration of the spawning period.

Cost effective methods for monitoring fecundity If egg escapement were adopted as a monitoring and management tool for the market squid fishery, a cost-effective method for monitoring fecundity of *L. opalescens* would be needed. A direct estimation of the standing stock of oocytes in an ovary by using a microscope and video system (as preformed in this study) is too time consuming for routine monitoring of the fishery because it takes about 4 hours per specimen.

Our first approach for an indirect estimator was to use the measurements routinely taken by CDF&G staff who sample the catch. These measurements were dorsal mantle length, mantle condition index, and an oviduct classification system for approximating the numbers of ova. To estimate the oocyte standing stock (E_Y) of the catch females, using only length and mantle condition, we fitted a nonlinear model to the data for all squid classed as mature (spawning individuals and pre-ovulatory) in our 1998 research survey data set. This yielded the equation

$$E_Y = 220.453e^{(1.99C + 0.0079L)}, \quad (17)$$

where L = dorsal mantle length; and
C = mantle condition index.

Equation 17 for E_Y explains only 33% of the variability within the survey data set (n=90) and therefore is rather imprecise. Using this model we estimated E_Y to average about 2221 oocytes in the ovaries of the mature females

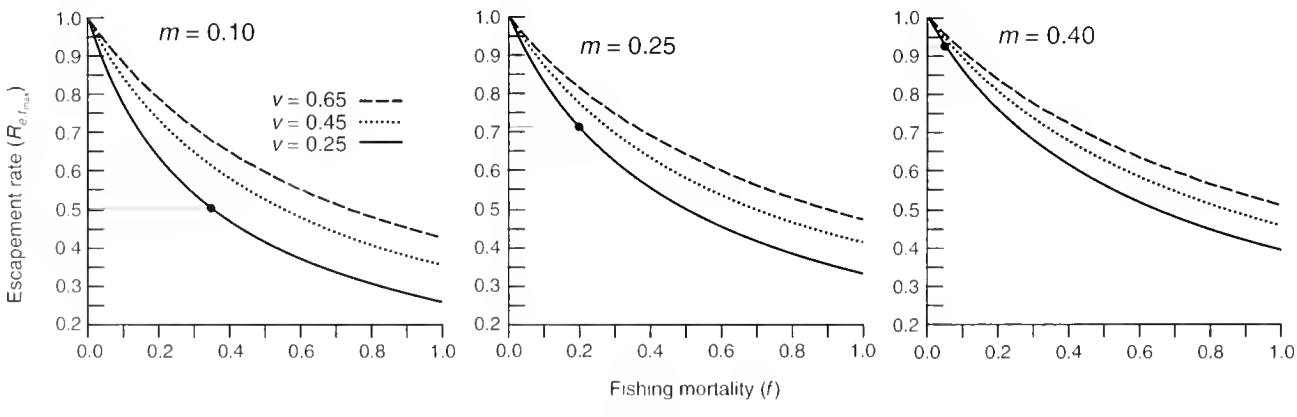

Figure 11

The egg escapement rate, $R_{e,t_{max}}$ (Eq. 12) of *L. opalescens* as a function of various daily natural adult mortality rates (m), daily egg deposition rates (v), and daily fishing mortality rates (f). In each panel, the solid circle indicates the f value for preferred values: z = 0.45 and v = 0.25.

(n=1275) sampled from catch during the period 1998–99 (Fig. 12); this estimate is equivalent to approximately 58% of the potential fecundity calculated from mean length (129 mm).

Our second approach was to estimate total fecundity (E_{YD}, standing stock of oocytes and ova) indirectly using the combined formalin wet weight of the ovary and the oviduct, in addition to mantle condition. Combining ovary and oviduct in one weight is more efficient than weighing them separately because much less time is required for dissection. Dorsal mantle length was also considered as a variable but it was not significant. The final equation for the total standing stock of oocytes and ova in a mature female squid is

$$E_{YD} = 378.28e^{(2.33C + 0.2447G - 0.24CG)}, \qquad (18)$$

where C = mantle condition index; and
G = gonad (ovary and oviduct) weight.

The predicted fecundity related well to the observed with a pseudo r^2 of 0.60 (df=143). We also used generalized additive models to estimate fecundity (GAM, pseudo r^2=0.64), as well as regression on the first principal component which explained 86% of the total variation (pseudo r^2=0.55). Although the GAM gave a slightly higher pseudo r^2 than the parametric nonlinear regression, we chose the later for easier interpretation and implementation. A pattern existed in the residuals from our model (Fig. 13); the model overestimated some fecundities at high mantle condition and underestimated fecundity at low mantle condition. This pattern in the residuals is probably related to the differences in density and size of oocytes in the ovary. Regardless of the minor problem with the residuals, this proxy (Eq. 18) for the standing stock of oocyte and ova is preferred because it gives a much more precise estimate at the minor additional cost of preserving and subsequently determining the combined weight of ovary and oviduct. Although formalin weight of ovary and oviduct are not presently monitored in the fishery, it is a variable that could be added to fishery protocols at a minor increase in cost. Another benefit of this more precise approach using E_{YD} is that oviduct is included in the estimate. If an estimate of the removal of fecundity by the fishery is needed, ova must be included. Because ova are not included in Equation 17, to add them requires using the oviduct classification system (Table 1) to estimate the average number of ova—a system that is imprecise but cheap. One could, of course, use Equation 17 for E_Y and either count the ova in the oviduct or weigh the oviduct, but that would take more work than applying Equation 18 for E_{YD}.

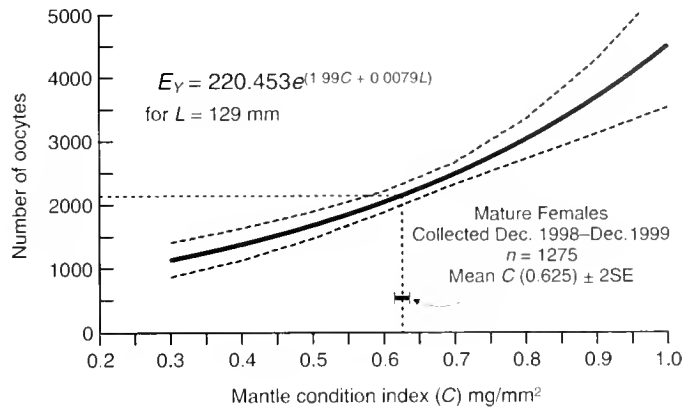

Figure 12

Standing stock of oocytes in the ovary (E_Y) as a function of mantle condition index (C) for a 129-mm mature female *L. opalescens* as predicted by Equation 17 (equation also given on top of panel; L is dorsal mantle length). Dashed lines are ±2SE. The mean E_Y for the females taken in the fishery was 2221 oocytes.

Discussion

Potential fecundity

Our estimate of *Loligo opalescens* potential fecundity is based on a regression of the standing stock of oocytes on dorsal mantle length for mature preovulatory females having yolked oocytes in their ovaries. The accuracy of this approach depends upon the assumption that these females are at the point in life when the standing stock of oocytes in their ovaries is equivalent to their potential lifetime fecundity. This key assumption would not hold if some of the mature squid classed histologically as preovulatory had in fact spawned. We do not know how long postovulatory follicles are distinguishable from atretic structures in the ovary of *L. opalescens* and, as far as we know, the rate of degeneration has not been determined for any loliginid. We know from our work on anchovy (Hunter and Goldberg, 1980; Hunter and Macewicz, 1985a), although it is not a cephalopod, that postovulatory follicles are distinguishable from atretic structures in the ovary of anchovy for about two to three days after spawning when the water temperature is about 16°C. This means that for undetected spawning to occur in *L. opalescens*, the interval between ovulation periods would likely need to exceed three days. This may be a minimum estimate because *L. opalescens* spawn at lower temperatures (9–13°C, Butler[2]) than do anchovy. Definitely a laboratory study on the rate of degeneration is necessary because postovulatory follicles in fish degenerate slower at lower temperatures (Fitzhugh and Hettler, 1995). In addition to the absence of postovulatory follicles, the oviduct must be empty for a spawning act to be undetected. Undetected ovulation and spawning seems unlikely because females with multiple stages of postovulatory follicles were common (87% of 247 mature females), females with only old postovulatory follicles were not detected, and the average life span on the spawning grounds may only be a few days.

Atretic losses of oocytes are another possible bias in estimating potential fecundity. Atresia (degeneration and resorption of an oocyte and its follicle) appears to be a

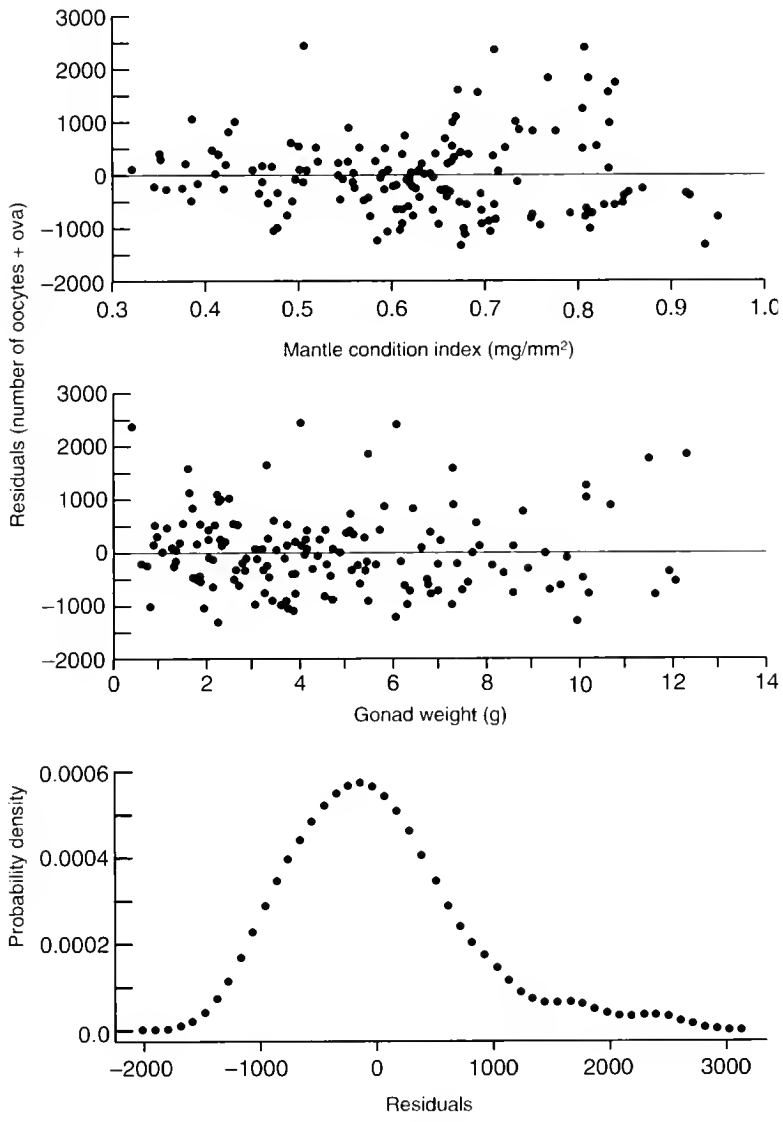

Figure 13

Residual plots of number of oocytes and ova from the equation $E_{YD} = 378.28e^{(2.33C + 0.2447G - 0.24CG)}$ (Eq. 18) where standing stock of oocytes and ova (E_{YD}) are predicted from mantle condition index (C) and gonad weight (G). Bottom panel shows probability density of residuals.

normal part of ovarian maturation in *L. oplaescens*, as it is the case for *L. v. reynaudii* (Melo and Sauer, 1998). Our evidence for this is that the standing stock of oocytes in immature female *L. opalescens* declines sharply as their ovaries mature (D increases, Fig. 7B). Clearly a narrow window of opportunity exists for an unbiased estimate of the potential fecundity of *L. oplaescens*. If the count is made too early in the ovarian maturation process, the count will either be low because extensive primary oogonia production may be still be occurring (64-mm female, Fig. 7A) or too high because additional oocytes will be absorbed before the female reaches maturity. If the count is made too late, it will be impossible to find a female that has not ovulated. Our selection criteria "presence of yolked oocytes" (which roughly begins at a oocyte size of about 1.1 mm) filtered out the very high counts of oocytes associated with immature ovaries.

From the practical standpoint, dealing with atretic losses that may continue into the spawning period is much less important for *L. opalescens* than for *L. v. reynaudii* (Melo and Sauer, 1998; Sauer et al., 1999) or *L. pealeii* (Maxwell and Hanlon, 2000). In these squid, where the spawning period may last weeks or months, atresia may seriously bias potential fecundity estimates. In the pres-

ent study all atretic losses would be attributed, of course, to ovulation and spawning but the chances of this being a major error seem low. Because we counted atretic as well as normal oocytes, atretic losses would be erroneously attributed to spawning only if atresia had proceeded to the point that the atretic structure could not be identified as that of an oocyte in whole-mount preparations under a light microscope (64× power). The time at stage for atretic oocytes in *L. opalescens* ovaries, as well as other squid, is unknown. The duration of alpha-stage atresia of yolked oocytes in anchovy is about a week at 16°C (Hunter and Macewicz, 1985b) and we suspect for the larger *L. opalescens* yolked oocyte that the alpha-stage duration may be even longer. The disappearance of unyolked atretic oocytes, as an oocyte-like structure that would be counted, is more difficult to dismiss because so little is known about this atretic stage and its duration. If our estimate of the average longevity of spawning female is only about 1.67 days, then atretic losses of even small unyolked oocytes is probably not an important bias. It would be useful if a way could be found to estimate oocyte resorption rates in squid although it may be very difficult. It seems more important to validate our preliminary estimate of the average longevity of spawning squid, because if true, any concerns regarding atresia could be dismissed.

Mature females without postovulatory follicles in their ovaries made up only 6% of the 247 females examined histologically. The rarity of these females in our collections reduced the precision of our potential fecundity estimate. Only thirteen of the fifteen females classed as a mature preovulatory female were usable for estimating potential fecundity, further reducing the sample size. Such a small sample size not only results in a low precision but raises the concern that the sample may not be representative of the stock as a whole. The fact that the average total fecundity of females with high mantle condition from the catch was close to the predicted value based on the thirteen females, indicates that the latter estimate may not be biased. Clearly a larger sample size is needed, particularly if egg escapement is used to monitor the fishery. It would be helpful, in obtaining more samples, if we knew the reason for the apparent rarity of mature preovulatory *L. opalescens* females. One possibility is that females might pass rapidly from the initial vitellogenesis to ovulation, perhaps in the course of a single day or some fraction of it, and ovulation might begin sometime in the evening when *L. opalescens* are the most vulnerable to fishing. Another possibility is that mature preovulatory females aggregate in regions not heavily fished by either our trawl or the fishery.

Egg escapement

A practical suggestion from this study is the idea of managing spawning-ground loliginid fisheries by monitoring the fecundity of the catch and computing the fraction of the potential fecundity spawned. Monitoring the escapement of eggs from the fishery is an attractive approach for *Loligo opalescens* because costs are moderate, unlike the high cost for monitoring egg beds that cover many locations offshore and occur at any time of the year, and because traditional fishery assessment models are difficult to apply or inappropriate at the present time (PFMC, 2002). To proceed with escapement fecundity as a management tool, it would be necessary to set a target level for egg escapement and to relate escapement to egg-per-recruit analysis so that fishing effort could be adjusted to alter egg escapement rates. Conceptual work along these lines has been completed (Maxwell[3]).

As mentioned earlier, as a practical matter in applying the egg escapement method, one would need to use Q_{SP}, the mean fraction of the potential fecundity escaping (Eq. 1), as a proxy for the more comprehensive and more useful measure of egg escapement $R_{e,t_{\max}}$, the fraction of the expected lifetime fecundity deposited (Eq. 12). Obviously, Q_{SP} will always be lower than $R_{e,t_{\max}}$ because the denominator of Q_{SP} (the fraction $\overline{E_{SP}}/\overline{E_P}$) is potential fecundity which will always be larger than the denominator for $R_{e,t_{\max}}$, which is expected lifetime fecundity (E). Although quite a different value, Q_{SP} is a useful proxy for $R_{e,t_{\max}}$. If natural mortality (m) and egg deposition rates (v) are constant, changes in fishing mortality will result in changes in Q_{SP} that are proportional to the change in $R_{e,t_{\max}}$.

However, changes will not be proportional if either v or m varies. If there is reason to believe that m and v are varying significantly, the use of Q_{SP} as a proxy for $R_{e,t_{\max}}$ should be undertaken with caution.

A point of concern in applying this method is that it may be difficult to substantially change escapement of eggs by regulating fishing effort. Our model indicated that egg escapement may be relatively insensitive to changes in fishing mortality if natural mortality rates are as high as we believe them to be. Of equal importance to management is the need to protect egg beds from damage by nets and to monitor the catch to prevent any change that might result in the capture of significant numbers of female *L. opalescens* before they begin to deposit eggs. Thus the fraction of the catch that is immature females must be monitored if the stock is managed by using the egg escapement method. For simplicity, our calculations of escapement were based on only mature females because immature females were only 2.6% of the females in the catch (1998–99) and their inclusion had little effect on parameter estimates. Egg escapement would decrease with an increase in the fraction of immature in the catch. As none of the fecundity of a captured immature female escapes the fishery, a relatively small increase in the fraction of immature animals in the catch can have significant consequences.

From the standpoint of fishery management, the most important unanswered question regarding the reproductive biology of *L. opalescens* is "how long do they remain on the spawning grounds?" or the equivalent question "what

[3] Maxwell, M. R., L. D. Jacobson, and R. Conser. Unpubl. data. Managing squid stocks using catch fecundity in an eggs-per-recruit model. Southwest Fisheries Science Center, National Marine Fisheries Service, 8604 La Jolla Shores Dr., La Jolla, CA 92037.

is the daily natural mortality of the spawners?" *Loligo opalescens* have only one spawning period in their life time (McGowan, 1954; Fields, 1965; Butler et al., 1999) but how long that period lasts remains unknown. Melo and Sauer (1999) concluded that the spawning period of *L. v. reynaudii* consisted of more than one spawning bout but neither the number of bouts nor the duration of each spawning period is known. In a laboratory study of *L. pealeii* (Maxwell and Hanlon, 2000), the number of bouts varied from one to ten, the interval between bouts was highly variable, and the life span after the first spawning bout was from 3 to 50 days. Our best guess for *L. opalescens* under fishing conditions was an average life on the spawning grounds of only 1.67 days and a maximum longevity of about 6 days. These estimates were based on a simple exponential model, constrained by various proxies for egg deposition rate, longevity, and the fraction of the potential fecundity in the catch (the only directly measured value). We believe that two of our estimates, 36% of the potential fecundity is deposited in the first 24 hours of spawning and minimum residual fecundity is about 22% of the potential fecundity, are on relatively firm ground but our estimate of the maximum longevity on the spawning grounds as 6 days is speculative. New information on mortality is needed because, over a wide range of daily mortality rates, our model yields values that are consistent with observed average fraction of potential fecundity in the catch. Because direct measurement of mortality on the spawning grounds may be difficult, it may be useful to develop some indirect approaches. For example, a laboratory study could be designed to generate an energy-based model that converts squid mantle tissue loss to deposited eggs. This mantle-to-egg conversion rate could be used to assign an age (time elapsed after first egg deposition) to modes of mantle condition from fishery samples. Mortality could then be computed by following modes of mantle condition through time.

Acknowledgments

This study was a cooperative project between the California Department of Fish & Game (CDF&G) and the National Marine Fisheries Service (NMFS) from start to finish. We worked closely with CDF&G personnel throughout the study with port-sampling data, cruise time, and partial financial support was provided by CDF&G. We worked particularly closely with M. Yaremko, A. Henry, and D. Hanan of CDF&G. J. Welsh assisted in the fecundity work. Others that contributed include J. Butler, T. Kudroschoff, N. Smith, A. Preti, K. Lazar, A. Cossio, and at sea K. Barsky, T. Bishop, S Charter, R. Dotson, D. Fuller, C. Graff, D. Griffith, P. Hamdorf, A. Hays, B. Horandy, M. Levy, I. Taniguchi, J. Ugoretz, and L. Zeidberg. We wish to thank the crews of the research vessels *Jordan* and *Mako*. We especially wish to thank diver J. Hyde who observed, collected, and photographed squid in La Jolla Canyon. M. Maxwell and two anonymous reviewers read the manuscript and provided constructive comments. R. Allen and H. Orr improved our illustrations.

Literature cited

Alheit, J.
1993. Use of the daily egg production method for estimating biomass of clupeoid fishes: a review and evaluation. Bull. Mar. Sci. 53:750–767.

Arkhipkin, A.
1993. Statolith microstructure and maximum age of *Loligo gahi* (Myopsida: Loliginidae) on the Patagonian shelf. J. Mar. Biol. Assoc. U.K. 73:979–982.

Arkhipkin, A., and N. Nekludova.
1993. Age, growth and maturation of the loliginid squids *Alloteuthis africana* and *A. subulata* on the west African shelf. J. Mar. Biol. Ass. U.K. 73:949–961.

Bower, J. R., and Y. Sakurai.
1996. Laboratory observations on *Todarodes pacificus* (Cephalopoda: Ommastrephidae) egg masses. Am. Malacological Bull. 13(1/2):65–71.

Boyle, P. R., and M. A. K. Ngoile.
1993. Assessment of maturity state and seasonality of reproduction in *Loligo forbesi* (Cephalopoda: Loliginidae) from Scottish waters. *In* Recent advances in fisheries biology (T. Okutani, R. K. O'Dor, and T. Kubodera, eds.), p. 37–48. Tokai Univ. Press, Tokyo, Japan.

Boyle, P. R., G. J. Pierce, and L. C. Hastie.
1995. Flexible reproductive strategies in the squid *Loligo forbesi*. Mar. Biol. 121:501–508.

Butler, J., D. Fuller, and M. Yaremko.
1999. Age and growth of market squid (*Loligo opolescens*) off California during 1998. Calif. Coop. Oceanic Fish. Invest. Rep. 40:191–195.

Coelho, M. L., J. Quintela, V. Bettencourt, G. Olavo, and H. Villa.
1994. Population structure, maturation patterns and fecundity of the squid *Loligo vulgaris* from southern Portugal. Fish. Res. 21:87–102.

Collins, M. A., G. M. Burnell, and P. G. Rodhouse.
1995. Reproductive strategies of male and female *Loligo forbesi* (Cephalopoda: Loliginidae). J. Mar. Biol. Assoc. U.K. 75:621–634.

Fields, W. G.
1965. The structure, development, food relations, reproduction, and life history of the squid, *Loligo opolescens* Berry. Calif. Dep. Fish Game Fish Bull. 131, 108 p.

Fitzhugh, G. R., and W.F. Hettler
1995. Temperature influence on postovulatory follicle degeneration in Atlantic menhaden, *Brevoortia tyrannus*. Fish. Bull. 93:568–572.

Guerra, A., and F. Rocha.
1994. The life history of *Loligo vulgaris* and *Loligo forbesi* (Cephalopoda: Loliginidae) in Galician waters (NW Spain). Fish. Res. 21:43–69.

Hatfield, E. M. C.
1991. Post-recruit growth of the Patagonian squid *Loligo gahi* (D'Orbigny). Bull. Mar. Sci. 49(1–2)349–361.
2000. So some like it hot? Temperature as a possible determinant of variability in the growth of the Patagonian squid, *Loligo gahi* (Cephalopoda: Loliginidae). Fish. Res. 47:27–40.

Hay, D. E., D. N. Outram, B. A. McKeown, and M. Hurlburt.
1987. Ovarian development and oocyte diameter as maturation criteria in Pacific herring (*Clupea harengus pallasi*). Can. J. Fish. Aquat. Sci. 44:1496–1502.

Hunter, J. R., and S. R. Goldberg.
1980. Spawning incidence and batch fecundity in northern anchovy, *Engraulis mordax*. Fish. Bull. 77:641–652.

Hunter, J. R., and N. C. H. Lo.
1997. The daily egg production method of biomass estimation: some problems and potential improvements. Ozeanografika 2:41–67.

Hunter, J. R., N. C. H. Lo, and R. J. H. Leong.
1985. Batch fecundity in multiple spawning fishes. *In* An egg production method for estimating spawning biomass of pelagic fish: application to the northern anchovy (*Engraulis mordax*) (R. Lasker, ed.), p. 67–77. NOAA Tech. Rep. NMFS 36.

Hunter, J. R., and B. J. Macewicz.
1985a. Measurement of spawning frequency in multiple spawning fishes. *In* An egg production method for estimating spawning biomass of pelagic fish: application to the northern anchovy (*Engraulis mordax*) (R. Lasker, ed.), p. 79–94. NOAA Tech. Rep. NMFS 36.
1985b. Rates of atresia in the ovary of captive and wild northern anchovy, *Engraulis mordax*. Fish. Bull. 83:119–136.

Hunter, J. R., B. J. Macewicz, N. C. H. Lo, and C. A. Kimbrell.
1992. Fecundity, spawning, and maturity of female Dover sole *Microstomus pacificus*, with an evaluation of assumptions and precision. Fish. Bull. 90:101–128.

Ikeda, Y., Y. Sakurai, and K. Shimazaki.
1993. Maturation process of the Japanese common squid *Todarodes pacificus* in captivity. *In* Recent advances in fisheries biology (T. Okutani, R. K. O'Dor, and T. Kubodera, eds.), p. 179–187. Tokai Univ. Press, Tokyo, Japan.

Jackson, G. D.
1993. Seasonal variation in reproductive investment in the tropical loliginid squid *Loligo chinensis* and the small tropical sepioid *Idiosepius pygmaeus*. Fish. Bull. 91:260–270.
1994. Statolith age estimates of the loliginid squid *Loligo opalescens* (Mollusca: Cephalopoda): corroboration with culture data. Bull. Mar. Sci. 54:554–557.

Jackson, G. D., A. I. Arkhipkin, V. A. Bizikov, and R. T. Hanlon.
1993. Laboratory and field corroboration of age and growth from statoliths and gladii of the loliginid squid *Sepioteuthis lessoniana* (Mollusca: Cephalopoda). *In* Recent advances in fisheries biology (T. Okutani, R. K. O'Dor, and T. Kubodera, eds.), p. 189–199. Tokai Univ. Press, Tokyo, Japan.

Jackson, G. D., J. W. Forsythe, R. F. Hixon, and R. T. Hanlon.
1997. Age, growth, and maturation of *Lolliguncula brevis* (Cephalopoda: Loliginidae) in the northwest Gulf of Mexico with a comparison of length-frequency versus statolith age analysis. Can. J. Fish. Aquat. Sci. 54:2907–2919.

Jackson, G. D., and J. Yeatman.
1996. Variation in size and age at maturity in *Photololigo* (*Mollusca: Cephalopoda*) from the northwest shelf of Australia. Fish. Bull. 94:59–65.

Kjesbu, O. S., P. R. Witthames, P. Solemdal, M. G. Walker.
1998. Temporal variations in the fecundity of Arcto-Norwegian cod (*Gadus morhua*) in response to natural changes in food and temperature. J. Sea Res. 40: 303–321.

Knipe, J. H., and R. D. Beeman.
1978. Histological observations on oogenesis in *Loligo opalescens*. *In* Biological, oceanographic, and acoustic aspects of the market squid, *Lolgio opalescens* Berry (C. W. Recksiek and H. W. Frey, eds.), p. 23–33. Calif. Dep. Fish Game Fish Bull. 169.

Laptikhovsky, V.
2000. Fecundity of the squid *Loligo vulgaris* Lamarck, 1798 (Myopsida, Loliginidae) off northwest Africa. Scientia Marina 64(3):275–278.

Lopes, S. S., M. L. Coelho, and J. P. Andrade.
1997. Analysis of oocyte development and potential fecundity of the squid *Loligo vulgaris* from the waters of southern Portugal. J. Mar. Biol. Assoc. U.K. 77:903–906.

Macewicz, B. J., and J. R. Hunter.
1994. Fecundity of sablefish, *Anoplopoma fimbria*, from Oregon coastal waters. Calif. Coop. Oceanic Fish. Invest. Rep. 35:160–174.

Maxwell, M. R., and R. T. Hanlon.
2000. Female reproductive output in the squid *Loligo peulei*: multiple egg clutches and implications for a spawning strategy. Mar. Ecol. Prog. Ser. 199:159–170.

McGowan, J. A.
1954. Observations on the sexual behavior and spawning of the squid, *Loligo opalescens*, at La Jolla, California. Calif. Fish Game Fish Bull. 40(1):47–55.

Melo, Y. C., and W. H. H. Sauer.
1998. Ovarian atresia in cephalopods. S. Afr. J. Mar. Sci. 20:143–151.
1999. Confirmation of serial spawning in the chokka squid *Loligo vulgaris reynaudii* off the coast of South Africa. Mar. Biol. 135:307–313.

Moltschaniwskyj, N. A..
1995. Multiple spawning in the tropical squid *Photololigo* sp.: what is the cost in somatic growth? Mar. Biol. 125:127–135.

Moltschaniwskyj, N. A., and J. M. Semmens.
2000. Limited use of stored energy reserves for reproduction by the tropical loliginid squid *Photololigo* sp. J. Zool. Lond. 251:307–313.

Natsukari, Y., and N. Komine.
1992. Age and growth estimation of the European squid, *Loligo vulgaris*, based on statolith microstructure. J. Mar. Biol. Assoc. U.K. 72:271–280.

PFMC
2002. Report of the Stock Assessment Review (STAR) panel for market squid, Appendix 3. *In*, Status of the Pacific Coast coastal pelagic species fishery and recommended acceptable biological catches: stock assessment and fishery evaluation—2002, 17 p. Pacific Fishery Management Council. Portland, OR

Quinn, T. J., and R. B. Deriso.
1999. Quantitative fish dynamics. Biological resource Mmanagement series, 542 p. Oxford Univ. Press, New York, NY.

Sauer, W. H. H., Y. C. Melo, and W. de Wet.
1999. Fecundity of the chokka squid *Loligo vulgaris reynaudii* on the southeastern coast of South Africa. Mar. Biol. 135:315–319.

Semmens, J. M., and N. A. Moltschaniwskyj.
2000. An examination of variable growth in the loliginid squid *Sepioteuthis lessoniana*: a whole animal and reductionist approach. Mar. Ecol. Prog. Ser. 193:135–141.

Woodhead, A. D.
1960. Nutrition and reproductive capacity in fish. Nutrition Society Proceedings 19:23–28.

Yang, W. T., R. F. Hixon, P. E. Turk, M. E. Krejci, W. H. Hulet, and R. T. Hanlon.
1986. Growth, behavior, and sexual maturation of the market squid, *Loligo opalescens*, cultured through the life cycle. Fish. Bull. 84:771–798.

Appendix I

Terms

E_P potential fecundity (standing stock of oocytes in the ovary of mature females prior to spawning)

$E_{SP,t}$ the total eggs deposited on the bottom up to time t (t in days)

E_C total number of eggs deposited by mature females in the catch or total number of eggs escaped

E_M total number of eggs deposited by mature females prior to death due to natural mortality

E_A total number of eggs deposited by females alive and not caught by fishery

E total number of eggs that would have been spawned during a squid's lifetime if no fishery existed

E_Y standing stock of oocytes in the ovary

E_D standing stock of ova in the oviduct

E_{YD} total fecundity, the sum of both the number of oocytes in the ovary and ova in the oviduct

E_{YD,t_k} stocking stock of oocytes in the ovary plus those ova in the oviduct after spawning has begun and up to the elapsed time t_k, where t_k is $\leq t_{\max}$

$t_{\max}$ maximum elapsed time with the time 0 being the time when mature females are about to ovulate or total elapsed time (in days) of spawners on the spawning ground

E_R standing stock of oocytes remaining in ovary at death

m daily adult natural mortality rate

f daily fishing mortality rate for adults

v daily egg deposition rate

$Q_{SP,t} = E_{SP,t}/E_P = 1 - e^{-vt}$ fraction of potential fecundity deposited up to time t

e^{-zt} mortality (survival) curve

N_0 number of mature females at time 0

N_t total number of spawners in the catch

R_{e,t_k} egg escapement rate = ratio of eggs deposited to total number of egg which would be spawned if there was no fishery, at a given elapsed time (t_k)

$R_{e,t_{\max}}$ egg escapement rate up to the maximum elapsed time ($t_{\max}$)

Appendix II

For any elapsed time t_k, formulas for E_C, E_M, E_A and E:

$$E_C = \overline{E_P} N_0 f \left[\frac{1-e^{-(m+f)t_k}}{m+f} - \frac{1-e^{-(m+f+v)t_k}}{m+f+v} \right]$$

$$E_M = \overline{E_P} N_0 m \left[\frac{1-e^{-(m+f)t_k}}{m+f} - \frac{1-e^{-(m+f+v)t_k}}{m+f+v} \right]$$

$$E_A = (\overline{E_P} - \overline{E_{YD,t_k}}) N_k = N_0 e^{-(m+f)t_k} \overline{E_P} (1-e^{-vt_k})$$

$$E = \overline{E_P} N_0 \left[\frac{v}{v+m} - e^{-mt_k} \left(1 - \frac{m}{v+m} e^{-vt_k} \right) \right].$$

The derivation for E_A is straight forward and the derivations for E_C, E_M, and E, similar among one another, are as follows:

$$E_C = \int_0^{t_k} \overline{E_{SP,t}} dC_t = \int_0^{t_k} \overline{E_P} (1-e^{-vt}) dC_t$$

$$= \overline{E_P} N_0 \int_0^{t_k} (1-e^{-vt}) e^{-(m+f)t} f dt,$$

where

$$C_t = N_0 \frac{f}{m+f} (1-e^{-(m+f)t})$$

is the number of removals of the cohort due to fishing up to time t (Quinn and Deriso, 1999).

$$E_M = \int_0^{t_k} \overline{E_{SP,t}} dD_{m,t} = \int_0^{t_k} \overline{E_P} (1-e^{-vt}) dD_{m,t}$$

$$= \overline{E_P} N_0 f \frac{v}{(m+f)(m+f+v)},$$

where

$$D_{m,t} = N_0 \frac{m}{m+f} \left(1-e^{-(m+f)t} \right)$$

is the number of removals of the cohort due to natural mortality up to time t (Quinn and Deriso, 1999) and E (when no fishing takes place):

$$E = \int_0^{t_k} \overline{E_{SP,t}} dD_t = \int_0^{t_k} \overline{E_P}(1-e^{-vt}) dD_t$$

$$= \overline{E_P} N_0 \int_0^{t_k} (1-e^{-vt}) e^{-mt} m dt,$$

where $D_t = N_0(1-e^{-mt})$ is the number of removals of the cohort due to natural mortality when no fishing takes place.

Abstract—The dusky rockfish (*Sebastes ciliatus*) of the North Pacific Ocean has been considered a single variable species with light and dark forms distributed in deep and shallow water, respectively. These forms have been subjected to two distinct fisheries separately managed by federal and state agencies: the light deep form is captured in the offshore trawl fishery; the dark shallow form, in the nearshore jig fishery. The forms have been commonly recognized as the light dusky and dark dusky rockfishes. From morphological evidence correlated with color differences in some 400 specimens, we recognize two species corresponding with these color forms. *Sebastes ciliatus* (Tilesius) is the dark shallow-water species found in depths of 5–160 m in the western Aleutian Islands and eastern Bering Sea to British Columbia. The name *Sebastes variabilis* (Pallas) is resurrected from the synonymy of *S. ciliatus* to apply to the deeper water species known from depths of 12–675 m and ranging from Hokkaido, Japan, through the Aleutian Islands and eastern Bering Sea, to Oregon. *Sebastes ciliatus* is uniformly dark blue to black, gradually lightening on the ventrum, with a jet black peritoneum, a smaller symphyseal knob, and fewer lateral-line pores compared to *S. variabilis*. *Sebastes variabilis* is more variable in body color, ranging from light yellow to a more usual tan or greenish brown to a nearly uniform dark dorsum, but it invariably has a distinct red to white ventrum. Synonymies, diagnoses, descriptions, and geographic distributions are provided for each species.

Manuscript approved for publication 22 December 2003 by Scientific Editor.

Manuscript received 20 January 2004 at NMFS Scientific Publications Office.

Fish. Bull. 102:328–348 (2004).

The dusky rockfishes (Teleostei: Scorpaeniformes) of the North Pacific Ocean: resurrection of *Sebastes variabilis* (Pallas, 1814) and a redescription of *Sebastes ciliatus* (Tilesius, 1813)

James W. Orr

Resource Assessment and Conservation Engineering Division
Alaska Fisheries Science Center
National Marine Fisheries Service, NOAA
7600 Sand Point Way NE
Seattle, Washington 98115
E-mail address: James.Orr@noaa.gov

James E. Blackburn

Alaska Department of Fish and Game
211 Mission Road
Kodiak, Alaska 99615-9988

Among the approximately 92 species of *Sebastes* found in the North Pacific, two commercially important species long identified under the name *Sebastes ciliatus* have been taxonomically problematic. The name *S. ciliatus* (Tilesius, 1813) has been commonly applied to specimens considered to represent a single variable species ranging from northern Japan to British Columbia (Barsukov, 1964; Westrheim, 1973; Shinohara et al., 1994; Mecklenburg et al., 2002), and the name *S. variabilis* (Pallas, 1814) has been treated as a junior synonym (Jordan and Gilbert, 1881; Eigenmann and Beeson, 1894; Jordan and Evermann, 1898; Blanc and Hureau, 1968). Two color forms within *S. ciliatus* have been reported and hypothesized to be distinct species (Quast and Hall, 1972; Eschmeyer et al., 1983; Kessler, 1985; Fig. 1). The typically light-colored form, commonly known as the light dusky rockfish, is often found in large aggregations over the outer continental shelf and upper slope at depths down to 675 m, and less frequently in nearshore habitats. The dark-blue to black form, commonly known as the dark dusky rockfish, is found in more shallow habitats from nearshore rocky reefs to depths no greater than 160 m.

These forms have been subjected to two distinct fisheries separately managed by U.S. federal and Alaska state agencies since 1998. The light-colored deep form is captured in the offshore trawl fishery and is the dominant species of the pelagic shelf rockfish fisheries complex regulated by the National Marine Fisheries Service (NMFS). Specific catch limits are set under the designation "dusky rockfish." The occasional catch of the dark form in these offshore waters has also been considered "dusky rockfish." The dark-colored shallow form is found commonly in the nearshore jig fishery regulated by the Alaska Department of Fish and Game. The dark form, routinely misidentified as *S. melanops*, may comprise up to 25% of the catch in the "black rockfish" jig fishery off Kenai Peninsula (Clausen et al.[1]) and is managed only as "other rockfish" bycatch within the fishery.

Early allozyme analyses (Tsuyuki et al., 1965, 1968) indicated significant genetic differences among samples identified as *S. ciliatus*. A more detailed analysis of several *Sebastes* species (Seeb, 1986) and a later study focused

[1] Clausen, D. M., C. R. Lunsford, and J. T. Fujioka. 2002. Pelagic shelf rockfish. *In* Stock assessment and fishery evaluation report for the groundfish resources of the Gulf of Alaska for 2002, p. 383–417. North Pacific Fishery Management Council, 605 W 4th Ave, Suite 306, Anchorage, AK 99501.

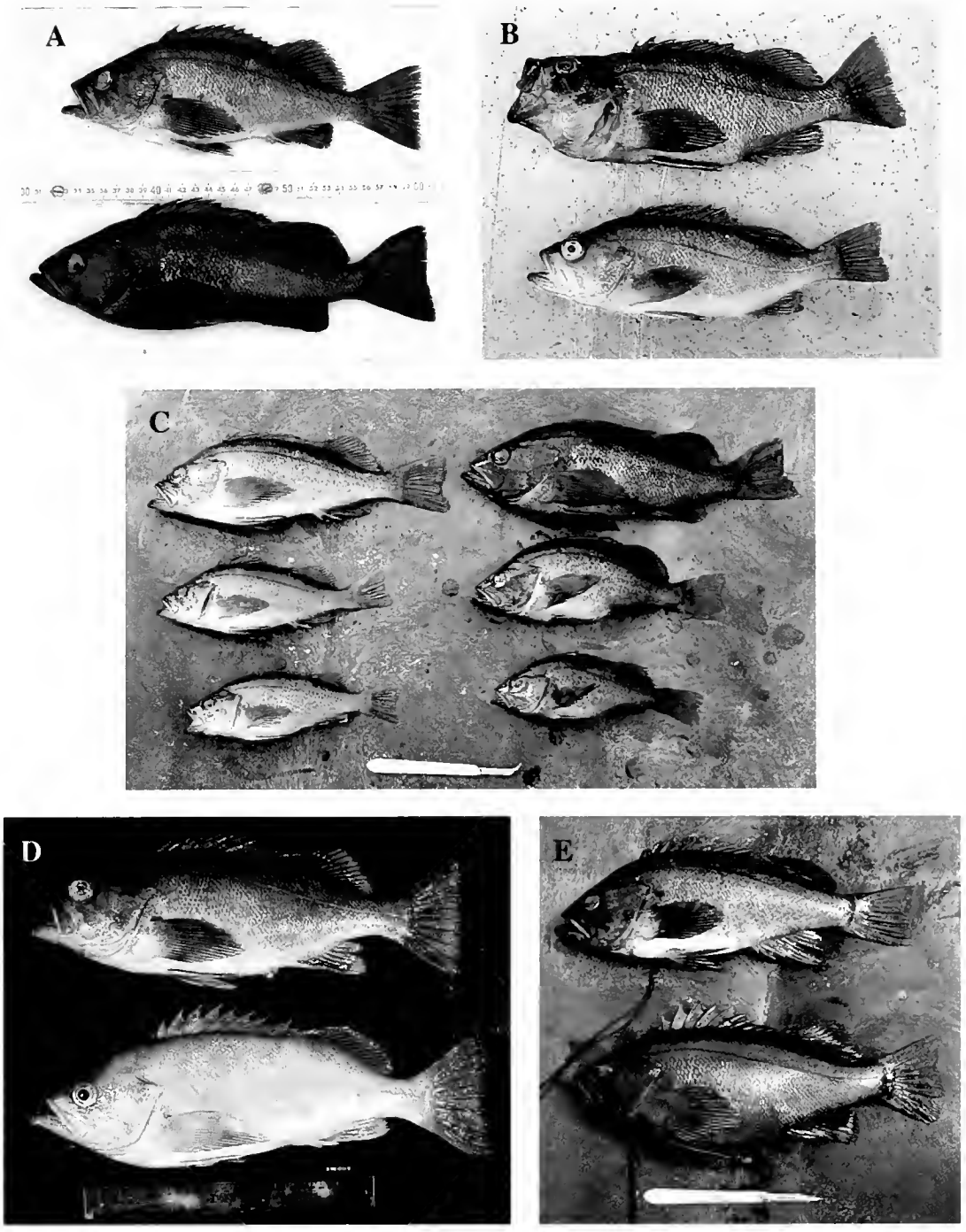

Figure 1

(**A**) *Sebastes variabilis* (top), UW 43494, 225.2 mm, and *S. ciliatus* (bottom), UW 43493, neotype, 266.4 mm, collected at 37 and 25 m depth, respectively, in Lynn Canal near Funter Bay, southeast Alaska. (**B**) *Sebastes ciliatus* (top), UW 45512, 235.2 mm, and *S. variabilis* (bottom), UW 45511, 206.2 mm, collected syntopically at 67 m depth in the northern Gulf of Alaska, 57.38061°N, 154.8009°W. (**C**) *Sebastes variabilis* (left), UW 43494, 150.6–225.2 mm, and *S. ciliatus* (right), UW 43492, 153.7–241.1 mm, collected at 37 and 25 m depth, respectively, in Lynn Canal near Funter Bay, southeast Alaska. (**D**) *Sebastes variabilis*, UW 43251, 390 mm (top) and 410 mm (bottom), northern Gulf of Alaska, 59.50446°N, 145.2262°W, 135 m depth. (**E**) *Sebastes melanops* (top), UW 43490, and *S. ciliatus* (bottom), UW 43484, 313 mm, collected at 25 m depth in Soapstone Cove, southeast Alaska.

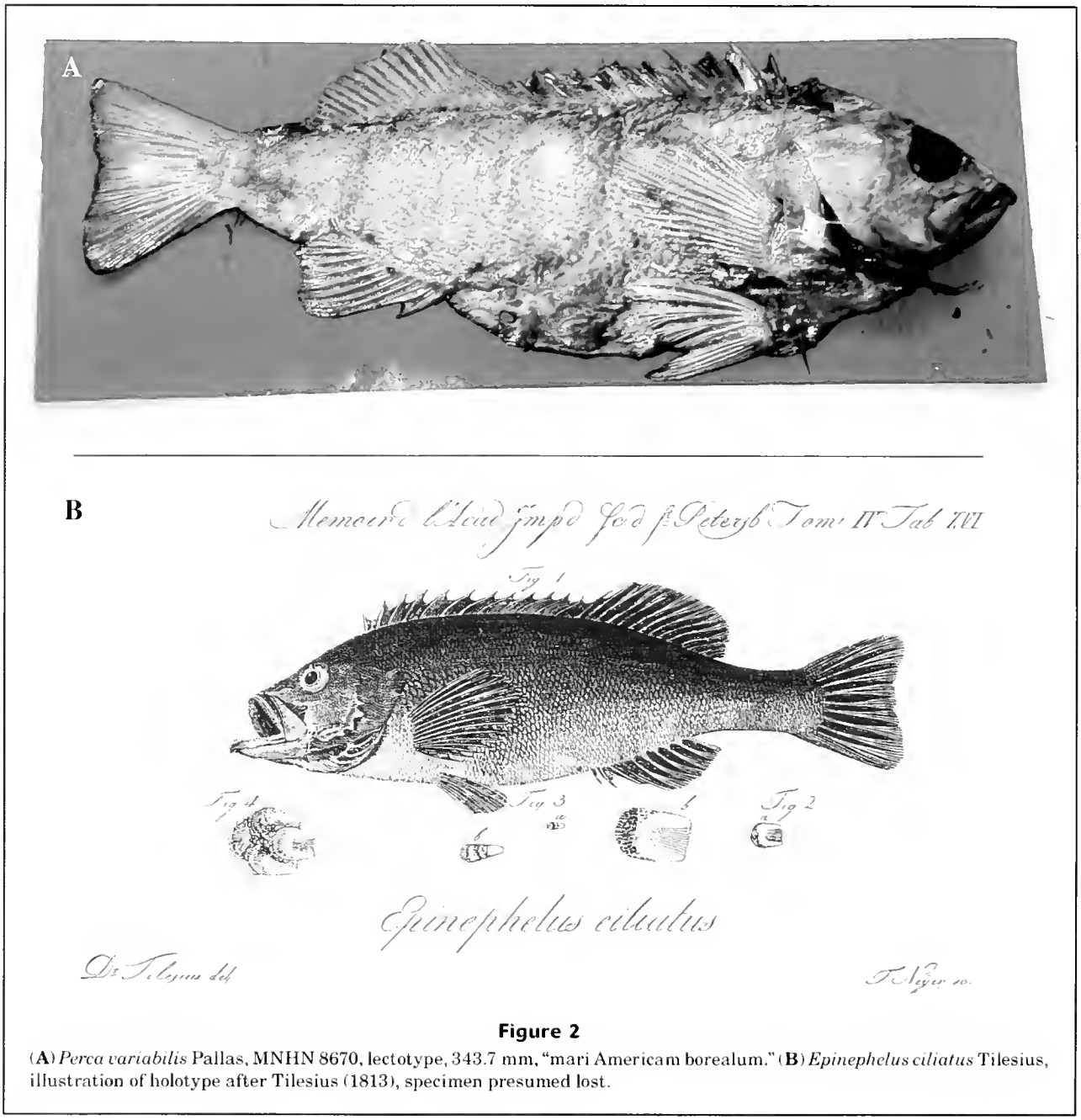

Figure 2

(**A**) *Perca variabilis* Pallas, MNHN 8670, lectotype, 343.7 mm, "mari Americam borealum." (**B**) *Epinephelus ciliatus* Tilesius, illustration of holotype after Tilesius (1813), specimen presumed lost.

on *S. ciliatus* (Westrheim and Seeb[2]) concluded that the two color forms were distinct sister species. Seeb's recent work with microsatellite DNA data has revealed discrete genetic differences between the two, as well as some evidence for infrequent hybridization (Seeb[3]). Sequence data from NADH dehydrogenase subunit regions of the mitochondrial genome, however, have not revealed differences between the two forms (López[4], Gray[5]), nor have sequence data from other work on closely related species of *Sebastes* (Bentzen et al., 1998; Sundt and Johansen, 1998; Roques et al., 2001).

[2] Westrheim, S. J., and L. W. Seeb. 1997. Unpubl. manuscript. Investigation of the *Sebastes ciliatus* species group, 36 p. Fisheries and Oceans Canada, Pacific Biological Station, Nanaimo, BC, Canada V9R 5K6.

[3] Seeb, L. W. 2002. Personal commun. Alaska Department of Fish and Game, 333 Raspberry Road, Anchorage, AK 99518-1599.

[4] López, J. A. 2000. Personal commun. Iowa State Univ., Ames, IA 50014.

[5] Gray, A. 2000. Personal commun. Fisheries Division, School of Fisheries and Ocean Sciences, Univ. Alaska Fairbanks, 11120 Glacier Highway, Juneau, AK 99801.

In this study, we provide morphological evidence from examination of about 400 specimens collected throughout the geographic and bathymetric range of the species to correlate color differences with meristic and shape differences. In thus recognizing two species, *S. ciliatus* and *S. variabilis*, previously referred to the name *S. ciliatus* (Tilesius, 1813), we discuss the nomenclatural consequences of this decision. Both species were originally described (as *Epinephelus ciliatus* Tilesius and *Perca variabilis* Pallas) on the basis of early Russian collections from along the Aleutian Islands (Svetovidov, 1978, 1981). The type series of one species is now represented by a single extant specimen (Fig. 2A) and the other by the illustration of a single, now lost, specimen (Svetovidov, 1978, 1981; Fig. 2B). Although workers since the turn of the century have associated the name *S. ciliatus* with the variably light-colored species (Jordan, 1896; Jordan and Evermann, 1898; Barsukov, 1964; Orr et al., 1998, 2000; Mecklenburg et al., 2002), the original description and accompanying illustration (Fig. 2B) appear to describe the uniformly dark species. We have also identified the remaining syntype (Fig. 2A) of *Perca variabilis* as the light species. Therefore, we refer the dark, shallow-water species (the dark rockfish) to *Sebastes ciliatus* (Tilesius, 1813) and resurrect the name *Sebastes variabilis* (Pallas, 1814) for the typically light, deeper-water species (the dusky rockfish).

Methods and materials

Counts and measurements follow Hubbs and Lagler (1958), except as noted below. Unless indicated otherwise, standard length (SL) is used throughout and was always measured from the tip of the snout. Depth at pelvic-fin base was measured from the origin of the dorsal fin to the base of the pelvic fins (at the articulation of the pelvic-fin spine); depth at anal-fin origin, from the base of the last dorsal-fin spine to the anal-fin origin; depth at anal-fin insertion, from dorsal-fin insertion to anal-fin insertion; body thickness, at pectoral-fin base; head thickness, at the posterior orbital rim; prepelvic- and preanal-fin length, from pelvic-fin base or anal-fin origin to the tip of the snout; pelvic-fin to anal-fin length from pelvic-fin base to anal-fin origin; caudal peduncle dorsal length from dorsal-fin insertion to caudal-fin base; caudal peduncle ventral length from anal-fin insertion to caudal-fin base. The small anterior notch in the orbit between the frontal bone and lateral ethmoid was excluded from orbit length and snout length measurements. Accessory scales are small scales located beyond the posterior field of major scales. The swimbladder musculature was examined after dissection according to the methods of Hallacher (1974). Institutional abbreviations follow Leviton et al. (1985) and Leviton and Gibbs (1988), as modified by Poss and Collette (1995).

Individuals were identified by body and peritoneum color (see species descriptions below) for grouping in ANOVA and ANCOVA, as well as for labeling individuals in graphs of principal components analysis scores. Univariate and multivariate analyses were conducted by using Statgraphics Plus 4.1 (Manugistics, Rockville, MD) and Splus 2000 (Mathsoft, Inc., Seattle, WA). Differences were considered significant at $P < 0.05$.

Arcsine-transformed morphometric ratios (with SL or head length as denominator) and meristic characters were tested to meet the assumptions of normality required for ANOVA. The following characters exhibited normal distributions and did not differ significantly in variance between species and were subjected to ANOVA: head length, orbit length, snout length, interorbital width, suborbital depth, gill-raker length, body thickness, pectoral-fin base width, pectoral-fin ray length, caudal peduncle ventral length, predorsal length, spinous dorsal-fin base, soft dorsal-fin base, and counts of lateral-line pores and gill rakers.

For morphometric characters, significant differences were also identified by using an analysis of covariance (ANCOVA) of log-10-transformed measurements with SL or head length (HL) as covariates when assumptions of normality and the homogeneity of slopes were satisfied. The ANCOVA model included species as a factor, SL or HL as a covariate, and a species/(SL or HL) interaction (e.g., $HL=C+Species+SL+(Species\times SL)$). A residual analysis was done for each model to determine the appropriateness of the model. Whenever the interaction was not significant (at the 5% level), a reduced model was used by dropping the interaction and forcing the slopes to be the same ($BD=C+Species+SL$). This removed the effect of SL and HL and allowed testing for significant differences between species. The following morphometric characters met the assumptions required for ANCOVA: head length, snout length, interorbital width, gill-raker length, pectoral-fin base width, pectoral-fin ray length, caudal peduncle ventral length, predorsal length, spinous dorsal-fin-base length, and soft dorsal-fin-base length.

On a dataset of specimens with all characters, sheared principal components analysis (SPCA) for a size-free analysis (Bookstein et al., 1985) was conducted by using morphometric characters, and a standard principal components analysis (PCA) was conducted by using all meristic characters. Raw morphometric data were log-transformed and the covariance matrix was subjected to SPCA, as was the correlation matrix of raw meristics. Differences between species were illustrated by plotting scores of sheared PC2 against sheared PC3 and sheared morphometric PC2 against the standard meristic PC1. Separate analyses were also conducted on three groupings: 1) each species by depth, 2) each species by sex, and 3) shallow-water populations of *S. ciliatus* and *S. variabilis* primarily collected in the vicinity of the Triplet Islands and Monashka Bay, on the northeast side of the Kodiak Island Archipelago, and the vicinity of Lynn Canal, Alaska. Shallow collections were defined as those made at less than 50 m depth, and deep collections were taken at depths greater than 50 m.

These plots were also examined for groupings indicative of geographic differences in body shape and meristics. Geographic areas were defined as follows: British Columbia, from the Straits of Juan de Fuca to Dixon Entrance; southeast Alaska, from Dixon Entrance to Chatham Strait; Gulf of Alaska, from Chatham Strait to the tip of the Alaska Pennisula; Aleutian Islands and Bering Sea,

Table 1

Proportional morphometrics and meristics of *Sebastes ciliatus* and *S. variabilis* from all depths and regions. Morphometric data are in %SL or %HL. X = statistically significant difference at 0.05 level, as evaluated by ANOVA and ANCOVA, when appropriate; ns = not statistically significant at 0.05 level. *n* = number of fish in sample.

	S. ciliatus			*S. variabilis*				
	n	Range	Mean ±SD	*n*	Range	Mean ±SD	ANOVA	ANCOVA
Meristics								
Dorsal-fin spines	138	12–14	13.0 ±0.2	194	13–14	13.0 ±0.1		
Dorsal-fin rays	138	13–17	15.0 ±0.5	194	13–16	15.0 ±0.4		
Anal-fin rays	139	7–9	7.9 ±0.4	195	7–9	7.9 ±0.4		
Pectoral-fin rays (left)	138	17–19	18.2 ±0.5	194	17–19	18.0 ±0.3		
Pectoral-fin rays (right)	137	16–19	18.2 ±0.4	195	16–19	18.0 ±0.4		
Unbranched pectoral-fin rays (left)	136	8–10	9.2 ±0.5	195	7–11	9.1 ±0.4		
Unbranched pectoral-fin rays (right)	108	8–11	9.2 ±0.5	188	7–11	9.1 ±0.5		
Lateral-line pores (left)	138	39–50	45.4 ±2.3	188	43–54	48.5 ±1.9	X	
Lateral-line pores (right)	125	40–54	45.3 ±2.4	172	42–54	48.5 ±1.9	X	
Lateral-line scales	132	44–60	50.6 ±2.7	177	47–63	52.8 ±2.7		
Gill rakers	137	32–37	34.8 ±1.1	184	32–37	34.7 ±0.9	X	

continued

from the tip of the Alaska Peninsula west and north into the Bering Sea.

Results

Color

Body color in life and in preservation differs consistently between *S. ciliatus* and *S. variabilis* (Fig. 1; see detailed description below). In life, *S. ciliatus* is uniformly bluish-black to gray, with slight gradual lightening on the belly; the peritoneum is invariably jet black. In contrast, *S. variabilis* varies in background color from golden yellow to greenish brown to dark gray, with a distinct break between the darker dorsum and the invariably white to pink ventrum, particularly at the base of the anal fin; the peritoneum is gray to black. In *S. variabilis* preserved for up to 30 years, the distinct break along the ventrum is retained and differs from the uniformly dark preserved color of *S. ciliatus*. This combination of characteristic body and peritoneum color was used initially to identify individuals as either *S. ciliatus* or *S. variabilis* as the basis for univariate statistical analyses.

Meristic characters

Lateral-line pore and gill-raker counts differed significantly between *S. ciliatus* and *S. variabilis* from all depths and regions, *S. ciliatus* having a lower range and mode of counts (Tables 1–3). In shallow water, only lateral-line pore counts showed significant differences (Table 4). Slight clinal variation was evident for lateral-line pores in *S. ciliatus* between southeast Alaska collections and northern Gulf of Alaska material (Table 2). In the PCA, counts of lateral-line pores, gill rakers, and pectoral-fin rays were most heavily loaded along the first PC axis, confirming that *S. ciliatus* has typically lower lateral-line pore and gill-raker counts and tends to have a higher pectoral-fin ray count (Tables 1–3, 5; Fig. 3B).

Morphometric characters

Among morphometric characters meeting statistical assumptions for ANOVA or ANCOVA, head length, interorbital width, suborbital depth, lower-jaw length, gill-raker length, body thickness, pectoral-fin base width, predorsal length, and soft-dorsal-fin-base length differed significantly between *S. ciliatus* and *S. variabilis* across all depths and regions (Table 1). Between shallow-water *S. ciliatus* and *S. variabilis*, all the above characters, except head length, interorbital width, and predorsal length, differed significantly (Table 4). No significant differences were found in analyses within species by depth or sex.

In the PCA for specimens collected across all regions and depths, clusters of *S. ciliatus* and *S. variabilis* showed broad overlap and only slight discrimination among individuals along the PC2 axis (Fig. 3A). Principal component 2, the primary shape component, described 1.8% of the total variation, and PC1, the size component having all loadings positive, described 96.4% of the variation. Characters loading most heavily along the PC2 axis included suborbital depth, gill-raker length, orbit length, body

Table 1 (continued)

	S. ciliatus			*S. variabilis*				
	n	Range	Mean ±SD	*n*	Range	Mean ±SD	ANOVA	ANCOVA
Morphometrics								
Standard length	132	83.8–340.0		192	77.7–430.8			
Head length/SL	113	28.7–35.5	32.9 ±1.2	129	28.1–36.2	32.5 ±1.2	X	ns
Orbit length/HL	111	21.5–30.6	25.6 ±2.0	121	20.6–33.5	25.6 ±2.1	ns	
Snout length/HL	111	18.2–26.0	21.4 ±1.6	121	17.1–27.1	21.4 ±1.8	ns	ns
Interorbital width/HL	111	22.9–29.3	25.9 ±1.3	121	22.5–30.4	26.4 ±1.4	X	X
Suborbital depth/HL	111	4.1–7.8	6.0 ±0.8	121	4.3–8.1	6.2 ±0.7	X	
Upper jaw length/HL	111	43.6–51.1	47.4 ±1.5	121	42.7–54.0	47.8 ±2.0		
Lower jaw length/HL	105	53.4–60.5	56.5 ±1.7	108	52.8–62.7	58.3 ±2.2	X	
Gill raker length/HL	98	11.3–20.7	15.0 ±1.6	110	11.6–19.9	15.5 ±1.7	ns	X
Depth at pelvic-fin base/SL	111	32.5–42.7	37.0 ±1.9	121	29.2–40.9	36.2 ±1.7		
Depth at anal-fin origin/SL	111	27.4–35.8	31.2 ±1.7	121	26.7–35.4	30.5 ±1.6		
Depth at anal-fin insertion/SL	109	13.8–18.5	15.9 ±1.0	116	13.1–18.0	15.4 ±0.9		
Body thickness/SL	111	14.9–22.3	18.0 ±1.2	120	12.9–20.9	17.3 ±1.5	X	
Pectoral-fin base width/SL	111	9.5–11.9	10.7 ±0.5	121	9.4–11.2	10.2 ±0.4	X	X
Pectoral-fin ray length/SL	111	24.6–31.8	28.5 ±1.3	121	23.5–31.0	28.2 ±1.4	ns	ns
Pectoral-fin length/SL	111	25.5–33.6	29.8 ±1.5	117	24.2–35.1	29.2 ±1.7		
Pelvic-fin ray length/SL	111	20.5–26.0	22.7 ±1.1	119	19.2–29.2	22.0 ±1.5		
Pelvic-fin ray/Pelvic-fin spine length	111	52.4–67.4	59.9 ±4.3	121	44.9–70.7	59.9 ±5.5		
Anal-fin spine I length/SL	83	3.6–9.1	5.2 ±0.9	107	3.3–8.8	5.3 ±1.0		
Anal-fin spine II length/SL	84	7.5–14.2	10.6 ±1.2	106	5.8–13.6	10.5 ±1.5		
Anal-fin spine III length/SL	84	10.0–14.6	12.4 ±1.1	107	9.5–15.6	12.2 ±1.3		
Anal-fin ray 1 length/SL	83	15.6–22.5	19.0 ±1.2	97	15.1–21.0	18.2 ±1.3		
Anal-fin ray 2 length/SL	84	14.5–23.4	20.2 ±1.2	97	15.3–23.1	19.5 ±1.3		
Caudal-fin length/SL	60	10.2–29.4	21.7 ±2.7	74	15.4–26.9	21.2 ±2.3		
Caudal peduncle depth/SL	111	9.3–13.7	11.4 ±0.7	121	9.5–12.2	10.9 ±0.5		
Caudal peduncle dorsal length/SL	111	11.9–16.2	13.8 ±0.8	121	12.6–16.4	14.1 ±0.8		
Caudal peduncle ventral length/SL	111	17.6–22.9	20.5 ±1.0	121	17.1–24.3	21.1 ±1.3	ns	ns
Preanal length/SL	111	60.0–77.4	68.7 ±2.5	121	59.4–77.9	68.1 ±2.6		
Pelvic- to anal-fin length/SL	105	26.1–43.2	32.5 ±3.1	111	25.9–41.7	31.6 ±2.9		
Predorsal length/SL	111	28.5–35.4	32.1 ±1.3	121	28.1–35.2	31.8 ±1.3	X	ns
Spinous dorsal-fin-base length/SL	111	32.1–43.6	37.2 ±2.1	121	31.6–41.9	37.0 ±2.1	ns	ns
Soft dorsal-fin-base length/SL	111	21.9–30.8	26.0 ±1.6	121	21.4–28.7	24.8 ±1.6	X	X
Anal-fin-base length/SL	111	13.9–18.9	16.5 ±1.0	121	13.1–18.4	16.3 ±1.0		
Prepelvic-fin length/SL	111	33.5–49.5	39.7 ±2.6	121	34.0–46.5	39.7 ±2.4		

thickness, caudal-peduncle dorsal length, and upper-jaw length (Table 6). No significant regional variation was observed within the overall PCA.

In the sheared PCA of differences in shape by depth, both species showed negligible differences within broadly overlapping clusters of individuals. In the depth analysis, loadings along the PC2 axis were strongest for suborbital depth, gill-raker length, and orbit length, and shallower individuals tended to have a greater suborbital depth, longer gill rakers, and longer orbit. In the combined morphometric and meristic shallow-water analysis, slight differences along the morphometric PC2 axis and the meristic PC1 axis reflected longer gill rakers and higher lateral-line pore counts in *S. variabilis*. No differences were found in the PCA comparing sex within species (Tables 7–8).

Table 2

Counts of lateral-line pores and gill rakers for *Sebastes ciliatus* and *S. variabilis* by region. AI or BS = Aleutian Islands or Bering Sea; GOA = Gulf of Alaska; SEAK = Southeast Alaska; BC = British Columbia.

		Lateral-line pores																		
Species	Region	39	40	41	42	43	44	45	46	47	48	49	50	51	52	53	54	*n*	Mean	SD
Sebastes ciliatus	AI or BS				2	3	8	4	8				1					26	44.73	1.66
	GOA	1		1	6	7	4	11	8	5	5	3	1					52	45.20	2.22
	SEAK					3	3	2	2	4	2	5	3					24	46.75	2.40
Sebastes variabilis	AI or BS							3	4	5	1	7	4	3				27	48.04	1.87
	GOA							5	4	14	11	15	13	8	3		1	74	48.68	1.95
	SEAK					1	1		3	5	9	5	14	4	2			44	48.75	1.94
	BC							1	3	1	2	3	4		1	1		16	48.63	2.25

		Gill rakers																		
Region		32	33	34	35	36	37											*n*	Mean	SD
Sebastes ciliatus	AI or BS	1	9	5	10	1												26	34.04	1.04
	GOA	2	17	23	7	2												51	33.80	0.87
	SEAK	1	1	6	13	3	1											25	34.77	0.92
Sebastes variabilis	AI or BS	3	1	10	8	2	1											25	34.22	1.13
	GOA	1	5	24	35	5												70	34.52	0.80
	SEAK		4	18	15	8	1											46	34.61	0.89
	BC		1	2	8	6												17	35.12	0.86

Systematics

Sebastes ciliatus (Tilesius, 1813)

Dark rockfish

Figs. 1–4; Tables 1–8

Epinephelus ciliatus Tilesius, 1813:406, pl. 16, figs. 1–4 (original description, one specimen: holotype apparently lost, sex unknown, approximately 413 mm TL, "Oceano orientali Camtschatcam et Americam alluenti").

Sebastichthys ciliatus: Jordan and Jouy, 1881:8 (in part, new combination).

Sebastodes ciliatus: Jordan and Gilbert, 1883:658 (in part, new combination).

Sebastostomus ciliatus: Eigenmann and Beeson, 1894:388 (in part, new combination).

Sebastes ciliatus: Westrheim, 1973:1230 (in part, new combination).

Sebastes sp. cf. *ciliatus*: Orr et al., 1998:26, 2000:26.

Neotype

UW 43493, 1(266.4 mm), Lynn Canal, north of Funter Bay, 58.2467°N, 134.899°W, 25 m depth, 13 July 1998.

Material examined

A total of 140 specimens, 83.8–340.0 mm, were examined, including the neotype above. See Appendix for catalog numbers and locality data.

Diagnosis

A species of *Sebastes* with the following combination of character states: body uniformly black to dark blue or gray, particularly at anal-fin base and ventral pectoral-fin rays; peritoneum jet black; symphyseal knob moderate to strong; extrinsic swimbladder muscle with anterior fascia separating sections of striated muscles, otherwise of type I (a–z) of Hallacher (1974); lateral-line pores 39–50, lateral-line scales 44–60; pectoral-fin (P1) rays 16–19; anal-fin (A) rays 7–9; dorsal-fin (D) rays 13–17; vertebrae 28 (11–12 + 16–17).

Description

D XII–XIV, 13–17; A III, 7–9; P1 16–19, 8–11 simple; lateral-line pores 39–50(54), scales 44–60; gill rakers 32–37 (10–11 + 22–27); vertebrae 28 (11–12 + 16–17). Meristic frequency and statistical data are presented in Tables 2–4.

Morphometric data and statistics are presented in Tables 1 and 4. Body relatively deep, especially at nape, depth at pelvic-fin base 32.5–42.7% SL; profile of dorsal margin of head steep from snout to nape above anterodorsal margin of gill slit, flattening to dorsal-fin origin; mouth large, with posterior end of maxilla extending between pupil and posterior rim of orbit, maxilla length 43.6–51.1% HL; symphyseal knob moderate to strong and having blunt tip, lower jaw length 53.4–60.5% HL; mandibular pores of moderate size. Cranial spines weak, in large adults covered by flesh, head smooth. Nasal spine invariably present; parietal ridge invariably present and small spine typically

Table 3

Counts of soft-dorsal-, anal-, and pectoral-fin rays for *Sebastes ciliatus* and *S. variabilis* by region. AI or BS = Aleutian Islands or Bering Sea; GOA = Gulf of Alaska; SEAK = Southeast Alaska; BC = British Columbia. *n* = number of fish in sample.

		Dorsal-fin rays							
Species	Region	13	14	15	16	17	*n*	Mean	SD
Sebastes ciliatus	AI or BS		2	21	3		26	15.04	0.45
	GOA	1	4	45	2		52	14.94	0.42
	SEAK		5	14	4	1	24	15.04	0.75
Sebastes variabilis	AI or BS			25	3		28	15.12	0.33
	GOA		7	54	9		70	15.03	0.49
	SEAK		4	40	3		47	14.98	0.39
	BC		1	16			17	14.94	0.24
		Pectoral-fin rays							
	Region	17	18	19			*n*	Mean	SD
Sebastes ciliatus	AI or BS	1	19	6			26	18.19	0.49
	GOA		44	8			52	18.16	0.37
	SEAK	2	16	6			24	18.17	0.56
Sebastes variabilis	AI or BS		23	4			27	18.17	0.38
	GOA	6	65				71	17.93	0.26
	SEAK	1	44	2			47	18.02	0.25
	BC		15	2			17	18.12	0.33
		Anal-fin rays							
	Region	7	8	9			*n*	Mean	SD
Sebastes ciliatus	AI or BS	4	21	1			26	7.88	0.43
	GOA	4	47				51	7.92	0.27
	SEAK	1	20	3			24	8.08	0.41
Sebastes variabilis	AI or BS	4	19	3			27	8.00	0.50
	GOA	8	63				71	7.88	0.32
	SEAK	5	41				46	7.89	0.31
	BC	1	15	1			17	8.00	0.35

present; postocular and tympanic spines absent or obsolete in adults (postocular present on at least one side in 23.2% and tympanic present on at least one side of 37.7% of specimens examined), most often present in juveniles. Interorbital region wide, 22.9–29.3% HL, strongly convex; parietal ridges weak, and area between ridges slightly convex; preopercular spines 5, directed posteroventrally; two opercular spines, upper spine directed posteriorly, lower spine directed posteroventrally; posttemporal and supracleithral spines present; lachrymal spines rounded, small; dorsal margin of opercle nearly horizontal; lower margin of gill cover with small spines: posteroventral tip of subopercle and anteroventral tip of interopercle rugose or with 1–2 small spines.

Dorsal-fin origin above anterodorsal portion of gill slit; dorsal fin continuous, gradually increasing in height to spine IV and decreasing in height to spine XII; spine XIII much larger, forming anterior support of soft dorsal fin; membranes of spinous dorsal fin moderately incised, less so posteriorly; soft dorsal fin with anterior rays longest, posterior rays gradually shortening. Anal-fin spine II shorter than III (7.5–14.2 vs. 10.0–14.6% SL), anterior rays longest on soft rayed portion of anal fin, posterior rays gradually shortening, posterior margin perpendicular to body axis or with slight posterior slant, anterior ray tips directly ventral to or forward of posterior tips, anterior tip of anal fin typically rounded. Pectoral fins with ray 10 longest, extending to or slightly anterior to vent, fin-ray length 24.6–31.8% SL, fin-base to ray-tip length 24.6–31.8% SL; fin-base width 9.5–11.9% SL. Pelvic fins extend about 60% of distance from pelvic-fin base to anal-fin origin, falling well short of vent, ray length 20.5–26.0% SL, spine length 52.4–67.4% ray length. Caudal fin shallowly emarginate, length 10.2–29.4% SL. Vent positioned below dorsal-fin spine 10, 1.6–5.8% SL from anal-fin origin.

Table 4

Selected proportional morphometrics and meristics of *Sebastes ciliatus* and *S. variabilis* from shallow-water collections. Morphometric data are in percent standard length (SL) or head length (HL). X = statistically significant difference at 0.05 level, as evaluated by ANOVA and ANCOVA, when appropriate; ns = not statistically significant at 0.05 level.

	S. ciliatus			*S. variabilis*				
	n	Range	Mean ±SD	*n*	Range	Mean ±SD	ANOVA	ANCOVA
Meristics	68			49				
Dorsal-fin rays		13–16	15.0 ±0.5		14–16	15.0 ±0.4	ns	
Anal-fin rays		7–9	7.9 ±0.4		7–9	8.0 ±0.3	ns	
Pectoral-fin rays (left)		17–19	18.1 ±0.5		17–19	18.0 ±0.2	ns	
Lateral-line pores (left)		40–50	45.2 ±2.1		42–51	47.9 ±2.0	X	
Gill rakers		32–37	34.3 ±1.1		32–36	34.6 ±1.0	ns	
Morphometrics								
Standard length		83.8–331.0			83.3–363.0			
Head length/SL		30.5–35.5	32.9 ±1.1		30.2–35.4	32.7 ±1.0	ns	ns
Orbit length/HL		21.5–30.6	25.6 ±2.1		23.6–30.0	26.4 ±1.6	ns	ns
Snout length/HL		18.2–26.0	21.3 ±1.6		18.2–24.0	20.9 ±1.4	ns	ns
Interorbital width/HL		22.9–28.2	25.6 ±1.2		23.0–28.8	25.8 ±1.1	ns	ns
Suborbital depth/HL		4.1–7.6	5.9 ±0.7		4.5–7.4	6.0 ±0.6	ns	ns
Upper jaw length/HL		43.6–50.4	47.3 ±1.5		43.9–54.0	47.3 ±2.0	ns	ns
Lower jaw length/HL		53.4–60.5	56.4 ±1.6		52.8–60.4	56.6 ±1.8	ns	X
Gill raker length/HL		11.8–20.7	15.2 ±1.5		13.3–19.9	16.1 ±1.6	X	X
Depth at pelvic–fin base/SL		34.0–40.8	36.7 ±1.5		33.7–38.6	36.2 ±1.2	ns	ns
Depth at anal–fin origin/SL		27.4–35.8	31.2 ±1.7		27.0–31.7	30.0 ±1.1	ns	ns
Body thickness/SL		14.9–21.3	17.9 ±1.2		12.9–20.9	17.1 ±1.8	X	ns
Pectoral-fin base width/SL		9.7–11.8	10.6 ±0.5		9.4–11.1	10.2 ±0.4	X	ns
Pectoral-fin ray length/SL		25.1–31.3	28.6 ±1.2		24.8–31.0	28.4 ±1.2	ns	ns
Caudal peduncle depth/SL		9.8–13.7	11.5 ±0.7		9.7–11.8	10.8 ±0.5	ns	ns
Caudal peduncle dorsal length/SL		11.9–16.2	14.0 ±0.8		12.6–15.3	13.9 ±0.7	ns	ns
Caudal peduncle ventral length/SL		18.2–22.5	20.6 ±1.0		17.1–24.3	21.3 ±1.5	X	X
Preanal length/SL		62.5–77.4	68.3 ±2.3		64.6–73.5	68.2 ±2.1	ns	ns
Predorsal length/SL		29.3–35.4	32.2 ±1.2		28.6–35.2	31.8 ±1.4	ns	ns
Spinous dorsal-fin-base length/SL		32.5–41.8	37.0 ±2.0		33.2–41.6	36.6 ±1.8	ns	ns
Soft dorsal-fin-base length/SL		22.1–29.6	26.2 ±1.4		21.4–28.7	25.0 ±1.6	X	X
Anal-fin-base length/SL		14.5–18.9	16.5 ±0.9		13.6–18.4	16.4 ±1.0	ns	ns
Prepelvic-fin length/SL		36.4–49.5	39.4 ±2.3		36.3–46.5	40.3 ±2.6	ns	ns

Table 5

Factor loadings for principal component (PC) analysis of meristic characters for *Sebastes ciliatus* and *S. variabilis* collected in all depths and regions.

	PC1	PC2	PC3
Lateral-line pores	−0.6139	−0.1000	−0.4151
Gill raker	−0.5993	0.1360	0.5217
Dorsal-fin rays	−0.2731	−0.5625	0.4739
Anal-fin rays	−0.0138	−0.7389	−0.3954
Pectoral-fin rays	0.4349	−0.3304	0.4180

Lateral body scales with many (ca. 5–7) accessory scales in posterior field. Maxilla and underside of mandible completely scaled; suborbital region scaled; branchiostegal rays scaled.

Gill rakers long, 11.3–20.7% HL, and slender on first arch, longest raker in joint between cerato- and hypobranchials, length of preceding and succeeding rakers progressively shorter; rudiments absent. Pseudobranchs 37–38.

Body color in life and after preservation dark, black to gray, lighter in deeper water, lightening ventrally on belly and occasional reddening from base of pectoral fin to base of anal fin, uniformly dark from soft dorsal fin to anal-fin base; vague darker mottling tapering from origin of soft

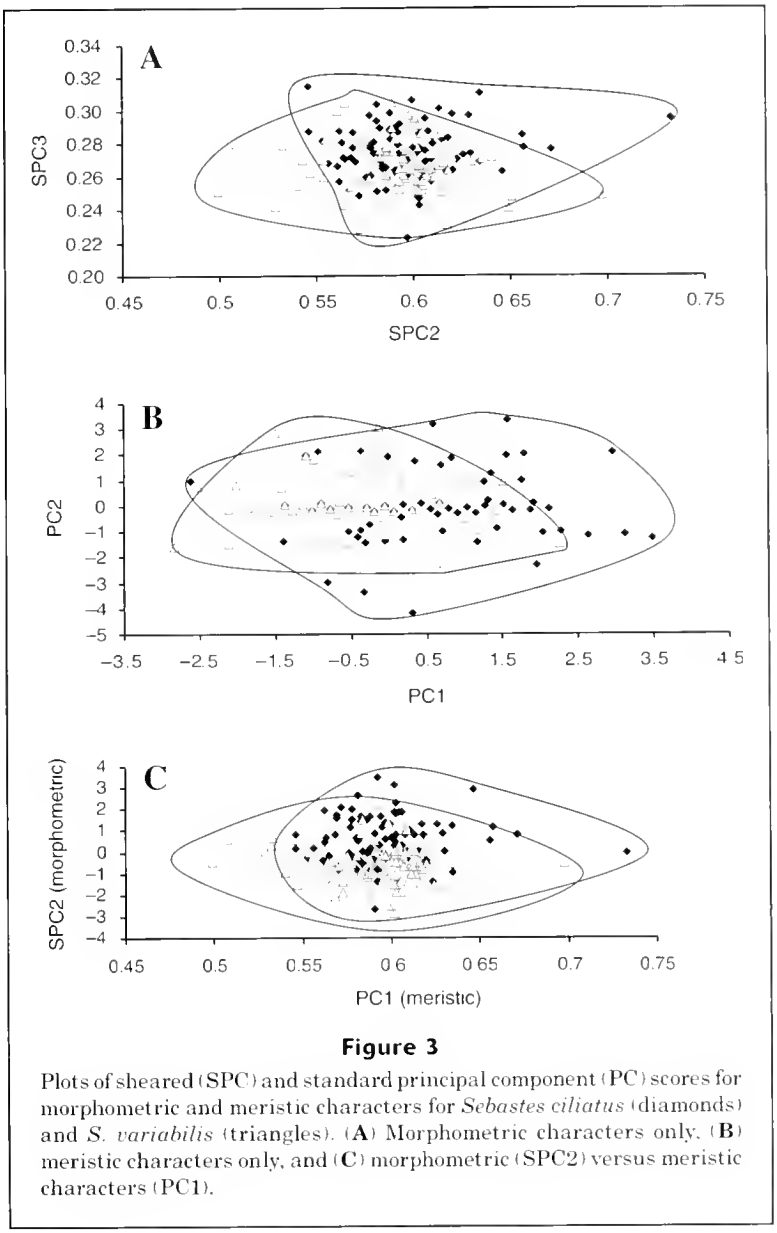

Figure 3

Plots of sheared (SPC) and standard principal component (PC) scores for morphometric and meristic characters for *Sebastes ciliatus* (diamonds) and *S. variabilis* (triangles). (**A**) Morphometric characters only, (**B**) meristic characters only, and (**C**) morphometric (SPC2) versus meristic characters (PC1).

dorsal fin ventrally and forward narrowing across lateral line, faint darker mottling also present farther posterior at soft dorsal-fin base. Head nearly uniformly dark, two faint bars extending from orbit to preopercle, a faint bar along anterior margin of maxilla. Median fins uniformly dark gray to black. Pectoral fins, including lower rays, gray to black. Pelvic fins dark. Peritoneum jet black; stomach, pyloric caeca, and intestines pale. See Figure 1 (A–C, E), and previously published color figures of Kessler (1985, "*S. ciliatus*, dark dusky rockfish"), Kramer and O'Connell (1986; "*S. ciliatus*, dark"), Kramer and O'Connell (1988, 1995; "*S. ciliatus*, Kodiak specimen," and "shallow water specimen"), Orr et al. (1998, 2000; "*S.* sp. cf. *ciliatus*, dark dusky rockfish"), Orr and Reuter (2002; "*S. ciliatus*, dark dusky"), and Mecklenburg et al. (2002; "*S. ciliatus*, dark phase"). Juveniles in life (Fig. 1C) similar to adults in general body color, often brassy on breast and head.

Largest specimen examined 340.0 mm (425 mm TL, 412 mm fork length; UW 46068). Maximum size confirmed 470 mm fork length (RACE Division[6]; Orr, personal observ.).

Distribution and natural history

The range of *Sebastes ciliatus* based on material examined extends from the western Aleutian Islands and east-

[6] RACE (Resource Assessment and Conservation Engineering) Division. 2002. Unpubl. data from RACE database. Alaska Fisheries Science Center, Natl. Mar. Fish. Serv., NOAA, 7600 Sand Point Way NE, Seattle, WA 98115.

Table 6

Factor loadings for sheared principal component (SPC) analysis of morphometric characters for specimens examined across all depths and regions for *Sebastes ciliatus* and *S. variabilis*.

	PC1	SPC2	SPC3
Head length	0.1526	0.1131	0.0416
Orbit length	0.1853	0.2090	0.0988
Depth at anal-fin origin	0.2564	0.1335	−0.0136
Snout length	0.2452	0.1109	0.0240
Interorbital width	0.5753	−0.8081	−0.0485
Suborbital depth	0.1905	0.1481	0.0675
Upper jaw length	0.1837	0.1394	0.0713
Lower jaw length	0.2332	0.2321	−0.9231
Gill raker length	0.1635	0.0768	0.0840
Body thickness	0.2045	0.1692	0.1404
Pectoral-fin base	0.2119	0.1146	0.1139
Pectoral-fin ray length	0.1551	0.0848	0.0105
Caudal peduncle depth	0.2113	0.1436	0.1757
Caudal peduncle dorsal length	0.1885	0.1561	0.0262
Caudal peduncle ventral length	0.1601	0.0829	0.0773
Pre-anal-fin length	0.1313	0.0732	0.0800
Predorsal-fin length	0.1516	0.1063	0.0456
Spinous dorsal-fin base length	0.1549	0.0976	0.0504
Soft dorsal-fin base length	0.1602	0.1271	0.1493
Anal-fin base length	0.1671	0.1266	0.1140

Table 7

Factor loadings for sheared principal component (SPC) analysis of morphometric characters for shallow water *Sebastes ciliatus* and *S. variabilis*.

	PC1	SPC2	SPC3
Head length	0.1149	0.0855	0.0497
Orbit length	0.1504	0.1223	0.0408
Depth at anal-fin origin	0.1876	0.1908	0.1111
Snout length	0.1586	0.0886	0.0687
Interorbital width	0.2465	0.1636	−0.0394
Suborbital depth	0.2428	0.1156	0.0024
Upper jaw length	0.5843	−0.8015	0.0042
Lower jaw length	0.1876	0.1565	0.0745
Gill raker length	0.2431	0.1866	−0.9189
Body thickness	0.1782	0.1386	0.0734
Pectoral-fin base	0.2103	0.1889	0.1819
Pectoral-fin ray length	0.2108	0.1308	0.1165
Caudal peduncle depth	0.1550	0.1033	0.0162
Caudal peduncle dorsal length	0.2126	0.1552	0.1930
Caudal peduncle ventral length	0.1854	0.1426	−0.0224
Pre-anal-fin length	0.1520	0.1098	0.0381
Predorsal-fin length	0.1499	0.1124	0.0603
Spinous dorsal-fin base length	0.1516	0.0953	0.0358
Soft dorsal-fin base length	0.1642	0.1395	0.1171
Anal-fin base length	0.1697	0.1061	0.1310

ern Bering Sea, through the Gulf of Alaska, to southeast Alaska. Other documented records extend its range south to Johnstone Strait, British Columbia (Peden and Wilson, 1976; Fig. 4). It is common throughout its range in shallow rocky habitats, and our material was collected at depths from 5 to 160 m, its total recorded depth range.

Sebastes ciliatus is commonly collected with *S. melanops* by trawl and hook-and-line gear in shallow waters, where *S. ciliatus* is commercially fished as part of the "black rockfish" fishery and has been often misidentified as *S. melanops*. In deeper (>100 m) trawls in Aleutian and Gulf of Alaska waters, *S. ciliatus* is commonly found in association with *S. alutus* (Pacific ocean perch), *S. polyspinis* (northern rockfish), and *S. variabilis* (dusky rockfish). Less frequently, *S. variegatus* (harlequin rockfish), *S. zacentrus* (sharpchin rockfish), and *S. proriger* (redstripe rockfish) are also captured with *S. ciliatus*. A large (320 mm; UW 47417) *S. ciliatus* was found in the stomach of a Pacific cod (*Gadus macrocephalus*) collected in the Aleutian Islands.

Females captured in summer (May–July) trawl surveys are most often ripe with eyed larvae. Near-term females and males were observed in July in shallow waters off southeast Alaska in contrast to individuals of *S. variabilis*, which were all immature at this time (Orr, personal observ.).

Table 8

Factor loadings for principal component (PC) analysis of meristic characters for shallow water *Sebastes ciliatus* and *S. variabilis*.

	PC1	PC2
Lateral-line pores	−0.5933	0.1677
Gill rakers	−0.4274	−0.6851
Dorsal-fin rays	−0.5742	−0.0777
Anal-fin rays	−0.3667	0.6191
Pectoral-fin rays	0.0325	−0.3364

Etymology

The specific name *ciliatus* is derived from the Latin word "cilium" for "eyelid" or "eyelash" and alludes to the numer-

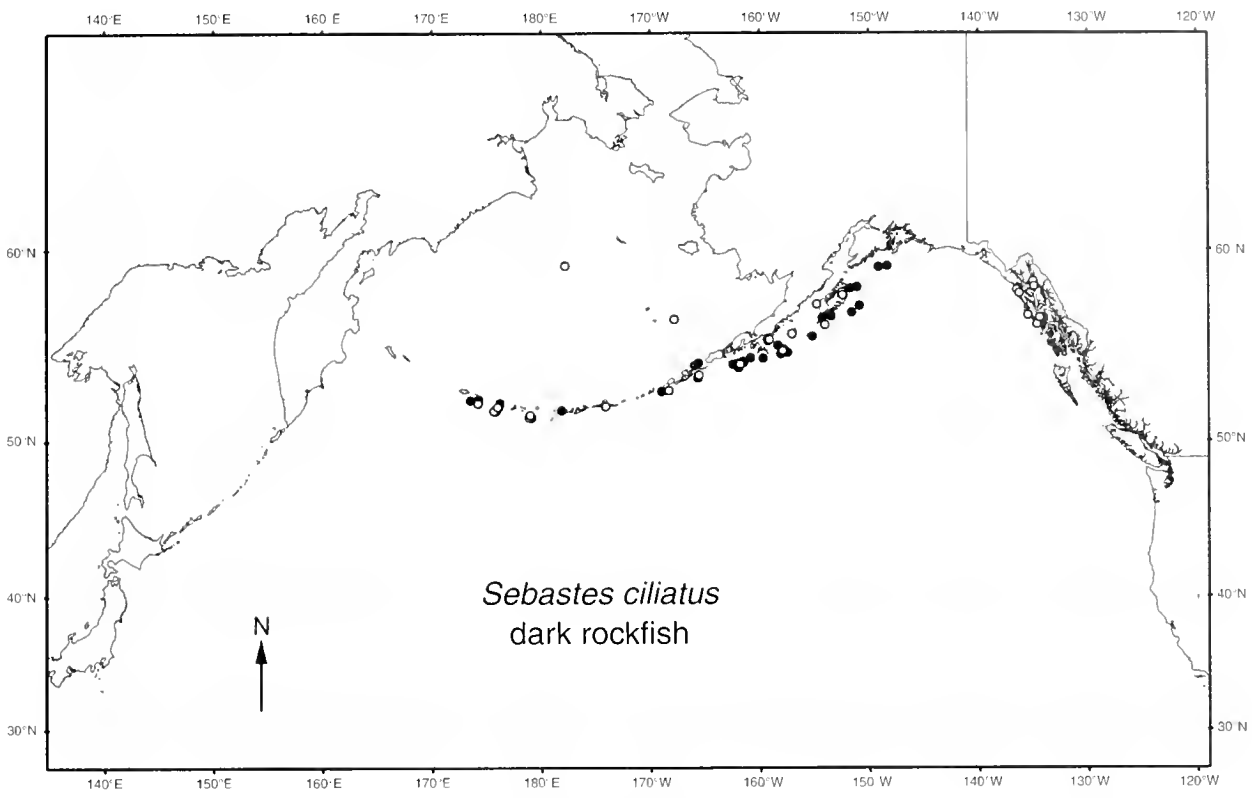

Figure 4

Distribution of *Sebastes ciliatus* based on material examined (open circles) and recent National Marine Fisheries Service survey data (closed circles) for the years 1999 to 2002. Each symbol may represent more than one capture.

ous accessory scales (similar to fringing eyelashes) that are found on the posterior field of the larger scales in most species of *Sebastes* (Tilesius, 1813).

Remarks

Tilesius (1813) based his description of *Epinephelus ciliatus* on a single specimen collected in the North Pacific "bordering Kamchatka and America," probably during the Krusenstern expedition of 1803–06 (Bauchot et al., 1997; Svetovidov, 1978, 1981; Pietsch, 1995). Although the illustration of the specimen was published (Tilesius, 1813; Fig. 2B), the specimen itself has since been lost, probably before the transfer of the Kunstkammer collection to the Zoological Museum of the Academy of Sciences, St. Petersburg (Svetovidov, 1978, 1981). Because *S. ciliatus* may easily be confused with other dark-colored *Sebastes* and *S. variabilis*, we have herein designated UW 43493, collected in Lynn Canal of southeast Alaska, as the neotype of *S. ciliatus*.

The illustration of the holotype of *E. ciliatus* Tilesius (1813) depicts a uniformly dark individual of *Sebastes*, and most of its reported meristics and other characters are consistent with both *S. ciliatus* and *S. variabilis*. However, its lateral-line pore count is low at 43, and although falling well within the range found in the material examined of *S. ciliatus*, the count is represented in only one individual of *S. variabilis* examined. Along with its low lateral-line pore count, a moderate symphyseal knob is illustrated, similar to that of *S. ciliatus*, excluding its identification as *S. melanops*, a common and similarly colored *Sebastes* found within the geographic range of *S. ciliatus*.

The anal-fin posterior margin of the specimen illustrated shows a moderate posterior slant, and tips of the posteriormost rays extend well past those of the anterior rays. *Sebastes ciliatus* may have an anal fin with a slight posterior slant, unlike *S. variabilis*, but it is never as pronounced as the illustration indicates. However, this character is not found in any other dark-colored species of *Sebastes* presently known from the Aleutian Islands and northern Gulf of Alaska west of Kodiak Island. *Sebastes entomelas* has an anal fin with a strong posterior slant to its posterior margin, but the northernmost record of this species is Kodiak Island (Allen and Smith, 1988; Love, 2002; Mecklenburg et al., 2002) where it is rare (RACE Division[6]). *Sebastes entomelas* also has a much higher count of lateral-line pores (50–60; Love et al., 2002).

One syntype of *Perca variabilis* was sent by Martin H. K. Lichtenstein (1780–1857), the director of the Berlin Zoological Museum in 1813, to Georges Cuvier at the Muséum National d'Histoire Naturelle in Paris, and has been preserved as MNHN 8670 (Svetovidov, 1981; Fig. 2A). Although originally from the collections of Carl Heinrich Merck (1761–1799; Svetovidov, 1981; Blanc and Hureau, 1968; Bauchot and Desoutter, 1986) and thus contempora-

neous with Tilesius's material, this specimen probably did not serve as the example for Tilesius's (1813) illustration. The illustration is of the left side of a whole fish, whereas MNHN 8670 is the dried skin and head of the right side. Counts and measurements taken from the original description and compared with the specimen indicate that it is improbable that the left side of this individual was the subject of the illustration. The counts provided by Tilesius (1813) include D XIII, (soft rays not given); A III, 8; P1 18; lateral-line pores 43. MNHN 8670 differs in counts of anal-fin rays (9) and in lateral-line pores (49). Although the symphyseal knob is reduced and the anal-fin margin is strongly slanted posteriorly in the Tilesius illustration, MNHN 8670 has a strong symphyseal knob and a perpendicular anal-fin margin with a distinctly pointed tip (Fig. 2, A and B).

Sebastes variabilis (Pallas, 1814)

Dusky rockfish

Figs. 1–3, 5; Tables 1–8

Perca variabilis Pallas, 1814:241 (original description, three? specimens; lectotype hereby designated, MNHN 8670, dried skin, sex unknown, 343.7 mm, "mari Americam borealum"; other syntypes apparently lost).

Sebastes variabilis: Cuvier, in Cuvier and Valenciennes, 1829:547 (new combination).

Sebastichthys ciliatus: Jordan and Jouy, 1881:8 (in part, new combination).

Sebastodes ciliatus: Jordan and Gilbert, 1883:658 (in part, new combination).

Sebastostomus ciliatus: Eigenmann and Beeson, 1894:388 (in part, new combination).

Sebastes ciliatus: Westrheim, 1973:1230 (in part, new combination).

Material examined

A total of 253 specimens, 48.0–430.8 mm, including the lectotype listed above, were examined. See Appendix for additional catalog numbers and locality data.

Diagnosis

A species of *Sebastes* with the following combination of character states: body light yellow to greenish brown to gray, typically greenish brown, with orange flecks variously present on sides, particularly light ventrally above anal-fin base and on ventral pectoral-fin rays; peritoneum light gray to jet black; symphyseal knob strong; extrinsic swimbladder muscle with a single section of striated muscle, lacking anterior fascia, otherwise of type 1 (a–z) of Hallacher (1974); lateral-line pores 43–54, lateral-line scales 47–63; pectoral-fin rays 16–19; anal-fin rays 7–9; dorsal-fin rays 13–16; vertebrae 28–29 (11–12 + 16–18).

Description

D XIII–XIV, 13–16; A III, 7–9; P1 16–19, 7–11 simple; lateral-line pores 43–54, scales 47–63; gill rakers 32–37 (10–11 + 22–26); vertebrae 28–29 (11–12 + 16–18) (one of ten specimens with 27 vertebrae, with one caudal vertebra bearing two neural and two haemal spines). Meristic frequency and statistical data are presented in Tables 2–4.

Morphometric data and statistics are presented in Tables 1 and 4. Body relatively deep, especially at nape, depth at pelvic-fin base 29.2–40.9% SL; profile of dorsal margin of head steep to nape above anterodorsal margin of gill slit, flattening to dorsal-fin origin. Mouth large, with posterior end of maxilla extending beyond pupil to or beyond posterior rim of orbit, maxilla length 42.7–54.0% HL; symphyseal knob strong with blunt tip, lower-jaw length 52.8–62.7% HL; mandibular pores of moderate size. Cranial spines weak, in large adults covered by flesh, head smooth. Nasal spines invariably present; parietal ridge invariably present and small spine typically present; postocular and tympanic spines typically absent or obsolete in adults (weak postocular spines present on at least one side in 29.7% and weak tympanic spines present on at least one side in 50.6% of specimens examined) are typically present in juveniles. Interorbital region wide, 22.5–30.4% HL, strongly convex; parietal ridges weak, and area between ridges slightly convex; preopercular spines 5, directed posteroventrally; two opercular spines, upper spine directed posteriorly, lower spine directed posteroventrally; posttemporal and supracleithral spines present; lachrymal spines rounded, small; dorsal margin of opercle nearly horizontal; lower margin of gill cover with small spines; posteroventral tip of subopercle and anteroventral tip of interopercle rugose or with 1 or 2 small spines.

Dorsal-fin origin above anterodorsal portion of gill slit; dorsal fin continuous, gradually increasing in height to spine IV or V and decreasing in height to spine XII; spine XIII much larger, forming anterior support of soft dorsal fin; membranes of spinous dorsal fin moderately incised, less so posteriorly; soft dorsal fin with anterior rays longest, posterior rays gradually shortening. Anal-fin spine II shorter than III (5.8–13.6 vs. 9.5–15.6% SL), anterior rays longest on soft rayed portion of anal fin, posterior rays gradually shortening, posterior margin perpendicular to body axis or with slight posterior slant, anterior ray tips directly ventral to posterior tips, anterior tip of anal fin typically pointed. Pectoral fins with ray 10 longest, extending to or slightly anterior to vent, fin-ray length 23.5–31.0% SL, fin base to ray tip length 24.2–35.1% SL; fin-base width 9.4–11.2% SL. Pelvic fins extend about 60% of distance from pelvic-fin base to anal-fin origin, falling well short of vent, ray length 19.2–29.2% SL, spine length 44.9–70.7% ray length. Caudal fin slightly emarginate, length 15.4–26.9% SL. Vent positioned below dorsal-fin spine 10, 2.2–7.0% SL from anal-fin origin.

Lateral body scales with many (ca. 5–7) accessory scales in posterior field. Maxilla and underside of mandible completely scaled; suborbital region scaled; branchiostegal rays scaled.

Gill rakers long, 11.6–19.9% HL, and slender on first arch, longest raker in joint between cerato- and hypobranchials, length of preceding and succeeding rakers progressively shorter; rudiments absent. Pseudobranchs 36–38.

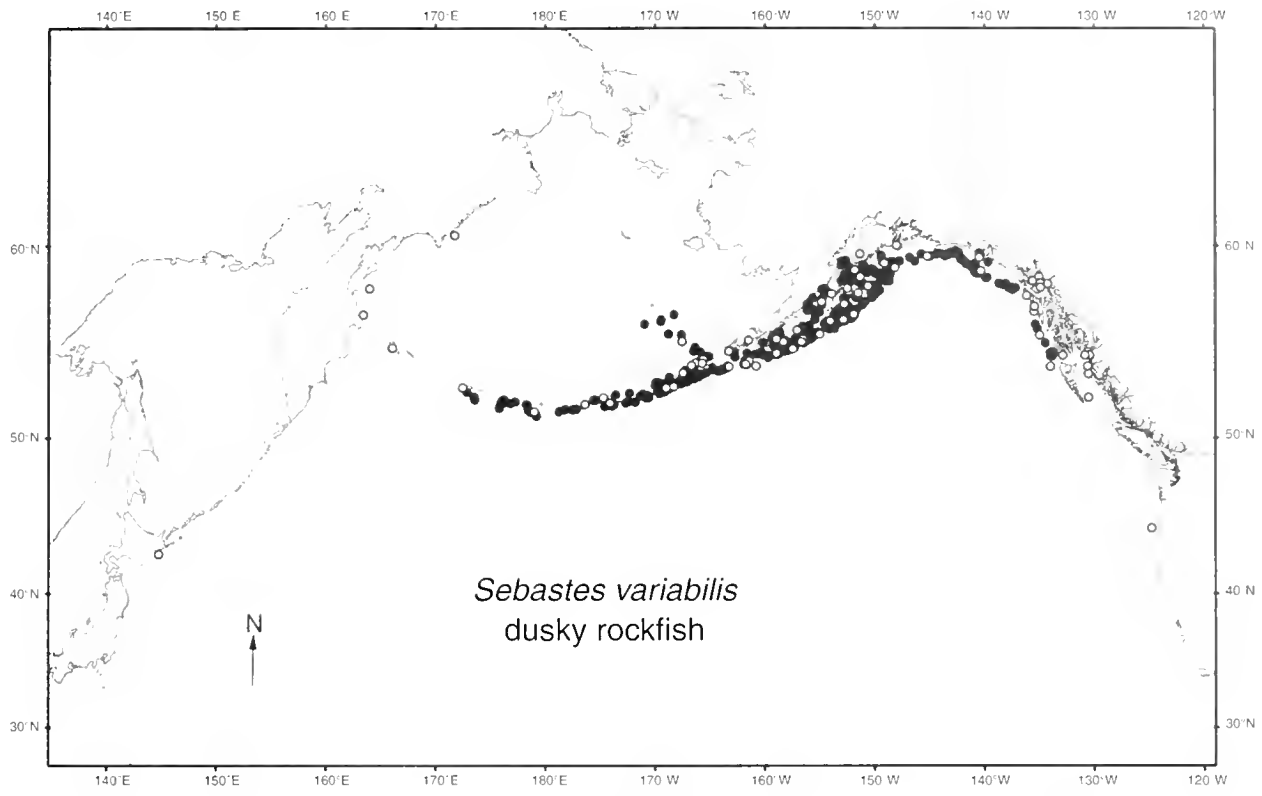

Figure 5

Distribution of *Sebastes variabilis* based on material examined (open circles) and recent National Marine Fisheries Service survey data (closed circles) for the years 1999 to 2002. Each symbol may represent more than one capture.

Body color in life variable (Fig. 1D); adults typically light, greenish-tan (Fig. 1B), often darker gray dorsally (Fig. 1D), rarely lighter yellow overall (Fig. 1D); invariably lightening ventrally to pinkish-white on head, belly, anal-fin base, and caudal peduncle; a clear demarcation between darker dorsum and light ventrum above anal-fin base; vague darker mottling tapering from origin of soft dorsal-fin ventrally and forward narrowing across lateral line, faint darker mottling also present farther posterior at soft dorsal-fin base, mottling most evident in tan individuals; brown to orange "flecks" present on sides of body on posterior fields of scales, appearing as darker speckling in juveniles. Head similar in background color to body, two prominent bars extending from orbit to preopercle, a prominent bar along anterior margin of maxilla in darker individuals (these bars obsolete in light individuals). Median fins and pelvic fins uniformly gray, lighter in light-bodied individuals. Pectoral fins brown to grayish pink; lower rays pink. Peritoneum light gray to jet black, typically dark gray; stomach, pyloric caeca, and intestines pale. See Figure 1 (A–D) and previously published color figures of Kessler (1985; "*Sebastes* sp., light dusky rockfish"), Kramer and O'Connell (1986; "*S. ciliatus*, light"), Kramer and O'Connell (1988, 1995; "*S. ciliatus*, light specimen"), Orr et al. (1998, 2000; "*S. ciliatus*, light dusky rockfish"), Orr and Reuter (2002; "light dusky"), Mecklenburg et al. (2002; "light phase").

Juveniles in life (Fig. 1C) lighter than adults, with dorsum light-brown to tan, background covered with orange-brown speckles, often with distinct dark band at base of soft dorsal fin; head brassy; ventrum pink on lower jaw, breast, and base of anal fin, lightening to white on belly.

Largest specimen examined 430.8 mm (527.7 mm fork length [FL], 541.3 mm TL; UW 44253). Maximum size reported 590 mm FL (RACE Division[6]).

Distribution and natural history

Sebastes variabilis is recorded from a single specimen off Hokkaido, Japan (Shinohara et al., 1994), and from other specimens collected from the east coast of Kamchatka to Cape Ol'utorskii (at 60°N) in the western Bering Sea, along the Aleutian Islands to 60°N in the eastern Bering Sea, through the Gulf of Alaska south to Johnstone Strait, British Columbia (Peden and Wilson, 1976; Richards and Westrheim, 1988; Fig. 5), and to central Oregon (based on a recently collected single specimen [UW 46575]). The earlier record of Schultz (1936) and Alverson and Welander (1952) from Washington at Neah Bay was reidentified by Westrheim (1968) as *S. entomelas*.

Although the depth of collection for material examined ranges from 6 to 370 m, and the species is recorded at depths to 675 m, large adults are commonly found along the edge of the continental shelf at depths of 100–300 m,

where the species is the target of commercial fisheries in the Gulf of Alaska. During trawl surveys, it is most commonly associated with *S. alutus* and *S. polyspinis*, and at greater depths with *S. aleutianus* (rougheye rockfish) throughout its range in Alaskan waters (Reuter, 1999; Ackley and Heifetz, 2001).

Females and males captured during summer (May–July) trawl surveys ranged widely in maturity state. Occasional ripe females were observed, although most females were maturing (Orr, personal observ.). A high percentage of females caught in trawl surveys during early April off southeast Alaska were releasing larvae, indicating that parturition occurs in the spring (Lunsford[7]). During July in shallower waters (ca. 40 m) of southeast Alaska, all *S. variabilis* collected were immature.

Etymology

The specific name *variabilis* is presumed to be a reference by Pallas (1814) to the wide range of body color in the species.

Remarks

Pallas (1814) described *Perca variabilis* from at least three specimens probably collected by Merck during the 1786–94 Billings expedition to the Russian Far East, including the Aleutian Islands, eastern Bering Sea, and northern Gulf of Alaska (Schmidt, 1950; Svetovidov, 1978, 1981; Pierce, 1990). One specimen was more completely described and used by him to obtain a set of counts and measurements. The other specimens were used to describe variation in the species, as in the following excerpt translated by the authors from the Latin text of Pallas (1814): "Body colored according to life and sex, varied, sometimes dark blue, belly white, fins blackish; female red below; those older wholly red or even purplish...." Pallas (1814) ultimately based the name *P. variabilis* on the supposed variability in color in this species.

Jordan and Evermann (1898) examined an individual from the Pallas collection, recognized by him as the "summer variety" of *P. variabilis* (ZMB 8145). They identified this "summer variety" as *Sebastes aleutianus* Jordan and Evermann (Jordan, 1884, 1885; Jordan and Evermann, 1898), a species easily distinguished from both *S. variabilis* and *S. ciliatus* by its full complement of eight pairs of strong cranial spines. These specimens have since been lost, probably during the destruction of the Berlin Zoological Museum during World War II (Paepke and Fricke, 1992). Although Jordan and Gilbert (1883) wrote that *S. proriger* was also confounded with *S. ciliatus*, Jordan (1885) and Jordan and Evermann (1898) corrected this statement, noting that only *S. ciliatus* and *S. aleutianus* were included within the material described as *E. ciliatus* and *P. variabilis* by Tilesius and Pallas.

[7] Lunsford, C. 2002. Personal commun. National Marine Fisheries Service, Auke Bay Laboratory, Alaska Fisheries Science Center, 11305 Glacier Highway, Juneau, AK 99801-8626.

Although MNHN 8670 (Fig. 2A) is from the Pallas collection (Svetovidov, 1978, 1981), it is apparently not the specimen used for the complete description. In his original account, Pallas (1814) listed the following meristic data (modified to standard notation): D XIII, 15; A III, 7; P1 17 (8 simple). Although the dorsal-fin ray count is identical with that of the MNHN 8670 specimen, both anal- and pectoral-fin ray counts differ. All elements are well preserved and easily counted.

Comparisons of proportions are more difficult to interpret because measurements had not been standardized at the time of the original description. However, of those measurements that can be readily compared, the following significant differences were found, providing additional evidence that this individual was not the specimen used for the primary description: total length (391.6 mm in Pallas [1814; "longitudo majoris speciminis"] vs. 414.0 mm taken from MNHN 8670), head length (101.6 mm ["capitis a summa maxilla ad operculum angulum"] vs. either 96.6 mm [standard head length] or 110.2 mm [head length to tip of lower jaw]). The specimen used by Pallas for the detailed meristics and morphometrics is presumed lost (Svetovidov, 1978).

Ayres (1854) misidentified *S. melanops* from the vicinity of San Francisco Bay as *S. variabilis*. Günther (1860) and Ayres (1862, 1863) placed *S. variabilis* of Ayres into the synonymy of *S. melanops*.

Comparisons

Sebastes variabilis is most similar to *S. ciliatus*; the latter is distinguished by its uniformly dark-blue to black color. *Sebastes ciliatus* is invariably dark at the base of the anal fin and on the lower pectoral rays, areas of lighter color in *S. variabilis* even in those individuals that have an overall dark body. The peritoneum of *S. ciliatus* is always jet black, unlike the usual gray peritoneum of *S. variabilis*, which however may often be dark or occasionally jet black. In combination with these color differences, a low count of 39–42 lateral-line pores will distinguish *S. ciliatus* from *S. variabilis*, although the total range of counts overlaps considerably.

The extrinsic morphological features of the swimbladder of both *S. ciliatus* and *S. variabilis* are of type I (a–z) of Hallacher (1974) in which the anterior muscle mass originates from the occipital region of the neurocranium, attaches to the pectoral girdle near the insertion of Baudelot's ligament, passes between the epineural and pleural ribs of vertebrae 3 and 4, passes ventral to the pleural rib of vertebrae 5, and continues posteriorly as three tendons that insert on the pleural ribs of vertebrae 8, 9, and 10. In *S. ciliatus* and not *S. variabilis*, the anterior striated muscle mass is separated into two sections by a thin fascia, similar to the condition reported in *S. paucispinis* alone among species of *Sebastes* (Hallacher, 1974). The morphological features of the complex differ significantly in *S. paucispinis*, however, in that the striated muscle does not attach to the pectoral girdle but bypasses it to insert by a single tendon into the posterior portion of the swimbladder. Only five specimens each of *S. ciliatus* and *S. varia-*

bilis were dissected in the present study to examine these muscles. Additional material should be examined to assess the intraspecific variability and systematic significance of this character complex.

Typical habitats of these two species also differ. Adult *S. ciliatus* are found in nearshore shallow habitats at maximum depths of 160 m and are abundant in protected coves on the outer coast of Alaska. *Sebastes variabilis*, in contrast, is found along the continental shelf margin at depths to 675 m. However, adult *S. variabilis* have also been collected in nearshore waters as shallow as 40 m (UW 43494). In areas of sympatry, such as the inside waters in Lynn Canal of southeast Alaska and Monashka Bay of Kodiak Island, *S. variabilis* is found at greater depths in stronger current, whereas *S. ciliatus* is found, often with *S. melanops*, among kelp (*Macrocystis*) on rocky ledges (Blackburn and Orr, personal observ.).

Other uniformly dark colored species of *Sebastes*, such as *S. melanops* and *S. mystinus*, may also be confused with *S. ciliatus* and darker individuals of *S. variabilis*, although both may be distinguished on the basis of color and morphological features. The body of *S. melanops* is dark bluish-black, has black speckling on the dorsum and lateral surfaces, and a distinctly white ventrum (in contrast with the slightly lighter ventrum of *S. ciliatus* [Fig. 1E]). Unlike *S. ciliatus*, in which the peritoneum is jet black, *S. melanops* has a white peritoneum. In *S. melanops*, five or six faint light blotches slightly larger than the orbit are present on the dorsum about midway between the lateral line and the dorsal-fin base. These blotches are especially prominent underwater, and in Alaska easily distinguish *S. melanops* from both *S. variabilis* and *S. ciliatus*, which lack blotches (Lauth[8]; see color figures of Love, 2002, and Stewart and Love, 2002). The symphyseal knob in *S. melanops* is obsolete, consisting only of a fleshy pad at the tip of the mandible, unlike the distinct bony knob of *S. ciliatus* and *S. variabilis*. Mandibular pores of *S. melanops* are obsolete, as compared with the larger, readily apparent pores of *S. ciliatus* and *S. variabilis*. Vertebral counts also differ, from 28–29 in *S. ciliatus* and *S. variabilis* to 26 in *S. melanops*. *Sebastes melanops* ranges from southern California to Atka Island in the Aleutian Islands (Mecklenburg et al., 2002) and the southern Bering Sea, where its presence is documented by a single recent collection (UW 47037). Most previous reports from the Bering Sea may be of *S. ciliatus*.

Sebastes mystinus is also similar to *S. ciliatus* but may be distinguished by the four distinct dark bars across its head and nape contrasting with its general body color of light mottled bluish-gray. The mouth of *S. mystinus* is smaller than that of *S. ciliatus*, and the maxilla extends only to the middle of the pupil rather than to the posterior portion of the orbit as in *S. ciliatus*. Like *S. melanops* and most Pacific *Sebastes*, *S. mystinus* has 26–27 vertebrae, compared to the 28–29 vertebrae of *S. ciliatus* and *S. variabilis*. *Sebastes mystinus* has been recorded from Sitka Harbor, Alaska (Kramer and O'Connell, 1995), to Punta Santo Tomas, northern Baja California (Hobson, 2002). Earlier reports from Kodiak Island, the Aleutian Islands, and Bering Sea are undocumented (Quast and Hall, 1972; Kramer and O'Connell, 1995; Mecklenburg et al., 2002) and probably refer to *S. ciliatus*.

Sebastes polyspinis is commonly caught in trawls and may be confused with *S. variabilis*, especially when preserved. It can be distinguished from *S. variabilis* by its modal count of 14 dorsal-fin spines and light (pink or white when live) oblique band across the lower rays of the pectoral fin, which remains prominent when recently preserved. In life, the overall color of *S. polyspinis* is reddish-orange to pink, overlaid with gray-green mottling and fine green spots. Evermann and Goldsborough (1907) considered the then undescribed *S. polyspinis* within the range of variation of "*S. ciliatus*," because at least one lot (USNM 6243) was misidentified by them as "*S. ciliatus*." They probably also confused *S. melanops* with *S. variabilis*, or possibly *S. polyspinis*, describing the color in life of *S. melanops* from Alaska as "olive-brown, blotched with dirty red." *Sebastes melanops* never has a trace of red, whereas the most common color pattern of *S. variabilis* could be adequately described by this phrase.

In the western Pacific, two species, the dark-colored *S. taczanowskii* and the light-colored *S. schlegelii*, may be confused with *S. ciliatus* and *S. variabilis*, respectively. Both may be distinguished from *S. ciliatus* and *S. variabilis* by modal counts of pectoral-fin rays (15 in *S. taczanowskii* and 17 in *S. schlegelii* vs. 18 in both *S. ciliatus* and *S. variabilis*) and vertebrae (26 in both *S. taczanowskii* and *S. schlegelii* vs. 28–29 in *S. ciliatus* and *S. variabilis*). *Sebastes schlegelii* may also be distinguished by its typical dorsal-fin spine count of 12 (vs. 13 in *S. ciliatus* and *S. variabilis*).

Implications for fisheries management

The dusky rockfish (*S. variabilis*) and the dark rockfish (*S. ciliatus*) have been subjected to two distinct fisheries separately managed by U.S. federal and Alaska state agencies: *S. variabilis* is captured in the offshore trawl fishery; *S. ciliatus*, in the nearshore jig fishery. Although the offshore fisheries for dusky rockfish only incidentally catch the dark rockfish and are managed for dusky rockfish, the nearshore fishery is not managed for dark rockfish, and instead the species has been routinely misidentified as black rockfish (*S. melanops*). *Sebastes ciliatus* has been found to comprise up to 25% of the catch in the "black rockfish" jig fishery of the northern Gulf of Alaska (Clausen et al.[1]).

Several differences in biologically significant parameters were evident from specimens examined in our study and from observations in survey data. The two species are typically found in different habitats, attain different maximum sizes, and show differences in reproductive seasonality. Recognizing the two as distinct species is the first step towards establishing a biologically based, species-specific management scheme.

[8] Lauth, R. R. 1998. Personal commun. Resource Assessment and Conservation Engineering Division, Alaska Fisheries Science Center, Natl. Mar. Fish. Serv., NOAA, 7600 Sand Point Way NE, Seattle, WA 98115.

Acknowledgments

We appreciate the early efforts of J. Geil and J. Westrheim to encourage this research through spirited discussion and by providing unpublished data, courtesy of Fisheries and Oceans Canada, Pacific Biological Station. We thank D. Clausen, C. Lunsford, T. W. Pietsch, D. E. Stevenson, and M. E. Wilkins for overall reviews and K. Mier for a statistical review. The care and transportation of specimens from Alaska is not a small task and we thank the many collectors who made this project possible: fisheries observers W. Benecki, M. Brown, K. Barber, T. Droz, J. Peeples, and J. Wiersema; personnel of the AFSC's RACE Division W. C. Flerx, R. Harrison, R. R. Lauth, G. R. Hoff, M. Martin, N. W. Raring, J. S. Stark, H. Zenger, and M. Zimmermann. For support of nearshore field work in southeast Alaska, we thank J. Fujioka, D. Clausen, and B. Wing. The University of Washington Fish Collection archived most of the fresh material examined for this study and we appreciate the support of the curator (T. W. Pietsch) and collections managers (K. E. Pearson and B. W. Urbain). We also thank the following curators and collections managers and their institutions for hosting visits for examination of material or for the loan of specimens: B. Wing (ABL), K. Sendall (BCPM), W. Eschmeyer, D. Catania (CAS), B. Sheiko (KIE), J.-C. Hureau, G. Duhamel, P. Pruvost (MNHN), D. F. Markle (OSU), and G. D. Johnson, S. Jewett, and S. J. Raredon (USNM).

Literature cited

Ackley, D. R., and J. Heifetz.
2001. Fishing practices under maximum retainable bycatch rates in Alaska's groundfish fisheries. Alaska Fish. Res. Bull. 8(1):22–44.

Allen, M. J., and G. B. Smith.
1988. Atlas and zoogeography of common fishes in the Bering Sea and northeastern Pacific. NOAA Tech. Rep. NMFS 66, 151 p.

Alverson, D. L., and A. D. Welander.
1952. Notes on the scorpaenid fishes of Washington and adjacent areas, with a key for their identification. Copeia 1952:138–143.

Ayres, W. O.
1854. [Descriptions of new species of California fishes.] Proc. Calif. Acad. Sci. 1:1–22.
1862. [Descriptions of fishes believed to be new.] Proc. Calif. Acad. Sci. 2:209–218.
1863. Notes on the sebastoid fishes occurring on the coast of California, U.S.A. Proc. Zool. Soc. London 26:390–402.

Barsukov, V. V.
1964. Key to the fishes of the family Scorpaenidae. Soviet Fisheries Investigations in the northeast Pacific. Soviet Fisheries Investigations in the northeast Pacific 53:226–262.

Bauchot, M.-L., J. Daget, and R. Bauchot.
1997. Ichthyology in France at the beginning of the 19th century: the histoire naturelle des poissons of Cuvier (1769–1832) and Valenciennes (1794–1865), p. 27–80. *In* Collection building in ichthyology and herpetology (T. W. Pietsch and W. D. Anderson Jr., eds.), 593 p. Am. Soc. Ichthyol. Herpetol. Spec. Publ. 3.

Bauchot, M.-L., and M. Desoutter.
1986. Catalogue critique des types de poissons du Muséum national d'Histoire naturelle. Sous-ordre des Percoidei (familles des Apogonidae, Centrachidae, Centropomidae, Dinolestidae, Glaucosomatidae, Grammatidae, Kuhliidae, Percidae, Percichthyidae, Plesiopidae, Priacanthidae, Pseudochromidae, Teraponidae). Bull. Mus. natl. Hist. nat., Paris, 4e sér., 8, sect. A, 4 suppl.: 51–130.

Bentzen, P., J. M. Wright, L. T. Bryden, M. Sargent, and K. C. T. Zwanenburg.
1998. Tandem repeat polymorphism and heteroplasmy in the mitochondrial control region of redfishes (*Sebastes*: Scorpaenidae). J. Hered. 89:1–7.

Blanc, M., and J. C. Hureau.
1968. Catalogue critique des types de poissons du Muséum national d'Histoire naturelle (poissons à joues cuirassées), 70 p. Publ. Diverces Mus. Natl. Hist. Nat. 23.

Bookstein, F. L., B. Chernoff, R. L. Elder, J. M. Humphries Jr., G. R. Smith, and R. E. Strauss.
1985. Morphometrics in evolutionary biology, 177 p. Acad. Nat. Sci. Spec. Publ. 15, Philadelphia, PA.

Cuvier, G., and A. Valenciennes.
1829. Histoire naturelle des poissons. Vol. 4, 518 p. Strasbourg.

Eigenmann, C. H., and C. H. Beeson.
1894. A revision of the fishes of the subfamily Sebastinae of the Pacific coast of America. Proc. U.S. Nat. Mus. 17:375–407.

Eschmeyer, W. N., E. S. Herald, and H. Hammann
1983. A field guide to Pacific coast fishes of North America. Houghton Mifflin Company, Boston, MA, 336 p.

Evermann, B. W., and E. L. Goldsborough.
1907. The fishes of Alaska. Bull. Bur. Fish. 26:219–360.

Gunther, A. C. G.
1860. Catalogue of the fishes in the British Museum. Catalogue of the acanthopterygian fishes in the collection of the British Museum. Gobiidae to Notacanthi. Cat. Fishes 3:1–586.

Hallacher, L. E.
1974. The comparative morphology of extrinsic swimbladder musculature in the scorpionfish genus *Sebastes* (Pisces: Scorpaenidae). Proc. Cal. Acad. Sci. 40:59–86.

Hobson, T.
2002. *Sebastes mystinus*. *In* Rockfishes of the northeast Pacific (M. Love, M. Yoklavich, and L. Thorsteinson, eds.), p. 215–218. Univ. California Press, Los Angeles, CA.

Hubbs, C. L., and K. F. Lagler.
1958. Fishes of the Great Lakes region, revised ed. Cranbrook Inst. Sci. Bull. 26, 213 p.

Jordan, D. S.
1883. Notes on American fishes preserved in the museums at Berlin, London, Paris, and Copenhagen. Proc. Acad. Nat. Sci. Phila. 1884:281–293.
1885. A catalogue of fishes known to inhabit the waters of North America, north of the Tropic of Cancer, with notes on the species discovered in 1883 and 1884. Rep. U.S. Fish Comm. 13:789–973.
1896. Notes on fishes, little known or new to science. Proc. Calif. Acad. Sci. 6:201–244.

Jordan, D. S., and B. W. Evermann.
1898. The fishes of North and Middle America: a descriptive catalogue of the species of fish-like vertebrates found in the waters of North America, north of the Isthmus of Panama. Part II. Bull. U.S. Natl. Mus. 47:i–xxx, 1241–2183.

Jordan, D. S., and C. H. Gilbert.
1881. Description of *Sebastichthys mystinus*. Proc. U.S. Natl. Mus. 4:70–72.
1883. Synopsis of the fishes of North America. Bull. U.S. Natl. Mus. 16:i-liv + 1–1018.
Jordan, D. S., and P. L. Jouy.
1881. Checklist of duplicates of fishes from the Pacific coast of North America, distributed by the Smithsonian Institution in behalf of the U.S. National Museum. Proc. U.S. Natl. Mus. 4:8.
Kessler, D. W.
1985. Alaska's saltwater fishes and other sea life, 358 p. Alaska Northwest Publishing Co., Anchorage, AK.
Kramer, D. E., and V. O'Connell.
1986. Guide to northeast Pacific rockfishes genera *Sebastes* and *Sebastolobus*. Alaska Sea Grant, Mar. Adv. Bull. 25, 78 p.
1988. Guide to northeast Pacific rockfishes genera *Sebastes* and *Sebastolobus*. [1st revision.] Alaska Sea Grant, Mar. Adv. Bull. 25, 78 p.
1995. Guide to northeast Pacific rockfishes genera *Sebastes* and *Sebastolobus*. [2nd revision.] Alaska Sea Grant, Mar. Adv. Bull. 25, 78 p.
Leviton, A. E., and R. H. Gibbs Jr.
1988. Standards in herpetology and ichthyology. Standard symbolic codes for institutional resource collections in herpetology and ichthyology. Suppl. no. 1: additions and corrections. Copeia 1988:280–282.
Leviton, A. E., R. H. Gibbs Jr., E. Heal, and C. E. Dawson.
1985. Standards in herpetology and ichthyology: part I. Standard symbolic codes for institutional resource collections in herpetology and ichthyology. Copeia 1985:802–832.
Love, M. S.
2002. *Sebastes entomelas*. *In* Rockfishes of the northeast Pacific (M. Love, M. Yoklavich, and L. Thorsteinson, eds.), p. 172–174. Univ. California Press, Los Angeles, CA.
Love, M. S., M. Yoklavich, and L. Thorsteinson (eds.).
2002. The rockfishes of the northeast Pacific, 405 p. Univ. California Press, Los Angeles, CA.
Mecklenburg, C. W., T. A. Mecklenburg, and L. K. Thorsteinson.
2002. Fishes of Alaska, 1037 p. Am. Fish. Soc., Bethesda, MD.
Orr, J. W., M. A. Brown, and D. C. Baker.
1998. Guide to rockfishes (Scorpaenidae) of the genera *Sebastes*, *Sebastolobus*, and *Adelosebastes* of the northeast Pacific Ocean. NOAA Tech. Memo. NMFS-AFSC-95, 46 p.
2000. Guide to rockfishes (Scorpaenidae) of the genera *Sebastes*, *Sebastolobus*, and *Adelosebastes* of the northeast Pacific Ocean, 2nd ed. NOAA Tech. Memo. NMFS-AFSC-117, 48 p.
Orr, J. W., and R. Reuter.
2002. *Sebastes ciliatus*. *In* Rockfishes of the northeast Pacific (M. Love, M. Yoklavich, and L. Thorsteinson, eds.), p. 151–153. Univ. California Press, Los Angeles, CA.
Paepke, H.-J., and R. Fricke.
1992. Critical catalog of the types of the fish collection of the Zoological Museum Berlin. Part 4: Scorpaeniformes. Mitt. Zool. Mus. Berl. 68:267–293.
Pallas, P. S.
1814. Zoographia Rosso-Asiatica, sistens omnium animalium in extenso Imperio Rossico et adjacentibus maribus observatorum recensionem, domocilia, mores et descriptiones, anatomen atque iconem plurimorum. Petrop., Acad. Sci., vol. 3, 428 p.
Peden, A. E., and D. E. Wilson.
1976. Distribution of intertidal and subtidal fishes of northern British Columbia and southeastern Alaska. Syesis 9:221–248.
Pierce, R. A.
1990. Russian America: a biographical dictionary. Alaska Historical Commission Studies in History, No. 132, 555 p. Limestone Press, Fairbanks, AK.
Pietsch, T. W. (ed.)
1995. Historical portrait of the progress of ichthyology, from its origins to our own time, by Georges Cuvier, 366 p. Edited and annotated by T. W. Pietsch, translated from the French by A. J. Simpson. Johns Hopkins Univ. Press, Baltimore, MD.
Poss, S., and B. B. Collette.
1995. Second survey of fish collections in the United States and Canada. Copeia 1995:48–70.
Quast, J. C., and E. L. Hall.
1972. List of fishes of Alaska and adjacent waters with a guide to some of their literature. NOAA Tech. Rep. NMFS SSRF-658, 47 p.
Reuter, R. F.
1999. Describing dusky rockfish (*Sebastes ciliatus*) habitat in the Gulf of Alaska using historical data. Unpubl. MS thesis, 83 p. California State Univ., Hayward, CA.
Richards, L. J., and S. J. Westrheim.
1988. Southern range extension of the dusky rockfish, *Sebastes ciliatus*, in British Columbia. Can. Field-Nat. 102:251–253.
Roques, S., J.-M. Sévigny, and L. Bernatchez.
2001. Evidence for broadscale introgressive hybridization between two redfish (genus *Sebastes*) in the North-west Atlantic: a rare marine example. Mol. Ecol. 10:149–165.
Schmidt, P. Y.
1950. Fishes of the Sea of Okhotsk. Academy of Sciences of the USSR, Transactions of the Pacific Committee, vol. 6, Moscow-Leningrad, 392 p. [In Russian, 1965 transl. by the Israel Prog. Sci. Trans. Available from the National Technical Information Service, Springfield, VA.]
Schultz, L. P.
1936. Keys to the fishes of Washington, Oregon and closely adjoining regions. Univ. Washington Publ. Biol. 2:103–228.
Seeb, L.
1986. Biochemical systematics and evolution of the scorpaenid genus *Sebastes*. Ph.D. diss., 176 p. Univ. Washington, Seattle, WA.
Shinohara, G., M. Yabe, and T. Honma.
1994. Occurrence of the scorpaenid fish, *Sebastes ciliatus*, from the Pacific coast of Hokkaido, Japan. Bull. Biogeogr. Soc. Japan 49:61–64.
Stewart, E., and M. Love.
2002. *Sebastes melonops*. *In* Rockfishes of the northeast Pacific (M. Love, M. Yoklavich, and L. Thorsteinson, eds.), p. 204–207. Univ. California Press, Los Angeles, CA.
Sundt R. C., and T. Johansen.
1998. Low level of interspecific DNA sequence variation of the mitochondrial 16S rDNA in north Atlantic redfish *Sebastes* (Pisces, Scorpaenidae). Sarsia 83:449–452.
Svetovidov, A. N.
1978. The types of the fish species described by P. S. Pallas in "Zoographi Rosso-Asiatica" (with a historical account of publication of this book). Nauka, Leningrad, 35 p. [In Russian.]
1981. The Pallas fish collection and the Zoographia Rosso-Asiatica: an historical account. Arch. Nat. Hist. 10:45–64.

Tilesius, W. G. von.
1813. Iconum et descriptionum piscium Camtschaticorum continuatio tertia tentamen monographiae generis Agoni Blochiani sistens. Mem. Acad. Imp. Sci. St. Petersb. 4:406–478.

Tsuyuki, H., E. Roberts, and W. E. Vanstone.
1965. Comparative zone electropherograms of muscle myogens and blood hemoglobins of marine and freshwater vertebrates and their application to biochemical systematics. J. Fish. Res. Board Canada 22:203–213.

Tsuyuki, H., E. Roberts, R. H. Lowes, W. Hadaway, and S. J. Westrheim.
1968. Contribution of protein electrophoresis to rockfish (Scorpaenidae) systematics. J. Fish. Res. Board Canada 25:2477–2501.

Westrheim, S. J.
1968. First records of three rockfish species (*Sebastodes aurora*, *S. ciliatus*, and *Sebastolobus altivelis*) from waters off British Columbia. J. Fish. Res. Board Canada 25: 2509–2513.
1973. Preliminary information on the systematics, distribution, and abundance of the dusky rockfish, *Sebastes ciliatus*. J. Fish. Res. Board Can. 30:1230–1234.

Appendix

Material examined

Sebastes ciliatus Bering Sea: UW 45488, 1(329.7 mm), 56.65°N, 167.8167°W, 100 m depth, 5 February 2001; UW 22474, 1(221.7 mm), 59.25°N, 177.8167°W, 160 m depth, 1987. Aleutian Islands: UW 43447, 1(290 mm), 51.2534°N, 179.2689°E, 165 m depth, 26 July 1997; UW 45588, 2(240–380 mm), Aleutian Is., FV *Vesteraalen*, 1997; ABL 69-13, 2(228.8–250.9 mm), Amchitka I., Constantine Harbor, 51.4°N, 179.3667°E, 6 September 1968; UW 46489 (UK T002383), 1(279.7 mm), 51.2707°N, 179.2118°E, 98 m depth, 26 July 1997; UW 45498, 1(318.5 mm), 51.9921°N, 174.1031°W, 93 m depth, 6 July 1997; UW 43039, 4(83.8–206.5 mm), Amchitka I., Constantine Harbor, off Kirilof, 7 December 1961; UW 43423, 2(295.1–315.9 mm), Amchitka I., 51.3833°N, 178.9°E, 88 m depth, 20 April 1993; UW 43436, 12(272–315 mm), 51.7552°N, 175.6726°E, 94 m depth, 1 August 1997; UW 14416, 1(183 mm), Amchitka I., Constantine Harbor, 5 September 1955; UW 43458, 5(263.9–288.6 mm), 51.2707°N, 179.2118°E, 98 m depth, 26 July 1997; UW 4766, 1(189 mm), Atka I., Atka village, 18 August 1938; UW 46483, 2(230–253 mm), 51.9730°N, 176.0841°E, 78 m depth, 20 July 2000; UW 46484, 2(275–293 mm), 51.9638°N, 176.0288°E, 64 m depth, 20 July 2000; UW 47417, 1(320 mm), Aleutian Is., recovered from stomach of *Gadus macrocephalus*. Gulf of Alaska: UW 43242, 6(320–390 mm), 53.7345°N, 165.5425°W, 89 m depth, 25 June 1996; UW 43272, 5(274–325.5 mm), 55.093°N, 157.8048°W, 76 m depth, 10 June 1996; UW 43420, 1(334.7 mm), 55.9042°N, 157.0751°W, 101 m depth, 18 June 1996; UW 45508, 2(242.4–292.6 mm), 55.1056°N, 157.9594°W, 78 m depth, 2 June 1999; UW 45512, 1(235.2 mm), 57.3806°N, 154.8009°W, 67 m depth, 7 June 1999; UW 45509, 1(298 mm), 54.3215°N, 161.8107°W, 72 m depth, 23 May 1999; UW 47412, 1(323.7 mm), 52.8953°N, 168.297°W, 99 m depth, 21 May 2001; UW 46488, 1(270 mm), 56.3686°N, 154.0495°W, 69 m depth, 24 June 2001; UW 46584, 1(295 mm), 55.1056°N, 157.9594°W, 78 m depth, 2 June 1999; UW 46485, 1(320.1 mm), 55.01862°N, 157.882°W, 76 m depth, 8 June 2001. Kodiak Island area: UW 43059, 1(200.7 mm), Kodiak I., Monashka Bay, SW of Trenton Pt., 57.8367°N, 152.4°W, 28 July 1977; UW 47289, 2(169–203.7 mm), Kodiak I., Monashka Bay, 5 m depth, 57.8383°N, 152.4283°W, 5 m depth, 31 July 1982; UW 44035, 2(216.7–274.5 mm), Kodiak I., Monashka Bay, 57.8367°N, 152.4°W, 18 m depth, 2 August 1982; UW 44036, 11(178.2–263.7 mm), Kodiak I., Monashka Bay, 57.8383°N, 152.4283°W, 12 m depth, 3 August 1982; UW 44045, 19(140.6–307.8 mm), Kodiak I., Monashka Bay, 57.8383°N, 152.4283°W, 15 m depth, 12 August 1982; UW 44049, 1(291.6 mm), Kodiak I., Monashka Bay, 57.8383°N, 152.4283°W, 12 m depth, 11 September 1982; UW 44050, 1(331 mm), NE of Kodiak I., Triplets Is., 57.98°N, 152.48°W, 18 m depth, 1 July 1983; UW 44051, 1(319.7 mm), Kodiak I., Monashka Bay, 57.8367°N, 152.4°W, 6 m depth, 14 October 1982. Southeast Alaska: ABL 60-7, 1(164 mm), Kuiu I., Washington Bay, ca. 5 mi W of Petersburg, 2 June 1960; ABL 62-105, 1(224.5 mm), Little Port Walter, SE tip of Baranoff I.; ABL 68-295, 1(214.1 mm), NW tip of Lincoln I., ca. 5 mi N of Pt. Retreat, Lynn Canal, 7.5 m depth, 4 July 1968; ABL 87-15, 1(111.8 mm), Port Althorp, 58.1317°N, 136.3333°W, 126–146 m depth, 18 July 1982; UW 43484, 17(202.8–315 mm), Cross Sound, Chichagof I., Soapstone Cove, 58.1°N, 136.5°W, 25 m depth, 11 July 1998; UW 43485, 19(124.4–264.7 mm), Lisianski Strait, 57.925°N, 136.288°W, 10 m depth, 12 July 1998; UW 43492, 3(153.7–241.1 mm), Lynn Canal, Funter Bay, 58.2467°N, 134.8983°W, 25 m depth, 13 July 1998; UW 22426, 2(134.8–169.4 mm), Alexander Archipelago, Biorka Channel, S. of Sitka, 33 m depth, 21 February 1982.

Sebastes variabilis Japan: HUMZ 125816, 1(334.0 mm), Pacific coast off Kushiro, Hokkaido, 42.6833°N, 144.7667°E, 200 m depth, 2 March 1993. Bering Sea: KIE 1277, 1(320.3 mm), east coast of Kamchatka off Cape Ol'utorskii, 60.4667°N, 171.75°E, 370 m depth, 18 August 1994; KIE 1409, 2(334.5–344.7 mm), Commander Is., Bering I., 55°N, 166.05°E, 90–120 m depth, 30 April 1996; KIE uncat, 1(324.5 mm), Karaginskiy Bay, 1 August 1998; UW 43500, 1(314.5 mm), 55.3179°N, 167.5503°W, 147 m depth, 3 July 1998; UW 43499, 1(370 mm), 56.7°N, 163.4°W, 77 m depth, 18 June 1998; UW 43498, 3(330–340 mm), 54.4763°N, 159.6925°W, 4 June 1996; UW 40308, 1(180 mm), 55.36°N, 163.44°W, 84 m depth, 7 May 1990; UW 40311, 1(187 mm), 55.55°N, 163.75°W, 84 m depth, 3 May 1990; UW 44166, 1(339.3 mm), Alaska, "2-1-92" at 1800 hours; UW 44182, 2(258.2–266 mm), FV *Yukon Challenger*, haul 105, 8 March 1993; UW 44253, 1(430.8 mm), Aleutian Is., 52.3°N, 173.8–174.7°W, 106–113 m depth, 10 April 1991; UW 44255, 1(375.7 mm), 56.4192°N, 152.853°W, 182 m depth, 24 March 1990; UW 44261, 1(331.1 mm), 57.3333°N, 151.4167°W, 128 m depth; UW

47411, 1(360 mm), Bering Sea, winter 2001, P. J. Sullivan. Aleutian Islands: UW 43480, 1(370 mm), 51.2522°N, 179.199°E, 173 m depth, 20 July 1997; UW 43460, 1(340 mm), Aleutian Is., FV *Dominator*, summer 1997; UW 43438, 5(330–370 mm), 51.9252°N, 176.3817°W, 122 m depth, 23 July 1997; UW 43455 (KU T002038), 1(275 mm), 51.2707°N, 179.2118°E, 98 m depth, 26 July 1997; UW 45499, 2(327–330 mm), 51.9921°N, 174.1031°W, 93 m depth; UW 45632, 3(83.3–126.1 mm), Amchitka I., NE of Sand Beach Cove, 51.5°N, 179°E, 36 m depth, 20 August 1971; UW 45460, 1(98.7 mm), 54.0386°N, 166.6406°W, 85 m depth, 22 May 2000; UW 43441, 2(380–381 mm), 54.17902°N, 166.3255°W, 240 m depth, 12 June 1997; UW 43442, 1(355 mm), 54.0386°N, 166.6572°W, 90 m depth, 13 June 1997; UW 43445, 2(315–340 mm), 54.3773°N, 165.608°W, 90 m depth, 11 June 1997; UW 43459 (KU T002038), 1(264.2 mm), 51.2707°N, 179.2118°E, 98 m depth, 26 July 1997; UW 43461, 1(330 mm), 53.6905°N, 167.2648°W, 112 m depth, 13 June 1997; UW 43416, 1(290 mm), 54.796°N, 163.2772°W, 89 m depth, 1 June 1996; UW 43443, 1(230 mm), 52.8589°N, 172.4586°E, 146 m depth, 5 August 1997; UW 43444, 1(220 mm), 52.8589°N, 172.4586°E, 146 m depth, 5 August 1997; UW 45588, 2(350–350 mm), Aleutian Is., FV *Vesteraalen*, summer 1997; UW 46482, 4(175–225 mm), 52.8280°N, 168.9904°W, 44 m depth, 20 May 2001. Gulf of Alaska: UW 43204, 7(350–420 mm), 55.4327°N, 158.9439°W, 155 m depth, 8 June 1996; UW 43200, 6(320–390 mm), 55.2924°N, 156.6652°W, 114 m depth, 12 June 1996; UW 43214, 1(190 mm), 57.3175°N, 154.8356°W, 82 m depth, 21 June 1996; UW 43212, 1(300 mm), 54.9351°N, 157.4668°W, 153 m depth, 12 June 1996; UW 43201, 8(290–380 mm), 54.1125°N, 161.7306°W, 111 m depth, 1 June 1996; UW 43203, 8(305–405 mm), 54.1125°N, 161.7306°W, 111 m depth, 1 June 1996; UW 43211, 2(380–410 mm), 54.6806°N, 158.9407°W, 95 m depth, 8 June 1996; UW 43213, 1(345 mm), 53.9849°N, 163.2663°W, 108 m depth, 30 May 1996; UW 43416, 1(290 mm), 54.7960°N, 163.2772°W, 89 m depth, 1 June 1996; UW 43417, 1(241.4 mm), 55.2898°N, 158.3123°W, 130 m depth, 10 June 1996; UW 43377, 1(356.4 mm), 55.6441°N, 134.9706°W, 202 m depth, 26 July 1996; UW 45587, 4(325.3–376.2 mm), 55.4351°N, 156.5458°W, 167 m depth, 15 June 1996; UW 44123, 1(85.3 mm), 57.2128°N, 152.7898°W, 135 m depth, 24 October 1997; KU T3178, 1(348.7 mm), 58.8191°N, 140.3303°W, 185 m depth, 14 July 1999; KU T003215, 1(324.3 mm), 58.8191°N, 140.3303°W, 185 m depth, 14 July 1999; KU T003216, 1(373.9 mm), 58.8191°N, 140.3303°W, 185 m depth, 14 July 1999; USNM 32014, 1(240.1 mm), Tolstoi Bay, October 1882; UW 45477, 2(351.5–352.8 mm), 59.1787°N, 149.1194°W, 157 m depth, 29 June 1999; UW 45510, 4(335–370 mm), 58.9658°N, 148.1749°W, 251 m depth, 14 July 1996; UW 45511, 3(206.2–213.4 mm), 57.3806°N, 154.8009°W, 67 m depth, 7 June 1999; UW 46487, 1(333.1 mm), 52.8953°N, 168.297°W, 99 m depth, 21 May 2001; UW 43427, 1(350 mm), 54.2758°N, 161.4326°W, 122 m depth, 3 June 1996; UW 43428, 1(315 mm), 55.9042°N, 157.0751°W, 101 m depth, 18 June 1996; UW 43466, 1(380 mm), 59.4469°N, 140.4849°W, 226 m depth, 30 July 1993; UW 43471, 1(371.7 mm), 58.0895°N, 150.5977°W, 141 m depth, 5 August 1993; UW 43473, 1(342 mm), 59.4469°N, 140.4849°W, 226 m depth, 18 July 1996; UW 22475, 2(240–270 mm), 54.0167°N, 160.8°W, 170 m depth, 4 November 1981; UW 40912, 1(213.6 mm), Prince William Sound, 60.5658°N, 147.5866°W, 70 m depth, 2 October 1989; UW 43214, 1(187.9 mm), 57.3175°N, 154.8356°W, 82 m depth, 21 June 1996; UW 43251, 8(320–420 mm), 59.5045°N, 145.2262°W, 135 m depth, 17 July 1996. Kodiak Island area: ABL 66-890, 1(103 mm), Marmot Bay, Kodiak I., 57.9333°N, 152.1167°W, 1964; UW 44052, 1(215.5 mm), Kodiak; UW 44032, 1(93.4 mm), Cook Inlet, Kachemak Bay, 59.6°N, 151.3°W, "<50 m" depth, 8 September 1981; UW 44033, 2(95.7–112 mm), Cook Inlet, Kachemak Bay, 59.6°N, 151.3°W, "<50 m" depth, 10 October 1981; UW 47148, 5(95.5–112 mm), Cook Inlet, Kachemak Bay, 59.6°N, 151.3°W, 10 October 1981; UW 44034, 1(363 mm), NE of Kodiak I., Triplets Is., 57.98°N, 152.48°W, 20–24 m depth, 1 July 1982; UW 44037, 1(335 mm), E of Kodiak I., 57.72–57.87°N, 151.8–152.2°W, crab pot, 18 August 1982; UW 44038, 2(275.3–310 mm), 57.975°N, 151.8433°W, 144 m depth, 19 August 1982; UW 44039, 3(266.7–300.4 mm), Kodiak I., Monashka Bay, 57.8367°N, 152.4°W, 15 m depth, 31 August 1982; UW 44040, 5(269.7–303.7 mm), Kodiak I., Monashka Bay, 57.8367°N, 152.4°W, 20 m depth, 14 October 1982; UW 44041, 1(281.1 mm), NE of Kodiak I., Triplets Is., 57.98°N, 152.48°W, 20 m depth, 2 July 1983; UW 43381, 1(340 mm), Triplets Is., hook and line, 57.98°N, 152.48°W, 34 m depth, 15 July 1993; UW 44042, 2(199.5–215.8 mm), Shelikof Strait off mouth of Uyak Bay, 57.7°N, 153.92°W, 100 m depth, 2 April 1984; UW 44043, 12(231.3–271.3 mm), Shelikof Strait; UW 44044, 2(229.6–257.8 mm), Kodiak I., Monashka Bay, jig, 57.8367°N, 152.4°W, 15 m depth, 12 August 1982; UW 44046, 1(302 mm), E of Kodiak I., 58.5217°N, 151.3333°W, 154 m depth, 21 August 1982; UW 44047, 1(321.7 mm), E of Kodiak I., 58.85°N, 151.8167°W, 113 m depth, 21 August 1982; UW 44048, 1(318.3 mm), Kodiak I., Monashka Bay, 57.8367°N, 152.4°W, 18 m depth, 11 September 1982; UW 46486, 1(278.5 mm), 56.6941°N, 151.9115°W, 59 m depth, 27 June 2001; UW 47362, 3(122–219 mm), 56.3686°N, 154.0495°W, 69 m depth, 24 June 2001. Southeast Alaska: UW 43495, 1(262 mm), Lynn Canal, N of Funter Bay, 58.03°N, 134.8967°W, 40 m depth, 13 July 1998; ABL 66-156, 1(269.4 mm), Barlow Cove, 19 mi NW of Juneau, 58.3197°N, 134.8967°W, 12 February 1967; ABL 68-301, 1(249.8 mm), Lynn Canal, off reef at N end of Little I., ca. 9 mi N of Pt. Retreat, 58.5417°N, 135.0433°W, 3 August 1968; ABL 69-116, 2(77.7–136.3 mm), Chichagof I., Ogden Passage between Khaz Bay and Portlock Harbor, 57.6333°N, 136.1617°W, 10 September 1969; ABL 69-122, 2(82–82.1 mm), Chichagof I., Icy Strait off SE end of Pleasant I., 58.3333°N, 135.6333°W; ABL 70-103, 1(173.2 mm), Gastineau Channel, Marmion I., ca. 9 mi. S of Juneau, 58.2°N, 134.2533°W, 10 July 1970; UW 43494, 11(150.7–225.2 mm), Lynn Canal, Funter Bay, 58.2467°N, 134.8988°W, 37 m depth, 13 July 1998; UW 44117, 26(153.8–272.7 mm), Funter Bay, 58.2467°N, 134.8983°N, 40 m depth, 13 July 1998; UW 44118, 5(151.9–190.0 mm),

Funter Bay, 58.2467°N, 134.8983°W, 40 m in depth, 13 July 1998; UW 46526, 12(48.0–93.5 mm), Sitka Sound, Middle I., 57.1°N, 135.45°W, 4 June 2001; UW 48866, 3(78.1–156.7 mm), Alexander Archipelago, Biorka Channel, S of Sitka, 33 m depth, 21 February 1982. British Columbia: BCPM 974-0623-001, 5(342–367 mm), Hecate Strait, Moresby Gully, RV *G. B. Reed*, 52.31°N, 130.4867°W, 185–199 m depth, 14 September 1974; BCPM 974-416, 1(154.7 mm), Dundas I., Brundige Inlet, reef at entrance to E arm, 1–5 m depth; BCPM 974-419, 1(124.8 mm), Dundas Is., Brundige Inlet, just N of island at entrance to E arm, 54.6043°N, 130.8612°W, 6–15 m depth, 19 June 1974; BCPM 974-434, 2(108.3–113.8 mm), mouth of Brundige Inlet E shore, 8–12 m depth; BCPM 974-447, 2(168.9–175.6 mm), Welcome Harbour channel, 54.0225°N, 130.6133°W, 6–12 m depth, 2 July 1974; BCPM 974-467, 2(127.9–162.1 mm), off Parkin Islets (E side), 54.6261°N, 130.4639°W, 6–8 m depth, 12 July 1974; BCPM 974-468, 1(120 mm), off N tip of Birnie Is., 54.6045°N, 130.4508°W, 6–12 m depth, 13 July 1974; BCPM 974-485, 1(129.9 mm), off island in Griffith Harbor, 53.6011°N, 130.5486°W, 5–8 m depth, 20 July 1974; BCPM 974-489, 2(145.8–151.5 mm), Safa Islets, 54.7733°N, 130.6067°W, 6–18 m depth, 28 July 1974. Oregon: UW 46575, 1(355 mm), 44.4°N, 124.783°W, 265 m depth, 17 May 2002.

Significant comparative material examined

Sebastes melanops USNM 342, syntypes, Cape Flattery, Washington, and Astoria, Oregon; UW 47037, 1(350 mm), Bering Sea, 55.2333°N, 164.65°W, 2 February 2002; UW 43490, 3(195–230 mm), Cross Sound, Chichagof I., Soapstone Cove, 58.1°N, 136.5°W, 25 m depth, 11 July 1998; UW 47288, 2(163–182 mm), Kodiak I., Monashka Bay, 5 m depth, 57.8383°N, 152.4283°W, 5 m depth, 2 August 1982.

Sebastes mystinus USNM 27031, syntype, 1(346 mm), Monterey, California; USNM 27085, syntype, 1(269 mm), Monterey, California; USNM 26971, syntype, 1(212 mm), Monterey, California.

Sebastes polyspinis USNM 60243, 2(75.3–141.3 mm), Alaska, Chignik Bay, 13.6 km S of Tuliumnit Point, 56°N, RV *Alabatross*, Sta. 4285, 57–108 m depth, 10 August 1903.

Recruitment as an evolving random process of aggregation and mortality

Joseph E. Powers

Southeast Fisheries Science Center
National Marine Fisheries Service, NOAA
75 Virginia Beach Drive
Miami, FL 33149

E-mail address: joseph.powers@noaa.gov

Abstract—The dynamics of the survival of recruiting fish are analyzed as evolving random processes of aggregation and mortality. The analyses draw on recent advances in the physics of complex networks and, in particular, the scale-free degree distribution arising from growing random networks with preferential attachment of links to nodes. In this study simulations were conducted in which recruiting fish 1) were subjected to mortality by using alternative mortality encounter models and 2) aggregated according to random encounters (two schools randomly encountering one another join into a single school) or preferential attachment (the probability of a successful aggregation of two schools is proportional to the school sizes). The simulations started from either a "disaggregated" (all schools comprised a single fish) or an aggregated initial condition. Results showed the transition of the school-size distribution with preferential attachment evolving toward a scale-free school size distribution, whereas random attachment evolved toward an exponential distribution. Preferential attachment strategies performed better than random attachment strategies in terms of recruitment survival at time when mortality encounters were weighted toward schools rather than to individual fish. Mathematical models were developed whose solutions (either analytic or numerical) mimicked the simulation results. The resulting models included both Beverton-Holt and Ricker-like recruitment, which predict recruitment as a function of initial mean school size as well as initial stock size. Results suggest that school-size distributions during recruitment may provide information on recruitment processes. The models also provide a template for expanding both theoretical and empirical recruitment research.

Manuscript approved for publication
10 December 2003 by Scientific Editor.

Manuscript received 20 January 2004
at NMFS Scientific Publications Office.

Fish. Bull. 102:349–365 (2004).

The study of recruitment processes has traditionally addressed mortality (predation and starvation) and the effects of patchiness on mortality (Vlymen, 1977; Beyer and Laurence, 1980; Hunter, 1984; Rothschild, 1986); hence the importance of aggregation and mortality in recruitment processes of marine fish populations has long been noted. Ecological processes of starvation, growth, and predation of larval fish, coupled with oceanographic factors show the inherent variability in these processes (Koslow, 1992; Mertz and Myers, 1994, 1995; Pepin, 1991; Rickman et al., 2000; Comyns et al., 2003). In particular Rickman et al. (2000) have indicated the importance of the magnitude of fecundity in the variability of egg and larval mortality. Indeed, Koslow (1992) argued that fecundity and the associated variability in egg and larval mortality will limit our ability to determine stock-recruitment relationships.

Stock-recruitment models have generally emphasized the static results of recruitment processes rather than the dynamics themselves. Indeed, although the classic stock-recruitment models such as the Beverton-Holt and Ricker have been related to microscale processes (Beverton and Holt, 1957; Ricker, 1958; Paulik, 1973; Harris, 1975), the dynamics at those scales were not explored, primarily because there was not a theoretical basis for doing so (Rothschild, 1986). Nevertheless, there is a need to develop a theoretical understanding of small-scale interaction processes during recruitment, particularly as they relate to group formation.

Group-formation (aggregation of fish into schools), schooling (shoaling) behavior, and the evolutionary motivations for formation of schools continue to be important research topics (Pitcher and Parrish, 1993; Landa, 1998). Schooling behavior has variously been attributed to predator-avoidance, predator-attack dilution, and hydrodynamic and foraging advantages (see Pitcher and Parrish, 1993, for a review). One of the first models for school formation was that of Anderson (1981) in which he empirically observed skewed distributions in which small schools were more prevalent than larger ones. Subsequently, Bonabeau and Dagorn (1995), Gueron and Levin (1995), Niwa (1998), and Bonabeau et al. (1999), developed group-size distribution models. In particular, Bonabeau et al. (1999) in comparing group-size distributions of tunas, sardinella, and buffalo suggested that power-law distributions may be quite generic. Niwa (1998) noted that Anderson's original model allowed for power-law distributions. Power-laws are termed scale-free because they exhibit no intrinsic scale. Similarly, existence of a power-law is often referred to as "scaling."

Recently, power-law distributions have arisen in studies of the physics of small-world and evolving networks (for example the world wide web, actor collaborations, scientific citations [Barabási and Albert,1999], biological cellular networks [Fell and Wagner, 2000], and ecosystem structure [Solé and Montoya, 2001]). In particular, Barabási and Albert (1999) demonstrated that a randomly evolving network would result in a scale-free degree distribution if the network is growing

(the number of nodes is increasing) and if the new nodes were linked to existing nodes by preferential attachment. Preferential attachment (or the "rich-get-richer" phenomenon) occurs when a new node is linked to an existing node with a probability proportional to the number of links already attached to that node. More formally, the Barabasi and Albert model is created by adding a new node at each time step and by randomly linking it to m existing nodes proportional to the number of links at the existing nodes. After a large number of time steps, the probability of a node having k links (the degree distribution) scales as a power-law $P(k) \sim k^{-\gamma}$, where $\gamma = 3$, independent of m. The Barabási and Albert result differs from the classic random network model of Erdös and Rényi (1960) in which nodes are linked randomly to existing nodes, leading to $P(k) \sim exp(-\lambda k)$. Subsequent research has expanded on the Barabási and Albert model to examine aging, removal and rewiring of nodes, removal of links, fitness and attractiveness of nodes, and local modifications to preferential attachment (see Albert and Barabási, 2002, for a review of these developments).

The generic occurrence of scale-free school-size distributions suggest that modeling of aggregation and mortality processes using the analogy of random networks may be fruitful. The approach may provide insight into recruitment dynamics and a theoretical basis for further investigation. This study attempts to do that and is organized in the following manner. First, a simulation model of the recruitment process is developed in which aggregation and mortality occur based upon some simple rules of preferential attachment and random attachment. Attachment rules are presented as metaphors for more complex behaviors. Next, analytical models are created that mimic the simulations, and results of the simulations and analytical models are compared. Finally, the implications for existing stock-recruitment models and investigation of recruitment processes are discussed.

Methods

Simulation of individuals in ecology and population dynamics (individual-based models) have become increasingly popular (McCauley et al., 1993). However, it is often difficult to understand the dynamics of large individually based models (Pascual and Levin, 1999). Thus, it is important to obtain models that describe dynamics of groups that incorporate individual behavior (Flierl et al., 1999). The models that are developed here include an individually based model (simulation model) and an analytical model that describes "mean-field" dynamics of the individuals behavior.

Simulation model

The recruiting fish of a year class may be modeled as a network of fish in which a fish "links" to other fish to form schools. (Note that in this context it is assumed that a "school" includes aggregations consisting of a single fish). Thus, the process of aggregation is a process of adding links to nodes (aggregation of schools). Similarly, mortality is the removal of nodes (fish) and, if there are no more fish in the school, then the removal of schools. A simulation model with simple rules of mortality and aggregation was created to examine the dynamics of these processes.

The simulation model followed individual fish and schools through a recruitment period, i.e., the passage of time until an arbitrary time of recruitment. During a recruitment period fish and schools undergo encounters of mortality and aggregation. Starting at time $t=0$ with S fish, $N_{t=0}$ schools and $k_{i,t=0}$ fish in school i ($i=1,2, \ldots, N_0$), simulations were conducted by randomly generating an encounter event (mortality or aggregation). If the event was a mortality, then a school was randomly selected by using the appropriate mortality rate model (m, discussed below). If the size of that school was greater than one, then that size was reduced by one. If the school size was equal to one, then the number of schools was reduced by one and this school was eliminated from the list.

If the event was an aggregation, then two distinct schools were randomly selected by using the appropriate aggregation rate model (w, also discussed below). The two schools were combined, leaving one school whose size was the sum of the two original ones and one fewer total number of schools. The probability of an event being a mortality was $m/(m+w)$ and the converse probability of an aggregation was $1-m/(m+w)$. Time increments of each event were computed using $\Delta t = m^{-1}$ for mortality events and $(mw)^{-1}$ for aggregation events. Results at time t were collated into the number of fish surviving to time t (denoted by R_t), the number of schools, N_t, the school size distribution, $P_t(k)$, and the average school size, $\bar{k}_t$. Note that $R_t = N_t \bar{k}_t$. Simulations were run until there were no fish left.

Encounter rates The encounter rates, m and w, were based upon random movements in statistical mechanics (Tolman, 1979) in which the encounter rate (U) of objects of type i with objects of type j is described by

$$U = (G_i + G_j) D_i D_j (v_i^3 + v_j^3)^{1/3}, \quad (1)$$

where G_i = the size of the detection space at which object detects object type j;
D_i = the density of objects of type i; and
v_i = the velocity (in three-dimensional space) at which object i moves in the environment.

For these simulations the G parameters were scaled to one and the velocity parameters (v's) were collapsed into two encounter rates: μ for mortality encounters (scaled to unity) and α for aggregation encounters.

Mortality rate In the simulations, mortality of fish is perpetrated by mortality agents. If the mortality agents randomly encounter schools of fish, then the probability of a successful mortality (the removal of a fish from the system) is proportional to the school size k. Under these conditions Equation 1 reduces to Equation 2 with

$$\begin{aligned} G_i = G_j = 1, (v_i^3 + v_j^3)^{\frac{1}{3}} &= \mu; \\ m &= 2\mu E N k, \end{aligned} \quad (2)$$

where E = the density of mortality agents; and
μ = the encounter rate of fish with mortality agents.

Note that on average Equation 2 reduces to $m = 2\mu E_t N_t \bar{k}_t = 2\mu E_t R_t = -dR/dt$. Hence, if the density of mortality agents is constant throughout the recruitment period, then mortality is density independent and mortality is proportional to abundance. An alternative interpretation of Equation 2 is that the mortality agents randomly encounter fish and that all encounters result in a successful mortality. The mortality model (Eq. 2) will be referred to as m_{di} (for density-independent). It is not expected that m_{di} is the most realistic, but rather it provides a basis for comparison.

A second mortality alternative is where mortality agents randomly encounter schools, whereupon they always perpetrate a successful mortality: $m_N = 2\mu E_t N_t$. This model, like m_{di}, assumes that the density of mortality agents are constant throughout the recruitment period.

For purposes of simulation, the density of mortality agents at the onset of the recruitment process was specified to be unity (E_0=1). For the two mortality models, m_{di} and m_N, this meant that E=1 throughout a simulation.

More realistic density-dependent mortality models are immediately suggested. The first is a density-dependent model in which the ratio of mortality-agent density to the number of schools remains constant throughout the recruitment period, i.e., E_t/N_t remains constant throughout the recruitment period. This leads to $m_{dN} = 2\mu N^2 k$, where E_t/N_t was set equal to one. In this model the ratio of mortality agents to schools is constant, agents and schools randomly encounter one another, and the probability of a successful mortality (given there is an encounter) is proportional to the number of fish that are in the school that is encountered (mortality success is related *preferentially* toward larger schools).

A second density-dependent model is where the mortality agent density is proportional to the number of fish (E_t/R_t is a constant set equal to one, $m_{dR}=2\mu R^2=2\mu N^2 k^2$). In this model the ratio of mortality agents to the number of fish in the population is constant; agents and schools randomly encounter one another; and the probability of a successful mortality (given there is an encounter) is proportional to the number of fish that are in the school that is encountered (mortality success related preferentially toward larger schools). Another interpretation of this model is that agents randomly encounter fish, at which time the fish suffers mortality at a probability independent of school-size characteristics.

A third density-dependent model depicts mortality-agent density proportional to school size (E_t/k_t is a constant set equal to one, $m_{dk}=2\mu Nk^2$). In this model the ratio of mortality agents to mean school size is constant, agents and schools randomly encounter one another, and the probability of a successful mortality (given that there is an encounter) is proportional to the number of fish that are in the school that is encountered. Another interpretation of this model is that agent density is proportional to the number of schools, agents encounter schools preferentially according to school size, and the probability of a successful mortality (given that there is an encounter) is proportional to the number of fish that are in the school that is encountered.

Subsequently it will be shown that the first density-dependent model is related to a Ricker-like stock-recruitment model and the second model is exactly equivalent to a Beverton-Holt model. Definitions of the mortality models are summarized in Table 1. Note that in the initial applications of these mortality models, it is assumed that a mortality encounter results in mortality of one fish. More detailed mortality models in which a number of fish greater than one are removed by mortality may be implemented in the future. Clearly, these would be more biologically realistic in many instances. However, the emphasis of this study is on the possible scaling behavior of school-size distributions. Barabasi and Albert (1999) showed that the scaling behavior of a growing random network is independent of the number of randomly selected links at each time step. With this analogy, simple increases in mortality per encounter are not expected to alter the scaling behavior of the school-size distributions. Therefore, the one-fish-per-mortality-encounter approach was used in these initial simulations.

Aggregation rate

Similar to mortality-rate encounters, aggregations were investigated as 1) random attachment of two unique schools ($w_N=2\alpha N(N-1)$) and 2) preferential attachment of two unique schools i and j ($w_{pa}=2\alpha N(N-1)k_i k_j$; [Table 1]). Note, the trivial alternative where there was no attachment, (α=0), results in equivalence between the mortality models m_{dN}, *and* m_{dR}; whereas m_{di} becomes a simple proportional mortality rate. Thus, results of models with α=0 are uninteresting in the context of this study and are not presented.

Initial conditions Each simulation was conducted with one of two alternative initial conditions. The first alternative was one of complete disaggregation in which simulations were initiated with S fish, S schools, and one fish in each school ($N_0=S$, $\bar{k}_0$=1). The second alternative initial condition was constructed from the population dynamics of a typical fish population. The main assertion of this alternative is that the eggs or larval fish produced by one female during spawning constitutes one school at the onset of the recruitment process. Thus, the fecundity per female at age is a measure of initial school size and the abundance of females at age is a measure of the frequency of schools of that size. More precisely, the initial condition was constructed for a population of females greater than five years of age (age of maturity), where their fecundity at age, F_{age}, is proportional to weight at age determined from a von Bertalanffy growth equation with parameters K=0.2 and L_∞=10, and an allometric parameter of 3: ($F_{age}=1000[(1-\exp(-\text{age}(0.2)))]^3$). Abundance at age, A_{age}, was computed with an instantaneous mortality rate of 0.2: $[A_{age}=X\exp(-0.2(\text{age}-5))]$. The scalar X was obtained from the approximate solution to $S=\Sigma F_{age} A_{age}$, where F and A were integer values and S was the initial number of fish

Table 1

Summary of definitons of the mortality models used in this study.

	Model	Definition
Mortality rates[1]:	$m_{dt} = 2\mu N k$	density-independent
	$m_{dN} = 2\mu N^2 k$	density-dependent, mortality agents proportional to N
	$m_{dR} = 2\mu N^2 k \bar{k}$	density-dependent, mortality agents proportional to R
	$m_{dk} = 2\mu N k \bar{k}$	density-dependent, mortality agents proportional to k
	$m_N = 2\mu N$	random encounters with schools
Aggregation rates:	$w_N = 2\alpha N(N-1)$	random encounters with schools
	$w_{pa} = 2\alpha N(N-1)k_i k_j$	preferential attachment of schools i and j
Initial conditions:	Disaggregated	$N_0 = S, \bar{k}_0 = 1$
	Aggregated	(see text and Table 2)

Mean field equivalents used in analytical model (see text):

$m_{dt} = 2\mu N\bar{k}$ $m_{dN} = 2\mu N\bar{k}^2$ $m_{dR} = 2\mu N^2\bar{k}^2$

$m_{dk} = 2\mu N\bar{k}^2$ $w_{pa} = 2N(N-1)\bar{k}^2$

Key to figures of simulation results:

Figure 1: *disaggregated*	m_{dt}	w_{pa}	$\alpha = 10^{-6}$	$S = 10^6$
Figure 2: *disaggregated*	m_{dt}	w_N	$\alpha = 10^{-6}$	$S = 10^6$
Figure 3: *aggregated*	m_{dt}	w_{pa}	$\alpha = 10^{-6}$	$S = 10^6$
Figure 4: *aggregated*	m_{dN}	w_{pa}	$\alpha = 1.5\times10^{-6}$	$S = 2\times10^6$
Figure 5: *aggregated*	m_{dN}	w_N	$\alpha = 1.5\times10^{-6}$	$S = 2\times10^6$

[1] In all simulations, μ was set equal to 1.

Table 2

The aggregated initial school-size distribution, when S = 1,000,000. Per capita female fecundity at age is a measure of school size, number of females at age is a measure of frequency of schools. See text for details of computation.

School size	Freq. of schools	Freq. × size	School size	Freq. of schools	Freq. × size
252	348	87,696	857	47	40,279
341	284	96,844	882	38	33,516
427	233	99,491	903	31	27,993
508	190	96,520	920	25	23,000
581	156	90,636	934	21	19,614
596	1	596	946	17	16,082
646	128	82,688	955	14	13,370
703	104	73,112	963	11	10,593
751	85	63,835	970	9	8730
793	70	55,510	975	7	6825
828	57	47,196	979	6	5874

Sum of freq. × size = S = 1,000,000.

of a simulation. Then one school of an appropriate magnitude, M, was added such that the $M + \Sigma F_{age} A_{age}$ was exactly equal to S. Note that under this construction the school sizes in the distribution do not vary with S (except for the one school of size M), whereas the frequency of schools by size do. An example of the initial distribution with the use of this construction is given in Table 2.

Analytical models

Analytical models of aggregation and recruitment are presented, where the models are developed from first principles and the parameters have an interpretation in the physics and biology of the recruitment process. Hopefully, the nature of the parameters can guide model selection,

and the estimates may provide a theoretical framework for empirical research on recruitment processes.

Noting that $R_t=N_t\bar{k}_t$, the recruitment dynamics depicted in the simulations may be modeled by using Equations 3–6 in which recruitment is dependent on the particular mortality and aggregation models that are chosen (m and w; Table 1):

$$dR_t/=-m=d(N_t\bar{k}_t")/dt=(d\bar{k}_t/dt")N_t+(dN_t/dt")\bar{k}_t \quad (3)$$

$$dN_t/dt=-w-m_1P_{1,t} \quad (4)$$

$$d\bar{k}_t/dt=m_1P_{1,t}\left[(\bar{k}_t-1)/(N_t-1)\right] -(m-m_1P_{1,t})/N_t+w\bar{k}_t/(N_{t-1}) \quad (5)$$

$$dP_{k,t}/dt=(m_{k+1}P_{k+1,t}-m_kP_{k,t})/N_t-w_kP_{k,t}/N_t \qquad k>1$$
$$+w\sum_{i=1}^{k-1}P_iP_{k-i}/N_t \quad (6)$$
$$=m_2P_{2,t}/N_t-m_1P_{1,t}(1-P_{1,t})/(N_t-1) \qquad k=1$$
$$-w_1P_{1,t}/N_t\ ,$$

where $P_{k,t}$ = the proportion of schools with k fish in them at time t.

Also, m_k and w_k denote encounter rates appropriate to schools of size k, whereas unsubscripted m and w denote mean field dynamics and, thus, the $k_{i,t}$'s are replaced by $\bar{k}_t$'s (see Table 1).

The first term in Equation 4 denotes the reduction in number of schools due to aggregation events; the second term denotes a reduction due to mortality events on schools with one fish in them. Similarly, the first term in the mean school-size equation (Eq. 5) describes the change in mean school size due to mortality events on schools of size equal to one; the second term is due to mortality events on schools of size greater than one; and the third term is due to aggregation events. Finally, the first term in Equation 6 describes the change in probability of school size k due to mortality; the second term describes loss due to aggregation; and the third describes gain due to aggregation. Of particular importance is $P_{1,t}$: when $P_{1,t}$ is zero, the loss of schools occurs only due to aggregation. When $P_{1,t}$ is positive, then loss of schools is accelerated due to mortality (Eq. 4).

The goal is to obtain solutions to Equations 3–6 as functions of α, μ, and the initial conditions. If one can be assured that there will not be a school composed of one fish during a particular recruitment period ($P_{1,t}=0$), then Equation 6 is eliminated, the $P_{1,t}$ terms drop out of Equations 4 and 5, and a numerical or analytical solution to the differential equations can be obtained, which is computationally feasible for use in fitting to stock-recruitment data. For example, when there is preferential aggregation ($w_{p\alpha}$) and mortality agents are proportional to schools (m_{dN}), the equations reduce to

$$dN_t/dt=-w_{p\alpha}=-2\alpha N_t(N_t-1)\bar{k}_1^2$$
$$d\bar{k}_t/dt=-m_{dN}/N_t+w_{p\alpha}\bar{k}_t(N_1-1)=-2\mu N_t\bar{k}_t+2\alpha N_t\bar{k}_t^3.$$

Analytical solutions were obtained for some of the mortality and aggregation models when $P_{1,t}=0$ throughout the recruitment process (Appendix 1). In particular for m_{dR} and $w_{p\alpha}$:

$$R_t=S/(1+2\mu tS) \quad (7)$$

$$N_t=N_0+(\alpha/\mu")\left[S-S/(1+2\mu tS")\right] \quad (8)$$

$$\bar{k}_t=\bar{k}_0/[1+2\mu tS+2\alpha tS\bar{k}_0], \quad (9)$$

which is the Beverton-Holt stock-recruitment model expanded to include equations for the number of schools and the mean school size. Interestingly, Equation 9 indicates that monitoring the school-size distribution two or more times during a recruitment procession would yield estimates of the stock-recruitment parameters without having direct measures of the number of surviving fish. Equation 7 predicts recruitment by using one parameter, μ_t, the rate of mortality encounters during the recruitment period. However, spawning stock biomass is often used as a surrogate for the number of initial stock, S. Thus, another parameter is needed to convert spawning stock biomass to S in Equation 7. In that case the recruitment model becomes $R_t=aS/(1+2\mu taS)$, where a is another parameter related to fecundity. The additional parameter will be needed for all the models discussed here, if spawning stock biomass is the measure of initial stock.

The assumption that $P_{1,t}=0$ for all t of a recruitment period may not be justified in all situations. An approximation was developed (Appendix 2) to be applied when the initial conditions are disaggregated and when there is preferential attachment. In this circumstance, the differential equation (Eq. 6) when $k=1$ is replaced by

$$dP_{1,t}/dt=-wP_{1,t}/N_t+m(1-P_{1,t})/N_t. \quad (10)$$

Results

Simulations

Several hundred simulations were conducted under various initial stock sizes (S), aggregation parameters (α), initial aggregation conditions, and mortality and aggregation models (m and w). An example set of results are presented in Figures 1–5 (a key to figures is in Table 1).

A typical example of the evolution of the school-size distribution is given in Figure 1 for the disaggregated initial condition, $\alpha=10^{-6}$, $S=10^6$, mortality model m_{dt} and aggregation model $w_{p\alpha}$. In this example both the mortality and aggregation models exhibit preferential attachment, and the school-size distribution approaches scale-free behavior $P(k)\sim k^{-\gamma}$, although γ evolves over time. Eventually, a so-called "giant cluster" is formed by the aggregation process, in which all the fish attach to one school. This has

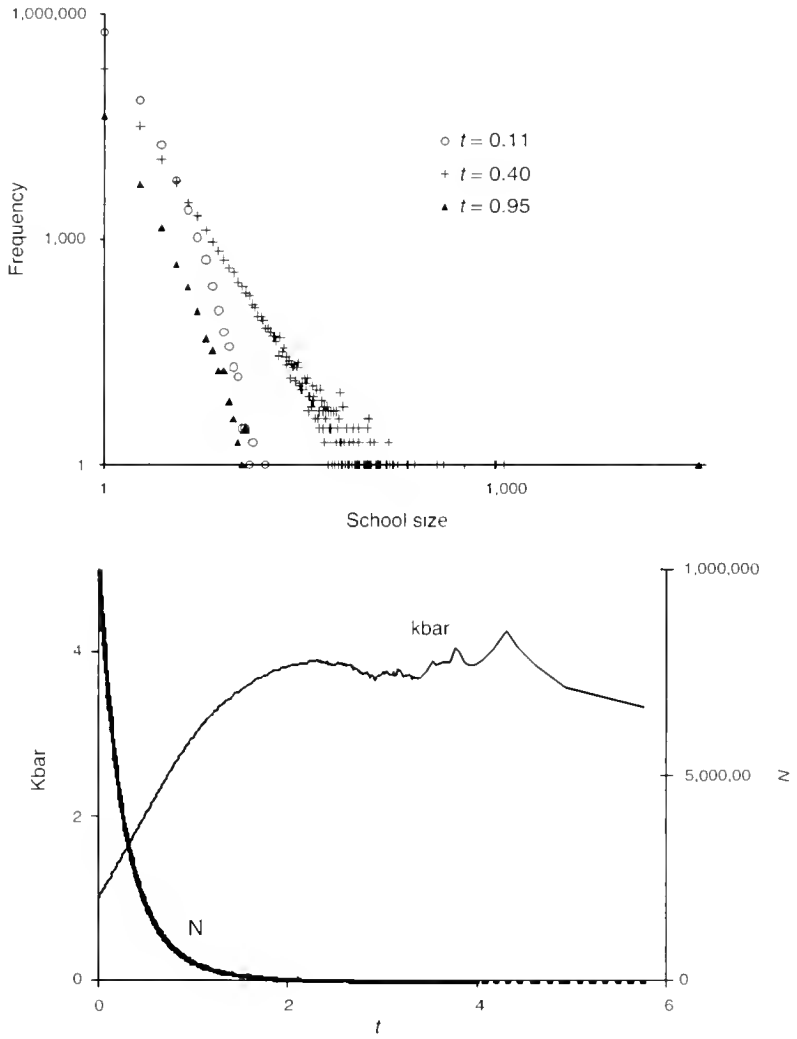

Figure 1

Simulated dynamics of school-size distributions with m_{dt} as the mortality model and w_{pa} as the aggregation model. This simulation started with disaggregated initial conditions (N_0=S), where S=10^6. The aggregation parameter was α=10^{-6}. The top panel shows school-size distributions (in log-log scale) at selected times (t). The lower panel gives the mean school size ($kbar$) and school abundance (N) versus time.

been shown to be an analog of Bose-Einstein condensation (Bianconi and Barabási, 2001; Dorogovtsev and Mendes, 2002) and gelation (Krapivsky et al., 2000). Greater mixing rates (α's) and larger densities (N's) accelerate the aggregation process and the formation of the giant cluster. The average size, $\bar{k}$, increases over time from the disaggregated initial condition until a giant cluster is formed. The number of schools declines over time because of both aggregation and the mortality of fish in schools that only have one fish in them.

When there is random aggregation beginning from a disaggregated initial condition (α=10^{-6}, S=10^6, m_{dt}, w_N; Fig. 2), the school-size distribution exhibits exponential behavior $P(k)$~exp$(-\lambda k)$, with λ evolving over time. This is equivalent to the Erdös and Rényi (1960) results for random graphs. A comparison of Figure 2 with Figure 1 shows the difference between preferential attachment and random attachment, i.e., the difference between scale-free and exponential models.

Aggregated initial conditions (Figs. 3–5) result in a transition from the initial distribution to either scale-free or exponential distribution. During the transition, the size of the smallest school gradually becomes smaller until there is a finite probability of schools with one fish in

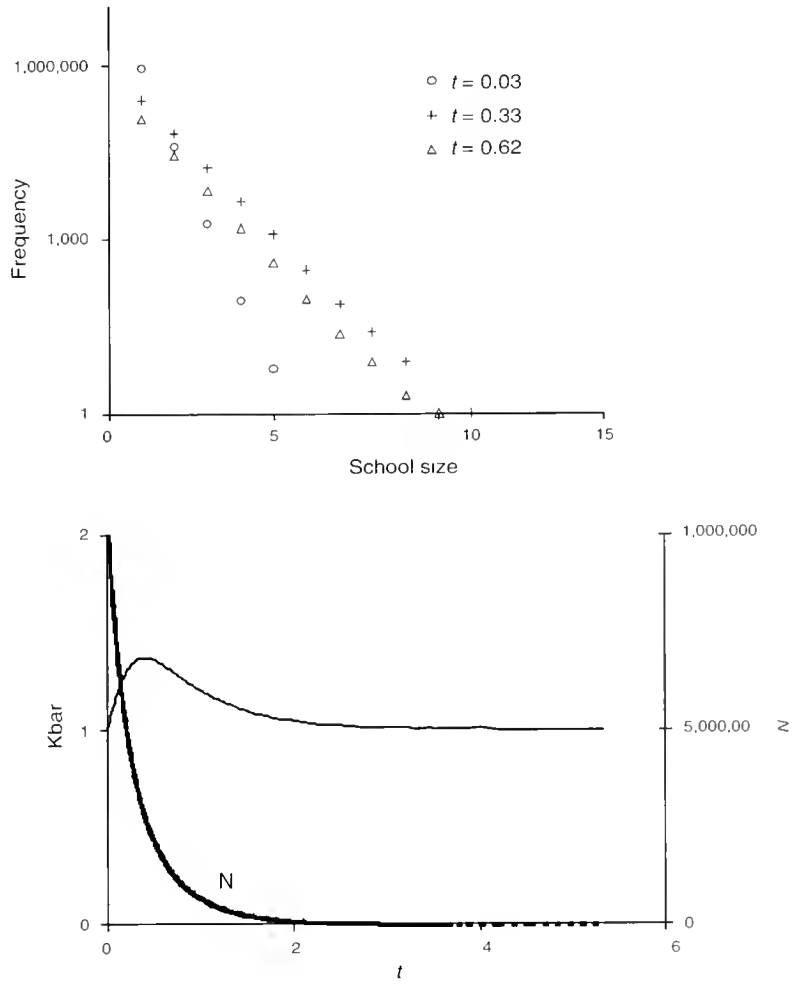

Figure 2

Simulated dynamics of school-size distributions with m_{dt} as the mortality model and w_N as the aggregation model. This simulation started with disaggregated initial conditions (N_0=S), where S=10^6. The aggregation parameter was α=10^{-6}. The top panel shows school-size distributions (frequency in log) at selected times (t). The lower panel gives the mean school size ($kbar$) and school abundance (N) versus time.

them. At this point the reduction in the number of schools is accelerated because of the mortality of fish that are in "schools" in which they are the only member, and because of the loss of schools attributed to aggregation.

Model comparisons

Numerical integration of Equations 3–5 matched the simulation results (Fig. 6, when $P_{1,t}$=0), indicating that the mathematical model describes the simulation dynamics. The numerical techniques are sufficiently efficient to be used in a curve-fitting context. Evaluations of the approximation (Appendix 2) indicate that the approximation may be useful for predictions of recruitment, when compared with the simulations. However, the components of recruitment, $\bar{k}_t$ and N_t, were biased (Fig. 7). Further research is needed to develop estimates of $P_{1,t}$ and, more generally, $P(k)$ under other models and initial conditions.

Recruitment was compared between mortality models and aggregation models (Fig. 8). If the mortality model was either m_{dt} or m_{dR}, then the mortality rate was not affected by the school-size distribution: random attachment and preferential attachment perform equally as well in terms of survival at a given time. But if mortality encounters proportional to school density (m_{dN}) were imposed, then there were better survival rates with preferential attachment than with random attachment (Fig. 8, A and B). Conversely, mortality encounters proportional to school

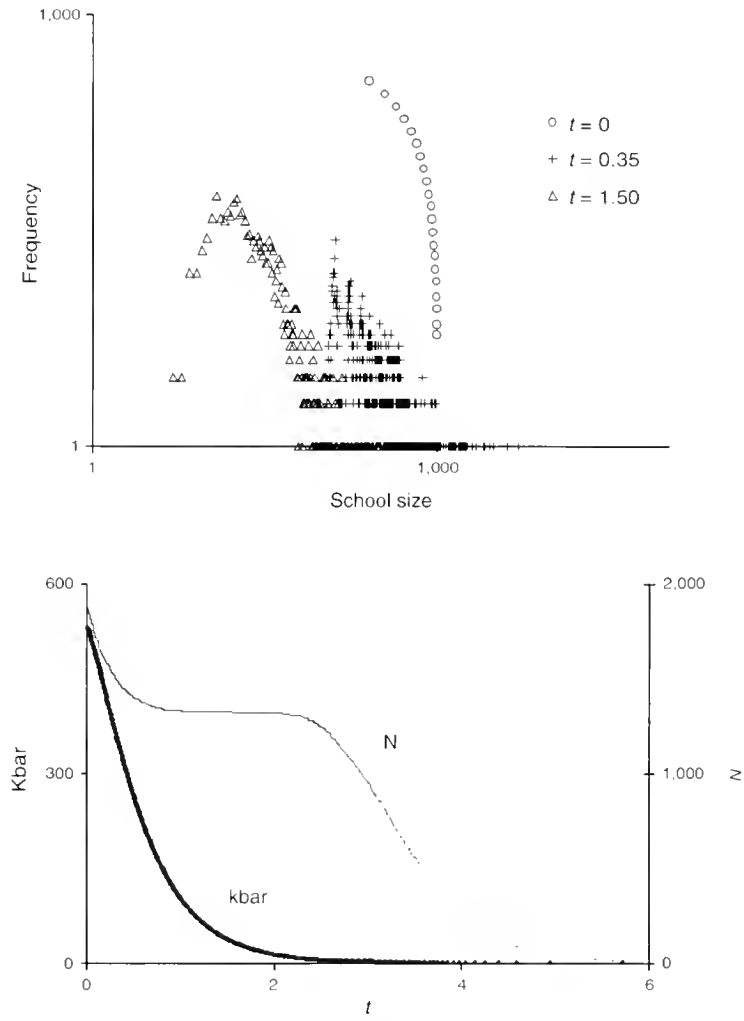

Figure 3

Simulated dynamics of school-size distributions using m_{dt} as the mortality model and w_{pa} as the aggregation model. This simulation started with aggregated initial conditions (S=10^6). The aggregation parameter was α=10^{-6}. The top panel shows school-size distributions (in log-log scale) at selected times (t). The lower panel gives the mean school size ($kbar$) and school abundance (N) versus time.

size (m_{dk}) led to poorer survival with preferential attachment (Fig. 8, C and D).

Discussion

Koslow (1992), Rickman et al. (2000), and others have commented on the inherent variability in stock-recruitment data and the limited predictive power of deterministic stock-recruitment models. Therefore, there is no expectation that one could select the models described here over other stock-recruitment models on the basis of fits to data. Although the aggregation-mortality models may be fitted to stock-recruitment data, the real usefulness is as a guide to selection of stock-recruitment models used in management, as a mechanism for integrating research on recruitment processes, and as a tool for exploring the structure of recruitment variability.

The aggregation-mortality models were introduced by using an analogy with evolving random networks (Barabási and Albert, 1999) and were shown to be analytically equivalent (Appendix 2). Modeled fish are subjected to competing forces of organization (aggregation) and decay (mortality), as in a network in which links to nodes in the network are created, destroyed, and rewired (Albert and Barabási, 2002). An important finding of Barabási and

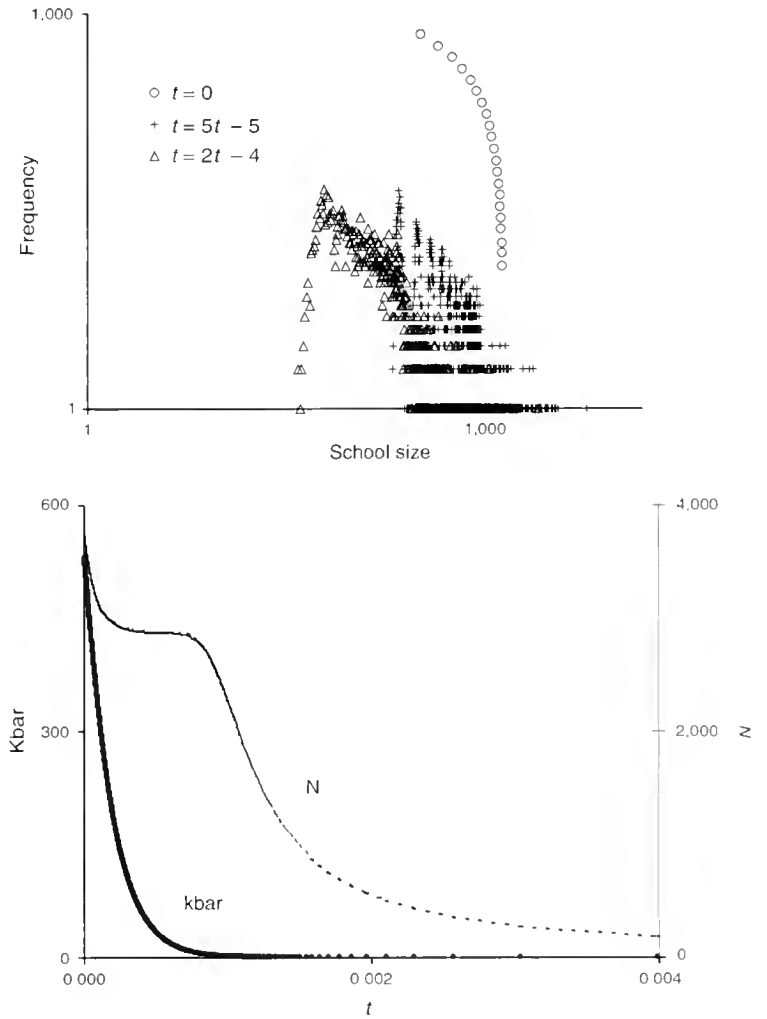

Figure 4

Simulated dynamics of school-size distributions using m_{dN} as the mortality model and w_{pa} as the aggregation model. This simulation started with aggregated initial conditions (S=2×10^6). The aggregation parameter was α=1.5×10^{-6}. The top panel shows school-size distributions (in log-log scale) at selected times (t). The lower panel gives the mean school size ($kbar$) and school abundance (N) versus time.

Albert (1999) was that scaling of the aggregate-size distribution was dependent on the type of aggregation, specifically preferential attachment. Bonabeau and Dagorn noted the generic occurrence of scaling of aggregation distributions in nature (Bonabeau and Dagorn, 1995) and this scaling of aggregation distributions motivated the development of the models presented here.

The emphasis of the aggregation models was on preferential attachment and on comparison of model results with results for models with random attachment strategies. The preferential attachment rule used in the simulations was that aggregation rates were proportional to the size of the school encountered. But, what is meant by preferential attachment and does preferential attachment occur in nature? Clearly, a fish, school or mortality agent has no global knowledge of the proportional size of a school that is encountered. However, preferential attachment in these models is a metaphor for aggregation strategies that are weighted toward larger school sizes. Indeed, studies of networks have shown that attachment may be proportional to a power of school size and still produce scale-free properties (Albert and Barabási, 2002). Also, network studies have shown that scale-free distributions occur when a wide number of attachment criteria are included, such as the "fitness" of the object being encountered and the attractiveness of local conditions (Bianconi and Barabási,

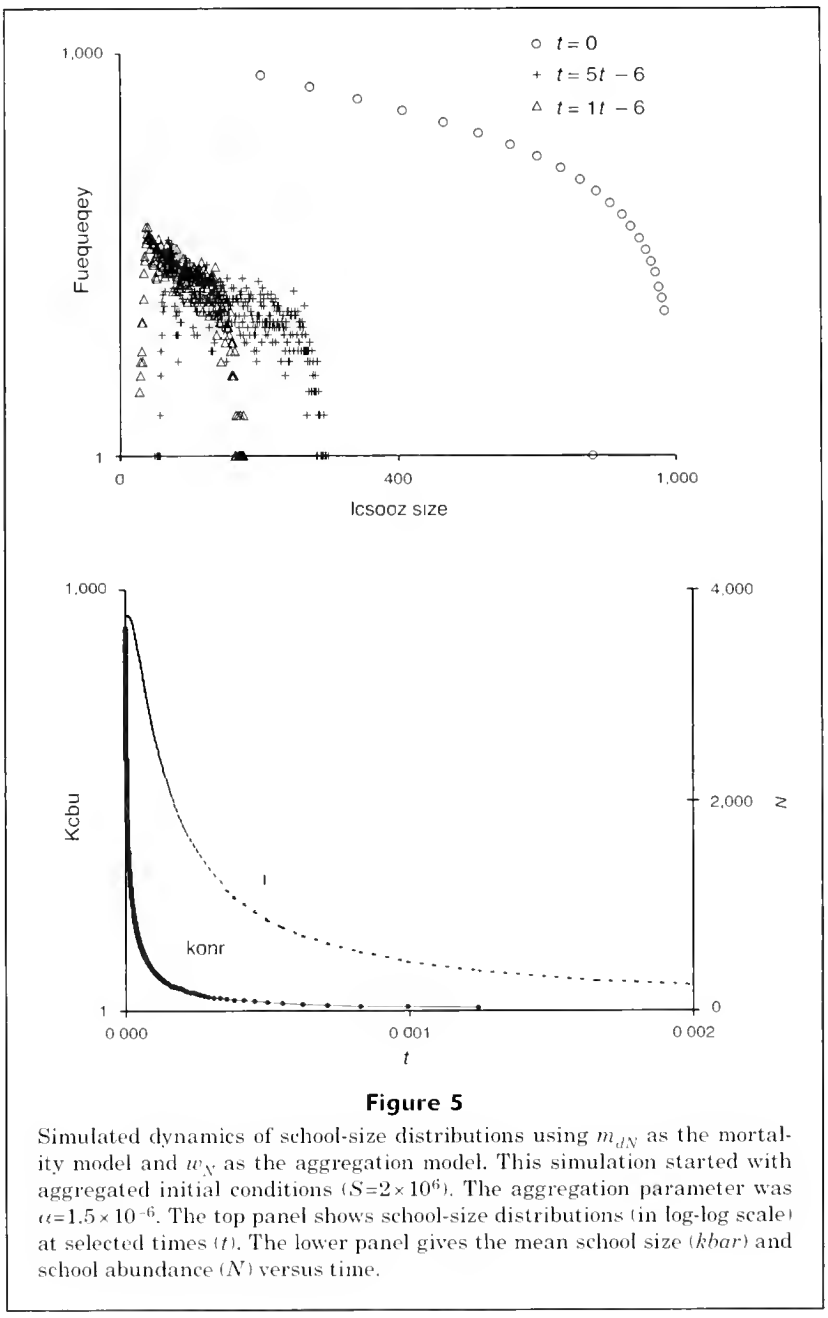

Figure 5

Simulated dynamics of school-size distributions using m_{dN} as the mortality model and w_N as the aggregation model. This simulation started with aggregated initial conditions (S=2×10^6). The aggregation parameter was α=1.5×10^{-6}. The top panel shows school-size distributions (in log-log scale) at selected times (t). The lower panel gives the mean school size (*kbar*) and school abundance (N) versus time.

2001; Calderelli et al., 2002; Vazquez, 2003). Biological concepts of fitness, feeding behavior, predator-avoidance behavior, and habitat suitability appear to fall within the attachment criteria examined in physics literature. Oceanographic stability (Myers and Pepin, 1994), assortative schooling by color patterns (Crook, 1999), chemosensory stimuli (Quinn and Busack, 1985), and larval fitness indices from RNA/DNA ratios (Pepin, 1991; Suneetha et al., 1999) may be mechanisms that directly or indirectly influence aggregation size and, thus, distribution.

The geometry of the school size itself may be sufficient to produce preferential attachment behavior, as well. In the models of this study, the detection spaces (G_i +G_j in Equation 1) were set to unity and assumed to be independent of school size. However, the detection space may be related to school size. For example, if a school of one fish has a spheroid detection space around itself with radius equal to 1, then using the geometry of an aggregation of k fish, the detection space of the aggregate would be proportional to $k^{1/3}$. Alternatively, if the detection space were a two-dimensional circle with a radius of 1, then the aggregate's detection space would be proportional to $k^{1/2}$. Substituting size-dependent detection spaces into the random mortality and aggregation models would be sufficient to induce pref-

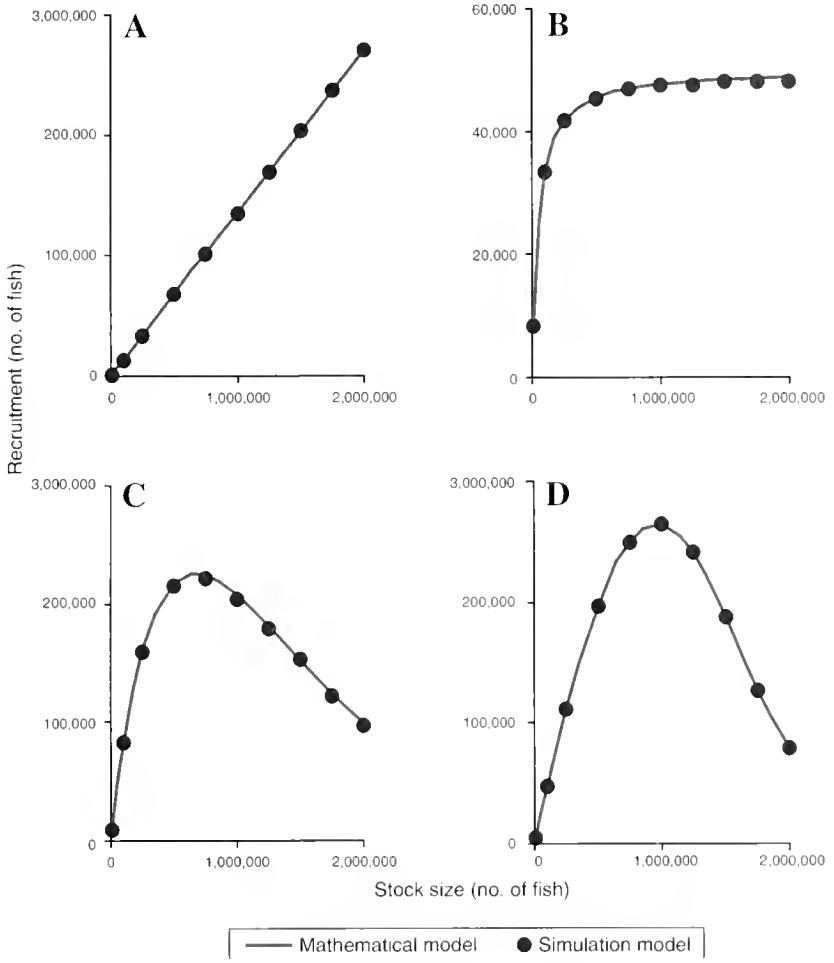

Figure 6

Stock-recruitment relationships from the mathematical models (Eqs. 3–5, aggregated initial conditions) compared with simulation results: (**A**) density-independent mortality (m_{dI}) and preferential attachment (w_{pa}) evaluated at t=1, α=10^{-9}, μ=1; (**B**) density-dependent mortality proportional to fish (m_{dR}) and preferential attachment (w_{pa}) evaluated at t=10^{-5}, α=3×10^{-5}, μ=1; (**C**) density-dependent mortality proportional to schools (m_{dN}) and preferential attachment (w_{pa}) evaluated at t=5×10^{-4}, α=1.5×10^{-6}, μ=1; and (**D**) density-dependent mortality proportional to school size (m_{dk}) and preferential attachment (w_{pa}) evaluated at t=10^{-3}, α=2×10^{-6}, μ=1.

erential interaction even when encounters are random: schools are randomly encountered, but the encounter event itself is weighted toward larger schools. Thus, the shape of the detection space may be another mechanism by which preferential attachment may be exhibited.

In the models presented, it is blithely assumed that mortality is caused by undefined mortality agents. However, most larval recruitment research has been directed at starvation and predation as determinants of recruitment variability (Lasker, 1975; Hunter, 1984; Bailey and Houde, 1989; Chambers and Trippel, 1997, for example). The mortality models used here clearly fit within the predation paradigm: mortality from predation results from encounters with mortality agents of specific density and size. Whereas, mortality from starvation ensues from a lack of encounters with prey agents of sufficient density and size. In certain situations starvation processes might be aptly described by the predation-encounter approach used in this study. However, further research is needed to evaluate their appropriateness and to develop alternative modifications to Equations 3–6. A mechanism to do this may be the inclusion of fragmentation of schools into the models. In the models as they are now characterized, new schools are not created, the number of schools only becomes smaller through either aggregation or through mortality on schools of a single fish. Fragmentation might

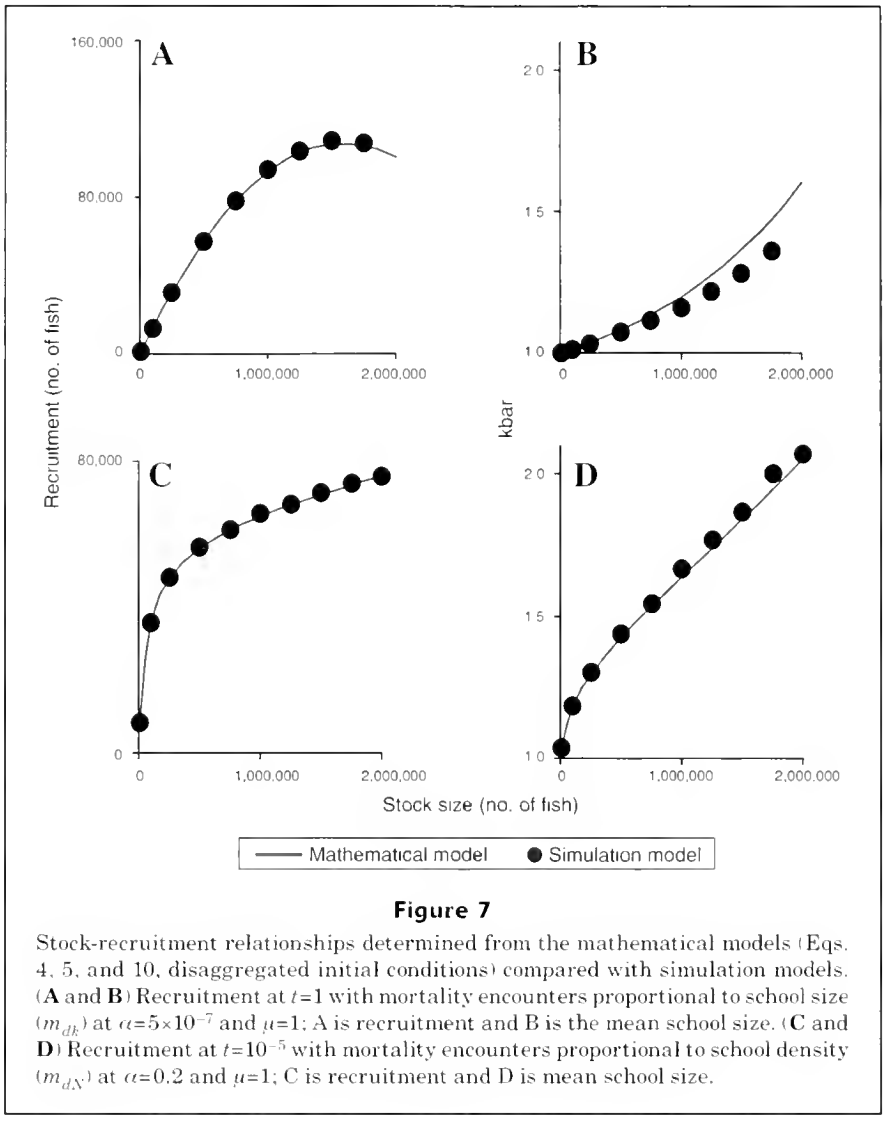

Figure 7

Stock-recruitment relationships determined from the mathematical models (Eqs. 4, 5, and 10, disaggregated initial conditions) compared with simulation models. (**A** and **B**) Recruitment at t=1 with mortality encounters proportional to school size (m_{dk}) at α=5×10^{-7} and μ=1; A is recruitment and B is the mean school size. (**C** and **D**) Recruitment at t=10^{-5} with mortality encounters proportional to school density (m_{dN}) at α=0.2 and μ=1; C is recruitment and D is mean school size.

occur due to secondary effects of mortality encounters, as well as other factors such as starvation. For example, Sogard and Olla (1997) have shown predation-risk and hunger to be related to group cohesion.

The formation of a giant cluster (a single school encompassing all the fish) is an important feature of the attachment process. The simulations showed that with preferential attachment the recruitment process passes through a phase where the size distribution is scale free, then a critical point is reached where a giant cluster is being formed, i.e. a single school begins to attract all the fish. Research on complex networks has shown the conditions for formation of the giant cluster (Aiello et al., 2000; Albert and Barabasi, 2002). This should be investigated for the school aggregation models because it is likely that the mortality models used in the present study would no longer be appropriate once the giant cluster is formed. Indeed in some fish stocks, schools may aggregate into giant clusters on a local scale and then aggregation may stop for reasons such as juveniles entering a benthic phase. The resulting distribution of school sizes may be the cluster distribution across benthic habitats. Spatial limitations of aggregation are an important feature of individually based models (Pascual and Levin, 1999). Again, this may be an important area for research.

What is the benefit of preferential attachment? If mortality encounters are proportional to school density, then recruitment survival rates are improved when there are fewer schools for a given number of fish, i.e. when preferential attachment is employed rather than random attachment (Fig. 8). Perhaps, preferential attachment strategies are a useful evolutionary hedge against uncertainty in the nature of the mortality dynamics. Conversely, when mortality encounters are proportional to school size, then better survival is achieved when schools are smaller, i.e. with random attachment (Fig. 8). If mortality by predators is related to larger schools, or if attainment of prey is inversely related to larger schools, then more solitary life

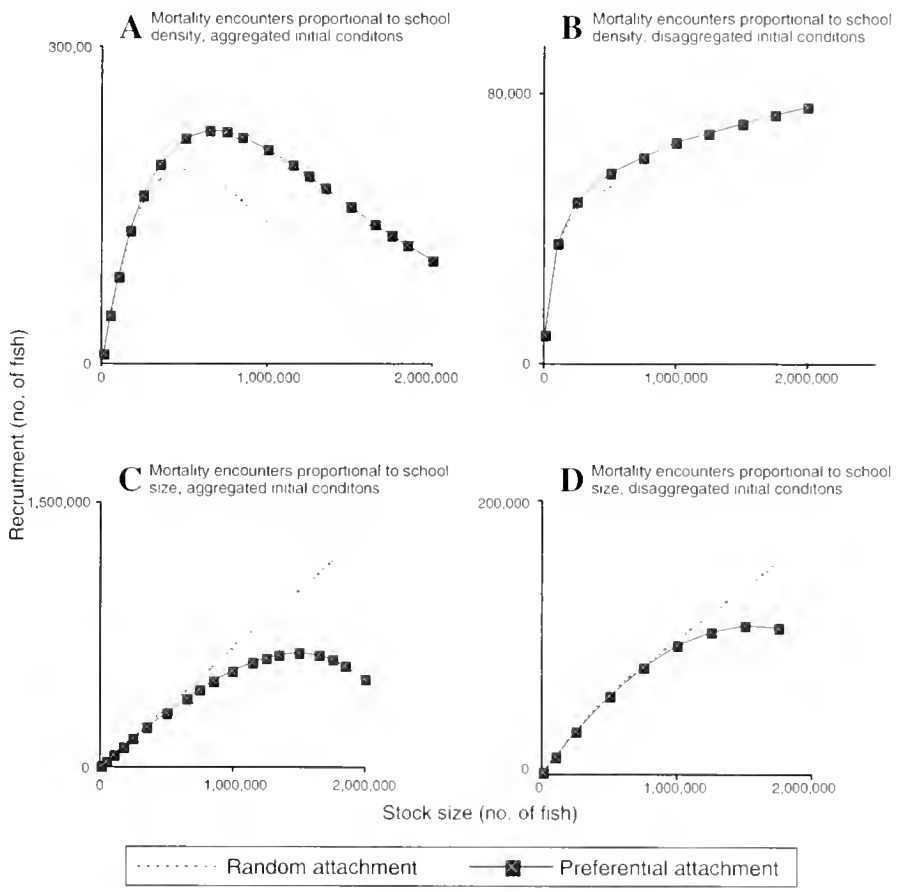

Figure 8

Stock-recruitment results with preferential attachment compared with random attachment (w_{pa} versus w_N). (**A**) Recruitment at t=1 with mortality encounters proportional to school density (m_{dN}) at $\alpha=10^{-9}$ and $\mu=5\times10^{-4}$ with an aggregated initial condition; (**B**) recruitment at $t=10^{-5}$ with mortality encounters proportional to school density (m_{dN}) at α=0.2 and μ=1 with a disaggregated initial condition; (**C**) recruitment at t=1 with mortality encounters proportional to school size (m_{dk}) at $\alpha=10^{-9}$ and $\mu=5\times10^{-4}$ with an aggregated initial condition; (**D**) recruitment at t=1 with mortality encounters proportional to school size (m_{dk}) at $\alpha=5\times10^{-7}$ and μ=1 with a disaggregated initial condition.

history strategies may evolve. Perhaps, the random aggregation model would be most effective for solitary predatory fish when their mortality is imposed by a m_{dk}-type model. For fish, this may be more likely to occur at later life stages than at recruitment. If mortality encounters are proportional to fish (m_{dR}), then results are intermediate and preferential attachment and random attachment perform equally as well.

The density-dependent mortality models implicitly incorporate a predator-prey interaction. Alternative predator-prey interactions examined were those in which predator density was proportional to fish, to schools, or to the number of fish within a school (school size) throughout a recruitment period. In reality mortality is perpetrated by a variety of agents at many different scales. Some agents act at the scale of the population ($N\bar{k}$), some at the scale of schools (N), some at the scale of mean school size ($\bar{k}$), and some at the scale of a local school (k_t). The mixture of predatory agents and their densities can cause various kinds of dynamics including oscillatory, chaotic, and stable behavior (Wilson 1996, Pascual and Levin 1999). Therefore, it is unlikely that the models in this study, in which predator-prey ratios are constant, would be predictive of anything other than average behavior during recruitment. However, the analytical approach allows changes in the scale of predator-prey interaction over time. We can model this as $m_t=2\mu N_t^a \bar{k}_t^b$, where a and b are dynamic (time-dependent) and, perhaps, correlated. Although we may wish to use the Beverton-Holt model ($a=b=2$) or the Ricker-like model ($a=2$, $b=1$) as a representation of average dynamics, it remains that recruitment variability will be influenced by the dynamics of the exponents, a and b. Numerical evalua-

tion of the differential equations by using random variates at each time step may be a mechanism to evaluate how the variability of a and b within a recruitment period are translated into the variability structure around a stock-recruitment relationship.

The model formulations used in the present study have been characterized from the underlying physical processes. By doing so, research may be directed at empirical and experimental measurement of specific stock-recruitment parameters, which opens the models to testing and verification. Additionally, results indicate that the school-size distribution contains a rich source of information on the mortality and aggregation processes and that monitoring of the distribution during recruitment could be useful for understanding recruitment variability and model structure.

Acknowledgments

I would like to thank the reviewers for their constructive comments and the National Marine Fisheries Service for allowing me the opportunity to conduct this research.

Literature cited

Aiello, W. F., F. Chung, and L. Lu.
2000. A random graph model for massive graphs. Proc 32nd ACM Symp. Theor. Comp., p. 171–180.

Albert, R., and A. Barabási.
2002. Statistical mechanics of complex networks. Rev. Mod. Phys. 74(1):47–98.

Anderson, J. J.
1981. A stochastic model for the size of fish schools. Fish. Bull. 79:315–323.

Bailey, K. M., and E. D. Houde.
1989. Predation on eggs and larvae of marine fishes and the recruitment problem. Adv. Mar. Biol. 25:1–83.

Barabási, A., and R. Albert.
1999. Emergence of scaling in random networks. Science 286:5098–512.

Bianconi, G., and A. Barabási.
2001. Bose-Einstein condensation in complex networks. Phys. Rev. Lett. 86:5632–5635.

Beverton, R. J. H., and S. J. Holt.
1957. On the dynamics of exploited fish populations. Fish. Invest. Lond. Ser. 2, 19 p.

Beyer, J. E., and G. C. Laurence.
1980. A stochastic model of larval fish growth. Ecol. Model. 8:109–132.

Bonabeau, E., and L. Dagorn.
1995. Possible universality in the size distribution of fish schools. Phys. Rev. E 51:R52220–R52223.

Bonabeau, E., L. Dagorn, and P. Freon.
1999. Scaling in animal group-size distributions. Proc. Natl. Acad. Sci. 96:4472–4477.

Caldarelli, G., A. Capocci, P. De Los Rios, and M.A. Munoz.
2002. Scale-free networks from varying vertex intrinsic fitness. Phys. Rev. Lett. 89, 258702.

Chambers, C., and E. A. Trippel.
1997. Early life history and recruitment in fish populations, 632 p. Chapman and Hall, London.

Comyns, B. H., R. F. Shaw, and J. Lyczkowski-Shultz.
2003. Small-scale spatial and temporal variability in growth and mortality of fish larvae in the subtropical northcentral Gulf of Mexico: implications for assessing recruitment success. Fish. Bull. 101:10–21.

Crook, A. C.
1999. Quantitative evidence for assortative schooling in a coral reef fish. Mar. Ecol. Prog. Ser. 176:17–23.

Dorogovtsev, S. N., and J. F. F. Mendes.
2000. Scaling behaviour of developing and decaying networks. Europhys. Lett. 52:33–39
2002. Evolution of networks. Adv. Phys. 51:1079–1187.

Erdos, P., and A. Rényi.
1960. On evolution of random graphs. Publ. Math. Inst. Hung. Acad. Sci. 5:17–61.

Fell, D. A., and A. Wagner.
2000. The small world of metabolism. Nat. Biotech. 18:1121–1122.

Flierl, G., D. Grunbaum, S.A. Levin, and D. Olson.
1999. From individuals to aggregations: the interplay between behavior and physics. J. Theor. Biol. 196:397–454.

Gueron, S., and S. A. Levin.
1995. The dynamics of group formation. Math. Biosci. 128:243–264.

Harris, J. G. K.
1975. The effect of density-dependent mortality on the shape of the stock and recruitment curve. J. Cons. Int. Explor. Mer 36:144–149.

Hunter, J. R.
1984. Inferences regarding predation on the early life stages of cod and other fishes. *In* The propagation of cod, *Gadus morhua* L. (E. Dahl, D. S. Danielssen, E. Moksness, and P. Solemdan, eds.), p. 533–562. Flodevigen Rapportser 1984.

Koslow, J. A.
1992. Fecundity and the stock-recruitment relationship. Can. J. Fish. Aquat. Sci. 49:210–217.

Krapivsky, P. L., S. Redner, and F. Leyvraz.
2000. Connectivity of growing random networks. Phys. Rev. Lett. 85:4629–4632.

Landa, J. T.
1998. Bioeconomics of schooling fishes: selfish fish, quasi-free riders, and other fishy tales. Environ. Biol. Fish. 53:353–364.

Lasker, R.
1975. Field criteria for survival of anchovy larvae: the relation between inshore chlorophyll maximum layers and successful first feeding. Fish. Bull. 73:453–462.

McCauley, E., W. G. Wilson, and A.M. de Roos.
1993. Dynamics of age-structured and spatially structured predator-prey interactions: individual-based models and population-level formulations. Am. Naturalist 142:412–442.

Mertz, G., and R. A. Myers.
1994. Match/mismatch predictions of spawning duration versus recruitment variability. Fish. Oceanogr. 3(4):236–245.
1995. Estimating the predictability of recruitment. Fish. Bull. 93:657–665.

Myers, R. A., and P. Pepin.
1994. Recruitment variability and oceanographic stability. Fish. Oceanogr. 3(4):246–255.

Niwa, H.-S.
1998. School size statistics of fish. J. Theor. Biol. 195:351–361.

Pascual, M., and S. A. Levin.
1999. From individuals to population densities: searching for the intermediate scale of nontrivial determinism. Ecology 80(7):2225–2236.
Paulik, G. J.
1973. Studies of the possible form of the stock-recruitment curve. Rapp. P.-v. Réun. Cons. Int. Explor. Mer 164: 303–315.
Pepin, P.
1991. Effect of temperature and size on development, mortality, and survival rates of early life history stages of marine fish. Can. J. Fish. Aquat. Sci. 48:503–518.
Pitcher, T. J., and J. K. Parrish.
1993. Functions of shoaling behaviour in teleosts. *In* Behaviour of teleost fishes (T. J. Pitcher, ed.), p. 363–439. Chapman and Hall, London.
Quinn, T. P., and C. A. Busack.
1985. Chemosensory recognotion of siblings in juvenile coho salmon *Oncorhynchus kisutch*. Anim. Behav. 33:51–56.
Ricker, W. E.
1958. Handbook of computations for biological statistics of fish populations, 119 p. Fish. Res. Board Can. Bull.
Rickman, S. J., N. K. Dulvy, S. Jennings, and J. D. Reynolds.
2000. Recruitment variation related to fecundity in marine fishes. Can. J. Fish. Aquat. Sci. 57:116–124.
Rothschild, B. J.
1986. Dynamics of marine fish populations, 269 p. Harvard Univ. Press, Cambridge, MA.
Sogard, S. M., and B. L. Olla.
1997. The influence of hunger and predation risk on group cohesion in a pelagic fish, walleye pollock *Theragra chalcogramma*. Environ. Biol. Fish. 50:405–413.
Solé, R. V., and J. M. Montoya.
2001. Complexity and fragility in ecological networks. Proc. R. Soc. London B. 268:2039–2045.
Suneetha, K.-B., A. Folkvord, and A. Johannessen.
1999. Responsiveness of selected condition measures of herring, *Clupea harengus*, larvae to starvation in relation to ontogeny and temperature. Environ. Biol. Fish. 54:191–204.
Tolman, R. C.
1979. The principles of statistical mechanics, 661 p. Dover Publs., New York, NY.
Vazquez, A.
2003. Growing networks with local rules: preferential attachment, clustering hierarchy and degree correlations. Phys. Rev. E 67:056104.
Vlymen, W. J.
1977. A mathematical model of the relationship between larval anchovy (*Engraulis mordax*) growth, prey microdistribution, and larval behavior. Environ. Biol. Fish. 2: 211–233.
Wilson, W. G.
1996. Lotka's game in predator-prey theory: linking populations to individuals. Theor. Pop. Biol. 50:368–393.

Appendix 1

Analytical solutions to Equations 3–5 for selected mortality and aggregation models. Solutions assume that $P_{1,t} = 0$ for all t evaluated and that the number of schools is large. No analytical solutions were found for (m_{dN},w_{pa}), (m_{dN}, w_{pa}), or (m_{dk},w_{pa}).

Mortality proportional to fish: m_{dR}
Preferential aggregation: w_{pa}

$$R_t = \frac{S}{1+2\mu St}$$

$$N_t = \frac{S}{\bar{k}_0} + \frac{\alpha}{\mu}\left(S - \frac{S}{1+2\mu St}\right)$$

$$\bar{k}_t = R_t / N_t = \frac{\bar{k}_0}{1+2\mu St + 2\alpha S\bar{k}_0 t}$$

Mortality proportional to fish: m_{dR}
Random aggregation: w_N

$$R_t = \frac{S}{1+2\mu St}$$

$$N_t = \frac{S}{S-(S-\bar{k}_0)e^{-2\alpha t}}$$

$$\bar{k}_t = R_t / N_t = \frac{S-(S-\bar{k}_0{}^{n}e^{-2\alpha t}}{\alpha+ 2\mu St}$$

Density-independent: m_{dt}
Preferential aggregation: w_{pa}

$$R_t = Se^{-2\mu t}$$

$$N_t = \frac{S}{\bar{k}_0} - \frac{S^2}{2}\frac{\alpha}{\mu}(1-e^{-4\mu t})$$

$$\bar{k}_t = R_t / N_t = \frac{\bar{k}_0 e^{-2\mu t}}{1-\frac{S\bar{k}_0}{2}\frac{\alpha}{\mu}(1-e^{-4\mu t})}$$

Density-independent: m_{dt}
Random aggregation: w_N

$$R_t = Se^{-2\mu t}$$

$$N_t = \frac{S}{S-(S-\bar{k}_0)e^{-2\alpha t}}$$

$$\bar{k}_t = R_t / N_t = e^{-2\mu t}\left(S-(S-\bar{k}_0)e^{-2\alpha t}\right)$$

Mortality proportional to schools: m_{dN}
Random aggregation: w_N

$$R_t = Se^{-2\mu t}\left\{\frac{\bar{k}_0}{S-(S-\bar{k}_0)e^{-2\alpha t}}\right\}^{\frac{\mu}{\alpha}}$$

$$N_t = \frac{S}{S-(S-\bar{k}_0)e^{-2\alpha t}}$$

$$\bar{k}_t = R_t / N_t = \frac{\bar{k}_0^{\mu/\alpha} e^{-2\mu t}}{\left[S-(S-\bar{k}_0)e^{-2\alpha t}\right]^{\frac{\mu}{\alpha}-1}}$$

Mortality proportional to school size: m_{dk}
Random aggregation: w_N

$$R_t = \frac{S}{1+2\mu St - \frac{\mu}{\alpha}(S-\bar{k}_0)[1-e^{-2\alpha t}]}$$

$$N_t = \frac{S}{S-(S-\bar{k}_0)e^{-2\alpha t}}$$

$$\bar{k}_t = R_t / N_t = \frac{S-(S-\bar{k}_0)e^{-2\alpha t}}{1+2\mu St - \frac{\mu}{\alpha}(S-\bar{k}_0)[1-e^{-2\alpha t}]}$$

Random mortality encounters: m_N
Random aggregation: w_N

$$R_t = S - \frac{\mu}{\alpha}\ln\left\{\frac{S}{\bar{k}_0}(e^{2\alpha t}-1)+1\right\}$$

$$N_t = \frac{S}{S-(S-\bar{k}_0)e^{-2\alpha t}}$$

$$\bar{k}_t = R_t / N_t$$

Appendix 2

Characteristics of school-size distribution under preferential attachment

Much of the recent literature on evolving complex networks has been directed at determining the degree distribution, i.e., the probability $P(k)$ of a node having k links (Albert and Barabási, 2002). When the network grows or declines proportional to k or when links are rewired to be proportional to k, then $P(k)$ can be determined by using continuum theory (Dorogovtsev and Mendes, 2000; Albert and Barabási, 2002) leading to scale-free degree distributions. Therefore, when preferential attachment and nonrandom mortality are used, then the model may be couched as a scale-free network in the manner of Barabasi and Albert (1999), Dorogovtsev and Mendes (2000) and Albert and Barabási (2002).

When the aggregation model is *preferential attachment* (w_{pa}) (ignoring for the moment the nonstationarity of N and R), then the partial differential of a school of size k_{it} with respect to R_t has been shown by Dorogovtsev and Mendes (2000) to asymptotically be

$$\partial k_{it} / \partial R_t = \beta_t (k_{it} / R_t), \tag{A1}$$

where β_t is the net rate of decay per each mortality event, i.e.,

$$\beta_t = 1 - w_{pa} / m. \tag{A2}$$

With specific-mortality models, β_t is

$$\begin{aligned}
m_{di}&: \ \beta_t = 1-(\alpha/\mu)(N_t-1)\bar{k}_t \approx 1-(\alpha/\mu)R_t \\
m_{dN}&: \ \beta_t = 1-(\alpha/\mu)(N_t-1)\bar{k}_t / N_t \approx 1-(\alpha/\mu)\bar{k}_t \\
m_{dR}&: \ \beta_t = 1-(\alpha/\mu)(N_t-1)/N_t \approx 1-(\alpha/\mu) \\
m_{dk}&: \ \beta_t = 1-(\alpha/\mu)(N_t-1) \approx 1-(\alpha/\mu)R_t/\bar{k}_t,
\end{aligned}$$

where the approximations on the right assume that the number of schools is large. The first term of (A2) denotes the removal of a fish proportional to school size for a mortality event; the second term denotes aggregation events proportional to school size. If β_t is independent of time ($\beta_t=\beta$), then Dorogovtsev and Mendes (2000) showed that under continuum conditions

$$P(k) \propto k^{-\gamma} \qquad \gamma = 1+1/\beta. \tag{A3}$$

Equation A3 is equivalent to the results of Dorogovtsev and Mendes (2000), Krapivsky et al. (2000), and Albert and Barabási (2002) and suggest that β_t may be a useful approximation for determining the power-law tail of the school-size distribution (Appendix Fig. 1).

The simulation results showed the dynamics of P_{kt}. When the aggregated initial condition was imposed, at the start of the simulations there were no schools with only one fish in them ($P_{1t}=0$). Eventually, as the number of schools and fish declined, P_{1t} became positive. Finally, as the distribution became scale-free, $-\partial P_{1t}/\partial k$ became negative and remained so throughout the remainder of the simulation or until a single giant cluster was formed (Appendix Fig. 1). Conversely, if the initial conditions began with schools being disaggregated, then $\partial P_{1t}/\partial k$ began as a negative number and remained so until either a giant cluster formed or there were no more fish remaining.

An approximation is suggested by the above results for circumstances when the initial conditions are disaggregated and when there is preferential attachment: the differential equation $dP_{k,t}/dt$ when $k=1$ (Eq. 6) is replaced by

$$dP_{1,t}/dt = -wP_{1,t}/N_t + m(1-P_{1,t})/N_t. \tag{A4}$$

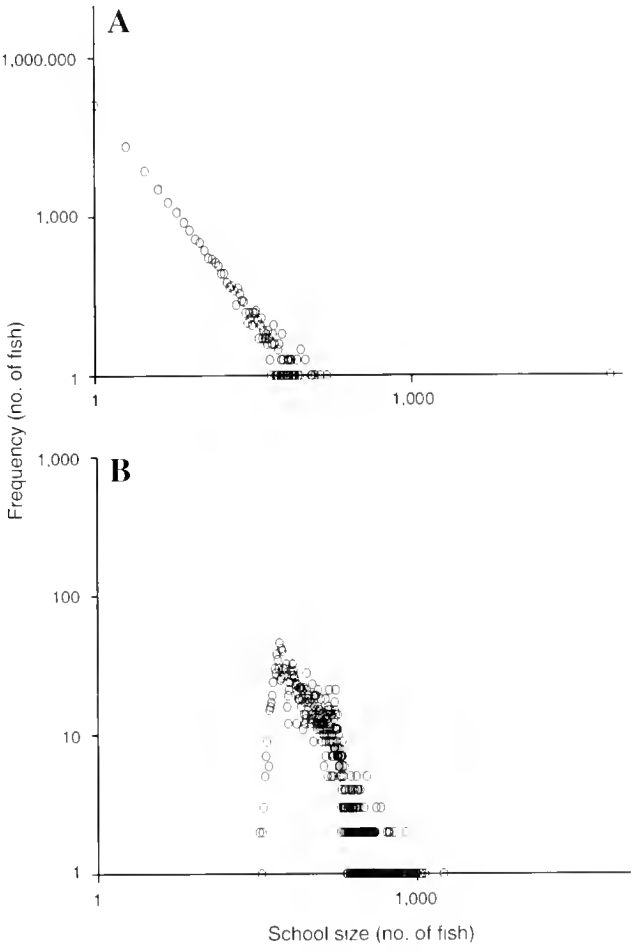

Appendix Figure 1

School-size distribution at selected times. (**A**) School-size distribution of a simulation starting with a disaggregated initial condition, $S=10^6$, $\alpha=10^{-6}$, where mortality is density-independent (m_{di}) and there is preferential attachment (w_{pa}). (**B**) Distribution starting with an aggregated initial condition, $S=2\times10^6$, $\alpha=1.5\times10^{-6}$, where mortality is density-dependent proportional to schools (m_{dN}) and with preferential attachment (w_{pa}). The dotted lines are the predictions of $\gamma=1+1/\beta$ from Equation A2, horizontally offset for viewing.

Abstract—We examined the diets and habitat shift of juvenile red snapper (*Lutjanus campechanus*) in the northeast Gulf of Mexico. Fish were collected from open sand-mud habitat (little to no relief), and artificial reef habitat (1-m^3 concrete or PVC blocks), from June 1993 through December 1994. In 1994, fish settled over open habitat from June to September, as shown by trawl collections, then began shifting to reef habitat—a shift that was almost completed by December as observed by SCUBA visual surveys. Stomachs were examined from 1639 red snapper that ranged in size from 18.0 to 280.0 mm SL. Of these, 850 fish had empty stomachs, and 346 fish from open habitat and 443 fish from reef habitat contained prey. Prey were identified to the lowest possible taxon and quantified by volumetric measurement. Specific volume of particular prey taxa were calculated by dividing prey volume by individual fish weight. Red snapper shifted diets with increasing size. Small red snapper (<60 mm SL) fed mostly on chaetognaths, copepods, shrimp, and squid. Large red snapper (60–280 mm SL) shifted feeding to fish prey, greater amounts of squid and crabs, and continued feeding on shrimp. We compared red snapper diets for overlapping size classes (70–160 mm SL) of fish that were collected from both habitats (Bray-Curtis dissimilarity index and multidimensional scaling analysis). Red snapper diets separated by habitat type rather than fish size for the size ranges that overlapped habitats. These diet shifts were attributed to feeding more on reef prey than on open-water prey. Thus, the shift in habitat shown by juvenile red snapper was reflected in their diet and suggested differential habitat values based not just on predation refuge but food resources as well.

Manuscript approved for publication 4 November 2003 by Scientific Editor.

Manuscript received 20 January 2004 at NMFS Scientific Publications Office.

Fish. Bull. 102:366–375 (2004).

Diet shifts of juvenile red snapper (*Lutjanus campechanus*) with changes in habitat and fish size

Stephen T. Szedlmayer

Marine Fish Laboratory
Department of Fisheries
Auburn University
8300 State Highway 104
Fairhope, Alabama 36532
E-mail address: sszedlma@acesag.auburn.edu

Jason D. Lee

Barry Vittor & Associates
8060 Cottage Hill Rd
Mobile, Alabama 36695

Larval red snapper (*Lutjanus campechanus*) spend approximately 26 days in the plankton, prior to metamorphosis and first appearance on benthic substrate. For the most part the fish settle on open substrate, where peaks in recruitment are observed in August and September, after which they may move to more structured habitat sometime within the first year (Szedlmayer and Conti, 1999). The apparent advantage of this habitat shift would be increased food resources and protection from predators. To help clarify the value of increased food resources on reef habitats, comparisons of diets from the two habitats are necessary. Also, because many fish species shift diets with increasing size (Sedberry and Cuellar, 1993; Burke, 1995; Rooker, 1995; Lowe et al., 1996), we need to distinguish possible ontogenetic diet differences from shifts that are due to habitat.

Previous red snapper diet studies have focused on larger individuals and on small sample sizes for fish <250 mm SL (Camber, 1955; Moseley, 1966; Bradley and Bryan, 1975). Camber (1955) described the diets of 15 "small red snapper" from Campeche Banks, and reported that 14 of the 15 stomachs contained small penaeid shrimps. Moseley (1966) described the diets of 45 "juvenile red snapper" collected off the coasts of Texas, and 28 off Louisiana. Louisiana fish fed on fishes, shrimps, detritus, and stomatopods, and Texas fish fed on shrimps, crabs, and mysid shrimps.

Perhaps the most comprehensive red snapper diet study to date has been that of Bradley and Bryan (1975) which described the diets, by season, of trawl-collected (open sand-mud habitat) and hook-and-line reef "rough bottom areas" fish off the Texas coast. They described the diets of 258 open-habitat and 190 reef red snapper and found that juvenile red snapper (25–325 mm FL) were dependent on shrimp, crabs, and other crustaceans and that adults (325–845 mm FL) were dependent on fish, crabs, and other crustaceans. They described a change in juvenile red snapper diet as fish size increased, "young red snapper depend almost exclusively upon invertebrates," and showed a gradual increase in vertebrate prey with growth. However, they did not separate out the proportions of their "juvenile" red snapper that were collected from reef versus open habitat. Thus, the shift from open to reef habitat is still poorly understood. If and when this shift occurs and whether this shift is accompanied with a diet shift that is independent of fish-size effects needs to be defined.

The purpose of the present study is to describe the diet of red snapper off the coast of Alabama—from the juvenile stage (just after settlement) to one-year old fish. We examined overall

ontogenetic shifts in red snapper diet with increasing size and possible changes in diet with habitat shifts from open substrate to structured habitat (artificial reefs).

Materials and methods

Red snapper were collected from open-flat substrate (sand and mud) and reef habitats (artificial reefs; Fig. 1). The open habitat was located approximately 6 km south of Mobile Bay, Alabama (30°06′N, 88°03′W), and ranged in depth from 12 to 20 m. Previous studies showed very high concentrations of age-0 red snapper from these areas (Szedlmayer and Shipp, 1994; Szedlmayer and Conti, 1999). The artificial reef habitats were located in the Hugh Swingle artificial reef area, approximately 20 km south of Mobile Bay, AL, and ranged in depth from 18 to 23 m (Szedlmayer and Shipp, 1994; Szedlmayer, 1997).

We collected fish from open substrate by trawl (7.62-m head rope, 2.54-cm mesh, 2-mm codend mesh). Samples were taken every two weeks from June to December 1994; however, time between samples was longer in the winter because of poor weather. Each trawl was fished for 10 min, and all age-0 and age-1 red snapper collected were placed on ice, returned to the laboratory, and frozen for later analysis. Bottom dissolved oxygen, salinity, and temperature were sampled with a Hydrolab Surveyor II at each location (Szedlmayer and Conti, 1999).

Prior to diet analysis, red snapper were thawed, weighed to the nearest 0.1 g, and measured to the nearest 0.1 mm SL. The whole fish was preserved in 10% formalin if SL was <50 mm, whereas for larger fish, stomachs were removed and preserved. After 48 hours in formalin, stomach samples were transferred to 75% isopropyl alcohol.

Concrete block and PVC artificial reefs (1 m^3) were placed in the Hugh Swingle reef area in August 1992 and July 1993 (Szedlmayer, 1997). "Reef" is used here for defining these artificial habitats. Reefs were not sampled for a minimum of 3 months after placement. Red snapper were collected from June 1993 through December 1994. Fish were collected from these reefs by SCUBA divers first placing a drop net (3.0 m radius, 1.3 cm square mesh) over the reef and then releasing rotenone into the enclosed area. Reef fish were placed on ice in the field and transported back to the laboratory. Approximately 12–18 h after collection all reef fish were weighed to the nearest 0.1 g and measured to the nearest 1.0 mm. Stomachs were fixed in 10% formalin, and after 24 h transferred to 75% isopropyl alcohol. Red snapper size classes were also estimated by SCUBA visual surveys in July and August 1994. On each visual survey, divers counted red snapper by 50-mm size intervals. Bottom dissolved oxygen, salinity, and temperature were sampled with a Hydrolab Surveyor II during each survey.

All stomachs were dissected and contents placed in petri dishes. All prey were counted and identified to the lowest possible taxon. Volume was calculated by using an adaptation of the method described by Hellawell and Able (1971). Each prey taxon from each stomach was placed into a glass well of a known depth. A cover slide was placed on the well,

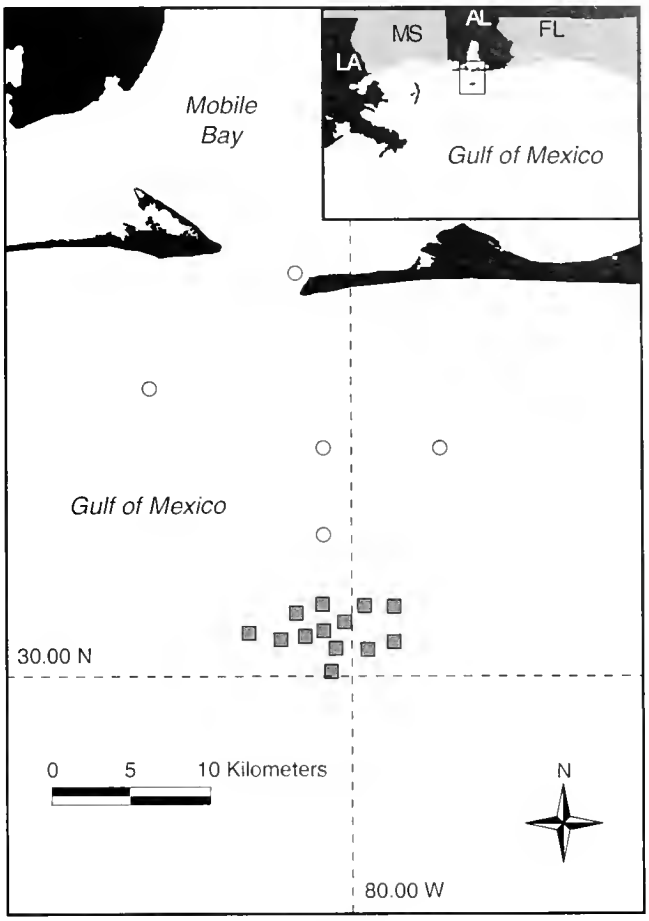

Figure 1

Collection sites for red snapper (*Lutjanus campechanus*) in the northern Gulf of Mexico. Open circles are open habitat trawl sites, and gray squares are 1-m^3 concrete or PVC artificial reefs.

depressing the prey taxon to a known depth (e.g., 1 mm). The prey were video taped with a high-8 Sony camera and images were digitized with Image Pro 2.0 software (Media Cybernetics, Silver Spring, MD). Image size was calibrated to 0.01 mm by a stage micrometer. The surface area of each preparation was measured by using Image Pro software. Volume was calculated by multiplying the surface area by the known depth. Specific volumes for particular prey taxa were calculated by dividing prey volume by individual fish weight (mm^3/fish wt g). Comparisons of diet shift by increasing fish size were made by grouping prey taxa into ten prey groups and by calculating specific volume for 10-mm-size intervals of red snapper.

A dissimilarity index (Bray-Curtis) was calculated from specific volumes of individual prey taxa, for overlapping size classes of red snapper both within and between habitats: Bray-Curtis = $\Sigma|Y_{ij}-Y_{ik}|/\Sigma(Y_{ij}+Y_{ik})$, where Y = specific volume of i^{th} species, and j and k are the samples being compared (Field et al., 1982). The dissimilarities were then used in a multidimensional scaling analysis (MDS; Schiffman et al., 1981). The MDS provided a two-dimensional "map" of the distances between samples (fish

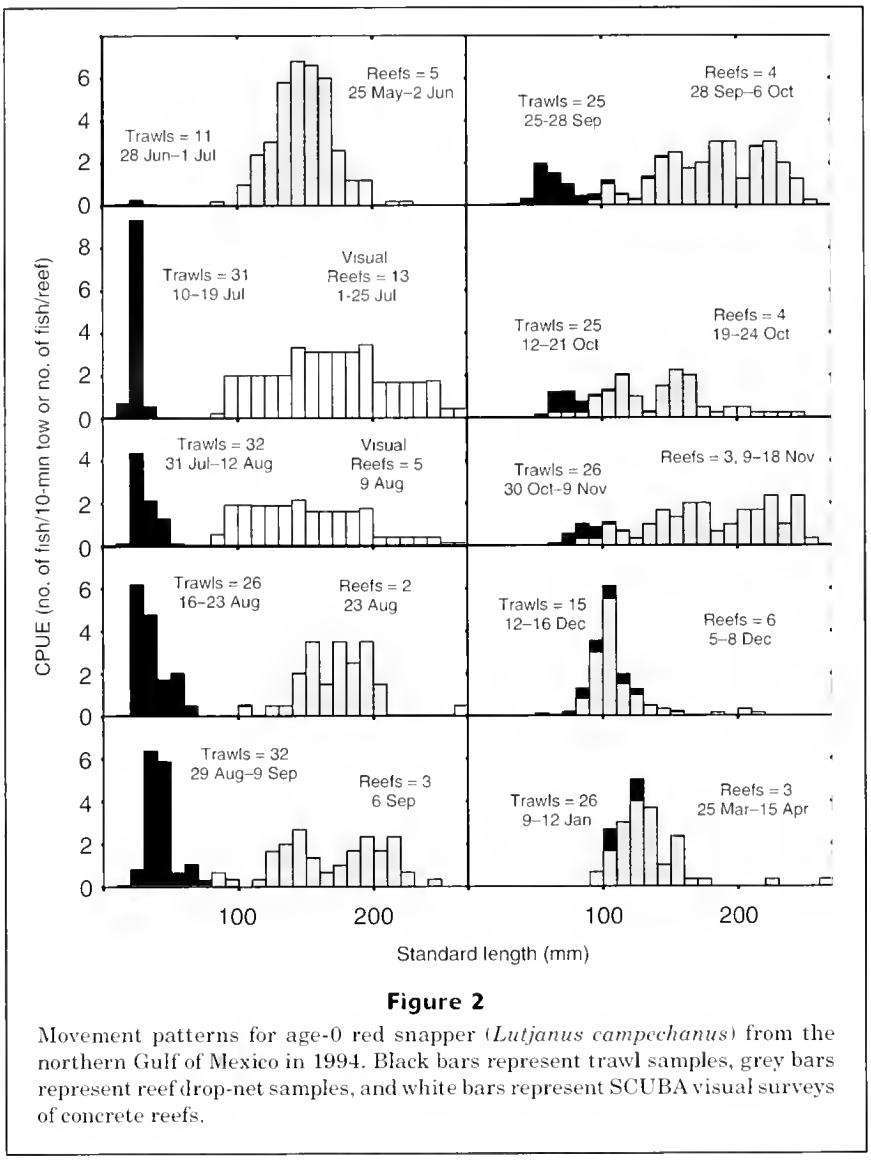

Figure 2

Movement patterns for age-0 red snapper (*Lutjanus campechanus*) from the northern Gulf of Mexico in 1994. Black bars represent trawl samples, grey bars represent reef drop-net samples, and white bars represent SCUBA visual surveys of concrete reefs.

size and habitat type) in Euclidian space based on the Bray-Curtis index. Thus, comparisons of red snapper diets were based on all prey taxa, yet independent of capture habitat and fish size.

Results

In the sampling areas during the summer and fall of 1994, salinity ranged from 30 to 35 ppt. Dissolved oxygen was 7 ppm in the early summer, decreased to 3 ppm in July and August, and increased to 7 ppm in the fall. Temperature was 22 C in June, increased to 28 C in late August, then dropped to just below 20 C by December. No significant differences were detected between trawl and reef sites for these environmental measures (t-test, $P \leq 0.05$).

Red snapper showed a clear shift in habitat during their first few months of life (Fig. 2). Fish first recruited to open habitat at the end of June, at sizes <40 mm SL. Fish continued to recruit to open habitat until early September, at which time they were larger (30 to 100 mm SL) and began shifting to more structured habitat. By mid-October most age-0 fish had moved to reef habitat. During the initial settlement no new recruits were collected or visually observed on the artificial habitats (Fig. 2). Overall, only red snapper <160 mm SL were collected from open habitat, whereas only red snapper >70 mm SL were collected from reef habitat. Size overlapped from 70.0 to 160 mm SL between habitats (Fig. 3).

A total of 1639 red snapper stomachs were analyzed: 570 from open substrate and 1069 from reef habitat. Prey were found in 789 (48%) of the total stomachs examined, 346 (61%) from the open habitat and 443 (41%) from the reef habitat (Fig. 3). Trawl-collected red snapper were mostly collected from site one, but sample sizes were also large (>30 with prey) at two other sites (Table 1). Total red

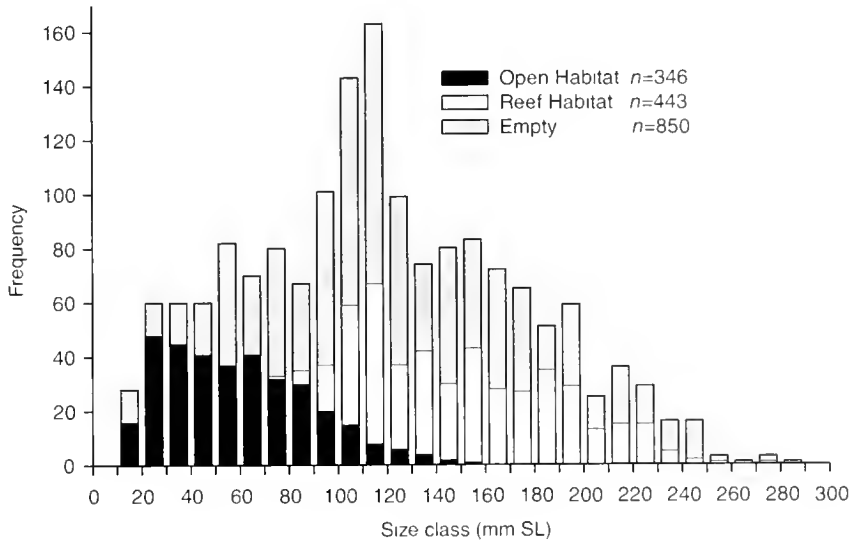

Figure 3

A comparison of red snapper (*Lutjanus campechanus*) length frequencies between open and reef habitats in the northern Gulf of Mexico. Gray bars = empty stomachs from both habitats.

Table 1

Number of red snapper (*Lutjanus campechanus*) stomachs sampled (*n*), and number of stomachs containing prey from open and reef habitat in the northeast Gulf of Mexico.

Open trawl sites		Reef habitats	
n	*n* with prey	*n*	*n* with prey
356	223	108	53
45	21	17	5
75	58	198	115
57	33	55	31
37	11	249	71
		50	23
		14	1
		89	45
		11	5
		209	74
		35	10
		22	4
		12	6

Table 2

Number of red snapper (*Lutjanus campechanus*) stomachs sampled (*n*), and number containing prey, by month and year, from open and reef habitat in the northeast Gulf of Mexico.

Open habitat			Reef habitat		
Month and year	*n*	*n* with prey	Month and year	*n*	*n* with prey
Jul 1994	56	43	Jun 1993	94	50
Aug 1994	169	109	Oct 1993	370	169
Sep 1994	187	98	May 1994	141	37
Oct 1994	97	52	Jun 1994	46	37
Nov 1994	16	12	Aug 1994	41	8
Dec 1994	45	32	Sep 1994	155	86
			Oct 1994	76	28
			Nov 1994	65	12
			Dec 1994	81	16

snapper collected from the reefs varied by site (from 11 to 249 fish), but large samples were collected from at least 6 different reefs (Table 1). Large sample sizes were collected during most months over open habitat, with the exception of November 1994 (n=12), and for most months (6 out of 9) from reef sites (Table 2). Only red snapper stomachs containing prey were used in our analyses.

Red snapper diets showed 55 different prey identified to the lowest possible taxon. In general, red snapper diets were dominated by fish (43%), squid (29.5%), shrimp (16.4%), and crabs (4.4%; Table 3). Specifically, the "shrimp" group included Mysidacea (mysid shrimps), Stomatopoda (mantis shrimps), Penaeidea (penaeid

Table 3

Specific volume (mm^3/fish weight g) for prey taxa from red snapper (*Lutjanus campechanus*). % = percent specific-volume of total volume, Habitat = prey habitat. General prey groups are noted in quotation marks. unid. = unidentified.

Prey taxa	Total volume	Percent	Lowest taxon	Specific volume	Percent	Habitat
Osteichthyes "fish"	5408.2	43.5	unid. fish	3465.9	27.9	
			Halichoeres spp.	650.4	5.2	reef
			Blenniidae	279.2	2.2	reef
			Serranidae	278.1	2.2	reef
			Serranus subligarius	240.8	1.9	reef
			Centropristis ocyurus	207.3	1.7	reef
			Engraulidae	117.9	0.9	open
			Ophichthidae	100.6	0.8	open
			Cynoglossidae	35.2	0.3	open
			Triglidae	20.8	0.2	open
			Ophichthus sp.	10.8	0.1	open
Cephalopoda "squid"	3665.6	29.5	Loliginidae	3665.6	29.5	open
Natantia "shrimp"	2033.7	16.4	unid. shrimp	544.6	4.4	
			Sicyoninae	359.6	2.9	reef
			Hippolytidae	345.7	2.8	reef
			Penaeidae	264.5	2.1	open
			Alpheidae	131.1	1.1	reef
			Sergestidae	24.2	0.2	open
			Luciferinae	22.6	0.2	open
			Ogyrididae	8.8	0.1	open
Stomatopoda "shrimp"			Squillidae	221.8	1.8	open
Mysidacea "shrimp"			Mysidacea	109.8	0.9	open
Reptantia "crabs"	550.8	4.4	Portunidae	302.0	2.4	mixed
			unid. crab	143.0	1.2	
			Diogeninae	51.6	0.4	open
			Leucosiidae	20.7	0.2	reef
			Xanthidae	16.7	0.1	reef
			Porcellanidae	7.3	0.1	reef
Chaetognatha	199.6	1.6	*Sagitta* spp.	199.6	1.6	open
Polychaeta	130.1	1.0	Polycheata	75.4	0.6	mixed
Polychaeta			Onuphidae	34.0	0.3	open
			Maldanidae	19.9	0.2	open
Ascidiacea "tunicate"	121.0	1.0	Ascidiacea	121.0	1.0	reef
Calanoida "copepod"	118.2	1.0	Calanoida	113.3	0.9	open
Octopodidae	93.6	0.8	*Octopus* sp.	93.6	0.8	reef
unid.	79.5	0.6	unid.	79.5	0.6	
Amphipoda	13.8	0.1	Amphipoda	9.4	0.1	mixed
Ostracoda	6.1	0.0	Ostracoda	6.1	0.0	open

shrimps), and Caridea (caridean shrimps). In addition, all Squillidae were probably *Squilla empusa*, according to Hopkins et al., (1987). Among fish, many were unidentified due to digestion, but if proportions of unidentified fish are similar to identified fish, then dominant fish prey included *Halichoeres* spp., (5.2%), Blenniidae (2.2%), and Serranidae (2.2%). Two prey fish were identified to species: *Serranus subligarius* (1.9%), and *Centropristis ocyurus* (1.7%).

Among the squid taxon, one genus dominated: *Lolliguncula* spp., (29.5%), but all squid were either *L. brevis* or *Loligo pealeii* (Hopkins et al., 1987). Among shrimp, dominant taxa included Sicyoninae (2.9%), Hippolytidae (2.8%), Penaeidae (2.1%), Squillidae (1.8%), and Alpheidae (1.1%). Among crabs, dominant taxa were mostly Portunidae (2.4%). Other groups showing greater than 1.0% included Chaetognatha (*Sagitta* sp. 1.6%), and Ascidiacea or tunicates (1.0%; Table 3).

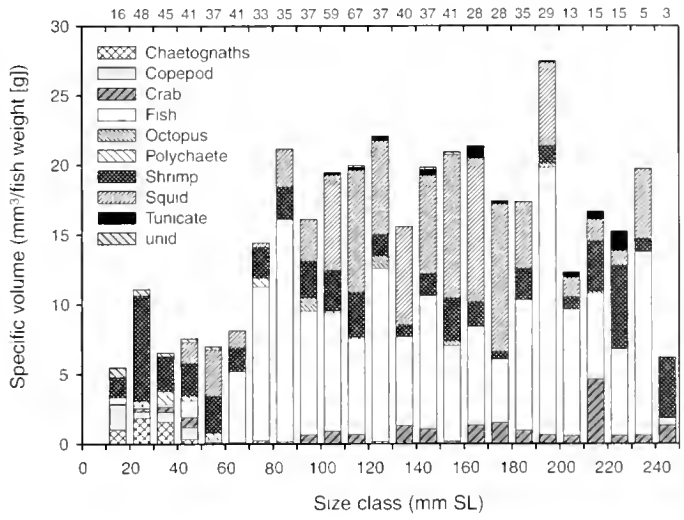

Figure 4

Stomach contents by specific-volume for ten higher taxonomic groups over 10-mm size classes of red snapper (*Lutjanus campechanus*) from both open and reef habitats in the northern Gulf of Mexico. Numbers on the upper axis are the number of red snapper that contained prey for each respective size class.

Red snapper shifted diets with increasing size. For red snapper <60.0 mm SL, diets were dominated by shrimp, chaetognaths, squid, and copepods. Large red snapper (60–280 mm SL) shifted to feeding on fish prey, greater amounts of squid and crabs, and continued feeding on shrimp (Fig. 4).

The diets of juvenile red snapper changed as they moved from open to reef habitats. Fish collected had overlapping sizes of 70.0 to 160.0 mm SL from both open and reef habitats, and the MDS analysis for this size range showed a clear separation of diets between the two habitats (Fig. 5). Two points that were outliers (R75, T155) were biased because they represented only one fish each, and the third outlier (R85) was difficult to explain.

The clear separation of red snapper diets shown by the MDS analysis can be attributed to several prey shifts that accompanied habitat shifts. For prey crabs, open-habitat red snapper diets were dominated by Xanthidae, and smaller amounts of Paguridae, Portunidae, Diogeninae, and Pinnotheridae (Fig. 6), whereas diets of red snapper from reef habitats shifted to a dominance by Portunidae and Diogeninae (Fig. 7). For prey shrimp, open habitat red snapper diets were dominated by Penaeidae and Mysidacea (Fig. 8), whereas diets from reef habitats shifted to a dominance of Sicyoninae, Hippolytidae, Alpheidae, and Squillidae (Fig. 9). For prey fish, open-habitat red snapper diets were dominated by Engraulidae (although most were unidentified; Fig. 10), whereas diets from reef habitat clearly reflected prey fish from reef habitats and included Blenniidae, Serranidae, and three prey fish identified to genera, *Centropristis* spp, *Halichoeres* spp., and *Serranus* spp. (Fig. 11).

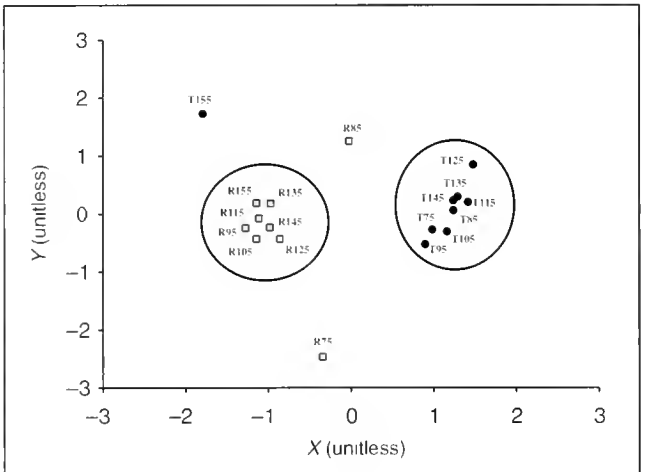

Figure 5

Multidimensional scaling of diets for red snapper (*Lutjanus campechanus*) based on the Bray-Curtis dissimilarity index computed for specific volume of prey taxa both within and between habitats for overlapping size classes (70.0 to 159.9 mm SL). The letter and number accompanying each point indicates the habitat and size class that each point represents (e.g., T = trawl, R = reef, 75 = 75 mm SL size class). Circles were drawn by hand. Axes are unitless.

Discussion

The present study provides a substantial sample size (n=1639) for red snapper diet analysis and a relatively

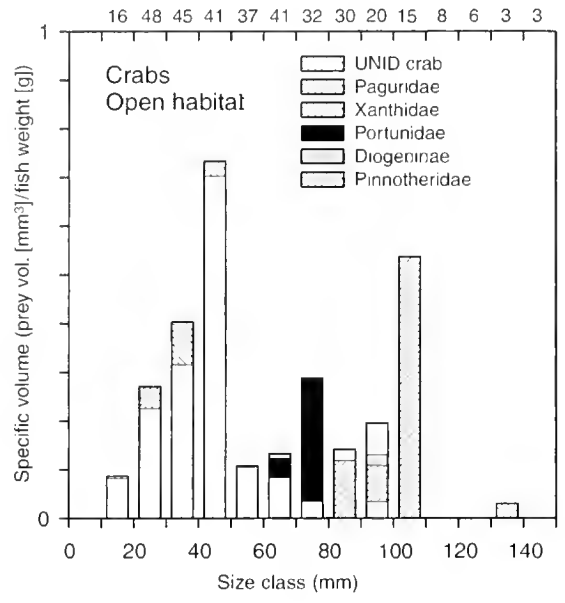

Figure 6

Crab prey from open habitat. Stomach contents by specific volume over 10-mm size classes of red snapper (*Lutjanus campechanus*) from the northern Gulf of Mexico. Numbers on the upper axis are the number of red snapper that contained prey for each respective size class.

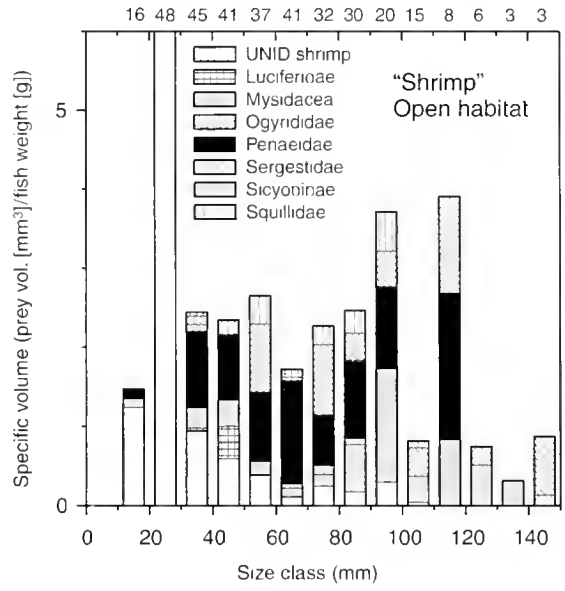

Figure 8

"Shrimp" prey from open habitat. Stomach contents by specific volume over 10-mm size classes of red snapper (*Lutjanus campechanus*) from the northern Gulf of Mexico. Numbers on the upper axis are the number of red snapper that contained prey for each respective size class.

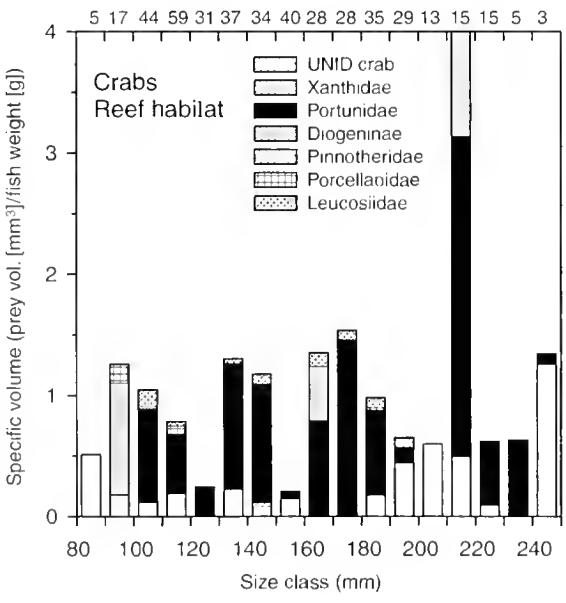

Figure 7

Crab prey from reef habitat. Stomach contents by specific volume over 10-mm size classes of red snapper (*Lutjanus campechanus*) from the northern Gulf of Mexico. Numbers on the upper axis are the number of red snapper that contained prey for each respective size class.

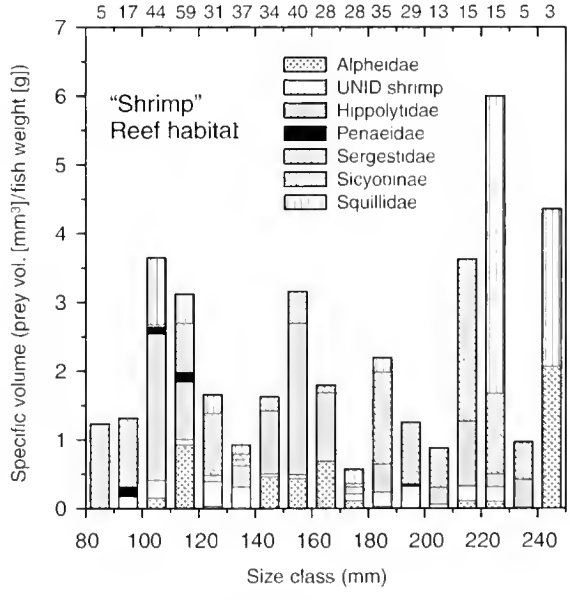

Figure 9

"Shrimp" prey from reef habitat. Stomach contents by specific volume over 10-mm size classes of red snapper (*Lutjanus campechanus*) from the northern Gulf of Mexico. Numbers on the upper axis are the number of red snapper that contained prey for each respective size class.

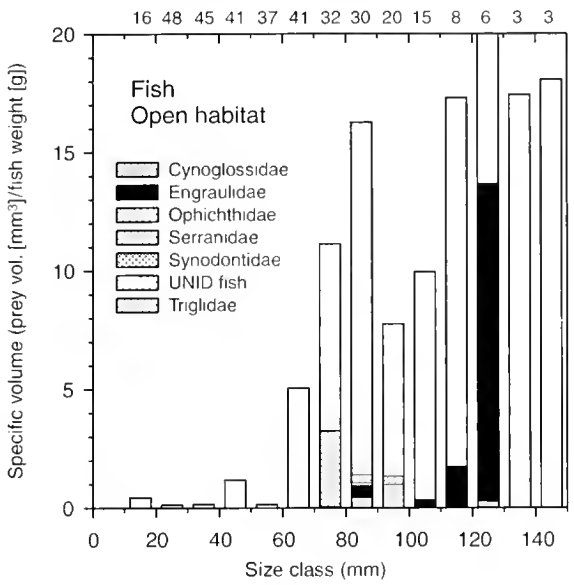

Figure 10

Fish prey from open habitat. Stomach contents by specific volume over 10-mm size classes of red snapper (*Lutjanus campechanus*) from the northern Gulf of Mexico. Numbers on the upper axis are the number of red snapper that contained prey for each respective size class.

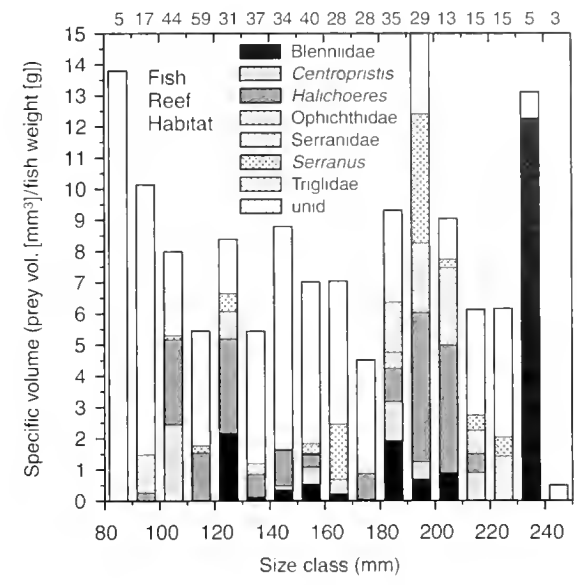

Figure 11

Fish prey from reef habitat. Stomach contents by specific volume over 10-mm size classes of red snapper (*Lutjanus campechanus*) from the northern Gulf of Mexico. Numbers on the upper axis are the number of red snapper that contained prey for each respective size class.

high percentage of stomachs with food (48%) compared to past studies. Rooker (1995) also showed a high percentage (69%; 312 out of 449 stomachs) of schoolmaster snapper (*Lutjanus apodus*) contained prey, when fish were collected from depths similar to those of the our study (1 to 27 m). The higher percentage of stomachs with prey found in our study compared to past studies of red snapper (Stearns, 1884; Camber,1955; Moseley, 1966) may be due to the shallower depths sampled (18 m; DeMartini et al., 1996).

Juvenile red snapper showed feeding patterns similar to many other marine fishes. After settlement, from approximately 20 to 60 mm SL, they showed a wide-ranging diet that included shrimp, copepods, chaetognaths, and squid. Prey fish were also found in the stomachs of the smallest red snapper collected (15–20 mm SL) but were not a dominant component. Sweatman (1993) reported similar results for the snapper *Lutjanus quinquelineatus*, ranging from 24 to 29 mm SL, i.e., piscivorous in the first few days after settlement. Above 60 mm SL, fish prey tended to dominate specific volume, but not by feeding less on shrimp because shrimp continued to be an important prey. Squid became another dominant component of red snapper diet at about 100 mm SL and also continued as an important prey up to 240 mm SL. Unfortunately, sample size was reduced above 230 mm SL, and it was difficult to estimate if squid and fish continued as dominant prey components above these size classes. Sedberry and Cuellar (1993) reported a similar shift in diets of reef-associated vermilion snapper (*Rhomboplites aurorubens*). This species shifted from small crustaceans to fishes and cephalopods over a size range similar to that of red snapper in the present study. Moseley (1966) reported a "slow transition from zooplankton to macro animals for red snapper sizes between 40 and 90 mm"—a transition that probably included fish prey that he did not specifically identify. Bradley and Bryan (1975), showed a shift in juvenile red snapper diets with size (25–325 mm FL). Their smallest red snapper keyed on invertebrates, then showed a sharp increase in dependency upon prey fish above 175 mm FL, when Batrachoididae (toadfish) became a dominant component. These shifts in diet are important in helping to identify fish habitat and are potentially key aspects of early survival.

Red snapper showed two major habitat shifts in their first year. Juvenile red snapper first settled from the plankton to benthic substrate near 20 mm SL (Szedlmayer and Conti, 1999). The present study showed a second shift from open habitat to reef habitat starting at about 70 mm SL (Fig. 3). No fish smaller than 70 mm were collected from the reefs, and smaller red snapper were rarely observed on these reefs from SCUBA visual surveys. No fish larger than 160 mm SL were caught from the open habitat but were present on the reefs. This finding suggested that red snapper had shifted to reef habitat by 160 mm SL but also may have avoided trawl gear as described earlier for age-0 red snapper (Bradley and Bryan, 1975) and age-0 summer flounder (*Paralichthys dentatus*) (Szedlmayer and Able, 1993). However, no large (150–300 mm) red

snapper were observed over open habitat by a SCUBA visual survey despite our observations that red snapper are attracted to SCUBA divers. Thus we suggest that a shift in habitat was more likely the cause of this absence than trawl avoidance.

The distinct diet shift as red snapper changed habitats was independent of increasing size and suggested that different benthic habitats play a critical role in the early life history of this species. This separation was completely independent of "a priori" knowledge of sample location and fish size. For example, the MDS analysis showed almost complete separation based on habitat rather then fish size (Fig. 5). These differences between open and reef habitat were readily apparent when prey taxa were separated into lower taxonomic categories. For example, fishes such as *Halichoeres* spp., *Serranus* spp., and *Centropristis* spp., were found only in the diets of reef-collected red snapper. These species are closely tied to reef structure (Nelson and Bortone, 1996). Prey shrimp also showed distinct differences in red snapper diets between habitats. Over open habitat, Mysidacea, Penaeidae, and Sergestidae were important components. After the shift to reef habitat, Mysidacea were absent and Penaeidae and Sergestidae were greatly reduced, and Sicyoninae, Hippolytidae, and Alpheidae became the dominant shrimp components. The latter are all families typically associated with reef habitats (Chance, 1970; Pequegnat and Heard, 1979). One exception was the increased feeding on Squillidae, an open habitat crustacean, at the largest size classes of this study (220–250 mm SL; Fig. 9). For crabs, the separation was not as clear, because of the dominance of Portunidae, which can be assigned to both open and reef habitats. However, increases in reef crabs were still apparent with habitat shift, i.e., Diogeninae, Porcellanidae, and Leucosiidae can all be considered reef prey. Although Bradley and Bryan (1975) pooled "juvenile" red snapper over open and reef habitats, they did show a marked increase in fish prey above 175 mm FL. This increase was almost exclusively due to Batrachoididae or toadfishes, which are typically found in reef habitat. We did not observe any toadfish prey in our juvenile red snapper collections, but its presence in this earlier study is consistent with present findings showing a shift to feeding on reef-habitat prey.

Red snapper diet shifted to greater percentages of reef-prey with movement to reef habitat, but with this shift they also continued feeding on other prey. This flexibility in feeding habits allows red snapper to take advantage of prey from wide-ranging habitats. Similar diet shifts related to habitat shifts have been shown in schoolmaster snapper, (*L. apodus*) (Rooker, 1995). The schoolmaster snapper shifted from nearshore mangroves to coral reef habitats near 70 mm SL; diets of fish ≤70.0 mm SL were dominated by crustaceans, particularly amphipods and crabs. Fish >70.0 mm SL fed on fishes and to a lesser extent crabs, shrimps, and stomatopods. Similar diet shifts were also shown for several fish species of Puget Sound. For example in pile perch (*Rhacochilus vacca*), striped seaperch (*Embiotoca lateralis*), and quillback rockfish (*Sebastes maliger*), the smallest juveniles preyed on open-habitat plankton and benthic fauna, and medium-size and larger fish (>121 mm) of all three species shifted their diets to include reef-associated prey (Hueckel and Stayton, 1982). However, at larger sizes these three species were not totally dependent on reef-associated prey.

We have examined red snapper diets based on specific volume of food. Although many other studies have used an index of relative importance (IRI; Pinkas et al., 1971; Cortes, 1997), we were specifically interested in the nutritional value of particular prey, and prey separation into open-habitat or reef-habitat. With IRIs these separations would be more difficult to define, e.g., pelagic prey with high numbers might be considered more important, but actually provide little nutritional value to red snapper diets (Macdonald and Green, 1983). Future studies on the effects of red snapper predation on prey distributions may be better suited for using IRIs.

In summary, red snapper diets from open habitat showed prey taxa associated with open sand-mud substrate and the planktonic environment. Open-habitat prey, such as chaetognaths, are known to be pelagic as well as benthic, as are sergestid shrimp, calanoid copepods, mysids, and stomatopods (Williams, 1968; Manning, 1969; Gosner, 1978; Stuck et al., 1979; Alldredge and King, 1985; Lindquist et al., 1994). Red snapper shifted diets to reef-associated prey with their habitat shift, and this diet shift was independent of fish size. These diet shifts were clearly apparent for both fish and shrimp prey but less so for crab prey. As shown with marine fish species from Puget sound, red snapper diets from reef habitat were not restricted to reef-associated prey. For example, squids were an important prey over both open and reef habitats in the present study and our findings agree with those of Bradley and Bryan (1975). The squids *Loligo* sp., and *Lolliguncula* sp. are both abundant in nearshore coastal waters and are not typically associated with reef structure (Gosner 1978; Laughlin and Livingston, 1982; Hopkins et al., 1987). Availability and ease in capture could be a key as to why squid are important for red snapper over size ranges of 40 to 240 mm SL. This flexibility in feeding habits allows red snapper to take advantage of prey from wide-ranging habitats, but clear shifts to additional reef prey supports the hypothesis that reef structure provides new prey resources.

Acknowledgments

We thank Joseph Conti, Kori M. Heaps, and Frank S. Rikard for help in field collections and invertebrate identification. This study was funded by NOAA, NMFS, MARFIN grant number USDC-NA47FF0018-0. This is a contribution of the Alabama Agricultural Station.

Literature cited

Alldredge, A. L., and J. M. King.
1985. The distance demersal zooplankton migrate above the benthos: implications for predation. Mar. Biol. 84:253–260.

Bradley, E., and C. E. Bryan.
1975. Life history and fishery of the red snapper (*Lutjanus campechanus*) in the northwestern Gulf of Mexico: 1970–1974. *In* Proceedings of the twenty-seventh Gulf and Caribbean Fisheries Institute, p. 77–106. Univ. Miami, Miami, FL.

Burke, J. S.
1995. Role of feeding and prey distribution of summer and southern flounder in selection of estuarine nursery habitats. J. Fish Biol. 47:355–366.

Camber, C. I.
1955. A survey of the red snapper fishery of the Gulf of Mexico, with special reference to the Campeche Banks. Florida State Board of Conservation Technical Series 12:1–64.

Chance, F. A., Jr.
1970. A new shrimp of the genus *Lysmata* (Decapoda: Hippolytidae) from the western Atlantic. Crustaceana 19:59–66.

Cortés, E.
1997. A critical review of methods of studying fish feeding based on analysis of stomach contents: application to elasmobranch fishes. Can. J. Fish. Aquat. Sci. 54:726–738.

DeMartini, E. E., F. A. Parrish, and D. M. Ellis.
1996. Barotrauma-associated regurgitation of food: implications for diet studies of Hawaiian pink snapper, *Pristipomoides filamentosus* (family Lutjanidae). Fish. Bull. 94:250–256.

Field, J. G., K. R. Clarke, and R. M. Warwick.
1982. A practical strategy for analyzing multispecies distribution patterns. Mar. Ecol. Prog. Ser. 8:37–52.

Gosner, K. L.
1978. A field guide to the Atlantic seashore, 329 p. Houghton Mifflin Company, Boston, MA.

Hellawell, J. M., and R. Able.
1971. A rapid volumetric method for the analysis of the food of fishes. J. Fish Biol. 3:29–37.

Hopkins, T. S., J. F. Valentine, and L. B. Lutz.
1987. An illustrated guide with key to selected benthic invertebrate fauna of the Northern Gulf of Mexico. Mississippi Alabama Sea Grant Publ. 087(10), Biloxi, MS.

Hueckel, G. S., and R. L. Stayton.
1982. Fish foraging on an artificial reef in Puget Sound, Washington. Mar. Fish. Rev. 44: 38–44.

Laughlin, R. A., and R. J. Livingston.
1982. Environmental and trophic determinants of the spatial/temporal distribution of the brief squid (*Lolliguncula brevis*) in the Apalachicola estuary (North Florida, USA). Bull. Mar. Sci. 32:489–497.

Lindquist, D. G., L. B. Cahoon, J. E. Clavijo, M. H. Posey, S. K. Bolden, L. A. Pike, S. W. Burk, and P. A. Cardullo.
1994. Reef fish stomach contents and prey abundance on a reef and sand substrata associated with adjacent artificial and natural reefs in Onslow Bay, North Carolina. Bull. Mar. Sci. 55:308–318.

Lowe, C. G., B. M. Wetherbee, G. L. Crow, and A. L. Tester.
1996. Ontogenetic dietary shifts and feeding behavior of the tiger shark, *Galeocerdo cuvier*, in Hawaiian waters. Environ. Biol. Fish. 47:203–211.

Macdonald, J. S., and R. H. Green.
1983. Redundancy of variables used to describe importance of prey species in fish diets. Can. J. Fish. Aquat. Sci. 40:635–637.

Manning, R. B.
1969. Stomatopod Crustacea of the Western Atlantic, 380 p. Univ. Miami Press, Miami, FL.

Moseley, F. N.
1966. Biology of the red snapper, *Lutjanus aya* Bloch, of the northwestern Gulf of Mexico. Publ. Inst. Mar. Sci. Univ. Texas 11:90–101.

Nelson, B. D., and S. A. Bortone.
1996. Feeding guilds among artificial-reef fishes in the northern Gulf of Mexico. Gulf Mex. Sci. 2:66–80.

Pequegnat, L. H., and R. W. Heard.
1979. *Synalpheus agelas*, new species of snapping shrimp from the Gulf of Mexico and Bahama Islands (Decapoda: Alpheidae). Bull. Mar. Sci. 29:110–116.

Pinkas, L., M. S. Oliphant, I. L. R. Iverson.
1971. Food habits of albacore, bluefin tuna, and bonito in California waters. Calif. Fish Game 152:1–105.

Rooker, J. R.
1995. Feeding ecology of the schoolmaster snapper, *Lutjanus apodus* (Walbum), from southwestern Puerto Rico. Bull. Mar. Sci. 56:881–894.

Schiffman, S. S., M. L. Reynolds, and F. W. Young.
1981. Introduction to multidimensional scaling, 413 p. Academic Press Inc., New York, NY.

Sedberry, G. R., and N. Cuellar.
1993. Planktonic and benthic feeding by the reef associated vermilion snapper, *Rhomboplites aurorubens* (Teleostei, Lutjanidae). Fish. Bull. 91:699–709.

Stearns, S.
1884. On the position and character of the fishing grounds of the Gulf of Mexico. Bull. U.S. Fish. Comm. 4:289–290.

Stuck, K. C., H. M. Perry, and R. W. Heard.
1979. An annotated key to the Mysidacea of the north central Gulf of Mexico. Gulf Res. Rep. 6: 225–238.

Sweatman, H. P. A.
1993. Tropical snapper (Lutjanidae) that is piscivorous at settlement. Copeia 1993:1137–1139.

Szedlmayer, S. T.
1997. Ultrasonic telemetry of red snapper, *Lutjanus campechanus*, at artificial reef sites in the northeast Gulf of Mexico. Copeia 1997:846–850.

Szedlmayer, S. T., and K. W. Able.
1993. Ultrasonic telemetry of age-0 summer flounder, *Paralichthys dentatus*, movements in a southern New Jersey estuary. Copeia 1993:728–736.

Szedlmayer, S. T., and J. Conti.
1999. Nursery habitats, growth rates, and seasonality of age-0 red snapper, *Lutjanus campechanus*, in the northeast Gulf of Mexico. Fish. Bull. 97:626–635.

Szedlmayer, S. T., and R. L. Shipp.
1994. Movement and growth of red snapper, *Lutjanus campechanus*, from an artificial reef area in the northeastern Gulf of Mexico. Bull. Mar. Sci. 55: 887–896.

Williams, A. B.
1968. Substrate as a factor in shrimp distribution. Limnol. Oceanog. 3:283–290.

Individual growth rates and movement of juvenile white shrimp (*Litopenaeus setiferus*) in a tidal marsh nursery*

Stacey Webb

Florida Department of Environmental Protection
Water Quality Standards and Special Projects Program
2600 Blair Stone Road, M.S. 3560
Tallahassee, Florida 32399
E-mail address: stacey.feken@dep.state.fl.us

Ronald T. Kneib

UGA Marine Institute
Sapelo Island, Georgia 31327

Abstract—We measured growth and movements of individually marked free-ranging juvenile white shrimp (*Litopenaeus setiferus*) in tidal creek subsystems of the Duplin River, Sapelo Island, Georgia. Over a period of two years, 15,974 juvenile shrimp (40–80 mm TL) were marked internally with uniquely coded microwire tags and released in the shallow upper reaches of four salt marsh tidal creeks. Subsequent samples were taken every 3–6 days from channel segments arranged at 200-m intervals along transects extending from the upper to lower reach of each tidal creek. These collections included 201,384 juvenile shrimp, of which 184 were marked recaptures. Recaptured shrimp were at large an average of 3–4 weeks (range: 2–99 days) and were recovered a mean distance of <0.4 km from where they were initially marked. Mean residence times in the creek subsystems ranged from 15.2 to 25.5 days and were estimated from exponential decay functions describing the proportions of marked individuals recaptured with increasing days at large. Residence time was not significantly correlated with creek length (Pearson=−0.316, P=0.684), but there was suggestive evidence of positive associations with either intertidal (Pearson r=0.867, P=0.133) or subtidal (Pearson r=0.946, P=0.054) drainage area. Daily mean specific growth rates averaged 0.009 to 0.013 among creeks; mean absolute growth rates ranged from 0.56–0.84 mm/d, and were lower than those previously reported for juvenile penaeids in estuaries of the southeastern United States. Mean individual growth rates were not significantly different between years (t-test, P>0.30) but varied significantly during the season, tending to be greater in July than November. Growth rates were size-dependent, and temporal changes in size distributions rather than temporal variation in physical environmental factors may have accounted for seasonal differences in growth. Growth rates differed between creeks in 1999 (t-test, P<0.015), but not in 1998 (t-test, P>0.5). We suggest that spatial variation in landscape structure associated with access to intertidal resources may have accounted for this apparent interannual difference in growth response.

Manuscript approved for publication 30 September 2003 by Scientific Editor.

Manuscript received 20 January 2004 at NMFS Scientific Publications Office.

Fish. Bull. 102:376–388 (2004).

In 2001, shrimp became the most popular seafood in the United States when per capita consumption (1.54 kg) surpassed that of canned tuna (1.32 kg) for the first time in recorded history (NOAA[1]). Although 77% of the catch is from the Gulf of Mexico, commercial fisheries in Atlantic coastal states of the southeastern United States also depend heavily on penaeid shrimp populations. Of the three most common estuarine-dependent penaeid species (*Litopenaeus setiferus*, *Farfantepenaeus aztecus*, and *F. duorarum*)[2] harvested in the South Atlantic Bight, white shrimp *Litopenaeus setiferus* dominate, comprising >70% of the catch in the region (North Carolina to the east coast of Florida) and 75–87% in South Carolina and Georgia (NMFS[3]).

Concerns over the possibility of depleting the resource as early as the 1930s led to intensive studies of the life cycle (Lindner and Anderson, 1956; Williams, 1984). The white shrimp has an annual life cycle that can be divided into offshore (oceanic) and inshore (estuarine) phases. Adults spawn in Atlantic waters in spring and the postlarvae migrate into estuaries, aided by flood tides and wind-generated currents (Lindner and Anderson, 1956; Wenner et al., 1998). Postlarvae penetrate into the shallow upper reaches of the nursery habitat where juveniles achieve a substantial portion of their adult body mass before moving into deeper creeks, rivers, and sounds where they approach maturity and emigrate seaward to spawning areas (Muncy, 1984; Williams, 1984).

Given the commercial importance and early interest in this species, surprisingly little research has focused on the juvenile stages within tidal marsh nursery habitats (Minello and Zimmerman, 1985; Zein-Eldin and Renaud, 1986; Knudsen et al., 1996; McTigue and Zimmerman, 1998). Seasonal migrations and ontogenetic movements of white shrimp between coastal ocean spawning grounds and estuarine nurseries are well known (Dall et al., 1990), as are the sometimes extensive migrations of adult shrimp along the Atlantic coast, primarily to the south during fall and early winter, and northward in late winter and early spring (Lindner and Anderson, 1956; Shipman, 1983). Within the estuary, juvenile white

*Contribution 921 of the Univerisity of Georgia Marine Institute, Sapelo Island, GA.

[1] NOAA (National Oceanic and Atmospheric Administration. 2002. Shrimp overtakes canned tuna as top U.S. seafood. Website: http://www.noaanews.noaa.gov/stories/s970.htm. [Accessed: 28 August 2002.]

[2] These species were all previously included in the genus *Penaeus*, but the subgenera were elevated to genera by Pérez-Farfante and Kensley (1997).

[3] NMFS (National Marine Fisheries Service). 2002. Unpubl. data. Website: http://www.st.nmfs.gov/st1/commercial/index.html. [Accessed 29 August 2002.]

shrimp, in contrast to other penaeid species, are found across a wider range of environmental conditions and habitats (Kutkuhn, 1966) and often make tidal excursions between subtidal and vegetated intertidal habitats to forage (Mayer, 1985; Kneib, 1995; 2000). However, relatively little is known about movements within subtidal creeks of the primary nursery areas, and the degree to which individuals exhibit fidelity to a particular tidal creek drainage system is unknown.

Direct measurement of juvenile shrimp growth rates within the nursery have also been rare. Most growth estimates for free-ranging juvenile shrimp are based on analyses of size-frequency data, which can be misleading (Loesch, 1965). Shrimp grow rapidly while in the estuarine nursery throughout the summer and early fall, and juveniles approach adult, or commercially harvestable size within 2–4 months after immigration to the estuary (Kutkuhn, 1966; Williams, 1984). Mean absolute growth rates of 0.7–1.1 mm/d are commonly reported for many penaeids (Dall et al., 1990). However, growth studies are difficult to compare because the rate of growth may vary between years and among seasons, as well as with size, age, and sex of individuals (Perez-Farfante, 1969). Growth estimates for *Litopenaeus setiferus* range widely, from 10 to 65 mm/month (Williams, 1984). Previous estimates were based on a variety of approaches including experimental studies in aquaria and ponds (Pearson, 1939; Johnson and Fielding, 1956), size distributions from tagging studies of adults (Lindner and Anderson, 1956), length-frequency distributions of juveniles in field samples (Gunter, 1950; Williams, 1955; Loesch, 1965; Harris, 1974; Mayer, 1985), mark-recapture of uniform size ranges of subadults and adults (Klima, 1974), and mark-recapture of shrimp in marsh ponds (Knudsen et al., 1996). Many estimates of growth for small (<80 mm TL) juvenile *L. setiferus* have been extrapolated from mark-recapture studies of larger (>100 mm TL) individuals (Lindner and Anderson, 1956; Harris, 1974; Klima, 1974). However, there is a paucity of empirical data on growth rates of small, free-ranging juvenile white shrimp within natural estuarine nursery habitats. The purpose of the present study was to provide reliable data on growth and movements of individual juvenile white shrimp within a natural estuarine nursery environment and to initiate an assessment of spatial variation in habitat quality in relation to tidal marsh landscape structure.

Recent innovations in tagging techniques have produced an effective way to obtain information on individual organisms through the use of sequentially numbered binary-coded microwire tags (Northwest Marine Technology, Inc. Shaw Island, WA). Microwire tags were first used in tagging experiments by Jefferts et al. (1963) and have since been used successfully to tag a variety of crustaceans including prawns (Prentice and Rensel, 1977), crayfish (Isely and Eversole, 1998), blue crabs (van Montfrans et al., 1986; Fitz and Weigert, 1991), and lobsters (Krouse and Nutting, 1990; Uglem and Grimsen, 1995). Results of these studies and others generally show that tag retention rates are high and tagging has little effect on the growth or survival of the fishes and crustaceans in which microwire tags have been used. In a laboratory study involving 240 juvenile white shrimp, Kneib and Huggler (2001) confirmed that tag retention was high (~98%), growth rates between tagged and control individuals were not significantly different, and the best location (based on tag retention and survival) for tag injection was in the muscle tissue of the abdomen. This type of tag allows for identification of individuals because each tag is etched with a unique number encoded in binary form. In addition, the tag is completely internal and inconspicuous, thus eliminating problems associated with external tags (e.g., streamer-type tags) that might interfere with molting or increase predation risk (Garcia and LeReste, 1981; van Montfrans et al., 1986; Isely and Eversole, 1998).

Materials and methods

Study area

All samples were collected from four tidal creek subsystems associated with the Duplin River on the west side of Sapelo Island, Georgia. The Duplin River tidal drainage (~11 km^2) includes almost 10 km^2 of tidal salt marsh that is inundated twice daily by unequal tides with a mean range of 2.1 m (Wadsworth, 1980). Smooth cordgrass (*Spartina alterniflora*) is the dominant vegetation in the intertidal marshes of this area. Seasonal water temperatures average between 10°C and 30°C, and salinity is characteristically polyhaline, ranging from 15 to 30 ppt (Kneib, 1995). Freshwater flow into the system is intermittent and originates largely from local upland runoff and indirect flows by several interconnected tidal channels from the Altamaha River about 8 km to the southwest (Ragotzkie and Bryson, 1955).

Tidal creeks included in this study were Post Office Creek (PO) and Stacey Creek (SC) in 1998, and the East and West forks (EF, WF, respectively) of the upper Duplin River in 1999 (Fig. 1). Logistical constraints precluded sampling shrimp populations from more than two creek systems within the same year, and different pairs of creeks were chosen in each of the two years to broaden the spatial coverage of the study. High-resolution black and white photographs (1:16000 scale) from an aerial survey of the region in December 1989 were used to measure broad-scale structural characteristics of the creek systems, including areal extent of the intertidal and subtidal portions of each drainage. The metrics and methods of extracting the information from the photographs are fully described elsewhere (see Webb and Kneib, 2002).

Field sampling

Shrimp were collected by cast net along the shallow (<1 m depth) edges of the subtidal portion of each creek system during low tide. Preliminary studies showed that 1.52-m diameter nets with ca. 1-cm mesh size collected the range of juvenile shrimp sizes (40–80 mm) targeted for marking in this study. All samples were collected within 2–3 hours of low tide to ensure that the shrimp popula-

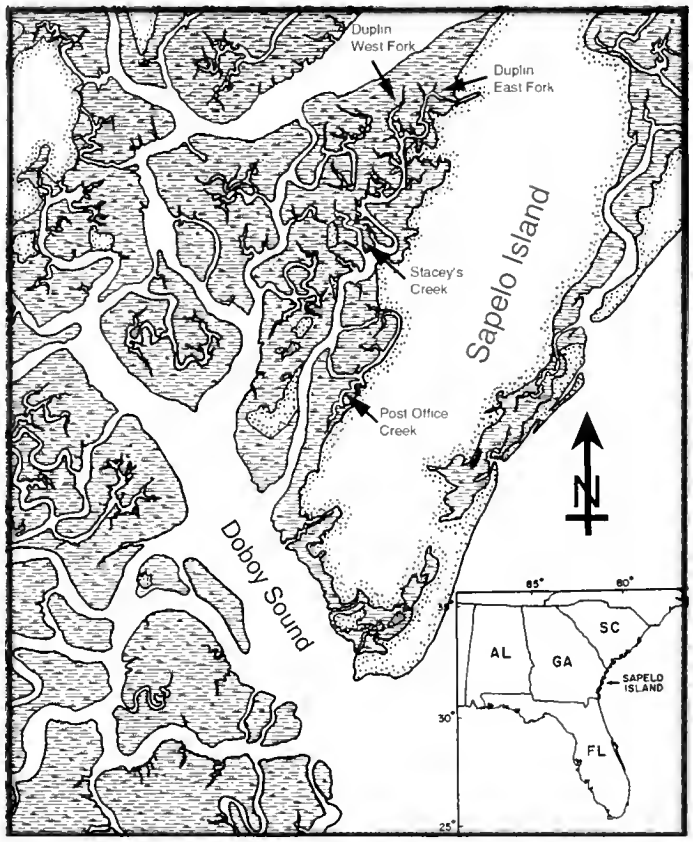

Figure 1

Map of the salt marsh estuary in the vicinity of Sapelo Island, Georgia, showing locations of the tidal creek subsystems within the tidal drainage of the Duplin River.

tion was restricted to the tidal creek channels and had no refuge in the intertidal vegetation. A series of stations, at intervals of approximately 200 m, was established along the length of the subtidal portion of each creek from the upper reaches to the mouth, so that the number of stations within a creek depended on the navigable length of the subtidal channel. There were 13 stations in PO, 11 in SC, 9 in EF, and 7 in WF. Salinity, water temperature, and dissolved oxygen were measured near the surface (<1 m depth) at the mouth of the tidal creek on each day of sampling by using a YSI model 85 meter (YSI, Inc. Yellow Springs, OH). Juvenile shrimp were marked with uniquely coded microwire tags (1.1 mm long×0.25-mm diameter, Northwest Marine Technology [NMT], Inc. Shaw Island, WA), which were injected into the muscle tissue of the first abdominal segment. We used a hand-held multishot injector (NMT) that was designed to cut, magnetize, and inject sequentially coded tags from a continuous stainless-steel wire spool. Each tag was etched with six lines of binary code that could be read under a microscope (25×) and translated into a set of numbered coordinates. Only three of the coded lines were required to identify a unique individual. A master line contained a distinguishing sequence code that was necessary to properly interpret codes on data lines designated D3 and D4. The numerical values associated with these coded lines were entered into a sequential tag conversion computer program (GR [Growth Rate], version 1.3, Northwest Marine Technology, Inc. Shaw Island, WA) that output the unique tag number corresponding to those coordinates.

A reference tag was archived for every shrimp marked in order that the code on either side of the tag injected into a shrimp was known with certainty. This was necessary to ensure positive identification of recaptured individuals because the injector was designed only to cut tags to a known length (1.1 mm) and did not distinguish between the beginning and end of sequential codes and often cut tags that included a portion of two adjacent codes. Prior to their release, marked shrimp were passed across a magnetometer (NMT) which signaled the presence of the ferromagnetic tag with an audible tone and flashing light. All shrimp collected after these marking sessions were scanned in the same manner and when a tag was detected, it was removed from the recaptured shrimp, cleaned and read under the microscope. The two reference tags bracketing the recovered tag were then located in the archive set to determine the date, location, and initial length at release of the marked shrimp. Thus the growth rate, time at large, and distance between points of release and recapture could be determined with certainty for individual shrimp.

Shrimp were marked and released only in the upper reaches of each tidal creek. During the marking process, small batches of shrimp (<50 individuals) were collected and held in insulated plastic coolers. Water in the coolers was exchanged each time a new batch of shrimp was collected. Only active individuals, 40–80 mm total length (TL, tip of the rostrum to end of the telson) and in apparently good condition, were candidates for marking. The marking process required a minimum field crew of two researchers. One measured shrimp and recorded data, while the other injected tags and released marked shrimp at the edge of the tidal creek.

We attempted to mark 1000 shrimp during a 3-day period in each tidal creek near the beginning of every month from July to November in both years. It was not possible to tag shrimp in both creeks simultaneously; therefore shrimp were marked and released in week 1 during the first week of the month, then in creek 2 during the second week of the month. The remainder of the month was spent collecting marked shrimp (Fig. 2). Inclement weather and mechanical problems with the tagging equipment sometimes prevented us from achieving the goal of tagging 1000 shrimp per creek within the first week of each month. In August 1998, the tag injector malfunctioned on the first day of tagging in SC and was unavailable for several weeks while it was being refurbished. Consequently, sampling was suspended in SC during that time. Although the same problem occurred while we attempted to mark shrimp from the EF in September 1999, we continued sampling in an attempt to recapture shrimp tagged in previous months.

A total of 6 sampling events after marking were planned in each creek per month (Fig. 2). A sample consisted of the combined contents of 10 haphazard casts of the net along the edge of the tidal creek within each station per sampling date. Shrimp populations were usually sampled at 3-day intervals for 21 days beginning from the midpoint of the marking period. A consistent exception was the second sample in the series, which occurred at a 6-day interval to accommodate the marking effort in the second creek and to keep the sampling effort consistent in all creeks. Inclement weather interrupted the sampling schedule on occasion and when unfavorable conditions persisted for more than 3 days, some of the planned sampling events after marking were cancelled; some months were represented by fewer than 6 sampling events. Sampling was terminated when, as a result of normal seasonal emigration from the nursery areas, shrimp densities declined to the point that they could no longer be consistently collected from the tidal creeks by cast net (19 November 1998 and 21 November 1999).

Catches of marked shrimp from each station were retained in separate plastic bags, placed on ice, and transported to the laboratory. A subsample of shrimp from each station (every tenth individual) was measured (TL, mm) to construct size distributions. If a sample included fewer than 100 shrimp, all were measured. Sex was not determined. All individuals were scanned for the presence of tags and when a marked shrimp was detected, it was measured (TL, mm) before the tag was removed and stored in a plastic vial for reading at a later date. For each recapture, we recorded date, creek, station of recapture (i.e., distance from original release site) and size of fish.

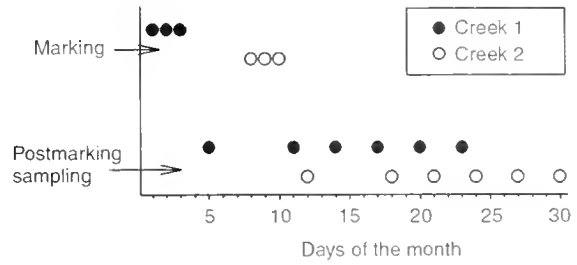

Figure 2

Schedule for monthly marking and postmarking field schedule for the juvenile white shrimp study.

Daily instantaneous (specific) growth rates (mm/[mm/d]) were calculated as

$$[(\ln L_2 - \ln L_1)/t],$$

where L_2 = total length (mm) of an individual on the date of recapture;
L_1 = initial total length (mm) on the date of tagging; and
t = number of days at large.

Daily absolute growth rates (mm/d) also were calculated (L_2-L_1/t) to facilitate comparison with estimates from previous studies. Displacement (distance moved) was determined by comparing the location of recapture with the original location at marking. Residence time within a tidal creek was determined from a plot of the proportion of recaptured individuals against time-at-large for each creek system. First, using the Regression Wizard in the computer program SigmaPlot® (version 8.0, SPSS, Inc. Chicago, IL), we fitted the data to an exponential decay function:

$$(y=a \times e^{-bt}),$$

where y = the proportion of total recaptures;
t = time at large; and
a and b = the estimated parameters.

Constraints imposed on the fit were $a=1$ (because the proportion of total recaptures could not exceed 1) and $b>0$ (because this was an exponential decay function). Mean residence time for shrimp in each creek was then estimated from the area below the fitted curves describing the proportion of recaptures with time at large. This was calculated with the macro function "area below curves" included in the "Toolbox" menu selection of SigmaPlot® (vers. 8.0, SPSS, Inc. Chicago, IL) which uses the trapezoidal rule to estimate the area under curves.

Statistical analyses

Most of the data analyses used statistical procedures in version 8.0 of the computer software package Systat®

(SPSS, Inc. Chicago, IL). When parametric tests were performed, residuals were analyzed to determine whether the data met the required assumptions (Sokal and Rohlf, 1995). Levene's test was used to evaluate conformity to the assumption of variance homogeneity among groups. When this assumption was violated, the data were transformed and retested. If the assumptions were still not met, then an appropriate nonparametric test was applied (e.g., Kruskal-Wallis one-way analysis of variance). Two sample *t*-tests were used to compare spatial and temporal variation in water temperature, salinity, and dissolved oxygen between creeks within a year and between years. August was omitted in comparisons of data between creeks in 1998, and between years because sampling in SC was suspended during August 1998. Regression analyses were performed to determine whether there were significant linear relationships between initial shrimp length and growth rates within each tidal creek. One-way ANOVA (controlling for the covariate initial length) was used to test for differences in growth rates between creeks within each year. A similar approach (controlling for initial size) was used to test for monthly (seasonal) differences in growth rate within years. If growth rates did not differ significantly between creeks, the data were pooled within year, otherwise creeks were treated separately. Only individuals at large for a month or less (to ensure that growth was representative of individual months) were included in the analyses.

Shrimp at large for fewer than 3 days were excluded from the statistical analyses to reduce certain anticipated biases associated with estimating growth rates. These included 1) measurement error (assumed to be at least 1 mm), which would likely represent a substantial proportion of the growth rate estimate when absolute change in size was small; 2) increments of growth associated with molting (Dall et al., 1990), which could either underestimate growth for shrimp that had been at large for a short time or had not molted since they were tagged or overestimate growth if shrimp were recaptured shortly after the first molt following marking; and 3) size-specific growth, where shrimp marked at a relatively small size and smaller shrimp exhibit a higher relative growth, so that early recaptures could represent larger than average growth rates.

Results

Physical parameters

Average water temperature, salinity, and dissolved oxygen (measured at the mouth of each tidal creek) were similar between creeks within years (see Table 1 in Webb and Kneib, 2002). In 1998, temperature ranged from 18.9 to 33.4°C, salinity from 18.2 to 28.0 ppt, and dissolved oxygen from 1.4 to 11.3 mg/L. In 1999, temperature ranged from 15.0 to 33.4°C, salinity from 23.9 to 32.5 ppt, and dissolved oxygen from 0.8 to 7.1 mg/L. Temperature followed expected seasonal patterns each year; mean values were highest in summer and declined toward autumn. Results of *t*-tests with separate variance estimates showed no significant differences between years in either mean temperature (t=0.14, df=134.0, P=0.80) or dissolved oxygen (t=1.82, df=115.9, P=0.07) but mean salinity was significantly (t=11.63, df=122.7, P<0.01) higher in 1999 (28.1 ppt) than in 1998 (24.8 ppt). Cumulative rainfall was 83.9 cm/yr in 1998 and 82.9 cm/yr in 1999 (Garbisch[4]). These values were indicative of drought conditions because they were well below the long-term mean annual precipitation value of ca. 132 cm/yr reported for Sapelo Island between May 1957 and March 2003 (Southeast Regional Climate Center[5]).

Growth

Shrimp collections during recapture efforts ranged from 20,077 to 78,724 individuals, but the proportion of marked individuals recaptured was low in both years, averaging just over 1% (Table 1). However, the recaptures included 184 individuals for which growth rates and net movements within the nursery were known precisely.

Daily absolute growth rates of individuals, which ranged from 0.25 to 2.5 mm, averaged 0.86, 0.78, 0.84, and 0.61 mm at PO, SC, WF and EF, respectively. The mean values are on the low end of the range reported in previous studies of juvenile *Litopenaeus setiferus* with other methods and conducted in different locations (Table 2). Daily specific growth rates were size-dependent in both years. Negative linear relationships between growth rate and initial size (i.e., smaller shrimp grew relatively faster) was the prevalent trend in all creeks (Fig. 3). No significant difference (t=1.19, df=74, P=0.237) in growth was detected between PO and SC, where mean (±SD) specific (instantaneous) daily growth rates were 0.014 ±0.006 and 0.012 ±0.007, respectively. In 1999, shrimp exhibited significantly (t=2.12, df=56, P=0.038) higher mean specific growth rates in the WF (0.014 ±0.008) compared to the EF (0.010 ±0.006) of the Duplin River. The physical environment was similar at these sites (Webb and Kneib, 2002), and there was no significant difference (t=1.43, df=81, P=0.156) in the mean final sizes of shrimp recaptured from these sites. However, the mean (±SD) initial size of marked shrimp at EF (61.3 ±8.3) was significantly (t=2.20, df=81, P=0.031) larger than at WF (56.0 ±10.9); therefore a lower specific growth rate was to be expected at EF.

On a finer temporal scale, seasonal variation in growth rates occurred in both years, more rapid growth early in the season, and a general increase in the mean size of individuals as the season progressed were evident (Fig. 4). The earlier observation that specific growth rate declined with size (Fig. 3) opens the possibility that seasonal variation in growth rates could be explained simply by

[4] Garbisch, J. Unpubl. data. Univ. Georgia Marine Institute Flume Dock Monitoring Station, NOAA, Sapelo Island National Estuarine Research Reserve. Univ. Georgia Marine Institute, Sapelo Island, GA 31327.

[5] Southeast Regional Climate Center. Unpubl. data. Website: http://water.dnr.state.sc.us/water/climate/sercc/climateinfo/historical/historical_ga.html. [Accessed 21 November 2003].

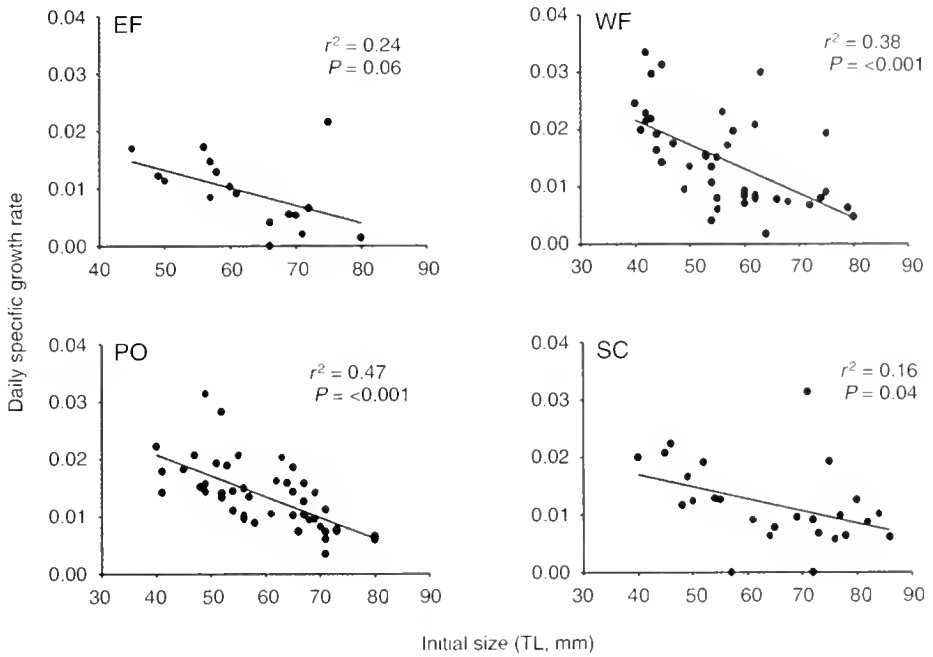

Figure 3

Scatter plots and linear regression results for the relationships between individual specific growth rates and initial sizes of recaptured juvenile shrimp in each tidal creek subsystem: EF = East Fork of Duplin River, WF = West Fork of Duplin River, PO = Post Office Creek, SC = Stacey Creek.

Table 1

Monthly summary of the number of shrimp tagged, number collected in subsequent sampling, and the number of tagged shrimp recaptured in each tidal creek.

Collection site and sampling process	July	August	September	October	November	Total
Post Office Creek						
Number tagged and released	1004	1077	1025	1000	779	4885
Number collected after tagging	7477	13,851	4730	8384	1298	35,740
Number of tags recaptured	13	16	16	22	1	68
Stacey Creek						
Number tagged and released	719	91	804	862	623	3099
Number collected after tagging	5877	0	5466	6376	2358	20,077
Number of tags recaptured	2	0	12	16	3	33
East Fork of Duplin River						
Number tagged and released	812	1000	0	1024	1003	3839
Number collected after tagging	23,080	14,490	11,020	14,804	3449	66,843
Number of tags recaptured	7	11	0	4	4	26
West Fork of Duplin River						
Number tagged and released	1008	1000	447	696	1000	4151
Number collected after tagging	32,130	17,926	10,954	10,600	7114	78,724
Number of tags recaptured	27	16	3	4	7	57

Table 2

Summary of estimated mean daily absolute growth rates for juvenile *Litopenaeus setiferus*. Growth rates were converted to mm/d if reported in other units.

Reference	Location	Growth rate (mm/d)	Method and notes
Gunter, 1950	Gulf of Mexico, Texas	0.8–1.3	Size frequency in field samples, juveniles 28–100 mm
Williams, 1955	coastal North Carolina	1.2	Size frequency in field samples, progression of maximum sizes of juveniles, 32–117 mm
Johnson and Fielding, 1956	Florida	1.3	Pond culture, juveniles
Lindner and Anderson, 1956	South Atlantic Bight and Gulf of Mexico	1.0–1.3	Extrapolated for juveniles 40–80 mm from Walford plot results using field mark-recapture (disc tags) data for individuals 70–205 mm
Loesch, 1965	Mobile Bay, Alabama	0.6–1.0	Size frequency from spring and summer field samples; progression of maximum sizes of juveniles 50–135 mm
		2.2	juveniles 15–70 mm
Klima, 1974	Galveston Bay, Texas	1.4–1.8	Extrapolated for juveniles 40–80 mm from Walford plot results determined from field mark-recaptured (stain-injected) subadults (117 mm)
	coastal Louisiana	1.0–1.3	Extrapolated for juveniles 40–80 mm from Walford plot results determined from field mark-recaptured (stain-injected) subadults (120 mm)
Mayer, 1985[1]	Sapelo Island, Georgia	0.9–1.5	Estimated from modal size-frequency data for juveniles 20–120 mm
Knudson et al., 1996	coastal Louisiana	0.3–0.7	Mark-recapture (injected pigments) of juveniles 45–58 mm (initial size) from coastal marsh ponds
This study	Sapelo Island, Georgia	0.6–0.9	Monthly mark-recapture (coded ferromagnetic tags) of juveniles 40–80 mm (initial size) from subtidal creeks

[1] Mean growth rates reported in Table 3 of Mayer (1985) were inconsistent with cohort data in Figure 8 of that thesis; rates reported here were derived directly from the data points shown in Figure 8 of Mayer's thesis.

changes in the average size of shrimp within the nursery over time.

We tested this hypothesis by comparing mean growth rates among months after controlling for initial length as a covariate. For these analyses, the 1998 data from PO and SC were pooled because there was no evidence of a difference in growth rates between these two creeks; the 1999 data from EF and WF were analyzed separately because mean growth rates differed between these two systems. After removing the effect of initial size, there was no significant difference among months in 1998, nor in 1999 at EF, but significant differences in mean growth remained detectable among months at WF (Table 3). The findings from WF also were unusual in that the covariate (initial length) was not a significant factor in the analysis. *Post hoc* multiple comparisons (Bonferroni, experiment-wise α=0.05) of mean growth rates among months (without accounting for the covariate) indicated that the specific growth rate in July (0.021) was significantly greater than that in the other months (0.007 to 0.011). This was the only statistically significant evidence of seasonal variation in growth apparently not associated with shrimp size distributions.

With respect to spatial variation in growth rates of juvenile shrimp, the most notable observation in this study was the relatively low mean growth rate observed at EF compared to the other sites. This difference could have resulted from the larger mean initial size of individuals tagged at EF (61.3 mm) compared with those at WF (56.0) in 1999. However, a similar difference in mean initial sizes of marked shrimp between tidal creek subsystems (SC, 64.2 mm; PO, 59.6 mm) in the previous year did not result in a significant difference in growth rates. When we considered the structural characteristics of each tidal creek at a landscape level, the EF subsystem had the largest tidal drainage area (119.5 ha.) compared to the other sites (58.6 to 104.9 ha.), but proportionally less of that area was intertidal drainage. There was a stronger correlation between mean growth rate (pooled across all individuals within a creek) and the proportion of the drainage area that was

Table 3

Summary of ANOVA results for the effects of month on specific growth rate of *Litopenaeus setiferus* after controlling for the covariate initial length. Only individuals at large between 3 and 32 days were included in the analyses. PO = Post Office Creek; SC = Stacey Creek; EF = East Fork of Duplin River; and WF = West Fork of Duplin River. Prob. = probability.

	1998 (PO and SC)			EF			WF		
Source	df	*F*-value	Prob.	df	*F*-value	Prob.	df	*F*-value	Prob.
Covariate (initial size)	1	30.77	<0.01	1	1.42	0.26	1	1.42	0.24
Month	4	1.25	0.30	3	0.74	0.55	4	4.32	<0.01
Error	70			11			36		

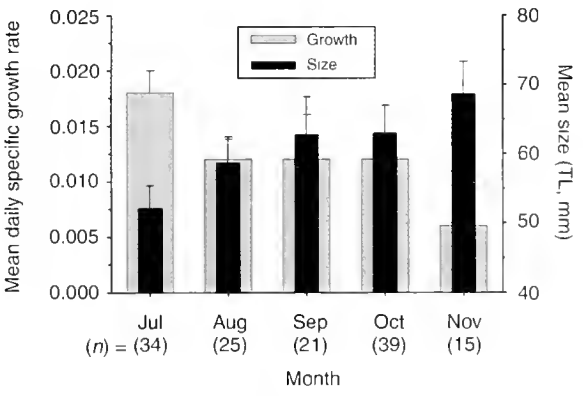

Figure 4

Mean daily specific growth rates and mean initial size of marked and recaptured juvenile white shrimp by month. Only individuals at large for 3 to 32 days were included. Error bars are 2 SEs and the number of observations are given in parentheses below each month.

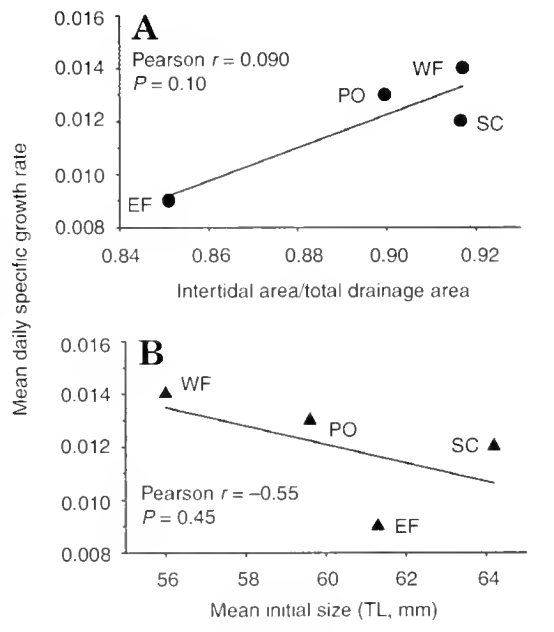

Figure 5

Correlations between mean daily specific growth rate in each tidal creek (PO=Post Office, SC=Stacey Creek, EF=East Fork of Duplin River, WF=West Fork of Duplin River). (**A**) The proportion of the tidal drainage area that is intertidal; (**B**) mean initial size of marked shrimp.

intertidal (Fig. 5A) than there was between growth and mean initial size (Fig. 5B) at the landscape level. There was almost no correlation between proportion of drainage area that was intertidal and initial mean size of marked shrimp (Pearson r=−0.18, P=1.0).

Residence time and movement of marked shrimp

Recaptured shrimp were at large for up to 99 days, but mean residence time for individuals marked in all four tidal creeks was between 15 and 26 days (Fig. 6). Mean residence time was greatest at EF and least at SC. During their time-at-large, net displacement (distance between mark and recapture sites) of the marked individuals ranged from 0 to 3000 m , but averaged 258–373 m in all creeks. There was no evidence of a significant relationship between time-at-large and mean net displacement (linear regression F=1.48; df=1,45; P=0.23), but movement was slightly related to shrimp size, and larger individuals showed greater displacement (Fig. 7). Variation in residence time among creek subsystems was not significantly correlated with length of the creek mainstem (Pearson r=−0.32, P=0.684), but there was evidence of positive associations with the amount of intertidal (Pearson r=0.87, P=0.133) and subtidal (Pearson r=0.95, P=0.054) drainage areas within each subsystem.

Most shrimp (93%) were recaptured in the same tidal creek subsystem in which they were originally marked, but there was some evidence of movement among creeks and between the subtidal and intertidal components of the shrimp nursery within creeks. The marked individual at large for the longest time (99 days) was recaptured at the same station where it was originally marked (net

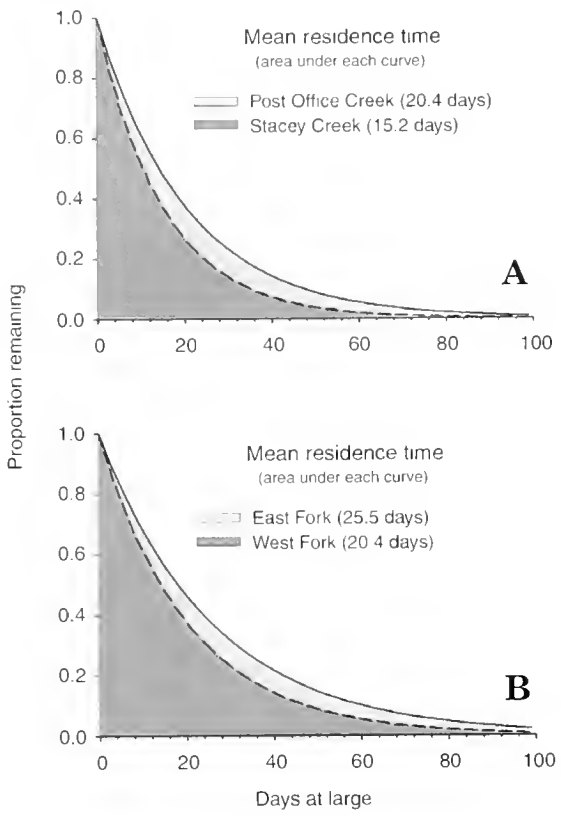

Figure 6

Estimates of mean residence times of marked shrimp in (**A**) tidal creeks sampled in 1998 and (**B**) creeks sampled in 1999. Estimates are based on the area under the curves describing the proportion of recaptured marked shrimp in each creek system that still remained to be captured after the indicated number of days-at-large.

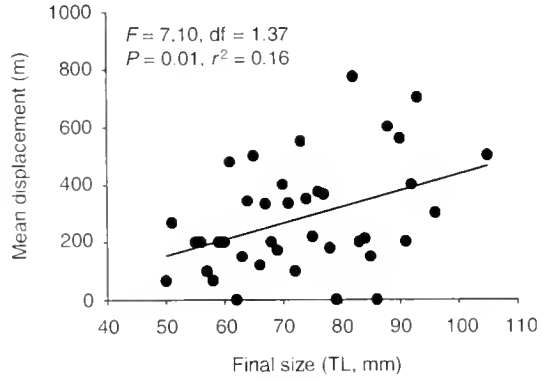

Figure 7

The effect of shrimp size at recapture on mean distance between mark and recapture locations (displacement). Summary results from the linear regression ANOVA performed on the data are shown. Values of mean displacement were based on data from 2–11 individuals within each size.

displacement=0 m). In contrast, one shrimp marked at PO demonstrated a net displacement of 3 km when it was recaptured at SC after 61 days at large. Nine shrimp (at large from 18 to 49 days) marked at WF were recaptured at EF, and two (at large 19 and 45 days) tagged at EF were recaptured at WF. It was not possible to determine precisely when these shrimp moved out of the creek in which they were tagged or how long they were present in the creek subsystem where they were ultimately recaptured. For the growth rate analyses, it was assumed that most growth occurred while the shrimp were in the creek and where individuals were marked. The mean (±SD) final size (mm, TL) of individuals that moved between creek subsystems was significantly (separate variance estimate t=2.62, df=16.9, P=0.018) larger (78.9 ±7.4) than that of the group tagged and recaptured in the same subsystem (71.3 ±13.1); the initial mean size of the two groups was nearly identical (57.5 ±10.8 and 57.7 ±10.4, respectively). Two shrimp (at large 7 and 17 days) tagged at EF were recaptured at high tide in flume weirs located 25 m into the interior of the intertidal marsh drained by that tidal creek subsystem. The flume weir samples were part of an ongoing study (Kneib, unpubl. data) to determine nekton use of the intertidal marsh surface (see Kneib, 1991, 1997; Kneib and Wagner, 1994).

Discussion

Growth

Mean growth rates of juvenile white shrimp measured in this study (0.6–0.9 mm/d) were near the lower end of the range of estimates previously reported for juvenile white shrimp along the U.S. Atlantic and Gulf coasts (Table 2). The principal difference between the present and previous studies is that the values presented in this study were based on direct measurements of free-ranging individual juvenile shrimp rather than on extrapolations from batch mark-recaptures of larger individuals or changes in modal size frequencies. The open nature of estuarine ecosystems, prolonged seasonal recruitment to the nursery, and ontogenetic differences in mortality and movement all may confound the interpretation of size-frequency data (Haywood and Staples, 1993). Given that our growth values were based on actual changes in the size of individuals rather than estimated from the apparent growth trajectories of cohorts, we are confident that the mean growth rates reported here accurately reflect those of free-ranging juvenile white shrimp (40–80 mm TL) in the polyhaline portion of the tidal marsh nursery habitat of coastal Georgia.

Temporal differences in observed growth rates in this study may have resulted from either variation in environmental conditions or spatial variation in habitat quality.

Penaeids are most abundant in tidal marsh nurseries when physical conditions (eg., temperature and salinity) appear optimal for their growth and survival (Zein-Eldin and Renaud, 1986), but environmental variability is characteristic of most estuaries and therefore is an obvious starting point for explaining observed differences in shrimp growth among sites or times. Salinity was the only environmental factor we measured that showed a significant difference between years but could not be associated with any interannual difference in mean growth rates.

Temperature may affect the growth and estuarine distribution of juvenile penaeids more than salinity (Vetter, 1983), and interactions between salinity and temperature may have even greater effects than variation in either factor alone (Zein-Eldin and Renaud, 1986). Mean temperatures throughout our study period (with the exception of November) in both years were largely within the optimum range for growth of white shrimp which, in the laboratory, was reported to be between 25° and 32.5°C (Zein-Eldin and Griffith, 1969). Higher temperatures generally contribute to faster growth in young penaeids (Perez-Farfante, 1969; Muncy, 1984), and therefore it seems reasonable to expect seasonal variation in temperature to be reflected in growth rates. However, this interpretation is confounded by the fact that growth rates also are size dependent (Fig. 3, Table 3) and that increases in mean size of juvenile white shrimp (Fig. 4) occurred while temperature in the nursery habitat was decreasing from the July maxima. It seems likely that growth rates of juvenile white shrimp were robust over the relatively narrow range of seasonal variation in temperature and salinity observed in the present study.

Alternatively, differences in growth between certain sites could be the result of spatial variation in habitat quality. This variation need not be a function of water quality, but rather a function of some structural aspect of the nursery habitat. There was a strong correlation between mean growth rates and the proportion of tidal creek drainage area that was intertidal. Only four creek subsystems were examined in ours study, and we recognize that this is an insufficient sample size to justify anything more than a suggestive hypothesis. However, evidence of relationships between the amount of intertidal habitat and penaeid shrimp production (Turner, 1977, 1992), as well as the amount of intertidal creek edge and juvenile shrimp abundance in adjacent subtidal creeks (Webb and Kneib, 2002), supports the contention that intertidal accessibility is an important component of nursery habitat quality for juvenile white shrimp. We propose that the ratio between intertidal and shallow subtidal habitat may be a key feature of white shrimp nursery habitat quality. When tidally inundated, the intertidal portion of marsh creek drainage systems is used extensively by juvenile white shrimp (Kneib, 1995, 2000), most likely as a rich foraging area (Kneib, 1997), and the shallow subtidal portion functions as a low tide refuge and corridor for the seasonal migration of postlarvae and subadults between the open estuary and coastal ocean spawning grounds and the juvenile nursery (Kneib, 1997, 2000).

Movement and residence time

Understanding the causes of broad-scale migration of penaeids has obvious implications for predicting commercial catches and therefore these causes have been the focus of research on shrimp movements for decades (Perez-Farfante, 1969; Muncy, 1984). However, finer-scale movements, which may affect growth and survival of juvenile shrimp within the estuary, are not as well known. Emigration of white shrimp from estuaries is determined by size, maturity, and environmental conditions (Muncy, 1984), and size plays a principal role (Dall et al., 1990). In the South Atlantic Bight, larger white shrimp (>100 mm TL) begin emigrating from the nursery to commercial fishing areas in the nearshore coastal ocean in August (Lindner and Anderson 1956, Shipman, 1983). We collected few shrimp >100 mm in the tidal marsh creeks, which is consistent with previous observations of ontogenetic migration to deeper waters. According to growth rates measured in this study, a shrimp of 40 mm TL would become large enough to emigrate from the estuary to the coastal ocean in 2–3 months (i.e., a shrimp tagged at 40 mm TL could reach 85–108 mm TL in 2.5 months).

The presence of high densities of small juvenile white shrimp in the upper reaches of Georgia's tidal marsh creeks (Harris, 1974; Hackney and Burbanck, 1976; Webb and Kneib, 2002) has supported the contention advanced by Weinstein (1979) that these areas are primary nurseries for juvenile fish and shellfish. However, it has been unclear whether these aggregations represent stable resident populations or are composed of tidal transients that constantly migrate among creek subsystems within the broader estuarine nursery. Young shrimp are known to move short distances to avoid unfavorable physiochemical conditions (Hackney and Burbanck, 1976; Dall et al., 1990) and routinely make tidally mediated excursions between subtidal and intertidal portions of the nursery to forage or escape predators (Kneib, 1995, 1997). Our findings showed that juvenile white shrimp also tended to remain resident in the upper reaches of tidal creeks where they were originally tagged until attaining a size (80–100 mm) at which they normally begin to emigrate from the nursery (Perez-Farfante, 1969).

Although there was some movement between tidal creek subsystems, the high level of site fidelity demonstrated by juvenile white shrimp was remarkable given the openness and degree of tidal flux in the Duplin River system (mean tide range=2.1 m). Data from the chemical analysis of shrimp tissue composition also suggest limited movements of juvenile penaeids within estuarine nurseries. Using the stable isotopes of carbon and nitrogen from muscle tissues of pink shrimp (*Farfantepenaeus duorarum*), Fry et al. (1999) traced shrimp movements within and between seagrass and mangrove habitats of southwestern Florida. They found distinct differences among individuals sampled from similar inshore habitat types separated by small (3–5 km) open water distances, indicating that individuals remained "resident" in specific portions of the estuary at least for several weeks. Noting a similar study in coastal Louisiana, Fry et al. (2003) suggested that

small juvenile brown shrimp (*Farfantepenaeus aztecus*) are more transient in suboptimal habitat (open bays and deeper channels) and exhibit less movement upon reaching optimal habitat (ponds and shallow channels).

The only study with which we can directly compare our findings on residence time and movements was conducted by Knudsen et al. (1996) near Calcasieu Lake, Louisiana, where tidal flux was considerably lower (mean tide range <0.6 m) and the system (marsh impoundments) was less open than that in the present study. Knudsen et al. (1996) marked batches of juvenile white shrimp (45–69 mm TL) by injection of colored pigments and released them into a pair of 35-ha. impoundments, each connected to the open estuary through a narrow channel that was fitted with screen deflectors and traps designed to collect all emigrating nekton. The mean time from release to emigration of juvenile white shrimp ranged from 30.2 to 59.9 days. Our estimates of tidal creek residence time for juvenile shrimp in Georgia tidal creeks was about half that reported for impoundments in Louisiana and may be explained by the differences in tidal flux and openness between the two systems. However, the values we observed were likely underestimates of the actual residence period of survivors within the creeks because they included losses due to mortality as well as emigration.

It seems clear from the studies conducted thus far that juvenile penaeids, once having entered the estuarine nursery, tend to remain within a limited spatial range where they are exposed to local conditions for several weeks. Our findings also provide evidence of spatial variation for both residence time and growth rate of juvenile white shrimp that is possibly attributable to structural differences in tidal creek subsystems. We suggest there may be an optimal value for the ratio of subtidal to intertidal drainage area within marsh creek systems that can achieve a favorable balance between suitable habitat (space) at low tide, which tends to enhance residence time and density of juvenile shrimp, while providing sufficient intertidal foraging habitat and predator refugia at high tide to promote high rates of juvenile shrimp growth and survival. Spatially explicit information on growth rates and the extent to which individual shrimp move within their estuarine nurseries are necessary initial steps toward meeting the challenge of maintaining quality nursery habitat for a sustainable shrimp fishery and satisfying other demands associated with human development in and around estuarine watersheds.

Acknowledgments

Several individuals provided field and laboratory assistance for this project, but we especially thank K. Feeley, J. Kneib, and J. Spicer for helping on a regular basis. The primary source of funding was a National Estuarine Research Reserve System Graduate Research Fellowship to S. Webb (NA870R0284) (Estuarine Reserves Division, Office of Ocean and Coastal Resource Management, NOS, NOAA), and matching funds provided by the University of Georgia Marine Institute. The Georgia Sea Grant College Program contributed funds for the purchase of an additional tag injector unit, which substantially improved the effectiveness of the mark-recapture program. The conceptual basis for this project was derived from research conducted under a grant from the National Science Foundation (DEB-9629621), which also contributed supplemental student support.

Literature cited

Dall, W., B. J. Hill, P. C. Rothlisberg, and D. J. Staples.
1990. The biology of the Penaeidae. *In* Advances in marine biology, vol. 27 (J. H. S. Blaxter and A. J. Southward, eds.), 489 p. Academic Press, London.

Fitz, H. C., and R. G. Weigert.
1991. Tagging juvenile blue crabs, *Callinectes sapidus*, with microwire tags: retention, survival, and growth through multiple molts. J. Crust. Biol. 11(2):229–235.

Fry, B., D. M. Baltz, M. C. Benfield, J. W. Fleeger, A. Gace, H. L. Haas, and Z. J.Quinones-Rivera.
2003. Stable isotope indicators of movement and residency for brown shrimp (*Farfantepenaeus aztecus*) in coastal Louisiana marshscapes. Estuaries 26:82–97.

Fry, B., P. L. Mumford, and M. B. Robblee.
1999. Stable isotope studies of pink shrimp (*Farfantepenaeus duorarum* Burkenroad) migrations on the southwestern Florida shelf. Bull. Mar. Sci. 65(2):419–430.

Garcia, S., and L. Le Reste.
1981. Life cycles, dynamics, exploitation and management of coastal penaeid shrimp stocks. FAO Fish. Tech. Paper 203, 215 p. FAO, Rome.

Gunter, G.
1950. Seasonal population changes and distributions as related to salinity, of certain invertebrates of the Texas coast, including the commercial shrimp. Publ. Inst. Mar. Sci., Univ. Texas 1:7–31.

Hackney, C. T., and W. D. Burbanck.
1976. Some observations on the movement and location of juvenile shrimp in coastal waters of Georgia. Bull. GA Acad. Sci. 34:129–136.

Harris, C. D.
1974. Observations on the white shrimp (*Penaeus setiferus*) in Georgia. Georgia Dep. Nat. Res. Contr. Ser. 27:1–47.

Haywood, M. D. E., and D. J. Staples.
1993. Field estimates of growth and mortality of juvenile banana prawn (*Penaeus merguiensis*). Mar. Biol. 116: 407–416.

Isely, J .J., and A. G. Eversole.
1998. Tag retention, growth, and survival of red swamp crayfish *Procambarus clarkii* marked with coded wire tags. Trans. Am. Fish. Soc. 127:658–660.

Jefferts, K. B., P. K. Bergmann, and H. F. Fiscusest.
1963. A coded wire identification system for macro-organisms. Nature 198:460–462.

Johnson, M. C., and J. R. Fielding.
1956. Propagation of the white shrimp, *Penaeus setiferus* (Linn.), in captivity. Tul. Stud. Zool. 2:49–56.

Klima, E. F.
1974. A white shrimp mark-recapture study. Trans. Am. Fish. Soc. 103(1):107–113.

Kneib, R. T.
1991. Flume weir for quantitative collection of nekton from vegetated intertidal habitats. Mar. Ecol. Prog. Ser. 75:29–38.

1995. Behaviour separates potential and realized effects of decapod crustaceans in salt marsh communities. J. Exp. Mar. Biol. Ecol. 193:239–256.

1997. The role of tidal marshes in the ecology of estuarine nekton. Oceanogr. Mar. Biol. Ann. Rev. 35:163–220.

2000. Salt marsh ecoscapes and production transfers by estuarine nekton in the southeastern United States. *In* Concepts and controversies in tidal marsh ecology (M. P. Weinstein and D. A. Kreeger, eds.), p. 267–291. Kluwer Academic Publishers, Dordrecht, The Netherlands.

Kneib, R. T., and M. C. Huggler.

2001. Tag placement, mark retention, survival and growth of juvenile white shrimp (*Litopenaeus setiferus* Pérez-Farfante, 1969) injected with coded wire tags. J. Exp. Mar. Biol. Ecol. 266:109–120.

Kneib, R. T., and S. L. Wagner.

1994. Nekton use of vegetated marsh habitats at different stages of tidal inundation. Mar. Ecol. Prog. Ser. 106:227–238.

Knudsen, E. E., B. D. Rogers, R. F. Paille, W. H. Herke, and J. P. Geaghan.

1996. Juvenile white shrimp growth, mortality, and emigration in weired and unweired Lousiana marsh ponds. North Am. J. Fish. Manag. 16:640–652.

Krouse, J. S., and G. E. Nutting.

1990. Evaluation of coded microwire tags inserted in legs of small juvenile American lobsters. *In* Fish-marking techniques (N. C. Parker, et al., eds.), p. 304–310. Am. Fish. Soc. Symp. 7, Bethesda, MD.

Kutkuhn, J. H.

1966. The role of estuaries in the development and perpetuation of commercial shrimp resources. Am. Fish. Soc. Spec. Publ. 3:16–36.

Lindner, M. J., and W. W. Anderson.

1956. Growth, migrations, spawning and size distribution of shrimp, *Penaeus setiferus*. Fish. Bull. 56:555–645.

Loesch, H.

1965. Distribution and growth of penaeid shrimp in Mobile Bay, Alabama. Publ. Inst. Mar. Sci., Univ. Texas 10:41–58.

Mayer, M. A.

1985. Ecology of juvenile white shrimp, *Penaeus setiferus* Linnaeus, in the Salt Marsh Habitat. M.S. thesis, 62 p. Georgia Inst. Technology, Atlanta, GA.

McTigue, T. A., and R. J. Zimmerman.

1998. The use of infauna by juvenile *Penaeus aztecus* Ives and *Penaeus setiferus* (Linnaeus). Estuaries 21:160–175.

Minello, T. J, and R. J. Zimmerman.

1985. Differential selection for vegetative structure between juvenile brown shrimp (*Penaeus aztecus*) and white shrimp (*Penaeus setiferus*), and implications in predator-prey relationships. Estuar. Coastal Shelf Sci. 20:707–716.

Muncy, R. J.

1984. Species profiles: life histories and environmental requirements of coastal fishes and invertebrates (South Atlantic)—white shrimp. U.S. Fish and Wildlife Service FWS/OBS-82/11.27, 19 p. U.S. Army Corps of Engineers TR EL-82-4, 19 p.

Pearson, J. C.

1939. The early life history of some American Penaeidae, chiefly the commercial shrimp *Penaeus setiferus* (Linn.). Fish. Bull. 30:1–73.

Perez-Farfante, I.

1969. Western Atlantic shrimps of the genus *Penaeus*. Fish. Bull. 67:461–591.

Perez-Farfante, I., and B. F. Kensley.

1997. Penaeoid and sergestoid shrimps and prawns of the world: keys and diagnoses for the families and genera. Memoires du Muséum National d'Historie Naturelle 175: 1–233.

Prentice, E. F., and J. E. Rensel.

1977. Tag retention of the spot prawn, *Pandalus platyceros*, injected with coded wire tags. J. Fish. Res. Board Can. 34:2199–2203.

Ragotzkie, R. A., and R. A. Bryson.

1955. Hydrography of the Duplin River, Sapelo Island, Georgia. Bull. Mar. Sci. Gulf Caribb. 5:297–314.

Shipman, S.

1983. Mark-recapture studies of penaeid shrimp in Georgia, 1978–1981. *In* Studies and assessment of Georgia's marine fisheries resources, 1977–1981 (S. Shipman, V. Baisden, and H. Ashley, eds.), p. 1–176. Georgia Dep. Nat. Res. Contr. Ser. 35.

Sokal, R. R., and F. J. Rohlf.

1995. Biometry: the principles and practice of statistics in biological research, 3rd ed., 887 p. W.H. Freeman and Co., New York, NY.

Turner, R. E.

1977. Intertidal vegetation and commercial yields of penaeid shrimp. Trans. Am. Fish. Soc. 106:411–416.

1992. Coastal wetlands and penaeid shrimp habitat. *In* Stemming the tide of coastal fish habitat loss (R. H. Stroud, ed.), p. 97–104 National Coalition for Marine Conservation, Savannah, GA.

Uglem, I., and S. Grimsen.

1995. Tag retention and survival of juvenile lobsters, *Hommarus gammarus*, marked with coded wire tags. Aquacult. Res. 26:837–841.

van Montfrans, J., J. Capelli, R. J. Orth, and C. H. Ryer.

1986. Use of microwire tags for tagging juvenile blue crabs (*Callinectes sapidus*). J. Crust. Biol. 6:370–376.

Vetter, E. A.

1983. The ecology of *Penaeus setiferus*: habitat selection, carbon and nitrogen metabolism, and simulation modeling. Ph.D. diss., 151 p. Univ. Georgia, Athens, GA.

Wadsworth, J. R.

1980. Geomorphic characteristics of tidal drainage networks in the Duplin River system, Sapelo Island, Georgia. Ph.D. diss., 247 p. Univ. Georgia, Athens, GA.

Webb, S. R., and R. T. Kneib.

2002. Abundance and distribution of juvenile white shrimp *Litopenaeus setiferus* within a tidal marsh landscape. Mar. Ecol. Prog. Ser. 232:213–223.

Weinstein, M. P.

1979. Shallow marsh habitats as primary nurseries for fishes and shellfish, Cape Fear River, North Carolina. Fish. Bull. 77:339–357.

Wenner, E. L., D. Knott, J. O. Blanton, C. Barans, and J. Amft.

1998. Roles of tidal and wind-generated currents in transporting white shrimp (*Penaeus setiferus*) postlarvae through a South Carolina (USA) inlet. J. Plank. Res. 20(12):2333–2356.

Williams, A. B.

1955. Contribution to the life histories of commercial shrimp (Penaeidae) in North Carolina. Bull. Mar. Sci. Gulf Caribb. 5:116–146.

1984. Shrimps, lobsters, and crabs of the Atlantic coast of the eastern United States, Maine to Florida, 550 p. Smithsonian Institution Press, Washington, D.C.

Zein-Eldin, Z. P., and G. W. Griffith.
1969. An appraisal of the effects of salinity and temperature on growth and survival of postlarval penaeids. FAO Fish. Rep. 57(3):1015–1026.

Zein-Eldin, Z. P., and M. L. Renaud
1986. Inshore environmental effects on brown shrimp, *Penaeus aztecus*, and white shrimp, *P. setiferus*, populations in coastal waters, particularly of Texas. Mar. Fish. Rev. 48(3):9–19.

Does the California market squid (*Loligo opalescens*) spawn naturally during the day or at night? A note on the successful use of ROVs to obtain basic fisheries biology data

John Forsythe

National Resource Center for Cephalopods
University of Texas Medical Branch at Galveston
301 University Blvd
Galveston, Texas 77555-1163
E-mail address: john.forsythe@utmb.edu

Nuutti Kangas

Roger T. Hanlon

Marine Resources Center
Marine Biological Laboratory
Woods Hole, Massachusetts 02543

The California market squid (*Loligo opalescens* Berry), also known as the opalescent inshore squid (FAO), plays a central role in the nearshore ecological communities of the west coast of the United States (Morejohn et al., 1978; Hixon, 1983) and it is also a prime focus of California fisheries, ranking first in dollar value and tons landed in recent years (Vojkovich, 1998). The life span of this species is only 7–10 months after hatching, as ascertained by aging statoliths (Butler et al., 1999; Jackson, 1994; Jackson and Domier, 2003) and mariculture trials (Yang, et al., 1986). Thus, annual recruitment is required to sustain the population. The spawning season ranges from April to November and spawning peaks from May to June. In some years there can be a smaller second peak in November. In Monterey Bay, the squids are fished directly on the egg beds, and the consequences of this practice for conservation and fisheries management are unknown but of some concern (Hanlon, 1998). Beginning in April 2000, we began a study of the *in situ* spawning behavior of *L. opalescens* in the southern Monterey Bay fishing area.

The prevailing thought is that the majority of spawning activity takes place at night because fishermen have observed these squids mating under their bright lights (which are used to attract and capture squids) and because television documentaries have revealed mating and spawning activity in large aggregations at night. The scientific literature on reproductive behavior is sparse. There are some cursory observations of actively spawning *L. opalescens* during diver surveys of egg beds (McGowan, 1954; Fields, 1965; Hobson, 1965; Hurley, 1977). Some daytime spawning has been seen both in southern and northern California but Fields (1965) and Hixon (1983) suggested indirectly that most spawning occurs at night. Shimek et al. (1984) also suggested night spawning by *L. opalescens* in Canada. Other loliginid squids whose natural behavior has been studied in the field were found to be daytime spawners (e.g., *L. pealeii*, *L. vulgaris reynaudii*, *Sepioteuthis sepioidea*; summarized in Hanlon and Messenger, 1996).

To help resolve this issue, we conducted three field expeditions (28 April–8 May 2000, 10–17 September 2000, and 16–21 August 2001) using remotely operated vehicles (ROVs) deployed either from the RV *John Martin* (Moss Landing Marine Laboratory) or the commercial squid FV *Lady J*. The ROVs were tethered vehicles with onboard video cameras and lights. Live video signals were transmitted by the tether to shipboard VCRs where observational data were viewed and recorded. For the first field trip, a large S4 Phantom ROV was used; it was outfitted with a video camera and zoom lens with tilt capability, and the video was recorded on Hi8 format video decks. For the second and third trips, a smaller S2 inspection-class Phantom ROV on loan from the NOAA Sustainable Seas Expeditions was used; this ROV had a customized fiber-optic tether and the video data were recorded on mini-digital video cassettes. Our goal was to make ROV dives each day from approximately dawn to dusk and to make a few comparable all-night surveys. A combination of adverse weather conditions and technical problems with the ROVs rarely allowed continuous video observations. During dives, if squids were encountered, we used video to conduct focal animal samples on females (which were paired) for as long as squids were present, or as long as we could keep track of the same individuals. Unless absolutely necessary to see the squids (for instance at night or at depths greater than 30 m in turbid daytime conditions), lights were not used for video taping in an effort to minimize their impact on the mating squids. Squids acclimated within minutes to the ROVs. After the expeditions, the videotapes were studied and the behavioral and biological data were quantified on a multimotion playback VCR.

By "mating" we refer to the peculiar mating behavior of this species that is unique among loliginid squids. The male firmly grasps the female from her ventral side and holds her for minutes or hours in a "copulatory embrace" in a nearly vertical position. Both copulation (i.e., transfer of spermatophores) and deposition of egg capsules occur in this posture. For example, as the female exudes a new egg capsule, the male and female lower themselves in unison to the egg bed where the female deposits the egg capsule in the sand. We have reported elsewhere on egg-

Manuscript approved for publication 20 January 2004 by Scientific Editor.

Manuscript received 25 January 2004 at NMFS Scientific Publications Office.

Fish. Bull. 102:389–392 (2004).

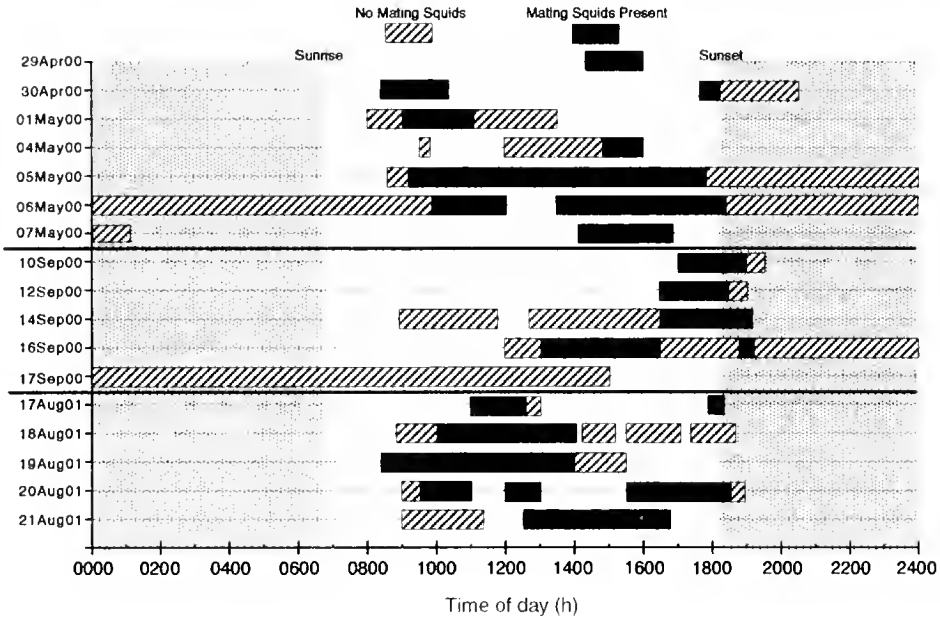

Figure 1

A summary of 154 spawning groups of *Loligo opalescens* showing the daily presence or absence of mating squids on egg beds in Monterey Bay, California. The horizontal bars represent the time periods when a ROV was on the bottom searching for mating squids during three different expeditions. Note three occasions in which operations were conducted continuously through the day and night, and also that spawning ceased at dusk.

laying frequency (Hanlon et al., in press). Only very rarely did we observe females laying eggs while unattended by a male; in these cases the female was moribund and laying her last few egg strands.

Results and discussion

We examined 28 hours of videotape recorded during 50 ROV dives over 18 days (divided into three expeditions). Figure 1 illustrates the relative presence or absence of mating *Loligo opalescens* throughout 24-hour periods. The large gaps in the daytime observation record were due to ROV problems. Although observation times varied daily, it is clear that normal mating and egg-laying behaviors were exclusively observed during daylight hours (ca. 0800–1800 hours but with some seasonal variation) and concluded near dusk. In all instances in Figure 1 where egg-laying extended into the early evening, these mating assemblages had formed during daylight hours and persisted slightly past sunset and the number of participating squids constantly decreased as sunset approached and passed. Observations were made throughout the night on three nights. Not only were no mating squids ever encountered around the egg beds at night, but generally no squids were encountered at all near the seabed, despite large aggregations that were present higher in the water column. Thus the 200–400 watt lights on the ROVs never induced any artificial spawning behavior because there were no squids present.

Figure 2 provides some quantification of Figure 1. This graph is based on 154 spawning groups that were videotaped and includes all three trips as well as the three "all night observations" illustrated in Figure 1. We were studying discrete groups of squids to examine mating dynamics and thus were sometimes biased to smaller groups of squids that could be kept in view. Overall, we observed that squids were present in greatest numbers in mid to late afternoon and absent during the night.

Our findings strongly indicate that the extensive egg beds produced at depths of 20–60 m in southern Monterey Bay (just beyond the kelp beds) are the result of daytime aggregations of mating *Loligo opalescens*. These benthic aggregations begin forming in the early morning hours and tend to be larger in the afternoon. Reproductive activity begins to wane toward sunset and comes to a near halt at sunset. We could find no evidence that egg laying occurs naturally during the night. All observations that we are aware of (mainly television documentaries) have occurred in the presence of artificial light sources near the surface provided either by fishermen or cinematographers. In the absence of artificial lighting, *L. opalescens* in South Monterey Bay does not aggregate into mating and spawning groups at night. Thus, we conclude that all significant egg deposition in the Monterey Bay fishery is the result of daytime aggregations of squids.

Two other ascribed characteristics of *L. opalescens* spawning are mass aggregations at the sea floor and subsequent die-offs after squids have spawned. Mass aggregations can be detected by standard fathometers used by commercial fishermen, who report that mass aggregations on the sea floor are rare in Monterey Bay. During our ROV operations we encountered only one large aggregation, which occurred on 21 August 2001. We estimated from our video recordings that there were approximately 3000–4000 squid in a 50-m^2 area on the sea floor and that intermittent egg laying was occurring over an area of ca. 2000 m^2 during a period of about 3 hours. Collectively, then, we recorded 154 very small spawning groups and one large spawning group. There was no mass die-off during or after this large spawning aggregation. Instead, we consistently observed in all spawning groups that females actively broke the embrace of the paired male and jetted strongly upwards away from the spawning groups and rejoined large schools in the upper water column. Thus, squids that dispersed from the egg beds were consistently in excellent condition—certainly not senescent or moribund. These observations corroborate the results of other studies on loliginid squids that spawn intermittently (Moltschaniwskyj, 1995; Maxwell and Hanlon, 2000). Twice we encountered large numbers of dead squids on the sea floor in the early morning, but in both instances the squid fishing fleet had been working in the same area the night before and it appeared as though these mortalities were associated with the purse-seine fishery; there were few eggs in those localities. McGowan (1954), Hobson (1965), and Cousteau and Diole (1973) reported that squids died after spawning in S. California. Various *Loligo* spp. are noted for flexible reproductive strategies (*cf.* Hanlon and Messenger, 1996) so it should not be surprising if *L. opalescens* occasionally engaged in large reproductive events. Our data suggest that small groups of squids (20–200 individuals) generally descend during the day and lay eggs for several hours before rejoining squids in the water column. We encourage other researchers to use ROVs or SCUBA without lights and with stealthy approaches to determine the natural diurnal spawning of *L. opalescens* throughout its range. Given our findings that active sexual selection processes are occurring during the day and that there is vertical migration between the large schools of squid in the water column and the small spawning groups at the substrate, it would be prudent, at the very least, to restrict daytime fishing directly over egg beds or to create protected spawning areas in southern Monterey Bay. This strategy would allow the complex mating system of *L. opalescens* to be played out without direct disruption by fishing activity. In such a short-lived species, annual recruitment to the population is necessary; thus sufficient eggs must be laid for each new generation to ensure a viable living resource.

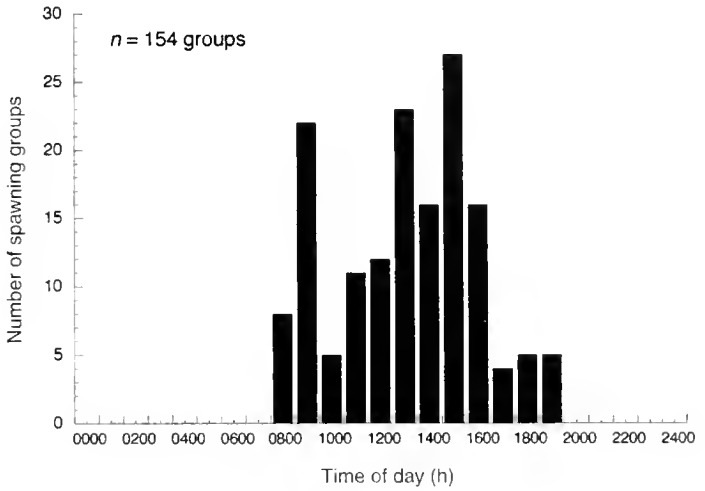

Figure 2

The number of squid spawning groups at the egg beds at different times of day (data pooled from three expeditions over 2 years; n=154 groups). A group is defined as a group of two or more mating pairs. These data correspond hour by hour with data in Figure 1.

Acknowledgments

We are most grateful for funding on NOAA grant UAF 98 0037 from the National Undersea Research Center (West Coast). Additional funding was provided by the David and Lucile Packard Foundation and the Sholley Foundation. J. Forsythe gratefully acknowledges financial support for travel from the National Institutes of Health, National Center for Research Resources (grant P40 RR0102423-23), and the Marine Medicine General Budget account of the Marine Biomedical Institute. N. Kangas gratefully acknowledges financial support from the Academy of Finland. We thank Sylvia Earle for loan of the Sustainable Seas ROV and we appreciate the professional efforts of Deep Ocean Exploration and Research (DOER) who supported the ROV operations. We especially thank John Rummel who helped begin this project, and Brett Hobson who kept it going at a critical juncture. We are thankful for expert shipboard assistance from the captains and crew of the RV *John Martin* and the FV *Lady J* (especially Captain Tom Noto). We benefitted from discussions with Bob Leos, Bill Gilly, Annette Henry, John Butler, Teirney Thies, and Sue Houghton.

Literature cited

Butler, J., D. Fuller, and M. Yaremko.
1999. Age and growth of market squid (*Loligo opalescens*) off California during1998. CalCOFI Rep. 40:191–195.

Cousteau J.-Y., and P. Diole.
1973. Octopus and squid: the soft intelligence, 304 p. Cassell, London.

Fields, W. G.
1965. The structure, development, food relations, reproduction, and life history of the squid *Loligo opalescens* Berry. Fish. Bull. 131:1–108.
Hanlon, R. T.
1998. Mating systems and sexual selection in the squid *Loligo*: How might commercial fishing on spawning squids affect them? CalCOFI Rep. 39:92–100.
Hanlon, R.T., N. Kangas, and J. W. Forsythe.
In press. Rate of egg capsule deposition, changing OSR and associated reproductive behavior of the squid *Loligo opalescens* on spawning grounds. Mar. Biol.
Hanlon, R. T., and J. B. Messenger.
1996. Cephalopod behaviour, 232 p. Cambridge Univ. Press, Cambridge.
Hixon, R. F.
1983. *Loligo opalescens*. *In* Cephalopod life cycles, vol. I, species accounts, 475 p. Academic Press, London.
Hobson, E. S.
1965. Spawning in the Pacific Coast squid. *Loligo opalescens*. Underwater Naturalist 3:20–21.
Hurley, A. C.
1977. Mating behavior of the squid *Loligo opalescens*. Mar. Behav. Physiol. 4:195–203.
Jackson, G. D.
1994. Statolith age estimates of the loliginid squid *Loligo opalescens*: corroboration with culture data. Bull. Mar. Sci. 54:554–557.
Jackson, G. D., and M. L. Domeier.
2003. The effects of an extraordinary El Nino/La Nina event on the size and growth of the squid *Loligo opalescens* off Southern California. Mar. Biol. 142:925–935.
Maxwell, M. R., and R. T. Hanlon.
2000. Female reproductive output in the squid *Loligo pealeii*: multiple egg clutches and implications for a spawning strategy. Mar. Ecol. Prog. Ser. 199:159–170.
McGowan, J. A.
1954. Observations on the sexual behavior and spawning of the squid, *Loligo opalescens*, at LaJolla, CA. Cal. Fish Game 40:47–54.
Moltschaniwskyj, N. A.
1995. Multiple spawning in the tropical squid *Photololigo* sp.: what is the cost in somatic growth? Mar. Biol. 124:127–135.
Morejohn, G. V., J. T. Harvey, and L. T.Krasnow.
1978. The importance of *Loligo opalescens* in the food web of marine vertebrates in Monterey Bay, California. *In* Biological, oceanographic, and acoustic aspects of the market squid, *Loligo opalescens* Berry (C. W. Recksiek and H. W . Frey, eds.), p. 67–98. Calif. Dep. Fish Game Fish Bull. 169.
Shimek, R. L., D. Fyfe, L. Ramsey, A. Bergey, J. Elliott, and S. Guy.
1984. A note on spawning of the Pacific market squid, *Loligo opalescens* (Berry, 1911), in the Barkley sound region, Vancouver Island, Canada. Fish. Bull. 82:445–446.
Vojkovich, M.
1998. The California fishery for market squid (*Loligo opalescens*). CalCOFI Rep. 39:55–60.
Yang, W. T., R. F. Hixon, P. E. Turk, M. E. Krejci, W. H. Hulet, and R. T. Hanlon.
1986. Growth, behavior, and sexual maturation of the market squid, *Loligo opalescens*, cultured through the life cycle. Fish. Bull. 84:771–798.

Incidental capture of loggerhead (*Caretta caretta*) and leatherback (*Dermochelys coriacea*) sea turtles by the pelagic longline fishery off southern Brazil

Jorge E. Kotas
IBAMA/Acordo Projeto TAMAR-
Instituto de Pesca/CPPM
Programa REVIZEE-SCORE SUL
Rodovia Osvaldo Reis 345 apt. 22 C
Itajaí-SC 88306-001, Brazil

Sílvio dos Santos
DTI-CNPq
Programa REVIZEE-SCORE SUL
Rua Ezio Testini 320
Santos-SP 11089-210, Brazil

Venâncio G. de Azevedo
DTI-CNPq
Programa REVIZEE-SCORE SUL
Av. Pavão 164
Caraguatatuba-SP 11676-520, Brazil

Berenice M. G. Gallo
Fundação Pró-TAMAR
Rua Antonio Athanásio 273
Ubatuba-SP 11680-000, Brazil

Paulo C. R. Barata
Fundação Oswaldo Cruz
Rua Leopoldo Bulhões 1480 - 8A
Rio de Janeiro - RJ 21041-210, Brazil
E-mail address (for P. C. R. Barata, contact author)
pbarata@alternex.com.br

back sea turtles by the surface longline fishery operating off the southern coast of Brazil, within Brazil's 200 mile exclusive economic zone (EEZ) and in international waters, and present catch-per-unit-of-effort (CPUE) data and estimates of average probability of death at capture for these species. Preliminary results of incidental captures of sea turtles by longliners during one longline trip in this area were presented by Barata et al.[2] In the present study we provide more detailed data from additional trips, including information concerning leatherback sea turtles, as well as analyses of these data. To our knowledge, this is the first detailed report about the incidental capture of sea turtles by the Brazilian commercial longline fleet.

Incidental capture in fishing gear is one of the main sources of injury and mortality of juvenile and adult sea turtles (NRC, 1990; Lutcavage et al., 1997; Oravetz, 1999). Six out of the seven extant species of sea turtles—the leatherback (*Dermochelys coriacea*), the green turtle (*Chelonia mydas*), the loggerhead (*Caretta caretta*), the hawksbill (*Eretmochelys imbricata*), the olive ridley (*Lepidochelys olivacea*), and the Kemp's ridley (*Lepidochelys kempii*)—are currently classified as endangered or critically endangered by the World Conservation Union (IUCN, formerly the International Union for Conservation of Nature and Natural Resources), which makes the assessment and reduction of incidental capture and mortality of these species in fisheries priority conservation issues (IUCN/Species Survival Commission, 1995).

Several studies have examined sea turtle bycatch by pelagic longline fisheries, especially in the North Atlantic and Pacific oceans (NRC, 1990; Nishemura and Nakahigashi, 1990; Tobias, 1991; Bolten et al., 1996; Williams et al., 1996; Lutcavage et al., 1997), but little is known about sea turtle bycatch in the South Atlantic. One of the most detailed reports on longline incidental captures in that area is that by Achaval et al. (2000), which documents the incidental capture of loggerhead and leatherback sea turtles in the southwestern Atlantic by longliners targeting swordfish (*Xiphias gladius*), tuna (*Thunnus obesus*), and other related species. Additional references, sometimes with scant detail, can be found in Weidner and Arocha (1999), Fallabrino et al. (2000), and Domingo et al.[1]

In this study, we report the incidental capture of loggerhead and leather-

Materials and methods

Observations were carried out by three of the authors (JEK, SS, and VGA) during three trips aboard Brazil-flagged commercial longline vessels based in Itajaí, State of Santa Catarina, southern Brazil (Fig. 1). The trips occurred in 1998, the first (10 sets) between 13 March and 12 April (summer–fall), the second (13 sets) between 15 June and 5 July (fall–winter), and the third (11 sets) between 28 September and 13 October (spring), and took place between latitudes 27°30′S and 34°30′S and longitudes 36°00′W and 52°00′W (Fig. 1). The

[1] Domingo, A., A. Fallabrino, R. Forselledo, and V. Quirici. 2002. Incidental capture of loggerhead (*Caretta caretta*) and leatherback (*Dermochelys coriacea*) sea turtles in the Uruguayan long-line fishery in Southwest Atlantic. Presented at the 22nd Annual Symposium on Sea Turtle Biology and Conservation, Miami, USA, 4–7 April 2002. [Available from A. Domingo: Dirección Nacional de Recursos Acuáticos, Constituyente 1497, C.P. 11.200, Montevideo, Uruguay.]

[2] Barata, P. C. R., B. M. G. Gallo, S. dos Santos, V. G. Azevedo, and J. E. Kotas. 1998. Captura acidental da tartaruga marinha *Caretta caretta* (Linnaeus, 1758) na pesca de espinhel de superfície na ZEE brasileira e em águas internacionais. *In* Resumos Expandidos da XI Semana Nacional de Oceanografia, Rio Grande, RS, outubro de 1998, p. 579–581. Editora Universitária-UFPel, Pelotas, RS, Brazil. [Available from FURG, Oceanologia, Av. Itália, km 8, Campus Carreiros, C.P 474, Rio Grande, RS 96201-900, Brazil.]

Manuscript approved for publication 22 December 2003 by Scientific Editor.
Manuscript received 20 January 2004 at NMFS Scientific Publications Office.
Fish. Bull. 102:393–399 (2004).

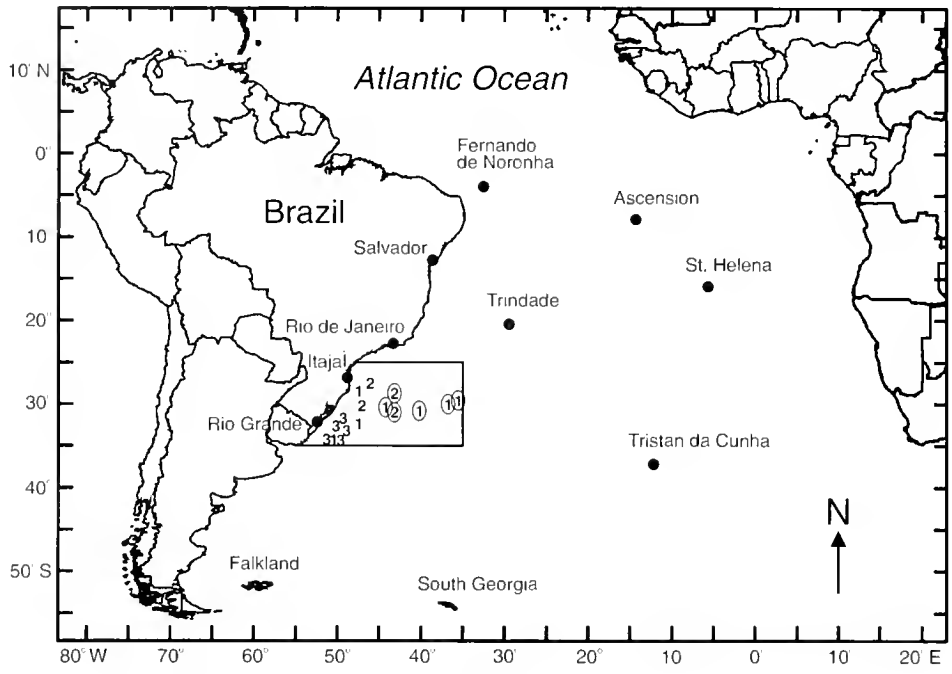

Figure 1

Fishing locations. Numbers 1, 2, and 3 indicate locations of the first, second, and third longline trips respectively; for each location, one or more sets were performed. Circled numbers indicate international waters outside the 200-mile Brazilian exclusive economic zone. The rectangular ocean area is limited by latitudes 25°S and 35°S and longitude 35°W. The fishing location farthest to the east is about 1320 km (713 nautical miles) from Itajaí, State of Santa Catarina, Brazil, the home port of the fishing vessels.

seabed in this area ranged from the continental shelf border to abyssal plains, including submarine elevations (e.g., Rio Grande). Operation depths, ranging from 170 to 4000 m, were obtained from nautical charts.

The first and second trips were aboard the *Yamaya III*, a 20.7-m, 325-hp engine, 30-t hold capacity, 10-crew longliner, and the third trip was aboard the *Basco*, a 24.4-m, 330-hp engine, 70-t hold capacity, 11-crew longliner. The vessels targeted swordfishes, sharks (mainly blue sharks, *Prionace glauca*) and tunas (*Thunnus albacares*, *T. alalunga* and *T. obesus*). Their fishing gear was the U.S.-style monofilament nylon longline, with 200–300 m sections between buoys, and each section contained four to five gangions set 40–60 m apart. Buoy dropper length ranged between 10 and 20 m, and gangion length ranged between 13 and 20 m. Each non-offset "J" hook (Swordfish 9/0) was baited with Argentine shortfin squid (*Illex argentinus*) and had a yellow chemical light stick hung over it. The average number of hooks per set was 1030, 992, and 950 on the first, second, and third trips, respectively.

On the first and second trips, the mainline was set off the stern by means of a line shooter so that a marked catenary was formed between buoys, allowing the hooks to operate at a greater depth. In this case, the maximum hook depth may have reached more than 40 m. On the third trip, the vessel *Basco* did not use a line shooter, and thus the hook depth for that trip may have been shallower. The longline gear was set around 5:30 PM, and was retrieved early in the morning. The average soak time was 7 h 30 min. For each set, the date, time, geographical position, number of hooks, and sea surface temperature were recorded. The species and condition (i.e., if the animal was alive or dead) of captured turtles were recorded; specimens with no apparent movement were considered dead.

Incidentally captured loggerhead turtles were taken aboard and hooks and lines were then removed. Whenever possible curved carapace length (CCL) and width were measured, and the turtles were double tagged (inconel tags style 681, National Band and Tag Co., Newport, KY), according to Projeto TAMAR's (Projeto Tartaruga Marinha, the Brazilian sea turtle conservation program) standard methods (Marcovaldi and Laurent, 1996). In some cases, it was not possible to bring loggerhead sea turtles on board the fishing vessel and, because of their great size, no leatherback sea turtles were brought on board. On these occasions, the turtles were pulled close to the boat and the gangions were then cut to free the turtles with the hooks still attached to them; however the length of the line remaining on the turtle was not recorded. None of these turtles was measured or tagged, although some of the leatherback sea turtles were filmed on video. No additional data and measurements, other than those presented in this study, were obtained.

Table 1

Data referring to fishing practices, sea surface temperature (°C), and capture of loggerhead and leatherback sea turtles, by trip. CPUE = catch-per-unit-of-effort (number of captured turtles/1000 hooks).

					Loggerheads				Leatherbacks			
Trip	Date	No. of sets	Average hooks/set	Average sea surface temperature	Alive (tagged)	Dead	Condition not recorded	CPUE	Alive	Dead	Condition not recorded	CPUE
1	13 Mar 98–12 Apr 98	10	1030	13.6	84 (17)	15	9	10.49	1	—	—	0.10
2	15 Jun 98–5 Jul 98	13	992	21.4	28 (12)	4	—	2.48	13	1	—	1.09
3	28 Sep 98–13 Oct 98	11	950	18.9	5 (5)	—	—	0.48	5	—	—	0.48
Total		34	990		117 (34)	19	9	4.31	19	1	—	0.59

CPUE (number of captured turtles/1000 hooks) was calculated separately for each species. Straight carapace lengths in published data were converted to CCL by using the formula in Teas (1993) to compare the CCL of captured loggerhead sea turtles to carapace length data found in the literature. To assess the significance of the difference in the proportion of dead loggerhead or leatherback sea turtles among trips, exact tests were applied, because ordinary chi-square tests are not reliable when expected cell frequencies are too small. The test statistics were $\chi^2 = \Sigma[(Observed - Expected)^2/Expected]$, and exact probabilities were computed for all tables with marginal frequencies fixed at the observed values (Lindgren, 1993, p. 376). These probability calculations were performed by a Turbo Pascal vers. 7 program (Borland International, Scotts Valley, CA). The confidence interval for overall probability of death at capture was calculated by the method in Zar (1996, p. 524). Ordinary chi-square tests and analysis of variance (ANOVA) tests followed Zar (1996) and were carried out with the software Systat vers. 9 (SPSS Inc., Chicago, IL). In the statistical tests, type-I error α was equal to 0.05. In the construction of Figure 2, to avoid overlapping of data points, the temperatures (but not the CPUEs) were jittered, that is, a small amount of uniform random noise was added to the temperature measurements (Cleveland, 1993).

Results

From a total of 34 sets and 33,650 hooks, 145 loggerhead (CPUE=4.31/1000 hooks) and 20 leatherback (CPUE=0.59/1000 hooks) sea turtles were captured. There was a significant difference in loggerhead CPUE among the trips (chi-square test, χ^2=137.3, P<0.001), but the proportion of dead loggerhead sea turtles was not significantly different among the trips (exact test, P=0.656). The average probability of death at capture for loggerhead sea turtles for the three trips was 0.140 (95% confidence interval=[0.086, 0.210]). For leatherback sea turtles, the difference in CPUE among the trips was significant (chi-square test, χ^2=9.76, P<0.01), and the proportion of dead leatherback sea turtles was not significantly different among the trips (exact test, P=1.000). The average probability of death at capture for leatherback sea turtles for the three trips was 0.050 (95% confidence interval=[0.001, 0.249]).

Table 2

Curved carapace length (CCL, cm) for loggerhead sea turtles, by trip.

Trip	Sample size	Average CCL	Standard deviation	Minimum	Maximum
1	19	56.9	7.3	46.0	70.0
2	30	57.2	7.5	46.0	68.0
3	5	67.0	5.9	58.0	73.0
Total	54	58.0	7.7	46.0	73.0

The average sea surface temperature (Table 1) was significantly different among the trips (ANOVA, n=34, F=55.37, P<0.001). The average temperature on the first trip was significantly lower than those on the second and third trips, and the average temperature on the second trip was significantly higher than that on the third trip (Tukey's *post hoc* test). For loggerhead sea turtles, CPUEs were generally higher on the first trip, which had the lowest average temperature (Fig. 2). For leatherback sea turtles, on the contrary, the lowest CPUEs were found on the first trip, on which only one leatherback sea turtle was captured (Table 1).

CCLs of captured loggerheads were in the range of 46–73 cm. Detailed loggerhead CCL data are presented in Table 2. There was a significant difference in average loggerhead CCL among the trips (Table 2); the average CCL on the third trip was greater than those on the first and second trips (ANOVA, n=54, F=4.209, P=0.020, Tukey's

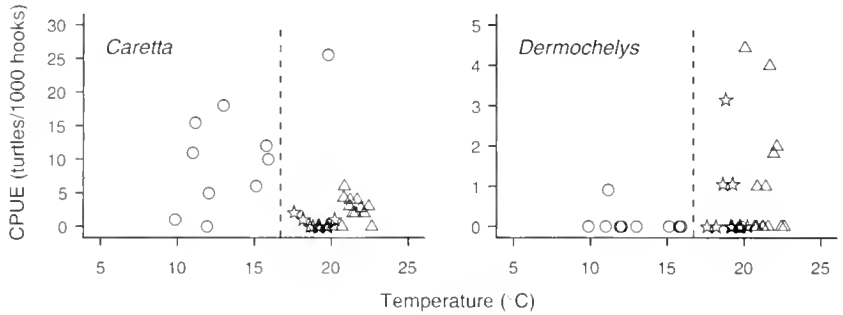

Figure 2

CPUE (number of captured turtles/1000 hooks) by sea surface temperature (°C) in each set, by species. Circles = first trip, triangles = second trip, stars = third trip. In each graph, the dashed vertical line, arbitrarily placed at 16.7 °C, marks a separation between the temperatures in the first trip and those in the second and third trips (except for one set in the first trip). Note that the two graphs have different vertical scales, and that, in the construction of this figure, temperature measurements (but not the CPUEs) have been jittered (see "Materials and methods" section).

post hoc test). Although leatherback sea turtles could not be hauled aboard for measurements, on board observations and video recordings indicated that they were subadult or adult animals.

Most of the loggerhead turtles were hooked through their mouths or esophagus, but a small number were hooked through their flippers or were found to be simply entangled in the lines. Loggerhead sea turtles taken aboard had their hooks removed, sometimes in a careless way that caused severe injury, and they were then returned to the sea. Leatherback sea turtles were found entangled in the lines or hooked either through the flippers or carapace or through the mouth. Because no leatherback sea turtle was hauled aboard, we could not tell if any were hooked in the esophagus.

Discussion

Achaval et al. (2000) reported data obtained from nine trips aboard two different longline vessels operating within the Uruguayan EEZ and in international waters in the South Atlantic in different seasons of the year, and employing different longline methods. Those authors reported that 28 loggerhead and 28 leatherback sea turtles were captured in 86 sets with 75,033 hooks in zones I and II, that correspond approximately to the fishing area covered in this study, yielding a CPUE of 0.37/1000 hooks for both loggerhead and leatherback sea turtles. For loggerhead sea turtles, there was a significant difference between our CPUE (Table 1) and that of Achaval et al. (chi-square test, χ^2=226.4, P<0.001); whereas for leatherback sea turtles no significant difference was found (chi-square test, χ^2=1.97, P=0.161).

Although the variations in CPUE observed in our study could be explained by differences in temperatures (Fig. 2), other physical, spatial, or temporal factors (or a combination of these factors) could be involved. The trips were carried out at different times of the year (Table 1); the third trip was more to the south and closer to the coast, and the first trip had sets more to the east (Fig. 1).

Our estimates of sea turtle mortality at capture may be lower than the actual mortality rates from longlines because our estimates do not consider postrelease deaths derived from 1) wounds caused by hooks removed from turtles on board, 2) embedded hooks and lines, and 3) stress caused by capture itself. Other researchers have also recognized that, because of factors such as these, there is great uncertainty in the estimates of mortality levels for sea turtles captured in longline gear (Balazs and Pooley, 1994; Eckert, 1994).

Captured loggerhead sea turtles were smaller (Table 2) than loggerhead sea turtles nesting in Brazil (minimum CCL=83.0 cm, average CCL= 103.0 cm, nesting season 1982–83 through nesting season 1999–2000; Projeto TAMAR[3]) and in several places in the North Atlantic and the Caribbean (minimum CCL=75.4 cm, average CCL in the range of 94.0–105.1 cm; Dodd, 1988). However, loggerhead sea turtles nesting in Cape Verde, in the northeastern Atlantic, are smaller than those nesting in those other places: minimum CCL=68.0 cm, average CCL=82.9 cm, data from 1998 (Cejudo et al., 2000). There is an overlap between the observed CCL range and that of adult Cape Verde loggerhead sea turtles (seven loggerhead turtles out of 54 observed, or 13.0%, had a CCL equal or greater than the minimum Cape Verde CCL), but the average CCL of the captured loggerhead sea turtles (Table 2) was well below that of loggerhead sea turtles nesting in Cape Verde. We estimate that the captured loggerhead sea turtles were generally juveniles, although a small number of them could have been adult turtles. However, size is

[3] Projeto TAMAR. 2000. Unpubl. data. Caixa Postal 2219, Salvador, BA 40210-970, Brazil.

not a reliable indicator of maturity or breeding status for sea turtles (Miller, 1997).

Along the southern coast of Brazil (between latitudes 23°S and 33°S), loggerhead sea turtles stranded or incidentally captured in fishing gear with CCLs as small as 32.5 cm have been observed (Projeto TAMAR[4]), but usually loggerhead sea turtles found in that region have CCLs greater than 50 cm, most commonly in the range of 60–90 cm (Pinedo et al., 1998; Bugoni et al., 2001; Projeto TAMAR[4]). Loggerhead sea turtles have also been found in Uruguay and Argentina (Frazier, 1984; Fallabrino et al., 2000). Their CCLs in those countries have been reported to be in the approximate range of 50–115 cm (Frazier, 1984). The loggerhead sea turtles reported here have an average CCL smaller than that usually observed for loggerhead sea turtles stranded or captured in southern Brazil, Uruguay, and Argentina, although most of the turtles (45 out of 54, or 83%) had CCLs equal to or greater than 50 cm, that is, they were within the size range for that region.

Cumulative evidence obtained from genetic and size-distribution data around oceanic basins, as well as tag returns, shows that the ontogenetic development of loggerhead sea turtles involves a pelagic juvenile stage (Carr, 1987; Musick and Limpus, 1997; Bolten et al., 1998). Transoceanic developmental migrations establishing a link between juveniles in feeding grounds and hatchlings from nesting beaches on opposite sides of the ocean basin have been demonstrated through genetic analysis for the North Atlantic and North Pacific (Bowen et al., 1995; Bolten et al., 1998). It has been suggested that a similar pattern may be expected for the South Atlantic (Bolten et al., 1998), where loggerhead sea turtles nest in Brazil and possibly in Africa (Marcovaldi and Laurent, 1996; Fretey, 2001). The incidental captures reported in our study, indicating the use of the pelagic environment by juvenile loggerhead sea turtles in the South Atlantic, support the hypothesis of transoceanic developmental migrations for those turtles in that ocean. Future genetic analysis of turtles incidentally captured in the South Atlantic would help to clarify their natal origin.

For leatherback sea turtles, there are important nesting grounds in the Atlantic, mainly in French Guiana and Suriname in South America, and Gabon and Congo in Africa (Spotila et al., 1996; Fretey, 2001). Leatherback sea turtles are known to travel long distances from their nesting beaches into pelagic waters (Goff et al., 1994; Morreale et al., 1996; Eckert and Sarti, 1997; Eckert, 1998). Satellite telemetry data indicate that leatherback sea turtles nesting in eastern South Africa can enter the South Atlantic (Hughes et al., 1998; Hughes[5]). In the southwestern Atlantic, leatherback sea turtles have been observed or captured in Brazil, Uruguay, and Argentina (Frazier, 1984; Pinedo et al., 1998; Achaval et al., 2000; Fallabrino et al., 2000; Bugoni et al., 2001).

Some measure of the significance of the three trips reported in the present study in terms of the potential for turtle capture and mortality in the South Atlantic longline fishery can be obtained by looking at information concerning the total fishing effort in the study area. In 1999, the Brazilian longline fleet consisted of 70 longliners (42 Brazilian and 28 leased foreign vessels); among them, 33 vessels were operating out of ports in southern Brazil, in the states of São Paulo, Santa Catarina, and Rio Grande do Sul. In that year, the total number of hooks of that longline fleet (both Brazilian and leased vessels) amounted to 13,598,260 hooks (ICCAT[6]). However, the southwestern Atlantic is fished not only by Brazil-based longliners, but also by longliners from Uruguay, Chile, Japan, Taiwan, and Spain (Folsom, 1997; Weidner and Arocha, 1999; Weidner et al., 1999). According to ICCAT's (International Commission for the Conservation of Atlantic Tunas) CATDIS data set (ICCAT)[7] longliners operating during 1995–97 in the area delineated by the present study (latitudes 25°S and 35°S and longitude 35°W, or eight ICCAT 5×5° statistical blocks, Fig. 1) had an average annual catch of tunas and swordfishes of 6885 metric tons (t) (the total hold capacity of the vessels on the three trips reported in this study was 130 t). However, due to unreported landings by vessels flying flags of convenience (FAO, 2001; FAO[8]) and other sources, the estimate obtained from ICCAT data should be considered a minimum estimate of the total annual tuna and swordfish catch (ICCAT[9]). Furthermore, because North Atlantic stocks of swordfishes and some species of tuna are considered overfished (NMFS[10]), quota or closure regulations (or both) in the North Atlantic may be driving longline fleets to the South Atlantic, increasing the risk of incidental capture of sea turtles there.

In Brazil, sea turtle capture is prohibited by federal legislation (Marcovaldi and Marcovaldi, 1999), and measures have been taken to address the problem of incidental capture by longlines and other kinds of fishing

[4] Projeto TAMAR. 2000. Unpubl. data. Rua Antonio Athanásio 273, Ubatuba, SP 11680-000, Brazil.

[5] Hughes, G. R. 2002. Personal commun. Ezemvelo KZN Wildlife, P O Box 13053, Cascades 3202, South Africa.

[6] ICCAT (International Commission for the Conservation of Atlantic Tunas). 2001. National report of Brazil. Report for biennial period, 2000–2001, part I (2000), vol. 1, English version, p. 312–315. Calle Corazón de María, 8, 28002 Madrid, Spain.

[7] ICCAT (International Commission for the Conservation of Atlantic Tunas). 2002. CATDIS dataset. Calle Corazón de María, 8, 28002 Madrid, Spain. [Available from http://www.iccat.org.]

[8] FAO (Food and Agriculture Organization of the United Nations). 2001. International plan of action to prevent, deter and eliminate illegal, unreported and unregulated fishing, 24 p. FAO, Rome. [Available from http://www.fao.org/docrep/003/y1224e/y1224e00.htm.]

[9] ICCAT (International Commission for the Conservation of Atlantic Tunas). 1999. Detailed report for swordfish, ICCAT SCRS swordfish stock assessment session (Madrid, Spain, September 27 to October 4, 1999), 176 p. Calle Corazón de María, 8, 28002 Madrid, Spain.

[10] NMFS (National Marine Fisheries Service). 2000. 2000 stock assessment and fishery evaluation for Atlantic highly migratory species, 150 p. U.S. Dep. Commer., NOAA, NMFS, Highly Migratory Species Management Division, 1315 East-West Highway, Silver Spring, MD 20910.

gear. Since 2001, Projeto TAMAR has been developing and implementing (through partnerships with other institutions) an action plan whose main objective is to reduce incidental sea turtle capture, including captures occurring in the open sea (Marcovaldi et al., 2002). The action plan includes, among other things, an assessment of fishery-related sea turtle mortality, the development of mitigation methods, and a proposal of adequate conservation and enforcement policies (Marcovaldi et al., 2002). However, because the longline fleet is composed of vessels from many nations, the reduction of incidental capture in the open sea calls for international cooperation (Eckert and Sarti, 1997; Trono and Salm, 1999; Crowder, 2000).

The observations reported in this study and the presence of a sizable longline fleet operating in the southwestern Atlantic indicate 1) the need for research to clarify habitat use by sea turtles in that part of the ocean (Eckert and Sarti, 1997; Bolten et al., 1998), 2) the need for continued research to quantify the impact of longline fishing on sea turtles in the pelagic realm of that ocean (Balazs and Pooley, 1994; Eckert, 1994), and 3) the implementation of conservation measures for sea turtles in that environment. We suggest the implementation of an International Observers Program on board longliners operating throughout the South Atlantic ocean.

Acknowledgments

This note is the result of observations made possible through an agreement between the REVIZEE Program (National Program for the Assessment of the Sustainable Fishing Potential of the Exclusive Economic Zone Live Resources, a Brazilian Government program) and Projeto TAMAR's station at Ubatuba, State of São Paulo. We would like to thank José Kowalsky of the Kowalsky fishing company and Marcelino Talavera (Itajaí, State of Santa Catarina), owners of the vessels *Yamaya III* and *Basco*, respectively, for kindly allowing access to the fishing vessels, and the crew of the two longliners, and also the fishing research center Centro de Pesquisa e Extensão Pesqueira do Sudeste-Sul–CEPSUL/IBAMA (Itajaí, State of Santa Catarina), and particularly Jorge Almeida de Albuquerque, for making this research possible. We also thank Larisa Avens and Matthew Godfrey for their generous reviews of the paper, and the two anonymous referees, whose suggestions helped to improve our work. Projeto TAMAR is affiliated with IBAMA (the Brazilian Institute for the Environment and Renewable Natural Resources), is co-managed by Fundação Pró-TAMAR, and officially sponsored by Petrobras. In Ubatuba, TAMAR is supported by Ubatuba's municipal government (Prefeitura Municipal de Ubatuba). S.S. and V.G.A. were supported by CNPq (Brazilian National Research Council).

Literature cited

Achaval, F., Y. H. Marin, and L. C. Barea.
2000. Captura incidental de tortugas con palangre pelágico oceánico en el Atlántico sudoccidental. *In* Captura de grandes peces pelágicos (pez espada y atunes) en el Atlántico Sudoccidental, y su interacción con otras poblaciones (G. Arena and M Rey, eds.), p. 83–88. Instituto Nacional de Pesca, Programa de las Naciones Unidas para el Desarrollo, Montevideo, Uruguay.

Balazs, G. H., and S. G. Pooley (comps.).
1994. Research plan to assess marine turtle hooking mortality: results of an expert workshop held in Honolulu, Hawaii, November 16–18, 1993. NOAA Tech. Memo. NOAA-TM-NMFS-SWFSC-201, 166 p.

Bolten, A. B., K. A. Bjorndal, H. R. Martins, T. Dellinger, M. J. Biscoito, S. E. Encalada, and B. W. Bowen.
1998. Transatlantic developmental migrations of loggerhead sea turtles demonstrated by mtDNA sequence analysis. Ecol. Appl. 8:1–7.

Bolten, A. B., J. A. Wetherall, G. H. Balazs, and S. G. Pooley (comps.).
1996. Status of marine turtles in the Pacific Ocean relevant to incidental take in the Hawaii-based pelagic longline fishery. NOAA Tech. Memo. NOAA-TM-NMFS-SWFSC-230, 167 p.

Bowen, B. W., F. A. Abreu-Grobois, G. H. Balazs, N. Kamezaki, C. J. Limpus, and R. J. Ferl.
1995. Trans-Pacific migrations of the loggerhead turtle (*Caretta caretta*) demonstrated with mitochondrial DNA markers. Proc. Natl. Acad. Sci. USA 92: 3731–3734.

Bugoni, L., L. Krause, and M. V. Petry.
2001. Marine debris and human impacts on sea turtles in southern Brazil. Mar. Pollut. Bull. 42:1330–1334.

Carr, A.
1987. New perspectives on the pelagic stage of sea turtle development. Conserv. Biol. 1: 103–121.

Cejudo, D., I. Cabrera, L. F. López-Jurado, C. Évora, and P. Alfama.
2000. The reproductive biology of *Caretta caretta* on the Island of Boavista (Republic of Cabo Verde, Western Africa). NOAA Tech. Memo. NMFS-SEFSC-443:244–245.

Cleveland, W. S.
1993. Visualizing data, 360 p. Hobart Press, Summit, NJ.

Crowder, L.
2000. Leatherback's survival will depend on an international effort. Nature 405:881.

Dodd, C. K., Jr.
1988. Synopsis of the biological data on the loggerhead sea turtle *Caretta caretta* (Linnaeus 1758). U.S. Fish Wildl. Serv. Biol. Rep. 88, 110 p.

Eckert, S. A.
1994. Evaluating the post-release mortality of sea turtles incidentally caught in pelagic longline fisheries. NOAA Tech. Memo. NMFS-SWFSC-201:106–110.
1998. Perspectives on the use of satellite telemetry and other electronic technologies for the study of marine turtles, with reference to the first year long tracking of leatherback sea turtles. NOAA Tech. Memo. NMFS-SEFSC-415:44–46.

Eckert, S. A., and M. L. Sarti.
1997. Distant fisheries implicated in the loss of the world's largest leatherback nesting population. Mar. Turtle Newsl. 78:2–7.

Fallabrino, A., A. Bager, A. Estrades, and F. Achaval.
2000. Current status of marine turtles in Uruguay. Mar. Turtle Newsl. 87:4–5.

FAO (Food and Agriculture Organization of the United Nations).
2001. Report of the second technical consultation on illegal,

unreported and unregulated fishing. Rome, 22–23 February 2001. FAO Fisheries Rep. 646, 38 p. FAO, Rome.

Folsom, W. B.
1997. World swordfish fisheries: an analysis of swordfish fisheries, market trends and trade patterns, vol. VI: Western Europe. NOAA Tech. Memo. NMFS-F/SPO-29, 324 p.

Frazier, J.
1984. Las tortugas marinas en el Atlántico sur occidental. *In* Serie divulgación no. 2, p. 2–21. Associacion Herpetologica Argentina, La Plata, Argentina.

Fretey, J.
2001. Biogeography and conservation of marine turtles of the Atlantic coast of Africa. CMS Technical Series Publ. no. 6, 429 p. UNEP/CMS Secretariat, Bonn, Germany.

Goff, G. P., J. Lien, G. B. Stenson, and J. Fretey.
1994. The migration of a tagged leatherback turtle, *Dermochelys coriacea*, from French Guiana, South America, to Newfoundland, Canada, in 128 days. Can. Field Nat. 108:72–73.

Hughes, G. R., P. Luschi, R. Mencacci, and F. Papi.
1998. The 7000 km oceanic journey of a leatherback turtle tracked by satellite. J. Exp. Mar. Biol. Ecol. 229: 209–217.

IUCN (International Union for Conservation of Nature and Natural Resources) Species Survival Commission.
1995. A global strategy for the conservation of marine turtles, 25 p. IUCN, Gland, Switzerland.

Lindgren, B. W.
1993. Statistical theory, 4th ed., 633 p. Chapman & Hall, New York, NY.

Lutcavage, M. E., P. Plotkin, B. Witherington, and P. L. Lutz.
1997. Human impacts on sea turtle survival. *In* The biology of sea turtles (P. L. Lutz and J. A. Musick, eds.), p. 387–409. CRC Press, Boca Raton, FL.

Marcovaldi, M. A., and A. Laurent.
1996. A six season study of marine turtle nesting at Praia do Forte, Bahia, Brazil, with implications for conservation and management. Chelonian Conserv. Biol. 2:55–59.

Marcovaldi, M. A., and G. G. dei Marcovaldi.
1999. Marine turtles of Brazil: the history and structure of Projeto TAMAR-IBAMA. Biol. Conserv. 91:35–41.

Marcovaldi, M. A., J. C. Thomé, G. Sales, A. C. Coelho, B. Gallo, and C. Bellini.
2002. Brazilian plan for reduction of incidental sea turtle capture in fisheries. Mar. Turtle Newsl. 96:24–25.

Miller, J. D.
1997. Reproduction in sea turtles. *In* The biology of sea turtles (P. L. Lutz and J. A. Musick, eds.), p. 51–81. CRC Press, Boca Raton, FL.

Morreale, S. J., E. A. Standora, J. R. Spotila, and F. V. Paladino.
1996. Migration corridor for sea turtles. Nature 384: 319–320.

Musick, J. A., and C. J. Limpus.
1997. Habitat utilization and migration in juvenile sea turtles. *In* The biology of sea turtles (P. L. Lutz and J. A. Musick, eds.), p. 137–163. CRC Press, Boca Raton, FL.

NRC (National Research Council).
1990. Decline of the sea turtles: causes and prevention. 259 p. National Academy Press, Washington, D.C.

Nishemura, W., and S. Nakahigashi.
1990. Incidental capture of sea turtles by Japanese research and training vessels: results of a questionaire. Mar. Turtle Newsl. 51:1–4.

Oravetz, C. A.
1999. Reducing incidental catch in fisheries. *In* Research and management techniques for the conservation of sea turtles (K. L. Eckert, K. A. Bjorndal, F. A. Abreu-Grobois, and M. Donnelly, eds.), p. 189–193. IUCN SSC Marine Turtle Specialist Group publication no. 4.

Pinedo, M. C., R. Capitoli, A. S. Barreto, and A. L. V. Andrade.
1998. Occurrence and feeding of sea turtles in southern Brazil. NOAA Tech. Memo. NMFS-SEFSC-412:117–118.

Spotila, J. R., A. E. Dunham, A. J. Leslie, A. C. Steyermark, P. T. Plotkin, and F.V. Paladino.
1996. Worldwide decline of *Dermochelys coriacea*: are leatherback turtles going extinct? Chelonian Conserv. Biol. 2:209–222.

Teas, W. G.
1993. Species composition and size class distribution of marine turtle strandings on the Gulf of Mexico and southeast United States coasts, 1985–1991. NOAA Tech. Memo. NMFS-SEFSC-315, 43 p.

Tobias, W.
1991. Turtles caught in Caribbean swordfish net fishery. Mar. Turtle Newsl. 53:10–12.

Trono, R. B., and R. V. Salm.
1999. Regional collaboration. *In* Research and management techniques for the conservation of sea turtles (K. L. Eckert, K. A. Bjorndal, F. A. Abreu-Grobois, and M. Donnelly, eds.), p. 224–227. IUCN SSC Marine Turtle Specialist Group publication no. 4.

Weidner, D. M., and F. Arocha.
1999. World swordfish fisheries: an analysis of swordfish fisheries, market trends and trade patterns. Vol. IV, Part A2b: Brazil. NOAA Tech. Memo. NMFS-F/SPO-35:237–628.

Weidner, D. M., F. J. Fontes, and J. Serrano.
1999. World swordfish fisheries: an analysis of swordfish fisheries, market trends and trade patterns. Vol. IV, part A2c: Urugnay, Paraguay and Argentina. NOAA Tech. Memo. NMFS-F/SPO-36:631–916.

Williams, P., P. J. Anninos, P. T. Plotkin, and K. L. Salvini (comps.).
1996. Pelagic longline fishery—sea turtle interactions. Proceedings of an industry, academic and government experts, and stakeholders workshop held in Silver Spring, Maryland, 24–25 May 1994. NOAA Tech. Memo. NMFS-OPR-7, 77 p.

Zar, J. H.
1996. Biostatistical analysis, 3rd ed., 662 p. Prentice Hall, Upper Saddle River, NJ.

Diet changes of Pacific cod (*Gadus macrocephalus*) in Pavlof Bay associated with climate changes in the Gulf of Alaska between 1980 and 1995

Mei-Sun Yang

Alaska Fisheries Science Center
National Marine Fisheries Service, NOAA
7600 Sand Point Way NE
Seattle, Washington 98115

E-mail address: mei-sun.yang@noaa.gov

The diet of Pacific cod (*Gadus macrocephalus*) in the area of Pavlof Bay, Alaska, was studied in the early 1980s by Albers and Anderson (1985). They found that the dominant prey species were forage species like pandalid shrimp, capelin (*Mallotus villosus*), and walleye pollock (*Theragra chalcogramma*). The shrimp fishery in Pavlof Bay began in 1968 and closed in 1980 because of low shrimp abundance (Ruccio and Worton[1]). Survey data indicate that, during the period between 1972 and 1997, the abundance of forage species such as pandalid shrimp and capelin declined and higher trophic-level groundfish such as Pacific cod increased. There is a general recognition that a long-term ocean climate shift in the Gulf of Alaska has been partially responsible for the observed reorganization of the community structure (Anderson and Piatt, 1999).

Because there has been an apparent shift in the abundance of both predators and prey in Pavlof Bay, it is important to understand how trophic relationships may also have changed. In order to partially address this question, stomach samples of Pacific cod and other groundfishes were taken in 1995. By performing a comparison of the diet of Pacific cod right after the climate shift with Pacific cod and other groundfishes well after the shift, this analysis may demonstrate how the relative abundance of prey in the Gulf of Alaska may have changed.

Methods

Stomachs of Pacific cod, walleye pollock, and arrowtooth flounder (*Atheresthes stomias*) were collected by National Marine Fisheries Service (NMFS) scientists on board the chartered vessel FV *Arcturus* conducting a trawl survey in Pavlof Bay, Alaska, (Fig. 1) from 5 August to 7 August 1995. The survey targeted shrimp and used a high-opening net with small mesh (32-mm stretched mesh). Each tow was about 1.2 km in length. The average depth of the 13 hauls where stomachs were collected was 108.9 (±9.5) m with a range from 90 to 123 m. When a sampled stomach was retained, it was put in a cloth stomach bag. A field tag with the species name, fork length (FL in cm) of the fish, and haul data (vessel, cruise, haul number, specimen number) was also put in the bag. All the samples collected were then preserved in buckets containing a 10% formalin solution. When the samples arrived at the laboratory, they were transferred into 70% ethanol before the stomach contents were analyzed. In the laboratory, the stomach was cut open, the contents were removed and blotted with a paper towel. Wet weight was then recorded to the nearest 0.1 g. After obtaining the total weight for a stomach's contents, the contents were placed in a Petri dish and examined under a microscope. Each prey item was classified to the lowest practical taxonomic level. Prey weights and numbers of commercially important fish were recorded. Standard lengths of prey fish and carapace width of crabs were also recorded. The diet of Pacific cod was summarized to show the percent frequency of occurrence, the percentage by number, and the percentage of the total weight of each prey item found in the stomachs. Stomach contents of walleye pollock and arrowtooth flounder were analyzed for comparisons.

Results

Of 130 Pacific cod stomachs analyzed, 129 contained food. Pacific cod sizes ranged from 40 to 80 cm FL (fork length); a mean size was 55.4 (SD ±7.2) cm.

Polychaetes, crangonid shrimp, pea crab, and clams were the most frequently found prey items in Pacific cod stomachs (Table 1). However, in terms of weight, eelpouts (zoarcids), Tanner crab (*Chionoecetes bairdi*), crangonid shrimp, hermit crab, and polychaetes were the most important prey of Pacific cod. Pandalid shrimp, spinyhead sculpin (*Dasycottus setiger*), pricklebacks (stichaeid), Pacific sandlance (*Ammodytes hexapterus*), arrowtooth flounder (*Atheresthes stomias*), and flathead sole (*Hippoglossoides classodon*) were minor prey.

Invertebrates (mainly crangonid shrimp, polychaetes, and crabs) were the principal prey of Pacific cod smaller than 60 cm (Fig. 2). There were nine prey categories as shown in Figure 2. The miscellaneous prey included Sipuncula, Echiura, fish offal (processed

[1] Ruccio, M. P., and C. L. Worton. 1999. Annual management report for the shellfish fisheries of the Alaska peninsula area, 1998. *In* Annual management report for the shellfish fisheries of the westward region, 1998. Regional Information Report 4K99-49, 312 p. Alaska Department of Fish and Game, Division of Commercial Fisheries, 211 Mission Road, Kodiak, Alaska 99615.

Manuscript approved for publication 24 December 2003 by Scientific Editor.

Manuscript received 20 January 2004 at NMFS Scientific Publications Office.

Fish. Bull. 102:400–405 (2004).

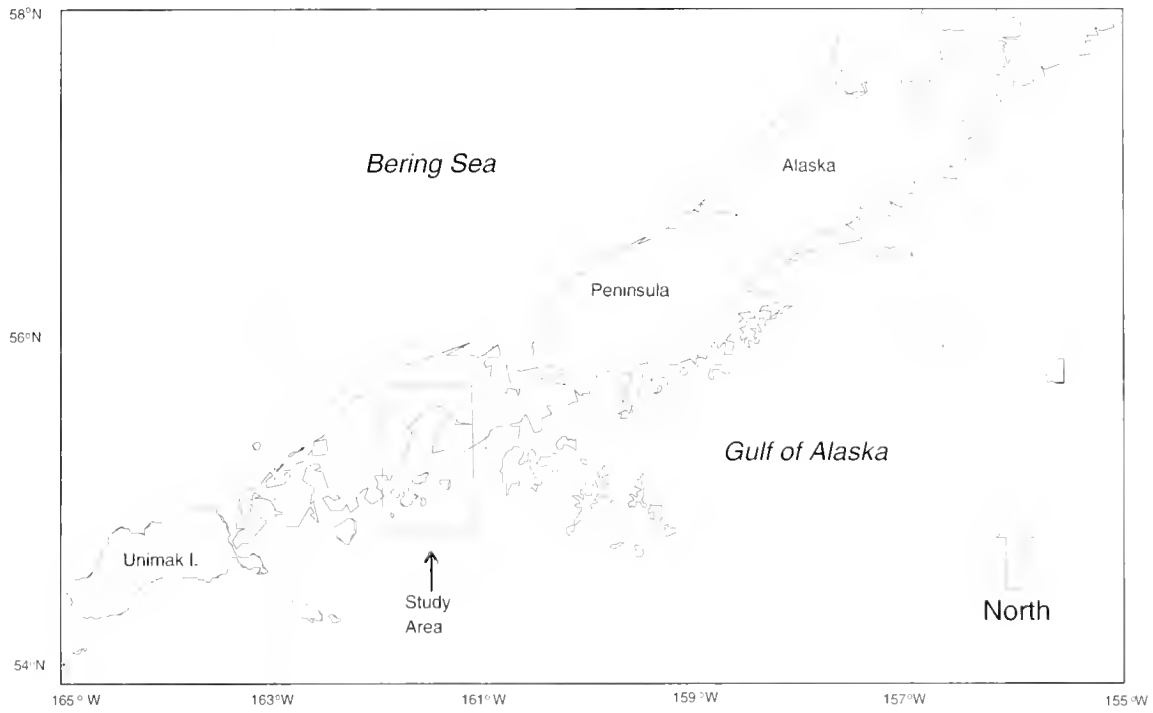

Figure 1

Location of study area in 1980, 1981, and 1995.

fish parts like head, tail, pyloric caeca, etc.), and all other prey organisms not included in the other eight prey categories. The importance of fish in the diet of Pacific cod increased after 60 cm FL. Walleye pollock were consumed only by Pacific cod ≥60 cm FL.

In general, Pacific cod ate prey of small individual size (Table 2). Tanner crabs (*Chionoecetes bairdi*) ranged from 4.5 to 42.3 mm carapace width. Eelpouts ranged in length from 36.2 to 256.6 mm standard length. Other fish prey ranged in length from 32.7 to 81.5 mm. Walleye pollock were consumed by Pacific cod but were not measurable.

In 1995, when Pacific cod stomachs were collected in Pavlof Bay, 218 walleye pollock and 80 arrowtooth flounder stomachs were also collected. Similar to the results for Pacific cod, pandalid shrimp and capelin were not important food of walleye pollock and arrowtooth flounder either (Fig. 3). These prey each comprised less than 3% of the total stomach content weight of walleye pollock and arrowtooth flounder. Instead, eelpouts, pricklebacks, euphausiids, and walleye pollock were important food of arrowtooth flounder, and euphausiids (83% by weight) were the main food of walleye pollock.

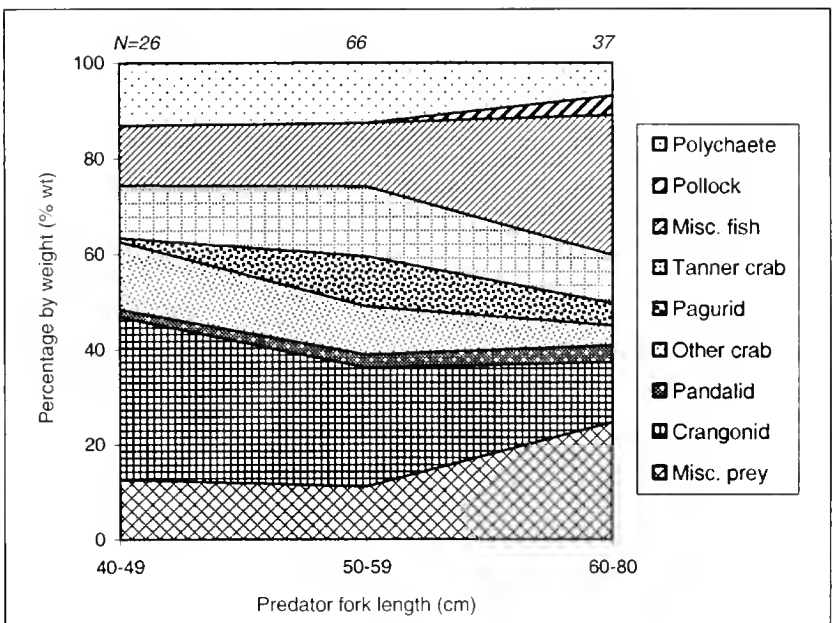

Figure 2

Variations in the main food items of Pacific cod, by predator size, in Pavlof Bay in 1995. *n*=sample size.

Discussion

This study shows that eelpouts, Tanner crabs, crangonids, hermit crabs, polychaetes, and echiuroids were the princi-

Table 1

Percent frequency of occurrence (%*F*), percentage by number (%*N*), and percentage by weight (%*W*) of prey items of Pacific cod collected in Pavlof Bay, Alaska, 1995.

Prey name	%*F*	%*N*	%*W*
Polychaeta (worm)	79.8	11.4	9.2
Gastropoda (snail)	14.0	0.8	0.4
Bivalvia (clam)	55.0	6.1	2.1
Cephalopoda (squid and octopus)	10.1	0.5	2.1
Copepoda	0.8	0.0	0.0
Peracarida Mysidacea (mysid)	31.8	11.5	0.2
Cumacea (cumacean)	13.2	0.9	0.0
Amphipoda (amphipod)	17.1	1.2	0.0
Euphausiacea (euphausiid)	15.5	10.0	0.7
Natantia (unidentified shrimp)	12.4	0.7	0.1
Caridea (shrimp)	12.4	1.2	1.2
Hippolytidae (shrimp)	17.8	1.2	0.2
Pandalidae (shrimp)	41.1	5.7	2.3
Crangonidae (shrimp)	76.0	18.9	13.3
Reptantia (unidentified crab)	11.6	0.5	1.9
Paguridae (hermit crab)	22.5	1.3	9.5
Decapoda Brachyura (crab)	0.8	0.0	0.1
Hyas sp. (lyre crab)	0.8	0.0	0.9
Hyas lyratus (lyre crab)	1.6	0.1	0.6
Chionoecetes sp. (snow and Tanner crab)	40.3	3.5	13.9
Pinnotheridae (pea crab)	1.6	0.1	0.1
Pinnixa sp. (pea crab)	68.2	8.4	3.2
Sipuncula (marine worm)	0.8	0.0	0.6
Echiura (marine worm)	24.0	1.4	6.6
Ophiuroidea (basket and brittle star)	9.3	0.7	0.1
Chaetognatha (arrow worm)	1.6	0.2	0.0
Rajidae (skate)	2.3	0.1	0.4
Osteichthyes Teleostei (fish)	12.4	1.1	0.6
Nongadoid fish remains	47.3	6.5	2.3
Gadidae (unidentified)	1.6	0.1	0.4
Theragra chalcogramma (walleye pollock)	2.3	0.1	1.4
Zoarcidae (eelpout)	16.3	0.9	14.0
Cottoidei (Sculpin)	2.3	0.1	0.2
Dasycottus setiger (spinyhead sculpin)	0.8	0.0	0.2
Stichaeidae (prickleback)	8.5	1.5	0.6
Lumpenus sp. (prickleback)	0.8	0.0	0.0
Ammodytes hexapterus (Pacific sand lance)	0.8	0.0	0.0
Pleuronectidae (flatfish)	2.3	0.2	0.2
Atheresthes stomias (arrowtooth flounder)	1.6	0.1	0.0
Hippoglossoides elassodon (flathead sole)	3.9	0.2	0.5
Unidentified organic material	10.1	0.5	0.6
Unidentified worm-like organism	5.4	0.3	0.5
Fish offal (processed fish parts, e.g., head, tail)	0.8	0.0	8.1
Total prey weight	2715 g		
Total stomachs	130		
Total empty stomachs	1		

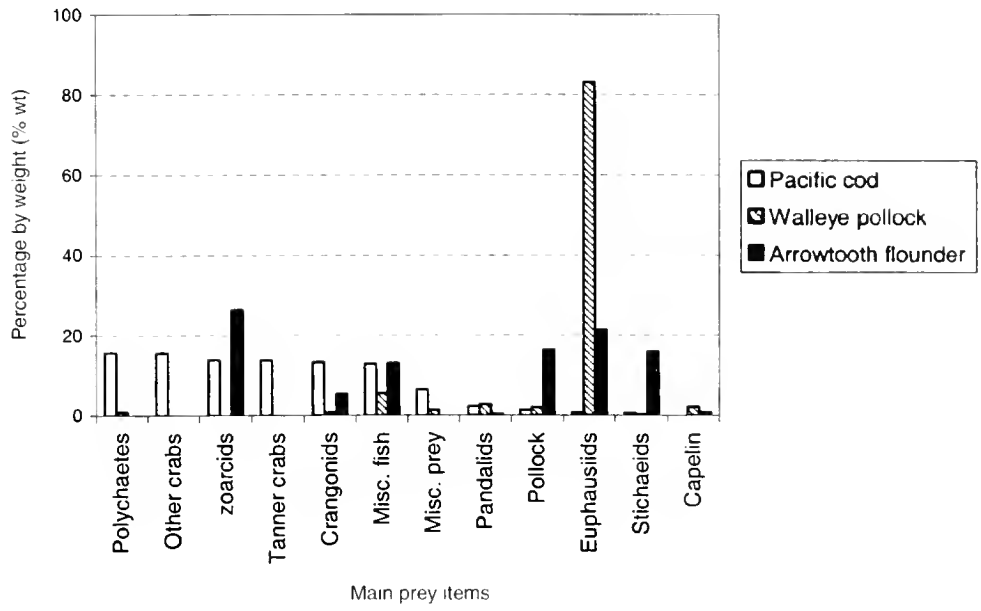

Figure 3

Percentage by weight of the main prey in the diet of Pacific cod (n=129), walleye pollock (n=216), and arrowtooth flounder (n=43) collected in Pavlof Bay in 1995.

pal prey of Pacific cod collected in Pavlof Bay in 1995. This is a large change in diet composition compared with that observed 15 years earlier (Albers and Anderson, 1985). In Albers and Anderson's (1985) study, pandalid shrimp, capelin, and walleye pollock were the main prey of Pacific cod (Fig. 4). The change in main prey from pelagic prey in the 1980s to benthic prey in 1995 corresponds to changes in species abundance trends in nearshore small-mesh trawl surveys observed by Anderson and Piatt (1999). In that study, they described that the community reorganization in the Gulf of Alaska was triggered by a shift in ocean climate during the late 1970s. They showed that the abundance of species such as pandalid shrimp and capelin declined while the abundance of predators such as Pacific cod, walleye pollock, and flatfish increased between 1972 and 1997.

The mean weight of pandalid shrimp consumed by Pacific cod in 1995 was only 0.5 g/cod. In contrast, the mean weights of undigested pink shrimp in Pacific cod stomachs ranged between 4.5 g/cod and 24.4 g/cod during 1980 and 1981. This finding corroborates those of Anderson (2000) and show that pandalid shrimp abundance continued to decrease in the late 1990s and Pacific cod abundance continued to increase during that same period.

The diet of Pacific cod in the present study was also compared with the diet of Pacific cod in the broader Gulf of Alaska shelf area (Fig. 5) (Yang and Nelson, 2000). The values of the percentage by weight of capelin in Pacific cod stomachs in the Gulf of Alaska in 1990, 1993, and 1996 were similar (all were less than 3%) to that in Pavlof Bay in 1995. However, pandalid shrimp were an important food item of Pacific cod throughout the Gulf of Alaska, comprising from 11% to 15% by weight of the total stomach contents of Pacific cod in the Gulf of Alaska in 3 years (1990, 1993, and 1996) (Yang and Nelson, 2000). These values are higher than that in Pavlof Bay (2% by weight). By comparing the depths of the sampling locations of the Pacific cod, high percentages of pandalid shrimp were found in the cod diet in deeper offshore areas of the Gulf of Alaska in 1990, 1993, and 1996, whereas low percentages of pandalid shrimp were found in cod diet in much

Table 2

Mean standard length (or carapace width), standard deviation, and the size range of prey consumed by Pacific cod in Pavlof Bay 1995.

Prey name	Mean (mm)	SD (mm)	Range (mm)	No. of individuals
Tanner crab	22.1	10.5	4.5–42.3	70
Zoarcid	86.4	73.5	36.2–256.6	15
Cottid	48.2	9.4	41.8–59	3
Stichaeid	46.9	19.6	32.7–81.5	5
Pacific sand lance	44.8	0.0	44.8–44.8	1
Arrowtooth flounder	39.1	7.4	33.8–44.3	2
Flathead sole	58.2	14.4	47.5–80.4	4

shallower areas in the Pavlof Bay area (Fig. 6). From the shrimp survey data, Anderson (2000) showed that pandalid shrimp occupying inshore and shallower water (e.g., Pavlof Bay area) declined to near extinction (<0.1 kg/km) from 1978 to 1982, while offshore and deepwater pandalid shrimp species maintained low population levels (>0.1 kg/km). The data from this study corroborates Anderson's (2000) results.

Anderson (2000) also reported that during the period of the decline of pandalid shrimp in inshore waters of the Gulf of Alaska, the abundance of some pleuronectids, Pacific cod, and walleye pollock increased. These species are predators of pandalid shrimp (Yang and Nelson, 2000). One hypothesis is that predators keep pandalid shrimp populations low. Albers and Anderson (1985) suggested that cod predation was one reason for the failure of the pink shrimp stock to rebuild in Pavlof Bay. In the Northwest Atlantic, Lilly et al. (2000) showed that the large increase in shrimp biomass seen in the 1990s was related to the collapse of cod (*Gadus morhua*) populations during the late 1980s and 1990s in the northeast Newfoundland shelf. The impact of cod on Barents Sea shrimp (*P. borealis*) was also reported by Berenboim et al. (2000). They found that when cod biomass is high, the shrimp frequency of occurrence in cod stomachs declines; there is a significant inverse correlation between the abundance of cod and shrimp.

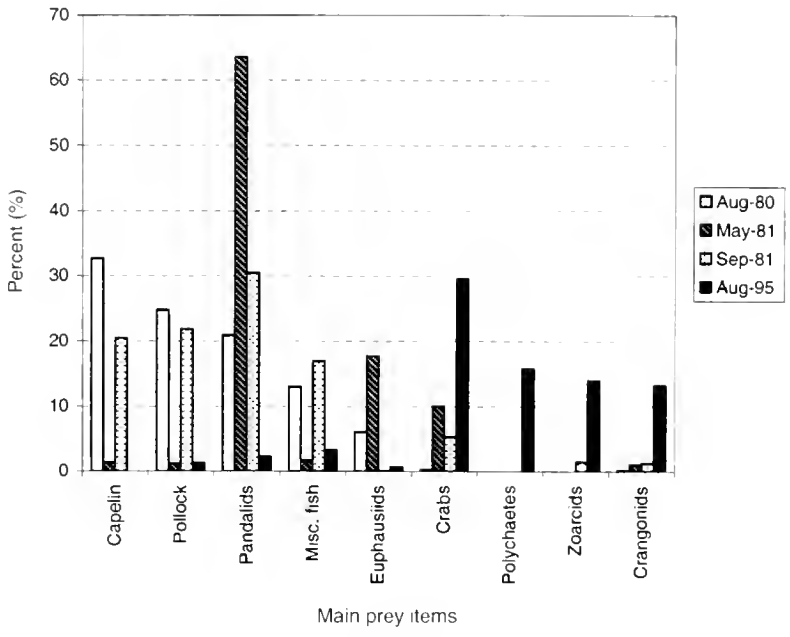

Figure 4

Percentage by volume (for the values in 1980s) and the percentage by weight (for the values in 1995) of the main prey items of Pacific cod collected in Pavlof Bay, Alaska.

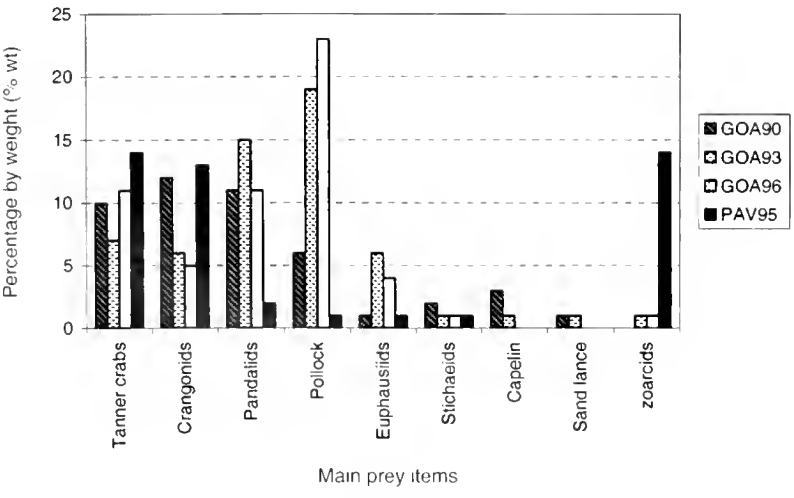

Figure 5

Percentage by weight of the main prey items in the diet of Pacific cod collected in 1990 (GOA90), 1993 (GOA93), and 1996 (GOA96) in the Gulf of Alaska and in 1995 (PAV95) in Pavlof Bay.

Tanner crabs consumed by Pacific cod in this study ranged from 5 to 42 mm carapace width (CW). In general, the size of Tanner crabs consumed increases as Pacific cod size increases. The size range of Tanner crabs consumed by Pacific cod in this study is similar to that (5–45 mm) found in Pacific cod stomachs in Albers and Anderson's (1985) study and is also similar to that (1–40 mm) found in Hunter's (1979) study near Kodiak Island.

Jewett's (1978) Pacific cod diet study around Kodiak Island from 1973 to 1976 showed that Tanner crabs were the most frequent (37%) prey of Pacific cod; pandalid shrimp occurred in 8–10% of the stomachs examined from 1973 to 1975; and walleye pollock were found in 4% of the stomachs examined. The importance of Tanner crabs as food of Pacific cod in Jewett's (1978) study is coincident with our study.

This study suggests that there were substantial differences between the diets of Pacific cod in Pavlof Bay between the early 1980s and 1995. In the 1980s, pandalid shrimp and capelin were the main food of Pacific cod, whereas benthic species (polychaetes,

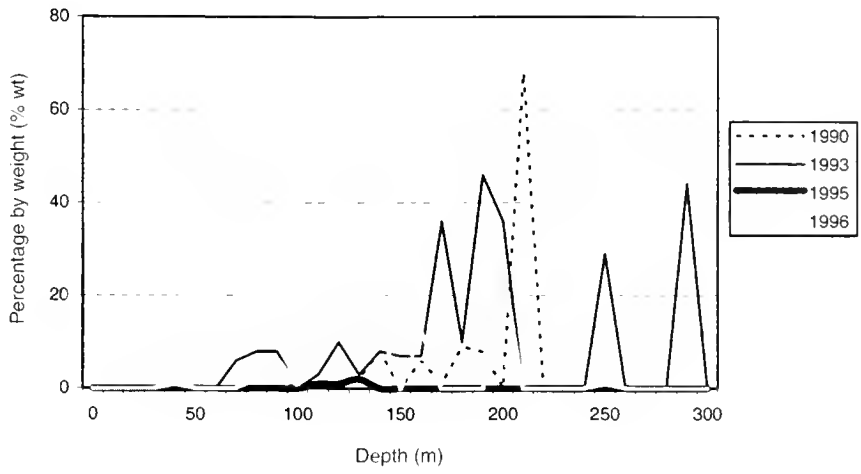

Figure 6

Pandalid shrimp consumed by Pacific cod sampled at different bottom depths (m) in Pavlof Bay in 1995, and in the Gulf of Alaska in 1990, 1993, and 1996.

hermit crabs, Tanner crabs, and eelpouts) were the dominant food in 1995. This change was probably due to the climate shift from cold to warm in the Gulf of Alaska.

Acknowledgments

I would like to thank Paul Anderson, Troy Buckley, and Patricia Livingston for reviewing the manuscript and for their very helpful suggestions. I also want to thank the two anonymous reviewers for their comments and suggestions.

Literature cited

Albers W. D., and P. J. Anderson.
1985. Diet of the Pacific cod, *Gadus macrocephalus*, and predation on the northern pink shrimp, *Pandalus borealis*, in Pavlof Bay, Alaska. Fish. Bull. 83:601–610.

Anderson, P. J .
2000. Pandalid shrimp as indicators of ecosystem regime shift. J. Northw. Atl. Fish. Sci. 27:1–10.

Anderson, P. J., and J. F. Piatt.
1999. Community reorganization in the Gulf of Alaska following ocean climate regime shift. Mar. Ecol. Prog. Ser. 189:117–123.

Berenboim, B. I., A. V. Dolgov, V. A. Korzhev, and N. A. Yaragina.
2000. The impact of cod on the dynamics of Barents Sea shrimp (*Pandalus borealis*) as determined by multispecies models. J. Northw. Atl. Fish. Sci. 27:69–75.

Hunter, M. A.
1979. Food resource partitioning among demersal fishes in the vicinity of Kodiak Island, Alaska. M.S. thesis, 120 p. Univ. Washington, Seattle, WA.

Jewett, S. C.
1978. Summer food of the Pacific cod, *Gadus macrocephalus*, near Kodiak Island, Alaska. Fish. Bull. 76:700–706.

Lilly, G. R., D. G. Parsons, and D. W. Kulka.
2000. Was the increase in shrimp biomass on the Northeast Newfoundland shelf a consequence of a release in predation pressure from cod? J. Northw. Atl. Fish. Sci. 27:45–61.

Yang, M-S., and M. W. Nelson.
2000. Food habits of the commercially important groundfishes in the Gulf of Alaska in 1990, 1993, and 1996. NOAA Tech. Memo. NMFS-AFSC-112, 174 p.

Fishery Bulletin

Guidelines for contributors

Content of papers

Articles

Articles are reports of 10 to 30 pages (double spaced) that describe original research in one or a combination of the following fields of marine science: taxonomy, biology, genetics, mathematics (including modeling), statistics, engineering, economics, and ecology.

Notes

Notes are reports of 5 to 10 pages without an abstract that describe methods and results not supported by a large body of data. Although all contributions are subject to peer review, responsibility for the contents of articles and notes rests upon the authors and not upon the editor or the publisher. It is therefore important that authors consider the contents of their manuscripts carefully. Submission of an article is understood to imply that the article is original and is not being considered for publication elsewhere. Manuscripts must be written in English. Authors whose native language is not English are strongly advised to have their manuscripts checked for fluency by English-speaking colleagues prior to submission.

Preparation of papers

Text

Title page should include authors' full names and mailing addresses (street address required) and the senior author's telephone, fax number, e-mail address, as well as a list of key words to describe the contents of the manuscript. **Abstract** must be less than one typed page (double spaced) and must not contain any citations. It should state the main scope of the research but emphasize the author's conclusions and relevant findings. Because abstracts are circulated by abstracting agencies, it is important that they represent the research clearly and concisely. **General text** must be typed in double-spaced format. A brief introduction should state the broad significance of the paper; the remainder of the paper should be divided into the following sections: Materials and methods, Results, Discussion (or Conclusions), and Acknowledgments. Headings within each section must be short, reflect a logical sequence, and follow the rules of multiple subdivision (i.e. there can be no subdivision without at least two subheadings). The entire text should be intelligible to interdisciplinary readers; therefore, all acronyms and abbreviations should be written out and all lesser-known technical terms should be defined the first time they are mentioned. The scientific names of species must be written out the first time they are mentioned; subsequent mention of scientific names may be abbreviated. Follow *Scientific style and format. CBE manual for authors, editors, and publishers* (6th ed.) for editorial style and the most current issue of the *American Fisheries Society's common and scientific names of fishes from the United States and Canada* for fish nomenclature. Dates should be written as follows: 11 November 1991. Measurements should be expressed in metric units, e.g. metric tons (t). The numeral one (1) should be typed as a one, not as a lower-case el (l).

Footnotes

Use footnotes to add editorial comments regarding claims made in the text and to document unpublished works or works with local circulation. Footnotes should be numbered with Arabic numerals and inserted in 10-point font at the bottom of the first page on which they are cited. Footnotes should be formatted in the same manner as citations. If a manuscript is unpublished, in the process of review, or if the information provided in the footnote has been conveyed verbally, please state this information as "unpubl. data," "manuscript in review," and "personal commun.," respectively. Authors are advised wherever possible to avoid references to nonstandard literature (unpublished literature that is difficult to obtain, such as internal reports, processed reports, administrative reports, ICES council minutes, IWC minutes or working papers, any "research" or "working" documents, laboratory reports, contract reports, and manuscripts in review). If these references are used, please indicate whether they are available from NTIS (National Technical Information Service) or from some other public depository. Footnote format: author (last name, followed by first-name initials), year; title of report or manuscript; type of report and its administrative or serial number; name and address of agency or institution where the report is filed.

Literature cited

The literature cited section comprises works that have been published and those accepted for publication (works in press) in peer-reviewed journals and books. Follow the name and year system for citation format. In the text, write "Smith and Jones (1977) reported" but if the citation takes the form of parenthetical matter, write "(Smith and Jones, 1977)." In the literature cited section, list citations alphabetically by last name of senior author: For example, Alston, 1952; Mannly, 1988; Smith, 1932; Smith, 1947; Stalinsky and Jones, 1985. Abbreviations of journals should conform to the abbreviations given in the *Serial sources for the BIOSIS previews database*. Authors are responsible for the accuracy and completeness of all citations. Literature citation format: author (last name, followed by first-name initials); year; title of report or article; abbreviated title of the journal in which the article was published, volume number, page numbers. For books, please provide publisher, city, and state.

Tables

Tables should not be excessive in size and must be cited in numerical order in the text. Headings in tables should be short but ample enough to allow the table to be intelligible on its own. All unusual symbols must be explained in the table legend. Other incidental comments may be footnoted (use italic arabic numerals for footnote markers). Use asterisks only to indicate probability in statistical data. Place table legends on the same page as the table data. We accept tables saved in most spreadsheet software programs (e.g. Microsoft Excel). Please note the following:

- Use a comma in numbers of five digits or more (e.g. 13,000 but 3000).
- Use zeros before all decimal points for values less than one (e.g. 0.31).

Figures

Figures include line illustrations, computer-generated line graphs, and photographs (or slides). They must be cited in numerical order in the text. Line illustrations are best submitted as original drawings. Computer-generated line graphs should be printed on laser-quality paper. Photographs should be submitted on glossy paper with good contrast. All figures are to be labeled with senior author's name and the number of the figure (e.g. Smith, Fig. 4). Use Helvetica or Arial font to label anatomical parts (line drawings) or variables (graphs) within figures; use Times Roman bold font to label the different sections of a figure (e.g. **A**, **B**, **C**). Figure legends should explain all symbols and abbreviations seen within the figure and should be typed in double-spaced format on a separate page at the end of the manuscript. We advise authors to peruse a recent issue of *Fishery Bulletin* for standard formats. Please note the following:

- Capitalize the first letter of the first word of axis labels.
- Do not use overly large font sizes to label axes or parts within figures.
- Do not use boldface fonts within figures.
- Do not create outline rules around graphs.
- Do not use horizontal lines through graphs.
- Do not use large font sizes to label degrees of longitude and latitude on maps.
- Indicate direction of degrees longitude and latitude on maps (e.g. 170 E).
- Avoid placing labels on a vertical plane (except on y axis).
- Avoid odd (nonstandard) patterns to mark sections of bar graphs and pie charts.

Copyright law

Fishery Bulletin, a U.S. government publication, is not subject to copyright law. If an author wishes to reproduce any part of *Fishery Bulletin* in his or her work, he or she is obliged, however, to acknowledge the source of the extracted literature.

Submission of papers

Send four printed copies (one original plus three copies)—clipped, *not stapled*—to the Scientific Editor, at the address shown below. Send photocopies of figures with initial submission of manuscript. Original figures will be requested later when the manuscript has been accepted for publication. Do not send your manuscript on diskette until requested to do so.

Dr. Norman Bartoo
National Marine Fisheries Service, NOAA
8604 La Jolla Shores Drive
La Jolla, CA 92037

Once the manuscript has been accepted for publication, you will be asked to submit a software copy of your manuscript. The software copy should be submitted in WordPerfect or Word format (in Word, save as Rich Text Format). Please note that we do not accept ASCII text files.

Reprints

Copies of published articles and notes are available free of charge to the senior author (50 copies) and to his or her laboratory (50 copies). Additional copies may be purchased in lots of 100 when the author receives page proofs.

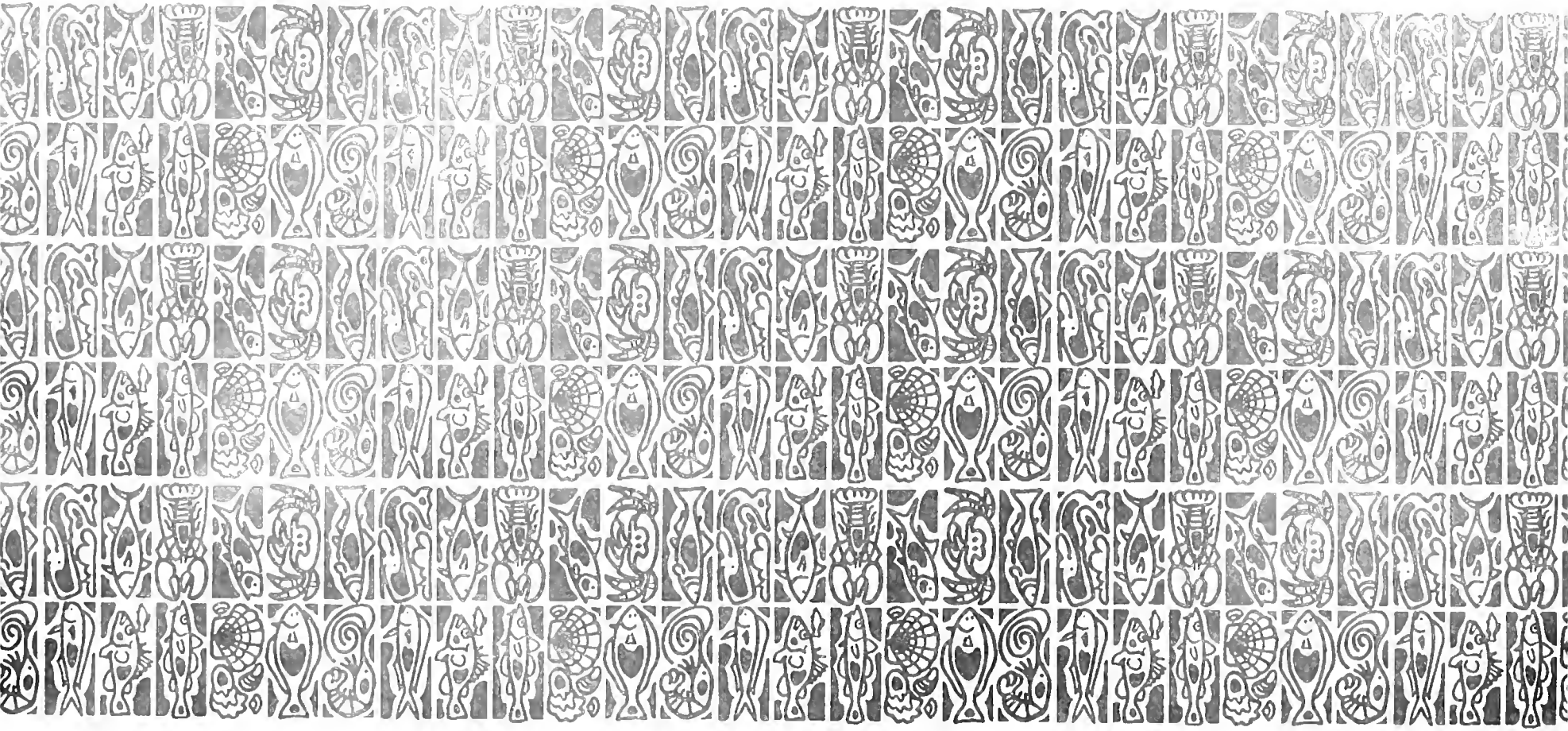

U.S. Department
of Commerce

Volume 102
Number 3
July 2004

Fishery Bulletin

The *Fishery Bulletin* (ISSN 0090-0656) is published quarterly by the Scientific Publications Office, National Marine Fisheries Service, NOAA, 7600 Sand Point Way NE, BIN C15700, Seattle, WA 98115-0070. Periodicals postage is paid at Seattle, WA and at additional mailing offices. POSTMASTER: Send address changes for subscriptions to Fishery Bulletin, Superintendent of Documents, Attn: Chief, Mail List Branch, Mail Stop SSOM, Washington, DC 20402-9373.

The Secretary of Commerce has determined that the publication of this periodical is necessary according to law for the transaction of public business of this Department. Use of funds for printing of this periodical has been approved by the Director of the Office of Management and Budget.

For sale by the Superintendent of Documents, U.S. Government Printing Office, Washington, DC 20402. Subscription price per year: $55.00 domestic and $68.75 foreign. Cost per single issue: $28.00 domestic and $35.00 foreign. **See back for order form.**

Fishery Bulletin

Fishery Bulletin web site: www.fishbull.noaa.gov

The *Fishery Bulletin* carries original research reports and technical notes on investigations in fishery science, engineering, and economics. It began as the Bulletin of the United States Fish Commission in 1881; it became the Bulletin of the Bureau of Fisheries in 1904 and the *Fishery Bulletin* of the Fish and Wildlife Service in 1941. Separates were issued as documents through volume 46; the last document was No. 1103. Beginning with volume 47 in 1931 and continuing through volume 62 in 1963, each separate appeared as a numbered bulletin. A new system began in 1963 with volume 63 in which papers are bound together in a single issue of the bulletin. Beginning with volume 70, number 1, January 1972, the *Fishery Bulletin* became a periodical, issued quarterly. In this form, it is available by subscription from the Superintendent of Documents, U.S. Government Printing Office, Washington, DC 20402. It is also available free in limited numbers to libraries, research institutions, State and Federal agencies, and in exchange for other scientific publications.

U.S. Department of Commerce
Seattle, Washington

Volume 102
Number 3
July 2004

Fishery Bulletin

Contents

Articles

Testicular development in migrant and spawning bluefin tuna (*Thunnus thynnus* (L.)) from the eastern Atlantic and Mediterranean

Francisco J. Abascal
César Megina
Antonio Medina

Departamento de Biología
Facultad de Ciencias del Mar y Ambientales
Universidad de Cádiz
Av República Saharaui
11510 Puerto Real
Cádiz, Spain

E-mail address (for A. Medina, contact author) antonio.medina@uca.es

Abstract—Testis histological structure was studied in bluefin tuna (*Thunnus thynnus*) from the eastern Atlantic and Mediterranean during the reproductive season (from late April to early June). Testicular maturation was investigated by comparing samples from bluefin tuna caught on their eastward reproductive migration off Barbate (Strait of Gibraltar area) with samples of bluefin tuna fished in spawning grounds around the Balearic Islands. Histological evaluations of cross sections showed that the testis consists of two structurally different regions, an outer proliferative region where germ cells develop synchronously in cysts, and a central region made up of a well-developed system of ducts that convey the spermatozoa produced in the proliferative region to the main sperm duct. Ultrastructural features of the different stages of the male germ cell line are very similar to those described in other teleost species. The bluefin tuna testis is of the unrestricted spermatogonial testicular type, where primary spermatogonia are present all along the germinative portion of the lobules. All stages of spermatogenesis were present in the gonad tissue of migrant and spawning bluefin tuna, although spermatids were more abundant in spawning fish. The testis size was found to increase by a factor of four (on average) during migration to the Mediterranean spawning grounds, whereas the fat bodies (mesenteric lipid stores associated with the gonads) became reduced to half their weight, and the liver mass did not change significantly with sexual maturation. Linear regression analysis of the pooled data of migrant and spawning bluefin tuna revealed a significant negative correlation between the gonad index (I_G) and the fat tissue index (I_F), and a weaker positive correlation between the gonad index (I_G) and the liver index (I_L). Our analyses indicate that the liver does not play a significant role in the storage of lipids and that mesenteric lipid reserves constitute an important energy source for gametogenesis in bluefin tuna.

Manuscript submitted 27 April 2003 to Scientific Editor's Office.

Manuscript approved for publication 25 March 2004 by the Scientific Editor.

Fish. Bull. 102:407–417 (2004).

The Atlantic northern bluefin tuna (*Thunnus thynnus thynnus* (L.)), is one of the most commercially valuable wild animals in the world. In the last two decades this species has been subject to intense over-fishing, which has caused a decline in both the eastern and western populations because of lowered recruitment (Mather et al., 1995; Sissenwine et al., 1998). The bluefin tunas (*T. thynnus* and *T. maccoyii*) are unique among tuna species in that they live mainly in cold waters and move into warmer waters to spawn (Olson, 1980; Lee, 1998; Schaefer, 2001); therefore the migratory pattern of these species depends substantially on reproduction. The eastern stock of Atlantic bluefin tuna spawns from June through August in the Mediterranean Sea, where natural conditions are apparently optimal for the survival of offspring. From late April to mid June, bluefin tuna breeding stocks migrate from the North Atlantic to spawning grounds in the Mediterranean (Mather et al., 1995; Ravier and Fromentin, 2001). A good understanding of the reproductive parameters (especially sexual maturation, fecundity, and spawning) of tunas is of paramount importance for population dynamics studies and the management of fisheries that target tunas. Nevertheless, "a very limited amount of scientifically useful information is available on the reproductive biology for most tunas" (Schaefer, 2001). Recent work has increased our knowledge on the reproductive biology of female *Thunnus thynnus* in the eastern Atlantic and the Mediterranean (Susca et al., 2000, 2001a, 2001b; Hattour and Macías, 2002; Medina et al., 2002; Mourente et al., 2002), but many questions remain still to be answered regarding male reproductive activity in this and other tuna species.

Histological examination of gonads is a useful tool for assessing the maturity state of fish. However, very few light-microscopy studies have been published on bluefin tuna and no ultrastructural studies of reproductive organs are yet available. The male reproductive cycle of *T. thynnus* has been characterized histologically by Santamaria et al. (2003), and Ratty et al. (1990) and Schaefer (1996, 1998) have reported valuable histological descriptions on male and female gonads of the Pacific albacore (*Thunnus alalunga*) and the yellowfin tuna (*Thunnus albacares*), respectively. In this article we report biometric and histological data on male *T. thynnus* caught during their reproductive migration and spawning period in order to provide further information on the biological aspects of reproduction for this species.

Materials and methods

Samples and condition indices

During the eastward migration, 62 adult male bluefin tuna weighing between 71 and 273 kg (mean 195.17 kg) were obtained from the trap fishery in the area of the Strait of Gibraltar (Barbate, Cádiz, southwestern Spain) from late April to early June 1999, 2000, and 2001. Thirty-four mature males, weighing between 19 and 349 kg (mean 115.11 kg), were sampled in June–July 1999–2001 from the purse-seine fleet operating in the Mediterranean spawning grounds of bluefin tuna off the Balearic Islands. Whenever possible, the total body weight (W) was recorded to the nearest kg. When individual body weights were not available, W was estimated from the fork length (L_F) measurements (recorded to the nearest cm), according to the formula: $W = 0.000019 \times L_F^3$ (Table VIII in Rodríguez-Roda, 1964). Following dissection, the liver, testes, and the fat bodies associated with the gonads were removed and weighed to the nearest g. The condition of the fish was assessed by three different indices. The gonad index (gonadosomatic index) (I_G) is indicative of the maturation state and was calculated as: $I_G = (W_G / W) \times 100$, where W_G = gonad weight. The liver index (hepatosomatic index) (I_L) and fat-body index (I_F) were calculated as $I_L = (W_L / W) \times 100$, and $I_F = (W_F / W) \times 100$ (where W_L and W_F represent liver and fat-body weights), respectively, and are considered as good indicators of the metabolic condition and energy reserves of the fish. All measurements are expressed as means ±SD.

Histology

For light microscopy, tissue samples from the central part of the testes were fixed for 48–96 hours in 10% formalin in phosphate buffer, 0.1 M, pH 7.2. After dehydration in ascending concentrations of ethanol, a part of each sample was embedded in paraffin wax and the remainder was embedded in plastic medium (2-hydroxyethyl-methacrylate). Paraffin sections (6 μm thick) were stained with haematoxylin-eosin, and plastic sections (3 μm thick) were stained with toluidine blue. These were examined and photographed on a Leitz DMR BE light microscope.

For electron microscopy, small fragments of testis were fixed for 3–4 hours in 2.5% glutaraldehyde buffered with 0.1 M sodium cacodylate buffer (pH 7.2). Following two 30-min washes in cacodylate buffer, they were postfixed for 1 hour at 4°C in cacodylate-buffered 1% osmium tetroxide, rinsed several times in buffer, dehydrated in ascending concentrations of acetone, and embedded in epoxy resin (either Epon 812 or Spurr). Thin sections (~80 nm thick) were picked up on copper grids, stained with uranyl acetate and lead citrate, and examined in a Jeol 1200 EX transmission electron microscope. Approximate dimensions provided for germ cells are measurements (means ±SD) of the largest cell diameters on electron micrographs.

Statistical analysis

The bluefin tuna specimens used in this study showed considerable variability in size, especially those caught by purse seine in Balearic waters, where weight ranged between 12 and 349 kg. The purse-seine fishery is, in fact, much less size-selective than are traps, which seldom catch small bluefin tuna (Rodríguez-Roda, 1964; Mather et al., 1995). Analysis of covariance (ANCOVA), with body weight as covariate, was used as the most suitable method (García-Berthou, 2001) to test interannual differences in the weight of the organs within the two sampling sites. ANCOVA was likewise applied to compare the weights of the three organs between both areas. All data were previously log-transformed to meet the prerequisites of normality and homoscedasticity (Zar, 1996). Linear least-squares regression analyses were performed to test possible correlations between I_G and the two other indices (I_L and I_F) by using the pooled data of Barbate and the Balearic Islands. In the regression between I_G and I_F, the Balearic samples corresponding to year 2001 were excluded because the reduced fat-body size (adipose tissue was almost nonexistent in the mesentery) of these small bluefin tuna did not permit an accurate weight measurements on board. The values of the indices were arcsine-transformed prior to the statistical analysis (Zar, 1996). A P-value ≤0.05 was considered statistically significant for all tests.

Results

Condition indices

ANCOVA did not reveal significant interannual differences in gonad, liver, and fat-body weight in the samples of Barbate as well as in those of the Balearic Islands. In contrast, a strongly significant difference in testicular size ($P<0.0001$) was found in comparing data of maturing bluefin tuna from Barbate (migrant tuna) with fully mature fish from the Balearic Islands (spawning fish). In fact, as shown in Figure 1, the average I_G was more than fourfold higher in the Balearic Islands than it was in Barbate (4.81 ±1.77 vs. 1.12 ±0.57). This finding may indicate a noticeable increase in sperm production during reproductive migration to the Mediterranean spawning grounds. Significant differences between maturing and spawning tuna were also found in fat-body weight, the volume of which dropped to about half by spawning time. Thus, I_F fell from 0.36 ±0.24 in migrating fish to 0.16 ±0.12 in spawning fish (see Fig. 1). The liver mass, however, did not differ significantly ($P=0.31$) between the two samples.

Figure 2 illustrates linear regression analysis between I_G and I_L, and between I_G and I_F. A significant negative correlation ($r^2=0.34$; $P<0.0001$) was found between I_G and I_F, indicating that the amount of mesenteric fat tissue decreases as the gonad matures. In contrast, there was a positive, though somewhat weak, correlation

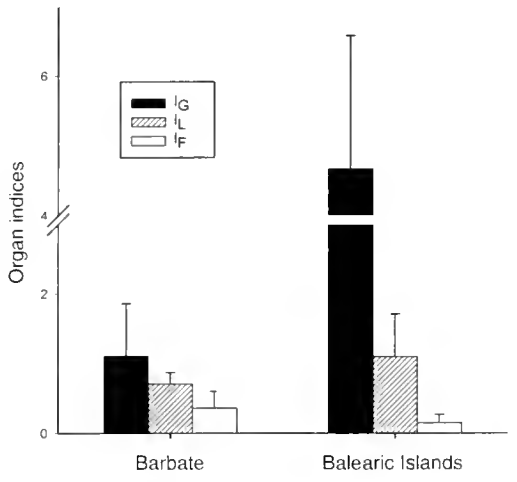

Figure 1

Differences in gonad index (I_G), liver index (I_L), and fat-body index (I_F) (means ±SD) between male bluefin tuna (*Thunnus thynnus*) from Barbate and male tuna from the Balearic Islands.

(r^2=0.21; P<0.0001) between I_G and I_L, which suggests a slight growth of the liver with sexual maturation.

Histology

The testes of *Thunnus thynnus* are paired, elongate organs that appear attached to the dorsal body wall by a mesentery. The fat body, which is closely associated with the gonad, consists of a variable amount of adipose tissue. The testis is composed of a dense array of lobules converging on the main sperm duct (vas deferens) and terminating blindly beneath the tunica albuginea at the periphery (Fig. 3, A and B). Two distinct zones can be distinguished in cross sections of the testes (Fig. 3A). At the outer region, the seminiferous lobules have a thick wall formed by the germinal epithelium, where germ cells develop in association with Sertoli cells; the lumina of the lobules are filled with spermatozoa that have been released after completion of the spermiogenetic process (Fig. 3, B and C). As a result of the release of mature sperm from spermatocysts into the lobule lumina, the germinal epithelium becomes discontinuous (Fig. 3B). The transition from the outer to the central region of the testis is marked by an abrupt change in the configuration of the testicular lobules, which lose the germinal epithelium and become ducts where lobule function has shifted from sperm production to sperm storage (Fig. 3C). Thus, the only sex cells that are found in the central part of the testis are mature spermatozoa, which fill the swollen lumina of the lobules. In this zone the testis ducts constitute an intricate network of channels that convey the spermatozoa produced in the proliferative region to the main sperm duct (Fig. 3, A and D), which is thick walled and located in the center of the testis (Fig. 3D).

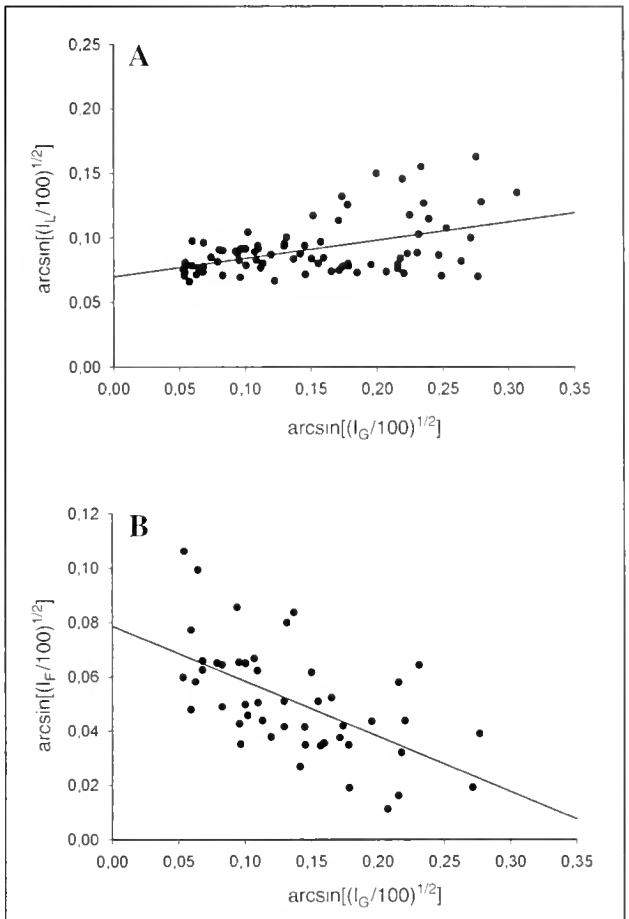

Figure 2

Linear regression between gonad index (I_G) and liver index (I_L) (**A**), and between gonad index (I_G) and fat body index (I_F) (**B**) (data were pooled from the two areas). In B, samples of bluefin tuna (*Thunnus thynnus*) collected off the Balearic Islands in 2001 were excluded.

The gametes develop in groups of isogenic cells called germinal cysts or spermatocysts, where the process of differentiation is synchronous (Fig. 4). Primary spermatogonia are large, single cells (Fig. 4A) that are distributed all along the germinal epithelium, as is characteristic of the teleost unrestricted testicular type. Spermatogonia B resulting from successive mitoses of spermatogonia A are found in small groups, whereas spermatocytes and spermatids are grouped within larger spermatocysts (Figs. 3, B and C, 4). The cysts containing late spermatids and spermatozoa, prior to spermiation, display a particular alveolar appearance due to the orientation of the spermatid heads facing the lobule walls and the bundles of flagella directed toward the seminiferous lobule lumen (Fig. 4, A, C, and D).

Active spermatogenesis was observed to occur both in migrant bluefin tuna from the Strait of Gibraltar (Fig. 4, A and B) and spawning fish from the Mediterranean (Fig. 4, C and D). In both cases, all stages of the male

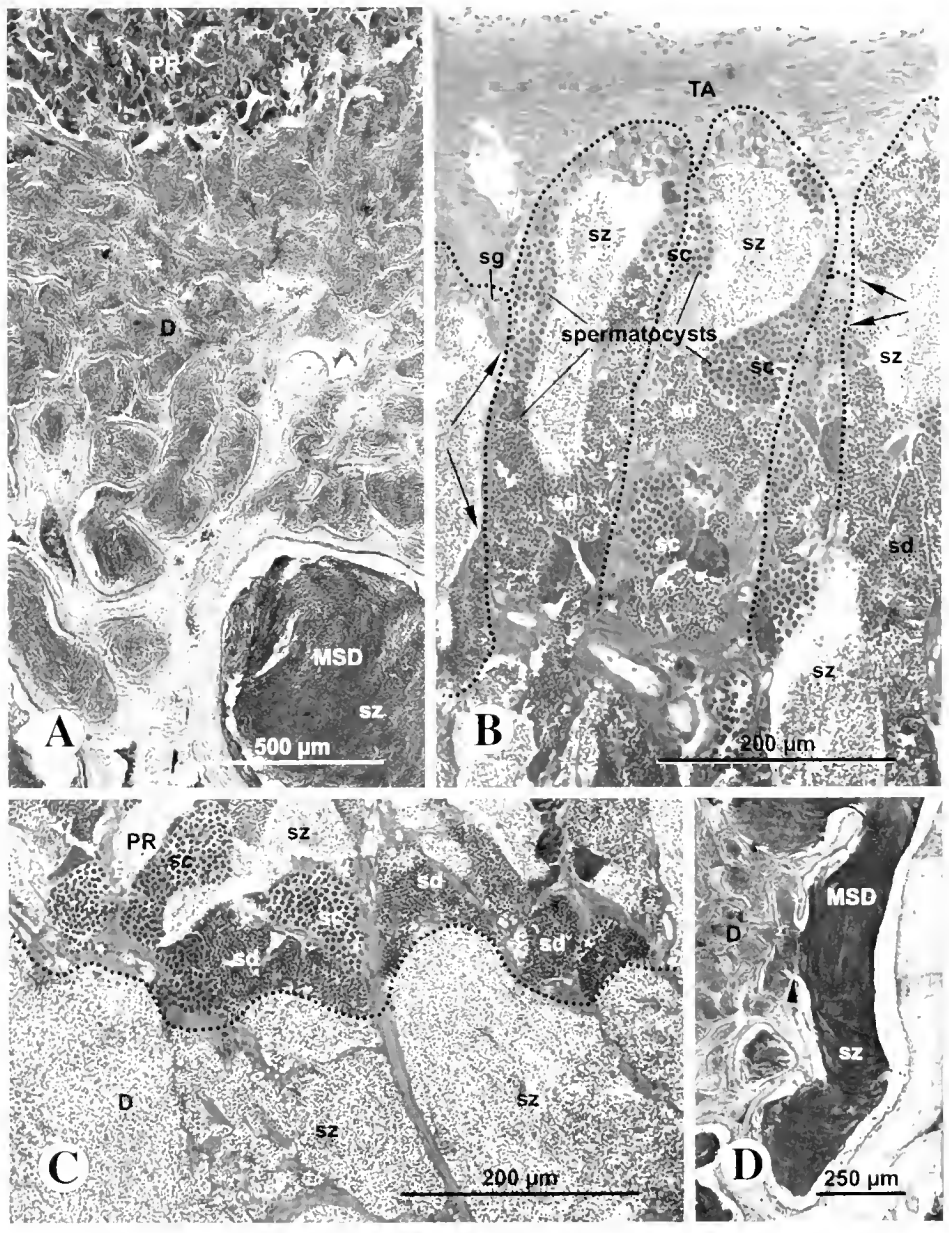

Figure 3

Light micrographs depicting the histological organization of the bluefin tuna (*Thunnus thynnus*) testis. (**A**) Transverse section showing the outer proliferative region (PR) of the testis and the inner region, which includes the testis duct system (D) and the main sperm duct (MSD). (**B**) Peripheral zone of the testis where the distal ends of some tubules (dotted lines) terminate beneath the tunica albuginea (TA). (**C**) Transition (dotted line) between the outer region (PR) of the testis, where the lobules contain developing germinal cysts, and the inner region (D), whose lobule walls enclose only mature spermatozoa. (**D**) Main sperm duct (MSD) filled with a compact mass of spermatozoa that are incorporated (arrowhead) from the testis ducts (D). Arrows = discontinuities in the germinal epithelium; sc = spermatocytes; sd = spermatids; sg = spermatogonia; sz = spermatozoa. All samples are from Barbate (A and D, paraffin-embedded sections stained with haematoxylin-eosin; B and C, toluidine-blue–stained plastic-embedded sections).

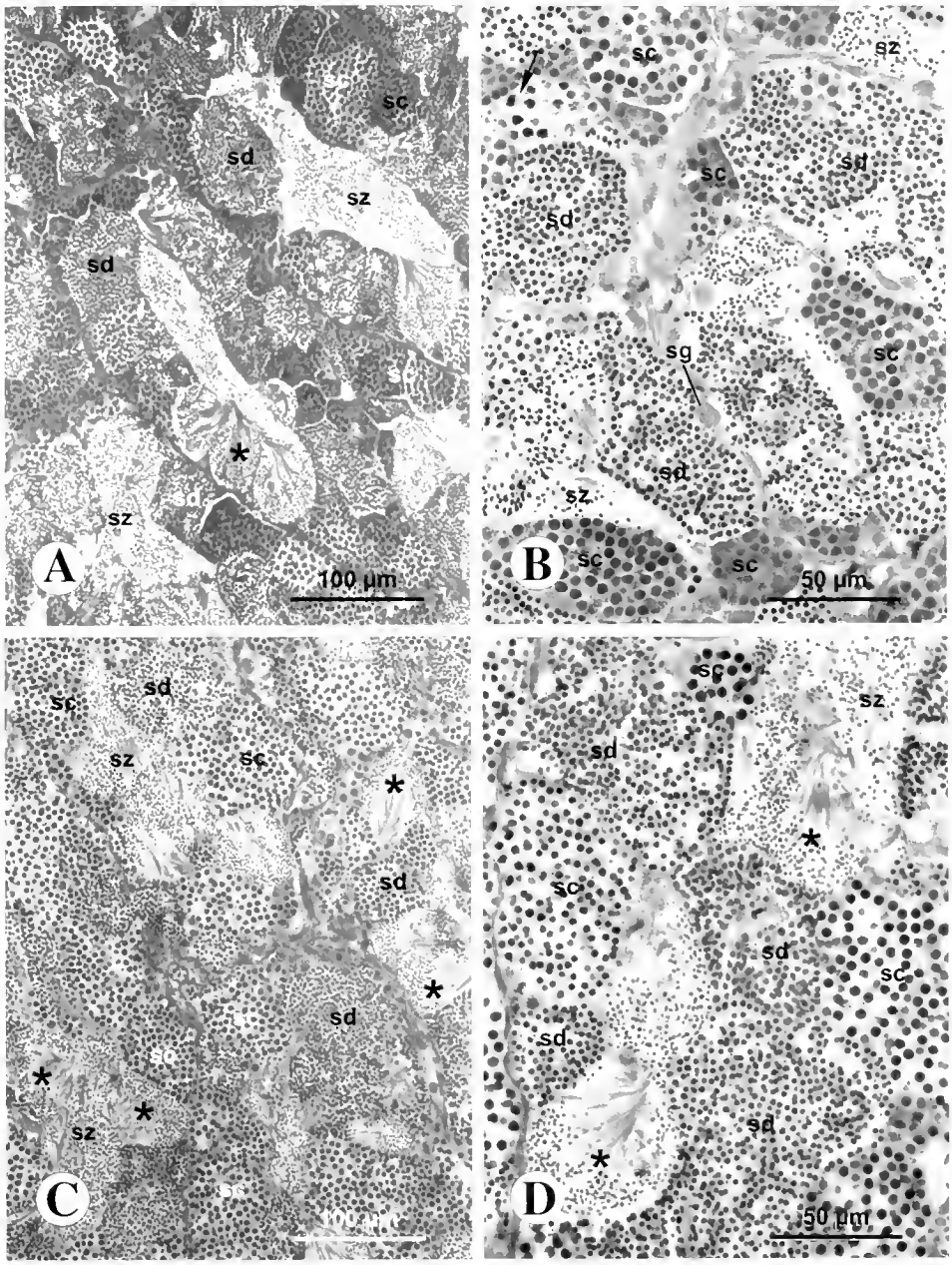

Figure 4

Spermatocysts in the testis proliferative region of bluefin tuna (*Thunnus thynnus*) from Barbate (**A** and **B**) and the Balearic Islands (**C** and **D**). All stages of spermatogenesis are present in both cases, although spermatid cysts containing late spermatids and spermatozoa (asterisks) are somewhat more abundant in specimens from the Balearic Islands. Arrow = dividing spermatocytes; sc = spermatocytes; sd = spermatids; sg = primary spermatogonion; sz = spermatozoa. Plastic-embedded sections (A–D) were stained with toluidine blue.

germ cell line were present in the gonads. In addition, large amounts of spermatozoa had accumulated in the central system of ducts and in the main sperm duct, both of which appear to function as reservoirs of sperm. In specimens from Barbate, spermatocytes and spermatids were abundant (Fig. 4B), whereas in most tuna collected in the Balearic area spermatids predominated over spermatocytes. Cysts containing late spermatids and spermatozoa were particularly common (Fig. 4, C and D).

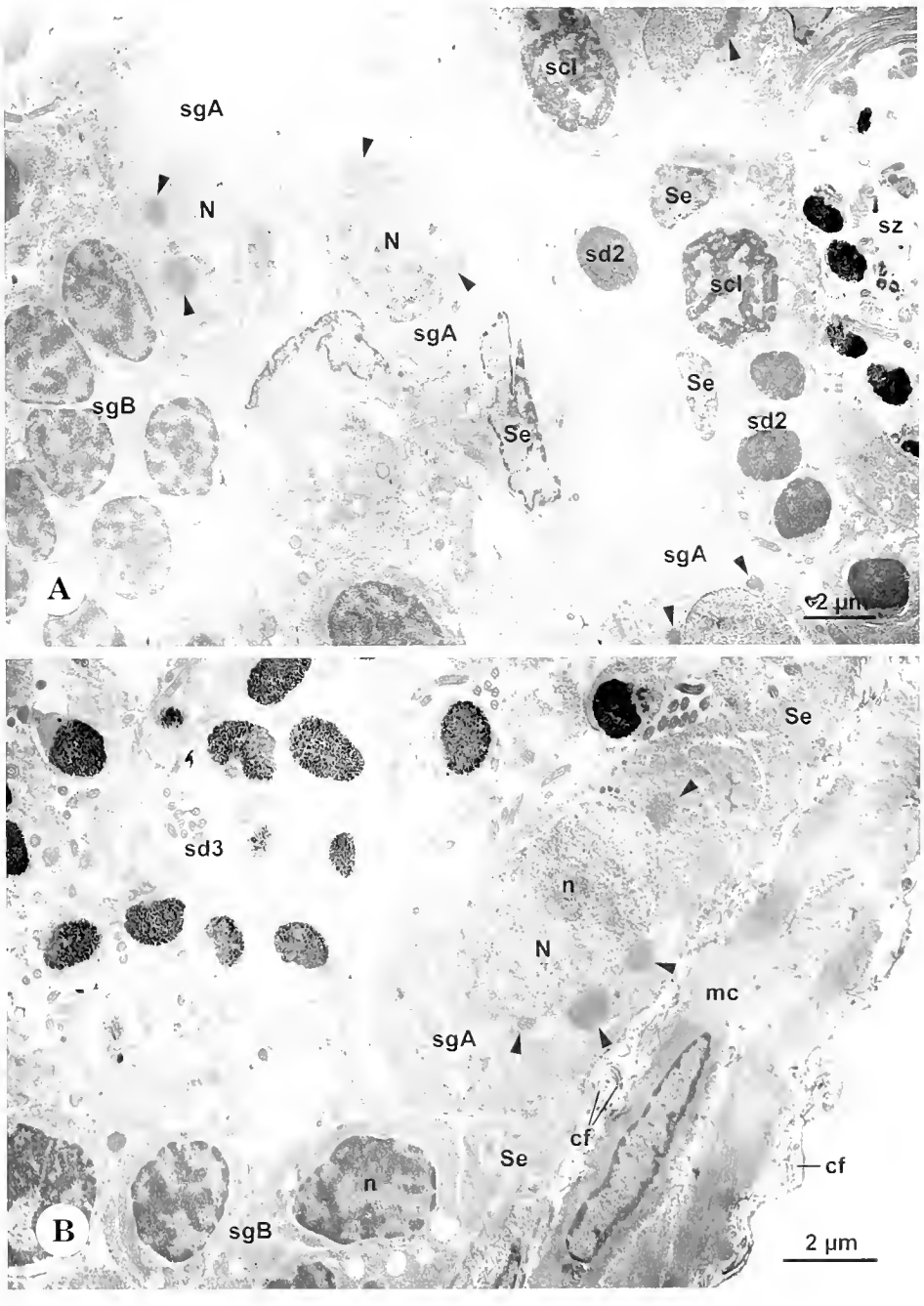

Figure 5

Electron micrographs of testicular tissue from bluefin tuna (*Thunnus thynnus*). (**A** and **B**) overviews displaying several spermatocyst types, including single primary spermatogonia (sgA), and clusters of spermatogonia B (sgB), primary spermatocytes (scl), mid spermatids (sd2), late spermatids (sd3), and spermatozoa (sz). The germ cells are surrounded by Sertoli cells (Se). Arrowheads = perinuclear bodies ("nuage"); N = nucleus; n = nucleolus; cf = collagen fibers; mc = myoid cell.

Ultrastructure

Primary spermatogonia are large, ovoid cells (8.55 ±1.07 µm) whose nucleus (>5 µm in its largest diameter) shows diffuse chromatin and a single central nucleolus. The cytoplasm contains free ribosomes, a few mitochondria, endoplasmic reticulum cisternae, and several masses

of electron-dense perinuclear material ("nuages") that indicate nucleocytoplasmic transport (Fig. 5, A and B). Such chromatoid bodies persist throughout spermatogenesis until the spermatid stage, but their size and number is far higher in primary spermatogonia. Spermatogonia B are grouped in clusters of a few cells. They are perceptibly smaller (6.75 ±0.37 µm) than spermatogonia A and their nucleus contains patchy chromatin (Fig. 5, A and B).

Spermatocytes form clusters in which the cells are interconnected by cytoplasmic bridges. Primary spermatocytes (4.84 ±0.45 µm) show a heterochromatic nucleus (~3.5 µm in diameter) that varies in appearance depending on the prophase-I stage. The cytoplasm contains free ribosomes (mostly polysomes), mitochondria, clear vesicles, and the diplosome (Figs. 5A, 6A). Synaptonemal complexes are clearly recognizable at pachytene (Fig. 6A). Secondary spermatocytes are apparently short-lived cells because they are rare in histological samples—a finding that suggests that the second meiotic division is triggered shortly after completion of the first division. Spermatocytes II are difficult to distinguish morphologically from early spermatids, although they are slightly larger (3.31 ±0.47 µm). The cytoplasm is more reduced than in spermatocytes I and the nucleus shows diffuse chromatin forming moderately electron-dense patches (Fig. 6B).

During spermiogenesis, the spermatid nucleus changes in shape and decreases in volume as the chromatin condenses. In early spermatids (2.39 ±0.28 µm) the spherical nucleus shows a dense chromatin with some electron-lucent areas (Fig. 6C). Then the chromatin becomes more homogeneous in mid spermatids (2.56 ±0.21 µm) (Figs. 5A, 6D), and eventually in late spermatids (1.81 ±0.32 µm) condenses into a coarse granular pattern, whereas the nucleus assumes an ovoid shape and forms a basal indentation over the proximal segment of the axoneme (Fig. 6E). Cytoplasmic changes involve elongation of the flagellum, reduction of the cytoplasmic mass, and coalescence of the mitochondria into a few large spherical units located around the proximal portion of the axoneme. Rotation of the nucleus does not take place during spermiogenesis, therefore the flagellum axis remains parallel to the base of the nucleus and the spermatozoon shows the typical ultrastructure of teleostean type-II sperm (Fig. 6F).

Discussion

Histologically, the bluefin tuna testis is of the unrestricted spermatogonial testicular type found in most teleosts, where spermatogonia occur along the greater part of the testicular tubules. In the restricted spermatogonial testicular type of the atheriniforms, on the other hand, the spermatogonia are confined to the distal end of the tubules, and spermatogenesis proceeds as the germ cells approach the efferent ducts (Grier et al., 1980; Grier, 1981). Efferent ducts are generally absent in unrestricted spermatogonial testes, so that germinal cysts form along the testicular tubule length (Grier et al., 1980; Grier, 1981; Lahnsteiner et al., 1994). However, in maturing and spawning bluefin tuna a well-developed network of ducts collects the sperm produced by the germinal epithelium and voids them into the main sperm duct. The central ducts of the testis are continuous with the proliferative segment of the testicular lobules, which lose the germinal epithelium in the innermost region of the testis and function as sperm storage structures. This process has been documented in the common snook (*Centropomus undecimalis*) (Grier and Taylor, 1998), the cobia (*Rachycentrum canadum*) (Brown-Peterson et al., 2002), and the swamp eel (*Synbranchus marmoratus*) (Lo Nostro et al., 2003). Grier et al. (1980) showed that in the atheriniform *Fundulus grandis* the efferent duct wall cells derive from Sertoli cells. A system of efferent ducts has been described in other species of teleosts possessing testes of the unrestricted spermatogonial type (Rasotto and Sadovy, 1995; Manni and Rasotto, 1997). As has been shown in other species of the genus (Ratty et al., 1990; Schaefer, 1996; 1998), the main sperm duct of *T. thynnus* has a thick wall and is located near the center of the testis, whereas in many other teleosts the main duct is dorsal (Grier et al., 1980).

Ultrastructural features of bluefin tuna spermatogenesis are comparable to those described extensively in teleosts (for examples of recent literature see Gwo and Gwo, 1993; Stoumboudi and Abraham, 1996; Quagio-Grassiotto et al., 2001; Huang et al., 2002; Koulish et al., 2002; Fishelson, 2003). The primary spermatogonia are the largest male germ cells and exhibit several conspicuous perinuclear ("nuage") bodies. After several divisions they give rise to cysts of secondary spermatogonia that enter meiosis to produce successively primary and secondary spermatocytes. Primary spermatocytes are abundant, particularly at the pachytene phase, and are therefore thought to be of long duration. In contrast, the spermatocyte-II stage is thought to be the shortest spermatogenetic step, because, as occurs in teleosts in general, it is the least frequent in histological samples. Spermiogenesis develops without the occurrence of rotation of the spermatid nucleus, resulting in a teleostean type-II spermatozoon (Mattei, 1970), in which the flagellar axis lies tangential to the nucleus instead of being inserted perpendicular to its base (Abascal et al., 2002).

Santamaria et al. (2003) divided the testicular cycle of *T. thynnus* caught in Mediterranean waters from February to September into five periods. Those developmental stages are similar to stages 2–6 classified by Grier (1981) for a generalized teleost annual reproductive cycle. Most probably, stage 1 (spermatogonial proliferation) occurs in Mediterranean bluefin tuna between October and January. More recently, annual histological changes in the germinal epithelium have been used to identify five distinct reproductive classes in males of several teleost species (Grier and Taylor, 1998; Taylor et al., 1998; Brown-Peterson et al., 2002; Lo Nostro et al., 2003). It is assumed that the most advanced maturation classes in males are characterized by the presence of a discontinuous germinal epithelium. According to this criterion, all

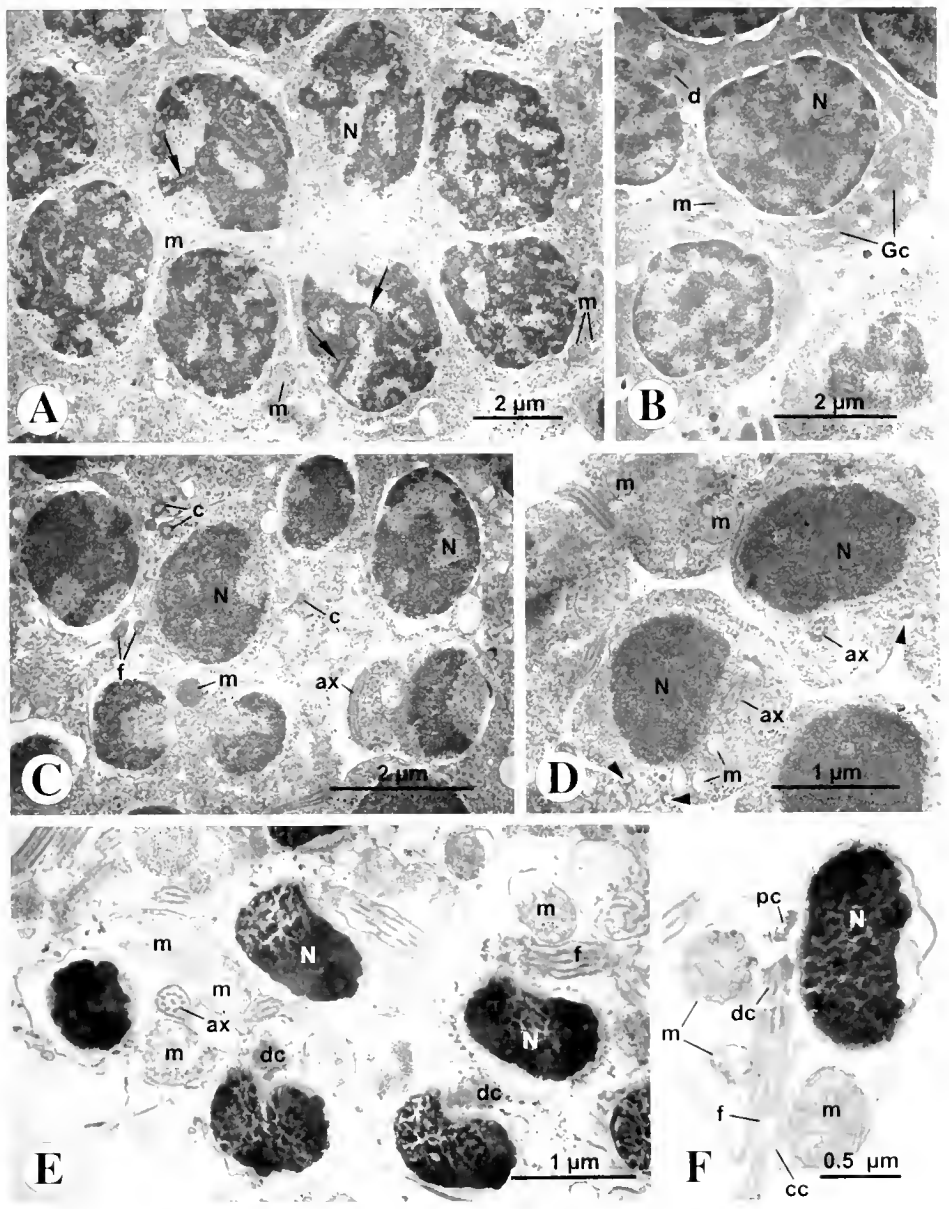

Figure 6

Electron micrographs of spermatocytes I (**A**), spermatocytes II (**B**), early spermatids (**C**), mid spermatids (**D**), late spermatids (**E**), and spermatozoon (**F**) from bluefin tuna (*Thunnus thynnus*). Arrows = synaptonemal complexes; arrowheads = cytoplasmic bridges between spermatids; ax = axoneme; c = centriole; cc = cytoplasmic canal; d = diplosome; dc = distal centriole; f = flagellum; Gc = Golgi complex; m = mitochondria; N = nucleus; pc = proximal centriole.

of the samples examined in the present study correspond to the mid- and late-maturation stages proposed by Grier and Taylor (1998), and Taylor et al. (1998). Testes at these stages become storage organs that are filled with sperm. The present study encompasses only a short period of the reproductive cycle, which comprises final gonad maturation. However, descriptions of the testicular histology throughout the annual cycle (Santamaria et al., 2003) appear to indicate that different maturation classes might be defined in the bluefin tuna based on histological examination of the germinal epithelium (see Taylor et al., 1998; Brown-Peterson et al., 2002).

Final sexual maturation involves a considerable increase in testis size, but no apparent remarkable histological changes, with the exception of a slightly higher frequency of the most advanced stages of spermatogen-

esis in fully mature bluefin tuna. The different testicular development of maturing and spawning tuna is reflected by their respective average I_G, which was fourfold higher in spawning fish. An equivalent gonad growth was found in the females collected in the same samplings (Medina et al., 2002), indicating a spatiotemporal parallelism in the gonad maturation cycle and a good synchronization of the reproductive peak in the two sexes. The maturation schedule differs between the two sexes, however, in that males are capable of generating mature spermatozoa while still on migration, whereas females do not appear to develop fully mature oocytes until they have reached the spawning grounds (Medina et al., 2002). Therefore, even though mature spermatozoa can be found in testicular ducts during prolonged periods throughout the reproductive cycle, it is unlikely that males are actually capable of spawning out of reproductive season.

The seasonal I_G profile of the bluefin tuna appears to be similar to that of the pelagic, highly migratory perciform *Rachycentron canadum* (Brown-Peterson et al., 2002), and the swamp eel (*Synbranchus marmoratus*) (Lo Nostro et al., 2003), in which peak I_G values occur when the reproductive activity is at a maximum. A different situation has been reported in the common snook (Taylor et al., 1998), where the highest I_G levels correspond with the mid maturation class and decrease during the latter part of the reproductive season. The biological significance of these different I_G profiles in terms of reproductive strategies is yet unknown because a very limited number of species have been examined so far.

Because spermatozoa are by far the most abundant cells in mature testes, the gonad weight becomes a good indicator of the quantity of sperm produced by a fish (Billard, 1986). Therefore, the significant increase in I_G that occurred between samplings off Barbate and the Balearic Islands would indicate that, during migration, bluefin tuna can raise several times the volume of sperm accumulated in the testes. The apparently high spermatogenetic activity observed in bluefin tuna caught on the spawning grounds suggests that bluefin tuna have the ability to regenerate testicular sperm stores. Continuous sperm production could be important because external fertilization requires the release of large amounts of sperm to ensure successful fertilization of eggs, especially when egg size is small. In addition, it should be noted that tunas spawn multiple times (June, 1953; Yuen, 1955; Buñag, 1956; Otsu and Uchida, 1959; Baglin, 1982; Stéquert and Ramcharrun, 1995) and can spawn almost daily throughout the reproductive season (Hunter et al., 1986; McPherson, 1991; Schaefer, 1996, 1998, 2001; Farley and Davis, 1998; Medina et al., 2002).

From histological examination of the sperm ducts, and based on the amount of sperm present and the staining of the epithelium, Schaefer (1998) proposed a spawning interval of 1.03 days for spawning male *Thunnus albacares* throughout the eastern Pacific Ocean. The spawning rate estimated for reproductively active females with the postovulatory-follicle method was 1.19 days (Schaefer, 1998), which coincides with the spawning interval estimated for female *T. thynnus* around the Balearic Islands (Medina et al., 2002). Unfortunately, we could not make a reliable estimation of the male spawning interval in our samples. Two possible reasons may account for this failure. One reason is that many of the samples of gonadal tissue did not include the main sperm duct. On the other hand, no clear evidence of spawning was identified by histological examination of those specimens processed that had sperm ducts. A plausible explanation for this fact is that recent sperm release can be detected only within 12 hours after the spawning event (Schaefer, 1996); hence for male spawning to be detected the fish would have to be sampled in a narrow range of times following spawning, which Schaefer (1996) established between 00.01 and 12.00 hours after spawning for *Thunnus albacares*. It would be worth conducting further research on bluefin tuna at their spawning grounds, by attempting to cover a broad range of sampling times in order to ensure collection of specimens shortly after gamete release. In this way, useful information would be obtained on such reproductive parameters as spawning schedules, fecundity, and the energy cost of spawning, which are essential for ecological assessments of the reproductive potential.

It is noteworthy that male tuna, as small as 20 kg in weight (~100 cm L_F), were caught on the spawning grounds in our study. They had gonad indices over 5% and histological features indicative of full maturity. These observations indicate that the eastern stock of Atlantic northern bluefin tuna can reach maturity at age 3 years and thus support conclusions of previous studies (Rodríguez-Roda, 1967; Hattour and Macías, 2002; Susca et al., 2001a, 2001b; Medina et al., 2002); western bluefin tuna, on the other hand, mature at an older age, which has been estimated at 6 years (Baglin, 1982).

Prior to sexual maturation, marine fish generally accumulate large lipid deposits, primarily triacylglycerols, which are subsequently mobilized to support gonad development and spawning migration (Bell, 1998). The major lipid storage sites are the mesenteric tissue, muscle, liver, and subdermal fat layers (Ackman, 1980). In bluefin tuna the liver does not appear to play an important role in lipid storage but is mainly involved in processing fatty acids mobilized from other bodily sources (Mourente et al., 2002). This metabolic pattern is consistent with our observations of weight modifications for liver and fat body from maturation through the spawning period. Although I_L increases only slightly with sexual maturation, I_F undergoes a marked decrease at the time of maximum gonad development. Thus, the regression analysis of the relationship between I_G and I_F shows a significant negative correlation, which reveals a depletion of mesenteric fat stores as the testes grow. The occurrence of a similar situation in females (Medina et al., 2002; Mourente et al., 2002) and in male and female *Thunnus alalunga* (Ratty et al., 1990) has led to the conclusion that fat-body lipid reserves provide an important energy source for gametogenesis in tunas.

Acknowledgments

This study has been funded by the Spanish government and the European Union (projects 1FD1997-0880-C05-04 and Q5RS-2002-01355). The authors wish to thank two anonymous reviewers for helpful recommendations. We also thank Pesquerias de Almadraba, S. J. and Ginés J. Méndez Alcalá (G. Méndez España, S. L.) for co-operation and assistance. The invaluable technical assistance of Agustín Santos and José Luis Rivero is greatly appreciated. G. Mourente lent useful help in our discussion on lipids.

Literature cited

Abascal, F. J., A. Medina, C. Megina, and A. Calzada.
2002. Ultrastructure of *Thunnus thynnus* and *Euthynnus alletteratus* spermatozoa. J. Fish Biol. 60:147–153.

Ackman, R. G.
1980. Fish lipids, part 1. *In* Advances in fish science and technology (J. J. Connell, ed.), p. 86–103. Fishing News Books Ltd., Farnham, England.

Baglin, R. E., Jr.
1982. Reproductive biology of western Atlantic bluefin tuna. Fish. Bull. 80:121–134.

Bell, J. C.
1998. Current aspects of lipid nutrition in fish farming. *In* Biology of farmed fish (K. D. Black and A. D. Pickering, eds.), p. 114–145. Sheffield Academic Press Ltd., Sheffield, England.

Billard, R.
1986. Spermatogenesis and spermatology of some teleost fish species. Reprod. Nutr. Dévelop. 26:877–920.

Brown-Peterson, N. J., H. J. Grier, and R. M. Overstreet.
2002. Annual changes in germinal epithelium determine male reproductive classes of the cobia. J. Fish Biol. 60:178–202.

Buñag, D. M.
1956. Spawning habits of some Philippine tuna based on diameter measurements of the ovarian ova. Philipp. J. Fish. 26:877–920.

Farley, J. H., and T. L. O. Davis.
1998. Reproductive dynamics of southern bluefin tuna, *Thunnus maccoyii*. Fish. Bull. 96:223–236.

Fishelson, L.
2003. Comparison of testes structure, spermatogenesis, and spermatocytogenesis in young, aging, and hybrid cichlid fish (Cichlidae, Teleostei). J. Morphol. 256:285–300.

García-Berthou, E.
2001. On the misuse of residuals in ecology: testing regression residuals vs. the analysis of covariance. J. Anim. Ecol. 70:708–711.

Grier, H. J.
1981. Cellular organization of the testis and spermatogenesis in fishes. Am. Zool. 21:345–357.

Grier, H. J., J. R. Linton, J. F. Leatherland, and V. L. De Vlaming.
1980. Structural evidence for two different testicular types in teleost fishes. Am. J. Anat. 159:331–345.

Grier, H. J., and R. G. Taylor.
1998. Testicular maturation and regression in the common snook. J. Fish Biol. 53:521–542.

Gwo, J.-C., and H.-H. Gwo.
1993. Spermatogenesis in the black porgy, *Acanthopagrus schlegeli* (Teleostei: Perciformes: Sparidae). Mol. Reprod. Dev. 36:75–83.

Hattour, A., and D. Macías.
2002. Bluefin tuna maturity in Tunisian waters: a preliminary approach. Col. Vol. Sci. Pap. ICCAT (International Commission for the Conservation of Atlantic Tunas) 54: 545–553.

Huang, J.-D., M.-F. Lee, and C.-F. Chang.
2002. The morphology of gonadal tissue and male germ cells in the protandrous black porgy, *Acanthopagrus schlegeli*. Zool. Stud. 41:216–227.

Hunter, J. R., B. J. Macewicz, and J. R. Sibert.
1986. The spawning frequency of skipjack tuna, *Katsuwonus pelamis*, from the South Pacific. Fish. Bull. 84:895–503.

June, F. C.
1953. Spawning of yellowfin tuna in Hawaiian waters. U. S. Fish and Wildlife Service, Fish. Bull. 54:47–64.

Koulish, S., C. R. Kramer, and H. J. Grier.
2002. Organization of the male gonad in a protogynous fish (Teleostei: Labridae). J. Morphol. 254:292–311.

Lahnsteiner, F., R. A. Patzner, and T. Weismann.
1994. Testicular main ducts and spermatic ducts in some cyprinid fishes I. Morphology, fine structure and histochemistry. J. Fish Biol. 44:937–951.

Lee, C. L.
1998. A study on the feasibility of the aquaculture of the southern bluefin tuna, *Thunnus maccoyii*, in Australia, 92 p. Agriculture Fisheries and Forestry-Australia (AFFA), Canberra, Western Australia.

Lo Nostro, F., H. Grier, L. Andreone, and G. A. Guerrero.
2003. Involvement of the gonadal germinal epithelium during sex reversal and seasonal testicular cycling in the protogynous swamp eel, *Synbranchus marmoratus* Bloch 1795 (Teleostei, Synbranchidae). J. Morphol. 257:107–126.

Manni, L., and M. B. Rasotto.
1997. Ultrastructure and histochemistry of the testicular efferent duct system and spermiogenesis in *Opistognathus whitehurstii* (Teleostei, Trachinoidei). Zoomorphol. 117:93–102.

Mather, F. J., III, J. M. Mason, and A. C. Jones.
1995. Historical document: life history and fisheries of Atlantic bluefin tuna. NOAA Tech. Memo. NMFS-SEFSC 370, 165 p.

Mattei, X.
1970. Spermiogenèse comparée des poissons. *In* Comparative spermatology (B. Baccetti, ed.), p. 57–69. Academic Press, New York, NY.

McPherson, G. R.
1991. Reproductive biology of yellowfin tuna in the eastern Australian fishing zone, with special reference to the north-western Coral Sea. Austr. J. Mar. Freshw. Res. 42:465–477.

Medina, A., F. J. Abascal, C. Megina, and A. Garcia.
2002. Stereological assessment of the reproductive status of female Atlantic northern bluefin tuna, *Thunnus thynnus* (L.), during migration to Mediterranean spawning grounds through the Strait of Gibraltar. J. Fish Biol. 60:203–217.

Mourente, G., C. Megina, and E. Diaz-Salvago.
2002. Lipids in female northern bluefin tuna (*Thunnus thynnus thynnus* L.) during sexual maturation. Fish Physiol. Biochem. 24:351–363.

Olson, R. J.
1980. Synopsis of biological data on the southern bluefin

tuna, *Thunnus maccoyii* (Castelnau, 1872). Inter-Am. Trop. Tuna Comm., Spec. Rep. 2:151–212.

Otsu, T., and R. N. Uchida.
1959. Sexual maturity and spawning of albacore in the Pacific Ocean. U. S. Fish and Wildlife Service, Fish. Bull. 59:287–305.

Quagio-Grassiotto, I., J. N. C. Negrão, E. D. Carvalho, and F. Foresti.
2001. Ultrastructure of spermatogenic cells and spermatozoa in *Hoplias malabaricus* (Teleostei, Characiformes, Erythrinidae). J. Fish Biol. 59:1494–1502.

Rasotto, M. B., and Y. Sadovy.
1995. Peculiarities of the male urogenital apparatus of two grunt species (Teleostei, Haemulidae). J. Fish Biol. 46:936–948.

Ratty, F. J., R. M. Laurs, and R. M. Kelly.
1990. Gonad morphology, histology, and spermatogenesis in south Pacific albacore tuna *Thunnus alalunga* (Scombridae). Fish. Bull. 88:207–216.

Ravier, C., and J.-M. Fromentin.
2001. Long-term fluctuations in the eastern Atlantic and Mediterranean bluefin tuna population. ICES (International Council for the Exploration of the Sea). J. Mar. Sci. 58:1299–1317.

Rodríguez-Roda, J.
1964. Biología del atún, *Thunnus thynnus* (L.), de la costa sudatlántica de España. Inv. Pesq. 25:33–146.

Rodríguez-Roda, J.
1967. Fecundidad del atún, *Thunnus thynnus* (L.), de la costa sudatlántica de España. Inv. Pesq. 31:33–52.

Santamaria, N., A. Corriero, S. Desantis, D. Zubani, R. Gentile, V. Sciscioli, M. de la Serna, and C. R. Bridges.
2003. Testicular cycle of the Mediterranean bluefin tuna (*Thunnus thynnus* L.). Cah. Opt. Med. 60:183–185.

Schaefer, K. M.
1996. Spawning time, frequency, and batch fecundity of yellowfin tuna, *Thunnus albacares*, near Clipperton Atoll in the eastern Pacific Ocean. Fish. Bull. 94:98–112.
1998. Reproductive biology of yellowfin tuna (*Thunnus albacares*) in the eastern Pacific Ocean. Inter-Am. Trop. Tuna Comm., Bull. 21:201–272.
2001. Reproductive biology of tunas. *In* Tuna: physiology, ecology and evolution (B. A. Block and E. D. Stevens, eds.), p. 225–270. Academic Press, London.

Sissenwine, M. P., P. M. Mace, J. E. Powers, and G. P. Scott.
1998. A commentary on western Atlantic bluefin tuna assessments. Trans. Am. Fish. Soc. 127:838–855.

Stéquert, B., and B. Ramcharrun.
1995. La fécondité du listao (*Katsuwonus pelamis*) de l'ouest de l'océan Indien. Aquat. Living Resour. 8:79–89.

Stoumboudi, M. Th., and M. Abraham.
1996. The spermatogenetic process in *Barbus longiceps*, *Capoeta damascina* and their natural sterile hybrid (Teleostei, Cyprinidae). J. Fish Biol. 49:458–468.

Susca, V., M. Deflorio, A. Corriero, C. R. Bridges, and G. De Metrio.
2000. Sexual maturation in the bluefin tuna (*Thunnus thynnus*) from the central Mediterranean Sea. *In* Proceedings of the 6th international symposium on the reproductive physiology of fish (B. Noberg, O. S. Kjesbu, G. L. Taranger, E. Andersson, and S. O. Stefansson, eds.), p. 105. Fish Symp. 99. Department of Fisheries and Marine Biology, Univ. Bergen, Bergen, Norway.

Susca, V., A. Corriero, C. R. Bridges, and G. De Metrio.
2001a. Study of the sexual maturity of female bluefin tuna: purification and characterization of vitellogenin and its use in an enzyme-linked immunosorbent assay. J. Fish Biol. 58:815–831.

Susca, V., A. Corriero, M. Deflorio, C. R. Bridges, and G. De Metrio.
2001b. New results on the reproductive biology of the bluefin tuna (*Thunnus thynnus*) in the Mediterranean. Col. Vol. Sci. Pap. ICCAT 52:745–751.

Taylor, R. G., H. J. Grier, and J. A. Whittington.
1998. Spawning rhythms of common snook in Florida. J. Fish Biol. 53:502–520.

Yuen, H. S. H.
1955. Maturity and fecundity of bigeye tuna in the Pacific. U.S. Fish and Wildlife Service Special Scientific Report: Fisheries 150, 30 p. Washington, D.C.

Zar, J. H.
1996. Biostatistical analysis, 662 p. Prentice-Hall, Upper Saddle River, NJ.

Abstract—From 1995 to 1998, we collected female black rockfish (*Sebastes melanops*) off Oregon in order to describe their basic reproductive life history and determine age-specific fecundity and temporal patterns in parturition. Female black rockfish had a 50% probability of being mature at 394 mm fork length and 7.5 years-of-age. The proportion of mature fish age 10 or older significantly decreased each year of this study, from 0.511 in 1996 to 0.145 in 1998. Parturition occurred between mid-January and mid-March, and peaked in February. We observed a trend of older females extruding larvae earlier in the spawning season and of younger fish primarily responsible for larval production during the later part of the season. There were differences in absolute fecundity at age between female black rockfish with prefertilization oocytes and female black rockfish with fertilized eggs; fertilized-egg fecundity estimates were considered superior. The likelihood of yolked oocytes reaching the developing embryo stage increased with maternal age. Absolute fecundity estimates (based on fertilized eggs) ranged from 299,302 embryos for a 6-year-old female to 948,152 embryos for a 16-year-old female. Relative fecundity (based on fertilized eggs) increased with age from 374 eggs/g for fish age 6 to 549 eggs/g for fish age 16.

Manuscript submitted 13 March 2003 to Scientific Editor's Office.

Manuscript approved for publication 30 March 2004 by the Scientific Editor.

Fish. Bull. 102:418–429 (2004).

Maturity, ovarian cycle, fecundity, and age-specific parturition of black rockfish (*Sebastes melanops*)

Stephen J. Bobko

Steven A. Berkeley

Department of Fisheries and Wildlife
Hatfield Marine Science Center
2030 SE Marine Science Drive
Oregon State University
Newport, Oregon 97365
Present address (for S. A. Berkeley, contact author): Long Marine Laboratory
University of California, Santa Cruz
100 Shaffer Rd
Santa Cruz, California 95060

E-mail address (for S. A. Berkeley, contact author): stevenab@cats.ucsc.edu

Many fish species in the North Pacific have a long reproductively active life span, which increases the likelihood of producing offspring during periods of favorable environmental conditions. This bet hedging reproductive strategy reduces the impact of environmental variation on reproductive success (Goodman, 1984; Leaman and Beamish, 1984; Schultz, 1989). In species with age-structured spawning schedules, a broad age distribution will maximize the length of the spawning season. The more protracted the reproductive period, the greater the likelihood that some spawning will occur during conditions favorable for larval survival (Lambert, 1990). Age-related differences in the timing of spawning have been observed in many fishes; usually larger, older fish spawn earlier (Simpson, 1959; Bagenal, 1971; Berkeley and Houde, 1978; Shepherd and Grimes, 1984; Lambert, 1987), but in some cases younger fish spawn earlier in the season (Hutchings and Myers, 1993).

Age truncation, an inevitable result of fishing, can increase recruitment variability by reducing the length of the spawning season or by selectively removing older, more fit individuals from the population. Factors that might affect individual reproductive success include the number of eggs produced, the quality of eggs (e.g., yolk or oil globule volume), and the size or health of eggs and larvae. Off the coast of Oregon, widow rockfish (*Sebastes entomelas*) have exhibited increased absolute fecundity, and more importantly have increased relative fecundity, with age (Boehlert et al., 1982). Individual populations of shortbelly rockfish (*Sebastes jordani*), have been found to produce larvae with differing lipid and protein compositions and consequently potentially differing rates of survival (MacFarlane and Norton, 1999). Zastrow et al. (1989) reported that striped bass eggs stripped from wild fish increase in quality with maternal age due to increased amounts of proteins and lipids, although relative concentrations remain unchanged.

Black rockfish (*Sebastes melanops*), like most other rockfish, are long-lived, moderately fecund livebearers with long reproductive life spans. Although their longevity and low rate of natural mortality is presumed to be an adaptation to allow successful reproduction over their lifespan despite long periods between favorable environmental conditions, it also makes them more susceptible to overexploitation. The objective of our research presented in the present article is twofold. First, we describe the basic reproductive life history of black rockfish, with an emphasis on the ovarian developmental cycle and maturity schedule. Second, we investigate age-specific fecundity and temporal patterns in parturition and

discuss their effect on reproductive success in a population undergoing truncation of the upper end of its age distribution.

Materials and methods

We collected female black rockfish during the months of peak female reproductive development, November through March, for three successive years from 1995–96 through 1997–98. Female black rockfish were primarily obtained from recreational charter boat landings in Newport, Depoe Bay, and Charleston, Oregon, in addition to some fish from commercial landings from Port Orford, Oregon (Fig. 1). We also collected fish by rod and reel and spearfishing. When possible, the sex of all available black rockfish was determined, and females were staged as immature or mature. Immature females were measured (FL), and mature females were returned to the laboratory. On extremely busy days when numerous charter boats were fishing, all mature females were collected, but immature fish were not measured. In total we collected 1643 female black rockfish. Immediately upon return to the laboratory, we recorded fork length, total weight when possible (most samples from charter boats were carcasses only), liver weight, and ovary weight. Ovaries were assigned a maturity stage based on macroscopic appearance and preserved in 10% buffered formalin. We initially followed the gross maturity stage scheme of Nichol and Pikitch (1994) for darkblotched rockfish (*Sebastes crameri*) but ultimately abandoned their classification of maturity stages in favor of the simplified maturity stages reported by Gunderson et al. (1980) (Table 1). Sagittal otoliths were removed and stored dry for age determination. All aging was done by an expert age reader from the Oregon Department of Fish and Wildlife (ODFW), who used the break-and-burn technique (Beamish and Chilton, 1982). Ten percent of the otoliths were randomly selected for a second reading to ensure consistency in interpretation of annuli. It should be noted that black rockfish ages have not been validated. However, ages have been validated for yellowtail rockfish (*Sebastes flavidus*), a closely related species (Leaman and Nagtegaal, 1987), by using otoliths; moreover, the break-and-burn aging method is widely accepted as valid for aging rockfish (MacLellan, 1997), and ages thus derived are routinely used in rockfish stock assessments. Because our sample included all mature females that we encountered, we used these data to estimate the age distribution of mature females in each time period, and the age distribution of parturition during each time interval.

Histological preparations were made from the ovaries of 175 females collected monthly from March 1996 through March 1997 to track seasonal ovarian development. Females collected in March 1996 and November 1996 through March 1997 were from our regular sampling program, whereas fish collected from April through October 1996 were obtained from Newport recreational charter boat landings. Females were randomly selected from each maturity stage observed each month and from as wide a range of ages as available (Table 2). Ovaries were embedded in paraffin, sectioned at 4–5 μm, and stained with gill-3 haematoxylin and eosin y solution.

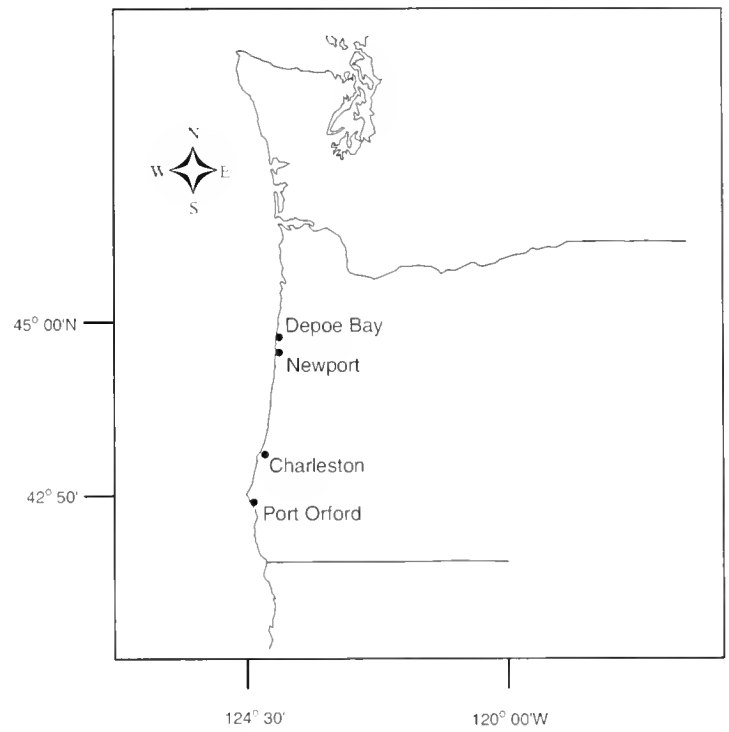

Figure 1

Map of the Oregon coast showing the study area where black rockfish (*Sebastes melanops*) were collected.

We determined stage-specific fecundity in black rockfish for females with unfertilized yolked oocytes (n=184) and fertilized eggs (n=85). Postfertilization ovaries were very fragile and tended to rupture easily and release embryos under the slightest pressure. Consequently, for estimating fecundity for these stages, we used only fish collected by ourselves so that we were certain that no eggs or larvae had been released during capture. To ensure that no eggs were lost after capture, these fish were immediately placed into plastic bags in order to retain any eggs that might be extruded before the ovary could be processed. Ovaries were processed following procedures modified from Lowerre-Barbieri and Barbieri (1993) to separate eggs and embryos from connective tissue. Briefly, fixed ovaries were manually manipulated and rinsed with water through a 1-mm square mesh sieve, which retained most of the connective tissue, into another sieve with 0.75-mm mesh. Ovary connective tissue was retained in the coarse sieve, and freed eggs were collected in the fine-mesh sieve. Freed eggs were patted dry, weighed (nearest 0.1 g), and three subsamples were collected, weighed (nearest 0.001 g), and placed in 10% buffered formalin.

Table 1

Macroscopic and histological descriptions of stages used to describe female black rockfish maturity.

Maturity stage	Macroscopic description	Histological description
1 Immature	Small and translucent ovary, pink during months without sexual activity and yellowish (except for very small fish) during months with reproductive activity.	Oocyte cytoplasm intensely basophilic. Densely packed oogonial nests and developing oocytes, with larger oocytes containing small clear vesicles.
2 Vitellogenesis	Ovary firm and yellow or occasionally cream in color. Large range of size, but all with visible opaque eggs.	Oogonia and developing oocytes still visible, but ovary dominated by large oocytes with numerous small red-staining yolk globules.
3 Fertilization	Eggs are golden and translucent. Ovary extremely large in relation to body cavity. Ovary wall thin and easily torn.	Fertilized eggs ovulated and found within the ovarian cavity. Eggs have a single pink-staining yolk mass and clear oil droplet.
4 Eyed larvae	Eyes of developing embryos visible, giving ovary an overall greyish color. Ovary fills a large portion of the body cavity.	Presence of developing larvae with black pigmented eyes. Yolk mass absorbed in late-stage larvae, but oil droplet usually present.
5 Spent	Ovary flaccid, purplish-red in color. Eyed larvae may still be visible.	Early-stage oocytes loosely associated. Extensive network of blood vessels. Possibility of encountering residual larvae.
6 Resting	Ovary again firm and pink in color. Black spots may be visible.	Similar appearance to immature fish. Ovary wall slightly thicker in early summer.

Table 2

Monthly ranges for age, length, and maturity stage of black rockfish collected off Oregon from March 1996 through March 1997 for histological analysis.

Month	Age (yr) range	FL (mm) range	Maturity stage range	n
March	7–25	375–510	1, 4–6	10
April	7–18	364–447	1, 5–6	12
May	7–13	340–465	1 and 6	15
June	5–13	349–432	1 and 6	15
July	5–13	360–475	1 and 6	14
August	5–11	357–493	1–2, 6	15
September	6–16	366–488	1 and 2	12
October	5–16	357–420	1 and 2	11
November	5–11	355–434	1 and 2	16
December	5–14	365–439	1 and 2	10
January	6–17	369–473	1–4	16
February	7–17	378–464	1–5	17
March	6–13	380–467	1, 5–6	12

The number of ova in the subsamples were counted and absolute fecundity was estimated by using the following algorithm:

$$AF = EW\left(\frac{\sum_{i=1}^{3} SSC_i}{\sum_{i=1}^{3} SSW_i}\right),$$

where AF = absolute fecundity, or the total number of eggs per female;
EW = weight of rinsed eggs (or larvae);
SSC_i = subsample count i, where i=1 to 3; and
SSW_i = subsample weight i, where i=1 to 3.

Relative fecundity (RF), based on gonad-free somatic weight was estimated by

$$RF = \frac{AF}{TW - GW},$$

where AF = absolute fecundity, or the total number of eggs per female;
TW = total weight; and
GW = gonad weight.

For our analyses of fecundity, we used only fish in which the number of eggs or larvae estimated from the three subsamples had coefficients of variation less than or equal to 5%, and for prefertilization eggs we used only females with average egg diameters of at least 450 μ to ensure inclusion of all developing oocytes. Only one cohort of developing oocytes is present in the ovary of

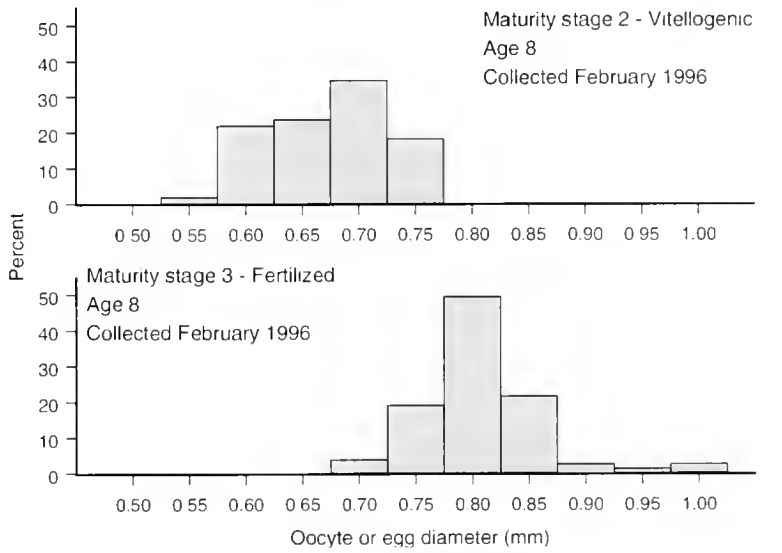

Figure 2

Prefertilization- and fertilized-egg–diameter frequency distributions showing a single mode of developing oocytes at both developmental stages.

black rockfish, either during development (stage 2) or after fertilization (stage 3) (Fig. 2). Analysis of covariance (ANCOVA) was used to test for annual effects in the relationship between prefertilization fecundity and age and a maturity-stage effect (prefertilization vs. fertilized-egg development stages) on both absolute and relative fecundity at age. We also used ANCOVA to test for a maturity stage effect in the relationship between absolute fecundity and fork length. All ANCOVA analyses were conducted by using multiple linear regression with the function lm in S-PLUS 2000 (MathSoft, Inc., Seattle, WA).

To predict the probability of a female black rockfish being mature based on its fork length, we fitted our maturity-at-length data to a logistic regression. During those months without reproductive activity, late spring through early fall, it was difficult to distinguish between immature and mature-resting ovaries. Consequently, only those females collected during the peak months of reproductive development and from sampling events where all fish, mature and immature, were collected were included in our analysis. Binary maturity observations (0=immature, 1=mature) and fork length were fitted to a logistic model by using the function glm, family = binomial of S-PLUS (S-PLUS 2000). The model used was

$$\pi(FL) = P(Y = 1 \mid FL) = \frac{e^{\beta 0 + \beta 1 FL}}{1 + e^{\beta 0 + \beta 1 FL}},$$

where $P(Y=1|FL)$ = probability of female black rockfish being mature at size FL; and

β_0 and β_1 = regression coefficients for the intercept and fork length, respectively.

For functional purposes, the response variable was interpreted as the percentage of female black rockfish mature at length. Assuming this relationship of fork length to maturity had not changed over time, we applied our logistic model to fork-length data from random sampling conducted by ODFW during the summers of 1992–2000 to calculate the percentage of female black rockfish caught by the recreational fishery off Newport that were mature in each year.

Fork length-at-age data for female black rockfish were fitted with the von Bertalanffy growth function (VBGF) by using the nonlinear function nls() in S-PLUS 2000. Age at 50% maturity was calculated by using our estimate of length at 50% maturity and a VBGF rearranged to the form

$$t_{50\%} = t_0 + \frac{1}{k}\left[\ln \frac{L_\infty}{L_\infty - l_{t50\%}}\right],$$

where $t_{50\%}$ = age at 50% maturity;
L_∞ = asymptotic length;
k = Brody growth parameter;
t_0 = age at zero length; and
$l_{t50\%}$ = length at 50% maturity.

Timing of parturition was estimated by microscopically determining embryo development stages for all females with fertilized eggs following Yamada and

Kusakari's (1991) stages of embryonic development for kurosoi (*Sebastes schlegeli*) modified to reflect the gestation period of 37 days for black rockfish (Boehlert and Yoklavich, 1984). Gestation period is likely to vary with water temperature. In determining gestation period, Boehlert and Yoklavich (1984) held black rockfish in the laboratory at 9–11°C. Mean water temperatures in our study area during the period of egg and larval development (December–April) were 10.9°, 10.1°, and 11.4°C in 1995–96, 1996–97, and 1997–98, respectively (http://co-ops.nos.noaa.gov/data). Even in the strong El Niño year of 1997–98, nearshore water temperature during the winter larval development period was only slightly outside this range. Therefore, we assumed a 37-day gestation period for all years of our study. Using the Boehlert and Yoklavich (1984) equation; ($stage\ duration = 0.0452 \times stage^{1.090}$) we solved for duration at each stage by adding 5 days to account for the time between hatching (stage 32) and parturition (also from Boehlert and Yoklavich, 1984). To calculate the time until parturition for each stage, we subtracted the previous stage durations from the total gestation period of 37. For example, at stage 1, parturition would occur in 37 days. At stage 2, parturition would take place in 37 days – stage-1 duration (~2 days) = 35 days.

For each year of our study, estimated parturition dates for all females in our sample were grouped into one-week time intervals and further subdivided into age categories: 6–8; 9–11; 12–14; and >15. These numbers were then multiplied by the appropriate value for age-class–specific fecundity based on fertilized eggs (Table 3) to estimate relative spawning output by week for each age class.

Table 3

Age group-specific absolute fecundity (based on fertilized eggs) and age distribution of mature females as a percentage of all mature females, used to estimate larval production. Calculated from data pooled from 1996 through 1998.

Age group (yr)	Absolute fecundity[1]	Percentage of all mature females represented by each age group
6–8	364,183.5	42.19
9–11	558,837.1	38.48
12–14	753,490.7	13.94
15 and older	948,144.3	5.39

[1] Absolute fecundity for each age group is the estimated fecundity (based on fertilized eggs) for ages 7, 10, 13, and 16, respectively.

Results

Ovarian development

Black rockfish off Oregon exhibited group-synchronous oocyte development; and females extruded only one brood of larvae per year (Fig. 2). Based on our observations of ovarian development from all three years of this study, parturition took place from mid-January through mid-March and peaked in February. Following parturition, unextruded larvae were quickly resorbed and the ovary lost much of its vascularization. From April through early August ovaries were in a resting state and contained oogonial nests and slightly larger oocytes with a basophilic cytoplasm and a maximum diameter of 50 μ. Also present at this time were developing oocytes ranging from 50 to 150 μ in diameter with small lipid vacuoles surrounding the nuclear membrane. Yolk deposition (vitellogenesis) began in late August and was observed through the third week of February. In the final stages of vitellogenesis, the largest oocytes were approximately 700 μ in diameter and had numerous oil vacuoles and yolk globules throughout the cytoplasm. The first female with fertilized eggs (stage 3) was observed during the second week of January, and stage-3 females were observed until the third week of February. Recently fertilized eggs were approximately 850 μ in diameter. The period of parturition as indicated by the occurrence of ovaries containing eyed larvae extended from the second week in January through the second week of March. Spent females were first collected during the last week of January and were most frequently collected in late February and early March.

Sexual maturity

Parameter values for the length-maturity logistic model were $\beta_0 = -26.73$ and $\beta_1 = 0.068$. The smallest mature female black rockfish we observed was 345 mm; all individuals were mature by 450 mm. Fifty percent of females were estimated to be mature at 394 mm fork length (Fig. 3). As reflected in our length-maturity logistic model, there was a decreasing trend in the percent maturity for female black rockfish in recreational landings from ODFW collections from 1992 through 2000 (Fig. 4). The von Bertalanffy parameter estimates for female black rockfish were $L_\infty = 442$ mm, $k = 0.33$, $t_0 = 0.75$ (Fig. 5). Using these estimates, along with the fork length at 50% maturity, we estimated the age at 50% maturity for female black rockfish to be 7.5 years. The median age of mature females decreased in each collection year from 10 years in 1996 to 9 in 1997 and to 7 years in 1998. In addition, we observed a significant decrease in the proportion of mature fish age 10 or older over the three years of our study (Pearson's $\chi^2 = 52.4$, df=2, $P<0.001$). The proportions decreased from 0.511 in 1996, to 0.318 in 1997, and 0.145 in 1998.

Fecundity

Absolute fecundity for prefertilization female black rockfish ranged from 482,528 oocytes for a 5-year-old female to 998,050 oocytes for a 19-year-old female. The results of ANCOVA (Table 4) over a common age

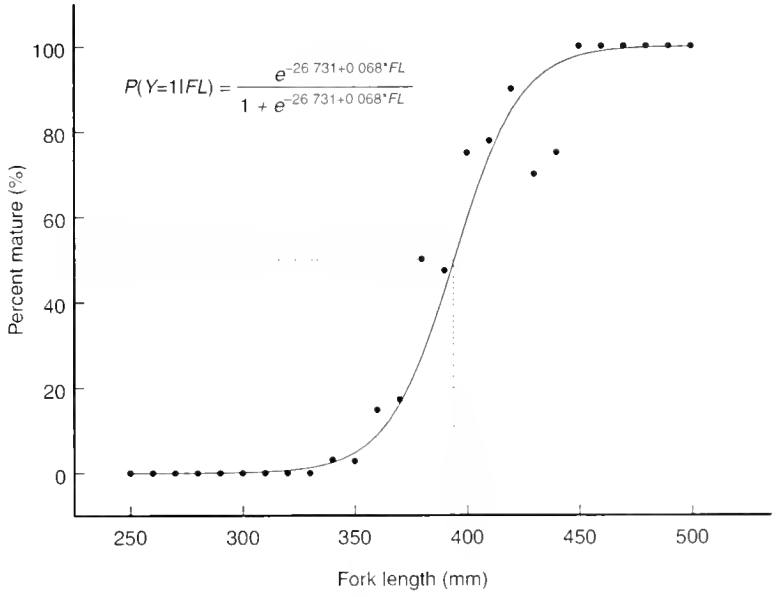

Figure 3

Logistic regression model for the estimated percentage of sexually mature female black rockfish as a function of fork length, with associated observed percent mature at 10-mm length intervals.

range showed no evidence of differences in slopes among the years 1996–98 ($P=0.161$). ANCOVA also showed no significant difference in elevations ($P=0.632$), indicating no annual effect and allowing one model to be fitted to the pooled data (Fig. 6). Absolute fecundity for females with fertilized eggs ranged from 299,302 embryos for a 6-year-old to 948,152 embryos for a 16-year-old. Because of the low number of females with developing embryos collected in 1996 and 1998, 19 and 4 females, respectively, and based on the results of prefertilization females, all data were pooled and fitted with one model (Fig. 7). Although we were able to pool the data for all years for fecundity-age regressions for both prefertilization females and fertilized females, there was evidence of interaction (i.e., unequal slopes) between stage-specific absolute fecundity and age (2-tailed t-test, $P=0.020$) requiring separate linear regressions to be fitted to the data (Fig. 8).

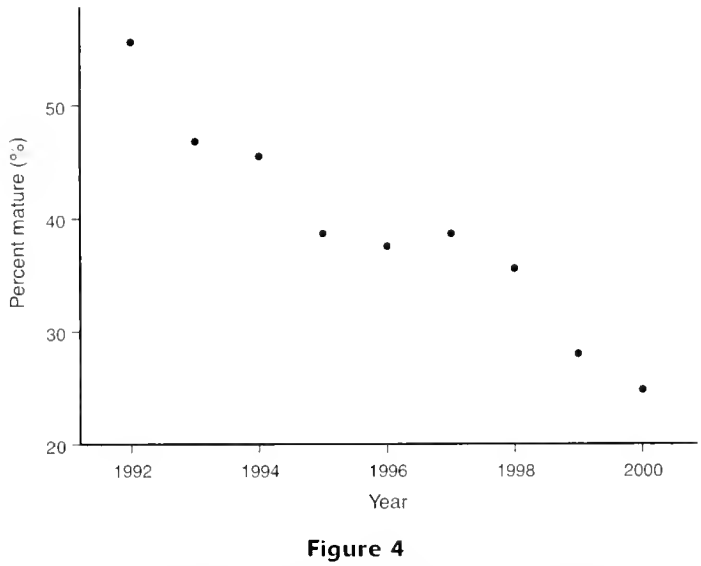

Figure 4

Estimated percent maturity for recreationally landed female black rockfish from Newport, Oregon, based on our logistic regression model of fork length on maturity. Data were from regular random summer port sampling conducted by the Oregon Department of Fish and Wildlife from 1992 through 2000.

Similar to the ANCOVA results for absolute fecundity, there were no differences in slopes or elevations for relative fecundity for prefertilization females for the years 1996–98 (Table 4). Again, based on the results of the ANCOVA for prefertilization females and due to the low number of fertilized females collected in 1996 and 1998, all relative fecundity data for females with fertilized eggs were pooled. Unlike the results for the relation between absolute fecundity and age there was no evidence of interaction (i.e., unequal slopes) between stage-specific relative fecundity and age (2-sided *t*-test

Table 4

Results of analyses of covariance testing for differences in slopes and elevations of annual absolute fecundity-age relation and annual relative fecundity-age relation. Response variables = AF and RF, treatment factors = year, and covariate = age.

Source of variation	df	Sum of squares	Mean square	F	P
Absolute fecundity (based on prefertilization oocytes)					
Equality of slopes	2	105,347	52,674	1.85	0.161
Error	160	4,564,320	28,527		
Equality of elevation	2	168,544	84,272	0.29	0.747
Error	162	3,459,048	288,254		
Relative fecundity (based on prefertilization oocytes)					
Equality of slopes	2	259.04	129.52	0.58	0.559
Error	160	35,452.22	221.58		
Equality of elevation	2	799.52	399.76	1.81	0.166
Error	162	35,711.26	220.44		

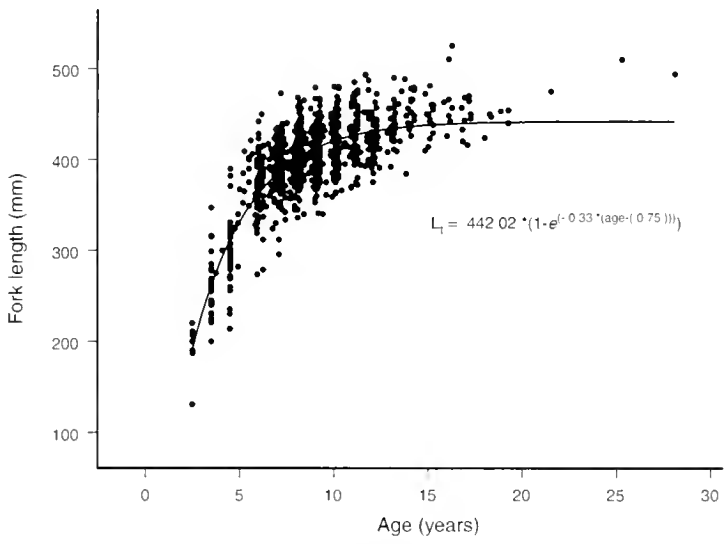

Figure 5

Fork length at age fitted to the von Bertalanffy growth model for female black rockfish.

P=0.096). There was, however, strong evidence (2-tailed t-test, P<0.001,) of a stage effect (i.e., unequal elevations) which necessitated that the data be fitted with a parallel-lines multiple linear regression model (Fig. 9).

Absolute fecundity for prefertilization female black rockfish ranged from 443,671 oocytes for a 381-mm-FL female to 1,135,457 oocytes for a 495-mm-FL female. For fertilized females, absolute fecundity ranged from 283,618 oocytes for a 381-mm-FL female to 1,073,356 oocytes for a 510-mm-FL female. The results of ANCOVA over a common size range showed no evidence of differences in slopes between maturity stages (2-sided t-test P=0.206). There was, however, strong evidence (2-tailed t-test, P<0.0001,) of a stage effect (i.e., unequal elevations) which necessitated that the data be fitted with a parallel-line multiple linear regression model (Fig. 10).

Temporal patterns in parturition

From 1996 through 1998 we estimated relative larval production for four age groups: 6–8; 9–11; 12–14; and 15 years and older (Fig. 11). In each year parturition took place from mid-January until mid-March, and older, larger fish extruded larvae earlier than younger fish. In 1996 and 1997, the 9–11 year-old fish dominated larval production, responsible for 60.1% and 49.6% of all larvae extruded, respectively (Table 5). In 1998 age 6–8 fish produced the largest percentage of larvae (65.3%). In all years, relative larval production was lowest for the oldest age group (15+), declining to near 0 by 1998.

Discussion

Ovarian development for black rockfish in Oregon was similar to the developmental cycles reported for other rockfish species (Moser, 1967; Bowers, 1992; Nichol and Pikitch, 1994) with the exception of seasonal timing and stage duration. Females underwent vitellogenesis for up to six months before fertilization, which occurred from December through February. In all three years, parturition off the Oregon coast occurred between mid-January and mid-March and peaked in February. Wyllie Echeverria (1987) observed similar timing for parturition of black rockfish off north-central California, with a peak in February but with parturition occurring through May.

All female black rockfish, except the smallest immature females, followed a seasonal cycle in which their ovaries developed an orange coloring during the months of reproductive activity—a pattern observed in olive rockfish (Love and Westphal, 1981). Similarly, Nichol and Pikitch (1994) observed darkblotched rockfish undergoing an "immature cycling" and even assigned these fish a maturity stage. After the reproductive season, the ovaries of immature black rockfish once again became pale pink in color. Because these fish were functionally immature and there was no way to project when they would become sexually mature, they were combined with those small, young females undergoing no seasonal ovarian development and were staged as immature.

Our estimate of fork length at 50% maturity for female black rockfish off Oregon was similar to the 400 mm estimate reported for north-central California females (Wyllie Echeverria, 1987), but lower than the estimate of 422 mm from Washington (Wallace and Tagart, 1994). Our estimated age at 50% maturity of 7.5 years was similar to the estimates of 7.9 and 7 years from Washington and north-central California, respectively. McClure (1982) reported that over 50% of examined female black rockfish collected off Depoe Bay, Oregon, were mature by age six. The difference between our estimate and McClure's was most likely due to using whole otoliths to age fish, which resulted in underestimates of age, and to assigning maturity stages only during summer months, which we have already described as problematic. Both absolute and relative fecundity increased with age for female black rockfish in Oregon waters, although there was a great deal of variation not accounted for by age. The low r^2 values for absolute fecundity regressions for pre- and postfertilization females (0.25 and 0.45 respectively) are due largely to the relatively poor correspondence between age and size (Fig. 5). Black rockfish, like many slow growing, long-lived fish grow slowly after sexual maturity. The rate of growth during their first few years can be quite variable depending on oceanographic conditions and food availability. As a result, young fish can be as large or larger than much older fish (Fig. 5). Length is a better predictor of fecundity than age as judged by the goodness-of-fit of the multiple linear regression model (Fig. 10; r^2=0.70).

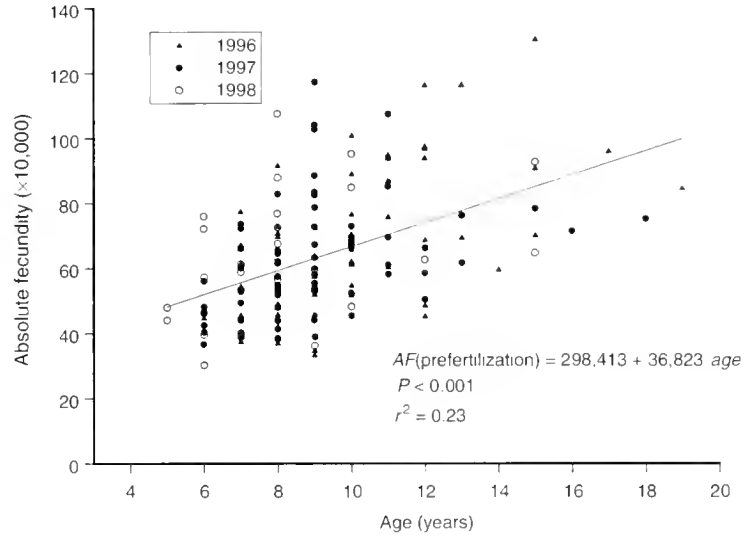

Figure 6

Scatter plot of black rockfish absolute fecundity (AF) (based on prefertilization eggs) on age by year (1996–98) with a fitted regression line from pooled data.

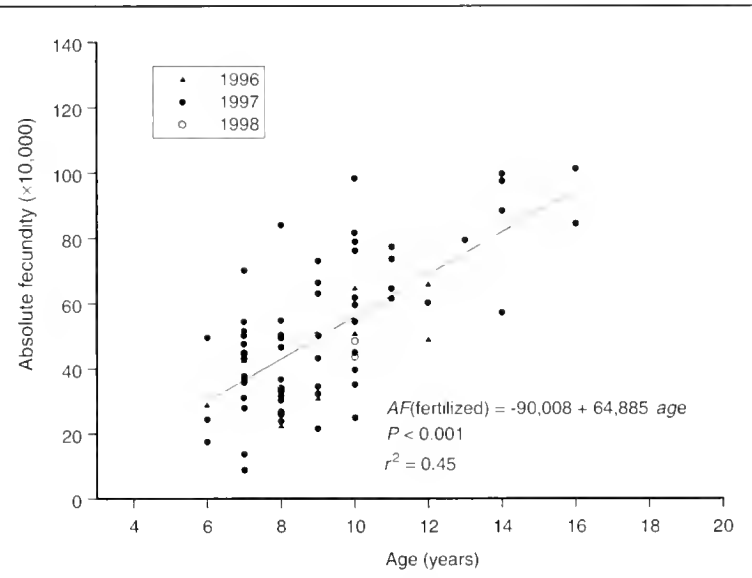

Figure 7

Scatter plot of black rockfish absolute fecundity (AF) (based on fertilized eggs) on age by year (1996–98) with a fitted regression line from pooled data.

An increase in absolute fecundity with age was observed in both prefertilization and postfertilization females, but they occurred at different rates. As illustrated in Figure 8, the absolute fecundity for a postfertilization 6-year-old black rockfish was only 58% of the estimated absolute fecundity for a prefertilization fish of the same age. By age 15 absolute fecundity

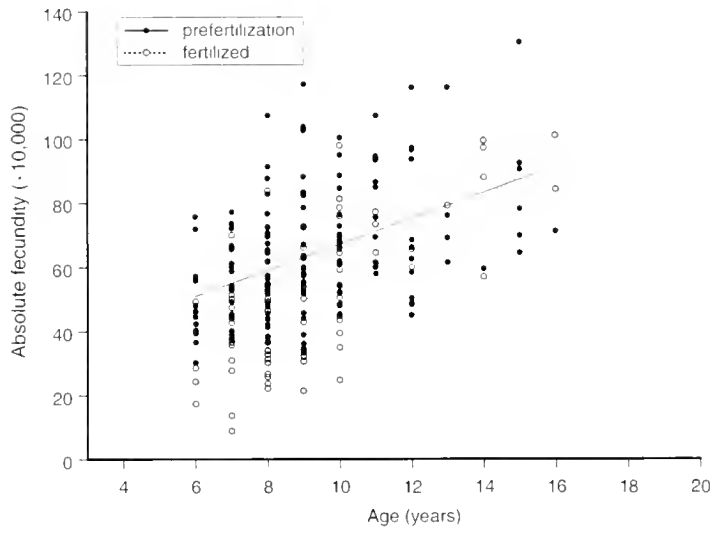

Figure 8

Separate-lines regressions fitted to absolute fecundity (based on prefertilization and fertilized eggs) on age for black rockfish in Oregon.

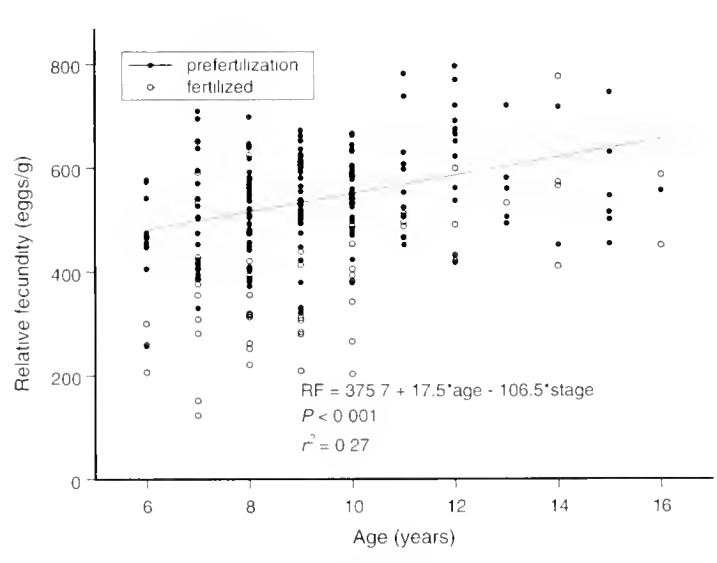

Figure 9

Parallel-lines model fitted to relative fecundity (based on prefertilization and fertilized eggs) on age for black rockfish in Oregon.

estimates for fertilized and prefertilization females were approximately equal. Yolked oocytes from older females were more successful in reaching the developing embryo stage. This may be attributed to higher rates of fertilization, greater viability of embryos, or a combination of both in older female black rockfish. Regardless of the mechanism there should have been signs of greater atresia in the ovaries of young fish, which we did not observe in our histological preparations. This may have been due to rapid resorption of unfertilized oocytes or an artifact of the fragile nature of fertilized ovaries, which made it difficult to obtain representative histological preparations. Nevertheless, these results suggest that fecundity in black rockfish is best described after fertilization, but care must be taken to minimize embryo loss. These results also suggest that current

estimates of reproductive potential, in which fecundity for prefertilization females is used, may overestimate actual larval production because an increasing proportion of the stock consists of young fish.

We observed a recurring trend of older, larger fish extruding larvae earlier in the reproductive season and larval output being increasingly dominated by younger and younger fish. Eldridge et al. (1991) reported that larger (and most likely older) yellowtail rockfish (*Sebastes flavidus*) spawned earlier in the season than smaller fish—a pattern also reported for darkblotched rockfish (*S. crameri*) by Nichol and Pikitch (1994). Reduced food availability has been suggested as a potential cause for delayed reproduction in *Sebastes* for smaller, younger individuals with high metabolic requirements for somatic growth (Larson, 1991). We feel that limiting the amount of energy that can be spent on reproductive development would cause lower fecundity or reduced yolk content, but not necessarily a delay in reproductive development that would result in suboptimal timing of parturition.

Stock assessments rarely consider changes in population age composition resulting from the removal of older age classes except to the extent that total egg and larval production is reduced. The decreasing representation of mature female black rockfish age 10 and older in the three years of our study indicates that age truncation is occurring in black rockfish in Oregon. This truncation not only removes biomass and potential larval production, but truncation of the upper end of the age distribution eliminates mature females with higher fecundity per individual, a greater success in carrying eggs through to the larval stage, and an age group that extends the overall parturition season. Further research is necessary to explore the controlling mechanisms of differential reproductive success with age and to determine how best to incorporate these findings into stock assessment models.

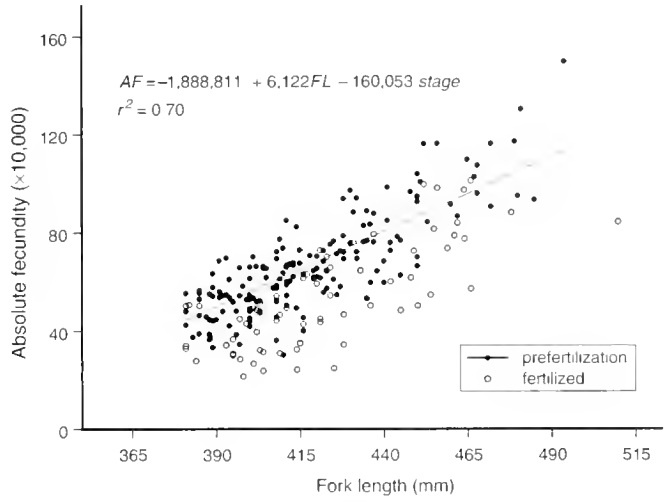

Figure 10

Parallel-lines model fitted to absolute fecundity (based on prefertilization and fertilized eggs) on age for black rockfish in Oregon.

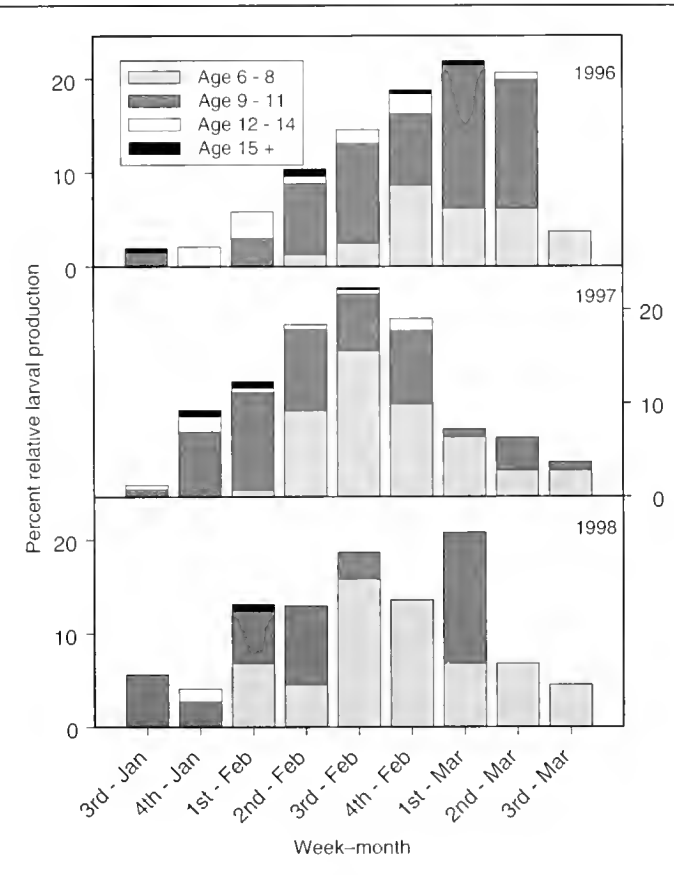

Figure 11

Percent relative larval production estimated from observations of larval development and age-group–specific absolute fecundity (based on fertilized eggs) for all mature females belonging to each age group of black rockfish collected in Oregon during 1996–98.

Acknowledgments

Many individuals contributed to the completion of this study. Tom Rippetoe provided many hours of expert assistance in all aspects of this research. Bob Mikus aged all of the adult black rockfish for this study. We thank him and the Oregon Department of Fisheries and Wildlife for all their support. We thank Dan Detman for his help and time in collecting black rockfish. We also thank Brock McLeod, Jason Castillo, David Stewart, and Michael Hogansen for all their help. We are especially grateful for all those unpaid volunteers who helped with fieldwork: Joe O'Malley, Mark Amend, Bill Pinnix, Wolfe Wagman, and Pat McDonald.

Table 5

Age group-specific relative larval production for 1996–98 for female black rockfish off Oregon.

	Percentage of relative larval production		
Age group	1996	1997	1998
6–8	26.4%	43.1%	65.3%
9–11	60.1%	49.6%	32.9%
12–14	11.3%	5.8%	1.8%
15 and older	2.2%	1.5%	0.0%

We thank the charter boat operators in Depoe Bay, Newport, and Charleston, Oregon, for their kindness, patience, and cooperation. Only through their assistance was this research possible. This research was partially supported by the NOAA Office of Sea Grant and Extramural Programs, U.S. Department of Commerce, under grant numbers NA36RG0451 (project no. R/OPF-46), and by appropriations made by the Oregon State legislature. Additional funding was provided through Hatfield Marine Science Center scholarships: the 1996 Barbara Schwantes Memorial Fellowship; the 1997 Mamie L. Markham Endowment Award; and the 1998 Bill Wick Marine Fisheries Award.

Literature cited

Bagenal, T. B.
1971. The interrelation of the size of fish eggs, the date of spawning and the production cycle. J. Fish Biol. 3:207–219.

Beamish, R. J., and D. E. Chilton.
1982. Preliminary evaluation of a method to determine the age of sablefish (*Anoplopoma fimbria*). Can. J. Fish. Aquat. Sci. 39:277–287.

Berkeley, S. A., and E. D. Houde.
1978. Biology of two exploited species of halfbeaks, *Hemiramphus brasiliensis* and *H. balao* from southeast Florida. Bull. Mar. Sci. 28:624–644.

Boehlert, G. W., W. H. Barss, and P. B. Lamberson.
1982. Fecundity of the widow rockfish, *Sebastes entomelas*, off the coast of Oregon. Fish. Bull. 4:881–884.

Boehlert, G. W., and M. M. Yoklavich.
1984. Reproduction, embryonic energetics, and the maternal-fetal relationship in the viviparous genus *Sebastes* (Pisces: Scorpaenidae). Biol. Bull. 167:354–370.

Bowers, M. J.
1992. Annual reproductive cycle of oocytes and embryos of yellowtail rockfish, *Sebastes flavidus* (family Scorpaenidae). Fish. Bull. 90:231–242.

Eldridge, M. B., J. A. Whipple, M. J. Bowers, B. M. Jarvis, and J. Gold.
1991. Reproductive performance of yellowtail rockfish, *Sebastes flavidus*. Environ. Biol. Fish. 30:91–102.

Goodman D.
1984. Risk spreading as an adaptive strategy in iteroparous life histories. Theoret. Popul. Biol. 25:1–20.

Gunderson, D. R., P. Callahan, and B. Goiney.
1980. Maturation and fecundity of four species of *Sebastes*. Mar. Fish. Rev. 42(3–4):1.

Hutchings, J. A., and R. A. Myers.
1993. Effect of age on the seasonality of maturation and spawning of Atlantic cod, *Gadus morhua*, in the northwest Atlantic. Can. J. Fish. Aquat. Sci. 50:2468–2474.

Lambert, T. C.
1987. Duration and intensity of spawning in herring *Clupea harengus* as related to the age structure of the mature population. Mar. Ecol. Prog. Ser. 39:209–220.

Lambert, T. C.
1990. The effect of population structure on recruitment in herring. J. Cons. Int. Explor. Mer. 47:249–255.

Larson, R. J.
1991. Seasonal cycles of reserves in relation to reproduction in *Sebastes*. Environ. Biol. Fish. 30:57–70.

Leaman, B. M., and R. J. Beamish.
1984. Ecological and management implications of longevity in some northeast Pacific groundfishes. Int. North Pac. Fish. Comm. Bull. 42:85–97.

Leaman, B. M., and D. A. Nagtegaal.
1987. Age validation and revised natural mortality rate for yellowtail rockfish. Trans. Am. Fish. Soc. 116(2): 171–175.

Love, M. S., and W. V. Westphal.
1981. Growth, reproduction, and food habits of olive rockfish, *Sebastes serranoides*, off central California. Fish. Bull. 79:533–545.

Lowerre-Barbieri, S. K., and L. R. Barbieri.
1993. A new method of oocyte separation and preservation for fish reproduction studies. Fish. Bull. 91:165–170.

MacFarlane, R. B., and E. C. Norton.
1999. Nutritional dynamics during embryonic development in the viviparous genus *Sebastes* and their application to the assessment of reproductive success. Fish. Bull. 97: 273–281.

Maclellan, S. E.
1997. How to age rockfish (*Sebastes*) using *S. alutus* as an example—the otolith burnts (*sic*) section technique. Canadian Tech. Rep. Fish. Aquat. Sci, 42 p.

McClure, R. E.
1982. Neritic reef fishes off central Oregon: aspects of life histories and the recreational fishery. M.S. thesis, 94 p. Oregon State Univ., Corvallis, OR.

Moser, H. G.
1967. Seasonal histological changes in the gonads of *Sebastodes paucispinis* (Ayres), and ovoviviparous teleost (family Scorpaenidae). J. Morph. 123:329–353.

Nichol, D. G., and E. K. Pikitch.
1994. Reproduction of darkblotched rockfish off the Oregon coast. Trans. Am. Fish. Soc. 123:469–481.

Schultz, D. L.
1989. The evolution of phenotypic variance with iteroparity. Evolution 43:473–475.

Shepherd, G. R., and C. B. Grimes.
1984. Reproduction of weakfish, *Cynoscion regalis*, in the New York Bight and evidence for geographically specific life history characteristics. Fish. Bull. 82(3):501–511.

Simpson, A. C.
1959. The spawning of plaice in the North Sea. Fish. Invest. M.A.F.F. London (Ser. 2) 22:1–111.

Wallace, F. W., and J. V. Tagart.
1994. Status of the coastal black rockfish stocks in Wash-

ington and northern Oregon in 1994. Appendix F in Status of the Pacific coast groundfish fishery through 1994 and recommended acceptable biological catches for 1995. Pacific Fisheries Management Council, Portland, OR.

Wyllie Echeverria, T.
1987. Thirty-four species of rockfishes: Maturity and seasonality of reproduction. Fish. Bull. 85:826–832.

Yamada, J., and M. Kusakari.
1991. Staging and time course of embryonic development in kurosoi, *Sebastes schlegeli*. Environ. Biol. Fish. 30:103–110.

Zastrow, C. E., E. D. Houde, and E. H. Saunders.
1989. Quality of striped bass, *Morone saxatilis*, eggs in relation to river source and female weight. Rapp. P.-V. Cons. Int. Explor. Mer 191:34–42.

Maori octopus (*Octopus maorum*) bycatch and southern rock lobster (*Jasus edwardsii*) mortality in the South Australian rock lobster fishery

Daniel J. Brock

South Australian Research and Development Institute (Aquatic Sciences)
2 Hamra Ave.
West Beach, South Australia 5024, Australia
Present address: Department of Soil and Water
Adelaide University
Adelaide, South Australia 5005, Australia
E-mail address: Brock.Daniel@saugov.sa.gov.au

Timothy M. Ward

South Australian Research and Development Institute (Aquatic Sciences)
2 Hamra Ave.
West Beach, South Australia 5024, Australia

Abstract—Octopuses are commonly taken as bycatch in many trap fisheries for spiny lobsters (Decapoda: Palinuridae) and can cause significant levels of within-trap lobster mortality. This article describes spatiotemporal patterns for Maori octopus (*Octopus maorum*) catch rates and rock lobster (*Jasus edwardsii*) mortality rates and examines factors that are associated with within-trap lobster mortality in the South Australian rock lobster fishery (SARLF). Since 1983, between 38,000 and 119,000 octopuses per annum have been taken in SARLF traps. Catch rates have fluctuated between 2.2 and 6.2 octopus/100 trap-lifts each day. There is no evidence to suggest that catch rates have declined or that this level of bycatch is unsustainable. Over the last five years, approximately 240,000 lobsters per annum have been killed in traps, representing ~4% of the total catch. Field studies show that over 98% of within-trap lobster mortality is attributable to octopus predation. Lobster mortality rates are positively correlated with the catch rates of octopus. The highest octopus catch rates and lobster mortality rates are recorded during summer and in the more productive southern zone of the fishery. In the southern zone, within-trap lobster mortality rates have increased in recent years, apparently in response to the increase in the number of lobsters in traps and the resultant increase in the probability of octopus encountering traps containing one or more lobsters. Lobster mortality rates are also positively correlated with soak-times in the southern zone fishery and with lobster size. Minimizing trap soak-times is one method currently available for reducing lobster mortality rates. More significant reductions in the rates of within-trap lobster mortality may require a change in the design of lobster traps.

Manuscript submitted 28 April 2003 to Scientific Editor's Office.

Manuscript approved for publication 2 March 2004 by the Scientific Editor.

Fish. Bull. 102:430–440 (2004).

Fishing traps are used throughout the world to target a wide range of crustaceans, fishes, and cephalopods. Commercial trap fisheries, especially those for decapod crustaceans, are often the most valuable fisheries within a region (Phillips et al., 1994). Traps are generally considered to be an efficient and benign form of fishing because they appear to cause relatively minor damage to benthic habitats, can be designed to target particular species and size ranges, and produce live catches in good condition while minimizing bycatch (Miller, 1990).

There are 49 species of spiny lobsters (Decapoda: Palinuridae) worldwide, 33 of which support commercial trap fisheries. The largest of these are in Cuba, South Africa, Mexico, Australia, and New Zealand (Williams, 1988). The main trap fisheries in Australia are for western rock lobster (*Panulirus cygnus*) in Western Australia and southern rock lobster (*Jasus edwardsii*) along the southern coastline. Octopuses constitute a significant component of the bycatch in both fisheries (Joll[1]; Knight et al.[2]).

In South Australia, *J. edwardsii* supports the State's most valuable commercial fishery. *Octopus maorum* is a significant bycatch species and is thought to be the major cause of lobster mortality in traps (Prescott et al.[3]).

Although the octopus bycatch of the South Australian rock lobster fishery (SARLF) is saleable, the commercial value of this product does not offset the value of the large number of lobsters that are killed in traps by octopus. Many fishermen are convinced that incidental mortality of octopus resulting from lobster fishing acts to control octopus numbers and that if these rates were reduced, octopus abundance and levels of within trap predation would increase.

Despite the prevalence of octopus bycatch in lobster fisheries, there have been only a few studies on the interaction between octopus and lob-

[1] Joll, L. 1977. The predation of trap-caught western rock lobster (*Panulirus Longipes cygnus*) by octopus. Department of Fisheries and Wildlife, Western Australia, Report 29, 58 p. [Available from Department of Fisheries, 168–170 St George's Terrace, Perth, Western Australia, 6000.]

[2] Knight, M. A., A. Tsolos, and A. M. Doonan. 2000. South Australian fisheries and aquaculture information and statistics report. Research Report Series 49, 69 p. [Available from SARDI Aquatic Science, 2 Hamra Avenue, West Beach, South Australia 5022.]

[3] Prescott, J., R. McGarvey, Y. Xiao, and D. Casement. 1999. Rock lobster. South Australian Fisheries Assessment Series 99/04, 35 p. [Available from SARDI Aquatic Science, 2 Hamra Avenue, West Beach, South Australia 5022.]

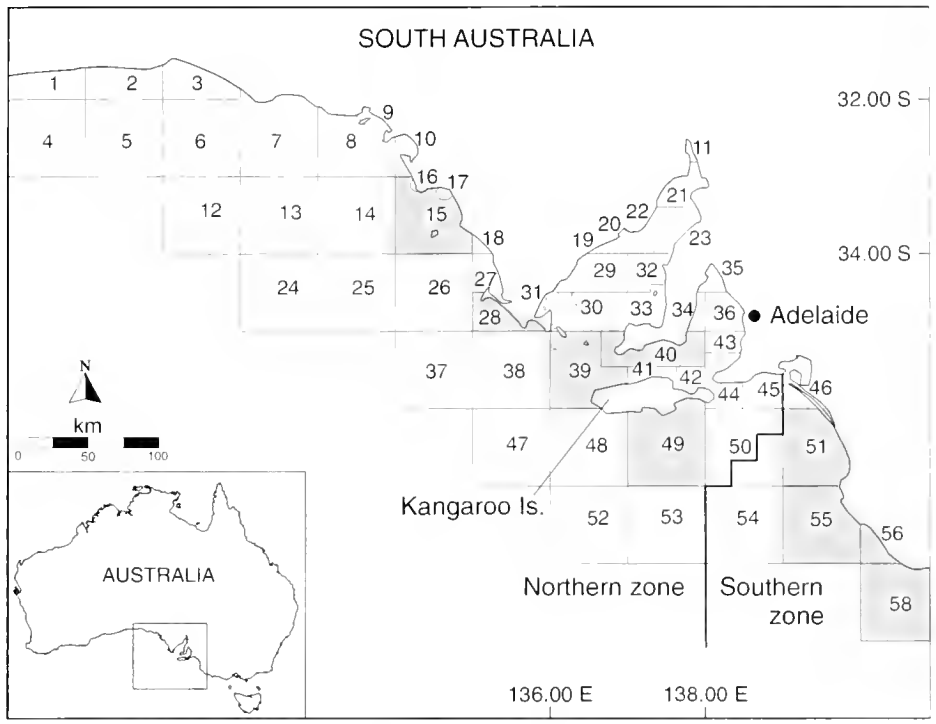

Figure 1

Map of the marine fishing areas (MFAs) of the South Australian rock lobster fishery. Shading shows the MFAs that were considered in this study and where most fishing effort is concentrated.

sters in traps (Joll[1]). Furthermore, there is a paucity of quantitative data on the impact of fishing on octopus populations, the proportion of lobster mortality that is attributable to octopus predation, or the long-term economic and ecological effects that octopus-induced mortality may have on lobster fisheries.

In this study, we examined the interaction between *O. maorum* and *J. edwardsii* in the South Australian rock lobster fishery (SARLF). The objectives were 1) to determine the number of lobsters and octopus caught and the number of lobsters killed in traps each year in the fishery; 2) to describe the interannual and seasonal patterns in lobster catch rate ($CPUE_L$), octopus catch rate ($CPUE_O$), and lobster mortality rate (M_L); 3) to examine some factors that may affect lobster mortality rates; 4) to estimate what proportion of the lobster mortality is attributable to octopus predation; and 5) to determine whether the rate of lobster mortality through octopus predation in traps is size dependent.

Materials and methods

South Australian rock lobster fishery

The SARLF is divided into a northern zone (NZ) and a southern zone (SZ), each of which is further divided into marine fishing areas (MFAs) for statistical purposes (Fig.1). There are 68 and 183 fishermen licensed to operate in the NZ and SZ respectively. The fishing season extends from November to May in the NZ and October to April in the SZ. A quota management system was introduced in the SZ in 1993, whereas the NZ is managed by gear restrictions and temporal closures.

Total annual catch and effort for the SARLF

Catch and effort data are recorded on a daily basis by all individual fishermen. Since 1983, a standardized logbook for recording catch and effort has been used across the fishery. Data provided by fishermen include MFA fished, average depth fished, number of trap-lifts, number and total weight of live lobsters, number of dead lobsters, and number and total weight of octopus. This information is stored in a South Australian rock lobster database that is managed by the South Australian Research and Development Institute, Aquatic Sciences.

Interannual and seasonal patterns in $CPUE_L$, $CPUE_O$, and M_L

Although commercial fishing for lobsters occurs along most of the South Australian coastline, the majority of effort is concentrated in only a few MFAs. In the NZ over the last 5 years about 72% of total trap-lifts were made in MFAs 15, 28, 39, 40, and 49. In the SZ over the same period 95% of trap-lifts were made in MFAs 51, 55, 56, and 58 (Fig. 1).

Data from the database were used to calculate catch rates of lobsters ($CPUE_L$), octopus ($CPUE_O$), and M_L on an annual and monthly basis for the nine major MFAs listed above. Catch rates from these MFAs for each fisherman were calculated according to the formula: *catch rate = catch number/(trap-lifts/day)*. Annual and seasonal trends in $CPUE_L$, $CPUE_O$, and M_L were calculated for each zone and MFA.

Factors that affect within-trap lobster mortality

Potential factors that affect within-trap lobster mortality were analysed by using a general linear model (type-3 sums of squares) under the assumption that the number of dead lobsters follows a log-normal distribution.

The number of dead lobsters/trap-lift/day/license (with a ln+1 transformation) was used as the measure of lobster mortality. A model of the following structure was used to examine factors that affect the numbers of dead lobster:

$$\begin{aligned} \textit{Dead lobster} = {} & \textit{License} + \textit{MFA} + \textit{Month} + \textit{Year} \\ & + \textit{Effort} + \textit{Depth} + \textit{Octopus} + \textit{Lobster catch} \\ & + \textit{Soak-time} + (\textit{License}\times\textit{Year}) + (\textit{License}\times\textit{Month}) \\ & + (\textit{Year}\times\textit{Month}) + (\textit{Year}\times\textit{MFA}) + (\textit{Soak-time}\times\textit{Year}) \\ & + (\textit{Soak-time}\times\textit{Month}). \end{aligned}$$

In the model, *License* represents an individual fisherman, *MFA* is the marine fishing area, *Month* accounts for seasonal variation and *Year* accounts for interannual variation, *Effort* is the number of trap-lifts/license each day, *Depth* is the average depth fished by each License on a particular day, *Octopus* and *Lobster* are the respective daily catches/license, and *Soak-time* is the number of days that the traps remained in the water since the previous trap-lift.

The interaction terms *License*×*Year* and *License*×*Month* account for variations in the catch characteristics of the individual licenses over time that result from changes in fishing practises and efficiency associated with different boats, license holders, and skippers. The interaction terms *Year*×*Month* and *Year*×*MFA* account for variation in the population dynamics of octopus and lobster over time in different locations that could result in differential trends in lobster mortality. The interaction terms *Soak-time*×*Year* and *Soak-time*×*Month* reflects the change in general fishing strategies over time. In quota-managed fisheries the average soak-time will be affected by a number of factors, for example, that may include price, weather, and the fishermen's perceived ability to catch their quota.

The analysis was run separately for the SZ (n=493,629 traps) and NZ (n=155,628 traps) because the respective zones have different fishing seasons and management structures. The relationship between the number of dead lobsters and the factors depth, soak-time,and number of octopuses and lobsters were presented graphically by the equation:

$$\textit{Lobsters killed in traps} \propto \textit{factor}^{-\alpha},$$

where α = the parameter estimated by use of the model.

Source of lobster mortality and size-dependent mortality

A sampling program was conducted on three commercial vessels from the SZ during the 2001–02 fishing season. Five days were spent on each vessel. All lobsters caught were measured (carapace length, mm), and the sex (male or female), maturity (mature or immature), status (dead or alive), and cause of death (octopus or other) were recorded.

The method used to distinguish between lobsters killed by octopus or other means followed that of Joll.[1] This suitability of this approach was confirmed through examination of the carcasses of over one hundred lobsters killed by octopus in aquarium trials (Brock et al.[4]). Lobsters with shells that were partly or completely separated at the juncture between abdomen and cephalothorax but were otherwise undamaged were deemed to have been killed by octopuses, whereas lobsters with shells without this separation and with evidence of bite marks were deemed to have been eaten by other predators (fish or cuttlefish).

Anecdotal evidence from fishermen suggests that larger lobsters are more susceptible to predation than smaller ones. The effect of CL on the probability of mortality was examined separately for males and females by generalized linear modeling. The probability of mortality at a given size was modeled with a logistic equation of the form:

$$P(sex,\ CL) = 1/(1+e^{-(a+bCL)}),$$

where P(sex, CL) = the probability of a lobster of a given sex at carapace length CL being dead; and
a and b are parameters to be estimated.

Results

Estimation of total lobster catch, octopus bycatch, and lobster mortality

In 1999, there were 1.6 million trap-lifts in the SARLF, and 70% of this total effort was in the SZ (Fig. 2). The number of traps-lifts in the SZ declined from 2.2 million in 1983 to 1.2 million in 1999 (Fig. 2A). In contrast, fishing effort in the NZ remained relatively consistent with 406,000 trap-lifts in 1983 and 480, 000 trap-lifts in 1999 (Fig 2B).

The total annual lobster catch has generally increased in each fishing zone since 1983 (Fig. 2, A and B).

[4] Brock, D. J., T. M. Saunders, and T. M. Ward. In review. A two-chambered trap with potential for reducing within-trap predation by octopus on rock lobster. Can. J. Fish. Aquat. Sci., 19 p. [Available from SARDI Aquatic Science, 2 Hamra Avenue, West Beach, South Australia 5022.]

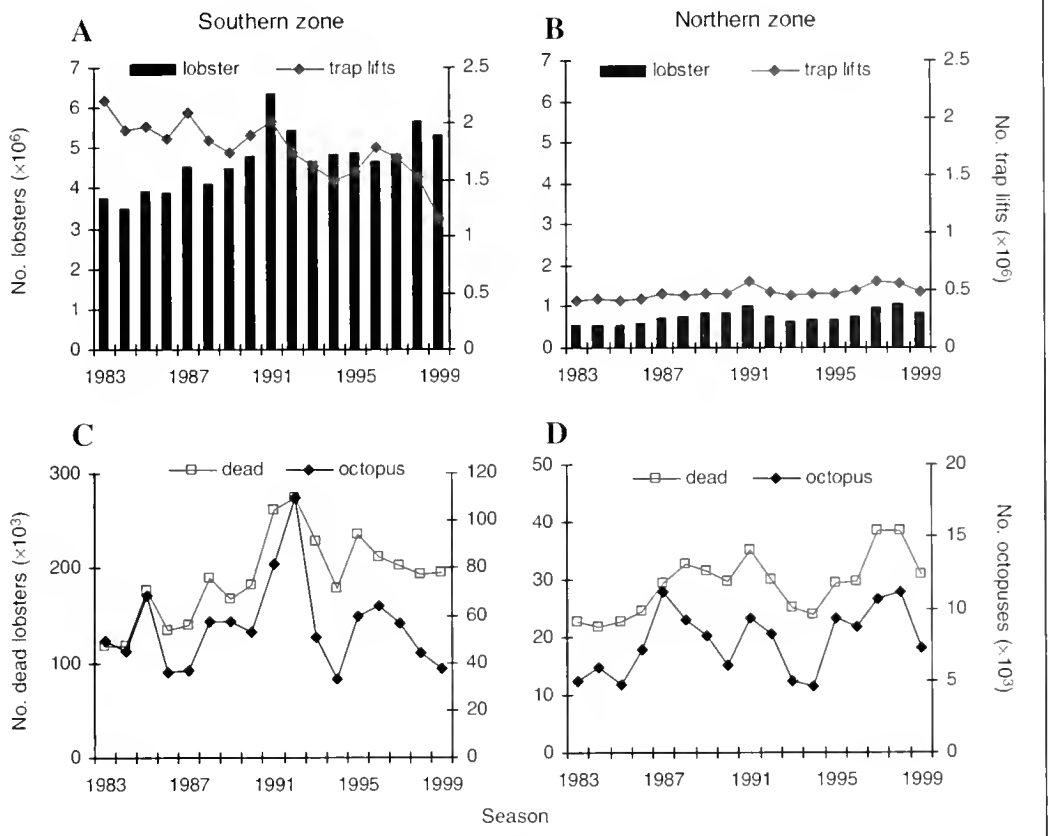

Figure 2

Annual total catch and effort for each zone of the South Australian rock lobster fishery for number of live lobsters caught (**A**), number of trap-lifts used (**B**), number of dead lobsters caught (**C**), and number of octopuses caught (**D**) (Note: change of scale in D).

In the SZ, the annual lobster catch rose from 3.8 million lobsters to a peak of 6.4 million lobsters in 1991 and was 5.4 million lobsters in 1999 (Fig. 2A). In the NZ, 560,000 lobsters were taken in 1983 compared to 850,000 in 1991 (Fig. 2B).

The total annual octopus catch varied among years in both zones, but between 70% and 90% of the total octopus catch were landed in the SZ (Fig. 2). The total number of octopus ranged from 36,000 in 1986 to 109,000 in 1992 (Fig. 2C) in the SZ, and from 4700 octopuses in 1985 to 11,200 in 1998 in the NZ (Fig. 2D).

In 1999, over 226,000 lobsters were killed in traps in the SARLF (Fig. 2). Since 1983, the mean proportion of dead lobsters out of the total catch has been approximately 4%. In the SZ, the number of lobsters killed in traps has generally increased from 118,000 in 1983 to 196,000 in 1999; a peak of 274,000 dead lobsters occurred in 1992 (Fig. 2C). In the NZ, there has also been a general increase in the number of lobster killed in traps each year; 24,000 dead lobsters were recorded in 1983, compared to 31,000 in 1999 and a peak of 39,000 dead lobsters recorded in 1998 (Fig. 2D).

Interannual and seasonal patterns in $CPUE_L$, $CPUE_O$, and M_L

Southern zone Mean annual $CPUE_L$ in the SZ increased from 175 to 466 lobsters/(100 trap-lifts/day) between 1983 and 1999, and the largest increase occurred between 1997 and 1999 (Fig. 3A). Mean annual $CPUE_O$ ranged from 1.8 to 6.2 octopus/(100 trap-lifts/day) in 1987 and 1992, respectively (Fig. 3C). Mean annual M_L rose from 5 to 17 dead lobster/(100 trap-lifts/day) between 1983 and 1999 (Fig. 3E). Peaks in both $CPUE_O$ and M_L occurred in 1985, 1992, and 1995.

Mean monthly $CPUE_L$ declined during the fishing season from 310 to 164 lobster/(100 trap-lifts/day) between October and April (Fig. 4A). In contrast, mean monthly $CPUE_O$ increased from 2.6 to 3.7 octopus/(100 trap-lifts/day) between October and December and declined to 1.8 octopus/(100 trap-lifts/day) in April (Fig. 4C). Similarly mean monthly M_L increased from 10.7 to 12.8 dead lobster/(100 trap-lifts/day) between October and November and declined to 6.7 dead lobster/(100 trap-lifts/day) in April (Fig. 4E).

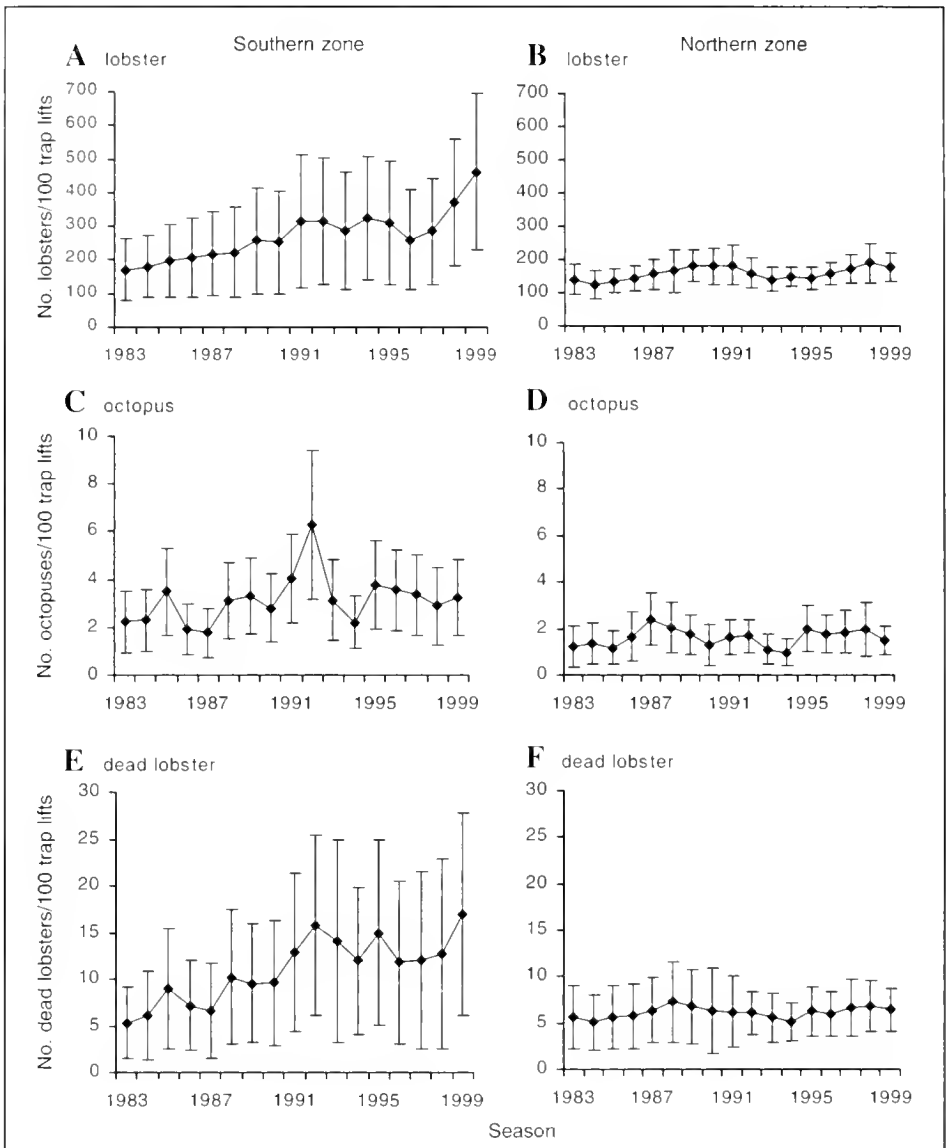

Figure 3

Annual catch rates in each fishing zone for lobsters ($CPUE_L$) (**A** and **B**), octopus ($CPUE_O$) (**C** and **D**), and dead lobsters (M_L) (**E** and **F**). Error bars are ±SD of mean.

Since 1983, mean annual $CPUE_L$ has increased in all MFAs, and has been consistently higher in MFAs 56 and 58 than in other areas (Fig. 5A). $CPUE_O$ has varied among years but has followed similar trends in different MFAs with consistent peaks in 1993 (Fig 5C). Prior to 1992, M_L was similar among MFAs but after 1992 was generally highest in MFAs 56 and 58 (Fig. 5E). M_L has increased over time in all MFAs.

Northern zone In the NZ, mean annual $CPUE_L$ rose from 135 to 179 lobsters/(100 trap-lifts/day) between 1983 and 1991, decreased to 138 lobsters/(100 trap-lifts/day) in 1993 and then rose again to 177 lobsters/(100 trap-lifts/day) in 1999 (Fig 3B). $CPUE_O$ ranged between 1.0 and 2.4 octopus/(100 trap-lifts/day) in 1987 and 1993 respectively (Fig. 3D). M_L ranged from 5.0 to 7.3 dead lobsters/(100 trap-lifts/day) in 1983 and 1988, respectively (Fig. 3F).

Mean monthly $CPUE_L$ declined from 196 to 88 lobster/100 trap-lifts/day between November and May (Fig. 4B). Mean monthly $CPUE_O$ was reasonably constant at between 1.43 and 1.7 octopus/100 trap-lifts/day for the first five months of the season before a decline to 1.0 octopus/100 trap-lifts/day in May (Fig. 4D). The mean monthly M_L declined from 7.5 to 3.4 dead lobster/100 trap-lifts/day between November and May (Fig. 4F).

Since 1983, mean annual $CPUE_L$ has been relatively low and stable in MFAs 15, 28, and 40 but has been

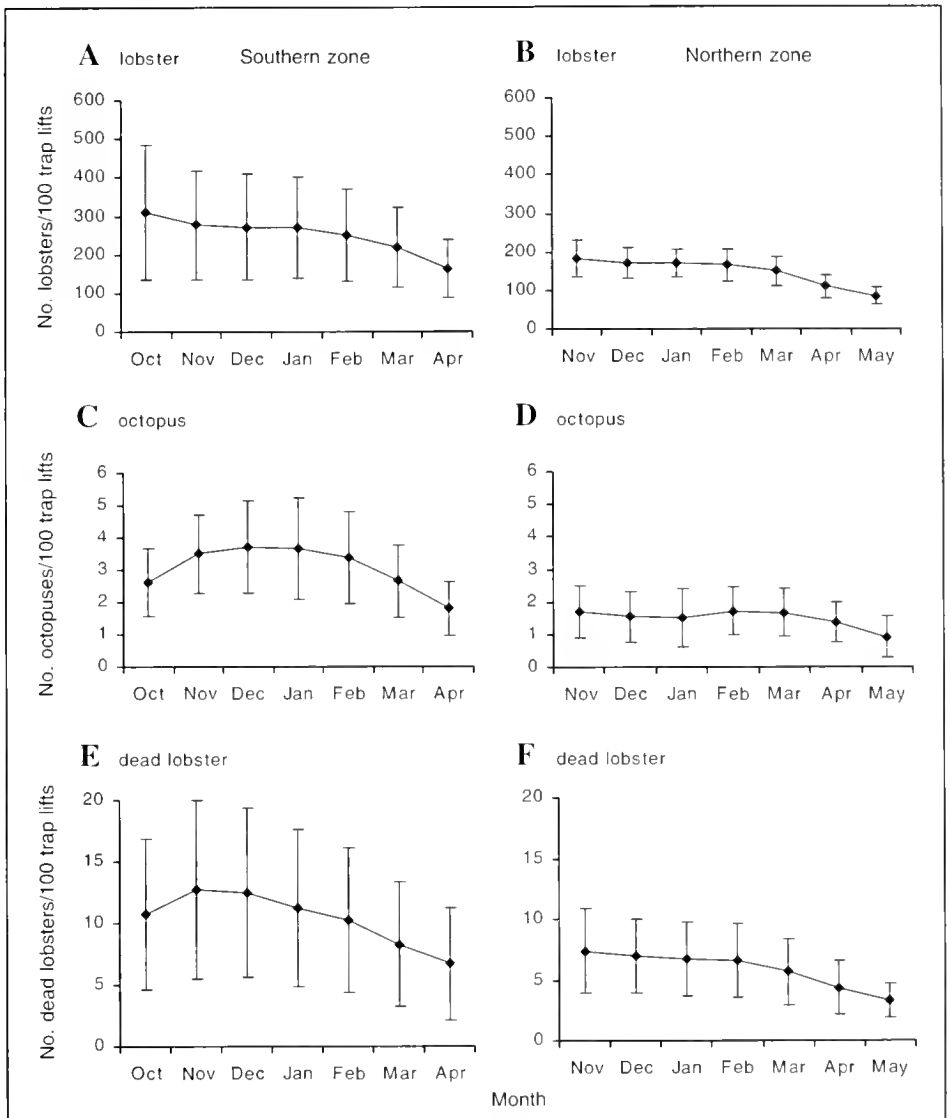

Figure 4

Mean monthly catch rates in each fishing zone for lobsters ($CPUE_L$) (**A** and **B**), octopus ($CPUE_O$) (**C** and **D**), and dead lobsters (M_L) (**E** and **F**). Error bars are ±SD of mean.

higher and more variable in MFAs 39 and 49 (Fig. 5B). There were large interannual fluctuations in $CPUE_O$ in each MFA, and these trends were similar among MFAs (Fig. 5D). M_L was highest in MFA 40, where a maximum of 12.5 dead lobsters/(100 traps lifts) was recorded 1998 and lowest in MFA 15 where the maximum was 5.2 dead lobsters/100 trap-lifts in 1997 (Fig. 5F). No clear long-term trends in M_L were apparent in any MFA.

Factors that affect within-trap lobster mortality

Based on the mean square values, the number of octopus had the greatest effect on lobster mortality in both zones (Table 1, A and B). The number of dead lobsters increased with both octopus and lobster catches and with soak-time and decreased as depth increased (Figs. 6 and 7). Based on the relative size of the mean square values, the factor with the greatest effect on the number of dead lobsters in the SZ was the number of octopus caught, followed by soak-time, number of lobsters caught, and depth. In the NZ, the number of octopus caught was also the most important factor, followed by the number of lobsters caught, depth, and soak-time.

Source of lobster mortality and size-dependent mortality

A total of 3627 lobsters from 635 trap-lifts were measured. In the sample there were 212 lobsters killed in traps of which 207 (98%) were killed by octopus and 5

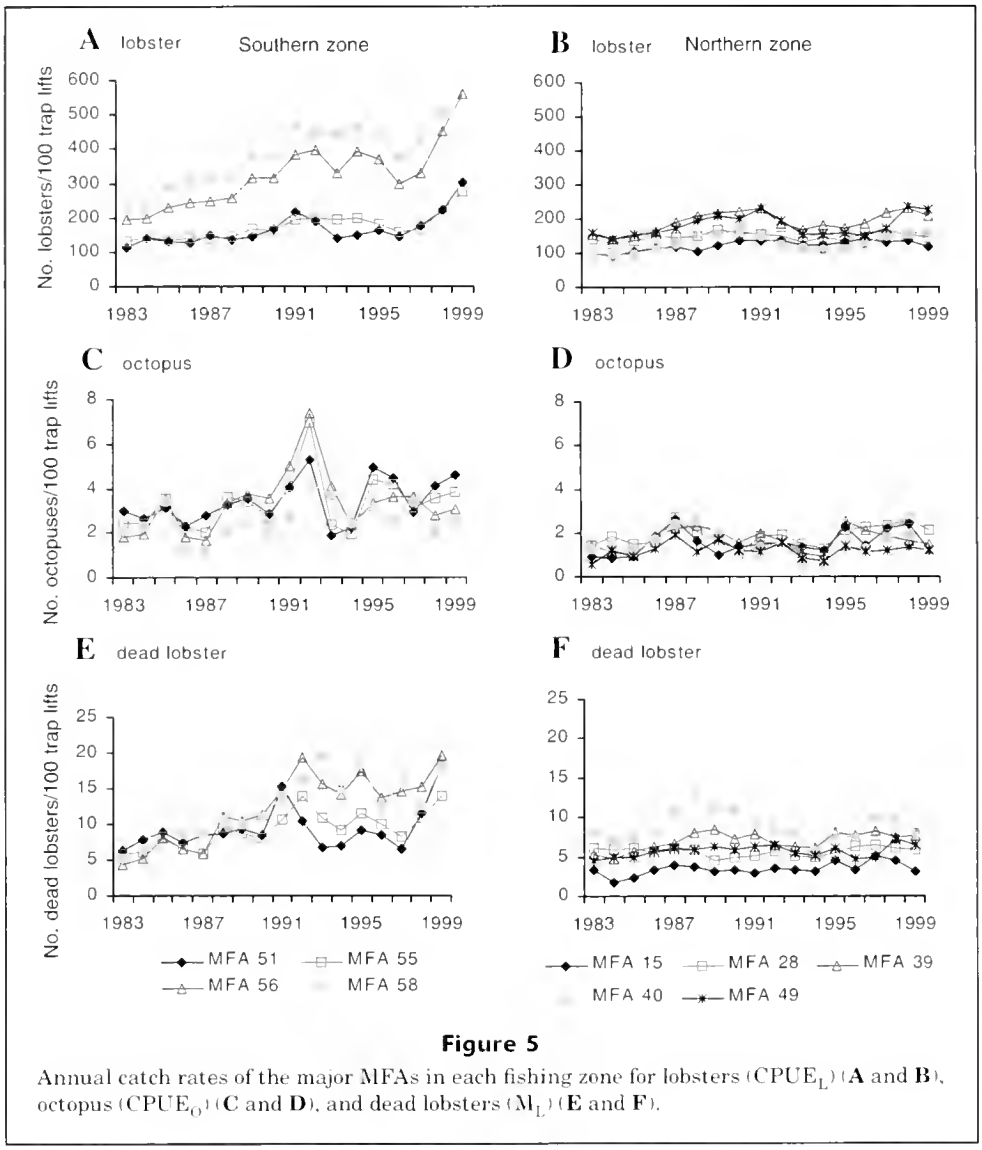

Figure 5

Annual catch rates of the major MFAs in each fishing zone for lobsters ($CPUE_L$) (**A** and **B**), octopus ($CPUE_O$) (**C** and **D**), and dead lobsters (M_L) (**E** and **F**).

by other predators. The mean CL of dead male lobsters was greater than live males (120 ±21.1(SD) vs. 110 ±18.3 (SD) mm, $P<0.001$). There was no significant difference in the mean size of live and dead female lobsters. For both sexes the probability of mortality increased with size according to the following relationships:

$$P(M_L, \text{males}) = 1/1+e^{-(-5.04+0.02CL)}$$
$$P(M_L, \text{females}) = 1/1+e^{-(-4.18+0.01CL)}.$$

Above 100 mm CL, the probability of mortality increased more sharply for male lobsters than for female lobsters (Fig. 8).

Discussion

Logbook data from the SARLF show that over the last five years approximately 240,000 lobsters have been killed in traps each year. Although there are numerous predators of trapped lobsters—such as seals, conger eels, and several species of finfish—the impacts of these taxa appear to be minor compared to the effects of predation by *O. maorum*. The field-sampling program conducted in the SZ in 2001–02 suggested that over 98% of within-trap mortality was attributable to *O. maorum*. Although the sampling program was spatially and temporally restricted, this finding, in conjunction with the strong correlations between annual, seasonal and spatial trends in the $CPUE_O$ and M_L, clearly demonstrates that *O. maorum* is the major predator of lobsters in SARLF traps.

The results of this study suggest that about 4% of the total annual catch of the SARLF is lost to predation by *O. maorum* in traps. Mortality rates attributable to octopuses in other Australian lobster fisheries range from 1% in the Western Australian fishery for *Panulirus cygnus*[1] (*O. tetricus*) to 5% in the Tasmanian fishery for

Table 1

Results of the general linear model of factors that affect lobster mortality (all data log transformed) for (**A**) southern zone (r^2=0.62), (**B**) northern zone (r^2=0.38).

A

Source	df	Squares	Mean square	*F*-value	*P*>*F*
Model	5319	314,536	59.13	147.41	<0.0001
Error	483,961	194,140	0.401		
Corrected total	489,280	508,677			

Source	df	Type-3 SS	Mean square	*F*-value	*P*>*F*
License	245	49158.1	200.6	500.2	<0.0001
MFA	3	9.6	3.2	8.0	<0.0001
Year	17	2494.6	146.7	365.8	<0.0001
MFA×Year	51	233.0	4.7	11.6	<0.0001
Month	6	2830.7	471.8	1176.1	<0.0001
Effort	1	229.6	229.6	572.4	<0.0001
Lobster catch	1	6728.7	6728.7	16773.4	<0.0001
Depth	1	1335.0	1335.0	3327.9	<0.0001
Octopus	1	35930.5	35930.5	89568.8	<0.0001
Soak-time	1	6842.1	6842.1	17056.1	<0.0001
Soak-time×Year	17	286.9	16.9	42.1	<0.0001
License×Year	3415	53019.8	15.5	38.7	<0.0001
License×Month	1460	5900.2	4.0	10.1	<0.0001
Year×Month	94	3760.4	40.0	99.7	<0.0001
Soak-time×Month	6	310.2	51.7	128.9	<0.0001

B

Source	df	Squares	Mean square	*F*-value	*P*>*F*
Model	2159	39,217	18.17	41.75	<0.0001
Error	148,731	64,713	0.435		
Corrected total	150,890	103,931			

Source	df	Type-3 SS	Mean square	*F*-value	*P*>*F*
License	95	3361.5	35.4	81.3	<0.0001
MFA	4	174.8	43.7	100.4	<0.0001
Year	17	241.2	14.2	32.6	<0.0001
MFA×Year	68	175.4	2.6	5.9	<0.0001
Month	7	317.3	45.3	104.2	<0.0001
Effort	1	27.1	27.1	62.3	<0.0001
Lobster catch	1	1299.7	1299.7	2987.2	<0.0001
Depth	1	391.3	391.3	899.3	<0.0001
Octopus	1	6305.1	6305.1	14491.0	<0.0001
Soak-time	1	210.8	210.8	484.4	<0.0001
Soak-time×Year	17	117.7	6.9	15.9	<0.0001
License×Year	1287	7275.6	5.7	13.0	<0.0001
License×Month	553	1170.7	2.1	4.9	<0.0001
Year×Month	95	275.9	2.9	6.7	<0.0001
Soak-time×Month	6	2.8	0.5	1.1	0.3743

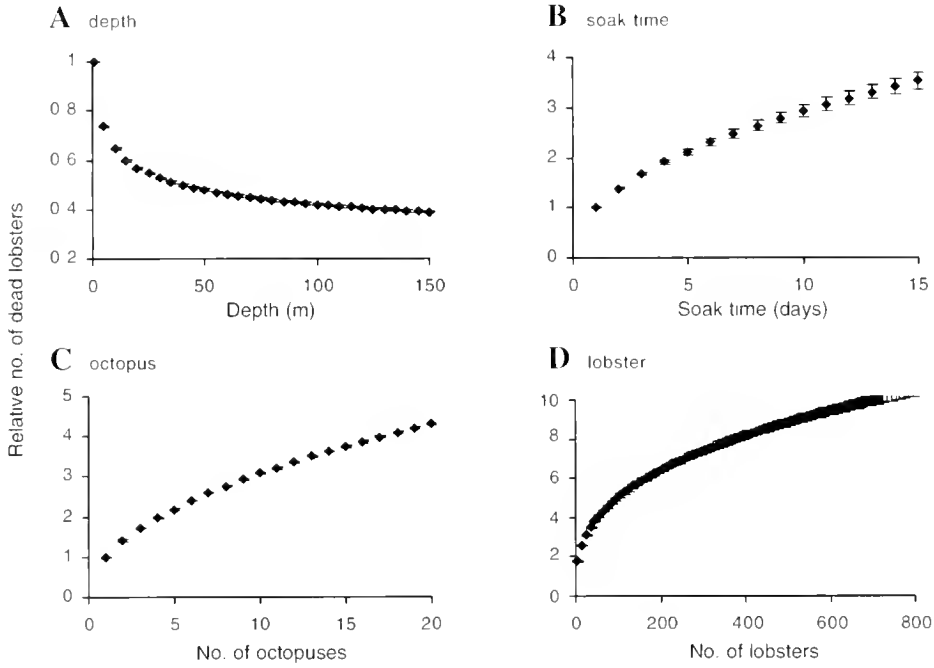

Figure 6

The relative number of dead lobster as a function of (**A**) depth, (**B**) soak-time, (**C**) number of octopus, and (**D**) no. of lobsters for the southern zone. Error bars are ±SD of mean.

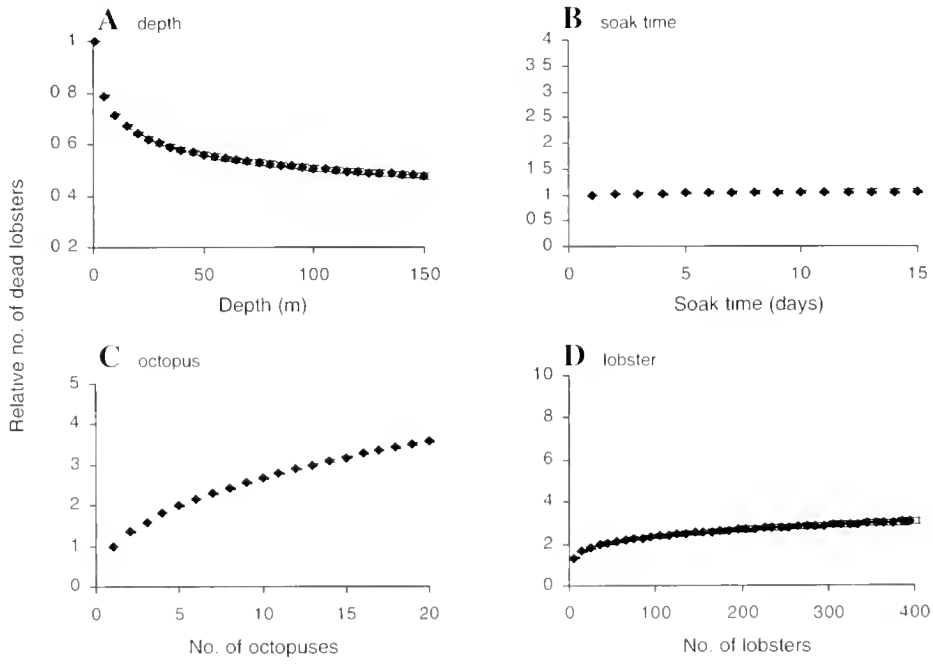

Figure 7

The relative number of dead lobster as a function of (**A**) depth, (**B**) soak-time, (**C**) number of octopus, and (**D**) number of lobsters for the northern zone. Error bars are ± SD of mean.

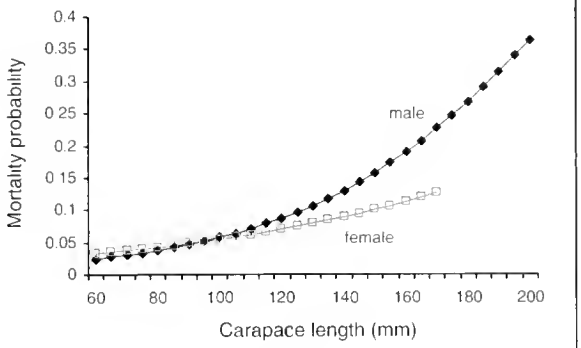

Figure 8

Size-dependent mortality of lobsters with respect to sex.

J. edwardsii (*O. maorum*), (Gardener[5]), and a localized study in the New Zealand fisheries for *J. edwardsii* (*O. maorum*) found the proportion of the lobster catch killed by octopus to be as high as 10% (Ritchie[6]). The estimates of lobster mortality from these other studies should be treated with caution however because the current study is the only one that documents within-trap lobster mortality from a fishery-wide data set.

The general linear modeling approach that we used to determine the factors associated with M_L has some limitations. For example, the logbook data for the SARLF, like the monitoring data for most other fisheries, are not completely independent, and interdependence among observations can bias estimates of parameters. Similarly, some of the factors in the model, notably $CPUE_L$ and $CPUE_O$ are partially correlated. In addition, the large number of observations and degrees of freedom tend to make most factors significant. We considered all of these issues when interpreting the results of the analyses and used the mean square (MS) values to rank the importance of factors.

In both zones, inter- and intra-annual fluctuations in M_L largely reflect the effects of $CPUE_O$ and $CPUE_L$. The broad trends in annual $CPUE_O$ have largely corresponded to those for M_L with peaks in both generally synchronous in both fishing zones. In the SZ, the general increase in M_L since 1983 appears to result from the increase in $CPUE_L$, which has more than doubled over this period. This assessment is supported by catch-rate data from individual MFAs. The two MFAs in the SZ that have had the greatest increases in $CPUE_L$ over the last 5 years (56 and 58) have also had the highest corresponding increase in M_L. Increases in $CPUE_L$ are likely to elevate M_L by both increasing the probability of octopus encountering traps containing lobsters and the number of lobsters in traps entered by octopus.

However, M_L is also positively correlated with soak-time, especially in the SZ. This finding is consistent with patterns observed in the New Zealand fishery for *J. edwardsii*[6] and reflects the increased opportunities for octopus predation when pots containing lobsters remain in the water for longer periods. In the SZ, fishermen return to port each day and choose to fish or not to fish each day according to factors such as weather and price; therefore, although a 24-h soak period is still most common, soak times can range from one to five days. In the NZ, fishermen remain at sea for extended periods and consequently soak times longer than 24 hours are rare.

There was considerable variation in the fishery data, especially in the southern zone. It is likely that much of this variation is related to the large geographical extent of the fishery as opposed to fishing practises. Across the fishery lobster growth rates and subsequent catch rates vary greatly (McGarvey et al., 1999a). For example, since 1991, the $CPUE_L$ in MFAs 56 and 58 have been twice those of MFAs 51 and 55 in the SZ. Although the variation in $CPUE_O$ between the zones has been similar, the higher variability in $CPUE_L$ in the SZ is reflected in the variation in M_L.

Data spanning 17 years and covering about 50,000 km^2 represent one of the few long-term and large-scale data sets on the distribution and abundance of an octopus species (Hernandez-Garcia et al., 1998; Quetglas et al., 1998). The paucity of octopus studies on these scales reflects the logistical constraints of fishery-independent surveys of octopus populations and the poor and inconsistent methods generally used to record fishery catch and effort data (Boyle and Boletsky, 1996). The few data that are available on the distribution patterns of octopus have been obtained mainly from small commercial fisheries and $CPUE_O$ has been included as a measure of relative abundance (Defeo and Castilla, 1998; Hernandez-Garcia et al., 1998). This approach has proven useful, but several potential biases must be considered when $CPUE_O$ data are being interpreted: these include 1) changes in fishing methods and efficiency over time; 2) the distribution pattern (e.g., random or aggregated) of the species under consideration; and 3) spatiotemporal fluctuations in catchability (Richards and Schnute, 1986; Rose and Kulka, 1999). There are several reasons why the data from the SARLF may provide a useful measure of the relative abundance of octopus over these spatial and temporal scales. Most importantly, the basic unit of effort in the fishery, the trap, has remained unchanged since 1983. Furthermore, although *O. maorum* is retained as bycatch and kills *J. edwardsii* in traps, it is neither targeted nor avoided by fishermen, and fishing effort is thus relatively independent of its distribution patterns because the economic effects of both the sale of octopus bycatch and the costs of lobster predation are relatively small compared to the primary

[5] Gardener, C. 2002. Personal commun. Tasmanian Aquaculture and Fisheries Institute, Private Bag 49, Hobart, Tasmania 7001.

[6] Ritchie, L. D. 1972. Octopus predation on trap-caught rock lobster—Hokianga area, N.Z. September–October 1972. New Zealand Marine Department. Fisheries Technical Report 81, 40 p. [Available from Ministry of Fisheries, 101–103 The Terrace, Wellington, New Zealand, 1020.]

economic driving force for the fishery, the lobster catch rates, and because the catch rates of octopus are difficult to predict. In addition, *O. maorum* is a solitary animal that tends to be dispersed randomly throughout areas of suitable habitat (Mather et al., 1985).

The higher total catches and catch rates of both lobster and octopus in the SZ, compared to the NZ, probably reflect the more extensive reef habitat and more intense nutrient-enrichment upwelling in this portion of the SARLF (Lewis, 1981). There have been large interannual fluctuations in $CPUE_O$ in both zones since 1983. Such fluctuations in population size are common among other cephalopods, especially squid, and may result from life history strategies that are characterized by rapid growth, short lifespan (<two years) and almost universal mortality after a single spawning event (Boyle and Boletsky, 1996). Despite these fluctuations, $CPUE_O$ has not declined noticeably in any MFA since 1983, which suggests that octopus mortality from fishing is consistent with little impact on octopus populations since the advent of fishing. This observation and the poor relationship between octopus catches and effort refute the belief of some SARLF fishermen that incidental fishing mortality acts to control octopus abundance.

This study, however, did confirm the view of fishermen that larger lobsters are killed more commonly by octopus than are smaller ones. This effect was most evident for male lobsters, which grow to larger sizes than females. There could be several reasons for the size-dependent mortality rates for rock lobsters. For example, octopus could actively select larger prey, or large lobsters could be captured more easily than small lobsters in traps by octopus. Because large lobsters can be worth more and produce more eggs than smaller lobsters, the increased mortality rates of large lobsters suggest that the total economic and ecological impacts of octopus predation in the SARLF are greater than indicated by the absolute number of lobsters killed.

Octopus predation of lobsters in traps is a significant problem in the SARLF. However, the economic effects vary between the zones. In the quota-managed SZ, additional lobsters are harvested to replace those killed in traps, which increases the time and costs of catch quotas, and imposes an impact on lobster abundance. In the input-controlled NZ, where there is no direct restriction on the quantity of lobsters taken, lobsters killed in traps represent both a direct economic loss and an impact on lobster abundance.

Like most fisheries for spiny lobsters, the SARLF is close to being fully exploited. Reducing rates of octopus predation provides one option available for increasing the value of the fishery. Some minor reductions in lobster mortality may be achieved by minimizing soak-times, especially in the SZ. More significant reductions in the rates of within-trap lobster mortality may be achieved by redesigning lobster traps (Brock et al.[4]).

Acknowledgments

This research was funded jointly by the Fisheries Research and Development Corporation, South Australian Rock Lobster Advisory Council, South Australian Research and Development Institute (Aquatic Sciences), and the University of Adelaide. The authors thank Thor Saunders for his support and assistance during the research. Jim Prescott provided advice for extracting data from the South Australian Rock Lobster Database. Yongshun Xiao provided statistical advice and assisted with the numerical modeling.

Literature cited

Boyle, R. F., and S. V. Boletsky.
1996. Cephalopod populations: definition and dynamics. Phil. Trans. R. Soc. Lond. 351:985–1002.

Defeo, O., and J. C. Castilla.
1998. Harvesting and economic patterns in the artisanal *Octopus mimus* (Cephalopoda) fishery in a northern Chile cove. Fish. Res. 38:121–130.

Hernandez-Garcia, V., J. L. Hernandez-Lopez, and J. J. Castro.
1998. The octopus (*Octopus vulgaris*) in the small-scale trap fishery off the Canary Islands (Central-East Atlantic). Fish. Res. 35:183–189.

Lewis, R. K.
1981. Seasonal upwelling along the south-eastern coastline of South Australia. Aust. J. Mar. Freshw. Res. 32:843–854.

Mather, J. A., S. Resler, and J. Cosgrove.
1985. Activity and movement patterns of *Octopus dofleini*. Mar. Behav. Physiol. 11:301–314.

McGarvey, R., G. Ferguson, and J. H. Prescott.
1999a. Spatial variation in mean growth rates of rock lobster, *Jasus edwardsii*, in South Australian waters. Mar. Freshw. Res. 50:333–342.

Phillips, B. F., J. S. Cobb, and J. Kittaka.
1994. Spiny lobster management, 550 p. Blackwell Scientific, London.

Quetglas, A., F. Alemany, A. Carbonell, P. Merella, and P. Sanchez.
1998. Biology and fishery of *Octopus vulgaris* Cuvier, 1797, caught by trawlers in Mallorca (Balearic Sea, Western Mediterranean). Fish. Res. 36:237–249.

Richards, L. J., and L. J. Schnute.
1986. An experimental and statistical approach to the question: Is CPUE an index of abundance? Can. J. Fish. Aquat. Sci. 43:1214–1227.

Rose, G. A., and D. W. Kulka.
1999. Hyperaggregation of fish and fisheries: how catch-per-unit-effort increased as the northern cod (*Gadus morhua*) declined. Can. J. Fish. Aquat. Sci. 56(suppl. 1):118–127.

Williams, A. B.
1988. Lobsters of the world—an illustrated guide, 186 p. Osprey Books, New York, NY.

Small-boat surveys for coastal dolphins: line-transect surveys for Hector's dolphins (*Cephalorhynchus hectori*)

Stephen Dawson[1]
Elisabeth Slooten[2]
Sam DuFresne[1]
Paul Wade[3]
Deanna Clement[2]

[1] Department of Marine Science
University of Otago
340 Castle Street
Dunedin, New Zealand
E-mail address: steve.dawson@stonebow.otago.ac.nz

[2] Zoology Department
University of Otago
340 Castle Street
Dunedin, New Zealand

[3] National Marine Mammal Laboratory
National Marine Fisheries Service
7600 Sand Point Way NE
Seattle, Washington 98115

Abstract—Management of coastal species of small cetaceans is often impeded by a lack of robust estimates of their abundance. In the Austral summers of 1997–98, 1998–99, and 1999–2000 we conducted line-transect surveys of Hector's dolphin (*Cephalorhynchus hectori*) abundance off the north, east, and south coasts of the South Island of New Zealand. Survey methods were modified for the use of a 15-m sailing catamaran, which was equipped with a collapsible sighting platform giving observers an eye-height of 6 m. Eighty-six percent of 2061 km of survey effort was allocated to inshore waters (4 nautical miles [nmi] or 7.4 km from shore), and the remainder to offshore waters (4–10 nmi or 7.4–18.5 km from shore). Transects were placed at 45° to the shore and spaced apart by 1, 2, 4, or 8 nmi according to pre-existing data on dolphin density. Survey effort within strata was uniform. Detection functions for sheltered waters and open coasts were fitted separately for each survey. The effect of attraction of dolphins to the survey vessel and the fraction of dolphins missed on the trackline were assessed with simultaneous boat and helicopter surveys in January 1999. Hector's dolphin abundance in the coastal zone to 4 nmi offshore was calculated at 1880 individuals (CV=15.7%, log-normal 95% CI=1384–2554). These surveys are the first line-transect surveys for cetaceans in New Zealand's coastal waters.

Manuscript submitted 27 April 2003 to Scientific Editor's Office.

Manuscript approved for publication 3 March 2004 by the Scientific Editor.

Fish. Bull. 201:441–451 (2004).

Several international workshops on cetacean bycatch problems have stated that a key impediment to the conservation of coastal and riverine small cetaceans is the lack of quantitative data on abundance (e.g., IWC, 1994). An important reason for this lack of data is that line-transect surveys are often conducted from large (>50 m) vessels (e.g. Barlow, 1988) and hence are extremely expensive ($US 10,000/day). Such costs usually put high-quality surveys such as those conducted for harbor porpoise in the U.S. (e.g., Carretta et al., 2001) beyond the reach of less affluent nations. The need for abundance estimates is especially great for the coastal and riverine species found in Asia, Africa, Australasia, and South America (Table 1). Several of these species have apparently small populations and restricted distributions, and all suffer from being taken as bycatch in fishing gear, principally in gill nets (IWC, 1994). In addition, it is difficult or impossible for large vessels to work close to shore, in shallow waters, where some of these species are most common.

The work described in this contribution had two aims: 1) to adapt ship-based line-transect methods (e.g., Barlow, 1988) to a 15-m catamaran, and 2) to provide an updated estimate of the abundance of Hector's dolphin (*Cephalorhynchus hectori*). Hector's dolphin, a small delphinid found only in the inshore waters of New Zealand, is subject to bycatch in gill nets throughout its range (Dawson et al., 2001). At least in the Canterbury region, and off the North Island west coast, recent catch levels are clearly unsustainable (Dawson and Slooten, 1993; Martien et al., 1999; Slooten et al., 2000; Dawson et al., 2001). Studies of mt-DNA indicate that the very small North Island population is distinct and that there are at least three separate populations in South Island waters (Pichler et al., 1998; Pichler and Baker, 2000; see also Baker et al., 2002). At the time of the present study the only quantitative population estimate was from a strip-transect survey conducted in 1984–85 (Dawson and Slooten, 1988), in which the offshore distribution, as well as the

proportion of dolphins detected within the strip, was estimated. A current, more robust estimate is needed for management. This study describes line-transect boat surveys conducted to estimate Hector's dolphin abundance on the north, east, and south coasts of the South Island of New Zealand.

Figure 1

Photograph of the observer platform on the catamaran *Catalyst*.

Materials and methods

Vessel choice and field methods

Displacement catamarans are inherently suitable for inshore surveys because of their resistance to rolling and their ability to sustain reasonably high cruising speeds with modest power. We based our surveys from a 15.3-m sailing catamaran (RV *Catalyst*), which is powered by two 50-hp diesel engines, and cruises at 9–10 knots while using <10 liters of fuel per hour. We fitted a collapsible aluminum sighting platform (~6 m eye height; Fig. 1) to increase the resolution with which observers could measure the downward angles to sightings (see Lerczak and Hobbs, 1998, for details) and to allow the observers to see animals farther away. The surveys were conducted with a crew of six (five observers, one skipper).

Three people stood on the platform at any given time; one scanned the surface waters to the right of the platform, and the other scanned to the left, and a third person (the recorder) recorded sightings dictated by the observers. Sightings made by the recorder were not used in our analyses because his or her sighting effort was unavoidably uneven (the recorder could not make sightings while recording another sighting). The recorder did not point out sightings to observers. Observers and data recorder rotated

Table 1

Examples of coastal and riverine species of special conservation concern.

Common name	Scientific name	Habitat
Vaquita	*Phocoena sinus*	Northern Gulf of California
Chilean dolphin	*Cephalorhynchus eutropia*	Inshore coastal Chile
Hector's dolphin	*Cephalorhynchus hectori*	Inshore coastal New Zealand
Commerson's dolphin	*Cephalorhynchus commersoni*	Inshore coastal Chile, Argentina, Falkland Is, Kerguelen Is.
Heaviside's dolphin	*Cephalorhynchus heavisidii*	Inshore coastal South Africa and Namibia
Peale's dolphin	*Lagenorhynchus australis*	Coastal Chile, Argentina, Falkland Is.
Finless porpoise	*Neophocoena phocaenoides*	Coastal and riverine Asia and Indonesia
Indo-Pacific humpbacked dolphins	*Sousa chinensis*	Inshore tropical and estuarine habitats in western Pacific and Indo Pacific
Burmeister's porpoise	*Phocoena spinipinnis*	Coastal Chile, Argentina, Uruguay, Brazil
Franciscana	*Pontoporia blainvillei*	Coastal Brazil and Argentina
Indus river dolphin	*Platanista minor*	Indus River
Ganges river dolphin	*Platanista gangetica*	Ganges, Bramaputra, Karnphuli, Meghna rivers
Boto	*Inia geoffrensis*	Amazon River
Tucuxi	*Sotalia fluviatilus*	Coastal and estuarine Atlantic Central and South America

every 30 minutes to avoid fatigue. Although Hector's dolphins are easily identified from other species, and group size is typically small (usually 2–8; Dawson and Slooten, 1988), in order to maintain even sighting effort on both sides of the trackline, observers did not confer during a sighting. Sighting information was entered into a custom-written program on a Hewlett-Packard 200LX palmtop computer on the sighting platform. Data recorded included horizontal sighting angle, downward angle to sighting (in reticles), species, group size, orientation of the animals when first sighted, depth, Beaufort sea state, swell height, glare, GPS fix, date, and time. The program also recorded survey effort by storing a GPS fix every 60 seconds. Weather conditions were recorded at the start of field effort, and whenever they changed.

Observers used reticle- and compass-equipped Fujinon 7×50 (WPC-XL) binoculars to make sightings and to measure the downward angle from the land, or horizon, to the sighting. If the former, the corresponding distance to land was measured with RADAR (Furuno 1720 model), or, if within a few hundred meters of shore, with a Bushnell lightspeed laser rangefinder (tested accuracy ±1 m from 12 to 800 m). We calibrated the accuracy of the RADAR by comparison with transit fixes and laser rangefinder measurements. Sighting angles were recorded by using angle boards (see Buckland et al., 1993) in the first season, and thereafter with the compasses in the binoculars. There were no ferrous metals or significant electrical fields within 6 m of the sighting platform.

Navigation was facilitated by the use of a Cetrek 343 GPS chartplotter with digitized C-MAP charts onto which transect waypoints were plotted. Depths were measured with a JRC JFV-850 echosounder (at 200 kHz).

At the start of each survey, several days were spent training observers at Banks Peninsula, where sighting rates are high. Training continued until we gained about 100 sightings (data gathered in this period were not used in the analyses). An observer manual (available from authors) specified scanning behavior and recording methods. To ensure a wide shoulder on the histograms of perpendicular sighting distances, observers were instructed to concentrate their effort within 45° of the trackline and to spend less time searching out to 90°. Observers spent about 85% of the time scanning with binoculars. Regular scans with the naked eye minimized fatigue and reduced the chance of missing groups close to the boat. To promote consistency, observers were asked to re-read the manual at least once a week throughout the survey.

While the survey was underway, exploratory data analyses were undertaken to assess data quality. These analyses showed that in the early stages of the first survey, observers were rounding angles of sightings close to the trackline to zero. The use of the angle boards was modified to minimize this problem, and they were not used in subsequent surveys. The data from these early lines were discarded and the survey lines repeated.

Survey effort was restricted to sea conditions of Beaufort 3 or less and swell heights of ≤2 meters. Transect lines were run down-swell and down-sun to minimize pitching and effects of glare. Deviations of up to 10° from the intended course were made if needed to further reduce pitching or glare. The inshore end of each line was surveyed to just outside the surf zone on open coasts, or until a 2 m depth was reached, or to within 50 m of rocky shores. All surveys were conducted in passing mode to minimize the extent of vessel attraction.

Line-transect data were collected in three surveys in three consecutive summer seasons, each focussing on a particular coastal area (Fig 2; Motunau to Timaru, 5 January–21 February 1998; Timaru to Long Point, 9 December 1998–16 February 1999; Farewell Spit to Motunau, 17 December 1999–28 January 2000).

Survey design

In order to obtain a clear picture of density and to minimize variance in encounter rate, Buckland et al. (1993) recommend placing transects across known density gradients. Because short-distance, alongshore movements are well-known for Hector's dolphins (Slooten and Dawson, 1994; Bräger et al., 2002) and the dolphins' density declines sharply with distance offshore (Dawson and Slooten, 1988), transects were placed at 45° to the coast. On curved coastlines (within strata) we divided the coastline into blocks, drew an imaginary baseline along the coast, and placed lines at 45° to that baseline. The starting point of the first line along the baseline was decided randomly; thereafter lines were spaced at regular intervals according to the sampling intensity required in that stratum (Fig. 2). Within harbors we placed lines at 45° to an imaginary line down the center of the harbor (Fig. 3). The aim of this scheme was to ensure that, within a stratum, any one point had the same chance of being sampled as any other.

Survey effort was stratified according to existing data on distribution, obvious habitat differences, and areas of intrinsic management interest. In summer, very few Hector's dolphins are seen beyond four nmi from shore (Dawson and Slooten, 1988); therefore most sampling effort was placed in this inshore zone (i.e. 45° lines at 2-, 4-, or 8-nmi spacings, approximately proportional to density as determined from previous surveys). Within harbors, transect spacings were either one or two nautical miles. In the offshore zone (from 4 to 10 nmi) we expected very low densities, and therefore used sparse transect spacing (~30 nmi apart). It was not our intention to estimate density in this offshore zone. A subsequent aerial survey was found to be better suited for this purpose (Rayment et al.[1]).

Our goal was to estimate effective half strip width (ESW) separately for strata with different exposure to wind and swell. Hence, in each survey we aimed to gain sufficient sightings to estimate ESW separately for harbors or protected waters, and open coasts. To reach

[1] Rayment, W., E. Slooten, and S. M. Dawson. 2003. Unpubl. data. Department of Marine Science, Univ. Otago, P.O. Box 56, Dunedin, New Zealand.

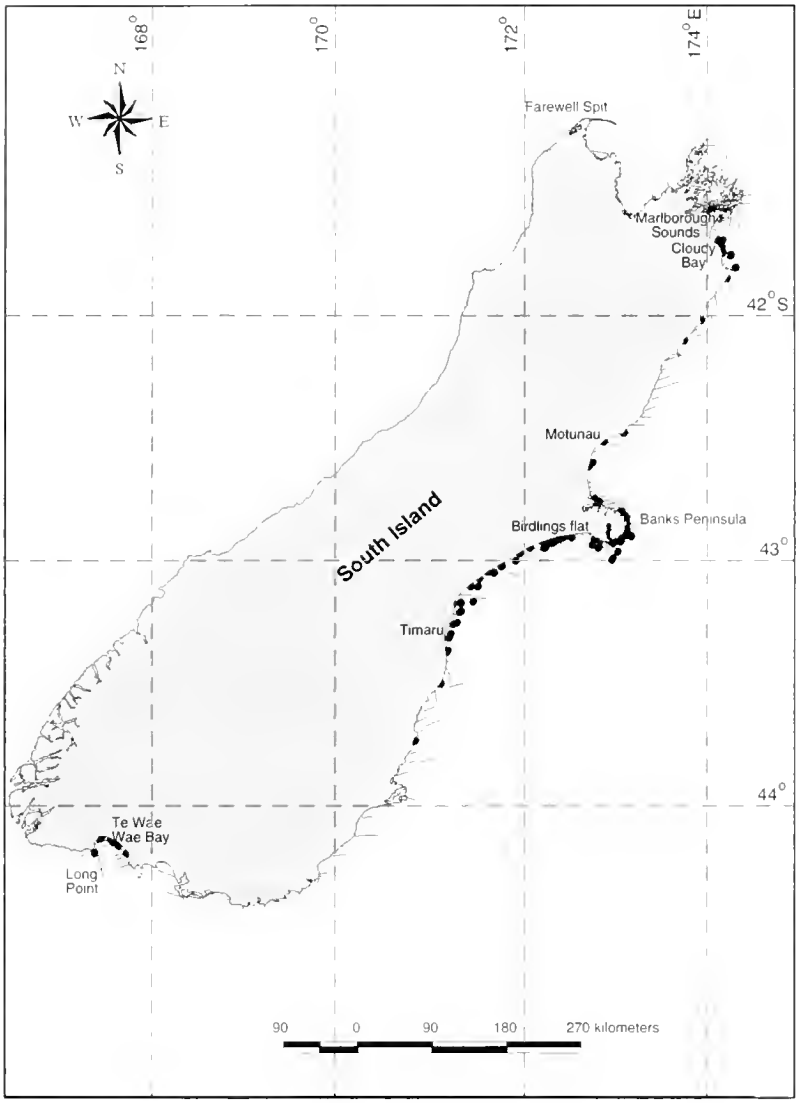

Figure 2

Map of New Zealand's South Island, showing transect lines and sightings of Hector's dophins (dots) 1997–2000.

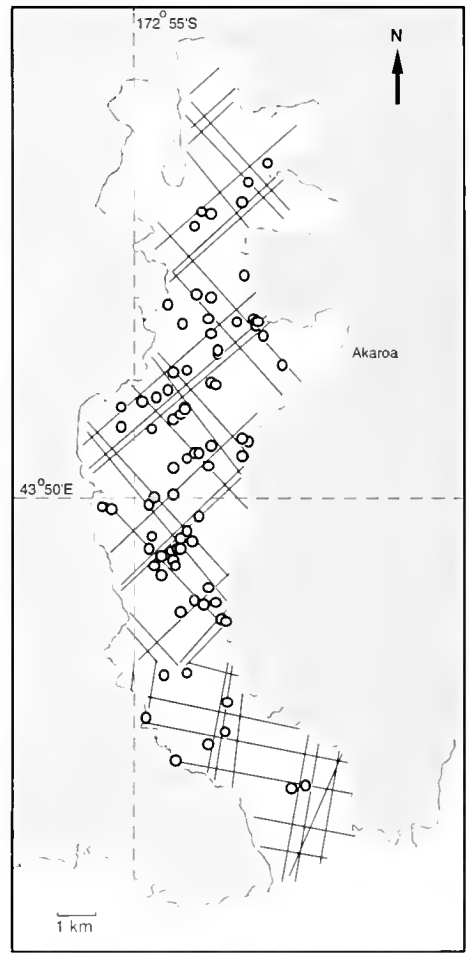

Figure 3

Example of transect layout in harbors (1997–98 Akaroa Harbor transect lines and sightings, showing three replicates).

Buckland et al.'s (1993) target of 60–80 detections for robust ESW estimation, in the 1997–98 survey we conducted replicate surveys (with a new set of lines each time) in the harbors and bays stratum (e.g., Fig. 3). Low sighting rates in the area surveyed in 1999–2000 would have required unrealistic effort levels to reach this target; therefore we gained extra sightings from areas with the same exposure but higher sighting rates (e.g., data used to calculate ESW for the Marlborough Sounds were supplemented by data gathered in Akaroa Harbour by the same observers, in the same summer). Hence different sample sizes were available to estimate density and ESW (Table 2). Because observers changed between surveys, we did not pool sightings across years for estimating ESW. Strata areas were measured from nautical charts with a digital planimeter.

Data analysis

Within each stratum, Hector's dolphin abundance (N_S) was estimated as (Buckland et al., 1993):

$$\hat{N}_S = \frac{AnS}{2LESW}, \quad (1)$$

where A = size of the study area;
n = number of groups seen;
S = expected group size;
L = length of transect line surveyed, and
ESW = the effective half strip width.

Because there was no significant relationship between group size and detection distance, expected group size was estimated as a simple mean group size.

Table 2

Survey effort by stratum. Number of sightings is the total number made before truncation and quality auditing (see "Vessel choice and field methods").

Survey zone	Stratum	Survey effort (km)	No. of sightings	Sightings per km
Motunau to Timaru (1997–98)	Banks Peninsula harbors and bays	223	89	0.399
	Banks Peninsula Marine Mammal Sanctuary (BPMMS) (excluding open coasts)	265	66	0.249
	<4 nmi offshore, to the north and south of BPMMS	174	21	0.121
	Offshore (4–10 nmi)	89	4	0.045
Timaru to Long Point (1998–99)	Timaru–Long Point (excluding Te Waewae Bay)	336	13	0.04
	Te Waewae Bay	101	14	0.14
	Offshore (4–10 nmi)	106	0	0
Motunau to Farewell Spit (1999–2000)	Farewell Spit–Stephens Island	120	0	0
	Marlborough Sounds (including Queen Charlotte Sound)	205	3	0.015
	Cape Koamaru–Port Underwood	68	0	0
	Cloudy Bay and Clifford Bay	89	13	0.146
	Cape Campbell–Motunau	192	5	0.026
	Offshore (4–10 nmi)	93	2	0.022

Using the program Distance 3.5 (Research Unit for Wildlife Population Assessment, University of St. Andrews, UK), we fitted detection functions to perpendicular distance data to estimate ESW (note that this value is derived directly from $f(0)$). Akaike's information criterion (AIC) was used to select among models fitted to the data. Models and adjustments were the following: hazard/cosine, hazard/polynomial, half-normal/hermite, half-normal/cosine, uniform/cosine (Buckland et al., 1993). Following Buckland et al. (1993), perpendicular sighting distances were truncated to eliminate the farthest 5% of sightings and binned manually for $f(0)$ estimation.

The coefficient of variation (CV) for the abundance estimate was calculated from the coefficients of variation of each variable element in Equation 1 above (Buckland et al., 1993):

$$CV(\hat{N}_s) = \sqrt{CV^2(n) + CV^2(S) + CV^2(ESW)}. \quad (2)$$

The $CV(n)$ was estimated empirically as recommended by Buckland et al. (1993):

$$CV(n) = \sqrt{\frac{\mathrm{var}(n)}{n^2}}, \quad (3)$$

where $$\mathrm{var}(n) = L\sum l_i (n_i / l_i - n/L)^2 / (k-1). \quad (4)$$

l_i = the length of transect line i;
n_i = the number of sightings on transect i; and
k = number of transect lines.

$CV(S)$ was estimated from the standard error of the mean group size. $CV(ESW)$ was estimated with the bootstrapping option in Distance 3.5 software. This process incorporates uncertainty in model fitting and model selection (Buckland et al., 1993).

Measuring the effect of attraction

Conventional line-transect estimates can be biased as a result of responsive movement of the target species and animals on or near the trackline being missed by observers (Buckland et al., 1993). Buckland and Turnock (1992) presented a method using co-ordinated boat and helicopter surveys to quantify and adjust for the combined effects of responsive movements of dolphins to the boat and to eliminate the bias from observers failing to see animals on or near the trackline. Their approach is better suited to the restricted space available on small boats than to a dual-platform approach (Palka and Hammond, 2001). Additionally, sightings can be made much farther ahead (reducing the possibility that the animals have already responded), and the two sighting teams are totally isolated from each other. For these reasons we adapted Buckland and Turnock's (1992) approach in our trials of 1998–99.

Simultaneous boat-and-helicopter surveys were carried out to the south of Banks Peninsula, predominantly between Birdlings Flat and the mouth of the Rakaia River. This area was chosen because it displayed representative and varying densities.

A Robinson R22 helicopter with pilot and one observer (ES) followed a zig-zag flight path approximately 1.5 km in front of the boat, traveling out to 1000 m on either side of the vessel's trackline at a height of 500 ft (152 m) (Fig. 4). To aid the process of tracking sightings from the air, sighting positions were marked with Rhodamine dye bombs.[2] The position of the helicopter in relation

[2] Dye bombs consisted of a tablespoon of Rhodamine dye in a paper cup 2/3 filled with sand. An additional (empty) paper cup was taped upside down on top of the first cup with paper-based masking tape. On impact the two cups broke apart, releasing the sand+dye mix into the water.

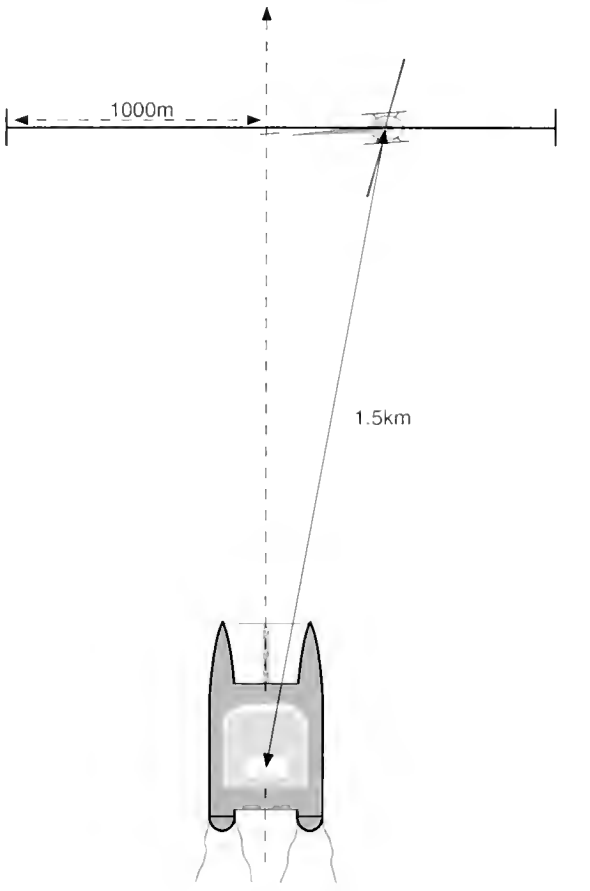

Figure 4

Schematic diagram of simultaneous helicopter-and-boat surveys for Hector's dolphins south of Bank Peninsula, South Island, New Zealand.

to the boat was determined with the boat's RADAR. The absolute position of the boat was determined to an accuracy of 2–5 m by differential GPS (Trimble GeoExplorer; postprocessed). Distances to land were obtained at the time of sighting with RADAR or during analysis by using GIS coastline data and the computer program "SDR Map" (Trimble Navigation, Christchurch, New Zealand).

Boat observers followed our standard sighting procedures (see above). On most occasions the helicopter was outside the field of view of the observers' binoculars because the observers were scanning the water surface, and the helicopter was well above what the observers could see through the binoculars. When it was within their view, observers made a conscious effort to remain unbiased by the movements of the helicopter. On making a sighting, the helicopter observer informed an independent observer located in the cabin (observers on the platform could not hear communications from the helicopter observer and vice versa). The helicopter then hovered briefly above the sighting while a range and bearing in relation to the boat was taken by RADAR. The helicopter then ceased hovering but tracked the group of dolphins either until the boat observers had sighted the group, or the group had passed abeam of the boat. A second range and bearing were then taken. Sightings lost by the helicopter observer during tracking were discarded in our analyses. The independent observer, in liaison with the helicopter observer and boat observers, determined whether the sighting was a duplicate (i.e., made by both helicopter and boat observers) by using information on location and group size. These decisions were checked again in analysis by inspection of plotted locations of sightings made from either platform or both platforms.

Following the approach of Buckland and Turnock (1992), let

$g_s(y)$ = the probability that a group detected from the helicopter at perpendicular distance y from the trackline of the ship is subsequently detected from the ship;

$$f_s(y) = g_s(y)/\mu, \text{ with } \mu = \int_0 g(y)dy$$

(area under helicopter detection function),

w = truncation distance for perpendicular distances y;

n_h = number of helicopter detections;

n_s = number of ship detections;

n_{hs} = number of detections made from both platforms (duplicate detections);

$f_h(y)$ = probability density function fitted to helicopter detection distances;

$f_{hs}(y)$ = probability density function fitted to duplicate detection distances as recorded from the helicopter;

$f(x)$ = probability density function fitted to perpendicular distances recorded from the ship;

L = length of transect line.

A conventional estimate of density of groups, assuming no responsive movement and $g(0) = 1$ (all animals on the trackline seen with certainty) is calculated as

$$\hat{D}_s = \frac{n_s \hat{f}(0)}{2L}. \quad (5)$$

A corrected estimate, allowing for responsive movement and including an estimate of $g(0)$ is given by

$$\hat{D}_c = \frac{n_s \hat{f}_s(0)}{2L\hat{g}_s(0)}, \quad (6)$$

where $$\hat{f}_s(0) = \frac{\hat{g}_s(0)}{\int_0^w \hat{g}_s(y)dy}, \quad (7)$$

$$\hat{g}_s(y) = \frac{n_{hs}\hat{f}_{hs}(y)}{n_h \hat{f}_h(y)}. \quad (8)$$

A correction factor for abundance estimates of Hector's dolphin groups can be estimated by

$$\hat{c} = \hat{D}_U / \hat{D}_S. \quad (9)$$

Using Distance 3.5, we fitted a half-normal model with cosine adjustments to estimate $f(0)$. The half-normal model was fitted to helicopter data to estimate $f_h(0)$ and the uniform model with cosine adjustments was used to estimate $f_{hs}(0)$. All were selected by using AIC. Potential model choices were the following: hazard/cosine, hazard/polynomial, half-normal/cosine, half-normal/hermite and uniform/cosine (Buckland et al., 1993). Truncation distance was 640 m for boat sightings, and 1000 m for helicopter and duplicate sightings. To ensure that only high-quality data were used to estimate effective half search widths, sightings for which range (radial distance) was estimated by eye and those made during Beaufort sea state >2 were removed before $f(0)$ estimation.

The error for the correction factor ($\hat{c}$) was estimated by bootstrapping on transect lines and applying the estimation procedure to each of 199 bootstrap data sets. The standard deviation of the bootstrap estimates was used as the standard error of $\hat{c}$.

Ideally, the correction factor would be estimated separately for each survey from separate sets of boat-and-helicopter trials conducted in areas of representative density. Financial and logistical constraints prevented this; therefore the correction factor estimated in 1998–99 was applied to each of the line-transect surveys reported in the present study. We note that this is not uncommon (e.g., Carretta et al., 2001).

Unbiased abundance estimates were calculated by

$$\hat{N}_U = \hat{c}\hat{N}_S. \quad (10)$$

The CVs of the corrected abundance estimates ($\hat{N}_U$) were calculated with the following equation (Turnock et al., 1995):

$$CV(\hat{N}_U) = \sqrt{CV^2(\hat{c}) + CV^2(\hat{N}_S)}, \quad (11)$$

where $CV(\hat{c}) = \frac{SE(\hat{c})}{\hat{c}}$. (12)

Upper ($\hat{N}_{UC}$) and lower ($\hat{N}_{LC}$) 95% confidence intervals for $\hat{N}_U$ were calculated by using the Satterthwaite degrees of freedom procedure outlined in Buckland et al. (1993). This procedure assumes a log-normal distribution of N_C, using

$$\hat{N}_{LC} = \hat{N}_L / C, \text{ and}$$
$$\hat{N}_{UC} = \hat{N}_U C, \quad (13)$$

where $C = \exp\left\{t_{df}(0.025)\sqrt{\log_e\left(1+\left[CV(\hat{N}_U)\right]^2\right)}\right\}$. (14)

The Satterthwaite degrees of freedom (df) for corrected abundance estimate confidence intervals were calculated by

Table 3

Summary of variables required for correction factor (boat-and-helicopter trials)

Parameter	Estimate
Length of transect, L (km)	308
Truncation distance, w (km)	1.0
Number of helicopter detections, n_h	58
Number of ship detections, n_s	126
Number of duplicate detections, n_{hs}	33
ESW of helicopter (km)	0.532
ESW for duplicates (km)	0.342
Apparent ESW of boat (km)	0.268
Apparent density estimate (groups/km^2)	0.7631
Corrected density estimate (groups/km^2)	0.3839
Boat detection probability "near" trackline	0.8861
Correction factor (c)	0.5032
Standard error, SE(c)	0.0912

$$df = \frac{CV^4(\hat{N}_U)}{\frac{CV^4(\hat{c})}{B-1} + \frac{CV^4(\hat{N}_S)}{df_S}}, \quad (15)$$

where B is the number of bootstrap samples, and df_S is the Satterthwaite degrees of freedom for the uncorrected abundance estimate, $\hat{N}_S$ (see Buckland et al., 1993).

The CV of combined abundance estimates ($\hat{N}_{U\Sigma}$) was computed by

$$SE(total) = \sqrt{\left\{SE^2(\hat{N}_{U1}) + SE^2(\hat{N}_{U2}) + \ldots + SE^2(\hat{N}_{U\Sigma})\right\}}, \quad (16)$$

and

$$CV(total) = \frac{SE(total)}{\hat{N}_U(total)}. \quad (17)$$

Results

The three line-transect surveys covered 2061 km of transect, and 231 sightings were used to estimate density (Table 2). Sighting rates were highest around Banks Peninsula (Table 3).

The simultaneous boat-and-helicopter surveys indicated that boat observers missed 11.4% of the dolphins on the trackline, but that strong responsive movement towards the boat resulted in apparent densities twice as high as they normally would be (Table 3). If the observers' attention was drawn to dolphin groups by the position of the helicopter, the results of these trials would be biased. This is unlikely, however, because several groups sighted by the helicopter observer subsequently passed within 200 m of the boat and were not seen by observers. We saw no evidence that the dolphins were affected by the helicopter.

Detection functions for boat-and-helicopter sightings (Fig. 5, C and D) are relatively smooth in comparison

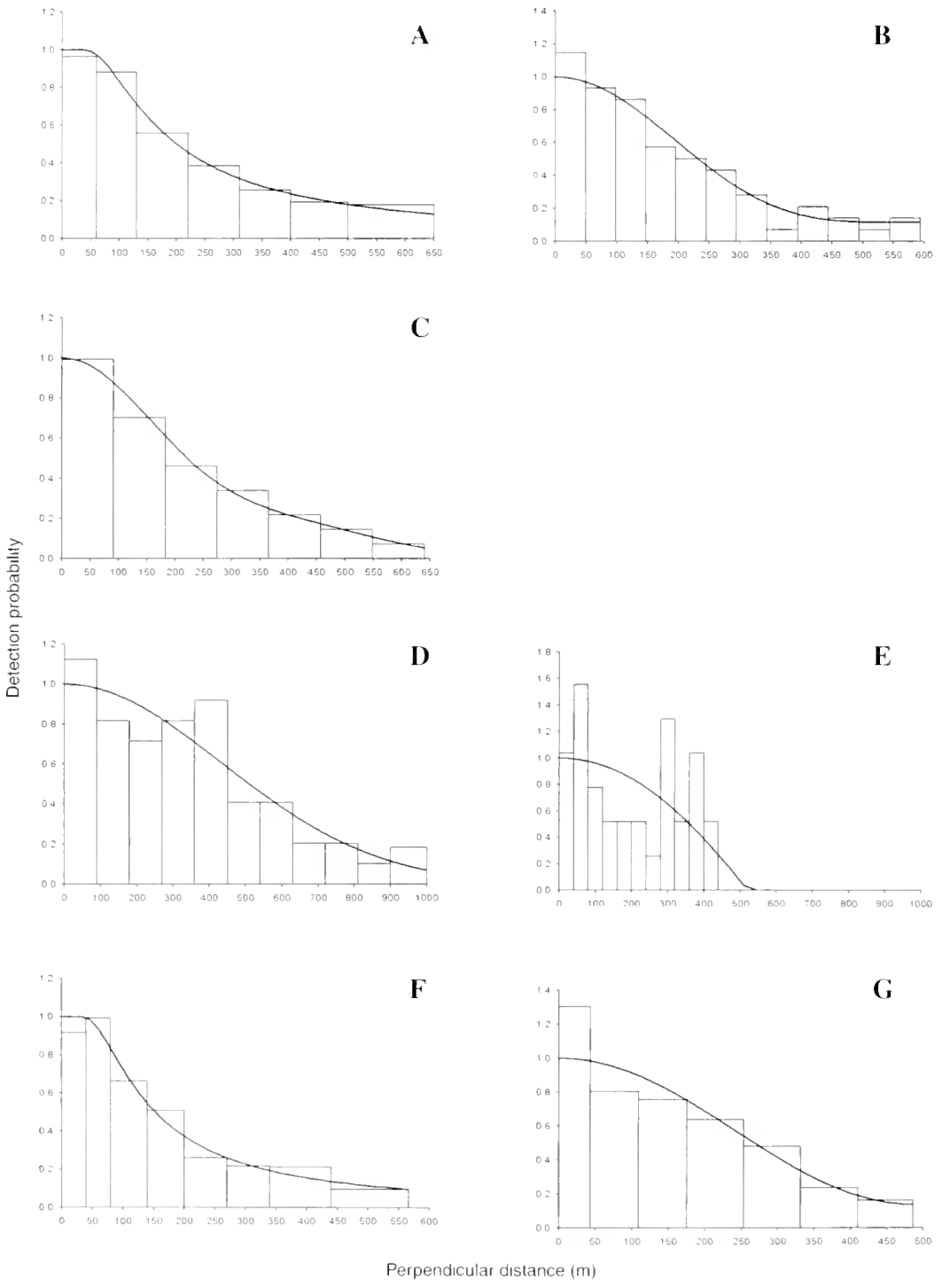

Figure 5

Histograms of perpendicular sighting distances, and their fitted detection functions as used to estimate effective strip width. n = number of sightings. The fitted model (hazard, cosine, uniform, or half normal) and any adjustments to it (cosine or none) are given in brackets. (**A**) 1997–98 harbors and bays (n=71; hazard/cosine); (**B**) 1997–98 open coasts (n=75; uniform/cosine); (**C**) 1998–99 open coasts (n=121; half-normal/cosine); (**D**) 1998–99 helicopter sightings (n=58; half-normal); (**E**) 1998–99 duplicate sightings (n=33; uniform/cosine); (**F**) 1999–2000 harbors and sounds (n=70; hazard/cosine); (**G**) 1999–2000 open coasts (n=89; uniform/cosine).

with those presented in Turnock et al. (1995). The detection function for the duplicate sightings (Fig. 5E) was more difficult to fit. Given the restricted sample size of duplicates (n=33), this result is not unexpected.

In the 1998–99 Timaru to Long Point and 1999–2000 Motunau to Farewell Spit surveys, robust estimation of ESW was facilitated by addition of extra sightings gained under similar sighting conditions at Banks Peninsula (Fig. 5, C, F, G). None of the three surveys showed significant evidence of larger groups being seen farther away. A broad pattern of abundance declining to the north and south of the Timaru–Banks Peninsula area is evident (Fig 2, Table 2). We made six sightings on 288 km of offshore lines (4–10 nmi offshore), confirming that densities in this zone are low.

Information on sea state is usually collected during boat line-transect surveys and sometimes used to poststratify data (e.g., Barlow, 1995). In our study this was not advantageous, for three reasons. 1) We avoided collecting data in conditions with whitecaps; therefore only a few sightings were collected in Beaufort 3. Hence variance estimates for this Beaufort state are large. 2) Differences among Beaufort states for key parameters such as sighting rate, average group size, and effective strip width were small and showed overlapping confidence intervals (we concede that statistical power is low because of reason 1 stated above). Note that data were pooled in the same way as for ESW estimation. 3) Stratification by Beaufort state does not produce abundance estimates that match the zones of intrinsic management interest (e.g., Banks Peninsula Marine Mammal Sanctuary; Dawson and Slooten, 1993).

Discussion

The catamaran survey platform was a near-ideal vessel for close inshore surveys. The sighting platform (Fig. 1) was a relatively inexpensive modification (~US$2000) that could be dismantled in about 10 minutes to allow sailing. The vessel's minimal draught allowed coverage of very shallow areas, which are an important part of the distribution of Hector's dolphin and many other inshore cetaceans. Although catamarans are inherently resistant to rolling, pitching can be a problem when motoring into a head sea or swell. We minimized this pitching by arranging lines so they could be run down-swell. The 45° placement of lines facilitated this reduction in pitching because it provided two alternative sets of lines (at 90° to one another). Further, these could be run inshore or offshore, allowing a choice of four options.

A significant advantage of vessels with low running costs is that the cost of training is low. We could afford to spend 7–10 days training before each survey. Further, waiting for weather to improve is inexpensive; therefore one does not need to gather data in marginal sighting conditions.

Estimated abundances (Table 4) were not significantly different from those estimated in the 1984–85 strip transect survey. Recent mark-recapture estimates of dolphin abundance at Banks Peninsula in 1996, based on photo-ID data, differed from the line-transect estimate for this area by less than 6% (Gormley, 2002; Jolly-Seber model allowing different capture probabilities between first and subsequent captures).

Our surveys confirmed previous work showing the patchy nature of Hector's dolphin distribution (Dawson and Slooten, 1988). Research at Banks Peninsula on the alongshore range of individually identified dolphins has shown a mean alongshore range of about 31 km (SE=2.43; Bräger et al., 2002). Despite wide-ranging surveys over 13 years, the most extreme sightings of any individual were 106 km apart. These data indicate very high site fidelity and indicate that even small-scale discontinuities in distribution may be long lasting. Lack of extensive movement along-shore, and hence limited contact with neighboring populations, is likely to be the mechanism by which Hector's dolphin has become segregated into genetically distinct populations (Pichler et al., 1998; Pichler and Baker, 2000).

The new abundance data, in combination with the genetic data indicating segregation of Hector's dolphin into four populations (Pichler and Baker, 2000) and modeling work indicating that the species is in decline in most of its range owing to bycatch in gill nets (Martien et al., 1999; Slooten et al., 2000), underscore the urgent need for better information on bycatch rates.

Despite strong evidence of bycatch throughout the species' range, observer coverage sufficient to estimate bycatch has been achieved only in one area (Canterbury) for one fishing season (1997–98; Baird and Bradford, 2000). During this season six Hector's dolphins were observed entangled in commercial gill nets (a further two were caught but released alive), resulting in a bycatch estimate of 17 individuals (Starr[3]). One mortality was observed in a trawl net, but very low observer coverage prevented any calculations of overall trawl bycatch (Baird and Bradford, 2000). No attempt was made to assess bycatch in recreational gillnetting during this period, but during a more recent summer (2000–01) five Hector's dolphin mortalities occurred in gill nets that were probably set by recreational fishermen (Department of Conservation and Ministry of Fisheries, 2001). It is not reasonable to assume that all mortalities in recreational gillnets are detected. In our opinion it is likely that combined commercial and recreational gillnet bycatch off Canterbury is about 15–30 individuals per year.

Hector's dolphin abundance on the north, east, and south coasts of the South Island estimated from the surveys reported in the present study is 1880 individuals (CV=15.7%). Hector's dolphins are more common on the

[3] Starr, P. 2000. Comments on "Estimation of the total bycatch of Hector's dolphins (*Cephalorhynchus hectori*) from the inshore trawl and setnet fisheries off the east coast of the South Island in the 1997–98 fishing year." Unpublished paper presented to Conservation Services Levy Working Group, 28 p. Department of Conservation, P.O. Box 10-420 Wellington, New Zealand.

Table 4

Corrected abundance estimates (only strata with sightings are listed). Number of sightings represents only those made in that stratum and used for density estimation. The number used for estimating effective half strip width (ESW) differs because it includes sightings from extra transects in areas of similar exposure and transects repeated on the same day (and hence not true replicates for the purposes of estimating density).

Survey zone	Stratum	No. of sightings	ESW (m) (n, CV%)	$N_{(c)}$ (CV%)	Lower 95% CI	Upper 95% CI
Motunau to Timaru (1997–98)	Akaroa harbor	56	275 (71, 22.6)	62 (33.9)	32	121
	Other harbors and bays	8	275 (71, 22.6)	14 (67.5)	3	79
	Banks Peninsula Marine Mammal Sanctuary (BPMMS) (excluding harbors and bays)	62	261 (75, 10.3)	821 (22.1)	535	1258
	<4 nmi offshore, to the north and south of BPMMS	19	261 (75, 10.3)	300 (36.5)	133	679
Timaru to Long Point (1998–99)	Timaru–Long Point (excluding Te Waewae Bay)	13	268 (121, 10.5)	310 (28.4)	201	478
	Te Waewae Bay	14	268 (121, 10.5)	89 (32.4)	36	218
Motunau to Farewell Spit (1999–2000)	Queen Charlotte Sound	3	214 (70, 20.2)	20 (100.5)	4	110
	Cloudy and Clifford Bay	13	277 (89, 6.1)	162 (55.4)	56	474
	Cape Campbell–Motunau	5	277 (89, 6.1)	102 (55.2)	34	305
Total				1880 (21.3)	1246	2843

South Island west coast, where an aerial survey of similar design resulted in an estimate of 5388 (CV=20.6%; Slooten et al., in press). Thus Hector's dolphin abundance in South Island waters is estimated at 7268 individuals (CV=15.8%). The North Island subspecies of Hector's dolphin, now considered critically endangered (IUCN[4]) remains to be surveyed quantitatively.

The new abundance estimates provide an empirical basis from which to calculate levels of take that would still allow the currently depleted populations to recover (e.g., Wade, 1998). These levels of take should be seen as short-term targets for bycatch reduction in gill and trawl nets. For the management of Hector's dolphin to be put on a rational basis, a more comprehensive and wide-ranging assessment of bycatch, including statistically robust observer programs in coastal fisheries, is urgently needed.

Acknowledgments

These surveys were funded principally by Department of Conservation Contracts SCO 3072, 3074, and 3075. Significant contributions to equipment used in the survey were made by the New Zealand Whale and Dolphin Trust and the University of Otago. We are very grateful for the hard work put in by the other observers: Laszlo Kiss, Nadja Schneyer, Gail Dickie, Niki Alcock, Lesley Douglas, James Holborow, Ellie Dickson, Guen Jones, Will Rayment, and Dan Cairney. Jay Barlow, Jeff Laake, Anne York, and Debbie Palka shared their thoughts on survey design and field methods. David Fletcher helped with aspects of variance estimation. Akaroa Harbour Cruises provided much appreciated field support. Daryl Coup wrote the sightings program we used to collect data in the field. Otago University's Department of Surveying very helpfully provided the GPS base-station data for postprocessing our GPS fixes.

[4] IUCN. 2000. IUCN red list of threatened species. International Union for Conservation of Nature and Natural Resources, Species Survival Commission. [Available at www.redlist.org.]

Literature cited

Baird, S. J., and E. Bradford.
2000. Estimation of the total bycatch of Hector's dolphins (*Cephalorhynchus hectori*) from the inshore trawl and setnet fisheries off the east coast of the South Island in the 1997–98 fishing year, 28 p. Published client report on contract 3024, funded by Conservation Services Levy, Department of Conservation, Wellington. Web site: http://csl.doc.govt.nz/CSL3024.pdf. [Accessed 8 March 2001.]

Baker, A. N., A. N. H. Smith, and F. B. Pichler.
2002. Geographical variation in Hector's dolphin: recognition of a new subspecies of *Cephalorhynchus hectori*. J Roy. Soc. N.Z. 32:713–727.

Barlow, J.
1988. Harbor porpoise, *Phocoena phocoena*, abundance estimation for California, Oregon, and Washington: I. Ship surveys. Fish. Bull. 86:417–432.
1995. The abundance of cetaceans in California waters. Part 1: Ship surveys in summer and fall of 1991. Fish. Bull. 93:1–14.

Bräger, S., S. M. Dawson, E. Slooten, S. Smith, G. S. Stone, and A. Yoshinaga.
2002. Site fidelity and along-shore range in Hector's dolphin, an endangered marine dolphin from New Zealand. Biol. Conserv. 108:–287.

Buckland, S. T., D. R. Anderson, K. P. Burnham, and J. L. Laake
1993. Distance sampling: estimating abundance of biological populations, 446 p. Chapman and Hall, New York, NY.

Buckland, S. T., and B. J. Turnock.
1992. A robust line transect method. Biometrics 48: 901–909.

Carretta, J. V., B. L. Taylor, and S. J. Chivers.
2001. Abundance and depth distribution of harbor porpoise (*Phocoena phocoena*) in northern California determined from a 1995 ship survey. Fish. Bull. 99:29–39.

Dawson, S. M., and E. Slooten.
1988. Hector's Dolphin *Cephalorhynchus hectori*: distribution and abundance. Rep. Int. Whal. Comm. (special issue) 9:315–324.
1993. Conservation of Hector's dolphins: the case and process which led to establishment of the Banks Peninsula Marine Mammal Sanctuary. Aquat. Cons. 3:207–221.

Dawson, S. M., E.. Slooten, F. Pichler, K. Russell, and C. S. Baker.
2001. North Island Hector's dolphins are threatened with extinction. Mar. Mamm. Sci. 17:366–371.

Department of Conservation and Ministry of Fisheries.
2001. Hector's dolphin and setnetting Canterbury Area: a paper for public comment, 9 p. [Available from Ministry of Fisheries, Private Bag 1926, Dunedin, New Zealand.]

Gormley, A.
2002. Mark-recapture abundance estimation in marine mammals. M.S. thesis., 105 p. Univ. Otago, Dunedin, New Zealand.

IWC (International Whaling Commission).
1994. Report of the International Whaling Commission workshop and symposium on the mortality of cetaceans in passive fishing nets and traps. Rep. Int. Whal. Comm. (special issue)15. 629 p.

Lerczak, J. A., and R. O. Hobbs.
1998. Calculating sighting distances from angular readings during shipboard aerial, and shore-based marine mammal surveys. Mar. Mamm. Sci. 14:590–599.

Martien, K. K., B. L. Taylor, E. Slooten, and S. M. Dawson.
1999. A sensitivity analysis to guide research and management for Hector's dolphin. Biol. Conserv. 90:183–191.

Palka, D. L., and P. S. Hammond.
2001. Accounting for responsive movement in line transect estimates of abundance. Can. J. Fish. Aquat. Sci. 58(4):777–787.

Pichler, F., and C. S. Baker.
2000. Loss of genetic diversity in the endemic Hector's dolphin due to fisheries-related mortality. Proc. Roy. Soc. (Lond), Series B. 267:97–102.

Pichler, F. B., S. M. Dawson, E. Slooten, and C. S. Baker.
1998. Geographic isolation of Hector's dolphin populations described by mitochondrial DNA sequences. Cons. Biol. 12:676–682.

Slooten, E., and S. M. Dawson.
1994. Hector's Dolphin. *In* Handbook of marine mammals, vol V (Delphinidae and Phocoenidae) (S. H Ridgway and R. Harrison, eds.), p. 311–333. Academic Press, New York, NY.

Slooten, E., S. M. Dawson, and W. J. Rayment.
In press. Aerial surveys for coastal dolphins: Abundance of Hector's dolphins off the South Island west coast, New Zealand. Mar. Mamm. Sci. 20(3).

Slooten, E., D. Fletcher, and B. L. Taylor.
2000. Accounting for uncertainty in risk assessment: Case study of Hector's dolphin mortality due to gillnet entanglement. Cons. Biol. 14:1264–1270.

Turnock, B. J., S. T. Buckland, and G. C. Boucher.
1995. Population abundance of Dall's porpoise (*Phocoenoides dalli*) in the Western North Pacific Ocean. Rep. Int. Whal. Comm. (special issue) 16:381–397.

Wade, P.
1998. Calculating limits to the allowable human-caused mortality of cetaceans and pinnipeds. Mar. Mamm. Sci. 14:1–37.

Description and growth of larval and pelagic juvenile pygmy rockfish (*Sebastes wilsoni*) (family Sebastidae)

Thomas E. Laidig
Keith M. Sakuma
Santa Cruz Laboratory
Southwest Fisheries Science Center
National Marine Fisheries Service, NOAA
110 Shaffer Rd.
Santa Cruz, California 95060
E-mail address: tom.laidig@noaa.gov

Jason A. Stannard
La Jolla Laboratory
Southwest Fisheries Science Center
National Marine Fisheries Service, NOAA
P. O. Box 271
La Jolla, California 92038

Abstract—A developmental series of larval and pelagic juvenile pygmy rockfish (*Sebastes wilsoni*) from central California is illustrated and described. *Sebastes wilsoni* is a noncommercially, but ecologically, important rockfish, and the ability to differentiate its young stages will aid researchers in population abundance studies. Pigment patterns, meristic characters, morphometric measurements, and head spination were recorded from specimens that ranged from 8.1 to 34.4 mm in standard length. Larvae were identified initially by meristic characters and the absence of ventral and lateral midline pigment. Pelagic juveniles developed a prominent pigment pattern of three body bars that did not extend to the ventral surface. Species identification was confirmed subsequently by using mitochondrial sequence data of four representative specimens of various sizes. As determined from the examination of otoliths, the growth rate of larval and pelagic juvenile pygmy rockfish was 0.28 mm/day, which is relatively slow in comparison to the growth rate of other species of *Sebastes*. These data will aid researchers in determining species abundance.

Manuscript submitted 9 June 2003 to Scientific Editor's Office.
Manuscript approved for publication 25 February 2004 by the Scientific Editor.
Fish. Bull. 102:452–463 (2004).

Rockfishes (genus *Sebastes*) form a diverse group comprising at least 72 species occurring in the northeastern Pacific (Love et al., 2002). Many of these species represent a substantial portion of the groundfish fishery off the west coast of North America, accounting for 20% of the groundfish landings in California in 2000 (Pacific Fishery Management Council, 2000). A few species are relatively abundant but are not harvested because of their small size. These species play vital roles in the community ecology, including providing prey for the larger, commercially important species. The pygmy rockfish (*Sebastes wilsoni*) having a maximum size of 23 cm total length, is among these small species (Love et al., 2002). Pygmy rockfish are common over sediment and rocky seafloor habitats at a depth of 30–274 m (Stein et al., 1992; Yoklavich et al., 2000). Stein et al. (1992) observed that pygmy rockfish were by far the most abundant fish species off Heceta Bank, Oregon, and Love et al. (1996) reported "clouds" of pygmy rockfish mixed with two other small species, squarespot rockfish (*S. hopkinsi*) and halfbanded rockfish (*S. semicinctus*) off southern California. In Soquel Canyon in central California, pygmy rockfish dominated fish assemblages in rock-boulder habitat at 75–175 m (Yoklavich et al., 2000).

Accurate identification of larval stages is critical. Biomass of rockfish populations can be estimated from larval production (Ralston et al., 2003) and larval and juvenile abundance studies (Moser and Butler, 1987; Hunter and Lo, 1993). If the larval and juvenile rockfish analyzed in these studies are not correctly identified, it could lead to either over- or underestimates of biomass or recruitment potential of a population. Identification of young stages of *Sebastes* has been accomplished through rearing studies and through descriptions based on developmental series of field-caught specimens of various sizes (Matarese et al., 1989; Moser, 1996). Otolith morphologies have been useful in discerning some *Sebastes* species (Laidig and Ralston, 1995; Stransky, 2001). Recently, molecular methods have proven to be an effective tool for the identification of *Sebastes* larvae (Seeb and Kendall, 1991; Rocha-Olivares, 1998; Rocha-Olivares et al., 2000).

In this study, we identify and describe the larvae and pelagic juveniles of pygmy rockfish based on morphometrics and pigmentation patterns, and estimate age and growth at two

developmental stages. Further, we examine otolith radius at time of larval extrusion to separate pygmy rockfish from other similarly pigmented *Sebastes* specimens. We also use mitochondrial DNA (mtDNA) sequence data to identify four putative pygmy rockfish specimens representing a continuum of late-larval through pelagic juvenile stages. The molecular results are used to confirm identifications based on morphological, meristic, and pigmentation characters and to assure that the assembled developmental series is monospecific.

Methods

Specimen collection

Specimens of larval and pelagic juvenile pygmy rockfish were obtained from research cruises conducted aboard the NOAA RV *David Starr Jordan* off central California. Specimens were collected in midwater (5–30 m) from mid-May to mid-June, 1990–92, between Bodega Bay (north of San Francisco) and Cypress Point (south of Monterey Bay) by using a 26 m×26 m modified Cobb midwater trawl (12.7-mm stretched-mesh codend liner). Specimens also were collected during early March, 1992–93, between Salt Point (north of San Francisco) and Cypress Point with a 5 m×5 m modified Isaacs-Kidd (MIK) frame trawl with 2-mm net mesh and 0.505-mm mesh codend. Specimens from the Cobb trawl were frozen and specimens from the MIK frame trawl were preserved in 95% ethanol for later analysis.

Meristics, morphometrics, and body pigmentation

We examined pigmentation patterns and physical characteristics of 122 pygmy rockfish larvae and pelagic juveniles. Standard length (SL) was measured for each individual and sizes ranged from 8.1 to 34.4 mm. Specimens greater than 19.9 mm were identified by using meristic characters (Chen, 1986; Matarese et al., 1989; Moreland and Reilly, 1991; and Laroche[1]), and pigment patterns were recorded. Specimens less than 20 mm were identified initially from pigment patterns from a series starting with the smallest (8.1 mm SL) identifiable individuals with complete fin-ray counts. Counts of dorsal-, anal-, and pectoral-fin rays, and the number of gill rakers on the first arch were recorded whenever possible and subsequently used in identifications. Gill raker counts were obtained only from fish larger than 15 mm SL.

We measured snout-to-anus length, head length, snout length, eye diameter, body depth at the pectoral fin base, body depth at anus, and pectoral-fin length on 16 specimens ranging from 8.1 to 29.6 mm SL, following Richardson and Laroche (1979). Head spination was examined on thirty-three specimens (8.1 to 29.6 mm SL) that were stained with alizarin red-s. Terminology for head spination follows Richardson and Laroche (1979). In the following descriptions, larval and juvenile lengths always refer to SL and pigmentation always refers to melanin.

Otolith examination

Sagittal otoliths were removed from 61 larval and pelagic juvenile pygmy rockfish (8.1–34.4 mm SL), and growth increments were counted beginning at the first increment after the extrusion check (the mark in the otolith formed when the larvae are released from their mother) by using a compound microscope at 1000× magnification (see Laidig et al., 1991). No validation of the these growth increments was performed during the present study, and none has been conducted by other researchers. However, we assumed that these growth increment counts corresponded to daily ages based on validation of daily growth increments in other co-occurring rockfishes, namely shortbelly rockfish, *S. jordani* (Laidig et al., 1991), black rockfish, *S. melanops* (Yoklavich and Boehlert, 1987), bocaccio, *S. paucispinis*, chilipepper, *S. goodei*, widow rockfish, *S. entomelas*, and yellowtail rockfish, *S. flavidus* (Woodbury and Ralston, 1991). The radius of the otolith was measured from the primordium to the postrostral edge of the extrusion check for comparison with similar measurements from other *Sebastes* spp. (as reported in Laidig and Ralston, 1995). Transformation from the larval stage to the pelagic juvenile stage was ascertained by the presence of accessory primordia (Laidig et al., 1991; Lee and Kim, 2000).

Molecular confirmation

Total genomic DNA was isolated from skeletal muscle tissue of four larval and juvenile putative pygmy rockfish specimens by using a CTAB and phenol-chloroform-isoamyl alcohol protocol (Winnepenninckx et al., 1993; Hillis et al., 1996). These four specimens ranged in length from 15 to 27 mm and had pigment patterns similar to the fish identified as pygmy rockfish in the present tudy. Polymerase chain reaction (PCR) amplifications and sequencing of partial mitochondrial DNA regions (cytochrome *b* [cyt-*b*] and control region [CR]) followed the methods of Rocha-Olivares et al. (1999a, 1999b). PCR products were verified on 2% agarose gels and purified by using a QIAquick™ PCR Cleanup Kit (Qiagen, Inc., Valencia, CA) following manufacturer protocols. Complementary strand sequence data were generated by using ABI PRISM™ DyeDeoxy™ terminator cycle sequence chemistry on an automated sequencer (Applied Biosystems, Model 377, Foster City, CA).

Cytochrome *b* sequence data (750 base pairs) from the four specimens were aligned with (previously generated) orthologous sequences from 119 individuals representing 61 species of *Sebastes* (Rocha-Olivares et al., 1999b). Species identifications, based on cyt-*b* data, were made by using distance-based cluster analyses in PAUP v4.0b2 (Phylogenetic Analysis Using Parsimony,

[1] Laroche, W. A. 1987. Guide to larval and juvenile rockfishes (*Sebastes*) of North America. Unpubl. manuscript, 311 p. Box 216, Enosburg Falls, VT 05450.

version 4, Sunderland, MA) and pairwise comparisons of sequence divergence (i.e., the number of nucleotide differences between two individuals expressed as a percentage). A secondary data set, which included an additional 450 base pairs of control region sequence, was generated for the four undetermined specimens and for a subgroup of known reference species with low levels of sequence divergence from the four putative pygmy rockfish specimens (Puget Sound rockfish [*S. emphaeus*], redstripe rockfish [*S. proriger*], harlequin rockfish [*S. variegatus*], sharpchin rockfish [*S. zacentrus*], and pygmy rockfish). Species identifications, based on this extended (cyt-*b* + CR) data subset, followed analyses described above.

Table 1

Frequency of occurrence (number of fish) of dorsal-, anal-, and pectoral-fin ray counts, and gill raker counts from 122 pygmy rockfish (*Sebastes wilsoni*).

Character	Count	Frequency of occurrence	Percent occurrence
Dorsal-fin rays	12	8	7
	13	110	91
	14	3	2
Anal-fin rays	5	2	2
	6	116	95
	7	4	3
Pectoral-fin rays	16	5	5
	17	92	90
	18	5	5
Gill rakers	36	11	14
	37	15	18
	38	22	28
	39	20	25
	40	10	13
	41	1	1
	42	1	1

Results

General development

All 122 fish had completed notochord flexion and possessed a full complement of segmented fin rays by 8.1 mm. The mode for dorsal-fin ray counts was 13, for anal-fin rays 6, and for pectoral-fin rays 17 (Table 1). The mode for gill raker counts was 38, and the range was 36–42. Anal- and dorsal-fin spines began to develop between 9.1 and 14.0 mm. Lateral line pores began to develop at 29 mm, although a full complement (37 to 46 pores) was not reached in our specimens. Morphometric measurements were taken from 16 individual pygmy rockfish of 8.1–29.6 mm (Table 2).

Head spination

At 8.1 mm, the postocular, parietal, nuchal, inferior posttemporal, supracleithral, superior opercular, preopercular (with the exception of the 2nd anterior), and 1st and

Table 2

Morphometric measurements (in mm) from 16 individuals of pygmy rockfish (*Sebastes wilsoni*).

SL	Snout–anus length	Head length	Snout length	Eye diameter	Body depth at pectoral base	Body depth at anus	Pectoral-fin length
8.1	5.2	3.3	0.8	1.3	2.8	2.3	1.5
9.0	5.3	3.0	1.0	1.5	3.0	2.3	1.7
10.8	6.5	4.2	1.2	1.7	3.5	2.8	2.3
12.1	7.0	4.3	1.3	2.0	3.8	2.8	2.5
12.8	7.7	4.8	1.3	2.2	3.7	3.0	2.5
14.2	8.3	4.7	1.3	2.2	4.3	3.5	3.3
15.2	9.2	5.7	1.7	2.0	4.2	3.5	3.5
16.2	9.7	5.2	1.5	2.0	4.5	3.8	3.8
17.5	10.8	6.2	2.0	2.3	5.0	3.8	4.2
18.6	11.5	6.0	2.0	2.7	5.5	4.3	5.0
20.7	12.7	6.2	2.0	2.7	6.2	5.2	5.0
22.3	14.2	6.7	2.2	2.8	6.8	5.7	6.2
23.8	14.5	6.7	2.0	3.2	7.3	6.3	5.9
24.3	14.2	7.0	2.2	2.7	7.0	5.8	6.3
28.9	17.0	8.0	2.6	3.3	8.5	7.3	7.0
29.6	16.9	7.8	2.6	3.5	8.7	7.5	6.9

2nd inferior and 1st superior infraorbital spines were present (Table 3). The nasal, pterotic, and 4th superior infraorbital first appeared at 10.8 mm. At 12.1 mm, the inferior opercular spine became evident. Between 14.2 and 17.5 mm, the preocular, tympanic, superior postemporal, 2nd anterior preopercular, and 3rd superior infraorbital spines formed. After 17.5 mm, no further changes in head spination were noted. The supraocular, coronal, 3rd inferior infraorbital, and 2nd superior infraorbital spines did not occur on any of the fish examined.

Body pigmentation

At 9.1 mm, pygmy rockfish had no pigment along the lateral and ventral body surfaces (Fig. 1A, Table 4). Pigment was heavy on the top of the head and present on the operculum. The dorsal midline surface had a few melanophores under the soft dorsal fin. The anterior lower jaw was pigmented on the tip and one to two melanophores were present on each side of the snout near the tip. Pigment also was present at the base and on the distal half of the pectoral fin.

By 14.0 mm, dense pigment along the dorsal midline stretched from the caudal peduncle to the first dorsal-fin spine (Fig. 1B, Table 4). The only lateral pigment on the body consisted of a few melanophores along the midline near the caudal peduncle. The ventral surface, including the anal and pelvic fins, remained unpigmented. Pigment on the pectoral fins had mostly disappeared by 11.0 mm and was rarely observed at 14.0 mm. Opercular and head pigment increased in density by 14.0 mm. Pigment along the lower edge of the orbit began to

Table 3

Development of head spines in individual pygmy rockfish (*Sebastes wilsoni*). "1" means spines present and "0" means spines absent.

	Standard length (mm)															
Spines	8.1	9.0	10.8	12.1	12.8	14.2	15.2	16.2	17.5	18.6	20.7	22.3	23.8	24.3	28.9	29.6
Nasal	0	0	1	1	1	1	1	1	1	1	1	1	1	1	1	1
Preocular	0	0	0	0	0	0	1	1	1	1	1	1	1	1	1	1
Supraocular	0	0	0	0	0	0	0	0	0	0	0	0	0	0	0	0
Postocular	1	1	1	1	1	1	1	1	1	1	1	1	1	1	1	1
Coronal	0	0	0	0	0	0	0	0	0	0	0	0	0	0	0	0
Tympanic	0	0	0	0	0	0	0	0	1	1	1	1	1	1	1	1
Parietal	1	1	1	1	1	1	1	1	1	1	1	1	1	1	1	1
Nuchal	1	1	1	1	1	1	1	1	1	1	1	1	1	1	1	1
Pterotic	0	0	1	1	1	1	1	1	1	1	1	1	1	1	1	1
Posttemporal																
Superior	0	0	0	0	0	0	1	1	1	1	1	1	1	1	1	1
Inferior	1	1	1	1	1	1	1	1	1	1	1	1	1	1	1	1
Supracleithral	1	1	1	1	1	1	1	1	1	1	1	1	1	1	1	1
Opercular																
Superior	1	1	1	1	1	1	1	1	1	1	1	1	1	1	1	1
Inferior	0	0	0	1	1	1	1	1	1	1	1	1	1	1	1	
Preopercular																
1st anterior	1	1	1	1	1	1	1	1	1	1	1	1	1	1	1	1
2nd anterior	0	0	0	0	0	1	1	1	1	1	1	1	1	1	1	1
3rd anterior	1	1	1	1	1	1	1	1	1	1	1	1	1	1	1	1
1st posterior	1	1	1	1	1	1	1	1	1	1	1	1	1	1	1	1
2nd posterior	1	1	1	1	1	1	1	1	1	1	1	1	1	1	1	1
3rd posterior	1	1	1	1	1	1	1	1	1	1	1	1	1	1	1	1
4th posterior	1	1	1	1	1	1	1	1	1	1	1	1	1	1	1	1
5th posterior	1	1	1	1	1	1	1	1	1	1	1	1	1	1	1	1
Infraorbital																
1st inferior	1	1	1	1	1	1	1	1	1	1	1	1	1	1	1	1
2nd inferior	1	1	1	1	1	1	1	1	1	1	1	1	1	1	1	1
3rd inferior	0	0	0	0	0	0	0	0	0	0	0	0	0	0	0	0
1st superior	1	1	1	1	1	1	1	1	1	1	1	1	1	1	1	1
2nd superior	0	0	0	0	0	0	0	0	0	0	0	0	0	0	0	0
3rd superior	0	0	0	0	0	0	0	1	1	1	1	1	1	1	1	1
4th superior	0	0	1	1	1	1	1	1	1	1	1	1	1	1	1	1

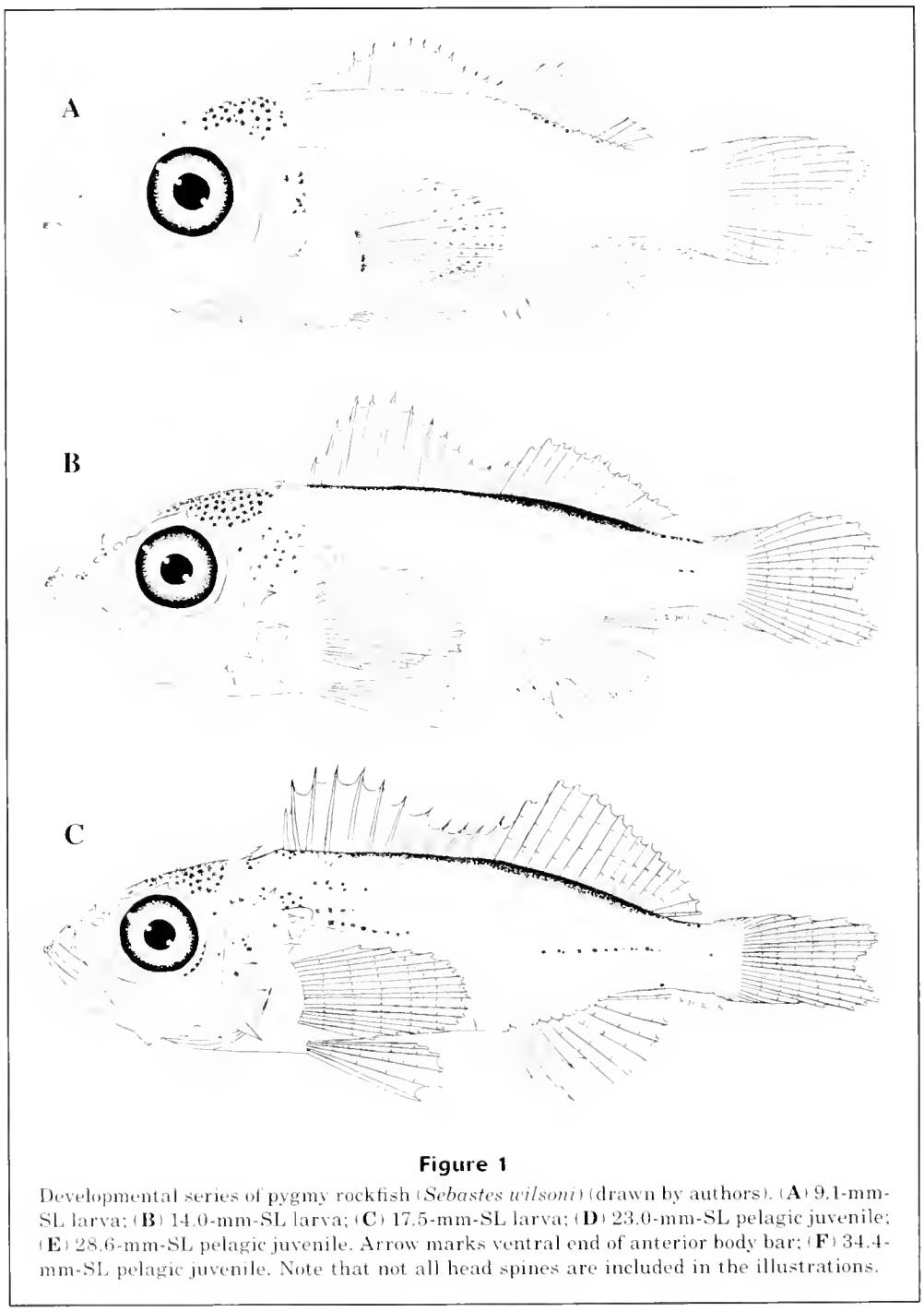

Figure 1

Developmental series of pygmy rockfish (*Sebastes wilsoni*) (drawn by authors). (**A**) 9.1-mm-SL larva; (**B**) 14.0-mm-SL larva; (**C**) 17.5-mm-SL larva; (**D**) 23.0-mm-SL pelagic juvenile; (**E**) 28.6-mm-SL pelagic juvenile. Arrow marks ventral end of anterior body bar; (**F**) 34.4-mm-SL pelagic juvenile. Note that not all head spines are included in the illustrations.

form in some specimens by 12.0 mm and was visible in most specimens by 14.0 mm (Fig. 1B). Snout pigment was represented by one or four melanophores. Anterior lower jaw pigment was heavy and confined to the tip of the jaw.

By 17.5 mm, the dorsal midline pigment had become much darker and denser (Fig. 1C, Table 4) and extended from the caudal fin to the head region, except for a gap where the nape pigment was beginning to form. All fins were unpigmented. Pigment along the ventral body midline began to form at 17.5 mm, with a few postanal melanophores. Lateral midline pigment formed in two locations. Melanophores near the peduncle increased anteriorly, and pigment began forming dorsal to the gut cavity and increased posteriorly toward the peduncle. A body bar began to form on the lateral surface above the pectoral fin between the spinous dorsal fin and the anterior lateral midline pigment. Opercular, eye, and head pigment all increased in density. Melanophores on the snout also became more prevalent between the tip of

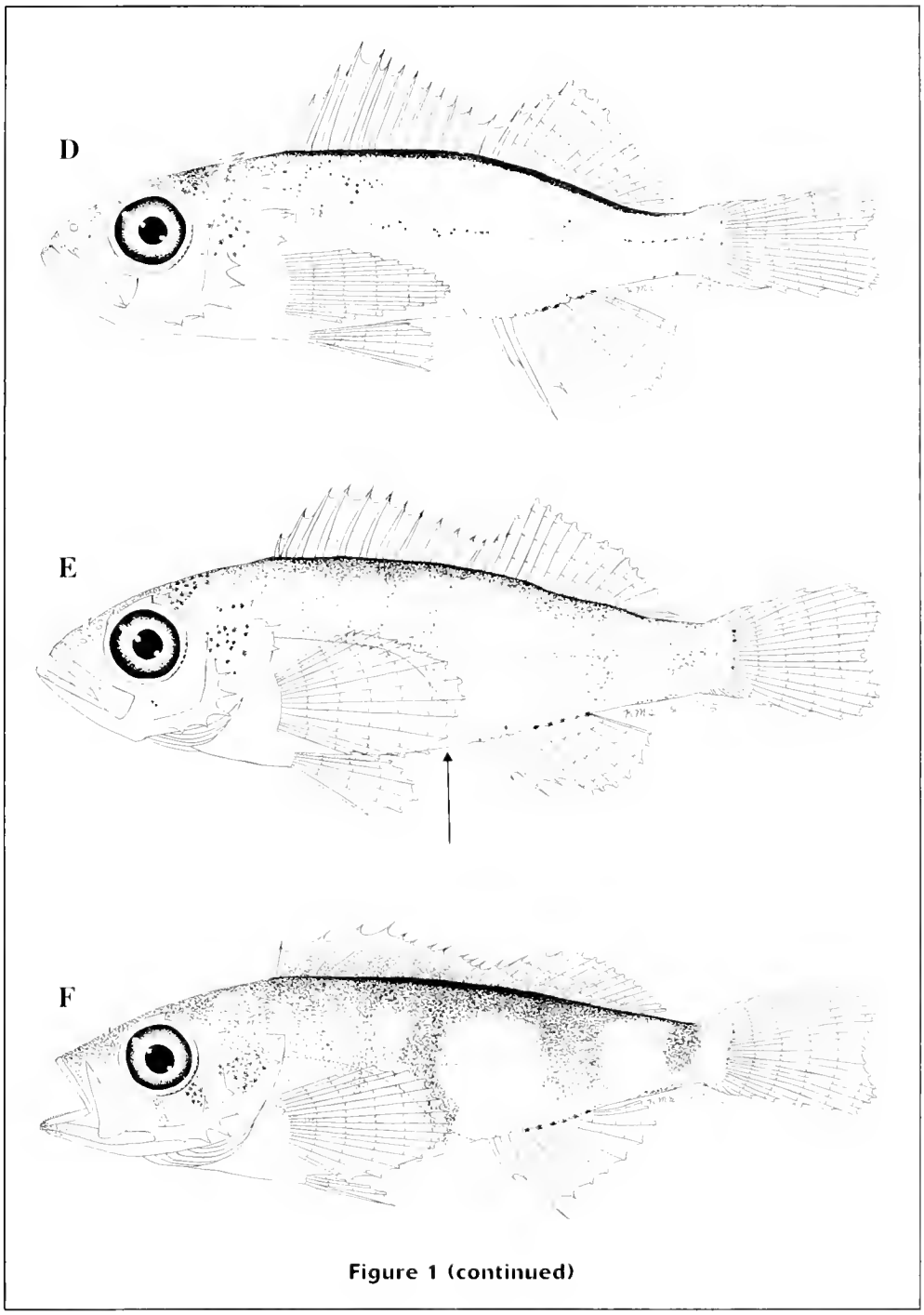

Figure 1 (continued)

the upper jaw and top of the head. Pigment on the tip of the lower jaw spread posteriorly and became denser than in smaller specimens.

When the pelagic juveniles reached 23.0 mm, the dorsal midline pigment was a dark strip extending from the caudal fin to the head (Fig. 1D, Table 4). Nape pigment almost merged with the head pigment, except for a small unpigmented area below the insertion of the parietal and nuchal spines. Hypural pigment was present distally in all individuals at this size and at larger sizes (n=30). Anterior and posterior lateral midline pigment merged to form a continuous line along the body. The number of melanophores increased on the ventral body surface, and a few melanophores were present at the anal-fin ray bases and along the ventral midbody posterior to the anal fin. The anterior body bar broadened and became more defined. A few melanophores on the flanks under the soft dorsal fin began to form a midbody bar. A third body bar began to form on the caudal peduncle. Pigment on the operculum, top of the

Table 4

Proportion of pygmy rockfish (*Sebastes wilsoni*) with melanophores present at various areas averaged over 1.0-mm size bins (range of ±1.0 mm). SL = standard length in mm, LJ = anterior tip of the lower jaw, EYE = posterior-ventral edge of the eye orbit, SNOUT = dorsal surface anterior to the eyes, OPER = operculum, CHK = radiating cheek bars, NAPE = nape pigment, DORS = dorsal body surface, VENT = ventral body surface, MID = along the lateral midline, HYP = hypural region, DFIN = spinous dorsal fin, PEC = blade of the pectoral fin, CAUD = caudal body bar, ANT = anterior body bar, MIDB = midbody bar, CANAL = clear area dorsal to anal fin, MAX = pigment on the side of the maxilla, UND = pigment under lower jaw.

SL	N	LJ	EYE	SNOUT	OPER	CHK	NAPE	DORS	VENT	MID	HYP	DFIN	PEC	CAUD	ANT	MIDB	CANAL	MAX	UND
8	2	1.0	0.0	1.0	1.0	0.0	0.0	1.0	0.0	0.0	0.0	0.0	1.0	0.0	0.0	0.0	0.0	0.0	0.0
9	3	1.0	0.0	1.0	1.0	0.0	0.0	0.7	0.0	0.0	0.0	0.0	1.0	0.0	0.0	0.0	0.0	0.0	0.0
10	6	1.0	0.0	1.0	1.0	0.0	0.0	1.0	0.0	0.0	0.0	0.0	1.0	0.0	0.0	0.0	0.0	0.0	0.0
11	10	1.0	0.0	1.0	1.0	0.0	0.0	1.0	0.0	0.0	0.0	0.0	0.9	0.0	0.0	0.0	0.0	0.0	0.0
12	5	1.0	0.2	1.0	1.0	0.0	0.0	1.0	0.0	0.0	0.0	0.0	0.4	0.0	0.0	0.0	0.0	0.0	0.0
13	7	1.0	0.1	1.0	1.0	0.0	0.0	1.0	0.0	0.0	0.0	0.0	0.4	0.0	0.0	0.0	0.0	0.0	0.0
14	8	1.0	0.9	1.0	1.0	0.0	0.0	1.0	0.3	0.5	0.0	0.0	0.4	0.0	0.0	0.0	0.0	0.0	0.0
15	6	1.0	0.8	1.0	1.0	0.0	0.0	1.0	0.3	0.7	0.2	0.0	0.2	0.0	0.0	0.0	0.0	0.0	0.0
16	7	1.0	0.9	1.0	1.0	0.0	0.0	1.0	0.1	0.9	0.3	0.0	0.3	0.0	0.0	0.0	0.0	0.0	0.0
17	8	1.0	0.8	1.0	1.0	0.0	0.3	1.0	0.3	0.8	0.4	0.0	0.0	0.0	0.0	0.3	0.0	0.0	0.0
18	14	1.0	1.0	1.0	1.0	0.0	0.8	1.0	0.6	1.0	0.7	0.0	0.0	0.0	0.0	0.8	0.0	0.0	0.0
19	7	1.0	1.0	1.0	1.0	0.0	0.6	1.0	0.3	1.0	0.3	0.0	0.0	0.1	0.0	0.7	0.0	0.0	0.0
20	2	1.0	1.0	1.0	1.0	0.0	1.0	1.0	1.0	1.0	1.0	0.0	0.0	0.5	0.0	1.0	0.0	0.0	0.0
21	6	1.0	1.0	1.0	1.0	0.0	0.8	1.0	0.8	1.0	0.5	0.0	0.0	0.3	0.3	0.7	0.0	0.0	0.0
22	4	1.0	1.0	1.0	1.0	0.0	1.0	1.0	0.8	1.0	0.5	0.0	0.0	0.5	0.3	1.0	0.0	0.0	0.0
23	1	1.0	1.0	1.0	1.0	0.0	1.0	1.0	1.0	1.0	1.0	0.0	0.0	1.0	1.0	1.0	0.0	0.0	0.0
24	5	1.0	1.0	1.0	1.0	0.0	1.0	1.0	1.0	1.0	1.0	0.0	0.0	1.0	0.8	1.0	0.2	0.0	0.0
25	1	1.0	1.0	1.0	1.0	0.0	1.0	1.0	1.0	1.0	1.0	0.0	0.0	1.0	1.0	1.0	0.0	0.0	0.0
26	1	1.0	1.0	1.0	1.0	0.0	1.0	1.0	1.0	1.0	1.0	1.0	0.0	1.0	1.0	1.0	1.0	0.0	0.0
27	2	1.0	1.0	1.0	1.0	0.0	1.0	1.0	1.0	1.0	1.0	1.0	0.0	1.0	1.0	1.0	1.0	0.0	0.0
28	3	1.0	1.0	1.0	1.0	0.7	1.0	1.0	1.0	1.0	1.0	1.0	0.0	1.0	1.0	1.0	1.0	0.7	0.7
29	6	1.0	1.0	1.0	1.0	0.8	1.0	1.0	1.0	1.0	1.0	1.0	0.3	1.0	1.0	1.0	1.0	0.7	1.0
30	3	1.0	1.0	1.0	1.0	0.7	1.0	1.0	1.0	1.0	1.0	1.0	0.7	1.0	1.0	1.0	1.0	0.7	1.0
31	3	1.0	1.0	1.0	1.0	0.7	1.0	1.0	1.0	1.0	1.0	1.0	0.7	1.0	1.0	1.0	1.0	0.7	1.0
32	3	1.0	1.0	1.0	1.0	1.0	1.0	1.0	1.0	1.0	1.0	1.0	1.0	1.0	1.0	1.0	1.0	1.0	1.0
33	1	1.0	1.0	1.0	1.0	1.0	1.0	1.0	1.0	1.0	1.0	1.0	1.0	1.0	1.0	1.0	1.0	1.0	1.0
34	1	1.0	1.0	1.0	1.0	1.0	1.0	1.0	1.0	1.0	1.0	1.0	1.0	1.0	1.0	1.0	1.0	1.0	1.0

head, and snout also increased in density, and pigment formed posteriorly along the upper and lower jaws. Melanophores posteriorly around the eye socket increased in number. The fins remained unpigmented.

Pygmy rockfish 28.6 mm long had dorsal pigment that stretched continuously from the jaws to the caudal fin (Fig. 1E, Table 4). Pigmentation was heavy along the dorsal midline, head, and nape. Snout pigmentation also intensified. More melanophores were present on the hypural margin. Pigment along the ventral body surface darkened, especially in the area posterior to the anal fin. More melanophores were observed at the anal-fin ray articulations than on smaller specimens. The three body bars increased in width and length and were better defined than on smaller specimens. The bar on the caudal peduncle began to exhibit a rectangular shape that is characteristic of the juvenile stage. The midbody bar also took on a rectangular shape, although the dorsal half was indented. The midbody bar and the caudal peduncle bars did not reach the ventral midline. The anterior body bar extended from the spinous dorsal fin to the vent (see arrow Fig. 1E). Anteriorly, the bar formed a more or less rectangular pattern on the dorsal half of the body above the pectoral fin. In general, the lateral body surface became more heavily pigmented, especially on the dorsal half. The lateral midbody pigment line began to be incorporated into the body bars. Opercular pigment became denser and merged with the nape pigment. The area anterior to the nape and operculum was less pigmented than the surrounding areas. Pigment along the posteroventral portion of the orbit became denser than in smaller specimens. A cheek bar began to form ventral to the eye (as evidenced by the two melanophores in Fig. 1E). Melanophores formed along the ventral surface of the lower jaw and covered the lateral surface of the upper jaw. Pigment began to develop on the membranes of the spinous dorsal fin, typically with some unpigmented areas between the dorsal fin pigment and the dorsal body pigment.

The largest specimen, 34.4 mm, had the densest and most distinctive pigmentation (Fig. 1F, Table 4). Pigment was present on most of the body. Along the dorsal surface, the pigment formed a complete line from the tip of the upper jaw to the caudal fin. The number of melanophores increased along the hypural region, the postanal ventral midline, and at the anal-fin articulations. The mid- and caudal body bars were rectangular and still did not reach the ventral midline, leaving an unpigmented ventrolateral area. The anterior body bar comprised heavy pigment extending posteriorly between dorsal-fin spines VIII–XI and the vent, a lighter area just anterior to this, and another heavily pigmented area stretching from about dorsal-fin spines III–VI almost to the middle of the gut cavity. Anterior to this bar was an area of mottled pigmentation. Pigment was visible just anterior to the base of the pectoral fin. Pigment covered both the spinous and soft dorsal fins, except along the distal edge. All other fins remained unpigmented. Opercular pigment was dense and merged with the nape pigment, but these were separated from the head and eye pigment by an area of low pigment density. Two cheek bars radiated from the lower margin of the orbit. Pigment occurred along both jaws and covered the snout and ventral portion of the lower jaw.

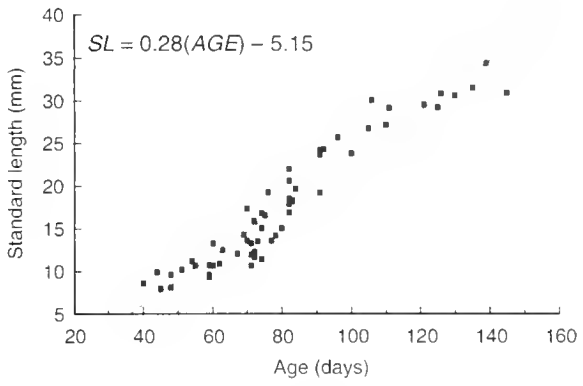

Figure 2

Standard length and age of pygmy rockfish (*Sebastes wilsoni*) (n=60). Solid line indicates predicted values from linear model.

Otolith examination

A linear relationship between standard length and age (as estimated from otolith increment counts) resulted in a good estimate of growth of pygmy rockfish (slope=0.28 mm/d; intercept=−5.15 mm; r^2=0.91; n=60; Fig. 2). The radius of the extrusion check ranged from 9.5 to 11.0 μm, averaging 10.5 μm (SD=0.29; n=60). Accessory primordia first appeared in a 19.8-mm specimen and were observed in otoliths from all larger specimens. Based on this character, transition from larval to pelagic juvenile stage occurs at around 20 mm SL.

Molecular confirmation

Interspecific levels of divergence, calculated among adult reference species, ranged from 0.13% (rougheye rockfish [*S. aleutianus*] vs. shortraker rockfish [*S. borealis*]) to 9.7% (black rockfish [*S. inermis*] vs. bocaccio) with an average of 4.1%. Two of the specimens (FT2 and FT3; Fig. 3A) were identical to one of the adult pygmy rockfish references (i.e. 0% sequence divergence) and differed from the other verified adult pygmy rockfish by a single nucleotide substitution (0.13% seq. div.). The remaining two specimens (FT1 and FT4; Fig. 3A) also were most similar to both adult pygmy rockfish references (0.13–0.40% seq. div.).

Although all four specimens were most similar to pygmy rockfish based on cytochrome *b* data, only a small number of nucleotide differences separated them from Puget Sound, redstripe, harlequin, and sharpchin rockfish (0.27–1.87%; Fig. 3A). A secondary data subset that included control region sequence (cyt-*b*+CR) yielded concordant results; all four larval specimens were

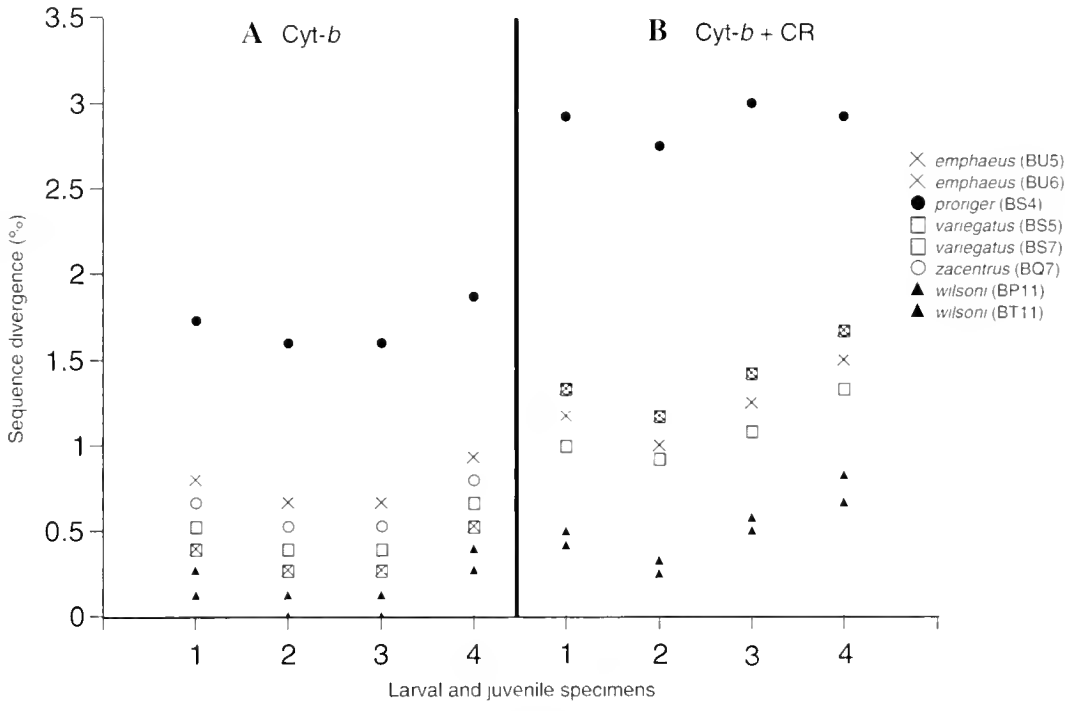

Figure 3

Percent sequence divergence based on the number of nucleotide differences in (**A**) cytochome *b* and (**B**) cytochrome *b* + control region between the four putative pygmy rockfish (*Sebastes wilsoni*) specimens (FT1–FT4) and five closely related reference species of *Sebastes*, including two adult *S. wilsoni*. Percent sequence divergence was calculated as the number of nucleotide differences over 750 base pairs (cyt-*b*) and 1200 base pairs (cyt-*b*+CR).

most similar to pygmy rockfish (0.25–0.83%; Fig. 3B). Increased levels of interspecific nucleotide variation, attributable to the faster evolving control region, resulted in more pronounced differences between the four specimens and the other species of *Sebastes* within the subset (range: 0.83–3.00%; Fig. 3B). Additionally, a distance-based analysis (UPGMA) of haplotypes (cyt-*b*+CR) clustered all four specimens with pygmy rockfish reference material.

Discussion

Postflexion larval pygmy rockfish can be identified through a combination of pigment and meristic characters. At approximately 8–10 mm, the larval pigment pattern is similar to only four of the 30 *Sebastes* species illustrated in the literature that occur within our geographic area (Matarese et al., 1989; Moser, 1996; Laroche[1]): yellowtail (*S. flavidus*), blue (*S. mystinus*), canary (*S. pinniger*), and sharpchin rockfish. Yellowtail and blue rockfish can be separated from pygmy rockfish because they exhibit ventral body and hypural pigment at this size—pigment that does not show up in pygmy rockfish until approximately 14 and 15 mm, respectively. In canary rockfish, the presence of ventral body pigment and dorsal midline pigment posterior to the soft dorsal fin (instead of at the base of the soft dorsal-fin rays as in pygmy rockfish) can help differentiate this species from pygmy rockfish. Pigmentation patterns of sharpchin rockfish are very similar to pygmy rockfish at 10 mm; however, sharpchin rockfish retain pigmented pelvic fins until 12.7 mm (Laroche and Richardson, 1981). Counts of anal-fin rays often can be used to differentiate these two species because pygmy rockfish have six rays and sharpchin have rockfish seven rays (Chen, 1986; Matarese et al., 1989; Moreland and Reilly, 1991; Laroche[1]). There is a small overlap in anal-fin ray counts (approximately 7%), and, because of this, 100% certainty of identification cannot be reached by anal-fin ray counts alone. Therefore, in order to increase confidence in identifications, a combination of pigmentation and fin-ray counts should be employed. After approximately 15 mm, a full complement of fin rays and gill rakers typically is present and can be used in combination with pigmentation patterns to differentiate pygmy rockfish from most other rockfish species. In these late-stage larvae, only three species (yellowtail, black (*S. melanops*), and blue rockfish) have a pigment pattern that could be confused with pygmy rockfish (Matarese et al., 1989; Moser, 1996; Laroche[1]),

but these patterns can be easily separated by using meristic characters.

Pelagic juvenile pygmy rockfish have a distinctive pigment pattern consisting of three body bars that can be used to discriminate this species from other *Sebastes* species. Yellowtail, halfbanded, and redstripe rockfish are the only species that have a similar three-barred pigment pattern (Matarese et al., 1989; Moser, 1996; Laroche[1]). Yellowtail rockfish can be distinguished by the lack of cheek bars and the presence of body bars that extend all the way to the ventral surface. Also, in yellowtail rockfish, the body bars form at a larger size than in pygmy rockfish. In halfbanded rockfish, the most anterior body bar is more densely pigmented than the other bars and typically forms a diamond shape. The caudal body bar is much wider and covers the entire peduncle. Redstripe rockfish are the most similar and are difficult to separate from pygmy rockfish by using pigmentation alone. However, these two species can be separated with greater than 90% certainty by using meristic counts. Pygmy rockfish have a mean anal-fin ray count of 6 (95% from the present study, and 93% from Laroche[1]), whereas redstripe rockfish have an average of 7 anal-fin rays (100% from Chen, 1986; 97% from Laroche[1]).

It should be noted that the only illustration of pygmy rockfish prior to our study was a 35.0-mm pelagic juvenile by Laroche,[1] which showed several pigment differences from our specimens of equivalent size. Laroche's illustrated specimen had only faint body barring, no cheek bars, and no ventral pigment, whereas all our specimens had prominent body barring, at least one cheek bar, and ventral pigment along the anal-fin articulations. At this time we cannot determine whether these differences were due to geographic variability in pigment patterns (Laroche's specimen probably was collected farther north than all of our specimens), or a misidentification of the original specimen illustrated by Laroche.[1]

The identification of larval and pelagic juvenile pygmy rockfish used in our study was confirmed by using DNA sequence analyses. Previous molecular identifications and subsequent descriptions of juvenile starry rockfish (*S. constellatus*) and swordspine rockfish (*S. ensifer*) also were based on mitochondrial cytochrome *b* data (Rocha-Olivares et al., 2000). In our study, orthologous cytochrome *b* sequence was sufficient for identification purposes, particularly for those specimens exhibiting exact haplotype matches to reference adult pygmy rockfish (e.g., FT2/FT3: 0.0% sequence divergence). Relatively low levels of interspecific genetic variation occurred between larval specimens and several reference species (pygmy, sharpchin, harlequin, and Puget Sound rockfish, and, to a lesser extent, redstripe rockfish). Rocha-Olivares et al. (1999a) used control region sequence, in addition to cytochrome *b*, to resolve phylogenetic relationships among recently diverged species of the *Sebastes* subgenus *Sebastomus*. In the present study, the control region sequence was used to increase divergence levels between species and to aid in insuring correct molecular identifications of specimens FT1 and FT4. Species assignment to pygmy rockfish was supported by the smallest divergence (based on cyt-*b* and cyt-*b*+CR) from reference pygmy rockfish compared with the other *Sebastes* species.

Larval and juvenile pygmy rockfish can also be separated from other *Sebastes* species by comparing the radius of the extrusion check on their otoliths. Of the fourteen other *Sebastes* species or species complexes with measured otolith extrusion check radii (Laidig and Ralston, 1995; Laidig et al., 1996; Laidig and Sakuma, 1998), only four species and two complexes have radii close to the average extrusion check radii for pygmy rockfish (10.5 μm, SD=0.3). Stripetail rockfish (*S. saxicola*) had an average extrusion check radius (11.6 μm, SD=0.5) that was larger than the largest radius for pygmy rockfish (11.0 μm). Quillback rockfish (*S. maliger*) had an average extrusion check radius of 9.1 μm (SD=0.1), which was smaller than the smallest radius for pygmy rockfish (9.5 μm). Species with extrusion check radii similar to pygmy rockfish were kelp rockfish (*S. atrovirens*) at 10.6 μm (SD=0.2), blue rockfish at 10.9 μm (SD=1.1), and the copper rockfish (*S. caurinus*, extrusion check radius=10.5 μm; SD=0.4) and gopher rockfish (*S. carnatus*, extrusion check radius=10.6 μm; SD=0.3) complexes (see Laidig et al., 1996, for complex definitions). Of these species, the only one that would be confused with pygmy rockfish, by pigmentation alone, would be blue rockfish at small sizes. However, pygmy rockfish and blue rockfish are easily separated by using meristic characters.

Growth rates of larval rockfish generally are slow during the first month of life and increase thereafter (Laidig et al., 1991; Sakuma and Laidig, 1995; Laidig et al., 1996). Because the youngest fish in our study was estimated to be 40 days old, our linear model can not be used to estimate early larval growth rates. For pygmy rockfish older than 40 days, the growth rate of 0.28 mm/day was somewhat slower than that observed for other *Sebastes*. Woodbury and Ralston (1991) found that, for fish older than 40 days, growth rates varied from 0.30 for widow rockfish (*S. entomelas*) to 0.97 mm/day for bocaccio. Other species exhibiting slightly faster growth rates after 40 days of age include stripetail rockfish (0.37 mm/day; Laidig et al., 1996), grass rockfish (*S. rastrelliger*; 0.36 mm/day; Laidig and Sakuma, 1998), and shortbelly rockfish (*S. jordani*; 0.53 mm/day; Laidig et al., 1991). Yellowtail rockfish had a more similar growth rate, ranging from 0.19 to 0.46 mm/day (Woodbury and Ralston, 1991). These differences in growth may reflect genetic variability or responses to environmental variables. Woodbury and Ralston (1991) suggested that annual variability in growth rates of juvenile rockfish was related to year-to-year changes in environmental conditions, especially temperature. Boehlert (1981) determined that temperature greatly affected growth rate of young splitnose rockfish (*S. diploproa*) in the laboratory. Boehlert and Yoklavich (1983) observed slower growth rates for black rockfish in colder temperatures. Lenarz et al. (1991) analyzed the vertical

distribution of late larval and pelagic juvenile rockfish and determined that pygmy rockfish were present on average in deeper, colder water than that favored by other rockfish species. This spatial separation of pelagic juvenile pygmy rockfish and other *Sebastes* spp. may explain the slower growth observed in pygmy rockfish.

Acknowledgments

We would like to thank the scientists and crew from the Southwest Fisheries Science Center (SWFSC) who collected the samples aboard the NOAA RV *David Starr Jordan*. We thank Geoff Moser and Bill Watson (NOAA, SWFSC) for examining some of our pygmy rockfish specimens. Reference sequences of *Sebastes* were generated and kindly provided by personnel at the Fisheries Resources Division of the SWFSC, La Jolla, CA (R. D. Vetter, A. Rocha-Olivares, B. J. Eitner, C. A. Kimbrell, and C. Taylor). In addition, we thank Mary Yoklavich for all her valuable comments and all the reviewers who contributed to this manuscript.

Literature cited

Boehlert, G. W.
1981. The effects of photoperiod and temperature on the laboratory growth of juvenile *Sebastes diploproa* and a comparison with growth in the field. Fish. Bull. 79:789–794.

Boehlert, G. W., and M. M. Yoklavich.
1983. Effects of temperature, ration, and fish size on growth of juvenile black rockfish, *Sebastes melanops*. Environ. Biol. Fish. 8:17–28.

Chen, L.
1986. Meristic variation in *Sebastes* (Scorpaenidae), with an analysis of character association and bilateral pattern and their significance in species association. NOAA Tech. Rep. NMFS-45, 17 p.

Hillis, D. M., B. K. Mable, A. Larson, S. K. Davis, and E. A. Zimmer.
1996. Nucleic acids IV: sequencing and cloning. Chapter 9 *in* Molecular systematics, 2nd ed. (D. M. Hillis, C. Moritz, and B. K. Mable, eds.), p. 321–381. Sinauer Associates, Sunderland, MA.

Hunter, J. R., and N. C.-H. Lo.
1993. Ichthyoplankton methods for estimating fish biomass introduction and terminology. Bull. Mar. Sci. 53:723–727.

Laidig, T. E., and S. Ralston.
1995. The potential use of otolith characters in identifying larval rockfish (*Sebastes* spp.). Fish. Bull. 93:166–171.

Laidig, T. E., S. Ralston, and J. R. Bence.
1991. Dynamics of growth in the early life history of shortbelly rockfish, *Sebastes jordani*. Fish. Bull. 89:611–621.

Laidig, T. E., and K. M. Sakuma.
1998. Description of pelagic larval and juvenile grass rockfish, *Sebastes rastrelliger* (Family Scorpaenidae), with an examination of age and growth. Fish Bull. 96:788–796.

Laidig, T. E., K. M. Sakuma, and M. M. Nishimoto.
1996. Description of pelagic larval and juvenile stripetail rockfish, *Sebastes saxicola* (family Scorpaenidae), with an examination of larval growth. Fish Bull. 94:289–299.

Laroche, W. A., and S. L. Richardson.
1981. Development of larvae and juveniles of the rockfishes *Sebastes entomelas* and *S. zacentrus* (Family Scorpaenidae) and occurrence off Oregon, with notes on head spines of *S. mystinus*, *S. flavidus*, and *S. melanops*. Fish. Bull. 79:231–257.

Lee, T.-W., and G.-C. Kim
2000. Microstructural growth in otoliths of black rockfish, *Sebastes schlegeli*, from prenatal larval to early juvenile stages. Ichthyol. Res. 47:335–341.

Lenarz, W. H., R. J. Larson, S. Ralston.
1991. Depth distributions of late larvae and pelagic juveniles of some fishes of the California Current. CalCOFI (California Cooperative Oceanic Fisheries Investigations) Rep. 32:41–46.

Love, M.
1996. Probably more than you wanted to know about the fishes of the Pacific coast, 381 p. Really Big Press, Santa Barbara, CA.

Love, M., M. Yoklavich, and L. Thorsteinson.
2002. The rockfishes of the northeast Pacific, 405 p. Univ. California Press, Berkeley, CA.

Matarese, A. C., A. W. Kendall Jr., D. M. Blood, and B. M. Vinter.
1989. Laboratory guide to early life history stages of northeast Pacific fishes. NOAA Tech. Rep. NMFS-80, 652 p.

Moreland, S. L., and C. A. Reilly.
1991. Key to the juvenile rockfishes of central California. *In* Methods used to identify pelagic juvenile rockfish (genus *Sebastes*) occurring along the coast of central California (T. E. Laidig and P. B. Adams, eds.), p. 59–180. NOAA Tech. Memo., NOAA-TM-NMFS-SWFSC-166.

Moser, H. G.
1996. The early stages of fishes in the California Current region. Calif. Coop. Oceanic Fish. Invest. Atlas no. 33, 1505 p.

Moser, H. G., and J. L. Butler.
1987. Descriptions of reared larvae of six species of *Sebastes*. *In* Widow rockfish: proceedings of a workshop, Tiburon, California, December 11–12, 1980 (W. H. Lenarz and D. R. Gunderson, eds.), p. 19–29. NOAA Tech. Rep. NMFS-48.

Pacific Fishery Management Council.
2000. Status of the Pacific coast groundfish fishery through 1999 and recommended acceptable biological catches for 2000, 165 p. Pacific Fishery Management Council, Portland, OR.

Ralston, S., J. R. Bence, M. B. Eldridge, and W. H. Lenarz.
2003. An approach to estimating rockfish biomass based on larval production, with application to *Sebastes jordani*. Fish. Bull. 101:129–146.

Richardson, S. L., and W. A. Laroche.
1979. Development and occurrence of larvae and juveniles of the rockfishes *Sebastes crameri*, *Sebastes pinniger*, and *Sebastes helvomaculatus* (Family Scorpaenidae) off Oregon. Fish. Bull. 77:1–46.

Rocha-Olivares, A.
1998. Multiplex haplotype-specific PCR: a new approach for species identification of the early life stages of rock-

fishes of the species-rich genus *Sebastes* Cuvier. J. Exp. Mar. Biol. Ecol. 231:279–290.

Rocha-Olivares, A., C. A. Kimbrell, B. J. Eitner, and R. D. Vetter.
1999a. Evolution of a mitochondrial cytochrome *b* gene sequence in the species-rich genus *Sebastes* (Teleostei, Scorpaenidae) and its utility in testing the monophyly of the subgenus *Sebastomus*. Mol. Phylogenet. Evol. 11:426–440.

Rocha-Olivares, A., H. G. Moser, and J. Stannard.
2000. Molecular identification and description of juvenile stages of the rockfishes *Sebastes constellatus* and *Sebastes ensifer*. Fish. Bull. 98:353–363.

Rocha-Olivares, A., R. H. Rosenblatt, and R. D. Vetter.
1999b. Molecular evolution, systematics, and zoogeography of the rockfish subgenus *Sebastomus* (*Sebastes*, Scorpaenidae) based on mitochondrial cytochrome *b* and control region sequences. Mol. Phylogenet. Evol. 11:441–458.

Sakuma, K. M., and T. E. Laidig.
1995. Description of larval and pelagic juvenile chilipepper, *Sebastes goodei* (family Scorpaenidae), with an examination of larval growth. Fish. Bull. 93:721–731.

Seeb, L. W., and A. W. Kendall Jr.
1991. Allozyme polymorphisms permit the identification of larval and juvenile rockfishes of the genus *Sebastes*. Environ. Biol. Fishes 30:191–201.

Stein, D. L., B. N. Tissot, M. A. Hixon, and W. Barss.
1992. Fish-habitat associations on a deep reef at the edge of the Oregon continental shelf. Fish. Bull. 90:540–551.

Stransky, C.
2001. Preliminary results of a shape analysis of redfish otoliths: comparison of areas and species, 9 p. North Atl. Fish. Org. Sci. Coun. Res. Doc. 01 14.

Winnepenninckx, B., T. Backeljau, and R. DeWachter.
1993. Extraction of high molecular weight DNA from mollusks. Trends Genet. 9:407.

Woodbury, D. P., and S. Ralston.
1991. Interannual variation in growth rates and back-calculated birthdate distributions of pelagic juvenile rockfishes (*Sebastes* spp.) off central California coast. Fish. Bull. 89:523–533.

Yoklavich, M. M., and G. W. Boehlert.
1987. Daily growth increments in otoliths of juvenile black rockfish, *Sebastes melanops*: An evaluation of autoradiography as a method of validation. Fish. Bull. 85:826–832.

Yoklavich, M. M., H. G. Greene, G. M. Cailliet, D. E. Sullivan, R. N. Lea, and M. S. Love.
2000. Habitat associations of deep-water rockfishes in a submarine canyon: an example of a natural refuge. Fish. Bull. 98:625–641

Estimating the emigration rate of fish stocks from marine sanctuaries using tag-recovery data

Richard McGarvey

Aquatic Sciences; South Australian Research and Development Institute (SARDI)
2 Hamra Avenue
West Beach, South Australia 5024, Australia
E-mail address: mcgarvey.richard@saugov.sa.gov.au

Abstract—A critical process in assessing the impact of marine sanctuaries on fish stocks is the movement of fish out into surrounding fished areas. A method is presented for estimating the yearly rate of emigration of animals from a protected ("no-take") zone. Movement rates for exploited populations are usually inferred from tag-recovery studies, where tagged individuals are released into the sea at known locations and their location of recapture is reported by fishermen. There are three drawbacks, however, with this method of estimating movement rates: 1) if animals are tagged and released into both protected and fished areas, movement rates will be overestimated if the prohibition on recapturing tagged fish later from within the protected area is not made explicit; 2) the times of recapture are random; and 3) an unknown proportion of tagged animals are recaptured but not reported back to researchers. An estimation method is proposed which addresses these three drawbacks of tag-recovery data. An analytic formula and an associated double-hypergeometric likelihood method were derived. These two estimators of emigration rate were applied to tag recoveries from southern rock lobsters (*Jasus edwardsii*) released into a sanctuary and into its surrounding fished area in South Australia.

Manuscript submitted 24 March 2003 to Scientific Editor's Office.

Manuscript approved for publication 5 March 2004 by the Scientific Editor.

Fish. Bull. 102:464–472 (2004).

Marine sanctuaries, also known as marine protected areas (MPAs), marine reserves, and no-take areas, are being widely promoted and implemented. Important for assessing the impact of these "no-take" sanctuaries (from which fishing has been excluded) on exploited populations is the rate of emigration of animals out into the remaining fished habitat.

The most widely available data for estimating movement rates of commercially or recreationally exploited populations are those from tagged and recovered fish (Hilborn, 1990). Animals are captured alive, a visible numbered tag is inserted and they are released back into the wild. Because the accuracy of tag-recovery studies relies on fishermen reporting recaptured tags, the quality of tag-recovery information is lower than that from a controlled experiment.

Tag-recovery experiments have three limitations for estimating movement rates of animals—the first two apply to most tagged populations, the third applies specifically to emigration from sanctuaries: 1) times at large (the numbers of days from when each animal is tagged and released to when it is subsequently recaptured in the fishery) are highly variable; 2) not all recaptured tags are reported to researchers by fishermen and this rate of tag nonreporting is often unknown; and 3) tag recoveries cannot be obtained from within sanctuaries for the simple reason that no fishing is allowed there.

If this last asymmetry (of recaptures from the sanctuary coming only from tagged animals that emigrate) is not accounted for in the estimation model, then the emigration rate out of the sanctuary will be overestimated. With previous movement estimators, tag releases and recaptures from all strata have been assumed. The aim of the present article is to develop an unbiased estimator of emigration rate from no-take areas by using data of tag releases both into the sanctuary and into the fished zone surrounding it, but where recoveries from nonmoving tagged animals are only possible from the fished zone. An estimate for the recovery rate (proportion of fish recaptured and their tags reported) in the fished zone was also obtained.

Materials and methods

Tag-recovery data

The data used to estimate the emigration rate from Gleesons Landing Lobster Sanctuary (Fig. 1) are tag recoveries from lobsters tagged and released both inside the sanctuary and into the fished zone surrounding the sanctuary. A large South Australian lobster tagging program was undertaken in 1993–96 throughout South Australian waters. T-bar tags (Hallprint, Victor Harbour, South Australia) were inserted into the ventral muscle at the first segment of the lobster abdomen. The rate of tag shedding was estimated from double tags at between 6% and 12% per year (Xiao[1]) and is incorporated in the recovery rate.

[1] Xiao Y. 2003. Personal commun. Aquatic Sciences, South Australian Research and Development Institute (SARDI), P.O. Box 120, Henley Beach, South Australia 5022, Australia.

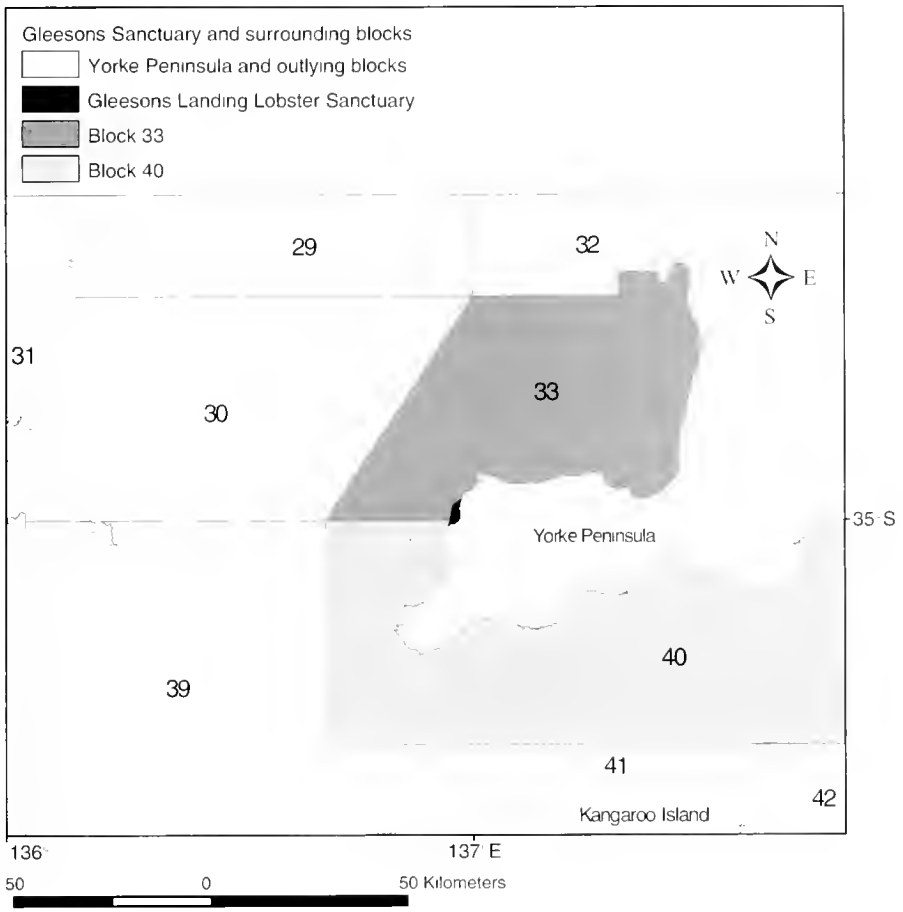

Figure 1

Location of Gleesons Landing Lobster Sanctuary (small dark area on the boundary of MFA blocks 33 and 40) along the west coast of the Yorke Peninsula in South Australia.

As part of this tagging program (Table 1), 3235 southern rock lobsters (*Jasus edwardsii*) were tagged and released into the "fished zone" surrounding Gleesons Sanctuary, namely into statistical reporting blocks 33 and 40 (Fig. 1). In January 1994, 413 lobsters were captured, tagged, and released inside the Gleesons Sanctuary. These lobsters were predominantly in the range of 80–120 mm carapace length (CL), around the size of maturity of about 100 mm CL; more lobsters below the legal minimum length (98.5 mm CL) were released in the fished zone.

Gleesons Landing Lobster Sanctuary (Fig. 1) is an area where lobster fishing has been prohibited since 1982. It lies along the Yorke Peninsula's western coast in an area of medium to low lobster catches. In width, this sanctuary extends 1–2 km from shore to seaward and runs 7–8 km north-south.

Nearly all tag recoveries were reported by commercial lobster fishermen who noticed tagged lobsters in their catch in the course of day-to-day fishing operations. Tag recoveries of lobsters released into both the sanctuary and the fished zone were, therefore, only possible from the fished zone. GPS coordinates, date, and carapace length were recorded for all tagged and recaptured lobsters. Longer-range movements from both sanctuary and fished zone were directed southwest towards the shelf edge.

Prescott et al.[2] previously described qualitative features of the movement of South Australian *Jasus edwardsii*: 1) nearly all longer-distance movements were directed offshore to deeper water and away from the coast; 2) in order of greater to lesser average distances moved, were i) immature females, ii) males, and iii) mature or egg-bearing females, for nearly all five South Australian regions analyzed; 3) movements were largely restricted to lobsters in a specific length range at time

[2] Prescott, J., R. McGarvey, G. Ferguson, and M. Lorkin. 1998. Population dynamics of the southern rock in South Australian waters. Fisheries Research and Development Corporation of Australia Report 93/086, p. 23–27. Aquatic Sciences, South Australian Research and Development Institute (SARDI), P.O. Box 120, Henley Beach, South Australia 5022, Australia.

Table 1

Tag-recovery data from Gleesons Landing lobster sanctuary and the surrounding fishing zone used in estimating yearly movement rates of southern rock lobsters.

Data	Variable name	Observed number of lobsters
Number of lobsters tagged and released into the sanctuary	$\tilde{N}^S_T$	413
Number of lobsters recovered that had moved (≥3 km) from the sanctuary into the fishing zone	$\tilde{N}^S_{M,R}$	29
Number of lobsters tagged and released into the surrounding fishing zone	$\tilde{N}^F_T$	3235
Number of lobsters recovered that had moved (≥3 km) within the fishing zone	$\tilde{N}^F_{M,R}$	89
Number of lobsters ecovered that had not moved (≥3 km) within the fishing zone	$\tilde{N}^F_{NM,R}$	277

of tagging, roughly 100–140 mm CL for females, and 100–150 mm CL for males, with a noticeable shift to smaller sizes for both sexes on the southeast coast of South Australia where growth and thus size of maturity are known to be lower; 4) overall, most lobsters in the fished areas did not move large distances, about 15% moving more than 5 km; 5) two areas stood out as being habitats from where significant movement occurred, the coastal zone off the Coorong and Yorke Peninsula; and 6) for Yorke Peninsula, higher than proportional numbers of tagged lobsters that moved significant distances were tagged and released inside Gleesons Sanctuary.

In the present study study, a lobster was classified as having undergone movement if its measured distance from point of tagging to point of recapture was greater than 3 km. This definition of lobster "movement" was chosen for two reasons. 1) The mean width of MPA coastal zone to be protected in the currently proposed state representative system is assumed to be 5 km wide; that is, it is assumed that sanctuary areas will extend from the shore outward to sea across the full 3 nmi (which is about 5 km) of state territorial waters. Thus, a 3-km movement would represent slightly more than the mean distance needed for lobsters to leave the state-protected territorial waters of the reserve and enter waters open for fishing. This assumption is strengthened by the knowledge that most longer-range movements of South Australian rock lobster are directed from inshore to offshore. 2) According to the geographical features of the present study, a 3-km movement seaward from any location in Gleesons Landing Sanctuary would place the tagged lobster well into the fished zone, i.e., it would constitute a movement out of the sanctuary. Of sanctuary-tagged lobsters, 4 of 33 recaptured lobsters in the first season after tagging exited the reserve but moved less than 3 km. These 4 recaptured lobsters were excluded from the data set. The mean distance moved by lobsters from the sanctuary was 37.4 km.

Because movement of South Australian lobsters is directed strongly away from the inshore zone, the immigration rate of lobsters back into the Gleesons Landing Sanctuary is likely to be quite low. Moreover, *Jasus edwardsii* seek shelter daily and remain on specific reefs through most of their life (MacDiarmid et al. 1991; Kelly 2001). Long-distance movements occur rarely more than once in a lifetime. Thus, in the fishing zone, where there is a continual removal of adult lobsters from reef habitat, the on-going creation of new shelter space is higher than in the sanctuary and thus lobsters that did stray inshore into the sanctuary would be less likely to find shelter, further reducing the probability of migration into the sanctuary. In the estimator presented below, only the emigration rate (the movement rate out of the sanctuary) is calculated.

The recapture data included lobsters at large for a wide range of times, many having been recaptured longer than one year after tag release. However, to estimate emigration rate, we sought the proportion of lobsters emigrating out per year. Therefore, subsets of recapture data were selected that had a mean time at large of one year. The temporal distributions of recaptured lobsters showed distinct modes around 1 year at large (recaptures between 0.5 and 1.5 years at large, Fig. 2), and the number of recaptures in these 1-year modes were used for estimating yearly movement rate (Table 1).

Some tagged and released lobsters were recaptured more than once. For these lobsters, the single recapture was selected and used for which the time at large was closest to one full year.

Notation

The information on movement in each set of tag releases is taken to be binary: each recaptured animal is classified as having moved or as having not moved during its approximately 1-year time at large (from time of tag release to time of recapture).

To carry out the movement-rate estimation, it is useful to consider the complete set of four possible outcomes for each tagged and released animal: 1) it moved and was recovered after one year (denoted M,R); 2) it did not move and was recovered after one year (NM,R); 3) it moved and was not recovered after one year (M,NR); 4) it did not move and was not recovered after one year (NM,NR). These four possible recapture outcomes applied to animals tagged and released in both strata,

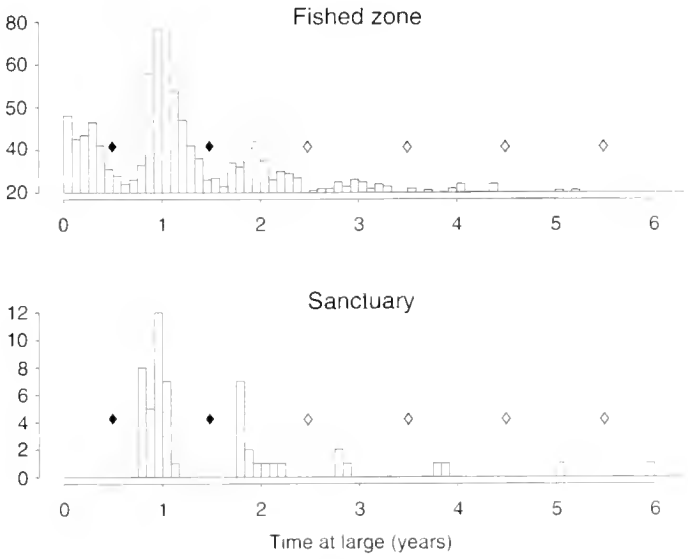

Figure 2

Histograms over time at large (in monthly bins) of recapture numbers from the fishing zone (MFA blocks 33 and 40) and from the Gleesons Landing Lobster Sanctuary. The diamond markers indicate divisions between modes at 0.5, 1.5, 2.5, etc. years at large; recaptures from the sanctuary and fishing zone that occurred between 0.5 and 1.5 years after release (between the black diamond markers) identify the subsets of data used to estimate yearly emigration rate from the sanctuary.

inside and outside the sanctuary. The tag-recovery data provided direct measures for only three of these eight possible numbers of recaptures.

We define "not recovered" to include both tagged animals that were not recaptured, as well as those that were recaptured by a fisherman but whose tag information (notably the location of recapture) was not reported back to researchers and therefore was not included in the tag-recovery database.

The movement-rate estimate is given in terms of the following data inputs: the number of lobsters tagged and released in 1) fished and 2) protected zones, and the numbers recovered that 3) moved (≥3 km) or 4) did not move from the fished zone over one year after tagging, and the 5) number that moved (≥3 km) from the sanctuary in one year.

Superscripts '*F*' and '*S*' denote fished zone and sanctuary, respectively, for the location of tag release. Let $N^F_{NM,R}$ and $N^F_{M,R}$ denote the numbers of animals that were recovered after a year and that moved or that did not move in the fished zone. From animals tagged and released inside the sanctuary, only the number that moved and were recovered ($N^S_{M,R}$) is available as an unbiased measure. In addition, we know the total number of animals originally tagged and released in the fished zone and sanctuary, N^F_T and N^S_T. Input quantities from the tag-recovery data set will henceforth be indicated by a tilde (~): $\{\tilde{N}^S_{M,R}, \tilde{N}^S_T, \tilde{N}^F_{NM,R}, \tilde{N}^F_{M,R}, \tilde{N}^F_T\}$ (Table 1).

Assumptions

Three assumptions were used to derive an emigration-rate estimate: 1) The two ways to define an estimate for the proportion that moved within the fished zone, namely as a proportion by using only recapture numbers, and as a proportion over the number originally tagged, can be set equal. 2) Recapture probabilities of animals that were tagged and released inside the sanctuary and that moved are assumed to equal those that were tagged and released into the fished zone and that also moved. (The first two assumptions were employed explicitly in steps 2 and 3 below.) 3) A third assumption is implicit in step 2, specifically in the recapture-conditioned movement proportion in the fished zone ($P^{F,R}_M$, Eq. 2): recapture probabilities of animals tagged and released in the fished zone that moved and of those that did not move are assumed to be equal. Assumptions 2 and 3 would both follow from assuming equal recapture probabilities for all lobsters in the fished zone.

Emigration rate: derivation of the estimate formula

In this section, an emigration-rate formula is derived. It provides a closed-form estimate of the yearly proportion of lobsters emigrating out of the sanctuary.

The proportion of animals moving can be estimated from tag-recovery data in two ways, namely as "tag-

conditioned" and "recapture-conditioned" proportions. A tag-conditioned movement proportion (Eq. 1) is the total number of lobsters that moved (≥3 km) divided by the number originally tagged and released. It includes, in the numerator, all tagged animals that moved, both those that were recovered, as well as those that were not recovered. With a recapture-conditioned movement-rate estimate (e.g., Eq. 2), only counts of recaptured lobsters are used. The estimate expresses the movement proportion as the number of tagged animals that were recaptured and that also moved (≥3 km) divided by the total number recaptured. These two definitions for the movement proportion will be used to derive an estimation formula in terms of the five data inputs.

Step 1 The derivation begins by writing the estimate for proportion of lobsters that moved (P_M^S) in tag-conditioned form:

$$P_M^S = \frac{\tilde{N}_{M,R}^S + N_{M,NR}^S}{\tilde{N}_T^S}. \tag{1}$$

This estimate of movement rate from the sanctuary is based on a tag-conditioned proportion because we have no observations of recaptured lobsters from the sanctuary that did not move (no unbiased measure of $N_{NM,R}^S$) which a recapture-conditioned movement proportion would have required. However we did have information about $N_{M,NR}^S$, the nonrecovery of tagged animals that emigrate from the sanctuary into the fished zone. It can be estimated (steps 2 and 3) with the second assumption that recovery rate for lobsters moving from the sanctuary equals that of lobsters moving (≥3 km) within the fished zone.

Step 2 Under assumption 1, the two ways in which movement proportion in the fished zone can be defined (as tag- and recapture-conditioned proportions) are equated. For fished zone releases, the recapture-conditioned ('*rc*') movement proportion is written

$$P_M^{F,rc} = \frac{\tilde{N}_{M,R}^F}{\tilde{N}_{NM,R}^F + \tilde{N}_{M,R}^F}. \tag{2}$$

For the recapture-conditioned estimate formula (Eq. 2), all three quantities on the right-hand side are given as data inputs. With only numbers of lobsters recovered, the formula is, in this sense, conditional on recapture.

The tag-conditioned ('*tc*') proportion of lobsters moving ≥3 km of those released in the fished zone is written

$$P_M^{F,tc} = \frac{\tilde{N}_{M,R}^F + N_{M,NR}^F}{\tilde{N}_T^F}. \tag{3}$$

The first assumption is

$$P_M^{F,rc} = P_M^{F,tc}. \tag{4}$$

Substituting Equations 2 and 3 into Equation 4 and solving for $N_{M,NR}^F$, the number of lobsters that moved ≥3 km within the fished zone but were not recovered, yields

$$N_{M,NR}^F = \tilde{N}_{M,R}^F \left\{ \frac{\tilde{N}_T^F}{\tilde{N}_{NM,R}^F + \tilde{N}_{M,R}^F} - 1 \right\}. \tag{5}$$

Step 3 Assumption 2 permits the derivation of a formula for $N_{M,NR}^S$. We first define the recovery proportions of animals that moved within the fished zone (F) as

$$f_M^F = \frac{\tilde{N}_{M,R}^F}{\tilde{N}_{M,NR}^F + \tilde{N}_{M,R}^F} \tag{6}$$

and from the sanctuary (S) as

$$f_M^S = \frac{\tilde{N}_{M,R}^S}{N_{M,NR}^S + \tilde{N}_{M,R}^S}. \tag{7}$$

Assumption 2, that the recovery rate (necessarily in the fished zone) for animals that were tagged and released in the sanctuary and that moved into the fished zone is the same as for animals that were both released and recaptured after moving within the fished zone becomes

$$f_M^F = f_M^S. \tag{8}$$

Substituting Equations 6 and 7 into Equation 8 and rearranging terms, we have

$$N_{M,NR}^S = \frac{\tilde{N}_{M,R}^S \left(N_{M,NR}^F + \tilde{N}_{M,R}^F \right)}{\tilde{N}_{M,R}^F} - \tilde{N}_{M,R}^S. \tag{9}$$

Step 4 Substituting Equation 5 into Equation 9 and substituting the result into Equation 1 yields a closed-form estimation formula for the quantity we seek, the proportion moving from the sanctuary in one year:

$$P_M^S = \frac{\tilde{N}_T^F \cdot \tilde{N}_{M,R}^S}{\tilde{N}_T^S \cdot \left(\tilde{N}_{NM,R}^F + \tilde{N}_{M,R}^F \right)}. \tag{10}$$

Numerical estimator: double-hypergeometric likelihood method

A likelihood formulation of this estimator was also constructed. The likelihood function describing a single tag-recapture experiment is hypergeometric (Seber, 1982; Rice, 1995) because sampling is without replacement. The set of possible outcomes from each of the two tagging experiments can be formulated as a 2×2 contingency table for the experimental populations of all lobsters originally tagged and released. The two pairs of outcomes represented in each contingency table are "moved" or "not moved" and "recovered" or "not recovered," yielding the four possible outcomes from both sets of tag releases (see "Notation" section).

In this study the data from two interacting tag-recovery experiments were used to generate an estimate of reserve emigration rate, namely of lobsters tagged and released into the sanctuary and into the fished zone. Thus, the product of a pair of linked hypergeometric probability mass functions, each corresponding to a 2-way contingency table, is the natural form of the likelihood function for P_M^S.

The derivation of Equation 10 was made with two assumptions, namely Equations 4 and 8. Incorporated in the likelihood, the two assumptions constrain the eight recapture numbers in the contingency tables. In the likelihood formulation, a third constraint was needed which is analogous to assumption 1 but which applies to sanctuary releases.

The derivation for constructing this likelihood from a pair of linked hypergeometric probability functions will proceed by 1) writing out the "raw" contingency tables in terms of the eight recapture numbers (N), as denoted in the "Tag-recovery data" and "Notation" sections, 2) algebraically re-expressing the elements of the tables so that the parameter to be estimated is explicit, 3) imposing the three constraints, and 4) writing out the likelihood, using the hypergeometric form for contingency tables.

For the lobsters tagged and released in the sanctuary, the raw contingency table is

	Recovered	Not recovered	Totals
Moved	$\tilde{N}^S_{M,R}$	$N^S_{M,NR}$	$\tilde{N}^S_{M,R}+N^S_{M,NR}$
Not moved	$N^S_{NM,R}$	$N^S_{NM,NR}$	$\tilde{N}^S_T-(\tilde{N}^S_{M,R}+N^S_{M,NR})$
Totals	$\tilde{N}^S_{M,R}+N^S_{NM,R}$	$\tilde{N}^S_T-(\tilde{N}^S_{M,R}+N^S_{NM,R})$	$\tilde{N}^S_T$

For the lobsters tagged in the fished zone:

	Recovered	Not recovered	Totals
Moved	$\tilde{N}^F_{M,R}$	$N^F_{M,NR}$	$\tilde{N}^F_{M,R}+N^F_{M,NR}$
Not moved	$N^F_{NM,R}$	$N^F_{NM,NR}$	$\tilde{N}^F_T-(\tilde{N}^F_{M,R}+N^F_{M,NR})$
Totals	$\tilde{N}^F_{M,R}+\tilde{N}^F_{NM,R}$	$\tilde{N}^F_T-(\tilde{N}^F_{M,R}+\tilde{N}^F_{NM,R})$	$\tilde{N}^F_T$

The two hypergeometric probability mass functions (pmfs) giving the model-predicted proportion of lobsters that moved and were recovered, based on the two contingency tables, are written as

$$P(\tilde{N}^S_{M,R})=\left(\frac{\binom{\tilde{N}^S_{M,R}+N^S_{M,NR}}{\tilde{N}^S_{M,R}}\binom{\tilde{N}^S_T-(\tilde{N}^S_{M,R}+N^S_{M,NR})}{N^S_{NM,R}}}{\binom{\tilde{N}^S_T}{\tilde{N}^S_{M,R}+N^S_{NM,R}}}\right). \quad (11)$$

$$P(\tilde{N}^F_{M,R})=\left(\frac{\binom{\tilde{N}^F_{M,R}+N^F_{M,NR}}{\tilde{N}^F_{M,R}}\binom{\tilde{N}^F_T-(\tilde{N}^F_{M,R}+N^F_{M,NR})}{\tilde{N}^F_{NM,R}}}{\binom{\tilde{N}^F_T}{\tilde{N}^F_{M,R}+\tilde{N}^F_{NM,R}}}\right). \quad (12)$$

Because the goal is to estimate the movement proportion, P_M^S (rather than any specific value of N), this proportion will need to be made explicit in the likelihood function as the sole freely varying parameter. Substituting from the definition of P_M^S (Eq. 1), we have

$$N^S_{M,NR}=P^S_M\cdot\tilde{N}^S_T-\tilde{N}^S_{M,R}. \quad (13)$$

Substituting for all occurrences of $N^S_{M,NR}$, Equation 11 becomes

$$P(\tilde{N}^S_{M,R})=\left(\frac{\binom{P^S_M\cdot\tilde{N}^S_T}{\tilde{N}^S_{M,R}}\binom{\tilde{N}^S_T\cdot(1-P^S_M)}{N^S_{NM,R}}}{\binom{\tilde{N}^S_T}{\tilde{N}^S_{M,R}+N^S_{NM,R}}}\right). \quad (14)$$

Writing the full joint-likelihood expression formed by the product of the two hypergeometric pmfs gives

$$L=\left(\frac{\binom{\tilde{N}^F_{M,R}+N^F_{M,NR}}{\tilde{N}^F_{M,R}}\binom{\tilde{N}^F_T-(\tilde{N}^F_{M,R}+N^F_{M,NR})}{\tilde{N}^F_{NM,R}}}{\binom{\tilde{N}^F_T}{\tilde{N}^F_{M,R}+\tilde{N}^F_{NM,R}}}\right)\times\left(\frac{\binom{P^S_M\cdot\tilde{N}^S_T}{\tilde{N}^S_{M,R}}\binom{\tilde{N}^S_T\cdot(1-P^S_M)}{N^S_{NM,R}}}{\binom{\tilde{N}^S_T}{\tilde{N}^S_{M,R}+N^S_{NM,R}}}\right).$$

As formulated, the value of $N^S_{NM,R}$ is still undetermined by data or constraint. A third constraint is therefore required. As with assumption 1 for the fished zone (Eq. 4), we apply the assumed equivalence of tag- and recapture-conditioned proportions to the sanctuary releases:

$$P^{S,rc}_M=\tilde{N}^S_{M,R}/(N^S_{NM,R}+\tilde{N}^S_{M,R})=P^{S,tc}_M=(\tilde{N}^S_{M,R}+N^S_{M,NR})/\tilde{N}^S_T.$$

In this application, $N^S_{NM,R}$ is understood as the number of lobsters that would have been taken if fishing had not been excluded from the sanctuary. Solving for $N^S_{NM,R}$ yields the third constraint,

$$N^S_{NM,R}=(\tilde{N}^S_{M,R}\cdot\tilde{N}^S_T)/(\tilde{N}^S_{M,R}+N^S_{M,NR})-\tilde{N}^S_{M,R},$$

Table 2

Intermediate calculated quantities from the numerical estimation. The equalities of $P_M^{F,rc}=P_M^{F,tc}$ and $f_M^F=f_M^S$ state assumptions 1 and 2.

Intermediate quantity	Variable name	Estimate
The proportions of lobsters tagged in the fishing zone that moved (≥3 km); recapture-conditioned ($P_M^{F,rc}$) or tag-conditioned ($P_M^{F,tc}$)	$P_M^{F,rc}=P_M^{F,tc}$	0.243
Number of lobsters that moved but were not recovered in the fishing zone	$N_{M,NR}^F$	697.7
Number of lobsters that moved from the sanctuary but were not recovered	$N_{M,NR}^S$	227.3
Number of lobsters that did not move and would have been recovered had there been equivalent levels of harvesting in the sanctuary	$N_{NM,R}^S$	17.7
Recovery proportions (in the fishing zone)—assumed to be equal for lobsters that moved inside the fishing zone f_M^F or from the sanctuary	$f_M^F=f_M^S$	0.113

without which this numerical estimator did not converge.

The factorial terms in the binomial coefficients of Equations 12 and 14 are defined only for natural numbers. However, in numerical minimization, factorials must be replaced with continuously varying approximations because the negative log-likelihood objective function is minimized by using numerical derivatives. The factorial z! was extended from natural numbers to the real line by using the gamma function, $\Gamma(z+1)$ and by using an asymptotic approximation formula for $\ln \Gamma(z)$ (Eq. 6.1.41 in Abramowitz and Stegun, 1965):

$$\ln\Gamma(z)=\left(z-\frac{1}{2}\right)\ln(z)-z+\frac{1}{2}\ln(2\pi)+\frac{1}{12z}-\frac{1}{360z^3}+\frac{1}{1260z^5}-\frac{1}{1680z^7}+\frac{1}{1188z^9}-\frac{691}{360360z^{11}}+\frac{1}{156z^{13}}. \quad (15)$$

The negative log likelihood was minimized numerically by using the AD Model Builder parameter estimation software (http://otter-rsch.com/admodel.htm).

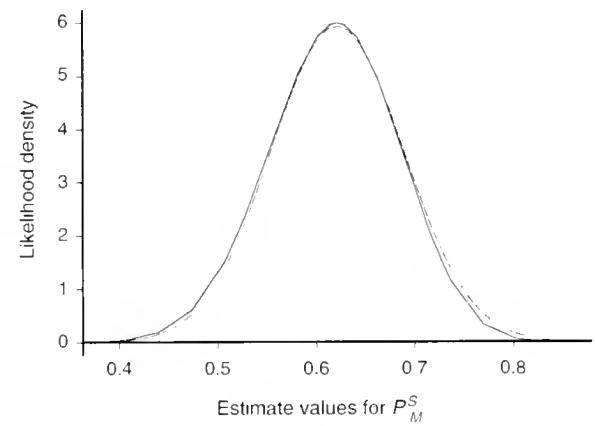

Figure 3

Profile likelihood (solid line) and asymptotic normal approximation (dashed line) for the likelihood confidence range about the estimate of P_M^S.

Results

The closed-form estimator for the proportion of lobsters that moved from the sanctuary (P_M^S) gave an estimate of 0.6206; i.e., about 62% of the lobsters tagged in Gleesons Sanctuary moved out in one year. The estimate obtained numerically, by maximizing the double-hypergeometric likelihood, yielded a value of 0.6212.

The small difference between the analytic and numerical estimates (0.09%) is presumably due to the use of the numerical approximation for the log-gamma function by the expansion of Equation 15. The close agreement suggests that the error introduced by that approximation is small.

The AD Model Builder parameter estimation software allows one to estimate confidence intervals of the movement-rate estimate in two ways: asymptotically, as diagonal elements of the covariance matrix, and by using a profile likelihood. Confidence intervals for the emigration rate estimate were thus obtained numerically from the hypergeometric likelihood by using both the asymptotic normal approximation and an exact profile likelihood. These gave 95% errors of 21.2% and 21.5% of the estimate, respectively. The approximate normal probability density function and the profile likelihood probability density function were also plotted (Fig. 3), yielding close agreement. Asymptotic confidence intervals therefore appear satisfactory for emigration proportion estimates not lying near the bounds of 0 and 1.

Intermediate calculation results (Table 2) included the recovery rate and movement rate (≥3 km) within the fished zone.

When independent estimates of exploitation rate are available, typically from stock assessment, the rate of tag reporting can be calculated from the tag-estimated recovery rate. The exploitation rate (yearly proportion of legal-size lobsters harvested) for the recapture year and

location of the present study (the 1995 northern zone rock lobster season) was estimated to be 26% (Ward et al.[3]) by using total yearly effort and catches by weight and number and a vector of weights at age. The tag-recovery rate of 11.3% (Table 2) is the estimated proportion of tagged lobsters that were captured and for which tags were reported. Thus the estimated tag-reporting rate (of those recaptured) is 0.113/0.26=43%. If tag shedding and natural mortality were also incorporated as additional causes for nonrecovery, the estimate would fall in the neighborhood of a 50% tag-reporting rate. This estimated level of tag-reporting falls within the range considered probable by fishermen. Thus, the recovery-rate estimate falls within a plausible range of values, adding confidence that the tag-recovery data are consistent with external estimates of exploitation rate.

Substantial movement of *Jasus edwardsii* out of a marine sanctuary was previously observed in New Zealand (Kelly and MacDiarmid, 2003) but not in Tasmania (Gardner and Ziegler[4]). Long-distance movement of this genus was also observed in New Zealand (Booth, 1997) but was much less common in Tasmanian *Jasus edwardsii* populations (Gardner et al., in press).

Discussion

The emigration-rate derivation above combined recapture-and tag-conditioned movement proportions. Both ways to define a movement rate were used to constrain the range of solutions for both analytic and numerical estimators. Equating these two definitions for movement proportion reduced the degrees of freedom by 1, thereby circumventing the absence of a count of recaptured lobsters from within the fished zone.

Previous estimators of movement rates among spatial cells from tag-recovery data have used either tag- or recapture-conditioned approaches. Hilborn (1990; see also Quinn and Deriso, 1999) developed a tag-conditioned movement-rate estimator. This estimator generally requires prior knowledge of the tag reporting rate. Schwarz et al. (1993) employed data consisting of simultaneous tag releases and recaptures repeated over a number of years at the same time each year to estimate movement, survival, and recovery rates in each spatial stratum. Schwarz et al. (1993) presented a general formulation for modeling this multiple yearly tag-recovery data set, extending a series of estimators for movement and survival (Arnason, 1972, 1973), and estimated the rate of tag recovery. Brownie et al. (1993) generalized the estimator of Schwarz et al. to non-Markovian movement rates. McGarvey and Feenstra (2002), following Hilborn, used the less costly and more commonly available single tag-recovery data employed in the present study but adopted a recapture-conditioned approach for estimating yearly movement rates. With "numbers recaptured" appearing in both the numerator and denominator, all nonspatially dependent sources of variation (such as tag reporting and shedding, short- and long-term tag-induced mortality, and natural mortality) cancel from the predicted recapture-conditioned likelihood proportions. This procedure permits a corresponding reduction in the prior information required to obtain unbiased movement estimates.

When recapture times vary, movement estimation is sensitive to spatial differences in mortality rate, notably between tag and recapture cells. Assuming that the nonreporting rate is unknown, mortality can be inferred from single tag-release information only imprecisely, for example by using mean tagged time at large. For this reason externally obtained mortality estimates, typically from stock-assessment models using fishery data, can be usefully combined with single tag recoveries in movement estimation. Hestbeck (1995) showed, when survival differs by cell, that ignoring the time of movement between yearly samples could bias movement estimates. McGarvey and Feenstra (2002) made explicit the variation in residence time and thus survival in source (tag-release) and destination (recapture) cells for each recaptured animal. By using prior knowledge of a migration season, migration source cell and destination cell residence times can be approximated as the time from the date of tag release to an assumed fixed (yearly) date of movement, and from that date to the date of recapture. These residence times are used in exponential survival factors that differ spatially given externally estimated fishing mortality rates in each cell.

For the data set available from Gleesons Landing, all tagged animals were released during the peak fishing season (mid-summer). Thus recoveries from the following fishing season had a mean and mode near the desired one-year-at-large. In future tag-recovery studies, where a yearly movement rate is sought, a similar choice for timing of tag releases, namely during the season of highest fishery catches, should yield a peak in recaptures a year later. Schwarz et al. (1993) employed this strategy with their multiple yearly tag-recovery data sets.

In the estimator presented above, variations in expected recovery numbers versus time, notably due to survival, were neglected. The small sample (33 recoveries between 0.5 and 1.5 years from the sanctuary) and lack of recaptures from within the sanctuary necessitated more modest estimation goals. Among data classes available for movement analysis, notably 1) multiple yearly tag recaptures by researchers in all cells, 2) multiple yearly tag recoveries where recapture is by fishermen (or

[3] Ward, T. M., R. McGarvey, Y. Xiao, and D. J. Brock. 2002. Northern zone rock lobster (*Jasus edwardsii*) fishery. South Australian Fisheries Assessment Series Report 2002/04b, 109 p. Aquatic Sciences, South Australian Research and Development Institute (SARDI); P.O. Box 120, Henley Beach, South Australia 5022, Australia.

[4] Gardner, C., and P. Ziegler. 2001. Are catches of the southern rock lobster *Jasus edwardsii* a true reflection of their abundance underwater? Tasmanian Aquaculture and Fisheries Institute Final Report. TAFI (Tasmanian Aquaculture and Fisheries Institute), University of Tasmania, Private Bag 49, Hobart TAS 7001, Australia.

hunters) in all cells, 3) single tag recoveries by fishermen in all cells, and 4) the data set employed in the present study of single-tag recoveries by fishermen in one of two cells, the latter represents the low end in quality and quantity of information about movement and survival.

A time-dependent approach could theoretically extend the approach of McGarvey and Feenstra (2002) to make explicit the residence times of each recaptured individual in the fishing zone and sanctuary, respectively, and thus make explicit differences in the predicted survival rate before and after movement. However without prior knowledge of when movement took place for each recaptured lobster, a modified likelihood method is called for, requiring integration over the probable movement times between tag release and recapture. This extension of residence-time-dependent movement estimators to variable times of movement remains a topic for future research.

Acknowledgments

I thank Hugh Possingham, André Punt, and two reviewers for comments on the draft manuscript. Lobsters were tagged and released into Gleesons Landing sanctuary by Greg Ferguson, together with fishermen Lenny and Murray Williams, under Fisheries Research and Development Corporation Project 93/086. This work was supported by the Australian Fisheries Research and Development Corporation Project No. 2000/195, and by the South Australian rock lobster industry.

Literature cited

Abramowitz, M., and I. R. Stegun.
1965. Handbook of mathematical functions, p. 257. Dover Publications, New York, NY.

Arnason, A. N.
1972. Parameter estimates from mark-recapture experiments on two populations subject to migration and death. Res. Popul. Ecol. (Kyoto) 13:97–113.
1973. The estimation of population size, migration rates, and survival in a stratified population. Res. Popul. Ecol. (Kyoto) 15:1–8.

Booth, J. D.
1997. Long-distance movements in Jasus spp. and their role in larval recruitment. B. Mar. Sci. 61(1): 111–128.

Brownie, C., J. E. Hines, J. D. Nichols, K. H. Pollock, and J. B. Hestbeck.
1993. Capture-recapture studies for multiple strata including non-Markovian transitions. Biometrics 49:1173–1187.

Gardner, C., S. Frusher, M. Haddon, and C. Buxton.
2003. Movements of the southern rock lobster *Jasus edwardsii* in Tasmania, Australia. Bull. Mar. Sci. 73(3): 653–671.

Hestbeck, J. B.
1995. Bias in transition-specific survival and movement probabilities estimated using capture-recapture data. J. Appl. Stat. 22:737–750.

Hilborn, R.
1990. Determination of fish movement patterns from tag recoveries using maximum likelihood estimators. Can. J. Fish. Aquat. Sci. 47:635–643.

Kelly, S.
2001. Temporal variation in the movement of the spiny lobster *Jasus edwardsii*. Mar. Freshw. Res. 53(3):323–331.

Kelly, S., and A. B. MacDiarmid.
2003. Movement patterns of mature spiny lobsters, *Jasus edwardsii*, from a marine reserve. N.Z. J. Mar. Freshw. Res. 37:149–158.

MacDiarmid, A. B., B. Hickey, and R. A. Maller.
1991. Daily movement patterns of the spiny lobster *Jasus edwardsii* (Hutton) on a shallow reef in northern New Zealand. J. Exp. Mar. Biol. Ecol. 147:185–205.

McGarvey, R., and J. E. Feenstra.
2002. Estimating rates of fish movement from tag recoveries: conditioning by recapture. Can. J. Fish. Aquat. Sci. 59:1054–1064.

Quinn, T. J. II, and R. B. Deriso.
1999. Quantitative fish dynamics, p. 414–419. Oxford Univ. Press, New York, NY.

Rice, J. A.
1995. Mathematical statistics and data analysis, p. 13–14, 39–40. Duxbury Press, Belmont CA.

Schwarz, C. J., J. F. Schweigert, and A. N. Arnason.
1993. Estimating migration rates using tag recovery data. Biometrics 49:177–193.

Seber, G. A. F.
1982. The estimation of animal abundance and related parameters, 2nd ed., p. 59–60. Griffin, London.

Reproductive dynamics of female spotted seatrout (*Cynoscion nebulosus*) in South Carolina*

William A. Roumillat

Marine Resources Research Institute
South Carolina Department of Natural Resources
217 Ft. Johnson Rd.
Charleston, South Carolina 29412
E-mail address roumillatb@mrd.dnr.state.sc.us

Myra C. Brouwer

South Atlantic Fishery Management Council
One Southpark Center; suite 306
Charleston, South Carolina 29407

Abstract—We describe reproductive dynamics of female spotted seatrout (*Cynoscion nebulosus*) in South Carolina (SC). Batch fecundity (BF), spawning frequency (SF), relative fecundity (RF), and annual fecundity (AF) for age classes 1–3 were estimated during the spawning seasons of 1998, 1999, and 2000. Based on histological evidence, spawning of spotted seatrout in SC was determined to take place from late April through early September. Size at first maturity was 248 mm total length (TL); 50% and 100% maturity occurred at 268 mm and 301 mm TL, respectively. Batch fecundity estimates from counts of oocytes in final maturation varied significantly among year classes. One-year-old spotted seatrout spawned an average of 145,452 oocytes per batch, whereas fish aged 2 and 3 had a mean BF of 291,123 and 529,976 oocytes, respectively. We determined monthly SF from the inverse of the proportion of ovaries with postovulatory follicles (POF) less than 24 hours old among mature and developing females. Overall, spotted seatrout spawned every 4.4 days, an average of 28 times during the season. A chronology of POF atresia for water temperature >25°C is presented. Length, weight (ovary-free), and age explained 67%, 65%, and 58% of the variability in BF, respectively. Neither RF (number of oocytes/g ovary-free weight) nor oocyte diameter varied significantly with age. However, RF was significantly greater and oocyte diameter was smaller at the end of the spawning season. Annual fecundity estimates were approximately 3.2, 9.5, and 17.6 million oocytes for each age class, respectively. Spotted seatrout ages 1–3 contributed an average of 29%, 39%, and 21% to the overall reproductive effort according to the relative abundance of each age class. Ages 4 and 5 contributed 7% and 4%, respectively, according to predicted AF values.

Manuscript submitted 13 May 2002 to Scientific Editor's Office.

Manuscript approved for publication 19 March 2004 by the Scientific Editor.

Fish. Bull. 102:473–487 (2004).

The spotted seatrout (*Cynoscion nebulosus*) is an estuarine-dependent member of the family Sciaenidae. Spotted seatrout are year-round residents of estuaries along the South Atlantic coast and spawning takes place inshore and in coastal areas (McMichael and Peters, 1989; Mercer[1]; Luczkovich et. al.[2]). As in many other sciaenids, spawning in this species occurs in the evening (Holt et al., 1985). Male spotted seatrout have the capacity to produce "drumming" sounds that are caused by the contraction of the swimbladder by specialized muscles that are seasonally hypertrophied from the abdominal hypaxialis muscle mass (Fish and Mowbray, 1970; Mok and Gilmore, 1983). Direct involvement of sound production with spawning has been shown for this and other sciaenids (Mok and Gilmore, 1983; Saucier et al., 1992; Saucier and Baltz, 1993; Luczkovich et al.[2]).

We have collected information on the spawning behavior of spotted seatrout in coastal South Carolina since 1990 (Saucier et al., 1992; Riekerk et al.[3]). Spawning aggregations were located by listening for drumming sounds from late afternoon until ~2300 h with passive hydrophone equipment. Spawning activity was subsequently verified through collections of newly spawned eggs and by the rearing of the larvae in the laboratory (Saucier et al., 1992).

Spotted seatrout are group-synchronous spawners with indeterminate fecundity and the protracted spawning season extends from April through September along the South Atlantic and Gulf of Mexico coasts (Overstreet, 1983; Brown-Peterson et al., 1988; McMichael and Peters, 1989; Saucier and Baltz, 1993; Brown-Peterson and Warren, 2001; Brown- Peterson et al., 2002; Nieland et al., 2002, Brown-

* Contribution 539 from the Marine Resources Research Institute of the South Carolina Department of Natural Resources, Charleston, SC 29422-2559.

[1] Mercer, L. P. 1984. A biological and fisheries profile of spotted seatrout, *Cynoscion nebulosus*. Special Scientific Report 40, 87 p. North Carolina Department of Natural Resources and Community Development, Division of Marine Fisheries, Morehead City, NC 28577.

[2] Luczkovich, J. J., H. J. Daniel III and M. W. Sprague. 1999. Characterization of critical spawning habitats of weakfish, spotted seatrout and red drum in Pamlico Sound using hydrophone surveys. Final report and annual performance report F-62-2 and F-62-2, p 65–68. North Carolina Department of Environment and Natural Resources, Division of Marine Fisheries, Morehead City, NC 28557.

[3] Riekerk, G. H. M., S. J. Tyree, and W. A. Roumillat. 1997. Spawning times and locations of spotted seatrout in the Charleston Harbor Estuarine System from acoustic surveys, 21 p. Final Report to Charleston Harbor Project, Bureau of Ocean and Coastal Resources Management, South Carolina Department of Health and Environmental Control, 1362 McMillan Ave., Charleston, SC 29405.

Peterson, 2003; Wenner et al.[4]). As in other indeterminate spawning fish, annual fecundity in this species is determined by the number of oocytes released during each spawning event (batch fecundity) and the number of spawning events occurring during the course of the spawning season (spawning frequency). Early efforts to estimate fecundity for spotted seatrout did not take into account the repetitive nature of spawning activities in this species (Pearson, 1929; Sundararaj and Suttkus, 1962; Overstreet, 1983) and only recently has an effort been made to coordinate batch fecundities with spawning frequencies (Brown-Peterson et al., 1988; Brown-Peterson and Warren, 2001; Nieland et al., 2002). This procedure is intuitively necessary to estimate the reproductive output for an entire spawning season and is made even more useful for fisheries management if separated by size class or age cohort within a population (Prager et al., 1987; Goodyear, 1993; Zhao and Wenner[5]).

An important component of assessment for management involves determining the spawning potential ratio (SPR), a measure of the effect of fishing on the reproductive potential of a stock (Goodyear, 1993). This value is usually calculated as the ratio of spawning stock biomass per recruit (SSBR) in the presence of fishing mortality (F) to the SSBR when F is equal to zero (Gabriel et al., 1989; Goodyear, 1993). Spawning potential ratio is currently used as a biological reference point for definition of recruitment overfishing (i.e., Vaughan et al., 1992). The calculation of SPR can be improved, however, by introducing egg production into the model. Fecundity is a much better predictor of reproductive potential than female biomass. Moreover, SPR calculations based on egg production may be more sensitive to the size-age composition of the spawning stock. However, accurate annual fecundity estimates for use in stock assessment do not exist for this or many other species in need of fisheries management. Therefore, our goal was to obtain batch fecundity (BF), spawning frequency (SF), and annual fecundity (AF) estimates for spotted seatrout by age class.

Materials and methods

Data to address the main objectives of this study were collected from late April through early September 1998–2000 as part of a long term monitoring effort (1991–present) to assess the relative abundance of age classes of recreationally important finfish in South Carolina estuaries. The study followed a monthly stratified random sampling design in three estuarine systems. The Cape Romain system comprised two strata: Romain Harbor and northern Bulls Bay. The Charleston Harbor system contained four strata: the Wando, Cooper, and Ashley Rivers, and Charleston Harbor. The Ashepoo-Combahee-Edisto (ACE) Basin system comprised a single stratum (Fig. 1). The number of sampling sites within each stratum ranged from 23 to 30. A subset of 12–14 sites was randomly selected each month. Sampling was conducted only during the daytime ebbing tide (0700–1800 h), primarily over mud and oyster shell substrates adjacent to the *Spartina alterniflora* marsh. At each site, we deployed a trammel net (182.8 m long by 2.4 m deep; outer walls: 17.8 cm square [35.6 cm stretch]; inner wall: 3.2 cm square [6.4 cm stretch]) from a rapidly moving shallow water boat in an arc against the shoreline at depths ranging from 0.5 to 2.0 m. We disturbed the water within the site in an effort to frighten fishes into the entrapment gear. We then hauled the trammel net back into the boat and removed the catch, which was kept alive in a 70-liter oxygenated holding tank. Spotted seatrout were measured for total length (TL) and standard length (SL) and a subsample of fish from each effort (5–10 individuals for each 20-mm size interval per month) were sacrificed, placed on ice, and transported to the laboratory for aging and reproductive data.

Specimens were processed in the laboratory 2–12 hours after capture. We recorded standard life-history parameters (TL, SL, fish weight, gonad weight, sex, and maturity) for each specimen. The following equation was used to convert lengths when necessary:

$$TL = 5.689 + 1.167(SL)\ (r^2=0.998) \qquad n=1191.$$

We removed sagittal otoliths for aging and preserved sections (<2% by weight) of each ovary in neutral buffered formalin for histological processing. The latter involved standard procedures for paraffin embedding and sectioning, and standard hematoxylin and eosin-y staining (Humason, 1972). Histological sections were viewed under a Nikon Labophot compound microscope equipped with a teaching head so that two readers could interpret sections simultaneously. Maturity estimation was modified from that of Wenner et al.[4] (Table 1).

Size at first maturity was histologically derived by first evidence of cortical alveoli stage oocytes. To arrive at estimates of 50% and 100% maturity, data were subjected to PROBIT analysis.

Age determination

The left sagittae were marked with a soft lead pencil through the core and embedded in epoxide resin. A transverse section (~0.5-mm thick) was taken through the core by using a low-speed saw equipped with a pair

[4] Wenner, C. A., W. A. Roumillat, J. E. Moran Jr., M. B. Maddox, L. B. Daniel III, and J. W. Smith. 1990. Investigations on the life history and population dynamics of marine recreational fishes in South Carolina: part 1. Final Report F-37, 177 p. Marine Resources Research Institute, Marine Resources Division, South Carolina Department of Natural Resources, 217 Ft. Johnson Rd., Charleston, SC 29412.

[5] Zhao, B., and C. A. Wenner. 1995. Stock assessment and fishery management of the spotted seatrout, *Cynoscion nebulosus*, on the South Carolina coast, 90 p. Marine Resources Research Institute, Marine Resources Division, South Carolina Department of Natural Resources, 217 Ft. Johnson Rd., Charleston, SC 29412.

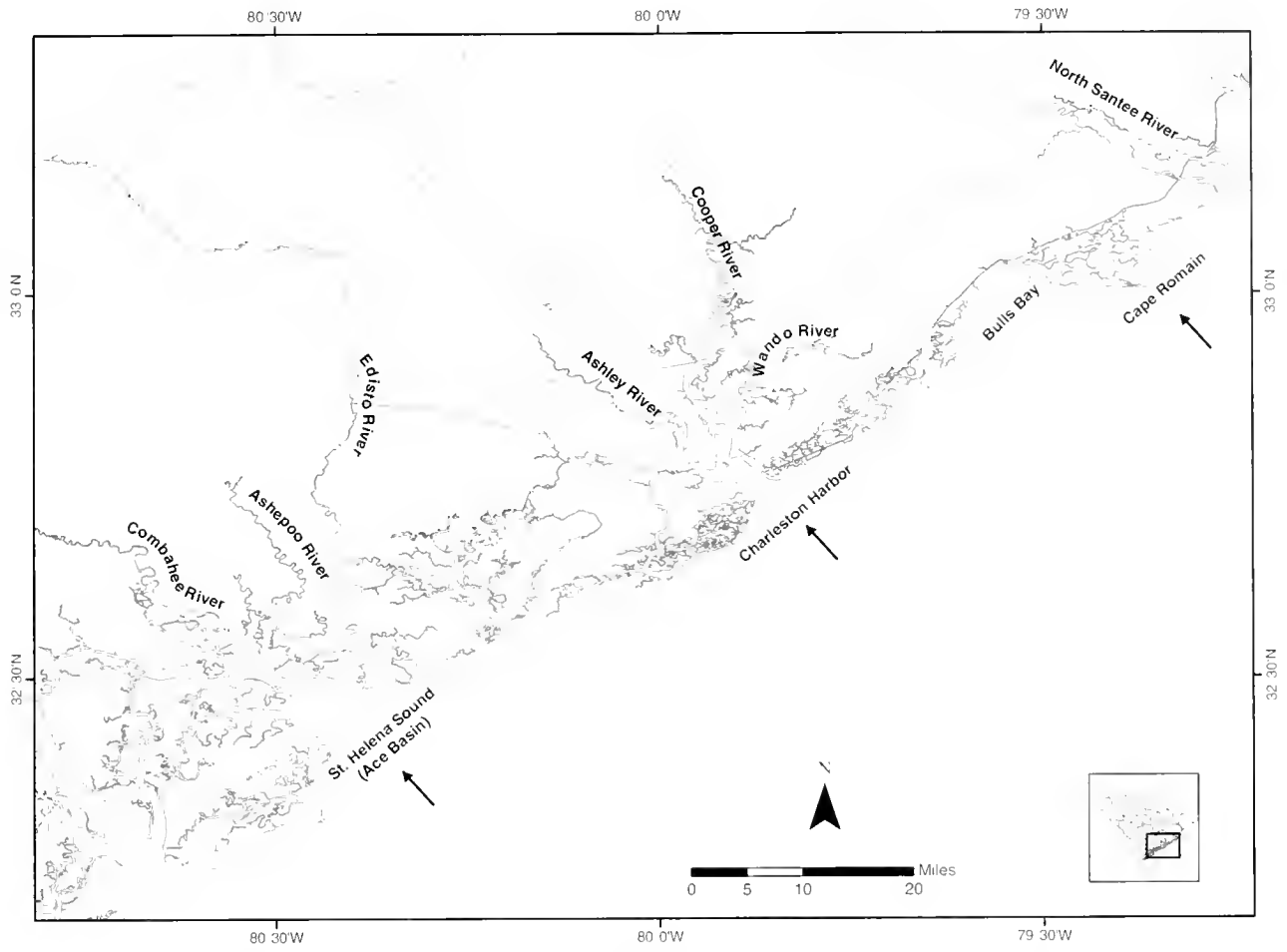

Figure 1

The three South Carolina estuarine systems (indicated by arrows) where *C. nebulosus* were collected.

Table 1

Criteria used for microscopic staging of *C. nebulosus* ovaries. FOM = final oocyte maturation; POF = postovulatory follicle.

Stage	Description
Immature	Ovary small in cross section. Early stage with only oogonia evident; later stage with small (<0.08 mm) primary oocytes, tightly packed. No evidence of early vitellogenesis.
Developing	First appearance of cortical alveoli stage oocytes through late vitellogenesis but no evidence of early FOM (lipid and yolk globule coalescence).
Ripe	Ovary containing oocytes demonstrating FOM (lipid and yolk coalescence through hydration).
Mature with day-0 POFs	Ovary exhibits POFs <24 h (see Table 2). Found at all water temperatures throughout the spawning season.
Mature with day-1 POFs	Ovary exhibits POFs >24 h consisting of closely packed granulosa cells (0.08–0.1 mm). Only identified in water < 25°C.
Spent	Ovary containing alpha- and beta-stage oocytic atresia.
Resting	Ovary containing small primary oocytes and oocytes with perinuclear nucleoli (<0.12 mm); usually some remnants of oocytic atresia.

of diamond wafering blades. The resulting section was mounted on a labeled microscope slide and examined with a Nikon SMZ-U microscope. A 1 January birth date was assumed for the process of aging. Spotted seatrout deposit an annulus in April or May (Murphy and Taylor, 1994; Wenner et al.[4]). Fish in the first three months of

Table 2

Criteria used for microscopic staging of *C. nebulosus* day-0 postovulatory follicles (POFs) in water temperatures above 25°C. Measurements represent longest axis of POFs.

POF chronology (in hours)	Description
0–4	Regular arrangement of granulosa-cell nuclei proximal to the basement membrane and obvious multiple layering as described by Hunter and Macewicz (1985). 200–300 μm (Fig. 4A).
5–8	Early signs of atresia, loss of the obvious layering, hypertrophy of granulosa cells, and a general compaction with an investment of blood vessels. 180–250 μm (Fig. 4B).
9–12	Well-defined lumen separating the internal granulosa cells from the outer wall of granulosa cells encompassed by theca. 150–200 μm (Fig. 4C).
13–24	Lumen reduced primarily by loss of granulosa tissue and proximity of peripheral layers. 130–175 μm (Fig. 4, D and E).

the year were aged by the addition of 1 year to the count of the number of annuli on the thin sections. In April or May, if the section had a large marginal increment, one was also added to the annular count. If the marginal increment was small or if the ring was detectable on the edge of the otolith section, age was equal to the number of annuli.

Seasonality

Spawning season for spotted seatrout in South Carolina was determined by using two techniques. The gonadosomatic index (GSI) was calculated as

$$(GW/OFWT) \times 100,$$

where GW = gonad weight (g); and
$OFWT$ = ovary-free weight (g).

For years prior to this study (1991–97), mean monthly GSI was obtained for all females by using data from the South Caroline Department of Natural Resources inshore fisheries archives (Wenner[6]). Reproductive seasonality among female spotted seatrout throughout the year was also examined by using histology (Table 1).

The first evidence of oocytes in final oocyte maturation (FOM) as evidenced by lipid and yolk coalescence; Brown-Peterson et al., 1988) or the occurrence of postovulatory follicles (POFs) defined the beginning of the spawning season. To determine the cessation of spawning, the percent occurrence of females in spawning condition (ripe and repeat spawners) and those in postspawning condition (spent and resting) were obtained for the months of August and September. To investigate the condition of females, we examined Fulton's condition factor (Ricker, 1975) over the spawning season using linear regression.

[6] Wenner, C. 2002. Unpubl. data. Marine Resources Research Institute, Marine Resources Division, South Carolina Department of Natural Resources, 217 Ft. Johnson Rd., Charleston, SC 29412.

Spawning frequency

We obtained samples for spawning frequency (SF) determination from 1 May through 31 August 1998, 1999 and 2000. Although samples were routinely collected throughout the year, only from early May through late August did we capture enough animals in the appropriate reproductive state for SF estimation. Spawning frequency was calculated as either the inverse of the proportion of ovaries with day-0 POFs (Hunter and Macewicz, 1985; Brown-Peterson et al., 1988) or with oocytes in FOM (Brown-Peterson et al., 1988; Lisovenko and Adrianov, 1991) among mature and developing females.

We designated two distinct morphological features of POFs based on time of specimen capture and water temperature. We interpreted the largest, least atrophied POFs to be <24 h old and termed them "day-0" POFs (Hunter and Macewicz, 1985). The presence of day-0 POFs in the ovary indicated that spawning had occurred the previous night. The second category comprised smaller POFs, which primarily consisted of closely packed granulosa cells determined to be >24 h old.

To complete the chronology of POF atresia we undertook round-the-clock sampling on 27–28 June and 26 July 2000. During these efforts, sampling continued beyond routine hours to encompass the period between dusk and dawn. The histological samples obtained allowed for the calibration of criteria used to age POFs (Table 2). To determine whether SF varied among months and age classes, Kruskal-Wallis tests were used. Because both factors (month and age) were fixed (model 1), it was not possible to test for their interaction by using a two-way parametric ANOVA without replication.

As a result of targeting fish for batch fecundity estimates (see below), we had available numerous specimens with oocytes in FOM with which to establish monthly SF. However, we knew that these specimens were disappearing from our shallow sampling sites into deeper spawning areas as the day progressed (Riekerk et al.[3]),

thus potentially adding bias to our SF estimates. Even though estimates of SF based on FOM were performed *a posteriori*, we chose to report them strictly for comparison to other studies with this method. Because sampling for females exhibiting FOM was accomplished in a directed fashion, statistical comparisons were not attempted.

Batch fecundity and relative fecundity

Observations taken over a decade of sampling the Charleston Harbor estuarine system showed that in females captured in shallow water (<1.5 m) during the spawning season, FOM began at about 1200 h (Wenner[6]). Similarly, Crabtree and Adams[7] reported FOM beginning in Florida spotted seatrout at about mid-day. Lowerre-Barbieri et al.[8] found hydrated females in shallow water in the vicinity of aggregations of drumming males in deeper water. We also speculated that from mid- to late afternoon hydrated females moved along the marsh edge toward deeper water spawning aggregations (8–25 m). Hydrophone surveys conducted in the Charleston Harbor area over several years (Riekerk et al.[3]; Wenner[6]) indicated that noise production typically began around 1800 h and ceased around 2200 h. Because this behavior has been associated with spawning in this and other sciaenids (Mok and Gilmore, 1983; Holt et al., 1985; Saucier et al., 1992; Saucier and Baltz, 1993), we assumed that spawning began at 1800 h and stopped at 2200 h. Thus we were able to target spotted seatrout in the mid- to late afternoon specifically to capture females with oocytes in the late stages of FOM for batch fecundity (BF) estimation. Because we have consistently identified recently spawned females in shallow areas, they apparently return to the marsh edge where they once again become available for capture with our sampling gear. Our stratified random sampling of estuarine areas along the coast (described previously) was designed to representatively sample these recently spawned females for SF estimation.

We conducted BF sampling during two consecutive afternoons fortnightly from the middle of April through the first week of September 1998, 1999, and 2000. We deployed a trammel net from a shallow water boat as described above at preselected sites in Charleston Harbor in depths ranging from 1.0 to 1.5 meters during the afternoon (1400–1800 h EDT) high tide.

Restricting our sampling to the hours immediately preceding the evening spawning event ensured that those females preparing to spawn were available for capture. Male spotted seatrout, identified by their drumming sounds, caught during this targeted effort were measured and released at the site of capture. We supplemented samples for BF estimation with specimens from local sportfishing tournaments held during summer months in the Charleston Harbor area.

We processed samples in the laboratory as previously described. If ovaries appeared by macroscopic examination to contain hydrated oocytes, they were fixed in 10% buffered seawater formalin for potential counts (Hunter et al., 1985). The appropriateness of these ovaries for BF counts was subsequently determined by examining the corresponding histological preparation.

To ensure that only those oocytes destined to be ovulated during the upcoming spawning event were counted, we chose to use only those oocytes undergoing FOM that could be easily separated by size from late vitellogenic oocytes (Nieland et al., 2002; Lowerre-Barbieri et al.[8]). If we observed numerous recent POFs in the histological sample, the corresponding whole ovary was not used for oocyte counts (because their presence indicated that ovulation had occurred). We reweighed ovaries (approximately 2 weeks after fixation) to the nearest 0.01 g and randomly extracted three 130–150 mg aliquots from eight potential locations in the ovary (each lobe was partitioned into quarters lengthwise). We stored subsamples in 50% isopropyl and counted oocytes under a Nikon SMZ-U dissecting microscope at 12× magnification. We counted each subsample twice by using a Bogorov tray and a hand-held counter and conducted a third count if the two initial counts were dissimilar by more than 10%. We used the mean number of oocytes in each subsample to calculate mean oocyte density (number of oocytes per gram preserved ovary weight) and total numbers of oocytes in the ovary. We compared mean oocyte densities among the four regions of each ovarian lobe and between the two lobes by using a two-way analysis of variance (ANOVA). Because our variances were heteroscedastic, we used nonparametric ANOVA (Kruskal-Wallis or ANOVA on ranks) for comparisons of mean BF among ages, months, and years. To investigate the relationships between BF and length, somatic weight (ovary-free body weight), and age, we used linear regression.

Relative fecundity (RF) was calculated as the number of oocytes per gram somatic weight (ovary-free). To select samples for inclusion in RF calculations, we looked for the presence of nuclear migration in histological preparations. We used this criterion to ensure that oocytes of similar morphological dynamics would be used, minimizing the potential for error. We used the Kruskal-Wallis test to investigate the effect of age on RF. Because sample sizes were quite uneven among months, we chose to compare RF between the beginning and end of the spawning season (May and August). This comparison was done by using a Mann-Whitney test. To corroborate any trends in RF, we also conducted diameter measurements on the preserved (10% buffered

[7] Crabtree R. E., and D. H. Adams. 1998. Spawning and fecundity of spotted seatrout, *Cynoscion nebulosus*, in the Indian River Lagoon, Florida. *In* Investigations into nearshore and estuarine gamefish abundance, ecology, and life history in Florida, p. 526–566. Tech. Rep. for Fed. Aid in Sport Fish Rest. Act Project F-59. Florida Marine Research Institute, Department of Environmental Protection, 100 Eighth Ave. SE, St. Petersburg, FL 33701.

[8] Lowerre-Barbieri, S. K., L. R. Barbieri, and J. J. Albers. 1999. Reproductive parameters needed to evaluate recruitment overfishing of spotted seatrout in the southeastern U.S. Final report to the Saltonstall-Kennedy (S-K) Grant Program (grant no. NA77FD0074), 23 p.

seawater formalin) oocytes. We used a video camera mounted on a Nikon SMZ-U dissecting microscope and coupled to a PC equipped with a frame-grabber and with OPTIMAS® Image Analysis software (version 6, Media Cybernetics, Bothell, WA). Two readers independently measured the diameter of approximately 30 preserved oocytes in each of three subsamples from 27 ovaries. To test for uniformity of size throughout the ovary, mean oocyte diameters were compared between ovarian lobes and among subsample locations within each lobe by using two-way ANOVA. We also compared mean oocyte diameters among months and ages by using two-way ANOVA.

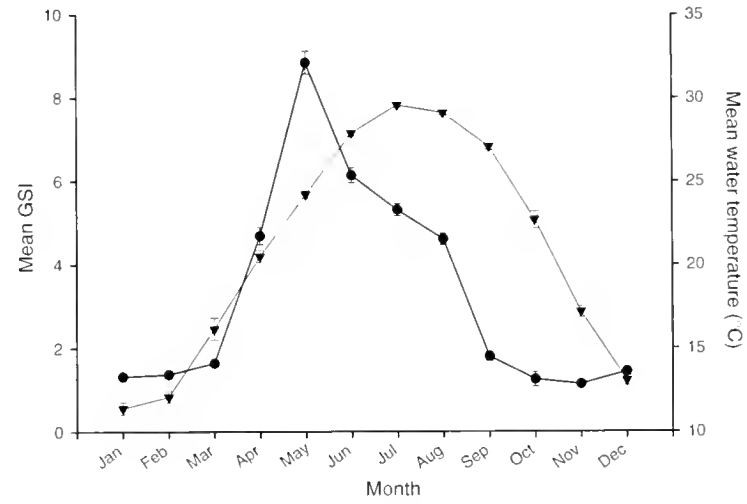

Figure 2

Mean monthly gonadosomatic index (GSI) for spotted seatrout in South Carolina for years 1991–2000 (circles). Mean water temperature for 1991–2000 (triangles). Error bars are standard errors. n = 1185.

Annual fecundity

Wiley (1996) demonstrated that spotted seatrout in South Carolina estuaries constitute a single population. Therefore, we felt justified in calculating monthly egg production (MEP) by multiplying the monthly SF (of specimens taken along the entire coast) by the mean monthly BF (of specimens from Charleston Harbor). Because not all age-1 female trout were mature at the beginning of the spawning season, the fraction of mature age-1 females obtained from previous work in South Carolina (Wenner[6]) was used to refine the MEP estimate. Because the latter was calculated by using SF obtained from data pooled across years, any comparison of MEP among years was deemed invalid. Kruskal-Wallis tests were used to determine whether MEP varied among months for each age class.

Monthly MEP estimates were summed to arrive at an annual fecundity (AF) estimate for each age class. Because the majority of individuals used in this study were aged 1–3, AF was estimated only for these age classes. We used linear regression to investigate the relationship between AF and age and thus predict AF for spotted seatrout aged 4 and 5. Using these predictions and the relative abundance of each age class in our samples, we estimated the contribution of each age class to the annual egg production.

All statistical analyses were conducted with the Statistical Package for the Social Sciences (version 9.0, SPSS Inc., Chicago, IL). The level of significance for all tests was 0.05.

Results

A total of 1038 spotted seatrout ranging in age from 1 to 5 was collected for this study. Because 97% of these belonged to age classes 1–3 we report reproductive parameters only for these ages. We examined a total of 941 mature and developing females, ranging in length from 248 mm to 542 mm TL, to determine spawning frequency (569, 285, and 87 for ages 1–3, respectively). Of these, 135 specimens (12 from sportfishing tournaments) were used to conduct oocyte counts (62, 52, and 21 for ages 1–3, respectively). These fish ranged in length from 268 to 530 mm TL. Minimum size at first maturity, as indicated by the presence of cortical alveoli stage oocytes in histological sections, was 248 mm TL. Size at 50% maturity was 268 mm, whereas 100% maturity was reached at 301 mm TL. Condition of females, as indicated by Fulton's condition factor, diminished over the course of the season (P<0.01, r^2=0.24).

Seasonality

Spawning in the Charleston Harbor area during the study period began in mid to late April as indicated by the presence of oocytes in late FOM or POFs in histological samples. During the study period, mean water temperatures ranged from 16° to 34°C. Highest temperatures were recorded during July and August for all three years of the study. The lowest documented water temperature when spawning began was 20 C. Cessation of spawning occurred when water temperature was 28°C. Mean monthly GSI for spotted seatrout captured along the South Carolina coast since 1991 (Fig. 2) showed a marked increase from 4.6 in April to 9.4 in May. Mean GSI in June declined to 6.3 and remained around 5.0 in July and August. A sharp decline was noted in September to 2.7, the lowest level for the season. Overall, mean gonadosomatic index (GSI) values followed the seasonal trend in water temperature (Fig. 2). Percent occurrence of females in spawning condition as evidenced from histological examination declined from approximately 87% in August to 12% in September. The percentage of

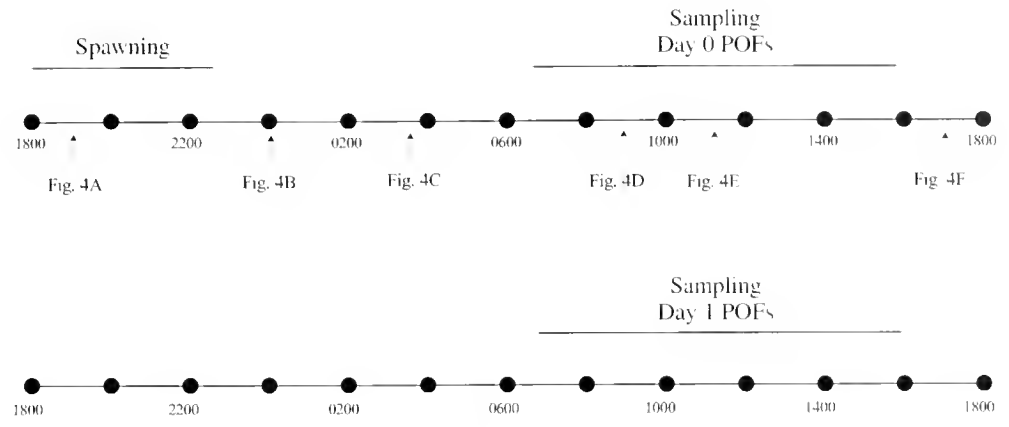

Figure 3

Forty-eight-hour chronological time line indicating *C. nebulosus* spawning time in Charleston Harbor, SC. Postovulatory follicles (POFs) observed at water temperatures >25 C were termed day-0 (<24 hours). Day-1 POFs (>24 hours) were observed only at water temperatures <25°C. Time of capture for specimens in Figure 4 are indicated.

post-spawning females increased from 9% in August to 91% in September. Thus, the spawning season for spotted seatrout in South Carolina extends from late April through early September.

Spawning frequency

Day-0 POFs were found through 1800 h of the day following a spawning event. Day-1 POFs were first observed in our routine samples when they were 36–37 hours old (the second day following a spawning event) only when water temperatures were below 25°C. Day-1 POFs were excluded from our analysis of SF because they did not provide evidence of a previous night's spawning event.

Figure 3 illustrates the time line for POF atrophy in spotted seatrout from 1–42 h after the onset of spawning at 1800 h. Because evidence of spawning for the first 12 h was documented only during a period when water temperatures were greater than 25°C, all of the examples shown are indicative of atrophy in warmer temperatures (Fig. 4). As indicated in Table 2, there was a time-dependent deterioration of POFs such that only those <24 h were detectable at water temperatures >25°C.

Small sample sizes prevented calculation of monthly SF for each age class by year. Therefore, we pooled data for all three years of this study to obtain a single monthly SF estimate by age class (Tables 3 and 4). The interaction between month and age on SF could not be statistically tested; however, age-3 fish spawned more frequently than younger fish (Kruskal-Wallis, $P<0.05$) and all seatrout spawned more frequently in June (Kruskal-Wallis, $P<0.05$). Peaks in SF observed for fish ages 2 and 3 in July and August, respectively (Tables 3 and 4), were not statistically significant.

Monthly SF values based on the occurrence of ovaries containing oocytes in FOM are also presented in Table 3. However, statistical comparisons were not feasible because of the nonrandom collection of specimens. Overall SF was estimated to be once every 4.4 days and once every 5.1 days with the POF and FOM methods, respectively.

Table 3

Spawning frequency (SF) expressed as the number of spawnings per month for *C. nebulosus* ages 1–3 for the spawning seasons of 1998–2000. Numbers in parentheses represent days between spawnings. *n* = number of fish in a sample. FOM = final oocyte maturation; POF = postovulatory follicle.

Age (yr)	Month	*n*	SF FOM method	SF POF method
1	May	89	4.53 (6.85)	4.18 (7.42)
	June	166	4.53 (6.62)	9.40 (3.13)
	July	185	4.68 (6.62)	6.54 (4.74)
	August	129	6.26 (4.95)	4.57 (6.79)
	Total	569	19.9 (6.18)	26.34 (4.67)
2	May	114	11.5 (2.78)	6.80 (4.56)
	June	79	5.70 (5.26)	7.60 (3.95)
	July	48	0.65 (47.62)	9.04 (3.43)
	August	44	9.87 (3.14)	6.34 (4.89)
	Total	285	30.67 (4.01)	29.36 (4.19)
3	May	46	10.10 (3.07)	7.42 (4.18)
	June	23	5.22 (5.75)	9.12 (3.29)
	July	10	3.10 (10.00)	3.10 (10.00)
	August	8	11.61 (2.67)	11.61 (2.67)
	Total	87	32.54 (2.67)	31.14 (3.95)
Overall		941	24.3 (5.06)	27.7 (4.44)

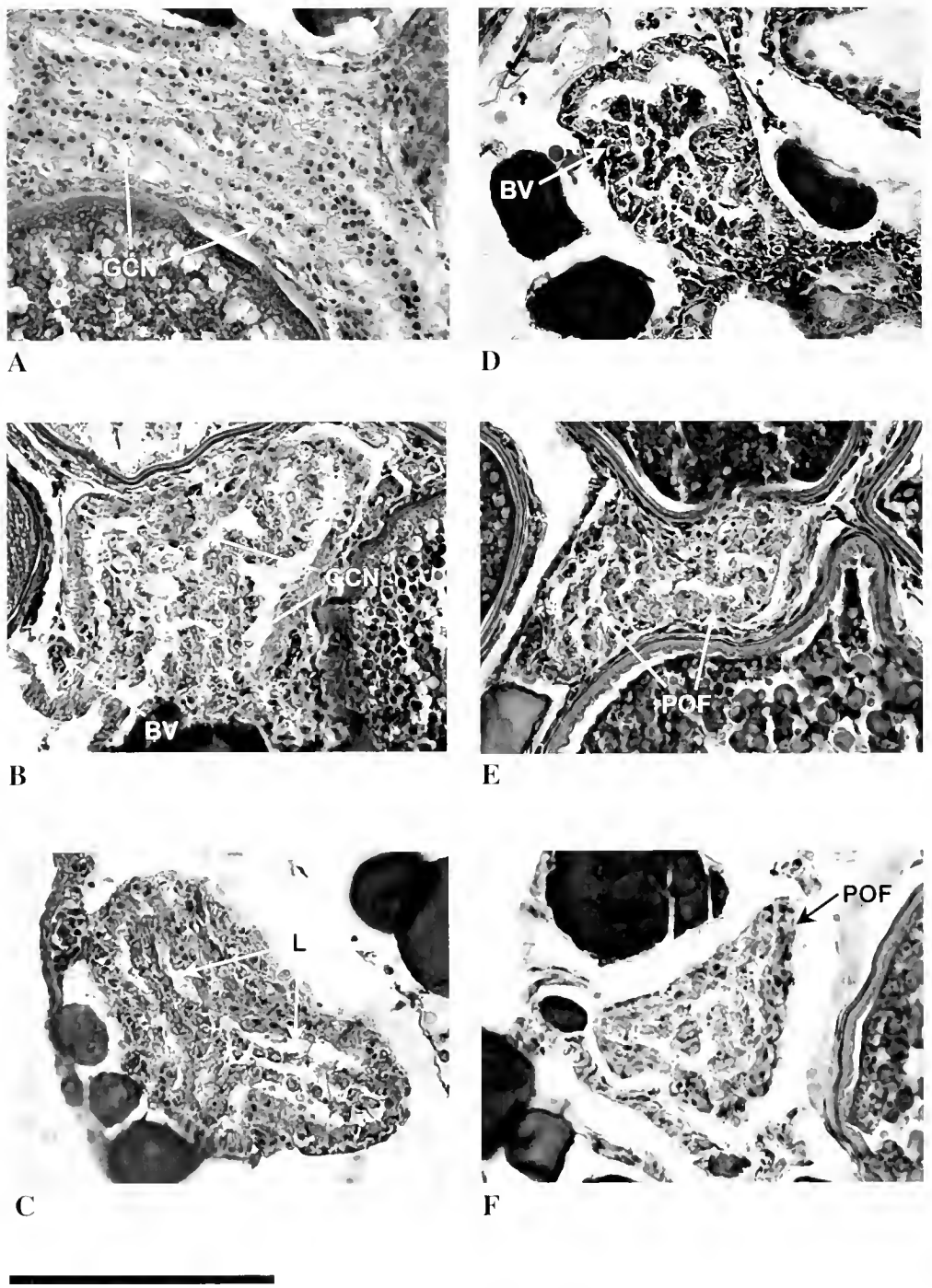

Figure 4

Photomicrographs of *C. nebulosus* postovulatory follicles (POFs) showing chronology of atresia at water temperatures >25 C. (**A**) 0–4 hours after spawning, (**B**) 5–8 hours after spawning, (**C**) 9–12 hours after spawning, (**D, E, F**) 13–24 hours after spawning.

Batch fecundity

As expected, we found a significant difference in mean BF among age classes (ANOVA on ranks, $P<0.05$). Age-1 spotted seatrout produced an average of 145,452 oocytes per batch spawned. Fish aged 2 and 3 spawned an average of 291,123 and 529,976 oocytes per batch, respectively. Therefore, mean BF was compared among months

Table 4

Fecundity parameters for *C. nebulosus* ages 1–3 from South Carolina estuaries. BF = batch fecundity in numbers of oocytes; SF = spawning frequency based on the postovulatory follicle (POF) method and expressed as the number of spawnings per month; MEP = monthly egg production = *(BF×SF)%mature*. Annual fecundity is the sum of mean monthly MEP values for each year class and represents the total number of oocytes produced by any given female from 1 May to 31 August. Numbers in parentheses indicate sample sizes.

Age (yr)	Month	Mean BF	SF	% mature	Mean MEP
1	May	117,760 (12)	4.18 (89)	78.6	386,897
	June	135,403 (16)	9.40 (166)	94.0	1,196,418
	July	141,237 (16)	6.54 (185)	97.0	895,978
	August	176,594 (18)	4.57 (129)	100	807,035
	Annual fecundity=3,286,328 oocytes				
2	May	280,724 (34)	6.80 (114)	100	1,908,926
	June	307,322 (10)	7.60 (79)	100	2,335,650
	July	370,170 (1)	9.04 (48)	100	3,346,337
	August	307,195 (7)	6.34 (44)	100	1,947,620
	Annual fecundity=9,538,533 oocytes				
3	May	487,475 (13)	7.42 (46)	100	3,617,061
	June	519,630 (4)	9.12 (23)	100	4,739,027
	July	765,911 (2)	3.1 (10)	100	2,374,325
	August	590,994 (2)	11.61 (8)	100	6,861,439
	Annual fecundity=17,591,852 oocytes				

Table 5

Monthly relative fecundity (number of oocytes /grams ovary-free weight) for *C. nebulosus* ages 1–3 for the spawning seasons 1998–2000. SD=standard deviation.

Month	Mean	Minimum	Maximum	SD	*n*
May	518.6	223.9	976.1	146.2	46
June	603.2	205.7	1306.1	241.8	20
July	820.9	662.2	1314.4	279.0	5
August	693.6	397.3	1021.8	207.9	12

and years for each age class separately (Table 4). There were no significant interannual or monthly variations in mean BF for any of the age classes (age-1: $P=0.59$, $n=62$; age-2: $P=0.17$, $n=52$; age-3: $P=0.07$, $n=21$). However, BF analysis for age-2 fish excluded the month of July because only one two-year-old specimen was captured that month during the study period. We investigated the relationship between BF and total length by using linear regression analysis. After pooling data across years, we found that total length explained 67% of the variability in spotted seatrout BF (Fig. 5A). Batch fecundity showed a similarly strong relationship to female somatic (ovary-free) weight (Fig. 5B) but did not relate to age as strongly (Fig. 5C). The equations below describe these relationships:

$BF = 2179.65(TL) - 520597$ $(r^2=0.67)$ $P<0.001$
$BF = 530.60(OFWT) + 18537.77$ $(r^2=0.65)$ $P<0.001$
$BF = 169398.21(Age) - 30956.33$ $(r^2=0.58)$ $P<0.001$.

Mean MEP was significantly different among months for age-1 spotted seatrout (Kruskal-Wallis, $P<0.05$). Age-1 fish spawned the least number of oocytes in May and most in June (Table 4). Statistical comparisons among months for ages 2 and 3 were inconclusive.

Relative fecundity

Relative fecundity among 83 spotted seatrout ages 1–3 ranged from 224 oocytes to 1314 oocytes/g OFWT (Table 5). Age did not have an effect on relative fecundity (Kruskal-Wallis, $P=0.75$). We found that spotted seatrout in South Carolina produced significantly more oocytes per gram ovary-free weight at the end than at the beginning of the spawning season (Mann Whitney, $P<0.05$). Mean oocyte diameters did not vary significantly between ovarian lobes or among locations within each lobe (ANOVA, $P=0.28$). A comparison among

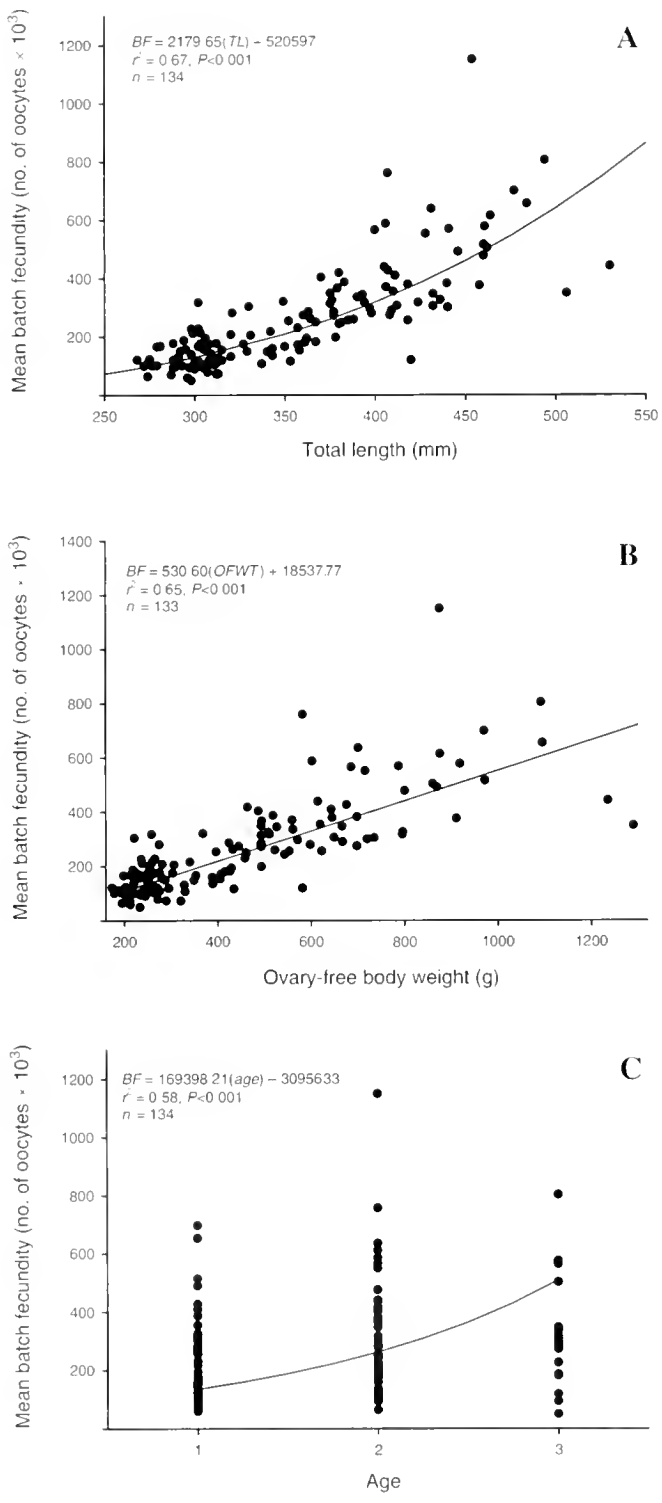

Figure 5

Relationship between batch fecundity (BF) and total length (TL) (**A**), between BF and ovary-free weight (OFWT) (**B**), and between BF and age (**C**) for *C. nebulosus* ages 1–3. Linear regression on data pooled for spawning seasons 1998–2000.

months and ages revealed that age had no effect on oocyte diameter (ANOVA, P=0.82). However, the effect of month corroborated the pattern of increasing RF as the spawning season progressed: oocytes were significantly smaller at the end of the season (ANOVA, P<0.05).

Annual fecundity

Annual fecundity estimates (summation of MEP) were approximately 3.2 million, 9.5 million, and 17.6 million oocytes for each age class, respectively (Table 4). The equation below describes the relationship between AF and age:

$$AF = 7152762(Age) - 4166620 \ (r^2=0.99) \ P<0.05.$$

From this relationship, the predicted AF for ages 4 and 5 were 24,444,430 and 31,597,190 oocytes, respectively. We expanded AF in relation to the abundance of each age class in our standard random samples for the three years of the study. We estimated that the overall average contribution from age-1 fish to the reproductive output for the season was approximately 29%, whereas fish aged 2 and 3 contributed 39% and 21% of oocytes, respectively. Ages 4–5 comprised less than 3% of specimens sampled and contributed 7% and 4% based on predicted AF values.

Discussion

Studies on the reproductive biology of *Cynoscion nebulosus* have established group-synchrony and indeterminate fecundity for this species throughout its range (i.e. Brown-Peterson et al., 1988; Brown-Peterson and Warren, 2001; Nieland et al., 2002; Mercer[1] and references therein). Fish with these features release gametes in several batches over a protracted spawning season and annual fecundity is not fixed prior to the onset of spawning (Wallace and Selman, 1981).

Based on mtDNA variation among spotted seatrout, the existence of two populations, one in the Gulf of Mexico and one in the South Atlantic, was established by Gold et al. (1999). However, variations in reproductive parameters have been suggested among geographic locations within the Gulf of Mexico (Brown-Peterson et al., 2002). Wiley (1996) suggested that spotted seatrout comprise a single stock in South Carolina; therefore reproductive parameters presented in the present study should be applicable only to the spotted seatrout population inhabiting coastal waters of this state. Further studies should be conducted to evaluate the applicability of these parameters to the entire southeast coast.

Other investigators (Brown-Peterson et al., 1988; Wieting, 1989; Brown-Peterson and War-

ren, 2001; Nieland et al., 2002; Lowerre-Barbieri et al.[8]) have used the gonadosomatic index (GSI) to delineate the spawning season in spotted seatrout. Even though the GSI provided a good approximation of the spawning season, histological data alone provided more precise evidence. Spotted seatrout in South Carolina began spawning near the end of April of each year and ceased by early September. Similarly, Lowerre-Barbieri et al.[8] reported that the spawning season for spotted seatrout in Georgia extended from late April to mid-September. We found histological evidence of initial spawning in specimens captured in 20°C water, although approximately 75% of spawning occurred when ambient water temperatures were greater than 25°C. In laboratory experiments, Brown-Peterson et al. (1988) found no successful spawning in water below 23°C but pointed out that others (McMichael and Peters, 1989) found eggs and larvae in 20.4°C water.

We found that females became mature approximately one full year after their birth. A female born in May of one year would be reproductively active in May of the following year. Females born later in the season would not be mature as the same successive season began; therefore, not all one-year-old females were mature when the spawning season began in May, but became mature before that season ended. This maturity schedule has also been reported for spotted seatrout in Louisiana (Nieland et al., 2002). However, Lowerre-Barbieri et al.[8] found that all one-year-old females were mature in coastal Georgia. A limited sample size or habitat segregation of mature and immature trout (Lowerre-Barbieri et al.[8]) may have contributed to their result.

The size at first maturity for spotted seatrout in this study was 248 mm TL. This size is comparable to what others have reported in other areas of the species' range (Brown-Peterson et al., 1988; Brown Peterson and Warren, 2001; Nieland et al., 2002; Mercer[1] and references therein; Lowerre-Barbieri et al.[8]). Our estimate of size at 50% maturity (268 mm TL) was larger than what Nieland et al. (2002) reported for 100% mature trout in Louisiana (250 mm TL). However, Nieland et al.'s (2002) statement that animals are 100% mature at 250 mm TL, does not agree with the growth equation they report for female trout when age = 1. Because we found size at 100% maturity among female spotted seatrout in South Carolina to be about 300 mm TL, we wonder whether Nieland et al.'s (2002) growth equation for female TL was meant to represent SL. Were this the case, they might have offered a different rationale for size at maturity among trout in Louisiana.

Brown-Peterson et al. (1988) and Brown-Peterson and Warren (2001) reported size at 100% maturity of 356 mm and 309 mm TL (using the SL-TL conversion found in our "Methods: section) for spotted seatrout in Texas and Mississippi, respectively. Brown-Peterson et al. (1988), however, chose a combination of gears that may not have sampled the trout population in Texas representatively for size-at-maturity estimation. In Mississippi, Brown-Peterson and Warren (2001) used a more appropriate gear for capture of late juvenile and early adult fish. Our estimate of size at 100% maturity was quite similar to theirs.

Spawning frequency

Determining the number of multiple spawning events during a single season for individual fish has been problematic. Initially, there was little understanding of the reproductive dynamics of spotted seatrout, and BF estimates were reported to represent the output for a whole season (Pearson, 1929; Sundararaj and Suttkus, 1962; Overstreet, 1983). Hunter et al. (1985) and Hunter and Macewicz (1985) developed techniques to overcome these limitations by providing protocols for the use of hydrated oocytes in determining BF and SF among group-synchronous species.

To use the techniques of Hunter (1985) and Hunter and Macewicz (1985) appropriately, it is critical to obtain a representative sample of the spawning population. DeMartini and Fountain (1981) and Lisovenko and Adrianov (1991) maintained that the relative occurrence of hydrated oocytes (as determined macroscopically) was an effective measurement of SF when the spawning population was sampled representatively. However, when sampling a species that spawns in aggregations at specific geographic locations, as do many of the sciaenids, it is inherently impossible to obtain a statistically representative sample of the spawning population for SF estimation based on FOM. Because the window of opportunity is temporally and spatially constrained, obtaining a sample that includes all sizes and ages involved is not feasible; the only choice in this situation is to sample in a directed fashion. This was the sampling strategy used to target females for BF counts; the majority of the animals captured whose oocytes evidenced FOM were obtained in a nonrandom fashion. Additionally, we assumed that fishes demonstrating FOM were moving toward deeper water spawning aggregations and away from our capture gear. For these reasons, we felt that our SF estimates based on the proportion of females with oocytes in FOM were biased and we excluded them from AF estimation. This is an important matter to keep in mind when comparing frequencies of spawning based on different methods.

Because obtaining representative numbers of animals with late-maturing oocytes is not often feasible, researchers have relied on the relative abundance of postovulatory follicles (POFs) to calculate SF (Brown-Peterson et al., 1988; Brown-Peterson and Warren, 2001; Nieland et al., 2002; Lowerre-Barbieri et al.[8]). The POF method lacks the limitations (described above) of the FOM method. Because the method we chose allowed us to sample all sizes and ages of fish in the estuary, obtaining representative numbers of animals with POFs was accomplished effectively. Therefore, we felt that our estimates of SF based on the POF method were more precise and we chose to use them in deriving AF.

The POF method depends on the ability to assess the disappearance of these structures. Hunter and Macewicz (1985) systematically sampled captive spawning anchovies to develop histological criteria for POF atrophy in

19°C water. Their criteria have been used by others to estimate rates of POF atrophy in other species and thereby determine the percentage of a population undergoing spawning over a discrete time period (Brown-Peterson et al., 1988; Fitzhugh et al., 1993; Taylor et al., 1998; Macchi and Acha, 2000; Brown-Peterson and Warren, 2001; Nieland et al., 2002). However, even though it has been demonstrated that the rate of POF atresia depends largely on ambient water temperature (Fitzhugh and Hettler, 1995), few (Brown-Peterson et al., 1988; Macchi and Acha, 2000; Nieland et al., 2002) have taken this into account when establishing the age of POFs for SF estimations. Our diurnal sampling of reproductively active spotted seatrout during warm water conditions enabled us to establish criteria to accurately estimate the age of POFs throughout the spawning season. Furthermore, we verified our assessments by sampling around the clock on two occasions to collect fish over the time period immediately following a spawning event.

Spotted seatrout ages 1–3 in SC spawned less frequently than those from the Indian River Lagoon, Florida (Crabtree and Adams[7]) but both studies showed that older fish spawned more frequently than younger animals. Our estimates for spotted seatrout aged 1–3 were 4.7, 4.2, and 4 days, respectively. Trout in these age classes in Florida were reported to spawn once every 4, 2.8, and 2.5 days, respectively. These differences probably not only reflect the distinct biological environments of each region but also indicate potential discrepancies in aging methods. No age-specific estimates of SF are available for other areas in the species' range. Brown-Peterson and Warren (2001) found SF among spotted seatrout in Biloxi Bay, MS, to be significantly lower than that of fish inhabiting the other two areas included in their study. They suggested that Biloxi Bay was a less conducive spawning habitat because of several factors, including shoreline development and a reduced amount of aquatic vegetation. However, because we found that SF varied significantly among age classes (age-3 fish spawned more frequently), the relative age composition of fish sampled by Brown-Peterson and Warren (2001) in the three estuaries might also have played a critical role in the determination of SF.

Batch fecundity

The best approach for estimating BF is to use only oocytes in FOM (Hunter et al., 1985; Brown-Peterson et al., 1988; Brown-Peterson and Warren, 2001; Brown-Peterson et al., 2002; Nieland et al., 2002; Lowerre-Barbieri et al.[8]). When it is not possible to obtain these, BF estimations can and have been carried out in some species by using the largest vitellogenic oocytes (Overstreet, 1983; Hunter et al., 1985; Wieting 1989). These efforts have the potential of being less accurate because isolating those oocytes destined to be spawned is difficult if the latter have not yet reached final maturation (Nieland et al., 2002). Inevitably this scenario would result in a nonmeasurable overestimation of female reproductive output. Brown-Peterson et al. (1988) and Brown-Peterson and Warren (2001) used a modification of this approach to estimate BF of spotted seatrout in Texas and Mississippi, respectively. However, even though the potential existed for overestimating BF, their estimates fell well below those presented in the present study, as did those presented by Nieland et al. (2002) for spotted seatrout ages 2–4 in Barataria Bay, Louisiana. Mean BF for ages 1–3 (170 thousand, 226 thousand, and 274 thousand oocytes, respectively) spotted seatrout in Indian River Lagoon, Florida (Crabtree and Adams[7]), also differed from those reported here. Our estimate took into account that not all age-1 females were mature at the beginning of the season. Crabtree and Adams,[7] however, did not adjust their estimate to reflect this discrepancy. Moreover, due to differences in aging methods, their age-1 and 2 cohorts possibly included ages 2 and 3, respectively. In addition, in the Florida study as well as in ours, relatively few numbers of older specimens were examined.

The relationships between BF and length, weight, and age in the present study were significant and predictive. Of these, TL exhibited the most predictive relationship. This fact may explain why age-1 and age-2 spotted seatrout in Georgia had mean BFs considerably higher than ours (175 thousand and 407 thousand, respectively; Lowerre-Barbieri et al.[8]): the size ranges for age-1 and age-2 in the Georgia study were greater than ours. Total length seems to be the most reliable predictor of BF among spotted seatrout in Georgia and SC (Lowerre-Barbieri et al.,[8] this study) and in Louisiana (Nieland et al., 2002). However, Crabtree and Adams[7] found that BF related best to ovary-free weight among spotted seatrout in Florida. We found ovary-free weight to be the second best predictor of BF. Overall, it appeared that TL and ovary-free weight were better predictors of BF than age for this species (Brown-Peterson, 2003).

As with SF, monthly egg production (MEP) estimates for SC spotted seatrout varied throughout the season. Because BF was not significantly different among months for any of our age classes, the variation in MEP resulted directly from the frequency of spawning. Monthly egg production estimates for age-1 fish were lowest in May and highest in June because SF was lowest in May and highest in June. Spawning frequency is a critical reproductive parameter because it seems to dictate annual reproductive output (DeMartini and Fountain, 1981; Brown-Peterson and Warren, 2001; Crabtree and Adams[7]); therefore, SF should be carefully considered, particularly for managed species.

Relative fecundity

We found that relative fecundity (RF), the number of oocytes per gram of somatic weight, did not show a significant relationship with female size. This finding was expected because dividing fecundity by ovary-free weight standardizes the values independently of size. However, this finding was in contrast to that of Brown-Peterson and Warren (2001). They collected specimens during the morning only, whereas we sampled ours throughout the day. This procedure allowed us to examine ovaries

over the entire range of maturation and to select only those clearly showing nuclear migration (based on histological observations) ensuring that only oocytes in the same phase of FOM (Brown-Peterson et al., 1988) were included in RF calculations. If sampling is conducted during a time period that is not close to active spawning (i.e., when oocytes are in different phases of FOM), then the number of oocytes per gram may be miscalculated.

As with BF, our RF estimates were higher than those reported for seatrout in the Gulf of Mexico (Brown-Peterson et al., 1988; Brown-Peterson and Warren, 2001), although spotted seatrout reproductive parameters appeared to vary considerably even within the Gulf of Mexico (Brown-Peterson et al., 2002). This was attributed to differential environmental conditions or food availability (or to both) (Brown-Peterson and Warren, 2001; Brown-Peterson et al., 2002). The significant seasonal increase in RF that we observed for spotted seatrout in South Carolina, however, has not been reported elsewhere. Brown-Peterson et al. (1988) found no differences in mean monthly RF among spotted seatrout in Texas. Brown-Peterson and Warren (2001) found significantly higher RF values in June than in August. In both instances, however, a small sample size may have biased their results.

Comparisons of mean oocyte diameters among months related the increase in RF to a general decrease in oocyte size over the course of the season. This phenomenon is widespread among marine pelagic spawners, and scientists have put forth several explanations to account for it (see Chambers, 1997). Bagenal (1971) suggested that egg size decreased over the spawning season owing to concurrent increased food availability for larvae. Others have suggested an inverse relationship between temperature and egg size (Ware, 1975; Wootton, 1994; Miller et al., 1995) or a seasonal decrease in egg size that is correlated to the condition of spawning females (DeMartini and Fountain, 1981; Chambers and Waiwood, 1996). The latter seems to apply to spotted seatrout in this study because a diminishing trend through the spawning season was observed in the condition factor of females.

Annual fecundity

Brown-Peterson (2003) presented AF estimates for spotted seatrout throughout their range. Our estimates were substantially below those for spotted seatrout in Indian River Lagoon (Crabtree and Adams[7]) but approximated those of Lowerre-Barbieri et al.[8] for trout in Georgia. A possible reason for the higher values in Florida was the more protacted spawning season in that area (50 days longer). No comparisons of AF estimates presented in this study and those of spotted seatrout in the Gulf of Mexico (Brown-Peterson, 2003) were made because they were not specific to age classes.

The main impetus behind the present study was to establish annual fecundity (AF) estimates by age class. We found that age-1 through age-3 spotted seatrout occurred abundantly in SC estuaries and that each of these age cohorts showed unique fecundity dynamics. The AF for an average age-1 fish was one-third that of age-2 (~3.28 million vs. 9.5 million). One year-old fish, however, constituted the majority of fish in our samples; their abundance was twice that of 2-year-olds and seven times that of 3-year-old fish. Even though the average age-3 trout produced almost twice as many oocytes during the season (17.5 million) as the average age-2 fish, their reduced abundance in our estuaries made their overall contribution only half that of 2 year-olds. Ages 4 and 5 were estimated to produce approximately 24.4 million and 31.6 million oocytes per female, respectively; however, the oocyte production by the predominant age groups overshadowed theirs. When analyzed in relation to the occurrence of the other age classes in our estuaries, age-2 fish contributed the greatest number of fertilizable oocytes to the environment (39%).

Reliable fecundities based on age and on length are optimal for stock assessment models (Williams[9]). This study provided AF estimates for three age classes that can be used in age-based models for the spotted seatrout population in South Carolina. Annual fecundity estimates based on length, however, have not been attempted even though length appears to be the best predictor of fecundity in spotted seatrout (see references in Brown-Peterson, 2003). Further analyses to investigate the relationship between egg production and fish length for each month of the spawning season would allow for more precise management efforts based on individual length-based estimates of AF.

Acknowledgments

We thank members of the Inshore Fisheries Section of the South Carolina Department of Natural Resources for assisting in field data collection throughout this study (C. Wenner, J. Archambault, H. von Kolnitz, W. Hegler, E. Levesque, L. Goss, C. McDonough, C. Johnson, A. Palmer). C. Wenner, H. von Kolnitz, and E. Levesque conducted age assessments. Histological processing was provided by C. McDonough, R. Evitt, A. Palmer, and W. Hegler. Assistance with oocyte counts was provided by C. McDonough, T. Piper, K. Maynard, and R. Evitt. Data management was coordinated by J. Archambault, C. Wenner, E. Levesque, and three anonymous reviewers provided helpful suggestions on the manuscript. Funding for this study was provided by the National Marine Fisheries Service under MARFIN grant no. NA77FF0550.

Literature cited

Bagenal, T. B.
1971. The interrelation of the size of fish eggs, the date of spawning, and the production cycle. J. Fish. Biol. 3:207–219.

[9] Williams, E. 2003. Personal commun. National Marine Fisheries Service, 101 Pivers Island, Rd., Beaufort, NC 28516.

Brown-Peterson, N. J.
2003. The reproductive biology of spotted seatrout. *In* Biology of the spotted seatrout (S. A. Bortone, ed.) p. 99–133. CRC Press, Boca Raton, FL.

Brown-Peterson, N. J., P. Thomas, and C. Arnold.
1988. Reproductive biology of the spotted seatrout, *Cynoscion nebulosus*, in South Texas. Fish. Bull. 86:3 73–387.

Brown-Peterson, N. J., M. S. Peterson, D. L. Nieland, M. D. Murphy, R. G. Taylor, and J. R. Warren.
2001. Reproductive biology of female spotted seatrout, *Cynoscion nebulosus*, in the Gulf of Mexico: differences among estuaries? Environ. Biol. Fish. 63:405–415.

Brown-Peterson, N. J., and J. R. Warren.
2002. The reproductive biology of spotted seatrout, *Cynoscion nebulosus*, along the Mississippi Gulf coast. Gulf. Mex. Sci. 19:61–73.

Chambers, R. C.
1997. Environmental influences on egg and propagule size in marine fishes. *In* Early life history and recruitment in fish populations (R. C. Chambers and A. E. Trippel, eds.), p. 93–102. Chapman and Hall, London.

Chambers, R. C., and K. G. Waiwood.
1996. Maternal and seasonal differences in egg sizes and spawning characteristics of captive Atlantic cod, *Gadus morhua*. Can. J. Fish. Aquat. Sci. 53:1986–2003.

DeMartini, E. E., and R. K. Fountain.
1981. Ovarian cycling frequency and batch fecundity in the queenfish, *Seriphus politus*: attributes representative of spawning fish. Fish. Bull. 79:547–560.

Fish, M. P., and W. H. Mowbray.
1970. Sounds of western North Atlantic fishes. A reference file of biological underwater sounds. The Johns Hopkins Press, Baltimore and London.

Fitzhugh, G. R., and W. F. Hettler.
1995. Temperature influence on postovulatory follicle degeneration in Atlantic menhaden, *Brevoortia tyrannus*. Fish. Bull. 93:568–572.

Fitzhugh, G. R., B. A. Thompson, and T. G. Snider.
1993. Ovarian development, fecundity and spawning frequency of black drum, *Pogonias cromis*, In Louisiana. Fish. Bull. 91:244–253.

Gabriel, W. L., M. P. Sissenwine, and W. J. Overholtz.
1989. Analysis of spawning stock biomass per recruit: an example for Georges Bank haddock. N. Am. J. Fish. Manag. 9:383–391.

Gold, J. R., L. R. Richardson, and C. Furman.
1999. Mitochondrial DNA diversity and population structure of spotted seatrout (*Cynoscion nebulosus*) in coastal waters of the Southeastern United States. Gulf Mex. Sci. 1:40–50.

Goodyear, C. P.
1993. Spawning stock biomass per recruit in fisheries management: foundation and current use. *In* Risk evaluation and biological reference points for fisheries management (S. J. Smith, J. J. Hunt, and D. Rivard, eds.), p. 67–81. Can. Spec. Publ. Fish. Aquat. Sci. 120.

Holt, G. J., S. A. Holt, and C. R. Arnold.
1985. Diel periodicity of spawning in sciaenids. Mar. Ecol. Prog. Ser. 27:1–7.

Humason, G. L.
1972. Animal tissue techniques. W. H. Freeman and Co. San Francisco and London.

Hunter, J. B., N. C. H. Lo, and R. J. H. Leong.
1985 Batch fecundity in multiple spawning fishes. *In* An egg production method for estimating spawning biomass of pelagic fish: application to the northern anchovy *Engraulis mordax* (R. Lasker, ed.), p. 67–77. NOAA Tech. Rep. NMFS 36.

Hunter, J. R., and B. J. Macewicz.
1985. Measurement of spawning frequency in multiple spawning fishes. *In* An egg production method for estimating spawning biomass of pelagic fish: application to the northern anchovy *Engraulis mordax* (R. Lasker, ed.), p. 79–94. NOAA Tech. Rep. NMFS 36.

Lisovenko, L. A., and D. P. Andrianov.
1991. Determination of absolute fecundity of intermittently spawning fishes. Voprosy ikhtiologii 31:631–641.

Macchi, G. J., and E. M. Acha.
2000. Spawning frequency and batch fecundity of Brazilian menhaden, *Brevoortia aurea*, in the Rio de la Plata estuary off Argentina and Uruguay. Fish. Bull. 98:283–289.

McMichael, R. H., and K. M. Peters.
1989. Early life-history of spotted seatrout, *Cynoscion nebulosus* (Pisces: Sciaenidae), in Tampa Bay, Florida. Estuaries 12:98–110.

Miller, T. J., T. Herra, and W. C. Leggett .
1995. An individual-based analysis of the variability of eggs and their newly hatched larvae of Atlantic cod (*Gadus morhua*) on the Scotian Shelf. Can. J. Fish. Aquat. Sci. 52:1083–1093.

Mok, H. K., and R. G. Gilmore.
1983. Analysis of sound production in estuarine aggregations of *Pogonias cromis*, *Bairdiella chrysoura*, and *Cynoscion nebulosus* (Sciaenidae). Bull. Inst. Zool., Acad. Sinica (Taipei) 22:157–186.

Murphy, M. D., and R. G. Taylor.
1994. Age, growth and mortality of spotted seatrout in Florida waters. Trans. Am. Fish. Soc. 123:482–497.

Nieland, D. L., R. G. Thomas, and C. A. Wilson.
2002. Age, growth and reproduction of spotted seatrout in Barataria Bay, Louisiana. Trans. Am. Fish. Soc. 131:245–259.

Overstreet, R. M.
1983. Aspects of the biology of the spotted seatrout, *Cynoscion nebulosus*, in Mississippi. Gulf Res. Rep. Suppl. 1:1–43.

Pearson, J. C.
1929. Natural history and conservation of the redfish and other commercial sciaenids on the Texas coast. Bull. U.S. Bur. Fish. 44:129–214.

Prager, M. H., J. F. O'Brien, and S. B. Saila.
1987. Using lifetime fecundity to compare management strategies: a case history for striped bass. Am. J. Fish. Manag. 7:403–409.

Ricker, W. E.
1975. Computation and interpretation of biological statistics of fish populations. Bull. Fish. Res. Board Can. 191:1–382.

Saucier, M. H., and D. M. Baltz.
1993. Spawning site selection by spotted seatrout, *Cynoscion nebulosus*, and black drum, *Pogonias cromis*, in Louisiana. Environ. Biol. Fish. 36:257–272.

Saucier, M. H., D. M. Baltz, and W. A. Roumillat.
1992. Hydrophone identification of spawning sites of spotted seatrout *Cynoscion nebulosus* (Osteichthys: Sciaenidae) near Charleston, South Carolina. N. Gulf Sci.12:141–145.

Sundararaj, B. I., and R. D. Suttkus.
1962. Fecundity of the spotted seatrout, *Cynoscion nebulo-*

sus (Cuvier), from Lake Borgne Area, Louisiana. Trans. Am. Fish. Soc. 91:84–88.

Taylor, R. G., H. J. Grier, and J. A. Whittington.
1998. Spawning rhythms of common snook in Florida. J. Fish Biol. 53:502–520.

Vaughan, D. S., G. R. Huntsman, C. S. Manooch III, F. C. Rohde, and G. F. Ulrich.
1992. Population characteristics of the red porgy, *Pagrus pagrus*, stock off the Carolinas. Bull. Mar. Sci. 50: 1–20.

Wallace, R. A., and K. Selman.
1981. Cellular and dynamic aspects of oocyte growth in teleosts. Am. Zool. 21:325–343.

Ware, D. M.
1975. Relation between egg size, growth, and natural mortality of larval fish. J. Fish. Res. Board Can. 32: 2503–512.

Wieting, D. S.
1989. Age, growth and fecundity of spotted seatrout (*Cynoscion nebulosus*) in Louisiana. M.S. thesis, 94 p. Louisiana State Univ., Baton Rouge, LA.

Wiley, B. A.
1996. Use of polymorphic microsatellites to detect population structure in spotted seatrout, *Cynoscion nebulosus* (Cuvier). M.S. thesis, 42 p. Univ. Charleston, Charleston, SC.

Wootton, R. J.
1994. Life histories as sampling devices: optimum egg size in pelagic fishes. J. Fish Biol. 45:1067–1077.

Estimating Dungeness crab (*Cancer magister*) abundance: crab pots and dive transects compared

S. James Taggart
Glacier Bay Field Station
Alaska Science Center
U.S. Geological Survey
3100 National Park Rd.
Juneau, Alaska 99801
E-mail address: jim_taggart@usgs.gov

Charles E. O'Clair
National Marine Fisheries Service
Auke Bay Laboratory
11305 Glacier Highway
Juneau, Alaska 99801

Thomas C. Shirley
Juneau Center, School of Fisheries & Ocean Sciences
University of Alaska Fairbanks
11120 Glacier Highway
Juneau, Alaska 99801

Jennifer Mondragon
Glacier Bay Field Station
Alaska Science Center
U.S. Geological Survey
3100 National Park Rd.
Juneau, AK 99801

Abstract—Dungeness crabs (*Cancer magister*) were sampled with commercial pots and counted by scuba divers on benthic transects at eight sites near Glacier Bay, Alaska. Catch per unit of effort (CPUE) from pots was compared to the density estimates from dives to evaluate the bias and power of the two techniques. Yearly sampling was conducted in two seasons: April and September, from 1992 to 2000. Male CPUE estimates from pots were significantly lower in April than in the following September; a step-wise regression demonstrated that season accounted for more of the variation in male CPUE than did temperature. In both April and September, pot sampling was significantly biased against females. When females were categorized as ovigerous and nonovigerous, it was clear that ovigerous females accounted for the majority of the bias because pots were not biased against nonovigerous females. We compared the power of pots and dive transects in detecting trends in populations and found that pots had much higher power than dive transects. Despite their low power, the dive transects were very useful for detecting bias in our pot sampling and in identifying the optimal times of year to sample so that pot bias could be avoided.

Manuscript submitted 13 March 2000 to Scientific Editor's Office.
Manuscript approved for publication 25 March 2004 by the Scientific Editor.
Fish. Bull. 102:488–497 (2004).

Reliable population assessments are fundamental to the management and conservation of commercially harvested crabs. Many crab populations are sampled with commercial crab pots to estimate population trends, to set harvest quotas, or to differentiate natural population fluctuations caused by anthropogenic changes to the ecosystem. Pots are used, for example, to assess the population status of blue crabs, *Callinectes sapidus* (Abbe and Stagg, 1996), red king crabs, *Paralithodes camtschaticus* (Zheng et al., 1993), snow crabs, *Chionoecetes opilio* (Dawe et al., 1996), and southern king crabs, *Lithodes santolla* (Wyngaard and Iorio, 1996).

The Dungeness crab (*Cancer magister*) fishery began in southeastern Alaska in 1916 and has been characterized by large fluctuations on annual and decadal scales (Orensanz et al., 1998). Large variation in the Dungeness crab harvest is not unique to Alaska; similar fluctuations have been documented in California and their causes are the subject of an ongoing debate (Higgins et al., 1997a, 1997b). It is not clear whether the processes that cause fluctuations in California are the same as those responsible for oscillations in Dungeness crab abundance in Alaska.

Most of the Dungeness crab fisheries in Alaska are managed by regulating the size and sex of the crabs caught, and, in some places, the season of the harvest. In southeastern Alaska, legal harvest is restricted to males with a carapace width greater than or equal to 165 mm (excluding the 10th anteriolateral spines) and the season is timed to avoid sensitive life

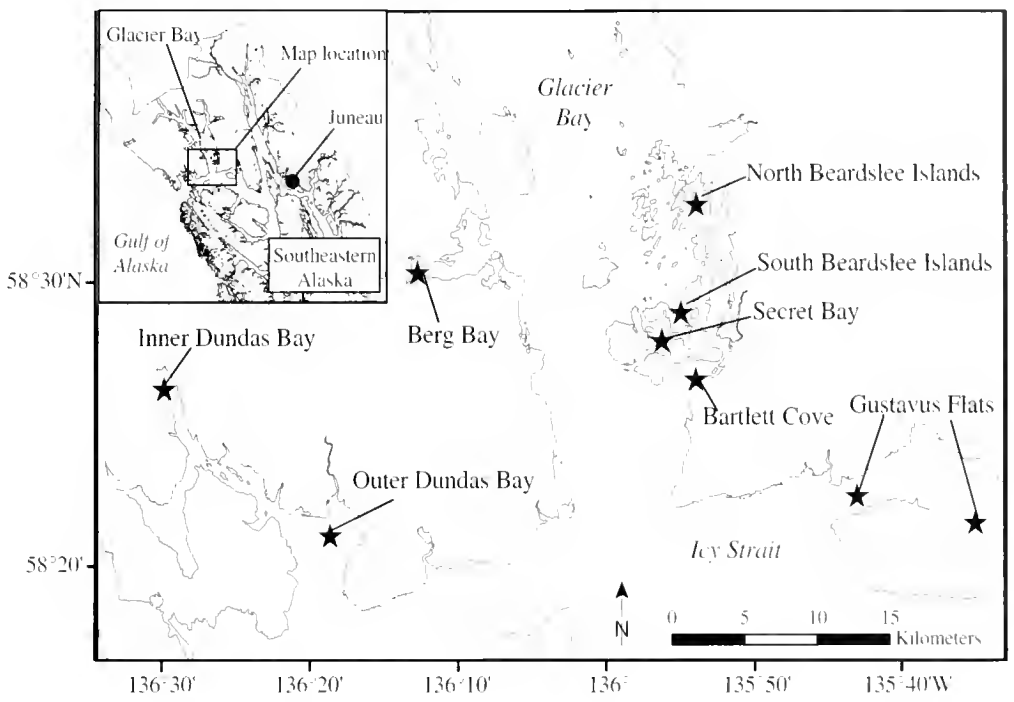

Figure 1

Map of study area showing eight study sites in or near Glacier Bay in southeastern Alaska.

history periods such as mating and molting (Kruse, 1993; Orensanz et al., 1998). Pre- and postseason stock assessment surveys using crab pots were initiated in southeastern Alaska in 2000 (Rumble and Bishop, 2002). The purpose of the latter management strategy is to assess the abundance of legal-size males before the fishing season, to estimate harvest rates, to define the timing of male and female mating and molting and to determine growth rate by tagging crabs.

The usefulness of surveys with pots for Dungeness crab population assessment, however, depends on the accuracy of these surveys in measuring population parameters. Factors that can bias catch per unit of effort (CPUE) and size-frequency estimates for Dungeness crabs are pot soak-time (Miller, 1974; High, 1976; Gotshall, 1978; Smith and Jamieson, 1989); freshness of bait (High, 1976; Smith and Jamieson, 1989); pot design (Miller, 1974; High, 1976; Smith and Jamieson, 1989); and agonistic interactions among conspecifics inside and at the entrance of pots (Caddy, 1979; Smith and Jamieson, 1989). Smith and Jamieson (1989) developed a standardized model to compensate for the effect of agonistic interactions, age of bait, and escapement. They also concluded that researchers could minimize these biases by measuring CPUE with standardized surveys with short soak times. These studies measured sampling bias with pots by comparing catch in pots among various experimental treatments. Opportunities for comparing surveys with pots to direct measures of abundance are rare. In our study, we compared the bias and power of CPUE estimates from surveys with pots to independent measures of abundance conducted by scuba divers on benthic dive transects.

Methods

Study area

The study area included eight sites in southeastern Alaska, near Glacier Bay: North Beardslee Islands (58°33′N 135°54′W), South Beardslee Islands (58°30′N 135°55′W), Berg Bay (58°31′N 136°13′W), Bartlett Cove (58°27′N 135°53′W), Gustavus Flats (58°23′N 135°43′W), Secret Bay (58°29′N 135°56′W), inner Dundas Bay (58°27′N 136°31′W), and outer Dundas Bay (58°21′N 136°18′W) (Fig. 1). All study sites were located within Glacier Bay National Park and Preserve, with the exception of Gustavus Flats, which was located adjacent to the Park boundary in Icy Strait.

Glacier Bay is a large (1312 km^2) glacial fjord system with high sedimentation rates of clay-silt particles from streams and tidewater glaciers (Cowan et al., 1988). The primarily unconsolidated rocky coastline is highly convoluted with numerous small bays. Dungeness crabs can be found throughout Glacier Bay; however the majority of the population are found in the lower 40 km of the estuary where our sites were located (Taggart et al., 2003). The shallow water in and around our study sites was primarily characterized by mud bottom, but sand, pebble, cobble, and shell substrates were also common (Scheding et al., 2001).

Table 1

Sampling dates for yearly spring and fall pot and dive surveys of Dungeness crabs (*Cancer magister*) in Glacier Bay, Alaska. Sample size (*n*) is listed for pots and dives for each sampling event.

	Spring sampling				Fall sampling			
Year	Pots	*n*	Dives	*n*	Pots	*n*	Dives	*n*
1992	7–12 April	248	7–12 April	69	17–22 Sept.	250	17–22 Sep.	75
1993	20–27 April	350	20–27 April	105	23–28 Sept.	250	23–28 Sep.	75
1994	20–27 April	350	23 April–1 May	105	13–18 Sept.	249	13–18 Sept.	75
1995	19–26 April	350	23 April–1 May	105	9–14 Sept.	236	15–19 Sept.	75
1996	15–21 April	350	22–28 April	105	13–18 Sept.	242	19–23 Sept.	73
1997	17–22 April	300	23–28 April	115	14–19 Sept.	298	20–25 Sept.	120
1998	—	—	—	—	9–14 Sept.	296	16–21 Sept.	91
1999	—	—	—	—	9–14 Sept.	299	17–22 Sept.	107
2000	—	—	—	—	9–14 Sept.	297	18–23 Sept.	60

Sampling dates

Sampling was conducted biannually, in April and September, from 1992 to 1997 and annually, in September, from 1998 to 2000 (Table 1). The spring and fall sampling periods were selected to coincide with crab life history events and to avoid sampling during commercial fishery operations. April sampling was scheduled to occur before larval hatching in May–June (Shirley et al., 1987) and before the summer commercial fishing season from 15 June to 15 August. September sampling began after the end of the fishing season (15 August) and ended before the beginning of the winter harvest (1 October to 30 November).

During 1992, the study sites were sampled with pots (referred to as "pot sampling") and by divers (referred to as "dive sampling") concurrently (Table 1). In 1993 and 1994, sampling was conducted on nearby study sites and the dive sampling usually one day ahead of the pot sampling. For logistical reasons, starting in 1995, we separated the pot sampling and the dive-transect sampling into two separate research cruises. The pot sampling was conducted on the first cruise and the dive sampling occurred on the second cruise; pot and dive sampling were separated at each location by 2 to 12 days.

Sampling with pots

Crabs were sampled with commercial crab pots (0.91 m in diameter, 0.36 m tall, with 5-cm wire mesh). Escape rings were sealed with webbing on each pot to retain smaller crabs. Pots were baited with hanging bait comprising salmon, cod, or halibut (depending on availability) and bait jars that were filled with chopped herring and squid. We found that cod was predictably available; therefore from 1996 on, we consistently used cod for hanging bait. Pots were soaked for 24 hours.

Within each study site, we set 25 pots in shallow water (0–9 m) and 25 pots in deep water (10–25 m). Each day we set 50 pots in one of the study sites and retrieved the 50 pots that had been set the previous day at one of the other study sites. The pots were set along strings parallel to shore at intervals of approximately 100 m. Within each study area, the strings of pots were located in prime Dungeness crab habitat determined by a local fisherman. We placed the pots at the same locations during subsequent sampling events by using a GPS (Rockwell PLGR+) with an accuracy of ±3 m. We estimate that the pots were set within 20 meters from the original waypoints. Water depth (standardized to mean lower low water), set and retrieval time, and GPS location were recorded for each pot. Water temperature and salinity profiles were measured at each study site during each sampling period with a SEABIRD SBE-19 Profiler.

As the pots were retrieved, we counted and identified all organisms. For all Dungeness crabs we recorded the sex, carapace width, shell condition, and damage to appendages. For female crabs we also recorded reproductive status. Carapace width was measured to the nearest millimeter immediately anterior to the 10th anterolateral spine with vernier calipers (Shirley and Shirley, 1988; Shirley et al., 1996). All organisms were returned to the water at the location where they were caught. A potential problem with returning the crabs to the water near the site of capture is the possibility that crabs could be resampled in subsequent pots, which would bias the catch per unit of effort. Beginning in April, 1995, all crabs collected in the South Beardslee Islands and Berg Bay were tagged with a sequentially numbered, double-T Floy tag (Floy Tag and Manufacturing Company, Seattle, WA) inserted along the posterolateral margin of the epimeral suture. Tags placed in this location are retained through ecdysis (Smith and Jamieson, 1989). Of the 5226 crabs tagged, only a single

crab was recovered during the same sampling event. Thus, the probability of resampling crabs by returning them to the water was very low.

Sampling by divers

Divers using scuba equipment censused crabs on 15 to 20, 2×100 m belt transects within each study site. Approximately one day of sampling was required at each study site. The dive transects were conducted perpendicular to the shoreline and they extended from the shallow subtidal (0 m, mean lower low water) to 18 m depth or to the end of the 100 m transect, whichever came first. Divers did not go below 18 m depth in an effort to reduce nitrogen accumulation in divers' blood and to reduce the surface intervals required between transects. From 1992 to 1997, transect locations were randomly selected in the same areas as the crab-pot sampling. The random locations selected in 1997 were resampled during the following years of the study.

Divers counted all Dungeness crabs located within 1 m of each side of the transect. An effort was made to locate buried crabs by swimming close to the bottom and looking for irregularities in the bottom or protruding crab eyestalks. Each crab was examined and the following were recorded: legal males ≥165 mm carapace width), sublegal males (<165 mm carapace width), ovigerous females, and nonovigerous females.

Data analysis

For each year, we calculated the average pot CPUE for each site by reproductive class (males, nonovigerous females, and ovigerous females). The number of pots sometimes deviated from 50 when a pot was lost or when the degradable cotton string securing the pot lid broke (range: 44–50 pots). The number of crabs counted on dive transects was averaged for each reproductive class by site for each year. All dive transects were conducted perpendicular to shore; thus the transects crossed the shallow habitat where the shallow string of pots was set and terminated at 18 m which was the center of the depth we targeted for the deep pot set. Because the deep pot set was at or slightly beyond the deep end of the transect, we may have sampled more crabs from deepwater habitats than from the shallower transects. However, we did not think this was a significant bias because we sampled crabs from a relatively large area. We, therefore, pooled the pots from both depth strata for analysis.

We tested for differences between April and September for the pot CPUE data and the dive density data with paired *t*-tests. CPUE and density data were not normally distributed; therefore we transformed the data with a square-root transformation $[Y=\sqrt{(Y+3/8)}]$ for statistical analyses (Zar, 1996). These analyses were conducted for males, nonovigerous females, and ovigerous females. Because seasonal increases in water temperature could drive differences in CPUE between April and September, we calculated mean water temperatures by averaging the water temperatures at the 5 m and 15 m depths at each site and year. This analysis was limited to years and sites where we collected samples in both April and September (1992–97, from five sites: North Beardslee Islands, South Beardslee Islands, Berg Bay, Bartlett Cove, and Gustavus Flats). We assessed how CPUE was influenced by two independent variables, water temperature and season, with stepwise regression. Because CPUE declined from 1992 to 1997 (Taggart et al., in press), we controlled for year so that it would not confound our analysis.

In order to assess sampling bias between pots and dive transects, the percentages of females (females/all crabs), nonovigerous females (nonovigerous females/all crabs), and ovigerous females (ovigerous females/all crabs) were calculated for each site and sampling time. We also compared the percentage of the male population that was legal size (legal-size male crabs/all male crabs) from the pots and from the dives. The percentage estimates from the pot data were compared to estimates from the dive transects with a paired sign test (Zar, 1996). If percentage estimates for pot data were unbiased when compared to estimates from dive data, the pot percentage estimates would have an equal chance of being higher or lower than the percentage estimates for the dive data. Because small sample sizes exaggerate percentage comparisons, we excluded samples where the total number of crabs collected was less than 25 crabs/site.

The power of pots and dive transects to detect trends in populations was compared with Monitor, a power analysis program (Gibbs and Melvin, 1997; Gibbs, 1998). For our analyses, we varied the number of transects and pots, compared males and nonovigerous females, and varied the duration of the study. For all analyses the following input parameters of the model were held constant: "survey occasions" = annual, "type" = linear, "significance level" = 0.05, "number of tails" = 2, "constant added" = 1, "trend variation" = 0, "rounding" = decimal, "trend coverage" = complete, and "replications" = 10,000.

To estimate power, the model requires "count" and "variance" for each plot across years for at least three years. Pot and transect data collected from 1992 to 1998 from five sites (North Beardslee Islands, South Beardslee Islands, Berg Bay, Bartlett Cove, and Gustavus Flats) were used for these analyses. The data were limited to September to avoid seasonal bias. The average across years was calculated for each transect and each pot. These averages were input into the model's variable called "plot count." For each pot and transect a linear regression was calculated among years (CPUE vs. year for pots; density vs. year for dive transects) and the residual mean square was the "plot variance" variable (Thomas and Krebs, 1997).

To estimate the effect of sample size on power we set the "number [surveys] conducted" to four and limited the analysis to males. We varied the number of "plots" (pots and transects). For pots, we randomly selected subsamples of the 250 pots and ran simulations from 25 pots to 250 pots in 25-pot increments. The number

of dive transects for which data were collected for multiple years was 75. For simulations with a sample size less than 75, we randomly subsampled the data in the same manner as we did with pots. For simulations with sample sizes greater than 75, we amplified the samples with simple bootstrapping to obtain samples from 100 to 250 transects in 25-transect increments (Wonnacott and Wonnacott, 1990). For each sample size, we modeled three annual rates of change (0.02, 0.03, and 0.05).

To evaluate how study duration affects power, we limited the analysis to males, varied study duration ("number [surveys] conducted") from two years to 12 years in two-year increments, and compared three annual rates of change (0.02, 0.03, and 0.05) for both pots and transects. To hold effort constant between the two sampling techniques, we set the pot and transect sample size to the number we could accomplish in a five-day research cruise (250 pots and 75 transects).

To explore the relationship between annual trend in population and power, we held effort constant (250 pots and 75 transects) and varied the annual trend (from −0.10 to +0.10 in 0.01 increments) for both males and nonovigerous females. It was not possible to conduct a power analysis for ovigerous females because a large proportion of the pots and transects had no ovigerous female crabs.

Results

The pot CPUE estimates for males, nonovigerous females, and ovigerous females was significantly different in April than in the following September (Fig. 2, A, C, and E). Male and nonovigerous female CPUE was higher in September (Fig. 2, A and C) and ovigerous female CPUE was lower in September (Fig. 2E). In contrast, April density estimates from dive transects were not significantly different from the following September density estimates for males (Fig. 2B). Dive density estimates for nonovigerous females were higher in September than in April (Fig. 2D); density estimates for ovigerous females were lower in September than in April (Fig. 2F).

When we tested the influence of temperature and season on male CPUE with stepwise regression, season was selected first; temperature was not selected because it did not have a significant additional effect (Table 2). Because no significant difference was found between the April and September density estimates from dive transects (Fig. 2B), we did not conduct a stepwise regression for the dive data.

Percentage estimates of females from sampling with pots were lower than percentage estimates from dive transects for a significant number of samples for both April and September (Fig. 3A); therefore pots were biased against sampling females. When females were split by reproductive status, no bias was detected for sampling nonovigerous females with pots (Fig. 3B). In contrast, the percentage estimates for ovigerous females remained biased and the magnitude of the bias increased (Fig. 3C). To test potential sampling bias

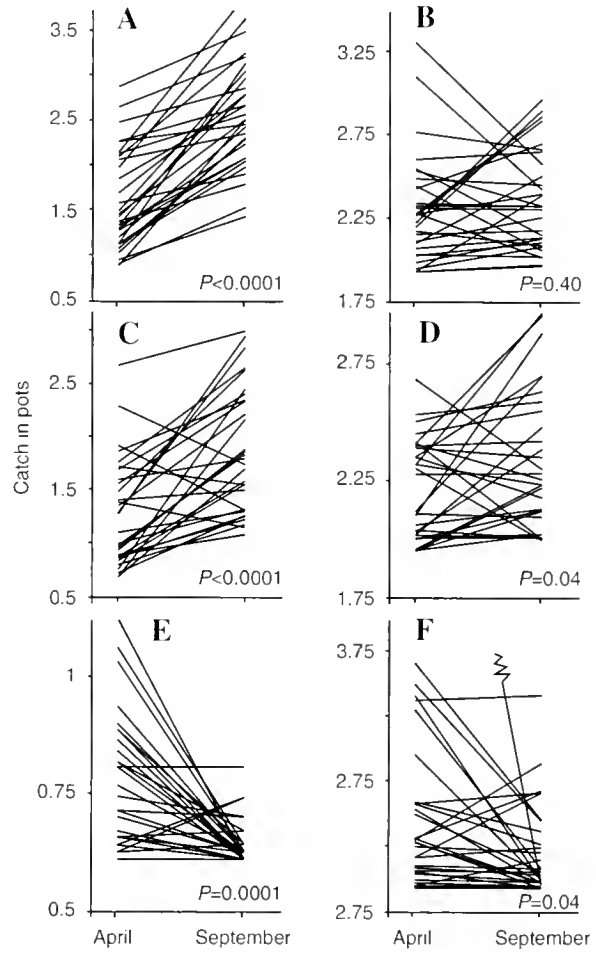

Figure 2

Within-year paired comparisons by site of catch in pots (left column) and density on dive transects (right column) for: (**A** and **B**) male Dungeness crabs (*Cancer magister*); (**C** and **D**) nonovigerous female crabs; and (**E** and **F**) ovigerous female crabs. Catch and density data were transformed with a square-root transformation. *P*-values indicate results from paired *t*-tests and significant results show differences between April and September. Lines on the graphs are parallel if measurements at sites were consistently higher or lower in April and September.

related to crab size, we compared the proportion of the male population that was legal size sampled with pots and dives (Fig. 4). There was no significant bias when pots and transects were compared with a sign test (April, $P>0.999$; September, $P=0.06$).

CPUE estimates from pots had a higher power than density estimates from dive transects for the same sample size (Fig. 5). Because more time is required to conduct a dive transect than to set and pull a crab pot, the power of transects compared to pots was even lower when effort was incorporated into the analysis (Fig 6). The power can be increased for both pots and

Table 2

Stepwise regression results of CPUE (male crabs/pot) versus three independent variables (year, season, and temperature).

Step	Model parameters	r^2	*P*-value (parameter)
1	*Year*	0.1493	0.001 (year)
2	*Year* and *month*	0.5589	0.04 (month)
3	*Year*, *month*, and *temperature*	0.5589	0.98 (temperature)

transects by increasing the study duration or increasing the amount of change in the population that the study is attempting to detect (Fig. 6). Although pots had more power than dive transects, there was only slightly more power to detect change in abundance of male crabs versus nonovigerous females (Fig. 7).

Discussion

For male Dungeness crabs, the density estimates from the dive transects showed no difference between April and September (Fig. 2B). The male CPUE estimates from pots, however, were consistently lower in April than in the following September (Fig. 2A). Because feeding rates of Dungeness crabs are correlated with temperature (Kondzela and Shirley, 1993), we thought that temperature was likely to explain the differences in CPUE between April and September. We found, however, that season had a larger effect than temperature (Table 2). This result suggests that seasonal factors other than temperature influence catchability. Stone and O'Clair (2001) followed the seasonal movements of Dungeness crabs in a glacial estuary in southeastern Alaska and reported that mean movement of male crabs was lower during the spring than in the late summer and fall. It is possible that our spring sampling schedule coincided with low male activity and male crabs were less likely to encounter a bait plume and be attracted to a pot. These results indicate that if pots are used for sampling, late summer and early fall is the time of year to conduct population assessment surveys of male crabs. Similar seasonal differences in CPUE have also been described for edible crabs (*Cancer pagurus*) and American lobsters (*Homarus americanus*) (Bennett, 1974). These data demonstrate the importance of controlling for season when comparing CPUE among years or sites.

The proportion of large crabs caught in pots increased with longer soak time for Dungeness crabs in British Columbia (Smith and Jamieson, 1989) and red king crabs in Britstol Bay, Alaska (Pengilly and Tracy, 1998). We found no bias when we measured the legal-size proportion of the male population caught in pots and compared it to the proportion sampled on dives (Fig. 4). We expect, however, that the bias observed in British Columbia and Bristol Bay would occur for our study sites if the soak time of pots were increased.

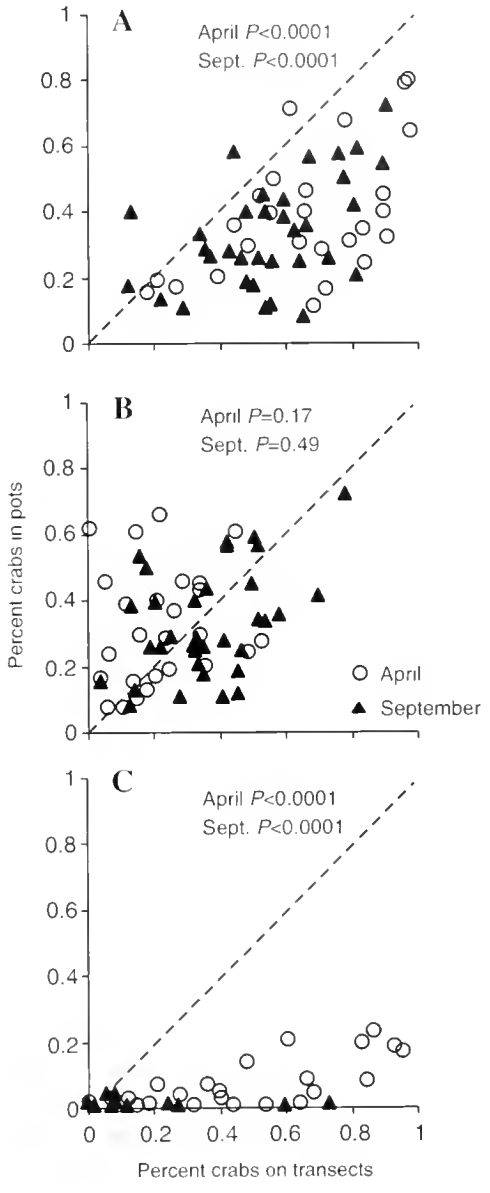

Figure 3

The percentage of (**A**) female Dungeness crabs (*C. magister*), (**B**) nonovigerous female crabs, and (**C**) ovigerous female crabs estimated from pots and from dive transects. The dashed line in each graph has a slope of 1; thus half of the data points should be above and half should be below the dashed line if percentage estimates for dives and pots are unbiased. Pot and dive transect data for each sex class and season were compared with a paired sign test and *P*-values are reported.

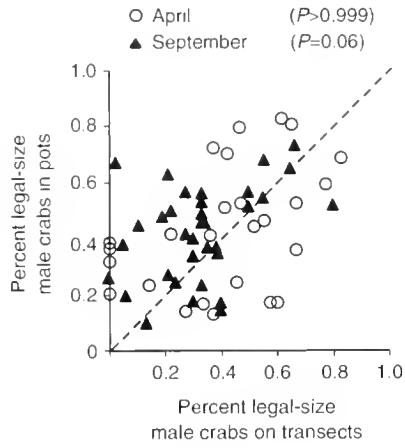

Figure 4

The percentage of male crabs of the Dungeness crab (*C. magister*) population that were legal size (≥165 mm) estimated from pots compared to the percentage of male crabs estimated from dive transects. Data from pots and dive transects were compared for each season with a paired sign test and *P*-values are reported

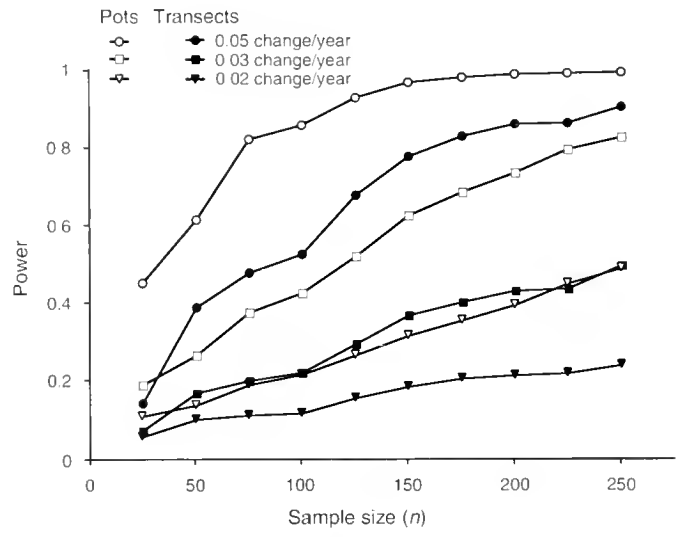

Figure 5

Relationship between power and sample size (*n*) in comparing catch from pots and density on dive transects for male Dungeness crabs (*C. magister*) at three levels of population change.

In both April and September, pot sampling was significantly biased against females (Fig. 3A). When females were categorized as ovigerous and nonovigerous, it was clear that ovigerous females accounted for the majority of the bias because pots were not biased against nonovigerous females (Fig. 3B). Similar results have been found for a closely related species, *Cancer pagurus*; female *C. pagurus* readily enter pots when they are in a nonovigerous reproductive state but are rarely captured when they are ovigerous (Bennett, 1995). Movement studies of Dungeness crabs tagged with sonic transmitters have demonstrated that ovigerous females move less frequently and move slower than males or nonovigerous females (O'Clair et al., 1990). Thus, one explanation for the bias against ovigerous female crabs is that their restricted movements make it less likely they will be able to locate and become entrapped in pots. In addition to being less mobile, ovigerous females may be less attracted to bait than nonovigerous crabs. In controlled feeding experiments, ovigerous females had lower feeding rates than nonovigerous females, and ovigerous females took longer to begin feeding (Schultz et al., 1996; Schultz and Shirley, 1997). Therefore, ovigerous females may be less responsive to the bait plume from a pot.

The estimate of nonovigerous females from both pot CPUE and dive transect density increased from April to September (Fig. 2, C and D). As with males, the increase in CPUE for nonovigerous females may be partly due to an increase in catchability in September. However, the fact that the density estimates from dives also increased suggests that the number of nonovigerous females actually increased between April and September. This explanation is supported by the decrease in ovigerous crabs from April to September for both CPUE (Fig. 2E) and density estimates (Fig. 2F).

The low catchability of ovigerous females makes it problematic to monitor relative abundance of females or changes in sex ratio through time. However, because pots were not biased against nonovigerous females (Fig. 3), the solution may be to estimate the relative abundance of females by sampling after females hatch their eggs and before they extrude a new clutch of eggs in the fall. In southeastern Alaska, most females are nonovigerous in late July and early August (Stone and O'Clair, 2001; Swiney et al., 2003); therefore this would be the optimal time of year to sample females or to measure sex ratio of Dungeness crab populations. Unfortunately, this timing coincides with the summer commercial fishing season, which could bias sampling if there was "competition" between survey pots and commercial pots.

For both males and females, the power analyses of the pot and dive data indicated that for most population assessment applications it would be extremely difficult to conduct enough dive transects to obtain sufficient statistical power. Even if it were possible to conduct as many dive transects as pot samples, the power of a dive transect was still lower than that of a pot; the higher power of the pots was due to lower variance among pots. Pots work by attracting crabs with a bait plume; thus the area and number of crabs sampled is

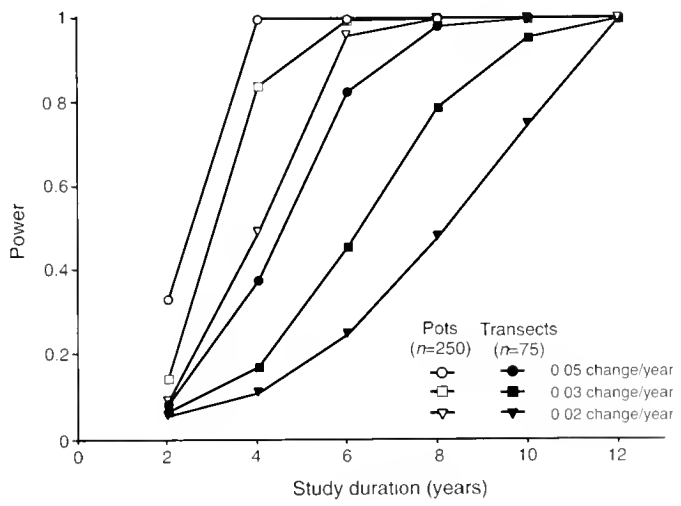

Figure 6

Relationship between power and study duration in comparing catch from crab pots and density on dive transects for male Dungeness crabs (*C. magister*) at three levels of population change. To hold effort constant, we set the sample size (n) to the number of pots and dives that could be accomplished in five days.

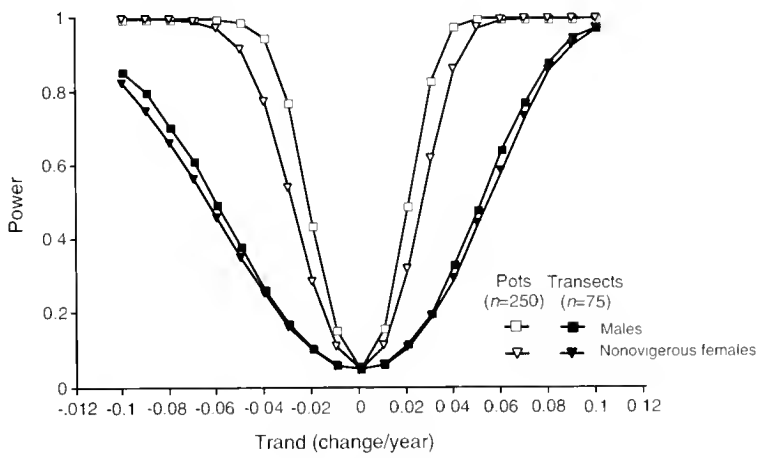

Figure 7

Relationship between power and trend in population in comparing catch in crab pots and density on dive transects for male and nonovigerous female Dungeness crabs (*C. magister*).

larger with pots than with transects and the variance with pots is lower.

Despite their low power, the independent measures of abundance provided by dives helped us identify bias in our Dungeness crab survey method. Our analysis of these two techniques demonstrates that it is possible to avoid most biases with pots if sampling is conducted at optimal times of year. Similar comparisons could be conducted in other areas to identify sampling biases so that they could be minimized and important parameters, such as abundance, size, and sex ratio, could be monitored effectively.

Acknowledgments

This long-term study was made possible by the support of a large number of people. J. de La Bruere made the field work efficient and enjoyable through his expert ability to operate the RV *Alaskan Gyre*. We thank A. Andrews for large efforts during the field work, data management, and analysis. G. Bishop, C. Dezan, E. Hooge, P. Hooge, E. Leder, J. Luthy, J. Nielsen, C. Schroth, D. Schultz, L. Solomon, and K. Swiney each participated in the project for several years. The manuscript was improved by comments from E. Mathews, E. Knudsen, and three anonymous reviewers. We thank M. Jensen, J. Brady, T. Lee, M. Moss, and S. Rice for their continued support. We especially thank the large number of unnamed graduate students, faculty, state and federal agency researchers—over 70 people total—who generously donated their time and efforts to this long-term project. This project was funded by the United States Geological Survey and the National Park Service.

Literature cited

Abbe, G. R., and C. Stagg.
1996. Trends in blue crab (*Callinectes sapidus* Rathbun) catches near Calvert Cliffs, Maryland, from 1968 to 1995 and their relationship to the Maryland commercial fishery. J. Shellfish Res. 15:751–758.

Bennett, D. B.
1974 The effects of pot immersion time on catches of crabs, *Cancer pagurus* L. and lobster, *Homarus gammarus* (L.). J. Cons. Int. Explor. Mer 35:332–336.
1995. Factors in the life history of the edible crab (*Cancer pagurus* L.) that influence modelling and management. ICES Mar. Sci. Symp. 199:89–98.

Caddy, J. F.
1979. Some considerations underlying definitions of catchability and fishing effort in shellfish fisheries, and their relevance for stock assessment purposes. Manuscript Report, 1489, 1–18 p. Department of Fisheries and Oceans Canada, Halifax, Nova Scotia, Canada.

Cowan, E. A., R. D. Powell, and N. D. Smith.
1988. Rainstorm-induced event sedimentation at the tidewater front of a temperate glacier. Geology 16: 409–412.

Dawe, E. G., D. M. Taylor, and J. M. Hoenig.
1996. Evaluating an index of snow crab (*Chionocetes opilio*) biomass from trapping surveys. *In* Proceedings of the international symposium on biology, management, and economics of crabs from high latitude habitats, Anchorage, Alaska, October 11–13, 1995, vol. 96-02, p. 301–314. Alaska Sea Grant College Program, Univ. Alaska, Anchorage, AK.

Gibbs, J. P.
1998. Monitoring populations of plants and animals. BioScience 48:935–940.

Gibbs, J. P., and S. M. Melvin.
1997. Power to detect trends in water bird abundance with call-response surveys. J. Wildl. Manag. 61(4): 1262–1267.

Gotshall, D. W.
1978. Catch-per-unit-of-effort studies of northern California Dungeness crabs, *Cancer magister*. Calif. Fish Game 64(3):189–199.

Higgins, K., A. Hastings, and L. W. Botsford.
1997a. Density dependence and age structure: nonlinear dynamics and population behavior. Am. Nat. 149(2):247–269.

Higgins, K., A. Hastings, J. N. Sarvela, and L. W. Botsford.
1997b. Stochastic dynamics and deterministic skeletons: population behavior of Dungeness crab. Science 276(5317):1431–1435.

High, W. L.
1976. Escape of Dungeness crabs from pots. Mar. Fish. Rev. 38(4):19–23.

Kondzela, C. M., and T. C. Shirley.
1993. Survival, feeding, and growth of juvenile Dungeness crabs from southeastern Alaska reared at different temperatures. J. Crustacean Biol. 13(1):25–35.

Kruse, G. H.
1993. Biological perspectives on crab management in Alaska. *In* Proceedings of the international symposium on management strategies for exploited fish populations (G. Kruse, D. M. Eggers, R. J. Marasco, C. Pautzke, and T. J. Quinn II, eds.), 355–384 p. Lowell Wakefield Fisheries Symposium. Alaska Sea Grant College Program Report 93-02, Univ. Alaska, Fairbanks, AK.

Miller, R. J.
1974. Saturation of crab traps: reduced entry and escapement. J. Cons. Int. Explor. Mer 38(3):338–345.

O'Clair, C. E., R. P. Stone, and J. L. Freese.
1990. Movements and habitat use of Dungeness crabs and the Glacier Bay fishery. *In* Second Glacier Bay science symposium, Glacier Bay National Park & Preserve, AK, Sept. 19–22, 1988 (A. M. Milner and J. D. Wood Jr., eds.), 74–77 p. U.S. National Park Service, Anchorage, AK.

Orensanz, J. M., J. Armstrong, D. Armstrong, and R. Hilborn.
1998. Crustacean resources are vulnerable to serial depletion—the multifaceted decline of crab and shrimp fisheries in the Greater Gulf of Alaska. Rev. Fish Biol. Fish. 8:117–176.

Pengilly, D., and D. Tracy.
1998. Experimental effects of soak time on catch of legal-sized and nonlegal red king crab by commercial king crab pots. Alaska Fish. Res. Bull. 5(2):81–87.

Rumble, J., and G. Bishop.
2002. Report to the Board of Fisheries, Southeast Alaska Dungeness Crab Fishery. Alaska Department of Fish and Game, Regional Information Report 1J02-45, p. 2.2–2.16. Alaska Dep. Fish and Game, Juneau, AK.

Scheding, K., T. C. Shirley, C. E. O'Clair, and S. J. Taggart.
2001. Critical habitat for ovigerous Dungeness crabs. *In* Spatial processes and management of fish populations October 27–30 (G. H. Kruse, N. Bez, A. Booth, M. W. Dorn, S. Hills, R. N. Lipcius, D. Pelletier, C. Roy, S. J. Smith, and D. Witherell, eds.), 431–446 p. Alaska Sea Grant, report AK-SG-01-02. Univ. Alaska, Fairbanks, AK.

Schultz, D. A., and T. C. Shirley.
1997. Feeding, foraging and starvation capability of ovigerous Dungeness crabs in laboratory conditions. J. Crustacean Res. 26:26–37.

Schultz, D. A., T. C. Shirley, C. E. O'Clair, and S. J. Taggart.
1996. Activity and feeding of ovigerous Dungeness crabs in Glacier Bay, Alaska. *In* High latitude crabs: biology, management, and economics, October 11–13, 1995, vol.

96-02, p. 411–424. Alaska Sea Grant College Program, AK-SG-96-02, Univ. Alaska, Anchorage, AK.

Shirley, S. M., and T. C. Shirley.
1988. Appendage injury in Dungeness crabs, *Cancer magister*, in southeastern Alaska. Fish. Bull. 86:156–160.

Shirley, T. C., G. Bishop, C. E. O'Clair, S. J. Taggart, and J. L. Bodkin.
1996. Sea otter predation on Dungeness crabs in Glacier Bay, Alaska. *In* High latitude crabs: biology, management, and economics, 563–576 p. Lowell Wakefield Fisheries Symposium. Alaska Sea Grant College Program Report 96-02, Univ. Alaska, Fairbanks, AK.

Shirley, S. M., T. C. Shirley, and S. D. Rice.
1987. Latitudinal variation in the Dungeness crab, *Cancer magister*: zoeal morphology explained by incubation temperature. Mar. Biol. 95(3):371–376.

Smith, B. D., and G. S. Jamieson.
1989. A model for standardizing Dungeness crab (*Cancer magister*) catch rates among traps which experienced different soak times. Can. J. Fish. Aquat. Sci. 46:1600–1608.

Stone, R. P., and C. E. O'Clair.
2001. Seasonal movements and distribution of Dungeness crabs, *Cancer magister*, in a glacial southeastern Alaska estuary. Mar. Ecol. Prog. Ser. 214:167–176.

Swiney, K. M., T. C. Shirley, S. J. Taggart, and C. E. O'Clair.
2003. Dungeness crab, *Cancer magister*, do not extrude eggs annually in southeastern Alaska: An *in situ* study. J. Crustacean Biol. 23(2):280–288.

Taggart, S. J., P. N. Hooge, J. Mondragon, E. R. Hooge, and A. G. Andrews.
2003. Living on the edge: the distribution of Dungeness crab, *Cancer magister*, in a recently deglaciated fjord. Mar. Ecol. Prog. Ser. 246:241–252.

Taggart, S. J., T. C. Shirley, C. E. O'Clair, and J. Mondragon.
In press. Dramatic increase in the relative abundance of large male Dungeness crabs, *Cancer magister*, following closure of commercial fishing in Glacier Bay, Alaska. *In* Aquatic protected areas as fisheries management tools (J. B. Shipley, ed.). Am. Fish. Soc., Bethesda, MD.

Thomas, L., and C. J. Krebs.
1997. A review of statistical power analysis software. Bull. Ecol. Soc. A. 78(2):128–139.

Wonnacott, T. H., and R. J. Wonnacott.
1990. Introductory statistics for business and economics, 815 p. John Wiley & Sons, New York, NY.

Wyngaard, J. G., and M. I. Iorio.
1996. Status of the southern king crab (*Lithodes santolla*) fishery of the Beagle Channel, Argentina. *In* Proceedings of the international symposium on biology, management, and economics of crabs from high latitude habitats, Anchorage, Alaska, October 11–13, 1995, vol. 96-02, 25–39 p. Alaska Sea Grant College Program, Univ. Alaska, Anchorage, AK.

Zar, J. H.
1996. Biostatistical analysis, 663 p. Prentice-Hall, Inc., Upper Saddle River, NJ.

Zheng, J., T. J. Quinn II, T. J., and G. H. Kruse.
1993. Comparison and evaluation of threshold estimation methods for exploited fish populations. *In* Proceedings of the international symposium on management strategies for exploited fish populations, Anchorage, Alaska, October 21–24, 1992 (G. H. Kruse, D. M. Eggers, R. J. Marasco, C. Pautzke, and T. J. Quinn II, eds.), vol. 93-02, 267–289 p. Alaska Sea Grant College Program, Anchorage, AK.

A method to improve size estimates of walleye pollock (*Theragra chalcogramma*) and Atka mackerel (*Pleurogrammus monopterygius*) consumed by pinnipeds: digestion correction factors applied to bones and otoliths recovered in scats

Dominic J. Tollit[1]
Susan G. Heaslip[1]
Tonya K. Zeppelin[2]
Ruth Joy[1]
Katherine A. Call[2]
Andrew W. Trites[1]

[1] Marine Mammal Research Unit, Fisheries Centre
University of British Columbia, Room 18, Hut B-3
6248 Biological Sciences Road
Vancouver, British Columbia, Canada, V6T 1Z4
E-mail address (for D. J. Tollit): tollit@zoology.ubc.ca

[2] National Marine Mammal Laboratory
Alaska Fisheries Science Center
National Marine Fisheries Service, NOAA
7600 Sand Point Way NE
Seattle, Washington 98115

Abstract—The lengths of otoliths and other skeletal structures recovered from the scats of pinnipeds, such as Steller sea lions (*Eumetopias jubatus*), correlate with body size and can be used to estimate the length of prey consumed. Unfortunately, otoliths are often found in too few scats or are too digested to usefully estimate prey size. Alternative diagnostic bones are frequently recovered, but few bone-size to prey-size correlations exist and bones are also reduced in size by various degrees owing to digestion. To prevent underestimates in prey sizes consumed techniques are required to account for the degree of digestion of alternative bones prior to estimating prey size. We developed a method (using defined criteria and photo-reference material) to assign the degree of digestion for key cranial structures of two prey species: walleye pollock (*Theragra chalcogramma*) and Atka mackerel (*Pleurogrammus monopterygius*). The method grades each structure into one of three condition categories; good, fair or poor. We also conducted feeding trials with captive Steller sea lions, feeding both fish species to determine the extent of erosion of each structure and to derive condition-specific digestion correction factors to reconstruct the original sizes of the structures consumed. In general, larger structures were relatively more digested than smaller ones. Mean size reduction varied between different types of structures (3.3–26.3%), but was not influenced by the size of the prey consumed. Results from the observations and experiments were combined to be able to reconstruct the size of prey consumed by sea lions and other pinnipeds. The proposed method has four steps: 1) measure the recovered structures and grade the extent of digestion by using defined criteria and photo-reference collection; 2) exclude structures graded in poor condition; 3) multiply measurements of structures in good and fair condition by their appropriate digestion correction factors to derive their original size; and 4) calculate the size of prey from allometric regressions relating corrected structure measurements to body lengths. This technique can be readily applied to piscivore dietary studies that use hard remains of fish.

Manuscript submitted 28 April 2003 to Scientific Editor's Office.
Manuscript approved for publication 25 March 2004 by the Scientific Editor.
Fish. Bull. 102:498–508 (2004).

Prey skeletal remnants from stomach samples and more recently from fecal (scat) samples are widely used to determine what pinnipeds eat (Pitcher, 1981; Olesiuk et al., 1990; Tollit and Thompson, 1996; Browne et al., 2002). Prey can usually be identified from taxon-specific hard remains, the sizes of which often correlate with the length and mass of the prey (Härkönen, 1986; Desse and Desse-Berset, 1996). In the past, sagittal otoliths were commonly used to estimate prey size (Frost and Lowry, 1981) but were recognized to erode or become completely digested (Prime and Hammond, 1987; Harvey, 1989). Thus, otolith measurements likely underestimated sizes and numbers of fish ingested (Jobling and Breiby, 1986), thereby preventing a reliable assessment of overlap of prey consumed with catch taken by commercial fisheries (Beverton, 1985). Accurate estimates of size of prey consumed by pinnipeds are also important in order to understand foraging behavior and to explain spatial and temporal variability in diet composition.

There are at least three potential ways to deal with the effect of digestion on estimates of prey size. One is to measure only relatively uneroded otoliths and assume that eroded otoliths are from the same size fish as uneroded otoliths (Frost and Lowry, 1986; Bowen and Harrison, 1994). Another is to apply a single species-specific digestion coefficient or correction factor (DCF), derived from feeding experiments with captive seals fed fish of known sizes and using measurements of all the eroded otoliths recovered in the scats produced (Prime and Hammond, 1987; Harvey, 1989). The third is to estimate and correct for the degree of digestion (based on defined losses of morphological features) of each recovered otolith by using estimates from reference material (Sinclair et al., 1994; Antonelis et al., 1997) or by applying condition-specific DCFs derived from fish fed in captive seal feeding studies (Tollit et al., 1997).

Of the three approaches to correctly estimate prey size from skeletal remains, there is the assumption with

the use of only uneroded otoliths that recovery and the degree of digestion is independent of otolith size, resulting in a potentially biased fraction. For certain species it can also result in a notable reduction in sample size because relatively few otoliths pass through the gut in good condition. The second approach of applying mean species-specific DCFs is an improvement to not accounting for size reduction (Laake et al., 2002); however, there is the assumption with this approach that all structures are reduced in size by the same amount. Consequently, mean fish mass may be overestimated if such correction factors are applied to relatively undigested otoliths, or they may be underestimated if applied to very digested otoliths (Hammond et al., 1994; Tollit et al., 1997). The third method accounts for the intraspecific variation in size reduction caused by digestion, reduces systematic error (see Hammond and Rothery, 1996), yields estimates of mass that compare favorably to those fed to captive animals (Tollit et al., 1997), and hence may well be the most promising approach to reconstructing prey size.

The dramatic decline of the western population of Steller sea lions (*Eumetopias jubatus*) in the 1980s (Loughlin et al., 1992; Trites and Larkin, 1996) has prompted a number of studies to determine what they eat and the extent of dietary overlap (prey consumed) with catch taken by commercial fisheries. Stomach contents analysis was used to determine diet until the late 1980s when scat analysis became the preferred method (e.g., Pitcher, 1981; Frost and Lowry, 1986; Sinclair and Zeppelin, 2002). However, unlike in stomachs, there is an overall sparsity of otoliths in Steller sea lion scats (Sinclair and Zeppelin, 2002) and, therefore there is a need to also use other skeletal structures to describe the size of prey consumed.

The following outlines a method (using defined criteria and photo-reference material) to assign the degree of digestion for otoliths and alternative key skeletal structures of walleye pollock (*Theragra chalcogramma*) and Atka mackerel (*Pleurogrammus monopterygius*) recovered from scats. We also present the results of a feeding study with captive Steller sea lions used to determine the extent of erosion and to derive condition-specific digestion correction factors to reconstruct the original sizes of the pollock and Atka mackerel structures consumed. Finally, we combine these DCFs with newly developed regression formulae that estimate fish length to derive a more accurate method of estimating size of pollock and Atka mackerel consumed by Steller sea lions and other pinnipeds (see Zeppelin et al., 2004, this issue; Tollit et al., 2004, this issue).

Materials and methods

Experimentally derived digestion correction factors

Feeding experiments were conducted with two 3-year-old female Steller sea lions: Steller sea lion 1 [SSL1] [ID no. F97HA], mean mass 129 kg; steller sea lion 2 [SSL2] [ID no. F97SI], mean mass 150 kg) between October 2000 and April 2002 at the Vancouver Aquarium Marine Science Centre. Over the experimental period, the sea lions were fed pollock for 52 days in 16 separate feeding experiments, and Atka mackerel for 31 days in 5 separate feeding experiments, at between ~4–8% of body mass per day. Fork length (FL) and weight of all fish were measured to ±0.1 cm and ±1 g. Sea lions were fed meals of pollock of three size categories (small, 28.5–32.5 cm FL; medium, 33.5–38.7 cm FL; large, 40–45 cm FL) and meals of Atka mackerel of one size category (30–36 cm FL). Fish of one particular size category were fed either as a single meal or as a seven-day block of meals. Full details of a typical experimental protocol can be found in Tollit et al. (2003). Size ranges for any category of fish fed within separate experiments were usually ≤3 cm. Fecal material was collected until no other remains of experimental meals were found (7 days after feeding), and was washed through a 0.5-mm sieve to remove hard parts. Each animal was maintained on whole Pacific herring (*Clupea pallasi*) between experiments at ~6% body mass per day.

The strong relationship between fish size and otolith size also exists for other skeletal structures (Desse and Desse-Berset, 1996). Thus, we quantified the types and numbers of the prey structures recovered in the scats of free-ranging Steller sea lions (from the collections of Trites et al.[1] and Sinclair and Zeppelin, 2000) and selected seven of the most commonly occurring structures for pollock and Atka mackerel. These were the sagittal otolith (OTO), as well as the interhyal (INTE), hypobranchial 3 (HYPO), pharyngobranchial 2 (PHAR), angular (ANGU), quadrate (QUAD), and the dentary (DENT). The structures selected also had particular morphological features that seemed to be relatively resistant to digestion and could effectively be used to estimate fish size (Figs. 1 and 2, Table 1).

Concurrent with our feeding study, we measured selected structures (Figs. 1 and 2) from randomly subsampled fresh fish and combined these data with unpublished NMFS data to generate allometric regression formulae relating structural measurements to fish length (see Zeppelin et al., this issue). Fork lengths (±0.1 cm) and weights (±1 g) of an extended subsample of pollock (8.3–47.7 cm FL) were measured to generate an appropriate regression formula for estimating fish mass from fork length estimates. All selected structures are located in the cranium as illustrated in Zeppelin et al. (2004, this issue). Naming of fish structures follows Rojo (1991).

Initial inspection of selected structures found in scats from the wild revealed high intraspecific variation in the degree of digestion, ranging from no apparent size reduction to about a 60% size reduction (heavily digested material). Consequently, we extended the condition-

[1] Trites, A. W., D. G. Calkins, and A. J. Winship. 2003. Unpubl. data. Marine Mammal Research Unit, Fisheries Centre, University of British Columbia, Hut B-3, 6248 Biological Sciences Road, Vancouver, B.C., Canada, V6T 1Z4.

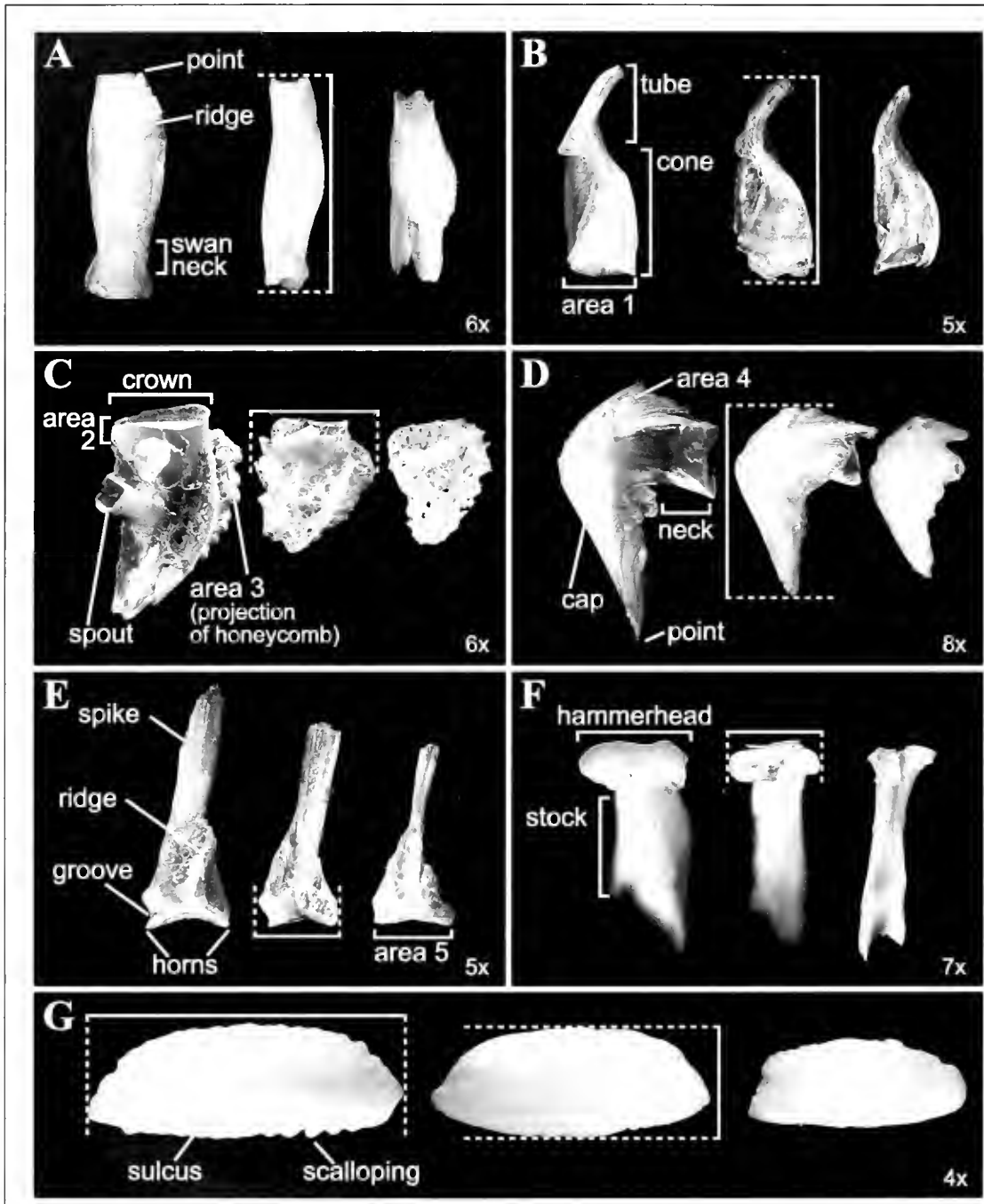

Figure 1

Photographs showing the changes in morphological features in seven cranial structures of walleye pollock (*Theragra chalcogramma*) resulting from digestion. Within each section of the figure three condition categories (good, fair, and poor) are represented from left to right for (**A**) interhyal (INTE), (**B**) hypobranchial 3 (HYPO), (**C**) pharyngobranchial 2 (PHAR), (**D**) angular (ANGU), (**E**) quadrate (QUAD), (**F**) dentary (DENT) and (**G**) sagittal otolith (OTO). Key features used in classification are labeled (see Table 1 for details), and the measurements taken to calculate fish length (solid line between dashed lines).

specific DCF technique described by Tollit et al. (1997). We began by examining the external morphological features and surface topography of selected structures from undigested fish (<12 cm to >53 cm) and compared these with the topography of the same structures recovered from scats collected from wild and captive animals

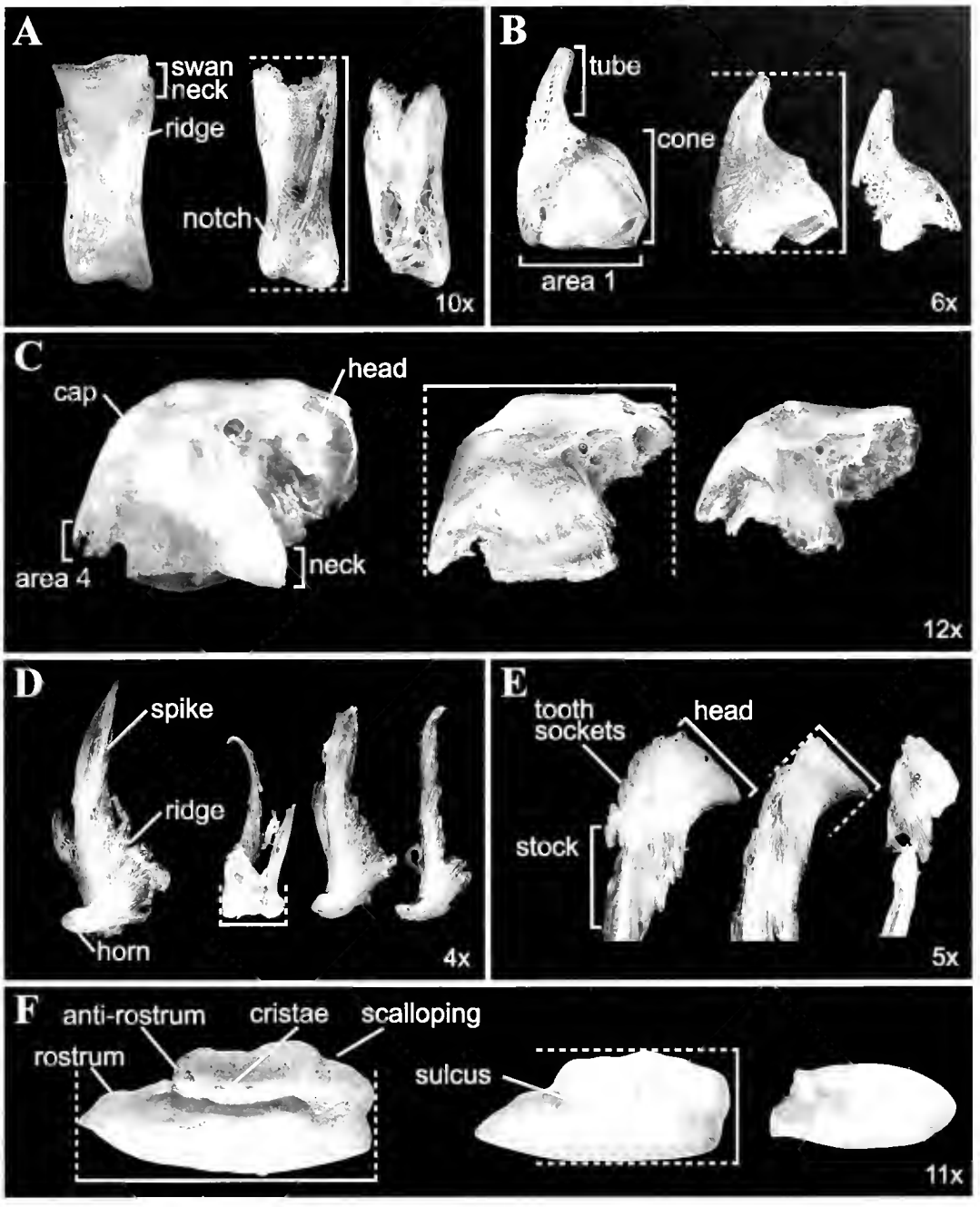

Figure 2

Photographs showing the changes in morphological features in seven cranial structures of Atka mackerel (*Pleurogrammus monopterygius*) resulting from digestion. Within each section of the figure three condition categories (good, fair, and poor) are represented from left to right for (**A**) interhyal (INTE), (**B**) hypobranchial 3 (HYPO), (**C**) angular (ANGU), (**D**) quadrate (QUAD), (**E**) dentary (DENT) and (**F**) sagittal otolith (OTO). Key features used in classification are labeled (see Table 1 for details) and measurements taken to calculate fish length (solid line between dashed lines).

(Figs. 1 and 2). The morphological features used to assess level of digestion showed no differences in relative shape, structure, or in proportion across the size range of fresh fish examined. We then devised a criteria-based method to assign a condition category to each structure depending on the degree of digestion. These criteria

take into account only the loss of size to the relevant feature being measured to estimate fish length (Figs. 1 and 2).

The grading criteria for otoliths (OTO) were based on the condition categories developed by Sinclair et al. (1996) to investigate prey selection by northern fur seals (*Callorhinus ursinus*). As seen in Sinclair et al. (1996) and other studies (Frost and Lowry, 1986; Tollit et al., 1997), external features such as lobation and the general shape and definition of the sulcus were found in our study to be good indicators of the degree of otolith digestion. For the remaining cranial bones, digestion indicators included the loss of definition or breakage of defined structural features such as the horns and ridge (QUAD), hammerhead and stock (DENT), swan neck, notch and ridge (INTE), honeycomb and crown (PHAR), cap, neck, and head (ANGU) and tube and cone (HYPO). We used changes in the described condition-category criteria (see Table 1 for full details) in tandem with photo-reference material (Figs. 1 and 2) to classify all structures into one of three digestion grades or condition categories: "good", "fair," or "poor."

Hard parts recovered from feeding experiments were sorted, and all selected cranial structures were assigned a condition category and measured with calipers to within ±0.01 mm. Because otoliths were often chipped or partly broken lengthwise, both length and width were measured. To test our grading technique, an independent observer (T.Z.) reassigned a random subsample of each condition category of pollock structures (n=158) in a blind test.

On initial investigation, high intraspecific variation was observed within the selected structures assigned in poor condition in our feeding study with captive Steller sea lions. Consequently, structures in poor condition were not used to calculate DCFs for this category. Our basis for exclusion was supported by the work of Sinclair et al. (1994) and Tollit et al. (1997). Captive sea lions in our study occasionally regurgitated prey in the swim tank. Recovered structures that we considered to have been regurgitated were excluded from DCF calculations (i.e., vertebrae still articulated, bones that had flesh attached or that were of a size to exclude passage through the pyloric sphincter).

Mean reduction (MR) in the metric of each structure (s) recovered from our feeding experiment was estimated for each remaining condition category (c) according to

$$MR_{s,c} = \left(1 - \frac{\bar{E}_{s,c}}{\bar{I}_s}\right) \times 100,$$

where the mean size of egested structures ($\bar{E}$) of each condition category was calculated from measurements of those recovered from the captive feeding experiments, and the mean size of each ingested structure ($\bar{I}_s$) was estimated from the fork length of fish fed by using inverse predictions of the regression formulae derived from fresh material (Zeppelin et al., 2004, this issue). Mean ingested size was estimated by using bootstrap simulations (1000 runs) that randomly sampled with replacement and selected the median (500th value) from the sorted bootstrapped values (Reynolds and Aebischer, 1991).

For pollock, mean reduction for each condition category was compared across size ranges by using a Kruskal-Wallis analysis of variance. A significance level of P<0.0056 was set based on the Bonferroni adjusted probability for nine multiple comparisons (Siegel and Castellan, 1988). Failing to find any significant differences resulted in pooling the data from each size range to calculate specific condition category MR values. Condition category DCFs were calculated for each selected structure as $\bar{I}_s/\bar{E}_{s,c}$ except for PHAR structures of Atka mackerel because too few elements were recovered from the scats of captive animals.

Estimating confidence limits around digestion correction factors

We used a bootstrap simulation to estimate upper and lower bounds of the 95% confidence interval (CI) given that the DCF is a ratio of two means (Reynolds and Aebischer, 1991). This technique allows different sources of error to be combined or partitioned. There were two major sources of error associated with calculating DCFs (Tollit et al., 1997). The first were those associated with the regression formulae used to calculate the mean size of structure ingested from the original fish fed, and the second were those associated with the errors around the mean size of egested structure (i.e., resampling errors).

We assessed errors associated with the regression formulae using a parametric bootstrapping procedure (Manly, 1997) that involved regressing structure size against fork length. This was repeated 1000 times and 95% confidence intervals were taken as the 25th and 975th values of the sorted bootstrapped regression coefficient values. Results were compared to those computed analytically by using the resultant standard error (Eq. 17.23 in Zar, 1984) and were found to be consistent (see Zeppelin et al., 2004, this issue).

We estimated resampling errors related to the variability in digestion of egested structures by repeatedly selecting n structures, at random, with replacement from the original sample set of n egested structures. Mean egested size was recalculated in this way 1000 times, as were a mean DCF and 95% CI as described above. Both regression and resampling errors were combined in sequence to derive overall 95% CIs around DCFs.

Our recommended procedure for applying our DCFs to cranial structures recovered from scats collected in the wild has four steps: 1) measure the recovered structures and grade the extent of digestion using defined criteria and photo-reference collection; 2) exclude structures graded in poor condition; 3) multiply measurements of structures in good and fair condition by their appropriate digestion correction factors to derive their original size; and 4) calculate the size of prey from allometric regressions relating corrected structure measurements to fish fork lengths (see also Tollit et al., 2004, this issue).

Results

A relatively objective method to estimate the degree of digestion of dominant structures of pollock and Atka mackerel was derived by using defined criteria (Table 1) and photo-reference material (Figs. 1 and 2). Condition-specific digestion correction factors (and derived confidence intervals) calculated for each structure augmented our method of estimating size of prey from bones and otoliths recovered in scats, as well as potentially from bones and otoliths taken from stomach contents.

Mean reduction (MR) in the size of pollock DENT and QUAD in good condition and ANGU, HYPO, INTE, OTO, and PHAR in fair condition were between 12.2–18.5%, and larger values were found for QUAD (22.8%) and DENT (24.7%) in fair condition (Table 2). Our overall 95% confidence intervals were generally symmetrical and converted to a mean range of ±2.2% (±0.5, SD) around MR values. Mean DCFs ranged between 1.14 and 1.33, and lower bounds of 95% CIs exceeded 1.11 in all instances, confirming that egested structures of these condition categories were significantly smaller than the size at which they were ingested (Table 2). Partitioning errors showed that resampling of egested structures was the major source of error (>73% across structures) within the overall total. Our overall 95% CIs resulted in a maximum total error of ±1.7 cm around an estimated mean of 40 cm for pollock.

Mean reduction in the size of Atka mackerel structures varied more widely (3.3–26.3%), leading to DCFs ranging between 1.03 and 1.36. QUAD in good condition provided the smallest DCF, and DENT in fair condition the largest. Overall, our 95% CIs converted to a mean range of ±2.4% (±0.6) around MR values, and all lower 95% CI bounds exceeded 1.0 (Table 2). As seen when errors were partitioned for pollock, errors owing to resampling of egested structures were the major source of error (>83% across structures) within the overall total for Atka mackerel. Our overall 95% CIs resulted in a maximum total error of ±1.2 cm around an estimated mean of 40 cm for Atka mackerel.

With the exception of the two largest skeletal structures (DENT and QUAD, Table 2), some selected structures (INTE, HYPO, PHAR, ANGU, and OTO) occurred in scats with no clear loss in size or loss of morphological features related to digestion. For these five structures, we ascribed the condition category good and assigned a DCF of 1.0 (i.e., no correction for partial size reduction due to digestion required).

Of the 158 structures in our blind test, 141 (89.2%) were assigned identical condition categories. Of the remaining 17 structures, 11 (65%) were noted as being borderline between categories. Angulars (ANGU) accounted for the majority (~60%) of all differences, with all but one re-assigned in good condition as opposed to fair condition. On review, differences in assigning angulars were mainly the result of differences in opinion on what constituted a well-defined and sharp point (Fig. 1, Table 1). Clarification through the additional use of reference material (including both pristine structures and examples of each condition category) is advised, particularly for angulars. Comparison of the same 158 bones between two observers (D.T. and S.H.) using the same structure reference collection resulted in assigning more than 93% (147/158) of structures to an identical category.

The regression formula for estimating pollock mass (M) from fork length (FL) estimates was best described by using an exponential equation ($M=0.0051\times FL^{3.11}$, $n=981$, $r^2=0.987$).

Discussion

The size of prey consumed by pinnipeds can usually be reliably estimated from otoliths recovered in scats if partial digestion is accounted for (Tollit et al., 1997). However, otoliths from Steller sea lion scats are often found in too few numbers, or are too digested or broken to be useful (Sinclair and Zeppelin, 2002; Tollit et al., 2004, this issue). It was, therefore, necessary to use alternative skeletal structures to estimate the size of prey selected by Steller sea lions. Zeppelin et al. (2004, this issue) documented good relationships ($r^2=0.78$–0.99) between the size of selected alternative structures and fork length for pollock and Atka mackerel. However, all skeletal structures are susceptible to digestion in the stomach (our study, and Murie and Lavigne, 1986). Thus, techniques are required to account for the degree of digestion of alternative structures prior to estimating prey size.

Reductions in the size of otoliths during passage through the digestive tract of pinnipeds have been widely reported (e.g., da Silva and Neilson, 1985; Prime and Hammond, 1987; Harvey, 1989; Tollit et al., 1997). Similarly, we found significant reduction in the sizes of all selected cranial structures from pollock and Atka mackerel. Size reduction also showed great variability. Relatively small structures were found with no obvious loss in size due to digestion, but were also frequently heavily eroded.

The degree of digestion on different otoliths and bones may be related to species, size of fish (Bowen, 2000), or even its shape, but seems to be random in any one meal (Murie and Lavigne, 1986). Degree of digestion likely depends on a range of factors such as meal size, meal frequency, meal composition, and method of consumption. In the face of these multiple factors we feel our method for classifying the degree of digestion into one of three condition categories is practical and relatively objective. However, our technique does not consider potential biases of enumeration associated with smaller prey being more susceptible to complete digestion than relatively larger prey, or of individual fish being counted more than once if all multiple structures are used. Nevertheless, resolution to these biases have been advocated (see Tollit et al., 1997; Laake et al., 2002; Tollit et al., 2003; Tollit et al., 2004, this issue). The category selections chosen with our criteria showed good agreement among independent observers.

Table 1

Distinctive external morphological features for defining the degree of digestion (condition category) as good (G), fair (F), and poor (P) for selected cranial structures of walleye pollock and Atka mackerel. Features are given in order of importance. See Table 2 for definition of structure codes and Figure 1 and 2 for illustrations. WP = walleye pollock.

Species and structure code	Category	Distinctive external morphological features
Walleye pollock		
INTE	G	1) Retains characteristic shape, notably the ridge and swan neck. 2) Both ends show no damage (except for the loss of the point and minor nicks) and do not affect length measurement.
	F	1) Ridge and swan neck clearly defined. 2) One end can show limited damage with <15% reduction. Minor nicks on opposite end acceptable, if there is no further loss in length measurement.
	P	1) Loss of characteristic shape, with ridge or swan neck (or both) ill defined. Body of structure contains holes. 2) Both ends show clear damage.
HYPO	G	1) Retains characteristic shape, with cone ~2× the length of the tube. 2) Tube end and area 1 show no damage (except for minor nicks) and do no affect the total length measurement. 3) Cone end angled when viewed from the front elevation (back elevation shown in Fig. 1).
	F	1) Tube end or area 1 shows limited damage (cone end no longer angled) clearly preventing an accurate length measurement.
	P	1) Both tube end and area 1 show damage, and a general loss of characteristic shape evident.
PHAR	G	1) Retains characteristic shape, notably a raised spout, honeycomb, and crown. 2) Crown clearly projects above honeycomb (front elevation) and is intact at area 2. 3) Clear projection of honeycomb (back elevation—see area 3). 4) No affect on measurement.
	F	1) No clear projection of honeycomb at area 3 or crown shows damage at area 2 (preventing an accurate width measurement). 2) Crown or spout (or both) can show minor damage.
	P	1) Characteristic shape lost, often only honeycomb present. 2) Honeycomb smooth, crown heavily eroded with areas 2 and 3 eroded or damaged. 3) Both ends show clear damage.
ANGU	G	1) Point sharp and well defined with no impact to measurement. 2) Area 4 in good condition and angled curve complete. 3) Neck present, but with minor damage. 4) Material of cap continues to point tip.
	F	1) Point no longer extensive or sharp or area 4 damaged and poorly defined. 2) Neck usually present, but with wear.
	P	1) Characteristic shape lost with neck often absent. 2) Point heavily eroded. 3) Area 4 shows damage or no definition.
QUAD	G	1) Groove defined from all angles and observable with the naked eye. 2) Horns rounded. 3) Angle of area 5 is clearly curvilinear. 4) Evidence of ridge and spike often observable.
	F	1) Groove unclear, forming only an indisctinct notch. 2) Horns have lost rounded definition and may be pointed or worn on one side. 3) Ridge and spike often only residual.
	P	1) Horns pointed, notch absent. 2) Ridge and spike often absent. 3) Angle of area 5 flattened. 4) Unable to determine side with assurance.
DENT	G	1) Hammerhead retains rounded end elevation features (note: both sides are not exactly symmetrical), allowing full width measurement. 2) Material in addition to the stock may be present. 3) Stock clearly curved from side elevation. 4) Width and breadth of "rounded" stock similar.
	F	1) Hammerhead shows erosion on one side, affecting full width measurement. 2) Breadth of stock reduced, but not flattened.
	P	1) Hammerhead eroded and flattened with both sides showing erosion. 2) Breadth of stock flattened, stock less rounded and less robust. 3) Unable to determine side with assurance.
OTO	P	1) Sulcus and scalloping (on most margins) well defined, and no obvious reduction in size due to digestion. 2) Able to determine side. 3) Inside strongly convex, retains characteristic shape.
	F	1) Sulcus worn but shows definition. 2) Able to determine side. 3) Scalloping worn but shows no reverse scalloping.
	P	1) Unable to determine side. 2) Scalloping worn completely smooth and reverse scalloping present. 3) Clearly broken, worn, flattened, and unable to obtain an accurate measurement.

continued

Table 1 (continued)

Species and structure code	Category	Distinctive external morphological features
Atka mackerel		
INTE	G	Like that of walleye pollock (WP) (except no point), with ridge, neck and notch clearly defined.
	F	1) Ridge present, but shows signs of wear. 2) Swan neck shows wear resulting in a "horseshoe" shape. 3) Notch shows only minor wear or chipping and does not prevent accurate measurement.
	P	1) Loss of characteristic ridge and neck with body worn (may contain holes). 2) Both neck and notch show clear damage.
HYPO	G	1) Cone rounded and complete, tube complete, retains characteristic shape. 2) Minor nicks on cone and tube may be present but do not impact total length measurement.
	F	Cone worn, loss of rounded shape, and area 1 shows minor chipping or damage or tip of tube is broken or clearly chipped.
	P	1) Cone body and area 1 show major wear, chips, and breaks. 2) Tube broken or absent entirely, unable to measure length.
ANGU	G	Like WP, additionally cap rounded and head shows only minor wear.
	F	Like WP, additionally 1) cap worn with loss of shape, 2) Head worn, chipped, and often has holes, 3) Ridge on dorsal side above neck worn smooth.
	P	Like WP, additionally 1) head shows major damage, wear, breaks, and holes, 2) Difficult to determine side with confidence.
QUAD	G	1) Horns rounded and in good condition, with angle between horns clearly curvilinear. (Note: Horns are of unequal size and shape and one side is more robust, rounded, and sloped.) 2) Evidence of ridge and spike observable, 3) Definition of left and right sides is easily achievable.
	F	1) Horns have lost rounded definition and may be pointed or worn on one side, making distinction between sides difficult. 2) Ridge and spike often only residual.
	P	Like WP, additionally no distinction between horns easily achievable.
DENT	G	Like WP (except no hammerhead), additionally 1) head retains characteristic features, tooth sockets present, 2) Ventral side of head a defined point.
	F	Like WP, additionally 1) head eroded or chipped with tooth sockets noticeably worn, 2) Point on ventral side of head eroded or chipped.
	P	Like WP, additionally head eroded or flattened with point often heavily eroded or badly chipped, accurate measurement unattainable.
OTO	G	1) Rostrum not chipped or broken. 2) Sulcus clearly defined, as are anterior and posterior colliculums. 3) Scalloping on antirostrum and posterior end clearly distinguishable. 4) No obvious wear or chipping with no obvious reduction in length (width). 5) Cristae of antirostrum forms a well-defined ridge.
	F	1) Rostrum shows some wear but remains unbroken and retains characteristic shape. 2) Sulcus still has definition despite wear, shown as a uniform channel, anterior and posterior colliculums indistinct. 3) Cristae and scalloping on antirostrum and posterior end worn smooth.
	P	1) Rostrum or posterior end broken or worn to such a degree that accurate measurement cannot be obtained. 2) Sulcus difficult to distinguish or worn smooth. 3) Cristae and scalloping on antirostrum and posterior end worn completely smooth. 4) Side cannot be easily obtained.

Nevertheless, we recommend that a hands-on reference collection be used.

The procedure we recommend to estimate fish length after classification involves excluding structures considered heavily digested (condition category poor) and applying specific condition-category DCFs (Table 2) to the remaining structure prior to calculating fish length from allometric regressions (see Tollit et al., 2004, this issue). The exclusion of structures in poor condition was necessary because of the large and variable size reduction observed in this category. Our technique uses changes noted in the morphological features of the structures themselves and is therefore not specific to Steller sea lions. Because structures are likely to erode in a predictable manner whatever the species of the stomach they are held within, it seems probable that they can also be classified into a particular condition category for use with DCFs. Consequently, our technique may be appropriate to marine piscivore dietary studies where prey size needs

Table 2

Condition-specific digestion correction factors (DCFs) for selected cranial structures of walleye pollock and Atka mackerel with associated condition categories good (G) and fair (F). Lower and upper bounds of the 95% confidence intervals (CIs) were calculated by using bootstrap resampling procedures.

Species and structure	Structure code	Grade	n	DCF	SD	CI	
						Lower	Upper
Walleye pollock							
Interhyal	INTE	F	54	1.1423	0.054	1.1168	1.1714
Hypobranchial 3	HYPO	F	22	1.1658	0.063	1.1343	1.1970
Pharyngobranchial 2	PHAR	F	39	1.2109	0.067	1.1717	1.2566
Angular	ANGU	F	85	1.2065	0.103	1.1670	1.2462
Quadrate	QUAD	G	20	1.2272	0.039	1.2025	1.2512
		F	27	1.2958	0.074	1.2623	1.3280
Dentary	DENT	G	17	1.1950	0.074	1.1546	1.2337
		F	31	1.3285	0.071	1.2941	1.3649
Otolith (length)	OTOL	F	37	1.1593	0.059	1.1400	1.1788
Otolith (width)	OTOW	F	49	1.2107	0.089	1.1901	1.2419
Atka mackerel							
Interhyal	INTE	F	37	1.0729	0.089	1.0374	1.1085
Hypobranchial 3	HYPO	F	23	1.1361	0.040	1.1160	1.1568
Angular	ANGU	F	40	1.1361	0.097	1.1053	1.1700
Quadrate	QUAD	G	23	1.0343	0.053	1.0070	1.0597
		F	23	1.0886	0.078	1.0551	1.1213
Dentary	DENT	G	34	1.2068	0.098	1.1666	1.2466
		F	37	1.3563	0.143	1.3063	1.4119
Otolith (length)	OTOL	F	109	1.1691	0.109	1.1459	1.1921
Otolith (width)	OTOW	F	115	1.2062	0.104	1.1837	1.2277

to be determined from partially digested prey hard remains.

Experimentally derived pollock DCFs were determined from three distinct size ranges of fish (28.5–45 cm FL), but the degree of erosion for each structure within each condition category did not show any significant differences across this range. We also found the relative shape, structure, and proportion of the morphological features used to estimate erosion were consistent for both smaller and larger fish. We therefore believe DCFs can be used for fish outside of the experimental size range of this study. Average size reduction varied between different pollock structures (12.2–24.7%) and also between condition categories, as they did for Atka mackerel (Table 2). We determined that pollock otoliths in fair condition were reduced by 14% in length, close to the 20% value estimated from reference material (Sinclair et al., 1994). Our criteria for defining a condition category of fair for pollock otoliths equates to a grade between low amounts and medium amounts of digestion as defined by Tollit et al. (1997) for Atlantic cod (which has a similar looking otolith). Our value of 14% lies midway between those determined for cod otoliths graded low and medium.

Jaw bones (DENT) were by far the largest structure used in our study but do not appear to pass through the pyloric sphincter without some level of digestion. Usually only the hammerhead and stock (representing less than a third of the whole structure) are recovered in scats. The large size accounts for the relatively greater percent mean reduction and hence higher DCF of DENT structures graded either in good or fair condition (Table 2). Although quadrates (QUAD) are also relatively large structures with a projecting ridge that is often much reduced when found in scats, we found QUAD structures of Atka mackerel recovered in scats from field studies and captive sea lion studies in relatively better condition than those of pollock, leading to differences in grading criteria and resulting DCFs (Tables 1 and 2). Part of the reason may be that the horns on a pollock QUAD project widthwise more than those of Atka mackerel, presenting a greater surface area for digestive erosion of the structural feature that is measured to estimate size (Fig. 1).

Our overall 95% confidence intervals around DCFs were generally narrow (Table 2), highlighting the tight fit of the regression formulae used and the benefits of partitioning the data into specific categories. Our bootstrap analysis suggests that resampling errors were the major source of error in calculating DCFs. Future research should concentrate on improving sample sizes for data on percentage size reduction of bones for each

category, rather than on improving regression formulae. For both prey species, QUAD in good condition and OTO in fair condition, in addition to pollock INTE in fair condition and Atka mackerel HYPO in fair condition, provided the most reliable estimates of prey size (Table 2). DENT in fair condition, particularly for Atka mackerel, provided the least reliable estimate of prey size (Table 2). Measurement error was relatively insignificant, but attention should be taken when measuring ANGU and HYPO (Tollit et al., 2004, this issue).

Companion studies by Tollit et al. (2004, this issue) and Zeppelin et al. (2004, this issue) demonstrate the feasibility of applying DCFs to structures other than otoliths and the need to consider the degree of digestion to correctly estimate the length of prey eaten by pinnipeds and other piscivores. Applying appropriate digestion correction factors will lead to more refined estimates of consumption (mass of prey) by marine mammals, as well as the extent of potential overlap (length of prey) with the length of fish caught by commercial fisheries.

Acknowledgments

Funding was provided to the North Pacific Universities Marine Mammal Research Consortium by the National Oceanographic Atmospheric Administration and the North Pacific Marine Science Foundation. We would like to thank the marine mammal trainers and staff of the Vancouver Aquarium Marine Science Centre, the contribution of personnel of the UBC Marine Mammal Research Unit of the UBC EM facility, J. L. Laake for statistical advice, T. J. Orchard, C. J. Gudmundson, S. J. Crockford, M. Wong, E. H. Sinclair, and two anonymous reviewers. We would also like to express gratitude to the organizations and companies that have donated fish to the project. Work was undertaken in accordance with UBC Animal Care Committee guidelines.

Literature cited

Antonelis, G. A., E. H. Sinclair, R. R. Ream, and B. W. Robson.
1997. Inter-island variation in the diet of female northern fur seals (*Callorhinus ursinus*) in the Bering Sea. J. Zool. (Lond.) 242(3):435–51.

Beverton, R. J. H.
1985. Analysis of marine mammal-fisheries interaction. *In* Marine mammals and fisheries (J. R. Beddington, R. J. H. Beverton, and D. M. Lavigne eds.), p. 3–33. George Allen & Unwin, Boston, MA.

Bowen, W. D.
2000. Reconstruction of pinniped diets: Accounting for complete digestion of otoliths and cephalopod beaks. Can. J. Fish. Aquat. Sci. 57:898–905.

Bowen, W. D., and G. D. Harrison.
1994. Offshore diet of grey seals *Halichoerus grypus* near Sable Island, Canada. Mar. Ecol. Prog. Ser. 112 (1–2):1–11.

Browne, P., J. L. Laake, and R. L. DeLong.
2002. Improving pinniped diet analyses through identification of multiple skeletal structures in fecal samples. Fish. Bull. 100:423–433.

da Silva, J., and J. D. Neilson.
1985. Limitations of using otoliths recovered in scats to estimate prey consumption in seals. Can. J. Fish. Aquat. Sci. 42:1439–1442.

Desse, J., and N. Desse-Berset.
1996. On the boundaries of osteometry applied to fish. Archaeofauna 5:171–179.

Frost, K. J., and L. F. Lowry.
1981. Trophic importance of some marine gadids in northern Alaska and their body-otolith size relationships. Fish. Bull. 79:187–192.
1986. Sizes of walleye pollock, *Theragra chalcogramma*, consumed by marine mammals in the Bering Sea. Fish. Bull. 84:192–197.

Hammond, P. S., A. J. Hall, and J. H. Prime.
1994. The diet of grey seals around Orkney and other island and mainland sites in North-eastern Scotland. J. Appl. Ecol. 31:340–350.

Hammond, P. S., and P. Rothery.
1996. Application of computer sampling in the estimation of seal diet. J. Appl. Stat. 23:525–533.

Härkönen, T.
1986. Guide to the otoliths of the bony fishes of the Northeast Atlantic, 256 p. Danbiu ApS. Biological Consultants, Hellerup, Denmark.

Harvey, J. T.
1989. Assessment of errors associated with harbor seal (*Phoca vitulina*) fecal sampling. J. Zool. (Lond.) 219:101–111.

Jobling, M., and A. Breiby.
1986. The use and abuse of fish otoliths in studies of feeding habits of marine piscivores. Sarsia 71:265–274.

Laake, J. L., P. Browne, R. L. DeLong, and H. R. Huber.
2002. Pinniped diet composition: a comparison of estimation models. Fish. Bull. 100:434–477.

Loughlin, T. R., A. S. Perlov, and V. A. Vladimirov.
1992. Range-wide survey and estimation of total number of Steller sea lions in 1989. Mar. Mamm. Sci. 8:220–239.

Manly, B. F. J.
1997. Randomization, bootstrap and Monte Carlo methods in biology, 2nd ed., 399 p. Chapman and Hall, New York, NY.

Murie, D. J., and D. M. Lavigne.
1986. Interpretation of otoliths in stomach content analyses of phocid seals quantifying fish consumption. Can. J. Zool. 64:1152–1157.

Olesiuk, P. F., M. A. Bigg, G. M. Ellis, S. J. Crockford, and R. J. Wigen.
1990. An assessment of the feeding habits of harbour seals (*Phoca vitulina*) in the Strait of Georgia, British Columbia, based on scat analysis. Can. Tech. Rep. Fish. Aquat. Sci. 1730, 135 p.

Pitcher, K. W.
1981. Prey of the Steller sea lion, *Eumetopias jubatus*, in the Gulf of Alaska. Fish. Bull. 79:467–472.

Prime, J. H., and P. S. Hammond.
1987. Quantitative assessment of gray seal diet from fecal analysis. *In* Approaches to marine mammal energetics (A. C. Huntley, D. P. Costa, G. A. J. Worthy, and M. A. Castellini, eds.), p. 165–181. Allen Press, Lawrence, KS.

Reynolds, J. C., and N. J. Aebischer.
1991. Comparison and quantification of carnivore diet by fecal analysis—a critique, with recommendations, based on a study of the fox *Vulpes vulpes*. Mamm. Rev. 21:97–122.

Rojo, A. L.
1991. Dictionary of evolutionary fish osteology, 273 p. CRC Press, Boca Raton.

Siegel, S., and N. J. Castellan.
1988. Nonparametric statistics for the behavioral sciences, 2nd ed., 399 p. McGraw-Hill, New York, NY.

Sinclair, E. H., G. A. Antonelis, B. W. Robson, R. R. Ream, and T. R. Loughlin.
1996. Northern fur seal, *Callorhinus ursinus*, predation on juvenile walleye pollock, *Theragra chalcogramma*. *In* Ecology of juvenile walleye pollock, *Theragra chalcogramma*. Papers from the workshop "The importance of prerecruit walleye pollock to the Bering Sea and North Pacific ecosystems" Seattle, WA, October 28–30, 1993 (R. D. Brodeur, P. A. Livingston, T. R. Loughlin, and A. B. Hollowed, eds.), p.167–178. NOAA Tech. Rep. NMFS 126. [NTIS No. PB97-155188.]

Sinclair, E., T. Loughlin, and W. Pearcy.
1994. Prey selection by northern fur seals (*Callorhinus ursinus*) in the eastern Bering Sea. Fish. Bull. 92:144–156.

Sinclair, E. H., and T. K. Zeppelin.
2002. Seasonal and spatial differences in diet in the western stock of Steller sea lions (*Eumetopias jubatus*). J. Mammal. 83(4):973–990.

Tollit, D. J., S. G. Heaslip, and A. W. Trites.
2004. Sizes of walleye pollock (*Theragra chalcogramma*) consumed by the eastern stock of Steller sea lions (*Eumetopias jubatus*) in Southeast Alaska from 1994 to 1999. Fish. Bull. 102:522–532.

Tollit, D. J., M. J. Steward, P. M. Thompson, G. J. Pierce, M. B. Santos, and S. Hughes.
1997. Species and size differences in the digestion of otoliths and beaks: implications for estimates of pinniped diet composition. Can. J. Fish. Aquat. Sci. 54:105–119.

Tollit, D. J., and P. M. Thompson.
1996. Seasonal and between-year variations in the diet of harbour seals in the Moray Firth, Scotland. Can. J. Zool. 74:1110–1121.

Tollit, D. J., M. Wong, A. J. Winship, D. A. S. Rosen, and A. W. Trites.
2003. Quantifying errors associated with using prey skeletal structures from fecal samples to determine the diet of the Steller's sea lion (*Eumetopias jubatus*). Mar. Mamm. Sci. 19(4):724–744.

Trites, A. W., and P. A. Larkin.
1996. Changes in the abundance of Steller sea lions (*Eumetopias jubatus*) in Alaska from 1956 to 1992: how many were there? Aquat. Mamm. 22:153–166.

Zar, J. H.
1984. Biostatistical analysis, 2nd ed., 718 p. Prentice-Hall, Englewood Cliffs, N.J.

Zeppelin, T. K., D. J. Tollit, K. A. Call, T. J. Orchard, and C. J. Gudmundson.
2004. Sizes of walleye pollock (*Theragra chalcogramma*) and Atka mackerel (*Pleuragrammus monopterygius*) consumed by the western stock of Steller sea lions (*Eumetopias jubatus*) in Alaska from 1998 to 2000. Fish. Bull. 102:509–521.

Sizes of walleye pollock (*Theragra chalcogramma*) and Atka mackerel (*Pleurogrammus monopterygius*) consumed by the western stock of Steller sea lions (*Eumetopias jubatus*) in Alaska from 1998 to 2000

Tonya K. Zeppelin[1]
Dominic J. Tollit[2]
Katherine A. Call[1]
Trevor J. Orchard[3]
Carolyn J. Gudmundson[1]

E-mail address Tonya Zeppelin@noaa.gov

[1] National Marine Mammal Laboratory
Alaska Fisheries Science Center
National Marine Fisheries Service, NOAA
7600 Sand Point Way NE
Seattle, Washington 98115

[2] Marine Mammal Research Unit
Fisheries Center, Room 18, Hut B-3
University of British Columbia
6248 Biological Sciences Road
Vancouver, British Columbia, Canada V6T 1Z4

[3] Department of Anthropology
University of Toronto
100 St. George Street
Toronto, Ontario, Canada M5S 3G3

Abstract—Prey-size selectivity by Steller sea lions (*Eumetopias jubatus*) is relevant for understanding the foraging behavior of this declining predator, but studies have been problematic because of the absence and erosion of otoliths usually used to estimate fish length. Therefore, we developed regression formulae to estimate fish length from seven diagnostic cranial structures of walleye pollock (*Theragra chalcogramma*) and Atka mackerel (*Pleurogrammus monopterygius*). For both species, all structure measurements were related with fork length of prey (r^2 range: 0.78–0.99). Fork length (FL) of walleye pollock and Atka mackerel consumed by Steller sea lions was estimated by applying these regression models to cranial structures recovered from scats (feces) collected between 1998 and 2000 across the range of the Alaskan western stock of Steller sea lions. Experimentally derived digestion correction factors were applied to take into account loss of size due to digestion. Fork lengths of walleye pollock consumed by Steller sea lions ranged from 3.7 to 70.8 cm (mean=39.3 cm, SD=14.3 cm, n=666) and Atka mackerel ranged from 15.3 to 49.6 cm (mean=32.3 cm, SD= 5.9 cm, n=1685). Although sample sizes were limited, a greater proportion of juvenile (≤20 cm) walleye pollock were found in samples collected during the summer (June–September) on haul-out sites (64% juveniles, n=11 scats) than on summer rookeries (9% juveniles, n=132 scats) or winter (February–March) haul-out sites (3% juveniles, n=69 scats). Annual changes in the size of Atka mackerel consumed by Steller sea lions corresponded to changes in the length distribution of Atka mackerel resulting from exceptionally strong year classes. Considerable overlap (>51%) in the size of walleye pollock and Atka mackerel taken by Steller sea lions and the sizes of these species caught by the commercial trawl fishery were demonstrated.

Manuscript submitted 28 April 2003 to Scientific Editor's Office.

Manuscript approved for publication 25 March 2004 by the Scientific Editor.

Fish. Bull. 102:509–521 (2004).

The western stock of Steller sea lions (*Eumetopias jubatus*) in the Gulf of Alaska and the Bering Sea has experienced dramatic and continued declines since the mid-1970s (Loughlin et al., 1992; Loughlin and York, 2000). It is likely that changes in prey availability linked to commercial fisheries and large-scale oceanographic changes are among the reasons for the continued decline (Loughlin and Merrick, 1989; NRC, 1996). The diet of the western stock of Steller sea lions has been recently assessed (Sinclair and Zeppelin, 2002), but discrete selection of prey by size has not been described. The size of prey is relevant for understanding the foraging behavior of the predator as well as the ecological role of the prey (e.g., mortality at a given life history stage). In the case of the Steller sea lion, prey-size selectivity is particularly important for understanding spatial and temporal changes in diet and is needed for making fishery management decisions.

Size of fish prey consumed by marine mammals has been estimated by using sagittal otoliths recovered from stomach and more recently scat samples (Pitcher, 1981; Frost and Lowry, 1986; Browne et al., 2002). Significant relationships have been demonstrated between fish fork length (FL) and otolith length (Templeman and Squires, 1956; Frost and Lowry, 1981; Harvey et al., 2000). The use of otoliths to describe the size of prey taken by Steller sea lions has proved useful in data collected from stomach samples (e.g., Pitcher, 1981; Calkins and Goodwin[1]). However, few

[1] Calkins, D. G., and E. Goodwin. 1988. Unpubl. report. Investigation of the declining sea lion population in the Gulf of Alaska, 76 p. Alaska Department of Fish and Game, 333 Raspberry Road, Anchorage, Alaska, 99518-1599.

otoliths are recovered from Steller sea lion scat, and measurements of otoliths recovered from scats likely underestimate prey size because of partial erosion from digestion (Prime and Hammond, 1987; Dellinger and Trillmich, 1988; Harvey, 1989). Because of the impracticality of collecting stomachs and the low number and poor quality of otoliths found in scats, alternative methods are needed to accurately describe the size of prey consumed by Steller sea lions.

Archaeological studies routinely use skeletal structures other than otoliths to estimate either fish length or mass (Keys, 1928; Casteel, 1976; Owen and Merrick, 1994; Desse and Desse-Berset, 1996). Wise (1980) used a regression of fish length on vertebrae length to estimate prey size from scat samples of otters (*Lutra lutra*) and mink (*Mustela vison*). The regression approach relies on the assumption that the overall size of a given fish and the size of skeletal structures are highly correlated. This assumption has been substantiated for cranial and skeletal structures other than otoliths in various North Pacific fish species (Orchard, 2001). Thus, the use of cranial structures appear to be a viable alternative to the use of otoliths for studying prey size of Steller sea lions.

Walleye pollock (*Theragra chalcogramma*) and Atka mackerel (*Pleurogrammus monopterygius*) rank among the top prey items of Steller sea lions (Sinclair and Zeppelin, 2002) as well as being valuable in the U.S. commercial fishery (NMFS, 2003). We estimated fork length for these two primary prey species from scats collected between 1998 and 2000 across the range of the Alaskan western stock of sea lions. Fish length was estimated by using regression formulae relating bone or otolith measurement to fork length for seven cranial structures found in sufficient quantities and in good and fair condition in scat samples. Experimentally derived digestion correction factors (Tollit et al., 2004b, this issue) were applied to bone and otolith measurements to account for loss of size due to erosion. The methods developed here proved to be an effective tool to estimate size of prey selected by Steller sea lions and are applicable for other marine mammal diet studies particularly where otoliths are highly eroded.

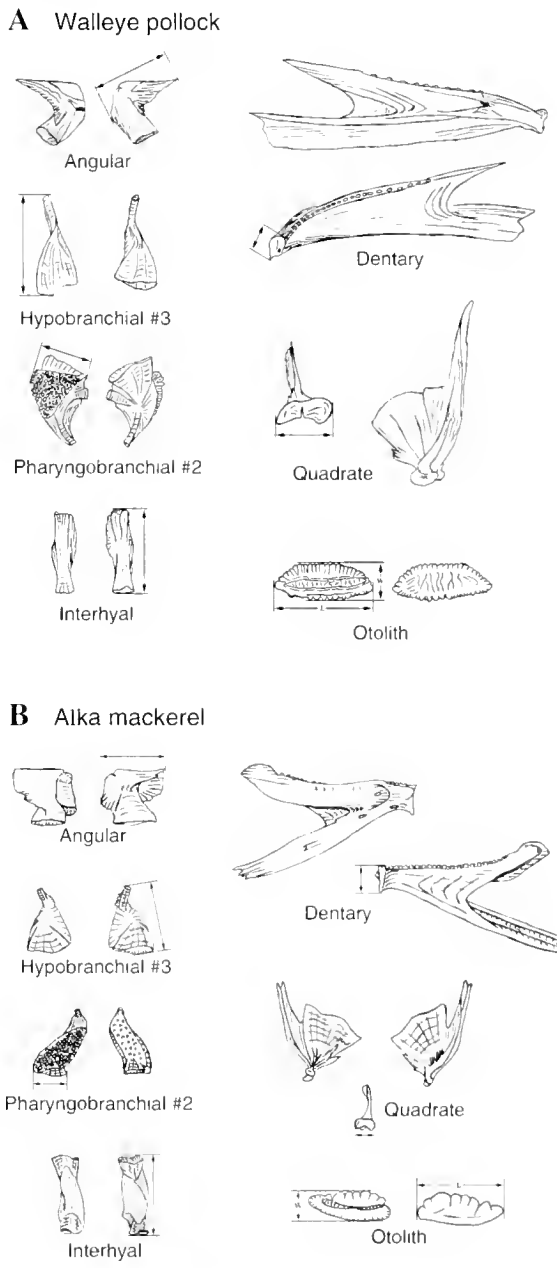

Figure 1

Illustrations of the various planes for bone and otolith measurements used to solve the bone-length to fish-length regression equations for (**A**) walleye pollock and (**B**) Atka mackerel. The structures from the right side of the body are shown for all structures except for quadrates.

Materials and methods

Development of regression formulae

Fork-length to bone and otolith-length regression equations were developed for seven cranial structures from walleye pollock and Atka mackerel. Bones and otoliths were selected according to species-specific features, predictability in condition, and prevalence in scats. Bones included the angular (ANG), quadrate (QUAD), interhyal (INTE), dentary (DENT), pharyngobranchial 2 (PHAR), and hypobranchial 3 (HYPO) (Fig. 1). Fork length regressions were developed for sagittal otolith length (OTOL), as well as for width (OTOW) measurements. All selected cranial structures were paired (having a left and right side) which allowed for enumeration of prey species. Only right-sided bones and otoliths were used to develop the regression equations.

In symmetrical fishes such as walleye pollock and Atka mackerel the left and right otoliths are mirror images of each other (Härkönen, 1986). We compared the left and right-sided measurements for all seven structures using a subsample of the structures used to develop the regression equations. There was no significant difference for either walleye pollock (paired t-test, $P<0.05$, $n=13$ for HYPO, 15 for QUAD, and 14 for all other structures) or Atka mackerel (paired t-test, $P<0.05$, $n=14$ for OTOS and 17 for all other structures).

Fish specimens used for regressions were collected from the Gulf of Alaska and Bering Sea. Standard length (SL) was converted to fork length for walleye pollock (when fork length was not available for a small number of otoliths included in the regressions) by using the following equation: $FL = 0.40+1.07(SL)$ (Wilson[2]). We chose to use FL over SL for the regressions because all fish were in good condition, thus allowing for accurate measurements. Additionally, FL is the standard used for commercial fishery and survey data by the National Marine Fisheries Service for direct comparisons. A partial analysis of these data was previously reported in Orchard (2001). We expanded the data set reported in Orchard (2001) to reflect the size range of bones found in Steller sea lion scats and included only fish specimens collected within our study area.

Linear regression models were fitted for most cranial structures by using the following equation:

$$Y = \alpha + \beta X,$$

where Y = the fork length of the fish;
X = the measurement of the cranial structure; and
α and β are constants that define the regression formula.

However, some cranial structures provided a better fit with the following quadratic regression equation:

$$Y = \alpha + \beta X + \beta X^2.$$

The strength of the relationship of the regression models was assessed by using a coefficient of determination (r^2).

Erosion is a potential source of bias when estimating prey body size from digested otoliths (Prime and Hammond, 1987; Dellinger and Trillmich, 1988; Harvey, 1989). We used condition-specific digestion correction factors (DCFs) developed by Tollit et al. (2004b, this issue) to correct for the high degree of variation in the erosion of cranial structures. DCFs were obtained from feeding experiments on captive juvenile Steller sea lions by using a subsample of fish collected for the regression analysis (Tollit et al., 2004b, this issue). Selected cranial structures from three size groups of pollock (28.5–45.0 cm FL) and one size group of Atka mackerel (30–36 cm FL) were used to develop the DCFs.

Estimation of size of walleye pollock and Atka mackerel consumed by Steller sea lions in the Bering Sea and Gulf of Alaska

Steller sea lion scats were collected from 1998 to 2000 along most of the U.S. range of the Alaskan western stock. Scats were collected from rookery (breeding) and haul-out (nonbreeding) sites in summer (June–September) and haul-out sites in winter (February–March). We assumed that scats collected on summer rookery sites primarily represent the diet of adult females because adult males present on rookeries usually fast during this time. Juveniles of both sexes come ashore on rookeries during summer and undoubtedly are represented in the data, but to a lesser degree than adult females. Scats from juvenile Steller sea lions are more likely to be sampled on haul-out sites during summer, where juveniles make up the greatest proportion of individuals. Scats collected on summer haul-out sites or any winter site presumably represent a greater cross-section of ages and sexes than collections from rookeries during summer.

Scats were rinsed through nested sieves of 4.8-, 1.4-, 0.7-, and 0.5-mm mesh. Bones and otoliths were identified to the lowest possible taxon by using reference collection specimens. All recovered otoliths and selected bones identified as either walleye pollock or Atka mackerel were given a condition grade based on the degree of erosion (Tollit et al., 2004b, this issue). In general, cranial structures considered in "good" condition had little or no erosion, "fair" were moderately eroded (generally up to about 20%), and "poor" were heavily digested (Tollit et al., 2004b, this issue). All structures that were given a condition grade of "good" or "fair" were identified as being from the left or right side and measured to the nearest 0.01 mm with digital calipers. Cranial structures graded as "poor" were not measured and excluded from further analyses because of high observed intraspecific variation (Tollit et al., 1997; Tollit et al., 2004b, this issue).

Fork-length estimates with and without DCFs applied were calculated for each cranial structure and for all structures combined. Otoliths were treated separately because most diet studies currently rely on otolith length to estimate fish fork length. Ninety-five percent confidence intervals around all mean size estimates were calculated by using parametric bootstrapping procedures (Manly, 1997) in which error associated with the regression equation and resampling error resulting from variability within correction factors, and variability in scats were taken into account. Full details of the bootstrapping procedure are presented in Tollit et al. (2004b, this issue).

The same fish may be represented by multiple cranial structures within a scat; therefore, in order to avoid pseudoreplication, we selected a minimum number of individuals (MNI; Ringrose, 1993) for each scat sample.

[2] Wilson, M. 2003. Personal commun. Alaska Fisheries Science Center, Natl. Mar. Fish. Serv., NOAA, Seattle, WA.

Table 1

Relationship between bone measurement and fish fork length (FL) in millimeters. For each equation the number of bones measured (n), coefficient of determination (r^2), standard error of the regression coefficient (SE and SE_x^2 for quadratic regression coefficients), range of fish lengths and mean of fork lengths are given. All measurements are given in millimeters.

Species	Structure code	Regression	r^2	n	SE, SE_x^2	Range of FL	Mean FL
Walleye pollock	INTE	$FL = 49.78x + 5.12$	0.98	49	1.12	83–477	201.61
	HYPO	$FL = 43.14x + 14.12$	0.99	49	0.78	83–477	231.58
	PHAR	$FL = 80.19x + 19.43$	0.95	51	2.58	83–477	204.37
	ANGU	$FL = 59.25x + 15.27$	0.96	44	1.82	83–477	208.75
	QUAD	$FL = 89.47x + 6.77$	0.99	59	1.32	83–477	203.92
	DENT	$FL = 108.46x - 1.52$	0.99	60	1.75	83–477	206.61
	OTOL	$FL = 0.50x^2 + 15.74x + 13.3$	0.99	504	0.68, 0.34	49–530	187.35
	OTOW	$FL = 2.32x^2 + 44.74x + 3.73$	0.99	508	1.54, 0.19	49–530	188.66
Atka mackerel	INTE	$FL = 57.38x + 95.57$	0.86	106	2.26	185–500	355.37
	HYPO	$FL = 38.58x$ 80.64	0.95	105	0.85	185–500	355.62
	PHAR	$FL = 81.32x + 70.40$	0.91	107	2.48	185–500	354.90
	ANGU	$FL = 58.38x + 73.86$	0.91	105	1.85	185–500	355.34
	QUAD	$FL = -8.90x^2 + 129.38x + 9.16$	0.96	108	7.07, 0.96	185–500	354.69
	DENT	$FL = -7.10x^2 + 115.83x - 21.68$	0.94	108	7.08, 0.73	185–500	354.69
	OTOL	$FL = 62.54x + 24.24$	0.83	165	2.19	185–500	349.82
	OTOW	$FL = 188.19x - 77.71$	0.78	170	7.71	185–500	350.09

Minimum number of individuals for each species in each scat was estimated by counting species-specific sided elements and choosing the greatest number of left or right elements. If more than one structure had the same number, the structure with the highest r^2 value in its regression on fork length (Table 1) was selected as a representative length estimate for that fish. If an equal number of left and right bones were present, right bones were selected.

Temporal variation in size of walleye pollock and Atka mackerel consumed by Steller sea lions

Temporal differences were assessed by grouping fish into stage-class categories. Stage-class categories were defined for pollock as follows: juvenile or 1-year-old fish (≤20 cm FL), adolescent (20.1–34 cm FL), subadult (34.1–45 cm FL), and adult (>45.1 cm FL; Dorn et al., 2001; Smith, 1981; Walline, 1983). Walleye pollock subadults are likely 3–4 years old, of which ~50% have matured and recruited into the fishery, whereas adults are sexually mature fish, likely 5 years or older. Stage-class categories for Atka mackeral were defined as follows: juvenile up to 2-year-old fish (≤30 cm), adolescent or 3-year-old fish (30.1–35.2 cm), subadult or 4-year-old fish (35.3–45 cm), and adults (>45.1 cm; Lowe et al., 2001; McDermott and Lowe, 1997). Atka mackerel adolescents are ~50% sexually mature and adult-size fish are fully mature.

A chi-squared contingency test was used to test for differences in the proportion of fish stage-classes occurring in scats among rookeries and haul-out sites, years, and seasons by using corrected fork-length estimates from all cranial structures (S-PLUS 2000, Mathsoft, Inc., Cambridge, MA). To avoid pseudoreplication, we used presence or absence of cranial elements of a stage class in a scat particilarily because multiple elements from the same stage-class within a sample may not be independent (Hunt et al., 1996). By using presence-absence data we also avoided the problems associated with the variability in passage and recovery rates of different size structures (Tollit et al., 1997). Because sample sizes were small, juvenile and adolescent walleye pollock stage classes and recruiting adult and adult Atka mackerel stage classes were combined for seasonal comparisons among years. Fisher's exact test was used for comparisons when samples sizes for any stage class were less than 5 (S-PLUS 2000, Mathsoft, Inc., Cambridge, MA).

We obtained size composition data from commercial bottom trawls of walleye pollock and Atka mackerel from the NMFS North Pacific Groundfish Observer Program. Data were divided into winter (January–April) and fall (August–November) seasons and compared with our seasonal scat data (February–March and June–September). The percentage of overlap in sizes of fish caught by the commercial groundfish fishery with sizes of fish consumed by Steller sea lions was calculated by comparing size-frequency distributions. Two-cm size bins were used for the overlap calculation and Steller sea lion prey-size data were rounded to the nearest integer to be consistent with the fishery data.

Results

Regression formulae

A total of 517 pollock and 191 Atka mackerel samples were used to develop the regression equations of bone and otolith measurement to fork length. The sample size and range of fish lengths used for the regressions varied between species and cranial structures (Table 1). No clear indications of sample size required for regression analysis are currently provided in the literature; however, Owen and Merrick (1994) recommend a minimum sample size of 30–40. Sample sizes used to develop equations presented here ranged from 44 to 508.

In general, linear models were used for regression equations; however, several cranial structures were best fitted with a quadratic model. For both species, all structures were strongly related to fork length (r^2 range: 0.78–0.99; Table 1). The regressions encompassed the majority of sizes of bones and otoliths found in Steller sea lion scat samples for this study. However, a small proportion of walleye pollock bones from scats were larger than those used to develop the regressions.

Frost and Lowry (1981) developed otolith linear regression equations for walleye pollock from the Bering Sea using a double-regression approach that produced an inflection point at 10 mm. We examined the double regression approach but found a higher degree of correlation using a quadratic regression model. We compared the results of our model with Frost and Lowry's (1981) model and found that estimated fork lengths of walleye pollock differed less than 2 cm across the length range in our samples.

Estimation of size of walleye pollock and Atka mackerel consumed by Steller sea lions in the Bering Sea and Gulf of Alaska

A total of 714 scats from 39 sites contained 3646 selected cranial elements from either walleye pollock or Atka mackerel. Of those, 212 scats contained 666 walleye pollock cranial elements with a condition grade of either "good" (n=236) or "fair" (n=430). The minimum number of individual pollock per scat ranged from 1 to 18 with a mean of 1.6 (SD=1.7). For Atka mackerel, 379 scats contained 1685 skeletal elements with condition grade of either "good" (n=755) or "fair" (n=930). The minimum number of individual Atka mackerel per scat ranged from 1 to 14 with a mean of 1.9 (SD=1.6).

The mean fork length of walleye pollock consumed by Steller sea lions in the Bering Sea and Gulf of Alaska estimated from uncorrected otoliths found in scats was 23.7 cm (SD=12.0; n=88). Application of the DCF increased the mean estimate to 28.4 cm (SD=14.75; n=88). The size distribution estimated from corrected otoliths had three modes: a major mode around 32 cm and minor modes around 5 cm and 13 cm (Fig. 2A). Confidence intervals for all grade-corrected estimates can be found in Table 1.

The mean fork length of walleye pollock estimated from all seven structures was 39.8% greater than the mean estimated from otoliths alone. The uncorrected mean was 33.1 cm. Applying the DCF increased the mean length of walleye pollock by 18.7% to 39.3 cm (paired t test, t_{665}=37.9, P<0.001). Mean grade-corrected size estimates for cranial structures other than otoliths ranged from 34.5 cm (PHAR) to 47.2 cm (HYPO) and 95% confidence intervals ranged from 25.2 to 50.6 cm (Table 2). The condition-specific DCFs increased length estimates between 6.8% (HYPO) and 28.3% (DENT). The size distribution estimated from all grade-corrected structures had three modes: a major mode around 44 cm and minor modes around 5 cm and 15 cm (Fig. 2A).

The mean fork length of Atka mackerel consumed by Steller sea lions in the Bering Sea and Gulf of Alaska estimated from uncorrected otoliths was 30.3 cm (SD=4.0; n=117). Application of the DCF increased the mean estimate to 34.7 (SD=4.8; n=117).

The mean fork length of Atka mackerel estimated from all structures (30.7 cm; SD=5.9 cm, corrected 32.3 cm; SD=5.9 cm, n=1685, paired t test, t_{1684}=39.1, P<0.001) was similar to the mean estimated from otoliths (6.9% less without a DCF and 1.3% less with a DCF; Fig. 2B). Mean grade-corrected size estimates for structures other than otoliths ranged from 26.6 cm (QUAD) to 34.2 cm (INTE) and 95% confidence intervals ranged from 24.0 cm (DENT) to 35.0 cm (INTE; Table 2). Use of the condition-specific DCFs increased length estimates between 2.1% (INTE) and 24.0% (DENT). Fork length estimates for all structures did not include PHAR because too few were recovered in scats in the feeding studies of captive Steller sea lions to develop a correction factor.

When mean prey size was calculated by using MNI, the mean corrected and uncorrected size estimate of both walleye pollock and Atka mackerel differed by less than 0.2 cm from estimates derived by using all structures. There was little difference in the standard deviations or distributions when MNI estimates were used compared with all structures (Table 2). Unsurprisingly, the use of MNI estimates did substantially reduce the sample size (336/666 for walleye pollock and 722/1685 for Atka mackerel).

Spatial and temporal variation in size of pollock and Atka mackerel consumed by Steller sea lions

No statistical difference was found in the proportion of pollock stage classes among years on summer rookery sites (P=0.29, χ^2=4.9, df=3) or winter haul-out sites (P=0.10; Fisher's exact test). Scats were collected only on summer haul-out sites during 2000. Although sample sizes were limited, we found significant differences in the proportion of pollock stage classes between summer rookery and haul-out scats (P=0.02; Fisher's exact test) and between summer and winter haul-out sites (P=0.018; Fisher's exact test) for year 2000. A greater proportion of juvenile pollock were found on summer haul-outs (64% juveniles, n=11 scats) than on summer rookeries (9% juveniles, n=132 scats) or winter haul-out sites (3% juveniles, n=69 scats, Fig. 3). No statistical difference

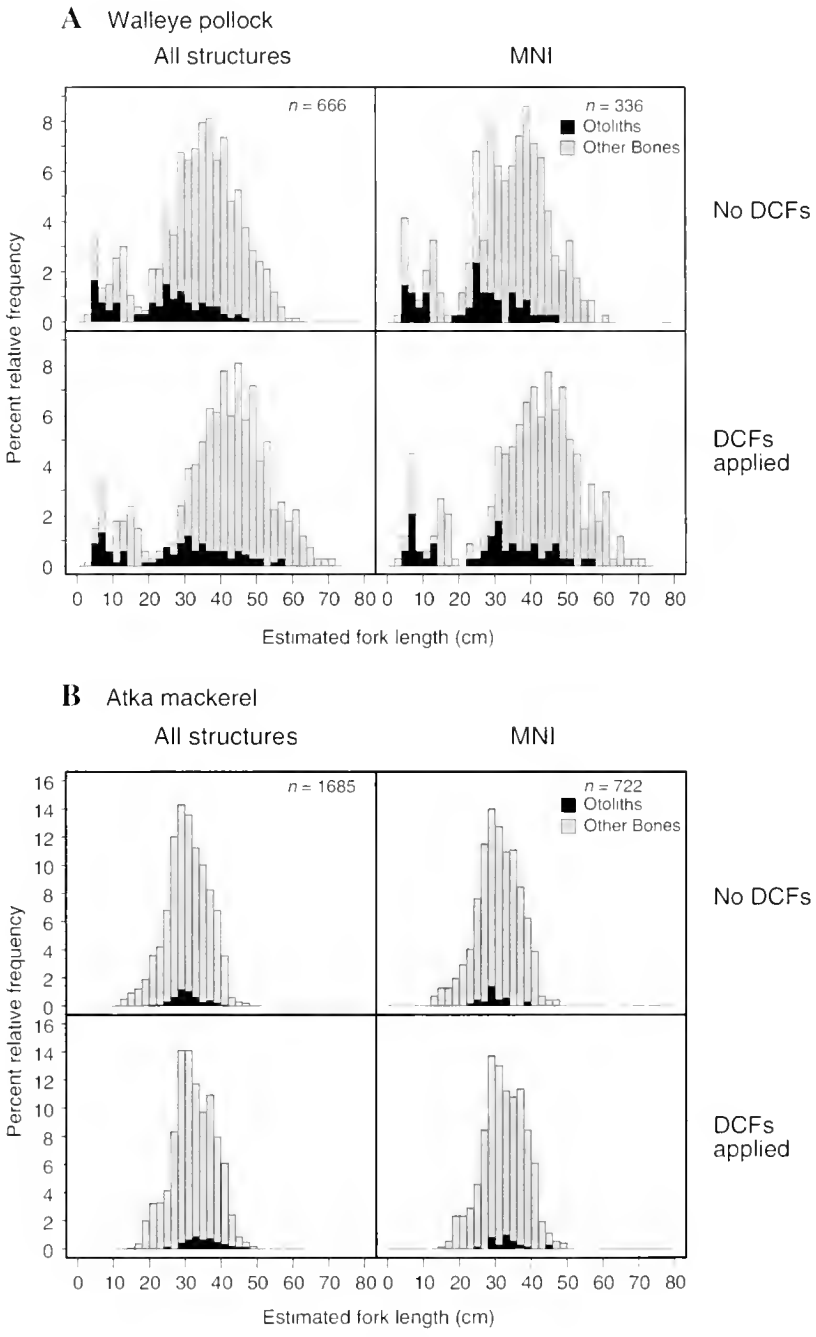

Figure 2

Relative frequency histograms of the estimated fork length of (**A**) walleye pollock and (**B**) Atka mackerel consumed by Steller sea lions. Fork lengths were predicted from cranial structures in good and fair condition. Comparisons were made on the application of correction factors (DCFs) which account for digestion and for using minimum number (MNI) estimates as a selection technique versus using all structures. Otoliths (black bars) are stacked beneath all other structures (gray bars).

was found in the proportion of stage classes between summer rookery (9.09% juvenile; 20.45% adolescent; 53.03% subadult; 65.15% adult) and winter haul-out (2.90% juvenile; 21.74% adolescent; 57.97% subadult; 46.38% adult) sites for all years combined (P=0.32, χ^2=2.3, df=2).

Table 2

Estimated mean fork length of walleye pollock and Atka mackerel consumed by Steller sea lions based on selected structures with or without application of condition-specific digestion correction factors (DCFs). Data sets exclude all structures graded as heavily digested. Remaining total sample sizes of elements (n^e) are given along with proportion of grade "good" structures (n^g). For data sets where DCFs were applied, 95% confidence intervals (95% CI) were estimated by using bootstrap resampling procedures (Tollit et al., 2004b, this issue).

Species	Structure code	DCF	n^e	n^g	Mean FL (cm)	SD (cm)	Range (cm)	95% CI
Walleye pollock	INTE	No	60	0.45	43.7	8.0	16.7–59.4	
		Yes	60	0.45	47.0	8.5	16.7–65.9	44.9–49.8
	HYPO	No	38	0.55	44.2	7.2	30.5–60.4	
		Yes	38	0.55	47.2	7.8	34.9–62.7	44.5–50.6
	PHAR	No	23	0.61	32.2	14.3	9.7–53.1	
		Yes	23	0.61	34.5	14.8	10.9–53.1	25.2–44.5
	ANGU	No	136	0.40	36.1	8.4	10.6–55.3	
		Yes	136	0.40	40.2	9.0	10.6–60.6	38.5–42.4
	QUAD	No	134	0.34	35.1	12.0	9.4–57.8	
		Yes	134	0.34	44.5	15.3	11.9–70.8	38.8–49.6
	DENT	No	187	0.37	28.6	11.8	3.1–57.2	
		Yes	187	0.37	36.7	15.1	3.7–70.2	30.3–42.4
	OTOL	No	88	0.03	23.7	12.0	4.6–46.8	
		Yes	88	0.03	28.4	14.8	4.6–57.1	17.0–32.4
	All	No	666	0.35	33.1	12.4	3.1–60.4	
		Yes	666	0.35	39.3	14.3	3.7–70.8	35.9–42.4
Atka mackerel	INTE	No	601	0.58	33.5	5.0	19.5–46.8	
		Yes	601	0.58	34.2	5.1	19.5–49.6	33.4–35.0
	HYPO	No	238	0.42	31.1	4.8	18.8–46.2	
		Yes	238	0.42	32.9	5.5	19.3–48.3	32.4–34.6
	ANGU	No	488	0.45	30.2	4.7	17.3–43.0	
		Yes	488	0.45	31.8	5.1	17.3–46.1	31.7–33.3
	QUAD	No	161	0.37	25.3	5.4	14.8–40.6	
		Yes	161	0.37	26.6	5.6	15.3–41.4	25.1–28.4
	DENT	No	80	0.28	22.5	7.7	13.0–38.7	
		Yes	80	0.28	27.9	8.0	17.7–44.1	24.0–33.0
	OTOL	No	117	0.06	30.3	4.0	21.2–40.6	
		Yes	117	0.06	34.7	4.8	21.2–47.0	33.5–35.8
	All	No	1685	0.45	30.7	5.9	13.0–46.9	
		Yes	1685	0.45	32.3	5.9	15.3–49.6	31.7–33.4

Significant differences were found in the proportion of Atka mackerel stage classes between 1998 and 1999 on summer rookery sites (P=0.05, χ^2 =6.0, df=2) and winter haul-out sites (P=0.01, χ^2=9.9, df=2) and between 1998 and 2000 winter haul-out sites (P=<0.01, Fisher's exact test). Significant seasonal differences were found only in 1998 (P=0.03, χ^2=7.1, df=2) which may be the result of the small sample size in winter 2000. In summer and winter, annual differences in size of Atka mackerel consumed by Steller sea lions corresponded to changes in the length distribution of Atka mackerel resulting from exceptionally strong year classes in 1995 and 1998 (Lowe et al., 2001). The 1995 year class is represented as a mode around 30 cm in 1998 (3-year-old fish), 35 cm in 1999 and >40 cm in 2000 (Fig. 4). The 1998 year class is represented most clearly as 2 year olds (mode 20–25 cm) in summer 2000 (Fig. 4). Strong annual modes found in our data match those recorded in surveys of Atka mackerel in the Bering Sea and Gulf of Alaska (Lowe et al., 2001).

For walleye pollock and Atka mackerel there was no difference in the mean size of fish caught by the commercial fishery among years (P>0.4, one-way ANOVA). There was a significant difference (P<0.05, one-way ANOVA) in the size of fish caught between seasons. This difference is likely due to aggregations of spawning adult fish caught during the roe fishery. In the winter there is a 56% overlap between the size of fish caught in the commercial pollock fishery and those taken by sea lions and a 54% overlap in the size taken by the Atka

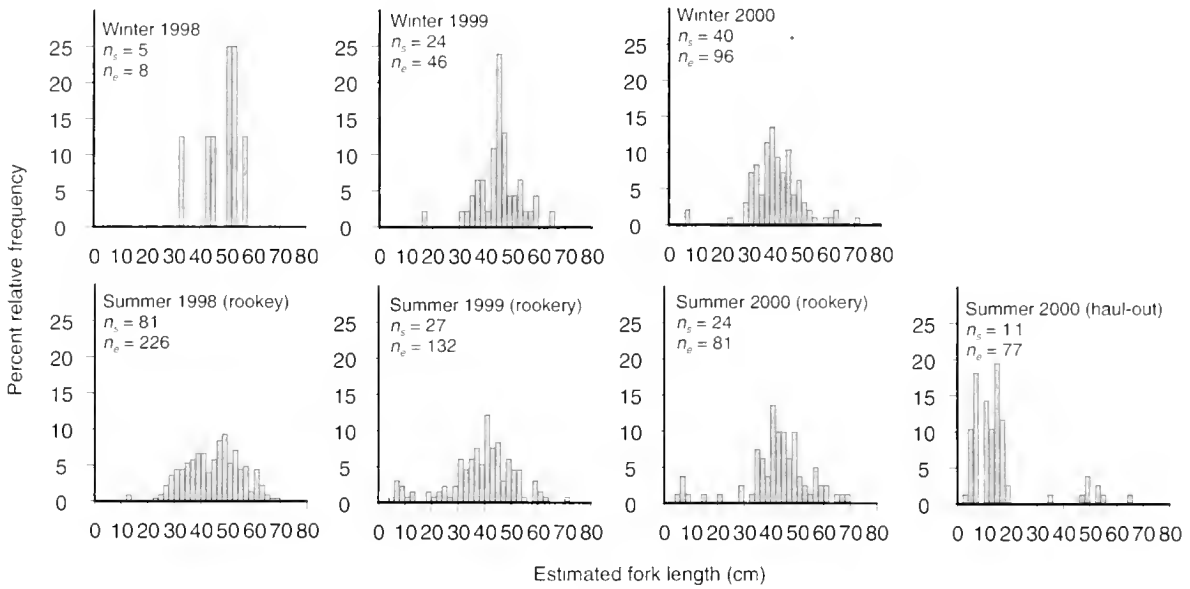

Figure 3

Relative frequency histograms of the estimated fork length of walleye pollock consumed by Steller sea lions across seasons and years for rookeries and haul-outs. Fork lengths are predicted from corrected cranial structures in good and fair condition. Sample sizes for cranial elements (n_e) and scats (n_s) are provided. All winter sites are considered haul-out sites.

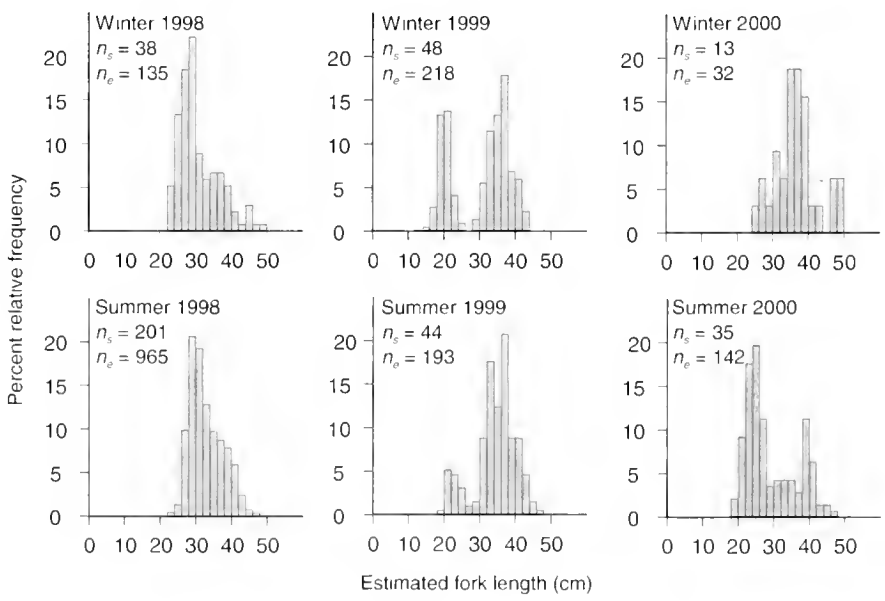

Figure 4

Relative frequency histograms of the estimated fork length of Atka mackerel of consumed by Steller sea lions by season and year. Fork lengths are predicted from corrected cranial structures in good and fair condition. Sample sizes for cranial elements (n_e) and scats (n_s) are provided. All summer sites are rookeries and winter sites are haul-out sites.

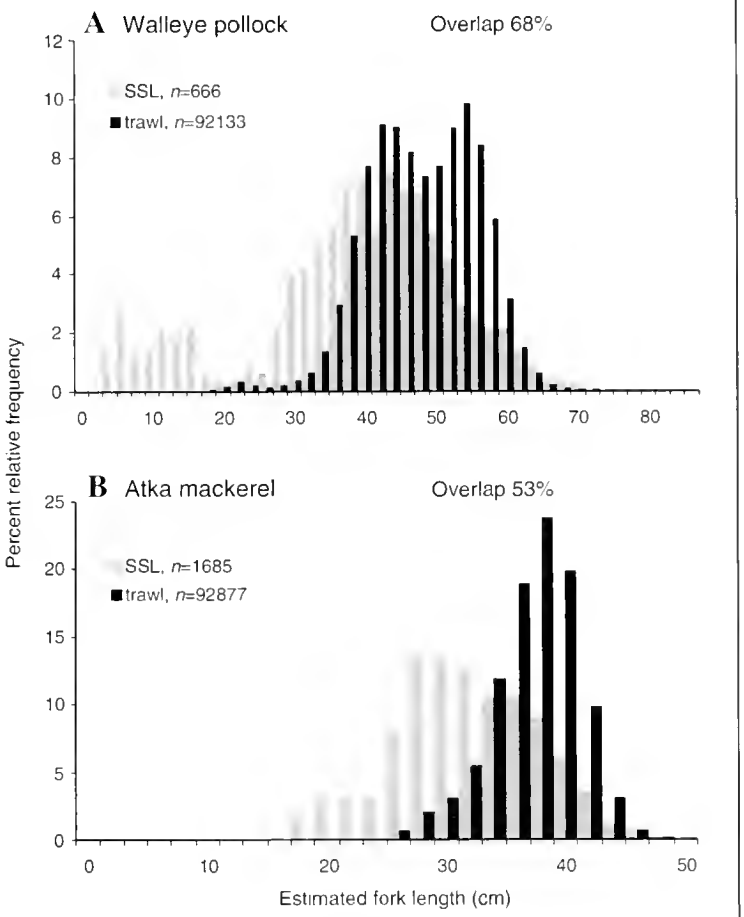

Figure 5

Relative frequency histograms of the estimated fork length of walleye pollock and Atka mackerel consumed by Steller sea lions (SSL) compared with relative frequency histograms of fish caught by the walleye pollock and Atka mackerel commercial trawl fishery.

mackerel fishery. In the summer the overlap in size of fish consumed by sea lions and the size of fish caught in the pollock fishery is 67% and there is a 51% overlap in the size of fish caught in the Atka mackerel fishery. When seasonal data were pooled, overlap between the size of fish caught in the commercial fishery and the size of fish consumed by sea lions was 68% for walleye pollock (Fig. 5A) and 53% for Atka mackerel (Fig. 5B).

Discussion

Regression formulae

Regressions of cranial structure measurement on fish fork length with the use of multiple structures was an effective tool for estimating size of fish consumed by Steller sea lions. Sample sizes of measurable prey remains from scats were enhanced by using a number of cranial structures in addition to otoliths. Body size estimates of only 13.2% of the pollock and 6.9% of the Atka mackerel prey in this study were based on otoliths alone. Fork-length estimates can be considered accurate regardless of which structure was used in the estimate because all r^2 values were high (range: 0.78–0.99). Likewise errors associated with the application of DCFs were consistent across structures (Tollit et al., 2004b, this issue). Confidence intervals around size estimates generally overlapped across structures; however, it was not surprising that different structures yielded slightly different mean sizes because different bones can originate from different scats.

The use of multiple cranial structures may also reduce bias resulting from variability in recovery and passage rates of structures from different species or sizes of fish (Pierce and Boyle, 1991; Browne et al.,

2002; Tollit et al., 2003). Even after applying a DCF, the estimated mean size of walleye pollock based on otoliths was 10.9 cm smaller than the mean size estimated by using all cranial structures. Because walleye pollock otoliths are relatively large and have a different composition than other cranial structures, the larger otoliths may be regurgitated, fully digested, or crushed by rocks in the stomach and not pass through in scat as readily as smaller otoliths or other cranial structures, thereby reducing their occurrence in scat and use in generating prey-size estimates. Atka mackerel otoliths are much smaller at older ages in relation to walleye pollock, which may explain why the size of prey estimated from otoliths was similar to the size estimated from other cranial structures.

The use of DCFs for all structures, including otoliths, to account for erosion increased mean size estimates for both walleye pollock (33.1 vs. 39.3 cm FL) and Atka mackerel (30.7 vs. 32.3 cm FL). The relatively small increase in the corrected size of Atka mackerel reflects that the structures from this species were found in better condition than those from pollock (Table 2), as well as that correction factors were found to be species-, structure-, and condition-specific (Tollit et al., 2004b, this issue). Overall, our results emphasize the importance of using appropriate condition-specific DCFs. Other studies with captive sea lions have also demonstrated that grade-specific DCFs can reduce systematic error and increase precision of body mass estimates (Tollit et al. 1997). For walleye pollock, there was no significant difference in the degree of erosion across the three size ranges for each structure within each condition category (Tollit et al., 2004b, this issue). We assume the DCFs can be used for fish outside of this size range because the relative shape, structure, and proportion of the morphological features are consistent for both smaller and larger fish (Tollit et al., 2004b, this issue). Further research is necessary to test whether there are differences across the size range for Atka mackerel.

Size of walleye pollock and Atka mackerel consumed by Steller sea lions in the Bering Sea and Gulf of Alaska

In general, Steller sea lions on summer rookery and winter haul-out sites consumed primarily subadult and adult-size walleye pollock and Atka mackerel year-round in 1998–2000. Steller sea lions typically forage near shore, in shallow water (<50 m) and at night (Raum-Suryan et al., 2002; Loughlin et al., 2003). Likewise, adult walleye pollock migrate vertically to shallower depths during the night (Smith, 1981). Adult-size Atka mackerel also are commonly found in nearshore coastal areas during their spawning season (Zolotov, 1993).

Juvenile walleye pollock were found in relatively high numbers only in scats collected on summer haul-out sites. Scats collected from summer haul-out sites likely represent a larger proportion of juvenile Steller sea lions than those collected on summer rookery or winter haul-out sites. Previous studies indicate that juvenile sea lions (<4 years old) consume smaller walleye pollock than adult sea lions (Pitcher, 1981; Frost and Lowry, 1986; Merrick and Calkins, 1996). Juvenile walleye pollock are often found at shallow depths in bays and near shore habitat (Smith, 1981). Likewise, Loughlin et al. (2003) reported that juvenile Steller sea lions are typically shallow divers and frequently make short range foraging trips (<15 km). Additional scat collections on summer haul-out sites are necessary to determine more conclusively prey-size selectivity for juvenile Steller sea lions.

Annual changes in the size-frequency distribution of Atka mackerel consumed by Steller sea lions followed changes in the size distribution of Atka mackerel resulting from exceptionally strong year classes. Merrick and Calkins (1996) also showed that the size of prey consumed by Steller sea lions can reflect the size distribution of the fish population. From the mid-1990s on, only 1999 was a strong recruitment year for walleye pollock in the Gulf of Alaska (Dorn et al., 2001), but we did not find a significantly greater proportion of juvenile fish eaten by Steller sea lions in 2000 than in 1999 or 1998 perhaps because sufficient numbers of larger size fish were available in regions where walleye pollock were consumed.

Historical studies of Steller sea lion prey size have primarily been based on measurements of walleye pollock otoliths found in stomach samples but often without application of correction factors for erosion (Pitcher, 1981; Merrick and Calkins, 1996; Calkins, 1998). Prey-size estimates based on stomach contents will likely differ from estimates derived from scats because of differences in digestion rates and breakage (Jobling and Breiby, 1986). However, results of studies examining the variability in prey size with sample type are variable. Sinclair et al. (1996) suggested that in northern fur seals (*Callorhinus ursinus*), another otariid, small otoliths tend to flush through the digestive system more quickly than larger ones, resulting in a possible bias in scats towards smaller otoliths. In contrast, experiments with captive sea lions have shown that smaller otoliths are recovered in lower relative frequencies than are larger ones (Tollit et al., 1997). Frost and Lowry (1980) found no significant difference between the size of otoliths obtained from stomach and intestines of ribbon seals. Overall, we believe useful comparisons of prey size consumed by Steller sea lions can be made between our study and earlier studies.

Steller sea lions have been reported to consume a wide size range of walleye pollock. However, in most prior studies a larger proportion of juvenile fish were found than what we estimated from scats. Otoliths from stomach samples collected from 1975 to 1978 in the Gulf of Alaska contained primarily juvenile age pollock (mean FL=29.8cm; SD= 11.6; Pitcher, 1981). Undigested otoliths from stomach samples collected between 1975 and 1981 in the Bering Sea also contained mostly juvenile fish (mean FL=29.3 cm) but had a distinct mode of adult-size pollock (48 cm FL; Frost and Lowry, 1986). Likewise, 43 stomach samples collected between 1985

and 1986 in the central Gulf of Alaska contained primarily juveniles (mean FL=25.4 cm; SD=12.4) and had a weak mode of adult-size fish (39–43 cm; Merrick and Calkins, 1996; Calkins and Goodwin[1]). Mostly adult-size fish were found in stomachs recovered from Steller sea lions caught in trawl nets in the central Gulf of Alaska (1983–84; Loughlin and Nelson, 1986) and in stomach samples collected from 1994 to 1995 in Japanese waters (Goto and Shimazaki, 1998). However, in both these studies the samples of prey size may have been biased by the selectivity of the fishing gear for larger fish.

Using identical methods to those of our study, Tollit et al. (2004a, this issue) estimated the size of walleye pollock consumed by the eastern stock of Steller sea lions between 1994 and 1999. The average size of walleye pollock consumed, estimated from all grade-corrected structures (mean=42.4 cm; SD=11.6), was similar to the average size found in our study of the western stock of Steller sea lions. Furthermore, Tollit et al. (2004a, this issue) also found a greater occurrence of adult pollock in scats collected on rookery sites than from scats collected on haul-out sites. However, Steller sea lions from the western stock consumed a greater proportion of juvenile and adolescent fish and less adult fish than those from the eastern stock during summer (June–July) and similar-size fish were consumed on haul-out sites in winter (March) in both regions. Neither study indicated the high occurrence of juvenile walleye pollock reported in the 1970s and 1980s. The greater occurrence of juvenile walleye pollock in historical studies may be a result of prey availability or differences in sampling methods.

By examining the relative size-frequency distributions of prey selected by Steller sea lions and those taken in the commercial trawl fishery, we found considerable overlap (68% walleye pollock and 53% Atka mackerel). Likewise, high levels of potential overlap in size were found between walleye pollock selected by Steller sea lions from the eastern stock and caught by the small commercial fishery bordering Southeast Alaska (Tollit et al., 2004a, this issue). The extent of overlap throughout the range of Steller sea lions between the size of prey consumed by sea lions and the size of fish targeted and taken by the pollock and Atka mackerel trawl fisheries could result in competition between fisheries and foraging sea lions if resources are limited.

Acknowledgments

Fish specimens for the regression equations were provided by the National Marine Fisheries Service, the University of Victoria, and the University of British Columbia bone reference collections. Fish remains were identified by Pacific Identifications, Victoria, BC. We thank J. Laake, A. York, and R. Joy for statistical advice, K. Chumbley, E. Sinclair, and S. Crockford for help in initiating the study, A. Browne and M. Wilson for walleye pollock otolith data, and S. Heaslip for graphics and laboratory assistance. Reviews by E. Sinclair, S. Melin, W. Walker, B. Robson, and three anonymous reviewers greatly improved this manuscript.

Literature cited

Browne, P., J. L. Laake, and R. L. DeLong.
2002. Improving pinniped diet analyses through identification of multiple skeletal elements in fecal samples. Fish. Bull. 100:423–433.

Calkins, D. G.
1998. Prey of Steller sea lions in the Bering Sea. Biosph. Cons. 1(1):33–44.

Casteel, R. W.
1976. Fish remains in archaeology and paleo-environmental studies, 180 p. Acad. Press, London.

Desse, J., and N. Desse-Berset,
1996. On the boundaries of osteometry applied to fish. Archaeofauna 5:171–179.

Dellinger, T., and F. Trillmich.
1988. Estimating diet composition from scat analysis in otariid: is it reliable? Can. J. Zool. 66:1865–1870.

Dorn, M., A. Hollowed, E. Brown, B. Megrey, C. Wilson, and J. Blackburn.
2001. Assessment of the walleye pollock stock in the Gulf of Alaska. *In* Stock assessment and fishery evaluation report for the groundfish resources of the Gulf of Alaska, 90 p. Prepared by the Gulf of Alaska Groundfish Plan Team, North Pacific Fishery Management Council, W 4th Avenue, Suite 306, Anchorage, Alaska 99501.

Frost, K. J., and L. F. Lowry.
1980. Feeding of ribbon seals (*Phoca fasciata*) in the Bering Sea in spring. Can. J. Zool. 58:1601–1607.
1981. Trophic importance of some marine gadids in Northern Alaska and their body-otolith size relationships. Fish. Bull. 84:192–197.
1986. Sizes of walleye pollock, *Theragra chalcogramma*, consumed by marine mammals in the Bering Sea. Fish Bull. 79:187–192.

Goto, Y., and K. Shimazaki.
1998. Diet of Steller sea lions off the Coast of Rausu, Hokkaido, Japan. Biosph. Cons. 1(2):141–148.

Härkönen, T.
1986. Guide to the otoliths of the bony fishes of the northeast Atlantic, 256 p. Danbiu Aps, Hellerup, Denmark.

Harvey, J. T.
1989. Assesment of errors associated with harbor seal (*Phoca vitulina*) fecal sampling. J. Zool. (London) 219: 101–111.

Harvey, J. T., Loughlin, T. R., Perez, M. A., and D. S. Oxman.
2000. Relationship between fish size and otolith length for 63 species of fishes from the eastern north Pacific Ocean, 36 p. NOAA Tech. Rep. NMFS 150.

Hunt., G. L., Jr., A. S. Kitaysky, M. B. Decker, D. E. Dragoo, and A. M. Springer.
1996. Changes in the distribution and size of juvenile walleye pollock, *Theragra chalcogramma*, as indicated by seabird diets at the Pribilof Islands and by bottom trawl surveys in the Eastern Bering Sea, 1975 to 1993. *In* Ecology of juvenile walleye pollock, *Theragra chalcogramma*. Papers from the workshop "The importance of prerecruit walleye pollock to the Bering Sea and North Pacific ecosystems" Seattle, WA, October 28–30, 1993 (R. D. Brodeur, P. A. Livingston, T. R. Loughlin,

and A. B. Hollowed, eds.), p. 125–139. NOAA Tech. Rep. NMFS 126. [NTIS no. PB97-155188.]

Jobling, M., and A. Breiby.
1986. The use and abuse of fish otoliths in studies of feeding habits of marine piscivores. Sarsia 71:265–274.

Keys, A. B.
1928. The weight-length relation in fishes. Proceedings of the National Academy of Sciences of the USA 14 (12):922–925.

Loughlin, T. R., and R. L. Merrick.
1989. Comparison of commercial harvest of walleye pollock and northern sea lion abundance in the Bering Sea and Gulf of Alaska, p. 679 –700. *In* Proceedings of the international symposium on the biology and management of walleye pollock, Nov. 14–16, 1988, Anchorage, Alaska. Alaska Sea Grant Report 89-1, Anchorage, AK .

Loughlin, T. R., and R. Nelson Jr.
1986. Incidental mortality of northern sea lions in Shelikof Strait, Alaska. Mar. Mamm. Sci. 2:14–33.

Loughlin T. R., A. S. Perlov, and V. A. Vladimirov.
1992. Range-wide survey and estimation of total number of Steller sea lions in 1989. Mar. Mamm. Sci. 83(3): 220–239.

Loughlin, T. R., J. T. Sterling, R. L. Merrick, J. L. Sease, and A. E. York.
2003. Diving behavior of immature Steller sea lions (*Eumetopias jubatus*). Fish. Bull. 101:566–582.

Loughlin, T. R., and A. E. York.
2000. An accounting of the source of Steller sea lion mortality. Mar. Fish. Rev. 62(4):40–45.

Lowe, S. A., R. F. Reuter, and H. Zenger.
2001. Assessment of Bering Sea /Aleutian Island Atka mackerel. *In* Stock assessment and fishery evaluation report for the groundfish resources of the Bering Sea /Aleutian Islands region, 44 p. Prepared by the Bering Sea and Aleutian Islands Groundfish Plan Team, North Pacific Fishery Management Council, W 4th Avenue, Suite 306, Anchorage, Alaska 99501.

Manly. B. F. J.
1997. Randomization, bootstrap and Monte Carlo methods in biology, 2nd ed., 399 p. Chapman and Hall, London; New York, NY.

McDermott, S. F., and S. A. Lowe.
1997. The reproductive cycle and sexual maturity of Atka mackerel, *Pleurogrammus monopterygius*, in Alaska waters. Fish. Bull. 95:231–333.

Merrick, R. L., and D. G. Calkins.
1996. Importance of juvenile walleye pollock in the diet of Gulf of Alaska Steller sea lions. *In* Ecology of juvenile walleye pollock, *Theragra chalcogramma* (R. D. Brodeur, P. A. Livingston, T. R. Loughlin, and A. B. Hollowed, eds.), p. 153–166. NOAA Tech. Rep. NMFS 126.

NMFS (National Marine Fisheries Service).
2003. Fisheries of the United States, 2002. Current Fishery Statistics No. 2002, 126 p. Fisheries Statistics and Economics Division, Natl. Mar. Fish. Serv., Silver Spring, MD.

NRC (National Research Council).
1996. The Bering Sea ecosystem, 307 p. National Academy Press. Washington, D.C.

Orchard, T. J.
2001. The role of selected fish species in Aleut paleodiet. M.A. thesis, 228 p. Univ. Victoria, Victoria, BC.

Owen, J. F., and J. R. Merrick.
1994. Analysis of coastal middens in south-eastern Australia: Sizing of fish remains in holocene deposits. J. of Archaeol. Sci. 21:3–10.

Pierce, G. J., and P. R. Boyle.
1991. A review of methods for diet analysis in piscivorous marine mammals. Oceanogr. Mar. Biol. Annu. Rev. 29:409–486.

Pitcher, K. W.
1981. Prey of the Steller sea lion, *Eumetopias jubatus*, in the Gulf of Alaska. Fish. Bull. 79:467–472.

Prime J. H., and P. S. Hammond.
1987. Quantitative assessment of gray seal diet from fecal analysis. *In* Approaches to marine mammal energetics (A. C. Huntley, D. P. Costa, G. A. J. Worthy and M. A. Castellini, eds.) p. 165–181. Allen Press, Lawrence, KS.

Raum-Suryan, K. L., K. W. Pitcher, D. G. Calkins, J. L. Sease, and T. R. Loughlin.
2002. Dispersal, rookery fidelity, and metapopulation structure of Steller sea lions (*Eumetopias jubatus*) in an increasing and a decreasing population in Alaska. J. Mammal. 18(3):746–764.

Ringrose, T. J.
1993. Bone counts and statistics: a critique. J. Archaeol. Sci. 20:121–157.

Sinclair, E. H., and T. K. Zeppelin.
2002. Seasonal and spatial differences in diet in the western stock of Steller sea lions (*Eumetopias jubatus*). J. Mammal. 83(4):973–990.

Sinclair, E. H., G. A. Antonelis, B. W. Robson, R. R. Ream, and T. R. Loughlin.
1996. Northern fur seal, *Callorhinus ursinus*, predation on juvenile walleye pollock, *Theragra chalcogramma*. *In* Ecology of walleye pollock, *Theragra chalcogramma* (R. D. Brodeur, P. A. Livingston, T. R. Loughlin, and A. B. Hollowed, eds.) p. 167–178. NOAA Tech. Rep., NMFS-126.

Smith, G. B.
1981. The biology of walleye pollock. *In* The eastern Bering Sea shelf: oceanography and resources, vol. 1 (D. W. Hood and J. A. Calder, eds.) p. 527–552. Univ. Wash. Press, Seattle, WA.

Templemann, W., and H. J. Squires.
1956. Relationship of otolith lengths and weights in the haddock, *Melanogrammus aeglefinus* (L.) to the rate of growth of the fish. J. Fish. Res. Board Can. 13: 467–487.

Tollit, D. J., S. G. Heaslip, and A. W. Trites.
2004a. Sizes of walleye pollock (*Theragra chalcogramma*) consumed by the eastern stock of Steller sea lions (*Eumetopias jubatus*) in Southeast Alaska from 1994 to 1999. Fish. Bull. 102:522–532.

Tollit, D. J., S. G. Heaslip, T. K. Zeppelin, R. Joy, K. A. Call, and A. W. Trites.
2004b. A method to improve size estimates of walleye pollock (*Theragra chalcogramma*) and Atka mackerel (*Pleurogrammus monopterygius*) consumed by pinnipeds: digestion correction factors applied to bones and otoliths recovered in scats. Fish. Bull. 102:498–508.

Tollit D. J., M. J. Steward, P. M. Thompson, G. J. Pierce, M. B. Santos, and S. Hughes.
1997. Species and size differences in the digestion of otoliths and beaks: implications for estimates of pinniped diet composition. Can. J. Fish Aquat. Sci. 54:105–119.

Tollit, D. J., M. Wong, A. J. Winship, D. A. S. Rosen, and A. W. Trites.
2003. Quantifying errors associated with using prey skeletal structures from fecal samples to determine the diet of the Steller sea lion (*Eumetopias jubatus*). Mar. Mamm. Sci. 19(4):724–744.

Walline, P. D.
1983. Growth of larval and juvenile walleye pollock related to year-class strength. Ph.D. diss., 144 p. Univ. Washington, Seattle, WA.

Wise, M. H.
1980. The use of fish vertebrae in scats for estimating prey size of otters and mink. J. Zool., Lond. 192:25–31.

Zolotov, O. G.
1993. Notes on the reproductive biology of *Pleurogrammus monopterygius* in Kamchatkan waters. J. Ichthyol. 33(4):25–37.

Sizes of walleye pollock (*Theragra chalcogramma*) consumed by the eastern stock of Steller sea lions (*Eumetopias jubatus*) in Southeast Alaska from 1994 to 1999

Dominic J. Tollit
Susan G. Heaslip
Andrew W. Trites

Marine Mammal Research Unit, Fisheries Centre
University of British Columbia
Room 18, Hut B-3, 6248 Biological Sciences Road
Vancouver, British Columbia, Canada, V6T 1Z4
E-mail (for D. J. Tollit): tollit@zoology.ubc.ca

Abstract—Lengths of walleye pollock (*Theragra chalcogramma*) consumed by Steller sea lions (*Eumetopias jubatus*) were estimated by using allometric regressions applied to seven diagnostic cranial structures recovered from 531 scats collected in Southeast Alaska between 1994 and 1999. Only elements in good and fair condition were selected. Selected structural measurements were corrected for loss of size due to erosion by using experimentally derived condition-specific digestion correction factors. Correcting for digestion increased the estimated length of fish consumed by 23%, and the average mass of fish consumed by 88%. Mean corrected fork length (FL) of pollock consumed was 42.4 ±11.6 cm (range=10.0–78.1 cm, n=909). Adult pollock (FL>45.0 cm) occurred more frequently in scats collected from rookeries along the open ocean coastline of Southeast Alaska during June and July (74% adults, mean FL=48.4 cm) than they did in scats from haulouts located in inside waters between October and May (51% adults, mean FL=38.4 cm). Overall, the contribution of juvenile pollock (≤20 cm) to the sea lion diet was insignificant; whereas adults contributed 44% to the diet by number and 74% by mass. On average, larger pollock were eaten in summer at rookeries throughout Southeast Alaska than at rookeries in the Gulf of Alaska and the Bering Sea. Overall it appears that Steller sea lions are capable of consuming a wide size range of pollock, and the bulk of fish fall between 20 and 60 cm. The use of cranial hard parts other than otoliths and the application of digestion correction factors are fundamental to correctly estimating the sizes of prey consumed by sea lions and determining the extent that these sizes overlap with the sizes of pollock caught by commercial fisheries.

Manuscript submitted 28 April 2003 to Scientific Editor's Office.

Manuscript approved for publication 25 March 2004 by the Scientific Editor.

Fish. Bull. 102:522–532 (2004).

The dramatic decline of the western population of Steller sea lions (*Eumetopias jubatus*) in the 1980s (Loughlin et al., 1992; Trites and Larkin, 1996) prompted a number of studies to determine what they eat and the extent of overlap of the fish consumed by Steller sea lions and fish caught by commercial fisheries. The eastern population of sea lions (east of longitude 144°) located mainly in Southeast Alaska and British Columbia gradually increased as the western population declined (e.g., Calkins et al., 1999), permitting insightful comparative studies to be undertaken (e.g., Merrick et al., 1995; Milette and Trites, 2003). Possible explanations for the different population trends include ocean climate, competition with fisheries, predation, and the amount or the sizes of pollock in the diets of sea lions in the two regions (Loughlin and York, 2000; Benson and Trites, 2002; NRC, 2003; Trites and Donnelly, 2003; Calkins and Goodwin[1]; Loughlin and Merrick[2]).

Reliable estimates of prey size are important not only to investigate prey selectivity and the extent of overlap in size of prey with size of the same species caught by commercial fisheries and by other marine piscivores but are also vital for accurately assessing prey numbers, biomass, and total consumption (Beverton, 1985; Ringrose, 1993; Laake et al., 2002). One means of estimating prey size is to measure hard parts recovered from fecal remains and to apply allometric regressions relating fork length to the size of otoliths (Frost and Lowry, 1981) and other bones (Zeppelin et al., 2004, this issue). However, the extent of digestion incurred by both otoliths and bones as they pass through the digestive tract must be accounted for to ensure that prey size is not underestimated (Tollit et al., 2004, this issue). Application of these two steps is integral to correctly estimate the size of prey consumed by Steller sea lions and other pinnipeds.

The goal of our study was to estimate the size of walleye pollock (*Theragra chalcogramma*) consumed by Steller sea lions in Southeast Alaska between 1994 and 1999 by using new methods outlined by Tollit et al. (2004, this issue) and Zeppelin et al. (2004, this issue). Previous size estimates for this region of Alaska are based on the analysis of only eight stomachs collected in 1986 (Calkins

[1] Calkins, D. G., and E. Goodwin. 1988. Unpubl. report. Investigation of the declining sea lion population in the Gulf of Alaska. 76 p. Alaska Department of Fish and Game, 333 Raspberry Rd, Anchorage, AK 99518.

[2] Loughlin, T. R., and R.L. Merrick. 1989. Comparison of commercial harvest of walleye pollock and northern sea lion abundance in the Bering Sea and Gulf of Alaska. *In* Proceedings of the international symposium on the biology and management of walleye pollock, Nov. 14–16, 1988, Anchorage, AK, p. 679–700. Alaska Sea Grant Rep. 89-01, Univ. Alaska Fairbanks, Fairbanks, AK.

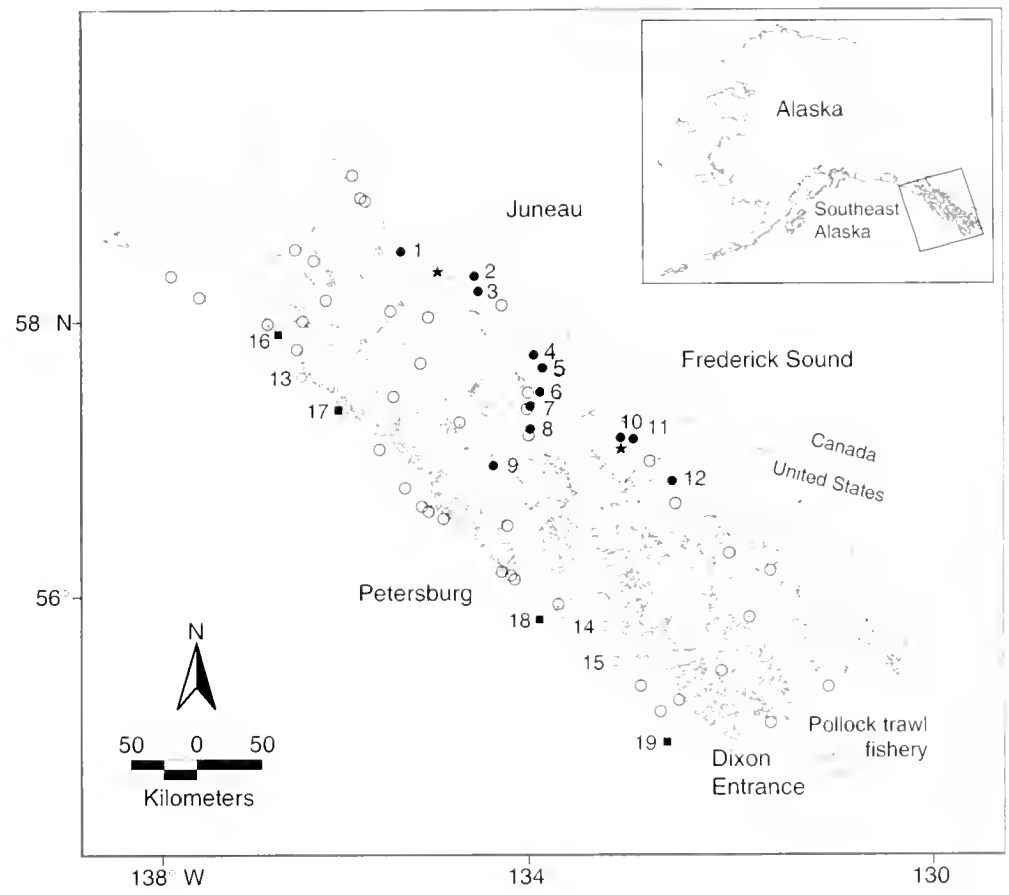

Figure 1

Location of Steller sea lion (*Eumetopias jubatus*) haul-outs and rookeries visited during 1994–99 to collect scats containing pollock hard remains. Symbols: haul-outs in inside waters (●), haul-outs in outside waters (◉), haul-outs where scats were not collected or sites at which no pollock hard remains were found (○), rookeries (■), and cities (★).

and Goodwin[1]). We sought to compare the sizes of pollock consumed in the 1990s with these earlier samples, as well as with the sizes consumed by the declining population of sea lions in the Gulf of Alaska and Bering Sea during the 1970s and 1980s (e.g., Pitcher, 1981; Merrick and Calkins, 1996) and between 1998 and 2000 (Zeppelin et al., 2004, this issue). We also wanted to evaluate the use of digestion correction factors (DCFs) and skeletal structures other than otoliths to estimate prey size, and to compare the different size estimates for fish consumed by sea lions in Southeast Alaska with sizes of fish caught by a nearby commercial trawl fishery.

Materials and methods

Estimating sizes of pollock consumed

Scats that contained pollock hard remains were collected from four rookeries and 16 haul-outs from both inside and outside waters of Southeast Alaska between 1994 and 1999 (Fig. 1 and Table 1). Scats from three haul-outs and four rookeries in outside waters were collected from May through October 1994–99, but most were collected from June and July. Scats from inside waters were collected at 13 haul-outs located in the straits and sounds between Juneau and Petersburg, Alaska (56.8–58.6°N, 132.8–134.9°W) (Fig. 1). The majority of these "inside" scats were collected from Frederick Sound (Fig. 1) between October 1995 and February 1997. Most were collected in the winter and spring, but some were collected in the summer of 1999 (Trites et al.[3]). In general, the haul-out sites visited to collect scats were those with relatively high numbers of animals across Southeast Alaska (Calkins et al., 1999; Sease et al., 2001).

Scats were washed and sieved (0.5 mm) and hard remains were identified by Pacific IDentifications Inc. (Univ. of Victoria, Victoria, B.C.). Seven commonly

[3] Trites, A. W., D. G. Calkins, and A. J. Winship. 2003. Unpubl. data. Marine Mammal Research Unit, Fisheries Centre, University of British Columbia, Room 18, Hut B-3, 6248 Biological Sciences Rd., Vancouver, B.C., Canada, V6T 1Z4.

Table 1

Steller sea lion scat collection sites in Southeast Alaska, as illustrated in Figure 1, giving details of the type (HO=haul-out), fish element sample size (n_f), and the estimated corrected mean fork length (mean FL, cm) of walleye pollock, based on seven cranial structures found in scats at each site.

Region	Site no.	Site name	Type	n_f	Mean FL	SD
Inside waters	1	Benjamin Island	HO	11	39.7	13.9
	2	Dorothy Island	HO	3	38.6	13.6
	3	Circle Point	HO	31	45.1	13.7
	4	Point League	HO	37	42.9	9.9
	5	Sunset Point	HO	196	37.4	10.3
	6	Sail Island	HO	36	35.5	10.0
	7a	W Brother Island	HO	8	40.9	14.7
	7b	SW Brother Island	HO	152	37.1	9.9
	8	Turnabout Island	HO	34	47.8	11.0
	9	Yasha Island	HO	19	44.8	5.3
	10	Sukoi Islets	HO	14	26.9	7.8
	11	Horn Cliffs	HO	19	44.3	12.7
	12	Liesnoi Island	HO	7	31.8	10.2
Outside waters	13	Cape Cross	HO	7	45.3	3.0
	14	Timbered Island	HO	5	39.3	8.7
	15	Point Addington	HO	1	53.5	—
	16	Graves Rock	Rookery	49	42.9	7.7
	17	White Sisters	Rookery	33	43.4	9.6
	18	Hazy Islands	Rookery	54	45.4	8.7
	19	Forrester Islands	Rookery	193	51.4	10.0

occurring, robust, and diagnostic pollock structures were removed from all scats containing pollock (see Tollit et al., 2004, this issue). All were from the cranium region (see Zeppelin et al., 2004, this issue) and included the sagittal otolith (OTO), as well as the interhyal (INTE), hypobranchial 3 (HYPO), pharyngobranchial 2 (PHAR), angular (ANGU), quadrate (QUAD), and the dentary (DENT). Each individual fish element was assigned one of three condition categories (good, fair, or poor) and was measured three times (±0.01 mm) at a specific location to calculate a mean estimate (see Tollit et al., 2004, this issue).

Fork lengths of pollock eaten by Steller sea lions in Southeast Alaska were first estimated by applying allometric regressions (Zeppelin et al., 2004, this issue) to otolith lengths (OTOL) without correcting for partial digestion (see Pitcher, 1981; Merrick and Calkins, 1996). We also measured and substituted otolith width (OTOW) when otoliths were broken lengthwise. We then applied appropriate DCFs and regression formulae to otoliths assigned in good and fair condition (Tollit et al., 2004, this issue). Finally, we applied allometric regressions (Zeppelin et al., 2004, this issue) to all elements of the remaining six cranial structures (bones) assigned to good or fair condition categories to provide estimates of fish size across structures both with and without applying the appropriate DCFs (Tollit et al., 2004, this issue). Structures in poor condition were excluded because of large intraspecific size variation noted from feeding experiments with captive sea lions (see also Sinclair et al., 1994; Tollit et al., 1997; Tollit et al., 2004, this issue).

To incorporate the major sources of error in our method, we calculated confidence intervals (95%) for fork-length estimates. First, we applied a random bootstrapped regression equation, followed by a bootstrapped correction factor applicable to each selected structure (see Tollit et al., 2004, this issue). For the five structures (INTE, HYPO, PHAR, ANGU, and OTO) in good condition for which Tollit et al. (this issue) recommended a DCF of 1.0 (no correction), we drew bootstrapped values from a discrete declining triangular probability distribution (◺) ranging from 1.0 to 1.05 (to simulate a limited degree of digestion). Finally, we bootstrapped individual scats at random, by selecting n scats with replacement from the original sample size n (to account for resampling variability across scats) and included only selected elements within those randomly bootstrapped scats. Bootstrap randomizations for these steps were done 1000 times and 95% confidence intervals were taken as the 25th and 975th values of the sorted bootstrapped values.

Finally, consideration was also given to whether an individual fish might be represented by different structures within a single scat. We therefore compared length estimates using all structures with those esti-

mated with the minimum number of individuals (MNI) technique (Ringrose, 1993; Browne et al., 2002). This technique is used to select structures within each scat that preclude pseudoreplication or double counting of fish. Within each scat, the structure with the greatest MNI was selected, and right-sided structures were selected over left-sided structures if both sides were found in equal number because right-sided structures are used in regression formulae. If two structures had the same MNI estimate, then selection was made on the structure with the larger regression determination coefficient, r^2 (OTO-W>OTO-L>QUAD>DENT>HYPO> INTER>ANGU>PHAR).

Geographical and temporal variation in sizes of prey consumed

All elements from the seven cranial structures in good or fair condition were used to compare size of pollock consumed by Steller sea lions in Southeast Alaska between regions (inside haul-outs versus outside rookeries), across years and across rookeries (with rookery data collected in June and July), and across months (with data collected from inside haul-outs). Biologically meaningful differences in FL of pollock were assessed by grouping corrected lengths into stage-class categories (juvenile or 1-year-old fish FL≤20 cm; adolescent 20<FL≤34 cm; subadult 34<FL≤45 cm; and adult FL>45 cm) (Smith, 1981; Walline, 1983; Dorn et al., 2001). Adults were considered to be mature fish ≥5 years old and targeted by fisheries (Smith, 1981). Subadults were likely 3 or 4 years old, of which only a proportion had matured or were targeted by the fishery. To avoid the possibility of pseudoreplication in our chi-squared comparisons, we used only the presence or absence of structures of each stage class in a scat because individual fish eaten by a sea lion may have come from an age-specific school and were therefore not independent (Hunt et al., 1996). Presence-absence data was chosen over MNI data because the former greatly reduces potential concerns regarding size-dependent recovery of cranial structures (Tollit et al., 1997). With the exception of our regional comparison, data from juvenile and adolescent stage-classes were pooled because of the low sample sizes of juvenile fish. A Fisher's exact test was used as an alternative test to chi-square comparisons when counts for a stage-class grouping were <5 (S-PLUS 2000, Mathsoft Inc., Seattle, WA).

Overlap of prey size with size of fish caught by fisheries

To assess the impact of using the new methods described and to compare the size of pollock consumed by sea lions with the size of pollock typically caught by fisheries, we obtained randomly subsampled size-frequency landing data from the Canadian commercial pollock fishery in Dixon Entrance (1993–1999) (Saunders[4]). This area is 115–135 km SE of the Forrester Island rookery on the southern border of Southeast Alaska (Fig. 1).

Results

Sizes of pollock consumed

The traditional method of estimating prey size from otoliths alone was not satisfactory because most otoliths were in poor condition (86%, n=247) or were broken lengthwise (>89%) (or were both broken and in poor condition). Cranial bones, on the other hand, occurred in higher numbers than otoliths and were therefore more useful for estimating prey size (Table 2).

Sixty-one percent of scats (1215 of 1987) collected from Southeast Alaska (1994–99) contained pollock remains, with an average MNI of 1.57 ±1.66 individual pollock per scat (range: 1–37 individuals). Many scats contained hard parts that were not useful for estimating prey size (e.g., gill rakers), leaving 531 scats (26%) with measurable selected structures. Of these, 303 scats contained 1746 elements in good (n=225), fair (n=684), and poor condition (n=837).

Applying digestion correction factors had a considerable effect on the estimated length and mass of fish consumed, and on the proportion that were deemed to be adults (Fig. 2). The estimated lengths of pollock calculated from all structures graded in good or fair condition (without accounting for digestion) was 34.4 ±9.7 cm (n=909, modal range: 32–40) (Table 2, Fig. 2). Lengths increased by 23% on average when appropriate DCFs were applied to each structure to account for the observed degree of digestion (mean FL=42.4 ±11.6 cm, modal range: 44–52, 95% CI=41.0–43.9) (paired t-test, t_{908}=67.1, P<0.001). A DCF of 1.0 (no correction required to account for digestion) was applied to 62 elements in good condition, resulting in a mean fork length of 39.6 ±11.9 cm estimated from those bones.

The size-frequency distribution of pollock consumed by sea lions also varied significantly following the application of DCFs (Kolmogorov-Smirnov, KS=176.2, P<0.001) and led to an increase in the proportion of fish thought to have been adult (>45 cm FL) from 16% to 44%. This result in turn reduced the proportion of fish thought to have been subadults (29%), adolescents (25%), and juveniles (<2%, ≤20 cm FL) (Fig. 2). The size range of pollock eaten ranged widely regardless of whether DCFs were applied (10–78 cm) or not (10–64 cm). When we calculated fork lengths using only elements selected according to MNI criteria, the means increased by just 0.5 cm for corrected and by just 0.3 cm for uncorrected lengths, with near identical standard deviations and distributions (Fig. 2) (Kolmogorov-Smirnov, uncorrected KS=0.33, P=0.89, corrected KS=0.032, P=0.91).

The use of all otoliths regardless of digestion state resulted in a mean fork length that was only about half of that derived by using all structures corrected for digestion (Table 2). Excluding otoliths in poor condition significantly reduced sample size (Table 2) but

[4] Saunders, M. 2002. Unpubl. data. Fisheries and Oceans Canada, 3190 Hammond Bay Road, Nanaimo, B.C., Canada, V9T 6N7.

Table 2

Estimated mean fork length (mean FL, cm) of walleye pollock consumed by Steller sea lions. Values were determined by using selected cranial structures with or without the application of condition-specific digestion correction factors (DCFs). Data sets exclude all structures graded in poor condition (with the exception of data sets marked with an asterisk). Fish element sample sizes (n_f) are given along with proportion of elements assigned condition category good (n^g). When DCFs were applied, 95% confidence intervals (95% CI) were estimated by using bootstrap resampling (see "Materials and methods").

Structure code	DCF	n	n^g	Mean FL	SD	Range	95% CI
INTE	No	37	0.35	44.0	8.0	28.0–54.5	—
	Yes	37	0.35	48.0	9.3	31.9–62.2	45.0–52.2
HYPO	No	47	0.19	35.3	8.9	19.0–52.0	—
	Yes	47	0.19	39.8	10.1	19.0–60.4	36.7–43.6
PHAR	No	20	0.25	38.1	8.5	20.4–50.3	—
	Yes	20	0.25	43.7	9.5	20.4–56.1	39.9–48.4
ANGU	No	207	0.16	34.0	10.2	10.0–62.8	—
	Yes	207	0.16	39.4	11.4	10.0–63.2	37.4–41.5
QUAD	No	238	0.36	33.1	10.4	14.0–63.8	—
	Yes	238	0.36	41.9	13.2	17.3–78.1	39.5–44.7
DENT	No	326	0.24	34.9	8.1	11.0–63.0	—
	Yes	326	0.24	45.1	9.8	14.7–75.3	43.3–46.8
OTOL	No	10	0.10	30.6	13.8	14.2–54.8	—
	Yes	10	0.10	36.6	17.6	16.7–67.2	27.0–51.1
OTOL or OTOW	No	34	0.03	27.2	16.1	10.8–54.8	—
	Yes	34	0.03	33.7	12.8	13.3–67.2	29.5–39.5
All structures	No	909	0.25	34.4	9.7	9.8–63.8	—
	Yes	909	0.25	42.4	11.6	10.0–78.1	41.0–43.9
OTOL*	No	27	0.04	23.3	11.9	7.9–54.8	—
OTOL or OTOW*	No	247	<0.01	20.2	9.7	5.0–58.0	—

increased our estimate of fork length by approximately 33%. Applying grade-specific DCFs increased these estimates by another 19% (to 36.6 cm) for otolith length and by 24% (to 33.7 cm) for a combination of otolith length and width (Table 2). All six remaining structures in good or fair condition provided larger corrected mean length estimates than did otoliths alone, but 95% confidence intervals derived from otoliths did overlap with other structures (Table 2). The smaller estimate provided by otoliths may reflect that >83% of grade corrected otoliths (n=34) came from the inside haulout sites, where animals seem to eat smaller fish (see following section). On the other hand, large pollock otoliths were observed to have been regurgitated in feeding studies on captive sea lions and also may be more easily crushed by rocks often found in the stomachs of Steller sea lions (Tollit et al., 2003). Regression formulae used in our study to predict pollock FL from otolith length were similar to those of Frost and Lowry (1981) for juvenile fish (<10 mm otolith length) but led to smaller fish size estimates (~1–1.7 cm) over the range of 30–50 cm.

The lengths of the biggest fish (corrected mean FL=48.0 cm) were estimated from measurements of INTE (Table 2), the structure with the lowest DCF. Dentary bones (the most abundant structure recovered) predicted mean (Table 2) and modes (FL 44–50 cm) similar to those predicted from all structures. Applying DCFs increased our length estimates by between 9% (INTE) and 29% (DENT) (paired t-tests, all P<0.001). Overall, corrected fork length estimates from elements in good condition were similar to those from elements in fair condition (Mann-Whitney U, P=0.47), but multiple comparisons indicated a significant difference (P<0.05) between condition categories for INTE and DENT (lengths were estimated to be longer from elements graded in fair condition).

Repeat measurements of individual elements were all within 0.04 mm of the mean, and 88.9–99.5% were within 0.02 mm. The highest variability was associated with ANGU, HYPO, and PHAR with 88.9%, 91.7%, and 94.9% of their respective measurements falling within 0.02 mm. A 0.02-mm measurement difference corresponded to only a 0.1–0.2 cm difference in fish length, depending on the structure used.

Small differences in estimates of fork lengths can have large effects on estimated body mass (given the exponential mass-length relationship, see Tollit et al., 2004, this issue) and can increase the mean mass of fish by more than sixfold depending on which method is used to estimate body length (all otoliths and no correction versus condition-corrected structures). The ap-

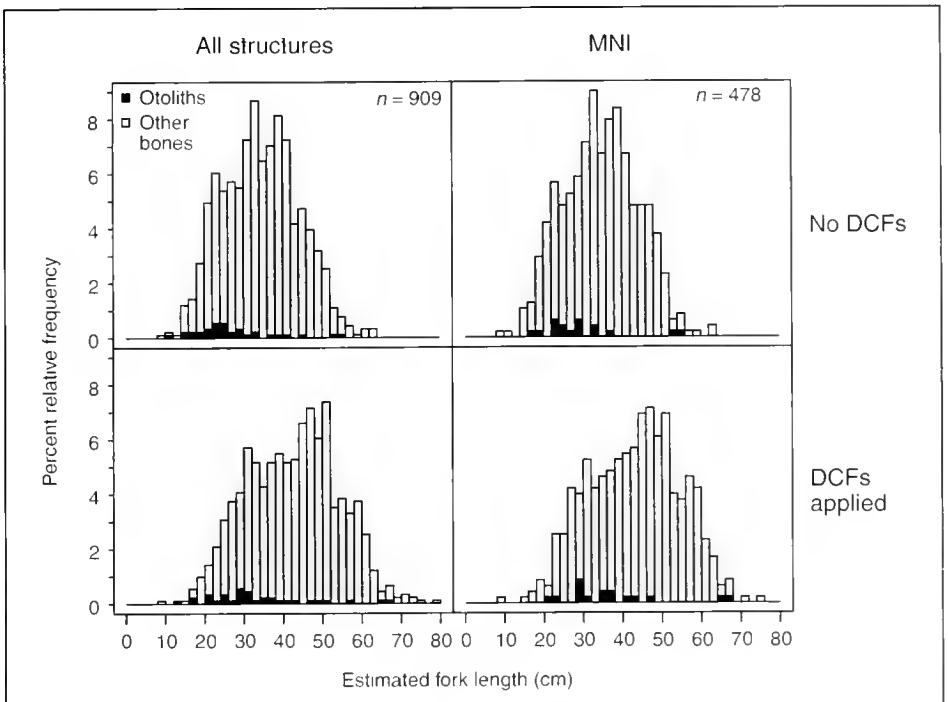

Figure 2

Relative frequency histograms of the estimated fork length of walleye pollock (*Theragra chalcogramma*) predicted from seven cranial structures in good and fair condition. Otoliths (black bars) are stacked beneath all other selected structures (gray bars). Comparisons were made with the application of digestion correction factors (DCFs) to take account of partial digestion and with the use of a selection technique (MNI) versus using all structures present in scats.

plication of our DCFs to all structures in good and fair condition increased the estimated mean mass of pollock consumed by 88% (from a mean of 388 g to 731 g). Thus, although we estimate that 44% of the number of pollock eaten by Steller sea lions were adults, based on length, their contribution, based on weight, increased to 74%. In contrast, the contribution of juvenile fish (in terms of mass) dropped to <0.1% (compared to <2% by number).

Geographical and temporal variation in sizes of pollock consumed

More pollock elements in good and fair condition were recovered from inside haul-outs (n=567) than from sites on the outside coastline (n=342) (Table 1). Upon investigation, we found the size of pollock consumed by Steller sea lions varied over time and across regions (Fig. 3). In particular, the frequency of occurrence of pollock stage classes differed significantly in the scats of sea lions resting at rookeries on the outside coastline of Southeast Alaska in summer (mean FL=48.4 cm, n=328, modal range: 44–50 cm, 95% CI=46.5–50.2, n_s=126 scats) compared to those collected between October and May at haul-outs in the waters of the inside passages (mean FL=38.4 cm, n=499, modal range: 30–34 cm, 95% CI=36.9–40.3, n_s=168 scats) (χ^2=45.2, P<0.001). Scats from these inside haul-outs contained a greater diversity of stage classes, and there was an equal probability of any given scat containing adults (51.2%), subadults (47.6%), and adolescents (53.0%), but a far less probability of containing juveniles (6.5%). In contrast, the pollock found in scats from the outside rookeries contained mostly adults (73.8%) and fewer occurrences of the remaining three stage classes (38.1%, 9.5%, and 3.2%, respectively). Notably, the stage-class comparison of summer 1999 with scats from inside versus outside waters was not significant (Fishers exact test, P=0.11).

Similar proportions of each pollock stage class were found in scats collected between years (Forrester, Fisher's exact test, P=0.54; Hazy, Fisher's exact test, P=0.16), and between rookeries (1994 only, Fisher's exact test, P=0.57; all years, Fisher's exact test, P=0.22). Scats from inside haul-outs collected in spring 1996 contained comparatively smaller fish than in other months and years examined (Fig. 3). However, there were no significant monthly differences in the proportions of age classes from October 1995 to February 1997 (χ^2=16.52, P=0.28) or when all monthly data (June and July 1999) were included from inside haul-outs (χ^2=23.4, P=0.10).

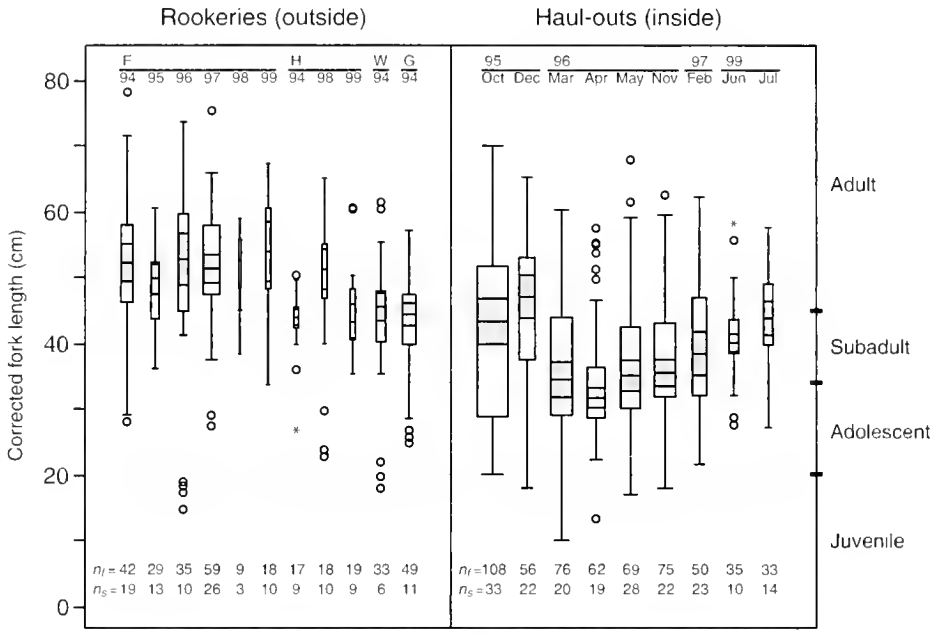

Figure 3

Box plots of corrected fork length of walleye pollock (*Theragra chalcogramma*) across months and years for haul-outs and rookeries in Southeast Alaska (Forrester Island, F; Hazy, H; White Sisters, W; Graves Rock, G). Box widths correspond to relative sample sizes for numbers of fish elements (n_f) and numbers of scats (n_s) are also provided, and stage-class categories are illustrated. Gray areas represent 95% confidence intervals, the whiskers bound 1.5× the interquartile range (boxes), the circles denote outliers, and the stars (*) denote extremes.

Overlap of size of pollock consumed by Steller sea lions with size of pollock caught by the fisheries

The Canadian commercial pollock trawl fishery in Dixon Entrance between 1993 and 1999 landed mostly (93%) adult fish (mean FL=52.2 ±5.9 cm, n=2103, modal range: 48–54 cm). The majority (79%) of scats containing pollock from the Forrester Island rookery in June and July also contained remains of adult pollock (mean corrected FL=51.4 ±10 cm, n=192, modal range: 46–52 cm, n_s=81 scats). Percentage overlap based on a comparison of size-frequency distributions totaled 75.1% for those fish eaten around Forrester Island and 52.1% for all fish eaten. However, the estimated overlap would have been assumed incorrectly to be half these values if DCFs had not been applied to the selected digested otoliths and bones (i.e., 36.7% overlap at Forrester and 24.1% for all areas combined). Clearly overlap levels would have been further underestimated if structures in poor condition had been included in our analyses.

Discussion

Only 57% of the scats (303 of 531) that contained suitable pollock remains had structures that were in good enough condition to be measured reliably. Numbers of elements in good or fair condition (n=909) averaged three per scat, and a very small fraction of these consisted of otoliths (<4%). The most numerous structures were DENT, QUAD, and ANGU (Table 1). This finding is inconsistent with feeding trials with captive Steller sea lions where otoliths were found to be the most commonly occurring structure (Cottrell and Trites, 2002; Tollit et al., 2003).

Different structures yielded somewhat different mean sizes of pollock, although 95% confidence intervals generally overlapped, ranging between 37 and 52 cm for bones (Table 2). Such discrepancy is not surprising given that different bones originate from different scats and possibly different fish (even within a single scat). Our comparison of estimates with all structures versus MNI selections indicates that the potential effect of double counting (and measuring) fish within a single scat is likely negligible with large sample sizes (Fig. 2). Although the use of all-structure data to estimate fish length results in a greatly increased sample size, there remains an underlying assumption that all structures are affected equally by digestion. Tollit et al. (2004, this issue) found no significant difference in the degree of erosion across the three size ranges (28.5–45.0 cm FL) for each structure within each condition category.

They also found that the relative shape, structure, and proportion of the morphological features used to estimate erosion were consistent for both smaller and larger fish. We therefore assumed that the DCFs in that study could be used reliably for the fish in our study outside of the experimental size range in which they were considered.

Applying DCFs increased mean fork length estimates by 23% (from 34.4 to 42.4 cm) on average and resulted in adult fish contributing 44% to the sea lion diet by number and 74% by mass. The contribution of juvenile fish was insignificant. Applying valid correction factors clearly provides better insights into prey-size selection and consequently niche overlap. It should also lead to more precise estimates of mass of prey consumed and the number of prey within a scat (Ringrose, 1993; Tollit et al., 1997; Laake et al., 2002).

Over 61 species of prey were identified in the diet of Steller sea lions in Southeast Alaska from 1993 to 1999 (Trites et al.[3]). The most common prey were walleye pollock, Pacific herring (*Clupea pallasi*), Pacific sand lance (*Ammodytes hexapterus*), salmon (*Oncorhynchus* spp.), arrowtooth flounder (*Reinhardtius stomias*), rockfish (*Sebastes* spp.), skates (*Raja* spp.), and cephalopods. During summer, gadids (most of which were pollock) made up 27% of the diet, and increased to 49–62% of the diet at other times of the year (Trites et al.[3]), confirming that pollock are a significant component of the diet.

Steller sea lions consumed a wide size range of pollock in Southeast Alaska; the bulk of fish fell between 20 and 60 cm and peaked between 44 and 52 cm (Fig. 2). The contribution of juvenile fish (≤20 cm) was insignificant. The only historical data to compare with these results are those from the stomach samples of eight Steller sea lions collected from Southeast Alaska in 1986 (Calkins and Goodwin[1]). Pollock lengths backcalculated from all otoliths found in the stomachs were generally shorter (mean FL=25.5 ±10.4 cm, range; 4.8–55.7cm, n=80) than our estimates from multiple structures found in scats collected during the 1990s (mean FL=42.4 ±11.6 cm, range: 10.0–78.1 cm, n=909). It should be noted that we derived our estimates after removing heavily eroded structures and applying DCFs, whereas Calkins and Goodwin[1] did not account for partial digestion. However our estimates of pollock length would have been similar to those of Calkins and Goodwin[1] if we had used only otoliths and had not corrected for digestion (Table 2). Although Frost and Lowry (1980) found no significant difference between the size of otoliths obtained from stomachs and intestines of ribbon seals, underestimates of fish size determined from otoliths from stomach samples will depend on the time since ingestion (i.e., on the extent of digestion).

One possible explanation for the virtual absence of juvenile pollock in the scats we examined is that the relatively smaller structures of smaller fish were more likely to be completely digested, and were therefore underrepresented in the scats (Tollit et al., 1997; Bowen, 2000). However, juvenile pollock otoliths and bones were found in large numbers in a number of scats collected from the western stock (Zeppelin et al., 2004, this issue). Clearly, the potential for underestimating smaller fish depends heavily on the balance between relative recovery rates and the number of different size fish consumed in a meal. For example, if an animal needs to eat 5 kg a day, then it would have to consume 195 15.5-cm pollock, but less than ten 41-cm pollock. Given that large pollock bones are at least three times more likely than small bones to pass through the digestive tract (Tollit et al., 2003; D. J. Tollit, unpubl. data), the sheer numbers of small pollock in this example would lead to a conclusion that smaller fish were more important numerically, when in fact they were equally important. Conversely, the relative proportion of large fish is likely to be overestimated if ten large and ten small pollock are consumed together. The generally low number of structures per scat provides little information to assess this balance. Hence we must assume that our results are representative and unbiased.

Steller sea lions in Southeast Alaska did not seem to eat fish over 65 cm. Whether or not sea lions do not target large fish, or whether large fish are harder to catch and handle, or are encountered at a lower rate is not known. However, large fish could be under-represented in scats if large fish cannot be swallowed whole, and head skeletal parts are lost while the fish is torn apart on the surface (Olesiuk et al., 1990; Wazenbock, 1995) or if bone regurgitation is size specific.

Regional, geographical, and temporal variation in sizes of pollock consumed

Stomach samples collected in 1975–78 and 1985–86 in the Gulf of Alaska contained substantial numbers of juvenile pollock, as well as larger fish (mode: 39–43 cm). In 1985, the distribution of sizes consumed by sea lions around Kodiak Island appeared to mimic that of the pollock population (Merrick and Calkins, 1996). However, juvenile sea lions ate significantly smaller and relatively more juvenile pollock than adult sea lions. Stomachs from the Gulf of Alaska contained an average of 49 pollock (1975–78) and 72 pollock (1985) compared with 1.6 pollock per scat in Southeast Alaska. In the Bering Sea, 90 stomachs were examined between 1975 and 1981 by using only non-eroded otoliths, and these also contained mainly (76%) juvenile pollock (mean FL=29.3 cm), but also some adult fish (Frost and Lowry, 1986).

Between 1998 and 2000, Steller sea lions across the range of the western population in Alaska consumed pollock averaging 39.3 ±14.3 cm (range: 3.7–70.8 cm, Zeppelin et al., 2004, this issue). This finding suggests that sea lions may have been less reliant on juvenile pollock than they were during the 1970s and 1980s. Apparent differences may reflect differences in pollock year-class strength, and thus differences in the dominant size classes that were available to be consumed. However, Zeppelin et al. (2004, this issue) reported that the size distribution of walleye pollock consumed by Steller sea lions between 1998 and 2000 did not appear to fluctuate with year-class strength, unlike the

sizes of Atka mackerel (*Pleurogrammus monopterygius*) consumed in western Alaska.

Comparing samples collected at rookeries from the eastern and western populations reveals that sea lions in the western stock ate significantly greater numbers of smaller pollock and fewer adults in summer than sea lions in Southeast Alaska (Zeppelin et al., 2004, this issue; and our study). However, both eastern and western stock sea lions using haul-outs in March (winter) ate similar size pollock. Adult pollock occurred more frequently in scats collected from rookeries along the open ocean coastline of Southeast Alaska during June and July (74% adults) than they did in scats from haul-outs located in inside waters between October and May (51% adults). Scats collected at rookeries can be considered to be from adult female sea lions and to a lesser extent from adult males, whereas those collected at haul-outs during other times of the year contain a more diverse mix of age groups, including greater numbers of younger sea lions. Thus it is uncertain whether observed size differences in pollock between these two groups are seasonal or due more to size preferences of different aged animals. Limited support for the former comes from the similar size pollock observed in the scats between the two groups in June and July of 1999. Overall, however, it is unknown whether the consumption patterns observed are a result of an actual size selection of prey or if they result from coincidental distributions of sea lions and prey-size classes. Some pinnipeds may select prey of particular sizes (Sinclair et al., 1994) and may encounter difficulties if they cannot switch to other sizes or species if the abundance of preferred prey is reduced. Fine-scale studies are now being undertaken to address such uncertainties.

There are few assessments of pollock stock size for the 1990s in Southeast Alaska (Martin, 1997). However the biomass is believed to have been low compared to other regions of Alaska. Juvenile pollock are known to congregate in the shallow inside waters of Southeast Alaska during winter (Sigler[5]) but are also known to occur in significant numbers in the summer in waters shallower than 200 meters on the outer coastline (Martin, 1997). Recruitment of 1-year-old fish was found to be high during acoustic studies in 1994 and 1999 in the Gulf of Alaska (Guttormsen et al., 2003).

Steller sea lions using rookeries in Southeast Alaska consumed mainly adult pollock between 1994 and 1999 and showed no evidence of tracking any abundant age class of pollock. However, the trend in increasing length estimates for inside haul-outs after 1995 (Fig. 3) does suggest that sea lions might be tracking a particular age class of prey. Certainly a greater range of age classes were consumed at these haul-outs (Fig. 3).

Scientific trawls in 1996 indicated that the larger pollock on the outside coastline occurred generally in waters 201–300 m deep during daylight hours (Martin, 1997) and that smaller pollock were present in shallower depths. Larger pollock tend to disperse and move to shallow waters to feed at night (Smith, 1981). Thus, the observed crepuscular and nighttime foraging by lactating Steller sea lions (Higgins et al., 1988; Trites and Porter, 2002) would be a logical foraging strategy to capture adult pollock. Other important factors, in addition to depth, that likely influence size selection include prey density and spatial distribution in relation to rookeries and haul-outs. Given both the greater mass and energy content of adults compared with juveniles (Perez, 1994; Anthony et al., 2000), the selection of adults would be an energy efficient strategy—all other things being equal.

Overlap in sizes of pollock consumed by Steller sea lions and sizes of pollock caught by fisheries

There was no commercial fishery for pollock in Southeast Alaska during the 1990s. However, a small fishery occurred in nearby Dixon Entrance, B.C., that might indicate sizes that could have been caught in Southeast Alaska if a fishery had occurred. Overlap in sizes of pollock caught by the B.C. fishery with those taken by Steller sea lions further north (our study) more than doubled after applying digestion correction factors (from 24% to 52%). Similarly, high levels of overlap were also found between the sizes of pollock consumed by the western stock (1998–2000) and those caught in the same region by fisheries (after our DCFs were applied to structures recovered from scats—Zeppelin et al., 2004, this issue). A high degree of overlap in size highlights a potential conflict between fisheries and sea lions, but this overlap cannot be considered indicative of competition unless the resource that fisheries and sea lions seek is limited across the space and time in question (Krebs and Davies, 1991).

Conclusions

Our study provides the first substantial description of the size of pollock eaten by Steller sea lions in Southeast Alaska. It also shows the benefits of using bones other than otoliths to estimate the sizes of prey eaten by Steller sea lions, and the importance of correcting for degree of digestion. Accurately reconstructing the sizes of bones and otoliths recovered from scats has a significant bearing, in turn, on accurately determining the mass of prey consumed, and on the extent of overlap of sizes of prey consumed and sizes of the same resource caught in commercial fisheries.

We found that Steller sea lions in Southeast Alaska consumed a large proportion of adult pollock and few juveniles between 1994 and 1999. Although greater proportions of juvenile and adolescent pollock were consumed over the same period, during the summer in the Gulf of Alaska and Bering Sea, larger size fish still were the most abundant prey item in the diet of sea lions. A comparison of these estimates with the lengths of pollock consumed during the 1970s and 1980s shows that

[5] Sigler, M. F. 2003. Unpubl. data. Auke Bay Lab, National Marine Fisheries Service, 11305 Glacier Highway, Juneau, AK 99801

Steller sea lions can consume a wide range of different size pollock (4–78 cm). Whether or not these differences in sizes of pollock consumed between regions and decades reflect differences in availability, size preferences, or year-class strength is not known and requires further study primarily with fine-scale data from scientific surveys and concurrent scat collections.

Acknowledgments

Funding was provided to the North Pacific Universities Marine Mammal Research Consortium by the National Oceanographic Atmospheric Administration and the North Pacific Marine Science Foundation. We would like to thank the contribution of personnel of the UBC Marine Mammal Research Unit, ADF&G, T. K. Zeppelin, K. A. Call, A. J. Winship, E. H. Sinclair, and two anonymous reviewers. We are also grateful to J. L. Laake and R. Joy for statistical advice.

Literature cited

Anthony, J. A., D. D. Roby, and K. R. Turco.
2000. Lipid content and energy density of forage fishes from the northern Gulf of Alaska. J. Exp. Mar. Biol. Ecol. 248:53–78.

Benson, A. J., and A. W. Trites.
2002. A review of the effects of regime shifts on the production domains in the eastern North Pacific Ocean. Fish and Fisheries 3:95–113.

Beverton, R. J. H.
1985. Analysis of marine mammal-fisheries interaction. *In* Marine mammals and fisheries (J. R. Beddington, R. J. H. Beverton, and D. M. Lavigne eds.), p. 3–33. George Allen & Unwin, Boston, MA.

Bowen, W. D.
2000. Reconstruction of pinniped diets: accounting for complete digestion of otoliths and cephalopod beaks. Can. J. Fish. Aquat. Sci. 57:898–905.

Browne, P., J. L. Laake, and R. L. DeLong.
2002. Improving pinniped diet analyses through identification of multiple skeletal structures in fecal samples. Fish. Bull. 100:423–433.

Calkins, D. G., D. C. McAllister, K. W. Pitcher, and G. W. Pendleton.
1999. Steller sea lion status and trend in Southeast Alaska: 1979–1977. Mar. Mamm. Sci. 15(2):462–477.

Cottrell, P. E., and A. W. Trites.
2002. Classifying prey hard part structures recovered from fecal remains of captive Steller sea lions (*Eumetopias jubatus*). Mar. Mamm. Sci. 18:525–539.

Dorn, M., A. Hollowed, E. Brown, B. Megrey, C. Wilson, and J. Blackburn.
2001. Assessment of the walleye pollock stock in the Gulf of Alaska. *In* Stock assessment and fishery evaluation report for the groundfish resources of the Gulf of Alaska, 90 p. Prepared by the Gulf of Alaska Groundfish Plan Team, North Pacific Fishery Management Council, W 4th Avenue, Suite 306, Anchorage, AK 99501.

Frost, K. J., and L. F. Lowry.
1980. Feeding of ribbon seals (*Phoca fasciata*) in the Bering Sea in spring. Can. J. Zool. 58:1601–1607.
1981. Trophic importance of some marine gadids in northern Alaska and their body-otolith size relationships. Fish. Bull. 79:187–192.
1986. Sizes of walleye pollock, *Theragra chalcogramma*, consumed by marine mammals in the Bering Sea. Fish. Bull. 84:192–197.

Guttormsen, M. A., C. D. Wilson, and S. Stienessen.
2003. Results of the February and March 2003 echo integration-trawl surveys of walleye pollock (*Theragra chalcogramma*) conducted in the gulf of Alaska, cruises MF2003-01 and MF2003-05. *In* Stock assessment and fishery evaluation report for the groundfish resources of the Gulf of Alaska, August 2003, 45 p. Prepared by the Gulf of Alaska Groundfish Plan Team, North Pacific Fishery Management Council, P.O. Box 103136, Anchorage, AK 99510.

Higgins, L. V., D. P. Costa, A. C. Huntley, and B. J. Le Boeuf.
1988. Behavioral and physiological measurements of maternal investment in the Steller sea lion, *Eumetopias jubatus*. Mar. Mamm. Sci. 4:44–58.

Hunt, G. L., Jr., A. S. Kitaysky, M. B. Decker, D. E. Dragoo, and A. M. Springer.
1996. Changes in the distribution and size of juvenile walleye pollock, *Theragra chalcogramma*, as indicated by seabird diets at the Pribilof Islands and by bottom trawl surveys in the Eastern Bering Sea, 1975 to 1993. *In* Ecology of juvenile walleye pollock, *Theragra chalcogramma*. Papers from the workshop "The importance of prerecruit walleye pollock to the Bering Sea and North Pacific ecosystems" Seattle, WA, October 28–30, 1993 (R. D. Brodeur, P. A. Livingston, T. R. Loughlin, and A. B. Hollowed, eds.), p. 125–139. NOAA Tech. Rep. NMFS 126. [NTIS no. PB97-155188.]

Krebs, J. R., and N. B. Davies.
1991. Behavioral ecology: an evolutionary approach, 3rd ed., 483 p. Blackwell Scientific, Boston, MA.

Laake, J. L., P. Browne, R. L. DeLong, and H. R. Huber.
2002. Pinniped diet composition: a comparison of estimation models. Fish. Bull. 100:434–477.

Loughlin, T. R., A. S. Perlov, and V. A. Vladimirov.
1992. Range-wide survey and estimation of total number of Steller sea lions in 1989. Mar. Mamm. Sci. 8:220–239.

Loughlin, T. R., and A. E. York.
2000. An accounting of the sources of Steller sea lion mortality. Mar. Fish. Rev. 62(4):40–45.

Martin, M. H.
1997. Data report: 1996 Gulf of Alaska bottom trawl survey. NOAA Tech. Memo. NMFS-AFSC-82, 235 p. [NTIS no. PB98-103930.]

Merrick, R. L., R. Brown, D. G. Calkins, and T. R. Loughlin.
1995. A comparison of Steller sea lion, *Eumetopias jubatus*, pup masses between rookeries with increasing and decreasing populations. Fish. Bull. 93(4):753–758.

Merrick, R. L., and D. G. Calkins.
1996. Importance of juvenile walleye pollock, *Theragra chalcogramma*, in the diet of Gulf of Alaska Steller sea lions, *Eumetopias jubatus*. *In* Ecology of juvenile walleye pollock, *Theragra chalcogramma*. Papers from the workshop "The importance of prerecruit walleye pollock to the Bering Sea and North Pacific ecosystems" Seattle, WA, October 28–30, 1993 (R. D. Brodeur, P. A. Livingston, T. R. Loughlin, and A. B. Hollowed, eds.), p. 153–166. NOAA Tech. Rep. NMFS 126. [NTIS no. PB97-155188.]

Milette, L. L., and A.W. Trites.
2003. Maternal attendance patterns of Steller sea lions (*Eumetopias jubatus*) from stable and declining populations in Alaska. Can. J. Zool. 81: 340–348.

NRC (National Research Council)
2003. Decline of the Steller sea lion in Alaskan waters: untangling food webs and fishing nets, 204 p. Prepared by the Committee on the Alaska Groundfish Fishery and Steller sea lions. National Academies Press, Washington, DC.

Olesiuk, P. F., M. A. Bigg, G. M. Ellis, S. J. Crockford, and R. J. Wigen.
1990. An assessment of the feeding habits of harbour seals (*Phoca vitulina*) in the Strait of Georgia, British Columbia based on scat analysis. Can. Tech. Rep. Fish. Aquat. Sci. 1730, 135 p.

Perez, M. A.
1994. Calorimetry measurements of energy value of some Alaskan fishes and squids. NOAA Tech. Memo. NMFS-AFSC-32, 32 p. [NTIS no. PB94-152907.]

Pitcher, K. W.
1981. Prey of the Steller sea lion, *Eumetopias jubatus*, in the Gulf of Alaska. Fish. Bull. 79:467–472.

Ringrose, T. J.
1993. Bone counts and statistics: a critique. J. Archaeol. Sci. 20:121–157.

Sease, J. L., W. P. Taylor, T. R. Loughlin, and K. W. Pitcher.
2001. Aerial and land-based surveys of Steller sea lions (*Eumetopias jubatus*) in Alaska, June and July 1999 and 2000. NOAA Tech. Mem. NMFS-ASFC-122, 52 p.

Sinclair, E. H., T. Loughlin, and W. Pearcy.
1994. Prey selection by northern fur seals (*Callorhinus ursinus*) in the eastern Bering Sea. Fish. Bull. 92: 144–156.

Smith, G. B.
1981. The biology of walleye pollock. *In* The eastern Bering Sea Shelf: oceanography and resources (D. W. Hood and J. A. Calder eds.), vol. 1, p. 527–551. Univ. Washington Press, Seattle, WA.

Tollit, D. J., S. G. Heaslip, T. K. Zeppelin, R. Joy, K. A. Call, and A. W. Trites.
2004. A method to improve size estimates of walleye pollock (*Theragra chalcogramma*) and Atka mackerel (*Pleurogrammus monopterygius*) consumed by pinnipeds: digestion correction factors applied to bones and otoliths recovered in scats. Fish. Bull. 102:498–508.

Tollit, D. J., M. J. Steward, P. M. Thompson, G. J. Pierce, M. B. Santos, and S. Hughes.
1997. Species and size differences in the digestion of otoliths and beaks: implications for estimates of pinniped diet composition. Can. J. Fish. Aquat. Sci. 54:105–119.

Tollit, D. J., M. Wong, A. J. Winship, D. A. S. Rosen, and A. W. Trites.
2003. Quantifying errors associated with using prey skeletal structures from fecal samples to determine the diet of the Steller sea lion (*Eumetopias jubatus*). Mar. Mamm. Sci. 19(4):724–744.

Trites, A. W., and L. P. Donnelly.
2003. The decline of Steller sea lions in Alaska: a review of the nutritional stress hypothesis. Mamm. Rev. 33:3–28.

Trites, A. W., and P. A. Larkin.
1996. Changes in the abundance of Steller sea lions (*Eumetopias jubatus*) in Alaska from 1956 to 1992: how many were there? Aquat. Mamm. 22:153–166.

Trites, A. W., and B. T. Porter.
2002. Attendance patterns of Steller sea lions (*Eumetopias jubatus*) and their young during winter. J. Zool. (Lond.) 256:547–556.

Walline, P. D.
1983. Growth of larval and juvenile walleye pollock related to year-class strength. Ph.D. diss., 144 p. Univ. Washington, Seattle, WA.

Wazenbock, J.
1995. Changing handling times during feeding and consequences for prey size selection of 0+ zooplanktivorous fish. Oecologia (Heidelb.) 104:372–586.

Zeppelin, T. K., D. J. Tollit, K. A. Call, T. J. Orchard, and C. J. Gudmundson.
2004. Sizes of walleye pollock (*Theragra chalcogramma*) and Atka mackerel (*Pleurogrammus monopterygius*) consumed by the western stock of Steller sea lions (*Eumetopias jubatus*) in Alaska from 1998 to 2000. Fish. Bull. 102:509–521.

Multidirectional movements of sportfish species between an estuarine no-take zone and surrounding waters of the Indian River Lagoon, Florida

Derek M. Tremain
Christopher W. Harnden
Douglas H. Adams
Florida Fish and Wildlife Conservation Commission
Florida Marine Research Institute
1220 Prospect Avenue, Suite 285
Melbourne, Florida 32901
Email Derek.Tremain@fwc.state.fl.us

Abstract—We examined movement patterns of sportfish that were tagged in the northern Indian River Lagoon, Florida, between 1990 and 1999 to assess the degree of fish exchange between an estuarine no-take zone (NTZ) and surrounding waters. The tagged fish were from seven species: red drum (*Sciaenops ocellatus*); black drum (*Pogonias cromis*); sheepshead (*Archosargus probatocephalus*); common snook (*Centropomus undecimalis*); spotted seatrout (*Cynoscion nebulosus*); bull shark (*Carcharhinus leucas*); and crevalle jack (*Caranx hippos*). A total of 403 tagged fish were recaptured during the study period, including 65 individuals that emigrated from the NTZ and 16 individuals that immigrated into the NTZ from surrounding waters of the lagoon. Migration distances between the original tagging location and the sites where emigrating fish were recaptured were from 0 to 150 km, and these migration distances appeared to be influenced by the proximity of the NTZ to spawning areas or other habitats that are important to specific life-history stages of individual species. Fish that immigrated into the NTZ moved distances ranging from approximately 10 to 75 km. Recapture rates for sportfish species that migrated across the NTZ boundary suggested that more individuals may move into the protected habitats than move out. These data demonstrated that although this estuarine no-take reserve can protect species from fishing, it may also serve to extract exploitable individuals from surrounding fisheries; therefore, if the no-take reserve does function to replenish surrounding fisheries, then increased egg production and larval export may be more important mechanisms of replenishment than the spillover of excess adults from the reserve into fishable areas.

Manuscript submitted 12 May 2003 to Scientific Editor's Office.
Manuscript approved for publication 20 January 2004 by the Scientific Editor.
Fish. Bull 102:533–544 (2004).

Fishery reserves or no-take sanctuaries, defined as areas where all fishing activities are prohibited, are increasingly proposed as an additional measure to traditional fishery management practices for protecting fish populations from overexploitation (PDT, 1990; Bohnsack and Ault, 1996). The American Fisheries Society recently issued a policy statement on the protection of marine fish stocks at risk of extinction and supported the development of large marine reserves to protect and rebuild vulnerable populations (Musick et al., 2000). Although reserves have been established primarily in reef or coastal marine habitats, the potential to apply similar management strategies in estuarine systems may also be possible (Johnson et al., 1999; Roberts et al., 2001).

Reserves in estuarine areas may help protect exploitable fishery species. Increases in species' sizes and densities within these reserves may also enhance adjacent fisheries by two separate mechanisms. Johnson et al. (1999) found that an existing estuarine no-take sanctuary on Florida's central east coast protected populations of larger, spawning-age sportfish species. As a result, they suggested that protection of populations in no-take sanctuaries could also lead to the replenishment of surrounding fisheries through increased egg production, larval export, and juvenile recruitment. Additionally, mark-recapture data have demonstrated that large juvenile and adult fishes emigrate from estuarine protected areas to surrounding waters (Bryant et al., 1989; Funicelli et al., 1989; Johnson et al., 1999; Roberts et al., 2001; Stevens and Sulak, 2001) and these data have been used to suggest that spillover of excess adult fish from estuarine reserve areas can directly supplement nearby fisheries. Roberts et al. (2001) concluded that the abundance of International Game Fish Association based on line-class-record catches in the vicinity of the estuarine no-take sanctuary on Florida's east coast resulted indirectly from protection and spillover of large adults to outlying waters.

It has also been suggested that reserves protect areas of undisturbed habitat (PDT, 1990), either by design or through cessation of destructive practices, and reserves are commonly established in areas of pristine, productive, or otherwise important habitats required by the species being protected (e.g., Russ, 1985). Furthermore, studies have shown that protecting fishery species can indirectly change the overall community structure (Cole and Keuskamp, 1998) and, under certain circumstances, can increase primary and secondary productivity (Sala and Zabala, 1996; Babcock et al., 1999). The influence of habitat quality on fish movements in relation to protected areas has not been investigated; however, reserve habitats that offer potential advantages in the form of improved habitat quality (Chapman and Kramer, 1999)

or increased food and habitat availability could be expected to attract, or at least retain, individuals that immigrate to the reserves from surrounding unprotected habitats. Reserve areas that attract and retain exploitable individuals from surrounding habitats at higher rates than they replenish the surrounding habitats could be considered to be sinks in terms of their ability to directly supplement adjacent fisheries through spillover of exploitable-size individuals. Fish emigration from reserve habitats and the replenishment of nearby fisheries is a commonly predicted benefit of harvest reserves (see reviews in Roberts and Polunin, 1991, and Rowley, 1994). However, there are currently no studies that simultaneously examine emigration and immigration in relation to estuarine reserves or that document the extent to which reserve areas may also function to withdraw individuals from surrounding fisheries. Without an assessment of net exchange, the interpretation of reserve benefits with respect to replenishment cannot be properly evaluated.

The National Aeronautics and Space Administration (NASA) closed a portion of the Indian River Lagoon at the Merritt Island National Wildlife Refuge (MINWR) on Florida's east coast for security purposes in 1962. A direct result of this closure was the effective creation of an estuarine no-take zone that remains to the present time. The proximity of this no-take zone to productive estuarine fisheries provided an opportunity to examine sportfish movements in the area with mark-recapture methods. Johnson et al. (1999) first documented sportfish migrations out of this no-take sanctuary, and in a related study, Stevens and Sulak (2001) provided more complete descriptions of movement patterns of individual species; each of these studies provided evidence that the restricted habitats protected fish populations and that adult sportfish egressed into surrounding waters open to fishing. However, because all tagged fish originated from within restricted habitats, in neither of these studies was it possible to consider the potential for the movements of fish into protected areas from surrounding waters. Therefore, we (sponsored by the Florida Fish and Wildlife Conservation Commission-Florida Marine Research Institute [hereafter referred to as FMRI] Fisheries-Independent Monitoring Program) tagged fish species throughout the northern Indian River Lagoon system, including both the MINWR no-take zone and the surrounding lagoon waters, from 1990 to 1999. We investigated the relationship between sportfish egress and ingress in relation to the MINWR no-take zone and offer a quantitative foundation for the discussion of net fish movements into or away from protected estuarine habitats.

Materials and methods

Study area

The Indian River Lagoon (IRL) is a shallow barrier island estuarine system spanning 253 km along the central east coast of Florida between Ponce de Leon Inlet in Volusia County and Jupiter Inlet in Palm Beach County. The lagoon is composed of three relatively isolated basins: Mosquito Lagoon, the Indian River proper, and the Banana River (Fig. 1). These three basins maintain hydrological connections with each other through narrow man-made channels at Haulover Canal and the Merritt Island Barge Canal (shown on Fig. 2) and through a natural channel at the southern end of the Banana River. Hydrodynamic exchange and fish passage between the lagoon and the Atlantic Ocean occur primarily through five inlets, which are concentrated in the southern half of the system. The hydraulic lock system located at Port Canaveral provides only an intermittent opportunity for exchange between the IRL and Atlantic Ocean. Gilmore et al. (1981) and Mulligan and Snelson (1983) have provided detailed descriptions of the lagoon and its habitats.

The no-take zone (NTZ) created by NASA and MINWR is located at the northern terminus of the Banana River basin of the lagoon. An earthen causeway defines the southern boundary of this no-access security area and contains only two openings that permit fish to migrate to and from adjacent waters. Much of the natural shoreline and saltmarsh habitats in the lagoon have been altered for mosquito control purposes. However, actual shoreline habitats surrounding MINWR—including the NTZ, the northern Banana River basin, the northern Indian River basin, and Mosquito Lagoon—remain relatively undeveloped in comparison to the urban shoreline development in the southern IRL. Detailed descriptions of the habitat composition within the NTZ and surrounding study area were provided by Johnson et al. (1999).

Data collection

Fish were tagged as part of several related FMRI projects (stratified-random, fixed-station, and directed sampling designs) in the northern IRL between 1990 and 1999 (FMRI[1]). In most cases, tagging was conducted opportunistically on healthy fish following capture in multipanel monofilament gill nets, nylon trammel nets, nylon haul seines, or on hook and line. In other cases, projects were designed specifically to assess tag-recapture information (Murphy et al., 1998). Because of the focus of our sampling programs in this area, the majority of our tagging efforts occurred north of Sebastian Inlet within the Indian and Banana River basins of the lagoon. A small percentage of tags were placed in fish captured south of Sebastian Inlet or in Mosquito Lagoon. Overall, our sampling collections in the NTZ

[1] FMRI (Florida Fish and Wildlife Conservation Commission). 1999. Florida Marine Research Institute, Fisheries-independent monitoring program, 1999 annual data summary report. In-house Report, Florida Fish and Wildlife Conservation Commission, Florida Marine Research Institute, 100 Eighth Ave. S.E., St. Petersburg, Florida, 33701.

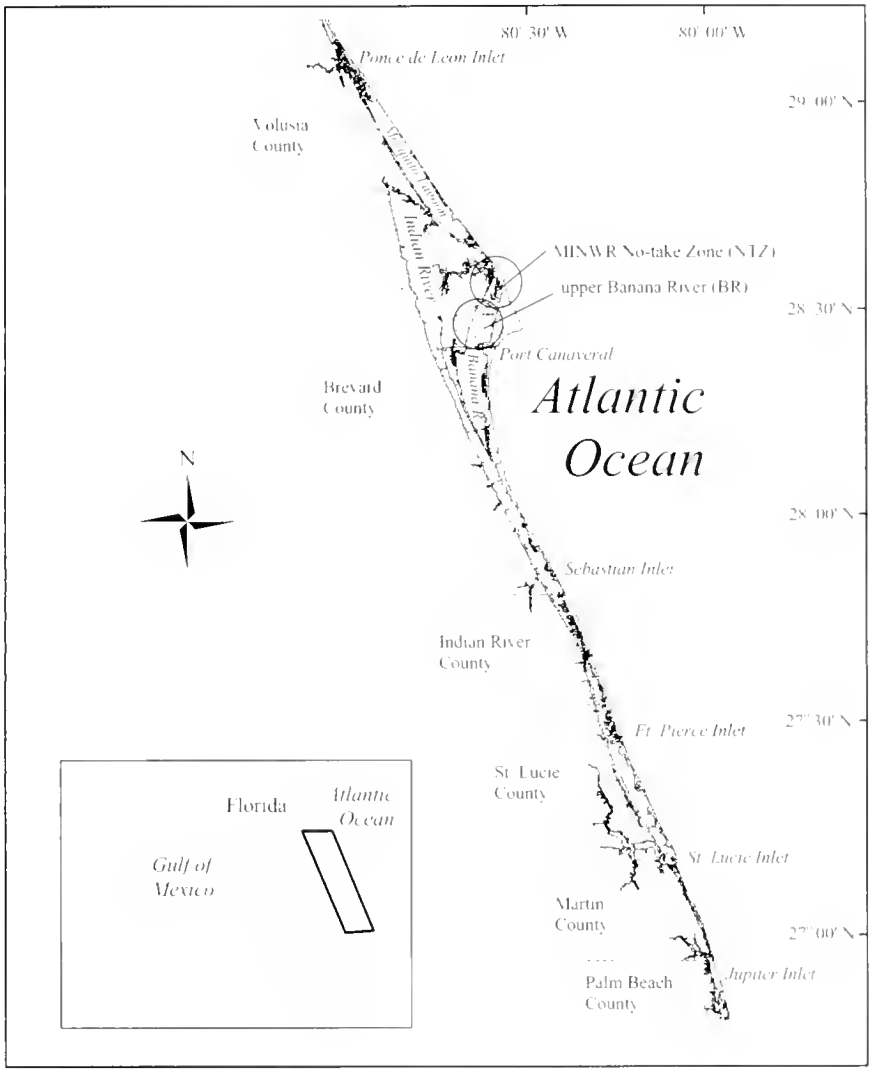

Figure 1

Map of Florida and the Indian River Lagoon study area.

accounted for approximately 20% of our total sampling efforts and averaged approximately 1–2 days/month over the study period.

Fish were tagged by inserting 50-mm, 70-mm, or 100-mm Hallprint dart tags (Halprint Ltd., Victor Harbor, South Australia) into the dorsal musculature; the plastic dart was lodged beneath the pterygiophores of the dorsal fin. Each tag contained a visible external streamer with a unique alphanumeric code and instructions for anglers to contact us with recapture information in order to collect a reward (five dollars or equivalent). Information recorded at the time of initial tagging included the tag number, species tagged, date, location (latitude and longitude), and fish length (standard, fork, and total lengths as appropriate for the species). Recapture information on tagged fish was collected through August 2000 from angler reports and from fish recaptured during FMRI sampling activities. Because of public-access prohibitions, recapture information from inside the MINWR NTZ was gathered exclusively through FMRI sampling efforts. Data requested for recaptured fish included the same information as that recorded at initial tagging; however, in several cases, length or precise location information returned from anglers was considered to be unreliable, which prevented accurate statistical comparisons of relationships involving recapture lengths or distances traveled. Therefore, reported length data are limited to initial tagging information only (total length; TL). To prevent problems with pseudoreplication for individuals recaptured on multiple occasions, we included only the initial tag recovery data in our calculations of recapture percentages.

Overall patterns of fish migrations, including general recapture locations and direction of movements into or away from the NTZ, were described by using data

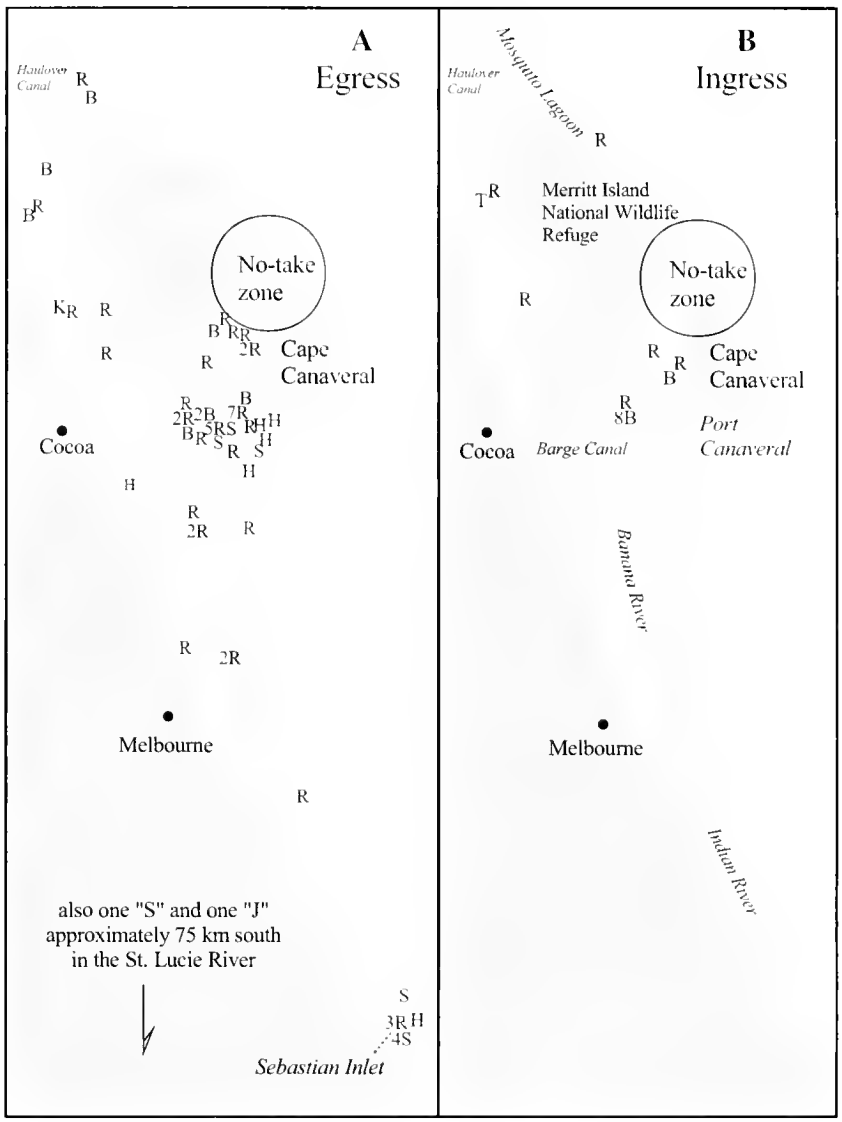

Figure 2

(**A**) Recapture locations of tagged fish that migrated out of the Merritt Island National Wildlife Refuge no-take zone. (**B**) Original tagging locations of fish that migrated into the Merritt Island National Wildlife Refuge no-take zone. R = red drum, B = black drum, S = common snook, H = sheepshead, T = spotted seatrout, J = crevalle jack, K = bull shark. Numbers before species codes (letters) indicate the number of individuals of that species that were captured at that location.

from all available recapture sources. In contrast, we calculated migration rates exclusively from the recapture data collected during FMRI sampling activities. Although this procedure excluded tag-return data from recreational anglers, it permitted a quantitative assessment of recapture rates based on standardized FMRI collection gear, comparable sampling effort, and 100% tag reporting rates. We resolved potential problems related to differences in habitat characteristics and sampling intensity by including only data from the NTZ and a fishable area of a similar size and habitat type in the adjacent Banana River (BR, Fig. 1). This BR zone corresponded precisely to the sampling zone used for population comparisons in Johnson et al. (1999), denoted as "FBR" (fished Banana River) in that study. Species that did not contribute any FMRI recapture information in either of these two areas were excluded from our analyses. Tag recovery and migration rates were calculated separately for the NTZ and BR. For our purposes, "migration" was defined as a directional fish movement across the NTZ boundary from the original tagging location, and we made the assumption that the migration patterns of recaptured fish represented the migration patterns of the overall population. Rela-

Table 1

Summary of tagging and recapture data for seven of the most common sportfish species tagged by FMRI scientists in the northern Indian River Lagoon study area. Locations where tag and recapture data were collected are separated into the no-take zone (NTZ) and the surrounding waters of the Indian River Lagoon (IRL).

	No-take zone			Indian River Lagoon				
		Recapture location			Recapture location			
Species	Tagged inside NTZ	NTZ	IRL	Tagged outside NTZ	NTZ	IRL	Total no. of fish tagged	Total no. recaptured and percent recaptured
Bull shark (*Carcharhinus leucas*)	1		1	24		1	25	2 (8.0)
Common snook (*Centropomus undecimalis*)	104	1	9	406		32	510	42 (8.2)
Crevalle jack (*Caranx hippos*)	55		1	59		1	114	2 (1.8)
Sheepshead (*Archosargus probatocephalus*)	597		6	520		26	1117	32 (2.9)
Spotted seatrout (*Cynoscion nebulosus*)	193	2		171	1	3	364	6 (1.6)
Black drum (*Pogonias cromis*)	637	4	8	831	9	32	1468	53 (3.6)
Red drum (*Sciaenops ocellatus*)	720	30	40	1344	6	190	2064	266 (12.9)
Total	2307	37	65	3355	16	285	5662	403 (7.1)

tive migration rates were calculated as the percentage of recaptured fish that migrated from their original tagging location. These migration rates and their reciprocal (retention rates) were compared between the NTZ and the BR to determine the relative potential for sportfish movements into or away from protected habitats. Chi-square contingency tests for frequency data (with Yates's correction for small sample sizes) were used to test the hypothesis that recapture location was independent of the tagging location.

Results

A total of 5951 fish of 27 species were tagged during FMRI sampling within the IRL between September 1990 and December 1999. However, because 95% of these fish were represented by only seven species (Table 1), which included all fish that migrated across the reserve boundaries, only these seven species were considered further in our analyses. Red drum (*Sciaenops ocellatus*) was the most commonly tagged species (n=2064), followed by black drum (*Pogonias cromis*, n=1468), sheepshead (*Archosargus probatocephalus*, n=1117), common snook, (*Centropomus undecimalis*, n=510), spotted seatrout (*Cynoscion nebulosus*, n=364), crevalle jack (*Caranx hippos*, n=114), and bull shark (*Carcharhinus leucas*, n=25). Approximately 41% (n=2307) of these fish were tagged inside the boundaries of the NTZ. The remainder (n=3355) were tagged in the surrounding lagoon. Through August 2000, 403 tagged fish (7.1% of total) were recaptured and reported either by FMRI staff sampling in the lagoon or by the public. Overall recapture rates were highest for red drum (12.9%), followed by those for common snook (8.2%), bull shark, (8.0%), black drum (3.6%), and sheepshead (3.0%).

Tagged fish were generally representative of the larger mobile members of the species and encompassed the legally exploitable size ranges for species with management restrictions (Table 2). For species except the bull shark and red drum, mean lengths of fish tagged inside the NTZ exceeded those of fish tagged outside the NTZ.

Approximately 25% (n=102) of the 403 total recaptured fish were fish originally tagged inside the NTZ (Table 1). Thirty-seven of these fish were also recovered inside the NTZ, including three red drum that were subsequently recaptured on multiple occasions in the protected area. The remaining 65 recaptured fish were caught after emigrating to outlying waters, including one red drum that was recaptured a second time outside the NTZ. Species that migrated out of the NTZ were red drum (n=40, mean TL=643 mm, SD=135 mm), common snook (n=9, mean TL=570 mm, SD=97 mm), black drum (n=8, mean TL=845 mm, SD=88 mm), sheepshead (n=6, mean TL=398 mm, SD=38 mm), bull shark (n=1, TL=789 mm), and crevalle jack (n=1, TL=628 mm). Recapture distances ranged from 0 km immediately outside the NTZ to approximately 150 km south in the St. Lucie River estuary, but recaptured fish were more abundant closer to the NTZ (Fig. 2A). Most of the recaptured fish were concentrated in areas of high fishing pressure, such as causeways, inlets, and waters near the boundary of the NTZ. Collectively, fish that emigrated from the NTZ did not appear to show a bias for any one direction of movement: recaptured fish were found both northward in the Indian River and southward throughout both the Indian River and Banana River basins of the lagoon. For individual species, red drum that emigrated were distributed throughout the lagoon system and coastal habitats, whereas black drum were predominantly recaptured in the northern

Table 2

Total length (TL) size ranges (in mm) and legal size limits (as of August 2000) for tagged sportfish species from the no-take zone and the outlying Indian River Lagoon study area.

	No-take zone			Indian River Lagoon			Legal size limits
Species	Mean (SD)	min	max	Mean (SD)	min	max	(mm TL)
Bull shark	789 (—)	789	789	974 (135)	684	1180	None
Common snook	570 (106)	330	844	506 (138)	227	944	660–864 (+ 1 over)
Crevalle jack	486 (140)	305	720	443 (113)	264	720	None
Sheepshead	398 (68)	235	614	365 (76)	171	594	305 minimum
Spotted seatrout	415 (129)	185	754	335 (111)	212	678	381–508 (+ 1 over)
Black drum	786 (129)	249	1156	742 (240)	225	1135	356–610 (+1 over)
Red drum	613 (166)	308	1245	624 (229)	203	1210	457–686

estuarine portion of the study area. Sheepshead and common snook were recaptured primarily to the south at inlets or in the adjacent Atlantic coastal waters outside the lagoon.

The remaining 75% (n=301) of the total recaptured fish were from fish originally tagged outside the NTZ (Table 1). The majority of these (n=285) were also recovered in outlying waters, including 16 red drum and 1 sheepshead that were subsequently recaptured on multiple occasions. Sixteen fish were recaptured after they had immigrated into the reserve. These recaptured fish were from three sciaenid species: predominantly black drum (n=9, mean TL=907 mm, SD=66 mm) and red drum (n=6, mean TL=656 mm, SD=170 mm), but also one spotted seatrout (TL=420 mm)(Fig. 2B). The longest migration distances into the NTZ were up to 75 km for red drum and spotted seatrout tagged in southern Mosquito Lagoon and the northern Indian River basins. All black drum that immigrated into the NTZ were tagged in the adjacent Banana River basin.

A relatively large number of red drum, common snook, and sheepshead that were tagged inside the NTZ or in the outlying waters were recaptured in close proximity (0 to 2.75 km distance) to inlet habitats. Recaptured red drum from inlet habitats (n=45, mean TL=647 mm, SD=135 mm) peaked during September through November. Recaptured common snook from inlet habitats (n=13, mean TL=598 mm, SD=111 mm) were distributed throughout much of the year but peaked in late fall. Few common snook were recaptured from inlet spawning habitats during the peak summer spawning months (June–August) when their fishery was closed. Recaptured sheepshead from inlet habitats (n=8, mean TL=373 mm, SD=53 mm) were concentrated in the winter and early spring.

Estimated migration rates were calculated by using only those fish that were tagged and recovered from FMRI sampling in the NTZ and the immediately adjacent upper Banana River (BR). The number of fish tagged in the NTZ (n=1654) was approximately 1.7 times the number tagged in the BR (n=965) (Table 3); however, the overall recapture rates of fish that were originally tagged in each of these two areas were equal (2.4%). Black drum and red drum made up the majority of tagged and recaptured fish in both areas and were the only species recaptured that had migrated both into and away from the NTZ in this comparison. For total sportfish (all species pooled), there was a significant relationship between the tagging location and the direction of fish movements ($\chi^2_{1,\,0.05}$=13.8, P=0.0002). A total of 40 fish originating from the NTZ were recaptured, but that number included only 2 fish (one red drum and one black drum) that emigrated to the BR (5% overall migration rate). In contrast, 23 fish originating in the BR were recaptured overall, including 12 that immigrated into the NTZ (52% overall migration rate). Species-specific migration rates were highest for black drum, and relative immigration rates (90%) were higher than emigration rates (25%). For this species, the frequency of immigration and emigration were statistically independent of tagging location ($\chi^2_{1,\,0.05}$=0.01, P=0.9039), which is probably due to the low number of recaptures of fish tagged inside the NTZ (Table 3). For red drum, relative immigration rates (27%) were also higher than emigration rates (3%), but in this case, there was a significant relationship between fish movements and tagging location ($\chi^2_{1,\,0.05}$=20.58, P<0.0001). Common snook, spotted seatrout, and sheepshead were also recaptured by FMRI scientists in these comparisons, but none of these recaptured fish represented evidence of migrations across the NTZ boundary from their original tagging location.

Discussion

This study demonstrated both the emigration and immigration of sportfish species across the boundaries of an estuarine no-take zone (NTZ). Legal-size large juveniles and adults of six of the recreationally valuable species tagged within NTZ boundaries—red drum, black drum, common snook, sheepshead, bull shark, and crevalle

Table 3

Summary of tag and recapture data from only the Florida Marine Research Institute sampling efforts in the no-take zone (NTZ) and the adjacent fished waters of the Banana River (BR). Species that did not contribute any recapture information were not included in calculations of totals or of migration percentages.

	No-take zone					Banana River				
	No. of fish tagged	No. fish recaptured			Percent that migrated	No. of fish tagged	No. fish recaptured			Percent that migrated
		NTZ	BR	Total			NTZ	BR	Total	
Red drum	720	32	1	33	3.3	176	3	8	11	27.3
Black drum	637	3	1	4	25.0	495	9	1	10	90.0
Common snook	104	1	0	1	0	62	0	1	1	0.0
Spotted seatrout	193	2	0	2	0	121	0	0	0	—
Sheepshead	597	0	0	0	—	232	0	1	1	0.0
Totals	1654	38	2	40	5.0	965	12	11	23	52.2
Tag recovery (%)				2.4					2.4	

jack—were documented to migrate out of the protected area. Johnson et al. (1999) and Stevens and Sulak (2001) also observed many of these same species emigrating from no-take zones within the same refuge system during the late 1980s, although the species with the highest recapture rates in their studies (common snook) differed from the current study (red drum). This difference may reflect an increase in the popularity of the red drum fishery on Florida's east coast during the current study period. Since 1989, when the recreational red drum fishery reopened under strict management regulations, there has been a significant increase in both the total red drum landings on the Atlantic coast and in the estimated number of fishing trips made by anglers seeking or catching red drum each year (Murphy[2]). Tagging studies in estuarine areas of the Everglades National Park have previously documented emigrations of striped mullet (*Mugil cephalus*), gray snapper (*Lutjanus griseus*), and spotted seatrout away from protected habitats (Bryant et al., 1989; Funicelli et al., 1989). Recent studies suggest that fish moving out of protected areas in the IRL may help to replenish nearby fisheries and may contribute to trophy fisheries in the surrounding system (Johnson et al., 1999; Roberts et al., 2001).

In our study, overall emigration rates were low, but many of the fish that emigrated from the estuarine NTZ moved comparatively large distances. The egress patterns of exploitable species may affect both the species' potential for protection and the degree to which fisheries located adjacent to protected reserves will be enhanced (DeMartini, 1993). In coastal marine and tropical reef systems, where the large majority of reserves have been established, long-distance movements greater than a few kilometers by demersal fishery species are limited to a very small percentage of individuals (Beaumariage, 1969; PDT, 1990 and references therein; Rowley, 1994), and the direct supplementation of nearby fisheries by exploitable species appears to be highly localized (Buxton and Allen, 1989; Russ and Alcala, 1996). The majority of fish that emigrated from the NTZ were recaptured between 10 and 75 km from the boundary, but fish were also recovered as far as 150 km from the NTZ boundary. Our observations on migration distances and recapture locations corresponded well with those reported from previous studies of fish movements out of this same reserve system (Johnson et al., 1999; Stevens and Sulak, 2001), although maximum recapture distances in earlier studies were even greater.

Many of the fish that emigrated from the NTZ—such as red drum, common snook, and sheepshead—were recaptured at inlet locations or in the nearshore coastal waters at sizes that were large enough to include reproductively mature adults (Murphy and Taylor, 1990; Render and Wilson, 1992; Taylor et al., 2000). The seasonality of inlet-associated recaptures was consistent with the seasonality of documented spawning and movement patterns for these species. In Florida, red drum typically spawn in nearshore coastal waters during the fall (Murphy and Taylor, 1990), although spawning within the IRL has also been documented (Johnson and Funicelli, 1991). Spawning by common snook may occur year-round on Florida's east coast (Gilmore et al., 1983), but most spawning takes place between May and October in or near major inlets to the Atlantic Ocean (Taylor et al., 1998). The limited number of common snook recaptured from inlet spawning habitats during the peak summer spawning season (June–August) was likely due to the fishery being closed during those months. Sheepshead move offshore with the onset of cool weather in the late fall (Gunter, 1945; Kelly, 1965), and spawning likely occurs in offshore waters during

[2] Murphy, M. D. 2002. A stock assessment of red drum, *Sciaenops ocellatus*, in Florida: status of the stocks through 2000, 32 p. Florida Fish and Wildlife Conservation Commission Report, Melbourne, FL.

the spring (Springer and Woodburn, 1960; Jennings, 1985; Tucker and Barbera, 1987). In the northern portion of the IRL, where the NTZ is located, the closest access to the coastal environment is through two inlets located approximately 75 km (Sebastian Inlet) and 100 km (Ponce de Leon Inlet) swimming distance away or through an intermittent lock opening at Port Canaveral approximately 12 km to the south. In order to reach nearshore or tidal-pass spawning habitats, species must first migrate to these locations. The coincidence of tag recoveries from these areas during identified spawning or migration periods likely indicated that the relatively long movement distances we observed resulted from a combination of geographical, environmental, and biological factors, including the proximity of the NTZ to habitats that are important for specific life-history requirements of individual species. From a management viewpoint, these relationships can affect the spatial extent of species' migrations in relation to protected habitats, as well as the degree of protection provided to individuals that are migratory, and should be considered carefully in the design of estuarine reserves.

This study documented the ingress of exploitable estuarine sportfish species into protected habitats and demonstrated that these movements can also cover substantial distances. Species moving towards the NTZ traveled distances of at least 10–75 km. The original tagging locations of these fish were distributed throughout the northern Indian and Banana rivers and southern Mosquito Lagoon, which paralleled the primary region of our tagging efforts. Whether or not fish from more southerly locations in the IRL system would migrate into the NTZ is largely unknown because of the lack of tagging effort in those areas. However, for tropical species such as the common snook, permit (*Trachinotus falcatus*), gray snapper, and others whose abundances increase seasonally in the northern lagoon habitats during the warmer months (Tremain and Adams, 1995), it seems probable that seasonal movements could bring them into contact with the protected habitats. In such cases, these species would benefit only temporarily from fishing protection until their return migrations made them again vulnerable to capture. In contrast, species observed migrating into the NTZ that typically have a high degree of site fidelity during specific life-history stages, such as the red drum (Beaumariage, 1969; Adams and Tremain, 2000), black drum (Murphy et al., 1998), and spotted seatrout (Moffett, 1961), should derive greater long-term benefits from reserve protection following immigration into protected areas.

Tagging studies that examine the transfer of fishery species between reserve and outlying habitats are rare, and we have found only one recent study on any fishery species, the American lobster (*Homarus americanus*), that investigated the effects that multidirectional species migrations may have upon protective reserve functions (Rowe, 2001). Studies in which fish movements have been examined, in both estuarine and marine protected areas, have focused exclusively on fish egress from reserve habitats (Bryant et al., 1989; Buxton and Allen, 1989; Funicelli et al., 1989; Holland et al., 1996; Zeller and Russ, 1998; Johnson et al., 1999, Stevens and Sulak, 2001) or on home ranges of species associated with reserve habitats (Eristhee and Oxenford, 2001; Starr et al., 2002). In the present study, we simultaneously examined both egress and ingress of sportfish in relation to a no-take reserve and the surrounding unprotected waters, and the results provide a starting point to quantitatively discuss the relationship between fish emigration and immigration, as well as the implications of such movements to the resulting functions of replenishment to or withdrawal from nearby estuarine fisheries. When all recapture sources were considered, the ratio of migrating to nonmigrating individuals was much higher for fish tagged inside the NTZ (1.58) than for those tagged outside the NTZ (0.05); this ratio implies that there is a spillover effect from the reserve. However, this difference is less apparent when measured against the large disparity between recapture effort from inside the NTZ (12–24 FMRI sampling days/year + 12–24 angler days/year) and recapture effort from the surrounding lagoon waters of Brevard County (50–100 FMRI sampling days/year + 114,000–181,000 angler days/year [FMRI, unpubl. data]). Furthermore, this direct comparison assumes that recapture potential was the same in protected and unprotected areas, which is unlikely given the differences between the primary recapture gear used in scientific research activities inside the reserve (nets) and the gear used in recreational angling outside the reserve (hook and line). There were no reliable estimates of sportfish species landings available for the limited study region that could have enabled us to intercalibrate for these differences; therefore, we limited further comparisons to only data recovered through FMRI sampling activities in the northern Banana River basin. This limitation came at the expense of important tag-recovery data collected by anglers or collected from more outlying areas of the lagoon but permitted a more quantitative comparison of migration potential that focused comparisons on immediately adjacent areas where the effects of spillover would most likely be realized (Buxton and Allen, 1989; Russ and Alcala, 1996). In these comparisons, a disproportionate number of fish were tagged inside the NTZ, but overall tag-recovery rates for fish originating in both the NTZ and the adjacent Banana River were equivalent. This finding indicated that tagged individuals from both areas were equally susceptible to recapture. However, there were substantial differences in the migration patterns of fish between the two areas. In the vicinity of the NTZ, the relative potential for overall sportfish migrations (primarily for red drum and black drum, which provided the greatest quantity of tag recovery data) towards the NTZ from unprotected habitats (52%) was greater than the potential for migrations out of the NTZ (5%).

Two potential limitations must be considered when comparing these migration rates. First, it is possible that recreational fishing in the upper Banana River could have reduced the number of tags available to FM-

RI sampling activities outside the NTZ, leading to lower tag recovery rates from this area. However, several fish from the Banana River study area were recaptured on multiple occasions—a common occurrence in this region where fish are caught and released in fishing practices. Although there is some postrelease cryptic mortality associated with catch-and-release practices, these releases likely limited the effects of local fishing on our analyses. Second, our assumption that the migration patterns of recaptured fish represented the migration patterns of the overall population may not be valid if the respective length frequencies were not also equally represented. The use of multiple gear types and sampling strategies to collect fish for tagging increased the likelihood that the length frequencies of species in our collections represented the available population. Reported recapture length frequencies closely approximated the population length frequencies in our collections for red drum, black drum, and sheepshead but over-represented the frequency of larger individuals for common snook and spotted seatrout. Because red drum and black drum were the principal species that displayed multidirectional migration patterns, we considered the potential for size bias to be minimal in our comparisons of estimated ingress and egress rates.

Ultimately, a determination of the net result of these migration patterns, in terms of replenishment to or withdrawal from adjacent fisheries, would require accurate assessments of species population abundances that were beyond the scope of this study. If there are large enough differences in population densities across the NTZ boundary, either as a result of increased production inside the reserve or high fishing mortality outside, then the relatively low emigration rates that we observed could still result in a net export of exploitable individuals to fished populations in surrounding waters. In trammel-net collections from this same reserve during the late 1980's, Johnson et al. (1999) estimated that in the protected habitats, relative abundances of red drum populations were 6.3 times greater and of black drum were 12.8 times greater than the relative abundances of these populations in adjacent unprotected areas. More recent shoreline haul-seine data from 1997–2000 show that these abundances were only 1.8 times greater for red drum and 1.5 times greater for black drum (FMRI, unpubl. data). To what extent the difference in abundance estimates between these two temporally separate studies is related to fish movements, to stringent changes in management regulations that have occurred, or to the difference in sampling methods used is undetermined. However, if we consider the more recent population level differences between the NTZ and adjacent waters, then the emigration and immigration rates observed in the present study indicate that there is a potential for more substantial movements by these species towards protected habitats than away from them.

One limitation of tag-recapture data is that such data provide only a snapshot view of overall fish movements, and the whereabouts of tagged individuals between the time of tagging and recapture are unknown. It is possible that the movements we observed for red drum and black drum in the vicinity of the NTZ were simply instantaneous views of a more complex series of movements between the NTZ and adjacent waters. One possibility is that these movements could be related to daily or seasonal home ranges that extend across reserve boundaries. Studies that attempt to quantify home ranges for these species at any temporal scale are limited. Carr and Chaney (1976) followed a single red drum, which was fitted with an ultrasonic transmitter, for up to two days after releasing it into the Intracoastal Waterway near St. Augustine, Florida. During that time, fish movements were oriented against the direction of tidal flow but remained within 2 km of the release point. Adams and Tremain (2000) found that large juvenile red drum repeatedly used or were continually associated with a 2-km section of a northern IRL tidal creek for periods of up to 18 months. Tagging studies from estuarine waters generally indicate that the majority of red drum and black drum do not make substantial movements from their release sites, although some individuals are capable of migrating up to several hundred kilometers (Beaumariage, 1969; Osburn et al. 1982; Music and Pafford, 1984; Murphy et al., 1998). During the present study, 20 red drum were recaptured on multiple occasions; however, none of these fish exhibited movements that could provide evidence for home ranges that overlapped the NTZ boundaries. Another possibility for the movement patterns we observed is that they are related to population equilibrium adjustments that occur when the relative attributes of the NTZ and surrounding areas change with respect to each other. For example, beginning in 1990 and coinciding with the onset of the present study, the Banana River adjacent to the NTZ (including much of our BR study area) was closed to motorized boat traffic. Although the area remained open to fishing, it became considerably more difficult to access by fishermen. If this limitation resulted in lower fishing pressure (i.e., predation) and fewer habitat disturbances, then the relative habitat value and rates of migration into this area may have increased during that time. There are no quantifiable estimates of migration rates prior to this study for comparison, but our results do not demonstrate an equilibrium adjustment toward potentially higher quality BR habitats during our study period. If species movements are not equilibrium adjustments, but rather are driven by an attraction to or retention within habitats that offer protective benefits, then ultimately reserve habitats should become saturated. Predicted equilibrium population sizes for queen conch (*Strombus gigas*) and spiny lobster (*Panulirus argus*) were achieved in just three years after the effective creation of a Caribbean reef harvest refuge, but models suggested that relatively minor changes in refuge area and boundary condition (i.e., permeability) could result in major population-level responses by exploited species, depending upon dispersal dynamics and habitat availability (Acosta, 2002). The estuarine no-take zone at

MINWR has been in effect for approximately 40 years, presumably long enough for fish populations to reach equilibrium levels, yet we observed a net movement of fish into protected habitats over the past decade.

A wide range of factors interact to determine the distributions of large mobile fish in the IRL, where physical environmental conditions (salinity, inlet distance, temperature, etc.) have a primary influence on the species' distributions over a lagoon-wide scale, and where species responses to biological variables (seagrass cover, depth, seasonality, etc.) act secondarily to influence distributions at smaller scales (Kupschus and Tremain, 2001). The specific mechanisms that lead to the greater ingress rates into the NTZ for red drum and black drum in the present study cannot be determined from our data. Possibilities include a behavioral attraction to the NTZ due to the interrelated influences of habitat preference, spawning, and social structure, or due to potentially higher retention rates after migration into the reserve. Red drum and black drum were routinely observed foraging in large schools within both the NTZ and surrounding waters, which suggested that food resources were available in each of these habitats; however, there are few studies that have attempted to quantify differences in resource availability between these areas. Johnson et al. (1999) described the habitat characteristics of their study areas within the same reserve system but found that protection from fishing, and not habitat difference, was the primary factor contributing to differences in the abundance of sportfish species between fished and unfished areas. The availability of suitable spawning habitats within the NTZ may also attract red drum and black drum to the reserve habitats. We observed indications of reproductive behavior by both of these species inside the NTZ that is common among members of the drum family, including concentrations of drumming fish (Mok and Gilmore, 1983) and repeated side-to-side contact among individual fish (Tabb, 1966) in the presence of ripe and running males. Although we did not directly observe these behaviors for either species outside of the NTZ, black drum and red drum are documented to spawn elsewhere within the IRL system (Mok and Gilmore, 1983; Johnson and Funicelli, 1991) and we cannot automatically presume that suitable spawning habitats do not also occur in the surrounding waters. If there is a behavioral attraction to protected habitats, then the subsequent retention of individuals that have immigrated into these areas may be prolonged by the limited boundary permeability of this reserve, which contains only two potential egress pathways back into the adjacent waters. In order to fully understand the protective functions of this estuarine reserve and others, it will be important to identify the biological, behavioral, and physical mechanisms that influence species movements in relation to the reserve boundaries.

The opportunistic nature of our tagging efforts within the design of a larger sampling program precluded statistically valid sample replication, and only one reserve and adjacent fished area were examined; therefore, the results of this study should not be generalized to other areas. Still, the IRL is typical of other bar-built estuaries where access by estuarine fishes to coastal waters through passes or inlets may be limited, and it is reasonable to expect that the geographical, environmental, and biological processes that influence species movements in the IRL would also be important in other estuaries of similar structure. Studies show that no-take areas in estuarine systems can have an effect on species' abundances and size distributions within these protected areas and may indicate that these areas protect species from the effects of fishing pressure (Johnson et al., 1999; FMRI unpubl. data). Whether or not these areas will actually increase fish abundance in adjacent waters or benefit surrounding fisheries through direct supplemental replenishment of exploitable species is less evident. Certainly, some individuals will migrate out of protected areas in response to environmental, biological, or physiological stimuli, and these individuals may contribute to trophy fisheries in surrounding waters (Roberts et al., 2001); however, our data indicated that within estuaries, reciprocal movements over relatively large distances into protected areas also occur and have the potential to extract exploitable individuals from surrounding fisheries. The overall impact of such withdrawals on these fisheries will depend on the degree of retention following migrations into protected areas. If retention rates are high, then increased egg production, larval export, and juvenile recruitment may be more important mechanisms for replenishment of nearby fisheries than spillover of exploitable species, but production and export will be limited unless reserves encompass spawning or nursery habitats (or both) that will support long-term protection and population growth. For estuarine-dependent coastal species that support estuarine fisheries, the benefits obtained within protected areas will be determined, in part, by their specific life-history characteristics, movement patterns, and the reserve design. Although the establishment and study of reserves in marine or coastal systems has increased in recent years, research on the effects of protected no-take reserves in estuarine habitats is still in its infancy. Information on the daily, seasonal, or annual movement patterns of estuarine-resident or estuarine-dependent coastal species is necessary for understanding and designing effective reserve areas in these habitats.

Acknowledgments

We wish to thank the crewmembers and volunteers at FMRI's Indian River Field Laboratory for collecting data and assisting in this study and the many fishermen who willingly provided us with recapture information. We are grateful to U.S. Fish and Wildlife Service personnel for providing access to sampling areas within restricted areas of the Merritt Island National Wildlife Refuge. This paper benefitted from reviews by R. Cody, J. Colvocoresses, L. French, J. Leiby, R. Paperno, J. Quinn,

T. Tuckey, and F. Vose, and two anonymous reviewers. This work was supported in part by funding from the Department of Interior, U. S. Fish and Wildlife Service, Federal Aid for Sport Fish Restoration Grant Number F-43, and by the State of Florida Recreational Saltwater Fishing License monies.

Literature cited

Acosta, C. A.
2002. Spatially explicit dispersal dynamics and equilibrium population sizes in marine harvest refuges. ICES J. Mar. Sci. 59:458–468.

Adams, D. H., and D. M. Tremain.
2000. Association of large juvenile red drum, *Sciaenops ocellatus*, with an estuarine creek on the Atlantic coast of Florida. Environ. Biol. Fish. 58:183–194.

Babcock, R. C., S. Kelly, N. T. Shears, J. W. Walker, and T. J. Willis.
1999. Changes in community structure in temperate marine reserves. Mar. Ecol. Prog. Ser. 189:125–134.

Beaumariage, D. S.
1969. Returns of the 1965 Schlitz tagging program including a cumulative analysis of previous results. Fla. Board Conserv. Mar. Res. Lab. Tech. Ser. 59, 38 p.

Bohnsack, J. A. and J. S. Ault.
1996. Management strategies to conserve marine biodiversity. Oceanography (9):73–82.

Bryant, H. E., M. R. Dewey, N. A. Funicelli, G. M. Ludwig, D. A. Meineke, and L. J. Mengal.
1989. Movement of five selected sports species of fish in Everglades National Park. Bull. Mar. Sci. 44:515.

Buxton, C. D., and J. A. Allen.
1989. Mark and recapture studies of two reef sparids in the Tsitsikamma Coastal National Park. Koedoe 32:39–45.

Carr, W. E. S., and T. Chaney.
1976. Harness for attachment of an ultrasonic transmitter to the red drum, *Sciaenops ocellatus*. Fish. Bull. 74:998–1000.

Chapman, M. R., and D. L. Kramer.
1999. Gradients in coral reef fish density and size across the Barbados Marine Reserve boundary: effects of reserve protection and habitat characteristics. Mar. Ecol. Prog. Ser. 181:81–96.

Cole, R. G., and D. Keuskamp.
1998. Indirect effects of predation from exploitation: patterns from populations of *Evechinus chloroticus* (Echinoidea) in northwestern New Zealand. Mar. Ecol. Prog. Ser. 173:215–226.

DeMartini, E. E.
1993. Modeling the potential of fishery reserves for managing Pacific coral reef fishes. Fish. Bull. 91: 414–427.

Eristhee, N., and H. A. Oxenford.
2001. Home range size and use of space by Bermuda chub *Kyphosis sectatrix* (L.) in two marine reserves in the Soufriere Marine Management Area, St. Lucia, West Indies. J. Fish Biol. 59:129–151.

Funicelli, N. A., D. A. Meineke, H. E. Bryant, M. R. Dewey, G. M. Ludwig, and L. S. Mengel.
1989. Movements of striped mullet, *Mugil cephalus*, tagged in Everglades National Park, Florida. Bull. Mar. Sci. 44:171–178.

Gilmore, R. G., Jr., C. J. Donohoe, and D. W. Cooke.
1983. Observations on the distribution and biology of the common snook, *Centropomus undecimalis* (Bloch). Fla. Sci. 46:313–336.

Gilmore, R. G., Jr., C. J. Donohoe, D. W. Cooke, and D. J. Herrema.
1981. Fishes of the Indian River Lagoon and adjacent waters. Harbor Branch Foundation Tech. Rep. No. 41, 64 p.

Gunter, G.
1945. Studies on marine fishes of Texas. Inst. Mar. Sci. Univ. Tex. 1:1–190.

Holland, K. N., C. G. Lowe, and B. M. Wetherbee.
1996. Movements and dispersal patterns of blue trevally (*Caranx melamgypus*) in a fisheries conservation zone. Fish. Res. 25:279–292.

Jennings, C. A..
1985. Species profiles: life histories and environmental requirements of coastal fishes and invertebrates (Gulf of Mexico)—sheepshead. U.S. Fish and Wildlife Service Biological Report 82(11.29) and U. S. Army Corps of Engineers, TR EL-82-4, 10 p.

Johnson, D. R., and N. A. Funicelli.
1991. Spawning of the red drum in Mosquito Lagoon, east-central Florida. Estuaries 14:74–79.

Johnson, D. R., N. A. Funicelli, and J. A. Bohnsack.
1999. Effectiveness of an existing no-take fish sanctuary within the Kennedy Space Center, Florida. N. Am. J. Fish. Manag. 19:436–453.

Kelly, J. R.
1965 A taxonomic survey of the fishes of the Delta National Wildlife Refuge with emphasis upon distribution and abundance. M.S. thesis, 133 p. Louisiana State Univ., Baton Rouge, LA.

Kupschus, S., and D. Tremain.
2001. Associations between fish assemblages and environmental factors in nearshore habitats of a subtropical estuary. J. Fish Biol., 58:1383–1403.

Moffett, A. W.
1961. Movement and growth of spotted seatrout, *Cynoscion nebulosus* (Cuvier), in west Florida., 35 p. Fla. Board Conserv. Mar. Res. Lab. Tech. Ser. No. 36.

Mok, H., and R. G. Gilmore.
1983. Analysis of sound production in estuarine aggregations of *Pogonias cromis*, *Bairdiella chrysoura*, and *Cynoscion nebulosus* (Sciaenidae). Bull. Inst. Zool, Academia Sinica (Taipei). 22:157–186.

Mulligan, T. J., and F. F. Snelson Jr.
1983. Summer-season populations of epibenthic marine fishes in the Indian River Lagoon system, Florida. Fla. Sci. 46:252–275.

Murphy, M. D., D. H. Adams, D. M. Tremain, and B. W. Winner.
1998. Direct validation of ages determined for adult black drum, *Pogonias cromis*, in east central Florida, with notes on black drum migration. Fish. Bull. 96:382–387.

Murphy, M. D., and R. G. Taylor.
1990. Reproduction, growth, and mortality of red drum *Sciaenops ocellatus* in Florida waters. Fish. Bull. 88:531–542.

Music, J. L., and J. M. Pafford.
1984. Population dynamics and life history aspects of major marine sportfishes in Georgia's coastal waters., 382 p. Georgia Department of Natural Resources, Contribution Series 38.

Musick, J. A., S. A. Berkeley, G. M. Cailliet, M. Camhi, G. Huntsman, M. Nammack, and M. L. Warren Jr.
2000. Protection of fish stocks at risk of extinction. Fisheries 25(3):6–8.

Osburn, H. R., G. C. Matlock, and A. W. Green.
1982. Red drum (*Sciaenops ocellatus*) movement in Texas bays. Contr. Mar. Sci., 25:85–97.

PDT (Plan Development Team).
1990. The potential of marine fishery reserves for reef fish management in the U.S. Southern Atlantic. NOAA Tech. Memo. NMFS-SEFC-261, 40 p.

Render, J. H., and C. A. Wilson.
1992. Reproductive biology of sheepshead in the northern Gulf of Mexico. Trans. Am. Fish. Soc. 121:757–764.

Roberts, C. M., J. A. Bohnsack, F. Gell, J. P. Hawkins, and R. Goodridge.
2001. Effects of marine reserves on adjacent fisheries. Science 294:1920–1923.

Roberts, C. M., and N. V. C. Polunin.
1991. Are marine reserves effective in management of reef fisheries? Rev. Fish Biol. and Fish. 1:65–91.

Rowe, S.
2001. Movement and harvesting mortality of American lobsters (*Homarus americanus*) tagged inside and outside no-take reserves in Bonavista Bay, Newfoundland. Can. J. Fish. Aquat. Sci. 58:1336–1346.

Rowley, R. J.
1994. Marine reserves in fisheries management. Aquat. Conserv. Mar. Freshwater Ecosyst. 4:233–254.

Russ, G. R.
1985. Effects of protective management on coral reef fishes in the central Philippines. Proc. of the 5th International Coral Reef Congress 4:219–224.

Russ, G. R., and A. C. Alcala.
1996. Do marine reserves export adult fish biomass? Evidence from Apo Island, central Philippines. Mar. Ecol. Prog. Ser. 132:1–9.

Sala, E., and M. Zabala.
1996. Fish predation and the structure of the sea urchin *Paracentrotus lividus* populations in the NW Mediterranean. Mar. Ecol. Prog. Ser. 140:71–81.

Springer, V. G., and K. D. Woodburn.
1960. An ecological study of the fishes of the Tampa Bay area. Fla. Board Conserv. Mar. Res. Lab. Prof. Pap. Ser. 1, 104 p.

Starr, R. M., J. N. Heine, J. M. Felton, and G. M. Cailliet.
2002. Movements of bocaccio (*Sebastes paucispinis*) and greenspotted (*S. chlorostictus*) rockfishes in a Monterey submarine canyon: implications for the design of marine reserves. Fish. Bull. 100:324–337.

Stevens, P. W., and K. J. Sulak.
2001. Egress of adult sport fish from an estuarine reserve within Merritt Island National Wildlife Refuge, Florida. Gulf Mex. Sci. 2:77–89.

Tabb, D. C.
1966. The estuary as a habitat for spotted seatrout *Cynoscion nebulosus*. Am. Fish. Soc. Special Publication 3:59–67.

Taylor, R. G., H. J. Grier, and J. A. Whittington.
1998. Spawning rhythms of common snook in Florida. J. Fish Biol. 53:502–520.

Taylor, R. G., J. A. Whittington, H. J. Grier, and R. E. Crabtree.
2000. Age, growth, maturation, and protandric sex reversal in common snook, *Centropomus undecimalis*, from the east and west coasts of South Florida. Fish. Bull. 98:612–624.

Tremain, D. M., and D. H. Adams.
1995. Seasonal variations in species diversity, abundance, and composition of fish communities in the northern Indian River Lagoon, Florida. Bull. Mar. Sci. 57:171–192.

Tucker, J. W., Jr., and P. A. Barbera.
1987. Laboratory spawning of sheepshead. Prog. Fish-Cult. 49:229–230.

Zeller, D. C., and G. R. Russ.
1998. Marine reserves: patterns of adult movement of the coral trout (*Plectropomus leopardus*) (Serranidae). Can. J. Fish. Aquat. Sci. 55:917–924.

Distribution, age, and growth of young-of-the-year greater amberjack (*Seriola dumerili*) associated with pelagic *Sargassum*

R. J. David Wells

Jay R. Rooker

Texas A&M University
Department of Marine Biology
5007 Avenue U
Galveston, Texas 77551
Present address (for R. J. D. Wells): Coastal Fisheries Institute
Louisiana State University
Baton Rouge, Louisiana 70803

E-mail address (for R. J. D. Wells): rwells4@lsu.edu

Abstract—Patterns of distribution and growth were examined for young-of-the-year (YOY) greater amberjack (*Seriola dumerili*) associated with pelagic *Sargassum* in the NW Gulf of Mexico. *Seriola dumerili* were collected off Galveston, Texas, from May to July over a two-year period (2000 and 2001) in both inshore (<15 nautical miles [nmi]) and offshore zones (15–70 nmi). Relative abundance of YOY *S. dumerili* (32–210 mm standard length) from purse-seine collections peaked in May and June, and abundance was highest in the offshore zone. Ages of *S. dumerili* ranged from 39 to 150 days and hatching-date analysis indicated that the majority of spawning events occurred from February to April. Average daily growth rates of YOY *S. dumerili* for 2000 and 2001 were 1.65 mm/d and 2.00 mm/d, respectively. Intra-annual differences in growth were observed; the late-season (April) cohort experienced the fastest growth in both years. In addition, growth was significantly higher for *S. dumerili* collected from the offshore zone. Mortality was approximated by using catch-curve analysis, and the predicted instantaneous mortality rate (Z) of YOY *S. dumerili* was 0.0045 (0.45%/d).

Manuscript submitted 9 December 2002 to Scientific Editor's Office.

Manuscript approved for publication 2 March 2004 by the Scientific Editor.

Fish. Bull. 102:545–554 (2004).

Recruitment of marine fishes is highly variable and closely linked to early life events (Houde, 1996; Cole, 1999). Early life survival is dependent upon several biological and environmental factors including spawning time, prey availability, predation pressure, growth, and physical transport mechanisms (Bricelj, 1993; Schnack et al., 1998). Recruitment success is commonly assessed by examining patterns of relative abundance (Sano, 1997), whereas estimates of growth and mortality are commonly used to index recruitment potential (Rilling and Houde, 1999; Rooker et al., 1999). Early life growth and mortality are linked because fishes with high growth rates often exhibit decreased size-specific predator vulnerability (Meekan and Fortier, 1996). As a result, estimates of juvenile abundance, growth, and mortality provide insight into patterns of nursery habitat quality and thus may be used to delineate essential fish habitat (EFH) (Pihl et al., 2000; Sullivan et al., 2000).

Greater amberjack (*Seriola dumerili*) is a reef-associated species with a circumglobal distribution in subtropical and temperate waters (Manooch and Potts, 1997a). In the Gulf of Mexico, *S. dumerili* is the largest carangid and supports important recreational and commercial fisheries (Thompson et al., 1999). Owing to increased fishing effort and landings, *S. dumerili* in the Gulf are currently assessed as overfished (NOAA, 2000). Consequently, detailed life history information is needed to effectively guide fishery management of this valuable resource. To date, available life history data on *S. dumerili* have almost entirely been based on assessments of subadults and adults (Manooch and Potts, 1997a, 1997b; Thompson et al.[1]). Despite the importance of early life processes, data on juvenile or young-of-the-year (YOY) *S. dumerili* are limited to qualitative surveys of pelagic *Sargassum* (Bortone et al., 1977; Settle, 1993).

The National Marine Fisheries Service has recently designated *Sargassum* as essential fish habitat (EFH) of several coastal migratory species including *S. dumerili* (NOAA, 1996). In response, the goal of this study was to examine the distribution and growth of *S. dumerili* associated with pelagic *Sargassum* mats in the NW Gulf of Mexico. Specifically, objectives of this research were to quantify spatial and temporal patterns of habitat use by *S. dumerili* and to determine age, hatching-date, growth, and mortality of *S. dumerili* by using otolith-based techniques.

[1] Thompson, B. A., C. A. Wilson, J. H. Render, M. Beasley, and C. Cauthron. 1992. Age, growth, and reproductive biology of greater amberjack and cobia from Louisiana waters. Final report NA90AA-H-MF722, 77 p. Marine Fisheries Initiative (MARFIN) program, National Marine Fisheries Service, NOAA, St. Petersburg, FL.

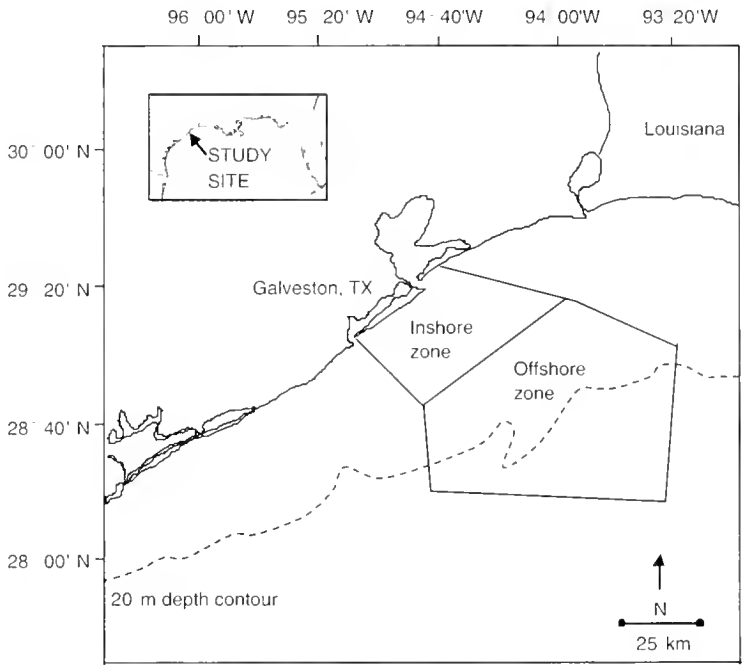

Figure 1

Map of sampling locations along the Texas Gulf coast for *S. dumerili*. Inshore (<15 nautical miles) and offshore (>15 nautical miles) zones off Galveston, TX, are shown.

Materials and methods

Field collections

Seriola dumerili associated with pelagic *Sargassum* mats were collected off Galveston, Texas, from May to July over a two-year period (2000 and 2001) (Fig. 1). Inshore (<15 nautical miles [nmi]) and offshore (15–70 nmi) zones were sampled to evaluate the potential importance of physiochemical conditions because inshore waters off the coast of Texas are heavily influenced by estuarine processes (Smith, 1980; Sahl et al., 1993). Replicate samples (3–5 per trip) in both the inshore and offshore zones were collected monthly by using a larval purse seine (20 m long×3.3 m deep, 1000-μm mesh). The purse seine was deployed into the water as the boat encircled a randomly chosen mat. The seine was pursed, the *Sargassum* was discarded, and fishes were funneled into the codend, collected, and frozen on dry ice. Distribution and abundance were expressed as relative abundance, and catch per unit of effort (CPUE) represented the number of fishes per purse-seine collection. In addition, a small number of YOY *S. dumerili* were collected with hook-and-line for age and growth information only. Standard lengths (SL) were measured to the nearest 0.1 mm, and weights to the nearest 0.1 g before otolith extraction. GPS locations and mat volume (length×width×depth) were recorded at each sample location. Environmental parameters measured included sea surface temperature, salinity, and dissolved oxygen. Daily sea surface temperature data were also taken from NOAA buoy 42035, 22 nmi offshore of Galveston, TX.

Otolith procedures

Sagittal otoliths were extracted from *S. dumerili*. Otoliths were measured to the nearest 0.001 mm and weighed to the nearest 0.0001 g. Left or right sagittae were randomly selected and mounted in epoxy resin (Spurr, 1969). Once mounted, a Buehler isomet low-speed saw equipped with a diamond wafering blade was used to transversely cut embedded otoliths. Otolith sections were then attached to petrographic slides with Crystalbond thermoplastic cement. Type A alumina powder (0.3 μm) and 400- and 600-grit sandpaper were used to grind both sides of the otolith, and a polishing cloth was used for final preparations.

Age was determined by counting growth increments along the sulcus from the core to the outer margin by using a Nikon Labophot-2 light microscope and Optimas 6.2 image analysis software (Media Cybernetics, Silver Spring, MD). Because of the difficulty of enumerating some inner increments near the otolith core, a relationship between age and otolith radius of several clear specimens was used to predict the number of increments within the unclear region. Age was determined by adding the correction factor to the increment count from the first identifiable increment to the otolith margin (Rooker and Holt, 1997). Correction factors consisting of more than five days were applied to 49%

of the fishes and the average correction accounted for 9.5% of the actual age estimate. Otolith readings with correction factors accounting for more than 20% of the predicted age were not used for estimates of growth. The following correction factor was used

$$Age\ (\text{d}) = 2.88 \times otolith\ radius\ (\mu\text{m}) - 0.096 \quad (r^2=0.88,\ n=20).$$

Additionally, all otolith counts were repeated twice to ensure adequate precision. Differences in readings of more than 20% were not incorporated into growth estimates.

Daily deposition of growth increments on sagittal otoliths was validated by using wild *S. dumerili* (n=14, 136–193 mm SL). Fishes caught in the wild were brought into the laboratory and placed in a circular holding tank (1.71 m diameter×0.75 m depth) for 48 hours. Fishes were then placed in a separate tank containing 80 liters of seawater with 100 mg/L of alizarin complexone for two hours (Thomas et al., 1995) and returned to the circular holding tank. Individuals were fed approximately 10% of their body weight daily. Fishes marked with alizarin were removed from the tank after 5 (n=5), 10 (n=5), and 15 (n=4) days. The number of otolith increments between the alizarin mark and outer edge were then counted for daily increment verification. Otolith slides were coded so that all readings were blind.

Hatching dates were determined for all individuals by subtracting daily age from date of capture. An age-specific mortality adjustment was made for individuals because larger *S. dumerili* have spent more time in the early life stages and hence individuals from these cohorts have experienced greater cumulative mortality. Because of the limited number of individuals in 2001, the mortality correction was calculated only for year 2000 collections and applied to hatching-date distributions in 2000 and 2001. Age-specific mortality adjustments were made according to the method described by Rooker and Holt (1997).

Growth and mortality of *S. dumerili* were estimated by using otolith-derived ages. Daily growth rates were estimated by using the linear growth equation

$$SL = slope\ (\text{age}) + y\text{-intercept}$$

and were reported as mm/d. Length-at-age data were also fitted with curvilinear growth models (von Bertalanffy, Laird-Gompertz). Percent variation in length explained by age for both curvilinear models was slightly better at times than the percent variation in length explained by age for the linear model; however, certain model parameters (i.e. L_∞) were biologically unrealistic and thus the linear model was deemed more appropriate. Moreover, when possible, L_∞ values were used to model length-at-age data and the nonlinear models were essentially linear over the limited size range examined. Mortality estimates for year 2000 *S. dumerili* were determined by using a regression on the decline in $\log_e$-transformed abundance on age. A regression coefficient (slope) was used to predict the instantaneous mortality rate:

$$\ln N_t = \ln N_0 - Zt,$$

where N_t = abundance at age t (expressed in days);
N_0 = an estimate of abundance at hatching; and
Z (slope) = the instantaneous mortality coefficient.

Mortality estimates were based upon 10-day cohort groupings. Individuals <40 days old were not included in the mortality regression because of an ascending catch curve and because there were too few individuals >139 days old in our sample—probably owing to gear avoidance or emigration (or both). Therefore, only *S. dumerili* between 40 and 139 days (45–192 mm) were used to estimate mortality.

Data analysis

Effects of location and date on CPUE and size estimates were examined by using a two-way analysis of variance (ANOVA). Levene's test and residual examination established if the homogeneity of variance assumption was met. Normality was evaluated by plotting residuals versus expected values. Abundance data were log (x+1) transformed when necessary to normalize data and reduce heteroscedasticity. Tukey's honestly significant difference (HSD) test was used to determine *a posteriori* differences among means. Comparisons of spatial and temporal variation in growth were performed by using analysis of covariance (ANCOVA). Prior to ANCOVA testing, the homogeneity of slopes assumption was examined using an interaction regression (Ott, 1993). If no significant interaction was detected, ANCOVA models were used to test for differences in length-at-age (y-intercepts) (Ott, 1993). Statistical analysis was carried out by using SYSTAT 8.0 (SYSTAT Software Inc., Richmond, CA), and significance was set at the alpha level of 0.05.

Results

Environmental conditions

Average temperatures from May to July ranged from 27.9 to 30.1°C in 2000 and from 24.5 to 30.4°C in 2001 (Fig. 2). Mean temperatures over the sampling period were 29.2°C and 27.9°C for 2000 and 2001, respectively. Zonal differences occurred: the inshore zone averaged 28.7°C (±0.3) in 2000 and 28.1°C (±0.9) in 2001, and the offshore zone averaged 29.8°C (±0.3) in 2000 and 27.6°C (±0.9) in 2001. Similar to temperature trends, mean salinity was higher in 2000 (34.6‰) than in 2001 (31.9‰) (Fig. 2). Average salinity values gradually increased from an average of 31.5‰ in May to 37.2‰ in July of 2000. A large drop in salinity occurred during

mid-summer of 2001, from 37.6‰ in May to 25.7‰ in June (owing to tropical storm Allison) and rose to 32.3‰ in July. Salinity values were lower and more variable within the inshore zone, ranging from 29‰ to 37‰ (33.4‰ average) in 2000 and from 15‰ to 37‰ (average 28.8‰) in 2001. In contrast, the offshore zone exhibited higher and more stable salinity values, ranging between 33‰ and 38‰ (36‰ average) in 2000, and between 28‰ and 36‰ (34.9‰ average) in 2001. Temperature and salinity values are likely to be influenced by variation in precipitation between years. Precipitation from January through July of 2000 (14.29 inches) was half that of 2001 (29.92 inches) and well below the 30-year average of 22.17 inches (National Weather Service, Dickinson, TX). Dissolved oxygen content was similar between years; values decreased throughout the summer months and were higher within the inshore zone.

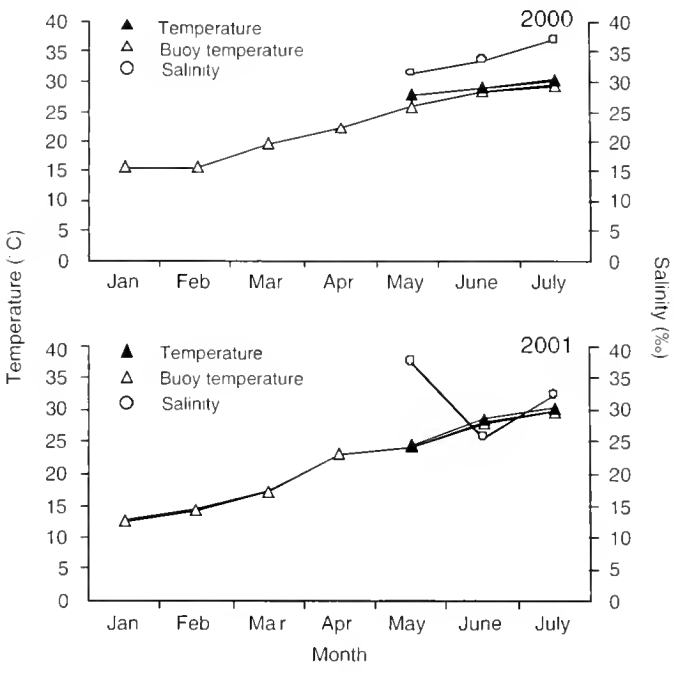

Figure 2

Environmental conditions from January to July of 2000 and 2001. Average temperature (°C) and salinity (‰) values. Open triangles represent temperature data from NOAA buoy 42035, located 22 nautical miles offshore of Galveston, TX.

Spatial and temporal distribution

A total of 181 YOY *S. dumerili* was collected from 42 purse seines over the two-year study period. CPUE values were fourfold higher in 2000 than in 2001, averaging 6.38 (±3.0) and 1.50 (±0.8) per seine, respectively (Fig. 3A). A significant year effect indicated that relative abundance was higher in 2000 (P=0.019). Additionally, CPUE values were higher in the offshore zone in both years (Fig. 3, B and C). However, no significant zonal difference existed in abundance between the inshore and offshore zones in 2000 (P=0.063) or 2001 (P=0.058). Temporal patterns indicated *S. dumerili* was highly abundant in May and June, declining in July in both years (Fig. 3A). A significant seasonal effect occurred for 2000 when highest relative abundance occurred in June with a CPUE of 16.2 (±0.8) (Tukey HSD, P<0.05).

Size comparison

Sizes of *S. dumerili* ranged from 33 to 210 mm SL (mean 125 mm SL ±3.8). Juveniles greater than 100 mm accounted for 68% of the total catch, whereas individuals less than 50 mm accounted for only 15%. Size differences of *S. dumerili* were observed between 2000 (average 125.5 mm) and 2001 (average 141.5 mm); significantly larger *S. dumerili* were collected from the offshore zone in 2001 (P=0.001). A significant interaction (year×month) occurred that indicated that the magnitude of size differences was variable over time. Sizes were also significantly different between zones in 2000; larger individuals were collected within the offshore zone (P=0.025). No zonal comparison was performed for 2001 because few individuals were collected from the inshore zone. In addition, a trend existed within both years: mean sizes significantly increased from May to June, then decreased in July (Tukey HSD, P<0.05).

Hatching-date distribution

Hatching-date distributions for *S. dumerili* were protracted in both 2000 and 2001. Fishes collected in 2000 exhibited hatching-dates from 29 January to 25 May (117 days), whereas those collected in 2001 hatched from 11 January to 30 May (139 days) (Fig. 4). In 2000, over 80% of the fishes appeared to result from spawning events in March and early April. The adjusted distributions from the age-specific mortality correction for both 2000 and 2001 were indistinguishable from those without the correction.

Age and growth

Results of the age-validation exercise indicated that juvenile *S. dumerili* deposit otolith increments on a daily basis (Fig. 5). Average increment counts at day 5, 10, and 15 were 4.8 (±0.2 SD), 9.2 (±0.4), and 14.0 (±0.7), respectively. A relationship between the observed versus expected increments was described by the following equation:

$$\textit{Observed increments} = 0.92\ (\textit{expected increments}) + 0.14 \quad (r^2=0.95)$$

where days after staining represent expected increment count.

Validation of daily growth increments has been observed in a similar study involving juvenile (0–60 days) *Seriola quinqueradiata* (Sakakura and Tsukamoto, 1997).

Age of *S. dumerili* was similar between years; estimated ages ranged from 41 to 150 days (35 to 210 mm SL) in 2000 and from 35 to 120 days (33 to 198 mm SL) in 2001 (Fig. 6). Interannual differences in growth were observed: 2000 (1.65 mm/d), 2001 (2.00 mm/d) (ANCOVA, slope, $P<0.001$) (Fig. 7). A significant cohort effect was also observed; the late-season (April) cohort experienced the fastest growth (ANCOVA, slopes, $P<0.001$) (Fig. 8). Average cohort-specific growth rates of *S. dumerili* spawned in February, March, and April of 2000 were 0.85 mm/d, 1.15 mm/d, and 2.76 mm/d, respectively. In addition, a significant difference in growth was observed for *S. dumerili* collected from inshore (1.55 mm/d) and offshore (1.65 mm/d) zones of 2000 (ANCOVA, slope, $P<0.001$) (Fig. 9). Again, the lack of individuals within the inshore zone in 2001 precluded a comparison between zones for that year.

Mortality

Owing to the limited number of *S. dumerili* collected in 2001, a single catch curve was developed for the 2000 year class, and the mortality coefficient (Z) was 0.0045 (0.45%/d) for individuals between 40 and 139 days (Fig. 10). Cumulative mortality was estimated for the 100-day period (40–139 days), resulting in an overall mortality of 36%.

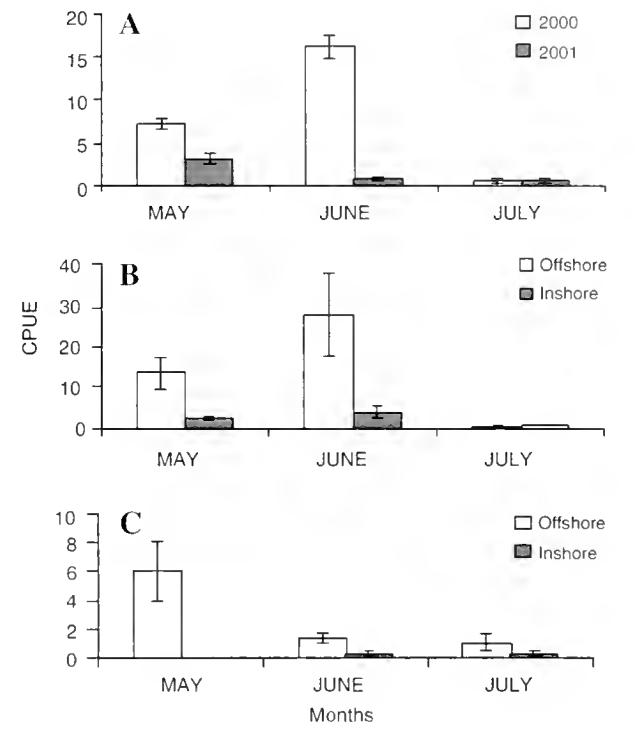

Figure 3

Relative abundance (number per purse seine) (±1 SE) of *S. dumerili* collected in association with *Sargassum* mats: (**A**) 2000 and 2001; (**B**) 2000 by zones; (**C**) 2001 by zones.

Discussion

The size range of *S. dumerili* collected in association with *Sargassum* ranged from approximately 30 to 210 mm (SL), and these sizes are similar to those reported in other studies investigating fish assemblages associated with pelagic *Sargassum*. Bortone et al. (1977) collected several small *S. dumerili* (12–72 mm SL) in the eastern Gulf, whereas individuals collected in the western Atlantic by Dooley (1972) ranged from 13 to 108 mm (SL). Cho et al. (2001) found juvenile *S. dumerili* (35–120 mm TL) associated with drifting *Sargassum* in the western Pacific. Additionally, Sakakura and Tsukamoto (1997) collected over 200 juvenile Japanese amberjack (*S. quinqueradiata*) (18–114 mm TL) associated with pelagic *Sargassum* in the East China Sea. Results of the present study and others indicate that pelagic *Sargassum* mats in the NW Gulf of Mexico serve as nursery habitat for *S. dumerili*.

The limited size range of *S. dumerili* associated with pelagic *Sargassum* indicates that a shift in habitat use may occur at approximately 5–6 months of age. Individuals greater than 210 mm (SL) have not been found in association with pelagic *Sargassum*, and larger *S. dumerili* (ca. 300 mm TL) are relatively common in the recreational headboat fishery in the Gulf of Mexico (Manooch and Potts, 1997a). As a consequence, *S. dumerili* may transition from a pelagic to a demersal existence at the late juvenile stage (between 200 mm SL and 300 mm TL). Pipitone and Andaloro (1995) found a shift in the diet of *S. dumerili*, from a diet predominately consisting of crustaceans toward one of fish >200 mm (SL), further supporting this hypothesis.

Seriola dumerili abundance was greater in the offshore zone than the inshore zone throughout the sampling period. These patterns of habitat use are consistent with earlier information that indicates *S. dumerili* is an offshore species (Hildebrand and Cable, 1930). The proximity to spawning grounds may contribute to the observed spatial patterns because *S. dumerili* are known to spawn in offshore areas (Fahay, 1975). Physiological preferences may also contribute to the dominance of *S. dumerili* in the offshore zone. In our study, salinity values were higher in the offshore zone but more variable within the inshore zone, suggesting that freshwater inflow influences conditions within the inshore zone. Chen et al. (1997) determined that optimum salinity conditions for *S. dumerili* larvae were between 32‰ and 35‰, and larvae remained inactive below a salinity of 30‰. Zonal differences in temperature and dissolved oxygen were also observed. Tzeng et al. (1997)

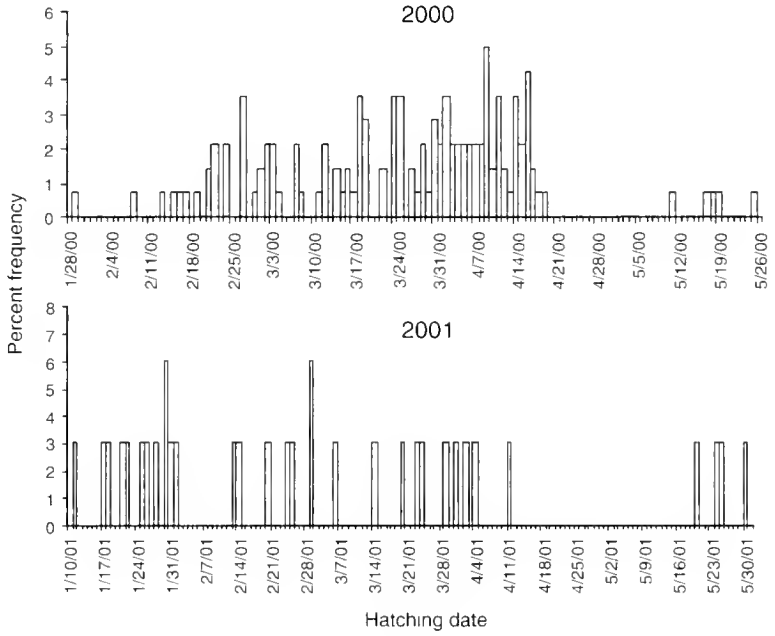

Figure 4

Hatch-date distributions of *S. dumerili* associated with *Sargassum* mats in 2000 and 2001.

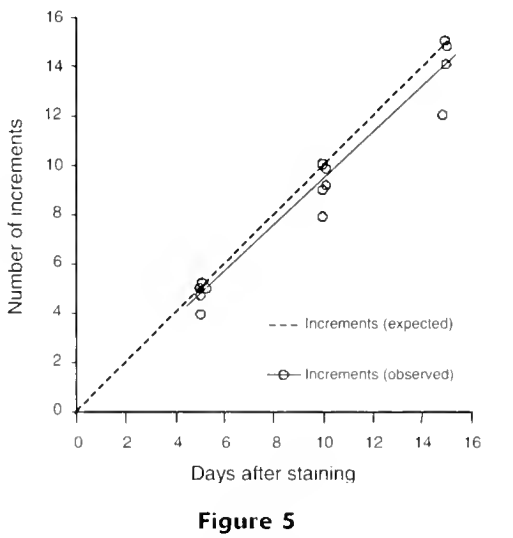

Figure 5

Linear regression of age verification for *S. dumerili*. Circles and solid line represent the number of daily increments observed after staining, and dotted line represents the number of increments expected.

attributed the distribution of fishes from nearshore to offshore stations to environmental factors, season, and life history strategies. Furthermore, the combination of available resources (i.e. food and habitat), seasons, and physiochemical tolerances may account for the observed spatial patterns of habitat use.

Temporal patterns of size-specific habitat use showed similar trends between years and appeared to be related to spawning season. Relative abundance of small *S. dumerili* was highest early in the season (May), declined in June, and further increased late into the season (July) for both 2000 and 2001. Nevertheless, small juveniles were collected during the entire collection period, which suggests that *S. dumerili* spawning in the NW Gulf is protracted. Previous studies have found that *S. dumerili* spawn throughout the spring and summer months (March–July) (Marino et al., 1995; Cummings and McClellan, 1996). In addition, Fahay (1975) suggested, on the basis of larval collections in the western Atlantic, that spawning occurs in the winter. Despite the limited duration of our collection efforts, our results are consistent with these findings with 63% of year-2000 *S. dumerili* and 36% of year-2001 fish resulting from spring spawning events. The remaining individuals were spawned January through early March.

Growth estimates indicated that *S. dumerili* have rapid growth throughout early life stages. Based on linear growth models, average growth of *S. dumerili* was 1.45 mm/d—an estimate similar to that of Manooch and Potts's (1997b) study in the Gulf (average growth of 1.17 mm/d for age-1 individuals). However, growth comparisons may be invalid because their study estimated growth based on counts of annuli and no temperature

data were presented. Because of the lack of studies investigating growth of YOY *S. dumerili*, we compared our estimates to those in Sakakura and Tsukamoto's (1997) study of YOY *S. quinqueradiata* where growth rates were estimated at 1.3 mm/d. Average temperature in their study was 21.2°C, which was considerably lower than the average during our study (28.6°C) and may account for their slower growth rates.

Variation in growth of *S. dumerili* was observed and rates were significantly higher in the offshore zone and greater for the late season cohort. Differences in water temperature may be partly responsible for observed differences in growth. Planes et al. (1999) suggested that spatial differences in growth of juvenile sparid fishes were a result of water temperature and currents. The proximity between zones in this study may have masked differences in hydrography; however, temperatures were higher in the offshore zone (29.8°C, CV=0.03) than in the inshore zone (28.7°C, CV=0.04), and warmer temperatures were likely contributing to faster growth rates in offshore waters. Intra-annual (cohort-specific) growth patterns indicated that the late-season cohort had the fastest growth. Similar to trends between zones, temperature was lowest for the slowest growing cohort (early season) and highest for the fastest growing cohort (late season). Although temperature may affect early life growth of *S. dumerili*, differences in growth may be attributed to other factors such as prey availability and predator activity (Houde, 1987; Paperno et al., 2000; Plaganyi et al., 2000). Moreover, a clear distinction exists in the size classes of YOY *S. dumerili* in comparisons of growth rates and these differences likely contribute to the observed results.

The mortality rate of YOY *S. dumerili* associated with pelagic *Sargassum* was estimated at 0.45 %/d for fishes collected in 2000. These findings are well below similar studies investigating mortality of YOY individuals. Nelson (1998) calculated a mortality estimate of 2.1–2.3%/d for pinfish in three different bay areas in the eastern Gulf of Mexico. In addition, Deegan (1990) estimated YOY menhaden mortality between 1.7 and 2.1%/d in the northern

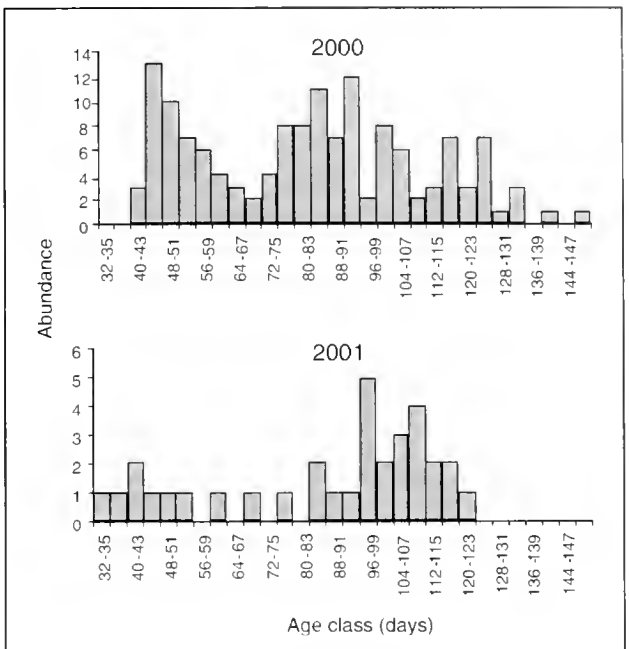

Figure 6

Age-frequency distribution of *S. dumerili* collected in association with *Sargassum* in 2000 and 2001.

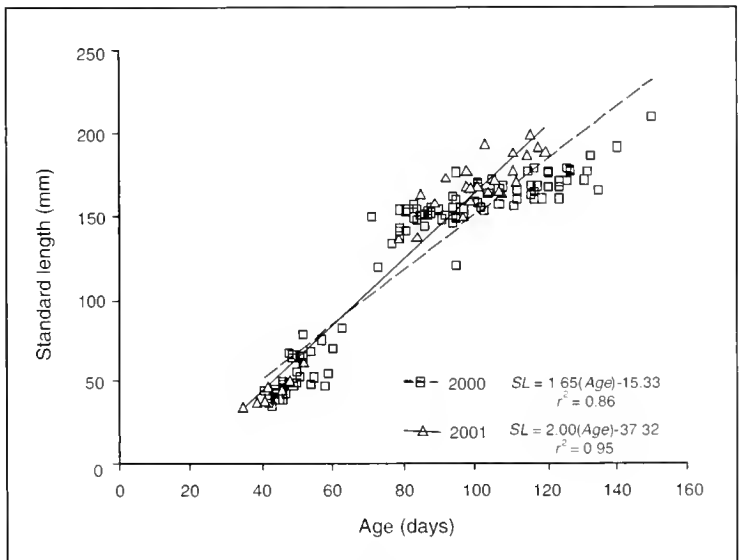

Figure 7

Age-length relationship of *S. dumerili* determined with linear growth curves for interannual comparison.

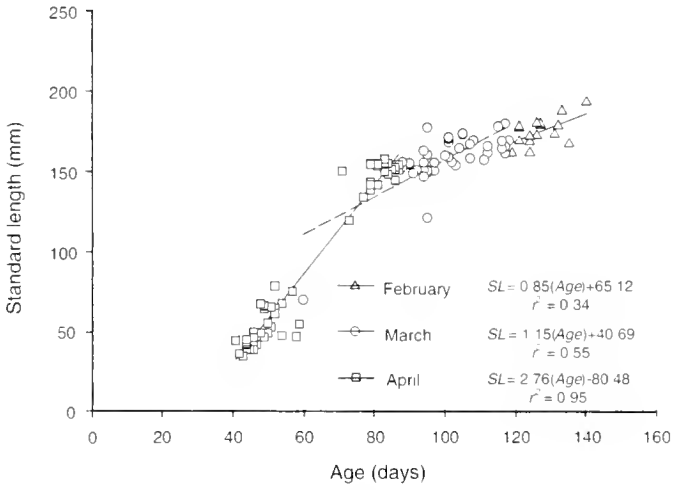

Figure 8

Age-length relationship of *S. dumerili* determined with linear growth curves for a comparison of cohorts of different hatching dates in 2000.

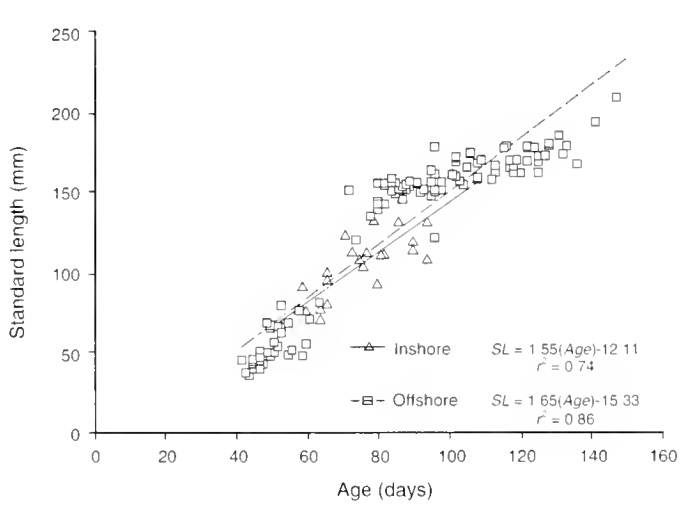

Figure 9

Age-length relationship of *S. dumerili* determined with linear growth curves for a comparison of zones in 2000.

Gulf. These studies included estuarine-dependent species and consisted of smaller individuals. Because our estimates were limited to age 40–139 d individuals, the lack of smaller fishes precluded any mortality estimates of younger *S. dumerili*. These estimates provide baseline information on mortality of YOY *S. dumerili*; however, more detailed studies will be needed to adequately determine mortality rates of YOY *S. dumerili*.

Based on observed patterns of distribution and growth in the NW Gulf of Mexico, early life survival of *S. dumerili* may depend on pelagic *Sargassum*. Results of this study suggest that *S. dumerili* are associated with this habitat over a limited size range and exhibit rapid growth during the first six months. Additionally, *S. dumerili* were more abundant and exhibited higher growth in offshore areas where potential spawning may occur. Thus, *Sargassum* appears to provide nursery habitat for YOY *S. dumerili*, and may influence the recruitment potential of this valuable fishery species.

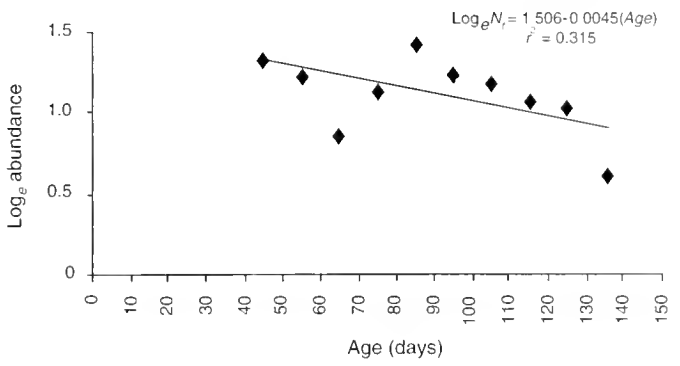

Figure 10

Mortality curve of *S. dumerili* based upon regression plot of $\log_e$ abundance on age of individuals collected in 2000.

Acknowledgments

We thank J. Harper, M. Lowe, B. Geary, J. Turner, and J. Wells for their assistance in the field. Funding for this project was provided by The Aquarium at Moody Gardens (grant 479005 to JRR). Top Hatt charters provided boat time offshore, and Kirk Winemiller and Jaime Alvarado offered constructive criticism and suggestions.

Literature cited

Bortone, S. A., P. A. Hastings, and S. B. Collard.
1977. The pelagic-*Sargassum* ichthyofauna of the eastern Gulf of Mexico. Northeast Gulf Sci. 1:60–67.

Bricelj, V. M.
1993. Aspects of the biology of the northern quahog, *Mercenaria mercenaria*, with emphasis on growth and survival during early life history. *In* Proceedings of the 2nd Rhode Island shellfish industry conference, p. 29–48. Sea Grant Progress report, Narragansett, RI.

Chen, C., R. Ji, J. Huang, H. He, and Z. Liao.
1997. The relationship between the salinity and the embryonic, early larval development in *Seriola dumerili*. J. Shanghai Fish. Univ. 6:5–10.

Cho, S-H., J-G. Myoung, and J-M. Kim.
2001. Fish fauna associated with drifting seaweed in the coastal area of Tongyeong, Korea. Trans. Am. Fish. Soc. 130:1190–1202.

Cole, J.
1999. Environmental conditions, satellite imagery, and clupeoid recruitment in the northern Benguela upwelling system. Fish. Oceanogr. 8:25–38.

Deegan, L. A.
1990. Effects of estuarine environmental conditions on population dynamics of young-of-the-year gulf menhaden. Mar. Ecol. Prog. Ser. 68:195–205.

Dooley, J. K.
1972. Fishes associated with the pelagic *Sargassum* complex, with a discussion of the *Sargassum* community. Contrib. Mar. Sci. 16:1–32.

Fahay, M. P.
1975. An annotated list of larval and juvenile fishes captured with surface-towed meter net in the South Atlantic Bight during four RV *Dolphin* cruises between May 1967 and February 1968. NOAA Tech. Rep. NMFS. SSRF-685:1–39.

Hildebrand, S. F., and L. E. Cable.
1930. Development and life history of fourteen teleostean fishes at Beaufort, N.C. Fish. Bull. 46:383–488.

Houde, E. D.
1987. Fish early life dynamics and recruitment variability. Am. Fish. Soc. Symp. 2:17–29.
1996. Evaluating stage-specific survival during the early life of fish. *In* Survival strategies in early life stages of marine resources (Y. Watanabe, Y. Yamashita, and Y. Oozeki, eds.), p. 51–66. AA Balkema, Rotterdam.

Leak, J. C.
1981. Distribution and abundance of carangid fish larvae in the eastern Gulf of Mexico, 1971–1974. Biol. Oceanogr. 1(1):1–28.

Manooch, C. S., III, and J. C. Potts.
1997a. Age, growth and mortality of greater amberjack from the southeastern United States. Fish. Res. 30:229–240.
1997b. Age, growth, and mortality of greater amberjack, *Seriola dumerili*, from the U.S. Gulf of Mexico headboat fishery. Bull. Mar. Sci. 61:671–683.

Marino, G., A. Mandich, A. Massari, F. Andaloro, S. Porrello, M. G. Finoia, and F. Cevasco.
1995. Aspects of reproductive biology of the Mediterranean amberjack (*Seriola dumerili* Risso) during the spawning period. J. Appl. Ichthyol. 11:9–24.

Meekan, M. G., and L. Fortier.
1996. Selection for fast growth during the larval life of Atlantic cod *Gadus morhua* on the Scotian Shelf. Mar. Ecol. Prog. Ser. 137:25–37.

Nelson, G. A.
1998. Abundance, growth, and mortality of young-of-the-year pinfish, *Lagodon rhomboides*, in three estuaries along the gulf coast of Florida. Fish. Bull. 96: 315–328.

NOAA (National Oceanic and Atmospheric Administration).
1996. Magnuson-Stevens Fishery Conservation and Management Act, as amended through Oct. 11, 1996. NOAA Tech. Mem. NMFS-F/SPO-23, 121 p.
2000. Stock assessments of Gulf of Mexico greater amberjack using data through 1998. Sustainable Fisheries Division, Southeast Fisheries Science Center, NMFS report 99/00-100, 27 p.

Ott, R. L.
1993. An introduction to statistical methods and data analysis, 4th ed., 1051 p. Duxbury Press, Belmont, CA.

Paperno, R., T. E. Targett, and P. A. Grecay.
2000. Spatial and temporal variation in recent growth, overall growth, and mortality of juvenile weakfish (*Cynoscion regalis*) in Delaware Bay. Estuaries 23:10–20.

Pihl, L., J. Modin, and H. Wennhage.
2000. Spatial distribution patterns of newly settled plaice (*Pleuronectes platessa* L.) along the Swedish Skagerrak archipelago. J. Sea. Res. 44:65–80.

Pipitone, C., and F. Andaloro.
1995. Food and feeding habits of juvenile greater amberjack, *Seriola dumerili* (Osteichthyes, Carangidae) in inshore waters of the central Mediterranean Sea. Cybium 19:305–310.

Plaganyi, E. E., L. Hutchings, and J. G. Field.
2000. Anchovy foraging: simulating spatial and temporal match/mismatches with zooplankton. Can. J. Fish. Aquat. Sci. 57:2044–2053.

Planes, S., E. Macpherson, F. Biagi, A. Garcia-Rubies, J. Harmelin, M. Harmelin-Vivien, J. Y. Jouvenel, L. Tunesi, L. Vigliola, and R. Galzin.
1999. Spatio-temporal variability in growth of juvenile sparid fishes from the Mediterranean littoral zone. J. Mar. Biol. Assoc. U.K. 79:137–143.

Rilling, G. C., and E. D. Houde.
1999. Regional and temporal variability in growth and mortality of bay anchovy, *Anchoa mitchilli*, larvae in Chesapeake Bay. Fish. Bull. 97:555–569.

Rooker, J. R., and S. A. Holt.
1997. Utilization of subtropical seagrass meadows by newly settled red drum *Sciaenops ocellatus*: patterns of distribution and growth. Mar. Ecol. Prog. Ser. 158:139–149.

Rooker, J. R., S. A. Holt, G. J. Holt, and L. A. Fuiman.
1999. Spatial and temporal variability in growth, mortality, and recruitment potential of postsettlement red drum, *Sciaenops ocellatus*, in a subtropical estuary. Fish. Bull. 97:581–590.

Sahl, L. E., W. J. Merrell, and D. C. Biggs.
1993. The influence of advection on the spatial variability of nutrient concentrations on the Texas-Louisiana continental shelf. Cont. Shelf. Res. 13:233–251.

Sakakura, Y., and K. Tsukamoto.
1997. Age composition in the schools of juvenile yellowtail *Seriola quinqueradiata* associated with drifting seaweeds in the East China Sea. Fish. Sci. 63:37–41.

Sano, M.
1997. Temporal variation in density dependence: Recruitment and postrecruitment demography of a temperate zone sand goby. J. Exp. Mar. Biol. Ecol. 214:67–84.

Schnack, D., St. John, R. Schneider, B. Klenz, A. Nissling, and E. Aro.
1998. 3rd European Mar. Sci. and Tech. Conf. (MAST). Fisheries and Aquaculture 5:181–185.

Settle, L. R.
1993. Spatial and temporal variability in the distribution and abundance of larval and juvenile fishes associated with pelagic *Sargassum*. M.S. thesis, 64 p. Univ. North Carolina-Wilmington, Wilmington, NC.

Smith, N. P.
1980. On the hydrography of shelf waters off the central Texas coast. J. Phys. Oceanogr. 10:806–813.

Spurr, A. R.
1969. A low-viscosity epoxy resin embedding medium for electron microscopy. J. Ultrastruct. Res. 26:31–43.

Sullivan, M. C., R. K. Cowen, K. W. Able, and M. P. Fahay.
2000. Spatial scaling of recruitment in four continental shelf fishes. Mar. Ecol. Prog. Ser. 207:141–154.

Thomas, L. M., S. A. Holt, and C. R. Arnold.
1995. Chemical marking techniques for larval and juvenile red drum (*Sciaenops ocellatus*) otoliths using different fluorescent markers. *In* Recent developments in fish otolith research, p. 703–717. The Belle W. Baruch Library in Marine Science, number 19. Univ. South Carolina Press, Columbia, SC.

Thompson, B. A., M. Beasley, and C. A. Wilson.
1999. Age distribution and growth of greater amberjack, *Seriola dumerili*, from the north-central Gulf of Mexico. Fish. Bull. 97:362–371.

Tzeng, W. N., Y. T. Wang, and Y. T. Chern.
1997. Species composition and distribution of fish larvae in Yenliao Bay, northeastern Taiwan. Zool. Stud. 36:146–158.

Identification of formalin-preserved eggs of red sea bream (*Pagrus major*) (Pisces: Sparidae) using monoclonal antibodies

Shingo Hiroishi
Yasutaka Yuki
Eriko Yuruzume
Faculty of Biotechnology
Fukui Prefectural University
1-1 Gakuen-cho
Obama City, 917-0003 Fukui, Japan
E-mail address (for S. Hiroishi): hiroishi@fpu.ac.jp

Yosuke Onishi
Tomoji Ikeda
Hironobu Komaki
Kansai Environmental Engineer Center
1-3-5 Azuchi-cho, Chuo-ku
Osaka City, 541-0052 Osaka, Japan

Muneo Okiyama
Ocean Research Institute
University of Tokyo
1-15-1 Minamidai, Nakano-ku,
Tokyo, Japan

Catches of important commercial fish such as red sea bream, flat fish, and yellowtail are decreasing in Japan. In order to sustain these species it is especially important that their distribution and biomass at all life stages are known. However, information on the early life stages of these species is limited because identifying the eggs and larvae of such fish is sometimes extremely difficult.

Mito (1960, 1979) and Ikeda and Mito (1988) developed methods for identifying pelagic fish eggs based on morphological features. However, their methods have limitations because many unidentified eggs have similar features. In addition, eggs are usually fixed in formaldehyde solution just after collection in the field. This procedure may alter several egg characteristics and therefore prevent identification (Ikeda and Mito, 1988), or make identification difficult when the egg diameter measures 0.8–1.0 mm because so many kinds of eggs fall in that range. Thus, an alternative identification method would be useful.

Effective genetic analyses for identifying fish eggs or larvae (or both) have been developed by Graves et al. (1989), Daniel and Graves (1994), and Shao et al. (2002). However, their methods may have limitations if samples are preserved in formaldehyde for several years or if DNA must be extracted from numerous samples. In addition, we are lacking the DNA sequences for many species sequences that are necessary for identifying eggs in the field.

We have successfully produced monoclonal antibodies to differentiate harmful marine phytoplankton species from morphologically similar harmless species (Hiroishi et al., 1988; Nagasaki et al., 1991b; Sako et al., 1993; Vrieling et al., 1993; Hiroishi et al., 2002) as well as *Microcystis*, a toxic fresh water bloom-forming cyanobacteria (Kondo et al., 1998). These antibodies were obtained from a culture supernatant solution of hybridoma cells that was produced by a cell fusion procedure between myeloma cells and antibody-producing spleen cells. The specific antibodies described above could be used to detect and quantify harmful bloom-forming microorganisms that react with the monoclonal antibodies and that secondarily react with fluorescein isothiocyanate conjugated goat anti-mouse Ig(G+M) antibody. With fluorescence microscopy with B-exciting light, yellowish fluorescein coronas around the cells of the toxic species were observed, confirming a positive reaction. These antibodies can recognize different molecules distributed on the cell surface, even when the organisms have similar morphological features. One of the molecules distributed on *Chattonella* was determined to be glycoprotein (Nagasaki et al., 1991a). This method would help us to differentiate small marine organisms like fish eggs.

Red sea bream (*Pagrus major*) (Table 1) eggs can easily be distinguished from those of other sparids also found in Japan, such as *Acanthopagrus latus*, by differences in egg size and spawning seasons, and from those of *Evynnis japonica* by differences in spawning seasons (Ikeda and Mito, 1988; Kinoshita, 1988; Hayashi, 2000). However, eggs of some sparids, such as *Acanthopagrus schlegeli*, *Sparus sarba*, and *Dentex tumifrons* are extremely difficult to distinguish from eggs of *P. major*. Therefore, we developed monoclonal antibodies that allow *P. major* eggs to be clearly identified by immunostaining, thus differentiating them from other similar sparids.

This technique may be a useful new tool for identifying fish eggs. Here, we report a method for identifying *P. major* eggs using monoclonal antibodies developed to react specifically with the eggs.

Materials and methods

Eggs of *P. major* were obtained from adult female fish that had spawned in

Manuscript submitted 4 April 2003
to Scientific Editor's Office.
Manuscript approved for publication
2 March 2004 by the Scientific Editor.
Fish. Bull. 102:555–560 (2004).

Table 1
Characteristics of Sparidae distributed in Japan.

Suborder	Species	Distribution	Spawning season	Egg size (mm)	Egg oil globule size (mm)
Pagrinae	*Pagrus major*	South of Hokkaido (Coastal)	Mar–May	0.90–1.03	0.19–0.25
	Evynnis japponica	South of Hokkaido (Coastal)	Oct–Dec	0.89–0.98	0.19–0.21
Sparinae	*Acanthopagrus schlegeli*	South of Hokkaido (Coastal)	Mar–Jun	0.83–0.91	0.20–0.22
	Acanthopagrus latus	South Japan (Coastal)	Oct–Nov	0.76–0.81	0.2
	Sparus sarba	South Japan (Coastal)	Apr–Jun	0.88–0.92	0.19–0.22
Denticinae	*Dentex tumifrons*	South Japan (Oceanic)	May–Jun	0.90–0.93	0.19

isolation tanks at several sea farming centers described in Table 2. Immediately after collection, fish eggs were fixed in a solution of 5% formaldehyde to sea water solution and stored. Before use, the eggs were thoroughly washed with distilled water and suspended in phosphate buffered saline (PBS) solution.

Monoclonal antibodies were developed according to the methods of Köhler and Milstein (1975), Garfré and Milstein (1981), and Hiroishi et al. (1984, 1988): 0.5 mL of egg suspension (200 eggs/PBS solution from Fukui Prefectural Sea Farming Center, Obama City, Fukui Prefecture) was mixed with 0.5 mL Freund's complete adjuvant (Nacalai Tesque, Inc., Kyoto, Japan). The mixture were then injected subcutaneously into BALB/c female mice (4 weeks of age). The female mice received second and third injections at 2-week intervals. For the final immunization, *P. major* eggs collected in the sea farming center of Kansai Environmental Engineering Center Co. (Miyazu City, Kyoto, Japan) were injected into the mouse after being emulsified with Freund's incomplete adjuvant (Nacalai Tesque, Inc.). Three days after the final immunization, the spleens of the mice were removed and passed through a mesh (mesh size: 100 μm). The spleen cells obtained by this procedure were fused with the myeloma cell line X63-AG8.653 at a ratio of 10:1 with 50% polyethylene glycol. After cell fusion, hybrid cells were incubated in a selective hypoxanthine-aminopterin-thymidine medium (Köhler, 1979; Garfré and Milstein, 1981).

The reactivity of the antibodies produced by the hybridomas was then determined. Eggs fixed with 5% formaldehyde in seawater were washed with PBS solution in a 96-well plate. Throughout the experiments, the principal eggs used were from the Fukui Prefectural Sea Farming Center. Normal horse serum solution (200 μL), diluted 100-fold with PBS, was added to the wells to prevent any nonspecific reactions. After incubation at room temperature for 20 minutes, the eggs were washed with 200 μL of PBS. After removing the PBS, 200 μL of the hybridoma culture supernatant solution was added to the wells and incubated at room temperature for 30 minutes. After washing with PBS (100 μL), biotinylated horse anti-mouse IgG (100 μL) was added to the wells and incubated at room temperature for 20 minutes. After the incubation, VECTASTAIN^{R} ABC reagent (avidin DH + biotinylated horseradish peroxidase/PBS, 100 μL) was added according to the direction of VECTASTAIN^{R} Elite ABC kit (ABC Mouse IgG Kit, Funakoshi Co., Tokyo, Japan). After immunostaining the eggs were observed by stereoscopic microscopy (SMZ-2T, Nikon Co., Tokyo, Japan). In a positive reaction, the surface of the fish egg was stained brown as a result of the oxidation of 3,3′-diaminobenzidine (substrate) by horseradish peroxidase bound to the egg surface by the antibody.

Unidentified pelagic fish eggs from open water were collected by using a plankton net (MTD net, NGG54 with mesh size of 0.344 mm, Rigo Co., Tokyo, Japan) from Wakasa Bay (Fukui Prefecture, Japan) in May 1997. They were fixed with 5% formaldehyde in sea water, either immediately or after incubation in seawater in finger bowls at 20°C for 24 hours, and identified by careful observation as described by Ikeda and Mito (1988) and Ikeda et al. (1991). The fixed eggs were transferred to net wells (mesh size 200 μm, diameter 24 mm, Corning Incorporated, Corning, NY) and washed with 10 mL of distilled water three times. Then the eggs in the netwells were immersed in 100 mL of PBS in a polystyrene tray (Corning Incorporated, Corning, NY) for 5 minutes. The egg suspension was placed into the wells of a six-well plate and incubated with 10 mL of normal horse serum solution for 20 minutes. After incubation, the eggs were incubated with 10 mL of MT-1 antibody solution (hybridoma culture supernatant) and then incubated with 10 mL of biotinylated horse anti-mouse IgG. The subsequent procedure was performed as described above.

The immunoglobulin subclass of monoclonal antibodies was determined according to the directions of the mouse monoclonal antibody isotyping kit (Amersham Pharmacia Biotech Co., Uppsala, Sweden) as follows: 3 mL of monoclonal antibodies solution (hybridoma supernatant solution) obtained in this study was added to 0.3 mL of horseradish peroxidase-conjugated anti-mouse IgG in the kit. An isotyping stick in the kit was incubated with the above solution at room tem-

perature for 15 minutes. Then the stick was washed with 0.1% Tween 20/PBS, and incubated with 4-chloro-1-naphthol solution (substrate of horseradish peroxidase in the kit) containing 0.1% H_2O_2 at room temperature for 15 minutes. The immunoglobulin subclass of the monoclonal antibodies was determined by observing the positions of bands that appeared on the stick.

Results and discussion

After cell fusion, hybridomas were grown in 42 wells of 96-well plates. Supernatant solutions of the cultures were used for the immunostaining assay to select hybridomas producing antibodies reactive to *P. major* eggs. After the assay, positive reactions were observed in six wells. These hybridomas were cloned by the limiting dilution method, and finally three clones producing monoclonal antibodies reactive with *P. major* were obtained. Those antibodies were named MT-1, MT-2, and MT-3. The subclass of all antibodies was IgG_1. Specificity of the antibodies was examined by using the eggs shown in Table 2. As a result, the antibodies were reactive with all the *P. major* eggs in both the early and late stages (before or after tail-bud stage), but not with eggs of other species (Table 3, Fig. 1). Thus, it becomes possible to identify *P. major* eggs. The immunostaining assay took 2.5 hours.

The oldest eggs of *P. major* (20 April, 1995) could react with the antibodies obtained as clearly as the recently collected eggs of *P. major*, indicating that egg samples preserved for up to 7 years could be analyzed by this method.

The method was also successful with 102 eggs collected from Wakasa Bay (Table 4), which had been immediately fixed with 5% formaldehyde in seawater. Among them, only 11 eggs were identified as *Callionymoidei* spp.

Table 2

Fish eggs used in the experiment

Egg no.	Species	Sampling location	Stage of eggs	Sampling day
1		Kansai Environmental Engineering Center (Miyazu, Kyoto Pref)	Early	20 Apr '95
2		Kansai Environmental Engineering Center (Miyazu, Kyoto Pref.)	Late	21 Apr '95
3		Fukui Prefectural Sea Farming Center (Obama, Fukui Pref.)	Early	2 Jun '95
4	*Pagrus major*	Fukui Prefectural Sea Farming Center (Obama, Fukui Pref.)	Late	2 Jun '95
5		Kyoto Prefectural Sea Farming Center (Miyazu, Kyoto Pref.)	Early	31 May '96
6		Kyoto Prefectural Sea Farming Center (Miyazu, Kyoto Pref.)	Early	31 May '96
7		Faculty of Agriculture, Kyushu University (Fukuoka, Fukuoka Pref.)	Early	6 Jun '96
8		Fukui Prefectural Sea Farming Center (Obama, Fukui Pref.)	Early and late	21 May '97
9		Osaka Prefectural Fisheries Station and Sea Farming Center (Osaka Pref.)	Early	11 May '95
10		Osaka Prefectural Fisheries Station and Sea Farming Center (Osaka Pref.)	Late	19 May '95
11	*Acanthopagrus schlegeli*	Faculty of Agriculture, Kyushu University (Fukuoka, Fukuoka Pref.)	Early	6 Jun '96
12		Osaka Prefectural Fisheries Station and Sea Farming Center (Osaka Pref.)	Early	19 May '97
13		Osaka Prefectural Fisheries Station and Sea Farming Center (Osaka Pref.)	Late	19 May '97
14	*Acanthopagrus latus*	Himedo, Amakusa, Kumamoto (Kumamoto Pref.)	Unknown	21 Nov '98
15	*Sparus sarba*	Faculty of Agriculture, Kyushu University (Fukuoka, Fukuoka Pref.)	Late	3–5 Jun '96
16	*Dentex tumifrons*	Ohara, Chiba (Chiba Pref.)	Unknown	Oct '98
17		Japan Sea-Farming Association (Miyazu, Kyoto Pref.)	Early	20 Apr '95
18	*Paralichthys olivaceus*	Japan Sea-Farming Association (Miyazu, Kyoto Pref.)	Late	21 May '97
19		Fisheries Laboratory of Kinki University (Kushimoto, Wakayama Pref.)	Late	15 Jan '97
20		Japan Sea-Farming Association (Miyazu, Kyoto Pref.)	Early and late	23 Apr '97
21	*Engraulis japonica*	Wakasa Bay (Fukui Pref.)	Unknown	May '97

(type II). The remaining 91 unidentified eggs were divided into three groups (types I, III, and IV) based on diameters. Of these 91, 51 type-II eggs reacted with MT-1. This finding is compatible with the possibility that the eggs were *P. major*, because the size was similar to that of *P. major* and each contained a single oil globule of a similar size (Tables 1 and 4). Another 43 eggs were collected from another area of Wakasa Bay (Table 5). None of the eggs fixed just after collection were morphologically identifiable. But, after incubation at 20°C for 24 hours until the late stage, all six eggs identified as *P. major* were reactive with the antibody MT-1, whereas the others were not. These findings strongly suggest that the method developed in this study is useful for identifying *P. major* eggs in seawater. Although only late stage eggs were used in this experiment, early stage eggs are also detectable because the antibody recognized both stages of *P. major* eggs from several sea farming centers (Table 2).

Compared to genetic analysis of fish eggs, this method has the advantage of being able to assay many eggs simultaneously without the need to separate individual eggs in tubes and without extracting DNA from the individual egg in each tube. Further, this method works with formalin-fixed eggs, whereas extraction of DNA from formalin-fixed material is problematic. Plankton samples from field studies are typically fixed in formalin-seawater solution.

There was no problem obtaining a large amount of the monoclonal antibody required when identifying *P. major* eggs. The antibody can be easily obtained by large-scale cultures of hybridoma cells. About 50 mL of antibody solution was obtained after two weeks of cultivation. There was no technical problem assaying 43 or 102 eggs from natural waters. However, one assay of a field sample cost about 20 U.S. dollars. To keep costs down an assay kit cheaper than the VECTASTAIN^{R} Elite ABC kit is needed when a large number of field samples are analyzed.

Table 3

Reactivity of monoclonal antibodies to fish eggs. + represents positive reaction; – represents negative reaction.

Egg no.	Species	Reactivity MT-1	MT-2	MT-3
1	*Pagrus major*	+	+	+
2		+	+	+
3		+	+	+
4		+	+	+
5		+	+	+
6		+	+	+
7		+	+	+
8		+	+	+
9	*Acanthopagrus schlegeli*	–	–	–
10		–	–	–
11		–	–	–
12		–	–	–
13		–	–	–
14	*Acanthopagrus latus*	–	–	–
15	*Sparus sarba*	–	–	–
16	*Dentex tumifrons*	–	–	–
17	*Paralichthys olivaceus*	–	–	–
18		–	–	–
19		–	–	–
20		–	–	–
21	*Engraulis japonica*	–	–	–

Acknowledgments

We would like to thank the following sea farming centers and universities for providing the fish eggs used in this study: Fukui Prefectural Sea Farming Center; Kyoto Prefectural Sea Farming Center; Faculty of Agriculture, Kyushu University; Osaka Prefectural Fisheries Station; Sea Farming Center of the Japan Sea-Farming Association; Fisheries Laboratory of Kinki University. We also thank Jeffrey M. Leis, Australian Museum, Sydney, Australia, for his kind advice during the writing of this manuscript.

Table 4

Reactivity of monoclonal antibody MT-1 to the pelagic eggs fixed with formaldehyde just after collection from Wakasa Bay. O.G. diameter = oil globule diameter

Fish egg type	Egg diameter (mm)	O.G. diameter (mm)	Reactivity (%) (positive egg no./ total egg no.)
I	0.72–0.79	0.16-0.19	0 (0/2)
II	0.75–0.82	no oil globule	0 (0/11)
III	0.81–1.02	0.19–0.28	58 (51/88)
IV	1.07	0.21	0 (0/1)

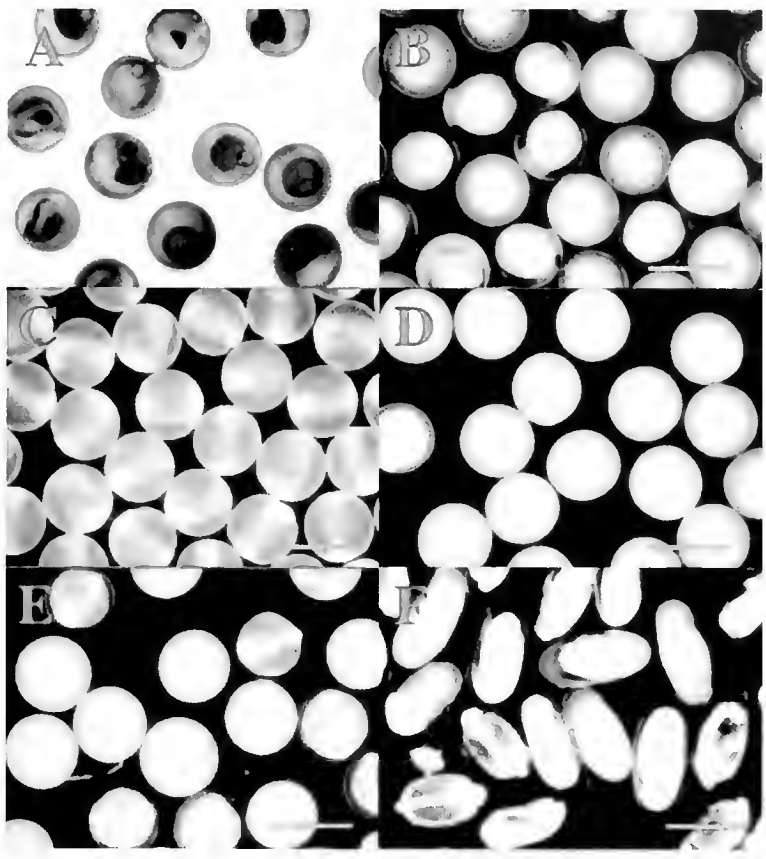

Figure 1

Reactivity of monoclonal antibody MT-1 to fish eggs detected by immunostaining. (**A**) *Pagrus major* (positive reaction); (**B**) *Pagrus major* (negative control reaction without primary antibody); (**C**) *Acanthopagrus shlegeli*; (**D**) *Sparus sarba*; (**E**) *Paralichthys olivaceus*; (**F**) *Engraulis japonica*. Bar represents 1 mm. Only the *P. major* eggs stained brown and showed a positive reaction.

Table 5

Reactivity of monoclonal antibody MT-1 to the pelagic eggs reared for 24 hours after collection from Wakasa Bay.

Egg	Species	Reactivity (%) (positive egg no./total egg no.)
Fish	*Pagrus major*	100 (6/6)
	Acanthopagrus shlegeli	0 (0/8)
	Paralichthys olivaceus	0 (0/1)
	Triglidae sp.	0 (0/1)
	Konosirus punctutus	0 (0/2)
	Soleoidei sp.	0 (0/7)
	Englauris japonicus	0 (0/13)
Decapod	*Enploteuthidae sp.*	0 (0/5)

Literature cited

Daniel III, L. B., and J. E. Graves.
1994. Morphometric and genetic identification of eggs of spring-spawning sciaenids in lower Chesapeake Bay. Fish. Bull. 92:254–261.

Garfré, G., and C. Milstein.
1981. Preparation of monoclonal antibodies: strategies and procedures. *In* Methods in enzymology (J. J. Langone and H. V. Vunakis, eds.), vol. 73, p.3–46. Academic press, New York, NY.

Graves, J. E. M. J. Curtis, P. S. Oeth, and R. S. Waples.
1989. Biochemical genetics of southern California basses of the genus *Paralabrax:* specific identification of fresh and ethanol-preserved individual eggs and early larvae. Fish. Bull. 88:59–66.

Hayashi, K.
2000. Sparidae. *In* Fishes of Japan with pictorial keys to the species (second ed.), T. Nakabo (ed.), p. 857–858. Tokai University Press, Tokyo. [In Japanese.]

Hiroishi, S., S. Matsuyama, T. Kaneko, Y. Nishimura, and J. Arita.
1984. Inhibition of cytotoxicity for screening a monoclonal antibody to HLA antigen. Preparation of a highly specific monoclonal antibody to HLA antigen. Tissue Antigens 24:307–312.

Hiroishi, S., R. Nakai, H. Seto,, T. Yoshida, and I. Imai.
2002. Identification of *Heterocapsa circularisquama* by means of antibody. Fisheries Sci. 68:627–628.

Hiroishi, S., A. Uchida, K. Nagasaki, and Y. Ishida.
1988. A new method for identification of inter- and intra-species of the red tide algae *Chattonella antiqua* and *Chattonella marina* (Raphidophyceae) by means of monoclonal antibodies. J. Phycol. 24:442–443.

Ikeda, T., S. Chuma, and M. Okiyama.
1991. Identification of pelagic eggs of marine fishes by rearing method. Jap. J. Ichthyol. 38:199–206. [In Japanese.]

Ikeda, T., and S. Mito.
1988. Identification of eggs and hatched larvae. *In* An atlas of the early stage fishes in Japan (M. Okiyama, ed.), p. 999–1119. Tokai Univ. Press, Tokyo. [In Japanese.]

Kinoshita, I.
1988. Sparidae. *In* An atlas of the early stage fishes in Japan (M. Okiyama, ed.), p. 527–536. Tokai University Press, Tokyo. [In Japanese.]

Köhler, G.
1979. Fusion of lymphocytes. *In* Immunological methods (I. Lefkovits and B. Pernis, eds.), p. 391–395. Academic press, New York.

Köhler, G., and C. Milstein.
1975. Continuous cultures of fused cells secreting antibody of predefined specificity. Nature (Lond.) 256: 495–497.

Kondo, R., G. Kagiya, Y. Yuki, S. Hiroishi, sand M. Watanabe.
1998. Taxonomy of a bloom-forming cyanobacterial genus *Microcystis*. Nippon Suisan Gakkaishi 64:291–292. [In Japanese.]

Mito, S.
1960. Keys to the pelagic fish eggs and hatched larvae found in the adjacent waters of Japan. The Science Bulletin of the Faculty of Kyushu University 18:71–94, pls. 2–17. [In Japanese.]
1979. Fish egg. Kaiyo kagaku 11:126–130. [In Japanese.]

Nagasaki, K, A. Uchida, S. Hiroishi, and Y. Ishida.
1991a. An epitope recognized by the monoclonal antibody MR-21 which is reactive with the cell surface of *Chattonella marina* type II. Fish. Sci. 57:885–890.

Nagasaki, K, A. Uchida, and Y. Ishida.
1991b. A monoclonal antibody which recognizes the cell surface of red tide alga *Gymnodinium nagasakiense*. Fish. Sci. 57:1211–1214.

Sako, Y., M. Adachi, Y. Ishida, C. Scholin, and D. M. Anderson.
1993. Preparation and characterization of monoclonal antibodies to *Alexandrium* species. *In* Toxic phytoplankton blooms in the sea (T. J. Smayda and Y. Shimizu, eds.) p. 87–93. Elsevier, New York, NY.

Shao, K.-T., K.-C. Chen, and J.-H. Wu.
2002. Identification of marine fish eggs in Taiwan using light microscopy, scanning electric microscopy and mt DNA sequencing. Mar. Freshw. Res. 53:355–365.

Vrieling, E., A. Draaijer, L. Van Zeiljl, W. Gieskes, and M. Veenhuis.
1993. The effect of labeling intensity, estimated by realtime confocal laser scanning microscopy, on flow cytometric appearance and identification of immunochemical labeled marine dinoflagellates. J. Phycol. 29:180–188.

Fishery Bulletin

Guidelines for contributors

Content of papers

Articles

Articles are reports of 10 to 30 pages (double spaced) that describe original research in one or a combination of the following fields of marine science: taxonomy, biology, genetics, mathematics (including modeling), statistics, engineering, economics, and ecology.

Notes

Notes are reports of 5 to 10 pages without an abstract that describe methods and results not supported by a large body of data. Although all contributions are subject to peer review, responsibility for the contents of articles and notes rests upon the authors and not upon the editor or the publisher. It is therefore important that authors consider the contents of their manuscripts carefully. Submission of an article is un-derstood to imply that the article is original and is not being considered for publication elsewhere. Manuscripts must be written in English. Authors whose native language is not English are strongly advised to have their manuscripts checked for fluency by English-speaking colleagues prior to submission.

Preparation of papers

Text

Title page should include authors' full names and mailing addresses (street address required) and the senior author's telephone, fax number, e-mail address, as well as a list of key words to describe the contents of the manuscript. **Abstract** must be less than one typed page (double spaced) and must not contain any citations. It should state the main scope of the research but emphasize the author's conclusions and relevant findings. Because abstracts are circulated by abstracting agencies, it is important that they represent the research clearly and concisely. **General text** must be typed in double-spaced format. A brief introduction should state the broad significance of the paper; the remainder of the paper should be divided into the following sections: Materials and methods, Results, Discussion (or Conclusions), and Acknowledgments. Headings within each section must be short, reflect a logical sequence, and follow the rules of multiple subdivision (i.e. there can be no subdivision without at least two subheadings). The entire text should be intelligible to interdisciplinary readers; therefore, all acronyms and abbreviations should be written out and all lesser-known technical terms should be defined the first time they are mentioned. The scientific names of species must be written out the first time they are mentioned; subsequent mention of scientific names may be abbreviated. Follow *Scientific style and format: CBE manual for authors, editors, and publishers* (6th ed.) for editorial style and the most current issue of the *American Fisheries Society's common and scientific names of fishes from the United States and Canada* for fish nomenclature. Dates should be written as follows: 11 November 1991. Measurements should be expressed in metric units, e.g. metric tons (t). The numeral one (1) should be typed as a one, not as a lower-case el (l).

Footnotes

Use footnotes to add editorial comments regarding claims made in the text and to document unpublished works or works with local circulation. Footnotes should be numbered with Arabic numerals and inserted in 10-point font at the bottom of the first page on which they are cited. Footnotes should be formatted in the same manner as citations. If a manuscript is unpublished, in the process of review, or if the information provided in the footnote has been conveyed verbally, please state this information as "unpubl. data," "manuscript in review," and "personal commun.," respectively. Authors are advised wherever possible to avoid references to nonstandard literature (unpublished literature that is difficult to obtain, such as internal reports, processed reports, administrative reports, ICES council minutes, IWC minutes or working papers, any "research" or "working" documents, laboratory reports, contract reports, and manuscripts in review). If these references are used, please indicate whether they are available from NTIS (National Technical Information Service) or from some other public depository. Footnote format: author (last name, followed by first-name initials), year, title of report or manuscript, type of report and its administrative or serial number, name and address of agency or institution where the report is filed.

Literature cited

The literature cited section comprises works that have been published and those accepted for publication (works in press) in peer-reviewed journals and books. Follow the name and year system for citation format. In the text, write "Smith and Jones (1977) reported" but if the citation takes the form of parenthetical matter, write "(Smith and Jones, 1977)." In the literature cited section, list citations alphabetically by last name of senior author. For example: Alston, 1952; Mundt, 1988; Smith, 1932; Smith, 1947; Stanisky and Jones, 1985. Abbreviations of journals should conform to the abbreviations given in the *Serial sources for the BIOSIS previews database*. Authors are responsible for the accuracy and completeness of all citations. Literature citation format: author (last name, followed by first-name initials), year, title of report or article, abbreviated title of the journal in which the article was published, volume number, page numbers. For books, please provide publisher, city, and state.

Tables

Tables should not be excessive in size and must be cited in numerical order in the text. Headings in tables should be short but ample enough to allow the table to be intelligible on its own. All unusual symbols must be explained in the table legend. Other incidental comments may be footnoted (use italic arabic numerals for footnote markers). Use asterisks only to indicate probability in statistical data. Place table legends on the same page as the table data. We accept tables saved in most spreadsheet software programs (e.g. Microsoft Excel). Please note the following:

- Use a comma in numbers of five digits or more (e.g. 13,000 but 3000).
- Use zeros before all decimal points for values less than one (e.g. 0.31).

Figures

Figures include line illustrations, computer-generated line graphs, and photographs (or slides). They must be cited in numerical order in the text. Line illustrations are best submitted as original drawings. Computer-generated line graphs should be printed on laser-quality paper. Photographs should be submitted on glossy paper with good contrast. All figures are to be labeled with senior author's name and the number of the figure (e.g. Smith, Fig. 4). Use Helvetica or Arial font to label anatomical parts (line drawings) or variables (graphs) within figures; use Times Roman bold font to label the different sections of a figure (e.g. A, B, C). Figure legends should explain all symbols and abbreviations seen within the figure and should be typed in double-spaced format on a separate page at the end of the manuscript. We advise authors to peruse a recent issue of *Fishery Bulletin* for standard formats. Please note the following:

- Capitalize the first letter of the first word of axis labels.
- Do not use overly large font sizes to label axes or parts within figures.
- Do not use boldface fonts within figures.
- Do not create outline rules around graphs.
- Do not use horizontal lines through graphs.
- Do not use large font sizes to label degrees of longitude and latitude on maps.
- Indicate direction of degrees longitude and latitude on maps (e.g. 170°E).
- Avoid placing labels on a vertical plane (except on y axis).
- Avoid odd (nonstandard) patterns to mark sections of bar graphs and pie charts.

Copyright law

Fishery Bulletin, a U.S. government publication, is not subject to copyright law. If an author wishes to reproduce any part of *Fishery Bulletin* in his or her work, he or she is obligated, however, to acknowledge the source of the extracted literature.

Submission of papers

Send four printed copies (one original plus three copies), clipped not stapled, to the Scientific Editor, at the address shown below. Send photocopies of figures with initial submission of manuscript. Original figures will be requested later when the manuscript has been accepted for publication. Do not send your manuscript on diskette until requested to do so.

Dr. Norman Bartoo
National Marine Fisheries Service, NOAA
8604 La Jolla Shores Drive
La Jolla, CA 92037

Once the manuscript has been accepted for publication, you will be asked to submit a software copy of your manuscript. The software copy should be submitted in WordPerfect or Word format (in Word, save as Rich Text Format). Please note that we do not accept ASCII text files. Color figures must be CMYK files.

Reprints

Copies of published articles and notes are available free of charge to the senior author (50 copies) and to his or her laboratory (50 copies). Additional copies may be purchased in lots of 100 when the author receives page proofs.

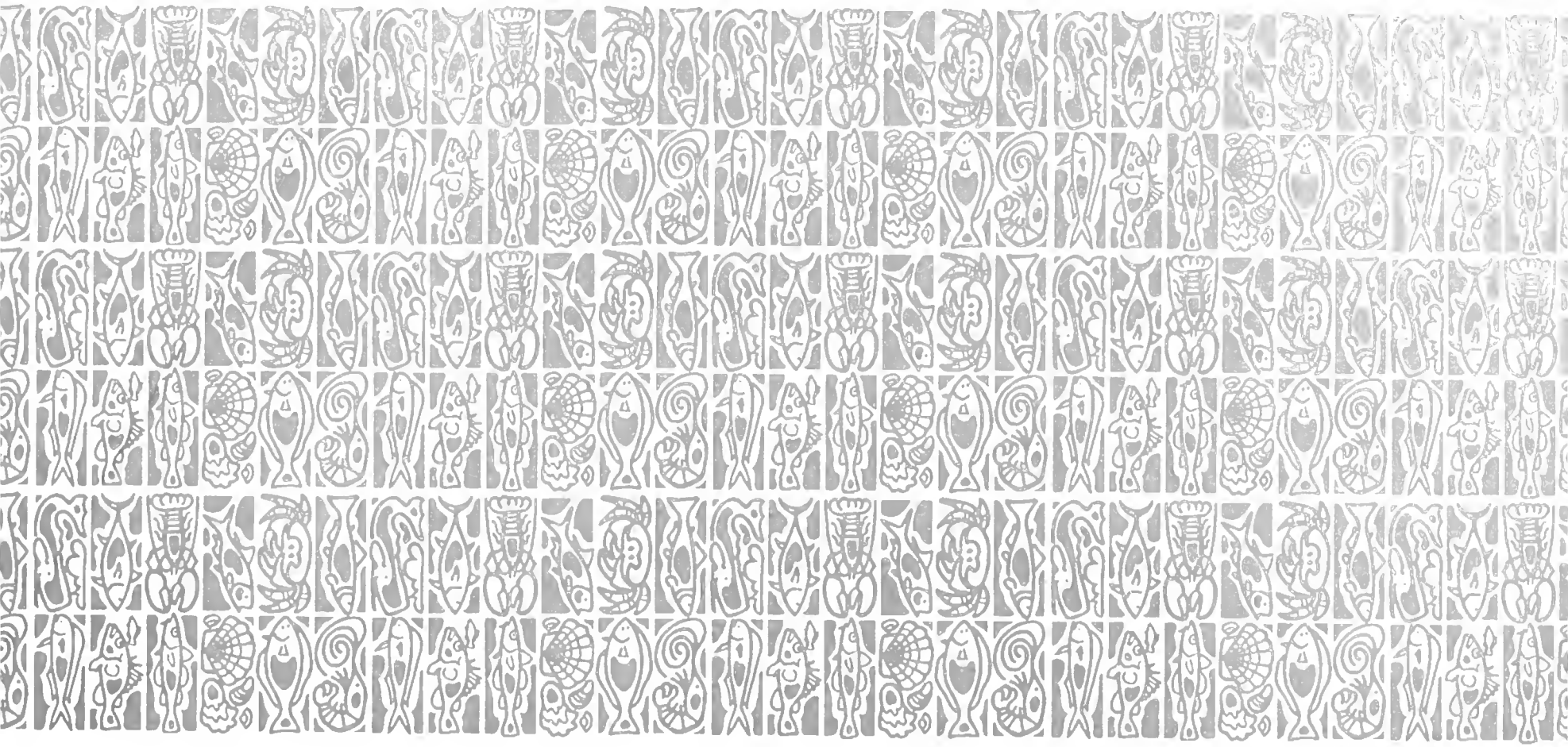

U.S. Department
of Commerce

Volume 102
Number 4
October 2004

Fishery Bulletin

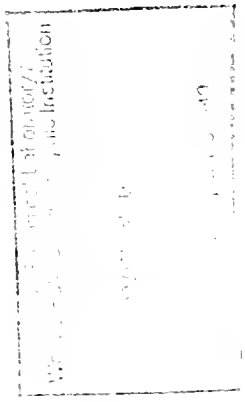

The *Fishery Bulletin* (ISSN 0090-0656) is published quarterly by the Scientific Publications Office, National Marine Fisheries Service, NOAA, 7600 Sand Point Way NE, BIN C15700, Seattle, WA 98115-0070. Periodicals postage is paid at Seattle, WA, and at additional mailing offices. POSTMASTER: Send address changes for subscriptions to Fishery Bulletin, Superintendent of Documents, Attn.: Chief, Mail List Branch, Mail Stop SSOM, Washington, DC 20402-9373.

The Secretary of Commerce has determined that the publication of this periodical is necessary according to law for the transaction of public business of this Department. Use of funds for printing of this periodical has been approved by the Director of the Office of Management and Budget.

For sale by the Superintendent of Documents, U.S. Government Printing Office, Washington, DC 20402. Subscription price per year: $55.00 domestic and $68.75 foreign. Cost per single issue: $28.00 domestic and $35.00 foreign. **See back for order form.**

Fishery Bulletin

***Fishery Bulletin* web site: www.fishbull.noaa.gov**

The *Fishery Bulletin* carries original research reports and technical notes on investigations in fishery science, engineering, and economics. It began as the Bulletin of the United States Fish Commission in 1881; it became the Bulletin of the Bureau of Fisheries in 1904 and the *Fishery Bulletin* of the Fish and Wildlife Service in 1941. Separates were issued as documents through volume 46; the last document was No. 1103. Beginning with volume 47 in 1931 and continuing through volume 62 in 1963, each separate appeared as a numbered bulletin. A new system began in 1963 with volume 63 in which papers are bound together in a single issue of the bulletin. Beginning with volume 70, number 1, January 1972, the *Fishery Bulletin* became a periodical, issued quarterly. In this form, it is available by subscription from the Superintendent of Documents, U.S. Government Printing Office, Washington, DC 20402. It is also available free in limited numbers to libraries, research institutions, State and Federal agencies, and in exchange for other scientific publications.

U.S. Department of Commerce
Seattle, Washington

Volume 102
Number 4
October 2004

Fishery Bulletin

Contents

Articles

Notes

Distribution and abundance of humpback whales (*Megaptera novaeangliae*) and other marine mammals off the northern Washington coast

John Calambokidis
Gretchen H. Steiger
David K. Ellifrit
Cascadia Research Collective
Waterstreet Building
218½ West Fourth Ave.
Olympia, Washington 98501
E-mail address (for J. Calambokidis) calambokidis@cascadiaresearch.org

Barry L. Troutman
Washington Dept. of Fish and Wildlife
600 Capitol Way
Olympia, Washington 98501

C. Edward Bowlby
Olympic Coast National Marine Sanctuary, NOAA
115 Railroad Ave E, Suite 301
Port Angeles, Washington 98362

Abstract—We examined the summer distribution of marine mammals off the northern Washington coast based on six ship transect surveys conducted between 1995 and 2002, primarily from the NOAA ship *McArthur*. Additionally, small boat surveys were conducted in the same region between 1989 and 2002 to gather photographic identification data on humpback whales (*Megaptera novaeangliae*) and killer whales (*Orcinus orca*) to examine movements and population structure. In the six years of ship survey effort, 706 sightings of 15 marine mammal species were made. Humpback whales were the most common large cetacean species and were seen every year and a total of 232 sightings of 402 animals were recorded during ship surveys. Highest numbers were observed in 2002, when there were 79 sightings of 139 whales. Line-transect estimates for humpback whales indicated that about 100 humpback whales inhabited these waters each year between 1995 and 2000; in 2002, however, the estimate was 562 (CV=0.21) whales. A total of 191 unique individuals were identified photographically and mark-recapture estimates also indicated that the number of animals increased from under 100 to over 200 from 1995 to 2002. There was only limited interchange of humpback whales between this area and feeding areas off Oregon and California. Killer whales were also seen on every ship survey and represented all known ecotypes of the Pacific Northwest, including southern and northern residents, transients, and offshore-type killer whales. Dall's porpoise (*Phocoenoides dalli*) were the most frequently sighted small cetacean; abundance was estimated at 181–291 individuals, except for 2002 when we observed dramatically higher numbers (876, CV=0.30). Northern fur seals (*Callorhinus ursinus*) and elephant seals (*Mirounga angustirostris*) were the most common pinnipeds observed. There were clear habitat differences related to distance offshore and water depth for different species.

Manuscript submitted 25 September 2003 to the Scientific Editor's Office.

Manuscript approved for publication 4 June 2004 by the Scientific Editor.

Fish. Bull. 102:563–580 (2004).

Marine mammals have had an important role in the history of the Olympic Peninsula for centuries. Many species, including sea otters (*Enhydra lutris*), harbor seals (*Phoca vitulina*), humpback whales (*Megaptera novaeangliae*), and gray whales (*Eschrichtius robustus*) were hunted by the Makah tribe (Swan, 1868; Huelsbeck, 1988). Much later, modern whalers targeted humpback whales in this region from stations at Bay City, Washington (1911–25, Scheffer and Slipp, 1948), and southern Vancouver Island, British Columbia (1905–43, Gregr et al., 2000). A small aboriginal hunt for gray whales resumed in these waters in 1998, and the Makah killed one gray whale in May 1999. Since the end of commercial whaling, marine mammals have been afforded protection under the Marine Mammal Protection Act of 1972. In addition, the waters off the northern Washington coast were designated as the Olympic Coast National Marine Sanctuary in 1994.

A number of studies have documented marine mammals in this region. Some surveys of broader areas have included the waters off northern Washington (Von Saunder and Barlow, 1999; Brueggeman[1]; Green et al.[2]). Species-specific studies also

[1] Brueggeman, J. J. 1992. Oregon and Washington marine mammal and seabird surveys. Final report of OCS Study MMS 91-0093 by Ebasco Environmental, Bellevue, Washington, and Ecological Consulting, Inc., Portland, Oregon, for the Minerals Management Service (MMS). 445 p. MMS, Pacific OCS Region, U.S. Dept. of Interior, 770 Paseo Camarillo, Camarillo, CA 93010.

[2] Green, G. A., M. A. Smultea, C. E. Bowlby, and R. A. Rowlett. 1993. Delphinid aerial surveys in Oregon and Washington offshore waters. Final report for contract 50ABNF200058 to the National Marine Mammal Laboratory, National Marine Fisheries Service, 100 p. Nat. Mar. Mamm. Lab., NMFS, 7600 Sand Point Way NE F/AKC3, Seattle, WA 98115.]

have been conducted on harbor porpoise (*Phocoena phocoena;* Barlow et al., 1988; Osmek et al., 1996; Calambokidis et al.[3]) and, to a limited degree, on humpback whales (Calambokidis et al., 1996, 2000) and gray whales (Darling, 1984; Green et al., 1995; Shelden et al., 2000; Calambokidis et al., 2002). Studies on pinnipeds and sea otters have also been conducted in this region (Jeffries et al., 2003; Jameson et al., 1982, 1986; Kvitek et al., 1992, 1998; Bowlby et al.[4]).

Information on humpback whales is of particular interest because they were the primary species hunted by whalers off Washington in the early 1900s. Since then, little has been known about their movements and distribution in this region. Photo-identification research has helped define the movements and stock structure of the humpback whales feeding off California (Calambokidis et al., 1990, 1996, 2000). Calambokidis et al. (1996) suggested that a demographic boundary exists between humpback whales that feed off the coasts of California, Oregon, and Washington and humpback whales feeding farther north off British Columbia and Alaska. The identity and degree of interchange of the whales that feed in this boundary area have been unclear.

Similarly for killer whales, photo-identification studies have revealed much about whale groups that frequent the inland waters of Washington and British Columbia (Bigg et al., 1990; Ford et al., 1994). Very little is known about their occurrence off the coast, in particular, about the "offshore" groups that are believed to be a distinct race (Ford et al., 1994) that are seen primarily offshore but occasionally also enter inland waterways.

We report here on the summer distribution of marine mammals off the northern Washington coast based on six ship line-transect surveys conducted between 1995 and 2002. These surveys were initiated to understand marine mammal distribution and abundance in the newly designated Olympic Coast National Marine Sanctuary, as well as to collect information on seabirds, oceanographic conditions, and juvenile fish. Each ship survey was conducted between mid-June and late July. Density estimates were made for the two most common species: humpback whales and Dall's porpoise. In addition, photo-identification data gathered during these ship surveys and from supplemental small boat surveys within the same area between 1989 and 2002 provided information on humpback and killer whale movements and stock structure.

Materials and methods

Ship surveys

Generally, ship surveys covered the area between the 20-m isobath and the landward margin of the continental shelf (200-m isobath) from the entrance to Strait of Juan de Fuca to the mouth of the Copalis River to include the boundaries of the Olympic Coast National Marine Sanctuary (Fig. 1). Although the northern extent of these waters is off southern British Columbia (Vancouver Island), the entire overlapping region will be referred to as northern Washington.

Fourteen east-west tracklines were selected, following permanent tracklines established by the NOAA ship *Miller Freeman* in 1989. Tracklines were spaced at 5-nmi intervals and were surveyed each year except in 2002, when only ten lines were surveyed (four southernmost lines were not included). Extra ship time allowed for replicate surveys of the northern survey legs in 1995, a short offshore extension of two lines in 1996 and 2000 (up to 17 nmi in 1986), the addition of three short east-west lines off southern Vancouver Island around La Perouse Bank in 1997, and one additional line that was surveyed south of the study area in 2000 (Fig. 1).

Ship surveys were conducted over a two-week period in late-June and July 1995, 1996, 1997, 1998, and 2000 (Table 1). In 2002, a shorter, one-week survey was done in mid-June. The marine mammal ship surveys were conducted by a single primary observer from the vessel's flying bridge (the sighting platform) with a viewing height of 10 m above the water level. All surveys were conducted from the NOAA ship *McArthur* (55 m) except during 2000, when the naval ship *Agate Passage* (33 m) was used. From these platforms, the primary observer scanned a 180-degree arc encompassing the area ahead of the ship and abeam to either side. Observers used reticle binoculars when possible and obtained measurements of distance to a sighting derived from the angle below the horizon (measured with graded reticles in the binoculars) and the known platform height. For sightings where the species could not be determined by the observer, animals were identified to a general taxonomic level (e.g., unidentified pinniped).

Photo-identification surveys

In addition, photo-identification data were examined that had been gathered within the survey area. Researchers took photographs directly from the survey ship, or from a *Zodiac* rigid-hulled inflatable that was launched when animals were sighted. In 1996, the last two days of vessel time on the *McArthur* were used to photograph whales for identification.

[3] Calambokidis, J., J. C. Cubbage, J. R. Evenson, S. D. Osmek, J. L. Laake, P. J. Gearin, B. J. Turnock, S. J. Jeffries, and R. F. Brown. 1993. Abundance estimates of harbor porpoise in Washington and Oregon waters. Report to the National Marine Mammal Laboratory, National Marine Fisheries Service, 55 p. Nat. Mar. Mamm. Lab., NMFS, 7600 Sand Point Way NE F/AKC3, Seattle, WA 98115.

[4] Bowlby, C. E., B. L. Troutman, and S. J. Jeffries. 1988. Sea otters in Washington: distribution, abundance, and activity patterns. Final report to National Coastal Resources Research and Development Institute, Hatfield Marine Science Center, 2030 S. Marine Dr., Newport, Oregon 97365, 131 p. Cascadia Research Collective, Wash. State Dept. of Wildlife, Olympia, WA.

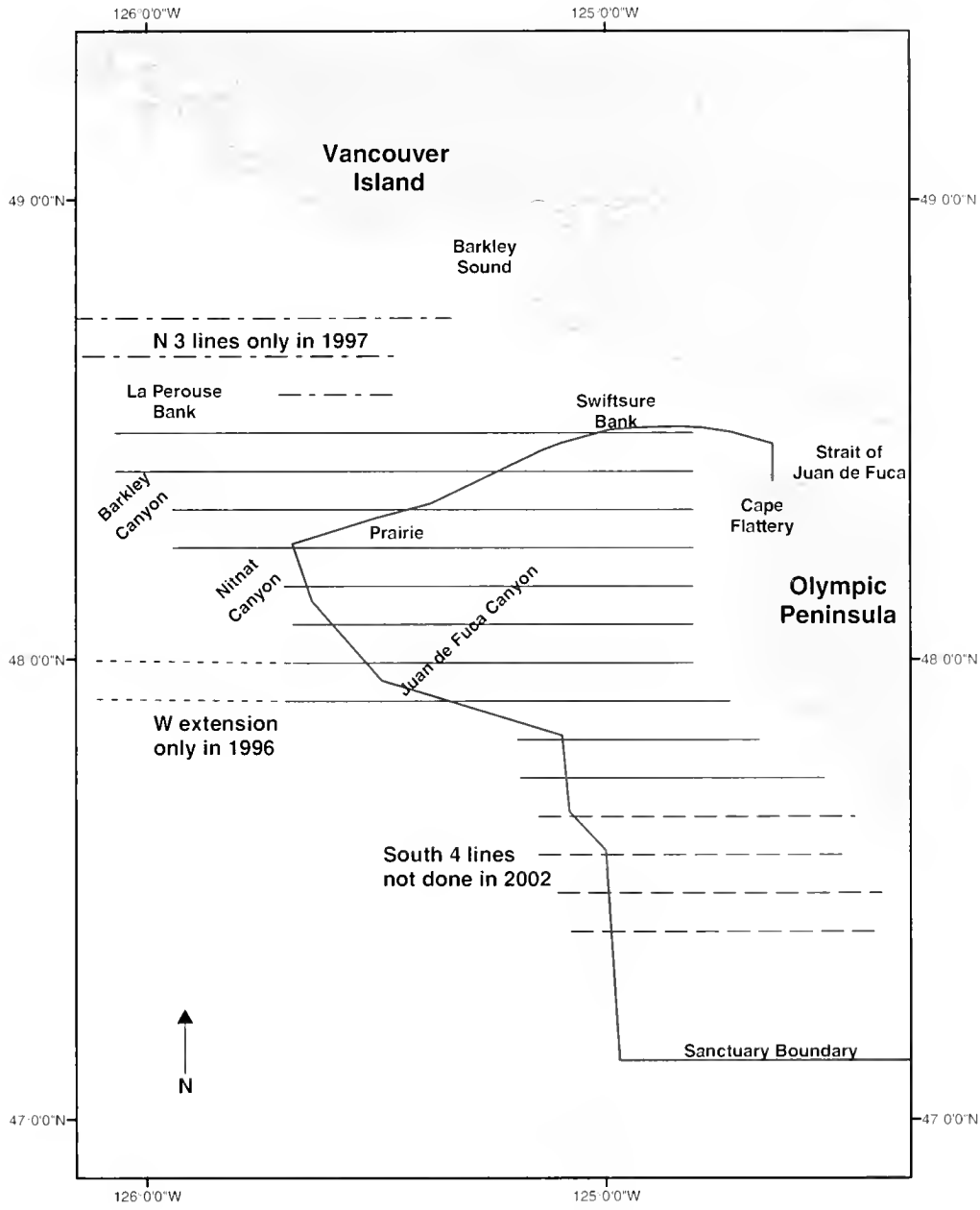

Figure 1

On-effort ship survey tracklines (horizontal lines) off the northern coast of Washington between 1995 and 2002. The Olympic Coast National Marine Sanctuary boundary is delineated and labeled. Dashed and dotted lines show three northern lines surveyed only in 1997, the western extension of two lines surveyed only in 1996, and the southern four lines missed in 2002.

In addition, dedicated photo-identification surveys were conducted by Cascadia Research scientists using a 5.3-m *Novurania* rigid-hulled inflatable that was launched from nearby ports and operated in areas where whales were concentrated. Photo-identification data in the present study includes data collected off the northern Washington coast between 1989 and 2002 (Table 2). It also includes photographs contributed by other researchers and boat operators taken in the area during this time (Table 2).

Generally, photographs were taken with Nikon 8008 35-mm cameras equipped with 300-mm Nikkor telephoto lenses. High-speed black-and-white film (Ilford HP 5+) was pushed 1½ stops so that exposure times were generally 1/1000 or 1/2000 of a second. Identification photographs were taken with standard procedures used

Table 1

Summary of ship survey effort off northern Washington (does not include small boat surveys).

Year	Dates of effort		No. of legs	Effort (h)	nmi on effort	Ship	Observers
	Start	End					
1995	21 Jul	27 Jul	10	46	546	*McArthur*	Troutman, Ellifrit
1996	28 Jun	5 Jul	14	46	540	*McArthur*	Troutman, Ellifrit
1997	9 Jul	18 Jul	17	52	513	*McArthur*	Troutman, Ellifrit
1998	25 Jun	4 Jul	14	55	572	*McArthur*	Troutman, Quan
2000	16 Jun	24 Jun	14	60	589	*Agate Passage*	Rowlett, Nelson
2002	12 Jun	18 Jun	10	32	315	*McArthur*	Troutman, Douglas
All years				291	3075		

Table 2

Photo-identification effort off the coast of northern Washington between 1989 and 2002. These data include whales identified from the ship or small boats launched from the ship, dedicated small boat surveys, and opportunistic photographs taken by others. Unique = number of different animals.

Year	Days IDs obtained			Humpback whales identified				Other sources of photographs
	No.	First	Last	No.	Unique	No. of mothers	No. of calves	
1989	1	1 Oct	1 Oct	1	1	0	0	
1990	3	25 Aug	6 Sep	10	10	1	1	Balcomb/Bloedel[1]
1991	4	23 Aug	4 Sep	14	13	0	0	Balcomb/Bloedel[1]
1993	1	15 Jul	15 Jul	3	3	0	0	
1994	3	25 Jun	15 Jul	20	16	0	0	G. Ellis,[2] R. Baird
1995	7	14 Jul	25 Jul	50	35	4	2	S. Mizroch[3]
1996	9	29 Jun	6 Oct	55	34	1	0	
1997	9	13 Jul	18 Oct	25	23	2	0	
1998	19	28 May	16 Oct	71	48	1	1	V. Deeke, B. Gisborne
1999	28	20 May	20 Oct	103	60	2	0	B. Gisborne
2000	12	2 Jun	4 Oct	56	40	2	1	B. Gisborne
2001	15	8 Jun	5 Oct	59	41	2	1	SWFSC,[4] B. Gisborne
2002	9	13 Jun	5 Sep	41	32	0	0	
Total	120			508	356	15	6	
Unique					191			

[1] Center for Whale Research, P.O. Box 1577, Friday Harbor, WA 98250.
[2] Dept. of Fisheries and Oceans, Pacific Biological Station, Nanaimo, BC, V9T 6N7, Canada.
[3] National Marine Mammal Laboratory, NMFS, 7600 Sand Point Way NE, Seattle, WA 98115.
[4] Southwest Fisheries Science Center, 8604 La Jolla Shores Dr., La Jolla, CA 92037.

in past research (Calambokidis et al., 1990). For humpback whales, photographs were taken of the ventral side of the tail flukes. For killer whales, the dorsal fin and surrounding saddle-patch area were photographed from both sides.

Photographs of individuals were first compared to those identified in the same region. To analyze interchange with other regions, we compared these individuals with existing catalogs to obtain sighting histories. For humpback whales, a catalog was used of over 1000 humpback whales identified since 1986 along the West Coast. The regions used for comparison were Oregon, northern California (Oregon-California border to Pt. Arena), northern central California (Pt. Arena to north of Monterey Bay), southern central California (north of Monterey Bay to Pt. Conception) and southern California (southern California Bight). For killer whales, whales were matched to existing catalogs (Bigg et al., 1987; Ford et al., 1994; Black et al., 1997). All identifications and group determinations were confirmed by one of the authors (DKE) or Graeme Ellis (Dept. of Fisheries and Oceans, Nanaimo, British Columbia).

Data analysis

For ship surveys between 1995 and 2000, position and oceanographic data (including depth, sea surface temperature) logged by the ship's computer were later reconciled with the sighting and effort data recorded by the observers. Sighting positions were analyzed for each species for water depth, distance from shore, distance from shelf edge (200-m depth contour) and sea surface temperature. Data analysis and mapping were conducted by using a geographic information system (GIS) with ArcInfo software (ESRI, Redlands, CA). Data from the shorter 2002 ship survey were included in the summary of sightings but were not available for the analyses of sightings related to oceanographic features.

Line-transect analysis to determine density and abundance was conducted for the two species with more than 30 sightings (humpback whales and Dall's porpoise). We used the program (Distance, version 3.5, Research Unit for Wildlife Population Assessment, University of St. Andrews, St. Andrews, UK) to conduct analyses. For these analyses, we used only effort and sightings from the regular east-west transect lines and did not include on-effort data from opportunistic lines or cross-tracks. We included sightings made by secondary as well as the primary observer. Although whales were reportedly seen out to 6 nmi, we truncated the sightings at 3 nmi for humpback whales and 2.5 nmi for Dall's porpoise. For humpback whales we included 16 sightings of unidentified whales (unidentified mainly because of distance). These were probably humpback whales because the only other large whales that were seen in the surveys were a few gray whales seen close to shore. Distance position data were incomplete for 13 of the 188 whale sightings and 14 of 82 Dall's porpoise sightings; for these the missing value was randomly selected from the observed measurements.

The Distance program was used to select the best model for sighting probability in relation to distance off the transect. We allowed the program to select among models (half-normal, uniform, hazard-rate, and negative exponential) and varying numbers of adjustment terms (cosine and simple polynomials) based on lowest Akaike's information criterion (AIC) score. All years were pooled for the model of sighting probability, but encounter rate and group size were calculated by year. An adjustment to group size was calculated if there was a significant group size bias with distance from the track line, which was not the case for humpback whales but was present in some years (1996 and 1997) for Dall's porpoise.

Area was calculated for abundance estimation based on the zone covered by the regularly scheduled transect lines covered in most years (study area was considered to encompass waters 2.5 nmi north of the northernmost line and 2.5 nmi south of the southernmost line). The only annual adjustment for area was for humpback whales in 2002. Surveys in that year did not cover the southern end of the study area (because of limited ship time), an area with a typically lower abundance of whales. To avoid extrapolating the higher density of whales from the northern portion of the study area to this region, we excluded this missed area from the abundance estimates.

Estimates of abundance for humpback whales were also calculated by using capture-recapture models (Seber, 1982; Hammond, 1986). We used identifications obtained in pairs of adjacent years taken from 1994 to 2002 to generate Petersen capture-recapture estimates. The Chapman modification of the Petersen estimate (Seber, 1982) was used because it was appropriate for sampling without replacement (Hammond, 1986).

Results

In total, there were 706 sightings of 2467 animals over the six ship surveys combined (Table 3). Fifteen different marine mammal species were seen: nine cetacean species, five pinniped species, and the sea otter were identified. Each year, 9 to 12 different species were seen, except in 2002 when only six species were observed. This 2002 survey, although shorter than those of the other years, showed a dramatic change in the species diversity and numbers of animals. We saw many more humpback and Dall's porpoise than in previous years. We also noted the absence of six regularly observed species: harbor porpoise, gray whales, Pacific white-sided dolphins (*Lagenorhynchus obliquidens*), Risso's dolphin (*Grampus griseus*), harbor seals, and California sea lions (*Zalophus californianus*).

Humpback whales

Of the large cetaceans, humpback whales were the most common species seen; there were 232 sightings of 402 animals during ship surveys (Table 3). Largest numbers of humpback whales were seen in 2002, when there were 79 sightings of 139 individuals during the one-week survey. Group sizes ranged from 1 to 8 animals (mean=1.7, SD=1.1). Only six calves were recorded from the ship surveys—probably because it was difficult to identify calves at the distance at which most sightings were made. Of these six sightings of mothers with calves, four sightings were outside the primary areas where other humpback whale groups were seen.

Sightings were concentrated in the northern part of the study area between Juan de Fuca Canyon and the outer edge of the continental shelf, an area known as "the Prairie" (Fig. 2). A small area east of the mouth of Barkley Canyon and north of the Nitnat Canyon where the water depth was 125–145 m had a high density of sightings in all years. A smaller number of humpback whales were also seen on Swiftsure Bank. Sightings in 2002 were not only more numerous but more broadly distributed; sightings were recorded in the areas described above and also farther south and closer to shore than those seen in previous years.

Line-transect estimates for humpback whales were very consistent in the first five surveys (1995 to

Table 3

Summary of marine mammal sightings by year during ship surveys off northern Washington. Opportunistic sightings (non-transect) are included.

	1995		1996		1997		1998		2000		2002		All years	
Species	No. of sightings	No. of animals	No. of sightings	No. of animals	No. of sightings	No. of animals	No. of sightings	No. of animals	No. of sightings	No. of animals	No. of sightings	No. of animals	No. of sightings	No. of animals
Baleen whales														
Humpback whale	25	40	54	86	23	44	27	36	24	57	79	139	232	402
Gray whale	1	1	2	3	2	3					5	7		
Minke whale	3	3	1	1	4	4								
Unidentified whale	4	8	3	3	11	12	1	1	3	3	4	6	26	33
Odontocetes														
Dall's porpoise	27	72	20	64	16	43	13	46	14	48	25	133	115	406
Harbor porpoise	4	10	11	20	2	5	14	43	7	11		38	89	
Pacific white-sided dolphin	4	596	16	149					4	369	4	19	28	1133
Northern right-whale dolphin					1	6		1	6					
Risso's dolphin	5	57	1	5	2	11	1	6		9	79			
Killer whale	3	16	2	38	2	21	2	5	3	36	2	8	14	124
Unidentified delphinid	6	9	8	56	2	4	3	5			4	18	23	92
Pinnipeds and otters														
Harbor seal	2	2	3	3	2	3	7	7	1	1			15	16
Elephant seal	6	6	10	10	2	2	2	2			20	20		
California sea lion	1	1	3	3			4	4						
Steller sea lion	3	5	1	1			4	6						
Northern fur seal	6	6	5	5	1	2	9	9	1	1	6	6	28	29
Sea otter	3	3	3	3										
Unidentified pinniped	4	4	3	3	1	2	4	4	1	1			13	14
Total sightings	94	772	141	495	65	146	91	179	66	545	125	330	706	2467

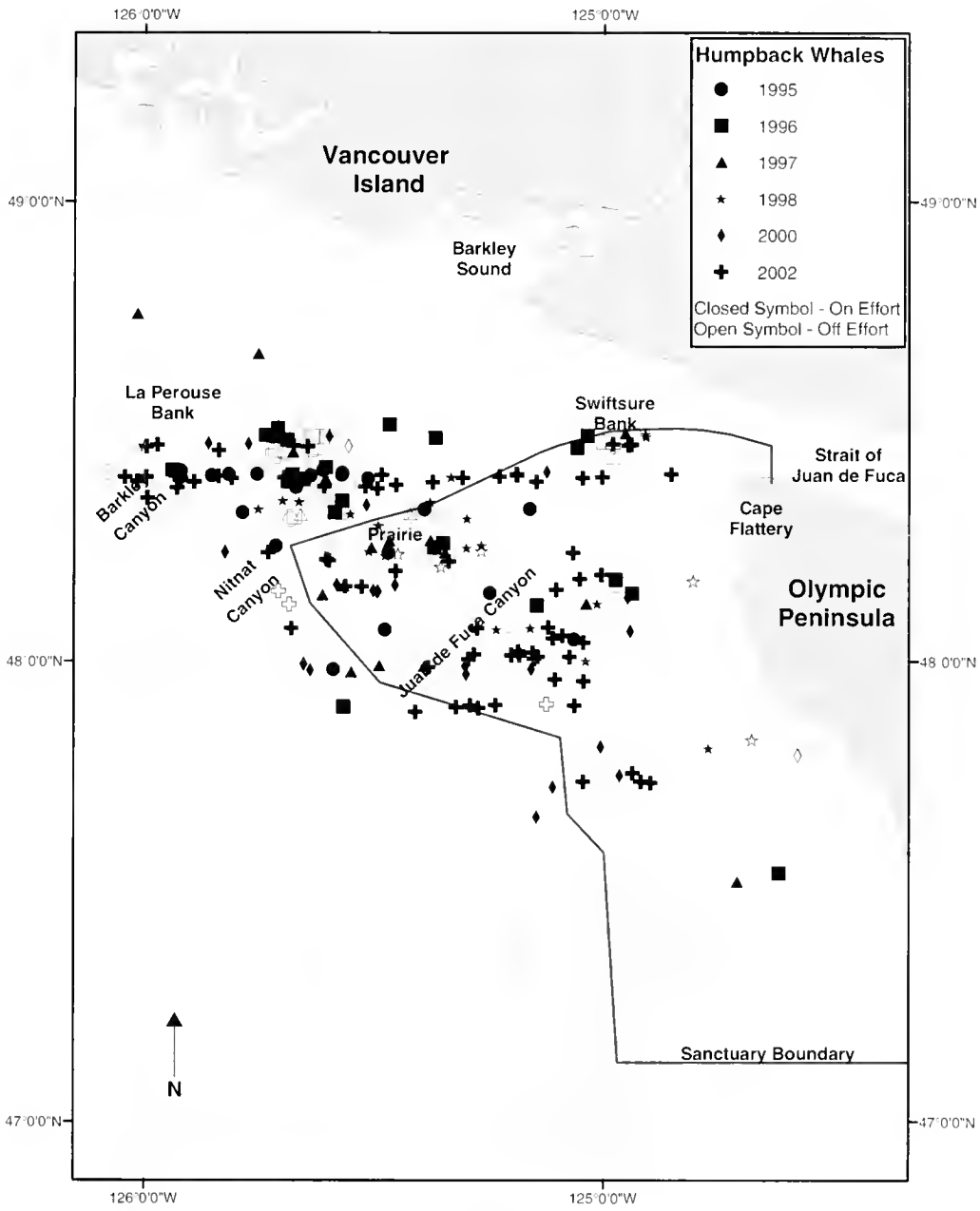

Figure 2

Locations (by year) for humpback whales (*Megaptera novaeangliae*) seen during ship surveys off the northern Washington coast between 1995 and 2002.

2000, Table 4, Fig. 3). The encounter rate of groups (0.046–0.053 sightings per nmi), density (0.034–0.050 whales per nmi^2), and abundance (85–125 individuals) were similar among these years. These data indicate that about 100 humpback whales used the study area during this period.

The sighting rate of humpback whales was dramatically higher in 2002 than in all previous years and was reflected in the line-transect estimates (Fig. 3). Estimated density (0.23 whales per nmi^2) was more than four times higher than any previous year. Applying this density to only the reduced area surveyed in 2002 (1953 instead of 2505 nmi^2) still yielded much higher estimates of abundance (562, CV=0.21) than in any previous year. These higher abundance estimates could not have been an artifact of random variation; the lower bound of the 95% confidence interval for the 2002 estimates was well above the upper confidence interval of any of the previous years (Table 4).

Of the humpback whales photographed during small boat surveys off the northern Washington-BC border between 1989 and 2002, 508 individuals were success-

Table 4

Results of line-transect analysis for humpback whales off northern Washington. On-effort sightings of humpback and unidentified large whales made during regular transects (not including deadheads [areas between transect lines] and opportunistic sightings) within 3 nmi of ship were used. Best detection model fit (AIC scores) was a negative exponential with 1 cosine adjustment yielding $f(0)$=1.05. Effective strip width was 0.95 nmi with CV=0.09.

Year	Sightings	Survey effort		Encounter rate	Group size	Density (per nmi^2)	Area (nmi^2)	Estimated abundance	CV	95% Conf. int.	
	n	lines	nmi							lower	upper
1995	23	58	438	0.053	1.48	0.041	2505	102	0.33	54	193
1996	24	59	474	0.051	1.54	0.041	2505	103	0.33	55	193
1997	26	92	493	0.053	1.62	0.045	2505	112	0.3	63	199
1998	20	62	432	0.046	1.40	0.034	2505	85	0.31	47	155
2000	23	70	504	0.046	2.09	0.050	2505	125	0.32	67	234
2002	72	43	305	0.236	1.81	0.224	1953	562	0.21	375	841
Total	188	384	2646								

fully identified of which 191 were unique individuals (Table 2). Of these 191, 83 (44%) had been seen in this area in more than one year within this time period. The proportion of animals seen more than one year changed over the course of the study (Fig. 4). The proportion of whales identified each year that had been seen in others years decreased annually (Fig. 4, regression r^2=0.63, P=0.002); the most dramatic drop occurred between 1998 and 1999.

Photographs of humpback whales documented animal movements within the study area and provided some insight into possible reasons for the high sighting rates during the 2002 ship surveys. On two occasions, the same humpback whale was identified on different days in a slightly different area and represented a duplicate sighting of this animal from the ship survey. It is possible that shifting humpback whale distribution during the course of the 2002 survey could have occurred in a manner that resulted in the same animals being encountered multiple times and that elevated the sighting rate and line-transect abundance estimate (Fig. 3). We cannot test this hypothesis because other animals may have shifted in a manner that they avoided being detected at all.

Abundance of humpback whales from capture-recapture models yielded estimates of 89 to 343 whales (Table 5, Fig. 3). These estimates tended to increase over the course of the study from a low of 89 whales for 1994–95 to a high of 343 for 2000–2001 and 230 for 2001–2002 (regression r^2=0.60, P=0.02). There was fairly good agreement between the capture-recapture and line-transect estimates until 2002 (Fig. 3).

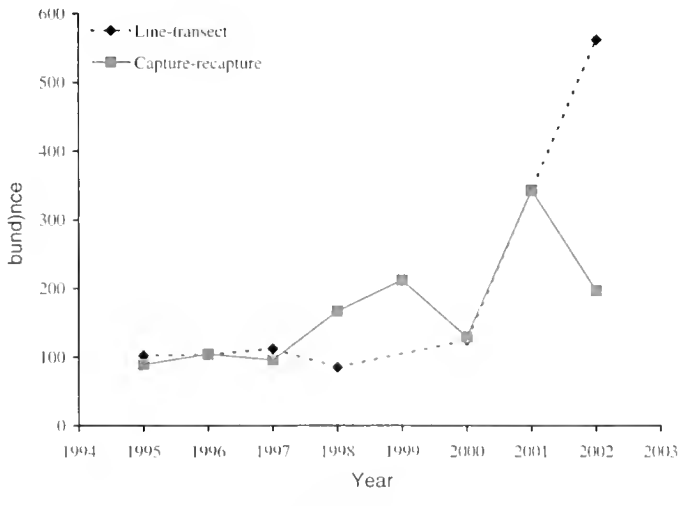

Figure 3

Line-transect (dashed line) and capture-recapture (solid line) estimates for humpback whale (*M. novaeangliae*) abundance between 1995 and 2002.

A total of 17 of the 191 (9%) whales that we identified off northern Washington had also been photographed off California and Oregon (Table 6). Interchange of whales seen off northern Washington and other feeding areas to the south decreased as distance among feeding areas increased. About 10% (10 of 105) of the whales that were identified off Oregon were also photographed off northern Washington. This rate of matching dropped below 3% (8 of 313) off northern California and continued to decrease to no interchange seen for whales photographed off southern California.

The proportion of whales that were seen in areas to the south appeared to change over the course of the study. From 1989 to 1998, when resighting rates between years within our study area were highest, we also had a higher proportion of interchange with feeding areas to the south (13 of 109 whales or 12%). From 1999 to 2002, after resightings within our region decreased, there was also a decrease

Table 5

Estimates of humpback whale abundance (Est.) off northern Washington obtained with the Petersen capture-recapture model. Each estimate was based on the identifications obtained (n) in each of two adjacent years.

	Sample 1		Sample 2				
Period	Year	n	Year	n	Match	Est.	CV
1994–95	1994	14	1995	35	5	89	0.27
1995–96	1995	35	1996	34	11	104	0.19
1996–97	1996	34	1997	21	7	95	0.24
1997–98	1997	23	1998	48	6	167	0.28
1998–99	1998	48	1999	60	13	213	0.19
1999–2000	1999	60	2000	31	14	129	0.16
2000–01	2000	40	2001	41	4	343	0.36
2001–02	2001	41	2002	32	5	230	0.32

in the proportion of these whales that had also been seen off California and Oregon (7 of 136 whales or 5%). This difference falls just short of statistical significance (χ^2=3.71, P<0.10) but is in the reverse direction from what would be expected if immigration from the south were to increase over time.

Between 1989 and 2002, 15 different mothers were seen with 16 calves (one mother seen with a calf in two different years). Mothers with calves represented 4.2% of the individual whales identified each year (15 of 356 unique annual identifications, Table 2). For each year only a small proportion of the calves were identified because calves raise their flukes less often.

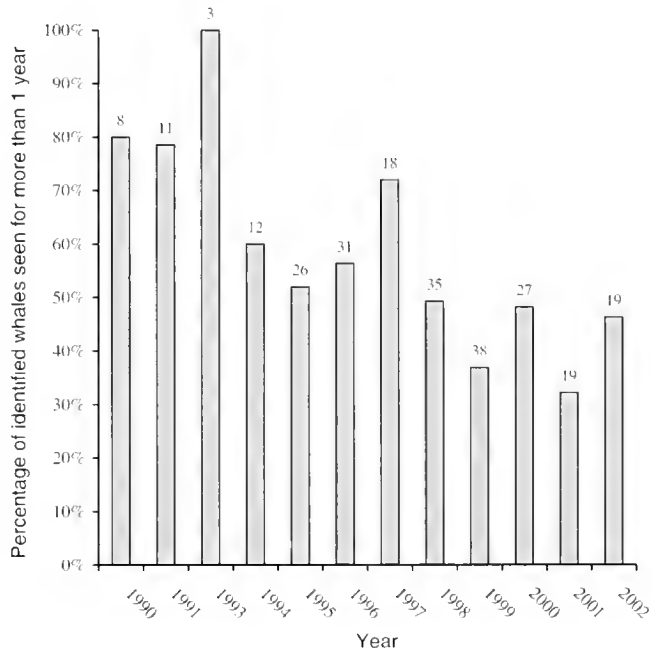

Figure 4

The proportion of humpback whales (*M. novaeangliae*) seen in more than one year during annual surveys off northern Washington from 1989 to 2002.

Killer whales

One other large cetacean species (killer whales) was also seen every year; there were a total of 14 sightings of 124 animals from ship surveys (Table 3). Three of these sightings were of large groups between 20 and 35 animals, and the rest were in groups fewer than ten (14 sightings, mean=8.9, SD=11.2). Killer whales were widely distributed across different habitats; there were sightings of animals both close to and far from shore and in fairly shallow and deep water (Fig. 5).

All three ecotypes of killer whales (namely, 1) southern and northern residents, 2) transients, and 3) offshore residents) were observed off the northern Washington coast. Of the 15 groups identified photographically between 1989 and 2002, there were sightings of animals from the southern resident (2 groups), northern resident (3), transient (5) and offshore (3) groupings (Table 7). Other sightings appeared to be northern residents (1) and offshore (1) animals but the quality of the photographs were too poor for us to be certain. Large groups of killer whales (20–40 animals) were seen on five occasions during small boat surveys.

Dall's porpoises

Dall's porpoises were the most frequently sighted small cetacean; there were 115 sightings of 406 animals and Dall's porpoises were observed every year (Table 3). No

Table 6

Number of humpback whales identified in different regions along the U.S. west coast and the number and percentage of these that matched with northern Washington. For northern Washington, we report the number of whales that were seen in that region in more than one year.

Region	No. of individuals	No. of matches with N. Wash.	% of whales that match with those in N. Wash.
Northern Washington	191	83	43.5%
Oregon	105	10	9.5%
N. California	313	8	2.6%
N. Central California	921	13	1.4%
S. Central California	666	3	0.5%
S. California	303	0	0.0%

Table 7

Summary of killer whale sightings off northern Washington between 1989 and 2002 where identifiable photographs were taken.

Date	No. of animals estimated	Lat. °N	Long. °W	Community	Pod or ID	Comments
13 Sep 89	3	48 23.0	124 48.5	Resident—southern	L10, L28,L41	
15 Jul 94	4	48 20.9	125 20.0	Transient	CA195	
25 Jul 95	7	47 49.8	124 59.5	Transient	CA195	
26 Jul 95	8	47 53.7	125 03.3	Transient	CA20,CA27	
17 Mar 96	6	46 58.2	124 15.7	Resident—southern	L26, L83	outside Grays Harbor
31 Mar 96	7	46 55.0	124 09.7	Transient—probably	T50?	Grays Harbor entrance
5 Jul 96	3	48 13.1	124 55.0	Transient	T185	
6 Jul 96	40	48 26.7	125 43.2	Resident—northern	C, D, G1s, G12s	
15 Jul 97	30	48 19.4	125 09.5	Offshore		
18 Jul 97	10	48 18.3	125 23.6	Offshore	CA105	
10 Aug 97	8	48 21.0	125 34.6	Transient	T36, T99, T36A?, T137?	
27 Aug 98	40	48 28.0	125 17.0	Offshore	O44,O30, O31,O172, O14, O158, O218	
10 Oct 99	30	48 22.0	125 38.1	Resident—northern	111	
18 Jun 00	20	48 03.8	125 04.3	Probably resident—northern		not southern residents
6 Sep 01	12	47 01.8	124 46.6	Resident—northern	G12s, G17s, G29s	

Table 8

Results of line-transect analysis for Dall's porpoise off northern Washington. All on-effort sightings during regular transects (not including deadheads [areas between transect lines] and opportunistic sightings) within 2.5 nmi of the ship were included. The best detection model fit (AIC scores) was the hazard rate with no cosine adjustment, yielding $f(0)$=2.60. Effective strip width of 0.38 nmi with CV=0.12. The group size for 96–97 was adjusted to account for a significant group size bias with distance from the trackline.

Year	Sightings n	Survey effort: lines	Survey effort: nmi	Encounter rate	Group size	Density (per nmi^2)	Area (nmi^2)	Estimated abundance	CV	95% Conf. int.: lower	95% Conf. int.: upper
1995	16	58	438	0.037	2.25	0.100	2505	268	0.32	143	501
1996	14	59	474	0.030	2.65	0.102	2505	255	0.32	138	472
1997	13	92	493	0.026	2.28	0.078	2505	197	0.38	95	405
1998	9	62	432	0.021	2.67	0.072	2505	181	0.49	72	453
2000	13	70	504	0.026	3.46	0.116	2505	291	0.42	132	644
2002	17	43	305	0.056	4.82	0.350	2505	876	0.3	487	1576
Total	82	384	2646								

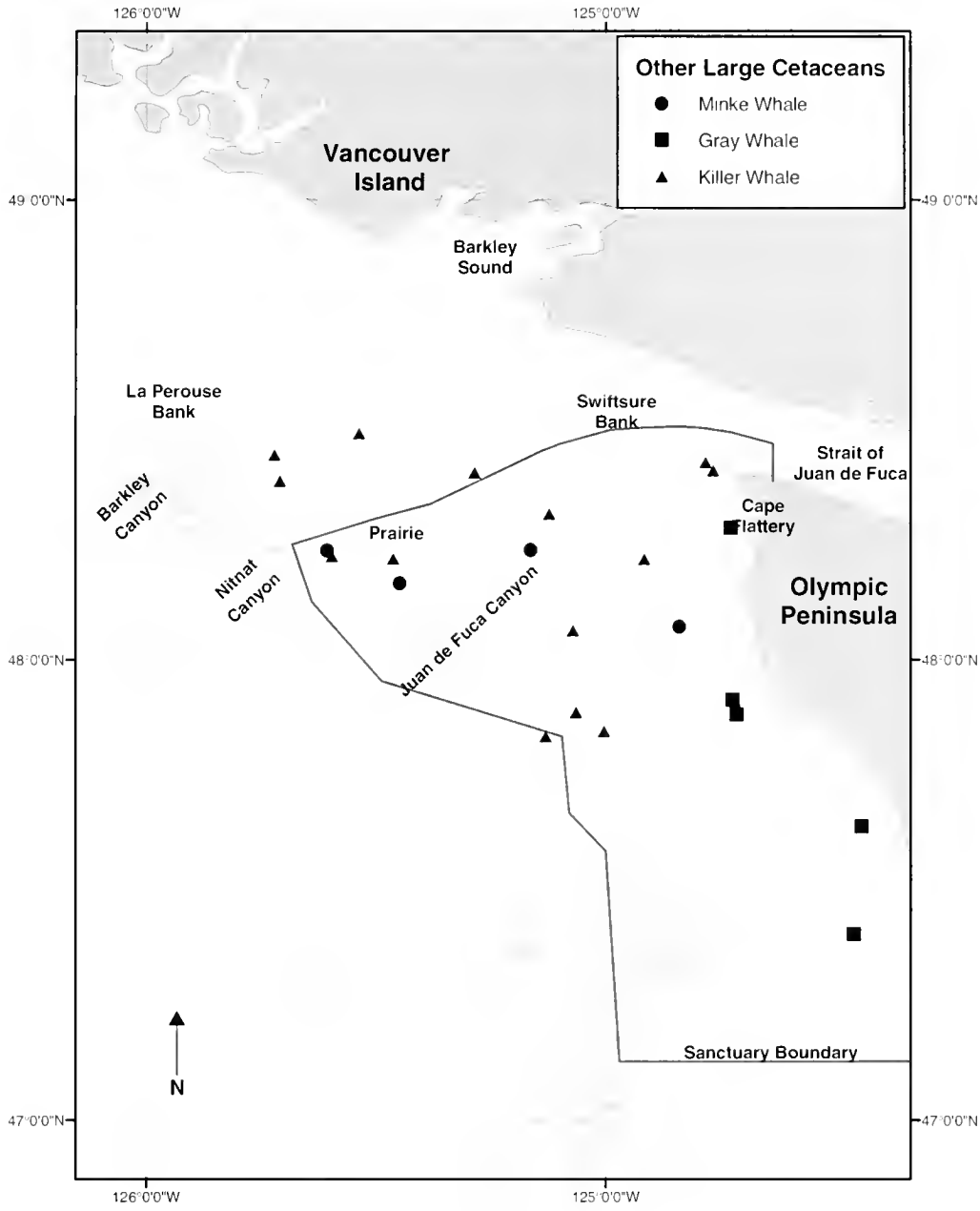

Figure 5

Locations of other large cetaceans seen during ship surveys off the northern Washington coast between 1995 and 2002.

calves were recorded during the surveys. Dall's porpoises were widely distributed in the study area but were not as commonly seen in more shallow coastal waters or in the southern portion of the study area (Fig. 6). Group size ranged between 1 and 12 individuals (mean=3.5, SD=2.2). Harbor porpoises were observed each year (except 2002) and there were a total of 38 sightings for the entire study period. Group size ranged between 1 and 6 individuals except for one sighting of a group of 20 animals (mean=2.3, SD=3.1). The distribution range for harbor porpoises was more restricted to coastal waters and showed only a small overlap with the distribution range for Dall's porpoises (Fig. 6).

Line-transect analysis allowed estimation of Dall's porpoise density and abundance (Table 8). Similar to those for humpback whales, results for Dall's porpoises were fairly consistent for the first five surveys (1995 to 2000): annual abundances were estimated between 181 and 291. For 2002, the encounter rate and corresponding density and abundances increased dramati-

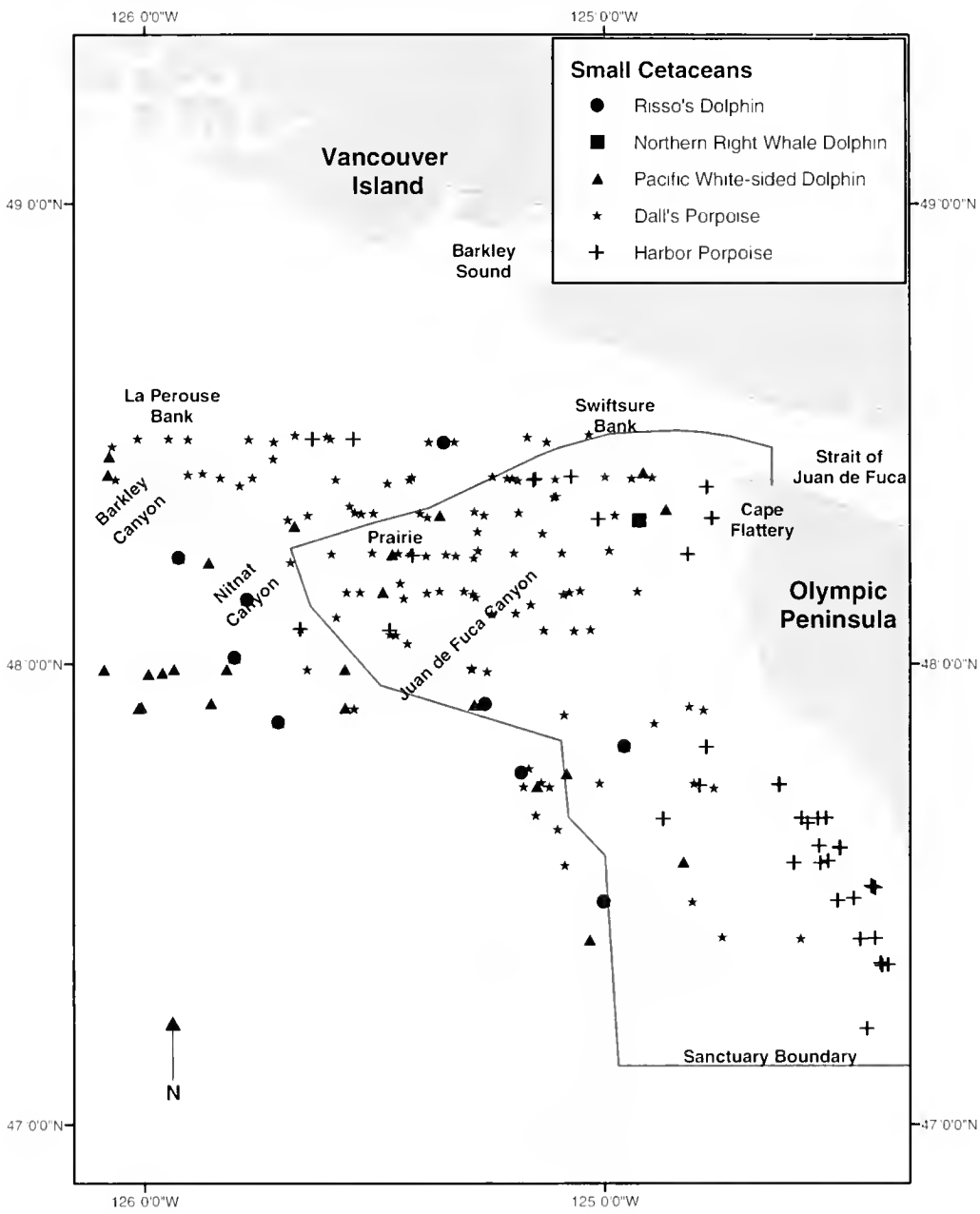

Figure 6

Locations of small cetaceans seen during ship surveys off the northern Washington coast between 1995 and 2002.

cally yielding an estimated abundance of 876 porpoises (CV=0.30, Table 8). Confidence intervals for some of the annual estimates overlapped among years.

Pinnipeds

Pinnipeds were not as frequently observed as cetaceans (Table 3, Fig. 7). The two most pelagic species observed in this region, northern fur seals and elephant seals, were the most commonly seen pinnipeds. Northern fur seals were observed every year except 2002 on a total of 28 occasions. All but one of these sightings were of a single animal. Elephant seals were seen in all years except 1998 and 2002.

Habitat differences

A number of broad habitat patterns emerged for different groups of species based on their association with water depth and distance from shore during the ship surveys from 1995 to 2000 (Table 9, data were not available for 2002). Five species were seen in shallow waters

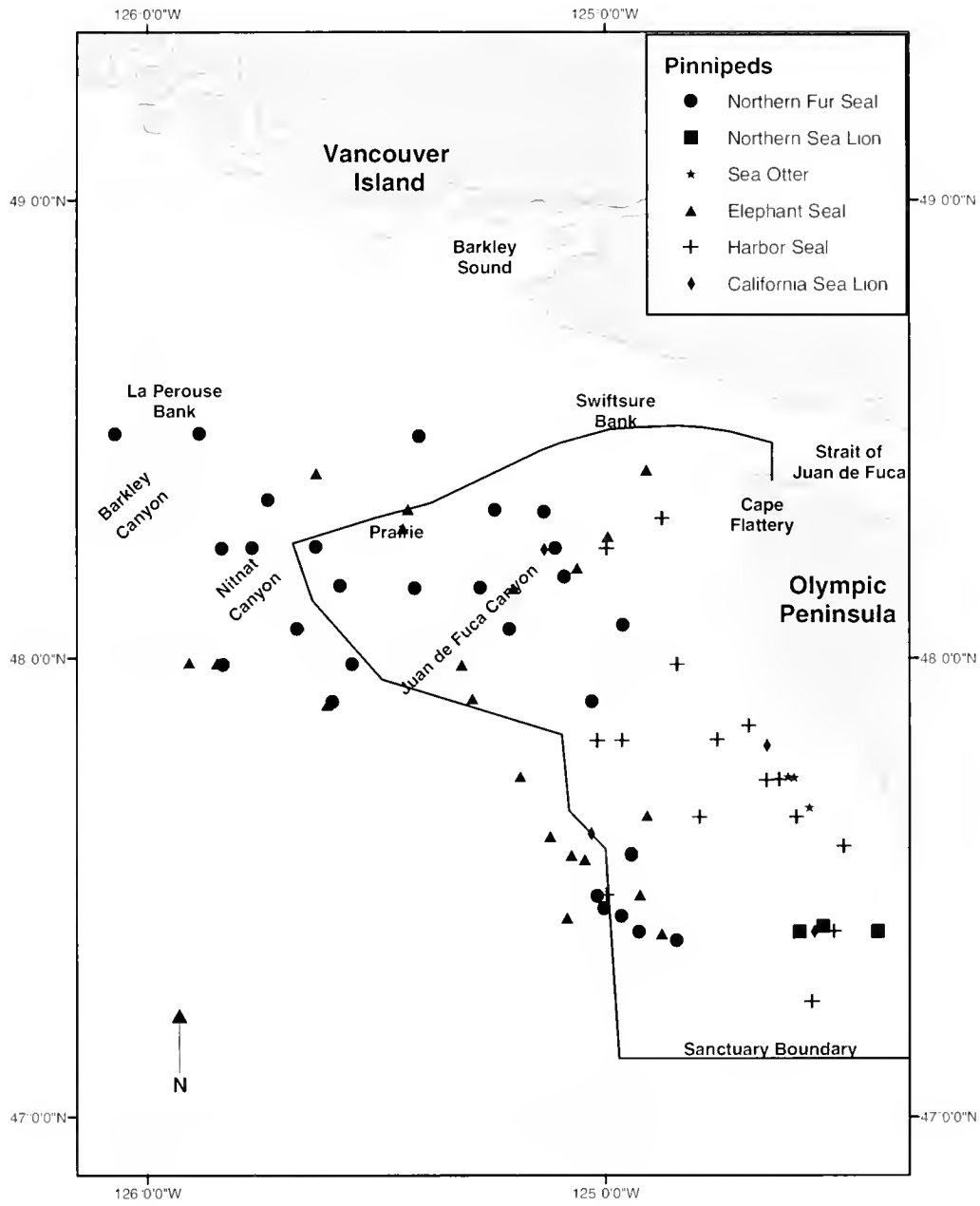

Figure 7

Locations of pinnipeds and sea otters (*Enhydra lutris*) seen during ship surveys off the northern Washington coast between 1995 and 2002.

(<100 m). Gray whales and sea otters were seen in the shallowest water of all species with average water depths of just 20 and 22 m, respectively; they also were the only two species for which sightings averaged less than 10 km from shore. The three other species—harbor porpoise, California sea lions, and northern sea lions (*Eumetopias jubatus*)—were seen in slightly deeper waters (averaging 34 to 91 m) and farther from shore (averaging 11 to 23 km). The five species that were predominantly found at mid-shelf depths (mean depths at 100–200 m) were humpback whales, killer whales, Dall's porpoises, harbor seals, and minke whales (*Balaenoptera acutorostrata*). Species seen far from shore (>40 km) and also in deepest waters (>200 m) included Pacific white-sided dolphins, Risso's dolphins, elephant seals, and northern fur seals. All of these species are known to feed along the continental slope or off the shelf.

Distances from the shelf break for different species did not fall into as clear a pattern as water depth and distance from shore (Table 9). This disparity may be the result of the varied habitat (with canyons cutting through the study area) and the lack of much effort off

Table 9

Summary of habitat and oceanographic parameters for sightings of different species during ship surveys from 1995 to 2000.

	Water depth (m)			Distance from shore (km)			Distance from shelf (km)			Sea surface temp. (°C)		
Species	*n*	Mean	SD	*n*	Mean	SD	*n*	Mean	SD	*n*	Mean	SD
Baleen whales												
Humpback whale	153	144	87	153	43.8	14.9	153	8.4	6.7	101	13.9	1.6
Gray whale	5	20	8	5	5.0	2.0	5	26.1	8.1	5	14.4	1.9
Minke whale	3	106	67	3	41.2	27.7	3	8.0	6.5	3	16.1	0.9
Unidentified large whale	21	189	280	21	40.5	18.4	21	8.0	7.3	18	15.4	1.3
Unidentified whale	1	197	—	1	36.3	—	1	0.1	—	1	13.0	—
Odontocetes												
Dall's porpoise	90	167	118	90	40.1	14.9	90	5.6	5.5	72	14.3	1.7
Harbor porpoise	38	58	70	38	16.3	15.6	38	17.2	11.6	29	13.9	1.7
Pacific white-sided dolphin	24	689	505	24	65.6	25.7	24	8.3	8.7	20	15.0	0.8
Northern right-whale dolphin	1	259	—	1	16.2	—	1	0.7	—			
Risso's dolphin	9	552	310	9	55.4	21.4	9	4.9	5.2	8	14.4	1.3
Killer whale	12	148	58	12	28.8	15.0	12	5.9	4.7	7	14.1	1.1
Unidentified delphinid	19	219	253	19	37.4	17.4	19	5.7	6.7	19	14.5	1.5
Pinnipeds and otters												
Harbor seal	15	102	154	15	17.3	11.0	15	15.5	12.0	14	14.2	1.4
Elephant seal	20	466	370	20	46.2	18.5	20	3.8	5.0	16	14.7	1.8
California sea lion	4	91	74	4	22.8	15.2	4	9.3	14.2	1	13.9	—
Steller sea lion	4	34	18	4	11.3	5.4	4	18.5	6.6	3	13.6	0.4
Northern fur seal	22	382	349	22	47.1	17.1	22	3.1	3.7	21	14.3	1.4
Sea otter	3	22	1	3	8.9	0.5	3	25.5	18.1	3	12.6	0.4
Unidentified pinniped	13	170	144	13	30.5	18.4	13	8.0	8.1	11	14.5	1.9
All sightings	457	205	251	457	39.1	20.1	457	8.4	8.4	352	14.3	1.6

the continental shelf. Despite most of our effort being on the continental shelf, the presence of several deep canyons in addition to the shelf edge, resulted in all species being an average of less than 11 km from the 200 m depth contour. The average surface water temperature for species that were seen also varied and was likely both a function of distance from shore and association with upwelling areas (Table 9). Sea otters were seen in the coldest waters (12.6°C) where they are predominantly found. Among the more offshore species, humpback whales, tended to be seen in colder waters (13.9°C) than most other offshore species, probably because of their association with offshore upwelling areas.

Discussion

Although humpback whales were the most abundant large cetacean seen in our study, their numbers of a few hundred still appear to be substantially lower than numbers found prior to whaling. Commercial hunting of humpback whales occurred in the 1900s from coastal whaling stations in northern California, Washington, and British Columbia. In these areas, thousands of humpback whales were killed over a relatively short time period (less than 10 years) before catches dropped precipitously with the depletion of the population. At the south end of our study area, 1933 humpback whales were taken from a station at Bay City (in Grays Harbor), Washington, from 1911 to 1925 (Scheffer and Slipp, 1948). To the north, 5638 humpback whales were taken from British Columbia stations from 1908 to 1967, of which 60% (3393) were taken from 1908 to 1917 from the two southernmost whaling stations on Vancouver Island closest to our study area (Gregr et al., 2000; Nichol et al., 2002). Additionally, 1871 humpback whales were taken from two stations in northern California from 1919 to 1926 (Clapham et al., 1997). Although these hunts encompassed areas larger than our study area, the number killed in short periods dwarfs even the sum of our abundance estimates for Washington and British Columbia and the estimate of under 1000 whales estimated in the 1990s for California, Oregon, and Washington (Calambokidis and Barlow, 2004). Moreover, humpback whales have not returned to some of the areas where they were once found prior to commercial

whaling; humpback whales were commonly observed in the inside waters of Washington and British Columbia (Scheffer and Slipp, 1948; Webb, 1988) and have not returned to these areas in any numbers (Calambokidis and Steiger, 1990).

The distribution of humpback whales within our study area was not uniform and indicated that some specific areas were important feeding habitat for this recovering species. The region between the Juan de Fuca Canyon and the shelf edge (the Prairie)—the mouth of Barkley Canyon and Swiftsure Bank—was the area where humpback whales were concentrated. In monthly aerial surveys in 1989–90 by Green et al.,[5] there were only a total of 13 sightings of 25 humpback whales along the entire Washington coast between July and September. Over half of those sightings were in the Prairie area.

Our line-transect estimates revealed that about 100 humpback whales inhabit the northern Washington coast waters each summer; substantially more (over 500), however, were present in 2002. Although this is a small number compared to estimates of just under 1000 humpback whales for California, Oregon, and Washington (Calambokidis and Barlow, 2004), our study area encompasses a relatively small area and reflects a high density of animals. Additionally our line-transect estimates were not corrected for any missed animals; therefore they are probably biased slightly downward.

Despite the relatively high density of humpback whales in this region, the photographic identification data indicated that a relatively small number of individuals use the area consistently. Both the line-transect and the photographic identification data (increasing capture-recapture estimates, as well as decreased proportions of animals sighted multiple years) showed that the number of whales using this region has increased in recent years. The growing number of whales in this region could be either the result of births or immigration into this area. Births alone could not account for this increase, especially because the proportion of whales that were mothers with calves seen in this region was not high. There did not appear to be a shift in distribution of animals from areas to the south because interchange with those areas dropped from 1999 to 2002. The most likely explanation for these changes is that there was a shift of animals from feeding areas from the north into this region beginning in the late 1990s.

This interchange of humpback whales with feeding areas to the south provides new insight into the structure of humpback whale feeding aggregations. In a study that examined interchange rates of humpback whales along the west coast, Calambokidis et al. (1996) identified northern Washington as a demographic boundary between the whales feeding area along California, Oregon, and Washington and those to the north. The larger sample reported here shows the same general pattern of decreasing interchange with distance from a feeding area as that reported previously for whales off California (Calambokidis et al., 1996). The decreasing rate of interchange with distance among feeding areas does not allow for a clear demarcation between feeding areas, however, as suggested by Calambokidis et al. (1996). Although humpback whales demonstrate site fidelity to specific feeding locations, their feeding aggregations may not have clear boundaries and may occupy overlapping ranges.

The commercial whaling data also tended to support the existence of somewhat discrete feeding areas off the west coast of the United States and British Columbia. Commercial whaling resulted in the depletion of humpback whales off British Columbia by 1917, whereas the numbers taken off Washington and California did not decline until the mid-1920s (Scheffer and Slipp, 1948; Clapham et al., 1997; Gregr et al., 2000).

The relatively small proportion of mothers with calves identified in our study is consistent with findings off California and Oregon (Steiger and Calambokidis, 2000). Steiger and Calambokidis reported reproductive rates along the California, Oregon, and Washington coasts that are lower than those reported for other regions in southeastern Alaska and the North Atlantic (Clapham and Mayo, 1987, 1990; Baker et al., 1992; von Ziegesar et al., 1994). In aerial transect surveys, no humpback whale calves were seen among the 68 humpbacks observed off the Oregon and Washington coasts in 1989–90 (Green et al.[5]). If geographic segregation is occurring by humpback mothers and calves, as was suggested by Steiger and Calambokidis (2000), this northern region is not the area where mothers and calves are congregated. It is interesting to note, however, that mothers and calves were distributed around the periphery of the main feeding region—a finding that suggests that a more local segregation may be occurring. A bias in sampling would occur if large concentrations of whales are targeted and mother with calves feeding on the perimeter of these groups were underrepresented.

In contrast to humpback whales, no other large rorquals (blue, fin, or sei whales) were observed during any of our ship or small boat surveys. Likewise, these species were absent in other recent surveys of Washington waters (Wahl, 1977; Von Saunder and Barlow, 1999; Shelden et al., 2000; Green et al.[5]), although they were seen in surveys farther offshore in surveys in July 1994 (Thomason et al.[6]). Fin whales were common

[5] Green, G. A., J. J. Brueggeman, R. A. Grotefendt, and C. E. Bowlby. 1992. Cetacean distribution and abundance off Oregon and Washington, 1989–1990. *In* Oregon and Washington marine mammal and seabird surveys (J. J. Brueggeman, ed.), 100 p. Final report of OCS Study MMS 91-0093 by Ebasco Environmental, Bellevue, Washington, and Ecological Consulting, Inc., Portland, Oregon, for the Minerals Management Service, Pacific OCS Region, U.S. Dept. of Interior, 770 Paseo Camarillo, Camarillo, CA 93010.

[6] Thomason, J., M. Dahlheim, S. E. Moore, J. Braham, K. Stafford, and C. Fox. 1997. Acoustic investigations of large cetaceans off Oregon and Washington: NOAA ship *Surveyor* (21 July–1 August 1994), 27 p. Final report by the National Marine Mammal Laboratory, 7600 Sand Point Way NE F/AKC3, Seattle, WA 98115.

in Washington waters in the early 1900s when they were the second most commonly killed species by Bay City whalers (Scheffer and Slipp, 1948). Blue and sei whales were less common, although they were present historically (Scheffer and Slipp, 1948). Although Bay City whaling stations (in Grays Harbor, Washington) were closed after humpback whales were depleted, serial depletion of whale populations continued off British Columbia waters, beginning with humpback and blue whales, then with fin and sperm whales, and finally with sei whales (Gregr et al., 2000).

No sperm whales or beaked whales were seen during our surveys, although our study area did not include the deeper waters where we would expect to find these species. Most of the sperm whales (90%) seen by Green et al.[5] off Washington and Oregon were present in deeper offshore waters outside of our study area.

The other cetacean species not seen in our surveys that have been reported to occur off Washington historically included northern right whale (*Eubalaena japonica*), pygmy sperm whale (*Kogia breviceps*), false killer whale (*Pseudorca crassidens*), short-finned pilot whale (*Globicephala macrorhynchus*), and striped dolphin (*Stenella coeruleoalba*) (Scheffer and Slipp, 1948). Sightings of northern right whales throughout the eastern North Pacific are scarce; there have been only a small number of sightings since the 1960s (Brownell et al., 2001). Several of these sightings, however, have been off the northern Washington coast (Fiscus and Niggol, 1965; Osborne et al., 1988; Rowlett et al., 1994). The primary reason for the paucity of sightings in the eastern North Pacific in recent decades is due to the illegal take of 372 right whales in the early to mid-1960s by the USSR (Brownell et al., 2001; Doroshenko[7]).

Although some small cetacean species such as Pacific white-sided dolphins and Risso's dolphins were sighted frequently on our surveys, they were not as common as in some previous surveys (Green et al.[5]), probably because our coverage was concentrated in shallower waters inside the shelf break. In contrast to our findings of a number of species seen near the shelf edge, Wahl (1977) reported that most marine mammal species off central Washington tended to be in either inshore or in deeper offshore waters and only killer whales and Dall's porpoises regularly used the slope waters (13–45 km offshore).

It is difficult to make abundance estimates of Dall's porpoise because of their proclivity to approach ships (Buckland and Turnock, 1992). If they begin to approach the ship before the observer sights them, the estimate is biased upwards, which would be the case with our estimate. Our estimate would also have a downward bias because we did not attempt to adjust for animals missed even if they were on the track line.

All three types of killer whales (residents [both northern and southern], transients, and offshore type) were identified in the waters off northern Washington. These sightings are interesting because of concerns about killer whale populations, especially the southern resident community that has declined in recent years. Although killer whales have been intensely studied in inside waters of the Pacific Northwest, little has been known about their use of outside waters, where they may spend large portions of their lives. Little is known about the offshore type of killer whales, which is believed to be a distinct race of killer whale that has only recently been described. These whales are believed to be found usually in large groups along the continental shelf but also have been seen in inland waters (Ford et al., 1994; Dahlheim et al., 1997). All three sightings of the offshore form were just west of the Juan de Fuca canyon on the Prairie; the closest sighting to shore was 37 km (30 animals on 15 July 1997).

Acknowledgments

We are grateful to those who assisted with this study. This work was supported by the Olympic Coast National Marine Sanctuary and Southwest Fisheries Science Center (Jay Barlow, COTR). Many people contributed to this study. Jennifer Quan, Richard Rowlett, Anne Nelson, and Annie Douglas worked on the ship surveys. We thank the ship personnel on board the *McArthur* and *Agate Passage*. Researchers who helped with small boat work included Joe Evenson and Todd Chandler. Photographs of whales from this area were also contributed by L. Baraff, R. Baird, P. Bloedel, V. Deeke, P. Ellifrit, G. Ellis, J. Evenson, B. Gisborne, B. Halliday, H. Hunt, S. Mizroch, K. Rasmussen, J. Wilson and SWFSC researchers. Permission to survey in Canadian waters was given by the Dept. of Fisheries and Oceans. Lisa Schlender, Kristin Rasmussen, and Annie Douglas organized and conducted the photographic matching with the help of many interns at Cascadia Research. DKE and Graeme Ellis identified the killer whales; Oscar Torres assisted with the photographic matching. Data analyses and mapping were conducted with the help of Scot McQueen at ESRI and Tom Williams.

Literature cited

Baker, C. S., A. Perry, and L. M. Herman.
1992. Population characteristics of individually identified humpback whales in southeastern Alaska: summer and fall 1986. Fish. Bull. 90:429–437.

Barlow, J., C. W. Oliver, T. D. Jackson, and B. L. Taylor.
1988. Harbor porpoise, *Phocoena phocoena*, abundance estimate for California, Oregon and Washington: II. Aerial surveys. Fish. Bull. 86:433–444.

Bigg, M. A., G. M. Ellis, J. K. B. Ford, and K. C. Balcomb.
1987. Killer whales. A study of their identification, genealogy and natural history in British Columbia and

[7] Doroshenko, N. V. 2000. Soviet whaling for blue, gray, bowhead and right whales in the North Pacific Ocean, 1961–1979. *In* Soviet whaling sata (1949–1979), p. 96–103. Center for Russian Environmental Policy, Vavilov St. 26, Moscow 117071, Russia.

Washington State, 79 p. Phantom Press and Publishers, Nanaimo, British Columbia, Canada.

Bigg, M. A., P. F. Olesiuk, G. M. Ellis, J. K. B. Ford, and K. C. Balcomb III.
1990. Social organization and genealogy of resident killer whales (*Orcinus orca*) in the coastal waters of British Columbia and Washington State. Rep. Int. Whal. Comm. (spec. issue 12):383–405.

Black, N. A., A. Schulman-Janiger, R. L. Ternullo, and M. Guerrero-Ruiz.
1997. Killer whales of California and western Mexico: a catalog of photo-identified individuals. NOAA Tech. Memo. NOAA-TM-NMFS-SWFSC-247, 174 p.

Brownell, R. L., Jr., P. J. Clapham, T. Miyashita, and T. Kasuya.
2001. Conservation status of North Pacific right whales. J. Cet. Res. Manag. (spec. issue 2):269–286.

Buckland, S. T., and B. J. Turnock.
1992. A robust line transect method. Biometrics 48:901–909.

Calambokidis, J., and J. Barlow.
2004. Abundance of blue and humpback whales in the eastern North Pacific estimated by capture-recapture and line-transect methods. Mar. Mamm. Sci. 20:63–85.

Calambokidis, J., J. C. Cubbage, G. H. Steiger, K. C. Balcomb, and P. Bloedel.
1990. Population estimates of humpback whales in the Gulf of the Farallones, California. Rep. Int. Whal. Commn (spec. issue 12):325–333.

Calambokidis, J., J. D. Darling, V. Deeke, P. Gearin, M. Gosho, W. Megill, C. M. Tombach, D. Goley, C. Toropova, and B. Gisborne.
2002. Abundance, range and movements of a feeding aggregation of gray whales (*Eschrichtius robustus*) from California to southeastern Alaska in 1998. J. Cet. Res. Manag. 4:267–276.

Calambokidis, J., and G. H. Steiger.
1990. Sightings and movements of humpback whales in Puget Sound, Washington. Northwestern Nat. 71:45–49.

Calambokidis, J., G. H. Steiger, J. R. Evenson, K. R. Flynn, K. C. Balcomb, D. E. Claridge, P. Bloedel, J. M. Straley, C. S. Baker, O. von Ziegesar, M. E. Dahlheim, J. M. Waite, J. D. Darling, G. Ellis, and G. A. Green.
1996. Interchange and isolation of humpback whales off California and other North Pacific feeding grounds. Mar. Mamm. Sci. 12:215–226.

Calambokidis, J., G. H. Steiger, K. Rasmussen, J. Urbán R., K. C. Balcomb, P. Ladrón de Guevara P., M. Salinas Z., J. K. Jacobsen, C. S. Baker, L. M. Herman, S. Cerchio, and J. D. Darling.
2000. Migratory destinations of humpback whales that feed off California, Oregon and Washington. Mar. Ecol. Prog. Ser. 192:295–304.

Clapham, P. J., and C. A. Mayo.
1987. Reproduction and recruitment of individually identified humpback whales, *Megaptera novaeangliae*, observed in Massachusetts Bay, 1979–85. Can. J. Zool. 65:2852–2863.
1990 Reproduction of humpback whales (*Megaptera novaeangliae*) observed in the Gulf of Maine. Rep. Int. Whal. Comm. (spec. issue 12):171–175.

Clapham, P. J., S. Leatherwood, I. Szczepaniak, and R. L. Brownell, Jr.
1996. Catches of humpback and other whales from shore stations at Moss Landing and Trinidad, California, 1919–1926. Mar. Mamm. Sci. 13:368–394.

Dahlheim, M. E., D. K. Ellifrit, J. D. Swenson.
1997. Killer whales of southeast Alaska: a catalogue of photo-identified individuals, 79 p. Day Moon Press, Seattle, WA.

Darling, J. D.
1984. Gray whales (*Eschrichtius robustus*) off Vancouver Island, British Columbia. *In* The gray whale, *Eschrichtius robustus* (M. L. Jones, S. Swartz, and S. Leatherwood, eds.), p. 267–287. Academic Press, Orlando, FL.

Fiscus, C. H., and K. Niggol.
1965. Observations of cetaceans off California, Oregon, and Washington. U.S. Fish and Wildl. Serv., Special Scientific Report-Fisheries 498, 27 p. U.S. Fish and Wildl. Serv., Washington, D.C.

Ford, J. K. B., G. M. Ellis, and K. C. Balcomb.
1994. Killer whales, 102 p. UBC Press, Vancouver, British Columbia.

Green, G. A., J. J. Brueggeman, R. A. Grotefendt, and C. E. Bowlby.
1995. Offshore distances of gray whales migrating along the Oregon and Washington coasts, 1990. Northwest Sci. 69:223–227.

Gregr, E. J., L. Nichol, J. K. B. Ford, G. Ellis, and A. W. Trites.
2000. Migration and populations structure of northeastern Pacific whales off coastal British Columbia: an analysis of commercial whaling records from 1908–1967. Mar. Mamm. Sci. 16:699–727.

Hammond, P. S.
1986. Estimating the size of naturally marked whale populations using capture-recapture techniques. Rep. Int. Whal. Comm. (spec. issue 8):253–282.

Huelsbeck, D. R.
1988. Whaling in the precontact economy of the central northwest coast. Arctic Anthropol. 25:1–15.

Jameson, R. J., K. W. Kenyon, S. Jeffries, and G. R. VanBlaricom.
1986. Status of a translocated sea otter population and its habitat in Washington. Murrelet 67:84–87.

Jameson, R. J., K. W. Kenyon, A. M. Johnson, and H. M. Wright.
1982. History and status of translocated sea otter populations in North America. Wildl. Soc. Bull. 10:100–107.

Jeffries, S., H. Huber, J. Calambokidis and J. Laake.
2003. Trends and status of harbor seals in Washington State: 1978–1999. J. Wildl. Manag. 67:201–219.

Kvitek, R. G., P. J. Iampietro, and C. E. Bowlby.
1998. Sea otters and benthic prey communities: a direct test of the sea otter as keystone predator in Washington state. Mar. Mamm. Sci. 14:895–902.

Kvitek, R. G., J. S. Oliver, A. R. DeGange, and B. S. Anderson.
1992. Sea otters and benthic prey communities in Washington State. Mar. Mamm. Sci. 5:266–280.

Nichol, L. M., E. J. Gregr, R. Flinn, J. K. B. Ford, R. Gurney, L. Michaluk, and A. Peacock.
2002. British Columbia commercial whaling catch data 1908 to 1967: a detailed description of the B.C. historical whaling database. Can. Tech. Rep. Fish. Aquat. Sci. 2396, vii +76 p.

Osborne, R., J. Calambokidis, and E. M. Dorsey.
1988. A guide to marine mammals of greater Puget Sound, 191 p. Island Publishers, Anacortes, WA.

Osmek, S., J. Calambokidis, J. Laake, P. Gearin, R. DeLong, S. Jeffries, and R. Brown.
1996. Assessment of the status of harbor porpoises (*Pho-*

coena phocoena) in Oregon and Washington waters. U.S. Dep. of Commerce, NOAA Tech. Memo., NMFS-AFSC-76, 46 p.

Rowlett, R. A., G. A. Green, C. E. Bowlby, and M. A. Smultea.
1994. The first photographic documentation of a northern right whale off Washington State. Northwestern Nat. 75:102–104.

Scheffer, V. B., and J. W. Slipp.
1948. The whales and dolphins of Washington State with a key to the cetaceans of the west coast of North America. Am. Midl. Nat. 39:257–337.

Seber, G. A. F.
1982. The estimation of animal abundance and related parameters, 2nd ed., 654 p. Griffin, London.

Shelden, K. E. W., D. J. Rugh, J. L. Laake, J. M. Waite, P. J. Gearin, and T. R. Wahl.
2000. Winter observations of cetaceans off the northern Washington coast. Northwestern Nat. 81:54–59.

Steiger, G. H., and J. Calambokidis.
2000. Reproductive rates of humpback whales off California. Mar. Mamm. Sci. 16:220–239.

Swan, J. G.
1868. The Indians of Cape Flattery, 109 p. Shorey Publications, Seattle, WA.

Von Saunder, A., and J. Barlow.
1999. A report of the Oregon, California and Washington line-transect experiment (ORCAWALE) conducted in West Coast waters during summer/fall 1996. NOAA Tech. Memo. NOAA-TM-NMFS-SWFSC-264, 49 p.

von Ziegesar, O., E. Miller, and M. E. Dahlheim.
1994. Impacts of humpback whales in Prince William Sound. *In* Marine mammals and the *Exxon Valdez* (T. R. Loughlin, ed.), p. 173–191. Academic Press, San Diego, CA.

Wahl, T. R.
1977. Sight records of some marine mammals offshore from Westport, Washington. Murrelet 58:21–23.

Webb, L. W.
1988. On the Northwest. Commercial whaling in the Pacific Northwest 1790–1967, 425 p. Univ. British Columbia Press, Vancouver, Canada.

Reproductive biology of male franciscanas (*Pontoporia blainvillei*) (Mammalia: Cetacea) from Rio Grande do Sul, southern Brazil*

Daniel Danilewicz

Grupo de Estudos de Mamíferos Aquáticos do Rio Grande do Sul (GEMARS)
Rua Felipe Neri, 382/203
Porto Alegre 90440-150, Brazil
Present address: Laboratório de Dinâmica Populacional–Pontifícia Universidade Católica do Rio Grande do Sul (PUCRS)
Av. Ipiranga, 6681
Porto Alegre 90619-900, Brazil
Email address (for D. Danilewicz): Daniel.Danilewicz@terra.com.br

Juan A. Claver

Alejo L. Pérez Carrera

Area Histología y Embriología Facultad de Ciencias Veterinarias
Universidad de Buenos Aires
Av. Chorroarín 280 C1427CWO
Buenos Aires, Argentina

Eduardo R. Secchi

Laboratório de Mamíferos Marinhos, Museu Oceanográfico "Prof. Eliézer C. Rios"
Fundação Universidade Federal do Rio Grande, Cx P. 379
Rio Grande 96200, Brazil

Nelson F. Fontoura

Laboratório de Dinâmica Populacional–Pontifícia Universidade Católica do Rio Grande do Sul (PUCRS)
Av. Ipiranga, 6681
Porto Alegre 90619-900, Brazil

Abstract—The reproductive biology of male franciscanas (*Pontoporia blainvillei*), based on 121 individuals collected in Rio Grande do Sul State, southern Brazil, was studied. Estimates on age, length, and weight at attainment of sexual maturity are presented. Data on the reproductive seasonality and on the relationship between some testicular characteristics and age, size, and maturity status are provided. Sexual maturity was assessed by histological examination of the testes. Seasonality was determined by changes in relative and total testis weight, and in seminiferous tubule diameters. Testis weight, testicular index of maturity, and seminiferous tubule diameters were reliable indicators of sexual maturity, whereas testis length, age, length, and weight of the dolphin were not. Sexual maturity was estimated to be attained at 3.6 years (CI 95%=2.7–4.5) with the DeMaster method and 3.0 years with the logistic equation. Length and weight at attainment of sexual maturity were 128.2 cm (CI 95%=125.3–131.1 cm) and 26.4 kg (CI 95%=24.7–28.1 kg), respectively. It could not be verified that there was any seasonal change in the testis weight and in the seminiferous tubule diameters in mature males. It is suggested that at least some mature males may remain reproductively active throughout the year. The extremely low relative testis weight indicates that sperm competition does not occur in the species. On the other hand, the absence of secondary sexual characteristics, the reversed sexual size dimorphism, and the small number of scars from intrassexual combats in males reinforce the hypothesis that male combats for female reproductive access may be rare for franciscana. It is hypothesized that *P. blainvillei* form temporary pairs (one male copulating with only one female) during the reproductive period.

Manuscript submitted 4 October 2002 to the Scientific Editor's Office.

Manuscript approved for publication 18 May 2004 by the Scientific Editor.

Fish. Bull. 102:581–592 (2004).

The franciscana (*Pontoporia blainvillei*) is a small dolphin endemic to the coastal waters of the southwestern Atlantic Ocean. The distribution of this species ranges from Golfo Nuevo (42°35′S; 64°48′W), Chubut Province, Argentina (Crespo et al., 1998) to Itaúnas (18°25′S; 30°42′W), Espírito Santo, southeastern Brazil (Moreira and Siciliano, 1991) (Fig. 1).

The franciscana's coastal habitat makes it vulnerable to being caught as incidental catch in gill nets and trammel nets throughout most of the species range (e.g., Praderi et al., 1989; Corcuera et al., 1994; Secchi et al., 2003). Because of its vulnerability as bycatch, the franciscana has been considered the most impacted small cetacean in the southwestern Atlantic Ocean (Secchi et al., 2002). In the Rio Grande do Sul coast, southern Brazil, this species has been subject to an intense bycatch in gill nets for at least three decades (Moreno et al., 1997; Secchi et al., 1997; Ott, 1998; Ott et al., 2002). The annual mortality of franciscanas in this region was estimated to range from several hundred up to about a thousand individuals (Ott et al., 2002). Simulations

*Contribution 012 from the Grupo de Estudos de Mamíferos Aquáticos do Rio Grande do Sul (GEMARS), Rua Felipe Neri, 382/203, Porto Alegre 90440-150, Brazil.

Figure 1

Map of the study area showing the locations along the southern coast of Brazil where franciscanas were caught as bycatch between 1992 and 1998.

studies on the effects of incidental captures on franciscanas in Rio Grande do Sul were carried out by using available data on vital rates, stock size, and bycatch estimates (e.g., Secchi, 1999; Kinas, 2002). All these studies showed that there is a decline in franciscana abundance in this region.

Although the reproductive biology of the female franciscanas have been studied in detail in Uruguay (Kasuya and Brownell, 1979; Harrison et al., 1981), Rio Grande do Sul (Danilewicz et al., 2000; Danilewicz, 2003), and Rio de Janeiro (Ramos, 1997), there are few data about male reproduction. Kasuya and Brownell (1979) presented information on male reproduction for Uruguay, although their small sample size precluded them from estimating age and size at attainment of sexual maturity.

In the Rio Grande do Sul coast, franciscanas are known to reproduce seasonally; births occur from October to early February (about 75% from October to December). Because the gestation period was estimated to last about 11.2 months, mating and conception may take place between November and early March (Danilewicz, 2003). Seasonal changes in testicular size and activity have been used to infer or corroborate mating seasons in some cetacean species (e.g., Neimanis et al., 2000). Nevertheless, it is not known if male franciscanas also undergo seasonal changes in the testicular activity.

In this study, we describe the reproductive biology of male franciscanas from Rio Grande do Sul and present evidences for the species' mating system.

Materials and methods

Sampling procedures

Data and samples collected from 121 specimens incidentally caught (88%) or beached (12%) along the Rio Grande do Sul coast between 1992 and 1998 were used for the analysis on reproduction of male franciscanas. The sampling of the incidentally caught animals was carried out through the monitoring of the commercial fishery fleet from Rio Grande (32°08′S; 52°05′W) and Tramandaí/Imbé (29°58′S, 50°07′W). Stranded dolphins were sampled from systematic beach surveys conducted in an area with an extension of 270 km of sandy beaches, between Torres (29°19′S, 49°43′W) and Lagoa do Peixe (31°15′S, 50°54′W).

Not all information could be collected from each carcass; therefore sample sizes varied among parameters. Standard length (SL, n=118) was measured by following the guidelines established by the American Society of Mammalogy (1961). The animals were weighed (n=97) and teeth were extracted and preserved dried or in a 1:1 mix of glycerin and alcohol (70%). Testes and epididymis were removed and fixed in 10% formalin.

Age determination

Age was estimated by counting the growth layer groups (GLGs) in thin, longitudinal sections of teeth (n=47). The teeth were decalcified in nitric acid or in RDO

(a commercial mixture of acids) and sectioned on a freezing microtome. The 15–20 μm sections were stained with Mayer's hematoxylin and mounted on microscope slides with Canadian balsam or in glycerin. Poor and off-center sections were discarded in favor of new preparations. Three readers counted independently the number of growth layer groups in both the dentine and cementum. When reader estimates differed, the sections were reexamined together and a best estimate was agreed upon. In this study, we considered one GLG to represent one year of age, which is the accepted model for the franciscana (Kasuya and Brownell, 1979; Pinedo, 1991; Pinedo and Hohn; 2000).

Reproduction

In the laboratory, the testes were separated from the epididymis, weighed to the nearest 0.01 g (n=107), and measured in three dimensions (length and two diameters perpendicular to each other in the middle of the testis) to the nearest 0.1 mm (n=104). The mean of these two diameters was called mean testis diameter. The weight of one of the gonads could not be recorded on some occasions (n=8) and we assumed that both testes had the same weight. Then, relative testis weight was determined as the ratio of the combined testis weight to the animal weight.

A 1-cm^3 subsample of each testis from the central portion of the organ was removed and examined by using standard histological preparations. The tissue was embedded in paraffin, sectioned in 4–10 μm thick slides through a manual microtome, and stained with hematoxylin and eosin (H&E). Male sexual maturity status was determined by examining the testicular sections at a magnification of 100×. In this study, we followed the classification criteria suggested by Hohn et al. (1985):

1 Immature—seminiferous tubules containing mainly spermatogonias. Abundant interstitial tissue present between the seminiferous tubules and lumen totally closed.
2 Pubertal—seminiferous tubules containing spermatogonias and spermatocytes. Less interstitial tissue present between the seminiferous tubules than in immature animals. The lumen is partially opened.
3 Mature—seminiferous tubules containing spermatogonias, spermatocytes, spermatids and, in many cases, spermatozoa. Interstitial tissue almost nonexistent between the seminiferous tubules. The lumen is totally opened.

The diameters of ten random circular seminiferous tubules were measured for each specimen (n=93) with a scale present in the lens of the microscope in order to calculate the seminiferous tubule mean diameter. A maturity index (MI) was calculated as the ratio of the combined testes weight by the combined testes length ($\Sigma W/\Sigma L$).

An analysis of the variation along the year of the values of relative and combined testes weight, and seminiferous tubule mean diameter, was employed to assess reproductive seasonality. Values of these parameters were compared between months when mating and conception occur ("reproductive months": November–March) and months when they not occur ("nonreproductive months": April–October). In order to increase the sample size of mature animals collected in reproductive months, data on testes weight from mature male franciscanas from Uruguay were included in the analysis (data supplied by Kasuya[1]).

The mean age at attainment of sexual maturity (ASM) was estimated through the DeMaster (1978) method and the logistic regression.

The DeMaster (1978) equation computes the mean as

$$ASM = \sum_{a=j}^{k} a(f_a - f_{a-1}),$$

where f_a = the fraction of sexually mature animals in the sample with age a;
j = the age of the youngest sexually mature animal in the sample; and
k = the age of the oldest sexually immature animal in the sample.

The variance of the DeMaster method estimate is calculated as

$$\mathrm{var}(ASM) = \sum_{a=j}^{k} \left[f_a(1-f_a)/N_a - 1 \right],$$

where N_a = the total number of animals aged a.

The logistic regression approach fits a sigmoid curve representing the probability that a franciscana of age a is sexually mature to the distribution of sexually mature and immature animals by age as

$$Y = 1/(1+e^{a+bx}) \quad \text{or} \quad \ln(1/Y-1) = a + bx,$$

where x = the age of the dolphin;
b = the slope of the regression; and
a = the intercept.

To obtain the age when 50% of the animals are sexually mature (Y=0.5), the last equation is simplified as $ASM = -a/b$.

Mean length and weight at sexual maturity was also estimated by the DeMaster (1978) method, by substituting age for length and weight, respectively. The method was slightly modified, as suggested by Ferrero and Walker (1993), and was calculated as

[1] Kasuya, T. 1970–73. Unpubl. data. Teikyo University of Science and Technology. Uenohara, Yamanashi Prefecture, 409-0193, Japan.

$$LSM = \sum_{Cmin}^{Cmax} L(f_t - f_{t-1}),$$

where $Cmax$ = the length or weight class of the largest or heaviest sexually immature animal;
$Cmin$ = the length or weight class of the smallest or lightest sexually mature animal;
L = the lower value of the length or weight class t; and
f_t = fraction of mature animals in the length or weight class t.

The specimens were pooled into length and weight intervals of 4 cm and 4 kg, respectively.

The estimated variance of this method is also modified and is calculated as

$$\mathrm{var}(MS) = w^2 \sum_{Cmin}^{Cmax} \left[(f_t(1-f_t)/N_t - 1 \right],$$

where N_t = the number of specimens in the length or weight class t; and
w = the interval width, a constant equal to 4 in these cases.

For estimating age, length, and weight at sexual maturity, pubertal animals were grouped together with immature animals.

Results

The weight and length of the left testes ranged from 0.23 to 10.42 g ($\bar{x}$=2.60 g) and from 15.7 to 59.7 mm ($\bar{x}$=33.6 mm), respectively. The weight and length of the right testes ranged from 0.17 to 9.98 g ($\bar{x}$=2.62 g) and from 17.9 to 60.0 mm ($\bar{x}$=34.5 mm), respectively. The relationship of testes weight and testes length resulted in significant regression (P<0.0001) and correlation (r^2=0.91; F=823.9; P<0.0001; y=0.000012$x^{3.33}$). The male with the heaviest relative testes weight was 141.6 cm in length and 31.2 kg in weight, and its combined-testes weight was 20.1 g, which is 0.064% of its total weight. The mean of the relative testes weight from 23 mature males was 0.036% of their total weight.

The testes of the franciscana are characterized by a high lateral symmetry. There was no statistically difference in weight (t=−0.09; P=0.93; n=71) and length (t=−0.4; P=0.69; n=100) between testes of the same animal. A strong correlation was found between left and right testes length (b=0.95; F=1073.0; r^2=0.92; P<0.0001; n=100; y=1.232 $x^{0.95}$) and between left and right testes weight (b=0.99; F=7262.8; r^2=0.99; P<0.0001; n=71; y=1.02$x^{1.0}$), where x and y represent values of the left and right testis, respectively.

Seminiferous tubule diameter

A nonlinear regression demonstrated positive allometry (b>0.333) of the seminiferous tubule diameter to the combined testicular weight (b=0.39; 95% CI=0.35–0.44) (Fig. 2), and a strong correlation between these two variables (F=343.6; r^2=0.86; P<0.0001; y=59.4$x^{0.39}$).

The relationship between the seminiferous tubule diameter and testes length is shown in Figure 3 and the relationship between the seminiferous tubule diameter and standard length is shown in Figure 4. In immature males, there was almost no increase in the seminiferous tubule diameter with the increase of standard length (0.26 μm/cm) and total weight (0.5 μm/kg). In mature males, however, seminiferous tubule diameter was significantly correlated with standard length (b=1.06; F=4.4; r^2=0.18; P=0.048; y=1.4775x−43.572) and there was no correlation with total weight (b=0.23; F=1.28; r^2=0.07; P=0.27; y=1.6132x+108.54).

The differences of the seminiferous tubule mean diameters were statistically significant between immature, pubertal, and mature male franciscanas (ANOVA, Fs=255.4; df=87; P<0.001).

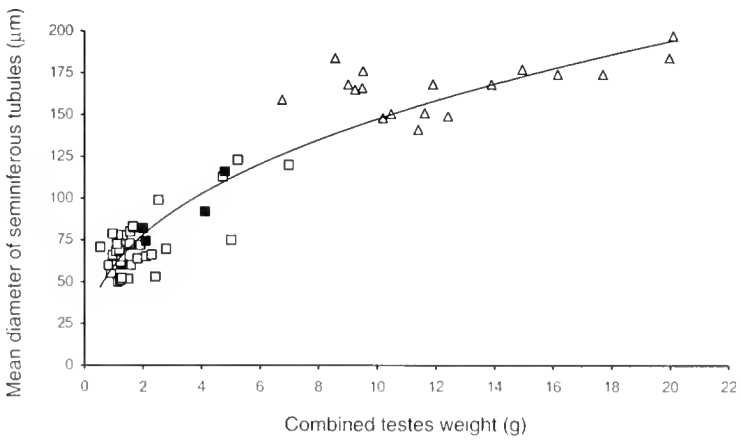

Figure 2

Relationship between combined-testes weight and mean seminiferous tubule diameter in immature (open boxes), pubertal (filled boxes), and mature (triangles) male franciscanas (*Pontoporia blainvillei*) from Rio Grande do Sul (n=59).

Combined-testes weight and length, and sexual maturity

There was almost no increment in mass of the combined-testes weight in immature dolphins. An increment of only about 2.0 g in the combined-testes mass was observed in animals of 70.0 to 125.0 cm in length. For dolphins about 120.0–130.0 cm in length, the combined-testes mass suddenly increased (Fig. 5), indicating the

attainment of sexual maturity. The rate of testes-mass gain was 0.05 g/cm for immature and 0.28 g/cm for mature dolphins. All animals with combined-testes weight higher than 5.0 g were sexually mature, and this finding may indicate that this parameter can be used as a reliable indicator of sexual maturity in male franciscanas from Rio Grande do Sul (Table 1). However, the large variation in testes weight after the attainment of sexual maturity precludes a correlation between testes mass and standard length.

Although testes length increases progressively as standard length increases (Fig. 6), there is no abrupt increase in testes length at the moment of attainment of sexual maturity, as observed in the testes mass. A nonlinear regression (exponential) best fits this relationship (y=4.5444 e0.0163x). As opposed to testes mass, there is a considerable overlap in the values of testes length of immature, pubertal, and mature franciscanas (Table 1), which makes testes length a less reliable predictor of sexual maturity than testes mass.

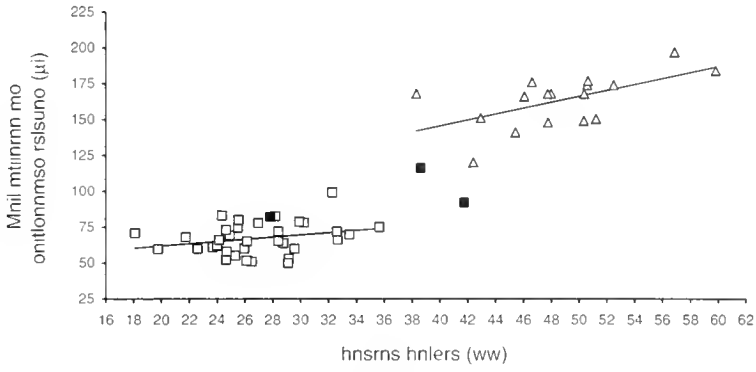

Figure 3

Relationship between testes length and mean diameter of seminiferous tubules in immature (open boxes), pubertal (filled boxes), and mature (triangles) male franciscanas (*Pontoporia blainvillei*) in Rio Grande do Sul (n=54). Data from pubertal animals are not included in the curves.

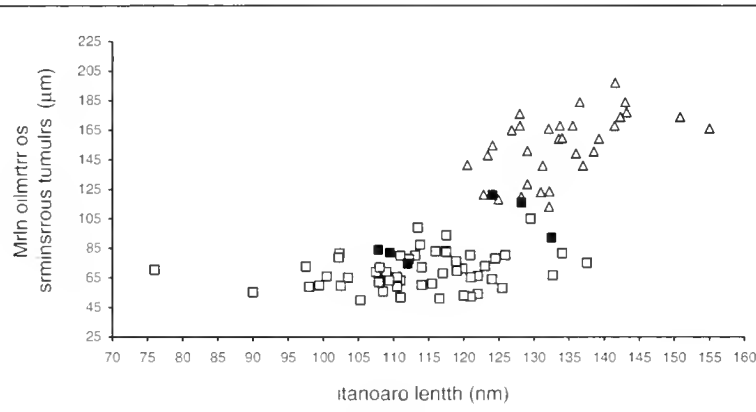

Figure 4

Relationship between standard length and mean diameter of seminiferous tubules in immature (open boxes), pubertal (filled boxes), and mature (triangles) male franciscanas (*Pontoporia blainvillei*) in Rio Grande do Sul (n=91).

Age, length, and weight at sexual maturity

Forty-seven specimens in the sample provided information on age and reproductive status (35 immature or pubertal, and 12 mature). The oldest immature animal was 5 years old and the youngest mature was 2 years old (Table 1). Average age at attainment of sexual maturity was estimated to be 3.6 years by the DeMaster method (SD=0.47; 95% CI =2.7–4.5) and 3.0 years by the logistic equation $Y = 1/(1+e^{0.74-2.23x})$. The age structure of the sample studied is presented in Figure 7.

Sexual maturity in relation to standard length was estimated for 110 males. The smallest mature and the largest immature males were 120.5 and 137.5 cm long, respectively. The average length at sexual maturity was 128.2 cm (SD=1.49; 95% CI=125.3–131.1 cm). Sexual maturity in relation to total weight was estimated for 90 males. The lightest mature and the heaviest immature males were 20.3 and 29.7 kg, respectively. The average weight at sexual maturity was 26.4 kg (SD=0.88; 95% CI=24.7–28.1 kg).

Index of testicular maturity

The differences of the mean index of testicular maturity between immature (0.03), pubertal (0.04), and mature (0.11) dolphins were statistically significant (ANOVA, Fs=210.0 df=101, P<0.001). There was almost no overlap in the values of this index between mature specimens and immature and pubertal specimens (Table 1). All males with an index value higher than 0.07 were sexually mature. These results indicate that the index of testicular maturity is a very good indicator of sexual maturity for franciscanas.

Reproductive seasonality

The null hypothesis that the combined and relative testis weight would be higher in the months when the females are reproductively active is rejected. No increase in the testes weight was observed during the months when most mating occurs (Fig. 8). There were no statistically significant differences in the combined-testes weight (ANOVA, Fs=2.28; df=34; P=0.48; n=35) and relative

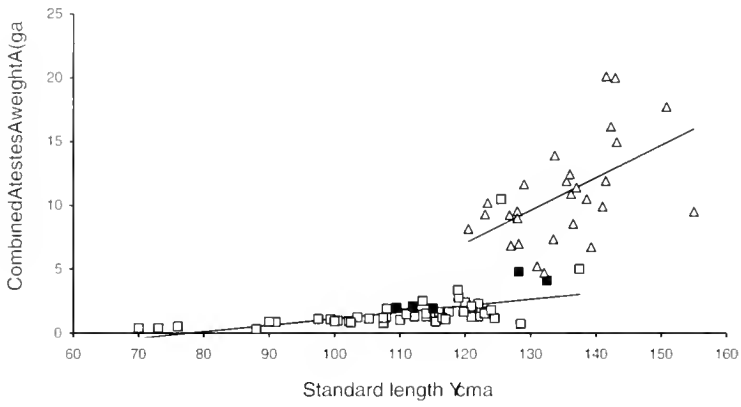

Figure 5

Relationship between standard length and combined-testes weight in immature (open boxes), pubertal (filled boxes), and mature (triangles) male franciscanas (*Pontoporia blainvillei*) in Rio Grande do Sul (n=79). Data from pubertal animals are not included in the curves.

testes weight (ANOVA, Fs=2.42; df=29; P=0.76; n=30) between reproductive and nonreproductive months.

The analyses of the variation in the diameter of the seminiferous tubules throughout the year also did not indicate that the testes undergo seasonal changes. However, it is important to view this result with caution because the sample size of mature males (and therefore the information on tubules diameter collected in reproductive months) was small (n=3). However, the presence of spermatids or spermatozoa (or both) in the seminiferous tubules may be also regarded as a direct evidence of testicular activity. Three mature males (11%) in the sample presented seminiferous tubules with spermatids or spermatozoa (or both) and were collected in nonreproductive months (May, June, and August). Although the epididymis of

Table 1

Summarized information on age, length, mass, and testicular characteristics for male franciscanas (*Pontoporia blainvillei*) in the Rio Grande do Sul at different sexual maturity stages.

Characteristics and maturity state	n	Mean	Standard deviation	Range
Age (years)				
Immature	31	1.29	1.01	0–5
Pubertal	4	2.0	0.82	1–3
Mature	12	3.8	1.14	2–6
Standard length (cm)				
Immature	62	111.2	13.62	70.0–137.5
Pubertal	7	118.5	9.75	107.8–132.5
Mature	37	133.7	7.71	120.5–155.0
Total mass (kg)				
Immature	53	19.0	5.6	4.95–29.7
Pubertal	6	21.4	4.62	17.1–28.0
Mature	30	29.9	5.22	20.25–41.5
Mean diameter of seminiferous tubules (μm)				
Immature	54	69.6	12.2	50.0–105.0
Pubertal	6	95.0	19.2	74.5–121.2
Mature	33	154.1	21.7	113.0–197.0
Combined testes mass (g)				
Immature	63	1.59	0.84	0.33–4.78
Pubertal	7	2.73	1.28	1.30–4.8
Mature	37	10.24	3.94	4.27–20.08
Testes length (mm)				
Immature	62	27.2	4.9	15.7–35.5
Pubertal	7	32.6	6.2	25.0–41.0
Mature	35	45.4	5.6	31.6–59.7
Index of testicular maturity				
Immature	61	0.03	0.01	0.01–0.06
Pubertal	7	0.04	0.01	0.02–0.06
Mature	36	0.11	0.03	0.05–0.18

a subsample of 10 mature males were examined histologically, we did not find any sign of spermatozoa.

Discussion

The high bilateral uniformity in testicular weight and length presented by the franciscana is a characteristic shared with many other cetacean species. Studies on the striped dolphin, *Stenella coeruleoalba* (Miyazaki, 1977), the common dolphin, *Delphinus delphis* (Collet and Saint Girons, 1984), the sperm whale, *Physeter macrocephalus* (Mitchell and Kozicki, 1984), and the dusky dolphin, *Lagenorhynchus obscurus* (van Waerebeek and Read, 1994), among others, demonstrate the same pattern of testis symmetry. Given the similar dimensions of both testes in franciscanas, it is possible to extrapolate the combined-testes weight by weighing only one testis without introducing bias in the analysis. It is recommended, however, that the weight of the testes should be presented without the epididymis weight, as it was presented in the most extensive comparative study on the subject (Kenagy and Trombulak, 1986).

There is a negative allometry of the seminiferous tubule diameter in relation to testis length, standard length, and total weight. This pattern is accentuated in immature males, in which the tubule diameters remain almost unchanged with the increase of the other variables. The lack of values for tubule diameters in the testes weight interval (2.5–6.0 g) and testes length interval (34–42 mm) just before the attainment of sexual maturity (Figs. 2 and 3) indicates that the increase in tubule size in relation to sexual maturity must occur very quickly, probably when the tubules are between 85 and 125 μm in diameter.

Attainment of sexual maturity

Length and weight at attainment of sexual maturity of male franciscanas in Rio Grande do Sul are very similar to those values estimated in previous estimates for Uruguay (Table 2). In contrast to the present study, Kasuya and Brownell (1979) calculated mean length at sexual maturity for Uruguay as the

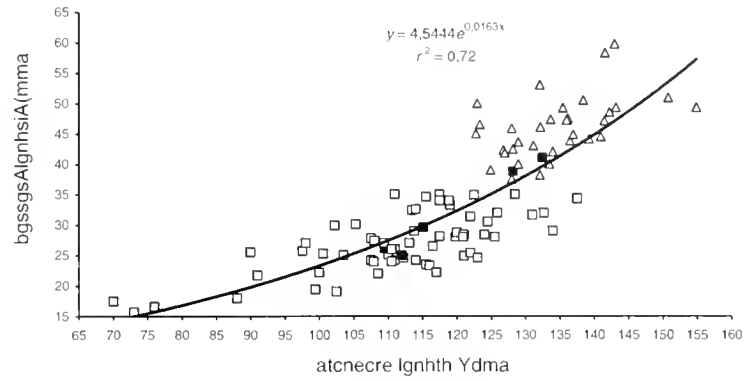

Figure 6

Relationship between standard length and testes length in immature (open boxes), pubertal (filled boxes), and mature (triangles) male franciscanas (*Pontoporia blainvillei*) in Rio Grande do Sul (n=99).

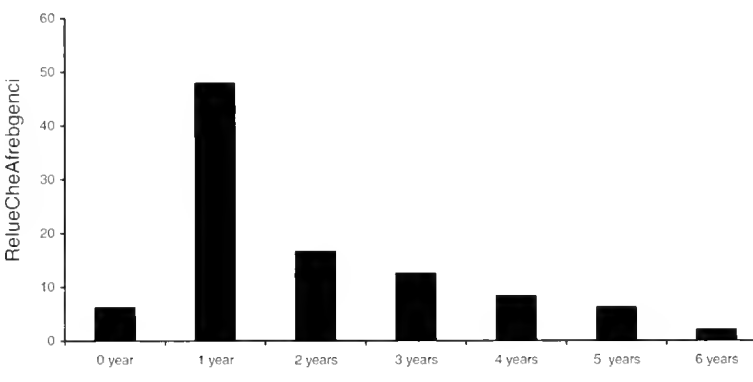

Figure 7

Age structure of male franciscanas (*Pontoporia blainvillei*) collected in Rio Grande do Sul (n=48).

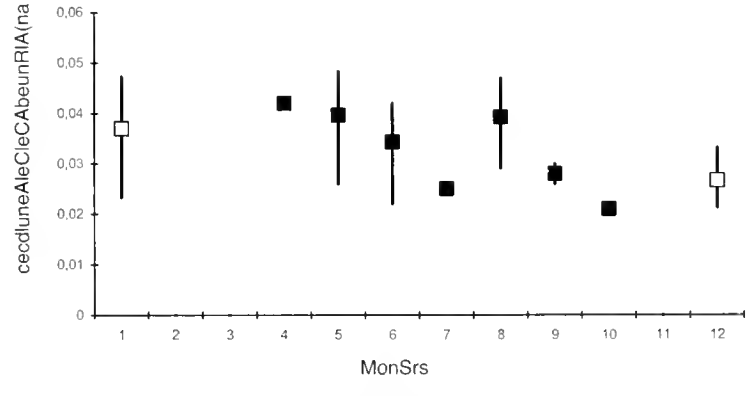

Figure 8

Relationship between month and relative testes weight in mature male franciscanas (*Pontoporia blainvillei*) (n=31) (1=January, 12=December; filled boxes=the nonreproductive months, open boxes=reproductive months). Bars indicate 25% and 75% percentiles.

Table 2

Comparison between average age, weight, and length at sexual maturity between male and female franciscanas from Rio Grande do Sul and Uruguay. The means of the animals from Rio Grande do Sul were estimated by using the DeMaster method (modified) and those from Uruguay were estimated by using a linear regression to determine the moment when 50% of the animals are mature.

	Rio Grande do Sul		Uruguay[1]	
	Males	Females[2]	Males	Females
Age	3.6	3.7	2–4	2.7
Weight (kg)	26.6	32.6	25.0–29.0	33.0–34.0
Length (cm)	127.4	138.9	131.4	140.3

[1] Data from Uruguay were compiled from Kasuya and Brownell (1979).

[2] Data from Danilewicz (2003).

length where 50% of the dolphins were mature through a linear regression. Applying this same approach, a LSM of 125.4 cm was estimated for Rio Grande do Sul—a value still very similar to the Uruguay estimate. Male franciscanas attain sexual maturity at less length and weight than do females in Rio Grande do Sul (Danilewicz, 2003), as observed previously in Uruguay (Kasuya and Brownell, 1979) and Rio de Janeiro (Ramos et al., 2000).

This is the first estimate of mean age at sexual maturity presented for male franciscanas. Kasuya and Brownell (1979) could not calculate ASM for Uruguay because of their small sample size (n=25). Nevertheless, Kasuya and Brownell suggested that sexual maturity is attained when males are between 2 and 4 years of age. Franciscanas from Rio de Janeiro were considered mature when they were older than 2 years of age and larger than 115.0 cm in length (Ramos et al., 2000). However, histological analysis of the testes was not performed and Ramos et al. employed indirect methods to determine sexual maturity. Nevertheless, despite the uncertainties produced by the use of different criteria to determine sexual maturity, it was evident that there was substantial difference in the size at maturity between males from Rio de Janeiro and those from Rio Grande do Sul and Uruguay. This difference is probably the result of the well-known distinct growth patterns of the franciscanas from these two regions (Pinedo, 1991) and does not necessarily reflect an early attainment of sexual maturity in males from the Rio de Janeiro population.

The trade-off between growth and reproduction is the best-documented phenotypic trade-off in nature (Stearns, 1992) and has been studied in a wide range of taxa. Because animals from Rio de Janeiro invest less in growth than do animals from Rio Grande do Sul, it is still an open question whether the franciscanas from the Rio de Janeiro have higher reproductive rates or start reproducing earlier than those from Rio Grande do Sul.

The oldest male and female franciscana ever aged were 16 and 21 years-old, respectively (Kasuya and Brownell, 1979; Pinedo, 1994). These ages contrasts with the age distribution found in the present study, where the oldest specimen analyzed was 6 years old. Similar to what is observed in catches for several other small cetacean species (e.g., Hector's dolphins—Slooten and Lad, 1991; harbor porpoise—Read and Hohn, 1995), a general feature of incidental catches for these species is the high entanglement rate of immature animals. In all fishing communities studied in Argentina, Uruguay, and Brazil, a large proportion (>50%) of the specimens caught were less than three years old (e.g., Kasuya and Brownell, 1979; Corcuera et al., 1994; Ott, 1998; Di Beneditto and Ramos, 2001). Although the precise reason for biased catch rates towards immature individuals is not well understood, it could be a combination of factors, including the imbalanced age-structure of local populations (where there are fewer older individuals because of an extensive history as bycatch) and a behavior-related higher vulnerability to bycatch for immature individuals (i.e., juveniles can be more inquisitive and have less ocean experience so that they rove into the area increasing the chances of being entangled). The typically low proportion of old animals in bycatches may explain the characteristics of the data used in this study.

Index of testicular maturity

An index of testicular maturity may be very useful in studies where it is necessary to know the sexual maturity of a large sample of animals without the need of histological analysis, which is time consuming and requires expertise. Although Hohn et al. (1985) recommended the investigation of the applicability of this indirect index of sexual maturity for male cetaceans, the research on this subject has shown no progress. To date, the index of sexual maturity has been calculated only for the common dolphin, *Delphinus delphis* (Collet and Saint Girons, 1984), and from the pantropical spotted dolphin, *Stenella attenuata* (Hohn et al., 1985). For both species, this index distinguished satisfactorily the mature from the immature and pubertal dolphins. Given the results presented, we also recommend the use of the index of testicular maturity as an alternative, nonhistological method, to determine the sexual maturity of male franciscanas. Males with index values lower than 0.05 can be safely classified as immature, and males with index values above 0.08 can be classified as mature. It is recommended that for animals with intermediate values their testes be analyzed histologically so that their reproductive status may be determined definitively.

Besides making intra- and inter-populational comparisons possible, the index of testicular maturity also permits interspecific comparisons because size differences between species are eliminated. The mean index of testicular maturity of mature franciscanas (0.12) is

considerably lower than mature pantropical spotted dolphins (1.9) (Hohn et al., 1985). This difference is a consequence of the relatively small increase of the testes weight of male franciscanas when sexual maturity is attained. Although male spotted dolphin show a marked increase of about 25-fold in testes weight at this moment, franciscanas show an increment in testes weight of about ninefold only.

Reproductive seasonality

The reproductive activities in male mammals are usually restricted to the periods when the females are in estrus (Lincoln, 1992). Reproductive seasonality in males has been reported for several cetacean species and populations through the identification of temporal variations in the testes weight and histological characteristics. In species where the reproductive period is restricted for a few months, as with the dusky dolphin (*Lagenorhynchus obscurus*) and the harbor porpoise (*Phocoena phocoena*), the testes weight presents marked fluctuations accompanying the reproductive period (Read, 1990; van Waerebeek and Read, 1994; Neimanis et al., 2000). Even in species with a diffuse reproductive period (i.e., with more than one peak for births per year) as in the case of dolphins of the genus *Stenella* in the tropical Pacific, it was possible to detect seasonal variation in the male reproductive rhythm (Perrin et al., 1976, Hohn et al., 1985).

Because of the known seasonality for births for franciscana (Kasuya and Brownell, 1979, Harrison et al., 1981, Danilewicz, 2003), it would be expected that the males would accompany the female rhythm, decreasing or even ceasing testicular activity in autumn and winter months. Kasuya and Brownell (1979) examined the seasonal change in testes weight in the months of January, June, and December. From our knowledge of the species' reproduction period, testes weight would be expected to be higher in December and January. However, the authors could not confirm this prediction and attributed the lack of seasonality to the small sample size of mature animals. Nevertheless, the lack of seasonality, even when the testes weight of the mature males from Rio Grande do Sul are included, may indicate what is occurring in the population, and not be a bias introduced by a small sample size.

In species that possess small testes, as in the case of the franciscana, the variation in the testicular activity may be better reflected by changes in the diameter of the seminiferous tubules and the rate of spermatogenesis rather than by changes in the testes weight. Nevertheless, the preliminary results about these characteristics (mature males with spermatids or spermatozoa [or both] in the seminiferous tubules in nonreproductive months and little monthly variation in the diameter of the seminiferous tubules) also do not support the hypothesis of a male reproductive seasonality. The combination of results presented here indicates that testicular activity is not completely interrupted in all males within the population, and that at least some of them may remain capable of fertilizing females during the year. This conclusion is supported by the observation of pregnancies outside the normal gestation season and that the births resulting from these pregnancies were estimated to take place in September and in late March (Danilewicz, 2003).

The hormone and sperm production by the testes during periods when the females are not able to reproduce may represent an unnecessary energetic expense by the male (Dewsbury, 1982) and may be an explanation for the period of reproductive inactivity for males of several mammal species. In species with large relative testes weight, the maintenance of high levels of sperm production in the testes is a considerable energetic cost for the individual. However, as discussed earlier, this is definitely not the case for the franciscana. For this reason, we suggest that the small energy investment in producing sperm all over the year, due to the small testicular mass, may be an evolutionary advantage for male franciscanas in case of the appearance of off-season reproductive females.

Franciscana reproductive strategy

Although important advances in the knowledge of franciscana behavior in the wild have been made (e.g., Bordino et al., 1999; Bordino, 2002), there is no information on the species' reproductive behavior and its mating strategy remains unknown. Relative testis weight, sexual size dimorphism, and secondary sexual characteristics may provide indirect clues regarding mating strategy in franciscana and are discussed below.

Relative testis weight In mammals, there is a functional relationship between relative testis weight and the species' mating system (Kenagy and Trombulak, 1986). Testes are relatively small in species presenting monogamy or extreme poliginy (several females + few males), i.e., where a male copulates with all females of a group or harem. Comparative studies have demonstrated that males tend to be larger than females and show secondary sexual characteristics in species presenting extreme poliginy. On the other hand, the relative testis weight is high and the sexual size dimorphism is reduced or nonexistent in species where several males copulate with only one estrus female (polyandry). In this case, the evolution for a large testis is attributed to the sperm competition in a system where different males attempt to fertilize the same female and where a higher copulatory frequency and higher levels of sperm production are required (Harcourt et al., 1981; Kenagy and Trombulak, 1986).

Using the data on 133 mammal species, Kenagy and Trombulak (1986) presented a function describing the relationship between body weight and combined-testes weight without epididymis. Applying their equation for the adult male franciscanas, we discovered that mature franciscanas have testes 3 to 12 times lighter than expected (mean=6 times) for a mammal of its body weight. Indeed, among the 133 species analyzed,

the relative testes weight of the franciscana is heavier than that of gorilla (*Gorilla gorilla*), humpback whales (*Megaptera novaeangliae*), and fin whales (*Balaenoptera physalus*), indicating that sperm competition does not occur in franciscanas.

Sexual size dimorphism Males are larger than females in most mammal species. Nevertheless, the reversed sexual size dimorphism (RSSD) (i.e., females are larger than males) is more common than previously thought and has been documented for 12 out of the 20 orders of mammals (Ralls, 1976, 1977). Among the odontocetes, four (Ziphidae, Pontoporiidae, Phocoenidae, and Delphinidae) out of the eight families present RSSD.

Although sexual selection may be the main reason why males are the larger sex in most mammal species, it has been systematically refused as an explanation in the cases where females are the larger sex (Ralls, 1976, 1977; Andersson, 1994). In species with RSSD, females do not mate with many males, they are not dominant, and are not more aggressive than males of the same species. Moreover, they do not show secondary sexual characteristics associated with intrasexual selection (e.g., horns in Artiodactyla and large canine teeth in Primates). Therefore, the occurrence of RSSD in mammals may be explained more satisfactorily by natural selection (Andersson, 1994).

Slooten (1991) proposed an interesting hypothesis for the occurrence of RSSD in cetaceans, suggesting that a minimum size may be necessary for a newborn cetacean to survive. In odontocetes, the smallest mean sizes at birth are about 70–80 cm. Because the size of the newborn is directly related to the size of the mother, in species of small dimensions the females would suffer a selective pressure to be a larger size, so that they could produce offspring with the minimum viable size. This hypothesis is reinforced by the fact that most of the odontocete species with RSSD (e.g., *Pontoporia blainvillei*, *Cephalorhynchus hectori*, *Cephalorhynchus commerssoni*, *Phocoena phocoena*, *Phocoena sinus*) are the smallest species within the group. Moreover, species presenting RSSD also have larger relative size at birth than the other species within the taxonomic group (Ralls, 1976).

The degree and direction of SSD (sexual size dimorphism) in mammals is the result of the difference of the sum of all selective pressures affecting the female's size and the sum of all selective pressures affecting the male's size (Ralls, 1976). Thus, it is very probable that more than one factor may act selectively on animals of both sexes in *Pontoporia*, molding the degree and direction of SSD. We propose that the requirement of a neonate minimum viable size (70–80 cm in length) is one of the main selective pressures acting on female franciscanas. It is important to emphasize that other factors may also be influencing SSD in franciscana, and in some species it was evident that different selective pressures could affect body size in opposing directions in males and females and in different age classes (Grant, 1986; Andersson, 1994). Among the factors that may be simultaneously acting on franciscana body size are intrinsic genetic and physiological limitations, and the requirement of maintaining an optimum size for the species' ecological niche.

Secondary sexual characteristics The presence and intensity of secondary sexual characteristics in males is a more precise indication of the degree of intrasexual selection than is body size (Andersson, 1994). In odontocete males, these characteristics are present in the form of "weapons," such as the tusk of the narwhal (*Monodon monoceros*) and the teeth in species of the genus *Grampus*, *Physeter*, *Berardius*, *Hyperoodon*, and *Mesoplodon* used in male-male combats (MacLeod, 1998). In species of these genus, the teeth were reduced in number, enlarged in size, and their form was modified (specially in males of Ziphiidae). The teeth of these species also lost their function in feeding because of a diet comprising almost exclusively cephalopods and were used uniquely in intrasexual combats. There is no evidence that the same evolutionary process occurred in male franciscanas because their teeth are very small and numerous (around 200), their diet is primarily fish, and the number of combat scars is apparently low. These characteristics support the hypothesis that male-male combat must be very rare or even nonexistent in franciscanas.

The sexual features presented in this study (extremely low testis weight, reversed sexual size dimorphism, absence of secondary sexual characteristics in males, and a low number of scars in males) indicate the absence of sperm competition in the franciscana, and these features differ drastically from those characteristics of odontocete species where males combat each other for copulation. This finding may indicate that franciscanas form temporary reproductive pairs during the reproductive period, where a male pairs and copulate with only one female. Recently, Valsecchi and Zanelatto (2003) provided molecular evidence suggesting that franciscanas may travel in kin groups that include mothers with their calves and the father of the youngest offspring. The authors also suggested that male franciscanas may prolong their bond with their reproductive partner, providing some form of paternal care. For a better understanding of franciscana social structure and mating system, the following suggestions are proposed: 1) an increase in the efforts of behavioral studies of free-ranging franciscanas; 2) quantification of the intraspecific teeth scars in franciscanas of different sexes and reproductive status in order to confirm the absence of intrassexual aggressions among males; 3) investigation of the relationship of relative testis weight, SSD, and reproductive strategies in cetaceans, by phylogenetic methods (see Harvey and Pagel, 1991) to understand the evolution of these characters in this group.

Acknowledgments

This study could not be made without the cooperation and friendship of the fishermen from Tramandaí/Imbé

and Rio Grande. Many people collaborated in the collection and necropsy of the dolphins, and the authors wish to thank Paulo Ott, Ignacio Moreno, Márcio Martins, Glauco Caon, Larissa Oliveira, Manuela Bassoi, Alexandre Zerbini, Luciana Möller, Luciano Dalla Rosa, Lilia Fidelix, and numerous volunteers for helping in this task. Gonad histology was partially done in Laboratório de Histologia e Embriologia Comparada of Universidade Federal do Rio Grande do Sul and we thank Sônia Garcia and Nivea Lothhammer for their instructions and encouragement on this subject. Paulo Ott, Enrique Crespo and Silvana Dans participated in the age determination procedures. Part of the age determination was also done in the Rio Grande and the first author thanks Cristina Pinedo and Fernando Rosas for their instruction. The authors also thanks Norma Luiza Würdig, Irajá Damiani Pinto (CECLIMAR-UFRGS), and Lauro Barcellos (Director of the Museu Oceanográfico) for their constant logistical support and for encouraging marine mammal studies in southern Brazil. Márcio Martins, Ignacio Moreno, Luiz Malabarba, and Mônica Muelbert reviewed an early draft of this paper. We wish to thank Renata Ramos and three anonymous reviewers for their suggestions regarding the manuscript. Financial support was given by Cetacean Society International, Fundação O Boticário de Proteção à Natureza, The MacCarthur Foundation, World Wildlife Fund, CNPq, UNEP, Yaqu Pacha Organization, and Whale and Dolphin Conservation Society. This paper is part of the first author's M.S. thesis, and The Coordenação de Aperfeiçoamento de Pessoal de Nível Superior (CAPES) has granted him a graduate fellowship. The Conselho Nacional de Desenvolvimento Científico e Tecnológico of the Brazilian Government (CNPq) has granted graduate fellowships to E.R. Secchi (Grant no. 200889/98-2).

Literature cited

American Society of Mammalogy.
1961. Standardized methods for measuring and recording data on the smaller cetaceans. J. Mamm. 42: 471–476.

Andersson, M.
1994. Sexual selection. Monographs in behavior and ecology, 599 p. Princeton Univ. Press. Princeton, NJ.

Bordino, P.
2002. Movement patterns of franciscana dolphin (*Pontoporia blainvillei*) in Bahia Anegada, Buenos Aires, Argentina. LAJAM (special issue) 1:71–76.

Bordino, P., G. Thompson, and M. Iñiguez.
1999. Ecology and behaviour of the franciscana (*Pontoporia blainvillei*) in Bahia Anegada, Argentina. J. Cetacean Res. Manag. 1 (2):213–222.

Collet, A., and H. Saint Girons.
1984. Preliminary study of the male reproductive cycle in common dolphins, *Delphinus delphis*, in the eastern North Atlantic. Rep. Int. Whal. Comm. (special issue) 6:355-360.

Corcuera, J., F. Monzon, E. A. Crespo, A. Aguilar, and J. A. Raga.
1994. Interactions between marine mammals and the coastal fisheries of Necochea and Claromecó (Buenos Aires Province, Argentina). Rep. Int. Whal. Comm. (special issue) 15:283–290.

Crespo, E. A., G. Harris, and R. González.
1998. Group size and distribution range of the franciscana, *Pontoporia blainvillei*. Mar. Mamm. Sci. 14 (4):845–849.

Danilewicz, D.
2003. Reproduction of female franciscana (*Pontoporia blainvillei*) in Rio Grande do Sul, southern Brazil. LAJAM 2 (2):67–78.

Danilewicz, D., E. R. Secchi., P. H. Ott, and I. B. Moreno.
2000. Analyses of the age at sexual maturity and reproductive rates of franciscanas (*Pontoporia blainvillei*) from Rio Grande do Sul, Southern Brazil. Comum. Mus. Ciênc. Tecnol. PUCRS 13(1):89–98.

DeMaster, D. P.
1978. Calculation of the average age of sexual maturity in marine mammals. J. Fish. Res. Board Can. 35 (6):912–15.

Dewsbury, D. A.
1982. Ejaculate cost and male choice. Am. Nat. 119: 601–610.

Di Beneditto, A. P. M., and R. M. A. Ramos.
2001. Biology and conservation of the franciscana (*Pontoporia blainvillei*) in the north of Rio de Janeiro State, Brazil. J. Cetacean Res. Manag. 3:185–192.

Ferrero R. C., and W. A. Walker.
1993. Growth and reproduction of the northern right whale dolphin, *Lissodelphis boreolis*, in the offshore waters of the North Pacific Ocean. Can. J. Zool. 71 (12):2335–2344.

Grant, P. R.
1986. Ecology and evolution of Darwin's finches. Princeton Univ. Press, Princeton, NJ.

Harcourt, A. H., P. H. Harvey, S. G. Larson, and R. V. Short.
1981. Testis weight, body weight and breeding system in primates. Nature 293:55–57.

Harrison, R. J., M. M. Bryden, D. A. McBrearty, and R. L. Brownell Jr.
1981. The ovaries and reproduction in *Pontoporia blainvillei* (Cetacea: Platanistidae). J. Zool. 193:563–580.

Harvey, P., and M. Pagel.
1991. The comparative method in evolutionary biology, 239 p. Oxford series in ecology and evolution. Oxford Univ. Press, Oxford, England.

Hohn, A., S. J. Chivers, and J. Barlow.
1985. Reproductive maturity and seasonality of male spotted dolphins, *Stenella attenuata*, in the eastern tropical Pacific. Mar. Mamm. Sci., 1(4):273–293.

Kasuya, T., and R. L. Brownell Jr.
1979. Age determination, reproduction, and growth of the franciscana dolphin, *Pontoporia blainvillei*. Sci. Rep. Whales Res. Inst. 31:45–67.

Kinas, P. G.
2002. The impact of the incidental kills by gillnets on the franciscana dolphin (*Pontoporia blainvillei*) in southern Brazil. Bull. Mar. Sci. 70:409–421.

Kenagy , G. K., and S. C. Trombulak.
1986. Size and function of mammalian testes in relation to body size. J. Mamm. 67(1):1–22.

Lincoln, G. A.
1992. Biology of seasonal breeding in deer. *In* The biology of deer (R. D. Brown, ed.), p. 565–574. Springer-Verlag, New York, NY.

MacLeod, C.D.
1998. Intraspecific scarring in odontocete cetaceans: an indicator of male 'quality' in agressive interactions? J. Zool. 244:71–77.
Mitchell, E. D., and V. M. Kozicki.
1984. Reproductive condition of male sperm whales, *Physeter macrocephalus*, taken off Nova Scotia. Rep. Int. Whal. Comm. (special issue) 6:243–48.
Miyazaki, N.
1977. Growth and reproduction of *Stenella coeruleoalba* off the Pacific coast of Japan. Sci. Rep. Whales Res. Inst. 29:21–48.
Moreira, L. M., and S. Siciliano.
1991. Northward extension range for *Pontoporia blainvillei*, p. 8. Abs. Ninth Bienn. Conf. Biol. Mar. Mamm. Chicago, IL.
Moreno, I. B., P. H. Ott, and D. Danilewicz.
1997. Análise preliminar do impacto da pesca artesanal costeira sobre *Pontoporia blainvillei* no litoral norte do Rio Grande do Sul, sul do Brasil. *In* Proceedings of the second workshop for the research coordination and conservation of the franciscana (*Pontoporia blainvillei*) in the Southwestern Atlantic (M. C. Pinedo A. and Barreto, eds.), p. 31–41. Editora da FURG, Rio Grande, Rio Grande do Sul, Brazil.
Neimanis, A. S., A. J. Read, R. A. Foster, and D. E. Gaskin.
2000. Seasonal regression in testicular size and histology in harbour porpoises (*Phocoena phocoena*, L.) from the Bay of Fundy and Gulf of Maine. J. Zool. 250:221–229.
Ott, P. H.
1998. Análise das capturas acidentais da toninha, *Pontoporia blaivillei*, no litoral norte do Rio Grande do Sul, sul do Brasil. MSc. Thesis, 120 p. Pontifícia Universidade Católica do Rio Grande do Sul, Porto Alegre, Brazil.
Ott, P. H., E. R. Secchi, I. B. Moreno, I.B., D. Danilewicz, E. A. Crespo, P. Bordino, R. Ramos, A. P. Di Beneditto, C. Bertozzi, R. Bastida, R. Zanelatto, J. Perez, and P. G. Kinas.
2002. Report of the working group of fishery interactions. LAJAM (special issue) 1:55–64.
Perrin, W. F., J. M. Coe, and J. R. Zweifel.
1976. Growth and reproduction of the spotted porpoise, *Stenella attenuata*, in the offshore eastern tropical Pacific. Fish. Bull. 74:229–269.
Pinedo, M. C.
1991. Development and variation of the franciscana, *Pontoporia blainvillei*. Ph.D. diss., 406 p. Univ. California, Santa Cruz, CA.
1994. Impact of incidental fishery mortality on the age structure of *Pontoporia blainvillei* in southern Brazil and Uruguay. Rep. Int. Whal. Comm. (spec. issue 15):261–264.
Pinedo, M. C., and A. Hohn.
2000. Growth layer patterns in teeth from the franciscana, *Pontoporia blainvillei*: developing a model for precision in age estimation. Mar. Mamm. Sci. 16 (1):1–27.
Praderi, R., M. C. Pinedo, and E. A. Crespo.
1989. Conservation and management of *Pontoporia blainvillei* in Uruguay, Brazil and Argentina. *In* Biology and conservation of river dolphins (W. F. Perrin, R. L. Brownell, Z. Kaya, and L. Jiankang (eds.), p. 52–56. Allen Press, Lawrence, KS.
Ralls, K.
1976. Mammals in which females are larger than males. Q. Rev. Biol. 51:245–276.
1977. Sexual dimorphism in mammals: avian models and unanswered questions. Am. Nat. 111:917–937.
Ramos, R.
1997. Determinação de idade e biologia reprodutiva de *Pontoporia blainvillei* e da forma marinha de *Sotalia fluviatilis* no litoral norte do Rio de Janeiro. M.S. thesis, 95 p. Universidade Estadual do Norte Fluminense, Rio de Janeiro, Brazil.
Ramos, R., A. P. Di Beneditto, and N. R. W. Lima.
2000. Growth parameters of *Pontoporia blainvillei* and *Sotalia fluviatilis* (Cetacea) in northern Rio de Janeiro, Brazil. Aquat. Mamm. 26 (1):65–75.
Read, A.
1990. Reproductive seasonality in harbour porpoises, *Phocoena phocoena*, from the Bay of Fundy. Can. J. Zool. 68:284–288.
Read, A., and A. Hohn.
1995. Life in the fast lane: the life history of the harbour porpoises from the Gulf of Maine. Mar. Mamm. Sci. 11:423–440.
Secchi, E. R.
1999. Taxa de crescimento potencial intrinseco de um estoque de franciscanas, *Pontoporia blainvillei* (Gervais & D'Orbigny, 1846) (Cetacea, Pontoporiidae) sob o impacto da pesca costeira de emalhe. M.S. thesis, 152 p. Fundação Universidade Federal do Rio Grande, Rio Grande, do Sul, Brazil. [In Portuguese.]
Secchi, E. R., A. N. Zerbini, M. Bassoi, L. Dalla Rosa, L. M. Moller, and C. C. Rocha-Campos.
1997. Mortality of franciscanas, *Pontoporia blainvillei*, in coastal gillnetting in southern Brazil. Rep. Int. Whal. Comm. 47:653–658.
Secchi, E. R., Ott, P. H., and Danilewicz, D.
2002. Report of the fourth workshop for the coordinated research and conservation of the franciscana dolphin (*Pontoporia blainvillei*) in the western South Atlantic. LAJAM (special issue) 1:11–20.
2003. Effects of fishing bycatch and the conservation status of the franciscana dolphin, *Pontoporia blainvillei*. *In* Marine mammals: fisheries, tourism and management issues (N. Gales, M. Hindell, and R. Kirkwood, eds.), p. 174–191. CSIRO Publishing, Collingwood, Victoria, Australia.
Slooten, E.
1991. Age, growth, and reproduction in Hector's dolphins. Can. J. Zool. 69:1689–1700.
Slooten, E., and F. Lad.
1991. Population biology and conservation of Hector's dolphin. Can. J. Zool. 69:1701–1707.
Stearns, S. C.
1992. The evolution of life histories, 249 p. Oxford, Univ. Press, New York, NY.
Valsecchi, E., and R. C. Zanelatto.
2003. Molecular analysis of the social and population structure of the franciscana (*Pontoporia blainvillei*): conservation implications. J. Cetacean Res. Manag. 5(1):69–75.
Van Waerebeek, K., and A. Read.
1994. Reproduction of dusky dolphins, *Lagenorhynchus obscurus*, from coastal Peru. J. Mamm. 75 (4):1054–1062.

Red snapper (*Lutjanus campechanus*) demographic structure in the northern Gulf of Mexico based on spatial patterns in growth rates and morphometrics

Andrew J. Fischer
Coastal Fisheries Institute
School of the Coast and Environment
Louisiana State University
Baton Rouge, Louisiana 70803-7503
E-mail address: afische@lsu.edu

M. Scott Baker Jr.
Coastal Fisheries Institute
School of the Coast and Environment
Louisiana State University
Baton Rouge, Louisiana 70803-7503

Charles A. Wilson
Coastal Fisheries Institute and
Department of Oceanography and Coastal Sciences
School of the Coast and Environment
Louisiana State University
Baton Rouge, Louisiana 70803-7503

Abstract—Red snapper (*Lutjanus campechanus*) in the United States waters of the Gulf of Mexico (GOM) has been considered a single unit stock since management of the species began in 1991. The validity of this assumption is essential to management decisions because measures of growth can differ for nonmixing populations. We examined growth rates, size-at-age, and length and weight information of red snapper collected from the recreational harvests of Alabama (n=2010), Louisiana (n=1905), and Texas (n=1277) from 1999 to 2001. Ages were obtained from 5035 otolith sections and ranged from one to 45 years. Fork length, total weight, and age-frequency distributions differed significantly among all states; Texas, however, had a much higher proportion of smaller, younger fish. All red snapper showed rapid growth until about age 10 years, after which growth slowed considerably. Von Bertalanffy growth models of both mean fork length and mean total weight-at-age predicted significantly smaller fish at age from Texas, whereas no differences were found between Alabama and Louisiana models. Texas red snapper were also shown to differ significantly from both Alabama and Louisiana red snapper in regressions of mean weight at age. Demographic variation in growth rates may indicate the existence of separate management units of red snapper in the GOM. Our data indicate that the red snapper inhabiting the waters off Texas are reaching smaller maximum sizes at a faster rate and have a consistently smaller total weight at age than those collected from Louisiana and Alabama waters. Whether these differences are environmentally induced or are the result of genetic divergence remains to be determined, but they should be considered for future management regulations.

Manuscript submitted 6 May 2003
to the Scientific Editor's Office.
Manuscript approved for publication
19 April 2004 by the Scientific Editor.
Fish. Bull. 102:593–603 (2004).

Red snapper (*Lutjanus campechanus*) in the United States waters of the Gulf of Mexico (GOM) are heavily exploited by both recreational and commercial fishermen (Wilson and Nieland, 2001; Shirripa and Legault[1]). Harvest, however, has not proceeded without detrimental affects on the population. Commercial landings have declined substantially from 6048 metric tons (t) in 1964 to 1207 t in 1990; recreational landings exhibited similar declines from 1937 t in 1981 to 481 t in 1990 (NMFS[2]). In 1991, harvest restrictions including reef fish permits, seasonal fishing, fish quotas, creel limits, and minimum size limits were placed upon the red snapper fishermen by the Gulf of Mexico Fishery Management Council (GMFMC[3]) to increase the spawning potential ratio to 20%, which is indicative of recovery. These regulations have also been adopted for state waters in Alabama, Louisiana, and Texas. Despite the management actions, GOM red snapper remain overfished (Goodyear[4]; Schirripa and Legault[1]).

[1] Shirripa, M. J., and C. M. Legault. 1999. Status of the red snapper in the U. S. waters of the Gulf of Mexico: updated through 1998, 44 p. + appendices. Contribution rep. SFD-99/00-75 from Sustainable Fisheries Division, Miami Laboratory, Southeast Fisheries Science Center, National Marine Fishery Service, 75 Virginia Beach Drive, Miami, FL 33149-1099. [Not available from NTIS].

[2] NMFS (National Marine Fisheries Service). 2003. Fisheries Statistics and Economics Division. Website: www.nmfs.noaa.gov.

[3] GMFMC (Gulf of Mexico Fishery Management Council). 1991. Amendment 3 to the reef fishery management plan for the reef fish resources of the Gulf of Mexico, 38 p. Gulf of Mexico Fishery Management Council, 3018 N. U.S. Hwy 301 Suite 1000, Tampa, FL. 33619-2272. [Not available from NTIS].

[4] Goodyear, C. P. 1995. Red snapper in U.S. waters of the Gulf of Mexico. Stock assesment report MIA-95/96-05, 171 p. Miami Laboratory, Southeast Fisheries Science Center, National Marine Fisheries Service, 75 Virginia Beach Dr., Miami, FL, 33149-1099. [Not available from NTIS].

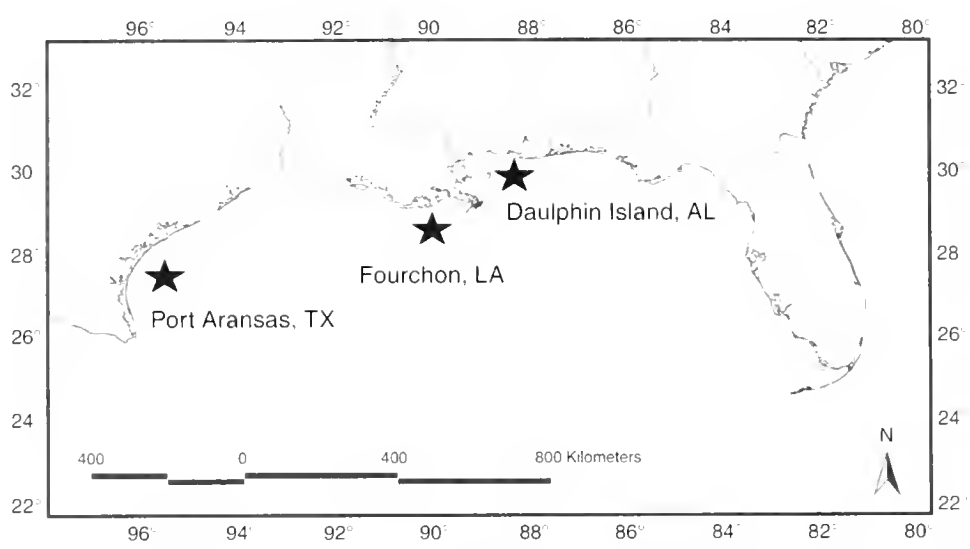

Figure 1

Map of the northern Gulf of Mexico showing the three red snapper (*Lutjanus campechanus*) sampling locations.

An underlying assumption crucial to a fishery management plan is that the fish species being managed is a unit stock (Gulland, 1965). A stock is defined as the part of a fish population that is under consideration as an actual or potential resource (Ricker, 1975). Since management began in 1991, red snapper in the northern GOM have been considered a unit stock. Genetic studies to date have shown that there is little evidence to dispute this assumption (Camper et al., 1993; Gold et al., 1997, Heist and Gold, 2000). On the other hand, tag-recapture studies indicate that red snapper have the capacity to move great distances, making it possible for separate stocks to develop (Patterson et al., 2001).

The validity of an assumption of a single stock of red snapper is essential to management decisions because measures of growth, natural mortality, reproductive capacity, and recruitment can differ among nonmixing populations. Should separate red snapper stocks exist, management plans would have to be enacted for each defined stock in order to follow federal guidelines. Even if a single large red snapper stock exists, management should be sensitive to both the diversity of habitats and user groups within the species area of occurrence. Because red snapper are arguably the most important recreational and commercial offshore fishery from Florida to southern Texas, every effort should be undertaken to develop the most effective and productive management plan.

The objective of this study was to evaluate the stock structure of GOM red snapper based on growth rates and size-at-age information. We hypothesized that red snapper sampled from across the northern GOM would be indistinguishable in their growth rates and size at age—a uniformity indicative of a single unit stock.

Methods and materials

Red snapper were collected from the recreational harvests of 1999, 2000, and 2001 from the northern GOM at Dauphin Island, Alabama, at Port Fourchon, Louisiana, and at Port Aransas, Texas (Fig. 1). A maximum of 75 fish were randomly selected and sampled from the daily catch of each charter boat or head boat while the captains and deck hands cleaned fish. These fish were not selected by size. Larger individuals (>6.8 kg) were opportunistically sampled from spear fishing and hook-and-line fishing tournaments in Alabama and Louisiana. In addition, a number of smaller fish (<406 mm, <457 mm during summer 1999) were randomly sampled during red snapper tagging cruises in Alabama. Morphometric measurements were recorded (fork length [FL] in mm, total weight [TW] in kg, and eviscerated body weight [BW] in kg), sex was determined by macroscopic examination of gonads, and both sagittal otoliths were removed, rinsed, and stored in coin envelopes until processed. Fish weights were not recorded for 1999 Texas samples.

A transverse thin section (containing the core) was taken from the left sagittal otolith of each individual. Sections were made with the Hillquist model 800 thin-sectioning machine equipped with a diamond embedded wafering blade and precision grinder (Cowan et al., 1995). When the left otolith was unavailable, the right otolith was sectioned. Examinations of otolith sections were made with a dissecting microscope with transmitted light and polarized light filter at 20× to 64× magnification Opaque annulus counts were made along the ventral side of the sulcus acousticus from the core to the proximal edge (Wilson and Nieland, 2001). Annulus counts were performed by two independent readers (AJF

and MSB) without knowledge of either date of capture or morphometric data. The appearance of the otolith section edge condition was coded as opaque or translucent after Beckman et al. (1989). Annuli were counted a second time when initial counts disagreed. In instances where a consensus between the two readers could not be reached, annulus counts of the more experienced reader (AJF) were used. Between-reader differences in annulus counts were evaluated with the coefficient of variation (CV), index of precision (D) (Chang, 1982), and average percent error (APE) (Beamish and Fournier, 1981). The periodicity of opaque zone formation was verified for each sampling location with edge analysis after Wilson and Nieland (2001). Ages of red snapper were estimated from opaque annulus counts and capture date with the equation described by Wilson and Nieland (2001):

$$Day\ age = -182 + (\text{opaque increment count} \times 365) + ((m-1) \times 30) + d,$$

where m = the ordinal number (1–12) of month of capture; and
d = the ordinal number (1–31) of the day of the month of capture.

The 182 days subtracted from each age estimate are to account for the uniform hatching date assigned for all specimens (Render, 1995; Wilson and Nieland, 2001). Age in years was assigned by dividing day age by 365.

Fork length–TW relationships were fitted with linear regression to the model $FL = a\ TW^b$ from $\log_{10}$-transformed data for Alabama, Louisiana, and Texas specimens. Analysis of covariance (ANCOVA) was used to compare slopes and intercepts among sampling locations (SAS, 1985). Variability in age, FL, and TW frequency distributions of red snapper were compared among states with the Komolgorov-Smirnov two-sample test (Tate and Clelland, 1957).

Growth of red snapper was modeled for FL and TW with the von Bertalanffy growth equations. Because of differences in sample population size among states, weighted mean FL and mean TW at age were fitted for each state with nonlinear regression in the forms:

$$FL_t = L_\infty(1 - e^{[-k(t)]})$$
$$TW_t = W_\infty(1 - e^{[-k(t)]})^b,$$

where FL_t = FL at age t;
TW_t = TW at age t;
L_∞ = the FL asymptote;
W_∞ = the TW asymptote;
k = the growth coefficient;
t = age in years; and
b = exponent derived from our length–weight regressions (SAS, version 5, 1985, SAS Inst, Cary, NC).

Because of a lack of smaller individuals in all sample populations, no y-intercepts for t_0 were specified and models were forced through 0. Larger individuals and juveniles selectively sampled by size were excluded from the models to more accurately reflect a random sample. Likelihood ratio tests (Cerrato, 1990) were used to test for differences among states in models and in growth parameter estimates. Differential growth was evaluated for red snapper in the first 10 years of life when somatic growth is most rapid (Szedlmayer and Shipp, 1994; Patterson et al., 2001; Wilson and Nieland, 2001). Linear regressions of mean FL and mean TW at age for fishes aged 1 to 10 years were compared among states with analysis of covariance (ANCOVA) and tested for homogeneity of slopes.

Table 1

Numbers of red snapper (*Lutjanus campechanus*) sampled from recreational sources by state and year.

State	Males	Females	Unknown sex	Total
Alabama				
1999	434	396	5	835
2000	355	415	7	777
2001	189	209	0	398
			Total	2010
Louisiana				
1999	367	339	31	737
2000	399	397	8	804
2001	160	179	25	364
			Total	1905
Texas				
1999	268	293	14	575
2000	278	284	22	584
2001	52	56	10	118
			Total	1277

Results

During the three-year study period, 5192 red snapper were sampled from the recreational harvest of the northern GOM (Table 1): 642 individuals from fishing tournaments, 71 undersize fish from tagging cruises, and 4479 random samples from recreational catches. The samples included 2502 males, 2568 females, and 122 individuals of undetermined sex. The resultant male-to-female ratios were 0.96:1 for Alabama, 1:0.99 for Louisiana, 0.94:1 for Texas, and 0.97:1 for all states combined. A chi-square test indicated no significant difference in the number of males to females (χ^2=0.78, P=0.38). Fork lengths ranged from 237 to 916 mm (Fig. 2A). Specimens from Alabama ranged from 237 to 916 mm FL, Louisiana specimens ranged from 282 to 913 mm FL, and Texas specimens ranged from 266 to 846 mm FL. The FL frequency distributions of the random samples were different among all states (AL and LA, maximum difference (MD)=5.26; AL and TX, MD=51.86; LA and TX, MD=51.77)(Fig. 2A).

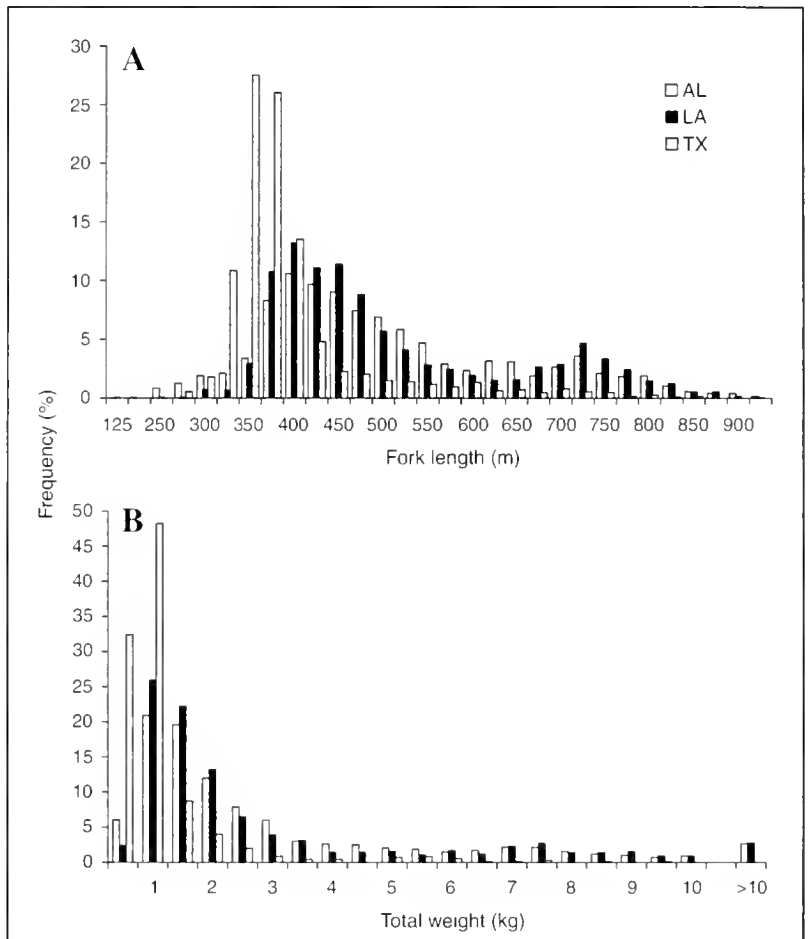

Figure 2

Distributions of (**A**) fork length in mm (n=5177) and (**B**) total weight in kg (n=4531) for red snapper (*Lutjanus campechanus*) sampled from the 1999–2001 recreational harvests of Alabama, Louisiana, and Texas.

Total weights of all fish sampled ranged from 0.11 to 17.35 kg (Fig. 2B). Specimens from Alabama ranged from 0.22 to 15.42 kg TW, Louisiana specimens were 0.42 to 17.35 kg TW, and Texas specimens ranged from 0.33 to 9.42 kg TW. Total weight-frequency distributions (in 0.5 kg increments) differed significantly between all states (AL and LA, MD=5.37; AL and TX, MD=53.68; and LA TX, MD=52.28)(Fig. 2B). Significant differences in red snapper FL-TW regression models were detected among states (ANCOVA test of homogeneity of slopes, $F_{5,\ 4522}$=23.36; P<0.001; r^2=0.98; ANCOVA test for equal intercepts, $F_{5,\ 4522}$=22.77, P<0.001, r^2=0.98); therefore, separate models were fitted for each state. The resultant equations were

$$AL\ TW = 1.51 \times 10^{-5}\ (FL^{3.03})$$
$$(F_{1,1965}=102740;\ P<0.0001;\ r^2=0.98);$$

$$LA\ TW = 1.02 \times 10^{-5}\ (FL^{3.09})$$
$$(F_{1,1856}=77981;\ P<0.0001;\ r^2=0.98);$$

$$TX\ TW = 2.88 \times 10^{-5}\ (FL^{2.92})$$
$$(F_{1,699}=13345;\ P<0.0001;\ r^2=0.95).$$

Ages were obtained from 5035 transverse otolith sections. Thirty fish had otolith sections deemed unreadable by both readers. The age estimates determined by the two readers were evaluated for reader agreement, precision, and average percent error for first and second readings of otolith sections by sample year. Table 2 gives APE, CV, D, percentage agreement (O), and percentages of differences in age estimates (±1, 2, and 3 years). The readers agreed on age estimates for 4053 otoliths (80.5%) after the initial reading. Re-examination of the 982 otolith sections for which annulus counts differed produced agreement for 5007 individuals.

We compared the timing of opaque annulus formation among red snapper sample sites by plotting the monthly occurrence of maximum and minimum proportions of opaque otolith edges. Sample limitations of red snapper in Texas, however, prevented meaningful comparisons of

opaque annulus formation for this state. However, minimum proportions of opaque edges during the months of April through October may indicate that red snapper from Texas form an opaque annulus during the winter months. Proportions of opaque edges for Alabama and Louisiana were essentially the same: maximum proportions of opaque edges during the months of February and March followed by a decrease to minimum proportions during the months of May through November (Fig. 3). These findings are consistent with previous age and growth studies on red snapper in the northern GOM (Patterson et al., 2001; Wilson and Nieland, 2001), indicating that the formation of one opaque annulus in the winter months is followed by the formation of one translucent annulus in summer. Annulus-based age estimates of red snapper from the northern GOM have also been validated to 55 years with otolith radiocarbon chronologies based on accelerator mass spectrometry ^{14}C measurements (Baker and Wilson, 2001).

Red snapper ages ranged from 1 to 45 years and the majority (90%) of individuals were between 2 and 6 years (Fig. 4). Alabama fish ranged from 1 to 35 years (n=1985), Louisiana fish ranged from 2 to 37 years (n=1864), and Texas fish ranged from 1 to 45 years (n=1186). Modal ages were 4 years for Alabama and 3 years for Louisiana and Texas red snapper. We found significant differences among age-frequency distributions from all states (AL and LA, MD=9; AL and TX, MD=33.84; and LA and TX, MD=24.84). Texas had a much higher proportion of younger individuals; 63% of sampled fish were aged at 3 years or less compared to only 30% of Alabama and 39% of Louisiana fish aged at 3 years or less.

Red snapper growth was modeled from weighted mean FL at age and mean TW at age by using the von Bertalanffy growth equation (Fig. 5, A and B). Resultant von Bertalanffy growth equations were

$$AL\ FL_{\infty} = 839(1 - e^{(-0.38(t))})$$
$$(F_{1;15} = 2824.9;\ P<0.0001;\ r^2=0.95);$$

$$LA\ FL_{\infty} = 847.8(1 - e^{(-0.25(t))})$$
$$(F_{1;13}=5024.4;\ P<0.0001;\ r^2=0.76);$$

$$TX\ FL_{\infty} = 778.2(1 - e^{(-0.49(t))})$$
$$(F_{1;19}=1452.1;\ P<0.001;\ r^2=0.85);$$

$$AL\ TW_{\infty} = 17.05(1 - e^{(-0.15(t))})^{3.03}$$
$$(F_{1;15}=457.9;\ P<0.0001;\ r^2=0.89);$$

$$LA\ TW_{\infty} = 12.61(1 - e^{(-0.32(t))})^{3.03}$$
$$(F_{1;14}=122.02;\ P<0.0001;\ r^2=0.18);$$

$$TX\ TW_{\infty} = 8.89(1 - e^{(-0.21(t))})^{2.84}$$
$$(F_{1;12}=613.01;\ P<0.0001;\ r^2=0.96).$$

Models of mean red snapper FL at age for Alabama and Louisiana were markedly similar with likelihood ratio tests indicating no significant differences between red snapper from the two states (Table 3). However, the Texas model differed from both Alabama and Louisiana models. The Texas model displayed significant differences from the other models in both L_{∞} and in k. A comparison of the models of mean TW at age indicated no significant differences between Alabama and Louisiana red snapper (Table 3). Differential growth in TW was found when comparing Alabama and Louisiana with the Texas model; significant differences were manifested in both W_{∞} and in k. The model failed to converge for estimating a common value of k for both Louisiana and Texas.

We recognized that the larger red snappers from Louisiana might bias the data; therefore we compared growth for fish from 2 to 10 years of age—a time period when red snapper have demonstrated rapid linear growth (Szedlmayer and Shipp, 1994; Patterson et al., 2001; Wilson and Nieland, 2001). Linear regressions of mean FL at age for all individuals 2 to 10 years (Fig. 6A) were compared among states. We found no significant differences among states (ANCOVA test of homogeneity of slopes, $F_{2;28}$=2.7; P=0.08; ANCOVA test for equal intercepts, $F_{2;28}$=0.52; P=0.6).

Table 2

Differences between two readers in average percent error (APE), coefficient of variation (CV), index of precision (D), and in percentages of agreement (O) for counts of opaque annuli in red snapper (*Lutjanus campechanus*) otoliths after first and second readings for each sample year. n=number of otoliths sampled.

Year	1st reading	2nd reading
1999 (n=2100)		
APE	0.483	0.499
CV	0.014	0.0008
D	0.010	0.0006
O	89.48%	99.43%
±1	8.62%	0.48%
±2	1.19%	0.095%
±3	0.71%	
2000 (n=2069)		
APE	0.487	0.499
CV	0.034	0.0006
D	0.024	0.0004
O	73.79%	99.47%
±1	22.49%	0.53%
±2	1.78%	
±3	1.93%	
2001 (n=866)		
APE	0.459	0.498
CV	0.032	0.0005
D	0.023	0.0003
O	74.73%	99.42%
±1	22.06%	0.58%
±2	2.27%	
±3	0.94%	

Mean TW at age was also examined among states for red snapper 2 to 10 years in age as above (Fig. 6B). No significant differences were found between Alabama and Louisiana (ANCOVA test of homogeneity of slopes, $F_{1,17}$= 0.1; P=0.75; ANCOVA test for equal intercepts, $F_{1,17}$= 0.26; P=0.66 for intercepts). However, a significant difference between slopes was detected when comparing Alabama and Texas red snapper (ANCOVA test of homogeneity of slopes, $F_{1,16}$=19.68; P<0.0007; ANCOVA test for equal intercepts, $F_{1,16}$=2.74; P<0.12). The same was found when comparing slopes for Louisiana and Texas red snapper (ANCOVA test of homogeneity of slopes, $F_{1,16}$=9.62; P<0.008) but not when comparing intercepts ($F_{1,16}$=0.64; P<0.44).

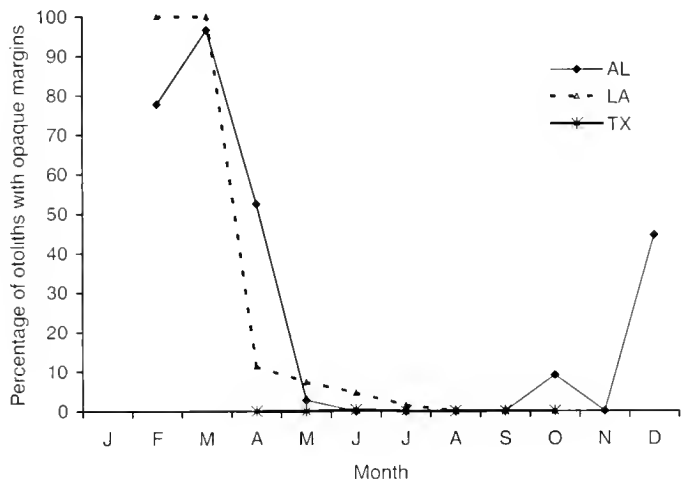

Figure 3

Marginal increment analysis of red snapper (*Lutjanus campechanus*) otoliths for specimens from Alabama (n=1985), Louisiana (n=1864), and Texas (n=1186).

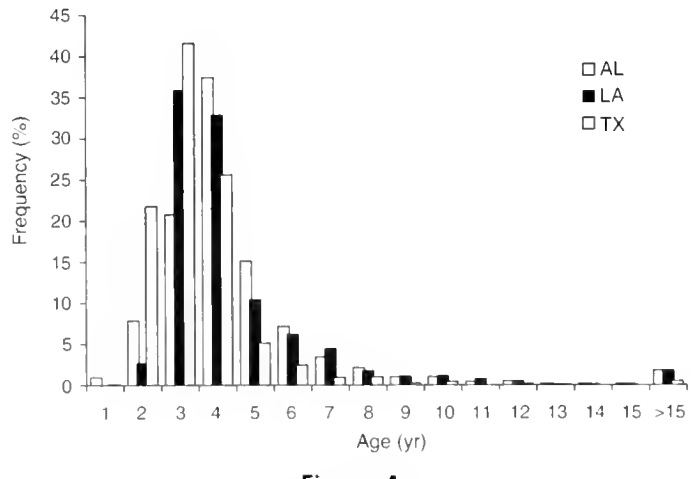

Figure 4

Age distributions for red snapper (*Lutjanus campechanus*) sampled from the 1999–2001 recreational harvests from Alabama, Louisiana, and Texas.

Discussion

Demographic variations in growth rates and in size-frequency distributions may indicate the existence of isolated management units of red snapper in the northern GOM. The recreational harvests of Alabama and Louisiana red snapper were dominated by individuals ranging from 375 to 425 mm FL, whereas the majority of Texas fish (69%) were 375 mm FL or less. It was within this size range (375–400 mm FL) that the significant differences in red snapper among states were detected. The FL distribution of red snapper sampled in Texas also differed from those for Alabama and Louisiana; there were very few large fish represented in the Texas sample population, partly because fishing tournaments (where larger individuals are targeted) were not sampled in Texas. Significant differences in TW frequencies among states were also detected at approximately 1 kg (the approximate weight of a red snapper 375–400 mm FL); 86% of Texas fish weighed 1 kg or less, compared to only 27% of Alabama fish and 28% of Louisiana fish in this size range.

One factor possibly contributing to the modal size class difference was the type of fishing vessel used to catch the fish. The majority of Texas specimens (~95%) were sampled from headboats; whereas Louisiana and Alabama fish were obtained almost exclusively from charterboats. This is not to say that charterboats were purposely excluded from the Texas survey. On the contrary, red snapper were sampled from any and all available recreational fishing parties at the three individual sampling locations. Differences in modal size and number of red snapper caught per person onboard charterboats versus headboats may be inconsequential considering that both trip types used similar gear and targeted similar or the same fishing locations. It should be noted however that in the Texas study area, charterboats routinely frequented a wider array of fishing spots (rigs, hardbottom, wrecks, etc.) than did headboats, which typically return to the same few rigs and large structures over and over again (Tolan[5]).

Our von Bertalanffy growth models on FL at age showed that red snapper from all three states exhibit a pattern of rapid, linear growth to approximately 10 years, after which maximum theoretical (asymptotic) FL is soon

[5] Tolan, J. 2003. Personal commun. Texas Parks and Wildlife Department, Resource Protection, 6300 Ocean Dr., Corpus Christi, TX 78412.

Table 3

Chi-square (χ^2), degrees of freedom (df), and *P*-values for likelihood ratio tests for comparing FL and TW von Bertalanffy growth models and parameters among sample locations (states). AL= Alabama; LA= Louisiana; and TX=Texas. n/a=not available.

	AL–LA	AL–TX			LA–TX		
	FL model	FL model	*L*	*k*	FL model	*L*	*k*
χ^2	2.54	5.14	13.67	21.53	5.8	10.16	9.8
df	1, 28	1, 34	1, 34	1, 34	1, 32	1, 32	1, 32
P	0.11	0.023	0.0002	3.48×10^{-6}	0.015	0.001	0.002
	TW model	TW model	*L*	*k*	TW model	*L*	*k*
χ^2	2.15	38.8	21.3	37.8	16.77	15.1	n/a
df	1, 29	1, 27	1, 27	1, 27	1, 26	1, 26	n/a
P	0.14	$4.7\cdot10^{-6}$	3.9×10^{-6}	$7.97\cdot10^{-10}$	4.2×10^{-5}	0.001	n/a

reached and growth in length becomes negligible. This pattern of rapid growth was similar to that reported in previous studies (Szedlmayer and Shipp, 1994; Manooch and Potts, 1997; Patterson, 1999; Wilson and Nieland, 2001). However, our models predicted smaller L_∞ and higher values of k. Because of the minimum size limits on the recreational fishery, very few fish under age 2 years (>300 mm FL) were included in our sample populations. We forced our models through $t_0=0$ to more accurately predict juvenile growth, which in turn increased our estimates of k. In addition, we had a much larger sample population that included more older, larger fish than most of the previously cited studies. These larger fish pulled the curve down, driving the lesser estimations of L_∞. The lack of significant differences in growth parameters between the Alabama and Louisiana models supports the findings of previous research, which indicates that Alabama and Louisiana red snapper grow at similar rates and reach comparable sizes (Patterson et al., 2001). However, values of L_∞ for Texas red snapper were significantly smaller than parameters predicted for Alabama and Louisiana red snapper. Interestingly, Texas had a value of k that was significantly larger then that for Alabama and Louisiana and this would indicate that Texas fish obtain a smaller maximum theoretical FL but reach it at a faster rate then fish from Alabama and Louisiana.

Von Bertalanffy growth models of mean weight at age produced similar results, indicating that Texas red snapper obtain significantly smaller maximum theoretical TW than fish from Alabama and Louisiana. Fish sampled from tournaments were excluded from all growth models to more accurately reflect

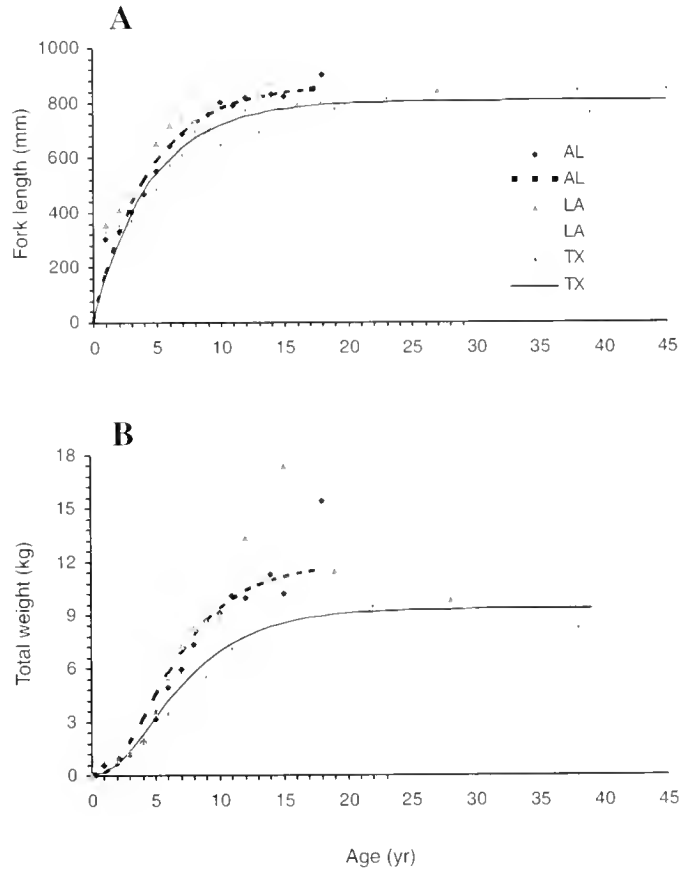

Figure 5

Observed (**A**) mean fork length (mm) at age and (**B**) mean total weight (kg) at age for red snapper (*Lutjanus campechanus*) from Alabama, Louisiana, and Texas. Plotted lines are weighted von Bertalanffy growth functions fitted to the data.

growth of a random population. Tournament anglers target large fish, possibly the fastest growing individuals at a given age, and their catches may bias growth estimates (Ottera, 1992; Vaughan and Burton, 1993; Goodyear, 1995). Without these tournament fish, however, the Alabama red snapper TW model did not reach an asymptote. Therefore the growth parameters for that model were poorly estimated. Notwithstanding, Alabama and Louisiana models did not differ significantly. Estimates of W_∞ and k predicted for Louisiana red snapper were slightly larger than previously reported for fish from the Louisiana commercial and recreational catches (Render, 1995). Although the Texas model predicted a value of W_∞ that was significantly less than those for both Alabama and Louisiana red snapper, Texas had a growth coefficient (k) that was larger then that for Alabama. It appears that, as in the length models, Texas fish reach a smaller theoretical maximum weight but at a faster rate than Alabama fish. Louisiana fish attained maximum weight at a faster rate than Alabama or Texas red snapper. Our growth models indicate that although Texas red snapper grow in mass at a faster rate than Alabama fish, Texas red snapper are consistently smaller at age and reach smaller maximum sizes than those from Alabama and Louisiana and that there is a veritable difference in size at age and growth rates among regions. Similar demographic variations in growth rates among populations have been previously noted for other marine fish species of the South Atlantic and GOM, such as gray snapper (Johnson et al., 1994; Burton 2001), and king mackerel (DeVries et al, 1990; DeVries and Grimes, 1997).

Linear regressions of mean FL and mean TW at age for red snapper aged one to 10 years indicated that only TW was significantly different among sample regions. Texas red snapper were shown to differ significantly from both Alabama and Louisiana red snapper in regressions of mean weight at age. Although comparisons of FL at age for all regions were not significantly different, Texas fish were significantly smaller in mass (TW) at age than fish from Alabama and Louisiana. This difference was observed in all age classes.

Our research efforts indicate that there is mounting evidence for discrete differences in size at age and in overall growth rates between red snapper sampled from the north central GOM (Louisiana and Alabama) and the southwest GOM (Texas). Texas red snapper are clearly reaching smaller maximum sizes and are consistently smaller (TW) at age than those collected from Louisiana and Alabama waters. Although the reasons behind these differences remain uncertain, logic indicates that factors such food availability, habitat preference, and actual population size may cause these differences between regions.

The more productive, nutrient-rich waters of the Mississippi River and north-central GOM off Louisiana and Alabama may be more conducive to faster growth than the less fertile waters off Texas. Approximately 70–80% of GOM fishery landings come from the waters surrounding the Mississippi River delta (Grimes, 2001). The western GOM (including the sampling area of Port Aransas, TX) is devoid of a contributing river system anything remotely similar to the Mississippi River. Draining 43% of the continental United States, the Mississippi River is the largest river system in North America and provides an enormous amount of nutrient-laden fresh water to the shallow continental shelf of the northern GOM. Although the mechanics by which the Mississippi River enhances fishery production remain uncertain, Grimes (2001) postulated that the discharge from the Mississippi primarily influences recruitment in the plume field. Increased growth rates associated with the Mississippi River plume compared with other regions of the GOM have been noted for a number of species, such as gulf menhaden (Warlen, 1988), king mackerel (DeVries et al., 1990), striped anchovy (Day, 1993), and yellowfin tuna (Lang et al., 1994).

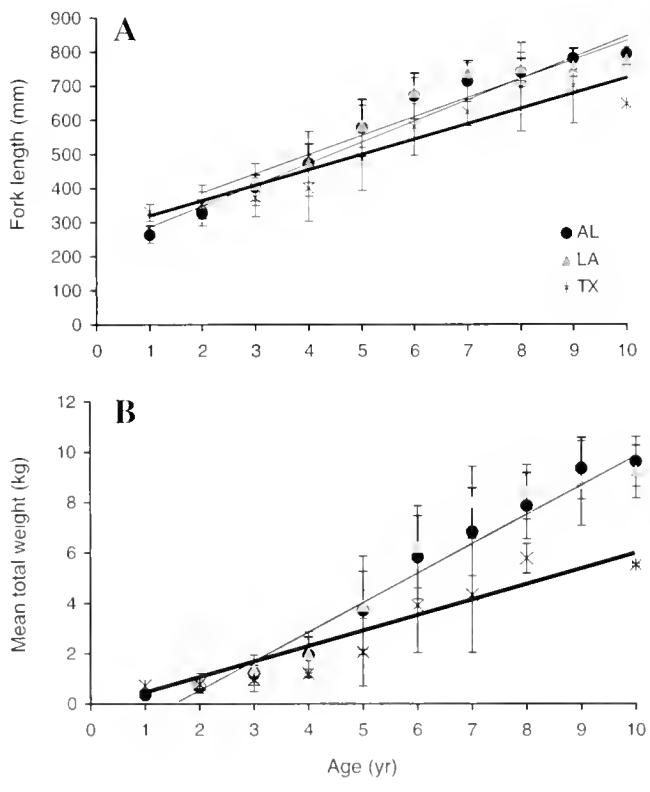

Figure 6

Scattergram with linear regression lines for relationships (**A**) between age (yr) and mean fork length (mm) and (**B**) age (yr) and mean total weight (kg) for red snapper (*Lutjanus campechanus*) aged 1 to 10 years from the 1999–2001 recreational harvests of Alabama, Louisiana, and Texas. Error bars represent standard deviations from the mean.

In addition to increased food availability off of the north-central GOM, the amount and condition of preferred habitat may have some effect on the observed differences in growth rates for Texas and those for Louisiana and Alabama. Approximately 95% of all Louisiana fishes sampled in this study were harvested from waters surrounding nearshore (<50 km) oil and gas platforms. Similarly, about 95% of all Alabama fishes sampled were caught over artificial reef sites. The fact that there was no detectable difference in size at age and overall growth rates between Louisiana and Alabama red snapper therefore is not surprising, given the similarity in the habitats sampled and the proximity of both locations to the Mississippi River discharge plume. Texas was the only area in which samples were routinely obtained from natural hard bottoms (40%), as well as from oil and gas platforms and artificial reefs (60%). Given that more than half of the Texas specimens were captured in the waters immediately surrounding artificial structures (i.e., oil and gas platforms), we can assume that habitat type is not be the sole source for the observed differences in growth rates among regions.

Despite the current acceptance of a unit stock hypothesis for GOM red snapper, the species is not, and to our knowledge never has been, uniformly distributed across the northern GOM. The fishery for red snapper began in northwest Florida approximately 20 years before the Civil War (Collins, 1887) and during that time period was centered between Mobile, AL, and Fort Walton, FL (Camber, 1955). One hundred years of landings data indicate that the fishery, and possibly the population, has undergone a major shift from the natural outcroppings of the West Florida Shelf to oil and gas platforms of the north-central portion of the GOM (Shirripa and Legault[1]). Fishery-dependent data indicate that currently there is a center of abundance of red snapper off southwest Louisiana and a second, smaller center off Alabama (Patterson et al., 2001; Goodyear[4]; Shirripa and Legault[1]). Patterson et al. (2001) stated that Louisiana and Alabama accounted for 32.6% and 11.4%, respectively, of the combined recreational and commercial GOM landings from 1981 to 1998. This is especially surprising for Alabama, considering that its coastline accounts for only 3% of the GOM coastline from the Texas-Mexico border to the southern tip if Florida (Patterson et al., 2001).

Red snapper have never been reported to be plentiful in Texas waters, despite the availability of suitable habitat in the form of natural hard bottom and the current high concentration of oil and gas platforms. In a historical report on red snapper fishing in the GOM, Camber (1995) reported that although a few red snapper were taken from the "Galveston Lumps" or the "Western" fishing grounds off Texas, the fishery never fully developed in this region during the latter part of the nineteenth century. Commercial landings for red snapper from the GOM indicated that Texas accounted for approximately only 18% of the total catch during the time period 1981–95 (Goodyear[6]). In a recent fishery-dependent survey of recreational headboat discards and landings in Texas coastal waters, red snapper less than the minimum legal size (15 inches) made up 64% of the catch (Dorf, 2000). In the latter study, Galveston, Port Aransas, and Port Isabel were surveyed to canvas a large portion of the Texas coast. Discard-to-landing ratios were as high as 211:1 in the waters off Galveston and were possibly indicative of the paucity of legal-size red snapper in Texas waters. Of the three sampling locations, Port Aransas had the lowest discard-to-landing ratio (5.2:1) and the largest mean fish length and weight (387 mm, 0.9 kg)—length and weight data that are consistent with a 3-yr-old fish from our Texas (Port Aransas) specimens. The majority of Texas fish (63%) were aged at 3 years or less. Age distribution, along with FL and TW distributions, may indicate that red snapper are being harvested from Texas waters just as they reach legal size. Given the vast differences in historical landings data between the northern and southwest GOM, the highly disproportionate discard-to-landing ratio reported for headboats in Texas waters (Dorf, 2000), and the large number of young fish sampled in Texas, it is not inconceivable to speculate that there are fewer red snapper available for harvest in Texas waters.

Demographic variation in growth rates may indicate the existence of separate management units of red snapper in the GOM. Our data indicate that the red snapper inhabiting the waters off Texas are reaching smaller maximum sizes at a faster rate, but are consistently smaller (TW) at age than those collected from Louisiana and Alabama waters. Whether these differences are environmentally induced or result from genetic divergence remains to be determined. The more productive, nutrient-rich waters of the Mississippi River and north-central GOM off Louisiana and Alabama may be more conducive to faster growth than the less fertile waters off Texas. Fishing pressure and its effects on population size may also be leading to the observed differences in growth rates. Fishery-dependent landing data and disproportionate discard-to-landing ratios in Texas waters loosely support the concept that fewer red snapper are available for harvest in the southwest GOM. Regardless of the cause, the existence of demonstrable demographic differences argues for the delineation of multiple red snapper management units in the GOM.

Acknowledgments

Funding for this research was provided by the U.S. Department of Commerce Marine Fisheries Initiative (MARFIN) program (grant number NA87FF0424). We

[6] Goodyear, C. P. 1996. An update of red snapper harvest in U.S. waters of the Gulf of Mexico. Report MIA-95/96-60, 21 p. Miami Laboratory, Southeast Fisheries Center, National Marine Fisheries Service, 75 Virginia Beach Dr. Miami, FL., 33149-1099. [Not available from NTIS].

thank Forrest Davis, John Gold, Jessica McCawley, Linda Richardson, Jim Tolan, Melissa Woods, Candace Aiken, and many others for help with sampling red snapper. We also thank Josh Maier and Brett Blackman for otolith sectioning. We thank Steve Tomeny and his boat captains and crew (Port Fourchon, LA), as well as all boat captains and crews in Dauphin Island, Alabama, and Port Aransas, Texas, for graciously allowing us to sample fish from their charter fishing vessels. We also thank Yvonne Allen for providing the map in Figure 1. Finally we would like to thank Dave Nieland for time spent fielding questions concerning statistical analysis and for a constructive review of this manuscript.

Literature cited

Baker, M. S. Jr., and C. A. Wilson.
2001. Use of bomb radiocarbon to validate otolith section ages of red snapper *Lutjanus campechanus* from the northern Gulf of Mexico. Limnol. Oceanogr. 46:1819–1824.

Beamish, R. J., and D. A. Fournier.
1981. A method for comparing the precision of a set of age determinations. Can. J. Fish. Aquat. Sci. 38:982–983.

Beckman, D. W., C. A. Wilson, and A. L. Stanley.
1989. Age and growth of red drum, *Sciaenops ocellatus*, from offshore waters of the northern Gulf of Mexico. Fish. Bull. 87:17–28.

Burton, M. L.
2001. Age, growth, and mortality of gray snapper, *Lutjanus griseus*, from the east coast of Florida. Fish. Bull. 99:254–265.

Camber, C. I.
1955. A survey of the red snapper fishery of the Gulf of Mexico, with special reference to the Campeche banks. Fla. Board Conserv. Tech. Ser. No. 12:1–64.

Camper, J. D., R. C. Barber, L. R. Richardson, and J. R. Gold.
1993. Mitochondrial DNA variation among red snapper (*Lutjanus campechanus*) from the Gulf of Mexico. Mol. Mar. Biol. Biotech. 2:154–161.

Cerrato, R. M.
1990. Interpretable statistical tests for growth comparisons using parameters in the von Bertalanffy equation. Can. J. Fish. Aquat. Sci. 47:1416–1426.

Chang, W. B.
1982. A statistical method for evaluating the reproducibility of age determination. Can. J. Aquat. Sci. 39:1208–1210.

Collins, J. W.
1887. Report on the discovery and investigation of fishing grounds made by the Fish Commision Steamer *Albatross* during a cruise along the Atlantic Coast and in the Gulf of Mexico. Rep. U.S. Comm. Fish. 13:217–311.

Cowan, J. H. Jr., R. L. Shipp, H. K Bailey IV, and D. W. Haywick.
1995. Procedure for rapid processing of large otoliths. Trans. Am. Fish. Soc. 124:280–282.

Day, G. R.
1993. Distribution, abundance, growth and mortality of striped anchovy, *Anchoa hepsetus*, about the discharge plume of the Mississippi River. M.S. thesis, 45 p. Univ. West Florida, Pensacola, FL.

DeVries, D. A., and C. B. Grimes.
1997. Spatial and temporal variation in age and growth of king mackerel, *Scomeromorus cavalla*, 1977–1992. Fish. Bull. 95:694–708.

Devries, D. A., C. B. Grimes, K. C. Lang, and D. B. White.
1990. Age and growth of king and Spanish mackerel larvae and juveniles from the Gulf of Mexico and U.S. south Atlantic. Environ. Biol. Fishes 29:135–143.

Dorf, B. A.
2003. Red snapper discards in Texas coastal waters: a fishery-dependent onboard survey of recreational headboat discards and landings. *In* Fisheries, reefs, and offshore development (D. R. Stanley and A. Scarborough-Bull, eds.), p. 155–166. Am. Fish. Soc. Symposium 36. Am. Fish. Soc., Bethesda, MD.

Gold J. R., F. Sun, and L. R. Richardson.
1997. Population structure of red snapper from the Gulf of Mexico as inferred from analysis of mitochondrial DNA. Trans. Am. Fish. Soc. 126:386–396.

Goodyear, C. P.
1995. Mean size at age: an evaluation of sampling strategies using simulated red grouper data. Trans. Am. Fish. Soc. 124:746–755.

Grimes, C. B.
2001. Fishery production and the Mississippi River discharge. Fisheries 26:7–26.

Gulland, J. A.
1965. Fish stock assessment: a manual of basic methods, 223 p. John Wiley & Sons, New York, NY.

Heist, E. J., and J. R. Gold.
2000. DNA microsatellite loci, and genetic structure of red snapper in the Gulf of Mexico. Trans. Am. Fish. Soc. 129:469–475.

Johnson, A. G., L. A. Collins, and C. P. Kelm.
1994. Age-size structure of gray snapper from the Southeastern United States: a comparison of two methods of back-calculating size at age from otolith data. Proc. Annu. Conf. Southeast Assoc. Fish and Wildl. Agencies 48:592–600.

Lang, K. L., C. B. Grimes, and R. F. Shaw.
1994. Variations in the age and growth of yellowfin tuna larvae, *Thunnus albacares*, collected about the Mississippi River plume. Environ. Biol. Fishes 39:259–270.

Manooch, C. S., III, and J. C. Potts
1997. Age and growth of red snapper, *Lutjanus campechanus*, *Lutjanidae*, collected along the southeastern United States from North Carolina through the east coast of Florida. J. Elisha Mitchell Sci. Soc. 113:111–122.

Ottera, H.
1992. Bias in calculating growth rates in cod (*Gadus morhua L.*) due to size selective growth and mortality. J. Fish Biol. 40:465–467.

Patterson, W. F. III.
1999. Aspects of the population ecology of red snapper *Lutjanus campechanus* in an artificial reef area off Alabama. Ph.D. diss., 164 p. Univ. South Alabama, Mobile, AL.

Patterson, W. F. III, James H. Cowan Jr., Charles A. Wilson, and Robert L. Shipp.
2001. Age and growth of red snapper, *Lutjanus campechanus*, from an artificial reef area off Alabama in the northern Gulf of Mexico. Fish. Bull. 99:617–627.

Render, J. H.
1995. The life history (age, growth, and reproduction) of red snapper (*Lutjanus campechanus*) and its affinity

for oil and gas platforms. Ph.D. diss., 76 p. Louisiana State Univ., Baton Rouge, LA.

Ricker, W. E.
1975. Computation and interpretation of biological statistics of fish populations, 382 p. Bull. Fish. Res. Board Can., Ottawa.

Szedlmayer, S. T., and R. L. Shipp.
1994. Movement and growth of red snapper, *Lutjanus campechanus*, from an artificial reef area in the northeastern Gulf of Mexico. Bull. Mar. Sci. 55(2–3): 887–896.

Tate, M. W., and R. C. Clelland.
1957. Non-parametric and shortcut statistics in the social, biological, and medical sciences, p. 93–94. Interstate Printers and Publishers, Inc., Danville, IL.

Vaughan, D. S., and M. L. Burton.
1993. Estimation of von Bertalanffy growth parameters in the presence of size-selective mortality: a simulated example with red grouper. Trans. Am. Fish. Soc. 123:1–8.

Warlen, S. M.
1988. Age and growth of larval gulf menhaden, *Brevoortia patronis*, in the northern Gulf of Mexico. Fish. Bull. 86:77–90.

Wilson, C. A., and D. L. Nieland.
2001. Age and Growth of red snapper, *Lutjanus campechanus*, from the northern Gulf of Mexico off Louisiana. Fish. Bull. 99:653–664.

Elemental signatures in otoliths of larval walleye pollock (*Theragra chalcogramma*) from the northeast Pacific Ocean*

Jennifer L. FitzGerald
Simon R. Thorrold
Biology Department, MS 35
Woods Hole Oceanographic Institution
Woods Hole, Massachusetts 02543
E-mail address (for J. L. FitzGerald): jfitzgerald@whoi.edu

Kevin M. Bailey
Annette L. Brown
NOAA Alaska Fisheries Science Center
7600 Sand Point Way NE
Seattle, Washington 91185

Kenneth P. Severin
Department of Geology and Geophysics
University of Alaska Fairbanks
P.O. Box 755780
Fairbanks, Alaska 99775-5780

Abstract—The population structure of walleye pollock (*Theragra chalcogramma*) in the northeastern Pacific Ocean remains unknown. We examined elemental signatures in the otoliths of larval and juvenile pollock from locations in the Bering Sea and Gulf of Alaska to determine if there were significant geographic variations in otolith composition that may be used as natural tags of population affinities. Otoliths were assayed by using both electron probe microanalysis (EPMA) and laser ablation inductively coupled plasma mass spectrometry (ICP-MS). Elements measured at the nucleus of otoliths by EPMA and laser ablation ICP-MS differed significantly among locations. However, geographic groupings identified by a multivariate statistical approach from EPMA and ICP-MS were dissimilar, indicating that the elements assayed by each technique were controlled by separate depositional processes within the endolymph. Elemental profiles across the pollock otoliths were generally consistent at distances up to 100 μm from the nucleus. At distances beyond 100 μm, profiles varied significantly but were remarkably consistent among individuals collected at each location. These data may indicate that larvae from various spawning locations are encountering water masses with differing physicochemical properties through their larval lives, and at approximately the same time. Although our results are promising, we require a better understanding of the mechanisms controlling otolith chemistry before it will be possible to reconstruct dispersal pathways of larval pollock based on probe-based analyses of otolith geochemistry. Elemental signatures in otoliths of pollock may allow for the delineation of fine-scale population structure in pollock that has yet to be consistently revealed by using population genetic approaches.

Manuscript submitted 4 August 2003 to the Scientific Editor's Office.
Manuscript approved for publication 28 May 2004 by the Scientific Editor.
Fish. Bull. 102:604–616 (2004).

The "stock" concept is a central tenet of modern fisheries science because it represents the fundamental management unit of marine fisheries (Begg and Waldman, 1999). This emphasis, in turn, places a premium on accurate identification of groups of fish whose population statistics are largely independent of other groups. However, stock identification has often proved problematic in marine fishes. For instance, the stock structure of walleye pollock (*Theragra chalcogramma*) across the North Pacific Ocean has been a topic of investigation for many years. Early studies were based on phenotypic characteristics of pollock, such as meristics and morphometrics (Serobaba, 1977; Hinckley, 1987; Temnykh, 1994). Other studies have focused on genotypic markers, such as DNA and allozyme analyses (Grant and Utter, 1980; Mulligan et al., 1992; Shields and Gust, 1995). These approaches resulted in only the broadest characterization of pollock stock structure but have been able to distinguish populations from the eastern and western Pacific (Bailey et al., 1999). Quasi-isolated subpopulations may be at least demographically isolated on smaller spatial scales. For instance, within the Gulf of Alaska, spawning pollock aggregate at specific locations in Shelikof Strait, Prince William Sound, and in the Shumagin Islands region (Bailey et al., 1999). However, the extent of larval dispersal from the spawning sites and the degree of spawning site fidelity of adult pollock to these locations remains unknown.

The difficulties associated with determining stock structure in fishes are essentially the same ones that currently limit our ability to determine population connectivity in marine systems (Thorrold et al., 2002). Tag-recapture studies using tags have limited applicability in the case of pollock. Adults are located deep in the water column and are sensitive to barotrauma during the process of being caught, brought to the surface, and tagged. Traditional population genetic approaches may be similarly

*Contribution 11219 from the Woods Hole Oceanographic Institution, Woods Hole, MA 02543.

ineffective because of the low level of exchange required to maintain genetic homogeneity, at least over ecological time scales, and the low level of genetic drift associated with large populations (Waples, 1998; Hellberg et al., 2002). However, preliminary studies have indicated that otolith geochemistry may prove to be a useful natural tag of population structure in walleye pollock (Severin et al., 1995). Otoliths are accretionary crystalline structures located within the inner ear of teleost fish. They are formed through concentric additions of alternating protein and aragonite layers around a central nucleus. The use of otoliths as natural geochemical tags is contingent on the metabolically inert nature of the otolith and the fact that once deposited, otolith material is neither resorbed nor metabolically reworked (Campana and Neilson, 1985; Campana, 1999). The chemical composition of otoliths also reflects to some degree the physicochemical characteristics of the ambient water (Bath et al., 2000). If the water where pollock reside has distinct oceanographic characteristics, then many of the elements incorporated into the otoliths should differ among locations. Migrations between water masses at some age will, therefore, be recorded in the chemical composition of the otolith at the appropriate daily increment. Natural geochemical signatures in otoliths may therefore be useful markers of environmental history throughout the life of the individual and in turn, fish stock composition (e.g., Campana et al., 1995).

The use of geochemical signatures in otoliths as natural tags requires accurate and precise assays of otolith composition. Electron probe micro-analysis (EPMA) has been commonly used for probe-based analyses of otolith chemistry (Gunn et al., 1992). However, detection limits of approximately 100 μg/g limit the technique to a relatively small number of minor elements in otoliths, including Na, Cl, K, and Sr (Campana et al., 1997). Most of the elements measured by EPMA are probably controlled by physiological rather than environmental factors, which may limit their usefulness in stock identification studies (Campana, 1999). Nonetheless, a number of researchers using EPMA have reported geographic differences in otolith chemistry (e.g., Thresher et al., 1994). More recently, attention has focused on inductively coupled plasma mass spectrometry (ICP-MS) to assay elements that are typically below the detection limits of EPMA. Laser ablation ICP-MS uses focused Nd:YAG or excimer lasers to ablate specific locations on the otolith. The vaporized material is then swept up by a carrier gas into a plasma torch and analyzed by mass spectrometry. Limits of detection of the technique are typically on the order of 0.1–1μg/g, allowing for quantification of several elements that cannot be assayed by using EPMA including Mg, Mn, Ba, and Pb (Thorrold et al., 1997; Thorrold and Shuttleworth, 2000). These observations led Campana et al. (1997) to conclude that EPMA and laser ablation ICP-MS were complementary and that there is little overlap in the elements that are accurately measured by the two techniques. Yet few studies of otolith geochemistry have attempted to use both approaches on the same samples.

The objectives of this study are to determine if larval walleye pollock from different geographic localities can be distinguished based on elemental signatures in their otoliths. By analyzing sagittal otoliths with both EPMA and laser ablation ICP-MS, we hoped to identify greater differences among locations than would have been possible by using either technique in isolation. If successful, the study may provide a powerful tool for determining stock structure and tracing migration pathways of walleye pollock in the north Pacific. These data could then be used by managers of one of the world's largest single species fisheries to direct the sustainable harvest of this considerable natural resource.

Materials and methods

All fish used in the study were collected in the spring and summer of 1999 from Alaska Fisheries Science Center research cruises in the Bering Sea and Gulf of Alaska (Fig. 1, Table 1). Fish of birth year 1999 were collected within three months of spawning time to minimize the likelihood of larval transport from other regions. In the case of the Yakutat samples, fresh juvenile pollock were removed from Pacific cod guts. Samples were collected only when the pollock were readily identifiable and heads were intact. Otoliths showed no visible sign of degradation from digestive processes. Juvenile pollock were frozen whole and transported to the laboratory for otolith removal.

Otoliths were removed from the fish and mounted on petrographic slides in LR White resin (acrylic, hard-grade). Larval otoliths were ground on one side to expose the nucleus by using 500-grit paper and were polished with 0.25-μm grit diamond paste. Juvenile otoliths were ground and polished in the sagittal plane on both sides to maximize clarity of the nucleus during microanalysis.

Electron probe microanalysis

After having been polished, the otoliths were cleaned with Formula 409® and coated with a 30-nm layer of carbon. They were subsequently analyzed with a Cameca SX-50 electron microprobe equipped with four wavelength dispersive spectrometers. A 15keV, 10 nA, 4-μm diameter beam was used for all analyses. Counting times, standards, detection limits, and analytical errors are summarized in Table 2. Although Mg was analyzed in all otoliths, in most cases it was below detection limits and was therefore not used in the statistical analysis.

Laser ablation ICP-MS

After having been ground and polished, otolith sections were decontaminated before elemental analysis by using laser ablation ICP-MS. Sections were rinsed in ultrapure water, scrubbed with a nylon brush in a solution of ultrapure H_2O, triple rinsed with ultrapure 1% HNO_3,

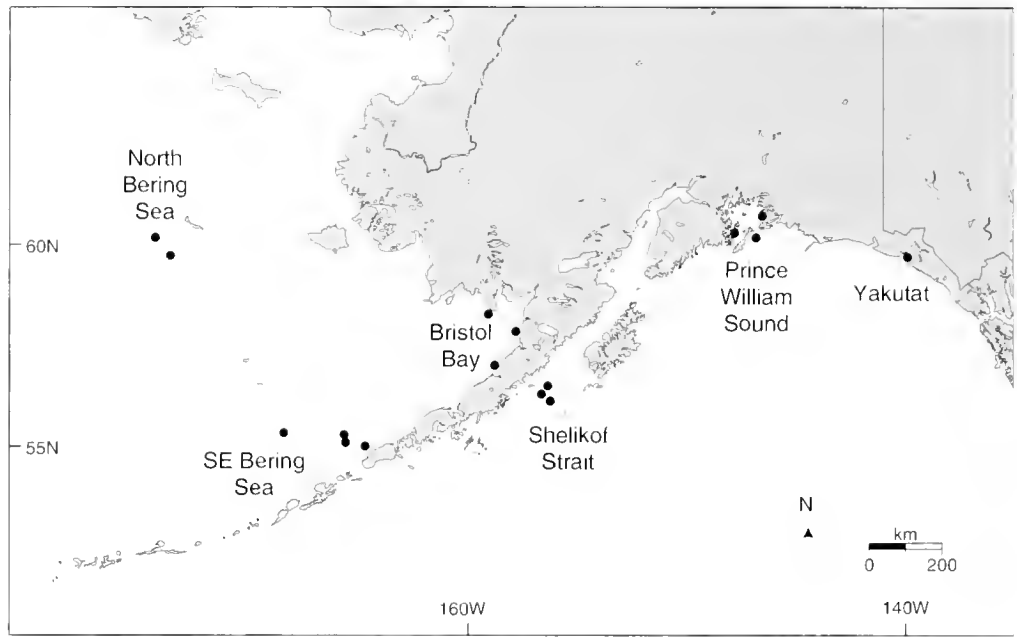

Figure 1

Locations of sampling sites for larval and juvenile walleye pollock (*Theragra chalcogramma*) in the Gulf of Alaska and Bering Sea.

sonified for 5 minutes in ultrapure H_20, and finally triple rinsed again with Milli-Q water. The section was dried under a positive flow hood for 24 hours and stored in a polyethylene bag.

Elemental analyses were conducted with a Finnigan MAT Element2 magnetic sector field ICP-MS and Merchantek EO LUV266X laser ablation system (Thorrold and Shuttleworth, 2000). Instrument set-up was similar to that outlined by Günther and Heinrich (1999). An Ar gas stream was used to carry ablated material from the laser cell to the ICP-MS. The carrier gas was then mixed with the Ar sample gas and a wet aerosol (1% HNO3) in the concentric region of the quartz dual inlet spray chamber. The wet aerosol was supplied by a self-aspirating PFA micro-flow (20 μL/min) nebulizer attached to a CETAC ASX100 autosampler. Diameter of the 266-nm laser beam was nominally 5 μm, repetition rate was 5 Hz, and the scanning rate was set at 5 μm/sec.

A typical run for an individual otolith consisted of a blank sample (1%HNO_3 only), a standard sample, five laser samples, and then another blank and standard. The number of laser samples in a run ranged from 5 to 15, depending upon the size of the otolith. All laser runs began with a 70 μm × 70 μm raster, centered on the otolith nucleus. The laser software was then used to trace out concentric lines, 720 μm in length and approximately 40 μm apart, which followed the contour of individual growth increments from the raster to the otolith edge. This approach produced reasonably high spatial resolution (30–50 μm) for life history scans across otoliths while allowing sufficient acquisition time to maintain measurement precision.

We examined Mn/Ca, Sr/Ca, and Ba/Ca ratios in the pollock otoliths by monitoring ^{48}Ca, ^{55}Mn, ^{86}Sr, and ^{138}Ba. Quantification followed the approach outlined by Rosenthal et al. (1999) for precise element/Ca ratios using sector field ICP-MS (Thorrold et al., 2001). Quality control was maintained by assaying a dissolved aragonite standard (Yoshinaga et al., 2000) every five samples. The standard was introduced at the appropriate time by moving the autosampler probe from the solution containing the 1% HNO_3 to the standard solution, while maintaining the carrier gas flow through the ablation cell. Elemental mass bias was calculated by reference to known values of the standard, and a correction factor was then interpolated and applied to the laser samples bracketed between adjacent standard measurements. Average (n=40) within-run precisions (RSD) of the standard measurements were all less than 1% (Mn/Ca: 0.16%, Sr/Ca: 0.16%, and Ba/Ca: 0.33%). Long-term (5-month) estimates of the standard measurements (n=40), again uncorrected for changes in mass bias over time, were less precise (Mn/Ca: 5.6%, Sr/Ca: 3.7%, and Ba/Ca: 5.6%). However, laser samples were corrected for changes in mass bias by using the laboratory standard. Precision of the technique was approximately 1% for all the ratios that we measured.

Statistical analyses

All elemental data were initially examined for normality and homogeneity of variance by using residual analysis (Winer, 1971) and were found to conform to the assumptions of ANOVA without the need for data transformation. We therefore assumed that require-

Table 1

Location, collection date, standard length range (mm), and sample sizes (n) of larval and juvenile walleye pollock (*Theragra chalcogramma*) captured from the southeast Bering Sea (SE Bering), North Bering Sea (N Bering), Bristol Bay, Shelikof Strait, Prince William Sound (PWS), and Yakutat, and analyzed by laser ablation ICP-MS (ICP-MS) and electron probe microanalysis (EPMA).

Area	Date	SL range (mm)	n (total)	n (ICP-MS)	n (EPMA)
SE Bering	23 May–27 July 1999	5.3–42.2	117	8	30
N Bering	18–23 July 1999	15.6–30.7	45	9	25
Bristol Bay	22–24 July 1999	85.1–135.7	75	11	28
Shelikof	27–28 May 1999	3.6–7.9	46	—	25
PWS	7 July–19 August 1999	35.2–66.0	11	4	6
Yakutat	15 July,1999	—	50	6	24

Table 2

Counting times for each element (time [seconds], standards, limits of detection [LOD, %weight, 99% confidence limits] and analytical errors [Error, %weight, 1 standard deviation]) for electron probe microanalysis (EPMA). Detection limits and analytical errors were calculated by following the procedures of Scott et al. (1995). N/A = not applicable.

Element	Time	Standard	LOD	Error
Na	60	Halite (CM Taylor)	0.029	0.023
Mg	60	Osumilite (USNM 143967)	0.019	0.022
P	60	Apatite (Wilberforce)	0.036	0.027
S	60	Gypsum (CM Taylor)	0.023	0.017
Cl	46	Halite (CM Taylor)	0.027	0.015
K	46	Osumilite (USNM 143967)	0.019	0.012
Ca	20	Calcite (NMNH 136321)	N/A	0.245
Sr	120	Strontianite (Smithsonian R-10065)	0.036	0.019

ments for the MANOVA were also met by the data. Among-location differences in the elemental composition of larval pollock in specific regions of the otoliths were compared by using one-factor multivariate analysis of variance (MANOVA) and one-factor analysis of variance (ANOVA). We treated location as a fixed factor in both MANOVA and ANOVA tests. Because of difficulties collecting pollock larvae, we were unable to achieve equal replication of sites within locations. We therefore pooled samples from collections within a location by randomly selecting fish from each location for subsequent analysis. However, the lack of replication at the within-location level necessarily restricted our ability to draw general conclusions concerning spatial variability in otolith composition beyond the samples analyzed in the present study. All *a posteriori* comparisons among locations were performed by using Tukey's honestly significant difference (HSD) test (experimentwise error rate=0.05). Multivariate differences in elemental signatures from the MANOVA were visualized by using canonical discriminant analyses (CDA). All analyses were conducting by using the SAS statistical program (SAS, version 6, 1990, SAS Inst. Inc., Cary, NC).

Comparisons of elemental profiles across otoliths were made with repeated measures ANOVA. We tested the following null hypotheses: 1) there was no variation in trace element profiles across individual otoliths (i.e., from the nucleus to the edge), 2) there were no differences in mean element concentrations among locations, determined by averaging data across individual otolith profiles, and 3) there were no differences in the pattern of element profiles across otoliths among locations. Otolith profiles with missing values were removed, and therefore we were able to use MANOVA for the repeated measures analysis. The multivariate approach to repeated measures is generally more conservative than univariate repeated measures analysis. However, the multivariate test does not assume sphericity of orthogonal components, requiring only that the data conform to multivariate normality with a common covariance matrix for individual larvae at each location (Littell et al., 1991). The approach still requires that adjacent points on the trajectories be equidistant. Therefore samples from EPMA were assigned to a distance category at intervals of 15 μm (0 μm, 15 μm, 30 μm , 45 μm, 60 μm, 75 μm, and 90 μm) across the otolith, to a distance of 90 μm from the nucleus. Samples were averaged when more than one measurement was available within a distance category. Laser ablation ICP-MS samples were assigned to a distance category at intervals of approxi-

Table 3

EPMA results of one-factor ANOVA (degrees of freedom [df]; sums of squares [SS]; mean square [MS]) at two positions (0–20 μm and 20–45 μm from the nucleus) in otoliths of larval walleye pollock (*Theragra chalcogramma*) collected from six locations: three locations in the Bering Sea (southeast Bering Sea [SB]; North Bering Sea [NB]; Bristol Bay [BB]) and three in the Gulf of Alaska (Prince William Sound [PW]; Shelikof Strait [SH]; and Yakutat [YK]). ***= significant at $\alpha = 0.05$; ns = nonsignificant. *A posteriori* multiple comparisons among locations were conducted by using Tukey's honestly significant difference (HSD). Locations are ordered (left to right) from lowest to highest concentrations, and lines link locations that are not significantly different (experimentwise error rate=0.05).

Element	Source	df	SS	MS	F	$P < F$	Tukey's HSD
0–20 μm							
Na	Location	5	24.7	4.9	16.37	***	PW BB YK NB SB SH
	Error	113	34.1	$3.0 \cdot 10^{-1}$			
P	Location	5	18.3	3.7	14.93	***	BB SH NB SB PW YK
	Error	113	27.7	2.5×10^{-1}			
S	Location	5	2.0	3.9×10^{-1}	5.04	***	PW BB NB YK SH SB
	Error	113	8.8	7.8×10^{-2}			
Cl	Location	5	10.2	2.0	3.93	***	PW NB BB YK SB SH
	Error	113	58.6	5.2×10^{-1}			
K	Location	5	2.4	4.8×10^{-1}	4.01	***	SH NB SB PW BB YK
	Error	113	13.51	1.2×10^{-1}			
Sr	Location	5	7.1	1.4	6.66	***	YK NB BB SH PW SB
	Error	113	24.1	2.1×10^{-1}			
20–45 μm							
Na	Location	4	15.9	4.0	26.66	***	BB PW YK SB NB
	Error	93	13.9	1.5×10^{-1}			
P	Location	4	14.9	3.7	17.07	***	BB NB SB PW YK
	Error	93	20.3	2.2×10^{-1}			
S	Location	4	1.1	2.8×10^{-1}	4.62	***	BB PW SB NB YK
	Error	93	5.7	6.1×10^{-2}			
Cl	Location	4	8.4×10^{-1}	2.1×10^{-1}	1.61	ns	PW SB NB BB YK
	Error	93	12.1	1.3×10^{-1}			
K	Location	4	1.9	4.7×10^{-1}	5.65	***	NB PW BB SB YK
	Error	93	7.7	8.3×10^{-2}			
Sr	Location	4	9.0×10^{-1}	2.2×10^{-1}	3.75	***	NB YK BB PW SB
	Error	93	5.6	6.0×10^{-2}			

mately 40 μm (nucleus, 40–80 μm, 80–120 μm, 120–160 μm, and 160–200 μm) across the otolith, to a distance of 200 μm from the nucleus.

Results

Electron probe microanalysis

A total of six elements (Na, P, S, Cl, K, and Sr) were quantified in the otoliths of pollock larvae by using EPMA. Average concentrations of the elements ranged from approximately 4 mg/g (otolith weight) for Na to less than 1 mg/g for Cl, S, and K. We found significant differences in the elemental composition both among sampling locations and across positions on the otoliths. Multivariate analyses of elemental signatures revealed significant differences among locations from samples 0–20 μm from the nucleus (MANOVA; Pillai's trace=1.18; $F_{30,560}$=5.74; P<0.0001), and 20–45 μm from the nucleus (MANOVA; Pillai's trace=1.47; $F_{24,364}$=8.86; P<0.0001).

Analysis of variance and Tukey's HSD *a posteriori* multiple comparison tests identified the individual elements contributing to differences in the multivariate signatures among locations. All six elements showed significant differences among locations at 0–20 μm from the otolith nucleus (Table 3). Multiple comparisons for each of the elements indicated relatively subtle differences among locations. Phosphorus concentrations were, however, significantly higher in samples from Yakutat than any of the other locations. Results of the ANOVA from samples at distances 20–45 μm from the nucleus were generally comparable with samples closer to the nucleus (Table 3). Although only Cl showed no significant variation among locations (Table 3), multiple comparisons of mean values for each element revealed little geographic patterns among locations. Note that Shelikof Strait samples were removed from this analysis because of a small sample size in this distance category.

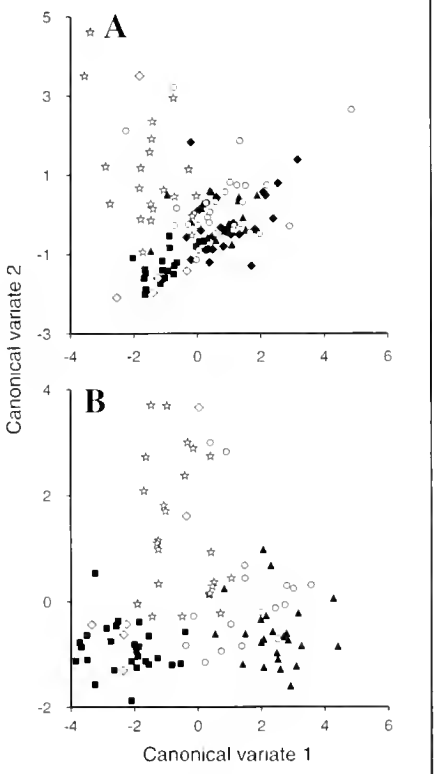

Figure 2

Plot of first two canonical variates contrasting multivariate elemental signatures in otoliths of walleye pollock (*Theragra chalcogramma*) determined by using electron probe microanalysis, at 0–20 μm from the nucleus (**A**) and 20-40 μm from the nucleus (**B**). Larvae were collected from the North Bering Sea (▲), southeast Bering Sea (○), Bristol Bay (■), Shelikof Strait (◆), Prince William Sound (◇), and Yakutat (☆).

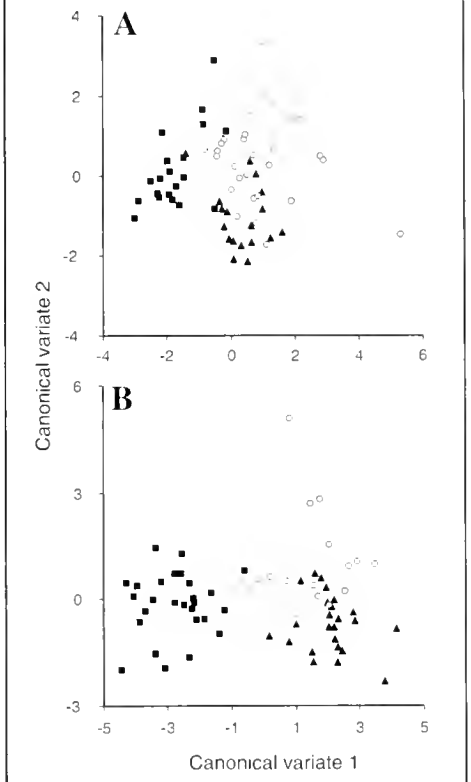

Figure 3

Plot of first two canonical variates contrasting multivariate elemental signatures in otoliths of walleye pollock (*Theragra chalcogramma*) determined by electron probe microanalysis at 0–20 μm from the nucleus (**A**) and 20–40 μm from the nucleus (**B**). Larvae were collected from the North Bering Sea (▲), southeast Bering Sea (○), and Bristol Bay (■).

We used CDA to visualize multivariate differences among locations in reduced dimensional space. Three groups were readily discernible in a plot of the first two canonical variates (Fig. 2). Samples from the North Bering Sea, the southeast Bering Sea, and Shelikof Strait formed one group separated from Yakutat, Bristol Bay, and Prince William Sound samples along the first canonical variate. The second canonical variate separated Yakutat samples from Bristol Bay and Prince William Sound individuals. Elemental signatures at 20–45 μm from the otolith nucleus were distributed similarly in canonical space to samples from the otolith nucleus (Fig. 2). Three groupings were apparent in the canonical plot, and Bering Sea larvae were separated from Bristol Bay and Prince William samples on canonical variate one, and Yakutat samples were separated from all other locations on canonical variate two. We then conducted a similar analysis with only samples from the southeast and North Bering Sea and Bristol Bay. Elemental signatures of larvae from the Bering Sea separated from Bristol Bay on canonical variate one. The southeast Bering Sea samples separated from the North Bering Sea along canonical variate two, although not as clearly as with the elemental signatures from the Bering Sea and Bristol Bay (Fig. 3).

Elemental profiles across otoliths varied significantly, as determined by repeated measures ANOVA, among the five locations for Na, P, S, and Sr (Table 4). Both S and Sr concentrations declined from high values at the nucleus to significantly lower values towards the edge of the otolith (Fig. 4). Repeated measures ANOVA also provided a test of the differences among locations when data were averaged over the otolith profiles. Significant differences among locations were detected for

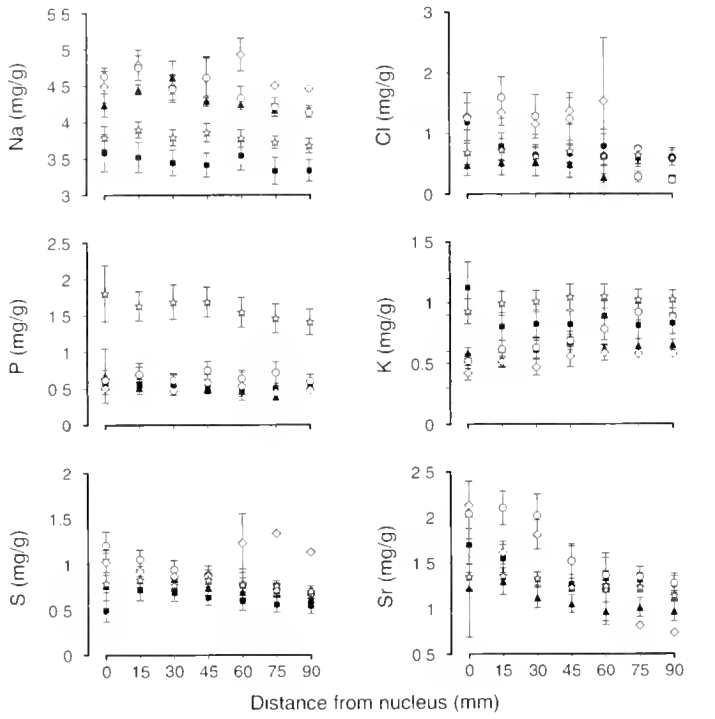

Figure 4

Profiles of elemental concentrations, determined by electron probe microanalysis, from the nucleus out to a distance of approximately 90 μm in the otoliths of larval walleye pollock (*Theragra chalcogramma*) collected from the North Bering Sea (▲), southeast Bering Sea (○), Bristol Bay (■), Prince William Sound (◇), and Yakutat (☆). Individual points are mean (±SE) values grouped at 15-μm intervals.

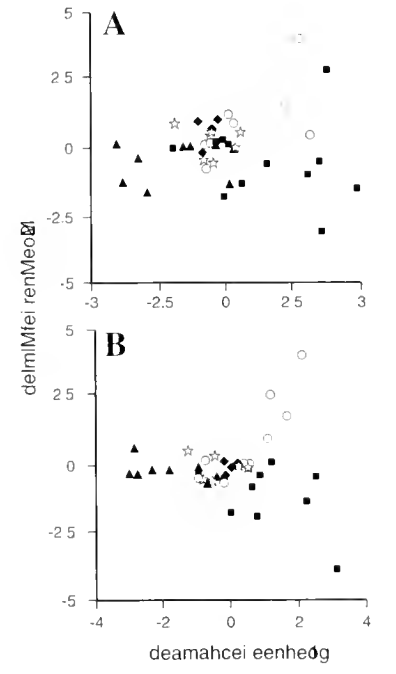

Figure 5

Plot of the first two canonical variates contrasting multivariate elemental signatures in otoliths of walleye pollock (*Theragra chalcogramma*) determined with laser ablation ICP-MS, at 0–40 μm from the nucleus (**A**) and 40–80 μm from the nucleus (**B**). Larvae and juveniles were collected from the North Bering Sea (▲), southeast Bering Sea (○), Bristol Bay (■), Prince William Sound (◆), and Yakutat (☆).

five elements (Sr, K, S, P, and Na). Finally, the interaction term (position×location) in the repeated measures ANOVA tested the hypothesis that the shape of the elemental profiles differed among locations. There was a significant interaction between profile and location for K.

Laser ablation ICP-MS

We quantified Mn/Ca, Sr/Ca, and Ba/Ca ratios in the otoliths of larval walleye pollock using laser ablation ICP-MS. Both Mn and Ba were found at trace levels in otoliths, with average values of approximately 3 μmol/mol and 6 μmol/mol, respectively. Strontium was present in the otoliths at an average concentration of approximately 2.2 mmol/mol. A MANOVA detected significant differences among locations from a raster centered on the nucleus (MANOVA; Pillai's trace=0.85; $F_{12,99}$=3.26; P<0.0005), and from the average values of lines 40–80 μm from the nucleus (MANOVA; Pillai's trace=0.99; $F_{12,99}$=4.1; P<0.0001).

Univariate ANOVA and *a posteriori* multiple comparisons by using Tukey's HSD revealed that Mn/Ca, Sr/Ca, and Ba/Ca ratios varied significantly among locations at the otolith nucleus and at positions 40–80 μm from the nucleus (Table 5). Samples from the North Bering Sea had consistently lower Sr/Ca and Ba/Ca ratios than those from the southeast Bering Sea at both positions. However, we noted only subtle differences among the Gulf of Alaska and Bristol Bay samples.

We found a total of three groupings in canonical plots of multivariate elemental signatures from the otoliths of larval walleye pollock (Fig. 5). Samples from the North Bering Sea and Bristol Bay were separated along canonical variate one. A third grouping, including larvae from the southeast Bering Sea, Prince William Sound, and Yakutat, clustered together in the center of the canonical plot. Samples from the nucleus and 40–80 μm outside the nucleus showed very similar geographic patterns.

Repeated measures ANOVA detected significant differences in both Mn/Ca and Ba/Ca profiles from the nu-

Table 4

EPMA results from repeated-measures ANOVA of elemental profiles across otoliths from walleye pollock (*Theragra chalcogramma*) larvae collected at five locations in the Bering Sea and the Gulf of Alaska. Within-subject effects (profile and profile×location) tested by using MANOVA (Pillai's trace), and between subjects effect (location) tested by using ANOVA (degrees of freedom [df]; sums of squares [SS]; mean squares [MS]). *** = significant at $\alpha = 0.05$; ns = nonsignificant.

Element	Source	df	Pillai's trace or SS	MS	F	$P < F$
Na	Profile	6, 41	4.9×10^{-1}		6.67	***
	Profile × location	24, 176	5.3×10^{-1}		1.12	ns
	Location	4	43.8	10.9	10.35	***
	Error	46	48.7	1.1		
P	Profile	6, 40	3.0×10^{-1}		2.91	***
	Profile × location	24, 172	4.6×10^{-1}		0.93	ns
	Location	4	55.0	13.8	8.07	***
	Error	45	76.8	1.7		
S	Profile	6, 41	3.6×10^{-1}		3.92	***
	Profile × location	24, 176	5.3×10^{-1}		1.12	ns
	Location	4	3.8	9.6×10^{-1}	4.56	***
	Error	46	9.7	2.1×10^{-1}		
Cl	Profile	6, 39	1.8×10^{-1}		1.41	ns
	Profile × location	24, 168	3.7×10^{-1}		0.72	ns
	Location	4	8.0	2.0	1.6	ns
	Error	44	55.3	1.3		
K	Profile	6, 41	8.3×10^{-2}		0.62	ns
	Profile × location	24, 176	8.5×10^{-1}		1.98	***
	Location	4	4.3	1.1	2.61	***
	Error	46	19.1	4.1×10^{-1}		
Sr	Profile	6, 40	4.5×10^{-1}		5.51	***
	Profile × location	24, 172	7.7×10^{-1}		1.72	ns
	Location	4	6.4	1.6	3.96	***
	Error	45	18.2	4.0×10^{-1}		

Table 5

Laser ablation ICP-MS results of one-factor ANOVA (degrees of freedom [df]; sums of squares [SS]; mean square [MS]) at two positions (0–40 μm and 40–80 μm from the nucleus) in walleye pollock (*Theragra chalcogramma*) otoliths collected at five locations: the southeast Bering Sea [SB], North Bering Sea (NB), Bristol Bay (BB), Prince William Sound (PW), and Yakutat (YK). ***= significant at $\alpha = 0.05$; ns=nonsignificant. Multiple comparisons among locations were conducted by using Tukey's honestly significant difference (HSD). Locations were ordered (left to right) from lowest to highest ratios; lines link locations that were not significantly different (α=0.05).

Element	Source	df	SS	MS	F	$P < F$	Tukey's HSD
0–40 μm (nucleus)							
Mn/Ca	Locations	4	19.3	4.82	3.5	***	PW NB SB YK BB
	Error	33	45.5	1.38			
Sr/Ca	Locations	4	1.07	0.27	3.43	***	NB YK BB PW SB
	Error	33	2.58	0.08			
Ba/Ca	Locations	4	219	54.8	3.35	***	NB BB PW YK SB
	Error	33	540	16.4			
40–80 μm							
Mn/Ca	Locations	4	30.7	7.68	3.24	***	NB PW SB YK BB
	Error	33	78.3	2.37			
Sr/Ca	Locations	4	0.99	0.25	3.70	***	NB YK PW BB SB
	Error	33	2.21	0.07			
Ba/Ca	Locations	4	397	99.2	5.50	***	NB BB PW YK SB
	Error	33	595	18.0			

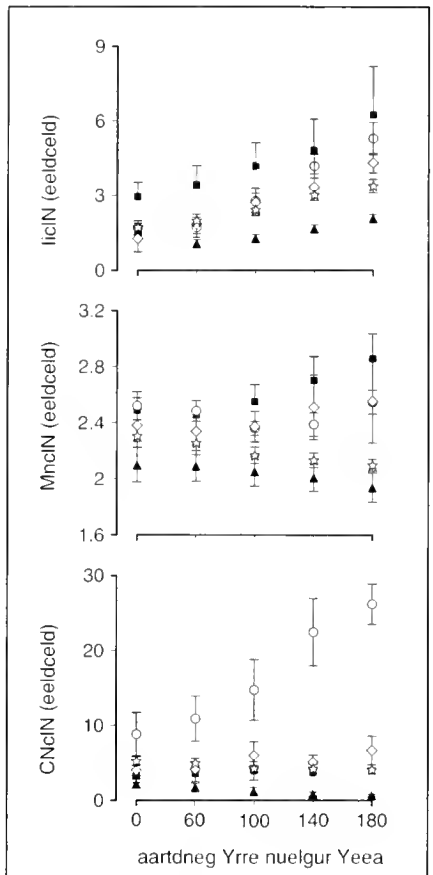

Figure 6

Profiles of elemental ratios, determined with laser ablation ICP-MS, from the nucleus out to a distance of approximately 200 μm in the otoliths of larval and juvenile walleye pollock (*Theragra chalcogramma*) collected from the North Bering Sea (▲), southeast Bering Sea (○), Bristol Bay (■), Prince William Sound (◇), and Yakutat (☆). Individual points are mean (±SE) values grouped at 40-μm intervals.

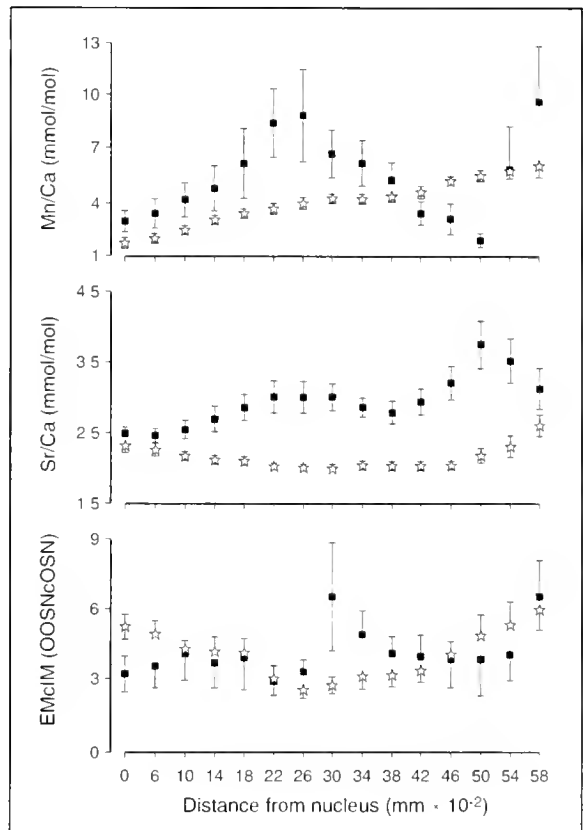

Figure 7

Profiles of elemental ratios, determined by using laser ablation ICP-MS, from the nucleus out to a distance of approximately 600 μm in the otoliths of juvenile walleye pollock (*Theragra chalcogramma*) collected from Bristol Bay (■) and Yakutat (☆). Individual points are mean (± SE) values grouped at 40-μm intervals.

cleus out to a distance of approximately 200 μm in the walleye pollock otoliths (Fig. 6, Table 6). The univariate test of location, averaged over the individual otolith profiles, was significant for both Sr/Ca and Ba/Ca. We also found significant interactions between profile and location for Mn/Ca, Sr/Ca, and Ba/Ca ratios (Table 6). Manganese values increased from the nucleus to the otolith edge at all locations, indicating that the significant interaction was generated by the observation that the profile from the North Bering Sea was considerably flatter than profiles from Bristol Bay and southeast Bering Sea. Strontium trajectories were more dynamic; profiles from some locations increased from the nucleus to the edge (Bristol Bay and Prince Williams Sound), profiles from other locations decreased (North Bering Sea and Yukatat), and a single location (southeast Bering Sea) showed no obvious trend. Finally, profile variations in Ba/Ca ratios among locations were dominated by a sharp increase in Ba/Ca ratios across the otoliths in the southeast Bering Sea samples. Profiles were effectively horizontal for the other four locations.

Otoliths in walleye pollock collected from Bristol Bay and Yakutat were significantly larger than those from the other four locations. We were, therefore, able to conduct extended profiles in these otoliths out to a distance of approximately 600 μm (Fig. 7). After starting at similar values at the nucleus, Mn/Ca and Sr/Ca profiles from the two locations quickly diverged and appeared to vary largely independently over the remaining time periods. The Ba/Ca profiles also appeared to be varying independently between the two locations, although the relative magnitude of differences between the two locations was smaller than for either Mn/Ca or Sr/Ca profiles.

Table 6

Laser ablation ICP-MS results from repeated-measures ANOVA of elemental profiles across otoliths from walleye pollock (*Theragra chalcogramma*) larvae collected at five locations in the Bering Sea and the Gulf of Alaska. Within-subject effects (profile and profile×location) were tested by using MANOVA (Pillai's trace), and between subjects effect (location) tested by using ANOVA (degrees of freedom [df]; sums of squares [SS]; mean squares [MS]). *** = significant at $\alpha = 0.05$; ns = nonsignificant.

Element	Source	df	Pillai's trace or SS	MS	F	$P < F$
Mn/Ca	Profile	4, 30	3.0×10^{-1}		17.1	***
	Position×location	16, 132	7.4×10^{-1}		1.9	***
	Location	4	1.99×10^{2}	49.7	2.49	ns
	Error	33	6.61×10^{-2}	20.1		
Sr/Ca	Profile	4, 30	2.18×10^{-1}		2.09	ns
	Position×location	16, 132	9.19×10^{-1}		2.46	***
	Location	4	1.05×10^{1}	2.62	6.02	***
	Error	33	1.44×10^{1}	0.44		
Ba/Ca	Profile	4, 30	6.92×10^{-1}		16.83	***
	Position×location	16, 132	1.04		2.9	***
	Location	4	5.83×10^{3}	1459	15.25	***
	Error	33	3.16×10^{3}	95.6		

Discussion

Quantifying dispersal pathways of larval fishes in marine environments is a difficult proposition. Marine fishes typically produce on the order of 10^4–10^6 eggs in a single spawning episode. These propagules are quickly dispersed in large volumes of seawater, making recovery of marked individuals difficult even if it were possible to introduce an artificial tag into the larvae at the time of spawning (Jones et al., 1999). Natural geochemical signatures in otoliths offer a useful alternative to artificial tagging approaches (Thorrold et al., 2002). The technique relies upon the assumption that larvae spawned at any given location retain a unique elemental or isotopic signature in their otoliths that can be recovered some time afterwards, and that variations in otolith geochemistry are sufficient to distinguish among geographic locations of interest. We found that elemental signatures in the otoliths of larval walleye pollock differed significantly geographically and with ontogeny. Samples at specific points on the otoliths, at the nucleus, and shortly after hatching, showed very similar patterns of variability, suggesting that the technique will likely be a robust method for identifying natal origins of walleye pollock after suitable groundtruthing of known spawning locations (e.g., Thorrold et al., 2001; Gillanders, 2002).

Elemental signatures in the otoliths of the larval pollock were assayed by using EPMA and laser ablation ICP-MS. Campana et al. (1997) noted that the two techniques were largely complementary in terms of elements that could be reliably assayed, and indeed only Sr was able to be quantified by both instruments in our study. Patterns of geographic variability presumably reflected the elements that were used in generating the multivariate signatures produced by each instrument. Elemental signatures from the EPMA data clustered into a Bering Sea group that included Shelikof Strait but excluded Bristol Bay, a coastal grouping that included Bristol Bay and Prince William Sound, whereas samples from Yakutat were separated from all other locations. Although sample sizes were smaller for the laser ablation ICP-MS assays, the data identified a grouping of locations in multivariate space that included the southeast Bering Sea, Prince William Sound, and Yakutat, whereas samples from both the north Bering Sea and Bristol Bay were separated from each other and the other locations. The observation that locations did not cluster into similar geographic groupings was probably a function of different mechanisms of elemental incorporation in otoliths. Elements assayed by ICP-MS in the present study substitute for Ca in the aragonitic lattice, and are believed to primarily reflect ambient physicochemical differences among natal locations (Bath et al., 2000; Milton and Chenery, 2001; Bath Martin et al, 2003). However, with the exception of Sr, the elements assayed by EPMA are likely under physiological regulation and therefore probably do not directly reflect either water chemistry or temperature (Campana, 1999). In either case, the application of elemental signatures in otoliths as natural tags of natal origins requires only that the signatures allow accurate classification of the natal origins of an unknown fish. A final caveat is necessary because it remains possible that preservation effects, particularly for labile elements that are not incorporated into the aragonite lattice, may also have contributed to at least some of the differences among locations (Milton and Chenery, 1998; Proctor et al., 1998). If present, such effects would clearly confound attempts to use elemental signatures as a natural tag of natal origins (Thresher, 1999).

It is important to note that although EPMA and laser ablation ICP-MS provided complementary information

on elemental composition, the spatial scale on which the data were gathered was different. Our laser ablation ICP-MS method required that we ablate a 70 μm × 70 μm raster, or a 720-μm line, in order to enable sufficient time to generate precise estimates of otolith composition. The EPMA analysis was less destructive than laser ablation ICP-MS, and therefore it was possible to sample individual points at a much finer spatial resolution (~5 μm), albeit with considerably less sensitivity and precision. For instance, using EPMA we were able to sample five points across a transect ending approximately 90 μm from the nucleus. In contrast, only a single raster could be sampled along this profile with laser ablation ICP-MS. Although the diameter of laser probes is approaching that of EPMA, ICP-MS is unlikely to match the spatial resolution of EPMA without further development of truly simultaneous mass analyzers such as time-of-flight ICP mass spectrometry (Mahoney et al., 1996). However, we were able to program the laser probe to trace out growth increments once the otolith radius had reached 120 μm and we found that the total length of a daily ring was approximately 700 μm. This finding, in turn, allowed us to construct elemental profiles at reasonable spatial resolution across the otoliths of larval pollock without sacrificing instrument precision by limiting acquisition times. Although it has not been used before with otoliths, our approach provides significant advantages over previous methods of using a raster to create elemental profiles (e.g., Thorrold et al., 1997; Thorrold and Shuttleworth 2000).

Previous work on pollock otolith chemistry was somewhat successful at distinguishing fish from locations in the Bering Sea and the Gulf of Alaska. Severin et al. (1995) used EPMA to sample the outer margin of otoliths from juvenile pollock collected along the Alaska Peninsula in the Gulf of Alaska and in Bristol Bay. We generated elemental profiles across otoliths from the nucleus out to approximately 90 μm for the EPMA samples, and up to 600 μm for the laser ablation ICP-MS assays. The profiles revealed some interesting differences between the elements assayed by each instrument. For instance, only one of the elements (K) from the EPMA analysis showed a significant interaction between profile and location, yet significant profile×location interactions were detected for Mn/Ca, Sr/Ca, and Ba/Ca ratios with laser ablation ICP-MS. We were also struck by the similarity of profiles from individuals sampled at the same location, as evidenced by the size of standard errors around mean values at specific distances across the otolith. For instance, the extended profiles from pollock collected in Bristol Bay and Yakutat show independent patterns of variation for all three elements from the nucleus out to 600 μm. Taken together, these data indicate that larvae from several spawning locations are indeed encountering water masses with differing physicochemical properties through their larval lives, and at approximately the same time. We lack, however, a sufficient understanding of the mechanisms controlling otolith chemistry to be able to relate the profiles to specific properties of different water masses in the study area. This knowledge will be necessary before it is possible to reconstruct dispersal pathways of larval pollock based on probe-based analyses of otolith geochemistry. Nonetheless, the among-location variability in elemental profiles revealed by both instruments is encouraging and justifies further investigations of otolith geochemistry in larval pollock.

Past attempts at identifying stock structure of walleye pollock in the North Pacific Ocean based on genetic techniques have been inconclusive (Bailey et al., 1999). In the most recent study, Olsen et al. (2002) were unable to distinguish between pollock from the Kamchatka Peninsula and several locations within the Gulf of Alaska based on three polymorphic microsatellite loci. Allozyme and MtDNA markers showed significant differences between North American and Asian populations, and among Gulf of Alaska locations. These data were difficult to reconcile because both markers showed temporal instability within locations. Adult tagging studies shed little light on the population structure of pollock because they address questions of repeat spawning, whereby adult fish return to the same area to spawn in subsequent years, rather than homing to natal spawning locations (Tsugi, 1989). It has proved impossible, except in rare circumstances (Jones et al., 1999), to artificially mark larvae before they are dispersed from spawning grounds, and therefore natural geochemical tags remain the most promising avenue for determining natal origins in walleye pollock. The ability to determine natal origins of individual fish is critical in the case of migratory marine fishes because it allows quantification of population connectivity through straying of adults as well as through larval dispersal (Thorrold et al., 2001). These data, in turn, identify the spatial extent of fish stocks that are demographically isolated or alternatively provide connectivity rates that are necessary to parameterize spatially explicit models if the species is usefully viewed as a metapopulation (Hanski and Gilpin, 1997; Smedbol and Wroblewski, 2002).

In summary, the elemental composition of otolith material deposited during early larval life in walleye pollock differed significantly among locations in the Gulf of Alaska and Bering Sea. These results imply that the larvae originated from different spawning locations, not that they constitute separate stocks. Nonetheless, these data represent the necessary first steps in using elemental signatures in otoliths as natural tags of natal origins in walleye pollock. Elemental profiles across otoliths were also unique to specific locations, suggesting that individuals collected at a location had experienced similar environmental conditions throughout their larval lives. This observation raised the possibility of reconstructing larval dispersal pathways based on high-resolution sampling of otolith chemistry. Although further work is needed to understand the processes influencing elemental uptake in pollock otoliths, we suggest that the potential information available from such studies would be invaluable for effective management of commercial pollock fisheries (Bailey et al., 1999). The approach appears to be particularly appropriate for in-

vestigating the potential existence of fine-scale population structure throughout the species range. Significant fine-scale population structure has been linked to the failure of northern cod stocks to recover from exploitation, even in the face of fishing moratoriums (Frank and Brickman, 2000; Hutchings, 2000). Analogous demographic processes acting in northern cod populations are clearly possible in walleye pollock, given the phyologenetic and life history similarities between the two species. The structure of pollock stock complexes within the major basins of the North Pacific Ocean remains, therefore, a critical gap in the knowledge necessary for the sustainable management of one of the world's largest marine fisheries.

Acknowledgments

This work was funded by North Pacific Marine Research Program to KMB, SRT and KPS, and was supported in part by NSF grants OCE-9871047 and OCE-0134998 to SRT. We thank the MACE, FOCI and groundfish task scientists who collected samples, and C. Latkoczy for assistance with the laser ablation ICP-MS analyses. This is Fisheries-Oceanography Coordinated Investigations collection number 0471-00A-0.

Literature cited

Bailey, K. M., T. J. Quinn, II, P. Bentzen, and W. S. Grant.
1999. Population structure and dynamics of walleye pollock, *Theragra chalcogramma*. Adv. Mar. Biol. 37:179–255.

Bath, G. E., S. R. Thorrold, C. M. Jones, S. E. Campana, J. W. McLaren, and J. W. H. Lam.
2000. Strontium and barium uptake in aragonitic otoliths of marine fish. Geochim. Cosmochim. Acta 64: 1705–1714.

Bath Martin, G. E., S. R. Thorrold, and C. M. Jones.
2004. The influence of temperature and salinity on strontium uptake in the otoliths of juvenile spot (*Leiostomus xanthurus*). Can. J. Fish. Aquat. Sci. 61:34–42.

Begg, G. A., and J. R. Waldman.
1999. An holistic approach to fish stock identification. Fish. Res. 43:1–3.

Campana, S. E.
1999. Chemistry and composition of fish otoliths: pathways, mechanisms and applications. Mar. Ecol. Prog. Ser. 188:263–297.

Campana, S. E., J. A. Gagne, and J. W. McLaren.
1995. Elemental fingerprinting of fish otoliths using ID-ICPMS. Mar. Ecol. Prog. Ser. 122:115–120.

Campana, S. E., and J. D. Neilson.
1985. Microstructure of fish otoliths. Can. J. Fish. Aquat. Sci. 42:1014–1032.

Campana, S. E., S. R. Thorrold, C. M. Jones, D. Guenther, M. Tubrett, H. Longerich, S. Jackson, N. M. Halden, J. M. Kalish, P. Piccoli, H. De Pontual, H. Troadec, J. Panfili, D. H. Secor.
1997. Comparison of accuracy, precision, and sensitivity in elemental assays of fish otoliths using the electron microprobe, proton-induced X-ray emission, and laser ablation inductively coupled plasma mass spectrometry. Can. J. Fish. Aquat. Sci. 54:2068–2079.

Frank, K. T., and D. Brinkman.
2000. Allee effects and compensatory population dynamics within a stock complex. Can. J. Fish. Aquat. Sci. 57:513–517.

Gillanders, B. M.
2002. Connectivity between juvenile and adult fish populations: do adults remain near their recruitment estuaries? Mar. Ecol. Prog. Ser. 240:215–223.

Grant, W. S., and F. M. Utter.
1980. Biochemical genetic variation in walleye pollock, *Theragra chalcogramma* population structure in the southeastern Bering Sea and the Gulf of Alaska. Can. J. Fish. Aquat. Sci. 37: 093–1100.

Gunn, J. S. H., I. R. Harrowfield, C. H. Proctor and R. E.Thresher.
1992. Electron probe microanalysis of fish otoliths--evaluation of techniques for studying age and stock discrimination. J. Exp. Mar. Biol. Ecol. 158:1–36.

Gunther, D., and C. A. Heinrich.
1999. Enhanced sensitivity in laser ablation-ICP mass spectrometry using helium-argon mixtures as aerosol carrier. J. Anal. At. Spectrom 14:1363–1368.

Hanski, I., and M. Gilpin (eds.).
1997. Metapopulation dynamics. Academic Press, San Diego, CA.

Hellberg, M. E., R. S. Burton, J. E. Neigel, and S. R. Palumbi.
2002. Genetic assessment of connectivity among marine populations. Bull. Mar. Sci. 70273–290.

Hinckley, S.
1987. The reproductive biology of walleye pollock, *Theragra chalcogramma*, in Bering Sea, with reference to spawning stock structure. Fish. Bull. 85:481–498.

Hutchings, J. A.
2000. Collapse and recovery of marine fishes. Nature 406:882–885.

Jones, G. P., M. J. Milicich, M. J. Emslie, and C. Lunow.
1999. Self-recruitment in a coral reef fish population. Nature 402:802–804.

Littel, R. C., R. J. Freund, and P. C. Spector.
1991. SAS systems for linear models, 3rd ed. SAS Inst., Inc., Cary, NC.

Mahoney, P. P., G. Li, and G. M. Hieftje.
1996. Laser ablation-inductively coupled plasma mass spectrometry with a time-of-flight mass analyzer. J. Anal. At. Spectrom. 11:401–405.

Milton, D. A., and S. R. Chenery.
1998. The effect of otolith storage methods on the concentrations of elements detected by laser-ablation ICPMS. J. Fish Biol. 53:785–794.
2001. Sources and uptake of trace metals in otoliths of juvenile barramundi (*Lates calcarifer*). J. Exp. Mar. Biol. Ecol. 264:47–65

Mulligan, T. J., R. W. Chapman, and B. L. Brown.
1992. Mitochondrial DNA analysis of walleye pollock, *Theragra chalcogramma* , the eastern Bering Sea and Shelikof Strait, Gulf of Alaska. Can. J. Fish. Aquat. Sci. 49:319–326.

Olsen, J. B., S. E. Merkouris, and J. E. Seeb.
2002. An examination of spatial and temporal genetic variation in walleye pollock (*Theragra chalcogramma*) using allozyme, mitochondrial DNA, and microsatellite data. Fish. Bull. 100:752–764.

Proctor, C. H. and R. E. Thresher.
1998. Effects of specimen handling and otolith prepara-

tion on concentration of element in fish otoliths. Mar. Biol. 131: 681–694.

Rosenthal, Y., P. M. Field, and R. M. Sherrell.
1999. Precise determination of element/calcium ratios in calcareous samples using sector field inductively coupled plasma mass spectrometry. Anal. Chem. 71:3248–3253.

Scott, V. D., G. Love, and S. J. B. Reed.
1995. Quantitative electron-probe analysis. Ellis Horwood Limited, Hemel Hempstead, Hertfordshire, England.

Serobaba, I. I.
1977. Data on the population structure of the walleye pollock, *Theragra chalcogramma*, from the Bering Sea. J. Ichthyol. 17:219–231.

Severin, K. P., J. Carroll and B. L. Norcross.
1995. Electron microprobe analysis of juvenile walleye pollock, *Theragra chalcogramma*, otoliths from Alaska: a pilot stock separation study. Environ. Biol. Fishes 43:269–283.

Shields, G. F., and J. R. Gust.
1995. Lack of geographic structure in mitochondrial DNA sequences of Bering walleye pollock, *Theragra chalcogramma*. Molecular Mar. Biol. Biotechnol. 4:69–82.

Smedbol, R. K., and J. S. Wroblewski.
2002. Metapopulation theory and northern cod population structure: interdependency of subpopulations in recovery of a groundfish population. Fish. Res. 55: 161–174.

Temnykh, O. S.
1994. Morphological differentiation of walleye pollock *Theragra chalcogramma* the western Bering Sea and Pacific Kamchatka waters. Voprosy ikhtiologii 34: no. 2.

Thorrold, S. R., C. M. Jones, and S. E. Campana.
1997. Response of otolith microchemistry to environmental variations experienced by larval and juvenile Atlantic croaker (*Micropogonias undulatus*). Limnol. Oceanogr. 42:102–111.

Thorrold, S. R., G. P. Jones, M. E. Hellberg, R. S. Burton, S. E. Swearer, J. E. Neigel, S. G. Morgan, and R. R. Warner.
2002. Quantifying larval retention and connectivity in marine populations with artificial and natural markers. Bull. Mar. Sci. 70:291–308.

Thorrold, S. R., C. Latkoczy, P. K. Swart, and C. M. Jones.
2001. Natal homing in a marine fish metapopulation. Science 291:297–299.

Thorrold, S. R., and S. Shuttleworth.
2000. In situ analysis of trace elements and isotope ratios in fish otoliths using laser ablation sector field inductively coupled plasma mass spectrometry. Can. J. Fish. Aquat. Sci. 57:232–242.

Thresher, R. E.
1999. Elemental composition of otoliths as a stock delineator in fishes. Fish. Res. 43:165–204.

Thresher, R. E., C. H. Proctor, J. S. Gunn, and I. R. Harrowfield.
1994. An evaluation of electron-probe microanalysis of otoliths for stock delineation and identification of nursery areas in a southern temperature groundfish, *Nemadactylus macropterus*. Fish. Bull. 92:817–840.

Tsugi, S.
1989. Alaska pollock population, *Theragra chalcogramma*, of Japan and its adjacent waters: Japanese fisheries and population studies. Mar. Behav. Physiol. 15:147–205.

Waples, R. S.
1998. Separating the wheat from the chaff: patterns of genetic differentiation in high gene flow species. J. Heredity 89:438–450.

Winer, B.
1971. Statistical principles in experimental design, 2nd ed. McGraw-Hill, New York, NY.

Yoshinaga, J., A. Nakama, M. Morita, and J. S. Edwards.
2000. Fish otolith reference material for quality assurance of chemical analyses. Mar. Chem. 69:91–97.

A sudden collapse in distribution of Pacific sardine (*Sardinops sagax*) off southwestern Australia enables an objective re-assessment of biomass estimates

Daniel J. Gaughan
Timothy I. Leary
Ronald W. Mitchell
Ian W. Wright

Western Australian Marine Research Laboratories
Department of Fisheries
West Coast Drive
Waterman, Western Australia 6020, Australia
E-mail address (for D. J. Gaughan): dgaughan@fish.wa.gov.au

Abstract—Fishery-independent estimates of spawning biomass (B_{SP}) of the Pacific sardine (*Sardinops sagax*) on the south and lower west coasts of Western Australia (WA) were obtained periodically between 1991 and 1999 by using the daily egg production method (DEPM). Ichthyoplankton data collected during these surveys, specifically the presence or absence of *S. sagax* eggs, were used to investigate trends in the spawning area of *S. sagax* within each of four regions. The expectation was that trends in B_{SP} and spawning area were positively related. With the DEPM model, estimates of B_{SP} will change proportionally with spawning area if all other variables remain constant. The proportion of positive stations (PPS), i.e., stations with nonzero egg counts—an objective estimator of spawning area—was high for all south coast regions during the early 1990s (a period when the estimated B_{SP} was also high) and then decreased after the mid-1990s. There was a decrease in PPS from the mid-1990s to 1999. The particularly low estimates in 1999 followed a severe epidemic mass mortality of *S. sagax* throughout their range across southern Australia. Deviations from the expected relationship between B_{SP} and PPS were used to identify uncertainty around estimates of B_{SP}. Because estimation of spawning area is subject to less sampling bias than estimation of B_{SP}, the deviation in the relation between the two provides an objective basis for adjusting some estimates of the latter. Such an approach is particularly useful for fisheries management purposes when sampling problems are suspected to be present. The analysis of PPS undertaken from the same set of samples from which the DEPM estimate is derived will help provide information for stock assessments and for the management of purse-seine fisheries.

Manuscript submitted 5 December 2002 to the Scientific Editor's Office.

Manuscript approved for publication 27 April 2004 by the Scientific Editor.

Fish. Bull. 102:617–633 (2004).

As a stock of small pelagic fish decreases, biomass assessment becomes problematic because of such factors as patchy distribution (Fletcher and Sumner, 1999) and continuing high catchability as a result of the schooling behavior of some fish (Uphoff, 1993). In these circumstances, ichthyoplankton surveys can provide a useful means of estimating spawning biomass, B_{SP}, for some pelagic fish species. Mangel and Smith (1990) used a technique that assessed the presence or absence of sardine (*Sardinops sagax*) eggs in a known spawning area. They found that changes in adult biomass were more accurately predicted by using presence-absence of eggs in sampling surveys than mean egg abundance because of misleading results arising from the spatial patchiness of eggs. In their presence-absence analysis, the spatial distribution of eggs is the key determinant of B_{SP} estimates and is used in a model with a series of other parameters to provide an estimate of B_{SP} (Mangel and Smith, 1990). Although this technique provides an objective indication of stock size that is not subjected to the inherent problems in estimating B_{SP} with the daily egg production method (DEPM, e.g., Ward et al., 2001), the modeling requires substantial prior knowledge of adult and egg production parameters. More recently, Zenitani and Yamada (2000) developed an optimal relationship between B_{SP} and spawning area for the Japanese sardine (*Sardinops melanostictus*) using a nonlinear model that assumed patchy egg distribution. In their case, biomass was estimated by using virtual population analysis with catch-at-age data from the commercial fishery.

The purse seine fishery for *Sardinops sagax* in Western Australia (WA) operates along the south coast around the port regions of Esperance, Bremer Bay, and Albany; and on the lower West Coast in the regions of Fremantle and Dunsborough (Fig. 1). A level of spatial distinctness among adult *Sardinops* populations necessitates that three south coast regions and the west coast region be managed as separate fisheries (Gaughan et al., 2002). Unlike the case with Japanese sardine (Zenitani and Yamada, 2000), it has not been possible to estimate the B_{SP} of *Sardinops* in each fishery in WA using only an age-based approach. Although Gaughan et al. (2002) considered the catch-at-age data for the WA *Sardinops* fisheries to be reasonable, the data span a relatively short time series, commencing in 1988 at Albany and Bremer Bay and later at the other regions. Therefore, both age-structure data and estimates of spawning biomass (B_{SP}) obtained with the DEPM have provided the biological basis for managing the *Sardinops* fisheries in WA for over a decade (Fletcher, 1991, 1995; Fletcher et al., 1996,

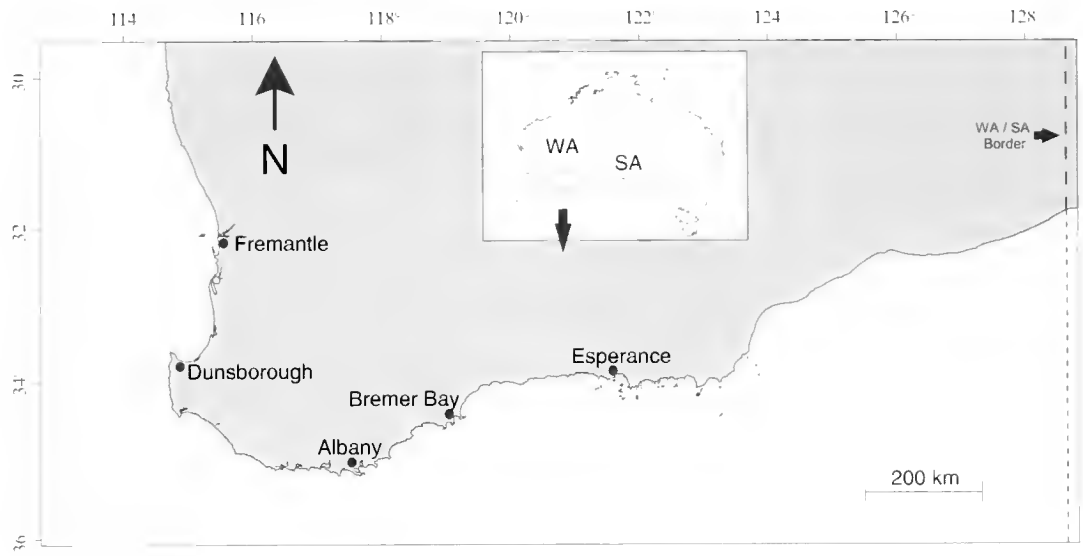

Figure 1

Map of southwestern Australia showing Pacific sardine fishing ports. North of Dunsborough to Fremantle constitutes the west coast fishery and the other regions constitute the south coast fishery. WA = Western Australia, SA = South Australia.

1996[1]; Cochrane[2]). A population model that integrates age-structure information and DEPM-derived estimates of B_{SP} ($B_{SP\text{-}DEPM}$) has recently been developed by Hall (2000) for each of the three south coast regions.

Although the DEPM is able to provide relatively robust estimates of B_{SP} for a variety of species (Alheit, 1993; Hunter and Lo, 1997), it is not without problems (Cochrane, 1999; Ward et al., 2001). The $B_{SP\text{-}DEPM}$ estimates for *Sardinops* in WA are presented at Management Advisory Committee (MAC) meetings and, in turn, are provided to the relevant government minister. The $B_{SP\text{-}DEPM}$ estimates therefore undergo critical scrutiny by industry representatives. The shortcomings of the DEPM (e.g., sensitivity of precision for small sample sizes) are well understood by the members of the management committee; industry recognizes that onshore infrastructure and fleet capacity must be matched to long-term average B_{SP} and that industry should not capitalize at levels that require maximal stock sizes to meet financial expectations. Inasmuch, a level of conservatism has been adopted by the Management Advisory Committee when setting quotas. Nonetheless, the accuracy of estimates has been a contentious issue; industry members typically believe that the scientific advice presented often underestimates the B_{SP}. Likewise, wide confidence intervals around biomass estimates introduce doubt in the minds of industry members regarding the reliability of scientific advice, which can therefore stall the implementation of management measures. However, the lack of a formal and objective means of dealing with suspect and imprecise $B_{SP\text{-}DEPM}$ estimates (e.g., because of problems with sampling spawning fish) has previously not been rigorously addressed.

Following the progression along the southern WA coast in early 1999 of a mass mortality of *Sardinops*, estimates of the quantity killed at Albany appeared to be very low (Gaughan et al., 2000). That is, very few dead *Sardinops* were found in comparison to the other regions where fisheries occur. Mortality rates for Esperance and Bremer Bay were 69.6% and 74.5% of the B_{SP}, respectively, whereas that for Albany was estimated to be only 2.4%. Estimates of the mortality rate of *Sardinops* in South Australia (SA, Fig. 1) for the same epizootic event were independently found to also be around 70% (Ward et al., 2001). The inconsistency with Albany could not be attributed to different weather conditions; the weather conditions at Albany were similar to those at Esperance and Bremer Bay and would be expected to result in equally visible evidence of mortality. Gaughan et al. (2000) contended that the true epizootic mortality rate of *Sardinops* in Albany was similar to that for the other regions, but that the very low mortality estimate was likely seen as such in view of the previous overestimation of B_{SP}.

In this study we aimed to address the problem of poor precision, while also developing a technique to identify particularly poor estimates of $B_{SP\text{-}DEPM}$, i.e., those for

[1] Fletcher, W. J., K. V. White, D. J. Gaughan, and N. R. Sumner. 1996. Analysis of the distribution of pilchard eggs off Western Australia to determine stock identity and monitor stock size. Final Report to Fisheries Research and Development Corporation. Project No. 92/95, 109 p. Department of Fisheries, Government of Australia, 168-170 St. Georges Tce, Perth, WA 6000, Australia.

[2] Cochrane, K. L. 1999. Review of Western Australia pilchard fishery, 12–16 April 1999. Fisheries Management Paper 129, 32 p. Department of Fisheries, Government of Western Australia, 168-170 St. Georges Tce, Perth, WA 6000, Australia.

Table 1

Estimates of spawning biomass (metric tons) of *Sardinops sagax* obtained by using the daily egg production method ($B_{SP\text{-}DEPM}$) for each of four regions in southwestern Australia. In those cases where data were sufficient to estimate a coefficient of variation (CV), the range around the $B_{SP\text{-}DEPM}$ estimate (Min./Max.) was calculated as ±1 standard deviation (SD); otherwise, the $B_{SP\text{-}DEPM}$ range was calculated by using assumed (AS) values for one or more of the DEPM parameters (see text). The numbers of adult *S. sagax* and plankton samples used in these calculations are shown.

Year	Min.	$B_{SP\text{-}DEPM}$	Max.	CV	±1 SD	Adult *n*	Plankton *n*
Albany							
1991	12,088	19,300	30,700	—	AS	10	41
1992	9006	16,994	24,981	0.44	±1 SD	10	31
1993	16,402	23,432	30,4620	0.30	±1 SD	9	61
1994	15,440	31,330	55,000	—	AS	10	107
1995	7720	17,544	27,368	0.56	±1 SD	10	83
1997	13,018	18,597	24,176	0.30	±1 SD	27	94
1999	0	89	531	4.99	±1 SD	2	263
Bremer Bay							
1992	12,000	19,280	79,000	—	AS	—	25
1993	16,170	44,010	63,608	—	AS	—	32
1994	15,700	28,458	42,500	—	AS	—	102
1999	2161	4156	6150	0.48	±1 SD	3	256
Esperance							
1993	14,326	32, 252	61, 800	—	AS	5	50
1994	10,700	20,080	40,100	—	AS	—	150
1995	10,900	31,900	45,647	—	AS	6	105
1999	3454	17,396	31,793	0.80	±1 SD	8	257
West coast							
1993	14,500	41,250	78,000	—	AS	—	55
1994	3100	8714	29,000	—	AS	—	133
1996	43,300	60,228	77,200	0.28	±1 SD	4	96
1998	9112	18,985	28,951	0.52	±1 SD	28	240
1999	3948	5275	6651	0.25	±1 SD	4	396

which accuracy was suspect. However, because of the small size of the fishery and the difficulty in securing additional research funds, no fishery-independent method of estimating biomass other than the DEPM was undertaken. We recognized that this study could not, therefore, unequivocally determine whether or not any improvement in accuracy had been achieved; therefore, we focused on improving the consistency between available data sets (in terms of the broader economic environment) in order to improve the decision-making process for what is a small-scale fishery.

We examine the relationship between relative trends in the $B_{SP\text{-}DEPM}$ and spawning area of *Sardinops* in each of four regional fisheries. We propose a method of using the relationship between spawning area and egg presence-absence data as an indicator of B_{SP} that is simpler than the methods of Mangel and Smith (1990) and Zenitani and Yamada (2000). We specifically chose to keep the retrospective analysis simple in recognition of data limitations, i.e., short time series and low numbers of samples for some DEPM surveys. In particular, our analyses did not rely on substantial knowledge of various parameters associated with estimating $B_{SP\text{-}DEPM}$. This investigation (an objective re-assessment of *Sardinops* $B_{SP\text{-}DEPM}$) was undertaken because of the contrast provided by the significant collapse in distribution, coupled with the sudden and substantial decrease in $B_{SP\text{-}DEPM}$ that followed mass mortality in 1998–99. Although problems in obtaining accurate B_{SP} estimates with the DEPM will not be resolved by the present study, greater consistency between indicators of the magnitude of B_{SP} and the development of a transparent and objective technique to identify apparent discrepancies between the two will facilitate better management of this key pelagic resource.

Methods

Estimates of spawning biomass with the DEPM

The estimates of B_{SP} used in this study (Table 1) were obtained by using the DEPM, which relies on ichthyoplankton surveys to estimate egg production and temporally concurrent samples of adult fish to estimate the adult parameters of fecundity, sex ratio, and weight.

The egg and adult data were subsequently combined in the DEPM model (Parker, 1985), as follows, to estimate spawning biomass:

$$B_{SP\text{-}DEPM} = (APWk)/(SFR),$$

where A = spawning area;
P = egg production (numbers of eggs before losses due to mortality);
W = weight of adult fish;
k = conversion factor to bring the various units to a value in metric tons;
S = spawning fraction; the proportion of females that spawn per day;
F = fecundity; number of eggs produced by a female; and
R = ratio of females to males by weight.

The DEPM provides a point estimate of spawning biomass, with upper and lower statistical bounds. In those individual surveys where all parameters could be estimated, estimates of coefficient of variation (CV) for $B_{SP\text{-}DEPM}$ were undertaken by using the delta method to sum the CV of the component parameters (Parker, 1985). In turn, the CV was used to provide an estimate of variability around the point estimate; specifically, we used ± 1 standard deviation to indicate the upper and lower bounds around the point estimates. In several surveys, particularly when the DEPM was initially being applied in WA, few adult samples meant that values for adult parameters (spawning fraction, sex ratio, fecundity, weight) could not be estimated and therefore a CV for the final estimate of $B_{SP\text{-}DEPM}$ could likewise not be estimated. Although sex ratio and weight could be reasonably estimated from the regular sampling of commercial catches around the survey period and fecundity could be estimated from a relatively small sample (e.g., 70–100 fish), estimating the spawning fraction was more difficult. In this latter case, the upper and lower bounds for the $B_{SP\text{-}DEPM}$ estimate were not based on a statistical measure but rather on what were thought to be likely low and high values of spawning fraction, respectively, for *Sardinops* from other surveys in WA and elsewhere (e.g., Alheit, 1993, Fletcher et al, 1996). Prior knowledge of likely $B_{SP\text{-}DEPM}$ values when applying the DEPM, specifically for the purpose of providing expert management advice, has recently been used successfully for *Sardinops* in South Australia (Ward et al. 2001).

Adult samples

Twenty DEPM surveys were conducted between 1991 and 1999 to identify stocks and to estimate spawning biomass of *Sardinops* of southwestern Australia (Fletcher et al., 1996a, 1996b; Fletcher et al.[3]; senior author's unpubl. data). The surveys were performed during the peak spawning months for *Sardinops* off the west coast, Albany, Bremer Bay, and Esperance regions. The timing of the DEPM survey cruises in each region was based on gonadosomatic indices for samples obtained from commercial catches, as described in Gaughan et al. (2002). The aim was to obtain samples from 35 catches of adult fish, as recommended by Alheit (1993), but this number was never achieved and in some cases no samples were obtained (Table 1). For each catch sampled, the ovaries from 15–50 females were immediately placed in 10% formalin and subsequently prepared histologically for microscopic examination. The remainder of the subsample was processed to obtain mean female weight and sex ratio by weight. Mature ovaries were retained for estimation of fecundity.

Plankton sampling and estimation of egg production

Plankton sampling extended from nearshore waters to the edge of the continental shelf (Fig. 2). Sampling stations were generally spaced uniformly, typically 2–4 nautical miles apart, along transects perpendicular to the shore. Analysis of *Sardinops* egg distribution from surveys conducted in the early 1990s indicated that these surveys sufficiently covered the distribution of the spawning stock (Fletcher and Tregonning, 1992; Fletcher et al., 1994), and later geostatistical analyses of *Sardinops* egg distribution patterns confirmed that the spacing of transects and stations were adequate to effectively represent the spatial distribution (Fletcher and Sumner, 1999). The earlier surveys were used to refine the spatial range of subsequent surveys. The number of plankton samples taken in each survey has generally increased since the early 1990s (Table 1).

Sardinops eggs were collected by using vertical tows that allowed the water column to be sampled from a maximum depth of 70 m to the surface; Fletcher (1999) showed that *Sardinops* eggs off southern Australia are typically restricted to the upper 70 m. Bongo nets with diameters of either 60 or 26 cm and constructed of either 500- or 300-micron mesh were used; the change to smaller nets was made to reduce sample volume and hence sorting time, whereas the change to smaller mesh was made to increase efficiency in capturing yolksac larvae; these changes did not affect the sampling efficiency for *Sardinops* eggs. Tow speed was standardized at 1 m/s. All samples were collected between 0630 and 1800 hours and immediately preserved in 5–10% formalin and seawater.

Plankton samples were examined under a dissecting microscope. *Sardinops* eggs were identified, classified into 12 developmental stages (White and Fletcher[4]), and

[3] Fletcher W. J., B. Jones, A. F. Pearce, and W. Hosja. 1997. Environmental and biological aspects of the mass mortality of pilchards (Autumn 1995) in Western Australia. Fisheries Research Report, Fisheries Department Western Australia 106, 115 p. Department of Fisheries, Government of Western Australia, 168-170 St. Georges Tce, Perth, WA 6000, Australia.

[4] White, K. V., and W. J. Fletcher. 1998. Identifying the developmental stages for eggs of the Australian pilchard, Sardinops sagax. Fisheries Research Division WA, Fisheries Research Report 103, 21 p. Department of Fisheries, Government of Western Australia, 168-170 St. Georges Tce, Perth, WA 6000, Australia.

Table 2

Correlations between 1) proportion of positive stations (PPS) and proportional spawning area (PSA) and 2) PPS and estimated spawning area (km^2) resulting from surveys of *Sardinops sagax* eggs at four regions in southwestern Australia. PPS is the proportion of the total number of plankton sampling stations that contained at least one *S. sagax* egg that had been spawned on the previous night. PSA is the proportion of the total survey area that consisted of spawning area. The values for spawning area are also provided.

	Survey	PPS	PSA (%)	Correlation I	Area (km^2)	Correlation II
Albany	Jul 91	0.46	37		1806	
	Jul 92	0.58	51		2686	
	Jul 93	0.52	36		2391	
	Jul 94	0.60	60		6672	
	Jul 95	0.33	28		1977	
	Jul 97	0.19	21		2224	
	Jul 99	0.15	1	0.94	107	0.68
Bremer Bay	Jul 92	0.61	64		2807	
	Jul 93	0.72	67		2809	
	Jul 94	0.70	71		4474	
	Jun 99	0.12	12	0.99	908	0.86
Esperance	Jul 93	0.50	44		5715	
	Jul 94	0.57	73		9796	
	Apr 95	0.61	36		5277	
	May 99	0.09	3	0.81	7840	0.83
West coast	Jul 93	0.53	62		8012	
	Jul 94	0.30	38		5199	
	Aug 96	0.23	16		2202	
	Aug 98	0.10	7		1835	
	Aug 99	0.12	10	0.98	1836	0.96

counted. Estimation of egg production was undertaken by fitting a negative exponential model (Picquelle and Stauffer, 1985) and was derived from the *y*-axis intercept of the regression model, representing time 0. The number of stages used to fit the model depended on the egg abundance for each stage; the best fitting model was chosen visually from an iterative sequence of fits. The best fit was not necessarily that with the smallest CV but rather that which intuitively did not violate our understanding of natural mortality rates as determined from the literature. For example, the slope of the regression model must be negative and egg mortality rates should fall within the broad range of 0.9–3.9/d (e.g., Smith et al., 1989).

Estimation of spawning area

According to water temperatures during each survey and the stage of egg development, *Sardinops* eggs were determined to have been spawned either the previous night ("day-1") or two nights previous ("day-2") as described by Fletcher et al. (1996). The total survey area was estimated by constructing a polygon around all stations. The spawning area was defined as the area in which day-1 *Sardinops* eggs were found (Fletcher et al., 1996a). The areas of the polygons around stations that had day-1 eggs, referred to as positive stations, were summed to estimate the spawning area for each zone. When positive stations occurred on the margin of the sampling area, polygons for these positive stations were drawn as for the embedded positive stations, but the areas of these polygons were extended by a standardized amount beyond the sampling areas (Wolf and Smith, 1986).

The proportion of positive stations (PPS) was calculated for each survey. The proportion of the survey area (PSA) that consisted of spawning area was also evaluated in each case. PPS and PSA were positively correlated at each region (Table 2); this result was expected and indicated that PPS provides a realistic representation of changes in spawning area. The relationships between PPS and the areal estimates of spawning area were not as strong, but these latter estimates suffered as potential predictors of biomass in our study because of the large differences in numbers of plankton samples collected between surveys (Table 1). PPS is thus not only an objective measure but can also be considered as an index of spawning area.

Modeling of spawning biomass

The collapse in distribution of *Sardinops* at each of four locations in southern Western Australia in 1999 is shown by the decline in spawning area (Fig. 2). The importance of this collapse in providing contrast for model fitting in otherwise poor data sets (few points with either flat or clumped distributions) is evident from linear fits of

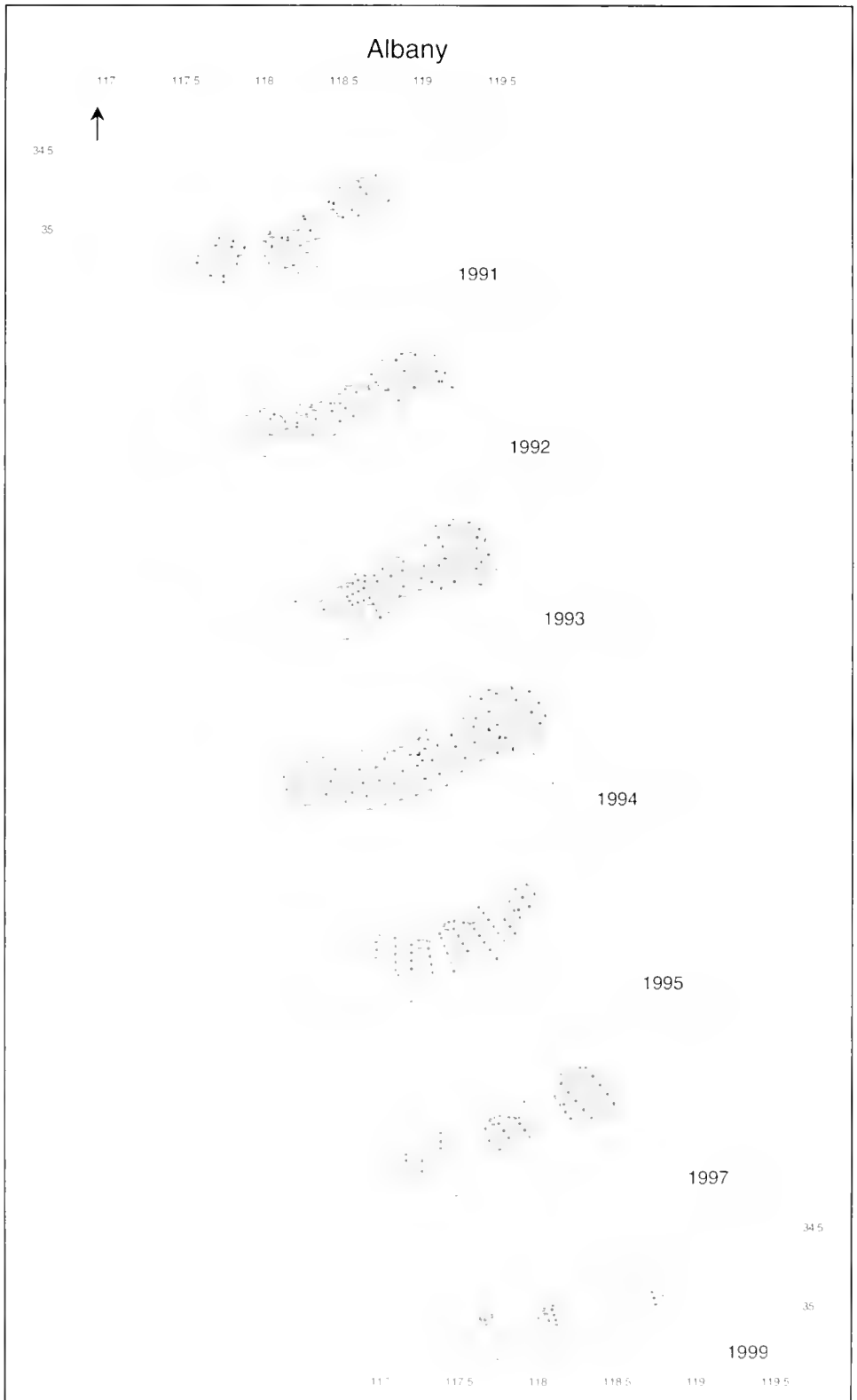

Figure 2

Sardinops sagax spawning area (distribution of eggs spawned on the night previous to sampling) from ichthyoplankton surveys conducted between 1991 and 1999 for Albany, Bremer Bay, Esperance, and west coast regions.

Figure 2 (continued)

$B_{SP\text{-}DEPM}$ against PPS for the south coast locations (Fig. 3). Because we wished to examine the relationship between trends in DEPM-based estimates of B_{SP} and PPS with the aim of improving estimates of B_{SP}, the development of an appropriate model is described here from first principles, followed by a selectivity analysis of error variance to choose the optimal estimator of B_{SP}. Given that we did not have a means of assessing the level of accuracy of the "adjusted" estimates, and the aim was therefore to improve consistency between data sets for the purpose of enhancing the decision-making process, our criteria in choosing an optimal estimator was to

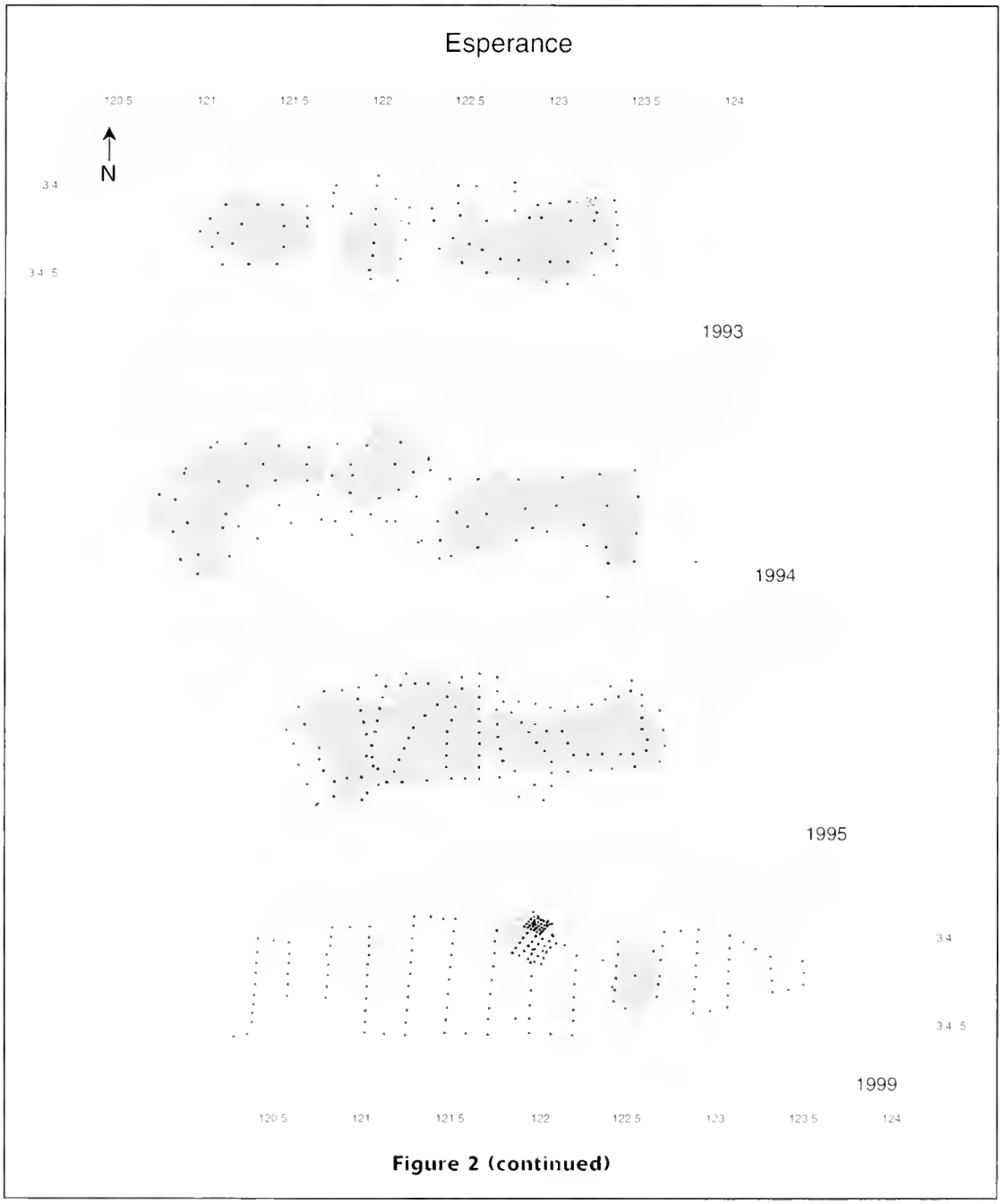

Figure 2 (continued)

minimize variance. In terms of improving management of the *Sardinops* fisheries in southwestern Australia, we considered this approach appropriate because of the relatively conservative exploitation rates that have been adopted by the Management Advisory Committee.

Model selection

The procedure used in the present study was to first invoke a general model and then use the data to drive a simplification process in order to avoid a specification error. Thus, for each of the fishery regions, we first considered the following general relationship between $B_{SP\text{-}DEPM}$ and PPS holding over time:

$$(B_{SP\text{-}DEPM})_t = \alpha_0 (PPS_t)^{\lambda} + \alpha_2 + e_t, \quad (1)$$

where λ is common for all areas, α_0 and α_2 are area specific constants, and the error term e_t is independent, homoscedastic and normal with a mean of zero. This model was chosen specifically in order to be amenable to Taylor series expansion during the simplification process. In satisfying dimensional and conservational

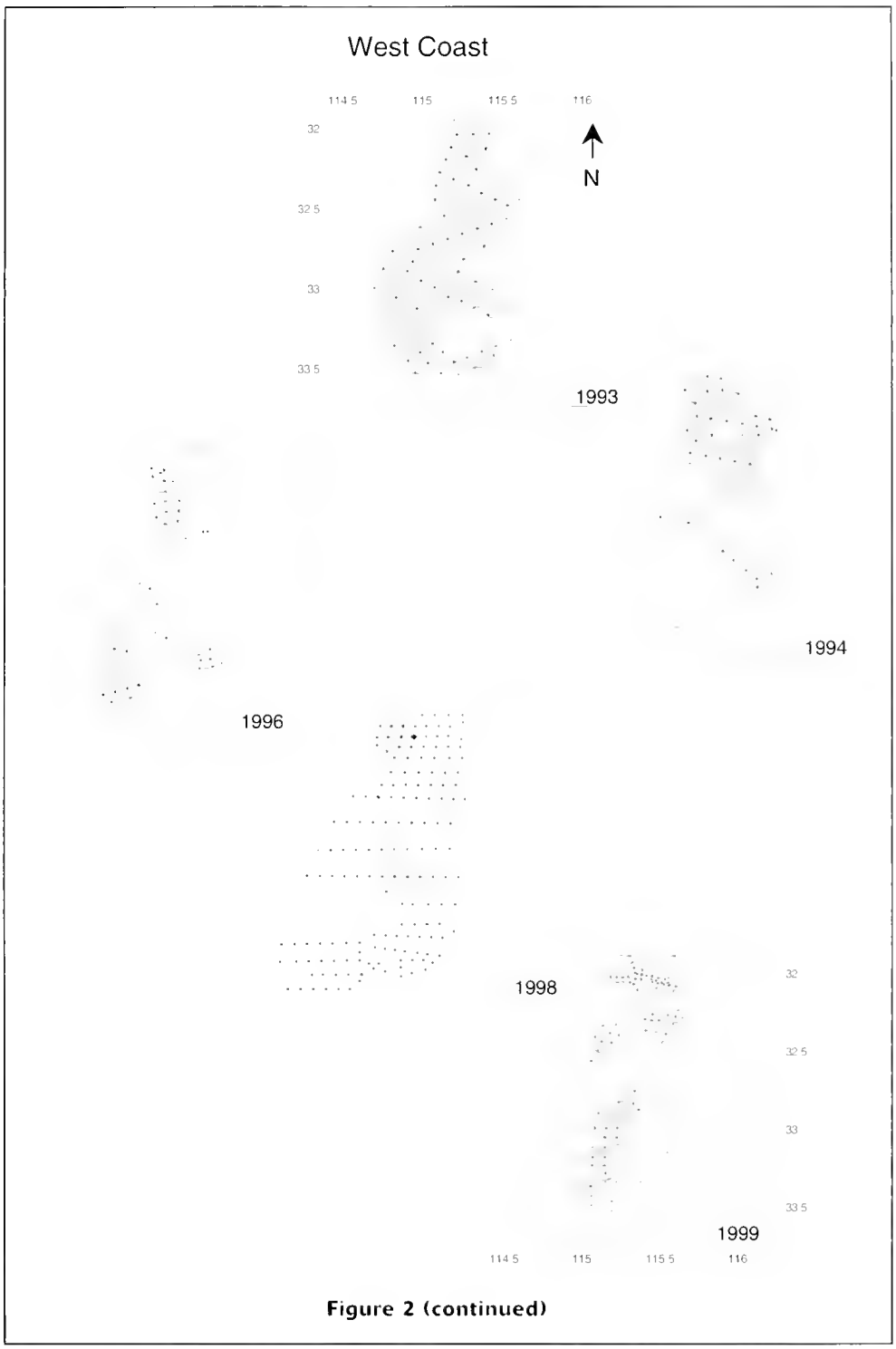

Figure 2 (continued)

arguments, α_2 must be zero; therefore the above family of models reduces to

$$(B_{SP\text{-}DEPM})_t = \alpha_0 (PPS_t)^{\lambda} + e_t \,. \qquad (2)$$

An attempt to fit the linear regression model, composed of the natural logarithms of either side of the above relation, to the observed data was unsuccessful because of heterogeneity of error variance.

Direct estimation of model II with a nonlinear regression procedure gave estimates of λ that were near 1 and with large standard errors on account of the small size of the data sets. However, residual diagnostics were satisfactory. Because the observed PPS values fell between

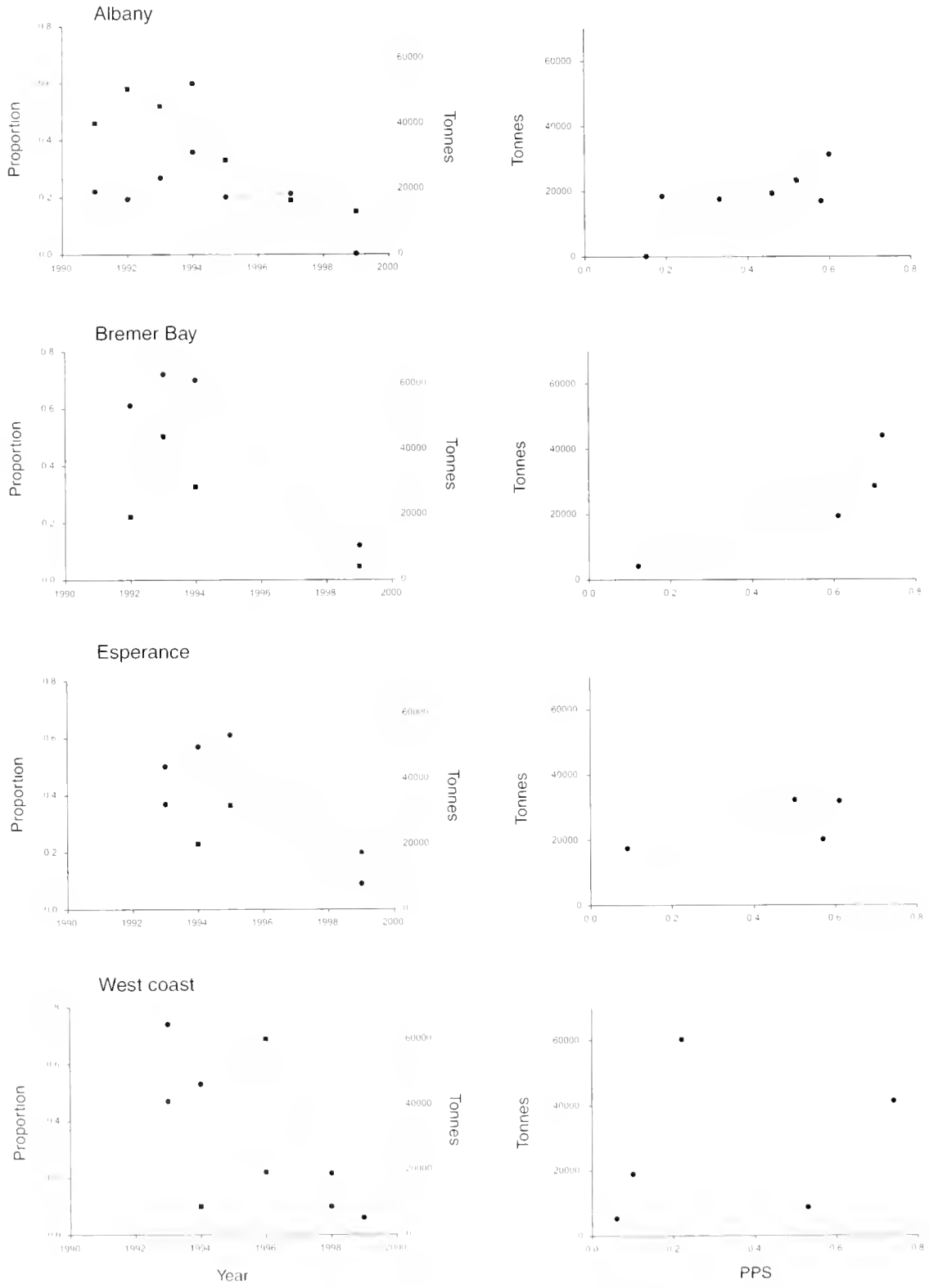

Figure 3

Plots of the proportions of positive stations (—●—) and $B_{SP\,DEPM}$ estimates (--■--) for the four *Sardinops sagax* fisheries in southwestern Australia. The right-hand panel shows linear fits of the relationship between proportion of positive stations and $B_{SP\,DEPM}$ estimates.

Table 3

Parameter estimates for two models (III and IV, see text for details) of *Sardinops sagax* spawning biomass, including tests for zero coefficients, at each of four regions in southwestern Australia.

Model III					Model IV				
Albany					Albany				
SE of estimate: 6011					SE of estimate: 6343				
	B_{SP}	*SE* of B_{SP}	$t(22)$	*P*-level		B_{SP}	*SE* of B_{SP}	$t(23)$	*P*-level
Intercept	−4597.15	2419.94	−1.90	0.070661	PPS	45,910.11	3552.36	12.92	4.96E-12
PPS	56,780.19	6638.90	8.55	1.91E-08					
Bremer Bay					Bremer Bay				
SE of estimate: 4016					SE of estimate: 3994				
	B_{SP}	*SE* of B_{SP}	$t(14)$	*P*-level		B_{SP}	*SE* of B_{SP}	$t(18)$	*P*-level
Intercept	−1436.88	1573.94	−0.91	0.37674	PPS	42,784	2308.30	18.53	9.47E-12
PPS	45,341.85	3638.2	12.46	5.75E-09					
Esperance					Esperance				
SE of estimate: 4639					SE of estimate: 10,214				
	B_{SP}	*SE* of B_{SP}	$t(20)$	*P*-level		B_{SP}	*SE* of B_{SP}	$t(21)$	*P*-level
Intercept	15,840.52	1751.38	9.045	0.000317	PPS	48,377.13	5095.09	9.49	4.76E-09
PPS	17,790.27	4097.73	4.34	1.66E-08					
West coast					West coast				
SE of estimate: 15,280					SE of estimate: 15,330				
	B_{SP}	*SE* of B_{SP}	$t(32)$	*P*-level		B_{SP}	*SE* of B_{SP}	$t(33)$	*P*-level
Intercept	5316.10	4826.58	1.10	0.278929	PPS	84,615.52	12,615.76	6.71	1.22E-07
PPS	63,192.69	23,161.29	2.73	0.010251					

zero and one, and λ was also close to 1, model II was able to be recast in a more tractable form by using the Taylor series expansion of the RHS of model II about PPS = 1, leading to the relationship

$$(B_{SP\text{-}PPS})_t = \alpha_0 PPS_t + \delta + e_t, \quad (3)$$

where the expected value of δ is approximately $-0.25\alpha_0(\lambda-1)$. Details of the derivation are provided in Appendix 1.

Fitting the regression model III to the DEPM-based estimates of B_{SP} gave the estimated coefficients shown in the left hand column of Table 3. Residual diagnostics showed that model III was satisfactory. Because none of the intercept terms were significantly different from zero, the parsimonious model

$$(B_{SP\text{-}PPS})_t = \alpha_0 (PPS)_t + e_t \quad (4)$$

was fitted, giving the results in the right hand column of Table 3. Residual diagnostics were also satisfactory for these models.

Optimal estimation of spawning biomass

We now have available two unbiased estimates of B_{SP}: estimator 1 (i.e., $B_{SP\text{-}DEPM}$) with associated error e', which has an expected value of 0 and variance $\mathrm{Var}(e') = \sigma_1^2$; and estimator 2 (i.e., $B_{SP\text{-}PPS}$) which model IV of the previous section fitted to the values of $B_{SP\text{-}DEPM}$ with error e, which had an expected value of 0 and variance $\mathrm{Var}(e) = \sigma^2$. Thus estimator 2 can be seen to be unbiased and with full error term $(e+e')$. In order to obtain an optimal predictor, i.e., with minimum variance, of spawning biomass ($B_{SP\text{-}Optimal}$), we considered the weighted average of the two estimators above:

$$B_{SP\text{-}Optimal} = (w)\ estimator\ 1 + (1-w)\ \text{estimator 2}),$$
$$\text{with weight } w\text{: } 0<w<1.$$

We must choose the weight w of estimator 1 in order to minimize the variance ($\mathrm{Var}(B_{SP\text{-}Optimal})$) of the estimator $B_{SP\text{-}Optimal}$.

$$\begin{aligned}\mathrm{Var}(B_{SP\text{-}Optimal}) &= \mathrm{Var}(we+(1-w)(e+e')) \\ &= \mathrm{Var}(e+(1-w)e') \\ &= \mathrm{Var}(e) + (1-w)^2\mathrm{Var}(e') + 2(1-w)\\ &\quad \mathrm{covariance}(e,e') \\ &= \sigma^2+(1-w)^2\sigma_1^2+2(1-w)\sigma\sigma_1\rho\end{aligned}$$

where ρ = correlation between e and e'. For Var ($B_{SP\text{-}Optimal}$) to be a minimum, the w derivative must be zero, yielding

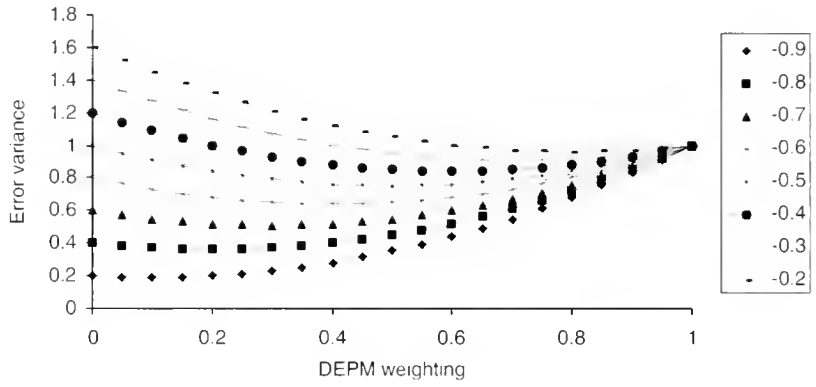

Figure 4

The relationship between error variance between the two estimators for spawning biomass ($B_{SP\text{-}DEPM}$ and $B_{SP\text{-}PPS}$) and the DEPM weighting required to give the optimally weighted estimate of B_{SP} (i.e., $B_{SP\text{-}OPTIMAL}$). Error variance is shown for a range of error correlations from $r = -0.9$ to -0.2.

$$0 = (1-w)\sigma_1 + \sigma\rho,$$

which requires $w = 1 + \sigma\rho/\sigma_1$.

In the event of $\rho = -\sigma_1/\sigma$, $B_{SP\text{-}Optimal}$ will have $w = 0$, i.e., the optimal estimator will just be estimator 2 alone.

The limited sample information available indicates that σ_1 is approximately equal to σ, which we therefore assume in order to simplify the next analysis. Because $B_{SP\text{-}PPS}$ is based on estimates of PPS, which can be estimated with more confidence than $B_{SP\text{-}DEPM}$, it must be expected that often, if not always, Variance($B_{SP\text{-}PPS}$) < Variance($B_{SP\text{-}DEPM}$).

i.e., $\mathrm{Var}(e+e') < \mathrm{Var}(e) + \varepsilon$, for small $\varepsilon > 0$;

i.e., $\sigma^2 + \sigma_1^2 + 2\rho\,\sigma_1\sigma < \sigma^2 + \varepsilon$;

i.e., $2\rho < (-\sigma_1^2 + \varepsilon)/\sigma_1\sigma$.

This requires $\rho < -0.5$ when $\sigma_1 = \sigma$, and ε is small. This relation has an important role in our decision of what is the best estimator.

In Figure 4 the error variance for the estimator $B_{SP\text{-}OPTIMAL}$ is shown for various DEPM weightings and a theoretical range of error correlations (i.e., between e and e') from $r = -0.9$ to -0.2. Our aim was to choose a DEPM weighting that provides minimal error variance along the most stable regions of the suite of error correlation curves, i.e., where the error correlation curves are flattest. The error correlation curves from -0.4 to -0.7 were the most stable and across these the DEPM weightings from 0.3 to 0.7 had the smallest error variance. Therefore we choose 0.5 as our preferred DEPM weighting, which lies centrally within a stable part of the range of theoretical error correlations.

Results

The decline in spawning area in each region (Fig. 2) corresponded to declines in $B_{SP\text{-}DEPM}$ (Table 1), which in turn were reflected by the $B_{SP\text{-}OPTIMAL}$ estimates (Fig. 5). We recognize that imbalance in the intensity of samples between years poses a problem for the interpolation of data between sampling stations but we contend that the collapse in distribution observed is of sufficient contrast to be a reliable reflection of the estimated 70% decrease in *Sardinops* biomass that resulted from the 1998–99 epidemic (Gaughan et al., 2000; Ward et al., 2001). Note that we have used Albany (Fig. 2A) as the primary support for this contention because of the larger data set. The same pattern was observed at all regions, although it was not so marked for the west coast *Sardinops* (Fig. 2D) because estimated B_{SP} (this term hereafter is used generically) had already declined substantially between 1996 and 1998.

Despite sometimes large intervals between consecutive surveys, there were two broad patterns in the trends for *Sardinops* B_{SP} during the 1990s (Fig. 5). Within each region on the south coast (Albany, Bremer Bay, and Esperance), $B_{SP\text{-}DEPM}$ remained relatively high in the early to mid 1990s before decreasing substantially by 1999. In contrast to the results from south coast DEPM surveys, the west coast estimated $B_{SP\text{-}DEPM}$ fluctuated widely (Table 1). This fluctuation resulted in a relatively poor fit of the optimal model and correspondingly wide CIs. Since 1996, when substantially more samples were routinely collected during each survey on the west coast, there has also been a decrease in B_{SP} consistent with that observed on the south coast.

Inconsistency in the determination of variability estimates around some $B_{SP\text{-}DEPM}$ estimates precludes any definitive statements about the relative precision of the

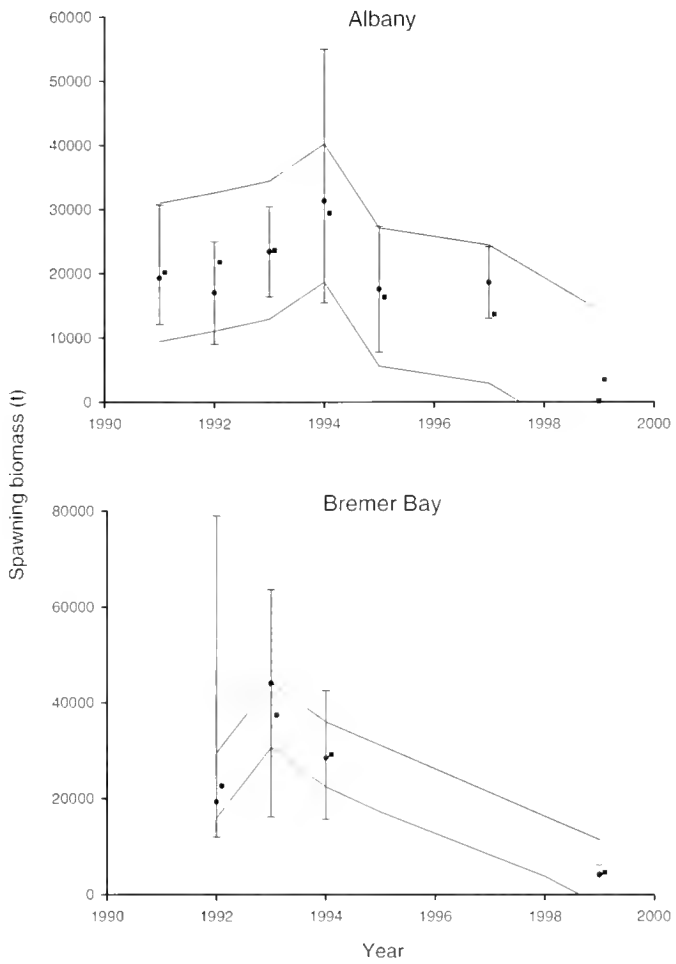

Figure 5

Sardinops sagax $B_{SP\text{-}DEPM}$ estimates (circles with error bars) and $B_{SP\text{-}OPTIMAL}$ estimates (squares with accompanying 95% confidence interval boundaries) at four regions of southwestern Australia. In each case the confidence intervals that extend below the *x*-axis have not been shown.

$B_{SP\text{-}OPTIMAL}$ estimates. Notwithstanding this, the CIs for the optimal estimates always encompassed the DEPM point estimates. Because the CIs were so broad in relation to the point estimates, only the point estimates for $B_{SP\text{-}DEPM}$ and $B_{SP\text{-}OPTIMAL}$ are further compared.

The estimated $B_{SP\text{-}OPTIMAL}$ indicates that for Albany the spawning biomasses were underestimated in 1992 and 1999 and overestimated in 1997 and that the difference between estimates in each case was greater than 25% (Fig. 5, Table 4). Although the DEPM estimated that the Albany B_{SP} remained steady between 1995 (17,544 t) and 1997 (18,597 t), the PPS almost halved from 0.33 to 0.19 for these same surveys (Tables 1 and 2). For Bremer Bay the estimates for $B_{SP\text{-}DEPM}$ and the $B_{SP\text{-}OPTIMAL}$ were within 20% (Fig. 5, Table 4). In Esperance the $B_{SP\text{-}OPTIMAL}$ estimate indicates that the DEPM underestimated B_{SP} by 19% in 1994, but overestimated B_{SP} by 37% in 1999.

The DEPM estimates of *Sardinops* B_{SP} on the west coast had the poorest fit against PPS. Thus, the optimal estimates of B_{SP} differed by >30% in four of the five DEPM-based B_{SP} estimates. In particular, the 1994 and 1999 DEPM estimates were too low, and those for 1996 and 1998 were too high.

Discussion

Egg presence-absence analysis, i.e., proportion of positive stations (PPS), was used to objectively assess changes in the spawning area of *Sardinops* along the south and lower west coasts of WA between 1991 and 1999. The

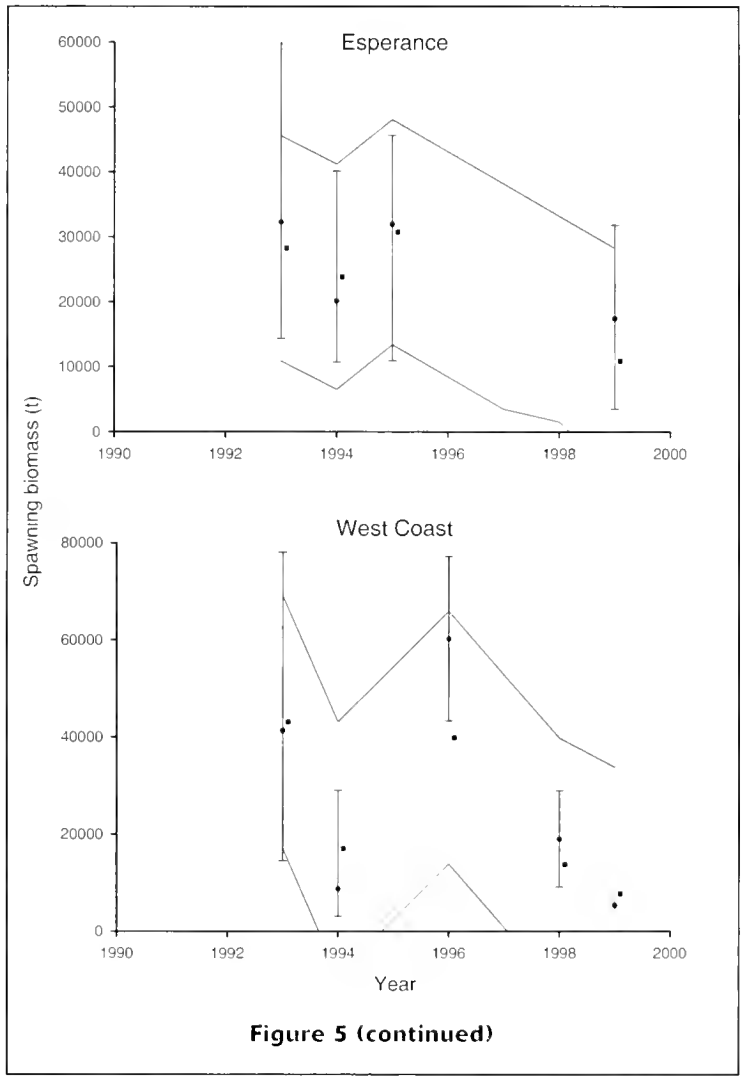

Figure 5 (continued)

collapse in distribution was evident in 1999 for three of the four regions examined and has been attributed to a combination of fishing mortality, several years of poor recruitment, and two mass mortality events (Murray and Gaughan, 2003). The spawning stock in Albany and Bremer Bay decreased to a point where the annual total allowable catch (TAC) in these fisheries was reduced to zero. The concurrent decreases in $B_{SP\text{-}DEPM}$ and PPS at the south coast regions in 1999, estimated shortly after the progression of an epidemic mass mortality (Gaughan et al., 2000), indicates a positive relationship between $B_{SP\ DEPM}$ and PPS. This widespread response provides support for the concept of using the PPS-$B_{SP\ DEPM}$ relationship to objectively detect, albeit retrospectively, particularly suspect estimates of $B_{SP\text{-}DEPM}$.

The marked decline in B_{SP} in 1999 to a very low level at Albany provided sufficient contrast in the time series of data to allow detection of an overestimation of spawning biomass in 1997. Although the difference may not appear to be overly large, the critical factor in this particular case is that the B_{SP} of 18,597 metric tons (t) was seen to be healthy, whereas an estimate of 13,660 t would have clearly indicated to the Management Advisory Committee a downward trend in *Sardinops* B_{SP}. In turn, such a result would have supported the contention that the stock was in decline, which was expected because of several years of poor recruitment, as evidenced by catch-at-age data (Gaughan et al., 2002). Furthermore, in 1998, during the 6 months prior to the mass mortality, the purse-seine fleet in Albany experienced significant difficulties in meeting catch expectations, which also indicated that the stock was at a low level. Although we cannot assess precision of the revised estimates of B_{SP}, it is likely that the $B_{SP\ OPTIMAL}$ for 1997 still overestimates the actual stock size.

The evidence for a decline in B_{SP} at Bremer Bay from 1994 to 1999, as suggested by the decline in PPS, was supported by trends in catch curves for that period, which showed very low levels of recruitment (Gaughan et al., 2002). The recruitment trends ensured that the annual TACs for Bremer Bay after the mid 1990s did not increase but instead were gradually reduced. The

Table 4

Comparison of estimates of spawning biomass for *Sardinops sagax* from four regions in southwestern Australia. Estimates obtained by using the daily egg production method (DEPM) were re-estimated by using a model that considered the proportion of positive stations (PPS, see text and Table 2) during each of the DEPM surveys. In turn, a weighted, or optimal, estimate was derived from the previous two estimates. The difference and ratio between the optimal and the DEPM estimates are provided for comparison. Optimal estimates that fall outside the 95% confidence intervals for the DEPM estimates and optimal:DEPM ratios that differ from 1 by greater than 0.25 are shown in bold type.

	DEPM estimate	PPS estimate	Optimal estimate	DEPM–PPS estimate	Optimal:DEPM
Albany					
1991	19,300	20,190	20,209	−890	1.05
1992	16,994	25,456	21,811	−8462	**1.28**
1993	23,432	22,823	23,653	609	1.01
1994	31,330	26,334	29,438	4996	0.94
1995	17,544	14,484	16,347	−1197	0.93
1997	18,597	8339	13,660	10,258	**0.73**
1999	89	6584	**3488**	−6495	**39.19**
Bremer Bay					
1992	19,280	21,346	22,689	−2066	1.18
1993	44,010	25,195	37,407	−6603	0.85
1994	28,458	24,495	29,204	3963	1.03
1999	4156	4199	4645	−43	1.12
Esperance					
1993	32,252	23,542	28,220	−4032	0.88
1994	20,080	26,838	23,827	−6758	1.19
1995	31,900	28,721	30,705	3179	0.96
1999	17,396	4238	10,875	13,158	**0.63**
West coast					
1993	41,250	48,318	43,048	−7068	1.04
1994	8714	27,350	17,049	−18,636	**1.96**
1996	60,228	20,968	**39,845**	39,260	**0.66**
1998	18,985	9117	13,723	9868	**0.72**
1999	5725	10,940	**7714**	−5665	**1.35**

very poor fit for Esperance may reflect the low sample size or may be indicative of a certain level of decoupling of B_{SP} and PPS not evident in the other south coast regions.

The 1996 estimate for the west coast was hampered by poor estimation of adult parameters resulting from a low number of adult samples obtained; the $B_{SP\text{-}DEPM}$ estimate for that year appeared to be much too high and, intuitively, was not used as the basis for making management decisions at that time. The precautionary decision to use the lower bound rather than the "best" estimate from the 1996 west coast DEPM survey was therefore justified. In contrast, the estimate of $B_{SP\text{-}DEPM}$ of 8714 t in 1994 for the west coast *Sardinops* stock appears to have been too low. The lack of an obvious collapse in distribution off the west coast was partly due to the marked changes in the intensity and distribution of sampling after 1996. Another contributing factor may have been a change in the distribution of the spawning adults because of the anomalously warm water in the Indian Ocean in the late 1990s (Webster et al., 1999) during the last major La Niña. The PPS of only 0.10 in 1998, before the epidemic mortality, may therefore have been the result of behaviorally mediated changes in the distribution of *Sardinops* in response to the warmer than average water temperatures (Gaughan et al., 2000). We recognize that other factors may also have influenced the distribution of *Sardinops* off the west coast but our relatively short time series of data precluded development of more definitive, alternative hypotheses at this time. The potential for unusual environmental conditions to influence spawning behavior applies equally to the south coast *Sardinops*; interpretation of PPS data therefore also requires consideration of environmental conditions in each case. As our time series of biomass estimates is extended through further DEPM surveys, hypotheses regarding the influence of the environment will be further developed. Preliminary hypotheses have already been presented to the Management Advisory Committee and thus form part of current management deliberations.

The results from this retrospective analysis will immediately be used to reassess the B_{SP} estimates obtained for *Sardinops* in WA during the 1990s before

refitting them to Hall's (2000) integrated models for the three adult assemblages on the south coast of WA. The integrated model is tuned with $B_{SP\text{-}DEPM}$ estimates. Therefore, replacing $B_{SP\text{-}DEPM}$ estimates with $B_{SP\text{-}OPTIMAL}$ estimates will result in a model that better simulates the size of the *Sardinops* stocks off southern WA. Although the changes may appear trivial, it is important that re-estimating the most deviant estimates of $B_{SP\text{-}DEPM}$ can be undertaken in a manner that satisfies demands by stakeholders, including industry, for openness and clarity in the provision of scientific advice.

As further DEPM surveys are conducted to assess the status of the *Sardinops* stocks in the five to six years following the 1998–99 mortality event, more reliable relationships between PPS and $B_{SP\text{-}DEPM}$ will be developed. To assist this process, the relative merits of the data for individual DEPM surveys can also be re-examined, particularly those data that this study has indicated to have resulted in poor estimates of $B_{SP\text{-}DEPM}$. An ongoing iterative approach that employs retrospective analyses will be undertaken in an attempt to continuously reduce the variance of the PPS-$B_{SP\text{-}DEPM}$ relationship. This approach will permit further refinement of Hall's (2000) integrated model, a process already in progress (Stephenson et al.[5]) and will therefore contribute to increased confidence in the scientific advice that is provided for management of the *Sardinops* fisheries in WA. Eventually, PPS alone may be sufficient to provide an indication of spawning biomass with an acceptable level of precision.

Besides contributing to the integrated model, the $B_{SP\text{-}OPTIMAL}$ point estimates obtained over nearly a decade in each of four management regions now provide a clearer indication of potential maximum biomass levels against which industry members can plan their businesses. Because of the highly variable recruitment of many small pelagic fish, purse-seine businesses that target fish such as *Sardinops* should not invest at levels that require an economic return based on maximum biomass sizes. For the purse-seine fishing zones in southern WA the maximum spawning biomass from which purse-seine industry members can expect their TACS to be determined are as follows: west coast 40,000 t, Albany 29,000 t, Bremer Bay 37,000 t, and Esperance 30,000 t. Although these values provide an upper limit to business planning, maximum biomasses should not represent investment targets. These values provide an indication of the maximum size for the industry but, because of the "natural and social disarray" that can result "from harvesting marine fish species at the crest of their production" (Smith 2000), the industry should be structured at a level that focuses on longer-term average biomass and that includes industry's ability to survive during periods of low stock size. Maximum and average B_{SP} for *Sardinops* at each of the four management regions in southwestern Australia will be further investigated during ongoing development of the integrated model and as more information becomes available.

Conclusion

Even large numbers of plankton samples can result in imprecise estimates of egg production for use in DEPM calculations (e.g., Mangel and Smith, 1990). Relative trends in spawning area that can be obtained from the same survey by using egg presence-absence analysis provide a secondary means of assessing trends in the status of stocks. This egg presence-absence analysis will be particularly useful for stocks already assessed by using DEPM surveys and more so for those that do not have large amounts of ancillary information, such as long time-series of catch-at-age data, or meaningful effort data.

Detection of either upwards or downwards bias in estimates of B_{SP} will be considered in the integrated model and also communicated to industry members to increase their understanding of the stock in each region. Although this review of biomass trends of *Sardinops* during the 1990s cannot change how *Sardinops* were managed during that period, an increased understanding of both the stock sizes and the science behind the biomass assessments will facilitate ongoing management processes.

Acknowledgments

The authors sincerely thank all Department of Fisheries staff involved with the collection and analysis of historical ichthyoplankton-survey data, in particular Stuart Blight, Gary Buckenara, Cameron Dawes-Smith, Rick Fletcher, Kieren Gosden, Matt Robinson, Rob Tregonning, Ken White, Bruce Webber, and other personnel on PV *Baudin* and PV *McLaughlan*. We also thank Kevern Cochrane (FAO) for a detailed review of an earlier version of this manuscript. We are grateful to the Fisheries Research and Development Corporation (Canberra) that provided funding through Project 92/25 for the earlier DEPM surveys.

Literature cited

Alheit, J.
1993. Use of the daily egg production method for estimating biomass of clupeoid fishes: a review and evaluation. Bull. Mar. Sci. 53:750–767.

Fletcher, W. J.
1991. A test of the relationship between otolith weight and age for the pilchard *Sardinops neopilchardus*. Can. J. Fish. Aquat. Sci. 48:35–38.
1995. Application of the otolith weight-age relationship for the pilchard, *Sardinops sagax neopilchardus*. Can. J. Fish. Aquat. Sci. 52:657–664.
1999. Vertical distribution of pilchard (*Sardinops sagax*)

[5] Stephenson, P., N. Hall, and D. Gaughan. 2004. Unpubl. data. Department of Fisheries, Western Australian Marine Laboratories, North Beach, Western Australia 6920, Australia.

eggs and larvae off southern Australia. Mar. Freshw. Res. 50:117–122.

Fletcher, W. J., N. C. H. Lo, E. A. Hayes, R. J. Tregonning, and S. J. Blight.
1996. Use of the daily egg production method to estimate the stock size of Western Australian sardines (*Sardinops sagax*). Mar. Freshw. Res. 47:819–825.

Fletcher W. J., and N. R. Sumner.
1999. Spatial distribution of sardine (*Sardinops sagax*) eggs and larvae: an application of geostatistics and resampling to survey data. Can. J. Fish. Aquat. Sci. 56:907–914

Fletcher, W. J., and R. J. Tregonning.
1992. The distribution and timing of spawning by the Australian pilchard (*Sardinops sagax neopilchardus*) off Albany, Western Australia. Aust. J. Mar. Freshw. Res. 46:1437–1449.

Fletcher, W. J., R. J. Tregonning, and G. J. Sant.
1994. Interseasonal variation in the transport of pilchard eggs and larvae off southern Western Australia. Mar. Ecol. Prog. Ser. 111:209–224.

Gaughan, D. J., W. J. Fletcher, and J. P. McKinlay.
2002. Functionally distinct adult assemblages within a single breeding stock of the sardine, *Sardinops sagax*: management units within a management unit. Fish. Res. 59:217–231.

Gaughan, D. J., R. W. Mitchell, and S. J. Blight.
2000. Impact of mortality, possibly due to herpes virus, on pilchard *Sardinops sagax* stocks along the south coast of Western Australia in 1998–99. Mar. Freshw. Res. 51:601–612.

Hall, N. G.
2000. Modelling for fishery management, utilising data for selected species in Western Australia. Ph.D. diss.,199 p. Murdoch Univ., Perth, Australia.

Hunter, J. R., and N. C. H. Lo.
1997. The daily egg production method of biomass estimation: some problems and potential improvements. Ozeanografika 2:41–69.

Mangel, M., and P. E. Smith.
1990. Presence-absence sampling for fisheries management. Can. J. Fish. Aquat. Sci. 47:1875–1887.

Murray, A. G., and D. J. Gaughan.
2003. Using an age-structured model to simulate the recovery of the Australian pilchard (*Sardinops sagax*) population following epidemic mass mortality. Fish. Res. 60:415–426.

Parker, K.
1985. Biomass model for the egg production model. *In* An egg production method for estimating spawning biomass of pelagic fish: application to the northern anchovy, *Engraulis mordax* (R. M. Lasker, ed.), p. 5–6. NOAA Tech. Rep. NMFS 36.

Picquelle, S., and G. Stauffer.
1985. Parameter estimation for an egg production method of anchovy biomass assessment. *In* An egg production method for estimating spawning biomass of pelagic fish: application to the northern anchovy, *Engraulis mordax* (R. M. Lasker, ed.), p. 7–15. NOAA Tech. Rep. NMFS 36.

Smith, P. E.
2000. Pelagic fish early life history: CalCOFI overview. *In* Fisheries oceanography: an integrated approach to fisheries ecology and management (P. J. Harrison and T. R. Parsons, eds.), p. 8–28. Blackwell Science, Oxford, UK.

Smith, P. E., H. Santander, and J. Alheit.
1989. Comparison of the mortality rates of pacific sardine, *Sardinop sagax*, and Peruvian anchovy, *Engraulis ringens*, eggs off Peru. Fish. Bull. 87:497–508.

Uphoff, J. H.
1993. Determining striped bass spawning stock status from the presence or absence of eggs in ichthyoplankton survey data. N. Am. J. Fish. Manag. 13:645–657.

Ward T. M., F. Hoedt, L. McLeay, W. F. Dimmlich, M. Kinloch, G. Jackson, R. McGarvey, P. J. Rogers, and K. Jones.
2001. Effects of the 1995 and 1998 mass mortality events on the spawning biomass of sardine, *Sardinops sagax*, in South Australian waters. ICES J. Mar. Sci. 58(4):865–875.

Webster P. J., A. M. Moore, J. P. Loschnigg, and R. R. Leben.
1999. Coupled ocean-atmosphere dynamics in the Indian Ocean during 1997–98. Nature 401:356–360.

Wolf, P., and P. E. Smith.
1986. The relative magnitude of the 1985 Pacific sardine spawning biomass off southern California. CalCOFI Rep. 27:25–31.

Zenitani, H., and S. Yamada.
2000. The relation between spawning area and biomass of Japanese pilchard, *Sardinops melanostictus*, along the Pacific coast of Japan. Fish. Bull. 98:842–848.

Appendix 1—Derivation of model III from model II

We start with model II

$$B_{SP\_DEPM} = \alpha_0 PPS^{\lambda} + e_i.$$

For brevity, y is used to denote PPS. We first note that $y^{\lambda}=yy^{(\lambda-1)}$. Now we obtain the Taylor series expansion of $y^{(\lambda-1)}$ about $y=1$ giving

$$y^{(\lambda-1)} = 1 + (\lambda-1)(y-1) + (\lambda-1)(\lambda-2)/2!(y-1)^2 + (\lambda-1)(\lambda-2)(\lambda-3)/3!(y-1)^3 + \ldots .$$

Multiplying this expression through by y gives

$$y^{\lambda} = y + y(y-1)(\lambda-1) + y[\text{terms involving second and higher powers of } (y-1)].$$

Because y is a proportion, it satisfies $0<y<1$ so that the higher powers of $(y-1)$ will be individually and collectively small. If y is close to 0.5, a further algebraic simplification of the second term is possible, giving the identity

$$y(y-1) = -0.25 + (y-0.5)^2.$$

When y is in the range $0.25<y<0.75$, the right-hand side of this identity remains close to -0.25. Thus model II may be simplified to

$$B_{SP\_PPS} = \alpha_0(PPS) - 0.25\alpha_0(\lambda-1) + e_i$$

which is the form of model III.

Abstract—Understanding recolonization processes of intertidal fish assemblages is integral for predicting the consequences of significant natural or anthropogenic impacts on the intertidal zone. Recolonization of experimentally defaunated intertidal rockpools by fishes at Bass Point, New South Wales (NSW), Australia, was assessed quantitatively by using one long-term and two short-term studies. Rockpools of similar size and position at four sites within the intertidal zone were repeatedly defaunated of their fish fauna after one week, one month, and three months during two short-term studies in spring and autumn (5 months each), and every six months for the long-term study (12 months). Fish assemblages were highly resilient to experimental perturbations—recolonizing to initial fish assemblage structure within 1–3 months. This recolonization was primarily due to subadults (30–40 mm TL) and adults (>40 mm TL) moving in from adjacent rockpools and presumably to abundant species competing for access to vacant habitat. The main recolonizers were those species found in highest numbers in initial samples, such as *Bathygobius cocosensis*, *Enneapterygius rufopileus*, and *Girella elevata*. Defaunation did not affect the size composition of fishes, except during autumn and winter when juveniles (<30 mm TL) recruited to rockpools. It appears that Bass Point rockpool fish assemblages are largely controlled by postrecruitment density-dependent mechanisms that indicate that recolonization may be driven by deterministic mechanisms.

Fish recolonization in temperate Australian rockpools: a quantitative experimental approach

Shane P. Griffiths

Environmental Science

and

Institute for Conservation Biology
University of Wollongong
Wollongong, New South Wales, Australia
Present address: CSIRO Marine Research
233 Middle Street
Cleveland, Queensland 4163 Australia

Email address: shane.griffiths@csiro.au

Ron J. West

Environmental Science
University of Wollongong
Wollongong, New South Wales, Australia

Andy R. Davis

Institute for Conservation Biology
University of Wollongong
Wollongong, New South Wales, Australia

Ken G. Russell

School of Mathematics and Applied Statistics
University of Wollongong
Wollongong, New South Wales, Australia

Manuscript submitted 28 April 2003 to the Scientific Editor's Office.

Manuscript approved for publication 5 May 2004 by the Scientific Editor.

Fish. Bull. 102:634–647 (2004).

Rocky intertidal fishes are faced with many biotic (competition and food availability) and abiotic (temperature and salinity) factors that can influence their distribution and abundance (Gibson, 1982). Despite occupying a dynamic environment, the fish assemblages in intertidal rockpools have been widely shown to remain persistent through time (Grossman, 1982, 1986; Collette, 1986). These communities can also rapidly return to their original state after major or even catastrophic perturbations (Moring, 1996). Such resilience is less common among assemblages of invertebrates (Connell, 1972; Astles, 1993) because recolonization of substrata is normally dependent upon successful larval settlement (Paine and Levin, 1981). In contrast, fish can rapidly colonize available habitat by larval recruitment from the plankton (Willis and Roberts, 1996, Beckley, 2000; Griffiths 2003a) but also by the relocation of subadults and adults from adjacent rockpools (Beckley, 1985a; Griffiths, 2003a). Under natural conditions rockpools can be defaunated by events such as hurricanes (Moring, 1996) and, in some regions, by seasonal freezing of rockpool water (Thomson and Lehner, 1976; Moring, 1990). These events can create new microhabitats or open existing ones for fish to colonize, and therefore have the potential to change fish assemblage structure.

Understanding recolonization processes of intertidal fish assemblages is integral for predicting the consequences of natural or anthropogenic impacts on the intertidal community. The role of disturbance and recolonization processes in structuring inter-

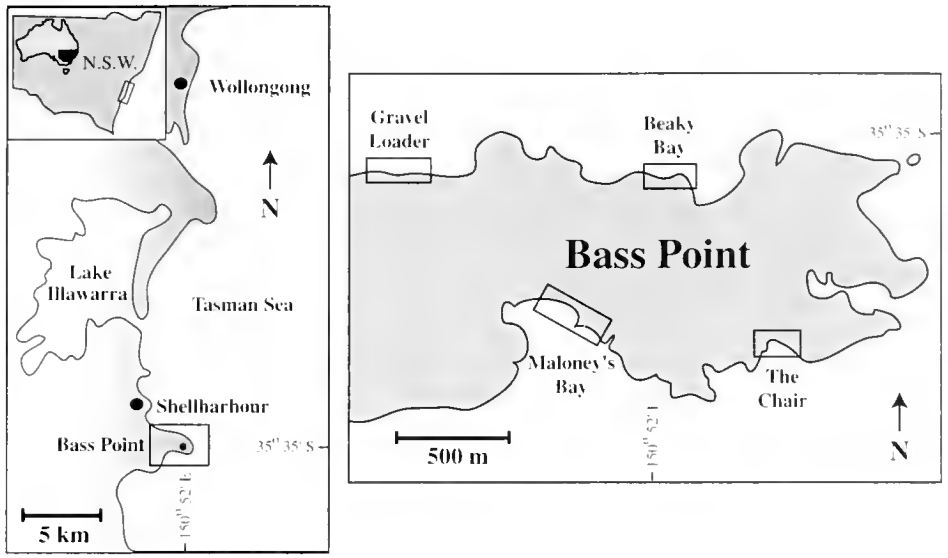

Figure 1

Map illustrating the four sampling sites at Bass Point and the location of the study location in the Illawarra region, New South Wales, Australia.

tidal rockpool fish assemblages has received considerable attention in many countries of the world (Bussing, 1972; Matson et al., 1986; Yoshiyama et al., 1986; Prochazka and Griffiths, 1992; Lardner et al., 1993; Prochazka, 1996; Faria and Almada, 1999; Silberschneider and Booth, 2001). Such studies have identified patterns in the rates of recovery, variation in species and size composition of recolonizing fish assemblages (Polivka and Chotkowski, 1998; Beckley, 2000), and homing abilities of many intertidal fishes (Green 1971; Yoshiyama et al., 1992; Griffiths, 2003b).

Rockpools can be regarded as "island' habitats (Underwood and Skilleter, 1996) among an inhospitable rocky landscape. Therefore, there is probably a balance between immigration (recruitment and relocation) and emigration (mortality) of fishes after a disturbance, *sensu* the equilibrium theory of island biogeography (MacArthur and Wilson, 1967). After a period of time, the number of species and individuals in a defaunated rockpool can be expected to reach an asymptote when a carrying capacity is reached. It is difficult to generalize about recolonization rates of rockpools by fishes from the current literature mainly owing to the diversity of methods used, their differing effectiveness in sampling fish, and the varying intensity of the sampling regime. For example, most studies have used only small sample sizes (<10 pools) and have sampled at a range of time intervals from days (Mistry et al., 1989; Matson et al., 1986; Polivka and Chotkowski, 1998) to years (Thomson and Lehner, 1976; Lardner et al., 1993; Mahon and Mahon, 1994). A second problem in measuring and comparing fish recolonization patterns between studies is that many researchers have sampled fish using an anesthetic (Mahon and Mahon, 1994; Pfister, 1995, 1997) or ichthyocide (Beckley, 1985a, 1985b, 2000; Willis and Roberts, 1996; Silberschneider and Booth, 2001), which may affect subsequent catches (Yoshiyama et al., 1986) and possibly result in fish assemblages never reaching preperturbation conditions (see Mok and Wen, 1985; Lockett, 1998).

Nonetheless, recolonization of rockpools by fishes is generally a rapid process, beginning within days, or even hours, after defaunation (Collette, 1986), and complete recolonization to preperturbation levels can take a few weeks (Collette, 1986; Faria and Almada, 1999) to several months (Mok and Wen, 1985; Willis and Roberts, 1996; Polivka and Chotkowski, 1998).

The aims of this study were to quantitatively determine 1) the period required for intertidal rockpools to recover to preperturbation levels, 2) the fish species (permanent residents, opportunist, or transients) responsible for recolonizing rockpools, 3) whether recolonization patterns differ between the four sites at Bass Point and between the times of year when defaunation took place, and 4) whether fish comprise different life-history stages before and after a disturbance (sampling)—by examination of length-frequency distributions.

Methods

Study site and experimental design

Spatial and temporal variation in fish recolonization patterns were investigated in three separate studies undertaken along the north- and south-facing rocky platforms at Bass Point (34°58'S, 150°93'E), New South Wales, Australia (Fig. 1). Bass Point is a large rocky headland that extends approximately 3 km into the Tasman Sea. Two short-term recolonization studies (each around 5

months in duration) were undertaken in spring–summer and autumn–winter (hereafter referred to as spring and autumn studies, respectively), and a long-term recolonization study spanned a 12-month period. Rockpools for each of the three studies were selected at four sites at Bass Point, NSW, which are named Maloney's Bay (MB), The Chair (TC), Gravel Loader (GL), and Beaky Bay (BB) (Fig. 1). Each of the four sites are separated by about 1 km. Rockpools were selected at each site (50–200 m apart) according to similar physical parameters (i.e., volume, surface area, and substrate type) and particularly according to their vertical elevation on the rock platform. Because higher pools might have less chance of fish recolonization because they are less frequently inundated by seawater (Griffiths et al., 2003), every effort was made to select pools located in the mid-intertidal zone (1–1.5 m above MLLW [mean lower low water]) and, although pools were visually similar, they varied in volume, ranging from 762 to 2160 liters (or 0.76–2.16 m^3). The bottom of the rockpools consisted of pebbles, cobbles, and small boulders.

For the short-term studies, four rockpools were sampled and fish removed at each of the four sites. In the spring study (beginning 7 September 1999), they were then resampled 1 week, 1 month, and 3 months after the preceding sampling date (referred to as the "1-week," "1-month," and "3-month" samples in this article). This study ended on 8 February 2000, after a period of 5 months. After this date a period of at least three months was given for pools to re-establish fish assemblages before beginning the autumn study on 15 May 2000. Rockpools were sampled in exactly the same manner as for the spring study, with sampling ending on 17 September 2000. For each study, 64 samples were taken giving a total of 128 samples for the short-term studies. It is important to note that although every effort was made to resample pools after exactly the same time intervals, this was not possible because of daily time and height of tides and wave heights. For example, for the "1 week" samples, the number of days between samples was actually between 7 and 10 days.

To determine whether frequent sampling in the short-term studies affected the structure of rockpool fish assemblages, a long-term study was undertaken by using four different rockpools at the same four sites that were sampled in the short-term studies. Four rockpools at each site were considered adequate because Griffiths (2003a) was able to detect significant differences in the numbers of fish species and individuals in rockpools between sites and months using four rockpools per site in the same region that was surveyed in our study. Rockpools were initially sampled on 22 September 1999 and then resampled twice at intervals of six months (20 April 2000 and 11 September 2000). A total of 48 samples were taken for this study.

Data collection

Fish were collected by hand after completely emptying each rockpool with a VMC 12V battery-powered bilge pump of 9029 L/h capacity by using the methods of Griffiths (2000). A thorough search of each pool was conducted by overturning all rocks and boulders, searching all crevices and shaking algal fronds until all fish that could be seen were removed. Fishes were identified and total lengths (TL) were measured. Fork length (FL) was also measured for economically significant species. Fish were categorized as being juveniles (<30 mm), subadults (30–40 mm), or adults (>40 mm). Fish were then released alive into rockpools or the shallow subtidal 10–30 m away from the rockpool being sampled, which was considered to be the approximate distance that fish may be displaced by waves and surge during significant natural disturbances, such as storms. Each species was categorized by its residential status in rockpool habitats according to the definitions of Griffiths (2003c) in order to better understand the types of fish responsible for recolonization. These categories were "permanent residents," "opportunists," and "transients."

Statistical analyses

A repeated-measures ANOVA (RM-ANOVA) was used (SPSS vers. 6.1; SPSS, Chicago, IL) to test for significant differences in the numbers of species and individuals between sampling intervals (within-subjects factor) and sites (among-subjects factor). Short- and long-term experiments were analyzed with two separate RM-ANOVAs. For the short-term study a third factor of season (i.e., spring or autumn; among-subjects factor) was added. All factors were considered fixed. Assumption of sphericity of the variance-covariance matrix was tested by using Mauchly's criterion and, if violated, F tests were performed with Greenhouse-Geisser–adjusted degrees of freedom. Student-Newman-Keuls (SNK) tests were used for *a posteriori* comparisons among means (numbers of species and individuals) in RM-ANOVAs.

Nonmetric multidimensional scaling (nMDS) was used to examine similarities in fish assemblage structure between sampling intervals and sites. Data were fourth-root transformed, to reduce the influence of highly abundant taxa, and a similarity matrix was constructed by using the Bray-Curtis similarity coefficient (Clarke, 1993). Stress values are given for all ordination plots; these values describe the quality of the representation of multidimensional relationships of the data in a two-dimensional plane. Stress factors of less than 0.2 (<0.2 is considered to give a good representation of sample "relatedness" and to prevent the prospect of drawing false inferences) were obtained for each ordination (Clarke, 1993).

Analysis of similarities (ANOSIM) was used to test whether fish assemblages in *a priori* groups differed statistically (Clarke, 1993). Abundance data for each species were pooled for the four rockpools at each site and time. Each ANOSIM comparison involved generating 4999 random permutations of the data to calculate the probability that observed differences in the structure of the fish assemblages among *a priori* groups could arise

by chance. Similarity percentages (SIMPER) were used to determine which species were responsible for differences between selected groups. This analysis involved calculating the average contribution of each species in each pair of groups and comparing this contribution to the overall dissimilarity of fish assemblages between the groups. All multivariate analyses were carried out with PRIMER (Plymouth routines in multivariate ecological research) software (version 5.2.2, PRIMER-E Ltd., Roborough, Plymouth, UK).

Results

Composition of rockpool fish assemblages

A total of 3658 fish representing 38 species and 19 families was caught in 176 samples from 32 rockpools at Bass Point between 7 September 1999 and 22 September 2000 (Table 1), corresponding to densities of 0.5 and 19 species/m^3 (mean 4.4 [±2.9] /m^3) and 0.5 and 80 fish/m^3 (mean 15.6 [±14.6] /m^3), respectively. The most numerically abundant taxa were permanent rockpool residents representing the families Gobiidae (*Bathygobius cocosensis*), Tripterygiidae (*Enneapterygius rufopileus*), Clinidae (*Heteroclinus whiteleggi* and *H. fosciatus*), Blenniidae (*Parablennius intermedius*), and Gobiesocidae (*Aspasmogaster costatus*), although the temporary resident *Girella elevata* was the third most abundant species. The ten most numerically abundant species represented 92% of the catch (Table 1). Three species, *G. elevata*, *Scorpis lineolatus*, and *Myxus elongatus*, represented by 504 fish were considered to be of economic significance. All economically important fishes were caught as juveniles in the rockpools and 89% of the fish measured less than 100 mm FL.

Numbers of species and individuals

For the short-term studies, the mean number of species differed significantly between sampling intervals and sites (RM-ANOVA, Table 2). With respect to the site factor, there were significantly more species caught at BB than at the other three sites and the latter three sites did not differ from each other (SNK test). Only the "1-week" samples accounted for significantly fewer species than the initial samples (Fig. 2). However, the mean number of species caught in the "1-month" and "3-month" samples did not differ significantly from the initial samples at all sites (Fig. 2).

The mean number of individuals differed significantly between sampling intervals and sites, although there was also a significant *time×site* interaction (RM-ANOVA, Table 2). A close investigation of the significant *interval×site* interaction, with primary interest in the interval factor, revealed that the number of individuals in the initial samples did not differ significantly from samples taken after three months at the exposed sites (MB and TC), but they did differ significantly at sheltered locations (GL and BB) (Fig. 2). It appeared that the

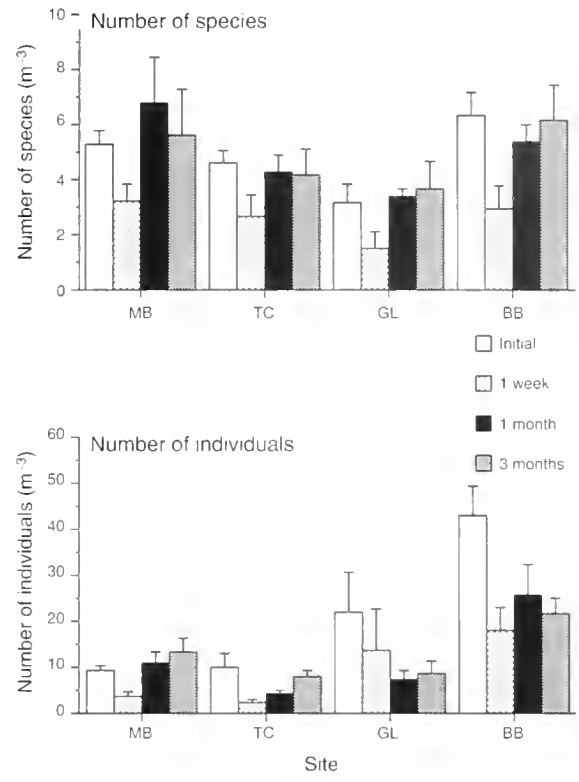

Figure 2

Mean (±SE) numbers of species and individuals (m^{-3}) caught in rockpools at Bass Point, New South Wales between 7 September 1999 and 17 September 2000 during the short-term recolonization studies (combined for spring and autumn) between sampling intervals separated by 1 week, 1 month, and 3 months. Key to sites: Maloney's Bay (MB), The Chair (TC), Gravel Loader (GL), Beaky Bay (BB).

Loader and Beaky Bay sites initially supported unusually high numbers of individuals and these high numbers may have accounted for significantly fewer individuals caught in the subsequent samples (Fig. 2).

For the long-term study, the number of individuals significantly differed among sampling times but did not for number of species (RM-ANOVA, Table 3). The significant difference in the mean number of individuals was due to fewer individuals caught in the "12-month" samples when fish numbers were pooled for all sites (SNK test, Fig. 3).

Variation in abundance of major recolonizing species

The rank abundances of the numerically dominant species were consistent for *B. cocosensis* and *E. rufopileus* across all sampling intervals for all studies, even though their relative abundances varied considerably (Table 4). In contrast, the ranks of the least common of the six species, namely *H. whiteleggi*, *P. intermedius*,

Table 1

Numbers of fish for each species caught from rockpools at four sites at Bass Point, NSW, during short-term (spring and autumn) and long-term recolonization studies conducted between 7 September 1999 and 22 September 2000. * = species of commercial or recreational significance (or both).

Family and scientific name	Spring study	Autumn study	Long-term study	Total
Muraenidae				
Gymnothorax prasinus	41	13	16	70
Gymnothorax cribroris	1	—	—	1
Plotosidae				
Cnidoglanis macrocephalus	1	—	—	1
Gobiesocidae				
Alabes dorsalis	—	2		2
Aspasmogaster costatus	134	41	65	240
Aspasmogaster liorhyncha	5	20	4	29
Syngnathidae				
Urocampus carinirostris	1	—	—	1
Scorpaenidae				
Scorpaena cardinalis	1	—	—	1
Serranidae				
Acanthistius ocellatus	33	35	16	84
Epinephelus daemeli	—	2	—	2
Plesiopidae				
Trachinops taeniatus	1	—	—	1
Girellidae				
Girella elevata	210	93	74	377
Scorpididae				
Microcanthus strigatus	1	—	—	1
*Scorpis lineolatus**	94	10	16	120
Pomacentridae				
Abudefduf vaigiensis	1	—	—	1
Parma microlepis	—	1	—	1
Chironemidae				
Chironemus marmoratus	30	11	10	51
Mugilidae				
*Myxus elongatus**	3	4	—	7
Labridae				
Halichoeres nebulosus	—	1	—	1
Notolabrus gymnogenis	—	1	—	1
Blennidae				
Parablennius intermedius	102	78	47	227
Istiblennius meleagris	8	10	4	22
Tripterygiidae				
Lepidoblennius haplodactylus	22	26	22	70
Norfolkia clarkei	7	4	3	14
Enneapterygius rufopileus	354	188	157	699
Clinidae				
Heteroclinus fasciatus	59	48	38	145
Heteroclinus nasutus	1	—	—	1
Heteroclinus heptacolus	24	—	1	25
Heteroclinus johnstoni	—	2	—	2
Heteroclinus whiteleggi	138	66	39	243
Ophiclinus gracilis	15	16	6	37

continued

Table 1 (continued)

Family and scientific name	Spring study	Autumn study	Long-term study	Total
Gobiidae				
Bathygobius cocosensis	583	293	285	1161
Callogobius depressus	6	2	7	15
Callogobius mucosus	1	—	—	1
Priolepis cincta	1	—	—	1
Gobiidae sp.	1	—	—	1
Microdesmidae				
Gunnellichthys monostigma	1	—	—	1
Tetraodontidae				
Torquigener pleurogramma	—	1	—	1
Totals	1880	968	810	3658

Table 2

Results of repeated-measures ANOVAs for significant differences in numbers of species and number of individuals (/m^3) caught at Bass Point during two short-term recolonization studies among sampling intervals (time) (within-subjects factor), seasons (spring and autumn) and sites (among-subjects factors). Both numbers of species and individuals data were $\log_{10}(x+1)$ transformed before analysis, which removed heteroscedasticity in the data. Mauchly's criterion for sphericity of variances was violated for number of species (P=0.025); therefore the analysis was performed with Greenhouse-Geisser–adjusted degrees of freedom. Mean squares (MS) and significance levels are shown and significant results are given in boldface. * = P<0.05; ** = P<0.01; *** = P<0.001.

	Number of species		Number of fish	
Source	df	MS	df	MS
Among subjects				
Season (*Se*)	1	14.94	1	1292.24
Site (*S*)	3	**46.80****	3	**2782.52****
S×*Se*	3	3.66	3	63.53
Residual	24	9.38	24	370.27
Within subjects				
Time (*T*)	2.16	**18.03*****	3	**825.70*****
T×*S*	6.47	2.93	9	**247.99****
T×*Se*	2.16	2.54	3	94.86
T×*S*×*Se*	6.47	1.89	9	137.84
Residual	51.75	1.41	72	79.71
Mauchly's criterion *W*		**0.569***		0.625

Table 3

Results of repeated-measures ANOVAs for significant differences in numbers of species and number of individuals (/m^3) caught at Bass Point during the long-term recolonization study among sampling intervals (within-subjects factor) and sites (among-subjects factors). Both numbers of species and individuals data were $\log_{10}(x+1)$ transformed before analysis, which removed heteroscedasticity in the data. Mean squares (MS) and significance levels are shown and significant results are given in bold. ** = P<0.01.

	Number of species		Number of individuals
Source	df	MS	MS
Among subjects			
Site (*S*)	3	86.93	176.18
Residual	12	27.49	169.67
Within subjects			
Time (*T*)	2	3.26	**451.38****
T×*S*	6	4.44	111.82
Residual	24	2.84	55.45
Mauchly's criterion *W*		0.622	0.705

and *A. costatus*, varied considerably among sampling intervals for each study. This result probably reflects their generally low abundances, because differences in ranks can be a result of a few incidences of low individual counts.

The mean number of the six most abundant recolonizing species showed considerable variability in space and time. For the short-term study, densities of these species differed significantly among sites and among time intervals or at least for higher order interactions containing these effects (Table 5). No definitive conclusions could be made regarding the effects of defaunation on these species because short-term recolonization patterns for each species were clearly variable within and among seasons (Fig. 4). However, the mean number of fish was generally highest in initial samples and low-

Table 4

Ranked abundances of the six most abundant species overall for each sampling interval in the spring, autumn, and long-term experiments. Total numbers of fish caught during each sampling occasion from 16 rockpools from four sites are shown in parentheses. 1=initial samples; 2=samples taken after 1 week; 3=samples taken after 1 month; 4=samples taken after 3 months. Species having equally ranked abundances are denoted by an "=" sign.

	Spring study				Autumn study				Long-term study		
Species	1	2	3	4	1	2	3	4	1	2	3
Bathygobius cocosensis	1 (153)	1 (69)	1 (73)	1 (59)	2 (81)	1 (20)	1 (58)	1 (41)	1 (115)	1 (114)	1 (63)
Enneapterygius rufopileus	2 (109)	2 (50)	4 (33)	2 (46)	1 (84)	2 (12)	2 (29)	3 (25)	2 (73)	2 (43)	2 (41)
Girella elevata	3 (46)	3 (36)	3 (40)	3 (38)	3 (34)	3 (10)	3 (16)	5 (13)	5 (5)	6 (3)	4 (12)
Heteroclinus whiteleggi	6 (11)	=4 (7)	2 (51)	5 (35)	6 (9)	=4 (5)	6 (7)	2 (37)	6 (4)	4 (27)	6 (8)
Parablennius intermedius	4 (27)	=4 (7)	6 (10)	6 (23)	=4 (14)	=4 (5)	4 (15)	4 (23)	4 (14)	5 (14)	3 (19)
Aspasmogaster costatus	5 (21)	=4 (7)	5 (13)	4 (36)	=4 (14)	6 (3)	5 (8)	6 (7)	3 (22)	3 (34)	5 (9)

est in the 1-week samples at each site for the majority of dominant species. For the long-term study only the mean number of *B. cocosensis* and *E. rufopileus* differed significantly among sampling times (Table 5), and this difference was due to lower numbers being caught in the 12-month samples (Fig. 4).

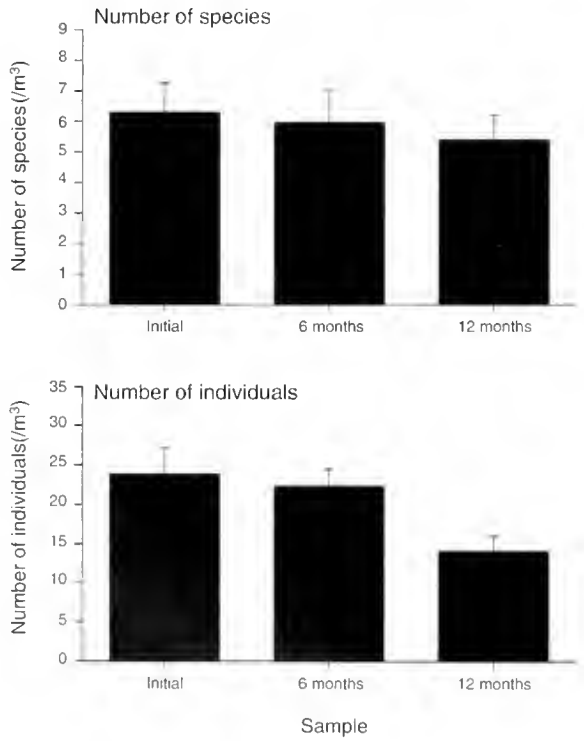

Figure 3

Mean (±SE) numbers of species and individuals (/m³) caught in rockpools at Bass Point, New South Wales, between 22 September 1999 and 11 September 2000 (pooled for all four sites) during the long-term recolonization study. Intervals between sampling for the long-term study were six months.

Fish assemblage structure

No clear patterns emerged in the nMDS ordination plots, with the exception of separation of the "1 week" samples from all other samples at BB during the autumn study (Fig. 5). ANOSIM supported these visual interpretations of ordination plots and revealed that fish assemblages did not differ significantly among sampling times at any of the four sites for the spring and long-term studies (Table 6) because abundant species *E. rufopileus*, *B. cocosensis*, *H. fasciatus*, and *P. intermedius* were common in all samples (SIMPER analysis). For the autumn study, the results of ANOSIM complemented those of RM-ANOVA in that significant differences among sampling intervals were detected only at BB (Table 6). At this site the initial samples and "1-week" samples differed significantly in their fish assemblages, which was due to higher numbers of *G. elevata* and *B. cocosensis* in the initial samples (SIMPER analysis).

Length-frequency distributions

Removal of fishes from rockpools did not have any apparent effects on the length-frequency distributions for at least two species (*B. cocosensis* and *E. rufopileus*) for which there were sufficient data to construct length-frequency histograms. Unfortunately, the less abundant recolonizing species, namely *P. intermedius*, *A. costatus*, and *H. whiteleggi*, were caught in too few numbers to ascertain the impacts of defaunation on their size compositions. Rockpools were mainly recolonized by subadults and adults for *B. cocosensis* and *E. rufopileus* in all three studies (Figs. 6 and 7). However, cohorts of small juveniles (15–30 mm) were evident in the "3-month" samples during spring and the initial autumn studies (February to June), which could then be clearly identified in subsequent samples (Figs. 6 and 7).

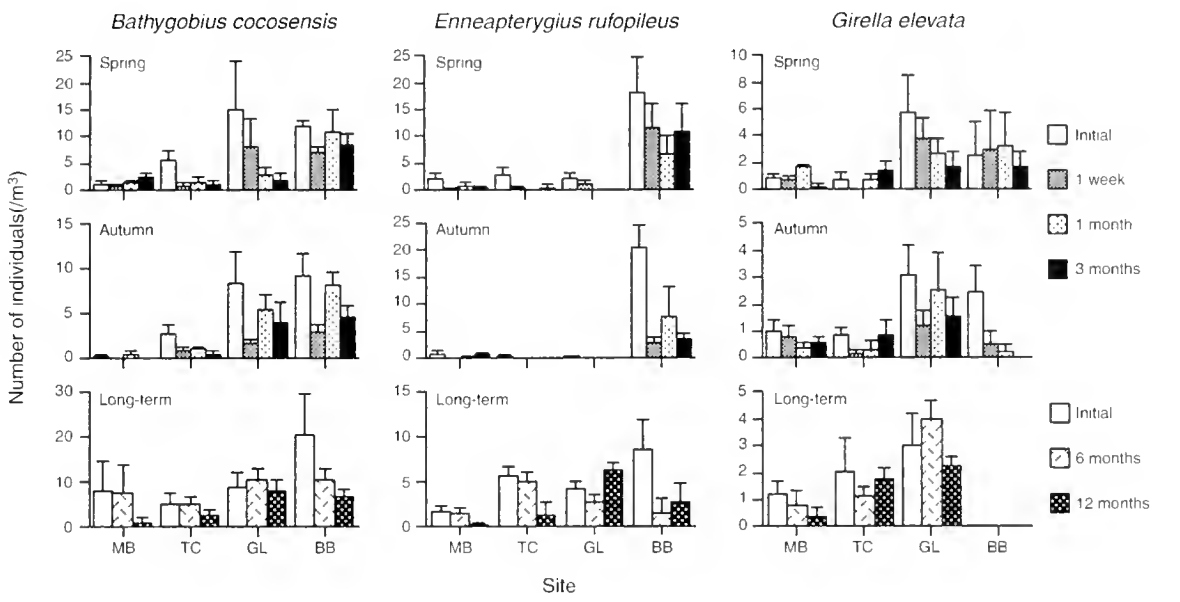

Figure 4

Mean (±SE) numbers of fish (/m³) for the six most abundant species caught from rockpools at four sites (MB=Maloney's Bay, TC=The Chair, GL=Gravel Loader, BB=Beaky Bay) during short-term (spring and autumn) (four sampling events) and long-term (three sampling events) recolonization studies undertaken between 7 September 1999 and 22 September 2000.

Table 5

Results of repeated-measures ANOVAs for significant differences in numbers of individuals (/m³) representing the six most abundant species caught at Bass Point during the short-term recolonization studies among sampling intervals (within-subjects factor) and sites and seasons (among-subjects factors). Data were $\log_{10}(x+1)$ transformed before analysis to remove heteroscedasticity in the data. Mauchly's criterion for sphericity of variances was violated ($P<0.001$) for species denoted by ^{G}; therefore analysis was performed using Greenhouse-Geisser–adjusted degrees of freedom. Greenhouse-Geisser degrees of freedom used for within-subjects factors where Mauchly's criterion for sphericity of variances was violated ($P<0.001$): *Time* (T) = 1.55; $Se \times T$ = 1.55; $S \times T$ = 4.64; $Se \times S \times T$ = 4.64; Residual = 34.14. Mean squares and significance levels are shown and significant results are given in bold. Degrees of freedom are shown in parentheses. * = $P<0.05$; ** = $P<0.01$; *** = $P<0.001$.

	Among-subjects factors				Within-subjects factors				
Species	Season (*Se*) (1)	Site (*S*) (3)	*Se*×*S* (3)	Residual (24)	Time (*T*) (3)	*Se*×*T* (3)	*S*×*T* (9)	*Se*×*S*×*T* (9)	Residual (72)
Bathygobius cocosensis^{G}	5.20	**24.50*****	3.62	2.18	**43.99*****	2.21	**10.68****	3.22	1.70
Enneapterygius rufopileus^{G}	0.66	**4.38*****	0.01	0.17	**0.70*****	0.05	**0.08***	**0.07***	0.04
Girella elevata	0.22	0.49	0.03	0.28	**0.12****	0.07	**0.05***	**0.07****	0.03
Heteroclinus whiteleggi^{G}	12.09	**20.77***	1.65	4.90	**18.99*****	**6.61***	**4.31***	4.22	1.72
Parablennius intermedius	0.00	**4.85***	0.20	1.20	**7.88****	0.20	1.92	0.29	1.07
Aspasmogaster costatus	0.37	**0.54****	0.15	0.10	**0.11***	0.09	0.03	**0.07***	0.03

Discussion

This study has shown that fish assemblages can quickly return to preperturbation levels after significant disturbance. This resilience appears to be driven mainly by postsettlement movements of fishes, although recruitment may periodically play a significant role in population replenishment. Not only does this provide an insight into the ecology of rockpool fish assemblages, but this information may also provide a basis for future sampling protocols where the confounding effects of sampling may be minimized.

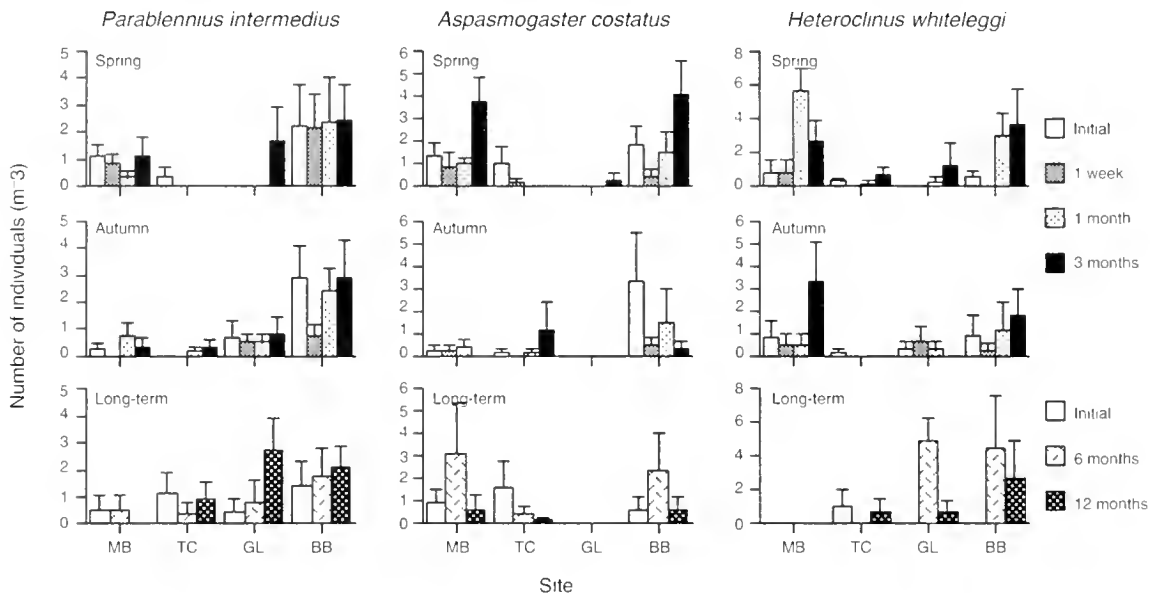

Figure 4 (continued)

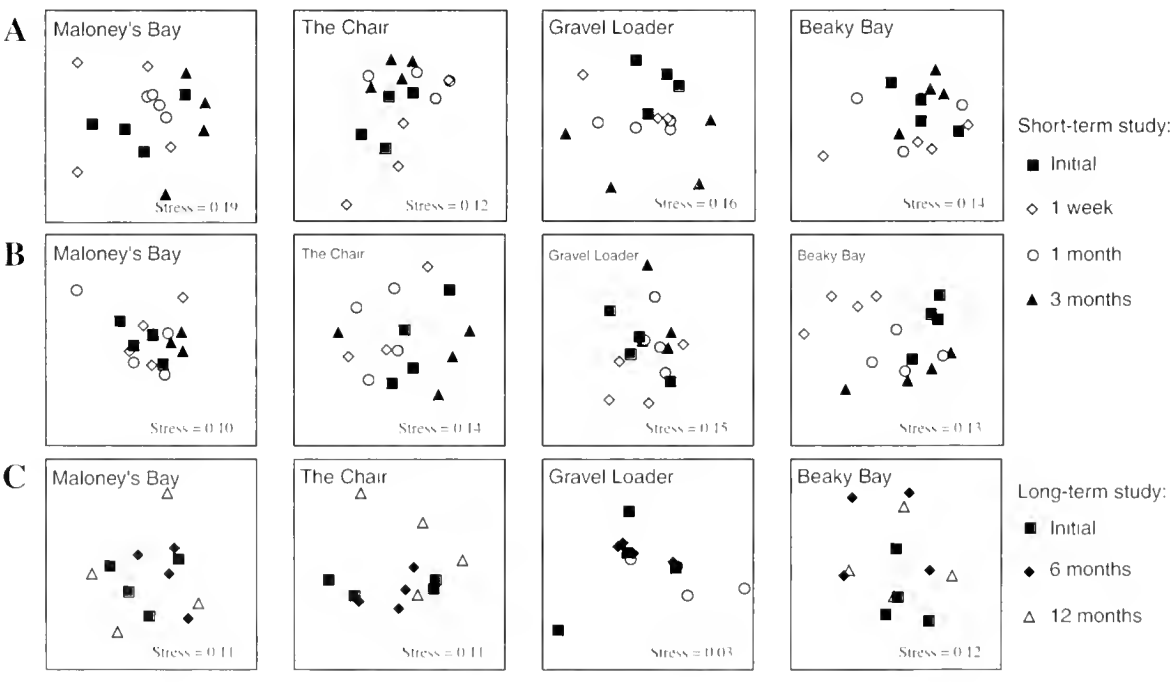

Figure 5

Nonmetric multidimensional scaling (MDS) plots for comparison of fish assemblages from four sites at Bass Point in respect to initial samples and those taken after 1 week, 1 month, and 3 months during (**A**) spring and (**B**) autumn short-term studies, and after 6 months and 12 months during (**C**) the long-term study. Each coordinate represents a single rockpool sample. Stress values are shown.

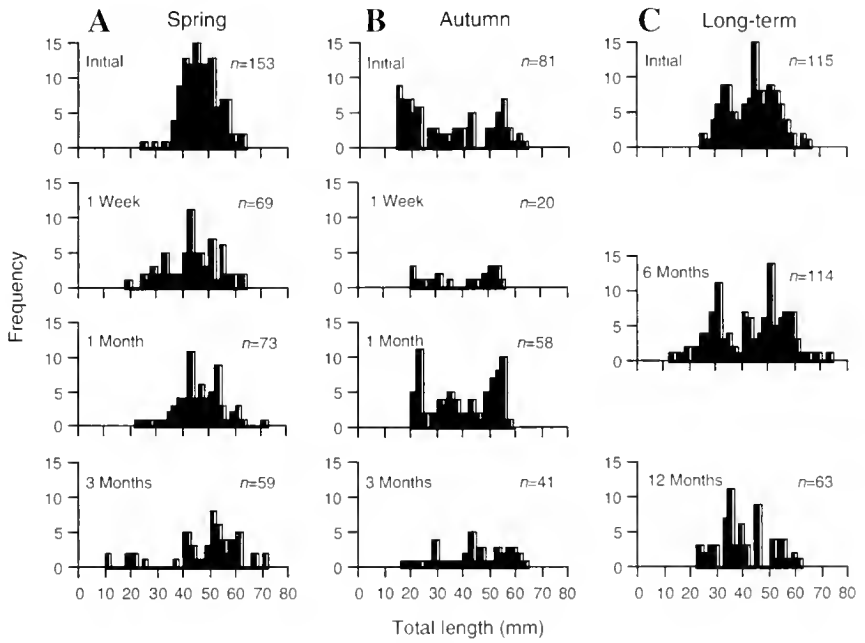

Figure 6

Length-frequency distributions (in 2-mm intervals) for *Bathygobius cocosensis* caught in the initial samples and after 1 week, 1 month, and 3 months later in the short-term study and caught in the initial sampling and 6 months and 12 months later in the long-term study. Samples were pooled for all sites during the (**A**) spring and (**B**) autumn short-term recolonization studies and for all sites during (**C**) the long-term recolonization study. Studies were conducted between 7 September 1999 and 22 September 2000. Samples sizes are shown.

Table 6

Results of ANOSIM testing for differences in fish assemblage structure among sampling intervals at four sites at Bass Point during the spring, autumn, and long-term recolonization studies. Significant results are shown in bold.

	Spring		Autumn		Long-term	
Site	*R*	*P* value	*R*	*P* value	*R*	*P* value
Maloney's Bay	0.002	0.474	0.029	0.393	−0.101	0.752
The Chair	0.185	0.057	0.014	0.422	0.063	0.284
Gravel Loader	0.083	0.165	0.027	0.389	0.190	0.051
Beaky Bay	0.025	0.383	0.726	**0.000**	0.044	0.348

For rockpool fish assemblages in southeastern Australia, a period of one week appears insufficient for recolonization of all species if fish are removed during sampling, whereas intervals of one to three months appear sufficient for rockpool fish assemblages at most Bass Point locations to recolonize to preperturbation levels. It is possible that recolonization times may be decreased if all fish are returned to rockpools immediately after sampling. However, this should not provide a foundation for subsequent studies with other defaunation methods, such as anesthetics or ichthyocides. The possible residual effects of these other sampling methods, such as the mortality of mobile and sessile invertebrates or the residues from chemical anesthetics and ichthyocides are possible factors that may complicate fish recolonization patterns (see Lockett, 1998) and certainly require additional investigation. Nonetheless, in recolonization studies with chemical sampling methods similar recolonization times as those of the present study were found. For example, recolonization of rockpools defaunated by ichthyocides was shown to be complete within 1 month (Grossman, 1982; Prochazka, 1996) and 3 months (Beckley, 1985a; Willis and Roberts, 1996; Polivka and Chotkowski, 1998).

Spatial variability in fish recolonization patterns was not definitive with regard to species composition

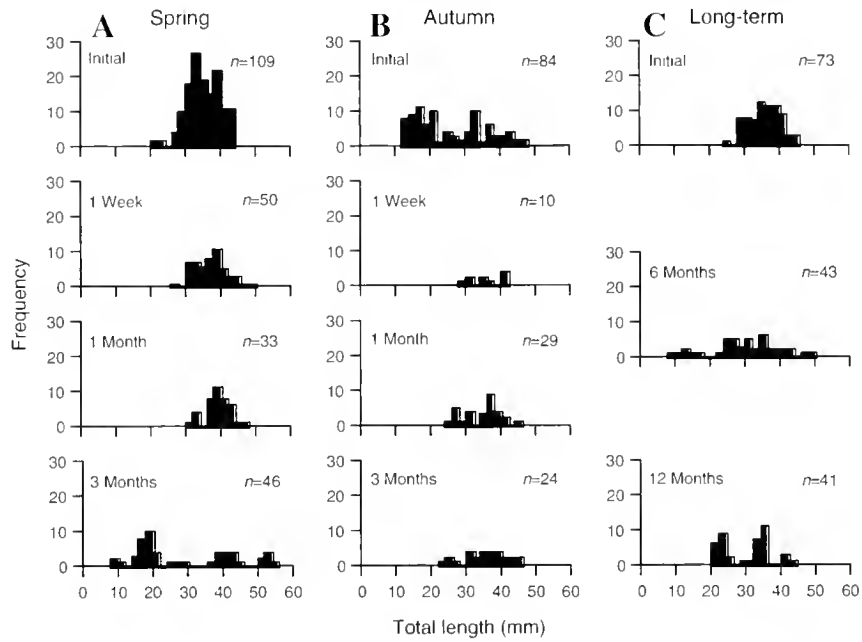

Figure 7

Length-frequency distributions (in 2-mm intervals) for *Enneapterygius rufopileus* caught in the initial samples and after 1 week, 1 month, and 3 months later in the short-term study and caught in the initial sampling and 6 months and 12 months later in the long-term study. Samples were pooled for all sites during the (**A**) spring and (**B**) autumn short-term recolonization studies and for all sites during (**C**) the long-term recolonization study. Studies were conducted between 7 September 1999 and 22 September 2000. Samples sizes are shown.

because samples were generally widely dispersed in nMDS ordination plots. The relatively low stress values (<0.2) indicate that high variability in fish assemblages at the level of individual rockpools is probably responsible for the patterns observed. However, some spatial variability in fish recolonization patterns was evident (Fig. 2) and appeared to be dependent to some extent on exposure of sites to predominant swell. There is evidence to suggest that wave exposure can affect the distribution of intertidal fishes (Gibson, 1972; Ibanez et al., 1989), although there is apparently no study that has investigated this effect in relation to fish recolonization in rockpools. In the present study, recolonization appeared more rapid at wave-exposed sites (MB and TC) compared to more sheltered sites. This may have been the result of the close distance between rockpools at exposed sites (within meters of each other), whereas at both sheltered sites, rockpools were significantly farther apart. Consequently, defaunated rockpools at exposed sites may recolonize more quickly if the major recolonizers are derived from neighboring rockpools as has been documented elsewhere (Beckley, 1985a; Polivka and Chotkowski, 1998).

Fish recolonization patterns were not influenced by the time of year that rockpools were defaunated in either short-term or long-term studies. The numbers of species and individuals consistently returned to pre-perturbation levels within a few weeks, but this return to previous levels may partially be a consequence of the relatively small number of species that are normally found in rockpools at any given time. In such situations a significant differences could only occur if large-scale changes in abundances were recorded. The lack of temporal variation in recolonization rates was surprising because recolonization was expected to be more rapid during summer, when the larvae of residents and warm water transients are expected to be available for settlement (Beckley, 1985a; Willis and Roberts, 1996). Recruitment was not the major mechanism driving fish recolonization in the present study because the majority of recolonizers were subadults and adults that would have relocated from nearby rockpools. Although many of the fish captured in each pool were tagged, the vast majority of fish caught in the same rockpool in subsequent sampling events were not tagged. Griffiths (2003b) showed that the common recolonizing species in the present study moved between a few rockpools within a limited home range. Therefore, postsettlement fishes from surrounding rockpools were probably moving into the study rockpools between each sampling event.

The movement of postsettlement fishes from adjacent rockpools also appears to control the resilience of rock-

pool fish assemblages. Therefore, the composition of species in newly recolonized rockpools is probably dependent upon the relative abundances of species in nearby rockpools. Species having the highest local abundances, such as *B. cocosensis* and *E. rufopileus*, are therefore more likely to be the primary recolonizers because vacant habitats have a higher probability of being located by these species during high-tide excursions throughout the intertidal zone (also see Polivka and Chotkowski, 1998). These species are also versatile and can exploit a range of microhabitats and, as a result, can occupy almost any rockpool within the intertidal zone (Griffiths et al., 2003). This is particularly true for *B. cocosensis*. In contrast, less abundant species such as *H. whiteleggi* often occupy more specific, and perhaps less abundant, microhabitats such as algal cover (see Marsh et al., 1978; Bennett and Griffiths, 1984) that may require longer periods to locate than more abundant habitats, such as cobble-covered substratum.

Processes regulating fish assemblages

The structure of multispecies assemblages can be regarded as being regulated by either deterministic or stochastic processes (see Grossman, 1982). Assemblages regulated by deterministic processes generally occur in environments where conditions are constant or fluctuate consistently over time. The structure of these assemblages is generally predictable. This can be maintained through a number of factors including partitioning of resources in finite supply (Schoener, 1974; Behrents, 1987) and interspecific competition, which prevents any single species being competitively dominant (Buss and Jackson, 1979).

In contrast, assemblages regulated by stochastic processes generally exist in unpredictable environments. Here, the resources are available on a random or periodic basis, which prevents superior competitors from dominating the assemblage (Sale, 1977, 1978). The success of particular species can be compared to winning a "lottery" for living space (Sale, 1977, 1978, 1982). Consequently, stochastically regulated assemblages are generally species rich (Sale, 1977).

Rockpool fish assemblages are often persistent for lengthy periods, even after catastrophic natural disturbances, such as hurricanes (Moring, 1996), and continual experimental eliminations (Grossman, 1982; Collette, 1986). For example, Collette (1986) found two species—*Pholis gunnellus* and *Tautogolabrus adspersus*—to be dominant over 19 years of study in two New England rockpools, whereas the rank of dominant species in the rockpools of Barbados showed no evidence of change over six years (Mahon and Mahon, 1994). Similar stability and persistence were evident in the present study, where *B. cocosensis*, *E. rufopileus* and *G. elevata* were consistently the highest ranked species in each collection for all three studies, regardless of the period between sampling. This finding may indicate that deterministic processes probably regulate the Bass Point fish assemblage. If this is the case, it may seem ironic because the intertidal zone is subjected to a high frequency of stochastic events. It would be easy to assume that such events could eliminate fishes from rockpools and thus leave microhabitats for other species to exploit. This kind of process has been documented for some sessile intertidal invertebrate assemblages that rely on the availability of vacant substrata for successful recruitment of larvae (see examples by Raffaelli and Hawkins, 1996). However, the locomotory capabilities and morphological and physiological adaptations of resident intertidal fishes allow them to cope with such disturbances by being able to cope temporarily with adverse conditions (Martin, 1995). As a result, the abundance of resident species may be little affected under normal disturbance regimes.

Conclusions

The results of this study have significantly increased an understanding of the patterns of recolonization of rockpools by fishes and some of the processes that underpin these patterns. Such an understanding of recolonization processes may improve our ability to predict the consequences of significant natural and anthropogenic disturbances on not only the fish assemblages but also on other intertidal community assemblages that may be maintained by the presence of fish (see Coull and Wells, 1983; Connell and Anderson, 1999).

On a more technical note, the recolonization rates observed in the present study may provide insight for other researchers aiming to study natural temporal variation of rockpool fish assemblages by minimizing the possibility of confounding effects of sampling. This may be particularly important for long-term monitoring programs, such as for marine protected areas (MPAs), that may require detection of changes in community structure over time. Finding sufficient numbers of similar-size pools at a single location for monitoring can be difficult; therefore repeated visits to the same rockpools may often be required. For southeastern Australian rockpools, we feel that a period of one to three months is required before resampling the same rockpools with the methods employed in this study. Although fish were not returned to rockpools immediately after sampling in the present study, we feel that this practice may significantly increase recolonization rates. However, the results of the present study should not provide a foundation for studies using other defaunation methods, such as anesthetics or ichthyocides, because other factors, such as chemical residues remaining in rockpools, may complicate fish recolonization patterns. Further investigation into these other factors will be necessary in the future.

Acknowledgments

We sincerely thank Jade Butler and Alan Griffiths for help with fieldwork. This paper is partly based upon

research included in a Ph.D. by S. P. Griffiths funded by an Australian Postgraduate Award. Additional funding was granted by the Institute for Conservation Biology, University of Wollongong, Shellharbour City Council, The Ecology Lab. Pty. Ltd., and Ocean Beach Hotel Fishing Club. S. P. Griffiths would like to thank CSIRO Marine Research for support during the preparation of this article.

Literature cited

Astles, K. L.
1993. Patterns of abundance and distribution of species in intertidal rockpools. J. Mar. Biol. Assoc. U.K. 73:555–569.

Beckley, L. E.
1985a. Tide-pool fishes: recolonization after experimental elimination. J. Exp. Mar. Biol. Ecol. 85:287–295.
1985b. The fish community of East Cape tidal pools and an assessment of the nursery function of this habitat. S. Afr. J. Zool. 20:21–27.
2000. Species composition and recruitment of tidal pools fishes in KwaZulu-Natal, South Africa. Afr. Zool. 35:29–34.

Behrents, K. C.
1987. The influence of shelter availability on recruitment and early juvenile survivorship of *Lythrypnus dalli* Gilbert (Pisces: Gobiidae). J. Exp. Mar. Biol. Ecol. 107:45–59.

Bennett, B. A., and C. L. Griffiths.
1984. Factors affecting the distribution, abundance and diversity of rock-pool fishes on the Cape Peninsula, South Africa. S. Afr. J. Zool. 19:97–104.

Buss, L. W., and J. B. C. Jackson.
1979. Competitive networks: nontransitive competitive relationships in cryptic coral reef environments. Am. Nat. 113:223–234.

Bussing, W. A.
1972. Recolonization of a population of supratidal fishes at Eniwetok Atoll, Marshall Islands. Atoll Res. Bull. 154:1–4.

Clarke, K. R.
1993. Non-parametric multivariate analyses of changes in community structure. Aust. J. Ecol. 18:117–143.

Collette, B. B.
1986. Resilience of the fish assemblage in New England tidepools. Fish. Bull. 84:200–204.

Connell, J. H.
1972. Community interactions on marine rock intertidal shores. Ann. Rev. Ecol. Syst. 3:169–192.

Connell, S. D., and M. J. Anderson.
1999. Predation by fish on assemblages of intertidal epibiota: effects of predator size and patch size. J. Exp. Mar. Biol. Ecol. 241:15–29.

Coull, B. C., and J. B. J., Wells.
1983. Refuges from fish predation: experiments with phytal meiofauna from the New Zealand rocky intertidal. Ecology 64:1599–1609.

Faria, C., and V. Almada.
1999. Variation and resilience of rocky intertidal fish in western Portugal. Mar. Ecol. Prog. Ser. 184:197–203.

Gibson, R. N.
1972. The vertical distribution and feeding relationships of intertidal fish on the Atlantic coast of France. J. Anim. Ecol. 41:189–207.
1982. Recent studies on the biology of intertidal fishes. Oceanogr. Mar. Biol. Ann. Rev. 20:363–414.

Green, J.M.
1971. High tide movements and homing behaviour of the tidepool sculpin *Oligocottus maculosus*. J. Fish. Res. Can. 28:383–389.

Griffiths, S. P.
2000. The use of clove oil as an anaesthetic and method for sampling intertidal rockpool fishes. J. Fish Biol. 57:1453–1464.
2003a. Spatial and temporal dynamics of temperate Australian rockpool ichthyofaunas. Mar. Freshw. Res. 54:163–176.
2003b. Homing behaviour of intertidal rockpool fishes in south-eastern New South Wales, Australia. Aust. J. Zool. 51:387–398.
2003c. Rockpool ichthyofaunas of temperate Australia: species composition, residency and biogeographic patterns. Estuar. Coast Shelf Sci. 58:173–186.

Griffiths, S. P., R. J. West, and A. Davis.
2003. Effects of intertidal elevation on the rockpool ichthyofaunas of temperate Australia. Environ. Biol. Fishes 68:197–204

Grossman, G. D.
1982. Dynamics and organisation of a rocky intertidal fish assemblage: the persistance and resilience of taxocene structure. Am. Nat. 119:611–637.
1986. Long term persistence in a rocky intertidal fish assemblage. Environ. Biol. Fishes 15:315–317.

Ibanez, M., I. Miguel, D. San Millan, and I. Ripa.
1989. Intertidal ichthyofauna of the Spanish Atlantic coast. Sci. Mar. 53:451–455.

Lardner, R., W. Ivantsoff, and L. E. L. M. Crowley.
1993. Recolonization by fishes of a rocky intertidal pool following repeated defaunation. Aust. Zool. 29: 85–92.

Lockett, M. M.
1998. The effect of Rotenone on fishes and its use as a sampling technique: a survey. Z. Fischkd. 5:13–45.

MacArthur, R. H., and E. O. Wilson.
1967. The theory of island biogeography, 224 p. Princeton Univ. Press, Princeton, NJ.

Mahon, R., and S. D. Mahon.
1994. Structure and resilience of a tidepool fish assemblage at Barbados. Environ. Biol. Fishes 41:171–190.

Marsh, B., T. M. Crowe, and W. W. Siegfried.
1978. Species richness and abundance of clinid fish (Teleostei: Clinidae) in intertidal rock pools. S. Afr. J. Zool. 13:283–291.

Martin, K. L. M.
1995. Time and tide wait for no fish: intertidal fishes out of water. Environ. Biol. Fishes 44:165–181.

Matson, R. H., C. B. Crabtree, and T. R. Haglund.
1986. Ichthyofaunal composition and recolonization in a central California tidepool. Calif. Fish and Game 72:227–231.

Mistry, S. D., E. K. Lizerbram, and E. R. Parton.
1989. Short-term ichthyofaunal recruitment in northern California tidepools. Copeia 1989:1081–1084.

Mok, H., and P. Wen.
1985. Intertidal fish community ecology on Lu Tao Island (Green Island), Taiwan. J. Taiwan Mus. 38:81–118.

Moring, J. R.
1990. Seasonal absence of fishes in tidepools of a boreal environment (Maine, USA). Hydrobiologia 194: 163–168.
Moring, J. R.
1996. Short-term changes in tidepools following two hurricanes. Hydrobiologia 328:155–160.
Paine, R. T., and S. A. Levin.
1981. Intertidal landscapes: disturbance and the dynamics of pattern. Ecol. Monogr. 47:37–63.
Pfister, C.A.
1995. Estimating competition coefficients from census data: a test with field manipulations of tidepool fishes. Am. Nat. 146:271–291.
1997. Demographic consequences of within year variation in recruitment. Mar. Ecol. Prog. Ser. 153: 229–238.
Polivka, K. M., and M. A.Chotkowski.
1998. Recolonization of experimentally defaunated tidepools by northeast Pacific intertidal fishes. Copeia:456–462.
Prochazka, K.
1996. Seasonal patterns in a temperate intertidal fish community on the west coast of South Africa. Environ. Biol. Fishes 45:133–140.
Prochazka, K., and C. L. Griffiths.
1992. The intertidal fish fauna of the west coast of South Africa—species, community and biogeographic patterns. S. Afr. J. Zool. 27:115–120.
Raffaelli, D., and S. Hawkins.
1996. Intertidal ecology, 372 p. Chapman and Hall, London.
Sale, P. F.
1977. Maintenance of high diverity in coral reef fish communities. Am. Nat. 111:337–359.
1978. Coexistance of coral reef fishes—a lottery for living space. Environ. Biol. Fishes 3: 85–102.
1982. Stock-recruit relationships and regional coexistance in a lottery competitive system: a simulation study. Am. Nat. 120:139–159.
Schoener, T. W.
1974. Resource partitioning in ecological communities. Science 185:27–39.
Silberschneider, V., and D. J., Booth.
2001. Resource use by *Enneapterygius rufopileus* and other rockpool fishes. Environ. Biol. Fishes 61:195–204.
Thomson, D. A., and C. E. Lehner.
1976. Resilience of a rocky intertidal fish community in a physically unstable environment. J. Exp. Mar. Biol. Ecol. 22:–29.
Underwood, A. J., and G. A. Skilleter.
1996. Effects of patch-size on the structure of assemblages in rock pools. J. Exp. Mar. Biol. Ecol. 197: 63–90.
Willis, T. J., and C. D. Roberts.
1996. Recolonization and recruitment of fishes to intertidal rockpools at Wellington, New Zealand. Environ. Biol. Fishes 47:329–343.
Yoshiyama, R. M., C. Sassaman, and R. N. Lea.
1986. Rocky intertidal fish communities of California: temporal and spatial variation. Environ. Biol. Fishes 17:23–40.
Yoshiyama, R. M., K. B. Gaylord, M. T. Philippart, T. R. Moore, J. R. Jordan, C. C. Coon, L. L. Schalk, C. J. Valpey, and I. Tosques.
1992. Homing behaviour and site fidelity in the intertidal sculpins (Pisces: Cottidae). J. Exp. Mar. Biol. Ecol. 160:115–130.

Factors influencing the timing and frequency of spawning and fecundity of the goldlined seabream (*Rhabdosargus sarba*) (Sparidae) in the lower reaches of an estuary

S. Alexander Hesp

Ian C. Potter

Centre for Fish and Fisheries Research
School of Biological Sciences and Biotechnology
Murdoch University
South Street
Murdoch, Western Australia 6150, Australia

E-mail address (for I. C. Potter, contact author): i.potter@murdoch.edu.au

Sonja R. M. Schubert

Ernst-Moritz Arndt Universitaet, Hansestadt Greifswald
F.-L.-Jahn Straße 15a
17487 Greifswald, Germany

Abstract—We have studied the reproductive biology of the goldlined seabream (*Rhabdosargus sarba*) in the lower Swan River Estuary in Western Australia, focusing particularly on elucidating the factors influencing the duration, timing, and frequency of spawning and on determining potential annual fecundity. Our results demonstrate that 1) *Rhabdosargus sarba* has indeterminate fecundity, 2) oocyte hydration commences soon after dusk (ca. 18:30 h) and is complete by ca. 01:30–04:30 h and 3) fish with ovaries containing migratory nucleus oocytes, hydrated oocytes, or postovulatory follicles were caught between July and November. However, in July and August, their prevalence was low, whereas that of fish with ovaries containing substantial numbers of atretic yolk granule oocytes was high. Thus, spawning activity did not start to peak until September (early spring), when salinities were rising markedly from their winter minima. The prevalence of spawning was positively correlated with tidal height and was greatest on days when the tide changed from flood to ebb at ca. 06:00 h, i.e., just after spawning had ceased. Because our estimate of the average daily prevalence of spawning by females during the spawning season (July to November) was 36.5%, individual females were estimated to spawn, on average, at intervals of about 2.7 days and thus about 45 times during that period. Therefore, because female *R. sarba* with total lengths of 180, 220, and 260 mm were estimated to have batch fecundities of about 4500, 7700, and 12,400 eggs, respectively, they had potential annual fecundities of about 204,300, 346,100 and 557,500 eggs, respectively. Because spawning occurs just prior to strong ebb tides, the eggs of *R. sarba* are likely to be transported out of the estuary into coastal waters where salinities remain at ca. 35‰. Such downstream transport would account for the fact that, although *R. sarba* exhibits substantial spawning activity in the lower Swan River Estuary, few of its early juveniles are recruited into the nearshore shallow waters of this estuary.

Manuscript submitted 9 June 2003 to the Scientific Editor's Office.

Manuscript approved for publication 28 April 2004 by the Scientific Editor.

Fish. Bull. 102:648–660 (2004).

The goldlined seabream (*Rhabdosargus sarba*) is an important recreational and commercial fish species in numerous regions throughout the Indo-west Pacific (van der Elst, 1988; El-Agamy, 1989; Kuiter, 1993). Although this species is a protandrous hermaphrodite in certain regions, e.g., the waters of Hong Kong and South Africa (Yeung and Chan, 1987; Garratt, 1993), it is a rudimentary hermaphrodite in a range of environments in Western Australia (Hesp and Potter, 2003). Rudimentary hermaphrodites are those species in which the juveniles possess gonads consisting of both immature testicular and ovarian tissues that, in adults, develop permanently into either functional testes with rudimentary ovarian tissue or functional ovaries with rudimentary testicular tissue (Buxton and Garratt, 1990). In Western Australia, *R. sarba* attains similar maximum lengths, i.e., 346–370 mm, in temperate marine coastal waters and the lower reaches of the Swan River Estuary on the lower west coast of Australia and in a large subtropical embayment ca. 800 km farther north (Hesp et al., 2004). However, the maximum age recorded for this species in the estuary, 7 years, was far less than that for the other two environments: temperate marine coastal waters (11 years) and a large subtropical embayment (13 years) (Hesp et al., 2004).

Although *R. sarba* is typically regarded as a marine species that frequently uses estuaries as a nursery area (e.g., Wallace, 1975; Potter and Hyndes, 1999; Smith and Suthers, 2000), it spawns in the lower Swan River Estuary as well as in coastal waters outside this estuary (Hesp and Potter, 2003). However, this sparid attains maturity later in the estuary than in those nearby coastal marine waters. If this indication that the onset of spawning for *R. sarba* in the Swan River Estuary is related to the attainment of higher salinities in the spring, it would parallel the situation recorded for the spotted seatrout (*Cynoscion nebulosus*) in the estuaries of the Gulf of Mexico where this species completes its entire life cycle (Brown-Peterson et al., 2002).

Despite the importance and widespread occurrence of *R. sarba*, and the great value of fecundity data for stock assessments (Hunter et al., 1992; Nichol and Acuna, 2001), only one attempt has apparently been made to estimate the annual fecundity of wild populations of this sparid (El-Agamy, 1989). Although El-Agamy (1989) recognized that *R. sarba* is a "fractional" spawner and has a

protracted spawning season, he recorded the fecundity of this species as the number of larger eggs (diameter >180 μm) estimated to be present in the ovaries of mature females just prior to the commencement of the spawning period. Thus, the very strong possibility that some eggs with diameters <180 μm would have been destined to have become fully mature and released at some stage during the protracted spawning season, i.e., the species has indeterminate fecundity, was not taken into account.

In species with indeterminate fecundity, the distribution of oocyte diameters essentially forms a continuum, reflecting the continuous maturation of oocytes throughout the spawning season and thus the progression through to maturity of some of the small and previtellogenic oocytes that were present at the beginning of the spawning period. Consequently, counts of the standing stock of larger oocytes found just prior to the onset of spawning will result in an underestimate of the potential annual fecundity of such species (Hunter et al., 1985, 1992; Lisovenko and Andrianov, 1991). Estimation of the annual fecundity of species with indeterminate fecundity thus requires a combination of data on batch fecundity and spawning frequency (Hunter et al., 1985). Batch fecundity, i.e., the number of oocytes released during a single spawning event, can be estimated by counting the number of hydrated oocytes present in ovaries immediately prior to that spawning (Hunter et al., 1985). The frequency with which a fish spawns during the spawning period can be determined from the frequency of mature female fish possessing ovaries with either hydrated oocytes or postovulatory follicles (POFs) of a known age (Hunter and Macewicz, 1985).

The spawning of many marine species of teleosts and invertebrates is correlated with lunar periodicity and the associated tidal cycles (e.g., Schwassmann, 1971; Taylor, 1984; Greeley et al., 1986; Hoque et al., 1999), with the spawning of such fish species typically peaking around the full or new moon (or both) (e.g., Johannes, 1978; Taylor and DiMichele, 1980; Greeley et al., 1986). Many fish and invertebrates with pelagic eggs spawn on high or ebb tides that enable eggs and the subsequent larval stages to be transported away from spawning areas, in which planktivorous predators are concentrated. This process thus reduces the likelihood of those early life cycle stages being subjected to predation (Taylor, 1984; Johnson et al., 1990; Morgan, 1990). The fact that there is very little recruitment of the early 0+ individuals of *R. sarba* into the lower Swan River Estuary, where extensive spawning occurs, indicates that tides transport the eggs of this species from spawning areas in the estuary into coastal marine waters (Hesp and Potter, 2003; Hesp et al., 2004).

This investigation, which involved a detailed study of the females of *R. sarba* in the lower Swan River Estuary, had the following aims: 1) to test the hypothesis that *R. sarba* has indeterminate fecundity; 2) to establish the period during the day when the oocytes of *R. sarba* become hydrated and when ovulation and spawning occur; 3) to establish whether *R. sarba* spawns mainly when salinities are high and thus approach those of the marine waters in which this species typically breeds and whether spawning is correlated with the strength and type (ebb vs flood) of tide in the lower reaches of the Swan River Estuary; 4) to estimate the average frequency of spawning for *R. sarba* during the spawning period; 5) and to determine the relationship between batch fecundity and fish length, and to use this relationship, in combination with the average spawning frequency, to calculate the potential annual fecundity of *R. sarba* of different sizes.

Materials and methods

Tide, lunar phase, and salinity

The maximum daily tidal heights at the mouth of the Swan River Estuary were calculated by using the tidal prediction data of the Coastal Data Centre at the Department of Planning and Infrastructure, Government of Western Australia (http://www.coastaldata.transport.wa.gov.au). The maximum tidal range at the mouth of the Swan River Estuary is small, i.e., ≤0.8 m, and tides can be diurnal or semidiurnal, depending on the time of year (Spencer, 1956). Salinity was measured on each sampling occasion by using a Yellow Springs Instruments salinity meter (YSI model number 30, Yellow Springs Instrument Co., Inc., Yellow Springs, OH).

Sampling

During 2001 and 2002, female *Rhabdosargus sarba* were collected by seine netting in nearshore shallow waters at distances of ca. 2.5 to 5 km from the mouth of the Swan River Estuary, and by rod and line fishing in water depths of 10–12 m at a distance of ca. 150 m from the shore (for details of sampling region and seine net, see Hesp and Potter, 2003). Sampling was undertaken at least once weekly between July and November, the period when *R. sarba* reach maturity in the lower Swan River Estuary (Hesp and Potter, 2003). It was restricted to the hours between dusk (ca. 18:00 h) and dawn (ca 06:00 h) because extensive seine netting and angling during the day in our earlier study failed to yield any *R. sarba*. The failure to capture *R. sarba* by these methods during daylight reflected the offshore movement of this species from the shallows prior to dawn and a far stronger targeting of bait by the large numbers of the banded toadfish (*Torquigener pleurogramma*) that feed in the offshore waters of the lower estuary during the day. Because the lower reaches of the Swan River Estuary act as a shipping harbor, alternative sampling methods, such as gill netting and spearing, could not be used to catch *R. sarba* during the day. The data for 2000 and 2001 were augmented by those derived from fish collected from the same location by using the same methods in 1998 and 1999 (Hesp and Potter, 2003). In total, the results of the present study are based on an examination of over 2000 *R. sarba*, of which 510 were

Table 1

Characteristics of each macroscopic stage in the development of the ovaries of *Rhabdosargus sarba*, and its corresponding histological characteristics. Adapted from Laevastu (1965). Terminology for oocyte stages follows Wallace and Selman (1989).

Stage	Macroscopic characteristics	Histological characteristics
I Virgin	Ovary is very small and strand-like.	*Rhabdosargus sarba* is a rudimentary hermaphrodite, *sensu* Hesp and Potter (2003). Thus, the gonads of small juveniles contain only connective tissue. Larger juveniles possess gonads (ovotestes) in which each ovarian lobe consists of an immature ovarian and testicular zone, separated by connective tissue. The ovotestes develop later into gonads containing almost entirely ovarian tissue (functional ovaries) or, in the case of males, gonads containing almost entirely testicular tissue (functional testes).
II Immature and resting	Small and transparent. Yellowish-orange in color. Oocytes not visible through ovarian wall.	Ovigerous lamellae highly organized. Chromatin nucleolar and perinucleolar oocytes dominate the complement of oocytes. Oogonia sometimes present. Chromatin nucleolar oocytes present in all subsequent ovarian stages.
III Developing	Slightly larger than stage II. Reddish color. Oocytes visible through ovarian wall.	Chromatin nucleolar, perinucleolar and cortical alveolar oocytes present.
IV Maturing	Larger than stage III. Reddish-orange in color. Yolk granule oocytes visible through ovarian wall.	Cortical alveolar and yolk granule oocytes abundant.
V Mature	Larger than stage IV, occupying half to two thirds of body cavity. Extensive capillaries visible in ovarian wall.	Yolk granule oocytes predominant.
VI Spawning	Hydrated oocytes visible through ovarian wall. Note that fish with ovaries in "spawning condition" can only be detected macroscopically when caught during the hydration period.	Migratory nucleus oocytes, hydrated oocytes, or postovulatory follicles present.
VII Spent	Smaller than V and VI and flaccid. Some yolk granule oocytes visible through ovarian wall.	Some remnant yolk granule oocytes present, all or almost all of which are typically undergoing atresia.
VIII Spent and recovering	Small and dark red.	Extensive scar tissue present. Ovarian lamellae becoming reorganized. No yolk granule oocytes present.

females with stage-V (mature) or stage-VI (spawning) ovaries (see Table 1 for definitions of these stages).

During the above sampling, *R. sarba* was collected for up to 2 hours at intervals commencing at 18:30, 21:30, 00:30, and 03:30 h on 1–2 September 2001 and for up to 2 hours at intervals commencing at 18:30 and 22:30 h on 13 September 2001. One of the ovarian lobes of up to five fish caught during each of these above time intervals was cut into several pieces, preserved in 10% neutrally buffered formalin solution and used for determining the distributions of oocyte diameters at the above different times. The other lobe was used for histology to determine the oocyte stages present in that lobe, and thus, by extrapolation, also the stages of the oocytes in the lobe that had been preserved in formalin. The resultant comparisons were used, in conjunction with data from other times, to elucidate the pattern of oocyte development during hydration and the duration of hydration and timing of ovulation.

Gonadal staging and histology of ovaries

The sex, total length (to the nearest 1 mm), and total weight and gonad weight (to the nearest 0.01 g) of each fish were recorded. From its macroscopic appearance, each gonad was assigned to one of the following stages in maturation, based on the scheme of Laevastu (1965), i.e., I = virgin, II = immature and resting, III = developing, IV = maturing, V = mature, VI = spawning, VII = spent, VIII = spent and recovering. The corresponding histological characteristics of each macroscopic stage are shown in Table 1. When hydrated oocytes could be seen through the ovarian wall of a fish, a note was made as to whether they were distributed throughout the ovary or were in

the ovarian duct and thus whether or not ovulation had commenced at the time of capture of that fish.

For all histological studies of the gonads, part of the mid region of one of the ovarian lobes was placed in Bouin's fixative for ca. 48 hours, dehydrated in a series of ethanols, embedded in paraffin wax, cut into 6-μm sections, and stained with Mallory's trichrome. The ovaries were fixed within 1–3 hours of capture of the fish.

To test the hypothesis that *R. sarba* has indeterminate fecundity, the diameters of 100 oocytes in histological sections of stage-VI ovaries of two fish caught during the spawning period were measured to the nearest 10 μm by using an eyepiece graticule in a compound microscope and the stage of each of those oocytes was recorded. Measurements were restricted to oocytes in which a nucleus was visible in their center to ensure that the oocytes had been sectioned through their center and that the diameters were thus measured accurately. This approach could not be used to measure the oocyte diameters of hydrated oocytes in histological sections because the nucleus of these oocytes undergoes germinal vesicle breakdown.

Histological sections of numerous ovaries were used to determine the timing of the formation and degeneration of postovulatory follicles (POFs). An age was assigned to the POFs found in ovaries of fish caught at different times of the day, based on the timing of ovulation and the degree to which those POFs had degenerated (Hunter and Goldberg, 1980; Hunter and Macewicz, 1985). Histological sections were also used to determine the relative abundance of the different stages of atresia in ovaries at different times during the spawning period.

The jars containing the ovarian lobes that had been preserved in formalin at the different time intervals on 1, 2, and 13 September 2001 (see earlier) were shaken until the oocytes of each ovary had become evenly suspended in the solution. The resultant solution from each ovary was then passed through a 125-μm sieve to remove the smallest oocytes, and we were able thus to focus our study more specifically on the vitellogenic oocytes. Comparisons of the appearance of the larger oocytes under a dissecting microscope with those of the different oocyte stages in histological sections of the other ovarian lobe of the same fish were used to allocate the oocytes observed under the dissecting microscope to a specific stage in oocyte development. Each oocyte in a representative subsample of 100 oocytes from each formalin-preserved ovarian lobe was measured under a dissecting microscope with an eyepiece graticule. This approach enabled the diameters of hydrated oocytes to be measured accurately, which was not possible with histological sections (see earlier).

Categorization of stages in atresia, fecundity estimates, and spawning frequency

On the basis of their histological characteristics, atretic oocytes were allocated to either the α or β stages, by using the criteria of Hunter and Macewicz (1985). Mature ovaries were categorized according to the proportions of their α and β atretic oocytes (Hunter and Macewicz, 1985). Thus, atretic state 0 = ovaries with yolked oocytes but no α atretic oocytes; atretic state 1 = ovaries in which less than 50% of the yolked oocytes are in the α stage of atresia; atretic state 2 = ovaries in which less than 50% of the yolked oocytes are α atretic and atretic state 3 = ovaries which contain no yolked oocytes but do possess β atretic oocytes. During the present study, atretic state 1 ovaries were further divided into three categories on the basis of the percentage of α atretic yolk granule oocytes in histological sections, namely early (<10%), mid (10–35%) and late (36–50%) atretic state 1, an approach similar to that adopted by Farley and Davis (1998).

The batch fecundities of 31 *R. sarba* were estimated from the number of hydrated oocytes in one of the ovarian lobes of fish that had been preserved in 10% neutrally buffered formalin. These fish were chosen because histological examination of their other ovarian lobe demonstrated that the ovaries were in atretic state 0 or early state 1, i.e., less than 10% of their yolk granule oocytes were atretic and newly formed POFs were not present (Hunter et al., 1992; Nichol and Acuna, 2001). The formalin-preserved ovarian lobe was dried with blotting paper and ca. 180–200 mg of tissue was removed from each of its anterior, middle, and posterior regions and weighed to the nearest 1 mg. These pieces of tissue were placed on separate slides, covered with 30% glycerol and examined under a dissecting microscope. The oocytes were then teased apart and the number of hydrated oocytes recorded. The number of hydrated oocytes in each of the three pieces of ovarian tissue of known weight were then used, in conjunction with the weight of both ovarian lobes, to estimate the total number of hydrated oocytes (=batch fecundity) that would have been present in the pair of ovarian lobes of each fish. The prevalence of spawning on any given night is expressed as the percentage of female fish with hydrated eggs (ovarian stage VI) among all female fish with stage-V (mature) and stage-VI (spawning) ovaries. These estimates were based on an examination of samples collected between 22:00 and 01:30 h, when it was possible to determine which female fish were going to spawn in the ensuing few hours (see Hunter et al., 1985, for further details of this method).

Results

Although mean monthly salinities in the lower Swan River Estuary in late spring to early winter were close to that of full strength sea water (35‰), they fell precipitously to a minimum of 23‰ (minimum individual value=14‰) in August, and then rose sharply in early to mid-spring (Fig. 1).

Staging of the ovaries and confirmation of indeterminate fecundity

The characteristics of each macroscopic stage of the ovaries of *R. sarba* and the corresponding histologi-

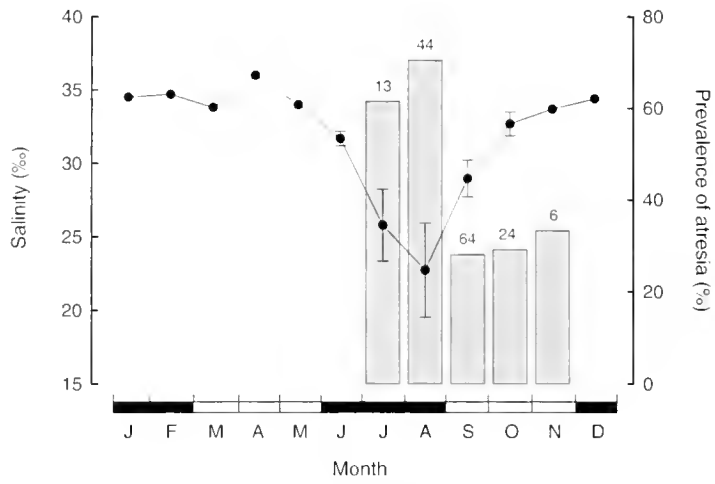

Figure 1

Mean monthly salinities (±1SE) at the bottom of the water column in the lower Swan River Estuary throughout the year and the prevalences of atresia in mature ovaries of *Rhabdosargus sarba* between July and November, which are shown as histograms, together with the number of fish examined. Closed rectangles on the horizontal axis refer to summer and winter months, and the open rectangles to autumn and spring months.

cal characteristics are presented in Table 1. Because stages V and VI could be distinguished macroscopically only during the period of oocyte hydration, the macroscopic data for these two stages had to be combined for other times. The diameters of the oocytes in histological sections of an ovarian lobe from each of two mature female *R. sarba* caught during the spawning season—oocyte diameters that were typical of those from mature *R. sarba* during this period—formed an essentially continuous distribution (Fig. 2). This distribution reflected the presence of oocytes at all stages in development from chromatin nucleolar oocytes to yolk granule oocytes and demonstrated that *R. sarba* has indeterminate fecundity *sensu* Hunter et al. (1985). Thus, the potential annual fecundity is not fixed prior to the commencement of the spawning period and consequently the potential annual fecundity of *R. sarba* has to be estimated by using a combination of batch fecundity and spawning frequency.

Period of hydration and spawning

The diameters of oocytes in ovaries of fish collected at intervals on 1–2 September 2001 and 13 September 2001 and which had been retained on the 125-μm sieve, produced a modal class that, for each time interval, fell between 420 and 600 μm (Fig. 3). At ca. 18:30 h on 1 September 2001, the oocyte diameters formed a single mode, and the vast majority of oocytes were less than 720 μm and produced a modal class at 420–539 μm (Fig. 3). However, by ca. 21:30 h on the same evening, the maximum diameter of the oocytes had increased markedly and the distribution of the oocyte diameters was beginning to become bimodal, with modal classes at 480–539 and 780–839 μm. By 00:30 h on 2 September, the oocyte diameter distributions had become markedly bimodal, and the modal diameter class of the largest oocytes at this time, and also at 03:30 h, lay between 840 and 959 μm (Fig. 3). The oocyte diameter frequencies on 13 September were essentially the same as those at similar times on 1 September; the distributions were unimodal at 18:30 h and bimodal at 22:30 h (Fig. 3). The oocyte diameters of each fish within a given time slot on 1, 2, and 13 September exhibited essentially the same distribution.

Histological sections showed that, at 18:30 h on 1 September 2001, most of the mature ovaries contained migratory nucleus stage oocytes, i.e., oocytes in which the nucleus was migrating towards the edge of the cytoplasm and a conspicuous lipid droplet was present in the cytoplasm (Fig. 4A). However, it was difficult at this time to distinguish migratory nucleus oocytes from yolk granule oocytes under a dissecting microscope (Fig. 4B). By 21:30 h, the yolk and lipid of the larger oocytes had begun to coalesce and the nucleus could sometimes be seen near the edge of the cytoplasm (Fig. 4C). Their relatively larger size, translucent appearance, and one's ability to detect their lipid droplet enabled these hydrating oocytes to be far more readily distinguished from yolk granule oocytes under a dissecting microscope than was the case earlier in the evening (cf. Fig. 4, B and D). By 00:30 h, the largest oocytes had increased

further in size and all of their lipid and yolk material had coalesced (Fig. 4E). Under the dissecting microscope, these hydrated oocytes were of similar appearance to the corresponding oocytes at 21:30 h (Fig. 4F). Although mature fish with ovaries containing the above stages in oocyte hydration were frequently found in nearshore shallow waters, the numbers of such fish in these waters declined markedly after about 00:30 h and none of the few fish caught there after this time contained recently formed POFs. However, fish with ovaries containing newly formed POFs were caught in offshore deeper waters.

Histological examination demonstrated that, when hydrated oocytes were present in the ovarian duct, the ovary contained recently formed POFs, which are formed by the thecal and granulosa layers of the oocytes that surround the zona radiata externa (Fig. 5A). Newly formed POFs (0–6 h old) possess a conspicuous lumen and their granulosa cells contain prominent darkly stained nuclei (Fig. 5B). These newly formed postovulatory follicles were first observed in the ovaries of females caught at ca. 01:30 h and were present in the ovaries of several fish caught in the ensuing four hours. In contrast, no newly formed POFs were found in the ovaries of *R. sarba* at dusk, i.e., ca. 18:30 h. At this time, the POFs comprised one of two morphological forms. The first and least degenerate form was less well organized than newly formed POFs and its nuclei were becoming pycnotic (Fig. 5C); the second form was smaller and highly degenerate and its nuclei had become far less visible or undetectable (Fig. 5D). The least degenerate of the two forms of POFs in ovaries of fish caught at ca. 22:00 and 01:00 h (Fig. 5, D and E) represents stages in degeneracy that are intermediate between those of the two different forms described above for the ovaries of fish caught at 18:30 h. These POFs were thus compact and, although some of their nuclei were still detectable, they were markedly pycnotic.

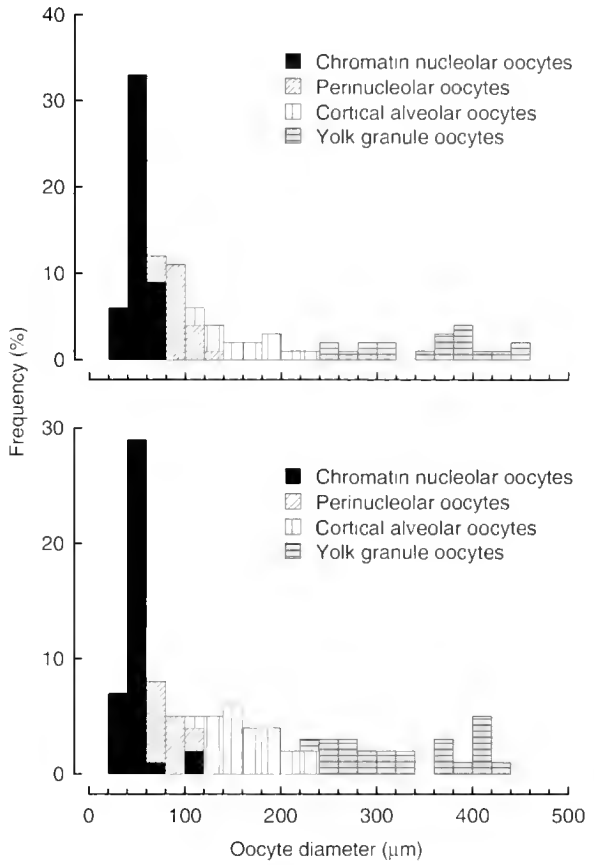

Figure 2

Percent frequency distributions for the oocyte diameters of different oocyte stages in histological sections of stage-VI ovaries of two female *Rhabdosargus sarba*.

Influence of salinity and tides on spawning

Both α and β atretic oocytes were frequently observed in the ovaries of *R. sarba*. The chorion (zona radiata) of the early α atretic vitellogenic oocyte was distorted, fragmented, and had moved inwards (Fig 6A). By the β atretic stage, the yolk and lipid had been resorbed and a large proportion of the oocyte volume was occupied by vacuoles (Fig. 6B).

Sixty-two percent and 72% of the stage-V and stage-VI ovaries sectioned in July and August, respectively, were at mid or late atretic state 1, i.e., 11–50% of their yolk granule oocytes were α atretic (Fig. 1). However, the prevalence of these mid-late state-1 ovaries declined precipitously to 28% in September, as salinities rose markedly, and remained at a similar level until the end of spawning in late November.

Histological sections showed that, in July and August, only 39% of the 57 pairs of ovarian lobes of *R. sarba* that were macroscopically assigned as stage V and stage VI contained migratory nucleus oocytes, hydrated oocytes, or POFs, i.e., were at stage VI. However, in the following two months, 76% of the 88 pairs of ovarian lobes of *R. sarba*, that were macroscopically assigned as stage V or stage VI, were shown by histology to be at stage VI.

During September, when spawning activity was greatest, the prevalence of spawning (PS) was positively correlated ($P<0.05$) with maximum daily tidal height (T). $PS = 91.72T + 20.73$ ($r^2=0.46$, number of sampling occasions=10) (Fig. 7A).

Data for the same days as those used to provide the points shown in Fig. 7A demonstrated that the prevalence of spawning (PS) is inversely correlated with the difference in hours between the time when spawning is believed to cease (ca. 06:00 h, see later) and the time of high tide. $PS = -8.26(T) + 78.22$ ($r^2=0.49$, number of sampling occasions=10) (Fig. 7B). Thus, the prevalence of these "spawning" females was greatest on those days when the time that the tide was about to change from flood to ebb coincided with the time when *R. sarba* is considered to cease spawning.

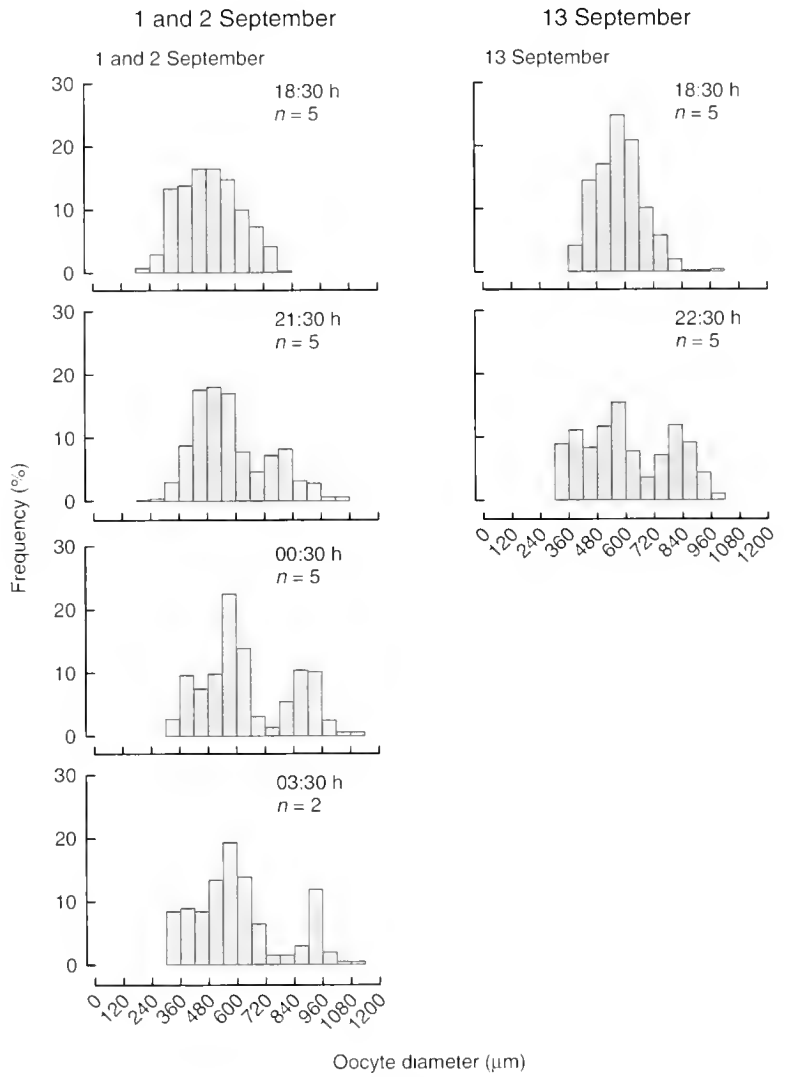

Figure 3

Frequency distributions for the oocyte diameters in mature ovaries of *Rhabdosargus sarba* caught on 1–2 and 13 September 2001. The ovaries had been preserved in formalin and their oocytes had been passed through a 125-µm sieve. The time of commencement of each 2-hour sampling interval is shown. *n* = number of fish used for oocyte diameter measurements.

Batch fecundity, spawning frequency, and potential annual fecundity

The relationship between batch fecundity (BF) and total length (TL) shown in Figure 8, and between batch fecundity and somatic weight (W) are described by the following equations:

$$\ln BF = 5.0025 \ln TL - 17.557 \quad (P<0.001;\ r^2=0.52,\ n=30),$$

$$BF = 1997 e^{0.0105W} \quad (P<0.001;\ r^2=0.55,\ n=30).$$

The batch fecundities of *R. sarba*, predicted by the above equations for fish with lengths of 180, 220, and 260 mm, were ca. 4500, 7700, and 12,400, eggs, respectively, and for fish with somatic weights of 100, 150, and 200 g were ca. 5700, 9600, and 16,300 eggs, respectively. The average daily prevalence of spawning during the spawning period was 36.5%. Thus, during this period, individual females spawned, on average, once every 2.7 days and therefore about 45 times during the spawning season. The potential annual fecundities of female *R. sarba* with lengths of 180, 220, and 260 mm were thus estimated to be ca. 204,300, 346,100, and 557,500 eggs, respectively.

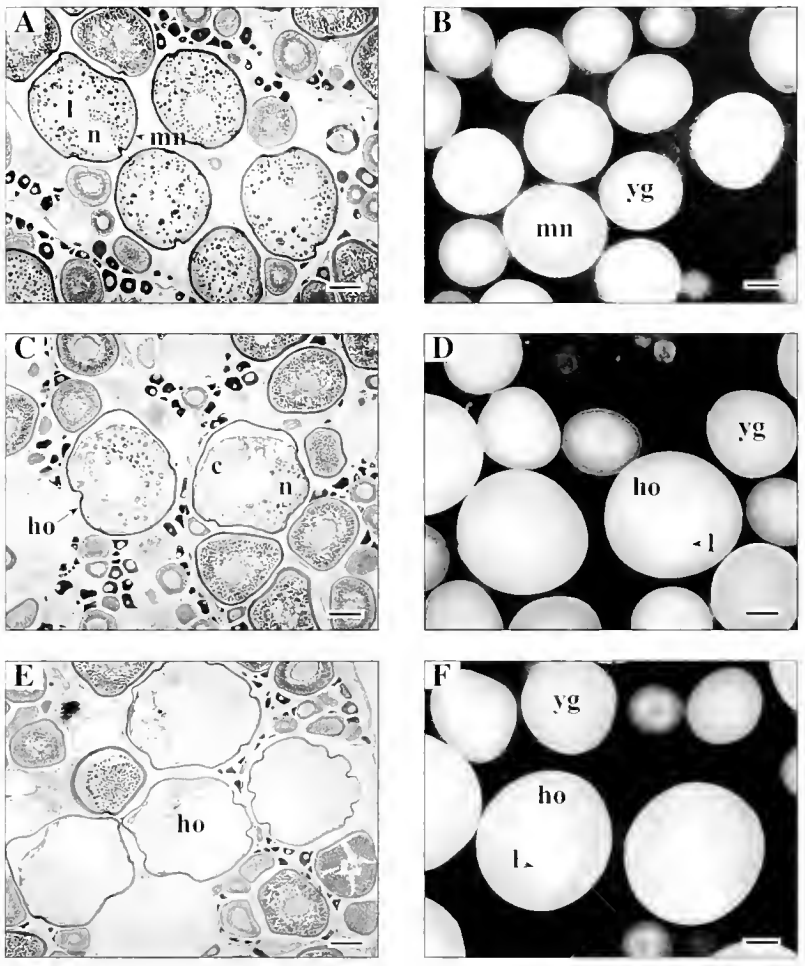

Figure 4

Histological sections of ovaries of individual *Rhabdosargus sarba* caught on 1 and 2 September 2001 at ca. 18:30 h (**A**), 21:30 h (**C**) and 00:30 h (**E**) and photographs of the oocytes from the other lobe of the ovary of the same three fish (**B, D ,F**). c=coalescing yolk and lipid; ho=hydrating oocyte; l=lipid droplet; mn=migratory nucleus oocyte; n=nucleus; yg=yolk granule oocyte. Scale bars = 200 μm in A, C, and D and 250 μm in B, D, and F.

Discussion

Oocyte hydration, ovulation, and spawning periods

Because histological studies showed that the ovaries of numerous fish caught on different occasions between 18:30 and 20:30 h did not contain recently formed POFs, we deduced that these fish had not spawned in the previous few hours. However, at this time, the ovaries of many fish, that were designated macroscopically as at stage V and stage VI, often contained numerous migratory nucleus-stage oocytes and, towards the end of this period, often a few oocytes in the early stages of hydration. Although the frequency distributions of the oocyte diameters of fish examined on both 1 and 13 September were still unimodal at 18:30 to 20:30 h, they had become bimodal by 21:30 to 23:30 h (Fig. 3), reflecting the fact that, by this time, numerous oocytes had become markedly enlarged through hydration. The above data demonstrate that hydration typically commences soon after dusk. Furthermore, because a number of *R. sarba* caught between 01:30 and 04:30 h, and particularly towards the end of this time interval, contained ovaries undergoing ovulation and had newly formed POFs, the period between the onset of hydration and commencement of ovulation typically lasts about 7–10 hours, which is very similar to the duration estimated for species such as the black sea anchovy (*Engraulis encrasicholus*) (Lisovenko and Andrianov, 1991) and ballyhoo (*Hemiramphus brasiliensis*) (McBride et al., 2003). Although we

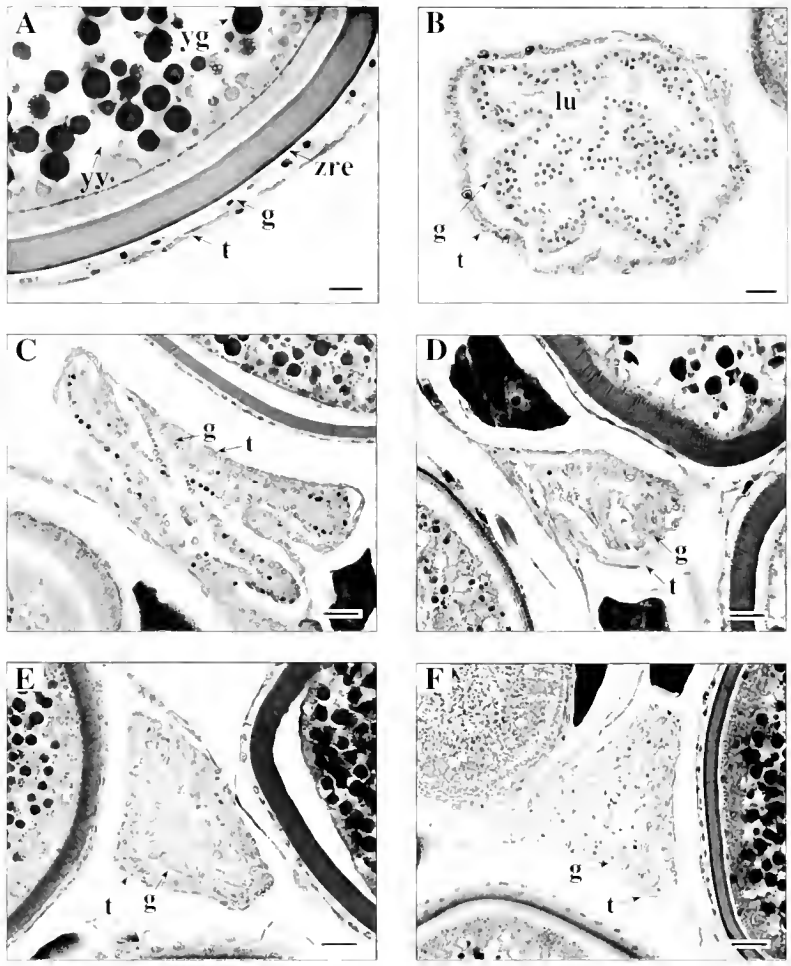

Figure 5

Histological sections through ovaries of *Rhabdosargus sarba* showing (**A**) the outer layers of a yolk granule oocyte, and postovulatory follicles in the ovaries of fish collected at (**B**) ca. 02:00, (**C** and **D**) ca. 18:30, (**E**) ca. 22:00 and ca. (**F**) 01:00 h. g=granulosa layer; lu=lumen; t=thecal layer; yg=yolk granule; yv=yolk vesicle; zre=zona radiata externa. Scale bars = 25 μm in A, and 50 μm in B–F.

caught several *R. sarba* with new POFs in their ovaries and hydrated oocytes in their oviducts, we were able to catch only one individual of this species in which the ovaries possessed new POFs and no hydrated oocytes. The latter fish, which had clearly just completed spawning, was caught between 05:00 and 06:00 h.

Several species are known typically to complete spawning in the 10–14 hours after the time when their oocytes commence hydration, e.g., the northern anchovy (*Engraulis mordax*) (Hunter and Macewicz, 1985), the spotted seatrout (*Cynoscion nebulosus*) (Brown-Peterson et al., 1988) and the horse mackerel (*Trachurus trachurus*) (Karlou-Riga and Economidis, 1997). Furthermore, spawning is typically completed 2–5 hours after the commencement of ovulation, e.g., the spotted seatrout (*Cynoscion nebulosus*) (Brown-Peterson et al., 1988), the Black Sea anchovy (*Engraulis encrasicholus*) (Lisovenko and Andrianov, 1991) and the weakfish (*Cynoscion regalis*) (Taylor and Villoso, 1994). These consistent data, when considered in conjunction with the similar duration of hydration of *R. sarba*, and the capture of a very recently spawned fish between 05:00 and 06:00 h, provide very strong circumstantial evidence that, in the lower Swan River Estuary, *R. sarba* spawns mainly between 02:00 and 06:00 h.

The newest POFs in the ovaries of *R. sarba* caught at dusk, i.e., at 18:30 h, had degenerated to an extent similar to those of ca. 12-h-old POFs in the ovaries of other species, e.g. the skipjack tuna (*Katsuwonus pelamis*) (Hunter et al., 1986) and the whitemouth croaker

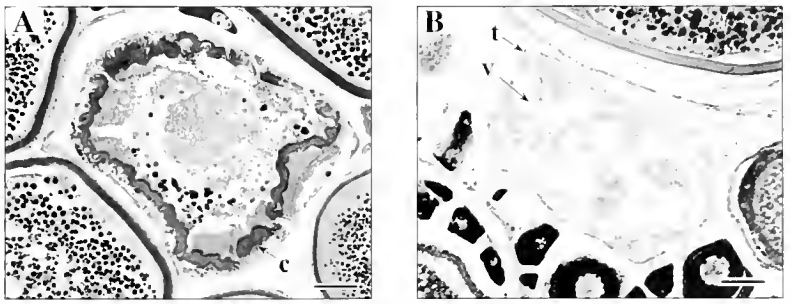

Figure 6

Histological sections of ovaries of *Rhabdosargus sarba* showing an oocyte at the (**A**) α and (**B**) β stages of atresia. c=chorion; t=thecal layer; v=vacuole. Scale bars = 100 μm in A and 50 μm in B.

(*Micropogonias furnieri*) (Macchi et al., 2003). This finding provides further evidence that *R. sarba* spawns close to dawn. Certainly, the state of degeneration of the newest POFs in mature ovaries of *R. sarba* at dusk provides very strong circumstantial evidence that spawning could not have occurred during at least most of the previous daylight hours.

Our results demonstrate that the prevalence of fish with ovaries at mid to late atretic state 1 declined precipitously as salinities increased from their winter minima in July and August and that this decrease was accompanied by an increase in the prevalence of migratory nucleus oocytes, hydrated oocytes or POFs. The implication that the oocytes of *R. sarba* are often inhibited from undergoing final oocyte maturation when salinities are low parallels the conclusions drawn for the influence of salinity on the gonadal development of *Cynoscion nebulosus* in estuaries entering the Gulf of Mexico (Brown-Peterson et al., 2002). The resorption of yolk granule oocytes by the ovaries of *R. sarba* in July and August would help conserve energy at a time when, if those oocytes progressed through to final maturation and were released, they would be exposed to salinities that are known to be lower than those required for optimal development (Mihelkakis and Kitajima, 1994).

Frequency of spawning

Because ovulation lasts for ca. 2–5 hours, the POFs that were present in ovulating ovaries and that showed no detectable signs of degeneration were presumably <3 hours old. It then follows that, when POFs at intermediate and advanced stages of degeneration were present in those same ovaries, those POFs were presumably ca. 24 and ca. 48 hours old, respectively. Thus, the presence of these three very distinct forms of POFs in the same ovary of a fish implies that individual *R. sarba* are capable of spawning on at least three successive days during that part of the month when spawning activity is greatest.

The estimated average frequency of spawning by *R. sarba*, i.e., once every 2.7 days, is essentially the same as that recorded for several other species, including e.g., spotted seatrout (*Cynoscion nebulosus*) (Brown-Peterson et al., 1988, 2002), red drum (*Sciaenops ocellatus*) (Wilson and Nieland, 1994), and common snook (*Centropomus undecimalis*) (Taylor et al., 1998). The resultant conclusion that *R. sarba* spawns about 45 times during a spawning period is comparable to that estimated for black sea anchovy (*Engraulis encrasicholus*) (Lisovenko and Andrionov, 1991) and cobia (*Rachycentron canadum*) (Brown-Peterson et al., 2001). However, spawning frequency does vary markedly among species.

Relationship between spawning time and tidal cycle

Although seine netting between 00:30 and 05:30 h on a number of days yielded no female *R. sarba* with newly formed POFs, rod-and-line angling in deeper water between 01:30 and 04:30 h yielded several females in which the ovaries contained both newly formed POFs and concentrations of hydrated oocytes in their oviducts, and also running ripe males. This finding provides strong circumstantial evidence that, just prior to ovulation, *R. sarba* moves from nearshore shallows to offshore deeper waters.

Because *R. sarba* typically spawns just prior to the commencement of a relatively strong ebb tide, the fertilized eggs would likely be transported downstream and out of the estuary. The conclusion that eggs are swept out of the estuary is supported by the fact that only 15 larvae of *R. sarba* were caught during extensive sampling of the lower Swan River Estuary and that virtually all of these larvae were caught at its mouth (Gaughan et al., 1990). A downstream movement of eggs would be further facilitated by *R. sarba* spawning in deeper waters, where the current is greatest. Emigration of eggs from the estuary would enhance the chances of survival of the eggs of this essentially marine species by ensuring that they would develop in

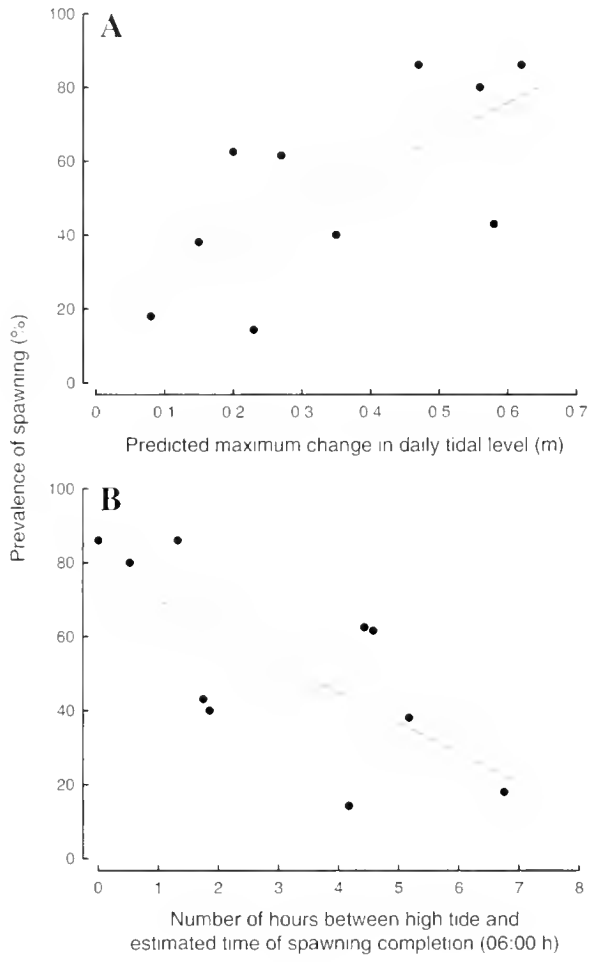

Figure 7

Relationship between prevalence of spawning and (**A**) the predicted maximum change in daily tidal level and (**B**) the difference between the time of high tide and the time at which spawning in *Rhabdosargus sarba* is estimated to be completed in the lower Swan River Estuary (06:00 h). Each point represents the data for a separate sampling occasion.

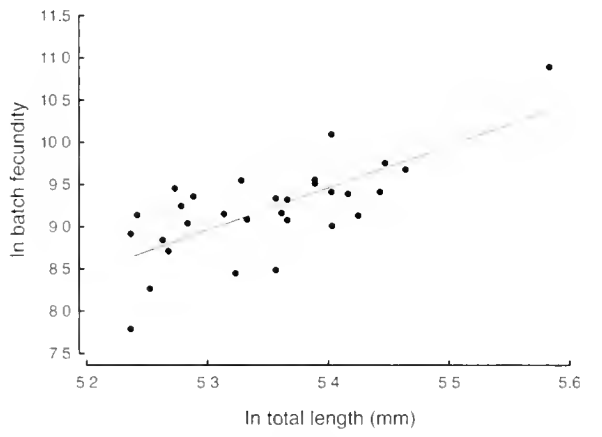

Figure 8

Relationship between batch fecundity (=number of hydrated oocytes) and total length (mm) for *Rhabdosargus sarba*.

a marine environment in which salinity remained constantly at ca. 35‰, rather than in one in which sudden rainfall could result in sudden marked declines in salinity. However, the possession of spawning cycles linked to lunar and tidal periodicities can reduce the likelihood of predation (Taylor, 1984). For example, Johannes (1978) pointed out that, because the spawning of many reef-dwelling fishes is synchronized with the lunar cycle and occurs on high or ebbing tides, their eggs would be transported away from reefs, where the concentration of predators is high, and consequently the likelihood of predation during the early stages of life would be reduced. Because planktivorous fishes are abundant in estuaries (Johnson et al., 1990; Morgan, 1990), including the Swan River Estuary where the planktivorous *Spratelloides robustus* was particularly numerous in some of our seine-net catches, a movement of the eggs of *R. sarba* out of the estuary would also enhance their chances of avoiding predation by that species.

A downstream transport of eggs would account for the relatively few young 0+ juveniles that are recruited into the nearshore shallow waters of the estuary (Hesp et al., 2004). Indeed, substantial recruitment into these nearshore waters, presumably as a result of immigration from coastal marine waters, does not occur until *R. sarba* is about one year old and about 140 mm in length (Hesp et al., 2004). Because *R. sarba* settles at a length of ca. 12 mm (Hesp et al., 2004) and ca. 30 days of age (Neira[1]), this immigration back into the estuary does not occur until 11 months after settlement. In contrast to the situation in the Swan River Estuary, *R. sarba* elsewhere typically spawns in marine waters and their larvae often enter estuaries on flood tides (e.g., Miskiewicz, 1986; Neira and Potter, 1992).

Potential annual fecundity

The estimates of potential annual fecundity derived for *R. sarba* during the present study, which ranged from 109,000 to 2,417,000 eggs for fishes of 188 and 266 mm total length, respectively, greatly exceed those of El-Agamy (1989), which ranged from 23,000 to 99,000 eggs for fishes of 170 and 260 mm total length, respectively. However, because El-Agamy (1989) based his estimates on the number of large oocytes present in the ovaries of individual *R. sarba*, he did not take into account the fact

[1] Neira, F. J. 2004. Personal commun. Australian Maritime College, Faculty of Fisheries and Marine Environment, PO Box 21, Beaconsfield, Tasmania 7270, Australia.

that this species has indeterminate fecundity. Thus, the values recorded for the annual fecundity of *R. sarba* in the Arabian Gulf almost certainly represent a marked underestimate of the true annual fecundity of this species in that region.

Acknowledgments

Our gratitude is expressed to colleagues and friends for help with sampling—to G. Thomson for preparing the histological sections, to F. J. Neira for information on the larval phase of *R. sarba*, and to D. Fairclough and two anonymous reviewers for invaluable comments on the manuscript. Financial support was provided by Murdoch University.

Literature cited

Brown-Peterson, N. J., R. M. Overstreet, J. M. Lotz, J. S. Francis, and K. M. Burns.
2001. Reproductive biology of cobia, *Rachycentron canadum*, from coastal waters of the southern United States. Fish. Bull. 99:15–28.

Brown-Peterson, N. J., M. S. Peterson, D. L. Nieland, M. D. Murphy, R. D. Taylor, and J. R. Warren.
2002. Reproductive biology of female spotted seatrout, *Cynoscion nebulosus*, in the Gulf of Mexico: differences among estuaries? Environ. Biol. Fishes 63:405–415.

Brown-Peterson, N., P. Thomas, and C. R. Arnold.
1988. Reproductive biology of the spotted seatrout, *Cynoscion nebulosus*, in south Texas. Fish. Bull. 86:373–388.

Buxton, C. D., and P. A. Garratt
1990. Alternative reproductive styles in seabreams (Pisces: Sparidae). Environ. Biol. Fishes 28:113–124.

El-Agamy, A. E.
1989. Biology of *Sparus sarba* Forskål from the Qatari water, Arabian Gulf. J. Mar. Biol. Assoc. India. 31:129–137.

Farley, J. H., and T. L. O. Davis.
1998. Reproductive dynamics of southern bluefin tuna, *Thunnus maccoyii*. Fish. Bull. 96:223–236.

Gaughan, D. J., F. J. Neira, L. E. Beckley and I. C. Potter.
1990. Composition, seasonality and distribution of the ichthyoplankton in the lower Swan Estuary, south-western Australia. Aust. J. Mar. Freshw. Res. 41:529–543.

Garratt, P. A.
1993. Comparative aspects of the reproductive biology of seabreams (Pisces: Sparidae). Ph.D. thesis, vol. 1, 175 p. Rhodes Univ., Grahamstown, South Africa.

Greeley, M. S., D. R. Marion, and R. MacGregor III.
1986. Semilunar spawning cycles of *Fundulus similes* (Cyprinodontidae). Environ. Biol. Fishes 17:125–131.

Hesp, S. A., N. G. Hall and I. C. Potter.
2004. Size-related movements of *Rhabdosargus sarba* in three different environments and their influence on estimates of von Bertalanffy growth parameters. Mar. Biol.

Hesp, S. A., and I. C. Potter.
2003. Reproductive biology of the tarwhine *Rhabdosargus sarba* (Sparidae) in Western Australian waters, in which it is a rudimentary hermaphrodite J. Mar. Biol. Assoc. U.K. 83:1333–1346.

Hoque, M. M., A. Takemura, M. Matsuyama, S. Matsuura, and K. Takano.
1999. Lunar spawning in *Siganus canaliculatus*. J. Fish Biol. 55: 1213-1222.

Hunter J. R., and S. R. Goldberg.
1980. Spawning incidence and batch fecundity in northern anchovy, *Engraulis mordax*. Fish. Bull. 77:641–652.

Hunter, J. R., N. C. H. Lo, and R. J. H. Leong.
1985. Batch fecundity in multiple spawning fishes. *In* An egg production method for estimating spawning biomass of pelagic fish: application to the northern anchovy (*Engraulis mordax*) (R. Lasker, ed.), p. 67–77. NOAA Tech. Rep. NMFS 36.

Hunter, J. R., and B. J. Macewicz.
1985. Measurement of spawning frequency in multiple spawning fishes. *In* An egg production method for estimating spawning biomass of pelagic fish: application to the northern anchovy (*Engraulis mordax*) (R. Lasker, ed.), p. 79–94. NOAA Tech. Rep. NMFS 36.

Hunter, J. R., B. J. Macewicz, L. N. Chyan-huei, and C. A. Kimbrell.
1992. Fecundity, spawning, and maturity of female Dover sole *Microstomus pacificus*, with an evaluation of assumptions and precision. Fish. Bull. 99:101–128.

Hunter J. R., B. J. Macewicz, and J. R. Sibert.
1986. The spawning frequency of skipjack tuna *Katsuwonus pelamis*, from the South Pacific. Fish. Bull. 84:895–903.

Johannes, R. E.
1978. Reproductive strategies of coastal marine fishes in the tropics. Environ. Biol. Fishes 3:65–84.

Johnson, W. S., D. M. Allen, M. V. Ogburn, and S. E. Stancyk.
1990. Short-term predation responses of adult bay anchovies *Anchoa mitchilli* to estuarine zooplankton availability. Mar. Ecol. Prog. Ser. 64:55–68.

Karlou-Riga C., and P. S. Economidis.
1997. Spawning frequency and batch fecundity of horse mackerel, *Trachurus trachurus* (L.), in the Saronikos Gulf (Greece). J. Appl. Ichthyol. 13:97–104.

Kuiter, R. H.
1993. The complete diver's and fishermen's guide to coastal fishes of south-eastern Australia, 437 p. Crawford House Press, Bathurst, Australia.

Laevastu, T.
1965. Manual of methods in fisheries biology. FAO, Rome.

Lisovenko, L. A., and D. P. Andrianov.
1991. Determination of absolute fecundity of intermittently spawning fishes. Vop. Ikhtiol. 31:631–641.

Macchi, G. J., E. M. Acha and M. I. Militelli.
2003. Seasonal egg production of whitemouth croaker (*Micropogonias furnieri*) in the Río de la Plata estuary, Argentina-Uruguay. Fish. Bull. 101:332–342.

McBride, R. S., J. R. Styer and R. Hudson.
2003. Spawning cycles and habitats for ballyhoo (*Hemiramphus brasiliensis*) and balao (*H. balao*) in south Florida. Fish. Bull. 101:583–589.

Mihelkakis, A., and C. Kitajima.
1994. Effects of salinity and temperature on incubation period, hatching rate, and morphogenesis of the silver sea bream, *Sparus sarba* (Forskål, 1775). Aquaculture 126:361–371.

Miskiewicz, A. G.
1986. The season and length at entry into a temper-

ate Australian estuary of the larvae of *Acanthopagrus australis*, *Rhabdosargus sarba* and *Chrysophrys auratus* (Teleostei: Sparidae). *In* Indo-Pacific fish biology: proceedings of the second international conference on Indo-Pacific fishes (T. Uyeno, A. R. Taniuchi and K. Matsuura, eds.), p. 740–747. Ichthyological Society of Japan, Tokyo.

Morgan, S. G.
1990. Impact of planktivorous fishes on dispersal, hatching, and morphology of estuarine crab larvae. Ecology 71:1639–1652.

Neira, F. J., and I. C. Potter.
1992. Movement of larval fishes through the entrance channel of a seasonally open estuary in Western Australia. Estuar. Coast. Shelf Sci. 35:213–224.

Nichol, D. G., and E. I. Acuna.
2001. Annual and batch fecundities of yellowfin sole, *Limanda aspera*, in the eastern Bering Sea. Fish. Bull. 99:108–122.

Potter, I. C., and G. A. Hyndes.
1999. Characteristics of the ichthyofauna of southwestern Australian estuaries, including comparisons with holarctic estuaries and estuaries elsewhere in temperate Australia: areview. Aust. J. Ecol. 24:395–421.

Schwassmann, H. O.
1971. Biological rhythms. *In* Fish physiology, vol. VI (W. S. Hoar and D. J. Randall, eds.), p 371–428. Academic Press Inc., New York, NY.

Smith, K. A., and I. M. Suthers.
2000. Consistent timing of juvenile fish recruitment to seagrass beds within two Sydney estuaries. Mar. Freshw. Res. 51:765–776.

Spencer, R. S.
1956. Studies in Australian estuarine hydrology. 2. The Swan River. Aust. J. Mar. Freshw. Res. 7:193–253.

Taylor, M. H.
1984. Lunar synchronisation of fish reproduction. Trans. Am. Fish. Soc. 113:484–493.

Taylor, M. H., and L. DiMichele.
1980. Ovarian changes during the lunar spawning cycle of *Fundulus heteroclitus*. Copeia 1980:118–125.

Taylor, M. H., and E. P. Villoso.
1994. Daily ovarian cycles in weakfish. Trans. Am. Fish. Soc. 123:9–14.

Taylor, R. G., H. J. Grier, and J. A. Whittington.
1998. Spawning rhythms in common snook in Florida. J. Fish Biol. 53:502–520.

van der Elst, R.
1988. A guide to the common sea fishes of Southern Africa, 2nd ed., 398 p. Struik Publishers, Cape Town, South Africa.

Wallace, J. H.
1975. The estuarine fishes of the east coast of South Africa. III. Reproduction. South African Association for Marine Biological Research, Oceanographic Research Institute, Investigational Report 41. The Oceanographic Research Inst., Durban, South Africa.

Wallace, R. A., and K. Selman.
1989. Cellular and dynamic aspects of oocyte growth in teleosts. Am. Zool. 21:325–343.

Wilson, C. A., and D. L. Nieland.
1994. Reproductive biology of red drum, *Sciaenops ocellatus*, from the neritic waters of the northern Gulf of Mexico. Fish Bull. 92:841–850.

Yeung, W. S. B., and S. T. H. Chan.
1987. The gonadal anatomy and sexual pattern of the protandrous sex-reversing fish, *Rhabdosargus sarba* (Teleostei: Sparidae). J. Zool. Lond. 212:521–532.

Fishery dynamics of the California market squid (*Loligo opalescens*), as measured by satellite remote sensing

Michael R. Maxwell
University of California
c/o Southwest Fisheries Science Center
8604 La Jolla Shores Drive
La Jolla, California 92037
Present address: Department of Biology
University of San Diego
5998 Alcalá Park
San Diego, California 92110
E-mail address maxwellm@sandiego.edu

Annette Henry
California Department of Fish and Game
8604 La Jolla Shores Drive
La Jolla, California 92037

Christopher D. Elvidge
NOAA National Geophysical Data Center
325 Broadway
Boulder, Colorado 80305

Jeffrey Safran
Vinita R. Hobson
Ingrid Nelson
Benjamin T. Tuttle
Cooperative Institute for Research in Environmental Sciences
University of Colorado
Boulder, Colorado 80303

John B. Dietz
Cooperative Institute for Research on Atmosphere
Colorado State University
Fort Collins, Colorado 80523

John R. Hunter
Southwest Fisheries Science Center
NOAA National Marine Fisheries Service
8604 La Jolla Shores Drive
La Jolla, California 92037

Abstract—Novel data on the spatial and temporal distribution of fishing effort and population abundance are presented for the market squid fishery *(Loligo opalescens)* in the Southern California Bight, 1992–2000. Fishing effort was measured by the detection of boat lights by the Defense Meteorological Satellite Program (DMSP) Operational Linescan System (OLS). Visual confirmation of fishing vessels by nocturnal aerial surveys indicated that lights detected by satellites are reliable indicators of fishing effort. Overall, fishing activity was concentrated off the following Channel Islands: Santa Rosa, Santa Cruz, Anacapa, and Santa Catalina. Fishing activity occurred at depths of 100 m or less. Landings, effort, and squid abundance (measured as landings per unit of effort, LPUE) markedly declined during the 1997–98 El Niño; landings and LPUE increased afterwards. Within a fishing season, the location of fishing activity shifted from the northern shores of Santa Rosa and Santa Cruz Islands in October, the typical starting date for squid fishing in the Bight, to the southern shores by March, the typical end of the squid season. Light detection by satellites offers a source of fine-scale spatial and temporal data on fishing effort for the market squid fishery off California, and these data can be integrated with environmental data and fishing logbook data in the development of a management plan.

Manuscript submitted 24 February 2003 to the Scientific Editor's Office.
Manuscript approved for publication 17 June 2004 by the Scientific Editor.
Fish. Bull. 102:661–670 (2004).

The market squid *(Loligo opalescens)* (also known as the opalescent inshore squid, FAO [Roper et al., 1984]) is currently the largest revenue fishery for California (Vojkovich, 1998; CDFG, 2000). The fishery's importance rose steadily in the 1980s and 1990s, in response to increased demand in Asia coupled with declines in other fisheries off the U.S. West Coast. Market squid is a short-lived species (Jackson, 1994; Butler et al., 1999) whose abundance appears to be readily impacted by environmental variability. For example, squid landings plummeted during the 1997–98 El Niño but reached a record high in the following year (CDFG, 2000). Considered an integral component of California's pelagic fishery, the market squid was included in the Coastal Pelagic Species Fishery Management Plan as approved by the Pacific Fisheries Management Council in 1998. In this plan, federal authority is invoked to monitor the fishery to ensure the provisions of the Magnuson-Stevens Fishery Conservation and Management Act of 1996. If a resource is estimated as overfished, the Council is to consider implementing active management measures.

The lack of records of fishing effort, such as vessel logbooks or observer data, hampered initial attempts to formulate a management plan for the market squid. The nature of the fishery, however, suggested an alternative measure of fishing effort: the detection of boat lights by satellites. The market squid is typically harvested on shallow nearshore spawning grounds in the Southern California Bight and Monterey Bay (Vojkovich, 1998). At night, specialized lightboats shine high intensity (c. 30,000 watt) lights on the water, which attract and congregate the squid near the surface. Seiner boats then capture the concentrated squid with purse-seine nets (Vojkovich, 1998). The lights of the fishing boats are detected and recorded by the U.S. Air Force Defense Meteorological Satellite Program (DMSP) Operational Linescan System (OLS).

DMSP-OLS satellites continuously orbit the planet, acquiring data on

meteorology and, incidentally, nighttime light sources (Croft, 1978; Elvidge et al., 1997, 2001b). Nighttime light detection by satellites has proven useful for various environmental questions, such as identifying the extent of forest fires (Elvidge et al., 2001a) and the effects of urban lighting on sea turtle nest selection and hatchling survivorship (Salmon et al., 2000). Compilation of light data for the global light-fishing squid fleet has contributed to examinations of the fishery's ecosystem impacts (Rodhouse et al., 2001). For local squid fisheries, the locations of boat lights over space and time are particularly valuable in cases where national boundaries pose constraints on the collection of effort data (e.g., *Illex argentinus* in the southwestern Atlantic, Waluda et al., 2002).

In this study, we used boat lights to quantify the spatial and temporal patterns of market squid fishing activity in the Southern California Bight over the period 1992–2000. The bight has come to represent the great majority of squid landings off California (Vojkovich, 1998; Butler et al., 1999; CDFG, 2000). An important component of our study is ground-truthing work that validates the feasibility of using light data as a measure of fishing effort. This estimate for fishing effort enables us to present novel landings-per-unit-of-effort (LPUE) data for the market squid. A companion paper analyzes the light detection properties of the DMSP-OLS satellites over the Southern California Bight (Elvidge et al.[1]).

Materials and methods

Light detection by satellites

The DMSP is a polar orbiting satellite system that acquires daytime and nighttime data during each orbit. The OLS is an oscillating scan radiometer designed for cloud imaging. A full technical description of image acquisition by the DMSP-OLS system, and the subsequent processing of images, appears in a companion paper (Elvidge et al.[1]). Briefly, the DMSP-OLS acquired nighttime data for over 2200 satellite orbits over the Southern California Bight (i.e., 117° to 122° W, 32°30′ to 34°30′N) between 26 April 1992 and 4 April 2001. Four different satellites were employed during this time. Three overlapped in operation dates, producing multiple images for some dates. On all dates, images were acquired between 18:30 and 22:00 Pacific Standard Time (PST), with 20:21 PST being the average time. The satellite images were processed into geo-referenced images of boat lights and clouds. This process involved superimposing a field of grid cells onto the satellite image, which quantified the satellite's "field of view," the extent of detected clouds, and the area available for light detection. Image pixels of lights were taken directly from the satellite image. Pixels were identified as lights by their visible band digital number. The images were subjected to quality-control procedures to correct for atmospheric noise and to eliminate images overly contaminated by solar glare, sunlight, heavy lunar illumination, or those containing missing data. Fixed sources of lights, such as city lights along the southern California coast, the city of Avalon (Santa Catalina Island), off-shore oil platforms, and naval installations, were masked from the light detection algorithm.

Data deliveries were irregular during 1992, resulting in gaps in the early part of the time series. For 1992–98, only data collected during the dark half of the lunar cycle were available. To control for lunar illumination throughout the time series, we restricted analysis of fishery data to images for which lunar illumination was less than 0.02 lux (lumens per square meter). Images for analysis were evaluated against additional criteria. For a given image, we calculated the number of total grid cells that were not used for light detection because of glare, missing data, or the masking of known nonboat lights. If the resulting number of grid cells left available for light detection was at least 50% of the original number of cells, we retained the image for analysis. Cloud coverage can obscure light sources[1]; therefore we used only images from nights when clouds covered less than 25% of the grid cells available for light detection. For nights with multiple acceptable images, we averaged the percent cloud coverage and the number of detected light pixels.

Ground-truthing: aerial observations of boat activity

To determine the relationship between detected light pixels and the number of squid fishing vessels on the water, 35 aerial surveys were conducted from 10 June 1999 to 18 May 2000. Each survey took place in a Cessna 337 Skymaster flown at an average altitude of 1160 m above sea level. The path of each survey covered the main areas of squid fishing activity within the Southern California Bight (Fig. 1): from San Diego, over the Channel Islands, to Point Conception, and back down the coastline to San Diego. Each survey took approximately four hours to complete, occurring between 18:00 h and midnight PST. These times encompassed the time that the DMSP-OLS satellites were over the bight. The 35 surveys produced 26 nights of usable data. Survey data were discarded if satellite images were unavailable, if flights were aborted because of weather, or if heavy fog obscured boat visibility. We note that, for this ground-truthing work, we did not restrict our analysis to nights with lunar illumination of less than 0.02 lux. Rather, we used all of the acceptable 26 nights, and quantified lunar illumination as a proportion of the moon's phase, where 0.00 denoted a new moon and 1.00 denoted a full moon.

All vessels on the water were identified by using Fujinon 10×50 gyroscopic binoculars, and the GPS positions of all vessels were recorded. Vessel type was identified as either a nonsquid vessel or as a squid fishing vessel.

[1] Elvidge, C. D., J. Safran, M. R. Maxwell, K. E. Baugh, A. Henry, and J. R. Hunter. Unpubl. data. Satellite based indices of lightboat fishing effort.

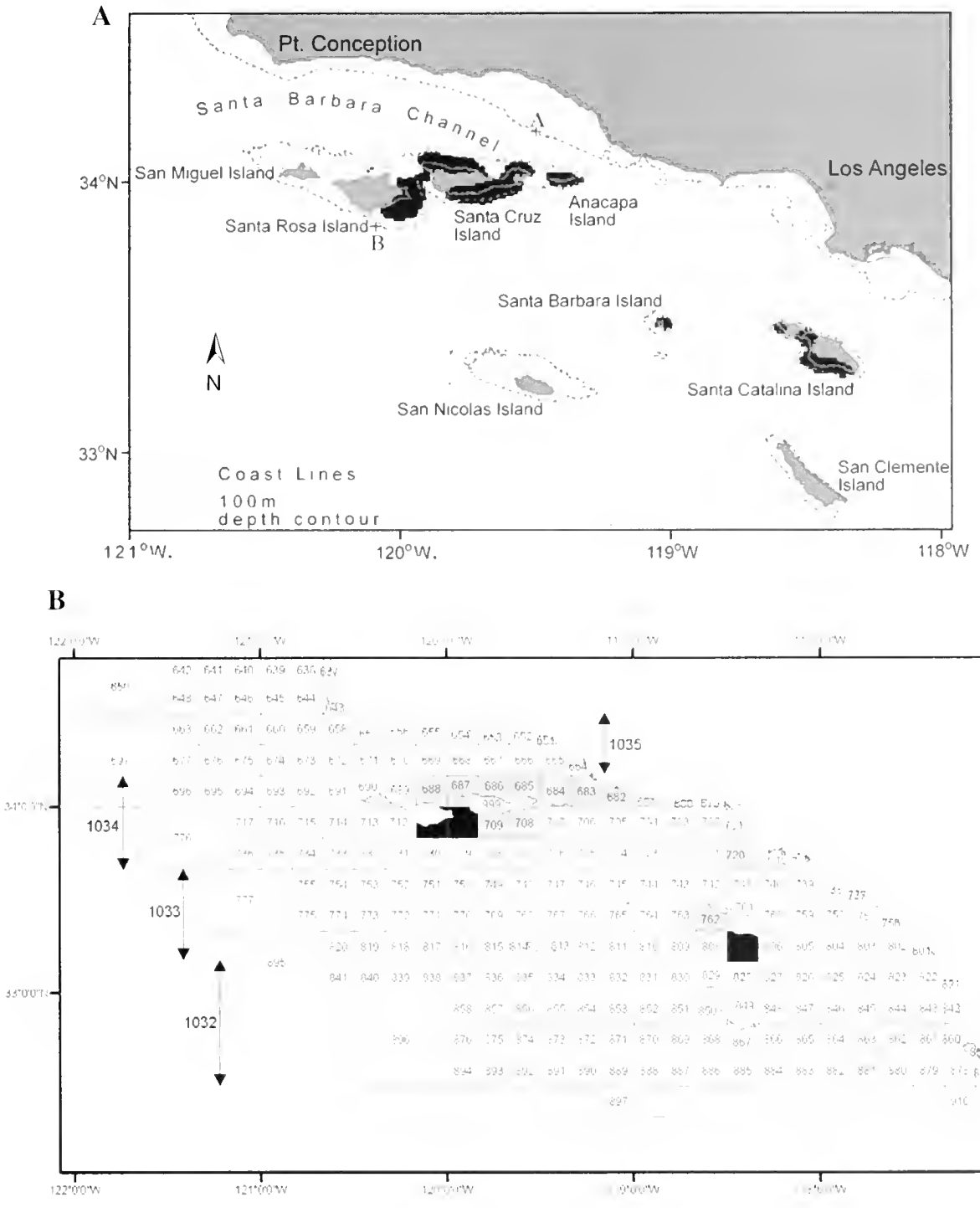

Figure 1

Fishing activity for the market squid in the Southern California Bight, from 26 April 1992 to 28 May 2000. (**A**) Composite satellite image of squid fishing vessel lights (black marks). Permanent sources of lights (e.g., city lights, offshore oil platforms, naval installations) are removed. CalCOFI stations 83.42 ("A"; 34.18° N, 119.51° W) and 83.51 ("B"; 33.88° N, 120.13° W) are indicated. (**B**) Squid landings as reported by California Dept. Fish and Game fishing blocks. Gray: blocks that account for 6.8 million kg (2%) or more of the landings from blocks 651–896. Black: blocks that account for 20.5 million kg (6%) or more. Latitudinal blocks 1032–1035 are indicated. Santa Cruz Island is marked "999" to aid correspondence with A.

Squid fishing vessels could not always be distinguished as light boats or seiners and therefore were recorded as "squid fishing vessels."

The numbers of squid fishing vessels showed large skew in their frequency distribution. These data were transformed by $x' = \log_{10}(x+1)$. Similarly, proportion lunar phase was transformed by $x' = \arcsin(\sqrt{x})$, and detected light pixels were transformed by $x' = \log_{10}(x+1)$ to correct for skew (Zar, 1984). These transformations produced normally distributed data acceptable for regression analysis. With these transformed variables, multiple stepwise regression (forward selection) was performed with the software S-Plus 2000 (MathSoft Inc., Cambridge, MA) to examine the effects of squid fishing vessels and the proportion lunar phase on detected light pixels. Squid fishing vessels and proportion lunar phase showed very little correlation (r=−0.09).

Fishery characteristics, 1992–2000

For quantitative analysis of the fishery data, we aggregated the nightly satellite data (i.e., light pixels detected on the water) into calendar quarters, as suggested by the within-year distribution of squid landings in the bight (Butler et al., 1999). To standardize conditions of light detection, we excluded all data after 28 May 2000, because this was the starting date of mandatory shielding of the high intensity lights of the lightboats. This regulation was enforced by California's Department of Fish and Game to reduce light pollution by the lightboats. The shields did not totally obscure the lightboats from detection by the satellites (authors' pers. obs.) but made the emitted light less bright, and, hence, less detectable by the satellites. Thus, our data for fishing effort spanned calendar quarters from Jul–Sep 1992 to Jan–Mar 2000. We included a quarter for analysis if it contained 10 or more nights of acceptable images. By these criteria, we described effort for 24 of the 31 calendar quarters. The mean number of nights per quarter was 26 (range=10–72 nights).

The quantity (kg) and location of landed market squid were recorded by California Department of Fish and Game (CDFG) throughout the 1992–2000 study period and were made available to the authors. During this study period, squid fishing in the bight occurred exclusively at night (Vojkovich, 1998). The squid were landed at port within several hours after being caught; therefore the landings for a given day corresponded to the previous night's effort. Squid fishermen reported the locations of their hauls by CDFG fishing blocks. We defined catch taken from the Southern California Bight as that from blocks 651–896 and 1032–1035 (Fig. 1). Blocks 651–896 are typically 10′ latitude × 10′ longitude and can be used to locate regions of high catch. Blocks 1032–1035 are large latitudinal bands, generally 30′ wide, that encompass blocks 651–896. We used blocks 1032–1035 in calculating the total catch in the bight, but not in depicting the location of the catch.

To construct the abundance index of landings per unit of effort (LPUE), we first estimated the number of squid fishing vessels for each night of satellite data, using the regression results of the ground-truthing work (see "Results" section). We then summed the nightly estimated number of vessels for each calendar quarter. For those nights for which we had estimated numbers of vessels, we also summed the landed catch within each calendar quarter. To arrive at LPUE for the quarter, we divided the summed landings by the corresponding summed effort.

Environmental data

We used the multivariate ENSO index (MEI) to indicate overall environmental conditions over the course of the 1992–2000 study period. The MEI is a multivariate index that incorporates sea level pressure, surface zonal and meridional wind components, sea surface temperature, surface air temperature, and cloudiness (Wolter and Timlin, 1998). The MEI index is calculated for the tropical Pacific (i.e., between 10°N and 10°S, from Asia to the Americas), and its monthly values appear on the website http://www.cdc.noaa.gov/~kew/MEI/table.html.[2]

Analysis of the location of fishing effort over the course of the traditional squid fishing season in the bight led to an investigation of oceanographic data for waters surrounding Santa Cruz Island in March. Specifically, we examined sea temperature from two sources. First, we obtained sea surface temperature for all satellite nights in March 1993–2000 from the Physical Oceanography Distributed Active Archive Center (PO.DAAC) at California Institute of Technology (Pasadena, CA). These data were reported for 18×18 km grids, which were approximately the size of the 10′×10′ fishing blocks. We selected the grid that covered block 686 to represent the northern shore of the island, and that which covered block 708 to represent the southern shore (Fig. 1B). For each year in the 1993–2000 period, we calculated mean March temperature for both blocks.

The second source of sea temperature was the database maintained by the California Cooperative Oceanic Fisheries Investigations (CalCOFI). Since 1950, the CalCOFI program has conducted quarterly survey cruises along transects perpendicular to the southern California coast. This system of transects incorporates 66 geographically fixed stations. At each station, a conductivity-temperature-depth (CTD) instrument is deployed. Details on survey methods appear on the website http://www-mlrg.ucsd.edu/calcofi.html,[3] along with the publicly accessible database. For April 1993–2000, we obtained temperatures at sea surface and at 75 meters depth at two stations (Fig. 1A): 83.42 (northeast of Santa Cruz Island; 34.18°N, 119.51°W) and 83.51 (southwest of Santa Cruz Island; 33.88°N, 120.13°W).

[2] NOAA-CIRES Climate Diagnostics Center website. [Accessed 3 November 2003.]

[3] California Cooperative Oceanic Fisheries Investigations website. [Accessed 3 November 2003.]

One measurement was made at each station at sea surface and at 75 meters depth during April (n=8 for both depths).

Results

Ground-truthing: aerial observations of boat activity

Nonsquid vessels used weak lights (i.e., much less than 30,000 watts), which did not show in the satellite images. On average, 23 squid fishing vessels were observed each night by the aerial surveys (range=0–64 vessels, n=26 nights). The 20:00-midnight observation period was the peak time for attraction of squid by the light boats. Although the squid vessels did change location during this time, they typically left their lights running to continue searching for squid. The number of squid vessels explained much of the variation in detected light pixels; proportion lunar phase failed to enter the analysis as a significant variable (Table 1). Detected light pixels increased with the number of squid vessels (Fig. 2).

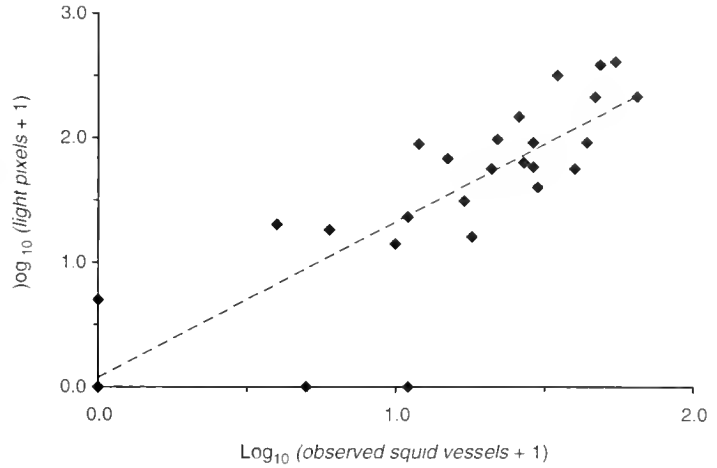

Figure 2

Plot of $\log_{10}$-transformed number of squid vessels and detected light pixels. Regression line taken from the statistics in Table 1.

The regression analysis yields the following simplified equation:

$$\log_{10}(p_t+1)=1.25\times\log_{10}(x_t+1), \quad (1)$$

where x_t = observed number of squid vessels; and
p_t = detected light pixels for night t.

We used inverse prediction to estimate the number of squid vessels for each satellite night ($\hat{E}_t$) in the 1992–2000 period (Zar, 1984). The estimated number of squid vessels was found by the equation

$$\hat{E}_t=10^{\log_{10}(p_t+1)/1.25}-1=\sqrt[1.25]{p_t+1}-1. \quad (2)$$

The ground sample distance of the satellite data is 2.7 km, which means that multiple squid vessels may potentially fit into one pixel of detected light. This could result in an underestimation of effort. The severity of this problem can be assessed by examining the coefficient of the simple linear regression of log-transformed variables represented by Equation 1. One of four scenarios is possible: 1) boats are not aggregated (coefficient=1), 2) boats are aggregated regardless of the number of boats on the water (coefficient=1), 3) boats are aggregated only when many boats are on the water (coefficient<1), or 4) boats are aggregated only when few boats are on the water (coefficient>1). The coefficient in Equation 1 is 1.25, which fails to significantly differ from 1.00 (t-test for regression coefficient: t = 1.305, β_0 = 1, df = 24, P > 0.2, two-tailed; power < 0.5, retrospectively calculated; Zar, 1984). This result suggests that very little clumping of the boats occurred (scenario 1), or that the degree of clumping was independent of the number of boats on the water (scenario 2). Although the statistical power of this t-test is not high (power<0.5), we conclude that the data provide more support for scenarios 1 and 2 over scenarios 3 and 4. Either scenario, 1 or 2, allows for a comparison of the relative values of estimated effort and LPUE within a time series.

Table 1

Multiple stepwise (forward selection) regression of detected light pixels on squid fishing vessels (transformed: $x'=\log_{10}(x+1)$ and proportion lunar phase (transformed: $x'=\arcsin(\sqrt{x})$. r^2=0.64; ANOVA: $F_{1,24}$=42.66, P<0.0001.

Variable	Coefficient ±SE	P
Squid fishing vessels	1.25 ±0.19	<0.0001
INTERCEPT	0.07 ±0.24	>0.75
Proportion lunar phase	not entered	not entered

Fishery characteristics, 1992–2000

A composite satellite image of all squid fishing activity in the Southern California Bight during the 1992–2000 study period revealed major concentrations of effort off the Channel Islands, especially Santa Rosa, Santa Cruz, Anacapa, and Santa Catalina (Fig. 1A). Squid fishing occurs close to the island shores and is bounded by the 100-m contour. During the study period, 379.2 billion kg of squid were landed in the bight: 341.2 billion from blocks 651–896 (Fig. 1B), and the remainder from the large blocks 1032–1035. The main areas of fishing activity, as indicated by satellite, are consistent with the blocks of high catch (Fig. 1B). We note that blocks 682

and 720, although areas of high catch, do not appear on the satellite composite because the mainland shore was excluded from light detection. Further, much activity was evident around Santa Barbara Island (block 765). Although this block represented 4.0 million kg (18th out of the 127 blocks), it did not rank highly enough for inclusion in Fig. 1B.

Analysis of temporal trends in the fishery showed peaks in landed catch for the bight in the fall and winter quarters (Oct–Dec and Jan–Mar, respectively; Fig. 3A). There was a near absence of catch during most of 1997–98 (Fig. 3A), which corresponded to the strong El Niño event during this period (Fig. 4). Effort data revealed surges in the Oct–Dec quarters before the 1997–98 El Niño (Fig. 3B). The Oct–Dec quarter of 1998 signalled a resumption of fishing effort following El Niño, but effort levels for 1999 and early 2000 were lower than pre-El Niño levels. Interestingly, squid abundance, as measured by landings per unit of effort (LPUE), showed a rapid increase from the El Niño lows, and squid abundance for 1999–2000 reached the highest values of the time series (Fig. 3C).

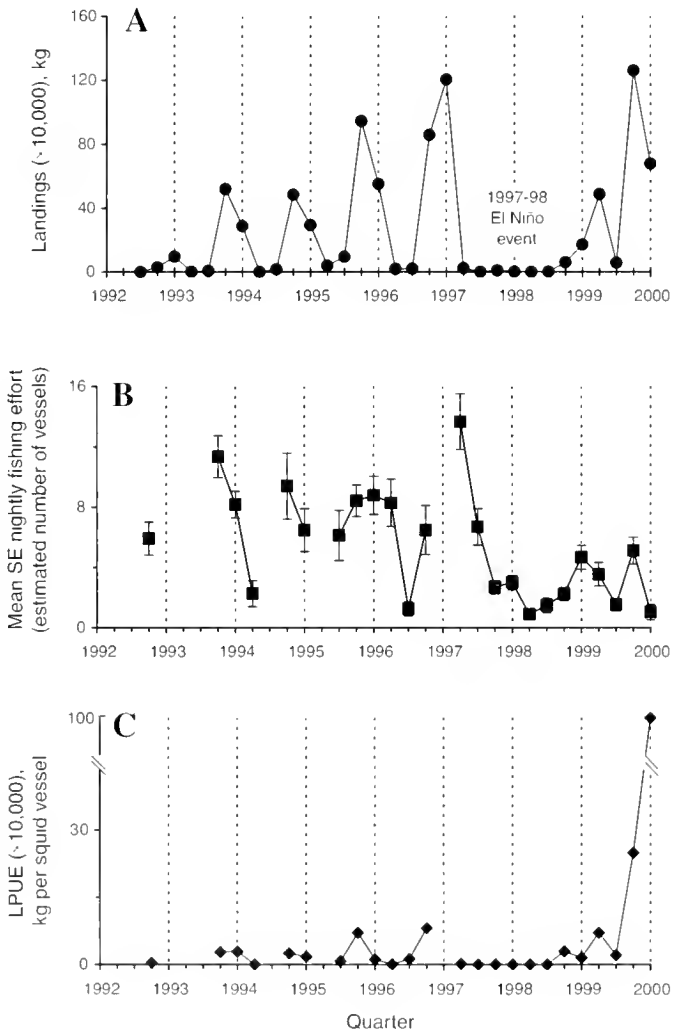

Figure 3

Time series of market squid fishery data in Southern California Bight, by calendar quarter (Jul–Sep 1992 to Jan–Mar 2000). The Jan–Mar quarters are marked by dashed vertical lines. (**A**) Landings are in kg (blocks 651–896, 1032–1035). (**B**) Mean ±SE nightly fishing effort, in estimated number of squid vessels. (**C**) Landings per unit of effort (LPUE): summed landings (kg) on satellite nights were divided by summed effort (estimated number of squid vessels) on the corresponding nights.

Analysis of boat locations along the Channel Islands revealed a shift over the course of the fishing season. Compiling the satellite data to yield composite images in multiyear sets, we found that fishing activity in October consistently included the north shore of Santa Cruz Island (Fig. 5, A,C,E). In contrast, fishing activity in March showed considerable reduction along the north side of Santa Cruz Is., but activity continued along the island's southern shore (Fig. 5, B,D,F). Composite images for December and January were also examined for all of the multiyear sets. December marked a transitional stage from the activity in October to reduction of fishing in March along the northern shores. In all multiyear sets, the December lights along northern Santa Cruz Island were more scattered and less dense than those in October. January images were very similar to those for March. Although data from March 1993–95 indicated little fishing activity, a composite image for January 1993–95 was very similar to that for March 1999–2000: light banks occurred off southern Santa Cruz, southeastern Santa Rosa, and around Anacapa, but were virtually absent from northern Santa Cruz and Santa Rosa.

Water temperatures around Santa Cruz Island did not consistently differ between northern and southern waters. March sea surface temperatures, measured by satellite, were very similar for the island's northern and southern shores (Table 2). April sea surface temperatures, measured at CalCOFI stations, were slightly warmer to the northeast of the island (Table 2). Temperatures at 75 meters, however, were nearly identical for the two CalCOFI stations (Table 2).

Discussion

The satellite images and landings data corroborated spatial and temporal patterns of fishing activity for the market squid. For the period 1992–2000, both data sets indicated intense harvesting along the Channel Islands of Santa Rosa, Santa Cruz, Anacapa, and Santa Catalina. The satellite images captured additional information, such as fishing activity being

Table 2

Water temperature (°C) for the northern and southern waters around Santa Cruz Island, March and April, 1993–2000.

	Northern waters				Southern waters			
Depth (m)	Location	Mean	Min	Max	Location	Mean	Min	Max
March sea surface temperature, as measured by satellite (PO.DAAC data)[1]								
0	Block 686	14.5	12.8	15.7	Block 708	14.7	13.2	15.9
April temperature, measured at CalCOFI stations[2]								
0	Station 83.42	13.6	11.6	16.7	Station 83.51	12.8	11.2	14.5
75	Station 83.42	9.9	9.3	11.2	Station 83.51	10.3	9.3	11.2

[1] Measurements made on multiple nights per month of March (range of measured nights per month of March: 6–26). "Mean" is the overall average of the mean March temperatures; "Min" is the minimum of the mean values, "Max is the maximum, of the mean values.

[2] One measurement made at each station at each depth per month of April (n=8 for both depths).

clearly delimited by the 100-m contour. The landings data, reported by fishing blocks, were much cruder in geographic scale and failed to catch this subtlety.

The ground-truthing work conducted by aerial surveys indicated that detected light pixels are useful in estimating the number of squid vessels in operation. This result is consistent with examination of the fishery for the squid *Illex argentinus* in the southwestern Atlantic, where vessels use powerful lamps to attract the squid to lures (Waluda et al., 2002). In the latter fishery, analysis of images acquired by the DMSP-OLS satellites revealed a good fit between the recorded number of vessels in operation on a given night and the number of light pixels detected (Waluda et al., 2002).

In the present study, the fishery data showed a strong response to the 1997–98 El Niño event, which was one of the strongest events on record (Wolter and Timlin, 1998). Fishing effort and landings tended to peak in the Oct–Dec and Jan–Mar quarters before the 1997–98 El Niño. Both data series dramatically dropped during the 1997–98 El Niño and showed recovery afterwards. Squid abundance, measured as LPUE, also showed a pronounced drop and rapid increase in response to the El Niño. It is interesting to note that another index of market squid abundance, the occurrence of squid beaks in the scat of sea lions, showed similar responses to earlier El Niño events (Lowry and Carretta, 1999). Squid beak occurrence dropped steeply during the strong 1983–84 El Niño, and increased afterwards. Beak occurrence also dipped and rose in response to a milder El Niño in 1992–93. Significantly, Lowry and Carretta (1999) examined southern Channel Islands: Santa Barbara, San Clemente, and San Nicolas. Our present study reflects squid abundance primarily around northern Channel Islands (e.g., Santa Rosa, Santa Cruz, Anacapa). Taken together, these studies may indicate that El Niño exerts a bight-wide influence on squid abundance.

We suggest that a strong El Niño event changes the reproductive conditions for the market squid in the

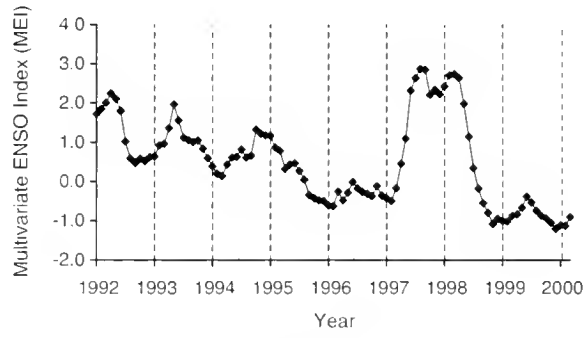

Figure 4

Multivariate ENSO index (MEI) for the tropical Pacific (between 10°N and 10°S), by month. Data were obtained from http://www.cdc.noaa.gov/~kew/MEI/table.html.

Southern California Bight. With regard to spawning, the spawning population becomes less abundant on the traditional shallow-water spawning grounds. Research on a congener, the South African chokka squid (*Loligo vulgaris reynaudii*), points to possible environmental influences on spawning for loliginid squid (Roberts and Sauer, 1994). Off South Africa, a strong El Niño can lead to reduced upwelling and increased turbidity. In normal years, upwelling, presumably detected by the squid as an influx of cold water, may trigger spawning behavior (Roberts and Sauer, 1994). In El Niño years off South Africa, reduced upwelling and increased turbidity on the inshore spawning grounds are thought to force the spawners into deeper water, beyond the reach of the fishery (Roberts and Sauer, 1994). In a recent study, catch for the chokka squid increased with strong easterly winds, which caused upwelling, and decreased with increased turbidity (Schön et al., 2002). In the California Current System, upwelling decreases during strong El Niño events (Schwing et al., 2000). Upwelling

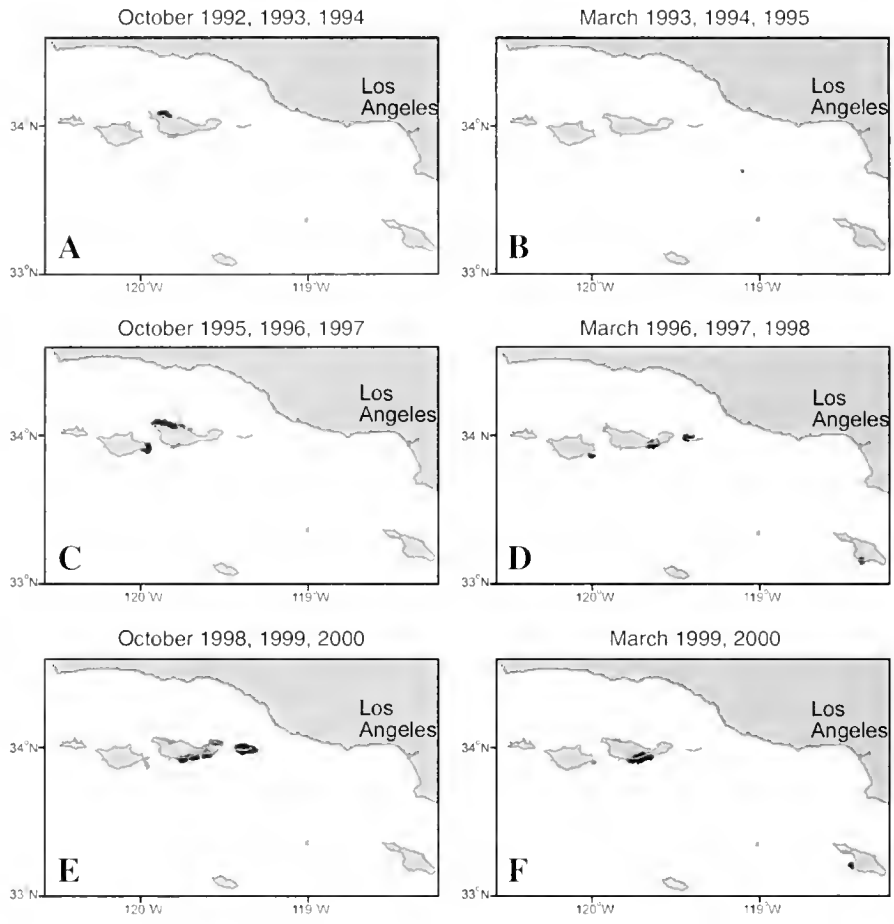

Figure 5

Location of fishing activity, as indicated by black areas, for the early (October) and late (March) parts of the traditional squid fishing season in the Southern California Bight, 1992–2000. For each month, a multiyear composite image is shown. (**A**) October 1992, 1993, 1994. (**B**) March 1993, 1994, 1995. (**C**) October 1995, 1996, 1997. (**D**) March 1996, 1997, 1998. (**E**) October 1998, 1999. (**F**) March 1999, 2000.

in the Southern California Bight was reduced during the 1997–98 El Niño (Hayward, 2000). It is not known how market squid adults respond to changes in water temperature or turbidity, or whether spawning fish shift to other habitats during El Niño events.

A strong El Niño event can also alter feeding and developmental conditions for squid. During the 1997-98 El Niño, macrozooplankton abundance substantially decreased in the Southern California Bight and off Baja California (Lynn et al., 1998; Hayward, 2000; Lavaniegos et al., 2002). Food availability affects growth rates of loligind squid (Jackson and Moltschaniwskyj, 2001). Recently, Jackson and Domeier (2003) indicated lower growth rates for the market squid in the Southern California Bight during the 1997–98 El Niño.

In the present study, fishing effort following the 1997–98 El Niño was generally below pre-El Niño levels. The subsequent high levels of catch in late 1999 and early 2000 may indicate that squid were in great abundance, thereby requiring less overall catch effort to meet market demand. A strong La Niña succeeded the 1997–98 El Niño (Lynn and Bograd, 2002; Schwing et al., 2002), with strong upwelling and high macrozooplankton abundance in the Southern California Bight by spring 1999 (Schwing et al., 2000; Hayward, 2000). Indeed, the high LPUE in the present study in late 1999 and early 2000 points to increased squid abundance in response to a more productive environment. Alternatively, one could argue that increased fishing efficiency, not increased squid abundance, resulted in high LPUE. One manifestation of higher fishing efficiency could be a contracted fishing range, where especially productive pockets are identified and targeted. An overall comparison of fishing location in October and March before and after El Niño did not support this explanation: the total spatial extent of fishing activity was not greatly

reduced in post-El Niño October or March. A noticeable concentration of fishing effort off the southern shore of Santa Cruz Island was evident in the post-El Niño period, however. The landings data may indicate that this southern shore, represented by blocks 708 and 709, was indeed productive. In the pre-El Niño period (1992–96), blocks 708 and 709 represented 3% of the landings in the bight. In the post-El Niño period (1999 to early 2000), these two blocks came to represent 12% of the landings.

The spatial distribution of fishing activity appears to shift over the course of the squid fishing season. In the Southern California Bight, October and March mark the traditional beginning and end of the squid fishing season, respectively (Butler et al., 1999). In the present study, fishing activity along the Santa Rosa and Santa Cruz Islands moved largely to the southern shores by March, leaving the northern shores relatively unfished. This spatial shift may reflect change in local squid habitat or changes in the fishermen's behavior. As a rough indicator of habitat quality, water temperature did not consistently differ between the northern and southern waters around Santa Cruz Island in March and April, both at sea surface and at 75 meters depth. Wind conditions, on the other hand, change considerably from October to March. The northern shores of Santa Rosa and Santa Cruz lie on the rim of the Santa Barbara Channel. Wind speed and wind stress are relatively low through the channel in the fall and early winter but increase significantly in March to remain high throughout the spring and summer (Winant and Dorman, 1997; Harms and Winant, 1998; Dorman and Winant, 2000). It remains unresolved whether the high winds in the Channel in March and April create ocean-floor turbulence and turbidity that discourage squid spawning (cf., Roberts and Sauer, 1994), or whether fishermen simply eschew the rocky Channel in favor of the southern shores of the islands.

Although satellite remote sensing can generate a "neutral party" record of fishing effort, we note three caveats associated with satellite data. First, large stationary sources of light, such as coastal cities, must be excluded when quantifying fishing vessel activity. The exclusion of urban light sources can result in underestimating effort, because boats that work near large light sources can be excluded from analysis. We were concerned that an underestimation of effort along the mainland coast would explain this study's post-El Niño increase in LPUE. Landings data, however, may indicate that effort in coastal blocks actually declined after the 1997–98 El Niño. Coastal blocks accounted for 19% of the landings in the pre-El Niño years (1992–96), dropping to 11% of landings in the post-El Niño years (1999 to early 2000).

Second, the spatial resolution of the satellite images may be large enough to allow multiple boats to fit into one "pixel" of detected light. Thus, effort may be underestimated. Analysis of the ground-truthing flyovers, however, did not indicate a strong interaction between boat aggregation and nightly fleet size. Boats may have indeed aggregated over the course of our study, but our analysis indicates that such aggregation was independent of nightly fleet size. In this case, the absolute values of estimated effort and LPUE would be underestimated across all dates. The relative values of effort and LPUE, however, will be only slightly affected within a time series; therefore we place confidence in our examinations of the temporal patterns of the effort-based data. A third caveat is specific to the present study. The ground-truthing work occurred during a period of relatively low fishing effort (1999–2000). Future fly-overs during periods of greater effort will be useful in corroborating our observed relationship between fly-over and satellite data.

The present study demonstrates that light detection by satellite remote sensing is useful for examining temporal and spatial patterns of fishing effort and population abundance, as measured by LPUE. Light detection by satellite has certain drawbacks, but these are not insurmountable. Importantly, geo-referenced satellite images provide an independent source of fishing effort, which can be feasibly integrated with environmental data through GIS analysis. With regard to market squid off California, satellite data can help provide fine-scale data on fishing location for this fishery's ongoing management efforts[4,5] (see also Mangel et al., 2002). Although mandatory shielding of the boat lights went into effect in May 2000, these lights are still detectable by the satellites (authors' pers. obs.). Recently, effort logbooks have become mandatory for squid fishermen off California. This requirement points to a unique opportunity to collect and corroborate fishery-dependent and independent measures of fishing effort.

Acknowledgments

We owe much gratitude to personnel of California's Department of Fish and Game for their assistance in the ground-truthing work. In particular, we thank the pilots Jeff Veal and Tom Evans, and the following aerial observers: D. Bergen, T. Bishop, S. Carner, D. Hanan, C. Kong, J. Kraus, A. Lohse, S. MacWilliams, D. Ono, M. Songer, J. Wagner, and E. Wilson. We also thank Paul Crone for collaboration on this project, Chris Reiss for extracting CalCOFI water temperature data, Rich Cosgrove for assistance with mapping, Kevin Hill for information about the Pacific Fisheries Management Council, and George Watters and anonymous reviewers for constructive comments. This project was funded by the California Department of Fish and Game and U.S. Department of Commerce (NOAA NESDIS Ocean Remote Sensing Program).

[4] California Department of Fish and Game. 2003. Draft: Market squid fishery management plan. [Available from: Calif. Dept. Fish Game, 4949 Viewridge Avenue, San Diego, CA 92123.]

[5] Maxwell, M. R., L. D. Jacobson, and R. Conser. Manuscript in review. Eggs-per-recruit model for management of the California market squid (*Loligo opalescens*) fishery.

Literature cited

Butler, J., D. Fuller, and M. Yaremko.
1999. Age and growth of market squid (*Loligo opalescens*) off California during 1998. Calif. Coop. Oceanic Fish. Invest. Rep. 40:191–195.

CDFG (California Department of Fish and Game).
2000. Review of some California fisheries for 1999: market squid, Dungeness crab, sea urchin, prawn, abalone, groundfish, swordfish and shark, ocean salmon, nearshore finfish, Pacific sardine, Pacific herring, Pacific mackerel, reduction, white seabass, and recreational. Calif. Coop. Oceanic Fish. Invest. Rep. 41:8–25.

Croft, T. A.
1978. Nighttime images of the earth from space. Sci. Am. 239:68–79.

Dorman, C. E., and C. D. Winant.
2000. The structure and variability of the marine atmosphere around the Santa Barbara Channel. Month. Weather Rev. 128:261–282.

Elvidge, C. D., K. E. Baugh, E. A. Kihn, H. W. Kroehl, and E. R. Davis.
1997. Mapping city lights with nighttime data from the DMSP Operational Linescan System. Photogram. Engin. Remote Sens. 63: 727–734.

Elvidge, C. D., V. R. Hobson, K. E. Baugh, J. Dietz, Y. E. Shimabukuro, Y. E. Krug, E. M. L. M. Novo, and F. R. Echavarria.
2001b. DMSP-OLS estimation of rainforest area impacted by ground fires in Roraima, Brazil: 1995 versus 1998. Int. J. Remote Sens. 22:2661–2673.

Elvidge, C. D., M. L. Imhoff, K. E. Baugh, V. R. Hobson, I. Nelson, J. Safran, , J. B. Dietz, and B. T. Tuttle.
2001a. Night-time lights of the world: 1994–1995. ISPRS J. Photogram. Remote Sens. 56:81–99.

Harms, S., and C. D. Winant.
1998. Characteristic patterns of circulation in the Santa Barbara Channel. J. Geophys. Res. 103:3041–3065.

Hayward, T. L.
2000. El Niño 1997–98 in the coastal waters of southern California: a timeline of events. Calif. Coop. Oceanic Fish. Invest. Rep. 41:98–116.

Jackson, G. D.
1994. Statolith age estimates of the loliginid squid *Loligo opalescens* (Mollusca: Cephalopoda): corroboration with culture data. Bull. Mar. Sci. 54:554–557.

Jackson, G. D., and M. L. Domeier.
2003. The effects of an extraordinary El Niño / La Niña event on the size and growth of the squid *Loligo opalescens* off Southern California. Mar. Biol. 142:925–935.

Jackson, G. D., and N. A. Moltschaniwskyj.
2001. The influence of ration level on growth and statolith increment width of the tropical squid *Sepioteuthis lessoniana* (Cephalopoda: Loliginidae): an experimental approach. Mar. Biol. 138:819–825.

Lavaniegos, B. E., L. C.-Perez, and G. Gaxiola-Castro.
2002. Plankton response to El Niño 1997–1998 and La Niña 1999 in the southern region of the California Current. Progress Oceanog. 54:33–58.

Lowry, M. S., and J. V. Carretta.
1999. Market squid (*Loligo opalescens*) in the diet of California sea lions (*Zalophus californianus*) in Southern California (1981–1995). Calif. Coop. Oceanic Fish. Invest. Rep. 40:196–207.

Lynn, R. J., T. Baumgartner, J. García, C. A. Collins, T. L. Hayward, K. D. Hyrenbach, A. W. Mantyla, T. Murphree, A. Shankle, F. B. Schwing, K. M. Sakuma, and M. J. Tegner.
1998. The state of the California Current, 1997–1998: transition to El Niño conditions. Calif. Coop. Oceanic Fish. Invest. Rep. 39:25–49.

Lynn, R. J., and S. J. Bograd.
2002. Dynamic evolution of the 1997–1999 El Niño-La Niña cycle in the southern California Current System. Progress Oceanog. 54:59–75.

Mangel, M., B. Marinovic, C. Pomeroy, and D. Croll.
2002. Requiem for Ricker: unpacking MSY. Bull. Mar. Sci. 70:763–781.

Roberts, M. J., and W. H. H. Sauer.
1994. Environment: the key to understanding the South African chokka squid (*Loligo vulgaris reynaudii*) life cycle and fishery? Antarctic Sci. 6:249–258.

Rodhouse, P. G., C. D. Elvidge, and P. N. Trathan.
2001. Remote sensing of the global light-fishing fleet: an analysis of interactions with oceanography, other fisheries and predators. Adv. Mar. Biol. 39:261–303.

Roper, C. F. E., M. J. Sweeney, and C. E. Nauen.
1984. Cephalopods of the world. An annotated and illustrated catalogue of species of interest to fisheries. FAO species catalogue, vol. 3, 277 p. FAO Fish Synop. 125.

Salmon, M., B. E. Witherington, and C. D. Elvidge.
2000. Artificial lighting and the recovery of sea turtles. *In* Sea turtles of the Indo-Pacific: research management and conservation (N. Pilcher and G. Ismail, eds.), p. 25–34. ASEAN Academic Press, London.

Schön, P-J., W. H. H. Sauer, and M. J. Roberts.
2002. Environmental influences on spawning aggregations and jig catches of chokka squid *Loligo vulgaris reynaudii*: a "black box" approach. Bull. Mar. Sci. 71:783–800.

Schwing, F. B., C. S. Moore, S. Ralston, and K. M. Sakuma.
2000. Record coastal upwelling in the California Current in 1999. Calif. Coop. Oceanic Fish. Invest. Rep. 41:148–160.

Schwing, F. B., T. Murphree, L. deWitt, and P. M. Green.
2002. The evolution of oceanic and atmospheric anomalies in the northeast Pacific during the El Niño and La Niña events of 1995–2001. Progress Oceanog. 54:459–491.

Vojkovich, M.
1998. The California fishery for market squid (*Loligo opalescens*). Calif. Coop. Oceanic Fish. Invest. Rep. 39:55–60.

Waluda, C. M., P. N. Trathan, C. D. Elvidge, V. R. Hobson, and P. G. Rodhouse.
2002. Throwing light on straddling stocks of *Illex argentinus*: assessing fishing intensity with satellite imagery. Can. J. Fish. Aquat. Sci. 59:592–596.

Winant, C. D., and C. E. Dorman.
1997. Seasonal patterns of surface wind stress and heat flux over the Southern California Bight. J. Geophys. Res. 102:5641–5653.

Wolter, K., and M. S. Timlin.
1998. Measuring the strength of ENSO events: how does 1997/98 rank? Weather 53:315–324.

Zar, J. H.
1984. Biostatistical analysis, 2nd edition, 718 p. Prentice-Hall, Englewood Cliffs, NJ.

Magnitude and distribution of sea turtle bycatch in the sea scallop (*Placopecten magellanicus*) dredge fishery in two areas of the northwestern Atlantic Ocean, 2001–2002

Kimberly T. Murray

Northeast Fisheries Science Center
National Marine Fisheries Service
166 Water Street
Woods Hole, Massachusetts 02543
E-mail address: Kimberly.Murray@noaa.gov

Abstract—In May 2001, the National Marine Fisheries Service (NMFS) opened two areas in the northwestern Atlantic Ocean that had been previously closed to the U.S. sea scallop (*Placopecten magellanicus*) dredge fishery. Upon reopening these areas, termed the "Hudson Canyon Controlled Access Area" and the "Virginia Beach Controlled Access Area," NMFS observers found that marine turtles were being caught incidentally in scallop dredges. This study uses the generalized linear model and the generalized additive model fitting techniques to identify environmental factors and gear characteristics that influence bycatch rates, and to predict total bycatch in these two areas during May–December 2001 and 2002 by incorporating environmental factors into the models. Significant factors affecting sea turtle bycatch were season, time-of-day, sea surface temperature, and depth zone. In estimating total bycatch, rates were stratified according to a combination of all these factors except time-of-day which was not available in fishing logbooks. Highest bycatch rates occurred during the summer season, in temperatures greater than 19°C, and in water depths from 49 to 57 m. Total estimated bycatch of sea turtles during May–December in 2001 and 2002 in both areas combined was 169 animals (CV=55.3), of which 164 (97%) animals were caught in the Hudson Canyon area. From these findings, it may be possible to predict hot spots for sea turtle bycatch in future years in the controlled access areas.

Manuscript submitted 1 December 2003 to the Scientific Editor's Office.

Manuscript approved for publication 27 May 2004 by the Scientific Editor.

Fish. Bull. 102:671–681 (2004).

Five species of sea turtles in the northwestern Atlantic Ocean are protected under the U.S. Endangered Species Act of 1973. The loggerhead turtle (*Caretta caretta*) is listed as a threatened species, and the leatherback (*Dermochelys coriacea*), hawksbill (*Eretmochelys imbricata*), Kemp's ridley (*Lepidochelys kempii*), and certain populations of the green sea turtle (*Chelonia mydas*) are listed as endangered. Populations of each of these species have declined principally as a result of human activities (NRC, 1990).

The incidental capture, or bycatch, of sea turtles in commercial fisheries is a major source of mortality (NRC, 1990; Turtle Expert Working Group, 2000). These turtles are captured incidentally in pelagic longlines (Lewison et al., 2004), trawls (Epperly, 2003), gill nets (Julian and Beeson, 1998), pound nets, weirs, pots, and traps (NMFS and USFWS, 1991; Allen, 2000). Such threats occur at various life stages of a population and at different intensities, and consequently have implications for management policy (Heppell et al., 2003).

The U.S. National Marine Fisheries Service (NMFS) has implemented management measures in both the Atlantic and the Pacific in the form of gear modifications or time and area closures to reduce sea turtle bycatch. For example, since the early 1990s, turtle excluder devices (TEDs) have been required in all inshore and offshore shrimp trawl nets in southeastern U.S. waters (Epperly, 2003) to reduce sea turtle mortality (Henwood and Stuntz, 1987). Bycatches of sea turtles in the U.S. pelagic longline fisheries for swordfish and tuna (Witzell, 1999) led to a year-round closure of a 2.6 million nmi^2 area in the northwestern Atlantic Ocean to these fisheries beginning in 2002.

In recent years, documented interactions have occurred between sea turtles and sea scallop dredges, a previously unidentified threat in recovery planning efforts (NMFS, 1991). During 2001 and 2002, fisheries observers aboard commercial sea scallop vessels documented the bycatch of sea turtles in two small regions of the Mid-Atlantic Bight (MAB). These areas, termed the "Hudson Canyon Controlled Access Area" (approximately 3150 km^2) and the "Virginia Beach Controlled Access Area" (approximately 900 km^2) were closed to scallop fishing in April 1998 but reopened in May 2001 on a conditional basis (Fig. 1). This study uses the generalized linear and generalized additive models to identify environmental factors and gear characteristics affecting the bycatch rate of sea turtles in these two areas and to predict total bycatch by sea scallop dredge vessels in these two areas in 2001 and 2002.

Methods

The fishery

In 2001 and 2002, 137 and 93 commercial vessels, respectively, participated in the Controlled Area Access Program sea scallop fishery. Although

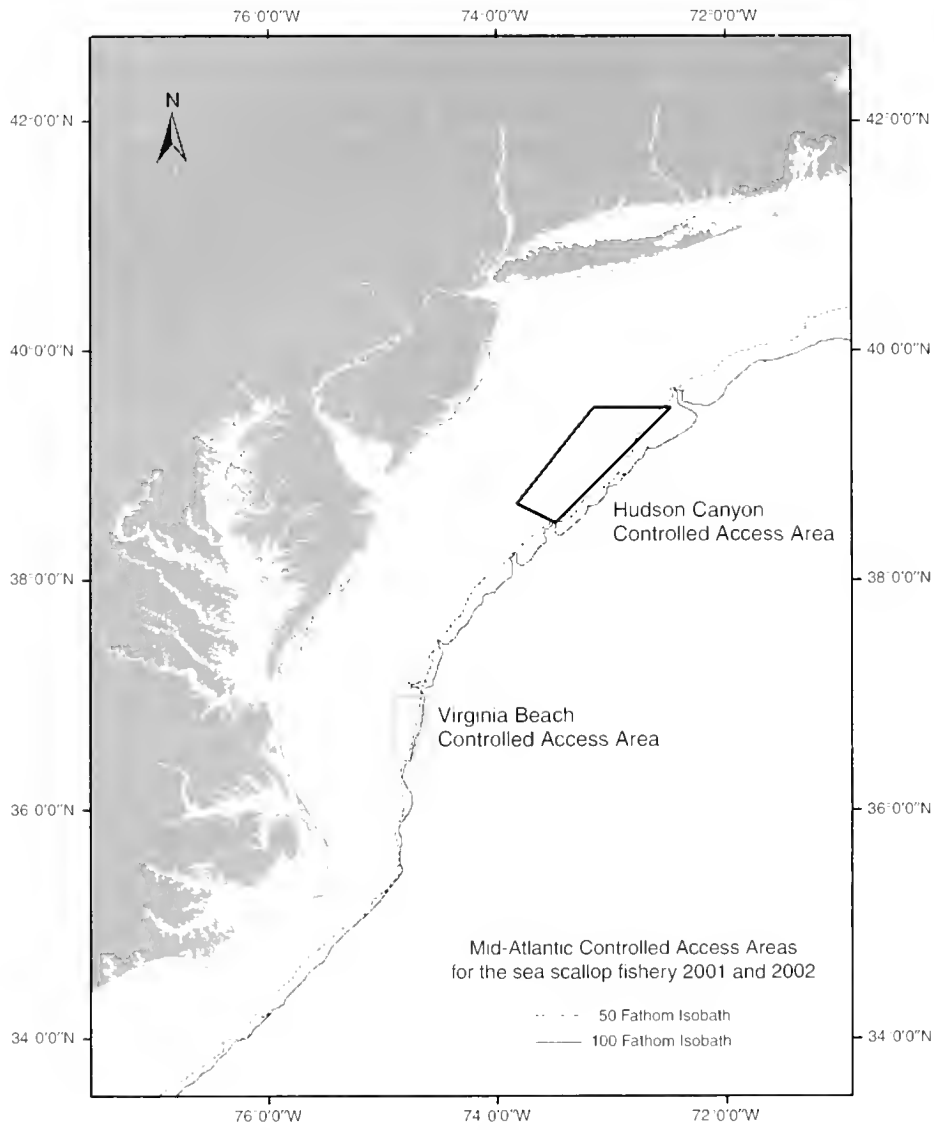

Figure 1

Mid-Atlantic controlled access areas for the sea scallop fishery 2001 and 2002.

the U.S. commercial scallop fishery operates year-round, the area access program in 2001 began on 1 May, and in 2002 on 1 March, and ended on 28 February following the respective fishing year (1 March–28 February). Vessels in the controlled access areas fished around the clock for approximately 5–12 days, accomplishing between 40 and 160 hauls per trip. Dredges in the controlled areas were generally fished at depths between 45 and 75 m. The average haul duration was about 1 hour. Most vessels fished two dredges simultaneously (one from each side of the vessel), which were generally either 3.9 or 4.5 m (13 or 15 ft) wide.

Vessels in the Mid-Atlantic typically fish with a New Bedford style scallop dredge equipped for soft-bottom substrates. In this configuration, tickler chains strung from the sweep chain run horizontally between the dredge frame and the ring bag and are designed to raise scallops off the bottom and into the bag. Turtles become entrapped in the ring bag or on the dredge frame. For dredging on hard bottom, such as in New England, vertical up and down chains hang over the tickler chains, preventing boulders from entering the ring bag (Smolowitz, 1998). New Bedford style scallop dredges have also been used in U.S. fisheries in the Pacific (PSMFC[1]).

[1] Pacific States Marine Fisheries Commission (PSMFC). 2003. Description of fishing gears used on the Pacific Coast. http://pcouncil.org/habitat/geardesc.pdf. [Accessed 6 April 2004.]

Data sources

Observer data Observers were placed on randomly selected vessels fishing in the controlled areas to record the bycatch of turtles and other protected species. From May to December in 2001 and 2002, observers sampled 11% of the commercial fishing effort in the Hudson Canyon region, and in October 2001, 16% of the effort in Virginia Beach. No trips were observed in the Virginia Beach region during 2002 because of low commercial fishing effort in the area. Observers were on- and off-watch on an irregular schedule throughout a 24-hour period, observing on average 65% of the hauls on a trip. When a dredge was hauled on board, observers recorded the haul location, time, depth, tow speed, tow duration, number of dredges observed, and the presence or absence of turtle bycatch. In 2001, observers identified 20% of the turtles that came aboard as loggerhead sea turtles but were unable to identify the remaining 80%. As a result of improved observer training (NMFS 2003), observers identified 88% of the turtles as loggerhead sea turtles in 2002, but they were unable to identify the remaining 12%. Given that observers document the loggerhead species most commonly in the Mid-Atlantic area, and that all sea turtles positively identified were loggerhead sea turtles, bycatch estimates in this analysis are considered to be those of loggerhead sea turtles. Although some turtles may have been released alive or injured, this analysis does not differentiate between live, dead, and injured animals.

Fishing effort data Under the 1982 Atlantic Sea Scallop Fishery Management Plan, all vessels targeting scallops must complete a vessel trip report (VTR) log (as of 1994) indicating area fished, kept and discarded catch, and fishing effort. These data were used to estimate the total fishing effort of the fleet. In calculating fishing effort, one unit of effort equals a single dredge haul because vessels may fish one or two dredges simultaneously on each haul. Because a preliminary analysis showed that tow duration or dredge length does not significantly affect the probability of turtle capture, dredge haul effort was not standardized for these two variables. All VTR trips from May to December in the controlled areas were used in the analysis. Because completion of vessel trip reports is mandatory and trips to the controlled areas were closely monitored, it was assumed that the VTR data represented 100% of total fishing effort.

Sea surface temperature Sea surface temperature at each position reported in the observer and VTR databases was extracted from NOAA AVHRR (advanced very high resolution radiometer) coastwatch satellite images. A Visual Basic (Microsoft Corp., Redmond, WA) routine was used to extract temperatures from 7-day composite images (3 days forward and backward from the haul date), by using a 3×3 cell window at 1-km resolution. Therefore, a 9-km^2 area of coverage around each coordinate position was used to extract sea surface temperature. Within the 3×3 cell search radius, the pixel representing the warmest temperature was used to avoid temperatures affected by cloud coverage.

Data analysis

Missing temperature data Sea surface temperature values could not be obtained for 33% of the VTR data and 10% of the observer data because of either missing coordinate positions on the VTR logs or bad satellite images. For these fishing events, sea surface temperature was predicted by using a linear regression based on year, month, and area. For the observer data, area was defined as either Hudson Canyon or Virginia Beach access areas (r^2=0.88). For the VTR data, the vessel's home state served as a proxy for area fished because most of the missing temperature values were due to missing coordinate positions (r^2=0.86).

Modeling approach Generalized linear model (GLM) and generalized additive model (GAM) fitting techniques were used to understand and predict bycatch rates of sea turtles in relation to environmental variables, fishing practices, and gear characteristics in the commercial sea scallop fishery. Unlike classic linear regression models, GLMs and GAMs allow for nonlinearity and nonconstant variance structures in the data (Guisan et al., 2002). GAMs differ from GLMs in that smooth functions replace the linear predictors in GLMs (Hastie and Tibshirani, 1990). Smooth functions, or "smoothers," summarize the trend of a response measurement as a function of multiple predictors (Hastie and Tibshirani, 1990) and therefore some form of parametric relationship between the response and explanatory variables is not assumed (Guisan et al. 2002). Both frameworks have been used to model abundance or probability events as a function of environmental variables (Frost et al., 1999; Denis et al., 2002; Guisan et al., 2002; Hamazaki, 2002).

A modeling approach to estimate bycatch of sea turtles in the sea scallop dredge fishery was preferred over the ratio method (Cochran, 1977) that has been used to estimate bycatch of marine mammals and turtles in other fisheries (Epperly et al., 1995; Rossman and Merrick, 1999). With the ratio method, the observed number of sea turtles divided by the observed effort is used to calculate a bycatch rate, and this rate is then multiplied by total commercial fishing effort to derive a bycatch estimate. Bycatch data in the sea scallop dredge fishery violate the underlying assumptions of the ratio method (Cochran, 1977), largely because sea turtle bycatch is binomially distributed with a nonconstant variance. An analyis of binary response data derived from a statistical model allows bycatch rates to be predicted by using factors that account for variability in bycatch. Moreover, stratifying bycatch rates according to these factors will reduce variability in total bycatch estimates. For the sea turtle data analyzed in the present study, the GLM approach provided a more accurate and less biased mortality estimate than that derived using the ratio method.

GAM smoothers Before a GLM was constructed, a GAM helped group continuous variables into categories. Fitting the GLM model with categorized variables was necessary to extrapolate bycatch rates in order to derive a total estimate of the bycatch of sea turtles in scallop dredges in the controlled access areas. All of the variables tested in the GLM model were first fitted to a GAM, in which the parameters of the continuous prediction variables were estimated by a smoothing spline. Variable values were grouped according to whether they had a positive or negative influence on the bycatch rate (i.e., the group explained more or less of the bycatch rate).

Development of a GLM bycatch model Because bycatch events were counts ranging from zero or one, a logistic regression was used to model the probability of sea turtle bycatch (GLM function, SPLUS 6.1, Seattle, WA). Each dredge haul is a data point and the response was whether turtle bycatch was zero or one. Probability of sea turtle bycatch (p) was calculated as

$$p = e^y / 1 + e^y$$
$$y = \beta_0 + \beta_1 x_1 + \beta_2 x_2 + \ldots + \beta_t x_t,$$

where β_t is a parameter coefficient;
x_t is a predictor variable; and
y is a sea turtle bycatch event.

Dredge hauls are assumed to be independent because turtles were never simultaneously caught in both dredges operating from a vessel during a single haul.

A forward stepwise selection method was used to determine the best fitting model. Model parameters were estimated by maximizing the log-likelihood function. The null model was the first model in the stepwise process and was specified with a single intercept term as

$$H_0: \log(turtle\ bycatch) = 1.$$

At each step, a new variable was added to the null model (Appendix 1) and tested against the former model formulation (ANOVA function, chi-square test) to determine the better fitting model. A preliminary assessment of a broad suite of gear characteristics and environmental factors indicated that 10 variables could significantly affect bycatch rates. The main effects of each variable were tested in the stepwise selection process as well as the interaction between season and temperature. Because the order of the predictor variables affects their significance, main effects were entered in various orders. If a P-value was less than 0.05, then the additional variable was considered to explain more of the variability in bycatch than a model without that variable. Each new model was also compared against the former model by using the Akaike information criterion (AIC), which is defined as

$$AIC = -2\log(L(\theta|y)) + 2K,$$

where $\log(L(\theta|y))$ = the numerical value of the log-likelihood at its maximum point; and
K = the number of estimable parameters (Burnham and Anderson, 2002).

The AIC is a measure of the level of parsimony, defined as a model that fits the data well and includes as few parameters as necessary (Palka and Rossman, 2001). If the AIC value decreases, the new combination of variables in the model fit the data better.

To investigate whether the bycatch data are over-dispersed, that is, where the sampling variance exceeds the theoretical variance, the GLM model was refitted by using a quasi-likelihood function. When data are over-dispersed, the estimated over-dispersion parameter is generally between 1 and 4 (Burnham and Anderson, 2002). The over-dispersion parameter fitted to the global model was 0.61, indicating these data were not over-dispersed and error assumptions of the binomial model were appropriate for analyzing these data.

Alias patterns in the final model were examined to assess correlation among the explanatory variables. The fit of the final model was assessed by plotting the observed turtle bycatch against the predicted turtle bycatch. The r^2 value indicated how well predictions from the linear model fit the actual data.

Bycatch rate estimates The spatial and temporal stratification of bycatch rates in each of the controlled access areas was determined by the explanatory variables in the best-fitting GLM. Parameter estimates from the model were used to predict the bycatch rate for each stratum.

The coefficient of variation (CV) for each bycatch rate was estimated by bootstrap resampling (Efron and Tibshirani, 1993). The resampling unit was a scallop dredge haul. Replicate bycatch rates were generated with the best-fitting GLM model, by sampling with replacement 1000 times from the original data set. The CV was defined as the standard deviation of the bootstrap replicate bycatch rates in a stratum divided by the bycatch rate for that stratum estimated from the original data. Variances and CVs of combined estimates were based on means weighted by their respective variances (Wade and Angliss, 1997).

Total bycatch The total estimated turtle bycatch in each stratum was calculated as the product of predicted bycatch per dredge haul (i.e., the predicted bycatch rate) for that stratum and the total number of dredge hauls accomplished by the commercial fishery in that stratum:

$$\frac{\sum Predicted\ bycatch}{\sum Dredge\ hauls_i} \times (Total\ dredge\ hauls)_i,$$

where i = stratum

Table 1

Analysis of deviance for significant factors affecting sea turtle bycatch. Significant factors were used to stratify bycatch rates and to contruct a model to predict total bycatch. AIC = Akaike information criterion.

Model	df	Deviance	Residual df	Residual deviance	*P* (chi)	AIC
null model only		18,071	405.29	407.2989		
null + year	1	−2.33	18,070	402.96	0.12626	406.9611
null + season	2	19.81	18,069	385.48	0.00004	391.4807
null + season + temp	1	9.34	18,068	376.13	0.00223	384.1319
null + season + temp + depth	2	17.23	18,066	358.89	0.00018	370.8983
null + season + temp + depth + time of day	1	7.86	18,065	351.03	0.00503	365.0318
null + depth + time of day + season (temp)	1	1.64	18,064	349.39	0.20011	365.3903
null + season + temp + depth + time of day + state	4	3.77	18,061	347.25	0.43746	369.2579
null + season + temp + depth + time of day + dredge frame width	2	3.27	18,063	347.76	0.19487	365.7611
null + season + temp + depth + time of day + number of up and down chains	1	0.54	18,064	350.48	0.45955	366.4849
null + season + temp + depth + time of day + number of tickler chains	1	3.18	18,064	347.84	0.07436	363.8480

Annual bycatch was the sum of the stratified bycatch estimates. The finite population correction factor (Cochran, 1977) was applied to bycatch estimates in stratas where the observer coverage was greater than 10%.

Number of dredge hauls in the VTR database without coordinate positions (32%) were prorated between the stratified areas according to the percentage of dredge hauls with known coordinates from the same year, state, and stratified areas.

Results

Observed bycatch

Nine and 16 turtle bycatch were observed in 2001 and 2002, respectively, in the Hudson Canyon controlled access area. Of the 25 turtles taken in the Hudson Canyon area across both years, 21 (84%) were taken during summer months. Two turtle bycatch were observed in the Virginia Beach access area during fall 2001—the only time when there was observer coverage in this area across both years.

GAM smoothers

Plots of the smoothed functions in the GAM revealed whether the continuous variable in the model explained any error in the bycatch rate estimates. For example, a plot of the smooth function for depth as a covariate revealed that bycatch rates may be higher between 49 m (27 fm) and 57 m (31 fm) and lower around this zone (Fig. 2). Likewise, a plot of the smooth function for temperature as a covariate revealed that bycatch rates may be higher above 19°C. These plots helped bin the continuous variables into categories (Appendix 1) which could then be tested in the GLM. All continuous variables in the GAM were categorized in a similar manner.

GLM bycatch model

Significant factors affecting sea turtle bycatch were season, sea surface temperature, depth zone, and time-of-day (Table 1). These variables were significant despite the order in which they were tested in the model. The model with the lowest AIC value was considered the "best" model, although time-of-day could not be included in the final model to predict bycatch rates. This level of information is not recorded in commercial fisheries logbooks; therefore bycatch rates based on time-of-day could not be extrapolated to total bycatch. Width of the scallop dredge frame, number of tickler chains, and number of up and down chains were not significant variables.

Model fit

The number of predicted sea turtle bycatch closely matched the observed bycatch in both years in all bycatch strata (Table 2). Strata were defined according to variables identified in the GLM as having a significant effect on bycatch rates. The relationship between actual and observed takes was strong (r^2=0.93), indicating that the predictions from the model fitted the data well.

Bycatch rate estimates

Bycatch rates were stratified by season, temperature interval, and depth zone (Table 3). Because year was not a

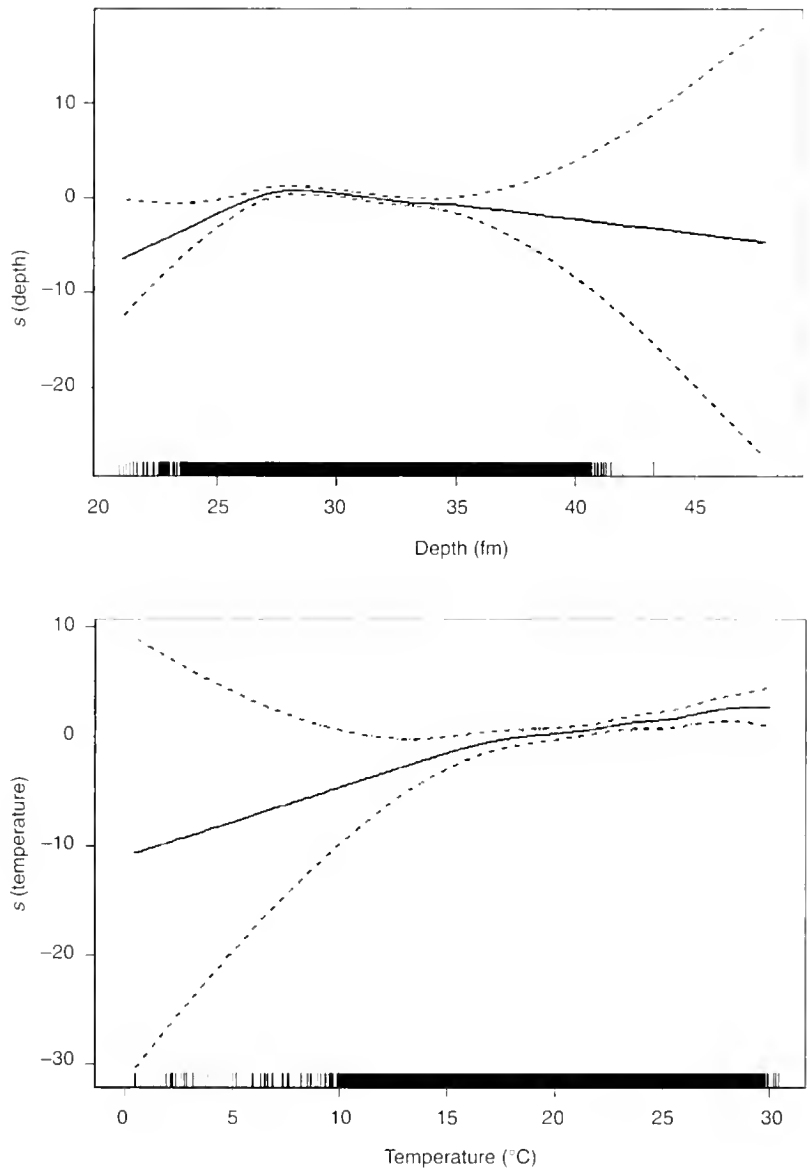

Figure 2

Partial fits for the general additive model (GAM) of sea turtle bycatch with depth and temperature as covariates, showing the relationship estimated by a smoothing spline. Depths between 27 fm (49 m) and 31 fm (57 m), and temperatures above 19 C, have a positive influence on the bycatch rate. 95% confidence bands are also shown. All continuous variables in the GAM were categorized in a similar manner. The "s" on the y-axis represents a smoothed function for each variable and explains the effect of each variable on sea turtle bycatch per haul.

significant factor in the final model, predicted bycatch rates were the same for 2001 and 2002. Highest sea turtle bycatch rates occurred during the summer season (Aug–Sep), in temperatures warmer than 19 C, in water depths from 49 to 57 m. Lowest bycatch rates occurred during the fall (Oct–Dec) and spring (May–June), in temperatures cooler than 19 C, and in water depths less than 49 m.

Total bycatch

The total estimated bycatch of sea turtles in the Mid-Atlantic controlled access areas in 2001 and 2002 combined was 169 animals (CV=55.3) (Table 4). Of this total, 164 animals (97%) were caught in the Hudson Canyon area: 69 (42%) in 2001 and 95 (58%) in 2002. Total esti-

Table 2

Observed versus predicted number of turtle bycatch, by stratum, 2001 and 2002. Obs.=observed; Pred.=predicted.

		Spring		Summer		Fall	
Water depth	Temp.	Number of obs. turtle bycatch	Number of pred. turtle bycatch	Number of obs. turtle bycatch	Number of pred. turtle bycatch	Number of obs. turtle bycatch	Number of pred. turtle bycatch
Shallow	High	0	0	0	0	0	0
	Low	0	0	0	0	0	0
Mid-depth	High	2	1	17	16	1	2
	Low	0	0	0	0	1	0
Deep	High	1	1	4	5	1	0
	Low	0	0	0	0	0	0

Table 3

Stratification of turtle bycatch rates with associated CVs. N.C.E.=no commercial effort.

Water depth	Temperature	Spring (May–June)	Summer (Aug–Sep)	Fall (Oct–Dec)
Shallow (<49 m)	High (>19°C)	0.0000027 (82.5)	0.0000052 (62.1)	0.0000030 (87.7)
	Low (<19°C)	0.0000002 (99.5)	N.C.E.	0.0000002 (106.6)
Mid-depth (49–57 m)	High (>19°C)	0.0032018 (64.9)	0.0061179 (25.4)	0.0035838 (57.2)
	Low (<19°C)	0.0002117 (95.4)	N.C.E.	0.0002371 (98.3)
Deep (>57 m)	High (>19°C)	0.0007578 (73.8)	0.0014512 (41.9)	0.0008485 (80.5)
	Low (<19°C)	0.0000500 (92.9)	N.C.E.	0.0000560 (103.8)

Table 4

Total bycatch estimates by year and season with weighted CVs (%) N.C.E.=no commercial effort.

		Spring	Summer	Fall	Total
Hudson Canyon	2001	10 (89.2)	50 (61.5)	9 (105.8)	69
	2002	13 (89.2)	78 (61.5)	4 (105.8)	95
Virginia Beach	2001	N.C.E.	N.C.E.	5 (105.8)	5
	2002	0	0	N.C.E.	0
Totals		23	128	18	169 (55.3)

mated bycatch of turtles in the Virginia Beach area was five animals in 2001 and zero animals in 2002.

Across both areas, the highest bycatches occurred in summer (128 turtles; 76%), followed by spring (23 turtles; 14%) and fall (18 turtles; 10%) (Table 5). One hundred thirty-two (78%) (CV=49.6) sea turtles were caught in the mid-depth zone from 49 to 57 m, whereas 37 (22%) (CV=59.6) sea turtles were caught in waters deeper than 57 m. One-hundred fifty-eight (93%) (CV=51.2) sea turtles were caught in waters warmer than 19°C, and 11 (7%) (CV=74.9) in waters cooler than 19°C.

Discussion

Use of bycatch models

Generalized linear and generalized additive models help to identify environmental variables or fishing practices that influence the probability of sea turtle bycatch. In estimating total mortality, bycatch rates can then be stratified according to these factors, reducing unexplained variability in the total estimate. Moreover, understanding factors that lead to a high or low

Table 5

Total bycatch estimates by season, depth, and temperature strata in Hudson Canyon and Virginia Beach controlled access areas in 2001 and 2002 with 95% confidence intervals. Spring=May–Jun; Summer=Jul–Sep; Fall=Oct–Dec. N.E.C.= no commercial effort; N.O.=no observer coverage.

		2001			2002			
Water depth	Temperature	Spring	Summer	Fall	Spring	Summer	Fall	Total
Shallow (<49 m)	High (>19°C)	0	0	0	0	0	0	0
	Low (<19°C)	0	N.O.	0	0	N.C.E.	0	0
Mid-Depth (49–57 m)	High (>19°C)	6 (0–13)	37 (21–59)	2 (0–5)	8 (0–21)	65 (34–96)	5 (0–9)	123
	Low (<19°C)	2 (0–8)	N.C.E.	4 (0–19)	1 (0–2)	N.C.E.	2 (0–10)	9
Deep (>57 m)	High (>19°C)	2 (0–5)	13 (4–25)	2 (0–5)	4 (0–11)	13 (4–24)	1 (0–1)	35
	Low (<19°C)	0 (0–1)	N.C.E.	1 (0–6)	0 (0–1)	N.C.E.	1 (0–2)	2
Total		10	50	9	13	78	9	169

probability of bycatch can motivate bycatch mitigation research. Finally, the ability to predict bycatch on the basis of explanatory variables allows one to examine the relative effectiveness of different management measures designed to reduce bycatch (Kobayashi and Polovina[2]). Ultimately this framework can improve the assessment of threats to turtles and broaden conservation options.

Magnitude of bycatch

During May–December in 2001 and 2002, an estimated 169 animals were captured incidentally by commercial sea scallop dredge vessels in two areas of the Mid-Atlantic Bight. Throughout the entire Mid-Atlantic Bight, the magnitude of bycatch was probably larger, particularly because the factors associated with the high bycatch rates were not specific to the controlled access areas. Of the 11 observed turtles measured for size, 9 (82%) were between 70–80 cm straight carapace length (the large juvenile stage). Stage class models indicate that the long-term survivability of loggerhead sea turtles is sensitive to mortality at this life stage (Crouse et al., 1987).

Factors influencing bycatch

The incidental capture of turtles occurs where there is overlap between fishing effort and turtle habitat. The elevated probability of turtle bycatch occurring in warm waters, during summer, at depths between 50 and 60 m is consistent with the habitat regime of loggerhead sea turtles in the Mid-Atlantic (Shoop and Kenney, 1992; Epperly et al., 1995; Coles and Musick, 2000). During the oceanic phase of their life cycle, sea turtles occupy habitats at specific temperatures or with bathymetric features that concentrate prey and other areas of enhanced productivity (Polovina et al., 2000). In Mid-Atlantic waters, high aggregations of loggerhead sea turtles have been observed in the summer, in waters 22–49 m deep, at temperatures from 20° to 24°C (Shoop and Kenney, 1992). In the Hudson Canyon and Virginia Beach controlled access areas, the bycatch of sea turtles was associated with habitat conditions rather than gear characteristics. From these findings, it may be possible to predict future hotspots for sea turtle bycatch in the controlled access areas where fishing effort and sea turtles overlap in time and space. These hotspots may be centered over the portion of the Hudson Canyon where depths are between 50 and 60 m, after waters warm to 19 C.

Because of the low amount of observer data in the Virginia Beach area, predicted bycatch rates for this area were based largely on conditions within the Hudson Canyon area. Sea scallop fishing effort occurs year-round both north and south of the Hudson Canyon, and high concentrations of loggerhead sea turtles (determined from migratory patterns) exist in spring and fall from North Carolina to northern Maryland (Shoop and Kenney, 1992). It is probable that the distribution of turtles and scallop fishing effort co-occur in other regions of the Mid-Atlantic, particularly south of the Hudson Canyon. The scallop dredge fishery in the Mid-Atlantic is a complex, dynamic system; there may be other factors influencing the bycatch of sea turtles in the fishery south of the Hudson Canyon that were not observed. However, without additional data on turtle interactions in these areas, it is unwise to extrapolate bycatch estimates beyond the scope of the data in this analysis.

Conservation management options

Time and area closures Models of turtle migrations can be used to predict interactions with fisheries in time and space to maximize the efficiency of time and area

[2] Kobayashi, D. R., and J. J. Polovina. 2000. Time/area closure analysis for turtle take reductions. Appendix C, Environmental Impact Statement, FMP for Pelagic Fisheries of the Western Pacific, 44 p. NMFS Honolulu, Hawaii, 96822.

closures (Morreale, 1996). The results of this analysis indicate that bycatch rates are affected by season, depth, and sea surface temperature. Within certain months and depth zones, therefore, the time when sea surface temperature reaches a threshold level may be the time to trigger an area closure. For example, this type of management approach has been taken in the southeastern United States to regulate turtle bycatch in the large-mesh gill-net fishery.[3] The timing of seasonally adjusted area closures is based upon analyzing sea surface temperatures in relation to the presence or absence of sea turtles throughout the area (Epperly et al., 1995; Epperly and Braun-McNeill[4]). In addition, temperature thresholds currently trigger area closures in the southern California driftnet fishery during El Niño conditions to prevent the incidental capture of loggerhead sea turtles.[5]

Results from the present study can be used to help evaluate potential bycatch reduction under different management scenarios, given certain assumptions. For example, had the portion of the Hudson Canyon controlled access area between depths of 49 and 57 m been closed after surface waters reached 19°C in the summer (the stratum with highest bycatch), the closure would have reduced bycatch by 39%. For this estimate, it is assumed that surface temperatures remain above 19°C throughout the summer and drop below 19°C thereafter. Further, this bycatch reduction scenario also assumes that fishing effort shifts proportionately to the fall and spring season within the same depth zone and that bycatch rates remain the same as those that are calculated. Alternatively, fishing effort could shift within a season to shallow and deep depth zones if scallop catch-per-unit-of-effort were not affected. Under this assumption, bycatch would be reduced by 60% under the same time and area closure. However, unless there are concurrent reductions in fishing effort, bycatch reductions achieved by these measures could well be offset by increases in bycatch in other depth strata and seasons.

Gear or fishing modifications Management actions to modify gear or fishing practices can be evaluated in a similar manner. For instance, this analysis indicates that bycatch rates are influenced by the time-of-day when dredges are in the water. Time-of-day was not used to stratify bycatch rates or to extrapolate total bycatch estimates because of limitations in the fishing effort data (VTR records). If time-of-day had been incorporated into the bycatch model, the model would have predicted higher bycatch rates when dredges were set between 4 am and 4 pm (day tows). If the stratum with the highest bycatch rate (summer, high surface temperatures, and depths between 49 and 57 m), had been further stratified by time-of-day, the model would have predicted a bycatch rate of 0.008 sea turtles/dredge hauls during the day, and 0.002 turtles/dredge hauls during the night. If all the commercial vessels had been fishing during the day in this stratum (n=6352 dredges in 2001), the estimated bycatch would have been 51 turtles. If the vessels had been fishing during the night, the total estimated bycatch would have been 13 turtles. According to these rates and effort, restricting vessels to night-time tows between the hours of 4 pm and 4 am has the potential to reduce bycatch by 75% in this particular stratum.

Although specific gear characteristics did not show a strong relationship to sea turtle bycatch in this analysis, further work should be conducted to evaluate whether specific gear characteristics could be modified to decrease bycatch. For example, the near significance with the model incorporating number of tickler chains (P=0.07) warrants further testing of this gear characteristic. Tickler chains cover the mouth of the dredge in a grid-like configuration with the vertical up and down chains. The number of chains on the bag and distance between the chains may help to prevent sea turtles from entering the dredge bag. This dredge configuration is currently being tested for sea turtle bycatch reduction in the Hudson Canyon area (DuPaul and Smolowitz[6]). Further research should also examine the behavior of sea turtles in relation to dredge gear for a more complete understanding of how and when turtles are entrapped.

Sea turtles and scallop dredge interactions cannot be viewed in isolation from other gear types and conservation measures. Some fisheries that co-occur with sea turtles may have an equal, if not greater, impact on turtles than do scallop dredges (e.g., the shrimp trawl fishery in the Gulf of Mexico [Henwood and Stuntz, 1987]). Changes in sea turtle abundance, or shifts in fishing effort, may increase the likelihood of encounters in both net and dredge fisheries. If environmental conditions associated with high bycatch rates in the Hudson Canyon and Virginia Beach areas are consistent across years, it may be possible to anticipate and deter future interactions from occurring.

Acknowledgments

I would like to thank Debra Palka and Marjorie Rossman for help with analytical and statistical approaches to bycatch estimation. Andy Solow and Andy Beet at the Marine Policy Center, Woods Hole Oceanographic Institute, also provided guidance in the statistical analysis. David Mountain provided invaluable help in acquiring

[3] Final Rule, FR 67: 71895-71900, 3 December 2002.

[4] Epperly, S. P. and J. Braun-McNeill. 2002. Unpubl. data. The use of AVHRR Imagery and the management of sea turtle interactions in the Mid-Atlantic Bight. NMFS Southeast Fisheries Science Center, Miami, Florida, 33149.

[5] Final Rule, FR 68: 69962-69967, 16 December 2003.

[6] DuPaul, W. P., and R. Smolowitz. 2003. Unpubl. data. Industry trials of a modified sea scallop dredge to minimize the catch of sea turtles. Virginia Institute of Marine Science, Gloucester Point, Virginia, 23062, and Coonamessett Farm, East Falmouth, Massachusetts, 02536.

sea surface temperature for the Observer and VTR data. Frederic Serchuk, Richard Merrick, Debra Palka, Marjorie Rossman, and Paul Rago at the Northeast Fisheries Science Center all provided initial reviews of the manuscript. Jeffrey Seminoff and two anonymous reviewers provided valuable comments during peer review. Finally, I wish to thank the observers who collected data on interactions between turtles and the sea scallop dredge fishery.

Literature cited

Allen, L. K.
2000. Protected species and New England fisheries: an overview of the problem and conservation strategies. Northeastern Naturalist 7(4):411–418.

Burnham, K. P. and D. R. Anderson.
2002. Model selection and multimodel inference: a practical information-theoretic approach, 2nd ed., 488 p. Springer-Verlag, New York, NY.

Cochran, W.G.
1977. Sampling techniques, 3rd ed., 428 p. John Wiley & Sons, New York, NY.

Coles, W. C. and J. A. Musick.
2000. Satellite sea surface temperature analysis and correlation with sea turtle distribution off North Carolina. Copeia 2:551–554.

Crouse, D. T., L. B. Crowder, and H. Caswell.
1987. A stage-based population model for loggerhead sea turtles and implications for conservation. Ecology 68(5):1412–1423.

Denis, V., J. Lejeune, and J. P. Robin.
2002. Spatio-temporal analysis of commercial trawler data using General Additive models: patterns of Loliginid (*sic*) squid abundance in the north-east Atlantic. ICES J. Mar. Sci., 59:633–648.

Efron, B. and R. J. Tibshirani.
1993. An introduction to the boostrap, 436 p. Chapman & Hall, New York, NY.

Epperly, S. P.
2003. Fisheries-related mortality and turtle excluder devices (TEDs). *In* The biology of sea turtles, vol. II (P. L. Lutz, J. A. Musick, and J. Wyneken, eds.), p. 339–353. CRC Press, Boca Raton, FL.

Epperly, S. P., J. Braun, A. J. Chester, F.A. Cross, J. V. Merriner, and P. A. Tester.
1995. Winter distribution of sea turtles in the vicinity of Cape Hatteras and their interactions with the summer flounder trawl fishery. Bull. Mar. Sci. 56(2): 547–568.

Frost, K. J., L. F. Lowry, and J. M. Ver Hoef.
1999. Monitoring the trend of harbor seals in Prince William Sound, Alaska, after the *Exxon Valdez* oil spill. Mar. Mamm. Sci. 15(2):494–506.

Guisan, A., T. C. Edwards, and T. Hastie.
2002. Generalized linear and generalized additive models in studies of species distributions: setting the scene. Ecol. Model. 157:89–100.

Hamazaki, T.
2002. Spatiotemporal prediction models of cetacean habitats in the mid-western North Atlantic ocean (from Cape Hatteras, North Carolina, USA to Nova Scotia, Canada). Mar. Mamm. Sci. 18(4):134–151.

Hastie, T. J., and R. J. Tibshirani.
1990. Generalized additive models, 329 p. Chapman and Hall, London.

Henwood, T. A., and W. E. Stuntz.
1987. Analysis of sea turtle captures and mortalities during commercial shrimp trawling. Fish. Bull. 85: 813–817.

Heppell, S. S., L. B. Crowder, D. T. Crouse, S. P. Epperly, and N. B. Frazer.
2003. Population models for Atlantic loggerheads. *In* Loggerhead sea turtles (A. Bolten and B. Witherington, eds.), pp. 255–273. Smithsonian Books, Washington, D.C..

Julian, F., and M. Beeson.
1998. Estimates of marine mammal, turtle, and seabird mortality for two California gillnet fisheries: 1990–1995. Fish. Bull. 96:271–284.

Lewison, R. L., S. A. Freeman, and L. B. Crowder.
2004. Quantifying the effects of fisheries on threatened species: the impact of pelagic longlines on loggerhead and leatherback sea turtles. Ecology Letters 7:221–231.

Morreale, S. J., E. A. Standora, J. R. Spotila, and F. V.Paladino.
1996. Migration corridor for sea turtles. Nature 384: 319–320.

NMFS (National Marine Fisheries Service).
2003. Fisheries observer program manual, 217 p. Northeast Fisheries Observer Program, Northeast Fisheries Science Center, Woods Hole, MA.

NMFS and USFWS (National Marine Fisheries Service and U.S. Fish and Wildlife Service).
1991. Recovery plan for U.S. population of loggerhead turtle, 64 p. National Marine Fisheries Service, Washington, D.C.

NCR (National Research Council).
1990. Decline of the sea turtles: causes and prevention, 259 p. National Academy Press, Washington, D.C.

Palka, D. L., and M. C. Rossman.
2001. Bycatch estimates of coastal bottlenose dolphin (*Tursiops truncatus*) in U.S. Mid-Atlantic gillnet fisheries for 1996–2000. Northeast Fisheries Science Center Reference Document 01-15, 77 p.

Polovina, J. J., D. R. Kobayashi, D. M. Parker, M. P. Seki, and G. H. Balazs.
2000. Turtles on the edge: movement of loggerhead turtles (*Caretta caretta*) along oceanic fronts, spanning longline fishing grounds in the central North Pacific, 1997–1998. Fish. Oceanogr. 9:71–82.

Rossman, M. C., and R. L. Merrick.
1999. Harbor porpoise bycatch in the Northeast multispecies sink gillnet fishery and the Mid-Atlantic coastal gillnet fishery in 1998 and during January–May 1999. Northeast Fish. Sci. Cent. Ref. Doc. 99-17, 36 p.

Shoop, R. C. and R. D. Kenney.
1992. Seasonal distributions and abundances of loggerhead and leatherback sea turtles in waters of the northeastern United States. Herpetol. Monogr. 6:43–67.

Smolowitz, R.
1998. Bottom tending gear used in New England. *In* Effects of fishing gear on the sea floor of New England (E. Dorsey and J. Pederson, eds.), p. 46–52. Conservation Law Foundation, Boston, MA.

Turtle Expert Working Group.
2000. Assessment update for the Kemp's ridley and loggerhead sea turtle populations in the western North Atlantic. U.S. Dep. Commer. NOAA Tech. Memo. NMFS-SEFSC-444, 115 p.

Wade, P. R., and R. P. Angliss.
1997. Guidelines for assessing marine mammal stocks: report of the GAMMS workshop April 3–5, 1996, Seattle, Washington. U.S. Dep. Commer., NOAA Tech. Memo. NMFS-OPR-12, 93 p.

Witzell, W. N.
1999. Distribution and relative abundance of sea turtles caught incidentally by the U.S. pelagic longline fleet in the western North Atlantic Ocean, 1992–1995. Fish. Bull. 97:200–211.

Appendix 1

Categorical variables examined in an analysis of factors affecting sea turtle bycatch in the sea scallop dredge fishery. Frequency of observed dredges in each category is also shown.

Variable	Category	Number of observed dredges in Hudson Canyon 2001	Number of observed dredges in Virginia Beach 2001	Number of observed dredges in Hudson Canyon 2002	Number of observed dredges in Virginia Beach 2002
Year	2001 or 2002	9493	520	8059	0
Season	Spring = May and June	3919	0	1987	0
	Summer = July, August, September	2719	0	3764	0
	Fall = October, November, December	2855	520	2308	0
State in which scallops were landed	Connecticut	199	0	595	0
	Massachusetts	4925	0	5628	0
	New Jersey	2849	0	740	0
	Rhode Island	112	0	474	0
	Virginia	1408	520	622	0
Frame width[1] category	Small = 3.0–3.9 m (10–13 ft)	560	0	443	0
	Medium = ≥3.9 m and <4.5 m (15 ft)	3987	122	3013	0
	Large = <4.5 m–4.8 m (15–16 ft)	4946	398	4603	0
Number of up and down chains used[2]	Code 1 = 0 chains	4256	520	2171	0
	Code 2 = 1–4 chains	4089	0	5378	0
	Code 3 = >4 chains	1148	0	510	0
Number of tickler chains used[3]	Code 1 = ≤2 chains	6890	520	4469	0
	Code 2 = >2 chains	2603	0	3590	0
Time-of-day	Day = 4 am–4 pm	5514	346	4854	0
	Night = 4 pm–4 am	3979	174	3205	0
Sea surface temperature	Hi = >19 °C	3910	518	4883	0
	Low = ≤19 °C	5583	2	3176	0
Depth	Shallow = 40–<49 m (22–27 fm)	1089	42	782	0
	Mid-Depth = 49–57 m (27–31 fm)	3371	280	3642	0
	Deep = >57–88 m (31–48 fm)	5033	198	3635	0

[1] Width of the dredge frame.

[2] Vertical chains attached to the sweep on the bottom of the dredge that prevent rocks from entering the chain bag. Number of up and down chains were influenced by bottom type.

[3] Horizontal chains attached to the sweep on the bottom of the dredge that help stir up contents of the sea bottom. Number of tickler chains were influenced by bottom type.

Validation and interpretation of annual skeletal marks in loggerhead (*Caretta caretta*) and Kemp's ridley (*Lepidochelys kempii*) sea turtles

Melissa L. Snover

Duke University Marine Laboratory
135 Duke Marine Lab Road
Beaufort, North Carolina 28516
Present addresss: Pacific Fisheries Environmental Laboratory
1352 Lighthouse Ave.
Pacific Grove, California 93950

E-mail address: melissa.snover@noaa.gov

Aleta A. Hohn

Center for Coastal Fisheries and Habitat Research
National Marine Fisheries Service, NOAA
101 Pivers Island Road
Beaufort, North Carolina 28516

Abstract—Numerous studies have applied skeletochronology to sea turtle species. Because many of the studies have lacked validation, the application of this technique to sea turtle age estimation has been called into question. To address this concern, we obtained humeri from 13 known-age Kemp's ridley (*Lepidochelys kempii*) and two loggerhead (*Caretta caretta*) sea turtles for the purposes of examining the growth marks and comparing growth mark counts to actual age. We found evidence for annual deposition of growth marks in both these species. Corroborative results were found in Kemp's ridley sea turtles from a comparison of death date and amount of bone growth following the completion of the last growth mark (n=76). Formation of the lines of arrested growth in Kemp's ridley sea turtles consistently occurred in the spring for animals that strand dead along the mid- and south U.S. Atlantic coast. For both Kemp's ridley and loggerhead sea turtles, we also found a proportional allometry between bone growth (humerus dimensions) and somatic growth (straight carapace length), indicating that size-at-age and growth rates can be estimated from dimensions of early growth marks. These results validate skeletochronology as a method for estimating age in Kemp's ridley and loggerhead sea turtles from the southeast United States.

Manuscript submitted 15 August 2003 to the Scientific Editor's Office.

Manuscript approved for publication 3 June 2004 by the Scientific Editor

Fish. Bull. 102:682–692 (2004).

The basic tenet of skeletochronology is that bone growth is cyclic and has an annual periodicity in which bone formation ceases or slows before new, relatively rapid bone formation resumes (Simmons, 1992; Castanet et al., 1993; Klevezal, 1996). This interruption of bone formation is evidenced within the primary periosteal compacta by histological features, which take two forms in decalcified and stained thin-sections. The most common form is a thin line that appears darker than the surrounding tissue, termed the "line of arrested growth" (LAG) (Castanet et al., 1977). The second, less-common form is a broader and less distinct line that also stains darker, referred to as an annulus (Castanet et al., 1977). Alternating with LAGs or annuli are broad zones that stain homogeneously light, and represent areas of active bone formation. Together, a broad zone followed by either a LAG or an annulus represents a skeletal growth mark (GM) (Castanet et al., 1993). To apply skeletochronology to a species, the annual periodicity of the GM must be validated.

Validation studies are necessary not only to confirm the annual nature of the GM but also to identify and interpret anomalous LAGs. Anomalous LAGs that are a common problem in skeletochronology studies of reptiles and amphibians include double (Chinsamy et al., 1995; El Mouden et al., 1997; Guarino et al., 1998), splitting (Guarino et al., 1995; 1998; Coles et al., 2001), and supplemental (Guarino et al., 1995; Lima et al., 2000; Trenham et al., 2000) lines. In addition to anomalous LAGs, there are two other difficulties typical in skeletochronology studies; compression of LAGs at the periphery of the bone and resorption of the innermost LAGs. In older animals the GMs are compressed at the outer periphery of the bone as a result of decreased growth. Francillon-Vieillot et al. (1990) term this phenomenon "rapprochement" and it is a problem when the LAGs become too close together to be differentiated —usually in the small phalangeal bones used in amphibian studies (Eggert and Guyetant, 1999; Lima et al., 2000; Leclair et al., 2000).

In addition to anomalous and compressed LAGs, the loss of early GMs through endosteal resorption is another problem with skeletochronology. Although this does not present a problem with most amphibian species (Kusano et al., 1995; Castanet et al., 1996; Sagor et al., 1998), the problem is extreme in skeletochronology studies of loggerhead (*Caretta caretta*; Klinger and Musick, 1995; Zug et al., 1995; Parham and Zug, 1997), green

Table 1

Species and history of known-age sea turtles analyzed in this study.

Sample	Species	History during captivity	Age (yr)
LK-1	*Lepidochelys kempii*	Captive for first year, then released	5.0
LK-2	*L. kempii*	Captive for first year, then released	6.5
LK-3	*L. kempii*	Captive for first year, then released	4.5
LK-4	*L. kempii*	Tagged and released after hatching	1.27
LK-5	*L. kempii*	Tagged and released after hatching	1.70
LK-6	*L. kempii*	Tagged and released after hatching	1.72
LK-7	*L. kempii*	Tagged and released after hatching	2.37
LK-8	*L. kempii*	Tagged and released after hatching	2.37
LK-9	*L. kempii*	Tagged and released after hatching	3.25
LK-10	*L. kempii*	Tagged and released after hatching	2.0
LK-11	*L. kempii*	Tagged and released after hatching	2.75
LK-12	*L. kempii*	Tagged and released after hatching	3.0
LK-13	*L. kempii*	Tagged and released after hatching	4.25
CC-1	*Caretta caretta*	Captive during entire life	29.4
CC-2	*C. caretta*	Captive for first two years, then released	8.0

(*Chelonia mydas*; Zug and Glor, 1998; Zug et al., 2002) and Kemp's ridley (*Lepidochelys kempii*; Zug et al., 1997) sea turtles. In each of these studies, the authors used various protocols to estimate the number of layers lost. Any protocol estimating the number of layers lost to resorption relies on the concept that the spatial pattern of the LAGs is representative of the growth of the animal. To confirm this assumption, researchers must establish a correlation between bone dimensions and body size (Hutton, 1986; Klinger and Musick, 1992; Leclair and Laurin, 1996).

Two of the studies that have applied skeletochronology to sea turtles have demonstrated annual GMs in both juvenile (Klinger and Musick, 1992) and adult (Coles et al., 2001) loggerhead sea turtles. Numerous additional studies have applied skeletochronology to sea turtles. To date, the technique has been applied to loggerhead (Zug et al., 1986; Zug et al., 1995; Bjorndal et al., 2003), green (Bjorndal et al., 1998; Zug and Glor, 1998; Zug et al., 2002), Kemp's ridleys (Zug et al., 1997), and leatherback (*Dermochelys coriacea*) (Zug and Parham, 1996) sea turtles. What is needed for the appropriate application of skeletochronology to sea turtle species is additional validation of annual GMs and a guide to their interpretation. Furthermore, because resorption is a problem in sea turtle bones, the validation of a proportional allometry between bone and somatic growth is necessary to enable back-calculation.

In this study, we address each of these issues for Kemp's ridley and loggerhead sea turtles by examining humeri from known-age animals. We analyzed each humerus without prior knowledge of the animal's age and we present the results of our analyses, including reinterpretations of bones for which we were incorrect in our age assessments. The purpose of this study was to use known-age samples both to validate the likelihood that GMs are annual and as a learning tool for the best guide to interpreting GM in wild animals.

Materials and methods

We obtained samples from two known-age loggerhead and 13 known-age Kemp's ridley sea turtles (Table 1). In addition, we collected samples from 240 wild loggerhead and 262 wild Kemp's ridley sea turtles. With the exception of one loggerhead, CC-1, all of the sea turtles died in the wild and samples were retrieved from the carcasses. Sample CC-1 died in captivity.

Sample preparation

Zug et al. (1986) analyzed skeletal elements of the cranium and right forelimb of loggerhead sea turtles and determined that the humerus was most suited to skeletochronology studies. Therefore, we also used the humerus. Specimens arrived as either dried bones or whole flippers. For flippers, we dissected out the humerus, which was then flensed, boiled, and air-dried for at least two weeks. We cross-sectioned each humerus at a site just distal to the deltopectoral crest. At this site, the ratio of cortical to cancellous bone is highest (Zug et al., 1986), and the region immediately distal to the insertion scar of the deltopectoral muscle on the ventral side of the bone maximizes that ratio (see Zug et al., 1986 for diagrams of the loggerhead sea turtle humerus). This site also provided a landmark that allowed us to section at equivalent sites on every humerus.

We removed 2–3 mm thick sections at that site using a Buehler® isomet low speed saw. This section was

fixed in 10% formalin then decalcified by using a commercial decalcifying agent (RDO, Apex Engineering Products Corporation, Calvert City, Kentucky). Time to decalcification varied with the size of the bone and the strength of the solution, usually between 12 and 36 hours. Following decalcification, 25-μm thick cross-sections were made by using a freezing-stage microtome. Sections were stained in Erlich's hematoxylin diluted 1:1 with distilled water (Klevezal, 1996) and mounted on slides in 100% glycerin.

Known-age sea turtles

We received the humeri from each of two captive, known-age loggerhead sea turtles after they died (Table 1). The first specimen, CC-1, was held in an outdoor tank during the summer months and inside a greenhouse during the winter months (this turtle was the same captive female noted in Swartz, 1997). The second, CC-2, was raised in captivity for two years then released from Panama City, Florida, into the Gulf of Mexico.

For the Kemp's ridley sea turtles, we received humeri from 13 dead known-age animals (Table 1). The head-start Kemp's ridleys were raised in captivity for one year, then released as part of a binational program operated jointly by state and federal U.S. agencies and the Instituto Nacional de la Pesca (INP) of Mexico (Klima and McVey, 1995). The coded-wire–tagged (CWT) Kemp's ridley sea turtles were tagged and released as hatchlings. This tagging program is operated jointly by the U.S. National Marine Fisheries Service (NMFS) Galveston Laboratory and the INP of Mexico as a means of gaining a better understanding of the early life history of the Kemp's ridley sea turtle (Caillouet et al., 1997).

Using the methods described previously, we prepared stained thin-sections from the humeri. Without prior knowledge of the animal's history, the number of visible LAGs was quantified for each bone and a minimum age estimated. Our age estimates were then compared to the age information available for each animal.

Indirect validation of annual growth marks

Peabody (1961) and Castanet et al. (1993) suggested that the correlation between the width of the last zone formed and the date of death provided an indirect means of validating that deposition of the LAG occurs annually and at the same time of year for an individual population. We applied this method to 76 wild Kemp's ridley sea turtles for which humeri displayed between one and five LAGs. Each of these animals had stranded dead along the Atlantic coast between Maryland and North Carolina. Thin-sections were prepared of the humeri as described above. We quantified the width of the last zone formed by measuring the outside diameter of the whole section (D_O) and the diameter of the last competed LAG (D_L), between the lateral edges of the bone on an axis parallel to the dorsal edge. The amount of bone growth after the last LAG (D_O–D_L) was plotted against the Julian stranding date, with the assumption that stranding date approximated date of death. Least-squares linear regressions were fitted to the data.

Validation of the relationship between LAG diameter and body size

In order to relate GM diameters to somatic growth rates, there must be a constant proportionality between bone growth and somatic growth (Chaloupka and Musick, 1997). To address this proportionality, we took eight morphometric measurements of 240 wild loggerhead and 262 wild Kemp's ridley humeri, using digital calipers or a tape measure when dimensions were beyond the range of the calipers. Measurements of maximum length, longitudinal length, proximal width, distal width, deltopectoral crest width, lateral diameter at sectioning site, ventral to dorsal thickness at sectioning site, and mass were recorded. We compared these measurements with the carapace length, measured as standard straight-line length (SCL) from the nuchal notch to the posterior end of the posterior marginal, using a least-squares linear regression. For mass, the data were natural-log transformed to form a linear regression.

Results

Known-age Kemp's ridley sea turtles

Three Kemp's ridley sea turtles captive for one year and then released were recovered 4.5 to 6.5 years after hatching (Table 1). Sample LK-1 had minimal resorption and four complete GMs, each comprising one zone followed by a LAG. An additional zone was seen at the periphery and the LAG that would complete this last GM was not yet visible at the outer edge of the humerus cross-section. From GM counts and death date, we estimated the age of this animal accurately at five years (Fig. 1). Sample LK-2 retained five completed and one incomplete GM; however, we observed a large area of resorption in the interior region of the cross-section that potentially obscured additional GMs. We aged this animal at a minimum of 5.5 years, the actual age being 6.5 years. Sample LK-3 displayed four completed GMs and one incomplete mark. Without prior knowledge of this animal's age, we estimated the age accurately at 4.5 years based on layer count and time of death.

Ten of the Kemp's ridley sea turtle samples were tagged and released after hatching, and no time was spent in captivity (Table 1). Results from these ten recovered animals allowed us the opportunity to study and interpret the early GM patterns in noncaptive animals. The first year mark for Kemp's ridley sea turtles appeared to be a poorly defined annulus, as evidenced by LK-4 (Fig. 2A). In turtles greater than two years old, similar first year marks also appeared more or less distinctly (Figs. 2B and 3). Additional marks, which can only be interpreted as supplemental lines given the age of the animal, appeared between GM one and the outer edge of the bone in LK-6 (Fig. 2B) and LK-10. Specimens

LK-7 and LK-8 were difficult to interpret and in our initial assessment we underestimated age by one year. In both of these samples, the LAG representing the end of the second GM was very close to the outer edge of the bone cross-section and was difficult to differentiate from the edge. Hence these samples were not counted in the initial assessment. Because both of these animals died in the fall, there would have been a full growing season, and hence a growth zone, following the completion of the second GM. Both of these animals were recovered dead in Cape Cod, Massachusetts, during the fall of 1999 when record numbers of cold-stunned sea turtles stranded in that region.

Humerus cross-sections from LK-9 through LK-13 (Fig. 3) showed poorly defined annuli at the end of the first GM—annuli similar to the poorly defined annulus in LK-4 (Fig.2A). Subsequent GMs in these humerus cross-sections contained well-defined LAGs. Without prior knowledge of these animals' history we accurately aged each of them from GM counts and stranding date. Specimens LK-9 through LK-13 demonstrated clearly that well-defined LAGs were deposited at the end of year two and in subsequent years, providing evidence that any lines between the year-one annulus and the year-two LAGs were supplemental.

Known-age loggerhead sea turtles

The first known-age loggerhead sea turtle, CC-1, was 29.4 years old. Eleven LAGs were discernible around the circumference of the bone cross-section (Fig. 4A), although the LAGs become too compressed on the lateral edges of the bone to be differentiated; hence counts were made on the ventral and dorsal edges.(Fig. 4). Tracing the LAGs from the lateral to the ventral edge of the bone, we observed that these LAGs at some point became bifurcating and splitting LAGs and we interpreted each branch as a separate LAG. An additional nine LAGs can still be seen within the resorption zone in most areas of the bone (Fig. 4B). On the dorsal side of the cross-section, at least four less-distinct LAGs or annuli could still be observed; these had been

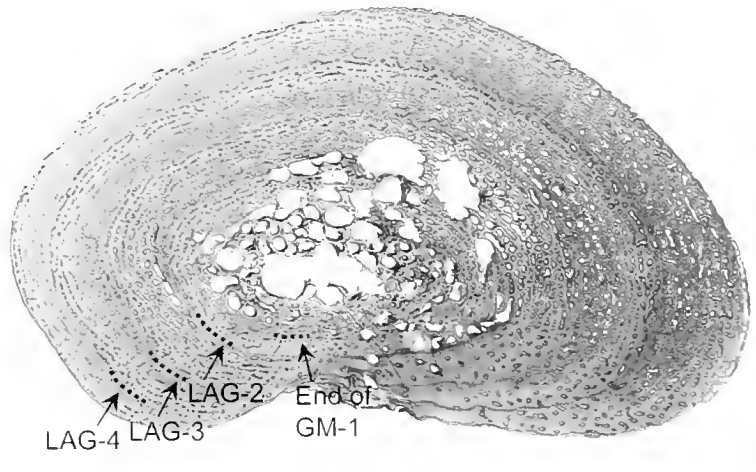

Figure 1

Image of a humerus cross-section from a headstart Kemp's ridley (*Lepidochelys kempii*, LK-1) sea turtle. GM-1 refers to growth mark one; LAG-2, LAG-3, and LAG-4 refer to the lines of arrested growth ending growth marks two, three, and four. Curved dashed lines highlight GM-1 and the LAG. Black bar represents 1 mm in length. This specimen was 5.0 years old.

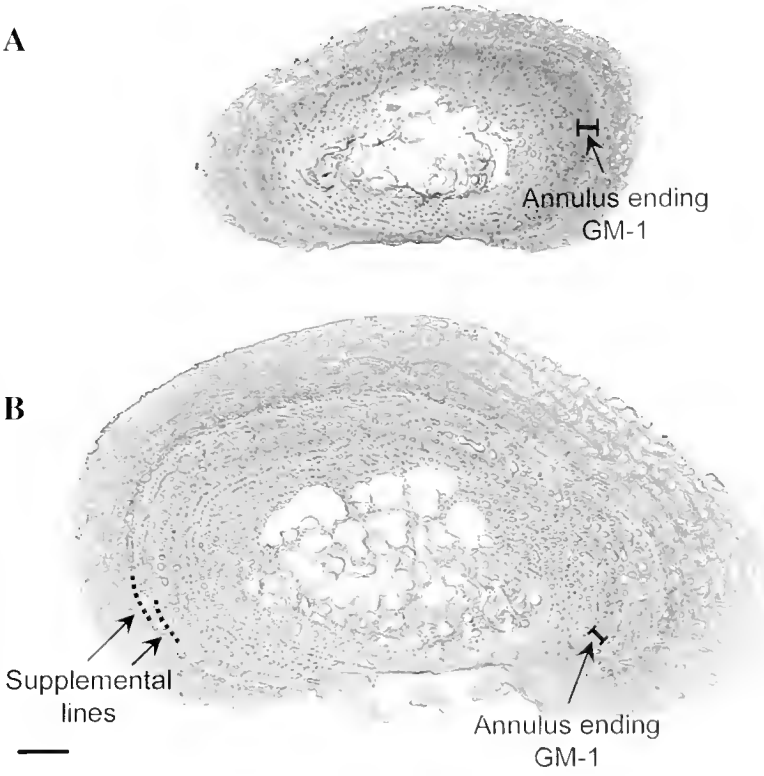

Figure 2

Images of humeri cross-sections of two coded-wire-tagged Kemp's ridley sea turtles (*L. kempii*). GM-1 refers to growth mark one. Black bar represents 1 mm for both images. (**A**) Specimen LK-4 was 1.27 years old. (**B**) Specimen LK-6 was 1.72 years old.

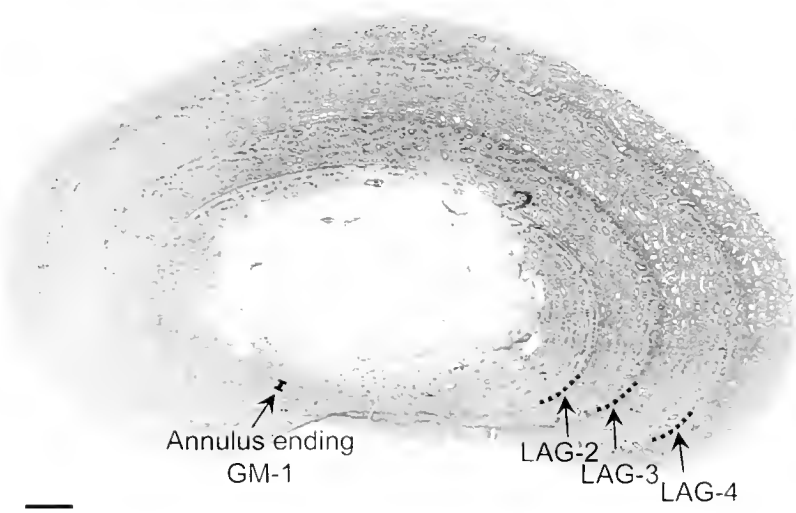

Figure 3

Image of humerus cross-section from a coded-wire–tagged Kemp's ridleys (*L. kempii*). Black bar represent 1 mm in length. GM-1 refers to growth mark one; LAG-2, LAG-3, and LAG-4 refer to the lines of arrested growth ending growth marks two, three, and four. Curved black lines highlight LAGs or annuli. This specimen, LK-13, was 4.75 years old.

resorbed in all other parts of the bone (Fig. 4C). There had been a great deal of remodeling within the bone and much of the inner portion of the bone had been resorbed. Summing all of these GMs, we gave a minimum age estimate of 24 years without prior knowledge of the history of the animal. The outermost 20 GMs contained well-defined LAGs that were spaced close together, whereas the four interior-most visible GMs contained LAGs or annuli that were spaced farther apart (Fig. 4). The number of layers completely resorbed was five.

A second known-age loggerhead sea turtle, CC-2, was eight years old. We assigned a minimum age estimate of five years. Just outside of the resorption area was a series of three LAGs that were very close together (Fig. 5). In our initial analysis, we assumed that three LAGs so close together could not each be deposited annually and we interpreted the triple LAGs as a single LAG with an anomalous appearance. We re-evaluated this assumption after learning its history. The animal was in captivity for two years and then released at 42.7 cm SCL in October 1994. Counting back from the outside of the bone, the outermost of the triplet LAGs would represent spring 1996. Given this evidence, our best interpretation of this bone section was that the innermost of the triplets of LAGs indicated release and was therefore not an annual mark. The next LAG was likely deposited the following spring (1995) and was likely an annual mark. The third of the closely spaced LAGs likely represented spring 1996, indicating that the animal did not grow significantly in its first year in the wild (Fig. 5). Following the three closely spaced LAGs, there were four additional indistinct LAGs or annuli that represented the remaining years at large. The outermost of these was very close to the edge of the bone, indicating that the animal did not grow much, if at all, during the last summer of its life.

Indirect validation of annual growth marks

For Kemp's ridley sea turtles, there was a significant increase in the amount of bone deposited after the last LAG from 20 June to 30 November (Fig. 6). The LAGs near the outer edges of the bones were fully visible in strandings that occurred after 20 June. Earlier detection of the outer LAGs was unlikely because a certain amount of bone formation must occur following the LAG before it can be discerned from the edge. There was not a significant relationship between bone growth and date from 1 December to 19 June. The slope of this regression was very close to zero (b=−0.003), indicating no trend, either increasing or decreasing, in the amount of bone deposited during this time (Fig. 6).

Validation of the relationship between LAG diameter and body size

The regressions of the eight morphometric measurements of loggerhead and Kemp's ridley sea turtle humeri against SCL revealed high correlations between bone dimension and body size (Table 2). Most importantly for purposes of back-calculation, the lateral diameter at the sectioning site of the humerus (distal to the insertion scar of the deltopectoral muscle) and the body length of the animal was highly correlated.

Discussion

Validation of the annual nature of growth marks

Our results supported annual deposition of GMs in loggerhead and Kemp's ridley sea turtles. The headstarted and older CWT Kemp's ridley sea turtles in particular highlighted the likelihood of annual marks. These animals displayed sharp and regularly spaced LAGs that were consistent with the actual ages of the animals. The results from the CWT Kemp's ridley sea turtles also emphasized the difficulties in interpreting early GMs. From these animals we concluded that in general Kemp's ridley sea turtles deposit a poorly defined annulus in their first year and well-defined LAGs starting with the end of the second year and in following years.

For loggerhead sea turtles, only CC-2 spent any time in the wild. The number of GMs deposited after the animal was released (determined from the appearance of the anomalous triplet of LAGs) was consistent with the number of years for which the animal was at large, considering that the first mark was deposited at release. This indicated that not less than one GM was deposited per year, and that additional or supplemental LAGs or annuli indistinguishable from annual lines may be deposited under extreme conditions, such as at the time of release into the wild. Fortunately, in this case, these extreme conditions were not frequent enough to have a serious impact on age estimates. For the life-time captive animal, CC-1, our estimated minimum age was five years shorter than the actual age of 29.4 years and clearly demonstrated that not more than one GM was deposited each year. Because of the relatively large size of the sea turtle humerus, in comparison to phalanges of amphibians, rapprochement did not appear to be a problem in our attempts to discern LAGs. This bone was similar in appearance to adult wild loggerhead and Kemp's ridleys sea turtles with rapprochement of the peripheral LAGs and resorption of most of the interior GMs. Although accurate age estimates cannot be made of these bones through skeletochronology, if rapprochement correlates to the timing of sexual maturity, counts of the compressed GMs can provide valuable information on postreproductive longevity and adult survival. This information can be combined with average age at reproductive maturation for piecing together the life history of sea turtles. Although our sample size for loggerhead sea turtles was very small (two), the size complements a tetracycline-injection study that previously validated annual GMs for juvenile loggerhead sea turtles from Chesapeake Bay (Klinger and Musick, 1992). In addition, an adult loggerhead sea turtle from that same study stranded dead 8.25 years after injection and provided evidence of annual deposition of growth marks in adults (Coles et al., 2001).

The indirect validation results for Kemp's ridley sea turtles highlighted the cyclic nature of bone growth; bone deposition increases from late spring through early summer to fall and no bone deposition occurs from December to spring. From this information we inferred that LAGs form annually in the spring for Kemp's ridley sea turtles that strand along the mid- to southeast U.S. Atlantic coast and that these LAGs are visible at the edges of the bones by late spring to early summer.

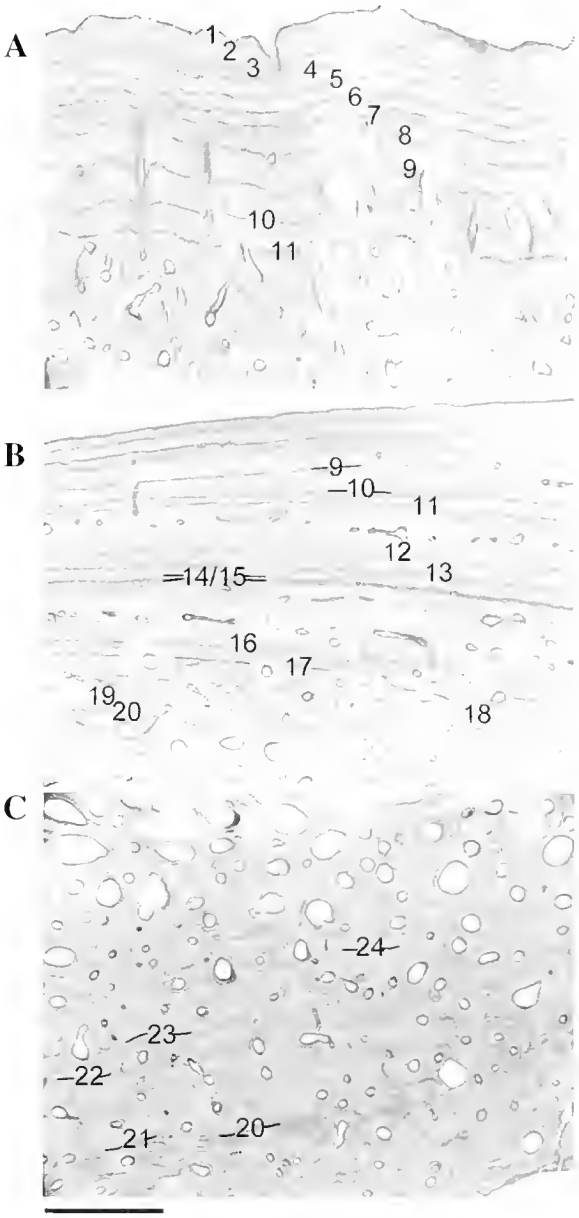

Figure 4

Images of different portions of the humerus cross-sections of CC-1 (*Caretta caretta*). Black bar represents 1 mm in length for all views. (**A** and **B**) The outer edge of the bone is at the top of the photo. (**C**) The outer edge of the bone is towards the bottom of the photo. For all views, lines of arrested growth (LAGs) are labeled with numbers; low numbers represent the most recently deposited LAGs (near the outer edge of the bone) and higher numbers represent the earlier LAGs.

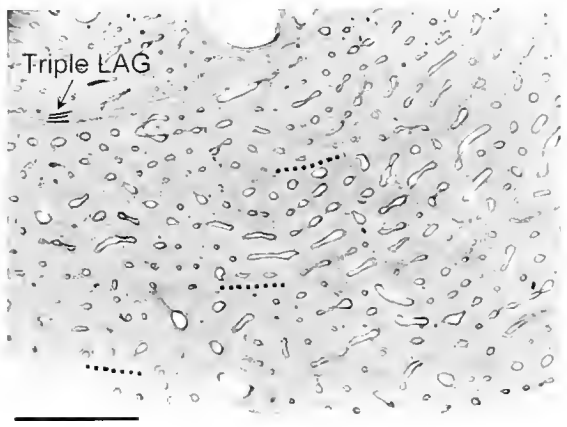

Figure 5

Image of a section of the humerus cross-section of CC-2 (*C. caretta*). Outer edge of bone is towards the bottom of the photo. Solid lines (upper left) highlight a series of triple lines of arrested growth (LAGs); curved dashed lines highlight the three diffuse LAGs. Black bar represents 1 mm in length.

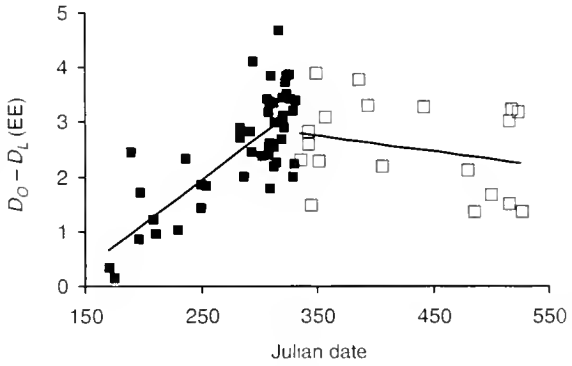

Figure 6

Julian date of stranding plotted against the amount of bone deposited peripherally to the last LAG in Kemp's ridley sea turtles (*L. kempii*; n=76). D_O represents the outside diameter of the humerus, D_L represents the diameter of the last LAG. Julian dates on x-axis equate to 20 June through 19 June; therefore numbers that are greater than 365 represent the Julian date plus 365. Solid lines represent linear regressions that were run separately for 6 months, 20 June to 31 November (filled squares) and 1 December to 19 June (open squares). The regression for the first six months was significant (P<0.006) and the regression for the second six months was not significant (P=0.27).

Most studied species of reptiles and amphibians deposit GMs within their bones (Castanet et al., 1993; Smirina, 1994). For some of these species, the annual nature of the GM has been validated (e.g., Tucker, 1997; de Buffrénil and Castanet, 2000; Trenham et al., 2000). For others, it is consistent with their ecology that the marks must represent annual events (Castanet et al., 1993). Growth marks observed in loggerhead (Zug et al., 1986; Zug et al., 1995; Coles et al., 2001), Kemp's ridley (Zug et al., 1997), and green (Zug and Glor, 1998; Zug et al., 2002) sea turtles are similar in structure to those observed in other species of reptiles and amphibians. Drawing on previous studies of reptiles and amphibians, validation studies on sea turtles, and the evidence presented in this article, we assert that GM in bones of sea turtles are likely deposited primarily with an annual periodicity.

Given these results, on the surface it seems contradictory that in two validation studies annual GMs could not be confirmed. For serpentine species, Collins and Rodda (1994) injected brown snakes with a fluorescent marker and kept them in captivity for one year under two different feeding regimes. Five or six GMs varying in distinctness were identified beyond the fluorescent marks in bone cross-sections. Statistical analyses showed that these marks may relate to shedding events. It is unclear if the GM pattern prior to captivity was similar to what was seen after the fluorescent mark. The forced feeding component of that study may have induced higher growth rates than would be found in nature, causing the shedding events to appear as histological marks in the bone.

In a sea turtle study, Bjorndal et al. (1998) did not find GMs in the humeri of green sea turtle bones. They suggested that the tropical marine habitat of the study population (approximately 21°07′N) allowed for continual activity and growth and inhibited GM formation. However, GMs have been clearly demonstrated in green sea turtles from the coastal waters of Florida (approximately 29°N) (Zug and Glor, 1998) and Hawaii (approximately 22°N) (Zug et al., 2002). Other studies of reptiles and amphibians in tropical and warm temporate climates have reported distinct GMs in species that remain active year-round (i.e., do not hibernate or estivate) (Patnaik and Behera, 1981; Estaban et al., 1996; Guarino et al., 1998).

Interpretation of anomalous LAGs

Although our sample sizes were small, especially for loggerhead sea turtles, several characteristics were noted in the analyses of the samples that would affect how anomalous LAGs are interpreted. Three interpretations of double and bifurcating LAGs are provided. The first interpretation is that if double LAGs appear frequently in individual bones and throughout the sample, they likely indicate an ecology that has two growth cycles per year (Castanet et al., 1993). In this case the two LAGs are distinct from each other over the entire bone cross-section. This pattern was observed in the newt *Triturus marmoratus* living at a high altitude where the animals had both winter and summer dormancy periods (Castanet and Smirina, 1990; Caetano et al., 1985; Caetano and Castanet, 1993). The second interpretation of double LAGs is that they result from a brief

Table 2

Regressions equations and statistics from correlations between dimensions of the humerus and notch-to-tip straight carapace length (SCL, cm) in loggerhead and Kemp's ridley sea turtles. All F statistics are significant at $P<0.005$.

Humeral measurement	Model equation	SE slope	F	r^2
Loggerhead sea turtles (n=243)				
Maximal length (ML, mm)	$SCL = 0.44 \times ML + 5.97$	0.0064	4814	0.95
Longitudinal length (LL, mm)	$SCL = 0.47 \times LL + 4.85$	0.0064	5381	0.96
Proximal width (PW, mm)	$SCL = 1.06 \times PW + 7.31$	0.015	4857	0.95
Deltopectoral crest width (DCW, mm)	$SCL = 1.69 \times DCW + 6.04$	0.026	4069	0.94
Site of sectioning width (SW, mm)	$SCL = 2.38 \times SW + 5.48$	0.037	4110	0.94
Site of sectioning thickness (ST, mm)	$SCL = 4.13 \times ST + 11.62$	0.080	2682	0.92
Distal width (DW, mm)	$SCL = 1.28 \times DW + 5.43$	0.021	3684	0.94
Mass (M, g)	$\ln(SCL) = 0.30 \times \ln(M) + 2.94$	0.0022	18905	0.99
Kemp's ridley sea turtles (n=262)				
Maximal length (ML, mm)	$SCL = 0.43 \times ML + 4.69$	0.0040	10970	0.98
Longitudinal length (LL, mm)	$SCL = 0.47 \times LL + 3.11$	0.0039	14772	0.98
Proximal width (PW, mm)	$SCL = 1.12 \times PW + 4.39$	0.010	12390	0.98
Deltopectoral crest width (DCW, mm)	$SCL = 1.69 \times DCW + 3.35$	0.017	10200	0.98
Site of sectioning width (SW, mm)	$SCL = 2.48 \times SW + 2.74$	0.033	5715	0.96
Site of sectioning thickness (ST, mm)	$SCL = 4.16 \times ST + 4.79$	0.072	3306	0.93
Distal width (DW, mm)	$SCL = 1.36 \times DW + 0.227$	0.013	11435	0.98
Mass (M, g)	$LN(SCL) = 0.30 \times LN(M) + 2.89$	0.0023	16305	0.98

interruption of hibernation (Hemelaar and van Gelder, 1980). In this instance little bone deposition would occur and the layers would not be distinct from each other over the entire bone, thus giving the appearance of a bifurcating LAG (Hemelaar and van Gelder, 1980). The third interpretation of double or bifurcating LAGs is that they result from extreme decreased growth over the active period, which places annual LAGs very close to each other and in some cases they appear to merge (de Buffrénil and Castanet, 2000).

With the first two interpretations, a double or bifurcating LAG would be counted as one for the purposes of age estimation, whereas the third interpretation would necessitate counting each LAG or bifurcating branch separately. Coles et al. (2001) interpreted a bifurcating LAG as one LAG in an adult loggerhead sea turtle that was recovered 8.25 years after it had been injected with oxytetracycline. In cross-sections of the humerus, Coles et al. (2001) reported seven LAGs following the tetracycline mark, six plus the bifurcating LAG. The animal was marked on 20 June 1989 and recovered dead on 22 September 1997. It is reasonable to assume that, as with Kemp's ridley sea turtles from the same region, the LAGs form in the spring, and Coles et al. (2001) showed that the oxytetracycline mark overlaid one of the LAGs—likely the LAG deposited in spring of 1989. Therefore, there should have been eight LAGs deposited after the tetracycline mark, not seven, each representing the spring of years 1990 through 1997. In this case, then, the bifurcating mark in this bone should be counted as two LAGs.

Similarly, for splitting LAGs, where numerous thinner LAGs branch out from what appears to be one thick LAG, Francillon-Vieillot et al. (1990) examined different bones from the same animal and determined whether each thin LAG comprising splitting LAGs should be counted as one LAG. In our analysis of the adult loggerhead sea turtle, CC-1, we observed several bifurcating and splitting LAGs, each of which eventually split into two or more thinner LAGs. We counted each of the thin LAGs as one. Because the LAG count was close to the actual age of the animal, this interpretation appears to have been appropriate for compressed LAGs in adult humeri.

The question remains as to whether this is the appropriate interpretation for double or bifurcating LAGs in juveniles. Wild loggerhead growth rates have been monitored in an ongoing mark-recapture study in Pamlico and Core Sounds in North Carolina (Epperly et al., 1995). Epperly et al. (1995) currently have 65 growth rates for 49 juvenile loggerhead sea turtles between 45.1 and 81.0 cm SCL at initial capture that were at-large for one year (±0.1 year). The mean annual growth rate for all of the animals is 2.09 cm/yr. However, of the 65 growth records, 11 of them displayed an annual increase of 0.3 cm or less in SCL (Braun-McNeill[1]). Hence it is not uncommon for juvenile loggerhead sea turtles to

[1] Braun-McNeill, J. 2004. Personal commun. Center for Coastal Fisheries and Habitat Research, National Marine Fisheries Service, NOAA, 101 Pivers Island Rd., Beaufort, NC 28516

grow little or not at all over the course of a year. Using the equation for width at sectioning site from Table 2, we found that the increase in bone diameter for these 11 animals was ≈0.13 mm or less, which places the LAGs very close together. Because it not uncommon for sea turtle to exhibit little or no growth over a year, LAGs spaced closely together very likely represent distinct years as also determined by de Buffrénil and Castanet (2000). Although the sample sizes are still small for a definitive answer, our results indicate that counting the LAGs individually is the correct interpretation of double or bifurcating LAGs in juvenile as well as adult loggerhead sea turtles.

Similarly, our results indicate the same interpretation for double or bifurcating LAGs in juvenile Kemp's ridley sea turtles. The CWT Kemp's ridley sea turtles, samples LK-7 and LK-8, displayed LAGs near the outer edge of the bone and a small amount of bone was deposited after the LAGs. These animals were each 2.25 years old and had one-year marks visible in the humeri but no LAGs or annuli other than those at the periphery. Other CWT samples clearly indicated that LAGs are deposited at the end of the second GM. The indirect validation results demonstrated that LAGs were visible in bone tissue by late spring or early summer. It seemed that the LAGs at the outer edge of the LK-7 and LK-8 bones were the LAGs ending the second GM and that very little growth occurred over the subsequent growing season. Both of these animals were recovered as dead strandings resulting from a major cold stun event in Cape Cod, Massachusetts, in 1999; hence their growth rates may have been anomalous in their last year of life. Had these animals survived the cold stun event, they would have deposited a year-three LAG very close to year two, giving the appearance of a double or bifurcating LAG.

Another anomaly in skeletochronology, supplemental lines, may form as a result of temporary stressful environmental events such as droughts. In support of this, Rogers and Harvey (1994) noted a supplemental line in 11 of 43 specimens of the toad *Bufo cognatus*, and in 10 of these animals the supplemental line was within a growth zone that corresponded to a drought year. Most skeletochronology studies that have noted the presence of supplemental lines have indicated that supplemental lines are easily identified as such because they are less distinct and do not appear around the entire circumference of the bone. In general, the same has been observed in sea turtles. Supplemental lines do appear but are generally easily differentiated from LAGs by appearance. An exception to this was the presence of supplemental marks in one- to two-year-old Kemp's ridley sea turtles. These marks were similar in appearance to the first year annuli. We were able to identify these marks as supplemental only by the observation of known-age animals. In addition, there appeared to be a supplemental line in CC-2 that represented when the animal was released; hence, highly stressful events may cause the deposition of nonannual lines, but these events are likely to be relatively rare in wild turtles and not likely to interfere significantly with age estimations.

Resorption of early growth marks

The loss of the early GMs due to endosteal resorption and remodeling of the interior region of the bone is a limiting factor in the application of skeletochronology to sea turtles. From our findings, it was possible to accurately age juvenile Kemp's ridley sea turtles up to at least 5 years from GM counts and this may be true for other sea turtle species (e.g., Bjorndal et al., 2003), with the possible exception of the leatherback sea turtle (Zug and Parham, 1996). Because sea turtles have distinct life-cycle stages, we suggest that in order to age a population of sea turtles, one must acquire an ontogenetic series of samples spanning all sizes and stages. Average duration can be determined for each ontogenetic stage and the approximate age of older animals with extreme resorption can be estimated. Because GM patterns appear to mimic somatic growth rates, once growth through each life-cycle stage is understood, backcalculation techniques can be used to estimate the number of layers resorbed.

Conclusions

For many species, skeletochronology is not a perfect method for age estimation. As GMs are histological expressions of variation in rates of osteogenesis (Castanet et al., 1993), external factors and individual variation will affect the appearance of the marks (Castanet et al., 1993, Esteban et al., 1996, Waye and Gregory, 1998). Endosteal resorption also serves to confound this technique and is the primary difficulty in the application of the technique to sea turtles. However, the evidence presented in the present study gives strong support to the concept that GMs are deposited on an annual basis in sea turtles and that the spatial pattern of the GMs correspond to the growth rates of the animal. The GMs therefore provide invaluable information on age and growth that cannot otherwise be easily obtained, and age determination by skeletocronology is valid and appropriate for the study of sea turtles.

Acknowledgments

We thank L. Crowder, S. Heppell, A. Read, and D. Rittschof for their valuable comments on earlier versions of this manuscript. A. Gorgone, B. Brown and J. Weaver provided assistance with the preparation of the humeri. Most of the humeri were received through the Sea Turtle Stranding and Salvage Network, a cooperative endeavor between the National Marine Fisheries Service, other federal and state agencies, many academic and private entities, and innumerable volunteers. We especially thank R. Boettcher and W. Teas. In addition, humeri were received from F. Swartz at the University of North Carolina–Chapel Hill Institute of Marine

Science, B. Higgins at the National Marine Fisheries Service–Galveston Lab, the Virginia Marine Science Museum Stranding Program, the Maryland Department of Natural Resources, and the Massachusetts Audubon Society in Wellfleet. Funding was provided by the National Marine Fisheries Service. All work was done under and complied with the provisions of the Sea Turtle Research Permit TE-676379-2 issued by the U.S. Fish and Wildlife Service.

Literature cited

Bjorndal, K. A., A. B. Bolten, R. A. Bennet, E. R. Jacobson, T. J. Wronski, J. J. Valeski, and P. J. Eliazar.
1998. Age and growth in sea turtles: limitations of skeletochronology for demographic studies. Copeia 1998: 23–30.

Bjorndal, K. A., A. B. Bolten, T. Dellinger, C. Delgado, and H. R. Martins.
2003. Compensatory growth in oceanic loggerhead sea turtles: response to a stochastic environment. Ecology 84:1237–1249.

Caetano, M. H., and J. Castanet.
1993. Variability and microevolutionary patterns in *Triturus marmoratus* from Portugal: age, size, longevity and individual growth. Amphibia-Reptilia 14:117–129.

Caetano, M. H., J. Castanet, and H. Francillon.
1985. Determination of the age of *Triturus marmoratus marmoratus* from the National Park of Peneda Geres, Portugal by means of skeletochronology. Amphibia-Reptilia 6:117–132.

Caillouet, C. W., B. A. Robertson, C. T. Fontaine, T. D. Williams, B. M. Higgins, and D. B. Revera.
1997. Distinguishing captive-reared from wild Kemp's ridleys. Marine Turtle News Letter 77:1–6.

Castanet, J., H. Francillon-Vieillot, and R. C. Bruce.
1996. Age estimation in desmognathine salamanders assessed by skeletochronology. Herpetologica 52:160–171.

Castanet, J., H. Francillon-Vieillot, F. J. Meunier, and A. De Ricqles.
1993. Bone and individual aging. *In* Bone, vol. 7: Bone growth B (B. B. K. Hall, ed.), p. 245–283. CRC press, Boca Raton, FL.

Castanet, J., F. J. Meumier, and A. de Ricqles.
1977. L'enregistrement de la croissance cyclique par le tissu osseux chez les Vertébrés poïkilothermes: données comparatives et essai de synthèse. Bull. Biol. Fr. Belg. 111:183–202.

Castanet, J., and E. Smirina.
1990. Introduction to the skeletochronological method in amphibians and reptiles. Ann. Sci. Nat. Zool. 11:191–196.

Chaloupka, M. Y., and J. A. Musick.
1997. Age, growth, and population dynamics. *In* The biology of sea turtles (P. L. Lutz and J. A. Musick, eds.) p. 233–276. CRC Press, New York.

Chinsamy, A., S. A. Hanrahan, R. M. Neta, and M. Seely.
1995. Skeletochronological assessment of age in *Angolosaurus skoogi*, a cordylid lizard living in an aseasonal environment. J. Herpetol. 29:457–460.

Coles, W. C., J. A. Musick, and L. A. Williamson.
2001. Skeletochronology validation from an adult loggerhead (*Caretta caretta*). Copeia 2001:240–242.

Collins, E. P., and G. H. Rodda.
1994. Bone layers associated with ecdysis in laboratory-reared *Boiga irregularis* (Colubridae). J. Herpetol. 28:378–381.

de Buffrénil, V., and J. Castanet.
2000. Age estimation by skeletochronology in the Nile monitor (*Varanus niloticus*), a highly exploited species. J. Herpetol. 34:414–424.

Eggert, C., and R. Guyetant.
1999. Age structure of a spadefoot toad *Pelobates fucus* (Pelobatidae) population. Copeia 1999:1127–1130.

El Mouden, P. E., H. Francillon-Vieillot, J. Castanet, and M. Znari.
1997. Âge individuel maturité, croissance et longévité chez l'agamidé nord-africain, *Agama impalcaris* Boettger, 1874, étudiés à l'aide de la squelettochronologie.

Epperly, S. P., J. Braun, and A. Veishlow.
1995. Sea turtles in North Carolina waters. Conserv. Biol. 9:384–394.

Esteban, M., M. Garcia-Paris, and J. Castanet.
1996. Use of bone histology in estimating the age of frogs (*Rana perezi*) from a warm temperate climate area. Can. J. Zool. 74:1914–1921.

Francillon-Vieillot, H., J. W. Arntzen, and J. Géraudie.
1990. Age, growth and longevity of sympatric *Triturus cristatus*, *T. marmoratus* and their hybrids (Amphibia, Urodela). A skeletochronological comparison. J. Herpetol. 24:13–22.

Guarino, F. M., F. Andreone, and F. Angelini.
1998. Growth and longevity by skeletochronological analysis in *Mantidactylus microtympanum*, a rainforest anuran from southern Madagascar. Copeia 1998:194–198.

Guarino, F. M., F. Angelini, and M. Cammarota.
1995. A skeletochronological analysis of three syntopic amphibian species from southern Italy. Amphibia-Reptilia 16:297–302.

Hemelaar, A. S. M., and J. J. van Gelder.
1980. Annual growth rings in phalanges of *Bufo bufo* (Anura, Amphibia) from the Netherlands and their use for age determination. Neth. J. Zool. 30:129–135.

Hutton, J. M.
1986. Age determination of living Nile crocodiles from the cortical stratification of bone. Copeia 1986: 332–341.

Klevezal, G. A.
1996. Recording structures of mammals: determination of age and reconstruction of life history, p. 49–52. A. A. Balkema, Rotterdam.

Klima, E. F., and J. P. McVey.
1995. Headstarting the Kemp's ridley turtle, *Lepidochelys kempi*. *In* The biology and conservation of sea turtles (K. A. Bjorndal, eds.), p. 481–487. Smithsonian Institution, Washington, D.C..

Klinger, R. C., and J. A. Musick.
1992. Annular growth layers in juvenile loggerhead turtles (*Caretta caretta*). B. Mar. Sci. 51:224–230.
1995. Age and growth of loggerhead turtles (*Caretta caretta*) from Chesapeake Bay. Copeia 1995:204–209.

Kusano, T., K. Fukuyama, and N. Miyashita.
1995. Age determination of the stream frog, *Rana sakurai*, by skeletochronology. J. Herpetol. 29:625–628.

Leclair Jr., R., and G. Laurin.
1996. Growth and body size in populations of mink frogs *Rana septentrionalis* from two latitudes. Ecography 19:296–304.

Leclair Jr., M. H. Leclair, J. Dubois, and J-L. Daoust.
2000. Age and size of wood frogs, *Rana sylvatica*, from Kuujjuarapik, Northern Quebec. Can. Field. Nat. 114:381–387.

Lima, V., J. W. Arntzen, and N. M. Ferrand.
2000. Age structure and growth pattern in two populations of the golden-striped salamander *Chioglossa lusitanica* (Caudata Salamandra). Amphibia-Reptilia 22:55–68.

Parham, J. F., and G. R. Zug.
1997. Age and growth of loggerhead sea turtles (*Caretta caretta*) of coastal Georgia: an assessment of skeletochronological age-estimates. B. Mar. Sci. 61:287–304.

Patnaik, B. K., and H. N. Behera.
1981. Age-determination in the tropical agamid garden lizard, *Calotes versicolor* (Daudin), based on bone histology. Exp. Gerontol. 16:295–307.

Peabody, F. E.
1961. Annual growth zones in vertebrates (living and fossil). J. Morphol. 108:11–62.

Rogers, K. L., and L. Harvey.
1994. A skeletochronology assessment of fossil and recent *Bufo cognatus* from south-central Colorado. J. Herpetol. 28:133–140.

Sagor, E. S., M. Ouellet, E. Barten, and D. M. Green.
1998. Skeletochronology and geographic variation in age structure in the wood frog, *Rana sylvatica*. J. Herpetol. 32:469–474.

Simmons, D. J.
1992. Circadian aspects of bone biology. *In* Bone, vol. 6: Bone growth A (B. B. K. Hall, ed.), p. 91–128. CRC press, Boca Raton, FL.

Smirina, E. M.
1994. Age determination and longevity in amphibians. Gerontology 40:133–146.

Swartz, F. J.
1997. Growth, maturity, and reproduction of a long-term captive male loggerhead sea turtle, *Caretta caretta* (Chelonia, Reptilia) in North Carolina. Elisha Mitchell Scientific Society 133:143–148.

Trenham, P. C., H. B. Shaffer, W. D. Koenig, and M. R. Stromberg.
2000. Life history and demographic variation in the California tiger salamander (*Ambystoma californiense*). Copeia 2000:365–377.

Tucker, A. D.
1997. Validation of skeletochronology to determine age of freshwater crocodiles (*Crocodylus johnstoni*). Mar. Freshw. Res. 48:343–351.

Waye, H. L., and P. T. Gregory.
1998. Determining the age of garter snakes (*Thamnophis* spp.) by means of skeletochronology. Can. J. Zool. 76:288–294.

Zug, G. R, G. H. Balazs, and J. A. Wetherall.
1995. Growth in juvenile loggerhead sea turtles (*Caretta caretta*) in the north Pacific pelagic habitat. Copeia 1995:484–487.

Zug, G. R., G. H. Balazs, J. A. Wetherall, D. M. Parker, and S. K. K. Murakawa.
2002. Age and growth of Hawaiian green sea turtles (*Chelonia mydas*): and analysis based on skeletochronology. Fish. Bull. 100:117–127.

Zug, G. R, and R. E. Glor.
1998. Estimates of age and growth in a population of green sea turtles (*Chelonia mydas*) from the Indian River lagoon system, Florida: a skeletochronological analysis. Can. J. Zool., 76:1497–1506.

Zug, G. R, H. J. Kalb, and S. J. Luzar.
1997. Age and growth in wild Kemp's ridley sea turtles *Lepidochelys kempii* from skeletochronological data. Biol. Conserv. 80:261–268.

Zug, G. R, and J. F. Parham.
1996. Age and growth in leatherback sea turtles, *Dermochelys coriacea* (Testudines, Dermochelyidae): a skeletochronological analysis. Chelonian Conserv. Biol. 2:244–249.

Zug, G. R., A. H. Wynn, and C. Ruckdeschel.
1986. Age determination of loggerhead sea turtles, *Caretta caretta*, by incremental growth marks in the skeleton. Smithsonian Institution, Contrib. Zool. 427, Washington D.C.

The Hudson-Raritan Estuary as a crossroads for distribution of blue (*Callinectes sapidus*), lady (*Ovalipes ocellatus*), and Atlantic rock (*Cancer irroratus*) crabs

Linda L. Stehlik
Robert A. Pikanowski
Donald G. McMillan

James J. Howard Marine Sciences Laboratory
Northeast Fisheries Science Center
National Marine Fisheries Service, NOAA
74 Magruder Road
Highlands, New Jersey 07732
E-mail address (for L. L. Stehlik): Linda.Stehlik@noaa.gov

Abstract—Blue (*Callinectes sapidus*) (Portunidae), lady (*Ovalipes ocellatus*) (Portunidae), and Atlantic rock (*Cancer irroratus*) (Cancridae) crabs inhabit estuaries on the northeast United States coast for parts or all of their life cycles. Their distributions overlap or cross during certain seasons. During a 1991–94 monthly otter trawl survey in the Hudson-Raritan Estuary between New York and New Jersey, blue and lady crabs were collected in warmer months and Atlantic rock crabs in colder months. Sex ratios, male: female, of mature crabs were 1:2.0 for blue crabs, 1:3.1 for lady crabs, and 21.4:1 for Atlantic rock crabs.

Crabs, 1286 in total, were subsampled for dietary analysis, and the dominant prey taxa for all crabs, by volume of foregut contents, were mollusks and crustaceans. The proportion of amphipods and shrimp in diets decreased as crab size increased. Trophic niche breadth was widest for blue crabs, narrower for lady crabs, and narrowest for Atlantic rock crabs. Trophic overlap was lowest between lady crabs and Atlantic rock crabs, mainly because of frequent consumption of the dwarf surfclam (*Mulinia lateralis*) by the former and the blue mussel (*Mytilus edulis*) by the latter. The result of cluster analysis showed that size class and location of capture of predators in the estuary were more influential on diet than the species or sex of the predators.

Manuscript submitted 27 November 2000 to the Scientific Editor's Office.

Manuscript approved for publication 4 May 2004 by the Scientific Editor.

Fish. Bull. 102:693–710 (2004).

The blue crab (*Callinectes sapidus*) (Portunidae), the lady crab (*Ovalipes ocellatus*) (Portunidae), and the Atlantic rock crab (*Cancer irroratus*) (Cancridae) are the largest and most common brachyuran crabs inhabiting both estuaries and inner continental shelves of the northeast coast of North America. The centers of abundance of these three species overlap in estuarine and coastal waters from New York to Virginia, although their ranges along the northwest Atlantic coast are broad. The blue crab is nearly always an estuarine resident, except during its larval stages, and ranges from the waters off Nova Scotia to Argentina (Williams, 1984). The northernmost estuaries where the species is abundant enough for commercial harvest are in New Jersey and New York (Briggs, 1998; Stehlik et al., 1998). The lady crab is distributed from the waters off Prince Edward Island to those off Georgia but it is most numerous from Georges Bank to Cape Hatteras (Williams, 1984). The Atlantic rock crab (referred to as "rock crab" in this article) is distributed in waters from off Labrador to Florida but is most common in estuaries from Nova Scotia to Virginia (Williams, 1984; Stehlik et al., 1991). Seasonal migrations are common for all three species. Although Jonah crabs (*Cancer borealis*) are present on the continental shelf, they are not included in the present study because they are rare within the Hudson-Raritan Estuary where our study was conducted.

Physiological tolerances and habitat preferences of these crabs have been extensively studied. In eastern United States estuaries the blue crab occurs in shallow to deep, sandy to muddy estuaries and tributaries along marsh edges, and in seagrass (Van Engel, 1958; Milliken and Williams, 1984; Hines et al., 1987; Wilson et al., 1990; van Montfrans et al., 1991; Rountree and Able, 1992). In the colder portions of its range, it becomes less active at about 15°C (Leffler, 1972), and buries itself, without eating, when the temperature is <5°C (Auster and DeGoursey, 1994). It survives at 34°C (Leffler, 1972) and at salinities from 0 to 50 ppt (Guerin and Stickle, 1992). The lady crab is most common on sand substrates (Williams, 1984). It is present on the inner continental shelf from off Cape Cod to off the Carolinas throughout the year (Stehlik et al., 1991). Its temperature tolerance is unknown, but it does not survive in <21 ppt (Birchard et al., 1982). The rock crab's optimum temperature range for activity is 14–22°C (Jeffries, 1966); thus the species avoids high summer temperatures. It is found on many substrates, such as sand, mud, bare rock, cobble, and algal beds.

The diet of the blue crab is generally mollusks, crabs, and fish, depending on crab size (Virnstein, 1977; Laughlin, 1982; Ryer, 1987; Hines et al., 1990). The diet of the lady crab is mainly bivalves such as *Mya arenaria* and *Spisula solidissima*, and some crustaceans (McDermott, 1983; Ropes, 1989; Stehlik, 1993). The rock crab consumes mollusks, small crustaceans, crabs, urchins, and fish (Scarratt and Lowe, 1972; Drummond-Davis et al., 1982; Hudon and Lamarche, 1989; Ojeda and Dearborn, 1991; Stehlik, 1993). In some of the aforementioned studies these crabs have been considered opportunistic and as such may be competitors for the same prey taxa. However, differences in maximum body size, chela structure, and the presence or absence of swimming appendages among blue, lady, and rock crabs indicate that they may have differences in diet (Warner and Jones, 1976; Williams, 1984).

Within the Hudson-Raritan Estuary, blue, lady, and rock crabs are all abundant, providing an opportunity to study partitioning of habitat and food resources by these species. The objectives of our study were to determine the temporal and spatial overlap of blue, lady, and rock crabs in this estuary and to differentiate the composition of their diets by the species, sex, and size of predators, and by location of collection.

This study has potential practical applications. Resource managers could use the results to consider when and where crabs depend upon certain locations to complete their life cycles, if dredging, filling, or sanctuaries were proposed. Dietary analysis of these crabs could indicate if they are a cause of mortality for young stages of commercially important species. For instance, the northern quahog (*Mercenaria mercenaria*) and the soft-shell clam (*M. arenaria*) recently have supported and presently support commercial and recreational harvests in the Hudson-Raritan Estuary (MacKenzie, 1990; 1997) and when young these clams are consumed by crabs. The blue crab supports lucrative fisheries in the estuary (Stehlik et al., 1998) and predation by various species of crabs upon blue crab juveniles may affect recruitment.

Materials and methods

Study area

The Hudson-Raritan Estuary, bordered by New Jersey on the south and Staten Island and Brooklyn, New York, on the north (Fig.1), has a surface area of about 280 km^2. The Hudson, Raritan, and Navesink-Shrewsbury rivers flow into the estuary from the north, west, and south, respectively. The study area is bounded on the west by the 74 15′ longitude line; on the east by a line between the northeast corner of Sandy Hook, NJ, and the tip of Rockaway Point, NY; and on all sides by the-3 m contour. The area was divided into nine strata according to physiographic features (Wilk et al.[1]). Sandy-bottom strata included Sandy Hook Bay (stratum 1), Raritan Bay south of Raritan Channel (stratum 2), and Lower Bay north of Raritan Channel (stratum 3). Eastern strata of more irregular depths were Romer Shoals (stratum 4), East Bank between Ambrose Channel and Rockaway, NY (stratum 5), and Gravesend Bay at the mouth of the Hudson River (stratum 6). Three strata were channels: Ambrose (stratum 7), Chapel Hill (stratum 8), and Raritan (stratum 9). Raritan Channel is maintained at a depth of 13.7 m, and the average depth of adjacent nonchannel stations is 7.1 m. Gravesend Bay is more than 13 m deep in its center.

The bottom of the Hudson-Raritan Estuary consists mostly of soft sediments (Jones et al., 1979; Coch, 1986; Wilber[2]). The substrates in semi-sheltered southern strata 1 and 2 are predominantly fine sand, silt, and clay; those of stratum 3 are mainly medium sand, with a mixture of sand, silt, and clay near channels; those of ocean-exposed strata 4, 5, 6, and 7 are gravel, sand, silt, broken shell, and have beds of blue mussels (*Mytilus edulis*). The bottom of Ambrose Channel is silt and clay near its head and fine sand toward the ocean. The sediments of the other two channels, and their immediate borders, are sand, silt, and clay. Based on physiographic form, temperature ranges, and sediments, strata 1, 2, 3, 8, and 9 were considered inner or riverward strata, whereas 4, 5, 6, and 7 were considered outer or oceanic-influenced strata.

Collections and analyses

Crabs were collected during monthly otter trawl surveys of the Hudson-Raritan Estuary from June 1991 to December 1994 (Wilk et al.[1]). Sampling was done from the 18-m research vessel *Gloria Michelle* by towing a 9.1-m otter trawl with a chain sewn to the bottom opening, and a 76-mm mesh net with a 51-mm codend liner. Wooden trawl doors were deployed to spread open the net. The net was towed once per station for 10 min at 5.6 km/h to cover a distance of approximately 1 km. All tows were made between 8 am and 2 pm. During 1991, fixed stations were towed (number of stations in 1991: 10 in June, 8 in July; 11 in August; 18 in September; 22 in October; 23 in November; 34 in December). Beginning in 1992, a stratified random sampling design was used, in which the nine strata were divided into 190 blocks of approximately 0.5 minutes latitude by 0.5 minutes longitude. Each month, 40 blocks were randomly sampled without replication, and the number of blocks in each stratum was proportional to the area of the stratum. Because of conflicting schedules, the vessel was not available in May or September 1992 or 1994. Temperature and salinity of water 1 m above the bottom were measured after each tow. During 1991

[1] Wilk, S. J., E. M. MacHaffie, D. G. McMillan, A. L. Pacheco, R. A. Pikanowski, and L. L. Stehlik. 1996. Fish, megainvertebrates, and associated hydrographic observations collected in the Hudson-Raritan Estuary, January 1992–December 1993, 95 p. Northeast Fish. Sci. Cent. Ref. Doc. 96-14, NMFS, Woods Hole, MA.

[2] Wilber, P. 2000. Unpubl. data. Coastal Services Center, National Ocean Survey, NOAA, 2234 Hobson Avenue, Charleston, SC, 29405.

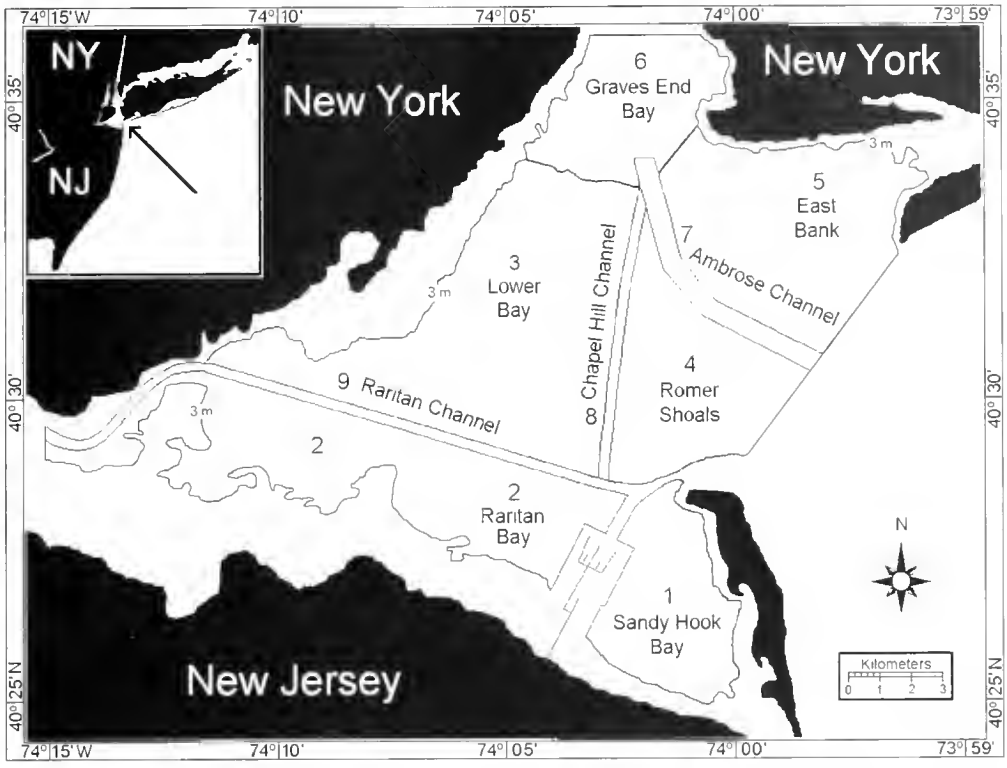

Figure 1

Hudson-Raritan Estuary, from New York to New Jersey, with 3-m contour, drawn boundaries, and the nine strata of the Hudson-Raritan Estuary trawl survey. The inset shows the location of the estuary on the United States coast off New York and New Jersey.

and 1992 temperature and salinity were determined by using a Niskin bottle, a thermometer, and an induction salinometer. Beginning in January 1993 a Hydrolab® Surveyor III multiprobe was used.

Fish and large invertebrates were counted, weighed, and measured (±1.0 cm), and sexes of the crabs were recorded. Catch per unit of effort or number per tow was used to estimate relative abundance. Crabs were measured by carapace width (CW) between the tips of the anterolateral teeth. Specimens were saved for dietary analysis from June 1991 through June 1992. These specimens were measured (±1.0 mm) and molt stages were classified as intermolt (hard-shelled), premolt (new skin separates easily from inside the carapace), soft-shelled, or postmolt (early and late papershell).

For some analyses, we separated crabs into two size classes based on maturity because preferred habitats, tolerances, or reproductive needs may be different for different life stages. Most researchers use a carapace width at which ≥50% or ≥80% of the individuals are mature (produce viable eggs or sperm) as a separation boundary. Maturity in males is determined by dissection or by allometric changes in growth of appendages (Hartnoll, 1978; Block and Rebach, 1998; de Lestang et al., 2003). Most female blue crabs in our study area and in Virginia had completed their pubertal molt and thus could reproduce by 12 cm CW (Van Engel, 1958; Fisher, 1999; Stehlik, unpubl. data). In Virginia, 80% of male blue crabs are mature by 11.9 cm (Van Engel, 1990). In lady crabs from the New York coast, nearly all males are mature at ≥6 cm, and females at about 5 cm (Briggs and Grahn[3]). In the middle-Atlantic portion of their range, male rock crabs mature at 5 cm (Haefner, 1976) and some females <5 cm bear eggs (Reilly and Saila, 1978). We chose the following CW boundaries for ≥80% maturity: blue crabs, ≥12 cm both sexes; lady crabs, ≥5 cm both sexes; and rock crabs, males ≥5 cm and females ≥4 cm.

Data on blue, lady, and rock crabs from NEFSC (Northeast Fisheries Science Center, NOAA) fall bottom trawl surveys on the northeast United States continental shelf, 1992–94, were used to expand the geographical viewpoint of our study. The presence of each species in each tow was plotted to show distributions in a representative year, 1992. The plots were made with Surfer® (version 6, Golden Software Inc., Golden, CO). Methods on the trawl surveys are described elsewhere (Azarovitz, 1981).

[3] Briggs, P. T., and C. M. Grahn. 1996. Aspects of the fishery biology of the lady crab (*Ovalipes ocellatus*) in New York waters, 8 p. An in-house paper, New York State Department of Environmental Conservation, 205 North Belle Mead Road, Suite 1, East Setauket, NY, 11733.

Foregut contents were analyzed as in Stehlik (1993). The foregut of each crab was removed and preserved in 70% ethanol. After opening the foregut, we estimated fullness of the gut (from 0% to 100%) visually, and prey items were identified to the lowest possible taxon. The proportion of the total volume of the foregut contents contributed by each prey taxon was estimated visually—a less labor-intensive modification of the methods of Williams (1981), Hyslop (1980), and Steimle et al. (1994). The volume of each prey taxon was multiplied by the percentage of gut fullness. Combining all foreguts, the volumes of prey taxa were listed in descending order. The top 12 prey categories on the list (with the exception of "unidentified" and nonexclusive categories such as Mollusca) were selected for use in most of the subsequent analyses. Foreguts that did not contain prey in any of the 12 categories were dropped from numerical analyses.

The dietary data were grouped in turn by predator species, sex, size class, and collection stratum, and the mean percentage volumes of each of the 12 mutually exclusive prey categories were calculated. For graphic representation of ontogenetic differences in diet, blue and rock crabs were grouped for convenience into 20-mm CW classes, and lady crabs were grouped in 10-mm CW classes because of their smaller size range. For numerical analyses, two maturity classes were used. We used Mann-Whitney tests to compare diets between sexes within predator species and between maturity stages within predator species. The test statistic was a chi square approximation.

Group average cluster analysis was used to graph the separation of diets by species, sexes, maturity stages, and strata by using the 12 prey categories as dependent variables. A Bray-Curtis similarity matrix was generated for each of the groupings, cluster analysis was performed by using Systat® (version 10, SPSS Inc., Chicago, IL), and dendrograms were generated by using the Bray-Curtis values as distance measures (Romesburg, 1984; Marshall and Elliott, 1997). A percent similarity level was chosen *a posteriori* that generated a reasonable number of classes.

Analysis of similarity (ANOSIM) was used to test for statistical significance of dietary differences among predator species and for sexes within species. Analysis of dissimilarity (SIMPER) was used to determine which prey taxa contributed most to the differences between species pairs (Clarke and Warwick, 1994).

Spatial, temporal, and trophic niche breadth and overlap indices were calculated from the number per tow (1992–94) and diets (June 1991–June 1992) of each crab species and sex. Temporal niche and overlap were calculated by month for combined years. Female rock crabs were dropped from consideration of trophic niche overlap due to low sample size.

Niche breadth (Colwell and Futuyama, 1971; Marshall and Elliot, 1997) is a measure of exploitation within a particular resource (for example, substrates or prey taxa within an estuary by a species). Niche breadth values are relative and can be compared only within one study. The highest value corresponds to the broadest niche, or to habitat or a diet generalist rather than to a specialist. Niche breadth (B) was calculated by the formula of Colwell and Futuyama (1971), and modified for measuring trophic niche breadth according to Hines et al. (1990):

$$B = 1 / \sum (p_{kj})^2 \text{ from } j = 1 \text{ to } n,$$

where $p_{kj} = N_{kj} / Y_k$ (p_{kj} is the proportion of crabs of species k associated with resource state j);
j = resource states (months, strata, diet categories);
n = number of resource states;
N_{kj} = catch per tow of species k at resource state j; and
Y_k = catch per tow of species k over all resource states.

When trophic niche breadth was calculated,

N_{kj} = total volume of diet category j consumed by predator k;
Y_k = total volume of all diet categories consumed by predator k.

Niche overlap is a measure of the joint use of a resource by two species (Colwell and Futuyama, 1971). Niche overlap (C_{hi}) between species h and i was calculated by the following formula (Colwell and Futuyama, 1971; Hines et al., 1990):

$$C_{hi} = 1 - 0.5\left(\sum | p_{hj} - p_{ij} |\right) \text{ from } j = 1 \text{ to } n,$$

where p_{hj} and p_{ij} are calculated in the same manner as p_{kj} above.

This index ranges from 0 (no overlap) to 1 (complete overlap) and is independent of sample size and differential resource availability (Eggleston et al., 1998).

Results

Temperature and salinity

Bottom water temperature in the study area followed a temperate seasonal cycle. The range during 1992–94 was from 0° to 26.6°C. Using the monthly mean temperature below or above 10°C, and migration cycles of the crabs, we grouped the months into two seasons: winter (November through April) and summer (May through October). The mean temperature in the winter months 1992–94 was 5.5°C, and that for summer was 18.9°C. Temperature nearest the estuary mouth was usually a few degrees lower in summer months and higher in the winter months each year, compared with the average throughout the estuary.

Bottom salinity in the study area ranged from 15.0 to 33.5 ppt. The majority of stations had salinities between

Table 1

Species, sex, number collected (*n*), and sex ratio (SR, male:female) of all crabs collected during the Hudson-Raritan Estuary trawl survey, June 1991–December 1994. Maturity boundaries are explained in the text. For the subsample examined for stomach contents (June 1991–June 1992), number (*n*), number of non-empty stomachs, and the mean and range of carapace width (CW, mm) are presented.

Crab species, sex	*n* collected	SR (m:f) immature	SR (m:f) mature	*n* stomachs opened	*n* not empty	Subsample CW	
						Mean	(Range)
Blue, male	2803	1:1.13	1:1.97	167	120	112	(35–185)
Blue, female	4816			272	208	129	(21–169)
Lady, male	14,903	1:1.30	1:2.12	173	124	60	(34–88)
Lady, female	29,681			255	228	55	(30–89)
Atlantic rock, male	15,503	4.65:1	21.43:1	400	281	92	(28–130)
Atlantic rock, female	822			19	14	51	(29–80)
Total	68,528			1286	975		

25 and 30 ppt. Salinity decreased with distance from the bay mouth and in any one month, the difference in salinity between stations at the estuary mouth and those at the westernmost part of the study area was approximately 5–10 ppt.

Catch by species, size, and sex

From June 1991 through December 1994, more than 68,000 blue, lady, and rock crabs were caught in 1200 otter trawl tows (Table 1). Other mega-invertebrates in the tows included the northern moonsnail (*Euspira heros*), the horseshoe crab (*Limulus polyphemus*), the American lobster (*Homarus americanus*), the portly spider crab (*Libinia emarginata*), the flatclaw hermit crab (*Pagurus pollicaris*), mud crabs (Xanthidae), and the sea star (*Asterias* sp.)

Catch per tow of crabs by size class increased as they became large enough to be retained by the mesh of the net (Fig. 2). Abundances of female blue and lady crabs in the study area were greater than those of the males. In rock crabs, males predominated (Table 1). Immature blue and lady crabs had sex ratios fairly close to 1:1 (male:female). Sex ratio in mature blue crabs, however, was 1:1.97, and in mature lady crabs, 1:2.12. In all sizes of rock crabs, sex ratio strongly favored males, particularly in mature crabs, in which the ratio was 21.43:1.

Temporal and spatial variation in catch

The maximum relative abundance of blue and lady crabs occurred during the warm months each year, whereas rock crabs were abundant only in the cold months (Fig. 3). Blue crabs were scarce in the otter trawls from January through May or June. We believe that many of them do remain in the study area, but are relatively inactive and are not accessible to otter trawls, as discussed below. Lady crabs migrated into the estuary in April and May and left in October and November.

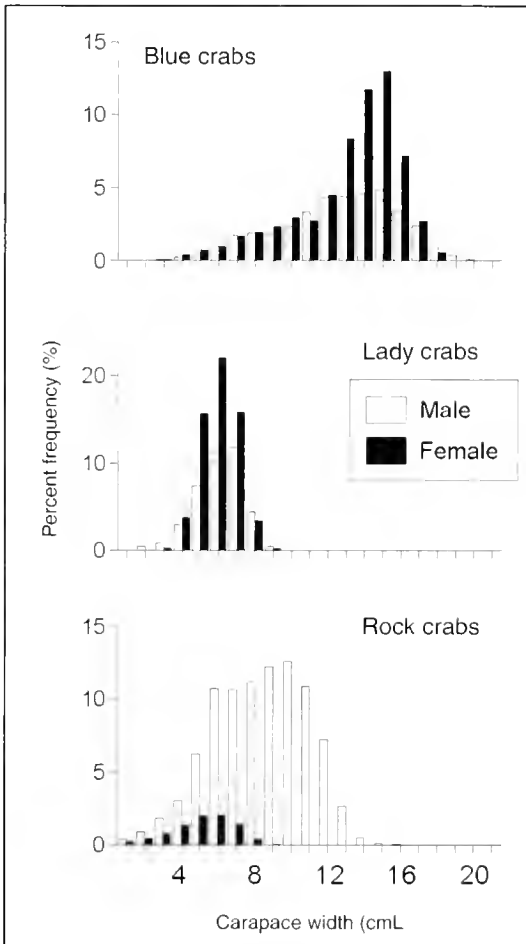

Figure 2

Carapace width (cm) frequencies for male and female blue, lady, and rock crabs collected during the Hudson-Raritan Estuary trawl survey, June 1991–December 1994, by percent frequency of the total catch of each species.

Rock crabs migrated into the estuary in November and gradually left during April, May, and June.

Hundreds of soft and postmolt male rock crabs were caught each winter in the study area (Fig. 4). The highest numbers of molting rock crabs were collected each December and January, and almost all of these crabs had completed molting by February. Very few molting or postmolt blue or lady crabs were caught.

The relative abundances of the three species varied by stratum (Fig. 5, A–C; Fig. 6). Blue crabs of both sexes were caught mainly in strata near river mouths (strata 1, 2, and 6), in the Chapel Hill and Raritan channels (strata 8 and 9) in summer, but mainly in stratum 6 and in the channels in winter. Lady crabs were widely distributed and were caught throughout the study area, including the outer strata close to the ocean. Male rock crabs were most frequently collected in and near the channels and in strata 1 and 6, whereas female rock crabs were sparsely scattered throughout the study area.

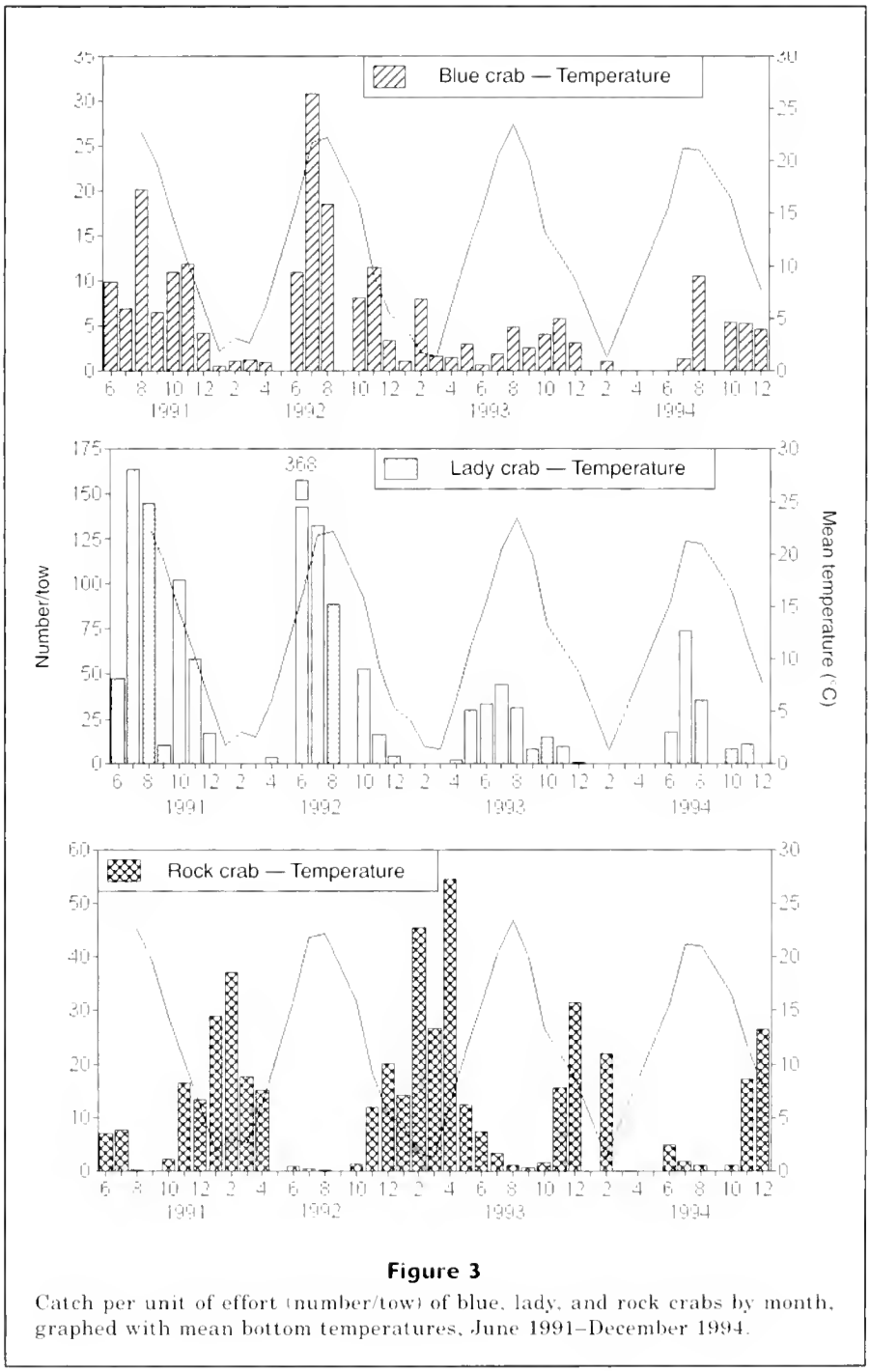

Figure 3

Catch per unit of effort (number/tow) of blue, lady, and rock crabs by month, graphed with mean bottom temperatures, June 1991–December 1994.

Foregut fullness

The total number of blue, lady, and rock crab foreguts examined was 1286. Foregut fullness varied by month in blue and rock crabs. The average fullness of blue crabs was 1% by volume from January through April, and 34% for the rest of the year. Ovigerous blue crabs (n=27) averaged 40% full. Lady crabs' average fullness was 41% during the months when they were present. The average fullness of rock crabs was 30% in all months when they were present; a minimum occurred in January when fullness was 7%. Of 419 rock crabs examined, intermolt crabs (n=293) were 33% full, premolt crabs (n=9) were empty, soft crabs (n=22) were empty, and postmolt crabs (n=95) were 20% full. Some rock crabs in the late postmolt stage were full even though their chelae were not completely calcified.

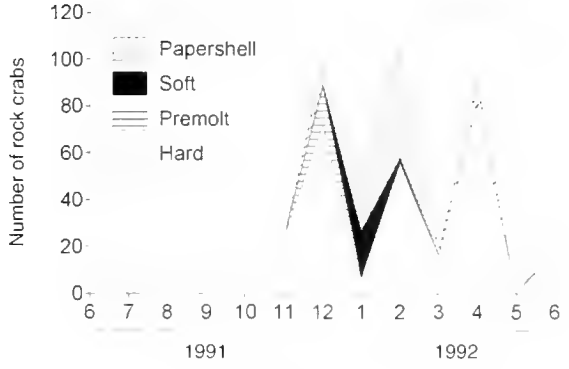

Figure 4

Number of rock crabs at each molt stage by month, 1991–92.

Diet composition

The number of crabs containing food was 975, and they consumed 44 identifiable taxa (Table 2). Most of the mollusks preyed upon were <15 mm in shell length. The crabs consumed were mud crabs (Xanthidae) and juvenile stages of other Anomura and Brachyura. When foreguts were only partially full, well-digested remains of prey frequently could be identified by pieces of shell or opercula, mandibles (for shrimp), or chela tips and carapace fragments (for crabs) (Elner et al., 1985). Recognizable prey taxa were grouped into 12 mutually exclusive categories (Table 3), which contributed 80.1% of the volume of all prey. The prey category "CRABS" represented pooled fragments of all crabs except Paguridae and Xanthidae. Crabs containing prey in one or more of the 12 categories numbered 713.

Differences in diet by predator species, sex, and size

Although the three predator species shared most prey taxa, there were differences in the proportions of the taxa consumed (Fig. 7). Mann-Whitney tests comparing diets of sexes within each species showed only two significant differences out of 36 comparisons. After cluster analysis upon the 12 prey types by species, sex, and size class (immature and mature), the resulting dendrogram showed that diets were most similar between size classes within a species (Fig. 8). Female rock crabs were not included because of their small sample size. When the diets of the three species were compared by analysis of similarity (ANOSIM) they were found to be different (P=0.067), but the data were extremely variable and not normally distributed. No significant differences were found between sexes within species and we therefore pooled sexes within species.

Pairwise comparisons of the species were performed by analysis of dissimilarity (SIMPER). Four taxa contributed significantly to the difference in diets of the first pair: the bivalves *M. edulis* and *M. lateralis* were more important in the diets of lady crabs, and Xanthidae and CRABS, were more important in the diets of blue crabs. The diets of blue crabs and rock crabs were significantly different in four taxa: CRABS and *M. lateralis* were more important for blue crabs, and *M. edulis* and Xanthidae for rock crabs.

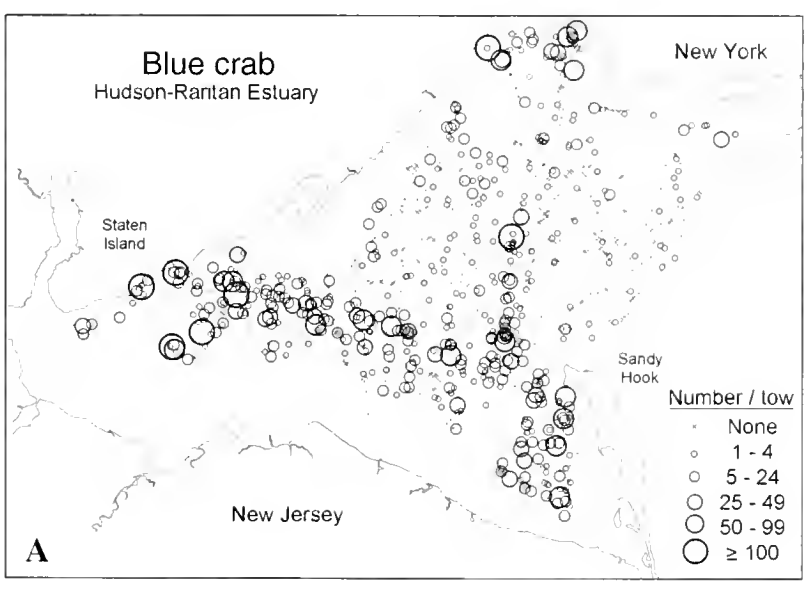

Figure 5

Catch per unit of effort of (**A**) blue, (**B**) lady, and (**C**) rock crabs, sexes combined, January 1992–December 1994, mapped by the midpoint of each tow.

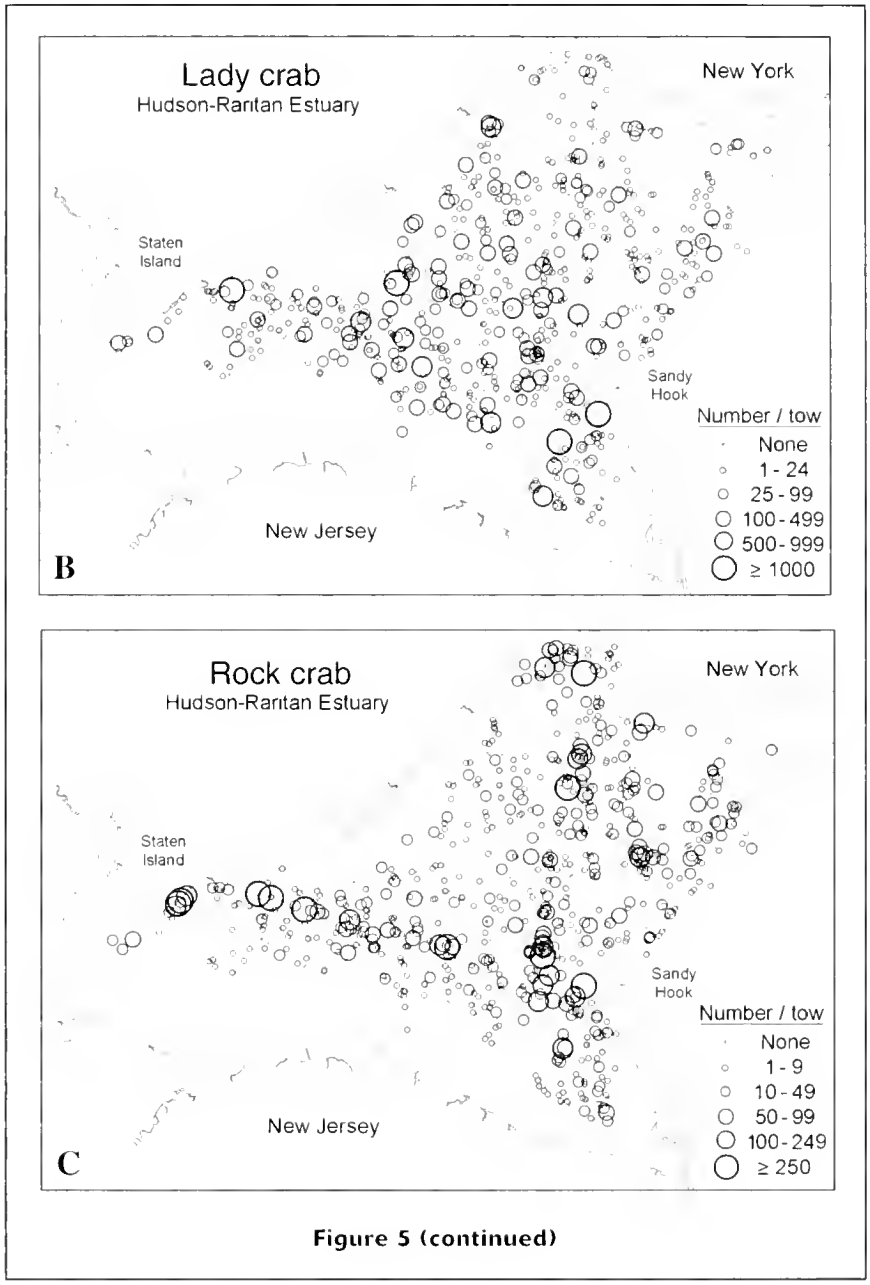

Figure 5 (continued)

The diets of lady crabs and rock crabs were significantly different in two taxa: *M. lateralis* for lady crabs and *M. edulis* for rock crabs.

Within the crab size ranges sampled adequately by our gear, we found some ontogenetic differences in diets (Fig. 9). Notably, amphipods and shrimp were consumed by smaller sizes of all three predators. Certain mollusks, such as *N. trivittatus* and the Atlantic jackknife clam (*Ensis directus*), increased in occurrence in foreguts with increasing crab size. Smaller lady crabs primarily fed upon *M. lateralis*, but larger ones broadened their diets to include other mollusks such as slippersnails (*Crepidula* spp.) and *M. edulis*. Blue and rock crabs exhibited two peaks in consumption of *M. edulis*: the foreguts of small crabs contained recently settled mussels, whereas those of large crabs contained shell fragments and meat of larger mussels. Xanthidae and Paguridae, small in body size, were eaten mostly by intermediate-size predators.

Mann-Whitney tests showed that amphipods were the only prey significantly different ($P<0.01$) between maturity classes for all three crab species.

Spatial variability in diets

Cluster analysis of the diets by species and stratum defined six groups at 50% similarity (Fig. 10). Group A consisted of lady and rock crabs caught at oceanward

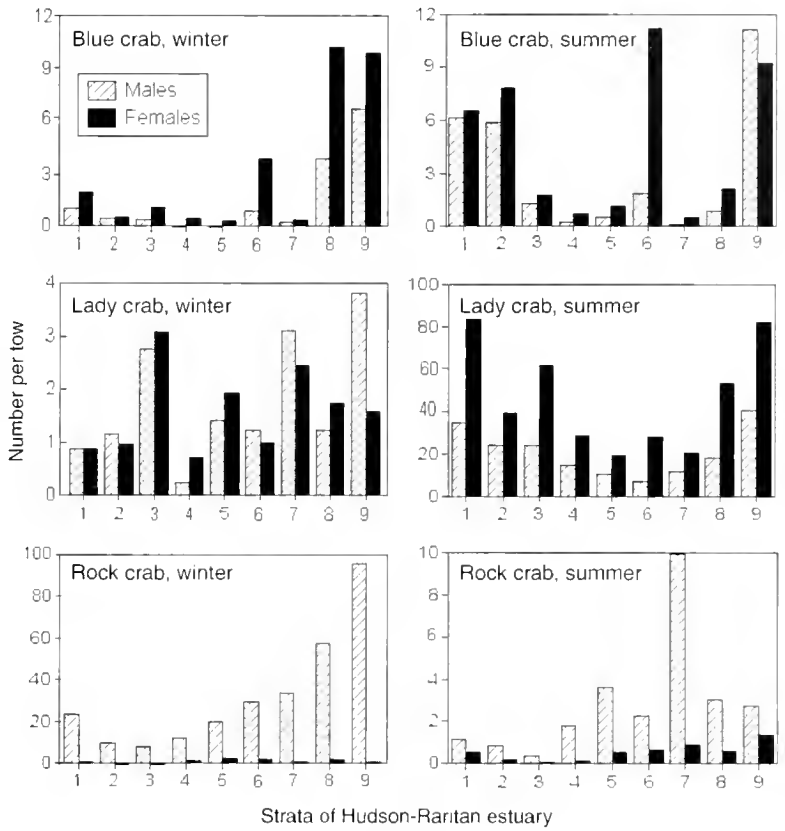

Figure 6

Catch per unit of effort for male and female crabs by seasons and strata, January 1992–December 1994. Note differences in scale among *y* axes.

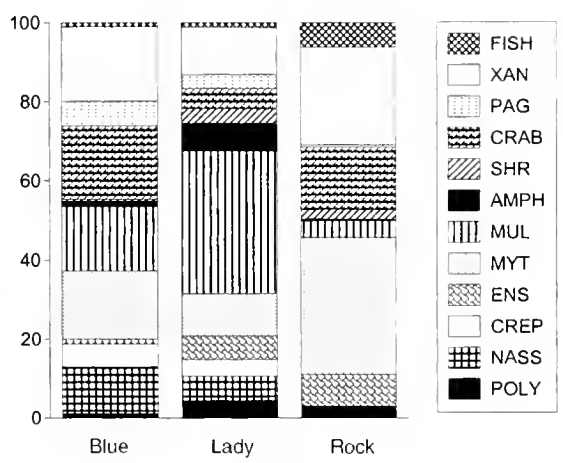

Figure 7

Percent volume of prey (of the 12 chosen categories) of blue, lady, and rock crabs from the Hudson–Raritan Estuary, including all strata and size classes, June 1991–June 1992. n=713. Codes for prey taxa are from Table 3.

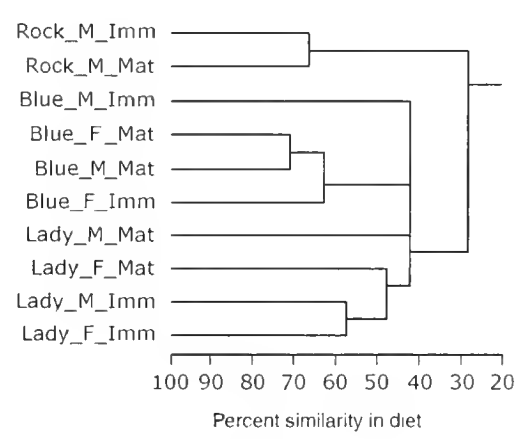

Figure 8

Cluster analysis dendrogram of similarities of the diets of species, sexes (M=male, F=female), and maturity stages (Imm=immature, Mat=mature) of blue, lady, and rock crabs, including all seasons and strata, June 1991–June 1992. Female rock crabs were not included because of the small sample size.

Table 2

Percent frequency of occurrence (%FRE) and percent volume (%VOL) of prey of blue, lady, and rock crabs collected during the trawl survey, June 1991–June 1992. Dashes mean that the dietary item was not found in any stomachs of that crab species. "Unid." means unidentified; "other" means uncommon identified taxa not listed below.

	Blue crab		Lady crab		Rock crab	
	%FRE	%VOL	%FRE	%VOL	%FRE	%VOL
Number of nonempty foreguts	328		352		295	
Plant material	1.5	<0.1	2.8	0.3	4.4	0.1
Hydrozoa	0.6	<0.1	1.4	<0.1	1.4	0.1
Mollusca, unid	6.7	0.9	3.4	0.9	12.3	14.2
Bivalvia, unid., other	12.2	1.4	11.1	1.6	7.8	4.6
Anadara transversa	—	—	0.3	0.1	—	—
Ensis directus	2.4	0.8	9.9	4.8	8.2	6.2
Lyonsia hyalina	—	—	0.3	<0.1	—	—
Mercenaria mercenaria	0.3	<0.1	0.3	<0.1	—	—
Mulinia lateralis	9.3	13.6	43.5	33.1	6.8	1.4
Mya arenaria	—	—	0.3	0.4	—	—
Mytilus edulis	19.6	14.3	13.9	9.8	28.7	27.3
Nucula proxima	3.4	0.4	5.1	0.6	0.7	0.1
Petricola pholadiformis	1.2	0.1	2.3	0.8	—	—
Pitar morrhuanus	—	—	0.3	<0.1	—	—
Spisula solidissima	—	—	1.7	0.5	—	—
Tellina agilis	4.6	1.5	9.4	2.1	1.4	0.2
Gastropoda, unid., other	6.4	0.7	4.0	0.2	1.0	0.1
Crepidula fornicata, convexa	8.6	2.5	5.4	2.8	0.3	<0.1
Crepidula plana	0.6	<0.1	0.3	<0.1	—	—
Nassarius obsoletus	1.5	1.2	0.3	0.2	0.3	<0.1
Nassarius trivittatus	20.8	6.8	15.6	4.6	0.3	<0.1
Naticidae	—	—	0.6	<0.1	—	—
Rictaxis punctostriatus	—	—	0.9	0.1	0.3	<0.1
Cephalopoda	0.3	0.8	0.6	0.3	—	—
Polychaeta, unid., other	2.4	0.2	4.3	0.3	2.7	0.9
Glyceridae	—	—	0.9	0.3	—	—
Hydroides dianthus	—	—	0.3	<0.1	—	—
Nephtyidae	—	—	0.9	0.3	—	—
Nereidae	1.5	0.3	1.7	0.1	0.7	0.3
Pherusa affinis	—	—	—	—	0.3	0.1
Pectinaria gouldii	2.4	0.8	15.9	2.4	0.7	<0.1
Polynoidae	—	—	0.3	<0.1	1.4	0.1
Insecta	0.3	<0.1	—	—	—	—
Crustacea, unid., other	4.9	0.6	3.4	0.3	5.8	1.4
Amphipoda, unid., other	2.8	0.6	7.7	1.4	1.4	0.2
Ampelisca sp.	1.5	0.6	6.8	1.3	0.7	0.4
Corophium sp.	0.6	0.2	1.7	0.7	—	—
Gammarus sp.	—	—	3.1	3.3	—	—
Mysidacea	—	—	0.3	<0.1	—	—
Caridean shrimp, unid., other	0.6	<0.1	2.0	0.1	0.7	<0.1
Crangon septemspinosa	2.8	0.6	6.0	2.3	3.1	2.0
Crabs unid., other[1]	17.7	7.4	8.8	2.7	11.3	4.2
Callinectes sapidus	0.3	<0.1	0.6	0.1	1.4	1.8
Cancer irroratus	1.5	1.0	2.3	0.5	2.0	1.4
Libinia sp.	0.9	0.6	0.9	0.6	1.0	0.5

continued

Table 2 (continued)

	Blue crab		Lady crab		Rock crab	
	%FRE	%VOL	%FRE	%VOL	%FRE	%VOL
Crabs unid., other[1] (cont.)	0.6	<0.1	2.0	0.1	0.7	<0.1
Ovalipes ocellatus	3.4	3.6	0.6	0.2	1.0	1.0
Pagurus longicarpus	2.1	1.5	1.7	0.6	—	—
Pagurus sp.	8.0	4.3	5.4	2.3	1.7	0.1
Xanthidae	21.1	20.8	15.9	10.6	21.2	18.4
Fish remains and scales	2.1	0.9	3.4	0.7	6.4	3.7
Inorganic debris, sand, mud	0.9	<0.1	0.9	0.2	0.7	0.1
Shell hash	2.4	1.5	—	—	—	—
Human-made objects	4.0	<0.1	4.8	<0.1	1.7	<0.1
Unid. organic matter	—	9.2	—	5.3	—	9.0
Mytilus byssus	1.8	<0.1	2.0	<0.1	3.1	0.2

Table 3

Twelve mutually exclusive prey categories that contributed 80% of the prey volume of all crabs examined. Codes are used in Figures 7 and 9. "Other" means uncommon identified taxa.

CODE	Category	Identifiable species
NASS	mud snails	*Nassarius trivittatus, N. obsoletus*
CREP	slipper shells	*Crepidula fornicata, C. convexa, C. plana*
ENS	razor clam	*Ensis directus*
MYT	blue mussel	*Mytilus edulis*
MUL	dwarf surfclam	*Mulinia lateralis*
POLY	Polychaeta	all
AMPH	Amphipoda	all
SHR	shrimp	*Crangon septemspinosa*, unid., other
CRAB	crabs	*Libinia* sp., *Cancer irroratus, Ovalipes ocellatus, Callinectes sapidus*, crab unid., and others excluding Paguridae or Xanthidae
PAG	hermit crabs	*Pagurus acadianus, P. longicarpus*, unid., other
XAN	mud crabs	Xanthidae: *Dyspanopeus sayi*, unid., other
FISH	fish, fish scales	all

outer strata (4, 5, and 7) that consumed large quantities of *M. edulis*. Clumps of recently settled and larger mussels were frequently collected in trawl nets in these strata. Group B contained crabs from Gravesend Bay, (stratum 6) that ate primarily *M. edulis* and *M. lateralis*. Group C contained crabs caught in the siltier southern strata and nearby channel (strata 1, 2, and 9) that consumed mainly *M. lateralis*, *M. edulis*, and CRABS. Group D consisted of rock crabs collected at inner strata (2, 3, and 8) that fed primarily upon *E. directus* and Xanthidae. *Ensis directus* was most common in diets in the northern sandier strata (strata 3, 5, 6, and 7). Groups E and F consisted of lady and rock crabs that consumed mainly *M. lateralis*. Four species-stratum combinations did not cluster with any groups.

Temporal, spatial, and trophic niche breadth and overlap

Niche breadth and overlap were calculated for both sexes of the three crab species (Table 4). Lady crabs of both sexes had the narrowest temporal niches (3.896 and 4.592), reflecting their presence in the estuary strictly in warm months. The temporal niche breadth of female blue crabs (8.187) was greatest, reflecting their year-long presence in the study area, even in the cold months when many males remain in rivers. The temporal overlaps of

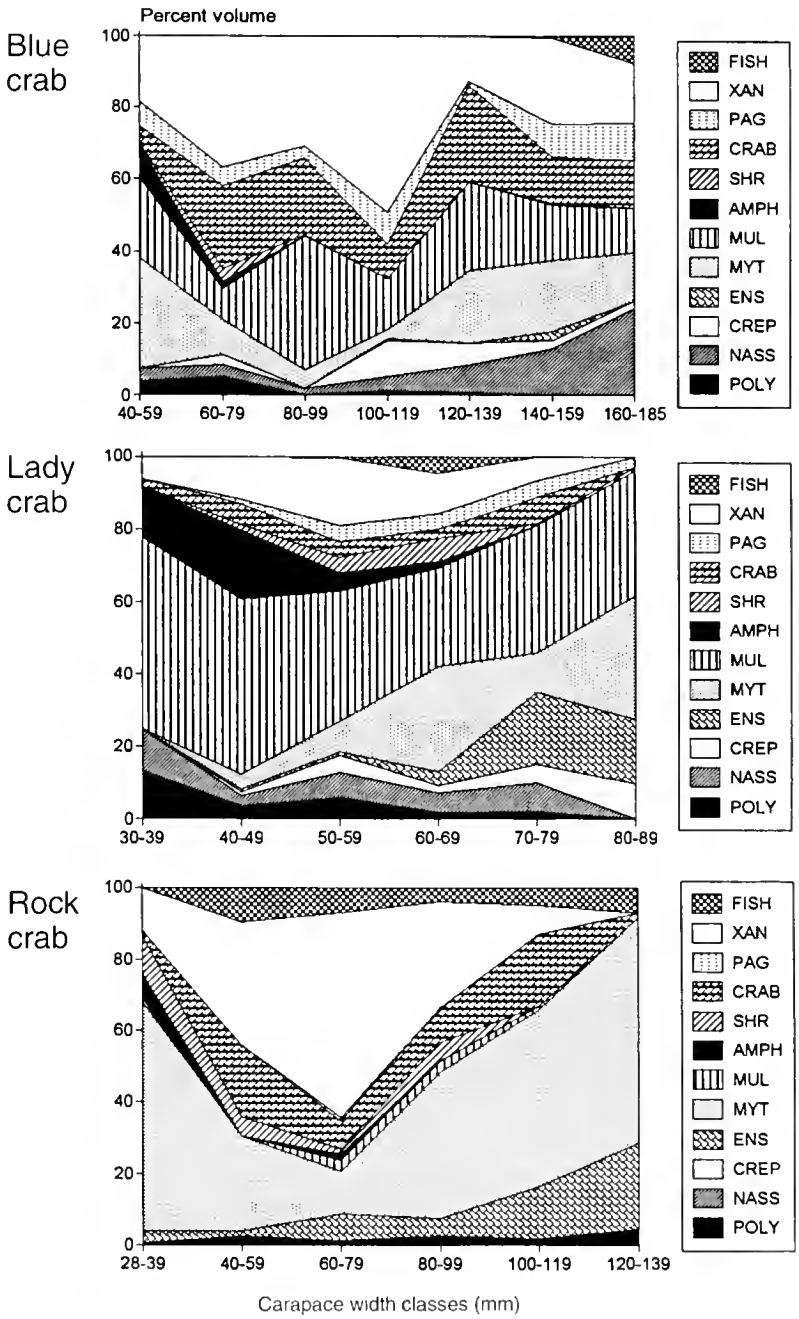

Figure 9

Percent volume of prey (of the 12 categories) by 10- or 20-mm size classes of blue, lady, and rock crabs, all seasons and strata. Codes for prey taxa are from Table 3.

male and female lady crabs with male rock crabs were the lowest in the matrix (0.149 and 0.186).

The spatial niche breadths of lady crabs were largest (7.320 and 7.324) (a result of their nonaggregative distribution throughout the study area), whereas the other two species tended to aggregate in certain locations, particularly in or near channels. Female rock crabs also had a broad spatial niche, although they were caught much less frequently than the other groups. Spatial overlap was highest within species, particularly between male and female lady crabs (0.908).

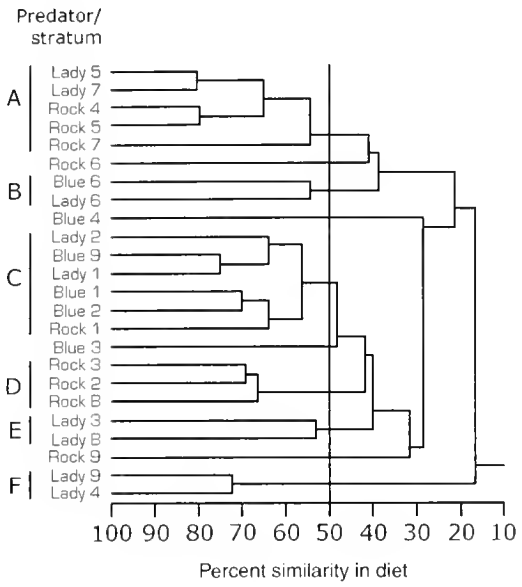

Figure 10

Cluster analysis dendrogram of the diets of blue, lady, and rock crabs from the nine strata of the Hudson-Raritan Estuary. The vertical line at 50% similarity defines groups A–F.

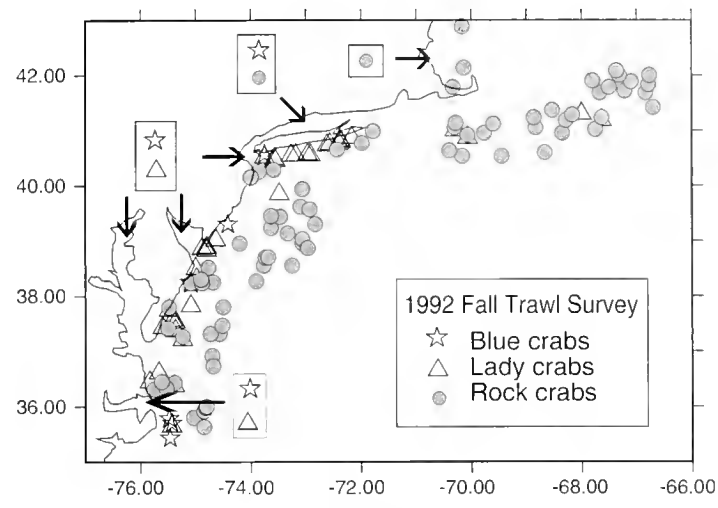

Figure 11

Presence of blue, lady, and rock crabs at stations from the fall 1992 bottom trawl survey, (Northeast Fisheries Science Center, Woods Hole, MA). Each point represents presence at a station. Occurrence inside the estuaries(boxed symbols) was derived from the literature cited in this article.

Trophic niche breadth was greatest in male and female blue crabs (5.234 and 6.563) and male lady crabs (6.166) (Table 4). It was narrowest for female rock crabs, but sample size was low. Overlap was highest within species: blue crab males and females (0.819), and lady crab males and females (0.861). Overlap was lowest between lady and rock crabs, sexes combined (0.427).

Discussion

Temporal and spatial overlap within the estuary

The scatter plots (Fig. 5) and spatial niche overlap indices indicate substantial likelihood of co-occurrence and encounter among blue, lady, and rock crabs in the Hudson-Raritan Estuary. However, the species were not all active in the study area at the same time. Seasonal migration and winter torpor are two mechanisms that, at times, prevent interspecies encounters. Rock crabs had low temporal overlaps with blue and lady crabs because when rock crabs migrate in from the coastal ocean, lady crabs migrate out and blue crabs become less active and sometimes bury themselves. Although otter trawling does not adequately sample buried blue crabs, commercial crab dredgers catch large numbers of overwintering blue crabs from December through March in and near the Raritan and Chapel Hill channels (Stehlik et al., 1998).

Temporal overlap between blue crabs and lady crabs was fairly high because of their co-occurrence in the warm months. It was expected that intra-estuarine spatial separation might minimize contact between these species because they are reported to prefer different substrates. The blue crab is known to occupy a variety of substrate types, including sand, mud, and submerged vegetation (Milliken and Williams, 1984; Wilson et al. 1990), whereas the lady crab is primarily collected on sand (Williams and Wigley, 1977). The lady crab buries itself in sand more readily than in mud (Barshaw and Able, 1990) and it is able to forage more efficiently in sand than in sand-gravel or sand-shell substrates (Sponaugle and Lawton, 1990). However, as shown in Figures 5 and 6, lady crabs were not confined to sandy strata but were most abundant on the fine-grained sediment strata 1, 2, and 9.

The pattern of seasonal estuarine use by blue and lady crabs is not unique to the Hudson-Raritan Estuary. Other estuaries in which the two Portunidae are abundant in summer months but uncommon in winter are Barnegat Bay, NJ (Milstein et al., 1977; pers. observ.), Delaware Bay (Winget et al., 1974), and Chesapeake Bay (Haefner and Van Engel, 1975).

Rock crabs undergo seasonal migrations from coastal waters into and out of estuaries, but the timing differs by latitude. In Canada, the Gulf of Maine, and northern Massachusetts, rock crabs are much more abundant in immediate coastal waters, estuaries, and in the intertidal zone in warmer months (Krouse, 1972; Scarratt and Lowe, 1972). Rock crabs are more numerous in Narragansett Bay, Rhode Island, in warmer months (Jeffries, 1966; Clancy[4]). Juveniles are present inside

[4] Clancy, M. 2002. Personal commun. Boston University, College of General Studies, Division of Natural Science, Boston, MA, 02115.

Table 4

Niche breadth and overlap for temporal, spatial, and trophic dimensions among blue, lady, and rock crabs. For temporal and spatial niches, all crabs (of all sizes) collected in 1992–94 are included. For trophic analyses, only the crabs containing one or more of the 12 prey categories were included. Female rock crabs were not included in trophic overlap because of the small sample size.

	Number of crabs	Mean CW, mm	Niche breadth		Overlap matrices				
Temporal niche									
(n=12 months, 1992–94)					BCF	LCM	LCF	RCM	RCF
Blue crab male (BCM)	2191	125	6.104	BCM	0.854	0.604	0.618	0.297	0.463
Blue crab female (BCF)	3483	129	8.187	BCF		0.649	0.576	0.376	0.564
Lady crab male (LCM)	11883	62	4.592	LCM			0.894	0.186	0.417
Lady crab female (LCF)	25312	61	3.896	LCF				0.149	0.339
Rock crab male (RCM)	14530	85	6.764	RCM					0.479
Rock crab female (RCF)	778	51	5.782						
Spatial niche									
(n=9 strata, 1992–94)					BCF	LCM	LCF	RCM	RCF
Blue crab male	2191	125	3.927	BCM	0.757	0.720	0.703	0.675	0.474
Blue crab female	3483	129	5.343	BCF		0.679	0.685	0.746	0.641
Lady crab male	11883	62	7.324	LCM			0.908	0.677	0.616
Lady crab female	25312	61	7.320	LCF				0.678	0.638
Rock crab male	14530	85	5.447	RCM					0.763
Rock crab female	778	51	7.191						
Trophic niche									
(n=12 prey categories, 1991–92)					BCF	LCM	LCF	RCM	
Blue crab male	84	111.0	5.234	BCM	0.819	0.570	0.580	0.576	
Blue crab female	139	127.9	6.563	BCF		0.629	0.651	0.609	
Lady crab male	98	59.4	6.166	LCM			0.861	0.437	
Lady crab female	200	54.9	4.655	LCF				0.417	
Rock crab male	181	88.8	4.139						
Rock crab female	11	53.7	2.620						
Trophic niche, sexes combined									
(n=12 prey categories, 1991–92)					LC	RC			
Blue crab (BC)	223	121.6	6.250	BC	0.628	0.623			
Lady crab (LC)	298	56.4	5.140	LC		0.427			
Rock crab (RC)	192	86.8	4.008						

that bay all year (Reilly and Saila, 1978). In contrast, in Delaware Bay and Chesapeake Bay they occur in coastal waters and estuaries mainly in colder months (Winget et al., 1974; Haefner and Van Engel, 1975; Haefner, 1976). Our data showed that rock crabs in the Hudson-Raritan Estuary conform to the pattern of migration typical of the latter southern bays.

A crossroads or overlap in distribution of the three crab species is more evident when a broader area on the continental shelf from Cape Cod to Cape Hatteras is considered. Crab presence was plotted by using data from the fall 1992 continental shelf trawl survey (Fig. 11). Fall surveys are done in September and October when waters are still warm. In the coastal waters off Raritan, Delaware, and Chesapeake Bays, blue and lady crabs were collected, whereas rock crabs were collected mainly on the central shelf. Estuarine presence in warm months, compiled from citations in the present study, is marked by symbols.

Sex ratios

In the Hudson-Raritan Estuary, sex ratios of blue, lady, and rock crabs were different from 1:1. In mature blue crabs, the sex ratio favored females because the study area is in the deeper oceanward portion of the estuarine system, where females release their eggs and overwinter. Many males spend their entire lives in water of relatively low salinity (Van Engel, 1958), such as is found in the nearby Hudson, Raritan, and Navesink-Shrewsbury rivers. In the Navesink River, the sex ratio of male to female blue crabs ≥12 cm over a two-year period was 2.6:1 (Meise and Stehlik, 2003).

In the Hudson-Raritan Estuary, female lady crabs ≥5 cm outnumbered males 2:1. Many of these females were ovigerous and therefore estuarine use may be related to reproduction. We were unable to locate published reports of lady crabs or other *Ovalipes* spp. mating locations, single-sex migrations, or locations of lar-

val release, any of which might be a reason for the use of the estuaries by female lady crabs.

The rock crabs that enter the estuary were predominantly males, and many females may never enter the estuary. Males use the estuary to molt, and possibly to avoid predators offshore. In comparison, on the northwest Atlantic continental shelf, the sex ratio in winter dredge collections was 1:2.2 males:females (Stehlik et al., 1991).

Feeding periodicity

Food consumption in crabs is affected by daily and seasonal cycles, temperature changes, reproductive rhythms, and molt (Warner, 1977; Stevens et al., 1982; Ryer, 1987; Mantelatto, 2001). In our study area, blue crabs ate little when inactive during the winter months, as reported above. Choy (1986) reported less feeding during egg-brooding in Portunidae, but in our study we found that fullness was about 40% in both egg-bearing and non-egg-bearing females in summer. A lack of feeding before and during molt, until calcification has sufficiently progressed, is typical of crabs (Warner, 1977). Empty stomachs in premolt and soft rock crabs in our study supported this observation.

Diet composition

We found that in the Hudson-Raritan Estuary, the most important prey items of blue crabs by volume were Xanthidae, then the mollusks *M. edulis* and *M. lateralis*, whereas only 2% of the prey volume was from cannibalism. In contrast, small blue crabs are of major importance in the diets of large blue crabs in Florida (Laughlin, 1982) and Maryland (Hines et al., 1990), and cannibalism is the source of more than 75% of the mortality of juveniles near estuarine shores (Hines and Ruiz, 1995). The major targets of cannibalism, early instars or molting juveniles, may be more abundant in rivers adjacent to our study area (Meise and Stehlik, 2003).

The diets of rock crabs in estuarine and coastal Canada and Maine usually contained a larger number of prey categories than did the diets in the present study (Scarratt and Lowe, 1972; Drummond-Davis et al., 1982; Hudon and Lamarche, 1989; Ojeda and Dearborn, 1991). These northern studies were done on rock, boulders, cobble, sand, and algal beds, where the diversity of habitats within a study area may offer a larger assortment of potential prey than the soft-bottom habitat of our estuary.

In the Hudson-Raritan Estuary, juveniles of commercially or recreationally harvested species were rarely consumed by the three species of crabs. Among mollusks, *M. arenaria* and *M. mercenaria* were scarce in crab stomachs, perhaps because other taxa such as *M. lateralis*, *N. trivittatus*, and Xanthidae provided abundant prey. The other commercially important species eaten by crabs was the blue crab juvenile, but infrequently as mentioned above.

Differences in diet among species, sexes, and size classes of predators

Our data did not support our hypotheses, based on existing studies, that blue, lady, and rock crabs would have different diets as a consequence of their species-specific body and chela structures. Blue and lady crabs (unlike rock crabs) swim, allowing them a greater foraging area than rock crabs. Chela structure affects the type and size of prey that can be crushed (Vermeij, 1978; Seed and Hughes, 1995; Behrens Yamada and Boulding, 1998). In Portunidae, the long chelae (in relation to their CW) have short muscle fibers better suited to quick grabbing than to prolonged crushing (Warner and Jones, 1976; Seed and Hughes, 1997). The chelae of Cancridae are monomorphic (same characteristics left and right sides), have relatively short, stout teeth, and close relatively slowly because of their muscle fibers (Warner and Jones, 1976). Chela crushing force (Newtons), measured with a force transducer, is positively correlated with chela height and thickness (Govind and Blundon, 1985; Block and Rebach, 1998). Although the chela structures of blue and rock crabs are quite different, the chelae of mature rock crabs (9–13.5 cm CW) generate crushing forces comparable to those of cutter and crusher chelae of mature male blue crabs (12–16 cm) (Govind and Blundon, 1985).

Chela crushing force in mature blue and rock crabs is likely to be more than sufficient for successful foraging upon all but the largest prey (Block and Rebach, 1998) and may not be a major determinant of diet. In fact, crabs often prey upon small or young bivalves rather than on large sizes, perhaps because the latter require more handling time and may damage chelae (Juanes, 1992; Seed and Hughes, 1995). Because Portunidae swim and have more versatile chelae, they may be expected to have broader trophic niches than Cancridae. In our study, blue crabs had the broadest trophic niche, lady crabs had an intermediate trophic niche, and rock crabs had the narrowest trophic niche.

We found no significant differences in diet by sex within species. Sexual dimorphism within a crab species accelerates after puberty (Hartnoll, 1978), but our study included many immature crabs. Some experimenters using force transducers found no significant difference in crushing force between the sexes of blue crabs of a broad size range (Blundon and Kennedy, 1982; Seed and Hughes, 1997), but in blue crabs >135 mm, males produced significantly more force than females (Eggleston, 1990). Sexual dimorphism is found in chela length, but not chela height, in lady crabs (significantly different slopes of CL/CW by regression; Stehlik, unpubl. data).

Carapace width and the proportion of chela height to carapace width are positively correlated with crushing force, which makes it possible for larger crabs to consume larger, harder-shelled mollusks or crustaceans (Hartnoll, 1978; Block and Rebach, 1998). The largest lady crabs do not grow to the carapace widths or chela lengths of mature blue crabs; therefore the force

of their chelae cannot match those of blue crabs. As they grow, Cancridae and Portunidae undergo shifts in diet, and may be divided into ontogenetically distinct trophic units (Laughlin, 1982; Stevens et al., 1982; Stoner and Buchanan, 1990; Rosas et al., 1994). In our study, larger crabs dropped amphipods and shrimp from their diets, but otherwise only minor changes occurred in prey identity and relative volumes of prey taxa among size classes (Fig. 9). An interesting ontogenetic shift was in the size of prey eaten: small crabs ate small individuals of prey taxa, such as *M. edulis*, and Xanthidae, and large crabs ate large individuals of the same taxa. Thus in our study the influence of physical structure upon diet was greater as body size increased within a species than among species.

Spatial variability and overlap in diets

The three predators were scattered throughout the cluster diagram of diet among strata of the estuary (Fig. 10), yet crabs from inner and outer groups of strata usually clustered separately. We concluded that location influenced diet more than did predator identity. The inner, outer, and channel strata differ in depth, sediment type, currents, and mean temperature, and therefore in benthic and epibenthic prey assemblages. Our results support the concept that these species are mainly opportunistic in diet, as was suggested for blue crabs (Laughlin, 1982), and rock crabs (Hudon and Lamarche, 1989). The Hudson-Raritan and other nearby coastal and estuarine areas from Long Island Sound to Chesapeake Bay are crossroads where blue, lady, and rock crabs share space and resources.

Acknowledgments

We thank those who helped design and carry out the Hudson-Raritan Estuary trawl surveys, especially Stuart Wilk, Anthony Pacheco, and Eileen MacHaffie. We also thank Fred Farwell, Sherman Kingsley, and the NOAA Corps captains and crew. Suellen Fromm was instrumental in obtaining data from NEFSC trawl surveys. We thank the scientists who shared their opinions and unpublished data. We are indebted to colleagues Mary Fabrizio, Clyde MacKenzie, John Manderson, Carol Meise, Frank Steimle, Allan Stoner, and anonymous reviewers who helped improve the manuscript. This paper is dedicated to the memory of Tony Pacheco.

Literature cited

Auster, P. J., and R. E. DeGoursey.
1994. Winter predation on blue crabs, *Callinectes sapidus*, by starfish *Asterias forbesi*. J. Shellfish Res. 13:361–366.

Azarovitz, T. A.
1981. A brief historical review of the Woods Hole Laboratory trawl survey time series. *In* Bottom trawl surveys (Doubleday, W.G., and D. Rivard, eds.), p. 62–67. Can. Spec. Publ. Fish. Aquat. Sci. 58.

Barshaw, D. E., and K. W. Able.
1990. Deep burial as a refuge for lady crabs, *Ovalipes ocellatus*: comparisons with blue crabs, *Callinectes sapidus*. Mar. Ecol. Prog. Ser. 66:75–79.

Behrens Yamada, S., and E. G. Boulding.
1998. Claw morphology, prey size selection and foraging efficiency in generalist and specialist shell-breaking crabs. J. Exp. Mar. Biol. Ecol. 220:191–211.

Birchard, G. F., L. Drolet, and L. H. Mantel.
1982. The effect of reduced salinity on osmoregulation and oxygen consumption in the lady crab, *Ovalipes ocellatus* (Herbst). Comp. Biochem. Physiol. 71A:321–324.

Block, J. D., and S. Rebach.
1998. Correlates of claw strength in the rock crab, *Cancer irroratus* (Decapoda, Brachyura). Crustaceana 71:468–473.

Blundon, J. A., and V. S. Kennedy.
1982. Mechanical and behavioral aspects of blue crab, *Callinectes sapidus* (Rathbun), predation on Chesapeake Bay bivalves. J. Exp. Mar. Biol. Ecol. 65:47–65.

Briggs, P. T.
1998. New York's blue crab (*Callinectes sapidus*) fisheries through the years. J. Shellfish Res. 17:487–491.

Choy, S. C.
1986. Natural diet and feeding habits of the crabs *Liocarcinus puber* and *L. holsatus* (Decapoda, Brachyura, Portunidae). Mar. Ecol. Prog. Ser. 31:87–99.

Clarke, K. R., and R. M. Warwick.
1994. Change in marine communities: an approach to statistical analysis and interpretation, 144 p. National Environmental Research Council, UK.

Coch, N. K.
1986. Sediment characteristics and facies distributions in the Hudson system. *In* Sedimentation in the Hudson system: the Hudson River and contiguous waterways (N. K.Coch and H. J. Bokuniewicz, eds.), p. 109–129. Northeastern Geology (spec. issue) 8.

Colwell, R. K., and D. J. Futuyama.
1971. On the measurement of niche breadth and overlap. Ecology 52:567–576.

de Lestang, S., N. G. Hall, and I. C. Potter.
2003. Reproductive biology of the blue swimmer crab (*Portunus pelagicus*, Decapoda: Portunidae) in five bodies of water on the west coast of Australia. Fish. Bull. 101:745–757.

Drummond-Davis, N. C., K. H. Mann, and R. A. Pottle.
1982. Some estimates of population density and feeding habits of the rock crab, *Cancer irroratus*, in a kelp bed in Nova Scotia. Can. J. Fish. Aquat. Sci. 39:636–639.

Eggleston, D. B.
1990. Functional responses of blue crabs *Callinectes sapidus* Rathbun feeding on juvenile oysters *Crassostrea virginica* (Gmelin): effects of predator sex and size, and prey size. J. Exp. Mar. Biol. Ecol. 143:73–90.

Eggleston, D. B., J. J. Grover, and R. N. Lipcius.
1998. Ontogenetic diet shifts in Nassau grouper: trophic linkages and predatory impact. Bull. Mar. Sci. 63:111–126.

Elner, R. W., P. G. Beninger, L. E. Linkletter, and S. Lanteigne.
1985. Guide to indicator fragments of principal prey taxa in the stomachs of two common Atlantic crab species: *Cancer borealis* Stimpson, 1859 and *Cancer irroratus* Say, 1817. Can. Tech. Rep. Fish. Aquat. Sci. 1403:1–20.

Fisher, M. R.
1999. Effect of temperature and salinity on size at maturity of female blue crabs. Trans. Am. Fish. Soc. 128:499–506.
Govind, C. K., and J. A. Blundon.
1985. Form and function of the asymmetric chelae in blue crabs with normal and reversed handedness. Biol. Bull. 168:221–231.
Guerin, J. L., and W. B. Stickle.
1992. Effect of salinity gradients on the tolerance and bioenergetics of juvenile blue crabs (*Callinectes sapidus*) from waters of different environmental salinities. Mar. Biol. 114:391–396.
Haefner, P. A., Jr.
1976. Distribution, reproduction and moulting of the rock crab, *Cancer irroratus* Say 1917, in the mid-Atlantic Bight. J. Nat. Hist. 10:377–397.
Haefner, P. A., Jr., and W. A. Van Engel.
1975. Aspects of molting, growth and survival of male rock crabs, *Cancer irroratus*, in Chesapeake Bay. Chesapeake Sci. 16:253–265.
Hartnoll, R. G.
1978. The determination of relative growth in Crustacea. Crustaceana 34:281–293.
Hines, A. H., R. N. Lipcius, and A. M. Haddon.
1987. Population dynamics and habitat partitioning by sex, size, and molt stage of blue crabs *Callinectes sapidus* in a subestuary of Chesapeake Bay. Mar. Ecol. Prog. Ser. 36:55–64.
Hines, A. H., A. M. Haddon, and L. A. Wiechert.
1990. Guild structure and foraging impact of blue crabs and epibenthic fish in a subestuary of Chesapeake Bay. Mar. Ecol. Prog. Ser. 67:105–126.
Hines, A. H., and G. M. Ruiz.
1995. Temporal variation in juvenile blue crab mortality: nearshore shallows and cannibalism in Chesapeake Bay. Bull. Mar. Sci. 57:884–901.
Hudon, C., and G. Lamarche.
1989. Niche segregation between American lobster *Homarus americanus* and rock crab *Cancer irroratus*. Mar. Ecol. Prog. Ser. 52:155–168.
Hyslop, E. J.
1980. Stomach contents analysis—a review of methods and their application. J. Fish. Biol. 17:411–429.
Jeffries, H. P.
1966. Partitioning of the estuarine environment by two species of *Cancer*. Ecology 47:477–481.
Jones, C. R., C. T. Fray, and J. R. Schubel.
1979. Textural properties of surficial sediments of Lower Bay of New York Harbor. Special Report 21, 113 p. Marine Sciences Research Center, State University of New York, Stony Brook, NY.
Juanes, F.
1992. Why do decapod crustaceans prefer small-sized molluscan prey? Mar. Ecol. Prog. Ser. 87:239–249.
Krouse, J. S.
1972. Some life history aspects of the rock crab, *Cancer irroratus*, in the Gulf of Maine. J. Fish. Res. Board Can. 29:1479–1482.
Laughlin, R. A.
1982. Feeding habits of the blue crab, *Callinectes sapidus* Rathbun, in the Appalachicola estuary, Florida. Bull. Mar. Sci. 32:807–822.
Leffler, C. W.
1972. Some effects of temperature on the growth and metabolic rate of juvenile blue crabs, *Callinectes sapidus*, in the laboratory. Mar. Biol. 14:104–110.
MacKenzie, C. L., Jr.
1990. History of the fisheries of Raritan Bay, New York and New Jersey. Mar. Fish. Rev. 52:1–45.
1997. The U. S. molluscan fisheries from Massachusetts Bay through Raritan Bay, N. J. and N. Y. *In* The history, present condition, and future of the molluscan fisheries of North and Central America and Europe. Volume 1, Atlantic and Gulf Coasts (C. L. MacKenzie, Jr., V. G. Burrell Jr., A. Rosenfield, and W. L. Hobart, eds.), p. 87–118. NOAA Tech. Rep. 127.
Mantelatto, F. L. M, and R. A. Christofoletti.
2001. Natural feeding activity of the crab *Callinectes ornatus* (Portunidae) in Ubatuba Bay (Sao Paulo, Brazil): influence of season, sex, size and molt stage. Mar. Biol. 138:585–594.
Marshall, S., and M. Elliott.
1997. A comparison of univariate and multivariate numerical and graphical techniques for determining inter- and intraspecific feeding relationships in estuarine fish. J. Fish Biol. 51:526–545.
McDermott, J. J.
1983. Food web in the surf zone of an exposed sandy beach along the mid-Atlantic coast of the United States. *In* Sandy beaches as ecosystems (A. McLachlan and T. Erasmus eds.), p. 529–538. Dr. W. Junk, The Hague, Netherlands.
Meise, C. J., and L. L. Stehlik.
2003. Habitat use, temporal abundance variability, and diet of blue crabs from a New Jersey estuarine system. Estuaries 26:731–745.
Milliken, M. R., and A. B. Williams.
1984. Synopsis of biological data on the blue crab, *Callinectes sapidus* Rathbun. NOAA Tech. Rep. NMFS 1, 39 p.
Milstein, C. B., D. T. Thomas, and associates.
1977. Summary of ecological studies for 1972–1975 in the bays and other waterways near Little Egg Inlet and in the ocean in the vicinity of the proposed site for the Atlantic Generating Station, New Jersey. Bull. 18, 757 p. Ichthyological Associates, Inc., Ithaca, NY.
Ojeda, F. P., and J. H. Dearborn.
1991. Feeding ecology of mobile benthic predators: experimental analyses of their influence in Atlantic rocky subtidal communities of the Gulf of Maine. J. Exp. Mar. Biol. Ecol. 149:13–44.
Reilly, P. N., and S. B. Saila.
1978 Biology and ecology of the rock crab, *Cancer irroratus* Say, 1817, in southern New England waters (Decapoda, Brachyura). Crustaceana 34:121–140.
Romesburg, H. C.
1984. Cluster analysis for researchers, 334 p. Lifetime Learning Publications, Belmont, CA.
Ropes, J. W.
1989. The food habits of five crab species at Pettaquamscutt River, Rhode Island. Fish. Bull. 87:197–204.
Rosas, C., E. Lazaro-Chavez, and F. Buckle-Ramirez.
1994. Feeding habits and food niche segregation of *Callinectes sapidus*, *C. rathbunae* and *C. similis* in a subtropical coastal lagoon of the Gulf of Mexico. J. Crustacean Biol. 14:371–382.
Rountree, R. A., and K. W. Able.
1992. Fauna of polyhaline subtidal marsh creeks in southern New Jersey: composition, abundance and biomass. Estuaries 15:171–185.

Ryer, C. H.
1987. Temporal patterns of feeding by blue crabs (*Callinectes sapidus*) in a tidal-marsh creek and adjacent seagrass meadow in the lower Chesapeake Bay. Estuaries 10:136–140.
Scarratt, D. J., and R. Lowe.
1972. Biology of the rock crab (*Cancer irroratus*) in Northumberland Strait. J. Fish. Res. Board Canada 29:161–166.
Seed, R., and R. N. Hughes.
1995. Criteria for prey size-selection in molliscivorous crabs with contrasting claw morphologies. J. Exp. Mar. Biol. Ecol. 193:177–195.
1997. Chelal characteristics and foraging behavior of the blue crab *Callinectes sapidus* Rathbun. Estuar. Coastal Shelf Sci. 44:221–229.
Sponaugle, S., and P. Lawton.
1990. Portunid crab predation on juvenile hard clams: effects of substrate type and prey density. Mar. Ecol. Prog. Ser. 67:43–53.
Stehlik, L. L.
1993. Diets of the brachyuran crabs *Cancer irroratus*, *C. borealis*, and *Ovalipes ocellatus* in the New York Bight. J. Crustacean Biol. 13:723–735.
Stehlik, L. L., C. L. MacKenzie Jr. and W. W. Morse.
1991 Distribution and abundance of four brachyuran crabs on the northwest Atlantic shelf. Fish. Bull. 89:473–492.
Stehlik, L. L., P. G. Scarlett, and J. Dobarro.
1998. Status of the blue crab fisheries of New Jersey. J. Shellfish Res. 17:475–485.
Steimle, F. W., D. Jeffress, S. A. Fromm, R. N. Reid, J. J. Vitaliano, and A. B. Frame.
1994. Predator-prey relationships of winter flounder, *Pleuronectes americanus*, in the New York Bight apex. Fish. Bull. 92:608–619.
Stevens, B. G., D. A. Armstrong, and R. Cusimano.
1982. Feeding habits of the Dungeness crab *Cancer magister* as determined by the index of relative importance. Mar. Biol. 72:135–145.
Stoner, A. W., and B. A. Buchanan.
1990. Ontogeny and overlap in the diets of four tropical *Callinectes* species. Bull. Mar. Sci. 46:3–12.
Van Engel, W. A.
1958. The blue crab and its fishery in Chesapeake Bay. Part 1—Reproduction, early development, growth, and migration. Commer. Fish. Rev. 20:6–17.
1990. Development of the reproductively functional form in the male blue crab, *Callinectes sapidus*. Bull. Mar. Sci. 46:13–22.
van Montfrans, J., C. H. Ryer, and R. J. Orth.
1991. Population dynamics of blue crabs *Callinectes sapidus* Rathbun in a lower Chesapeake Bay tidal marsh creek. J. Exp. Mar. Biol. Ecol. 153:1–14.
Vermeij, G. J.
1978. Biogeography and adaptation, 332 p. Harvard University Press, Cambridge, MA.
Virnstein, R. W.
1977. The importance of predation by crabs and fishes on benthic infauna in Chesapeake Bay. Ecology 58:1199–1217.
Warner, G. F.
1977. The biology of crabs, 202 p. Van Nostrand Reinhold Co., New York, NY.
Warner, G. F., and A. R. Jones.
1976. Leverage and muscle type in crab chelae (Crustacea: Brachyura). J. Zool., Lond. 180:57–68.
Williams, A. B.
1984. Shrimps, lobsters, and crabs of the Atlantic coast of the eastern United States, Maine to Florida, 550 p. Smithsonian Institution Press, Washington, DC.
Williams, A. B., and R. L. Wigley.
1977. Distribution of decapod Crustacea off northeastern United States based on specimens at the Northeast Fisheries Center, Woods Hole, MA. NOAA Tech. Rep. NMFS Circ. 407, 44 p.
Williams, M. J.
1981. Methods for analysis of natural diet in portunid crabs (Crustacea, Decapoda, Portunidae). J. Exp. Mar. Biol. Ecol. 52:103–113.
Wilson, K. A., K. W. Able, and K. L. Heck Jr.
1990. Habitat use by juvenile blue crabs: a comparison among habitats in southern New Jersey. Bull. Mar. Sci. 46:105–114.
Winget, R. R., D. Maurer, and H. Seymour.
1974. Occurrence, size composition and sex ratio of the rock crab, *Cancer irroratus* Say and the spider crab, *Libinia emarginata* Leach in Delaware Bay. J. Nat. Hist. 8:199–205.

Radiometric validation of age, growth, and longevity for the blackgill rockfish (*Sebastes melanostomus*)

Melissa M. Stevens
Allen H. Andrews
Gregor M. Cailliet
Kenneth H. Coale

Moss Landing Marine Laboratories
8272 Moss Landing Road
Moss Landing, California 95039
E-mail address (for A. H. Andrews, contact author): andrews@mlml.calstate.edu

Craig C. Lundstrom

Department of Geology
University of Illinois–Urbana Champaign
255 Natural History Bldg.
1301 W. Green Street
Urbana, Illinois 61801

Abstract—As nearshore fish populations decline, many commercial fishermen have shifted fishing effort to deeper continental slope habitats to target fishes for which biological information is limited. One such fishery that developed in the northeastern Pacific Ocean in the early 1980s was for the blackgill rockfish (*Sebastes melanostomus*), a deep-dwelling (300–800 m) species that congregates over rocky pinnacles, mainly from southern California to southern Oregon. Growth zone-derived age estimates from otolith thin sections were compared to ages obtained from the radioactive disequilibria of ^{210}Pb, in relation to its parent, ^{226}Ra, in otolith cores of blackgill rockfish. Age estimates were validated up to 41 years, and a strong pattern of agreement supported a longevity exceeding 90 years. Age and length data fitted to the von Bertalanffy growth function indicated that blackgill rockfish are slow-growing (k=0.040 females, 0.068 males) and that females grow slower than males, but reach a greater length. Age at 50% maturity, derived from previously published length-at-maturity estimates, was 17 years for males and 21 years for females. The results of this study agree with general life history traits already recognized for many *Sebastes* species, such as long life, slow growth, and late age at maturation. These traits may undermine the sustainability of blackgill rockfish populations when heavy fishing pressure, such as that which occurred in the 1980s, is applied.

Manuscript submitted 9 June 2003 to the Scientific Editor's Office.

Manuscript approved for publication 18 June 2004 by the Scientific Editor.

Fish. Bull. 102:711–722 (2004).

The blackgill rockfish (*Sebastes melanostomus*) is a deep-water rockfish that is found mainly along the continental slope between 300 and 800 m depth off central and southern California (Moser and Ahlstrom, 1978; Cross, 1987; Williams and Ralston, 2002). Although not as heavily targeted in relation to other commercially important rockfish species, a directed commercial fishery for blackgill rockfish has existed since the mid-1970s, beginning off southern California (Point Conception area) and spreading northward (Monterey area) as stocks of other heavily fished rockfishes declined (Butler et al., 1999). Using acoustic sonar and set nets, the commercial fleet was able to catch large aggregations of previously unexploited blackgill rockfish. Landings peaked in 1983 with 1346 metric tons (t) caught coast-wide, but declined over the next decade, presumably because of the disappearance of the large concentrations that could be located with acoustical gear (Butler et al., 1999). In 2001, 141 t were reportedly landed along the entire west coast (PacFIN[1])—less than half of the allowable catch (343 t; NOAA, 2001) for blackgill rockfish that year.

The first stock assessment of blackgill rockfish was made by Butler et al. (1999). One objective of this assessment was to determine age and growth characteristics, which were then applied to estimate age-at-maturity, natural mortality, and stock biomass. Using conventional aging methods (i.e., otolith increments), we estimated that blackgill rockfish live at least 87 years and reach full (100%) maturity from 13 to 26 years for females, and from 13 to 24 years for males. Although such estimates are useful and should be considered whenever available, validation of the age-estimation procedure is needed to be certain of accurate age estimates (Beamish and McFarlane, 1983; Campana, 2001). Inaccurate age determinations in some cases have led to overharvesting of stocks such as Pacific ocean perch (*Sebastes alutus*)

[1] PacFIN (Pacific Fisheries Information Network). 2002. Commercial fisheries landing data. http://www.PacFIN.org. [Accessed 9 August 2002].

and orange roughy (*Hoplostethus atlanticus*; Beamish, 1979; Archibald et al., 1983; Mace et al., 1990). These historical examples of fishery collapses necessitate that age validation be achieved before age and growth information is applied to management.

In the last decade, radiometric age validation has been applied successfully to over 20 species of rockfishes and other marine teleosts (Burton et al., 1999; Kastelle et al., 2000; Andrews et al., 2002). The most common technique uses the disequilibria between two radioisotopes, radium-226 (^{226}Ra) and lead-210 (^{210}Pb), present in the otolith (Bennett et al., 1982; Smith et al., 1991). Radium-226 is a naturally occurring radioisotope and calcium analogue that is incorporated from the surrounding seawater into the aragonitic crystalline matrix of fish otoliths. Radium-226 decays through a series of short-lived radioisotopes to ^{210}Pb. Because the half-lives of these isotopes are known, the ratio of activity between them (^{210}Pb:^{226}Ra) gives a measure of elapsed time since the initial incorporation of ^{226}Ra into the otolith (Campana et al., 1990). Radium-226 decays very slowly (a 1600 year half-life) in relation to ^{210}Pb (a 22 year half-life), allowing the activity ratio of these radioisotopes to build into secular equilibrium (1:1 ratio; Smith et al., 1991). Based on this relationship (also referred to as ingrowth), the ^{210}Pb: ^{226}Ra activity ratio is suitable for age determination in fishes up to 5 half-lives of ^{210}Pb, or approximately 120 years of age (Andrews et al., 1999b; Campana, 2001). This approach is therefore ideally suited to the blackgill rockfish, whose longevity has been estimated at almost 90 years (Butler et al., 1999).

The objectives of this study were 1) to estimate age from otolith growth zone counts, 2) to describe growth, and 3) to validate the annual periodicity of growth zones used to estimate longevity for the blackgill rockfish with the radiometric aging technique. An ancillary objective was to create a reliable predictive relationship between average otolith weight and estimated age for use as a timesaving tool in the management of this species. Growth zones quantified in sectioned otoliths were used to estimate age, and growth was described by using the von Bertalanffy growth function. Final age estimates were directly compared to radiometric ages to evaluate agreement between the two methods and ultimately were used to validate age estimation procedures, age-at-maturity, and longevity for this species.

Materials and methods

Approximately 1210 blackgill rockfish sagittal otoliths were available for this study. Otoliths were collected by National Marine Fisheries Service (NMFS) personnel from commercial vessels in 1985 at ports along the California coastline (Long Beach to Fort Bragg), and during NMFS research surveys from 1998 to 2000 from central California to the Oregon-Washington border. Thirty-two juvenile blackgill rockfish, collected from spot prawn traps along the central California coast, were provided by Robert Lea of the California Department of Fish and Game (CDFG). Fish total length (TL; cm or mm), catch area (port or geographic location), and otolith weights (right and left, 1985 samples only) were provided. Otoliths were first considered for age estimation (sectioning), and the remainder were reserved for radiometric analysis. Otolith weights (left and right, male and female) were measured to the nearest milligram and compared with *t*-tests to determine if significant differences in mass existed between sides or sexes.

Estimation of age and growth

Based on previous aging studies and the need to conserve samples for radiometric analysis, approximately 310 otoliths (25% of the collection) were assumed to be sufficient for age estimation. The left otolith from 5 to 30 fish, depending upon the number available in each 50-mm size class (ranging from 100 mm to 600 mm), was randomly chosen by using a basic resampling tool. Otoliths were thin-sectioned and mounted onto glass slides. Approximately 50 otoliths were damaged in the sectioning process, leaving 260 otoliths available for age estimation.

Sections were viewed by three readers under magnification (25 and 40×) with transmitted or reflected light. Each reader obtained age estimates by inspecting all available growth axes, choosing the most discernible axis, and reading it three times consecutively. A growth zone (here termed an "annulus") was defined as one pair of translucent (winter-forming) and opaque (summer-forming) bands. A final age, based on each reader's most confident estimate, was chosen. Precision between and within readers was compared by using average percent error (APE; Beamish and Fournier, 1981), index of precision (D) and coefficient of variation (CV; Chang, 1982). Percent agreement among readers was also calculated. Reader 1 (author) determined the final age estimate for each section as described in Mahoney (2002). Ages that could not be confidently resolved (through re-examination or discussion) were removed from analysis.

Length and age estimates for males, females, and sexes combined were fitted to the von Bertalanffy growth function (VBGF). A small portion of juvenile samples (n=16) were included in each function. Because there was strong agreement between facility aging techniques (MLML and NMFS, La Jolla, Butler et al. 1999), additional aged samples were added to strengthen the VBGF and age prediction models (n=119). Estimates of age at first, 50%, and 100% maturity were calculated by inserting existing size at maturity data (Echeverria, 1987) into the VBGF and solving for age (t).

Age prediction, age group determination, and core extraction

Campana et al. (1990) was the first to circumvent the assumption of constant ^{226}Ra uptake throughout the life of the fish by eliminating younger growth layers from adult otoliths, leaving just the oldest layers of

otolith growth (i.e., the core, representing the first few years of life). Radium-226 is present at such low activity levels, however, that many otolith cores from fish of a similar age and same sex must be pooled to acquire the mass of material needed for detection (~0.5 to 1 gram; Andrews et al., 1999a, 1999b). Because we possessed a limited number of blackgill rockfish otoliths (~1200), an age prediction model was created to conserve otolith material for radiometric analysis. It was appropriate to assume from the results of Francis (2003) that within-sample heterogeneity with respect to otolith age and mass growth rate was negligible in the core material.

To determine age groups for radiometric analyses, final ages for fish whose otoliths were sectioned, along with their corresponding average otolith weight (left and right, n=2), were used to predict age for the remaining fish in the collection. Several parameters were regressed to determine a predictive relationship between average otolith weight (henceforth termed "otolith weight") and estimated age (i.e., section age). The following regressions were compared to estimated age by using Kruskal-Wallis (nonnormal) ANOVA: 1) otolith weight (to the nearest 0.001 g), 2) otolith weight and fish length (to the nearest 1 mm), and 3) otolith weight plus otolith length (to the nearest 0.001 mm) multiplied by otolith weight (as an interaction term). A power function was also investigated but did not result in a better fit than that provided by a simple linear regression (either log-transformed or normal). A paired sample t-test and student's t-test for slopes were used to determine if a significant difference existed between male and female otolith weight, and between male and female otolith weight-to-age regressions, respectfully. The final regression equations were applied to the average otolith weight for all individual remaining fish to obtain a predicted age. Age groups were created if there was sufficient otolith material from fish of the same sex and of a similar predicted age.

The predicted age range for each group was kept as narrow as possible while permitting enough material for analysis; approximately 25 to 50 otoliths were needed at a target core weight of 0.02 g. Fish that had both otoliths intact (not sectioned or broken) were preferred to reduce the number of fish for each radiometric sample. To better insure sample conformity, 90% confidence intervals with respect to fish length and otolith weight were used to eliminate from each group dissimilar fish that may have varied significantly from predicted age. In addition to this discriminating technique, groups were further confined by capture year and location. Only samples caught in the same year and similar geographic location (based on the majority of port locations within 300 miles) were included in the same group.

Core size was determined by viewing several whole juvenile blackgill rockfish otoliths with estimated ages between 1 and 7 years. The first annulus was determined to be approximately 2 mm wide, and a 3-year-old otolith was measured at 3 mm wide, 4 mm long, and 1 mm thick, and having a weight of 0.02 g. These dimensions were chosen as the target core size because a core of this size could be easily extracted, yet was young enough to minimize the possible error associated with variable ^{226}Ra uptake in the first few years of growth. Otoliths from adult fish were ground down to the target core size with a lapping wheel and 80- to 120-grit silicon-carbide paper. Otoliths from selected juveniles, if older than age 3 (core size), were also ground to the target core size.

Radiometric analysis

The radiometric analysis was conducted as described in Andrews et al. (1999a, 1999b). Because previous studies have revealed extremely low levels of ^{210}Pb and ^{226}Ra in otolith samples, trace metal precautions were employed throughout sample cleaning and processing (Bennett et al., 1982; Campana et al., 1990; Andrews et al.,1999a). Acids were double distilled (GFS Chemicals®, Powell, OH) and all dilutions were made using Millipore® filtered Milli-Q water (18 MΩ/cm). Samples were thoroughly cleaned, dried, and weighed to the nearest 0.0001 g prior to dissolution. Whole juvenile otoliths groups were analyzed first to determine if exogenous ^{210}Pb was a significant factor, and to determine baseline levels of ^{226}Ra activity.

Because of the low-level detection problems associated with (beta) β-decay of ^{210}Pb, the activity ^{210}Pb was quantified through the autodeposition and (alpha) α-spectrometric determination of its daughter proxy, polonium-210 (^{210}Po, half-life=138 days; Flynn, 1968). In preparation for ^{210}Po analysis, samples were dissolved in acid and spiked with a calibrated yield tracer, ^{208}Po, estimated to be 5 times the activity of ^{210}Po in the otolith sample. Polonium isotopes from the sample were autodeposited onto a purified silver planchet (A.F. Murphy Die and Machine Co., North Quincy, MA) held in a rotating Teflon™ holder over a 4-hour period (Flynn, 1968). The activity of ^{208}Po and ^{210}Po on the planchets was measured with ion-implant detectors in a Tennelec (Oak Ridge, TN) TC256 α-spectrometer interfaced with a multichannel analyzer and an eight channel digital multiplexer. Counts were recorded with Nucleus® software (Nucleus Personal Computer Analyzer II, The Nucleus Inc., Oak Ridge, TN) on an IBM computer. Counts measured over periods that ranged from 28 to 50 days accumulated from 160 to 919 total counts. Lead-210 activity, along with uncertainty, was calculated in a series of equations that corrected for background and reagent counts, as well as error associated with count statistics and procedure (pipetting error, yield-tracer uncertainty, etc; Andrews et al., 1999a). The remaining sample was dried and conserved for ^{226}Ra analysis.

Determination of ^{226}Ra employed an elemental separation procedure followed by isotope-dilution thermal ionization mass spectrometry (TIMS) as described in Andrews et al. (1999a, 1999b). The sample was spiked with a known amount of ^{228}Ra yield tracer estimated to produce a ^{226}Ra:^{228}Ra atom ratio close to one. The samples were dissolved in strong acid and dried repeatedly (~90–100°C) until the sample color was bright

white, indicating that most organic material had been removed. A three-step elemental separation procedure was used to remove calcium and barium, elements that interfere with the detection of radium in the TIMS process. This involved passing the samples through three cation exchange columns, two containing a slurry of BioRad AG® 50W-X8 resin (first and second column), and one containing EiChroM Sr® resin (third column). The samples were introduced to a highly acidic medium within the columns, which separated the elements according to elution characteristics (Andrews et al., 1999b).

Radiometric age for each group was determined by inserting the measured ^{210}Pb and ^{226}Ra activities into the secular equilibrium model (Smith et al., 1991) and correcting for the elapsed time between capture and autodeposition. Because these activities were measured from the same sample, the calculation was independent of sample mass (Andrews et al., 1999a, 1999b). Propagated uncertainty associated with the final ^{210}Pb activity was based on count statistics, and procedural error and uncertainty for the final ^{226}Ra activity was based on procedural error and an instrumental TIMS analysis routine (Wang et al., 1975; Andrews et al., 1999b). The combined errors were used to calculate high and low radiometric ages.

Accuracy of age estimates

Measured ^{210}Pb:^{226}Ra activity ratios for each age group, along with their total sample age (predicted age + time since capture), were plotted with the expected ^{210}Pb:^{226}Ra growth curve. Each age group range was widened by multiplying the minimum and maximum age in the range by the age estimate CV, which was determined from the variability in age estimates among three readers. Agreement between the measured ratio with respect to estimated age and the expected ratio (ingrowth curve) provided an indication of the age estimate accuracy. Radiometric age was compared to the average predicted age for each group by using two tests: 1) a paired sample *t*-test to determine if a significant difference existed between the two age estimates for the groups and 2) predicted age was plotted against radiometric age and the correlation was compared to a hypothetical agreement line (slope of 1) by using *t*-tests for slope and elevation.

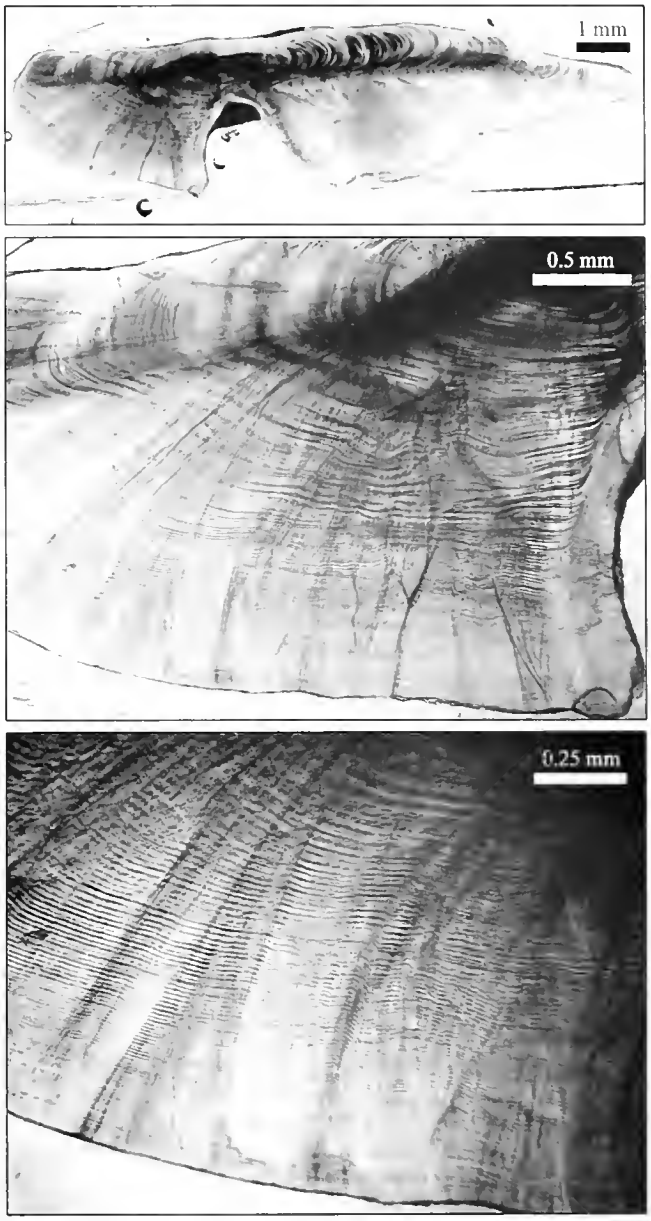

Figure 1

Three images of a blackgill rockfish (*Sebastes melanostomus*) otolith section viewed with transmitted light at 25× magnification (top), 40× (center), and 80× magnification (bottom). This section was aged most consistently as 90 years under a microscope, but because of finer digital resolution and contrast, the section pictured can be aged as high as 102 years.

Results

Estimation of age and growth

Growth zones observed within otolith sections of most blackgill rockfish were difficult to interpret. Distinction of the first annulus was often ambiguous, and the banding pattern during the first several years (1 to ~10) of growth was, in some sections, wide and inconsistent. After approximately 8 to 12 growth zones, the zone width transitioned to a narrower zone, which became extremely compressed after 20–40 growth zones. In some sections, these older zones were beyond optical resolution, whereas in others they were remarkably clear (Fig. 1).

Table 1

Comparison of von Bertalanffy growth function parameters for this study and Butler et al. (1999; in parentheses), for combined sexes, females, and males. All lengths are total lengths (mm). Note that the sample size for females and males does not sum to 332 because the same juvenile samples (n=16) were used for each sex, and only once for combined sexes. N.R.= not reported.

	Combined sexes	Females	Males
L_∞ (mm)	509 (524[1])	548 (554[1])	448 (467[1])
95% CI	491–528 (N.R.)	520–576 (N.R.)	434–462 (N.R.)
k	0.045 (0.040)	0.040 (0.040)	0.068 (0.060)
95% CI	0.038–0.052	0.033–0.047	0.058–0.078
t_0	−4.86 (−5.02)	−4.49 (−4.66)	−2.37 (−2.98)
95% CI	−6.60 to −3.12	−6.30 to −2.67	−3.55 to −1.19
n	332 (335)	181 (98)	167 (78)
r^2	0.81 (0.79)	0.87 (0.90)	0.87 (0.92)

[1] Total lengths from some samples in Butler et al., 1999 were estimated from fork length (FL in mm) by using an equation from Echeverria and Lenarz (1984).

The most consistent axis in the otolith section for which confident interpretations could be made was along either the sulcus ridge, or along the dorsoventral margin. Final age estimates were resolved for 197 fish, or approximately 76% of the 260 successfully sectioned otoliths. Agreement among readers was relatively low: approximately 24% of age estimates were within ±1 year, 61% were within ±5 years, and 87% were within ±10 years. The mean difference in age estimates between readers was 2.9 ±4.0 years. Among the three readers, APE was 10.7%, D was 8.4%, and CV was 14.6%. Average percent error, D, and CV estimates were comparable within readers; reader 1 APE was 5.2%, D was 4.1%, and CV was 7.0%. The two oldest fish to be aged were a 90-year-old male (450 mm TL) collected in 1999 and an 87-year-old female (546 mm TL) collected in 1985. Both individuals were caught south of Point Conception, California.

The VBGF fitted to age and length data resulted in distinct growth curves for male and female blackgill rockfish (Fig. 2). This difference is also represented by non-overlapping confidence intervals with respect to the primary VBGF parameters (L_∞, k; Table 1). The growth coefficient, k, ranged from 0.040 (±0.007, female) to 0.068 (±0.010, male), and asymptotic length was 448 ±14 mm for males to 548 ±28 mm for females. The asymptotic length for females was 32 mm less than the largest female fish sampled (580 mm TL), and for males, was 74 mm less than the largest male sampled (522 mm TL). The fit for all three functions was satisfactory (r^2=0.81, 0.87; Table 1, Fig. 2). Estimated ages at first, 50%, and 100% maturity, derived from inserting published estimates of length-at-maturity (Echeverria, 1987) into the growth model for each sex, were 15, 21, and 22 years for females and 13, 17, and 28 years for males (Table 2).

Table 2

Age at maturity estimates, in years, for male and female blackgill rockfish (95% confidence intervals are in parentheses). Maturity estimates were derived by inserting published estimates of length at maturity into the von Bertalanffy growth function.

	First maturity	50% maturity	100% maturity
Females	15 (12–22)	21 (16–31)	22 (17–33)
Length at maturity[1] (mm)	300	350	360
Males	13 (11–15)	17 (14–20)	27 (22–35)
Length at maturity[1] (mm)	290	330	390

[1] Echeverria (1987).

Age prediction, age group determination, and core extraction

A paired sample t-test indicated that there was a significant difference between male and female average otolith weight (t=4.54, P<0.001), and a student's t-test for slopes indicated a significant difference between male and female average otolith weight-to-age regressions (t_{crit}=1.967, t=2.87, P<0.05). Therefore, male and female age estimates and regressions were treated separately. There was no statistical difference between regressions involving fish length and average otolith weight (Kruskal-Wallis one-way ANOVA on ranks, H=4.834, P=0.089). A simple linear regression, with average otolith weight as the independent variable and estimated

age as the dependent variable, was sufficient to predict age. Log normalizing the regressions to stabilize the variance in older age estimates was unsuccessful (Cochran's test: α=0.05, 36 df, C=0.4748, P=0.486). The final regressions are given in Figure 3.

Fourteen age groups based on the predicted ages of unsectioned otoliths were chosen. These groups consisted of four juvenile groups, and five male and five female adult groups (Table 3). Fish lengths ranged from 82 mm to 580 mm TL, and predicted age ranged from 1 to 69 years. The number of otolith cores per age group ranged from 11 to 59, representing 7 to 32 fish per group. Total sample weight for each age group ranged from 0.4649 g to 1.6424 g. Whole otolith weight ranged from 0.041 to 0.842 g, and average individual core weight for the adult age groups ranged from 0.025 g to 0.028 g. The process of extracting the core inadvertently destroyed some otoliths in the grinding process, leading to smaller samples for some groups.

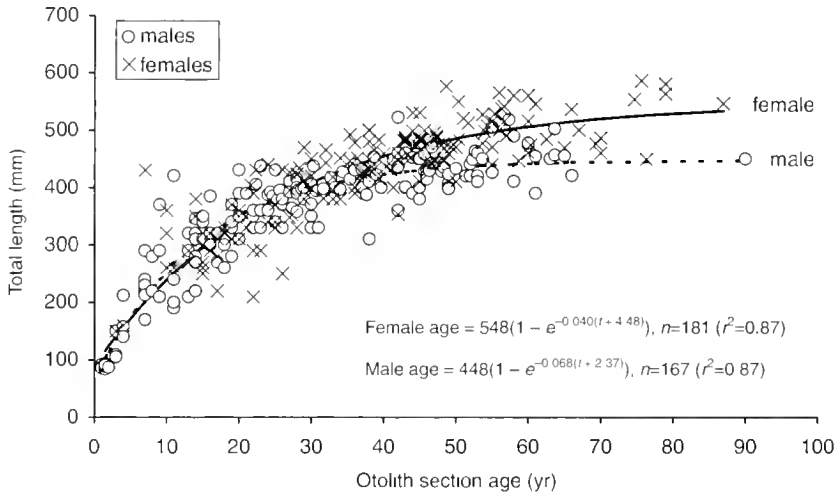

Figure 2

Blackgill rockfish (*Sebastes melanostomus*) von Bertalanffy growth functions plotted for males and females. Observed and expected values, as well as the parameters of the equations, are given. Note that the same juvenile samples (n=16) were included in both male and female equations.

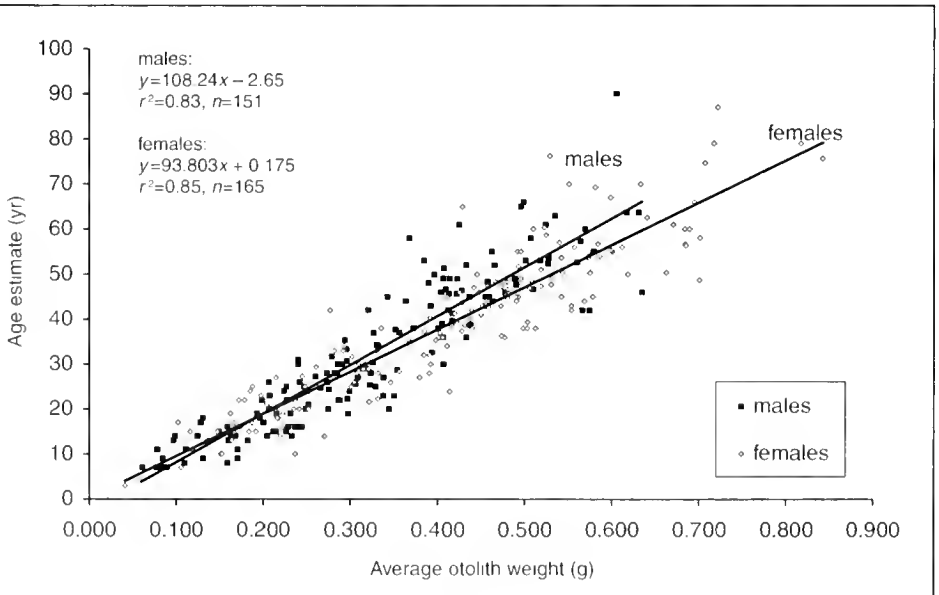

Figure 3

Predictive relationship between average otolith weight and estimated age for blackgill rockfish (*Sebastes melanostomus*). These regression equations were used to predict the age of fish whose otoliths were reserved for radiometric analysis.

Radiometric analysis

Radiometric analysis of all age groups (n=14) resulted in the successful determination of ^{210}Pb activity for all samples, and limited success for ^{226}Ra (Table 4). Activities of ^{210}Pb increased, as expected, fivefold from juvenile to adult age groups, and ranged from near 0.01 dpm/g for the juvenile samples to over 0.05 dpm/g for the oldest age groups. Error associated with these measurements ranged from 3.7 to 9.2 % (1s). The detection of ^{226}Ra activity was met with some technical difficulties. Because of poor radium recovery, radium measurements were unreliable in three samples and radium was lost in four samples. Therefore, an average of the reliable ^{226}Ra measurements was used because of the relative consistency of levels measured in these samples (0.0643 ±0.0035 dpm/g, n=7). The use of a single estimate for ^{226}Ra activity was acceptable prior to refinement of the technique (Andrews et al., 1999b). Calculated ^{210}Pb:^{226}Ra ratios increased as expected from 0.172 to 0.845 and 0.912 for the oldest groups (Table 4).

Age estimate accuracy

Radiometric ages were in agreement with predicted ages, as evidenced by concordance of ^{210}Pb:^{226}Ra activity

Table 3

Summary data for 14 pooled otolith age groups of blackgill rockfish. The age range and sample weight of each age group was based on the age prediction model and otolith availability. Groups were confined by year of capture, and for the 1985 samples, by port location. Mean total length (±1 standard deviation) of individuals per group is provided, along with the number of fish and otoliths, total sample weight, and average core weight.

Sample number	Age group (yr)	Sex	Capture year	Mean length ±σ (TL mm)	Number of fish,[1] number of otoliths	Sample weight (g)	Avg. core weight (g)
BG1	1–3	Juvenile	1998	154 ±26	7, 11[2]	0.4649	0.042
BG2	4	Juvenile	1998	200 ±8	10, 8[2]	1.1687	0.065
BG3	4–5	Juvenile	1999	217 ±9	15,19[2]	1.6630	0.088
BG4	1–7	Juvenile	2000	119 ±37	25, 36[2]	0.7854	0.022
BG5	29–31	Female	1985	400 ±20	25, 46	1.2510	0.027
BG6	26–28	Male	1985	379 ±19	22, 35	0.8866	0.025
BG7	11–17	Female	1998	276 ±20	22, 33	0.9018	0.027
BG8	39–41	Female	1985	458 ±22	31, 53	1.3332	0.025
BG9	48–54	Male	1985	459 ±21	25, 48	1.2491	0.026
BG10	60–69	Female	1985	525 ±30	19, 30	0.8254	0.028
BG11	19–23	Male	1998	329 ±16	21, 39	1.0313	0.026
BG12	56–59	Female	1985	502 ±28	13, 25	0.6989	0.028
BG13	39–41	Male	1985	428 ±24	31, 59	1.6424	0.028
BG14	42–47	Male	1998	423 ±26	32, 54	1.4267	0.026

[1] Both otoliths were not available for every fish chosen.

[2] Whole juvenile otoliths.

Table 4

Summary of radiometric results for pooled otolith age groups. Samples are listed in order of increasing age-group range. Activities are expressed as disintegrations per minute, per gram (dpm/g). Radium-226 activity was averaged among samples with low analytical error (<10%; n=7) and was determined to be 0.0643 (±0.0035) dpm/g. This value was then applied to all samples to gain an estimate of ^{226}Ra activity and radiometric age. Agreement between radiometric age and predicted age was qualified by the degree of overlap between the two age ranges. Radiometric age incorporates the time between capture and analysis.

Sample number	^{210}Pb activity (dpm/g) ±%s[1]	^{210}Pb:^{226}Ra activity ratio	Radiometric age (yr)	Radiometric age range (yr)	Predicted age group range[2]	Average age[3] (yr)	Age range agreement[4]
BG1	0.0154 ±8.6	0.234	7.1	5.4–8.7	0–3	2	Exceeds
BG2	0.0124 ±6.7	0.193	5.5	4.3–6.5	4–5	4	Overlaps
BG3	0.0118 ±5.5	0.184	5.5	4.5–6.4	4–6	4.5	Overlaps
BG4	0.0111 ±9.2	0.172	6.0	5.3–6.7	0–8	3.5	Encompasses
BG7	0.0300 ±5.6	0.467	18.0	15.2–21.4	9–19	14	Overlaps
BG11	0.0276 ±5.8	0.430	15.7	13.2–18.7	16–26	21	Overlaps
BG6	0.0440 ±4.7	0.684	22.3	16.2–30.3	22–32	27	Overlaps
BG5	0.0439 ±4.4	0.683	22.1	16.2–30.3	25–35	30	Overlaps
BG13	0.0481 ±3.8	0.749	29.3	21.8–40.4	33–47	40	Overlaps
BG8	0.0494 ±4.0	0.769	32.1	23.7–45.1	33–47	40	Overlaps
BG14	0.0499 ±3.8	0.777	45.8	37.3–59.1	36–54	45	Overlaps
BG9	0.0560 ±3.7	0.871	50.7	35.8–85.1	41–62	51	Encompasses
BG12	0.0586 ±4.7	0.912	62.9	40.7–undef.	48–67	57	Encompasses
BG10	0.0543 ±4.4	0.845	44.8	31.6 – 71.6	51–79	65	Overlaps

[1] Error calculation based on the standard deviation of ^{210}Pb activity (Wang et al., 1975).

[2] Predicted age range was extended by 14.6% of coefficient of variation (CV) associated with growth-zone–derived age estimates.

[3] The average predicted age of each radiometric age group.

[4] Definition of terms: Exceeds = radiometric age range is greater than predicted age range; Overlaps = radiometric age range partially agrees with predicted age range; Encompasses = radiometric age range was in agreement with predicted age range.

in otolith cores with expected ingrowth curves through time (Fig. 4). Of the 14 pooled otolith groups, three had radiometric age ranges that fully encompassed the predicted age range, ten resulted in overlapping age ranges, and one exceeded predicted age (Table 4). In addition, radiometric ages were in close agreement with predicted ages in a direct comparison (r^2=0.88; Fig. 5). Further t-tests indicated no significant difference in slope (t=1.92, P=0.092) or elevation (t=0.163, P=2.201) between the regression and a hypothetical agreement line (slope of 1), confirming the close agreement of radiometric age and predicted age.

Discussion

Estimation of age and growth

The growth pattern present in otoliths of blackgill rockfish was often difficult to interpret. Complications inherent to the growth pattern were the following: obscure growth zones up to age 10–15 (the ages when the otolith begins to thicken laterally), rapid transition to slower growth, conflicting or ambiguous growth patterns, and poor resolution of extremely compressed zones in old-age fish. Irregular patterns may have led to enumeration of false growth zones (checks), and the compression of the outer layers may have concealed growth zones present in older fish. This finding has been consistent among previous studies of rockfishes (Chilton and Beamish, 1982).

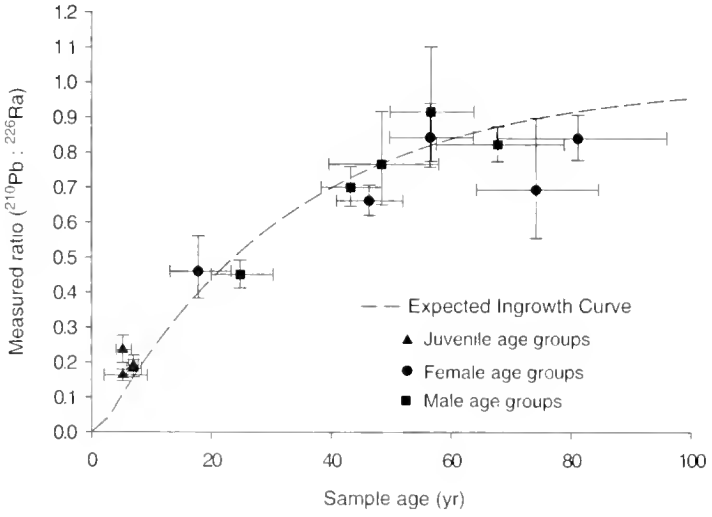

Figure 4

Measured ^{210}Pb:^{226}Ra ratio plotted against total sample age (mean predicted age plus time since capture) of blackgill rockfish (*Sebastes melanostomus*), with respect to the expected ^{210}Pb:^{226}Ra activity ratio. Horizontal error bars represent the predicted age range (based on age prediction model extended by 14.6% CV). Vertical error bars represent high and low activity ratios based on the analytical uncertainty associated with ^{210}Pb and ^{226}Ra measurements.

Because of the difficulty involved in interpreting growth patterns, aging of blackgill rockfish otoliths involved a high degree of individual subjectivity, as evidenced by the relatively low precision (D=8.4%) and high variation (CV=15%) between readers. However, there were some remarkably clear otoliths and for these we were highly confident of age estimates (Fig. 1). Overall, 87% of between-reader age estimates were within 10 years, emphasizing that although the method of interpretation of growth can be imprecise, it provides a reasonable indication of the growth characteristics and longevity of this species.

The von Bertalanffy growth parameters for male and female blackgill rockfish appear to indicate that blackgill rockfish possess distinct patterns of growth (Table 1). Female blackgill rockfish exhibited a slower growth rate than males up to approximately 25–30 years of age (Fig. 2). At this point, the male growth rate slows and approaches an asymptotic length of 448 mm, but females continue to grow in length, reaching an asymptotic length of 548 mm. This trend of slower growing, but ultimately larger females has been observed in other slope-dwelling *Sebastes* species, such as the darkblotched (*S. crameri*; Rogers et al., 2000), and splitnose (*S. diploproa*; Wilson and Boehlert, 1990) rockfishes. For both sexes, the growth coefficient is low (k=0.040–0.068) when compared to shallower-dwelling (50–200 m) rockfishes, such as the greenstriped (*S. elongates*, 0.10–0.12; Love et al., 1990) and widow (*S. entomelas*, 0.20–0.25; Williams et al., 2000) rockfishes, but very similar to other deep-dwelling, long-lived species, such as the shortspine thornyhead (*Sebastolobus alaseanus*, k=0.020; Cailliet et al., 2001), yelloweye (*S. ruberrimus*, k=0.046; Andrews et al., 2002), and bank (*S. rufus*, k=0.041; Cailliet et al., 2001) rockfishes.

Previous maturity estimates for blackgill rockfish (7–9 yr males, 6–10 yr females; Echeverria 1987), based on whole otolith counts, were much lower than estimates obtained from section ages in the present study (Table 2). Maturity estimates from our study support those derived by Butler et al. (1999), largely because the aging protocol was the same between facilities. Although our growth model included some age estimates (37%) from Butler et al. (1999), our results further confirm age at maturity (Table 2). Compared to other species of the genus, blackgill rockfish have a late maturity that resides at the upper end of the range for rockfishes (Cailliet et al., 2001; Love et al., 2002).

Extraordinarily old ages in average-size fish exhibited by the blackgill rockfish should not be dismissed as an anomaly. In this study the oldest blackgill rockfish was a 90-year-old male (aged as high as 102 years) that was 450 mm TL. This fish was 160 mm less than the maximum reported

length (Love et al., 2002). According to an experienced rockfish age and growth researcher, "some of the oldest specimens [rockfish] are rarely the largest (lengthwise), and most, if not all, are males." (Munk[2]) The reasons for this age-length pattern are beyond the scope of this study, but the implications for stock dynamics and management are that it is worthy of further consideration.

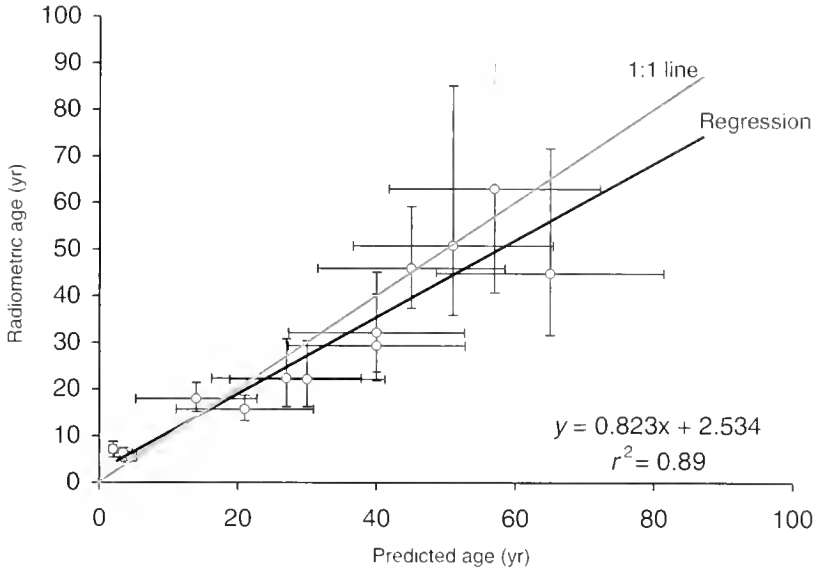

Figure 5

Direct comparison of mean predicted age and radiometric age for 14 pooled otolith age groups for blackgill rockfish (*Sebastes melanostomus*). A regression of the data points and 1:1 line of agreement are included for comparison. Horizontal error bars represent the error associated with age estimation (average predicted age multiplied by 14.6% CV), plus the standard error of the regression (1*s*) used to predict age for radiometric samples. Vertical error bars represent high and low radiometric age estimates based on the analytical uncertainty associated with ^{210}Pb and ^{226}Ra measurements.

Age prediction, age-group determination, and core extraction

The use of otolith weight as a proxy for age has benefits over conventional otolith aging methods by reducing cost, increasing sample size, and allowing greater objectivity (Boehlert, 1985; Pawson, 1990; Fletcher, 1991; Pilling et al., 2003). In this study, predicting ages from otolith weight increased the number of unsectioned otoliths that could be used in the radiometric analysis, but the prediction model also amplified the uncertainty associated with estimates of age, especially in older fish. The variance around the regression line increased with otolith weight, and log normalizing the data did not eliminate this problem. Older predicted ages, therefore, were more uncertain than younger ages (Fig. 3). Although limited to a specific otolith weight range, the prediction model presented here may provide managers with a more efficient and less costly way to investigate the age structure of blackgill rockfish stocks.

In an ideal study, otoliths from the entire estimated age range for blackgill rockfish would be available in the sample set. Otoliths from fish with predicted ages greater than 70 years, however, were not present in our study in sufficient numbers to allow age determination by radiometric methods. This was so, even though more than half of the 1200 otolith pairs obtained for ourstudy were sampled directly from commercial fishing vessels in 1985 along the coast of central and southern California, where the bulk of the fishery occurred. Because fishermen often target adult aggregations, the absence of these older individuals may be an indication that the population had already experienced depletion of older age classes at the time of sample collection, particularly if natural mortality is thought to be low for most rockfishes (Bloeser[3]). However, it is possible that the largest, oldest fish are naturally rare, even at the start of an intensive commercial fishery. Knowledge of blackgill rockfish pre-exploitation stock structure and population dynamics would help to elucidate which (depletion of older age classes or a natural situation of low numbers of older fish) is the more likely scenario.

Radiometric analysis

In previous studies the analytical uncertainty of ^{226}Ra was the limiting factor in radiometric age determination (Andrews et al., 1999a). Typically, TIMS determination of ^{226}Ra reduces error to less than 1–3% of the determined value, but technical difficulties (improperly mixed nitric acid) led to poor recovery and loss of radium in seven samples. The remaining seven samples were deemed reliable because of relatively high radium recovery, longer run times, and low analytical uncertainty as determined by the TIMS analysis routine. The ^{226}Ra activity determined for these samples was consistent

[2] Munk, K. 2002. Personal commun. Alaska Department of Fish and Game, P.O. 25526, Juneau, AK 99802.

[3] Bloeser, J. A. 1999. Diminishing returns: the status of West Coast rockfish, 94 p. Pacific Marine Conservation Council, P.O. Box 59, Astoria, OR 97103.

enough that we could assume that ^{226}Ra activities were similar among all samples and that use of an average was valid (0.0643 [±0.0035] dpm/g). This approach is acceptable because ^{226}Ra activities measured in previous radiometric studies on Pacific rockfishes were relatively constant. For example, the activity of cored yelloweye rockfish (*S. ruberrimus*) otoliths had a mean ^{226}Ra activity of 0.0312 (±0.0026) dpm/g (n=18; Andrews et al., 2002), and the rougheye rockfish (*S. aleutianus*), another deepwater species (to 730 m; Love et al., 2002), had a similar otolith core ^{226}Ra activity averaging 0.065 (±0.003) dpm/g (Kastelle et al., 2000).

Accuracy and uncertainty of ages estimates

Radiometric activities measured in blackgill rockfish otoliths generally agreed with expected activity ratios for ^{210}Pb and ^{226}Ra (Fig. 4), confirming the validity of growth-zone–derived age estimates. In addition, a direct comparison between radiometric age and predicted age resulted in a strong agreement (r^2=0.89; Fig. 5), which was further supported by slope and elevation tests that revealed no significant difference from a 1:1 agreement line.

The most critical sources of error involved in age estimation, prediction, and radiometric age determination were the following: 1) age estimate uncertainty, 2) regression error associated with predicted ages, and 3) analytical uncertainty associated with the radiometric aging technique (TIMS and α-spectrometry). Conventional aging techniques are inherently subjective (Boehlert, 1985; Campana, 2001) and thus create uncertainty associated with an estimated age. This uncertainty is transferred to the prediction model, where the natural variability associated with individual otolith weight must also be considered. For most samples, however, the error bars either overlapped or were in contact with the agreement line (Figs. 4 and 5), further confirming the concordance of radiometric age with predicted age.

Implications for management

When considering the longevity of rockfishes for which a maximum age has been reported (Munk, 2001; Cailliet et al., 2001), a longevity exceeding 90 years places the blackgill rockfish within the top 20% of long-lived rockfishes. There is a trend for rockfishes that may indicate that longevity increases as maximum depth of occurrence increases, and physiological adaptations to the environmental conditions of deep-sea living could provide an explanation (Cailliet et al., 2001). The confirmed longevity and the maximum depth of occurrence (~800 m) for the blackgill rockfish provide further support for this concept.

Longevity in the rockfishes has been central to its evolutionary success in relation to other marine teleosts. The suite of life history characters implicit with a long lifespan (slow adult growth, late age-at-maturity, low adult natural mortality) represent a "slow and steady" adaptive strategy, whereby the energy allocated towards individual growth is prolonged, eventually contributing to greater fecundity (due to larger size at maturity) over the lifespan of the individual. This reproductive strategy serves to propagate genetic material across several generations, as well as to diffuse the effect of mortality associated with each reproductive event (Leaman, 1991). In this sense, longevity may act to buffer the species against short-term (El Niño) and long-term environmental change (Pacific Decadal Oscillations), and the stochasticity inherent in the Pacific Ocean system (Moser et al., 2000).

In the absence of fishing pressure, the genetic contribution of a slow-growing, longer-lived species may be more conserved in the collective species' gene pool (Munk[2]). In the presence of fishing pressure, however, this "slow and steady" adaptation may be detrimental (Musick, 1999). Although modeling fish populations for the purpose of management typically involves some or all of these parameters, the focus is often on determining sustainable biomass and this approach largely ignores the unknown effects of changes in age structure due to removal of the oldest individuals from the population (Craig, 1985), as well as a loss of genetic diversity that could prevent full recovery of severely depleted populations (Hauser et al, 2002). Given the current depressed condition of many heavily fished rockfish stocks, species-specific life history characteristics, such as longevity, growth rate, and age-at-maturity estimates, should be given thorough consideration in the development of an effective management strategy. Management regulations that account for these characteristics, such as a limited fishing season, or designation of harvest refugia (Yoklavich, 1998), would provide a stronger basis for conservation and sustainability of the resource.

Acknowledgments

We wish to thank John Butler, Don Pearson, and Cindy Taylor of the Southwest Fisheries Science Center, Mark Wilkins, Jerry Hoff, Waldo Wakefield, and Bob Lauth of the Alaska Fisheries Science Center, and Bob Lea of CDFG for donating specimens for this study. Mary Yoklavich (NMFS), Di Tracey and Larry Paul (NIWA, New Zealand), Kristen Munk (ADFG), Don Pearson (NMFS), Tom Laidig (NMFS), and Steve Campana (DFO, Canada) provided valuable insight into blackgill rockfish growth patterns. Patrick McDonald of the Oregon Department of Fish and Wildlife aged otolith sections. Pete Holden at the University of California, Santa Cruz, measured radium in the refined samples using TIMS. The comments and suggestions of three anonymous reviewers were greatly appreciated. This work was supported by the National Sea Grant College Program of the U.S. Department of Commerce's National Oceanic and Atmospheric Administration under NOAA Grant number NA06RG0142, project number R/F-182, through the California Sea Grant College Program; and in part by the California State Resources Agency.

Literature cited

Andrews, A. H., G. M. Cailliet, and K. H. Coale.
1999a. Age and growth of the Pacific grenadier (*Coryphaenoides acrolepis*) with age estimate validation using an improved radiometric ageing technique. Can. J. Fish. Aquat. Sci. 56:1339–1350.

Andrews, A. H., K. H. Coale, J. Nowicki, C. Lundstrom, A. Palacz, and G. M. Cailliet.
1999b. Application of an ion-exchange separation technique and thermal ionization mass spectrometry to ^{226}Ra determination in otoliths for radiometric age determination of long-lived fishes. Can. J. Fish. Aquat. Sci. 56:1329–38.

Andrews, A. H., G. M. Cailliet, K. H. Coale, K. M. Munk, M. M. Mahoney and V. M. O'Connell.
2002. Radiometric age validation of the yelloweye rockfish (*Sebastes ruberrimus*) from south-eastern Alaska. Mar. Freshw. Res. 53:1–8.

Archibald, C. P., D. Fournier, and B. M. Leaman.
1983. Reconstruction of stock history and development of rehabilitation strategies for Pacific ocean perch in Queen Charlotte Sound, Canada. N. Am. J. Fish. Manag. 3:283–294.

Beamish, R. J.
1979. New information on the longevity of Pacific ocean perch (*Sebastes alutus*). J. Fish. Res. Board Can. 36:1395–1400.

Beamish, R. J., and D. A. Fournier.
1981. A method for comparing the precision of a set of age determinations. Can. J. Fish. Aquat. Sci. 38:982–983.

Beamish, R. J., and G. A. McFarlane.
1983. The forgotten requirement for age validation in fisheries biology. Trans. Am. Fish. Soc. 112(6):735–743.

Bennett, J. T., G. W. Boehlert, and K. K. Turekian.
1982. Confirmation of longevity in *Sebastes diploproa* (Pisces: Scorpaenidae) from ^{210}Pb/^{226}Ra measurements in otoliths. Mar. Biol. 71:209–215.

Boehlert, G. W.
1985. Using objective criteria and multiple regression models for age determination in fishes. Fish. Bull. 83:103–117.

Burton, E. J., A. H. Andrews, K. H. Coale, and G. M. Cailliet.
1999. Application of radiometric age determination to three long-lived fishes using ^{210}Pb:^{226}Ra disequilibria in calcified structures: a review. *In* Life in the slow lane: ecology and conservation of long-lived marine animals (J. A. Musick, ed.,), p. 77–87. Am. Fish. Soc. Symp. 23.

Butler, J. L., L. D. Jacobson, and J. T. Barnes.
1999. Stock assessment for blackgill rockfish. *In* Appendix to the status of the Pacific coast groundfish fishery through 1998 and recommended acceptable biological catches for 1999: stock assessment and fishery evaluation, 93 p. Pacific Fishery Management Council, 2130 SW Fifth Avenue, Suite 224, Portland, Oregon, 97201.

Cailliet, G. M., A. H. Andrews, E. J. Burton, D. L. Watters, D. E. Kline, and L. A. Ferry-Graham.
2001. Age determination and validation studies of marine fishes: do deep-dwellers live longer? Exp. Gerontology 36:739–764.

Campana, S. E.
2001. Accuracy, precision and quality control in age determination, including a review of the use and abuse of age validation methods. J. Fish Biology 59:197–242.

Campana, S. E., K. C. Zwanenburg, and J. N. Smith.
1990. ^{210}Pb/^{226}Ra determination of longevity in redfish. Can. J. Fish. Aquat. Sci. 47:163–165.

Chang, W. Y. B.
1982. A statistical method of evaluating the reproducibility of age determination. Can. J. Fish. Aquat. Sci. 48:734–750.

Chilton, D. E., and R. J. Beamish.
1982. Age determination methods for fishes studied by the Groundfish Program at the Pacific Biological Station, 102 p. Can. Spec.Pub. Fish. Aquat. Sci. 60.

Craig, J. F.
1985. Aging in fish. Can. J. Zoology 63:1–8.

Cross, J. N.
1987. Demersal fishes of the upper continental slope off southern California. CalCOFI Report 28:155–167.

Echeverria, T. W.
1987. Thirty-four species of California rockfishes: maturity and seasonality of reproduction. Fish. Bull. 85:229–249.

Echeverria, T. W., and W. H. Lenarz.
1984. Conversions between total, fork, and standard length in 35 species of *Sebastes* from California. Fish. Bull. 82:249–251.

Fletcher, W. J.
1991. A test of the relationship between otolith weight and age for the pilchard *Sardinops neopilchardus*. Can. J. Fish. Aquat. Sci. 48:35–38.

Flynn, W. W.
1968. The determination of low levels of polonium-210 in environmental materials. Anal. Chimica Acta. 43: 221–227.

Francis, R. I. C. C.
2003. The precision of otolith radiometric ageing of fish and the effect of within-sample heterogeneity. Can. J. Fish. Aquat. Sci. 60:441–447.

Hauser, L., G. J. Adcock, P. J. Smith, J. H. Bernal Ramirez, and G. R. Carvalho.
2002. Loss of microsatellite diversity and low effective population size in an overexploited population of New Zealand snapper (*Pagrus auratus*). Proc. Nat Acad. Sci. 99(18):11742–11747.

Kastelle, C. R., D. K. Kimura, and S. R. Jay.
2000. Using Pb^{210}/Ra^{226} disequilibrium to validate conventional ages in Scorpaenids (*sic*) (genera *Sebastes* and *Sebastolobus*). Fish. Res. 46:299–312.

Leaman, B. L.
1991. Reproductive style and life history variables relative to exploitation and management of *Sebastes* stocks. Environ. Biol. Fishes 30: 253–271.

Love, M. S., P. Morris, M. McCrae, and R. Collins.
1990. Life history aspects of 19 rockfish species (Scorpaenidae: Sebastes) from the southern California Bight, 38 p. NOAA Technical Report. NMFS 87.

Love, M. S., M. M. Yoklavich, L. Thorsteinson, and J. Butler.
2002. The rockfishes of the Northeast Pacific, 405 p. Univ. California Press, Berkeley, CA.

Mace, P. M., J. M. Fenaughty, R. P. Coburn, and I. J. Doonan.
1990. Growth and productivity of orange roughy (*Hoplostethus atlanticus*) on the north Chatham Rise. New Zealand J. Mar. Fresh. Res. 24:105–109.

Mahoney, M. M.
2002. Age, growth and radiometric age validation of the blackgill rockfish, *Sebastes melanostomus*. M.Sc. thesis, 70 p. California State Univ., San Francisco, CA. [Available from: Moss Landing Marine Labora-

tories, 8272 Moss Landing Road, Moss Landing, CA 95039.]

Moser, H. G., and E. H. Ahlstrom.
1978. Larvae and pelagic juveniles of blackgill rockfish, *Sebastes melanostomus*, taken in midwater trawls off southern California and Baja California. J. Fish. Res. Board Can. 35:981–996.

Moser, H. G. R. L. Charter, W. Watson, D. A. Ambrose, J. L. Butler, S. R. Charter, and E. M. Sandknop.
2000. Abundance and distribution of rockfish (*Sebastes*) larvae in the southern California Bight in relation to environmental conditions and fishery exploitation. CalCOFI Report 41:132–147.

Musick, J. A.
1999. Ecology and conservation of long-lived marine animals. *In* Life in the slow lane: ecology and conservation of long-lived marine animals (J. A. Musick, ed.), p. 1–10. Am. Fish. Soc. Symp. 23.

Munk, K. M.
2001. Maximum ages of groundfishes in waters off Alaska and British Columbia and considerations of age determination. Alaska Fish. Res. Bull. 8(1):12–21.

NOAA (National Oceanic and Atmospheric Administration).
2001. Magnuson-Stevens Act Provisions; Fisheries off West Coast states and in the western Pacific; Pacific coast groundfish fishery; annual specifications and management measures. Federal Register 66:8, 2338–2355.

Pawson, M. G.
1990. Using otolith weight to age fish. Fish. Biol. 36:521–531.

Pilling, G. M., E. M. Grandcourt, and G. P. Kirkwood.
2003. The utility of otolith weight as a predictor of age in the emperor *Lethrinus mahsena* and other tropical fish species. Fish. Res. 60:493–506.

Rogers, J. B., R. D. Methot, T. L. Builder, K. Piner, and M. Wilkins.
2000. Status of the darkblotched rockfish (*Sebastes crameri*) resource in 2000. *In* Appendix to the status of the Pacific Coast groundfish fishery through 2000 and recommended acceptable biological catches for 2001: stock assessment and fishery evaluation, 79 p. Pacific Fishery Management Council, 2130 SW Fifth Ave., Suite 224, Portland, OR 97201.

Smith, J. N., R. Nelson, and S. E. Campana.
1991. The use of Pb-210/Ra-226 and Th-228/Ra-228 disequilibria in the ageing of otoliths of marine fish. *In* Radionuclides in the study of marine processes (P. J. Kershaw and D. S. Woodhead, eds.), p. 350–359. Elsevier Applied Science, New York, NY.

Wang, C. H., D. L. Willis, and W. D. Loveland.
1975. Radiotracer methodology in the biological, environmental, and physical sciences, 480 p. Prentice Hall, Englewood Cliffs, NJ.

Williams, E. H., A. D. MacCall, S. V. Ralston, and D. E. Pearson.
2000. Status of the widow rockfish resource in 2000. *In* Appendix to the status of the Pacific Coast groundfish fishery through 1999 and recommended acceptable biological catches for 2000, 75 p. Pacific Fishery Management Council, 2130 SW Fifth Ave., Suite 224, Portland, OR 97201.

Williams, E. K., and S. R. Ralston.
2002. Distribution and co-occurrence of rockfishes (family: Sebastidae) over trawlable shelf and slope habitats of California and southern Oregon. Fish. Bull. 100:836–855.

Wilson, C. D., and G. W. Boehlert.
1990. The effects of different otolith ageing techniques on estimates of growth and mortality for the splitnose rockfish, *Sebastes diploproa*, and canary rockfish, *S. pinniger*. Calif. Fish Game 76:146–160.

Yoklavich, M. (ed).
1998. Marine harvest refugia for West Coast rockfish: a workshop, 162 p. NOAA-Tech. Memo. NMFS-SWFSC-255.

Descriptions of larval, prejuvenile, and juvenile finescale menhaden (*Brevoortia gunteri*) (family Clupeidae), and comparisons to gulf menhaden (*B. patronus*)

James M. Tolan

Texas Parks and Wildlife Department
6300 Ocean Dr., NRC 2501
Corpus Christi, Texas 78412
E-mail address: James.Tolan@tpwd.state.tx.us

David A. Newstead

Center for Coastal Studies
Texas A&M University–Corpus Christi
6300 Ocean Dr., NRC 3216
Corpus Christi, Texas 78412

Abstract—Larval and juvenile development of finescale menhaden (*Brevoortia gunteri*) is described for the first time by using wild-caught individuals from Nueces Bay, Texas, and is compared with larval and juvenile development of co-occurring gulf menhaden (*B. patronus*). Meristics, morphometrics, and pigmentation patterns were examined as development proceeded. An illustrated series of finescale menhaden is presented to show changes that occurred during development. For finescale menhaden, transformation to the juvenile stage was completed by 17–19 mm standard length (SL). By contrast, transformation to the juvenile stage for gulf menhaden was not complete until 23–25 mm SL. Characteristics useful for separating larval and juvenile finescale menhaden from gulf menhaden included 1) the presence or absence of pigment at the base of the insertion of the pelvic fins; 2) the standard length at which medial predorsal pigment occurs; 3) differences in the number of dorsal fin ray elements; and, 4) the number of vertebrae.

Manuscript submitted 9 September 2003 to the Scientific Editor's Office.

Manuscript approved for publication 14 June 2004 by the Scientific Editor.

Fish. Bull. 102:723–732 (2004).

Finescale menhaden (*Brevoortia gunteri* Hildebrand), one of three recognized species of menhaden (Reintjes, 1969; Hettler, 1984) found in the Gulf of Mexico, occurs in the northern and western Gulf of Mexico, from Chandeleur Bay, Louisiana, to Campeche Bay, west of Punto Morros (McEachran and Fechhelm, 1998). Despite their common occurrence in coastal and estuarine waters along the Texas and Mexico coasts (Simmons, 1957; Hellier, 1962; Hoese, 1965; Whitehead, 1985; Castillo-Rivera and Kobelkowsky, 2000), their early development has not been described. Early development of gulf menhaden (*B. patronus* Goode), on the other hand, has been well described (Suttkus, 1956; Hettler, 1984; Ahrenholz, 1991).

In coastal waters of the western Gulf of Mexico, finescale menhaden are spatially and temporally sympatric with gulf menhaden (Castillo-Rivera et al., 1996). Gulf menhaden are found throughout the northern gulf from Florida Bay to Campeche Bay. Yellowfin menhaden (*B. smithi* Hildebrand) are found in the eastern gulf from the Mississippi River Delta to Cape Lookout, North Carolina, and co-occur with finescale menhaden only in its extreme western range (Dahlberg, 1970; Hoese and Moore, 1977). A large amount of hybrid introgression occurs between gulf and yellowfin menhaden, although finescale hybrids (either finescale×gulf menhaden or finescale×yellowfin menhaden) have not been reported (Ahrenholz, 1991).

Both finescale and gulf menhaden are estuarine-dependent species inhabiting shallow nursery areas for their early development (Gunter, 1945; Shaw et al., 1985; Castillo-Rivera and Kobelkowsky, 2000). Gulf menhaden are intermittent or multiple spawners (Christmas and Waller, 1975; Lewis and Roithmayr, 1981), and adults move offshore in late summer and early fall. Spawning off the coast of Texas is protracted, and the spawning season begins at the end of August and continues through April (Shaw et al., 1985). Estuarine immigration of gulf menhaden ranging in size from 10 to 32 mm TL has been observed from late October through April (Copeland, 1965; Gallaway and Strawn, 1974; Allshouse, 1983). In Nueces Bay, the greatest densities of gulf menhaden larvae are seen from late February to early May, and the peak immigration of 19–26 mm TL individuals occurs from late April and early May (Newstead, 2003). Finescale menhaden spawn in estuarine or nearshore areas (Gunter, 1945; Simmons, 1957) and their spawning season has been reported from November to March (Ahrenholz, 1991). Hellier (1962) reported 25-mm-TL specimens taken from the Upper Laguna Madre

on the lower Texas coast during February, and Gunter (1945), Simmons (1957), and Hoese (1965) have reported postlarval finescale menhaden from the middle and lower Texas coasts from January to May. Gulf menhaden have received considerable attention in fishery science because of their large population sizes and resulting ecological and economic importance in the northern Gulf of Mexico (Nelson and Ahrenholz, 1981; Smith, 1991), whereas finescale menhaden are less numerous and not directly sought by any recognized fishery (Ahrenholz, 1991). Our study describes for the first time the development of postflexion (late larval), prejuvenile, and juvenile finescale menhaden.

Materials and methods

A total of 170 wild-caught finescale menhaden larvae and juveniles were used to describe early development. All specimens came from ichthyoplankton collections in Nueces Bay, Texas (27.87°N, 97.51°W), during May and June 2003. Individuals were collected in the tidal channels of Nueces Delta with a side-mounted push net (60-cm ring net, 0.505-mm mesh). For comparison, 357 wild-caught gulf menhaden larvae and juveniles collected during May and June of 1999, 2000, and 2002 from two nearby stations outside the delta (less than 1.5 km away), in addition to the tidal channel collections of 2003, were also studied. All individuals were initially fixed in either 10% formalin or 95% ethanol and transferred to fresh 95% ethanol after 48 hours.

Pigment patterns were recorded and specimens of finescale menhaden were illustrated. Gulf menhaden were not illustrated because the figures in Hettler (1984) are adequate.

Morphometrics

Body measurements were made to the nearest 0.1 mm with an ocular micrometer fitted to a dissecting microscope. All individuals collected were postflexion, prejuvenile, or juvenile stage as defined in Leis and Rennis (1983), and standard length (SL) was measured as the distance from the tip of the snout along the midline to a vertical line through the posterior edge of the hypural plate. All lengths are SL unless otherwise noted. Definitions and other terms are as follows:

BD = body depth; vertical depth at the pectoral symphysis.
CP = caudal peduncle; horizontal distance from the posterior edge of the dorsal fin base to the posterior edge of the hypural plate.
EYE = eye diameter; horizontal distance between the anterior and posterior edges of the fleshy orbit.
PAL = preanal length; distance from the tip of the snout to the origin of the anal fin, measured along the midline.

Ratios of these four body proportion measurements in relation to SL were fitted by means of nonlinear least squares regression techniques (SigmaPlot, version 5.0, SPSS Inc., Chicago, IL) in order to graphically illustrate any development differences between the two species. Increasing ratios (BD/SL, CP/SL, and EYE/SL) were described with an exponential rise-to-maximum equation:

$$y = a(1 - e^{-bx}),$$

whereas, the decreasing ratio of PAL/SL measurements were described with a exponential decay equation:

$$y = ae^{-bx}.$$

In both equations, y = body proportion ratio; x = SL; a = intercept; and b = SL specific exponential rate of change.

Meristics

Each specimen was examined to determine whether scale formation had been initiated, and a total count of ventral scutes for specimens in which they were sufficiently developed was obtained. A total of 37 finescale and 48 gulf menhaden from the 2003 collections were cleared and stained according to Potthoff (1984) and used for fin-ray and vertebrae counts. Because of the difficulty in accurately counting myomeres in transforming clupeids (Hettler, 1984; Ditty et al., 1994), we chose to count total vertebrae and use the number of postdorsal and preanal vertebrae instead of postdorsal and preanal myomeres as a potential diagnostic character. Fin-ray counts included dorsal, anal, and caudal fins (both principal and procurrent rays).

Results

Morphological development

Finescale menhaden larvae were first collected at 9.7 mm and ranged to 22.5 mm as transforming juveniles (Fig. 1). Transformation from the larval to the juvenile form began around 14 mm and was completed by around 20 mm (Fig 2). Ratios of body depth, caudal peduncle, and eye diameter all increased in relation to standard length as larvae grew, whereas snout-to-anal length decreased (Table 1). The decrease in snout-to-anal length reflected the transformation from the elongate fusiform shape of the larvae to the laterally compressed deep-bodied shape of the juvenile. Scales began to form at around 15 mm on the caudal peduncle region and progressed forward along the ventral and lateral surfaces towards the dorsal surface. None of the individuals examined had the enlarged and fringed median scales preceding the dorsal fin, which are an adult characteristic of the genus *Brevoortia*. Ventral scutes also began forming around 15 mm, and the full complement of 27–31 scutes (McEachran and Fechhelm, 1998) was found by 19 mm.

Gulf menhaden ranged from 11.7 mm as larvae to 40.4 mm juveniles. For gulf menhaden, body depth,

Table 1

Proportional measurements in relation to standard length (SL) used to describe finescale menhaden (*Brevoortia gunteri*) larval development.

Length class (mm, SL)	Number of specimens	Body depth: SL	Preanal length: SL	Caudal peduncle: SL	Eye diameter: SL
<11.0	1	0.100	0.804	0.256	0.054
11.1–12.0	2	0.108	0.798	0.259	0.059
12.1–13.0	5	0.119	0.778	0.251	0.059
13.1–14.0	15	0.139	0.764	0.263	0.064
14.1–15.0	28	0.136	0.756	0.269	0.062
15.1–16.0	25	0.168	0.735	0.281	0.074
16.1–17.0	23	0.208	0.711	0.302	0.082
17.1–18.0	17	0.220	0.705	0.311	0.085
18.1–19.0	3	0.239	0.700	0.327	0.080
19.1–20.0	2	0.219	0.700	0.304	0.078
>20.1	1	0.318	0.690	0.304	0.093

caudal peduncle, and eye diameter ratios all similarly increased in relation to standard length as larvae grew, whereas snout-to-anal length decreased (Table 2). Scale initiation in gulf menhaden was not seen until 19 mm, and ventral scutes did not begin forming until around 18 mm. The full complement of scutes (28–32 scutes; McEachran and Fechhelm, 1998) was seen by around 25 mm. No enlarged median dorsal scales were noted from the gulf menhaden individuals examined.

With little overlap in the 15–20 mm size range (see Fig. 1) and a limited number of juvenile-size finescale menhaden (SL>20 mm), it was not possible to effectively separate finescale and gulf menhaden morphometrically on the basis of BD:SL, PAL:SL, CP:SL, and EYE:SL ratios (Fig 3). By 25 mm, proportional body measurements had become nearly constant for gulf menhaden whereas body measurements were still changing for finescale menhaden even though they appeared to be fully transformed. For a fish of given size, finescale menhaden typically had a greater body depth, a shorter preanal length, and a greater caudal peduncle length than gulf menhaden.

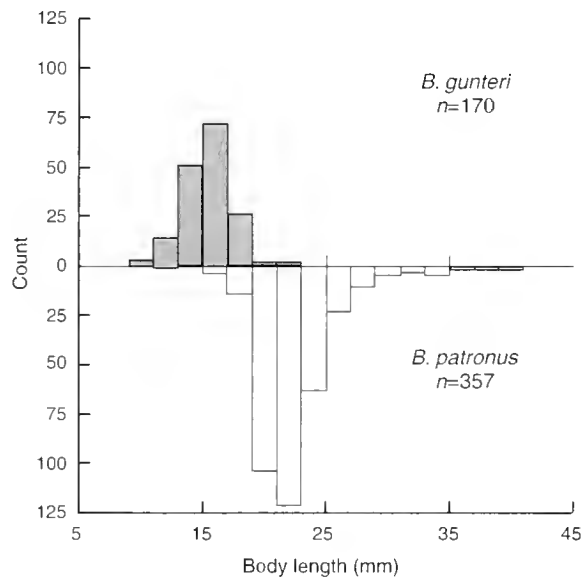

Figure 1

Length-frequency histograms for *Brevoortia gunteri* and *B. patronus* derived from ichthyoplankton collections in Nueces Bay, Texas, during May and June (1999–2003).

Meristic features

No recently hatched or preflexion finescale menhaden were examined and all postflexion individuals followed the fin development sequence identified for other clupeids (Houde et al., 1974; Hettler, 1984; Ditty et al., 1994). The caudal and dorsal fins are first to develop, followed by the pelvic fins, whereas the pectoral fins are the last to fully develop even though the pectorals are the first fins to form as nonrayed buds. Only vertebrae and dorsal-fin ray counts were useful in separating finescale and gulf menhaden, because most other meristics overlapped (Table 3). Finescale menhaden had fewer total vertebrae (=43 vs. 46) and fewer dorsal-fin rays (median value=18 vs. 21) than gulf menhaden. Postdorsal and preanal vertebrae also showed a high degree of overlap between the two species (Table 3). The forward movement of the anal fin in relation to the dorsal fin was most evident in fully transformed gulf menhaden, and the number of postdorsal-preanal vertebrae decreased from 4 to −3. The relative placement of the anal fin also

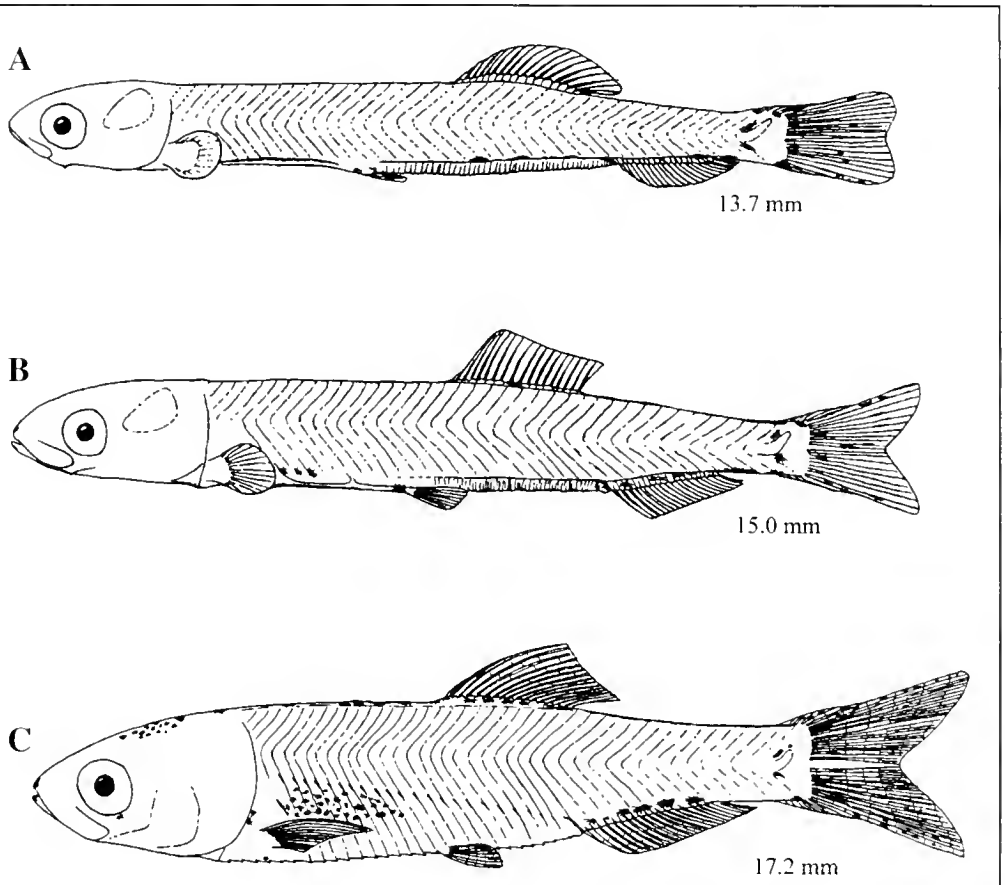

Figure 2

Developmental stages of *Brevoortia gunteri*. (**A**) Postflexion larva, 13.7 mm. (**B**) Postflexion larva, 15.0 mm. (**C**) Transforming larva, 17.2 mm. (**D**) Transforming larva, 19.0 mm. (**E**) Transformed juvenile, 23.9 mm.

Table 2

Proportional measurements relative to standard length (SL) used to describe gulf menhaden (*Brevoortia patronus*) larval development.

Length class (mm, SL)	Number of specimens	Body depth: SL	Preanal length: SL	Caudal peduncle: SL	Eye diameter: SL
<14.0	1	0.086	0.829	0.229	0.061
14.1–15.0	1	0.119	0.786	0.238	0.061
15.1–16.0	3	0.136	0.764	0.261	0.063
16.1–17.0	4	0.136	0.764	0.261	0.063
17.1–18.0	5	0.144	0.749	0.257	0.065
18.1–19.0	13	0.169	0.733	0.265	0.067
19.1–20.0	26	0.183	0.725	0.274	0.074
20.1–21.0	22	0.176	0.735	0.271	0.068
21.1–22.0	17	0.236	0.719	0.282	0.084
22.1–24.0	9	0.286	0.709	0.298	0.095
24.1–26.0	2	0.337	0.730	0.313	0.103
26.1–29.0	11	0.352	0.730	0.299	0.098
29.1–32.0	4	0.356	0.740	0.308	0.100
>32.1	3	0.380	0.736	0.294	0.097

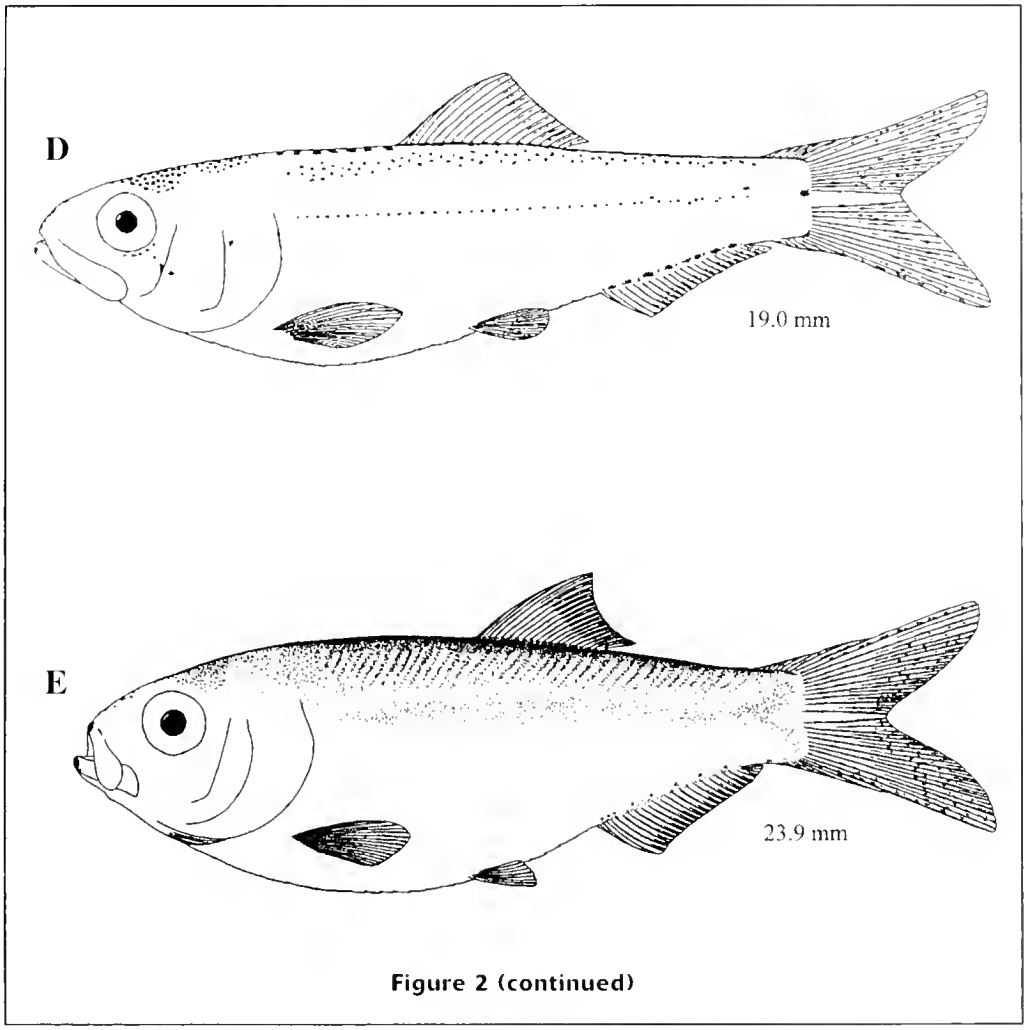

Figure 2 (continued)

Table 3

Meristics in finescale menhaden, *Brevoortia gunteri*, (37 specimens) and in gulf menhaden, *B. patronus*, (48 specimens). Median values are given in parentheses.

			Number in full complement	
Meristic	*B. gunteri*	*B. patronus*	*B. gunteri*	*B. patronus*
Caudal-fin rays				
Principal (dorsal)	10	10		10–11
(ventral)	9	9		9–10
Procurrent (dorsal)	7–9 (8)	8–9 (8)		8–9
(ventral)	7–8 (7)	5[1]–8 (7)		7–8
Dorsal-fin rays	17–20 (18)	16[1]–23 (21)	17–20	21–23
Anal-fin rays	18–24 (22)	20–23 (21)	20–25	18–22
Vertebrae	43–44 (43)	40[1]–46 (46)	42–44	45–46
Postdorsal and preanal vertebrae	0–3 (2)	–3[2]–4 (1)		2–4[3]

[1] *B. patronus* larva SL=11.7 mm.

[2] *B. patronus* fully transformed individual SL=40.4 mm.

[3] Postdorsal and preanal myomere counts in larvae 10–15 mm SL (Ditty et al., 1994)

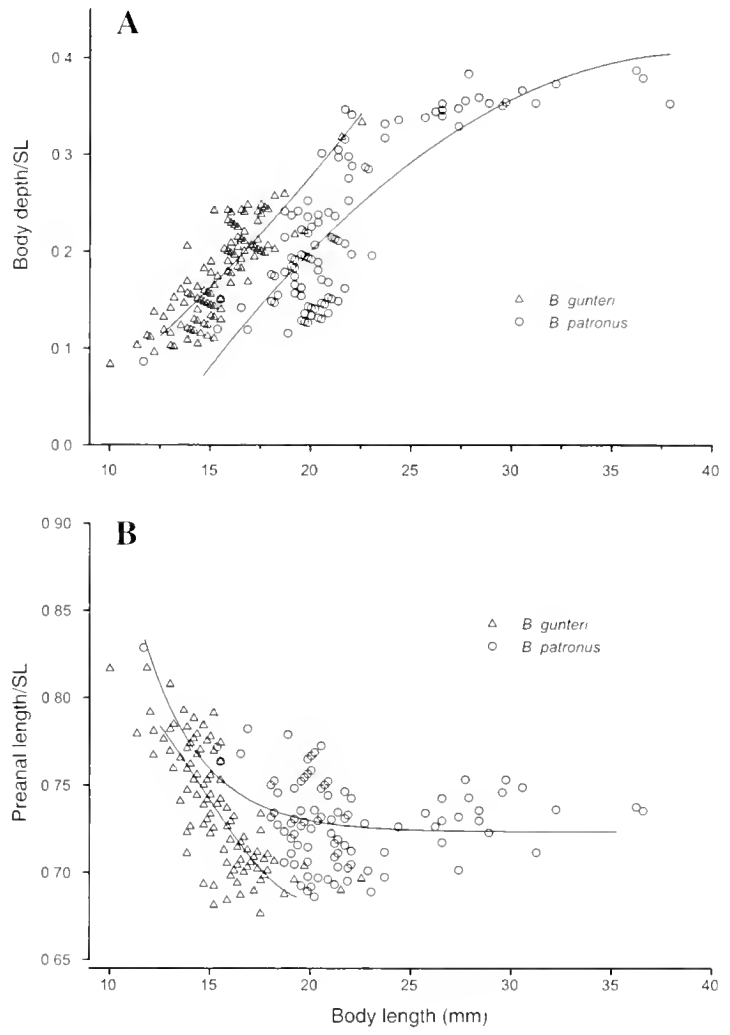

Figure 3

Morphometric comparisons (shown as a percentage of standard length [SL]) for wild-caught *Brevoortia gunteri* and *B. patronus*. (**A**) BD/SL. (**B**) PAL/SL. (**C**) CP/SL. (**D**) EYE/SL. Best fit nonlinear regression lines were fitted by least squares estimation.

changed in finescale menhaden, although the number of postdorsal-preanal vertebrae only decreased from three to zero.

Pigmentation

Early pigmentation patterns in finescale menhaden (Fig. 2) were similar, but not identical, to the pigmentation described for gulf menhaden (Suttkus, 1956; Hettler, 1984). Both dorsal and ventral notochord tip pigment, which are diagnostic for the genus *Brevoortia* (Fig. 2), were found in all individuals examined. In specimens <14 mm, pigmentation was sparse and found primarily along the ventral margin of the caudal peduncle, the base of the anal fin, at the end of the gut near the vent, and ventrally as two lines beginning at the pectoral fin bases below the foregut. Along the dorsal margin of the hindgut, 3–6 fine melanophores were usually present. At the base of the pelvic fins, 1–2 small, paired stellate melanophores were present. Additionally, all individuals had a medial melanophore along the isthmus (ventral midline anterior to the cleithrum) and most had an internal melanophore at the nape. Other pigment present in the smallest finescale larvae included a series of paired melanophores anterior to the dorsal fin base (seen in 26% of the larvae examined). This predorsal mid-line pigment series increased both in size and number as the larvae grew. The head was unpigmented.

By 16 mm, pigment increased along the dorsal surface of the hindgut, the base of the dorsal fin, and the

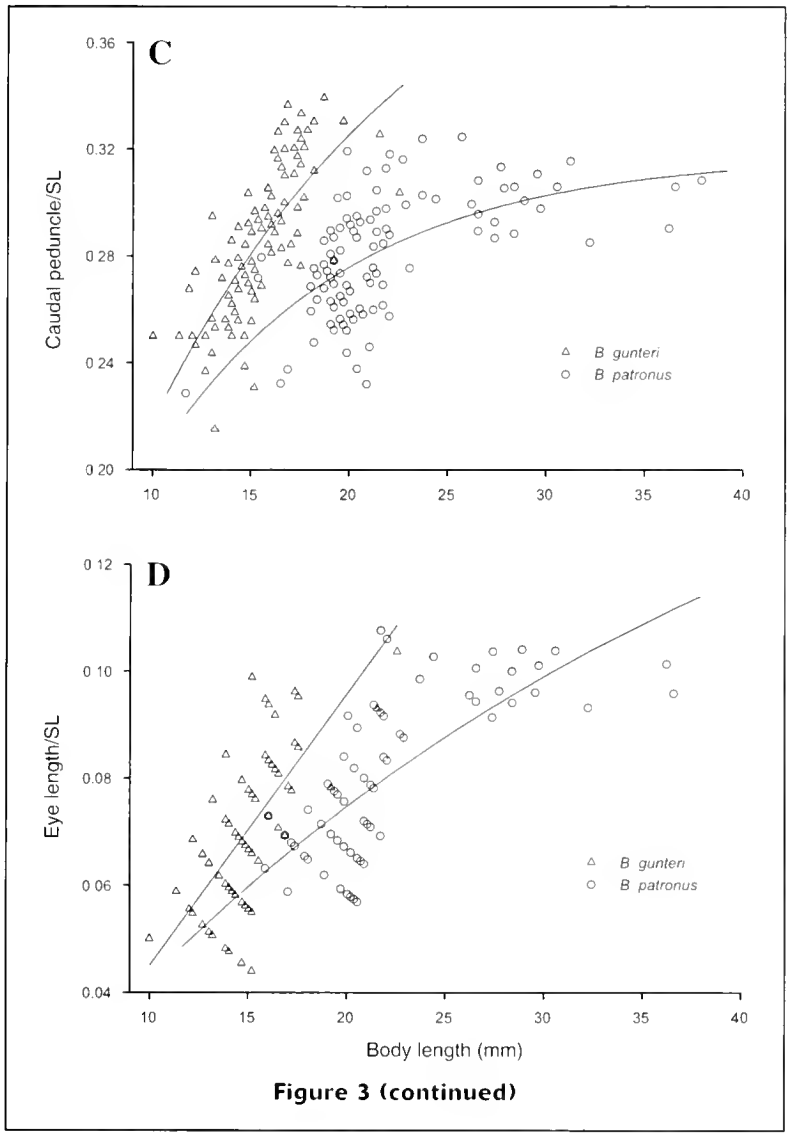

Figure 3 (continued)

base of the anal fin (Fig. 2). The predorsal midline melanophores series was more prominent (51% of the individuals displayed this pigment pattern). Additional pigmentation included paired lateral melanophores near the dorsal region of the brain cavity, internal pigment above the notochord from the posterior margin of the base of the dorsal fin to the caudal fin, and internal pigment over the gas bladder. A large melanophore was also present above the base of the pectoral fin.

By 18 mm, the dorsal surface of the head became highly pigmented with up to 25 small melanophores. The snout, lower jaw, and pelvic fins were also pigmented by this size. The dorsal and ventral surfaces of the caudal peduncle, as well as the medial predorsal region became more densely pigmented. Outstanding features at this size included 2–9 ventrolateral melanophores in a series along the digestive tract level with the pectoral fins, and isthmus pigment was separated into two spots in many individuals. By 20 mm, the head region was heavily pigmented and the mid-line predorsal pigment progressed fully to the head. Ventrolaterally, 10–30 melanophores forming a triangular pattern covered much of the digestive tract. New pigmentation features at this size included 1–3 small melanophores at the base of the eye and an internal series below the notochord from the base of the dorsal fin to the caudal fin. Pigmentation at the pelvic fin insertion was lost in some specimens, although it was still visible internally in all but one of the cleared and stained specimens. Isthmus pigmentation was also lost at this size.

Living juveniles (>20 mm) are silvery in color over most of the body. The head, back, and dorsal and caudal fins are all pigmented. In preservation, two dark, slash-like pigments spots were present on the posterior lateral body above and below the urostyle. In nearly all other aspects, juvenile finescale menhaden closely

resembled adults by this size. No humeral spots were noted in the two individuals examined.

Discussion

Finescale menhaden larvae resemble the larvae of other clupeids (Houde and Fore, 1973; Jones et al., 1978; McGowan and Berry, 1983; Hettler, 1984; Ditty et al., 1994) in having elongate, slender bodies, light pigmentation, and a small head lacking spines. They have a long, straight gut, often with striations along the hindgut, posteriorly placed dorsal and anal fins, and the vent is always posterior to the dorsal fin base (Jones et al., 1978). Hettler (1984) discussed the separation of individual species of *Brevoortia*, and Ditty et al. (1994) presented a synopsis of characters to separate clupeid larvae (<15 mm) based on meristic, morphometrics, and pigmentation. Finescale menhaden have 43–44 vertebrae, whereas gulf menhaden have 44–46. Yellowfin menhaden are reported to have 45–47 vertebrae (Houde and Swanson, 1975). The number of vertebrae, which should approximate the number of myomeres in larvae much smaller than those collected in this study, in conjunction with pigment differences have been shown to be useful in separating clupeid species complexes (Ditty et al., 1994). In the western gulf, counts of 43–44 vertebrae (=myomeres) would separate finescale menhaden from other clupeid larvae such as *Sardinella aurita* (45–47 vertebrae; Ditty et al., 1994), *Etrumeus teres* (48–50 vertebrae; Fahay, 1983), and *Opisthonema oglinum* (45–46 vertebrae; Richards et al., 1974). Species from the western gulf with similar vertebral counts (*Harengula jaguana*, 39–42; Houde et al., 1974; and *Jenkinsia lamprotaenia*, 39–42; Powles, 1977) can be distinguished from finescale menhaden by their larger PAL:SL ratio (>85% at 15 mm for *Harengula* vs. <85% for finescale menhaden, Table 1) and fewer anal rays (13–14 for *Jenkinsia* vs. 18–24 for finescale menhaden, Table 3). Although vertebral counts were used successfully in distinguishing finescale menhaden from gulf menhaden, the time necessary to clear and stain larvae makes this method impractical for distinguishing between large numbers of menhaden.

In larval and prejuvenile stages, finescale and gulf menhaden are morphologically very similar. Proportional body measurements overlapped too greatly to reliably distinguish the two species. Only the presence of medial predorsal pigment prior to transformation, stellate melanophores at the pelvic fin base, and the size at transformation were useful characters in distinguishing the two species. Hettler (1984) noted that gulf menhaden lack paired melanophores in the predorsal region until initiation of transformation. Pigment at the pelvic fin base appears to be a diagnostic character for the small-scale menhadens because Houde and Swanson (1975) also reported a similar feature in yellowfin menhaden as small as 12.3 mm. Although the presence of this pigment at the pelvic fin base is proposed to be diagnostic for the small-scale menhadens (present study), Hettler's (1984) illustration of a 16.5-mm gulf menhaden shows this pigment. Pigmentation descriptions for developing gulf menhaden have not specifically addressed melanophores at the pelvic fin insertion (Hettler, 1984). Finescale menhaden transform at a smaller size (17–19 mm) than any of the other Gulf of Mexico menhadens. Gulf menhaden did not complete transformation until around 25 mm, which is in agreement with the reported lengths of 25–28 mm for both laboratory reared and wild-caught individuals (Suttkus, 1956; Hettler, 1984). Yellowfin menhaden reach transformation at an intermediate size (20–23 mm; Houde and Swanson, 1975).

Even as adults, finescale menhaden very closely resemble gulf menhaden (Hoese and Moore, 1977) and few reliable characters effectively separate them. Only the absence of striations on the margin of the operculum, a single humeral spot (with no hint of trailing spots along the lateral margins), and more scale rows (60–77 in finescale vs. 36–50 in gulf menhaden; Hoese and Moore, 1977; McEachran and Fechhelm, 1998) distinguish finescale from gulf menhaden. All other meristics overlap greatly; i.e., counts of dorsal-fin rays, anal-fin rays, pectoral-fin rays, pelvic-fin rays, gill-raker counts, and ventral scutes. Although externally similar, significant differences in internal structure between finescale and gulf menhaden have been documented. Finescale menhaden have fewer branchiospinules and shorter intermediate gill rakers than gulf menhaden and, as such, filter mainly zooplankton from the water column; gulf menhaden, in contrast, feed primarily on phytoplankton and detritus (Castillo-Rivera et al., 1996).

Based on length-frequency differences seen between the two species (Fig. 1), the reported spawning season for finescale menhaden along the middle Texas coast could be extended to late May. We still do not know of characters that would distinguish finescale menhaden eggs, and yolksac, preflexion, and flexion larvae from other species in the genus *Brevoortia*. In order to fully describe the development of finescale menhaden, laboratory spawning and rearing experiments are needed to fully describe these early-life stages. Houde (1973) presented relatively simple rearing techniques that allow descriptions of the developmental stages of larval fish (from egg through transformation of larvae to the juvenile stage). These methods have been used successfully for Atlantic, gulf, and yellowfin menhaden, and presumably, finescale menhaden could be reared with these same techniques if their eggs could be obtained. The rearing of finescale menhaden would also allow the effectiveness of the proposed pigment characters used to separate finescale menhaden from gulf menhaden to be tested.

Acknowledgments

This work was performed with funding from the Coastal Bend Bays & Estuaries Program under contract 0203. The Texas Parks and Wildlife Department, Coastal

Studies Program, Resource Protection Division provided additional interagency cooperation in the form of equipment and field logistical support. This manuscript was improved by comments from two anonymous reviewers.

Literature cited

Ahrenholz, D. W.
1991. Population biology and life history of the North American menhadens, *Brevoortia* spp. Mar. Fish. Rev. 53(4):3–19.

Allshouse, W. C.
1983. The distribution of immigrating larval and postlarval fishes into the Aransas-Corpus Christi Bay complex. M.S. thesis, 118 p. Corpus Christi State Univ., Corpus Christi, Texas.

Castillo-Rivera, M., and A. Kobelkowsky.
2000. Distribution and segregration of two sympatric *Brevoortia* species (Teleostei:Clupeidae). Estuar. Coast. Shelf Sci. 50:593-598.

Castillo-Rivera, M., A. Kobelkowsky, and V. Zamayoa.
1996. Food resource partitioning and trophic morphology of *Brevoortia gunteri* and *B. patronus*. J. Fish Biol. 49:1102–1111.

Christmas, J. Y., and R. S. Waller.
1975. Location and time of menhaden spawning in the Gulf of Mexico, 20 p. Gulf Coast Res. Lab., Ocean Springs, MS.

Copeland, B. J.
1965. Fauna of the Aransas Pass Inlet, Texas: I. Emigration as shown by tide trap collections. Publ. Inst. Mar. Sci. Univ. Tex. 10:9–21.

Dahlberg, M. D.
1970. Atlantic and Gulf of Mexico menhadens, genus *Brevoortia* (Pisces:Clupeidae). Bull. Fla. State Mus., Biol. Sci. 15:91–162.

Ditty, J. G., E. D. Houde, and R. F. Shaw.
1994. Egg and larval development of Spanish sardine, *Sardinella aurita* (Family Clupeidae), with a synopsis of characters to identify clupeid larvae from the northern Gulf of Mexico. Bull. Mar. Sci. 54(2):367–380.

Fahay, M. P.
1983. Guide to the early stages of marine fishes occurring in the western North Atlantic Ocean, Cape Hatteras to the southern Scotian shelf. J. Northwest Atl. Fish. Sci. 4:1–423.

Gallaway, B. J., and K. Strawn.
1974. Seasonal abundance and distribution of marine fisheries at a hot-water discharge in Galveston Bay, Texas. Contr. Mar. Sci. 18:71–137.

Gunter, G.
1945. Studies on marine fishes of Texas. Publ. Inst. Mar. Sci. 1(1):1–190.

Hellier, T. R., Jr.
1962. Fish production and biomass studies in relation to photosynthesis in the Laguna Madre of Texas. Publ. Inst. Mar. Sci. Univ. Tex. 8:1–22.

Hettler, W. F.
1984. Description of eggs, larvae, and early juveniles of gulf menhaden, *Brevoortia patronus*, and comparisons with Atlantic menhaden, *B. tyrannus*, and yellowfin menhaden, *B. smithi*. Fish. Bull. 82:85–95.

Hoese, H. D.
1965. Spawning of marine fishes in the Port Aransas, Texas, area as determined by the distribution of young and larvae. Ph.D. diss., 144 p. Univ. of Texas, Austin, TX.

Hoese, H. D., and R. H. Moore.
1977. Fishes of the Gulf of Mexico: Texas, Louisiana, and adjacent waters, 327 p. Texas A&M Univ. Press, College Station.

Houde, E. D.
1973. Some recent advances and unsolved problems in the culture of marine fish larvae. Proc. World Mariculture Soc. 3:83–112.

Houde, E. D., and P. L. Fore.
1973. Guide to identify eggs and larvae of some Gulf of Mexico clupeid fishes. Fla. Dep. Nat. Resour. Mar. Res. Lab. Leafl. Ser. 4 (part 1, no. 23). 14 p.

Houde, E. D., W. J. Richards, and V. P. Sakensa.
1974. Descriptions of eggs and larvae of the scaled sardine, *Harengula jaguana*. Fish. Bull. 72:1106–1122.

Houde, E. D., and L. J. Swanson Jr.
1975. Descriptions of eggs and larvae of yellowfin menhaden, *Brevoortia smithi*. Fish. Bull. 73:660–673.

Jones, P. W., F. D. Martin, and J. D. Hardy Jr.
1978. Development of fishes of the Mid-Atlantic Bight: an atlas of egg, larvae, and juvenile stages. Vol. 1: Acipenseridae through Ictaluridae, 340 p. U.S. Dep. Inter., Biol. Serv. Prog.

Leis, J. M., and D. S. Rennis.
1983. The larvae of Indo-Pacific coral reef fishes, 269 p. Univ. Hawaii Press, Honolulu, HI.

Lewis, R. M., and C. M. Roithmayr.
1981. Spawning and sexual maturity of gulf menhaden, *Brevoortia patronus*. Fish. Bull. 78:947–951.

McEachran, J. D., and J. D. Fechhelm.
1998. Clupeidae. *In* Fishes of the Gulf of Mexico. Vol. 1: Myxiniformes to Gasterosteiformes, p. 328–346. Univ. Texas Press, Austin, TX.

McGowan, M. F., and F. H. Berry.
1983. Clupeiforms: development and relationships. *In* Ontogeny and systematics of fishes, p. 108–126. Am. Soc. Ichthyol. Herpetol., Special Publ. 1.

Nelson, W. R., and D. W. Ahrenholz.
1981. Population and fishery characteristics of gulf menhaden, *Brevoortia patronus*. Fish. Bull. 84:311–325.

Newstead, D. J.
2003. Larval fish recruitment to isolated nursery grounds in Nueces Bay, Texas. M.S. thesis, 61 p. Texas A&M Univ.-Corpus Christi, Corpus Christi, TX.

Potthoff, T.
1984. Clearing and staining techniques. *In* Ontogeny and systematics of fishes, p. 35–37. Am. Soc. Ichthyol. Herpetol., Special Publ. 1.

Powles, H.
1977. Description of larval *Jenkinsia lamprotaenia* (Clupeidae, Dussumieriinae) and their distribution off Barbados, West Indies. Bull. Mar. Sci. 27:788–801.

Reintjes, J. W.
1969. Synopsis of the biological data on Atlantic menhaden, *Brevoortia tyrannus*, 30 p. U.S. Dep. Inter., Fish Wildl. Ser., Circ. 320.

Richards, W. J., R. V. Miller, and E. D. Houde.
1974. Egg and larval development of the Atlantic thread herring, *Opisthonema oglinum*. Fish. Bull. 72:1123–1136.

Shaw, R. F., J. H. Cowan and T. L. Tillman.
1985. Distribution and density of *Brevoortia patronus*

(gulf menhaden) eggs and larvae in the continental shelf waters of western Louisiana. Bull Mar. Sci. 36(1):96–103.

Simmons, E. G.
1957. An ecological survey of the upper Laguna Madre of Texas. Publ. Inst. Mar. Sci. Univ. Tex. 4:156–200.

Smith, J. W.
1991. The Atlantic and gulf menhaden purse seine fisheries: origins, harvesting technologies, biostatistical monitoring, recent trends in fisheries statistics, and forecasting. Mar. Fish. Rev. 53(4):28–41.

Suttkus, R. D.
1956. Early life history of the gulf menhaden, *Brevoortia patronus*, in Louisiana. Trans. North Am. Wild. Conf. 21:390–407.

Whitehead, P.J .
1985. FAO species catalogue. Vol. 7. Clupeoid fishes of the world. An annotated and illustrated catalogue of the herrings, sardines, pilchards, sprats, anchovies and wolfherrings. Part 1: Chirocentridae, Clupeidae and Pristigasteridae. FAO Fish. Synop. 125, vol 7, pt 1, 303 p. FAO, Rome.

Diet of the minimal armhook squid (*Berryteuthis anonychus*) (Cephalopoda: Gonatidae) in the northeast Pacific during spring

Kazuhisa Uchikawa

National Research Institute of Far Seas Fisheries
5-7-1 Shimizu-Orido
Shizuoka, 424-8633, Japan
E-mail address: stomyct@affrc.go.jp

John R. Bower

Northern Biosphere Field Science Center, Hakodate Branch
Hokkaido University
3-1-1 Minato-cho, Hakodate
Hokkaido 041-8611, Japan

Yasuko Sato

Department of Agriculture, Forestry and Fisheries, Niigata Prefecture
Agriculture Affairs Division
Shinko-cho
Niigata 950-8570, Japan

Yasunori Sakurai

Graduate School of Fisheries Sciences
Hokkaido University
3-1-1 Minato-cho, Hakodate
Hokkaido 041-8611, Japan

Abstract—The stomach contents of the minimal armhook squid (*Berryteuthis anonychus*) were examined for 338 specimens captured in the northeast Pacific during May 1999. The specimens were collected at seven stations between 145–165°W and 39–49°N and ranged in mantle length from 10.3 to 102.2 mm. Their diet comprised seven major prey groups (copepods, chaetognaths, amphipods, euphausiids, ostracods, unidentified fish, and unidentified gelatinous prey) and was dominated by copepods and chaetognaths. Copepod prey comprised four genera, and 86% by number of the copepods were from the genus *Neocalanus*. *Neocalanus cristatus* was the most abundant prey taxa, composing 50% by mass and 35% by number of the total diet. *Parasagitta elegans* (Chaetognatha) occurred in more stomachs (47%) than any other prey taxon. Amphipods occurred in 19% of the stomachs but composed only 5% by number and 3% by mass of the total prey consumed. The four remaining prey groups (euphausiids, ostracods, unidentified fish, and unidentified gelatinous prey) together composed <2% by mass and <1% by number of the diet. There was no major change in the diet through the size range of squid examined and no evidence of cannibalism or predation on other cephalopod species.

The squid family Gonatidae plays an important role in the ecosystems of the North Pacific. In the Sea of Okhotsk, the annual production of gonatid squids is more than half that of fish production (Lapko, 1996), and in the western and central Bering Sea, gonatid production is thought to exceed that of the dominant fish families (Radchenko, 1992). In the subarctic North Pacific, the gonatids are an important link in the pelagic food web (Brodeur et al., 1999). To better understand the food web in the North Pacific and the processes influencing the production of gonatid squids in this region, information is needed on the feeding behavior of these squids.

The minimal armhook squid (*Berryteuthis anonychus*) (also known as the "smallfin gonate squid" [Roper et al., 1984]) is a small gonatid (maximum mantle length=150 mm) distributed mainly in the northeast Pacific (Roper et al., 1984; Bower et al., 2002). It is a major prey for fishes, squids, seabirds, and marine mammals (Ogi et al., 1980; Pearcy et al., 1988; Pearcy, 1991; Kuramochi et al., 1993; Pearcy et al., 1993; Ohizumi et al., 2003) but is not targeted by any fishery. Despite the importance of *B. anonychus* in the food web of the subarctic North Pacific, the only published reports on its feeding behavior are two abstracts in the Russian literature (Lapshina, 1988; Didenko, 1990). In this article, we provide further information on the feeding behavior of *B. anonychus* by describing the diet of a wide size range of squid collected from the northeast Pacific during late spring.

Methods

Berryteuthis anonychus was collected during a United States National

Manuscript submitted 2 September 2003 to the Scientific Editor's Office.

Manuscript approved for publication 29 June 2004 by the Scientific Editor.

Fish. Bull. 102:733–739 (2004).

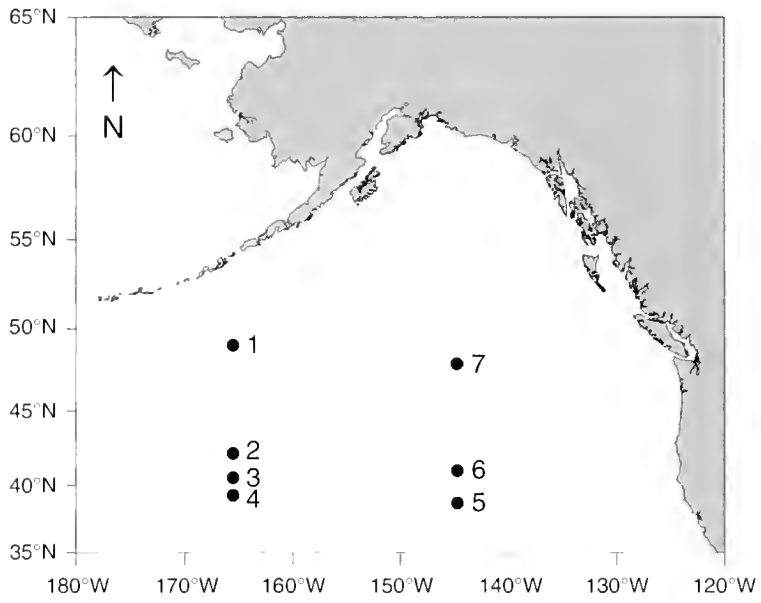

Figure 1

Sampling stations in the northeast Pacific where *Berryteuthis anonychus* were collected during May 1999. Numbers indicate station numbers.

Marine Fisheries Service (NMFS) survey of salmon in the northeast Pacific (Carlson et al., 1999; Bower et al., 2002). Samples were collected during 6–17 May 1999 at seven stations between 145–165°W and 39–49°N (Fig. 1). At each station, a midwater trawl modified to fish at the surface was towed for 1 hour. The trawl was 198 m long and had hexagonal mesh in its wings and body, and a 1.2-cm mesh liner was used in the codend. Trawling speeds were 7–9 km/h, and the average net dimensions while fishing were 16 m vertical spread and 45 m horizontal spread.

Squid samples were frozen on board to –20°C and preserved in 50% isopropyl alcohol in the laboratory. The mantle length (ML) of each squid was measured to the nearest 0.1 mm, and each squid was weighed to the nearest 0.01 g. The stomach contents of 338 squid (167 males, 144 females, 27 undetermined) ranging in ML from 10.3 to 102.2 mm (Fig. 2) were examined under a stereomicroscope. A total of 359 squid were collected during the survey (Bower et al., 2002), but 21 of these specimens were either damaged or lost, and thus excluded from our analyses. Most prey items were fragmented; therefore prey identification was usually based on diagnostic body parts as described in Brodsky (1950), Miller (1988), Baker et al. (1990), and Vinogradov et al. (1996), and by comparison with zooplankton specimens collected in the same area. The prey items were counted and weighed to the nearest 0.01 mg. These wet mass measurements presumably underestimated the initial wet masses because mass loss occurs in invertebrate samples preserved in isopropyl alcohol (e.g., Howmiller, 1972), and it was assumed all prey taxa were equally affected by the preservation. The numbers of individuals of each

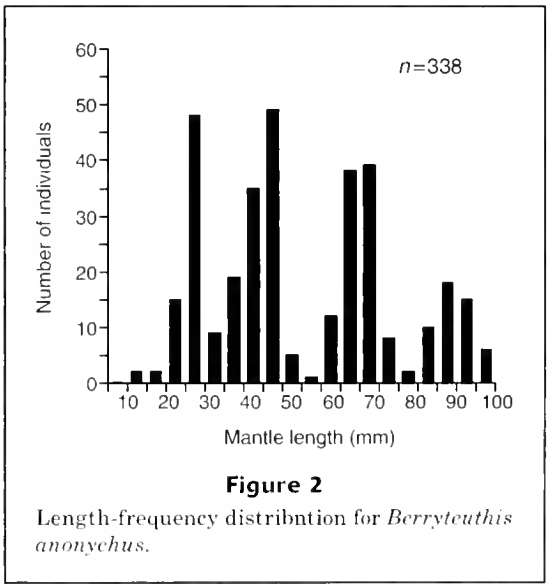

Figure 2

Length-frequency distribution for *Berryteuthis anonychus*.

prey taxon were estimated from the numbers of prey parts, such as copepod mandibles, amphipod heads and chaetognath seizing hooks. Because of the difficulty in distinguishing the copepods *Neocalanus plumchrus* and *N. flemingeri*, they were grouped as a single taxon, *N. plumchrus+flemingeri*. Some calanoid copepods that could not be identified to genus level were identified as either a "specialized form" or a "generalized form"; characters of the specialized form included appendages that were greatly enlarged or strongly developed with chelae, spines on the posterior corners of the terminal thoracic segment,

Table 1

Numbers of *Berryteuthis anonychus* stomachs with identifiable prey remains, without identifiable remains, and without remains from the northeast Pacific. Station numbers refer to those shown in Figure 1.

Station no.	With identifiable remains	Without identifiable remains	Without remains	Total
1	25	0	0	25
2	29	19	45	93
3	33	0	2	35
4	12	1	2	15
5	51	9	6	66
6	44	18	16	78
7	26	0	0	26
Total	220	47	71	338

and an asymmetrically swollen genital segment. The generalized form included calanoid copepods of the *Calanus* type that did not share any of these characters.

A stomach-contents index (SCI, %) was calculated as *SCI=(wet mass of total stomach contents/wet body mass)*×100. For each prey taxon, the percentages by number (*N*) and wet mass (*WM*) of the total prey, and the percentage frequency of occurrence (*F*) were determined. An index of relative importance (IRI) was calculated for each prey taxon as $IRI_i = F_i \times (N_i + WM_i)$ (Pinkas et al., 1971), where *i* denotes the taxon. The *IRI* for each major group of prey taxa was then standardized to *%IRI* (Cortés, 1997):

$$\%IRI_i = 100 \times IRI_i / \sum_{i}^{n} IRI_i ,$$

where *n* is the total number of groups collected.

Copepod mandible size is directly related to the carapace length of several calanoid copepods in the North Atlantic (Karlson and Båmstedt, 1994); therefore mandible width was used as an indicator of relative prey size to compare copepod prey size with squid mantle size. A total of 87 mandibles were measured from the stomachs of 10 squid measuring 29–102 mm ML.

Results

Of the 338 stomachs examined, 267 (79%) contained prey, and 220 (65%) contained identifiable prey (Table 1). Individual SCI values ranged from 0% to 8.0% (station mean=1.0%). SCI values varied significantly among sampling times (Kruskal-Wallis test, $P<0.001$), and the two highest SCI values occurred in the afternoon and just after sunset (Fig. 3).

The diet of *B. anonychus* comprised seven major prey groups and was dominated by copepods (*N*=70%, *WM*=85%, *F*=74%, *%IRI*=87%) and chaetognaths (*N*=24%, *WM*=11%, *F*=48%, *%IRI*=12%) (Table 2). The five other prey groups (amphipods, euphausiids, ostracods, unidentified fish, and unidentified gelatinous prey) each had a *%IRI* value ≤1%.

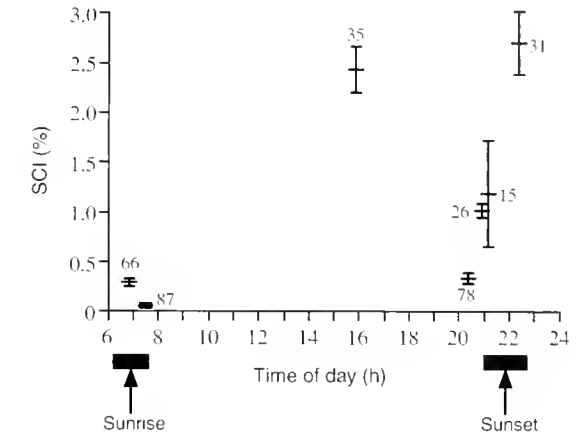

Figure 3

Mean stomach contents index (SCI) of *Berryteuthis anonychus* collected in the northeast Pacific during May 1999 at different times of day. SE = standard error of the mean. Numbers indicate squid sample size for each sampling.

Copepod prey comprised four genera, and 86% by number of the copepods were from the genus *Neocalanus*. *Neocalanus cristatus* was the most abundant prey taxa, composing 50% by mass and 35% by number of the total diet. The three *Neocalanus* taxa (*Neocalanus* spp., *N. plumchrus+flemingeri*, and *N. cristatus*) composed 85% by mass and 68% by number of the diet. *Neocalanus cristatus* was identified based on the presence of the head crest, which develops at the C5 copepodite stage (Brodsky, 1950). Thus, this taxon comprises only the C5 and C6 stages, and possible members of the *Neocalanus* spp. taxon include *N. plumchrus*, *N. flemingeri*, and earlier stages (C1–C4) of *N. cristatus*. Squid ≥60 mm ML fed mainly on *Neocalanus cristatus* (*N*=39%, *WM*=53%, *F*=50%) and *Neocalanus* spp. (*N*=29%, *WM*=31%, *F*=40%), whereas those <60 mm ML fed mainly on *Neocalanus* spp. (*N*=43%, *WM*=53%, *F*=29%) and *Neocalanus plumchrus+flemingeri* (*N*=8%, *WM*=10%, *F*=14%), and consumed few C5–C6 *Neocalanus cristatus* (*N*=4%, *WM*=4%, F=6%). The mandible size of copepod prey showed a clear positive relationship with ML (Fig. 4), indicating that the squid fed on larger copepods as the squid grew. Taxa from other copepod genera (i.e., *Candacia*, *Metridia*, and *Pleuromamma*) composed 0.5% of the total prey number and 0.1% of the total wet mass (Table 2).

Parasagitta elegans, the only identified chaetognath, occurred in more stomachs (47%) than any other prey taxon and in 58% of the stomachs from squid ≥60 mm

Table 2

Prey items identified from stomach contents of *Berryteuthis anonychus* collected in the northeast Pacific during May 1999. %IRI: standardized index of relative importance. *%IRI* values in parentheses are those for <60 mm ML and ≥60 mm ML squid. Frequency of occurrence was calculated from the number of stomachs containing food. "—" means prey taxon was not present in stomachs.

Taxon	Number (%)	Wet mass (%)	Frequency of occurrence (%)	*%IRI* (<60 mm ML, ≥60 mm ML)
Copepoda	70.2	85.3	74.2	86.5 (80.9, 84.8)
Candacia columbiae	0.2	0.1	1.9	
Candacia sp.	<0.1	<0.1	0.4	
Metridia pacifica	0.2	<0.1	2.2	
Neocalanus cristatus	35.0	50.4	23.2	
Neocalanus plumchrus+flemingeri	3.1	1.8	12.4	
Neocalanus spp.	30.0	32.3	33.3	
Pleuromamma spp.	0.1	<0.1	1.9	
Calanoida (generalized form)	0.5	0.3	4.9	
Calanoida (specialized form)	0.1	0.1	0.4	
Unidentified Calanoida	0.9	0.3	14.2	
Unidentified Copepoda	0.1	0.1	2.6	
Chaetognatha	23.9	10.8	47.6	12.4 (18.1, 13.9)
Parasagitta elegens	23.8	10.7	47.2	
Unidentified Chaetognatha	0.1	0.1	1.1	
Amphipoda	4.6	2.5	19.1	1.0 (1.0, 1.3)
Hyperia medusarum	0.8	0.9	2.2	
Themisto pacifica	2.5	0.9	7.5	
Unidentified Hyperiidae	0.4	0.5	0.7	
Unidentified Physocephalata	<0.1	<0.1	0.4	
Unidentified Hyperiidea	0.7	0.2	7.5	
Unidentified Amphipoda	0.1	<0.1	1.9	
Euphausiacea	0.5	0.9	4.5	<0.1 (<0.1, 0.1)
Euphausia pacifica	<0.1	0.4	0.5	
Thysanoessa sp.	<0.1	<0.1	0.4	
Unidentified Euphausiacea	0.5	0.5	3.7	
Ostracoda	<0.1	<0.1	1.1	<0.1 (<0.1, —)
Unidentified fish	<0.1	0.8	0.4	<0.1 (—, <0.1)
Unidentified gelatinous prey	<0.1	<0.1	0.4	<0.1 (<0.1, —)
Unidentified crustacea	0.1	<0.1	1.1	
Unidentified material	0.6	0.1	18.7	

Neocalanus plumchrus and *N. flemingeri* were grouped as a single taxon (*N. plumchrus+flemingeri*) because of difficulty in distinguishing these species in partly digested materials.

Neocalanus cristatus comprises stages C5 and C6 only.

Neocalanus spp. = *N. cristatus* (stages C1–C4), *N. plumchrus*, and *N. flemingeri*.

Calanoida (specialized form) = unidentified individuals with markedly enlarged appendages, strongly developed chelae, a spine on the posterior corner of the terminal thoracic segment, or asymmetrically swollen genital segments.

Calanoida (generalized form) = unidentified *Calanus*-type individuals that share none of the characters of the specialized form.

ML. *P. elegans* was the third most abundant prey taxon, composing 24% by number and 11% by mass of the total diet (Table 2).

Amphipods (mainly *Themisto pacifica* and *Hyperia medusarum*) were consumed by 19% of the squid but composed only 5% by number and 3% by wet mass of the total prey consumed. The four other prey groups combined composed <2% by mass and <1% by number of the diet. There were no major changes in *%IRI* values through the size range of squid examined (Table 1) and no evidence of cannibalism or predation on other cephalopod species.

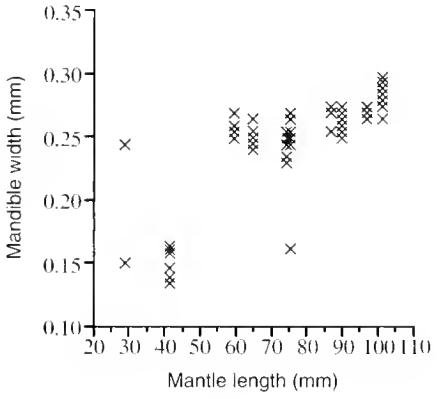

Figure 4

Relationship between mandible width of copepod prey and mantle length of *Berryteuthis anonychus*.

Discussion

The diet of *Berryteuthis anonychus* collected in the northeast Pacific during May was dominated by calanoid copepods and chaetognaths. During early July in this area, *B. anonychus* larger than those examined in the present study (ML: 75–127 mm vs. 10–102 mm) fed on a wider variety of prey, including primarily calanoid copepods, hyperiid amphipods, pteropods, and euphausiids (Lapshina, 1988). Possible causes for this change in diet include seasonal change in prey availability and an ontogenetic change in the squid's ability to capture prey.

The zooplankton composition in the upper 150 m of the subarctic North Pacific is highly seasonal. *Neocalanus* copepods, the major prey of *B. anonychus*, dominate the epipelagic zooplankton community during spring and early summer (Mackas and Tsuda, 1999). They then descend from the upper layer to spend the late summer, autumn, and early winter at 400–2000 m, well below the depth range of *B. anonychus* (0–200 m; Nesis, 1997). As a result of this ontogenetic descent, the upper ocean zooplankton biomass decreases greatly, and the community is then dominated by a different group of species. This group includes euphausiids (Mackas and Tsuda, 1999), which are consumed by more *B. anonychus* in July (28%; Lapshina, 1988) than in May (5%; present study). Other prey that show a large increase in frequency of occurrence between May and July are amphipods (19% in May, 52% in July) and pteropods (0% in May, 40% in July).

Oceanic squids such as *B. anonychus* generally feed on small crustaceans as juveniles and then shift their diet to larger fish and other cephalopods as they grow (Rodhouse and Nigmatullin, 1996). We observed no such ontogenetic shift within the size range examined, but copepod prey size was found to increase with growth. These data are consistent with those for other squids in that prey size increases during development (Nixon, 1987; Hanlon and Messenger, 1996). Most gonatids undergo ontogenetic vertical descent (Roper and Young, 1975; Nesis, 1997), and a clear shift in the diet can accompany this habitat shift (e.g., as seen in *Berryteuthis magister*; Nesis, 1997). Nesis (1997), however, suggested that *B. anonychus* does not undergo ontogenetic descent; therefore no such habitat-change–related shift in diet would be expected to occur in this species.

Highest feeding intensities were recorded in the afternoon and just after sunset, which would indicate that *B. anonychus* feeds both day and night. Such a feeding scenario is supported by the high overlap in depth distributions of *B. anonychus* (day: 50–200 m, night: 0–150 m; Nesis, 1997) and its main prey, *Neocalanus cristatus*; during spring, *N. cristatus* occurs mainly at 50–150 m, and like the other *Neocalanus* species, shows no evidence of diel vertical migration (Mackas et al., 1993). Therefore *B. anonychus* and *N. cristatus* occupy nearly the same depth range both day and night.

The chaetognath *Parasagitta elegans* was the third most abundant prey taxon and was consumed by more squid than any other taxon. *Parasagitta elegans* forms an important fraction of the springtime macrozooplankton community in the North Pacific (Brodeur and Terazaki, 1999) and inhabits mainly the epipelagic layer (0–200 m) (Kotori, 1976; Terazaki and Miller, 1986); therefore predation on *P. elegans* could also occur both day and night. Another gonatid squid, *Gonatus modokai*, has also been found to prey on *Parasagitta* sp. (Kubodera and Okutani, 1977).

There was no evidence of cannibalism, which commonly occurs in many gonatids, particularly *Berryteuthis magister* and *Gonatopsis borealis* (Lapko, 1996; Nesis, 1997). Cannibalism in squids appears to occur less frequently when prey are abundant (Shchetinnikov, 1992; Santos and Haimovici, 1997), as is the case in the North Pacific during spring. In addition, at nearly every station sampled, squid of a small size range were collected (Bower et al., 2002); therefore it seems that opportunities for intercohort cannibalism were limited.

The large stock size of *B. anonychus* in the North Pacific (Nesis, 1997) and its importance in the diet of higher predators may indicate that the food chain from copepods through squids and these higher predators is an important trophic pathway in the pelagic food web of the Subarctic Pacific during spring. The large seasonality in zooplankton composition in the upper 150 m may indicate that these trophic pathways will show similar seasonal variations.

Acknowledgments

We thank the late H. Richard Carlson for providing us with squids collected during the May 1999 NMFS salmon survey aboard the FV *Great Pacific*. We also thank Chingis Nigmatullin and the late Kir Nesis for translating two Russian abstracts into English, H. Sugi-

saki and M. Terazaki for helping identify prey, K. Ichige for helping in the laboratory, and the three anonymous reviewers of the manuscript.

Literature cited

Baker A. de C., B. P. Boden, and E. Brinton.
1990. A practical guide to the euphausiids of the world, 96 p. Natural History Museum, London.

Bower, J. R., J. M. Murphy, and Y. Sato.
2002. Latitudinal gradients in body size and maturation of *Berrytetuhis anonychus* (Cephalopoda: Gonatidae) in the northeast Pacific. Veliger 45:309–315.

Brodeur, R. D., and M. Terazaki.
1999. Springtime abundance of chaetognaths in the shelf region of the northern Gulf of Alaska, with observations on the vertical distribution and feeding of *Sagitta elegans*. Fish. Oceanogr. 8:93–103.

Brodeur, R., S. McKinnell, K. Nagasawa, W. Pearcy, V. Radchenko, and S. Takagi.
1999. Epipelagic nekton of the North Pacific subarctic and transition zones. Prog. Oceanogr. 43:365–397.

Brodsky, K.A.
1950. Calanoida of the far eastern seas and Polar basin of the U.S.S.R. Dokl. Akad. Nauk. SSSR. 35:1–442. USSR Israel Program Scient. Transl. (1967), Jerusalem. Transl. No. TT-65-51200, 440 p.

Carlson, H. R., J. M. Murphy, C. M. Kondzela, K. W. Myers, and T. Nomura.
1999. Survey of salmon in the northeastern Pacific Ocean, May 1999. North Pacific Anadromous Fish Commission, Document 450, 37 p. Natl. Mar. Fish. Serv., Juneau, AK.

Cortes, E.
1997. A critical review of methods of studying fish feeding based on analysis of stomach contents: application to elasmobranch fishes. Can. J. Fish. Aquat. Sci. 54:726–738.

Didenko, V. D.
1990. Prospects of fishery for the squid *Berryteuthis anonychus* in the north-eastern Pacific. *In* "Vth all-USSR conference on commercial invertebrates, Minsk-Naroch. Abstracts of Communications," p. 82–83. [In Russian.] VNIRO Publishing, Moscow, Russia.

Hanlon, R. T., and J. B. Messenger.
1996. Cephalopod behaviour, 232 p. Cambridge Univ. Press, Cambridge, UK.

Howmiller, R. P.
1972. Effects of preservatives on weights of some common macrobenthic invertebrates. Trans. Am. Fish. Soc. 101:743–746.

Karlson, K., and U. Bamstedt.
1994. Planktivorous predation on copepods. Evaluation of mandible remains in the predator guts as a quantitative estimate of predation. Mar. Ecol. Prog. Ser. 108:79–89.

Kotori, M.
1976. The biology of Chaetognatha in the Bering Sea and the northern North Pacific Ocean, with emphasis on *Sagitta elegans*. Mem. Fac. Fish. Hokkaido Univ. 23:95–183.

Kubodera, T., and T. Okutani.
1977. Description of a new species of gonatid squid, *Gonatus madokai* n.sp. from the north-west Pacific, with notes on morphological changes with growth and distribution in immature stages (Cephalopoda: Oegopsida). Venus Jap. J. Malacol. 36(3):123–151.

Kuramochi, T., T. Kubodera, and N. Miyazaki.
1993. Squids eaten by Dall's porpoises, *Phocoenoides dalli* in the northwestern North Pacific and in the Bering Sea. *In* Recent advances in cephalopod fisheries biology (T. Okutani, R. K. O'Dor, and T. Kubodera, eds.), p. 229–240. Tokai Univ. Press, Tokyo.

Lapko, V. V.
1996. The role of squids in the Sea of Okhotsk communities. Oceanology 35:672–677.

Lapshina, V. I.
1988. On the feeding of the squid *Berryteuthis anonychus* Pearcy and Voss from the area of north-eastern Pacific. Deposited MS, Dep. VINITI 25.10.88, No. 7673-B 88, 1–5. [In Russian.]

Mackas, D. L., H. Sefton, C. B. Miller, and A. Raich.
1993. Vertical habitat partitioning by large calanoid copepods in the oceanic subarctic Pacific during spring. Prog. Oceanogr. 32:259–294.

Mackas, D. L., and A. Tsuda.
1999. Mesozooplankton in the eastern and western subarctic Pacific: community structure, seasonal life histories, and interannual variability. Prog. Oceanogr. 43:335–363.

Miller, C. B.
1988. *Neocalanus flemingeri*, a new species of Calanidae (Copepoda: Calanoida) from the subarctic Pacific Ocean, with a comparative redescription of *Neocalanus plumchrus* (Marukawa) 1921. Prog. Oceanogr. 20:223–273

Nesis, K. N.
1997. Gonatid squids in the subarctic North Pacific: ecology, biogeography, niche diversity and role in the ecosystem. Adv. Mar. Biol. 32:243–324.

Nixon, M.
1987. Cephalopod diets. *In* Cephalopod life cycles, vol. II: comparative reviews (P. R. Boyle, ed.), p. 201–219. Academic Press, London.

Ogi, H., T. Kubodera, and K. Nakamura.
1980. The pelagic feeding ecology of the short-tailed shearwater *Puffinus tenuirostris* in the subarctic Pacific region. J. Yamashina Inst. Ornithol. 12:157–182.

Ohizumi, H., T. Kuramochi, T. Kubodera, M. Yoshioka, and N. Miyazaki.
2003. Feeding habits of Dall's porpoises (*Phocoenoides dalli*) in the subarctic North Pacific and the Bering Sea basin and the impact of predation on mesopelagic micronekton. Deep-Sea Res. (I Oceanogr. Res. Pap.). 50:593–610.

Pearcy, W. G.
1991. Biology of the transition region. *In* Biology, oceanography, and fisheries of the North Pacific Transition Zone and Subarctic Frontal Zone (J. A. Wetherall, ed.), p. 39–55. NOAA Tech. Rep. NMFS 105.

Pearcy, W. G., R. D. Brodeur, J. M. Shenker, W. W. Smoker, and Y. Endo.
1988. Food habits of Pacific salmon and steelhead trout, midwater trawl catches and oceanographic conditions in the Gulf of Alaska, 1980–1985. Bull. Ocean Res. Inst. Univ. Tokyo. 26:29–78.

Pearcy, W. G., J. P. Fisher, and M. M. Yoklavich.
1993. Biology of the Pacific pomfret (*Brama japonica*) in the North Pacific Ocean. Can. J. Fish. Aquat. Sci. 50:2608–2625.

Pinkas L., M. S. Oliphant, and I. L. K. Iverson.
1971. Food habits of albacore, bluefin tuna, and bonito in California waters. Calif. Dep. Fish Game Fish. Bull. 152:1–105.

Radchenko, V. I.
1992. The role of squids in the pelagic ecosystem of the Bering Sea. Oceanology 32:762–767.

Rodhouse, P. G., and Ch. M. Nigmatullin.
1996. Role as consumers. Phil. Trans. R. Soc. Lond. B. 351:1003–1022.

Roper, C. F. E., and R. E. Young.
1975. Vertical distribution of pelagic cephalopods. Smithson. Contrib. Zool. 209:1–51.

Roper, C. F. E., M. J. Sweeney, and C. E. Nauen.
1984. FAO species catalogue. Vol. 3. Cephalopods of the world. An annotated and illustrated catalogue of species of interest to fisheries. FAO Fish. Synop. 125, vol. 3, 277 p. FAO, Rome.

Santos, R. A., and M. Haimovici.
1997. Food and feeding of the short-finned squid *Illex argentinus* (Cephalopoda: Ommastrephidae) off southern Brazil. Fish. Res. 33:139–147.

Shchetinnikov, A. S.
1992. Feeding spectrum of squid *Sthenoteuthis oualaniensis* (Oegopsida) in the eastern Pacific. J. Mar. Biol. Assoc. U.K. 72:849–860.

Terazaki, M., and C. B. Miller.
1986. Life history and vertical distribution of pelagic chaetognaths at Ocean Station P in the subarctic Pacific. Deep-Sea Res. 33:323–337.

Vinogradov, M. E., A. F. Volkov, and T. N. Semenova.
1996. Hyperiid amphipods (Amphipoda, Hyperiidea) of the world oceans (D. Siegel-Causey, ed.), 632 p. Science Publishers, Lebanon, NH.

Capture probability of a survey trawl for red king crab (*Paralithodes camtschaticus*)

Kenneth L. Weinberg
Alaska Fisheries Science Center
National Marine Fisheries Service, NOAA
7600 Sand Point Way N.E.
Seattle, Washington 98115
E-mail address: ken.weinberg@noaa.gov

Robert S. Otto
Kodiak Fisheries Research Center
National Marine Fisheries Service, NOAA
301 Research Court
Kodiak, Alaska 99615

David A. Somerton
Alaska Fisheries Science Center
National Marine Fisheries Service, NOAA
7600 Sand Point Way N.E.
Seattle, Washington 98115

Abstract—The relative abundance of Bristol Bay red king crab (*Paralithodes camtschaticus*) is estimated each year for stock assessment by using catch-per-swept-area data collected on the Alaska Fisheries Science Center's annual eastern Bering Sea bottom trawl survey. To estimate survey trawl capture efficiency for red king crab, an experiment was conducted with an auxiliary net (fitted with its own heavy chain-link footrope) that was attached beneath the trawl to capture crabs escaping under the survey trawl footrope. Capture probability was then estimated by fitting a model to the proportion of crabs captured and crab size data. For males, mean capture probability was 72% at 95 mm (carapace length), the size at which full vulnerability to the survey trawl is assigned in the current management model; 84.1% at 135 mm, the legal size for the fishery; and 93% at 184 mm, the maximum size observed in this study. For females, mean capture probability was 70% at 90 mm, the size at which full vulnerability to the survey trawl is assigned in the current management model, and 77% at 162 mm, the maximum size observed in this study. The precision of our estimates for each sex decreased for juveniles under 60 mm and for the largest crab because of small sample sizes.

In situ data collected from trawl-mounted video cameras were used to determine the importance of various factors associated with the capture of individual crabs. Capture probability was significantly higher when a crab was standing when struck by the footrope, rather than crouching, and higher when a crab was hit along its body axis, rather than from the side. Capture probability also increased as a function of increasing crab size but decreased with increasing footrope distance from the bottom and when artificial light was provided for the video camera.

Manuscript submitted 5 September 2003 to the Scientific Editor's Office.

Manuscript approved for publication 28 April 2004 by the Scientific Editor.

Fish. Bull. 102:740–749 (2004)

Regulations limit the annual harvest of Bristol Bay red king crab (RKC; *Paralithodes camtschaticus*) to males ≥135 mm in carapace length[1] (6.5 inches carapace width), and the size of the harvest is dependent upon the estimated biomasses of mature males and females. For stock assessments of RKC, area-swept abundance estimates are determined from the data from annual eastern Bering Sea (EBS) bottom trawl surveys conducted by the National Marine Fisheries Service, Alaska Fisheries Science Center (AFSC), and these estimates are used as input into a length-based assessment model (Zheng et al., 1995) to compute the total allowable catch for each annual fishing season.

It is assumed with the current assessment model that all male RKC ≥95 mm and all female RKC ≥90 mm within the path of the survey trawl (wingtip to wingtip) are captured. This assumption seems reasonable because the survey trawl uses a small diameter footrope designed to stay close to the bottom and red king crab are quite large. However, video photography taken following the 2000 EBS survey revealed that a considerable number of large (≥90 mm) RKC pass under the footrope of the survey trawl.

To assess the potential impact of escaping crab on the calculation of crab biomass, we conducted an experiment to estimate the size-related capture efficiency of the standard survey bottom trawl for Bristol Bay RKC. In this experiment, crab passing beneath the survey trawl were subsequently captured with an auxiliary net that was attached underneath and behind the footrope of the survey trawl (Engås and Godø, 1989; Walsh, 1992). Experimental nets like the one used for this study have been used previously in trawl efficiency studies for flatfish (Munro and Somerton, 2002), as well as for snow (*Chionoecetes opilio*) and Tanner (*C. bairdi*) crabs (Somerton and Otto, 1999). Trawl catch data alone, however, tell little about the details involved with escapement. Therefore, we deployed a video camera on the trawl to observe crab behavior and analyzed a combination of trawl-per-

[1] All references to measured crab lengths are carapace length.

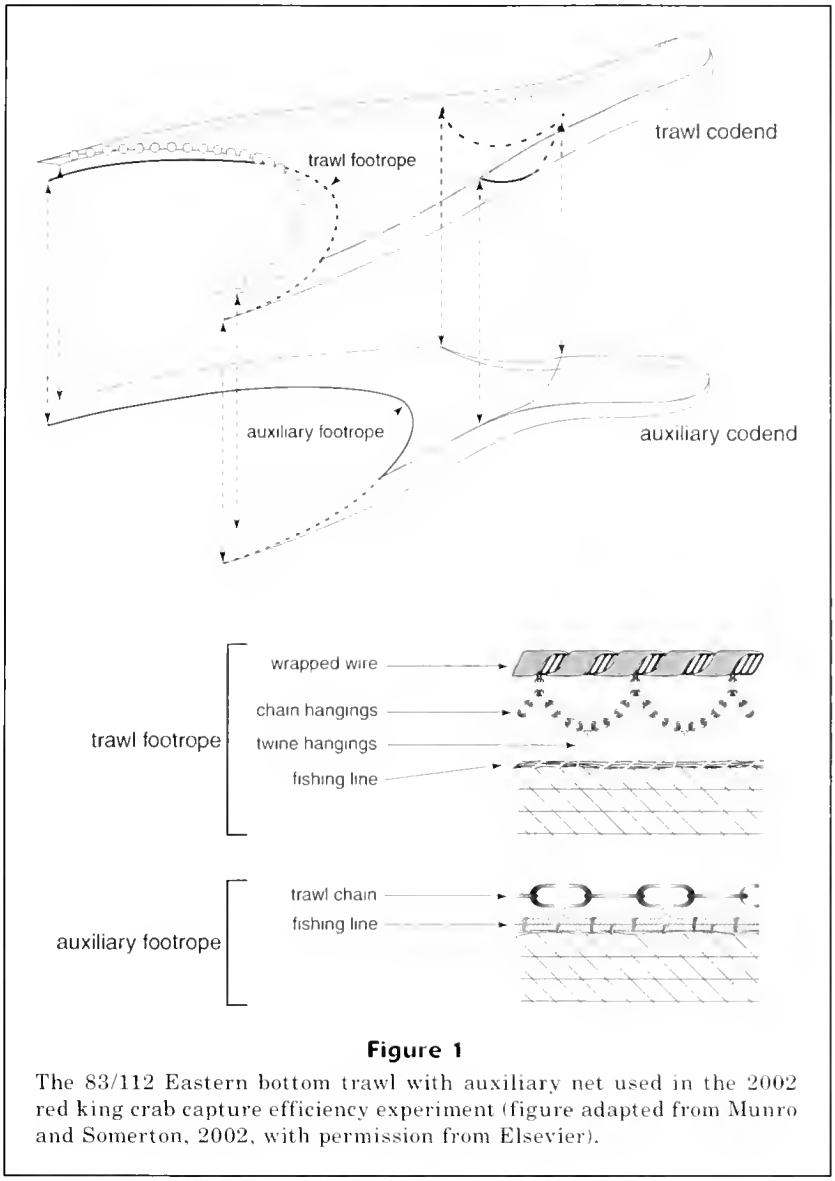

Figure 1

The 83/112 Eastern bottom trawl with auxiliary net used in the 2002 red king crab capture efficiency experiment (figure adapted from Munro and Somerton, 2002, with permission from Elsevier).

formance and crab-behavioral variables to help us understand the escapement process.

Materials and methods

Description of trawl gear

The 83/112 Eastern bottom trawl has been used by the AFSC in annual surveys to assess EBS crab and shelf groundfish stocks since 1982 (Armistead and Nichol, 1993). For the present experiment, an auxiliary net with an independent footrope constructed of heavy chain-link and a separate codend were attached to the bottom of the survey trawl to capture epibenthic animals passing beneath the trawl footrope (Fig. 1). Briefly, the 83/112 Eastern is a low-rise trawl that has a 25.3-m long headrope strung with 48 floats giving it approximately 102 kg of lift and a 34.1 m long, 5.2-cm diameter footrope constructed of 1.6-cm stranded wire rope protected with a single wrap of polypropylene line and split rubber hose. The net is constructed with nylon twine: 10.1-cm stretch mesh throughout the wing and throat sections; 8.9-cm stretch mesh in the intermediate section; a double layer of 8.9-cm stretch mesh in the codend; and a 3.1-cm stretch mesh liner in the codend. It is fished with a pair of 1.8×2.7-m steel V-doors weighing approximately 816 kg apiece.

The auxiliary net attaches to the wingtips and to the bottom of the survey trawl so that the bottom panel of the trawl serves as the top panel of the auxiliary net up to the beginning of the intermediate section. At this point, the two nets part and the auxiliary net then has a top panel of 8.9-cm stretch mesh and a double layer

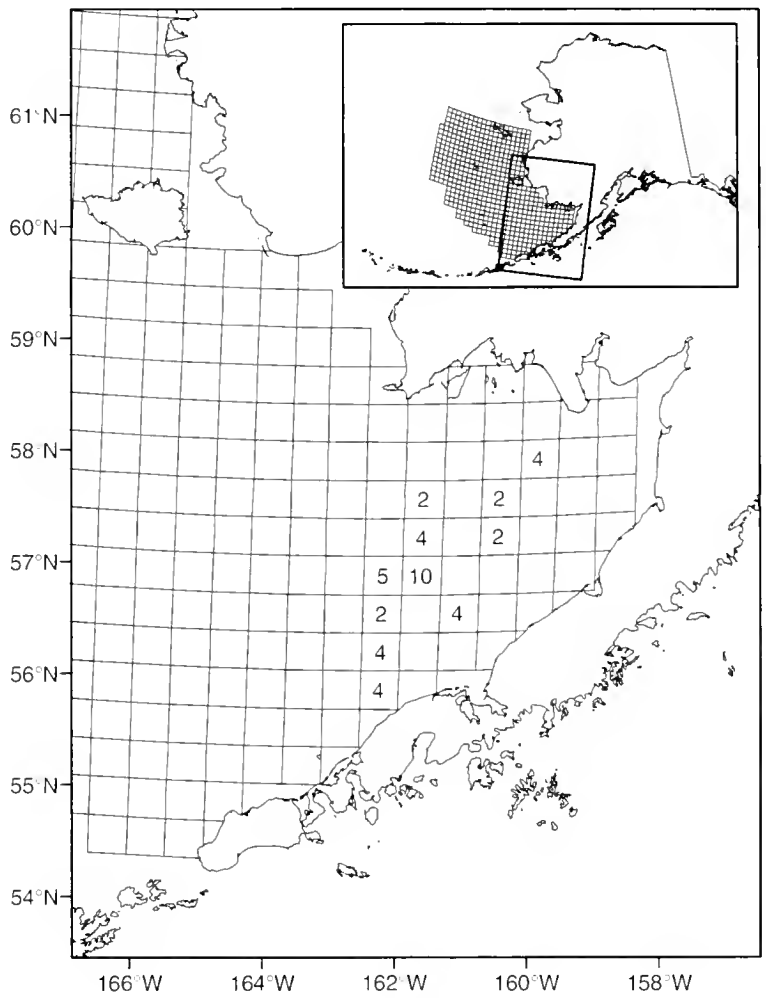

Figure 2

The annual eastern Bering Sea survey station grid showing the number of successful tows per station block made during the 2002 red king crab capture efficiency study. Each block represents a 400-nmi^2 area.

codend with a 3.1-cm stretch mesh liner. The 38.2 m long auxiliary footrope constructed of heavy 16-mm-long link trawl chain was designed to drag through soft bottom and presumably captures all escaping crabs. Munro and Somerton (2002) provided detailed construction plans of this experimental gear in their appendices.

Experimental design

Operations were conducted from 21 to 29 July 2002, aboard the FV *Arcturus*, one of two commercial stern trawlers chartered by the AFSC since 1993 to carry out annual Bering Sea groundfish surveys. Trawling took place in Bristol Bay (Fig. 2) at depths from 41 to 77 m and followed standardized survey protocols that included towing during daylight hours at a 1.5 m/sec (3 knots) vessel speed and using locked winches and standardized lengths of trawl warp (scope) at each towing depth. Acoustic net mensuration equipment was used to measure wing spread for each tow. Bottom contact sensors were used on the centers of both the trawl and auxiliary footropes to measure the distance (in centimeters) between the footropes and the bottom (Somerton and Weinberg, 2001). A silicon-intensified tube (SIT) camera, which uses ambient light, was attached to the center of the trawl to view RKC interaction with the footrope. On some of our trial tows, however, a 30-W quartz halogen light was also used to increase contrast between ambient light and the sea floor.

Two departures from standardized survey protocol were necessary for this experiment. First, 27.5-m long bridles were used instead of the survey standard 55-m long bridles to help offset the loss of wing spread caused by the added drag of the auxiliary net (Munro and Somerton, 2002). Second, tow length was shortened from the survey standard of 30 min to 20 min to minimize the decrease of path width over time due to increased drag from large catches in the auxiliary net.

Towing sites were selected according to catch rates and carapace lengths obtained from the recently completed 2002 EBS survey (Stevens[2]). Tows were made in pairs, one in a northerly direction, the other in a southerly direction and were offset to the east or west by a minimum of 0.1 nmi; the initial direction was chosen randomly in order to mitigate any bias that the current flow might have on footrope contact with the bottom (Weinberg, 2003). Increased effort was given to sites producing favorable numbers and crab lengths by adding additional towing pairs. For each tow the total catch of all species from each net was first weighed before all RKC were removed from the catch, weighed, coded by sex, and measured to the nearest millimeter.

Data analysis

Trawl geometry Trawl geometry for standard survey nets and experimental nets was measured to confirm that the two gear types fished similarly. Average wing spreads and footrope heights off-bottom for experimental tows were compared to those from 33 standard survey gear tows taken at the same or nearby sampling locations. Because the depth of sampling varied, wing spread and footrope height were linearly regressed on scope, a factor variable indicating gear type (i.e., survey or experimental), and their interaction. Two-tailed *t*-tests were used to test for the difference in the slopes and the intercepts between gear types. Significance of the interaction term indicated that slopes differed between gear types. For nonsignificant interaction, significance of the intercepts indicated that wing spread or footrope height differed between gear types by a constant amount.

Capture probability Capture probability for the experimental gear was estimated from catch data of the trawl and the auxiliary net as a function of carapace length (L) for both male and female crab. Based on the assumption that the auxiliary net allows no escapement, the probability of capture at the footrope was modeled as a logistic function (Munro and Somerton, 2002) by using SPLUS software (version 6.1, Insightful Corporation, Seattle, WA). Two models were considered: the first, a two-parameter model which reaches an asymptotic maximum of 1 (unity):

$$P(L) = \frac{1}{1+e^{-(\alpha+\beta L)}}; \quad (1)$$

and the second, a three-parameter model which reaches an asymptotic maximum less than 1:

$$P(L) = \frac{\gamma}{1+e^{-(\alpha+\beta L)}}. \quad (2)$$

[2] Stevens, B. G., R. A. Macintosh, J. A. Haaga, C. E. Armistead, and R. S. Otto. 2002. Report to industry on the 2002 eastern Bering Sea crab survey. AFSC Proc. Rep. 2002-5, 59 p. Alaska Fish. Sci. Cent., Natl. Mar. Fish. Serv., NOAA, Kodiak Fishery Research Center, 301 Research Court, Kodiak AK 99615.

Because crab capture at the footrope is a binomial process (i.e., crabs are either captured or they escape), the models were fitted to the capture and length data by using maximum likelihood (Millar, 1992; Munro and Somerton, 2001) and the data were pooled across tows. For each sex, both models were fitted to the data, and the best of the competing models was selected according to the lowest obtained value of the Akaike information criterion (AIC; Burnham and Anderson, 1998), defined as

$$AIC = -2(\log likelihood) + 2(number\ of\ parameters).$$

After choosing a model for each sex, we examined whether the capture probability curves differed between sexes by fitting a model to the data for both sexes combined, and then comparing the value of AIC for this model to the sum of the AIC values for the models fitted to each sex, again using the minimum AIC value to objectively select the better of the two models.

Bootstrapped confidence intervals were constructed for the mean capture probability for each 1-mm length category, between the smallest and the largest individuals (Efron and Tibshirani, 1993) by resampling the catch-at-size data from individual hauls 1000 times. Empirical 95% confidence intervals were then determined as the range between the 25th highest and the 25th lowest of the bootstrap capture probability estimates.

Video data analyses

To understand the factors associated with crab escapement under the footrope, a video camera was mounted on the trawl to observe RKC interaction with the center of the trawl footrope. These *in situ* video observations included tows made in 2000 on the standard trawl and in 2002 on the experimental trawl. Artificial light was provided for all of the 2000 tows, and for some of the 2002 trial tows made before the capture efficiency experiment began. All the 2002 experimental tows were made under natural light conditions. RKC encounters observed on the videotapes were counted from the time the footrope settled to the bottom until the time the footrope was lifted off-bottom at the end of the tow. The probability of capture was predicted as a function of several explanatory variables. Variables observed and codes (in parentheses) for each individual included the following:

1 the capture event—the crab escaped beneath the footrope (0) or was captured (1);
2 use of artificial light—the tow was made with (0) or without artificial light (1);
3 estimated mean footrope height above the sea floor over the course of the entire tow was based on the bottom contact sensor and was expressed in centimeters (0–5);
4 body height—the crab was observed to be crouching with its legs either tucked beneath the carapace or stretched out so that the carapace was very close to the bottom (0) or standing upright on its dactyls (1);

Table 1

Regression coefficients of wing spread (width) and footrope distance from the bottom (footrope) as a function of scope and gear type based on tows from the capture efficiency experiment and tows using standard survey gear. Also provided are the results of two-tailed *t*-tests testing for the difference in intercept between gear types.

		Intercept		
	Slope	Experimental gear (n=43)	Standard gear (n=33)	P intercept
Width (m)	0.0038	15.3206	16.0713	<0.0000
Footrope (cm)	0.0087	−1.2582	−0.4241	0.0023

5 body orientation at the point of contact with the footrope—footrope contact occurred along the body axis (1) or from the side (2);
6 crab size—small (0), medium (1), or large (2), where size is expressed as an approximation based on visual comparison of carapace length to the dimensions of trawl parts, such as mesh or chain links. Corresponding length intervals were approximately ≤90 mm, 90–135 mm, and ≥135 mm.

As a general rule, crabs could be seen in the videos 1–2 seconds prior to contact with the footrope. Assignment of codes was typically straightforward. However, in some instances, several reviews of the encounter were necessary in order to determine a crab's position or orientation in relation to the footrope.

The probability of capture was estimated by using stepwise generalized linear modeling (GLM; Venables and Ripley, 1994) to fit a logistic model describing the probability of capture as a function of crab size, where body height, body orientation, average footrope distance from the bottom during the tow, the use of artificial light, and all possible first order interactions were considered as additional potential terms. The model fitting procedure (with data from crabs for which all variables were observed) entailed a stepwise backward model selection process. The process began with fitting the model to all interaction terms less one, and then calculating and comparing the resulting AIC values. The interaction producing the largest decrease in AIC was subsequently eliminated. Next, the procedure was repeated with the remaining terms until no interaction term could be eliminated without increasing the AIC. Then, the above process was repeated for the main effects. For the main effects having an interaction term, both the main effects and the interaction term were eliminated together as a unit. The final model chosen contained those terms that produced the minimum AIC value.

Results

Effect of the auxiliary net on trawl geometry

Regressions of wing spread and footrope height on scope, gear type, and their interaction were compared to determine how closely the two gear types fished. The interaction term was not significant for wing spread (P=0.08) nor for footrope height (P=0.82), indicating that the slopes did not differ between gear types. However, tests of the intercepts were significant for both wing spread and footrope height and indicated that trawl geometry differed between survey and experimental trawls (Table 1). Predicted standard survey wing spreads for the minimum (137 m), median (229 m), and maximum (320 m) scopes used were 16.6, 16.9, and 17.3 m —approximately 0.8 m more than the experimental gear at the same scopes. Predicted footrope distances off the bottom were 0.8, 1.6, and 2.4 cm, at the above three scope values—approximately 0.8 cm greater than the experimental gear. Although we detected statistical differences in the trawl geometry between the two gear types, the actual difference in physical measurements was small and presumably had only a nominal effect on the results of the capture efficiency experiment.

Our assumption that the auxiliary net caught all escaping crabs was reinforced by two observations: 1) the data from the bottom contact sensor on the chain footrope indicated consistent contact with the sea floor; and 2) the auxiliary net consistently had large catches of benthic organisms other than crab, such as starfish and shells, and produced enough drag on the system to reduce wing spread. The effectiveness of the auxiliary footrope at capturing escaping crab is in part due to its weight and small diameter that enable it to sweep beneath the crabs and in part due to the suspension of benthic organisms initiated by the turbulence created by the passing of the first footrope.

Length-based capture probability

Capture probability was estimated from length measurements (n=3233) collected from 43 successful experimental tows (21 north, 22 south) made within 11 standard EBS survey station blocks (Fig. 2). Male samples (n=1667) ranged in size from 23 to 184 mm (Fig. 3). Female samples (n=1566) ranged in size from 51 to 162 mm.

The two-parameter model (model 1) of capture probability was selected over the three-parameter model (model 2) because it had a lower AIC value for both male and female RKC (Table 2). For the comparison of

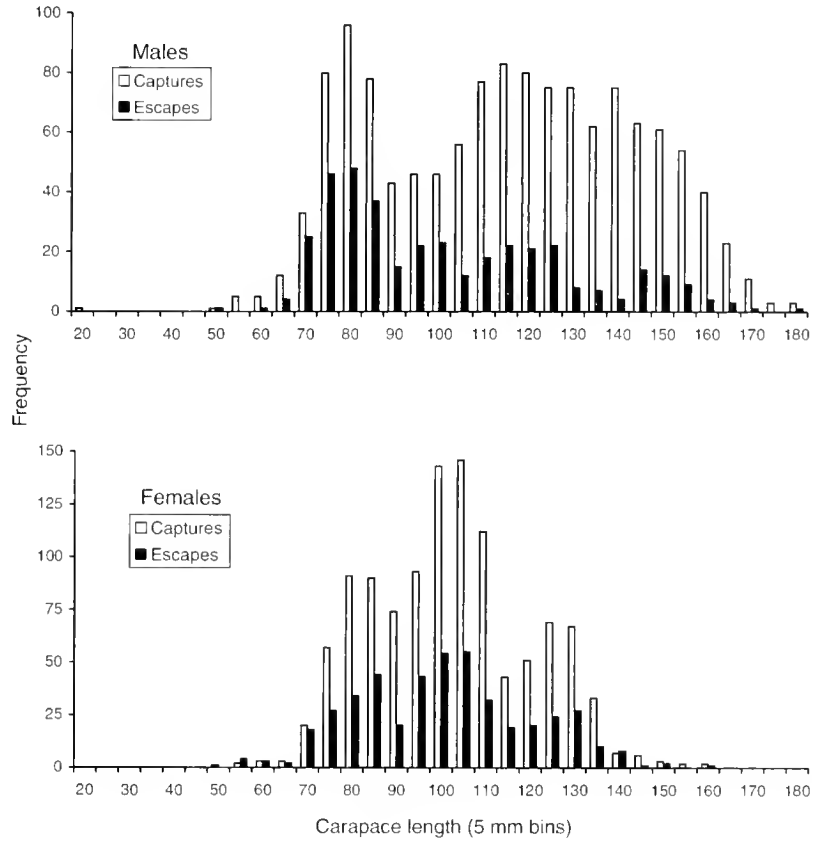

Figure 3

Size frequency of red king crabs taken in the survey trawl (captures) and the auxiliary net (escapes) during the 2002 capture efficiency study. Crab have been binned into 5-mm carapace length intervals.

Table 2

Estimated parameter and Akaike's information criterion (AIC) values for the maximum likelihood fit of the 2-parameter and the 3-parameter logistic models for males, females, and for sexes combined. Parameter variance estimates based on bootstrapping 1000 replicates are provided for the final model used to estimate red king crab capture probability for the 83/112 Eastern survey bottom trawl.

Sex	Model	α	β	γ	AIC	Var α	Var β	Covariance $\alpha\beta$
Male	$1/(1+e^{-(\alpha+\beta l)})$	−0.7366	0.0178	—	1725.3	0.113	1.28×10^{-5}	-1.14×10^{-3}
	$\gamma/(1+e^{-(\alpha+\beta l)})$	−0.8826	0.0209	0.9622	1727.1	—	—	—
Female	$1/(1+e^{-(\alpha+\beta l)})$	0.3540	0.0054	—	1875.7	0.279	2.58×10^{-5}	-2.63×10^{-3}
	$\gamma/(1+e^{-(\alpha+\beta l)})$	0.3540	0.0054	0.9999	1877.7	—	—	—
Combined sexes	$1/(1+e^{-(\alpha+\beta l)})$	−0.4569	0.0143	—	3612.7	—	—	—

selectivity curves for males and females with model 1, we found the summed AIC for separate curves to be lower than the AIC for sexes combined. Consequently, separate selectivity curves were estimated for males and females (Table 2).

The fitted model predicted male capture probability to be 41.9% at 23 mm (size of the smallest male observed); 72.2% at 95 mm (size at which full vulnerability to the survey trawl is assigned in the current management model); 80.2% at 120 mm (size assigned

in the current management model for male maturity); 84.1% at 135 mm (legal size for males); and 92.7% at 184 mm (size of the largest male crab encountered in our experiment [Fig. 4]). The fitted model predicted female capture probability to be 65.2% at 51 mm (size of the smallest female observed); 69.8% at 90 mm (size at which both full vulnerability to the survey trawl and 50% female maturity are assigned in the current management model); 74.7% at 135 mm (same size at which males enter the fishery); and 77.4% at 162 mm (size of the largest female crab encountered in our experiment [Fig. 5]). Estimated capture probability for both male and female crab was equal at 88 mm (69.9%). Model variability, as indicated by the 95% confidence bounds, was greatest at the extremes of our size ranges because of low sample frequency. This was especially true for small crabs, and the uncertainty was so large that extrapolation of the capture probability functions to either males or females below <60 mm is not recommended.

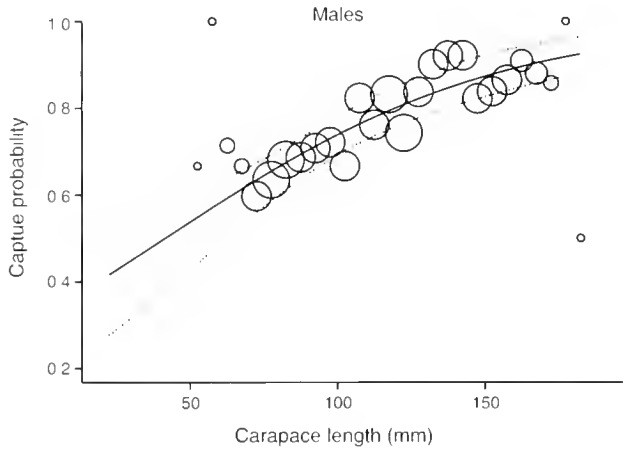

Figure 4

A 2-parameter logistic model (solid line) and 95% confidence bounds (dashed lines) estimating male red king crab capture probability for the 83/112 Eastern survey bottom trawl. Symbols are scaled to the sample length frequency summed over all tows and binned into 5-mm carapace length intervals. Symbols range in size from the smallest circle representing a single individual to the largest circle representing 138 males.

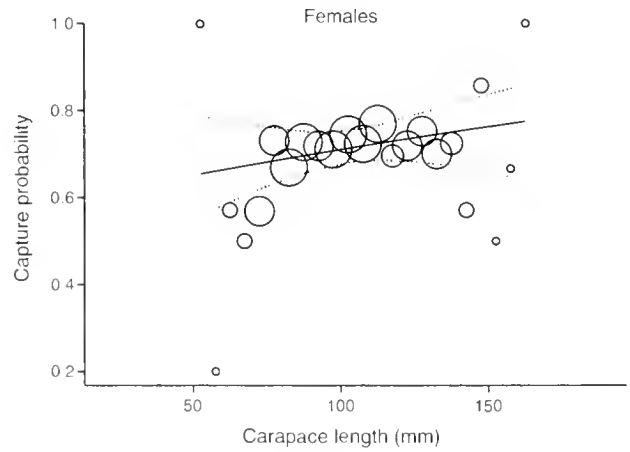

Figure 5

A 2-parameter logistic model (solid line) and 95% confidence bounds (dashed lines) estimating female red king crab capture probability for the 83/112 Eastern survey bottom trawl. Symbols are scaled to the sample length frequency summed over all tows and binned into 5-mm carapace length intervals. Symbols range in size from the smallest circle representing two individuals to the largest circle representing 206 females.

Factors influencing escapement

Modeling the effect of various factors on capture probability was based on observations of RKC (n=248) from videotapes collected during 28 EBS tows. Approximately two-thirds of the counted crabs were captured. The influence of artificial lighting, body height, footrope distance from the bottom, crab size, body orientation, and the interaction of body height and body orientation were significant (Table 3). Capture probability decreased when lights were used and when the distance between the footrope and the bottom increased. Capture probability increased when crabs were standing up on their legs, with increased body size, and when the footrope contact was made along the body axis rather than from the side of the crab.

Capture probability, based on direct observation, was predicted by the fitted logistic models to illustrate how the various explanatory variables affect the capture outcome. We present two examples. In the first case, capture probability in natural light

Table 3

Model coefficients for predicting red king crab capture probability from counts obtained with a trawl-mounted video camera.

	Value	Standard error
Intercept	−2.014	0.676
Light variable	−0.959	0.526
Body height variable	3.789	0.624
Body orientation variable	0.207	0.613
Crab size variable	1.506	0.315
Footrope height variable	−0.286	0.197
Body height and orientation interaction	−1.436	0.785

conditions and when crab are oriented sideways to the oncoming footrope, was predicted as a function of footrope distance off the bottom for each size class, and for both standing and crouching crab (Fig. 6). For all size groups, capture probability decreased with increasing footrope height from the bottom. The importance of whether a crab was standing or crouching diminishes with decreasing crab size because the footrope is more likely to pass completely over smaller crab. In contrast, the importance of standing was higher for large crab because they were more likely to be undercut by the footrope and captured, whereas crouching crab were more susceptible to having their legs first pinned down by the footrope, which exerted a downward pressure on their carapace and allowed the footrope to pass over the crab. Capture probability of medium-size individuals, which included a large proportion of egg-bearing females, was more dependent upon the body height of the crab. Footrope contact below the carapace typically resulted in capture; however contact above the legs often forced the crab's carapace down, causing the crab to roll forward and pass beneath the footrope.

In the second case, capture probability was predicted for natural light conditions when the footrope is 1 cm off-bottom, as a function of crab size, by body orientation to the footrope, and for standing and crouching individuals (Fig. 7). Under these conditions, capture probability was greater for crab contacted along their body axis than for crab hit from the side. In addition, capture probability increased with crab size for both standing and crouching crab, regardless of whether the footrope first contacted the crab along their body axis or from the side. When the footrope was 1 cm off bottom, the difference in the body-orientation effect on capture probability for standing crab was greater for smaller crab than for medium and larger individuals, but relatively equal for crouching crab of all sizes.

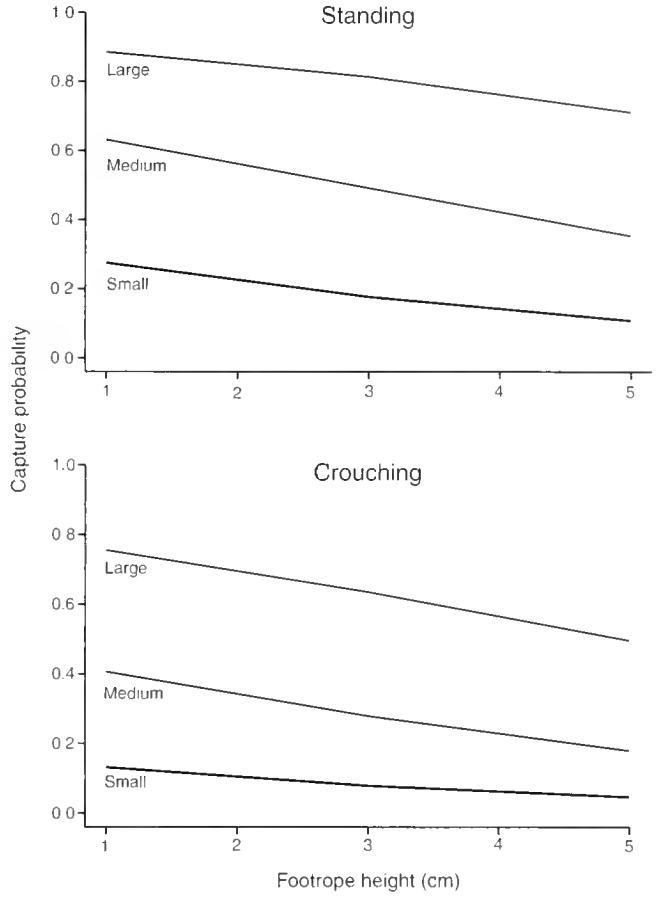

Figure 6

Estimated red king crab capture probability (based on direct observations) by size class as a function of footrope height above the bottom for standing and crouching individuals. For this model, it was assumed that no artificial light was used for the camera and that crab were oriented sideways to the footrope upon initial contact.

Discussion

Our observations confirmed that adult Bristol Bay red king crab can escape beneath the footrope of the AFSC's 83/112 Eastern survey bottom trawl under normal towing conditions. Capture probability increased with size but did not reach 100% for the largest crab caught. For the current management model used for RKC stock assessments, 100% capture probability is assumed for adult crabs and should be revised. A recruitment ogive is used in the calculation of the total spawning biomass for defining overfishing under the Magnuson-Stevens Fishery Conservation and Management Act (Stevens[2]). Revised computations of vulnerability will be required for this purpose as well. Survey trawl selectivity, although similar between the two sexes at prerecruit sizes, was generally 15% higher for legal-size males than for equal-size females. This between-sex difference in capture probability may be explained by behavioral differences (for instance, egg-bearing females stand differently from large males). Unfortunately, crab, when viewed from above, mask their gender; thus sex was excluded from our modeling exercise of video data.

Survey catch statistics for RKC are routinely included in the management modeling procedure to estimate the abundance of legal-size males (≥135 mm), male prerecruits (95–134 mm), the effective spawning biomass of males (≥120 mm), and the spawning biomass of females (≥90 mm, as determined from size at 50% maturity). We estimated capture probability for legal-size males (up to 184 mm) to range from 84% to 93%, for prerecruit males from 73% to 84%, and for the mature portion of the male spawning population (up to 184 mm) from

80% to 93% Our estimated capture probability for the survey trawl on the female portion of the spawning RKC population ranged from 70% to 77% for crab up to 162 mm. A review of the AFSC database for EBS crab surveys showed that the largest male and female crabs taken were 200 mm and 172 mm. Corresponding capture probabilities estimated by the model for these size crabs were 94% and 78%, respectively.

Two main factors affect the overall capture efficiency of epibenthic species by a bottom trawl: 1) horizontal herding, defined as movement into the path of the trawl between the wingtips in response to stimuli produced by the doors or bridles; and 2) escapement, defined as the avoidance of capture once the crab is within the path of the trawl. We believe herding is negligible because our observations of crab movement, which were consistent with those reported by Rose (1999), indicated that RKCs are slow-moving animals that can travel only slight distances before being overtaken by a trawl approaching at 1.5 m/sec. Our video observations of the trawl bridle revealed that RKCs consistently passed over the top of the bare cable, with one exception—where a few crabs were seen sliding along the bridle, legs entangled, to the wingtip before being cast outside the path of the trawl. Escapement is likely restricted to footrope escapement because mesh escapement is impeded by the spiny surface and long legs of the crab and could only occur for the smallest individuals, which we encountered in low numbers and which could not be predicted reliably by our model.

We recognize from the analysis of our *in situ* data that capture probability is influenced not only by trawl performance but also by crab behavior. For instance, crabs standing upright, such as moving or migrating individuals, are more susceptible to capture than those with their bodies resting on the substrate. Crab density could also affect capture probability as seen for some species of fish (Godo et al., 1999). The crabs we observed with our video cameras were fairly dispersed and the maximum number of crabs seen in any single video frame was two (twice observed). Crabs in relatively low abundance are likely to react directly to the gear, but in areas of high abundance, crabs may react to each other in response to the stimuli from the approaching gear, causing them to crouch or conversely move away from perceived danger. Both of these responses would result in a different capture probability.

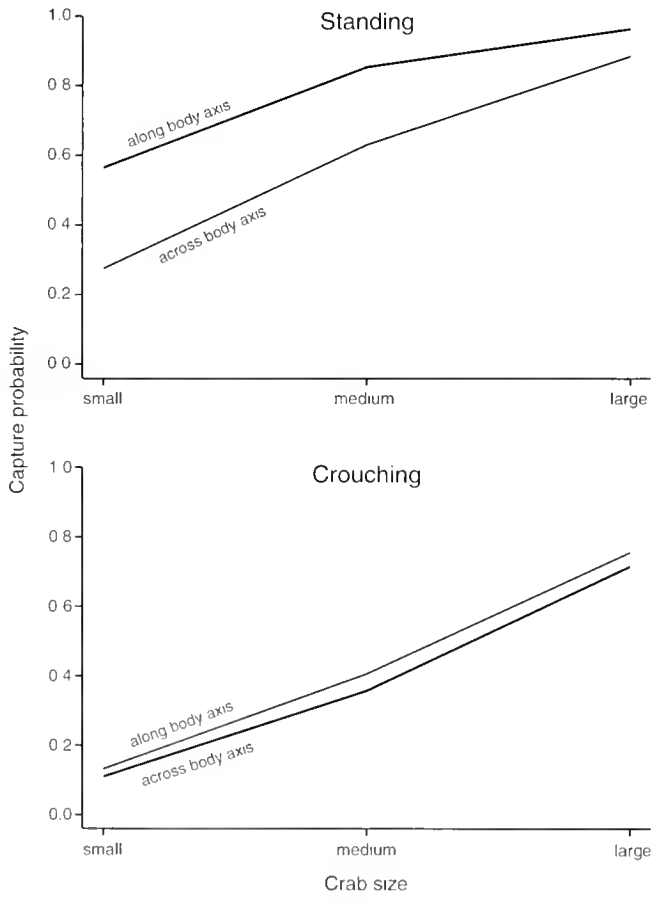

Figure 7

Estimated red king crab capture probability (based on direct observations) by body orientation at the time of footrope contact as a function of crab size for standing and crouching individuals. For this model, it was assumed that no artificial light was used for the camera and that the footrope was 1 cm off bottom.

Our estimates of capture probability apply to the conditions in which the EBS survey is conducted; that is, relatively disperse offshore populations encountered during daylight hours on sandy bottom during the summer months. There are other behavioral factors or environmental conditions that we did not consider in the present study but which could affect the efficiency of the survey trawl. These include, but are not limited to, the following: trawling where the substrate is substantially different; crabs that are either aggregated into pods or are buried (Dew[3]); and temperatures or tidal currents that would affect the migratory or feeding behavior, and therefore the body height of crab (Dew, 1990). Our estimates of capture probability are also based on the assumption that the auxiliary net is 100% efficient at capturing crab escaping beneath the footrope of the survey trawl. We have no direct evidence to believe otherwise. However, if crabs also escaped the auxiliary net, then our estimates of capture probability would be too large.

In conclusion, we wish to clarify to users of our findings that, although these experimentally determined selectivity models indicate an upward correction in spawning biomass of red king crab may be in order, we find no reason

[3] Dew, C. B. 2003. Personal commun. Alaska Fisheries Science Center, 7600 Sand Point Way NE, Seattle, WA 98115.

to claim that the stock is in any better condition than the condition that was determined by the most recent assessment. The foremost utility of the AFSC annual EBS surveys is to monitor distribution and abundance trends through time. The survey accomplishes this by maintaining strict protocols and consistency in trawling methods, in computation of area-swept abundance, and in nonenvironmentally affected trawl efficiency. The survey times series is designed to detect changes in abundance, signaling advances in the population's rebuilding processes, regardless of whether crab are 100% or 80% vulnerable to the survey trawl. We advocate that careful consideration be given to the other factors that drive the management model, along with the results of our capture efficiency experiment, to ensure that the stock rebuilding process remains uninterrupted.

Acknowledgments

We are thankful to Captain Glenn Sullivan and the crew of the FV *Arcturus* for their professional attitudes and relentless attention to detail; to scientists Chris Johnston, Frank Shaw, and Kerim Aydin for their assistance at sea following the 2002 survey; to Craig Rose and Scott McEntire for technical support; to Dave King and Jim Smart for preparation of the experimental trawl gear; and to Gary Walters, Braxton Dew, Doug Pengilly, Jie Zheng, and our anonymous reviewers for their helpful comments during the manuscript review process.

Literature cited

Armistead, C. E., and D. G. Nichol.
1993. 1990 bottom trawl survey of the eastern Bering Sea continental shelf. NOAA Tech. Memo. NMFS-AFSC-7, 190 p.

Burnham, K. P., and D. R. Anderson.
1998. Model selection and inference: a practical information-theoretic approach, 353 p. Springer-Verlag, New York, NY.

Dew, C. B.
1990. Behavioral ecology of podding red king crab, *Paralithodes camtschatica*. Can. J. Fish. Aquat. Sci. 47:1944–1958.

Efron, B., and R. Tibshirani.
1993. An introduction to the bootstrap, 436 p. Chapman and Hall, New York, NY.

Engås, A., and O. R. Godø.
1989. Escape of fish under the fishing line of a Norwegian sampling trawl and its influence on survey results. J. Cons. Int. Explor. Mer 45:269–276.

Godo, O. R., S. J. Walsh, and A. Engås.
1999. Investigating density-dependent catchability in bottom trawl surveys. ICES J. Mar. Sci. 56:292–298.

Millar, R. B.
1992. Estimating the size-selectivity of fishing gear by conditioning on the total catch. J. Am. Stat. Assoc. 87:962–968.

Munro, P. T., and D. A. Somerton.
2001. Maximum likelihood and non-parametric methods for estimating trawl footrope selectivity. ICES J. Mar. Sci. 58:220–229.
2002. Estimating net efficiency of a survey trawl for flatfishes. Fish. Res. 55:267–279.

Rose, C. R.
1999. Injury rates of red king crab, *Paralithodes camtschaticus*, passing under bottom-trawl footropes. Mar. Fish. Rev. 61(2):72–76.

Somerton, D. A., and R. S. Otto.
1999. Net efficiency of a survey trawl for snow crab, *Chionoecetes opilio*, and Tanner crab, *C. bairdi*. Fish. Bull. 97:617–625.

Somerton, D. A., and K. L. Weinberg.
2001. The affect of speed through the water on footrope contact of a survey trawl. Fish. Res. 53:17–24.

Venables, W. N., and B. D. Ripley.
1994. Modern applied statistics with S-plus, 452 p. Springer-Verlag, New York, NY.

Walsh, S. J.
1992. Size-dependent selection at the footgear of a groundfish survey trawl. N. Am. J. Fish. Manag. 12:625–633.

Weinberg, K. L.
2003. Change in the performance of a Bering Sea survey trawl due to varied trawl speed. Alaska Fish. Res. Bull. 10(1):42–49.

Zheng, J., M. C. Murphy, and G. H. Kruse.
1995. A length-based population model and stock-recruitment relationships for red king crab, *Paralithodes camtschaticus*, in Bristol Bay, Alaska. Can. J. Fish. Aquat. Sci. 52 (6):1229–1246.

Evidence of shark predation and scavenging on fishes equipped with pop-up satellite archival tags

David W. Kerstetter
School of Marine Science
Virginia Institute of Marine Science
College of William and Mary
Gloucester Point, Virginia 23062
E-mail address: bailey@vims.edu

Jeffery J. Polovina
Pacific Islands Fisheries Science Center
National Marine Fisheries Service
Honolulu, Hawaii 96822

John E. Graves
School of Marine Science
Virginia Institute of Marine Science
College of William and Mary
Gloucester Point, Virginia 23062

Over the past few years, pop-up satellite archival tags (PSATs) have been used to investigate the behavior, movements, thermal biology, and postrelease mortality of a wide range of large, highly migratory species including bluefin tuna (Block et al., 2001), swordfish (Sedberry and Loefer, 2001), blue marlin (Graves et al., 2002), striped marlin (Domeier and Dewar, 2003), and white sharks (Boustany et al., 2002). PSAT tag technology has improved rapidly, and current tag models are capable of collecting, processing, and storing large amounts of information on light level, temperature, and pressure (depth) for a predetermined length of time before the release of these tags from animals. After release, the tags float to the surface, and transmit the stored data to passing satellites of the Argos system.

A problem noted by several authors using early PSAT models was the occasional occurrence of tags that did not transmit data. Clearly, a tag attached to a moribund fish that would sink to a depth exceeding the pressure limit of the tag casing would be destroyed. To prevent the loss of tags due to mortality events, tag manufacturers and researchers have developed mechanisms that release tags from dead or dying fish before the structural integrity of the tag is compromised at depth. These mechanisms include both mechanical devices that sever the monofilament tether that attaches the tag to the fish upon reaching a given depth and internal software subroutines that activate the normal electronic release mechanism if the tag either reaches a certain depth or maintains a constant depth for a predetermined length of time.

Despite the addition of these release mechanisms to PSATs, some tags still fail to transmit data. Such failure could result from any of the following events or conditions: mechanical failure of a critical tag component; destruction by fishing crews unaware of or not participating in the present research; excessive epifaunal growth that makes the tag negatively buoyant or prevents the tag from floating with the antenna in a vertical position; or fouling of the tag on the fish, fishing gear, or flotsam. Another cause of failure is that the tags could be lost as a result of ingestion. For example, a free-swimming white marlin (*Tetrapturus albidus*) was observed mouthing and almost swallowing a free-floating PSAT off the Dominican Republic in May 2002 (Graves, personal observ.). Alternately, the tag could be ingested incidentally with part of the tagged fish, as described by Jolley and Irby (1979) who reported that an acoustic tag on a sailfish (*Istiophorus platypterus*) was eaten along with the fish by an undetermined species of shark. In this note, we present data from PSATs deployed on two white marlin in the western North Atlantic Ocean and on an opah (*Lampris guttatus*) in the central Pacific; the data from these tags indicate that the tags were consumed by sharks.

Materials and methods

White marlin 1 (WM1)

At approximately 10:00 am local time on 1 September 2002, a white marlin was observed on pelagic longline gear set during the night near the southeastern edge of Georges Bank. The fish, which had been caught on a slightly offset, straight-shank J-style hook (size 9/0), was manually guided with the leader alongside the vessel. A PTT-100 HR model PSAT (Microwave Telemetry, Inc., Columbia, MD) was attached to the dorsal musculature approximately 5 cm below the base of the dorsal fin with a large nylon anchor according to the procedure and tether design described in Kerstetter et al. (2003). The tag was activated shortly after the white marlin was first identified, although approximately one hour is required following activation for this tag model to begin collecting data. The tag was programmed to record point measurements of temperature, light, and pressure (depth) in four-minute time intervals and to detach from the animal after 10 days. After release from the fish, the positively buoyant tag was expected to float to the surface and transmit stored and real-time data. For both white marlin

Manuscript submitted 27 April 2003
to the Scientific Editor's Office.
Manuscript approved for publication
7 June 2004 by the Scientific Editor.
Fish. Bull. 102:750–756 (2004).

Table 1

Comparison of depths and temperatures recorded by three pop-up satellite archival tags (PSATs) before and after the tags were ingested by an organism.

	Before ingestion					After ingestion				
Animal	Depth range (m)	Depth mean (SD)	Temp. range (°C)	Temp mean (SD)	*n*	Depth range (m)	Depth mean (SD)	Temp range (°C)	Temp mean (SD)	*n*
WM1	145.2	145.2 (±0.00)	11.6–11	11.7 (±0.07)	179	0–564.9	130.0 (±237.50)	12.1–26.5	24.1 (±0.84)	2755
WM2	0–26.9	5.9 (±4.44)	19.8–27.8	24.7 (± 0.91)	207	0–699.3	131.0 (±162.61)	18.9–29.5	27.3 (±1.20)	1683
Opah	32–456	221.81 (±92.20)	8–25.6	16.68 (±4.21)	360	0–524	170.56 (±133.83)	26.2–30.6	28.64 (±0.67)	168

tags, minimum straight-line distances were calculated between the point of release and the first clearly transmitted location of the tag following its release (pop-off) (Argos location codes 0–3).

At the time of tagging, the longline hook used to capture the fish was not visible in the mouth of the white marlin. The leader was therefore cut as close as possible to the fish before the fish was released, following the standard operating procedure for the domestic pelagic longline fleet. The fish was maintained alongside the vessel for less than three minutes for the application of the PSAT and a conventional streamer tag. Although the white marlin was initially active at the side of the vessel, some light bleeding from the gills was noted. After release, the fish swam away slowly under its own power.

White marlin 2 (WM2)

At 9:05 am on 2 August 2003, a white marlin was observed on pelagic longline gear with the same configuration in the same approximate area of Georges Bank as WM1. The fish was caught by a circle hook (size 16/0) in the right corner of the mouth, and although the stomach was everted, the fish appeared to be in excellent physical condition. A PTT-100 HR tag had been activated at 6:30 am that morning, and was therefore collecting data at the time of tagging. After the fish was brought to the side of the vessel, both the PSAT and a conventional streamer tag were attached to this fish in less than three minutes by using the same protocol as that described for WM1, and the fish swam strongly away from the vessel after release without any evident bleeding.

Opah

At 5:52 pm local time on 21 November 2002, a female opah was observed on pelagic longline gear set during the day east of the Island of Hawaii. The fish was brought to the side of the fishing vessel and a Wildlife Computers (Redmond, WA) PAT2 model tag was attached through the dorsal musculature with a Wildlife Computers titanium anchor. The tag was programmed to record the temperature and depth occupied by the fish in binned histograms, and the minimum and maximum temperatures and depths for 12-hour time periods. However, these 12-hour bins encompassed both day and night periods. The tag was programmed to be released six months after deployment. In the event of a premature release, the tag was programmed to begin transmitting stored data if it remained at the surface for longer than three days. The opah was lively and quickly dived after it was released.

Results

WM1

Release of the PSAT was expected to occur on 10 September 2002 and the tag was expected to begin transmitting data on that date, but the first transmission was not received until almost two days later. At the time of first transmission, the PSAT was 81.3 km (43.9 nmi) west-southwest of the tagging location. A total of 81.5% of the archived light level, temperature, and pressure (depth) data was recovered.

The light level, temperature, and pressure (depth) readings over time are presented in Fig. 1 (A–C) and summarized in Table 1. The first light level measurements indicated that the fish was already in relatively dark waters within one hour following its release. Light levels continued to drop to almost zero during the next ten hours and remained at that level for the next nine days (Fig. 1A). During the next seven-day surface transmission period, the tag recorded real-time day and night differences in light levels, which indicated that the light sensor was functioning properly.

Sea surface temperatures in the area where the gear was set and hauled back, varied from 25.2° to 26.7°C (D. Kerstetter, unpubl. data) and the first temperature

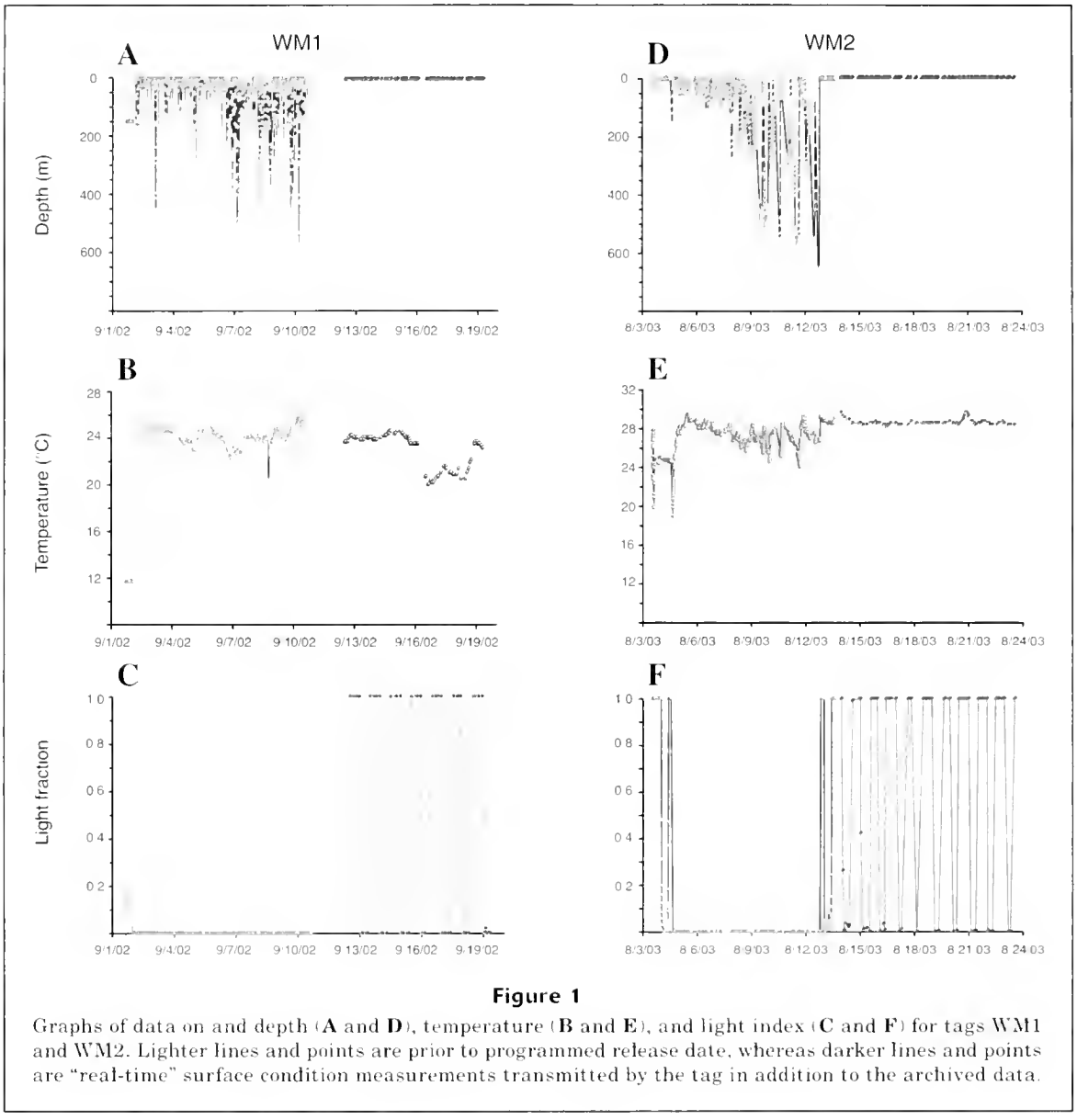

Figure 1

Graphs of data on and depth (**A** and **D**), temperature (**B** and **E**), and light index (**C** and **F**) for tags WM1 and WM2. Lighter lines and points are prior to programmed release date, whereas darker lines and points are "real-time" surface condition measurements transmitted by the tag in addition to the archived data.

recording by the PSAT (one hour after activation) was 11 C (Fig. 1B). The temperature remained fairly constant at 11°C for a period of approximately ten hours after which there was a rapid rise to 25 C. The temperature of the PSAT remained between 22.5° and 26.5 C for the next nine days (until the programmed release date), with the exception of one brief decrease to 20 C on 8 September. When the tag began transmitting on 12 September, the real-time surface temperature was 23.6°C.

The pressure data (Fig. 1C) indicated that the tag was at a depth of approximately 145 m at one hour following release. The PSAT remained at this depth for a little more than ten hours after which the data suggested that there was a rapid rise to the surface. For the next nine days, the tag reported considerable vertical movement between the surface and depths to 565 m. The tag was at the surface when it began transmitting both archived and real-time data on 12 September.

WM2

The tag reported data as expected on 13 August 2003 and transmitted 57.3% of the archived data. At the time of first transmission, the PSAT was 600.1 km (324.0 nmi) east-southeast of the tagging location. Summary depth and temperature data recorded by the PSAT are included in Table 1.

From the depth and temperature data, it appears that the fish survived for approximately 24 hours after release, at which point the light readings dropped to zero (see Fig. 1D) and remained at that level for

the next eight days. The depth record following this change in light level was marked by several discrete diving events, and depths (see Fig. 1F) ranged between the surface and over 699 m. Recorded temperatures for this period varied between 18.9° and 29.5°C, although sea surface temperatures in the area where gear was set and hauled back varied from 20.9° to 26.0°C (Kerstetter, unpubl. data). On 12 August, the light level returned to its maximum value and the tag remained at the surface for approximately one day until its scheduled release date (13 August) when it began transmitting data.

Opah

The PAT2 satellite tag was expected to pop-up 6 months after deployment, but the first transmission was received after only 34 days from a location about 330 km (178 nmi) northwest of the deployment site. All the archived binned light level, temperature, and pressure (depth) data from this period were recovered (see Table 1). This tag model collected eight temperature and depth samples during each 12-hour period, resulting in 16 values per day or 528 total values for the deployment period. The two 12-hour blocks were removed from all analyses to more accurately represent the differences in data between specimens: 1) the 12-hour block after tagging in order to allow for the recovery of the animal, and 2) the 12-hour block during which the predation event putatively occurred in order to clarify the potentially distant depth and temperature characteristics of the ingesting animal.

The measured sea surface temperature during the tagging of the opah was 25.9°C. The ranges of dive depths, temperature, and light based on minimum and maximum values over the 12-hour day and night periods showed two distinct patterns (Fig. 2). During the first period (23 days), the dive depths ranged from about 32 to 456 m (Fig. 2A). Water temperatures encountered by the tag during this period ranged from 8.0° to 25.6°C (Fig. 2B) and the light index values ranged from about 50 to 150 (Fig. 2C). During the second period (11 days), the dive depths ranged from 0 to 524 m, temperature ranged from 26.2° to 30.6°C (higher than the 24.2–24.8°C SST recorded by the tag after it was released from the fish), and the light index recorded persistently low values.

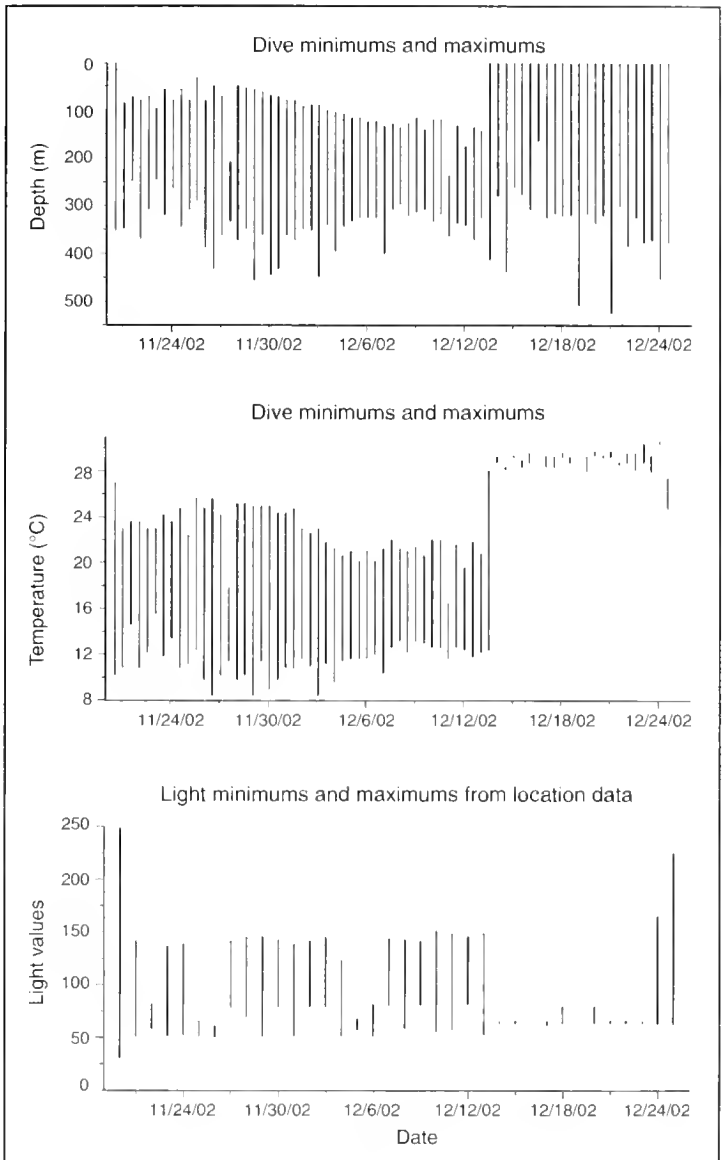

Figure 2

Graphs of depth (**A**), temperature (**B**), and light index (**C**) for the opah PAT tag from deployment until transmission.

Discussion

WM1

Our interpretation of these data is that the PSAT on WM1 was ingested by an animal scavenging the marlin carcass. The first PSAT readings for WM1, recorded about one hour after its release, indicated that the marlin was already dead or moribund by that time and was descending to the ocean floor. For the next ten hours, the tag and carcass remained at a constant depth of 145 m (the depth of the nearest sounding at the site of release, according to NOAA depth chart 13003 [1998], was approximately 160 m) and at a temperature of 11°C. The light level steadily decreased at approximately 4:30 pm, corresponding to changes in ambient light from the setting of the sun. At approximately 9:00 pm local time, there was a dramatic change in conditions when temperature rapidly rose to near 26°C and depths began to vary between the surface and 600 m.

We cannot attribute these changes to a resuscitation of the fish for three reasons. 1) The measured light levels indicated that the tag was in complete darkness for a period of ten days, even though it was at the surface during daylight hours. A malfunctioning light sensor cannot explain this observation because the tag recorded day and night differences in light levels at the surface during the seven-day transmission period after it was released from the fish. 2) After a rapid increase, the temperature remained relatively constant, between 23° and 26°C, even when the tag was at depths in excess of 300 m. Although dive behavior may be affected by location-specific conditions, previous PSAT observations of more than 20 other white marlin indicated that temperature ranges of individual dive events rarely exceed 8°C when, it is assumed, animals make foraging dives to depth (Horodysky et al., in press). 3) The PSAT recorded several dives in excess of 400 m, and previous observations of white marlin have revealed no dives in excess of 220 m (Horodysky et al., in press). Finally, the PSAT was scheduled to be released from WM1 after ten days on 10 September. Although archiving of light, temperature, and pressure data ceased on that date, the tag did not begin transmitting until 12 September.

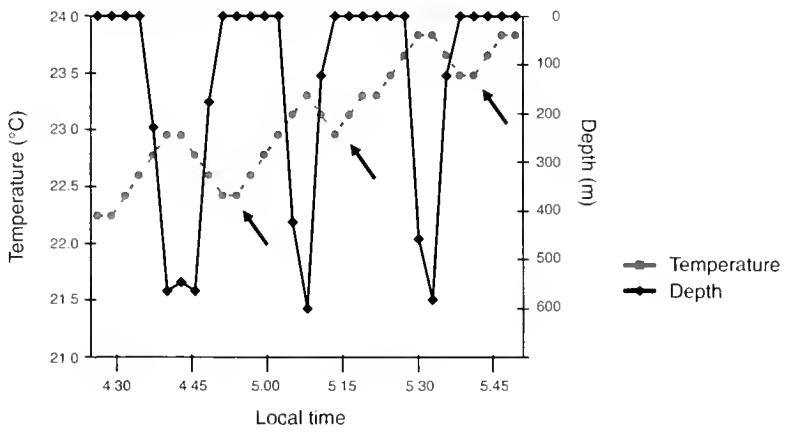

Figure 3

Delayed temperature changes recorded by tag WM1 following deep dive events on the morning of 2 September 2002. Arrows indicate the lowest temperatures recorded in association with a movement of the animal to depth; note that these temperatures were often recorded while the animal was at or near the surface and therefore represent a delay between depth and temperature.

WM2

The shallow dive patterns reported by this fish may indicate that it survived for approximately 24 hours following its release. Between 12:45 and 3:07 pm (local time), the light level fell abruptly from the maximum light level value to zero. At 3:08 pm, the temperature was 19.8°C at 166 m depth; by 4:37 pm, the temperature was above 24°C and remained above this value for the remainder of the deployment period. At 5:58 pm on 12 September, the light levels returned to maximum strength from zero—an indication that the tag had likely been egested. For the 19 hours remaining of the programmed deployment period prior to pop-off, the depth, light, and temperature data all indicated that the tag was floating at the surface.

Opah

Based on recovered data, our conjecture is that the tag was attached to the live opah for the first 23 days. Then, sometime during the 12-hour period from 2:00 pm 13 December to 2:00 am 14 December the tag was ingested. From our data, we cannot discern whether 1) the tag was detached prematurely from the opah and was floating on the surface when it was ingested, 2) an animal attacked the opah and ingested the tag incidentally, or 3) an animal ingested the tag alone. However, it is unlikely that the opah died, sank to the ocean floor, and was scavenged because the ocean floor in the area where the opah was tagged is below 2000 m. We have observed from other tags on opahs what we believe are mortalities; these occur shortly after tagging and show that the tag reaches depths in excess of 1000 m before detaching when the emergency pressure release in the tag is triggered. We did not observe depths below 600 m at any time during this record, and therefore the pressure-induced detachment mechanism on the tag was not triggered.

The ingestion hypothesis for the failure of these three tags to transmit data is supported by several lines of evidence. First, the light level readings were consistent with a tag residing in the complete darkness of an alimentary canal. Second, although temperature variations occurred during the deployment period, the delay in temperature changes during dives to depths indicates that the tags were not directly exposed to ambient water (see Fig. 3 for an example from WM1, as well as the comparisons in Table 1) and further may indicate that the scavenger was either endothermic or of large enough size to mitigate heat loss at depth.

There are several organisms that could have eaten these PSATs, whether by scavenging a carcass or attacking a moving fish. Clearly, each of these organisms was sufficiently large to ingest the tag without seriously damaging it. It is unlikely that a cetacean was responsible for any of these events because internal temperatures for odontocete whales (including killer whales, *Orcinus orca*) range between approximately 36° and 38°C (Whittow et al., 1974)—well above the range of temperatures recorded by the PSATs.

The only other natural predators of large pelagic fishes are various species of sharks. Several species of lamnid sharks maintain elevated body temperatures, including the shortfin mako (*Isurus oxyrinchus*) and the white shark (*Carcharodon carcharias*), both of which are found in the area of Georges Bank (Cramer, 2000) and the Central Pacific (Compagno, 1984). Several shortfin makos were caught by the same longline vessel during the week following each white marlin PSAT deployment (WM1: n=4, 95–189 cm FL; WM2: n=3, 94–199 cm FL) (Kerstetter, unpubl. data). The opah tag record closely resembles the relatively constant temperature noted for lamnid sharks, despite the independence of stomach temperature with ambient water for these endothermic sharks as reported by Carey et al. (1981). It is also interesting to note that although precipitous temperature fluctuations were generally absent, a rapid drop in temperature from 24° to 20°C was observed with tag WM1 on 8 September at 32.3 m depth—a fluctuation that could have resulted from another feeding event that brought cool food matter into the stomach. Similar reductions in stomach temperatures due to feeding have been noted for white sharks (McCosker, 1987). The range of temperatures recorded by each of the two white marlin tags appears rather broad for an endothermic shark, however, and although the temperature at depth was not measured, the delay in stomach temperature closely resembles the pattern of blue shark internal temperatures (*Prionace glauca*) measured in the Mid-Atlantic (Carey and Scharold, 1990).

The diving behavior recorded by the three tags also corroborates ingestion of the tags by sharks. Carey et al. (1982) reported that a tagged white shark off Long Island, New York, made frequent dives to the bottom during a 3.5-day acoustic tracking period. White sharks are known to dive to depth while scavenging whale carcasses (Dudley et al., 2000; Carey et al., 1982). A juvenile white shark also tracked by Klimley et al. (2002) spent far more extended times at depth than either white marlin tag. Although the programming of the tag on the opah precludes such fine-scale analyses of diving behavior, the available data are not inconsistent with the mako tracks in the study of Klimley et al. (2002). However, the short duration dives with frequent returns to the surface seen with the two white marlin tags most closely resemble those of blue sharks (Carey and Scharold, 1990) and were notably missing from the tracks of three shortfin makos observed by Klimley et al. (2002).

If sharks were indeed the scavenging animals, it is likely that the tags were regurgitated, rather than egested through the alimentary canal, whereupon the PSAT floated to the surface and was able to transmit the archived data. The narrow diameter of the spiral valve in the elasmobranch gastrointestinal tract would likely be too narrow to allow the undamaged passage of an object the size of a PSAT, even for a large shark. Although the available literature describing regurgitation abilities of pelagic sharks is rather limited, Hazin et al. (1994) reported that 35% of blue sharks brought aboard for scientific study had everted and protruding stomachs. Economakis and Lobel (1998) also stated their belief that regurgitation of ingested ultrasonic tags was the primary cause of lost tracks for grey reef sharks (*Carcharhinus amblyrhynchos*) on Johnston Atoll in the central Pacific Ocean.

Conclusions

The temperatures and dive depths recorded by the opah tag and both white marlin tags after apparent ingestion share similarities, yet also contain sufficient information to indicate the different identities of the ingesting organisms. The dive depths in all cases ranged from the surface to over 500 m, whereas the temperatures remained relatively constant at several degrees above the background SST, even during deep dive events. Temperature ranges alone strongly indicate sharks rather than odontocete whales were the ingesting organisms. However, limited literature on the internal stomach temperatures of the various pelagic sharks forces us to rely on telemetered diving behavior data for further species identification, which we used in the present study to suggest that blue sharks ingested the two white marlin tags (on account of the broad range of recorded temperatures) and that an endothermic shark ingested the opah tag.

It is not possible to account for all of the factors that may result in the failure of satellite tags to transmit data, but the results from these three PSATs indicated that biological activities such as predation and scavenging may play an important role. We believe that the most consistent explanation for the data transmitted by these three tags is that they were ingested by large sharks. One cannot calculate the probability that a tag could be engulfed whole without physical damage to the tag, survive for several days in the caustic environment of a digestive system, and be regurgitated with sufficient battery power to transmit data to the Argos satellites, but we suspect that the probability is not very great. We expect that a far greater number of tags may have had similar fates, that is to say, they were damaged by predation or scavenging and digestion processes or were regurgitated later in the transmission cycle, when the PSAT batteries had insufficient remaining power for successful data transmission. The failure of satellite tag to transmit data is frequently considered to be the result of internal tag malfunction or user error. However, these three data sets clearly indicate that the failure of PSATs to function may also be due to predation or scavenging events.

Acknowledgments

The authors would like to thank the Captain of the FV *Sea Pearl* and Captain Greg O'Neill of the FV *Carol Ann*, Don Hawn (University of Hawaii), who deployed the tag on the opah, Evan Howell (PIFSC) for analyses of the opah data, Andrij Horodysky (VIMS), who provided a critical review of the manuscript, Melinda Braun (Wild-

life Computers), who suggested the predation hypothesis to explain the opah data, and Lissa Werbos (Microwave Telemetry, Inc.), who independently suggested the scavenging hypothesis for the WM1 data. This research was supported in part by the National Marine Fisheries Service, the NOAA Ocean Exploration Program, and the University of Hawaii Pelagic Fisheries Research Program (PFRP).

Literature cited

Block, B. A., H. Dewar, S. B. Blackwell, T. D. Williams, E. D. Prince, C. J. Farwell, A. Boustany, S. L. H. Teo, A. Seitz, A. Walli, and D. Fudge.
2001. Migratory movements, depth preferences and thermal biology of Atlantic bluefin tuna. Science 293:1310–1314.

Boustany, A. M., S. F. Davis, P. Pyle, S. D. Anderson, B. J. LeBoeuf, and B. A. Block.
2002. Expanded niche for white sharks. Nature 415: 35–36.

Carey, F. G., J. W. Kanwisher, O. Brazier, G. Gabrielson, J. G. Casey, and H. L. Pratt.
1982. Temperature and activities of a white shark, *Carcharodon carcharias*. Copeia 1982(2):254–260.

Carey, F. G., and J. V. Scharold.
1990. Movements of blue sharks (*Prionace glauca*) in depth and course. Mar. Biol. 106:329–342.

Carey, F. G., J. M. Teal, and J. W. Kanwisher.
1981. The visceral temperatures of mackerel sharks (Lamnidae). Physiol. Zool. 54(3):334–344.

Compagno, L. J. V.
1984. Sharks of the world: an annotated and illustrated catalogue of shark species known to date. Part 1. Hexanchiformes to Lamniformes. U.N. FAO species synopsis 125, vol. 4, pt. I, 249 p. FAO, Rome.

Cramer, J.
2000. Species reported caught in the U.S. commercial pelagic longline and gillnet fisheries from 1996 to 1998. NMFS Sustainable Fisheries Division SFD-99/00-78:1–33.

Domeier, M. L., and H. Dewar.
2003. Post-release mortality rate of striped marlin (*Tetrapterus audax*) caught with recreational tackle. Mar. Freshw. Res., 54(4):435–445.

Dudley, S. F. J., M. D. Anderson-Reade, G. S. Thompson, and P. B. McMullen.
2000. Concurrent scavenging off a whale carcass by great white sharks, *Carcharodon carcharias*, and tiger sharks, *Galeocerdo cuvier*. Fish. Bull. 98:646–649.

Economakis, A. E., and P. S. Lobel.
1998. Aggregation behavior of the grey reef shark, *Carcharhinus amblyrhynchos*, at Johnston Atoll, central Pacific Ocean. Environ. Biol. Fishes 51(2):129–139.

Graves, J. E., B. E. Luckhurst, and E. D. Prince.
2002. An evaluation of pop-up satellite tags for estimating post-release survival of blue marlin (*Makaira nigricans*) from a recreational fishery. Fish. Bull. 100:134–142.

Hazin, F., R. Lessa, and M. Chammas.
1994. First observations on stomach contents of the blue shark, *Prionace glauca*, from southwestern equatorial Atlantic. Revista Brasileira de Biologia 54(2):195–198.

Horodysky, A. Z., D. W. Kerstetter, and J. E. Graves.
In press. Habitat preferences and diving behavior of white marlin (*Tetrapturus albidus*) released from the recreational rod-and-reel and commercial pelagic longline fisheries in the western North Atlantic: implications for habitat-based stock assessment models. International Commission for the Conservation of Atlantic Tunas, Coll. Vol. Sci. Pap., SCRS 2003/033.

Jolley, J. W., Jr., and E. W. Irby Jr.
1979. Survival of tagged and released Atlantic sailfish (*Istiophorus platypterus*: Istiophoridae) determined with acoustical telemetry. Bull. Mar. Sci. 29(2):155–169.

Kerstetter, D. W., B. E. Luckhurst, E. D. Prince, and J. E. Graves.
2003. Use of pop-up satellite archival tags to demonstrate survival of blue marlin (*Makaira nigricans*) released from pelagic longline gear. Fish. Bull. 101(4):939–948.

Klimley, A. P., S. C. Beavers, T. H. Curtis, and S. J. Jorgensen.
2002. Movements and swimming behavior of three species of sharks in La Jolla Canyon, California. Environ. Biol. Fishes 63:117–135.

McCosker, J. E.
1987. The white shark, *Carcharodon carcharias*, has a warm stomach. Copeia 1987(1):195–197.

NOAA (National Oceanographic and Atmospheric Administration).
1998. Atlantic coast chart 13003: Cape Sable to Cape Hattaras. National Ocean Service, Washington, D.C.

Sedberry, G. R., and J. K. Loefer.
2001. Satellite telemetry of swordfish, *Xiphias gladius*, off of the eastern United States. Mar. Biol. 139:355–360.

Whittow, G. C., I. F. G. Hampton, D. T. Matsuura, C. A. Ohata, R. M. Smith, and J. F. Allen.
1974. Body temperature of three species of whales. J. Mammol. 55(3):653–656

Survival rates for rays discarded by the bottom trawl squid fishery off the Falkland Islands

Vladimir V. Laptikhovsky

Falkland Islands Government Fisheries Department
P.O. Box 598
Stanley, FIQQ 1ZZ
Falkland Islands
E-mail address: vlaptikhovsky@fisheries.gov.fk

Waters off the Falkland Islands are subject to a specialized multispecies ray fishery and were first fished by a Korean fleet in 1989. More than twenty different rajid species have been recorded from catches around the islands, and five species accounted for 87.04% of the total catch during 1993–2002. Catches peaked in 1993 at 8523 metric tons, and specific fishing licenses—R (second season) and F (first season)—were first introduced in 1994 and in 1995, respectively (Agnew et al. 2000; Falkland Islands Government, 2002; Wakeford et al., in press).

In addition to the licensed ray fishery, rays are taken as bycatch in the bottom trawl fishery that targets the squid *Loligo gahi* and, to a lesser extent, by the trawl fishery that targets finfish. A 10% bycatch of nontarget species is allowed in both these fisheries. In 2000–2002, the reported ray bycatch of trawlers not licensed to catch rays represented between 20.2% and 31.9% of the total ray catch. However, under-reporting of elasmobranch bycatch is a common practice for trawl fisheries where sharks and rays are discarded (Stevens et al., 2000), and the reported chondrichthyan catch is only about half of the estimated actual global catch (Bonfil, 1994). The actual ray bycatch in Falkland waters may be much higher than reported because only large rays are processed (and therefore, reported) onboard trawlers. This situation makes ray fishery management in the Falkland Islands, which is already difficult because of the nature of the multispecies target, even more complicated. However, good management is of primary importance because sharks and rays appear to be particularly vulnerable to over-exploitation because of their late attainment of sexual maturity, long life span, both low fecundity and natural mortality, and close relationship between recruitment and parental stock (Stevens et al., 2000). In the Falkland trawl fisheries (which includes most trawlers licensed to catch rays), rays smaller than approximately 30 cm disk width are discarded after spending between 5 min and 4 hours in the fish bin and passing through the factory sorting line together with other catch. Some rays that have been caught, stored, and then discarded still show signs of life. In contrast to other marine organisms whose survival after being discarded has been investigated, ray survival has been studied only in Australian waters (Stobutzki et al., 2002). The aim of this study was to investigate the survival rates of discarded rays onboard trawlers in the Falkland waters.

Materials and methods

The research was conducted onboard the Falkland Islands registered trawler *Sil* (length of 78.5 m, gross tons (GRT) of 2156 t, net tons (NT) of 647 t). The vessel used a bottom trawl with a vertical opening of 5 m, horizontal opening of 30 m, and a codend mesh size of 110 mm. Trawling speed varied between 3.8 and and 4.2 kn. Fishing occurred at a depth of 80–190 m during the day and the early part of the night. The surface temperature was 8.7–9.2°C; the near bottom temperature was 6.8–7.6°C. Up to four hauls occurred daily. Each catch was released from the codend into the fish bin, which had a continuous supply of sea water, and the catch immediately began to be sorted on a conveyor belt. Squids and commercial fish were separated from the noncommercial discarded bycatch and were frozen. Of a total of 4306.2 kg of rays caught during the observed period, 67.0% were discarded and only the large rays were processed. The time taken to sort the catch was between 1 and 3 hours.

A total of 66 rays that had been discarded by fishermen were sampled randomly from the conveyor belt and put into a 40-liter (44×35×26 cm) or a 60-liter (31×76×26 cm) fish box that contained running seawater. For each animal, the species and sex was identified and total length (TL) and disk width (DW) were measured within 1 cm. Their "stamina index" was assigned according to four major categories:

A alive, flapping wings.

I immobile, but alive, reacting to irritation, spiracles beginning to work actively after being placed in seawater.

D dead; immobile, but spiracles begin to move slowly and irregularly after being placed in seawater.

DD dead; paralyzed, body stiffened and wings curved but may resume breathing after being placed in seawater.

Each ray (including those evidently dead) was kept in these boxes either until its death was evident (no breathing) or it fully recovered and began to try to swim actively. In some rays the rate of spiracle contractions was episodically recorded.

Manuscript submitted 5 June 2003
to the Scientific Editor's Office.
Manuscript approved for publication
30 June 2004 by the Scientific Editor.
Fish. Bull. 102:757–759 (2004).

Table 1

Species composition and survival of sampled rays. DW= disk width.

Species	*n*	TL, cm	DW, cm	Time spent in fish bin (min.)	Survival rate (%)
Bathyraja albomaculata	14	36–61	26–44	20–110 (mean 45)	71.4
B. brachiurops	11	15–67	9–49	31–145 (mean 72)	54.6
B. griseocauda	3	62–83	47–60	30–75 (mean 60)	0.0
B. macloviana	2	36–42	24–29	70–135	0.0
B. magellanica	5	30–44	20–30	50–125 (mean 90)	60.0
Bathyraja sp.	16	24–104	21–74	5–120 (mean 52)	75.0
Psammobatis sp.	15	29–47	18–33	30–200 (mean 98)	60.0

Table 2

Ray survival (S%), mean recovery time (RT, min.), and occurrence of the four "stamina index" categories after different periods of time (T, min.) spent in the fish bin. T=time (minutes). A=alive; I=immobile; D=presumed dead; DD=dead.

				Occurrence of categories (%)			
T	*n*	S	RT	A	I	D	DD
5–30	16	87.5	38.2	18.75	25	18.75	37.5
31–60	20	75.0	55.5	10.0	30.0	40.0	20.0
65–120	24	41.7	102.2	0	20.8	50.0	29.2
125–200	6	16.7	20[1]	0	16.7	83.3	0

[1] Only one individual (*Psammobathis* sp.).

Results

The sampled rays belonged to eight species (Table 1). Of the 66 sampled rays, a total of 21 were dead at sampling, four recovered breathing but then died, and 39 survived. Two rays recorded as category DD in the "stamina index" were released before full recovery after being held for 4 to 9 hours in running water. Even though these individuals were still breathing, both were considered dead because they still had stiffened bodies and curved wings. If they had been in such a state for a long time in their natural habitat, they almost certainly would have been consumed by scavengers or caught again by another trawler. The overall survival rate was 59.1%, female survival rate was 66.7%, and male survival rate was 56.4%.

All five rays assigned to the "stamina index" category A were sampled between 5 and 30 min (mean 20 min) after the catch was poured into the fish bin. All five individuals began immediately to breathe normally and recovered within 5 to 20 minutes.

Of a total of 18 rays assigned to the "stamina index" category I, which were sampled between 15 and 145 min (mean 55.7 min) after haul, 88.9% (n=16) survived. The breathing of these specimens at the time of sampling was usually slow, although occasionally normal. Spiracle contraction rates gradually increased from an initial rate of 5–15 bit/min to 25–28 bit/min for *B.brachiurops* specimens and to 35–38 bit/min for individuals of *B. albomaculata* and *Bathyraja* sp. Upon attaining normal breathing, they remained immobile, but fully recovered between 15 minutes and 3 hours.

The survival rate of 28 rays that were assigned to the "stamina index" category D was 39.3% (n=11). Of the remaining individuals, two rays died after 15 and 45 minutes after being placed in running seawater and 15 rays were dead at the time of sampling. The skates were sampled between 30 and 200 min (mean 84.2 min) after the haul. Those that survived took 5–80 minutes to recover normal breathing and between 15 and 315 minutes to attain full recovery.

A total of 15 rays were assigned the "stamina index" category DD. However seven of them (46.7%) survived. These individuals were sampled between 20 and 115 minutes (mean 63.9 min.) after the haul and fully recovered within 40 to 150 minutes.

Survival rate varied substantially among the eight species sampled (Table 1). In general, ray survival drastically decreased and recovery time increased with the time spent in the fish bin (Table 2). The critical duration in the fish bin appeared to be between one and two hours; only one *Psammobathis* sp. survived more than two hours in the fish bin and exhibited a surprisingly fast recovery.

Discussion

The survival of discarded rays during trawling operations in the Falkland waters is quite important. Although 65.2% of the individuals were initially assigned as dead, the actual mortality was 40.9%, although it took some rays up to six hours to recover. Survival of shallow-water shelf species such as *Psammobatis* sp., in particular, but also *B. brachiurops* and *B. magellanica,* was somewhat higher than relatively deep-water species such as *B. albomaculata*, *B. griseocauda*, and *Bathyraja* sp., which inhabit the shelf edge and upper part of the slope. This survival rate was most likely related to the greater resilience to environmental changes for shallow-water species, whose habitat is more changeable both seasonally and spatially. Male survival was lower, which is in accordance with data for rays and skates obtained in northern Australian waters (Stobutzky et al., 2002).

Recent data from a tropical prawn fishery off northern Australia showed that on average 44% of individuals of a number of ray and shark species survived a trawling event (Stobutzky et al., 2002). The Falkland ray survival rate was higher. This difference may be due either to the higher metabolic rates of tropical ray species (and therefore a higher vulnerability to asphyxia), or to an overestimation of their mortality, which was assessed immediately after individuals where landed on deck (unlike the recovery time allowed in the present study). The latter factor is more probable because in the present study 41.9% of rays initially recorded as dead (D and DD) eventually recovered.

Despite the demonstrated ability of skates to survive after being caught and stored in fish bins, their continued survival is not guaranteed once they are discarded. They may fall prey to the hundreds of albatrosses and other scavenging birds that are associated with trawlers (author's pers. obs.). The consumption of different discarded fish species and squids from trawlers in Falkland waters by seabirds, primarily by black-browed albatrosses, has been studied (Thompson, 1992), but it is not known whether rays are also taken by sea birds and to what extent. Despite the great abundance of seabirds around vessels in the Southwest Atlantic, it is likely that they consume a minor part of discards as found in Australia (Hill and Wassenberg, 2000). Most of the discarded fish probably fall to the sea floor and attract and are consumed by bottom scavengers and bottom dwellers (Laptikhovsky and Fetisov, 1999; Laptikhovsky and Arkhipkin, 2003). Consequently, even after recovering and successfully avoiding the seabirds, the discarded skates may be consumed or mortally injured by these bottom scavengers during the recovery time, which appears to be about 0.5–1.5 hours.

Acknowledgments

I would like to thank the crew of FV *Sil* for their valuable help during sampling procedures and their hospitality onboard; the Director of Fisheries, John Barton, for supporting this work; A. I. Arkhipkin and an anonimous reviewer for valuable comments; and Helen Otley (FIFD) for language editing.

Literature cited

Agnew, D. J., C. P. Nolan, J. R. Beddington, and R. Baranovski.
2000. Approaches to the assessment and management of multispecies skate and ray fisheries using the Falkland Islands fishery as an example. Can. J. Fish. Aquat. Sci. 57:429–440.

Bonfil, R.
1994. Overview of world elasmobranch fisheries. FAO Fish. Tech. Pap. 341, 119 p.

Falkland Islands Government.
2002. Fisheries Department fisheries statistics, 7, 1993–2002. Falkland Islands Government Fisheries Department, Stanley, Falkland Islands.

Hill, B. J., and T. J. Wassenberg.
2000. The probably fate of discards from prawn trawlers fishing near coral reefs. A study in northern Great Barrier Reef, Australia. Fish. Res. 48:277–286.

Laptikhovsky, V., and A. Arkhipkin .
2003. An impact of seasonal squid migrations and fishery on the feeding spectra of subantarctic notothenioids *Patagonotothen ramsayi* and *Cottoperca gobio* around the Falkland Islands. J. Appl. Ichthyol. 19:35–39.

Laptikhovsky, V., and A. Fetisov
1999. Scavenging by fish of discards from the Patagonian squid fishery. Fish. Res. 41:93–97.

Stevens, J. D., R. Bonfil, N. K. Dulvy, and P. A. Walker.
2000. The effects of fishing on sharks, rays and chimaeras (chondrichthyans), and the implication for marine ecosystems. ICES J. Mar. Sci. 57:476–494.

Stobutzki, I. C., M. J. Miller, D. S. Heales, and D. T. Brewer.
2002. Sustainability of elasmobranchs caught as bycatch in a tropical prawn (shrimp) trawl fishery. Fish. Bull. 100:800–821.

Thompson K. R.
1992. Quantitative analysis of the use of discards from squid trawlers by black-browed albatrosses *Diomedea melanophris* in the vicinity of the Falkland Islands. Ibis 134:11–21.

Wakeford, R .C., D. A. J. Middleton, D. J. Agnew, J. H. W. Pompert, and V. V. Laptikhovsky.
In press. Management of the Falkland Islands multispecies ray fishery: addressing sustainability and diversity. Can. J. Fish. Aquat. Sci.

Acknowledgment of reviewers

The editorial staff of *Fishery Bulletin* would like to acknowledge the scientists who reviewed articles published in 2003–2004. Their contributions have helped ensure the publication of quality science.

Dr. G.R. Abbe
Dr. Pere Abello
Mr. Douglas H. Adams
Dr. Vera N. Agostini
Dr. Juergen Alheit
Dr. Robert J. Allman
Mr. Michael D. Arendt
Dr. Alexander I. Arkhipkin
Dr. David A. Armstrong
Dr. Colin Attwood
Ms. Larisa Avens

Mr. M. Scott Baker Jr.
Dr. Donald M. Baltz
Dr. A. Banner
Dr. Jay Barlow
Dr. Steve Berkeley
Dr. Eric P. Bjorkstedt
Dr. James A. Bohnsack
Ms. Genevieve Briand
Dr. Richard W. Brill
Dr. Alejandro M. Brockmann
Dr. Fiona M. Brook
Dr. Elizabeth Brooks
Dr. Nancy Brown-Peterson
Dr. Jay Burnett
Mr. Michael Burton
Dr. Morgan S. Busby

Dr. Michael Canino
Dr. John K. Carlson
Dr. Milani Y. Chaloupka
Dr. David M. Checkley Jr.
Dr. Susan J. Chivers
Dr. Phillip J. Clapham
Dr. William Coles
Mr. L. Alan Collins

Dr. Craig Dahlgren
Dr. Marilyn E. Dahlheim
Dr. Louis B. Daniel III
Dr. Jana L.D. Davis
Dr. Earl G. Dawe
Dr. Edward E. DeMartini
Dr. Heidi Dewar

Dr. Robert W. Elner
Dr. Tomo Eguchi
Dr. Charles E. Epifanio
Dr. Sheryan P. Epperly

Dr. S. Frantini
Dr. Gregory L. Fulling

Ms. Moira Galbraith
Dr. Francisco J. Garcia-Rodriguez
Mr. Bert Geary
Dr. Harry J. Grier
Dr. Churchill B. Grimes
Dr. Donald R. Gunderson

Dr. Chris Habicht
Dr. Lewis J. Haldorson
Dr. J. Mark Hanson
Dr. E. Brian Hartwick
Dr. James T. Harvey
Dr. Jonathan Heifetz
Dr. Kevin T. Hill
Dr. Simeon Hill
Dr. David B. Holts

Dr. J. Jeffrey Isely

Dr. George D. Jackson
Ms. Nadine Johnston
Dr. Lindsay Joll

Dr. Michel J. Kaiser
Mr. Craig R. Kastelle
Dr. Izhar A. Khan
Dr. J. King
Dr. A. Peter Klimley
Dr. Suzanne Kohin

Dr. Thomas E. Laidig
Dr. Richard W. Langton
Ms. Amy Lapolla
Dr. Robert N. Lea
Dr. Christopher M. Legault
Dr. Steven T. Lindley
Dr. Romuald Lipcius
Dr. Kwang Ming Liu
Dr. Kai Lorenzen
Dr. Milton S. Love
Mr. Mark S. Lowry
Dr. Mark Luckenbach

Dr. R. Bruce MacFarlane
Dr. William K. Macy
Dr. Richard McBride
Dr. Susanne McDermott
Ms. Kitty Mecklenburg
Dr. David A. Milton

Dr. T.J. Minello
Mr. Karl W. Mueller
Dr. Ashley Mullen
Dr. Keith D. Mullin
Dr. Michael D. Murphy
Dr. Kate Myers

Dr. Wallace J. Nichols

Dr. Peter F. Olesiuk

Dr. Ernst Peebles
Dr. Karl M. Polivka
Dr. Kenneth H. Pollock
Dr. Allyn B. Powell

Dr. Hans-Joachim Raetz
Dr. Stephen Ralston
Mrs. Tone Rasmussen
Dr. Sherrylynn Rowe
Dr. Peter Rubec
Mr. D.E. Ruzzante

Dr. Yvonne Sadovy
Dr. Bernard Sainte-Marie
Dr. Kurt M. Schaefer
Dr. George R. Sedberry
Dr. Jeffrey Seminoff
Mr. Lawrence Settle
Dr. James B. Shaklee
Dr. Alan Sinclair
Dr. Oscar Sosa-Nishizaki
Dr. Gretchen Steiger
Dr. David L. Stein
Dr. Allan W. Stoner
Dr. D.P. Swain
Dr. Yonat Swimmer

Dr. Yuji Tanaka
Dr. Sven Thatje
Dr. A.M. Tokranov
Dr. M.J. Tremblay
Dr. Marc Trudel

Dr. Fred M. Utter

Dr. Peter Van Tamelen

Dr. Michael Vecchione

Dr. Claire M. Waluda
Mr. William Watson
Dr. George Watters
Dr. Elizabeth L. Wenner
Mr. A.J. Winship
Dr. Sabine Petra Wintner
Dr. Bernd Wursig

Dr. Orio Yamamura
Dr. Richard E. Young

Fishery Bulletin Index

Volume 102(1–4), 2004

List ot titles

Fishery Bulletin Index

Volume 102(1–4), 2004

List of authors

Fishery Bulletin Index

Volume 102(1–4), 2004

List ot subjects

This statement is required by the Act of August 12, 1970, Section 3685, Title 39, U.S. Code, showing ownership, management, and circulation of the *Fishery Bulletin*, publication number 366-370, and was filed on 02 September, 2004. The *Bulletin* is published quarterly (four issues annually) with an annual subscription price of $55.00 (sold by the Superintendent of Documents, U.S. Government Printing Office, Washington, DC 20402). The complete mailing address of the office of publication is NMFS Scientific Publications Office, NOAA, 7600 Sand Point Way NE, BIN C15700, Seattle, WA 98115. The complete mailing address of the headquarters of the publishing agency is National Marine Fisheries Service, NOAA, Department of Commerce, 1335 East-West Highway, Silver Spring, MD 20910. The name of the publisher is Willis Hobart and the managing editor is Sharyn Matriotti; their mailing address is: NMFS Scientific Publications Office, 7600 Sand Point Way NE, BIN 15700, Seattle, WA 98115. The owner is the U.S. Department of Commerce, 14th St. N.W., Washington, DC 20230; there are no bondholders, mortgages, or other security holders. The purpose, function, and nonprofit status of the organization (agency) and the exempt status for Federal income tax purposes has not changed during the preceding 12 months. The extent and nature of circulation is as follows: total number of copies (A) (average number of copies of each issue during the preceding 12 months) was 1371 and the actual number of copies of the single issue published nearest to the filing dates was 1382. Paid circulation (B) is handled by the U.S. Government Printing Office, Washington, DC 20402, and the total number printed for sales (mail subscriptions and individual sales) was 475 for the average number of copies each issue during the preceding 12 months and 475 the actual number of copies of the single issue published nearest to the filing date (C). Free distribution (D) by mail, samples, complimentary and other free copies (average number of copies each issue during the preceding 12 months) was 792 and the actual number of copies of the single issue published nearest to the filing date was 761. Free distribution outside the mail (E) by carriers or other means was 0 for both average number of copies and actual number of copies. Total free distribution (F) was 0 for both average number of copies and actual number of copies of the single issue published nearest the filing date. The total distribution (G, sum of D and B) (average number of copies each issue during the preceding 12 months) was 1267 and the actual number of copies of the single issue published nearest to the filing date was 1236. There were 65 copies (avg. annual) not distributed (H). The total (I, sum of G and H) is equal to the net press run figures shown in Item A, 1332 and 1301 copies, respectively. I certify that the statements made by me above are correct and complete: (Signed) Willis Hobart, Publisher.

Fishery Bulletin

Guidelines for contributors

Content of papers

Articles

Articles are reports of 10 to 30 pages (double spaced) that describe original research in one or a combination of the following fields of marine science: taxonomy, biology, genetics, mathematics (including modeling), statistics, engineering, economics, and ecology.

Notes

Notes are reports of 5 to 10 pages without an abstract that describe methods and results not supported by a large body of data. Although all contributions are subject to peer review, responsibility for the contents of articles and notes rests upon the authors and not upon the editor or the publisher. It is therefore important that authors consider the contents of their manuscripts carefully. Submission of an article is un-derstood to imply that the article is original and is not being considered for publication elsewhere. Manuscripts must be written in English. Authors whose native language is not English are strongly advised to have their manuscripts checked for fluency by English-speaking colleagues prior to submission.

Preparation of papers

Text

Title page should include authors' full names and mailing addresses (street address required) and the senior author's telephone, fax number, e-mail address, as well as a list of key words to describe the contents of the manuscript. **Abstract** must be less than one typed page (double spaced) and must not contain any citations. It should state the main scope of the research but emphasize the author's conclusions and relevant findings. Because abstracts are circulated by abstracting agencies, it is important that they represent the research clearly and concisely. **General text** must be typed in double-spaced format. A brief introduction should state the broad significance of the paper; the remainder of the paper should be divided into the following sections: Materials and methods, Results, Discussion (or Conclusions), and Acknowledgments. Headings within each section must be short, reflect a logical sequence, and follow the rules of multiple subdivision (i.e. there can be no subdivision without at least two subheadings). The entire text should be intelligible to interdisciplinary readers; therefore, all acronyms and abbreviations should be written out and all lesser-known technical terms should be defined the first time they are mentioned. The scientific names of species must be written out the first time they are mentioned; subsequent mention of scientific names may be abbreviated. Follow *Scientific style and format: CBE manual for authors, editors, and publishers* (6th ed.) for editorial style and the most current issue of the *American Fisheries Society's common and scientific names of fishes from the United States and Canada* for fish nomenclature. Dates should be written as follows: 11 November 1991. Measurements should be expressed in metric units, e.g. metric tons (t). The numeral one (1) should be typed as a one, not as a lower-case el (l).

Footnotes

Use footnotes to add editorial comments regarding claims made in the text and to document unpublished works or works with local circulation. Footnotes should be numbered with Arabic numerals and inserted in 10-point font at the bottom of the first page on which they are cited. Footnotes should be formatted in the same manner as citations. If a manuscript is unpublished, in the process of review, or if the information provided in the footnote has been conveyed verbally, please state this information as "unpubl. data," "manuscript in review," and "personal commun.," respectively. Authors are advised wherever possible to avoid references to nonstandard literature (unpublished literature that is difficult to obtain, such as internal reports, processed reports, administrative reports, ICES council minutes, IWC minutes or working papers, any "research" or "working" documents, laboratory reports, contract reports, and manuscripts in review). If these references are used, please indicate whether they are available from NTIS (National Technical Information Service) or from some other public depository. Footnote format: author (last name, followed by first-name initials); year; title of report or manuscript; type of report and its administrative or serial number; name and address of agency or institution where the report is filed.

Literature cited

The literature cited section comprises works that have been published and those accepted for publication (works in press) in peer-reviewed journals and books. Follow the name and year system for citation format. In the text, write "Smith and Jones (1977) reported" but if the citation takes the form of parenthetical matter, write "(Smith and Jones, 1977)." In the literature cited section, list citations alphabetically by last name of senior author: For example, Alston, 1952; Mannly, 1988; Smith, 1932; Smith, 1947; Stalinsky and Jones, 1985. Abbreviations of journals should conform to the abbreviations given in the *Serial sources for the BIOSIS previews database*. Authors are responsible for the accuracy and completeness of all citations. Literature citation format: author (last name, followed by first-name initials); year; title of report or article; abbreviated title of the journal in which the article was published, volume number, page numbers. For books, please provide publisher, city, and state.

Tables

Tables should not be excessive in size and must be cited in numerical order in the text. Headings in tables should be short but ample enough to allow the table to be intelligible on its own. All unusual symbols must be explained in the table legend. Other incidental comments may be footnoted (use italic arabic numerals for footnote markers). Use asterisks only to indicate probability in statistical data. Place table legends on the same page as the table data. We accept tables saved in most spreadsheet software programs (e.g. Microsoft Excel). Please note the following:

- Use a comma in numbers of five digits or more (e.g. 13,000 but 3000).
- Use zeros before all decimal points for values less than one (e.g. 0.31).

Figures

Figures include line illustrations, computer-generated line graphs, and photographs (or slides). They must be cited in numerical order in the text. Line illustrations are best submitted as original drawings. Computer-generated line graphs should be printed on laser-quality paper. Photographs should be submitted on glossy paper with good contrast. All figures are to be labeled with senior author's name and the number of the figure (e.g. Smith, Fig. 4). Use Helvetica or Arial font to label anatomical parts (line drawings) or variables (graphs) within figures; use Times Roman bold font to label the different sections of a figure (e.g. **A**, **B**, **C**). Figure legends should explain all symbols and abbreviations seen within the figure and should be typed in double-spaced format on a separate page at the end of the manuscript. We advise authors to peruse a recent issue of *Fishery Bulletin* for standard formats. Please note the following.

- Capitalize the first letter of the first word of axis labels.
- Do not use overly large font sizes to label axes or parts within figures.
- Do not use boldface fonts within figures.
- Do not create outline rules around graphs.
- Do not use horizontal lines through graphs.
- Do not use large font sizes to label degrees of longitude and latitude on maps.
- Indicate direction of degrees longitude and latitude on maps (e.g. 170°E).
- Avoid placing labels on a vertical plane (except on y axis).
- Avoid odd (nonstandard) patterns to mark sections of bar graphs and pie charts

Copyright law

Fishery Bulletin, a U.S. government publication, is not subject to copyright law. If an author wishes to reproduce any part of *Fishery Bulletin* in his or her work, he or she is obliged, however, to acknowledge the source of the extracted literature.

Submission of papers

Send four printed copies (one original plus three copies)—clipped, *not stapled*—to the Scientific Editor, at the address shown below. Send photocopies of figures with initial submission of manuscript. Original figures will be requested later when the manuscript has been accepted for publication. Do not send your manuscript on diskette until requested to do so.

Dr. Norman Bartoo
National Marine Fisheries Service, NOAA
8604 La Jolla Shores Drive
La Jolla, CA 92037

Once the manuscript has been accepted for publication, you will be asked to submit a software copy of your manuscript. The software copy should be submitted in WordPerfect or Word format (in Word, save as Rich Text Format). Please note that we do not accept ASCII text files. Color figures must be CMYK files.

Reprints

Copies of published articles and notes are available free of charge to the senior author (50 copies) and to his or her laboratory (50 copies). Additional copies may be purchased in lots of 100 when the author receives page proofs.